N70-34702

NASA SP-7035

NASA

Scientific and Technical Reports and Publications for 1969

A Selected Listing

CASE FILE
COPY

NATIONAL AERONAUTICS AND SPACE ADMINISTRATION

PUBLISHED BY:
UNITED STATES GOVERNMENT
NATIONAL AERONAUTICS AND SPACE ADMINISTRATION
OFFICE OF TECHNOLOGY UTILIZATION
SCIENTIFIC AND TECHNICAL INFORMATION DIVISION

NASA Scientific and Technical Reports and Publications for 1969—A Selected Listing (NASA SP-7035) is prepared by the NASA Scientific and Technical Information Facility operated for the National Aeronautics and Space Administration by Informatics Tisco, Inc.

CASE FILE
COPY

ERRATA

NASA SP-7035

NASA

SCIENTIFIC AND TECHNICAL REPORTS
AND PUBLICATIONS FOR 1969

A Selected Listing

May 1970

Page I-417: The accession numbers listed on this page of the Accession Number Index are in error. All numbers should have an "A" prefix rather than the "N" prefix. For example, N69-27400 should be listed as A69-27400. The other data are correct.

Issued: November 1970

NASA SP-7035

NASA Scientific and Technical Reports and Publications for 1969

A Selected Listing

Scientific and Technical Information Division
OFFICE OF TECHNOLOGY UTILIZATION
NATIONAL AERONAUTICS AND SPACE ADMINISTRATION
Washington, D.C.

MAY 1970

For sale by the Superintendent of Documents, U.S. Government Printing Office, Washington, D.C. 20402 Price $7.50

INTRODUCTION

WHAT NASA SCIENTIFIC AND TECHNICAL REPORTS AND PUBLICATIONS FOR 1969 IS

NASA Scientific and Technical Reports and Publications for 1969, a Selected Listing, (NASA SP-7035) combines in a single publication a selective listing of NASA reports which were printed and widely distributed and announced in *Scientific and Technical Aerospace Reports (STAR)* and significant articles which were announced in *International Aerospace Abstracts (IAA).* The documents listed from *STAR,* which abstracts report literature for the aerospace sciences, include the following NASA report series: Special Publications (NASA SP-), Technical Reports (NASA TR R-), Technical Notes (NASA TN D-), Technical Memorandums (NASA TM X-), Technical Translations (NASA TT F-), and Contractor Reports (NASA CR-). The documents listed from *IAA,* which abstracts journal literature for the aerospace sciences, include those which carry an author affiliation from NASA Headquarters or a NASA Center, or which were basic documents for a conference or symposium in which a NASA-authored paper was included. NASA-generated reports and articles announced in *STAR* or *IAA* during 1969 but omitted from this volume can be located through the annual indexes to *STAR* and *IAA.*

HOW NASA SCIENTIFIC AND TECHNICAL REPORTS AND PUBLICATIONS FOR 1969 IS ORGANIZED

The arrangement of abstracts in this publication is similar to that of *STAR* and *IAA,* i.e., by NASA subject categories. In each subject category, *IAA* references are arranged in accession number order followed by *STAR* references also in accession number order. The first section contains the bibliographic citations and abstracts; the second section contains five indexes (subject, personal author, corporate source, report/accession number, and accession/report number), each arranged with the "A" accessions before the "N" accessions.

STAR Entries

AVAILABILITY OF DOCUMENTS

Documents listed are available on initial distribution without charge to:

1. NASA Offices, Centers, contractors, subcontractors, grantees, and consultants:
2. Other U.S. Government agencies and their contractors:
3. Libraries in the United States that have arrangements with NASA to maintain collections of NASA documents for public use;
4. Other organizations in the United States having a need for NASA documents in work related to the aerospace program; and
5. Foreign government or academic organizations that have established appropriate reciprocal arrangements with NASA.

NASA documents that have been microfiched(1) (identified by the # sign in the citation) are available on microfiche without charge at any time to the same organizations, described above, that are eligible to receive full-sized copy on initial distribution.

HOW TO OBTAIN MICROFICHE

If you are registered with NASA and eligible to receive reports as described above, send the completed *Document Request* (Facility Form 492) to:

NASA Scientific and Technical Information Facility
P.O. Box 33
College Park, Maryland 20740

If you are not registered with NASA and wish to receive information concerning registration, request *Registration Form—Technical Publications* (Facility Form 713) from the NASA Scientific and Technical Information Facility at the address given above. Others may obtain microfiche copies by purchase as described in the following paragraphs.

(1) A microfiche is a transparent sheet of film, 105 × 148 mm in size, containing up to 72 pages of information reduced to micro images (not to exceed 20:1 reduction).

PUBLIC SALE OF DOCUMENTS

All documents listed with a Clearinghouse for Federal Scientific and Technical Information (CFSTI) availability statement or a Superintendent of Documents, U.S. Government Printing Office (GPO) availability statement in the citation may be purchased from the U.S. Government sales agency cited, at the address given below.

Publications with a CFSTI availability statement are sold in hard copy and in microfiche copy by:

Clearinghouse for Federal Scientific and Technical Information
(CFSTI)
Springfield, Virginia 22151

The following unit price has been established by CFSTI: $3 for hard copy, $0.65 for microfiche.

Publications with a GPO availability statement in the citation are sold in hard copy by:

Superintendent of Documents, U.S. Government Printing Office
(GPO)
Washington, D.C. 20402.

NASA documents available from GPO are also available from CFSTI at the GPO price given in the citation.

COSATI SUBJECT CATEGORY CODE

In the citation of each document is a code, e.g., CSCL 25A, that indicates the subject category assigned to it from the *COSATI Subject Category List* (first edition, December 1964) published by the Committee on Scientific and Technical Information of the Federal Council for Science and Technology.

IAA Entries

All cited documents are available from the AIAA Technical INFORMATION Service as follows: Paper copies are available at $3.00 per document up to a maximum of 20 pages. The charge for each additional page is $0.25. Microfiche are available at the rate of $0.50 per microfiche for documents identified by the symbol # following the accession number. A number of publications, because of their special characteristics, are available only for reference in the AIAA Technical Information Service Library. Minimum air-mail postage to foreign countries is $1.00.

Please refer to the accession number, e.g., A69-13193, when requesting documents. Address all inquiries and requests to:

Technical Information Service
American Institute of Aeronautics and Astronautics, Inc.
750 Third Avenue, New York, N.Y. 10017

INDEXING VOCABULARY

The Preliminary Edition of the *NASA Thesaurus* (December 1967) (NASA SP-7030) is used as the authority for the indexing vocabulary that appears in the subject index. The *NASA Thesaurus* should be consulted in examining the current indexing vocabulary, including associated cross-reference structure. Only the subject terms that have been selected to describe the documents abstracted in this publication appear in the subject index. Copies of the *NASA Thesaurus* may be obtained from the Clearinghouse for Federal Scientific and Technical Information or the Superintendent of Documents, U.S. Government Printing Office at $8.50 for the three-volume set.

TABLE OF CONTENTS

Subject Categories

Abstracts in the journal are grouped under the following categories:

page:

01 AERODYNAMICS
Includes aerodynamics of bodies, combinations, internal flow in ducts and turbomachinery; wings, rotors, and control surfaces. For applications see: 02 Aircraft and 31 Space Vehicles. For related information see also: 12 Fluid Mechanics; and 33 Thermodynamics and Combustion. 1

02 AIRCRAFT
Includes fixed-wing airplanes, helicopters, gliders, balloons, ornithopters, etc; and specific types of complete aircraft (e.g., ground effect machines, STOL, and VTOL); flight tests; operating problems (e.g., sonic boom); safety and safety devices; economics; and stability and control. For basic research see: 01 Aerodynamics. For related information see also: 31 Space Vehicles; and 32 Structural Mechanics. 25

03 AUXILIARY SYSTEMS
Includes fuel cells, energy conversion cells, and solar cells; auxiliary gas turbines; hydraulic, pneumatic and electrical systems; actuators; and inverters. For related information see also: 09 Electronic Equipment; 22 Nuclear Engineering; and 28 Propulsion Systems. 41

04 BIOSCIENCES
Includes aerospace medicine, exobiology, radiation effects on biological systems; physiological and psychological factors. For related information see also: 05 Biotechnology. 65

05 BIOTECHNOLOGY
Includes life support systems, human engineering; protective clothing and equipment; crew training and evaluation, and piloting. For related information see also: 04 Biosciences. 81

06 CHEMISTRY
Includes chemical analysis and identification (e.g., spectroscopy). For applications see: 17 Materials, Metallic; 18 Materials, Nonmetallic; and 27 Propellants. 99

07 COMMUNICATIONS
Includes communications equipment and techniques; noise; radio and communications blackout; modulation telemetry; tracking radar and optical observation; and wave propagation. For basic research see: 23 Physics, General; and 21 Navigation. 107

08 COMPUTERS
Includes computer operation and programming; and data processing. For basic research see: 19 Mathematics. 129

09 ELECTRONIC EQUIPMENT
Includes electronic test equipment and maintainability; component parts, e.g., electron tubes, tunnel diodes, transistors; integrated circuitry; microminiaturization. For basic research see: 10 Electronics. For related information see also: 07 Communications and 21 Navigation. 139

10 ELECTRONICS
Includes circuit theory; and feedback and control theory. For applications see: 09 Electronic Equipment. For related information see: Specific Physics Categories. 153

11 FACILITIES, RESEARCH AND SUPPORT
Includes airports; lunar and planetary bases including associated vehicles; ground support systems; related logistics; simulators; test facilities (e.g., rocket engine test stands, shock tubes, and wind tunnels); test ranges; and tracking stations. 159

12 FLUID MECHANICS
Includes boundary-layer flow; compressible flow; gas dynamics; hydrodynamics; and turbulence. For related information see also: 01 Aerodynamics; and 33 Thermodynamics and Combustion. 175

13 GEOPHYSICS
Includes aeronomy; upper and lower atmosphere studies; oceanography; cartography; and geodesy. For related information see also: 20 Meteorology; 29 Space Radiation; and 30 Space Sciences. 195

14 INSTRUMENTATION AND PHOTOGRAPHY
Includes design, installation, and testing of instrumentation systems; gyroscopes; measuring instruments and gages; recorders; transducers; aerial photography; and telescopes and cameras. 217

15 MACHINE ELEMENTS AND PROCESSES
Includes bearings, seals, pumps, and other mechanical equipment; lubrication, friction, and wear; manufacturing processes and quality control; reliability; drafting; and materials fabrication, handling, and inspection. 235

16 MASERS
Includes applications of masers and lasers. For basic research see: 26 Physics, Solid-State. 259

17 MATERIALS, METALLIC
Includes cermets; corrosion; physical and mechanical properties of materials; metallurgy; and applications as structural materials. For basic research see : 06 Chemistry. For related information see also: 18 Materials, Nonmetallic; and 32 Structural Mechanics. 261

18 MATERIALS, NONMETALLIC
Includes corrosion; physical and mechanical properties of materials (e.g., plastics); and elastomers, hydraulic fluids, etc. For basic research see: 06 Chemistry. For related information see also: 17 Materials, Metallic; 27 Propellants; and 32 Structural Mechanics. 275

19 MATHEMATICS
Includes calculation methods and theory; and numerical analysis. For applications see: 08 Computers. 283

20 METEOROLOGY
Includes climatology; weather forecasting; and visibility studies. For related information see also: 13 Geophysics; and 30 Space Sciences. 289

21 NAVIGATION
Includes guidance; autopilots; star and planet tracking; inertial platforms; and air traffic control. For related information see also: 07 Communications. 295

22 NUCLEAR ENGINEERING
Includes nuclear reactors and nuclear heat sources used for propulsion and auxiliary power. For basic research see: 24 Physics, Atomic, Molecular, and Nuclear. For related information see also: 03 Auxiliary Systems; and 28 Propulsion Systems. 307

23 PHYSICS, GENERAL
Includes acoustics, cryogenics, mechanics, and optics. For astrophysics see: 30 Space Sciences. For geophysics and related information see also: 13 Geophysics, 20 Meteorology, and 29 Space Radiation. 315

24 PHYSICS, ATOMIC, MOLECULAR, AND NUCLEAR
Includes atomic, molecular and nuclear physics. For applications see: 22 Nuclear Engineering. For related information see also: 29 Space Radiation. 321

25 PHYSICS, PLASMA
Includes magnetohydrodynamics. For applications see: 28 Propulsion Systems. 333

26 PHYSICS, SOLID-STATE
Includes semiconductor theory; and superconductivity. For applications see: 16 Masers. For related information see also: 10 Electronics. 343

27 PROPELLANTS
Includes fuels; igniters; and oxidizers. For basic research see: 06 Chemistry; and 33 Thermodynamics and Combustion. For related information see also: 28 Propulsion Systems. 351

28 PROPULSION SYSTEMS
Includes air breathing, electric, liquid, solid, and magnetohydrodynamic propulsion. For nuclear propulsion see: 22 Nuclear Engineering. For basic research see: 23 Physics, General; and 33 Thermodynamics and Combustion. For applications see: 31 Space Vehicles. For related information see also: 27 Propellants. 355

29 SPACE RADIATION
Includes cosmic radiation; solar flares; solar radiation; and Van Allen radiation belts. For related information see also: 13 Geophysics; and 24 Physics, Atomic, Molecular, and Nuclear. 371

30 SPACE SCIENCES
Includes astronomy and astrophysics; cosmology; lunar and planetary flight and exploration; and theoretical analysis of orbits and trajectories. For related information see also: 11 Facilities, Research and Support; and 31 Space Vehicles. 389

31 SPACE VEHICLES

Includes launch vehicles; manned space capsules; clustered and multistage rockets; satellites; sounding rockets and probes; and operating problems. For basic research see: 30 Space Sciences. For related information see also: 28 Propulsion Systems; and 32 Structural Mechanics. 443

32 STRUCTURAL MECHANICS

Includes structural element design and weight analysis; fatigue; thermal stress; impact phenomena; vibration; flutter; inflatable structures; and structural tests. For related information see also: 17 Materials, Metallic; and 18 Materials, Nonmetallic. 461

33 THERMODYNAMICS AND COMBUSTION

Includes ablation, cooling, heating, heat transfer, thermal balance, and other thermal effects; and combustion theory. For related information see also: 12 Fluid Mechanics; and 27 Propellants. 483

34 GENERAL

Includes reports of a broad nature related to industrial applications and technology, and to basic research; defense aspects; law and related legal matters; and legislative hearings and documents. 501

SUBJECT INDEX I-1

PERSONAL AUTHOR INDEX I-275

CORPORATE SOURCE INDEX I-377

REPORT/ACCESSION NUMBER INDEX I-403

ACCESSION/REPORT NUMBER INDEX I-413

TYPICAL CITATION AND ABSTRACT FROM IAA

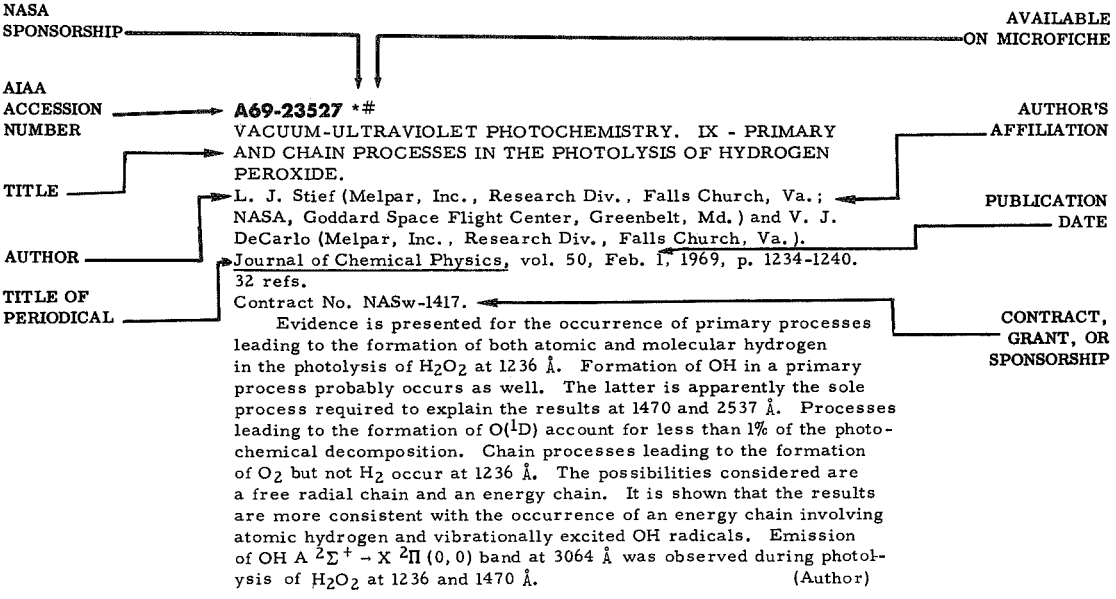

TYPICAL CITATION AND ABSTRACT FROM STAR

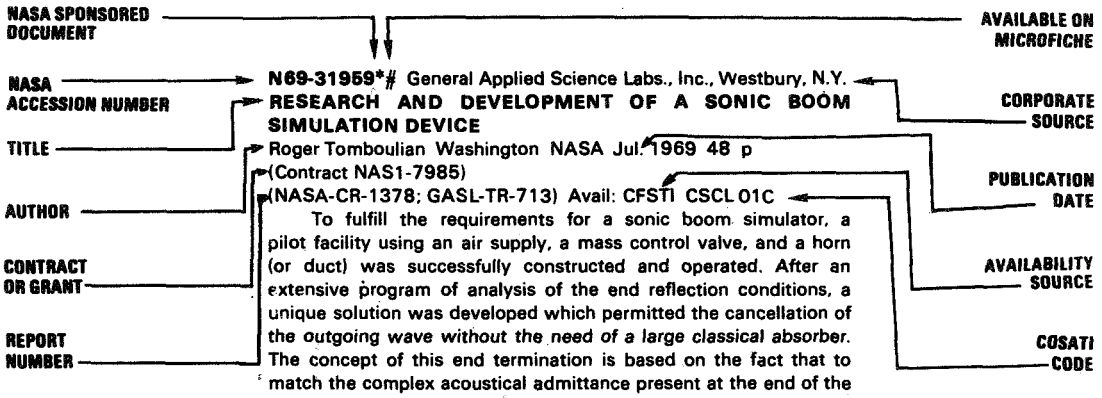

NASA Scientific and Technical Reports and Publications for 1969

a selected listing

MAY 1970

01

AERODYNAMICS

Includes aerodynamics of bodies, combinations, internal flow in ducts and turbomachinery; wings, rotors, and control surfaces. For applications see: 02 Aircraft and 31 Space Vehicles. For related information see also: 12 Fluid Mechanics; and 33 Thermodynamics and Combustion.

A69-12520 *#
HYPERSONIC VISCOUS INTERACTION ON SLENDER CONES.
C. C. Horstman and M. I. Kussoy (NASA, Ames Research Center, Moffett Field, Calif.).
(American Institute of Aeronautics and Astronautics, Aerospace Sciences Meeting, 6th, New York, N. Y., Jan. 22-24, 1968, Paper 68-2.)
AIAA Journal, vol. 6, Dec. 1968, p. 2364-2371. 34 refs.

Results of an experimental investigation conducted to obtain surface measurements and flowfield properties about slender cones in the viscous interaction regime. The measurements, obtained for the most part on a 3° half-angle cone in helium at Mach 41, included surface pressures and heat transfer, shock-wave shapes, and detailed shock-layer surveys (to obtain velocity and density profiles) at angles of attack up to 15°. Surface pressures were successfully correlated with published data for a wide range of test conditions by means of a strong interaction parameter. At angle of attack the pressure and heat-transfer distribution on the sharp 3° cone displayed a blunted-cone type of overexpansion on the windward side. Measured density and pitot pressure profiles through the shock layer indicated pressures were below the Rankine-Hugoniot values over the entire model length at zero and 10° angle of attack on the leeward side. At zero angle of attack, measured velocity profiles deviated from the usual calculated laminar boundary-layer profiles. Surface heat-transfer measurements at zero angle of attack fell significantly below both weak and strong interaction predictions but were successfully correlated with previous published merged flow results. (Author)

A69-12522 *#
FLOW PHENOMENA AND SEPARATION OVER DELTA WINGS WITH TRAILING-EDGE FLAPS AT MACH 6.
Allen H. Whitehead, Jr. and J. Wayne Keyes (NASA, Langley Research Center, Hampton, Va.).
(American Institute of Aeronautics and Astronautics, Aerospace Sciences Meeting, 6th, New York, N. Y., Jan. 22-24, 1968, Paper 68-97.)
AIAA Journal, vol. 6, Dec. 1968, p. 2380-2387. 26 refs.

Results of an experimental investigation conducted to obtain surface measurements and flowfield properties about slender cones in the viscous interaction regime. The measurements, obtained for the most part on a 3° half-angle cone in helium at Mach 41, included surface pressures and heat transfer, shock-wave shapes, and detailed shock-layer surveys (to obtain velocity and density profiles) at angles of attack up to 15°. Surface pressures were successfully correlated with published data for a wide range of test conditions by means of a strong interaction parameter. At angle of attack the pressure and heat-transfer distribution on the sharp 3° cone displayed a blunted-cone type of overexpansion on the windward side. Measured density and pitot pressure profiles through the shock layer indicated pressures were below the Rankine-Hugoniot values over the entire model length at zero and 10° angle of attack on the leeward side. At zero angle of attack, measured velocity profiles deviated from the usual calculated laminar boundary-layer profiles. Surface heat-transfer measurements at zero angle of attack fell significantly below both weak and strong interaction predictions but were successfully correlated with previous published merged flow results. (Author)

A69-14714 *#
AERODYNAMICS OF BODIES OF REVOLUTION IN CONING MOTION.
Murray Tobak, Lewis B. Schiff (NASA, Ames Research Center, Moffett Field, Calif.), and Victor L. Peterson (NASA, Ames Research Center, Hypersonic Aerodynamics Branch, Moffett Field, Calif.).
(American Institute of Aeronautics and Astronautics, Aerospace Sciences Meeting, 6th, New York, N. Y., Jan. 22-24, 1968, Paper 68-20.)
AIAA Journal, vol. 7, Jan. 1969, p. 95-99. 9 refs.

Nonlinear functional analysis is used to show that the moments for an arbitrary motion about the center of gravity may be compounded of the sum of contributions from four simple motions, three of which are standard. The fourth, lunar motion, is investigated experimentally with an apparatus designed to reproduce the lunar motion in a wind tunnel. Photographs of the vortices on the leeward side of the body reveal that they become asymmetrically disposed with respect to the angle-of-attack plane during lunar motion. This makes them a potent source of "Magnus-type" moment. The contribution of the vortices to Magnus moment appears to be proportional to their contribution to pitching moment during steady planar motion multiplied by the turning rate of the angle-of-attack plane during lunar motion. The moment is a potential causative agent in the occurrence of large-amplitude circular limit motions. (Author)

A69-18052 *#
SOME TOPICS IN HYPERSONIC BODY SHAPING.
E. S. Love (NASA, Langley Research Center, Aero-Physics Div., Hampton, Va.), W. C. Woods, G. C. Ashby, Jr. (NASA, Langley Research Center, Aero-Physics Div., Hypersonic Fluid Mechanics Branch, Hampton, Va.), and R. W. Rainey (NASA, Langley Research Center, Aero-Physics Div., Hypersonic Aerodynamics

Branch, Hampton, Va.).
American Institute of Aeronautics and Astronautics, Aerospace Sciences Meeting, 7th, New York, N.Y., Jan. 20-22, 1969, Paper 69-181. 19 p. 36 refs.
Members, $1.00; nonmembers, $1.50.

Some topics related to hypersonic body shaping for minimum drag and improved performance are presented. Implications of the most frequently assumed pressure laws are reviewed from the view of practical flight regimes, and solutions expressed in exponential residuals are presented for inviscid minimum drag power-law bodies (simple and complex) for a wide range of fineness ratios. Experimental results from Mach 6 to 20 are presented for a series of trapezoidal bodies; the cross-section of the body giving best lift-drag ratio differs from that indicated in earlier work. A simple "$\sin^2$-deficiency method" is presented for predicting pressures on blunt shapes; the method appears to yield results comparable to more elaborate methods requiring machine computation. (Author)

A69-18161 *#
A NEW METHOD FOR EXTRACTING AERODYNAMIC COEFFICIENT FROM FREE-FLIGHT DATA.
Gary T. Chapman and Donn B. Kirk (NASA, Ames Research Center, Moffett Field, Calif.).
American Institute of Aeronautics and Astronautics, Aerospace Sciences Meeting, 7th, New York, N.Y., Jan. 20-22, 1969, Paper 69-134. 7 p. 7 refs.
Members, $1.00; nonmembers, $1.50.

Description of a method for obtaining aerodynamic coefficients from the observed motion of a body in flight. The method eliminates the need for closed-form solutions by employing numerical solutions to the equations of motion. This makes possible a far more general treatment. A least-squares technique employing differential corrections must be used; for this purpose, partial derivatives of each dependent variable with respect to each unknown coefficient, including all initial conditions, must be known accurately at every data station. Application of the method of parametric differentiation yields the required accuracy in these partial derivatives, and rapid convergence of the solution is usually obtained. The method is applied to four examples of varying complexity, and the diversity of its application is demonstrated. M.G.

A69-18167 *#
ON THE SINGULARITY METHOD OF SUBSONIC LIFTING-SURFACE THEORY.
Siegfried Wagner (NASA, Ames Research Center, Moffett Field, Calif.).
American Institute of Aeronautics and Astronautics, Aerospace Sciences Meeting, 7th, New York, N.Y., Jan. 20-22, 1969, Paper 69-37. 14 p. 16 refs.
Members, $1.00; nonmembers, $1.50.

Extension of the lifting-surface theory at steady subsonic flow [due to Multhopp (1955) and Truckenbrodt (1953)] to the leading edge of wings. An optimal number of integration stations for spanwise integration is calculated. The positions of these integration stations are not identical with the spanwise distribution of the control points where the tangential flow condition is fulfilled. The new integration procedure, along with an accurate treatment of the singularities, allows an improved prediction of the loading of wings with complicated planforms such as double-delta and variable-sweep wings. A method for calculating the spanwise distribution of the leading-edge-suction force and of the induced drag is developed and is applied to the computation of the loading of a variable-sweep wing. A comparison with measurements and existing theories shows that the spanwise distribution of lift, pitching moment, induced drag, and leading-edge-suction force can be computed more accurately by the present method. M.G.

A69-18176 *#
THEORETICAL AND EXPERIMENTAL STUDY OF SUPERSONIC STEADY FLOW AROUND INCLINED BODIES OF REVOLUTION.
John V. Rakich and Joseph W. Cleary (NASA, Ames Research Center, Moffett Field, Calif.).
American Institute of Aeronautics and Astronautics, Aerospace Sciences Meeting, 7th, New York, N.Y., Jan. 20-22, 1969, Paper 69-187. 10 p. 20 refs.
Members, $1.00; nonmembers, $1.50.

Description of a three-dimensional method of characteristics and critical assessment of numerical results by comparison with the results of hypersonic wind-tunnel experiments. Calculations for a 15° half-angle sphere-cone have been performed for angles of attack up to $\alpha = 20°$, and have been carried downstream 45 nose radii for $\alpha = 10°$. Comparisons with pointed-cone calculations show that effects of bluntness persist at this distance. Pitot-pressure distributions in the flowfield are in good agreement with experiment except on the leeward side of the body far from the nose, where low-energy, viscous fluid accumulates. Oil-film studies of surface streamlines demonstrate the large viscous crossflow in the boundary layer. Theoretical upwash angles around a Sears-Haack body are compared with classical slender-body theory, indicating nonlinearities due to Mach number, which may reduce the interference lift of wing-body combinations. (Author)

A69-18184 *#
CONE DRAG IN RAREFIED HYPERSONIC FLOW.
M. I. Kussoy and C. C. Horstman (NASA, Ames Research Center, Moffett Field, Calif.).
American Institute of Aeronautics and Astronautics, Aerospace Sciences Meeting, 7th, New York, N.Y., Jan. 20-22, 1969, Paper 69-140. 7 p. 17 refs.
Members, $1.00; nonmembers, $1.50.

Experimental drag coefficients for spheres and sharp cones in rarefied hypersonic air flow are presented. These data were obtained using a free-flight technique in a shock tunnel. The test conditions were: (1) Mach number from 15 to 24.3, (2) Reynolds number per inch from 480 to 2730, (3) mean free path from 0.016 to 0.127 in., and (4) cone semivertex angles from 2.5 to 25°. When compared with hypersonic viscous interaction and near-free molecule theories (both computed for the present range of test conditions), the cone drag is over-estimated. However, applying the viscous-interaction parameter of Mirels and Ellinwood, a correlation of cone drag for each cone angle in terms of Mach number and free-stream Reynolds number is developed. A correlation of average local skin-friction coefficient (deduced from the present data) for individual cone angles is also developed in terms of Mach number and free-stream Reynolds number. The ratio of skin friction to heat-transfer coefficient is shown to be a function only of cone angle. (Author)

A69-21972 *#
NEW FEATURES OF THE METHOD OF INTEGRAL RELATIONS FOR THE BLUNT BODY PROBLEM.
Jerry C. South, Jr. (NASA, Langley Research Center, Applied Mechanics Branch, Hampton, Va.).
AIAA Journal, vol. 7, Feb. 1969, p. 369-371. 5 refs.

Description of two new features of the one-strip method of integral relations in its application to the inviscid, supersonic blunt-body problem. The features are: (1) the adaptation of the method to blunt power-law bodies with infinite curvature at the nose, and (2) the use of intermediate parameter perturbations to aid in the construction of highly unstable saddle-point solutions. The present study considers the adaptation of the simplest (one-strip) approximation of the method to hypersonic, ideal-gas flow over axisymmetric power-law bodies. B.H.

A69-22495 *#
PROGRAMS FOR COMPUTATION OF VELOCITIES AND STREAMLINES ON A BLADE-TO-BLADE SURFACE OF A TURBOMACHINE.
Theodore Katsanis and W. D. McNally (NASA, Lewis Research Center, Cleveland, Ohio).
American Society of Mechanical Engineers, Annual Gas Turbine Conference and Products Show, 14th, Cleveland, Ohio, Mar. 9-13, 1969, Paper 69-GT-48. 8 p. 13 refs.
Members, $0.75; nonmembers, $1.50.

Description of Fortran programs that give the solution to the two-dimensional, subsonic, nonviscous flow problem on a blade-to-

blade surface of revolution of a turbine. Flow may be axial, radial, or mixed. There may be a change in stream channel thickness in the through-flow direction. Either single, tandem, or slotted blades may be handled as well as blade rows with splitter vanes. Also, small regions may be magnified to give more detail where desired, such as around a leading or trailing edge or through a slot. The method is based on a finite-difference solution of the stream-function equations. Numerical examples are shown to illustrate the type of blades which can be analyzed, and to show results which can be obtained. Results are compared with experimental data. (Author)

A69-22521 *#
SOME MEASUREMENT PROBLEMS ENCOUNTERED WHEN DETER MINING THE PERFORMANCE OF CERTAIN TURBINE STATOR BLADES FROM TOTAL PRESSURE SURVEYS.
Thomas P. Moffitt, Herman W. Prust, Jr., and Harold J. Schum (NASA, Lewis Research Center, Cleveland, Ohio).
American Society of Mechanical Engineers, Annual Gas Turbine Conference and Products Show, 14th, Cleveland, Ohio, Mar. 9-13, 1969, Paper 69-GT-103. 8 p.
Members, $0.75; nonmembers, $1.50.

Discussion of the problems encountered in determining turbine stator blade performance from total-pressure surveys downstream of the blade row. The stator blades were suitable for turbine cooling and incorporated thick trailing edges having a large included wedge angle between the suction and pressure surfaces. Blade performance was rated in terms of kinetic energy loss coefficients, which relate the frictional and mixing losses to the ideal kinetic energy that could be developed at a given overall pressure ratio. The loss coefficients were calculated from the results of total-pressure surveys and flow conditions as determined by measurements at the inlet and outlet of the blade row. For the type of blading involved, it was determined that these loss coefficients were sensitive to the size of support stem of the total-pressure probe used and the size and axial location of the probe sensing element. The effect of these variables on the results obtained are presented, and desirable manners of taking survey data for this type of blading are discussed. (Author)

A69-25378 *#
A CLOSED-FORM SOLUTION TO OBLIQUE SHOCK-WAVE PROPERTIES.
Vincent R. Mascitti (NASA, Langley Research Center, Advanced Configuration Group, Hampton, Va.).
Journal of Aircraft, vol. 6, Jan.-Feb. 1969, p. 66.

Development of a method for direct computation of oblique shock-wave properties with freestream Mach numbers and flow-deflection angle as the independent variables. It is shown that this problem has an explicit solution, which is presented in general terms. F.R.L.

A69-26762 *#
REINGESTION CHARACTERISTICS AND INLET FLOW DISTORTION OF V/STOL LIFT-ENGINE FIGHTER CONFIGURATIONS.
Jerry V. Kirk and Jerry P. Barrack (NASA, Ames Research Center, Full-Scale and Systems Research Div., Moffett Field, Calif.).
(American Institute of Aeronautics and Astronautics, Aerospace Sciences Meeting, 6th, New York, N.Y., Jan. 22-24, 1968, Paper 68-78.)
Journal of Aircraft, vol. 6, Mar.-Apr. 1969, p. 116-122.

Study of short-path reingestion of exhaust gas and inlet-flow distortion in V/STOL lift engines. Reingestion during hover was studied on a static-test facility and inlet-flow distortion was studied in a 40 x 80 ft wind tunnel. Factors affecting exhaust-gas reingestion, engine surge, and hover performance are presented and discussed. Inlet-flow distortion and total pressure recovery during transition from hover to wing-supported flight are shown for two types of lift-engine configurations. The effects of an inlet vane and engine tilt are shown for a range of flight speeds, power settings, and aircraft angles of attack. R.B.S.

A69-31881 *#
UNUSUAL BOUNDARY-LAYER TRANSITION RESULTS ON CONES IN HYPERSONIC FLOW.
George G. Mateer and Howard K. Larson (NASA, Ames Research Center, Moffett Field, Calif.).
(American Institute of Aeronautics and Astronautics, Aerospace Sciences Meeting, 6th, New York, N.Y., Jan. 22-24, 1968, Paper 68-40.)
AIAA Journal, vol. 7, Apr. 1969, p. 660-664. 16 refs.

Nonablating, 5° and 15° half-angle cones were tested as part of a program to study the effects of subliming ablation on boundary-layer transition. The results of wind-tunnel tests showed that the measured transition Reynolds numbers (1) were independent of the local unit Reynolds number, (2) were equal to those usually observed or higher, and (3) decreased as the boundary-layer edge Mach number increased from 5 to 6.8. The first two of these unusual results may be due in part to a unique feature of the wind tunnel: a low-molecular weight helium-air boundary layer. Data are presented which show a significant effect of wind-tunnel boundary-layer molecular weight on model boundary-layer transition. In addition, a new correlation of transition results for cones is presented which shows that the dependence of transition on boundary-layer edge Mach number extends over a range of edge Mach numbers from 3 to 8. These tests were conducted at nominally constant values of free-stream Mach number (7.4), wall-to-total temperature ratio (0.4), and total temperature (1500°R). The only tunnel condition varied was total pressure, 200 to 1800 psia, which produced a corresponding variation in free-stream unit Reynolds number of $0.9\text{-}8.0 \times 10^6$ per foot. Transition was defined from measurements of heat transfer to the model surface. Preliminary results from 5° camphor cones indicate no significant effect of camphor ablation on transition at an edge Mach number of 6.8. (Author)

A69-32769 *#
FLIGHT AND WIND TUNNEL INVESTIGATION OF INSTALLATION EFFECTS ON SUPERSONIC CRUISE EXHAUST NOZZLES AT TRANSONIC SPEEDS.
Fred A. Wilcox, Nick E. Samanich, and Bernard J. Blaha (NASA, Lewis Research Center, Cleveland, Ohio).
American Institute of Aeronautics and Astronautics, Propulsion Joint Specialist Conference, 5th, U.S. Air Force Academy, Colorado Springs, Colo., June 9-13, 1969, Paper 69-427. 8 p. 5 refs.
Members, $1.00; nonmembers, $1.50.

Discussion of a combination wind tunnel and flight research program, initiated by the NASA Lewis Research Center, for the purpose of investigating the effect of the location of power plants in aft-mounted wing nacelles in future supersonic-cruise aircraft. This investigation is based on the use of an F-106 aircraft which has been modified to carry two aft-mounted nacelles housing J-85 afterburning turbojet engines. Flight tests are now underway with a variety of exhaust nozzle concepts. Some of the significant results obtained from the flight and wind tunnel program are discussed. P.v.T.

A69-33250
BALLISTICS RANGE BOUNDARY-LAYER TRANSITION MEASUREMENTS ON CONES AT HYPERSONIC SPEEDS.
Norman W. Sheetz, Jr. (U.S. Navy, Naval Ordnance Laboratory, Corona, Calif.).
IN: VISCOUS DRAG REDUCTION; PROCEEDINGS OF THE SYMPOSIUM, DALLAS, TEX., SEPTEMBER 24, 25, 1968. [A69-33247 17-12]
Symposium sponsored by the U.S. Navy and NASA.
Edited by C. S. Wells.
New York, Plenum Press, 1969, p. 53-83. 38 refs.

Investigation of the effect of a number of parameters on the boundary-layer transition on conical bodies. These parameters include Mach number, cone angle, nose bluntness, and the ratio of wall-to-recovery temperature. The tests were conducted on 3, 5, 6.3, and 9° half-angle cones. The test Mach number varied from 3 to 15, while the ambient temperature ranged from 80 to 800°F. The free-stream Reynolds number based on tip radius varied from near

zero to 10^5. The data show a stabilizing, and apparently linear, effect on the boundary layer as the free-stream Mach number is increased. B.H.

A69-33251
AMPLIFIED LAMINAR BOUNDARY LAYER OSCILLATIONS AND TRANSITION AT THE FRONT ATTACHMENT LINE OF A 45° SWEPT FLAT-NOSED WING WITH AND WITHOUT BOUNDARY LAYER SUCTION.
W. Pfenninger and J. W. Bacon, Jr. (Northrop Corp., Beverly Hills, Calif.).
IN: VISCOUS DRAG REDUCTION; PROCEEDINGS OF THE SYMPOSIUM, DALLAS, TEX., SEPTEMBER 24, 25, 1968. [A69-33247 17-12]
Symposium sponsored by the U.S. Navy and NASA.
Edited by C. S. Wells.
New York, Plenum Press, 1969, p. 85-105. 8 refs.

Discussion of experiments performed in the Northrop 7 x 10 ft tunnel, in which transition at the attachment line of a 45° swept flat-nose wing was observed. For a wing with suction through closely spaced chordwise slots, the wind tunnel screen turbulence was found to induce regular amplified attachment-line boundary layer oscillations. The oscillations were generally modulated and superimposed on random low-frequency oscillations induced by free-stream large-scale eddies. The high-frequency boundary-layer velocity fluctuations arising near the attachment line were found to grow, leading finally to turbulent spots in combination with the random low-frequency oscillations. Without suction, transition started at attached line transition Reynolds numbers of 240 and 310 at potential flow velocity/kinematic viscosity ratios of 5.5×10^6 and 3.5×10^6, respectively. V.P.

A69-33290 *#
NONGRAY RADIATING FLOW ABOUT SMOOTH SYMMETRIC BODIES WITH LARGE BLOWING.
W. B. Olstad (NASA, Langley Research Center, Gas Physics Section, Hampton, Va.).
American Institute of Aeronautics and Astronautics, Thermophysics Conference, 4th, San Francisco, Calif., June 16-18, 1969, Paper 69-637. 14 p. 16 refs.
Members, $1.00; nonmembers, $1.50.

Modification of a simplified flowfield technique developed by Maslen (1964) to account for radiation and large blowing. Radiation cooling and nongray absorption (including the contribution of atomic lines) were taken into account. Results were obtained for a series of blunted cones traveling at speeds from 10.7 to 15.2 km/sec at an altitude of 60.96 km in the earth atmosphere. It is shown that the radiative heating distributions depend strongly on whether the primary source of radiation is the entropy layer or the flow external to the entropy layer. It is also shown that the entropy layer can be significantly affected by radiation cooling. The reduction of radiative heating by blowing cold air from the body surface is also discussed. (Author)

A69-33463 *#
EFFECTS OF MASS ADDITION OF VARIOUS GASES ON THE HEAT TRANSFER AND SURFACE PRESSURES ON A BLUNT CONE IN HYPERSONIC FLOW.
C. C. Pappas and George Lee (NASA, Ames Research Center, Moffett Field, Calif.).
American Institute of Aeronautics and Astronautics, Fluid and Plasma Dynamics Conference, San Francisco, Calif., June 16-18, 1969, Paper 69-716. 5 p.
Members, $1.00; nonmembers, $1.50.

Surface effects of uniform mass addition of the gases helium, air, argon, helium-argon mixtures, and three freons (with molecular weight to 200). Surface heat transfer and pressure were obtained over the whole length of the blunt conical body. Tests were conducted on a cold porous wall in a hypersonic air stream of Mach number 13.4, total enthalpy 2100 Btu/lb, and Reynolds number of 31,000 per foot. The effect of lowering molecular weight was to decrease the heat transfer everywhere and increase surface pressure on the afterbody, except for the freon gases which show little effect of molecular weight on heat transfer. Agreement between theory and experiment was good for the stagnation point heat transfer, except for the freon gases. A nonsimilar boundary-layer theory coupled to an inviscid surface pressure prediction was in good agreement with experimental heat transfer and pressure. (Author)

A69-34407 *#
AERODYNAMIC AND FLIGHT CHARACTERISTICS OF SEVERAL VARIABLE GEOMETRY ENTRY SPACECRAFT DURING SUBSONIC WING DEPLOYMENT AND LANDING.
B. J. Kuchta (General Dynamics Corp., Convair Div., San Diego, Calif.) and B. Spencer, Jr. (NASA, Langley Research Center, Hampton, Va.).
American Institute of Aeronautics and Astronautics and Canadian Aeronautics and Space Institute, Subsonic Aero- and Hydro-Dynamics Meeting, Ottawa, Canada, July 2, 3, 1969, AIAA Paper 69-742.
17 p. 5 refs.
Members, $1.00; nonmembers, $1.50.

Flight characteristics during landing and wing deployment are presented for three lifting entry spacecraft concepts having hypersonic (L/D)s of approximately 1.0, 2.0, and 3.0. The types of variable geometry studied include foldout; switchblade; and a single-pivot, two-position skewed wing. Detailed static subsonic wind-tunnel data obtained on each vehicle were used to estimate the dynamic stability characteristics. Wind-tunnel data were obtained for various wing deployment positions. The spacecraft concepts studied are dynamically stable throughout the subsonic flight envelope, but stability augmentation is required to provide acceptable handling qualities with the center of gravity of the vehicles located by detailed preliminary design. Wing deployment transients are minor and the piloting task during wing deployment consists of a simple push-over maneuver. For the configurations investigated, landing characteristics are comparable to present day high-performance fighter aircraft. (Author)

A69-35226
AERODYNAMICS OF ROTARY WING AND V/STOL AIRCRAFT; CORNELL AERONAUTICAL LABORATORY AND U.S. ARMY AVIATION MATERIEL LABORATORIES, SYMPOSIUM, 3RD, BUFFALO, N.Y., JUNE 18-20, 1969, PROCEEDINGS. VOLUME 2 - WIND TUNNEL TESTING, NEW CONCEPTS IN ROTOR CONTROL.
Buffalo, N.Y., Cornell Aeronautical Laboratory, Inc., 1969. 318 p.
Price of three volumes, $10.00.

CONTENTS:

FOREWORD. A. Ritter (Cornell Aeronautical Laboratory, Inc., Buffalo, N.Y.) and J. E. Yeates (U.S. Army, Aviation Materiel Command, Fort Eustis, Va.). 2 p.

WIND TUNNEL TESTING.

MODEL VS. FULL SCALE ROTOR TESTING. J. P. Rabbott, Jr. (United Aircraft Corp., Stratford, Conn.). 38 p. 14 refs. [See A69-35227 18-11]

THE FLOW THROUGHOUT A WIND TUNNEL CONTAINING A ROTOR WITH A SHARPLY DEFLECTED WAKE. H. H. Heyson (NASA, Langley Research Center, Hampton, Va.). 45 p. 42 refs. [See A69-35228 18-11]

COMMENTS ON V/STOL WIND TUNNEL DATA AT LOW FORWARD SPEEDS. W. H. Rae, Jr. and S. Shindo (Washington, University, Seattle, Wash.). 31 p. 14 refs. [See A69-35229 18-11]

PROBLEMS ASSOCIATED WITH WIND TUNNEL TESTS OF HIGH DISK LOADING SYSTEMS AT LOW FORWARD SPEEDS. F. A. Lazzeroni and L. W. Carr (U.S. Army, Aeronautical Research Laboratory, Moffett Field, Calif.). 28 p. 7 refs. [See A69-35230 18-11]

NEW CONCEPTS IN ROTOR CONTROL.

SOME RESEARCH ON ROTOR CIRCULATION CONTROL. R. M. Williams (U.S. Naval Material Command, Washington, D.C.). 36 p. 12 refs. [See A69-35231 18-01]

THE AERODYNAMICS OF A CIRCULATION-CONTROLLED ROTOR. M. C. G. Smith (Ministry of Technology, National Gas Turbine Establishment, Pyestock, Hants., England). 49 p. [See A69-35232 18-01]

HIGHER HARMONIC PITCH CONTROL. J. C. Balcerak, J. C. Erickson, Jr. (Cornell Aeronautical Laboratory, Inc., Buffalo, N.Y.), and J. H. McGarvey (U.S. Army, Aviation Materiel Laboratories, Fort Eustis, Va.). 30 p. 18 refs. [See A69-35233 18-01]

THE CONTROLLABLE TWIST ROTOR. A. F. Smith (Kaman Corp., Bloomfield, Conn.). 45 p. 7 refs. [See A69-35234 18-01]

A69-35636 * #

DATA CORRELATION FROM INVESTIGATIONS OF A HIGH-SUBSONIC SPEED TRANSPORT AIRCRAFT MODEL IN THREE MAJOR TRANSONIC WIND TUNNELS.

Stuart L. Treon, Frank W. Steinle, William R. Hofstetter (NASA, Ames Research Center, Moffett Field, Calif., and John R. Hagerman (USAF, Aeronautical Systems Div., Systems Engineering Group, Wright-Patterson AFB, Ohio).

American Institute of Aeronautics and Astronautics, Aircraft Design and Operations Meeting, Los Angeles, Calif., July 14-16, 1969, Paper 69-794. 8 p. 6 refs.

Members, $1.00; nonmembers, $1.50.

Results of a series of investigations involving a 0.0226-scale Lockheed C-5A aircraft model conducted in the Ames Research Center, NASA, 11- by 11-ft, Arnold Engineering Development Center 16-ft, and Cornell Aeronautical Laboratory 8-ft Transonic Wind Tunnels at high subsonic speeds. The objectives of the investigations were to: (1) identify areas of agreement and disagreement in the data from the different facilities; (2) determine corroborative explanations where differences existed; (3) prescribe and verify test and data reduction procedures to improve the quality of wind-tunnel test results; and (4) identify problems requiring further research. Of significance, the identical wing-fuselage combination was maintained throughout the initial test entries in the three facilities, along with the same sting and balance combination. Standard test techniques at each facility were employed. Comparisons of static force, moment, and model base pressure for the wing-fuselage configuration are presented. In spite of precautions taken, procedural errors were experienced. Beyond corrections for the procedural errors, however, there remain significant differences in the data from the three facilities. An analysis of factors influencing the quality of data from the Ames facility is suggestive of the need for continuing critical appraisal of generally accepted test procedures, instrumentation tolerances, and corrections to wind-tunnel data. (Author)

A69-37155 * #

EXPERIMENTAL AERODYNAMICS OF A ROTOR ENTRY VEHICLE.

Alan D. Levin and Ronald C. Smith (NASA, Ames Research Center, Moffett Field, Calif.).

(American Institute of Aeronautics and Astronautics, Aerodynamic Deceleration Systems Conference, El Centro, Calif., Sept. 23-25, 1968, Paper 68-950.)

Journal of Aircraft, vol. 6, July-Aug. 1969, p. 330-335. 11 refs.

An unpowered rotor entry vehicle model has been tested at Mach numbers 0.10 to 3.54 at angles of attack from 15° to 90°. The tests included variations of blade collective and cyclic pitch angles. A summary of the autorotative equilibrium rotor speed, forces, and moments is presented. The results indicate that adding the rotor to the capsule improved vehicle performance throughout most of the Mach number range. Maximum lift-to-drag ratio was substantially improved at low Mach numbers. Large pitching moments were produced by the rotor requiring the use of flaps for longitudinal trim. Control phasing was unusual compared to the predicted response of an "ideal rotor," but did not change grossly with forward flight speed. (Author)

A69-37185 * #

EXPERIMENTAL INVESTIGATION OF SEPARATED FLOW OVER A CAVITY AT HYPERSONIC SPEED.

Mansop Hahn (NASA, Ames Research Center, Moffett Field, Calif.).

(American Institute of Aeronautics and Astronautics, Fluid and Plasma Dynamics Conference, Los Angeles, Calif., June 24-26, 1968, Paper 68-672.)

AIAA Journal, vol. 7, June 1969, p. 1092-1098. 13 refs.

Research supported by the National Research Council and NASA.

An experimental investigation of flow details (velocity and temperature) and wall heat transfer within the separated flow region of an annular cavity at a free-stream Mach number of 7.3 is discussed. Tests were conducted at a total temperature of 1110 K and a wall-to-total temperature ratio of 0.26. Free-stream Reynolds number per meter ranged from 1.6 to 6.3×10^{6}. Effects of Reynolds number and cavity length-to-depth ratio on the distribution of temperature and heat-transfer rate are examined for both separated laminar and transitional flows. For laminar flow, typical results show that the velocity along the dividing streamline gradually increases downstream and approaches 35% of the outer-edge velocity. For both laminar and transitional flows, cavity gas temperature increased toward the reattachment region, which was consistent with the measured distribution of the heat-transfer rate on the cavity wall. The magnitude of the temperature varied with Reynolds number and cavity length-to-depth ratio. The ratio of integrated heat-transfer rate in laminar separated flow to that in corresponding attached flow was less than the theoretical limiting value of Chapman and varied with Reynolds number and cavity length-to-depth ratio. (Author)

A69-39237 * #

CENTER-OF-GRAVITY REQUIREMENTS FOR TRIM OF SEVERAL AXISYMMETRIC BODIES.

Robert W. Rainey and Peter T. Bernot (NASA, Langley Research Center, Hampton, Va.).

Journal of Spacecraft and Rockets, vol. 6, Apr. 1969, p. 509-511.

Evaluation of axisymmetric configurations for manned spacecraft which provide higher hypersonic lift-to-drag ratios. It is shown that the cone-conical-frustrum configurations, although simple, offer numerous advantages including better volume utilization and generally easier center-of-gravity requirements on the bases examined. Z.W.

A69-41369

AERODYNAMICS OF ROTARY WING AND V/STOL AIRCRAFT; CORNELL AERONAUTICAL LABORATORY AND U.S. ARMY AVIATION MATERIEL LABORATORIES, SYMPOSIUM, 3RD, BUFFALO, N.Y., JUNE 18-20, 1969, PROCEEDINGS. VOLUME 3—PANEL SESSION ON RECOMMENDATIONS FOR FUTURE AERODYNAMIC RESEARCH, PANEL SUMMARIES AND FEATURED SPEAKERS.

Buffalo, N.Y., Cornell Aeronautical Laboratory, Inc., 1969. 148 p. Price of three volumes, $10.00.

CONTENTS:

FOREWORD. A. Ritter (Cornell Aeronautical Laboratory, Inc., Buffalo, N.Y.) and J. E. Yeates (U.S. Army, Aviation Materiel Laboratories, Fort Eustis, Va.). 2 p.

WELCOMING REMARKS. W. O. Breuhaus (Cornell Aeronautical Laboratory, Inc., Buffalo, N.Y.). 2 p.

WELCOMING REMARKS. E. Soler (U.S. Army, Aviation Materiel Laboratories, Fort Eustis, Va.). 3 p.

KEYNOTE ADDRESS. A. Gessow (NASA, Office of Advanced Research and Technology, Washington, D.C.). 6 p.

RECOMMENDATIONS FOR FUTURE AERODYNAMIC RESEARCH.

NOW IS THE TIME FOR AERODYNAMICS TO COME TO THE AID OF THE HARDWARE. E. S. Carter (United Aircraft Corp., Stratford, Conn.). 17 p. (See A69-41370 23-02)

RECOMMENDATIONS FOR FUTURE AERODYNAMIC RESEARCH. C. W. Ellis (Boeing Co., Morton, Pa.). 28 p. (See A69-41371 23-01)

NOTES ON ROTOR AERODYNAMIC RESEARCH. F. B. Gustafson (NASA, Langley Research Center, Hampton, Va.). 10 p.

01 AERODYNAMICS

(See A69-41372 23-01)

SUGGESTIONS TOWARD A CO-ORDINATED APPROACH TO AERODYNAMIC RESEARCH. J. M. Harrison (Lockheed Aircraft Corp., Burbank, Calif.). 6 p. (See A69-41373 23-11)

FUTURE AERODYNAMICS RESEARCH. R. R. Lynn (Bell Aerospace Corp., Fort Worth, Tex.). 6 p. (See A69-41374 23-01)

AERODYNAMIC RESEARCH RELATED TO PROPELLER DRIVEN V/STOL AIRCRAFT. O. E. Michaelsen (Canadair, Ltd., Montreal, Canada). 13 p. (See A69-41375 23-02)

PANEL DISCUSSION–QUESTION AND ANSWER PERIOD.

SOME PROBLEMS IN THE NUMERICAL SOLUTION OF VORTEX MOTION EQUATIONS. J. P. Jones and M. Noak (Southampton, University, Southampton, England). 27 p. (See A69-41376 23-12)

A69-41372 * #

NOTES ON ROTOR AERODYNAMIC RESEARCH.

F. B. Gustafson (NASA, Langley Research Center, Hampton, Va.).

IN: AERODYNAMICS OF ROTARY WING AND V/STOL AIRCRAFT; CORNELL AERONAUTICAL LABORATORY AND U.S. ARMY AVIATION MATERIEL LABORATORIES, SYMPOSIUM, 3RD, BUFFALO, N.Y., JUNE 18-20, 1969, PROCEEDINGS. VOLUME 3–PANEL SESSION ON RECOMMENDATIONS FOR FUTURE AERODYNAMIC RESEARCH, PANEL SUMMARIES AND FEATURED SPEAKERS. (A69-41369 23-01)

Buffalo, N.Y., Cornell Aeronautical Laboratory, Inc., 1969. 10 p.

Discussion of three fields of rotor aerodynamic research–namely, comparison of theoretical and experimental data, rotor-blade flow visualization, and development of ways of using more blade-section camber. More thorough theory/data comparisons are recommended. It is suggested that a technique for obtaining flow visualization in cross sections around the retreating blade should be devised for use in solving high tip-speed ratio, high section angle-of-attack rotor aerodynamic problems. It is stressed that improved aerodynamic characteristics might be obtained by making the trailing edge "self-adaptive" (flexible) and thus permitting increased camber. P.G.

A69-41886 * #

HYPERSONIC VISCOUS INTERACTION ON SHARP AND BLUNT INCLINED PLATES.

Joseph H. Kemp, Jr. (NASA, Ames Research Center, Moffett Field, Calif.).

(American Institute of Aeronautics and Astronautics, Fluid and Plasma Dynamics Conference, Los Angeles, Calif., June 24-26, 1968, Paper 68-720.)

An approximate analysis is presented for the effect of arbitrarily distributed blowing on the laminar boundary-layer flow and pressure distribution around two-dimensional or axisymmetric hypersonic blunt bodies. The analysis is based on a simplified integral method solution coupled with a Newtonian model of the inviscid flow around the effective body shape defined by the dividing streamline between the blown and free-stream gas. Numerical results for a hemispherically blunted cone with various injection levels, including the case of strong blowing, are given for three different types of blowing distributions encountered in practice. Significant increases in the local pressure are found when blowing is continued around the nose into the afterbody region. (Author)

A69-43588 * #

DOWNSTREAM COOLING EFFECTIVENESS OF MASSIVE UPSTREAM TRANSPIRATION FROM A SLENDER CONE.

James C. Dunavant (NASA, Langley Research Center, Aerophysics Div., Hampton, Va.) and James C. Mulligan (North Carolina State University, Mechanical and Aerospace Engineering Dept., Raleigh, N.C.).

AIAA Journal, vol. 7, Sept. 1969, p. 1796, 1797.

Results of measurements of the radiation equilibrium temperature downstream of a transpiration-cooled gas flow section near a slender-cone vertex in a continuous flow hypersonic tunnel with the blowing rate exceeding blowoff and with a nominal freestream Mach number of 10. A simple lumped parameter formulated from approximate theoretical considerations is shown to provide a basis for the correlations characterizing the cooling effectiveness of such a system. A comparison of the experimental and theoretical results shows a fair agreement for a helium flow at low- and middle-range Reynolds numbers. V.Z.

N69-10054*# National Aeronautics and Space Administration. Langley Research Center, Langley Station, Va.

CALCULATED AND EXPERIMENTAL HINGE MOMENTS ON A TRAILING-EDGE FLAP OF A 75° SWEPT DELTA WING AT MACH 6

J. Wayne Keyes and George C. Ashby, Jr. Washington Dec. 1967 28 p refs

(NASA-TN-D-4268) Avail: CFSTI CSCL 01A

The hinge moment characteristics of a trailing-edge flap on a 75° swept delta wing have been investigated at a Mach number of 6.0 and a Reynolds number of 4.03×10^6 (based on the root chord of the delta wing). This investigation was conducted at angles of attack from 30° to 90° and flap-deflection angles from 0° to 30°. The boundary layer in the area of the wing–flap junction was considered to be transitional for angles of attack up to approximately 60° and laminar for angles of attack from 60° to 90°. Both a sharp and blunt leading-edge wing and two flap aspect ratios were used in the investigation. Although the flow on the wing and flap was found to be complex, a meaningful analysis of the data can be made for the nonseparated case if the local flow regime over the wing and flap is properly classified (subsonic or supersonic) for each angle of attack and flap-deflection angle. The slope of the hinge moment curves changed at approximately the same angle of attack that the flow regimes were predicted to change when tangent–cone and oblique shock theories were used. Boundary layer separation over the flap was not extensive for flap deflections less than 20°. The type of boundary layer could have a strong influence on the hinge moments for flap deflection angles large enough to cause boundary layer separation. Author

N69-10215*# National Aeronautics and Space Administration. Langley Research Center, Langley Station, Va.

A METHOD FOR DETERMINING SURFACE PRESSURES ON BLUNT BODIES OF REVOLUTION AT SMALL ANGLES OF ATTACK IN SUPERSONIC FLOW

Charlie M. Jackson, Jr., Wallace C. Sawyer, and Rudeen S. Smith Washington Nov. 1968 104 p refs

(NASA-TN-D-4865) Avail: CFSTI CSCL 01A

Existing theoretical techniques have been modified and combined to provide a method for computing surface pressure distributions on blunt bodies with spherical nose caps and arbitrary afterbody shapes. The method consists basically of modified Newtonian theory in the stagnation region with second-order shock-expansion theory used when the surface flow becomes supersonic. The second-order shock-expansion theory is most conveniently applied to rotationally symmetric bodies; therefore, to use this theory at small angles of attack, the body meridian lines are used to generate equivalent bodies of revolution from which the meridian pressure distributions are obtained. A complete, consistent set of experimental surface pressure data is presented for two typical blunt reentry configurations to permit evaluation. The test conditions provide surface pressure distributions for six Mach numbers from 1.50 to 4.63 and four angles of attack from 0° to 12° for each model. A comparison of the present theoretical method with these experimental data indicates that this method gives adequate engineering estimates of the surface pressures on

blunt bodies at moderate angles of attack except where flow separation or detached secondary shock waves are present. Author

N69-10294*# National Aeronautics and Space Administration. Lewis Research Center, Cleveland, Ohio.
EFFECT OF POROUS BLEED IN A HIGH PERFORMANCE AXISYMMETRIC, MIXED COMPRESSION INLET AT MACH 2.50
Robert W. Cubbison, Edward T. Meleason, and David F. Johnson Washington Nov. 1968 37 p refs
(NASA-TM-X-1692) Avail: CFSTI CSCL 01C

A study to determine the effect of boundary layer bleed location and the amount of total bleed flow on the performance of a mixed compression, axisymmetric, reflecting-shock inlet was conducted in the Lewis 10- by 10-Foot Supersonic Wind Tunnel at Mach 2.498. Best overall inlet performance was obtained with 2.5 percent supercritical bleed located just downstream of the last cowl and centerbody shock reflection points in the supersonic diffuser. Critical pressure recovery was 0.899 with 16.5 percent distortion, and the subcritical operating range was 7.8 percent of engine corrected airflow. Distortion considerations may dictate either more bleed or use of vortex generators. Author

N69-10343*# McDonnell-Douglas Co., Long Beach, Calif.
A NUMERICAL SOLUTION FOR THE MINIMUM INDUCED DRAG, AND THE CORRESPONDING LOADING, OF NONPLANAR WINGS Final Report
J. L. Lundry Washington NASA Nov. 1968 39 p refs
(Contract NAS1-7484)
(NASA-CR-1218; DAC-66900) Avail: CFSTI CSCL 20D

A numerical procedure has been developed for the accurate computation of the minimum induced drag, and the associated loading, of nonplanar wings. The minimum induced drag and the loading are determined by the solution of a potential problem about the shed vortex wake in the Trefftz plane. The potential problem is analyzed in an auxiliary mapping plane that is related to the physical plane by the Schwarz–Christoffel transformation; the procedure can therefore be applied to configurations with front views that can be approximated by straight line segments. The success of the method depends on an iteration that converges satisfactorily for most cases. Comparisons of results of the method with results of known test cases show that errors in the minimum induced drag and in the corresponding loading are of the order of 10^{-4} when the method is programmed in single precision arithmetic for an IBM 7094. Author

N69-10558*# National Aeronautics and Space Administration. Lewis Research Center, Cleveland, Ohio.
EFFECT OF VARIABLE STATOR AREA ON PERFORMANCE OF A SINGLE-STAGE TURBINE SUITABLE FOR AIR COOLING. 6: TURBINE PERFORMANCE WITH 70-PERCENT DESIGN STATOR AREA
Harold J. Schum, Edward M. Szanca, and Herman W. Prust, Jr. Washington Nov. 1968 24 p refs
(NASA-TM-X-1697) Avail: CFSTI CSCL 21E

The performance of this turbine is compared with those obtained for the design and the 130-percent design-stator-area turbines. Whereas the design turbine yielded an efficiency of 0.923 at its equivalent design operating condition, the closed turbine produced an efficiency of only 0.840 at the same operating point. This compares with 0.897 for the open turbine. The large loss of efficiency for the closed turbine is attributed mainly to the high velocities at the stator exit, incidence to the rotor, and substantially reduced reaction across the rotor. Author

N69-10732*# National Aeronautics and Space Administration. Langley Research Center, Langley Station, Va.
AERODYNAMIC CHARACTERISTICS OF 0.25-SCALE MODEL OF TOMAHAWK LAUNCH VEHICLE AT MACH NUMBERS FROM 2.30 TO 4.63
Lloyd S. Jernell Washington Nov. 1968 62 p refs
(NASA-TM-X-1684) Avail: CFSTI CSCL 01A

An investigation of several configurations of a 0.25-scale model of the Tomahawk launch vehicle has been conducted in the Langley Unitary Plan wind tunnel at Mach numbers from 2.30 to 4.63. The investigation included the effects of body fineness ratio, fin planform geometry, and fin cant angle for an angle of attack range of about $-4°$ to $21°$ at roll angles from $0°$ to $67°$. The results indicate that for the moment reference center employed, each configuration experienced pitch-up at angles of attack of approximately $8°$ to $10°$ at a Mach number of 2.30, with the angle of pitch-up decreasing with increasing Mach number. The larger fins delay pitch-up to a slightly higher angle of attack at all test Mach numbers. Canting the basic fins $1°$ was effective in producing rolling moment throughout the ranges of angle of attack and Mach number. Varying the roll angle resulted in large variations in the lateral force and moments above angles of attack of about $4°$ because of the effects of the forebody vortices acting on the fins. Author

N69-10789*# National Aeronautics and Space Administration. Ames Research Center, Moffett Field, Calif.
EFFECTS OF ANGLE OF ATTACK AND BLUNTNESS ON THE SHOCK-LAYER PROPERTIES OF A 15° CONE AT A MACH NUMBER OF 10.6
Joseph W. Cleary Washington Nov. 1968 40 p refs
(NASA-TN-D-4909) Avail: CFSTI CSCL 01A

An experimental investigation was conducted to determine the effects of varying angle of attack and nose bluntness ratio on the shock layer properties of a typical conical entry body. Distributions of pitot and static pressures were measured across the shock layer of a cone with $15°$ semiapex. The measurements were obtained from wing-tunnel tests in air at a Mach number of 10.6 and a free stream unit Reynolds number of 1.2×10^6 per foot. Results are presented at fore and aft axial positions for several circumferential angles when at angle of attack. Pitot pressure distributions demonstrate that the flow over the sharp cone was essentially conical except for the separated-flow region on the leeward side. Increasing bluntness ratio not only caused progressive deviations from conical flow but also affected the leeward flow separation pattern. Comparisons with inviscid theory show that because of bluntness, the flow remained attached on the lee side for an axial distance of several nose radii while farther aft, the flow separated in a manner similar to that of the sharp cone. On the windward side where the boundary layer was thin, inviscid theory accurately predicts the more salient properties of shock layers for both sharp and blunted cones. Author

N69-11009*# National Aeronautics and Space Administration, Langley Research Center, Langley Station, Va.
HEAT-TRANSFER AND PRESSURE DISTRIBUTIONS INSIDE THE HINGE-LINE GAP OF A WEDGE-FLAP COMBINATION AT MACH NUMBER 10.4
J. David Dearing and H. Harris Hamilton Washington Nov. 1968 57 p refs
(NASA-TN-D-4911) Avail: CFSTI CSCL 01A

Aerodynamic heating inside the gap separating a control flap from the adjacent support structure has been measured at a nominal free stream Mach number of 10.4. The model, a 10-percent-thick wedge, was fitted with a simple flap whose chord

was 20 percent of the wedge chord. Angle of attack was varied to change the entrance-to-exit pressure ratio and resulted in local Mach numbers ahead of the gap entrance of from 5.9 to 7.9. Laminar, transitional, and turbulent boundary layers on the wedge near the entrance were obtained by combined variations in local Mach numbers and local Reynolds number. The heating in the gap always decreased from entrance to exit and at the gap center never exceeded one-half that on the wedge at the entrance. In general, the gap heating increased with gap width and flap deflection, and rounding the gap entrance and exit lip tended to increase the overall level of heating in the gap over that for the sharp-lip configuration. Author

N69-11634*# National Aeronautics and Space Administration. Langley Research Center, Langley Station, Va.

THE PATH OF A JET DIRECTED AT LARGE ANGLES TO A SUBSONIC FREE STREAM

Richard J. Margason Washington Nov. 1968 54 p refs
(NASA-TN-D-4919) Avail: CFSTI CSCL 20D

An investigation was made of the path and general shape of the wake from a single jet exiting at large angles to the free stream through a range of effective velocity ratios (square root of the ratio of the free-stream dynamic pressure to the jet dynamic pressure). The jet-exit deflection angles ranged, in 30° increments, from 30° to 180° from the free stream. Photographs taken of the wake, which was a mixture of compressed air and water vapor, showed that the jet paths were essentially the same when the jet was exiting upward or downward as well as when the jet was located adjacent to a large surface or located away from adjacent surfaces. The primary variables determining the jet path are the deflection angle of the jet exit and the effective velocity ratio. The results were compared with equations for the jet path from other investigations, and the best empirical fit to these data was determined. Author

N69-12286* McDonnell-Douglas Co., Long Beach, Calif.

A NUMERICAL SOLUTION FOR THE MINIMUM INDUCED DRAG, AND THE CORRESPONDING LOADING, OF NONPLANAR WINGS. 1: USER'S MANUAL FOR COMPUTER PROGRAM 55VD. 2: DESCRIPTIVE MANUAL FOR COMPUTER PROGRAM 55VD

J. L. Lundry Washington NASA Nov. 1968 390 p
(Contract NAS1-7484)
(NASA-CR-1218-Suppl; DAD-66898; DAD-66899) Avail: CFSTI CSCL 01A

A numerical procedure has been developed for the accurate computation of the minimum induced drag, and the associated load distribution, of nonplanar wings. As is well known, the minumum induced drag may be determined by analyzing a potential problem in the Trefftz plane. The procedure solves the potential problem in an auxiliary mapping plane related to the physical plane by the Schwarz–Christoffel transformation for configurations with front views that may be approximated by straight line segments. Previously, the main computational difficulty had been the determination of the mapping constants. The procedure presented here offers a choice of two methods to determine these constants. The procedure has been applied to seven nonplanar lifting configurations, resulting in the development of computer program 55VD in the FORTRAN 4 language for use on an IBM 7094. Program 55VD has been converted to FORTRAN 2.0 for use on the Langley Research Center's CDC 6000 series digital computers. This report is a user's manual for the FORTRAN 2.0 version of program 55VD. Author

N69-13154*# National Aeronautics and Space Administration. Lewis Research Center, Cleveland, Ohio.

PRELIMINARY INVESTIGATION OF DISTORTION DYNAMICS IN A MACH 3 MIXED COMPRESSION INLET

Robert E. Coltrin and Glenn A. Mitchell Washington Dec. 1968 22 p refs
(NASA-TM-X-1706) Avail: CFSTI CSCL 01A

The inlet was operated at critical and supercritical conditions while at 0° angle of attack in the 10- by 10-foot supersonic wind tunnel. The cowl lip diameter was 45.98 cm. Total-pressure sensors with a flat response to 200 Hz were distributed at several diffuser exit locations. The amplitude probability density functions for the total pressures were nearly Gaussian. Frequency analysis showed that the amplitude of the power spectral densities for these pressures dropped by half from 0 to 100 Hz, but was nearly constant at higher frequencies. No periodic components were observed. Author

N69-13218*# National Aeronautics and Space Administration. Langley Research Center, Langley Station, Va.

HYPERSONIC AERODYNAMIC CHARACTERISTICS OF A MODEL OF A LOW-FINENESS-RATIO VARIABLE GEOMETRY LOGISTICS SPACECRAFT CONCEPT

Bernard Spencer, Jr. Washington Dec. 1968 44 p refs
(NASA-TM-X-1701) Avail: CFSTI CSCL 01A

An investigation has been made in the Langley 15-inch hypersonic flow apparatus at a Mach number of 10.03 to determine the static aerodynamic characteristics of a model of a low fineness ratio variable geometry logistics spacecraft concept designed for hypersonic lift drag ratios near 1.0. The variable geometry feature envisioned for the configuration is a fold-down-type wing, stowed in the triangular side areas of the body during entry and deployed at subsonic speeds for improvement in subsonic performance. The variable geometry feature is considered to be retracted for the present hypersonic tests. Author

N69-13238*# National Aeronautics and Space Administration. Lewis Research Center, Cleveland, Ohio.

AN ESTIMATE OF THE SUPERSONIC FLOW FIELD ABOUT AN AXISYMMETRIC BODY WITH AN N WAVE PRESSURE TRACE

Roger W. Luidens Washington Dec. 1968 28 p refs
(NASA-TN-D-4935) Avail: CFSTI CSCL 01A

Linearized flow assumptions and the conservation equations of mass, momentum, and energy are used to estimate the flow field at all distances from a body which produces an N wave pressure trace. The analytical results show good agreement with experimental results for cones and axisymmetric bodies with convex profiles. The influence of the shock wave entropy increase on the attenuation of the shock wave static pressure rise with distance from the body is illustrated. Author

N69-13621*# General Motors Corp., Indianapolis, Ind. Allison Div.

EXPERIMENTAL INVESTIGATION OF ADVANCED CONCEPTS TO INCREASE TURBINE BLADE LOADING. 3: PERFORMANCE EVALUATION OF TANDEM ROTOR BLADE

H. G. Lueders Washington NASA Dec. 1968 43 p refs
(Contract NAS3-7902)
(NASA-CR-1254) Avail: CFSTI CSCL 20D

The overall performance of a single-stage turbine designed with a tandem rotor blade and negative rotor hub reaction was investigated over a range of equivalent speeds and expansion ratios. Surveys of total pressure, flow angle, temperature, and hot-wire data were taken at the rotor trailing edge. The performance of the turbine is compared with the performance of a plain rotor blade turbine. Both turbines have the same design requirements and were tested with the same stator. Author

N69-14000*# National Aeronautics and Space Administration. Langley Research Center, Langley Station, Va.

WIND-TUNNEL INVESTIGATION OF A LARGE JET TRANSPORT MODEL EQUIPPED WITH AN EXTERNAL-FLOW JET FLAP

Lysle P. Parlett, Marvin P. Fink, and Delma C. Freeman, Jr. Washington Dec. 1968 86 p refs

(NASA-TN-D-4926) Avail: CFSTI CSCL 20D

A wind tunnel investigation was carried out to determine the aerodynamic characteristics of a model of a large jet transport aircraft equipped with an external-flow jet-augmented flap. The tests were conducted in the Langley full-scale tunnel by using a model powered by scaled nitrogen-driven, fan-jet engines. The results of the investigation were analyzed for the case of an airplane having a thrust-weight ratio of 0.30 for both takeoff and landing. These results indicated that the model with the external-flow jet flap could achieve a maximum trimmed lift coefficient of approximately 4.0 with this thrust-weight ratio. When this maximum lift coefficient was examined with consideration of reasonable operational safety margins based on flight experience with several powered-lift airplanes, it appeared that a safe operational approach lift coefficient was about 2.2. Based on this analysis, it appeared that the use of the jet flap would provide increases in operational lift coefficient of the airplane and would give substantial improvements in takeoff and landing performance. Static longitudinal stability and trim could be achieved over the entire lift range by the use of a horizontal tail with an area of 22 percent of the wing area. The out-of-trim moments caused by operation with the critical engine out could be trimmed throughout the entire lift range by the use of conventional rudder, aileron, and spoiler controls. Author

N69-14001*# National Aeronautics and Space Administration. Langley Research Center, Langley Station, Va.

THEORY FOR COMPUTING SPAN LOADS AND STABILITY DERIVATIVES DUE TO SIDESLIP, YAWING, AND ROLLING FOR WINGS IN SUBSONIC COMPRESSIBLE FLOW

M. J. Queijo Washington Dec. 1968 78 p refs

(NASA-TN-D-4929) Avail: CFSTI CSCL 20D

A method of computing span loads and some of the resulting aerodynamic derivatives for wings in sideslip, yawing, and rolling flight is derived. The method is applicable to wings of arbitrary planform, and accounts for compressibility effects. The span-load computations require that angle-of-attack span-load distributions be available for the wing under consideration. The theory developed is a consistent approach, based on the use of a vortex system, for determining the various wing parameters. Author

N69-14075*# National Aeronautics and Space Administration. Lewis Research Center, Cleveland, Ohio.

EFFECT OF BLEED-SYSTEM BACK PRESSURE AND POROUS AREA ON THE PERFORMANCE OF AN AXISYMMETRIC MIXED-COMPRESSION INLET AT MACH 2.50

Bobby W. Sanders and Robert W. Cubbison Washington Dec. 1968 33 p refs

(NASA-TM-X-1710) Avail: CFSTI CSCL 21E

Two bleed geometries that had about a 2.75 to 1 ratio in total porous area were tested with different bleed-exit areas to provide various back pressures. With bleed-exit areas providing the same supercritical bleed mass flow, the higher porous-area configuration provided higher total-pressure recovery at critical inlet operation. For the same supercritical bleed mass flow the more porous configuration also obtained a reduction in bleed drag of 42.5 percent but at a complete loss of subcritical stability margin. However, by proper control of the bleed-exit areas, the engine corrected airflow could be decreased 13.18 percent from that at critical operation without incurring an unstart. Author

N69-14211*# General Motors Corp., Indianapolis, Ind. Allison Div.

EXPERIMENTAL INVESTIGATION IN AN ANNULAR CASCADE SECTOR OF HIGHLY LOADED TURBINE STATOR BLADING. VOLUME 1: ANALYSIS AND DESIGN

James L. Bettner Washington NASA Dec. 1968 169 p refs

(Contract NAS3-9404)

(NASA-CR-1219) Avail: CFSTI CSCL 21E

An analytical and experimental program was initiated to investigate the application of boundary layer control concepts to highly loaded turbine stator blades in an annular cascade. A plain blade was designed which forms the performance base line for the program. Four boundary layer control concepts were investigated—vortex generators, tangential jet blowing, tandem airfoils, and jet flap. The stator blades were designed to a suction surface diffusion factor of 0.4. Author

N69-14289*# National Aeronautics and Space Administration. Lewis Research Center, Cleveland, Ohio.

A MATHEMATICAL ANALYSIS OF SUPERSONIC INLET DYNAMICS

Ross G. Willoh Washington Dec. 1968 45 p refs

(NASA-TN-D-4969) Avail: CFSTI CSCL 21E

An approximate mathematical analysis of supersonic inlet dynamics is presented. The subsonic duct is subdivided into constant-area sections which are represented by one-dimensional wave equations. The movable normal shock is used as the upstream boundary condition, and a choked station is assumed for the downstream boundary condition. The analysis leads to a closed-form matrix solution for the shock-position transfer function. Analytical results are presented and compared with experimental data. Author

N69-14385*# National Aeronautics and Space Administration. Lewis Research Center, Cleveland, Ohio.

BACK FLOW FROM JET PLUMES IN VACUUM

Norman T. Grier Washington Jan. 1969 20 p refs

(NASA-TN-D-4978) Avail: CFSTI CSCL 20D

Approximate calculations were performed to determine the increase in particle density at points surrounding a jet nozzle due to the exhausted gas in the jet plume. The calculations were made for helium, argon, and nitrogen for a nozzle throat radius of 1 cm. The chamber density ranged from 10^{-8} to 1 g per cc. The plume flow is assumed radial with the source point at the nozzle exit on the nozzle axis. Author

N69-14566*# National Aeronautics and Space Administration. Lewis Research Center, Cleveland, Ohio.

DESIGN OF SUPERSONIC INLETS BY A COMPUTER PROGRAM INCORPORATING THE METHOD OF CHARACTERISTICS

Bernhard H. Anderson Washington Jan. 1969 118 p refs

(NASA-TN-D-4960) Avail: CFSTI CSCL 20D

A FORTRAN IV computer program which incorporates the method of characteristics was written to assist in the design of supersonic inlets. The computer program was written with the intention of studying many types of inlet configurations with a minimum of computer time. Particular attention was given to a discussion of a reformulation of the boundary value problem to introduce throat Mach number and flow angle as direct program input quantities. Comparison between the computer results and experimental data indicates good agreement for a number of different configurations. Author

01 AERODYNAMICS

N69-14872*# National Aeronautics and Space Administration. Langley Research Center, Langley Station, Va.
EFFECT OF UNIT REYNOLDS NUMBER, NOSE BLUNTNESS, ANGLE OF ATTACK, AND ROUGHNESS ON TRANSITION ON A 5° HALF-ANGLE CONE AT MACH 8
P. Calvin Stainback Washington Jan. 1969 78 p refs
(NASA-TN-D-4961) Avail: CFSTI CSCL 01A

A 5° half-angle cone has been tested at a nominal free-stream Mach number of 8 over a range of local, sharp cone unit Reynolds numbers from about 4.5×10^6 per meter (1.3×10^6 per foot) to 4.5×10^7 per meter (1.3×10^7 per foot) in a conventional blowdown tunnel. The nominal ratio of wall temperature to free-stream total temperature was about 0.4. The purpose of the investigation was to determine the effect of unit Reynolds number, nose bluntness, angle of attack, and roughness on the beginning of transition and on laminar and turbulent heating. The results obtained with the smooth models indicated that there was an increase in the transition Reynolds number with increasing unit Reynolds number and a rearward movement of the location of transitions with increasing nose bluntness and angle of attack for the windward ray. Although the hypersonic laminar boundary layer could be tripped with various types of roughness elements, large three-dimensional elements caused circumferential nonuniformities in the heat-transfer distribution around the cone for large distances into the turbulent boundary-layer region. The local transition Reynolds numbers for all bluntnesses (including the sharp tip cone) were correlated reasonably well as a single function of local unit Reynolds number if the local flow quantities were obtained from boundary-layer solutions with variable stream entropy effects included. Also, the agreement between laminar transfer data and theory, in the form of Stanton number as a function of Reynolds number, appeared to be improved if variable-entropy effects were taken into account. Author

N69-16121*# National Aeronautics and Space Administration. Langley Research Center, Langley Station, Va.
PRELIMINARY STUDY OF EFFECTS OF REYNOLDS NUMBER AND BOUNDARY-LAYER TRANSITION LOCATION ON SHOCK-INDUCED SEPARATION
James A. Blackwell, Jr. Washington Jan. 1969 27 p refs
Paper presented at AGARD Specialists' Meeting on Transonic Aerodyn., Paris, Sep. 1968; sponsored by AGARD
(NASA-TN-D-5003) Avail: CFSTI CSCL 20D

A two-dimensional experimental and theoretical investigation was conducted on an airfoil to determine the effect of Reynolds number and transition location on shock-induced separated flow. The experimental investigation was conducted in the 8-foot transonic pressure tunnel at Mach numbers from 0.60 to 0.80, angles of attack from 0° to 4°, and Reynolds numbers from 3.0×10^6 to 16.8×10^6. Transition locations from 0.05 to 0.50 chord were utilized. The results indicate that variation of the Reynolds number from full-scale values to the usual wind-tunnel values results in substantial changes in the shock location, trailing-edge pressure recovery, and boundary-layer losses at the trailing edge. By properly fixing the boundary-layer transition point on the wind-tunnel model, full-scale results can be simulated at the usual wind-tunnel Reynolds numbers. The required location of the transition point can be predicted theoretically with acceptable accuracy by simulating the boundary-layer characteristics at the airfoil trailing edge. Author

N69-16180*# National Aeronautics and Space Administration. Langley Research Center, Langley Station, Va.
PREDICTION OF LIFT AND DRAG FOR SLENDER SHARP-EDGE DELTA WINGS IN GROUND PROXIMITY
Charles H. Fox, Jr. Washington Jan. 1969 36 p
(NASA-TN-D-4891) Avail: CFSTI CSCL 01A

A method of predicting the lift and drag of slender planar sharp-edge delta wings in ground proximity is described, and the results are compared with experimental data. The method utilizes a vortex-lattice computer program incorporating an image technique to compute the potential-flow normal-force and axial-force characteristics of delta wings in ground proximity. A recently published vortex-lift concept in free air based on a leading-edge-suction analogy is utilized, and a method is presented for combining it with the results of the potential-flow theory in ground proximity. A comparison of the theoretical and experimental lift and drag for delta wings with a wide range of aspect ratios is presented at selected angles of attack. The comparison indicates that this method provides a reasonably good prediction of the lift and drag in ground proximity for aspect ratios less than 2.0 in the angle-of-attack range from 5° to 16° Author

N69-16209*# National Aeronautics and Space Administration. Langley Research Center, Langley Station, Va.
EXPERIMENTAL SURFACE-PRESSURE DISTRIBUTIONS ON A 9° SPHERICALLY BLUNTED CONE AT MACH NUMBERS FROM 1.50 TO 4.63
Wallace C. Sawyer and Rudeen S. Smith Washington Jan. 1969 60 p refs
(NASA-TM-X-1730) Avail: CFSTI CSCL 20D

An investigation was conducted in a wind tunnel to determine the pressure distributions on a 9° spherically blunted cone at Mach numbers from 1.50 to 4.63 with Reynolds numbers of 2.25×10^6 and 3.00×10^6 per foot (7.38×10^6 and 9.84×10^6 per meter). Angle of attack was varied from 0° to 12°. The surface pressures were integrated in order to obtain forebody forces and moments. The experimental surface pressures and integral forces and moments were compared with an existing theoretical method which predicts surface pressures and aerodynamic characteristics. Comparison of the experimental and theoretical results showed good agreement for surface pressures at moderate angles of attack except at the lower Mach numbers. Comparison of the results for forces and moments generally showed good agreement. The process of integrating surface pressures has been programmed for high speed digital computation. The program is written so that it will apply to arbitrary bodies of revolution. For convenience, the program is presented with the necessary operating details. Author

N69-16460*# National Aeronautics and Space Administration. Langley Research Center, Langley Station, Va.
ROUGHNESS DRAG DUE TO TWO-DIMENSIONAL FABRICATION-TYPE SURFACE ROUGHNESS ON AN OGIVE CYLINDER FROM FORCE TESTS AT TRANSONIC SPEEDS
K. R. Czarnecki and William J. Monta Washington Jan. 1969 48 p refs
(NASA-TN-D-5004) Avail: CFSTI CSCL 20D

An investigation has been made in the transonic Mach number range from 0.70 to 1.20 and over a range of free stream Reynolds number per foot from about 0.8×10^6 to 6.0×10^6 (2.6×10^6 to 19.7×10^6 per meter) to determine by means of force tests the roughness drag due to essentially two dimensional fabrication-type surface roughness immersed in a turbulent boundary layer. Six types of surface roughness, including step, wave, crease, and swept configurations, were investigated. The tests were made on an ogive cylinder of fineness ratio 12.2, the roughness elements covering the cylindrical portion of the models. Some force test data obtained previously on the these models at Mach numbers of 1.61 and 2.01 have been included as an aid to the analysis, and a comparison is made of the force test results with those results obtained from the pressure distribution investigations and with supersonic wave drag theory. The investigation indicated that roughness elements submerged in a turbulent boundary layer had drag characteristics very much like those of bodies in a uniform free stream as the Mach number was increased or the roughness sweep angle was changed. There was, however, a strong influence of change in Reynolds number of boundary layer thickness on the drag characteristics when substantial wave drag was present. Author

N69-16467*# National Aeronautics and Space Administration. Marshall Space Flight Center, Huntsville, Ala.

DEVELOPMENT OF AIR BEARING LIFT PADS

Dan H. Dane and Herman T. Blaise Washington Jan. 1969 21 p (NASA-TM-X-1724) Avail: CFSTI CSCL 01C

If a loaded air pad would float 0.317 cm (0.125 in.) above the floor, the drag would be almost zero, and the floor surface would not affect the performance of the air pad. Raising a precision air bearing or bladder air bearing higher than the air film layer by supplying more air to the pads produces unacceptable vibrations. Lowering the volume of air from a ground effects machine to get the desired effect produces statically unstable conditions. To provide a frictionless lift capacity on rough floors, a mathematical model of an air bearing lift pad (air pad) that floats 0.317 cm off the surface was devised, manufactured, and successfully tested. Three of these air bearing lift pads were assembled into a cushion air pad platform that had a load carrying capacity exceeding 45.4 kg (100 lb) over a rough floor with less than 0.284 N (1 oz) friction drag. Seven upgraded units were designed and manufactured to support 136 kg (300 lb) for the serpentuator testing program and for general simulation use. Author

N69-17289*# National Aeronautics and Space Administration. Langley Research Center, Langley Station, Va.

A PARAMETRIC STUDY OF BLADE-MOTION STABILITY BOUNDARIES FOR AN ARTICULATED ROTOR

Julian L. Jenkins, Jr. Washington Feb. 1969 29 p refs (NASA-TN-D-5032) Avail: CFSTI CSCL 01C

The blade-motion stability and response sensitivity of a fully articulated rotor (flapping and lead-lag degrees of freedom) was examined by using a numerical solution to the coupled, nonlinear, rigid-blade equations of motion. The effect of initial conditions on the tip-speed ratio for divergent motion is indicated by varying the initial azimuth angle for introducing a disturbance and by varying the disturbance amplitude at the critical aximuth angle. Methods of extending the divergence boundary of an articulated rotor are examined. The effects of blade-root pocket cutout, hinge restraint (spring and damping), flapping-hinge cant angle, and hinge offset are evaluated individually, and a representative combination of these parameters was chosen to indicate the overall effectiveness on blade-motion stability and response. Author

N69-17304*# National Aeronautics and Space Administration. Langley Research Center, Langley Station, Va.

AERODYNAMIC FORCES ON A STATIONARY AND OSCILLATING CIRCULAR CYLINDER AT HIGH REYNOLDS NUMBERS

George W. Jones, Jr., Joseph J. Cincotta (Martin Co., Baltimore, Md.), and Robert W. Walker Washington Feb. 1969 65 p refs (NASA-TR-R-300) Avail: CFSTI CSCL 20D

A wind-tunnel investigation was made of the steady drag and unsteady lift forces on a stationary and oscillating circular cylinder in two-dimensional flow at high Reynolds numbers and at Mach numbers up to 0.6. The experimental data were obtained in the Langley transonic dynamics tunnel from tests of a 3-foot diameter cylinder instrumented to measure directly the unsteady lift and mean drag forces on the cylinder. The cylinder could be held fixed or oscillated laterally to the flow at frequencies from 3 to 20 hertz. For the stationary cylinder, the static pressure distributions, the mean drag coefficients at M 0.2, and the Strouhal number of the unsteady lift forces follow the trends established by previous investigators up to the limits of Reynolds number investigated. At higher Reynolds numbers, each of these parameters remains essentially constant. The unsteady lift force can be categorized into three regimes dependent upon Reynolds number: wide-band random, narrow-band random, and quasi-periodic. Oscillation of the cylinder in the lift direction has no significant effect on the mean drag coefficient. An unsteady lift due to cylinder motion, exists only when the cylinder is oscillated at or relatively near the aerodynamic Strouhal frequency for the stationary cylinder. Author

N69-17312*# National Aeronautics and Space Administration. Langley Research Center, Langley Station, Va.

***AERODYNAMIC DATA ON LARGE SEMISPAN TILTING* WING WITH 0.4-DIAMETER CHORD, SINGLE-SLOTTED FLAP, AND SINGLE PROPELLER 0.22 CHORD BELOW WING**

Marvin P. Fink Washington Jan. 1969 205 p refs (NASA-TN-D-5016) Avail: CFSTI CSCL 20D

A study was made in the full-scale tunnel to determine the longitudinal aerodynamic characteristics of a large-scale semispan V/STOL tilt-wing configuration with a single propeller which was tested for modes of rotation. The wing had a ratio of chord to propeller diameter of 0.4, a 40-percent-chord single-slotted flap, an aspect ratio of 6.14 (3.07 for the semispan), a taper ratio of 1.0, and an NACA 4420 airfoil section. The direction of propeller rotation was found to have a very significant effect on the lift and descent capability (as determined from drag-lift ratios attainable without stalling of any part of the wing within the propeller slipstream) and that up-at-the-tip rotation gave the more favorable results. The use of flow-control devices was very effective in increasing the descent capability and lift for down-at-the-tip propeller rotation where the characteristics without such devices were poor but was much less effective for up-at-the-tip propeller rotation. For the most favorable combination of the configuration variables, descent angles of nearly 27° were achieved over the entire test range of power conditions. Author

N69-17392*# National Aeronautics and Space Administration. Lewis Research Center, Cleveland, Ohio.

ANALYTICAL INVESTIGATION OF THE EFFECT OF COOLING AIR ON TWO-STAGE TURBINE PERFORMANCE

Warren J. Whitney Washington Jan. 1969 24 p refs (NASA-TM-X-1728) Avail: CFSTI CSCL 21E

Turbine efficiency is determined as a function of inlet temperature by using the isolated-flow analytical method. The parameters that are varied are coolant total-pressure coefficient, coolant to inlet temperature ratio, and velocity-diagram type. The general results are used to determine the efficiency-temperature trend for two example turbine applications. Author

N69-17398*# National Aeronautics and Space Administration. Langley Research Center, Langley Station Va.

PERFORMANCE OF A TOWED, 48-INCH-DIAMETER (121.92-cm) BALLUTE DECELERATOR TESTED IN FREE FLIGHT AT MACH NUMBERS FROM 4.2 TO 0.4

J. W. Usry Washington Feb. 1969 34 p refs Film supplement number L-1002 to this report is available on loan from NASA. Langley Research Center, Langley Station, Va. (NASA-TN-D-4943) Avail: CFSTI CSCL 01C

A ballute decelerator inflated by ram air was tested in free flight to determine the inflation, drag, and stability characteristics. The decelerator has a 40-inch (101.6-cm) envelope equatorial diameter and a 10-percent burble fence. It was towed 13.5 feet (4.12 m) aft of a cone-cylinder-flare payload with a maximum diameter of 18.21 inches (46.25 cm). The decelerator was deployed at an altitude of 115,000 feet (35.1 km) at a velocity of 4400 ft/sec (1342 m/sec) and inflated at a Mach number of 4.2 and a free-stream dynamic pressure of 163 lb/ft^2 (7.8 kN/m^2). The time from the beginning of inflation of the decelerator to full inflation was 0.42 second. Longitudinal loads during inflation were of the same order of magnitude as the steady-state drag load. The decelerator appeared to have excellent stability characteristics in pitch and yaw during and after inflation. Roll rates of both bodies increased after deployment from a minimum of about 2.6 radians/sec just prior to inflation to a maximum of about 6.8 radians/sec for the decelerator and about 5.8 radians/sec for the payload. The drag coefficient of the decelerator varied from about 1.45 at a Mach number of 1.25 to 0.67 at a Mach number of 4.2 Author

01 AERODYNAMICS

N69-17816*# National Aeronautics and Space Administration. Lewis Research Center, Cleveland, Ohio.

TWO DIMENSIONAL INVISCID JET FLOW FROM TWO NOZZLES AT AN ANGLE TO A PLANE SURFACE

Marvin E. Goldstein and Robert Siegel Washington Feb. 1969 45 p refs

(NASA-TN-D-5064) Avail: CFSTI CSCL 20D

Conformal mapping was used to obtain the free streamlines and wall pressure coefficient for jets issuing from two nozzles and striking a surface. The jet nozzle exit planes are at an angle to the surface and can be spaced an arbitrary distance apart and an arbitrary distance from the surface. The effect of nozzle position and tilt angle on the extent of the flow back between the nozzles is shown. The back flow results from a collision between part of the flow from each jet that has been turned by striking the plate. Author

N69-17818*# National Aeronautics and Space Administration. Langley Research Center, Langley Station, Va.

FORTRAN PROGRAMS FOR CALCULATING WIND-TUNNEL BOUNDARY INTERFERENCE

Harry H. Heyson Washington Feb. 1969 74 p refs

(NASA-TM-X-1740) Avail: CFSTI CSCL 20D

Boundary-interference programs, developed in NASA TR R-302, are presented without comment. These programs should be utilized only after careful consideration of the assumptions and procedures given in that report. A systematic computer procedure is developed for calculating the wind tunnel interference factors for arbitrary configurations from the interference calculations for a vanishingly small model. The method is not limited to any one tunnel configuration since it is necessary only to substitute a subroutine appropriate to the tunnel for that given herein. The underlying theory (subroutine DLTAS) in the present computer programs is directly applicable to models which produce large wake deflections, such as V/STOL models. These programs may also be used directly for more conventional testing at moderate lift coefficients by means of the few simple modifications. No sample calculations or check cases are provided. Author

N69-17831*# National Aeronautics and Space Administration. Lewis Research Center, Cleveland, Ohio.

THEORETICAL ANALYSIS OF FLOW IN VTOL LIFT FAN INLETS WITHOUT CROSSFLOW

Norbert O. Stockman and Seymour Lieblein Washington Feb. 1969 39 p refs

(NASA-TN-D-5065) Avail: CFSTI CSCL 20D

A method based on the Douglas incompressible potential-flow computer program has been used for the theoretical analysis of the axisymmetric flow in VTOL lift fan or engine inlets in static operation (no crossflow). The usefulness of the method for predicting flow in real inlets without flow separation was indicated by good agreement between theoretical results and limited available experimental compressible data. Example solutions were given for several different inlet configurations in which shroud curvature and depth, centerbody size and location, and inlet boundaries (type of installation) were varied. The application of the method to the design of an actual fan-in-wing inlet was given in some detail. Author

N69-19027*# National Aeronautics and Space Administration. Langley Research Center, Langley Station, Va.

TUFT-GRID SURVEYS AT LOW SPEEDS FOR DELTA WINGS

John D. Bird Washington Feb. 1969 33 p refs

(NASA-TN-D-5045) Avail: CFSTI CSCL 20D

Tuft-grid surveys were made along the chord and in the near wake of 60°, 75°, 82.5°, and 86.5° delta wings at low speeds in the Langley stability tunnel to show the nature of the flow in the vicinity of such wing planforms. The results are presented without a detailed discussion in that the photographs of the flow patterns are felt to be largely self-explanatory. An unusual wake pattern which gave evidence of three asymmetrically arranged trailing vortices was obtained for the 86.5° delta wing at an angle of attack of 25° and zero sideslip. Author

N69-19028*# National Aeronautics and Space Administration. Langley Research Center, Langley Station, Va.

USE OF SUPERPOSITION IN DIGITAL COMPUTERS TO OBTAIN WIND TUNNEL INTERFERENCE FACTORS FOR ARBITRARY CONFIGURATIONS, WITH PARTICULAR REFERENCE TO V/STOL MODELS

Harry H. Heyson Washington Feb. 1969 114 p refs

(NASA-TR-R-302) Avail: CFSTI CSCL 20D

A superposition method utilizing a digital computer is developed to obtain wall interference for arbitrary configurations. A variety of specific configurations are treated. Sample numerical results indicate that a large number of variables, such as wind-tunnel configuration, model configuration, wake deflection, model location, span of wing and tail, load distribution, sweep, angle tail height, may individually or collectively produce substantial effects on wall interference. Interference is particularly severe at the rear rotor of tandem systems; the maximum size of such systems for reasonable wall effects is discussed. Author

N69-19130*# National Aeronautics and Space Administration. Lewis Research Center, Cleveland, Ohio.

PERFORMANCE CHARACTERISTICS FROM MACH 2.58 TO 1.98 OF AN AXISYMMETRIC MIXED-COMPRESSION INLET SYSTEM WITH 60-PERCENT INTERNAL CONTRACTION

Robert W. Cubbison, Edward T. Meleason, and David F. Johnson Washington Feb. 1969 64 p refs

(NASA-TM-X-1739) Avail: CFSTI CSCL 20D

A study has been made in the Lewis 10 by 10 foot supersonic wind tunnel to determine the performance characteristics of an axisymmetric, mixed compression inlet system designed for Mach 2.5. Inlet performance is presented for 0° and maximum unstart angle of attack. Diffuser static pressure distributions and compressor face total pressure profiles are shown for several operating conditions. Data presented show effects of Mach number, Reynolds number, bypass flow, and vortex generators on performance. Performance during restart cycles and required area ratios for restart are presented. Author

N69-19243*# National Aeronautics and Space Administration. Langley Research Center, Langley Station, Va.

FULL-SCALE INVESTIGATION OF THE AERODYNAMIC CHARACTERISTICS OF A SAILWING OF ASPECT RATIO 5.9

Marvin P. Fink Washington Feb. 1969 32 p refs

(NASA-TN-D-5047) Avail: CFSTI CSCL 20D

An investigation was conducted to determine the aerodynamic characteristics of a full-scale model employing a sailwing having a wing aspect ratio of 5.9. The wing had a rigid leading-edge spar, rigid root and wing-tip ribs, a trailing-edge cable stretched between these ribs, and a fabric covering stretched between the leading and trailing edges. Included in the investigation were tests to determine the effect of a round leading edge as well as a D-spar leading edge on the aerodynamic characteristics of the model. Also, the effects of geometric dihedral on the lateral characteristics were determined. The aerodynamic characteristics of the sailwing compared favorably with those of a conventional wing in terms of maximum lift and maximum lift-drag ratio. The round-spar leading-edge configuration had higher lift coefficients but lower values of maximum lift-drag ratio than those of the D-spar configuration. Increased dihedral caused a decrease in maximum lift for both configurations, produced the expected increase in effective dihedral, and gave little effect on the directional stability characteristics. Author

N69-19641*# National Aeronautics and Space Administration. Langley Research Center, Langley Station, Va.

A NUMERICAL METHOD FOR EVALUATION AND UTILIZATION OF SUPERSONIC NACELLE-WING INTERFERENCE

Robert J. Mack Washington Mar. 1969 27 p refs

(NASA-TN-D-5057) Avail: CFSTI CSCL 01A

A numerical method for calculating (1) the inviscid flow nacelle-wing interference loads on a warped wing surface, (2) a load-compensating reflex camber surface for optimization purposes, and (3) the interference-lift effective-area contribution to sonic-boom pressure disturbances are presented and discussed. Within the limitations of a modified supersonic linearized theory, the numerical method can provide reasonable good estimations of the loads imposed on a wing surface by nacelles mounted nearby. Author

N69-19826*# National Aeronautics and Space Administration. Langley Research Center, Langley Station, Va.

EXPERIMENTAL PRESSURE DISTRIBUTIONS ON A 120° CONE AT MACH NUMBERS FROM 2.96 TO 4.63 AND ANGLES OF ATTACK FROM 0° TO 20°

Robert L. Stallings, Jr. and Dorothy H. Tudor Washington Mar. 1969 77 p refs

(NASA-TN-D-5054) Avail: CFSTI CSCL 01A

A sharp and a blunt 120° cone configuration were tested. The blunt configuration consisted of a spherical segment with a radius of 1/8 the base diameter and which faired into a 120° cone frustum. The tests were conducted at Mach 2.96, 3.95, and 4.63 over a range of angles of attack from 0° to 20°. Pressure distributions and shock shapes obtained on both the sharp and blunt cones at an angle of attack (α) of 0° were in good agreement with an approximate theoretical solution based on the one-strip method of integral relations. Mach number had no effect on pressure distributions expressed in the form of local measured pressures divided by the free-stream pitot pressure ($p_l/p_{t,2}$) for either the shapr or blunt configurations at $\alpha = 0°$. At $\alpha > 0°$, the Mach number effect was confined to the leeward side of both configurations and consisted of a decrease in $p_l/p_{t,2}$ with increasing Mach number. Pressure distributions on the cone frustum of the blunt and sharp configurations were essentially the same throughout the range of test variables. An approximate technique involving a tangent-cone concept is presented for predicting the windward and leeward pressures for $\alpha > 0°$. Results from this method are in fair agreement with experimental results both in the form of pressure distributions and force coefficients. For $\alpha > 0°$, the local pressures around the circumference of both the sharp- and blunt-cone configurations, nondimensionalized by the pressure measured along the windward ray, were in good agreement with an empirically derived second-order polynomial. Author

N69-19925*# National Aeronautics and Space Administration. Langley Research Center, Langley Station, Va.

A METHOD FOR DETERMINING THE TOTAL DRAG OF A POINTED BODY OF REVOLUTION IN SUPERSONIC FLOW WITH TURBULENT BOUNDARY LAYER

Charlie M. Jackson, Jr. and Rudeen S. Smith Washington Mar. 1969 67 p refs

(NASA-TN-D-5046) Avail: CFSTI CSCL 01A

An approximate mathematical model of the inviscid and viscid flow field about a body of revolution was developed by utilizing modifications of the second-order shock-expansion theory and of a theoretical analysis of compressible boundary layer growth with pressure gradient. The area of application of this model is intended to be restricted to the attached bow-shock condition in the supersonic flow region with an all turbulent boundary layer. The viscid–inviscid interaction is accounted for by iteration between the respective theories. The solution of the mathematical model including the iteration and the integration of surface conditions to give wave and friction drags was programmed for digital computation, and the program is included. The viscid and inviscid solutions including interactions were applied to several body shapes over a wide range of test conditions and the resulting total drag estimates generally agreed with the reported experimental values to within 5 percent. In view of the difficulty involved in obtaining precise experimental data, it is believed that the present method is generally as accurate as the current experimental testing techniques. Author

N69-19926*# National Aeronautics and Space Administration. Langley Research Center, Langley Station, Va.

EFFECTS OF CONE ANGLE, BASE FLARE ANGLE, AND CORNER RADIUS ON MACH 3.0 AERODYNAMIC CHARACTERISTICS OF LARGE-ANGLE CONES

William D. Deveikis and James Wayne Sawyer Washington Mar. 1969 47 p refs

(NASA-TN-D-5048) Avail: CFSTI CSCL 01A

A wind tunnel investigation was conducted on large angle cones to determine the effects on static aerodynamic characteristics of cone angles from 110° to 150°, base flare angles from 65° to 90°, and base corner radii to 20 percent of the base radius. The tests were conducted at angles of attack to 12° and at Reynolds numbers, based on maximum body diameter, of approximately 1.1 $\times 10^6$ and 3.0 $\times 10^6$ in a Mach 3.0 stream. All models were statically stable, and aerodynamic centers were located downstream from the base. The static stability was relatively insensitive to cone angle but decreased as the flare angle and corner radius increased. The axial force coefficient increased with cone angle and flare angle but decreased with increasing corner radius. Author

N69-20016*# National Aeronautics and Space Administration. Langley Research Center, Langley Station, Va.

WIND-TUNNEL DATA FROM A 0.16-SCALE V/STOL MODEL WITH DIRECT-LIFT AND LIFT-CRUISE JETS

Matthew M. Winston Washington Mar. 1969 72 p refs

(NASA-TM-X-1758) Avail: CFSTI CSCL 01C

Investigations were conducted on a 0.16-scale V/STOL model in the 17-foot (5.18-meter) test section of the Langley 300-mph 7- by 10-foot tunnel. Six cold-air ejectors were used to simulate four direct-lift and two lift-cruise jet engines. Longitudinal and lateral-directional aerodynamic characteristics were investigated for various model configurations, forward speeds, and power conditions in the transition and cruise flight ranges. In addition to control-effectiveness studies, the effects of power variations for different lift-nozzle settings and the effects of height above the ground were investigated. Author

N69-20873*# National Aeronautics and Space Administration. Flight Research Center, Edwards, Calif.

WIND-TUNNEL FORCE AND PRESSURE TESTS OF ROCKET-ENGINE NOZZLE EXTENSIONS ON THE 0.0667-Scale X-15-2 MODEL AT SUPERSONIC AND HYPERSONIC SPEEDS

Earl J. Montoya and Jack Nugent Washington Mar. 1969 65 p refs

(NASA-TM-X-1759) Avail: CFSTI CSCL 01A

Wind-tunnel force and pressure test results of nozzle extensions on the 0.0667-scale X-15-2 model over the free-stream Mach number range from 2.3 to 8.0 at angles of attack from $-5°$ to 18° and Reynolds numbers of 2.0 $\times 10^6$ per foot (6.56 $\times 10^6$ per meter) and 3.4 $\times 10^6$ per foot (1.12 $\times 10^7$ per meter) are presented. The effects of the presence of an aft-mounted ramjet shape and control-surface deflections are shown. Force data indicate that the addition of the nozzle extensions did not appreciably affect

the overall drag or static margin of the model. On the basis of these results as well as other considerations, a nozzle with an internal expansion ratio of 22.1 was deemed most suitable. The presence of this nozzle extension slightly increased the model base pressure. Fuselage afterbody flows impinged on the nozzle extension and formed a shock wave at the impingement point. Large longitudinal and circumferential pressure variations existed on the nozzle extension. Deflecting the speed brakes and horizontal tails significantly affected the nozzle pressures; whereas, the addition of the model ramjet did not have an effect. Author

N69-20914*# National Aeronautics and Space Administration. Lewis Research Center, Cleveland, Ohio.
CHARACTERISTICS STUDY OF A BICONE MIXED-COMPRESSION INLET FOR MACH 1.80 TO 2.50
Bernhard H. Anderson Washington Mar. 1969 35 p ref
(NASA-TN-D-5084) Avail: CFSTI CSCL 01A

A theoretical design study was made to evaluate the behavior of a bicone mixed compression inlet over the Mach number range 1.800 to 2.500 and to explore the possibilities in overall performance that may be realized by modifications of the external and internal geometries. For the inlet operating on-design, the results indicate three characteristics are required for favorable surface compression distributions and low flow distortion near the throat at off-design Mach numbers. These are (1) low-contour curvature of the internal surfaces, (2) nearly equal compression rates on the cowl and centerbody surfaces, and (3) generally low distortion levels in the flow field upstream of the throat. Author

N69-21000*# National Aeronautics and Space Administration. Langley Research Center, Langley Station, Va.
EXPLORATORY INVESTIGATION OF FLOW FIELD RESULTING FROM FORWARD-FACING NOZZLES EXHAUSTING NEAR A LARGE CYLINDRICAL BODY AT FREE-STREAM MACH NUMBERS OF 3.0 AND 6.0
Robert J. McGhee and James A. Martin Washington Mar. 1969 40 p refs
(NASA-TN-D-5030) Avail: CFSTI CSCL 01A

The investigation showed that the resulting flow field contained extensive regions of boundary layer separation and mixing adjacent to the cylindrical body. The extent of flow separation on the body depended upon the ratio of jet-exit static pressure to free-stream static pressure, jet-exit Mach number, and free-stream Mach number. An extensive wake region, caused by the limited expansion of the jet exhaust flow at the nozzle lip, was observed around the nozzles and body base at all test conditions. Increasing the angle of attack from 0° to 4° had only a minor effect on the flow field. Large local surface pressures resulted from the initial impingement of the nozzle exhaust on the body. The pressure coefficient on the body just forward of the nozzle exit, when based on jet-exit conditions, was independent of the ratio of jet-exit static pressure to free-stream static pressure and free-stream Mach number. Author

N69-21106*# National Aeronautics and Space Administration. Langley Research Center, Langley Station, Va.
ANTENNA EFFECTS ON THE AERODYNAMIC CHARACTERISTICS OF A 0.410-SCALE MODEL OF THE CAJUN ROCKET AT MACH NUMBERS FROM 2.30 TO 4.63
Lloyd S. Jernell Washington Mar. 1969 56 p ref
(NASA-TM-X-1771) Avail: CFSTI CSCL 01A

The effects of several proposed antenna configurations on the aerodynamic characteristics of a 0.410-scale model of the Cajun rocket were investigated in a wind tunnel at Mach numbers form 2.30 to 4.63. Data were obtained at angles of attack to approximately 12° for roll angles of 0°, 22.5°, and 45°. The results indicate that the antenna configurations investigated have no significant effects on either the normal force or pitching moment parameters. The turnstile and Dovap antennas contribute appreciably to the axial force coefficient. The greater values of the induced lateral characteristics are generally produced by the quadraloop and Dovap antennas. Author

N69-21477*# Lockheed-Georgia Co., Marietta.
MODEL TESTS OF JET INDUCED LIFT EFFECTS ON A VTOL AIRCRAFT IN HOVER
P. K. Shumpert and J. G. Tibbetts Washington NASA Mar. 1969 129 p refs
(Contract NAS1-7891)
(NASA-CR-1297) Avail: CFSTI CSCL 01A

Lift losses and jet decay profiles were measured for 18 nozzle configurations and various airframe configurations at nozzle pressure ratios from 1.4 to 2.3 and at heights from landing gear height to infinity. Outboard-hinged nozzle doors greatly increased the lift losses except near the ground. Increasing nozzle lateral spacing reduced the near-ground losses. Other changes had lesser lift effects. The lift losses out of ground effect correlated well with a jet decay parameter which reflected the amount of jet mixing and the corresponding strength of the induced flow field. After correcting for the effects of differences in the jet decay parameter, the results of the present tests also correlated well with the results of a previous NASA test program which used a similar model. Author

N69-21811*# National Aeronautics and Space Administration. Lewis Research Center, Cleveland, Ohio.
FORTRAN PROGRAM FOR CALCULATING VELOCITIES AND STREAMLINES ON A BLADE-TO-BLADE STREAM SURFACE OF A TANDEM BLADE TURBOMACHINE
Theodore Katsanis and William D. McNally Washington Mar. 1969 114 p refs
(NASA-TN-D-5044) Avail: CFSTI CSCL 20D

A Fortran 4 computer program was written that gives the blade-to-blade solution of the two dimensional, subsonic, compressible (or incompressible), nonviscous flow problem for a circular or straight infinite cascade of tandem or slotted turbomachine blades. The blades may be fixed or rotating. The flow may be axial, radial, or mixed. The results include streamline coordinates, velocity magnitude and direction throughout the passage, and the blade surface velocities. This method is based on the stream function using an iterative solution of nonlinear finite difference equations. Author

N69-22553*# National Aeronautics and Space Administration. Lewis Research Center, Cleveland, Ohio.
REVISED FORTRAN PROGRAM FOR CALCULATING VELOCITIES AND STREAMLINES ON A BLADE TO BLADE STREAM SURFACE OF A TURBOMACHINE
Theodore Katsanis and William D. McNally Washington Apr. 1969 59 p refs
(NASA-TM-X-1764) Avail: CFSTI CSCL 01A

An existing FORTRAN IV computer program for blade-to-blade aerodynamic analysis of turbomachine blades was revised to obtain a simpler program consistent with related programs. The analysis is for two-dimensional, subsonic, compressible or incompressible,

nonviscous flow in a circular or straight infinite cascade of blades, which may be fixed or rotating. The flow may be axial, radial, or mixed, and the stream channel thickness may change in the through-flow direction. The results include streamline coordinates, velocity magnitude and direction throughout the passage, and the blade-surface velocities. This report includes a complete description of the input required by the program and the program listing. Author

N69-22554*# National Aeronautics and Space Administration. Langley Research Center, Langley Station, Va.

EXPERIMENTAL STAGNATION POINT VELOCITY GRADIENTS AND HEAT TRANSFER COEFFICIENTS FOR A FAMILY OF BLUNT BODIES AT MACH 8 AND ANGLES OF ATTACK

James C. Ellison Washington Apr. 1969 24 p refs
(NASA-TN-D-5121) Avail: CFSTI CSCL 01A

Local pressure and heat-transfer measurements were obtained on a family of blunt, axisymmetric bodies having a range of ratios of body radius to nose radius from 0 to 0.707, and ratios of corner radius to body radius of 0 to 0.40. The experimental data were obtained at a Mach number of 8.0 and a Reynolds number of 1.37 $\times$ 10^6, over a range of angles of attack from 0° to 20°. An effective nose radius was determined for each body and employed to calculate the stagnation-point values of the heat-transfer coefficient. The results indicated that the stagnation-point heat-transfer coefficient for a given body geometry varies with the angle of attack, except for the flat-faced body having the largest corner radius. Author

N69-22938*# National Aeronautics and Space Administration. Lewis Research Center, Cleveland, Ohio.

FORTRAN PROGRAM FOR CALCULATING VELOCITIES IN A MAGNIFIED REGION ON A BLADE TO BLADE STREAM SURFACE OF A TURBOMACHINE

Theodore Katsanis and William D. McNally Washington Apr. 1969 83 p refs
(NASA-TN-D-5091) Avail: CFSTI CSCL 20D

A Fortran IV computer program was written to obtain a local detailed solution around a leading or trailing edge or in a slot region for compressible, subsonic, nonviscous flow on a blade-to-blade surface between turbomachine blades. This program allows a coarse-mesh solution for an entire blade-to-blade region to be magnified in a small rectangular region. The results include detailed surface velocities, velocity magnitude and direction, and stream-function values throughout the magnified region. The method is based on the stream function and uses the iterative solution of nonlinear finite-difference equations. Author

N69-23538*# National Aeronautics and Space Administration. Langley Research Center, Langley Station, Va.

WIND TUNNEL INVESTIGATION OF INFLATION OF DISK-GAP-BAND AND MODIFIED RINGSAIL PARACHUTES AT DYNAMIC PRESSURES BETWEEN 0.24 AND 7.07 POUNDS PER SQUARE FOOT

Charles H. Whitlock Washington May 1969 7 p refs
(NASA-TM-X-1786) Avail: CFSTI CSCL 01C

Exploratory wind-tunnel tests of the disk-gap-band and modified ringsail parachute con figurations have been conducted at dynamic pressures between 0.24 and 7.07 lb/ft^2 (11 and 339 N/m^2). Both parachutes exhibited positive inflation characteristics over the range of the tests within technique limitations. The disk-gap-band configuration required less time and distance to inflate than the modified ringsail configuration did. Author

N69-23769*# National Aeronautics and Space Administration. Lewis Research Center, Cleveland, Ohio.

OVERALL PERFORMANCE OF A TANDEM-BLADED INDUCER TESTED IN WATER

Richard F. Soltis, Donald C. Urasek, and Max J. Miller Washington May 1969 39 p refs
(128-31-32-12-22)
(NASA-TN-D-5134) Avail: CFSTI CSCL 01A

A 6.5-inch (16.5-cm) diameter inducer composed of tandem blades was tested. Design values of head rise coefficient and flow coefficient were 0.303 and 0.109, respectively. At design flow the noncavitating measured head rise coefficient was 0.278 at a hydraulic efficiency of 0.88. Cavitation caused the head rise to drop off at a suction specific speed of approximately 20,000. It is speculated that cavitation performance could be improved by reducing the blade thickness in the leading edge regions of both blades. The occurrence of cavitation is illustrated in still photographs and the visual observations are correlated with measured results. Small changes to slot geometry were made and resulted in relatively small changes in performance. Author

N69-23781*# National Aeronautics and Space Administration. Langley Research Center, Langley Station, Va.

WIND-TUNNEL INVESTIGATION OF THE AERODYNAMIC CHARACTERISTICS OF A TWIN-KEEL PARAWING

George M. Ware Washington May 1969 30 p refs
(NASA-TN-D-5199) Avail: CFSTI CSCL 01A

An investigation was conducted in the Langley full scale tunnel to determine the performance and the static stability and control characteristics of a twin keel parawing. The model was essentially an all flexible single keel parawing configuration with a rectangular panel added to form a center section between the triangular outboard panels. The tests showed that the model had a maximum lift-drag ratio of 3.4. The model was longitudinally stable from the minimum angle of attack attainable before nose collapse up to the stall angle, an angle of attack range of about 15°. Changing the length of the aft keel and wing tip lines was effective in trimming the model over the entire unstalled angle of attack range and resulted in a modulation in lift-drag ratio from 2.2 to 3.4. The model was directionally stable, had positive effective dihedral over the unstalled angle of attack range in which the configuration could be trimmed, and had longitudinal stability. At angles of attack above the stall, however, the model became directionally unstable and had negative effective dihedral. Differential deflection of the wing tips produced positive rolling moments and negative yawing moments over the test range of angle of attack when the lines were changed in a direction to lower the right wing tip. Author

N69-23892*# General Motors Corp., Indianapolis, Ind.

EXPERIMENTAL INVESTIGATION IN AN ANNULAR CASCADE SECTOR OF HIGHLY LOADED TURBINE STATOR BLADING. VOLUME 3: PERFORMANCE OF TANDEM BLADE

James L. Bettner Washington May 1969 73 p refs
(Contract NAS3-9404)
(NASA-CR-1341) Avail: CFSTI CSCL 01A

A tandem blade consisting of two airfoils was tested in a six blade annular cascade. The performance of this blade was evaluated and compared with that of a plain blade designed to the same set of velocity triangles and tested in the same cascade. The solidity of the tandem airfoil was approximately 91% of the plain blade. By all modes of performance evaluation, the tandem blade met or exceeded the design requirements. Because of flow separation effects, the plain blade consistently fell short of satisfying the design requirements. The tandem blade surface velocity distribution

and blade loads agreed well with theoretical values. Suction surface diffusion factor requirements were met or exceeded. High speed flow visualization studies showed that flow separation was prevented to the trailing edge of the tandem secondary airfoil. The tandem hub, mean, and tip blade sections were 1.2, 6.2, and 2.7%, respectively, in excess of satisfying the required change in tangential velocity across the blade row, while the comparable plain blade sections were 9.0, 8.5, and 11.1% deficient. Author

N69-23926*# National Aeronautics and Space Administration. Ames Research Center, Moffett Field, Calif.

NEWTONIAN AERODYNAMICS FOR CIRCULAR CONES MODIFIED TO PRODUCE LIFT AT ZERO ANGLE OF ATTACK

Barbara J. Short Washington May 1969 32 p refs

(NASA-TN-D-5193) Avail: CFSTI CSCL 01A

A parametric study was conducted to determine the theoretical aerodynamic characteristics of right circular cones modified to produce lift at zero angle of attack. In the modification, portions of the cone lying above and behind an inclined plane surface were removed. Newtonian impact theory was used to express force and moment coefficients as functions of the manner in which the cone is terminated by this cutting plane at the base. In addition, relationships were formed that allow limits of acceptable design and performance characteristics to be imposed, such as lower limits of useful volume and lift-drag ratios, assurance of maintaining supersonic flow over the trailing edges, and the permissible range of center-of-gravity locations to assure trim at zero angle of incidence. The configurations studied suggest that it is practical to trim cones at a useful level of lift-drag ratio without inclining the axis of the basic cone relative to the airstream. Author

N69-23927*# National Aeronautics and Space Administration. Langley Research Center, Langley Station, Va.

INVESTIGATION OF A CLASS OF BODIES THAT GENERATE FAR-FIELD SONIC BOOM SHOCK STRENGTH AND IMPULSE INDEPENDENT OF BODY LENGTH AND VOLUME

Raymond L. Barger and Frank L. Jordan, Jr. Washington May 1969 16 p refs

(NASA-TN-D-5148) Avail: CFSTI CSCL 01A

A design method is studied which provides a means of continually increasing the volume of a body without increasing the maximum overpressure or impulse. A sequence of three sonic-boom-generating bodies having length ratios of 1:2.5:4 and volume ratios of 1:7.6:16.6 was designed and tested. The results of the experiments, together with theoretical considerations, indicate that in the far field, the essential signature characteristics (maximum overpressure and impulse) are virtually the same for all three bodies. Author

N69-24764*# National Aeronautics and Space Administration. Langley Research Center, Langley Station, Va.

PRESSURE DISTRIBUTIONS ON 140°, 160°, and 180° CONES AT MACH NUMBERS FROM 2.30 TO 4.63 AND ANGLES OF ATTACK FROM 0° TO 20°

James F. Campbell and Dorothy H. Tudor Washington May 1969 148 p refs

(NASA-TN-D-5204) Avail: CFSTI CSCL 01A

Surface pressure distributions were experimentally obtained on spherically blunted cones with apex angles of 140°, 160°, and 180° (flat disk). The 140° and 160° cones had a ratio of nose radius to base radius of 0.25. Results indicate that an increase in cone angle or angle of attack or both leads to an increase in pressure windward of the measured stagnation point; a decrease in cone angle or an increase in angle of attack leads to a decrease in pressure leeward of the measured stagnation point. Mach number has little effect on the pressure distributions for the cones at zero angle of attack. At angles of attack greater than zero, an increase in Mach number results in a decrease in pressure on the leeward side of all the configurations. A correlation parameter successfully correlates the stagnation point locations for the entire range of test Mach number, cone angle, and angle of attack; an empirical representation of this correlation agrees with the experimental results. Pressure distributions at zero angle of attack agree with a theoretical solution based on the one-strip method of integral relations. Circumferential pressure distributions on large-angle conical bodies can be approximated by second-order polynomials. Author

N69-25244*# National Aeronautics and Space Administration. Langley Research Center, Langley Station, Va.

TRANSONIC AERODYNAMIC CHARACTERISTICS OF HYPERSONIC LOW-WAVE-DRAG ELLIPTICAL BODY-TAIL COMBINATIONS AS AFFECTED BY CHANGES IN STABILIZER CONFIGURATION

Charles H. Fox, Jr. and Bernard Spencer, Jr. Washington May 1969 61 p refs

(NASA-TM-X-1789) Avail: CFSTI CSCL 01A

An investigation has been made in the Langley high-speed 7- by 10-foot tunnel at Mach numbers of 0.89, 0.95, and 1.17 to determine systematically the effects of various combinations of outboard-stabilizer and vertical-tail configurations on the longitudinal and lateral-directional stability and the aerodynamic performance of an elliptical hypersonic low-wave-drag body. The longitudinal area distribution of the body conformed to the theoretical shape required to minimize the zero-lift hypersonic pressure drag under the geometric constraints of given length and volume. The body had an elliptical cross section with a semiaxis ratio of 2 (major axis horizontal) and had an equivalent fineness ratio of 6.14. Base-mounted outboard stabilizers were tested at various dihedral angles alone and in combination with either a single center-line vertical tail or with a vee-tail. The angle of attack was varied from approximately $-4°$ to $18°$ at sideslip angles of 0 and -5 The results of the study indicate that the maximum untrimmed lift-drag ratio is improved considerably by the addition of the outboard stabilizers. The resultant performance is, however, sensitive to changes in the stabilizer dihedral for a given tail configuration. Author

N69-25327*# General Motors Corp., Indianapolis, Ind. Allison Div.

EXPERIMENTAL INVESTIGATION IN AN ANNULAR CASCADE SECTOR OF HIGHLY LOADED TURBINE STATOR BLADING. VOLUME 2: PERFORMANCE OF PLAIN BLADE AND EFFECT OF VORTEX GENERATORS

James L. Bettner Washington NASA May 1969 148 p refs (Contract NAS3-9404)

(NASA-CR-1323; EDR-5315-Vol-2) Avail: CFSTI CSCL 21E

An annular cascade of six blades was designed and fabricated to exhibit the following aerodynamic characteristics: (1) equivalent weight flow per passage, (2) equivalent change in tangential velocity, (3) blade suction surface diffusion factor, Ds: 0.4. The plain blade was tested and the program base-line level of experimental performance was determined. Both flow visualization studies and aerodynamic measurements determined that flow separation occurred on the plain blade suction surface. The region of separated flow on the blade surface exhibited strong radial and circumferential variations. All of the blade configurations of the experimental program were designed for a radially constant suction surface diffusion factor of 0.4; however, plain blade diffusion factors of only

0.330, 0.332 and 0.312 were realized experimentally at the hub, mean, and tip sections, respectively. Also, the hub, mean, and tip sections were 9.0, 8.5, and 11.1% deficient in achieving the required change in tangential velocity across the blade row. Author

N69-25391*# National Aeronautics and Space Administration. Langley Research Center, Langley Station, Va.
CHARTS FOR INTERPOLATION OF LOCAL SKIN FRICTION FROM EXPERIMENTAL TURBULENT VELOCITY PROFILES
Jerry M. Allen and Dorothy H. Tudor Washington 1969 42 p refs
(NASA-SP-3048) Avail: CFSTI CSCL 01A

Charts which allow the easy and rapid determination of local skin friction from experimental turbulent velocity profiles taken in air on smooth surfaces are presented. The charts, calculated from the Fenter–Stalmach law of the wall, cover Mach number range from 0 to 5 and are good for all Reynolds numbers and total temperature levels. Caution should be employed when using these charts with profiles taken under conditions of large heat transfer or pressure gradient because of the lack of reliable experimental verification of the theory under these test conditions. The use of these charts requires that the experimental profile be plotted on translucent paper to the same scale as the charts presented in this report and overlaid on the proper chart. Author

N69-26271*# National Aeronautics and Space Administration. Langley Research Center, Langley Station, Va.
HYPERSONIC FLUTTER ANALYSIS USING MEASURED STATIC AERODYNAMIC DERIVATIVES, AND COMPARISON WITH EXPERIMENT
Robert C. Goetz Washington May 1969 52 p refs
(NASA-TN-D-5233) Avail: CFSTI CSCL 01A

A two-part investigation was conducted, the final intent being to evaluate a quasi-steady flutter analysis technique, using measured static aerodynamic derivatives, at hypersonic speeds. In the first part, static force and moment data were obtained for a series of square-planform double-wedge airfoils with both sharp and circularly blunted leading edges. Aerodynamic characteristics were obtained in helium flow over an angle-of-attack range of $-2°$ to 8° at Mach numbers of 6.8 and 15.3. The results indicate that increasing the leading-edge bluntness greatly increases the drag and decreases the lift at a given angle of attack at both Mach numbers. At a Mach number of 6.8 the aerodynamic center was found to shift forward with increase in bluntness, while at a Mach number of 15.3 there was a slight rearward shift. In the second part of the investigation, a two-degree-of-freedom quasi-steady flutter analysis, including rate terms, is formulated for these airfoils in terms of the experimentally determined slope of the lift curve and location of the aerodynamic center. These comparisons indicate that the pitch-rate term has a significant effect upon the flutter solution and should be included in the quasi-steady analysis. Author

N69-26312*# National Aeronautics and Space Administration. Lewis Research Center, Cleveland, Ohio.
EXPERIMENTAL DATA FOR TWO 1400-FEET PER SECOND TIP SPEED COMPRESSOR ROTORS OPERATED WITH INLET FLOW DISTORTIONS
Everett E. Bailey and Robert S. Ruggeri Washington May 1969 74 p refs Avail: CFSTI CSCL 01A

Data for two 1400-feet-per-second tip speed rotors operated with radial and circumferential flow distortions are presented for a range of equivalent rotor speeds from .50 to 100 percent. Rotor design pressure ratios were 1.6 and 1.76. Data are presented mostly in tabular form, and include radial and circumferential distributions of inlet and discharge total pressures and temperatures, and various wall static pressure measurements along the hub and outer casing. Uniform inlet flow data are included for comparison. Observations of flow conditions at near-stall, with and without distortion, are made. The desirability of comparing distortion data at zero stall margin is discussed. Author

N69-26976*# National Aeronautics and Space Administration. Lewis Research Center, Cleveland, Ohio.
JET EFFECTS ON BOATTAIL PRESSURE DRAG OF ISOLATED EJECTOR NOZZLES AT MACH NUMBERS FROM 0.60 TO 1.47
Douglas E. Harrington Washington May 1969 88 p refs
(NASA-TM-X-1785) Avail: CFSTI CSCL 20D

The cylindrical ejector nozzles were operated over a range of pressure ratios from approximately 1.0 (jet off) to 11 Results were obtained with both 15°and 10°boattail angles. The 15°configurations utilized different radii of curvature at the boattail juncture with a cylindrical forebody. Subsonically, the jet caused large reductions in boattail pressure drag whether the jet was under or overexpanded. A jet boundary simulator was effective in duplicating a fully expanded jet with an exit static-pressure ratio of one. Author

N69-28112*# National Aeronautics and Space Administration. Langley Research Center, Langley Station, Va.
EXPERIMENTAL INVESTIGATION OF THE TURBULENT BOUNDARY LAYER ON A TYPICAL SUBSONIC TRANSPORT FUSELAGE
Richard D. Samuels Washington Jun. 1969 88 p refs
(NASA-TN-D-5242) Avail: CFSTI CSCL 01A

It was determined that the velocity profile can be approximated by use of the widely accepted two-dimensional power-law representation. The velocity index reflects the effects of longitudinal pressure gradient, unit Reynolds number, angle of attack, and to an undetermined degree both the inviscid and the boundary-layer cross flow. The fuselage was more nearly axisymmetric at the forward stations than at the aft stations; consequently, there was little difference found in the boundary-layer parameters with respect to circumferential locations over the forward portions of the fuselage but large deviations in the parameters were noted over the aft portion. For the small angles of attack ($-2°$ to 2°), the various boundary-layer thicknesses varied linearly with angle of attack along the top and bottom center lines of the fuselage, but no definite trends were established for stations along the side. No regions of separated flow were detected on the fuselage. Nash's method for calculating the turbulent boundary layer on a body of revolution when applied to a body having a circumference equal to that of the actual fuselage gave reasonable agreement at an angle of attack of 0° with experiment for all the boundary-layer parameters at all stations for which measurements were made. Author

N69-29027*# National Aeronautics and Space Administration. Manned Spacecraft Center, Houston, Tex.
AERODYNAMIC CHARACTERISTICS DETERMINED DURING DEVELOPMENT OF THE APOLLO LAUNCH ESCAPE VEHICLE CONFIGURATION
William C. Moseley, Jr. and Francis Evans Bowen Washington Jun. 1969 89 p refs
(NASA-TN-D-5208) Avail: CFSTI CSCL 01A

Wind tunnel studies were conducted in the development of the Apollo launch escape vehicle to determine the effect of

configuration changes on the aerodynamic characteristics of the vehicle. Results indicate that changes in escape tower and rocket-body length had only slight effects on the static stability. Author

N69-29154*# National Aeronautics and Space Administration. Langley Research Center, Langley Station, Va.
AERODYNAMIC INVESTIGATION OF SHARP CONE-CYLINDER SPIKES ON 120 DEGREE BLUNTED CONES AT MACH NUMBERS OF 3.00, 4.50, AND 6.00
Robert J. McGhee and W. Frank Staylor Washington Jun. 1969 42 p refs
(NASA-TN-D-5201) Avail: CFSTI CSCL 01A

Some effects of sharp cone-cylinder spikes located at the apex of two 120° spherically blunted cones were investigated at free stream Mach numbers of 3.00, 4.50, and 6.00 at angles of attack of 0°, 2°, and 5°. Spikes of various lengths, diameters, and tip angles were tested, and surface-pressure distributions and schlieren photographs were obtained for the models. The free-stream Reynolds numbers were 6.89, 2.95 and 3.64 $\times$ 10^6 per meter at free-stream Mach numbers of 3.00, 4.50, and 6.00, respectively. Several distinct types of flow which occurred on the spikes were found to be a function of the parameter l/δ, the ratio of the spike-cylinder length to the bow-shock stand-off distance at the stagnation point. For spike lengths of $l/\delta < 0.8$, subsonic steady flow existed over the entire model with a small region of separated flow near the spike. The bow shock was detached and unsteady in the vicinity of the spike for $0.8 < l/\delta < 1.0$. The bow shock attached to the spike tip at about $l/\delta = 1.1$ and remained steady until flow oscillation again occurred at $l/\delta > 2.2$. A region of relatively low pressure separated flow occurred behind the attached bow shock and was followed by a high reattachment pressure near the intersection of the attached spike shock and detached body shock. Author

N69-29231*# National Aeronautics and Space Administration. Langley Research Center, Langley Station, Va.
TRANSONIC AERODYNAMIC CHARACTERISTICS OF TWO HYPERSONIC CRUISE CONFIGURATIONS
Richard A. Langhans Washington Jun. 1969 98 p refs
(NASA-TM-X-1816) Avail: CFSTI CSCL 01A

An investigation was conducted in the 8-foot transonic pressure tunnel to determine the aerodynamic characteristics of two hypersonic cruise airplane configurations. The investigation was conducted at Mach numbers ranging from 0.80 to 1.20, angles of attack from approximately $-5°$ to 15°, and constant Reynolds number per meter of 13.12 $\times$ 10^6. The results of the investigation show the distinct wing-body configuration is longitudinally unstable for the chosen center-of-gravity location and has a pitch-up tendency. This configuration is directionally stable and has positive effective dihedral. The blended wing-body configuration is longitudinally stable at Mach numbers greater than 0.90 and unstable at Mach numbers from 0.80 to 0.90. This configuration is directionally stable and has positive effective dihedral. Author

N69-29269*# National Aeronautics and Space Administration. Ames Research Center, Moffett Field, Calif.
AN EXPERIMENTAL AND THEORETICAL INVESTIGATION OF A SYMMETRICAL AND A CAMBERED DELTA WING CONFIGURATION AT MACH NUMBERS FROM 2.0 TO 10.7
Walter P. Nelms, Jr., Ralph L. Carmichael, and Charles R. Castellano Washington Jun. 1969 34 p refs
(NASA-TN-D-5272) Avail: CFSTI CSCL 01A

The effect of wing camber on the longitudinal aerodynamic characteristics was studied for a configuration representative of an airplane designed to cruise at hypersonic speeds. A 70° swept delta wing with a symmetrical section and 4-percent thickness ratio was compared to one of identical planform and thickness which was cambered so as to have a flat lower surface. Experiment data were obtained at eight Mach numbers from 1.99 to 10.70 and compared with estimates from three different theoretical procedures. It was found that a configuration with a flat-bottomed wing was in no way superior to a similar configuration with a symmetrical wing section. In fact, at the lowest Mach numbers of this study the flat-bottomed wing had a large negative pitching moment at zero lift, which would indicate fairly substantial values of trim drag. The characteristics could be predicted with fair accuracy by the tangent-wedge/tangent-cone procedure. Author

N69-29270*# National Aeronautics and Space Administration. Langley Research Center, Langley Station, Va.
USE OF TETRAFLUOROMETHANE TO SIMULATE REAL-GAS EFFECTS ON THE HYPERSONIC AERODYNAMICS OF BLUNT VEHICLES
Robert A. Jones and James L. Hunt Washington Jun. 1969 134 p refs
(NASA-TR-R-312) Avail: CFSTI CSCL 01A

An experimental and theoretical study was made of the use of CF_4 in low hypersonic flows as a means of simulating the flow field over the forebody of blunt configurations in hypersonic flight where dissociation of the gas in the shock layer gives large density ratios across the shock wave. A pilot model hypersonic CF_4 blowdown tunnel was built and studied. With this facility a normal-shock density ratio of 12.1 was obtained at a Mach number of 6 with stagnation conditions of 1650 N/cm^2 and 736°K. The results indicate that flow fields over the forebody of blunt configurations for real-gas conditions resulting in normal-shock density ratios up to 17 can be simulated by this method. A computer program for isentropic flow of CF_4 as well as flow across normal and oblique shocks was set up. Plots of various flow parameters are presented as a function of free-stream Mach number for various stagnation temperatures. A method for computing axisymmetric nozzle contours which includes a correction for boundary-layer displacement thickness is described. Author

N69-29318*# National Aeronautics and Space Administration. Langley Research Center, Langley Station, Va.
MEASUREMENTS OF MUTUAL INTERFERENCE HEATING FOR A PROBE ANTENNA MOUNTED ON AN APOLLO REENTRY CONFIGURATION
Robert A. Jones and James L. Hunt Washington Jun. 1969 38 p refs
(NASA-TM-X-1787) Avail: CFSTI CSCL 01A

A study was made at a Mach number of 8 to determine the interference heating effects of a probe antenna located on the windward afterbody of an Apollo model at a 25° angle of attack and protruding ahead of the undisturbed main bow shock. The interference heating effects were observed to occur only on the windward part of the afterbody. The presence of the probe antenna resulted in peak heating rated as large as 23 times the local value for a model without a probe or 2.3 times the reference heat transfer coefficient, which was the calculated heat transfer at the stagnation point of the Apollo model at an angle of attack of 0° This interference heating to the afterbody was very sensitive to Reynolds number with the highest heating rates occurring at the highest Reynolds numbers. The maximum interference heating rates to the probe occurred at the point where the slip-flow line emanating from the intersection of the body bow shock and the probe shock impinged on the lower edge of the probe. The value of this maximum heat transfer rate to the probe was 15.5 times

the reference value or 1.3 times the estimated value for the probe leading edge subjected to the undistrubed local flow conditions immediately behind the body bow shock. Author

N69-29479*# National Aeronautics and Space Administration. Lewis Research Center, Cleveland, Ohio.
ANALYSIS OF TWO DIMENSIONAL INVISCID MODEL OF JET IMPINGEMENT UNDER VERTICAL-TAKEOFF AIRPLANE
Robert Siegel and Marvin E. Goldstein Washington Jul. 1969 36 p refs
(NASA-TN-D-5288) Avail: CFSTI CSCL 01A

Conformal mapping was used to obtain the free streamline pattern and surface pressure distribution for downward jet flow issuing from two parallel slot nozzles. After striking the ground, a portion of the flow from each jet moves along the ground toward the centerline between the jets. When these two portions collide, an upflow results which strikes a plate above the ground simulating the undersurface of an airplane fuselage. Typical flow patterns are shown to illustrate the effect on the free streamlines of nozzle height, nozzle spacing, plate height, plate width, and plate angle. Author

N69-30060*# National Aeronautics and Space Administration. Lewis Research Center, Cleveland, Ohio.
CHARACTERISTIC DESIGN STUDY OF MIXED-COMPRESSION TWO-DIMENSIONAL INLETS WITH LOW-ANGLE COWLS FOR THE MACH NUMBER RANGE 2.70 TO 1.80
Bernhard H. Anderson Washington Jul. 1969 37 p refs
(NASA-TN-D-5330) Avail: CFSTI CSCL 01A

An analytical study was performed to evaluate the effects of several design variables at off-design Mach numbers. Major improvements were realized in overall surface Mach number distributions at off-design conditions by decreasing the internal compression rate in two ways: (1) extending the overall supersonic compression length to avoid surface inflection point, and (2) requiring greater compressive turning by the cowl lip shock. Decreasing the compression rate provided nearly equal cowl and centerbody Mach numbers and Mach number gradients on design. Author

N69-30063*# National Aeronautics and Space Administration. Langley Research Center, Langley Station, Va.
INFLATION AND PERFORMANCE OF THREE PARACHUTE CONFIGURATIONS FROM SUPERSONIC FLIGHT TESTS IN A LOW-DENSITY ENVIRONMENT
Charles H. Whitlock and Richard J. Bendura Washington Jul. 1969 53 p refs
(NASA-TN-D-5296) Avail: CFSTI CSCL 01C

Ten flight tests of modified-ringsail, disk-gap-band, and cross parachute configurations with deployment initiated at Mach numbers and dynamic pressures corresponding to conditions expected during entry into a Martian atmosphere have been completed. Comparison of flight results indicates that theoretical snatch force values were never exceeded when the deployment techniques of these tests were used. Opening loads showed no definite trend with Mach number. Values for filing times compared favorably with generally accepted empirical curves based on 15-percent geometric porosity. Canopy stability was good when Mach numbers were below 1.4 for the modified-ringsail and disk-gap-band configurations. At higher Mach numbers, one test of the disk-gap-band configuration showed canopy fluctuations. The cross-parachute canopies did not achieve a stable configuration during the data period. Comparison of the drag coefficients indicates that the cross parachute produced the highest values and the modified-ringsail values were slightly higher than those of the disk-gap-band configuration. Author

N69-30609*# Michigan Univ., Ann Arbor. Dept. of Aerospace Engineering.
SUBSONIC SPHERE DRAG MEASUREMENTS AT INTERMEDIATE REYNOLDS NUMBERS
Kenneth R. Sivier and J. A. Nicholls Washington NASA Jul. 1969 79 p refs
(Grant NGR-23-005-003)
(NASA-CR-1392) Avail: CFSTI CSCL 01A

The drag of spheres, at subsonic Mach numbers and Reynolds numbers from 25 to 4000, was studied in a continuous wind tunnel using a one-component, magnetic support-and-balance system. The low turbulence incompressible results verified this experimental approach, especially at Reynolds numbers below 300 where the spherical models were not disturbed by unsteady lateral forces. Measurements were also made to evaluate the effects of compressibility, slip flow (Knudsen numbers up to 0.04), sphere surface roughness, and free-stream turbulence (intensities up to 8%). Author

N69-30632*# National Aeronautics and Space Administration. Lewis Research Center, Cleveland, Ohio.
TWO-DIMENSIONAL CASCADE INVESTIGATION OF A TURBINE TANDEM BLADE DESIGN
Stanley M. Nosek and John F. Kline Washington Jul. 1969 18 p refs
(NASA-TM-X-1836) Avail: CFSTI CSCL 01B

Static pressures were measured on the surfaces, and total pressures were surveyed downstream of the trailing edge. The objective was to determine the surface flow characteristics and the trailing edge wake characteristics. Also overall performance in terms of kinetic energy loss was determined. Tests were with a six-bladed (five-passage) cascade in a tunnel open to atmosphere at the inlet. The inlet-total to exit-static-pressure ratios were over a range from 1.2 to 1.5. Author

N69-30722*# National Aeronautics and Space Administration. Ames Research Center, Moffett Field, Calif.
INVESTIGATION OF A 0.3-SCALE JET-TRANSPORT MODEL HAVING A JET-AUGMENTED *BOUNDARY-LAYER-CONTROL* FLAP WITH *DIRECT-LIFT* CONTROL CAPABILITY
Kiyoshi Aoyagi, Stanley O. Dickinson, and Paul T. Soderman (Army Aeron. Res. Lab.) Washington Jul. 1969 86 p refs
(NASA-TN-D-5129) Avail: CFSTI CSCL 01B

An investigation was conducted to define a trailing edge flap system for a large scale subsonic jet transport model that would provide high lift at low-thrust-to-weight ratios (0.05 to 0.10) and direct lift control. The model has a 35° swept wing of aspect ratio 6.43 and four pod-mounted engines under the wing. The flap system was externally jet-augmented from the exhaust of the inboard jet engines. The flap system consisted of a main flap with blowing boundary layer control and a small auxiliary flap for providing direct lift control. Results were obtained with three boundary layer control arrangements and two different auxiliary flap chords at several main and auxiliary flap deflections. Three-component longitudinal data and descent capabilities of the model with the resultant flap system are presented. The results of descent performance computations indicate that the resultant flap system is capable of providing ±0.2 g incremental acceleration normal to the flight path at an approach speed of 117 knots(1 g flight wing loading = 53 psf) or a 4° change in flight-path angle with a thrust-to-weight ratio of 0.05. Author

N69-30878*# National Aeronautics and Space Administration. Lewis Research Center, Cleveland, Ohio.

A STUDY OF HELIUM PENETRATION AND SPREADING IN A MACH 2 AIRSTREAM USING A DELTA WING INJECTOR

Louis A. Povinelli, Frederick P. Povinelli, and Martin Hersch Washington Jul. 1969 17 p refs

(NASA-TN-D-5322) Avail: CFSTI CSCL 01B

Experiments were conducted to determine if vortices could aid the penetration and spreading of helium in a Mach 2 airstream. A half-delta-wing injector, having a 30° semiapex angle and a 12° angle of attack, was used. This delta configuration was designed to produce leading edge vortices into which helium was injected. A flat plate of the same blockage area and at the same angle of attack was also run for comparison. Measured helium concentration showed that the half-delta injector was more effective than the angled flat plate in achieving greater penetration along the vortex position. The spreading was also larger with the delta injector. Author

N69-31228*# National Aeronautics and Space Administration. Ames Research Center, Moffett Field, Calif.

SHOCK SHAPES AND PRESSURE DISTRIBUTIONS FOR LARGE ANGLE POINTED CONES IN HELIUM AT MACH NUMBERS OF 8 AND 20

David A. Stewart and Mamoru Inouye Washington Jul. 1969 22 p refs

(NASA-TN-D-5343) Avail: CFSTI CSCL 01A

Bow-wave shapes and surface pressures were measured in helium at Mach numbers 8 and 20 on pointed cones with semivertex angles from 52° to 90°. For large cone angles ($\geq 65°$) the bow wave was nearly spherical, the bow-wave shape and surface pressure distribution were predicted adequately by both the method of integral relations and the method of Kaattari, and the bow-wave shape was not influenced by cone angle or a small amount of bluntness. For cone angles approaching shock attachment (attachment $< \sigma < 65°$) where the bow wave was no longer spherical, the method of integral relations adequately predicted the shock shape and surface pressure distribution. The Kaattari method was not applicable for these conditions. Author

N69-31337*# National Aeronautics and Space Administration. Langley Research Center, Langley Station, Va.

A FINITE-STEP METHOD FOR CALCULATION OF THEORETICAL LOAD DISTRIBUTIONS FOR ARBITRARY LIFTING SURFACE ARRANGEMENTS AT SUBSONIC SPEEDS

James A. Blackwell, Jr. Washington Jul. 1969 42 p refs

(NASA-TN-D-5335) Avail: CFSTI CSCL 01A

A simple theoretical method has been developed to compute the load distribution in subsonic compressible flow of arbitrary wings and lifting-surface arrangements. A finite-step method was used in the analysis. The results of the theoretical method have been compared with experiment and show good agreement. Author

N69-31360*# National Aeronautics and Space Administration. Lewis Research Center, Cleveland, Ohio.

ANALYTICAL INVESTIGATION OF TWO-DIMENSIONAL LOSS CHARACTERISTICS OF SUPERSONIC TURBINE STATOR BLADES

Louis J. Goldman and Michael R. Vanco Washington Jul. 1969 22 p refs

(NASA-TM-X-1823) Avail: CFSTI CSCL 01A

An analysis was conducted to determine the loss characteristics of two-dimensional, minimum length, supersonic nozzles with sharp-edged throats. Boundary layer characteristics were calculated and used to obtain the conditions downstream of the nozzles after the flow had mixed to a uniform state. Subsonic, sonic, and supersonic aftermixing axial Mach number solutions were obtained for this model. The loss characteristics were investigated for nozzles designed over an exit Mach number range of 1.5 to 5.0. The effect of nozzle flow angle, throat Reynolds number, and specific heat ratio on losses were studied. Author

N69-31875*# National Aeronautics and Space Administration. Langley Research Center, Langley Station, Va.

EFFECTS OF WING PLANFORM ON THE STATIC AERODYNAMICS OF A CRUCIFORM WING-BODY MISSILE FOR MACH NUMBERS UP TO 4.63

M. Leroy Spearman and Charles D. Trescot, Jr. Washington Jul 1969 140 p refs

(NASA-TM-X-1839) Avail: CFSTI CSCL 01A

Wind tunnel tests were made to determine the longitudinal and lateral aerodynamic characteristics of a cruciform wing–body missile configuration with various wing planforms. The planforms included a family of delta wings and a family of rectangular wings having a constant root chord but varying spans. In addition, a cranked-tip planform was included, and some limited tests were made to determine the longitudinal location effects for a rectangular wing. All configurations were tested at Mach numbers from 1.50 to 4.63 and, in addition, limited transonic results were obtained in the 8-foot transonic pressure tunnel for the body alone and the body with one of the rectangular wing planforms. The results are summarized in the form of various pertinent aerodynamic parameters as a function of Mach number. The summary of results is useful in demonstrating the importance of certain parameters, and should be useful in providing a source of systematic experimental data for future correlation with analytical techniques. Author

N69-32299*# National Aeronautics and Space Administration. Langley Research Center, Langley Station, Va.

EXPERIMENTAL FLOW PROPERTIES IN THE WAKE OF A 120° CONE AT MACH NUMBER 2.20

James F. Campbell and Josephine W. Grow Washington Jul. 1969 55 p refs

(NASA-TN-D-5365) Avail: CFSTI CSCL 01A

An investigation has been conducted to obtain flow properties in the wake of a 120° cone at a free-stream Mach number of 2.20 Free-stream Reynolds number based on model (base) diameter was 0.66×10^6 for the study. Measured total and static pressures were used to calculate the appropriate flow properties which are presented in tabular form. Results typical of the tabulated data indicate that the largest gradients in the flow properties occur at the location in the wake near the neck-down or recompression region. The wake profiles tend to smooth out farther downstream to the extent that static pressure becomes essentially constant across the wake. Velocity distributions at these distances were predicted empirically by considering velocity as a power-law function of longitudinal distance from the cone and as an exponential function of radial distance from the wake center. Author

N69-32338*# National Aeronautics and Space Administration. Langley Research Center, Langley Station, Va.

A NUMERICAL ANALYSIS OF THE USE OF PERFORATED WALLS TO CONTROL SHOCK LOCATION AND MOVEMENT IN AN INTERNAL COMPRESSION SUPERSONIC INLET

Clarence W. Matthews Washington Jul. 1969 53 p refs

(NASA-TR-R-317) Avail: CFSTI CSCL 01A

This paper presents an analysis of the ability of a perforated

wall in an internal-compression super-sonic inlet to control the motion of the shock due to variety of transients in the flow values at the engine face. The method of one-dimensional unsteady-flow characteristics was used to calculate the shock motion. The perforated walls were found to contain the shock within the inlet for appreciably larger transient magnitudes than was possible with solid walls. Author

N69-33210*# National Aeronautics and Space Administration, Langley Research Center, Langley Station, Va.
EFFECTS OF JET EXHAUST LONGITUDINAL AERODYNAMIC CHARACTERISTICS OF A JET V/STOL MODEL
Arthur W. Carter Washington Jul. 1969 135 p refs
(NASA-TN-D-5333) Avail: CFSTI CSCL 01A

A wind tunnel investigation of the jet location interference effects on the longitudinal aerodynamic characteristics of a jet V/STOL model has been made for an unswept untapered wing with an aspect ratio of 6 and 30 percent chord slotted flaps. The effects of jet location were explored systematically from several wing chord lengths ahead to several chord lengths behind the wing. Various vertical locations were also investigated. Aerodynamic and pressure data are presented. Author

N69-33237*# National Aeronautics and Space Administration. Langley Research Center, Langley Station, Va.
SUPERSONIC AERODYNAMIC CHARACTERISTICS AND SHOCK STANDOFF DISTANCES FOR LARGE-ANGLE CONES WITH AND WITHOUT CYLINDRICAL AFTERBODIES
James F. Campbell Washington Aug. 1969 97 p refs
(NASA-TN-D-5334) Avail: CFSTI CSCL 01A

Results of this study indicated that all the cone configurations were statically stable with the moment center located at the cone base. Addition of cylindrical afterbody sections resulted in increases in stability throughout the Mach number range. Axial force increased as cone semiapex angle was increased, a maximum being approached for the flat disk. Throughout the angle-of-attack range, addition of cylindrical afterbody sections resulted in reductions in axial force that were not more than 4 percent for all combinations of cone semiapex angles and cylinder lengths and were less than 3 percent for most combinations. Normal force and lift decreased as cone semiapex angle was increased, minimum values being obtained for the flat disk; an increase in these forces resulted when cylindrical afterbody sections were added. Shock standoff distance for any body with a detached shock wave appeared to be uniquely dependent on the inverse square of the density ratio across a normal shock. This dependence allowed shock standoff distance for the conical bodies to be adequately predicted within the test range of cone semiapex angles and Mach numbers. Author

N69-33275*# National Aeronautics and Space Administration. Langley Research Center, Langley Station, Va.
WIND-TUNNEL INVESTIGATION OF AN STOL AIRCRAFT CONFIGURATION EQUIPPED WITH AN EXTERNAL-FLOW JET FLAP
Lysle P. Parlett and James P. Shivers Washington Aug. 1969 86 p refs
(NASA-TN-D-5364) Avail: CFSTI CSCL 01A

The present investigation was performed to provide information on the static longitudinal and lateral characteristics of a proposed short take-off and landing (STOL) transport configuration utilizing the jet-flap principle. Longitudinal tests were conducted at engine gross-thrust coefficients of from 0 to 3.4 through a range of angle of attack which included the stall; and lateral tests were made, both power-off and power-on, through a sideslip range of $\pm 30^\circ$ at angles of attack of 0° and 10°. Untrimmed lift coefficients up to 7.8 were attained at a gross-thrust coefficient of 2.83 in the tail-off condition. With the tail on, nearly all high-lift conditions were characterized by a marked longitudinal instability which began at an angle of attack of 7°. The instability was apparently caused by the tip vortices which, under the influence of the highly loaded center section of the wing, were drawn into the region of the horizontal tail. The tail-on configuration was directionally stable and had positive dihedral effect at all flap and power settings tested; and in the take-off and landing conditions increasing power increased directional stability and decreased dihedral effect. With one outboard engine not operating, the model could be trimmed laterally and directionally up to lift coefficients of 4.2 in the take-off condition and 5.7 in the landing condition. Author

N69-33302*# National Aeronautics and Space Administration. Langley Research Center, Langley Station, Va.
AERODYNAMIC INTERFERENCE EFFECTS CAUSED BY PARALLEL-STAGED SIMPLE AERODYNAMIC CONFIGURATIONS AT MACH NUMBERS OF 3 AND 6
John P. Decker Washington Aug. 1969 85 p refs
(NASA-TN-D-5379) Avail: CFSTI CSCL 01A

A wind tunnel investigation has been conducted to examine the aerodynamic interference effects associated with simple three dimensional aerodynamic configurations placed parallel and in close proximity to each other. The configurations were 10° half-cone bodies that varied in length and were tested with and without simple delta wings. The flat surfaces of the configurations were adjacent to each other during testing. The effects of vertical spacing and relative incidence angle between the configurations were measured, and the resulting data were used to determine the influence of relative body size, nose bluntness, and lifting surfaces on the longitudinal aerodynamic characteristics of the lower configuration at Mach numbers of 3 and 6. Increasing the size of the upper configuration generally caused a progressive decrease in the normal-force-curve slope and a progressive decrease in the static longitudinal stability of the lower configuration. For the upper configuration larger than the lower configuration, the data suggest some form of progressive blanketing since the normal-force-curve slope decreases to zero and even negative values at some of the vertical spacings investigated. Increasing the incidence angle of the upper configuration generally caused nose-up increments in the pitching-moment coefficient and negative increments in the normal-force coefficient of the lower configuration. Author

N69-34703*# Northrop Corp., Hawthorne, Calif.
RECIRCULATION EFFECTS PRODUCED BY A PAIR OF HEATED JETS IMPINGING ON A GROUND PLANE
Gordon R. Hall and Kenneth H. Rogers Washington NASA May 1969 115 p refs
(Contract NAS1-7834)
(NASA-CR-1307) Avail: CFSTI CSCL 01A

An experimental investigation of the recirculation effects resulting from the interaction of a pair of heated jets, a quiescent environment, a ground plane, and a pair of inlets was performed. Upwash blockage surfaces were also used for selected tests. Inlet temperature rise and upwash flow characteristics were determined for a wide range of model geometries and inlet/nozzle flow conditions. Details of the near flow field structure were obtained. Inlet temperature rise and induced aerodynamic forces have been related to the character of the near flow field. The results of the investigation lead to several significant conclusions which relate directly to model simulation of full scale recirculation phenomena. Author

N69-34986*# National Aeronautics and Space Administration. Langley Research Center, Langley Station, Va.
AERODYNAMIC CHARACTERISTICS IN PITCH OF A 1/7-SCALE MODEL OF A TWO- AND THREE-STAGE ROCKET CONFIGURATION AT MACH NUMBERS OF 0.4 TO 4.63
William F. Hinson, Richard A. Langhans, and Roger H. Fournier Washington Aug. 1969 40 p refs
(NASA-TM-D-5378) Avail: CFSTI CSCL 01A

An investigation has been conducted to determine the longitudinal stability characteristics of the upper two- and three-stage combinations of a four-stage solid-propellant unguided rocket research vehicle. The stages tested were stabilized by trapezoidal cruciform fins. Test Mach number range for the three-stage configuration was 0.4 to 1.0; for the two-stage configuration, 0.4 to 4.63. Angle-of-attack range was approximately -4^0 to 14^0. Reynolds number ranged from 1.5×10^6 to 3.4×10^6 per foot (4.92×10^6 to 11.14×10^6 per meter). The general aerodynamic characteristics of normal-force, pitching-moment, and drag coefficients as a function of angle of attack and Mach number are presented. Author

N69-35300*# National Aeronautics and Space Administration. Langley Research Center, Langley Station, Va.
EXPERIMENTAL PRESSURE DISTRIBUTIONS FOR A FAMILY OF BLUNT BODIES AT MACH NUMBERS FROM 2.49 TO 4.63 AND ANGLES OF ATTACK FROM 0 DEG TO 15 DEG
Robert L. Stallings, Jr. and Dorothy T. Howell Washington Aug. 1969 87 p refs
(NASA-TN-D-5392) Avail: CFSTI CSCL 01A

A family of blunt bodies of revolution having variable nose and shoulder radii and cylindrical afterbodies were tested ranging in shape from a hemisphere cylinder to a flat face cylinder. Included is a complete tabulation of the experimental data and a discussion of the more significant findings. Author

N69-35521*# Lockheed Missiles and Space Co., Sunnyvale, Calif.
AERODYNAMIC EFFECTS OF BULBOUS BASES
Lars E. Ericsson and J. Peter Reding Washington NASA Aug. 1969 116 p refs
(Contract NAS1-6450)
(NASA-CR-1339; LMSC-4-17-68-4) Avail: CFSTI CSCL 01A

An exploratory study has been made of the effect that a bulbous base can have on the aerodynamic characteristics of blunt space capsules and slender reentry bodies. It is found that the base has a profound effect and can cause drastic loss of dynamic stability. A careful examination of available experimental data reveals that the often complex effects of bulbous bases can be explained using quasi-steady separated flow concepts. In general, a bulbous base adversely affects the vehicle dynamics but increases the static stability. Support interference is a serious problem that can prevent simulation in dynamic wind tunnel tests of full-scale vehicle dynamics. A possible means of measuring and correcting for this dynamic sting interference is outlined. Author

N69-35855*# National Aeronautics and Space Administration. Langley Research Center, Langley Station, Hampton, Va.
PRESSURES AND HEAT TRANSFER ON A 75 DEGREE SWEPT DELTA WING WITH TRAILING-EDGE FLAP AT MACH 6 AND ANGLES OF ATTACK TO 90 DEGREES
J. Wayne Keyes Washington Sep. 1969 46 p refs
(NASA-TN-D-5418) Avail: CFSTI CSCL 01A

An investigation has been made of the effects of deflecting a flap on the flow field on a 75° swept delta wing with sealed gap for angles of attack from 0° to 90°. Pressure and heat-transfer measurements were made with the free-stream Reynolds number (based on wing root chord) varying from 1.3×10^6 to 5.6×10^6 for 0° angle of attack and at 3.4×10^6 for angles greater than 0°. Flap deflections from 0° to 40° were investigated. In general, center line calculations based on existing two-dimensional methods were in good agreement with the trends of the pressure and heat-transfer distributions if the flow pattern characteristic of the angle-of-attack range and the type of boundary layer are taken into account. Author

N69-36699*# National Aeronautics and Space Administration. Langley Research Center, Langley Station, Va.
BODIES OF REVOLUTION HAVING MINIMUM TOTAL DRAG IN HYPERSONIC FLOW
Waldo I. Oehman and Sylvia A. Wallace Washington Sep. 1969 53 p
(NASA-TN-D-5438) Avail: CFSTI CSCL 01A

The calculus of variations was used to study minimum-drag bodies in hypersonic flow. Newton's formula for pressure drag was assumed, and viscous drag was formulated by use of a variable local skin-friction coefficient. Numerical results are included to assess the effect of the viscous drag for bodies having either given length and base height or given length and volume. The computer program is included for convenience. Author

N69-37521*# National Aeronautics and Space Administration. Lewis Research Center, Cleveland, Ohio.
FORTRAN PROGRAM FOR CALCULATING TRANSONIC VELOCITIES ON A BLADE-TO-BLADE STREAM SURFACE OF A TURBOMACHINE
Theodore Katsanis Washington Sep. 1969 99 p refs
(NASA-TN-D-5427) Avail: CFSTI CSCL 01A

A method was developed to obtain a transonic flow solution on a blade-to-blade surface of a turbomachine. The blade may be fixed or rotating. The flow may be axial, radial, or mixed. The results include velocities on the blade surface and throughout the passage. The transonic solution is obtained by a velocity-gradient method, using information obtained from a finite-difference stream-function solution at a reduced weight flow. Author

N69-38065*# National Aeronautics and Space Administration. Flight Research Center, Edwards, Calif.
FLIGHT-MEASURED AERODYNAMIC DRAG OF TWO LARGE EXTERNAL TANKS ATTACHED TO THE X-15-2 AIRPLANE AT MACH NUMBERS OF 1.6 TO 2.3
David F. Fisher Washington Oct. 1969 15 p refs
(NASA-TM-X-1895) Avail: CFSTI CSCL 01A

Full-scale power-on flight lift and drag measurements were made on the X-15-2 airplane just before and just after two large external fuel tanks were ejected. By subtracting the drag of the airplane after tank ejection from the drag of the airplane before tank ejection, the incremental drag due to the tanks was determined. Analysis of the data showed that the percentage increase of incremental drag due to the tanks was almost equal to the percentage increase in cross-sectional area caused by the tanks. A buildup drag estimate based on free-stream conditions agreed well with the flight data; whereas, the wind -tunnel data, although they had the same general trend of tank drag coefficient with Mach number, were lower than both the estimate and the flight data. Author

N69-38612*# National Aeronautics and Space Administration. Langley Research Center, Langley Station, Va.
EFFECT OF HYPERSONIC RESEARCH ENGINE INSTALLATION ON AERODYNAMIC CHARACTERISTICS OF 0.0667-SCALE MODEL OF X-15A-2 AIRPLANE AT MACH NUMBERS FROM 1.75 TO 4.63

Ernald B. Graves Washington Aug. 1969 186 p ref
(NASA-TM-X-1840) Avail: CFSTI CSCL 01A

An investigation was conducted in a wind tunnel to determine the effect of the proposed hypersonic research engine (HRE) installation on the aerodynamic characteristics of a 0.0667-scale model of the X-15A-2 research vehicle. Test Mach numbers ranged from 1.75 to 4.63 at a constant Reynolds number of 3.0×10^6 per foot (9.84×10^6 per meter). The angle of attack range was from about $-5°$ to $20°$ and the angle of sideslip range was from about $-4°$ to $9°$. Test results indicate that the installation of the hypersonic research engine on the X-15A-2 research vehicle will not generally produce any significant adverse effects on the static stability and control characteristics of the airplane. As expected, there is a small drag increase due to the presence of the engine. Shock patterns emanating from the leading edges of the wing and landing skid appear to be interacting with the flow field forward of the HRE inlet. This interaction would significantly influence the performance of the HRE. Author

N69-38670*# National Aeronautics and Space Administration, Washington, D.C.

AERODYNAMICS AND FLIGHT DYNAMICS OF TURBOJET AIRCRAFT

T. I. Ligum Sep. 1969 248 p refs Transl. into ENGLISH of the book "Aerodinamika i Dinamika Poleta Turboreaktivnykh Samoletov" Moscow, 1967 p 1-246
(NASA-TT-F-542) Avail: CFSTI CSCL 01A

The physical bases of high-speed aerodynamics, and the influence of air compressibility on the aerodynamic characteristics of wings and aircraft are presented. Primary attention is turned to passenger jets. The following areas are covered: takeoff characteristics of jets and methods of improving them; best climbing modes; horizontal flight; the descent; the landing approach; turns and corners; controllability and stability; icing and its influence on flying characteristics; and the characteristics of modern jet engines. Author

N69-38768*# National Aeronautics and Space Administration, Langley Research Center, Langley Station, Va.

DEVELOPMENT OF THREE-DIMENSIONAL PRESSURE-DISTRIBUTION FUNCTIONS FOR LIFTING SURFACES WITH TRAILING-EDGE CONTROLS BASED ON THE INTEGRAL EQUATION FOR SUBSONIC FLOW

Alfredo Navarro Crespo and Herbert J. Cunningham Washington Oct. 1969 74 p refs
(NASA-TN-D-5419) Avail: CFSTI CSCL 01A

For partial-span control surfaces of the trailing-edge flap type with leading-edge hinge and sealed gaps, a series of lifting pressure distributions are developed for deflected and deformed flaps on thin, swept, tapered wings for use in aeroelastic analysis. Solutions for the steady case are presented that overcome the fundamental problem of determining the nature and distribution of the pressure singularity along the flap leading edge and provide an advanced basis for extension to the oscillating case of flutter. Author

N69-38775*# National Aeronautics and Space Administration, Ames Research Center, Moffett Field, Calif.

LARGE-SCALE WIND-TUNNEL INVESTIGATION OF AN M1-L LIFTING BODY WITH AN INFLATABLE AND A RIGID AFTERBODY

Kenneth W. Mort and Michael D. Falarski (Army Aeron. Res. Lab.) Washington Oct. 1969 29 p refs
(NASA-TN-D-5468; A-2894) Avail: CFSTI CSCL 01A

The M1-L lifting body concept employs a high volumetric efficiency forebody and an inflatable afterbody that is deployed to provide lift-to-drag ratios sufficient for horizontal landings. The purpose of the investigation described here was to determine the low-speed aerodynamic characteristics of a large-scale model with an inflatable afterbody. In addition, a model with a rigid afterbody was tested as a datum for aeroelastic characteristics. Deployment of the inflatable afterbody increased the maximum lift-to-drag ratio (L/D) from less than 1 to slightly more than 2. This value was about 15 to 20 percent less than that for the model with the rigid afterbody. Because a maximum L/D of about 2-1/2 is the minimum value required to accomplish a horizontal landing, this 20-percent reduction appeared to be the most significant effect of flexibility. Studies indicated that deployment of the inflatable afterbody is mechanically feasible. Author

N69-40026*# National Aeronautics and Space Administration. Langley Research Center, Langley Station, Va.

SUPERSONIC LIFTING CAPABILITIES OF LARGE-ANGLE CONES

James F. Campbell and Dorothy T. Howell Washington Oct. 1969 66 p refs
(NASA-TN-D-5499) Avail: CFSTI CSCL 01A

Experimental data were obtained on wind-tunnel models at Mach numbers from 1.41 to 4.63 for a Reynolds number of 0.8×10^6 based on model base diameter. Cone semiapex angles ranged from $40°$ to $90°$ (disk). Results indicated that transverse displacement of the center of gravity vertically from the vehicle longitudinal center line is an effective method of producing trim lift on large-angle cones, the trim lifting capability increasing with increase in cone semiapex angle. An increase in cone semiapex angle decreases the transverse center-of-gravity displacement required to achieve a given value of trim lift-drag ratio, and correspondingly lowers trim angle of attack, and increases trim drag. Transverse displacement of the center of gravity up to 4 percent of the base diameter from the longitudinal center line results in continual decreases in trim drag to values that are about 80 percent of the trim drag obtained for the center of gravity located on the longitudinal center line. For all combinations of cone semiapex angle and transverse center-of-gravity location, trim drag is essentially constant at Mach numbers greater than 2. Rearward longitudinal displacement of the center of gravity from the cone base to 10 percent of the base diameter has little or no effect on the trim aerodynamic characteristics obtained by transverse center-of-gravity shift for cones with semiapex angles equal to or greater than $70°$. Author

N69-40345*# National Aeronautics and Space Administration. Manned Spacecraft Center, Houston, Tex.

WIND-TUNNEL INVESTIGATION OF THE AERODYNAMIC PRESSURES ON THE APOLLO COMMAND MODULE CONFIGURATION

William C. Moseley, Jr. and B. J. Wells (Federal Electric Corp., Houston, Tex.) Washington Oct. 1969 76 p refs
(NASA-TN-D-5514) Avail: CFSTI CSCL 01A

A program of wind-tunnel tests was conducted at Mach numbers from 0.4 to 19.0 to determine the pressure distribution of the Apollo command module. Data are presented for the angle-of-attack range from $0°$ to $180°$. Results of these tests are presented as pressure coefficients plotted against the physical positions of the orifices. Author

N69-40876*# National Aeronautics and Space Administration. Langley Research Center, Langley Station, Va.

PRESSURE DISTRIBUTION OF A LARGE SEMISPAN TILTING WING WITH 0.4-DIAMETER-CHORD, SINGLE-SLOTTED FLAP, AND A SINGLE PROPELLER 0.22 CHORD BELOW WING

Marvin P. Fink and Charles C. Smith, Jr. Washington Oct. 1969

01 AERODYNAMICS

380 p refs
(NASA-TN-D-5481) Avail: CFSTI CSCL 01A

The model consisted of a semispan wing-propeller combination and half fuselage. The tests were made for both up-at-the-tip modes of propeller rotation, with and without a leading edge slat and with and without fences. The tests consisted of the measurement of the wing surface pressures over a range of angles of attack from 5° to 80° for thrust coefficients of 0.90, 0.80, 0.60, and 0.30 for flap deflections at 0°, 20°, 40°, and 60°. The data are presented in tabulated form with only a minimum of analysis. Author

02

AIRCRAFT

Includes fixed-wing airplanes, helicopters, gliders, balloons, ornithopters, etc; and specific types of complete aircraft (e.g., ground effect machines, STOL, and VTOL); flight tests; operating problems (e.g., sonic boom); safety and safety devices; economics; and stability and control. For basic research see: 01 Aerodynamics. For related information see also: 31 Space Vehicles; and 32 Structural Mechanics.

A69-13367 *

AIRCRAFT WITHOUT WINGS.

C. A. Syvertson (NASA, Ames Research Center, Moffett Field, Calif.).

Science Journal, vol. 4, Dec. 1968, p. 46-51.

Discussion of the M2-F1 and M2-F2 wingless aircraft, which will enable astronauts to make their own landings at an airport of their own choice. These aircraft are of the lifting-body type, and the basic shape from which they were evolved was a cone. At modest cost, these vehicles are capable of reconciling the very different demands of hypersonic atmosphere entry and conventional airfield landing. It is suggested that the lifting body aircraft offers an attractive, proven alternative to purely ballistic manned capsules.

F. R. L.

A69-14930 *

TRAILING VORTEX HAZARD.

William A. McGowan (NASA, Aeronautical Vehicles Div., Washington, D. C.).

Society of Automotive Engineers, Business Aircraft Meeting, Wichita, Kan., Apr. 3-5, 1968, Paper 680220. 15 p. 19 refs.

Members, $0.75; nonmembers, $1.00.

Light aircraft that encounter the trailing vortex system generated by heavy transport aircraft can experience high roll rates, loss of altitude, and large structural loads. Envelopes of vortex system velocities, duration, and movement for various wind conditions have been determined. Specific operational procedures for the takeoff, landing, and en route phases of flight are suggested to enable the light aircraft pilot to avoid the wake turbulence of heavy aircraft.

(Author)

A69-15563 *

V/STOL SESSION INTRODUCTORY AND REVIEW PAPER.

John P. Campbell (NASA, Langley Research Center, Hampton, Va.).

(New York Academy of Sciences, International Congress on Subsonic Aeronautics, New York, N.Y., Apr. 3-6, 1967.)

New York Academy of Sciences, Annals, vol. 154, Nov. 22, 1968, p. 843-855. 7 refs.

Description of the basic characteristics of V/STOL aircraft with emphasis on propeller, ducted fan, and turbojet types. An illustration of the basic tradeoffs between hovering capability and cruising speed is given for the various V/STOL types. It is shown that the compound helicopter achieves higher speeds by unloading the rotor and using an additional means of propulsion for cruising flight. It is concluded that the various V/STOL types afford a wide range of capabilities to satisfy a variety of mission requirements and that at least two or three V/STOL types in addition to the helicopter will eventually see wide-spread operational use.

B.H.

A69-15568 *

NASA RESEARCH ON FLEXIBLE WINGS.

Francis M. Rogallo (NASA, Langley Research Center, Hampton, Va.).

(New York Academy of Sciences, International Congress on Subsonic Aeronautics, New York, N.Y., Apr. 3-6, 1967.)

New York Academy of Sciences, Annals, vol. 154, Nov. 22, 1968, p. 953-961. 16 refs.

Review of the presently known characteristics and possible future applications of flexible wings. Among the various flexible wings, the all-flexible wing is exciting much interest because - for the same gross weight and steady sink speed - it requires only 1/10 as much area as the conventional parachute. Stiffened high-performance flexible wings show promise of becoming economical, lightweight, rugged, stowable wings for cargo tow gliders, and a variety for sports gliders; they may also be useful in the recovery of boosters and hypersonic aircraft. Attempts to use stiffened flexible wings were not encouraging because a greater performance is needed than that provided by the rigid or inflated frame of wings of conical shape used. Wind-tunnel results show that the maximum lift-drag ratio of the single-keel wing is about 2-1/2 while that of the twin-keel wing is about 3.

G.R.

A69-15571 *

LIFTING-BODY RESEARCH VEHICLES IN A LOW-SPEED FLIGHT TEST PROGRAM.

John G. McTigue and Bertha M. Ryan (NASA, Flight Research Center, Edwards AFB, Calif.).

(New York Academy of Sciences, International Congress on Subsonic Aeronautics, New York, N.Y., Apr. 3-6, 1967.)

New York Academy of Sciences, Annals, vol. 154, Nov. 22, 1968, p. 1014-1032.

Discussion of a multiphased flight study to determine the handling qualities of lifting-body entry vehicles. Although manned orbital experience with ballistic shapes has been successful, the recovery of such vehicles leaves much to be desired. The maneuverability footprint at the time of retrofire for the Mercury and Gemini vehicles is extremely limited in comparison to the larger footprint of a lifting body with a maximum hypersonic lift-to-drag ratio of 1 to 1.3. In addition, the lifting body would provide a horizontal landing capability on prepared landing sites anywhere within the continental U.S. on a single orbit. Predictions based on small-scale wind-tunnel data are not always satisfactory, while predictions based on data obtained in full-scale wind tunnels with the actual flight vehicles are closer to the flight data for low-speed conditions. Fourteen glide flights on the M2-F2 have shown that the longitudinal handling qualities are good. It is hoped that the use of lifting bodies for space missions can be recommended within two years.

G.R.

A69-18058 *#

EXPERIENCE USING BALAKRISHNAN'S EPSILON TECHNIQUE TO COMPUTE OPTIMUM FLIGHT PROFILES.

Lawrence W. Taylor, Jr., Harriet J. Smith, and Kenneth W. Iliff (NASA, Flight Research Center, Edwards AFB, Calif.).

American Institute of Aeronautics and Astronautics, Aerospace Sciences Meeting, 7th, New York, N.Y., Jan. 20-22, 1969, Paper 69-75. 8 p. 12 refs.

Members, $1.00; nonmembers, $1.50.

Grant No. NGR-05-007-122.

A technique for computing optimum profiles is developed which differs from the classical gradient method in that a term representing the constraint of satisfying the equations of motion is included in the cost function to be minimized. Although the number of unknown independent functions is increased to include the state variables, the dimensionality of the gradient of the modified cost is greatly re-

duced, resulting in considerable savings in complexity and time. The unknown control and state variables are expressed in a functional expansion to facilitate solution by means of Newton's method. The effects of weighting terms and the number of functions on the convergence properties are discussed. Comparisons are made of solutions using the classical gradient method, dynamic programming, and Balakrishnan's epsilon technique. (Author)

A69-19546 *#
THE DYNAMIC RESPONSE OF A FLEXIBLE ROTOR BLADE TO A TIP-VORTEX INDUCED MOVING FORCE.
John F. Ward and William J. Snyder (NASA, Langley Research Center, Hampton, Va.).
American Institute of Aeronautics and Astronautics and American Helicopter Society, VTOL Research, Design, and Operations Meeting, Georgia Institute of Technology, Atlanta, Ga., Feb. 17-19, 1969, AIAA Paper 69-203. 15 p. 9 refs.
Members, $1.00; nonmembers, $1.50.

Approximate analytical solution of the dynamic response of a flexible rotor blade to a radially moving force. The results are interpreted specifically in terms of helicopter rotor-blade vibration characteristics associated with tip-vortex impingement. These results indicate that low-frequency mode resonant amplification of repetitive impulse loadings can be encountered at moderate to high forward speeds on lifting rotor systems. The resonant conditions are encountered in sequence with increasing forward speed. For blades of conventional design, the resonant frequencies are encountered at noninteger multiples of rotor rotational speed. (Author)

A69-19764 •
NASA AND FLIGHT SAFETY RESEARCH.
Charles W. Harper (NASA, Office of Advanced Research and Technology, Washington, D.C.).
Air Line Pilot, vol. 38, Feb. 1969, p. 10, 11.

Review of NASA flight safety research programs, most of which relate to situations in which an aircraft should not be found. The research takes two forms: finding means to avoid the unpleasant situation, and dealing with it when it cannot be avoided. The effect of very large size on aircraft handling qualities is discussed. It is suggested that safety will be realized by having a built-in and predetermined response to all failure modes. F.R.L.

A69-22379 *#
A COMPARISON OF NEWTON-RAPHSON AND OTHER METHODS FOR DETERMINING STABILITY DERIVATIVES FROM FLIGHT DATA.
Lawrence W. Taylor, Jr., Kenneth W. Iliff, and Bruce G. Powers (NASA, Flight Research Center, Edwards AFB, Calif.).
American Institute of Aeronautics and Astronautics, Flight Test, Simulation, and Support Conference, 3rd, Houston, Tex., Mar. 10-12, 1969, Paper 69-315. 16 p. 8 refs.
Members, $1.00; nonmembers, $1.50.

A new technique of determining stability derivatives from flight data is formulated and compared with the simple equations, analog matching, least squares, and Shinbrot methods of analysis. It is shown that the new technique, termed Newton-Raphson, is superior to the others whether flight data or a statistical model is used. Although the new method uses the Newton-Raphson technique, it is also similar to quasi-linearization. The Newton-Raphson technique has been developed to enable the use of a priori (wind tunnel) information and to automatically adjust bias terms and initial conditions to compensate for errors. The technique has been successfully applied to the X-15, XB-70, F-111, and HL-10 vehicles and has application to many other system identification problems. (Author)

A69-26872 *
THE X-15 PROGRAM IN RETROSPECT.
John V. Becker (NASA, Langley Research Center, Aero-Physics Div., Hampton, Va.).
Raumfahrtforschung, vol. 13, Mar.-Apr. 1969, p. 45-53. 21 refs.
USAF-supported research.

Review of the principal results of 199 flights of the X-15 research aircraft against a background of the original plans and goals. Noteworthy results were obtained in aerospace piloting problems, in validation of ground research and developmental testing facilities, and in the study of heat transfer in the presence of complex flow fields. The ability of the X-15 system to fly out of the atmosphere for a few minutes of space flight, followed by a steep reentry, produced additional data of value to the space program. Considerable detailed research and development efforts in many areas were given impetus, new and unsuspected problems were identified, and new technology was developed in time for urgent but initially unforeseeable applications. F.R.L.

A69-29702 *
FLIGHT INVESTIGATION OF THE WING-ROTOR LIFT-SHARING CHARACTERISTICS OF A HINGELESS ROTOR COMPOUND HELICOPTER.
Perry L. Deal and Julian L. Jenkins, Jr. (NASA, Langley Research Center, Hampton, Va.).
Society of Experimental Test Pilots, Technical Review, vol. 9, no. 3, 1969, p. 78-85.

Results of a NASA flight test program utilizing the Army/Lockheed hingeless rotor compound aircraft to determine the lift-sharing characteristics of the wing and rotor in both level and maneuvering flight. The data show that there is an inherent reduction in rotor lift as level flight airspeed is increased. The rotor overspeed tendencies could require constant attention during maneuvering flight. F.R.L.

A69-30369 *
SONIC BOOMS - FUNDAMENTAL CHARACTERISTICS.
Harry W. Carlson (NASA, Langley Research Center, Hampton, Va.).
IN: MAN IN HIS ENVIRONMENT; INSTITUTE OF ENVIRONMENTAL SCIENCES, ANNUAL TECHNICAL MEETING AND EQUIPMENT EXPOSITION, 15TH, ANAHEIM, CALIF., APRIL 20-24, 1969, PROCEEDINGS. [A69-30356 15-11]
Mt. Prospect, Ill., Institute of Environmental Sciences, 1969, p. 185-188.

Description of the nature of the aircraft-created pressure patterns which are responsible for the sound commonly referred to as the sonic boom. Experimental and theoretical studies dealing with the problem are reported. It is pointed out that analytic and wind-tunnel studies have also served in the establishment of aircraft design techniques for sonic-boom minimization. G.R.

A69-30480 *#
THE POTENTIAL OF NUCLEAR POWER FOR HIGH-SPEED OCEAN-GOING AIR-CUSHION VEHICLES.
Frank E. Rom and Albert F. Kascak (NASA, Lewis Research Center, Cleveland, Ohio).
American Institute of Aeronautics and Astronautics, Advanced Marine Vehicles and Propulsion Meeting, 2nd, Seattle, Wash., May 21-23, 1969, Paper 69-416. 17 p. 11 refs.
Members, $1.00; nonmembers, $1.50.

Investigation of the performance potential of air cushion vehicles powered with nuclear power plants based on nuclear aircraft technology. It is shown that aircraft nuclear power plants would be more than ten times lighter than current nuclear marine power plants. Based on a simplified cost analysis, the nuclear air cushion vehicle can carry payloads at the rate of 2 to 5 cents per ton mile. The cargo carrying capacity and the cost of hauling cargo in terms of cents per mile is independent of the range. The unrefueled range for these vehicles is expected to be of the order of 1 to 2 million miles. B.H.

A69-35639 * #
A STEERABLE LANDING GEAR FOR VEHICLES WITH MAIN GEAR SKIDS.
Upshur T. Joyner (NASA, Langley Research Center, Hampton, Va.).
American Institute of Aeronautics and Astronautics, Aircraft Design and Operations Meeting, Los Angeles, Calif., July 14-16, 1969, Paper

69-790. 11 p. 8 refs.
Members, $1.00; nonmembers, $1.50.

Description of a proposed steering system for lifting body spacecraft, consisting of a freely castoring corotating wheel nose gear with an axle that can be tilted right or left under pilot control, and skids on the main gear. A prototype gear used in research has developed a maximum usable steer force, or side force, of about 500 lb with an applied vertical load of 2000 lb. This amount of steer force is shown to be sufficient to prevent the HL-10 vehicle from leaving the side of a 150-ft-wide runway following touchdown on center line with a lateral drift rate of 25 ft per second. (Author)

A69-35648 * #
FUTURE TECHNOLOGY TRENDS IN AIRBREATHING PROPULSION.
James F. Dugan, Jr. (NASA, Lewis Research Center, Propulsion Section, Cleveland, Ohio).
American Institute of Aeronautics and Astronautics, Aircraft Design and Operations Meeting, Los Angeles, Calif., July 14-16, 1969, Paper 69-774. 11 p. 34 refs.
Members, $1.00; nonmembers, $1.50.

For subsonic jet transports, noise control is a very pressing problem. The means to control this noise at its source (the engine) are assessed. These include designing for high bypass ratio, lining the ducts with acoustic material, using resonators, choking the engine airflow in the inlet or compressor guide vanes, and rotor-stator blade spacing. Further advances in lower SFC and engine weight are forthcoming through higher turbine inlet temperature, higher bypass ratios, new fuels, and advanced materials. The current trends in turbine-blade cooling are discussed along with the use of blowing and suction techniques for achieving higher stage loading in compressors and turbines to reduce their size and weight. The propulsion systems for a possible nuclear-powered subsonic cargo aircraft are briefly reviewed. For V/STOL aircraft, a wide variety of propulsion systems are being evaluated in prototype aircraft. The major types and tradeoffs among engine weight, low fuel consumption, and noise are illustrated. The major trends in hypersonic airbreathing propulsion are in engines that operate in two or more modes and in supersonic combustion. (Author)

A69-35649 * #
RECENT STUDIES ON EFFECTS OF RUNWAY GROOVING ON AIRPLANE OPERATIONS.
Upshur T. Joyner, W. Pelham Phillips, and Thomas J. Yager (NASA, Langley Research Center, Hampton, Va.).
American Institute of Aeronautics and Astronautics, Aircraft Design and Operations Meeting, Los Angeles, Calif., July 14-16, 1969, Paper 69-773. 15 p. 14 refs.
Members, $1.00; nonmembers, $1.50.

Runway grooving is a significant way of improving tire traction in adverse weather conditions, and this technique has been under study by NASA. Various groove patterns have been evaluated for wet traction; one of the better groove patterns (with grooves 1/4 in. wide and 1/4 in. deep on 1 in. centers) was installed on a research runway. Full-scale traction studies were made using a Convair 990A transport and an F-4D fighter aircraft. Braking traction values obtained on the wet grooved runway were substantially higher than those obtained on the wet ungrooved runway. The results from these investigations were used as the basis for calculations of the effects of grooving on aircraft landing field length and takeoff balanced field length under wet conditions. Grooving is shown to be very beneficial on both counts. (Author)

A69-35952 * #
SOME TEST RESULTS FROM THE NASA PLANETARY ENTRY PARACHUTE PROGRAM.
Harold N. Murrow and John C. McFall, Jr. (NASA, Langley Research Center, Hampton, Va.).
(American Institute of Aeronautics and Astronautics, Aerodynamic Deceleration Systems Conference, 2nd, El Centro, Calif., Sept. 23-25, 1968, Paper 68-934.)
Journal of Spacecraft and Rockets, vol. 6, May 1969, p. 621-623. 16 refs.

Results are summarized from the 13-flight test program designed to furnish data applicable to decelerators for use on Mars. During the series, deployment was initiated at Mach numbers between 1.15 and 3.16 in the altitude region of 122,000 to 159,000 ft. Two techniques were employed to achieve the test conditions, one using a rocket vehicle and the other a large helium-filled balloon. The rocket-launched tests were conducted to obtain basic information on the candidate types and the balloon-launched tests to investigate their deployment performance in the wake of a large aeroshell. Three parachute types with diameters from 30 to 85 ft and a 15-ft-diam Ballute were tested. Deployment characteristics and loadings, drag values, and stability characteristics are summarized. Effects of porosity, sterilization, and mortar-type deployments are discussed. A unique "post-reefing" system for minimization of descent time after the data period is described. (Author)

A69-37154 * #
INFLUENCE OF DRAG ON THE MISSION PERFORMANCE OF HYPERSONIC AIRCRAFT.
Lionel L. Levy, Jr. (NASA, Ames Research Center, Moffett Field, Calif.).
Journal of Aircraft, vol. 6, July-Aug. 1969, p. 326-329. 6 refs.

The variations of drag during the climb and cruise phases of representative hypersonic-cruise transport missions were examined in detail for several possible hypersonic aircraft to assess the influence of drag on mission performance. During cruise, the drag due to lift has the most influence on estimates of performance, independent of configuration and altitude. During climb, the dominant drag component depends on configuration and/or flight path. In some cases, the friction drag was estimated to be 20 to 40 per cent of the total, a percentage great enough so that erroneous estimates would significantly affect performance estimates. Increasing the cruise Mach number increases the drag due to lift during both climb and cruise, and decreasing the allowable sonic-boom overpressure increases the drag due to lift during climb. Significant gains in performance can be realized for reasonably small reductions in drag. In one case, it was found that the payload capacity could be increased from 187 to 231 passengers by reducing the total drag 10 per cent throughout the mission. (Author)

A69-39015 * #
DEVELOPMENT STATUS OF ATTACHED INFLATABLE DECELERATORS.
Martin M. Mikulas, Jr. and Herman L. Bohon (NASA, Langley Research Center, Hampton, Va.).
(American Institute of Aeronautics and Astronautics, Aerodynamic Deceleration Systems Conference, 2nd, El Centro, Calif., Sept. 23-25, 1968, Paper 68-929.)
Journal of Spacecraft and Rockets, vol. 6, June 1969, p. 654-660. 6 refs.

An extensive research program encompassing both structural and aerodynamic disciplines has demonstrated the potentiality and workability of attached inflatable decelerators (AIDs) for supersonic application. An AID consists of an inflatable fabric afterbody attached to a payload which can be deployed at supersonic speeds to provide a sizable increase in drag. An analysis for the determination of constant tension (isotensoid) AID shapes and masses is presented, and results are given in the form of plots. Performance data obtained from both subsonic drop tests and supersonic wind-tunnel tests of models designed from the analysis are presented. The most significant results are those obtained in the AEDC 16-S propulsion wind tunnel on two 5-ft-diam models deployed at Mach numbers 2.2 and 3. Both models deployed successfully and experienced flutter-free flight. The internal pressure and total drag agreed well with values obtained from the analysis. (Author)

A69-39413 * #
DESIGN, DEVELOPMENT, AND FLIGHT TEST EXPERIENCE WITH LIFTING BODY STABILITY AUGMENTATION SYSTEMS.
Ronald P. Kotfilia (Sperry Rand Corp., Phoenix, Ariz.) and Weneth D. Painter (NASA, Flight Research Center, Edwards, Calif.).
American Institute of Aeronautics and Astronautics, Guidance, Control, and Flight Mechanics Conference, Princeton, N.J., Aug. 18-20, 1969, Paper 69-887. 13 p. 7 refs.
Members, $1.00; nonmembers, $1.50.

Description of the design and development of lifting body stability augmentation systems, and discussion of the ground test techniques that were used for their evaluation. Test criteria and procedures are established for various ground tests, such as frequency response, limit cycle, and structural resonance. Ground test results are compared with subsequent flight test data. Z.W.

A69-40803
EARTH OBSERVATIONS FROM BALLOONS; AMERICAN SOCIETY OF PHOTOGRAMMETRY, SYMPOSIUM, WASHINGTON, D.C., FEBRUARY 6, 7, 1969, PROCEEDINGS.
Falls Church, Va., American Society of Photogrammetry, 1969. 180 p.
Members, $5.00; nonmembers, $10.00.

CONTENTS:

METEOROLOGICAL CONSIDERATIONS FOR TETHERED AND HOVERING FREE BALLOONS. G. F. Nolan (USAF, Cambridge Research Laboratories, Bedford, Mass.), p. 5-18. (See A69-40804 22-02)

AGRICULTURAL AND FORESTRY APPLICATIONS OF BALLOONS. A. B. Park (U.S. Department of Agriculture, Washington, D.C.), p. 19-27. (See A69-40805 22-34)

BALLOON FLIGHTS TO TEST REMOTE SENSORS. A. P. Colvocoresses (U.S. Geological Survey, Washington, D.C.), p. 30-35. (See A69-40806 22-02)

SECONDARY EXPERIMENT SPACE AVAILABLE ON BALLOON FLIGHTS—1969. J. C. McFall, Jr. (NASA, Langley Research Center, Hampton, Va.), p. 38-43. (See A69-40807 22-02)

REPORT ON A TEST OF A HOT-AIR BALLOON AS A PLATFORM FOR MARINE OBSERVATIONS. R. R. Green, F. J. Hester, J. Rockwell, Jr. (U.S. Bureau of Commercial Fisheries, La Jolla, Calif.), and R. R. Whitney (U.S. Bureau of Sports Fisheries and Wildlife; Washington, University, Seattle, Wash.), p. 45-63.

MONITORING WATER POLLUTION FROM AN AIRBORNE PLATFORM. J. I. Bregman (U.S. Department of the Interior, Washington, D.C.), p. 65-80.

STATIONARY BALLOONS FOR USE IN THE BUREAU OF LAND MANAGEMENT. G. B. Torbert (U.S. Department of the Interior, Washington, D.C.), p. 81-90.

TETHERED BALLOON FOR STUDY OF COASTAL DYNAMICS. C. J. Sonu (Louisiana State University, Baton Rouge, La.), p. 91-102. (See A69-40808 22-02)

A SURVEY OF THE POTENTIAL OF BEAMED MICROWAVE POWER FOR BALLOONS. J. C. Graham (Raytheon Co., Sudbury, Mass.), p. 103-112. (See A69-40809 22-03)

A UNIQUE APPROACH TO BALLOON STATION KEEPING. E. R. Bourke (Raytheon Co., Waltham, Mass.), p. 113.

THE HOT AIR BALLOON AS AN OBSERVATIONAL PLATFORM. J. A. Winker (Raven Industries, Inc., Sioux Falls, S. Dak.), p. 115-127. (See A69-40810 22-02)

ADVANCED BALLOON SYSTEMS AS PHOTOGRAPHIC PLATFORMS. R. S. Ross (Goodyear Aerospace Corp., Akron, Ohio), p. 129-154. (See A69-40811 22-02)

THE CURRENT STATE OF THE ART OF PLASTIC BALLOONS. J. Nelson (Winzen Research, Inc., Minneapolis, Minn.), p. 155-161. (See A69-40812 22-02)

PERFORMANCE CHARACTERISTICS OF A TETHERED BALLOON SYSTEM. M. N. Silbert (NASA, Wallops Station, Wallops Island, Va.), p. 163-187. 10 refs. (See A69-40813 22-02)

A69-40807 * #
SECONDARY EXPERIMENT SPACE AVAILABLE ON BALLOON FLIGHTS—1969.
John C. McFall, Jr. (NASA, Langley Research Center, Applied Materials and Physics Div., Hampton, Va.).
IN: EARTH OBSERVATIONS FROM BALLOONS; AMERICAN SOCIETY OF PHOTOGRAMMETRY, SYMPOSIUM, WASHINGTON, D.C., FEBRUARY 6, 7, 1969, PROCEEDINGS. (A69-40803 22-02)
Falls Church, Va., American Society of Photogrammetry, 1969, p. 38-43.

Provision of information to new experimenters on secondary payload space availability on balloon flights, indicating the steps to follow in obtaining use of this space. There are three launching agencies: the USAF, the National Center for Atmospheric Research (NCAR), and the USN. Experiments should be autonomous, and weigh around 30 lb. The procedure for obtaining "hitch-hike" space is outlined, and the names and addresses of representatives of the launch agencies are given. F.R.L.

A69-40813 * #
PERFORMANCE CHARACTERISTICS OF A TETHERED BALLOON SYSTEM.
Mendel N. Silbert (NASA, Wallops Station, Vehicle Analysis Section, Wallops Island, Va.).
IN: EARTH OBSERVATIONS FROM BALLOONS; AMERICAN SOCIETY OF PHOTOGRAMMETRY, SYMPOSIUM, WASHINGTON, D.C., FEBRUARY 6, 7, 1969, PROCEEDINGS. (A69-40803 22-02)
Falls Church, Va., American Society of Photogrammetry, 1969, p. 163-187. 10 refs.

Description of tests determining the aerostatic and aerodynamic characteristics of the Dart Vee balloon. The physical properties of four Dart Vee balloons (nominal volumes range from 250 to 750 cubic feet) are presented, and their flight characteristics are evaluated. Results of the aerostatic analysis indicate that, due to the permeability of the gas envelope to helium, the balloon experienced a complete loss of super pressure and a loss of approximately ten per cent of its initial usable free lift in a 24 hour period. The results of the aerodynamic analysis indicate that the Dart Vee balloon has a lift to drag ratio of approximately 1.5 and a stall angle of 16.5 degrees. The balloon exhibited a static lift of 7.5 pounds and an aerodynamic lift of 70 pounds measured just prior to an observed instability which occurred at an airspeed of 18 miles per hour. P.G.

A69-41127
FLIGHT SAFETY FOUNDATION, ANNUAL INTERNATIONAL AIR SAFETY SEMINAR, 21ST, ANAHEIM, CALIF., OCTOBER 8-11, 1968, TECHNICAL SUMMARY.
Arlington, Va., Flight Safety Foundation, Inc., 1968. 249 p.
$5.00.

CONTENTS:

HOW GOES IT, p. i.

WHAT SIGNIFICANCE—STATISTICS. M. W. Eastburn (American Airlines, Inc., New York, N.Y.), p. 1-10. (See A69-41128 22-34)

RELIABILITY APPROACH TO AIRCRAFT SAFETY. I. Bazovsky (Genge Industries, Inc., Scientific and Consulting Div.), p. 10-12. (See A69-41129 22-02)

OVERALL WORLD STATISTICS. W. W. Moss (Pan American World Airways, Inc., New York, N.Y.), p. 12-28. (See A69-41130 22-34)

PLANNING FOR THE SUPERSONIC FUTURE. O. Bakke (Federal Aviation Administration, Washington, D.C.), p. 29-34. (See A69-41131 22-34)

SAFETY ELEMENTS OF ADVANCED AIRCRAFT DESIGN. T. F. Laughlin, Jr. (Lockheed Aircraft Corp., Burbank, Calif.), p. 35-43. (See A69-41132 22-02)

DESIGN FOR SAFETY–THIRD GENERATION AND AHEAD. A. G. Heimerdinger (McDonnell Douglas Corp., St. Louis, Mo.), p. 44-48. (See A69-41133 22-02)

DESIGN FOR SAFETY. D. James (British Aircraft Corp., Ltd., London, England), p. 42-57. (See A69-41134 22-02)

SAFETY ASSURANCE PROGRAM FOR THE B-747. J. N. Funk (Boeing Co., Seattle, Wash.), p. 58-72. (See A69-41135 22-02)

747 ENGINEERING PROGRAM, p. 72-78. (See A69-41136 22-34)

ADVANCED TRAINING CONCEPTS IN SIMULATION. R. E. Flexman (Illinois, University, Urbana, Ill.), p. 79-90. (See A69-41137 22-11)

HUMAN FACTORS IN FLIGHT TRAINING. A. Burrows (McDonnell Douglas Corp., Long Beach, Calif.), p. 91-97. 13 refs. (See A69-41138 22-05)

WHAT'S IMPORTANT IN SIMULATION? J. P. Reeder (NASA, Langley Research Center, Hampton, Va.), p. 98-116. 10 refs. (See A69-41139 22-11)

THE BUREAU OF AVIATION SAFETY AND THE ACCIDENT PREVENTION SYSTEM. C. O. Miller (National Transportation Safety Board, Washington, D.C.), p. 117-126. 7 refs. (See A69-41140 22-02)

THE SST ENVIRONMENT. N. A. Lieurance (ESSA, Washington, D.C.), p. 127-144. 12 refs. (See A69-41141 22-02)

SURVIVAL ASPECTS–THIRD GENERATION JETS. G. Bates (Federal Aviation Administration, Washington, D.C.), p. 145-156. (See A69-41142 22-34)

LESSONS FROM THE B-70 TO BE APPLIED TO SST SAFETY. F. Fulton (NASA, Edwards, Calif.), p. 157-169. (See A69-41143 22-02)

AIRLINE PILOTS LOOK AT THE FUTURE. C. Ruby (Air Line Pilots Association, Washington, D.C.), p. 170-187. (See A69-41144 22-34)

FLIGHT PERFORMANCE ANALYSIS. J. Nicholl (British Overseas Aircraft Corp., Hounslow, Middx., England), p. 188-190. (See A69-41145 22-02)

MEDICAL PROBLEMS FACING AIR CARRIER PILOTS TODAY AND IN THE FUTURE. E. Carter (Mayo Clinic, Rochester, Minn.), p. 191-198. (See A69-41146 22-05)

SATELLITES AND AIR SAFETY. R. Anderson, p. 199-205. (See A69-41147 22-07)

ADVANCED RECRUITING AND TRAINING METHODS. G. F. S. Hinckley (Overseas National Airways, Jamaica, N.Y.), p. 206-216. (See A69-41148 22-34)

THE COCKPIT TEAM AS PART OF THE COMPANY. R. Stone (United Air Lines, Inc., Chicago, Ill.), p. 217-222. (See A69-41149 22-34)

NEW CONCEPTS IN IN-FLIGHT MONITORING. J. Ferrarese (Federal Aviation Administration, Washington, D.C.), p. 223-228. (See A69-41150 22-05)

THE SOLUTION OF SAFETY PROBLEMS THROUGH RESEARCH AND DEVELOPMENT. R. L. Simpkins (Trans World Airlines, Inc., Kansas City, Mo.), p. 229-237. (See A69-41151 22-02)

LIST OF ATTENDEES, p. 238-240.

A69-41143 * #
LESSONS FROM THE B-70 TO BE APPLIED TO SST SAFETY.
Fitzhugh Fulton (NASA, Edwards, Calif.).
IN: FLIGHT SAFETY FOUNDATION, ANNUAL INTERNATIONAL AIR SAFETY SEMINAR, 21ST, ANAHEIM, CALIF., OCTOBER 8-11; 1968, TECHNICAL SUMMARY. (A69-41127 22-02)
Arlington, Va., Flight Safety Foundation, Inc., 1968, p. 157-169.

Discussion of the North American Rockwell XB-70 aircraft, a very valuable research vehicle that has produced important data that are particularly applicable to the SST program. The XB-70 is a large, delta-wing aircraft with dual vertical tail surfaces, a movable canard surface with trailing-edge flaps, and a movable nose ramp to provide acceptable visibility at low speed and reduced drag at high speed. It has been flown at Mach 3 and at altitudes above 70,000 ft. Flight characteristics vs wind tunnel predictions are compared. The cockpit instrumentation is described in detail and is evaluated. The XB-70 has vertical-tape flight instruments and round-dial engine instruments. Overspeed operation, inlet operation, and flying qualities are considered. Aspects of operation during deceleration and descent are treated, as well as questions of landing-gear reliability and hydraulic-system operation. F.R.L.

A69-42831 * #
FLIGHT EVALUATION OF RADAR-INERTIAL SYSTEMS.
Ronald J. Madigan (NASA, Electronics Research Center, Cambridge, Mass.).
American Astronautical Society and Operations Research Society of America, Joint National Meeting, Denver, Colo., June 17-20, 1969, AAS Paper 69-401. 31 p.

Review of the NASA-ERC program for the development of guidance, navigation, and flight control technology for aircraft. The technical approach includes in-flight evaluation of radio-inertial hybrid systems based initially on helicopter flight tests at Wallops Station, Va. Future plans for development and evaluation of advanced navigation and control systems and components are considered. Initial flight tests results of a radar-updated Gemini inertial navigation system during the approach and landing phase are presented. These results describe a range of performance based on deliberate variations of the system up-date and inertial system performance parameters. (Author)

A69-43279 *
APPLICATION OF QUADRATIC OPTIMIZATION TO HELICOPTER FLIGHT CONTROL.
Donald L. Gray, Paul S. Rempfer, and Lloyd Stevenson (NASA, Electronics Research Center, Cambridge, Mass.).
IN: AMERICAN AUTOMATIC CONTROL COUNCIL, JOINT AUTOMATIC CONTROL CONFERENCE, 10TH, UNIVERSITY OF COLORADO, BOULDER, COLO., AUGUST 5-7, 1969, PREPRINTS OF TECHNICAL PAPERS. (A69-43267 24-10)
New York, American Institute of Chemical Engineers, 1969, p. 240-247. 6 refs.

Application of steady-state linear quadratic optimal control results to flight control of a set of linearized helicopter equations of motion. A commanded step input is to be tracked quickly and smoothly with zero steady-state error, and all feedback gains are assumed to be constant. Potter's (1966) method of finding the steady-state solution to the matrix Riccati equation is used, with simple repeated roots present. The closed-loop system eigenvectors are used as a tool in adjusting the performance index. The resulting optimal feedback control system is simplified to create a suboptimal control feeding back only available state variables. These systems are compared with one designed by the classical means. (Author)

A69-43715 * #
STATUS OF RESEARCH ON PARAWING LIFTING DECELERATORS.
William C. Sleeman, Jr. and Thomas G. Gainer (NASA, Langley Research Center, Full-Scale Research Div., Hampton, Va.).
(American Institute of Aeronautics and Astronautics, Aerodynamic Deceleration Systems Conference, 2nd, El Centro, Calif., Sept. 23-25, 1968, Paper 68-967.)
Journal of Aircraft, vol. 6, Sept.-Oct. 1969, p. 405-409. 7 refs.

A significant amount of research information on all-flexible parawings has been obtained in wind-tunnel and flight-test investigations. The paper briefly summarizes some of the most important results obtained in these investigations in the key areas of performance and deployment technology. The parawing research areas currently receiving attention are reviewed, and some details of the technology development for recovery of manned space vehicles and for personnel escape systems for aircraft are presented. (Author)

N69-10087*# National Aeronautics and Space Administration. Langley Research Center, Langley Station, Va.
DEVELOPMENT OF SONIC-BOOM SIGNATURES IN A STRATIFIED ATMOSPHERE .
Raymond L. Barger Washington Nov. 1968 17 p refs
(NASA-TN-D-4890) Avail: CFSTI CSCL 01B

Equations describing the development of the pressure signature of a supersonic projectile or equivalent body of an airplane in straight steady level flight in an atmosphere having vertical gradients of temperature, pressure, and wind have been derived. The analytical method utilizes results of ray tube calculations for a stratified atmosphere in the context of an analysis by Whitham. Author

N69-10371*# National Aeronautics and Space Administration. Langley Research Center, Langley Station, Va.
FLIGHT TESTS OF A DIRECT LIFT CONTROL SYSTEM DURING APPROACH AND LANDING
Joseph W. Stickle, James M. Patton, and Robert C. Henry Washington Nov. 1968 46 p refs
(NASA-TN-D-4854) Avail: CFSTI CSCL 01B

The National Aeronautics and Space Administration has recently completed a flight program to evaluate the use of direct lift control (DLC) as an aid to flight path control during approach and landing. The program utilized a U.S. Navy F8-C airplane modified to incorporate symmetrically variable ailerons to augment the primary longitudinal control system. The airplane was also equipped with an airspeed sensing autothrottle and a commercially available cross-pointer-type instrument landing system. Approximately 230 approaches were made along various single- and two-segment approach paths, guidance being provided by a modified AN/GSN-5 radar and instrument landing system data link. Comparisons of flight path deviations and touchdown dispersion between the basic F8-C control system and the direct lift control system were made. The results indicate that direct lift control provides a better control of small flight path errors than the conventional F8-C control system. Direct lift control with a controlled pitch attitude change, provided through an aileron to horizontal tail interconnect, improved piloting performance and reduced workload during the approach and landing task. Author

N69-10495*# National Aeronautics and Space Administration. Ames Research Center, Moffett Field, Calif.
CALCULATED AND FLIGHT MEASURED HANDLING-QUALITIES FACTORS OF THREE SUBSONIC JET TRANSPORTS
Walter E. McNeill Washington Nov. 1968 32 p refs
(NASA-TN-D-4832) Avail: CFSTI CSCL 01D

As part of a NASA intercenter study of jet transport stability and control problems in severe turbulence, several calculated and flight-measured handling qualities factors of three current jet transports have been reviewed, and compared with various handling qualities criteria. The longitudinal and lateral handling qualities parameters were calculated by means of a digital computer program, for several typical flight conditions within the normal operating envelopes, using aerodynamic and physical data supplied by the manufacturers of the aircraft as the most reliable information available. The calculations did not take account of effects of yaw dampers and automatic pitch trim devices. On the basis of the current military specification and other published criteria, all three transports had satisfactory or acceptable predicted or flight measured longitudinal short period frequency and damping characteristics in the flignt conditions of interest. Except for some cases of speed instability associated with disengagement of Mach trim compensation devices, acceptable longitudinal phugoid characteristics also were calculated for these transports. Author

N69-10733*# National Aeronautics and Space Administration. Langley Research Center, Langley Station, Va.
LOW SUBSONIC FLIGHT AND FORCE INVESTIGATION OF A SUPERSONIC TRANSPORT MODEL WITH A VARIABLE-SWEEP WING
Delma C. Freeman, Jr. Washington Nov. 1966 84 p refs
Film supplement number L-1008 to this report is available on loan
(NASA-TN-D-4726) Avail: CFSTI CSCL 01C

An investigation was conducted in the Langley full scale tunnel to determine the low speed static and dynamic longitudinal and lateral-directional stability characteristics of a 1/20 scale model of a variable sweep wing supersonic commercial air transport configuration. The results of the investigation showed that the dynamic longitudinal stability and control characteristics of the model were generally satisfactory over the test angle of attack range except for the landing configuration at high angles of attack where the model was statically longitudinally unstable. The effects of power were found to be very large and stabilizing on the longitudinal stability of the model. In the wing sweep range from 20° to 42°, the model generally had good lateral-directional characteristics except for flights at the highest lift coefficients where the model diverged in yaw. The angles of attack at which these divergences occurred, were in the range where there was extensive stalling of the movable wing panels, and the airplane would not ordinarily be operated. As the sweep was increased past 42°, there was a marked deterioration in both lateral control effectiveness and Dutch roll damping, and at maximum sweep (Λ = 72°) an unstable Dutch roll oscillation together with very weak roll control made flight almost impossible. Author

N69-10935*# National Aeronautics and Space Administration. Langley Research Center, Langley Station, Va.
AERODYNAMIC CHARACTERISTICS OF TWIN PROPELLER DEFLECTED SLIPSTREAM STOL AIRPLANE MODEL WITH BOUNDARY LAYER CONTROL ON INVERTED V-TAIL
Richard J. Margason and Garl L. Gentry, Jr. Washington Nov. 1968 181 p refs
(NASA-TN-D-4856) Avail: CFSTI CSCL 01C

This report presents stability and control data for a small deflected-slipstream short take-off and landing (STOL) airplane model which had an inverted V-tail equipped with boundary-layer control. The results of the static wind tunnel investigation are promising and indicate that with further development, an inverted V-tail with boundary layer control can be designed which would produce the longitudinal and directional trim required for an engine-out situation with no control input by the pilot. The data also show that the lateral control required for an engine-out situation can be obtained from a spoiler with the attendant lift loss. The airplane can be trimmed with both engines operating with or without the boundary layer control on the tail when the flaps are retracted (0° flap deflection); however, when the flaps are deflected (45° flap deflection), the boundary layer control is needed to obtain trim up to a thrust coefficient of 2.10. The rudder is capable of producing large increments of yawing moment without changing directional stability and without causing cross coupling with rolling moment for both the flaps-retracted and the flaps-deflected configuration. Both flap configurations (flaps retracted and flaps deflected) with and without the boundary layer control on the tail have positive dihedral effect and are directionally stable through most of the test ranges of angles of attack and sideslip. Author

N69-11542*# National Aeronautics and Space Administration, Washington, D. C.
PROGRESS OF NASA RESEARCH RELATING TO NOISE ALLEVIATION OF LARGE SUBSONIC JET AIRCRAFT
1968 691 p refs Conf. held at Hampton, Va., 8–10 Oct. 1968
(NASA-SP-189) Avail: CFSTI CSCL 01B

The presented conference papers cover research progress in control and reduction of jet aircraft noise. Evaluated are noise reduction techniques for engines and nacelles currently in use, the possibility of steeper approach angles, and the development of less noise producing engines. For individual titles see: N69-11543 through N69-11581.

N69-13185*# *Cornell Aeronautical Lab., Inc., Buffalo, N. Y.*
SYNTHESIS METHODS FOR MANUAL AEROSPACE CONTROL SYSTEMS WITH APPLICATIONS TO SST DESIGN
Walter W. Wierwille and James R. Knight Washington NASA Dec. 1968 144 p refs
(Contract NAS1-7141)
(NASA-CR-1208; CAL-IM-2429-B-1) Avail: CFSTI CSCL 01D

Two synthesis approaches were studied: a programming approach and a man-machine performance approach. The programming approach places emphasis on moving the poles or eigenvalues of a closed-loop flight control system toward positions considered most desirable from a handling qualities point of view. These poles or eigenvalues are functions of each adjustable parameter in the compensators and various sensor feedback paths. To adjust the various parameters optimally, a programming procedure was developed that was implemented by means of digital computer programs. Three programs have been developed. The first performs synthesis in a single flight regime, determining optimum fixed values for the adjustable parameters. The second performs synthesis in an arbitrary number of flight regimes simultaneously, again determining a single set of fixed-values for the adjustable parameters. The third program also performs synthesis in an arbitrary number of flight regimes simultaneously, but allows specified parameters to vary from one regime to another. The programming approach was applied to the longitudinal dynamics of an SST for six flight regimes. It was found that all three programs operated effectively in moving the closed-loop system poles. Author

N69-13252*# National Aeronautics and Space Administration. Ames Research Center, Moffett Field, Calif.
FLIGHT TESTS UNDER IFR WITH AN STOL TRANSPORT AIRCRAFT
Robert C. Innis, Curt A. Holzhauser, and Richard P. Gallant Washington Dec. 1968 65 p refs
(NASA-TN-D-4939) Avail: CFSTI CSCL 01B

An STOL transport was studied in instrument flight. This aircraft was flown on 7-1/2° and 2-1/2° ILS approaches. It could be flown comfortably and accurately on the 7-1/2° ILS at 60 knots to 200 feet above the runway. The descent and deceleration capabilities were more than adequate in the approach and landing configuration, but were not sufficient in the preapproach configuration. The handling characteristics during instrument flight were generally satisfactory, except for moderate heading excursions at low speeds and moderate angle-of-attack excursions at the rear center of gravity. These characteristics, while not satisfactory, were acceptable and are considered general problems of STOL aircraft operations. Author

N69-14008*# National Aeronautics and Space Administration. Langley Research Center, Langley Station, Va.
FLYING QUALITY FACTORS CURRENTLY LIMITING HELICOPTER NAP OF THE EARTH MANEUVERABILITY AS IDENTIFIED BY FLIGHT INVESTIGATION
Henry L. Kelley, Robert J. Pegg, and Robert A. Champine Washington Dec. 1968 49 p refs
(NASA-TN-D-4931) Avail: CFSTI CSCL 01B

A flight investigation utilizing two modern lightweight helicopters was conducted to study the effects of flying qualities on nap-of-the-earth maneuver capability. Variation in flying qualities was provided by the markedly different stability and control characteristics which resulted from the basically different rotor systems of the two test vehicles. Several tasks were used to provide a realistic basis on which to determine the parameters most pertinent to maneuver capability. The results indicate that the initial angular response characteristics about the roll axis and the sensitivity of the height control are of primary importance. For example, the tightness of the initial roll response, as determined by the magnitude of roll-control sensitivity in combination with angular-velocity damping, had a significant influence on the pilot's ability to attain quickly, precisely, and consequently safely, those bank angles necessary to perform the tasks smoothly. Wind velocity and direction, stick-fixed maneuver stability gradients, angular-velocity and control-system coupling, vibration, and power-governing-system characteristics were other factors that significantly influenced the pilot's ability to maneuver the helicopters. Author

N69-14504*# National Aeronautics and Space Administration. Manned Spacecraft Center, Houston, Tex.
A MATHEMATICAL MODEL FOR CALCULATING THE FLIGHT DYNAMICS OF A GENERAL PARACHUTE-PAYLOAD SYSTEM
Joe D. Gamble Washington Dec. 1968 34 p refs
(NASA-TN-D-4859) Avail: CFSTI CSCL 01A

An analysis yielding six-degree-of-freedom equations of motion is presented for predicting the dynamic behavior of a general parachute-payload system. The parachute canopy and associated air-mass are approximated as a rigid body, and separate equations of motion are derived for the canopy and payload subject to the constraint of the risers and suspension lines. The analysis determines the forces and the response of various riser and suspension-line geometries subjected to large displacements, under the assumption that these lines are linearly elastic. The equations are readily adaptable to computer solutions and should be of interest in analyzing the dynamic performance of lifting-parachute payload systems. Author

N69-14729*# Litchford Systems, Northport, N. Y.
STUDY OF ADVANCED ELECTRONIC APPLICATIONS TO AERONAUTICAL DISPLAY AND CONTROL PROBLEMS
G. B. Litchford Washington NASA Jan. 1969 140 p refs
(Contract NASw-1541)
(NASA-CR-1240) Avail: CFSTI CSCL 01D

Electronic aids for navigation, ATC, and collision avoidance in the field of general aviation are discussed, with the aim of accomodating the pilot with minimum IFR capability. Low cost electronic air and ground aids are outlined, and time shared VHF Omnirange (VOR) area coverage is evaluated. Data transmission techniques are discussed as to potential, cost, and effectiveness. General aviation use of the national Secondary Surveillance Radar System (SSR) is treated in light of increased air traffic, both commericial airline and general aviation, in altitudes less than 10,000 feet and the corresponding increase in collision potential. Recent developments in the SSR system include a low cost modified airborne transponder which could be installed in general aviation aircraft to effectively combat the risk of collision in dense airspace. Electronic simulation of very low visibility landing guidance and instrument displays is discussed as to presently available equipment and the need for more flexible and complex systems. A summary of the general requirements of computer generated low visibility landing systems concludes the study. A.C.R.

N69-14763*# Stencel Aero Engineering Corp., Asheville, N. C.
HUMAN SURVIVAL IN AIRCRAFT EMERGENCIES
Charles A. Yost and Ronald W. Oates Washington NASA Jan. 1969 61 p refs
(Contract NASw-1530)
(NASA-CR-1262) Avail: CFSTI CSCL 01B

A general study was performed to outline methods for the improvement of human survival in civilian aircraft emergencies. Survival condition criteria, accident statistics and human tolerance limits were surveyed with respect to those aircraft used in two categories: certificated air carriers and general-private aviation (including official executive aircraft). The methods presented for aircraft occupant survival improvement fall into the general areas of occupant protection through seat design and occupant restraint improvement to withstand impact accelerations which are applied to the aircraft. Author

N69-16384*# National Aeronautics and Space Administration. Ames Research Center, Moffett Field, Calif.

LARGE SCALE WIND TUNNEL INVESTIGATION TO IMPROVE THE LOW SPEED LONGITUDINAL STABILITY AT HIGH LIFT OF A SUPERSONIC TRANSPORT WITH VARIABLE-SWEEP WINGS

Anthony M. Cook and Dale G. Jones Washington Jan. 1969 57 p refs

(NASA-TN-D-5005) Avail: CFSTI CSCL 01A

An investigation has been made in the Ames 40- by 80-Foot Wind Tunnel to develop techniques to improve the longitudinal stability for a supersonic transport. The model had a wing pivot outboard of the fuselage, a high aspect ratio movable wing panel, and a highly swept, fixed, inboard wing portion (strake). Special efforts were made to minimize the adverse effects of the vortex flow from the highly swept strake leading edge. Flow control devices tested on the strake included increased leading edge radius, leading edge (Krueger-type) flaps, and upper surface vortex generators. Fences on both strake and movable wing panel were also tested. The results show the basic model with a sharp strake leading edge to have pitch-up at an angle of attack as low as 5°. The use of a larger strake leading edge radius together with a strake leading edge flap and a wing fence produced essentially linear pitching moment characteristics to 18° angle of attack, with a stable break at stall. A combination of vortex generators on the strake upper surface, and a wing fence outboard of the pivot also produced acceptable pitching moment characteristics. Author

N69-17257*# National Aeronautics and Space Administration. Langley Research Center, Langley Station, Va.

SUPERSONIC TRANSPORT OPERATING PRACTICES DURING SIMULATED OPERATIONS IN FUTURE AIR TRAFFIC CONTROL SYSTEM ENVIRONMENTS

Milton D. McLaughlin and Richard H. Sawyer Washington Feb. 1969 65 p refs

(NASA-TN-D-5018) Avail: CFSTI CSCL 01B

Operating practices of the supersonic transport (SST) during simulated operations in air traffic control (ATC) system environments conceived for the time period for introduction of the SST into service are presented. An SST flight simulator and the Federal Aviation Administration ATC simulation facilities were used to create the real-time simulations. The SST flight simulator was operated by airline crews and the ATC simulation facilities by experienced air traffic controllers. The test program included departure and arrival operations under instrument flight rule conditions in the New York and Los Angeles terminal areas with two design study configurations of the SST. The design study configurations were representative of variable-sweep and fixed-wing designs. Both designs had a variable-incidence forebody. Author

N69-17279*# National Aeronautics and Space Administration. Langley Research Center, Langley Station, Va.

VARIABILITY IN SONIC-BOOM SIGNATURES MEASURED ALONG AN 8000-FOOT LINEAR ARRAY

Domenic J. Maglieri, Vera Huckel, Herbert R. Henderson, and Norman J. McLeod Washington Feb. 1969. 58 p refs

(NASA-TN-D-5040) Avail: CFSTI CSCL 20A

Systematic measurement studies designed to minimize all effects other than those of the local atmosphere are presented to document the variability of sonic-boom signatures at ground level. Measurements from an 8000-foot (2438-meter) linear microphone array indicate that wavelike overpressure patterns in which the signature shapes progress from peaked to rounded vary with time. Such variations are believed to be attributable to the atmosphere rather than to the airplane motion. Analyses of data for the same instruments, test array, time period, airplane altitude, and airplane type, and for Mach numbers of 1.3 and 1.6, suggest that less variability in pressure, impulse, period, and rise time exists for the Mach number 1.6 data. The probability of equaling or exceeding the ratio of measured to calculated over-pressure, impulse, and time durations for the F-104 fighter airplane has been determined from a sample of more than 2500 data points for different operating conditions, geographical locations, and climatic conditions. The results suggest that the logarithms of these quantities follow a normal distribution. Author

N69-17303*# National Aeronautics and Space Administration. Langley Research Center, Langley Station, Va.

FULL-SCALE WIND-TUNNEL INVESTIGATION OF STATIC LONGITUDINAL AND LATERAL CHARACTERISTICS OF A LIGHT TWIN-ENGINE AIRPLANE

Marvin P. Fink and Delma C. Freeman, Jr. Washington Jan. 1969 217 p refs

(NASA-TN-D-4983) Avail: CFSTI CSCL 01B

An investigation was conducted in the Langley full-scale tunnel to determine the static longitudinal and lateral stability and control characteristics of a full-scale light twin-engine airplane. Hinge moments were also measured for all control and flap surfaces during the investigation. In general, the airplane was found to have stick-fixed longitudinal stability through the stall, but stick-fixed instability could be encountered at some lift coefficients with rearward center of gravity location. The airplane has stick-free stability through the stall, however, for all power, flap, and center of gravity conditions investigated. At angles of attack below the stall, the airplane is directionally stable, has positive effective dihedral, and the variation of the lateral coefficients is fairly linear. At angles of attack above the stall, the airplane is directionally stable, and has positive effective dihedral for all conditions except at a thrust coefficient of 0. However, rolling and yawing moments greater than those produced by full opposite control occur at zero sideslip because of asymmetrical wind stall. Aileron and rudder effectiveness is maintained through the stall. Author

N69-17700*# National Aeronautics and Space Administration, Langley Research Center, Langley Station, Va.

INVESTIGATION OF OPENING CHARACTERISTICS OF AN ALL-FLEXIBLE PARAWING

Thomas G. Gainer Washington Feb. 1969 32 p refs

(NASA-TN-D-5031) Avail: CFSTI CSCL 01C

Opening forces for an all flexible parawing were measured during deployments made in the 17 foot section of a wind tunnel. The wing tested had a nominal keel length of 5 feet, a flat pattern leading edge sweep of 45°, and equal length leading edges and keel. Lift and drag coefficient time histories were obtained by measuring three components of the total force on the wing. Tunnel dynamic pressure was varied from 0.5 to 2.0 pounds per square foot. Two slotted versions of the wing were also tested and some exploratory tests of a reefing technique of shortening one of the keel suspension lines were made. The results indicated that as the wing opened, there was a buildup in both lift and rage coefficient to large values. The ratio of maximum resultant force coefficient to steady state resultant force coefficient (shock factor) was about 3.0. When the resultant force reached a maximum, it was inclined about 48° to the airstream. For the infinite mass conditions of the tests, filling time was about 2.5 times the ratio of keel length to velocity. The complete force time history, including both the opening force and the forces during the transition to steady state angle of attack, could be nondimensionalized with respect to filling time. Opening forces for a 5 foot wing calculated by using the wind-tunnel data were in excellent agreement with drop test data. Author

N69-19950*# National Aeronautics and Space Administration. Manned Spacecraft Center, Houston, Tex.

EXPERIMENTAL VERIFICATION OF SCALE FACTORS FOR PARAWING OPENING CHARACTERISTICS WITH DIMENSIONAL RATIOS FROM 1:1.3 TO 1:3

Robert H. Moore, David L. Eichblatt, and Theodore F. Hughes

Washington Mar. 1969 41 p refs
(NASA-TN-D-5071) Avail: CFSTI CSCL 01C

Verification of an analytical scaling technique by experimental drop tests under controlled conditions is presented in which opening characteristics of full scale flexible parawing and an intermediate scale model are predicted from results of model testing. Two methods of scaling are considered, dynamic similarity and wing loading. Dynamic similarity is derived from comparing similar forces in the equation of motion of scale models to those of a prototype. Wing loading is similar but differs by requiring the payload-weight-per-canopy area of all parawings to be the same. Three scaled, all flexible parawings with keel lengths of 8, 18, and 24 feet were tested at initial opening velocities ranging from 46 to 90 feet per second. Results are presented in the form of comparisons of actual and predicted tension, acceleration, velocity, and distance time histories. Author

N69-20848*# San Diego Aircraft Engineering, Inc., Calif.
POTENTIAL STRUCTURAL MATERIALS AND DESIGN CONCEPTS FOR LIGHT AIRCRAFT
Washington Mar. 1969 142 p refs
(Contract NAS2-4423)
(NASA-CR-1285) Avail: CFSTI CSCL 01C

An investigation of various areas associated with the design of light aircraft and a study of structural materials and concepts is presented. The primary objectives of this two-phase study were: (1) to make a comparative evaluation of a wide variety of materials and structural concepts, presently and potentially available for application to light aircraft, by investigating the affect of design, manufacturing, operational, and material requirements on the cost of this class of aircraft; (2) to apply the more promising materials and structural concepts to the conceptual design of light aircraft; and (3) to identify key problem areas where additional research may increase the potential of promising materials or concepts. This report summarizes the results of the comparative evaluation and shows how these results may be applied to the structural design studies of light aircraft. Author

N69-21020*# National Aeronautics and Space Administration. Ames Research Center, Moffett Field, Calif.
LARGE-SCALE TESTS OF AN AIRPLANE MODEL WITH A DOUBLE-DELTA WING, INCLUDING LONGITUDINAL AND LATERAL CHARACTERISTICS AND GROUND EFFECTS
Victor R. Corsiglia, David G. Koenig, and Joseph P. Morelli
Washington Mar. 1969 82 p refs
(NASA-TN-D-5102) Avail: CFSTI CSCL 01C

A wind-tunnel investigation has been undertaken to determine the lateral directional, and longitudinal aerodynamic characteristics of a supersonic transport configuration with a double-delta wing of aspect ratio 1.66. Ground effects were also investigated. There was no large reduction in static longitudinal stability at high angles of attack. The trimmed lift coefficient in ground effect, at gear height, was 1.25 times that out of ground effect at the angle of attack for takeoff or landing. Calculations of takeoff performance showed that the takeoff distance can be reduced by increasing the speed beyond that corresponding to the ground limit value of angle of attack. To improve the lift-drag ratio in the takeoff climb, it is desirable to accelerate after lift-off, because the speed for maximum L/D is about 250 knots relative to a takeoff speed of about 190 knots. The improved L/D results in reduced noise at distances greater than 3 miles from brake release and results in more efficient flight. Author

N69-22539*# National Aeronautics and Space Administration. Ames Research Center, Moffett Field, Calif.
THE USE OF PILOT RATING IN THE EVALUATION OF AIRCRAFT HANDLING QUALITIES
George E. Cooper and Robert P. Harper, Jr. (Cornell Aeron. Lab.)
Washington Apr. 1969 54 p refs
(NASA-TN-D-5153) Avail: CFSTI CSCL 01A

Pilot rating scales and their use in assessing aircraft handling qualities are reviewed historically, and objections that have been raised to limitations of earlier scales are considered in the development of a revised scale. Terminology used in the evaluation of handling qualities is reviewed and new definitions are proposed to improve communication and international understanding. Of particular significance is the new definition of handling qualities, which emphasizes the importance of factors that influence the selection of a rating other than stability and control characteristics. The experimental use of pilot rating is discussed in detail, with special attention devoted to (1) clarifying the difference between mission and task, (2) identifying what the rating applies to, (3) considering the pilot's assessment criteria, and (4) defining the simulation situation. The important elements of the report are then summarized in a suggested Briefing Guide, designed for guidance in planning and executing handling qualities experiments. Author (F.S.)

N69-22546*# Aeronautical Research Associates of Princeton, Inc., N. J.
SONIC BOOM PROPAGATION IN A STRATIFIED ATMOSPHERE, WITH COMPUTER PROGRAM
Wallace D. Hayes, Rudolph C. Haefeli, and H. E. Kulsrud
Washington NASA Apr. 1969 50 p refs
(Contract NAS1-7721)
(NASA-CR-1299) Avail: CFSTI CSCL 20A

This analysis, to some extent a synthesis of established theory but with many new features, is given in sufficient detail to serve as an algorithm for the computation of sonic boom pressure signatures. This algorithm is realized in a FORTRAN computer program. Required inputs include atmospheric properties and horizontal winds as functions of altitude, information on the flight path of the maneuvering aircraft, and aircraft F-functions. Ray tube areas are computed according to geometric acoustic theory, and nonlinear effects are accounted for through an appropriate age variable. The output includes midfield pressure signatures at any altitude. Results from sample calculations are presented and discussed. Author

N69-22572*# *National Aeronautics and Space Administration.* Ames Research Center, Moffett Field, Calif.
AN INVESTIGATION OF A DIRECT SIDE-FORCE MANEUVERING SYSTEM ON A DEFLECTED JET VTOL AIRCRAFT
Terrell W. Feistel, Ronald M. Gerdes, and Emmett B. Fry
Washington Apr. 1969 15 p refs
(NASA-TN-D-5175) Avail: CFSTI CSCL 01C

A series of flight and simulator tests were conducted using the X-14A variable stability jet, VTOL research aircraft and an all-axis motion simulator to determine the acceptability of a direct side-force vane for sideward maneuvering without changing bank angle. The side-force vane, immersed in the jet exhaust of the X-14A just below the diverters, deflected the jet sideways through a small angle and was controlled by a device on the pilot's control stick, which could provide either proportional or on-off control. The side-force vane with proportional control was evaluated in flight for the performance of lateral offset maneuvers of 1 to 2 wing spans translation distance. For this task, the use of the vane for translation was preferred over roll when only a low value of roll control power was available, with a higher control power available in roll; the two methods were equally acceptable. Author

N69-23449*# National Aeronautics and Space Administration. Langley Research Center, Langley Station, Va.
HEAVE RESPONSE OF A PLENUM AIR CUSHION INCLUDING PASSIVE AND ACTIVE CONTROL CONCEPTS
Jack D. Leatherwood, Grayson V. Dixon, and David G. Stephens

Washington, May 1969 44 p refs
(NASA-TN-D-5202) Avail: CFSTI CSCL 01C

An analytical and experimental investigation was conducted to determine the heave (vertical) response characteristics of an open-plenum air cushion suspension to simulated guideway inputs. In addition, passive and active control concepts for attenuating undesirable heave responses were considered. Analog computer solutions of the linear and nonlinear equations of motion were obtained and compared with experimental data. Results of analysis and experiment defined cushion resonant response conditions at which guideway inputs may be greatly amplified in the absence of cushion control. With control, however, the analysis suggests that heave responses may be significantly attenuated for a relatively wide range of guideway inputs. Author

N69-24761*# National Aeronautics and Space Administration, Washington, D.C.
DYNAMICS OF THE SPATIAL MOTION OF AN AIRCRAFT
G. S. Byushgens et al Apr. 1969 221 p refs Transl. into ENGLISH of the publ. "Dinamika Prostranstvennogo Dvizheniya Samoleta" Moscow, Mashinostr. Press. 1967
(NASA-TT-F-555) Avail: CFSTI CSCL 01C

Discussed are original concepts of the theory of spatial motion of an aircraft by taking into account cross couplings. Criteria are given here for stabilizing the motion of an aircraft during maneuvers involving intense rolling. To describe the characteristics of aircraft dynamics during spatial maneuvers, the authors employ several concepts and methods involving the qualitative theory of differential equations. The qualitative results obtained in the analysis are illustrated by the results of calculating the aircraft dynamics on digital computers and simulators. Considerable attention is paid to a physical explanation of the results obtained and to a description of the mechanics of aircraft motion in the most common cases of controlled flight. Detailed analysis is given of the reasons and conditions for appearance of the phenomenon of "inertial rotation" of an aircraft involving losses in effective lateral control. Author

N69-26194*# National Aeronautics and Space Administration. Ames Research Center, Moffett Field, Calif.
TECHNIQUE FOR CALCULATING OPTIMUM TAKEOFF AND CLIMBOUT TRAJECTORIES FOR NOISE ABATEMENT
Heinz Erzberger and Homer Q. Lee Washington May 1969 25 p refs
(NASA-TN-D-5182) Avail: CFSTI CSCL 01C

A procedure was developed for determining optimum takeoff and climbout trajectories for jet aircraft that minimize the noise produced during overflight of communities located along the ground track of the climbout path. The procedure enables one to compute optimum takeoff trajectories for noise abatement for a particular aircraft operating from a particular airport subject to prescribed operational constraints. An important part of the procedure consists in defining appropriate criteria for noisiness of a trajectory. Two criteria are proposed and are used as a basis for calculating noise optimum trajectories: (1) the perceived noise level (in PNdB) measured after a power reduction at the beginning of the noise-sensitive area, and (2) the perceived noise level, averaged along the noise-sensitive ground track of a climbout trajectory. Calculating trajectories that minimize the chosen criterion for noisiness is interpreted as an optimum control problem. The procedure was applied to the calculation of optimum trajectories for a typical, currently in-service jet transport. Author

N69-27177*# National Aeronautics and Space Administration. Langley Research Center, Langley Station, Va.
EVALUATION OF A CONTACT-ANALOG DISPLAY IN LANDING APPROACHES WITH A HELICOPTER
Robert W. Sommer and R. Earl Dunham, Jr. Washington Jun. 1969 25 p refs
(NASA-TN-D-5241) Avail: CFSTI CSCL 01D

The contact-analog presentation included an inclined pathway, fixed in a ground-coordinate system, that provided information for slope and course guidance. The tests were conducted along a 6° glide slope at approach speeds of about 30 knots to a breakout that was followed by a visual slowdown to hover. The tests of the display showed that because of the limited horizontal view of the contact analog (24°) and an incorrect generation of the lateral movement of the pathway, the pilots were constrained to fly within ±100 feet (±30.48 m) laterally of the path center line. The use of the pathway for slope control was found to be difficult because of the limited vertical view of the contact analog (18°) and the necessity of flying an appreciable distance above the pathway to prevent inversion of the pathway. For the slope offset of the present tests (50 feet (15.24 m)), the nearest visible part of the pathway was a considerable distance ahead of the helicopter; thus slope deviations were difficult to detect. The display also presented an unrealistic quality because of the relative motions of the ground grid and the pathway tip. Author

N69-28044*# National Aeronautics and Space Administration. Langley Research Center, Langley Station, Va.
A WIND-TUNNEL AND ANALYTICAL STUDY OF THE CONVERSION FROM WING LIFT TO ROTOR LIFT ON A COMPOSITE-LIFT V/TOL AIRCRAFT
Robert J. Huston and James P. Shivers Washington Jun. 1969 58 p refs
(NASA-TN-D-5256) Avail: CFSTI CSCL 01C

The principal problem associated with the conversion from wing-borne to rotor-borne flight is the possibility of a large attitude disturbance during the first revolution of the rotor. The aircraft disturbance is due to an oscillation of the lift center of pressure in a longitudinal and lateral direction at a frequency that is simply the number of blades multiplied by the rotor rotational speed. The results of a wind tunnel study indicate that large amplitude cyclic pitch is one means of eliminating the source of the aircraft disturbance for a three-bladed rotor/wing aircraft. In addition, the selection of four blades on a rotor-wing aircraft may so substantially reduce the disturbing moments that cyclic pitch is not required to eliminate the moments. The results of an analytical investigation indicate that the disturbance may also be reduced in magnitude by a rapid initial rotor acceleration or by the use of an oscillation of the horizontal tail surfaces (elevons) at the frequency of the lift center of pressure oscillation. However, simultaneous use of the elevons for longitudinal and lateral control will increase the minimum conversion speeds. Author

N69-28097*# National Aeronautics and Space Administration. Langley Research Center, Langley Station, Va.
WIND-TUNNEL INVESTIGATION OF STEADY-STATE AERODYNAMICS OF A COMPOSITE-LIFT VTOL AIRCRAFT MODEL
Matthew M. Winston and Robert J. Huston Washington Jun. 1969 40 p refs
(NASA-TN-D-5232) Avail: CFSTI CSCL 01C

An investigation of a composite-lift VTOL aircraft model with three different rotor/wing configurations was conducted in the Langley full-scale tunnel. The aircraft configuration was one which employed a three-bladed lifting rotor for helicopter flight which could be stopped to become a fixed wing for airplane cruise flight. The aerodynamic and control characteristics were obtained for helicopter flight, and the cruise aerodynamics were obtained for airplane flight. The results indicate only small differences between the three configurations for most of the helicopter-mode operating conditions. Need for improvements in blade design is indicated, and a potential roll control problem at high tip-speed ratios is identified. The results of the airplane-mode cruise investigation indicate the

importance of careful design of composite lifting surfaces in order to achieve good efficiency in both rotary wing and fixed wing flight. Author

N69-29232*# National Aeronautics and Space Administration. Langley Research Center, Langley Station, Va.
A FLIGHT INVESTIGATION OF A LIGHTWEIGHT HELICOPTER TO STUDY THE FEASIBILITY OF FIXED-COLLECTIVE-PITCH AUTOROTATIONS
Robert J. Pegg Washington Jun. 1969 17 p refs
(NASA-TN-D-5270) Avail: CFSTI CSCL 01C

A flight investigation of a lightweight teetering rotor helicopter was conducted to explore the limitations encountered in power-off flight with the collective pitch stick held in the trim level flight position. The results indicate that with the collective pitch stick fixed in the trim level flight position, autorotation is possible under selected conditions with attendant gains in helicopter performance. Aircraft vibrations limited successful use of this technique to airspeeds between 25 and 80 knots. Author

N69-30633*# National Aeronautics and Space Administration. Langley Research Center, Langley Station, Va.
STATIC STABILITY CHARACTERISTICS OF A 0.16-SCALE MODEL OF A JET-LIFT; V/STOL RESEARCH AIRPLANE IN CRUISE
Matthew M. Winston Washington Jul. 1969 23 p refs
(NASA-TM-X-1835) Avail: CFSTI CSCL 01C

The investigation was conducted in the 17-foot test section of the 300 mph 7-by-10-foot tunnel. The longitudinal characteristics of the basic configuration indicate a need for improved stability in cruise. The effects of adding auxiliary horizontal-tail surfaces are shown. Also, the characteristics of the model with an alternate horizontal-tail arrangement are discussed. The effects of these modifications on the basic lateral directional characteristics of the model and the effects of cruise power on all configurations are included. Author

N69-30727*# National Aeronautics and Space Administration. Langley Research Center, Langley Station, Va.
AN EXPERIMENTAL INVESTIGATION OF THE MIXING OF COMPRESSIBLE-AIR JETS IN A COAXIAL CONFIGURATION
James M. Eggers and Marvin G. Torrence Washington Jul. 1969 52 p refs
(NASA-TN-D-5315) Avail: CFSTI CSCL 01B

An experimental investigation was made to obtain data on the mixing of parallel, circular, compressible-air jets in a coaxial configuration. A Mach 1. 3 outer jet and a near-sonic central jet, both exhausting to a quiescent atmosphere were studied. Data were also obtained with both jets operating at subsonic Mach numbers. Radial distributions of total pressure, static pressure, and mass fraction concentration (air in air)of the central jet gas were determined at downstream axial stations both in the near-jet jet and far-jet flow fields. Concentration measurements were made by using a tracer-gas technique. The central-jet gas was a 1% mixture of ethylene in air. At each test condition, the total temperature of both jets was approximately 300° K. The Reynolds numbers for the supersonic and subsonic outer-jet flow were approximately 42.1×10^6 and 13.9×10^6 per meter, respectively. Results of the investigation indicate that good correlation with the experimental air mixing data can be obtained by using an eddy viscosity model based on a representative width of the mixing zone and on the center-line mass flow per unit area. The concentration decay in the region well downstream of the concentration potential core was found to be inversely proportional to the square of the axial coordinate. The accuracy of the concentration measurements was found to be significantly affected by sampling technique and sampling probe design. Author

N69-31874*# National Aeronautics and Space Administration. Langley Research Center, Langley Station, Va.
A LABORATORY INVESTIGATION OF N-WAVE FOCUSING
W. D. Beasley, J. D. Brooks, and R. L. Berger Washington Jul. 1969 19 p refs
(NASA-TN-D-5306) Avail: CFSTI CSCL 01C

A laboratory investigation of the focusing of an N-wave at a point and along a line was conducted. The N-wave was created by a spark at the focus of a parabolic mirror which reflected the N-wave as a plane wave and directed it toward the focusing mirror. Microphone traces of the signature were obtained for various positions of the wave relative to the focus, and schlieren photographs of the passage of the N-wave through the line focus were obtained. The results indicated that the wave underwent a componentwise phase shift of $\pi/2$ radians on passing through a line focus and a corresponding shift of π radians on passing through a point focus, in a manner similar to the focusing of light. Author

N69-31917*# Aztec School of Languages, Inc., Acton, Mass. Research Translation Div.
CRITICAL REGIMES OF SUPERSONIC JET AIRCRAFT-STALL AND SPIN
M. G. Kotik Washington NASA Jul. 1969 215 p refs Transl. into ENGLISH of the book "Kriticheskiye Rezhimy Sverkhzvukovogo Samoleta-Svalivaniye i Shtopor" Moscow, Mashinostr. Press, 1967
(Contract NASw-1692)
(NASA-TT-F-526) Avail: CFSTI CSCL 01C

The results of theoretical and experimental studies of phenomena connected with stall and spin, and with the escape of aircraft from those regimes which involve complex nonstationary motion of an aircraft in space, are presented. Particular attention is paid to the results of flight experiments (tests) of modern aircraft for stall and spin. The conditions for supersonic jet aircraft entering critical (turbulent) regimes are examined, as well as the characteristics of stability and maneuverability at large angles of attack and the effect on these characteristics of a number of factors: angular velocities for banking aircraft, Mach number, and flight altitude. Author

N69-31959*# General Applied Science Labs., Inc., Westbury, N.Y.
RESEARCH AND DEVELOPMENT OF A SONIC BOOM SIMULATION DEVICE
Roger Tomboulian Washington NASA Jul. 1969 48 p
(Contract NAS1-7985)
(NASA-CR-1378; GASL-TR-713) Avail: CFSTI CSCL 01C

To fulfill the requirements for a sonic boom simulator, a pilot facility using an air supply, a mass control valve, and a horn (or duct) was successfully constructed and operated. After an extensive program of analysis of the end reflection conditions, a unique solution was developed which permitted the cancellation of the outgoing wave without the need of a large classical absorber. The concept of this end termination is based on the fact that to match the complex acoustical admittance present at the end of the duct, both the resistive and inertial components of the pressure wave must be cancelled. The initial results obtained using this impedance matching device on the end of the duct indicate that the approach is conceptually sound and that a simulator device of reasonable length can be made and yet produce full-scale sonic boom signatures. The initial results obtained from this facility are discussed. Author

N69-31962*# National Aeronautics and Space Administration. Ames Research Center, Moffett Field, Calif.
FLIGHT-DETERMINED AERODYNAMIC PROPERTIES OF A JET-AUGMENTED, AUXILIARY-FLAP,

DIRECT-LIFT-CONTROL SYSTEM INCLUDING CORRELATION WITH WIND-TUNNEL RESULTS

L. Stewart Rolls, Anthony M. Cook, and Robert C. Innis Washington Jul. 1969 41 p refs Revised
(NASA-TN-D-5128-Rev) Avail: CFSTI CSCL 01C

Flight tests were conducted on the modified Boeing 367-80 prototype, jet-transport aircraft to determine the aerodynamic characteristics of an externally blown auxiliary-flap system. These flight data are compared with data from a similarly modified one-third scale model in the Ames 40- by 80-foot wind tunnel. Flight data for dynamic steps of the auxiliary flaps indicate a lower peak normal acceleration capability than that indicated by the flight data for static steps; the lower peak is attributed to a rate limit of the flap actuator. The pilots reported an improvement in the landing flare and touchdown tasks resulting from the increased vertical response of the direct-lift-control system. Author

N69-32110*# National Aeronautics and Space Administration. Langley Research Center, Langley Station, Va.

SIMULTANEOUS USAGE OF ATTITUDE CONTROL FOR VTOL MANEUVERING DETERMINED BY IN-FLIGHT SIMULATION

Frank R. Niessen Washington Jul. 1969 12 p refs
(NASA-TN-D-5342) Avail: CFSTI CSCL 01C

The amount of simultaneous control a pilot would use in performing various operational tasks in a vehicle with control response characteristics similar to those of a jet VTOL aircraft was measured. The simulation technique used in this study eliminated trim and disturbance effects. The simultaneous control usage for maneuvering was analyzed in terms of relative bleed-air demands. The results indicate that whenever high total usage did occur, it lasted for only a few tenths of a second. No simultaneous complete control demands occurred during any of the maneuvers; furthermore, the largest simultaneous control demands were significantly less than the sum of the individual maximum control demands. Author

N69-32284*# National Aeronautics and Space Administration. Flight Research Center, Edwards, Calif.

FLIGHT MEASUREMENTS OF CANARD LOADS, CANARD BUFFETING, AND ELEVON AND WING TIP HINGE MOMENTS ON THE XB-70 AIRCRAFT INCLUDING COMPARISONS WITH PREDICTIONS

Jerald M. Jenkins, V. Michael DeAngelis, Edward L. Friend, and Richard C. Monaghan Washington Aug. 1969 29 p refs
(NASA-TN-D-5359) Avail: CFSTI CSCL 01A

Flight-test data are presented from Mach 0.40 to Mach 3.00. The data are compared with the manufacturer's rigid and aeroelastic predictions, wind-tunnel airfoil data, or results derived from flight tests of other comparable aircraft. Author

N69-32337*# National Aeronautics and Space Administration. Langley Research Center, Langley Station, Va.

ANALYSIS OF LATERAL DIRECTIONAL STABILITY CHARACTERISTICS OF A TWIN JET FIGHTER AIRPLANE AT HIGH ANGLES OF ATTACK

Joseph R. Chambers and Ernie L. Anglin Washington Aug. 1969 48 p refs
(NASA-TN-D-5361) Avail: CFSTI CSCL 01C

An investigation was conducted to determine the factors producing a directional divergence at high angles of attack for a twin-jet swept-wing fighter airplane. The study consisted of static wind tunnel tests, tuft-flow visualization tests, and calculations of the dynamic lateral directional stability characteristics of the airplane. Several modifications to the basic configuration were evaluated in an attempt to delay or eliminate the instability. Author

N69-34915*# Michigan Univ., Ann Arbor.

LABORATORY EXPERIMENTS ON REVERTED RUBBER FRICTION

G. H. Nybakken, R. J. Staples, and S. K. Clark Washington NASA Aug. 1969 58 p refs
(Grant NGR-23-005-010)
(NASA-CR-1398; TR-7) Avail: CFSTI 01C

Laboratory experiments were carried out to explain the mechanism of reverted rubber skidding as was observed on aircraft tires. It was determined that surface heat generation is the cause of this rubber degradation, and that such reverted rubber exhibits remarkably low friction coefficients on wet surfaces, at all speeds, compared to unreverted rubber on dry surfaces. The process of reverted rubber sliding can take place at ambient temperatures, and is not dependent on the simultaneous presence of heat. It is believed to be caused by a thin water film between the soft reverted rubber and the rigid roadway. Author

N69-34988*# National Aeronautics and Space Administration. Langley Research Center, Langley Station, Va.

SPIN-TUNNEL INVESTIGATION OF A 1/20-SCALE MODEL OF A STRAIGHT-WING, TWIN-BOOM, COUNTER-INSURGENCY AIRPLANE

Henry A. Lee Washington Aug. 1969 28 p ref
(NASA-TM-X-1602) Avail: CFSTI CSCL 01C

An investigation has been made to determine the erect and inverted spin and recovery characteristics of a 1/20-scale dynamic model of a straight-wing, twin-boom, counter-insurgency airplane. Tests were made for the normal loading with the center of gravity at 28-percent mean aerodynamic chord and for a forward and rearward position at 17-percent and 30-percent mean aerodynamic chord, respectively. The landing configuration for the normal loading was also investigated. Additional tests were made to determine the effect of the sponsons, the external wing-tip-mounted missiles, external rocket pods, and an external gun pod. The use of rockets as an emergency recovery device was also investigated. The test results indicate that the airplane will spin in the erect attitude for all loading conditions and will spin inverted only for aileron-with control settings. The optimum control technique for recovery from all spins is movement of the rudder to against the spin followed about one-half turn later by neutralization of the longitudinal and lateral controls. Stores mounted on the wings and sponsons will have no appreciable effect on the spin and recovery characteristics. Author

N69-35762*# National Aeronautics and Space Administration. Flight Research Center, Edwards, Calif.

FIXED-BASE SIMULATOR PILOT RATING SURVEYS FOR PREDICTING LATERAL-DIRECTIONAL HANDLING QUALITIES AND PILOT RATING VARIABILITY

Lawrence W. Taylor, Jr., and Kenneth W. Iliff Washington Aug. 1969 115 p refs
(NASA-TN-D-5358) Avail: CFSTI CSCL 01C

Pilot ratings of lateral-directional handling qualities were collected for a wide range of simplified aircraft characteristics through the use of a simple fixed-base simulator with a color contact analog display. The results of the general survey were obtained with an engineer as the subject and are contained in 45 plots involving five parameters. In another survey, utilizing the same simulation, ratings were obtained from many pilots in order to study the variability in pilot ratings among pilots and the differences in pilot rating that result from changes in mission. The standard deviation of individual pilot ratings ranged from 1.0 at the "good" end of the scale to 2.0 in the middle of the scale. Ratings for specific missions were generally numerically higher (more adverse) than those for the general mission for the same vehicle characteristics. Author

N69-35861*# Flight Safety Foundation, Inc., Arlington, Va.
GENERAL-AVIATION PILOT REACTIONS TO AND OPINIONS ON GROOVED RUNWAYS
George E. Cranston Washington NASA Aug. 1969 27 p
(Contract NAS1-8668)
(NASA-CR-1428) Avail: CFSTI CSCL 01C

At the time the survey was performed, there were four commercial airports in the continental United States that had at least one grooved runway. Personal interviews were conducted between general-aviation pilots and aviation safety specialists at these sites by using a prepared questionnaire to obtain the data discussed in this paper. The results of the survey and study show that the grooving of runways has a pronounced beneficial effect and provides increased safety for high-speed general-aviation aircraft operations by the reduction of hydroplaning and increasing braking action during wet runway conditions. Pilots operating light, low-speed aircraft did not generally realize these benefits as the runway lengths and widths at these airports far exceeded their operational requirements under all anticipated circumstances involved with this problem. Author

N69-36258*# National Aeronautics and Space Administration. Langley Research Center, Langley Station, Va.
STATIC AND DYNAMIC STABILITY DERIVATIVES OF A MODEL OF A JET TRANSPORT EQUIPPED WITH EXTERNAL-FLOW JET-AUGMENTED FLAPS
Delma C. Freeman, Jr., Sue B. Grafton, and Richard D'Amato Washington Sep. 1969 52 p refs
(NASA-TN-D-5408) Avail: CFSTI CSCL 01C

A wind-tunnel investigation has been made to determine the static and dynamic stability derivatives of a model of a large jet transport equipped with external-flow jet-augmented flaps. The tests were conducted in the Langley full-scale tunnel, and a model powered by scale-model, compressed-air-driven turbofan engines was used. The results of the investigation showed that blowing on the flap system increased the lift curve slope, delayed the stall, and increased the maximum lift coefficient. The data also showed that all model configurations generally had static longitudinal stability over the test angle-of-attack range except those at the higher flap-deflection angles where the effects of power were destabilizing. The results also showed that the model had positive damping in pitch, roll, and yaw throughout the test angle-of-attack range up to and slightly beyond the stall for all test conditions. The application of power in the flap system resulted in appreciable increases in roll damping but produced essentially no effects in pitch and yaw damping. There were essentially no effects due to oscillation frequency on the damping derivatives. Author

N69-36326*# National Aeronautics and Space Administration, Washington, D.C.
INVESTIGATION OF VIBRATION AND STABILITY OF AIRCRAFT ENGINE COMPONENTS [ISSLEDOVANIYE VIBRATSII PROCHNOSTI DETALEY AVIADVIGATELEY]
G. S. Skubachevskiy ed. Aug. 1969 12 p refs Transl. into ENGLISH from Trans. Moscow Aviation Inst. (Moscow), no. 172, 1967
(NASA-TT-F-547) Avail: CFSTI CSCL 01C

CONTENTS:

1. THE SHAPE OF THE ELASTIC CURVE OF A WEIGHTLESS ROTATING SHAFT CARRYING ECCENTRICALLY LOCATED POINT MASSES OR DISKS A. N. Ogurechnikov p 1–19 (See N69-36327 21-15)

2. THE OPTIMUM HYDRAULIC DAMPING AMOUNT FOR A TURBINE ROTOR K. A. Kryukov p 20–47 refs (see N69-36328 21-28)

3. DYNAMIC COMPLIANCES IN A SYSTEM WITH FRICTION V. M. Balepin p 48–52 refs (See N69-36329 21-15)

4. FORCED VIBRATIONS OF A FREE SHAFT WITH FRICTION Ye. A. Artemov p 53–70 refs (See N69-36330 21-15)

5. SELF-INDUCED VIBRATIONS OF AXIAL-COMPRESSOR BLADES I. M. Movshovich p 71–82 refs (See N69-36331 21-01)

6. COMPUTATION OF VIBRATIONS OF VARIABLE-THICKNESS DISKS BY THE RITZ METHOD A. V. Karpov p 82–88 refs (See N69-36332 21-32)

7. THE HYDROSTATIC BEARING AS A SOURCE OF VIBRATIONS G. A. Ivanov p 89–92 refs (See N69-36333 21-15)

8. STABILITY OF THREE-LAYER CYLINDRICAL SHELLS BEYOND THE ELASTIC LIMIT V. V. Serdyukov p 93–104 refs (See N69-36334 21-32)

9. THE APPLICATION OF CONFORMAL MAPPING TO PROBLEMS OF THE THEORY OF ELASTICITY V. G. Gorlov p 105–110 refs (See N69-36335 21-19)

10. STABILITY OF THREE-LAYER CYLINDRICAL SHELLS IN THE ELASTIC AND INELASTIC REGIONS I. A. Yefimov p 111–117 refs (See N69-36336 21-32)

N69-36807*# National Aeronautics and Space Administration. Langley Research Center, Langley Station, Va.
ANALYSIS OF THE FLAT-SPIN CHARACTERISTICS OF A TWIN-JET SWEPT-WING FIGHTER AIRPLANE
Joseph R. Chambers, James S. Bowman, Jr., and Ernie L. Anglin Washington Sep. 1969 35 p refs
(NASA-TN-D-5409) Avail: CFSTI CSCL 01C

An investigation was conducted to determine the significant factors affecting the flat-spin characteristics of a contemporary high-performance fighter airplane having horizontal tail surfaces with negative geometric dihedral (droop). Various phases of the study included static and forced-oscillation wind-tunnel tests, rotary-balance tests, single-degree-of-freedom autorotation tests, and free-spinning tests of a dynamically scaled model. Author

N69-37976*# National Aeronautics and Space Administration. Langley Research Center, Langley Station, Va.
SPIN-TUNNEL INVESTIGATION OF A 1/30-SCALE MODEL OF A SUBSONIC ATTACK AIRPLANE
Henry A. Lee Washington Aug. 1969 29 p ref
(NASA-TM-X-1788) Avail: CFSTI CSCL 01C

Spin and recovery characteristics of a single-engine swept-wing model were tested. Several combat loading conditions were tested for a range of center-of-gravity positions. The effects of external stores, assymetrical loading conditions, and dive brakes were determined as well as parachute size requirements for emergency spin recovery. The results indicate that erect spins can be obtained for all normal loading conditions. Satisfactory recoveries can be obtained by the optimum control technique, i.e. simultaneous movement of the rudder to full against the spin, the ailerons to full with the spin (stick left in a left spin), and the elevator to full up (stick back). With dive brakes open, the airplane may not spin. For the asymmetric loading, spins will be possible only when most of the weight of the external stores is on the outboard wing (right wing for a left spin), and recoveries by optimum control will be unsatisfactory. The airplane will spin inverted, but spins may be difficult to obtain. The optimum control technique for recovery from an inverted spin is to neutralize all controls and then move the rudder to oppose the yawing motion. A parachute 25 feet in diameter (laid out flat) with a drag coefficient of 0.48 (based on the laid-out-flat diameter) and a towline length of 27 feet will suffice for emergency spin recovery. Author

N69-38104*# National Aeronautics and Space Administration. Flight Research Center, Edwards, Calif.

VARIATION IN ENGINE NOISE FOR TWO LANDING-APPROACH CONFIGURATIONS OF A JET TRANSPORT AIRCRAFT

Elmor J. Adkins, Norman J. McLeod, and Paul L. Lasagna Washington, D.C. Oct. 1969 15 p refs

(NASA-TM-X-1896) Avail: CFSTI CSCL 01C

A limited flight investigation was conducted to determine the effect of reduced flap deflections on power required and the resulting engine noise for a subsonic jet transport aircraft. Noise levels were measured during level flight at an altitude of 400 feet (122 meters) at approach speeds. Data were obtained during flybys with flap deflections of 50° and 36°. The maximum overall sound pressure level (OASPL) from flybys with 36° of flap deflection averaged 3 decibels (ref. 0.00002 newtons/meter^2) lower than for flybys with 50° of flap deflection. Buffet intensity was reduced by the use of lower-flap deflections. Author

N69-38598*# National Aeronautics and Space Administration. Langley Research Center, Langley Station, Va.

RESULTS OF A FREE-FLIGHT TEST TO DETERMINE THE PERFORMANCE CHARACTERISTICS OF A TOWED, CONICAL DECELERATOR

J. W. Usry Washington 1969 34 p refs Film supplement number L-1049 to this report is available on loan from Langley Research Center

(NASA-TM-X-1833) Avail: CFSTI CSCL 01C

An inflatable fabric decelerator was tested in free flight to determine its drag and stability characteristics. The inflated decelerator approximated an 80° cone with a 48-inch (121.9-cm) base and was towed behind a cone–cylinder–flare payload at a distance of 13.6 feet (4.15 m) from the payload base. The payload had a maximum flare diameter of 18.21 inches (46.25 cm). The decelerator was deployed at an altitude of 112 000 feet (34.14 km) and a velocity of 4560 ft/sec; 1390 m/sec). Inflation occurred at a Mach number of 4.31 and a dynamic pressure of 130 lb/ft^2 (6224 N/m^2). The snatch force after deployment was not more than 500 pounds (2224 N); this low force indicated that the towline assembly design could be simplified for future flights by eliminating the two snubber lines and the nylon sleeve. The shock force due to inflation was 5600 pounds (24.9 kN). After inflation the force in the towline varied between 300 and 1600 pounds (1334 and 7117 N). The oscillatory motion of the decelerator had a high frequency, and the amplitude increased with time. The test was terminated about 1 second after inflation because of a failure at the attachment point of the towline to the decelerator. The results indicated that the decelerator system was unstable and not suitable for use as a supersonic decelerator with the payload used in this experiment under the conditions of the test. A drag coefficient of 0.75 at a Mach number of 4.2 was estimated from the mean value of the force in the towline prior to the failure. Author

N69-38657*# Boeing Co., Seattle, Wash. Commercial Airplane Div.

A FLIGHT INVESTIGATION OF SYSTEMS DEVELOPED FOR REDUCING PILOT WORKLOAD AND IMPROVING TRACKING ACCURACY DURING NOISE-ABATEMENT LANDING APPROACHES

Clarence C. Flora, Gerhard K. L. Kriechbaum, and Wayne Willich Washington NASA Oct. 1969 70 p refs

(Contract NAS2-4200)

(NASA-CR-1427) Avail: CFSTI CSCL 01C

A two-phase flight test program was conducted using the Boeing 367-80 airplane. Concurrently, a supplemental ground-based flight simulator program was performed. This study was directed at evaluating various systems developed to reduce the pilot workload while maintaining tracking accuracy under simulated instrument conditions during noise-abatement landing approaches. Preliminary results showed that steeper than normal approaches could not be performed at the same pilot workload level as a conventional approach without improvements in the path guidance system, flight instrument displays, and automatic flight controls. The results of further flight evaluations showed that when the pilot was given an appropriate combination of systems aids he was able to perform steep, two-beam or decelerating approaches with workloads and accuracies comparable to those of conventional approaches. Author

N69-38770*# National Aeronautics and Space Administration. Langley Research Center, Langley Station, Va.

THREE-TRACK RUNWAY AND TAXIWAY PROFILES MEASURED AT INTERNATIONAL AIRPORTS A AND B

Albert W. Hall Washington Sep. 1969 102 p ref

(NASA-TN-D-5444) Avail: CFSTI CSCL 01E

Three-track runway and taxiway profiles are presented for use in studies of airplane response to ground roughness. This report presents the tabulated and plotted data for two international airports. Author

N69-38807*# National Aeronautics and Space Administration. Ames Research Center, Moffett Field, Calif.

FLIGHT EVALUATION OF TIP-TURBINE-DRIVEN FANS FOR LATERAL CONTROL IN A HOVERING VTOL AIRCRAFT

L. Stewart Rolls and Ronald M. Gerdes Washington Oct. 1969 18 p refs

(NASA-TN-D-5491; A-3299) Avail: CFSTI CSCL 01C

A flight evaluation was made of small tip-turbine-driven fans as a means of augmenting the lateral control characteristics of a VTOL aircraft in hover. Two 12.8-inch-diameter fans were designed, constructed, and tested on the X-14A VTOL test vehicle. Although the fans used less bleed air for a given thrust output, they were unacceptable because of the high time constants of the control system. The time constant reductions which can be provided by closing the control loop with rpm feedback are eliminated when a full command is required. Author

N69-38819*# Boeing Co., Seattle, Wash.

FLIGHT TEST RESULTS OF A TRAILING EDGE FLAP DESIGNED FOR DIRECT-LIFT CONTROL

Charles R. Taylor, Jr. Washington NASA Oct. 1969 84 p refs

(Contract NAS2-4200)

(NASA-CR-1426) Avail: CFSTI CSCL 01C

A flight test investigation was conducted with the Boeing 707 prototype to obtain the performance characteristics of a trailing edge flap for direct-lift control (DLC). The flap system consisted of a main flap with blowing boundary layer control (BLC) and a slotted aft auxiliary flap for DLC. The auxiliary flap had a deflection range of 10° up and 30° down with respect to a faired position with the main flap. The DLC-null angle was 10° down from the faired position. Steady-state aerodynamic characteristics of the flap system were obtained from steady trimmed flight at several speeds plus slow deceleration to the stall. Airplane response and dynamics were obtained from step inputs to the auxiliary flap from their null setting. Similar maneuvers using wing spoilers for DLC also were accomplished. The steady-state results showed that lift coefficient increments (ΔC_L) of about 0.30 to 0.40 generally were obtained with 40° of auxiliary flap travel, while increments of 0.52 to 0.60 were noted with 15° of spoiler travel. Thrust impingement and BLC both tended to increase the ΔC_L's of the flaps, whereas higher main flap settings decreased them. Incremental normal accelerations on the order of +0.10 and −0.12 g were obtained with ±20° flap steps from the null flap. Spoiler steps of ±8° from the null spoiler gave +0.22 and −0.10 g increments. Author

N69-39188*# National Aeronautics and Space Administration. Langley Research Center, Langley Station, Va.
OPERATIONAL LIMITATIONS IN FLYING NOISE-ABATEMENT APPROACHES
Richard H. Sawyer and William T. Schaefer, Jr. Washington Oct. 1969 44 p refs
(NASA-TN-D-5497; L-6260) Avail: CFSTI CSCL 01C

An investigation of the capability of jet transport airplanes to be operated on steep noise-abatement profiles under simulated 200-foot-ceiling (60.96 meter) instrument flight conditions was conducted. Six airplanes ranging in type from a twin-engine turbojet executive transport to a four-engine turbofan intercontinental commercial transport were used. Both single-segment glide-slope (up to 7°) and two-segment glide-slope (up to 9°) profiles were investigated. Author

N69-40439*# Lockheed-Georgia Co., Marietta.
EFFECT OF JET TEMPERATURE ON JET AND PURE TONE NOISE RADIATION
Harry E. Plumblee, George A. Wynne, and Ben T. Zinn Washington NASA Nov. 1969 73 p refs
(Contract NAS1-8443)
(NASA-CR-1472) Avail: CFSTI CSCL 01C

A model jet nozzle was tested over a temperature range of 540°R to 1100°R, and sound pressure was measured at enough positions in the far field to calculate sound power. From these tests, the effect of temperature on total sound power was isolated. A prediction technique for sound pressure was modified to sound power and was verified over the temperature test range of this program. The prediction method was then used to determine the effect of temperature, as high as 3500°R, on radiated sound power. It was determined that jet sound power is a nonlinear function of temperature. At high temperatures, significant reductions in jet noise may be achieved. The changes in fan noise characteristics were also measured as the noise propagates through a high-temperature region in the fan duct and subsequently radiates into an ambient medium. It was shown that increasing temperature increases higher-order acoustic duct mode cut-on frequencies. Increasing temperature possibly reduces radiated pure tone noise. Design studies were made concerning the changes required to modify an existing engine to test the jet-heating concept. A combustion instability analysis for annular duct geometry was performed and used in designing components such as the combustion chamber and flameholders, to reduce high frequency combustion instability. Author

N69-40937*# National Aeronautics and Space Administration. Langley Research Center, Langley Station, Va.
EVALUATION OF A TECHNIQUE FOR DETERMINING AIRPLANE AILERON EFFECTIVENESS AND ROLL RATE BY USING AN AEROELASTICALLY SCALED MODEL
Irving Abel Washington Nov. 1969 40 p refs
(NASA-TN-D-5538; L-6695) Avail: CFSTI CSCL 01C

Wind-tunnel studies of an aeroelastically and dynamically scaled model of a multijet cargo airplane have been conducted to measure aileron-control characteristics at Mach numbers up to 0.93. A successful technique has been demonstrated for determining the aileron effectiveness, reversal boundary, and flight roll rates below the reversal boundary based on measured values of damping in roll. Author

03

AUXILIARY SYSTEMS

Includes fuel cells, energy conversion cells, and solar cells; auxiliary gas turbines; hydraulic, pneumatic and electrical systems; actuators; and inverters. For related information see also: 09 Electronic Equipment; 22 Nuclear Engineering; and 28 Propulsion Systems.

A69-10606 *

STRIKING CHARACTERISTICS AND TIME LAGS OF THE MAGNETRON GAUGE IN HELIUM FROM 1.9×10^{-7} TORR TO 7×10^{-10} TORR.

William S. Lassiter (NASA, Langley Research Center, Hampton, Va.).

Journal of Vacuum Science and Technology, vol. 5, Sept.-Oct. 1968, p. 147-151. 6 refs.

Experimental measurement of the lower limits of operation of the magnetron ionization gauge in helium over the pressure range from 1.9×10^{-7} to 7×10^{-10} torr. The dependence of the striking voltage on the striking magnetic field at the upper branches of the striking characteristic curves deviates slightly from the parabolic dependence predicted by theory. On the lower branches of the striking characteristic curves, the results show that below 10^{-8} torr, the minimum striking voltage decreases with a decrease in pressure instead of increasing, as predicted by theory. Striking time lags are measured below 10^{-8} torr. The time lags increase with a decrease in pressure and are shown to contribute no significant error in the measurements of the striking characteristics. M.G.

A69-11396 *#

LUNAR POWER SYSTEMS - A LONG VIEW.

Fred Schulman (NASA, Nuclear Power Systems Branch) and A. H. Smith (California Institute of Technology, Jet Propulsion Laboratory, Pasadena, Calif.).

Astronautics and Aeronautics, vol. 6, Nov. 1968, p. 62-69. 32 refs.

Discussion of various technology options for lunar-surface power plants, assuming that a Saturn-V-class vehicle is the mode of transportation to the moon. The amount of power that can then be made available on the moon per launch is expected to be that which can be generated by a power plant weighing up to 30,000 lb and packaged in a Saturn V vehicle. In view of the present state of power technology, it is anticipated that the development and delivery of such systems to the moon will be both difficult and costly. It is contended that many years will be required before any of these advanced systems can be made available for lunar uses, unless the present rate of national investment in space power technology is increased. V.Z.

A69-11762 *

PULSE MOTOR FOR SPACECRAFT ATTITUDE CONTROL.

David Suddeth (NASA, Goddard Space Flight Center, Greenbelt, Md.) and David Blackwood (Talley Industries, Inc., Mesa, Ariz.).

IN: SPACE PROJECTIONS FROM THE ROCKY MOUNTAIN REGION; PROCEEDINGS OF THE SYMPOSIUM, DENVER, COLO., JULY 15, 16, 1968. VOLUME 3. [A69-11755 02-11]

Symposium sponsored by the American Astronautical Society and the American Institute of Aeronautics and Astronautics.

Tarzana, Calif., American Astronautical Society, 1968. 19 p.

Discussion of design details and development test results for a micropulse solid-propellant rocket motor and firing logic wafer. These components, when combined, form a multipulse thruster module for spacecraft attitude control. Thruster module design and development have been to the requirements of NASA's Contract No. NAS 7-553. Emphasis is placed on the solid-propellant micropulse rocket motor and, to a lesser extent, on the electronic components. M.M.

A69-13074 *#

OBSERVATIONS ON CdS SOLAR CELL STABILITY.

A. E. Spakowski and A. F. Forestieri (NASA, Lewis Research Center, Cleveland, Ohio).

Institute of Electrical and Electronics Engineers, Photovoltaic Specialists Conference, Pasadena, Calif., Nov. 19-21, 1968, Paper. 10 p. 8 refs.

Results of thermal cycling tests conducted to study the stability of CdS solar cells. Early 1968 CdS solar cells are more stable than cells tested previously. The improvement appears to result from the general upgrading of process quality control and from tighter performance specifications. It is not believed that mechanical stresses induced during thermal cycling are the primary cause of cell degradation. The degradation however is a strong function of how the cells are electrically loaded during the test. It is believed that this load effect is often responsible for the differences observed when seemingly identical cells are tested. (Author)

A69-13075 *#

IMPURITY PROFILE AND ENERGY BAND DIAGRAM FOR THE Cu_2S-CdS HETEROJUNCTION.

Henry W. Brandhorst, Jr. (NASA, Lewis Research Center, Cleveland, Ohio).

Institute of Electrical and Electronics Engineers, Photovoltaic Specialists Conference, Pasadena, Calif., Nov. 19-21, 1968, Paper. 7 p. 12 refs.

Based on the impurity profile in the CdS layer determined from capacitance measurements and on the Hall and electron microprobe data for the Cu_2S layer, a band structure for the Cu_2S-CdS heterojunction was assembled. There are apparently four regions in the device: (1) n^+CdS, (2) nCdS:Cu, (3) pCu_2S:Cd, and (4) p^+Cu_2S. The band structure supports a model which has the Cu_2S contributing significantly to the red response, optically active copper centers in the CdS, and a maximum voltage of 0.85 V (V_D). (Author)

A69-13076 *#

SOLAR CELL PERFORMANCE AT JUPITER TEMPERATURE AND SOLAR INTENSITY.

Curt H. Liebert (NASA, Lewis Research Center, Cleveland, Ohio).

Institute of Electrical and Electronics Engineers, Photovoltaic Specialists Conference, Pasadena, Calif., Nov. 19-21, 1968, Paper. 7 p. 8 refs.

Measurement of the photovoltaic properties of two typical CdS thin-film solar cells and five flight-type silicon cells under conditions simulating earth and Jupiter. The efficiency of the best silicon cells near Jupiter was about 1.4 times greater than that achieved at earth. The efficiency at Jupiter for the CdS thin-film cells was about 1.1 times greater than at earth. P.v.T.

A69-13125 *#

SHEATH STRUCTURE IN THE UNIGNITED MODE.

Peter M. Sockol (NASA, Lewis Research Center, Cleveland, Ohio).

Institute of Electrical and Electronics Engineers, Thermionic Conversion Specialists Conference, Framingham, Mass., Oct. 21-23, 1968, Paper. 10 p. 10 refs.

A kinetic theory model of the plasma-sheath transition is used to analyze the sheath structure in the unignited mode of a thermionic converter. The study is confined to conditions in which the mean-free-paths and Debye length are small compared to the diode spacing. The emitter sheath structure is found to be the same as in the isothermal diode. The collector sheath varies from completely continuum to completely collisionless with a noncontinuum presheath as the local Debye length varies from much larger to much smaller than the mean-free-path. Theoretical current-voltage characteristics are compared with experimental ones. (Author)

03 AUXILIARY SYSTEMS

A69-13126 *#
A COMPARISON OF THE PERFORMANCE OF TWO RHENIUM, NIOBIUM CYLINDRICAL THERMIONIC CONVERTERS.
Richard M. Williams and Thomas J. Kascak (NASA, Lewis Research Center, Cleveland, Ohio).
Institute of Electrical and Electronics Engineers, Thermionic Conversion Specialists Conference, Framingham, Mass., Oct. 21-23, 1968, Paper. 10 p. 6 refs.

The performances of two rhenium, niobium thermionic converters are compared. The major difference between the converters was the surface preparation of the vapor-deposited rhenium emitters: one emitter was mechanically polished, the other was electroetched. The Rasor-Warner correlation was used to compare the emitter work functions, which in each case were within ±0.1 eV of the 5.0 eV vacuum work function curve. Steady-state electrode efficiency and power density measurements were obtained for each converter. The performance of the mechanically polished emitter was superior to that of the electroetched emitter. This indicates that electroetching of vapor-deposited rhenium does not guarantee a performance improvement. (Author)

A69-13127 *#
ELECTRON COOLING AND PLASMA HEATING OF THERMIONIC CONVERTERS.
Roland Breitwieser (NASA, Lewis Research Center, Cleveland, Ohio).
Institute of Electrical and Electronics Engineers, Thermionic Conversion Specialists Conference, Framingham, Mass., Oct. 21-23, 1968, Paper. 12 p. 14 refs.

An expression is developed that describes electron cooling of the emitter as modified by the return of energy from the interelectrode plasma. The semiempirical relation provides good agreement with experiment in the various modes of operation of a thermionic converter. Included in the expression are the effects of plasma density, diode spacing, and the surface potential difference across the converter. The technique of extracting the terms used in the expression from current-voltage information is also presented. (Author)

A69-15299 *
HIGH-TEMPERATURE CAPACITORS FROM PYROLYTIC BORON NITRIDE.
R. E. Stapleton and R. A. Lindberg (Westinghouse Electric Corp., Aerospace Electrical Div., Advanced Systems Dept., Lima; NASA, Lewis Research Center, Space Power Systems Div., Cleveland, Ohio).
Space/Aeronautics, vol. 50, Dec. 1968, p. 75, 76.

Results of a research program conducted to evaluate the feasibility of fabricating a high-temperature (1100°F) capacitor comparable in size, weight, and electrical characteristics to conventional lower-temperature capacitors. Four high-temperature, high-purity dielectric materials were tested, including single-crystal aluminum oxide, polycrystalline aluminum oxide, hot-pressed beryllium oxide, and pyrolytic boron nitride. Pyrolytic boron nitride was selected as the optimum material yielding the thinnest wafers. The use of alternatingly interconnected thin-film electrodes resulted in a nearly maximum capacitance for a given volume. A high-capacitance unit was fabricated by stacking five wafers on top of each other. Data are given for the dissipation factor and capacitance change with temperature. T.M.

A69-15310 *
THE EFFECT OF OXYGEN-SUPPLY IMPURITIES ON THE PERFORMANCE OF A HYDROGEN-OXYGEN FUEL CELL.
J. C. Jones (NASA, Manned Spacecraft Center, Houston, Tex.) and J. E. Cox (Houston, University, Houston, Tex.).
Energy Conversion, vol. 8, Nov. 1968, p. 113-115. 7 refs.

Experimental evaluation of the effect of inert diluent impurities in the reactant oxygen supply on the performance of a hydrogen-oxygen fuel cell. The experimental method involved the operation of single cells with three reactant oxygen supply purity levels. Constant load was maintained and change in cell performance was measured as voltage degradation with time during the test run. Inert blanketing of the oxygen electrode may be responsible for the voltage degradation. After each test run, significant immediate voltage recovery was observed when the oxygen electrode was purged. (Author)

A69-16158 *#
STATUS OF PHOTOVOLTAIC POWER TECHNOLOGY.
Arvin Smith (NASA, Washington, D.C.).
American Society of Mechanical Engineers, Winter Annual Meeting and Energy Systems Exposition, New York, N.Y., Dec. 1-5, 1968, Paper 68-WA/Sol-1. 12 p. 76 refs.
Members, $0.75; nonmembers, $1.50.

Review of the status of photovoltaic power technology primarily from the viewpoint of current and future applications to the exploration and use of space. The photovoltaic-solar cell technology has shown steady improvement in reliability, increased efficiency, reduced cost, increased power per unit of hardware weight, and ability to withstand extremes of the space environment. New developments are underway to increase solar-cell and array size, to reduce stowage volume during boosting into orbit, and to improve resistance to space radiation and thermal cycling. Silicon-cell electrical contacts and interconnections, low-energy proton damage to small exposed cell areas, and instability of CdS thin-film solar cells are examples of problems receiving attention at this time. M.M.

A69-16359 *#
THE PERFORMANCE OF A RHENIUM, NIOBIUM CYLINDRICAL THERMIONIC CONVERTER.
Thomas J. Kascak and Richard M. Williams (NASA, Lewis Research Center, Cleveland, Ohio).
Institute of Electrical and Electronics Engineers, Thermionic Conversion Specialists Conference, Framingham, Mass., Oct. 21-23, 1968, Paper. 10 p. 8 refs.

A cylindrical thermionic converter with a vapor-deposited rhenium emitter and a niobium collector, with a 10 mil interelectrode spacing, was tested under steady-state conditions. The efficiency and power density were measured over an emitter temperature range of 1600 to 2050 K and over a collector temperature range of 873 to 1173 K. The results show that the maximum electrode efficiency increased from 5.2 to 13.4%, and the power density at maximum efficiency increased from 1.2 to 8.1 W/cm^2 as the emitter temperature ranged from 1600 to 2050 K. The maximum power density increased from 1.4 to 8.8 W/cm^2, and the electrode efficiency at maximum power density increased from 4.9 to 12.8% over the emitter temperature range from 1600 to 2050 K. (Author)

A69-21034
ELECTROCHEMICAL GENERATORS FOR SPACE APPLICATIONS; CENTRE NATIONAL D'ETUDES SPATIALES, INTERNATIONAL CONVENTION, PARIS, FRANCE, DECEMBER 4-7, 1967, PROCEEDINGS [LES GENERATEURS ELECTROCHIMIQUES POUR APPLICATIONS SPATIALES; CENTRE NATIONAL D'ETUDES SPATIALES, COLLOQUE INTERNATIONAL, PARIS, FRANCE, DECEMBER 4-7, 1967, PROCEEDINGS].
Paris, Dunod Editeur. 1968. 272 p. In French, English, and Russian.
$22.

CONTENTS:

FOREWORD [AVANT-PROPOS]. 1 p.

FUEL CELL SYSTEMS FOR MANNED SPACECRAFT. H. McBryar (NASA, Manned Spacecraft Center, Houston, Tex.), p. 1-18. [See A69-21035 08-03]

SPACE APPLICATIONS OF ELECTROCHEMICAL GENERATORS [APPLICATIONS SPATIALES DES GENERATEURS ELECTROCHIMIQUES]. H. Daspet and D. Coudot (Centre National d'Etudes Spatiales, Brétigny-sur-Orge, Essonne, France), p. 19-32. 6 refs. [See A69-21036 08-03]

FUNDAMENTAL PROBLEMS RELATIVE TO LOW-TEMPERATURE FUEL CELLS USING CARBON FUELS [PROBLEMES FONDAMENTAUX RELATIFS AUX PILES A BASSE TEMPERATURE UTILISANT DES COMBUSTIBLES CARBONES]. M. Bonnemay, G. Bronoël, E. Devos, and D. Doniat (Centre National de la Recherche Scientifique, Bellevue, Hauts-de-Seine, France), p. 33-46. 8 refs. [See A69-21037 08-03]

SPECIAL FEATURES OF ELECTRODES FOR FUEL CELLS OPERATING UNDER WEIGHTLESSNESS CONDITIONS [PARTICULARITES DES ELECTRODES POUR PILES A COMBUSTIBLE FONCTIONNANT EN CONDITIONS D'APESANTEUR]. V. S. Bagotskii (Akademiia Nauk SSSR, Institut Elektrokhimii, Moscow,

USSR), p. 47-55. [See A69-21038 08-03]

COLD HYDROGEN AND BASIC ELECTROLYTE CELLS AT THE RESEARCH CENTER OF THE CGE [LES PILES FROIDES A HYDROGENE ET A ELECTROLYTE BASIQUE AU CENTRE DE RECHERCHES DE LA C. G. E.]. C. Edon (Compagnie Générale d'Electricité de Paris, Marcoussis, Essonne, France), p. 57-70. [See A69-21039 08-03]

THE 200-W MEMBRANE CELL "ABEPAC" [LA PILE A MEMBRANE DE 200W "ABEPAC"]. C. Vanleugenhaghe, A. Clauss, and C. Beaudet (Société d'Etudes, de Recherches et d'Applications pour l'Industrie, Brussels, Belgium), p. 71-78. [See A69-21040 08-03]

A COMPACT HYDROGEN-OXYGEN CELL [PILE HYDROGENE-OXYGENE COMPACTE]. R. Vic (Compagnie Industrielle des Piles Electriques, Argenteuil, Val-d'Oise, France) and Y. Breelle (Institut Français du Pétrole, Rueil-Malmaison, Hauts-de-Seine, France), p. 79-89. [See A69-21041 08-03]

ION-EXCHANGE FUEL CELLS AS A SOURCE OF ENERGY ON BOARD BALLOONS FOR EXPLORATION OF THE UPPER ATMOSPHERE [LES PILES A COMBUSTIBLE A MEMBRANE ECHANGEUSE D'IONS COMME SOURCE D'ENERGIE A BORD DES BALLONS D'EXPLORATION DE LA HAUTE ATMOSPHERE]. P. Demange (Compagnie Française Thomson Houston-Hotchkiss Brandt, Chatou, Yvelines, France), p. 91-98. [See A69-21042 08-03]

ELECTRODIALYTIC REGENERATION OF ALKALINE ELECTROLYTES IN FUEL CELLS. E. Justi, A. Kalberlah, K. Mund, and P. Tomczak (Braunschweig, Technische Hochschule, Braunschweig, West Germany), p. 99-111. 21 refs. [See A69-21043 08-03]

LATERAL-DIFFUSION GAS ELECTRODES FOR ELECTROCHEMICAL GENERATORS [ELECTRODES A GAZ A DIFFUSION LATERALE POUR GENERATEURS ELECTROCHIMIQUES], p. 113-120. 17 refs. [See A69-21044 08-03]

SOME PROBLEMS OF THE OPERATION OF FUEL CELL OXYGEN ELECTRODES. N. A. Shumilova (Akademiia Nauk SSSR, Institut Elektrokhimii, Moscow, USSR), p. 121-133. 12 refs. [See A69-21045 08-03]

MEDIUM-TEMPERATURE FUEL CELLS [PILES A COMBUSTIBLES A MOYENNE TEMPERATURE]. J. Laroche (EMC, Toulouse, France) and G. Billaud (Office National Industriel de l'Azote, Toulouse, France), p. 135-142. [See A69-21046 08-03]

THE VARTA FUEL CELL SYSTEM. H. H. v. Döhren, J. Euler, and A. Winsel (Varta AG, Frankfurt am Main, West Germany), p. 143-162. 15 refs. [See A69-21047 08-03]

BEHAVIOR OF A ZINC ELECTRODE IN ALKALINE MEDIA [COMPORTEMENT D'UNE ELECTRODE DE ZINC EN MILIEU ALCALIN]. F. Jolas (Société Les Piles Wonder, St. Ouen, Seine-St-Denis, France), p. 163-169. 13 refs. [See A69-21048 08-06]

TYPES OF ELECTROCHEMICAL GENERATORS USING A ZINC ELECTRODE IN AN ALKALINE MEDIUM [TYPES DE GENERATEURS ELECTROCHIMIQUES UTILISANT UNE ELECTRODE DE ZINC EN MILIEU ALCALIN]. A. Saada (Société Les Piles Wonder, St. Ouen, Seine-St-Denis, France), p. 171-182. [See A69-21049 08-03]

STUDY OF ZINC OXIDATION IN WEAKLY ALKALINE SOLUTIONS [ETUDE DE L'OXYDATION DU ZINC DANS LES SOLUTIONS FAIBLEMENT BASIQUES]. J. C. Sohm, J. Augustynski, and F. Dalard (Grenoble, Université, Grenoble, France), p. 183-191. [See A69-21050 08-06]

NICKEL-CADMIUM AND SILVER-CADMIUM STORAGE BATTERIES FOR SPACE APPLICATIONS [BATTERIES D'ACCUMULATEURS NICKEL-CADMIUM ET ARGENT-CADMIUM POUR APPLICATIONS SPATIALES]. J. du Plessix (Société des Accumulateurs Fixes et de Traction, Romainville, Seine-St-Denis, France), p. 193-205. [See A69-21051 08-03]

STUDY OF ELECTROCHEMICAL OXIDATION OF HYDROCARBONS ON PLATINUM [ETUDE DE L'OXYDATION ELECTROCHIMIQUE DES HYDROCARBURES SUR LE PLATINE]. M. Bonnemay, G. Bronoël, D. Doniat, and E. Levart (Centre National de la Recherche Scientifique, Bellevue, Hauts-de-Seine, France), p. 207-216. 10 refs. [See A69-21052 08-06]

PROTON DIFFUSION IN SOLIDS - APPLICATION TO FUEL CELLS [DIFFUSION DES PROTONS DANS LES SOLIDES - APPLICATIONS AUX PILES A COMBUSTIBLE]. M. Christen (Compagnie Générale d'Electricité de Paris, Marcoussis, Essonne, France), p. 217-232. 15 refs. [See A69-21053 08-06]

DIRECT ELECTROCHEMICAL CONVERSION OF THE ENERGY OF A RADIOACTIVE ELEMENT [CONVERSION ELECTROCHIMIQUE DIRECTE DE L'ENERGIE D'UN RADIOELEMENT]. C. Eyraud, J. Lenoir, and P. Jenin (Lyon, Université, Lyon; Direction des Recherches et Moyens d'Essais, Paris, France), p. 233-243. 6 refs. [See A69-21054 08-06]

HYDROGEN-OXYGEN FUEL CELLS WITH HYDROPHOBIC TYPE ELECTRODES AND AN ALKALINE ELECTROLYTE [PILES A COMBUSTIBLE HYDROGENE-OXYGENE A ELECTRODES D'UN TYPE HYDROPHOBE A ELECTROLYTE ALCALIN]. N. S. Lidorenko, T. N. Toroptseva, V. E. Dmitrenko, and F. R. Iuppets (Akademiia Nauk SSSR, Institut Elektrokhimii, Moscow, USSR), p. 251-259. [See A69-21055 08-03]

HIGH-ENERGY-DENSITY ELECTROCHEMICAL GENERATORS USING NONAQUEOUS MEDIA [GENERATEURS ELECTROCHIMIQUES A HAUTE DENSITE D'ENERGIE UTILISANT DES MILIEUX NON AQUEUX]. G. Gerbier (Société des Accumulateurs Fixes et de Traction, Poitiers, France), p. 261-268. [See A69-21056 08-03]

A69-21035 *

FUEL CELL SYSTEMS FOR MANNED SPACECRAFT.
Hoyt McBryar (NASA, Manned Spacecraft Center, Houston, Tex.).
IN: ELECTROCHEMICAL GENERATORS FOR SPACE APPLICATIONS; CENTRE NATIONAL D'ETUDES SPATIALES, INTERNATIONAL CONVENTION, PARIS, FRANCE, DECEMBER 4-7, 1967, PROCEEDINGS [LES GENERATEURS ELECTROCHIMIQUES POUR APPLICATIONS SPATIALES; CENTRE NATIONAL D'ETUDES SPATIALES, COLLOQUE INTERNATIONAL, PARIS, FRANCE, DECEMBER 4-7, 1967, PROCEEDINGS]. [A69-21034 08-03]
Paris, Dunod Editeur, 1968, p. 1-18.

Description of the requirements for manned-spacecraft electrical power systems. Considerations that led to the selection of fuel cells for Gemini and Apollo - i.e., weight and volume limitations and high-energy yield requirements for payload compatibility are discussed. The Gemini and Apollo fuel cell system design and configuration are presented, with cutaway views showing mounting locations within the respective equipment bays. The interrelations between the fuel cells and other subsystems such as the thermal control (radiator) system and life support system (water production for metabolic use, etc.) are shown and described. The ion-exchange membrane and the Bacon fuel cell concepts are described with illustrations showing fuel cell elements and performance. The crew-critical aspects relative to the fuel cell are given for the Apollo program. M. G.

A69-21806

INSTITUTE OF ELECTRICAL AND ELECTRONICS ENGINEERS, ANNUAL THERMIONIC CONVERSION SPECIALIST CONFERENCE, 7TH, FRAMINGHAM, MASS., OCTOBER 21-23, 1968, CONFERENCE RECORD.
New York, Institute of Electrical and Electronics Engineers, Inc., 1968. 354 p.
Members, $10.00; nonmembers, $15.

CONTENTS:

INDEX TO AUTHORS, p. v.

SURFACES AND MATERIALS.

EFFECTIVE WORK FUNCTION DETERMINATIONS OF RHENIUM AND MOLYBDENUM. D. L. Jacobson and A. E. Campbell (Electro-Optical Systems, Inc., Pasadena, Calif.), p. 1-9. 6 refs. [See A69-21807 09-26]

MEASUREMENTS OF THE WORK FUNCTION AND DESORPTION ENERGY OF CESIUM AND POTASSIUM ON (100) TUNGSTEN. D. L. Fehrs (NASA, Electronics Research Center, Cambridge, Mass.), T. J. Lee, and R. E. Stickney (Massachusetts Institute of Technology, Cambridge, Mass.), p. 10-17. 14 refs. [See A69-21808 09-26]

THE EFFECT OF TEMPERATURE ON THE WORK FUNCTION MINIMUM OF CESIATED TUNGSTEN SURFACES. T. J. Lee (Massachusetts Institute of Technology, Cambridge, Mass.) and B. J. Hopkins (Southampton, University, Southampton, England), p. 18-22. 14 refs. [See A69-21809 09-26]

SURFACE CHARACTERIZATION STUDIES ON CVD TUNGSTEN.

J. R. Thompson, J. C. Danko, T. L. Gregory (General Electric Co., Pleasanton, Calif.), and H. F. Webster (General Electric Co., Schenectady, N.Y.), p. 23-30. [See A69-21810 09-26]

PREFERRED CRYSTAL ORIENTATION EVALUATION AND VACUUM WORK FUNCTION MEASUREMENTS ON CHEMICALLY VAPOR-DEPOSITED TUNGSTEN EMITTERS. L. Yang, R. G. Hudson, T. Tagami (Gulf General Atomic, Inc., San Diego, Calif.), and J. W. R. Creagh (Gulf General Atomic, Inc., San Diego, Calif.; NASA, Lewis Research Center, Cleveland, Ohio), p. 31-40.

PARTIAL ROLE FIGURES FROM CYLINDRICAL AND PLANAR TUNGSTEN SPECIMENS. L. van Someren and E. W. Sprenkle (Thermo Electron Corp., Waltham, Mass.), p. 41-46. 5 refs. [See A69-21811 09-26]

THE THERMIONIC EMISSION FROM RHENIUM AND CHEMICALLY VAPOR DEPOSITED RHENIUM IN CESIUM VAPOR. E. L. Burgess (Sandia Corp., Albuquerque, N. Mex.), p. 47-50.

CHEMICAL VAPOR DEPOSITION OF TUNGSTEN. J. Chin and J. Horsley (Gulf General Atomic, Inc., San Diego, Calif.), p. 51-59.

THE OPTICAL GONIOMETER AS A TOOL IN THE STUDY OF ROUGH SURFACES. L. van Someren (Thermo Electron Corp., Waltham, Mass.), p. 60-63.

OXYGEN EFFECTS IN TANTALUM THERMIONIC EMITTERS. S. S. Luebbers (California Institute of Technology, Pasadena, Calif.) and J. G. De Steese (McDonnell Douglas Corp., Richland, Wash.), p. 64-68. 7 refs. [See A69-21812 09-03]

HIGH-TEMPERATURE COMPATIBILITY TESTING OF ISOTOPE FUEL CONTAINER SYSTEMS. R. L. Andelin and J. D. Watrous (McDonnell Douglas Corp., Richland, Wash.), p. 69-78.

CESIUM SORPTION IN MATERIALS FOR INTEGRAL RESERVOIRS. M. K. Yates and G. O. Fitzpatrick (Gulf General Atomic, Inc., San Diego, Calif.), p. 79-87.

EVALUATION OF CARBON AND GRAPHITE INSULATIONS FOR THERMIONIC APPLICATIONS. K. A. Gasper and J. S. Holmgren (McDonnell Douglas Corp., Richland, Wash.), p. 88-95.

REACTOR TESTS OF ISOTHERMAL IRRADIATORS. C. V. Weaver and W. A. Ranken (California, University, Los Alamos, N. Mex.), p. 96-98.

CONVERTER TESTING.

REPRODUCIBILITY OF THERMIONIC PERFORMANCE. P. K. Shefsiek (Thermo Electron Corp., Waltham, Mass.), p. 99-102. [See A69-21813 09-03]

CORRELATION OF FIXED-SPACING THERMIONIC CONVERTER PERFORMANCE WITH VARIABLE-SPACING TEST VEHICLE DATA. O. S. Merrill (California Institute of Technology, Pasadena, Calif.), p. 103-112. [See A69-21814 09-03]

FIXED-SPACE PLANAR THERMIONIC DIODE WITH COLLECTOR GUARD RING. T. O. Speidel (Thermo Electron Corp., Waltham, Mass.) and R. M. Williams (NASA, Lewis Research Center, Cleveland, Ohio), p. 113-117. [See A69-21815 09-03]

A COMPARISON OF THE PERFORMANCE OF TWO RHENIUM, NIOBIUM CYLINDRICAL THERMIONIC CONVERTERS. R. M. Williams and T. J. Kascak (NASA, Lewis Research Center, Cleveland, Ohio), p. 118-122. 6 refs. [See A69-21816 09-03]

THE PERFORMANCE OF A RHENIUM, NIOBIUM CYLINDRICAL THERMIONIC CONVERTER. T. J. Kascak and R. M. Williams (NASA, Lewis Research Center, Cleveland, Ohio), p. 123-127. 8 refs. [See A69-21817 09-03]

LARGE CYLINDRICAL THERMIONIC DIODE WITH RHENIUM EMITTER FOR DIODE KINETIC EXPERIMENTS. M. Peelgren (California Institute of Technology, Pasadena, Calif.) and T. Speidel (Thermo Electron Corp., Waltham, Mass.), p. 128-133. [See A69-21818 09-03]

PERFORMANCE OF CHLORIDE AND FLUORIDE VAPOR-DEPOSITED TUNGSTEN EMITTERS IN THERMIONIC CONVERTERS. C.-C. Wang (Thermo Electron Corp., Waltham, Mass.) and J. J. Ward (NASA, Lewis Research Center, Cleveland, Ohio), p. 134-140. [See A69-21819 09-03]

EMISSION CHARACTERISTICS OF A DUPLEX VAPOR-DEPOSITED TUNGSTEN EMITTER. F. Rufeh and D. Lieb (Thermo Electron Corp., Waltham, Mass.), p. 141-150. [See A69-21820 09-03]

PERFORMANCE COMPARISON OF FOUR CYLINDRICAL DIODES WITH VARIOUS TYPES OF TUNGSTEN EMITTERS. D. M. Ernst (Thermo Electron Corp., Waltham, Mass.), p. 151-154. [See A69-21821 09-03]

SIDE-WALL CURRENTS IN UNIGNITED HARDWARE-TYPE THERMIONIC ENERGY CONVERTERS. K. Shimada (California Institute of Technology, Pasadena, Calif.), p. 155-158. [See A69-21822 09-03]

ELECTRICAL TESTING OF A SIX-CONVERTER GENERATOR. G. Stapfer and K. Shimada (California Institute of Technology, Pasadena, Calif.), p. 159-163. [See A69-21823 09-03]

METALLOGRAPHY OF THERMIONIC CONVERTERS. P. Rouklove (California Institute of Technology, Pasadena, Calif.), p. 164-171. 10 refs. [See A69-21824 09-03]

OPERATION OF A THREE-DIODE FLAME-FIRED THERMIONIC POWER SUPPLY. P. Shefsiek, L. Lazaridis (Thermo Electron Corp., Waltham, Mass.), and I. Shai (Atomic Energy Commission, Israel), p. 172-174.

INVESTIGATIONS ON SEMICONDUCTING COLLECTOR MATERIALS. H. Albrecht, W. Kluge, H. Rapp, and H. Strecker (Stuttgart, Technische Universität, Stuttgart, West Germany), p. 175-177. [See A69-21825 09-26]

PLASMA STUDIES.

THERMIONIC RESEARCH AT STRESA (A REVIEW). L. K. Hansen (North American Rockwell Corp., Canoga Park, Calif.), p. 178-187.

ELECTRON DENSITY AND TEMPERATURE MEASUREMENTS OF THE IGNITED MODE PLASMA IN A THERMIONIC CONVERTER. R. J. Andersen (United Aircraft Corp., East Hartford, Conn.), p. 188-194. 18 refs. [See A69-21826 09-03]

THE LOW-VOLTAGE ARC. C. Warner (North American Rockwell Corp., Canoga Park, Calif.), p. 195-201.

ISOTHERMAL DIODE '68. J. F. Morris (NASA, Lewis Research Center, Cleveland, Ohio), p. 202-208. 48 refs. [See A69-21827 09-03]

SHEATH STRUCTURE IN THE UNIGNITED MODE. P. M. Sockol (NASA, Lewis Research Center, Cleveland, Ohio), p. 209-215. 10 refs. [See A69-21828 09-03]

THE DENSITY OF POSITIVE IONS TRAPPED IN THE EMITTER SHEATH. D. DeMichele and M. V. Davis (Arizona, University, Tucson, Ariz.), p. 216-223.

FISSION FRAGMENT GENERATED PLASMAS FOR THERMIONIC DIODES - AN ASSESSMENT. F. E. Jamerson, F. E. Gifford, C. B. Leffert, and D. B. Rees (General Motors Corp., Warren, Mich.), p. 224-229. 9 refs. [See A69-21829 09-03]

IONIC SPECIES PRESENT IN ARGON-CESIUM AND CESIUM DISCHARGES. H. Held, J. L. Gilkinson, and L. M. Chanin (Minnesota, University, Minneapolis, Minn.), p. 230-234. 22 refs. [See A69-21830 09-03]

ELECTRON COOLING AND PLASMA HEATING OF THERMIONIC CONVERTERS. R. Breitwieser (NASA, Lewis Research Center, Cleveland, Ohio), p. 235-241. 14 refs. [See A69-21831 09-03]

FREE AREA FOR TRANSLATION CALCULATED BY MONTE-CARLO SIMULATION OF SURFACE MIGRATIONS. C. Y. Fleck (RAND Corp., Santa Monica, Calif.), p. 242-246.

EFFECT OF DIODE GEOMETRY ON SATURATED ION CURRENT. E. A. Guignard and T. H. Pigford (California, University, Berkeley, Calif.), p. 247-253. [See A69-21832 09-03]

HEAT TRANSFER.

HEAT PIPE STUDIES AT THERMO ELECTRON CORPORATION. D. M. Ernst, E. K. Levy, and P. K. Shefsiek (Thermo Electron Corp., Waltham, Mass.), p. 254-257. [See A69-21833 09-03]

COMPATIBILITY OF VARIOUS HIGH-TEMPERATURE HEAT PIPE ALLOYS WITH WORKING FLUIDS. G. D. Johnson (McDonnell Douglas Corp., Richland, Wash.), p. 258-265.

ULTIMATE HEAT PIPE PERFORMANCE. J. E. Kemme (California, University, Los Alamos, N. Mex.), p. 266-271.

THE CALCULATION OF EMITTER SUPPORT CONDUCTION LOSS. P. Brosens and I. Shai (Thermo Electron Corp., Waltham, Mass.), p. 272-276.

HEAT TRANSFER IN MULTICOMPONENT MONATOMIC GASES IN THE LOW, INTERMEDIATE AND HIGH PRESSURE REGIME. W. R. Lloyd, D. R. Wilkins, and P. R. Hill (General Electric Co., Pleasanton, Calif.), p. 277-285.

THERMIONIC BOUNDARY CONDITIONS FOR TWO-DIMENSIONAL THERMAL ANALYSIS OF CONVERTERS. M. J. Abbate and A. Schock (Fairchild Hiller Corp., Farmingdale, N.Y.), p. 286-289. [See A69-21834 09-03]

DEVICES AND SYSTEMS.

FAST CRITICAL EXPERIMENTS IN SUPPORT OF THERMIONIC REACTOR PHYSICS. S. C. Cohen, R. A. Moore, J. L. Russell, Jr., D. A. Sargis, and R. Sharp (Gulf General Atomic, Inc., San Diego, Calif.), p. 290-298. 11 refs. [See A69-21835 09-03]

AN IMPROVED OUT-OF-CORE THERMIONIC REACTOR FOR LOW POWER. S. Dagbjartsson, M. Groll, O. Schlörb, and R. Pruschek (Stuttgart, Technische Universität, Stuttgart, West Germany), p. 299-304. [See A69-21836 09-03]

OPTIMIZATION OF SERIES-CONNECTED THERMIONIC CONVERTERS WITH DIFFERENT HEAT INPUT. E. Wolf and W. Haug (Stuttgart, Technische Universität, Stuttgart, West Germany), p. 305-312.

EFFECT OF CESIUM PRESSURE ON THERMIONIC STABILITY. A. Schock (Fairchild Hiller Corp., Farmingdale, N.Y.), p. 313-317. [See A69-21837 09-03]

THERMAL STABILITY AS A FUNCTION OF CONVERTER PERFORMANCE. D. Lieb and F. Rufeh (Thermo Electron Corp., Waltham, Mass.), p. 318-322. [See A69-21838 09-03]

THEORETICAL LIMITS TO USE AN ADSORPTION SYSTEM AS CESIUM RESERVE IN THERMIONIC CONVERTER. P. Defranould (Compagnie Française Thomson Houston-Hotchkiss Brandt, Bagneux, Hauts-de-Seine, France), p. 323-330. [See A69-21839 09-03]

THEORY OF GAS BREAKDOWN IN HOT CRACKS WITH APPLICATION TO THERMIONIC TRILAYER INSULATION. A. Kniazzeh (NASA, Electronics Research Center, Cambridge, Mass.), p. 331-341. 12 refs. [See A69-21840 09-03]

POSSIBLE INSTABILITIES IN A THERMIONIC REACTOR WITH ALL NEGATIVE REACTIVITY COEFFICIENTS. C. A. Heath (Gulf General Atomic, Inc., San Diego, Calif.), p. 342-347. [See A69-21841 09-03]

A69-21819 *

PERFORMANCE OF CHLORIDE AND FLUORIDE VAPOR-DEPOSITED TUNGSTEN EMITTERS IN THERMIONIC CONVERTERS.
Chi-Chung Wang (Thermo Electron Corp., Waltham, Mass.) and James J. Ward (NASA, Lewis Research Center, Cleveland, Ohio).
IN: INSTITUTE OF ELECTRICAL AND ELECTRONICS ENGINEERS, ANNUAL THERMIONIC CONVERSION SPECIALIST CONFERENCE, 7TH, FRAMINGHAM, MASS., OCTOBER 21-23, 1968, CONFERENCE RECORD. [A69-21806 09-03]
New York, Institute of Electrical and Electronics Engineers, Inc., 1968, p. 134-140.
NASA-sponsored research.

Six planar geometry thermionic converters with chloride and fluoride vapor-deposited tungsten emitters, niobium collectors, and 8-mil interelectrode spacing were tested to compare performance characteristics. The investigated temperatures range from 1600 to 2000 K. The results show that for emitter temperatures above 1800 K the chloride vapor deposited tungsten emitters which have (110) preferred orientation offer approximately a 50% higher power density than that of the fluoride vapor-deposited tungsten emitters which have (100) preferred orientation. For emitter temperatures lower than 1700 K the chloride vapor-deposited tungsten emitters offer better performance only at low output-voltage. Chemical etching of the fluoride vapor-deposited tungsten improves its performance to the level of chloride vapor-deposited tungsten. A qualitative correlation was observed for the chloride emitter between the degree of orientation, the cesiated work functions, and converter performance. Converter life tests are proceeding to determine performance stability. Approximately 3000 hr have been attained with the fluoride tungsten emitter at 1900 K, 1600 hr on an etched fluoride tungsten emitter at 1900 K and approximately 4000 hr on a chloride tungsten emitter at 2000 K. The life test program is not yet complete. (Author)

A69-21827 *

ISOTHERMAL DIODE '68.
James F. Morris (NASA, Lewis Research Center, Cleveland, Ohio).
IN: INSTITUTE OF ELECTRICAL AND ELECTRONICS ENGINEERS, ANNUAL THERMIONIC CONVERSION SPECIALIST CONFERENCE, 7TH, FRAMINGHAM, MASS., OCTOBER 21-23, 1968, CONFERENCE RECORD. [A69-21806 09-03]
New York, Institute of Electrical and Electronics Engineers, Inc., 1968, p. 202-208. 48 refs.

Discussion of the isothermal diode as a basis for the study of the internal complex that controls thermionic energy conversion. Nottingham's (1962) theory, which places a sheath with arbitrary exponential variations of charge concentrations between an equilibrium plasma and a field-modified emitter of electrons, ions, and atoms, is discussed. It is shown that in current isothermal-diode theory the self-consistent interactions of the electrode and the ionized gas build the sheath, which strongly affects particle emissions through arrival rates and fields at the emitter face. The improved theory is shown to reveal a need for a virtual Schottky emitter to give equal absolute sheath drops for positive and negative charges, and to prevent net currents at equilibrium. Near-equilibrium calculations are given, showing that the emission sheath properties correlate with the work function minus the plasma potential, the plasma-electron concentration, and the electrode temperature. Parametric results emphasize the great increase in total cesium arrival rates that positive-ion sheaths can cause. The computed trends for cesium and polycrystalline tungsten show some near-equilibrium effects of this system on emitter and sheath functions. B.H.

A69-21828 *

SHEATH STRUCTURE IN THE UNIGNITED MODE.
Peter M. Sockol (NASA, Lewis Research Center, Cleveland, Ohio).
IN: INSTITUTE OF ELECTRICAL AND ELECTRONICS ENGINEERS, ANNUAL THERMIONIC CONVERSION SPECIALIST CONFERENCE, 7TH, FRAMINGHAM, MASS., OCTOBER 21-23, 1968, CONFERENCE RECORD. [A69-21806 09-03]
New York, Institute of Electrical and Electronics Engineers, Inc., 1968, p. 209-215. 10 refs.

A kinetic theory model of the plasma-sheath transition is used to analyze the sheath structure in the unignited mode of a thermionic converter. The study is confined to conditions in which the mean-free-paths and Debye length are small compared to the diode spacing. The emitter sheath structure is found to be the same as in the isothermal diode. The collector sheath varies from completely continuum to completely collisionless with a noncontinuum presheath as the local Debye length varies from much larger to much smaller than the mean-free-path. Theoretical current-voltage characteristics are compared with experimental ones. (Author)

A69-21840 *

THEORY OF GAS BREAKDOWN IN HOT CRACKS WITH APPLICATION TO THERMIONIC TRILAYER INSULATION.
Alfredo Kniazzeh (NASA, Electronics Research Center, Cambridge, Mass.).
IN: INSTITUTE OF ELECTRICAL AND ELECTRONICS ENGINEERS, ANNUAL THERMIONIC CONVERSION SPECIALIST CONFERENCE, 7TH, FRAMINGHAM, MASS., OCTOBER 21-23, 1968, CONFERENCE RECORD. [A69-21806 09-03]
New York, Institute of Electrical and Electronics Engineers, Inc., 1968, p. 331-341. 12 refs.

Brief discussion of a new theory for gas breakdown in hot cracks, where the theory is specifically applied to the breakdown of a cesium vapor-filled crack in an insulator such as might be found in the trilayer of a thermionic fuel element. The thermionic insulator analysis includes the effect on breakdown caused by certain parameters which might change over extended mission lifetimes or by a change in insulator material. The intent is to produce a breakdown model which (1) can eventually be used to inexpensively screen proposed insulator materials and gas environments and (2) can extrapolate short-term experimental data to long-term mission requirements. The novel feature of the model presented is the inclusion of surface interactions in the equations describing the electron-energy distribution function. This permits the inclusion of thermionic emission from the insulating walls and the absorption and scattering of high-energy electrons by the wall. M.M.

A69-23993 *

AUXILIARY ELECTRODE CHARGE CONTROL.
Floyd E. Ford (NASA, Goddard Space Flight Center, Greenbelt, Md.).
IN: U.S. ARMY ELECTRONICS COMMAND, ANNUAL POWER SOURCES CONFERENCE, 22ND, ATLANTIC CITY, N.J., MAY 14-16, 1968, PROCEEDINGS. [A69-23990 10-03]
Red Bank, N.J., Power Sources Conference Publications Committee,

1968, p. 53-57. 5 refs.

Discussion of signal-electrode charge control of nickel-cadmium batteries. It is pointed out that this type of control offers some unique advantages over previous methods. Being in intimate association with the electrochemical process of the cell, the signal-electrode signals the onset of oxygen pressure within a cell and provides a voltage that is linearly related to pressure over a limited region. This signal voltage can provide a unique method for overcharge control. Use of a selected number of signal-electrode-type cells in each battern provides signals that can be used to maintain the capacity of the battery above the rated value and thus optimize overcharge. G. R.

A69-26497 *#

HIGH-FIELD CRYOGENIC MAGNETS WITH PURE ALUMINUM CONDUCTOR.

Gerald V. Brown (NASA, Lewis Research Center, Cleveland, Ohio).

University of California, Symposium on Engineering Problems of Fusion Research, Los Alamos, N. Mex., Apr. 8-11, 1969, Paper. 8 p. 7 refs.

Discussion of the use of very pure aluminum conductors in high-current-density cryogenic magnets. The need to limit the strain in the aluminum by appropriate structure strength is analyzed. The conclusion is that aluminum with a resistivity ratio above 10,000 could be effectively used if the strain is limited to a few tenths of a percent. Magnetoresistance is a more serious problem at high fields than is strain resistivity. It is shown that average current densities needed to produce fields of 300 kG and over could be obtained even though large amounts of structure are needed to keep the strain low. An examination of the forces in a tape-wound solenoid shows that the problem of the low yield stress of pure aluminum can be solved by making the conductor thin and thus preventing excessive accumulation of force within the conductor. The amount of structure needed in a tape-wound coil is analyzed in terms of a nondimensional parameter containing the conductor current density and the Young's modulus of the structure. The advantage of a high-modulus structure is emphasized. (Author)

A69-26498 *#

VARIABLE-VOLTAGE, DIRECT-CURRENT POWER SUPPLIES FOR ENERGIZING CRYOGENICALLY COOLED AND SUPERCONDUCTIVE ELECTROMAGNETS.

J. C. Laurence, E. H. Meyn, and R. J. Jirberg (NASA, Lewis Research Center, Cleveland, Ohio).

University of California, Symposium on Engineering Problems of Fusion Research, Los Alamos, N. Mex., Apr. 8-11, 1969, Paper. 10 p.

Power supplies for energizing cryogenically cooled and superconductive electromagnets, and their control circuitry are described. The first is a dc generator of the homopolar type with a continuous rating of 0 to 60,000 A at 38 V. Overloads of up to three times the continuous current output are available for a duty cycle of 2 min. Control circuitry provides for complete reversal of the output voltage by reversing the direction of the exciter field. This feature is useful for discharging an electromagnet in the shortest possible time. The second of these converts three-phase, 440 V, 60-Hz power into a variable-voltage (0 to 45 V) direct current (0 to 15,000 A continuous rating). The fundamental ripple frequency is 360 Hz and its peak-to-peak amplitude is less than 18% of the dc output voltage. Variations in the preset dc output voltage under continuous load are limited to ±1% when the ac input power variations are regulated to ±5%. (Author)

A69-28855 *#

FLAT CONDUCTOR CABLE TECHNOLOGY.

Wilhelm Angele (NASA, Marshall Space Flight Center, Astrionics Laboratory, Huntsville, Ala.).

American Society of Mechanical Engineers, Design Engineering Conference and Show, New York, N.Y., May 5-8, 1969, Paper 69-DE-67. 15 p.
Members, $0.75; nonmembers, $1.50.

Short report on the status of flat conductor cable (FCC) technology as of Autumn 1968. The basic design and manufacturing principles are briefly mentioned. Standards and specifications are listed. The highlights of FCC properties, advantages, and limitations are given. FCC harness design, assembly, and installation methods are presented, as well as the results of a large application study. Proposals for future development efforts and an outlook concerning the expanded use and application of FCC are also included. (Author)

A69-32405

ELECTROCHEMICAL GENERATORS FOR SPACE APPLICATIONS; CENTRE NATIONAL D'ETUDES SPATIALES, INTERNATIONAL CONFERENCE, PARIS, FRANCE, DECEMBER 4-7, 1967, PROCEEDINGS [LES GENERATEURS ELECTROCHIMIQUES POUR APPLICATIONS SPATIALES; CENTRE NATIONAL D'ETUDES SPATIALES, COLLOQUE INTERNATIONAL, PARIS, FRANCE, DECEMBER 4-7, 1967, PROCEEDINGS].

Paris, Dunod Editeur, 1968. 262 p. In French, English, and Russian. $22.

CONTENTS:

FOREWORD [AVANT-PROPOS]. 1 p.

FUEL CELL SYSTEMS FOR MANNED SPACECRAFT. H. McBryar (NASA, Manned Spacecraft Center, Houston, Tex.), p. 1-18. [See A69-32406 16-03]

SPACE APPLICATIONS OF ELECTROCHEMICAL GENERATORS [APPLICATIONS SPATIALES DES GENERATEURS ELECTROCHIMIQUES]. H. Daspet and D. Coudot (Centre National d'Etudes Spatiales, Brétigny-sur-Orge, Essonne, France), p. 19-32. 6 refs. [See A69-32407 16-03]

BASIC PROBLEMS OF LOW TEMPERATURE CELLS USING CARBON-CONTAINING FUELS [PROBLEMES FONDAMENTAUX RELATIFS AUX PILES A BASSE TEMPERATURE UTILISANT DES COMBUSTIBLES CARBONES]. M. Bonnemay, G. Bronoël, E. Devos, and D. Doniat (Centre National de la Recherche Scientifique, Bellevue, Hauts-de-Seine, France), p. 33-46. 8 refs. [See A69-32408 16-03]

PARTICULARS CONCERNING ELECTRODES FOR FUEL CELLS OPERATING UNDER WEIGHTLESS CONDITIONS [PARTICULARITES DES ELECTRODES POUR PILES A COMBUSTIBLE FONCTIONNANT EN CONDITIONS D'APESANTEUR]. V. S. Bagotzkii (Akademiia Nauk SSSR, Institut Elektrokhimii, Moscow, USSR), p. 47-55. [See A69-32409 16-03]

HYDROGEN AND BASIC ELECTROLYTE COLD CELLS AT THE CGE RESEARCH CENTER [LES PILES FROIDES A HYDROGENE ET A ELECTROLYTE BASIQUE AU CENTRE DE RECHERCHES DE LA C.G.E.]. C. Edon (Compagnie Générale d'Electricité de Paris, Marcoussis, Essonne, France), p. 57-70. [See A69-32410 16-03]

THE 200-W "ABEPAC" MEMBRANE CELL [LA PILE A MEMBRANE DE 200W "ABEPAC"]. C. Vanleugenhaghe, A. Clauss, and C. Beaudet (Société d'Etudes, de Recherches et d'Applications pour l'Industrie, Brussels, Belgium), p. 71-78. [See A69-32411 16-03]

COMPACT HYDROGEN-OXYGEN CELL [PILE HYDROGENE-OXYGENE COMPACTE]. R. Vic (Compagnie Industrielle des Piles Electriques, Argenteuil, Val-d'Oise, France) and Y. Breelle (Institut Français du Pétrole, Rueil-Malmaison, Hauts-de-Seine, France), p. 79-89. [See A69-32412 16-03]

ION-EXCHANGE MEMBRANE FUEL CELLS AS A POWER SOURCE FOR BALLOONS EXPLORING THE UPPER ATMOSPHERE [LES PILES A COMBUSTIBLE A MEMBRANE ECHANGEUSE D'IONS COMME SOURCE D'ENERGIE A BORD DES BALLONS D'EXPLORATION DE LA HAUTE ATMOSPHERE]. Ph. Demange (Compagnie Française Thomson Houston-Hotchkiss Brandt, Châtou, Yvelines, France), p. 91-98. [See A69-32413 16-03]

ELECTRODIALYTIC REGENERATION OF ALKALINE ELECTROLYTES IN FUEL CELLS. E. Justi, A. Kalberlah, K. Mund, and P. Tomczak (Braunschweig, Technische Universität, Braunschweig, West Germany), p. 99-111. 12 refs. [See A69-32414 16-03]

LATERAL DIFFUSION GAS ELECTRODES FOR ELECTROCHEMICAL GENERATORS [ELECTRODES A GAZ A DIFFUSION LATERALE POUR GENERATEURS ELECTROCHIMIQUES], p. 113-120. 17 refs. [See A69-32415 16-03]

SOME PROBLEMS OF THE OPERATION OF FUEL CELL OXYGEN ELECTRODES. N. A. Shumilova (Akademiia Nauk SSSR, Institut Elektrokhimii, Moscow, USSR), p. 121-133. 12 refs. [See A69-32416 16-03]

MEDIUM TEMPERATURE FUEL CELLS [PILES A COMBUS-

TIBLES A MOYENNE TEMPERATURE]. J. Laroche and G. Billaud (EMC - Office National Industriel de l'Azote, Toulouse, France), p. 135-142. [See A69-32417 16-03]

THE VARTA FUEL CELL SYSTEM. H. H. v. Dŏhren, J. Euler, and A. Winsel (Varta AG, Frankfurt am Main, West Germany), p. 143-162. 15 refs. [See A69-32418 16-03]

BEHAVIOR OF A ZINC ELECTRODE IN AN ALKALINE MEDIUM [COMPORTEMENT D'UNE ELECTRODE DE ZINC EN MILIEU ALCALIN]. F. Jolas (Société Les Piles Wonder, St. Ouen, Seine-St-Denis, France), p. 163-169. 13 refs. [See A69-32419 16-03]

TYPES OF ELECTROCHEMICAL GENERATORS UTILIZING A ZINC ELECTRODE IN AN ALKALINE MEDIUM [TYPES DE GENERATEURS ELECTROCHIMIQUES UTILISANT UNE ELECTRODE DE ZINC EN MILIEU ALCALIN]. A. Saada (Société Les Piles Wonder, St. Ouen, Seine-St-Denis, France), p. 171-182. [See A69-32420 16-03]

STUDY OF THE OXIDATION OF ZINC IN WEAKLY BASIC SOLUTIONS [ETUDE DE L'OXYDATION DU ZINC DANS LES SOLUTIONS FAIBLEMENT BASIQUES]. J. C. Sohm, J. Augustynski, and F. Dalard (Grenoble, Université, Grenoble, France), p. 183-191. [See A69-32421 16-03]

NICKEL-CADMIUM AND SILVER-CADMIUM STORAGE BATTERIES FOR SPACE APPLICATIONS [BATTERIES D'ACCUMULATEURS NICKEL-CADMIUM ET ARGENT-CADMIUM POUR APPLICATIONS SPATIALES]. M. Jochaud du Plessix (Société des Accumulateurs Fixes et de Traction, Romainville, Seine-St-Denis, France), p. 193-205. [See A69-32422 16-03]

STUDY OF ELECTROCHEMICAL OXIDATION OF HYDROCARBONS ON PLATINUM [ETUDE DE L'OXYDATION ELECTROCHIMIQUE DES HYDROCARBURES SUR LE PLATINE]. M. Bonnemay, G. Bronoël, D. Doniat, and E. Levart (Centre National de la Recherche Scientifique, Bellevue, Hauts-de-Seine, France), p. 207-216. 10 refs. [See A69-32423 16-03]

DIFFUSION OF PROTONS IN SOLIDS - APPLICATIONS TO FUEL CELLS [DIFFUSION DES PROTONS DANS LES SOLIDES - APPLICATIONS AUX PILES A COMBUSTIBLE]. M. Christen (Compagnie Générale d'Electricité de Paris, Marcoussis, Essonne, France), p. 217-232. 15 refs. [See A69-32424 16-03]

DIRECT ELECTROCHEMICAL CONVERSION OF THE ENERGY OF A RADIOELEMENT [CONVERSION ELECTROCHIMIQUE DIRECTE DE L'ENERGIE D'UN RADIOELEMENT]. C. Eyraud, J. Lenoir, and P. Jenin (Lyon, Université, Lyons; Direction des Recherches et Moyens d'Essais, Paris, France), p. 233-243. 6 refs. [See A69-32425 16-03]

HYDROGEN-OXYGEN FUEL BATTERIES BASED ON HYDROPHOBIC-TYPE ELECTRODES WITH AN ALKALINE ELECTROLYTE [TOPLIVNYE VODORODNO-KISLORODNYE BATAREI NA OSNOVE ELEKTRODOV GIDROFOBNOGO TIPA S SHCHELOCHNYM ELEKTROLITOM]. N. S. Lidorenko, T. N. Toroptseva, V. E. Dmitrenko, and F. R. Iuppets (Akademiia Nauk SSSR, Institut Elektrokhimii, Moscow, USSR), p. 245-249. [See A69-32426 16-03]

HIGH-ENERGY-DENSITY ELECTROCHEMICAL GENERATORS USING NONAQUEOUS MEDIA [GENERATEURS ELECTROCHIMIQUES A HAUTE DENSITE D'ENERGIE UTILISANT DES MILIEUX NON AQUEUX]. G. Gerbier (Société des Accumulateurs Fixes et de Traction, Poitiers, France), p. 261-268. [See A69-32427 16-02]

A69-32406 *

FUEL CELL SYSTEMS FOR MANNED SPACECRAFT.

Hoyt McBryar (NASA, Manned Spacecraft Center, Houston, Tex.). IN: ELECTROCHEMICAL GENERATORS FOR SPACE APPLICATIONS; CENTRE NATIONAL D'ETUDES SPATIALES, INTERNATIONAL CONFERENCE, PARIS, FRANCE, DECEMBER 4-7, 1967, PROCEEDINGS [LES GENERATEURS ELECTROCHIMIQUES POUR APPLICATIONS SPATIALES; CENTRE NATIONAL D'ETUDES SPATIALES, COLLOQUE INTERNATIONAL, PARIS, FRANCE, DECEMBER 4-7, 1967, PROCEEDINGS]. [A69-32405 16-03] Paris, Dunod Editeur, 1968, p. 1-18.

Description of the requirements for manned-spacecraft electrical power systems. Considerations that led to the selection of fuel cells for Gemini and Apollo (i.e., weight and volume limitations and high energy yield requirements for payload compatibility) are discussed. The Gemini and Apollo fuel cell system design and configuration are presented, with cutaway views showing mounting locations within the respective equipment bays. The interrelationships of the fuel cells with other subsystems are shown and described. The ion-exchange membrane and the Bacon fuel cell concepts are described with illustrations showing fuel cell elements and performance. Operational and flight-control requirements are described for each system, with distinction being made between astronaut control and monitoring functions, and ground control and monitoring functions. A summary of the Gemini Program is given relative to the fuel cell. Salient elements of the Apollo lunar landing mission are described, supported by a view showing the earth and moon and the trajectory path with significant events indicated along the way. The crew-critical aspects relative to the fuel cell are given.

(Author)

A69-32709 *#

DEVELOPMENT OF ELECTRIC POWER SUPPLIES FOR ELECTRIC PROPULSION.

Carl E. Johnson (U.S. Atomic Energy Commission, Washington, D.C.), Arvin H. Smith, and Fred Schulman (NASA, Washington, D.C.).

American Institute of Aeronautics and Astronautics, Propulsion Joint Specialist Conference, 5th, U.S. Air Force Academy, Colorado Springs, Colo., June 9-13, 1969, Paper 69-826. 23 p. 14 refs. Members, $1.00; nonmembers, $1.50.

Discussion of developments in solar and nuclear electric power technology for electric propulsion. Solar cell fold-out arrays weighing 50 lb/kWe in full sunlight at 1 AU are now technology ready in size ranges up to 50 kWe. Up to 10 kWe rollout arrays weighing 30 lb/kWe (oriented in full sun at 1 AU) will be technology ready in 1971; 10 lb/kWe in full sun at 1 AU looks like a reasonable technology goal for 10 years from now. In the late 1970s, the technology of nuclear electric power supplies will become available to extend electric propulsion to the 100 to 300 kWe power range. It is noted that this nuclear power technology should achieve specific weights in the 20 to 50 lb/kWe range and retain this weight at large distances from the sun.

M.M.

A69-35176 *#

AN EXPERIMENTAL INVESTIGATION OF SEVERAL LOW-AREA-RATIO WATER JET PUMPS.

Nelson L. Sanger (NASA, Lewis Research Center, Cleveland, Ohio). American Society of Mechanical Engineers, Applied Mechanics and Fluids Engineering Conference, Chicago, Ill., June 16-19, 1969, Paper. 46 p. 20 refs.

Experimental evaluation of several low-area-ratio jet pumps in water. The principal geometrical variables investigated were area ratio, throat length, and nozzle spacing. Diffuser geometry was also varied, but to a lesser degree. Experimental values of efficiency and head ratio were compared to a one-dimensional theoretical prediction method previously found to be applicable to moderate- and high-area-ratio pumps. Two related cavitation prediction parameters were developed and compared to experimental data.

(Author)

A69-35678

INSTITUTE OF ELECTRICAL AND ELECTRONICS ENGINEERS, PHOTOVOLTAIC SPECIALISTS CONFERENCE, 7TH, PASADENA, CALIF., NOVEMBER 19-21, 1968, CONFERENCE RECORD.

New York, Institute of Electrical and Electronics Engineers, Inc., 1968. 285 p.

Members, $8.00; nonmembers, $12.

CONTENTS:

BASIC STUDIES.

IMPURITY PHOTOVOLTAIC EFFECT IN SILICON. G. Güttler and H. J. Queisser (Frankfurt, Universität, Frankfurt am Main, West Germany), p. 1-8. 15 refs. (See A69-35679 19-26)

PHOTOVOLTAIC EFFECTS IN GRADED-BAND-GAP STRUCTURES. Y. Marfaing and J. Chevallier (Centre National de la Recherche Scientifique, Meudon-Bellevue, Hauts-de-Seine, France), p. 9-15. 13 refs. (See A69-35680 19-26)

GALLIUM PHOSPHIDE DEVICES FOR USE AT HIGH

TEMPERATURES. Y. Nannichi and G. L. Pearson (Stanford University, Stanford, Calif.), p. 16-21. (See A69-35681 19-26)

THE PHOTOVOLTAIC EFFECT IN THE Cu-Cd-S SYSTEM. A. E. vanAerschot, J. J. Capart, K. H. David, M. Fabbricotti, K. H. Heffels, K. K. Reinhartz (European Space Research Organization, Noordwijk, Netherlands), and J. J. Loferski (European Space Research Organization, Noordwijk, Netherlands; Brown University, Providence, R.I.), p. 22-32. 17 refs. (See A69-35682 19-26)

IMPURITY PROFILE AND ENERGY BAND DIAGRAM FOR THE Cu_2S-CdS HETEROJUNCTION. H. W. Brandhorst, Jr. (NASA, Lewis Research Center, Cleveland, Ohio), p. 33-38.

THE MECHANISM OF THE PHOTOVOLTAIC EFFECT IN HIGH EFFICIENCY CdS THIN-FILM SOLAR CELLS. L. R. Shiozawa, G. A. Sullivan, and F. Augustine (Clevite Corp., Cleveland, Ohio), p. 39-46. 48 refs. (See A69-35683 19-03)

PHOTOVOLTAIC EFFECT AT COPPER SULFIDE-CADMIUM SULFIDE HETEROJUNCTIONS. W. D. Gill, P. F. Lindquist, and R. H. Bube (Stanford University, Stanford, Calif.), p. 47-53. 5 refs. (See A69-35684 19-26)

CONTRIBUTIONS TO CADMIUM SULFIDE-COPPER SULFIDE SOLAR CELL STUDIES. W. Palz (Centre National d'Etudes Spatiales, Brétigny-sur-Orge, Essonne, France), G. C. Solal, J. Vedel (Centre National de la Recherche Scientifique, Paris, France), J. Fremy, D. T. Nguyen, and J. Valerio (Société Anonyme de Télécommunications, Paris, France), p. 54-57. 9 refs. (See A69-35685 19-03)

EFFECT OF BIAS LIGHT ON THE SPECTRAL RESPONSE OF Cu_2S-CdS CELLS. A. E. Potter, Jr., R. L. Schalla, H. W. Brandhorst, Jr., and L. Rosenblum (NASA, Lewis Research Center, Cleveland, Ohio), p. 62-65.

NEW DEVELOPMENTS AND APPLICATIONS.

ALUMINUM CONTACT DEPOSITION AND TESTING FOR SILICON SOLAR CELLS. R. Sudbury, K. Stirrup, and D. Smith (Ion Physics Corp., Burlington, Mass.), p. 66-69. (See A69-35686 19-03)

NEW ASPECTS FOR THE CHOICE OF CONTACT MATERIALS FOR SILICON SOLAR CELLS. H. Fischer and R. Gereth (Telefunken AG, Heilbronn, West Germany), p. 70-76. 11 refs. (See A69-35687 19-03)

HIGH-TEMPERATURE ANNEALABLE SOLAR ARRAY. D. R. Clarke (Boeing Co., Seattle, Wash.), p. 77-81. 5 refs. (See A69-35688 19-03)

HARDENED SOLAR CELLS. W. P. Rahilly (USAF, Systems Command, Wright-Patterson AFB, Ohio), p. 82-84. 5 refs. (See A69-35689 19-03)

MULTI-JUNCTION SOLAR CELLS. J. R. Davis, D. L. Barrett, P. Rai-Choudhury, and J. E. Johnson (Westinghouse Electric Corp., Pittsburgh, Pa.), p. 85-91. (See A69-35690 19-03)

SOLAR CELL PERFORMANCE AT JUPITER TEMPERATURE AND SOLAR INTENSITY. C. H. Liebert (NASA, Lewis Research Center, Cleveland, Ohio), p. 92-96.

CHARACTERISTICS OF SOLAR CELLS AT LOW TEMPERATURES. R. J. Lambert (U.S. Navy, Office of Naval Research, Washington, D.C.), p. 97-100. (See A69-35691 19-03)

LITHIUM DOPED SOLAR CELLS.

STATUS OF LITHIUM SOLAR CELL DEVELOPMENT. P. A. Berman (California Institute of Technology, Pasadena, Calif.), p. 101-107. 11 refs. (See A69-35692 19-03)

BETA IRRADIATION OF LITHIUM DOPED SOLAR CELLS. D. L. Reynard and D. B. Orvis (Philco-Ford Corp., Palo Alto, Calif.), p. 108-112. 8 refs. (See A69-35693 19-03)

GAMMA IRRADIATION OF LITHIUM SILICON SOLAR CELLS. P. H. Fang (NASA, Electronics Research Center, Cambridge, Mass.), p. 113-116. (See A69-35694 19-03)

EFFECTS OF LITHIUM ON SOLAR CELL PROPERTIES. P. A. Iles (Globe-Union, Inc., Milwaukee, Wis.), p. 117-124. (See A69-35695 19-03)

PHOTOCONDUCTIVITY STUDY OF ANNEALING OF RADIATION DEFECTS IN LITHIUM-DOPED SILICON. J. C. Bochet, J. Capart, K. H. David, K. H. Heffels, A. Atzei (European Space Research Organization, Noordwijk, Netherlands), and J. J. Loferski (European Space Research Organization, Noordwijk, Netherlands; Brown University, Providence, R.I.), p. 125-130. 5 refs. (See A69-35696 19-26)

LONG TERM STABILITY OF LITHIUM-DOPED SOLAR CELLS IRRADIATED WITH ELECTRONS, PROTONS, OR NEUTRONS. T. J. Faith, G. J. Brucker, A. G. Holmes-Siedle, and J. Wysocki (Radio Corporation of America, Princeton, N.J.), p. 131-145. 24 refs. (See A69-35697 19-03)

INJECTION-LEVEL EFFECTS IN IRRADIATED, LITHIUM-CONTAINING SOLAR CELLS. G. J. Brucker, T. Faith, and A. Holmes-Siedle (Radio Corporation of America, Princeton, N.J.), p. 146-154. 15 refs. (See A69-35698 19-03)

RADIATION AND ENVIRONMENTAL EFFECTS.

OBSERVATIONS ON C_DS SOLAR CELL STABILITY. A. E. Spakowski and A. F. Forestieri (NASA, Lewis Research Center, Cleveland, Ohio), p. 155-160.

ENVIRONMENTAL ASSESSMENT OF THIN SILICON SOLAR CELLS FROM PILOT PRODUCTION. R. L. Crabb (Ministry of Technology, Royal Aircraft Establishment, Farnborough, Hants., England) and D. Basnett (Ferranti, Ltd., Hollinwood, Lancs., England), p. 161-174. 9 refs. (See A69-35699 19-03)

ATTITUDE CONTROL ROCKET EXHAUST PLUME EFFECTS ON SOLAR CELLS. L. D. Massie (USAF, Aero Propulsion Laboratory, Wright-Patterson AFB, Ohio) and P. J. Martinkovic (USAF, Rocket Propulsion Laboratory, Edwards AFB, Calif.), p. 175, 176. (See A69-35700 19-03)

LOW ENERGY PROTON DAMAGE IN SILICON SOLAR CELLS. R. L. Statler (U.S. Navy, Naval Research Laboratory, Washington, D.C.) and D. J. Curtin (Communications Satellite Corp., Washington, D.C.), p. 177-183. 9 refs. (See A69-35701 19-03)

AN EXPLORATORY STUDY OF THE INTERPLANETARY ENVIRONMENTAL EFFECTS ON SOLAR-CELL COVER GLASSES. A. C. Wilbur and D. L. Anderson (NASA, Ames Research Center, Moffett Field, Calif.), p. 184-188. 5 refs. (See A69-35702 19-03)

ACCELERATED UV DEGRADATION TO SOLAR CELL COATINGS. J. E. Vesel and D. R. Lott (Lockheed Aircraft Corp., Sunnyvale, Calif.), p. 189-194. (See A69-35703 19-03)

SOLAR CELL RADIATION DAMAGE ON SYNCHRONOUS SATELLITE ATS-I. R. C. Waddel (NASA, Goddard Space Flight Center, Greenbelt, Md.), p. 195-205. 14 refs. (See A69-35704 19-03)

IRRADIATION STUDIES ON STATE-OF-THE-ART CADMIUM SULFIDE CELLS. D. J. Curtin (Communications Satellite Corp., Washington, D.C.), p. 206-213. 9 refs. (See A69-35705 19-03)

SOLAR ARRAY TECHNOLOGY.

TEMPERATURE AND HUMIDITY EFFECTS ON SILICON SOLAR CELLS. W. Luft, C. C. McCraven, and L. A. Aroian (TRW Systems Group, Redondo Beach, Calif.), p. 214-225. (See A69-35706 19-03)

LARGE SOLAR ARRAY DEVELOPMENT IN U.K. F. C. Treble (Ministry of Technology, Royal Aircraft Establishment, Farnborough, Hants., England), p. 226-233. 6 refs. (See A69-35707 19-03)

SOLAR ARRAYS UTILIZING LARGE AREA SILICON SOLAR CELLS. J. D. Gum, E. D. Steele, R. L. Oliver, and E. L. Ralph (Textron, Inc., Sylmar, Calif.), p. 234-242. (See A69-35708 19-03)

ELECTRICAL OUTPUT OF SHADOWED SOLAR ARRAYS. H. S. Rauschenbach (TRW Systems Group, Redondo Beach, Calif.), p. 243-252. 15 refs. (See A69-35709 19-03)

INTEGRATED CdS SOLAR CELL ARRAY. J. H. Martin (Martin Marietta Corp., Denver, Colo.) and F. A. Shirland (Clevite Corp., Cleveland, Ohio), p. 253-257. 5 refs. (See A69-35710 19-03)

LARGE RETRACTABLE SOLAR CELL ARRAY. J. F. Wise (USAF, Aero Propulsion Laboratory, Wright-Patterson AFB, Ohio), p. 258-261. 9 refs. (See A69-35711 19-03)

LATE NEWS SESSION.

SOLAR CELL CALIBRATION EXPERIMENTS ON LES-6. F. W. Sarles, Jr., A. G. Stanley, and C. Burrowes (Massachusetts Institute of Technology, Lexington, Mass.), p. 262-268. 8 refs. (See A69-35712 19-03)

SOLAR CELL DEGRADATION EXPERIMENTS ON LES-4 AND -5. F. W. Sarles, Jr. and L. P. Cox (Massachusetts Institute of Technology, Lexington, Mass.), p. 269-273. (See A69-35713 19-03)

A69-35694 *

GAMMA IRRADIATION OF LITHIUM SILICON SOLAR CELLS.

P. H. Fang (NASA, Electronics Research Center, Cambridge, Mass.).

IN: INSTITUTE OF ELECTRICAL AND ELECTRONICS ENGINEERS, PHOTOVOLTAIC SPECIALISTS CONFERENCE, 7TH, PASADENA, CALIF., NOVEMBER 19-21, 1968, CONFERENCE RECORD. (A69-35678 19-03)

New York, Institute of Electrical and Electronics Engineers, Inc., 1968, p. 113-116.

Radiation damage and recovery properties of various lithium-diffused silicon p-n solar cells were investigated by measuring photovoltaic parameters as a function of the gamma radiation fluence. The 1-MeV electron equivalent flux was roughly equal to a severe radiation condition in space. Two groups of cells were irradiated: one group at 65 deg C and the second group at 35 deg C. In both cases, a continuous degradation was observed. The rate of degradation is, in general, slower than the conventional n-p solar cells. With the variation of the concentration profile of lithium, it is expected that the result will be modified. However, the present knowledge does not seem to provide sufficient information to compare directly the superiority of different types of silicon solar cells. (Author)

A69-35702 *

AN EXPLORATORY STUDY OF THE INTERPLANETARY ENVIRONMENTAL EFFECTS ON SOLAR-CELL COVER GLASSES.

A. C. Wilbur and D. L. Anderson (NASA, Ames Research Center, Moffett Field, Calif.).

IN: INSTITUTE OF ELECTRICAL AND ELECTRONICS ENGINEERS, PHOTOVOLTAIC SPECIALISTS CONFERENCE, 7TH, PASADENA, CALIF., NOVEMBER 19-21, 1968, CONFERENCE RECORD. (A69-35678 19-03)

New York, Institute of Electrical and Electronics Engineers, Inc., 1968, p. 184-188. 5 refs.

Exploratory investigation of interplanetary space environment effects on solar-cell cover glasses to study the feasibility of predicting response so that optimum cover-glass systems can be selected for specific space missions. Effects of 3-MeV protons on Corning 0211 microsheet, Corning 7940 silica, antireflection coating, blue interference filters, and blue-red interference filters have been measured. Effects of temperature and of concurrent illumination on radiation damage were investigated. The effects of 2-keV protons on antireflection coatings were also measured. Results are presented as optical transmission spectra. (Author)

A69-35704 *

SOLAR CELL RADIATION DAMAGE ON SYNCHRONOUS SATELLITE ATS-I.

Ramond C. Waddel (NASA, Goddard Space Flight Center, Spacecraft Technology Div., Greenbelt, Md.).

IN: INSTITUTE OF ELECTRICAL AND ELECTRONICS ENGINEERS, PHOTOVOLTAIC SPECIALISTS CONFERENCE, 7TH, PASADENA, CALIF., NOVEMBER 19-21, 1968, CONFERENCE RECORD. (A69-35678 19-03)

New York, Institute of Electrical and Electronics Engineers, Inc., 1968, p. 195-205. 14 refs.

Results of a study in which various types of solar cells were monitored during 416.8 days in synchronous orbit on satellite ATS 1. Judging by the remaining percentage of initial maximum power, qualified conclusions were that (1) degradation was greater than expected; (2) optimum base resistivity was 10 ohm-cm; (3) optimum shield thickness was 6 mils; (4) sapphire and silica shields were comparable; (5) silica shields were superior to glass; (6) boron and aluminum doping were comparable; and (7) it was necessary to presume some radiation damage, some drop in illumination, and a development of series resistance to account for the results. (Author)

A69-42236

AMERICAN INSTITUTE OF CHEMICAL ENGINEERS, INTERSOCIETY ENERGY CONVERSION ENGINEERING CONFERENCE, 4TH, WASHINGTON, D.C., SEPTEMBER 22-26, 1969, PROCEEDINGS.

Conference co-sponsored by the American Institute of Aeronautics and Astronautics, the American Nuclear Society, the American Society of Mechanical Engineers, the American Chemical Society, the Institute of Electrical and Electronics Engineers, and the Society of Automotive Engineers.

New York, American Institute of Chemical Engineers, 1969. 1186 p. Members, $30; nonmembers, $40.

CONTENTS:

SUMMARIES OF SESSIONS, p. xv-xxxiii.

DYNAMIC CYCLES—RANKINE. I.

ORGANIC RANKINE CYCLE WITH RECIPROCATING ENGINE. D. T. Morgan, E. F. Doyle, and S. S. Kitrilakis (Thermo Electron Corp., Waltham, Mass.), p. 1-10. (See A69-42237 23-03)

JET CONDENSER DEVELOPMENT FOR AN ORGANIC RANKINE-CYCLE POWER CONVERSION SYSTEM. R. Garcia (Aerojet-General Corp., Azusa, Calif.), p. 11-20. (See A69-42238 23-03)

DESIGN OF A PRACTICAL HYDROCARBON BOILER. J. P. Norton (American Air Filter Co., Inc., St. Louis, Mo.), p. 21-25. (See A69-42239 23-03)

SPACE POWER. I.

COMPUTER ANALYSIS OF SPACE POWER SYSTEMS FOR MISSION ANALYSIS. R. D. Arno (NASA, Office of Advanced Research and Technology, Moffett Field, Calif.), p. 26-32. (See A69-42240 23-03)

COMPUTER SIMULATION OF SATELLITE ELECTRIC POWER SYSTEMS. P. Bauer (TRW Systems Group, Redondo Beach, Calif.), p. 33-41.

PERFORMANCE ANALYSIS OF SATELLITE ELECTRIC POWER SYSTEMS BY COMPUTER SIMULATION. M. Schwartzburg (TRW Systems Group, Redondo Beach, Calif.), p. 42-50. (See A69-42241 23-03)

SOLAR CELL POWER SYSTEMS FOR MANNED SPACE STATIONS. H. Weiner (McDonnell Douglas Corp., Santa Monica, Calif.), p. 51-60. 8 refs. (See A69-42242 23-03)

OPTIMIZATION OF BATTERY SUBSYSTEMS FOR EARTH SATELLITE LIFETIMES OF GREATER THAN 5 YEARS. M. Koslover (TRW Systems Group, Redondo Beach, Calif.), p. 61-73. (See A69-42243 23-03)

POWER SYSTEMS FOR THE APOLLO APPLICATIONS PROGRAM. D. L. Daubert, W. H. Gross (Martin Marietta Corp., Denver, Colo.), C. B. Graff (NASA, Marshall Space Flight Center, Huntsville, Ala.), and J. D. Murrell (NASA, Manned Spacecraft Center, Houston, Tex.), p. 74-83. (See A69-42244 23-03)

BIOMEDICAL POWER. I.

ENERGY SYSTEM REQUIREMENTS FOR A HEART ASSIST-DEVICE. P. M. Newgard and G. J. Eilers (Stanford Research Institute, Menlo Park, Calif.), p. 84-88.

ENERGY TRANSMISSION THROUGH INTACT SKIN. L. A. Heimlich, F. H. Christiansen (United Aircraft Corp., Farmington, Conn.), and T. Sato (Yale University, New Haven, Conn.), p. 89-94.

ELECTROMECHANICAL ENERGY CONVERSION FOR ARTIFICIAL HEARTS—A NEW CONCEPT UTILIZING A NUTATING MOTOR. W. S. Kelly and R. D. Crosier (Battelle

Memorial Institute, Richland, Wash.), p. 95-100.

NUCLEAR ELECTRIC POWER SOURCES FOR BIOMEDICAL APPLICATIONS. D. E. Knapp, A. Bennett, J. G. DeStesse, L. C. Olsen, E. W. Saaski, B. I. Griffin, and K. A. Gasper (McDonnell Douglas Corp., Richland, Wash.), p. 101-106.

DEVELOPMENT OF AN IMPLANTABLE ARTIFICIAL HEAT POWER SOURCE EMPLOYING A THERMOCOMPRESSOR. W. R. Martini (McDonnell Douglas Corp., Richland, Wash.), p. 107-114.

DEVELOPMENT OF A STIRLING CYCLE POWER SYSTEM FOR ARTIFICIAL HEARTS. K. E. Buck (Aerojet-General Corp., San Ramon, Calif.), p. 115-121.

THERMIONIC POWER. I.

THERMIONIC REACTOR CONCEPTS. L. K. Price (U.S. Atomic Energy Commission, Washington, D.C.), p. 122-130. 11 refs. (See A69-42245 23-22)

THERMIONIC FUEL ELEMENT DEVELOPMENT. D. S. Beard (U.S. Atomic Energy Commission, Washington, D.C.), p. 131-136. (See A69-42246 23-22)

FRENCH THERMIONIC PROGRAM AND ACCOMPLISHMENTS. B. Devin (Commissariat à l'Energie Atomique, Gif-sur-Yvette, Essonne, France), p. 137-145. 9 refs. (See A69-42247 23-03)

NUCLEAR POWER AND HYBRIDS.

SNAP-21 10-WATT THERMOELECTRIC POWER SYSTEM. F. K. Fox (3M Co., Roseville, Minn.) and L. R. Niendorf (Union Carbide Corp., Linde Div.), p. 146-152. (See A69-42248 23-03)

SNAP-27 PROGRAM REVIEW. A. A. Pitrolo (General Electric Co., Philadelphia, Pa.), B. J. Rock (U.S. Atomic Energy Commission, Washington, D.C.), W. Remini (NASA, Manned Spacecraft Center, Houston, Tex.), and J. A. Leonard (Sandia Corp., Albuquerque, N. Mex.), p. 153-170. (See A69-42249 23-22)

THE ROLE OF NUCLEAR POWER ENERGY CENTERS IN DEVELOPING ECONOMY. J. M. Holmes (Oak Ridge National Laboratory, Oak Ridge, Tenn.), p. 171-175.

CONTROLLED THERMONUCLEAR POWER. B. Myers, R. W. Werner, J. D. Lee, and P. B. Mohr (California, University, Livermore, Calif.), p. 176-187.

THE WESTERN COAL DEPOSITS—A NATIONAL SOURCE OF POWER AND URANIUM. M. Steinberg, J. Powell, and B. Manowitz (Brookhaven National Laboratory, Upton, N.Y.), p. 188-206.

DYNAMIC CYCLES—RANKINE. II.

EFFECT OF PRESSURE RATIO ON THE PERFORMANCE OF SUPERSONIC TURBINE-NOZZLES. R. E. Barber (Barber-Nichols Engineering Co., Arvada, Colo.), p. 207-225. 12 refs. (See A69-42250 23-28)

COMPARATIVE PERFORMANCE ANALYSIS OF SUPER-CRITICAL FLUID POWER CYCLES. A. V. Pradhan, p. 226-236.

OPTIMIZING A 5 BHP STEAM TURBINE DESIGN. P. F. Swenson, Jr. (Swenson Research, Inc., Bedford Heights, Ohio) and E. N. Poulos (Prototherm Research Laboratories, Inc., Cleveland, Ohio), p. 237-252.

DESIGN OF VAPOR TURBINES INCLUDING EFFECTS OF SUPERSATURATION. K. E. Boyd, E. A. Mock, and R. A. Rackley (Garrett Corp., Phoenix, Ariz.), p. 253-260. 13 refs. (See A69-42251 23-22)

ROTARY STEAM ENGINE. P. O. Tauson (Westinghouse Electric Corp., Pittsburgh, Pa.), p. 261-270. (See A69-42252 23-03)

SPACE POWER. II.

IMPACTABLE POWER SUBSYSTEMS FOR MARS LANDERS. M. Swerdling (California Institute of Technology, Pasadena, Calif.), p. 271-283. 10 refs. (See A69-42253 23-03)

THERMAL MODEL OF A 75 WATT(E) SPACE POWER-PLANAR RTG SYSTEM. A. J. Parker, Jr. (Hittman Associates, Inc., Columbia, Md.) and W. S. West (NASA, Goddard Space Flight Center, Greenbelt, Md.), p. 284-299. (See A69-42254 23-03)

STATUS REPORT ON SMALL REACTOR-THERMOELECTRIC POWER SYSTEMS FOR UNMANNED SPACE APPLICATIONS. J. D. Gylfe and J. H. VanOsdol (North American Rockwell Corp., Canoga Park, Calif.), p. 300-307. (See A69-42255 23-22)

25 KWE REACTOR-THERMOELECTRIC POWER SYSTEM FOR MANNED ORBITING SPACE STATIONS. J. D. Gylfe, R. A. Johnson (North American Rockwell Corp., Canoga Park, Calif.), R. A. DuVal (U.S. Atomic Energy Commission, Canoga Park, Calif.), and L. W. Brantley (NASA, Marshall Space Flight Center, Huntsville, Ala.), p. 308-320. (See A69-42256 23-22)

THE COMPACT Co-60 KERNEL FOR SPACE POWER. W. Ruehle and D. L. Forrest (Aerojet-General Corp., San Ramon, Calif.), p. 321-329. (See A69-42257 23-22)

BIOMEDICAL POWER. II.

THE NEW MERCURIC OXIDE-CADMIUM (MERCAD) BATTERY SYSTEM FOR MEDICAL AND IMPLANTATION APPLICATIONS. M. Eisenberg (Electrochimica Corp., Menlo Park, Calif.), p. 330-338.

STUDIES OF IMPLANTABLE NICKEL CADMIUM-CELLS FOR HEART ASSIST DEVICES. R. P. Hamlen, E. G. Siwek (General Electric Co., Schenectady, N.Y.), G. Rampel (General Electric Co., Gainesville, Fla.), L. D. Wechsler, and J. Zampini (General Electric Co., Syracuse, N.Y.), p. 339-345.

AN IMPLANTABLE BIOLOGICAL FUEL CELL WITH AN AIRBREATHING CATHODE. A. J. Appleby, D. Y. C. Ng (Institute of Gas Technology, Chicago, Ill.), S. K. Wolfson, Jr. (Michael Reese Hospital Medical Center, Chicago, Ill.), and H. Weinstein (Illinois Institute of Technology, Chicago, Ill.), p. 346-353.

LIMITATIONS OF BLOOD PLASMA AS A FUEL CELL ELECTROLYTE. M. Beltzer and J. S. Batzold (Esso Research and Engineering Co., Linden, N.J.), p. 354-360.

TROPHICALLY POWERED FUEL CELL POWER SUPPLY FOR THE ARTIFICIAL HEART. S. Messinger and R. F. Drake (American Hospital Supply Corp., Everett, Mass.), p. 361-369.

THERMIONIC POWER. II.

PRESENT STATUS OF DEVELOPMENT OF THERMIONIC DIODES AND THERMIONIC REACTORS IN THE FEDERAL REPUBLIC OF GERMANY. K. Einfeld (Internationaler Atomreaktorbau GmbH, Bensberg, West Germany), p. 370-382. 23 refs. (See A69-42258 23-22)

THE USE OF ION SPUTTERING IN MAKING ELECTRODES FOR THERMIONIC ENERGY CONVERTERS. J. Kramar (Výzkumný Ústav Silnoproudé Elektrotechniky, Běchovice, Czechoslovakia), p. 383-385. (See A69-42259 23-15)

THERMOELECTRIC POWER.

SILICON GERMANIUM AIR-VAC TECHNOLOGY—A STATUS REPORT. R. E. Berlin, L. H. Gnau, and R. S. Nelson (Radio Corporation of America, Harrison, N.J.), p. 386-394.

DESIGN AND PERFORMANCE ANALYSIS OF SILICON-GERMANIUM RTG's. V. Raag (Resalab Scientific, Menlo Park, Calif.), p. 395-399. 6 refs. (See A69-42260 23-22)

PRACTICAL APPLICATIONS OF MULTI-LAYER INSULATIONS. F. Notaro, G. E. Nies (Union Carbide Corp., Tonawanda, N.Y.), and R. Hedel (Radio Corporation of America, Harrison, N.J.), p. 400-407.

THE MULTI-FOIL THERMAL INSULATION DEVELOPMENT PROGRAM—A STATUS REPORT. M. L. Paquin (Thermo Electron Corp., Waltham, Mass.), p. 408-415.

LIFE AND PERFORMANCE CHARACTERISTICS OF Pb-Te COUPLES IN HYDROCARBON FIRED SYSTEMS. A. Herchakowski (U.S. Army, Electronics Command, Fort Monmouth, N.J.), p. 416-419.

FURTHER DEVELOPMENT OF THE STAR THERMOELECTRIC PANEL. N. C. Miller (North American Rockwell Corp., Canoga Park, Calif.), p. 420-424. (See A69-42261 23-22)

A MODEL TO DESCRIBE LONG-TERM PERFORMANCE CHARACTERISTICS OF PRESSURE CONTACTED LEAD-TELLURIDE THERMOELECTRIC GENERATORS. D. R. Field and G. W. Bunde (3M Co., St. Paul, Minn.), p. 425-435. 16 refs. (See A69-42262 23-22)

THE PERFORMANCE EVALUATION AND LIFE TESTING

OF THERMOELECTRIC GENERATORS AT THE JET PROPULSION LABORATORY. P. Rouklove and V. Truscello (California Institute of Technology, Pasadena, Calif.), p. 436-446. (See A69-42263 23-22)

DYNAMIC CYCLES–RANKINE. III.

AN ORGANIC RANKINE CYCLE FOR MANNED SPACE APPLICATIONS. S. D. Diamond and A. M. Taylor (McDonnell Douglas Corp., Santa Monica, Calif.), p. 447-455. 5 refs. (See A69-42264 23-22)

ZIRCONIUM HYDRIDE REACTOR-ORGANIC RANKINE POWER SYSTEMS. J. H. VanOsdol, F. R. Wilson (North American Rockwell Corp., Canoga Park, Calif.), and R. E. Niggemann (Sundstrand Corp., Rockford, Ill.), p. 456-464. (See A69-42265 23-22)

STUDY OF A 300 kWe RANKINE CYCLE ADVANCED NUCLEAR-ELECTRIC SPACE POWER SYSTEM. J. A. Heller, T. A. Moss, and G. J. Barna (NASA, Lewis Research Center, Cleveland, Ohio), p. 465-483. 19 refs. (See A69-42266 23-22)

DESIGN AND PERFORMANCE OF A MOBILE WASTE HEAT ORGANIC RANKINE CYCLE SYSTEM PROVIDING ELECTRIC POWER AND ENVIRONMENTAL CONTROL. E. Kaplan and E. Lodwig (Fairchild Hiller Corp., Bay Shore, N.Y.), p. 484-493. (See A69-42267 23-03)

SPACE POWER. III.

RADIOISOTOPE THERMAL ENERGY SOURCES FOR SPACE STATION LIFE SUPPORT SYSTEMS. R. V. Elms, Jr. and H. H. Greenfield (Lockheed Aircraft Corp., Sunnyvale, Calif.), p. 494-504. 5 refs. (See A69-42268 23-22)

ELECTRICAL/THERMAL INTEGRATION OF DYNAMIC POWER AND LIFE SUPPORT SYSTEMS FOR MANNED SPACECRAFT. C. H. Shinbrot and J. V. Coggi (McDonnell Douglas Corp., Santa Monica, Calif.), p. 505-514. 14 refs. (See A69-42269 23-22)

ISOTEC THERMOELECTRIC GENERATOR FOR SPACE POWER. E. J. Steeger and J. E. Cruver (Gulf General Atomic, Inc., San Diego, Calif.), p. 515-521. (See A69-42270 23-22)

ELECTROCHEMICAL POWER. I.

NEW LOW TEMPERATURE BATTERIES. N. T. Wilburn and A. L. Almerini (U.S. Army, Electronics Command, Fort Monmouth, N.J.), p. 522-524.

RESERVE TYPE ORGANIC ELECTROLYTE BATTERIES. K. H. M. Braeuer (U.S. Army, Electronics Command, Fort Monmouth, N.J.), p. 525-527.

HIGH ENERGY LITHIUM-ORGANIC ELECTROLYTE BATTERIES FOR WIDE TEMPERATURE RANGE APPLICATIONS. M. Eisenberg (Electrochimica Corp., Menlo Park, Calif.), p. 528-537.

SECONDARY CELLS WITH LITHIUM ANODES AND PASTE ELECTROLYTES. H. Shimotake, A. K. Fischer, and E. J. Cairns (Argonne National Laboratory, Argonne, Ill.), p. 538-547.

LONG LIFE THERMAL CELL. J. R. Moser, H. J. Goldsmith, and R. L. Blucher (Catalyst Research Corp., Baltimore, Md.), p. 548-554.

PHOTOVOLTAIC POWER. I.

CHARACTERISTICS OF GaAs PHOTOVOLTAIC DIODES AT LOW IRRADIANCE. R. Kalibjian and K. Mayeda (California, University, Livermore, Calif.), p. 555-560.

A TECHNIQUE FOR IDENTIFYING THE CAUSE OF PERFORMANCE DEGRADATION IN CADMIUM SULFIDE SOLAR CELLS. K. L. Kennerud (Boeing Co., Seattle, Wash.), p. 561-566. (See A69-42271 23-03)

EVALUATION OF INTEGRAL COVERS ON SILICON SOLAR CELLS. J. W. Fairbanks (NASA, Goddard Space Flight Center, Greenbelt, Md.), p. 567-574. 6 refs. (See A69-42272 23-03)

THE "HOT SPOT" FAILURE MODE FOR SOLAR ARRAYS. F. A. Blake and K. L. Hanson (General Electric Co., Philadelphia, Pa.), p. 575-581. (See A69-42273 23-09)

TEMPERATURE CYCLING EFFECTS ON SOLAR PANELS. W. Luft and E. Maiden (TRW Systems Group, Redondo Beach, Calif.), p. 582-589. (See A69-42274 23-03)

CHEMICAL AND PHYSICAL SYSTEMS.

A DEMONSTRATION OF THE FEASIBILITY OF ALL-SOLID, EXOTHERMIC REACTIONS AS CHEMICAL HEAT SOURCES SUITABLE FOR SPACECRAFT THERMAL CONTROL. R. W. Riebling (California Institute of Technology, Pasadena, Calif.), p. 590-598. 5 refs. (See A69-42275 23-03)

THE DYNAMIC PERFORMANCE OF A THERMODYNAMIC CYCLE USING A CHEMICALLY REACTIVE GAS. C. H. Wolgemuth (Pennsylvania State University, University Park, Pa.), p. 599-605.

A WIND ENERGY STORAGE AND CONVERSION SYSTEM FOR USE IN UNDERDEVELOPED COUNTRIES. R. Ramakumar, H. J. Allison, W. L. Hughes, and K. A. McCollom (Oklahoma State University, Stillwater, Okla.), p. 606-613.

USING THE RANKINE POWER CYCLE FOR FLUID EVALUATION. O. E. Buxton, Jr. (Ohio State University, Columbus, Ohio), p. 614-623. 8 refs. (See A69-42276 23-33)

ANALYSIS OF AN OSCILLATING ENGINE FOR POWER GENERATION BASED ON THE "DRINKING BIRD" PRINCIPLE. S. S. Shergill and R. P. Morgan (Missouri, University, Columbia, Mo.), p. 624-638; Appendix, J. P. Fraser (General Electric Co., Schenectady, N.Y.), p. 639-641.

DYNAMIC CYCLES–BRAYTON, STIRLING. IV.

CLOSED BRAYTON CYCLE POWER SYSTEM APPLICATIONS. A. Pietsch (Garrett Corp., Phoenix, Ariz.), p. 642-651. 12 refs. (See A69-42277 23-03)

BRAYTON-B POWER SYSTEM–A PROGRESS REPORT. W. J. Brown (NASA, Lewis Research Center, Cleveland, Ohio), p. 652-658. 6 refs. (See A69-42278 23-03)

HOT PERFORMANCE CHARACTERISTICS OF A GAS BEARING BRAYTON CYCLE TURBOALTERNATOR. J. C. Wood, M. E. Valgora, and H. B. Tryon (NASA, Lewis Research Center, Cleveland, Ohio), p. 659-667. 12 refs. (See A69-42279 23-03)

ANALOG COMPUTER STUDIES OF A 2 TO 10 KILOWATTS ELECTRIC BRAYTON CYCLE SPACE POWER SYSTEM INCLUDING STARTUP AND SHUTDOWN. D. A. Cantoni and R. L. Thomas (NASA, Lewis Research Center, Cleveland, Ohio), p. 668-678. (See A69-42280 23-03)

THE RADIOISOTOPE ENERGIZED STIRLING ENGINE FOR SPACECRAFT AUXILIARY ELECTRIC POWER IN THE 250 TO 500 W(e) POWER RANGE. C. E. Leach and B. C. Fryer (Battelle Memorial Institute, Richland, Wash.), p. 679-691. (See A69-42281 23-22)

UNDERWATER POWER.

ECONOMIC SELECTION OF UNDERSEA POWERPLANTS. R. N. Edwards, J. A. Hill, and M. E. Cohen (General Electric Co., Philadelphia, Pa.), p. 692-698.

A LONG LIVED SEA WATER BATTERY. C. L. Opitz (Lockheed Aircraft Corp., Plainfield, N.J.), p. 699-704.

ELECTROCHEMICAL POWER.

PARAMETRIC CHARGE STUDIES FOR AEROSPACE NICKEL-CADMIUM BATTERIES. K. E. Preusse, R. C. Shair, F. E. Betz, and J. Sylvia (Gulton Industries, Inc., Metuchen, N.J.), p. 705-709. (See A69-42282 23-03)

ELECTRICAL CHARACTERISTICS OF A SEALED NICKEL-CADMIUM BATTERY HAVING A BIPOLAR CONSTRUCTION. H. N. Seiger, S. Charlip, and S. Lerner (Gulton Industries, Inc., Metuchen, N.J.), p. 710-714. 5 refs. (See A69-42283 23-03)

THE APPLICATION OF BENCH TESTS IN THE DEVELOPMENT OF HEAT-STERILIZABLE BATTERY SEPARATORS. W. von Hartmann (California Institute of Technology, Pasadena, Calif.), p. 715-720. 10 refs. (See A69-42284 23-03)

TWO YEAR FLIGHT PERFORMANCE OF THE LOCKHEED TYPE XI NICKEL-CADMIUM BATTERY. M. J. Teresa and R. E. Corbett (Lockheed Aircraft Corp., Sunnyvale, Calif.), p. 721-729. 5

refs. (See A69-42285 23-03)

PHOTOVOLTAIC POWER. II.

ATM SOLAR CELL MODULE PERFORMANCE TESTING. J. Bruno (Martin Marietta Corp., Denver, Colo.), p. 730-735. (See A69-42286 23-03)

EVALUATION OF THE PERFORMANCE OF SOLAR ARRAYS ON INTELSAT SPACECRAFT AT SYNCHRONOUS ALTITUDE. D. J. Curtin and J. F. Stockel (Communications Satellite Corp., Washington, D.C.), p. 736-742. (See A69-42287 23-03)

ADVANCED DESIGN MODULES FOR LUNAR SURFACE SOLAR ARRAY POWER SYSTEMS. J. E. Boretz (TRW Systems Group, Redondo Beach, Calif.) and J. L. Miller (NASA, Marshall Space Flight Center, Huntsville, Ala.), p. 743-753. 7 refs. (See A69-42288 23-03)

SOLAR ARRAY CONFIGURATIONS AND PERFORMANCE ON THE MARTIAN SURFACE. M. Swerdling and A. Hasbach (California Institute of Technology, Pasadena, Calif.), p. 754-762. 7 refs. (See A69-42289 23-03)

40 WATTS/POUND SPACECRAFT SOLAR ARRAYS. P. A. Dillard (TRW Systems Group, Redondo Beach, Calif.), p. 763-771. 7 refs. (See A69-42290 23-03)

LIGHTWEIGHT LARGE AREA SOLAR ARRAYS. D. D. Abbott (Boeing Co., Seattle, Wash.), p. 772-777. 20 refs. (See A69-42291 23-03)

TRANSPORTATION. I.

GROUND TRANSPORTATION ENERGY TRANSFER. E. J. Ward and K. L. Lawson (U.S. Department of Transportation, Washington, D.C.), p. 778-794.

LINEAR INDUCTION MOTOR FOR HIGH SPEED TRACKED VEHICLES. K. M. Chirgwin, C. H. Lee (Garrett Corp., Torrance, Calif.), and P. J. Larsen (U.S. Department of Transportation, Washington, D.C.), p. 795-806.

ELECTRIC PROPULSION SYSTEM FOR LINEAR INDUCTION MOTOR TEST VEHICLE. G. P. Kalman, D. Irani, and A. U. Simpson (Garrett Corp., Torrance, Calif.), p. 807-817.

A CONTRIBUTION OF THE LIQUID-METAL INDUCTION-MHD-CONVERTER-THEORY TO THE CALCULATIONS OF THE LINEAR MOTOR FOR VERY HIGH SPEED GROUND-VEHICLES. C. Carpetis, A. Gann, and W. Peschka (Deutsche Forschungs- und Versuchsanstalt für Luft- und Raumfahrt, Stuttgart, West Germany), p. 818-825.

POWER CONDITIONING. I.

HIGH QUALITY ELECTRIC POWER PROGRAM. H. H. Kajihara (U.S. Naval Civil Engineering Laboratory, Port Hueneme, Calif.), p. 826-829.

MODULARIZATION OF HIGH-POWER INVERTERS AND CONVERTERS. F. Gourash (NASA, Lewis Research Center, Cleveland, Ohio), P. F. Pittman (Westinghouse Electric Co., Pittsburgh, Pa.), and J. F. Heins (Westinghouse Electric Corp., Lima, Ohio), p. 830-838. 5 refs. (See A69-42292 23-03)

A DUTY CYCLE GENERATOR FOR SWITCHING REGULATORS. A. Schloss (California Institute of Technology, Pasadena, Calif.) and P. Gutknecht (Westinghouse Electric Corp., Pittsburgh, Pa.), p. 839-843. 8 refs. (See A69-42293 23-03)

POWER PROCESSING AND CONTROL FOR MILITARY MANPACK FUEL CELL POWER SOURCES. W. B. Kempler and M. E. Cannon (U.S. Army, Electronics Command, Fort Monmouth, N.J.), p. 844-853.

1 KVA THREE-PHASE DC-AC INVERTER WITH DIGITAL CONTROL. M. Knight (U.S. Naval Air Systems Command, Washington, D.C.) and R. Torkildsen (General Electric Co., Lynn, Mass.), p. 854-860. (See A69-42294 23-03)

HEAT PIPES. I.

HEAT PIPE THERMIONIC CONVERTER RESEARCH IN EUROPE. C. A. Busse (EURATOM and Comitato Nazionale per l'Energia Nucleare, Ispra, Italy), p. 861-872. 47 refs. (See A69-42295 23-03)

THE HEAT PIPE—A PROGRESS REPORT. G. Y. Eastman (Radio Corporation of America, Lancaster, Pa.), p. 873-878. (See A69-42296 23-03)

HEAT PIPE DEVELOPMENT FOR THERMIONIC APPLICATIONS. P. K. Shefsiek and D. M. Ernst (Thermo Electron Corp., Waltham, Mass.), p. 879-887. 10 refs. (See A69-42297 23-03)

EXPERIMENTAL DETERMINATION OF WICK PROPERTIES FOR HEAT PIPE APPLICATIONS. R. A. Freggens (Radio Corporation of America, Lancaster, Pa.), p. 888-897. (See A69-42298 23-03)

ELECTROCHEMICAL POWER. III.

DEVELOPMENT OF NEW MATERIALS OF CONSTRUCTION FOR FUEL CELLS. R. R. Sayano, R. A. Mendelson, M. E. Kirkpatrick, E. T. Seo, and H. P. Silverman (TRW Systems Group, Redondo Beach, Calif.), p. 898-903. (See A69-42299 23-03)

AN ALUMINUM-HYDROGEN PEROXIDE POWER SOURCE. S. Zaromb (Zaromb Research Corp., Passaic, N.J.), p. 904-910.

HIGH RATE PERFORMANCE OF ZINC-AIR BATTERIES. N. I. Palmer, B. E. Jagid, and F. J. Staudinger (Leesona Corp., Lake Success, N.Y.), p. 911-919.

PURGE DYNAMICS OF FUEL CELLS. D. Gidaspow and S. S. Sareen (Institute of Gas Technology, Chicago, Ill.), p. 920-932. 14 refs. (See A69-42300 23-03)

TRANSPORTATION. II.

ENERGY CONVERSION DEVICES IN GROUND TRANSPORTATION. G. G. Leeth (General Electric Co., Santa Barbara, Calif.), p. 933-939.

ENERGY TRANSFORMATIONS IN TUBEFLIGHT PROPULSION. J. V. Foa (Rensselaer Polytechnic Institute, Troy, N.Y.), p. 940-952.

MAGNETICALLY SUSPENDED TRAINS FOR VERY HIGH SPEED TRANSPORT. J. R. Powell and G. T. Danby (Brookhaven National Laboratory, Upton, N.Y.), p. 953-963.

LINEAR INDUCTION MOTOR FOR HIGH SPEED GROUND TRANSPORTATION. T. C. Wang (National Taiwan University, Taiwan, China), p. 964-974.

POWER CONDITIONING. II.

POWER CONDITIONING DEVELOPMENT FOR THE SERT II ION THRUSTOR. A. C. Hoffman (NASA, Lewis Research Center, Cleveland, Ohio), R. W. Briggs, E. F. Swiderski, S. F. Bauer, and R. M. Weger (Westinghouse Electric Corp., Lima, Ohio), p. 975-986. 8 refs. (See A69-42301 23-03)

HIGH FREQUENCY CAPABILITIES OF A NEW POWER THYRISTOR. R. L. Davies (General Electric Co., Auburn, N.Y.), p. 987-991.

ULTRA-RELIABLE POWER PROCESSOR FOR HYDROCARBON-AIR FUEL CELL POWER SYSTEMS. M. S. Kosmin (U.S. Army, Electronics Command, Fort Monmouth, N.J.), p. 992-999.

HIGH-EFFICIENCY BOOST REGULATOR DESIGN FOR PLANETARY SPACECRAFT. D. J. Hopper (California Institute of Technology, Pasadena, Calif.), p. 1000-1003. (See A69-42302 23-03)

TRACKING SOLAR ARRAY MAXIMUM POWER BY SENSING ARRAY TEMPERATURE. M. Sussman (NASA, Langley Research Center, Hampton, Va.), p. 1004-1009. 7 refs. (See A69-42303 23-03)

HEAT PIPES. II.

DEVELOPMENT OF AN ADVANCED SPACE RADIATION SYSTEM. J. T. Peters and R. G. Hannah (Isotopes, Inc., Baltimore, Md.), p. 1010-1015. (See A69-42304 23-22)

AVIONIC APPLICATION OF A HEAT PIPE. A. T. Calimbas and R. H. Hulett (Philco-Ford Corp., Palo Alto, Calif.), p. 1016-1024. 8 refs. (See A69-42305 23-03)

EXPERIMENTS WITH A TWO-FLUID HEAT PIPE. K. T. Feldman, Jr. (New Mexico, University, Albuquerque, N. Mex.) and G. L. Whitlow (Energy Conversion Systems, Inc., Albuquerque, N. Mex.), p. 1025-1032. 7 refs. (See A69-42306 23-33)

HEAT PIPES FOR TEMPERATURE CONTROL. W. Bienert (Dyna-Therm Corp., Cockeysville, Md.), p. 1033-1041. 9 refs. (See

A69-42307 23-33)

ELECTROCHEMICAL POWER. IV.

ECONOMIC HIGH-PRESSURE HYDROGEN-OXYGEN REGENERATIVE FUEL-CELL SYSTEMS. H. J. Allison, R. Ramakumar, and W. L. Hughes (Oklahoma State University, Stillwater, Okla.), p. 1042-1047. 10 refs. (See A69-42308 23-03)

AMMONIA-AIR FUEL CELL SYSTEM. P. L. Terry and O. J. Adlhart (Engelhard Minerals and Chemicals Corp., Newark, N.J.), p. 1048-1051.

THE HYDRAZINE-AIR BI CELL, A SIMPLIFIED FUEL CELL SYSTEM. J. Perry, Jr. and L. J. Rogers (U.S. Army, Electronics Command, Fort Monmouth, N.J.), p. 1052-1056.

A CIRCULATING ELECTROLYTE HYDROGEN/AIR FUEL CELL SYSTEM. C. G. Clow and J. G. Bannochie (Energy Conversion, Ltd., Basingstoke, England), p. 1057-1064.

HIGH POWER DENSITY FUEL CELL. B. Durante (USAF, Aero Propulsion Laboratory, Wright-Patterson AFB, Ohio), J. K. Stedman, and C. Z. Bushnell (United Aircraft Corp., South Windsor, Conn.), p. 1065-1071. (See A69-42309 23-03)

USER REQUIREMENTS.

STRATEGIES FOR A NATIONAL NUCLEAR ENGINEERING PROGRAM. C. Starr and C. B. Smith (California, University, Los Angeles, Calif.), p. 1072-1080.

SUBJECT INDEX, p. 1083-1115.

AUTHOR INDEX, p. 1116-1131.

A69-42240 *

COMPUTER ANALYSIS OF SPACE POWER SYSTEMS FOR MISSION ANALYSIS.

Roger D. Arno (NASA, Office of Advanced Research and Technology, Mission Analysis Div., Moffett Field, Calif.).

IN: AMERICAN INSTITUTE OF CHEMICAL ENGINEERS, INTERSOCIETY ENERGY CONVERSION ENGINEERING CONFERENCE, 4TH, WASHINGTON, D.C., SEPTEMBER 22-26, 1969, PROCEEDINGS. (A69-42236 23-03)

Conference co-sponsored by the American Institute of Aeronautics and Astronautics, the American Nuclear Society, the American Society of Mechanical Engineers, the American Chemical Society, the Institute of Electrical and Electronics Engineers, and the Society of Automotive Engineers.

New York, American Institute of Chemical Engineers, 1969, p. 26-32.

The sensitivity of a space power system weight to various mission parameters is examined for an automated satellite repair vehicle and, very briefly, for three generations of manned space stations. Primary batteries, solar cells, fuel cells, radioisotope thermoelectric generators, and secondary battery characteristics are described for the low power, short duration repair vehicle. A comparison is made between solar cells, isotope Brayton, reactor Rankine, reactor Brayton, reactor thermoelectric, and advanced reactor systems for a range of mission dates and power levels for space stations. A computer program is used which allows the description of a wide variety of space power systems over a range of mission parameters. (Author)

A69-42244 *

POWER SYSTEMS FOR THE APOLLO APPLICATIONS PROGRAM.

D. L. Daubert, W. H. Gross (Martin Marietta Corp., Denver, Colo.), C. B. Graff (NASA, Marshall Space Flight Center, Huntsville, Ala.), and J. D. Murrell (NASA, Manned Spacecraft Center, Houston, Tex.).

IN: AMERICAN INSTITUTE OF CHEMICAL ENGINEERS, INTERSOCIETY ENERGY CONVERSION ENGINEERING CONFERENCE, 4TH, WASHINGTON, D.C., SEPTEMBER 22-26, 1969, PROCEEDINGS. (A69-42236 23-03)

Conference co-sponsored by the American Institute of Aeronautics and Astronautics, the American Nuclear Society, the American Society of Mechanical Engineers, the American Chemical Society, the Institute of Electrical and Electronics Engineers, and the Society of Automotive Engineers.

New York, American Institute of Chemical Engineers, 1969, p. 74-83.

Fuel cell/battery and solar array/battery systems satisfy major power demands of the manned Apollo Applications Program (AAP) space vehicles. This description of major power system design considerations and features provides information for a general understanding of these systems and how they satisfy AAP power requirements. Mission characteristics, spacecraft attitudes, vehicle configurations, and power requirements are major design considerations influencing configuration and operation of the systems. Modular design, multi-kilowatt power capabilities, and long life are distinguishing features of the AAP power systems, which are capable of generating and conditioning power for subsequent distribution to electrical equipment. (Author)

A69-42254 *

THERMAL MODEL OF A 75 WATT(E) SPACE POWER-PLANAR RTG SYSTEM.

Andrew J. Parker, Jr. (Hittman Associates, Inc., Columbia, Md.) and William S. West (NASA, Goddard Space Flight Center, Greenbelt, Md.).

IN: AMERICAN INSTITUTE OF CHEMICAL ENGINEERS, INTERSOCIETY ENERGY CONVERSION ENGINEERING CONFERENCE, 4TH, WASHINGTON, D.C., SEPTEMBER 22-26, 1969, PROCEEDINGS. (A69-42236 23-03)

Conference co-sponsored by the American Institute of Aeronautics and Astronautics, the American Nuclear Society, the American Society of Mechanical Engineers, the American Chemical Society, the Institute of Electrical and Electronics Engineers, and the Society of Automotive Engineers.

New York, American Institute of Chemical Engineers, 1969, p. 284-299.

Contract No. NAS 5-10441.

Description of the preliminary work accomplished on an advanced thermoelectric design concept for NASA. This concept has possible application to deep space missions and may offer additional flexibility in the integration of a power supply with spacecraft. The concept differs from conventional omnidirectional thermal radiator devices in that it uses a planar unidirectional or bidirectional radiator. The accomplishments include design, fabrication, and test of a full size thermal model to establish feasibility of the concept. (Author)

A69-42272 *

EVALUATION OF INTEGRAL COVERS ON SILICON SOLAR CELLS.

John W. Fairbanks (NASA, Goddard Space Flight Center, Greenbelt, Md.).

IN: AMERICAN INSTITUTE OF CHEMICAL ENGINEERS, INTERSOCIETY ENERGY CONVERSION ENGINEERING CONFERENCE, 4TH, WASHINGTON, D.C., SEPTEMBER 22-26, 1969, PROCEEDINGS. (A69-42236 23-03)

Conference co-sponsored by the American Institute of Aeronautics and Astronautics, the American Nuclear Society, the American Society of Mechanical Engineers, the American Chemical Society, the Institute of Electrical and Electronics Engineers, and the Society of Automotive Engineers.

New York, American Institute of Chemical Engineers, 1969, p. 567-574. 6 refs.

Description of three integral coverslip developmental efforts for silicon solar cells. The initial approach involved fusing a borosilicate glass on the cell surface. In the other approaches, two types of sputtering were developed: radio frequency sputtering and high-vacuum-ion-beam sputtering. Sputtering work was concentrated on fused silica. Cells coverslipped by these three techniques were subjected to solderability, temperature-humidity, and radiation tests. All cells were solderable by conventional techniques. Several rf sputtered coverslipped cells fractured during temperature-humidity testing. Tests indicate that all sputtered silica coverslips have internal stresses built into the coverslip. These stresses are possibly tolerable in film thicknesses up to 3 mils. Current efforts are directed toward alleviating the problem. (Author)

03 AUXILIARY SYSTEMS

A69-42278 *
BRAYTON-B POWER SYSTEM--A PROGRESS REPORT.
William J. Brown (NASA, Lewis Research Center, Cleveland, Ohio).
IN: AMERICAN INSTITUTE OF CHEMICAL ENGINEERS, INTERSOCIETY ENERGY CONVERSION ENGINEERING CONFERENCE, 4TH, WASHINGTON, D.C., SEPTEMBER 22-26, 1969, PROCEEDINGS. (A69-42236 23-03)
Conference co-sponsored by the American Institute of Aeronautics and Astronautics, the American Nuclear Society, the American Society of Mechanical Engineers, the American Chemical Society, the Institute of Electrical and Electronics Engineers, and the Society of Automotive Engineers.
New York, American Institute of Chemical Engineers, 1969, p. 652-658. 6 refs.

Description of progress on the 2-to-10 kW Brayton-B power system under investigation by NASA, Lewis Research Center. All power conversion component hardware has been built, and initial component testing has begun. A Brayton-B power system with an electric heat source is ready for test at the Plum Brook Space Power Facility. Analysis, based on preliminary test data, shows that the power conversion unit can provde 2-to-15 kWe at high system efficiencies from 0.17 to 0.30. (Author)

A69-42279 *
HOT PERFORMANCE CHARACTERISTICS OF A GAS BEARING BRAYTON CYCLE TURBOALTERNATOR.
James C. Wood, Martin E. Valgora, and H. B. Tryon (NASA, Lewis Research Center, Cleveland, Ohio).
IN: AMERICAN INSTITUTE OF CHEMICAL ENGINEERS, INTERSOCIETY ENERGY CONVERSION ENGINEERING CONFERENCE, 4TH, WASHINGTON, D.C., SEPTEMBER 22-26, 1969, PROCEEDINGS. (A69-42236 23-03)
Conference co-sponsored by the American Institute of Aeronautics and Astronautics, the American Nuclear Society, the American Society of Mechanical Engineers, the American Chemical Society, the Institute of Electrical and Electronics Engineers, and the Society of Automotive Engineers.
New York, American Institute of Chemical Engineers, 1969, p. 659-667. 12 refs.

Description of the design and testing of a turboalternator built for a Brayton cycle space power system. The turbine was designed to operate on argon with an inlet temperature of 1225 deg F. The turboalternator shaft is supported by gas-lubricated bearings. Major areas of investigation were: (1) starting and stopping shaft rotation without bearing damage while the journal bearings operated hydrodynamically; (2) maintaining proper bearing clearance during the startup thermal transient; and (3) having good shaft stability under the loads imposed by the alternator magnetic field. Stability is important because gas bearings have very low damping capability. Previous testing at turbine inlet temperatures up to 200 deg F was extended by running the temperature up to 1225 deg F for a total of 1165 hours. Starts and stops, full-load stop transients, short circuits, and loads of 3.5 times rated were investigated with the bearings operating hydrodynamically. (Author)

A69-42292 *
MODULARIZATION OF HIGH-POWER INVERTERS AND CONVERTERS.
Francis Gourash (NASA, Lewis Research Center, Cleveland, Ohio), P. F. Pittman (Westinghouse Electric Corp., Research Laboratories, Pittsburgh, Pa.), and J. F. Heins (Westinghouse Electric Corp., Research Laboratories, Lima, Ohio).
IN: AMERICAN INSTITUTE OF CHEMICAL ENGINEERS, INTERSOCIETY ENERGY CONVERSION ENGINEERING CONFERENCE, 4TH, WASHINGTON, D.C., SEPTEMBER 22-26, 1969, PROCEEDINGS. (A69-42236 23-03)
Conference co-sponsored by the American Institute of Aeronautics and Astronautics, the American Nuclear Society, the American Society of Mechanical Engineers, the American Chemical Society, the Institute of Electrical and Electronics Engineers, and the Society of Automotive Engineers.
New York, American Institute of Chemical Engineers, 1969, p. 830-838. 5 refs.

Description of techniques for modularizing static inverters and converters into "building blocks" or modules which can be paralleled to increase the power capacity of aerospace electrical power conditioning systems. Inverter and converter modules provide dc and three-phase, 400-Hz ac power at 2.5 kW per module. Circuit functions include automatic paralleling, control, protection, annunciation, power switching, and high-frequency pulse-width modulation; these circuits can be separately packaged into interchangeable submodules. The circuits and performance test results of two experimental breadboard ac and dc modules, and their applications to modular systems are presented and discussed. (Author)

A69-42301 *
POWER CONDITIONING DEVELOPMENT FOR THE SERT II ION THRUSTOR.
A. C. Hoffman (NASA, Lewis Research Center, Cleveland, Ohio), R. W. Briggs, E. F. Swiderski, S. F. Bauer, and R. M. Weger (Westinghouse Electric Corp., Aerospace Electrical Div., Lima, Ohio).
IN: AMERICAN INSTITUTE OF CHEMICAL ENGINEERS, INTERSOCIETY ENERGY CONVERSION ENGINEERING CONFERENCE, 4TH, WASHINGTON, D.C., SEPTEMBER 22-26, 1969, PROCEEDINGS. (A69-42236 23-03)
Conference co-sponsored by the American Institute of Aeronautics and Astronautics, the American Nuclear Society, the American Society of Mechanical Engineers, the American Chemical Society, the Institute of Electrical and Electronics Engineers, and the Society of Automotive Engineers.
New York, American Institute of Chemical Engineers, 1969, p. 975-986. 8 refs.

Description of the design of a power conditioner for operating with a mercury ion thrustor. The power conditioner converts 54 to 75 dc from a solar cell array into nine different electrical outputs for the thrustor. Total delivered power is approximately 1100 W, with nominal operation at approximately 900 W. The major amount of electric power is delivered at 3000 V, 0.25 A dc. Specific weight of the power conditioner is 18 pounds per kilowatt. Nominal load efficiency is 87.5 per cent. (Author)

A69-42303 *
TRACKING SOLAR ARRAY MAXIMUM POWER BY SENSING ARRAY TEMPERATURE.
Merton Sussman (NASA, Langley Research Center, Hampton, Va.).
IN: AMERICAN INSTITUTE OF CHEMICAL ENGINEERS, INTERSOCIETY ENERGY CONVERSION ENGINEERING CONFERENCE, 4TH, WASHINGTON, D.C., SEPTEMBER 22-26, 1969, PROCEEDINGS. (A69-42236 23-03)
Conference co-sponsored by the American Institute of Aeronautics and Astronautics, the American Nuclear Society, the American Society of Mechanical Engineers, the American Chemical Society, the Institute of Electrical and Electronics Engineers, and the Society of Automotive Engineers.
New York, American Institute of Chemical Engineers, 1969, p. 1004-1009. 7 refs.

Description of a straightforward technique in which a spacecraft solar cell array is constrained to operate close to its maximum power point over a wide range of environmental conditions. The output of an array temperature sensor is used to vary the duty cycle of a pulse-width-modulated impedance regulator so that array voltage tracks its optimum value. A resistance-type temperature sensor was found to be applicable on most spacecraft missions. However, a solar cell used as a temperature sensor has the advantage of negligible transient errors on lightweight arrays for orbiting spacecraft.(Author)

N69-10068*# National Aeronautics and Space Administration. Lewis Research Center, Cleveland, Ohio.

DESIGN AND ANALYSIS OF A MODULAR SERVOAMPLIFIER FOR FAST-RESPONSE ELECTROHYDRAULIC CONTROL SYSTEMS

John R. Zeller Washington Nov. 1968 23 p refs

(NASA-TN-D-4898) Avail: CFSTI CSCL 09E

A low cost three stage servoamplifier has been developed for use in fast response research servosystems. This device has the capability of improving the low frequency dynamics of the inductive coils of torque motor devices in electrohydraulic servovalves. In addition, this amplifier provides other servosystem functions such as summing, gain (adjustable), and compensation. A dynamic model of the amplifier-coil combination has been included to assist in analytical evaluation. The flexibility of the modular configuration has been demonstrated in several operational research installations. Author

N69-10088#* National Aeronautics and Space Administration. Lewis Research Center, Cleveland, Ohio.

SUMMARY OF ELECTRICAL COMPONENT DEVELOPMENT FOR A 400-HERTZ BRAYTON ENERGY CONVERSION SYSTEM

Charles S. Corcoran and Le Roy J. Yeager Washington Nov. 1968 33 p refs

(NASA-TN-D-4874) Avail: CFSTI CSCL 10B

The major electrical components of a 400 hertz Brayton cycle system are the alternator, the voltage regulator-exciter, and the parasitic loading speed controller. Unique design features of the components are described. The experimental evaluation of the components and subsystem indicates that the alternator has an efficiency of 91.5 percent at design and that the steady stage and transient performance is suitable for a space power system. In addition, bearing reactions caused by magnetic unbalance resulting from an unsymmetrical gap were determined experimentally. The data show that the reactions consist primarily of a constant and a pole frequency component. Author

N69-10708*# National Aeronautics and Space Administration. Langley Research Center, Langley Station, Va.

CALORIMETRIC, OPTICAL, AND VIBRATION INVESTIGATIONS OF STRETCH-FORMED ALUMINUM SOLAR CONCENTRATORS

Marvin D. Rhodes and Conrad M. Willis Washington Nov. 1968 45 p refs

(NASA-TN-D-4889) Avail: CFSTI CSCL 10B

Three stretch-formed aluminum solar concentrators were evaluated. The models represent three phases of a program; all were 1.52-m-diam paraboloids with a nominal rim angle of $\pi/3$ rad. Calorimetric tests were made on each model to determine the improvement in model performance caused by changes in model design and fabrication. Model 3 was superior to the other models in both geometrical accuracy and specular reflectance and is considered suitable for thermionic applications. Optical-ray-trace tests were performed on models 1 and 2 to determine the magnitude and location of surface slope errors. The largest slope errors occurred near the gore seams but the region of high error was only about 8% of the total area. Ray-trace data were also used to calculate geometric efficiency by three methods. Only the random error method gave reasonable results for both models. Vibration tests on model 1 caused failure in the welds of the rim support ring structure, but subsequent calorimetric tests revealed little or no reduction in concentrator efficiency. Author

N69-11373*# General Electric Co., Cincinnati, Ohio.

Cb-1Zr PUMPED SODIUM LOOP

E. E. Hoffman and J. Holowach Washington, D. C. NASA Nov. 1968 264 p refs

(Contract NAS3-2547)

(NASA-CR-1135) Avail: CFSTI CSCL 14B

A forced circulation Cb-1Zr pumped sodium loop was operated for 2650 hours at a maximum circuit temperature of 2065°F. The single phase sodium test was conducted to evaluate a number of components and test procedures prior to the construction and operation of the Cb-1Zr Rankine system corrosion test loop, a two-loop Cb-1Zr facility in which sodium was circulated in the primary or heater circuit and potassium was boiled and circulated in a two-phase secondary loop. Components which were evaluated included metering and isolation valves, slack diaphragm and stressed diaphragm pressure transducers, electrical feedthroughs, and electromagnetic helical induction pump. Detailed chemical and metallurgical evaluations revealed no evidence of corrosion or significant contamination, either from the sodium or the vacuum chamber environment. The specifications, procedures, fabrication techniques, and testing methods employed for the Cb-1Zr pumped sodium loop test were confirmed to be adequate for the Cb-1Zr Rankine system corrosion test loop test system. Author

N69-12575*# National Aeronautics and Space Administration. Lewis Research Center, Cleveland, Ohio.

SELECTED TECHNOLOGY FOR THE ELECTRIC POWER INDUSTRY

Washington 1968 334 p refs Proc. of a Technol. Util. Conf., Cleveland, 11-12 Sep. 1968

(NASA-SP-5057) Avail: CFSTI CSCL 10

CONTENTS:

1. NUCLEAR REACTOR HEAT SOURCES FOR FUTURE POWER GENERATION S. J. Kaufman, D. Bogart, J. V. Miller, and R. E. Gluyas p 1-34 refs (See N69-12576 02-22)

2. TOPICS ON RANKINE CYCLE POWER SYSTEMS TECHNOLOGY M. J. Saari, J. A. Heller, R. G. Dorsch, P. L. Stone, H. G. Hurrell et al p 35-89 (See N69-12577 02-03)

3. BRAYTON CYCLE SYSTEMS W. L. Stewart, W. A. Benser, A. J. Glassman, D. C. Guentert, and R. O. Hickel p 91-137 (See N69-12578 02-03)

4. RELIABILITY S. C. Himmel p 139-156 (See N69-12579 02-15)

5. AUTOMATIC CHECKOUT AND CONTROL J. N. Sivo p 157-171 (See N69-12580 02-31)

6. INSTRUMENTATION I. Warshawsky p 173-202 (See N69-12581 02-14)

7. BEARING AND SEAL TECHNOLOGY W. J. Anderson and L. P. Ludwig p 203-220 (See N69-12582 02-15)

8. ENGINEERING MECHANICS AND MATERIALS G. M. Ault p 221-258 refs (See N69-12583 02-17)

9. CRYOGENICS AND SUPERCONDUCTIVITY D. L. Nored and J. C. Laurence p 259-280 (See N69-12584 02-26)

10. DIRECT ENERGY CONVERSION H. J. Schwartz and J. J. Ward p 281-303 (See N69-12585 02-03)

11. SUMMARY OF CONFERENCE B. Lubarsky p 305-307 (See N69-12586 02-03)

12. INFORMATION SOURCES AND PROGRAMS J. E. Burnett p 309-321 (See N69-12587 02-08)

N69-13246*# National Aeronautics and Space Administration. Lewis Research Center, Cleveland, Ohio.

EVALUATION OF A FLUIDIC OSCILLATOR AS A

MOLECULAR WEIGHT SENSOR FOR GAS MIXTURES
Milton J. LeRoy, Jr. Washington Dec. 1968 15 p refs
(NASA-TM-X-1698) Avail: CFSTI CSCL 10B

A fluidic oscillator was tested to determine its performance as a molecular-weight sensor for flowing gas mixtures. A linear relation between inverse frequency squared and molecular weight was obtained over the test range. It was also determined that the temperature of the gas and pressure drop across the oscillator must be kept constant. Author

N69-14312*# National Aeronautics and Space Administration. Lewis Research Center, Cleveland, Ohio.
ANALOG SIMULATION OF CLOSED LOOP BRAYTON CYCLE TEST FACILITY
Hugh Klassen Washington Dec. 1968 29 p refs
(NASA-TM-X-1715) Avail: CFSTI CSCL 14B

The performance of a Brayton cycle test loop, which contained an experimental turbocompressor, was simulated with an analog computer. The working fluid was argon. The results of actual and simulated test runs were compared. The variation of rotative speed with time during injection starts is shown as a function of injection rate, turbine inlet temperature, and loop volume. The operating characteristics of the compressor are shown during injection starts. Author

N69-14397*# American Cyanamid Co., Stamford, Conn. Research Labs.
HIGH-PERFORMANCE LIGHT-WEIGHT ELECTRODES FOR HYDROGEN-OXYGEN FUEL CELLS
D. Gershberg, W. P. Colman, K. E. Olson, and E. W. Schmitz Washington NASA Dec. 1968 188 p refs
(Contract NAS3-8524)
(NASA-CR-1216) Avail: CFSTI CSCL 10B

This report covers work done with electrodes in alkaline, matrix-type fuel cells operating on hydrogen and oxygen. The principal objective was to determine and recommend preferred matrix materials and operating conditions under which these electrodes would be capable of 2000-hour performance in a total module having a weight to-power ratio substantially lower than those presently available for space environment. The experimental program included evaluation of potentially suitable matrix materials and life testing in small and in battery-size cells. Author

N69-14518*# National Aeronautics and Space Administration. Lewis Research Center, Cleveland, Ohio.
EXPERIMENTAL INVESTIGATION OF THE DYNAMICS OF WATER REJECTION FROM A MATRIX TYPE OF HYDROGEN-OXYGEN FUEL CELL
Paul R. Prokopius and Robert W. Easter Washington Dec. 1968 24 p refs
(NASA-TN-D-4956) Avail: CFSTI CSCL 10B

An experimental study of water-rejection dynamics was conducted on a matrix type of hydrogen-oxygen fuel cell which employs a hydrogen stream to extract the product water. Step transients were introduced in the hydrogen inlet humitity and in the rate of electrochemical water production. The resulting water-rejection transients were measured as changes in hydrogen outlet humidity. The transient response data were compared to the responses of a mathematical model developed for a Bacon type of cell. Data are presented which illustrate the effects that various initial operating conditions have on the outlet humidity responses for step transients in both inlet humidity and the rate of water production. Author

N69-15382*# Radio Corp. of America, Harrison, N. J.
SUPERCONDUCTIVE MAGNET SYSTEM, 14-TESLA, 15-cm-BORE
E. R. Schrader and P. A. Thompson Washington NASA Jan. 1969 55 p refs
(Contract NAS3-7101)
(NASA-CR-1260) Avail: CFSTI CSCL 09A

A description is presented of the design and construction of a 14-tesla (140-kilogauss) electromagnet with a 15-cm bore and using Nb_3Sn ribbon. A support system was developed in parallel with magnet design and construction. This system contains a standard research helium dewar and commercially available power supplies. A control console and interconnecting cables complete the entire magnet system. The magnet has four electrically separated groups of windings, the power to which can be supplied and controlled individually. This arrangement provides for a wide range of sequential and synchronized control of the electrical modules. Such control is necessary when optimum powering of the magnet is obtained and field produced by the electromagnet is maximized. Author

N69-15397*# National Aeronautics and Space Administration. Lewis Research Center, Cleveland, Ohio.
EFFECTS OF SAMPLE PREPARATION ON PHOTOMICROGRAPHS OF CADMIUM SULFIDE THIN-FILM SOLAR CELLS
John M. Bozek Washington Jan. 1969 14 p
(NASA-TM-X-1722) Avail: CFSTI CSCL 10B

Cross-section photomicrographs of thin film CdS solar cells revealed large, lamellar cracks in the CdS layer. Investigation of these cracks showed that they were caused, or at least aggravated, by the mounting and polishing techniques used, particularly by the absence of firm mounting of the cell sample. Use of an aluminum mechanical sandwich or of a slab epoxy mounting technique yielded cross sectional photomicrographs of the CdS thin film solar cells showing no large, lamellar cracks in the CdS layer. Author

N69-16379*# Westinghouse Electric Corp., Lima, Ohio.
INVERTER-CONVERTER PARALLEL OPERATION
G. W. Ernsberger, H. R. Howell, and J. L. Klingenberger Washington NASA Jan. 1969 107 p refs
(Contract NAS3-2792)
(NASA-CR-1224) Avail: CFSTI CSCL 10B

Mathematical analysis of circuit operation for harmonic-neutralized, static inverters operating in parallel have been developed and experimentally verified. Inverters can be operated in parallel provided that: (a) all inverters operate at exactly the same frequency; (b) the internal voltages of all inverters are in phase at all times; (c) all nominal regulated output voltages are the same; and (d) circuit provisions in each inverter insure load division. Static converters can be operated in parallel provided that: (a) all converters have the same nominal regulated output voltage, and (b) circuit provisions are provided in each voltage regulator circuit to cause the converters to share load current. Author

N69-17225*# National Aeronautics and Space Asministration. Lewis Research Center, Cleveland, Ohio.
A METHOD FOR REDUCING THE EQUIVALENT SINK TEMPERATURE OF A VERTICALLY ORIENTED RADIATOR ON THE LUNAR SURFACE
Darl D. Bien and Donald C. Guentert Washington Jan. 1969 17 p refs
(NASA-TM-X-1729) Avail: CFSTI CSCL 13A

An aluminized plastic cover sheet over the lunar surface immediately surrounding a vertical radiator offers a simple, light-weight method for reducing the radiator equivalent sink temperature. A simplified analysis predicts equivalent sink temperature as a function of cover surface coating properties, cover length, and radiator elevation for a radiator in the lunar equatorial plane. Results indicate that equivalent sink temperature can be reduced from over 600°R (333°K) (no cover) to about 400°R (200°K) (with cover). The corresponding reduction in required radiator area

is about 50 percent for a radiator temperature of 700°R (389°K). The effect of operation off the lunar equator is also discussed. *Author*

N69-17765*# Westinghouse Electric Corp., Lima, Ohio.
EVALUATION OF MAGNETIC MATERIALS FOR STATIC INVERTERS AND CONVERTERS
R. M. Frost, R. E. McVay, and D. M. Pavlovic Washington NASA Feb. 1969 175 p refs
(Contract NAS3-2792)
(NASA-CR-1226) Avail: CFSTI CSCL 10B

Magnetic materials for use in static inverters and converters were tested under dc excitation and under 400 to 3200 Hz square-wave voltage excitation. Materials evaluated included: 4%Mo–79%Ni–17%Fe, 50%Ni–50%Fe, magnetically annealed 49%Co–2%V–49%Fe, singly and doubly grain-oriented silicon steel, the latter both stress-relief annealed and magnetic field annealed. Magnetization curves, hysteresis loops, core loss and apparent power were determined for temperatures from −55° to +250°C; constant current flux reset data were obtained at room ambient. The effects of both vacuum exposure at 250°C and several conventional processing steps on magnetic properties were evaluated. *Author*

N69-18042*# TRW Systems, Redondo Beach, Calif.
BATTERIES FOR SPACE POWER SYSTEMS
Paul Bauer Washington NASA 1968 314 p refs
(NASA-SP-172) Avail: CFSTI CSCL 10C

A summary of all NASA sponsored work on batteries and related electrochemistry is given. Basic processes in a galvanic cell and operational and test problems of all types of batteries are outlined and data requirements for the design of sophisticated, high-efficiency space electric-power systems are analyzed. The validity and usefulness of individual battery systems for spacecraft applications are evaluated with emphasis on battery selection and integration into high efficiency electric-power systems. G.G.

N69-18885*# Electro-Optical Systems, Inc., Pasadena, Calif.
HYDROGEN-OXYGEN ELECTROLYTIC REGENERATIVE FUEL CELLS
M. Klein and R. Astrin Washington NASA Feb. 1969 356 p
(Contract NAS3-2781)
(NASA-CR-1244) Avail: CFSTI CSCL 10A

A research and development program to develop an electrolytic regenerative hydrogen-oxygen fuel cell concentrated on the development of a capillary matrix bipolar pile fuel cell stack with integral gas storage tankage. Tasks were undertaken to select and develop electrodes and matrix materials for the regenerative fuel cell. A cell stack employing an oxygen electrode, a potassium titanate matrix, and a hydrogen electrode consisting of a platinized sintered porous nickel plaque was found to comprise the best cell construction. Such cells were cycled on a 35-minute discharge/65-minute charge test regime and attained life-times in the 500 to 1000 cycle range with minimal deterioration. A 500-watt 34-cell prototype, assembled at the end of the program, was subjected to a limited number of test cycles and yielded approximately 15 watt hours per pound. The program demonstrated the potential of the regenerative hydrogen-oxygen fuel cell concept and it is apparent that increases in cycle life and energy density can be achieved with additional development. *Author*

N69-19799*# National Aeronautics and Space Administration. Lewis Research Center, Cleveland, Ohio.
DESCRIPTION AND EVALUATION OF DIGITAL-COMPUTER DESIGN-ANALYSIS PROGRAM FOR HOMOPOLAR INDUCTOR ALTERNATORS
David S. Repas and Gary Bollenbacher Washington Mar. 1969 93 p refs
(NASA-TN-D-5072) Avail: CFSTI CSCL 10A

A digital computer program for analyzing the electromagnetic design of homopolar inductor alternators is presented. The program, which is written in FORTRAN 4 programming language, is described in general terms. The calculational methods are either outlined briefly or appropriate references are cited. Instructions for using the program are given, and typical program input and output for a 15-kVA alternator are shown. Calculated results for this and two nearly identical 80-kVA alternators are compared with experimental data. In general, considering the many assumptions and approximations which are made in the calculational methods, it is felt that reasonable agreement was obtained between the test data and calculated results. *Author*

N69-19829*# National Aeronautics and Space Administration. Lewis Research Center, Cleveland, Ohio.
A FORTRAN 4 PROGRAM TO ESTIMATE THE OFF-DESIGN PERFORMANCE OF RADIAL-INFLOW TURBINES
Carroll A. Todd and Samuel M. Futral, Jr. Washington Mar. 1969 49 p refs
(NASA-TN-D-5059) Avail: CFSTI CSCL 10A

This program computes conventional performance parameters at required combinations of speeds and flow rates. Necessary input information consists of flow areas, diameters, blade angles, and an estimate of design point performance. The flow equations and corresponding computer listings are given. A set of example calculations is included. *Author*

N69-20780*# National Aeronautics and Space Administration. Lewis Research Center, Cleveland, Ohio.
DYNAMIC ANALYSIS OF PERMANENT MAGNET STEPPING MOTORS
David J. Robinson Washington Mar. 1969 65 p refs
(NASA-TN-D-5094) Avail: CFSTI CSCL 09C

A dynamic analysis of permanent magnet stepping motors for multistep operation is described. Linearized transfer function for single-step responses are developed. Multistep operation, when the motor is driven by a current source, is analyzed by using phase plane techniques. Failure of the motor to operate for fixed stepping rates and load torques is discussed. Dimensionless curves showing maximum stepping rate as a function of motor parameters and load torque are developed and experimentally verified. The curves allowed the maximum stepping rate of a motor with viscous, inertial, and torque loads to be predicted from simple measurements of the motor parameters. *Author*

N69-20797*# National Aeronautics and Space Administration. Lewis Research Center, Cleveland, Ohio.
NONCAVITATING AND CAVITATING PERFORMANCE OF SEVERAL LOW AREA RATIO WATER JET PUMPS HAVING THROAT LENGTHS OF 3.54 DIAMETERS
Nelson L. Sanger Washington Mar. 1969 35 p refs
(NASA-TN-D-5095) Avail: CFSTI CSCL 10B

Performance of several jet pumps was determined having diffuser included angles of 2.5° and 6° over a range of spacings of the nozzle exit from the throat entrance of 0 to 3.0 throat diameters. The throat length was found to be too short to permit matching with a conventional diffuser (6° included angle) because significant mixing continued into the diffuser entrance. However, due to the low rate of diffusion the pump having the 2.5° diffuser achieved the relatively high efficiencies of 31.5 percent for a nozzle-to-throat area ratio of 0.066, and 38.7 percent for an area ratio of 0.197. *Author*

03 AUXILIARY SYSTEMS

N69-20828*# National Aeronautics and Space Administration. Lewis Research Center, Cleveland, Ohio.

PERFORMANCE OF THE SNAP-8 LUBRICATION AND COOLANT SUBSYSTEM

H. B. Block, R. Kruchowy, and J. D. Gallagher Washington Mar. 1969 29 p refs

(NASA-TM-X-1731) Avail: CFSTI CSCL 08N

A SNAP-8 system containing all major prototype components except the nuclear reactor and the radiator was assembled and tested for 1445 hours at Lewis Research Center. The overall system consisted of five subsystems. One subsystem lubricated and/or cooled the other four SNAP-8 subsystems. Lubrication and coolant subsystem pump parameters, and component endurance data were examined. Data indicated no degradation in pump performance during the test. Fluid was supplied to the SNAP-8 components at the required flow rate and temperature. None of these components experienced a failure or significant degradation caused by lack of lubrication or cooling. Proper cooling of the mercury pump and the turbine alternator space seals resulted in a very low oil and mercury leakage to the space vacuum simulator. Author

N69-20852*# National Aeronautics and Space Administration. Lewis Research Center, Cleveland, Ohio.

COMPARISON OF BRAYTON AND RANKINE CYCLE MAGNETOGASDYNAMIC SPACE-POWER GENERATION SYSTEMS

Lester D. Nichols Washington Mar. 1969 59 p refs

(NASA-TN-D-5085) Avail: CFSTI CSCL 10B

Idealized Brayton- and Rankine-MHD cycles are considered for use in space. The Brayton-MHD cycle uses neon as the working fluid; the Rankine-MHD uses lithium. Both are seeded with cesium. The systems are restricted to a specified generator length and specific radiator area. It is shown that generally an entrance Mach number of 1.0 provides maximum power output; for the same value of Hall parameter the Rankine-MHD system may be used at a lower temperature than the Brayton-MHD; but at the same maximum temperature the Brayton-MHD generates more power than the Rankine-MHD. Subsonic entrance Mach number is recommended for Brayton-MHD, and supersonic for Rankine-MHD. Author

N69-20868*# National Aeronautics and Space Administration. Lewis Research Center, Cleveland, Ohio.

PERFORMANCE OF AN EXPERIMENTAL SNAP-8 POWER CONVERSION SYSTEM

Robert P. Macosko, William T. Hanna, Sol H. Gorland, and Kent S. Jeffries Washington Mar. 1969 30 p refs

(NASA-TM-X-1732) Avail: CFSTI CSCL 18N

A SNAP-8 experimental power system was operated for 1445 hours over a time span of 1463 hours. Approximately 1100 hours of continuous system operation were achieved. Steady-state system performance did not degrade with time. All SNAP-8 prototype components performed satisfactorily throughout the test with the exception of the parasitic load resistor. Three automatic shutdowns occurred during the course of the test. The automatic protective system employed functioned properly. There was no oil contamination of the mercury loop as a result of the shutdowns. Author

N69-20883*# National Aeronautics and Space Administration. Lewis Research Center, Cleveland, Ohio.

EFFECT OF ROTOR TIP CLEARANCE ON THE PERFORMANCE OF A 5-INCH SINGLE STAGE AXIAL FLOW TURBINE

Donald E. Holeski and Samuel M. Futral, Jr. Washington Mar. 1969 20 p refs

(NASA-TM-X-1757) Avail: CFSTI CSCL 10A

Turbine efficiency decreased linearly with increasing rotor tip clearance. Static efficiency decreased 20 percent (0.79 to 0.63) as rotor tip clearance was increased from 1.2 to 8.0 percent of passage height. Rotor exit flow survey data are presented in addition to performance data. Comparison of data with three reference turbines substantiated the results obtained and indicated that rotor tip clearance effects are larger for a reaction turbine than for an impulse turbine. Author

N69-20913*# National Aeronautics and Space Administration. Lewis Research Center, Cleveland, Ohio.

RESULTS OF ENDURANCE TESTS OF A SNAP 8 TURBINE-ALTERNATOR

Armen S. Asadourian, Robert J. Frye, Robert P. Macosko, and Richard W. Vernon Washington Mar. 1969 20 p refs

(NASA-TM-X-1741) Avail: CFSTI CSCL 18N

The SNAP-8 turbine-alternator was tested with mercury vapor in a system endurance run. Considerable long term endurance and performance information was obtained. The turbine-alternator accumulated 1445 hours (1110 hr continuous) and was subjected to four starts and stops. During the test period, the electrical power output ranged between 36.8 and 45.6 kW. Prolonged operation of the turbine-alternator did not reveal any degradation in performance or operating characteristics. Author

N69-20937*# National Aeronautics and Space Administration. Lewis Research Center, Cleveland, Ohio.

COLD PERFORMANCE EVALUATION OF 4.97-INCH RADIAL-INFLOW TURBINE DESIGN FOR SINGLE-SHAFT BRAYTON CYCLE SPACE-POWER SYSTEM

William J. Nusbaum and Milton G. Kofskey Washington Mar. 1969 24 p refs

(NASA-TN-D-5090) Avail: CFSTI CSCL 10A

Tests were conducted in argon over a range of turbine inlet pressures from 2.95 to 16.40 psia (2.03 to 11.31 N/cm^2 abs) corresponding to a Reynolds number range from 34,950 to 175,800 at equivalent design speed and pressure ratio. Results are presented to show the effect of this change in Reynolds number on turbine performance. Results are also presented in terms of equivalent specific work, mass flow, torque, and efficiency for operation at the design Reynolds number of 76 200 and at speeds ranging from 0 to 110 percent of equivalent design speed with inlet-total- to exit-static-pressure ratios of 1.33 to 2.01. Author

N69-21016*# National Aeronautics and Space Administration. Lewis Research Center, Cleveland, Ohio.

PERFORMANCE OF N/P SILICON AND CADMIUM SULFIDE SOLAR CELLS AS AFFECTED BY HYPERVELOCITY PARTICLE IMPACT

Robert L. Bowman, Michael J. Mirtich, and John R. Jack Washington Mar. 1969 16 p refs

(NASA-TN-D-5133) Avail: CFSTI CSCL 10A

A shock tube was used to accelerate particles to hypervelocities for the purpose of simulating micrometeoroid exposure. Various solar cells were then exposed to this simulated environment. The electrical characteristic curves of the cells before and after exposure were measured. The degradation of N/P Si solar cells covered by the thinnest quartz (6 mils or 0.15 mm) was greatly reduced from that suffered by cells without covers. The studies also demonstrated that encapulated CdS solar cells performed as well as protected silicon for exposure energies less than 0.5 J despite evidence of particle penetration of the encapsulant. Author

N69-21088*# National Aeronautics and Space Administration. Langley Research Center, Langley Station, Va.

CALORIMETRIC EVALUATION OF TWO CONE-COLUMN SOLAR-ENERGY CONCENTRATIONS

Marvin D. Rhodes and Conrad M. Willis Washington Mar. 1969 25 p refs

(NASA-TN-D-5109) Avail: CFSTI CSCL 10B

Two cone-column solar-energy concentrators were evaluated in this investigation. Both models had a rim angle of 0.79 radian and an effective radius of 76 cm. The first model was a simplified version of the cone-column with a rigidized cone. This model had a calorimetric efficiency of about 0.55 at an aperture radius of 8.16 solar-image radii. If this efficiency could be attained with a model utilizing a low-mass membrane cone. The cone-column would be competitive with a petalous concentrator designed for use with a Rankine cycle system. The second model was constructed to study some of the problems associated with the fabrication of an accurate membrane cone. However, the efficiency of this model was only about 0.28 at an aperture radius of 8.16 solar-image radii. The low efficiency of this model is due to markoff and interference of cone gores. The variation in efficiency for misalinement of the concentrator axis with the solar rays indicated that the performance of the cone-column was similar to that of a paraboloid. In addition, it was shown that small variations in misalinement can be compensated for by transverse displacements of the heat receiver. Author

N69-21771*# Pratt and Whitney Aircraft, East Hartford, Conn.

HIGH PERFORMANCE TURBOALTERNATOR AND ASSOCIATED HARDWARE. 1: DESIGN OF TURBOALTERNATOR

R. Cohen, W. K. Gilroy, and W. B. Spencer Washington NASA Mar. 1969 215 p refs

(Contract NAS3-6013)

(NASA-CR-1290; PWA-3070-Vol-1) Avail: CFSTI CSCL 10B

The National Aeronautics and Space Administration is conducting an evaluation of Brayton cycle turbomachinery configurations. As part of this program, a turboalternator has been designed incorporating a two stage axial flow turbine driving an inductor alternator supported on gas bearings. The gas bearing rotor support system was successfully tested in a gas bearing dynamic simulator and in the turboalternator under electrical load and fault conditions to impose magnetic unbalance forces. A total of about 300 hours of operation was accumulated on the gas bearings with about 200 hours under electrical load. A backup gas bearing system was designed and various experimental investigations were conducted to verify certain areas of the turboalternator design in addition to the gas bearing testing. The turboalternator was successfully tested at design conditions in a high temperature loop. Author

N69-22896*# National Aeronautics and Space Administration. Lewis Research Center, Cleveland, Ohio.

DESIGN AND PERFORMANCE OF TWO INTEGRATED CIRCUITS FOR FLUIDIC-CONTROLLED PNEUMATIC STEPPING MOTOR SYSTEM

Miles O. Dustin and Robert E. Wallhagen Washington Apr. 1969 50 p refs

(NASA-TN-D-5155) Avail: CFSTI CSCL 10B

Typical sizing calculations are demonstrated for determining the interconnecting line sizes. The integrated circuits control a nutator stepping motor up to 300 steps per second with a maximum output torque of 90 in.-lb (1020 cm-N) at zero speed. Author

N69-22940*# National Aeronautics and Space Administration. Lewis Research Center, Cleveland, Ohio.

EFFECTS OF TEMPERATURE AND ELECTROLYTE CONCENTRATION ON PERFORMANCE OF A FUEL CELL OF THE BACON TYPE

Robert E. Post Washington Apr. 1969 31 p refs

(NASA-TN-D-5154) Avail: CFSTI CSCL 10B

Performance was studied in terms of voltage-current data for temperatures ranging from 300° to 460°F (422 to 511K), KOH concentrations ranging from 70 to 82 wt. %, and reactant pressures of 22.4 psia ($1.54\times10^5 N/m^2$). The effect of increased concentration appeared as an upward displacement of the voltage-current curve and was two or more times that calculated from thermodynamic considerations. The effect of temperature appeared to be consistent with rate-process principles, in that it increased with current and decreased as equilibrium conditions were approached. Author

N69-23356*# National Aeronautics and Space Administration. Langley Research Center, Langley Station, Va.

A PARAMETRIC ANALYSIS OF SURFACE TEMPERATURES OF PARABOLOIDAL SOLAR CONCENTRATORS IN SPACE

Robert J. Platt, Jr. Washington Apr. 1969 68 p refs

(NASA-TN-D-5144) Avail: CFSTI CSCL 10B

A parametric analysis was made of the surface temperatures of a paraboloidal mirror in space and aimed at the sun. The problem is simplified by the assumption of steady-state conditions, the paraboloidal mirror (solar concentrator) being located directly between the earth and the sun. Surface temperatures are plotted for a range of the important parameters for altitudes up to 35,000 kilometers. Additional temperature plots are presented for the case of a solar concentrator approaching the sun. The results indicate that at an irradiance of one solar constant, a concentrator of very low thermal conductance may experience a front surface temperature of 600°K in space, unless a front surface coating is used to increase the emittance. The temperature difference between the front and rear surfaces, which causes thermal distortion of the mirror, may be greatly reduced by proper selection of thermal control surfaces if the concentrator is near the earth. At irradiances of many solar constants, as in the case of a concentrator used with a solar probe, metal construction and high emittance coatings appear to be needed to reduce the front surface temperature and to minimize thermal distortion. Author

N69-23643*# National Aeronautics and Space Administration. Washington, D. C.

INDUCTION HEATING ADVANCES: APPLICATIONS TO 5800°F

A. F. Leatherman and D. E. Stutz 1969 46 p refs

(NASA-SP-5071) Avail: SOD $0.30 CSCL 13A

Induction furnace design and basic heating principles are discussed. Vacuum reaction, vacuum brazing, and protective atmosphere furnaces are described, and radiant heat shielding designs are included. Theoretical considerations are given to induced currents and skin effects, operating frequency, heating coils, and power requirements. Various equipment arrangements are illustrated, and characteristics of components are given. Some of the more important advantages of induction heating are identified as no contact between work load and heat source, very high temperature capability, rapid heating, simplified control of processing, high efficiency, production capabilities, localization of heat, choice of vacuum or atmospheres, and cooler and cleaner working conditions. N.E.N.

03 AUXILIARY SYSTEMS

N69-28123*# National Aeronautics and Space Administration. Langley Research Center, Langley Station, Va.
CALORIMETRIC EVALUATION OF THREE 1.5-METER-DIAMETER INFLATABLE RIGIDIZED SOLAR CONCENTRATORS
Marvin D. Rhodes Washington Jun. 1969 35 p refs
(NASA-TN-D-5234) Avail: CFSTI CSCL 10B

The calorimetric efficiency of two 1.52-meter-diameter inflatable rigidized solar concentrators has been determined in order to evaluate their potential use with solar dynamic-cycle power systems. The membranes for these models were fabricated by different construction techniques and rigidized in a simulated space-vacuum environment with different foam materials (polyurethane and epoxy). Neither model was capable of satisfying typical design requirements of dynamic-cycle systems. The polyurethane-foam model had the higher calorimetric efficiency of the two models (0.61 at an aperture ratio of 7.6 as compared with 0.43 for the epoxy-syntactic-foam model); however, both models had about the same contour accuracy. In addition, these two models were compared with an epoxy–fiber - glass model rigidized at atmospheric pressure. Failure of all three models to meet the typical design requirements of the Brayton and Rankine cycle systems is due to low geometrical accuracy and low specular reflectance. Author

N69-29555*# National Aeronautics and Space Administration. Lewis Research Center, Cleveland, Ohio.
EFFECTS OF THERMAL-SHOCK CYCLING ON THIN-FILM CADMIUM SULFIDE SOLAR CELLS
John J. Smithrick Washington Jun. 1969 14 p refs
(NASA-TM-X-1819) Avail: CFSTI CSCL 10B

Thermal-shock cycling of Kapton, copper, and molybdenum substrate thin-film cadmium suflide (CdS) solare cells was conducted in an inert atmosphere by heating the cells to 65°C (338°K) and dipping them into liquid nitrogen. The Kapton substrate cells split in the CdS and delaminated. The open-circuit voltage and fill factor did not change; the shortcircuit current and maximum power decreased in direct proportion to the area by delamination. The single copper substrate cell tested did not delaminate or degrade after 1352 cycles. The single molybdenum cell tested did not delaminate after 1352 cycles but did degrade;however, comparable molybdenum substrate cells degrade on shelf storage also. The mode of degradation under thermal shock cycling was different from that observed, by others, under thermal cycling more realistic earth orbit simulation. Author

N69-29707*# National Aeronautics and Space Administration. Lewis Research Center, Cleveland, Ohio.
PRELIMINARY PERFORMANCE CHARACTERISTICS OF A GAS-BEARING TURBOALTERNATOR
James C. Wood, Martin E. Valgora, Roman Kruchowy, Joseph S. Curreri, Dennis A. Perz et al Henry B. Tryon Washington Jun. 1969 22 p refs
(NASA-TM-X-1820) Avail: CFSTI CSCL 10A

This report presents a preliminary evaluation of a Brayton cycle turboalternator using gas-lubricated bearings and operating on argon at a turbine inlet temperature of 1225°F (936°K). The turboalternator was operated successfully through steady-state and transient modes for 1165 total hours, during which time it was started and stopped 24 times. The alternator output was 8.8 kilowatts electric. The temperatures in the turboalternator did not exceed the predicted values when the turboalternator was operating at design conditions. The bearings always operated within the design clearance limits during both steady-state and transient testing. Largest clearance changes were experienced with the thrust bearings during full-load electrical transient tests. Author

N69-29977*# National Aeronautics and Space Administration. Lewis Research Center, Cleveland, Ohio.
DYNAMIC PERFORMANCE ANALYSIS OF A FUEL-CONTROL VALVE FOR USE IN AIRBREATHING ENGINE RESEARCH
Peter G. Batterton and John R. Zeller Washington July 1969 29 p refs
(NASA-TN-D-5331) Avail: CFSTI CSCL 13K

The analysis of a fast-response fuel-control valve for use in turbojet engine research is presented. This analysis includes cases where the valve is (1) closely coupled to the engine spray nozzles, and (2) located some distance from the engine, thus requiring connection by a hydraulic transmission line. The analysis results in a complete nonlinear model and an equivalent linearized model for both cases. The dynamic performance of the analytical models is presented and compared against corresponding experimental fuel-flow response data. A discussion is included which demonstrates how operating conditions affect fuel-flow frequency response. Author

N69-30945*# National Aeronautics and Space Administration. Goddard Space Flight Center, Greenbelt, Md.
A BRUSHLESS DC TORQUER-DRIVEN REACTION WHEEL FOR SPACECRAFT ATTITUDE CONTROL
R. Fulcher Washington Jul. 1969 20 p refs
(NASA-TN-D-5265) Avail: CFSTI CSCL 10B

A further development of electromechanical direct drive systems for space applications, dc photoelectronic (brushless) commutation techniques have been applied to the design of a reaction wheel. The resulting prototype hardware, which also incorporates optimized mechanical features, is shown to compare favorably on a weight/power basis with currently used ac torquer-driven reaction wheels. Furthermore, full utilization of the brushless commutator has simplified and improved control systems by providing, within the reaction wheel itself, the control electronic functions of bidirectional rotation, torque level control, and power amplification. A test control system using a prototype, brushless reaction wheel on a single-axis platform demonstrated excellent dynamic response and high pointing accuracy (within a few seconds of arc). Life testing of prototype hardware has been underway for 2 years. Author

N69-31844*# National Aeronautics and Space Administration. Lewis Research Center, Cleveland, Ohio.
EFFECTS OF NICKEL ON THE PERFORMANCE OF N ON P SILICON SOLAR CELLS
Cosmo R. Baraona Washington Aug. 1969 18 p refs
(NASA-TN-D-5366) Avail: CFSTI CSCL 10B

Nickel was added to 10-ohm-cm boron-doped silicon by a floating-zone technique. The calculated nickel concentrations were about 10^{14} atoms/cm^3. Solar cells were made by a standard process. Diffusion length, spectral response, and current-voltage characteristics were measured before and after bombardments by 1-MeV electrons with fluences ranging from 1×10^{14} to 1.5×10^{16} per cm^2. Nickel decreases the initial solar cell performance and does not improve the radiation resistance of the cell. The decreased performance is probably caused by nickel precipitation. Author

N69-32553*# General Electric Co., Schenectady, N.Y. Research and Development Center.
CHARACTERISTICS OF A THERMIONIC CONVERTER WITH A CHLORIDE VAPOR DEPOSITED TUNGSTEN EMITTER (110) AND A NICKEL COLLECTOR

V. C. Wilson and S. P. Podkulski Washington NASA Aug. 1969 37 p refs
(Contract NAS3-8511)
(NASA-CR-1416; GESP-9001) Avail: CFSTI CSCL 10A

A chloride vapor-deposited (110) tungsten emitter with a vacuum work function of 4.96 eV was built into a 0.005-inch-spaced converter with a nickel collector. The I–V curves for emitter temperatures of 1673°K to 2153°K are presented. The output power versus emitter temperature is compared with three other similar converters. This converter yielded almost the same output power as a converter with a single-crystal (110) tungsten emitter, 0.002-inch spacing and a molybdenum collector. The vapor-deposited (110) tungsten surface was found to be extremely stable. The collector work function was observed to decrease when the device was left at room temperature for one month. Author

N69-34652*# National Aeronautics and Space Administration. Lewis Research Center, Cleveland, Ohio.
ANALYSIS OF DYNAMIC PERFORMANCE LIMITATIONS OF FAST RESPONSE (150 to 200 Hz) ELECTROHYDRAULIC SERVOS
John R. Zeller Washington Aug. 1969 25 p refs
(NASA-TN-D-5388) Avail: CFSTI CSCL 13L

Fast response (150 to 200 Hz) electrohydraulic valve-controlled piston servo systems are used as research tools in experimental dynamics and controls studies. The components within these systems must operate at their limits of capability to achieve these high rates of response. A detailed nonlinear analytical model of these systems was formulated. The accuracy of this model was verified by comparing model dynamic performance against actual experimental data for a specific application. The analysis has led to a new generalized design criterion which in specific applications assists in determining a maximum region of dynamic performance capability. Author

N69-35537*# National Aeronautics and Space Administration. Lewis Research Center, Cleveland, Ohio.
PERFORMANCE CHARACTERISTICS OF A 14.3-KILOVOLT-AMPERE MODIFIED LUNDELL ALTERNATOR FOR 1200 HERTZ BRAYTON-CYCLE SPACE-POWER SYSTEM
David S. Repas and Richard A. Edkin Washington Sept. 1969 28 p refs
(NASA-TN-D-5405) Avail: CFSTI CSCL 10A

The measured performance of the alternator is presented. Test results include alternator saturation curves, losses and efficiency, voltage unbalance, harmonic analysis, machine reactances, and time constants. The peak electromagnetic efficiency of the alternator was 93.6 percent for a unity power factor load of 9.5 kW. For an output of 14.3 kVA at 0.75 power factor lagging, the alternator electromagnetic efficiency was 90.3 percent. Author

N69-35689*# General Electric Co., Schenectady, N.Y.
CHARACTERISTICS OF A THERMIONIC CONVERTER WITH A FLUORIDE VAPOR DEPOSITED TUNGSTEN EMITTER ETCHED TO PREFERENTIALLY EXPOSE THE 110 CRYSTAL PLANES
V. C. Wilson and J. Lawrence Washington NASA Aug. 1969 117 p refs
(Contract NAS3-8511)
(NASA-CR-1381; GEST-2107) Avail: CFSTI CSCL 10A

A variable spaced planar thermionic converter was built with a tungsten emitter, a niobium collector and a niobium guard ring. The tungsten emitting surface was a 0.020-inch-thick layer of fluoride vapor deposited tungsten. X-ray analysis and etch pit studies showed this surface was oriented with a (100) plane parallel to the bulk surface. The surface was etched to expose the (110) planes which are inclined 45 degrees to the (100) planes. The surface was then a mass of peaks, ridges and valleys several microns in depth, and had an exposed area about 40 percent greater than the plane surface. The initial output performance of this surface at low cesium pressures and also at large spacings was better than unetched (100) tungsten. The most output was obtained at 10 mils spacing or more for emitter temperatures from 1700°K to 2000°K. Operation for 21.8 hours at 2155°K reduced the sharpness of the points and ridges and the output performance decreased, particularly at larger spacings. Author

N69-35763*# National Aeronautics and Space Administration. Lewis Research Center, Cleveland, Ohio.
THE IMPROVEMENT OF AN ELECTRONIC POWER SUPPLY FOR GREATER RELIABILITY IN AEROSPACE USE
John P. Quitter and J. W. Schaelchlin (Gen. Dyn./Convair, San Diego, Calif.) Washington Sep. 1969 47 p refs
(NASA-TM-X-1875) Avail: CFSTI CSCL 10A

This report is a brief account of an upgrading program for electronic equipment. Serious design obstacles were overcome that led to the successful development of a highly reliable electronic component for space use. The component discussed is an inverter that provides three-phase 400-Hz power to the Centaur space vehicle. Because of early ground failure and design deficiencies, the inverter has received much engineering attention. This report is concerned with general upgrading of all piece parts used in the inverter, as well as improved mechanical and thermal design. Weaknesses of original piece parts are described, and rationale presented for the choice of better parts. Author

N69-36411*# General Electric Co., Schenectady, N.Y. Tube Dept.
REDUCTION OF RECOVERY TIME IN HIGH-TEMPERATURE CESIUM VAPOR THYRATRONS
A. W. Coolidge, Jr. Washington NASA Sep. 1969 47 p refs
(Contract NAS3-9423)
(NASA-CR-1417) Avail: CFSTI CSCL 10B

An existing cesium vapor thyratron design was modified with the goal of reducing the recovery time from 300 to 100 microseconds. The approach taken was to facilitate ion-electron recombination by reducing the path lengths traversed by the ions after the cessation of current conduction. This included reduction of grid-to-anode spacing, grid-to-cathode spacing, and a reduction in the width of the grid slots. Although the tubes fabricated with these modifications were more difficult to fire and exhibited slightly increased voltage drop, stable operation was achieved for extended time periods in an inverter circuit. Author

N69-36758*# National Aeronautics and Space Administration. Lewis Research Center, Cleveland, Ohio.
EFFECTS OF SIMULATED SPACE ENVIRONMENT ON FULL, HALF, AND QUARTER-SIZE CADMIUM SULFIDE THIN-FILM SOLAR CELLS
Anthony F. Ratajczak, Thomas M. Klucher, and Clifford K. Swartz Washington 16 p refs
(NASA-TM-X-1884) Avail: CFSTI CSCL 10B

Full-, half-, and quarter-size CdS thin film solar cells were subjected to a simulated space environment to test the effect of cell size on performance degradation. The test data indicate that there is more variation in degradation among common size cells than between different size cells and that cell degradation does not appear to be substantially affected by cell size. Author

N69-36829*# Whittaker Corp., San Diego, Calif.
ELECTROCHEMICAL CHARACTERIZATION OF NONAQUEOUS SYSTEMS FOR SECONDARY BATTERY

03 AUXILIARY SYSTEMS

APPLICATION
Manny Shaw, O. A. Paez, and Frank A. Ludwig Washington NASA Sep. 1969 229 p refs
(Contract NAS3-8509)
(NASA-CR-1434) Avail: CFSTI CSCL 10B

Approximately one thousand electrode-organic electrolyte combinations have been characterized relative to their use as rechargeable battery systems, using the method of cyclic voltammetry. Electrode systems consisted of silver, copper, nickel, cobalt, zinc, cadmium, indium, iron, molybdenum, chromium, manganese, vanadium, lithium, calcium, and magnesium. In general, the most promising positive metals were silver, copper, zinc, cadmium, and indium. A large majority of the nickel, cobalt, and iron systems exhibited no discharge peaks at all, and in most cases negligible discharge current. Twenty-four recommended systems comprising silver, copper, zinc, and cadmium, were further characterized by constant-current charge and discharge of sintered electrodes. Author

N69-36843*# General Electric Co., Schenectady, N.Y. Tube Dept.
DEVELOPMENT AND INVERTER TESTING OF HIGH TEMPERATURE CESIUM-VAPOR THYRATRONS
A. W. Coolidge, Jr. Washington NASA Sep. 1969 47 p refs
(Contract NAS3-9423)
(NASA-CR-1435) Avail: CFSTI CSCL 09E

Cesium vapor thyratrons were developed for operation at 200° C to 300° C, in a vacuum environment. The tubes were rated 15 amperes average current, 250 volts peak forward and inverse. A major effort consisted of reducing the recovery time from over 300 microseconds to less than 100 microseconds. The tubes were endurance tested over 3000 hours in an inverter circuit. Author

N69-37827*# National Aeronautics and Space Administration. Lewis Research Center, Cleveland, Ohio.
DIFFUSION LENGTHS IN SILICON OBTAINED BY AN X-RAY METHOD
John H. Lamneck, Jr. Washington Oct. 1969 9 p refs
(NASA-TM-X-1894) Avail: CFSTI CSCL 10B

The necessity for a rapid method of measuring diffusion lengths of silicon solar cells in radiation damage and subsequent annealing studies led to the development of a new procedure utilizing a standard X-ray machine. After the machine was calibrated with cells of known diffusion lengths, measurements on test cells could be made at the rate of one every 2 min with a standard deviation of less than 2 percent. Author

N69-37883*# National Aeronautics and Space Administration, Lewis Research Center, Cleveland, Ohio.
EFFECT OF ELECTROTHERMAL INSTABILITIES ON BRAYTON- AND RANKINE-CYCLE MAGNETOHYDRODYNAMIC SPACE-POWER GENERATION SYSTEMS
Allan R. Bishop and Lester D. Nichols Washington Oct. 1969 18 p refs
(NASA-TN-D-5461) Avail: CFSTI CSCL 10B

Plane wave electrothermal instabilities are included in the analysis of idealized Brayton- and Rankine-cycle magnetohydrodynamic generators. It is shown that the instabilities cause an increase in Joule heating and a reduction in output power. An increase in the magnetic field can compensate for the reduction in output power. Author

N69-38767*# National Aeronautics and Space Administration. Lewis Research Center, Cleveland, Ohio.
ELECTRICAL CHARACTERISTICS OF A LARGE AREA THIN FILM CdS SOLAR CELL
Ernie W. Spisz and John R. Jack Washington Oct. 1969 25 p refs
(NASA-TM-X-1899) Avail: CFSTI CSCL 10B

The electrical characteristics of a large area (54.7 cm^2) thin film CdS solar cell were obtained over a range of temperatures and radiant intensity levels at atmospheric conditions and in an ultrahigh vacuum simulation facility. The electrical characteristics were obtained over the temperature range from 20° to 90°C at radiant intensity levels of 0.014, 0.070, 0.140, and 0.245 W/cm^2. By applying the conventional "lumped constants" photovoltaic equation to the data, the effect of temperature on the reverse saturation current of the diode and the effect of temperature and radiant intensity level on the series resistance were determined. Author

N69-39238*# National Aeronautics and Space Administration. Lewis Research Center, Cleveland, Ohio.
PRELIMINARY INVESTIGATION OF A SINGLE-SHAFT BRAYTON ROTATING UNIT DESIGNED FOR A 2- TO 10-KILOWATT SPACE POWER GENERATION SYSTEM
Robert Y. Wong, Hugh A. Klassen, Robert C. Evans, and Charles H. Winzig Washington Oct. 1969 39 p refs
(NASA-TM-X-1869; E-5130) Avail: CFSTI CSCL 10B

A 525-hour hot test at design thermal conditions was made. The results indicated that the performance of the turbine, compressor, and alternator are close to design specifications; no evidence of major design flaws; that the gas bearings had no short term operational problems; and that alternator armature winding temperatures were higher than anticipated. Author

N69-39335*# National Aeronautics and Space Administration, Lewis Research Center, Cleveland, Ohio.
COLD AIR INVESTIGATION OF A TURBINE WITH STATOR-BLADE TRAILING-EDGE COOLANT EJECTION. PART 1: OVERALL STATOR PERFORMANCE
Warren J. Whitney, Edward M. Szanca, and Frank P. Behning Washington Oct. 1969 21 p refs
(NASA-TM-X-1901; E-5182) Avail: CFSTI CSCL 01A

Overall stator performance was obtained with ratios of coolant to primary mass flow of 0, 0.02, 0.035, 0.05, and 0.07. The effects of coolant on the performance parameters, mass flow characteristic and outlet flow angle, were determined experimentally. These effects were also determined theoretically for the condition of design primary mass flow. Author

N69-40440*# National Aeronautics and Space Administration. Lewis Research Center, Cleveland, Ohio.
MOTOR-STARTING CHARACTERISTICS OF TWO INDUCTOR ALTERNATORS
Charles S. Corcoran, David S. Repas, and Martin E. Valgora Washington Oct. 1969 13 p refs
(NASA-TM-X-1912) Avail: CFSTI CSCL 10B

Two inductor alternators were started as induction motors. One machine had a 5.2-inch (13.2-cm) diameter rotor with amortisseur windings and laminated pole tips; the other had a 7.38-inch (18.7-cm) diameter rotor with solid poles. Armature current, field voltage, and rotational speed were measured as functions of time. Torque was computed and is presented as a function of speed. The machine starting performance is compared to the requirements of a typical Brayton cycle generating system. Author

N69-40787*# National Aeronautics and Space Administration. Lewis Research Center, Cleveland, Ohio.
CONCEPTUAL DESIGN AND STRUCTURAL MODEL OF A

560-WATT THIN-FILM SOLAR-CELL ARRAY

Francis J. Stenger Washington Oct. 1969 14 p refs
(NASA-TM-X-1913) Avail: CFSTI CSCL 10B

A structural model of a cadmium sulfide thin-film solar-cell array was constructed with a deployment structure weight of 0.12 lb/ sq ft (0.59 kg/m^2) of panel area and a projected power output of from 15.5 to 19.4 W/lb (34.2 to 42.7 W/kg) using available CdS solar cells. The rollout, nonretractable array used a 40-ft (12.2-m) long storable boom as the basic structural element. The boom stiffness was tested using two simple mechanical suspensions. Author

04

BIOSCIENCES

Includes aerospace medicine, exobiology, radiation effects on biological systems; physiological and psychological factors. For related information see also: 05 Biotechnology.

A69-11073
LIFE SCIENCES AND SPACE RESEARCH VI; COSPAR, PLENARY MEETING, 10TH, OPEN MEETING OF WORKING GROUP V, LONDON, ENGLAND, JULY 27, 28, 1967, PROCEEDINGS.
Meeting sponsored by COSPAR, the International Union of Biochemistry, the International Union of Biological Sciences, and the International Union of Physiological Sciences.
Edited by A. H. Brown and F. G. Favorite.
Amsterdam, North-Holland Publishing Co., 1968. 206 p. In English and French.
$12.60.

CONTENTS:

PREFACE. A. H. Brown and F. G. Favorite, p. v, vi.

THE MEDICAL LEGACY OF GEMINI. C. A. Berry (NASA, *Manned Spacecraft Center, Houston, Tex.*), p. 1-19. 7 refs. [See A69-11074 01-04]

LIFE SUPPORT FOR MAN IN SPACE.

LIFE IN THE SPACECRAFT AND PLANETARY STATION. B. A. Adamovich, Iu. G. Nefedov, A. S. Ushakov, and S. V. Chizhov, p. 23-26. [See A69-11075 01-05]

MAN AS THE MAIN COMPONENT OF THE CLOSED ECOLOGICAL SYSTEM OF THE SPACECRAFT OR PLANETARY STATION. V. V. Parin and B. A. Adamovich, p. 27-31. [See A69-11076 01-05]

EXPERIMENTAL BIOLOGICAL LIFE SUPPORT SYSTEM. I - CONTINUOUS CULTIVATION OF ALGAE AS A LINK OF A CLOSED ECOSYSTEM. L. V. Kirenskii, I. A. Terskov, I. I. Gitelson, G. M. Lisovskii, B. G. Kovrov, and Iu. N. Okladnikov, p. 32-36. 10 refs. [See A69-11077 01-05]

EXPERIMENTAL BIOLOGICAL LIFE SUPPORT SYSTEM. II - GAS EXCHANGE BETWEEN MAN AND MICROALGAE CULTURE IN A 30-DAY EXPERIMENT. L. V. Kirenskii, I. A. Terskov, I. I. Gitelson, G. M. Lisovskii, B. G. Kovrov, and Iu. N. Okladnikov, p. 37-40. [See A69-11078 01-05]

PROBLEM OF REPRODUCTION OF FOOD PROTEIN BY AUTOTROPHIC ORGANISMS IN EXTRATERRESTRIAL CONDITIONS. V. I. Fofanov, A. S. Ushakov, N. S. Kliushkina, and K. V. Smirnov, p. 41-44. [See A69-11079 01-05]

SETTING PROTEIN LIMITS FOR SPACE DIETS. D. H. Calloway and S. Margen (California, University, Berkeley, Calif.), p. 45, 46.

HYDROGENOMONAS EUTROPHA AS A SPACE FOOD SOURCE. C. I. Waslien and D. H. Calloway (California, University, Berkeley, Calif.), p. 47, 48.

A LIFE SUPPORT SYSTEM FOR SATELLITE EXPERIMENTS OVER ONE YEAR. R. G. A. Lotz (Frankfurt, Universität, Frankfurt am Main, West Germany), p. 49-55. [See A69-11080 01-05]

THE EFFECT OF EXTREME ENVIRONMENTS ON TERRESTRIAL LIFE.

CORRELATION OF DOSE RATE AND SPECTRAL MEASUREMENTS IN THE INNER VAN ALLEN BELT. A. L. Thede and G. E. Radke (USAF, Systems Command, Kirtland AFB, N. Mex.), p. 59-68. 9 refs. [See A69-11081 01-29]

PSYCHOMOTOR REACTIONS AMONG PRIMATES PUT INTO BALLISTIC FLIGHT IN ROCKETS [REACTIONS PSYCHOMOTRICES CHEZ DES PRIMATES PLACES EN VOL BALISTIQUE EN FUSEES]. R. Grandpierre and G. Chatelier, p. 69-78. [See A69-11082 01-04]

RESISTANCE OF ORGANISMS TO EXTREME INFLUENCES IN RELATION TO SOME EXOBIOLOGICAL PROBLEMS. L. K. Lozina-Lozinskii (Akademiia Nauk SSSR, Moscow, USSR), p. 79-86. 28 refs. [See A69-11083 01-04]

WEIGHTLESSNESS AND THE DEVELOPING FROG EGG. R. S. Young (NASA, Washington, D.C.) and J. W. Tremor (NASA, Ames Research Center, Moffett Field, Calif.), p. 87-93. [See A69-11084 01-04]

ON THE INTERRELATIONS BETWEEN ULTRAVIOLET AND VISIBLE LIGHT DURING THEIR SIMULTANEOUS ACTION ON THE CELL. E. I. Zaar (Akademiia Nauk SSSR, Leningrad, USSR), p. 94-99. 40 refs. [See A69-11085 01-04]

THE BIOLOGICAL EFFECTIVENESS OF SOLAR ELECTROMAGNETIC RADIATION IN SPACE. P. R. Lorenz, C. L. Hemenway, and J. Hotchin (Union University; New York State, Dept. of Health, Albany, N.Y.), p. 100-107. 12 refs. [See A69-11086 01-04]

THE SURVIVAL OF TERRESTRIAL MICROORGANISMS IN SPACE AT ORBITAL ALTITUDES DURING GEMINI SATELLITE EXPERIMENTS. J. Hotchin, P. Lorenz, and C. L. Hemenway (New York State, Dept. of Health; Union University, Albany, N.Y.), p. 108-114. 5 refs. [See A69-11087 01-04]

MICROBIOLOGICAL STUDIES ON THE RADIATION ENVIRONMENT OF THE IONOSPHERE AND STRATOSPHERE. E. Petras and K. Bisa (Fraunhofer Gesellschaft zur Förderung der angewandten Forschung, Grafschaft, West Germany), p. 115-122. 6 refs. [See A69-11088 01-04]

THE EFFECT OF EXTREME COOLING ON GLOBULAR AND FIBRILLAR PROTEINS. M. A. Khenokh and V. P. Pershina (Akademiia Nauk SSSR, Moscow, USSR), p. 123-129. 11 refs. [See A69-11089 01-04]

LIFE DETECTION.

CHAIRMAN'S REPORT ON THE COSPAR SYMPOSIUM ON STERILIZATION TECHNIQUES FOR INSTRUMENTS AND MATERIALS AS APPLIED TO SPACE RESEARCH. P. H. A. Sneath (Leicester University, Leicester, England), p. 133-135.

RELATIONSHIP OF PLANETARY QUARANTINE TO BIOLOGICAL SEARCH STRATEGY. E. C. Levinthal, J. Lederberg (Stanford University, Stanford, Calif.), and C. Sagan (Harvard University; Smithsonian Institution, Cambridge, Mass.), p. 136-145. 11 refs. [See A69-11090 01-05]

PROBABILITY OF GROWTH (p_G) OF VIABLE MICROORGANISMS IN MARTIAN ENVIRONMENTS. E. J. Hawrylewicz, C. A. Hagen, V. Tolkacz, B. T. Anderson, and M. Ewing (IIT Research Institute, Chicago, Ill.), p. 146-156. 11 refs. [See A69-11091 01-04]

APPLICATIONS OF CAPILLARY MICROSCOPY IN EXOBIOLOGICAL RESEARCH. J. B. Opfell, G. P. Zebal, and J. L. Shannon (Philco-Ford Corp., Newport Beach, Calif.), p. 157-169. 10 refs. [See A69-11092 01-05]

A COMPARATIVE EVALUATION OF DIFFERENT METHODS FOR DETECTION OF EXTRATERRESTRIAL LIFE. A. A. Imshenetskii, S. A. Butenko, L. A. Kuzjurina, M. Mukhin, G. G. Sotnikov, and R. I. Redorova (Akademiia Nauk SSSR, Moscow, USSR), p. 170-182. [See A69-11093 01-05]

PHOTOLYSIS OF ALIPHATIC AMINO ACIDS IN THE PRESENCE OF SALT IONS. M. A. Khenokh and N. P. Bogdanova (Akademiia Nauk SSSR, Moscow, USSR), p. 183-190. 20 refs. [See A69-11094 01-06]

PHOTOLYSIS OF ALIPHATIC AMINO ACIDS IN THE PRESENCE OF METAL OXIDES. M. A. Khenokh and N. P. Bogdanova (Akademiia Nauk SSSR, Moscow, USSR), p. 191-197. 6 refs. [See A69-11095 01-06]

IS VENUS HABITABLE? C. Sagan (Harvard University; Smithsonian Institution, Cambridge, Mass.), p. 198.

AUTHOR INDEX, p. 199.

A69-11074 *
THE MEDICAL LEGACY OF GEMINI.
Charles A. Berry (NASA, Manned Spacecraft Center, Houston, Tex.).
IN: LIFE SCIENCES AND SPACE RESEARCH VI; COSPAR, PLENARY MEETING, 10TH, OPEN MEETING OF WORKING GROUP V, LONDON, ENGLAND, JULY 27, 28, 1967, PROCEEDINGS. [A69-11073 01-04]
Meeting sponsored by COSPAR, the International Union of Biochemistry, the International Union of Biological Sciences, and the International Union of Physiological Sciences.
Edited by A. H. Brown and F. G. Favorite.
Amsterdam, North-Holland Publishing Co., 1968, p. 1-19. 7 refs.

The Mercury and Gemini space flights have provided approximately 2,000 manhours of weightless exposure which can be used in comparing flight results with the predicted effects of manned space flight. In general the environmental hazards and the effects upon man appear to be of less magnitude than originally anticipated. The effects noted on the various body systems are summarized. The principal physiologic changes noted were orthostatism for some 50 hr after the flight, reduced red cell mass, and reduced X-ray density in the os calcis and the small finger. Much was learned about man's ability to work in a pressurized suit in the extravehicular condition. All of these findings are of importance in relation to the planning for future long duration missions. (Author)

A69-11084 *
WEIGHTLESSNESS AND THE DEVELOPING FROG EGG.
R. S. Young (NASA, Washington, D.C.) and J. W. Tremor (NASA, Ames Research Center, Moffett Field, Calif.).
IN: LIFE SCIENCES AND SPACE RESEARCH VI; COSPAR, PLENARY MEETING, 10TH, OPEN MEETING OF WORKING GROUP V, LONDON, ENGLAND, JULY 27, 28, 1967, PROCEEDINGS. [A69-11073 01-04]
Meeting sponsored by COSPAR, the International Union of Biochemistry, the International Union of Biological Sciences, and the International Union of Physiological Sciences.
Edited by A. H. Brown and F. G. Favorite.
Amsterdam, North-Holland Publishing Co., 1968, p. 87-93.

Description of the results of the flight of fertilized frog eggs in the manned orbital flights Gemini 8 and Gemini 12. The experiment was designed to determine the effect of weightlessness or near weightlessness on the ability of the cell to divide normally and on subsequent differentiation and embryogenesis. Eggs were fixed periodically in flight so that recovered material could be carefully compared to simultaneous ground controls with respect to gross morphology and histology. Some embryos were recovered alive after 4 days in orbit. In general, no abnormalities were detected which were inconsistent with the controls. Death, shortly after recovery, of the embryos recovered alive in Gemini 12, remains unexplained. The protocol of the experiment and the experimental hardware are described. (Author)

A69-11770 *
SOME BIOLOGICAL PROBLEMS IN THE SEARCH FOR EXTRATERRESTRIAL LIFE.
Harold P. Klein (NASA, Ames Research Center, Moffett Field, Calif.).
(International Symposium on Bioastronautics and the Exploration of Space, 4th, San Antonio, Tex., June 27, 1968.)
IN: SPACE PROJECTIONS FROM THE ROCKY MOUNTAIN REGION; PROCEEDINGS OF THE SYMPOSIUM, DENVER, COLO., JULY 15, 16, 1968. VOLUME 3. [A69-11755 02-11]
Symposium sponsored by the American Astronautical Society and the American Institute of Aeronautics and Astronautics.
Tarzana, Calif., American Astronautical Society, 1968. 21 p. 44 refs.

General discussion of the possible existence of extraterrestrial life forms in the solar system. The various components of the Martian atmosphere are reviewed on the basis of data obtained from the Mariner 4 flyby of 1965. It is suggested that the factor most prohibitive to the existence of life on Mars would be the almost total lack of water vapor. The adaptation of terrestrial organisms to simulated Martian atmospheres is briefly discussed. Some problems in planning "life detection" experiments to be used on unmanned Mars probes are also treated. M.G.

A69-11866 *
CHARACTERIZATION OF RIBULOSE DIPHOSPHATE CARBOXYLASE AND PHOSPHORIBULOKINASE FROM THIOBACILLUS THIOPARUS AND THIOBACILLUS NEAPOLITANUS.
R. D. MacElroy, E. J. Johnson, and M. K. Johnson (NASA, Ames Research Center, Exobiology Div., Moffett Field, Calif.).
Archives of Biochemistry and Biophysics, vol. 127, Sept. 1968, p. 310-316. 24 refs.

Investigation of two enzymes involved in the fixation of CO_2 by the chemosynthetic autotrophs Thiobacillus thioparus and Thiobacillus neapolitanus. Both of these enzymes, ATP:D-ribulose-5-phosphate 1-*phosphotransferase* (phosphoribulokinase) and D-ribulose-1,5-diphosphate carboxylase (ribulose diphosphate carboxylase) appear to sediment at identical rates in sucrose density gradients and to have similar characteristics during gel filtration. In addition to the major peak of ribulose diphosphate carboxylase activity observed in sucrose density gradients, an additional lighter peak of activity, suggestive of a subunit, has been observed. The relationship of these enzymes to those found in Fraction I protein of plant tissue is discussed, and it is suggested that both enzymes from the chemoautotrophs may be part of the same moiety. M.M.

A69-12804 *
THE SEARCH FOR LIFE - PLANETARY EVOLUTION.
Richard S. Young (NASA, Washington, D.C.).
IN: SPACE PROJECTIONS FROM THE ROCKY MOUNTAIN REGION; PROCEEDINGS OF THE SYMPOSIUM, DENVER, COLO., JULY 15, 16, 1968. VOLUME 1. [A69-12801 02-30]
Symposium sponsored by the American Astronautical Society and the American Institute of Aeronautics and Astronautics.
Tarzana, Calif., American Astronautical Society, 1968. 19 p.

Discussion of the two primary objectives of the NASA Planetary Exploration Program - namely, to gain data concerning the origin of the solar system and the origin of life. These two objectives are actually so interwoven as to be essentially indistinguishable from each other. If present theories concerning the sequence of events which led to the origin of life on earth are correct, then it is clear that the very early environment of any given planet is critical to the ability of that planet to produce and sustain a living system. Thus the physics and chemistry of planetary formation and early evolution are of the utmost importance to an understanding of the origin of life. It is believed that the likelihood of life on the moon, Venus, and Jupiter is considerably less than for Mars, but that much can be learned about planetary evolution from each of them. P.v.T.

A69-13433 *
UPTAKE AND INCORPORATION OF EXOGENOUS LEUCINE IN BACTERIAL CELLS UNDER HIGH OXYGEN TENSION.
Ho Lee Young (NASA, Ames Research Center, Moffett Field, Calif.).
Nature, vol. 219, Sept. 7, 1968, p. 1068, 1069. 8 refs.

Investigation of the relationship between the transport and the incorporation of amino acids, and net synthesis of protein at high oxygen tension in cells of Pseudomonas saccharophila. The results indicate that the ratio of endogenous to exogenous leucine is greater in cells grown in oxygen than in cells grown in air during incubation, and not the reverse. The results also suggest that high oxygen tension has little direct effect on the incorporation of leucine into protein, but that it strongly inhibits the leucine uptake. M.M.

A69-13498 *
EFFECTS OF ACUTE EXPOSURE TO HIGH-ENERGY PROTONS ON PRIMATES.
S. Tom Taketa, Bruce L. Castle, Wayne H. Howard, Charles C. Conley, Webb Haymaker (NASA, Ames Research Center, Moffett Field, Calif.), and Charles A. Sondhaus (California, University, Lawrence Radiation Laboratory, Berkeley, Calif.).
(Workshop Conference on Space Radiation Biology, University of California, Berkeley, Calif., Sept. 7-10, 1965.)
Radiation Research Supplement, no. 7, 1967, p. 336-359. 45 refs.

Discussion of data from collaborative studies to determine the biological effectiveness of protons as compared with other types of radiation, specifically ^{60}Co gamma radiation. The study, which used 43 rhesus monkeys, demonstrated the phenomena of dose buildup from the action of high-energy protons to be independent of

the Bragg peak effect and to be related to the distance traversed by the primary protons. Data based on midpoint air dose, midpoint tissue dose, and average body dose were used for the evaluation. Protons appeared to be as effective or slightly more effective than gamma rays when the comparisons were based improperly on midpoint air dose, but less effective when based on absorbed tissue dose. Appearance, radiation syndrome symptoms, and pathological changes were essentially similar in both groups. Silver impregnation in the brains of 15 animals revealed glial activation in most of them and was considered a radiation effect. G.V.

A69-13700 *#
EXTRATERRESTRIAL BIOLOGY - PROSPECTS AND PROBLEMS IN THE EARLY 1970'S.
Richard D. Johnson and Harold P. Klein (NASA, Ames Research Center, Moffett Field, Calif.).
American Institute of Aeronautics and Astronautics, Annual Meeting and Technical Display, 5th, Philadelphia, Pa., Oct. 21-24, 1968, Paper 68-1122. 7 p. 17 refs.
Members, $1.00; nonmembers, $1.50.

The scientific rationale and experimental strategy for the biological exploration of Mars are discussed in terms of the chemical and biological experiments planned for these missions in the early 1970's. The experimental concepts and hardware development are treated in conjunction with the various mission constraints. Specifically, the chemical experiments are discussed in terms of the specificity of the analysis as applied to extraterrestrial samples, the experimental complexity with respect to sample processing, and the various types of analysis with respect to the detectors. The biological experiments are discussed in terms of growth and reproduction, metabolism, enzyme activity, and microscope scanning. Problems associated with growth media, water availability, and interference from soil are treated in terms of the experiment design The evolution and integration of the various separate experiments into more complex instruments is discussed as a prospect for later missions. (Author)

A69-13897 *
CRITICAL TEMPERATURE FOR INTRACRANIAL SELF-STIMULATION IN WHITE RATS.
Pava Popovic, A. B. Silver, and V. P. Popovic (Emory University, Dept. of Physiology, Atlanta, Ga.).
American Journal of Physiology, vol. 214, Apr. 1968, p. 801-803. 12 refs.
Grant No. NGR-11-001-009.

Evaluation of experiments made with white rats in order to ascertain the critical temperature for self-stimulation. Bipolar stainless steel electrodes were chronically implanted in the hypothalamic supramammillary area ("pleasure center") of 18 white rats which were trained to press a lever for intracranial self-stimulation Each rat pressed the lever 40 to 60 times per minute whenever it was placed for 1 hr in the box. When the body temperature reached 22 to 23°C, the rats eventually stopped pressing the lever. This point represents the "critical body temperature" for intracranial self-stimulation. P.v.T.

A69-14692 *
DISPERSION AND ATTENUATION OF SMALL ARTIFICIAL PRESSURE WAVES IN THE CANINE AORTA.
Max Anliker, Eric Ogden (Stanford University, Dept. of Aeronautics and Astronautics, Stanford; NASA, Ames Research Center, Div. of Environmental Biology, Moffett Field, Calif.), and Michael B. Histand.
Circulation Research, vol. 23, Oct. 1968, p. 539-551. 36 refs.
Grant No. NGR-05-020-223.

Description of a method for determining the elastic behavior of large blood vessels in the canine aorta in terms of their transmission characteristics for small sinusoidal pressure signals. The method is new insofar as it uses transient signals of the form of finite trains of sine waves that are superimposed on the naturally occurring pressure fluctuations and are generated by an electrically driven impactor or by a pump. Its application to the thoracic aortas of 18 mature mongrel dogs anesthetized with pentobarbital has shown that dispersion and attenuation data for frequencies between 40 and 200 cps can be obtained without requiring either Fourier-transform computations or resolution of reflection interference. M.M.

A69-15332 *
MAGNITUDE ESTIMATES OF ROTATIONAL VELOCITY DURING AND FOLLOWING PROLONGED INCREASING, CONSTANT, AND ZERO ANGULAR ACCELERATION.
Brant Clark and John D. Stewart (NASA, Ames Research Center, Moffett Field, Calif.).
Journal of Experimental Psychology, vol. 78, no. 2, 1968, p. 329-339. 24 refs.

Description of an experiment in which velocity of rotation was observed by ten observers in a rotating simulator during and following accelerations about a vertical axis which varied between .5° to 1.5°/sec^2 and .006 to .030°/sec^3 and continued for 2 to 3 min. Trials with zero acceleration were also included. Magnitude estimates of velocity of rotation increased and then declined during the constant accelerations, while more complex effects occurred during increasing accelerations. Aftereffects and an autokinetic effect were also observed. The current theory of vestibular function is discussed in the light of these results. M.G.

A69-15333 *
CELLULAR LOCALIZATION OF ACETYL-COENZYME A SYNTHETASE IN YEAST.
Harold P. Klein and Linda Jahnke (NASA, Ames Research Center, Exobiology Div., Moffett Field, Calif.).
Journal of Bacteriology, vol. 96, Nov. 1968, p. 1632-1639. 23 refs.

Study of the subcellular sites of the enzyme acetyl-CoA synthetase which is involved in lipid synthesis in Saccharomyces cerevisiae. Direct assays are performed for the enzyme in the microsomal fraction of the cells of Saccharomyces cerevisiae. The data suggest that during aerobic, but not anaerobic, growth on glucose, the enzyme moves from the microsomal fraction into the mitochondrial fraction. It is further suggested that the enzyme leaves the mitochondria when the cells become older, but while they are still viable. M.G.

A69-15969 *
COMPARISON OF THREE METHODS TO DETERMINE THRESHOLDS FOR PERCEPTION OF ANGULAR ACCELERATION.
John D. Stewart (NASA, Ames Research Center, Moffett Field, Calif.) and Brant Clark.
American Journal of Psychology, vol. 81, June 1968, p. 207-216. 13 refs.

Comparative study of three psychophysical methods used to determine thresholds for the perception of angular acceleration in man. Sixteen men with normal vestibular function were studied using three random forced-choice procedures with a simulator rotating the subject about a vertical axis. The constant method, using a 10-sec constant acceleration, was found to be the most reliable, and there was a high correlation between thresholds determined by a forced-choice random double-staircase method and the constant method. The constantly increasing accelerations of the ramp method were found to produce unreliable, equivocal results. The thresholds determined by the constant and staircase methods for the 16 subjects varied between 0.07 and 1.19 deg/sec^2. G.V.

A69-15983 *
EFFECTS OF PROGRESSIVE HYPOHYDRATION ON MAXIMAL ISOMETRIC MUSCULAR STRENGTH.
J. S. Bosco, R. L. Terjung (San Jose State College, San Jose, Calif.), and J. E. Greenleaf (NASA, Ames Research Center, Moffett Field, Calif.).
Journal of Sports Medicine and Physical Fitness, vol. 8, June 1968,

p. 81-86. 15 refs.

Experimental investigation in which nine male college students between the ages of 20 and 29, who had previous athletic experience and were physically active, were hypohydrated for two one-week periods. During the third week of the diet, a general decrease was evident in all the isometric strength measures except knee extension, paralleled with a mean weight loss of 2.5%. In general, the maximal strengths exhibited decreasing trends but only elbow flexion was significantly decreased at up to 3.1% hypohydration. M.M.

A69-17105 *

IDENTITY BETWEEN THE GROWTH HORMONE DEGRADING ACTIVITY OF THE PITUITARY GLAND AND PLASMIN.

S. Ellis, J. M. Nuenke, and R. E. Grindeland (NASA, Ames Research Center, Environmental Biology Div., Moffett Field, Calif.).

Endocrinology, vol. 83, Nov. 1968, p. 1029-1042. 63 refs.

Investigation confirming the identity between plasmin and the esterase contaminating the growth hormone. Degradation products have been found in highly purified preparations of growth hormone. The degradation of the growth hormone and its electrophoretic behavior is presumably caused by a trypsin-like peptidase present in pituitary extracts. The effect could be duplicated with human plasmin during the investigations. Several other tests were performed to establish the identity between plasmin and the esterase. G.R.

A69-19429 *

IN VIVO UTILIZATION OF ACETATE-1-C^{14} IN CENTRIFUGED RATS.

E. D. Neville and D. D. Feller (NASA, Ames Research Center, Environmental Biology Div., Moffett Field, Calif.).

Aerospace Medicine, vol. 40, Feb. 1969, p. 164-167. 13 refs.

Fed and fasted male rats were centrifuged at 5 g for 1, 3, and 24 hr. After this exposure, the metabolism of the rat was followed for a 3-hr period by measuring plasma glucose, plasma FFA, expired $C^{14}O_2$ and CO_2 patterns, and recovery of C^{14} in plasma lipids from acetate-1-C^{14}. Centrifugation caused a significant rise in plasma glucose and FFA in both fasted and fed rats. Plasma glucose remained elevated during the 3-hr postcentrifugation period while plasma FFA returned to normal values. Lipid synthesis increased in the intact rat as measured by an increased plasma C^{14}-lipid content. The observed increase of acetate incorporation into plasma lipids of rats previously exposed to centrifugation stress supports the previous observation, on isolated tissues, that this stress enhances lipogenesis. The relative roles of plasma glucose and FFA in energy relations of stressed animals are discussed. (Author)

A69-19481 *

STUDIES OF THE ELECTRON TRANSPORT CHAIN OF EXTREMELY HALOPHILIC BACTERIA. I - SPECTROPHOTOMETRIC IDENTIFICATION OF THE CYTOCHROMES OF HALOBACTERIUM CUTIRUBRUM.

J. K. Lanyi (NASA, Ames Research Center, Exobiology Div., Moffett Field, Calif.).

Archives of Biochemistry and Biophysics, vol. 128, Dec. 1968, p. 716-724. 11 refs.

Room temperature and liquid nitrogen difference spectra of H. cutirubrum extracts show evidence of two b-type, two c-type, and one a-type cytochrome. A scheme for electron transport involving these components is suggested whereby, at pH 7.2, the electron flow proceeds through cytochrome b(559), cytochrome c(555), and cytochrome a(592). At pH 9.4, however, it appears that an alternate pathway through cytochrome b(563) and cytochrome c(550) is opened. DPNH and α-glycerophosphate reduce both b-type cytochromes, while succinate reduces only cytochrome b(559). After overnight incubation, cytochrome b(563) is inactivated and can no longer be reduced enzymically. (Author)

A69-19726 *

TRANSMISSION CHARACTERISTICS OF AXIAL WAVES IN BLOOD VESSELS.

M. Anliker, W. E. Moritz (Stanford University, Dept. of Aeronautics and Astronautics, Stanford, Calif.), and E. Ogden (NASA, Ames Research Center, Environmental Biology Div., Moffett Field, Calif.).

(Society for Experimental Stress Analysis, Spring Meeting, Albany, N.Y., May 7-10, 1968, Paper 1350.)

Journal of Biomechanics, vol. 1, Dec. 1968, p. 235-246. 23 refs.

Grant No. NGR-05-020-223.

Determination of the phase velocities and damping of sinusoidal axial waves in the carotid artery of anesthetized dogs using an electrooptical tracking system. For frequencies between 25 and 150 Hz, the speed of the axial waves ranged between 20 and 40 m/sec and generally increased with frequency, while the natural pressure wave traveled at a speed of about 10 m/sec. It is noted, however, that on the basis of an isotropic wall model, the axial wave speed should be approximately 5 times higher than the pressure wave speed. This discrepancy can be interpreted as an indication of anisotropic behavior of the carotid wall. The carotid artery appears to be more elastic in the axial than in the circumferential direction. M.M.

A69-20374 *

ADRENAL EPINEPHRINE AND PHENYLETHANOLAMINE N-METHYL TRANSFERASE (PNMT) ACTIVITY IN THE RAT BEARING A TRANSPLANTABLE PITUITARY TUMOR.

Joan Vernikos-Danellis (NASA, Ames Research Center, Environmental Biology Div., Moffett Field, Calif.), R. Ciaranello, and J. Barchas (NASA, Ames Research Center, Environmental Biology Div., Moffett Field; Stanford University, School of Medicine, Palo Alto, Calif.).

Endocrinology, vol. 83, Dec. 1968, p. 1357, 1358. 12 refs.

NIH Grants No. HD-02881; No. MH-13259; Grant No. NGR-05-020-168.

Determination of plasma corticosterone and adrenal phenylethanolamine N-methyl transferase (PNMT) in rats bearing a transplantable pituitary tumor for six weeks. Ten male Fischer rats were fed commercial rat chow and water and were maintained at a constant temperature of 24°C. Half the rats were implanted with tumor tissue suspended in saline and injected intramuscularly into the right hind leg. The rats were decapitated six weeks after tumor implantation. It was found that there was a 350% increase in adrenal PNMT and a 160% increase in adrenal epinephrine in the tumor-implanted animals as compared to the controls. G.R.

A69-23158 *

PLASMA ENZYME RESPONSES TO BLOOD WITHDRAWAL IN CHICKENS.

C. M. Winget, G. H. Bond, and L. S. Rosenblatt (NASA, Ames Research Center, Environmental Biology Div., Moffett Field, Calif.).

Comparative Biochemistry and Physiology, vol. 27, 1968, p. 827-833. 17 refs.

Description of the effect of repeated sampling (blood withdrawal) on the plasma cholinesterase, acid phosphatase, and alkaline phosphatase over an 8-hr period in the domestic chicken (Gallus domesticus). Hematocrit ratios were affected by the volume of blood removed as well as the sequence of the sample taken. (Author)

A69-25460 *

POTENTIAL EFFECTS OF RECENT FINDINGS ON SPACECRAFT STERILIZATION REQUIREMENTS.

S. Schalkowsky, R. C. Kline (Exotech, Inc., Washington, D.C.), and L. B. Hall (NASA, Washington, D.C.).

Space Life Sciences, vol. 1, Mar. 1969, p. 520-530. 6 refs.

Contracts No. NASw-1558; No. NASw-1666.

Discussion of an extended analytical model (accommodating information which has been developed in the past year or which is currently being evolved) for an assessment of spacecraft sterilization requirements. The probability of a release of viable organisms from the spacecraft is evaluated as a function of: (1) impact velocity magnitudes and the probability of their occurrence; (2) the degree of equipment fracturing at impact velocities; and (3) the number of viable organisms in spacecraft materials. It is concluded that the results of work now in progress on spacecraft material fracturing,

on the estimation of buried contamination loads, and on microbial resistance on mated surfaces, may lead to less severe dry-heat sterilization of planetary spacecraft than had been considered necessary in the past. G.R.

A69-25643 *

ESTIMATING THE SIZE AND CONCENTRATION OF UNICELLULAR MICROORGANISMS BY LIGHT SCATTERING.

Edward L. Merek (NASA, Ames Research Center, Exobiology Div., Moffett Field, Calif.).

Applied Microbiology, vol. 17, Feb. 1969, p. 219-221. 6 refs.

The optical density of suspensions of microorganisms was measured at two different positions in a spectrophotometer cuvette compartment. From these two measurements, the particle size and the particle concentration could be estimated. Estimates of particle numbers were not significantly different from those obtained by direct microscopic counting. (Author)

A69-26557 *

RAT BODY COMPOSITION - SENSOR IMPLANTATION AND LIGHTING EFFECTS.

Grover C. Pitts, T. Robert Bullard, John W. Tremor, Paul D. Sebesta, Franz Halberg, and Walter Nelson (Virginia, University, School of Medicine, Charlottesville, Va.; NASA, Ames Research Center, Moffett Field, Calif.; Minnesota, University, Medical School, Minneapolis, Minn.).

Aerospace Medicine, vol. 4, Apr. 1969, p. 417-420. 14 refs.
Contracts No. NAS 2-1554; No. NAS 2-2738.

The effects of transensor-implantation, sham-implantation, or no implantation and three lighting regimens (continuous light, or darkness, or 12 hr of each per day) on body composition of 54 adult female Sprague-Dawley rats were evaluated by analysis of variance with a factorial design. Body composition involved chemical fractionation into lipid, water, protein-nitrogen, and ash of eviscerated carcass and viscera treated separately. Statistically significant results included: (1) percent fat in eviscerated carcass reduced in presence of transensor, (2) percent fat in viscera reduced after sham operation, (3) percent water in fat-free viscera increased in presence of the transensor (probably edema evoked by transensor as an irritant), and (4) percent fat in eviscerated carcass increased with daily dark-fraction, probably reflecting effect of lighting regimen on feeding activity. (Author)

A69-27909 *

LUNAR MEDICINE.

Charles A. Berry (NASA, Manned Spacecraft Center, Houston, Tex.).

Science Journal, vol. 5, May 1969, p. 103-107.

Analysis of medical problems connected with space travel and the exploration of the moon. Man, adapted to living in an earth environment, is exposed to entirely different conditions in a space vehicle and on the lunar surface. Medical findings obtained from previous space missions are evaluated, and measures are described which are designed to ensure that astronauts will be able to meet the demands of the exploration programs contemplated. G.R.

A69-30036 *

CONTROL OF ATP-DEPENDENT CO_2 FIXATION IN EXTRACTS OF HYDROGENOMONAS FACILIS - NADH REGULATION OF PHOSPHORIBULOKINASE.

R. D. MacElroy (NASA, Ames Research Center, Exobiology Div., Moffett Field, Calif.), E. J. Johnson, and M. K. Johnson (NASA, Ames Research Center, Exobiology Div., Moffett Field, Calif.; Tulane University, Medical School, Dept. of Microbiology, New Orleans, La.).

Archives of Biochemistry and Biophysics, vol. 131, Apr. 1969, p. 272-275. 8 refs.
NSF Grant No. GB-7492.

The role of NADH in stimulating ATP-dependent CO_2 fixation has been examined in crude extracts of Hydrogenomonas facilis. It has been found that the stimulation cannot be attributed to reduction of the product, 3-phosphoglyceric acid, and consequent regeneration of substrate. Rather, NADH appears to specifically affect phosphoribulokinase, probably by causing an allosteric transition of this regulatory enzyme. The kinetics of the NADH effect on CO_2 fixation suggest cooperative binding of the effector. A similar cooperative response of the enzyme to ATP has been noted. It is suggested that the control of CO_2 fixation is mediated by allosteric regulation of phosphoribulokinase activity. (Author)

A69-30444 *

DIFFERENCES BETWEEN RADIATION-INDUCED LIFE SHORTENING AND NATURAL AGING IN DROSOPHILA MELANOGASTER.

Henri Atlan (NASA, Ames Research Center, Moffett Field, Calif.), Jaime Miquel, and Rosemarie Binnard.

Journal of Gerontology, vol. 24, Jan. 1969, p. 1-4. 7 refs.

Study of the mortality kinetics of Drosophila melanogaster showing essential differences between gamma radiation-induced life shortening and normal aging. Gamma irradiation of Drosophila melanogaster imagoes 1 to 20 days of age resulted in death at a constant time after exposure. Age at irradiation influenced survival time only when the flies were irradiated 30 to 90 days after eclosion. These results suggest that the life-shortening effects of gamma radiation on Drosophila are the result of a radiation syndrome which, at least for 1 to 20 day old flies, is unrelated to aging. P.v.T.

A69-31336 *#

MECHANISMS OF ACTION OF LIGHT ON CIRCADIAN RHYTHMS IN THE MONKEY.

C. M. Winget, L. S. Rosenblatt, C. W. DeRoshia, and N. W. Hetherington (NASA, Ames Research Center, Environmental Biology Div., Moffett Field, Calif.).

COSPAR, Plenary Meeting, 12th, Prague, Czechoslovakia, May 11-24, 1969, Paper. 25 p. 18 refs.

Description of changes in deep body temperature (DBT) and locomotor activity (LMA) phase relationships as well as alterations in the DBT waveform in response to changing photoperiods in two species of subhuman primates (Macaca nemestrina and Cebus albifrons). It has been demonstrated that DBT and LMA rhythmicity are stable in the subhuman primate. Asymmetrical DBT waveforms retained their inherent shapes over a relatively long time period and were perhaps entrained to the 12L:12D cycle. Maxima were exhibited during light and minima in the dark with a range of oscillation in DBT of 2 to 3°C. G.R.

A69-31539 *

IDENTIFICATION OF SUGARS AS THEIR TRIFLUOROACETYL POLYOL DERIVATIVES.

Jacob Shapira (NASA, Ames Research Center, Biotechnology Div., Moffett Field, Calif.).

Nature, vol. 222, May 24, 1969, p. 792, 793. 14 refs.

Description of a method which successfully solves the problems inherent in the identification of mixtures of sugars by gas-liquid chromatography (GLC). The method involves the sodium borohydride reduction of the sugar or sugar mixture to the corresponding polyol(s) and GLC of the trifluoroacetyl derivative. G.R.

A69-32967

EXOBIOLOGY: THE SEARCH FOR EXTRATERRESTRIAL LIFE; AMERICAN ASTRONAUTICAL SOCIETY AND AMERICAN ASSOCIATION FOR THE ADVANCEMENT OF SCIENCE, SYMPOSIUM, NEW YORK, N.Y., DECEMBER 30, 1967, PROCEEDINGS.

Edited by M. M. Freundlich (Cutler-Hammer, Inc., Airborne

Instruments Laboratory Div., Deer Park, N.Y.) and B. M. Wagner (Columbia University, College of Physicians and Surgeons, New York, N.Y.).
Tarzana, Calif., American Astronautical Society (AAS Science and Technology Series. Volume 19), 1969. 183 p.
Members, $7.35; nonmembers, $9.75.

CONTENTS:

INTRODUCTION. M. M. Freundlich (Cutler-Hammer, Inc., Deer Park, N.Y.) and B. M. Wagner (Columbia University, New York, N.Y.), p. ix, x.

FRONTIERS IN SOLAR SYSTEM EXOBIOLOGY. C. Sagan (Cornell University, Ithaca, N.Y.), p. 1-11. [See A69-32968 17-04]

AUTOMATED MICROBIAL METABOLISM LABORATORY. G. V. Levin (Biospherics Research, Inc., Washington, D.C.), p. 13-28. [See A69-32969 17-05]

LIFE DETECTION TECHNIQUES. R. S. Young (NASA, Washington, D.C.), p. 29-35. [See A69-32970 17-05]

TECHNIQUES OF INTERSTELLAR COMMUNICATION. E. M. Hafner (Rochester, University, Rochester, N.Y.), p. 37-62. [See A69-32971 17-30]

THE ORIGIN OF MICROBIAL LIFE ON EARTH AND ITS IMPLICATIONS FOR EXTRATERRESTRIAL FORMS. H. D. Isenberg (Long Island Jewish Hospital, New Hyde Park; New York, State University, Brooklyn, N.Y.), p. 63-95. 34 refs. [See A69-32972 17-04]

BIOCHEMICAL BASES FOR LIFE IN EXTRATERRESTRIAL ENVIRONMENTS. W. Vishniac (Rochester, University, Rochester, N.Y.), p. 97-116. 5 refs. [See A69-32973 17-04]

SOCIOLOGICAL ASPECTS OF EXOBIOLOGY. B. M. Wagner (Columbia University, New York, N.Y.), p. 117-130. [See A69-32974 17-34]

DISCUSSIONS, p. 131-172.

A69-33173 *

CHROMOSOME ANALYSES OF GEMINI ASTRONAUTS.

P. C. Gooch (Oak Ridge National Laboratory, Biology Div., Oak Ridge, Tenn.) and C. A. Berry (NASA, Manned Spacecraft Center, Medical Research and Operations Directorate, Houston, Tex.).

Aerospace Medicine, vol. 40, June 1969, p. 610-614. 15 refs.
NASA Contract No. R-104.

Pre- and postflight leukocyte chromosome aberration analyses were carried out on the Gemini astronauts. No large chromosomal effects of spaceflight were demonstrated. The small postflight increases in aberration levels observed after some of the missions could not be correlated with flight duration, isotope injection, or extravehicular activity. (Author)

A69-33746 *

CHANGES IN GROWTH AND BODY COMPOSITION OF MICE EXPOSED TO CHRONIC CENTRIFUGATION.

Lanny C. Keil (NASA, Ames Research Center, Environmental Biology Div., Moffett Field, Calif.).

Growth, vol. 33, 1969, p. 83-88. 14 refs.

Mature and weanling mice were centrifuged at 4.7 g for one and two months. After centrifugation, the animals were sacrificed, and their body composition was determined and compared to that of noncentrifuged controls. Centrifuged animals showed a significant reduction in body mass and body fat. Differences in water and protein content between the control and experimental animals may be due to a repression of growth imposed by centrifugation. Increases were seen in the total body calcium of the weanling males, while centrifuged females showed a reduction in calcium after two months of centrifugation. (Author)

A69-35291 *

EFFECT OF SALTS AND ORGANIC SOLVENTS ON THE ACTIVITY OF HALOBACTERIUM CUTIRUBRUM CATALASE.

Janos K. Lanyi and Joann Stevenson (NASA, Ames Research Center, Exobiology Div., Moffett Field, Calif.).

Journal of Bacteriology, vol. 98, May 1969, p. 611-616. 11 refs.

Observation that catalase in extracts of the extreme halophile Halobacterium cutirubrum exhibits up to threefold stimulation by 0.5 to 1.5 M monovalent salts and by 0.1 M divalent salts, while inhibition of enzyme activity occurs at higher concentrations. The inhibitory effect, and to some extent the stimulation, is salt-specific; the effectiveness of a salt in inhibiting enzyme activity depends on both cation and anion. Aqueous solutions of ethylene glycol, glycerol, and dimethyl sulfoxide containing no ions influence enzyme activity in the same manner as do salts. F.R.L.

A69-35976 *

CONVERSION OF ACETATE-2-^{14}C TO $^{14}CO_2$ AND ^{14}C-FATTY ACIDS IN THE PARTIALLY HEPATECTOMIZED RAT (33627).

E. D. Neville, K. S. Talarico, and D. D. Feller (NASA, Ames Research Center, Environmental Biology Div., Moffett Field, Calif.).

Society for Experimental Biology and Medicine, Proceedings, vol. 130, 1969, p. 643-651. 17 refs.

Results of an experiment in which 67% of the liver of male rats was removed to determine the relationship of the changes occurring in the oxidation of acetate to changes in fatty acid synthesis. Control rats were exposed to sham surgery, in which the liver was removed, handled, and returned intact to the abdominal cavity. The liver weight and fatty acid content of the liver at various times after surgery are compared for the two groups. The results suggest that in addition to deposition via transport, the fatty acid content of the regenerating liver is increased by synthesis in situ, during the premitotic phase as well as the mitotic phase. B.H.

A69-36458 *

CHANGES IN PERCEIVED SIZE OF HIGH LUMINANCE TARGETS.

Richard F. Haines (NASA, Ames Research Center, Moffett Field, Calif.).

Aerospace Medicine, vol. 40, July 1969, p. 754-758. 24 refs.

Investigation of the relationship between target luminance, shape, and size and its apparent size. Various diffuse white targets were foveally fixated by three highly trained male observers. Target luminances ranged from 0 to 13,000 foot Lamberts, and target sizes ranged from 39 min of arc to 2 deg, 35 min of arc in width. An unilluminated (black) background was used. The observer moved a point source of light behind the target along each of four meridians until it just disappeared at the target's apparent edge. An apparent expansion of the target occurred between the unilluminated and the illuminated conditions which averaged over 5 min of arc. However, when a filter was used across the entire field of view to reduce the luminance of the point source and the target by the same amount, no regular relationship was found between target luminance or size and its apparent size. All observers remarked that the square target appeared enlarged and quite round under high luminance conditions. Possible explanations for and applications of these data are given. (Author)

A69-37567 *

ATP ASSAY OF TERRESTRIAL SOILS—A TEST OF AN EXOBIOLOGICAL EXPERIMENT.

N. H. MacLeod, E. W. Chappelle, and A. M. Crawford (NASA, Goddard Space Flight Center, Greenbelt, Md.).

Nature, vol. 223, July 19, 1969, p. 267, 268. 13 refs.

Determination of the adenosine triphosphate (ATP) content of a variety of soils in order to define some of the problems associated with the measurement of ATP in soil-like material which may be encountered on Mars, for example. The ATP content of 25 terrestrial soil samples was estimated by the firefly luciferase assay, which is considered to be a feasible tool for exobiological work. ATP, the central molecule of bioenergetic reactions, occurs in all terrestrial organisms. F.R.L.

A69-37577 *
NEW OBSERVATIONS ON THE SUBSTRATE SPECIFICITY OF CATHEPSIN C (DIPEPTIDYL AMINOPEPTIDASE I) INCLUDING THE DEGRADATION OF β-CORTICOTROPIN AND OTHER PEPTIDE HORMONES.
J. Ken McDonald, Benjamin B. Zeitman, Thomas J. Reilly, and Stanley Ellis (NASA, Ames Research Center, Environmental Biology Div., Moffett Field, Calif.).
Journal of Biological Chemistry, vol. 244, May 25, 1969, p. 2693-2709. 65 refs.

Experimental investigation of the substrate specificity of cathepsin C derived from rat liver. It was found that, compared to bovine spleen cathepsin C in acrylamide gel electrophoresis, the rat liver enzyme behaved as a more acidic protein, and showed evidence of a polymeric structure as indicated by its apparent dissociation to subunits in the presence of sodium dodecyl sulfate. M.M.

A69-37612
LIFE SCIENCES AND SPACE RESEARCH VII; COSPAR, PLENARY MEETING, 11TH, OPEN MEETING OF WORKING GROUP V AND SYMPOSIUM ON BIOLOGICAL EFFECTS OF RADIATION IN SPACE, TOKYO, JAPAN, MAY 14-16, 1968 AND MAY 10, 1968, PROCEEDINGS.
Meeting and symposium co-sponsored by the International Union of Biochemistry, the International Union of Biological Sciences, the International Union of Physiological Sciences, and the International Union of Pure and Applied Biophysics.
Edited by Wolf Vishniac (Rochester, University, Rochester, N.Y.) and F. G. Favorite.
Amsterdam, North-Holland Publishing Co., 1969. 220 p.
$14.10.

CONTENTS:

PREFACE. W. Vishniac (Rochester, University, Rochester, N.Y.) and F. G. Favorite, p. v, vi.

COMPARATIVE METHODOLOGY FOR STUDY OF NONTERRESTRIAL LIFE.

RISK AND YIELD—A COMPARISON OF EXOBIOLOGICAL TECHNIQUES. W. Vishniac (Rochester, University, Rochester, N.Y.), p. 1.

A COMPARATIVE EVALUATION OF METHODS FOR THE SEARCH FOR LIFE ON MARS. A. A. Imshenetskii (Akademiia Nauk SSSR, Institut Mikrobiologii, Moscow, USSR), p. 2-8. (For abstract see issue 15, page 2857, Accession no. A68-31989)

CONTAMINATION AND STERILIZATION.

THE EFFECTS OF HIGH INTENSITY VISIBLE AND ULTRAVIOLET LIGHT ON THE DEATH OF MICROORGANISMS. C. O. Chichester and W. A. Maxwell (California, University, Davis, Calif.), p. 11-18. 9 refs. (See A69-37613 20-04)

RELEASE OF MICROBIAL CONTAMINATION FROM FRACTURED SOLIDS. N. J. Petersen (U.S. Public Health Service, Phoenix, Ariz.), R. G. Cornell (Florida State University, Tallahassee, Fla.), and J. R. Puleo (U.S. Public Health Service, Cape Kennedy, Fla.), p. 19, 20. (See A69-37614 20-04)

DISCUSSION OF A POSSIBLE CONTAMINATION OF SPACE WITH TERRESTRIAL LIFE. H. Bücker and G. Horneck (Frankfurt, Universität, Frankfurt am Main, West Germany), p. 21-27. 9 refs. (See A69-37615 20-04)

POTENTIAL EFFECTS OF RECENT FINDINGS ON SPACECRAFT STERILIZATION REQUIREMENTS. S. Schalkowsky, R. C. Kline (Exotech, Inc., Washington, D.C.), and L. B. Hall (NASA, Washington, D.C.), p. 28.

METEORITES.

ORGANIC GEOCHEMICAL INVESTIGATIONS IN RELATION TO THE ANALYSES OF RETURNED LUNAR ROCK SAMPLES. B. Nagy and H. C. Urey (California, University, La Jolla, Calif.), p. 31-46. 20 refs. (See A69-37616 20-04)

RESULTS OF RECENT BIOLOGICAL EXPERIMENTS IN SPACE FLIGHT.

BIOSATELLITE II MISSION. O. E. Reynolds (NASA, Washington, D.C.), p. 49-61. (For abstract see issue 15, page 2861, Accession no. A68-31978)

EFFECTS OF RADIATION DURING SPACE FLIGHT ON MICROORGANISMS AND PLANTS ON THE BIOSATELLITE II AND GEMINI XI MISSIONS. F. J. de Serres (Oak Ridge National Laboratory, Oak Ridge, Tenn.), p. 62-66. (See A69-37617 20-04)

SURVIVAL OF RNA AND DNA VIRUSES IN SPACE ON THE GEMINI XII SATELLITE. J. Hotchin, F. D. Baker, and L. Benson (New York State, Dept. of Health, Albany, N.Y.), p. 67, 68.

RADIATION-INDUCED CHROMOSOME ABERRATIONS AND RHYTHMS IN ROOTS OF GRAVITY-COMPENSATED VICIA. S. A. Gordon and E. M. Buess (Argonne National Laboratory, Argonne, Ill.), p. 69.

MUTATIONAL RESPONSES OF INSECTS IN THE BIOSATELLITE II EXPERIMENT. R. C. von Borstel, R. H. Smith, A. R. Whiting (Oak Ridge National Laboratory, Oak Ridge, Tenn.), D. S. Grosch (North Carolina State University, Raleigh, N.C.), L. S. Browning (William Marsh Rice University, Houston, Tex.), I. I. Oster (Bowling Green State University, Bowling Green, Ohio), J. V. Slater, and B. Buckhold (California, University, Berkeley, Calif.), p. 70-76. 12 refs. (See A69-37618 20-04)

BIOSATELLITE II—PHYSIOLOGICAL AND SOMATIC EFFECTS ON INSECTS. B. Buckhold (California, University, Berkeley, Calif.), p. 77-83. 6 refs. (See A69-37619 20-04)

WEIGHTLESSNESS EXPERIMENTS ON BIOSATELLITE II. B. F. Edwards (Emory University, Atlanta, Ga.), p. 84-92. (For abstract see issue 15, page 2723, Accession no. A68-31956)

RECIPROCITY IN GEOTROPIC RESPONSE AND ACCELERATION CONSTRAINTS OF THE BIOSATELLITES. J. S. Miller (Argonne National Laboratory, Argonne, Ill.), p. 93, 94. (See A69-37620 20-04)

GENETIC EFFECTS PRODUCED BY THE SPACE ENVIRONMENT. I. I. Oster (Bowling Green State University, Bowling Green, Ohio), p. 95, 96.

PHYSIOLOGICAL ADAPTIVE MECHANISMS OF MAN (AND ANIMALS) TO SPACE FLIGHT CONDITIONS.

STUDIES OF HUMAN ADAPTATION TO SPACE FLIGHT EFFECTS UNDER LOW-CALORIE DIET CONDITIONS. P. P. Ivanov, Iu. G. Nefiodov, A. S. Ushakov, L. I. Kakurin, K. A. Lariecheva, I. G. Vysotskii, and Iu. V. Latova, p. 99-101. (See A69-37621 20-04)

INTESTINAL HYDROGEN AND METHANE OF MEN FED SPACE DIET. D. H. Calloway and E. L. Murphy (California, University, Berkeley, Calif.), p. 102-109. (See A69-37622 20-05)

THE EFFECTS OF POSITIVE ACCELERATION ON THE CENTRAL NERVOUS SYSTEM. G. Mitarai, T. Nagasaka, S. Mori, and S. Takagi (Nagoya University, Nagoya, Japan), p. 110-120. (For abstract see issue 15, page 2719, Accession no. A68-31950)

REGENERATION LIFE SUPPORT SYSTEM.

CURRENT RESEARCH ON REGENERATIVE SYSTEMS. J. Shapira, A. D. Mandel, P. D. Quattrone, and N. L. Bell (NASA, Ames Research Center, Moffett Field, Calif.), p. 123-129. 11 refs. (See A69-37623 20-04)

THE PROBLEM OF STERILIZING A LIFE-SUPPORT SYSTEM IN BIOSATELLITE EXPERIMENTS OVER ONE YEAR. R. G. A. Lotz (Frankfurt, Universität, Frankfurt am Main, West Germany), p. 130-133. 5 refs. (See A69-37624 20-04)

OXYGEN SUPPLY AND CARBON DIOXIDE ABSORPTION IN LONG-TERM LIFE-SUPPORT SYSTEMS. R. G. A. Lotz and M. E. A. Fuchs (Frankfurt, Universität, Frankfurt am Main, West Germany), p. 134-137. (See A69-37625 20-04)

EXOBIOLOGY.

PHOTOSENSITIZING EFFECT OF CATIONS ON AMINO ACIDS AND PEPTIDES. N. P. Bogdanova and M. A. Khenokh, p. 141-148. 10 refs. (See A69-37626 20-04)

RESISTANCE OF THE PROTOZOON COLPODA MAUPASI TO MARTIAN CONDITIONS OF ATMOSPHERIC PRESSURE AND LOW PARTIAL PRESSURE OF OXYGEN. L. K. Lozina-Lozinskii and V. N. Bychenkova, p. 149-155. (See A69-37627 20-04)

SYMPOSIUM ON BIOLOGICAL EFFECTS OF RADIATIONS IN SPACE.

EARLY RESPONSE OF MAN TO WHOLE-BODY IONIZING RADIATION. D. Grahn (Argonne National Laboratory, Argonne, Ill.), p. 159.

CHARACTERISTICS OF BIOLOGICAL EFFECTS OF COSMIC RADIATION, MODEL INVESTIGATIONS. V. V. Parin, Iu. G. Grigoriev, E. E. Kovalev, N. I. Ryzhov, N. N. Derbeneva, V. I. Popov, and M. G. Petrovnin, p. 160-170. 7 refs. (See A69-37628 20-04)

STUDIES OF THE EFFECTS OF PHYSIOLOGICALLY DAMAGING DOSES OF RADIATION ON THE PERFORMANCE LEVEL OF TRAINED PRIMATES. J. F. Spalding, D. N. Farrer, and W. H. Langham (USAF, Aeromedical Research Laboratory, Holloman AFB, N. Mex.; California, University, Los Alamos, N. Mex.), p. 171, 172.

VESTIBULAR ANALYZER AS A CRITICAL ORGAN IN THE EVALUATION OF RADIATION HAZARDS DURING SPACE FLIGHTS. Iu. G. Grigoriev, p. 173-185. (For abstract see issue 15, page 2719, Accession no. A68-31952)

RBE VALUES FOR FAST NEUTRONS IN CONNECTION WITH ESTIMATES OF THE RADIATION BURDEN IN SPACE. E. H. Graul, H. Krüger, W. Rüther, and D. Piroth (Marburg, Universität, Marburg an der Lahn, West Germany), p. 186-194. 19 refs. (See A69-37629 20-04)

A RADIATION SOURCE FOR TESTING OPTICAL SOLAR RADIATION EFFECTS. W. Völker (Frankfurt, Universität, Frankfurt am Main, West Germany), p. 195-200. (See A69-37630 20-11)

PREDICTION OF INTERINDIVIDUAL DIFFERENCES IN RADIOSENSITIVITY IN MAMMALS. Y. Ueno (Kyoto University, Kyoto, Japan), p. 201-206. (For abstract see issue 15, page 2719, Accession no. A68-31969)

SOME RESULTS OF RADIOBIOLOGICAL STUDIES PERFORMED ON COSMOS-110 BIOSATELLITE. V. V. Antipov, N. L. Delone, M. D. Nikitin, G. P. Parfionov, and P. P. Sakhonov, p. 207-209.

INDEX OF AUTHORS, p. 210.

A69-37623 •

CURRENT RESEARCH ON REGENERATIVE SYSTEMS.

Jacob Shapira, Adrian D. Mandel, Phillip D. Quattrone, and Nancie L. Bell (NASA, Ames Research Center, Biotechnology Div., Moffett Field, Calif.).

IN: LIFE SCIENCES AND SPACE RESEARCH VII; COSPAR, PLENARY MEETING, 11TH, OPEN MEETING OF WORKING GROUP V AND SYMPOSIUM ON BIOLOGICAL EFFECTS OF RADIATION IN SPACE, TOKYO, JAPAN, MAY 14-16, 1968 AND MAY 10, 1968, PROCEEDINGS. (A69-37612 20-04)

Meeting and symposium co-sponsored by the International Union of Biochemistry, the International Union of Biological Sciences, the International Union of Physiological Sciences, and the International Union of Pure and Applied Biophysics.

Edited by Wolf Vishniac and F. G. Favorite.

Amsterdam, North-Holland Publishing Co., 1969, p. 123-129. 11 refs.

Summary of multiple studies directed toward the development of a regenerative life support system, showing that easily synthesized organic compounds and microbiological materials are potentially capable of being used as foods for long-duration space missions. The organic compounds presently believed to offer the greatest potential are glycerol, simple glycerol derivatives such as triacetin, and formose sugars. Laboratory studies indicate that glycerol can be synthesized from formaldehyde, which in turn is obtained by the direct catalytic oxidation of methane, a by-product of the Sabatier reaction used in spacecraft atmosphere control systems. Formose sugars are derived from the self-condensation of formaldehyde. Mixtures of glycerol and triacetin have been shown to be suitable as a major component of diets fed to weanling rats for prolonged periods. These compounds do not exist as stereoisomers and therefore offer advantages over the formose sugars. An automated system for the continuous autotrophic production of Hydrogenomonas eutropha bacteria is in operation, and the nutritional requirements for growth in the system using urea as a nitrogen source, are being studied. Nutritional evaluation of Hydrogenomonas bacteria has shown that they are capable of supplying the total protein requirement of growing rats for prolonged periods. The potential and problems of these regenerative systems and the prospects for the accomplishment of a totally regenerative food system will be discussed. (Author)

A69-39871 •

SENSITIVITY OF THE ADRENAL CORTICOSTERONE RESPONSE TO ACTH AS A FUNCTION OF TIME AFTER HYPOPHYSECTOMY.

Joan Vernikos-Danellis (NASA, Ames Research Center, Environmental Biology Div., Moffett Field, Calif.).

Endocrinology, vol. 84, June 1969, p. 1507, 1508. 5 refs.

Comparison of the sensitivity of the increase in adrenal corticosterone concentration in rats in response to ACTH at various time intervals after removal of the pituitary gland. The animals were most sensitive 2 and 4 hr after removal of the pituitary, and the sensitivity of this response decreased progressively at intervals of 12 hr or longer after hypophysectomy. (Author)

A69-40974 •

PRESSURE-DIAMETER RELATIONS OF CAPILLARIES AND SMALL BLOOD VESSELS IN FROG LUNG.

J. E. Maloney and B. L. Castle (NASA, Ames Research Center, Biotechnology Div., Moffett Field, Calif.).

Respiration Physiology, vol. 7, Aug. 1969, p. 150-162. 10 refs.

Static pressure-diameter measurements were made on the small pulmonary blood vessels of the frog lung, and the change in the septal area occupied by capillaries was investigated at intravascular pressures of 1 to 27 cm water. Over this pressure range, the smallest arteries (30 to 50 microns) increased their radius by 27 per cent, while the change for veins of the same size was 6 per cent. Medium size arteries and veins (50 to 150 microns) showed a similar pattern of increase in radius by 30 per cent, while the largest arteries (150 to 400 microns) increased their radius by 50 per cent, over the complete pressure range. Capillaries occupied 79 per cent of the alveolar septum at low intracapillary (1 cm water) pressures and less than 80.5 per cent at higher intracapillary pressures (27 cm water). These results indicate that the small arterial blood vessels of the lung are highly compliant and capable of large alterations in blood volume and resistance with changes in intravascular pressure. (Author)

A69-41077 •

STUDIES OF THE ELECTRON TRANSPORT CHAIN OF EXTREMELY HALOPHILIC BACTERIA. III--MECHANISM OF THE EFFECT OF SALT ON MENADIONE REDUCTASE.

Janos K. Lanyi (NASA, Ames Research Center, Exobiology Div., Moffett Field, Calif.).

Journal of Biological Chemistry, vol. 244, Aug. 10, 1969, p. 4168-4173. 12 refs.

Description of the effects of monovalent and divalent cations and of polyamines on the menadione reductase activity for the purpose of exploring the mechanism of the salt dependence of this enzyme. There is no menadione reductase activity in the absence of

salt. This activity increases with salt concentration to a maximum at 2 mol or higher concentrations of sodium chloride. The enzyme activity lost at low salt concentrations can be restored by adding 2 mol NaCl. Z.W.

A69-41404 *
COMPENSATORY HYPERTROPHY AND PHENYLETHANOLAMINE N-METHYL TRANSFERASE (PNMT) ACTIVITY IN THE RAT ADRENAL.
Roland D. Ciaranello, Jack D. Barchas, and Joan Vernikos-Danellis (Stanford University, Dept. of Psychiatry, Stanford; NASA, Ames Research Center, Moffett Field, Calif.).
Life Sciences, vol. 8, Apr. 1, 1969, p. 401-407. 9 refs.
NIH Grant No. HD-02881; Contract No. NR-102-715; Grant No. NGR-05-020-168.

Investigation of the hypothesis that physiological as opposed to pharmacological conditions (exogenous adrenocorticotrophic hormone) might raise adrenal PNMT further in nonhypophysectomized rats. The data obtained show that enzyme activity increases 1.5 times over sham operated controls 40 days after surgery. It is noted that the possibility exists that chronic low levels of pituitary-adrenal stimulation might be more effective in increasing enzyme activity than acute, high levels. P.G.

A69-42021 *
VIRUSLIKE PARTICLES IN THE FAT BODY, OENOCYTES, AND CENTRAL NERVOUS TISSUE OF DROSOPHILA MELANOGASTER IMAGOES.
D. E. Philpott, J. Weibel, H. Atlan, and J. Miquel (NASA, Ames Research Center, Moffett Field, Calif.).
Journal of Invertebrate Pathology, vol. 14, July 1969, p. 31-38. 7 refs.

A viruslike particle has been found in the nucleus of fat-body cells and oenocytes of *Drosophila melanogaster* imagoes 15, 76, and 91 days old. The particle has also been observed in glial cells of the cephalic ganglionic center of 91-day-old flies and in glial cells of 29-day-old flies that were exposed to 50 kr of gamma radiation when they were one day old. (Author)

A69-42701
CIRCADIAN RHYTHMS IN NONHUMAN PRIMATES; INTERNATIONAL CONGRESS OF PRIMATOLOGY, 2ND, SYMPOSIUM, EMORY UNIVERSITY, ATLANTA, GA., JULY 2, 1968, PROCEEDINGS.
Edited by F. H. Rohles (Kansas State University of Agriculture and Applied Science, Institute for Environmental Research, Manhattan, Kan.).
Basel, Switzerland, S. Karger AG (Bibliotheca Primatologica, No. 9), 1969. 136 p.
$7.90.

CONTENTS:

PREFACE. F. H. Rohles (Kansas State University of Agriculture and Applied Science, Manhattan, Kan.), p. IX, X.

ILLUMINATION INTENSITY AND BEHAVIORAL CIRCADIAN RHYTHMS. D. N. Farrer and J. W. Ternes (USAF, Systems Command, Holloman AFB, N.Mex.), p. 1-7. 7 refs. (See A69-42702 24-04)

CENTRAL NERVOUS, CARDIOVASCULAR AND METABOLIC DATA OF A MACACA NEMESTRINA DURING A 30-DAY EXPERIMENT. T. Hoshizaki, W. R. Adey, J. P. Meehan, D. O. Walter, J. I. Berkhout, and E. Campeau (California, University, Los Angeles, Calif.), p. 8-38. 11 refs. (See A69-42703 24-04)

SOCIAL ENTRAINMENT OF BIORHYTHMS IN RHESUS MONKEYS. F. H. Rohles and G. Osbaldiston (Kansas State University of Agriculture and Applied Science, Manhattan, Kan.), p. 39-51. 8 refs. (See A69-42704 24-04)

A BIGEMINUS PATTERN IN SOCIAL BEHAVIOR. J. S. Thach, Jr. (U.S. Navy, Naval Aerospace Medical Institute, Pensacola, Fla.), p. 52-63. 30 refs. (See A69-42705 24-04)

PHASE RELATIONSHIPS BETWEEN CIRCADIAN RHYTHMS AND PHOTOPERIODISM IN THE MONKEY. C. M. Winget (NASA, Ames Research Center, Moffett Field, Calif.), D. F. Rahlmann, and N. Pace (California, University, Berkeley, Calif.), p. 64-74. 12 refs. (See A69-42706 24-04)

CIRCADIAN VARIATIONS OF PHYSIOLOGICAL VARIABLES IN ISOLATED AND NON-ISOLATED MACACA NEMESTRINA. R. E. Smith (California, University, Davis, Calif.) and D. R. Wekstein (Kentucky, University, Lexington, Ky.), p. 75-90. 23 refs. (See A69-42707 24-04)

BIOLOGIC RHYTHM CORRELATES OF DISTURBED BEHAVIOR IN THE RHESUS MONKEY. C. F. Stroebel (Institute of Living Hospital, Hartford, Conn.), p. 91-105. 18 refs. (See A69-42708 24-04)

CIRCADIAN SYSTEM OF NONHUMAN PRIMATES—SUMMARY OF A SYMPOSIUM IN 1968 AND OF SOME EARLIER WORK. F. Halberg (Minnesota, University, Minneapolis, Minn.), p. 106-127. 30 refs. (See A69-42709 24-04)

A69-42706 *
PHASE RELATIONSHIPS BETWEEN CIRCADIAN RHYTHMS AND PHOTOPERIODISM IN THE MONKEY.
C. M. Winget (NASA, Ames Research Center, Environmental Biology Div., Moffett Field, Calif.), D. F. Rahlmann, and N. Pace (California, University, Dept. of Physiology, Berkeley, Calif.).
IN: CIRCADIAN RHYTHMS IN NONHUMAN PRIMATES; INTERNATIONAL CONGRESS OF PRIMATOLOGY, 2ND, SYMPOSIUM, EMORY UNIVERSITY, ATLANTA, GA., JULY 2, 1968, PROCEEDINGS. (A69-42701 24-04)
Edited by F. H. Rohles.
Basel, Switzerland, S. Karger AG (Bibliotheca Primatologica, No. 9), 1969, p. 64-74. 12 refs.

Study of the phase relationships of circadian rhythms of heart rate, locomotor activity, and deep body temperature (DBT) in unrestrained *Cebus albifrons* and *Macaca nemestrina* in response to photoperiods of various lengths. The primates were maintained unrestrained for relatively long periods (as long as 18 months). For each experiment, the animals were placed in individual cages in a relatively constant environment. The circadian rhythm of DBT was determined by hermetically sealed miniature radio transmitters implanted retroperitoneally on the right side of the abdominal cavity. Although the results do not indicate which physiological mechanisms are responsible for the circadian rhythms of DBT, locomotor activity, and heart rate in the nonhuman primates, they do show that the relationships involved are nonlinear. G.R.

A69-43369
INTERNATIONAL CONGRESS OF AEROSPACE MEDICINE, 18TH, AMSTERDAM, NETHERLANDS, SEPTEMBER 15-18, 1969, FREE COMMUNICATIONS.
The Hague, Inter Scientias, 1969. 578 p. In English and French.

CONTENTS:

THE EFFECT OF SUPERSONIC FLYING ON THE URINARY CATECHOLAMINE EXCRETION IN PILOTS. R. Debijadji, L. Perović, and V. Varagić (Institute of Aviation Medicine, Zemun, Yugoslavia), p. 5-12. 17 refs. (See A69-43370 24-04)

THE EFFECT OF POSITIVE PRESSURE BREATHING ON THE CEREBRAL CIRCULATION AND THE CONTENT OF CATECHOLAMINES IN HYPOTHALAMUS AND ADRENALS. R. I. Aleksandar, D. M. Jovan, and D. Vukosava (Institute of Aviation Medicine, Zemun, Yugoslavia), p. 15-27. 21 refs. (See A69-43371 24-04)

THE CENTRIFUGE AS A THERAPEUTIC DEVICE. R. Pelligra, S. Stein, J. Dickson, K. Skrettingland (NASA, Ames

Research Center, Moffett Field, Calif.), J. Markham, P. Lippe (NASA, Ames Research Center, Moffett Field; Stanford University, Stanford, Calif.), and J. Noyes (NASA, Ames Research Center, Moffett Field; O'Connor Hospital, San Jose, Calif.), p. 31-39, 41, 43 (7 ff.). (See A69-43372 24-04)

OCULOBULBAR VERGENCE CHANGES INDUCED BY M-1 VALSALVA MANEUVERS. L. M. Fenning, p. 61-77. 13 refs. (See A69-43373 24-04)

METHODS FOR THE STUDY OF THE BEHAVIOUR OF HUMAN CIRCADIAN RHYTHMS IN KIDNEY FUNCTION BEFORE, DURING AND AFTER GLOBAL FLIGHTS. F. Gerritzen, p. 81, 82. (See A69-43374 24-04)

OBSERVATION OF SOME CIRCULATORY REACTIONS AFTER CUMULATION OF VEGETATIVE STIMULI. Botka, Moučka, Horáček, and Novák, p. 87-91. (See A69-43375 24-04)

PITFALLS IN THE DIAGNOSIS OF LATENT DIABETES. G. F. Catlett and G. J. Kidera (United Air Lines, Inc., Chicago, Ill.), p. 95, 96.

F-5 COCKPIT FOGGING IN SOUTH VIETNAM. D. X. Giu (South Vietnamese Air Force, Saigon, South Vietnam), p. 99-102. (See A69-43376 24-05)

CARDIOLOGICAL REPORT AND FLYING PERSONNEL—THEIR MAIN DIFFICULTIES (EXPERTISE CARDIOLOGIQUE ET PERSONNEL NAVIGANT—SES PRINCIPALES DIFFICULTES). R. Carre, J. C. Richart, J. Salvagniac, and F. Plas, p. 105-107.

THE WOLFF-PARKINSON AND WHITE SYNDROME AND THE APTITUDE ON FLYING PERSONNEL (SYNDROME DE WOLFF-PARKINSON ET WHITE ET APTITUDE AU PERSONNEL NAVIGANT). R. Carre, J. C. Richart, J. Salvagniac, and F. Plas, p. 111-113.

COMMENTS ON ICAO RECOMMENDATIONS CONCERNING HEARING REQUIREMENTS FOR FLIGHT PERSONNEL (A PROPOS DES RECOMMANDATIONS DE L'O.A.C.I. SUR LES NORMES AUDITIVES DU PERSONNEL NAVIGANT TECHNIQUE). J. Pasquet and J. Lavernhe (Compagnie Nationale Air France, Paris, France), p. 117-122. (See A69-43377 24-05)

PSYCHOTHERAPY AND CHEMOTHERAPY IN AVIATION MEDICINE (PSYCHOTHERAPIES ET CHIMIOTHERAPIES EN MEDECINE AERONAUTIQUE). C. J. Blanc and R. J. Digo (Compagnie Nationale Air France, Paris, France), p. 125-131. (See A69-43378 24-04)

THE ROLE OF RADIOLOGY IN MEDICAL INVESTIGATIONS AFTER EJECTION OF MILITARY JET PILOTS (LA PART DE LA RADIOLOGIE DANS L'ENQUETE MEDICALE APRES EJECTION DES PILOTES MILITAIRES D'AVIONS A REACTION). R.-P. Delahaye, G. Gueffier, H. Seris, and R. Auffret, p. 135-150. (See A69-43379 24-04)

HUMAN RESISTANCE TO ACCELERATIONS OF HIGH INTENSITY AND SHORT DURATION—MECHANICAL AND CIRCULATORY EFFECTS (RESISTANCE DU CORPS HUMAIN AUX ACCELERATIONS ELEVEES DE COURTE DUREE—EFFETS MECANIQUES ET HEMODYNAMIQUES). R. Auffret, H. Seris, J. Demange, and R. P. Delahaye, p. 153-162. 12 refs. (See A69-43380 24-04)

THE EFFECTS OF MILD ACUTE PHYSICAL STRESS ON DELIVERY AND NEONATAL MORTALITY IN RATS. M. F. Foley, C. R. Huie, and C. E. Billings, p. 165-168. (See A69-43381 24-04)

HEAT TOLERANCE IN THE CASE OF VENTILATION FAILURE IN A SUPERSONIC TRANSPORT AIRCRAFT (TOLERANCE A LA CHALEUR DANS LE CAS DE PANNE DE LA CLIMATISATION SUR AVION DE TRANSPORT SUPERSONIQUE). J. Colin, C. Boutelier, and J. Timbal (Centre d'Essais en Vol, Brétigny-sur-Orge, Essonne, France), p. 171-179. 7 refs. (See A69-43382 24-05)

IN-FLIGHT MEDICAL DISORDERS IN THE FRENCH AIR FORCE—ANALYTICAL STUDY FROM 1961 TO 1968 (LES MALAISES EN VOL DANS L'ARMEE DE L'AIR FRANCAISE—ETUDE ANALYTIQUE DE 1961 A 1968). P. Pesquies, P. M. Pingannaud, J. Nathie, and J. Borsarello, p. 183-191. (See A69-43383 24-05)

SCIENCE AND COMMUNICATION (AS APPLIED TO AEROSPACE MEDICINE). L. van der Reis, p. 195, 196.

A SPECIFIC PHYSICAL TRAINING AND THE ACCELERATION TOLERANCE LEVEL. Z. Jethon, P. Stechni, and L. Zaleski (Wojskowy Instytut Medycyny Lotniczej, Warsaw, Poland), p. 199, 200.

INFLUENCE OF ALTITUDE ON HUMAN HEAT EXCHANGE (INFLUENCE DE L'ALTITUDE SUR LES ECHANGES THERMIQUES DE L'HOMME). J. Timbal, J. Colin, and Ch. Boutelier (Centre d'Essais en Vol, Brétigny-sur-Orge, Essonne, France), p. 203-210. 7 refs. (See A69-43384 24-04)

OSCILLATIONS IN EXPIRATORY GAS FLOW DURING PERFORMANCE OF FORCED VITAL CAPACITY. D. H. Glaister (Royal Air Force, Farnsborough, Hants., England), p. 213-215.

EFFECTS OF PROLONGED POSITIVE ACCELERATIONS (+3 G_z) ON THE VARIATIONS OF HUMAN CARDIAC OUTPUT (EFFETS DES ACCELERATIONS POSITIVES PROLONGEES (+3 Gz) SUR LES VARIATIONS DU DEBIT CARDIAQUE HUMAIN). J. M. R. Demange (Centre d'Essais en Vol, Brétigny-sur-Orge, Essonne, France), p. 219-227. (See A69-43385 24-04)

A STUDY OF SIMULATED AIRLINE PILOT INCAPACITATION. C. R. Harper, G. J. Kidera, and J. F. Cullen (United Air Lines, Inc., Chicago, Ill.), p. 231-243. (See A69-43386 24-05)

CIRCADIAN PERIODICITY OF REACTION-TIMES. J. C. Aschoff (Ulm, University, Ulm, West Germany), p. 247-254. (See A69-43387 24-04)

FREQUENCY OF URINARY LITHIASIS AMONG AIRCREWS (LITHIASE URINAIRE ET PERSONNEL NAVIGANT). R. Pannier, G. Leguay, and A. Didier (Ministère des Armées, Versailles, France), p. 257-270. (See A69-43388 24-04)

HYPERCAPNIA IN AIR CREWS (L'HYPERVENTILATION DANS LE PERSONNEL NAVIGANT). R. Pannier, G. Leguay, A. Didier, and A. Sarrazin (Ministère des Armées, Versailles, France), p. 273-275.

HYPNOTICS AND JET-AGE TRAVEL. J. Snyder (Hoffmann-La Roche, Inc., Nutley, N.J.), p. 279-284. 15 refs. (See A69-43389 24-05)

NORMS FOR QUANTITATIVE VECTORCARDIOGRAPHY WITH SPECIAL EMPHASIS ON THE MEDICAL EVALUATION OF FLYING PERSONNEL. P. Rijlant, I. Ruttkay, J. Cernohorsky, and A. Allard, p. 287-292. 9 refs. (See A69-43390 24-05)

RECENT EXAMINATIONS ON PULSE-WAVE-VELOCITY AND ITS SIGNIFICANCE IN AVIATION MEDICINE. H. W. Kirchhoff and K. Burkhart (Bundesministerium der Verteidigung, Fürstenfeldbruck, West Germany), p. 295, 296.

MEDICAL WASTAGE OF MILITARY AND CIVIL AIRCREW IN GREAT BRITAIN 1963-68. G. Bennett (Board of Trade, London, England) and P. J. O'Connor (Royal Air Force, Farnborough, Hants., England), p. 299-305. (See A69-43391 24-05)

PREVENTION OF FOOD-BORN DISEASES IN CIVIL AVIATION. D. A. A. Mossel and J. Hoogendoorn, p. 309-313. (See A69-43392 24-05)

BRAZILIAN AIR FORCE MEDICAL SERVICES. W. de Oliveira Freitas (Brazilian Air Force, Rio de Janeiro, Brazil), p. 317-330.

UNSCHEDULED LANDINGS FOR MEDICAL REASONS—A FIVE-YEAR SURVEY OF THE EXPERIENCE AT AMERICAN AIRLINES. V. Schocken and L. G. Lederer, p. 333-339. (See A69-43393 24-05)

EVALUATION OF THE THERAPEUTIC VALUE OF DIMETHYL SULFOXIDE (DMSO) IN ACUTE STRAINS AND SPRAINS, BURSITIS, AND TENDONITIS, BY DOUBLE BLIND CLINICAL INVESTIGATION. J. H. Brown, p. 343, 344.

INVESTIGATION ON THE DISPLACEMENT OF PLASMA PROTEINS OF RATS BLOOD WHEN EXPOSED TO THE INFLUENCE OF ACCELERATIONS AND HYPOKINESIA. B. Stanislaw and W. Mieczyslaw (Wojskowy Instytut Medycyny Lotniczej, Warsaw, Poland), p. 347-349.

OCULAR HOMOEOSTASIS IN HYPERBARIC CIRCUMSTANCES AT HIGH ALTITUDES (L'HOMEOSTASIE OCULAIRE EN L'HYPOBARISME DES GRANDES ALTITUDES). M. P. Popescu (Medico-Pharmaceutical Institute, Bucharest, Rumania), p.

353, 354.

A MINIATURIZED PUMP OXYGENERATOR FOR EVALUATION OF PERIPHERAL CIRCULATORY CHANGES INDUCED BY LONGTERM WEIGHTLESSNESS IN RATS. V. Popovic and P. Popovic (Emory University, Atlanta, Ga.), p. 357-360. (See A69-43394 24-05)

ELECTRONEURAL METHOD FOR SEDATION AND SLEEP IN AVIATION MEDICINE. S. A. Ziemnowicz-Radvan (Brain Research Foundation, Washington, D.C.), p. 363, 364.

CHINA'S LEGACY TO THE EXPLORATION OF SPACE. C. D. J. Generales, Jr., p. 367-397.

PSYCHIATRICAL AND PSYCHOLOGICAL APPROACH. H. Gartmann, p. 401-407. 6 refs. (See A69-43395 24-05)

MEDICAL PROBLEMS IN SPACE. D. E. Busby (Continental Air Lines, Inc., Los Angeles, Calif.), p. 411-418. (See A69-43396 24-05)

THE SPINAL COLUMN OF PILOTS AND THE SEAT. de Sambucy and G. Clerc, p. 421, 422.

EXOBIOLOGY. A. W. Schwarz (Nijmegen, Catholic University, Nijmegen, Netherlands), p. 425, 426.

BACTERIAL ACTIVITY IN LOW AMBIENTAL PRESSURE. F. M. Merayo, p. 429-437. 20 refs. (See A69-43397 24-04)

FACTORS INFLUENCING THE TIME OF SAFE UNCONSCIOUSNESS (TSU) FOR COMMERCIAL JET PASSENGERS FOLLOWING CABIN DECOMPRESSION. J. G. Gaume (McDonnell Douglas Corp., Long Beach, Calif.), p. 447-457. 5 refs. (See A69-43398 24-05)

EVALUATION OF THE SKIAGRAM. F. Rempt, J. Hoogerheide, and W. P. H. Hoogenboom (National Aeromedical Centre, Soesterberg, Netherlands), p. 461-464. (See A69-43399 24-04)

ACQUIRED MYOPIA IN YOUNG PILOTS. J. Hoogerheide, F. Rempt, and W. P. H. Hoogenboom (National Aeromedical Centre, Soesterberg, Netherlands), p. 467-470. (See A69-43400 24-04)

LAMBDA WAVES IN EEG OF NORMAL ADULTS AND THEIR RELATION TO COMPLEXITY OF VISUAL IMAGERY. D. N. J. Donker (National Aeromedical Centre, Soesterberg, Netherlands) and J. F. Smits (Utrecht, State University, Utrecht, Netherlands), p. 473-478. (See A69-43401 24-04)

THE PROBLEM OF AMOEBIASIS AMONG FOREIGN CREW IN SOUTHEAST ASIA, p. 481-484.

U.S. AIRCRAFT HIJACKINGS–EPIDEMIOLOGICAL CONSIDERATIONS, p. 487, 488.

BASIC STUDIES ON HIRUDO MEDICINALIS FOR A SPACE EXPERIMENT. I. R. G. A. Lotz, M. E. A. Fuchs, and P. E. A. Moyat (Frankfurt, Universität, Frankfurt am Main, West Germany), p. 491-498. 9 refs. (See A69-43402 24-04)

BASIC STUDIES ON HIRUDO MEDICINALIS FOR A SPACE EXPERIMENT. II. R. G. A. Lotz and G. H. Bowman (Frankfurt, Universität, Frankfurt am Main, West Germany), p. 501-507. (See A69-43403 24-04)

THE URINARY EXCRETION OF HORMONAL METABOLITES BEFORE, DURING AND AFTER INTERCONTINENTAL FLIGHTS. Th. Strengers (O. L. Vr. Gasthuis, Amsterdam, Netherlands), p. 511-514. 5 refs. (See A69-43404 24-04)

REDUCTION OF THE OXYGEN CONSUMPTION DURING ANOXIA (ABAISSEMENT DE LA CONSOMMATION D'OXYGENE AU COURS DE L'ANOXIE). M.-V. Strumza and D. Zaoui (Paris, Université, Paris, France), p. 517.

SELECTIVE G-FORCE APPLICATION IN THE TREATMENT OF RETINAL DETACHMENT. J. ten Doesschate, R. Hoppenbrouwers, and M. P. Lansberg (National Aeromedical Centre, Soesterberg, Netherlands), p. 521-525. (See A69-43405 24-04)

THE RELATIONSHIP BETWEEN SOME PHYSIOLOGICAL AND PSYCHOLOGICAL VARIABLES. L. Pannekoek and L. K. F. Njio, p. 529-531. (See A69-43406 24-04)

CIRCADIAN RHYTHM AND PERFORMANCE. M. v. Zoeren, J. H. H. Thijssen, and L. Pannekoek (National Aeromedical Centre, Soesterberg, Netherlands), p. 535-539. (See A69-43407 24-04)

A PECULIAR CLINICAL CASE BOTH OF HYPOXIA AND HYPOTHERMIA STUDIED IN A 18 YEARS OLD STOWAWAY FROM HABANA TO MADRID. J. M. Pajares (Gran Hospital; Madrid, University, Madrid, Spain), p. 543, 544.

PECULIARITIES OF THE RESPONSE OF THE ACOUSTIC ANALYZER OF MAN DURING PROLONGED NOISE EFFECT IN A YEAR-LONG MEDICO-ENGINEERING EXPERIMENT. T. N. Krupina, E. I. Mantsev, V. Ya. Levanov, M. A. Vytchikova, and I. Ya. Yakovleva, p. 547-549. (See A69-43408 24-05)

GROUP PSYCHOPHYSIOLOGICAL METHODS OF SELECTION AND RECRUITMENT OF FLYING CREWS. M. A. Novikov and A. A. Gerasimovich, p. 553, 554.

PHARMACOLOGICAL CORRECTION OF CHANGES IN WATER-SALT AND PROTEIN METABOLISM DURING A 120-DAY BED REST EXPERIMENT. T. N. Krupina, G. P. Mikhailovsky, M. M. Korotaev, E. I. Sokolov, A. Ya. Tizul, Z. P. Pak, V. P. Bychkov, and I. Ya. Yakovleva, p. 557, 558.

METHODS OF RECORDING PHYSIOLOGICAL PARAMETERS DURING SOYUZ SPACE FLIGHTS. L. I. Kakurin, I. S. Shadrintsev, and A. G. Zerenin, p. 561.

DYNAMIC RESPONSE OF THE HUMAN CENTRAL NERVOUS SYSTEM TO THE EFFECTS OF CLOSED VOLUME AND HYPOKINESIA. E. V. Kukolevskaya, p. 565, 566.

DIAGNOSTICS OF EARLY FORMS OF ATHEROSCLEROSIS AND LATENT CORONARY INSUFFICIENCY IN FLIGHT CREWS. B. L. Gelman, I. M. Pishugin, G. L. Strongin, L. I. Kuznetsova, and A. A. Shishova, p. 569.

MEDICAL QUESTIONS IN THE ACTIVITY OF TECHNICAL PERSONNEL OF CIVIL AVIATION. V. V. Levashov, p. 573, 574.

PREFLIGHT MEDICAL INSPECTION OF FLIGHT CREWS. A. I. Kraftsov and G. N. Druzhinina, p. 577, 578.

A69-43372 * #

THE CENTRIFUGE AS A THERAPEUTIC DEVICE.

R. Pelligra, S. Stein, J. Dickson, K. Skrettingland (NASA, Ames Research Center, Moffett Field, Calif.), J. Markham, P. Lippe (NASA, Ames Research Center, Moffett Field; Stanford University, Stanford, Calif.), and J. Noyes (NASA, Ames Research Center, Moffett Field; O'Connor Hospital, San Jose, Calif.).

IN: INTERNATIONAL CONGRESS OF AEROSPACE MEDICINE, 18TH, AMSTERDAM, NETHERLANDS, SEPTEMBER 15-18, 1969, FREE COMMUNICATIONS. (A69-43369 24-04)

The Hague, Inter Scientias, 1969, p. 31-39, 41, 43 (7 ff.).

Description of a therapeutic application of centrifugation by which a 10 by 6 by 4 mm bullet fragment floating freely in the ventricular system of the human brain was moved to a fixed safe position where it was embedded in the posterolateral wall of the left lateral ventricle. The patient was briefly exposed to increased accelerations in a centrifuge with five degrees of freedom at the NASA Ames Research Center. He has remained symptom-free without an apparent neurological deficit over a period of six months following this procedure. V.Z.

A69-43565 *

EFFECTS OF HYPEROXIA AND HYPOXIA ON MITOSIS IN THE NORMAL AND REGENERATING RAT LIVER.

K. S. Talarico, D. D. Feller, and E. D. Neville (NASA, Ames Research Center, Environmental Biology Div., Moffett Field, Calif.).

Society for Experimental Biology and Medicine, Proceedings, vol. 131, 1969, p. 430-434. 9 refs.

Demonstration of the effects of hyperoxia and hypoxia on mitotic activity in the regenerating and normal rat liver by exposing partially hepatectomized and unoperated rats to hyperoxic and normobaric, hyperoxic and hypobaric, normoxic and hypobaric, and hypoxic and hypobaric environments. When exposed to 100 per cent oxygen at various pressures for various time periods up to 34 hr, no change was noted in the animals. When exposed to a hypoxic condition (air, 380 mm Hg) for the same time periods, the partially hepatectomized group showed a delay in the initiation of mitosis, while the unoperated group showed a reduction in mitotic activity due to the hypoxic environment. F.R.L.

04 BIOSCIENCES

A69-43750 *
SYNTHESIS OF ACYCLIC ISOPRENOIDS BY THE γ-IRRADIATION OF ISOPRENE.
Colin Munday, Katherine Pering, and Cyril Ponnamperuma (NASA, Ames Research Center, Exobiology Div., Moffett Field, Calif.).
Nature, vol. 223, Aug. 23, 1969, p. 867, 868. 18 refs.

Discussion of experiments in which it was shown that branched chain acyclic polymers can be produced from isoprene under plausible geochemical conditions. Two series of experiments were conducted. In the first, isoprene was irradiated by cobalt 60 gamma rays in sealed tubes. In the second, isoprene was adsorbed onto the surface of vermiculite before irradiation. The products were then extracted from the vermiculite with 10 ml of freshly distilled isoprene. Excess solvent was removed under vacuum. A portion of the products of each series was hydrogenated in hexane at atmospheric pressure, using hydrogen with 5 per cent palladium as a catalyst. The products before and after hydrogenation were analyzed by gas chromatography and mass spectrometry. Parallel studies of the isoprene and the vermiculate before irradiation showed that they were free of the compounds sought. V.P.

N69-10444*# National Aeronautics and Space Administration, Washington, D. C.
BIOLOGY OF HARD TISSUE
Ann M. Budy, ed. 1968 399 p refs Proc. of Conf. Held at Pacific Palisades, Calif., 6–9 Mar. 1966
(NASA-SP-161) Avail: SOD $1.75; CFSTI CSCL 06C

CONTENTS:
1. HOMEOSTASIS OF CALCIUM p 13–82 (See N69-10445 01-04)
2. LOCAL (NONHORMONAL) FACTORS CONTROLLING BONE RECONSTRUCTION p 83–133 (See N69-10446 01-04)
3. CELLULAR DIFFERENTIATION IN BONE p 135–204 (See N69-10447 01-04)
4. SYSTEM DISEASES OF BONE p 205–254 (See N69-10448 01-04)
5. GENERAL SESSION 1 p 255–326 (See N69-10449 01-04)
6. GENERAL SESSION 2 p 327–357 (See N69-10450 01-04)

N69-11056*# National Aeronautics and Space Administration. Langley Research Center, Langley Station, Va.
A MICRO LAGOON TECHNIQUE FOR THE CULTURE AND OBSERVATION OF ISOLATED MAMMALIAN CELLS
Clarence D. Cone, Jr. and Kathryn M. Peddrew Washington Nov. 1968 26 p refs
(NASA-TN-D-4906) Avail: CFSTI CSCL 06A

A technique for physically partitioning a monolayer of cells into micro regions on a culturing surface is described. The method consists of forming a thin grease layer into a field of tiny ponds or lagoons in which small numbers of cells or other microbiological specimens can be confined for purposes of growth, manipulation, and microscopic observation. Special instruments and procedures which have been developed for lagoon-field formation are described in detail, as are the characteristics of various formation materials which have been evaluated. Factors and problems affecting various aspects of lagoon-field suitability for cytological purposes are discussed, and the details of special culturing vessels and lagoon-inoculation procedures which have been developed by the authors for particular types of experiments are presented. A number of cytological applications, particularly in the field of time-lapse cinephotography, in which the technique has proven to be exceptionally valuable are outlined. The basic micro lagooning techniques described have considerable flexibility for adaptation and should thus prove to be useful for a wide range of cytological applications where simple micro isolation is a prime requirement. Author

N69-11695*# National Aeronautics and Space Administration. Washington, D. C.
AEROSPACE MEDICINE AND BIOLOGY: A CONTINUING BIBLIOGRAPHY WITH INDEXES
Oct. 1968 83 p refs
(NASA-SP-7011(55) Avail: CFSTI CSCL 06

Subject coverage concentrates on the biological, physiological, psychological, and environmental effects to which man is subjected during and following simulated or actual flight in the earth's atmosphere or in interplanetary space. References describing similar effects on biological organisms of lower order are also included. Such related topics as sanitary problems, pharmacology, toxicology, safety and survival, life support systems, exobiology, and personnel factors receive appropriate attention. Each entry consists of a standard citation accompanied by its abstract. Author

N69-12434*# Lovelace Foundation for Medical Education and Research, Albuquerque, N. Mex.
COMPENDIUM OF HUMAN RESPONSES TO THE AEROSPACE ENVIRONMENT. VOLUME 1: SECTIONS 1–6
Emanuel M. Roth, ed. Washington NASA Nov. 1968 506 p refs
(Contract NASr-115)
(NASA-CR-1205(I)) Avail: CFSTI CSCL 06S

CONTENTS:
1. MICROWAVE RADIATION E. M. Roth 26 p refs (See N69-12435 02-04)
2. LIGHT ENVIRONMENT: A. VISIBLE LIGHT. B. ULTRAVIOLET LIGHT E. M. Roth and S. Finkelstein 160 p refs (See N69-12436 02-04)
3. IONIZING RADIATION E. M. Roth 117 p refs (See N69-12437 02-04)
4. MAGNETIC FIELDS D. E. Busby 8 p refs (See N69-12438 02-04)
5. ELECTRIC CURRENT S. Finkelstein and E. M. Roth 23 p refs (See N69-12439 02-04)
6. THERMAL ENVIRONMENT T. A. Bottomley (Bellcomm. Inc.) and E. M. Roth 148 p refs (See N69-12440 02-04)

N69-12588*# Lovelace Foundation for Medical Education and Research, Albuquerque, N. Mex.
COMPENDIUM OF HUMAN RESPONSES TO THE AEROSPACE ENVIRONMENT. VOLUME 2: SECTIONS 7–9
Emanuel M. Roth, ed. Washington NASA Nov. 1968 507 p refs
(Contract NASr-115)
(NASA-CR-1205(II)) Avail: CFSTI CSCL 06S

CONTENTS:
1. ACCELERATION W. G. Teichner, R. L. Craig (Harvard School of Public Health), and E. M. Roth 222 p refs (See N69-12589 02-04)
2. VIBRATION A. N. Chambers (Bellcomm, Inc.) and E. M. Roth 95 p refs (See N69-12590 02-04)
3. SOUND AND NOISE A. N. Chambers (Bellcomm, Inc.) and E. M. Roth 83 p refs (See N69-12591 02-04)

N69-12592*# Lovelace Foundation for Medical Education and Research, Albuquerque, N. Mex.
COMPENDIUM OF HUMAN RESPONSES TO THE AEROSPACE ENVIRONMENT. VOLUME 3: SECTIONS 10–16
Emanuel M. Roth, ed. Washington NASA Nov. 1968 552 p refs
(NASr-115)
(NASA-CR-1205(III)) Avail: CFSTI CSCL 06S

CONTENTS:
1. OXYGEN-CO_2-ENERGY E. M. Roth 77 p refs

(See N69-12593 02-04)

2. INERT GAS E. M. Roth 40 p refs (See N69-12594 02-04)

3. PRESSURE E. M. Roth 40 p refs (See N69-12595 02-04)

4. CONTAMINANTS STANDARDS W. H. Teichner, A. O. Mirarchi (Harvard School of Public Health), and E. M. Roth 94 p refs (See N69-12596 02-04)

5. NUTRITION E. M. Roth 43 p refs (See N69-12597 02-04)

6. WATER E. M. Roth 27 p refs (See N69-12598 02-04)

7. ANTHROPOMETRY AND TEMPORO-SPATIAL ENVIRONMENT E. M. Roth 97 p refs (See N69-12599 02-04)

N69-12600*# Lovelace Foundation for Medical Education and Research, Albuquerque, N. Mex.

COMPENDIUM OF HUMAN RESPONSES TO THE AEROSPACE ENVIRONMENT. VOLUME 4: CONVERSION TABLES ALPHABETIC INDEX

Emanuel M. Roth, ed. Washington NASA Nov. 1968 188 p (Contract NASr-115)

(NASA-CR-1205(IV)) Avail: CFSTI CSCL 06S

Conversion tables are presented for the multiple systems of units and measures used in the basic biological, physical, and engineering sciences. Directions for the use of the tables are included. A.C.R.

N69-14387*# National Aeronautics and Space Administration, Washington, D. C.

AEROSPACE MEDICINE AND BIOLOGY

Nov. 1968 191 p

(NASA-SP-7011(56)) Avail: CFSTI CSCL 06

Subject coverage concentrates on the biological, physiological, psychological, and environmental effects to which man is subjected during and following simulated or actual flight in the earth's atmosphere or in interplanetary space. References describing similar effects on biological organisms of lower order are also included. Such related topics as sanitary problems, pharmacology, toxicology, safety and survival, life support systems, exobiology, and personnel factors receive appropriate attention. Each entry consists of a standard citation accompanied by its abstract. Author

N69-14860*# National Aeronautics and Space Administration, Washington, D. C.

NASA CONTRIBUTIONS TO BIOINSTRUMENTATION SYSTEMS—A SURVEY

Gershon Weltman, Moshe Klagsbrun, Donald Ukkestad, and Ben Ettelson 1968 101 p refs Prepared by Spacelabs, Inc.

(NASA-SP-5054) Avail: SOD $1.00; CFSTI CSLC 06B

Advances in bioinstrumentation devices and techniques achieved by the National Aeronautics and Space Administration are described to facilitate use of NASA contributions in medicine and the bioinstrumentation industry. Accordingly, the survey is directed largely toward two groups: those in medicine who plan, specify, and utilize advanced bioinstrumentation systems; and those in engineering who design, develop, and manufacture them. The objectives are to stress the correspondence between spaceflight and nonaerospace applications and to lay the groundwork for subsequent extrapolation of NASA's experiences by the reader. Five main areas of NASA bioinstrumentation system development are identified: (1) *Planning*—The techniques to establish information requirements and equipment specification for system development are outlined. (2) *Sensing and signal conditioning*—Detection of physiological signals under aerospace conditions and design of advanced electronic instrumentation to process and transmit these signals are discussed. (3) *Medical monitoring and data processing*—Significant NASA contributions to data processing, including acquisition techniques, computation of derived parameters, and methods of data display are included. (4) *Measurements in the field*—Solutions to some difficult problems of making laboratory-quality measurements in the field are treated. (5) *Manufacture*—NASA contributions to bioinstrumentation fabrication and quality assurance are presented. Author

N69-16537*# National Aeronautics and Space Administration, Washington, D. C.

AEROSPACE MEDICINE AND BIOLOGY A CONTINUING BIBLIOGRAPHY WITH INDEXES

Dec. 1968 187 p refs

(NASA-SP-7011(57)) Avail: CFSTI CSCL 06

The abstracts and annotated indexes were selected from those introduced into the NASA Information System during November 1968. The references were previously announced by the Library of Congress, the American Institute of Aeronautics and Astronautics, and NASA. Emphasis is placed on the biological, physiological, psychological, and environmental effects to which man is subjected during the following simulated or actual flight in the earth's atmosphere or in interplanetary space. A.L.

N69-17248*# National Aeronautics and Space Administration, Langley Research Center, Langley Station, Va.

MITOTIC SYNCHRONIZATION OF L-STRAIN FIBROBLASTS WITH 5-AMINOURACIL AS DETERMINED BY TIME-LAPSE CINEPHOTOGRAPHY

Clarence D. Cone, Jr. and Max Tongier, Jr. Washington Feb. 1969 28 p refs

(NASA-TN-D-5021) Avail: CFSTI CSCL 06A

A technique for producing mitotically synchronous cultures of L-strain fibroblasts by treatment with 5-aminouracil (an analog of thymine) is presented along with a detailed description of a procedure for determining the resulting degree of synchrony by use of time-lapse cinephotography. Several sets of representative experimental results illustrating the mitotic synchronization effectiveness of 5-aminouracil as determined by the time-lapse technique are presented and are interpreted on the basis of previous results for plant and animal cells. Basic effects on the validity of experimental results, caused by deviations of synchronized experimental cultures from ideal or perfect synchrony are also discussed, and a quantitative index for expressing the relative degree of synchrony attainable with various agents is defined. Author

N69-17782*# National Aeronautics and Space Administration, Langley Research Center, Langley Station, Va.

OSMOTICALLY INDUCED COALESCENCE OF SARCOMA CELLS THROUGH INTERCELLULAR BRIDGES IN VITRO

Clarence D. Cone, Jr., and Max Tongier, Jr. Washington Feb. 1969 24 p refs

(NASA-TN-D-5022) Avail: CFSTI CSCL 06R

A relatively detailed description is presented of a microtechnique by which cells possessing true intercellular bridges *in vitro* can be induced to coalesce into single mono- and multinucleate giant cells. The technique consists in the carefully controlled perfusion of a cell field with a hypotonic solution, which causes osmotic swelling and thereby induces connected cells to coalesce through expansion of the connecting bridge. Details of the perfusion system and methodology are discussed, along with the system of time lapse cinemicorgraphy used for recording the coalescence process. Principal features of an alternate coalescence technique utilizing a movable micropipet are also outlined. Representative photographic sequences reproduced from time lapse film recordings are presented to illustrate the basic nature of the coalescence phenomenon for the case of L-strain fibroblasts. An interpretation of the implications of coalescence in indicating cytoplasmic continuity of intercellular bridges, and other aspects of intercellular communication at the molecular level, is included.

Finally, a brief mention is made of several additional cytological applications of the osmotic swelling procedure. Author

N69-18722*# Bolt, Beranek, and Newman, Inc., Van Nuys, Calif.
COMBINATION EFFECTS OF TONE AND DURATION PARAMETERS ON PERCEIVED NOISINESS
Karl S. Pearsons Washington NASA Feb. 1969 49 p refs
(Contract NAS1-7461)
(NASA-CR-1283) Avail: CFSTI CSCL 06P

Three series of judgment tests were conducted to investigate the effects on perceived noisiness of tone content and duration parameters. Time patterns for the stimuli employed in the tests were triangular in shape to simulate aircraft flyover time histories. Stimuli for the first test included durations of 4, 12, and 32 seconds measured 10 dB below the maximum level of the stimulus. Tone-to-noise ratios in 1/3 octave bands for the stimuli at 2000 and 4000 Hz were varied to include 10 and 25 dB and no tone. In the second test stimuli included recordings of test stand turbofan engine noise using the same time history shape and durations mentioned above. The third test utilized pure-tone and broadband noise spectra like those used in the first Test, however, the duration of the tone differed from the duration of the noise, and the maximum level of the tone did not always occur at the same point in time as the maximum level of the noise. Author

N69-19023*# National Aeronautics and Space Administration, Washington, D. C.
AEROSPACE MEDICINE AND BIOLOGY: A CONTINUING BIBLIOGRAPHY WITH INDEXES, DECEMBER 1968
Jan. 1969 195 p refs
(NASA-SP-7011(58)) Avail: CFSTI CSCL 06

Subject coverage concentrates on the biological, physiological, psychological, and environmental effects to which man is subjected during and following simulated or actual flight in the earth's atmosphere or in interplanetary space. References describing similar effects on biological organisms of lower order are also included. Such related topics as sanitary problems, pharmacology, toxicology, safety and survival, life support systems, exobiology, and personnel factors receive appropriate attention. Each entry consists of a standard citation accompanied by its abstract. Author

N69-19115*# National Aeronautics and Space Administration. Langley Research Center, Langley Station, Va.
AN ANALYSIS OF THE OPERATION OF A MASS MEASURING SYSTEM IN AN ORBITING SPACECRAFT
Bruce A. Conway Washington Feb. 1969 29 p refs
(NASA-TN-D-5039) Avail: CFSTI CSCL 06B

An analysis of the operation of a mass measuring system, which is based on the oscillating spring mass principle, aboard a spacecraft is made. This analysis considers the dynamic effects of the oscillating device on an uncontrolled spacecraft by developing the equations of motion for the system. An approximate solution of these equations is then deduced, and a simple analytic expression for the maximum attitude error is found. Numerical integration of the equations of motion was performed on a digital computer for some typical measurement operations. Comparison between the approximate and exact solutions for these cases was very close. Results showed small (less than 0.02°) attitude errors arising from the operation of this device. Author

N69-19714*# National Aeronautics and Space Administration. Washington, D. C.
AEROSPACE MEDICINE AND BIOLOGY. A CONTINUING BIBLIOGRAPHY WITH INDEXES
Feb. 1969 198 p
(NASA-SP-7011(60)) Avail: CFSTI CSCL 06

Subject coverage is concentrated on biological, psychological, physiological, and environmental effects to which man is subjected during and following simulated or actual flight in the earth's atmosphere or in interplanetary space. References describing similar effects on biological organisms of lower order are included as well as such related topics as sanitary problems, pharmacology, toxicology, safety and survival, life support systems, exobiology, and personnel factors. Applied research is emphasized, but references to fundamental studies and theoretical principles related to experimental development also qualify for inclusion. Each entry is accompanied by its abstract. K.W.

N69-22637*# Systems Technology, Inc., Hawthorne, Calif.
DYNAMICS OF THE VESTIBULAR SYSTEM AND THEIR RELATION TO MOTION PERCEPTION, SPATIAL DISORIENTATION, AND ILLUSIONS
Richard A. Peters Washington NASA Apr. 1969 249 p refs
(Contract NAS2-3650)
(NASA-CR-1309; TR-168-1) Avail: CFSTI CSCL 06P

In piloting tasks, visual observation of instrument indicators and of the visual field and sensations of motion, provide the sensible signals upon which the pilot bases his control of the aircraft. Variations of the gravitational-inertial force environment during the flight of an aircraft affect the pilot's motion sensors in his vestibular system and through them affect his control of the vehicle, his visual process, and his sense of orientation. A study is made of the basic physiology of the human vestibular system and its interconnection with the oculomotor system. The dynamic functions of the semicircular canals and utricles (otolith organs) and the relation between subjective perceptions of motion and the accelerations which produce them are studied. Mathematical models of the dynamic functions of the vestibular system are presented. The various illusions experienced by pilots of aircraft are related to the accelerations which produce them and to the dynamics of the vestibular sensors involved. Author

N69-23126*# National Aeronautics and Space Administration, Washington, D. C.
AEROSPACE MEDICINE AND BIOLOGY: A CONTINUING BIBLIOGRAPHY WITH INDEXES
Mar. 1969 138 p refs
(NASA-SP-7011/61/) Avail: CFSTI CSCL 05B

Subject coverge concentrates on the biological, physiological, psychological, and environmental effects to which man is subjected during and following simulated or actual flight in the earth's atmosphere or in interplanetary space. References describing similar effects on biological organisms of lower order are also included. Such related topics as sanitary problems, pharmacology, toxicology, safety and survival, life support systems, exobiology, and personnel factors receive appropriate attention. Each entry consists of a standard citation accompanied by its abstract. Author

N69-24752*# National Aeronautics and Space Administration, Washington, D. C.
AEROSPACE MEDICINE AND BIOLOGY: A CUMULATIVE INDEX TO THE 1968 ISSUES OF A CONTINUING BIBLIOGRAPHY
Jan. 1969 882 p refs Supersedes SP-7011(47) through SP-7011(58); see N69-20026, N68-20027, N68-22882, N68-25844, N68-28246, N68-32707, N68-35069, N68-38051, N69-11695, N69-14387, N69-16537, N69-19023
(NASA-SP-7011(59); NASA-SP-7011(47); NASA-SP-7011(48) NASA-SP-7011(49); NASA-SP-7012(50); NASA-SP-7011(51); NASA-SP-7011(52); NASA-SP-7011(53); (NASA-SP-7011(54) NASA-SP-7011(55); NASA-SP-7011(56); NASA-SP-7011(57); NASA-SP-7011(58)) Avail: CFSTI CSCL 05B

A cumulative index of documents pertaining to the biological, psychological, and environmental effects to which man is subjected during and following simulated or actual flight in the earth's atmosphere or in interplanetary space is presented. References

describing similar effects on biological organisms of lower order are also included. Such related topics as sanitary problems, pharmacology, toxicology, safety and survival, life support systems, exobiology, and personnel factors receive appropriate attention. Author

N69-24822*# National Aeronautics and Space Administration. Washington, D. C.

AEROSPACE MEDICINE AND BIOLOGY. A CONTINUING BIBLIOGRAPHY WITH INDEXES, MARCH 1969

Apr. 1969 170 p refs

(NASA-SP-7011(62)) Avail: CFSTI CSCL 05B

Subject coverage concentrates on the biological, physiological, psychological, and environmental effects to which man is subjected during and following simulated or actual flight in the earth's atmosphere or in interplanetary space. References describing similar effects on biological organisms of lower order are also included. Such related topics as sanitary problems, pharmacology, toxicology, safety and survival, life support systems, exobiology, and personnel factors receive appropriate attention. Each entry consists of a standard citation accompanied by its abstract. Author

N69-29195*# National Aeronautics and Space Administration. Langley Research Center, Langley Station, Va.

A PROCESS FOR IMPRINTING MICRO LAGOON FIELDS IN PLASTIC SURFACES FOR USE IN CELL AND TISSUE CULTURE

Clarence D. Cone, Jr. and Edward N. Fleenor, Jr. Washington Jun. 1969 33 p refs

(NASA-TN-D-5255) Avail: CFSTI CSCL 06C

The process involved the fabrication of a metal impression die possessing a raised image anvil of the micro lagoon field on its surface, and the impressment of the heated die into the surface of suitable plastic vessels. Details of the die fabrication process are given, including the techniques used for photo transference of the basic lagoon-field image to the metal die surface and the development of the anvil imprint image on the die surface by chemical etching. The process used for imprinting the lagoon-field image into the plastic culturing surfaces of various culture vessel types is also described. Photomicrographs of typical lagoon fields formed by the process are presented, along with an analysis of factors in the die-fabrication process which affect the dimensional accuracy of the resulting lagoons. Time-lapse studies of actual cell growth in lagoons produced by the impression process, using L-strain fibroblasts, indicate that the lagoons are of excellent optical quality and are very effective in preventing both the escape of cells from the lagoons and the intrusion of external cells into the lagoons. Author

N69-29723*# National Aeronautics and Space. Ames Research Center, Moffett Field, Calif.

TOXICITY PROBLEMS IN PLASTIC HARDWARE DESIGNED FOR BIOLOGICAL SPACE-FLIGHT EXPERIMENTS

Richard Willoughby Washington Jun. 1969 7 p refs

(NASA-TM-X-1818) Avail: CFSTI CSCL 06C

In the development of hardware for biological space flight, various plastic materials were found to be toxic to sea urchin sperm and unfertilized eggs. Glass control chambers were not. Acrylic and polycarbonate plastics were tested as material for the hardware body, while fluorocarbon elastomer rubber, nitrile, three silicone rubbers, butyl rubber, and ethylene propylene were tested as O ring materials. Fertilized frog eggs were found to be compatible with ethylene propylene and acrylic plastic after careful treatment, principally outgassing by vacuum exposure, but no treatment was discovered which would sufficiently detoxify plastic hardware so that it would maintain sea urchin sperm and unfertilized eggs. Author

N69-31356*# Aztec School of Languages, Inc., Maynard, Mass. Research Translation Div.

COORDINATION OF THE VOLUNTARY MOVEMENTS OF MAN IN A ZERO GRAVITATIONAL FIELD (UNDER WEIGHTLESSNESS) [KOORDINATSIYA PROIZVOL'NYKH DVIZHENIY CHELOVEKA V NULEVOM GRAVITATSIONNOM POLE (V NEVESOMOSTI]

L. V. Chkhaidze Washington NASA Jul. 1969 34 p Transl. into ENGLISH of the book "Koordinatsiya Proizvol'nykh Dvizheniy Cheloveka v Usloviyakh Kosmicheskogo Poleta" Moscow, Nauka Press, 2d. ed., 1966

(Contract NASw-1692)

(NASA-TT-F-578) Avail: CFSTI CSCL 06S

The coordination of the voluntary movements of man in a zero gravitational field (weightlessness) is analyzed on the basis of observational data accumulated under conditions of temporary weightlessness and in flights of artificial manned satellites. The general biomechanical rules of movements performed under weightlessness conditions are derived from tests carried out according to cyclographic method. The discussions regarding coordination during weightlessness are supplemented by the personal reports of Soviet cosmonauts, as well as the American astronaut John Glenn. It is concluded that even prolonged weightlessness causes no serious or lasting disorders in an invididual's movement coordination if he has been properly and adequately trained. However, certain changes should be expected in the dimensionality of the dynamic components of the coordination structure of skills performed in an altered gravitational field, and the limits to the decrease of the elements of the movement structure can reach 50%. Author

N69-31401*# Israel Program for Scientific Translations, Ltd., Jerusalem.

THE OXYGEN REGIME OF THE ORGANISM AND ITS REGULATION (SYMPOSIUM)

N. V. Lauer ed. and A. Z. Kolchinskaya ed. 1969 372 p refs Transl. into ENGLISH of the book "Kislorodnyi Rezhim Organizma I Ego Regulirovanie (Materialy Simpoziuma)" Kiev, Naukova Dumka, 1966 Published for NASA and NSF *Its* IPST Cat. No. 5275

(NASA-TT-F-501; TT68-50302) Copyright. Avail: CFSTI CSCL 06P

Presented are various studies of respiration and its regulation. Evaluated are the effects of breathing, circulation, and oxygen metabolism in the organism and the role of oxygen parameters in the regulation of autonomic functions governing the gas exchange. For individual titles, see N69-31401 through N69-31444.

N69-31923*# National Aeronautics and Space Administration, Washington, D.C.

AEROSPACE MEDICINE AND BIOLOGY: A CONTINUING BIBLIOGRAPHY WITH INDEXES

Jul. 1969 154 p

(NASA-SP-7011(65)) Avail: CFSTI CSCL 06S

Subject coverage concentrates on the biological, physiological, psychological, and environmental effects to which man is subjected during and following simulated or actual flight in the earth's atmosphere or in interplanetary space. References describing similar effects on biological organisms of lower order are also included. Such related topics as sanitary problems, pharmacology, toxicology, safety and survival, life support systems, exobiology, and personnel factors receive appropriate attention. Each entry consists of a standard citation accompanied by its abstract. Author

N69-32131*# Aztec School of Languages, Inc., Maynard, Mass. Research Translation Div.

PROBLEMS OF SPACE BIOLOGY. VOLUME 8: ADAPTATION TO HYPOXIA AND RESISTANCE OF AN ORGANISM [PROBLEMY KOSMICHESKOY BIOLOGII. TOM 8: ADAPTATSIYA K GIPOKSII I USTOYCHIVOST ORGANIZMA]

Chernigovskiy, ed. Washington NASA Jul. 1969 p 255 refs Transl. into ENGLISH from Nauka Press (Moscow), 1968 p 5-146, 151-157, 166-181, 188-211, 230-243, 254-261

(Contract NASw-1692)

(NASA-TT-F-580) Avail: CFSTI CSCL 06S

Data are presented on the adaptation of animal and human organisms to lowered barometric pressure, under natural and simulated high altitude conditions; behavioral characteristics of first-time and experienced mountain climbers; and the role of physical exercise in adaptation to hypoxia. For individual titles, see N69-32132 through N69-32158.

N69-37062*# Princeton Univ., N.J.

SECOND-ORDER WAVE STRUCTURE IN SUPERSONIC FLOWS

David A. Caughey Washington NASA Sep. 1969 87 p refs (Grant NGR-31-001-119)

(NASA-CR-1438) Avail: CFSTI CSCL 20D

Second-order effects upon the wave systems associated with bodies in uniform supersonic flight are considered. An appropriate scaling of the independent variables is introduced to take into account the locally small, but cumulative, nonlinearities which determine the validity of the classical perturbation theories at large distances from the body. Predicted shock angles for the flow over slender wedges (planar flow) and cones (Axisymmetric flow) are compared with exact inviscid calculations to show the improvement afforded by inclusion of second-order effects. Inclusion of the full second-order solution is required to achieve appreciable improvement over the first-order theory for the conical case. Author

N69-37887*# National Aeronautics and Space Administration, Washington, D.C.

AEROSPACE MEDICINE AND BIOLOGY Continuing Bibliography with Indexes, Aug. 1969

Sep. 1969 79 p refs

(NASA-SP-7011(67)) Avail: CFSTI CSCL 06C

Subject coverage concentrates on the biological, physiological, psychological, and environmental effects to which man is subjected during and following simulated or actual flight in the earth's atmosphere or in interplanetary space. References describing similar effects on biological organisms of lower order are also included. Such related topics as sanitary problems, pharmacology, toxicology, safety and survival, life support systems, exobiology, and personnel factors receive appropriate attention. Each entry consists of a standard citation accompanied by its abstract. Author

N69-37909*# National Aeronautics and Space Administration, Washington, D.C.

AEROSPACE MEDICINE AND BIOLOGY Continuing Bibliography with Indexes, Jul. 1969

Aug. 1969 172 p refs

(NASA-SP-7011(66)) Avail: CFSTI CSCL 06C

The contents of this ussue are comprised of abstracts relating to biological, physiological, psychological, and environmental effects to which man is exposed during and following simulated or actual flight in the earth's atmosphere or interplanetary space. Included are such related topics as sanitary problems, pharmacology, toxicology, safety and survival, life support systems, exobiology, and personnel factors. References describing similar effects on lower biological organisms are also considered. G.G.

N69-38235*# National Aeronautics and Space Administration, Washington, D.C.

AEROSPACE MEDICINE AND BIOLOGY A Continuing Bibliography with Indexes, Apr. 1969

May 1969 198 p refs

(NASA-SP-7011(63)) Avail: CFSTI CSCL 06C

Subject coverage concentrates on the biological, physiological, psychological, and environmental effects to which man is subjected during and following simulated or actual flight in the earth's atmosphere or in interplanetary space. References describing similar effects on biological organisms of lower order are also included. Such related topics as sanitary problems, pharmacology, toxicology, safety and survival, life support systems, exobiology, and personnel factors receive appropriate attention. Each entry consists of a standard citation accompanied by its abstract. Author

N69-38242*# National Aeronautics and Space Administration, Washington, D.C.

AEROSPACE MEDICINE AND BIOLOGY A Continuing Bibliography with Indexes, May 1969

Jun. 1969 166 p refs

(NASA-SP-7011(64)) Avail: CFSTI CSCL 06C

Subject coverage concentrates on the biological, physiological, psychological, and environmental effects to which man is subjected during and following simulated or actual flight in the earth's atmosphere or in interplanetary space. References describing similar effects on biological organisms of lower order are also included. Such related topics as sanitary problems, pharmacology, toxicology, safety and survival, life support systems, exobiology, and personnel factors receive appropriate attention. Each entry consists of a standard citation accompanied by its abstract. Author

N69-40324*# National Aeronautics and Space Administration, Washington, D.C.

CONCENTRATION OF MATTER AND ACTION OF ENZYMES IN COACERVATES

T. N. Yevreinova Oct. 1969 223 p refs Transl. into ENGLISH of the book "Kontsentrirovaniye Veshchestv i Deystviye Fermentov v Koatservatkh" Moscow, Nauka Press, 1966 p 3-186

(NASA-TT-F-525) Avail: CFSTI CSCL 06C

The book brings together published data and the author's own experimental findings on coacervate systems consisting of compounds formed biogenically: proteins, nucleic acids, enzymes, carbohydrates, and other biopolymers and low molecular compounds included in the composition of living organisms. Most attention is given to the main property of coacervation, i.e., the concentration of compounds in individua coacervate drops both during their formation and during their absorption of substances, including enzymes, from the surrounding solution. It is shown that coacervate drops constitute very suitable models which can be used to elucidate and reproduce many of the phenomena characteristic of protoplasm, and to approach the solution of the most important problem in biology, the artifical synthesis of living matter. Author

N69-40955*# Union Carbide Corp., Tonawanda, N.Y. Linde Div. Research Lab.

BIOCHEMICAL AND METABOLIC EFFECTS OF A SIX-MONTH EXPOSURE OF SMALL ANIMALS TO A HELIUM-OXYGEN ATMOSPHERE

Robert W. Hamilton, Jr., Janis D. Cohen, Gerald F. Doebbler, Lorenzo F. Exposito, John M. King, et al Washington NASA Oct. 1969 90 p refs

(Contract NAS2-3900)

(NASA-CR-1372) Avail: CFSTI CSCL 04C

Selected biochemical analyses were made on the parent and two successive generations of mice. These included blood indices; electrophoretically separated tissue protein patterns from liver, skeletal muscle, and cardiac muscle; quantitative determinations of LDH, MDH, and G6PDH from the same tissues; serum insulin; and semi-quantitative histochemical estimates of liver glycogen. No cases of statistically significant difference or consistent trends were seen between the experimental environmental groups. Additional analyses of liver nucleotides and redox-coenzymes also failed to show a significant difference. The relative weights of liver, heart, kidney, and diaphragm (wet and dry) were the same in both groups. Histopathological examination of kidney and adrenal tissue produced unremarkable findings and none that were attributable to the nature of the gaseous environment. It must be concluded that prolonged exposure to helium-oxygen, relative to air, does not produce detectable changes in several key subcellular factors which might be altered by serious metabolic disturbances, and therefore the helium exposure is well tolerated. Author

05

BIOTECHNOLOGY

Includes life support systems, human engineering; protective clothing and equipment; crew training and evaluation, and piloting. For related information see also: 04 Biosciences.

A69-11335 *

DYNAMIC RESPONSE OF THE HUMAN BODY TO VIBRATION WHEN COMBINED WITH VARIOUS MAGNITUDES OF LINEAR ACCELERATION.

Hubert C. Vykukal (NASA, Ames Research Center, Moffett Field, Calif.).

Aerospace Medicine, vol. 39, Nov. 1968, p. 1163-1166.

To determine the effects of vibration combined with higher linear accelerations on human body dynamics, a study was conducted whereby four subjects, in a semisupine position, were exposed to vibration (±0.4 g at 2-1/2 to 20 cps in 1/2 cps increments) combined with linear accelerations of 1, 2-1/2, and 4 g. The mechanical impedance of each subject was measured. A vibration device developed for use with various motion generators was utilized in the investigation. Results show significant changes in both impedance magnitude and body resonance. The effects of higher linear accelerations on the human body dynamics are increased stiffness, reduced damping of the whole body, and higher energy transmission to internal organs. Resonances at higher frequencies became more predominant in magnitude because of increased coupling of the body system when immersed in a high g environment. (Author)

A69-11865

A NEUTRAL BUOYANCY MICRO-ELECTRODE FOR PROLONGED RECORDING FROM SINGLE NERVE UNITS.

Torquato Gualtierotti and Pearl Bailey (NASA, Ames Research Center, Instrumentation Div., Neurobiology Branch, Moffett Field, Calif.).

Electroencephalography and Clinical Neurophysiology, vol. 25, 1968, p. 77-81. 7 refs.

Description of a new electrode which allows continuous recording from single neurones or nerve fibers for an extended period of time. It also allows recording during gross movement and high acceleration and vibration. The basic principle of such an electrode is that its density equals that of the surrounding tissue. Moreover, to avoid standing oscillations, the electrode is counterbalanced against torque momentum and is floating. A miniaturized voltage-follower to be used with the microelectrode is also described. M.M.

A69-11950 *

MEASUREMENT OF PILOT DESCRIBING FUNCTIONS FROM FLIGHT TEST DATA WITH AN EXAMPLE FROM GEMINI X.

Rodney C. Wingrove and Frederick G. Edwards (NASA, Ames Research Center, Moffett Field, Calif.).

(NASA, Annual University Conference on Manual Control Systems, 4th, University of Michigan, Ann Arbor, Mich., Mar. 25, 1968.)

IEEE Transactions on Man-Machine Systems, vol. MMS-9, Sept. 1968, p. 49-55. 11 refs.

Theoretical analysis of a technique for reducing the error in identifying the pilot-describing function from routine flight-test records due to the fact that the pilot's output noise is correlated with the input error signal. The error can be reduced in the computer processing by shifting the input signal by an amount equivalent to the pilot's time delay. This technique for reducing the identification error is analyzed with theory and is demonstrated with the identification of a simulated pilot model. The technique is applied to flight-test records obtained from the retrofire phase of the Gemini X mission. M.M.

A69-11953 *

INSTANT MODULAR 3-D MOCKUP FOR CONFIGURING CONTROL AND DISPLAY EQUIPMENT.

Charles C. Kubokawa (NASA, Ames Research Center, Moffett Field, Calif.).

IEEE Transactions on Man-Machine Systems, vol. MMS-9, Sept. 1968, p. 72-81. 18 refs.

A modular three-dimensional mockup technique was developed as a method for economizing and facilitating the design of control and display equipment. The integral parts of the mockup include modular easy-to-assemble console bays and panels, simulated magnetic backed three-dimensional controls and displays of actual size, various writing shelf configurations, fast assembly clamps, storage cabinet with casters, and a Polaroid camera. Human engineering constraints were designed into the mockup parts- i.e., optimum reach, height, view, and control limits - so that the designers could not deviate from human engineering inputs, facilitating optimum operating conditions. (Author)

A69-12216 *

THE EFFECT OF BREATHING 100% OXYGEN ON FOVEAL THRESHOLDS.

Mary M. Connors (NASA, Ames Research Center, Moffett Field, Calif.).

Human Factors, vol. 10, Aug. 1968, p. 377-384. 18 refs.

This study examined the effects of breathing 100% oxygen at sea level on the luminance thresholds necessary for perception of red (642 nm), green (521 nm), blue (468 nm), and yellow (584 nm), and the chromatic and absolute thresholds associated with these dominant wavelengths. Using two highly trained observers, thresholds were measured for one target size and exposure duration by the method of constant stimuli. For the foveal thresholds investigated, no differences were found between the condition of breathing 100% oxygen and breathing normal room air at sea level. There is at least some physiological basis for thinking that vision may improve in a high oxygen environment. At the other extreme, breathing high concentrations of oxygen under pressure is known to degrade vision. Evidence relating to the visual effects of high oxygen concentrations is evaluated and conclusions are drawn with reference to the findings of this and other studies. (Author)

A69-12498 *

PROTECTION AGAINST TOXIC ROCKET FUELS.

Wallace B. Frierson (SysteMed Corp.; NASA, Marshall Space Flight Center, Medical Center, Huntsville, Ala.).

American Industrial Hygiene Association Journal, vol. 29, Sept.-Oct. 1968, p. 456-460.

Description of a detailed treatment procedure for acute exposures to toxic rocket fuels or oxidizers. Other aspects of a preventive program are outlined. These cover construction of the facility, preparation and use of operating procedures, environmental health surveys, and inspections and monitoring of exposed employees. Among the toxic chemicals considered are UDMH, Aerozine 50, N_2O_4, fluorine derivatives, and the boranes. B.H.

A69-12987 *#

WATER ELECTROLYSIS - PROSPECT FOR THE FUTURE.

T. Wydeven (NASA, Ames Research Center, Moffett Field, Calif.) and R. W. Johnson (NASA, Langley Research Center, Hampton, Va.).

(AVIATION AND SPACE: PROGRESS AND PROSPECTS; PROCEEDINGS OF THE ANNUAL AVIATION AND SPACE CONFERENCE, BEVERLY HILLS, CALIF., JUNE 16-19, 1968, p. 93-102.)

ASME, Transactions, Series B - Journal of Engineering for Industry, vol. 90, Nov. 1968, p. 531-540. 13 refs.

A hard space suit suitable for use on planetary surfaces and for other extravehicular activities has been designed and fabricated. Except for the use of soft gloves, the suit is constructed completely of hard materials and allows for exceptional mobility with low

torques and leakage. There are no restoring torques in the constant volume joints - i.e., the joints are neutrally stable in any position in which they are placed. (Author)

A69-12993 *#
ADVANCED DEVELOPMENTS IN HARD SPACE SUIT TECHNOLOGY.
H. C. Vykukal (NASA, Ames Research Center, Moffett Field, Calif.).
(AVIATION AND SPACE: PROGRESS AND PROSPECTS; PROCEEDINGS OF THE ANNUAL AVIATION AND SPACE CONFERENCE, BEVERLY HILLS, CALIF., JUNE 16-19, 1968, p. 86-92.)
ASME, Transactions, Series B - Journal of Engineering for Industry, vol. 90, Nov. 1968, p. 577-583.

Survey of oxygen generators for spacecraft based on water electrolysis. The water electrolysis cells surveyed are predominantly prototype units including both liquid and vapor feed cells. Cell design, operational performance, gas purity, and problems encountered during testing are discussed. Suggestions are given as to where future research might be concentrated in order to solve some of the more general problems associated with water electrolysis. (Author)

A69-13441 *
MICROBIOLOGICAL STUDIES ON A WATER MANAGEMENT SUBSYSTEM FOR MANNED SPACE FLIGHT.
Judd R. Wilkins and David C. Grana (NASA, Langley Research Center, Hampton, Va.).
Society of Automotive Engineers, Aeronautic and Space Engineering and Manufacturing Meeting, Los Angeles, Calif., Oct. 7-11, 1968, Paper 680718. 7 p.
Members, $0.75; nonmembers, $1.00.

Currently under investigation at the Langley Research Center in Hampton, Va., is a research test chamber to study and test life support subsystems for long-duration space missions. This system is designed to support four men for a period of one year in a near-earth circular orbit with resupply at a 90-day interval. Critical life support subsystems include the recovery of water from urine, waste management, and personal hygiene. Microbiological studies in support of the development and testing of a wick evaporator, water management subsystem are reported. The goal of this program is to produce water meeting the recommended standard of "essential sterility," that is, no more than a sum total of 10 microorganisms per ml. Modification of the wick evaporator system to permit the use of heat for sterilization will be described. Microbiological and chemical results obtained during research and development on a bench model and from two units inside the Integrated Life Support System (ILSS) test chamber are presented. The multidisciplinary approach used in this program and the background philosophy behind water standards for space missions are discussed. The laboratory techniques used for the microbiological examination of samples from the water management system are reviewed. (Author)

A69-15388 *#
SPACE FLIGHT NUTRITION [NAHRUNG FÜR DEN WELTRAUMFLUG].
John R. Bannister (NASA, Goddard Space Flight Center, Greenbelt, Md.).
Weltraumfahrt Raketentechnik, vol. 19, Nov.-Dec. 1968, p. 167-171. In German.

Discussion of biological, psychological, and technological requirements in the creation of nutrition programs for astronauts. Preservation and reconstitution techniques, such as dehydration and freeze-drying are examined, and the disposal of wastes is considered. It is concluded that, apart from technological considerations, the major requirement of future space flight diets will be to achieve as close an approximation to "normal" earth diets as possible, in terms of nutritional balance, appetite appeal, and psychological satisfaction. Space diets of the various flights are reviewed and evaluated from all these points of view. B.H.

A69-15934
STERILIZATION TECHNIQUES FOR INSTRUMENTS AND MATERIALS AS APPLIED TO SPACE RESEARCH; COSPAR, SYMPOSIUM, LONDON, ENGLAND, JULY 18-22, 1967, PROCEEDINGS (COSPAR Technique Manual Series. Number 4).
Edited by P. H. A. Sneath (Leicester, University, Leicester, England).
Paris, COSPAR Secretariat, 1968. 302 p.

CONTENTS:

PREFACE. P. H. A. Sneath (Leicester, University, Leicester, England), p. V.

INTRODUCTION.

THE IMPORTANCE OF STERILIZATION TECHNIQUES IN SPACE EXPLORATION. L. B. Hall (NASA, Washington, D.C.), p. 3-18. 23 refs. [See A69-15935 05-05]

THE VALUE OF AGREED STANDARDS OF STERILITY. C.-G. Heden (Karolinska Institute; Medical Research Council, Stockholm, Sweden), p. 19-34. 8 refs. [See A69-15936 05-05]

STERILIZATION ENDPOINTS AND PROTECTION.

EFFICIENCY OF STERILANTS IN TERRESTRIAL AND EXTRATERRESTRIAL ENVIRONMENTS. S. D. Rubbo and J. F. Gardner (Melbourne, University, Melbourne, Australia), p. 37-50. 13 refs. [See A69-15937 05-05]

SOME OBSERVATIONS REGARDING FACTORS IMPORTANT IN DRY HEAT STERILIZATION. I. J. Pflug (Minnesota, University, Minneapolis, Minn.), p. 51-58. 9 refs. [See A69-15938 05-05]

PROTECTIVE MECHANISMS AFFECTING DRY-HEAT STERILIZATION. R. Angelotti (U. S. Public Health Service, Cincinnati, Ohio), p. 59-74. 21 refs. [See A69-15939 05-05]

ETHYLENE OXIDE STERILIZATION RATES AND PROTECTIVE INFLUENCES. R. K. Hoffman (U.S. Army, Fort Detrick, Md.), p. 75-86. 12 refs. [See A69-15940 05-04]

ESTIMATION OF MICROBIAL SURVIVAL IN HEAT STERILIZATION. S. Schalkowsky and R. Wiederkehr (Exotech, Inc., Washington, D.C.), p. 87-100. 14 refs. [See A69-15941 05-04]

THE AGE OF BACILLUS SUBTILIS SPORES AND THEIR RESISTANCE TO ETHYLENE OXIDE. M. Bomar (Universita 17. Listopadu, Prague, Czechoslovakia), p. 101-108.

DETERMINATION OF TERMINAL STERILIZATION PROCESS PARAMETERS. J. A. Stern and A. R. Hoffman (California Institute of Technology, Pasadena, Calif.), p. 109-120. 7 refs. [See A69-15942 05-05]

COMBINED STERILIZATION TECHNIQUES.

THE POSSIBILITY OF USING HYDROGEN PEROXIDE MIXED WITH A DETERGENT TO REDUCE MICROBIAL CONTAMINATION. V. I. Vashkov, E. N. Nikiforova, and Iu. F. Shumaeva (Academy of Sciences, Moscow, USSR), p. 123-126. [See A69-15943 05-05]

IMPARTING ANTIMICROBIAL PROPERTIES TO VARIOUS MATERIALS. V. I. Vashkov and G. V. Shcheglova (Academy of Sciences, Moscow, USSR), p. 127-131. [See A69-15944 05-05]

SYNERGISTIC EFFECTS OF ETHYLENE OXIDE AND OTHER AGENTS. S. Kaye, p. 133-140. [See A69-15945 05-05]

STERILIZATION BY LOW TEMPERATURE STEAM AND FORMALDEHYDE UNDER SUB-ATMOSPHERIC PRESSURES AT 80°C. V. G. Alder (United Bristol Hospitals, Bristol, England), p. 141-155. 16 refs. [See A69-15946 05-05]

THE PLACE OF RADIATION STERILIZATION IN COMBINED TECHNIQUES. L. O. Kallings (National Bacteriological Laboratory, Stockholm, Sweden), p. 157-166. 53 refs. [See A69-15947 05-05]

SYNERGISM IN ETHYLENE OXIDE-METHYL BROMIDE STERILIZATION OF VERY DRY SPORE AND STAPHYLOCOCCAL POPULATIONS. J. B. Opfell, J. L. Shannon, and J. T. Brady (Philco-Ford Corp., Newport Beach, Calif.), p. 167.

SUPPORTING TECHNIQUES.

PLANETARY QUARANTINE - TECHNIQUES FOR THE PREVENTION OF CONTAMINATION OF THE PLANETS BY UNSTERILE SPACEFLIGHT HARDWAVE. C. W. Craven (California Institute of Technology, Pasadena, Calif.) and R. P. Wolfson (General Electric Co., Valley Forge, Pa.), p. 171, 172.

TECHNIQUES FOR THE LIMITATION OF BIOLOGICAL LOADING OF SPACECRAFT BEFORE STERILIZATION. J. J. McDade (Lovelace Foundation for Medical Education and Research, Albuquerque, N. Mex.), W. J. Whitfield, C. A. Trauth, Jr., and H. D. Sivinski (Sandia Corp., Albuquerque, N. Mex.), p. 173-206. 37 refs. [See A69-15948 05-05]

AN EXPERIMENT TO DETERMINE THE EFFECTS OF SOLID AND LIQUID ROCKET ENGINE COMBUSTION ON THE VIABILITY OF MICROORGANISMS. A. F. Oberta, J. R. Gillis, M. G. Koesterer, and R. P. Wolfson (General Electric Co., Philadelphia, Pa.), p. 207-232. 14 refs. [See A69-15949 05-05]

TECHNIQUE FOR STERILE INSERTION AND REPAIR OF SPACECRAFT. P. C. Trexler (Royal Veterinary College, London England) and A. A. Rothstein (Martin Marietta Corp., Denver, Colo.), p. 233-238. 9 refs. [See A69-15950 05-05]

LABORATORY INVESTIGATIONS RELATED TO A SYSTEMS ANALYSIS APPROACH TO PLANETARY QUARANTINE. R. L. Olson (Boeing Co., Seattle, Wash.) and R. H. Green (Boeing Co., Seattle, Wash.; California Institute of Technology, Pasadena, Calif.), p. 239, 240.

SAMPLING AND VERIFICATION TECHNIQUES.

PANSPERMIA REVISITED, OR HAVE WE ALREADY CONTAMINATED MARS? J. Hotchin (New York State, Dept. of Health, Albany, N.Y.), p. 243-254. 11 refs. [See A69-15951 05-05]

SAMPLING AND VERIFICATION IN LARGE-SCALE STERILIZATION PROCEDURES. J. H. Brewer (Becton and Dickinson Co., Rutherford, N.J.), p. 255-262. 7 refs. [See A69-15952 05-05]

CONTROL AND SAMPLING IN STERILE ROOMS. G. Sykes (Boots Pure Drug Co., Ltd., Nottingham, England), p. 263-268. 5 refs. [See A69-15953 05-05]

FACTORS INFLUENCING THE DETECTION AND ENUMERATION OF MICROBIAL CONTAMINANTS ON SPACE HARDWARE. M. S. Favero (U.S. Public Health Service, Phoenix, Ariz.), p. 269-285. 12 refs. [See A69-15954 05-05]

AUTHOR INDEX, p. 287.

A69-15935 *#

THE IMPORTANCE OF STERILIZATION TECHNIQUES IN SPACE EXPLORATION.

Lawrence B. Hall (NASA, Washington, D.C.).

IN: STERILIZATION TECHNIQUES FOR INSTRUMENTS AND MATERIALS AS APPLIED TO SPACE RESEARCH; COSPAR, SYMPOSIUM, LONDON, ENGLAND, JULY 18-22, 1967, PROCEEDINGS (COSPAR Technique Manual Series. Number 4). [A69-15934 05-05]
Edited by P. H. A. Sneath.

Paris, COSPAR Secretariat, 1968, p. 3-18. 23 refs.

Summary of the present state of spacecraft sterilization to prevent viable terrestrial organisms from being transported to other planets. Mathematical models have been developed to define the scope and details of planetary quarantine. The COSPAR Resolution of 1964 provided a framework consisting essentially of three elements: a model of the principal parameters and their interrelation, agreements as to which parameters should serve as basic standards, and the selection of quantitative values for a chosen parameter. The possibility of contamination by nonlanding vehicles is considered. Microbial load estimation and control is discussed, as well as microbial survival and growth probabilities. G.R.

A69-17215 *

DETECTION TIME TO A POINT SOURCE OF LIGHT APPEARING ON A STAR FIELD BACKGROUND WITH AND WITHOUT A GLARE SOURCE PRESENT.

Richard F. Haines (Michigan State University, East Lansing, Mich.; NASA, Ames Research Center, Moffett Field, Calif.).

Human Factors, vol. 10, Oct. 1968, p. 523-529. 30 refs.

One hundred and twenty seven untrained observers were tested in a planetarium in order to determine how long it takes to detect the onset of a point source of light appearing at different locations within a star field with and without a veiling glare source present. Results indicated that detection time was shortest when test spots were flashed in a totally dark visual environment. Introduction of a simulated star field produced significantly longer detection times as did the introduction of a star field and glare source. These results are related to findings from previous investigations as well as to certain sighting situations performed in the aerospace environment. (Author)

A69-17642

INTERNATIONAL ASTRONAUTICAL FEDERATION, INTERNATIONAL ASTRONAUTICAL CONGRESS, 18TH, BELGRADE, YUGOSLAVIA, SEPTEMBER 24-30, 1967, PROCEEDINGS. VOLUME 4 - LIFE IN SPACECRAFT.
Edited by Michał Łunc.

Oxford, Pergamon Press, Ltd.; Warsaw, Państwowe Wydawnictwo Naukowe, 1968. 208 p. In English, Russian, and French.
Price of four volumes, $90.

CONTENTS:

CONTRIBUTORS. p. v, vi.

LIFE SUPPORT.

SPACECRAFT ENVIRONMENT AND TOLERANCE TO HYPOXIA [USLOVIIA OBITANIIA V GERMOKABINAKH I PERENOSIMOST' GIPOKSII]. N. A. Agadzhanian, I. N. Zakharova, L. V. Kaliuzhnyi, and A. V. Sergienko (Ministerstvo Zdravookhraneniia, Moscow, USSR), p. 1-10. [For abstract see issue 23, page 4352, Accession no. A68-44090]

BIOENGINEERING PROBLEMS ASSOCIATED WITH THE HABITABILITY OF SPACECRAFT AND PLANETARY STATIONS [BIOLOGO-TEKHNICHESKIE VOPROSY OBITAEMOSTI KOSMICHESKIKH KORABLEI I PLANETNYKH STANTSII]. B. A. Adamovich and Iu. G. Nefedov (Ministerstvo Zdravookhraneniia, Moscow, USSR), p. 11-16. [For abstract see issue 23, page 4358, Accession no. A68-44089]

INVESTIGATION OF THE LONG-TERM EFFECT OF A LOW-PRESSURE OXYGEN ATMOSPHERE ON ANIMALS AND HUMAN BEINGS [ISSLEDOVANIE DLITEL'NOGO VOZDEISTVIIA NA ZHIVOTNYKH I CHELOVEKA KISLORODNOI ATMOSFERY S PONIZHENNYM DAVLENIEM]. A. M. Genin, S. G. Zharov, E. Ia. Kaplan, V. V. Ogleznev, and V. I. Solov'ev (Akademiia Nauk SSSR, Moscow, USSR), p. 17-25. [For abstract see issue 23, page 4352, Accession no. A68-44087]

ADVANCED PROTECTION SYSTEMS FOR ASTRONAUT EXTRAVEHICULAR ACTIVITY. D. L. Richardson (Arthur D. Little, Inc., Cambridge, Mass.), p. 27-38. 10 refs. [See A69-17643 06-05]

ENERGY EFFICIENCY OF LIFE-SUPPORT SYSTEMS [OB ENERGETICHESKOI EFFEKTIVNOSTI SISTEM ZHIZNEOBESPECHENIIA]. A. B. Rubin (Moskovskii Gosudarstvennyi Universitet, Moscow, USSR), p. 39-43. 5 refs. [See A69-17644 06-05]

SPACE PHYSIOLOGY.

HUMAN PHYSIOPATHOLOGY IN FACE OF RADIATION AND HYBERNATION. M. Nieto (Academia de Ciencias Médicas de Barcelona, Barcelona, Spain), p. 45-47. [See A69-17645 06-04]

FURTHER INVESTIGATIONS OF THE COMPLEX EFFECT OF IONIZING RADIATION AND ACCELERATIONS ON AN ORGANISM IN ASSOCIATION WITH SPACE FLIGHTS [DAL'NEISHEE ISSLEDOVANIE KONPLEKSNOGO VOZDEISTVIIA NA ORGANIZM IONIZIRUIUSHCHEGO IZLUCHENIIA I USKORENIIA V SVIAZI S KOSMICHESKIMI POLETAMI]. V. V. Antipov, B. I. Davydov, E. F. Panchenkova, and P. P. Saksonov (Akademiia Nauk SSSR, Moscow, USSR), p. 49-57. [For abstract see issue 24, page 4113, Accession no. A67-42393]

POSSIBLE MECHANISMS OF THE INFLUENCE OF CHANGING GRAVITATION CONDITIONS ON BLOOD CIRCULATION IN THE BRAIN [VOZMOZHNYE MEKHANIZMY VLIIANIIA USLOVII IZMENNOI GRAVITATSII NA SISTEMU MOZGOVOGO KROVOOBRASHCHENIIA]. Iu. E. Moskalenko (Akademiia Nauk SSSR, Leningrad, USSR), p. 59-69. 20 refs. [See A69-17646 06-04]

GASTRIC SECRETION IN CATS AFTER INTENSIVE IRRADIATION CONNECTED WITH PREVIOUS AND SIMULTANEOUS HYPOXIA. J. Kaulbersz, A. Barylak, and T. Radecki (Akademia Medyczna, Kraków, Poland), p. 71-73.

CERTAIN VISUAL FEEDBACK MECHANISMS IN SIMULATED HIGH-ALTITUDE CONDITIONS [CERTAINS MECANISMES OCULAIRES DE FEED BACK DANS LES CONDITIONS DES GRANDES ALTITUDES SIMULEES]. M. P. Popescu, M. Stefan, I. Pintilie, and D. Pavel (Institut Médico-Pharmaceutique de Bucarest; Centre Médical de l'Aviation, Bucharest, Rumania), p. 75-80. 38 refs. [See A69-17647 06-05]

GENERAL. I - HYPODYNAMIA.

EFFECT OF 62-DAY HYPODYNAMIA ON THE HUMAN ORGANISM [VLIIANIE 62-SUTOCHNOI GIPOKINEZII NA ORGANIZM CHELOVEKA]. T. V. Benevolenskaia, N. M. Boglevskaia, M. M. Korotaev, T. N. Krupina, I. A. Maslov, G. P. Mikhailovskii, T.

A. Petrova, K. V. Smirnov, and I. Ia. Iakovleva (Akademiia Nauk SSSR, Moscow, USSR), p. 81-86. [For abstract see issue 23, page 4352, Accession no. A68-44091]

IS THERE A COMMON GEOTROPIC DEPENDENCY IN ORGANISMS? W. Briegleb (Deutsche Versuchsanstalt für Luft- und Raumfahrt, Institut für Flugmedizin, Bad Godesberg, West Germany), p. 87-90.

THE EFFECTIVENESS OF WEIGHTLESS SIMULATORS FOR OBTAINING MAINTAINABILITY CRITERIA FOR SPACE SYSTEMS. C. B. May (NASA, Marshall Space Flight Center, Huntsville, Ala.), p. 91-114. [See A69-17648 06-05]

PSYCHOMOTOR REACTIONS DURING BALLISTIC ROCKET FLIGHTS [REACTIONS PSYCHOMOTRICES AU COURS DE VOLS BALISTIQUES EN FUSEES]. R. Grandpierre and G. Chatelier (Centre d'Enseignement et de Recherches de Médecine Aéronautique, Paris, France), p. 115-121. [See A69-17649 06-04]

CHANGES IN HUMAN TOLERANCE TO TRANSVERSE ACCELERATIONS FOLLOWING HYPODYNAMIA OF VARYING DURATION [IZMENENIE PERENOSIMOSTI CHELOVEKOM POPERECHNYKH PEREGRUZOK POSLE GIPODINAMIKI RAZLICHNOI PRODOLZHITEL'NOSTI]. A. R. Kotovskaia, R. A. Vartbaronov, and S. F. Simpura (Akademiia Nauk SSSR, Moscow, USSR), p. 123-131. [For abstract see issue 23, page 4352, Accession no. A68-44084]

CYTOPHYSIOLOGICAL AND CYTOCHEMICAL ASPECTS OF HYPOKINESIA - EXPERIMENTAL STUDY [TSITOFIZIOLOGICHESKIE I TSITOKHIMICHESKIE ASPEKTY IZUCHENIIA GIPOKINEZII - EKSPERIMENTAL'NOE ISSLEDOVANIE]. V. V. Portugalov, O. G. Gazenko, E. I. Il'ina-Kakueva, V. B. Malkin, T. B. Artiukhina, I. A. Bukaeva, V. Ia. Gotlib, K. D. Rokhlenko, N. A. Roshchina, and V. I. Starostin (Akademiia Nauk SSSR, Moscow, USSR), p. 133-142. [For abstract see issue 03, page 375, Accession no. A68-13950]

GENERAL. II.

MANNED SPACE FLIGHT SAFETY. E. B. Konecci (Texas, University, Austin, Tex.), p. 143-160. 19 refs. [See A69-17650 06-05]

HEART RATE RHYTHM AS AN INDICATOR OF HUMAN ORGANISM NEUROENDOCRINE REGULATION IN SPACE FLIGHT [RITM SERDECHNYKH SOKRASHCHENII KAK INDIKATOR SOSTOIANIIA NEIRO-ENDOKRINNOI REGULIATSII ORGANIZNA V USLOVIIAKH KOSMICHESKOGO POLETA]. V. V. Parin, R. M. Baevskii, and G. A. Nikulina (Akademiia Nauk SSSR, Moscow, USSR), p. 161-169. [For abstract see issue 03, page 376, Accession no. A68-13951]

CURRENT STATE AND PROSPECTS OF STUDYING THE HUMAN CARDIOVASCULAR SYSTEM IN SPACE FLIGHTS [SOVREMENNOE SOSTOIANIE I PERSPEKTIVY ISSLEDOVANII SERDECHNO-SOSUDISTOI SISTEMY CHELOVEKA V KOSMICHESKIKH POLETAKH]. I. T. Akulinichev, V. A. Degtiarev, and D. G. Maksimov (Akademiia Nauk SSSR, Moscow, USSR), p. 171-178. [For abstract see issue 23, page 4352, Accession no. A68-44088]

INVESTIGATION OF VISUAL WORK CAPACITY IN SPACE FLIGHT [ISSLEDOVANIE ZRITEL'NOI RABOTOSPOSOBNOSTI V KOSMICHESKOM POLETE]. E. A. Ivanov, V. A. Popov, and L. S. Khachatur'iants (Akademiia Nauk SSSR, Moscow, USSR), p. 179-186.

PSYCHO-PHYSIOLOGICAL CORRELATIONS OF THE SPACE-GRAVITATIONAL PERCEPTIONS IN FLYING PERSONNEL. V. Ceauşu, S. Sigal, and V. Teodorescu (Medical Center for Aviation, Bucarest, Rumania), p. 187-192. [For abstract see issue 23, page 4358, Accession no. A68-44086]

A69-17648 *

THE EFFECTIVENESS OF WEIGHTLESS SIMULATORS FOR OBTAINING MAINTAINABILITY CRITERIA FOR SPACE SYSTEMS.
C. B. May (NASA, Marshall Space Flight Center, Huntsville, Ala.). IN: INTERNATIONAL ASTRONAUTICAL FEDERATION, INTERNATIONAL ASTRONAUTICAL CONGRESS, 18TH, BELGRADE, YUGOSLAVIA, SEPTEMBER 24-30, 1967, PROCEEDINGS. VOLUME 4 - LIFE IN SPACECRAFT. [A69-17642 06-05]
Edited by Michal Lunc.
Oxford, Pergamon Press, Ltd.; Warsaw, Państwowe Wydawnictwo Naukowe, 1968, p. 91-114.

Discussion of criteria relative to the operational problem, equipment design, man/machine interface, and interior and exterior layouts for weightlessness simulators. The nonparametric experimental design approach is used to obtain data relative to the performance of a representative removal and replacement task in the simulators. An air filled G4-c suit pressurized to 3.5 psi is used by three experienced subjects. The task utilized both power and hand tools in a one hand and a one hand plus knee attached mode. Scaling factors (considering the shirt-sleeve environment as the baseline) are presented for shirt-sleeve, pressurized 1-g, aircraft simulator, six-degree-of-freedom machines, and for underwater simulators.
M. G.

A69-18202 *#

APOLLO 4 AND 6 RADIATION ANALYSIS.
Timothy T. White and Alva C. Hardy (NASA, Manned Spacecraft Center, Space Physics Div., Houston, Tex.).
American Institute of Aeronautics and Astronautics, Aerospace Sciences Meeting, 7th, New York, N.Y., Jan. 20-22, 1969, Paper 69-17. 7 p. 15 refs.
Members, $1.00; nonmembers, $1.50.

Analysis of radiation measurements inside the Apollo 4 and 6 command modules while passing through the most intense portions of the trapped radiation belts. Measurements of the integrated radiation dose behind shields of 0.015 and 0.9 in. of aluminum were made inside the command modules on both missions. Dose-rate measurements behind similar shielding were obtained in the Apollo 6 command module during the ascent to apogee. Dose calculations were made with Manned Spacecraft Center computer codes, using analytical shielding descriptions, models of the radiation environment, and radiation-transport data. The calculated mission doses were within a factor of 2.5 of the measured doses, with better agreement in the calculations for the more thinly shielded sensors. The differences between the calculated and measured doses were, for the most part, attributed to errors in the model environment. The analysis of the Apollo 4 and 6 data indicated that dose calculations for manned lunar missions which pass through the more intense portion of the trapped radiation belt are reliable and that the expected doses are well below the planning operational dose limits set by NASA. (Author)

A69-22542 *

PRELIMINARY CLINICAL REPORT OF THE MEDICAL ASPECTS OF APOLLOS VII AND VIII.
Charles A. Berry (NASA, Manned Spacecraft Center, Houston, Tex.).
Aerospace Medicine, vol. 40, Mar. 1969, p. 245-254.

Preliminary clinical report of the significant medical data gathered on the missions of Apollo 7 and 8. Preventive medical activities in the preflight period and inflight treatment procedures are discussed. Cardiovascular findings and hematological and biochemical analyses conducted during both pre- and postflight examinations are reported. It is concluded that the Apollo spacecraft is capable of supporting man adequately in the space environment from a physiological point of view, and that radiation levels have not been proven to be significant in the flights thus far. B.H.

A69-23879 *

MOTION CUES IN MAN-VEHICLE CONTROL.
Richard S. Shirley (NASA, Electronics Research Center, Office of Control Theory and Application, Cambridge, Mass.) and Laurence R. Young (Massachusetts Institute of Technology, Dept. of Aeronautics and Astronautics, Cambridge, Mass.).
IEEE Transactions on Man-Machine Systems, vol. MMS-9, Dec. 1968, p. 121-128. 5 refs.
Grant No. NsG-577.

Investigation of the human operator's use of roll-motion cues for man-vehicle control in a compensatory tracking task with a disturbance input. Extensive data for the human operator's describing function are taken for a wide range of vehicle dynamics under conditions of visual cues only, roll-motion cues only, and simultaneous visual and roll-motion cues. Addition of roll-motion cues to visual cues permits the human operator to increase his phase lead at frequencies above 3 rad/sec. This makes it possible for him to increase the system open-loop gain without a loss of system stability, and thus to reduce the system tracking error. Experimental results indicate that in a compensatory system with a disturbance input, any condition in which additional human operator lead at frequencies above 3 rad/sec would be useful is a condition in which roll-motion cues would aid. P.v.T.

A69-23880 •
HUMAN INFORMATION PROCESSING RATES DURING CERTAIN MULTIAXIS TRACKING TASKS WITH A CONCURRENT AUDITORY TASK.
Thomas E. Wempe and Daniel L. Baty (NASA, Ames Research Center, Moffett Field, Calif.).
IEEE Transactions on Man-Machine Systems, vol. MMS-9, Dec. 1968, p. 129-138. 7 refs.

Description of experiments conducted to determine the information processing rates of several subjects performing one- and two-axis compensatory tracking tasks with a secondary auditory task. The experimental variables were the order of controlled element dynamics, the forcing function, and the addition of a secondary task. Human information processing rates decreased slightly on each tracking channel with the addition of the second tracking channel or the secondary auditory task. Other than this effect, the information processing rates were additive until a limit in the total information processing rate was reached. This limit was related to the order of the controlled element. (Author)

A69-24795 *#
AUDITORY TEMPORAL MASKING AND THE PERCEPTION OF ORDER.
J. L. Homick (NASA, Manned Spacecraft Center, Houston, Tex.), L. F. Elfner, and G. G. Bothe (Florida State University, Tallahassee, Fla.).
Acoustical Society of America, Journal, vol. 45, Mar. 1969, p. 712-718. 7 refs.
NSF-supported research.

An investigation of the effects of frequency, intensity, and time on the perception of temporal order and the amount of temporal masking produced under conditions of a short burst (12 msec) of tone separated temporally from a narrow-band noise indicates a similarity of function underlying the two phenomena. Temporal masking is greater and the perception of temporal order is more difficult when the signal is centered in the band of noise. Temporal masking is greater and the perception of temporal order is more difficult for a weak signal than for a more intense signal. The observed temporal masking can be interpreted in terms of a cochlear model. The relationship between temporal masking and the perception of temporal order is discussed in terms of a hierarchy of level of perception brought about by temporal cues. (Author)

A69-25642 *
SINGLE-CHANNEL PRESSURE TELEMETRY UNIT.
Harold Sandler, Thomas B. Fryer (NASA, Ames Research Center, Moffett Field, Calif.), and Boris Datnow (Mayo Clinic, Dept. of Pathology, Rochester, Minn.).
Journal of Applied Physiology, vol. 26, Feb. 1969, p. 235-238. 8 refs.

Description of a single-channel pressure telemetry unit which is capable of chronic implantation. Reliable function of these units has been obtained up to 6 months. Recent units have been modified to include a magnetic latching or radio frequency switch. Small size and low power consumption have been achieved without sacrificing accuracy and reliability. This approach is advocated for experimental situations requiring pressure measurements in free-ranging animals or in experimental animals in hostile environments. (Author)

A69-26235 *
AN ANALYTIC ELASTIC-VISCOELASTIC MODEL FOR THE SHAPE AND THE FORCES IN THE LEFT VENTRICLE.
Dhanjoo N. Ghista and Harold Sandler (NASA, Ames Research Center, Moffett Field, Calif.).
Journal of Biomechanics, vol. 2, Mar. 1969, p. 35-47. 7 refs.

An analytic model of the human left ventricle is presented, which incorporates the three-dimensional shape of the left ventricle and the effects of ventricular wall thickness. The model resembles a thick-walled ellipsoid of revolution, a shape chosen because its volume most closely approximates the volume of postmortem left ventricular chambers when compared with volumes estimated by other regular three-dimensional figures of equivalent dimensions. The shape and size parameters of the model are determined from ventricular dimensions obtained from single plane cineangiocardiography. The model is equilibrated by a uniform internal normal stress, corresponding to the measured pressure in the ventricle cavity, and zero stress on the outer surface. Elastic and quasi-static viscoelastic solutions (for stresses and strains) that provide for shear in the ventricular wall are obtained for uniform isotropic wall material. (Author)

A69-26553 *
EEG SENSING AND TRANSMITTING SYSTEM CONTAINED IN A FLIGHT HELMET.
Richard M. Westbrook and Joseph J. Zuccaro (NASA, Ames Research Center, Moffett Field, Calif.).
Aerospace Medicine, vol. 4, Apr. 1969, p. 392-396.

Taking EEG data from human subjects participating in aircraft or flight simulator programs is often impractical because the technique of applying the electrodes in slow and tedious and often abrasive to the subject's scalp. An EEG monitor helmet has been developed in which the electrodes can be applied quickly and easily because they require no special preparation of the subject's scalp. A pilot's flight helmet is used to hold the prepositioned electrodes. Electrical contact is made between scalp and electrodes by means of a paste electrolyte. All of the electronics, including the rf transmitter, are an integral part of the helmet's shell. This system has been tested in the laboratory and in flight. It provides excellent EEG data. (Author)

A69-28298 *#
DEVELOPMENT OF METEOROID PROTECTION FOR EXTRA-VEHICULAR-ACTIVITY SPACE SUITS.
William E. McAllum (NASA, Manned Spacecraft Center, Space Physics Div., Meteoroid Sciences Branch, Houston, Tex.).
American Institute of Aeronautics and Astronautics, Hypervelocity Impact Conference, Cincinnati, Ohio, Apr. 30-May 2, 1969, Paper 69-366. 10 p. 8 refs.
Members, $1.00; nonmembers, $1.50.

The space suit used during extravehicular activities requires meteoroid protection during the space exposure to prevent perforation of the pressure bladder. The development of protective cover-layers for the Gemini and lunar-surface EVA suits is described. The meteoroid mass, which must be absorbed in the coverlayer to satisfy the mission exposure time and the reliability requirements, was simulated by a hypervelocity glass projectile of equal penetrating energy. Textiles or "soft goods" that were compatible with suit fabrication techniques were impacted with the laboratory projectile to determine response to impact and resistance to penetration. An effective projectile breakup was achieved with nylon cloth; therefore, the bumper concept that was developed previously for metallic sheets was applied to the suit protection. Two configurations were developed, one of which used nylon felt and the other used neoprene as the primary energy absorber. (Author)

A69-30394 *
MANNED TEST OPERATIONS RELATED TO THE APOLLO LUNAR MODULE IN THE SIMULATED SPACE ENVIRONMENT.
O. L. Pearson (NASA, Manned Spacecraft Center, Houston, Tex.) and P. R. Gauthier (Boeing Co., Seattle, Wash.).
IN: MAN IN HIS ENVIRONMENT; INSTITUTE OF ENVIRONMENTAL SCIENCES, ANNUAL TECHNICAL MEETING AND EQUIPMENT EXPOSITION, 15TH, ANAHEIM, CALIF., APRIL 20-24, 1969, PROCEEDINGS. [A69-30356 15-11]

Mt. Prospect, Ill., Institute of Environmental Sciences, 1969, p. 459-474.

Description of a series of tests conducted to confirm spacecraft performance in the thermal vacuum (TV) environment and to verify flight operating procedures related to the Apollo lunar module. Tests were conducted of a representative spacecraft, manufactured and checked out in the same manner as the flight spacecraft. To simulate the mission time lines, it was necessary to seek a thermal similarity and introduce the two crewmen at that point. The test crewmen entered the spacecraft cabin under TV conditions and energized the vehicle systems in much the same manner as is planned in flight. G.R.

A69-31459 *#

FOOD TECHNOLOGY PROBLEMS RELATED TO SPACE FEEDING.

H. A. Hollender, Mary V. Klicka (U.S. Army, Natick Laboratories, Natick, Mass.), and M. C. Smith (NASA, Houston, Tex.).

COSPAR, Plenary Meeting, 12th, Prague, Czechoslovakia, May 11-24, 1969, Paper. 19 p. 7 refs.

Discussion of technological problems connected with feeding the astronaut in space, and summary of NASA criteria for space foods. Except for contingency purposes, these criteria eliminated foods in metal tubes and directed development effort to the dehydrated foods. Two approaches to the use of dehydrated foods were pursued. Bite-size foods (to be eaten dry) and precooked dehydrated foods (to be reconstituted with water by the astronaut before consumption) were developed. The subjects discussed include thermostabilized wet meat products, packaging, human factors, and controls on food production and development. G.R.

A69-31472 *#

SPACECRAFT STERILIZATION BY DESTRUCTIVE HEATING.

Byron L. Swenson (NASA, Ames Research Center, Moffett Field, Calif.) and Lawrence B. Hall (NASA, Washington, D.C.).

COSPAR, Plenary Meeting, 12th, Prague, Czechoslovakia, May 11-24, 1969, Paper. 15 p.

Study of the problem of sterilization of spacecraft by destructive heating before entering a planet's atmosphere. It is concluded that a spacecraft can theoretically be sterilized in space by heating to destruction with thermite or similar agents, but heavy weight and design penalties must be accepted. A danger of contamination lies in microbes entrapped within plastic pieces surviving entry, since the low diffusivity of such materials protects them from experiencing high internal temperatures. Z.W.

A69-32810 *

ORTHOSTATIC INTOLERANCE AFTER ARTIFICIAL HEAT ACCLIMATIZATION IN PHYSICALLY FIT SUBJECTS.

J. E. Greenleaf and J. S. Bosco (NASA, Ames Research Center, Biotechnology Div., Moffett Field, Calif.).

Nature, vol. 222, May 31, 1969, p. 891. 5 refs.

Experimental study of the effects of artificial heat acclimatization on orthostatic tolerance in men exposed to the combined stresses of heat, exercise, and dehydration. Three out of four test persons showed marked orthostatic intolerance, although analysis of fluid losses and levels of total body dehydration does not reasonably explain the effect. P.G.

A69-32970 *

LIFE DETECTION TECHNIQUES.

Richard S. Young (NASA, Washington, D.C.).

IN: EXOBIOLOGY: THE SEARCH FOR EXTRATERRESTRIAL LIFE; AMERICAN ASTRONAUTICAL SOCIETY AND AMERICAN ASSOCIATION FOR THE ADVANCEMENT OF SCIENCE, SYMPOSIUM, NEW YORK, N.Y., DECEMBER 30, 1967, PROCEEDINGS. [A69-32967 17-04]

Edited by M. M. Freundlich and B. M. Wagner. Tarzana, Calif., American Astronautical Society (AAS Science and Technology Series. Volume 19), 1969, p. 29-35.

Discussion of the rationale for life detection, including the reasons for the approaches that are taken. The problem of detecting life on an extraterrestrial body requires some degree of experimental sophistication. The single long-shot experiment is considered unlikely to produce unequivocable data, so that a multiple experiment approach is recommended. A discussion is presented of the types of experiments most likely to produce data interpretable as a function of life processes. These experiments include chemical analyses, identification of metabolic activity and evidence for growth and replication at the molecular and/or cellular level. All of these experiments are considered in the light of the realities of planetary mission capability. A discussion is offered concerning the problems of integrating such varied experiments into a single multipurpose laboratory concept. (Author)

A69-33303 *#

EVALUATION OF LITHIUM PEROXIDE FOR OXYGEN SUPPLY AND CARBON DIOXIDE CONTROL.

R. Norman Prince (NASA, Manned Spacecraft Center, Crew Systems Div., Houston, Tex.) and Kenneth J. Dresser (United Aircraft Corp., Hamilton Standard Div., Windsor Locks, Conn.).

American Institute of Aeronautics and Astronautics, Thermophysics Conference, 4th, San Francisco, Calif., June 16-18, 1969, Paper 69-620. 12 p.

Members, $1.00; nonmembers, $1.50.

Contract No. NAS 9-8159.

Results of a series of 54 tests conducted to evaluate the feasibility of utilizing lithium peroxide for oxygen supply and carbon dioxide control in advanced extravehicular portable life support systems. The test data generated by these tests show a definite potential for significant weight and volume savings in portable life support systems and space vehicles supporting extravehicular excursions. For example, a lithium peroxide/oxygen system may be up to 11% smaller and 23% lighter than a comparable lithium hydroxide/oxygen system for a 4-hr 2000-Btu/hr (average) mission. This savings becomes even more significant for a vehicle that must support multiple excursions. The program objectives included the generation of system design data, as well as the evaluation of various chemical densities, chemical catalysts, bed temperature, and bed geometry. The most promising chemical form is a low-bulk density lithium peroxide catalyzed by 2% nickel sulfate. The most critical operating parameter was the temperature of the lithium peroxide bed which, under certain test conditions, exceeded 600°F. Although excessive bed temperatures reduce carbon dioxide removal, high temperatures enhance oxygen evolution due to thermal decomposition of the lithium peroxide. (Author)

A69-38388 *

VENTILATION-PERFUSION INEQUALITY AND OVERALL GAS EXCHANGE IN COMPUTER MODELS OF THE LUNG.

John B. West (NASA, Ames Research Center, Biotechnology Div., Moffett Field, Calif.).

***Respiration Physiology,* vol. 7, June 1969, p. 88-110. 23 refs.**

Study of the effects of increasing ventilation-perfusion inequality on overall gas exchange in digital computer models of the lung. Ventilation/unit volume and perfusion/unit volume were distributed log normally with respect to lung volume. Ventilation-perfusion inequality was found to affect the transfer of carbon dioxide nearly as much as oxygen. The reasons for the misconception that inequality does not interfere with carbon dioxide transfer are discussed. The effects of changing overall ventilation, blood flow, inspired oxygen, hemoglobin concentration, and the acid-base status of the blood were investigated when oxygen uptake and carbon dioxide output were held constant at normal values. In general, mismatch of ventilation and blood flow in a lung caused the arterial oxygen tension to fall and the carbon dioxide to rise. Increasing overall ventilation rapidly restored blood carbon dioxide tensions to normal but improved oxygen tensions little. M.M.

A69-39170 *
CARBON DIOXIDE BUILD-UP CHARACTERISTICS IN SPACE-SUITS.
E. L. Michel, H. S. Sharma, and R. E. Heyer (NASA, Manned Spacecraft Center, Houston, Tex.).
(Aerospace Medical Association, Annual Scientific Meeting, 39th, Miami Beach, Fla., May 6-9, 1968.)
Aerospace Medicine, vol. 40, Aug. 1969, p. 827-829.

Description of a method for monitoring carbon dioxide levels in spacesuit research. Summaries of spacesuit carbon dioxide levels obtained in the laboratory during predetermined activity are presented for various spacesuit configurations, indicating that spacesuit carbon dioxide levels can be maintained within physiologically acceptable limits during energy expenditures up to 2000 BTU per hr. B.H.

A69-40163 *
DISCRIMINANT ANALYSIS IN AVERAGE EVOKED RESPONSE STUDIES—THE STUDY OF SINGLE TRIAL DATA.
Emanuel Donchin (NASA, Ames Research Center, Moffett Field, Calif.).
Electroencephalography and Clinical Neurophysiology, vol. 27, Sept. 1969, p. 311-314. 8 refs.

Approach to the measurement of the similarity of an EEG segment following the onset of a specific stimulus to a given average evoked potential. The data obtained suggest that it is possible to make meaningful comparisons between EEG records obtained with a single presentation of the stimulus and the average evoked potential. The technique for measuring evoked response similarity assumes that each record represents a point in a multidimensional space, and similarity is defined as the Euclidean distance in this space. P.G.

A69-40370 * #
ENGINEERING AND OPERATIONAL EXPERIENCES RELATED TO LUNAR-SURFACE THERMAL-VACUUM QUALIFICATION OF THE APOLLO EXTRAVEHICULAR MOBILITY UNIT.
R. E. Sanders, J. P. Vincent, and H. E. Maples (NASA, Manned Spacecraft Center, Space Environment Test Div., Houston, Tex.).
American Institute of Aeronautics and Astronautics, American Society for Testing and Materials, and Institute of Environmental Sciences, Space Simulation Conference, 4th, Los Angeles, Calif., Sept. 8-10, 1969, AIAA Paper 69-992. 12 p. 6 refs.
Members, $1.00; nonmembers, $1.50.

Description of manned testing of extravehicular activity equipment in a high-fidelity thermal-vacuum environment. This testing was the qualification of the Apollo extravehicular mobility unit for a simulated lunar-surface thermal-vacuum environment. For this testing, unique systems, equipment, and techniques were developed because of the extravehicular-mobility-unit design and the high fidelity required of the simulated environment. These systems and equipment included a lunar-surface thermal simulator, a simulated lunar-thermal environment, a solar-beam fold mirror, a weight-relief and falling-restraint system for the crewman and his extravehicular-mobility-unit, and an environmental control system. (Author)

A69-40371 * #
A REAL-TIME PROCESSING SYSTEM FOR DETERMINATION OF METABOLIC RATES OF A SUITED ASTRONAUT.
Russell J. Kelly (Boeing Co., Houston, Tex.), George F. Humbert, and David G. Billingsley (NASA, Manned Spacecraft Center, Houston, Tex.).
American Institute of Aeronautics and Astronautics, American Society for Testing and Materials, and Institute of Environmental Sciences, Space Simulation Conference, 4th, Los Angeles, Calif., Sept. 8-10, 1969, AIAA Paper 69-993. 7 p.
Members, $1.00; nonmembers, $1.50.

The metabolic rate and total energy expenditure of a suited astronaut were estimated during thermal-vacuum crew-training tests and extravehicular-mobility-unit lunar qualification tests. The crewman was configured in the Apollo space suit with a portable life-support system, and his metabolic rate was estimated by using the electrocardiogram and the portable-life-support-system oxygen-bottle pressure decay as received from telemetry. These parameters were processed by the Acceptance Checkout Equipment Spacecraft computer in real time, and the results were displayed on an alpha numeric CRT. An accurate method for determining the heart rate from the electrocardiogram under conditions of strenuous exercise is presented. Comparisons of heart rate and oxygen utilization methods for the calculation of total energy expenditure are made with posttest analysis of carbon dioxide production. Constraints and limitations of each method are discussed. (Author)

A69-41674 *
EFFECTS OF ANGULAR ACCELERATION ON MAN—THRESHOLDS FOR THE PERCEPTION OF ROTATION AND THE OCULOGYRAL ILLUSION.
Brant Clark (San Jose State College, San Jose, Calif.) and John D. Stewart (NASA, Ames Research Center, Moffett Field, Calif.).
Aerospace Medicine, vol. 40, Sept. 1969, p. 952-956. 32 refs.
Grant No. NGL-05-046-002.

Investigation of the sensitivity of normal human observers to angular acceleration about their yaw axis, using the perception of rotation and the oculogyral illusion as indicators. The data were obtained for 53 normal men, using a one-degree-of-freedom simulator that could produce angular accelerations with narrow limits of error. A forced-choice, random, double staircase method was used to present the 10-sec stimuli. Thresholds for the perception of rotation for these 53 men were found to vary from 0.05 to 2.20 deg per sec per sec with a mean of 0.41 deg per sec per sec. The thresholds for the oculogyral illusion for 32 men were significantly below these figures, the thresholds varying from 0.04 to 0.28 deg per sec per sec with a mean of 0.11 deg per sec per sec. These data show that normal men are extremely sensitive to angular acceleration about their yaw axis under optimum testing conditions. The results are discussed in relation to the psychophysiological mechanisms involved and to their implications for spatial orientation and the precision of control tasks in flight. (Author)

A69-41675 *
FLIGHT RESEARCH PROGRAM. XIV—LANDING PERFORMANCE IN JET AIRCRAFT AFTER THE LOSS OF BINOCULAR VISION.
Charles E. Lewis, Jr. and Gary E. Krier (NASA, Flight Research Center, Edwards, Calif.).
Aerospace Medicine, vol. 40, Sept. 1969, p. 957-963. 15 refs.

Thirteen pilots were studied in a T-33A jet trainer during a series of touch-and-go landings. Each flight included landing approaches with full binocular vision, followed by approaches with first the left and then the right eye covered. Both lateral and longitudinal miss-distance were photooptically measured from a specified touchdown point. Performance on final approach was analyzed with respect to airspeed control, sink rate, and the approach angle. Landing errors were clearly shown not to increase significantly during approaches made with one eye covered. The pilots were free to select any angle of descent during approach that they desired. Steeper approaches were consistently observed when vision was restricted to one eye than those flown with normal vision. One pilot was studied for three consecutive weeks during which his dominant eye was patched. Landing performance was analyzed during three flights (including thirty-five landings) and was compared with control data. Analysis of these data revealed no significant difference in landing performance with vision restricted to one eye over the entire period. (Author)

05 BIOTECHNOLOGY

A69-41679 •
EFFECTS OF VARIOUS RESPIRATORY MANEUVERS ON THE PHYSIOLOGICAL RESPONSE TO ANGULAR ACCELERATION.
Jose G. Lipana (NASA, Flight Research Center, Lovelace Foundation Field Laboratory, Edwards, Calif.), John Fletcher (Systems Research Laboratories, Inc., San Antonio, Tex.), William Brown, and George Cohen (Systems Research Laboratories, Inc., San Antonio; USAF, School of Aerospace Medicine, Biodynamics Branch, Brooks AFB, Tex.).
(Aerospace Medical Association, Annual Scientific Meeting, San Francisco, Calif., May 5-8, 1969.)
Aerospace Medicine, vol. 40, Sept. 1969, p. 976-980. 8 refs.
Contract No. AF 41(609)-2897.

Study of the effects of breath holding, M1, Valsalva, and Mueller's maneuvers on healthy males during static condition at various postures and during pure axis rotations. The subject was seated inside a hollow spherical simulator. Rotation was at the rate of 6 rpm with the axis of rotation through the body. Heart rates, ECG, blood pressures, respiratory rates and voice were monitored by telemetry. The characteristics of the response pattern were dependent on the kind of maneuver, the instantaneous posture, and the time the maneuver was initiated. Early obliteration of the pulse pressures were notable with Mueller's and Valsalva maneuvers. On repeated performance, all of the maneuvers studied provoked nausea, vomiting, and syncopal symptoms of varying degrees. The onset of these symptoms limited the duration for which the subject can normally withstand prolonged rotation. Unlike the M1 maneuver, which had beneficial effect during linear positive acceleration, none of these maneuvers was protective against angular acceleration. On the contrary, performance of any of these maneuvers jeopardizes man's tolerance to this spectrum of acceleration. (Author)

A69-41683
PHYSICAL FITNESS AND TOLERANCES TO ENVIRONMENTAL EXTREMES.
K. E. Klein, H. M. Wegmann, H. Brüner, and L. Vogt (Deutsche Forschungs- und Versuchsanstalt für Luft- und Raumfahrt, Institut für Flugmedizin, Bad Godesberg, West Germany).
Aerospace Medicine, vol. 40, Sept. 1969, p. 998-1001. 33 refs.

During "submaximum" loading tests of 20-30 min duration at simulated altitude (312 mm Hg), during acceleration, and during exercise at sea level and at moderate simulated altitude (578 mm Hg), heart rates were significantly lower for highly trained athletes (20-25 per cent) than in nonathletes. In maximum tolerance tests, however, there was a significant difference between the two groups only for maximum oxygen uptake at physical exercise, but no indication was seen for a positive cross-adaption effect of physical exercise training on the other stressors. Statistical analysis of the correlation between heart rate responses to the different stressors and the corresponding tolerances proved negligible relationships only; whereas heart rates were always highly dependent on sea level maximum oxygen uptake. The results do not support the idea of an improvement of human tolerance to environmental extremes by physical exercise training. (Author)

A69-41800 *
PRESCRIPTION OF EXERCISE FOR THE HYPOKINETIC AIRLINE PILOT.
L. E. Morehouse (NASA, Manned Spacecraft Center, Dept. of Preventive Medicine, Houston, Tex.; California, University, Dept. of Physical Education, Human Performance Laboratory, Los Angeles, Calif.), W. L. Marxer, and E. D. Warren (NASA, Manned Spacecraft Center, Dept. of Preventive Medicine, Houston, Tex.; Federal Aviation Administration, Los Angeles, Calif.).
IN: AVIATION AND SPACE MEDICINE; PROCEEDINGS OF THE SEVENTEENTH INTERNATIONAL CONGRESS, OSLO, NORWAY, AUGUST 5-8, 1968. (A69-41783 23-05)
Edited by Birger Hannisdahl and C. W. Sem-Jacobsen.
Oslo, Universitetsforlaget, 1969, p. 146-153.

Discussion of the recent advances in exercise physiology and instrumentation which have made it possible to establish standards for evaluation of exercise tolerance, to define personal training loads, and to prescribe exercise for the hypokinetic airline pilots in accordance with their needs and interests. The signs of hypokinesis in airline pilots, due mostly to lack of physical exercise, the prescriptions of physical exercise in accurate doses, the pertinent predictive tests and their evaluation, are described. A number of methods and means of controlling the heart rate are reviewed. The procedures used in calibration tests to establish the current level of the pilot's most vigorous regular physical activity and the maximum work rate at which exercise is well tolerated, as well as the respective metered training regimens, are commented on in detail. O.H.

A69-42850 * #
EVA MANEUVERING UNIT COMPARISON.
Allwin E. Wudell, William H. Tobey (Martin Marietta Corp., Space Operations Section, Research Dept., Denver, Colo.), and C. E. Whitsett, Jr. (NASA, Manned Spacecraft Center, Houston, Tex.).
American Astronautical Society and Operations Research Society of America, Joint National Meeting, Denver, Colo., June 17-20, 1969, AAS Paper 69-516. 46 p.
Contracts No. AF 33(615)-68-C-1175; No. NAS 9-9109.

Description of two studies on the comparison, through simulation, of three maneuvering units for space tasks. The maneuvering units considered are: (1) an unstabilized astronaut maneuvering unit (AMU), (2) a hand-held maneuvering unit (HHMU), and (3) an integrated maneuvering and life support system (IMLSS). The test subject was suspended in the gimbaled head of the six-degree-of-freedom servo-driven moving-base simulator. The simulation technique involves computation of the problem dynamics on a hybrid computer that then determines the commands for the moving base. Instrument maneuvering unit hand controller mockups are used by the test subject. Signals from the hand controller mockups are used in the hybrid program to introduce the thrust histories. The performance comparison data for the AMU and HHMU, as well as for four configurations of the IMLSS, are established. Z.W.

A69-42876 * #
RECENT ADVANCES IN CLOSED LIFE SUPPORT SYSTEM CONCEPTS.
Jacob Shapira (NASA, Ames Research Center, Biotechnology Div., Moffett Field, Calif.).
American Astronautical Society and Operations Research Society of America, Joint National Meeting, Denver, Colo., June 17-20, 1969, AAS Paper 69-143. 12 p. 23 refs.

The logistics of long duration manned space missions demands that effective systems be developed for the recovery of useful materials from metabolic and other wastes. The order of priority is water, oxygen, and food. The current state of development is also in the same order. This work discusses those approaches to these problems which are currently under most intensive investigation in this country. Water is most conveniently recovered by a combination of vacuum distillation and multifiltration. Carbon dioxide is removed by absorption and is subsequently reduced to methane with hydrogen to produce additional water. Oxygen can be produced from water by electrolysis of recovered liquid water or directly from the vapor phase. Bioregenerative food systems may have utility, but physicochemical methods appear to offer many advantages. (Author)

A69-42983 * #
A MULTIPURPOSE VENTRICULAR ACTUATING SYSTEM.
John A. Webb, Jr. and Vernon D. Gebben (NASA, Lewis Research

Center, Cleveland, Ohio).
International Federation for Medical and Biological Engineering, International Conference on Medical and Biological Engineering, 8th, and Annual Conference on Engineering in Medicine and Biology, 22nd, Chicago, Ill., July 19-25, 1969, Paper. 11 p.

Description of the design of a pneumatic driving system for heart assist or total heart replacement pumps. The system provides square pressure waveforms to drive the heart assist and uses feedback control to regulate a total heart replacement pump. A pneumatic square wave generator was developed to serve as a flexible tool for studying various cardiac assist techniques. This generator can be synchronized with the natural heart using the R-wave of the electrocardiogram as a trigger. The addition of feedback control to regulate a total heart replacement is discussed and data are given.
(Author)

N69-10813*# California Univ., San Diego.
EXPERIMENTS ON VISUAL ACUITY AND THE VISIBILITY OF MARKINGS ON THE GROUND IN LONG-DURATION EARTH-ORBITAL SPACE FLIGHT
S. Q. Duntley, R. W. Austin, J. L. Harris, and J. H. Taylor Washington NASA Nov. 1968 231 p refs
(Contract NAS9-5095)
(NASA-CR-1134; SIO-Ref-68-6) Avail: CFSTI CSCL 06S

Visual acuity experiments conducted during the Gemini program are discussed. The report sets forth the evolution of the experimental design, the preparatory experiments, the equipments constructed, the training of flight crews and teams of experimenters, the selection of ground sites, their preparation and operation, the inflight experiments on Gemini 5 and Gemini 7, the resulting data and their interpretation, the conclusions and their meaning in terms of the Apollo mission and other future spaceflights, as well as certain suggestions for future inflight tests of human visual capabilities in space. Author

N69-11675*# Case Western Reserve Univ., Cleveland, Ohio.
A LUNAR GRAVITY SIMULATOR, VOLUME 1
Washington NASA Nov. 1968 34 p
(Contract NAS1-7459)
(NASA-CR-1233-vol-1) Avail: CFSTI CSCL 14B

A prototype lunar gravity simulator using magnetic air bearing supports with constant force spring motors, and specially designed harness is described. The system is suspended from a steel ceiling. The subject, wearing a crash helmet and boots, rides in a three axis gimbaled harness. The harness system is suspended from the center of a spider ring which is supported by cables that wind and unwind by constant force spring motors. The system supports approximately 5/6 of the subject's weight, and permits freedom of movement. The simulator is designed to accommodate subjects weighing from 168 to 264 pounds. Testing results, precautions regarding operation, and details of the harness are presented.
F.O.S.

N69-13161*# Lockheed Missiles and Space Co., Sunnyvale, Calif.
VISUAL SENSING OF SPACECRAFT GUIDANCE INFORMATION. EARTH ORBIT RENDEZVOUS MANEUVERS
S. Seidenstein, W. K. Kincaid, Jr., G. L. Kreezer, and D. H. Utter Washington NASA Dec. 1968 257 p refs
(Contract NAS1-6801)
(NASA-CR-1214) Avail: CFSTI CSCL 06B

An analysis of each orbit rendezvous in terms of maneuver geometry served as a basis for establishing the requirements for visually sensed rendezvous guidance information. Analysis of the physical environment supported an evaluation of the sensory basis for visually deriving the desired information. Visual capabilities were then examined in terms of sensitivity, cross range motion perception, range, and range rate determinations. Estimates of sensitivity and variability are presented where available. Conclusions are drawn regarding the adequacy of available data, and recommendations are given for future areas of study. Author

N69-13202*# Webb Associates, Malibu, Calif.
PRELIMINARY EVALUATION TEST OF THE LANGLEY CARDIOVASCULAR CONDITIONING SUIT CONCEPT
B. V. Blockley and S. L. Friedlander Washington NASA Dec. 1968 70 p refs
(Contract NAS1-6004)
(NASA-CR-1206) Avail: CFSTI CSCL 06K

Two experiments were conducted, each two weeks in duration, in which the same subject spent the major portion of each day immersed in water and the remainder of the time in bed. The man remained completely horizontal except when submerged. In the control experiment, a simple waterproof garment was worn over ordinary long underwear during water immersion; in the second experiment the man was dressed in a specially constructed pressure suit designed to prevent or retard the deconditioning of weightlessness (cardiovascular conditioning suit or CVCS). The cardiovascular conditioning suit successfully prevented the deterioration in orthostatic tolerance, impairment in tolerance for brief mild exercise, and reduction in maximum work capacity which had been observed in the control experiment. During the initial 5 days, when pressurization time in the suit was less than one hour per day, venous compliance increased roughly 2-fold, but had fallen again to the initial value by the morning of the 11th day. Venous compliance appears to be an excellent predictor of tilt-table response. In the experiment in which the CVCS was used there was essentially no difference in venous compliance between pre- and post-exposure, and the tilt responses were the same except for a slight elevation of diastolic pressures during the post-exposure tilt.
Author

N69-13926*# Michigan Univ., Ann Arbor.
SKILL TRAINING FOR THE PRODUCTION OF A MEMORIZED MOVEMENT PATTERN
Margaret Robb and Richard W. Pew Washington NASA Dec. 1968 37 p refs
(Contract NASR-54(06))
(NASA-CR-1251) Avail: CFSTI CSCL 05H

Based on the assumption that man may be regarded as an information processing system, experiments were conducted to assess the efficacy of several kinds of feedback information. Five groups of subjects were trained under different feedback conditions in the execution of a distinctive movement pattern. In a subsequent test condition, all groups attempted to reproduce the movement pattern without the aid of any external concurrent feedback. The training conditions, reflecting different modes of feedback, were blanked, vision, vision–blanked, passive–active, and slow–standard. The main variables were the types of terminal and concurrent feedback administered to the subjects through internal and external modes. Performance was compared in terms of integrated absolute error scores and in terms of a more detailed performance criterion that attempted to separate out performance precision with respect to amplitude and timing accuracy. The results are graphically depicted and it is hypothesized that the stage during training at which augmented feedback is introduced may be important. M.G.J.

N69-13969*# Lovelace Foundation for Medical Education and Research, Albuquerque, N. Mex.
RAPID (EXPLOSIVE) DECOMPRESSION EMERGENCIES IN PRESSURE-SUITED SUBJECTS
Emanuel M. Roth Washington Nov. 1968 129 p
(Contract NASr-115)
(NASA-CR-1223) Avail: CFSTI CSCL 06S

A review is presented of the biomechanical factors determining lung damage following explosive decompression of space suits in vacuum test chambers. Critical variables, such as ratio of free volume of suit to area of orifice, pressure ratio, and pressure differential, are outlined. Calculations were made of orifices caused by catastrophic disruption of typical soft and hard space suits at seal sites, and predictions were made as to the likelihood of lung

damage, based on the location of the seal disruption and open/closed glottis conditions. It was concluded that all seal areas should be designed for slow propagation of disruptive processes, and that preparation of therapeutic devices and facilities for handling explosive decompression emergencies would be advisable. It was found that use of gases other than 3.7 psia O_2 in the suits alters the hazard; the higher the percentage of helium in the mixture, the less is the hazard. Also, since the maximum possible amplitude of transmural pressure is determined by the pressure difference, the higher the initial pressure in the suit, the more hazardous the exposure. The pathological physiology of explosive decompression was reviewed, followed by a summary of the most recent ideas in selection and testing of subjects to reduce the hazard and the treatment of individual syndromes and conditions. Author

N69-14094*# Kentucky Univ., Lexington.
AN INVESTIGATION OF THE SUITABILITY OF WHITE RATS FOR SUB-ORBITAL STUDIES OF BEHAVIOR IN A GRAVITY FIELD
A. B. Broderson and K. O. Lange Washington NASA Dec. 1968 102 p refs
(Grant NsG-456)
(NASA-CR-1255) Avail: CFSTI CSCL 06C

Techniques were developed for evaluating the Spraque Dawley rat as a subject for the first of four in-flight gravity preference experiments to be launched into suborbital trajectories by Aerobee 150A rockets. Special configuration centrifuges were developed and used to experimentally determine the locomotion behavior of rats in fields of simulated gravity. Techniques were developed for investigating the effect of rocket launch stress on this behavior, and an environmental simulation system was developed and used to routinely prepare rats for the confinement, acceleration, spin, noise, and vibration of an Aerobee launch. The suitability of the subject and the effectiveness of the environmental simulation routine were verified by the satisfactory behavior demonstrated in the first flight experiment. Author

N69-14145*# Bolt, Beranek, and Newman, Inc., Cambridge, Mass.
HUMAN VISUAL SAMPLING PROCESSES: A SIMULATION VALIDATION STUDY
John W. Senders, Jaime R. Carbonell, and Jane L. Ward Washington NASA Jan. 1969 110 p refs
(Contract NAS1-5059)
(NASA-CR-1258; BBN-1681) Avail: CFSTI CSCL 05H

The results obtained in some fundamental investigations strongly support the notion that the behavior of the pilot or controller/monitor is largely determined by, and calculable on, the basis of physical characteristics of the system. Based on the results a validation study more nearly approaching operational situations was undertaken. This study used an instrumented flight simulator, operational pilots, and complete measuring, recording, and analysis techniques to validate and improve the methods offered by the theory. The applied goal of the program was to make possible an a priori evaluation of the work load which any set of information sources to be monitored and controlled will place on the man. The following results were obtained: a measure of the goodness of prediction of the Nyquist models, and the development and a measure of goodness of prediction of a new queueing/cost-effectiveness model. Author

N69-14212*# Systems Technology, Inc., Hawthorne, Calif.
SMALL PERTURBATION DYNAMICS OF THE NEUROMUSCULAR SYSTEM IN TRACKING TASKS
Raymond P. Magdaleno, Duane T. Mc Ruer, and George P. Moore Washington NASA Dec. 1968 133 p refs
(Contract NAS2-2824)
(NASA-CR-1212; TR-154-1) Avail: CFSTI CSCL 05H

Existing physiological data and human operator describing function data are synthesized by providing models which are compatible with the overall human operator's input/output characteristics, as well as with the individual components of the neuromuscular system in tracking situations. Of interest are recent anatomical and physiological data for the muscle spindle and input/output studies of the muscle which indicate that quasi-linear models can describe the basic behavior of these elements in tracking tasks. Two key developments are reported: 1) variation in muscle system parameters as a function of average muscle tension or operating point, and 2) the role of the muscle spindle both as an adaptive equalization element and in its effect on setting muscle tone or average tension. The pertinent whole human data include the covariation of high and low frequency describing function phase data and the variation of high frequency phase with set tension changes interpreted from force disturbance experiments. Author

N69-14213*# Case Western Reserve Univ., Cleveland, Ohio.
A LUNAR GRAVITY SIMULATOR, VOLUME 3
Dennis A. Millett Washington NASA Dec. 1968 252 p refs
(Contract NAS1-7459)
(NASA-CR-1235) Avail: CFSTI CSCL 14B

Magnetic air bearings for use as low friction overhead support fixtures in a vertical lunar gravity simulator were investigated. This device consists of a flat magnetic disc with a central air orifice. The theoretical analyses of the air bearing are in good agreement with experiment. Theoretical magnet force ranged from 15% to 35% above the experimental value. Disc ceramic magnets were theoretically optimized based on maximum force-to-weight ratio and design curves are presented. Author

N69-14345*# Louisville Univ., Ky.
EFFECTS OF PRACTICE AND WORK LOAD ON THE PERFORMANCE OF A CODE TRANSFORMATION TASK (COTRAN)
Earl A. Alluisi and Ben B. Morgan, Jr. Washington NASA Dec. 1968 73 p refs
(Grant NGR-18-002-008)
(NASA-CR-1261) Avail: CFSTI CSCL 05H

Results are presented on the effects of practice and operator work load on the acquisition and performance of a code-transformation (COTRAN) task, which was developed to obtain performance measurements of that part of intellectual functioning which is typically called non verbal mediation; it follows the problem-solving paradigm. During the acquisition phase, 27 COTRAN problems were solved on each of four (Group-4, with four subjects), eight (Group-8, with twenty subjects), or twelve (Group-12, with four subjects) successive days. Performance reached asymptotic levels in four to six sessions, in general, and the differences in final levels of performance of the three groups (4, 8, and 12) were not statistically significant. During the transfer phase, each of the 28 subjects solved 27 COTRAN problems of each of five successive days while time-sharing the COTRAN task with different combinations of tasks selected from a multiple-task performance battery. The results indicated that skilled COTRAN performance is sensitive to at least two or three levels of work-load stress, and that different subjects may tend to adopt different strategies in time-sharing the COTRAN task with other tasks. Author

N69-14478*# Dunlap and Associates, Inc., Darien, Conn.
PERIPHERAL VISION DISPLAYS, PHASE 2 REPORT
Leroy L. Vallerie Washington NASA Dec. 1968 49 p refs
(Contract NAS12-88)
(NASA-CR-1239; BSD-68-643) Avail: CFSTI CSCL 05H

Two commercially available display systems were investigated in conjunction with other concepts involving the use of flicker to

encode airspeed signals and differential brightness to enhance the discriminability of input signals. Tracking information was presented in three control dimensions: viz., pitch, roll and airspeed. An adaptive loop simulator was employed to evaluate operator performance. The results clearly indicated that effective control can be exercised using peripheral displays employing changes in motion as the primary encoding stimulus. A higher level of performance was achieved with one system which contained a single display for presenting integrated pitch and roll signals. The addition of airspeed was found to degrade performance in pitch and roll under all display conditions. Performance could not be enhanced by means of differential brightness. Further evidence was provided for the use of motion as a very effective means for encoding displays designed for viewing in the periphery. Author

N69-14768*# Michigan Univ., Ann Arbor.
PROPRIOCEPTIVE CUES AND THEIR INFLUENCE ON OPERATOR PERFORMANCE IN MANUAL CONTROL
James Herman Herzog Washington NASA Jan. 1969 178 p refs
(Contract NASr-54(06))
(NASA-CR-1248) Avail: CFSTI CSCL 05H

The neuromuscular control system of the human upper limb was investigated as an auxiliary source of sensory information. Analysis of a functional block diagram of the human operator indicated that a control system with interesting characteristics could be devised if the control stick were constructed to be a mechanical analog of the plant being controlled. This is called the matched manipulator control technique, in which the control force applied to the plant is a scalar multiple of the reaction force experienced by the operator. The operator is in a particularly advantageous position to formulate control strategies to emphasize either accurate control performance or minimum use of control effort. Experimentation with several human operators indicated that performance with the matched manipulator technique was consistently superior to control of the same plants with position type control sticks. This technique seems to offer an interesting and useful means of altering the interface between the human operator and his electro-mechanical surroundings in order to improve the system performance. Author

N69-14979*# Case Western Reserve Univ., Cleveland, Ohio.
A LUNAR GRAVITY SIMULATOR, VOLUME 2
Richard J. Morgen Washington NASA Dec. 1968 142 p refs
(Contract NAS1-7459)
(NASA-CR-1234) Avail: CFSTI CSCL 14B

The design of a vertical lunar gravity simulator is presented. The simulation technique involves negating the various limb segments separately using constant-force negator springs. Overhead support is provided by magnetic air pads which offer negligible resistance to horizontal movement. The torso harness that is used provides for six degrees of freedom over a wide range of movements. The dynamic behavior of the lunar gravity simulator is considered. Indications are that low fatigue-life negator coils mounted back-to-back will be suitable as constant-force, long-deflection springs. A conical drum, adjustable-force negator unit is optimized for minimum weight. A technique for determing the mass and center of mass of the various body segments is also presented. An analysis to determine the correct attachment points for negating the limbs and torso is presented. It is recommended that negator coils of the lowest rated fatigue life be used as constant-force, long-deflection spring elements. Author

N69-15372*# Systems Technology, Inc., Hawthorne, Calif.
MEASUREMENT OF PILOT DESCRIBING FUNCTIONS IN SINGLE-CONTROLLER MULTILOOP TASKS
Robert L. Stapleford, Samuel J. Craig, and Jean A. Tennant Washington NASA Jan. 1969 109 p refs
(Contract NAS2-3144)
(NASA-CR-1238; TR-167-1) Avail: CFSTI CSCL 05H

Problems of measuring pilot describing functions in multiloop tasks with one controller (i.e., where the pilot is controlling two, or more, response variables with a single manipulator are considered. Both direct and implicit measurement techniques were considered and tested experimentally. The experimental task used was attitude and altitude control with elevator of an aircraft in a simulated landing approach. Experimental results show that the measurement of multiloop describing functions is feasible, although the techniques are considerably more complex than those required for single-loop compensatory tasks. However, there are fundamental limitations on the accuracy of some of the results. These are discussed in detail. The experimental data also provide a spot check on the existing multiloop pilot model. The results support the current model and, in particular, show that the inner-loop (attitude) closure is quite similar to that for single-loop attitude tracking. Author

N69-15629*# National Aeronautics and Space Administration. Langley Research Center, Langley Station, Va.
POTENTIAL PROBLEMS RELATED TO WEIGHTLESSNESS AND ARTIFICIAL GRAVITY
Ralph W. Stone, Jr. and William M. Piland Washington Jan. 1969 60 p refs
(NASA-TN-D-4980) Avail: CFSTI CSCL 06S

A study has been made of many publications to provide planners of future space missions with a summary of the pertinent problems associated with the weightless environment of space. Based on this study, a review is presented of the possible adverse effects of weightlessness on the astronaut's physiological processes and his performance in space. Techniques and devices which are potentially capable of counteracting the adverse effects of weightlessness are discussed. These counteractive measures include lower-body negative pressure devices, pressure cuffs, anti-g suits, the cardiovascular conditioning suit, exercise apparatus, and artificial gravity. The impact of additional weight and crew involvement in the inclusion of these devices on a particular mission is also discussed. The effects of these devices range from minor increases in launch weight and crew activity to significant vehicle-configuration complexity and astronaut involvement. Results are presented of research on the therapeutic value of the counteractive devices for weightlessness. Where an insufficient assessment of these devices exists, further research is recommended which could influence a decision on their use. Primarily, it is important to determine whether the effects of simulated weightlessness are progressive beyond that which has been experienced to date or whether the effects plateau at a specific level of physiological adaptation. Author

N69-16212*# Michigan Univ., Ann Arbor.
A STUDY OF HUMAN OPERATOR PERFORMANCE USING REGRESSION ANALYSIS
August Llewellyn Burgett Washington NASA Jan. 1969 192 p refs
(Contract NASr-54(06))
(NASA-CR-1259) Avail: CFSTI CSCL 05I

The regression analysis technique is used to analyze the performance of human operators in low order compensatory manual control systems. This study is based on two experiments in which the subjects controlled single and double integrator dynamical systems with an input which was low frequency noise. In modeling the human operator system the crossover model is used. This model expresses the entire forward-loop of the compensatory control system as a series of operators: a gain K, a time-delay τ, and a single integration. The study takes the form of obtaining estimates of the parameters K and τ for twenty-five 20-second intervals for each day of testing. From an analysis of these parameter values, inferences are made about the performance of the human operators. Author

05 BIOTECHNOLOGY

N69-17738*# Michigan Univ., Ann Arbor.
A FUNDAMENTAL STUDY OF PREDICTIVE DISPLAY SYSTEMS
John De Shon Warner Washington NASA Feb. 1969 200 p refs
(Contract NASr-54(06))
(NASA-CR-1274) Avail: CFSTI CSCL 05H

The particular predictive technique considered utilizes a repetitive, fast time, on-line computation scheme which provides a predicted response of the controlled element to the human operator based on certain assumptions about future control inputs and disturbances. An in depth discussion is provided on the various characteristics that are important in any predictive display application. The problem of performance measurement is discussed. An experimental investigation on the effects of the controlled element dynamics on performance with three display forms (exploratory prediction, on-line prediction, and no prediction) in a time vs. error format is reported. A minimum time terminal control task for a pure inertia system driven by a fixed three state relay controller was chosen for the study. The system is described by several independent parameters which are hypothesized as being important in a variety of manual control situations. These parameters are varied systematically to determine their effect on performance with the three display forms. Several new performance measures are developed for use in minimum-time terminal control tasks. Author

N69-17814*# National Aeronautics and Space Administration. Flight Research Center, Edwards, Calif.
HUMAN TRANSFER CHARACTERISTICS IN FLIGHT AND GROUND SIMULATION FOR A ROLL TRACKING TASK
Fred D. Newell (Cornell Aeron. Lab., Inc.) and Harriet J. Smith
(NASA-TN-D-5007) Avail: CFSTI CSCL 05H

Pilot transfer characteristics for three pilots were measured in flight and in ground based simulators for a compensatory roll tracking task with small bank angle disturbances. The forcing function, in each case, consisted of the sum of ten sine waves with a bandwidth of 1.5 radians per second. A variable stability T-33 airplane was used to obtain the flight measurements. Ground based simulator measurements were obtained with both the T-33 airplane and a general purpose simulator which used a contact analog color display. Three different controlled elements were used, two of which were simple single degree of freedom controlled elements that were studied previously. The third was a multiple degree of freedom element representative of an airplane with good handling qualities and was considered and controlled as a single degree of freedom configuration in roll. The results of the simple controlled element experiments agreed reasonably well with previous results. For the multiple degree of freedom controlled element experiment, a noticeable effect of display was found. For this experiment, which was restricted to a small disturbance bank angle tracking task with good controlled element dynamics, nonvisual motion cues appeared to be of less importance than visual cues. Author

N69-19902*# Environmental Research Associates, Randallstown, Md.
CORRELATION STUDY OF THE SIMULATION OF GEMINI EXTRAVEHICULAR ACTIVITY WITH FLIGHT RESULTS
Harry L. Loats, Jr., G. Samuel Mattingly, and G. M. Hay Washington NASA Feb. 1969 199 p refs
(Contract NAS1-7142)
(NASA-CR-1146; ERA-67-7) Avail: CFSTI CSCL 22A

The water immersion simulation of the Gemini EVA utilized full-scale mockups of the Gemini vehicle including portions of the Agena target vehicle with valid replicas of ancillary EVA equipment such as tools, astronaut maneuvering unit, etc. All important items were maintained in a neutrally bouyant condition. Bio-instrumentation was incorporated into the Gemini flight suits and continuous voice and film records were obtained. The water immersion simulation of the Gemini extravehicular activity provided a valid training time line for performance of complex extravehicular tasks and provided adequate measures of the level of work entailed. A second capability evidenced as a result of the program was the method for evaluating various competitive hardware concepts such as tools and motion restraints. The technique used in the preflight evaluation and training was to perform the simulation run with ERA subjects prior to actual performance of the training run by the astronaut. This technique permitted pre-evaluation of hardware in a repetitive manner and served to assess the validity of the water simulation mode. Factors such as drag-damping and orientational stability were compensated by variation of the mockup orientation and configuration. Author

N69-21478*# National Aeronautics and Space Administration, Washington, D. C.
TELEOPERATOR CONTROL An AEC-NASA Technology Survey
William R. Corliss and Edwin G. Johnsen Dec. 1968 169 p refs
(NASA-SP-5070) Avail: CFSTI CSCL 06B

A comprehensive survey on engineering problems in teleoperator control and man machine integration is given. The various technical chapters are divided into: (1) control theory; (2) man-machine interface; (3) control hardware; and (4) displays. Design principles and configurations cover the wide range between hot-cell master slaves to walking machines and their varying electronic subsystems. G.G.

N69-21501*# National Aeronautics and Space Administration. Marshall Space Flight Center, Huntsville, Ala.
SIMULATION OF PACKAGE TRANSFER CONCEPTS FOR SATURN 1 ORBITAL WORKSHOP
Charles B. Nelson Washington Mar. 1969 15 p
(NASA-TN-D-5111) Avail: CFSTI CSCL 06B

Investigated was the problem of manual transferring massive packages in a zero-g environment from the Saturn docking adapter into the crew quarter areas of the Saturn stage. Only a single handrail was to be used to assist the astronaut during package manipulation. Preliminary transfer simulation studies with a six degree of freedom simulator established the efficiency of the pole and the basic man/package transfer technique. Analysis and correlation of data from the simulations indicated that a combination of package parameter size and mass (moment of inertia) effected package maneuverability; a package with a moment of inertia 3.4 to 4.0 N–m-sec^2 (300 to 350 in.–lbf–sec^2) appeared to be the upper limit for one man to transfer within a reasonable time frame. G.G.

N69-21773*# National Aeronautics and Space Administration. Lewis Research Center, Cleveland, Ohio.
PERFORMANCE AND CAVITATION DAMAGE OF AN AXIAL-FLOW PUMP IN 1500° F (1089 K) LIQUID SODIUM
Dean C. Reemsnyder, Walter S. Cunnan, and Carl Weigel Washington Apr. 1969 25 p refs
(NASA-TN-D-5138) Avail: CFSTI CSCL 13L

A low headrise axial flow pump was operated in liquid sodium at temperatures to 1500° F for 558 hr to investigate pump performance and blade cavitation damage in alkali metals. The research rotor had nine insertable blades of three different materials, a blade tip diffusion factor of 0.40, and a hub tip radius ratio of 0.77. Overall performance was obtained, and a 200 hr cavitation endurance test was conducted in 1500° F sodium at 3450 rpm. Post-test blade inspection indicated that there was slight cavitation damage and that the Ni–Cr-base superalloy (René 41) was more cavitation damage resistant to high temperature sodium than either 316 or 318 stainless steel. Author

N69-22766*# Battelle Memorial Inst., Columbus, Ohio.
SYSTEMS APPROACH TO EVALUATING HYDROGENOMONAS CULTURES
John F. Foster and John H. Litchfield Washington NASA Apr. 1969 48 p refs
(Contract NAS2-4270)
(NASA-CR-1296) Avail: CFSTI CSCL 06M

Cultures of *Hydrogenomonas eutropha* are confirmed as a stable process operating at room temperature for waste conversion, to consume the metabolic wastes carbon dioxide and urea; and the hydrogen by-product from water electrolysis. Environmental measurements with feedback controls can balance consumption of these wastes by individual makeups at the same rates as consumption. In this manner, a stable culture with constant conversión rates can be maintained in steady state growth for long periods and is suitable for consideration as a continuous waste conversion process. The growth rate indicated by careful experimental measurements is a fractional increase of 0.33 per hour of the weight of bacterial cells in the culture, which is harvested continuously from a cellular culture maintained at a constant concentration of 6.1 g (dry weight) per liter of liquid culture. These values can be used for calculating the maximum production rate of cellular material in evaluating potential practical applications. Author

N69-22990*# National Aeronautics and Space Administration. Manned Spacecraft Center, Houston, Tex.
THE RELATIONSHIP BETWEEN OPTICAL DISTORTION AND BINOCULAR DEPTH PERCEPTION
L. R. Loper and R. C. Stout Washington Apr. 1969 10 p refs
(NASA-TN-D-5162) Avail: CFSTI CSCL 06B

Binocular depth perception, a vital function during spacecraft docking and lunar landing, could be degraded by any spacecraft system optical transparency. A study of the relationship between binocular depth perception and optical distortion in the Apollo pressure suit helmets and visors was made to aid in setting optical distortion limits for the helmets and visors. Data obtained from the study indicated that all the helmets and visors which were tested degraded binocular depth perception. As measured by the Howard–Dolman apparatus, there is evidently a systematic effect of optical distortion in the Apollo helmets and visors on binocular stereoscopic depth perception. A program for studying this problem in greater depth is outlined. Author

N69-23842*# National Aeronautics and Space Administration. Ames Research Center, Moffett Field, Calif.
A TECHNIQUE FOR IDENTIFYING PILOT DESCRIBING FUNCTIONS FROM ROUTINE FLIGHT-TEST RECORDS
Rodney C. Wingrove and Frederick G. Edwards Washington May 1969 33 p refs
(NASA-TN-D-5127) Avail: CFSTI CSCL 06B

The problem of identifying the input-output relationship of the pilot by use of measured data from routine flight operations in which the pilot provides feedback control is considered. The problem in using the measured input and output data directly is that any extraneous output noise by the pilot causes an error in identification. This problem is solved by the development of a computer processing technique that, under certain conditions, yields an estimate relatively free from identification error. A theoretical analysis to show that this technique will reduce the identification error is presented. The simulation and identification of several known system elements are included to compare with the theory and to illustrate the use of this technique. Also, results obtained from the retrofire phase of the Gemini X mission are presented to demonstrate the application of this technique to routine flight-test records. Author

N69-26259*# National Aeronautics and Space Administration. Langley Research Center, Langley Station, Va.
THE EQUIPOTENTIAL SPACE SUIT DESIGN CONCEPT AND ITS APPLICATION TO A SPACE SUIT ELBOWJOINT
Donald E. Barthlome Washington May 1969 43 p ref
(NASA-TN-D-5221) Avail: CFSTI CSCL 06K

Space-suit design studies indicate that a high operational feasibility exists for a concept involving a nonconstant-volume space-suit elbow joint, a joint-assist mechanism, and a space-suit pressure stabilizer. The space-suit pressure stabilizer serves to limit pressure changes within the joint to ± 0.05 psi (0.035 N/cm^2). The joint-assist mechanism, or joint assist, is a modified constant-force spring mounted on a soft space-suit joint. The cross section of the spring has been altered so that most of the energy required to bend the joint is provided by the joint assist. The joint and stabilizer, both of which exhibit relatively high degrees of elasticity, store most of this energy and return it to the joint assist as the joint and stabilizer return to their initial configurations. Therefore, if friction is neglected, the joint, joint assist, and stabilizer constitute a system with a total potential energy that remains constant (regardless of the angle of bend) and equal to the initial potential energy given to the assist during installation on the joint. Test results show that the maximum bending moment required by the joint was reduced from 1.40 lbf-ft (1.90 N-m) without the assist to 0.10 lbf-ft (0.14 N-m) with the assist, a reduction of 14 to 1. Author

N69-26455*# Aztec School of Languages, Inc., Acton, Mass.
PERCEPTION OF SPACE AND TIME IN OUTER SPACE
A. A. Leonov et al Washington NASA May 1969 111 p refs Transl. into ENGLISH of the book "Vospriyatiye Prostranstva i Vremeni v Kosmose" Moscow, Nauka Press, 1968 p 1–115
(Contract NASw-1692)
(NASA-TT-F-545) Avail: CFSTI CSCL 06S

The characteristic dynamics of spacecraft flight are explained as well as the role of astronauts in the "man-spacecraft" system. The authors describe how the conditions of existence and the psychophysiological mechanisms of perception of space and time outside the earth change during a flight in outer space. The effect of weightlessness, prolonged isolation in a small area, emotional tension, and other factors of space flight on human perception of time are explained. Author

N69-27266*# Garrett Corp., Los Angeles, Calif.
A STUDY OF ASTRONAUTS' EXTRAVEHICULAR WORK CAPABILITIES IN WEIGHTLESS CONDITIONS
E. C. Wortz, W. Schreck, W. Robertson, G. Lamb, and L. Browne Washington NASA May 1969 247 p
(Contract NAS1-7571)
(NASA-CR-1334) Avail: CFSTI CSCL 05E

Exploratory experiments were conducted on methods of erection and assembly of large modules, transportation of cargo modules, and crew rescue during weightless simulation by neutral buoyancy techniques. A formal experiment was conducted on four typical restraint systems during the performance of various tasks with varying work envelopes. Data were collected on energy expenditures, reactive loads, and performance times. Conclusions are drawn about various aspects of extravehicular activity work and the efficacy of restraint systems. Author

N69-27577*# Aztec School of Languages, Inc., Acton, Mass.
ELECTROMEDICAL APPARATUS: PRINCIPLES OF OPERATION, INSTALLATION, AND USE
N. M. Liventsev Washington NASA May 1969 430 p Transl. into ENGLISH of the book "Elektromeditsinskaya Apparatura; Printsip Deystviya, Ustroystvo, Ekspluatatsiya" Moscow, Meditsina Press, 1964
(Contract NASw-1692)
(NASA-TT-F-523) Avail: CFSTI CSCL 06B

This expanded and updated edition covers the following: (1) phototherapeutic appartus, including the use of optical radiation,

lamps for infrared and photothermal radiation, and lamps for ultraviolet radiation; (2) electrocardiographs powered by battery and line voltage, and low-frequency amplifiers; (3) dc and low-frequency electrotherapeutic apparatus; (4) electrotherapeutic apparatus using high-frequency currents; (5) apparatus for ultrasonic therapy; and (6) organization and operation of electrical phototherapeutic departments. K.W.

N69-28024*# National Aeronautics and Space Administration. Langley Research Center, Langley Station, Va.
SIMULATION OF GEMINI EXTRAVEHICULAR TASKS BY NEUTRAL-BUOYANCY TECHNIQUES
Otto F. Trout, Jr., Gary P. Beasley, and Donald L. Jacobs (NASA Manned Spacecraft Center) Washington Jun. 1969 92 p refs
(NASA-TN-D-5235) Avail: CFSTI CSCL 05E

Neutral-buoyancy simulation techniques were applied to investigate experimentally the astronaut's extravehicular tasks in the Gemini flight program. The preflight hardware, procedures, modes of performance, and data developed during the neutral-buoyancy tests are described and compared with those pertaining to the extravehicular activities in the Gemini flights. Continuing development of the simulation during this investigation showed that the techniques are useful in assessing procedures and supporting hardware, obtaining a reasonable estimate of the subject's energy expenditure, and developing realistic time lines in training the astronaut for the extravehicular tasks in space. Author

N69-28071*# Systems Technology, Inc., Hawthorne, Calif.
EXPERIMENTS AND A MODEL FOR PILOT DYNAMICS WITH VISUAL AND MOTION INPUTS
Robert L. Stapleford, Richard A. Peters, and Fred R. Alex Washington NASA May 1969 126 p refs
(Contract NAS2-3650)
(NASA-CR-1325; TR-168-2) Avail: CFSTI CSCL 05H

This report describes the results of a simulator program to investigate the effects of motion cues on a manual-control tracking task. The experimental variables were controlled-elements dynamics, linear motion characteristics, and angular motion characteristics. The data obtained include: pilot describing functions, both overall (combined visual and motion feed-backs) and separate (independent visual and motion pathways); remnant characteristics; and tracking performance. These data are also compared with previous experimental results. A multimodality pilot model for both visual and motion feedbacks is derived. The dynamics of the two (angular and linear) motion feedback paths and the integration of visual and motion feedbacks are discussed. The implications of the experimental data and the multimodality pilot model on the design requirements for moving-base simulators are also reviewed. Author

N69-28099*# Westinghouse Electric Corp., Pittsburgh, Pa.
SOLID ELECTROLYTE SYSTEM FOR OXYGEN REGENERATION
L. Elikan and J. P. Morris Washington NASA Jun. 1969 180 p refs
(Contract NAS1-7306)
(NASA-CR-1359) Avail: CFSTI CSCL 05E

High efficiency multi-cell batteries employing $(ZrO_2)_{0.9}(Y_2O_3)_{0.1}$ electrolyte were constructed and operated for periods exceeding 100 days. Three five-cell batteries were life-tested; their lives were 152, 112, and 77 days. A continuous carbon deposition reactor in which the CO in the $CO–CO_2–H2–H_2O$ mixture produced by electrolysis was decomposed to form solid C and CO_2, was operated for 100 days without interruption and without decline in catalyst activity. Over 60% conversion was obtained throughout the test. The carbon produced was dry, free flowing, and non-clogging. Palladium foils were found to be an effective means of removing H_2 from a CO, CO_2, $H_2.H_2O$ mixture. Operated 800°C and above, no carbon deposition was observed on the foil. Based on the performance of the multi-cell electrolysis battery, carbon deposition reactor, and palladium foils tested, it is estimated that a solid electrolyte oxygen system can be built for a 4-man, 100-day mission which will weigh 121 pounds and require 1160 watts of power. Author

N69-30168*# Harvard Univ., Boston, Mass. School of Public Health.
PREDICTING HUMAN PERFORMANCE IN SPACE ENVIRONMENTS
Warren H. Teichner and Diane Olson Washington NASA Jun. 1969 186 p refs
(Grant NGR-22-007-070)
(NASA-CR-1370) Avail: CFSTI CSCL 06L

An attempt is made to provide a systematic framework which can be used for predicting the effects of the physical environment on human performance. The nature of the approach was: (1) to develop a general classification scheme for the description of tasks; (2) to develop postulates from the basic literature of psychology so as to formulate a quantitative model of wide scope representing fundamental behavioral processes assumed to underlie performance at the tasks; (3) to develop relationships between environmental conditions and major physiological effects known or thought to result from them; (4) to postulate relationships between selected ones of the underlying behavioral processes and the physiological effects, and then to use these relationships along with the performance model to predict the effects of the environment on performance; and (5) to develop a general criterion for determining the environmental conditions which should be considered limiting. Author

N69-32044*# Scripta Technica, Inc., Washington, D.C.
PROBLEMS OF SPACE BIOLOGY. VOLUME 7: OPERATIONAL ACTIVITY, PROBLEMS OF HABITABILITY AND BIOTECHNOLOGY
V. N. Chernigovskiy, ed. NASA May 1969 527 p refs Transl. into ENGLISH of the book "Problemy Kosmicheskoy Biologii. Vol. 7: Rabochaya Deyatelnost, Voprosy Obitayemosti i Biotekhnologiya" Moscow, Nauk, 1967
(Contract NASw-1694)
(NASA-TT-F-529) Avail: CFSTI CSCL 06S

In the papers presented, three problems are examined: psychophysiological aspects of operational activity, questions relating to the habitability and hygiene of spacecraft cabins, and the problem of biotechnology. For individual titles, see N69-32045 through N69-32106.

N69-33260*# National Aeronautics and Space Administration. Manned Spacecraft Center, Houston, Tex.
A REVIEW OF SPACECRAFT WASTE-MANAGEMENT SYSTEMS
W. W. Kemmerer, Jr. and Jon W. Morar Washington Aug. 1969 14 p
(NASA-TM-X-1851) Avail: CFSTI CSCL 05E

This document reviews the design requirements, development, and use of the waste-management systems for Project Mercury and for the Gemini Program. A review of the use of these systems during actual missions is included. Author

N69-33775*# National Aeronautics and Space Administration. Lewis Research Center, Cleveland, Ohio.
CLEAN ROOM TECHNOLOGY
James W. Useller Washington 1969 66 p refs
(NASA-SP-5074) Avail: SOD $0.35; CFSTI CSCL 06L

The clean room requirements are studied to control contamination for component reliability in industry and the space program. Contaminants are classified in four general categories: (1) particulate: dust, chips, fibers, etc.; (2) chemical: gases, liquids, oily films, etc.; (3) biological: bacteria, virus, fungi, spores, etc.; and (4) energy or changes of state. The controlling factors for clean rooms are facility design, equipment, procedures, activities, and maintenance. The operation and monitoring procedures are discussed. F.O.S.

N69-35024*# National Aeronautics and Space Administration. Ames Research Center, Moffett Field, Calif.
EFFECTS OF DIFFERING AMOUNTS OF TRAINING AND OF MONOCHROMATIC TARGETS ON SEXTANT SIGHTING PERFORMANCE
Emmett C. Lampkin and Robert J. Randle Washington Aug. 1969 10 p refs
(NASA-TN-D-5190) Avail: CFSTI CSCL 05I

Sighting performance using a standard marine, gimbal mounted sextant with a special telescope substituted for the eyepiece was studied in combinations of simulated monochromatic stars. The stars were simulated by projecting a point source of light onto a parabolic mirror. The point source was provided by placing a lamp behind a 0.0005-inch-diameter aperture and positioning it at the focal point of the parabolic mirror. The collimated image of the aperture being projected was perceived as a star at infinity. The combinations of stars studied were: red-red, white-white, and red-green. It is concluded that five days of training are sufficient for achieving a performance asymptote; and monochromatic stars may be used for sextant sightings, with performance being more consistant from the red end of the spectrum. A discussion of the results is presented. F.O.S.

N69-35540*# McDonnell-Douglas Co., Huntington Beach, Calif.
REQUIREMENTS STUDY FOR A BIOTECHNOLOGY LABORATORY FOR MANNED EARTH ORIBTING MISSIONS. VOLUME 2: SUMMARY OF INDIVIDUAL EXPERIMENTS REQUIREMENTS
L. T. Kail Washington NASA Aug. 1969 205 p refs
(Contract NAS7-518)
(NASA-CR-1409; DAC-58156) Avail: CFSTI CSCL 06S

This volume summarizes the requirements of each experiment used in establishing the biotechnology requirements described in Volume I of this report. The requirements for each experiment are presented in four sections: (1) biomedical and human research; (2) behavioral research; (3) bioscience research; and (4) life support and protective systems. The experiment title, category, and assigned number relate directly to the research program discussed in Volume 1, Section 2. Author

N69-35541*# McDonnell-Douglas Co., Huntington Beach, Calif.
REQUIREMENTS STUDY FOR A BIOTECHNOLOGY LABORATORY FOR MANNED EARTH ORBITING MISSIONS. VOLUME 1: RESULTS, RECOMMENDATIONS AND REQUIREMENTS
L. T. Kail Washington NASA Aug. 1969 169 p
(Contract NAS7-518)
(NASA-CR-1408; DAC-58155) Avail: CFSTI CSCL 06S

The objective of the study presented here was to expand and incorporate the results of past studies, into an all-encompassing life science research program (gap-filling as required) to identify manned Earth-orbital life science laboratory equipment requirements for the 1970's. Another objective of the study was to identify and integrate requirements that are common to the four life science research fields of biomedicine and human research, behavior, bioscience, and life support systems. An elementary sketch of a concept for a biotechnology laboratory as part of a multipurpose space station is shown. The individual equipment items required in the "laboratory area" are described. The centrifuge shown relates to requirements of experiments considered in this report and represents another program currently under study by NASA for life sciences research. This study has addressed itself to the total research activities and equipment encompassed by such a laboratory. The results of the study provide a basis for further definition of a facility. Author

N69-36271*# AiResearch Mfg. Co., Los Angeles, Calif. Dept. of Life Sciences.
MAN'S CAPABILITY FOR SELF-LOCOMOTION ON THE MOON. VOLUME 2: SUMMARY REPORT
E. C. Wortz, W. G. Robertson, L. E. Browne, and W. G. Sanborn Washington NASA Sep. 1969 85 p refs Revised
(Contract NAS1-7053)
(NASA-CR-1043; Rept-68-4262-Vol-2-Rev-1) Avail: CFSTI CSCL 06S

A comprehensive study of man's self-locomotive capabilities in simulated lunar gravity is presented. An inclined-plane and a gimbal-vertical simulator equipped with treadmills were used to simulate lunar gravity. Man's locomotive characteristics and the metabolic costs of walking, running, and loping at velocities from 2 to 12.8 km/hr were determined for subjects in pressurized Gemini-4C suits. The results showed that the energy cost of locomotion in simulated lunar gravity is considerably less than that in earth gravity. Ascending grades caused large increases in metabolic cost over that of level walking where the magnitude of the cost depends on the simulation technique used. Increasing the load carried from 75 to 400 earth pounds had a small and inconsistent effect on metabolic costs. Changing the smooth, hard walking surface to sandy soil caused a large increase in the metabolic cost at the higher locomotion rates. Author

N69-36709*# Environmental Research Associates, Randallstown, Md.
STUDY OF THE ASTRONAUT'S CAPABILITIES TO MAINTAIN LIFE SUPPORT SYSTEMS AND CABIN HABITABILITY IN WEIGHTLESS CONDITIONS
Harry L. Loats, Jr., George M. Hay, and Edwin Morris Washington NASA Aug. 1969
(Contract NAS1-7887)
(NASA-CR-1405; ERA-68-1) Avail: CFSTI CSCL 06S

The main emphasis during the program was to determine the applicability of various restraint and locomotion aids related to the performance of a variety of critical intravehicular tasks. Although the exact nature of future space station missions and hardware is not fully defined at present, certain important characteristics are indicated. Specific characteristics of the tasks were investigated and included: maintenance and repair of life support systems; working at a work bench, a standup platform, a work station, and a control console: locomotion about the interior of the compartment, data collection tasks including writing and calculations, cargo handling and storage, and general and housekeeping tasks. Author

N69-36925*# Dunlap and Associates, Inc., Darien, Conn.
DIFFERENTIAL THRESHOLDS FOR MOTIONS IN THE PERIPHERY
James M. Link and Leroy L. Vallerie Washington NASA Sep. 1969 22 p refs
(Contract NAS12-88)
(NASA-CR-1439; BSD-69-701) Avail: CFSTI CSCL 06N

A study was conducted to determine the differential thresholds for rotary and linear motion in the periphery. Isograms were developed based on threshold estimates obtained from ten subjects using the psychophysical method of limits. The results of this study indicated that differential thresholds for rotary and linear motion

were found to increase as a linear function of eccentricity angle. Threshold isograms for both types of motion are elliptical in shape with the horizontal axis approximately twice as long as the vertical axis. Based on statistical analysis, there appears to be no real difference between rotary and linear motion. Subjects, however, reported a preference for rotary motion. Thresholds decreased logarithmically as a function of changing speed. Age of the subject appears to be a highly significant factor which influences the perception of motion. At high display velocities, subjects reported the occurrence of interference factors such as blur, fusion, strobing and flicker. These factors were particularly noticeable with the linear display. Author

N69-37517*# Texas Technological Coll., Lubbock.
REMOVAL OF ACID GASES AND OXIDES OF NITROGEN FROM SPACECABIN ATMOSPHERES
A. J. Gully, R. M. Bethea, R. R. Graham, and M. C. Meador Washington NASA Jul. 1969 148 p
(Contract NAS1-7584)
(NASA-CR-1388) Avail: CFSTI CSCL 06K

The methods of removal of oxides of nitrogen and of the acid gases sulfur dioxide, hydrogen chloride, hydrogen fluoride, and chlorine in low concentrations from air as part of the effort to develop an effective atmospheric purification subsystem for long-term manned space missions were studied. Methods investigated were: (1) reaction with basic solid materials, (2) adsorption, and (3) for oxides of nitrogen, catalytic reduction of nontoxic to less toxic gases. Adsorption at ambient temperature of both chlorine and nitrogen dioxide on activated carbon was found to be rapid with sulfur dioxide being adsorbed to a lesser extent. In exploratory work, nickel oxide and copper oxide were found to exhibit appreciable activity in the catalytic decomposition of nitrogen dioxide. Maximum decomposition of nitrogen dioxide observed (nickel oxide catalyst at 482°C) was 53%. Nitric oxide was the major decomposition product. Solid-gas reaction was found to be the most generally effective method of contaminant removal. The solid reactants tested included sodium carbonate, sodium bicarbonate, barium carbonate, calcium carbonate, lithium carbonate, and manganese dioxide. Author

N69-37964*# AiResearch Mfg. Co., Los Angeles, Calif.
MAN'S CAPABILITY FOR SELF-LOCOMOTION ON THE MOON. VOLUME 1: DETAILED REPORT
E. C. Wortz, W. G. Robertson, L. E. Browne, and W. G. Sanborn Washington NASA Sep. 1969 408 p refs Revised
(Contract NAS1-7053)
(NASA-CR-1402; Rept-68-3986-Rev-1) Avail: CFSTI CSCL 06S

Results are presented on a comprehensive study of man's self-locomotive capabilities in simulated lunar gravity. An inclined-plane and a gimbal-vertical simulator equipped with treadmills were used to simulate lunar gravity. Man's locomotive characteristics and the metabolic costs of walking, running, and loping at velocities from 2 to 12.8 km/hr were determined for subjects in pressurized Gemini-4C suits. The results showed that the energy cost of locomotion in simulated lunar gravity is considerably less than that in earth gravity. Ascending grades caused large increases in metabolic cost over that of level walking where the magnitude of the cost depends on the simulation technique used. Increasing the load carried from 75 to 400 earth-pounds had a small and inconsistent effect on metabolic costs. Changing the smooth, hard walking surface to sandy soil caused a large increase in the metabolic cost at the higher locomotion rates. Author

N69-38491*# TRW Systems Group, Redondo Beach, Calif.
HEAT PIPE DEVICES FOR SPACE SUIT TEMPERATURE CONTROL Research Report, 30 Jun. 1966 - 1 Sep. 1968
Arnold P. Shlosinger Washington NASA Oct. 1969 56 p refs
(Contract NAS2-3817)
(NASA-CR-1400; TRW-06462-6005-R0-00) Avail: CFSTI CSCL 06K

Investigations performed to develop techniques for control of temperature in extravehicular space suits have provided technological knowledge of general applicability to temperature control systems. This report summarizes this knowledge. Other reports, referenced in this report, deal with the specific application to space suits and the related materials research performed. A heat pipe thermal switching device is described, and test results presented. Techniques for bonding of capillary structures to solid substrates are discussed. Recommendations for suitable bonding techniques are provided. Heat pipes of flexible materials are described, and data resulting from experimentation with flexible heat pipes presented. Concepts for preventing freezing or for restart of frozen heat pipes are discussed and experiments, demonstrating feasibility of one of these concepts, are described and data presented. Author

N69-38600*# Michael Reese Hospital and Medical Center, Chicago, Ill.
ANALYSES AND MEASUREMENTS OF BLOOD SAMPLES
Eric Reiss Washington NASA Oct. 1969 16 p
(Contract NAS2-4757)
(NASA-CR-1395) Avail: CFSTI CSCL 06P

Details of experimental procedures are given. The radioimmunoassay for parathyroid hormone (PTH) yielded reliable and reproducible measurements in man, and the methods developed in our laboratory are applicable for the investigation of calcium metabolism during weightlessness in space flight. Despite substantial accomplishments, many problems remain. These problems are spelled out in detail. They emphasize the need for ongoing investigations and improvement in currently employed technics. Author

N69-38701*# Aztec School of Languages, Acton, Mass. Research Translation Div.
PROBLEMS OF SPACE BIOLOGY, VOLUME 6
N. M. Sisakyan, ed. Washington NASA Jul. 1969 557 p refs Transl. into ENGLISH of the book "Problemy Kosmicheskoy Biologii, Tom. 6" Moscow, Nauka, 1967 p 1-528
(Contract NASw-1692)
(NASA-TT-F-528) Avail: CFSTI CSCL 06C

Presented are various studies on space biology and aerospace medicine. The effects of altered gravitation on humans and organisms and the biological action of radiation are investigated. For individual titles, see N69-38701 through N69-38759.

N69-39183*# National Aeronautics and Space Administration. Langley Research Center, Langley Station, Va.
APPLICATION OF HUMAN TRANSFER FUNCTIONS TO SYSTEM ANALYSIS
James J. Adams and Maxwell W. Goode Washington Oct. 1969 32 p refs
(NASA-TN-D-5478; L-6382) Avail: CFSTI CSCL 05E

An analytical study was made of a full-scale, manually controlled lunar landing simulator by using analytical transfer functions for the pilot control response along with the analytical representation for the mechanisms. The results of this study show that some of the dynamic characteristics of the simulator were in a range to influence the response of the manually controlled systems that were to be tested. Tests were made in which the dynamic response of the simulator was varied over a limited range of characteristics. The results confirm the conclusion of the analytical study in that the change did influence the piloted response. Author

N69-39210*# National Aeronautics and Space Administration. Marshall Space Flight Center, Huntsville, Ala.

ROTATING SPACE STATION STABILIZATION CRITERIA FOR ARTIFICIAL GRAVITY

Carl A. Larson Washington Oct. 1969 46 p refs

(NASA-TN-D-5426) Avail: CFSTI CSCL 06S

An understanding of man's dependency on a gravity field is an area where research has yielded limited results, thereby, prompting space station designers to include provisions for providing an artificial gravity field capability. A rotogravic environment, though satisfying certain of man's physiological requirements, can introduce other complicated requirements. Therefore, this investigation was devoted to obtaining, for space station designers, insight into how man's physiological tolerances and range of adaptability can be used to define operational and configurational design criteria. Author

N69-39211*# Stanford Research Inst., Menlo Park, Calif.

CHARACTERISTICS OF THE TACTILE INFORMATION CHANNEL

J. C. Bliss, J. W. Hill, and B. M. Wilber Washington NASA Oct. 1969 181 p refs

(Contract NAS2-4582)

(NASA-CR-1389) Avail: CFSTI CSCL 06S

Experiments with multiple-point tactile and visual stimulus fields are described. A number of the experiments involved a brief presentation of between 2- and 12-point stimuli randomly distributed in a 3 by 8 matrix. The subject's task was to specify the location of each point stimulated in the entire matrix (whole report) or in the subset of the matrix indicated by a marker (partial report). In some of these latter experiments all stimulators were activated after the point stimuli, forming an erasure field which interfered with the perception of the stimuli. Analogous visual and tactile experiments were performed. The experiments with the erasure post-field indicated that information is transferred in parallel, rather than sequentially, to higher centers. A model for both visual and tactile information processing is proposed. In another series of experiments the point stimuli were presented sequentially rather than simultaneously. The results indicated a strong dependence of the number of positions perceived in the correct spatial location with a minimum occurring in the range of 50 to 100 ms. Author

N69-39212*# Honeywell, Inc., Lexington, Mass. Radiation Center.

LABORATORY OCULOMETER

John Merchant Washington NASA Oct. 1969 100 p refs

(Contract NAS12-531)

(NASA-CR-1422) Avail: CFSTI CSCL 06B

The oculometer is an electro-optical device that measures the direction of pointing of the human eye. It is not attached to the subject, and operates with essentially invisible infrared radiation. The oculometer can find application in cases where eye direction is to be measured with a minimum of interference to the subject for: (1) psychological and physiological monitoring; and (2) eye control, that is the direct control of target acquisition/tracking systems by oculometer signals defining the direction of pointing of operator's eye. Author

06

CHEMISTRY

Includes chemical analysis and identification (e.g., spectroscopy). For applications see: 17 Materials, Metallic; 18 Materials, Nonmetallic; and 27 Propellants.

A69-10588 *

CALCULATION OF COMPLEX CHEMICAL EQUILIBRIA.

Frank J. Zeleznik and Sanford Gordon (NASA, Lewis Research Center, Cleveland, Ohio).

I & EC - Industrial and Engineering Chemistry, vol. 60, June 1968, p. 27-57. 93 refs.

Review of the calculation of complex chemical equilibria, with equal emphasis on both thermodynamic fundamentals and numerical analysis. Considerable attention is given to multipurpose schemes used to obtain solutions of the system of simultaneous equations describing chemical equilibrium, and special purpose schemes are treated in outline. The literature is surveyed, and some of the advantages and disadvantages of the various equilibrium computation schemes proposed are indicated. The application of equilibrium computations to typical problems is discussed. The two alternate, but equivalent, formulations of the conditions of chemical equilibrium are contrasted: first as a minimization of the Gibbs free energy and second as a set of equilibrium constant relations. I.P.

A69-10893 *

FLUORESCENCE SPECTRA OF HOMOGENEOUS AND MIXED EUROPIUM COMPLEXES.

Nicolae Filipescu (George Washington University, Dept. of Chemistry, Washington, D.C.), K. Moorjani, N. McAvoy, S. Bjorklund, C. R. Hurt, and J. Zumoff (NASA, Goddard Space Flight Center, Greenbelt, Md.).

Applied Spectroscopy, vol. 22, Sept.-Oct. 1968, p. 513-519. 28 refs. Grant No. NsG-603.

High-resolution emission spectra of several europium complexes with β-diketones, dipyridyl, and plenanthroline have been examined at 77 K in microcrystals. The Stark splitting of the ^7F levels in the ground multiplet and the relative intensities of the individual $^5D_0 \rightarrow {}^7F$ transitions can be used for theoretical correlation with the ligand field parameters, transition probabilities, molecular structure, and Eu-ligand bonding. The fluorescence spectra of the bis-aqua, tris, tris-aqua, tetrakis, and mixed chelates with the bidentate ligands are discussed in relation to molecular configuration. (Author)

A69-11285 *

KINETICS OF THE REACTION BETWEEN LITHIUM HYDRIDE AND LIQUID AMMONIA AT -78°C.

Irving Warshawsky (NASA, Lewis Research Center, Cleveland, Ohio).

Electrochemical Society, Journal, vol. 115, Oct. 1968, p. 1045, 1046. 8 refs.

Study of the reaction rate and the mechanism for the reaction between lithium hydride and liquid ammonia at -78°C. It is suggested that, once the reaction is underway, its continuation necessitates a chemisorption process in which ammonia dissociates at the lithium amide/liquid ammonia interface into a proton and an amide ion. M.G.

A69-11603 #

RELIABILITY IN THE ELIMINATION OF MULTIVALUEDNESS IN PHASE MEASUREMENTS [O NADEZHNOSTI USTRANENIIA MNOGOZNACHNOSTI FAZOVYKH IZMERENII].

G. I. Skrypnik, A. A. Serova, and D. I. Ataev.

Radiotekhnika i Elektronika, vol. 13, Oct. 1968, p. 1753-1761. 6 refs. In Russian.

Description of an algorithm for resolving the ambiguity arising in the two-scale method of phase measurements. The method of the greatest probability for white Gaussian noise interference is used to formulate the algorithm. A relationship is established between the reliability of eliminating the multivaluedness and the basic characteristics of the system in the presence of a parasitical shift between the scales. The results are extended to the case of multiscale measurements. I.P.

A69-14862 *

TRANSIENT ELECTRO-OSMOSIS IN CAPILLARY TUBES.

W. T. Hanna (Carnegie-Mellon University, Pittsburgh, Pa.; NASA, Lewis Research Center, Cleveland, Ohio) and J. F. Osterle (Carnegie-Mellon University, Pittsburgh, Pa.).

Journal of Chemical Physics, vol. 49, Nov. 1, 1968, p. 4062-4068. 10 refs.

Transient electroosmosis of water in glass capillary tubes is treated analytically. The usual selective ion adsorption mechanism is assumed. The analysis is restricted to tube radii greater than about 3×10^{-5} m for which the effects of fluid compressibility and electrical capacitance and inductance are negligible. The problem considered is the transient response of the system to a step change in either pressure or voltage under various external loading conditions. The resulting time histories of the induced force (voltage or pressure) and the fluid flow and electrical current are solved for. A Laplace transform technique is employed. Coupling coefficients are established in the Laplace domain relating the electrical current and fluid flow rate to the electric field and pressure gradient. The cross-coupling coefficients are shown to obey the reciprocal relations for nonsteady-state irreversible processes. (Author)

A69-16493 *

TRANSITIONS IN GLASSES AT LOW TEMPERATURES.

Robert A. Haldon, William J. Schell, and Robert Simha (Southern California, University, Dept. of Chemistry, Los Angeles, Calif.). IN: CRYOGENIC PROPERTIES OF POLYMERS; PROCEEDINGS OF THE NASA-CASE CONFERENCE ON THE PROPERTIES OF POLYMERS AT CRYOGENIC TEMPERATURES, NASA LEWIS RESEARCH CENTER AND CASE-WESTERN-RESERVE UNIVERSITY, CLEVELAND, OHIO, APRIL 25-27, 1967. [A69-16485 05-18] Edited by T. T. Serafini and J. L. Koenig.

New York, Marcel Dekker, Inc., 1968, p. 137-153. 31 refs. Grant No. NsG-343.

Results of length-temperature measurements from -180°C to the glass transition temperature for a poly(vinyl alkyl ether) series, poly(ethylene terephthalate), and a tetrafluoroethylene-trifluoropropylene copolymer series. The glass-glass transitions of these materials in both amorphous and crystalline states are determined. The relation between the transition temperature and the structure of the glasses studied is examined. Z.W.

A69-16497 *

DEVELOPMENT OF VULCANIZABLE ELASTOMERS SUITABLE FOR USE IN CONTACT WITH LIQUID OXYGEN.

P. D. Schuman, E. C. Stump, and G. Westmoreland (Peninsula ChemResearch, Inc., Gainesville, Fla.).

IN: CRYOGENIC PROPERTIES OF POLYMERS; PROCEEDINGS

OF THE NASA-CASE CONFERENCE ON THE PROPERTIES OF POLYMERS AT CRYOGENIC TEMPERATURES, NASA LEWIS RESEARCH CENTER AND CASE-WESTERN-RESERVE UNIVERSITY, CLEVELAND, OHIO, APRIL 25-27, 1967. [A69-16485 05-18]
Edited by T. T. Serafini and J. L. Koenig.
New York, Marcel Dekker, Inc., 1968, p. 263-278. 37 refs.
Contract No. NAS 8-5352.

An account is given of research concerned with the preparation of polymers which are compatible with and have usable mechanical properties in the presence of liquid oxygen. The effect of structure on polymer glass transition temperatures is discussed, and the synthesis and characterization of some fluorocarbon vinyl ethers and their polymers are described. (Author)

A69-16498 *

SYNTHESIS OF FLUORINATED POLYURETHANES.
R. Gosnell and J. Hollander (Whittaker Corp., Narmco Research and Development Div., San Diego, Calif.).
IN: CRYOGENIC PROPERTIES OF POLYMERS; PROCEEDINGS OF THE NASA-CASE CONFERENCE ON THE PROPERTIES OF POLYMERS AT CRYOGENIC TEMPERATURES, NASA LEWIS RESEARCH CENTER AND CASE-WESTERN-RESERVE UNIVERSITY, CLEVELAND, OHIO, APRIL 25-27, 1967. [A69-16485 05-18]
Edited by T. T. Serafini and J. L. Koenig.
New York, Marcel Dekker, Inc., 1968, p. 279-298.
NASA-sponsored research.

The purpose of the investigation described was to develop LOX-compatible adhesive systems which have structural utility at cryogenic temperatures. Work was concentrated on the preparation of fluorinated polyurethanes. Initial efforts were directed at highly fluorinated aliphatic and aromatic diamines. Several diamines were prepared and all were studied in their reaction with phosgene to prepare the corresponding diisocyanates. A unique chlorocarbonylation technique was developed for the synthesis of these fluorinated diisocyanates resulting in higher yields and less byproducts than conventional phosgenation. Using a conventional approach to polyurethanes, highly fluorinated hydroxyl-terminated polyester and polyether oligomers were sought for reaction with the several isocyanates. Simple polymers were prepared and tested in LOX, three of which were shown to be LOX-compatible. Efforts were made to determine structural effects on LOX-compatibility. (Author)

A69-18111 *#

HIGH TEMPERATURE DECOMPOSITION OF AMMONIUM PERCHLORATE USING CO_2 LASER-MASS SPECTROMETRY.
G. L. Pellett and W. R. Cofer, III (NASA, Langley Research Center, Hampton, Va.).
American Institute of Aeronautics and Astronautics, Aerospace Sciences Meeting, 7th, New York, N.Y., Jan. 20-22, 1969, Paper 69-143. 15 p. 15 refs.
Members, $1.00; nonmembers, $1.50.

Description of a CO_2 laser pyrolysis/mass spectrometry technique wherein ammonium perchlorate (AP) was rapidly pyrolyzed at heating rates up to 222 cal/cm^2-sec within the low-pressure ion-source chamber of a mass spectrometer. By using single square-wave heating pulses, and cinephotography of oscilloscope-displayed mass spectra, time-correlated analyses of pyrolysis products and their evolution rates were obtained during consecutive periods of transient heatup and growth, quasi-steady decomposition, and transient cooldown. Laser pyrolyses of doped-AP samples exhibited widely variable relative species contributions due to condensed-phase (CP) decomposition. Mechanistic features of CP decomposition are discussed, and their possible relevance to solid-propellant combustion is considered. M.M.

A69-18419 *

ELECTRON MICROPROBE ANALYSIS OF VANADIUM IN THE PRESENCE OF TITANIUM.
Kenneth G. Snetsinger, T. E. Bunch, and Klaus Keil (NASA, Ames Research Center, Space Sciences Div., Moffett Field, Calif.).
American Mineralogist, vol. 53, Sept.-Oct. 1968, p. 1770-1773. 8 refs.

Description of a special method of electron microprobe analysis of vanadium in the presence of titanium by compositional studies of chromite in chondritic meteorites. This procedure involves the determination of the ratio of the intensity of $TiK_{\alpha 1,\,2}$ to that of $TiK_{\beta 1,\,3}$, the latter value being measured at the wavelength of $VK_{\alpha 1,\,2}$, pure rutile (TiO_2) being used for this determination. Then titanium and vanadium are measured on a standard chromite and on the unknown chromite, the $TiK_{\alpha 1,\,2}/TiK_{\beta 1,\,3}$ ratio obtained from rutile being used to correct the $VK_{\alpha 1,\,2}$ intensity for interference from $TiK_{\beta 1,\,3}$ in the standard and the unknown. Z. W.

A69-19775 •

SOME PARAMETERS AFFECTING AUGER AND PHOTOELECTRON SPECTROSCOPY AS AN ANALYTICAL TECHNIQUE.
L. I. Yin, I. Adler, and R. Lamothe (NASA, Goddard Space Flight Center, Greenbelt, Md.).
Applied Spectroscopy, vol. 23, Jan.-Feb. 1969, p. 41-50. 28 refs.

Various possibilities of Auger and photoelectron spectroscopy as an analytical technique are discussed. In some applications, simple electrostatic analyzers with coarse resolution may suffice and even be preferable. Typical spectra obtained with a hemispherical electrostatic analyzer of 0.6% energy resolution are presented and discussed. Such factors as sample thickness, sample potential, surface contamination, and incident angle of the exciting X rays have been found to affect the quality and character of the observed spectra. These results characterize some of the features, problems, and capabilities of applied Auger and photoelectron spectroscopy. (Author)

A69-20535 *

ROTATIONAL SPECTRUM OF ETHYLENE EPISULFOXIDE.
W. F. White (NASA, Langley Research Center, Hampton, Va.) and J. E. Wollrab (McDonnell Douglas Corp., Research Div., St. Louis, Mo.).
Chemical Physics Letters, vol. 3, Jan. 1969, p. 25, 26. 6 refs.

Use of the rotational spectrum of ethylene episulfoxide to determine the molecular structure of this compound and, in particular, the orientation of the SO bond with respect to the C_2S ring. It is found that the ground state rotational spectrum of ethylene episulfoxide agrees with NMR and Raman data in predicting a molecule with C_s symmetry. A dipole moment of 3.66 D is obtained. P.v.T.

A69-23127 *

FACTORS AFFECTING THE CATION REQUIREMENT OF A HALOPHILIC NADH DEHYDROGENASE.
Lawrence I. Hochstein and Bonnie P. Dalton (NASA, Ames Research Center, Exobiology Div., Moffett Field, Calif.).
Biochimica et Biophysica Acta, vol. 167, 1968, p. 638-640. 7 refs.

Brief description of results of studies on an NADH dehydrogenase derived from the NADH oxidase. It was observed that the cation concentration required for stability and maximum activity could be varied over a wide range depending on the cation and the buffer in which the enzyme was maintained. The experimental results point to the complexity of the cation requirement for one putatively halophilic enzyme in that whether the enzyme is halophilic or not depends on factors other than the enzyme per se. M.M.

A69-23371 *

THE GROWTH OF SINGLE CRYSTALS BY CONTROLLED DIFFUSION IN SILICA GEL.
Bernard Rubin (NASA, Electronics Research Center, Cambridge, Mass.).
AIChE Journal, vol. 15, Mar. 1969, p. 206-208. 9 refs.

Single crystals of calcium tartrate tetrahydrate, neodymium-doped calcium tartrate tetrahydrate, and cuprous chloride have been grown by controlled diffusion in silica gel using both metathetical and decomplexation reactions. Conditions for the optimum growth of the crystals are given, and it is shown how the pH of the gel, the temperature of its formation, the concentration of the reactants which make up the gel, and the concentration of the reactants which result in the crystal are important in attaining good single-crystal products. Crystals have been grown up to 11 mm on edge in three to four weeks, and in many cases take on a form which seems to have been cut and polished. (Author)

A69-23527 *#
VACUUM-ULTRAVIOLET PHOTOCHEMISTRY. IX - PRIMARY AND CHAIN PROCESSES IN THE PHOTOLYSIS OF HYDROGEN PEROXIDE.
L. J. Stief (Melpar, Inc., Research Div., Falls Church, Va.; NASA, Goddard Space Flight Center, Greenbelt, Md.) and V. J. DeCarlo (Melpar, Inc., Research Div., Falls Church, Va.).
Journal of Chemical Physics, vol. 50, Feb. 1, 1969, p. 1234-1240. 32 refs.
Contract No. NASw-1417.

Evidence is presented for the occurrence of primary processes leading to the formation of both atomic and molecular hydrogen in the photolysis of H_2O_2 at 1236 Å. Formation of OH in a primary process probably occurs as well. The latter is apparently the sole process required to explain the results at 1470 and 2537 Å. Processes leading to the formation of $O(^1D)$ account for less than 1% of the photochemical decomposition. Chain processes leading to the formation of O_2 but not H_2 occur at 1236 Å. The possibilities considered are a free radial chain and an energy chain. It is shown that the results are more consistent with the occurrence of an energy chain involving atomic hydrogen and vibrationally excited OH radicals. Emission of OH $A\ ^2\Sigma^+ \rightarrow X\ ^2\Pi$ (0, 0) band at 3064 Å was observed during photolysis of H_2O_2 at 1236 and 1470 Å. (Author)

A69-25641 *
INTERACTION OF URANYL IONS WITH PHOSPHOLIPID AND CHOLESTEROL MONOLAYERS.
Dinesh O. Shah (NASA, Ames Research Center, Exobiology Div., Moffett Field, Calif.).
(Biophysical Society, Annual Meeting, 12th, Pittsburgh, Pa., Feb. 19-21, 1968.)
Journal of Colloid and Interface Science, vol. 29, Feb. 1969, p. 210-215. 20 refs.
NSF Grant No. GB-5273.

Determination of surface pressures and potentials of egg and dipalmitoyl lecithins, dipalmitoyl phosphatidic acid, cholesterol, cholestanol, and eicosanyl trimethylammonium monolayers on subsolutions of uranyl acetate and NaCl. Among these films only lecithin monolayers were influenced by the presence of uranyl acetate in the subsolution. It is evident from surface potential measurements that uranyl ions interact with phosphate groups in lecithin monolayers but not in phosphatidic acid monolayers. G.R.

A69-27762 *
CHEMICAL REACTIONS OF DUCTILE METALS DURING COMMINUTION.
Alan Arias (NASA, Lewis Research Center, Cleveland, Ohio).
Metallurgical Society of AIME, Transactions, vol. 245, Apr. 1969, p. 685-695. 15 refs.

Investigation of the behavior of metal powders during ball milling either in pure water or in oxygenated water in order to gain an insight into the grinding mechanism. It is found that zirconium, tantalum, iron, and stainless-steel powders ground in pure water were extensively comminuted and simultaneously oxidized with hydrogen release, whereas nickel, copper, and silver powders did not react with water and their particle sizes increased. On grinding nickel, copper, and silver in water pressurized with oxygen, nickel and copper became extensively comminuted and were oxidized, whereas silver did not react with oxygen and its particle size increased. From these results and other considerations, it is hypothesized that for extensive comminution of ductile metals and alloys to occur on grinding they must react with the grinding media. Z.W.

A69-28439 *
THE EFFECT OF TIME OF HEATING ON THE THERMAL POLYMERIZATION OF L-LYSINE.
Milton R. Heinrich, Duane L. Rohlfing, and Ester Bugna (NASA, Ames Research Center, Exobiology Div., Moffett Field, Calif.).
Archives of Biochemistry and Biophysics, vol. 130, Mar. 1969, p. 441-448. 28 refs.

Investigation of several parameters of the thermal polymerization of L-lysine free base at 195°C over the time period from 15 min to 4 hr. Free lysine disappeared within 1 hr. The concentration of α-aminocaprolactam and of oligomers of several sizes reached a maximum after 30 to 45 min, and subsequently decreased. Molecular size, as judged by biuret color intensity and by gel filtration, increased rapidly and, in part, ultimately exceeded 100,000. Racemization was extensive and paralleled the disappearance of free lysine. Catalytic activity for the decarboxylation of oxaloacetic acid increased rapidly and reached a maximum after 2 hr. Dinitrophenylation and subsequent hydrolysis indicated that the polymers were branched, and that the linear portions contained more ε- than α-peptide bonds. A partial understanding of the method of chain growth can thus be inferred. M.G.

A69-30442 *
THERMAL DECOMPOSITION OF YTTRIUM-DOPED SILVER CARBONATE.
T. Wydeven and E. Rand (NASA, Ames Research Center, Moffett Field, Calif.).
Journal of Catalysis, vol. 12, Nov. 1968, p. 271-277. 9 refs.

Study of the decomposition kinetics of yttrium-doped silver carbonate powder and pressed pellets by isothermogravimetric analysis from 155 to 185°C. The extent of decomposition at constant temperature increased significantly when powdered samples were decomposed in the presence of water vapor. When pellets of pressed powder were decomposed, good agreement was found between the experimental decomposition rate and the rate predicted by the Polanyi-Wigner equation, thus providing evidence that yttrium-doped silver carbonate decomposes by the interface mechanism. Preirradiation (10^6) of doped silver carbonate only slightly increased the decomposition rate. P.v.T.

A69-31807 *
DIFFERENTIAL THERMAL ANALYSIS OF SOME BIOLOGICAL SPECIMENS, PROTEINS, AND STARCHES.
V. I. Oyama (California Institute of Technology, Jet Propulsion Laboratory, Pasadena; NASA, Ames Research Center, Moffett Field, Calif.) and George K. Estok (California Institute of Technology, Jet Propulsion Laboratory, Pasadena, Calif.).
Texas Journal of Science, vol. 20, Apr. 1969, p. 355-360.

Dynamic differential thermal analysis, with helium flow, of various dried plant and animal specimens and related substances yields discrete decomposition peaks of the exothermic type, suitable as valuable monitors of the pyrolysis process prior to analysis of volatile decomposition products by gas-liquid chromatography. Two main peaks are generally observed, one in the region of 350°C and the other more variable between 450 and 600°C. Undifferentiated soil organisms give generally similar patterns, whereas more highly organized plant and metazoan animal forms vary appreciably with phylum. (Author)

A69-31808 *
STUDIES ON THE FORMATION AND TRANSFORMATION OF ESTERS. LXXX.
Joseph Rabinowitz, Sherwood Chang, J. M. Hayes, and Fritz Woeller (NASA, Ames Research Center, Exobiology Div., Moffett Field, Calif.).
Journal of Organic Chemistry, vol. 34, Feb. 1969, p. 372-376. 5 refs.

Study of various reactions involving hydrazinoethanol and its sulfate monoester, hydrazinoethyl hydrogen sulfate. Reactions of hydrazinoethanol and hydrazinoethyl hydrogen sulfate with phenyl isothiocyanate take place at the substituted nitrogen atom. The corresponding monophenylthiocarbamoyl derivatives undergo ring closure in hydrochloric acid and sodium hydroxide, respectively. Monothiocarbamoylation of hydrazinoethyl hydrogen sulfate with o-methoxycarbonylphenyl isothiocyanate occurs at the unsubstituted nitrogen atom. Monophenylcarbamoylation of hydrazinoethanol or hydrazinoethyl hydrogen sulfate takes place at the substituted nitrogen atom. G.R.

A69-32312 *
TEMPERATURE DEPENDENCE OF THE RATE CONSTANTS FOR THE REACTIONS $O^+ + O_2 \rightarrow O_2^+ + O$ AND $O^+ + N_2 \rightarrow NO^+ + N$.
Peter Stubbe (NASA, Goddard Space Flight Center, Laboratory for

Space Sciences, Greenbelt, Md.).
Planetary and Space Science, vol. 17, June 1969, p. 1221-1231. 23 refs.

The dependence of the rate constant k_r for the reactions $O^+ + O_2 \rightarrow O_2^+ + O$ (k_1) and $O^+ + N_2 \rightarrow NO^+ + N$ (k_2) on the gas temperature T, the vibrational temperature T_v of the molecular reactant, and the relative flow velocity v_s between the gases, is studied theoretically by means of a collision theory approach. The resulting expression for k_r contains the two unknown parameters A (activation energy) and P_0 (scaling factor) which have to be determined empirically. $k_1(T)$ is found to have a minimum at about 650°K and a nearly linear increase for temperatures above 750°K. For the second reaction, the rate constant is presented as a function of T and A, since uncertainties in the experimental results do not allow a reliable determination of A. The increase rate of k_2 with $T_v(N_2)$, the vibrational temperature of N_2, falls off strongly with increasing gas temperature. (Author

A69-33651 *
DETERMINATION OF THE WATER-SOLUBLE DINITROPHENYL-AMINO ACIDS BY ION-EXCHANGE CHROMATOGRAPHY.
M. R. Heinrich and Ester Bugna (NASA, Ames Research Center, Exobiology Div., Moffett Field, Calif.).
Analytical Biochemistry, vol. 28, Apr. 1969, p. 1-5. 16 refs.

Application of ion-exchange chromatography to the determination of free lysine and DNP derivatives. Using the ninhydrin color reaction, the eluate, with a pH 5.00 buffer, is first passed through a flow cell into a spectrometer or colorimeter for recording its absorbance and subsequent analysis as an amino acid. The calculation of concentration was made from the peak height and width in the usual manner. The lower limits for analysis are approximately 0.01 to 0.05 μmole, using standard Technicon equipment. V.P.M.

A69-34184 *
ALICYCLIC HYDROCARBONS FROM AN UNUSUAL DEPOSIT IN DERBYSHIRE, ENGLAND - A STUDY IN POSSIBLE DIAGENESIS.
Katherine Pering and Cyril Ponnamperuma (NASA, Ames Research Center, Exobiology Div., Moffett Field, Calif.).
Geochimica et Cosmochimica Acta, vol. 33, Apr. 1969, p. 528-532. 10 refs.

Gas chromatographic and mass spectrometric analyses of the alicyclic hydrocarbons extractable from two morphologically dissimilar types of organic material from a localized deposit of hydrocarbons in the Carboniferous limestone of North Derbyshire, England revealing distinct variations in the distribution pattern of the alkanes. The two forms may have different origins or evolutionary histories. (Author)

A69-34443 *#
APPARENT ACTIVATION ENERGY OF CHEMICAL REACTIONS AT HIGH TEMPERATURE.
C. Frederick Hansen (NASA, Ames Research Center, Moffett Field, Calif.).
Physics of Fluids, vol. 12, May 1969, pt. 1, p. 1127, 1128. 10 refs.

According to the usual form of measured cross sections, the slope of an Arrhenius plot differs from the activation energy by an electron volt or so at high temperature. Thus, cross-section shape is needed before activation energy can properly be deduced from rate data. (Author)

A69-37101 *
STUDIES OF THE ELECTRON TRANSPORT CHAIN OF EXTREMELY HALOPHILIC BACTERIA. II—SALT DEPENDENCE OF REDUCED DIPHOSPHOPYRIDINE NUCLEOTIDE OXIDASE.
Janos K. Lanyi (NASA, Ames Research Center, Exobiology Div., Moffett Field, Calif.).
Journal of Biological Chemistry, vol. 244, June 10, 1969, p. 2864-2869. 16 refs.

Characterization of the electron transport chain of Halobacterium cutirubrum, and examination of the role of b-type cytochromes in the oxidation of DPNH. The results suggest a main branch of electron transport which includes a flavoprotein, reduced by DPNH, and a subsidiary branch consisting of flavoproteins and cytochrome b(559), reduced by DPNH and succinate. The branches join at the c-type cytochromes. The relation of DPNH oxidase activity to NaCl concentration, and the irreversible inactivation of the enzyme in the absence of salt reflect the behavior of a single component of the system, DPNH dehydrogenase. The place of the b-type cytochromes in a proposed electron transport system based on these findings is confirmed through the determination of salt dependence curves. B.H.

A69-38277 *
HEATS OF ADSORPTION OF CARBON DIOXIDE ON SILVER (I) OXIDE AND COPPER (II) OXIDE AS DETERMINED BY GAS CHROMATOGRAPHY.
T. Wydeven and M. Leban (NASA, Ames Research Center, Moffett Field, Calif.).
Journal of Chromatographic Science, vol. 7, July 1969, p. 445-448. 15 refs.

Determination of the heats of adsorption of carbon dioxide on silver (I) oxide and copper (II) oxide. The heats of adsorption were derived from relative retention time *vs* temperature data. (Author)

A69-39706 *#
THE FLUORINATION OF METALS.
Patricia M. O'Donnell (NASA, Lewis Research Center, Cleveland, Ohio).
Gordon Research Conference, New London, N.H., July 21-25, 1969, Paper. 33 p. 37 refs.

Results of kinetic studies on the reaction of elemental fluorine with nickel, copper, iron, titanium, beryllium, aluminum, zirconium, and silver. The data are described by various rate laws which are dependent on the variables, temperature, pressure, and film thickness. Rate constants are given for the reactions as well as calculated activation energies. The migrating species in several of the reactions has been identified by radioactive tracer experiments and cross-section analysis of marker experiments. For the silver system, diffusion coefficients are plotted. Exposure to either vacuum or moisture is shown to effect the passivity of the metal fluoride films. (Author)

A69-40932 *
DETERMINATION OF OXYGEN IN LITHIUM BY THE VACUUM DISTILLATION METHOD.
Randall F. Gahn (NASA, Lewis Research Center, Cleveland, Ohio).
Analytical Chemistry, vol. 41, Aug. 1969, p. 1303-1306. 6 refs.

Application to lithium of the vacuum distillation method for determining oxygen in alkali metals. In this method the nonvolatile impurities, assumed to be lithium monoxide, are separated from the volatile lithium by heating the lithium sample in high vacuum. The alkalinity or the lithium content of the impurities is then converted to an oxygen concentration. Method reproducibility was determined at the 30- and 80-ppm oxygen levels. Method accuracy was evaluated through quantitative oxygen additions and recoveries, estimation of the method blank, and identification of the distillation residue from the lithium-oxygen system. (Author)

A69-42557 *
TRACE PORPHYRIN COMPLEXES—FLUORESCENCE DETECTION BY DEMETALLATION WITH METHANESULFONIC ACID.
G. W. Hodgson, Etta Peterson, and B. L. Baker (NASA, Ames Research Center, Moffett Field, Calif.; Research Council of Alberta, Edmonton, Alberta, Canada).
Mikrochimica Acta, vol. 4, 1969, p. 805-814. 11 refs.

Description of a method for the detection and spectral examination of traces of porphyrin complexes by controlled demetallation and spectrofluorometry. It is noted that, by carrying out the demetallation with methanesulfonic acid in the optical cell, difficulties connected with handling losses and introduction of contamination are minimized. The method is sensitive to quantities

as low as 0.05 ng, which is about two orders of magnitude greater than the sensitivity of direct absorption spectrophotometry. P.G.

N69-10126*# National Aeronautics and Space Administration. Lewis Research Center, Cleveland, Ohio.

OBSERVATIONS ON PERMEATION OF POLYTETRAFLUOROETHYLENE BY COMPOUNDS OF RHENIUM, MOLYBDENUM, AND TUNGSTEN

Harold Leibecki Washington Nov. 1968 16 p refs

(NASA-TN-D-4886) Avail: CFSTI CSCL 07B

Observations of diffusion of rhenium, molybdenum, and tungsten hexafluorides into polytetrafluorethylene and hydrolysis of the resultant material are reported. Exposure of *polytetrafluoroethylene to rhenium or molybdenum hexafluoride*, followed by hydrolysis, results in impregnation of the plastic with a metal compound. Tungsten hexafluoride was observed to grow a fibrous product (composition unresolved) on the surface of the plastic during ambient air hydrolysis. Rhenium hexafluoride hydrolysis yielded a mixture of rhenium oxides. The polytetrafluoroethylene sample was investigated for electrical conduction and was found to be substantially more conductive than the pure plastic. The hydrolysis product of molybdenum hexafluoride impregnation was postulated to be a mixture of molybdenum oxides. The electrical conduction properties of the product were not investigated. Author

N69-14180*# National Aeronautics and Space Administration. Lewis Research Center, Cleveland, Ohio.

EVALUATION OF THE RESULTS OF A ROUND ROBIN ANALYSIS FOR OXYGEN fN POTASSIUM AND SODIUM

Glenn R. Zellars and Charles A. Barrett Washington Dec. 1968 39 p refs

(NASA-TN-D-4971) Avail: CFSTI CSCL 07D

Analysts from 17 laboratories analyzed tube samples of *high-purity potassium and sodium for oxygen*. Most oxygen analyses were determined by the mercury amalgamation method and several by vacuum distillation; one value of oxygen in potassium was obtained by neutron activation analysis. Analytical results submitted by the participating laboratories gave a mean value for oxygen in potassium of 14.7 ppm with a standard deviation of 5.08 ppm. For dodium, the mean value was 10.7 ppm with a standard deviation of 4.70. The oxygen results for each alkali metal showed variations significantly in excess of the experimental error. Statistical techniques were applied to the oxygen data to identify the most likely sources of variability. Author

N69-18962*# National Aeronautics and Space Administration. Ames Research Center, Moffet Field, Calif.

SOLVENT PURIFICATION PROCEDURES USED IN ORGANIC GEOCHEMISTRY LABORATORIES

Keith A. Kvenvolden and J. M. Hayes Washington Feb. 1969 15 p refs

(NASA-TM-X-1746) Avail: CFSTI CSCL 07D

As organic and inorganic solvents are often a source of contamination in organic geochemistry, questionnaires were sent to *organic chemical laboratories on the use and purification of solvents*. An analysis of the replies shows: (1) Analytical reagent grade solvents generally are unacceptable for organic geochemical use unless they are purified by some kind of column chromatography or distillation. (2) In some applications, spectroscopic grade and pesticide or nanograde quality solvents were used successfully as received from the manufacturers. (3) Pretreatment of solvents before distillation is not a common practice. (4) Laboratories reporting successful distillation techniques use simple distillation setups with good fractionating columns operated under high reflux ratios. (5) In a few instances, the level of residue contamination in solvents used for analyses was reported and varied from 10^{-7} to 10^{-9} gm/ml. (6) Techniques of fractional crystallization and zone melting seem to provide higher purity solvents than can be prepared by distillation. Author

N69-19129*# National Aeronautics and Space Administration. Lewis Research Center, Cleveland, Ohio.

THE DISSOCIATION ENERGY OF GASEOUS TITANIUM MONONITRIDE

Carl A. Stearns and Fred J. Kohl Washington Feb. 1969 20 p refs

(NASA-TN-D-5027) Avail: CFSTI CSCL 07D

The titanium nitride molecule has been identified in the vapor phase over solid $TiN_{0.78}$ at temperatures above 2250°K. *The Knudsen effusion method was used in conjunction with a* double-focusing mass spectrometer. The high resolution of the spectrometer made possible the identification of the TiN molecule. From experimentally determined partial pressures, the enthalpy for the reaction $TiN(g) = Ti(g) + 0.5\ N_2(g)$ has been calculated as $\Delta H^o_{298} = -1.8 \pm 7$ kcal/mole (-7.5 ± 29 kJ/mole). This reaction enthalpy yields thermodynamic properties for gaseous TiN when combined with published thermodynamic data: (1) $TiN(g) = Ti(g) + N(g)$, $D^o_{298} = 111.2 \pm 8$ kcal/mole (465.3 ± 33 kJ/mole); (2) TiN(s) = TiN(g), $\Delta H^o_{s,298} = 195.5 \pm 9$ kcal/mole (818.0 ± 38 kJ/mole); and (3) $Ti(s) + 0.5\ N_2(g) = TiN(g)$, $\Delta H^o_{f,298} = 114.8 \pm 8$ kcal/mole (480.3 ± 33 kJ/mole). Author

N69-20775*# National Aeronautics and Space Administration. Electronics Research Center, Cambridge, Mass.

EFFECTS OF LITHIUM AND OXYGEN LOSSES ON THE MAGNETIC AND CRYSTALLOGRAPHIC PROPERTIES OF SPINEL LITHIUM FERRITE

D. H. Ridgley, H. Lessoff, and J. D. Childress Washington Mar. 1969 31 p refs

(NASA-TR-R-305) Avail: CFSTI CSCL 07B

A study of the effects of sintering temperatures and cooling rates on the magnetic and crystallographic properties of spinel *lithium ferrite shows that both the magnetic moment and lattice* parameter increase with sintering temperature. Either annealing at lower temperatures or slow cooling under oxygen causes reoxidation of the Fe^{+2} formed at higher temperatures with attendent decreases in moment and lattice parameter and gradual precipitation of α–Fe_2O_3 as a second phase. The various products formed were shown to be equivalent to solid solutions of spinel lithium ferrite with Fe_3O_4 on rapid cooling and to solid solution of lithium ferrite and γ–Fe_2O_3 with precipitation of α–Fe_2O_3 on slow cooling. Lithium losses and α–Fe_2O_3 precipitate amounts are calculated. The magnetic moment and lattice parameter of stoichiometric lithium ferrite were determined: magnetic moment at 25°C = 3736±20G; lattice parameter at 28°C = 8.3293±0.0005Å. Author

N69-20801*# National Aeronautics and Space Administration. Lewis Research Center, Cleveland, Ohio.

A COMPARISON OF TWO SPECTROPHOTOMETRIC METHODS FOR THE DETERMINATION OF PALLADIUM IN TITANIUM-BASE ALLOYS

Warren F. Davis Washington Mar. 1969 28 p refs

(NASA-TM-X-1767) Avail: CFSTI CSCL 07D

This report compares extraction procedures using 1–nitroso 2–naphthol and dimethylglyoxime for the spectrophotometric determination of palladium in titanium-base alloys. Dimethylglyoxime has greater selectivity but lower sensitivity, similar precision (about 25 ppm at the 0.2 percent level), is faster, and covers a wider range of palladium contents than does 1–nitroso 2–naphthol. The dimethylglyoxime procedure has no interferences by any of the common or potential alloying elements, for example, cobalt, niobium, and tantalum; thus it is well suited to the determination of 0.1 *to 1.0 percent palladium in titanium-base alloys*. Selectivity is improved by the presence of nitrate. Author

06 CHEMISTRY

N69-20853*# National Aeronautics and Space Administration. Lewis Research Center, Cleveland, Ohio.
PRELIMINARY DEVELOPMENT OF SPECTROCHEMICAL ANALYSIS OF SUPERALLOYS WITH THE LIQUID-LAYER SOLID-SAMPLE SPARK TECHNIQUE
Ramon M. Barnes Washington Mar. 1969 23 p refs
(NASA-TM-X-1753) Avail: CFSTI CSCL 07D

A comparison study is made, for the spectrochemical analysis of cobalt-base superalloys, between the liquid-layer solid-sample spark technique and the conventional point-to-plane spark analysis in air. The changes of analytical concentration curves are indicated for alloying constituents of two developmental cobalt-base alloys, and correlation of the changes to preliminary microscopic, metallographic, and spectroscopic phenomena are hypothesized. Author

N69-22991*# National Aeronautics and Space Administration. Lewis Research Center, Cleveland, Ohio.
ANALYSIS OF LIGHT-SCATTERING DATA FROM POLYMER SOLUTIONS
James A. Ryan Washington Apr. 1969 18 p refs
(NASA-TN-D-5177) Avail: CFSTI CSCL 07D

An analysis was made of various factors affecting the analytical fitting of curves to a Zimm plot of light scattering data from dilute polymer solutions. The use of a computer to completely fit the data analytically was not feasible. However, a procedure was developed whereby the computer calculates the points on the limiting tangent. This tangent is then extrapolated graphically to zero concentration. A computer program was written which incorporates this method. Author

N69-23353*# National Aeronautics and Space Administration. Lewis Research Center, Cleveland, Ohio.
THE SYNTHESIS OF A NOVEL POLYIMIDE PRECURSOR
Peter Delvigs, Li-Chen Hsu, and Tito T. Serafini Washington Apr. 1969 16 p refs
(NASA-TN-D-5184) Avail: CFSTI CSCL 07C

A novel blocked polymide precursor was synthesized by using diethylamine as the blocking reagent. The structure of the blocked precursor is the bis(n,N-diethylamide) of the polyamic acid derived from pyromellitic dianhydride and 4,4'-diaminodiphenyl ether. The blocked precursor was more resistant to thermal imidization than the corresponding polyamic acid. The weight average, molecular weight of the blocked precursor could be increased by solid-state polymerization. However, the molecular weight of the polyamic acid could not be changed from its initial value. Furthermore, the blocked precursor was still completely soluble after solid-state polymerization. The solvolytic stability of the blocked precursor in anhydrous N,N-dimethylacetamide was superior to that of the polyamic acid. Author

N69-23706*# National Aeronautics and Space Administration. Lewis Research Center, Cleveland.
DETERMINATION OF OXYGEN IN LITHIUM BY THE VACUUM DISTILLATION METHOD
Randall F. Gahn Washington May 1969 13 p refs
(NASA-TN-D-5197) Avail: CFSTI CSCL 07B

The vacuum distillation method for determining oxygen in alkali metals was applied to lithium. In this method the nonvolatile impurities, assumed to be lithium monoxide, are separated from the volatile lithium by heating the lithium sample in high vacuum. The alkalinity or the lithium content of the impurities is then converted to an oxygen concentration. Method reproducibility was determined at the 30 and 80 ppm oxygen levels. Method accuracy was evaluated through quantitative oxygen additions and recoveries, estimation of the method blank, and characterization of the distillation residue from the lithium-oxygen system. Author

N69-24940*# National Aeronautics and Space Administration. Lewis Research Center, Cleveland, Ohio.
RADIATION INDUCED REDUCTION OF AMMONIACAL NICKEL (2) SULFATE TO METALLIC NICKEL
Warren H. Philipp and Stanley J. Marsik Washington May 1969 14 p refs
(NASA-TN-D-5213) Avail: CFSTI CSCL 07C

Aqueous ammoniacal nickel (II) sulfate solutions containing a variety of soluble organic compounds were irradiated with 2MeV electrons. When this organic additive was either a primary alcohol, secondary alcohol, or cyclic ether, the divalent nickel was reduced to elemental nickel powder. The reaction mechanism involves the decomposition of water by the ionizing radiation into hydrogen atoms and hydroxyl radicals. The organic additive scavenges the hydroxyl radicals by reducing them, and the remaining hydrogen atoms then reduce the divalent nickel to the free metal powder. Author

N69-33493*# Avco Corp., Lowell, Mass.
STUDY OF FERROMAGNETIC LIQUID
Robert Kaiser and Ronald E. Rosensweig Washington NASA Aug. 1969 100 p refs
(Contract NASw-1581)
(NASA-CR-1407) Avail: CFSTI CSCL 07D

It is possible to induce substantial magnetic forces in ferrofluids. These are stable micro-dispersions formed by grinding a ferromagnetic powder in the presence of a surfactant solution. Novel hydrocarbon base ferrofluids with increased magnetization and improved thermal stability have been prepared. Water, fluorocarbon and nonvolatile ester base ferrofluids have also been synthesized. Physical properties of numerous magnetite base ferrofluids were measured. For these systems the particle size is less than 150 Å. Magnetic properties can be accounted for by superparamagnetic theory and particle concentration. The maximum attainable concentration of particles varies as a function of the ratio of the stabilizing layer thickness to the particle diameter. A minimum value of 30 Å was observed. Ferrofluid viscosity increases as a function of carrier liquid viscosity, particle concentration, and the stabilization ratio. Author

N69-36413*# Rocketdyne, Canoga Park, Calif. Research Div.
PROPERTIES OF NONAQUEOUS ELECTROLYTES
Rudolf Keller, James N. Foster, Douglas C. Hanson, John F. Hon, and James S. Muirhead Washington NASA Aug. 1969 253 p refs
(Contract NAS3-8521)
(NASA-CR-1425; R-7703) Avail: CFSTI CSCL 07D

Aprotic electrolytes with and without dissolved cupric fluoride and cupric chloride were studied. The electrolytes were based on four solvents: propylene carbonate, dimethyl formamide, acetonitrile, and methyl formate. Characterized components were used to prepare the solutions. Structural studies were performed utilizing nuclear magnetic resonance and electron paramagnetic resonance techniques. Various physical properties were determined including solubility, heat of solution, vapor pressure, viscosity, density, sonic velocity, conductance, diffusion coefficient, and dielectric constant. Author

N69-40240*# National Aeronautics and Space Administration. Lewis Research Center, Cleveland, Ohio.
ELECTROCHEMICAL BEHAVIOR OF THE ALUMINUM ELECTRODE IN MOLTEN SALT ELECTROLYTES
Betty S. DelDuca Washington Oct. 1969 30 p refs
(NASA-TN-D-5503) Avail: CFSTI CSCL 07D

The kinetics for dissolution and deposition of solid aluminum in molten $AlCl_3$-NaCl and $AlCl_3$-$(LiCl\text{-}KCl)_{eut}$ electrolytes were studied by means of galvanostatic and potentio-static techniques over a temperature range of 175° to 313°C (448 to 586 K). The apparent exchange currents varied from 1 to 56 mA/cm^2. Surface diffusion was found to be the rate-determining step at low overpotentials, and charge transfer the rate-determining step at high

overpotentials. The most probable anodic rate-determining step was found to be $Al \rightarrow Al^{+} + e^{-}$; the most probable cathodic rate-determining step was $Al^{+++} + e^{-} \rightarrow Al^{++}$ in $AlCl_3$-$(LiCl\text{-}KCl)_{eut}$ electrolyte and $Al^{++} + e^{-} \rightarrow Al^{+}$ in $AlCl_3 \cdot NaCl$ electrolyte. Current efficiencies for dissolution were close to 100 percent. Author

07

COMMUNICATIONS

Includes communications equipment and techniques; noise; radio and communications blackout; modulation telemetry; tracking radar and optical observation; and wave propagation. For basic research see: 23 Physics, General; and 21 Navigation.

A69-10556 *

RADIATION MODELS USING DISCRETE RADIATOR ENSEMBLES. S. Karp (NASA, Electronics Research Center, Cambridge, Mass.), Robert M. Gagliardi, and Irving S. Reed (Southern California, University, Dept. of Electrical Engineering, Los Angeles, Calif.). IEEE, Proceedings, vol. 56, Oct. 1968, p. 1704-1711. 14 refs. Grant No. AF AFOSR 496-67.

In recent literature, radiation emitted or reflected from a body or surface has been modeled as equivalent radiation from a collection of individual discrete radiators. This model has application to the analysis of forward and backscatter from rough surfaces, clutter and chaff models for radar, and cavity emissions at optical frequencies. The present work investigates radiation using a generalization of the above radiator ensemble. Some degree of coupling is assumed to exist between individual radiators, and each radiator emits random energy bursts as a Poisson process. Analysis is confined to power spectral densities and first-order statistics of the resulting scalar radiation field. The results indicate that the pulsed radiator model can account for many properties of radiation. A by-product of the analysis is a filter model for dispersive channels, applicable to radar design problems. (Author)

A69-13176

EASCON '68; INSTITUTE OF ELECTRICAL AND ELECTRONICS ENGINEERS, ELECTRONICS AND AEROSPACE SYSTEMS CONVENTION, WASHINGTON, D.C., SEPTEMBER 9-11, 1968, RECORD. New York, Institute of Electrical and Electronics Engineers, Inc., 1968. 624 p.
Members, $12.50; nonmembers, $17.50.

CONTENTS:

CHAIRMAN'S MESSAGE. D. L. Coddington, p. 3.

SPACE COMMUNICATIONS.

CHARACTERIZATION AND CODING OF DCSP SATELLITE COMMUNICATION CHANNELS. R. M. Langelier (U.S. Army, Materiel Command, Fort Monmouth, N.J.), D. Quagliato, and J. Quigley (U.S. Army, Electronics Command, Fort Monmouth, N.J.), p. 9-13. 6 refs. [See A69-13177 03-07]

SYNTHESIS OF DIGITAL PHASE-LOCKED LOOPS. W. E. Larimore (Communications and Systems, Inc., Paramus, N.J.), p. 14-20. 12 refs. [See A69-13178 03-07]

AN EFFICIENT TDMA SYSTEM FOR USE BY EMERGING NATIONS WITH THE INTELSAT IV SATELLITE. W. G. Schmidt (Communications Satellite Corp., Washington, D.C.), p. 21-27. 7 refs. [See A69-13179 03-07]

TECHNIQUES FOR ASSURING HIGH RELIANCE THROUGH ACCEPTANCE TESTING ON IDCSP SATELLITES. E. T. Bobak, E. I. Roberts (Aerospace Corp., El Segundo, Calif.), and P. C. McLellan, p. 28-34.

SOME COMMUNICATION SYSTEM CONSIDERATIONS FOR USE OF A LIBRATION POINT SATELLITE TO SUPPORT AN APOLLO LUNAR FAR-SIDE MISSION. B. L. McQuaid (Hughes Aircraft Co., Culver City, Calif.), p. 35-46. 9 refs. [See A69-13180 03-07]

RADAR SYSTEMS. I.

HIGH RANGE RESOLUTION BY MEANS OF PULSE TO PULSE FREQUENCY SHIFTING. K. Ruttenberg and L. Chanzit (United Aircraft Corp., Norwalk, Conn.), p. 47-51. 6 refs. [See A69-13181 03-07]

IMPROVED MULTIFUNCTION ARRAY RADAR PERFORMANCE WITH MULTIFREQUENCY OPERATIONS. D. E. Hunt (Texas Instruments, Inc., Dallas, Tex.), p. 52-59. 10 refs. [See A69-13182 03-07]

RADAR ATTITUDE SENSING SYSTEM. E. Burcher (NASA, Washington, D.C.) and E. Rupp (Bell Aerospace Corp., Buffalo, N.Y.), p. 60-63. [See A69-13183 03-07]

GEODESIC LENSES FOR RADAR ANTENNAS. R. C. Johnson and R. M. Goodman, Jr. (Georgia Institute of Technology, Atlanta, Ga.), p. 64-69. 6 refs. [See A69-13184 03-09]

CLUTTER REJECTION USING A CODED BURST WAVEFORM. C. P. Rasmussen (General Electric Co., Aerospace Electronics Dept.), p. 70-78. 6 refs. [See A69-13185 03-07]

OPTICAL CORRELATION FOR FAST ACQUISITION OF PSEUDO RANDOM RANGING CODES. J. L. de Montlivault (Centre National d'Etudes Spatiales, Paris, France), p. 79-82. 7 refs. [See A69-13186 03-07]

SYSTEMS SUPPORT AND TESTING TECHNIQUES.

EVALUATION CRITERION FOR AUTOMATIC TEST EQUIPMENT. R. F. Barry (Radio Corporation of America, Burlington, Mass.), p. 83-87. [See A69-13187 03-14]

INSTRUMENTATION SYSTEM EVALUATION WITH PSEUDO-NOISE. L. R. Malling (Massachusetts Institute of Technology, Lexington, Mass.), p. 96-101. 11 refs. [See A69-13188 03-09]

AUTOMATIC TEST EQUIPMENT AND ITS APPLICATION TO TESTING PROBLEMS PRESENTED BY TODAY'S COMPLEX COMMUNICATION EQUIPMENT. A. M. Greenspan (Radio Corporation of America, Burlington, Mass.), p. 102-107. [See A69-13189 03-11]

PROBLEMS IN R & D AUTOMATIC SUPPORT SYSTEMS DEVELOPMENT. D. L. Reed (Emerson Electric Co., St. Louis, Mo.), p. 108-112. [See A69-13190 03-11]

COMMUNICATIONS - IDEAS, APPLICATIONS, AND PERFORMANCE.

MULTI-MODE PROPAGATION COMMUNICATION SYSTEM. W. J. Richter, Jr. and R. L. Hawkins (Melpar, Inc., Falls Church, Va.), p. 113-120. [See A69-13191 03-07]

HIGH SPEED DIGITAL TRANSMISSION TESTS AT 35 GHZ. C. K. H. Tsao, J. T. deBettencourt, R. Savage (Raytheon Co., Lexington, Mass.), and D. T. Worthington (U.S. Defense Communications Agency, Washington, D.C.), p. 121-124. 6 refs. [See A69-13192 03-07]

ATMOSPHERIC LIMITATIONS FOR LASER COMMUNICATIONS. M. Subramanian (Bell Telephone Laboratories, Inc., Whippany, N.J.), p. 125-133. 16 refs. [See A69-13193 03-07]

A COMPARISON OF OPTICAL RECEIVERS FOR DEEP SPACE COMMUNICATIONS. J. I. Bowen and J. N. Lahti (Bell Telephone Laboratories, Inc., Whippany, N.J.), p. 134-141. 10 refs. [See A69-13194 03-07]

AN AGRICULTURAL REMOTE SENSING INFORMATION SYSTEM. R. A. Holmes (Purdue University, Lafayette, Ind.), p. 142-149. [See A69-13195 03-08]

RADAR SYSTEMS. II.

A DIGITAL MODIFIED DISCRETE FOURIER TRANSFORM DOPPLER RADAR PROCESSOR. E. L. Hall, D. D. Lynch, and R. E. Young (Emerson Electric Co., St. Louis, Mo.), p. 150-159. 8 refs. [See A69-13196 03-07]

AN AUTOMATIC SEQUENTIAL DETECTOR FOR NONCOHERENT MTI RADAR. D. N. Thomson (General Atronics Corp., Philadelphia, Pa.), p. 160-167. 12 refs. [See A69-13197 03-07]

MTI PERFORMANCE DEGRADATION CAUSED BY LIMITING. H. R. Ward and W. W. Shrader (Raytheon Co., Wayland, Mass.), p. 168-174. 7 refs. [See A69-13198 03-07]

COMPUTER GENERATION OF RADAR RETURN SIGNALS.

C. E. Suyo (McDonnell Douglas Corp., St. Louis, Mo.), p. 175-180 6 refs. [See A69-13199 03-14]

ECM/ECCM SYSTEM SIMULATION PROGRAM. D. H. Cook (Vitro Corporation of America, West Orange, N.J.), p. 181-186. [See A69-13200 03-08]

SIGNAL PROCESSING. I - PHASE AND FREQUENCY DOMAIN TECHNIQUES.

INTERFERENCE REJECTION IN A PHASE-LOCKED LOOP WITH DECISION FEEDBACK. F. D. Natali and W. J. Walbesser (New York, State University, Buffalo, N.Y.), p. 187-192. [See A69-13201 03-10]

QUANTIZED SECOND ORDER FREQUENCY LOCKED LOOP. D. T. Hess and K. K. Clarke (Brooklyn, Polytechnic Institute, Brooklyn, N.Y.), p. 193-197. [See A69-13202 03-07]

PRACTICAL PHASE REFERENCE DETECTORS FOR FULLY MODULATED PSK SIGNALS. S. Riter (Texas Agricultural and Mechanical University, College Station, Tex.) and W. Hon (Houston, University, Houston, Tex.), p. 198-205. 9 refs. [See A69-13203 03-09]

A DIGITAL SIMULATION OF A CARRIER DEMODULATOR/TRACKING PHASE-LOCKED LOOP IN A NOISY, MULTIPATH ENVIRONMENT. A. E. Smith and R. S. Johnson (Radio Corporation of America, Moorestown, N.J.), p. 206-216. 14 refs. [See A69-13204 03-07]

SYSTEM SIMULATION - AN APPROACH TO THE OPTIMIZATION OF SIGNAL PROCESSING AND CODING FOR VLF CHANNELS. H. M. Morozumi and M. M. McCormick (General Electric Co., Syracuse, N.Y.), p. 217-224. 8 refs. [See A69-13205 03-07]

A SOLID-STATE SYNCHRONOUS FILTER. V. A. Richley (Youngstown State University, Youngstown, Ohio) and A. W. Revay, Jr. (Florida Institute of Technology, Melbourne, Fla.), p. 225-232. 11 refs. [See A69-13206 03-09]

NAVIGATION, SURVEILLANCE AND TRACKING. I.

XX CENTURY NAVIGATION. P. V. H. Weems, p. 233, 234. [See A69-13207 03-21]

A SHORT-BASELINE RADIATING INTERFEROMETER NAVIGATION SATELLITE CONCEPT INCORPORATING METHODS TO ELIMINATE SYSTEMATIC NAVIGATION ERROR. P. I. Klein (Pennsylvania, University, Philadelphia, Pa.), p. 235-246. 11 refs. [See A69-13208 03-21]

WORLD'S MOST POWERFUL VHF TRANSMITTING STATION. L. D. Breetz (U.S. Navy, Office of Naval Research, Washington, D.C.), p. 247-251. [See A69-13209 03-11]

AN ADVANCED LONG-RANGE NAVIGATION CAPABILITY CONCEPT FOR A 1979 INITIAL OPERATIONAL CAPABILITY. W. B. Wrigley (Lockheed Aircraft Corp., Marietta, Ga.), p. 252-254. 5 refs. [See A69-13210 03-21]

A NON-ORTHOGONAL MULTI-SENSOR STRAPDOWN INERTIAL REFERENCE UNIT. J. P. Gilmore (Massachusetts Institute of Technology, Cambridge, Mass.), p. 255-262. 8 refs. [See A69-13211 03-14]

ON OPTIMIZING THE OMEGA RADIONAVIGATION SYSTEM. D. W. Haney (General Precision Systems, Inc., Silver Spring, Md.), p. 263-270. [See A69-13212 03-21]

NAVIGATION, SURVEILLANCE AND TRACKING. II.

MATHEMATICAL MODELING OF LONG TERM GYRO DRIFT RATE. A. S. Oravetz (U. S. Naval Material Command, Brooklyn, N. Y.), S. J. Jakimczyk, and H. J. Sandberg (Dynamics Research Corp., Stoneham, Mass.), p. 271-278. [See A69-13213 03-21]

APPROACH GUIDANCE PLANET TRACKER. M. K. Cohen (Kollsman Instrument Corp., Elmhurst, N.Y.) and M. Gorstein (NASA, Electronics Research Center, Cambridge, Mass.), p. 279-289. [See A69-13214 03-21]

SIGNAL PROCESSING. II - TIME DOMAIN TECHNIQUES.

A NONCOHERENT DETECTOR WITH IMPROVED IMMUNITY TO FADING. M. N. Woinsky (Bell Telephone Laboratories, Inc., New York, N.Y.) and L. Kurz (New York University, New York, N.Y.), p. 290-295. 8 refs. [See A69-13215 03-07]

A SAMPLED-DATA DELAY-LOCK LOOP FOR SYNCHRONIZING TDMA SPACE COMMUNICATIONS SYSTEMS. R. J. Huff and K. L. Reinhard (Ohio State University, Columbus, Ohio), p. 296-305. 9 refs. [See A69-13216 03-07]

A 10,000:1 PULSE COMPRESSION FILTER USING A TAPPED DELAY LINE LINEAR FILTER SYNTHESIS TECHNIQUE. R. D. Haggarty, L. A. Hart, and G. C. O'Leary (Mitre Corp., Bedford, Mass.), p. 306-314. 11 refs. [See A69-13217 03-09]

AN EXPERIMENTAL MEASUREMENT OF THE DETECTION CAPABILITY OF A LINEAR FM PULSE COMPRESSION SYSTEM. D. J. Belknap (Mitre Corp., Bedford, Mass.), p. 315-318. 10 refs. [See A69-13218 03-07]

CHANNEL IDENTIFICATION CODING FOR DATA COMPRESSORS. S. A. Sheldahl (Martin Marietta Corp., Denver, Colo.), p. 319-324. 7 refs. [See A69-13219 03-07]

DIGITAL DATA COMPRESSION BUFFER QUEUE CONTROL. W. A. Stevens and L. A. Pownall (Martin Marietta Corp., Denver, Colo.), p. 325-332.

A STORED PROGRAM DATA COMPRESSION DEVELOPMENTAL SYSTEM. L. A. Pownall (Martin Marietta Corp., Denver, Colo.), p. 333-338. [See A69-13220 03-08]

ENVIRONMENTAL SCIENCES AND SYSTEMS.

A LUNAR-SURFACE ELECTRIC-FIELD DETECTOR. B. W. Sherman (Missouri, University, Columbia, Mo.), R. H. Manka (NASA, Manned Spacecraft Center, Houston, Tex.), H. R. Anderson (William Marsh Rice University, Houston, Tex.), M. C. Terry, and J. D. Droppleman (Lockheed Aircraft Corp., Houston, Tex.), p. 339-344. [See A69-13221 03-14]

THE USE OF THE STARK EFFECT IN ELECTRIC-FIELD MEASUREMENT. P. K. Shumaker and B. W. Sherman (Missouri, University, Columbia, Mo.), p. 345-350. [See A69-13222 03-14]

EVALUATION OF NOMAD BUOY TELEMETRY SYSTEM. R. K. Franklin (U. S. Naval Oceanographic Office, Washington, D.C.) and J. L. Kelly (Page Communications Engineers, Inc., Washington, D.C.), p. 351-356. [See A69-13223 03-07]

SOLAR X-RAY CONTROL OF THE D-LAYER OF THE IONOSPHERE. P. R. Sengupta (Iowa, University, Iowa City, Iowa), p. 357-363. 10 refs. [See A69-13224 03-29]

ROCKET AND SATELLITE STUDIES OF SOLAR X-RAY FLARES. P. R. Sengupta (Iowa, University, Iowa City, Iowa), p. 364-375. 28 refs. [See A69-13225 03-29]

AN UNMANNED GEOPHYSICAL OBSERVATORY FOR ANTARCTICA. J. A. Jenny (Stanford University, Stanford, Calif.), p. 376-381.

SIGNAL PROCESSING. III - DIGITAL AND SAMPLE DATA TECHNIQUES.

LINEAR PROCESSING OF DIGITAL COMMUNICATION SIGNALS. J. W. Bayless (Southern Methodist University, Dallas; LTV Electrosystems, Inc., Greenville, Tex.) and S. C. Gupta (Southern Methodist University; Collins Radio Co., Dallas, Tex.), p. 382-385. 8 refs. [See A69-13226 03-07]

COEFFICIENT SENSITIVITY AND GENERALIZED DIGITAL FILTER SYNTHESIS. I. M. Langenthal (Signal Analysis Industries Corp., Copiague, N.Y.), p. 386-392. [See A69-13227 03-09]

ON ADAPTIVE SYNCHRONOUS DETECTION WITH FINITE MEMORY. R. L. Spooner (Bolt, Beranek and Newman, Inc., Washington, D. C.) and D. Jaarsma (Michigan, University, Ann Arbor, Mich.), p. 393-401. [See A69-13228 03-08]

A SHIFT-AND-ADD PROPERTY FOR MAJORITY COMBINED COMPOSITE CODES. J. A. Colligan (Michigan, University, Ann Arbor, Mich.), p. 402-406. [See A69-13229 03-07]

ACCURATE DIGITAL DETECTION OF ANGLE-MODULATED SIGNALS. F. D. Natali (Philco-Ford Corp., Palo Alto, Calif.), p. 407-413. 5 refs. [See A69-13230 03-07]

OPTIMIZATION OF THE REPRESENTATION OF SAMPLED DATA SIGNALS ON ORTHONORMAL BASES. M. T. Clark (Department of Defense, Washington, D.C.), p. 414-421. 7 refs. [See A69-13231 03-07]

SYSTEMS ENGINEERING.

EXPLORER 33 AND 35 - RELIABILITY ACHIEVEMENT BY DESIGN. R. H. Broadhurst (Bird Engineering-Research Associates, Inc.), p. 422-430. 7 refs. [See A69-13232 03-31]

OPTIMIZATION OF DIGITAL COMPUTER SYSTEMS. T. L. Collins (Boeing Co., Seattle, Wash.), p. 431-437. [See A69-13233 03-08]

SATELLITE SYSTEMS FOR NAVIGATION AND TRAFFIC CONTROL.

SPOT - A VERSATILE NAVIGATION/TRAFFIC CONTROL SATELLITE SYSTEM FOR TRANSOCEANIC AIRCRAFT AND

MARINE TRAFFIC. M. W. Mitchell, J. D. Barnla, and L. J. Tangradi (Radio Corporation of America, Camden, N.J.), p. 438-447. [See A69-13234 03-21]

SYNTHESIS OF AN AERONAUTICAL SERVICE SATELLITE SYSTEM. R. E. Jorasch, C. L. Murphy, and D. G. Middlebrook (Philco-Ford Corp., Palo Alto, Calif.), p. 448-455. [See A69-13235 03-21]

TRANSOCEANIC AIR TRAFFIC CONTROL USING SATELLITES. R. E. Anderson (General Electric Co., Schenectady, N.Y.), p. 456-464. [See A69-13236 03-21]

IMPROVED NORTH ATLANTIC AIR NAVIGATION USING AN AERONAUTICAL SATELLITE. R. J. Adams (Hughes Aircraft Co., El Segundo, Calif.), p. 465-476. 13 refs. [See A69-13237 03-21]

INTERNATIONAL SATELLITE SYSTEM FOR AIRCRAFT COMMUNICATIONS AND AIR TRAFFIC CONTROL. Q. C. Wilson, W. T. Brandon, and A. G. Cameron (Mitre Corp., Bedford, Mass.), p. 477-484. 10 refs. [See A69-13238 03-21]

APPLICATIONS TECHNOLOGY SATELLITES.

DESIGN EVOLUTION OF MECHANICALLY DESPUN ANTENNAS FROM ATS TO INTELSAT. L. Blaisdell, F. Donnelly, J. Killian, and O. Mahr (Sylvania Electric Products, Inc., Waltham, Mass.), p. 485-495. [See A69-13239 03-09]

WEFAX - WEATHER DATA RELAY COMMUNICATIONS EXPERIMENT. S. Wishna (NASA, Goddard Space Flight Center, Greenbelt, Md.), p. 496-500. [See A69-13240 03-11]

USE OF A DATA RELAY SATELLITE SYSTEM WITH ATS. M. Fashano and R. J. Rechter (Hughes Aircraft Co., El Segundo, Calif.), p. 501-513. 16 refs. [See A69-13241 03-07]

RADIO FREQUENCY INTERFERENCE EXPERIMENT DESIGN FOR THE APPLICATIONS TECHNOLOGY SATELLITE. V. F. Henry (NASA, Goddard Space Flight Center, Greenbelt, Md.) and J. J. Kelleher (NASA, Washington, D.C.), p. 514-520. 6 refs. [See A69-13242 03-07]

THE SDP-3 - A COMPUTER FOR USE ON BOARD SMALL SCIENTIFIC SPACECRAFT. R. A. Cliff (NASA, Goddard Space Flight Center, Greenbelt, Md.), p. 521-527. [See A69-13243 03-08]

FUTURE AVIONICS FOR GENERAL AVIATION.

AN AIRCRAFT ROAD SYSTEM VIA A COCKPIT PPI DISPLAY OF GROUND RADAR DATA ON TRANSPONDER EQUIPPED AIRCRAFT BROADCAST IN A 10 KC BANDWIDTH DIGITAL CODE. R. McFee (Syracuse University, Syracuse, N.Y.), p. 528-530. [See A69-13244 03-21]

RESULTS OF VOR PATH STABILITY INVESTIGATIONS. R. H. McFarland and F. J. Kiko (Ohio University, Athens, Ohio), p. 531-536. 8 refs. [See A69-13245 03-07]

AN AIRBORNE VIDEO TAPE NAVIGATIONAL DISPLAY. W. G. Mulley (U. S. Naval Material Command, Johnsville, Pa.) and J. J. Stein (Pennsylvania State University, University Park, Pa.), p. 537-542. [See A69-13246 03-21]

SSR "LISTEN-IN" FEATURE FOR PROXIMITY WARNING. G. B. Litchford, p. 543-552. [See A69-13247 03-21]

SIGNAL PROCESSING. IV - ANALYTIC TECHNIQUES.

SUBOPTIMUM, PHYSICALLY REALIZABLE DETECTION PROCEDURES FOR A CLASS OF NONGAUSSIAN PROCESSES WITH DEPENDENT SAMPLES. D. R. Klose and L. Kurz (New York University, Bronx, N.Y.), p. 553-560. 12 refs. [See A69-13248 03-07]

THE FAST FOURIER-HADAMARD TRANSFORM AND ITS USE IN SIGNAL REPRESENTATION AND CLASSIFICATION. J. E. Whelchel, Jr. and D. F. Guinn (Melpar, Inc., Falls Church, Va.), p. 561-573. 29 refs. [See A69-13249 03-07]

ON THE MINIMUM MEAN SQUARE ERROR OBTAINABLE IN PAM-FM. G. Tartara (Milano, Politecnico, Milan, Italy), p. 574-580. 7 refs. [See A69-13250 03-07]

DELAY-LINE BANDWIDTH REDUCTION TECHNIQUES. E. M. Drogin and A. E. Ruvin (Cutler-Hammer, Inc., Deer Park, N.Y.), p. 581-584. [See A69-13251 03-07]

THE PARAMETRIC SEQUENTIAL CLASSIFICATION OF SPECTRAL PATTERNS WITH APPLICATION TO SIGNAL DETECTION AND EXTRACTION. N. L. Owsley (Duke University, Durham, N.C.), p. 585-592. 10 refs. [See A69-13252 03-07]

THE TWO-INPUT ERF CORRELATOR. M. H. Burke (Communications Satellite Corp., Washington, D.C.) and J. S. Lee (George Washington University, Washington, D.C.), p. 593-599. 12 refs. [See A69-13253 03-09]

DIOMEDE - A PSEUDO-RANDOM RANGING SYSTEM USING OPTICAL CORRELATION. R. Picciotto and C. Skenderoff (Compagnie Française Thomson Houston-Hotchkiss Brandt, Paris, France), p. 600-606. [See A69-13254 03-07]

RESULTS OF AN EXPERIMENTAL STUDY OF COHERENT PSK IN A MULTIPATH ENVIRONMENT. J. F. Balcewicz (Radio Corporation of America, Princeton, N.J.) and J. C. Blair, p. 607-614. 7 refs. [See A69-13255 03-07]

ABSTRACTS, p. 615-618.

A69-13183 *

RADAR ATTITUDE SENSING SYSTEM.
Eugene Burcher (NASA, Washington, D.C.) and Edward Rupp (Bell Aerospace Corp., Bell Aerosystems Co., Buffalo, N.Y.).
IN: EASCON '68; INSTITUTE OF ELECTRICAL AND ELECTRONICS ENGINEERS, ELECTRONICS AND AEROSPACE SYSTEMS CONVENTION, WASHINGTON, D.C., SEPTEMBER 9-11, 1968, RECORD. [A69-13176 03-07]
New York, Institute of Electrical and Electronics Engineers, Inc., 1968, p. 60-63.

A radar attitude sensing system for use in earth orbital and lunar orbital vehicles is described. This is a multipurpose flight control instrument which employs radar data to obtain vehicle roll, pitch, yaw, altitude, and velocity. It uses a lightweight radar with an electronically steered antenna to provide an all solid-state sensor with no moving parts. The system employs a monopulse antenna configuration whose sum beam illuminates the terrain about the vehicle nadir. The radar return on the sum beam and two pairs of difference beams provides all of the measurement information. Operation is described at the block-diagram level. Theoretical performance is determined and is compared with results from an aircraft flight test program. These results are extrapolated to orbital altitudes and velocities. (Author)

A69-13242 *

RADIO FREQUENCY INTERFERENCE EXPERIMENT DESIGN FOR THE APPLICATIONS TECHNOLOGY SATELLITE.
Varice F. Henry (NASA, Goddard Space Flight Center, Greenbelt, Md.) and John J. Kelleher (NASA, Washington, D.C.).
IN: EASCON '68; INSTITUTE OF ELECTRICAL AND ELECTRONICS ENGINEERS, ELECTRONICS AND AEROSPACE SYSTEMS CONVENTION, WASHINGTON, D.C., SEPTEMBER 9-11, 1968, RECORD. [A69-13176 03-07]
New York, Institute of Electrical and Electronics Engineers, Inc., 1968, p. 514-520. 6 refs.

Description of the design of experiments to provide data on mutual rf interference between satellite and terrestrial telecommunications systems. The proposed experiment is designed to measure and evaluate the amount of mutual interference between communication satellite and terrestrial microwave relay systems at the shared common-carrier frequency bands of 6 and 4 GHz. It is proposed to measure terrestrial-to-satellite interference at 6 GHz and satellite-to-terrestrial interference at 4 GHz. To implement the technical requirements of this experiment, it is necessary to use a satellite of the type planned for the ATS F and G programs. These spacecraft, each carrying a 30-ft parabola as the prime antenna, will be capable of 0.1^{o} pointing accuracy and full earth-scanning coverage. It is postulated that measurements will be made of several parameters relevant to a fuller understanding of existing conditions with respect to such interference. M.M.

A69-13721 *

MILLIMETER WAVELENGTHS FOR SPACE COMMUNICATIONS?
John J. Kelleher (NASA, Washington, D.C.) and William O. Binkley (NASA, Goddard Space Flight Center, Systems Div., Extra High Frequency Technology Section, Greenbelt, Md.).
Microwave Journal, vol. 11, Nov. 1968, p. 30, 32, 34, 36.

Discussion of new short-wave bands to meet the growing needs of proliferating space services. Migration to bands above 10 GHz, where the spectrum is not so crowded, is suggested. Their utilization will depend on technical feasibility and adequate hardware. It is considered to be reasonably certain that millimeter wavelengths can be used for earth/space communications, provided that systems are designed to compensate for propagation anomalies and that frequency bands are made available. B.H.

07 COMMUNICATIONS

A69-13900 *#
CHARACTERISTICS OF LOW-LATITUDE VLF EMISSIONS.
Tadanori Ondoh (NASA, Goddard Space Flight Center, Greenbelt, Md.) and Susumu Isozaki.
Radio Research Laboratories, Journal, vol. 15, May 1968, p. 133-146. 13 refs.

Study of vlf emissions at 2, 5, and 21 kHz, which were observed since March 1966, August 1964, and December 1966, respectively, at Hiraiso (geomagnetic latitude 26.2° N), located well below the latitude of peak occurrence of vlf emissions. The diurnal variation of the 2-kHz emission is similar to those at mid-latitudes and high latitudes. However, the diurnal variation of the 5-kHz emission at Hiraiso is different from those at high latitudes. As for simultaneous occurrence of vlf emissions at 2 and 5 kHz, power fluxes observed at Hiraiso are always larger at 2 than at 5 kHz. This characteristic is similar to the broadband vlf emissions observed in the auroral zone. The rate occurrence of 21-kHz vlf emissions at low latitudes suggests that 21-kHz vlf emissions may be generated relatively near the ionosphere on geomagnetic lines of force starting from the auroral zone. F.R.L.

A69-14917 *#
A MATHEMATICAL TECHNIQUE FOR PROGRAMMING AUTOMATIC PICTURE TRANSMISSION TRACKING ANGLES.
David E. Pitts (NASA, Manned Spacecraft Center, Houston, Tex.).
Journal of Applied Meteorology, vol. 7, Dec. 1968, p. 1036-1038.

A computer can be used to calculate look angles for automatic picture transmission (APT) receiving stations. This method eliminates the laborious use of the plotting board and overlays, and enables the APT operator to have all possible orbit types preprogrammed and available a very short time after a new APT satellite is placed in orbit. The necessary coordinate transformations are presented in a form that makes them adaptable for use with very small computers. (Author)

A69-18944 *
CONDUCTIVE EMI - RESPONSIBILITY AND CONTROL.
Gary Harris (NASA, Goddard Space Flight Center, Solar Physics Branch, Greenbelt, Md.).
Frequency Technology, vol. 7, Feb. 1969, p. 22-25.

Discussion of electromagnetic interference (EMI) problems created by the coupling of noise from one subassembly to another by means of conductive paths. The discussion is primarily aimed at spacecraft but the information is equally appropriate when applied to ship-board installations, aircraft, and other environments. It is suggested that the overall responsibility for the control of an EMI program should rest with some central authority within the systems management organization. G.R.

A69-19092
INTERNATIONAL TELEMETERING CONFERENCE, LOS ANGELES, CALIF., OCTOBER 8-11, 1968, PROCEEDINGS.
Conference sponsored by the International Foundation for Telemetering.
Tarzana, Calif., International Foundation for Telemetering (ITC Proceedings. Volume 4), 1968. 660 p.
$21.

CONTENTS:

PCM THEORY AND APPLICATION.

A MAXIMUM LIKELIHOOD BIT SYNCHRONIZER. P. Mallory (Dynatronics, Inc., Orlando, Fla.), p. 1-16. [See A69-19093 07-09]

THE EFFECT OF CODING ON RATE EQUALIZATION OF DIGITAL CHANNELS. S. Butman (California Institute of Technology, Pasadena, Calif.), p. 17-21. 7 refs. [See A69-19094 07-07]

RICIAN INTERSYMBOL INTERFERENCE IN FREQUENCY SHIFT KEYING. J. J. Vencill (McDonnell Douglas Corp., Huntington Beach, Calif.), p. 22-33. 6 refs. [See A69-19095 07-07]

PERFORMANCE OF BLOCK-CODING SYSTEMS WHEN TRANSMITTING THROUGH A N-ARY DISCRETE CHANNEL IN THE PRESENCE OF WHITE GAUSSIAN NOISE. R. W. Okkes (European Space Research Organization, Noordwijk, Netherlands), p. 34-62. 9 refs. [See A69-19096 07-07]

OPTIMUM AND SUB-OPTIMUM DETECTION OF DIGITAL SEQUENCES CORRUPTED BY WHITE NOISE. J. K. Holmes and S. Butman (California Institute of Technology, Pasadena, Calif.), p. 63-78. [See A69-19097 07-07]

PERFORMANCE OF A BANDWIDTH LIMITED PCM/PSK/PM TELEMETRY SYSTEM. G. E. Miller and V. A. Jennings (Boeing Co., Seattle, Wash.), p. 79-106. [See A69-19098 07-07]

A PCM-TELEMETRY SYSTEM FOR SOUNDING ROCKET PAYLOADS. R. Hommel (Deutsche Versuchsanstalt für Luft- und Raumfahrt, Oberpfaffenhofen, West Germany), p. 107-115. [See A69-19099 07-07]

TELEMETRY SYSTEMS AND APPLICATIONS.

SINGLE RF CARRIER TIME-SHARING BY REMOTE LOCATIONS. S. L. Stadler (United Aircraft Corp., Tevose, Pa.), p. 116-133. [See A69-19100 07-07]

MULTIFUNCTION RECEIVER SYSTEM FOR INTEGRATED TRACKING, TELEMETRY AND RANGING DATA ACQUISITION. H. W. Shaffer (NASA, Goddard Space Flight Center, Greenbelt, Md.) and E. L. King (General Dynamics Corp., Rochester, N.Y.), p. 134-148. [See A69-19101 07-07]

A DATA RECORDING SYSTEM FOR DEEP SEA LOGGING. S. Ben-Yaakov (California, University, Los Angeles, Calif.), p. 149-160.

CRACKED SOLDER JOINT MECHANISM IN DISCRETE COMPONENT ASSEMBLIES. H. P. Estes and P. E. Theobald, p. 161-179. [See A69-19102 07-15]

A 100 KHz SYSTEM WITH AUTOMATIC OPERATION - THE OMEGA IV TELEMETRY PROCESSOR. T. R. Norton and J. I. Norworth (Stellarmetrics, Inc., Santa Barbara, Calif.), p. 180-187. [See A69-19103 07-09]

HIGH RELIABILITY TAPE RECORDERS FOR SATELLITE, AIRCRAFT & DRONE APPLICATIONS. S. Wiig, R. Santee (Borg-Warner Corp., Santa Ana, Calif.), and E. D. Lucas, Jr. (Best Electronics, Tustin, Calif.), p. 188-199. [See A69-19104 07-14]

RF TELEMETRY FROM A HIGH SPEED SUBTERRAIN. T. W. H. Caffey and W. R. Hale (Sandia Corp., Albuquerque, N. Mex.), p. 200-211.

DIGITAL TELEMETRY SYSTEMS.

DIGITAL FM - TUTORIAL. J. Salz (Florida, University, Gainesville, Fla.), p. 212-232. 21 refs. [See A69-19105 07-07]

WIDEBAND PCM-FM BIT ERROR PROBABILITY USING DISCRIMINATOR DETECTION. J. J. Hayes, C. H. Chen, and W. J. Kubicki (Avco Corp., Wilmington, Mass.), p. 233-247. 8 refs. [See A69-19106 07-07]

EXPECTED NUMBER OF SPIKES OF PHASE LOCKED LOOP DEMODULATORS. P. W. Osborne and D. L. Schilling (Brooklyn, Polytechnic Institute, Brooklyn, N.Y.), p. 248-258. 6 refs. [See A69-19107 07-07]

DIGITAL-DATA TRANSITION TRACKING LOOPS. W. C. Lindsey (Southern California, University, Los Angeles, Calif.) and T. O. Anderson (California Institute of Technology, Pasadena, Calif.), p. 259-271. [See A69-19108 07-07]

PERFORMANCE OF BINARY PSK COMMUNICATION SYSTEMS. J. F. Oberst and D. L. Schilling (Brooklyn, Polytechnic Institute, Brooklyn, N.Y.), p. 272-289. [See A69-19109 07-07]

L- AND S-BAND ANTENNAS AND SYSTEMS.

A TWO-CHANNEL MONOPULSE TELEMETRY AND TRACKING ANTENNA FEED. R. R. Yaminy (Radiation Systems, Inc., McLean, Va.), p. 290-306. [See A69-19110 07-09]

MINIATURE CURRENT DISCONTINUITY DEVICE ANTENNAS. B. J. Bittner (Kaman Sciences Corp., Colorado Springs, Colo.), p. 307-316. [See A69-19111 07-09]

DESIGN OF AIRBORNE S-BAND TELEMETRY ANTENNAS. H. D. Weinschel (New Mexico State University, University Park, N. Mex.), p. 317-329. [See A69-19112 07-09]

THE SUN AS A CALIBRATION SIGNAL SOURCE FOR L- AND S-BAND TELEMETRY. W. R. Hedeman (Aerospace Corp., San Bernardino, Calif.), p. 330-342. 11 refs. [See A69-19113 07-07]

AN ADAPTIVE AIRBORNE VLF/UHF TRANSMITTER SYSTEM. E. B. Franke and W. F. Trover (Teledyne, Inc., Huntsville, Ala.), p. 343-358. [See A69-19114 07-09]

MINIATURE POWER AMPLIFIER FOR TELEMETRY TRANSMITTERS. R. H. Winkler (Teledyne, Inc., Mountain View, Calif.), p. 359-367. [See A69-19115 07-09]

RESULTS OF THE UHF TELEMETRY SYSTEM R&D FLIGHT TESTS AT WHITE SANDS MISSILE RANGE. B. Chin and J. W.

Hamilton (U.S. Army, White Sands Missile Range, N. Mex.), p. 368-377. 6 refs. [See A69-19116 07-07]

RECORDING AND PCM.

COMPATIBILITY REQUIREMENTS AND CONSIDERATIONS OF RANGE TELEMETRY TAPE. G. H. Schulze (Pan American World Airways, Inc., Cocoa Beach, Fla.), p. 378-391. [See A69-19117 07-14]

THE EFFECTS, MEASUREMENT, AND ANALYSIS OF FLUTTER IN INSTRUMENTATION RECORDERS. L. Moore (Micom, Inc., Palo Alto, Calif.), p. 392-398. [See A69-19118 07-14]

CAUSE AND EFFECT OF TIME BASE ERRORS IN COHERENT DEMODULATION OF A SUPPRESSED CARRIER AM MULTIPLEX. F. J. Schmitt (Lockheed Aircraft Corp., Plainfield, N.J.) and M. H. Nichols, p. 399-406. 6 refs. [See A69-19119 07-07]

PERFORMANCE CHARACTERISTICS AND SPECIFICATION OF PCM BIT SYNCHRONIZER/SIGNAL CONDITIONERS. B. Peavey (NASA, Goddard Space Flight Center, Greenbelt, Md.), p. 407-419. 5 refs. [See A69-19120 07-09]

BIT ERROR RATES IN THE PRESENCE OF UNTRACKED TIME BASE FLUCTUATION. P. Mallory (Dynatronics, Inc., Orlando, Fla.) and A. O. Roche, p. 420-429. [See A69-19121 07-07]

THE SIGNAL-TO-NOISE RATIO ESTIMATION TECHNIQUES FOR PCM SIGNALS. J. Y. Sos (NASA, Goddard Space Flight Center, Greenbelt, Md.), p. 430-439. [See A69-19122 07-07]

SPACE APPLICATIONS.

SYNTHESIS OF HIGH DATA RATE COHERENT TELEMETRY SYSTEMS. L. N. Ma, M. S. Stone, and D. P. Sullivan (TRW Systems Group, Redondo Beach, Calif.), p. 440-454. [See A69-19123 07-07]

COMMUNICATIONS FOR THE APOLLO APPLICATIONS PROGRAM. S. W. Fordyce (NASA, Office of Manned Space Flight, Washington, D.C.), p. 455-464. [See A69-19124 07-07]

A HIGH-RATE TELEMETRY SYSTEM FOR THE MARINER 1969 MISSION. R. C. Tausworthe, M. F. Easterling, and A. J. Spear (California Institute of Technology, Pasadena, Calif.), p. 465-480. 5 refs. [See A69-19125 07-07]

THE SMALL ASTRONOMY SATELLITE (SAS) PROGRAM. M. R. Townsend (NASA, Goddard Space Flight Center, Greenbelt, Md.), p. 481-502. [See A69-19126 07-31]

ANALOG TELEMETRY.

OUTPUT SNR OF AN FM DISCRIMINATOR WITH NON-IDEAL LIMITING. D. L. Schilling (Brooklyn, Polytechnic Institute, Brooklyn, N.Y.) and J. J. Refi (Bell Telephone Laboratories, Inc., Baltimore, Md.), p. 503-512. [See A69-19127 07-09]

FREQUENCY FEED-FORWARD - AN OPEN LOOP APPROACH FOR EXTENDING THE THRESHOLD AND LINEARITY OF FM DEMODULATORS. M. G. Pelchat and S. B. Boor (Radiation, Inc., Melbourne, Fla.), p. 513-529. [See A69-19128 07-09]

PRESAMPLING FILTERING. D. D. McRae and R. C. Davis (Radiation, Inc., Melbourne, Fla.), p. 530-543. [See A69-19129 07-07]

ERRORS RESULTING FROM CHANNEL FILTERS AND ADJACENT CHANNEL CROSSTALK IN DSB/SC TELEMETRY SYSTEMS. W. E. Salter (Sperry Rand Corp., New York, N.Y.) and W. O. Frost (NASA, Marshall Space Flight Center, Huntsville, Ala.), p. 544-559. 6 refs. [See A69-19130 07-07]

A DOUBLE SIDEBAND-QUADRATURE CARRIER MULTIPLEX TELEMETRY SYSTEM. J. M. Gutwein and J. F. Annese (ADCOM, Inc., Cambridge, Mass.), p. 560-580. [See A69-19131 07-07]

FLIGHT AND LABORATORY TESTING OF A DOUBLE SIDEBAND FM TELEMETRY SYSTEM. R. B. Richardson and P. F. Harney (NASA, Flight Research Center, Edwards AFB, Calif.), p. 581-596. [See A69-19132 07-07]

MEDICAL AND BIOLOGICAL TELEMETRY APPLICATIONS.

TRANSMISSION OF CARDIOVASCULAR DATA FROM DOGS. R. Rader, J. P. Meehan, J. P. Henry, R. Krutz, and R. Trumbo (Southern California, University, Los Angeles, Calif.), p. 597-606. 6 refs. [See A69-19133 07-05]

LASER APPLICATIONS TO BIOLOGY AND MEDICINE. D. E. Rounds (Pasadena Foundation for Medical Research, Pasadena, Calif.), p. 607-613.

ENVIRONMENTAL TELEMETRY.

COMMUNICATIONS BETWEEN SATELLITE AND BALLOONS FOR THE EOLE MISSION. J. P. Bourdeau, P. Debray, and X. Namy (Centre National d'Etudes Spatiales, Brétigny-sur-Orge, Essonne, France), p. 614-630. [See A69-19134 07-07]

PRELIMINARY EXPERIMENT RESULTS FROM THE OMEGA POSITION LOCATION EQUIPMENT (OPLE). H. S. Horiuchi (NASA, Goddard Space Flight Center, Greenbelt, Md.), p. 631-638. [See A69-19135 07-21]

TELEMETRY WITH UNRESTRAINED ANIMALS. H. A. Baldwin and D. L. Brumbaugh (Sensory Systems Laboratory, Tucson, Ariz.), p. 639-649. 8 refs. [See A69-19136 07-05]

BUOY TELEMETRY FOR ENVIRONMENT PREDICTION IN FISHERIES RESEARCH. W. B. McAlister (Bureau of Commercial Fisheries, Seattle, Wash.), p. 650-657.

A69-19101 *

MULTIFUNCTION RECEIVER SYSTEM FOR INTEGRATED TRACKING, TELEMETRY AND RANGING DATA ACQUISITION.

H. W. Shaffer (NASA, Goddard Space Flight Center, STADAN Operations Div., Greenbelt, Md.) and E. L. King (General Dynamics Corp., Electronics Div., Rochester, N.Y.).

IN: INTERNATIONAL TELEMETERING CONFERENCE, LOS ANGELES, CALIF., OCTOBER 8-11, 1968, PROCEEDINGS. [A69-19092 07-07]

Conference sponsored by the International Foundation for Telemetering.

Tarzana, Calif., International Foundation for Telemetering (ITC Proceedings. Volume 4), 1968, p. 134-148.

Contract No. NAS 5-10555.

Description of the rationale, concepts, background requirements, and technical justifications leading to the decision by NASA/Goddard Space Flight Center to develop the Multifunction Receiver System. Attention is given to multiple network operation and mission and cost effectiveness. A specific design approach used to satisfy the requirements of this program is examined. Z.W.

A69-19122 *

THE SIGNAL-TO-NOISE RATIO ESTIMATION TECHNIQUES FOR PCM SIGNALS.

John Y. Sos (NASA, Goddard Space Flight Center, Information Processing Div., Greenbelt, Md.).

IN: INTERNATIONAL TELEMETERING CONFERENCE, LOS ANGELES, CALIF., OCTOBER 8-11, 1968, PROCEEDINGS. [A69-19092 07-07]

Conference sponsored by the International Foundation for Telemetering.

Tarzana, Calif., International Foundation for Telemetering (ITC Proceedings. Volume 4), 1968, p. 430-439.

The paper describes three potentially practical methods for estimating the SNR in a PCM signal. One method, referred to as the "spectral null" method, uses spectral characteristics of PCM signals to estimate the SNR; the other two use statistical properties of the signal - i.e., its mean value and variance. These two methods are known as "variance estimation" and "null zone." The implementation of each method is discussed. The spectral null method takes the least amount of equipment, but is more difficult to calibrate and operate over a wide range of bit rates than the other two systems. All three approaches, however, are uncomplicated enough to be included in almost any existing PCM data-handling system. Performance characteristics of each system are analyzed. It is shown that the variance estimation method is the most versatile. It can reliably estimate the SNR to within 1.5 dB over a range of SNRs from 0 to +10 dB. (The SNR is defined as the ratio of signal energy per bit/noise power density.) Under certain conditions all three methods can provide estimates to within 1 dB, especially over a SNR range from +3 to +10 dB. (Author)

A69-19124 *

COMMUNICATIONS FOR THE APOLLO APPLICATIONS PROGRAM.

Samuel W. Fordyce (NASA, Office of Manned Space Flight, Washington, D.C.).

IN: INTERNATIONAL TELEMETERING CONFERENCE, LOS ANGELES, CALIF., OCTOBER 8-11, 1968, PROCEEDINGS. [A69-19092 07-07]

Conference sponsored by the International Foundation for Telemetering.

Tarzana, Calif., International Foundation for Telemetering (ITC Proceedings. Volume 4), 1968, p. 455-464.

Description of the communications for the Apollo Applications Program (AAP), which will consist of a series of extended-duration manned missions in low earth orbit. The initial missions are based upon equipment and techniques proved in previous space flight missions. This is especially true of the communications systems, which rely on the Gemini, Saturn, and Apollo communications hardware operating with the manned space flight network. Following AAP missions may include new spacecraft developments involving television, teleprinters, satellite relays, and spacecraft data management systems. These developments are described briefly, but many of them are concepts only in early development stages. Z.W.

A69-19130 *

ERRORS RESULTING FROM CHANNEL FILTERS AND ADJACENT CHANNEL CROSSTALK IN DSB/SC TELEMETRY SYSTEMS.
W. E. Salter (Sperry Rand Corp., New York, N.Y.) and W. O. Frost (NASA, Marshall Space Flight Center, Huntsville, Ala.).
IN: INTERNATIONAL TELEMETERING CONFERENCE, LOS ANGELES, CALIF., OCTOBER 8-11, 1968, PROCEEDINGS. [A69-19092 07-07]
Conference sponsored by the International Foundation for Telemetering.
Tarzana, Calif., International Foundation for Telemetering (ITC Proceedings. Volume 4), 1968, p. 544-559. 6 refs.

The waveform distortion resulting from adjacent channel crosstalk and from amplitude and phase nonlinearity in channel filters limits the minimum channel spacing and, hence, the bandwidth utilization efficiency of a double sideband/suppressed carrier (DSB/SC) telemetry link. The paper presents results of an analysis defining the minimum achievable mean-square error when Butterworth filters are used in the DSB demodulator/demultiplexer. With data inputs consisting of band-limited random signals, solutions are given for various combinations of data order, filter order, channel spacing, and filter cutoff. The tradeoff between waveform distortion and channel spacing is illustrated, and optimum locations for the filter cutoff are defined. The irremovable error based on Weiner optimum filter theory is presented as an interesting basis for comparison. (Author)

A69-19132 *

FLIGHT AND LABORATORY TESTING OF A DOUBLE SIDEBAND FM TELEMETRY SYSTEM.
Robert B. Richardson and Paul F. Harney (NASA, Flight Research Center, Edwards AFB, Calif.).
IN: INTERNATIONAL TELEMETERING CONFERENCE, LOS ANGELES, CALIF., OCTOBER 8-11, 1968, PROCEEDINGS. [A69-19092 07-07]
Conference sponsored by the International Foundation for Telemetering.
Tarzana, Calif., International Foundation for Telemetering (ITC Proceedings. Volume 4), 1968, p. 581-596.

Discussion of the laboratory tests and preliminary flight evaluation of a double-sideband suppressed carrier constant-bandwidth telemetry system that will be used as an airborne high-frequency data recorder. Some practical limitations are illustrated, and laboratory and flight-test results are compared. No attempt is made to compare this system with systems using other forms of modulation. Results obtained using an rf link are compared with magnetic tape recording of data. Calibration requirements are included for each system. (Author)

A69-20045 *

CONJUGATE ECHOES IN ALOUETTE-2 TOPSIDE-SOUNDER DATA.
Jayaram Ramasastry, Edward J. Walsh (NASA, Electronics Research Center, Cambridge, Mass.), and John R. Herman (Lowell Technological Institute, Research Foundation, Lowell, Mass.).
IEEE Transactions on Antennas and Propagation, vol. AP-16, Nov. 1968, p. 771-774.

Three types of ionograms containing symmetric conjugate echo traces which appear frequently in the Alouette 2 satellite topside-sounder data are presented and explained in terms of multiple reflections between conjugate points of the field line passing through the satellite. Such symmetric traces have not been previously reported in the literature. The high intensity of these traces gives credence to the existence of magnetospheric waveguides along which signals can propagate with very little attenuation. (Author)

A69-23279 *

FM/AM TELEMETRY TO MEASURE IMPACT ACCELERATIONS.
Dean R. Harrison (NASA, Ames Research Center, Moffett Field, Calif.).
IN: INSTRUMENTATION IN THE AEROSPACE INDUSTRY. VOLUME 14 - INSTRUMENT SOCIETY OF AMERICA, INTERNATIONAL AEROSPACE INSTRUMENTATION SYMPOSIUM, 14TH, BOSTON, MASS., JUNE 3-5, 1968, PROCEEDINGS. [A69-23245 10-11]
Edited by John Leak.
Pittsburgh, Instrument Society of America, 1968, p. 221-224. 8 refs.

An FM/AM telemetry system has been designed which provides three-axis acceleration measurements during impact tests of models of soft-landing structures. The system was designed to employ a three-axis piezoelectric accelerometer working into three separate FM/AM telemetry circuits. Each carrier was received and detected by a separate receiver at the ground station. The subcarrier output of the receiver was recorded directly on magnetic tape. The frequency of the subcarrier was preset to the center frequency of the tape recorder FM electronics to facilitate demodulation of the recorded subcarrier during playback of the tape. During calibration, drop-test acceleration wave forms were recorded by both telemetry and direct wire techniques. Wave-form comparisons showed close correlation for each axis tested. (Author)

A69-24993 *

ANALYSIS OF APERTURE RADIATION FROM AN AXIALLY SLOTTED CIRCULAR CONDUCTING CYLINDER USING GEOMETRICAL THEORY OF DIFFRACTION.
C. A. Balanis (NASA, Langley Research Center, Hampton, Va.) and L. Peters, Jr. (Ohio State University, Dept. of Electrical Engineering, Columbus, Ohio).
IEEE Transactions on Antennas and Propagation, vol. AP-17, Jan. 1969, p. 93-97. 8 refs.

The wedge-diffraction theory in combination with the creeping-wave theory is used to compute the radiation pattern of an axial slot on a circular conducting cylinder. The slot is excited by a parallel-plate waveguide operating in the TEM mode. The total field in the "lit" region is obtained by the superposition of the wedge-diffracted and creeping-wave fields. The total field in the "shadow" region is obtained solely from the creeping-wave contribution. (Author)

A69-25288

INSTITUTE OF ELECTRICAL AND ELECTRONICS ENGINEERS, ANNUAL REGION III CONVENTION, 7TH, COCOA BEACH, FLA., NOVEMBER 18-20, 1968, RECORD.
New York, Institute of Electrical and Electronics Engineers, Inc., 1968. 433 p.
Members, $12; nonmembers, $18.

CONTENTS:

ADVANCED TECHNOLOGIES.
ON THE SOLUTIONS OF PERIODICALLY-VARYING SYSTEMS. H. F. VanLandingham (Virginia Polytechnic Institute, Blacksburg, Va.), p. S1-1p1, S1-1p2. [See A69-25289 11-19]
ASYMPTOTIC STABILITY WITH OUTPUT CONSTRAINTS. P. M. Julich (Louisiana State University, Baton Rouge, La.), p. S1-2p1 to S1-2p6. 8 refs. [See A69-25290 11-19]
SOME RESULTS IN MINIMUM-ENTROPY FEATURE EXTRACTION. R. C. Gonzalez and J. T. Tou (Florida, University, Gainesville, Fla.), p. S1-3p1 to S1-3p10. 8 refs. [See A69-25291 11-19]
A DIGITALLY CONTROLLED FORMANT GENERATOR FOR A TERMINAL ANALOG SPEECH SYNTHESIZER. J. A. Dickerson (International Business Machines Corp., Research Triangle Park, N.C.), p. S1-4p1 to S1-4p9. [See A69-25292 11-09]
LIQUID CRYSTALS - THEIR APPLICATION TO NONDESTRUCTIVE TESTING. T. A. Simcox (General Electric Co., Cocoa Beach, Fla.), p. S1-5p1 to S1-5p15. 6 refs. [See A69-25293 11-15]

UNDERSEA TECHNOLOGY.
A STUDY OF SIGNAL PERTURBATION EFFECTS IN A SHALLOW

WATER ENVIRONMENT. H. N. Dawirs (Florida State University, Tallahassee, Fla.) and J. H. Hammond (U.S. Navy, Mine Defense Laboratory, Panama City, Fla.), p. S2-1pl to S2-1p8.

CONTRIBUTION OF TEMPERATURE COEFFICIENTS ON ACCURACY OF OCEANOGRAPHIC INSTRUMENTATION. L. Chase and J. E. Boyd (U.S. Naval Oceanographic Office, Washington, D.C.), p. S2-2pl.

SUITCASE OCEANOGRAPHY. A. H. Haynes and B. L. Avery (U.S. Naval Oceanographic Office, Washington, D.C.), p. S2-3pl, S2-3p2.

AN ELECTRICAL TRANSDUCER SYSTEM FOR MEASURING OCEAN CURRENTS. G. G. Miler, Jr. (Florida Institute of Technology, Melbourne, Fla.), p. S2-4pl to S2-4p8.

SPACE ELECTRONICS.

THE COMPONENT NEEDS OF ADVANCED COMMERCIAL COMMUNICATIONS SATELLITES. E. Podraczky (Communications Satellite Corp., Washington, D.C.), p. S3-1pl.

A HIGH-GAIN SELF-STEERING MICROWAVE REPEATER. W. H. Kummer and R. A. Birgenheier (Hughes Aircraft Co., Culver City, Calif.), p. S3-2pl to S3-2p8. 7 refs. [See A69-25294 11-07]

SPACE DATA RELAY. P. L. Suttler, Jr. (USAF, Systems Command, Los Angeles, Calif.), p. S3-3pl to S3-3pll. [See A69-25295 11-07]

DATA RELAY SATELLITES FOR SUPPORT OF NASA R&D MISSIONS. P. F. Barritt (NASA, Office of Tracking and Data Acquisition, Washington, D.C.), p. S3-4pl to S3-4p5. [See A69-25296 11-07]

TELEMETRY.

AN APPROACH TO ADAPTIVE THRESHOLD DETECTION. M. J. Bouvier, Jr. (Louisiana State University, Baton Rouge, La.) p. S4-1pl to S4-1p7. 10 refs. [See A69-25297 11-07]

A DIGITAL SIMULATION OF A PHASED LOCKED RECEIVER IN A FADING MULTIPATH ENVIRONMENT. A. E. Smith and R. S Johnson (Radio Corporation of America, Moorestown, N.J.), p. S4-2pl to S4-2pl3. 14 refs. [See A69-25298 11-07]

A COMPUTER-AIDED MEASUREMENT OF SNR EMPLOYING A TIME INTERVAL COUNTER. C. E. Smith, F. R. McDevitt, and E. R. Graft (Auburn University, Auburn, Ala.), p. S4-3pl to S4-3p4. 5 refs. [See A69-25299 11-07]

TELEMETRY SYSTEM PERFORMANCE TESTS AT THE EASTERN TEST RANGE. E. T. Johnson (Radio Corporation of America, Patrick AFB, Fla.), p. S4-4pl to S4-4p8. [See A69-25300 11-07]

MEASURING MICROWAVE NOISE - A SERIES OF NOTES. W. E. Pastori (Cutler-Hammer, Inc., Deer Park, N.Y.), p. S4-5pl to S4-5p8. 16 refs. [See A69-25301 11-07]

EDUCATION.

COOPERATIVE ENGINEERING EDUCATION. E. M. Corlew and C. H. Weaver (Tennessee, University, Knoxville, Tenn.), p. S5-1pl to S5-1p6.

TOWARD A MORE FLEXIBLE ELECTRICAL ENGINEERING CURRICULUM. W. H. Chen (Florida, University, Gainesville, Fla.), p. S5-2pl to S5-2p7.

REPORT ON CURRENT PROGRAMS IN CONTINUING ENGINEERING STUDIES FOR GREATER BOSTON. I. Katz (Northeastern University, Boston, Mass.), p. S5-3pl to S5-3pl5.

PREDICTING GRADES AT A SOUTHERN TECHNICAL INSTITUTE AND SOME PROBLEMS IN PREDICTING GRADES IN GENERAL. E. Marks (Georgia Institute of Technology, Atlanta, Ga.), p. S5-4pl to S5-4p4.

ENGINEERING EDUCATION AND THE COMPUTER. W. H. Niehoff (International Business Machines Corp., Endicott, N.Y.), p. S5-5pl to S5-5p4.

POWER.

REAL TIME/PROCESS COMPUTER INTERFACE WITH POWER SYSTEMS. T. M. Urban (General Electric Co., Cape Canaveral, Fla.), p. S6-1pl to S6-1pl5. [See A69-25302 11-34]

OUT OF A WILDERNESS - HISTORY OF TURKEY POINT POWER PROJECT. G. Kinsman (Florida Power and Light Co., Miami, Fla.), p. S6-2pl to S6-2p4.

CRYSTAL RIVER NUCLEAR PLANT ELECTRICAL DESIGN CONCEPTS. W. A. Szelistowski (Florida Power Corp., St. Petersburg, Fla.), p. S6-3pl to S6-3p7.

NUCLEAR POWER GENERATION - THE UNIVERSITY'S ROLE. R. E. Uhrig (Florida, University, Gainesville, Fla.), p. S6-4pl.

ELECTROGASDYNAMICS - ENERGY OF THE FUTURE! K. R. Rao (Texas, University, Arlington, Tex.), p. S6-5pl to S6-5p6.

MANAGEMENT.

ISOLATION - THE MAJOR BARRIER TO THE INTELLECTUAL CROSS-FERTILIZATION OF SCIENTIFIC PERSONNEL IN AN AIR FORCE-INDUSTRY RESEARCH AND DEVELOPMENT PROGRAM. J. A. Angelo, Jr. (USAF, Systems Command, Los Angeles, Calif.), p. S7-1pl to S7-1p8. 5 refs. [See A69-25303 11-34]

THE PERILS OF PROPHECY OR TECHNOLOGICAL FORECASTING FOR THE MANAGER. H. Winter (Research Associates, Inc., Silver Spring, Md.), p. S7-2pl to S7-2p5.

INTEGRATED MANAGEMENT INFORMATION SYSTEM (IMIS). G. H. Boos (General Electric Co., League City, Tex.), p. S7-3pl to S7-3pl0. [See A69-25304 11-34]

MANAGEMENT TRAINING FOR EXECUTIVE DEVELOPMENT. J. H. Hinton (Bendix Corp., Cape Kennedy, Fla.), p. S7-4pl to S7-4p7. 8 refs. [See A69-25305 11-34]

MANAGER TRAINING. G. H. Turpin, p. S7-5pl to S7-5p4.

MICRO-ELECTRONICS.

LOW FREQUENCY NOISE SOURCES IN INTEGRATED CIRCUIT TRANSISTORS. R. C. Jaeger, A. J. Brodersen, and E. R. Chenette (Florida, University, Gainesville, Fla.), p. S8-1pl.

EXTENSIONS OF PN JUNCTION THEORY. D. D. Kleppinger and F. A. Lindholm (Florida, University, Gainesville, Fla.), p. S8-2pl to S8-2pl3. 14 refs. [See A69-25306 11-26]

APPROXIMATE EQUIVALENT LINEAR CIRCUITS FOR THE STEP RESPONSE OF DIFFUSED AND THIN FILM RESISTORS. H. P. Weber (Florida Institute of Technology, Melbourne, Fla.), p. S8-3pl.

A MONOLITHIC GERMANIUM IMAGING MOSAIC. M. A. Schuster and J. M. Saboe (Westinghouse Electric Corp., Baltimore, Md.), p. S8-4pl to S8-4pl0. 7 refs. [See A69-25307 11-26]

APPLICATIONS OF ANALYTICAL TECHNIQUES.

AN EXPERIMENTAL INVESTIGATION OF ATMOSPHERIC EFFECTS ON AN OPTICAL PCM DATA RELAY. R. E. Blue (International Business Machines Corp., Cape Canaveral, Fla.) and D. T. Sze (International Business Machines Corp., Poughkeepsie, N.Y.), p. S9-1pl to S9-1pl0. 17 refs. [See A69-25308 11-14]

A SIMULATION OF AIRBORNE ANTENNA DESIGNATION FUNCTIONS. J. W. McRary and B. W. Koeppel (Pan American World Airways, Inc., Patrick AFB, Fla.), p. S9-2pl to S9-2pl5. [See A69-25309 11-07]

COMPUTER-AIDED DESIGN - ROOT LOCUS. D. R. Dunn and J. F. Pierce (Tennessee, University, Knoxville, Tenn.), p. S9-3pl to S9-3p8.

AN INVESTIGATION OF THE DECOUPLING EFFECTS IN A MAGNETIC FORMING BERYLLIUM COIL ASSEMBLY. M. E. Davis, J. W. Rogers, D. D. Wier (Mississippi State University, State College, Miss.), and J. D. Bennight (NASA, Marshall Space Flight Center, Huntsville, Ala.), p. S9-4pl to S9-4p6. 8 refs. [See A69-25310 11-14]

NONLINEAR MAGNETIC FIELD SOLUTIONS FOR NONHOMOGENEOUS ISOTROPIC CURRENT-FREE REGIONS. F. O. Simons, Jr. (Florida, University, Orlando, Fla.) and W. A. Walter (Florida, University, Daytona Beach, Fla.), p. S9-5pl to S9-5p8. 12 refs. [See A69-25311 11-14]

TELEPHONY.

EFFECT OF DATA LOADING ON RADIO AND CARRIER SYSTEMS. J. B. Berry, Jr. (Southern Bell Telephone and Telegraph Co., Atlanta, Ga.), p. S10-1pl to S10-1p9.

RAYLEIGH-FADING SIGNAL IN A MULTI-CHANNEL REPEATER. C. F. Eaton (Mitre Corp., Bedford, Mass.), p. S10-2pl to S10-2p3.

USE OF COMPUTER TECHNIQUES IN DESIGNING WIRE COMMUNICATIONS. J. T. Cates, Jr. (Southern Bell Telephone and Telegraph Co., Atlanta, Ga.), p. S10-3pl to S10-3p9.

MICROWAVE RADIO INTERFERENCE STUDIES BY COMPUTER. C. H. Roggenkamp (Southern Bell Telephone and Telegraph Co., Atlanta, Ga.), p. S10-4pl to S10-4p8. 5 refs. [See A69-25312 11-07]

COMPUTERIZATION OF RADIO ENGINEERING FUNCTIONS.

J. D. Creel (South Central Bell Telephone Co., Birmingham, Ala.), p. S10-5pl to S10-5p5. [See A69-25313 11-07]

COMMUNITY ANTENNA TELEVISION SYSTEMS DESIGN AND OPERATION. H. C. Irby (Southern Bell Telephone and Telegraph Co., Atlanta, Ga.), p. S10-6pl to S10-6p8.

ANTENNAS.

THE DEVELOPMENT OF COMPACT ANTENNA RANGE TECHNIQUES. R. C. Johnson (Georgia Institute of Technology, Atlanta, Ga.), p. S11-1pl to S11-1p8. 7 refs. [See A69-25314 11-09]

LOADED TRAVELING WAVE ANTENNA ELEMENTS OF REDUCED SIZE. G. G. Rassweiler (Radiation, Inc., Melbourne, Fla.), p. S11-2pl to S11-2pl2. 18 refs. [See A69-25315 11-09]

DUAL-REFLECTOR ANTENNA DESIGN TECHNIQUES FOR LOW NOISE APPLICATIONS. F. Rouffy (U.S. Army, Huntsville, Ala.), p. S11-3pl to S11-3p8. 19 refs. [See A69-25316 11-09]

SYMMTRAC I AND SYMMTRAC L FEEDS FOR LOW NOISE ANTENNAS. L. Blaisdell (Sylvania Electric Products, Inc., Waltham, Mass.) and R. Rubin (Mitre Corp., Bedford, Mass.), p. S11-4pl to S11-4pl0. [See A69-25317 11-09]

THE ZEROTH-ORDER APPROXIMATION TO THE CURRENT DISTRIBUTION ON THE ELEMENTS OF CIRCULAR ARRAYS OF TANGENTIAL DIPOLES. J. D. Tillman, S. B. Roberts (Tennessee, University, Knoxville, Tenn.), and E. R. Graf (Auburn University, Auburn, Ala.), p. S11-5pl to S11-5p9. 5 refs. [See A69-25318 11-09]

COMPUTERS.

ENGINEERING ASPECTS OF COMPUTER-ASSISTED INSTRUCTIONAL SYSTEMS. R. W. Avery (Radio Corporation of America, Palo Alto, Calif.), p. S12-1pl to S12-1p6.

DESIGNING THE HUMAN "COMPONENT" INTO A TOTAL COMMUNICATION SYSTEM. G. P. Livingston (International Business Machines Corp., Research Triangle Park, N.C.), p. S12-2pl to S12-2p5.

APPLICATIONS OF COMPUTER SIMULATION IN ELECTRONICS. F. F. Martin (Hughes Aircraft Co., Fullerton, Calif.), p. S12-3pl to S12-3p5. 20 refs. [See A69-25319 11-08]

ADVANCED COMPUTER FOR BOOSTER/SATELLITE APPLICATION. R. J. Starbuck (USAF, Systems Command, Los Angeles, Calif.), p. S12-4pl to S12-4p5. [See A69-25320 11-08]

PROGRAMMED FOR SERVICE. P. E. Williamson (Southern Bell Telephone and Telegraph Co., Atlanta, Ga.), p. S12-5pl, S12-5p2.

A69-25296 *#

DATA RELAY SATELLITES FOR SUPPORT OF NASA R&D MISSIONS.

Paul F. Barritt (NASA, Office of Tracking and Data Acquisition, Washington, D.C.).

IN: INSTITUTE OF ELECTRICAL AND ELECTRONICS ENGINEERS, ANNUAL REGION III CONVENTION, 7TH, COCOA BEACH, FLA., NOVEMBER 18-20, 1968, RECORD. [A69-25288 11-07]

New York, Institute of Electrical and Electronics Engineers, Inc., 1968, p. S3-4pl to S3-4p5.

For the past three years, NASA has been studying the potential use of satellites in synchronous orbit for direct communication between other, low-altitude spacecraft and the mission control centers. Requirements for tracking and data acquisition service which could be provided by a data relay satellite system (DRSS) range from voice and low data for the operation of a manned earth orbital mission up to several megahertz of video data from an Earth Resources Technology Satellite. The range of requirements results in conflicts in technological approaches - for example, in the choice of operating frequency. For one set of requirements, a low frequency should be selected, while another set of requirements suggests a very high frequency. NASA is continuing its study efforts toward defining a DRSS which will meet the Agency's requirements in hopes of getting a development program underway in the near future. In the meantime, work is proceeding on the development of technology that has potential application to a DRSS. (Author)

A69-25933 *

COMMUNICATIONS FOR SPACE RESEARCH.

Gerald Truszynski (NASA, Washington, D.C.).

Signal, vol. 23, Apr. 1969, p. 19-22.

Review of developments in tracking and communications networks which are essential for a successful space mission. To support the broad spectrum of requirements stemming from the variety of missions, NASA has developed three functionally oriented tracking and data acquisition networks, together with a worldwide communications system which ties the networks and the control centers together to form an integrated entity for support of any specific mission. Data processing capacity is studied, and results obtained from the new 210-ft antenna currently in use at Goldstone are discussed. Attention is given to the Unified S-band System, which is the heart of the Manned Space Flight Net. It is basically the same communications system developed initially by the Jet Propulsion Laboratory for the Deep Space Net. It is considered that a high state of perfection has been achieved in communications systems. The possibilities of a Data Relay Satellite System are being studied. F.R.L.

A69-26965 *

THE APPLICATION OF THE IMAGE ORTHICON TELEVISION SYSTEM TO ROCKET TRAJECTORY DETERMINATION.

J. D. Stolarik, K. Burrows (NASA, Goddard Space Flight Center, Greenbelt, Md.), and M. Miller (NASA, Goddard Space Flight Center, Greenbelt, Md.; Vitro Corporation of America, New York, N.Y.).

Planetary and Space Science, vol. 17, Mar. 1969, p. 579-584. 7 refs.

During darkness or twilight, the high optical sensitivity of the image orthicon TV camera tube can be used to track a light source carried on board a rocket and hence, by relating the position of the light to a star background, the rocket's trajectory can be determined. The technique is considerably simpler and potentially more accurate than standard radar and Doppler methods currently in use. A method of computing trajectory from one TV site, in conjunction with very limited radar data is described. (Author)

A69-26976 *#

MICROWAVE RADIOMETRIC CAPABILITIES AND TECHNIQUES.

H. I. Ewen (Ewen Knight Corp., East Natick, Mass.), F. Haneman (Cutler-Hammer, Inc., Airborne Instruments Laboratory Div., Melville, N.Y.), R. M. Kalafus, R. Mailloux (NASA, Electronics Research Center, Cambridge, Mass.), M. E. Louapre (Aerojet-General Corp., El Monte, Calif.), and D. H. Steinbrecher (Massachusetts Institute of Technology, Cambridge, Mass.).

IN: SYMPOSIUM ON REMOTE SENSING OF ENVIRONMENT, 5TH, UNIVERSITY OF MICHIGAN, ANN ARBOR, MICH., APRIL 16-18, 1968, PROCEEDINGS. [A69-26974 12-14]

Symposium sponsored by the U.S. Navy, the U.S. Air Force, the U.S. Army, the U.S. Geological Survey, and the Department of Agriculture.

Ann Arbor, Michigan, University, Willow Run Laboratories, 1968, p. 9-58. 121 refs.

Grant No. NGR-22-009-163.

Discussion of the principles of operation and present capabilities of microwave radiometric sensors. Antennas and radiometric receivers are treated at length as the two major functional subsystems of the sensor. Scanning antennas are useful where rapid successive measurements are to be made, as in mapping applications. For airborne application, power and weight requirements allow schemes such as Sperry Rand's AN/AAR-33, which consists of three parabolic dishes rotating continually about an axis along the length of the aircraft. Each antenna is connected for $\pm 55^{\circ}$ of angular scan. The prime function of the receiver in a microwave radiometric sensor is to measure the antenna temperature. The method by which this is achieved is described. Projected capabilities offered by near-future solid-state component advances are discussed. P.v.T.

A69-27001 *#

OPTICAL RADAR STUDIES OF THE ATMOSPHERE.

J. D. Lawrence, Jr., M. P. McCormick, S. H. Melfi (NASA, Langley Research Center, Hampton, Va.), and D. P. Woodman (College of William and Mary, Williamsburg, Va.).

IN: SYMPOSIUM ON REMOTE SENSING OF ENVIRONMENT, 5TH, UNIVERSITY OF MICHIGAN, ANN ARBOR, MICH., APRIL 16-18, 1968, PROCEEDINGS. [A69-26974 12-14]

Symposium sponsored by the U.S. Navy, the U.S. Air Force, the U.S. Army, the U.S. Geological Survey, and the Department of Agriculture.

Ann Arbor, Michigan, University, Willow Run Laboratories, 1968, p. 609-616. 13 refs.

Discussion of the use of optical radar (lidar) to study the lower atmosphere. Rigorous Mie theory calculations of clear-atmosphere volume backscattering cross sections are presented for four laser wavelengths. Ruby laser radar measurements of the atmosphere are compared to a scattering model. In addition, laser radar observations of meteorological phenomena are described. G.R.

A69-29489 *

SYNTHESIS TECHNIQUES FOR A CLASS OF SSB-AM-PM SIGNALS.
John H. Painter (NASA, Langley Research Center, Hampton, Va.).
IEEE Transactions on Aerospace and Electronic Systems, vol. AES-5, May 1969, p. 450-456.

This paper develops synthesis techniques for a particular type of single-sideband sinusoidal carrier which is phase modulated by a subcarrier. Mathematical expressions for signal efficiency, sensitivity of design to parameter variation, and ratio of peak to average power are derived and incorporated in a computer program. Given the desired power ratios for modulated signal components, the program solves for the corresponding modulation parameters and evaluates signal efficiency, design sensitivity, and peak to average power ratio. A sample signal design is presented for clarity. (Author)

A69-31694 *#

ENHANCEMENT OF PHOTON-BUNCHING EFFECTS.
Melvin D. Aldridge (NASA, Langley Research Center, Hampton, Va.).
Journal of Applied Physics, vol. 40, Mar. 15, 1969, p. 1720-1727. 16 refs.

Analysis showing that photon-bunching effects in a spatially coherent noise field can be enhanced by the superposition of a monochromatic coherent "signal" and/or by shaping the spectrum of the incident noise. For a Lorentz spectral shape, the addition of "signal" to noise is shown to increase bunching effects by a factor no greater than 4. By changing the noise spectrum from a Lorentz to a rectangular shape, bunching effects are shown to increase by a factor of 2 despite the fact that total incident noise power decreases. In all cases, the ratio of bunching noise to shot noise is proportional to the average number of detected noise photons per cycle of noise bandwidth. For the specific problem analyzed, the maximum value of the ratio of bunching noise to shot noise is determined. In the absence of "signal," the results are found to agree with the exact distribution of Bèdard (1966). (Author)

A69-33371 *

TRACKING AND DATA ACQUISITION FOR SPACE EXPLORATION.
Robert J. Coates (NASA, Goddard Space Flight Center, Greenbelt, Md.).
Space Science Reviews, vol. 9, May 1969, p. 361-418. 75 refs.

The tracking and data acquisition systems provide the key link between the remote spacecraft and the scientific experimenter on the ground. The operation of the space experiment takes place through the links of command, telemetry, and tracking. The evolution from the early very simple spacecraft missions toward more complex and sophisticated missions has been paralleled by a similar evolution in the tracking and data acquisition systems. The early Minitrack interferometer tracking system still carries the major tracking workload for space missions; however, greater tracking accuracy requirements for more recent missions, such as OGO and the Apollo mission, have brought about the development of unified tracking and data acquisition systems which utilize hybrid pseudo-random code/sidetone ranging techniques. The data acquisition has evolved from analog telemetry systems to the present-day heavy use of PCM digital telemetry. Likewise the command systems have evolved from early simple "on/off" command systems into PCM digital command data systems. The trend is toward greater real time control of more complex functions on board the spacecraft. Newer spacecraft are incorporating computer-type systems in the spacecraft which require programming and memory load through the ground command link. The most attractive concept for the next generation network for tracking and data acquisition is a network consisting of synchronous-orbit Tracking and Data Relay Satellites for covering launches and low-orbit earth satellites plus a few selected ground stations for supporting spacecraft in high earth orbit and lunar orbit. (Author)

A69-35940 *#

RADIO PROPAGATION EXPERIMENTS WITH INTERPLANETARY SPACECRAFT.
Glenn A. Reiff (NASA, Office of Space Science and Applications, Washington, D.C.).
(American Institute of Aeronautics and Astronautics, Aerospace Sciences Meeting, 6th, New York, N.Y., Jan. 22-24, 1968, Paper 68-35.)
Journal of Spacecraft and Rockets, vol. 6, May 1969, p. 551-557. 18 refs.

Results of the Mariner 5 development and flight near Venus in 1967 are highlighted in this summary of the scientific findings provided by spacecraft radio propagation experiments. Description of the work required to adapt these experiments for the exploration of Venus provides a good example of the unexpected, subtle interactions that can arise when developing a specific spacecraft mission. In conducting radio propagation investigations, effects of the transmission medium on frequency, phase, and amplitude of electromagnetic waves are used to measure properties of the medium. The scientific data obtained from the Pioneers and Mariners have been the source of new information concerning the environments of the sun, Mars, and Venus. Dual-frequency propagation experiments and S-band occultation experiments are described. (Author)

A69-35996 •

FLIGHT AND LABORATORY TESTS OF AN "L-BAND" TELEMETRY RF SYSTEM.
R. Bruce Richardson and Robert W. Borek (NASA, Flight Research Center, Edwards AFB, Calif.).
Telemetry Journal, vol. 4, June-July 1969, p. 21-24.

Discussion of laboratory and flight test results for an airborne solid-state uhf telemetry transmitter. Worst-case conditions showed the minimum rf output power to be 5 W, with a dc-to-rf power conversion efficiency of 7.8%. The transmitter met all other specified requirements with the exception of the vibration tests. A brief flight-test program to verify operational characteristics was satisfactorily completed. Continuous telemetry data acquisition was accomplished to an average distance equal to 95% of the theoretical horizon range. G.R.

A69-36237

NTC 69; INSTITUTE OF ELECTRICAL AND ELECTRONICS ENGINEERS, NATIONAL TELEMETERING CONFERENCE, WASHINGTON, D.C., APRIL 22-24, 1969, RECORD.
New York, Institute of Electrical and Electronics Engineers, Inc., 1969. 336 p.
Members, $17.50; nonmembers, $20.

CONTENTS:

AEROSPACE TELEMETRY. I—RADIO LINKS.

A SOLID STATE S-BAND TO VHF CONVERTER FOR 1970. M. Kizner and I. Kuzminsky (Mu-Del Electronics, Inc., Wheaton, Md.), p. 9-14. 6 refs. (See A69-36238 19-07)

NONLINEAR EFFECTS IN TELEMETRY TRANSMITTER-RECEIVER RF LINKS. C. S. Johnson and R. M. Caster (Sandia Corp., Albuquerque, N. Mex.), p. 15-21. (See A69-36239 19-07)

LOW NOISE BROADBAND 4GHz PARAMETRIC AMPLIFIER. U. Rutulis (Northern Electric Co., Ltd., Ottawa, Canada), p. 22-25. (See A69-36240 19-07)

PREDETECTION COMBINER FOR TELEMETRY DIVERSITY APPLICATIONS. R. G. Cease (Raytheon Co., Norwood, Mass.), p. 26-30. (See A69-36241 19-07)

STADAN PCM DATA HANDLING SYSTEMS. H. J. Franks, Jr. (NASA, Goddard Space Flight Center, Greenbelt, Md.), p. 31-33. (See A69-36242 19-07)

BIOMEDICAL TELEMETRY. I—ANIMAL TELEMETRY.

RATS—THEIR COMINGS AND GOINGS. W. S. Friauf (National Institutes of Health, Bethesda, Md.), p. 34-38. (See A69-36243 19-04)

AN OSCILLATOR HAVING NO REACTIVE COMPONENTS FOR USE AS AN INTEGRATED CIRCUIT BIOTELEMETER. A.

R. Martin (California, University, Los Angeles, Calif.), p. 39-42. 9 refs. (See A69-36244 19-05)

PCM BIT-SYNCHRONIZATION THEORY.

AN APPLICATION OF NON-LINEAR FILTER THEORY TO PCM BIT SYNCHRONIZATION. G. Lee (McDonnell Douglas Corp., St. Louis, Mo.) and J. Komo (McDonnell Douglas Corp., St. Louis; Missouri, University, Columbia, Mo.), p. 43-48. 11 refs. (See A69-36245 19-07)

NONLINEAR ANALYSIS OF AN ABSOLUTE VALUE TYPE OF EARLY-LATE-GATE BIT SYNCHRONIZER. M. K. Simon (California Institute of Technology, Pasadena, Calif.), p. 49-55. 6 refs. (See A69-36246 19-07)

SIGNAL CONDITIONING, BIT SYNCHRONIZATION AND GROUP SYNCHRONIZATION FOR HIGH BIT RATE PCM. J. S. Gray (Radiation, Inc., Melbourne, Fla.), p. 56-62. (See A69-36247 19-07)

METHOD FOR THE MEASUREMENT OF SIGNAL-TO-NOISE RATIO IN A PCM BIT SYNCHRONIZER. P. Anglade (Service des Equipements de Champ de Tir Arcueil, France), J. Girault (Thomson-CSF, Issy-les-Moulineaux, Hauts-de-Seine, France), and T. Hawkes (Thomson-CSF, Vélizy-Villacoublay, Yvelines, France), p. 63-66. (See A69-36248 19-07)

ON THE PERFORMANCE OF A CLASS OF PCM BIT SYNCHRONIZERS. J. J. Stiffler (Raytheon Co., Lexington, Mass.), p. 67-70. (See A69-36249 19-07)

AEROSPACE TELEMETRY. II—ANTENNAS AND PROPAGATION.

LOW DATA RATE TELEMETRY—A MATCH FOR THE METEOR-BURST CHANNEL. D. N. March (Montana State University, Bozeman, Mont.), p. 71-76. 25 refs. (See A69-36250 19-07)

BACKFIRE ANTENNAS FOR TELEMETRY AND TRACKING APPLICATIONS. L. R. Dod (NASA, Goddard Space Flight Center, Greenbelt, Md.), p. 77-84. 15 refs. (See A69-36251 19-07)

QUASI-ISOTROPIC PATTERN CRITERION FOR S-BAND TM ANTENNAS OF SOUNDING ROCKETS. B. T. Buller (New Mexico State University, University Park, N. Mex.), p. 85-91. 7 refs. (See A69-36252 19-07)

INTERFEROMETER-CONTROLLED TELEMETRY TRACKING SYSTEM. W. K. Cooper (New Mexico State University, University Park, N. Mex.), p. 92-96. (See A69-36253 19-07)

A PERFORMANCE EVALUATION OF A TWO-ELEMENT LARGE APERTURE ANTENNA ARRAY. L. F. Deerkoski (NASA, Goddard Space Flight Center, Greenbelt, Md.), p. 97-103. 5 refs. (See A69-36254 19-07)

INDUSTRIAL TELEMETRY. I—APPLICATIONS.

TELEMETERING BY THE REFLEX KLYSTRON ACCELEROMETER AND SEISMOMETER. G. A. Sawyer and T. K. Ishii (Marquette University, Milwaukee, Wis.), p. 104-108. (See A69-36255 19-07)

TELEMETRIC CONTROL OF URBAN TRANSPORTATION AND LAW ENFORCEMENT. R. W. Franks (Lockheed Aircraft Corp., Sunnyvale, Calif.), p. 109-113. (See A69-36256 19-07)

OIL AND GAS TELEMETRY SYSTEMS. E. W. Kassor (Raytheon Co., Norwood, Mass.), p. 114-116.

LASER LINK MODULATION MEANS FOR WIDE SPECTRUM TELEMETRY WORLD WIDE AND URBAN COMMUNICATIONS SYSTEMS. I. Kamen (Laser Link Corp.) and J. Vogelman (Chromalloy American Corp., New York, N.Y.), p. 117-123. (See A69-36257 19-07)

INDUSTRIAL, SCIENTIFIC AND COMMERCIAL APPLICATIONS OF NASA DEVELOPED TELEMETRY TECHNOLOGY. E. S. Teltscher (Digicom, Inc., Roslyn, N.Y.), p. 124-131. 69 refs. (See A69-36258 19-34)

SURVEYING EARTH RESOURCES WITH REMOTE SENSORS. J. D. Koutsandreas (NASA, Washington, D.C.), p. 132-144. 15 refs. (See A69-36259 19-14)

COMMUNICATION TECHNOLOGY. II—DATA COMPRESSION.

BUFFER CONSIDERATIONS FOR DATA COMPRESSION OF NON-STATIONARY VIDEO DATA. D. J. Popp (McDonnell Douglas Corp., St. Louis, Mo.), p. 145-150. 5 refs. (See A69-36260 19-07)

EFFECT OF TRANSMISSION ERRORS IN IMAGE DATA COMPRESSION TECHNIQUES. T. L. Belver (General Electric Co., Philadelphia, Pa.), p. 151-156. (See A69-36261 19-07)

CODING SCHEMES FOR RUN-LENGTH INFORMATION BASED ON POISSON DISTRIBUTION. W. W. Happ (NASA, Electronics Research Center, Cambridge, Mass.), p. 157-161. 12 refs. (See A69-36262 19-07)

THE COMPUTER-EVALUATION OF WILD-POINT REJECTION FOR TELEMETRY DATA COMPRESSORS. J. E. Medlin (Lockheed Aircraft Corp., Sunnyvale, Calif.), p. 162-171. 8 refs. (See A69-36263 19-07)

A MAXIMUM RMS ERROR COMPARISON OF SEVERAL REDUNDANCY REDUCTION TECHNIQUES. J. N. Breaux (Boeing Co., New Orleans, La.), p. 172-175. (See A69-36264 19-07)

AEROSPACE TELEMETRY. III—COMPUTATION AND CODING.

THE IMP-I COMPUTER EXPERIMENT. R. A. Cliff and S. Paull (NASA, Goddard Space Flight Center, Greenbelt, Md.), p. 176-183. (See A69-36265 19-08)

COMPARISON OF A CORRELATION VERSUS A PROBABILITY DETECTION MEASURE IN A CODED, SEQUENTIAL DETECTION TM SYSTEM. T. V. Saliga (Honeywell, Inc., St. Petersburg, Fla.), p. 184-190. 11 refs. (See A69-36266 19-07)

DATA HANDLING EQUIPMENT REQUIREMENTS FOR CONVOLUTIONAL PCM TELEMETRY. J. Y. Sos (NASA, Goddard Space Flight Center, Greenbelt, Md.), p. 191-194. (See A69-36267 19-07)

BIOMEDICAL TELEMETRY. II—PERSONAL TELEMETRY.

EEG MONITORING DURING THE TREATMENT OF DECOMPRESSION ILLNESS ("BENDS"). J. R. Zweizig, J. Hanley, A. Cockett, P. Hahn, W. R. Adey, and E. Ruspini (California, University, Los Angeles, Calif.), p. 195-200. 11 refs. (See A69-36268 19-05)

THE GENERAL DESIGN CONSIDERATIONS FOR A WIRELESS TELEMETRY SYSTEM IN THE MEDICAL DIAGNOSIS OF HUMANS. L. N. Ziecheck (Lewis Associates, Inc., Bethesda, Md.), p. 201-206. 5 refs. (See A69-36269 19-05)

A MINIATURIZED TELEMETRY DEVICE FOR THE TRANSMISSION OF THE ELECTRICAL ACTIVITY OF SINGLE NERVE CELLS IN THE BRAIN. J. G. McElligott, J. R. Zweizig, and R. T. Kado (California, University, Los Angeles, Calif.), p. 207-210. 5 refs. (See A69-36270 19-05)

EKG TRANSMISSION FROM EMERGENCY VEHICLES. R. J. Huszar and J. Haloburdo (Saint Francis Hospital, Hartford, Conn.), p. 211-214. 9 refs. (See A69-36271 19-05)

A BIOMEDICAL TELEMETRY SYSTEM FOR CLINICAL APPLICATIONS. G. D. Summers and A. J. Temps, Jr. (Fairchild Hiller Corp., Farmingdale, N.Y.), p. 215-221. (See A69-36272 19-05)

ROUTINE TELEMETRY OF ELECTROCARDIOGRAMS AND COMPUTER ANALYSIS. P. R. Amlinger (Missouri, University, Columbia, Mo.), p. 222-227. 11 refs. (See A69-36273 19-05)

COMMUNICATION TECHNOLOGY. III—FM TECHNIQUES.

AN INTEGRATED FM MULTIPLEX RECEIVER/GENERATOR. H. R. Camenzind and A. B. Grebene (Signetics Corp., Sunnyvale, Calif.), p. 228-233. 11 refs. (See A69-36274 19-07)

COMPUTER OPTIMIZATION OF FM/FM TELEMETRY SYSTEMS. C.-H. Chen (Avco Corp., Wilmington; Southeastern Massachusetts Technological Institute, North Dartmouth, Mass.), R. J. D'Auteuil, and R. O'Keeffe (Avco Corp., Wilmington, Mass.), p. 234-240. (See A69-36275 19-07)

BASEBAND AGC IN AM/FM SYSTEMS. R. S. Simpson and W. H. Tranter (Alabama, University, University, Ala.), p. 241-246. 7 refs. (See A69-36276 19-07)

COMPOUND PHASE-LOCKED LOOP RECEIVER. V. Z. Viskanta (TRW Systems Group, Redondo Beach, Calif.), p. 247-253. 6 refs. (See A69-36277 19-07)

FM/FM TELEMETRIC TECHNIQUES APPLIED TO EDU-

CASTING. H. R. Walker (Educasting Systems, Inc., New York, N.Y.), p. 254-261.

OCEANIC TELEMETRY. I—OCEANIC PROGRAMS AND APPLICATIONS.

TELEMETRY REQUIREMENTS FOR NATIONAL DATA BUOY SYSTEMS. M. E. Gilbert (U.S. Coast Guard, Washington, D.C.), p. 262-265.

COMMUNICATIONS FOR THE MAKAI UNDERSEA TEST RANGE. L. W. McMahon (Bendix Corp., North Hollywood, Calif.), p. 266-270.

ELECTROMECHANICAL CABLE—DATA LINK FOR FISHING GEAR. L. D. Lusz (Bureau of Commercial Fisheries, Seattle, Wash.), p. 271-276.

AN ANALOG DEVICE FOR COMPUTING TEN MINUTE PEAK AND AVERAGE WIND SPEED. C. K. Miller (Technical Communications Corp., Lexington, Mass.), p. 277-279. (See A69-36278 19-14)

AEROSPACE TELEMETRY. V—STORED-PROGRAM DATA SYSTEMS.

THE TITAN III REMOTE MULTIPLEXED INSTRUMENTATION SYSTEM. D. E. Miller (Aerospace Corp., El Segundo, Calif.) and G. W. Cantrell (Space Craft, Inc., Huntsville, Ala.), p. 280-284. (See A69-36279 19-07)

THE STORED PROGRAM DATA PROCESSOR FOR POST-APOLLO APPLICATIONS. W. E. Mallary (NASA, Manned Spacecraft Center, Houston, Tex.) and M. C. Smith (Space Craft, Inc., Huntsville, Ala.), p. 285-291. (See A69-36280 19-07)

COMMUNICATION TECHNOLOGY. V—OPTIMIZATION TECHNIQUES IN COMMUNICATION SYSTEMS.

AN APPLICATION OF NONLINEAR FILTER THEORY TO BINARY PROCESSES IN DIGITAL TELEMETRY. A. L. McBride (Texas Instruments, Inc., Dallas, Tex.) and A. P. Sage (Southern Methodist University, Dallas, Tex.), p. 292-298. 11 refs. (See A69-36281 19-07)

OPTIMUM TRANSMISSION OF DIGITAL DATA BY PULSE CODE MODULATION. B. R. N. Murthy and P. A. Wintz (Purdue University, Lafayette, Ind.), p. 299-305. 7 refs. (See A69-36282 19-07)

OPTIMUM POWER ALLOCATION FOR PHASE AND SYNCHRONIZATION ERROR IN A TWO CHANNEL SYSTEM. J. R. Sergo and J. F. Hayes (Purdue University, Lafayette, Ind.), p. 306-310. 7 refs. (See A69-36283 19-07)

DIGITAL COMPENSATION OF TAPE RECORDER TIME-BASE ERROR. R. C. Houts, R. S. Simpson, and D. W. Burlage (Alabama, University, University, Ala.), p. 311-314. 5 refs. (See A69-36284 19-14)

THE ROLE OF FRICTION FORCES ON MAGNETIC TAPE CONTACT AREAS. V. W. Vodicka (Applied Magnetics Corp., Goleta, Calif.), p. 315-320. 7 refs. (See A69-36285 19-14)

SECOND ORDER TRACKING LOOP STATISTICS AND OPTIMUM RECEIVER DESIGN. M. Y. Rhee and F. H. Hussein (Virginia Polytechnic Institute, Blacksburg, Va.), p. 321-325. 7 refs. (See A69-36286 19-07)

A69-36242 *
STADAN PCM DATA HANDLING SYSTEMS.
Henry J. Franks, Jr. (NASA, Goddard Space Flight Center, Greenbelt, Md.).
IN: NTC 69; INSTITUTE OF ELECTRICAL AND ELECTRONICS ENGINEERS, NATIONAL TELEMETERING CONFERENCE, WASHINGTON, D.C., APRIL 22-24, 1969, RECORD. (A69-36237 19-07)
New York, Institute of Electrical and Electronics Engineers, Inc., 1969, p. 31-33.

Description of the capabilities of the PCM data handling system used in the NASA Space Tracking and Data Acquisition Network (STADAN). As there is a considerable number of scientific satellites that must be decommutated by STADAN, the output capabilities of these systems are explained rather than the group synchronizer capabilities. The work shows how one user, the BIOSAT project, utilizes these systems to aid in the mission. (Author)

A69-36251 *
BACKFIRE ANTENNAS FOR TELEMETRY AND TRACKING APPLICATIONS.
Louis R. Dod (NASA, Goddard Space Flight Center, Advanced Development Div., Greenbelt, Md.).
IN: NTC 69; INSTITUTE OF ELECTRICAL AND ELECTRONICS ENGINEERS, NATIONAL TELEMETERING CONFERENCE, WASHINGTON, D.C., APRIL 22-24, 1969, RECORD. (A69-36237 19-07)
New York, Institute of Electrical and Electronics Engineers, Inc., 1969, p. 77-84. 15 refs.

Results of tests of four backfire antennas with lengths of 0.5, 1.0, 1.5, and 2.0 wavelengths at the 1500-MHz test frequency for radiation characteristics as a function of the physical dimensions. Gains of 3 to 4.5 dB over conventional endfires have been measured. Based upon the design data, a five-element array has been modeled and tested. The results of the array measurements and the application of the antennas to tracking and telemetry are discussed.(Author)

A69-36254 *
A PERFORMANCE EVALUATION OF A TWO-ELEMENT LARGE APERTURE ANTENNA ARRAY.
Leonard F. Deerkoski (NASA, Goddard Space Flight Center, Greenbelt, Md.).
IN: NTC 69; INSTITUTE OF ELECTRICAL AND ELECTRONICS ENGINEERS, NATIONAL TELEMETERING CONFERENCE, WASHINGTON, D.C., APRIL 22-24, 1969, RECORD. (A69-36237 19-07)
New York, Institute of Electrical and Electronics Engineers, Inc., 1969, p. 97-103. 5 refs.

Description of a two-element adaptively phased array with element gains of 18 dB assembled and evaluated at 136 MHz. The gain improvement of the system over that of a single element was measured while tracking ATS-C. The measured gain improvement fell within 0.5 dB of the theoretical maximum 90 per cent of the time, corresponding to a normalized improvement of 2.5 dB for the two-element array. The relative phase between array elements was measured while tracking Relay 2 and ESSA spacecraft, and analysis of the data from several array baselines showed the phase noise to be essentially independent for element separations greater than 400 ft. (Author)

A69-36262 *
CODING SCHEMES FOR RUN-LENGTH INFORMATION BASED ON POISSON DISTRIBUTION.
W. W. Happ (NASA, Electronics Research Center, Cambridge, Mass.).
IN: NTC 69; INSTITUTE OF ELECTRICAL AND ELECTRONICS ENGINEERS, NATIONAL TELEMETERING CONFERENCE, WASHINGTON, D.C., APRIL 22-24, 1969, RECORD. (A69-36237 19-07)
New York, Institute of Electrical and Electronics Engineers, Inc., ENGINEERS, NATIONAL TELEMETERING CONFERENCE, WASHINGTON, D.C., APRIL 22-24, 1969, RECORD. (A69-36237 19-07)
New York, Institute of Electrical and Electronics Engineers, Inc., 1969, p. 285-291.

The stored-program data processor (SPDP) is a flexible, programmable-format, PCM data-acquisition system which has the capacity and flexibility to satisfy a wide range of both operational and experimental spacecraft data-handling requirements. The programmable memory and system timing allow channel-sampling rates, format sizing, and bit rates to be tailored to measurement and bandwidth requirements. The SPDP can be programmed into three operational modes and has input-output buffers which enable it to

A69-36267 *
DATA HANDLING EQUIPMENT REQUIREMENTS FOR CONVOLUTIONAL PCM TELEMETRY.
John Y. Sos (NASA, Goddard Space Flight Center, Information

Processing Div., Greenbelt, Md.).
IN: NTC 69; INSTITUTE OF ELECTRICAL AND ELECTRONICS ENGINEERS, NATIONAL TELEMETERING CONFERENCE, WASHINGTON, D.C., APRIL 22-24, 1969, RECORD. (A69-36237 19-07)
New York, Institute of Electrical and Electronics Engineers, Inc., 1969, p. 191-194.

Description of the characteristics of ground data handling equipment for convolutional telemetry in the 100 to 3200 bits per second range; i.e., the bit rate of most Explorer satellites. The performance of commercially-available, bit and frame synchronizers and magnetic tape recorders is considered. It is shown that for rate one-half codes, such equipment can be specified. For lower rate codes, however, special development will be required. The performance of sequential decoders is also discussed. It is shown that for a 16-time processing speed-up of the 1.6 kHz bit rate, a special-purpose hardware sequential decoder is required. The IMP-1 spacecraft's convolutional PCM telemetry system is used as an example throughout the paper. (Author)

A69-36280 *
THE STORED PROGRAM DATA PROCESSOR FOR POST-APOLLO APPLICATIONS.
William E. Mallary (NASA, Manned Spacecraft Center, Houston, Tex.) and Mark C. Smith (Space Craft, Inc., Huntsville, Ala.).
IN: NTC 69; INSTITUTE OF ELECTRICAL AND ELECTRONICS ENGINEERS, NATIONAL TELEMETERING CONFERENCE, WASHINGTON, D.C., APRIL 22-24, 1969, RECORD. (A69-36237 19-07)
New York, Institute of Electrical and Electronics Engineers, Inc., 1969, p. 285-291.

The stored-program data processor (SPDP) is a flexible, programmable-format, PCM data-acquisition system which has the capacity and flexibility to satisfy a wide range of both operational and experimental spacecraft data-handling requirements. The programmable memory and system timing allow channel-sampling rates, format sizing, and bit rates to be tailored to measurement and bandwidth requirements. The SPDP can be programmed into three operational modes and has input-output buffers which enable it to interface with a variety of data-handling, computational, and control equipment. (Author)

A69-37865 *
COMPARISONS BETWEEN TOPSIDE AND GROUND-BASED SOUNDINGS.
John E. Jackson (NASA, Goddard Space Flight Center, Greenbelt, Md.).
IEEE, Proceedings, vol. 57, June 1969, p. 976-985. 20 refs.

Review of past observations which show that electron density profiles derived from topside ionograms have a tendency to be slightly too low. This problem is then examined in the light of more recent and better controlled experiments in which vertical electron density profiles were obtained essentially simultaneously by topside and ground-based soundings. These new measurements confirmed past observations and indicated that the error had a tendency to increase with satellite altitude. From a study of the ground echoes, which are often seen on topside ionograms, it is shown that the above discrepancies can be partially attributed to systematic errors (0 to 30 km) in the topside ionogram height markers. Horizontal electron density gradients can also contribute to this discrepancy. The errors found in the N(h) profile (although systematic) are usually too small to detract significantly from the general usefulness of topside ionograms. Also, the portion of the error due to incorrect height markers can often be calculated from a ground trace analysis, and the ionogram data can be corrected accordingly. (Author)

A69-37892 *
FREQUENCY SHIFTS OBSERVED IN THE ALOUETTE II CYCLOTRON HARMONIC PLASMA RESONANCES.
Robert F. Benson (NASA, Goddard Space Flight Center, Laboratory for Space Sciences, Greenbelt, Md.).
IEEE, Proceedings, vol. 57, June 1969, p. 1139-1142. 8 refs.

Investigation of the cyclotron harmonic plasma resonances observed by Alouette 2 using a technique that yielded frequency measurements with an accuracy of the order of 1 kHz. A comparison of earlier Alouette 1 results with the present Alouette 2 results indicates that the bulk of the original excitation volume associated with the higher cyclotron harmonic resonances is confined to a region considerably less than one antenna length in radius from the antenna, that the size of this region decreases with increasing harmonic number, and that it increases significantly as the radiating antenna becomes parallel to the direction of the earth's magnetic field. M.M.

A69-39437
INSTITUTE OF ELECTRICAL AND ELECTRONICS ENGINEERS, ANNUAL SOUTHWESTERN CONFERENCE AND EXHIBITION, 21ST, SAN ANTONIO, TEX., APRIL 23-25, 1969, RECORD.
New York, Institute of Electrical and Electronics Engineers, Inc., 1969. 835 p.
Members, $16.; nonmembers, $20.

CONTENTS:

INTEGRATED SYSTEMS TESTING FOR ASSURANCE OF ELECTROMAGNETIC COMPATIBILITY OF UNMANNED SPACECRAFT. M. R. Mesnard (Martin Marietta Corp., Denver, Colo.), p. 1 C 1-1 C 8. (See A69-39438 21-09)

SHIELDED ENCLOSURE MEASUREMENTS CAN BE ACCURATE. G. N. Van Steenberg, W. C. Dolle (Southwest Research Institute, San Antonio, Tex.), and J. F. Willman (Texas, University, Austin, Tex.), p. 1 E 1-1 E 7. (See A69-39439 21-09)

PROCESSING BIOMEDICAL INFORMATION BY OPTICAL METHODS. W. L. Anderson, L. S. Berger, R. W. Ware, and R. L. Bond (Southwest Research Institute, San Antonio, Tex.), p. 6 A 1-6 A 4. (See A69-39440 21-05)

PHYSIOLOGICAL RECORDING WITH DRY ELECTRODES. A. E. Schulze, T. C. Carr, and D. M. Hickman (Space Craft, Inc., Houston, Tex.), p. 6 B 1-6 B 8. (See A69-39441 21-05)

QRS DISCRIMINATION FROM NOISY ELECTROCARDIOGRAMS. C. A. Braun (Tracor, Inc., Austin, Tex.), C. W. Van Ryswyk (White Instruments, Inc., Austin, Tex.), and F. B. Vogt (Texas, University, Austin, Tex.), p. 6 C 1-6 C 8. 6 refs. (See A69-39442 21-05)

ELECTROCARDIOGRAM R-WAVE AMPLITUDE DETECTOR. B. L. Steadman and T. W. Morris (USAF, School of Aerospace Medicine, Brooks AFB, Tex.), p. 6 D 1-6 D 8. (See A69-39443 21-05)

TWO ELECTRONIC STETHOSCOPES FOR USE IN HIGH NOISE LEVEL ENVIRONMENTS. H. L. Brammell, M. A. Hunt (USAF, Washington, D.C.), and J. E. Allred, p. 6 E 1-6 E 6. (See A69-39444 21-05)

LASER INDUCED BREAKDOWN IN HIGH PRESSURE GASES. G. W. Haynes, O. M. Friedrich, Jr., and A. A. Dougal (Texas, University, Austin, Tex.), p. 7 A 1-7 A 8. 9 refs. (See A69-39445 21-16)

A LABORATORY WATER VAPOR LASER. R. N. Chandler and R. K. Likuski (Texas, University, Austin, Tex.), p. 7 B 1-7 B 7. 8 refs. (See A69-39446 21-16)

POLARIZATION MODULATION USING THE MACALUSO-CORBINO EFFECT. V. C. West, M. Kristiansen, and M. O. Hagler (Texas Technological College, Lubbock, Tex.), p. 7 D 1-7 D 8. 6 refs. (See A69-39447 21-16)

TWO-WAVELENGTH, SINGLE-EXPOSURE HOLOGRAPHIC INTERFEROMETRY. F. Weigl, O. M. Friedrich, Jr., and A. A. Dougal (Texas, University, Austin, Tex.), p. 7 E 1-7 E 7. 6 refs. (See A69-39448 21-14)

OPTIMUM FILTER DESIGN FOR NOISY FEEDBACK SYSTEM. S. Z. H. Taqvi and N. M. Shehadeh (Houston, University, Houston, Tex.), p. 8 A 1-8 A 8. 6 refs. (See A69-39449 21-10)

ON FILTERING PRIOR TO LIMITING DIGITAL SIGNALS IN STRONG NOISE. J. H. Painter (NASA, Langley Research Center, Hampton, Va.), p. 8 C 1-8 C 8. (See A69-39450 21-07)

TRANSMISSION CHARACTERISTICS OF SPLIT-PHASE PCM CODES. B. H. Batson (NASA, Manned Spacecraft Center, Houston,

Tex.), N. M. Shehadeh, and R. Van Cleave (Houston, University, Houston, Tex.), p. 8 F 1-8 F 8. (See A69-39451 21-07)

SOLID STATE AMPLIFIERS OPERATING AT AND BEYOND 10 GHz. E. P. Schelonka (U.S. Air Force Academy, Colorado Springs, Colo.), p. 9 A 1-9 A 8. (See A69-39452 21-09)

AN X-BAND OSCILLATOR USING A SUPERCONDUCTING CAVITY. J. L. Stone, G. L. Baker, and W. H. Hartwig (Texas, University, Austin, Tex.), p. 9 B 1-9 B 8. 8 refs. (See A69-39453 21-09)

A UNILATERAL TRANSFORMER. B. Rabinovici (Northeastern University, Boston, Mass.) and C. A. Renton (NASA, Electronics Research Center, Cambridge, Mass.), p. 9 F 1-9 F 6. (See A69-39454 21-09)

INVESTIGATION OF HARMONIC ION CYCLOTRON WAVE PROPAGATION AND DAMPING IN A PLASMA. N. B. Dodge, J. G. Melton, O. M. Friedrich, Jr., and A. A. Dougal (Texas, University, Austin, Tex.), p. 11 B 1-11 B 8. 5 refs. (See A69-39455 21-25)

HF DIRECTION FINDING DURING MULTIMODE PROPAGATION CONDITIONS. C. Dodge and P. E. Martin (Southwest Research Institute, San Antonio, Tex.), p. 15 D 1-15 D 8. (See A69-39456 21-07)

PRACTICAL LIMITATIONS TO THE RANGING ACCURACY ACHIEVABLE WITH A MODULATED CW LASER. J. L. Bowie and W. L. Kuriger (Oklahoma, University, Norman, Okla.), p. 15 E 1-15 E 7. 5 refs. (See A69-39457 21-16)

AN APPLICATION OF PATTERN RECOGNITION THEORY TO WEATHER PREDICTION USING QUANTIZED RADAR DATA. J. H. Horwedel and W. L. Kuriger (Oklahoma, University, Norman, Okla.), p. 15 F 1-15 F 8. 9 refs. (See A69-39458 21-08)

ELECTROMAGNETIC WAVE SCATTERING FROM A LAYER WITH PLANE INTERFACE IN FRONT AND A ROUGH INTERFACE IN BACK. K. Krishen and W. W. Koepsel (Kansas State University, Manhattan, Kan.), p. 15 G 1-15 G 8. (See A69-39459 21-07)

A STUDY OF STATE VARIABLE FEEDBACK IN NON-LINEAR SYSTEMS. J. L. Melsa and H. B. Parekh (Southern Methodist University, Dallas, Tex.), p. 16 D 1-16 D 7. 7 refs. (See A69-39460 21-10)

LASER PROFILOMETER. W. S. Olsen (Texas, University, Austin, Texas), p. 18 F 1-18 F 7. (See A69-39461 21-16)

OPTIMAL PROCESSING OF SATELLITE DOWN-LINKED DATA. C. N. Kelly and E. O. Brigham (LTV Electrosystems, Inc., Greenville, Tex.), p. 19 B 1-19 B 8. 7 refs. (See A69-39462 21-07)

SIMPLIFIED PARAMETER QUANTIZATION PROCEDURE FOR ADAPTIVE ESTIMATION. R. L. Sengbush and D. G. Lainiotis (Texas, University, Austin, Tex.), p. 19 C 1-19 C 8. (See A69-39463 21-10)

PROPERTIES OF METAL-POLYMER-SILICON THIN FILM STRUCTURES. E. T. Fitzgibbons, L. C. Wang, Y. S. Chuang, and W. H. Hartwig (Texas, University, Austin, Tex.), p. 20 F 1-20 F 8. 5 refs. (See A69-39464 21-26)

INDEX TO AUTHORS, p. a-c.

A69-39450 *
ON FILTERING PRIOR TO LIMITING DIGITAL SIGNALS IN STRONG NOISE.
John H. Painter (NASA, Langley Research Center, Hampton, Va.).
IN: INSTITUTE OF ELECTRICAL AND ELECTRONICS ENGINEERS, ANNUAL SOUTHWESTERN CONFERENCE AND EXHIBITION, 21ST, SAN ANTONIO, TEX., APRIL 23-25, 1969, RECORD. (A69-39437 21-07)
New York, Institute of Electrical and Electronics Engineers, Inc., 1969, p. 8 C 1-8 C 8.

Examination of the problem of optimizing the filter prior to limiting a digital signal in strong noise. In particular, the case for choosing the noise bandwidth of a single-pole low-pass filter is treated in detail. The optimization criterion adopted is that of maximizing the expected gain of a simple feedback system which tracks the limited digital signal. A closed-form mathematical model, applicable to the strong-noise case, is solved by use of a digital computer to obtain the "optimum" bandwidth. A comparison of results is made for the case of a periodic square-wave signal and for the case of a weakly periodic (pseudorandom) digital signal. (Author)

A69-39451 *
TRANSMISSION CHARACTERISTICS OF SPLIT-PHASE PCM CODES.
B. H. Batson (NASA, Manned Spacecraft Center, Houston, Tex.), N. M. Shehadeh, and R. Van Cleave (Houston, University, Houston, Tex.).
IN: INSTITUTE OF ELECTRICAL AND ELECTRONICS ENGINEERS, ANNUAL SOUTHWESTERN CONFERENCE AND EXHIBITION, 21ST, SAN ANTONIO, TEX., APRIL 23-25, 1969, RECORD. (A69-39437 21-07)
New York, Institute of Electrical and Electronics Engineers, Inc., 1969, p. 8 F 1-8 F 8.

Determination of certain transmission characteristics of a carrier which is amplitude-shift-keyed (ASK), phase-shift keyed (PSK), or frequency-shift-keyed (FSK) by a split-phase PCM code. The ensemble-average autocorrelation function and the power spectral density (Fourier transform of the ensemble-average autocorrelation function) are determined for each modulation scheme. All the calculations assume a random bit pattern with equally likely ones and zeros. It is also assumed that the modulation is noncoherent—i.e., that the phase of the PCM modulating sequence is not related to the phase of the carrier. B.H.

A69-41588 *
EQUATORIAL PLANE PATTERN OF AN AXIAL-TEM SLOT ON A FINITE SIZE GROUND PLANE.
C. A. Balanis (NASA, Langley Research Center, Hampton, Va.) and L. Peters, Jr. (Ohio State University, Dept. of Electrical Engineering, Columbus, Ohio).
IEEE Transactions on Antennas and Propagation, vol. AP-17, May 1969, p. 351-353. 5 refs.

Discussion of the edge diffraction effects in a TEM-mode axially slotted ground plane of finite width and length in an analysis of the scattered and radiated wave fields in waveguides of different geometries. The diffractions from the edges of the ground plane and their contributions to the overall radiation pattern are calculated. A diffraction superimposition procedure is applied to radiation pattern calculations. V.Z.

A69-41734
INTERNATIONAL FOUNDATION FOR TELEMETERING, INTERNATIONAL TELEMETERING CONFERENCE, WASHINGTON, D.C., SEPTEMBER 15-17, 1969, PROCEEDINGS.
Woodland Hills, Calif., International Foundation for Telemetering (ITC Proceedings. Volume 5), 1969. 620 p.
$15.
CONTENTS:
ON-BOARD COMPUTATION AND DATA PROCESSING.

USE OF COMPUTERS AND PROGRAMMABLE TELEMETRY SYSTEMS ON SCIENTIFIC SATELLITES. P. Feinberg, M. Maxwell, and J. R. Silverman (NASA, Goddard Space Flight Center, Greenbelt, Md.), p. 1-13. (See A69-41735 23-08)

AN ON-BOARD PROCESSOR FOR OAO-C. C. E. Trevathan, R. Hartenstein, and T. D. Taylor (NASA, Goddard Space Flight Center, Greenbelt, Md.), p. 14-22. 5 refs. (See A69-41736 23-08)

RECENT IMPROVEMENTS IN THE SDP-3 COMPUTER. R. A. Cliff (NASA, Goddard Space Flight Center, Greenbelt, Md.), p. 23-48. 5 refs. (See A69-41737 23-08)

COSMIC RAY EXPERIMENTS SOURCE-ENCODING IN THE IMP-I SPACECRAFT. C. A. Cancro and P. J. Janniche, Jr. (NASA, Goddard Space Flight Center, Greenbelt, Md.), p. 49-71. (See A69-41738 23-07)

A COMPLEMENTARY MOS SPACECRAFT DATA HANDLING SYSTEM. F. J. Link and R. J. Lesniewski (NASA, Goddard Space Flight Center, Greenbelt, Md.), p. 72-77. (See A69-41739 23-08)

TRANSMITTERS.

07 COMMUNICATIONS

USE OF L- AND S-BAND TRANSMITTERS FOR OUTER SPACE APPLICATIONS. P. A. Updike (Teledyne, Inc., Huntsville, Ala.), p. 78-82. (See A69-41740 23-09)

THE REALIZATION OF TELEMETRY TRANSMITTERS WITH VERY WIDE BANDWIDTHS. R. H. Roberts (Bertea Corp., Irvine, Calif.), p. 83-93. (See A69-41741 23-07)

AN EXACT SOLUTION OF INJECTION PHASE-LOCKING. C. C. Wang (TRW Systems Group, Redondo Beach, Calif.), p. 94-104. 9 refs. (See A69-41742 23-07)

A POWER COMBINER FOR STEP LEVEL HIGH POWER UHF SOLID STATE TRANSMITTERS. B. E. Rose (Hughes Aircraft Co., Culver City, Calif.), p. 105-112. (See A69-41743 23-09)

DATA TRANSMITTER COUPLING METHODS—DC VERSUS AC. A. A. Viggiano (Lockheed Aircraft Corp., Sunnyvale, Calif.), p. 113-122. (See A69-41744 23-07)

CODING AND DATA FORMATTING.

CODING—AN ENGINEERING TOOL FOR THE DIGITAL TELEMETRY LINK. R. M. Muller (NASA, Goddard Space Flight Center, Greenbelt, Md.), p. 123-135. 7 refs. (See A69-41745 23-07)

RECENT DEVELOPMENTS IN ALGEBRAIC DECODING. R. T. Chien (Illinois, University, Urbana, Ill.), p. 136-148. 18 refs. (See A69-41746 23-07)

ON PUNCTUATING ERROR-CORRECTING CODES. J. J. Stiffler (Raytheon Co., Sudbury, Mass.), p. 149.

APPLICATION OF NONLINEAR ENCODING TO PICTURE TRANSMISSION. L. W. Gardenhire (Radiation, Inc., Melbourne, Fla.), p. 150-156. (See A69-41747 23-07)

FLEXIBLE FORMAT ADAPTIVE TELEMETRY ENCODER. R. S. Cooperman (Communications Satellite Corp., Washington, D.C.), p. 157-165. (See A69-41748 23-07)

STORED PROGRAM DECOMMUTATION TECHNIQUES. R. J. Galpin and R. C. Mabe (International Business Machines Corp., Gaithersburg, Md.), p. 166-173. (See A69-41749 23-08)

ANTENNA SYSTEMS.

A HIGH POWER VERSATILE FEED SYSTEM FOR COMMUNICATION SATELLITE USAGE. R. W. Hurlburt, L. L. Reiser, and R. R. Yaminy (Radiation Systems, Inc., McLean, Va.), p. 174-188. (See A69-41750 23-07)

S-BAND PHASED ARRAY TELEMETRY RECEIVER. R. C. Kent (Ryan Aeronautical Co., San Diego, Calif.), p. 189-202. (See A69-41751 23-07)

A 17:1 DUAL BAND CIRCULARLY POLARIZED FOCUSED TWO-CHANNEL MONOPULSE TRACKING SYSTEM. P. A. Lantz (NASA, Goddard Space Flight Center, Greenbelt, Md.), G. G. Chadwick, R. W. Hurlburt, and R. R. Yaminy (Radiation Systems, Inc., McLean, Va.), p. 203-217. 8 refs. (See A69-41752 23-07)

S-BAND ANTENNA SYSTEMS FOR MISSILES. J. E. Hill (Granger Associates, Chatsworth, Calif.), p. 218-231. 9 refs. (See A69-41753 23-09)

ANTENNA PATTERN ANALYSIS—A COMPUTER METHOD. F. M. Wolff (Atlantic Research Corp., Alexandria, Va.), p. 232-247. 7 refs. (See A69-41754 23-08)

DATA RELAY SATELLITE SYSTEMS.

TRACKING AND DATA RELAY SATELLITE SYSTEM. P. F. Barritt and A. M. G. Andrus (NASA, Washington, D.C.), p. 248, 249, 251 (4 ff). (See A69-41755 23-07)

SATELLITE RELAY SYSTEMS. H. Nakamura (Aerospace Corp., El Segundo, Calif.), p. 258.

SATELLITE SYSTEMS FOR DATA RELAY. R. A. Stampfl (NASA, Goddard Space Flight Center, Greenbelt, Md.) and N. Sirri (California Institute of Technology, Pasadena, Calif.), p. 259.

COMPARISON BETWEEN A DATA RELAY SATELLITE SYSTEM AND A GROUND-BASED MISSION SUPPORT NETWORK IN TERMS OF MISSION SUPPORT CAPABILITY, SUPPORT EFFECTIVENESS AND SYSTEM AND MISSION SPACECRAFT REQUIREMENTS. J. A. Delaney (TRW Systems Group, Redondo Beach, Calif.), p. 260-286. (See A69-41756 23-07)

RFI CHARACTERISTICS OF A DELAY RELAY SATELLITE SYSTEM. J. W. Bryan (NASA, Goddard Space Flight Center, Greenbelt, Md.), p. 287-294. (See A69-41757 23-07)

PSEUDO-NOISE SPREAD SPECTRUM TECHNIQUES FOR COMBATTING MULTIPATH AND RFI. C. R. Cahn and J. N. Birch (Magnavox Co., Torrance, Calif.), p. 295.

10.6-MICROMETER LASER COMMUNICATION SYSTEM EXPERIMENT FOR ATS-F AND ATS-G. J. H. McElroy, H. L. Richards, N. McAvoy, T. E. McGunigal, W. E. Richards, and H. Yagelowich (NASA, Goddard Space Flight Center, Greenbelt, Md.), p. 296-305. 7 refs. (See A69-41758 23-07)

THE S-BAND TELEMETRY, TRACKING, AND COMMAND EXPERIMENT. R. H. Pickard, P. E. Schmid, and P. J. Heffernan (NASA, Goddard Space Flight Center, Greenbelt, Md.), p. 306-323. 14 refs. (See A69-41759 23-07)

PROGRAMMABLE DATA LINKS AND ANALYSIS.

CONCEPTS OF INTEGRATED ADAPTIVE DATA TRANSMISSION SYSTEMS. R. F. Filipowsky (International Business Machines Corp., Huntsville, Ala.), p. 324-356. 16 refs. (See A69-41760 23-07)

PERMUTATION AND CIRCULANT MATRICES AND THE FAST FOURIER TRANSFORM. N. I. Heenan (Mitre Corp., Bedford, Mass.), p. 357-377. 5 refs. (See A69-41761 23-19)

FLEXIBLE FORMAT GENERATOR DESIGN TECHNIQUES. W. M. Rathbone (Lockheed Aircraft Corp., Plainfield, N.J.), p. 378-390. (See A69-41762 23-08)

MAP, A MODULAR DESIGN CONCEPT FOR RECOVERABLE SCIENTIFIC ROCKET-BORNE EXPERIMENTS. W. W. Wright (Southwest Center for Advanced Studies, Dallas, Tex.), p. 391-397. (See A69-41763 23-31)

DATA REDUCTION SYSTEM FOR THE MODULAR AURORAL PROBE. N. Eaker (Southwest Center for Advanced Studies, Dallas, Tex.), p. 398-402. (See A69-41764 23-08)

BIOTELEMETRY TECHNIQUES.

EVALUATION OF PROTECTIVE MASKS BY USE OF RADIO TELEMETRY. R. J. Redd (U.S. Army, Defense Development and Engineering Laboratories, Edgewood Arsenal, Md.), p. 403-415. (See A69-41765 23-07)

BIOTELEMETRY OF EKG SIGNALS WITHIN A SMALL, CLOSED CHAMBER. F. C. Carpenter, Jr. (McDonnell Douglas Corp., Huntington Beach, Calif.), p. 416-425. 7 refs. (See A69-41766 23-05)

APOLLO EXTRAVEHICULAR COMMUNICATION TELEMETRY SUBSYSTEM. J. J. Weippert and R. E. Donaghy (Sonex, Inc., Philadelphia, Pa.), p. 426-437. (See A69-41767 23-07)

LOW COST WATER QUALITY MONITORING BY RADIO TELEMETRY. D. S. Woffinden and A. D. Kartchner (Utah State University, Logan, Utah), p. 438-443.

WIDEBAND FIBEROPTIC ANALOG INFORMATION LINK. K. Avicola (Union Carbide Corp., Santa Monica, Calif.) and R. A. Churchill (North American Rockwell Corp., Anaheim, Calif.), p. 444-460. 8 refs. (See A69-41768 23-07)

TELEMETRY STANDARDS AND DATA QUALITY ASSURANCE.

WHY DATA SYSTEM STANDARDS? W. B. Poland, Jr., R. T. Fitzgerald, and R. J. Coates (NASA, Goddard Space Flight Center, Greenbelt, Md.), p. 461-469. (See A69-41769 23-08)

IRIG TELEMETRY STANDARDS 1969. R. S. Reynolds (Sandia Corp., Albuquerque, N. Mex.), p. 470-473, 475, 477. (See A69-41770 23-07)

TRANSMISSION AND RECORDING TECHNIQUES AND PERFORMANCE.

DOPPLER JITTER VERSUS DIGITAL ERROR RATE. C. L. Weber (Southern California, University, Los Angeles, Calif.), p. 479-491. 14 refs. (See A69-41771 23-07)

PERFORMANCE OF PARTIALLY COHERENT BINARY RECEPTION. R. W. Okkes (European Space Research Organization, Noordwijk, Netherlands), p. 492-504. (See A69-41772 23-07)

A NEW BANDLIMITED M-ARY NON-COHERENT TELEMETRY SYSTEM. M. S. Stone (TRW Systems Group, Redondo Beach,

Calif.), p. 505-511. 6 refs. (See A69-41773 23-07)

FILTERING EFFECTS IN A SPREAD-SPECTRUM COMMUNICATION SYSTEM. W. H. Harman (TRW Systems Group, Redondo Beach, Calif.), p. 512-522. (See A69-41774 23-07)

DIGITAL TIME-BASE ERROR COMPENSATOR FOR WIDEBAND TELEMETRY RECORDER/REPRODUCERS. M. S. Klein and S. Tomback (Communications and Systems, Inc., Paramus, N.J.), p. 523-531. (See A69-41775 23-09)

THE HIGH SPEED TAPE TRANSPORT. J. G. Isabeau and C. A. Vogel (Newell Industries, Inc., Sunnyvale, Calif.), p. 532-551. 6 refs. (See A69-41776 23-14)

UHF TELEMETRY.

FREQUENCY DIVERSITY FOR UHF TELEMETRY. W. K. Kinkead (General Electric Co., Philadelphia, Pa.), p. 552-560. (See A69-41777 23-07)

DEVELOPMENT OF THE CV-2138 (XAN-1) TELEMETRY AND MDI UHF DOWN CONVERTER. H. Lilienkamp (U.S. Navy, Naval Avionics Facility, Indianapolis, Ind.), p. 561-566. (See A69-41778 23-09)

A PHASE-LOCKED UHF TELEMETRY TRANSPONDER FOR MISSILE SCORING APPLICATIONS. J. R. Delbauve (U.S. Navy, Naval Avionics Facility, Indianapolis, Ind.), p. 567-578. (See A69-41779 23-09)

UHF TM SYSTEM COVERAGE PREDICTIONS OVER WATER. W. L. Wuster (U.S. Navy, Naval Avionics Facility, Indianapolis, Ind.), p. 579-592. 8 refs. (See A69-41780 23-07)

TELEMETRY-SCORING RECEIVERS. K. Burgess (U.S. Navy, Naval Avionics Facility, Indianapolis, Ind.), p. 593-602. (See A69-41781 23-09)

EIGHTH ANNUAL REPORT OF THE TELEMETERING STANDARDS COORDINATION COMMITTEE. L. W. Gardenhire (Radiation, Inc., Melbourne, Fla.), p. 605-611. (See A69-41782 23-34)

A69-41738 *

COSMIC RAY EXPERIMENTS SOURCE-ENCODING IN THE IMP-I SPACECRAFT.

Ciro A. Cancro and Paul J. Janniche, Jr. (NASA, Goddard Space Flight Center, Spacecraft Technology Div., Greenbelt, Md.).

IN: INTERNATIONAL FOUNDATION FOR TELEMETERING, INTERNATIONAL TELEMETERING CONFERENCE, WASHINGTON, D.C., SEPTEMBER 15-17, 1969, PROCEEDINGS. (A69-41734 23-07)

Woodland Hills, Calif., International Foundation for Telemetering (ITC Proceedings. Volume 5), 1969, p. 49-71.

Description of the design and operation of three separate detectors for covering a wide range of cosmic-ray events on the IMP-I spacecraft. These devices are the medium-energy detector (MED), the low-energy detector (LED), and the very low energy detector (VLED). A cross section of each detector is presented, and the events analyzed in each particular detector are outlined. The source encoding associated with each detector receives output pulse signals from its detector, identifies and analyzes events of interest, monitors event rates, selects results to be telemetered, and feeds these results to accumulators and then to storage registers in the spacecraft central encoder. Since there are many other experiments on the spacecraft, the central encoder transfers the data from the registers to the telemetry at the appropriate times in accordance with the PCM format. Z.W.

A69-41745 *

CODING—AN ENGINEERING TOOL FOR THE DIGITAL TELEMETRY LINK.

Ronald M. Muller (NASA, Goddard Space Flight Center, Greenbelt, Md.).

IN: INTERNATIONAL FOUNDATION FOR TELEMETERING, INTERNATIONAL TELEMETERING CONFERENCE, WASHINGTON, D.C., SEPTEMBER 15-17, 1969, PROCEEDINGS. (A69-41734 23-07)

Woodland Hills, Calif., International Foundation for Telemetering (ITC Proceedings. Volume 5), 1969, p. 123-135. 7 refs.

Discussion of various digital coding techniques from an engineer's and user's points of view. Each technique is displayed in a uniform way which measures performance against the best possible (Schannon) channel. Encoding-decoding complexity and other system merits and drawbacks of each technique are discussed. The reader is introduced to coding by drawing analogies with an everyday and familiar coded communication channel-spoken English. Bit, word, and block error detection and correction techniques are then presented. A concatenated block code scheme which combines these techniques is developed. Z.W.

A69-41752 *

A 17:1 DUAL BAND CIRCULARLY POLARIZED FOCUSED TWO-CHANNEL MONOPULSE TRACKING SYSTEM.

Paul A. Lantz (NASA, Goddard Space Flight Center, Greenbelt, Md.), George G. Chadwick, Roderic W. Hurlburt, and Roger R. Yaminy (Radiation Systems, Inc., McLean, Va.).

IN: INTERNATIONAL FOUNDATION FOR TELEMETERING, INTERNATIONAL TELEMETERING CONFERENCE, WASHINGTON, D.C., SEPTEMBER 15-17, 1969, PROCEEDINGS. (A69-41734 23-07)

Woodland Hills, Calif., International Foundation for Telemetering (ITC Proceedings. Volume 5), 1969, p. 203-217. 8 refs.

Description of a dual circularly polarized feed system for operation in incremental bands over the frequency range from 136 to 2300 MHz. The characteristics of a 60-ft parabola excited by the feed system are discussed. Tracking data for this system have also been obtained using a helicopter, the Apollo 8 vehicle, and Cassiopeia A. It is shown that the two-channel monopulse technique allows the use of antenna feeds which, in turn, provide sidelobes of greater than -20 dB relative to the main lobe peak for all frequencies. This sidelobe performance reflects the fact that the feed is approximately focused at all frequencies. The characteristics of a similar feed used in the Apollo Range Instrumented Aircraft are also described. P.G.

A69-41755 *

TRACKING AND DATA RELAY SATELLITE SYSTEM.

P. F. Barritt and A. M. G. Andrus (NASA, Washington, D.C.).

IN: INTERNATIONAL FOUNDATION FOR TELEMETERING, INTERNATIONAL TELEMETERING CONFERENCE, WASHINGTON, D.C., SEPTEMBER 15-17, 1969, PROCEEDINGS. (A69-41734 23-07)

Woodland Hills, Calif., International Foundation for Telemetering (ITC Proceedings. Volume 5), 1969, p. 248, 249, 251 (4 ff).

Discussion of the Tracking and Data Relay Satellite System (TDRSS), using satellites in synchronous orbit to relay data between a low-altitude earth orbital spacecraft (both manned and automated) and the various mission control centers. It is shown that such a system would improve mission reliability, contribute immeasurably to the safety and morale of the crews of manned spacecraft, enable experimenters to monitor their experiments in real time, and relieve constraints on mission planning and operations that are imposed by the short duration of ground-based tracking and data acquisition facilities. The benefits outlined are realizable upon the implementation of an operational TDRSS consisting of three satellites and their supporting ground stations. P.G.

A69-41757 *

RFI CHARACTERISTICS OF A DELAY RELAY SATELLITE SYSTEM.

John W. Bryan (NASA, Goddard Space Flight Center, Greenbelt, Md.).

IN: INTERNATIONAL FOUNDATION FOR TELEMETERING, INTERNATIONAL TELEMETERING CONFERENCE, WASHINGTON, D.C., SEPTEMBER 15-17, 1969, PROCEEDINGS. (A69-41734 23-07)

Woodland Hills, Calif., International Foundation for Telemetering (ITC Proceedings. Volume 5), 1969, p. 287-294.

Determination of the effect of RFI caused by earth-based emitters on the operation of geosynchronous satellites for relay of data from near-earth orbiting satellites. The information presented is based upon known frequency assignments and known equipment

capabilities. All data and analyses given are for the continental U.S. only. A survey of the space command band from 148 to 155 MHz discovered over 15,000 potential RFI sources. While most of these sources do not emit at the NASA command frequencies, their combined spectral density is sufficiently great to cause concern over adjacent channel interference. Z.W.

A69-41758 *

10.6-MICROMETER LASER COMMUNICATION SYSTEM EXPERIMENT FOR ATS-F AND ATS-G.

J. H. McElroy, H. L. Richards, N. McAvoy, T. E. McGunigal, W. E. Richards, and H. Yagelowich (NASA, Goddard Space Flight Center, Greenbelt, Md.).

IN: INTERNATIONAL FOUNDATION FOR TELEMETERING, INTERNATIONAL TELEMETERING CONFERENCE, WASHINGTON, D.C., SEPTEMBER 15-17, 1969, PROCEEDINGS. (A69-41734 23-07)

Woodland Hills, Calif., International Foundation for Telemetering (ITC Proceedings. Volume 5), 1969, p. 296-305. 7 refs.

Description of the first intersatellite laser communication experiment using a laser communication system weighing 30 lb and consuming 30 W on board the ATS-F and ATS-G satellites. A 6-in. aperture optical antenna, with a 92 dB antenna gain, and a 500 mW carrier provide a minimum 23 dB carrier-to-noise ratio for a 5-MHz bandwidth system. This experiment will permit analysis of laser communication systems as a base line for future operational system designs. O.H.

A69-41759 *

THE S-BAND TELEMETRY, TRACKING, AND COMMAND EXPERIMENT.

R. H. Pickard, P. E. Schmid, and P. J. Heffernan (NASA, Goddard Space Flight Center, Greenbelt, Md.).

IN: INTERNATIONAL FOUNDATION FOR TELEMETERING, INTERNATIONAL TELEMETERING CONFERENCE, WASHINGTON, D.C., SEPTEMBER 15-17, 1969, PROCEEDINGS. (A69-41734 23-07)

Woodland Hills, Calif., International Foundation for Telemetering (ITC Proceedings. Volume 5), 1969, p. 306-323. 14 refs.

The ATS-F S-band Telemetry, Tracking and Command Experiment is designed to develop and demonstrate critical aspects of the technology necessary for an operational tracking and data relay satellite (TDRS) system within the framework of existing applications flight programs. The experiment involves the implementation and operation of a two-way radio link between a synchronous satellite (ATS-F) and a near-earth orbiting satellite (Nimbus E). The link will be used for precision range and range-rate tracking of Nimbus E from ATS-F, relay of Nimbus E telemetry to the ground via ATS-F, and command of Nimbus E from the ground through ATS-F. The basic purpose of the experiment is to gain experience in the implementation and operation of real time telemetry, tracking, and command links using a synchronous satellite relay. A specific major program goal is to establish the extent to which it is possible to determine the orbit of a near-earth orbiting spacecraft using tracking data obtained from a synchronous satellite. (Author)

A69-42500

INSTITUTE OF ELECTRICAL AND ELECTRONICS ENGINEERS, INTERNATIONAL CONFERENCE ON COMMUNICATIONS, BOULDER, COLO., JUNE 9-11, 1969, CONFERENCE RECORD.

New York, Institute of Electrical and Electronics Engineers, Inc. (IEEE ICC Conference Publications. Volume 5), 1969. 818 p. Members, $10.00; nonmembers, $20.

CONTENTS:

PREFACE. R. C. Kirby and W. F. Utlaut, p. iii.

PERFORMANCE OF SELF-SYNCHRONIZED PSK SYSTEMS. J. F. Oberst and D. L. Schilling (Brooklyn, Polytechnic Institute, Brooklyn, N.Y.), p. 4-1 to 4-8. 5 refs. (See A69-42501 23-07)

RADIO SPECTRUM UTILIZATION IN AEROSPACE COMMUNICATION SYSTEMS. J. M. Clarke (NASA, Electronics Research Center, Cambridge, Mass.), R. J. Otero, and W. C. Wanbaugh (IIT Research Institute, Annapolis, Md.), p. 5-13 to 5-18. (See A69-42502 23-07)

SUPPRESSION OF INTERFERENCE IN A CONGESTED SPECTRUM. E. J. Ferrari and J. M. Gutwein (ADCOM, Inc., Cambridge, Mass.), p. 5-19 to 5-30. (See A69-42503 23-07)

NOISE REDUCTION IN WIDEBAND ATMOSPHERIC RECEIVING SYSTEMS. W. L. Taylor, H. M. Burdick, and L. W. Eichacker (ESSA, Boulder, Colo.), p. 5-31 to 5-34. 5 refs. (See A69-42504 23-07)

RANGE DIFFERENCE ERROR DUE TO THE PRESENCE OF IONOSPHERIC ELECTRONS. C. C. Chen (TRW Systems Group, Redondo Beach, Calif.), p. 7-1 to 7-5. 5 refs. (See A69-42505 23-07)

CHARACTERIZATION OF MILLIMETER WAVE EARTH-SPACE LINK COMMUNICATIONS CHANNELS. E. Brookner (Raytheon Co., Sudbury, Mass.), p. 7-7 to 7-14. 16 refs. (See A69-42506 23-07)

PROJECTED REQUIREMENTS FOR DEEP SPACE COMMUNICATIONS. R. C. Tausworthe (California Institute of Technology, Pasadena, Calif.), p. 7-15 to 7-20. 7 refs. (See A69-42507 23-07)

AN ANALYSIS OF THE TELECOMMUNICATIONS PERFORMANCE OF A LUNAR RELAY SATELLITE SYSTEM. G. D. Arndt, B. H. Batson, and S. W. Novosad (NASA, Manned Spacecraft Center, Houston, Tex.), p. 7-21 to 7-27. 6 refs. (See A69-42508 23-07)

SHORT TERM FREQUENCY STABILITY MEASUREMENTS OF THE APPLICATIONS TECHNOLOGY SATELLITE #1 MULTIPLE ACCESS COMMUNICATION SYSTEM. G. K. Kuegler and R. Martel (Westinghouse Electric Corp., Baltimore, Md.), p. 7-29 to 7-37. 10 refs. (See A69-42509 23-07)

A TDMA/PCM EXPERIMENT ON APPLICATIONS TECHNOLOGY SATELLITES. Y. Suguri (Ministry of Posts and Telecommunications, Nakaminato, Japan), H. Doi (Nippon Telegraph and Telephone Public Corp., Tokyo, Japan), and E. Metzger (NASA, Goddard Space Flight Center, Greenbelt, Md.), p. 15-1 to 15-6. (See A69-42510 23-07)

MAT-1—A 700-CHANNEL TIME-DIVISION MULTIPLE-ACCESS SYSTEM WITH DEMAND-ASSIGNMENT FEATURES. W. G. Schmidt, O. G. Gabbard, E. R. Cacciamani, W. G. Maillet, and W. W. Wu (Communications Satellite Corp., Washington, D.C.), p. 15-7 to 15-12. 12 refs. (See A69-42511 23-07)

A NEW MULTIPLE ACCESS TECHNIQUE FOR USE WITH SATELLITE NETWORKS. E. Thomas (Page Communications Engineers, Inc., Washington, D.C.), p. 15-13 to 15-18. (See A69-42512 23-07)

DIGITAL TRANSITION TRACKING SYMBOL SYNCHRONIZER FOR LOW SNR CODED SYSTEMS. W. J. Hurd and T. O. Anderson (California Institute of Technology, Pasadena, Calif.), p. 20-1 to 20-8. (See A69-42513 23-07)

AN ANALYSIS OF THE STEADY-STATE PHASE-NOISE PERFORMANCE OF A DIGITAL-DATA-TRANSITION TRACKING LOOP. M. K. Simon (California Institute of Technology, Pasadena, Calif.), p. 20-9 to 20-15. (See A69-42514 23-07)

DISTRIBUTED COMMUNICATIONS FOR A GLOBAL SATELLITE NETWORK. W. P. McKee, Jr. (McDonnell Douglas Corp., Santa Monica, Calif.), p. 28-1 to 28-6. 8 refs. (See A69-42515 23-07)

BIOLOGIC EFFECTS OF RADIO AND MICROWAVES—PRESENT KNOWLEDGE; FUTURE DIRECTIONS. A. M. Burner (USAF, Systems Command, Brooks AFB, Tex.), p. 32-1 to 32-6. (See A69-42516 23-04)

EARTH STATION ANTENNA SIDELOBE ENVELOPE ANALYSIS. G. Hyde and R. W. Kreutel, Jr. (Communications Satellite Corp., Washington, D.C.), p. 32-7 to 32-14. (See A69-42517 23-09)

S-BAND PIN-DIODE SWITCH FOR HIGH CW POWER. P. J. Meier (Cutler-Hammer, Inc., Deer Park, N.Y.), p. 33-3 to 33-7. (See A69-42518 23-09)

ON THE APPLICATION OF SEMICONDUCTOR PHASE-SHIFTING FOR INERTIALESS ELECTRONIC ANTENNA SCANNING AT MICROWAVE TO MILLIMETER WAVE FRE-

QUENCIES—INSERTION LOSS LIMITATIONS. E. A. Graham (ONERA, Châtillon-sous-Bagneux, Hauts-de-Seine, France), p. 33-9 to 33-14. 5 refs. (See A69-42519 23-09)

PCM TELEVISION VIA SATELLITE RELAY. J. C. Balan (ITT Space Communications, Inc., Ramsey, N.J.), M. A. Epstein, and L. Feit (International Telephone and Telegraph Corp., Nutley, N.J.), p. 37-1 to 37-9. 8 refs. (See A69-42520 23-07)

EXTENSION OF THE CONCEPT OF SATELLITE COMMUNICATION SYSTEM CAPACITY TO A TWO DIMENSIONAL MODEL. P. L. Bargellini (Communications Satellite Corp., Washington, D.C.), p. 37-25 to 37-29. (See A69-42521 23-07)

TEST AND PRELIMINARY FLIGHT RESULTS ON THE SEQUENTIAL DECODING OF CONVOLUTIONAL ENCODED DATA FROM PIONEER IX. D. R. Lumb (NASA, Ames Research Center, Moffett Field, Calif.), p. 39-1 to 39-8. (See A69-42522 23-07)

A HIGH SPEED SEQUENTIAL DECODER FOR SATELLITE COMMUNICATIONS. G. David Forney, Jr. (Codex Corp., Watertown, Mass.) and R. M. Langelier (U.S. Navy, Office of the Chief of Naval Operations, Washington, D.C.), p. 39-9 to 39-17. 10 refs. (See A69-42523 23-07)

ALGORITHMS FOR TEST PATTERNS IN MULTITERMINAL DEVICES WITH SYMMETRY CONSTRAINTS. W. W. Happ and A. S. Weitzenfeld (NASA, Electronics Research Center, Cambridge, Mass.), p. 41-13 to 41-18. 14 refs. (See A69-42524 23-08)

RESPONSE OF A CASCADE CONNECTED LIMITER AND PHASE DETECTOR TO PM SIGNAL. J. C. Chang (Lockheed Aircraft Corp., Houston, Tex.), p. 45-7 to 45-12. 8 refs. (See A69-42525 23-07)

DATA COMPRESSION WITH BOUNDED ERRORS. E. C. Posner and E. R. Rodemich (California Institute of Technology, Pasadena, Calif.), p. 47-1 to 47-2. (See A69-42526 23-08)

SPACE VEHICLE MULTIBEAM ANTENNA SYSTEM DESIGN. E. A. Graham (ONERA, Châtillon-sous-Bagneux, Hauts-de-Seine, France), p. 49-1 to 49-8. 10 refs. (See A69-42527 23-09)

AUTHOR INDEX, p. I-1 to I-6.

A69-42502 •

RADIO SPECTRUM UTILIZATION IN AEROSPACE COMMUNICATION SYSTEMS.

J. M. Clarke (NASA, Electronics Research Center, Cambridge, Mass.), R. J. Otero, and W. C. Wanbaugh (IIT Research Institute, Systems Sciences Research Div., Annapolis, Md.).

IN: INSTITUTE OF ELECTRICAL AND ELECTRONICS ENGINEERS, INTERNATIONAL CONFERENCE ON COMMUNICATIONS, BOULDER, COLO., JUNE 9-11, 1969, CONFERENCE RECORD. (A69-42500 23-07)

New York, Institute of Electrical and Electronics Engineers, Inc. (IEEE ICC Conference Publications. Volume 5), 1969, p. 5-13 to 5-18.

Discussion of a few of the important areas being examined in a spectrum engineering and management program initiated by NASA. NASA radio spectrum use (both present and planned) is considered, and potential spectrum-sharing problems are discussed. An outline is provided of the other areas and objectives which form a part of the NASA program. G.R.

A69-42508 *

AN ANALYSIS OF THE TELECOMMUNICATIONS PERFORMANCE OF A LUNAR RELAY SATELLITE SYSTEM.

G. D. Arndt, B. H. Batson, and S. W. Novosad (NASA, Manned Spacecraft Center, Information Systems Div., Houston, Tex.).

IN: INSTITUTE OF ELECTRICAL AND ELECTRONICS ENGINEERS, INTERNATIONAL CONFERENCE ON COMMUNICATIONS, BOULDER, COLO., JUNE 9-11, 1969, CONFERENCE RECORD. (A69-42500 23-07)

New York, Institute of Electrical and Electronics Engineers, Inc. (IEEE ICC Conference Publications. Volume 5), 1969, p. 7-21 to 7-27. 6 refs.

Investigation of the performance characteristics of two lunar relay satellite system (LRSS) configurations proposed recently for providing a communications capability between the earth and a lunar orbiter situated behind the moon. The expected communications capabilities are determined for operations with the present Apollo communications system and with a conceptual modified Apollo communications system. Positive circuit margins are expected with both LRSS configurations for the full-downlink phase-modulated mode when using the present and the modified Apollo spacecraft high-gain antennas. Both LRSS configurations also provide a satisfactory performance for wideband downlink modes and all uplink modes when using the spacecraft high-gain antennas of the modified Apollo system. Recommendations for obtaining maximum use of the LRSS configurations are outlined. V.Z.

A69-42522 *

TEST AND PRELIMINARY FLIGHT RESULTS ON THE SEQUENTIAL DECODING OF CONVOLUTIONAL ENCODED DATA FROM PIONEER IX.

Dale R. Lumb (NASA, Ames Research Center, Moffett Field, Calif.).

IN: INSTITUTE OF ELECTRICAL AND ELECTRONICS ENGINEERS, INTERNATIONAL CONFERENCE ON COMMUNICATIONS, BOULDER, COLO., JUNE 9-11, 1969, CONFERENCE RECORD. (A69-42500 23-07)

New York, Institute of Electrical and Electronics Engineers, Inc. (IEEE ICC Conference Publications. Volume 5), 1969, p. 39-1 to 39-8.

Discussion of tests and preliminary flight results of the Pioneer 9 deep space probe with a telemetry link operated for about a month in the coded mode with sequential decoding of a rate-½, 25-bit constraint-length convolutional code. A comparison of the decoding-computation for the subcarrier channel and rf channel levels of testing with computer-simulation data revealed that the Pioneer demodulator/bit synchronizer was responsible for the principal disagreement between the system and simulation test results for the three highest Pioneer data rates. Close agreement is obtained between the preliminary Pioneer flight data and the test results. V.Z.

A69-42549 •

A NOTE ON THE EFFECTS OF THE IONOSPHERE ON SATELLITE ORBITAL CORRECTIONS IN NEAR-REAL TIME.

A. D. Poularikas (Rhode Island, University, Kingston, R.I.) and T. S. Golden (NASA, Goddard Space Flight Center, Greenbelt, Md.).

IEEE Transactions on Aerospace and Electronic Systems, vol. AES-5, Sept. 1969, p. 865-867. 7 refs.

Investigation of the influence of ionospheric irregularities on the accurate determination of the position of a satellite. A method is presented whereby these effects are easily accounted for in near-real time without the need to know their detailed structure. (Author)

N69-10885*# National Aeronautics and Space Administration. Langley Research Center, Langley Station, Va.

RADIOFREQUENCY TRANSMISSION CHARACTERISTICS OF SEVERAL ABLATION MATERIALS

Melvin C. Gilreath, William F. Croswell, and Stark L. Castellow, Jr. Washington Nov. 1968 41 p refs

(NASA-TN-D-4879) Avail: CFSTI CSCL 20N

An experimental investigation was conducted to determine the transmission loss, and effects upon the radiation patterns and impedance of typical antennas, produced by thermally degraded ablation materials. A cone-shaped model was used, which consisted of a truncated aluminum substructure with flush-mounted antennas over which a thermal-protection test material was bonded. Measurements of transmission loss through several thermal protection materials were made at 2.66 GHz and 9.60 GHz. The dielectric properties of all virgin materials were measured at room temperature. In addition, antenna radiation patterns, voltage standing wave ratios (VSWR), and gain were determined before and after the materials were subjected to the thermal test. It was concluded that, in general, materials which form and retain continuous conductive char layers during thermal exposure produce very high transmission losses. Also, it is shown that antennas which are

covered with such high-loss materials may exhibit extreme perturbations in the radiation patterns that are not present when the antenna is covered with the virgin material. The antennas used for this test program experienced an increase in VSWR when covered with the high-loss materials; however, the loss attributable to this mismatch was less than 2 dB. Author

N69-11011*# National Aeronautics and Space Administration. Goddard Space Flight Center, Greenbelt, Md.
RELATIONSHIP BETWEEN COMPLEX- AND ENVELOPE-COVARIANCE FOR RICIAN FADING COMMUNICATION CHANNELS
Erwin Mondre Washington Nov. 1968 33 p refs
(NASA-TN-D-4825) Avail: CFSTI CSCL 09D

In practice, the measurement of the covariance function (which characterizes a time and frequency selective fading communication channel) involves envelope detecting the received signals before correlating. Envelope covariance is insufficient for an accurate evaluation of system performance and rather a complex covariance is needed. This paper presents a study of these two covariances for Rician statistics. The general properties of the Rician distribution are discussed. The relationship between complex covariance and covariance of the envelopes of a complex Rician fading communication channel is derived. It includes the well known case of Rayleigh fading. For the assumption of symmetric spectrum of the narrow band random process there exists a monotonic relationship which allows the evaluation of the complex covariance once the envelope covariance is measured. An extension to unsymmetric spectrum is given. The results obtained show that the envelope covariance represents a lower bound of the magnitude of the complex covariance. Author

N69-13155*# National Aeronautics and Space Administration. Manned Spacecraft Center, Houston, Tex.
OPTIMUM DESIGN OF COMMUNICATION LINKS WITH NOISY PHASE REFERENCE
William E. Zrubek Washington Dec. 1968 25 p refs
(NASA-TN-D-4895) Avail: CFSTI CSCL 17B

A binary communication link is analyzed, and an expression is obtained for bit error probability when the phase reference is noisy. Graphical results are presented which allow selection of modulation index to minimize the error probability. Author

N69-13158*# National Aeronautics and Space Administration. Langley Research Center, Langley Station, Va.
RADIOFREQUENCY TRANSMISSION CHARACTERISTICS OF CANDIDATE ABLATION MATERIALS FOR PLANETARY-ENTRY-VEHICLE HEAT SHIELDS
Melvin C. Gilreath, Andreq J. Chapman, and Douglas M. Hatcher Washington Dec. 1968 62 p refs
(NASA-TN-D-4920) Avail: CFSTI CSCL 22B

An experimental investigation was conducted to determine the radiofrequency properties of several candidate ablation materials for planetary-entry-vehicle heat shields. The radiofrequency transmissibility of each ablative material was determined by the real-time measurement of the attenuation of a 35 GHz signal while each sample was exposed to a simulated planetary entry environment. The simulated planetary environment was produced by providing a heating rate, pressure, and free-stream Mach number in an arc-heated supersonic wind tunnel. Recordings of the transmission loss obtained through each material during the arc-tunnel test and photographs of all test specimens before and after thermal exposure are presented. In addition to the transmission loss measurements, the dielectric properties of most virgin materials were measured at room temperature and are also presented. Author

N69-13301*# National Aeronautics and Space Administration. Manned Spacecraft Center, Houston, Tex.
LUNAR SURFACE TRANSMISSION LOSS FOR THE APOLLO ASTRONAUT
Jefferson F. Lindsey, III Washington Dec. 1968 28 p refs
(NASA-TN-D-4915) Avail: CFSTI CSCL 17B

Radio-wave propagation theory is reviewed with emphasis on point-to-point communications on the lunar surface. The geometric optics solutions for both a plane surface and a spherical surface are presented. The transmission loss is found to slope at 40 dB/decade of distance at the longer distances for which the path difference between the direct and the reflected wave is less than one-half wavelength. The Bremmer series for radio-wave diffraction solution is presented for calculation of the transmission loss near the line of sight when the geometric optics solution does not apply. In addition to smooth-surface effects, the roughness effects of knife-edge diffraction and of small hills are used to obtain a combined-effects transmission loss plot. Finally, measured data are presented which confirm that the maximum astronaut-to-lunar-module range will be at least 8200 feet and that the maximum astronaut-to-astronaut range will be at least 6000 feet. Author

N69-14973*# Aztec School of Languages, Inc., Acton, Mass. Research Translation Div.
RADIO BRIDGE: "EARTH-MOON-EARTH" [RADIOMOST: 'ZEMLYA-LUNA-ZEMLYA']
V. Ye. Demidov Washington NASA Jan. 1969 47 p refs Transl. into ENGLISH from Russian
(Contract NASw-1692)
(NASA-TT-F-527) Avail: CFSTI CSCL 17B

Problems in providing a reliable communications system for passage of signals from the earth to the moon and back are examined. Selection of the appropriate type of modulation, and the elimination of noise; the selection of optimal frequencies, and systems for coding transmission are considered. The use of the earth–moon–earth radio link, as a means of communications with space stations and isolated points on the earth, is investigated. F.O.S.

N69-15373*# National Aeronautics and Space Administration. Electronics Research Center, Cambridge, Mass.
EXAMPLES OF CODING SCHEMES BASED ON STRATEGIC VALUE
W. W. Happ Washington NASA Jan. 1969 18 p refs
(NASA-TN-D-4962) Avail: CFSTI CSCL 09D

Procedures are developed to construct variable-length codes for alphabets containing messages with assigned weighted-information content. Criteria specifying the strategic value of a code are defined, and codes are examined on the basis of alphabets containing messages with weighted-information content. Figures-of-merit are established and utilized to compare different types and possible trade-offs for simple codes. Algorithms governing these codes are established and examined on the basis of representative examples. Author

N69-16162*# National Aeronautics and Space Administration. Langley Research Center, Langley Station, Va.
ERROR ANALYSIS OF INPUT-NOISE-TEMPERATURE MEASUREMENTS OF LOW-NOISE AMPLIFIERS
Hans-Juergen C. Blume Washington Jan. 1969 41 p refs
(NASA-TN-D-4997) Avail: CFSTI CSCL 09C

The method presented provides means of determining all effects which significantly influence measurement of the output-noise-power ratio (Y-factor) of a typical low-noise-amplifier test setup. The error analysis of the Y-factor method illustrates the error propagation which occurs in the derivations of the input noise temperature and gives an estimate of the maximum error. The general concepts used in determining these influences and the error propagation are applied to reflection-type amplifiers. Numerical examples demonstrate the value in considering all elements which (1) affect the calibrated noise power along the transfer path from the noise source to the amplifier under test, and (2) add noise power along the path from the amplifier to the noise indicator. The error analysis applied to the examples revealed that for minimization of the input-noise-temperature error, accurate knowledge of the losses and temperatures is more important than obtaining extremely

high ratios of the hot- to cold-noise source temperatures. A comparison between the input noise temperature determined by considering all influencing effects and the input noise temperature determined without considering these effects for a typical low-noise measuring system for reflection-type amplifiers revealed a considerable difference. Author

N69-16196*# National Aeronautics and Space Administration. Goddard Space Flight Center, Greenbelt, Md.

A COMPARSION OF SEQUENTIAL DECODING METRICS BY COMPUTER SIMULATION

Thomas V. Saliga (M.S. Thesis—Md. Univ., College Park, 1968) Washington Jan. 1969 56 p refs

(NASA-TR-R-294) Avail: CFSTI CSCL 17B

This paper determines a sequential decoder's performance and metric sensitivity by means of a computer simulation using two metrics: (1) A log-a-posteriori probability metric, and (2) A cross-correlation metric. Both metrics are defined, derived, and tabulated for the memoryless gaussian channel. Simulations of a rate 1/2, constraint-length 32 coded data system are made using 16 level quantized metrics. When good metric and decoder parameters have been found, the decoder's computational load, overflow probabilities, and error probability are found as a function of channel signal-to-noise ratio, using at least 500 simulated telemetry frames per data point. It is shown that the correlation metric is inferior to the probability metric by at least 1.5 decibels and suffers a higher error rate. In addition, the correlation metric decoder degrades intolerably with 0.5 decibel signal-amplitude fluctuations, whereas the probability metric decoder is negligibly affected. Author

N69-19025*# National Aeronautics and Space Administration. Lewis Research Center, Cleveland, Ohio.

FEASIBILITY STUDIES OF DIRECT VOICE BROADCAST SATELLITES

Perry W. Kuhns Washington Feb. 1969 22 p refs

(NASA-TM-X-1747) Avail: CFSTI CSCL 17B

The results of two voice broadcast satellite studies undertaken in 1966–67 are summarized. These studies included audience and receiver analyses, conceptual spacecraft configurations, technological evaluations, cost evaluations, and data of indigenous noise surveys. Author

N69-19114*# National Aeronautics and Space Administration. Langley Research Center, Langley Station, Va.

THE ADMITTANCE OF A PARALLEL-PLATE APERTURE ILLUMINATING A DISPLACED DIELECTRIC–DIELECTRIC BOUNDARY

J. Earl Jones Washington Feb. 1969 60 p refs

(NASA-TN-D-5038) Avail: CFSTI CSCL 09F

The variational method is used to determine the admittance of a transverse-electromagnetic-mode excited, parallel-plate aperture having an infinite flange and illuminating a displaced dielectric–dielectric boundary. The results are applied to provide insight into two problems of interest: (a) the effect of an air gap on the admittance of dielectric coated aperture antennas and (b) the admittance of an aperture antenna coated with an underdense plasma slab. Numerical computations for the air gap problem are verified experimentally. For either problem, the most significant changes in the admittance occur for displacements less than 0.25 wavelength. (The wavelength referred to is the free space wavelength divided by the square root of the relative permittivity of the medium between the boundary and the aperture.) For the dielectric coated slot antenna, changes in the admittance due to an air gap are enhanced if either the slot width is reduced or the permittivity is increased. For a slot antenna coated with a thin underdense plasma slab, the admittance becomes more sensitive to changes in the layer thickness as the plasma becomes more dense. As observed theoretically for both the air gap problem and the underdense-plasma problem, the admittance is not influenced by the presence of surface waves. Experimental verification of this result is given for the air gap problem. Author

N69-22949*# National Aeronautics and Space Administration. Electronics Research Center, Cambridge, Mass.

A REVIEW OF RADIOMETRIC MEASUREMENTS OF ATMOSPHERIC ATTENUATION AT WAVELENGTHS FROM 75 CENTIMETERS TO 2 MILLIMETERS

William I. Thompson, III and George G. Haroules Washington Apr. 1969 20 p refs

(NASA-TN-D-5087) Avail: CFSTI CSCL 17B

Published values of vertical attenuation resulting from radiometric measurements of absorption and emission of the Earth's atmosphere in the wavelength range from 75 cm (0.4 GHz) to 2 mm (150 GHz) are presented. The literature search included a review of several hundred publications. These data emphasize the need for further theoretical and experimental work in the calculation and measurement of attenuation in this portion of the spectrum. Author

N69-22951*# National Aeronautics and Space Administration. Electronics Research Center, Cambridge, Mass.

RADIOMETRIC TECHNIQUES APPLICABLE TO THE MEASUREMENT OF SOLAR ACTIVITY AND ATMOSPHERIC ATTENUATION AT MILLIMETER WAVELENGTHS

George G. Haroules Washington Apr. 1969 21 p refs

(NASA-TR-R-306) Avail: CFSTI CSCL 17B

The available dynamic range for measurements of this type is determined by the brightness temperature of the sun and the sky noise fluctuation level at the frequency of observation. During the period of measurement, it is assumed that the solar flux intensity is constant and that all apparent variations in solar intensity are associated with atmospheric effects. Similar radiometric measurement instruments are used for the determination of solar radiation characteristics at millimeter wavelengths. Useful data are limited to those periods when the weather conditions are relatively mild. Here, the assumption is made that all apparent variations in solar intensity are associated with the radiation characteristics of the sun itself. The most useful data concerning solar radiation characteristics are obtained under clear weather conditions; that concerning atmospheric attenuation is obtained under adverse weather conditions. Author

N69-23163*# National Aeronautics and Space Administration. Goddard Space Flight Center, Greenbelt, Md.

THE LOG-A-POSTERIORI PROBABILITY METRIC FOR USE IN SEQUENTIAL DECODING

T. V. Saliga Washington Apr. 1969 25 p refs

(861-51-75-01-51)

(NASA-TN-D-4930) Avail: CFSTI CSCL 17B

Convolutional encoding with sequential decoding is one of the best coded communications systems available for spacecraft telemetry. When implementing a sequential decoder, a decoding confidence measure based upon the received signal probabilities is used. The best known measure is the log-a-posteriori probability metric. Tabulations of the metric for various telemetry system parameters are given. Both a continuous and a quantized metric are treated for various symbol signal-to-noise ratios on a Gaussian channel. Quantized symbol metrics are tabulated for 2, 4, 8, and 16 levels, and it is shown that the quantized LAP metric is an approximation of the ideal continuous metric. Author

N69-23317*# National Aeronautics and Space Administration. Goddard Space Flight Center, Greenbelt, Md.

SOLAR EFFECTS ON VHF COMMUNICATIONS BETWEEN A SYNCHRONOUS SATELLITE RELAY AND EARTH GROUND STATIONS

Sheldon Wishna and James R. Greaves (Allied Res. Associates, Inc., Concord, Mass.) Washington Apr. 1969 11 p

(NASA-TN-D-5100) Avail: CFSTI CSCL 17B

An investigation has been performed to correlate VHF interference, as reported by participating ground stations, with the occurrence of certain solar phenomena. The participating ground stations were taking part in the Weather Facsimile (WEFAX) experiment, which utilizes the Applications Technology Satellite

(ATS)-1 to relay processed meteorological data from a central weather station to the ground stations. The VHF communication system, located on board the satellite, is an active frequency translator with an uplink receive frequency of 149.22 MHz and a downlink transmit frequency of 135.6 MHz. The data were transmitted to the satellite from the ATS ground station located at Mojave, California. The ATS-1 satellite is at an altitude of 19,300 nautical miles and is located over the equator at 151° West longitude. Approximately 50 ground stations located in an area extending from the east coast of the United States to Australia and Japan participated in the program. The analysis was conducted over an 8-month period beginning on January 2, 1967 and continuing through August of the same year. Author

N69-23642*# National Aeronautics and Space Administration. Goddard Space Flight Center, Greenbelt, Md.

PARAMETRIC ANALYSIS OF MICROWAVE AND LASER SYSTEMS FOR COMMUNICATION AND TRACKING: A SUMMARY

F. Kalil Washington Apr. 1969 97 p refs

(NASA-TR-R-309) Avail: CFSTI CSCL 17B

A comparative analysis was made of laser and microwave telecommunication systems for space applications. Parametric families of curves are presented that give the weights and telecommunications capabilities of spaceborne communication systems. These curves permit the mission planner and designer to compare various sytems and select the one that best meets their requirements. A sample case demonstrates the use of these curves. The sample calculation and concluding remarks point out the advantages of a computerized method that uses the calculus of maxima and minima for selecting the optimum spaceborne communication system configuration that can provide the specified information rate for the least spaceborne weight penalty and/or cost. Author

N69-23882*# National Aeronautics and Space Administration. Manned Spacecraft Center, Houston, Tex.

PERFORMANCE CHARACTERISTICS OF THE APOLLO ASTRONAUT BACKPACK ANTENNA

Jefferson F. Lindsey, III Washington May 1969 22 p refs

(NASA-TN-D-5081) Avail: CFSTI CSCL 09E

Antenna patterns and voltage-standing-wave ratio measurements were made, including both surface reflection effects and free space data. The antenna pattern data were taken at frequencies of 259.7, 279.0, and 296.8 megahertz, with surface reflection effects included. The voltage standing wave ratio in this range were under 2.0:1, and the gains with surface reflection effects and the astronaut standing ranged from the worst case null of −5 decibels at 259.7 megahertz to +2 decibels at 279.0 megahertz. In the bending over and lying down positions, the gains range from −28 to +1 decibels. As a result, no height gain correction factor in the transmission loss is required in the circuit margin calculations for the bending over and lying down positions. Author

N69-24051*# National Aeronautics and Space Administration. Electronics Research Center, Cambridge, Mass.

FIRST-ORDER SOLUTIONS FOR MUTUAL COUPLING BETWEEN WAVEGUIDES WHICH PROPAGATE TWO ORTHOGONAL MODES

R. J. Mailloux Washington May 1969 26 p refs

(NASA-TN-D-5180) Avail: CFSTI CSCL 17B

A theoretical and experimental study of closely spaced open-ended waveguides radiating through a conducting ground plane is described. The waveguides are large enough in some cases to allow two orthogonally polarized propagating modes in each waveguide. A first-order analysis is presented which is based upon the method of moments and uses of a single-mode approximation to the aperture field for each polarization. An improved first-order analysis is also presented which uses a higher order mode solution for the self admittances. Close agreement with experiment is demonstrated. Author

N69-24059*# Ohio State Univ., Columbus.

THE Te-01 MODE REFLECTION COEFFICIENT OF A GROUND-PLANE MOUNTED PARALLEL-PLATE WAVEGUIDE ILLUMINATING A REFLECTING SHEET

L. L. Tsai and R. C. Rudduck Washington NASA May 1969 27 p refs

(Grant NGR-36-008-005)

(NASA-CR-1327; TR-1691-30) Avail: CFSTI CSCL 17B

The TE_{01} mode reflection coefficient is analyzed for a symmetric parallel-plate waveguide terminated in a ground plane and radiating into a perfectly reflecting sheet oriented normal to the guide axis. The method of analysis and calculated results are similar to those of the TEM mode analysis. The transmission between two identical waveguides facing each other is also analyzed. Author

N69-26272*# National Aeronautics and Space Administration. Goddard Space Flight Center, Greenbelt, Md.

RADIO FREQUENCY INTERFERENCE EXPERIMENT DESIGN FOR THE APPLICATIONS TECHNOLOGY SATELLITE

Varice F. Henry and John J. Kelleher Washington May 1969 15 p refs

(NASA-TN-D-5041) Avail: CFSTI CSCL 17B

The proposed experiment described herein is designed to measure and evaluate the amount of mutual interference between communications-satellite and terrestrial microwave relay systems at the shared common carrier frequency bands of 6 and 4 GHz. It is proposed to measure terrestrial-to-satellite interference at 6 GHz and satellite-to-terrestrial interference at 4 GHz. To meet the technical requirements of this experiment, it is necessary to utilize a satellite of the type planned for the ATS F and G program. These spacecraft, each carrying a 30-foot parabola as the prime antenna, will be capable of 0.1-degree pointing accuracy and full earth-scanning coverage. Measurements will be made of several parameters to obtain a fuller understanding of existing conditions related to such interference. Parametric measurements will include transmitted and received power levels, propagation-path loss and variations as a function of range, elevation angle, RF polarization, and geographical location of interference sources. Author

N69-26273*# Ohio State Univ., Columbus.

SLOPE DIFFRACTION ANALYSIS OF TEM PARALLEL-PLATE GUIDE PATTERNS

D. C. F. Wu and R. C. Rudduck Washington NASA May 1969 52 p refs

(Grant NGR-36-008-005)

(NASA-CR-1326; TR-1691-29) Avail: CFSTI CSCL 09E

The radiation pattern of a TEM mode parallel plate waveguide is analyzed by wedge diffraction theory in conjunction with a slope correction term. This slope correction term is the diffraction by a conducting wedge due to an incident wave with sinusoidal amplitude variation over the wave front. Such a wave is referred to as a slope wave. The slope diffraction takes into account the nonuniform wave in calculating second order diffractions for the open ended guide. The slope correction term provides an improvement in the accuracy of the pattern in the region near the plane of the aperture as compared to the previous wedge diffraction calculations. Author

N69-28223*# North American Rockwell Corp., Downey, Calif.

THEORETICAL FLOW FIELD CALCULATIONS FOR PROJECT RAM

H. Webb, Jr., H. Dresser, K. Korkan, and R. Raparelli Washington NASA May 1969 153 p refs

(Contract NAS1-8172; Proj. RAM)

(NASA-CR-1308) Avail: CFSTI CSCL 17B

Theoretical flow fields for seven flight conditions for the RAM-C blunted cone configuration are presented. Both viscous and inviscid flow regions are considered in an analysis leading to predictions of nonequilibrium chemical effects within the entire flow field. Special emphasis is placed on the presence of free electron

concentrations which are responsible for the phenomena of radio attenuation. The flight investigation of these effects is the purpose of the RAM Project. Nonequilibrium flow is predicted by using a one-dimensional analysis along streamlines both in the boundary layer region and in the inviscid flow region. For two of the flight conditions, calculations were performed to evaluate the influence of a larger nose radius on the flow field. This change in geometry occurs when the beryllium nosecap is ejected. Very small plottable differences were found on outer streamlines for the lower speed flight condition when comparisons were made on similarly located normals. Author

N69-29230*# National Aeronautics and Space Administration. Langley Research Center, Langley Station, Va.

ANALYTIC FUNCTION MODELS OF NOISE AND MODULATION

John H. Painter, Someshwar C. Gupta, (Southern Methodist Univ.), and Jon W. Bayless (Southern Methodist Univ.) Washington Jun. 1969 32 p refs

(NASA-TR-R-314) Avail: CFSTI CSCL 17B

The theory of complex analytic time functions are applied to a representation of stochastic and deterministic time processes. By using analytic notation, noise and modulated signals are represented in the same manner. A mathematically rigorous method of transition from real to analytic processes is given. By use of the theory of distributions, the rotating vector, or phasor, method is generalized to arbitrary functions and stochastic processes. The advantages of analytic time function notation are exploited to derive correlation and spectral functions for both signal and noise processes. The polar and quadrature forms for band pass processes are derived. Author

N69-31985*# National Aeronautics and Space Administration, Washington, D.C.

WEATHER SATELLITE PICTURE RECEIVING STATIONS: INEXPENSIVE CONSTRUCTION OF AUTOMATIC PICTURE TRANSMISSION GROUND EQUIPMENT

Charles H. Vermillion 1969 107 p refs

(NASA-SP-5080) Avail: CFSTI CSCL 17B

A description is given of how one can procure or build the antenna, FM receivers, and other components for the automatic picture transmission (APT) ground station. A facsimile video enchancement device is also described, along with the direct readout infrared (DRIR) adapter unit which can convert the APT system to receive nighttime as well as daytime cloudcover data. The DRIR system takes advantage of the NIMBUS 3 high resolution infrared radiometer (HRIR) which transmits pictures over the same frequencies used by the APT system in the daytime. Detailed drawings and parts lists are included for each system. Installation, alignment, and operation of the complete APT ground station are also described. The APT ground stations are inexpensive and reliable. They can be built from surplus parts for under $500 or procured for as low as $5000. With them, scientists, local weather stations, amateurs, and others can receive satellite-taken photographs of the earth as APT-equipped satellites pass overhead. Author

N69-32721*# Aerochem Research Labs., Inc., Princeton, N.J.

VAPORIZATION AND DECOMPOSITION KINETICS OF CANDIDATE RE-ENTRY BLACKOUT SUPPRESSANTS IN LOW-PRESSURE FLAMES

Shelby C. Kurzius and Fredrik H. Raab Aug. 1969 65 p refs

(Contract NAS1-7169)

(NASA-CR-1330; TP-181) Avail: CFSTI CSCL 17B

This study provides the first experimental measurements of thermal accommodation coefficients between liquids and high-temperature gas. Beams of uniformly sized droplets were sent across 5 and 10 torr $H_2/CO/O_2$/air flames and their evaporation rates were photographically determined. Droplet sizes were on the order of the mean free path in the flames. From the observed evaporation rates, the following translational thermal accommodation coefficients were obtained for combustion gases at about 2500 K: water, 0.76 ± 0.14; perfluoro–octane, 0.17 ± 0.04; Freon E–8, 0.22 ± 0.10. Apparently, only translational energy is effectively transferred from the gas to the liquid; the measured accommodation coefficients are in agreement with predictions based on Baule's classical theory, in which the surface of the condensed phase is regarded essentially as a super-dense gas. Additionally, measurements of the decomposition kinetics of sulfur hexafluoride and perfluoro–octane vapors in 10, 20, 40, and 100 torr $H_2/CO/O_2$/air flames are reported. Author

N69-37602*# National Aeronautics and Space Administration. Langley Research Center, Langley Station, Va.

APPLICATIONS OF ANALYTIC FUNCTION THEORY TO ANALYSIS OF SINGLE-SIDEBAND ANGLE-MODULATED SYSTEMS

John H. Painter Washington Sep. 1969 42 p refs

(NASA-TN-D-5446) Avail: CFSTI CSCL 17B

The theory and notation of complex analytic time functions and stochastic processes are applied to the investigation of the single-sideband angle-modulation process. Low-deviation modulation and linear product detection in the presence of noise are carefully examined for the case of sinusoidal modulation. Modulation by an arbitrary number of sinusoids or by modulated subcarriers is considered. Also treated is a method for increasing modulation efficiency. An examination of the asymptotic (low-noise) performance of nonlinear detection of a single-sideband carrier which is heavily frequency modulated by a Gaussian process is discussed. Author

N69-39176*# National Aeronautics and Space Administration. Electronics Research Center, Cambridge, Mass.

COMMUNICATION SYSTEM DESIGN

Louis A. Frasco Washington Oct. 1969 32 p refs

(NASA-TN-D-5472) Avail: CFSTI CSCL 17B

A general system design philosophy palatable to both analog and digital communication engineers is presented. The method of presentation is novel and some new results and calculations are presented. An attempt is made to establish the relevance of the more theoretical aspects of communication system design (i.e., statistical communication theory, information theory and coding, etc.) to the work of the practicing system design engineer in evaluating real systems. Consideration of the fidelity of the overall system, from source characterization to user requirements, is of prime importance. The use of the computer in system management of hybrid analog/digital systems is also discussed. In addition, optimum bounds on performance are calculated for the space channel and compared with the performance of some existing systems. Author

N69-39264*# National Aeronautics and Space Administration. Electronics Research Center, Cambridge, Mass.

COMMUNICATION EFFICIENCY OF QUANTUM SYSTEMS

Sherman Karp Washington Sep. 1969 24 p refs

(NASA-TR-R-320; C-78) Avail: CFSTI CSCL 17B

This report presents a method for evaluating the theoretical performance of quantum communication systems based on the communication efficiency parameter, $\beta = P/N_0R$. For Gaussian systems, β represents the minimum average amount of energy required to decipher a bit of information, with zero error, in the presence of white noise of spectral density N_0. For certain quantum systems, the Gaussian result is directly applicable with N_0 replaced by $h\nu$. In general, β is recognized to be the minimum number of average (photon) events required to decipher a bit of information with zero error. To make comparisons with Gaussian systems, the parameter κ is introduced with $h\nu/\kappa$ becomes the effective Gaussian spectral density of the quantum system. Several systems are considered in addition to the capacity bound for the narrow-band quantum channel introduced by Gordon. Unlike the Gaussian channel, there is no lower bound on β as the bandwidth-to-data-rate ratio, α, is increased. Thus β can be continually decreased at the

expense of average data rate. For large values of α, PPM direct detection asymptotically approaches the lower bound for β. Author

N69-39282*# Mississippi State Univ., State College. Dept. of Electrical Engineering.

A STUDY OF 2 GHz ELECTROMAGNETIC WAVE PROPAGATION OVER OPTICAL PATHS IN THREE GEOGRAPHICAL REGIONS OF THE UNITED STATES

J. O. Hebert, Jr., F. M. Ingels, D. F. Fitzgerald, E. E. Gross, and S. Y. Lee Washington NASA Oct. 1969 135 p refs Revised (Grant NGR-25-001-007)

(NASA-CR-1442) Avail: CFSTI CSCL 17B

Statistical signal level distributions are used to derive an empirical relationship between electromagnetic wave propagation *reliability, fade margin, path length, and geographical location*. This procedure allows the microwave systems designer to calculate the fade margin required for a particular optical path and a given reliability for operating frequencies in the 2 GHz region. Cross correlations of microwave signal fading over selected paths and the fading obtained over a high elevation angle path are included. G.G.

N69-40099*# National Aeronautics and Space Administration. Langley Research Center, Langley Station, Va.

PULSE-RESPONSE CURVES OF CONVENTIONAL LOW-PASS FILTERS

William D. Stanley (Old Dominion Univ.) and Doris M. Higgins Washington Oct. 1969 116 p refs

(NASA-TN-D-5494) Avail: CFSTI CSCL 17B

A catalog of 100 different pulse responses of conventional low-pass filters is presented. The pulse responses were obtained by a computer simulation of a general digital filter whose characteristics could be varied to correspond very closely with the various analog filter functions. The standard Butterworth, the Chebyshev (with various ripples), and the Bessel filter functions are considered. Filter orders from 1 to 5 are included. For each filter type and order, responses corresponding to four different products of bandwidth and pulse width are considered. Author

08

COMPUTERS

Includes computer operation and programming; and data processing. For basic research see: 19 Mathematics.

A69-13243 *

THE SDP-3 - A COMPUTER FOR USE ON BOARD SMALL SCIENTIFIC SPACECRAFT.

R. A. Cliff (NASA, Goddard Space Flight Center, Spacecraft Technology Div., Flight Data Systems Branch, Greenbelt, Md.).

IN: EASCON '68; INSTITUTE OF ELECTRICAL AND ELECTRONICS ENGINEERS, ELECTRONICS AND AEROSPACE SYSTEMS CONVENTION, WASHINGTON, D.C., SEPTEMBER 9-11, 1968, RECORD. [A69-13176 03-07]
New York, Institute of Electrical and Electronics Engineers, Inc., 1968, p. 521-527.

The SDP-3 is a general-purpose stored-program computer which has been designed for use as the core of the data system of a small scientific spacecraft. It is a serial, two's complement, 16-bit-word machine. It has one level of indirect addressing and one hardware index register. To facilitate time-sharing operation there is a 16-level priority interrupt system and a real-time clock. The 4K memory is divided into 16 pages of 256 words each. There is a user and a monitor mode. Interpage access is prohibited in user mode. (Author)

A69-14858 *

AN ALGORITHM FOR DERIVING THE EQUATIONS OF MATHEMATICAL PHYSICS BY SYMBOLIC MANIPULATION.

James C. Howard and Howard Tashjian (NASA, Ames Research Center, Moffett Field, Calif.).

ACM, Communications, vol. 11, Dec. 1968, p. 814-818, 826. 6 refs.

A method is described whereby a digital computer can be used to derive the equations of mathematical physics in any curvilinear coordinate system requested by the user. The effectiveness of the technique is demonstrated by using it to derive the Navier-Stokes equations of fluid motion and the continuity equation. To derive these equations by this method, the user need know only the coordinate transformation equations relating the curvilinear coordinates of interest to an orthogonal Cartesian triad. When this program is used and the coordinate transformation equations are supplied as input, the computer will derive the Navier-Stokes equations and the continuity equation. The equations obtained will be relative to the curvilinear coordinate system specified by the transformation equations used as input. In the paper, the emphasis is on theoretical considerations and methodology rather than on programming details. (Author)

A69-15472 *

THE SDP-1 STORED-PROGRAM COMPUTER.

Rodger A. Cliff (NASA, Goddard Space Flight Center, Greenbelt, Md.).

IEEE Transactions on Aerospace and Electronic Systems, vol. AES-4, Nov. 1968, p. 864-870.

A stored-program computer could be used to advantage on small scientific spacecraft because of its flexibility. The paper describes the design and programming of a stored-program computer specifically adapted to this particular application. In order to be suitable for use in a small scientific spacecraft, a computer must have the following characteristics: reliability, low power drain, light weight, small size, problem-solving power, and flexibility. To meet these requirements, a computer was designed that has 1024 words of program memory and 512 words of data memory. The words are 12 bits in length and both memories are randomly accessed. In order to protect the program, the program memory is of the nondestructive read-out type. The data memory is the conventional read/write variety. The computer is organized such that the power drain is small and less hardware is required by restricting parallel gating of information, number of registers, and number and complexity of instructions. Considerable effort has been devoted to programming the computer. Analysis shows that it takes on the order of 2 msec to perform one of the floating-point operations. These limitations should be acceptable; the computer is not expected to be required to perform extremely complex or lengthy computations. (Author)

A69-29004 *#

COHORT-II - A MONTE CARLO GENERAL PURPOSE SHIELDING COMPUTER CODE.

Leonard Soffer and Lester C. Clemons, Jr. (NASA, Lewis Research Center, Cleveland, Ohio).

American Nuclear Society, Conference on the Effective Use of Computers in the Nuclear Industry, Knoxville, Tenn., Apr. 21-23, 1969, Paper. 17 p. 10 refs.

COHORT II integration into a single package with more flexible geometry and biasing. Written completely in FORTRAN-IV for the IBM-7094 computer, it represents a major revision and modernization of the original COHORT code. The code method is the conventional one in which "particles" are generated, tracked and analyzed. The allowed shielding geometry is flexible, with space divided into homogeneous regions bounded by surfaces describable by a general quadratic equation. Spherical, cylindrical, and rectangular parallelepipeds are allowed for the source regions. Biasing options include selection of source particles from preferred locations, energies and directions. The exponential transform can also be used during particle tracking, and secondary gammas can be generated and placed on tape during a neutron problem to be tracked during a subsequent computer run. Output includes number fluxes in energy bins at arbitrarily located point detectors and average over regions. Energy-integrated quantities such as dose rates are also obtainable. Checkout calculations are performed for point isotropic neutron and gamma sources in polyethylene and aluminum, and for two duct problems. B.H.

A69-33106 *#

USE OF TIME-SHARING COMPUTER TO SUPPORT SEVERAL LARGE TEST FACILITIES.

Charles W. Putt and Fredric N. Goldberg (NASA, Lewis Research Center, Cleveland, Ohio).

Instrument Society of America, National Aerospace Instrumentation Symposium, 15th, Las Vegas, Nev., May 5-7, 1969, Paper. 10 p.

Discussion of a central data system connected to a large time-shared computer for recording data from the test facilities of the Lewis Research Center of NASA. Time-sharing typewriter terminals connected to the central computer are located in the test facility control rooms. This system enables the central computer to provide computed results at each test facility within minutes of recording. G.R.

A69-33108 *#

A DEVICE FOR PRINTING ALPHANUMERIC LISTINGS AND DIGITAL DATA PLOTS.

John W. Oglesbee (NASA, Lewis Research Center, Cleveland, Ohio).

Instrument Society of America, National Aerospace Instrumentation Symposium, 15th, Las Vegas, Nev., May 5-7, 1969, Paper. 16 p.

A commercially available high-speed printer has been modified to perform x-y plotting of digital data. The resulting device performs the dual function of printing and plotting at relatively low cost. The basic printing mechanism and its modification to a plotting device are described. A small digital computer is required as a control device, and the special software developed for this application is discussed. In the plotting mode, the device is capable of producing a typical (7" square) plot in less than 25 sec. Any number of points can be plotted in this time, with a resolution of 1 part in 500. Several variables can be plotted simultaneously using a different symbol for each variable. The plotter generates any one

of a number of different grid patterns, complete with titles, axes labels, and numerical scales. When not plotting, the device can be used as a 300 character per second printer. (Author)

A69-33745 *#
STUDY OF A GLOBAL SEARCH ALGORITHM FOR OPTIMAL CONTROL.
Elwood C. Stewart, William P. Kavanaugh, and David H. Brocker (NASA, Ames Research Center, Moffett Field, Calif.).
International Association for Analog Computation, Meeting, 5th, Lausanne, Switzerland, Aug. 28-Sept. 2, 1967, Paper. 25 p.; Discussion, O. W. Kolbe (Stuttgart, Technische Universität, Stuttgart, West Germany), p. 24. 8 refs.

Feasible method of implementing the maximum principle, based on an adaptive random search algorithm which utilizes direct measurements of the boundary cost-function hypersurfaces. No restrictions are placed on the continuity of the surfaces or the number of valleys. The adaption enhances convergence by varying the mean and variance of a probability distribution as a function of past performance. The algorithm has both local and global search properties so that "hanging up" in local valleys is avoided. A hybrid computer implementation of the algorithm is discussed. The usefulness of the algorithm is investigated experimentally for a fifth-order nonlinear minimum-fuel orbit-transfer problem. Convergence is generally obtained within several thousand iterations (1 to 2 min). Details are given on the manner in which the system iterates, typical solutions obtained for a wide range of situations, and the convergence properties of several variations of the basic algorithm. Cross sections through the boundary hypersurfaces reveal the striking irregularities which high-order systems can have and, hence, demonstrate the effectiveness of the adaptive random search approach in coping with them. (Author)

A69-35099 *#
THE IMPACT OF SPEECH COMMUNICATION WITH COMPUTER.
Wayne A. Lea (NASA, Electronics Research Center, Man-Computer Systems Branch, Cambridge, Mass.).
IN: SPACE, TECHNOLOGY, AND SOCIETY; CANAVERAL COUNCIL OF TECHNICAL SOCIETIES, SPACE CONGRESS, 6TH, COCOA BEACH, FLA., MARCH 17-19, 1969, PROCEEDINGS. VOLUME 1. [A69-35070 18-34]
Edited by L. E. Jones, III.
Cape Canaveral, Fla., Canaveral Council of Technical Societies, 1969, p. 15-19 to 15-31. 47 refs.

Discussion of the possibilities of speech communication with computers with regard to studies in a number of related fields such as acoustics, phonetics, linguistics, language learning, speech and hearing physiology, psychology, bionics, communication theory, human engineering, and computer science. It is noted that, among the several possible modalities of man-computer communication, speech is particularly promising, especially for manned space flight. The many specific advantages of speech justify a comprehensive program in automatic speech recognition and synthesis, segmentation and production of natural-flowing continuous speech, and development of relevant physiological and linguistic models. It is noted that mechanisms for aiding the deaf, blind, and other physically handicapped may result from efforts to mechanically analyze or synthesize speech. P. G.

A69-36265 *
THE IMP-I COMPUTER EXPERIMENT.
Rodger A. Cliff and Stephen Paull (NASA, Goddard Space Flight Center, Greenbelt, Md.).
IN: NTC 69; INSTITUTE OF ELECTRICAL AND ELECTRONICS ENGINEERS, NATIONAL TELEMETERING CONFERENCE, WASHINGTON, D.C., APRIL 22-24, 1969, RECORD. (A69-36237 19-07)
New York, Institute of Electrical and Electronics Engineers, Inc., 1969, p. 176-183.

The SDP-3 computer was designed to serve as the core of the data system of a small unmanned spacecraft. It is a 16-bit serial machine with 4096 words of memory. The computer will be flown as an engineering experiment on IMP 1. In this application, it will handle control and data compression for four scientific experiments. Interface between the computer and the experiments is accomplished by experiment interface packages which are located within the experiment package. These experiment packages are supplied to the experiment builder by the computer builder. The experiment interface packages are constructed from a line of standard interface modules, which in turn are built of the same ICs used in the SDP-3. An adaptive format consisting of data tagged with identification and word count is used for data transmission. (Author)

A69-37377
ONBOARD COMPUTERS ON ROCKETS AND SATELLITES; CENTRE NATIONAL D'ETUDES SPATIALES, INTERNATIONAL CONFERENCE, PARIS, FRANCE, DECEMBER 3-6, 1968, PROCEEDINGS (CALCULATEURS EMBARQUES SUR FUSEES ET SATELLITES; CENTRE NATIONAL D'ETUDES SPATIALES, COLLOQUE INTERNATIONAL, PARIS, FRANCE, DECEMBER 3-6, 1968, PROCEEDINGS).
Paris, Centre National d'Etudes Spatiales, 1969. 443 p. In French and English.
$14.

CONTENTS:

FOREWORD (AVANT-PROPOS), p. VII.

INTRODUCTION (INTRODUCTION). H. Felix (Centre Spatial de Toulouse, Toulouse, France), p. IX, X.

CRITERIA OF CHOICE (CRITERES DE CHOIX).

SPECIAL ARITHMETICAL TECHNIQUES AND ONBOARD COMPUTERS (TECHNIQUES ARITHMETIQUES SPECIALES ET CALCULATEURS EMBARQUES). J. Chinal (Paris, Université, Paris, France), p. 1-6. 13 refs. (See A69-37378 20-08)

TRENDS IN THE DESIGN OF AEROSPACE DIGITAL COMPUTERS. D. O. Baechler (Bellcomm, Inc., Washington, D.C.), p. 7-36.

SELECTION CRITERIA FOR THE DESIGN OF A COMPUTER CARRIED ON BOARD A SATELLITE AND FOR ITS PROGRAMMING LANGUAGE AS A FUNCTION OF SPECIAL REQUIREMENTS (CRITERES DE CHOIX DE L'ARCHITECTURE D'UN CALCULATEUR EMBARQUE SUR SATELLITE ET DE SON LANGAGE DE PROGAMMATION EN FONCTION DES BESOINS PARTICULIERS). Y. Gautier and A. B. Samoun (IBM France, S.A., Paris, France), p. 37-43. (See A69-37379 20-08)

"ASTRE"—A PROGRAMMING LANGUAGE DIRECTED TOWARD A BETTER UTILIZATION OF MEMORY (UN LANGAGE DE PROGRAMMATION ORIENTE VERS UNE MEILLEURE UTILISATION DE LA MEMOIRE—"ASTRE"). M. Ritout (Société d'Economie et de Mathématiques Appliquées, Paris, France), p. 45-54.

ANALOGIES AND DIFFERENCES BETWEEN COMPUTERS CARRIED ON MISSILES AND SATELLITES (ANALOGIES ET DIFFERENCES ENTRE CALCULATEURS EMBARQUES SUR LANCEURS ET SUR SATELLITES). G. Collot (Société pour l'Etude et la Réalisation d'Engins Balistiques, S.A., Puteuax, Hauts-de-Seine, France), p. 55-64. (See A69-37380 20-08)

DESIGN SELECTION CRITERIA FOR AN ONBOARD AIRCRAFT COMPUTER (CRITERES DE CHOIX DE L'ARCHITECTURE D'UN CALCULATEUR EMBARQUE SUR AVION). G. La Rosa (Délégation Ministérielle pour l'Armement, Paris, France), p. 65-68. (See A69-37381 20-08)

COMPOSITION AND DEFINITION OF A PROCESSING SYSTEM ON BOARD MISSILES—CHARACTERISTICS OF THE COMPUTER—EXAMPLES OF COMPUTERS (COMPOSITION ET DEFINITION D'UN SYSTEME DE TRAITEMENT EMBARQUE SUR ENGINS—CARACTERISTIQUES DU CALCULATEUR—EXEMPLES DE CALCULATEURS). A. Cote, M. Darchen, and Ch. Meraud (Société d'Applications Générales d'Electricité et de Mécanique, Paris, France), p. 69-79.

DESCRIPTION OF DEVELOPMENTS (DESCRIPTION DE REALISATIONS).

ROLE OF A COMPUTER IN AN ONBOARD PCM TELEMETRY SYSTEM (INTERET D'UN CALCULATEUR DANS UN SYSTEME DE TELEMESURE PCM EMBARQUE). M. Renaud (Société Intertechnique, Plaisir, Yvelines, France), p. 81-91. (See A69-37382 20-08)

ON BOARD PROCESSOR FOR DIGITAL FILTERING AND DATA COMPRESSION. V. Cappellini (Consiglio Nazionale delle Ricerche, Florence, Italy), p. 93-107. 9 refs. (See A69-37383 20-08)

ON-BOARD PROCESSOR. I—PHILOSOPHY, DESIGN AND OPERATION. R. M. Muller (NASA, Goddard Space Flight Center, Greenbelt, Md.), p. 109-118. 5 refs. (See A69-37384 20-08)

THE SDP-3—A COMPUTER DESIGNED FOR DATA SYSTEMS OF SMALL SCIENTIFIC SPACECRAFT. R. A. Cliff (NASA, Goddard Space Flight Center, Greenbelt, Md.), p. 119-137. (See A69-37385 20-08)

ON BOARD DATA PROCESSING SYSTEM FOR THE FIRST SWEDISH SATELLITE PROJECT. L. Lubeck (SOLNA, Sweden), p. 139-146. (See A69-37386 20-08)

DATA PROCESSOR FOR THE SWEDISH SATELLITE PROJECT. B. Jiewertz (SAAB Aktiebolag, Linköping, Sweden), p. 147-154. (See A69-37387 20-08)

USE OF AN ONBOARD COMPUTER FOR ACCOMPLISHING "PROJECT ROSEAU" EXPERIMENTS (UTILISATION D'UN CALCULATEUR EMBARQUE POUR LA REALISATION D'EXPERIENCES SCIENTIFIQUES—"PROJET ROSEAU"). G. Malleus (Centre National d'Etudes des Télécommunications, Issy-les-Moulineaux, Hauts-de-Seine, France), p. 155-159. (See A69-37388 20-08)

ONBOARD COMPUTER PROJECT ON THE ROSEAU SATELLITE (PROJET DE CALCULATEUR EMBARQUE SUR LE SATELLITE ROSEAU). H. Felix (Centre National d'Etudes Spatiales, Brétigny-sur-Orge, Essonne, France), p. 161-173. (See A69-37389 20-08)

AN OUTLINE OF THE FERRANTI DATA HANDLING SYSTEM PROPOSED BY THE SUD-AVIATION GROUP FOR PROJECT L.A.S. J. E. Remington, R. A. Williams, and R. E. Wright (Ferranti, Ltd., Bracknell, Berks., England), p. 175-218. (See A69-37390 20-08)

THE ELLIOTT MCS 920 M COMPUTER WITH PARTICULAR REFERENCE TO ITS APPLICATION TO THE INERTIAL GUIDANCE OF THE CECLES-ELDO LAUNCHER. A. H. Cairns (Elliott Space and Weapon Automation, Ltd., Camberley, Surrey, England), p. 219-233. (See A69-37391 20-08)

COMPUTERS FOR MISSILES—APPLICATIONS TO SATELLITES (CALCULATEURS POUR ENGINS—APPLICATIONS AUX SATELLITES). G. Yelloz (Laboratoire Central de Télécommunications, Paris, France), p. 235-254. (See A69-37392 20-08)

DISCRETE CONTROL SYSTEM SIMULATION METHOD FOR SPACECRAFT. L. N. Lupichev, Iu. K. Hodarev, and I. V. Shamanov (Akademiia Nauk SSSR, Moscow, USSR), p. 255-266. (See A69-37393 20-08)

DESIGN OF TESTS FOR SELF-DIAGNOSABLE CONTROL DIGITAL COMPUTERS. A. F. Volkov, V. A. Vedeshenkov, I. N. Vasil'ev, and V. A. Petrov, p. 267-282. 5 refs. (See A69-37394 20-08)

SIMULATION (SIMULATION).

SIMULATION OF A COMPUTER AND ITS ENVIRONMENT (SIMULATION D'UN CALCULATEUR ET DE SON ENVIRONNEMENT). J. Arnould (Société d'Etudes des Systèmes d'Automation, Paris, France), p. 283-296. (See A69-37395 20-08)

SIMULATION OF THE "ROSEAU" COMPUTER (SIMULATION DU CALCULATEUR "ROSEAU"). J. Cazemajou (Centre National d'Etudes Spatiales, Brétigny-sur-Orge, Essonne, France), p. 297-302. (See A69-37396 20-08)

ASSEMBLY LANGUAGE OF THE "ROSEAU" COMPUTER (LANGAGE ASSEMBLEUR DU CALCULATEUR "ROSEAU"). P. Charlemagne (Centre National d'Etudes Spatiales, Brétigny-sur-Orge, Essonne, France), p. 303-306. (See A69-37397 20-08)

COMPUTER SIMULATION OF AN ONBOARD NAVIGATION COMPUTER (SIMULATION SUR ORDINATEUR D'UN CALCULATEUR DE NAVIGATION EMBARQUE). M. T. Doucet (Société Crouzet, Valence, Drôme, France), p. 307-311. (See A69-37398 20-08)

FORMAL DESCRIPTION OF A HARDWARE-ORIENTED LANGUAGE—"CASSANDRA" (DESCRIPTION FORMELLE D'UN LANGAGE ORIENTE VERS LE HARDWARE—"CASSANDRE"). J. Mermet (Grenoble, Université, St-Martin-d'Hères, Isère, France), p. 313-353.

SYSTEM OF PROCESSING DESCRIPTIONS IN THE "CASSANDRA" LANGUAGE—APPLICATION TO SIMULATION (SYSTEME DE TRAITEMENT DES DESCRIPTIONS EN LANGAGE "CASSANDRE"—APPLICATION A LA SIMULATION). F. Anceau and P. Liddell (Grenoble, Université, St-Martin-d'Hères, Isère, France), p. 355-363.

RELIABILITY (FIABILITE).

RECONFIGURATION AND SELF-REPAIR OF ONBOARD SATELLITE COMPUTERS (RECONFIGURATION ET AUTO-DEPANNAGE DES CALCULATEURS EMBARQUES SUR SATELLITES). F. P. Maison (Electronique Marcel Dassault, S.A., Saint-Cloud, Hauts-de-Seine, France), p. 365-387. (See A69-37399 20-08)

THE PROBLEM OF THE FUNCTIONAL RELIABILITY OF ONBOARD COMPUTERS (LE PROBLEME DE LA FIABILITE FONCTIONNELLE DES CALCULATEURS EMBARQUES). J. P. Vedel (Electronique Marcel Dassault, S.A., Saint-Cloud, Hauts-de-Seine, France), p. 389-406. (See A69-37400 20-08)

ASSEMBLY TECHNIQUES FOR DIGITAL CIRCUITS (TECHNIQUES D'ASSEMBLAGE DE CIRCUITS DIGITAUX). P. Romand (Société Crouzet, Valence, Drôme, France), p. 407-412. (See A69-37401 20-08)

MEMORIES (MEMOIRES).

PERMANENT TOROIDAL MEMORY (MEMOIRE PERMANENTE A TORES). G. Mary (Société Crouzet, Valence, Drôme, France), p. 413-419. (See A69-37402 20-08)

STUDY AND DEVELOPMENT OF A WIRE-TYPE SPACE MEMORY (ETUDE ET REALISATION D'UNE MEMOIRE A FILS SPATIALE). G. Grunberg, G. Antier, L. Chabanas, I. Melnick, and G. Nicolas (Commissariat à l'Energie Atomique, Grenoble, France), p. 421-435. (See A69-37403 20-08)

A69-37384 *

ON-BOARD PROCESSOR. I—PHILOSOPHY, DESIGN AND OPERATION.

Ronald M. Muller (NASA, Goddard Space Flight Center, Greenbelt, Md.).

IN: ONBOARD COMPUTERS ON ROCKETS AND SATELLITES; CENTRE NATIONAL D'ETUDES SPATIALES, INTERNATIONAL CONFERENCE, PARIS, FRANCE, DECEMBER 3-6, 1968, PROCEEDINGS (CALCULATEURS EMBARQUES SUR FUSEES ET SATELLITES; CENTRE NATIONAL D'ETUDES SPATIALES, COLLOQUE INTERNATIONAL, PARIS, FRANCE, DECEMBER 3-6, 1968, PROCEEDINGS). (A69-37377 20-08)

Paris, Centre National d'Etudes Spatiales, 1969, p. 109-118. 5 refs.

Description of the basic design and principles of operation of an onboard spacecraft computer. Structured around a dual bussing system, the computer has a variable memory size up to a maximum of 65K words in 4096 word increments. It has a provision for the incorporation of standby redundant central processing units and input/output devices as needed for enhanced reliability during a long mission. A dynamic memory protection feature is implemented to ensure that writing occurs only in desired memory areas. Program control over interrupt priority is provided. The location of the binary point may also be specified in the program, and scaling is automatic. This provides some of the features of floating point without the hardware and memory penalties. V.P.M.

A69-37385 *

THE SDP-3—A COMPUTER DESIGNED FOR DATA SYSTEMS OF SMALL SCIENTIFIC SPACECRAFT.

Rodger A. Cliff (NASA, Goddard Space Flight Center, Spacecraft Technology Div., Flight Data Systems Branch, Greenbelt, Md.).

IN: UNBOARD COMPUTERS ON ROCKETS AND SATELLITES; CENTRE NATIONAL D'ETUDES SPATIALES, INTERNATIONAL CONFERENCE, PARIS, FRANCE, DECEMBER 3-6, 1968, PROCEEDINGS (CALCULATEURS EMBARQUES SUR FUSEES ET SATELLITES; CENTRE NATIONAL D'ETUDES SPATIALES, COLLOQUE INTERNATIONAL, PARIS, FRANCE, DECEMBER 3-6, 1968, PROCEEDINGS). (A69-37377 20-08)
Paris, Centre National d'Etudes Spatiales, 1969, p. 119-137.

Description of a general-purpose stored-program computer which has been designed for use as the core of the onboard data system of a small scientific spacecraft. It is a serial, two's complement, 16-bit-word machine. It has one level of indirect addressing and one hardware index register. To facilitate time-sharing operation, there is a 16-level priority interrupt system and a real time clock. The 4K memory is divided into 16 pages of 256 words each. There is a user and a monitor mode. Interpage access is prohibited in user mode. The computer has been simulated on an IBM 1800 computer. V.P.M.

A69-39604 •
PROGRAMMED TEST PATTERNS FOR MULTITERMINAL DEVICES.
Francis J. McIntosh and W. W. Happ (NASA, Cambridge, Mass.).
IN: AMERICAN FEDERATION OF INFORMATION PROCESSING SOCIETIES, SPRING JOINT COMPUTER CONFERENCE, BOSTON, MASS., MAY 14-16, 1969, PROCEEDINGS. VOLUME 34. (A69-39601 21-08)
Montvale, N.J., AFIPS Press, 1969, p. 229-240. 15 refs.

Development of a computer program for generating and listing the many distinct configurations of a multiterminal network or device, realizable through a suitable arrangement of the terminals or accessible test points. Combinatorial techniques are utilized to generate all the nonredundant subnetwork configurations derivable from an asymmetrical network or device. The prime advantage of the program lies in the fact that for large networks of seven or eight terminals, thousands of unique configurations can be realized which is not possible with hand enumeration. The program is applicable to testing and network analysis. V.P.M.

A69-39921 *
ON-BOARD SPACECRAFT PROCESSOR.
C. Trevathan, R. Hartenstein, M. Tharpe, J. Novello, and T. Taylor (NASA, Goddard Space Flight Center, Greenbelt, Md.).
Instruments and Control Systems, vol. 42, Aug. 1969, p. 63-66.

Description of an onboard processor (OBP) which is being developed to service individual sensors of a spacecraft. The system will be programmable from the ground, with high computational capacity, to maximize data reduction. Thus the vehicle may be launched with a single data format and, as characteristics of phenomena and behavior of instruments in orbit are ascertained, additional degrees of data processing can be implemented. The OBP will control sampling and formatting of telemetry data, provide storage, and process experiment, control, and other spacecraft signals. The memory will store instructions for action on command or after specified time intervals. M.M.

A69-40335 * #
CONCEPT OF AN INTERACTIVE SYSTEM AS AN EXPERIMENTER.
Leo C. Driscoll and Carl A. Kalinowski (NASA, Electronics Research Center, Computer Research Laboratory, Cambridge, Mass.).
American Institute of Aeronautics and Astronautics, Aerospace Computer Systems Conference, Los Angeles, Calif., Sept. 8-10, 1969, Paper 69-953. 7 p. 16 refs.
Members, $1.00; nonmembers, $1.50.

Discussion of some design implications of an interactive experimenter computer system both from software and hardware standpoints. Three major design areas are considered. In one approach, the astronaut/experimenter and the machine/experimenter play interchangeable roles of question answering. In another, the astronaut/experimenter and the machine/experimenter converse in terms of shared-inference that tend to make the experimental environment more transparent. In the third approach, the astronaut/experimenter and the machine/experimenter share an experimental context and mutual language of context that will enhance the selectivity of experiment design. P.G.

A69-40339 * #
CLASP, COMPUTER LANGUAGE FOR AERONAUTICS AND SPACE PROGRAMMING.
Raymond J. Rubey (Logicon, Inc., San Pedro, Calif.) and Edward H. Bersoff (NASA, Electronics Research Center, Cambridge, Mass.).
American Institute of Aeronautics and Astronautics, Aerospace Computer Systems Conference, Los Angeles, Calif., Sept. 8-10, 1969, Paper 69-957. 8 p.
Members, $1.00; nonmembers, $1.50.
Contract No. NAS 12-2005.

Description of the NASA computer language CLASP, whose development was coordinated with the evolution of SPL (Space Programming Language). CLASP's data declaration and arithmetic control features enable the coding of fixed-point calculations, while relieving the programmer of much of the burden of scaling determination. The programmer is also provided control over hardware operations and the type of optimization, while the compiler is given greater flexibility in meeting his specifications. B.H.

A69-40344 * #
MEMORY REDUCTION THROUGH HIGHER LEVEL LANGUAGE HARDWARE.
H. Kerner (NASA, Marshall Space Flight Center, Huntsville, Ala.) and L. Gellman (Computer Sciences Corp., Huntsville, Ala.).
American Institute of Aeronautics and Astronautics, Aerospace Computer Systems Conference, Los Angeles, Calif., Sept. 8-10, 1969, Paper 69-963. 12 p. 13 refs.
Members, $1.00; nonmembers, $1.50.

Evaluation of traditional assignment of computer functions to logic and memory on the basis of trends in their cost and mission characteristics. The higher information content of a higher-level language is exploited for the savings of memory. An instruction set was selected from the directly executable statements of FORTRAN, and the remaining statements were identified for compilation. Programs written in this language occupied 75 per cent less memory than those obtained by compilation. A computer for the execution of the selected FORTRAN statements was functionally designed in order to estimate the corresponding logic hardware effort. The tradeoff between costs saved through memory reduction and expenditures for the additional logic hardware considered development, manufacturing, power, and weight costs. The proposed concept shows a cost advantage for missions with a high weight penalty and large memory requirements. Another advantage is the higher execution speed inherent in this organization. (Author)

A69-40363 * #
RAE-A ATTITUDE DETERMINATION GROUND SUPPORT SYSTEM.
Philip J. Bonomo, William J. Budurka (International Business Machines Corp., Federal Systems Div., Federal Systems Center, Gaithersburg, Md.), and Roger D. Werking (NASA, Goddard Space Flight Center, Computations Div., Greenbelt, Md.).
American Institute of Aeronautics and Astronautics, Aerospace Computer Systems Conference, Los Angeles, Calif., Sept. 8-10, 1969, Paper 69-983. 15 p. 15 refs.
Members, $1.00; nonmembers, $1.50.
Contract No. NAS 5-10022.

Description of a disk-oriented programming system designed to support all attitude-dependent portions of the Radio Astronomy

Explorer-A (RAE-A) mission. RAE-A is a gravity-gradient stabilized spacecraft characterized by four 750-ft long experimental booms. Functions performed by the attitude support system, during both spin and despin mission phases, include: reduction and calibration of telemetry data; determination, prediction, and command of spacecraft attitude; simulation of data for test purposes; and system maintenance. Design constraints imposed by mission requirements, spacecraft sensors, and existing ground support equipment (computers and tracking stations) are discussed. Summary descriptions of major program modules are given, including descriptions of use and typical mission support performance. All significant attitude-related events that occurred during support of the RAE-A mission, including apogee motor ignition and real-time observation of total spacecraft attitude during boom deployment maneuvers, are discussed. (Author)

A69-41735 *
USE OF COMPUTERS AND PROGRAMMABLE TELEMETRY SYSTEMS ON SCIENTIFIC SATELLITES.
Paul Feinberg, Marvin Maxwell, and Joseph R. Silverman (NASA, Goddard Space Flight Center, Greenbelt, Md.).
IN: INTERNATIONAL FOUNDATION FOR TELEMETERING, INTERNATIONAL TELEMETERING CONFERENCE, WASHINGTON, D.C., SEPTEMBER 15-17, 1969, PROCEEDINGS. (A69-41734 23-07)
Woodland Hills, Calif., International Foundation for Telemetering (ITC Proceedings. Volume 5), 1969, p. 1-13.

Description of the major design features of programmable data handling and telemetry systems on scientific satellites. The characteristics of each system are described, and relative advantages and disadvantages are compared. Comments are made on specific potential problem areas such as system checkout, experiment and spacecraft integration, software, and ground data processing. The applications, capabilities, and the system and physical characteristics of each unit are tabulated. Z.W.

A69-41736 *
AN ON-BOARD PROCESSOR FOR OAO-C.
C. E. Trevathan, R. Hartenstein, and T. D. Taylor (NASA, Goddard Space Flight Center, Greenbelt, Md.).
IN: INTERNATIONAL FOUNDATION FOR TELEMETERING, INTERNATIONAL TELEMETERING CONFERENCE, WASHINGTON, D.C., SEPTEMBER 15-17, 1969, PROCEEDINGS. (A69-41734 23-07)
Woodland Hills, Calif., International Foundation for Telemetering (ITC Proceedings. Volume 5), 1969, p. 14-22. 5 refs.

Description of the design of a stored program computer for spacecraft use and its application on the fourth Orbiting Astronomical Observatory (OAO-C). The computer is a medium scale, parallel machine and has a memory capacity of 16,384 words of 18 bits each. It possesses a comprehensive instruction repertoire and operates on 45 W of power (including the dc to dc converter). The machine operates at a 667 KHz rate and executes an add instruction in 7.5 microseconds. The primary functions of this computer include auxiliary command storage, spacecraft monitoring and malfunction reporting, data compression and status summary, and emergency corrective action for certain anomalous situations. Z.W.

A69-41737 *
RECENT IMPROVEMENTS IN THE SDP-3 COMPUTER.
R. A. Cliff (NASA, Goddard Space Flight Center, Spacecraft Technology Div., Greenbelt, Md.).
IN: INTERNATIONAL FOUNDATION FOR TELEMETERING, INTERNATIONAL TELEMETERING CONFERENCE, WASHINGTON, D.C., SEPTEMBER 16-17, 1969, PROCEEDINGS. (A69-41734 23-07)
Woodland Hills, Calif., International Foundation for Telemetering (ITC Proceedings. Volume 5), 1969, p. 23-48. 5 refs.

Description of the SDP-3, a small serial computer which will be flown as an engineering experiment on the IMP-I spacecraft. In this application it will handle data acquisition for four of the scientific experiments. Modifications to the SDP-3 which improve its operation with little change in hardware complexity include: (1) permitting full-word indirect addressing in user mode for all instructions which do not modify the contents of memory, (2) extending output channel capability to cover all of memory, (3) a new subroutine linkage instruction, (4) a conditional skip on memory zero instruction, (5) byte-oriented instructions, and (6) improved index register manipulation instructions. The use of 8-bit MSI shift registers produces a significant hardware and power saving at the expense of deleting all left-shifting instructions. Further hardware savings are realized with a special multiplication instruction which allows the MQ (multiplier quotient) register to be deleted. As a result of these and other modifications the power dissipation of the SDP-3 has been decreased by 2/3 W and the number of ICs by 260, while in most respects operation has either been unchanged or improved. (Author)

A69-41739 *
A COMPLEMENTARY MOS SPACECRAFT DATA HANDLING SYSTEM.
Fred J. Link and Robert J. Lesniewski (NASA, Goddard Space Flight Center, Spacecraft Technology Div., Greenbelt, Md.).
IN: INTERNATIONAL FOUNDATION FOR TELEMETERING, INTERNATIONAL TELEMETERING CONFERENCE, WASHINGTON, D.C., SEPTEMBER 15-17, 1969, PROCEEDINGS. (A69-41734 23-07)
Woodland Hills, Calif., International Foundation for Telemetering (ITC Proceedings. Volume 5), 1969, p. 72-77.

Description of an on-board data handling system for a 1970 earth orbiting spacecraft, using medium scale integration, complementary MOS arrays. The organization can be divided into several distinct parts: a 512-word by 16-bit memory, a logarithmic data compressor, five rate counter/registers, an address switcher, and a control block. The system contains random access 64-bit memory arrays, 8-bit preset counters, and 8-bit parallel load shift registers. The smallest of these arrays contains over 200 active devices. The rest of the scheme is composed of multiinput NAND and NOR arrays, D type flip-flops, and seven-stage binary ripple counters. Z.W.

A69-41769 *
WHY DATA SYSTEM STANDARDS?
W. B. Poland, Jr., R. T. Fitzgerald, and R. J. Coates (NASA, Goddard Space Flight Center, Greenbelt, Md.).
IN: INTERNATIONAL FOUNDATION FOR TELEMETERING, INTERNATIONAL TELEMETERING CONFERENCE, WASHINGTON, D.C., SEPTEMBER 15-17, 1969, PROCEEDINGS. (A69-41734 23-07)
Woodland Hills, Calif., International Foundation for Telemetering (ITC Proceedings. Volume 5), 1969, p. 461-469.

Discussion of some ideas about data system standards which have been developed at the Goddard Space Flight Center (GSFC) of NASA over a period of about nine years, mainly as the result of experience gained in using the Space Tracking and Data Acquisition Network (STADAN), a collection of tracking, command, and telemetry stations for ground support of scientific satellites. As the purposes and uses of data system standards are often misunderstood, a description is given of the growth and current implementation of the working approach to standards at GSFC. This approach is conditioned by the operating environment and by a number of administrative decisions, which are discussed. The areas included in the existing GSFC standards and some of those planned for future coverage are described, and some considerations bearing on the feasibility of combining GSFC and other data systems are examined. O.H.

A69-42524 *
ALGORITHMS FOR TEST PATTERNS IN MULTITERMINAL DEVICES WITH SYMMETRY CONSTRAINTS.

W. W. Happ and A. S. Weitzenfeld (NASA, Electronics Research Center, Cambridge, Mass.).
IN: INSTITUTE OF ELECTRICAL AND ELECTRONICS ENGINEERS, INTERNATIONAL CONFERENCE ON COMMUNICATIONS, BOULDER, COLO., JUNE 9-11, 1969, CONFERENCE RECORD. (A69-42500 23-07)
New York, Institute of Electrical and Electronics Engineers, Inc. (IEEE ICC Conference Publications. Volume 5), 1969, p. 41-13 to 41-18. 14 refs.

Description of procedures developed to identify unique test patterns for multiterminal devices with specified symmetry. Combinatorial concepts and coding procedures are defined by examining in detail an illustrative example: the unique three-terminal two-ports which result from a four-terminal passive network with symmetry. Algorithms are developed to derive nonredundant one-ports from an N-terminal parent network with specified symmetry. Applications are examined in (1) failure diagnostics of microcircuits, (2) generation of useful network functions for multiterminal thin-film devices, (3) partitioning of large systems into smaller subsystems, and (4) modelling with preassigned accuracy. (Author)

A69-42621 *
CENTRAL DATA SYSTEM CONCEPTS FOR SPACECRAFT DATA MANAGEMENT.
Richard O. Fimmell (NASA, Ames Research Center, Data Systems Branch, Moffett Field, Calif.), Alexander Egger, and Louis M. Bello (TRW Systems Group, Electronic Data Systems Laboratory, Data Systems Electronics Dept., Redondo Beach, Calif.).
Telemetry Journal, vol. 4, Aug.-Sept. 1969, p. 63-72.

Discussion of the design concepts of a central data system (CDS) for more efficient, flexible data management, and description of its application in an advanced deep space solar probe. The design features high data sampling rates, programmable data processing, bulk data storage capability (for data sampled during periods of noncommunication), and standard experiment package/CDS interfaces. The basic system concept is based upon sampling each data point at a high rate in a fixed sequence and allowing a central processor to select, process, and format sampled data into a highly efficient format for transmission. The CDS is programmable so that data formulating and processing may be programmed via the command link to optimize data transmission for unexpected conditions. Preliminary design efforts have indicated that a CDS to process data from seven particle and fields experiments can be designed, using present state-of-the-art components, to weigh 16.5 lb and consume 5.4 W from the dc/dc converter. (Author)

N69-10098*# National Aeronautics and Space Administration. Lewis Research Center, Cleveland, Ohio.
COMPUTE—A TIME-SHARING DESK CALCULATOR PROGRAM
Paul Swigert Washington Nov. 1968 24 p
(NASA-TN-D-4917) Avail: CFSTI CSCL 09B

Introductory details are presented on the COMPUTE program, written primarily in FORTRAN 4, which operates under the IBM 360/67 Time-Sharing System (TSS). The program allows the TSS user to perform various numerical calculations without writing FORTRAN programs. The user may thus solve various numerical problems while at the TSS terminal by simply communicating with COMPUTE. It is anticipated that the user will obtain from this introduction the information necessary to begin using COMPUTE. More specific information about the capabilities of COMPUTE can be derived from the actual use of the program. This is possible because of numerous error, warning, and information messages generated by COMPUTE and printed at the terminal. Author

N69-10316*# Rensselaer Polytechnic Inst., Troy, N. Y.
ADAPTIVE SIMULATION USING MODE IDENTIFICATION
Rob Roy, C. H. Schley, and A. R. Axelrod Washington NASA Nov. 1968 70 p refs
(Grant NGR-33-018-014)
(NASA-CR-1179) Avail: CFSTI CSCL 12B

An input-output process model is formulated using only the process operating record: the processes considered have a finite settling time. As the structure of the process is not known, nonlinear and linear processes fall within the class of processes studied. Since the process parameters are not monitored, the overall cause-effect relationship of the model must change, based only on the on-line operating record of the process. The problems of process identification and pattern recognition are examined in relation to the procedures for assigning a given input pattern to a particular category. Methods for adaptive modal construction are described, and some results are presented on the application of the modal learning technique to both linear and nonlinear systems. Adaptive simulation by the method of potential functions is described, along with the method of realizing the algorithm. Aizerman's proof of the convergence of the algorithm for the two-category case is extended to R categories. M.G.J.

N69-11470*# Ohio State Univ., Columbus.
PREPROCESSING ELECTRONIC SATELLITE OBSERVATIONS
Joseph E. Gross, III Washington NASA Nov. 1968 200 p refs
(Contract NGR-36-008-093)
(NASA-CR-1183) Avail: CFSTI CSCL 09B

Detailed description of the preprocessing procedures currently used in the reduction of electronic data from geodetic satellites is presented. A general, non-technical description of the four major electronic satellite tracking methods currently used for geodetic purposes is also presented. Author

N69-13566*# National Aeronautics and Space Administration. Lewis Research Center, Cleveland, Ohio.
A SET OF 360 FORTRAN (LEVEL G OR H) SUBROUTINES FOR GENERATING PRINTED PLOTS
Lois T. Dellner Washington 1968 71 p refs
(NASA-TM-X-1700) Avail: CFSTI CSCL 09B

A set of subroutines, written in 360 FORTRAN IV (level G or H), easy for the FORTRAN programmer to use, provides printed plots as part of normal output. These subroutines are simplified so that no choices must be made and generalized so that choices may be made by the programmer of the plotting characters, the scales, the appearance of the grid, and other options. The FORTRAN routines generate ordinary output records (up to 132 characters) suitable for on- or off-line printing. Author

N69-16140*# Stanford Research Inst., Menlo Park, Calif.
HUMAN INTELLECT AUGMENTATION TECHNIQUES Final Report
D. C. Engelbart Washington NASA 1969 78 p refs
(Contract NAS1-5904)
(NASA-CR-1270) Avail: CFSTI CSCL 09B

A multiproject program that is exploring the value of computer aids to augmenting human intellectual capability is discussed. Outlined briefly are the background and the "bootstrapping" nature of the program (e.g., the report was produced with the experimental computer aids) and its status at the start of this project. Advances during the project were in the programming system (CRT on-line debugging, etc.),in both off-line and on-line computer-aided text-manipulation systems implemented on a CDC 3100, and in specifications, designs, and nearly completed implementation of a time-shared system on the SDS 940, which will be committed to serving 12 on-line CRT consoles for this program. Special features of the design included commercial-TV display consoles, special equipment to reduce CPU overhead to a few percent for servicing I/O, a new machine-oriented, systems programmer compiler language,

a compiler-compiler, and a Control Metalanguage Translator for compiling the interactive part of the on-line system from a special Control Metalanguage description. Author

N69-18954*# National Aeronautics and Space Administration. Lewis Research Center, Cleveland, Ohio.
A CONVERSATIONAL APPROACH TO MATRIX CALCULATIONS, CONCEPTS AND IMPLEMENTATION
R. Bruce Canright, Jr. Washington Feb. 1969 42 p refs
(NASA-TM-X-1749) Avail: CFSTI CSCL 09B

The conversational use of computers makes user-oriented languages desirable. A computer program was developed which enables users to do matrix calculations conversationally, without knowledge of computers or programming languages. The program converses in a brief command language, which provides for input/output, matrix arithmetic, forming of the transpose, inverse, determinant, and eigenvalues, and exponentiation. Details of the program language and logic are given, with a sample user program conversation. Technical details and FORTRAN program listings are also presented. Author

N69-21119*# National Aeronautics and Space Administration. Electronics Research Center, Cambridge, Mass.
APPLICATION OF A MODIFIED FAST FOURIER TRANSFORM TO CALCULATE HUMAN OPERATOR DESCRIBING FUNCTIONS
Richard S. Shirley Washington Mar. 1969 30 p refs
(NASA-TM-X-1762) Avail: CFSTI CSCL 09B

A modified fast Fourier transform (FFT) is used in a hybrid computer program to permit processing of tracking data during a run to yield the human operator's describing function almost immediately after the data-taking period. The computer processing time is substantially reduced at no cost in accuracy. Author

N69-21527*# System Development Corp., Santa Monica, Calif.
HAND-PRINTED INPUT FOR ON-LINE SYSTEMS
M. I. Bernstein and H. L. Howell Washington NASA Mar. 1969 114 p refs
(Contract NAS12-526)
(NASA-CR-1284) Avail: CFSTI CSCL 09B

This document describes a program for recognizing hand-printed information in real time, which provides on-line computer users with a means of inputting two-dimensional information as simply as writing with pen and paper. The program operates under the time-sharing system and uses a RAND Tablet for input and a CRT display for output. Each user of the program builds a unique character dictionary, based on samples of his own input characters. For each user, the program currently recognizes about 100 different characters, which are chosen from a larger alphabet by the individual user. This document describes how the recognition program interfaces with the time-sharing system; what functions the program performs in recognizing hand-drawn input; and how the character dictionary is constructed and tested. Author

N69-22935*# National Aeronautics and Space Administration. Electronics Research Center, Cambridge, Mass.
COMPUTER PROGRAM FOR DIMENSIONAL ANALYSIS
A. D. Sloan and W. W. Happ Washington Apr. 1969 31 p refs
(NASA-TN-D-5165) Avail: CFSTI CSCL 09B

In order to scale models of devices (ships, space capsules, integrated circuits, etc.) and phenomena (nuclear detonations, space-charge widening, sloshing in fuel tanks, etc.), it is necessary to determine nondimensional groupings of variables. A computer program establishes sets of invariant or nondimensional sets of variables and searches for an optimum set under specified optimization criteria. This Fortran IV program is based on algorithms of integer programming. Typical running times are 2 minutes for 10^4 sets of equations. Author

N69-23381*# Lockheed Missiles and Space Co., Palo Alto, Calif.
REMOTE INFORMATION RETRIEVAL FACILITY
Roger K. Summit Washington NASA Apr. 1969 48 p
(Contract NASw-1454)
(NASA-CR-1318; N-07-68-1) Avail: CFSTI CSCL 09B

A summary of work performed is given, including the installation of a remote terminal base at Ames Research Center, California, for the use of engineers and scientists in conducting on-line searches on the NASA collection of machine-readable document citations, and the later relocation of the terminal at NASA headquarters in Washington, D. C. The file conversion process is described, along with the system operation at each terminal. The DIALOG information retrieval language used and the computer environment within which the set of programs operates are discussed, with details on command language modifications and on the major hardware components of the IBM 360/30. A comparative analysis of system utilization during the two separate operational phases is presented, with reference to search characteristics and user reaction. Individual search summaries from the first phase are included. P.A.B.

N69-26193*# National Aeronautics and Space Administration. Goddard Space Flight Center, Greenbelt, Md.
PREPROCESSING OF MINITRACK DATA
Edward R. Watkins, Jr. Washington May 1969 24 p refs
(NASA-TN-D-5042) Avail: CFSTI CSCL 09B

The principles embodied in the Minitrack system are summarized for classification of the reduction process. The use of computers for tracking-data processing necessitates the transition of principles into algorithms; where applicable, the development of algorithms is included. The current procedures for preparing Minitrack data messages, and the current computer processing procedures, are presented with emphasis on a description of the IBM 360 computer program designed and developed on the basis of past experience with Minitrack data reduction. Author

N69-29478*# National Aeronautics and Space Administration. Goddard Space Flight Center, Greenbelt, Md.
A SPACECRAFT ANALOG-TO-DIGITAL CONVERSION SYSTEM EMPLOYING MOSFETS
Donald C. Lokerson Washington Jul 1969 29 p refs
(NASA-TN-D-5228) Avail: CFSTI CSCL 09B

The analog-to-digital conversion systems used in past Interplanetary Monitoring Platform spacecraft are reviewed to indicate why a new voltage-controlled oscillator is required and what characteristics are desirable for the new oscillator. Since the system developed employs metal oxide semiconductor field effect transistors (MOSFETS), this type of transistor is described. Analysis, design, and developmental innovations are described in detail for the system, which is composed of an analog commutator, a voltage-to-frequency oscillator, an internal voltage regulator, and a digital storage register. The system performance using special calibration equipment is described in detail for the operation over a nominal 0 to +5 volt input with a 5-millisecond sample time. The linearity is within ±0.5 percent of the 6-kHz to 46-kHz frequency range. Tests indicate long-term stability is about ±0.2 percent over a three-month period, whereas short-term stability is ±0.5 percent after warmup. The system described can be adapted to permit measurements at hundreds of megohms impedance. The time constants can be changed to allow a wide range of frequencies and sample times. Author

08 COMPUTERS

N69-29592*# National Aeronautics and Space Administration. Flight Research Center, Edwards, Calif.
A SIMPLE TECHNIQUE FOR AUTOMATIC COMPUTER EDITING OF BIODATA
Ram Swaroop, (Computing and Software, Inc., Greenbelt, Md.) Kenneth A. West, (Computing and Software, Inc., Greenbelt, Md.), and Charles E. Lewis, Jr. Washington Jul. 1969 20 p refs
(NASA-TN-D-5275) Avail: CFSTI CSCL 09B

Before any data are statistically analyzed, it is always necessary to edit the data to some extent. Furthermore, when large quantities of data are collected, the editing must be performed by automatic means. One common task in the editing process is the identification of observations which deviate markedly from the rest of the sample, commonly known as outliers. A simple statistical technique for identifying the outliers and the necessary computer program is presented. The program requires as input only the data set, sample size, and preselected levels of significance at which outliers are to be identified. It is assumed that the data set is a random sample of size larger than two from a normal population. Two examples are presented to illustrate applications of the described technique. Author

N69-30014*# National Aeronautics and Space Administration. Ames Research Center, Moffett Field, Calif.
A COMPILATION OF CURRENT COMPUTER PROGRAMS FOR LOW-THRUST TRAJECTORY ANALYSIS
Alfred C. Mascy Washington Jul. 1969 68 p
(NASA-TM-X-1824) Avail: CFSTI CSCL 09B

A catalog of brief descriptions of current low-thrust trajectory and mass computation programs is presented. All known sources were contacted, and questionnaires were sent to those who indicated that they possessed such codes. A total of 59 descriptions of computer programs pertinent to this discipline are compiled. They are capable of generating flyby and rendezvous trajectories with their associated mass computation. Included in the codes are those capable of variable thrust trajectory as well as constant thrust with coast trajectory calculations. No attempt is made to evaluate any computer code or in any way compare programs; rather, the descriptions of existing codes are presented. Further details concerning a particular program may be obtained from the organization shown on each description. Author

N69-32350*# Tennessee Univ., Tullahoma, Space Inst.
AN EXPERIMENTAL AND THEORETICAL INVESTIGATION OF STRIATIONS IN A He-Ne LASER
T. B. Carlson, F. M. Shofner, and C. W. Bray Washington NASA Jul. 1969 60 p refs
(Grants NGR-43-001-056; NSF GK-1638)
(NASA-CR-1387) Avail: CFSTI CSCL 20E

This investigation shows that striation oscillations in the He–Ne discharge occur over significant ranges of pressure and current with respect to the optimum values for maximum laser power. This instability, which is of the order of 500 KHz in frequency, effectively modulates the coherent light output of the He–Ne laser as well as the discharge tube voltage and current. A theoretical analysis has been modified to predict the striation frequency pressure and radius dependences for the single constituent gas. The experimental results for the He–Ne laser show good correlation with the functional dependence predicted. One practical design consideration is that striation effects can be minimized by using small diameter tubes which have characteristically higher striation frequencies and modulate the coherent output less effectively. Author

N69-32556*# National Aeronautics and Space Administration. Lewis Research Center, Cleveland, Ohio.
TAGGED ARITHMETIC
Paula J. Bettinger, Andrew M. Manos and Betty Jo Armstead Washington Aug. 1969 21 p
(NASA-TN-D-5370) Avail: CFSTI CSCL 09B

A special tagged arithmetic system has been developed for use with FORTRAN programs written to process experimental data. The tagged arithmetic system carries a condition code with every numerical value and uses a special output to call attention to answers computed by using questionable input data. The questionable input data may result from instrumentation or data recording system malfunctions, which can cause ill-conditioned calculations that result in process-time faults or error conditions. Author

N69-32685*# National Aeronautics and Space Administration. Lewis Research Center, Cleveland, Ohio.
IMPLEMENTATION AND STRUCTURE OF COMPUTE, A TIME-SHARING CALCULATOR PROGRAM
R. Bruce Canright, Jr. and Paul Swigert Washington Jul. 1969 91 p refs
(NASA-TN-D-5350) Avail: CFSTI CSCL 09B

The computer program, COMPUTE, written primarily in FORTRAN 4 and operating under the IBM 360/67 time-sharing system allows users to perform various numerical calculations solely by interacting with COMPUTE. This report gives details on the computer system, and outlines the structure of the computer program. This report is intended to serve as a guide for adapting and implementing COMPUTE. Complete source listings are included. Author

N69-35569*# National Aeronautics and Space Administration. Lewis Research Center, Cleveland, Ohio.
FORTRAN PROGRAM FOR MACHINE COMPUTATION OF GROUP TABLES OF FINITE GROUPS
Gabriel Allen, David D. Evans, and Paul Swigert Washington Sep. 1969 43 p refs
(NASA-TN-D-5402) Avail: CFSTI CSCL 09B

A FORTRAN program has been written for machine computation of group tables for finite groups. The use of the method depends on the fact that every finite group of order n is isomorphic to some subgroup of the symmetric group S_n. The procedure for using the program is as follows: After the proper isomorphism has been established, the appropriate elements of S_n are entered into the program as input data. The program computes and prints out the group table for these elements of S_n. Then the translation is made from the elements back to the original group elements. Two examples are shown. Author

N69-35613*# Wolf Research and Development Corp., Bladensburg, Md.
A SURVEY OF CURRENT DEBUGGING CONCEPTS
Wallace Kocher Washington NASA Aug. 1969 89 p refs
(Contract NAS5-9756-99)
(NASA-CR-1397) Avail: CFSTI CSCL 09B

The debugging of computer programs is analysed in terms of the localization and correction of errors. Current debugging concepts are presented with only logical and clerical errors considered. The computer program for the Interplanetary Monitoring Platform is documented with emphasis placed on the error diagnostic procedures. Proposals for developing software that will allow debugging to be conducted using the same language as the source program are included. F.O.S.

N69-35816*# Sperry Rand Corp., Huntsville, Ala. Space Support Div.
COMPUTER-AIDED FILTER DESIGN MANUAL
Sidney Gussow and Glenn Weathers Washington NASA 1969 106 p refs
(Contract NAS8-20055)

(NASA-SP-3049) Avail: CFSTI CSCL 09B

A computerized filter design procedure to provide a simplified and accurate method of design and synthesis for engineers having minimum experience in this area is described. It may also be utilized by experienced personnel to perform laborious and complex calculations. The procedure consists of selection, analysis and synthesis of electric wave filters for telemetry applications. Filter selection includes the use of charts to assist in rapid choice of a suitable configuration. Passive synthesis programs calculate the component circuit values required for the specific filter; use realization techniques for singly and doubly loaded networks, and assist the designer in tuning. Active synthesis is accomplished through active quadratic networks which are connected in cascade, and it is reported that the active design is not satisfactorily accurate for narrow bandwidth requirements or for a frequency much beyond 500 kHz. The analysis programs calculate filter response characteristics, including amplitude, phase, time delay, and group delay responses. A.C.R.

N69-36918*# National Aeronautics and Space Administration Lewis Research Center, Cleveland, Ohio.

HARDWARE (OR SOFTWARE) PROVISIONS FOR MULTIPLE PRECISION FLOATING-POINT ARITHMETIC

L. Richard Turner Washington Sep. 1969 9 p

(NASA-TM-X-1885) Avail: CFSTI CSCL 09B

A variant of floating-point arithmetic is described which permits the easy realization of indefinite precision within the framework of the floating-point arithmetic. The principal difference of this arithmetic involves the details of floating-point addition. It has been realized in hardware and also simulated. It is proposed that this feature be considered as an option or mode for future computers. Author

N69-38654*# National Aeronautics and Space Administration. Lewis Research Center, Cleveland, Ohio.

A DEVICE FOR PRODUCING BOTH HARD COPY ALPHANUMERIC LISTINGS AND DIGITAL DATA PLOTS

John W. Oglesbee Washington. Oct. 1969 25 p

(NASA-TN-D-5474; E-4863) Avail: CFSTI CSCL 09B

A high-speed printer was modified to perform the additional function of x−y plotting of digital data. The basic printing mechanism and its modification to a plotting device are discussed. A small digital computer was selected as a control device, and the special software developed for this application is described. In the plotting mode, the device is capable of producing a typical (7-in.-square) plot in about 25 seconds. The plot is constructed from a matrix of dots, with a resolution of 500 dots across the width of the plot. When not plotting, the device can be used as a 300-character-per-second printer. Author

09

ELECTRONIC EQUIPMENT

Includes electronic test equipment and maintainability; component parts, e.g., electron tubes, tunnel diodes, transistors; integrated circuitry; microminiaturization. For basic research see: 10 Electronics. For related information see also: 07 Communications and 21 Navigation.

A69-10193 *

DESIGN CONSIDERATIONS FOR AN INTEGRATED 1.8-GHZ PARAMETRIC AMPLIFIER.

P. Bura, Raymond Camisa, Wen Y. Pan, Shui Yuan (Radio Corporation of America, Advanced Communications Laboratory, West Windsor, N.J.), and Arthur Block (NASA, Goddard Space Flight Center, Greenbelt, Md.).

IEEE Journal of Solid-State Circuits, vol. SC-3, June 1968, p. 86-90.

Contract No. NAS 5-10558.

A hybrid-integrated parametric amplifier has been fabricated in a microstrip transmission-line configuration. General design considerations and their implementation in a microstrip medium are discussed. The amplifier exhibited a power gain of 10 dB and 50-MHz half-power bandwidth with a noise figure of 2.0 dB. It was pumped at X-band frequency and required only 10 mW of pump power. The integrated pump source consisted of the transistor oscillator and a varactor quadrupler stage. (Author)

A69-10564 *

A PASSIVE ISOLATING TRANSFORMER OF REPEATED POSITIVE OR NEGATIVE VOLTAGE PULSES.

Janis M. Niedra (NASA, Lewis Research Center, Cleveland, Ohio).

IEEE, Proceedings, vol. 56, Oct. 1968, p. 1754, 1755.

Description of a passive circuit which can transform the voltage, either up or down, of indefinitely repeated positive or negative pulses. The circuit is made of transistors, diodes, and magnetic cores and can provide direct current isolation between multiple loads and between a load and the source. M.G.

A69-11000 *

A STEPPING MOTOR DRIVE CIRCUIT USING MAGNETIC CORE LOGIC.

Joseph C. Thornwall (NASA, Goddard Space Flight Center, Greenbelt, Md.).

IEEE Transactions on Aerospace and Electronic Systems, vol. AES-4, Sept. 1968, p. 672-679.

Description of a new magnetic core circuit used to supply power in the proper phase and time sequence to a bidirectional stepping motor. This circuit will power a standard voltage stepping motor from a nonstandard voltage power supply and includes a means for maintaining a constant energy pulse excitation over a wide range of dc power supply input voltage, a means for supplying power to the winding of the motor on pairs of isolated conductors, and a means for conductively isolating the low-level logic circuits from the high-level power circuits. (Author)

A69-12328 *

THE ADMITTANCE OF A PARALLEL-PLATE WAVEGUIDE APERTURE ILLUMINATING A METAL SHEET.

J. Earl Jones, C. T. Swift (NASA, Langley Research Center, Hampton, Va.), L. L. Tsai, R. C. Rudduck, and W. D. Burnside (Ohio State University, ElectroScience Laboratory, Columbus, Ohio).

IEEE Transactions on Antennas and Propagation, vol. AP-16, Sept. 1968, p. 528-535. 20 refs.

Research sponsored by Ohio State University; Grants No. NsG-448; No. NGR-36-008-048.

The admittance of a parallel-plate waveguide aperture having an infinite flange and illuminating a metal sheet is determined by two separate methods: (1) wedge diffraction theory; and (2) an integral transform solution. Numerical computations obtained by either method are in excellent agreement and are verified experimentally. A Smith chart is employed to show that, for a given aperture width, the admittance locus coalesces about the half-space value as the metal sheet recedes to infinity. A strong interaction between the aperture and the metal sheet occurs for distances in the vicinity of integral multiples of one half-wavelength. The interaction becomes much more localized with respect to distance as the distance to the sheet is increased; however, the admittance is always infinite at these distances. (Author)

A69-16562 *

EFFECTS OF ELECTRIC FIELDS ON ANNEALING OF RADIATION DAMAGE IN MOSFET'S.

Vitaly Danchenko, Upendra D. Desai, Joseph M. Killiany (NASA, Goddard Space Flight Center, Greenbelt, Md.), and Sidney S. Brashears (Electro-Mechanical Research, Inc., College Park, Md.).

IEEE Transactions on Electron Devices, vol. ED-15, Oct. 1968, p. 751-756. 16 refs.

Radiation damage in p-channel MOS devices by 1.5 MeV electrons has been studied by thermal annealing in conjunction with electric fields between the metallic gate and the substrate. Both positive and negative gate biases retard the process of annealing. Annealing with negative gate bias reveals: (1) that during thermal annealing the majority of the electrons that recombine with the positive charge in the oxide originate from the conduction band of the silicon, and (2) that during irradiation a great number of ionized electrons that remain in the oxide do not recombine with the holes, but are trapped in weakly bound states. The effect of positive bias on annealing of radiation damage is obscured by the positive charge induced due to positive bias-temperature treatment alone. No effect of drain-to-source potential on annealing has been observed. (Author)

A69-17708 *#

AUTOMATIC DISTORTIONLESS CONTROL OF MAGNETIC FIELD MODULATION.

Russell J. Jirberg (NASA, Lewis Research Center, Cleveland, Ohio).

Review of Scientific Instruments, vol. 40, Jan. 1969, p. 173, 174.

Description of a design for maintaining magnetic field modulation at a desired level. A closed-loop mode of control is used. The system utilizes a light-sensitive resistor as one leg of an attenuator which adjusts the driving signal fed to the modulation amplifier. With appropriate control of the illumination incident upon the photocell, changes in core magnetization with field can be automatically compensated for. G.R.

A69-17773 *#

REFLECTIONS OF ELECTRON BEAMS IN THERMIONIC DIODES.

James F. Morris (NASA, Lewis Research Center, Cleveland, Ohio)

Journal of Applied Physics, vol. 39, Dec. 1968, p. 6099, 6100. 9 refs.

Discussion of plasma collisional effects on positive-ion sheaths at emitters and on net currents in cesium diodes. To represent possible current reductions by collisions, the discussion relies on a kinetic reflection coefficient (due to Baksht et al., 1967) for electron beams. Results of the study indicate that kinetic reflections appear to affect sheath structures and transport only trivially in cesium diodes. Hence calculations for positive-ion sheaths in thermionic converters require no corrections for plasma scattering of emitted electron beams back to the emitters. M.G.

A69-18420
MOGA 68; INTERNATIONAL CONFERENCE ON MICROWAVE AND OPTICAL GENERATION AND AMPLIFICATION, 7TH, HAMBURG, WEST GERMANY, SEPTEMBER 16-20, 1968, PROCEEDINGS [MOGA 68; INTERNATIONALE TAGUNG ÜBER ERZEUGUNG UND VERSTÄRKUNG VON SCHWINGUNGEN IM OPTISCHEN UND MIKROWELLENBEREICH, 7TH, HAMBURG, WEST GERMANY, SEPTEMBER 16-20, 1968, PROCEEDINGS].
Berlin, VDE-Verlag GmbH (Nachrichtentechnische Fachberichte. Volume 35), 1968. 814 p. In German, English, and French. $15.

CONTENTS:

AUTHOR INDEX [AUTORENVERZEICHNIS], p. X-XII.
INTRODUCTION [ZUR EINFÜHRUNG]. F. W. Gundlach, p. 1-3.

ELECTRONIC TUBES [ELEKTRONENRÖHREN].
THE USE OF ELECTRONIC TUBES IN SPACE FLIGHT [DIE ELEKTRONENRÖHRE IN DER RAUMFAHRT]. A. Prommer (Siemens AG, Munich, West Germany), p. 5-10. [See A69-18421 07-09]
LARGE SIGNAL THEORY OF AMPLITUDE AND PHASE NONLINEARITIES IN TRAVELING WAVE TUBES. S. O. Wallander (Chalmers University of Technology, Göteborg, Sweden), p. 11-15. [See A69-18422 07-09]
EFFICIENCY ENHANCEMENT OF TRAVELING WAVE TUBES BY VELOCITY RESYNCHRONIZATION. O. Sauseng (Hughes Aircraft Co., Torrance, Calif.), p. 16-29. [See A69-18423 07-09]
R-F DEFOCUSING IN HIGH-POWER TRAVELING-WAVE AMPLIFIERS. H. K. Detweiler (California Institute of Technology, Pasadena, Calif.) and J. E. Rowe (Michigan, University, Ann Arbor Mich.), p. 30-35. 5 refs. [See A69-18424 07-09]
DESIGN AND PERFORMANCE OF THE X-BAND 10-KW CW TRAVELING-WAVE TUBE. S. Nishida (Tokyo Shibaura Electric Co. Ltd., Kawasaki, Japan), p. 36-41. [See A69-18425 07-09]
A HIGH POWER CW RING-BAR TRAVELLING WAVE TUBE. M. O. Bryant and F. E. Wray (Ministry of Defence /Navy/, Harlow, Essex, England), p. 42-47.
POWER TRAVELING WAVE TUBES IN GROUND STATIONS FOR THE INTELSAT 3 SYSTEM [LEISTUNGSWANDERFELDROEHREN FUER BODENSTATIONEN FUER DAS INTELSAT-III-SYSTEM]. P. Meyerer and K. Pöbl (Siemens AG, Munich, West Germany), p. 48-54. [See A69-18426 07-09]
HIGH POWER TWT FOR SATELLITE COMMUNICATION. W. A. Harman, K. W. Slocum, and J. A. Ruetz (Varian Associates, Palo Alto, Calif.), p. 55-60. [See A69-18427 07-09]
COMPARISON OF DELAY LINES IN HIGH-POWER TRAVELING-WAVE TUBES [VERGLEICH VON VERZÖGERUNGSLEITUNGEN FÜR HOCHLEISTUNGSWANDERFELDRÖHREN]. F. Gross, K. Pöbl, and W. Veith (Siemens AG, Munich, West Germany), p. 61-66. [See A69-18428 07-09]
THE SYMMETRICAL ROD COUPLED CIRCUIT FOR HIGH POWER TRAVELLING WAVE TUBES. R. C. M. King (English Electric Valve Co., Ltd., Chelmsford, Essex, England), p. 67-73.
SUITABILITY OF RING- AND SLAT-TYPE DELAY LINES IN CONTACT-COOLED SYSTEMS FOR POWER TRAVELING-WAVE TUBES [EIGNUNG VON RING- UND STEG-VERZÖGERUNGSLEITUNGEN IN KONTAKTGEKÜHLTEN SYSTEMEN FÜR LEISTUNGS-WANDERFELDRÖHREN]. P. Malzahn (Telefunken AG, Ulm, West Germany), p. 74-79.
APPROXIMATE THEORY OF THE ROUND WIRE HELIX SLOW WAVE STRUCTURE. O. Nilsson (Chalmers University of Technology, Göteborg, Sweden), p. 80-85.
TL 4002 SATELLITE TRAVELING-WAVE TUBES FOR THE SYMPHONIE COMMUNICATION SATELLITE [DIE SATELLITEN-WANDERFELDRÖHRE TL 4002 FÜR DEN NACHRICHTENSATELLITEN "SYMPHONIE"]. J. Bretting, H. Pöchmüller, and H. Luksch (Telefunken AG, Konstanz, West Germany), p. 86-92. [See A69-18429 07-09]
AN ELECTROSTATICALLY FOCUSED BWO. A. M. Alekseenko (Ministry of Electronic Industry, Moscow, USSR), p. 93-98.
FREQUENCY- AND POWER-STABLE BACKWARD-WAVE OSCILLATORS AS ENERGY PUMPS FOR MOLECULAR AND PARAMETRIC AMPLIFIERS [FREQUENZ- UND LEISTUNGSSTABILE RÜCKWÄRTSWELLEN-OSZILLATOREN ALS ENERGIEPUMPEN FÜR MOLEKULAR- UND PARAMETRISCHE VERSTÄRKER]. F. Gross and F. Hanf (Siemens AG, Munich, West Germany), p. 99-104. [See A69-18430 07-09]
A 3-MM BACKWARD-WAVE TUBE WITH A WIDE TUNING RANGE [EINE 3 MM RÜCKWÄRTSWELLENRÖHRE MIT GROSSEM DURCHSTIMMBEREICH]. G. Bolz (Berlin, Technische Universität, Berlin, West Germany), p. 105-109.
CENTIPEDE TWYSTRON AMPLIFIERS AND TRAVELING WAVE TUBES FOR BROADBAND, HIGH-EFFICIENCY, SUPER-POWER AMPLIFICATION. T. Roumbanis (Varian Associates, Palo Alto, Calif.), p. 110-114.
NEW APPROACH IN THE DESIGN OF COUPLED-CAVITY EXTENDED-INTERACTION OUTPUT RESONATORS FOR KLYSTRON AMPLIFIERS. E. L. Lien (Varian Associates, San Carlos, Calif.), p. 115-120. [See A69-18431 07-09]
THE DOUBLE-GAP CATCHER, A MEANS FOR IMPROVING THE EFFICIENCY OF KLYSTRONS. J. R. Hechtel (Varian Associates, San Carlos, Calif.), p. 121-128. 11 refs. [See A69-18432 07-09]
HIGH-POWERED MICROWAVE INTERACTIONS IN A PULSED ELECTRON BEAM-PLASMA KLYSTRON. A. H. Beck, R. Tannenbaum, and T. P. R. Linnecar (Cambridge University, Cambridge, England), p. 129-134. [See A69-18433 07-09]
UHF HIGH POWER KLYSTRONS FOR DESY. P. Palluel, P. Aucouturier (Compagnie Générale de Télégraphie Sans Fil, Paris, France), and H. Musfeldt (Deutsches Elektronen-Synchrotron, Hamburg, West Germany), p. 135-139. [See A69-18434 07-09]
HIGH-PERVEANCE 80-KW KLYSTRON OPERATING IN THE S BAND [KLYSTRON 80 KW CRETE A HAUTE PERVEANCE FONCTIONNANT EN BANDE S]. G. Faillon (Thomson-Varian, Paris, France), p. 140-144.
KILOWATT CW KLYSTRON AMPLIFIERS AT Ku AND Ka BANDS. B. G. James and L. T. Zitelli (Varian Associates, Palo Alto, Calif.), p. 145-150.
NON-LINEAR BEHAVIOUR IN KLYSTRONS FOR U.H.F. TELEVISION. C. J. Edgecombe and R. Heppinstall (English Electric Valve Co., Ltd., Chelmsford, Essex, England), p. 151-156.
SIGNAL DISTURBANCES BY IONS, SLOW ELECTRONS, AND MULTIPACTOR CHARGES IN KLYSTRONS FOR TELEVISION [SIGNALSTÖRUNGEN DURCH IONEN, LANGSAME ELEKTRONEN UND MULTIPACTORENTLADUNGEN BEI UHF-FERNSEHKLYSTRONS]. H. Bohlen and V. Dubravec (Valvo GmbH, Hamburg, West Germany), p. 157-164.
A KLYSTRON FREQUENCY MULTIPLIER FOR SUBMILLIMETRE WAVES, GENERATING ITS OWN DRIVING POWER. B. B. van Iperen, W. Kuypers, and H. Tjassens (Philips' Gloeilampenfabrieken, Eindhoven, Netherlands), p. 165-171.
METHODS OF CONTROLLING REFLEX KLYSTRONS IN SHOCK AND VIBRATION - APPLICATION TO A 2-WATT X-BAND DRIVER TUBE [METHODES DE CONTROLE DES KLYSTRONS REFLEX EN CHOCS ET EN VIBRATIONS - APPLICATION A UN TUBE ENGIN 2 WATTS BANDE X]. J. G. Boissière (Thomson-Varian, Paris, France), p. 172-179.
INVESTIGATION OF SYNCHRONOUS-WAVE R-F TO D-C CONVERSION. R. W. Grow (Utah, University, Salt Lake City, Utah), C. C. Johnson (Washington, University, Seattle, Wash.), and D. C. Watson, p. 180-183.
GENERATION OF HOLLOW BEAMS WITH A CONSISTENT VELOCITY ALONG A LONGITUDINAL MAGNETIC FIELD [ÜBER DIE ERZEUGUNG VON HOHLSTRAHLEN MIT EINHEITLICHER LÄNGSGESCHWINDIGKEIT IM LONGITUDINALEN MAGNETISCHEN GLEICHFELD]. H. J. Linn, K. Pöschl, and W. Veith (Siemens AG, Munich, West Germany), p. 184-190.
COMPARISON OF THE RIGIDITY OF NONHOLLOW AND HOLLOW BEAMS [VERGLEICH DER STEIFHEIT VON VOLL- UND HOHLSTRAHLEN]. H. Seunik (Siemens AG, Munich, West Germany), p. 191-199.
PERIODIC ELECTROSTATIC FOCUSING OF HIGH-PERVEANCE ELECTRON BEAMS. H. L. Hartnagel (Sheffield, University, Stafford, England), p. 200-207.
TWO ASPECTS OF MAGNETIC BEAM FOCUSING. H. K. Kwan (Hong Kong, University, Hong Kong), F. J. Newland, and T. E. Swain (M-O Valve Co., Ltd., Wembley, England), p. 208-223.
QUASI-PERIODIC FOCUSING OF HIGH-POWER KLYSTRONS WITH PERMANENT MAGNETS [QUASIPERIODISCHE FOKUSSIERUNG VON HOCHLEISTUNGSKLYSTRONS MIT PERMANENTMAGNETEN]. V. Dubravec (Valvo GmbH, Hamburg, West

Germany), p. 224-234.

ELECTRON VELOCITY MEASUREMENT IN ANNULAR ELECTRON BEAMS. H. L. Nattrass and H. B. Gers (Natal, University, Natal, Republic of South Africa), p. 235-240.

PROBLEMS OF HIGH-VACUUM ELECTRICAL BREAKDOWNS PERTAINING TO HIGH-VOLTAGE MICROWAVE ELECTRON TUBES. S. A. Zusmanovskii, V. G. Karmazin, and A. L. Radionovskii (Ministry of Electronic Industry, Moscow, USSR), p. 241-247.

A BROADBAND-WAVEGUIDE WINDOW FOR HIGH POWER MICROWAVE TUBES. P. H. Cross (Ministry of Defence /Navy/, Harlow, Essex, England), p. 248-252. [See A69-18435 07-09]

SPIRALING ELECTRON BEAM INTERACTION WITH FAST WAVE CIRCUITS. P. R. McIsaac (Cornell University, Ithaca, N.Y.), p. 253-258. 8 refs. [See A69-18436 07-10]

AN EXPERIMENT IN THE PARALLEL OPERATION OF HIGH POWER MAGNETRONS. P. F. Lewis (English Electric Valve Co., Ltd., Chelmsford, Essex, England), p. 259-263.

IMPROVEMENT OF THE STABILITY OF C.W. MAGNETRONS AGAINST LOAD REFLECTIONS BY METHODS OUTSIDE THE TUBE. W. Golombek (Valvo GmbH, Hamburg, West Germany) and F. Timmermans (Philips' Gloeilampenfabrieken, Eindhoven, Netherlands), p. 264-274.

THE EFFECT OF GAS ATMOSPHERES ON THE SECONDARY EMISSION OF MAGNETRON CATHODES. C. E. Maloney and F. J. Weaver (English Electric Valve Co., Ltd., Chelmsford, Essex, England), p. 275-282.

THE CARPITRON - TRANSMITTER TUBE FOR SPACE TELECOMMUNICATIONS STATIONS [LE CARPITRON - TUBE EMETTEUR POUR STATIONS DE TELECOMMUNICATIONS SPATIALES]. Y. Peyrard (Compagnie Générale de Télégraphie Sans Fil, Paris, France), p. 283-287. [See A69-18437 07-09]

A NEW TYPE OF MAGNETRON AMPLIFIER [EIN NEUER MAGNETRON-VERSTÄRKERTYP]. I. V. Lebedev, O. V. Betskii, and V. G. Alybin (Moskovskii Energeticheskii Institut, Moscow, USSR), p. 288-293.

NONLINEAR SINGLE-CHARGE THEORY OF CROSSED-FIELD INTERACTION AND ITS APPLICATION TO CFA'S AND NOISE GENERATORS. J. M. Osepchuk (Raytheon Co., Waltham, Mass.), p. 294-302.

MEASUREMENTS ON A CONTROLLED DELAY CROSSED FIELD TUBE. G. Kantorowicz (Compagnie Générale de Télégraphie Sans Fil, Orsay, France), p. 303-307.

THE STABILITY OF THICK CROSSED FIELD BEAMS. G. Smol (M-O Valve Co., Ltd., Wembley, England), p. 308-313.

ELECTRON VELOCITY DISTRIBUTION IN QUASI BRILLOUIN FLOW. P. A. Lindsay (London, University, King's College, London, England), p. 314, 315.

BEAM INSTABILITY IN CROSSED FIELD AMPLIFIERS. A. Reddish, D. J. Smith, G. Smol, R. Tannenbaum, and D. W. Ward (M-O Valve Co., Ltd., Wembley, England), p. 316-321.

GROWTH PROCESSES AND INTER-LINE NOISE IN PULSED MAGNETRONS. B. Vyse and M. A. Hulley (M-O Valve Co., Ltd., Wembley, England), p. 322-326.

BEHAVIOR OF A PLANE SPACE-CHARGE DIODE WITH MAXWELLIAN VELOCITY DISTRIBUTION IN THE CASE OF OSCILLATIONS AND NOISE IN THE TRANSIT TIME REGION [DAS VERHALTEN DER EBENEN RAUMLADUNGSDIODE MIT MAXWELLSCHER GESCHWINDIGKEITSVERTEILUNG BEI WECHSEL- UND RAUSCHGRÖSSEN IM LAUFZEITGEBIET]. H. Hubert (Siemens AG, Erlangen, West Germany), p. 327-332.

HIGH-POWER NOISE SOURCES [SOURCES DE BRUIT A GRANDE PUISSANCE]. J. Arnaud (Bell Telephone Laboratories, Inc., Holmdel, N.J.), M. Progent, W. Sobotka, and L. Teyssier (Compagnie Générale de Télégraphie Sans Fil, Orsay, France), p. 333-336.

COMPARATIVE NOISE MEASUREMENTS IN KLYSTRON OSCILLATORS [VERGLEICHENDE RAUSCHMESSUNGEN AN OSZILLATORKLYSTRONS]. G. Feldmann and K. H. Rathsmann (Telefunken AG, Konstanz, West Germany), p. 337-341. 6 refs. [See A69-18438 07-09]

EQUIVALENT TWO-PORT OF A TRAVELING-WAVE TUBE AMPLIFIER [DAS ÄQUIVALENTE RAUSCHZWEITOR EINES WANDERFELDRÖHRENVERSTÄRKERS]. K. Fischer (Aachen, Technische Hochschule, Aachen, West Germany), p. 342-346.

ELECTRON BEAM NOISE REDUCTION THROUGH EXPLOITATION OF HIGH ENERGY-STORAGE SENSITIVITIES NEAR LIMITING PERVEANCE. J. C. Twombly (Colorado, University, Boulder, Colo.) and J. A. Valent (International Business Machines Corp., Boulder, Colo.), p. 347-354.

NON LINEAR EFFECTS IN PLASMA RESONANCES. Y. Archambault, G. Mourier, and P. Vesin (Compagnie Générale de Télégraphie Sans Fil, Orsay, France), p. 355-357.

A COUPLING SCHEME FOR BEAM-PLASMA AMPLIFIERS. A. Singh, K. C. Gupta, and G. Singh (Central Electronics Engineering Research Institute, Pilani, Rajasthan, India), p. 358-363.

PARAMETRIC AMPLIFICATION OF CYCLOTRON HARMONIC WAVES IN PLASMA. K. J. Harker and F. W. Crawford (Stanford University, Stanford, Calif.), p. 364-367. 6 refs. [See A69-18439 07-25]

THE CHARACTERISTICS OF BEAM-PLASMA DISCHARGE. Iu. G. Iaremenko, V. M. Deev, S. M. Eremin, K. I. Palatov, I. F. Kharchenko, and E. G. Shustin (Akademiia Nauk SSSR, Institut Radiotekhniki i Elektroniki, Moscow, USSR), p. 368-377.

SEMICONDUCTORS [HALBLEITER].

MICROWAVE SEMICONDUCTOR DEVICES. C. A. P. Foxell (Associated Semiconductor Manufacturers, Ltd., Wembley, Middx., England), p. 378-384. [See A69-18440 07-09]

MICROWAVE INTEGRATED CIRCUITS. H. Sobol and D. R. Carley (Radio Corporation of America, Somerville, N.J.), p. 385-387. [See A69-18441 07-09]

TRANSFERRED-ELECTRON OSCILLATORS AND AMPLIFIERS. B. G. Bosch (Telefunken AG, Ulm, West Germany), p. 388-400. 79 refs. [See A69-18442 07-09]

OBSERVATIONS OF CURRENT WAVEFORMS OF THE TRANSFERRED-ELECTRON OSCILLATORS. T. Ikoma, H. Toritsuka, and H. Yanai (Tokyo, University, Tokyo, Japan), p. 401-406. [See A69-18443 07-09]

HIGH POWER HYBRID MODE OSCILLATIONS IN GaAs. B. Jeppsson, P. Jeppesen, and L. F. Eastman (Cornell University; Cayuga Associates, Inc., Ithaca, N.Y.), p. 407-413. [See A69-18444 07-26]

PULSE POWER FROM LSA DEVICES AT CENTIMETER THROUGH MILLIMETER WAVELENGTHS. W. K. Kennedy, Jr., B. Jeppsson, and L. F. Eastman (Cayuga Associates, Inc., Ithaca, N.Y.), p. 414-418. [See A69-18445 07-09]

THE EFFECT OF INHOMOGENEITIES ON LIMITED SPACE-CHARGE ACCUMULATION (L.S.A.) IN N-TYPE GALLIUM ARSENIDE. G. A. Acket (Philips' Gloeilampenfabrieken, Eindhoven, Netherlands), p. 419-422. 6 refs. [See A69-18446 07-26]

AN EXPERIMENTAL STUDY OF HIGH PEAK POWER GUNN EFFECT OSCILLATORS. J. S. Heeks, H. K. Au, and A. D. Woode (International Telephone and Telegraph Corp., Harlow, Essex, England), p. 423-428. [See A69-18447 07-09]

STABLE NEGATIVE R-F CONDUCTANCE AND OSCILLATION CONDITIONS IN GaAs. W. R. Curtice (Michigan, University, Ann Arbor, Mich.), p. 429-435. 6 refs. [See A69-18448 07-26]

COMPUTER MODEL OF THE GUNN DIODE. D. P. Dizhur, M. E. Levinstein, D. N. Nasledov, M. S. Shur, and A. F. Ioffe (Akademiia Nauk SSSR, Fiziko-Tekhnicheskii Institut, Leningrad, USSR), p. 436-439. [See A69-18449 07-09]

A CONTRIBUTION TO THE EXPLANATION OF THE GUNN DIODE SUB-THRESHOLD BEHAVIOUR. J. Pokorný (Československá Akademie Věd, Prague, Czechoslovakia), p. 441-446. 10 refs. [See A69-18450 07-09]

SOLUTION REGROWTH EPITAXIAL GALLIUM ARSENIDE FOR GUNN, HYBRID AND LSA DEVICES. S. I. Long, B. Jeppsson, and E. Johnson (Cornell University, Ithaca, N.Y.), p. 447-453. 10 refs. [See A69-18451 07-26]

MICROWAVE OSCILLATION AND AMPLIFICATION IN A LONG BULK GaAs WITH $BaTiO_3$ SHEETS ON THE SURFACE. S. Kataoka, H. Tateno, M. Kawashima, and Y. Komamiya (Ministry of International Trade and Industries, Tokyo, Japan), p. 454-460. [See A69-18452 07-26]

MICROWAVE LOGIC WITH GUNN DIODES. H. L. Hartnagel (Sheffield, University, Sheffield, England), p. 461-466. 8 refs. [See A69-18453 07-09]

FRANZ-KELDYSH EFFECT IN GUNN DOMAINS AND RELATED PHENOMENA. P. Guetin (Radiotechnique-Compelec, Suresnes, Hauts-de-Seine, France), p. 467-469. 6 refs. [See A69-18454 07-26]

A MICROSTRIP CIRCUIT MODULE FOR THE GUNN OSCILLATOR. M. P. Wasse, A. Pearson, and G. King (International

Telephone and Telegraph Corp., Harlow, Essex, England), p. 470-474.

MAGNETICALLY TUNABLE GUNN OSCILLATORS USING A YIG SPHERE. J. Magarshack and R. Spitalnik (Radiotechnique-Compelec, Suresnes, Hauts-de-Seine, France), p. 475-478.

A MECHANICALLY AND ELECTRONICALLY TUNABLE RESONATOR FOR DRIVING IMPATT AND GUNN DIODES [EIN MECHANISCH UND ELEKTRONISCH ABSTIMMBARER RESONATOR ZUM BETRIEB VON IMPATT- UND GUNN-DIODEN]. P. Olfs (Siemens AG, Munich, West Germany), p. 479-482. [See A69-18455 07-09]

IMPEDANCE RELATIONS IN A DIODE WAVEGUIDE MOUNT. B. B. van Iperen (Philips' Gloeilampenfabrieken, Eindhoven, Netherlands), p. 483-486.

DETAILED ANALYSIS OF A TEM TRANSMISSION-LINE RESONATOR FOR SOLID STATE MICROWAVE OSCILLATOR APPLICATION. R. Engelmann and H. Pollmann (Telefunken AG, Ulm, West Germany), p. 487-492.

TRANSISTORIZED MICROWAVE POWER OSCILLATORS WITH ELECTRONIC WIDEBAND TUNING [TRANSISTORIERTE MIKROWELLEN-LEISTUNGSOSZILLATOREN MIT ELEKTRONISCHER BREITBAND-DURCHSTIMMUNG]. H.-N. Toussaint (Siemens AG, Munich, West Germany), p. 493-495.

WIDEBAND TUNABLE TRANSISTORIZED FUNDAMENTAL-WAVE AND HARMONIC OSCILLATORS FROM 1 TO 4 GHZ [BREITBANDIG DURCHSTIMMBARE TRANSISTOR-GRUND- UND OBERWELLENOSZILLATOREN VON 1 BIS 4 GHZ]. J. Gier (Siemens AG, Munich, West Germany), p. 496-499.

SUPPRESSION OF FREQUENCY NOISE IN TRANSISTORIZED OSCILLATORS BY INJECTION SYNCHRONIZATION [UNTERDRÜCKUNG DES FREQUENZRAUSCHENS IN TRANSISTOROSZILLATOREN DURCH INJEKTIONSSYNCHRONISIERUNG]. W. E. Heinlein and C. J. Müller (Siemens AG, Munich, West Germany), p. 500-506.

RECENT DEVELOPMENTS ON AVALANCHE DIODE OSCILLATORS. B. Hoefflinger (Cornell University, Ithaca, N.Y.), p. 507-519. 24 refs. [See A69-18456 07-09]

HIGH CURRENT DENSITY OPERATION AND ANALYSIS OF AVALANCHE TRANSIT-TIME DIODES. C. P. Snapp and B. Hoefflinger (Cornell University, Ithaca, N.Y.), p. 520-529. 7 refs. [See A69-18457 07-09]

LARGE-SIGNAL ANALYSIS OF AVALANCHE-DIODE OSCILLATORS. P. T. Greiling and G. I. Haddad (Michigan, University, Ann Arbor, Mich.), p. 530-534. [See A69-18458 07-09]

THERMALLY INDUCED FREQUENCY VARIATIONS DURING AN OSCILLATION PULSE IN AVALANCHE TRANSIT-TIME DIODES [THERMISCH BEDINGTE FREQUENZVARIATION WÄHREND DES SCHWINGUNGSIMPULSES BEI LAWINEN-LAUFZEITDIODEN]. C. Wünsche (Siemens AG, Munich, West Germany), p. 535-539. 6 refs. [See A69-18459 07-09]

EXAMINATION OF BULK SEMICONDUCTOR DEVICES IN THE TIME-RESOLVED SCANNING ELECTRON MICROSCOPE. G. Y. Robinson, R. M. White, and N. C. MacDonald (California, University, Berkeley, Calif.), p. 540-542.

MICROWAVE AMPLIFIER WITH SEMICONDUCTORS [MIKROWELLEN-VERSTÄRKER MIT HALBLEITERN]. K. Garbrecht (Siemens AG, Munich, West Germany), p. 543-557.

HELIUM-COOLED PARAMETRIC AMPLIFIER FOR SATELLITE GROUND STATIONS WITH 500 MHZ BANDWIDTH. H. Brüntrup, U. Scherner, and D. Roth (Siemens AG, Munich, West Germany), p. 558-560. [See A69-18460 07-09]

1,4 GHZ PARAMETRIC AMPLIFIER WITH CLOSED-CYCLE COOLING FOR RADIO ASTRONOMY. E. Schuegraf and D. Roth (Siemens AG, Munich, West Germany), p. 561-563. [See A69-18461 07-09]

A LOW NOISE WIDEBAND PARAMETRIC AMPLIFIER FOR SATELLITE COMMUNICATIONS. C. S. Aitchison, E. L. Hentley, S. R. Longley, and J. C. Williams (Mullard, Ltd., Redhill, Surrey, England), p. 564-569. [See A69-18462 07-09]

WIDEBAND UNCOOLED PARAMETRIC AMPLIFIERS WITH VERY LOW NOISE TEMPERATURE [AMPLIFICATEURS PARAMETRIQUES LARGE BANDE NON REFROIDIS A TRES BASSE TEMPERATURE DE BRUIT]. P. Boutelant (Compagnie Générale d'Electricité de Paris, Marcoussis, Essonne, France), p. 570-576. [See A69-18463 07-09]

TRANSISTORIZED AMPLIFIER FOR INPUT STAGES IN THE RANGE FROM 2 TO 3 GHZ [TRANSISTORVERSTÄRKER FÜR EINGANGSSTUFEN IM BEREICH VON 2 BIS 3 GHZ]. H. Bogatzky (Siemens AG, Munich, West Germany), p. 577-583.

TUNNEL DIODE AMPLIFIERS FOR COMMUNICATION SATELLITES IN THE 5.5 TO 6.5-GHZ RANGE [TUNNELDIODENVERSTÄRKER FÜR NACHRICHTENSATELLITEN IM BEREICH VON 5,5 - 6,5 GHZ]. M. Niemeyer (Siemens AG, Munich, West Germany), p. 584-589. [See A69-18464 07-09]

HYSTERESIS LOSSES IN FREQUENCY MULTIPLIERS WITH STORAGE DIODE [HYSTERESEVERLUSTE BEI FREQUENZVERVIELFACHERN MIT SPEICHERDIODE]. K. Schünemann (Braunschweig, Technische Universität, Braunschweig, West Germany), p. 590-593.

VARACTOR-LOADED LADDER LINES. V. K. Tripathi (Oklahoma, University, Norman, Okla.) and G. I. Haddad (Michigan, University, Ann Arbor, Mich.), p. 594-599.

MAGNETO-PLASMA WAVES IN SEMICONDUCTORS. H. Pötzl (Wien, Technische Hochschule, Vienna, Austria), p. 600-607. 24 refs. [See A69-18465 07-26]

ACOUSTIC AMPLIFICATION AT MICROWAVE FREQUENCIES IN PIEZOELECTRIC SEMICONDUCTORS. C. W. Turner (California, University, Berkeley, Calif.), p. 608-611.

MICROWAVE EMISSION FROM InSb AVALANCHE PLASMA UNDER A MAGNETIC FIELD. S. Kataoka and M. Tacano (Ministry of International Trade and Industries, Tokyo, Japan), p. 612-617. 9 refs. [See A69-18466 07-26]

NONISOTHERMAL WAVE PROPAGATION AND INSTABILITIES IN INDIUM ANTIMONIDE. J. E. Rowe (Michigan, University, Ann Arbor, Mich.) and J. E. King (Royal Institute of Technology, Stockholm, Sweden), p. 618-621. 5 refs. [See A69-18467 07-26]

MAGNETO-ACOUSTIC AMPLIFICATION IN InSb. C. Hammar and P. Weissglas (Royal Institute of Technology, Stockholm, Sweden), p. 622-627.

INTERPRETATION OF THE MICROWAVE EMISSION OF n-InSb. W. Harth and R. Jaenicke (München, Technische Hochschule, Munich, West Germany), p. 628-632.

INTERACTION OF SPIN WAVES WITH ELECTRONS. B. Schneider and H. J. Schmitt (Deutsche Philips GmbH, Hamburg, West Germany), p. 633-636.

A STABLE, 100 MW, Q-BAND SOLID STATE SOURCE. C. S. Aitchison, C. D. Corbey, S. R. Longley, A. R. Lusted, and B. H. Newton (Mullard, Ltd., Redhill, Surrey, England), p. 637-644.

QUANTUM ELECTRONICS [QUANTENELEKTRONIK].

SOME TRENDS IN QUANTUM ELECTRONICS. M. Bernard (Centre National d'Etudes des Télécommunications, Issy-les-Moulineaux, Hauts-de-Seine, France), p. 645-655. 39 refs. [See A69-18468 07-16]

NEAR INFRARED PARAMETRIC DEVICES USING LITHIUM NIOBATE. M. J. Colles, R. C. Smith, and C. R. Stanley (Southampton, University, Southampton, England), p. 656-662.

EFFICIENT FREQUENCY DOUBLING WITH A HIGH REPETITION RATE YAG - ND-GIANT PULSE LASER. U. Deserno and G. Zeidler (Siemens AG, Munich, West Germany), p. 663-666. [See A69-18469 07-16]

RESONANT EMISSION OF DIFFERENCE FREQUENCY DUE TO OPTICAL MIXING IN ACTIVE QUANTUM SYSTEM UNDER LASER OSCILLATION. H. Inaba and T. Hidaka (Tohoku University, Sendai, Japan), p. 667-672. 8 refs. [See A69-18470 07-16]

OFF-RESONANCE FREQUENCY DOUBLING USING RUBY. D. Roth and G. Schollmeier (Siemens AG, Munich, West Germany), p. 673-676. [See A69-18471 07-16]

SIGNAL CONVERSION BY MULTIPLE MODULATION IN OPTICAL COMMUNICATION SYSTEMS. G. Schiffner, W. Leeb, and H. Kindl (Wien, Technische Hochschule, Vienna, Austria), p. 677-682. 5 refs. [See A69-18472 07-07]

EXPERIMENTAL STUDIES OF A WEAKLY ANISOTROPIC GAS LASER. W. M. Doyle and M. B. White (Philco-Ford Corp., Newport Beach, Calif.), p. 683-688. 5 refs. [See A69-18473 07-16]

CONSIDERATION ON THE LONG LIFE OF GAS LASERS. M. Miya (Nippon Electric Co., Ltd., Kawasaki, Japan), p. 689-694. [See A69-18474 07-16]

STABILIZED SINGLE-MODE IONIZED ARGON LASER [LASER ARGON IONISE A MODE UNIQUE, STABILISE]. P. Martinot-Lagarde and C. Coumes (Compagnie Générale de Télégraphie Sans Fil, Levallois, France), p. 695-702. [See A69-18475 07-16]

ATTEMPTS TO INCREASE THE POWER OF A CLOSED CO_2 LASER BY SPINNING THE FILLING GAS [VERSUCHE ZUR

LEISTUNGSSTEIGERUNG EINES ABGESCHLOSSENEN CO_2-LASERS DURCH UMWÄLZEN DES FÜLLGASES]. E. Klement and D. Rosenberger (Siemens AG, Munich, West Germany), p. 703-708. [See A69-18476 07-16]

SYNTHESIS OF TRAVELLING-WAVE MICROWAVE AND OPTICAL RESONATORS. J. R. Fontana (California, University, Santa Barbara, Calif.), p. 709-717. [See A69-18477 07-16]

OPTIMALLY DESIGNED RESONANCE MODULATORS IN THE MICROWAVE REGION [OPTIMAL *DIMENSIONIERTE RESONANZ*-MODULATOREN IM MIKROWELLENBEREICH]. B. Hill and G. Wencker (Aachen, Technische Hochschule, Aachen, West Germany), p. 718-723.

MOLECULAR INTERACTIONS IN THE AMMONIA MASER [INTERACTIONS MOLECULAIRES DANS LA MASER A AMMONIAC]. G. Descornet (Bruxelles, Université Libre, Brussels, Belgium), p. 724-738. 11 refs. [See A69-18478 07-16]

SIDEBAND AMPLIFICATION AT 258 GHZ USING A SATURATED GAS RESONANCE. H. J. Liebe (ESSA, Boulder, Colo.) and B. Senitzky (Brooklyn, Polytechnic Institute, Farmingdale, N.Y.), p. 739-744. 10 refs. [See A69-18479 07-16]

OPTICALLY PUMPED MILLIMETER WAVE MASER. J. C. Clark (EG&G, Inc., Goleta, Calif.) and R. W. Grow (Utah, University, Salt Lake City, Utah), p. 745-749. 5 refs. [See A69-18480 07-16]

FREQUENCY TRANSFORMATION IN MULTI-LEVEL QUANTUM SYSTEMS. E. G. Soloviev, A. V. Startsev, and K. K. Pukhov, p. 750-753. [See A69-18481 07-16]

THEORY AND DESIGN OF SUBMILLIMETER-WAVE GAS LASERS FOR WAVELENGTHS BETWEEN 0.1 AND 0.774 MM [THEORIE UND KONSTRUKTION VON SUBMILLIMETERWELLEN-GASLASERN *FUER WELLENLAENGEN ZWISCHEN* 0,1 MM UND 0,774 MM]. F. Kneubühl (Eidgenössische Technische Hochschule, Zurich, Switzerland), p. 754-756.

METHODS FOR THE MEASUREMENT OF FREQUENCY AND STABILITY OF LASER GENERATORS IN THE INFRARED. L. Frenkel (NASA, Electronics Research Center, Cambridge, Mass.) and M. A. Pollack (Bell Telephone Laboratories, Inc., Holmdel, N.J.), p. 757-763. 12 refs. [See A69-18482 07-16]

DESIRED LASER CHARACTERISTICS FOR SPACE COMMUNICATIONS. M. Ross (McDonnell Douglas Corp., St. Louis, Mo.), p. 764-769. 5 refs. [See A69-18483 07-16]

He-Ne LASER FOR OPTICAL CORRECTION AND GUIDE-BEAM TECHNIQUES [He-Ne LASER FÜR OPTISCHE JUSTIER- UND LEITSTRAHLVERFAHREN]. O. Hintringer (Siemens AG, Munich, West Germany), p. 770-776. [See A69-18484 07-16]

DIAGNOSTIC OF PLASMAS USING LASER BEAMS. A. R. M. Rashad (South Florida, University, Tampa, Fla.), p. 777-781. 6 refs. [See A69-18485 07-14]

FLUORESCENCE METHOD OF DETERMINING OF LASER PARAMETERS. V. R. Belan, V. V. Grigoriants, and M. E. Zhabotinski (Akademiia Nauk SSSR, Institut Radiotekhniki i Elektroniki, Moscow, USSR), p. 782-786.

PRODUCTION OF A GIANT PULSE BY COHERENT PUMPING [PRODUCTION D'UNE IMPULSION GEANTE A L'AIDE D'UN POMPAGE COHERENT]. G. Briquet, J. M. Jego, and J. Kerdiles (Commissariat à l'Energie Atomique, Paris, France), p. 787-790. [See A69-18486 07-16]

TANDEM AMPLIFIER SYSTEM OF GLASS AND $SeOCl_2$ LIQUID LASERS DOPED WITH NEODYMIUM. C. Yamanaka, T. Yamanaka, G. Yamaguchi, T. Sasaki, and S. Nakai (Osaka University, Osaka, Japan), p. 791-796. 5 refs. [See A69-18487 07-16]

SYNCHRONISATION OF TWO Q-SWITCHED SOLID STATE LASERS. G. Chartier and A. Koster (Paris, Université, Orsay, Essonne, France), p. 797-802. 5 refs. [See A69-18488 07-16]

A69-18905 *#

PHOTOSENSITIVE BARIUM TITANATE SCHOTTKY DIODES.
David E. Sawyer (NASA, Electronics Research Center, Component Technology Laboratory, Cambridge, Mass.).
Applied Physics Letters, vol. 13, Dec. 1, 1968, p. 392, 393. 5 refs.

Observation of photocurrents generated in Schottky barrier diodes on Remeika-grown reduced barium titanate. Photon-to-electron conversion efficiencies of 5% at 0.3μ are measured, suggesting that the effect may be large enough for employment in practical devices. P.v.T.

A69-19120 *

PERFORMANCE CHARACTERISTICS AND SPECIFICATION OF PCM BIT SYNCHRONIZER/SIGNAL CONDITIONERS.
B. Peavey (NASA, Goddard Space Flight Center, Greenbelt, Md.).
IN: INTERNATIONAL TELEMETERING CONFERENCE, LOS ANGELES, CALIF., OCTOBER 8-11, 1968, PROCEEDINGS. [A69-19092 07-07]
Conference sponsored by the International Foundation for Telemetering.
Tarzana, Calif., International Foundation for Telemetering (ITC Proceedings. Volume 4), 1968, p. 407-419. 5 refs.

Discussion of the test data obtained on synchronizers used at the Goddard Space Flight Center and its satellite tracking and data acquisition network stations. The test data indicate that there is no single synchronizer excelling in all respects. It is shown that bit error rate alone does not wholly characterize the synchronizers, particularly when operating with low (less than 7 dB) SNRs plus jitter. Definitions of performance parameters which would uniformly and unambiguously describe and specify synchronizers are suggested and discussed. Z.W.

A69-19582 *

X-RAY FLUORESCENCE AND ELECTRON MICROPROBE TECHNIQUES FOR DETERMINATION OF THIN-FILM THICKNESSES.
James E. Cline (NASA, Electronics Research Center, Cambridge, Mass.).
IN: PHYSICAL MEASUREMENT AND ANALYSIS OF THIN FILMS.
Edited by F. M. Murt and W. G. Guldner.
London, Plenum Press (Progress in Analytical Chemistry. Volume 2), 1969, p. 83-92. 5 refs.

Discussion of two methods for determining the thickness of thin films: X-ray fluorescence and electron microprobe techniques. For X-ray fluorescence, a linear relationship is obtained between the function $-\log(1 - I_t/I_0)$ and the mass thickness of the thin film, where I_t is the intensity of the characteristic X-rays from the thin film and I_0 is the limiting intensity from thick layers. For electron-microprobe techniques, a more complex relationship is found due to the variation of the effective electron excitation function, which reaches a maximum at a penetration depth depending on the electron-beam voltage of the characteristic X-rays emitted. A method is described for the simultaneous determination of both gold and molybdenum thicknesses in a laminated metallization system used for integrated circuits. (Author)

A69-22433

NATIONAL ELECTRONICS CONFERENCE, 24TH, CHICAGO, ILL., DECEMBER 9-11, 1968, PROCEEDINGS.
Conference sponsored by the Illinois Institute of Technology, the Institute of Electrical and Electronics Engineers, Northwestern University, and the University of Illinois.
Oak Brook, Ill., National Electronics Conference, Inc., 1968. 960 p.
$10.00.

CONTENTS:

PRESIDENT'S MESSAGE. R. M. Janowiak, p. iii.

INDEX OF TECHNICAL PAPERS, p. xxxvii-xlviii.

GUIDANCE AND CONTROL COMPONENTS FOR SPACE APPLICATIONS. C. Janow (NASA, Washington, D.C.), p. 30-35. 14 refs. [See A69-22434 09-14]

A VIBRATING MOMENTUM EXCHANGE DEVICE. D. F. Sellers (LTV Electrosystems, Inc., Dallas, Tex.) and M. G. Rekoff, Jr. (Texas Agricultural and Mechanical University, College Station, Tex.), p. 48-51. [See A69-22435 09-21]

ERROR BOUNDS FOR OPTIMUM SMOOTHING ALGORITHMS. R. E. Griffin and A. P. Sage (Southern Methodist University, Dallas, Tex.), p. 58-63. 6 refs. [See A69-22436 09-19]

ESTIMATION IN LINEAR DISCRETE SYSTEMS WITH TIME DELAY. R. Priemer and A. G. Vacroux (Illinois Institute of Technology, Chicago, Ill.), p. 64-66. [See A69-22437 09-10]

KALMAN FILTER WITH DELAYED STATES AS OBSERVABLES. R. G. Brown and G. L. Hartmann (Iowa State University of Science and Technology, Ames, Iowa), p. 67-72. 5 refs. [See A69-22438

09-10]

TRAJECTORY SENSITIVITY OF A LARGE LAUNCH BOOSTER CONTROL SYSTEM. J. Y. S. Luh and M. Maguiraga (Purdue University, Lafayette, Ind.), p. 77-82. 5 refs. [See A69-22439 09-10]

A DYNAMIC PROGRAMMING COMPUTATIONAL APPROACH TO OPTIMIZATION WITH STATE VARIABLE DISCONTINUITIES. J. L. Melsa (Southern Methodist University, Dallas, Tex.) and C. J. McLennan (Ryan Aeronautical Co., San Diego, Calif.), p. 83-87. 10 refs. [See A69-22440 09-10]

ANALYSIS OF AN ADAPTIVE CONTROL ALGORITHM FOR LINEAR SYSTEMS. A. E. Pearson (Brown University, Providence, R.I.), p. 88-91. 6 refs. [See A69-22441 09-10]

CONJUGATE DIRECTION METHODS FOR NONLINEAR OPTIMIZATION PROBLEMS. S. S. Tripathi and K. S. Narendra (Yale University, New Haven, Conn.), p. 125-129. 10 refs. [See A69-22442 09-10]

ON THE DESIGN OF SPECIFIC OPTIMAL CONTROLLERS. S. Murtuza (Western Electric Co., Inc., Princeton, N.J.), p. 136-141. 7 refs. [See A69-22443 09-10]

THEORY OF ONE-PORT COUPLED MICROWAVE OSCILLATORS. G. E. Raue and T. K. Ishii (Marquette University, Milwaukee, Wis.), p. 143-147. 8 refs. [See A69-22444 09-09]

OPTICAL PULSE COMPRESSION. J. W. Hansen (Bell Telephone Laboratories, Inc., Murray Hill, N.J.), p. 148-151. 7 refs. [See A69-22445 09-16]

A HIGHLY RELIABLE MULTI-CHANNEL MICROWAVE AMPLIFIER. H. P. Gregor (Syracuse University Research Corp., Syracuse, N.Y.) and A. T. Adams (Syracuse University, Syracuse, N.Y.), p. 158-162. 5 refs. [See A69-22446 09-09]

CUTOFF-COUPLED MICROWAVE FILTERS. J. R. Brauer and E. H. Scheibe (Wisconsin, University, Madison, Wis.), p. 163-168. 5 refs. [See A69-22447 09-09]

ANALYSIS OF PERIODICALLY-RESPONDING NONLINEAR SYSTEMS BY METHODS STEMMING FROM THE CALCULUS OF VARIATIONS. R. S. Marleau and T. J. Higgins (Wisconsin, University, Madison, Wis.), p. 169-174. 7 refs. [See A69-22448 09-10]

BOUNDEDNESS IN NONLINEAR SYSTEMS. R. E. Fitts (U.S. Air Force Academy, Colorado Springs, Colo.), p. 175-180. 5 refs. [See A69-22449 09-19]

CASCADED PHASE LOCKED LOOPS. C. L. Weber and J. J. Stein (Southern California, University, Los Angeles, Calif.), p. 181-186. 10 refs. [See A69-22450 09-10]

SYSTEM PARTITIONING FOR LSI. H. J. Thamhain and P. J. Molenda (General Electric Co., Syracuse, N.Y.), p. 200-205. 7 refs. [See A69-22451 09-09]

MICROELECTRONIC FILTERS FOR FREQUENCY DIVISION MULTIPLEX. R. G. Hove, C. C. Myrick, and B. B. Woo (Boeing Co., Seattle, Wash.), p. 210-215. 5 refs. [See A69-22452 09-09]

MODERN MICROELECTRONICS FOR DIGITAL ADAPTIVE CONTROL SYSTEMS. S. A. White (North American Rockwell Corp., Anaheim, Calif.), p. 268-273. 6 refs. [See A69-22453 09-10]

DC TO DC CONVERTER REGULATED BY A CONSTANT-FREQUENCY DUTY-CYCLE GENERATOR. I. M. H. Bábaá (Bell Telephone Laboratories, Inc., Winston-Salem, N.C.), T. G. Wilson (Duke University, Durham, N.C.), and Y. Yu (TRW Systems Group, Redondo Beach, Calif.), p. 291-296. 7 refs. [See A69-22454 09-03]

POWER GENERATION WITH AVALANCHE DIODES. K. K. N. Chang (Radio Corporation of America, Princeton, N.J.), p. 318-321. 9 refs. [See A69-22455 09-09]

SILICON VIDICON - AN IMAGE TUBE FOR THE VIEWING OF NEAR INFRARED AND VISIBLE RADIATION. F. L. Skaggs (Texas Instruments, Inc., Dallas, Tex.), p. 339-342. [See A69-22456 09-09]

ANALYSIS OF AN OPTICAL MOTOR SYSTEM ENERGIZED WITH A LASER. R. H. Johnson, A. P. Szews, and T. K. Ishii (Marquette University, Milwaukee, Wis.), p. 377-381. [See A69-22457 09-03]

nTH ORDER REDUNDANCY REDUCTION. L. C. Wilkins and P. A. Wintz (Purdue University, Lafayette, Ind.), p. 389-391. [See A69-22458 09-19]

POWER ALLOCATION - RAPIDLY VARYING PHASE ERROR. J. F. Hayes (Purdue University, Lafayette, Ind.) and W. C. Lindsey (California Institute of Technology, Pasadena, Calif.), p. 392-395. 5 refs. [See A69-22459 09-07]

A SATELLITE COMMUNICATION SYSTEM USING PN CODES. D. R. Anderson and P. A. Wintz (Purdue University, Lafayette, Ind.), p. 427-430. 15 refs. [See A69-22460 09-07]

SCINTILLATION FADING OF VHF BEACONS ON SYNCHRONOUS SATELLITES. H. E. Whitney, R. S. Allen, and J. Aarons (USAF, Cambridge Research Laboratories, Bedford, Mass.), p. 437-439. [See A69-22461 09-07]

EFFICIENT SPACE-GROUND DATA TRANSMISSION. S. Shapiro (General Precision Systems, Inc., Wayne, N.J.) and W. Shapiro (Bendix Corp., Teterboro, N.J.), p. 440-443. [See A69-22462 09-07]

A SIMPLIFIED OPTIMUM SELECTION OF MODULATION INDICES FOR MULTITONE PHASE MODULATION. I. Kadar (Grumman Aircraft Engineering Corp., Bethpage, N.Y.), p. 444-449. [See A69-22463 09-07]

AN FMFB DEMODULATOR FOR SATELLITE COMMUNICATIONS. J. F. Marchese, S. L. Anema (International Business Machines Corp., Gaithersburg, Md.), and M. Malinowski (U.S. Satellite Communications Agency, Washington, D.C.), p. 450-455. [See A69-22464 09-07]

HYBRID DIGITAL TRANSMISSION SYSTEMS. I - JOINT OPTIMIZATION OF ANALOG AND DIGITAL REPEATERS. R. W. Chang and S. L. Freeny (Bell Telephone Laboratories, Inc., Holmdel, N.J.), p. 456-461. [See A69-22465 09-07]

GLOBAL SYSTEM OF COMMERCIAL SATELLITE COMMUNICATIONS. F. J. D. Taylor and R. C. Barthle (Communications Satellite Corp., Washington, D.C.), p. 479-484. [See A69-22466 09-07]

POSSIBLE LARGE CAPACITY DOMESTIC SATELLITE SYSTEM. L. C. Tillotson (Bell Telephone Laboratories, Inc., Holmdel, N.J.), p. 485-487. [See A69-22467 09-07]

COMMUNICATION SYSTEMS USING SYNCHRONOUS AND NEAR SYNCHRONOUS SATELLITES. E. Hoo, K. Ekeland, and R. Coen (Hughes Aircraft Co., Fullerton, Calif.), p. 488-493. [See A69-22468 09-07]

THE AUSTRALIAN COMMERCIAL SATELLITE COMMUNICATION STATION. R. L. Kaiser, J. M. Thornell, and G. F. Mansur (Collins Radio Co., Dallas, Tex.), p. 494-497. [See A69-22469 09-07]

LOW-NOISE RECEIVER FOR SATELLITE COMMUNICATION GROUND TERMINALS. R. Hendricks, P. Lombardo, and S. Okwit (Cutler-Hammer, Inc., Deer Park, N.Y.), p. 498-502. [See A69-22470 09-07]

ADAPTIVE RECEIVER TECHNIQUES FOR DIGITAL COMMUNICATION THROUGH SELECTIVE FADING CHANNELS. C. C. Bailey (Bell Telephone Laboratories, Inc., Holmdel, N.J.) and J. C. Lindenlamb (Purdue University, Lafayette, Ind.), p. 507-512. [See A69-22471 09-07]

A SIGNAL PROCESSING TECHNIQUE FOR PREDETECTION COMBINING. W. J. Bickford (Raytheon Co., Norwood, Mass.), p. 513-517. 5 refs. [See A69-22472 09-07]

WIDEBAND TECHNIQUE FOR IMPROVING FSK RECEPTION IN ATMOSPHERIC NOISE. H. F. Hartley (Westinghouse Electric Corp., Leesburg, Pa.), p. 528-532. 7 refs. [See A69-22473 09-07]

CONSTANT ENVELOPE THRESHOLD DETECTOR. J. L. Sundry and W. F. Paul (Westinghouse Electric Corp., Baltimore, Md.), p. 533-538. [See A69-22474 09-07]

APPLICATION OF HELIUM-NEON LASER FOR PROCESS DIMENSIONAL CONTROL. S. Minkowitz (Perkin-Elmer Corp., Wilton, Conn.), p. 854-858. [See A69-22475 09-16]

EVAPORATION PROCESSES BY LASER BEAMS. P. D. Zavitsanos, L. E. Brewer, and W. E. Sauer (General Electric Co., King of Prussia, Pa.), p. 864-869. 11 refs. [See A69-22476 09-16]

ADAPTIVE SIGNAL TRACKING SYSTEM. J. E. Thompson (Westinghouse Electric Corp., Baltimore, Md.), p. 903-905. [See A69-22477 09-07]

INDEX OF AUTHORS, p. 907-913.

A69-22786 *

SMALL-SIGNAL AND SATURATION CHARACTERISTICS OF AN X-BAND CYCLOTRON-RESONANCE OSCILLATOR.

B. Kulke and R. W. Wilmarth (NASA, Electronics Research Center, Microwave Circuits Branch, Cambridge, Mass.).

IEEE, Proceedings, vol. 57, Feb. 1969, p. 219, 220.

Design information and operating characteristics are given for an experimental X-band cyclotron-resonance oscillator. Saturated power levels near 3 W, at 0.8% efficiency, are reported. Qualitative agreement with theory has been observed under small-signal, zero-space-charge conditions. (Author)

A69-22787 *

A SiC BACKWARD DIODE.

Richard Farrell (NASA, Electronics Research Center, Cambridge, Mass.).

IEEE, Proceedings, vol. 57, Feb. 1969, p. 221, 222.

SiC backward diodes which operate between 77 and 1000 K have been developed. Figures of merit ($\gamma\sqrt{R}$) of 19, 300, 3960, and 15 at 12.5 MHz, 50 MHz, and 8.8 GHz, respectively, have been measured with detector area on the order of 10^{-5} cm^2. These results are compatible with a prior analysis which predicted an upper frequency limit of between 0.1 and 1.0 GHz for SiC backward diodes. (Author)

A69-24740

INSTITUTE OF ELECTRICAL AND ELECTRONICS ENGINEERS, CONFERENCE ON TUBE TECHNIQUES, 9TH, NEW YORK, N.Y., SEPTEMBER 17, 18, 1968, CONFERENCE RECORD.

New York, Institute of Electrical and Electronics Engineers, Inc. 1968. 299 p.

Members, $7.00; nonmembers, $10.50.

CONTENTS:

FOREWORD. K. Garoff. 1 p.

LASER BEAM JOINING OF CRITICAL COMPONENTS FOR HIGH RELIABILITY. D. K. Davis and L. R. Falce (Varian Associates, Palo Alto, Calif.), p. 72-80. [See A69-24741 11-16]

HIGH TEMPERATURE SEALANTS FOR VACUUM SYSTEMS. R. K. E. Weebe (Hughes Aircraft Co., Torrance, Calif.), p. 113-116. [See A69-24742 11-18]

MATERIALS AND TECHNIQUES FOR GAS LASERS. W. B. Bridges (Hughes Aircraft Co., Malibu, Calif.), p. 117-124. 25 refs. [See A69-24743 11-16]

DEVELOPMENT OF HIGH TEMPERATURE THYRATRONS FOR LARGE NUCLEAR ELECTRICAL SPACE POWER SYSTEMS. N. D. Jones (General Electric Co., Schenectady, N.Y.), p. 137-144. [See A69-24744 11-09]

FUTURE MICROWAVE TUBE TECHNOLOGY. J. M. Osepchuk (Raytheon Co., Waltham, Mass.), p. 145-153. 37 refs. [See A69-24745 11-09]

AN ELECTRICALLY INSULATED HEAT PIPE FOR DEPRESSED COLLECTORS. A. Basiulis and J. C. Dixon (Hughes Aircraft Co., Torrance, Calif.), p. 176-181. 14 refs. [See A69-24746 11-09]

COOLING OF A HIGH-POWER ELECTRON TUBE IN A SPACE VEHICLE. E. C. Conway (General Electric Co., King of Prussia, Pa.) and R. W. Wilmarth (NASA, Electronics Research Center, Cambridge, Mass.), p. 182-190. 12 refs. [See A69-24747 11-09]

NONELECTRIC CATHODE HEATING. E. C. Conway, M. J. Kelley (General Electric Co., King of Prussia, Pa.), R. W. Wilmarth (NASA, Electronics Research Center, Cambridge, Mass.), and J. E. Beggs (General Electric Co., Schenectady, N.Y.), p. 191-195. [See A69-24748 11-09]

A NEW MEANS FOR CONTROL OF SECONDARY ELECTRON REDISTRIBUTION AT IMAGE TUBE STORAGE TARGETS. R. C. Hergenrother (Raytheon Co., Waltham, Mass.), p. 236-239. [See A69-24749 11-09]

A69-24747 *

COOLING OF A HIGH-POWER ELECTRON TUBE IN A SPACE VEHICLE.

E. C. Conway (General Electric Co., Missile and Space Div., King of Prussia, Pa.) and R. W. Wilmarth (NASA, Electronics Research Center, Cambridge, Mass.).

IN: INSTITUTE OF ELECTRICAL AND ELECTRONICS ENGINEERS, CONFERENCE ON TUBE TECHNIQUES, 9TH, NEW YORK, N.Y., SEPTEMBER 17, 18, 1968, CONFERENCE RECORD. [A69-24740 11-09]

New York, Institute of Electrical and Electronics Engineers, Inc., 1968, p. 182-190. 12 refs.

Contract No. NAS 12-565.

Description of a thermal control system built to provide cooling for a traveling wave tube (TWT) mounted in a spacecraft. The system was designed to demonstrate the capability of heat pipes to provide high thermal conductance paths for 750 W (dissipated at the TWT collector) to flow to a flat plate radiator where the heat can be radiated to space. The evaporators of four heat pipes and the TWT collector are attached to a block located at the center of the radiator. The heat pipe condensers, placed along the diagonals of the square radiator plate, maintain the diagonals very nearly isothermal, thus keeping the fin effectiveness high. Test results are included, showing the system thermal performance in several modes of operation for varying power dissipations. The results of failure of one, two, three, or all four pipes are presented. Also included is an analytical investigation of the weight and area requirements of both passive and heat-pipe space radiators. This analysis serves as a general guide in judging the effect of temperature limits and power dissipation on the thermal control system. (Author)

A69-24748 *

NONELECTRIC CATHODE HEATING.

E. C. Conway, M. J. Kelley (General Electric Co., King of Prussia, Pa.), R. W. Wilmarth (NASA, Electronics Research Center, Cambridge, Mass.), and J. E. Beggs (General Electric Co., Research and Development Center, Schenectady, N.Y.).

IN: INSTITUTE OF ELECTRICAL AND ELECTRONICS ENGINEERS, CONFERENCE ON TUBE TECHNIQUES, 9TH, NEW YORK, N.Y., SEPTEMBER 17, 18, 1968, CONFERENCE RECORD. [A69-24740 11-09]

New York, Institute of Electrical and Electronics Engineers, Inc., 1968, p. 191-195.

Contract No. NAS 12-565.

Description of a vacuum tube which has been constructed to obtain more efficient utilization of heat than is provided by thermoelectric or thermionic devices. The vacuum tube is such that its cathode is directly heated by a radioisotope source external to the tube. The tube design incorporates a heat pipe to provide almost isothermal transfer of heat from the external source to the cathode. Test results demonstrate operation with an external electrical heater and a radioisotope heat source. M.M.

A69-24984 *

RADIATION AND NEAR-FIELD COUPLING BETWEEN TWO COLLINEAR OPEN-ENDED WAVEGUIDES.

Robert J. Mailloux (NASA, Electronics Research Center, Cambridge, Mass.).

IEEE Transactions on Antennas and Propagation, vol. AP-17, Jan. 1969, p. 49-55. 22 refs.

Description of an experimental and theoretical study of closely spaced collinear coupled waveguides radiating through a common perfectly conducting ground plane. The problem is formulated as a set of simultaneous integral equations and is solved approximately by expanding the aperture field in a Fourier series. The special case of a single isolated waveguide is treated first, and the results are compared with experiment as well as with the approximate results of Lewin (1951). Attention is given to the edge singularities. The more general case of two collinear coupled waveguide slots is solved by the same numerical method using the symmetrical properties of the geometry. Phase and amplitude of the mutual coupling are evaluated and compared with experiment. Agreement is excellent. (Author)

A69-24986 *

THE INFLUENCE OF AIR-GAP TOLERANCES ON THE ADMITTANCE OF A DIELECTRIC-COATED SLOT ANTENNA.

J. Earl Jones (NASA, Langley Research Center, Hampton, Va.). (Institute of Electrical and Electronics Engineers, International Antenna and Propagation Symposium, Boston, Mass., Sept. 9-11, 1968.)

IEEE Transactions on Antennas and Propagation, vol. AP-17, Jan. 1969, p. 63-68. 9 refs.

The admittance of a TEM mode-excited parallel-plate aperture having an infinite flange and illuminating a displaced dielectric

boundary is determined by the variational method. The results are applied to provide insight into the following two problems of interest: (1) the effect of an air gap on the admittance of dielectric-coated aperture antennas, and (2) the admittance of an aperture antenna coated with an underdense plasma slab. Numerical computations for the air-gap problem are verified experimentally. (Author)

A69-28042
ANNUAL NATIONAL RELAY CONFERENCE, 17TH, OKLAHOMA STATE UNIVERSITY, STILLWATER, OKLA., APRIL 22, 23, 1969, PROCEEDINGS.
Conference sponsored by the National Association of Relay Manufacturers and Oklahoma State University.
Scottsdale, Ariz., National Association of Relay Manufacturers, 1969. 271 p.
$5.00.

CONTENTS:

PREFACE. 1 p.

THE ENGINEERING APPROACH TO FAILURE ANALYSIS OF SWITCHING DEVICES. H. D. Sauter (American Machine and Foundry Co., Princeton, Ind.), p. 2-1 to 2-18. [See A69-28043 13-09]

RELIABILITY vs COST. R. G. Schubert and P. J. McPherson (Leach Corp., Los Angeles, Calif.), p. 3-1 to 3-4. 5 refs. [See A69-28044 13-09]

GUIDELINES FOR RELIABLE RELAY APPLICATION AND SELECTION. L. W. Wendling (U.S. Naval Air Systems Command, Washington, D.C.) and E. U. Thomas (Grumman Aircraft Engineering Corp., Bethpage, N.Y.), p. 10-1 to 10-35. 21 refs. [See A69-28045 13-09]

REQUIREMENTS FOR RELAYS IN SPACECRAFT HAVING MAGNETIC FIELD CONSTRAINTS. J. L. Swyler (NASA, Goddard Space Flight Center, Greenbelt, Md.), p. 11-1 to 11-12. 6 refs. [See A69-28046 13-09]

SYSTEMS APPLICATION OF LATCHING REED RELAYS IN SCIENTIFIC SATELLITE INSTRUMENTATION. R. S. Cuikay (USAF, Cambridge Research Laboratories, Bedford, Mass.), p. 12-1 to 12-4. [See A69-28047 13-09]

RELAY COIL TEMPERATURE RISE AT SIMULATED OUTER SPACE PRESSURE LEVELS. R. J. Backe (Sperry Rand Corp., New York, N.Y.; NASA, Goddard Space Flight Center, Greenbelt, Md.), p. 13-1 to 13-23. 18 refs. [See A69-28048 13-09]

THE DEVELOPMENT OF A HIGH PERFORMANCE MICRO-MINIATURE LATCHING RELAY. M. Hurter (Bourns, Inc., Riverside, Calif.), p. 20-1 to 20-6. [See A69-28049 13-09]

A69-28046 *
REQUIREMENTS FOR RELAYS IN SPACECRAFT HAVING MAGNETIC FIELD CONSTRAINTS.
James L. Swyler (NASA, Goddard Space Flight Center, Quality Assurance Div., Greenbelt, Md.).
IN: ANNUAL NATIONAL RELAY CONFERENCE, 17TH, OKLAHOMA STATE UNIVERSITY, STILLWATER, OKLA., APRIL 22, 23, 1969, PROCEEDINGS. [A69-28042 13-09]
Conference sponsored by the National Association of Relay Manufacturers and Oklahoma State University.
Scottsdale, Ariz., National Association of Relay Manufacturers, 1969, p. 11-1 to 11-12. 6 refs.

Outline of the background required by the relay user and designer alike for a better understanding of the requirements of spacecraft with magnetic field constraints. The fields of various relay types are compared. Spacecraft instruments and stabilization systems are described, as well as techniques for minimizing the effects of operational and permanent fields and methods for measuring these fields. The overall problem of spacecraft magnetic cleanliness and the effect of a relay on this problem is briefly touched upon.
P.v.T.

A69-28048 *
RELAY COIL TEMPERATURE RISE AT SIMULATED OUTER SPACE PRESSURE LEVELS.
Richard J. Backe (Sperry Rand Corp., New York, N.Y.; NASA, Goddard Space Flight Center, Greenbelt, Md.).
IN: ANNUAL NATIONAL RELAY CONFERENCE, 17TH, OKLAHOMA STATE UNIVERSITY, STILLWATER, OKLA., APRIL 22, 23, 1969, PROCEEDINGS. [A69-28042 13-09]
Conference sponsored by the National Association of Relay Manufacturers and Oklahoma State University.
Scottsdale, Ariz., National Association of Relay Manufacturers, 1969, p. 13-1 to 13-23. 18 refs.

Study of the problem of the increase in the temperature rise of relay coils when air is removed from the ambience outside and inside the relay case. The space environment and relay applications are described. The normal thermal considerations for relays are discussed and the data obtained are evaluated. The conclusions drawn from this study are: (1) the temperature rise of a sealed or unsealed relay increases substantially and continuously as pressures are varied from sea level to the range equivalent to 250, 000 to 350, 000 ft; (2) for altitudes over 50, 000 to 100, 000 ft, these increases cannot be deduced from published convection derating curves; gaseous conduction is an important phenomenon at these levels; (3) at pressures equivalent to orbiting altitudes, maximum average coil temperatures of sealed relays are generally around 150°C, while those of unsealed relays frequently exceed 200°C; (4) radiation is an important factor in relay cooling at altitudes above 200, 000 ft and is the principal factor at 500, 000 ft; and (5) black- or gray-painting the relay cans will substantially increase emissivity, resulting in much lower coil temperatures at high altitudes. P.v.T.

A69-31618 *
THERMAL INSTABILITIES LIMITING POWER DISSIPATION IN TRANSISTORS.
S. M. Spitzer (NASA, Electronics Research Center, Cambridge, Mass.).
Solid-State Electronics, vol. 12, May 1969, p. 433-437. 8 refs.

Explanation of the development of second breakdown and other thermal instabilities using solutions to the heat flow equation. Stability criteria in cases where the multiplication factor can be assumed to be unity are presented in terms of α_T, the thermal coefficient of the emitter-base junction. It is found that simple Ebers-Moll theory does not contain information about base resistance and its stabilizing effects on device operation. An experimental parameter, α_T', contains this base resistance information, and yields stability criteria predicting reduced power dissipation capability for the transistor at low current levels. The calculation of α_T' is developed, and the application of this calculation is discussed. (Author)

A69-31851 *
HOW RELIABLE ARE MOS IC's? AS GOOD AS BIPOLARS, SAYS NASA.
Leon C. Hamiter, Jr. (NASA, Huntsville, Ala.).
Electronics, vol. 42, June 23, 1969, p. 106-110.

Results of an MOS IC reliability study conducted by NASA, including a discussion of the causes of device degradation and failure. Thousands of MOS ICs from a single manufacturer were tested at 25°C operating life, 85°C operating life, 125°C reverse bias, 125°C storage, and 150°C storage. Some 4, 339, 000 circuit hours were accumulated in this group of tests alone, with only three failures - a failure rate of 0.095% per 1000 hours at maximum stress. This test experience is comparable to NASA's experience with operational systems using MOS ICs. It was found that MOS and bipolar ICs of equal complexity offer approximately the same failure rates. A complex MOS circuit offers a lower total failure rate than discrete parts or less complex ICs that must be assembled on printed-circuit boards and interconnected to perform the equivalent function.
G.R.

A69-32889 *
THE EFFECTS OF DIELECTRIC OVERCOATING ON ELECTROMIGRATION IN ALUMINUM INTERCONNECTIONS.
Stuart M. Spitzer and Seymour Schwartz (NASA, Electronics Research Center, Cambridge, Mass.).
(Institute of Electrical and Electronics Engineers, Annual Reliability of Physics Symposium, 7th, Washington, D.C., Dec. 2-4, 1968.)
IEEE Transactions on Electron Devices, vol. ED-16, Apr. 1969, p. 348-350. 12 refs.

Study of the effects of dielectric overcoating as a function of aluminum thickness. It is seen that surface treatment is effective for aluminum less than 5000 Å thick. It is pointed out that for aluminum thickness greater than 6000 Å, surface passivation will have no effect with respect to electromigration. It is shown that the type of aluminum deposition technique and deposition and post-deposition heat treatment is critical in obtaining the maximum bulk component of the activation energy. The dielectric overcoating, in combination with optimal bulk properties, increases the mean time between failure of the aluminum stripes by one to two orders of magnitude, at high current densities and elevated ambients, over that found in many conventional integrated circuits. M. M.

A69-32893 *

THERMAL EFFECTS ON THE INTEGRITY OF ALUMINUM TO SILICON CONTACTS IN SILICON INTEGRATED CIRCUITS.

Robert J. Anstead and Samuel R. Floyd (NASA, Goddard Space Flight Center, Greenbelt, Md.).

(Institute of Electrical and Electronics Engineers, Annual Reliability of Physics Symposium, 7th, Washington, D. C., Dec. 2-4, 1968.) IEEE Transactions on Electron Devices, vol. ED-16, Apr. 1969, p. 381-386.

Observations of serious discontinuities in aluminum interconnections at contact windows of integrated circuits, by means of the scanning electron microscope. In some instances the discontinuities have produced catastrophic failure. Two types of discontinuities have been observed, and simulation of one type has been possible through exposure to temperatures 25 to 50°C below the aluminum-silicon eutectic of 577°C. A preliminary electron probe analysis has revealed the presence of silicon in the interconnection regions overlying the silicon dioxide steps bordering the contact windows. M. M.

A69-34802 *

REFLECTION COEFFICIENT OF A TEM MODE SYMMETRIC PARALLEL-PLATE WAVEGUIDE ILLUMINATING A DIELECTRIC LAYER.

W. D. Burnside, R. C. Rudduck, L. L. Tsai (Ohio State University, ElectroScience Laboratory, Columbus, Ohio), and J. E. Jones (NASA, Langley Research Center, Hampton, Va.).

Radio Science, vol. 4, June 1969, p. 545-556. 18 refs.

Grant No. NGR-36-008-005.

The reflection coefficient of a symmetric parallel-plate waveguide operating in the TEM mode and illuminating a lossless dielectric layer is analyzed by wedge-diffraction and geometrical-optics techniques. The interactions between the waveguide and the dielectric layer are treated in terms of iterative bounce waves. The *reflection from the dielectric layer and the scattering from the* waveguide for cylindrical wave incidence are both represented by resultant component cylindrical waves. Thus each interacting bounce wave between the guide and the dielectric layer becomes the superposition of a finite number of cylindrical wave components. The reflection coefficient of the guide is then obtained by adding the various bounce wave contributions to the guide's free-space reflection coefficient. For the two geometries considered (the thin-walled guide and the ground-plane guide) calculated results are in excellent agreement with those measured. (Author)

A69-35293 *

LINEAR OPERATION OF A P-N-P-N TETRODE.

Nicholas C. Voulgaris (NASA, Electronics Research Center, Cambridge, Mass.) and Edward S. Yang (Columbia University, Dept. of Electrical Engineering, New York, N. Y.).

IEEE Transactions on Electron Devices, vol. ED-16, May 1969, p. 468-478. 15 refs.

NSF Grant No. GK-1550; Grant No. NGR-33-008-090.

Model of a four-terminal p-n-p-n device operating as a semiconductor tetrode amplifier. The equations characterizing this *model are based on the physical structure of a commercially* available silicon planar p-n-p-n tetrode; they are use (1) to derive the device terminal characteristics; (2) to synthesize small-signal equivalent circuits suitable for lf operation (h-parameter circuit) and for hf operation (bridged hybrid-π circuit); (3) to study the dependence of short-circuit gains of the tetrode on the dc biasing currents and frequency; and (4) to obtain a stability condition which must be satisfied to ensure that the operation of the device is restricted in its OFF state where it can function as a small-signal linear amplifier. The theoretical results are in close agreement with experimental values. (Author)

A69-35781

INSTITUTE OF ELECTRICAL AND ELECTRONICS ENGINEERS, ANNUAL SEMINAR ON FAILURE ANALYSIS, 2ND, UNIVERSITY OF PENNSYLVANIA, PHILADELPHIA, PA., MAY 22, 1969, PROCEEDINGS.

Philadelphia, Institute of Electrical and Electronics Engineers, Inc., 1969. 51 p.

$5.00.

CONTENTS:

ACHIEVING RELIABILITY ASSURANCE THROUGH CAUSE-AND-EFFECT FAILURE ANALYSIS. S. A. Rosenthal (Kollsman Instrument Corp., Syosset, N.Y.), p. 1-4. (See A69-35782 19-34)

IMPROVING COMMUNICATION EQUIPMENT RELIABILITY THROUGH TESTING AND FAILURE ANALYSIS. N. R. Wheelock (Radio Corporation of America, Camden, N.J.), p. 5-9. (See A69-35783 19-09)

IMPROVING AVIONIC EQUIPMENT RELIABILITY VIA TEST AND FAILURE ANALYSIS. J. J. Bussolini and G. Friedenreich (Grumman Aircraft Engineering Corp., Bethpage, N.Y.), p. 11-15. (See A69-35784 19-09)

USING TESTS AND ANALYSES TO ACHIEVE RELIABLE MICROWAVE EQUIPMENT. H. H. Anderson, Jr. and V. Stachejko (Radio Corporation of America, Moorestown, N.J.), p. 17-20. (See A69-35785 19-09)

MICROELECTRONIC DEVICE STANDARDIZING SPECIFICATIONS—EIA MED-50 COMMITTEE REPORT. C. H. Zierdt, Jr. (Bell Telephone Laboratories, Inc., Allentown, Pa.), p. 21.

AUTOMATIC TESTING OF COMPLEX INTEGRATED CIRCUITS. H. Hellman (Radio Corporation of America, Camden, N.J.), p. 23.

DETAILED FAILURE ANALYSIS TECHNIQUES AND THEIR USE IN DERIVING SCREENING TESTS. E. A. Doyle (USAF, Rome Air Development Center, Griffiss AFB, N.Y.), p. 25.

INTEGRATED CIRCUIT FAILURE MECHANISMS AND THEIR DETECTION THROUGH FAILURE ANALYSIS—1969 SURVEY. C. D. Root, R. T. Brown, and J. Gaffney (Raytheon Co., Sudbury, Mass.), p. 27-36. (See A69-35786 19-09)

FAILURE MECHANISMS AND ANALYSES IN LARGE-SCALE INTEGRATED CIRCUITS. G. L. Schnable, E. S. Schlegel, and R. S. Keen (Philco-Ford Corp., Blue Bell, Pa.), p. 37-40. (See A69-35787 19-09)

IMPURITY ANALYSIS OF SILICON DIOXIDE PASSIVATION LAYERS BY ION BEAM MASS SPECTOMETRY. H. C. Gorton (Battelle Memorial Institute, Columbus, Ohio), p. 41-43.

CURRENT STATUS OF SCANNING ELECTRON MICROSCOPY IN SEMICONDUCTOR DEVICE RELIABILITY PHYSICS. R. J. Anstead and S. R. Floyd (NASA, Goddard Space Flight Center, Greenbelt, Md.), p. 45-55. (See A69-35788 19-26)

A69-36676 *

DESIGN OF A LONG-LIFE RELIABLE NUCLEAR EXPERIMENT FOR SPACE FLIGHT.

James H. Trainor and Donald J. Williams (NASA, Goddard Space Flight Center, Greenbelt, Md.).

IEEE Transactions on Geoscience Electronics, vol. GE-7, Apr. 1969, p. 74-77. 9 refs.

Description of an experiment which has been developed for flight on OGO-F in polar orbit. Measurements will be made of the electron flux and spectra above 30 keV, both for precipitating and locally mirroring electrons as well as atmospheric backscatter. The scientific purposes, detector and electronic systems, packaging, thermal design, internal calibration, and test philosophy are discussed. This work emphasizes the design features and philosophy used in the development, fabrication, and testing of the experiment in order to ensure a long, useful lifetime in space. (Author)

A69-37299 *
DESIGN PARAMETERS FOR OVERDRIVEN VARACTOR FREQUENCY DOUBLERS USING PUNCH-THROUGH OR BIMODE VARACTORS.
Alfred I. Grayzel (NASA, Electronics Research Center, Cambridge, Mass.).
IEEE Transactions on Microwave Theory and Techniques, vol. MTT-17, June 1969, p. 345-347. 7 refs.

Description of design parameters for realizable punch-through or bimode varactor doublers. A charge-voltage relationship is obtained for the overdriven case. Using this relationship, a computer program for a varactor doubler was written, and the design parameters at the maximum efficiency point were found as a function of the voltage at the break point. G.R.

A69-38530 *
A FUNDAMENTAL MULTIPLEXER THEOREM.
Alfred I. Grayzel (NASA, Electronics Research Center, Cambridge, Mass.).
IEEE, Proceedings, vol. 57, May 1969, p. 847,848. 5 refs.

Proof of a fundamental multiplexer theorem and description of a synthesis procedure for Butterworth networks. The theorem states that one can choose m minus 1 frequencies between zero and infinity and then synthesize m filters with passbands which, when connected either in series or in parallel, will have an input impedance of 1 plus j0 for all frequencies. G.R.

A69-39454 *
A UNILATERAL TRANSFORMER.
B. Rabinovici (Northeastern University, Boston, Mass.) and C. A. Renton (NASA, Electronics Research Center, Cambridge, Mass.).
IN: INSTITUTE OF ELECTRICAL AND ELECTRONICS ENGINEERS, ANNUAL SOUTHWESTERN CONFERENCE AND EXHIBITION, 21ST, SAN ANTONIO, TEX., APRIL 23-25, 1969, RECORD. (A69-39437 21-07)
New York, Institute of Electrical and Electronics Engineers, Inc., 1969, p. 9 F 1-9 F 6.

Description of a transformer having the property of unidirectional transfer of energy. It is made from a single domain, uniaxial permalloy film. The theory of its operation is presented, experimental results are given, and applications are discussed. (Author)

A69-40697 *
AN OMNIDIRECTIONAL MICROWAVE ANTENNA FOR USE ON SPACECRAFT.
William F. Croswell and Capers R. Cockrell (NASA, Langley Research Center, Hampton, Va.).
IEEE Transactions on Antennas and Propagation, vol. AP-17, July 1969, p. 459-466. 17 refs.

Description of the qualitative theory, design, and development of a parallel-plate waveguide-fed antenna, suitable for flush-mounted broad-band spacecraft applications. The antenna makes use of wedge-like metal posts placed uniformly about the periphery of the feed plates to provide both structural strength and practical interconnection routes for cables without disrupting the antenna impedance and patterns. Measurements taken on the antenna, which is mounted on spheroids up to 50 wavelengths in circumference, are presented. Equatorial patterns are omnidirectional within plus or minus 0.25 dB, and polar patterns have beam widths similar to a half-wave dipole. (Author)

A69-40698 *
RADIATION CHARACTERISTICS OF A CAVITY-BACKED CYLINDRICAL GAP ANTENNA.
Calvin T. Swift, Thomas G. Campbell (NASA, Langley Research Center, Hampton, Va.), and Henri Hodara (Tetra Tech, Inc., Pasadena, Calif.).
(Institute of Electrical and Electronics Engineers, Plasma Sheath Symposium, 3rd, Boston, Mass., Sept. 21-23, 1965.)
IEEE Transactions on Antennas and Propagation, vol. AP-17, July 1969, p. 467-477. 6 refs.
Contract No. NAS 1-4623.

The input impedance and the equatorial radiation patterns of a vhf cavity-backed cylindrical gap antenna are derived and compared with experiments. The experiments generally support the computations, provided that the gap dimension is neither larger than about one hundreth of a wavelength, nor so thin that mechanical tolerances in the feed design become important. The results show that the tuning, impedance bandwidth, and the radiation patterns of this antenna can be controlled very accurately by adjusting the internal radius and height of the cavity. Salient points of this antenna are its wide-band characteristics (10-per cent bandwidth), its pattern circularity, and particularly the fact that it can be made an integral part of a space vehicle. (Author)

A69-40703 *
APERTURE RADIATION FROM AN AXIALLY SLOTTED ELLIPTICAL CONDUCTING CYLINDER USING GEOMETRICAL THEORY OF DIFFRACTION.
Constantine A. Balanis (NASA, Langley Research Center, Hampton, Va.) and Leon Peters, Jr. (Ohio State University, Dept. of Electrical Engineering, Columbus, Ohio).
IEEE Transactions on Antennas and Propagation, vol. AP-17, July 1969, p. 507-513. 18 refs.

Computation of the equatorial radiation pattern of a parallel-plate TEM mode axial slot on an infinite cylinder of elliptical cross section, using wedge-diffraction and creeping-wave theory. The wedge-diffracted fields are obtained by the diffraction interaction from a set of infinite wedges approximating the parallel-plate-cylinder geometry. Surface-wave propagation on curved bodies, commonly used in scattering, is employed for the creeping-wave contribution. The total field in the lit region is approximated using superposition of wedge-diffracted and creeping-wave fields and in the shadow region solely by creeping-wave fields. The computed patterns are compared with experimental results since boundary-value solutions are not readily available. Good agreement between theory and experiment is indicated. (Author)

A69-41224 *
OPTIMUM DESIGN OF GERMANIUM MICROWAVE BACKWARD DIODES.
John B. Hopkins (NASA, Electronics Research Center, Cambridge, Mass.).
IEEE, Proceedings, vol. 57, Aug. 1969, p. 1458-1460. 7 refs.

Computer calculation to obtain data to serve as guidelines in the fabrication of optimum germanium backward diode microwave detectors. Curves are presented indicating obtainable performance for varying junction diameter, impedance level (determined by the size and impurity concentration), and operating frequency. Z.W.

A69-41228 * #
APPLICATION OF A VARIABLE RESISTANCE TO ARREST OSCILLATIONS IN A PULSED CAPACITOR DISCHARGE CIRCUIT.
Dah Yu Cheng (NASA, Ames Research Center, Moffett Field, Calif.).
Review of Scientific Instruments, vol. 40, Sept. 1969, p. 1153-1157. 5 refs.

Kirchhoff's equation for the current flow from a capacitor connected in series with an inductance and a resistance (that varies with current) is solved by an iterative integration scheme. The resistance of the circuit is assumed to increase during the discharge due to Joule heating. The conditions for over-, under-, and critical damping are derived and used to design a circuit that has a short risetime and a long decay time without current oscillation. The realistic nature of the circuit is verified experimentally. (Author)

A69-41589 *
ADMITTANCE OF A WAVEGUIDE-FED APERTURE LOADED WITH A DIELECTRIC PLUG.
Calvin T. Swift (NASA, Langley Research Center, Hampton, Va.).
IEEE Transactions on Antennas and Propagation, vol. AP-17, May 1969, p. 356-359.

The admittance of a rectangular aperture antenna, loaded with a dielectric plug, was previously formulated as a boundary-value problem and the results are summarized. Calculations and supporting measurements show that a TE_{03} mode can be strongly excited in the plug, resulting in a resonant perturbation of the admittance. (Author)

A69-41590 *
A SIMPLE ANTENNA WITH GOOD CIRCULAR POLARIZATION.
L. C. Van Atta, Robert J. Mailloux, and M. M. Levenson (NASA, Electronics Research Center, Cambridge, Mass.).
IEEE Transactions on Antennas and Propagation, vol. AP-17, May 1969, p. 360, 361.

Description of a circularly polarized antenna of simple design with good circularity over a wide sector of space. The antenna geometry is illustrated, and an example of the normalized orthogonal field distributions is given. Various slot combinations are considered. It is shown that the range of 3-dB beamwidths over which good circular polarization can be maintained using this technique lies between 60 and 85 deg. P.G.

A69-42215
INSTITUTE OF ELECTRICAL AND ELECTRONICS ENGINEERS, ELECTROMAGNETIC COMPATIBILITY SYMPOSIUM, 11TH, ASBURY PARK, N.J., JUNE 17-19, 1969, RECORD.
New York, Institute of Electrical and Electronics Engineers, Inc., 1969. 355 p.
Members, $6.00; nonmembers, $12.

CONTENTS:

CHAIRMAN'S MESSAGE. J. J. O'Neil. 1 p.

INTERFERENCE PROPAGATION.

THE COMPATIBILITY OF MAN IN THE MICROWAVE ENVIRONMENT. L. P. Inglis (North American Rockwell Corp., Canoga Park, Calif.), p. 7-11. 8 refs. (See A69-42216 23-05)

INTERFERENCE SOURCES.

THE DIMENSIONS OF RADIO NOISE. E. N. Skomal (Aerospace Corp., San Bernardino, Calif.), p. 18-28. 39 refs. (See A69-42217 23-07)

THE PROPERTIES OF THE RADIATION BELOW 1 GHz FROM GAP-TYPE ELECTRICAL DISCHARGES ON ELECTRIC POWER DISTRIBUTION LINES. J. P. German (Texas Agricultural and Mechanical University, College Station, Tex.), p. 35-42. (See A69-42218 23-07)

AN EVALUATION OF THE DIFFERENT TYPES OF DIGITAL INTEGRATED CIRCUITS AS SOURCES OF ELECTROMAGNETIC INTERFERENCE. R. R. Grim (Honeywell, Inc., Annapolis, Md.), p. 43-48. (See A69-42219 23-09)

INTERFERENCE SHIELDING AND FIXES.

ACTIVE PRESELECTION FILTER TECHNIQUES FOR ADJACENT CHANNEL INTERFERENCE SUPPRESSION AT UHF. H. W. Denny and R. A Byers (Georgia Institute of Technology, Atlanta, Ga.), p. 55-61. (See A69-42220 23-09)

INTERFERENCE BLANKER FOR HF RECEIVERS. G. J. Palladino and R. H. Sugarman (American Electronic Laboratories, Inc., Colmar, Pa.), p. 62-67. (See A69-42221 23-09)

THE SHIELDING OF ELECTROMAGNETIC PULSES BY USE OF MAGNETIC MATERIALS. R. R. Ferber and F. J. Young (Westinghouse Electric Corp., Pittsburgh, Pa.), p. 73-79. (See A69-42222 23-09)

INTERFERENCE PREDICTION.

INTERFERENCE PREDICTIONS—PHILOSOPHIES, OBJECTIVES, AND FUTURE DIRECTIONS. R. D. Wetherington, E. E. Donaldson, and R. W. Moss (Georgia Institute of Technology, Atlanta, Ga.), p. 80-84. (See A69-42223 23-07)

AIRCRAFT ANTENNA-COUPLED INTERFERENCE ANALYSIS. M. D. Siegel (McDonnell Douglas Corp., St. Louis, Mo.), p. 85-90. (See A69-42224 23-09)

RADIATED INTERFERENCE AND SUSCEPTIBILITY CHARACTERISTICS OF UNSHIELDED LINES. R. J. Mohr (Cutler-Hammer, Inc., Deer Park, N.Y.), p. 91-99. (See A69-42225 23-09)

INTERFERENCE MEASUREMENT TECHNIQUES.

PRELIMINARY INTERPRETATION OF NEAR-FIELD EFFECTS ON MEASUREMENT ACCURACY IN SHIELDED ENCLOSURES. C. W. Stuckey, W. R. Free, and D. W. Robertson (Georgia Institute of Technology, Atlanta, Ga.), p. 119-127. 6 refs. (See A69-42226 23-09)

INTERFERENCE MANAGEMENT.

AN ANALYTICAL APPROACH TO QUANTIFYING EMC IN SYSTEM EFFECTIVENESS. R. B. Schulz (Boeing Co., Seattle, Wash.), p. 143-154. (See A69-42227 23-10)

A TIME-SHARING SCHEME TO ALLEVIATE INTERFERENCE IN COLLOCATED RADIO EQUIPMENTS. J. Perini (Syracuse University, Syracuse, N.Y.) and J. F. Spina (USAF, Rome Air Development Center, Griffiss AFB, N.Y.), p. 167-172. (See A69-42228 23-09)

A FREQUENCY ASSIGNMENT GUIDE FOR TACTICAL FM RADIOS IN THE 30- TO 76-MHz FREQUENCY BAND. C. W. Milligan and I. J. Sorkin (Bell Aerospace Corp., Tucson, Ariz.), p. 177-181. (See A69-42229 23-07)

INTERFERENCE MEASUREMENT EQUIPMENT.

PULSE INTERFERENCE EFFECTS IN A PHASE-LOCK LOOP. J. M. Clarke (NASA, Electronics Research Center, Cambridge, Mass.), R. J. Otero, and W. C. Wanbaugh (IIT Research Institute, Annapolis, Md.), p. 207-214. (See A69-42230 23-10)

INTERFERENCE FILTERS.

UNIQUE FABRICATION TECHNIQUE FOR WAVEGUIDE BELOW CUT OFF HIGH PASS FILTERS. R. E. Rabe (USAF, Rome Air Development Center, Griffiss AFB, N.Y.), p. 227-232. 5 refs. (See A69-42231 23-15)

INTERFERENCE MEASUREMENT PROBLEMS AND SOLUTIONS.

EMC FIGURE OF MERIT FOR RECEIVERS. W. G. Duff (Atlantic Research Corp., Alexandria, Va.), p. 257-262. (See A69-42232 23-09)

ACHIEVING FILTER EFFECTIVENESS AND INSURING RELIABILITY. J. P. Demetry and L. N. Pasquino (International Business Machines Corp., Owego, N.Y.), p. 290-297. (See A69-42233 23-09)

INTERFERENCE PREVENTION AND CONTROL.

THE STRUCTURES EMC ENGINEER—SOMETHING NEW ON THE HORIZON. V. C. Plantz (Boeing Co., Everett, Wash.), p. 312-318. (See A69-42234 23-02)

INTERFERENCE EMISSION FILTERING IN HIGH POWER MICROWAVE TRANSMITTERS. F. O. Johnson (Varian Associates, Palo Alto, Calif.), p. 336-341. 9 refs. (See A69-42235 23-09)

A69-42536 *
A 60-GHz MULTIFREQUENCY RADIOMETRIC SENSOR FOR DETECTING CLEAR AIR TURBULENCE IN THE TROPOSPHERE.
George G. Haroules and Wilfred E. Brown (NASA, Electronics Research Center, Microwave Laboratory, Cambridge, Mass.).

IEEE Transactions on Aerospace and Electronic Systems, vol. AES-5, Sept. 1969, p. 712-723. 14 refs.

The temperature profile in a horizontal path forward of an aircraft can be sensed with a multichannel 5-mm passive radiometric receiving system. The characteristic signature of the multichannel radiometric output as a function of time would provide a measure of the range to the region of temperature discontinuity forward of the aircraft. Applicability to clear air turbulence (CAT) detection is predicated on the assumption that temperature discontinuities, at least in some cases, are associated with regions of such turbulence. It is therefore concluded that such a device has potential application as a CAT detector. Preliminary calculations indicate that the presence of a CAT region could be detected approximately 5 to 6 min before penetration, assuming an aircraft speed of 600 mph. A description is given of the design and construction of a two-frequency instrument which will be used to support the measurement program for determining the correlation between the meteorological parameters that are associated with the phenomenon called CAT. A multifrequency multibeam system is also described as the detector system for future supersonic aircraft. (Author)

N69-10250*# National Aeronautics and Space Administration. Lewis Research Center, Cleveland, Ohio.

THE EFFECTS OF REACTOR RADIATION ON 22-VOLT SILICON VOLTAGE REGULATOR DIODES

Suzanne T. Weinstein Washington Nov. 1968 24 p refs

(NASA-TN-D-4923) Avail: CFSTI CSCL 09A

Twenty-five silicon voltage regulator (Zener) diodes (S1N2985B) were exposed to reactor radiation to a total fast neutron fluence of 8.2×10^{13} neutrons per square centimeter and a gamma dose of 6.3×10^{7} rads carbon. The Zener voltage remained essentially constant and the breakdown knee was somewhat softened. The forward and reverse-leakage currents increased, and the forward voltage drop at high forward currents increased. The junction capacitance remained unchanged. Author

N69-14256*# ITT Industrial Labs., Fort Wayne, Ind.

RESEARCH AND DEVELOPMENT OF A SINGLE GUN COLOR CRT, PHASE 1 Final Report

Thomas E. Sisneros, Paul A. Faeth, and Joseph A. Davis Washington NASA Dec. 1968 72 p refs

(Contract NAS12-534)

(NASA-CR-1228) Avail: CFSTI CSCL 09A

The feasibility of producing cathode-ray tubes which have a current density-dependent color variation at constant accelerating voltage has been demonstrated. The screens for these tubes were prepared by combining superlinear phosphors with linear or sublinear phosphors. The preparation of phosphors having a superlinear intensity versus current density behavior was studied. Phosphors having superlinear behavior in the current density range normally used for CRT operation were prepared by partially poisoning (ZnCd)S:Ag with a few ppm of Ni. A number of experimental screens and tubes were prepared utilizing various combinations of experimental phosphors. Color shifts from reddish-orange to yellow and from yellowish-green to yellow to orange have been obtained. Author

N69-15441# Michigan Univ., Ann Arbor. Electron Physics Lab.

E-TYPE PHOTODEMODULATORS FOR COHERENT LIGHT SIGNALS Final Technical Report

John L. Mason Aug. 1968 47 p refs

(Contract DA-ARO-D-31-124-G634)

(AD-677374; REPT-07094-1-F) Avail: CFSTI CSCL 9/1

The theoretical studies are summarized and an experimental investigation is reported for an E-type traveling-wave phototube. The principal feature of such a device is the centrifugal electrostatic focusing of the electron beam. The theoretical study yields a small-signal power theorem, the types of waves propagating along a thin E-type beam, and a small-signal analysis of the traveling-wave phototube. An expression for the equivalent resistance of the device is derived, with numerical results given for the case of zero circuit loss, zero space charge, and synchronous beam velocity. For comparison, equivalent resistance values are given for O-type phototubes. The experimental investigation involved a phototube designed to operate at S-band. Design considerations and measurement techniques are discussed. Experimental curves for the equivalent resistance are presented and compared with the theoretical results. Author (TAB)

N69-18761*# IIT Research Inst., Chicago, Ill. Thermal Measurement Section.

EVALUATION OF VACUUM UV DETECTOR-SPECTROSCOPY SYSTEMS FOR CAPSULE REENTRY MEASUREMENTS

Ronald L. Ohlhaber, Mark W. P. Cann and Harold V. Watts Washington NASA Feb. 1969 167 p refs

(Contract NAS1-7481)

(NASA-CR-1268; IITRI-V6045) Avail: CFSTI CSCL 20F

Various vacuum ultraviolet detector-spectroscopy systems that could be employed for spectroscopic measurement of the shock wave created ahead of a capsule experiencing hypervelocity reentry conditions were analyzed and evaluated. A generalized set of measurement requirements and environmental conditions was established for a 50,000 ft/sec entry velocity. These conditions are then used to evaluate such detector-spectroscopy systems as ion chambers, proportional counters, Geiger-Mueller tubes, photoelectric tubes, wavelength shifters, photoconductive cells, photovoltaic cells, reverse biased diodes, miniature photodiode arrays, and photoelectric cathode with retardation grid analyzers. The most favorable system appears to be a wavelength dispersing device (grating) followed by an electronically scanned miniature detector array. The array elements could be chosen from either photodiodes, phototransistors, or photoconductors, whichever shows the best vacuum ultraviolet response. Author

N69-20888*# National Aeronautics and Space Administration. Langley Research Center, Langley Station, Va.

PARAMETERS AFFECTING FIRING TIME OF SIMULTANEOUSLY TRIGGERED TRIGATRON SPARK GAP SWITCHES

Michael D. Williams Washington Mar. 1969 31 p refs

(NASA-TN-D-5077) Avail: CFSTI CSCL 09E

The investigation was conducted primarily to determine how the variation of each of several spark gap parameters affects the firing-time differences (switch jitter) of simultaneously triggered trigatron spark gap switches. These parameters were switch voltage (15 to 20 kV), peak trigger voltage (14 to 20 kV), and the curvature of the edge of the trigger electrode hole. The firing times were measured by using the light emitted from the switches. The more significant conclusions are (1) By inference, the physical differences in the members of a switch group create firing-time differences like a component of true switch jitter and only higher switch voltages (of the parameters investigated) significantly diminish their magnitude; (2) true switch jitter is more sensitive to changes in switch voltage than to changes in peak trigger voltage; (3) increased peak trigger voltage is not very effective in reducing switch jitter; (4) the curvature of electrode hole edges does not significantly affect switch jitter in the fast mode of switch operation; and (5) the curves of the firing distributions are not Gaussian integrals as previously believed. Author

N69-23225*# Texas Instruments Inc., Dallas.

RELIABILITY HANDBOOK FOR SILICON MONOLITHIC MICROCIRCUITS. VOLUME 1: APPLICATION OF MONOLITHIC MICROCIRCUITS

William C. Weger et al Washington NASA Apr. 1969 235 p refs

(Contract NAS8-20639)

(NASA-CR-1346; Rept-03-67-04-Vol-1) Avail: CFSTI CSCL 09A

Described are: (1) typical problems that were experienced with certain applications and modes of operation for several families of digital and linear microcircuits; (2) the most reliable and trouble free methods of use or application of each type of circuit presented; (3) how to obtain maximum information from manufacturers' data sheets; (4) a method for derating the devices in actual use, and a method by which to assess the gain (or loss) in circuit performance and reliability which results from the application of the derating method; (5) the characteristics, advantages, and disadvantages of the various types of packages now available, and a method by which the user can evaluate the available packages and select the one most suitable for the intended application; and (6) methods for the interconnection of packages and assembly of circuits into components and systems. Author

N69-23226*# Texas Instruments Inc., Dallas.
RELIABILITY HANDBOOK FOR SILICON MONOLITHIC MICROCIRCUITS. VOLUME 2: FAILURE MECHANISMS OF MONOLITHIC MICROCIRCUITS
William O. Shurtleff Washington NASA Apr. 1969 35 p refs
(Contract NAS8-20639)
(NASA-CR-1347; Rept-03-67-04-Vol-2) Avail: CFSTI CSCL 09A

Defects are enumerated that are introduced into monolithic microcircuits during the various processes of manufacture; the impact of these defects on microcircuit failure rates and the techniques that are used to correct or remove the defects from the processes are considered. The techniques of processing that are used in the manufacture of monolithic microcircuits are sophisticated, numerous, and complex. There is a finite probability that defects are introduced at each step of the manufacturing process. These defects are of concern to both the manufacturer and the user of monolithic microcircuits in two major respects: (1) Defects reduce the effective yield of the manufacturer, thereby increasing the cost of each microcircuit bought by the user, and (2) Defects may cause microcircuit reliability problems which adversely affect the user's end product and the reputation of the microcircuit manufacturer. Author

N69-23556*# National Aeronautics and Space Administration. Electronics Research Center, Cambridge, Mass.
DEVELOPMENT OF AN EXPERIMENTAL SILICON CARBIDE BACKWARD DIODE OPERABLE TO 1000°K
Richard Farrell Washington Apr. 1969 7 p refs
(NASA-TN-D-5183) Avail: CFSTI CSCL 09A

Silicon carbide backward diodes which operate between 77°K and 1000°K were developed. Figures of merit ($\gamma \sqrt{R}$) of 19,300, 3,960, and 15 at 12.5 MHz, 50 MHz, and 8.8 GHz, respectively, were measured with detector areas on the order of 10^{-5} cm^2. These results are compatible with a prior analysis which predicts an upper frequency limit of between 0.1 and 1.0 GHz for SiC backward diodes. Author

N69-25328*# Texas Instruments, Inc., Dallas.
RELIABILITY HANDBOOK FOR SILICON MONOLITHIC MICROCIRCUITS. VOLUME 3: FAILURE ANALYSIS OF MONOLITHIC MICROCIRCUITS
Wilton L. Workman Washington NASA Apr. 1969 196 p refs
(Contract NAS8-20639)
(NASA-CR-1348; TI-03-67-04) Avail: CFSTI CSCL 09E

The purpose of the handbook is to provide aid in determining the most effective application and understanding of monolithic microcircuits, and the most effective quality and reliability assurance controls for the circuits. This volume describes the following topics: (1) effective failure analysis methods; (2) a step-by-step procedure for performing failure analysis; (3) how to identify failure mechanisms and their causes; and (4) how to assess the results of a failure analysis and to establish a relationship between the findings and the affected parameters or characteristics. For Volumes I and II of this publication see N69-23225 and N69-23226 respectively. Author

N69-27841*# National Aeronautics and Space Administration. Lewis Research Center, Cleveland, Ohio.
CAVITATION PERFORMANCE OF 80.6° HELICAL INDUCER IN LIQUID HYDROGEN
Phillip R. Meng and Royce D. Moore Washington Jun. 1969 14 p refs
(NASA-TM-X-1808) Avail: CFSTI CSCL 09E

The cavitating and noncavitating performance of an 80.6° helical inducer was evaluated in liquid hydrogen over a temperature range from 31.0° to 40.2° R (17.2 to 22.3 K). The inducer was operated at 30 000 rpm at flow coefficients from 0.08 to 0.12. The net positive suction head requirements decreased with increasing liquid temperature; at constant temperature, these requirements increased rapidly with flow coefficient. At the lower values of flow coefficient and the higher liquid temperatures, the inducer produced a useful head rise even with vapor at the inducer inlet. Author

N69-36706*# National Aeronautics and Space Administration. Electronics Research Center, Cambridge, Mass.
FABRICATION AND CHARACTERISTICS OF MICROWAVE BACKWARD DIODES IN INDIUM ARSENIDE
John B. Hopkins Washington Sep. 1968 25 p refs
(NASA-TN-D-5401) Avail: CFSTI CSCL 09A

The many advantages of backward diodes for microwave mixing and detecting – zero bias, low local oscillator power, low $1/f$ noise, and environmental insensitivity – are significantly offset by the high capacitance associated with a narrow tunneling junction. This either severely limits high-frequency operation or requires small-area junctions which are fragile and susceptible to burnout at low power levels. This limitation can be reduced considerably by selection of a semiconductor with small band-gap and low carrier effective mass, with consequent high tunneling probability and reduced capacitance per unit area. Thus, a device of given size permits higher frequency operation, or equivalent electrical performance with larger area, leading to improved ruggedness and resistance to burnout. Computer-aided studies of the characteristics of tunneling junctions have confirmed the initial estimate that, among elemental and III-V semiconductors, InAs offers optimum improvement of detector performance. Author

N69-36710*# National Aeronautics and Space Administration. Lewis Research Center, Cleveland, Ohio.
TRANSISTOR PERFORMANCE IN INTENSE MAGNETIC FIELDS
Wayne R. Hudson, Erwin H. Meyn, and Clarence W. Schultz (Conn. Univ.) Washington Sep. 1969 14 p refs
(NASA-TN-D-5428) Avail: CFSTI CSCL 09A

The forward current transfer ratio ($h_{FE} = (\Delta I_{collector}/\Delta I_{base})$) of a germanium junction transistor operating in the common emitter mode is reduced by the application of a magnetic field. This reduction is greatest when the magnetic field vector is perpendicular to the direction of minority carrier motion through the base region. The base thickness is also an important variable. Transistors with smaller base (planar diffused) regions are less affected by magnetic fields. Author

N69-38597*# National Aeronautics and Space Administration. Electronics Research Center, Cambridge, Mass.
LEAK DETECTION IN HERMETICALLY SEALED DEVICES
I. Litant Washington Oct. 1969 13 p refs
(NASA-TN-D-5457) Avail: CFSTI CSCL 09A

A method for detecting leaks in a hermetically sealed device was developed. The method comprises the introduction of a low-boiling halogenated liquid into the device through the leaks, and detecting the vaporizing liquid as it escapes from the leaks by the use of a halogen detector. The leaks may thus be pinpointed, and the leak rate determined. Author

N69-38774*# National Aeronautics and Space Administration.

Electronics Research Center, Cambridge, Mass.

A METHOD FOR SEPARATING A SEMICONDUCTOR WAFER INTO INDIVIDUAL CHIPS

I. Litant Washington Oct. 1969 13 p refs

(NASA-TM-X-1892; C-85) Avail: CFSTI CSCL 09E

A method has been devised to improve the breaking of a semiconductor single-crystal wafer into chips. A scribed wafer placed face-up on a convex surface is contacted rapidly by a rubber diaphragm under air pressure. A stress is thereby applied uniformly in all directions at once causing essentially complete breakage along prescribed lines. Dust and debris are minimized. Author

N69-38776*# National Aeronautics and Space Administration. Lewis Research Center, Cleveland, Ohio.

A TRANSFORMER OF CLOSELY SPACED PULSED WAVEFORMS HAVING A NONZERO AVERAGE VALUE

Janis M. Niedra Washington Oct. 1969 27 p refs

(NASA-TN-D-5473; E-5185) Avail: CFSTI CSCL 09E

With the use of diodes, transistors, and magnetic cores, a passive circuit was constructed that transformed the voltage, either up or down, of repeated positive or negative pulses. This circuit combined a pulse transformer with switching devices to effect a resonant flux reset. It could transform various pulsed waveforms that had a nonzero average value and were relatively closely spaced in time. The circuit provided direct current isolation between multiple loads and between a load and the source, similar to a conventional transformer. Several experimental circuits were tested. Author

N69-38852*# National Aeronautics and Space Administration. Langley Research Center, Langley Station, Va.

A NAVIGATION-AIDS IDENTIFICATION DECODER AND DISPLAY FOR GENERAL-AVIATION AIRCRAFT

Charles W. Meissner, Jr. Washington Oct. 1969 14 p refs

(NASA-TN-D-5445) Avail: CFSTI CSCL 09F

A device has been designed to interpret and display the Morse code identifier for very high frequency omnirange stations and other navigation aids. It is intended to reduce the workload of the general-aviation pilot and to aid in safe navigation. A prototype device has been fabricated which can be readily mounted in an aircraft instrument panel. The input signal is obtained from the aircraft audio bus. It in no way affects the operation of other avionic equipment on the aircraft. Author

N69-40079*# National Aeronautics and Space Administration. Langley Research Center, Langley Station, Va.

APPLICATION OF PRESSURIZED LIQUID NITROGEN INSIDE PARAMETRIC-AMPLIFIER STRUCTURES FOR INPUT-NOISE-TEMPERATURE IMPROVEMENT

Hans-Juergen C. Blume Washington Oct. 1969 31 p refs

(NASA-TN-D-5509) Avail: CFSTI CSCL 09E

The temperature rise caused by power dissipation in lossy capacitance diodes in cooled parametric amplifiers, especially in monostatic high-power radar systems, diminished the noise-reduction effect of the coolant. To obtain good heat conduction from the diode so that it would remain at ambient temperature, liquid nitrogen helium gas under pressure was employed as dielectric material surrounding the lossy diode. All adjustments for optimum performance of a 400-MHz amplifier were accomplished at room temperature before immersion into liquid nitrogen by using calculated and measured values from curves that showed resonant frequency variation of each circuit due to the change of the relative dielectri c constant from 1 to 1.435, the slight change of the physical dimension caused by thermal contraction, and the change of the operating frequency at high gain. Author

N69-41208*# National Aeronautics and Space Administration. Electronics Research Center, Cambridge, Mass.

ENERGY DISTRIBUTION OF A SPIRALING ELECTRON BEAM

Bernhard Kulke Washington Nov. 1969 25 p refs

(NASA-TN-D-5490) Avail: CFSTI CSCL 09A

A retarding-field analyzer was used to investigate the energy conversion and the energy spread of a spiraling electron beam, where the trajectory is generated from a magnetic corkscrew-magnetic ramp combination. It was found that in the absence of space-charge effects, a relatively narrow, near rectangular energy distribution will be generated by the corkscrew when the axial magnetic field is tuned to cyclotron resonance. The normalized width of this distribution is approximately independent of the degree of energy conversion, in agreement with the theory, and the mean transverse energy varies as the square of the corkscrew current. The magnetic ramp amplifies both the mean transverse energy and the energy spread linearly. Both these quantities also can be estimated by using the mirroring effect of the magnetic ramp, in conjunction with variable corkscrew current. Author

10

ELECTRONICS

Includes circuit theory; and feedback and control theory. For applications see: 09 Electronic Equipment. For related information see: Specific Physics Categories.

A69-13073 *

LOGARITHMIC VARIATION CRITERIA FOR THE STABILITY OF SYSTEMS WITH TIME-VARYING GAINS.

M. Freedman (NASA, Electronics Research Center, Cambridge, Mass.) and G. Zames.

SIAM Journal of Control, vol. 6, Aug. 1968, p. 487-507. 14 refs.

Derivation of a new stability condition for a feedback system consisting of a linear element H(s) and a time-varying gain k(t). It is shown that if k(t) lies in an interval [a + ε, b - ε], and if the shifted Nyquist diagram $H(j\omega - \sigma_{sh})$ does not intersect a critical interval of the complex plane and encircles it a number of times equal to the number of poles of H(s) in the region Re {s} > $-\sigma_{sh}$, then the closed-loop system is stable, provided that the average logarithmic variation $\hat{k}$ satisfies a particular inequality. M. M.

A69-14693

STOCHASTIC PROBLEMS IN CONTROL; AMERICAN AUTOMATIC CONTROL COUNCIL, JOINT AUTOMATIC CONTROL CONFERENCE, UNIVERSITY OF MICHIGAN, ANN ARBOR, MICH., JUNE 26, 1968, PROCEEDINGS.

New York, American Society of Mechanical Engineers, 1968. 124 p. *Members, $4.00; nonmembers, $5.00.*

CONTENTS:

PREFACE. B. Friedland. 1 p.

MATHEMATICAL MODELING OF STOCHASTIC PROCESSES. T. Kailath and P. Frost (Stanford University, Stanford, Calif.), p. 1-38. 24 refs. [See A69-14694 04-19]

A SURVEY OF STABILITY OF STOCHASTIC SYSTEMS. F. Kozin (Brooklyn, Polytechnic Institute, Brooklyn, N.Y.), p. 39-86. 65 refs. [See A69-14695 04-19]

RECENT RESULTS IN LINEAR AND NON-LINEAR FILTERING. R. S. Bucy (Southern California, University, Los Angeles, Calif.), p. 87-105. 25 refs. [See A69-14696 04-10]

OPTIMAL STOCHASTIC CONTROL. W. M. Wonham (NASA, Electronics Research Center, Cambridge, Mass.), p. 107-120. [See A69-14697 04-10]

A69-14697 *

OPTIMAL STOCHASTIC CONTROL.

W. M. Wonham (NASA, Electronics Research Center, Cambridge, Mass.).

IN: STOCHASTIC PROBLEMS IN CONTROL; AMERICAN AUTOMATIC CONTROL COUNCIL, JOINT AUTOMATIC CONTROL CONFERENCE, UNIVERSITY OF MICHIGAN, ANN ARBOR, MICH., JUNE 26, 1968, PROCEEDINGS. [A69-14693 04-10]

New York, American Society of Mechanical Engineers, 1968, p. 107-120.

Brief survey of results obtained from investigations of stochastic control, which has evolved largely within the framework of dynamic programming. Only system models where stochastic elements are featured explicitly are considered. The survey is restricted to small dynamic systems described by random differential equations, the "large" systems of operations research being ignored. The solvable stochastic version of the well-known linear-quadratic regulator problem is presented. The so-called separation theorem is presented and discussed. A system designed to operate partly open-loop, as is the case with some guidance systems, and where corrections are applied only at certain preassigned points along the trajectory is also examined. M. G.

A69-16598 *

L_2-STABILITY OF TIME-VARYING SYSTEMS - CONSTRUCTION OF MULTIPLIERS WITH PRESCRIBED PHASE CHARACTERISTICS.

M. I. Freedman (NASA, Electronics Research Center, Cambridge, Mass.).

SIAM Journal on Control, vol. 6, Nov. 1968, p. 559-578. 6 refs.

Investigation of a system consisting of a linear element G(s) and a time-varying gain n(·). It is shown that the system is stable for all n(·) in a sector [0, k) if it is assumed that the system is stable for all constant gains in that sector. The proof employs a "multiplier" operator. However, a method is used to eliminate any "multiplier" dependence from the final results, so that these results are explicit and geometric. The techniques developed are believed to show promise of eliminating the multiplier dependence from many recent stability results. G. R.

A69-16601 *

ON A MATRIX RICCATI EQUATION OF STOCHASTIC CONTROL.

W. M. Wonham (NASA, Electronics Research Center, Cambridge, Mass.).

SIAM Journal on Control, vol. 6, Nov. 1968, p. 681-697. 7 refs.

NSF Grant No. GK-967; Grant No. AF AFOSR 693-67.

Discussion of a generalized version of the matrix Riccati and matrix quadratic equations which arise in problems of stochastic control and filtering. The generalization consists in the addition of a linear positive operator to the linear terms of the standard Riccati equation and, in certain cases, a weakening of the usual hypothesis of complete observability to observability of unstable modes. The proofs given are simple applications of Bellman's principle of quasi-linearization and of a known monotone convergence property of symmetric matrices. Applications to control and filtering are indicated. G. R.

A69-17939 *

SUBOPTIMAL STATE ESTIMATION FOR CONTINUOUS-TIME NONLINEAR SYSTEMS FROM DISCRETE NOISY MEASUREMENTS.

Michael Athans (Massachusetts Institute of Technology, Dept. of Electrical Engineering, Cambridge, Mass.), Richard P. Wishner, and Anthony Bertolini (Massachusetts Institute of Technology, Lincoln Laboratory, Lexington, Mass.).

(AMERICAN AUTOMATIC CONTROL COUNCIL, JOINT AUTOMATIC CONTROL CONFERENCE, 9TH, UNIVERSITY OF MICHIGAN, ANN ARBOR, MICH., JUNE 26-28, 1968, *PROCEEDINGS*, p. 364-382.)

IEEE Transactions on Automatic Control, vol. AC-13, Oct. 1968, p. 504-514. 28 refs.

Research supported by the Massachusetts Institute of Technology and ARPA; Grant No. NGR-22-009-124.

Derivation of the dynamical equations of a "second-order" filter which estimates the states of a nonlinear plant on the basis of discrete noisy measurements. The filter equations contain terms involving the second-order partial derivatives of the plant and output equations. Simulation results are presented which yield a comparison of the performance of the first- versus the second-order filter. It is demonstrated that the use of second-order terms in the Taylor series expansion to correct bias errors can improve the performance of a filter which is to estimate the state variables of a nonlinear plant. M. G.

10 ELECTRONICS

A69-17947 *

ON THE STABILIZATION OF CONTROLLABLE SYSTEMS.

William A. Wolovich (NASA, Electronics Research Center, Office of Control Theory and Application, Cambridge, Mass.).

IEEE Transactions on Automatic Control, vol. AC-13, Oct. 1968, p. 569-572. 12 refs.

Conditions are obtained for the asymptotic stabilization of linear dynamical systems through the use of linear state-variable feedback. The procedures developed rely on uniform controllability of the given systems, and yield explicit expressions for the transition matrices of the stabilized systems. As a consequence of the treatment, explicit expressions are obtained for Liapunov transformations which reduce the stabilized systems to canonical (phase-variable) form. Results are given for time-varying multivariable (multiinput) systems. (Author)

A69-19853 *

ANALYSIS OF COMMUTATED NETWORKS EMPLOYING FEEDBACK CIRCUITS.

Michael T. Borelli (NASA, Marshall Space Flight Center, Huntsville, Ala.).

IEEE Transactions on Aerospace and Electronic Systems, vol. AES-5, Jan. 1969, p. 39-45. 5 refs.

A method of analysis has been developed for feedback systems employing commutated networks in the forward loop and linear transfer functions in the feedback loop. The method handles single-phase and polyphase commutated networks as well as coupled and uncoupled networks. Although commutated networks are linear from the superposition theory viewpoint, linear feedback theory is shown to be not applicable because of the harmonics present in the feedback. Techniques for simplifying the analysis of commutated networks by the use of equivalent block diagrams provide additional insights into commutated network operation. (Author)

A69-21327 *#

DOMAIN ANALYSIS AND MEASUREMENT TECHNIQUES FOR DISTRIBUTED RC STRUCTURES. I - ANALYSIS IN THE RECIPROCAL TIME DOMAIN.

W. W. Happ (NASA, Electronics Research Center, Cambridge, Mass.) and S. C. Gupta (Southern Methodist University, Dallas, Tex.).

Journal of Applied Physics, vol. 40, Jan. 1969, p. 109-117. 18 refs.

The impulse response in distributed-parameter systems results in a spectrum of delta functions in the time domain for LC structures. It is shown that for RC structures the impulse response results in a spectrum of Poisson-derived functions in the reciprocal time domain. This isomorphism is exploited for the analysis of RC devices to establish a calculus of Poisson-derived functions and a transform technique which is essentially the Laplace transform. Applications of this technique to thin-film devices and minority-carrier devices are examined and lead to the determination of the transient response for one-ports and two-ports that are subject to a wide range of terminations. Illustrative examples of excitations include the impulse, the step, and the ramp, as well as signals generated by the distributed parameter devices themselves. Significant advantages accrue from a spectral description of RC devices in the reciprocal time domain. (Author)

A69-22567 *

OPTIMAL STOCHASTIC CONTROL.

W. M. Wonham (NASA, Electronics Research Center, Cambridge, Mass.).

(American Automatic Control Council, Joint Automatic Control Conference, 9th, University of Michigan, Ann Arbor, Mich., June 26-28, 1968.)
Automatica, vol. 5, Jan. 1969, p. 113-118. 112 refs.

General discussion of the present status and future direction of research in optimal stochastic control. System models where stochastic elements are featured explicitly are discussed. Only small dynamic systems, described by random differential equations are treated, and the larger systems of operations research are ignored. The solvable stochastic version of the well-known linear-quadratic regulator problem is reviewed. A brief survey of the problem involved in attempting to formulate and to solve optimal stochastic control problems is then presented. M. G.

A69-25450 *

STABILITY OF SYSTEMS WITH SECTOR NONLINEARITIES - A COMPARISON OF VARIOUS INEQUALITIES.

G. Zames (NASA, Electronics Research Center, Cambridge, Mass.).

IEEE Transactions on Automatic Control, vol. AC-13, Dec. 1968, p. 709-711.

Discussion of a common method of deriving stability conditions of the multiplier-type. This method involves two steps: (1) the feedback equation is transformed into a new equation containing a pair of positive operators; and (2) an appropriate multiplier is introduced. Depending on which of these steps is performed first, two different results are obtained, and it has not been clear in the past whether either result is preferable to the other. It is shown that, under suitable hypotheses, it is preferable to perform step (1) first - i.e., a better stability condition is obtained if the transformation into positive operators is performed before the multiplier is introduced. M. M.

A69-30601 *

A COMPUTATIONAL APPROACH TO OPTIMAL CONTROL OF STOCHASTIC SATURATING SYSTEMS.

W. M. Wonham and W. F. Cashman (NASA, Electronics Research Center, Cambridge, Mass.).

International Journal of Control, First Series, vol. 10, July 1969, p. 77-98. 20 refs.

Digital computation of a suboptimal nonlinear feedback control for a time-variant linear system subject to additive white noise. The cost functional is the expectation, under stochastically stationary conditions, of a quadratic function of state and control variables. The design of an eighth-order attitude control and of a second-order tracking system are given as examples. For the latter system, the elliptical differential equation of dynamic programming is solved by finite differences to yield the true optimal control, and results are compared with those for the suboptimal control. The procedure can be modified if the observations of the state include additive noise. B. H.

A69-32899 *

DIGITAL SIMULATION STABILITY CRITERION.

Carl F. Lorenzo and Leslie L. Scalzott (NASA, Lewis Research Center, Cleveland, Ohio).

Instruments and Control Systems, vol. 42, Apr. 1969, p. 113-117. 6 refs.

Discussion of a criterion for computer stability analysis. A digital stability scheme is presented which is premised on the use of only perturbed transient responses. The stability analysis block in the program should be capable of handling any time function (continuous or discontinuous, oscillatory or nonoscillatory, periodic or aperiodic) and any system, linear or nonlinear. The criterion developed is essentially an approximation to asymptotic stability (which requires ultimate state boundedness of the output). G.R.

A69-34671

ASILOMAR CONFERENCE ON CIRCUITS AND SYSTEMS, 2ND, PACIFIC GROVE, CALIF., OCTOBER 30-NOVEMBER 1, 1968, CONFERENCE RECORD.

Conference sponsored by the U.S. Naval Postgraduate School and the University of Santa Clara.
New York, Institute of Electrical and Electronics Engineers, Inc., 1969. 631 p.
Members, $20.; nonmembers, $30.

CONTENTS:

FOREWORD. S. R. Parker (U.S. Naval Postgraduate School, Monterey, Calif.) and R. C. Dorf (Santa Clara, University, Santa Clara, Calif.), p. 3.

COMPUTER AIDED DESIGN OF LINEAR AND SATURATING SERVOMECHANISMS. E. W. Van Winkle and D. S. Levine (Bendix Corp., Teterboro, N.J.), p. 16-20. 5 refs. [See A69-34672 18-10]

STOCHASTIC SERVOMECHANISM DESIGN VIA OPTIMAL FILTER THEORY. S. Fagin, A. Graefe, and E. Grinoch (Sperry Rand Corp., Great Neck, N.Y.), p. 40-45. [See A69-34673 18-10]

REGIONS OF EXPONENTIAL BOUNDEDNESS FOR THE PROBLEM OF LUR'E. D. Šiljak and S. Weissenberger (Santa Clara, University, Santa Clara, Calif.), p. 61-63. 6 refs. [See A69-34674 18-19]

SENSITIVITY ANALYSIS OF DISCRETE KALMAN FILTERS. F. L. Sims and D. G. Lainiotis (Texas, University, Austin, Tex.), p. 147-152. 7 refs. [See A69-34675 18-10]

ADAPTIVE FILTERING IN SATELLITE ORBIT ESTIMATION. A. H. Jazwinski (Analytical Mechanics Associates, Inc., Lanham, Md.), p. 153-158. 15 refs. [See A69-34676 18-10]

ONE-SWITCHING OPTIMAL CONTROL FOR PITCH MOTION OF A SATELLITE. E. P. Hofer (Stuttgart, Technische Universität, Stuttgart, West Germany), p. 168-172. [See A69-34677 18-31]

SUB-OPTIMAL CLOSED-LOOP CONTROL OF NONLINEAR SYSTEMS USING INVARIANT IMBEDDING TECHNIQUES. W. J. Steinway and J. L. Melsa (Southern Methodist University, Dallas, Tex.), p. 188-191. 7 refs. [See A69-34678 18-10]

MULTILOOP DISTRIBUTED RC ACTIVE NETWORKS FOR LOW PARAMETER SENSITIVITY WITH LOW AMPLIFIER GAIN. C. V. Shaffer (NASA, Ames Research Center, Moffett Field, Calif.; Florida, University, Gainesville, Fla.) and W. J. Kerwin (NASA, Ames Research Center, Moffett Field, Calif.), p. 197-201. [See A69-34679 18-10]

A CIRCUIT ANALYSIS PROGRAM FOR EDUCATIONAL USE. R. E. Bach, Jr., G. F. Currin, and P. A. Olendzenski (Northeastern University, Boston, Mass.), p. 255-259. 14 refs. [See A69-34680 18-10]

APPLICATION OF OPTIMAL CONTROL THEORY TO CONTROLLERS WHICH EXHIBIT OTHER THAN "BANG-BANG" TIME RESPONSES. D. J. Hampton (Sperry Rand Corp., Phoenix, Ariz.) p. 336-339. [See A69-34681 18-02]

PERIODICALLY SWITCHED LOSSLESS NETWORKS - SYSTEM FUNCTIONS AND POWER RELATIONS. M. Awipi and H. E. Meadows (Columbia University, New York, N.Y.), p. 358-362. 11 refs. [See A69-34682 18-10]

DEVELOPING AN ATTITUDE CONTROL SYSTEM FOR THE APOLLO TELESCOPE MOUNT. S. M. Seltzer (Lockheed Aircraft Corp., Sunnyvale, Calif.), p. 371-375. 6 refs. [See A69-34683 18-21]

A SIMPLE MOMENTUM CONTROL SYSTEM FOR SATELLITE MANEUVERING. M. G. Lyons and J. J. Rodden (Lockheed Aircraft Corp., Sunnyvale, Calif.), p. 376-381. [See A69-34684 18-31]

STATE SPACE APPROACH TO MIXED BOUNDARY VALUE PROBLEMS. C. F. Chen (Houston, University, Houston, Tex.) and M. M. Chen (Boston University, Boston, Mass.), p. 382-385. [See A69-34685 18-19]

STATE-SPACE STRUCTURE OF MODEL-REFERENCE ADAPTIVE CONTROL FOR A NOISY SYSTEM. M. G. Currie (McDonnell Douglas Corp., Santa Monica, Calif.) and E. B. Stear (California, University, Los Angeles, Calif.), p. 401-405. 15 refs. [See A69-34686 18-10]

A TECHNIQUE FOR CORRECTING COEFFICIENT QUANTIZATION ERRORS IN HYBRID CONTROL SYSTEMS. D. L. Chenoweth, C. L. Phillips, and J. C. Johnson (Auburn University, Auburn, Ala.), p. 444-447. 7 refs. [See A69-34687 18-10]

OPTIMIZATION OF SLOWLY-VARYING SYSTEMS BY MINIMIZATION OF THE EXPECTED VALUE OF A QUADRATIC PERFORMANCE INDEX. L. B. Patrick (North American Rockwell Corp., Anaheim, Calif.) and H. D'Angelo (Denver, University, Denver, Colo.), p. 542-546. 7 refs. [See A69-34688 18-10]

AN ANALYTIC TEST FOR ABSOLUTE STABILITY AND POSITIVE REALNESS. D. Šiljak (Santa Clara, University, Santa Clara, Calif.), p. 580, 581. [See A69-34689 18-10]

AUTHOR INDEX, p. 631, 632.

A69-34679 *

MULTILOOP DISTRIBUTED RC ACTIVE NETWORKS FOR LOW PARAMETER SENSITIVITY WITH LOW AMPLIFIER GAIN.

C. V. Shaffer (NASA, Ames Research Center, Moffett Field, Calif.; Florida, University, Gainesville, Fla.) and W. J. Kerwin (NASA, Ames Research Center, Moffett Field, Calif.).

IN: ASILOMAR CONFERENCE ON CIRCUITS AND SYSTEMS, 2ND, PACIFIC GROVE, CALIF., OCTOBER 30-NOVEMBER 1, 1968, CONFERENCE RECORD. [A69-34671 18-10]

Conference sponsored by the U.S. Naval Postgraduate School and the University of Santa Clara.

New York, Institute of Electrical and Electronics Engineers, Inc., 1969, p. 197-201.

Study showing that the use of multiloop feedback provides a considerable reduction in sensitivity and in the gain-sensitivity product in active distributed RC networks as compared to single-loop circuits. Design equations are presented allowing various optimizations depending on the specific requirements. It is concluded that the use of a single RC line provides zero Q sensitivity to passive element variation and allows tuning, for example, by varying the dc bias on a depletion-layer capacity in a monolithic distributed RC structure without any effect on the resonant Q. P.G.

A69-42230 *

PULSE INTERFERENCE EFFECTS IN A PHASE-LOCK LOOP.

J. M. Clarke (NASA, Electronics Research Center, Cambridge, Mass.), R. J. Otero, and W. C. Wanbaugh (IIT Research Institute, Systems Sciences Research Div., Annapolis, Md.).

IN: INSTITUTE OF ELECTRICAL AND ELECTRONICS ENGINEERS, ELECTROMAGNETIC COMPATIBILITY SYMPOSIUM, 11TH, ASBURY PARK, N.J., JUNE 17-19, 1969, RECORD. (A69-42215 23-09)

New York, Institute of Electrical and Electronics Engineers, Inc., 1969, p. 207-214.

Contracts No. NAS 12-639; No. NASw-1729.

Study of the ability of a phase-lock loop (PLL) demodulator to acquire and remain locked on a desired signal in the presence of receiver noise and pulse interference such as that generated by radar equipments. Measurements were conducted over a wide range of PLL operating conditions for a typical space instrumentation receiver. The PLL and interference signal parameters varied during the test included the desired signal-to-noise ratio, the signal-to-interference ratio, the offset of the pulse carrier frequency from the desired signal, the pulse width and pulse repetition rate of the interference signal, and the receiver tracking bandwidth. G.R.

A69-43267

AMERICAN AUTOMATIC CONTROL COUNCIL, JOINT AUTOMATIC CONTROL CONFERENCE, 10TH, UNIVERSITY OF COLORADO, BOULDER, COLO., AUGUST 5-7, 1969, PREPRINTS OF TECHNICAL PAPERS.

New York, American Institute of Chemical Engineers, 1969. 1025 p. Members, $40.; nonmembers, $50.

CONTENTS:

ANALYSIS OF PROPORTIONAL FLUID AMPLIFIERS IN CASCADE AND WITH FEEDBACK. Q. B. Chou, E. C. Hind (Worthington /Canada/, Ltd., Canada), E. C. Hind, J. Y. Harrison, and R. A. A. Bryant (New South Wales, University, Sydney, Australia), p. ix-xviii. 6 refs. (See A69-43268 24-03)

SEPARATION THEOREM FOR NONLINEAR MEASUREMENTS. R. E. Curry (Cornell University, Ithaca, N.Y.), p. 1-4. 7 refs. (See A69-43269 24-10)

TRANSFORMATION TECHNIQUE FOR OPTIMAL CONTROL PROBLEMS WITH A STATE VARIABLE INEQUALITY CONSTRAINT. D. H. Jacobson and M. M. Lele (Harvard University, Cambridge, Mass.), p. 52-59. 24 refs. (See A69-43270 24-10)

ON-OFF LIMIT-CYCLE CONTROLLERS FOR REACTION-JET CONTROLLED SYSTEMS. I—ANALYSIS AND SYNTHESIS. J. M. Mendel (McDonnell Douglas Corp., Santa Monica, Calif.), p. 65-73. 5 refs. (See A69-43271 24-10)

STEADY-STATE ANALYSIS OF THE HUMAN RESPIRATORY SYSTEM. H. T. Milhorn, Jr. and D. R. Brown (Mississippi, University, Jackson, Miss.), p. 141, 142. 10 refs. (See A69-43272 24-05)

AN INFORMATION PROCESSING MODEL FOR TACTILE PERCEPTION. J. C. Bliss (Stanford Research Institute, Menlo Park, Calif.), p. 144, 145. 7 refs. (See A69-43273 24-05)

VESTIBULAR MODELS. L. R. Young (Massachusetts Institute of Technology, Cambridge, Mass.), p. 146, 147. 8 refs. (See A69-43274 24-05)

APPLICATIONS OF A SIMPLIFIED MULTIDIMENSIONAL STOCHASTIC APPROXIMATION ALGORITHM. D. F. Elliott (North American Rockwell Corp., Anaheim, Calif.) and D. D. Sworder (Sothern California, University, Los Angeles, Calif.), p. 148-154. 7 refs. (See A69-43275 24-10)

DETERMINISTIC THEORY OF ESTIMATION AND CONTROL. G. W. Johnson (International Business Machines Corp., Cambridge, Mass.), p. 155-160. 11 refs. (See A69-43276 24-10)

AN ATTITUDE CONTROL SYSTEM FOR LARGE LAUNCH VEHICLES. S. M. Seltzer (Lockheed Aircraft Corp., Sunnyvale, Calif.), p. 228-231. (See A69-43277 24-31)

STATE VARIABLE SYNTHESIS OF A CONTROL SYSTEM FOR A LAUNCH VEHICLE WITH SEVERE MODE INTERACTION. R. L. Swaim (Purdue University, Lafayette, Ind.), p. 232-239. 6 refs. (See A69-43278 24-31)

APPLICATION OF QUADRATIC OPTIMIZATION TO HELICOPTER FLIGHT CONTROL. D. L. Gray, P. S. Rempfer, and L. Stevenson (NASA, Electronics Research Center, Cambridge, Mass.), p. 240-247. 6 refs. (See A69-43279 24-02)

QUASI-OPTIMUM DESIGN OF AN AIRCRAFT LANDING CONTROL SYSTEM. C. K. Ling (Singer-General Precision, Inc., Little Falls, N.J.), p. 248-256. (See A69-43280 24-02)

THE COMPUTATION OF OPTIMAL APOLLO-TYPE REENTRY TRAJECTORIES. B. D. Tapley, W. T. Fowler, and W. E. Williamson (Texas, University, Austin, Tex.), p. 281, 282. 7 refs. (See A69-43281 24-30)

SINGULAR OPTIMAL CONTROL PROBLEMS. D. H. Jacobson (Harvard University, Cambridge, Mass.), p. 283, 284. 8 refs. (See A69-43282 24-10)

A TECHNIQUE FOR OPTIMIZING THE SELECTION OF QUANTIZED COEFFICIENTS IN DIGITAL CONTROLLERS. D. L. Chenoweth (LTV Aerospace Corp., Dallas, Tex.), C. L. Phillips, and J. C. Johnson (Auburn University, Auburn, Ala.), p. 312-317. 10 refs. (See A69-43283 24-10)

ON THE STOCHASTIC FUEL-REGULATOR PROBLEM. H. D. Gilbert and G. N. Saridis (Purdue University, Lafayette, Ind.), p. 318-325. 15 refs. (See A69-43284 24-10)

SUBOPTIMAL CLOSED-LOOP CONTROLLER DESIGN FOR MINIMUM PROBABILITY OF INEQUALITY CONSTRAINTS VIOLATION. J. Y. S. Luh and M. P. Lukas (Purdue University, Lafayette, Ind.), p. 326-334. 13 refs. (See A69-43285 24-10)

ON COMPUTATIONAL SOLUTIONS OF STATE CONSTRAINED OPTIMIZATION PROBLEMS. W. F. Hamilton, Jr. and A. J. Koivo (Purdue University, Lafayette, Ind.), p. 384-393. 18 refs. (See A69-43286 24-10)

ON THE FREQUENCY RESPONSE OF VISCOUS COMPRESSIBLE FLUIDS AS A FUNCTION OF THE STOKES NUMBER. F. R. Goldschmied (Westinghouse Electric Corp., West Lafayette, Ind.), p. 394-409. 6 refs. (See A69-43287 24-12)

THE FREQUENCY RESPONSE OF VOLUME-TERMINATED PNEUMATIC LINES WITH CIRCULAR AND RECTANGULAR CROSS SECTIONS. M. E. Franke, R. W. Wilda, R. N. Miller, and C. V. Fada (USAF, Air University, Wright-Patterson AFB, Ohio), p. 410-415. 17 refs. (See A69-43288 24-12)

DYNAMIC MODELS FOR VISCOUS FLUID TRANSMISSION LINES. C. R. Gerlach (Southwest Research Institute, San Antonio, Tex.), p. 416-424. 11 refs. (See A69-43289 24-12)

SYNTHESIS OF FLUID LOGIC CONTROL CIRCUITS. J. H. Cole (Arkansas, University, Fayetteville, Ark.) and E. C. Fitch, Jr. (Oklahoma State University, Stillwater, Okla.), p. 425-432. (See A69-43290 24-10)

OPTIMAL ESTIMATION OF ROTATION-COUPLED FLEXURAL OSCILLATIONS. J. L. Farrell, J. K. Newton, J. A. Miller, and J. J. Connelly (Westinghouse Electric Corp., Baltimore, Md.), p. 433-441. 10 refs. (See A69-43291 24-31)

QUASI-OPTIMUM PROPORTIONAL NAVIGATION. E. I. Axelband and F. W. Hardy (Hughes Aircraft Co., Culver City, Calif.), p. 444-450. (See A69-43292 24-21)

DESIGN OF TIME LAG SYSTEMS WITH SENSITIVITY CONSTRAINTS. J. Tal and S. J. Kahne (Minnesota, University, Minneapolis, Minn.), p. 459-462. (See A69-43293 24-10)

OPTIMAL INPUTS FOR PARAMETER ESTIMATION IN DYNAMIC SYSTEMS WITH WHITE OBSERVATION NOISE. N. E. Nahi (Southern California, University, Los Angeles, Calif.) and D. E. Wallis, Jr. (Northrop Corp., Hawthorne, Calif.), p. 506-513. 12 refs. (See A69-43294 24-10)

POLICIES AND CONTROLLER DESIGN FOR A PURSUING VEHICLE. D. M. Salmon (Wolf Management Services, Palo Alto, Calif.), p. 522-529. (See A69-43295 24-19)

FORMAL SOLUTIONS FOR A CLASS OF STOCHASTIC PURSUIT-EVASION GAMES. W. W. Willman (Harvard University, Cambridge, Mass.), p. 530-534. 9 refs. (See A69-43296 24-19)

FLUIDIC SUN SENSOR FOR SOLAR-POINTING FLUIDIC ATTITUDE CONTROL. W. V. Miller (TRW Systems Group, Redondo Beach, Calif.), p. 545-553. (See A69-43297 24-21)

TRISTABLE FLUID AMPLIFIERS. J. Santos, J. Santamarina, J. Giunta, and H. Arango (Universidad Nacional del Sur, Bahía Blanca, Buenos Aires, Argentina), p. 554-558. (See A69-43298 24-03)

DESIGN BASIS FOR VORTEX-TYPE FLUID AMPLIFIERS OPERATING IN THE INCOMPRESSIBLE FLOW REGIME. D. N. Wormley and H. H. Richardson (Massachusetts Institute of Technology, Cambridge, Mass.), p. 568-577. 12 refs. (See A69-43299 24-03)

A "FLUIDIC TRANSMITTER." R. T. Johnson (Missouri, University, Rolla, Mo.) and J. M. Trummel (Iowa, University, Iowa City, Iowa), p. 578-583. (See A69-43300 24-03)

APPLICATION OF A NEW METHOD IN ADAPTIVE CONTROL. L. G. Hofmann (Systems Technology, Inc., Princeton, N.J.), p. 584-592. 10 refs. (See A69-43301 24-31)

ON THE CORRECTION OF COEFFICIENT QUANTIZATION ERRORS IN HYBRID CONTROL SYSTEMS. D. L. Chenoweth (LTV Aerospace Corp., Dallas, Tex.), C. L. Phillips, and J. C. Johnson (Auburn University, Auburn, Ala.), p. 613, 614. 8 refs. (See A69-43302 24-10)

THE STABILITY OF DISTRIBUTED PARAMETER SYSTEMS. J. C. Willems (Massachusetts Institute of Technology, Cambridge, Mass.), p. 621, 622. 11 refs. (See A69-43303 24-10)

AN APPROXIMATE MINIMAL TIME CLOSED-LOOP CONTROLLER FOR PROCESSES WITH BOUNDED CONTROL AMPLITUDES AND RATES. J. Y. S. Luh (Purdue University, Lafayette, Ind.) and J. S. Shafran (TRW Systems Group, Redondo Beach, Calif.), p. 623-632. 18 refs. (See A69-43304 24-10)

ON THE OPTIMAL GAIN PROBLEM AND ITS APPLICATIONS. S. J. Asseo (Northrop Corp., Hawthorne, Calif.), p. 645-659. 12 refs. (See A69-43305 24-10)

OPTIMIZATION OF CONTROL SYSTEMS WITH DISCONTINUITIES AND TERMINAL CONSTRAINTS. P. Dyer and S. R. McReynolds (California Institute of Technology, Pasadena, Calif.), p. 660-668. 10 refs. (See A69-43306 24-10)

A COMPUTER PROGRAM FOR THE SYNTHESIS OF DECOUPLED MULTIVARIABLE FEEDBACK SYSTEMS. E. G. Gilbert and J. R. Pivnichny (Michigan, University, Ann Arbor, Mich.), p. 677-684. 12 refs. (See A69-43307 24-10)

PERFORMANCE EQUIVALENCE IN A TWO LEVEL SYSTEM. V. Jurdjevic (Case-Western-Reserve University, Cleveland, Ohio), p. 685-689. 9 refs. (See A69-43308 24-10)

FREQUENCY DOMAIN STABILITY CRITERIA FOR DISTRIBUTED PARAMETER SYSTEMS. H. C. Khatri (Catholic University of America, Washington, D.C.), p. 719-728. 13 refs. (See A69-43309 24-10)

PARALLEL OPERATION OF VALVE-CONTROLLED HYDRAULIC SERVO MOTORS. R. E. Lang (Raytheon Co., Wayland, Mass.), p. 742-748. (See A69-43310 24-03)

OPTIMAL ALLOCATION OF TRACKING PULSES FOR AN ARRAY RADAR. H. Heffes and S. Horing (Bell Telephone Laboratories, Inc., Whippany, N.J.), p. 815-821. 6 refs. (See A69-43311 24-07)

QUASI-OPTIMIZATION OF A LOCALIZER ACQUISITION SYSTEM. D. MacKinnon (Massachusetts Institute of Technology, Cambridge, Mass.), p. 822-830. 14 refs. (See A69-43312 24-21)

QUASI-OPTIMUM CONTROL FOR MINIMUM-TIME RENDEZVOUS IN A CENTRAL FORCE FIELD. S. Welt and B. Friedland (Singer-General Precision, Inc., Little Falls, N.J.), p. 831-842. (See A69-43313 24-21)

ON THE STRUCTURE OF MULTIVARIABLE SYSTEMS. W. A. Wolovich (NASA, Electronics Research Center, Cambridge, Mass.) and P. L. Falb (Brown University, Providence, R.I.), p. 860-868. 9

refs. (See A69-43314 24-10)

STATE VARIABLE FEEDBACK DECOUPLING AND DESIGN OF MULTIVARIABLE SYSTEMS. C. R. Slivinsky (Missouri, University, Columbia, Mo.) and D. G. Schultz (Arizona, University, Tucson, Ariz.), p. 869-876. 11 refs. (See A69-43315 24-10)

SOME RESULTS ON THE L_p-STABILITY OF LINEAR TIME-VARYING SYSTEMS. J. C. Willems (Massachusetts Institute of Technology, Cambridge, Mass.), p. 913-917. 5 refs. (See A69-43316 24-10)

PATH INTEGRALS AND LIAPUNOV FUNCTIONALS. M. Gruber (Massachusetts Institute of Technology, Lexington, Mass.), p. 918-929. 19 refs. (See A69-43317 24-10)

LIMIT CYCLE OSCILLATIONS IN PULSE-MODULATED SYSTEMS. R. N. Clark (Washington, University, Seattle, Wash.) and G. F. Franklin (Stanford University, Stanford, Calif.), p. 930-936. 7 refs. (See A69-43318 24-10)

ESTIMATION OF THE PARAMETERS OF SAMPLED-DATA SYSTEMS BY MEANS OF STOCHASTIC APPROXIMATION. C. B. Neal (Hughes Aircraft Co., Culver City, Calif.) and G. A. Bekey (Southern California, University, Los Angeles, Calif.), p. 977, 978. (See A69-43319 24-10)

HUMAN OPERATOR CHARACTERISTICS BASED ON AN ANALOG COMPUTER ORIENTED PARAMETER IDENTIFICATION TECHNIQUE. A. L. Burgett (South Florida, University, Tampa, Fla.), p. 988, 989. 6 refs. (See A69-43320 24-05)

N69-10755*# National Aeronautics and Space Administration. Marshall Space Flight Center, Huntsville, Ala.

ANALYSIS OF COMMUTATED NETWORKS EMPLOYING FEEDBACK CIRCUITS

Michael T. Borelli Washington Nov. 1968 93 p refs

(NASA-TN-D-4893) Avail: CFSTI CSCL 09E

The development of advanced automatic control systems often requires new and unusual circuits, components, techniques, and other such items, to provide the necessary control to accomplish a specific mission. An adaptive automatic flight control system for large space booster vehicles has been developed that uses tracking-notch filters composed of commutated networks (CN's) From this successful application and others cited in the literature, it appears that these networks are particularly well suited for use in tracking filters. In this investigation of CN's and in most practical cases, the reactive elements are capacitors. The commutation action in a resistor–capacitor CN can transform the frequency response characteristics of a low pass filter into that of a highly selective band pass filter. Effective low-frequency band pass or band elimination filters can be realized without the use of magnetic elements. These and other transformations of a network's basic characteristics provide very interesting properties that are useful for some special applications. The methods of analysis are those employing full-wave balanced commutation and include: (1) classical method; (2) difference equations; (3) modulation equivalents; and (4) Laplace transforms. Author

N69-16198*# National Aeronautics and Space Administration. Lewis Research Center, Cleveland, Ohio.

ANALYSIS AND DESIGN OF INDUCTORS FOR PROTECTING POWER TRANSISTORS AGAINST CURRENT SURGES IN INVERTER BRIDGE CIRCUITS

Francis Gourash Washington Jan. 1969 46 p refs

(NASA-TN-D-4995) Avail: CFSTI CSCL 09A

An analysis of transistor inverter and converter bridge circuits shows that surge currents exist during the switching time interval. These currents result from transistor unequal turnon and turnoff switching characteristics. The surge currents are limited only by the resistance of the power source and the saturated resistance of the transistors. They can reach peak values which exceed the transistor's maximum current rating by an order of magnitude. Inductors avoid transistor failure by limiting the current surges to safe levels. They also substantially reduce the circuit power loss due to the surge currents. A technique for the design of inductors with the proper inductance is presented. Author

N69-19003*# Westinghouse Electric Corp., Lima, Ohio.

INVERTER-CONVERTER AUTOMATIC PARALLELING AND PROTECTION

C. L. Doughman, B. A. Marino, and N. D. Lenhart Washington NASA Feb. 1969 164 p refs

(Contract NAS3-2792)

(NASA-CR-1225) Avail: CFSTI CSCL 09E

Electrical control and protection circuits are developed for a multi-channel, paralleled ac system and for a multi-channeled, paralleled dc system. Electrical control for each of the two systems consists of automatic paralleling circuits and electrical contactor control circuits. Protection circuits for the ac system include overvoltage, undervoltage, overfrequency, underfrequency, frequency reference protection, overcurrent, load division and differential current. Protection circuits for the dc system are the same as for the ac system except that no frequency protection circuits are included. Test results verify and demonstrate the developed technology. Author

N69-21123*# National Aeronautics and Space Administration. Electronics Research Center, Cambridge, Mass.

A SUBOPTIMAL APPROXIMATION TO THE KALMAN FILTER

Leon Bess Washington Mar. 1969 28 p refs

(NASA-TN-D-5082) Avail: CFSTI CSCL 09C

A suboptimal estimation scheme similar to the Kalman filter is described which makes use of scalar weighting factors instead of matrix factors. It is shown that the accuracy degradation of the suboptimal estimator is not too great for most cases of practical interest. Moreover, it readily lends itself to physical interpretation. Author

N69-22919*# National Aeronautics and Space Administration. Electronics Research Center, Cambridge, Mass.

SYMBOL-ORIENTED FAILURE ANALYSIS IN MULTICOMPONENT SYSTEMS

Milton C. Weinstein and W. W. Happ Washington Apr. 1969 16 p refs

(NASA-TN-D-5112) Avail: CFSTI CSCL 09F

Computer oriented procedures are developed to assess the error in performance of electronic circuits and similar quasilinear systems if one element in a multicomponent system fails. A tutorial introduction to tagging techniques is provided to make the presentation self-contained. Author

N69-24918*# National Aeronautics and Space Administration. Lewis Research Center, Cleveland, Ohio.

NOISE IN AXISYMMETRIC CONVERGENT ELECTRON BEAMS

H. G. Kosmahl and L. U. Albers Washington May 1969 62 p refs

(NASA-TN-D-5212) Avail: CFSTI CSCL 09E

The noise along axisymmetric convergent electron beams used in O-type high power microwave tubes was investigated analytically as a function of several tube design parameters. The computations and investigations were carried out for magnetically fully confined flow, Brouillon flow, and electrostatically focused flow for power levels near 1 kW and perveances from 0.1×10^{-6} to 1.0×10^{-6}. The computed minimum noise figures ranged between 20 and 60 db depending on voltage, perveance, area convergence, and gun design. Author

N69-28121*# National Aeronautics and Space Administration. Electronics Research Center, Cambridge, Mass.

DESIGN CONSIDERATIONS FOR CYCLOTRON RESONANCE OSCILLATORS

Bernhard Kulke Washington Jun. 1969 38 p refs

10 ELECTRONICS

(NASA-TN-D-5237) Avail: CFSTI CSCL 09E

From the linearized kinetic theory of stimulated cyclotron radiation, and from related physical arguments, some design criteria are deduced for spiraling-beam cyclotron-resonance oscillators for possible use at millimeter-wave frequencies. While an optimum choice of the geometry of the interaction region is important, the most essential design problem is the control and minimization of the axial velocity spread on the spiraling beam. Author

11

FACILITIES, RESEARCH AND SUPPORT

Includes airports; lunar and planetary bases including associated vehicles; ground support systems; related logistics; simulators; test facilities (e.g., rocket engine test stands, shock tubes, and wind tunnels); test ranges; and tracking stations.

A69-11755
SPACE PROJECTIONS FROM THE ROCKY MOUNTAIN REGION; PROCEEDINGS OF THE SYMPOSIUM, DENVER, COLO., JULY 15, 16, 1968. VOLUME 3.
Symposium sponsored by the American Astronautical Society and the American Institute of Aeronautics and Astronautics.
Tarzana, Calif., American Astronautical Society, 1968. 378 p.
Price of three volumes, $10.00.

CONTENTS:

TEST TECHNIQUES AND OPERATIONS.

HYPERSONIC PROPULSION FACILITY AT OGDEN, UTAH. R. O. Boe (Marquardt Corp., Van Nuys, Calif.). 17 p. [See A69-11756 02-11]

SPACE SIMULATION TESTS OF PLANETARY SPACECRAFT. B. Hartel (Martin Marietta Corp., Denver, Colo.). 20 p. 5 refs. [See A69-11757 02-11]

RESIDUAL GAS ANALYZER FOR MONITORING SUBLIMATION FROM SPACECRAFT MATERIALS. R. W. Jackman (Ball Brothers Research Corp., Boulder, Colo.). 15 p. [See A69-11758 02-11]

ACQUISITION OF DATA FOR THE APOLLO APPLICATIONS PROGRAM CREW MOTION EXPERIMENT. W. J. Maes and C. H. Murrish (Martin Marietta Corp., Denver, Colo.). 22 p. 5 refs. [See A69-11759 02-05]

A TRAILING CAMERA TECHNIQUE FOR STUDYING PROJECTILE PENETRATION INTO EARTH MATERIALS. J. L. Colp and W. B. Pepper (Sandia Corp., Albuquerque, N. Mex.). 36 p. 7 refs. [See A69-11760 02-11]

WHITE SANDS MISSILE RANGE - A ROCKY MOUNTAIN REGIONAL SPACE AND MISSILE TEST FACILITY. A. L. Vick (U.S. Army, Performance Evaluation Office, White Sands Missile Range, N. Mex.). 17 p. [See A69-11761 02-11]

MECHANICAL AND PROPULSION TECHNOLOGY.

PULSE MOTOR FOR SPACECRAFT ATTITUDE CONTROL. D. Suddeth (NASA, Goddard Space Flight Center, Greenbelt, Md.) and D. Blackwood (Talley Industries, Inc., Mesa, Ariz.). 19 p. [See A69-11762 02-03]

SPACE APPLICATIONS OF BERYLLIUM PROPELLANTS. C. R. Voris (Thiokol Chemical Corp., Brigham City, Utah). 13 p. [See A69-11763 02-27]

TESTING A STERILIZABLE LIQUID PROPULSION SYSTEM. J. B. Keough (Martin Marietta Corp., Denver, Colo.). 15 p. [See A69-11764 02-11]

OPTICAL MEASUREMENTS THROUGH A ROCKET PLUME. J. Pernicka (Martin Marietta Corp., Denver, Colo.). 14 p. 13 refs. [See A69-11765 02-14]

SPACE MECHANISM LUBRICATION. B. J. Perrin and R. W. Mayer (Ball Brothers Research Corp., Boulder, Colo.). 18 p. [See A69-11766 02-15]

PENETRATION OF TERRESTRIAL MATERIALS BY INSTRUMENTED PROJECTILES. J. L. Colp (Sandia Corp., Albuquerque, N. Mex.). 59 p. 16 refs. [See A69-11767 02-11]

THE MAGNETOTROPOMETER. R. P. Woolley (Ball Brothers Research Corp., Boulder, Colo.). 12 p. [See A69-11768 02-14]

EXOBIOLOGY AND STERILIZATION.

DESIGN EVOLUTION OF THE WOLF TRAP LIFE DETECTOR. D. E. Buckendahl (Ball Brothers Research Corp., Boulder, Colo.). 12 p. [See A69-11769 02-05]

SOME BIOLOGICAL PROBLEMS IN THE SEARCH FOR EXTRATERRESTRIAL LIFE. H. P. Klein (NASA, Ames Research Center, Moffett Field, Calif.). 21 p. 44 refs. [See A69-11770 02-04]

NON-EXISTENCE OF A BIOTA-CLOUD RECONTAMINATION HAZARD FOR A PLANETARY LANDER. J. F. Vandrey (Martin Marietta Corp., Baltimore, Md.). 13 p. 5 refs. [See A69-11771 02-05]

DETERMINATION OF THE TERMINAL STERILIZATION CYCLE FOR A POSSIBLE MARS CAPSULE. A. R. Hoffman (California Institute of Technology, Pasadena, Calif.). 30 p. 9 refs. [See A69-11772 02-05]

NEW FAST TECHNIQUES FOR BIO-ASSAY. L. L. Salomon and M. A. Rothenberg (Dugway Proving Ground, Dugway, Utah). 19 p. [See A69-11773 02-05]

BIOLOGICAL MONITORING OF A FULL SCALE SIMULATED MARS LANDER. A. A. Rothstein (Martin Marietta Corp., Denver, Colo.) and H. Kaufman (Highland Laboratories, Costa Mesa, Calif.). 14 p. [See A69-11774 02-05]

A69-12379 *#
FLIGHT TEST EVALUATION OF A SMALL ONE-MAN LUNAR FLYING DEVICE.
Maxwell W. Goode (NASA, *Langley Research Center, Space* Mechanics Div., Hampton, Va.) and Lee H. Person, Jr. (NASA, Langley Research Center, Flight Mechanics and Technology Div., Hampton, Va.).
(American Institute of Aeronautics and Astronautics, Flight Test, Simulation and Support Conference, 2nd, Los Angeles, Calif., Mar. 25-27, 1968, Paper 68-240.)
Journal of Spacecraft and Rockets, vol. 5, Dec. 1968, p. 1468-1472.

Initial test evaluation of a small one-man flying device referred to as "POGO," and discussion of the feasibility of the vehicle control concept, the piloting differences between earth and lunar gravity, and the impact of pressure suits on vehicle handling qualities. The concept of direct manual control of a thrust vector (proportional acceleration command system) appears to be feasible. Pitch and roll control sensitivities were too high - resulting in a disharmony between attitude and translational capabilities. The test results have indicated that the effects of the pressure suits on the handling qualities of the vehicle did not present any major problems. The piloting differences between earth and lunar gravity operations are sufficient to warrant training of astronauts in simulated lunar gravity.
M.G.

A69-12385 *#
AUTOMATIC CONTROLS FOR FACILITIES AND MERCURY ION THRUSTERS IN DURABILITY TESTING.
C. R. Nichols (NASA, Lewis Research Center, Research Facilities Section, Cleveland, Ohio) and S. J. Obloy (NASA, Lewis Research Center, Electronics Section, Cleveland, Ohio).
(American Institute of Aeronautics and Astronautics, Propulsion Joint Specialist Conference, 4th, Cleveland, Ohio, June 10-14, 1968, Paper 68-576.)
Journal of Spacecraft and Rockets, vol. 5, Dec. 1968, p. 1484-1486. 7 refs.

Description of design alterations in several vacuum chamber systems of Lewis Research Center, carried out as a result of three-year durability tests, to provide for automatic shutdown during unattended operation. These alterations and the use of thruster-control circuits permitted a vacuum-chamber operation with reduced support manpower. The 8.5 to 850-m^3 chambers use normal roughing, oil-diffusion, and cryopumping systems. Chamber pressure, with thrusters operating, is typically in the 10^{-7}-torr range. Also described are thruster controls allowing continuous testing of ion thrusters for almost three months with only one man per shift.
V.Z.

11 FACILITIES, RESEARCH AND SUPPORT

A69-13240 *
WEFAX - WEATHER DATA RELAY COMMUNICATIONS EXPERIMENT.
Sheldon Wishna (NASA, Goddard Space Flight Center, Greenbelt, Md.).
IN: EASCON '68; INSTITUTE OF ELECTRICAL AND ELECTRONICS ENGINEERS, ELECTRONICS AND AEROSPACE SYSTEMS CONVENTION, WASHINGTON, D.C., SEPTEMBER 9-11, 1968, RECORD. [A69-13176 03-07]
New York, Institute of Electrical and Electronics Engineers, Inc., 1968, p. 496-500.

Description of WEFAX (abbreviation for Weather Facsimile), an experiment designed to explore the operational feasibility of direct transmission, via a satellite relay, of meteorological data from a central weather station source to widely scattered remote weather stations or receiving units. The transmission media used for the experiment are the vhf communication facilities of the ATS-1 (Applications Technology Satellite), while the receiving stations cooperating in this program are the network of APT (Automatic Picture Transmission) ground stations. The WEFAX experiment has been highly successful in demonstrating the feasibility of transmitting weather data via a synchronous satellite. Usable receptions can be assured nearly 95% of the time. M.M.

A69-15572 *
FACTORS INFLUENCING THE CHOICE OF FACILITIES AND TECHNIQUES FOR AERONAUTICAL DEVELOPMENT.
Richard E. Kuhn (NASA, Langley Research Center, Hampton, Va.).
(New York Academy of Sciences, International Congress on Subsonic Aeronautics, New York, N.Y., Apr. 3-6, 1967.)
New York Academy of Sciences, Annals, vol. 154, Nov. 22, 1968, p. 1036-1054. 25 refs.

Examination of factors in the development of aeronautical tools such as wind tunnels, tow-test rigs, etc. As an example of how the nature of the system to be tested can affect the nature of the test itself, it is noted that the large deflections of the air flow that V/STOLs produce have required that oversized wind-tunnels and specialized towed rigs be used. The introduction of variable sweep required a reevaluation of the entire longitudinal-stability area. Work with the jumbo jets highlighted another problem area: the gap between the Reynolds number capability of existing tunnels and the actual flight Reynolds numbers. A number of specialized facilities have been developed for the determination of aerodynamic derivatives necessary in the study of the dynamic motions of aircraft. Operational considerations as noise and IFR traffic control are also discussed. G.R.

A69-15574 *
WIND-TUNNEL WALL EFFECTS AT EXTREME FORCE COEFFICIENTS.
Harry H. Heyson (NASA, Langley Research Center, Hampton, Va.).
(New York Academy of Sciences, International Congress on Subsonic Aeronautics, New York, N.Y., Apr. 3-6, 1967.)
New York Academy of Sciences, Annals, vol. 154, Nov. 22, 1968, p. 1074-1093. 37 refs.

Study of wall constraints at extreme force coefficients, the magnitude of which in V/STOL testing has been shown experimentally to be large and to differ from the effects noted in conventional testing. A progress report on theoretical work now being conducted by NASA, the University of Washington, and the Boeing Company is presented. Some of the real effects encountered in wind-tunnel testing are also discussed. These include the requirements for moving belts in ground-effect testing, and the recirculation limits on minimum speed which have been discovered in tests at the University of Washington. F.R.L.

A69-15575 *
A REVIEW OF FACILITIES AND TEST TECHNIQUES USED IN LOW-SPEED FLIGHT.
Seth B. Anderson and Laurel G. Schroers (NASA, Ames Research Center, Moffett Field, Calif.).
(New York Academy of Sciences, International Congress on Subsonic Aeronautics, New York, N.Y., Apr. 3-6, 1967.)
New York Academy of Sciences, Annals, vol. 154, Nov. 22, 1968, p. 1094-1114. 11 refs.

Discussion of the means by which new facilities, developed to support flight-test programs, and new flight techniques, devised to help explore problem areas, have been applied. The relative merits and limitations of each facility and technique are pointed out, and future needs are discussed. Principal attention is given to the facilities and test techniques for studying low-speed problems of handling qualities, stability and control, and performance. A typical problem has been chosen to illustrate the relationship between facilities. F.R.L.

A69-15992 *
UNIFORMITY OF PROTON BEAMS AVAILABLE AT THE NASA SYNCHROCYCLOTRON (SREL).
Gerald F. Hill, William C. Honaker, and K. H. Kim (NASA, Langley Research Center, Hampton, Va.).
(Radiological Society of North America, Scientific Assembly and Annual Meeting, Chicago, Ill., Nov. 26-Dec. 1, 1967.)
Radiology, vol. 91, Sept. 1968, p. 562-567. 6 refs.

Summary of approximately 30 beam configurations which are available with a 600 MeV proton synchrocyclotron used in space-radiation research. Attention is given to such parameters as proton beam energy, energy spread, intensity, intensity profile, repeatability, and area. The results are primarily related to large-area beams, which are of interest to experimenters studying the radiation effects of protons on animals. Uniformity of several large-area beams is discussed in terms of dose-rate (rads/min) in muscle. B.H.

A69-17705 *#
CHARACTERISTICS OF COMPOSITE CARBON RESISTORS USED FOR MEASURING ACCELERATOR TERMINAL VOLTAGES.
F. R. Stevenson and D. J. Gauntner (NASA, Lewis Research Center, Cleveland, Ohio).
Review of Scientific Instruments, vol. 40, Jan. 1969, p. 140-144. 16 refs.

Investigation of a voltage divider board composed of 1152, 22 MΩ composite carbon resistors used to measure the terminal voltage of a 3 MeV Dynamitron. The board was calibrated in situ using the ^{9}Be and D photoneutron threshold reactions and a magnetic analyzer. The present calibration of the divider board, which was made after over 5 years of extensive accelerator usage, agrees within 2% with the original factory calibration. The linear temperature coefficient of resistance was measured to be $+(0.85 \pm 0.10) \times 10^{-3}/^{\circ}C$ in the range 25 to 35°C. The divider board resistance decreased linearly with voltage ($-1.1 \times 10^{-5}\%/V$) up to 2 MeV which corresponds to 1750 V on each resistor. The results show that composite carbon resistors and the techniques described can be applied with confidence to the measurement of high voltage. (Author)

A69-22008 *#
IN SITU VACUUM TESTING - A MUST FOR CERTAIN ELASTOMERIC MATERIALS.
John P. Mugler, Jr. (NASA, Langley Research Center, Space Environment Branch, Hampton, Va.), Lawrence R. Greenwood, William S. Lassiter (NASA, Langley Research Center, Hampton, Va.), and Robert A. Comparin (Virginia Polytechnic Institute, Blacksburg, Va.).
(SPACE SIMULATION CONFERENCE, 3RD, SEATTLE, WASH., SEPTEMBER 16-18, 1968, PROCEEDINGS, p. 85-89.)
Journal of Spacecraft and Rockets, vol. 6, Feb. 1969, p. 219-221.

An experimental program has been conducted to measure the vacuum-induced changes in the mechanical and thermal properties of several filled elastomers wherein both in-situ and before-and-after tests were conducted. The results from the in-situ tests showed that vacuum exposure caused substantial increases in maximum stress and modulus of solid rocket fuel and decreases in thermal conductivity of heat-shield material even though the vacuum weight loss was small. A comparison of the results from the in-situ and before-and-after tests showed that in-situ vacuum testing was necessary to obtain valid measurements of the vacuum-induced changes because reexposure of the materials to the atmosphere caused the properties to substantially or fully revert to their preexposure values. (Author)

A69-23026 *
A PYROTECHNIC-ACTIVATED CALORIMETER FOR FLIGHT RESEARCH AT LUNAR RETURN VELOCITY.
Don D. Davis, Jr. and Clotaire Wood (NASA, Langley Research Center, Hampton, Va.).
IN: USE OF PYROTECHNIC AND EXPLOSIVE ELEMENTS IN SPACE SYSTEMS; CENTRE NATIONAL D'ETUDES SPATIALES, INTERNATIONAL CONFERENCE, TARBES, HAUTES-PYRENEES, FRANCE, JULY 9-12, 1968, PROCEEDINGS [UTILISATION DES ELEMENTS PYROTECHNIQUES ET EXPLOSIFS DANS LES SYSTEMES SPATIAUX; CENTRE NATIONAL D'ETUDES SPATIALES, COLLOQUE INTERNATIONAL, TARBES, HAUTES-PYRENEES, FRANCE, JULY 9-12, 1968, PROCEEDINGS]. [A69-23003 10-27]
Paris, Dunod Editeur, 1969, p. 369-378.

Discussion of a rather unique application of a pyrotechnic device to solve a problem that was encountered in the design of the reentry package for Project Fire. Project Fire was undertaken by NASA to investigate the heating environment of vehicles entering the earth's atmosphere at velocities slightly greater than lunar return velocities. The primary object was to obtain onboard measurements that would define the hot-gas radiance and the total heating on a blunt-nosed body of fairly large scale. These results, on a firmly established basis, were needed to test various theoretical and empirical heat-transfer prediction techniques that had been proposed by individual research scientists, as well as others that would be proposed in the future. P.v.T.

A69-23245
INSTRUMENTATION IN THE AEROSPACE INDUSTRY. VOLUME 14 - INSTRUMENT SOCIETY OF AMERICA, INTERNATIONAL AEROSPACE INSTRUMENTATION SYMPOSIUM, 14TH, BOSTON, MASS., JUNE 3-5, 1968, PROCEEDINGS.
Edited by John Leak (Boeing Co., Vertol Div., Seattle, Wash.).
Pittsburgh, Instrument Society of America, 1968. 345 p.
Members, $12.; nonmembers, $15.

CONTENTS:

FOREWORD. J. Leak (Boeing Co., Seattle, Wash.). 1 p.

ACCIDENT FLIGHT DATA RECORDING.
FLIGHT RECORDERS. E. Sigg (Flight Safety Foundations, Inc., Arlington, Va.), p. 1-5. [See A69-23246 10-14]
FLIGHT DATA RECORDERS. F. B. Lemmon (Lockheed Aircraft Corp., Ontario, Calif.), p. 6-12. 23 refs. [See A69-23247 10-14]
CRASH PROTECTION OF DATA RECORDERS. J. C. Crosby (United Control Corp., South El Monte, Calif.), p. 13-19. [See A69-23248 10-14]

INSTRUMENTATION FOR HIGH SPEED ROTATING MACHINERY.
KINEMATIC MONITORING SYSTEMS FOR ROTATING EQUIPMENT INSTRUMENTATION. F. F. Reed and W. J. Rizzi (United Aircraft Corp., Trevose, Pa.), p. 20-34. [See A69-23249 10-14]
TURBOPUMP VIBRATION MEASUREMENTS AT CRYOGENIC TEMPERATURES. B. W. Washburn (California, University, Los Alamos, N. Mex.), p. 35-37. [See A69-23250 10-14]
MINIATURE TELEMETRY. C. H. Hoeppner (Industrial Electronetics Corp., Satellite Beach, Fla.), p. 38-42. [See A69-23251 10-07]
A DYNAMIC TORSIOGRAPH SYSTEM FOR HIGH-SPEED MACHINERY. E. K. Yager (General Dynamics Corp., San Diego, Calif.), p. 43-47. [See A69-23252 10-14]
MONITORING EQUIPMENT FOR TURBINE ENGINE DEVELOPMENT. R. F. Brown, R. D. House, and J. O. Roebuck (United Aircraft Corp., East Hartford, Conn.), p. 48-53. [See A69-23253 10-14]

ATMOSPHERIC MEASUREMENTS.
AN AIR-LAUNCHED WINDSONDE. S. F. Rohrbough, L. E. Koehler, and J. G. Ballinger (Honeywell, Inc., St. Paul, Minn.), p. 54-57. [See A69-23254 10-14]
APPLICATION OF PULSE TECHNIQUES TO SONIC ANEMOMETRY. A. Bisberg (Cambridge Systems, Inc., Newton, Mass.) and R. M. Peirce (USAF, Cambridge Research Laboratories, Bedford, Mass.), p. 58-63. 8 refs. [See A69-23255 10-14]
ELECTRONIC INSTRUMENTATION FOR THE MEASUREMENT OF CHARGED PARTICLES BY AN AC VOLTAGE METHOD. R. S. Cuikay (USAF, Cambridge Research Laboratories, Bedford, Mass.), R. E. Sprague, and J. Fay (Northeastern University, Boston, Mass.), p. 65 to 66-B. [See A69-23256 10-09]
THE USE OF TRANSPONDERSONDES FOR ATMOSPHERIC SOUNDINGS. E. J. Georgian (USAF, Cambridge Research Laboratories, Bedford, Mass.), p. 67-72. 5 refs. [See A69-23257 10-14]

AUTOMATION OF TEST FACILITIES.
AUTOMATION OF ROCKET ENGINE TEST FACILITIES. G. N. Kapandritis (Aerojet-General Corp., Sacramento, Calif.), p. 73-81. [See A69-23258 10-11]
FINAL CONTROL ELEMENTS FOR THE DIRECT DIGITAL CONTROL OF TEST STANDS. H. Friedland, A. W. Langill (Proces Systems Instrumentation, Sacramento, Calif.), and R. S. Hutton (Minneapolis Moline, Minneapolis, Minn.), p. 82-91. [See A69-23259 10-11]
CONSIDERATIONS INVOLVED IN AUTOMATION OF TEST FACILITIES. B. W. Washburn (California, University, Los Alamos, N. Mex.), p. 92-98. [See A69-23260 10-11]

MAINTENANCE RECORDING SYSTEMS FOR FLEET AIRCRAFT.
MAINTENANCE RECORDING SYSTEMS FOR A FLEET OF AIRCRAFT (AN OVERVIEW). W. J. Gabriel (General Dynamics Corp., Fort Worth, Tex.), p. 99-101. [See A69-23261 10-11]
AIRBORNE INTEGRATED DATA SYSTEM. W. J. Mozak, Jr. (Curtiss-Wright Corp., Caldwell, N.J.), p. 102-104. [See A69-23262 10-08]
HOWELL ENGINE HOT SECTION ANALYZER AND ITS APPLICATIONS. J. S. Howell (Howell Instruments, Inc., Fort Worth, Tex.), p. 105-109. [See A69-23263 10-11]
AIRBORNE INTEGRATED DATA SYSTEMS. F. B. Lemmon (Lockheed Aircraft Corp., Ontario, Calif.), p. 110-114. [See A69-23264 10-08]

WIND TUNNEL INSTRUMENTATION.
A SEMICONDUCTOR STRAIN GAGE BALANCE FOR USE IN CONVENTIONAL WIND TUNNELS. J. F. Reed (Sandia Corp., Albuquerque, N. Mex.) and S. B. Moore (LTV Aerospace Corp., Dallas, Tex.), p. 115-120. 5 refs. [See A69-23265 10-11]
NONINTERFERENCE WIND TUNNEL INSTRUMENTATION. W. E. Beyermann, W. H. Buford, Jr., J. B. Merzenich (Marquardt Corp., Van Nuys, Calif.), and K. Bernstein, p. 121-128. 11 refs. [See A69-23266 10-11]
SECOND-ORDER SYSTEM APPROXIMATIONS FOR DESCRIBING PNEUMATIC INSTRUMENTATION LINE TRANSFER FUNCTIONS. R. D. Samuelson (Aerojet-General Corp., Sacramento, Calif.), p. 129-134. [See A69-23267 10-14]
THE ELECTROLYTIC BUBBLE LEVEL TO OBTAIN MODEL ATTITUDE ACCURACY DURING WIND TUNNEL TESTS. R. W. Cotter (Cornell Aeronautical Laboratory, Inc., Buffalo, N.Y.), p. 135-140. [See A69-23268 10-11]

TELEMETRY SYSTEMS FOR REAL TIME FLIGHT TESTING.
C-5 FLIGHT TEST TELEMETRY DATA PROCESSING SYSTEM. P. J. Germond (Weston Instruments, Inc., Sarasota, Fla.), p. 141-146. [See A69-23269 10-08]
READINESS TESTING FOR A REAL TIME TELEMETRY SYSTEM. D. J. Lemke (International Business Machines Corp., White Sands Missile Range, N. Mex.), p. 147-152. [See A69-23270 10-08]
AN APPLICATION OF THIRD GENERATION GROUND STATION CONCEPTS. D. R. Schropp (Boeing Co., Renton, Wash.), p. 153-161. 5 refs. [See A69-23271 10-02]

ADVANCES IN AIRCRAFT FLIGHT TEST INSTRUMENTATION.
PROPOSED SPECIFICATION FOR ERROR SIGNALS RESULTING FROM COMMON MODE VOLTAGE IN PASSIVE SIGNAL HANDLING EQUIPMENT. W. J. Moore (Johns Hopkins University, Silver Spring, Md.), p. 162-167. [See A69-23272 10-07]
USE OF THE ANGULAR ACCELEROMETER FOR STABILIZATION AND CONTROL. P. G. Leigh (Systron-Donner Corp., Concord, Calif.), p. 168-173. [See A69-23273 10-02]
A COMPUTER APPROACH TO ANALYZE AEROELASTIC STABILITY. W. F. Wenzlaff and C. P. Dennis (Boeing Co., Wichita, Kan.), p. 174-184. 10 refs. [See A69-23274 10-02]
C5 AIRCRAFT FLIGHT TEST PCM MULTIPLEXER/ENCODER.

J. R. Gadway (Weston Instruments, Inc., Sarasota, Fla.), p. 185-199. [See A69-23275 10-14]

AIRCRAFT AND MISSILE CONTROL INSTRUMENTATION.
ON-BOARD AIRCRAFT WEIGHING SYSTEMS. B. H. Shapiro (BLH Electronics, Inc., Waltham, Mass.), p. 200-203. [See A69-23276 10-14]
BORESIGHT SHIFT ANALYSIS FOR THE APOLLO LM AND CSM TRACKING SYSTEMS. C. C. Wang (TRW Systems Group, Redondo Beach, Calif.), p. 204-215. 11 refs. [See A69-23277 10-11]
HIGH RESPONSE IMPULSE TESTING OF LOW THRUST PROPULSION DEVICES. R. D. Steger (Lockheed Aircraft Corp., Sunnyvale, Calif.), p. 216-220. [See A69-23278 10-11]

MINIATURIZED TELEMETRY SYSTEMS.
FM/AM TELEMETRY TO MEASURE IMPACT ACCELERATIONS. D. R. Harrison (NASA, Ames Research Center, Moffett Field, Calif.), p. 221-224. 8 refs. [See A69-23279 10-07]
MINIATURE TELEMETRY SYSTEMS FOR GUN-LAUNCHED INSTRUMENTATION. W. H. Mermagen (U.S. Army, Ballistic Research Laboratory, Aberdeen Proving Ground, Md.), p. 225-235. 14 refs. [See A69-23280 10-07]
IN-FLIGHT BALLISTIC RANGE MEASUREMENTS WITH A RUGGEDIZED TELEMETRY SYSTEM. L. E. Moir (Canadian Armament Research and Development Establishment, Quebec, Canada), p. 236-245. [See A69-23281 10-07]
A MICROCIRCUIT A-TO-D CONVERTER FOR AEROSPACE ENVIRONMENT. A. A. Molinari, Jr. (Sprague Electric Co., Worcester, Mass.), p. 246-251. [See A69-23282 10-03]
MICROELECTRONIC DATA AND CONTROL TRANSMISSION SYSTEM FOR DYNAMIC WIND-TUNNEL TESTING. J. H. Schrader and C. D. Nichols (NASA, Langley Research Center, Hampton, Va.), p. 252-256. [See A69-23283 10-11]

ON-LINE COMPUTER DATA ACQUISITION SYSTEMS.
DATA SYSTEM FOR TURBINE ENGINE DEVELOPMENT. J. R. Hosking, J. D. MacKinnon, and P. C. Searle (United Aircraft Corp., Hartford, Conn.), p. 257-266. [See A69-23284 10-08]
COMPUTERIZED SHAKE FACILITY FOR TESTING THE SATURN V MOON ROCKET. A. F. Batzinger and A. L. Garey (Systems Engineering Laboratories, Inc., Fort Lauderdale, Fla.), p. 267-269. [See A69-23285 10-11]
A WIND TUNNEL DATA ACQUISITION AND CONTROL SYSTEM R. H. Croll, Jr., J. F. Reed, and F. E. Forsythe (Sandia Corp., Albuquerque, N. Mex.), p. 270-278. [See A69-23286 10-11]
MISSISSIPPI TEST FACILITY HARDWIRE DATA ACQUISITION SYSTEM ERROR ANALYSIS. W. R. Walker and J. E. Queen (General Electric Co., Bay Saint Louis, Miss.), p. 279-296. [See A69-23287 10-11]

DATA PROCESSING AND REDUCTION TECHNIQUES.
THE OPTIMUM CALIBRATION INTERVAL PROGRAM. W. H. Webb and A. F. Holder (North American Rockwell Corp., Anaheim, Calif.), p. 297-301. [See A69-23288 10-15]
INCREASED ACCURACY OF A "DUAL INERTIA" FLUTTER CORRECTING MAGNETIC TAPE RECORDER/REPRODUCER. A. Brand (Consolidated Electrodynamics Corp., Pasadena, Calif.), p. 302-306. 7 refs. [See A69-23289 10-14]
COMPUTER DATA PROCESSING FOR ABLATION MEASUREMENT. R. J. D'Auteuil (Avco Corp., Wilmington, Mass.), p. 307-312. [See A69-23290 10-08]
A TELEMETRY CHANNEL FREQUENCY RESPONSE CORRECTION TECHNIQUE. J. S. Wakefield (Boeing Co., New Orleans, La.), J. J. Merkel (Collins Radio Co., Newport Beach, Calif.), P. J. Haddican (Lockheed Aircraft Corp., Houston, Tex.), and C. Jolissaint (Stanford University, Stanford, Calif.), p. 313-327. 7 refs. [See A69-23291 10-07]
CONDITIONING OF DIGITAL SAMPLED DATA SPECTRA. B. W. Washburn (California, University, Los Alamos, N. Mex.), p. 328-335. [See A69-23292 10-07]
AUTHOR INDEX, p. 337, 338.

A69-23283 *
MICROELECTRONIC DATA AND CONTROL TRANSMISSION SYSTEM FOR DYNAMIC WIND-TUNNEL TESTING.
James H. Schrader and C. D. Nichols (NASA, Langley Research Center, Hampton, Va.).
IN: INSTRUMENTATION IN THE AEROSPACE INDUSTRY. VOLUME 14 - INSTRUMENT SOCIETY OF AMERICA, INTERNATIONAL AEROSPACE INSTRUMENTATION SYMPOSIUM, 14TH, BOSTON, MASS., JUNE 3-5, 1968, PROCEEDINGS. [A69-23245 10-11]
Edited by John Leak.
Pittsburgh, Instrument Society of America, 1968, p. 252-256.
Description of a microelectronic data and control transmission system designed for use in a wind tunnel where access to the test model is not practical during a relatively long period of time covering a series of test conditions. It provides for remote control of various electromechanical transducers in the model, and ensures complete remote setup capability on the data system. The overall system is capable of transmitting up to 20 high-response data signals from the model and up to 54 auxiliary control functions to the model over a single 1/16-in. diameter cable. (Author)

A69-25081 *
ONBOARD CHECKOUT SYSTEM CONCEPT AND PHILOSOPHY.
Oscar Cabra, Jr. (NASA, Manned Spacecraft Center, Houston, Tex.).
IN: INSTITUTE OF ELECTRICAL AND ELECTRONICS ENGINEERS, AUTOMATIC SUPPORT SYSTEMS SYMPOSIUM FOR ADVANCED MAINTAINABILITY, ST. LOUIS, MO., NOVEMBER 12-14, 1968, PROCEEDINGS. [A69-25059 11-11]
New York, Institute of Electrical and Electronics Engineers, Inc., 1968, p. 5C-1 to 5C-17.
Summary of the requirements, underlying considerations, and techniques for system selection, concept development, and description of an onboard checkout system. The onboard checkout is designed for factory, prelaunch, and inflight checkout and for the monitoring of electronic, electrical, and electromechanical networks of manned spacecraft experiments and development subsystems. The design effort was directed by the Checkout Systems Branch of the NASA Manned Spacecraft Center, Houston, and conducted by the Martin-Marietta Corporation, Denver, Colo., under a NASA contract. (Author)

A69-25768 *
APOLLO MISSION SIMULATION WITH VISUAL PRESENTATION.
Riley David McCafferty (NASA, Manned Spacecraft Center, Kennedy Space Center, Fla.) and Lawrence W. Lockwood (General Electric Co., Apollo Systems Dept., Houston, Tex.).
Society of Motion Picture and Television Engineers, Technical Conference, 105th, Miami Beach, Fla., Apr. 20-25, 1969, Paper 105-74. 16 p.
$0.50.
Description of the command module simulator for the Apollo Program, and delineation of the onboard computer system and the dynamically controlled visual presentation. All simulated systems functions are originated in computer software packages, which functionally tie the onboard computer, and the guidance, navigation, and orbital mechanics together with a dynamic visual presentation via an infinity-optics display to supply composite training capability. Realistic visual simulation of the views which would be seen from the spacecraft at any portion of the mission is provided to the astronauts in the simulator trainer. M.M.

A69-26265 *
FOUR-GIMBAL SYSTEMS FOR SIMULATION DISPLAY.
John W. Wilson (NASA, Langley Research Center, Hampton, Va.).
Simulation, vol. 12, Mar. 1969, p. 115-120. 8 refs.
Discussion of a driving law for the fourth angle for two different four-gimbal systems. The first system has advantages in design and implementation for platform isolation. The second is specifically designed to minimize occlusion in visual display systems. In each system, the fourth-angle driving law is a direct consequence of maximizing the angle between the two axes causing the singularity. Thus, a necessary differential constraint is found to maintain a nonsingular solution. A sufficiency condition for a nonsingular solution is also found. The second four-gimbal system that minimizes occlusion has the interesting result that the maximum angle between the singularity-forming axes is not always 90°. G.R.

A69-26499 *#
A SOLUTION TO TRITIUM PUMP CONTAMINATION FOR SMALL ACCELERATORS.
Robert Steinberg and Donald L. Alger (NASA, Lewis Research Center, Cleveland, Ohio).
American Nuclear Society, Conference on Small Accelerators, New York, N.Y., Apr. 8, 9, 1969, Paper. 9 p.

Description of a method for reducing tritium contamination in a small 200-kV, 15-mA positive ion accelerator designed primarily for the production of neutrons. The vacuum system associated with the small accelerator is designed for reducing problems arising because: (1) the diffusion pump exhausts tritium to the surrounding area through the roughing pump, and (2) after prolonged pumping of tritium, the getter-ion pump becomes unstable, necessitating the changing or cleaning of its elements accompanied by a release of tritium. A solution to these problems is suggested which involves the separation of the static (beam) and dynamic (beam on) pumping functions and the incorporation of a titanium bulk sublimator into the vacuum system. The system permanently buries tritium in the pump chamber walls, thus reducing the problem of uncontrolled tritium release. Separation of the pumping functions has the advantage that the sublimator provides considerable pumping speed in the 1×10^{-4} to 2×10^{-3} torr range where start-up can be difficult for a getter-ion pump alone. M.G.

A69-26796 *#
LIGHTWEIGHT, HIGH-THERMAL-CAPACITY FORCE MODELS FOR USE IN ARC TUNNELS.
James G. Fowke and James N. Mueller (NASA, Langley Research Center, Hampton, Va.).
Journal of Spacecraft and Rockets, vol. 6, Mar. 1969, p. 326, 327.

Discussion of lightweight, high-heat-capacity uncooled models for satisfying model-balance compatibility during force tests in high-enthalpy hypersonic arc tunnels at high simulated altitudes. The models discussed are made of copper or beryllium coated with pure cobalt. G.R.

A69-27906 *
THE LUNAR COLONY.
R. W. Johnson (NASA, Advanced Manned Missions Program Office, Washington, D.C.).
Science Journal, vol. 5, May 1969, p. 82-88.

Description of the various stages of development of a lunar colony. The stages described comprise the use of the Lunar Module for the first scientific studies, the establishment of semipermanent bases, and finally a permanent colony. The construction of large permanent lunar bases is discussed in detail, taking account of the solution of special problems connected with the supply of oxygen, food, water, power, and transportation. Convincing reasons why such a colony should be established to support a lunar scientific observatory are cited. G.R.

A69-27947 *
A PROGRAM PLAN FOR EARTH ORBITAL SPACE ASTRONOMY.
Jean R. Olivier (NASA, Marshall Space Flight Center, Huntsville, Ala.) and Harry L. Wolbers (McDonnell Douglas Corp., McDonnell Douglas Astronautics Co., Huntington Beach, Calif.).
IEEE Transactions on Aerospace and Electronic Systems, vol. AES-5, Mar. 1969, p. 242-252.

Manned space flight offers the opportunity to couple the astronaut/scientist's ability to select and process data and to calibrate, modify, and repair instruments with the vantage point for astronomical observations provided by a platform located above the earth's atmosphere. The role which manned space flight may play in the 1970-1990 time period in meeting astronomical research needs is examined. The instruments and facilities that appear feasible for that period are described. (Author)

A69-28271 *#
APPLICATIONS OF A TUBE WIND TUNNEL IN SUPERSONIC TESTING.
William J. Sheeran, Kenneth C. Hendershot (Cornell Aeronautical Laboratory, Inc., Hypersonic Facilities Dept., Buffalo, N.Y.), and Homer B. Wilson, Jr. (NASA, Marshall Space Flight Center, Thermal Environment Branch, Huntsville, Ala.).
American Institute of Aeronautics and Astronautics, Aerodynamic Testing Conference, 4th, Cincinnati, Ohio, Apr. 28-30, 1969, Paper 69-335. 16 p. 17 refs.
Members, $1.00; nonmembers, $1.50.

Discussion of the operation and applications of the short-duration tube wind tunnel at the Cornell Aeronautical Laboratory. This facility has been in operation for a number of years and is capable of providing supersonic test environments at freestream Reynolds numbers of up to 4×10^7 ft^{-1}. The facility is a modification of the Ludwieg pressure-tube type of wind tunnel and has a steady flow duration of approximately 40 msec when using room-temperature air as the test gas. This test period is more than adequate to establish the model flowfields and to make the desired measurements. Base-heating tests involving a Saturn S-IC model are described, as well as base-burning investigations conducted with a scale-model solid propellant rocket. The use of this facility in basic investigations of rocket plumes and the evaluation of blast-wave effects is also discussed. (Author)

A69-28278 *#
THE AMES COMBINED HEATING FACILITY.
Forrest E. Gowen and Frank H. Nichols (NASA, Ames Research Center, Moffett Field, Calif.).
American Institute of Aeronautics and Astronautics, Aerodynamic Testing Conference, 4th, Cincinnati, Ohio, Apr. 28-30, 1969, Paper 69-342. 7 p. 10 refs.
Members, $1.00; nonmembers, $1.50.

The paper describes a facility that can be used for testing ablative heat-shield material models with diameters as large as 10 cm, in a combined convective and radiative heating environment with constant or transient heating conditions. With this size model, convective heating rates as large as 1000 W/cm^2 coupled with radiative heating rates up to about 900 W/cm^2 are available. Data from initial tests conducted in the facility are presented. They include results from calibrations of the convective and radiative heating systems as well as results from the first transient heating tests, with heating cycles which simulate realistic manned entry heating environments. (Author)

A69-28844 *#
MANNED AEROSPACE SIMULATION.
Donald C. Dust, Ronald D. Denison, and Robert E. Coate (NASA, Ames Research Center, Moffett Field, Calif.).
American Society of Mechanical Engineers, Design Engineering Conference and Show, New York, N.Y., May 5-8, 1969, Paper 69-DE-27. 7 p.
Members, $0.75; nonmembers, $1.50.

Description of the techniques and equipment used at NASA-Ames for manned aerospace simulation to produce research results applicable to the design and development of aerospace vehicles. How these same techniques and equipment can be applied to research applicable to other types of manned vehicles is discussed. Why and how simulators are useful in research are explained. The equipment required to provide a useful simulation system is divided into four main areas which include the computing, motion, visual, and audio systems. The requirements and specifications of these various systems and how they add to the realism of the simulator and the validity of the research results are shown. (Author)

A69-29029 *
EXPLORATORY INVESTIGATION ON THE MEASUREMENT OF SKIN FRICTION BY MEANS OF LIQUID CRYSTALS.
E. J. Klein and A. P. Margozzi (NASA, Ames Research Center, Moffett Field, Calif.).
(Israel Journal of Technology, vol. 7, no. 1-2, 1969, p. 173-180.)
IN: ISRAEL ANNUAL CONFERENCE ON AVIATION AND ASTRONAUTICS, 11TH, TEL-AVIV AND HAIFA, ISRAEL, MARCH 5, 6, 1969, PROCEEDINGS. [A69-29011 14-12]
Jerusalem, Weizmann Science Press of Israel, 1969, p. 173-180.
5 refs.

New method proposed for the direct measurement of local skin

friction in aerodynamic testing makes use of thin coatings of cholesteric liquid crystal mixtures which respond to shearing forces by changes in their wavelength of maximum light scattering. A calibration of shear versus wavelength was obtained for a sample substance; a static calibration was made to measure the effects of temperature, pressure, and angle of viewing; and the behavior of the substance was observed in a pipe-flow experiment. Preliminary results showed that the method appears feasible. However, for such a method to become widely applicable in wind-tunnel testing, further research will be needed - i.e., to obtain liquid crystal mixtures sensitive over appropriate ranges on the shear scale, to prevent the occurrence of roughness on the surface of liquid crystal coating subjected to aerodynamic shear forces, and to develop a suitable optical measuring technique for data acquisition. (Author)

A69-30356
MAN IN HIS ENVIRONMENT; INSTITUTE OF ENVIRONMENTAL SCIENCES, ANNUAL TECHNICAL MEETING AND EQUIPMENT EXPOSITION, 15TH, ANAHEIM, CALIF., APRIL 20-24, 1969, PROCEEDINGS.
Mt. Prospect, Ill., Institute of Environmental Sciences, 1969. 665 p. Members, $12.; nonmembers, $18.

CONTENTS:

AUTHOR'S INDEX, p. XIII-XV.

A MULTIPLE SHAKER GROUND VIBRATION TEST SYSTEM TO SIMULATE INFLIGHT LEVELS IN A TANDEM ROTOR HELICOPTER. P. S. Skopowski (Boeing Co., Morton, Pa.), p. 6-13. 7 refs. [See A69-30357 15-11]

A NEW APPROACH TO MODAL VIBRATION TESTING OF COMPLEX AEROSPACE STRUCTURES. R. W. Budd (Hughes Aircraft Co., Space Simulation Laboratory), p. 14-20. [See A69-30358 15-11]

REAL TIME, WIDE BAND SHOCK RESPONSE ANALYSIS. R. G. Irvine, p. 25-30. 9 refs. [See A69-30359 15-15]

SHOCK PULSE TIME HISTORY GENERATOR. R. T. Fandrich, Jr. (Radiation, Inc., Melbourne, Fla.), p. 31-36. [See A69-30360 15-11]

A MAGNETICALLY SUSPENDED ROCKET SLED. D. Williams, Jr. (Sandia Corp., Albuquerque, N. Mex.), p. 37-43. 7 refs. [See A69-30361 15-11]

ESTABLISHING FLIGHT WORTHINESS OF MISHANDLED ELECTRONIC EQUIPMENT. T. M. Good, A. F. Bonetti, A. Giuglianotti, and J. W. Tinney (International Business Machines Corp., Owego, N.Y.), p. 44-65. [See A69-30362 15-09]

LOAD HISTORY EFFECTS IN STRUCTURAL FATIGUE. H. Akaike (Institute of Statistical Mathematics, Tokyo, Japan) and S. R. Swanson (MTS Systems Corp.), p. 66-77. 9 refs. [See A69-30363 15-32]

FAILURE MECHANISMS IN MATERIALS-STRUCTURES SUBJECTED TO SHORT-TIME LOADINGS. W. C. Lyons and F. R. Tuler (Sandia Corp., Albuquerque, N. Mex.), p. 78-91. 106 refs. [See A69-30364 15-17]

TIME DEPENDENCE OF THE MAXIMUM STRUCTURAL RESPONSE UNDER RANDOM LOADING. R. L. Barnoski (Measurement Analysis Corp., Marina Del Rey, Calif.), p. 92-97. 9 refs. [See A69-30365 15-32]

WEAR-DEPENDENT FAILURE RATES AND SYSTEM WEAROUT RELIABILITY PREDICTION UNDER NONGAUSSIAN RANDOM LOADING. T. I. Smits (Catholic University of America, Washington, D.C.), p. 98-108. 40 refs. [See A69-30366 15-32]

DYNAMIC EFFECTS OF VIBRATION ON GUIDANCE AND CONTROL SYSTEM PERFORMANCE. D. Sargent (TRW Systems Group, Redondo Beach, Calif.), p. 109-120. 33 refs. [See A69-30367 15-14]

DERIVATION OF DESIGN AND TEST CRITERIA. R. E. Blake and W. S. Baird (Lockheed Aircraft Corp., Palo Alto, Calif.), p. 128-138. 16 refs. [See A69-30368 15-15]

SONIC BOOMS - FUNDAMENTAL CHARACTERISTICS. H. W. Carlson (NASA, Langley Research Center, Hampton, Va.), p. 185-188. [See A69-30369 15-02]

SONIC BOOM DAMAGE TO STRUCTURES. J. H. Wiggins, Jr. (J. H. Wiggins Co.), p. 189-197. 5 refs. [See A69-30370 15-11]

A SURVEY OF SONIC BOOM SIMULATION TECHNIQUES AND UNMANNED MONITORING DEVICES. J. K. Power (Federal Aviation Administration, Washington, D.C.), p. 198-210. [See A69-30371 15-11]

JET NOISE SUPPRESSION (A STATUS REPORT). J. B. Large (Boeing Co., Renton, Wash.), p. 211-214. 8 refs. [See A69-30372 15-28]

AIRPORT NOISE - AN ENVIRONMENTAL PROBLEM. J. O. Powers (Federal Aviation Administration, Washington, D.C.), p. 215-230. 10 refs. [See A69-30373 15-11]

COMMUNITY RESPONSE TO ATMOSPHERIC NOISE. R. C. Casperson (Dunlop and Associates, Inc., Darien, Conn.), p. 231-236. 12 refs. [See A69-30374 15-34]

INTERFERENCE MEASURING INSTRUMENT CALIBRATION. F. R. Hume (North American Rockwell Corp., Downey, Calif.), p. 253-258. [See A69-30375 15-09]

SOME ASPECTS OF INTERPLANETARY EARTH-ENTRY SIMULATION. E. M. Sullivan, W. D. Erickson, G. L. Smith, and J. T. Suttles (NASA, Langley Research Center, Hampton, Va.), p. 269-275. 15 refs. [See A69-30376 15-30]

INVESTIGATION OF PLASMAS AT VERY HIGH PRESSURE. E. E. Soehngen and U. Bauder (USAF, Aerospace Research Laboratories, Wright-Patterson AFB, Ohio), p. 276-280. 7 refs. [See A69-30377 15-25]

OPERATING CHARACTERISTICS OF A MULTI-MEGAWATT ARC HEATER USED WITH THE AFFDL 50 MEGAWATT FACILITY. R. T. Smith and J. L. Folck (USAF, Flight Dynamics Laboratory, Wright-Patterson AFB, Ohio), p. 281-294. 14 refs. [See A69-30378 15-11]

WIDE RANGE HEAT FLUX MEASUREMENTS USING SURFACE TEMPERATURE SENSORS. D. W. Grunditz and D. H. Smith (McDonnell Douglas Corp., Santa Monica, Calif.), p. 295-300. [See A69-30379 15-33]

THE NUCLEAR ENVIRONMENT AGAINST WHICH EQUIPMENT MUST BE HARDENED. C. N. Davidson and W. P. Schneider (U.S. Army, Combat Development Command, Fort Bliss, Tex.), p. 301-308. [See A69-30380 15-22]

ANALYTICAL DESCRIPTIONS OF THE NUCLEAR WEAPON ENVIRONMENT AND EFFECTS. R. T. Castle (Battelle Memorial Institute, Columbus, Ohio), p. 319-322. 5 refs. [See A69-30381 15-22]

GENERATION OF LOW MAGNETIC FIELD ENVIRONMENT FOR STUDY OF SPACE NULL MAGNETIC FIELD EFFECTS ON MAN. D. E. Beischer (U.S. Naval Aviation Medical Center, Pensacola, Fla.), p. 342-346. 13 refs. [See A69-30382 15-11]

THE DESIGN AND PERFORMANCE OF A VERSATILE 25 SOLAR CONSTANT SIMULATOR. J. P. Kirkpatrick (NASA, Ames Research Center, Moffett Field, Calif.), L. F. Polak, and J. H. Beauchene (Aerospace Controls Corp., Los Angeles, Calif.), p. 347-353. [See A69-30383 15-11]

PERFORMANCE AND VERSATILITY OF A 20-KW XENON LAMP SOLAR SIMULATOR AT LINCOLN LABORATORY. G. A. Gallagher (Massachusetts Institute of Technology, Cambridge, Mass.), p. 354-359. 14 refs. [See A69-30384 15-11]

SOLAR SIMULATOR USING A PULSED XENON ARC TUBE. D. Creed (Hughes Aircraft Co., Culver City, Calif.), p. 363-369. [See A69-30385 15-11]

EXPERIENCES WITH A LARGE SPACE ENVIRONMENT SIMULATION FACILITY. D. H. Orbock and B. Peterson (Sperry Rand Corp., Huntsville, Ala.), p. 376-386. 6 refs. [See A69-30386 15-11]

A DIGITALLY CONTROLLED VIBRATION OR ACOUSTICS TESTING SYSTEM. I - ADVANTAGES AND BASIC CONCEPTS. C. P. Chapman (California Institute of Technology, Pasadena, Calif.), p. 387-393. 5 refs. [See A69-30387 15-11]

A DIGITALLY CONTROLLED VIBRATION OR ACOUSTICS TESTING SYSTEM. II - STATISTICAL REQUIREMENTS AND SPECTRUM SHAPING TECHNIQUES. J. Shipley (California Institute of Technology, Pasadena, Calif.), p. 394-402. [See A69-30388 15-11]

A DIGITALLY CONTROLLED VIBRATION OR ACOUSTICS TESTING SYSTEM. III - HARDWARE REQUIREMENTS AND IMPLEMENTATION. C. L. Heizman (TIME/DATA Corp., Palo Alto, Calif.), p. 403-409. [See A69-30389 15-11]

TEST FACILITY FOR SIMULATION OF SYSTEM-ENVIRONMENT INTERACTION DURING MARTIAN ENTRY. E. Heer, J. A. Garba, F. W. Orlik, and G. A. Berry (California Institute of Technology, Pasadena, Calif.), p. 410-418. [See A69-30390 15-11]

SPACE SIMULATION QUALIFICATION OF A SPIN STABILIZED

SYNCHRONOUS ORBIT COMMUNICATIONS SATELLITE. M. B. Levine (Hughes Aircraft Co., Space Simulation Laboratory), p. 419-424. [See A69-30391 15-11]

A LARGE, SELECTIVELY PUMPED, THERMAL VACUUM TEST FACILITY. A. A. Edwards (Lockheed Aircraft Corp., Sunnyvale, Calif.), p. 446-450. [See A69-30392 15-11]

THE DESIGN OF THE COMSAT THERMAL VACUUM CHAMBER. A. W. Clark (Communications Satellite Corp., Washington, D.C.) and W. F. Mitchell (CGS Scientific Corp., Southampton, Pa.), p. 451-458. [See A69-30393 15-11]

MANNED TEST OPERATIONS RELATED TO THE APOLLO LUNAR MODULE IN THE SIMULATED SPACE ENVIRONMENT. O. L. Pearson (NASA, Manned Spacecraft Center, Houston, Tex.) and P. R. Gauthier (Boeing Co., Seattle, Wash.), p. 459-474. [See A69-30394 15-05]

REFRIGERATION OF SPACE FLIGHT CRYOGENIC GAS STORAGE SYSTEMS. E. L. Dunning (Southern Illinois University, Carbondale, Ill.), p. 475-478. [See A69-30395 15-11]

EXPERIMENTAL SIMULATION OF TWO-PHASE VENTING TO A SPACE ENVIRONMENT. A. B. Walburn (General Dynamics Corp., San Diego, Calif.) and E. A. Evans, p. 479-483. [See A69-30396 15-31]

PRESSURE CONTROL OF FLIGHT CONFIGURATION CRYOGENIC CONTAINERS DURING HEAT LEAK EVALUATION TESTS. D. Beck (McDonnell Douglas Corp., St. Louis, Mo.), p. 484-489. [See A69-30397 15-31]

TESTING AS A TEAM - THE COLLABORATION OF GOVERNMENT AND INDEPENDENT TESTING LABORATORIES. W. P. McLean (Dayton T. Brown, Inc.), p. 546-550. [See A69-30398 15-34]

INTEGRATED STRUCTURAL AND DYNAMIC TESTING PLANS FOR A LARGE INTERPLANETARY SPACECRAFT. S. M. Kaplan (General Electric Co., Philadelphia, Pa.), p. 565-572. 19 refs. [See A69-30399 15-11]

A NEW TECHNIQUE FOR INTEGRATED TESTING UTILIZING CONFIDENCE LEVELS. W. C. Stolp (McDonnell Douglas Corp., Huntington Beach, Calif.) and E. H. Welch (U.S. Army, Missile Command, Redstone Arsenal, Ala.), p. 573-576. [See A69-30400 15-15]

COST-EFFECTIVENESS OF TEST SELECTION. H. Hecht (Aerospace Corp., El Segundo, Calif.), p. 577-583. 11 refs. [See A69-30401 15-34]

MANAGEMENT OF THE INDEPENDENT TESTING LABORATORY. B. M. Bleak (Wyle Laboratories, Systems Group), p. 589-592. [See A69-30402 15-34]

THE PROCUREMENT OF THE BOEING A-7000 (7 MODULE) SOLAR SIMULATOR. R. T. Jessen, Jr. and A. R. Lunde (Boeing Co., Seattle, Wash.), p. 597-604. [See A69-30403 15-11]

ANALYSIS AND DESIGN OF RESONANT FIXTURES TO AMPLIFY VIBRATOR OUTPUT. J. Verga (Hazeltine Corp., Little Neck, N.Y.), p. 619-625. [See A69-30404 15-11]

SIMULATION OF THE SATURN V BOOST-PHASE ENVIRONMENT ON MAJOR APOLLO SPACECRAFT STAGES. D. R. Reese (Wyle Laboratories, Huntsville, Ala.) and A. N. Levine (NASA, Manned Spacecraft Center, Houston, Tex.), p. 629-643. [See A69-30405 15-11]

A69-30383 *

THE DESIGN AND PERFORMANCE OF A VERSATILE 25 SOLAR CONSTANT SIMULATOR.

J. P. Kirkpatrick (NASA, Ames Research Center, Moffett Field, Calif.), L. F. Polak, and J. H. Beauchene (Aerospace Controls Corp., Los Angeles, Calif.).

IN: MAN IN HIS ENVIRONMENT; INSTITUTE OF ENVIRONMENTAL SCIENCES, ANNUAL TECHNICAL MEETING AND EQUIPMENT EXPOSITION, 15TH, ANAHEIM, CALIF., APRIL 20-24, 1969, PROCEEDINGS. [A69-30356 15-11]

Mt. Prospect, Ill., Institute of Environmental Sciences, 1969, p. 347-353.

Contract No. NAS 2-3921.

Description of a versatile high-intensity solar radiation simulator currently being used for both high- and low-intensity testing. Designed for thermal balance tests, power conversion studies, and material degradation experiments, it uses a 20-kw xenon lamp and a 5-kw krypton lamp as sources and may be run in three basic optical modes: (1) a 4-5/8-in.-diam target plane with radiant intensities from 10 to 40 solar constants; (2) a 12-in. target plane with intensities up to 8 solar constants; and (3) a 30-in. target plane with intensities up to 2 solar constants. In addition, operation with the krypton source only provides solar intensities as low as 1/25 of a solar constant without any modification of the optical system. The maximum variations in uniformity throughout the target planes for the three modes are approximately ±2.5%, ±3.0%, and ±3.5%, respectively. The optical, mechanical, and electrical design of the system is described in detail. System performance for the first 450 hr of operation is presented. F.R.L.

A69-31917 *#

MULTIPLE-FUNCTION PROBE FOR AIRFLOW RESEARCH.

George E. Glawe, Lloyd N. Krause, and Thomas J. Dudzinski (NASA, Lewis Research Center, Cleveland, Ohio).

AIAA Journal, vol. 7, Apr. 1969, p. 776, 777.

Description of the design and testing of a small combination probe for use in compressor and turbine research. The probe combines a high-recovery shielded thermocouple for sensing total temperature, a total-pressure sensing tube, and a flow-direction sensing wedge having a 60° included angle. The flow-direction sensing hole indication may also be used to obtain static pressure. M.G.

A69-33471 *#

PROBLEMS OF FLOW SIMULATION IN WIND TUNNELS.

J. Lloyd Jones (NASA, Ames Research Center, Aeronautics Div., Moffett Field, Calif.).

American Institute of Aeronautics and Astronautics, Fluid and Plasma Dynamics Conference, San Francisco, Calif., June 16-18, 1969, Paper 69-660. 9 p. 18 refs.

Members, $1.00; nonmembers, $1.50.

Illustration of flow-simulation problems that are generated or amplified as a result of recent trends in aircraft design that require more detailed attention to local flow conditions on models in wind-tunnel tests to assure that the test results can be used to predict adequately the aerodynamic characteristics of the aircraft. Because the effects of viscosity are fundamental in the proper modeling of local flows in wind-tunnel tests, the boundary layer and its coupling with the external flow are key features in the examples cited. These examples include problems of providing known boundary-layer-flow characteristics and problems resulting from flow separation and shock-boundary-layer interactions. Test techniques to resolve some of these simulation problems are discussed, and limitations of existing wind-tunnel facilities are examined in relation to these problems. (Author)

A69-35228 *#

THE FLOW THROUGHOUT A WIND TUNNEL CONTAINING A ROTOR WITH A SHARPLY DEFLECTED WAKE.

Harry H. Heyson (NASA, Langley Research Center, Hampton, Va.).

IN: AERODYNAMICS OF ROTARY WING AND V/STOL AIRCRAFT; CORNELL AERONAUTICAL LABORATORY AND U.S. ARMY AVIATION MATERIEL LABORATORIES, SYMPOSIUM, 3RD, BUFFALO, N.Y., JUNE 18-20, 1969, PROCEEDINGS. VOLUME 2 - WIND TUNNEL TESTING, NEW CONCEPTS IN ROTOR CONTROL. [A69-35226 18-01]

Buffalo, N.Y., Cornell Aeronautical Laboratory, Inc., 1969. 45 p. 42 refs.

Examination of the flowfield throughout a wind tunnel of a rotor with sharply deflected blades, using modified NASA TR R-124 and TR R-302 computer programs. The general nature of the computed flowfield is verified by flow studies. The predominant effect at low speed is a region of reversed flow in front of the wake near the floor. This region initiates large-scale vortices in the flow which are the apparent cause of the minimum-speed V/STOL testing limits. V.P.M.

11 FACILITIES, RESEARCH AND SUPPORT

A69-35714
ICIASF '69; INTERNATIONAL CONGRESS ON INSTRUMENTATION IN AEROSPACE SIMULATION FACILITIES, 3RD, POLYTECHNIC INSTITUTE OF BROOKLYN, FARMINGDALE, N.Y., MAY 5-8, 1969, RECORD.
New York, Institute of Electrical and Electronics Engineers, Inc., (IEEE Publication 69 C 19-AES), 1969. 338 p. In English and French.
Members, $12.50; nonmembers, $15.

CONTENTS:
ELECTROSTATIC PROBES.
ION PROBES IN CONVENTIONAL AND MAGNETICALLY DRIVEN SHOCK TUBES. W. E. Scharfman and W. C. Taylor (Stanford Research Institute, Menlo Park, Calif.), p. 11-19. 8 refs. (See A69-35715 19-11)
OBSERVATIONS ON ELECTROSTATIC PROBE BEHAVIOR IN COLLISION-DOMINATED IONIZED TURBULENT GAS FLOWS IN BALLISTIC RANGES. A. Cantin, A. Emond, and D. Heckman (Canadian Armament Research and Development Establishment, Valcartier, Quebec, Canada), p. 20-33. 41 refs. (See A69-35716 19-11)
CALIBRATION AND USE OF ELECTROSTATIC PROBES FOR HYPERSONIC WAKE DIAGNOSTICS. I. P. French, R. A. Hayami, T. E. Arnold, M. Steinberg (General Motors Corp., Santa Barbara, Calif.), J. P. Appleton, and A. A. Sonin (Massachusetts Institute of Technology, Cambridge, Mass.), p. 34-42. 21 refs. (See A69-35717 19-11).
FIELD TRACING WITH ELECTROSTATIC PROBES IN LOW DENSITY SLIGHTLY IONIZED FLOWS. S. Lederman, M. H. Bloom, and G. F. Widhopf (Brooklyn, Polytechnic Institute, Brooklyn, N.Y.), p. 43-50. 9 refs. (See A69-35718 19-11)
THEORY AND CALIBRATION OF SMALL CONTINUUM ELECTROSTATIC PROBES IN AN IONIZED FLOW. J. K. Dukowicz (Cornell Aeronautical Laboratory, Inc., Buffalo, N.Y.), p. 51-62. 13 refs. (See A69-35719 19-14)

FLOW DIAGNOSTICS. I.
FLASH X-RAY TECHNIQUE FOR RECESSION MEASUREMENTS IN ABLATING MODELS. P. C. Kassel, Jr. (NASA, Langley Research Center, Hampton, Va.), p. 63-67. (See A69-35720 19-11)
NANOSECOND PHOTOGRAPHY WITH SUPER RADIANT LIGHT, X RAYS OR ELECTRONS. J. L. Brewster, J. P. Barbour, W. P. Dyke, and F. J. Grundhauser (Field Emission Corp., McMinnville, Ore.), p. 68-71. (See A69-35721 19-14)
ELECTRON BEAM FLOW VISUALIZATION IN HYPERSONIC HELIUM FLOW. L. M. Weinstein, R. D. Wagner, Jr., A. Henderson, Jr., and S. L. Ocheltree (NASA, Langley Research Center, Hampton, Va.), p. 72-78. 18 refs. (See A69-35722 19-11)
QUANTITATIVE VISUALIZATION OF LOW DENSITY FLOW FIELDS USING THE ELECTRON BEAM EXCITATION TECHNIQUE. B. L. Maguire, E. P. Muntz, and J. R. Mallin (General Electric Co., Valley Forge, Pa.), p. 79-85. 6 refs. (See A69-35723 19-11)

CALIBRATION AND ERROR ANALYSIS.
PHOTOMULTIPLIER AREA SENSITIVITY MEASUREMENTS USING A MULTICOLOR DISPLAY TECHNIQUE. O. Youngbluth, Jr. (NASA, Langley Research Center, Hampton, Va.), p. 86-91, 321-325. (See A69-35724 19-14)
CALIBRATION APPARATUS FOR SURFACE THERMOCOUPLES. E. H. Schulte, E. O. Puronen, and W. P. Dixon (McDonnell Douglas Corp., St. Louis, Mo.), p. 92-95. (See A69-35725 19-11)
CALIBRATION METHOD USED AT ONERA FOR HOTSHOT AND SHOCK TUBE HEAT TRANSFER TRANSDUCERS. J. Maulard (ONERA, Châtillon-sous-Bagneux, Hauts-de-Seine, France), p. 96-106. 6 refs. (See A69-35726 19-14)
MULTI-CHANNEL PRESSURE TELEMETRY SYSTEM FOR BASE PRESSURE MEAUREMENTS ON SMALL MODELS. G. S. Pick and S. E. Dawson (U.S. Naval Material Command, Ship Research and Development Center, Carderock, Md.), p. 107-115. (See A69-35727 19-14)
AN ANALYSIS OF SOURCES OF ERROR IN TYPICAL PRESSURE MEASUREMENTS IN A BLOWDOWN SUPERSONIC TUNNEL. P. G. Pugh and J. Peto (Ministry of Technology, Teddington, Middx., England), p. 116-125. 9 refs. (See A69-35728 19-11)

FLOW DIAGNOSTICS. II.
FUNDAMENTALS OF HOLOGRAPHIC VELOCIMETRY. F. M. Shofner, R. W. Menzel, T. H. Gee, and R. O. Webb (Tennessee, University, Tullahoma, Tenn.), p. 126-135. 19 refs. (See A69-35729 19-14)
PROCESSING HOLOGRAPHIC VELOCIMETRY DATA. F. M. Shofner, R. W. Menzel, T. H. Gee, and R. O. Webb (Tennessee, University, Tullahoma, Tenn.), p. 136-144. 13 refs. (See A69-35730 19-14)
PULSED LASER HIGH-SPEED PHOTOGRAPHY. R. E. Rowlands (IIT Research Institute, Chicago, Ill.) and C. E. Taylor (Illinois, University, Urbana, Ill.), p. 145-159. 42 refs. (See A69-35731 19-14)
LASER PHOTOGRAPHIC SYSTEM FOR AEROBALLISTIC RANGE PHOTOGRAPHY. P. H. Dugger and J. W. Hill (ARO, Inc., Arnold Air Force Station, Tenn.), p. 160-167. (See A69-35732 19-14)
A TECHNIQUE FOR PARTICLE SIZING IN MOVING STREAMS. W. D. Hall and E. B. Champagne (KMS Industries, Inc., Ann Arbor, Mich.), p. 168-172. (See A69-35733 19-14)

FORCES AND STRAINS.
BALANCE FOR MEASURING SKIN FRICTION IN THE PRESENCE OF HEAT TRANSFER. J. R. Bruno, W. J. Yanta (U.S. Navy, Naval Ordnance Laboratory, Silver Spring, Md.), and D. B. Risher (U.S. Navy, Ordnance Systems Command, Washington, D.C.), p. 173-177. (See A69-35734 19-11)
BALANCE FOR MEASURING SKIN FRICTION IN THE PRESENCE OF ABLATION. J. R. Bruno (U.S. Navy, Naval Ordnance Laboratory, Silver Spring, Md.), p. 178-183. (See A69-35735 19-11)
STRAIN GAGE INSTRUMENTATION FOR A LIGHT GAS GUN. P. D. Flynn (U.S. Army, Pitman-Dunn Research Laboratories, Philadelphia, Pa.), p. 184-189. 7 refs. (See A69-35736 19-14)
ACCELEROMETER FORCE BALANCE TECHNIQUES. G. R. Duryea and W. J. Sheeran (Cornell Aeronautical Laboratory, Inc., Buffalo, N.Y.), p. 190-197. 6 refs. (See A69-35737 19-11)
THE MAGNETIC SUSPENSION SYSTEM AS A WIND TUNNEL DYNAMIC BALANCE. M. Judd (Massachusetts Institute of Technology, Cambridge, Mass.), p. 198-206. 10 refs. (See A69-35738 19-11)

FLOW DIAGNOSTICS. III.
ANALYSIS OF THE VISCOUS WAKE OF AN ABLATING SPHERE WITH THE AID OF AN IMAGE CONVERTER CAMERA. H. Fagot and J. Vauvrecy (Institut Franco-Allemand de Recherches, Saint-Louis, Haut-Rhin, France), p. 207-213. (See A69-35739 19-14)
STRIOSCOPIC METHODS FOR MEASURING MASS VOLUME IN HYPERSONIC WAKES IN A HOT-SHOT TUNNEL (METHODES STRIOSCOPIQUES DE MESURE DES MASSES VOLUMIQUES DANS LES SILLAGES HYPERSONIQUES EN TUNNEL DE TIR). P. Smigielski, L. Oudin, A. Kalt, F. Albe, M. Devaud, and A. Stimpfling (Institut Franco-Allemand de Recherches, Saint-Louis, Haut-Rhin, France), p. 214-222. 19 refs. (See A69-35740 19-11)
QUANTITATIVE SCHLIEREN MEASUREMENTS BY THE PHOTOMULTIPLIER TECHNIQUE. B. W. Hannah and R. G. Dale, Jr. (Cincinnati, University, Cincinnati, Ohio), p. 223-228. 7 refs. (See A69-35741 19-14)
TWO-WAVELENGTH LASER INTERFEROMETRY OF HYPERSONIC IONIZED FLOWS. F. H. Oertel and J. H. Spurk (U.S. Army, Ballistics Research Laboratories, Aberdeen Proving Ground, Md.), p. 229-234. 8 refs. (See A69-35742 19-14)
NANOSECOND PULSE DOPPLER RADAR FOR THE INVESTIGATION OF TURBULENT WAKES IN SHOCK TUNNELS

AND BALLISTIC RANGES. M. C. Young and B. R. Tripp (Cornell Aeronautical Laboratory, Inc., Buffalo, N.Y.), p. 235-242. 12 refs. (See A69-35743 19-11)

DATA ACQUISITION AND PROCESSING.

A 500,000 SAMPLE PER SECOND DIGITAL RECORDER FOR THE AMES ELECTRIC ARC SHOCK TUNNEL. H. L. Seegmiller and Louis Mazer (NASA, Ames Research Center, Moffett Field, Calif.), p. 243-247. (See A69-35744 19-11)

A HIGH-SPEED DIGITAL DATA ACQUISITION SYSTEM. F. G. Reinagel and B. R. Tripp (Cornell Aeronautical Laboratory, Inc., Buffalo, N.Y.), p. 248-251. (See A69-35745 19-14)

DYDRA-DATA LOGGER FOR DYNAMIC MEASUREMENTS. P. H. Fuijkschot and L. J. M. Joosten (Nationaal Luchtvaartlaboratorium, Amsterdam, Netherlands), p. 252-261. (See A69-35746 19-11)

A NEW METHOD FOR THE QUICK ANALYSIS OF TRANSIENT PHENOMENA. J. Fiquet, J. Dupé, and F. Mescam (ONERA, Châtillon-sous-Bagneux, Hauts-de-Seine, France), p. 262-268. (See A69-35747 19-11)

THERMAL EFFECTS.

A HIGH HEAT FLUX SENSOR EMPLOYING SEMICONDUCTORS. E. H. Schulte and R. F. Kohl (McDonnell Douglas Corp., St. Louis, Mo.), p. 269-277. 21 refs. (See A69-35748 19-14)

A NEW FERROELECTRIC TRANSDUCER FOR USE IN HEAT TRANSFER AND FLOW STUDIES. K. R. Jolls and P. M. Sforza (Brooklyn, Polytechnic Institute, Brooklyn, N.Y.), p. 278-286. 13 refs. (See A69-35749 19-14)

HIGH ENERGY RECOVERY PRESSURE AND ENTHALPY SENSOR. A. Wortman (Northrop Corp., Hawthorne, Calif.), p. 287-294. 7 refs. (See A69-35750 19-14)

MINIATURE TOTAL TEMPERATURE PROBE FOR BOUNDARY LAYER MEASUREMENTS IN SHORT RUNNING TIME HYPERSONIC FACILITIES. J. H. Perry (Rolls Royce, Ltd., Derby, England) and R. A. East (Southampton, University, Southampton, England), p. 295-302. 12 refs. (See A69-35751 19-11)

FLOW DIAGNOSTICS. IV.

SPECTROSCOPIC DETERMINATION OF HIGH VELOCITY FLOW FIELD STATIC TEMPERATURES. H. J. Unger, F. K. Hill, and N. G. Paul (Johns Hopkins University, Silver Spring, Md.), p. 303-308. 13 refs. (See A69-35752 19-11)

A GAS-CAP RADIATION PROBE FOR THE DETECTION OF DRIVER GAS IN THE TEST SECTION OF A HYPERSONIC SHOCK TUNNEL. D. J. McCaa and C. E. Rogers (Cornell Aeronautical Laboratory, Inc., Buffalo, N.Y.), p. 309-314. (See A69-35753 19-11)

INSTRUMENTATION FOR EXPERIMENTAL INVESTIGATION OF MICROWAVE INTERACTION WITH REACTING TURBULENT BOUNDARY LAYERS. F. G. Reinagel (Cornell Aeronautical Laboratory, Inc., Buffalo, N.Y.), p. 315-318. 5 refs. (See A69-35754 19-11)

A69-35720 *
FLASH X-RAY TECHNIQUE FOR RECESSION MEASUREMENTS IN ABLATING MODELS.
P. C. Kassel, Jr. (NASA, Langley Research Center, Hampton, Va.).
IN: ICIASF '69; INTERNATIONAL CONGRESS ON INSTRUMENTATION IN AEROSPACE SIMULATION FACILITIES, 3RD, POLYTECHNIC INSTITUTE OF BROOKLYN, FARMINGDALE, N.Y., MAY 5-8, 1969, RECORD. (A69-35714 19-11)
New York, Institute of Electrical and Electronics Engineers, Inc. (IEEE Publication 69 C 19-AES), 1969, p. 63-67.

A commercial flash X-ray unit, in conjunction with one of two special film transport devices, has been used to obtain sequenced dynamic radiographs of ablating models during reentry simulation tests at an arc jet facility. A technique is described for obtaining, from these radiographs, the location of the surface and the char-virgin material interface of the model as a function of time. (Author)

A69-35722 *
ELECTRON BEAM FLOW VISUALIZATION IN HYPERSONIC HELIUM FLOW.
Leonard M. Weinstein, Richard D. Wagner, Jr., Arthur Henderson, Jr., and Stewart L. Ocheltree (NASA, Langley Research Center, Hampton, Va.).
IN: ICIASF '69; INTERNATIONAL CONGRESS ON INSTRUMENTATION IN AEROSPACE SIMULATION FACILITIES, 3RD, POLYTECHNIC INSTITUTE OF BROOKLYN, FARMINGDALE, N.Y., MAY 5-8, 1969, RECORD. (A69-35714 19-11)
New York, Institute of Electrical and Electronics Engineers, Inc. (IEEE Publication 69 C 19-AES), 1969, p. 72-78. 18 refs.

An electron-beam fluorescence probe and the afterglow associated with it have been investigated for visualizing hypersonic helium flowfields. Although densities were generally too high for quantitative measurements with the electron beam, the qualitative visualization allows flow structure to be observed. The value and versatility of the method is demonstrated by the results obtained during several research projects in which the fluorescence probe and afterglow were used. (Author)

A69-35744 *
A 500,000 SAMPLE PER SECOND DIGITAL RECORDER FOR THE AMES ELECTRIC ARC SHOCK TUNNEL.
H. Lee Seegmiller and Louis Mazer (NASA, Ames Research Center, Moffett Field, Calif.).
IN: ICIASF '69; INTERNATIONAL CONGRESS ON INSTRUMENTATION IN AEROSPACE SIMULATION FACILITIES, 3RD, POLYTECHNIC INSTITUTE OF BROOKLYN, FARMINGDALE, N.Y., MAY 5-8, 1969, RECORD. (A69-35714 19-11)
New York, Institute of Electrical and Electronics Engineers, Inc., (IEEE Publication 69 C 19-AES), 1969, p. 243-247.

Description of a 500,000 sample per second digital data acquisition system for the Ames electric arc shock tunnel. As many as 24 analog input signals can be accepted, and full-scale output may be obtained from input voltages in 10 ranges between 0.5 and 500 mV. Bipolar 8-bit information is stored in four parallel magnetostrictive delay lines during a 10 msec period and is recirculated for nondestructive interrogation. Examples of model pressure and heat-transfer data obtained in the expanding nozzle flow of the shock tunnel are presented. The shielding and grounding arrangement are also described. (Author)

A69-36022 *
THE IMPACT OF FAILURE DATA ON MANAGEMENT OF A LAUNCH OPERATIONS RELIABILITY PROGRAM.
Robert E. Cato, Jr. (NASA, Kennedy Space Center, Cocoa Beach, Fla.) and Wallace C. Wheadon (General Electric Co., Cocoa Beach, Fla.).
IN: ANNALS OF ASSURANCE SCIENCES; PROCEEDINGS OF THE EIGHTH RELIABILITY AND MAINTAINABILITY CONFERENCE, DENVER, COLO., JULY 7-9, 1969. (A69-35999 19-15)
Conference sponsored by the American Institute of Aeronautics and Astronautics, the Society of Automotive Engineers, and the American Society of Mechanical Engineers.
New York, Gordon and Breach, Science Publishers, Inc., 1969, p. 238-243.

Discussion of efforts which have been made to conduct a responsible launch-operations reliability program with existing failure data. The basic reliability organization and requirements are discussed, and the corrective action program which is one potential source of field-failure data is reviewed. Reliability problems which occured as a result of poor data are discussed. Recovery plans to obtain acceptable field-failure data and the manner in which such data could be used to upgrade the existing program are treated. M.M.

A69-37704 *
ANALYSIS OF A MULTIPLICATIVE FEED SYSTEM FOR MONOPULSE TRACKING APPLICATIONS.

Hugh P. Taylor (Ewen Knight Corp., East Natick, Mass.), George G. Haroules, and Wilfred E. Brown (NASA, Electronics Research Center, Cambridge, Mass.).
IEEE Transactions on Aerospace and Electronic Systems, vol. AES-5, July 1969, p. 581-588.

In angle tracking antenna applications, the angle sensing boresight accuracy capabilities are important. The ability of an antenna to precisely determine the bearing angle to a point source is determined by the slope of the control function pattern at boresight. In the presence of extraneous interference, the magnitudes of the sidelobe and backlobe responses are important. Control pattern slope (angular sensitivity) is primarily a function of aperture illumination. It can be described by a current distribution in intensity and phase at every point. Once distribution is defined, lobe structure is defined by the associated transform. When more than one feed is used, the distribution will be a vector sum of the individual feed distributions. The resulting secondary pattern can be defined in terms of the amplitude distribution and the phase center locations of the contributing feeds. With a four-horn monopulse configuration, the feed phase centers are displaced from the boresight axis. Placing the phase centers on the boresight axis by rotating the feeds through 45 deg results in a different set of intensity and phase values. A quite different secondary pattern results. The control function obtained by the subtraction of the powers from a paired set of on-axis feeds results in a lower sidelobe level than that obtained with a conventional monopulse combiner for a given feed taper. (Author)

A69-38181 •
SPACECRAFT LOADER HAS ALL-HYDRAULIC, ALL-DIRECTION POSITIONING.
Edwin J. Skolka (NASA, Goddard Space Flight Center, Greenbelt, Md.).
Hydraulics and Pneumatics, vol. 22, Feb. 1969, p. 89-92.

Description of a 50,000 lb all hydraulic-powered, self-propelled, six-degree-of-freedom loading vehicle capable of moving a 40,000 lb test assembly to a test chamber and positioning it with such accuracy that it can be inserted into and attached to the test chamber. The vehicle has precise flow controls and an unusual but simple suspension and leveling system, which is illustrated in a block diagram. The operation of the six-degree-of-freedom positioning control system is described in detail. B.H.

A69-38271 *
ENVIRONMENTAL CONTROL FOR RADIATION TESTING OF LUNAR ROCK SAMPLES.
W. C. Anderson (Union Carbide Corp., Nuclear Div., Oak Ridge, Tenn.), J. G. Griffith, K. A. Richardson (NASA, Manned Spacecraft Center, Houston, Tex.), and J. C. Little.
Heating, Piping and Air Conditioning, vol. 41, July 1969, p. 79-88. 6 refs.

Detailed description of the mechanical design concept of the NASA Lunar Receiving Laboratory, an underground center for examining lunar samples by gamma ray spectrometry for induced radioactive nuclides and naturally occurring isotopes. The facility includes provisions for room isolation, triple filtration of air with HEPA filters, radon adsorption with activated charcoal at -112 deg F, and pressure control between sensitive areas. B.H.

A69-38894 *
HANDBOOK OF SOLAR SIMULATION FOR THERMAL VACUUM TESTING.
John Arvesen (NASA, Ames Research Center, Moffett Field, Calif.), F. N. Benning, J. A. Castle (Textron, Inc., Spectrolab Div., Sylmar, Calif.), Robert Fink (Hughes Aircraft Co., Culver City, Calif.), J. S. Griffith (California Institute of Technology, Jet Propulsion Laboratory, Pasadena, Calif.), Peter Lenn (U.S. Army, Materiel Command, Washington, D.C.), Malcolm Lillywhite (Martin Marietta Corp., Friendship International Airport, Md.), L. A. Nelson (McDonnell Douglas Corp., St. Louis, Mo.), A. F. Matel (Hughes Aircraft Co., Culver City, Calif.), and C. W. Quillin (Textron, Inc., Spectrolab Div., Sylmar, Calif.).
Mt. Prospect, Ill., Institute of Environmental Sciences, 1968. 165 p. 107 refs.
Members, $5.00; nonmembers, $9.00.

This handbook is a compilation of the most useful information on solar simulation for simulator operators, designers of facilities, spacecraft thermal designers, and others connected with space simulation testing. A further purpose is to aid in communication between workers in the field; hence there are sections on nomenclature, test requirements, system parameters, and other subjects. The space environment is described, with emphasis on the thermally important properties of space. The handbook emphasizes solar simulators used for thermal vacuum testing. Since system integration tests require essentially the same environment as thermal balance testing, and the tests frequently are run concurrently, the handbook in practice covers the facility requirements of this type of testing as well. Brief attention is given to other types of space simulation testing and their individual requirements. The tentative standard for space and solar simulation, MIL-STD-810B, Test Method 517, which proposes a somewhat idealized requirement, is discussed. A scale of requirements with various degrees of simulation accuracy is provided. Solar simulators themselves are discussed with reference to systems, sources, and components. Parameters of good solar simulators and components are given, with numerous examples. Solar simulator effects on thermal control coatings are considered. Solar instrumentation and current methods of measuring spectral irradiance are described, as well as the necessary cold shroud and vacuum requirements. Suggestions on operation and maintenance are provided. F.R.L.

A69-38896 •
PHYSICAL, CHEMICAL, AND BIOLOGICAL ACTIVITIES AT THE LUNAR RECEIVING LABORATORY.
W. W. Kemmerer, Jr., J. A. Mason, and B. C. Wooley (NASA, Manned Spacecraft Center, Lunar Receiving Laboratory, Houston, Tex.).
BioScience, vol. 19, Aug. 1969, p. 712-715.

Description of the quarantine and release policies for crew and lunar samples followed in the NASA Lunar Receiving Laboratory. The activities of the three functional areas of the laboratory—namely, the sample operations area, the crew reception area, and the administration and support area—are described. The first two areas are confined within the unit-biological-barrier system and assume the following major tasks: (1) physico-chemical testing of lunar samples, (2) time-critical and scientific investigations that must be completed within the proposed quarantine examination of lunar samples, (3) biological examination of the astronauts, (4) permanent storage under vacuum of a portion of the samples, and (5) sample distribution to the scientific community. The physico-chemical test laboratory provides detailed microscopic, limited petrographic, and compositional data on selected lunar samples. Microbiological, zoological, and botanical testing is discussed in detail, and the radiation counting laboratory is described. B.H.

A69-40191 *
APOLLO LUNAR SAMPLE ANALYSIS PROGRAM—A PROGRESS REPORT.
V. R. Wilmarth (NASA, Washington, D.C.).
IN: THE APPLICATION OF MODERN PHYSICS TO THE EARTH AND PLANETARY INTERIORS; PROCEEDINGS OF THE NATO ADVANCED STUDY INSTITUTE, UNIVERSITY OF NEWCASTLE-UPON-TYNE, NEWCASTLE-UPON-TYNE, ENGLAND, MARCH 29-APRIL 4, 1967. (A69-40172 22-30)
Edited by S. K. Runcorn.
London and New York, Wiley-Interscience, 1969, p. 533-546.

Description of the Apollo program of lunar sample collection and subsequent analysis. The schedule of the astronauts' activity on the moon and their equipment for geological studies are described. The tools and packaging facilities are discussed in detail, and the

types of samples which are expected to be collected on the lunar surface are considered. The facility which is destined to carry out the investigations on the samples is described, and the various laboratories are briefly mentioned, including the counting room for radioactive investigations, the gas analysis laboratory, and the preliminary examination laboratory. The international scientific program for the investigation of lunar samples is outlined together with mineralogic, petrologic, chemical, isotopic, biochemical, and organic analyses. P.G.

A69-40323 * #
DESCRIPTION OF A REAL-TIME DIGITAL FULL-SCALE CMG CONTROL SYSTEM SIMULATION FOR MANNED SPACECRAFT.
Robert G. Kyle and Claude R. Keckler (NASA, Langley Research Center, Hampton, Va.).
American Institute of Aeronautics and Astronautics, Aerospace Computer Systems Conference, Los Angeles, Calif., Sept. 8-10, 1969, Paper 69-940. 12 p.
Members, $1.00; nonmembers, $1.50.

Description of a real-time digital computer-hardware simulation of the Apollo Telescope Mount (ATM) mission. The simulation has been developed and employed to evaluate full-scale control moment gyro (CMG) system performance in providing stabilization and control for the ATM cluster configuration. The full-scale CMG system is linked to a digital computer program representing the ATM spacecraft, and the simulation operates in a real-time mode. System-stability and gimbal-rate limit cycling problems were encountered during initial simulation operations. These problems and solutions are discussed, and typical simulation data of spacecraft and CMG system response are presented. Future computer system hardware simulations to be employed in CMG technology development are outlined and include use of a control flight test bed to reproduce the spacecraft motion and examine CMG system-spacecraft interactions. (Author)

A69-40352 * #
A NEW APPROACH TO TELEMETRY DATA PROCESSING—THE DATA REDUCTION LABORATORY.
J. J. Quann, B. A. Walton, and F. A. Keipert (NASA, Goddard Space Flight Center, Greenbelt, Md.).
American Institute of Aeronautics and Astronautics, Aerospace Computer Systems Conference, Los Angeles, Calif., Sept. 8-10, 1969, Paper 69-972. 7 p.
Members, $1.00; nonmembers, $1.50.

Description of the designation, tasks, and possibilities of the data reduction laboratory attached to the NASA Goddard Space Flight Center. It is noted that, with the aid of the facilities available in the laboratory, relatively complicated processes can be written, checked out, and put into operation in terms of hours. Anomalies can be observed and compensated for, and data correlations are facilitated. It is stressed that the time lag between launch and final analysis is considerably shortened. P.G.

A69-40373 * #
THE ORBITING ASTRONOMICAL OBSERVATORY THERMAL TEST PROGRAM.
P. Caruso, Jr., C. Dan, Jr., E. Young (NASA, Goddard Space Flight Center, Greenbelt, Md.), and D. Mengers (Grumman Aerospace Corp., Bethpage, N.Y.).
American Institute of Aeronautics and Astronautics, American Society for Testing and Materials, and Institute of Environmental Sciences, Space Simulation Conference, 4th, Los Angeles, Calif., Sept. 8-10, 1969, AIAA Paper 69-995. 28 p. 29 refs.
Members, $1.00; nonmembers, $1.50.

The Orbiting Astronomical Observatory thermal test and evaluation program consisted of an Alzak heater skin thermal balance study, a radiation model test, a solar array test, several thermal balance and electronic functional tests on the spacecraft experiment packages, a thermal model test, and two combined thermal-vacuum electrical functional checks on the integrated spacecraft. The significant results of the test program, a review of the thermal evaluation methods employed, and the problems encountered in assessing the Observatory thermal performance are presented. (Author)

A69-40386 * #
APPLICATION OF THE LINE-SOURCE TECHNIQUE FOR VACUUM THERMAL CONDUCTIVITY MEASUREMENTS.
Lawrence R. Greenwood (NASA, Langley Research Center, Hampton, Va.) and Robert A. Comparin (Virginia Polytechnic Institute, Blacksburg, Va.).
American Institute of Aeronautics and Astronautics, American Society for Testing and Materials, and Institute of Environmental Sciences, Space Simulation Conference, 4th, Los Angeles, Calif., Sept. 8-10, 1969, AIAA Paper 69-1013. 5 p. 5 refs.
Members, $1.00; nonmembers, $1.50.

Experimental study of the accuracy of the line-source technique for measuring the thermal conductivity of an ablative heat-shield material. The technique was then used to determine the thermal conductivity of the material in a vacuum. The thermal conductivity of the same samples was measured first by using the guarded hot-plate technique, and then by using the line-source technique. The results showed that the average thermal conductivity measured by the line-source technique was within 2 per cent of the other value with a maximum deviation for any one sample of less than 7 per cent. Vacuum measurements using the line-source technique showed a 15-per cent decrease in thermal conductivity after exposure to the vacuum for 24 hours. After reexposure to the atmosphere, the thermal conductivity returned to its original value. (Author)

A69-40390 * #
EFFECTS OF MISSION ENVIRONMENTS ON THE MECHANICAL PROPERTIES OF DACRON PARACHUTE MATERIAL.
David C. Spence (NASA, Langley Research Center, Hampton, Va.).
American Institute of Aeronautics and Astronautics, American Society for Testing and Materials, and Institute of Environmental Sciences, Space Simulation Conference, 4th, Los Angeles, Calif., Sept. 8-10, 1969, AIAA Paper 69-1018. 6 p. 10 refs.
Members, $1.00; nonmembers, $1.50.

Study of the effects of mission environments on the mechanical properties of two groups of tensile samples of Dacron-55 parachute material. The first group was exposed to the mission environments of ethylene oxide decontamination, dry heat sterilization, vacuum, and a simulated Martian atmosphere, and was tensile tested in situ. The second group was a control group and was stored and tested at a temperature of 75 deg F and 45 per cent relative humidity. The results indicate that the sequential exposure of Dacron parachute material to these mission environments will induce changes in the mechanical properties of this material, not to exceed minus 7.7 per cent in maximum stress, minus 18.0 per cent in elongation, minus 17.4 per cent in total energy, minus 9.9 per cent for initial modulus, and plus 4.5 per cent for final modulus. (Author)

A69-40392 * #
AN IN SITU FACILITY FOR THE DETERMINATION OF THE EFFECTS OF A SPACE ENVIRONMENT ON THE SOLAR ABSORPTANCE OF MATERIALS.
M. S. Cridlin, C. A. Nicoletta, and J. D. Mann (NASA, Goddard Space Flight Center, Greenbelt, Md.).
American Institute of Aeronautics and Astronautics, American Society for Testing and Materials, and Institute of Environmental Sciences, Space Simulation Conference, 4th, Los Angeles, Calif., Sept. 8-10, 1969, AIAA Paper 69-1021. 6 p. 9 refs.
Members, $1.00; nonmembers, $1.50.

Description of a laboratory facility for measuring total solar absorptance in the space environment. The use of a vacuum

integrating sphere allowing for an absolute absorptance value eliminates the difficulties encountered in optical measurements through a window. Four samples can be mounted in the facility at the same time but irradiated individually. The space environment consists of ultrahigh vacuum, low energy protons and electrons, from 1 to 30 kev, and solar electromagnetic radiation. All radiation doses are measured at the sample position. Sample temperatures are controlled and recorded during preirradiation, irradiation, and optical measurement phases. The facility should prove an accurate and dependable tool for determining the qualifications of thermal control coatings when exposed to a space environment. M.M.

A69-40393 * #
EFFECTS OF SIMULATED MARS DUST EROSION ENVIRONMENT ON THERMAL CONTROL COATINGS.
G. L. Adlon, E. L. Rusert (McDonnell Douglas Corp., St. Louis, Mo.), and W. S. Slemp (NASA, Langley Research Center, Applied Materials and Physics Div., Hampton, Va.).
American Institute of Aeronautics and Astronautics, American Society for Testing and Materials, and Institute of Environmental Sciences, Space Simulation Conference, 4th, Los Angeles, Calif., Sept. 8-10, 1969, AIAA Paper 69-1023. 11 p. 7 refs.
Members, $1.00; nonmembers, $1.50.

Evaluation of thermal control coatings, windows, and mirrors for application on the proposed 1973 Mars Viking Lander vehicles, under simulated Martian surface conditions. Such parameters as weight and thickness losses, solar absorptance, IR emittance, reflectance, and transmission changes were measured. Ten thermal control materials, two mirrors, and two window materials were exposed to different dust densities at 45 and 90 degree angles and exposure times of 2 to 4 hours. Large increases in solar absorptance were measured for the majority of the coatings exposed to the simulated environment. The hard materials (flame sprayed coatings and glass reference slides) and the soft aluminum-silicate pigmented glass resin coating lost the most coating weight. After 10 minutes of exposure, the fused silica and the alumino-silicate window materials were rendered unusable from a transmittance standpoint. (Author)

A69-40401 • #
PRESSURE MEASUREMENTS AND GAS-FLOW ANALYSIS IN CHAMBERS A AND B DURING THERMAL VACUUM TESTS OF SPACECRAFT 2TV-1 AND LTA-8.
H. K. F. Ehlers (NASA, Manned Spacecraft Center, Space Environment Effects Section, Houston, Tex.).
American Institute of Aeronautics and Astronautics, American Society for Testing and Materials, and Institute of Environmental Sciences, Space Simulation Conference, 4th, Los Angeles, Calif., Sept. 8-10, 1969, AIAA Paper 69-1033. 8 p.
Members, $1.00; nonmembers, $1.50.

During several thermal-vacuum tests of two manned spacecraft, pressures and gas flows in various locations and in various directions in two large vacuum chambers were studied to determine whether the vacuum of space was simulated sufficiently to meet the test objectives. An attempt was made to identify and locate gas sources inside the vacuum chambers and to determine the effect of the gases on the simulation. The study consisted of a theoretical analysis based on a simple mathematical model, and an experimental analysis based on measurements taken with several regular tubulated ion gauges in fixed positions. The results show that the vacuum of space was adequately simulated, even in the presence of numerous gas leaks. The effects and the detection of several gas leaks are described.
(Author)

A69-41139 * #
WHAT'S IMPORTANT IN SIMULATION?
John P. Reeder (NASA, Langley Research Center, Flight Mechanics and Technology Div., Hampton, Va.).
IN: FLIGHT SAFETY FOUNDATION, ANNUAL INTERNATIONAL AIR SAFETY SEMINAR, 21ST, ANAHEIM, CALIF., OCTOBER 8-11, 1968, TECHNICAL SUMMARY. (A69-41127 22-02)
Arlington, Va., Flight Safety Foundation, Inc., 1968, p. 98-116. 10 refs.

Discussion of simulation requirements to reduce aircraft flight time for training to a minimum. It is noted that fixed-base piloted flight simulators have proved very useful in advanced vehicle research, in navigation and traffic control studies, and in procedural training. However, a high degree of interpretation by trained pilots is often required to predict the suitability of aircraft behavior or actual aircraft controllability from fixed-base simulation. Consequently, the interpretation of fixed-base simulation may often be wrong. The various problems of flight simulation, such as the need for motion, characteristics of the control system and instrumentation, visual simulation, and motion in critical maneuvers are considered. Factors which are missing in simulation (such as the "pucker factor") are discussed, and it is shown how these factors alter the emphasis in piloting performance in an aircraft. It is concluded that simulation cannot wholly replace flight training in the aircraft concerned, but that it may markedly reduce the amount of flight training required.
P.G.

A69-42120
STRUCTURES TECHNOLOGY FOR LARGE RADIO AND RADAR TELESCOPE SYSTEMS; PROCEEDINGS OF THE INTERNATIONAL SYMPOSIUM, MASSACHUSETTS INSTITUTE OF TECHNOLOGY, CAMBRIDGE, MASS., OCTOBER 18-20, 1967.
Symposium sponsored by the U.S. Navy and the Massachusetts Institute of Technology.
Edited by J. W. Mar and Harold Liebowitz.
Cambridge, MIT Press, 1969. 546 p.
$30.

CONTENTS:

THE DESIGN OF A 300-FT RESEARCH ANTENNA. A. B. Youmans (U.S. Navy, Naval Research Laboratory, Sugar Grove, W.Va.), p. 5-12. 10 refs. (See A69-42121 23-11)

THE 100-M RADIO TELESCOPE OF THE MAX PLANCK INSTITUTE FOR RADIO ASTRONOMY IN BONN. O. Hachenberg (Max-Planck-Institut für Radioastronomie, Bonn, West Germany), p. 13-27. (See A69-42122 23-11)

DESIGN STUDIES FOR A 440-FT-DIAMETER RADIO AND RADAR TELESCOPE. H. G. Weiss (Massachusetts Institute of Technology, Lexington, Mass.), p. 29-54. 16 refs. (See A69-42123 23-11)

THE NANÇAY RADIO TELESCOPE. M. Ginat (Paris, Observatoire, Paris, France), p. 55-63. 5 refs. (See A69-42124 23-11)

SOME CONSIDERATIONS OF WIND EFFECTS ON LARGE STRUCTURES. C. Scruton (Ministry of Technology, Teddington, Middx., England), p. 65-88. 36 refs. (See A69-42125 23-32)

POINTING AND TRACKING ACCURACY—RECOMMENDED STANDARDS. L. V. Smith, Jr. (Communications Satellite Corp., Washington, D.C.), p. 89-99. (See A69-42126 23-07)

LOSS CALCULATION ON METAL SPACE FRAME RADOMES. J. Ruze (Massachusetts Institute of Technology, Lexington, Mass.), p. 101-112. 9 refs. (See A69-42127 23-11)

THE CONSTRUCTIVE SCHEMES OF MULTISUPPORT STEERABLE PARABOLIC ANTENNAS. P. D. Kalachev and A. D. Kuzmin (Akademiia Nauk SSSR, Fizicheskii Institut, Moscow, USSR), p. 113-120. (See A69-42128 23-11)

DETERMINATION OF THE APPROXIMATE STRUCTURAL PARAMETERS OF A LARGE STEERABLE ANTENNA. H. A. Cress and S. G. Talbert (Battelle Memorial Institute, Columbus, Ohio), p. 121-134. (See A69-42129 23-32)

STRUCTURAL PERFORMANCE OF THE PARKES 210-FT PARABOLOID. H. C. Minnett, D. E. Yabsley, and M. J. Puttock (Commonwealth Scientific and Industrial Research Organization, Canberra, Australia), p. 135-149. 7 refs. (See A69-42130 23-32)

DESIGN OF THE HAYSTACK ANTENNA AND RADOME. H. G. Weiss, W. R. Fanning, F. A. Folino, and R. A. Muldoon (Massachusetts Institute of Technology, Lexington, Mass.), p. 151-184. 16 refs. (See A69-42131 23-11)

TECHNIQUES USED TO EVALUATE THE PERFORMANCE OF THE NASA/JPL 210-FT-REFLECTOR STRUCTURE UNDER ENVIRONMENTAL LOADS. M. S. Katow (California Institute of Technology, Pasadena, Calif.), p. 185-200. 14 refs. (See A69-42132 23-32)

ROSMAN I DYNAMIC ANALYSIS. T. G. Butler (NASA, Goddard Space Flight Center, Greenbelt, Md.), p. 201-217. (See A69-42133 23-32)

CONSTRUCTION AND PERFORMANCE OF THE 150-FT NRC ANTENNA AT ALGONQUIN RADIO OBSERVATORY, ONTARIO, CANADA. M. H. Jeffery (Freeman Fox and Partners, London, England), p. 219-240. (See A69-42134 23-11)

COMPUTER-AIDED DESIGN OF A LARGE STEERABLE ANTENNA STRUCTURE. W. Weaver, Jr. (Stanford University, Stanford, Calif.), p. 241-271. 5 refs. (See A69-42135 23-32)

MAINTAINING SURFACE ACCURACY OF LARGE RADIO TELESCOPES BY ACTIVE COMPENSATION. H. Rothman and F. K. Chang (Ammann and Whitney, Inc., New York, N.Y.), p. 273-286. (See A69-42136 23-11)

CONTROL OF RMS SURFACE ERROR IN LARGE ANTENNA STRUCTURES. P. Weidlinger, p. 287-309. (See A69-42137 23-11)

HOMOLOGOUS DEFORMATIONS OF TILTABLE TELESCOPES. S. von Hoerner (National Radio Astronomy Observatory, Green Bank, W.Va.), p. 311-333. 9 refs. (See A69-42138 23-32)

METAL SPACE FRAME RADOME DESIGN. R. D'Amato (Massachusetts Institute of Technology, Lexington, Mass.), p. 335-367. 25 refs. (See A69-42139 23-32)

INSTABILITY IN RETICULATED SPHEROIDS—EXPERIMENTAL RESULTS AND THE EFFECTS OF NODAL IMPERFECTIONS. D. T. Wright (Committee on University Affairs, Toronto, Canada), p. 369-379. 11 refs. (See A69-42140 23-32)

AUTOMATED LARGE DEFLECTION AND STABILITY ANALYSIS OF THREE-DIMENSIONAL BAR STRUCTURES. L. Berke (USAF, Flight Dynamics Laboratory, Wright-Patterson AFB, Ohio) and R. H. Mallett (Bell Aerospace Corp., Buffalo, N.Y.), p. 381-419. 18 refs. (See A69-42141 23-32)

ANALYSIS OF GEOMETRICALLY NONLINEAR FRAMED STRUCTURES. J. Connor, Jr. (Massachusetts Institute of Technology, Cambridge, Mass.), p. 421-443. 10 refs. (See A69-42142 23-32)

BUCKLING TESTS ON SPACE FRAME RADOME. S. D. Lewis and E. A. Witmer (Massachusetts Institute of Technology, Cambridge, Mass.), p. 445-464. (See A69-42143 23-32)

ASTRA—BOEING'S ADVANCED STRUCTURAL ANALYZER. B. E. Greene, E. D. Herness, M. W. Ice, W. L. Salus, and D. R. Strome (Boeing Co., Seattle, Wash.), p. 465-498. 29 refs. (See A69-42144 23-32)

APPLICATION OF THE NASA GENERAL PURPOSE STRUCTURAL ANALYSIS PROGRAM TO LARGE RADIO TELESCOPES. C. W. McCormick (MacNeal-Schwendler Corp., San Marino, Calif.), p. 499-514. (See A69-42145 23-32)

ICES STRUDL—AN INTEGRATED APPROACH TO A STRUCTURAL COMPUTER SYSTEM. R. D. Logcher (Massachusetts Institute of Technology, Cambridge, Mass.), p. 515-536. 9 refs. (See A69-42146 23-08)

INDEX, p. 537, 538.

A69-43044 * #
THE SIMULATOR TO MATCH THE TRANSPORTS TO COME.
Maurice D. White and John C. Dusterberry (NASA, Ames Research Center, Moffett Field, Calif.).
Astronautics and Aeronautics, vol. 7, Sept. 1969, p. 54-60.

Description of a new flight simulator for advanced transport aircraft. The large lateral motion of the simulator is emphasized. It is stated that the simulator developed is expected to extend simulation capabilities significantly beyond those of existing aircraft research simulators. The equipment is provided with motions large enough so that by systematically limiting them it can be learned what motions training simulators need. Factors contributing to the pilot's confidence in his evaluation are considered. Problems arising from the length of the fuselage of large aircraft are discussed. It is noted that asymmetric loss of engine thrust at supersonic speeds on a supersonic transport could whip the cockpit through quite large and confusing movements and that a simulator should reproduce the accelerations expected during these maneuvers with reasonable fidelity. P.G.

N69-10888*# National Aeronautics and Space Administration. Marshall Space Flight Center, Huntsville, Ala.
BLAST SHIELDS TESTING
Walter V. Medenica Washington Nov. 1968 68 p refs
(NASA-TN-D-4894) Avail: CFSTI CSCL 20K

Several types of protective steel shields were exposed to explosive blasts of RP-1 and liquid oxygen (LOX) or liquid hydrogen (LH_2) and LOX combinations, as a ride-along project of the Pyro Project. They included: solid arched plates, angle deflectors, wire screen No. 1 (65.3% open area), wire screen No. 2 (48% open area), solid flat plates, and wire screen No. 3 (27% open area). The first four of the above shields were instrumented with strain gauges and pressure transducers. Author

N69-11371*# National Aeronautics and Space Administration. Langley Research Center, Langley Station, Va.
ANALYSIS OF NUMERICAL INTEGRATION TECHNIQUES FOR REAL-TIME DIGITAL FLIGHT SIMULATION
John W. Wilson and George G. Steinmetz Nov. 1968 98 p refs
(NASA-TN-D-4900) Avail: CFSTI CSCL 22A

Low order numerical integration techniques are analyzed and established as adequate for digital simulation of man in the loop nonaerodynamic rigid body problems. In addition to low order integration techniques, a Green's function approach is presented for the solution of the gyroscope equations. This approach yields an exact solution to the gyroscope output for the simulated forcing function with virtually no limitation on the integration interval size. Effects of roundoff error are shown to be marginal for the translational dynamics with solution rates on the order of 32 solutions per second on a floating point machine with a 27-bit fractional part. Two example problems were solved by using the techniques established. A Gemini–Agena eleven degree of freedom problem was programed in FORTRAN and then modified to a Gemini–Agena elastically coupled system. Primary concern was given to minimizing the time required of the arithmetic unit. The results of these problems indicate the utility of the IBM 7094 class of computers for this type of problem since only a small fraction of the memory and arithmetic processing time was used (10 to 15 percent each). This study strongly supports the desirability of multiprograming to alleviate inefficiency on a more sophisticated machine. Author

N69-14507*# National Aeronautics and Space Administration. Marshall Space Flight Center, Huntsville, Ala.
ACCEPTANCE TESTING LUNAR AND PLANETARY VEHICLES (A CONCEPT)
Fritz Kramer Washington Dec. 1968 24 p
(NASA-TN-D-4924) Avail: CFSTI CSCL 22D

This report presents the least known of the two concepts which allow us to study the effects of lunar or planetary gravitation on the full-size prototype vehicle with respect to vehicle dynamics and driving characteristics, and to familiarize the astronauts with the behavior of surface vehicles under different gravitations. The concept is explained and illustrated for lunar application because the moon exhibits relative to Earth the smallest gravitational attraction, and causes, therefore, the greatest deviation of the vehicle's behavior from its behavior on Earth. However, the principle and its implementation are applicable without restriction or degradation to any other magnitude of gravitational acceleration. Author

11 FACILITIES, RESEARCH AND SUPPORT

N69-15633*# National Aeronautics and Space Administration. Ames Research Center, Moffett Field, Calif.

ANALYSIS OF NONEQUILIBRIUM AIR STREAMS IN THE AMES 1-FOOT SHOCK TUNNEL

Robert S. Hiers, Jr. and John O. Reller, Jr. Washington Jan. 1969 27 p refs

(NASA-TN-D-4985) Avail: CFSTI CSCL 14B

An analysis and the results of a preliminary calibration of nonequilibrium test streams in the Ames 1-foot shock tunnel are presented. The facility is combustion driven and is normally operated in the tailored-interface mode to provide a nominal reservoir enthalpy of 9,100 J/gm and pressure of 275 atm. In addition, the shock tunnel is operated in the equilibrium-interface mode to provide enthalpies between 6,000 J/gm and 15,000 J/gm at a nominal reservoir pressure of 275 atm. Results are presented for three typical operating conditions. Static pressure, pitot pressure, velocity, mass flow, and stagnation point heat transfer were measured in the test stream. These data are compared with numerically integrated and sudden-freeze models for air undergoing both chemical and vibrational relaxation. It is shown that the sudden-freeze model is satisfactory for calibrating the test stream if certian frozen-flow parameters are determined using experimental data. An added advantage of this approach is that flow properties in the test stream may be obtained without specifying the relaxation rates. Author

N69-20451*# National Aeronautics and Space Administration. Washington, D. C.

PAVEMENT GROOVING AND TRACTION STUDIES

1969 512 p refs Conf. held at Hampton, Va., 18–19 Nov. 1968 Film supplement numbers L-775, L-944, and L-947 to this report are available on loan from NASA. Langley Research Center

(NASA-SP-5073) Avail: CFSTI CSCL 01E

The effectiveness of runway grooving as a means for increasing tire traction was discussed at the conference in terms of aircraft performance, aircraft operational problems, results of skid correlation studies, and pavement grooving and surface treatments to improve tire traction on highways. For individual titles, see N69-20452 through N69-20478.

N69-22629*# National Aeronautics and Space Administration. Langley Research Center, Langley Station, Va.

A RENDEZVOUS AND STATION-KEEPING SIMULATOR WITH FLY AROUND CAPABILITY AND VIRTUAL IMAGE VIEWING

William M. Kahlbaum, Richard E. Bardusch, and John J. Stumpf Washington Apr. 1969 40 p refs

(NASA-TN-D-5123) Avail: CFSTI CSCL 14B

A screen-type-refractive-virtual-image rendezvous simulator has been designed and built at the Langley Research Center. In this simulator, the test subject views combined images of a celestial background, a featureless earth horizon, and a rendezvous target vehicle through a circular window with a 30° field of view. The virtual images of the horizon and stars appear to be at infinity, while the target-vehicle image appears to be at some closer distance. The three elements of the display are rear projected on screens by means of separate gimbaled projectors. The horizon and star images are generated optically, while the target-vehicle image is generated by a closed-circuit television system. The observed size of the target-vehicle image varies as a function of problem range. Range changes within 160 meters of the observer are simulated by moving the television camera along a range bed. Range changes beyond 160 meters with satisfactory television line resolution are simulated by continuously shrinking the raster on the television projection tube. Since the problem requires three degrees of continous rotational freedom for the observer, a central computer program generates attitude information (by means of quaternion rate equations) and presents this information to the simulator in the form of direction cosine matrices. Author

N69-22989*# National Aeronautics and Space Administration. Ames Research Center, Moffett Field, Calif.

EXPLODING WIRE INITIATION AND ELECTRICAL OPERATION OF A 40-kV SYSTEM FOR ARC-HEATED DRIVERS UP TO 10 FEET LONG

Robert E. Dannenberg and Anthony F. Silva Washington Apr. 1969 41 p refs

(NASA-TN-D-5126) Avail: CFSTI CSCL 14B

This report describes an energy storage and electric arc driver system for shock driven facilities. Energy for the arc is supplied from a capacitor bank rated at 1 MJ at an operating voltage of 40 kV. Results are presented for arc discharge lengths of 54 and 116 inches with peak currents of 600 kA. The entire arc strike sequence of exploding wire initiation, dwell period, and subsequent bank discharge is discussed. The effect of different wire types on arc initiation is also discussed. The composition of the driver gas is shown to be a factor limits the discharge of stored energy from the capacitor bank. Author

N69-23194*# National Aeronautics and Space Administration. Flight Research Center, Edwards, Calif.

VISUAL SIMULATION IMAGE GENERATION USING A FLYING-SPOT SCANNER

Charles A. Wagner Washington Apr. 1969 58 p refs

(NASA-TN-D-5151) Avail: CFSTI CSCL 14B

The flying-spot scanner television camera used as a video signal generator for visual flight simulation is analyzed. A description of the technique is included as well as a detailed theoretical analysis of the quality of the video that can be produced. A commercially available flying-spot scanner designed for flight simulation was tested, and its capabilities are presented. Discussion is limited to the television camera; display devices such as monitors are not included. The flying-spot scanner was found to be a low-cost device which can simulate all motions of an aircraft except roll. Large excursions at high rates are easily achieved. It is limited to a relatively small field of view, a fixed forward visibility, and simulation of flat terrain. The quality of the video is adequate over a moderate range of altitudes; very high and very low altitudes result in poor performance. Possible approaches to increasing the useful altitude range are discussed. Author

N69-24089*# Michigan Univ., Ann Arbor.

MAGNETIC FIELD PROPERTIES RELATED TO THE DESIGN OF A ONE-COMPONENT MAGNETIC SUPPORT-AND-BALANCE SYSTEM

K. R. Sivier Washington NASA May 1969 50 p refs

(Grant NGR-23-005-003)

(NASA-CR-1352) Avail: CFSTI CSCL 14B

Calculations have been made of the magnetic performance characteristics of air-cored solenoids applied to a one-component magnetic support-and-balance system. These characteristics include field strength, field gradients, static stability derivatives for a ferromagnetic body in the solenoid field, and the solenoid power required to produce given field strengths and to levitate a magnetic body. These characteristics were calculated only in the vicinity of the solenoid axis and are shown to be related simply to four fundamental, shape dependent, dimensionless parameters (and to several ratios of these parameters). Author

N69-25343*# Michigan Univ., Ann Arbor.

ONE COMPONENT, MAGNETIC, SUPPORT AND BALANCE SYSTEM FOR WIND TUNNEL MODELS

K. R. Sivier and M. Henderson Washington NASA May 1969 83 p refs

(Grant NGR-23-005-003)

(NASA-CR-1353) Avail: CFSTI CSCL 20D

Sphere drag at subsonic Mach numbers and Reynolds numbers from about 25 to 4000 was measured by the instrumentation. The

system was used with a vertical wind tunnel and incorporated a simple error-rate type of feedback control system to hold the model vertically. The natural radial stability of the system was used to hold the model on or near the axes of the solenoids and the wind tunnel. The system performed well, especially at Reynolds numbers where unsteady lateral aerodynamic forces were absent or very small. Author

N69-28095*# Michigan Univ., Ann Arbor.
EXPERIMENTAL EVALUATION OF A SUBSONIC EXPANSION TUBE
Philip C. Malte and Kenneth R. Sivier Washington NASA Jun. 1969 88 p refs
(Grant NGR-23-005-003)
(NASA-CR-1354) Avail: CFSTI CSCL 01A

An experimental study of a subsonic expansion tube was carried out to determine its utility as a test facility for studying the drag of small spherical particles at subsonic Mach numbers and Reynolds numbers below 1000. Of particular interest were the length of steady flow achieved, the steadiness of this flow, the tube geometry needed to optimize the flow quality, and the growth of the unsteady boundary layer on the tube walls. It was found that a 15 ft long tube was capable of providing useful flows for at least 15 msec for Mach numbers up to about 0.7. Author

N69-29737*# National Aeronautics and Space Administration. Lewis Research Center, Cleveland, Ohio.
SPECTRAL AND OPERATIONAL CHARACTERISTICS OF A HIGH-INTENSITY CARBON ARC SOLAR SIMULATOR
Ernie W. Spisz and John R. Jack Washington Jul. 1969 18 p refs
(NASA-TM-X-1825) Avail: CFSTI CSCL 14B

A commercially avialable high intensity carbon arc solar simulator was evaluated to determine its suitability as a finely controlled radiant source for experimentally determining the solar absorptance of various materials. The spectral distribution of the radiant intensity is determined over the wavelength range from 0.36 to 2.1 μm, and the stability and uniformity of the radiant beam are evaluated. A control system which provides both a constant radiant intensity and a slowly varying sinusoidal perturbation of the radiant intensity is also discussed. Author

N69-29981*# National Aeronautics and Space Administration. Langley Research Center, Langley Station, Va.
DESCRIPTION OF THE HIGH-ENTHALPY ARC TUNNEL AT THE LANGLEY RESEARCH CENTER INCLUDING TEST STREAM CONDITIONS AT SELECTED OPERATING POINTS
William L. Wells Washington Jul. 1969 52 p refs
(NASA-TN-D-5295) Avail: CFSTI CSCL 14B

The high-enthalpy arc tunnel consists of a 4-megawatt direct current power supply, a 75,000-foot^3 pump-down vacuum system, a commercial long-axial-arc gas heater, a free jet test section, and necessary high-pressure cooling water and test gas systems. Three supersonic conical nozzle lengths are used to provide a wide range of test stream parameters. The nozzle exit radii are 1.00 inch, 2.30 inches, and 3.82 inches. The arc gas heater was operated at chamber pressures from 1.2 to 3.3 atm with corresponding air mas-flow rates from about 0.02 to 0.08 lb/sec. Stagnation pressures behind the normal shock measured at the stream center line cover a range from about 0.03 to 0.72 atm and cold-wall heating rates range from about 200 to 903 Btu/ft^2-sec on a 1-inch diameter flat-faced probe. Calculated enthalpies based on these measurements range from about 10,000 to 13,000 Btu/lb. In all three nozzles, measurements were made of pressure and heating-rate distributions on a specific probe shape. Graphical comparisons show reasonably good agreement between the measured heating-rate distributions and theory and between the measured pressure distributions and data from a tunnel where the flow is known to be smooth and uniform. Author

N69-35359*# National Aeronautics and Space Administration. Ames Research Center, Moffett Field, Calif.
USE OF A SIX-DEGREES-OF-FREEDOM MOTION SIMULATOR FOR VTOL HOVERING TASKS
Emmett B. Fry, Richard K. Greif, and Ronald M. Gerdes Washington Aug. 1969 26 p refs
(NASA-TN-D-5383) Avail: CFSTI CSCL 14B

A piloted, six degrees of freedom motion simulator has been evaluted with regard to its ability to simulate VTOL visual hovering tasks. Characteristics of the variable stability jet lift Bell X-14A aircraft were simulated, and results for the roll and pitch axes were compared with flight data. The roll axis data were also compared with data from two and single degree of freedom simulators. Control power and damping requirements for the roll and pitch axes compared very well with flight data. The simulator's motion quality was considered outstanding for VTOL hovering flight. Its travel limits were large enough to simulate hover/maneuver tasks on a one to one scale. Roll lateral motions (two degrees of freedom motions) gave essentially the same results as six degrees operation for evaluation of roll axis maneuvers. Author

N69-36224*# National Aeronautics and Space Administration. Flight Research Center, Edwards, Calif.
NASA HIGH TEMPERATURE LOADS CALIBRATION LABORATORY
Walter J. Sefic and Karl F. Anderson Washington Sep. 1969 13 p refs
(NASA-TM-X-1868) Avail: CFSTI CSCL 14B

The NASA High Temperature Loads Calibration Laboratory and the equipment it contains for simulating the loading and heating of aircraft or their components are described. Particular emphasis is placed on various fail-safe devices which are built into the equipment to minimize the possibility of damage to flight vehicles. The data-acquisition system is described. This system involves on-site pickup of data and signal conditioning coupled with conversion from analog to digital data and transmission to a central area for recording on magnetic tape and distribution to real-time displays. Instrumentation available in the facility for measuring load, position, and strain is also discussed. Author

N69-37022*# Chrysler Corp., Detroit, Mich.
EXPERIMENTAL VERIFICATION OF SURFACE VEHICLE DYNAMICS
B. D. Van Deusen, J. M. Sneyd, C. H. Hoppe, and R. F. Hughes Washington NASA Sep. 1969 139 p refs
(Contract NASw-1607)
(NASA-CR-1399) Avail: CFSTI CSCL 13F

Techniques were developed to allow prediction of the dynamic response of vehicles traversing yielding and nonyielding rough surfaces. Virgin terrestrial and extraterrestrial surfaces were classified according to their frequencies and amplitude distribution. An attempt to verify these conditions was undertaken. A four wheeled truck and a specially designed single wheel trailer were instrumented and driven (pulled) across both yielding and nonyielding surfaces. The surface profile was measured on both surfaces and soil parameters were measured on the yielding surface. With this input information the theoretical prediction was compared with the physical measurements in a statistical fashion. The analog computer simulation was converted to a digital computer simulation to allow a more useful and versatile prediction technique. Author

12

FLUID MECHANICS

Includes boundary-layer flow; compressible flow; gas dynamics; hydrodynamics; and turbulence. For related information see also: 01 Aerodynamics; and 33 Thermodynamics and Combustion.

A69-13137 *
INTERACTION OF LINEAR WAVES WITH OBLIQUE SHOCK WAVES
J. F. McKenzie (California, University, Dept. of Applied Electrophysics, La Jolla, Calif.) and K. O. Westphal (NASA, Ames Research Center, Moffett Field, Calif.).
Physics of Fluids, vol. 11, Nov. 1968, p. 2350-2362. 19 refs.

Derivation of formulas for the amplitudes of waves that diverge from a shock as a result of any given incident disturbance. It is shown that in an ideal gas (where the Mach number M is large), that the pressure amplitude and the component of the energy flux normal to the shock of a transmitted sound wave are of O (M^2) greater than those in the incident sound wave. Furthermore, if the impinging sound wave is incident near the critical angle, the ratio of the pressure amplitude of the transmitted sound wave to that of the incident one is of O (M^3). It is also shown that incident entropy-vorticity waves can generate intense sound waves behind a strong shock. The dependence of the transmission, reflection, and generation coefficients for sound waves on the Mach number and the angle of incidence is depicted in a series of graphs. The results are applied to the amplification of small disturbances in the solar wind on passage through the bow shock of the earth. M. G.

A69-13138 *
IONIZING SHOCK STRUCTURE IN A MONATOMIC GAS.
Donald L. Chubb (Columbia University, New York, N. Y.; NASA, Lewis Research Center, Cleveland, Ohio).
Physics of Fluids, vol. 11, Nov. 1968, p. 2363-2376. 27 refs.
Contract No. AF 49(638)-1634.

The structure of an ionizing shock front in a monatomic gas is described. Both atom-atom and electron-atom collisional ionization are considered. The ionization rates for either of these processes are assumed to be controlled by the rate of excitation from the ground state to the first excited level. In the front part of the shock, called the atom-atom shock, atom collisional dissipative mechanisms (viscosity and thermal conductivity) determine the shock structure. A bimodal Mott-Smith velocity distribution function is assumed for the atoms in this region, which has a thickness of the order of the atom-atom viscosity mean free path. In the rear part of the shock front, called the relaxation zone, the collisional ionization processes determine the structure. For this region, which has a thickness proportional to the electron-atom ionization mean free path, Maxwellian velocity distributions are assumed for the electrons, ions, and atoms. It is found that for Mach numbers of 30 or more the atom-atom shock is of comparable thickness to the relaxation zone, and the degree of ionization behind the atom-atom shock is of the order of 10^{-1}. (Author)

A69-14510 *#
A NUMERICAL SOLUTION OF UNSTEADY FLOW IN A TWO-DIMENSIONAL SQUARE CAVITY.
L. F. Donovan (NASA, Lewis Research Center, Cleveland, Ohio).
American Institute of Chemical Engineers, Annual Meeting, 61st, Symposium on Fundamental Research in Fluid Mechanics, Part I, Los Angeles, Calif., Dec. 1-5, 1968, Paper 25 C. 18 p. 13 refs.
$0.50.

Numerical solution of the continuity equation and unsteady Navier-Stokes equations for two-dimensional flow in a square cavity. The fluid is initially at rest, and the upper surface of the cavity moves with constant velocity throughout the calculations such that the Reynolds number is 100, based on the length and velocity of the moving surface and the viscosity of the fluid. Good agreement is shown between the calculated position of the vortex center at large times and both the position of an experimentally determined vortex center and the position of the vortex center calculated from an extant solution of the steady Navier-Stokes equations. Velocity profiles at large times are in excellent agreement with those calculated from an extant solution of the steady Navier-Stokes equations. Another method of presenting the results of the calculations is also used to illustrate the results more clearly. M. M.

A69-15791 *#
A JET PUMP CAVITATION PREDICTION PARAMETER.
Nelson L. Sanger (NASA, Lewis Research Center, Cleveland, Ohio).
American Society of Mechanical Engineers, Fluids Engineering Conference, Philadelphia, Pa., May 6-8, 1968, Paper. 5 p. 7 refs.

Derivation of a parameter which predicts jet pump head-rise deterioration due to cavitation, and comparison of this parameter to existing methods of prediction. The cavitation prediction parameter correlates jet pump cavitation from two different experimental investigations, and it is shown that the predicted deterioration conforms well with empirically derived data. It is suggested that the use of the parameter appears justified over a wide range of spacings of the nozzle exit from the throat entrance. G. V.

A69-18094 *#
A STUDY OF THE NONSIMILAR NATURE OF THE LAMINAR BOUNDARY LAYER IN A REGION OF ADVERSE PRESSURE GRADIENT.
William F. Gallo, Joseph G. Marvin, and A. Vernon Gnos (NASA, Ames Research Center, Moffett Field, Calif.).
American Institute of Aeronautics and Astronautics, Aerospace Sciences Meeting, 7th, New York, N. Y., Jan. 20-22, 1969, Paper 69-35. 9 p. 13 refs.
Members, $1.00; nonmembers, $1.50.

Study of the effect of including the streamwise history or nonsimilar terms in the usual transformed laminar boundary-layer equations at three locations on a typical, blunted, compression surface. The locations represent regions of mildly positive pressure gradient, mildly negative pressure gradient, and strongly negative pressure gradient. Theoretical boundary-layer solutions were obtained at the three stations by numerically solving the laminar boundary-layer equations both with and without the streamwise history terms included. Both solutions are compared with experimental boundary-layer data. The results indicate that in the presence of a strong negative pressure gradient the solutions exhibit a significant difference when the streamwise history terms are considered. The largest differences appear in velocity profile and displacement thickness, with the data confirming the validity of the fully nonsimilar solution. (Author)

A69-18213 *#
HYPOTHESIS FOR THE ORIGIN OF CROSS-HATCHING.
Murray Tobak (NASA, Ames Research Center, Moffett Field, Calif.).
American Institute of Aeronautics and Astronautics, Aerospace Sciences Meeting, 7th, New York, N. Y., Jan. 20-22, 1969, Paper 69-11. 8 p. 21 refs.
Members, $1.00; nonmembers, $1.50.

Cross-hatching is hypothesized to be caused by spatially periodic fluctuations in surface pressure, the origin of which is the presence in the boundary layer of an array of regularly spaced counterrotating longitudinal vortices. The vortices originate from surface irregularities near the leading edge; the probability of their appearance

is enhanced by the presence of a local region of concave curvature in the boundary-layer streamlines. Surface ablation is not a necessary condition for the presence of the pressure fluctuations that lead to cross-hatching, but may be the mechanism causing the streamline curvature. For cross-hatching to appear, the boundary layer aft of the concavity must be turbulent and the local flow must be supersonic. (Author)

A69-18317 *#
INTEGRATION OF THE EQUATIONS GOVERNING THE ONE-DIMENSIONAL FLOW OF A CHEMICALLY REACTIVE GAS.
H. E. Bailey (NASA, Ames Research Center, Moffett Field, Calif.).
Combustion Institute and University of California, Specialists' Session on Chemical Kinetics Calculations, University of California, Berkeley, Calif., Oct. 30, 1968, WSCI Paper 68-46. 35 p. 11 refs.

Introduction of the concept of parasitic eigenvalues in the numerical solution of sets of ordinary differential equations. The use of an implicit method is proposed for the solution of differential equations containing such parasitic eigenvalues. These ideas are then applied to the integration of the equations which govern the one-dimensional flow of a chemically reactive gas. In particular, results are given for the flow downstream of a normal shock wave and for the flow in a converging-diverging nozzle. The conditions under which the more complicated computations required by the implicit method appear justified are delineated. M. M.

A69-21480 *#
THE EFFECT OF ACCELERATION ON HEAT TRANSFER IN A TURBULENT BOUNDARY LAYER.
Robert W. Graham (NASA, Lewis Research Center, Cleveland, Ohio).
University of Minnesota, Heat Transfer Seminar, University of Minnesota, Minneapolis, Minn., Feb. 18, 1969, Paper. 17 p. 5 refs.

Review of some recent research concerning acceleration effects on forced convection in a turbulent boundary layer. The results obtained show that for accelerated turbulent flow, the heat-transfer levels are generally below the unaccelerated values. The following conclusions are made: (1) conventional turbulent-flow heat-transfer correlations overpredict at the throat; (2) momentum boundary-layer history is relatively unimportant, while thermal boundary-layer history is very important; (3) for subsonic and sonic conditions the energy thickness integral approach is useful in predicting local heat-transfer rates; and (4) little information exists concerning the nature of the turbulence structure in accelerating flow. Much has to be learned about production and dissipation of turbulence. M. M.

A69-21995 *#
MEASUREMENT OF MEAN DROP SIZES FOR SPRAYS FROM SUPERHEATED WATERJETS.
Paul B. Gooderum and Dennis M. Bushnell (NASA, Langley Research Center, Aero-Physics Div., Hampton, Va.).
Journal of Spacecraft and Rockets, vol. 6, Feb. 1969, p. 197, 198. 11 refs.

Investigation of the mean drop size generated in the lowest ambient pressure mode of dispersion, usually referred to as the vapor pressure breakup regime. The results obtained indicate that for vapor pressure breakup of liquid water jets under low Weber number conditions the final resultant mean drop size depends only on the temperature of the injected water and the orifice diameter. M. M.

A69-25282 *#
DIRECTION OF MAXIMUM TURBULENT VORTICITY IN A SHEAR FLOW.
R. G. Deissler (NASA, Lewis Research Center, Cleveland, Ohio).
Physics of Fluids, vol. 12, Feb. 1969, p. 426, 427. 7 refs.

Derivation of an equation for the direction of maximum turbulent vorticity in a turbulent shear flow. For a weak homogeneous turbulent field with a uniform transverse velocity gradient, that direction is found to be reasonably close to (but different from) the direction of maximum mean strain rate for a range of velocity gradients. The degree of alignment of the turbulent vortices is also determined. (Author)

A69-26013 *#
APPROXIMATE EQUATIONS OF MOTION FOR GASES AND LIQUIDS.
John A. Dutton (Pennsylvania State University, Dept. of Meteorology, University Park, Pa.) and George H. Fichtl (NASA, Marshall Space Flight Center, Huntsville, Ala.).
Journal of the Atmospheric Sciences, vol. 26, Mar. 1969, p. 241-254. 14 refs.
NSF Grant No. GA-1595X.

Development of a set of conditions which justify the application of the Boussinesq approximation to compressible fluids. Two cases are found and compared. In the first, in which the vertical scale of the motion can be of the same order of magnitude as the scale height of the medium, the perturbation momentum must be nondivergent and the effects of perturbations of pressure appear in several places. In the other case, where the vertical scale of the motion is much less than the scale height, the perturbation velocities are nondivergent and the perturbation pressure appears only in the pressure gradient force. The approximate equations lead to linearized equations controlling the stability of wave motion which are formally equivalent to those for the same problem in the flow of a stratified medium which is incompressible in the sense that the flow is solenoidal. Various properties of the approximate equations are investigated, and it is shown that acoustic modes are not permitted. M. G.

A69-28212 *#
UNDEREXPANDED JET NOISE REDUCTION USING RADIAL FLOW IMPINGEMENT.
Darshan S. Dosanjh (Syracuse University, Syracuse, N. Y.) and Francis J. Montegani (NASA, Lewis Research Center, Cleveland, Ohio).
(American Institute of Aeronautics and Astronautics, Aerospace Sciences Meeting, 6th, New York, N. Y., Jan. 22-24, 1968, Paper 68-81.)
AIAA Journal, vol. 7, Mar. 1969, p. 458-464. 14 refs.
Grant No. NsG-431.

Noise from high-speed jet flows was investigated using the impingement of a radial annular jet flow on the first shock-cell region of a moderately underexpanded axisymmetric converging main jet flow. Acoustical data and the spark shadowgraphs of the interacting jet flows were recorded in an anechoic chamber. Different nozzle arrangements were used, and the operating main jet total pressure, the percent impingement, and the impingement location were varied. Under all operating conditions, a characteristic variation of the total acoustic power level with percent impingement was observed. Moreover, under selected operating conditions the total acoustic power emitted by the interacted jet flows was lower than that emitted by the main jet flow alone. A maximum sound pressure level reduction of 3-1/2 db was achieved. As a result of interaction of two impinging jet flows, the strong shock pattern in the main underexpanded jet flow is modified, and the emergence of new repetitive shock structure interposed between the original repetitive shock pattern of the main jet flow is observed in the interacted jet flows. The shadowgraphs of the interacting jet flows also reveal almost spherical acoustic emissions originating from individual sources located near each oblique shock tip. An acoustic model based on a finite number of wideband acoustic monopole sources distributed on a line is proposed. The results of the analysis agreed qualitatively with those obtained experimentally. (Author)

A69-28280 *#
USE OF PRESTON TUBES FOR MEASURING HYPERSONIC TURBULENT SKIN FRICTION.
Earl R. Keener and Edward J. Hopkins (NASA, Ames Research Center, Moffett Field, Calif.).
American Institute of Aeronautics and Astronautics, Aerodynamic Testing Conference, 4th, Cincinnati, Ohio, Apr. 28-30, 1969,

Paper 69-345. 11 p. 27 refs.
Members, $1.00; nonmembers, $1.50.

A brief review is made of supersonic Preston-tube correlations which account for the effects of Mach number and Reynolds number for adiabatic surfaces. Experimental results are presented which show that two of these correlations are applicable to nonadiabatic surfaces in an airstream at M = 7. Direct measurements with a skin-friction balance were used for the calibrations. The Reynolds number ranged from 4 to 14 million, and the ratio of wall-to-adiabatic-wall temperature ranged from 0.3 to 0.5. The major conclusion is that the correlation can be simplified and made independent of the boundary-layer-edge condition, by basing the correlation factors on only three measurements, namely wall temperature, wall pressure, and Preston-tube pressure. (Author)

A69-29011

ISRAEL ANNUAL CONFERENCE ON AVIATION AND ASTRONAUTICS, 11TH, TEL-AVIV AND HAIFA, ISRAEL, MARCH 5, 6, 1969, PROCEEDINGS.
Conference convened by the Israel Society of Aeronautics and Astronautics; the Technion - Israel Institute of Technology, Department of Aeronautical Engineering; the Israel Ministry of Transport, Civil Aviation Administration; the Israel National Committee for Space Research; and Tel-Aviv University, Institute of Planetary and Space Science.
Conference supported by the Israel Ministry of Transport; the Israel Ministry of Defence; the Information Services in the Prime Minister's Office; the National Council for Civil Aviation; the Technion - Israel Institute of Technology; Tel-Aviv University; the Paz Oil Co., Paz Aviation Service; and the Israel Airlines, El-Al.
(Israel Journal of Technology, vol. 7, no. 1-2, 1969.)
Jerusalem, Weizmann Science Press of Israel, 1969. 209 p.
$4.00.

CONTENTS:

THEORY OF COUPLED HEAT AND MASS TRANSFER WITH ZERO-ORDER REACTIONS IN TWO-PHASE SYSTEMS. L. L. Tavlarides (Pittsburgh, University, Pittsburgh, Pa.) and B. Gal-Or (Technion - Israel Institute of Technology, Haifa, Israel; Pittsburgh, University, Pittsburgh, Pa.), p. 1-14. 26 refs. [See A69-29012 14-33]

ASYMPTOTIC SOLUTIONS OF THE STABILITY OF ONE-DIMENSIONAL INCOMPRESSIBLE INVISCID FLOWS. E. Wasserstrom (Technion - Israel Institute of Technology, Haifa, Israel), p. 15-21. 14 refs. [See A69-29013 14-12]

CARBON DIOXIDE BLUE CONTINUUM EMISSION AT HIGH TEMPERATURES. D. Weihs and Y. Manheimer-Timnat (Technion - Israel Institute of Technology, Haifa, Israel), p. 23-29. 13 refs. [See A69-29014 14-11]

DEVELOPMENT OF VISCOUS CHANNEL FLOW WITH SUCTION. S. Abarbanel (Tel-Aviv University, Tel-Aviv, Israel), p. 31-34. [See A69-29015 14-12]

TRANSIENT BURNING OF SPHERICAL SYMMETRIC FUEL DROPLETS. A. Chervinsky (Princeton University, Princeton, N.J.), p. 35-42. 12 refs. [See A69-29016 14-33]

AN EXPERIMENTAL INVESTIGATION OF THE NEAR WAKE IN AN AXISYMMETRIC SUPERSONIC FLOW WITH AND WITHOUT BASE INJECTION. V. Zakkay and R. Sinha (New York University, New York, N.Y.), p. 43-53. 15 refs. [See A69-29017 14-01]

ON THE MEASUREMENT OF LOW LEVEL TURBULENCE USING A PAIR OF SENSORS. M. Poreh, I. Landa, and I. Kidron (Technion - Israel Institute of Technology, Haifa, Israel), p. 55-60. 5 refs. [See A69-29018 14-14]

SPACE DYNAMICS AND THE FOUNDATIONS OF CLASSICAL AND RELATIVISTIC THERMODYNAMICS. B. Gal-Or (Technion - Israel Institute of Technology, Haifa, Israel; Pittsburgh, University, Pittsburgh, Pa.), p. 61-72. 35 refs. [See A69-29019 14-33]

HYPERSONIC FLOW PAST AN OSCILLATING SLENDER CONE. M. Hanin (Technion - Israel Institute of Technology, Haifa, Israel) and D. Golan (Israel Air Force, Tel-Aviv, Israel), p. 73-77. [See A69-29020 14-01]

SOLUTION OF LINEAR COMBUSTION INSTABILITY PROBLEMS USING THE GALERKIN METHOD. B. T. Zinn (Georgia Institute of Technology, Atlanta, Ga.) and E. A. Powell, p. 79-89. 16 refs. [See A69-29021 14-33]

EXPERIMENTAL STUDIES OF THE EFFECT OF GENERAL IMPERFECTIONS ON THE ELASTIC STABILITY OF THIN SHELLS. W. H. Horton and J. I. Craig (Georgia Institute of Technology, Atlanta, Ga.), p. 91-103. 19 refs. [See A69-29022 14-32]

LINEARIZED ANALYSIS OF FLOW OF INCOMPRESSIBLE LAMINAR JET CONTAINED BETWEEN SIDE WALLS. I. Greber (Case-Western-Reserve University, Cleveland, Ohio), p. 105-110. 5 refs. [See A69-29023 14-12]

STABILITY OF HETEROGENEOUS ORTHOTROPIC CYLINDRICAL SHELLS IN AXIAL COMPRESSION. Y. Stavsky and S. Friedland (Technion - Israel Institute of Technology, Haifa, Israel), p. 111-119. 19 refs. [See A69-29024 14-32]

SYSTEMATIC COMPUTATION OF LUMPED WEIGHT AND INERTIA REPRESENTATIONS OF ARBITRARY STRUCTURES. D. Bendavid (Boeing Co., Seattle, Wash.), p. 121-133. 10 refs. [See A69-29025 14-32]

IMPULSIVE SOUND PROPAGATION IN A FLUID SPHERE OF VARIABLE INTERNAL FRICTION. Z. S. Alterman and J. Aboudi (Tel-Aviv University, Tel-Aviv, Israel), p. 135-147. [See A69-29026 14-23]

ELASTIC-PLASTIC IMPACT OF PLATES. S. Hanagud, B. Ross, and G. Sidhu (Stanford Research Institute, Menlo Park, Calif.), p. 149-161. 11 refs. [See A69-29027 14-32]

THE SEMI-EMPIRICAL PARAMETERS USED IN THE DIVIDING STREAMLINE AND THE MOMENTUM INTEGRAL ANALYSES FOR SEPARATED FLOWS. J. Rom (Technion - Israel Institute of Technology, Haifa, Israel) and E. Levi, p. 163-171. 5 refs. [See A69-29028 14-01]

EXPLORATORY INVESTIGATION ON THE MEASUREMENT OF SKIN FRICTION BY MEANS OF LIQUID CRYSTALS. E. J. Klein and A. P. Margozzi (NASA, Ames Research Center, Moffett Field, Calif.), p. 173-180. 5 refs. [See A69-29029 14-11]

AN EXPERIMENTAL STUDY OF THE LOCAL BUCKLING OF RING-STIFFENED CYLINDERS SUBJECT TO AXIAL COMPRESSION. D. J. Tenerelli (Lockheed Aircraft Corp., Palo Alto, Calif.) and W. H. Horton (Georgia Institute of Technology, Atlanta, Ga.), p. 181-194. 17 refs. [See A69-29030 14-32]

WAKE RECIRCULATION FLOWS GENERATED BY FLOWS (M > 1) OVER REARWARD FACING STEPS AND BLUNT BASES. M. G. Scherberg (USAF, Aerospace Research Laboratories, Wright-Patterson AFB, Ohio), p. 195-198. 6 refs. [See A69-29031 14-01]

SUMMARIES, p. 199, 200.

A69-30478 *#

ANALYTICAL PREDICTION OF THE INCOMPRESSIBLE TURBULENT BOUNDARY LAYER WITH ARBITRARY PRESSURE DISTRIBUTION.
George S. Deiwert (NASA, Ames Research Center, Moffett Field, Calif.) and Douglas E. Abbott (Purdue University, School of Mechanical Engineering, Lafayette, Ind.).
American Institute of Aeronautics and Astronautics, Advanced Marine Vehicles and Propulsion Meeting, 2nd, Seattle, Wash., May 21-23, 1969, Paper 69-397. 10 p. 16 refs.
Members, $1.00; nonmembers, $1.50.
NASA-Army-supported research.

The boundary layer equations for incompressible two-dimensional turbulent flows with arbitrary pressure distributions are solved by the method of weighted residuals. The method is capable of predicting skin friction, boundary layer integral parameters, and velocity profiles. The analytical technique contains a theoretical convergence criterion, and enables computations to be made to any desired accuracy (subject to the accuracy of the selected turbulence model). To obtain solutions, a mixing length model for the turbulent shear description is used in conjunction with initial profile data modified by orthogonal functions. Analytical results are compared with three experimental cases: (1) the Schubauer and Klebanoff flow over an airfoil-like body which includes favorable and adverse pressure gradients and leads to separation, (2) the equilibrium flow with an adverse pressure gradient of Bradshaw, and (3) the favorable pressure gradient equilibrium flow of Herring and Norbury. In all three cases excellent agreement is obtained. The method is sufficiently rapid to permit its use as a subprogram in analyses of broader extent. (Author)

A69-31908 * #
VELOCITY FLUCTUATION INTENSITIES IN A HYPERSONIC TURBULENT BOUNDARY LAYER.
William D. Harvey and Dennis M. Bushnell (NASA, Langley Research Center, Aero-physics Div., Gas Dynamics Section, Hampton, Va.).
AIAA Journal, vol. 7, Apr. 1969, p. 760-762. 11 refs.
Estimate of the intensity of the velocity fluctuations in a hypersonic turbulent boundary layer, based directly on the fluctuation data of Wallace (1968). A mixing length approach is evaluated for computing indirectly the magnitude and trends of density and velocity fluctuations from measurements of mean flow quantities. P.v.T.

A69-33247 *
VISCOUS DRAG REDUCTION; PROCEEDINGS OF THE SYMPOSIUM, DALLAS, TEX., SEPTEMBER 24, 25, 1968.
Symposium sponsored by the U.S. Navy and NASA.
Edited by C. S. Wells (Ling-Temco-Vought, Inc., Research Center, Dallas, Tex.).
New York, Plenum Press, 1969. 510 p.
$22.50.

CONTENTS:

FOREWORD. C. S. Wells (Ling-Temco-Vought, Inc., Dallas, Tex.), p. v.

BOUNDARY LAYER TRANSITION, PREDICTION AND CONTROL.
ON THE MANY FACES OF TRANSITION. M. V. Morkovin (Illinois Institute of Technology, Chicago, Ill.), p. 1-31. 65 refs. [See A69-33248 17-12]
BOUNDARY-LAYER TRIPPING WITH EMPHASIS ON HYPERSONIC FLOWS. E. L. Morrisett, D. R. Stone, and A. H. Whitehead Jr. (NASA, Langley Research Center, Hampton, Va.), p. 33-51. 22 refs. [See A69-33249 17-12]
BALLISTICS RANGE BOUNDARY-LAYER TRANSITION MEASUREMENTS ON CONES AT HYPERSONIC SPEEDS. N. W. Sheetz, Jr. (U.S. Navy, Naval Ordnance Laboratory, Corona, Calif.), p. 53-83. 38 refs. [See A69-33250 17-01]
AMPLIFIED LAMINAR BOUNDARY LAYER OSCILLATIONS AND TRANSITION AT THE FRONT ATTACHMENT LINE OF A 45° SWEPT FLAT-NOSED WING WITH AND WITHOUT BOUNDARY LAYER SUCTION. W. Pfenninger and J. W. Bacon, Jr. (Northrop Corp., Beverly Hills, Calif.), p. 85-105. 8 refs. [See A69-33251 17-01]

DRAG REDUCTION WITH POLYMER ADDITIVES.
STUDIES OF VISCOUS DRAG REDUCTION WITH POLYMERS INCLUDING TURBULENCE MEASUREMENTS AND ROUGHNESS EFFECTS. J. G. Spangler (Ling-Temco-Vought, Inc., Dallas, Tex.), p. 131-157. 20 refs. [See A69-33252 17-12]
EXPLORATORY DRAG REDUCTION STUDIES IN NON-POLAR SOAP SYSTEMS. I. Radin, J. L. Zakin, and G. K. Patterson (Missouri, University, Rolla, Mo.), p. 213-231. 24 refs. [See A69-33253 17-12]

APPLICATIONS OF POLYMER DRAG REDUCTION.
AN ANALYSIS OF UNIFORM INJECTION OF A DRAG-REDUCING FLUID INTO A TURBULENT BOUNDARY LAYER. C. S. Wells (Ling-Temco-Vought, Inc., Dallas, Tex.), p. 361-382. 18 refs. [See A69-33254 17-12]

WALL TURBULENCE.
A MODEL FOR LARGE EDDY CONTRIBUTIONS IN INCOMPRESSIBLE TURBULENT BOUNDARY LAYERS. J. L. Gaddis and J. P. Lamb (Texas, University, Austin, Tex.), p. 427-445. 19 refs. [See A69-33255 17-12]
NORMAL-STRESS EFFECTS IN DRAG-REDUCING FLUIDS. R. I. Tanner (Brown University, Providence, R.I.), p. 463-474. 18 refs. [See A69-33256 17-12]
RELATIONSHIP BETWEEN FLOW PATTERN, CONSTITUTIVE EQUATION AND MOLECULAR STRUCTURE. F. W. Boggs (Pennsylvania State University, University Park, Pa.), p. 475-493. 15 refs. [See A69-33257 17-12]
AUTHOR INDEX, p. 495.
SUBJECT INDEX, p. 496-500.

A69-33248
ON THE MANY FACES OF TRANSITION.
Mark V. Morkovin (Illinois Institute of Technology, Chicago, Ill.).
IN: VISCOUS DRAG REDUCTION; PROCEEDINGS OF THE SYMPOSIUM, DALLAS, TEX., SEPTEMBER 24, 25, 1968. [A69-33247 17-12]
Symposium sponsored by the U. S. Navy and NASA.
Edited by C. S. Wells.
New York, Plenum Press, 1969, p. 1-31. 65 refs.
Contracts No. AF 44(620)-69-0022; No. AF 33(615)-67-C-1662.
In seeking a rational approach to the variety of transitional behavior, the author conjectures that many instability paths to turbulence are admissible and that their effectiveness hinges on whether the given mechanism supplies the proper scales, intensity level, and three-dimensional phase relations needed for self-regeneration. Conceptual lessons are drawn from a recently completed critical survey of the literature on transition to turbulence, and a number of unifying conjectures are advanced for subsonic speeds. The roles of linear amplification, nonlinear limiting, and secondary instability inducted by unsteady nonlinear effects are illustrated for a number of transitional flows, including those in presence of roughness and streamwise vorticity. A clarification is advanced for the question of fast vs slow transition. An overall model of the linear and nonlinear processes leading to transition is proposed. (Author)

A69-33249 *
BOUNDARY-LAYER TRIPPING WITH EMPHASIS ON HYPERSONIC FLOWS.
E. Leon Morrisette, David R. Stone, and Allen H. Whitehead, Jr. (NASA, Langley Research Center, Hampton, Va.).
IN: VISCOUS DRAG REDUCTION; PROCEEDINGS OF THE SYMPOSIUM, DALLAS, TEX., SEPTEMBER 24, 25, 1968. [A69-33247 17-12]
Symposium sponsored by the U.S. Navy and NASA.
Edited by C. S. Wells.
New York, Plenum Press, 1969, p. 33-51. 22 refs.
Experiments on the effect of trip geometry, size, and location on the position of transition at local Mach numbers up to 8.5. The pressure drag of the trip is investigated at local Mach numbers of 4.7 and 5.5. Based on test results, a flow model was constructed which includes trip-produced multiple vortex filaments similar to those found at supersonic speeds that are assumed to be responsible for introducing the disturbances that lead to transition. The Reynolds number based on the distance from the leading edge to the roughness position as well as Mach number and wall-to-total temperature ratio should be considered in choosing the smallest effective trip size. The effect of trip shape on the position of transition at hypersonic speeds is small; however, certain shapes exhibit the advantageous characteristic of having drag coefficients which were relatively independent of roughness height over a restricted range of the variables tested. (Author)

A69-33252 *
STUDIES OF VISCOUS DRAG REDUCTION WITH POLYMERS INCLUDING TURBULENCE MEASUREMENTS AND ROUGHNESS EFFECTS.
J. G. Spangler (Ling-Temco-Vought, Inc., Research Center, Dallas, Tex.).
IN: VISCOUS DRAG REDUCTION; PROCEEDINGS OF THE SYMPOSIUM, DALLAS, TEX., SEPTEMBER 24, 25, 1968. [A69-33247 17-12]
Symposium sponsored by the U.S. Navy and NASA.
Edited by C. S. Wells.
New York, Plenum Press, 1969, p. 131-157. 20 refs.
Research supported by the Ling-Temco-Vought Independent Research and Development Funds; Contract No. NASw-729.
Recent results of turbulence measurements in very effective drag-reducing fluids. Effects of the polymer on turbulence intensity are found not to be directly related to friction reduction. Turbulence intensity is found to be a function of Reynolds number, polymer concentration, and location in the flowfield and may be locally higher or lower than for Newtonian flow. Turbulence spectral measurements show moderate effects in both macroscale and microscale for polymer

solutions, suggesting a possible elasticity effect which is not related to the drag-reduction phenomenon. Friction factors for flow of a very effective drag-reducing dilute polymer solution in uniformly rough pipes are presented. The onset of "fully rough" effects is found to occur at higher Reynolds numbers in the polymer solution than in water, in accordance with predictions based on the sublayer thickening effect of the polymer. The friction factors are found to be less for the polymer than for water in the roughness transition regime, but there is an indication that in the fully rough regime no drag reduction will be realized. The data are analyzed in terms of a roughness function based on the effects of the polymer and the roughness on the law of the wall velocity profile. (Author)

A69-33253 *

EXPLORATORY DRAG REDUCTION STUDIES IN NON-POLAR SOAP SYSTEMS.

I. Radin, J. L. Zakin, and G. K. Patterson (Missouri, University, Rolla, Mo.).

IN: VISCOUS DRAG REDUCTION; PROCEEDINGS OF THE SYMPOSIUM, DALLAS, TEX., SEPTEMBER 24, 25, 1968. [A69-33247 17-12]
Symposium sponsored by the U.S. Navy and NASA.
Edited by C. S. Wells.
New York, Plenum Press, 1969, p. 213-231. 24 refs.
Grant No. NGR-26-003-003.

Effects of concentration, flow rate, and tube diameter on drag reduction in nonpolar soap solutions. Aluminum dioleate in toluene solutions were used in pressure drop measurements at concentrations of 0.2, 0.5, 0.75, and 1.0%. Pressure drop measurements were made in tube diameters ranging from 0.01 to 2.0 in. A few such measurements were also made with an aluminum palmitate soap in toluene. The results of these measurements differed from those observed in aqueous systems. Higher concentrations (0.75%) were required before drag reduction occurred. No critical upper shear stress was observed. While little mechanical degradation was observed after an initial holding period, the solutions degraded on aging. Thus, while aqueous soap systems have appeared to be at equilibrium and have shown reversible shear effects, the changes in viscosity with time for these nonpolar systems indicate that they were not at equilibrium. It is believed that the differences in the nature of the soap structure in solution for the two types of systems cause the observed differences in the turbulent flow behavior. (Author)

A69-33254

AN ANALYSIS OF UNIFORM INJECTION OF A DRAG-REDUCING FLUID INTO A TURBULENT BOUNDARY LAYER.

C. Sinclair Wells (Ling-Temco-Vought, Inc., Research Center, Dallas, Tex.).

IN: VISCOUS DRAG REDUCTION; PROCEEDINGS OF THE SYMPOSIUM, DALLAS, TEX., SEPTEMBER 24, 25, 1968. [A69-33247 17-12]
Symposium sponsored by the U.S. Navy and NASA.
Edited by C. S. Wells.
New York, Plenum Press, 1969, p. 361-382. 18 refs.
Research supported by Ling-Temco-Vought.

Evaluation of the mass flux requirements for drag reduction by uniform injection of a high molecular weight polymer solution into a turbulent boundary layer on a flat plate or slender body of revolution. This evaluation is necessary in order to determine the feasibility of using polymer solutions to reduce skin friction drag on marine vehicles. Uniform injection is chosen for analysis since it raises the additive concentration to the drag reducing level in the wall region only, where recent experiments have shown that it is needed. Calculations of skin friction reduction and mass flux required are plotted for conditions of interest for marine vehicles. Distributed injection is compared with slot injection and is found to require between 40 and 140 times less additive solution than does slot injection to maintain equivalent drag reduction. A "specific additive consumption" is defined and compared with specific fuel consumption of several underwater propulsion units. The comparison shows slot injection of a 1000 ppm solution to be of marginal value, while porous wall injection would give more performance increase than adding an equal amount of fuel. It is noted that there is considerably more performance advantage to be gained from a continuous ablating additive coating than from additional fuel, if it could be made to ablate at the optimum rate. (Author)

A69-33255

A MODEL FOR LARGE EDDY CONTRIBUTIONS IN INCOMPRESSIBLE TURBULENT BOUNDARY LAYERS.

J. L. Gaddis and J. P. Lamb (Texas, University, Austin, Tex.).

IN: VISCOUS DRAG REDUCTION; PROCEEDINGS OF THE SYMPOSIUM, DALLAS, TEX., SEPTEMBER 24, 25, 1968. [A69-33247 17-12]
Symposium sponsored by the U.S. Navy and NASA.
Edited by C. S. Wells.
New York, Plenum Press, 1969, p. 427-445. 19 refs.

Incompressible turbulent boundary layer analysis based on a two-region characterization for eddy viscosity. The eddy viscosity for the inner region is described with Spalding's generalized function, whereas the outer region, characterized by large eddy scales, is treated through an application of Prandtl's eddy viscosity model for free shear flows. A similarity solution for the outer region is obtained for a linearized motion equation and suitably joined to the inner solution by requiring continuity of shear stress and eddy viscosity. The present matching criteria for the two regions result in the preservation of the velocity profile shape in the defect plane, while simultaneously yielding the correct longitudinal development of all layer parameters such as momentum thickness and wall shear stress. The present model is extended to the low Reynolds number regime where the wake strength is greatly diminished. It is suggested that interfacial conditions are, collectively, the particular feature of incompressible flow which may serve as the point of reference for variable density transformations. (Author)

A69-33256 *

NORMAL-STRESS EFFECTS IN DRAG-REDUCING FLUIDS.

R. I. Tanner (Brown University, Providence, R.I.).

IN: VISCOUS DRAG REDUCTION; PROCEEDINGS OF THE SYMPOSIUM, DALLAS, TEX., SEPTEMBER 24, 25, 1968. [A69-33247 17-12]
Symposium sponsored by the U.S. Navy and NASA.
Edited by C. S. Wells.
New York, Plenum Press, 1969, p. 463-474. 18 refs.
Grant No. NGR-40-002-009.

Demonstration that some viscoelastic fluid theories show an increased "resistance" to nonviscometric (or nonshearing) deformations due to "normal-stress effects," but no upper limit on stretch rate is discernible. Using this fact on a one-dimensional Burgers-type model of "weak turbulence," drag reduction is predicted. Some observations on transition in solutions of polyethylene-oxide (Polyox) were made using a water table. It was found that (1) the rate of spread of turbulent "spots" is reduced; (2) a fine-grained wavy structure covered the surface and waviness increased with concentration; and (3) turbulent spot generation at sharp edges was reduced. (Author)

A69-33257 *

RELATIONSHIP BETWEEN FLOW PATTERN, CONSTITUTIVE EQUATION AND MOLECULAR STRUCTURE.

Fitzhugh W. Boggs (Pennsylvania State University, Ordnance Research Laboratory, University Park, Pa.).

IN: VISCOUS DRAG REDUCTION; PROCEEDINGS OF THE SYMPOSIUM, DALLAS, TEX., SEPTEMBER 24, 25, 1968. [A69-33247 17-12]
Symposium sponsored by the U.S. Navy and NASA.
Edited by C. S. Wells.
New York, Plenum Press, 1969, p. 475-493. 15 refs.
Navy-NASA-sponsored research.

In developing the constitutive equation for an arbitrary fluid on a purely phenomenological basis, it has been shown that the stress tensor can be represented as a generalized functional depending on a Finger rate of strain tensor. If only the first derivative with respect to time and only a single quadratic term are retained in the general equation, then the second-order fluid results. From the phenomenological point of view, there is no a priori reason why the coefficients in the second-order fluid should be related to each other. However, it has been found experimentally that, for the second-order fluid, the two second-order coefficients can, to a good approximation, be expressed in terms of one of them. This has been shown to lead to equations which differ from the Navier-Stokes equation by a term which depends only on the Weissenberg number. The theory of viscosity of polymeric solutions (Kirkwood, 1948, 1954), or theories closely related to it, have been able to explain

the linear viscoelastic properties of polymeric solutions quite well. It is shown that it is possible to develop a constitutive equation which includes nonlinear as well as viscoelastic terms from these same assumptions. The coefficients of the acceleration tensors are found to depend only on the concentration and intrinsic viscosity for a wide variety of polymers. It suggests, as does the Weissenberg conjecture, that in dilute polymer solutions, nonlinearity and viscoelasticity are always present together. Their relative importance will depend on the nature of the flow. (Author)

A69-33436 *#
A NEW MOMENTUM-INTEGRAL METHOD FOR TREATING MHD AND SIMPLE HYDRODYNAMIC ENTRANCE FLOWS.
Richard E. Schwirian (NASA, Lewis Research Center, Cleveland, Ohio).
American Institute of Aeronautics and Astronautics, Fluid and Plasma Dynamics Conference, San Francisco, Calif., June 16-18, 1969, Paper 69-724. 10 p. 15 refs.
Members, $1.00; nonmembers, $1.50.

New momentum integral method for describing the incompressible flow of a conducting fluid in the entrance of an MHD channel. The method is distinctive in that an "edge" stress is permitted to exist at the boundary layer-free stream interface. The edge stress exerts a drag force on the free stream and mathematically accounts for the development of viscous stresses in the free-stream flow as the fluid enters the channel. By a prudent choice of the edge stress variation, the governing differential equation is forced to yield an asymptotic solution with the correct wall stress. The edge stress method allows accurate analytical solutions for the friction factor and pressure variation in laminar entrance flows to be obtained for all Hartmann numbers. This accuracy exists at all points in the flow, both near the entrance and arbitrarily far downstream. Nonmagnetic turbulent flow is described. (Author)

A69-33437 *#
VORTEX ENHANCEMENT OF JET PENETRATION IN SUPERSONIC FLOW.
Louis A. Povinelli, Frederick P. Povinelli, and Martin Hersch (NASA, Lewis Research Center, Cleveland, Ohio).
American Institute of Aeronautics and Astronautics, Fluid and Plasma Dynamics Conference, San Francisco, Calif., June 16-18, 1969, Paper 69-664. 7 p. 7 refs.
Members, $1.00; nonmembers, $1.50.

Investigation of the effect of vortex motion on jet penetration and spreading. Experiments were conducted in a Mach 2 airstream. Two injector configurations were used. The first was a half-delta wing with a 30° semiapex and a 12° angle of attack. Helium was injected from the upper surface in line with the mean position of the vortex. The second injector was a flat plate at the same angle of attack and equal projected frontal area. Measurements of the helium concentration profiles at various downstream distances indicated that penetration into the free stream was at least twice as large with the delta injector. This increase in penetration is based on measurements made relative to the injection orifice and along the vortex position. Comparison of the penetration at other angular positions may not yield the same degree of enhancement. The spread of helium in the lateral direction was found to occur over twice the angular range with the delta injector as with the angled flat plate. The experimental measurement of the jet boundary (along the vortex angle) was found to be in reasonable agreement with the mean vortex position near the trailing edge of the injector. (Author)

A69-33441 *#
PRELIMINARY RESULTS FROM AN EXPERIMENTAL INVESTIGATION OF NOZZLE WALL BOUNDARY LAYER AT MACH NUMBERS RANGING FROM 27 TO 47.
Joseph H. Kemp, Jr. and A. K. Sreekanth (NASA, Ames Research Center, Moffett Field, Calif.).
American Institute of Aeronautics and Astronautics, Fluid and Plasma Dynamics Conference, San Francisco, Calif., June 16-18, 1969, Paper 69-686. 8 p. 19 refs.
Members, $1.00; nonmembers, $1.50.

Results from pitot-pressure and total-temperature surveys of the boundary layer in the nozzle of the Ames M-50 helium tunnel. Included are data from four nozzle stations with Re_θ ranging from 1200 to 8100. From the measured values, velocity profiles, density profiles, momentum thickness, displacement thickness, and wall-friction coefficient are determined. Results indicate that the boundary layer has a very thick (30% to 65% of the 2.5- to 12-in. total thickness) inner region with laminar-like characteristics and an outer region with turbulent-like characteristics. The n value obtained by representing the turbulent region with a power law relationship varies from 9 to 20 depending on the density ratio across the boundary layer. The momentum thickness, displacement thickness, and wall-friction coefficient provide reasonable extensions to data obtained at lower Mach number. (Author)

A69-33453 *#
INFLUENCE OF MEASURED FREE-STREAM DISTURBANCES ON HYPERSONIC BOUNDARY-LAYER TRANSITION.
R. D. Wagner, Jr., D. V. Maddalon, L. M. Weinstein, and A. Henderson, Jr. (NASA, Langley Research Center, Hampton, Va.).
American Institute of Aeronautics and Astronautics, Fluid and Plasma Dynamics Conference, San Francisco, Calif., June 16-18, 1969, Paper 69-704. 19 p. 24 refs.
Members, $1.00; nonmembers, $1.50.

Results of a study of transition in hypersonic flow over a wide range of test conditions in the Langley M = 20 helium tunnel. Direct measurements of the facility free-stream disturbances have been made with a constant current anemometer which has a frequency response capability of 500 kHz. In unheated flow, fluctuation mode diagrams identify the disturbances as sound waves produced by moving sources of sound (the turbulent nozzle wall boundary layer). The test section disturbance levels can be quite high with a maximum of about 3.5% rms mass flow fluctuation (which corresponds to about 6% rms static pressure fluctuation) when transition of the nozzle wall boundary layer occurs in the portion of the nozzle which can influence the test section disturbance level via direct acoustic radiation. For the same range of test conditions, transition measurements have been made on a 10° half-angle wedge. A strong correlation between the movement of transition on the model and the free-stream disturbance level is observed; transition appears to be dominated by the intense sound radiation of the nozzle wall boundary layer. The results show that the free-stream disturbances are a major contributor to the unit Reynolds number effect on transition Reynolds number. Heat-transfer transition data using heated flow (as opposed to unheated) indicated a significant effect of heating the flow, the transition Reynolds number decreasing with heated flow. (Author)

A69-33462 *#
INTEGRAL BALANCE OF FORCES AND MOMENTA IN ACCELERATED BOUNDARY LAYERS.
Newell D. Sanders (NASA, Lewis Research Center, Cleveland, Ohio).
American Institute of Aeronautics and Astronautics, Fluid and Plasma Dynamics Conference, San Francisco, Calif., June 16-18, 1969, Paper 69-666. 6 p. 7 refs.
Members, $1.00; nonmembers, $1.50.

Analysis and classification of accelerated boundary layers in terms of the balance of pressure force, inertia force, entrainment momentum, and wall friction force. These quantities are defined in terms of a reference velocity U_b, a reference thickness δ_b, and a reference density ρ_b (or temperature t_b). These reference parameters are defined in terms of the flow deficiency, momentum deficiency, and enthalpy deficiency integrals and characterize a one-dimensional model boundary layer. A useful short-cut estimate of boundary layer development in a severe pressure gradient is illustrated and extended to the estimation of separation in adverse gradients. This method is used to discuss the diffusion factor D which is commonly used in compressor and cascade analysis. A method for classifying boundary layers according to the balance of integral forces is presented. (Author)

A69-33474 *#
CALCULATION OF NONEQUILIBRIUM HYPERSONIC TURBULENT BOUNDARY LAYERS AND COMPARISONS WITH EXPERIMENTAL DATA.
Dennis M. Bushnell and Ivan E. Beckwith (NASA, Langley Research

Center, Hampton, Va.).
American Institute of Aeronautics and Astronautics, Fluid and Plasma Dynamics Conference, San Francisco, Calif., June 16-18, 1969, Paper 69-684. 22 p. 44 refs.
Members, $1.00; nonmembers, $1.50.

Solution, by a finite-difference procedure, of compressible turbulent boundary-layer equations. The Reynolds stress is modeled by an eddy viscosity function where the mixing length is assumed to depend on the distance from the wall and the boundary-layer thickness except in the near wall region where Van Driest's exponential damping function is used. For applications to wall blowing cases, comparisons with data show that the damping factor should be taken as a function of the blowing rate as determined from incompressible data. Nonequilibrium effects could be approximately accounted for by assuming that the mixing length in the midregion of the boundary layer is a function of a velocity profile shape factor. This shape factor is identical to the incompressible form factor, and the functional relation between it and the mixing length was based on incompressible data. The nearly quadratic relation between total temperature and velocity that is observed in wall boundary layers of hypersonic nozzles could be obtained in the calculations only by using values for the total turbulent Prandtl number of 1.5 or more. Tentative models for the fluctuating density terms were used in some of the calculations. The results indicated that these terms may have large effects on low-density, hypersonic boundary layers. (Author)

A69-33476 *#
COMBINED EFFECTS OF MASS ADDITION AND NOSE BLUNTNESS ON BOUNDARY-LAYER TRANSITION.
Joseph G. Marvin and Clifford M. Akin (NASA, Ames Research Center, Moffett Field, Calif.).
American Institute of Aeronautics and Astronautics, Fluid and Plasma Dynamics Conference, San Francisco, Calif., June 16-18, 1969, Paper 69-706. 10 p. 11 refs.
Members, $1.00; nonmembers, $1.50.

Transition measurements on a 5° half-angle cone, obtained from heat-transfer data. The cone, consisting of a short solid tip (sharp or blunt) followed by a uniformly porous section, was tested in a 3.5-ft wind tunnel at $M_{\infty} = 7.4$ and free-stream Reynolds numbers of 3×10^6 and 4.7×10^6, based on model length. The effects of argon, air, and helium injection (mass rates between 0 and 2.5% of free-stream rates) through the porous skin are determined. A significant decrease in transition Reynolds number was observed with increasing mass injection. The magnitude of the decrease is shown to depend on injection rate and molecular weight. For the same mass injection rate, the lighter injectant resulted in a greater decrease. Small nose bluntness moved transition location rearward, but the amount it moved depended on the injection rate and molecular weight. At the highest injection rates, transition location was the same as for the sharp cone. (Author)

A69-37208 * #
A MODIFIED MODEL FOR VIBRATION-DISSOCIATION COUPLING PHENOMENA.
N. M. Reddy (NASA, Ames Research Center, Moffett Field, Calif.).
AIAA Journal, vol. 7, June 1969, p. 1179, 1180. 7 refs.

Study of the effect of allowing the parameter U, in a model discussed by Marrone and Treanor (1963), to vary with kinetic temperature. The variation is assumed to occur in such a way that the average energy of dissociating molecules corresponds to the energy of a critical vibrational level below the dissociation limit. The coupling between vibration and dissociation is discussed. The effect of letting U vary was studied by computing the flow quantities behind normal shock waves in oxygen. G.R.

A69-39674 *
ON THE O.D.E. OF STAGNATION POINT FLOWS OF POWER LAW FLUIDS.
Robert A. Spinelli (NASA, Goddard Space Flight Center, Goddard Institute for Space Studies, New York, N.Y.).
Zeitschrift für angewandte Mathematik und Physik, vol. 20, July 25, 1969, p. 479-486.

Development of a rigorous proof that solutions of the third-order quasi-linear ordinary differential equation governing steady two-dimensional stagnation point flows of non-Newtonian power law fluids, which have continuous third derivatives, do not exist for powers equal to or greater than two. A simple numerical technique is described for calculating the solution in all cases where n is greater than zero. Some numerical results are given. B.H.

A69-43367 * #
SHOCK IONIZATION KINETICS OF PURE NITROGEN.
S. B. Bentley (NASA, Ames Research Center, Moffett Field, Calif.).
Physics of Fluids, vol. 12, Sept. 1969, p. 1939-1941. 5 refs.

Study of the ionization rate limiting processes behind strong shock waves in pure nitrogen. The parameters of these processes are determined by varying the terms which represent these processes in the fluid dynamic equations. Also varied are the coefficients representing a propagating one-dimensional shock wave. Diagrams are plotted to show the electron density profiles produced by electron impact ionization behind shock waves in pure nitrogen flows. V.Z.

N69-10070*# National Aeronautics and Space Administration. Lewis Research Center, Cleveland, Ohio.
PREDICTION OF THERMODYNAMIC EFFECTS OF DEVELOPED CAVITATION BASED ON LIQUID-HYDROGEN AND FREON-114 DATA IN SCALED VENTURIS
Royce D. Moore and Robert S. Ruggeri Washington Nov. 1968 25 p refs
(NASA-TN-D-4899) Avail: CFSTI CSCL 20M

Cavity-pressure-depression measurements made in cavitated regions of hydrogen and Freon-114 (dichlorotetrafluoroethane) in two scaled venturis were used to evaluate experimental exponents of previously reported equations for the prediction of thermodynamic effects of cavitation for venturis. This prediction method accounts for changes in liquid, temperature, flow velocity, cavity length, and venturi scale. Use of the method requires similarity of body and cavity and a known cavity-pressure depression at one operating condition. The experimental data used included a velocity range of 20 to 205 feet per second (6.1 to 62.5 m/sec) and cavity lengths from 0.2 to 2.7 free stream diameters. Author

N69-10293*# National Aeronautics and Space Administration. Lewis Research Center, Cleveland, Ohio.
WATER FLOW AND CAVITATION IN CONVERGING–DIVERGING BOILER-INLET NOZZLE
James R. Stone and Nick J. Sekas Washington Nov. 1968 23 p refs
(NASA-TM-X-1689) Avail: CFSTI CSCL 20D

Experimental flow-pressure relations were determined for water flowing through a 0.025-inch throat diameter converging-diverging conical nozzle. The nozzle was tested with and without a plug and wire helix insert downstream of the throat. Such nozzles are being studied for possible use as inlets for single tube once through Rankine cycle boilers. The test nozzle is made of transparent plastic. Cavitating and noncavitating data are reported for throat velocities from 49 to 94 ft/sec and temperatures from 57° to 171° F. In well-developed cavitation, the flow is insensitive to nozzle exit pressure, thus minimizing the possibility of feed-system-boiler coupling instability. The plug and wire helix insert reduces the tendency for slugging. Author

N69-10443*# National Aeronautics and Space Administration. Langley Research Center, Langley Station, Va.
REAL-HELIUM HYPERSONIC FLOW PARAMETERS FOR PRESSURES TO 3600 ATMOSPHERES AND TEMPERATURES

TO 15,000°K
Charles G. Miller, III and Sue E. Wilder Washington Nov. 1968 43 p refs
(NASA-TN-D-4869) Avail: CFSTI CSCL 20D

The virial form of the equation of state is used to derive a method for determining reservoir, nozzle-throat, free-stream, and normal-shock conditions for real-helium flow. This method is derived primarily to meet the needs of hotshot-type wind tunnels where the basic input data are measured reservoir pressure and stagnation pressure behind a normal shock. However, the method is derived to include an additional measurement of free-stream density, free-stream velocity, or reservoir temperature. The method is applied for reservoir pressures to 3600 atmospheres, temperatures to 15,000°K, and a range of free-stream Mach numbers from 10 to 100, and the results are presented in the form of nondimensionalized reservoir thermodynamic and nozzle-throat parameters and as simple correction factors which may be applied to ideal-helium flow parameters. These calculations are restricted to reservoir densities less than the critical density of helium and to theoretically uncondensed free-stream flow. Author

N69-10472*# National Aeronautics and Space Administration. Langley Research Center, Langley Station, Va.
USE OF BARONTI-LIBBY TRANSFORMATION AND PRESTON TUBE CALIBRATIONS TO DETERMINE SKIN FRICTION FROM TURBULENT VELOCITY PROFILES
Jerry M. Allen Washington Nov. 1968 41 p refs
(NASA-TN-D-4853) Avail: CFSTI CSCL 20D

A large number of velocity profiles with corresponding local skin friction measurements have been used to investigate the validity of the Baronti-Libby transformation as a skin friction measuring technique over a wide range of test conditions. The possibility of using existing Preston tube calibrations to calculate skin friction from velocity profiles is investigated, and a computational procedure is developed so that a Clauser-type determination of skin friction from velocity profiles can be accomplished without the necessity of plotting. The principal conclusions that result from this study are that the Baronti-Libby transformation gives good results for adiabatic flow but does not predict the correct trend with heat transfer and that using the Fenter-Stalmach law only as a Preston tube calibration is unduly restrictive since it is shown that the law can be used to calculate local skin friction from conventional velocity profiles with results that are comparable with those of the more complex Baronti-Libby method. Author

N69-10693*# National Aeronautics and Space Administration, Washington, D. C.
SOME FLUID MECHANICAL PROBLEMS RELATED TO SUBSONIC AND SUPERSONIC AIRCRAFT
John T. Howe, ed. 1968 24 p refs
(NASA-SP-183) Avail: CFSTI CSCL 01A

Some of the problems connected with modern subsonic and supersonic aircraft and which have their origin in fluid mechanical phenomena are reviewed. The following topics are discussed and found to require further study: 1. Turbulent boundary layers, including the effects of three dimensionality and adverse pressure gradients; 2. Separated flows, such as are due to adverse pressure gradients, to shock boundary layer interactions including the transonic problem, and to concavities; 3. Vortex flows, such as arise from wings and fuselages at angles of attack; 4. Correlation of wind tunnel measurements with flight data and other wind tunnel data; and 5. Transonic flows, including two dimensional airfoil design, integration of wings and fuselage, and methods of increasing the critical Mach number. Author

N69-10788*# National Aeronautics and Space Administration. Langley Research Center, Langley Station, Va.
BLUNT BODY STAGNATION REGION FLOW WITH NONGRAY RADIATION HEAT TRANSFER: A SINGULAR PERTURBATION SOLUTION
Walter B. Olstad Washington Nov. 1968 83 p refs
(NASA-TR-R-295) Avail: CFSTI CSCL 20D

A singular perturbation solution to the blunt-body stagnation region flow of an inviscid, radiating gas has been obtained by means of the Poincare-Lighthill-Kuo, or perturbation-of-coordinates, method. A number of results for a gray gas have been presented in order to provide some physical insight into the effects of various parameters on the shock-layer enthalpy profiles and the radiant heat-transfer rates. A nongray absorption coefficient model was developed which includes, in an approximate way, the important vacuum ultraviolet contributions of bound-free and line transitions. This model was used to obtain solutions pertinent to the case of reentry into the earth's atmosphere. While the results are restricted to small values of the radiation cooling parameter, which characterized the relative importance of radiation and convection as energy transport mechanisms, they cover broad ranges of vehicle velocity, altitude, and nose radius, which are of practical interest. Author

N69-10804*# National Aeronautics and Space Administration. Langley Research Center, Langley Station, Va.
HEAT TRANSFER AND PRESSURE DISTRIBUTIONS DUE TO SINUSOIDAL DISTORTIONS ON A FLAT PLATE AT MACH 20 IN HELIUM
James P. Arrington Washington Nov. 1968 49 p refs
(NASA-TN-D-4907) Avail: CFSTI CSCL 01A

An experimental investigation was conducted to determine the effects of a two-dimensional repetitive sine-wave distortion on the pressure and heat-transfer distributions. Tests were made on a sharp flat plate with a distorted section in a relatively thick boundary layer which changed from laminar to transitional for certain test conditions. The tests were conducted in helium at free-stream Mach numbers of about 20, over a range of length Reynolds numbers varying from 2.72×10^6 to 8.80×10^6 with the flat-plate surface at angles of inclination of 0°, 5°, and 10°. The results of the present tests were similar to results obtained in air at lower free-stream Mach numbers and Reynolds numbers with relatively thinner boundary layers. The pressure and heat-transfer distributions were greatly altered in the distorted section (oscillating from maximum to minimum values) with the heating distribution being affected the most. The magnitude of these pressure and heat-transfer oscillations also depended on whether the flow was laminar or transitional. However, the values generally approached the undisturbed flat-plate results a short distance downstream of the distorted region. Author

N69-13945*# National Aeronautics and Space Administration. Langley Research Center, Langley Station, Va.
USE OF PHOTOIONIZATION IN MEASURING VELOCITY PROFILE OF FREE-STREAM FLOW IN LANGLEY PILOT MODEL EXPANSION TUBE
Wilfred J. Friesen Washington Dec. 1968 46 p refs
(NASA-TN-D-4936) Avail: CFSTI CSCL 20D

Free-stream velocity profile measurements were made of expansion tube flows for flow core velocities of the order of 6300 m/sec, for flow core densities ρ/ρ_0 (where ρ is the gas density and ρ_0 is the gas density at standard conditions) from 3×10^{-4} to 2×10^{-3}, and over flow time intervals of about 150 μsec. The method of measurement was based on identifying a region of the flowing test gas by photoionization and, after a delay of a few microseconds, photographing the displaced position of the region by the light emitted when an electrical current was passed through it. The main conclusions reached are that there is a flow core with a radius between 50 and 60 percent of the tube radius, in which the velocity is uniform to within 5 percent, and that the method of measurement is a useful technique for obtaining velocity profiles within the range of test gas density. Author

N69-14095*# IIT Research Inst., Chicago, Ill.
FLOW IN A TWO-DIMENSIONAL CHANNEL WITH A RECTANGULAR CAVITY
Unmeel B. Mehta and Zalman Lavan Washington NASA Jan. 1969 89 p refs
(Grants NGR-14-004-028; NsG-694)
(NASA-CR-1245) Avail: CFSTI CSCL 20D

The steady state flow characteristics in a rectangular cavity located in the lower wall of a two-dimensional channel whose upper wall was moved with a uniform velocity, were investigated by solving the complete Navier–Stokes equations for laminar imcompressible fluid in terms of the stream function and vorticity. Numerical results were determined for a range of Reynolds numbers from 1 to 500 and for cavity aspect ratios of 0.5, 1.0 and 2.0. A circulating flow extending the whole height was observed for shallow and square cavities. For deep cavity a secondary vortex near the bottom of the cavity was also noticed. Time dependent solutions for the vortex flow in a square cavity bounded by three motionless walls and a fourth moving in its plane were obtained. Author

N69-14314*# National Aeronautics and Space Administration. Manned Spacecraft Center, Houston, Tex.
THE STAGNATION-POINT BOUNDARY LAYER WITH SUCTION AND INJECTION IN EQUILIBRIUM DISSOCIATING AIR
Kenneth C. Weston Washington Dec. 1968 89 p refs
(NASA-TN-D-3889) Avail: CFSTI CSCL 20D

Calculations for the compressible, equilibrium dissociating stagnation point boundary layer with suction and injection were performed using a digital computer. Results are shown which reproduce both the perfect gas, linear viscosity-temperature relation calculations of Cohen and Reshotko, and the dissociating air results of Fay and Riddell. Calculations for the dissociated air boundary layer with air injection indicate significantly higher heating rates than those obtained for the perfect gas, linear viscosity-temperature relation model. A procedure is indicated which allows application of the results for air injection to engineering calculations for cases of foreign-gas injection. Author

N69-14316*# National Aeronautics and Space Administration. Lewis Research Center, Cleveland, Ohio.
INVISCID FLOW ANALYSIS OF TWO PARALLEL SLOT JETS IMPINGING NORMALLY ON A SURFACE
Richard T. Gedney and Robert Siegel Washington Dec. 1968 32 p refs
(NASA-TN-D-4957) Avail: CFSTI CSCL 20D

Conformal mapping was applied to obtain the flow pattern for two parallel jets of finite width originating from infinity and impinging normally on a plate. The ratio of the half spacing between the jets to the jet width (S/H) is the single parameter governing the flow. Analytical expressions and graphs are given for the free streamlines, internal streamlines, and pressure coefficient along the plate for various values of the S/H ratio. A portion of each jet flows outward along the plate and the remaining flow is a recirculation back toward infinity along the axis between the jets. The amount of recirculation is given as a function of the S/H ratio. Author

N69-14483*# National Aeronautics and Space Administration. Lewis Research Center, Cleveland, Ohio.
NONLINEAR DECAY OF A DISTURBANCE IN AN UNBOUNDED VISCOUS FLUID
Robert G. Deissler Washington Dec. 1968 29 p refs
(NASA-TN-D-4947) Avail: CFSTI CSCL 20D

The nonlinear decay of a disturbance was calculated by an iterative solution to the Navier–Stokes equations. The general expressions obtained for successive approximations were suitable for machine computations, within the limitations of the computer capacity. For the initial condition, a three dimensional cosine distribution with two harmonic terms was assumed. The nonlinear interaction of these harmonic terms then produced new harmonics. As the iteration process proceeded, a large number of harmonics, at wave numbers higher than, lower than, or the same as the original ones were generated. This process appeared to be similar to that occurring in the early stages of the development of turbulence by flow through a grid. Author

N69-15371*# National Aeronautics and Space Administration. Lewis Research Center, Cleveland, Ohio.
EMPIRICAL CHARACTERIZATION OF SOME PRESSURE WAVE SHAPES IN STRONG TRAVELING TRANSVERSE ACOUSTIC MODES
Marcus F. Heidmann Washington NASA Jan. 1969 12 p refs
(NASA-TM-X-1716) Avail: CFSTI CSCL 20D

Pressure wave shapes measured at the wall of a short cylindrical cavity containing a relatively pure traveling transverse acoustic mode were evaluated for harmonic content. The empirical relation $p' = \epsilon \cos t + \epsilon^2 \cos 2t + \epsilon^3 \cos 3t + \ldots$, was found to adequately represent wave shapes for peak-to-peak pressure amplitudes approaching the mean cavity pressure. The relation is relatively simple and provides a convenient method of characterizing strong wave shapes for many analytical and experimental purposes. Author

N69-15473*# National Aeronautics and Space Administration. Lewis Research Center, Cleveland, Ohio.
OBSERVATIONS OF INTERFACE BEHAVIOR DURING INFLOW TO AN ELLIPTICAL ENDED CYLINDER IN WEIGHTLESSNESS
Eugene P. Symons and Ralph C. Nussle Washington Jan. 1969 17 p refs
(NASA-TM-X-1719) Avail: CFSTI CSCL 20D

An experimental investigation was conducted during which liquid was pumped into a 4-cm-diameter cylindrical tank, initially void of liquid, in a weightless environment. The tank bottom, an inverted ellipse, was scaled from the Centaur propellant tank, as was the inlet line location. Three inlet diameters (0.2, 0.4, and 0.8 cm) were studied. The liquid–vapor interface during inflow became increasingly distorted as inflow velocity was increased. Furthermore, any increase in the ratio of inlet diameter to tank diameter necessitates lowering of inlet velocity to maintain a stable liquid–vapor interface. Author

N69-15630*# National Aeronautics and Space Administration. Ames Research Center, Moffett Field, Calif.
ANALYSIS OF THE STABILITY OF A THIN LIQUID FILM ADJACENT TO A HIGH-SPEED GAS STREAM
Philip R. Nachtsheim Washington Jan. 1969 34 p refs
(NASA-TN-D-4976) Avail: CFSTI CSCL 20D

Oblique wave formation in the melt layer of a body entering the atmosphere is examined. The three-dimensional disturbance equations of the liquid including the effects of viscosity are formulated. The disturbance motion of the gas is taken into account neglecting viscosity. The Tollmien–Schlichting type of instability in the liquid is excluded and only those modes are considered for which the phase velocity of the disturbance is greater than the velocity of the basic liquid flow at the gas-liquid interface. Numerical and approximate analytic results are presented for waves in the liquid with supersonic flow over their crests. A comparison with the numerical solutions shows that the approximate analytic solutions are accurate for solving the eigenvalue problem when the Reynolds number of the liquid film is small, that is, for a highly viscous melt layer. The approximate solutions are obtained in closed form. It is demonstrated that the mechanism of liquid wave generation is supersonic wave drag. The relation between the wavelength of the disturbance and the other parameters involved in the eigenvalue problem is determined and is presented for a wide range of these parameters. Author

12 FLUID MECHANICS

N69-15631 *# National Aeronautics and Space Administration. Langley Research Center, Langley Station, Va.

PRELIMINARY INVESTIGATION OF MOMENTUM DIFFUSION BETWEEN TWO SUPERSONIC AIRSTREAMS IN THE PRESENCE OF SHOCK WAVES

John P. Weidner and Carl A. Trexler Washington Jan. 1969 79 p refs

(NASA-TN-D-4974) Avail: CFSTI CSCL 20D

An experimental study of compressible two-dimensional mixing between two parallel supersonic airstreams passing through oblique shock waves has been performed, and the results have been compared with those of a computerized theoretical method. This experiment was restricted to measurements of momentum diffusion in the near region, with the purpose of the study being to determine the effect of the oblique shock waves on mixing. The model consisted of a two-dimensional rectangular duct mounted in a Mach 4 airstream operating at ambient temperature. The Mach 4 stream was the primary air through the duct, while the secondary air was injected at a higher total pressure and Mach number through three isentropic nozzles set into the bottom surface of the duct. The nozzles were oriented at such an angle relative to the primary stream as to create a set of shock waves each having a turning angle of about 6.0°. Total pressure measurements were taken across the mixing zone at several stations on either side of two crossing shock waves and were reduced to velocity profiles through the mixing zone. Average Mach numbers measured in the two streams were 3.5 and 4.4 ahead of the shock waves and 2.9 and 3.7 behind the shock waves. The theoretical solution indicated an increase in eddy viscosity in the vicinity of the shock waves. Author

N69-16098 *# National Aeronautics and Space Administration. Lewis Research Center, Cleveland, Ohio.

REAL-GAS EFFECTS IN CRITICAL FLOW THROUGH NOZZLES AND THERMODYNAMIC PROPERTIES OF NITROGEN AND HELIUM AT PRESSURES TO 300 TIMES 10^5 NEWTONS PER SQUARE METER (APPROX. 300 ATM)

Robert C. Johnson Washington 1968 204 p refs

(NASA-SP-3046) Avail: CFSTI CSCL 20D

A critical-flow factor for gaseous nitrogen and helium flowing through critical-flow nozzles was calculated. This factor provides a convenient means for determining the mass-flow rate of these gases through critical-flow nozzles. In addition, the results include the nozzle throat velocity, the compressibility factor, the entropy, the enthalpy, the specific heat, the specific-heat ratio, the speed of sound, and the critical pressure, density, and temperature ratios. These results are tabulated as functions of the plenum pressure and temperature. The pressure range is 300 $\times$ 10^5 newtons per square meter (approx. 300 atm). For nitrogen, the temperature range is from 100° to 400°K. For helium, the range is from 15° to 400°K. The FORTRAN 4 subroutines used to calculate these results are also included. These routines permit three different sets of independent variables. In addition to the plenum pressure and temperature, the other independent variable is either the nozzle exit pressure, the nozzle exit Mach number, or the nozzle exit temperature. Author

N69-17751 *# Pratt and Whitney Aircraft, East Hartford, Conn.

ANALYTICAL AND EXPERIMENTAL STUDY OF THE DYNAMICS OF A SINGLE-TUBE COUNTERFLOW BOILER

H. L. Hess, J. R. Hooper, and S. L. Organ Washington NASA Feb. 1969 196 p refs

(Contract NAS3-9420)

(NASA-CR-1230) Avail: CFSTI CSCL 20D

An analytical and experimental study of a single tube counterflow boiler was conducted. The boiler geometry simulated one of the tubes of a typical boiler for a Rankine cycle space powerplant. Steady state, frequency response, and step response tests were conducted using water as the working fluid. The frequency response and step response tests were conducted by perturbing the boiling fluid flow rate at the inlet to the boiler. Experimental transfer functions were obtained from the frequency response test results. A linearized analysis of the boiler dynamics was performed to derive a theoretical expression for the boiling fluid exit pressure transfer function. A comparison was made between the theoretical and experimental transfer functions. Author

N69-17779 *# National Aeronautics and Space Administration. Lewis Research Center, Cleveland, Ohio.

FREQUENCY RESPONSE OF A FORCED FLOW SINGLE TUBE BOILER WITH INSERTS AND EXIT RESTRICTION

Grady H. Stevens, Eugene A. Krejsa, and Jack H. Goodykoontz Washington Feb. 1969 43 p refs

(NASA-TN-D-5023) Avail: CFSTI CSCL 20M

The frequency response technique was used to measure some of the dynamic properties of a heat exchanger boiler. The boiling fluid, Freon-113, exhausted through an orifice to a constant pressure. The boiling fluid inlet flow rate was varied sinusoidally about a mean value. The magnitude and phase of the perturbations of the boiler inlet flow, inlet pressure, and orifice pressure drop were measured. The data were used to compute the boiler inlet impedance (the complex ratio of the perturbations of inlet pressure and inlet flow) and the transfer impedance (the complex ratio of the perturbations of orifice pressure drop and boiler inlet flow). Author

N69-17827 *# National Aeronautics and Space Administration. Lewis Research Center, Cleveland, Ohio.

THE ELLIPSOIDAL VELOCITY DISTRIBUTION FUNCTION

N. Stankiewicz Washington Feb. 1969 18 p refs

(NASA-TN-D-5026) Avail: CFSTI CSCL 20D

An ellipsoidal velocity distribution function is found as the result of maximizing the entropy with constraints on the number density, the mean velocity, and the stress energy tensor. The relation of this function to the macroscopic flow equations (continuity, momentum, etc.) is studied. The special case of one dimensional channel flow is analyzed. It is shown that the ellipsoidal distribution function gives a consistent description of viscous flow. That is, the parabolic flow profile and Newton's law of viscosity become natural consequences of the macroscopic flow equations. Author

N69-19112 *# National Aeronautics and Space Administration. Lewis Research Center, Cleveland, Ohio.

LATERAL SLOSHING IN CYLINDER UNDER LOW-GRAVITY CONDITIONS

Jack A. Salzman and William J. Masica Washington Feb. 1969 35 p refs

(NASA-TN-D-5058) Avail: CFSTI CSCL 20D

An experimental investigation was conducted to determine liquid sloshing characteristics in cylinders with hemispherical bottoms under low Bond number conditions. Static contact angles were restricted to near 0° so that the equilibrium liquid surface was nearly hemispherical at very low Bond numbers. The experiments were conducted in both normal and low gravity environments. Data were obtained at Bond numbers ranging from 0 to greater than 800. The natural frequency and damping of the fundamental asymmetric sloshing mode at deep liquid depths were correlated in terms of known system parameters. The natural frequency data at shallow liquid depths were compared with existing theoretical studies. All results were compared with previous normal gravity experimental sloshing studies. Author

N69-20794*# National Aeronautics and Space Administration. Lewis Research Center, Cleveland, Ohio.

EFFECT OF FLOW RATE ON THE DYNAMIC CONTACT ANGLE FOR WETTING LIQUIDS

Thom A. Coney and William J. Masica Washington Mar. 1969 22 p refs

(NASA-TN-D-5115) Avail: CFSTI CSCL 20D

Experimental measurements were made of the dynamic contact angle over a previously wetted liquid surface as a function of interface velocity and liquid properties. The experiments were conducted in a weightless environment using glass tubing with a rectangular cross section. All liquids exhibited zero degree static contact angles. The study showed that existing theory adequately predicted the contact angle dependence on interface velocity and liquid properties. In addition, qualitative agreement was obtained between the theoretical and experimental interface shapes. Author

N69-21400*# National Aeronautics and Space Administration. Lewis Research Center, Cleveland, Ohio.

VISCOUS FLOW IN A SHORT CYLINDRICAL VORTEX CHAMBER WITH A FINITE SWIRL RATIO

Robert W. Hornbeck Washington Mar. 1969 34 p refs

(NASA-TN-D-5132) Avail: CFSTI CSCL 20D

The laminar incompressible viscous flow in a short cylindrical vortex chamber is analyzed numerically. The flow is assumed to enter the chamber periphery with an arbitrary ratio of tangential to radial velocity components and to exit at a line sink at the chamber axis. The numerical technique permits consideration of both the tangential and radial momentum equations. Comparisons are made with solutions available for the limiting cases of zero swirl and infinite swirl. Results are presented for a wide variety of swirl ratios, Reynolds numbers, and chamber aspect ratios. The results include radial and tangential velocity profiles, pressure distributions, and points of radial flow reversal. Author

N69-21653*# Nielsen Engineering and Research, Inc., Palo Alto, Calif.

CALCULATION OF COMPRESSIBLE TURBULENT BOUNDARY LAYERS WITH PRESSURE GRADIENTS AND HEAT TRANSFER

Larry L. Lynes, Jack N. Nielsen, and Gary D. Kuhn Washington NASA Mar. 1969 141 p refs

(Contract NAS2-4391)

(NASA-CR-1303; NEAR-TR-6) Avail: CFSTI CSCL 20D

The method of integral relations has been applied to the calculation of compressible turbulent boundary layer characteristics under the action of pressure gradients. In order to solve the problem it was necessary to specify an eddy-viscosity model. A computer program was developed to do the calculations for a class of two dimensional or axisymmetric configurations from low speeds to hypersonic speeds. At hypersonic speeds, comparisons were made between predicted and measured boundary layer quantities for curved plates and flat plates with and without oblique shock wave impingement. The computer program has been applied to a hypersonic axisymmetric configuration composed of a hollow cylinder culminating in a compression flare. A simple method is presented for estimating the magnitude of the normal pressure gradients and of adjusting the displacement and momentum thicknesses predicted by boundary layer theory for the gradients. Author

N69-23085*# National Aeronautics and Space Administration. Langley Research Center, Langley Station, Va.

FORCES AND MOMENTS DUE TO AIR JETS EXHAUSTING PARALLEL TO LARGE FLAT PLATES IN A NEAR VACUUM

Joseph J. Janos and Sherwood Hoffman Washington Apr. 1969 26 p refs

(NASA-TN-D-5147) Avail: CFSTI CSCL 20D

Three flat plates of equal length but with width-length ratios of 0.25, 0.50, and 1.0 were tested. The nozzles used were conical and had nominal exit Mach numbers of 1.0, 3.0, and 5.0. The locations of the nozzles were varied longitudinally and vertically. The plate widths were 48, 96, and 192 throat diameters. The ratios of total pressure to ambient pressure varied from 22×10^6 to 15.5×10^6, and the ratios of jet exit pressure to ambient pressure varied from 11.6×10^6 to 3.2×10^5. The pressure altitude was 312,000 feet (95 km). The impingement forces, moments, and center-of-pressure trends were similar for all three plates. The magnitudes of the impingement parameters were decreased by reducing the plate width or effective plate length, raising the nozzle location, increasing the exit Mach number, or decreasing the jet flow turning angle. For the nozzle positions surveyed, the normal force on the plate was as high as 47.5 percent of the thrust for a nozzle close to the widest plate and as low as 4.8 percent of the thrust for a nozzle relatively high above the narrowest plate. Author

N69-23467*# National Aeronautics and Space Administration. Langley Research Center, Langley Station, Va.

THE LEADING-EDGE EFFECTS ON THE LAMINAR FLATPLATE BOUNDARY LAYER AND THE AERODYNAMIC HEATING AT MACH 10.4

Howard W. Stone Washington May 1969 34 p refs

(NASA-TN-D-5160) Avail: CFSTI CSCL 20D

Wall pressure and heat transfer distributions and boundary layer impact pressure profiles were obtained on a flat plate with both sharp and cylindrically blunted leading edges. The range of free stream Reynolds number based on leading edge thickness was from 73 to 70,000. Although the boundary layer displacement effects behind a sharp leading edge are known to increase the wall pressure and heat transfer in the weak interaction regime, these tests show that boundary layer displacement effects result in only a slight change in the impact pressure and velocity profiles. Slight blunting of the leading edge had little effect on the pressure distribution but, with the boundary layer growing in an entropy gradient, the heat transfer was reduced. Large leading edge bluntness increased the heat transfer relative to the sharp leading edge. Author

N69-24058*# IIT Research Inst., Chicago, Ill.

EFFECT OF FREE STREAM TURBULENCE ON COAXIAL MIXING

R. A. Kulik, J. J. Leithem, and H. Weinstein Washington NASA May 1969 48 p refs

(Grant NsG-694)

(NASA-CR-1336) Avail: CFSTI CSCL 20D

The effects of free stream turbulence and boundary layer trip devices on mixing in a co-axial jet stream are presented. A screen of fine mesh placed in the outer infinite free stream effected both a boundary layer separation where screen and inner duct met, and a lowering of the free stream turbulence level. To determine the dominate effect of the screen, a boundary layer trip device was used to effect the boundary layer separation without reducing the free stream turbulence. Both air and air-Freon-12 systems with density ratios of 1 and 4 respectively, were studied. The outer stream velocity was kept constant at 51 ft/sec and the mass average velocity ratios varied from 2 to 20. Data are presented for the relative axial turbulence intensities as well as velocity, concentration, and mass holdup. Comparison of the screen and boundary layer trip device data taken without any such devices indicated that both devices effected the same preservation of the inner-stream integrity. Mixing is retarded by a factor of 2 to 4 for low velocity ratios. Author

12 FLUID MECHANICS

N69-24800*# National Aeronautics and Space Administration. Lewis Research Center, Cleveland, Ohio.

PHOTOGRAPHIC STUDY OF A BROMINE JET FLOWING IN A COAXIAL AIRSTREAM AND IMPINGING ON A STAGNATION SURFACE

Charles C. Masser and Maynard F. Taylor Washington May 1969 22 p refs

(NASA-TN-D-5209) Avail: CFSTI CSCL 20D

A photographic study is made of a bromine jet issuing into a coaxially flowing airstream and impinging on a stagnation surface. The objective is to determine if the amount of bromine in the near jet region can be increased by the insertion of a stagnation surface in the jet. The diameter, shape and distance of the stagnation surface from the bromine injection point was varied. Several cases showed that a stagnation surface did slightly reduce the erratic behavior of the jet, and in other cases slightly increased the amount of bromine in the near jet region. However, no substantial increase of bromine in the near jet region was found by using a stagnation surface. Author

N69-24877*# Cornell Univ., Ithaca, N. Y. Dept. of Thermal Engineering.

COMMENTS ON THE NATURE OF THE OUTSIDE BOUNDARY LAYER ON A LIQUID SPHERE IN A STEADY, UNIFORM STREAM

Brice S. Sumner and Franklin K. Moore Washington NASA May 1969 19 p refs

(Grant NGR-33-010-042)

(NASA-CR-1362) Avail: CFSTI CSCL 20D

An analytical and experimental investigation was made to determine in a qualitative way the nature of the boundary layer on the outside of a liquid sphere in a steady, uniform stream at high Reynolds number. The results indicate that the small perturbation boundary layers assumed by some are not justified when the densities and viscosities of the fluids inside the sphere and outside of it are comparable. Author

N69-24917*# National Aeronautics and Space Administration. Lewis Research Center, Cleveland, Ohio.

VAPOR INGESTION PHENOMENON IN WEIGHTLESSNESS

Kaleel L. Abdalla and Steven G. Berenyi Washington May 1969 32 p refs

(NASA-TN-D-5210) Avail: CFSTI CSCL 20D

An experimental program was conducted in which the vapor ingestion phenomenon during draining from flat-bottom, cylindrical tanks was studied in both weightlessness and normal gravity. The vapor ingestion phenomenon in weightlessness was correlated with the Weber number using the critical liquid height prior to vapor ingestion as the significant dimension. The normal gravity data agreed with a theoretical analysis predicting a Froude number correlation. Liquid residuals were generally higher in weightlessness than in normal gravity. Effects of initial liquid height and liquid properties on the vapor ingestion phenomenon and comparisons of vapor ingestion heights for both environments are also presented. Author

N69-24926*# Cornell Univ., Ithaca, N. Y. Dept. of Thermal Engineering.

HYDRODYNAMIC STABILITY OF INVISCID ROTATING COAXIAL JETS

S. Leibovich Washington NASA May 1969 39 p refs

(Grant NGR-33-010-042)

(NASA-CR-1363) Avail: CFSTI CSCL 20D

The inviscid hydrodynamic stability of a swirling coaxial jet to axisymmetric disturbances is investigated when the flow is incompressible but density stratified. The axial and swirl velocity components and the density profiles are all allowed to be arbitrary functions of radius. Flow with a cylindrical vortex sheet is examined. The discontinuity sheet introduces an instability which cannot be stabilized by rotation as in the continuous case. Nevertheless, the presence of rotation reduces the growth rates of disturbances. The case of rapid rotation outside, and no rotation inside, is particularly simple to treat. Author

N69-24935*# National Aeronautics and Space Administration. Marshall Space Flight Center, Huntsville, Ala.

EXPERIMENTAL INVESTIGATION OF BASE FLOW FIELD AT HIGH ALTITUDE FOR A FOUR ENGINE CLUSTERED NOZZLE CONFIGURATION

Edwin B. Brewer and Charles E. Craven (Lockheed Missile and Space Co.) Washington NASA May 1969 100 p refs

(NASA-TN-D-5164) Avail: CFSTI CSCL 20D

Surveys of the base flow were made with static and pitot pressure probes, a constant current anemometer, condenser microphones, and wind vanes. The reverse flow was confined to the proximity of the model centerline and appeared to be an axisymmetric jet decaying from supersonic to subsonic flow. This reverse jet impinged on the center of the heat shield and spread out, forming a wall jet. A slowly circulating separated flow region was present in the base region formed from the viscous pumping of the nozzle jet plumes, the axisymmetric reverse jet, and the base wall jet. The static pressure in the circulating region was very nearly ambient. Hot-wire measurements indicated that the flow of the reverse jet had a relatively low turbulence level. The reverse jet originates from the detached shock portion of the inviscid plume–plume impingement line rather than the oblique shock recompression portion; therefore, the shear layer type of analysis for calculating the reverse flow is not applicable. Author

N69-24958*# Cornell Univ., Ithaca, N. Y.

ON MINIMIZING THE WAKE OF DROPLETS

Franklin K. Moore Washington NASA May 1969 18 p refs

(Grant NGR-33-010-042)

(NASA-CR-1368) Avail: CFSTI CSCL 20D

The inviscid flow inside and outside a moving droplet is analyzed, allowing the shape to be nonspherical subject to surface tension. Specifically, the Weber number-drag relationship is sought which seems to assure the least tendency to form a separated wake. Two conditions of continuous velocity derivatives are imposed at the rear stagnation point for this purpose. The results give reasonable changes of shape (flattening) and reasonable but somewhat too low values of Weber number for minimum wake. Even rather small departures from spherical shape dramatically suppress internal circulation. Author

N69-26504*# National Aeronautics and Space Administration. Langley Research Center, Langley Station, Va.

INVISCID RADIATING SHOCK LAYERS ABOUT SPHERES TRAVELING AT HYPERBOLIC SPEEDS IN AIR

Richard W. Barnwell Washington May 1969 75 p refs

(NASA-TR-R-311) Avail: CFSTI CSCL 20D

Time-dependent finite-difference techniques are used to obtain numerical solutions for the problem of the inviscid flow of radiating equilibrium air past spheres traveling at hyperbolic speeds. The effects of absorption are included, and results are presented for both gray and nongray absorption coefficient models for spheres with different radii. It is shown that the nondimensional heat-flux distributions for the gray and nongray models are similar and that these distributions are weak functions of the radius of the sphere and the altitude and strong functions of the flight velocity. Author

N69-26956*# National Aeronautics and Space Administration. *Ames Research Center, Moffett Field, Calif.*

EXPLORATORY INVESTIGATION ON THE MEASUREMENT OF SKIN FRICTION BY MEANS OF LIQUID CRYSTALS

Enrique J. Klein and Angelo P. Margozzi Washington May 1969 12 p refs

(NASA-TM-X-1774) Avail: CFSTI CSCL 20D

A new method is proposed for directly measuring local skin friction in aerodynamic testing. It makes use of thin coatings of cholesteric liquid crystal mixtures that respond to shearing forces by changes in the wavelength of maximum light scattering. A calibration of shear versus wavelength was obtained for a sample substance; a static calibration was made to measure the effects of temperature, pressure, and angle of viewing; and the behavior of the substance was observed in a pipe-flow experiment. Preliminary results showed that the method appears feasible. Author

N69-26987*# National Aeronautics and Space Administration, Washington, D.C.

COMPRESSED GAS HANDBOOK

John S. Kunkle, ed., Samuel D. Wilson, ed., and Richard A. Cota, ed. 1969 572 p

(NASA-SP-3045) Avail: SOD $4.75; CFSTI CSCL 20D

A complete source of the theory and data required to analyze high pressure compressible flow systems found in space vehicle ground support equipment is provided. The theoretical equations of fluid flow by derivation are developed. Practical problem solving is treated qualitatively. In the section on applications, the theory is presented without the supporting derivations and treats practical problems quantitatively. It is intended as a ready reference for analysis. A feature is the full size working charts for the rapid solution of common compressible flow problems. A selection of basic thermodynamic data for air, nitrogen, oxygen, helium, and hydrogen is appended. The data range is as wide as possible for completeness, and special emphasis is given to data up to 6000 psig, and from +150°F to −100°F. Author

N69-27168*# Israel Program for Scientific Translations, Ltd., Jerusalem.

NONLINEAR PROBLEMS OF COMPRESSIBLE FLOW

A. G. Bagdoev 1969 172 p refs Transl. into ENGLISH of the publ. "Nekotorye Nonlineinye Zadachi o Dvizhenii Szhimaemoi Zhidkosti" Erevan, Izd. AN Arm. SSR, 1967 Published for NASA and NSF *Its* Cat. NO. 5436

(NASA-TT-F-560; TT-69-55023) Copyright. Avail: CFSTI CSCL 20D

The motion of a half-space of ideal compressible fluid due to an arbitrary pressure front moving over its surface is considered. Physically, such a situation arises in an explosion on or above the surface of a fluid. Since a liquid is a considerably denser medium than air, the pressure in the air may be considered as in the reflection of a shock wave from a rigid wall. Consequently, the pressure at the liquid surface will be known as a function of the time and coordinates. The problem consists in finding a solution of the gas dynamic equations for given discontinuity conditions at the boundary. For a liquid under pressures of the order of several hundreds of atmospheres, the parameter determining the liquid motion will be small, and a linear theory can be used. The linear theory, however, gives an incorrect picture in the vicinity of the sound wave, as well as near the free surface and at large time. It is also worthwhile to calculate approximations higher than the first. Here the problem is formulated nonlinearly for the pressure, a small parameter is introduced and an isentropic approximation used. It is shown that the linear theory can be greatly improved by using only the linear solution. Various methods of improving the linear solution are studied, and the pressure is determined in the second approximation. Author

N69-27954*# National Aeronautics and Space Administration. Lewis Research Center, Cleveland, Ohio.

THE LIQUID-VAPOR INTERFACE DURING OUTFLOW IN WEIGHTLESSNESS

Steven G. Berenyi and Kalell L. Abdalla Washington Jun. 1969 23 p refs

(NASA-TM-X-1811) Avail: CFSTI CSCL 20D

An experimental program was conducted to determine the effect of outflow from a tank on the behavior of the liquid-vapor interface in weightlessness. A previously determined correlation was extended to larger tank models in a high Weber number flow region. The tests were conducted with two separate tank shapes and two test liquids, and at various initial fillings. Author

N69-29144*# National Aeronautics and Space Administration. Ames Research Center, Moffett Field, Calif.

SUMMARY AND CORRELATION OF SKIN-FRICTION AND HEAT-TRANSFER DATA FOR A HYPERSONIC TURBULENT BOUNDARY LAYER ON SIMPLE SHAPES

Edward J. Hopkins, Morris W. Rubesin, Mamoru Inouye, Earl R. Keener, George C. Mateer et al Thomas E. Polek Washington Jun. 1969 29 p refs

(NASA-TN-D-5089) Avail: CFSTI CSCL 01A

Local skin-friction and heat-transfer data were directly measured in air for turbulent boundary layers on flat plates, cones, and a wind-tunnel wall. The Mach number at the edge of the boundary layer ranged between 5 and 7.4 and the wall to adiabatic wall temperature ratio varied bwtween 0.1 and 0.6. The skin-friction and heat-transfer data are compared with other data obtained by direct measurement of surface shear with balances and accompanied by boundary layer surveys. The use of momentum thickness Reynolds number in the skin-friction comparison avoids arbitrary location of the virtual origin of the turbulent boundary layer. Adiabatic and cold wall data are employed to assess four theories for predicting turbulent skin friction. Analysis of the skin-friction data indicates that the theory of Van Driest II or Coles gives the best predictions for wall to adiabatic wall temperature ratios above 0.3. At wall to adiabatic wall temperature ratios below 0.3, none of the theories give the proper trend with wall to adiabatic wall temperature ratio. The heat-transfer analysis for nonadiabatic conditions generally substantiates the skin-friction analysis. Author

N69-29235*# Techtran Corp., Glen Burnie, Md.

HIGH-VELOCITY HYDRODYNAMICS, NO. 4

I. L. Rozovskiy, ed. Washington NASA Jun. 1969 165 p refs Transl. into ENGLISH of the publ. "Gidrodinamika Bolshikh Skorostey" Kiev, Naukova Dumka Press, 1968

(Contract NASw-1695)

(NASA-TT-F-577) Avail: CFSTI CSCL 12A

The problem of complete approximation in some region of the Euclidian space of a new boundary value problem is discussed. The criteria for a uniform approximation are satisfied by allowing freedom in the selection of the mapping of the Euclidian space into the new space as well as in the choice of the new differential operator, the boundaries of the region and the boundary conditions. The complete approximation in the new space yields a linear problem which leads to satisfactory results in physical space for sufficiently large perturbation parameters. The Poincare–Lighthill–Go method is an example of a procedure based on the idea of complete approximation. Problems in hydrodynamics which may be solved by this method are examined. Author

N69-29608*# National Aeronautics and Space Administration. Langley Research Center, Langley Station, Va.

HEAT TRANSFER TO THE WINDWARD SIDE OF A FINENESS-RATIO-2.9 CYLINDER WITH NEARLY SPHERICAL

ENDS AT A MACH NUMBER OF 6 AND ANGLES OF ATTACK OF 50°, 70°, AND 90°

James L. Hunt Washington Jul. 1969 45 p refs
(NASA-TN-D-5251) Avail: CFSTI CSCL 20D

An investigation was conducted in the Langley 20-inch Mach 6 tunnel to define the heat transfer to a fineness-ratio-2.9 cylinder with nearly spherical ends. Heat transfer data and schlieren photographs were obtained at a nominal Reynolds number, based on model diameter, of 1×10^6 at sweep angles of 0°, 20°, and 40°. Beckwith's laminar swept infinite-cylinder theory, small-cross-flow theory, and local similarity theory with Libby's three-dimensional stagnation-point theory were used piecewise to predict the laminar heat transfer with acceptable accuracy. Local flat-plate approximations for turbulent heat transfer, calculated by the method of Spalding and Chi, agreed with the data obtained in the turbulent flow regions. Author

N69-30071*# National Aeronautics and Space Administration. Langley Research Center, Langley Station, Va.

FLOW-FIELD MEASUREMENTS DOWNSTREAM OF TWO PROTUBERANCES ON A FLAT PLATE SUBMERGED IN A TURBULENT BOUNDARY LAYER AT MACH 2.49 AND 4.44

Lana M. Couch Washington Jul. 1969 136 p refs
(NASA-TN-D-5297) Avail: CFSTI CSCL 20D

Pilot pressure, static pressure, and total temperature distributions were obtained on a flat plate and on the portion of a flat plate downstream of a plate-mounted cylinder and of a plate-mounted fairing at free-stream Mach numbers of 2.49 and 4.44. Velocity gradients adjacent to the plate surface downstream of both models were greater than those obtained on the plate surface and indicate higher shearing stress and heat transfer to the plate surface within the model wakes. The extent of mixing downstream of both models, as indicated by velocity profiles, decreased with increasing Mach number. Increasing the unit Reynolds number by a factor of 2 had only a negligible effect on the profiles obtained on the flat plate. Flow patterns on the plate surface (as shown by oil-flow photographs) downstream of both models indicated some regions of similarity. Author

N69-30728*# IIT Research Inst., Chicago, Ill.

TURBULENCE IN THE MIXING REGION BETWEEN DUCTED COAXIAL STREAMS

J. J. Leithem, R. A. Kulik, and H. Weinstein Washington NASA Jul. 1969 48 p refs
(Grant NsG-694SC)
(NASA-CR-1335) Avail: CFSTI CSCL 20D

An experimental investigation of both homogeneous and heterogeneous compound ducted jets is presented for axially symmetric coflowing streams. The flow system considered in one of a circular 3 inch inner stream issuing into a circular 6 inch, faster moving, outer stream. Air was used for the outer stream gas and both air and Freon-12 were used for the inner jet. This gave density ratios of 1 and 4, inner to outer stream, respectively. The velocity ratio was varied from 4.19 to 30.0 for both cases with absolute velocities of 1.5 to 40 ft/sec. All data were taken with a constant temperature hot wire anemometer system. Average velocity, radial and axial turbulence intensity profiles both near and far downstream are presented for the homogeneous cases. Average velocity, density and axial turbulence intensity profiles as well as mass holdup data both near and far downstream are presented for the heterogeneous cases. The ratio of axial to radial turbulence intensity was about 1.5, the same as found for unconfined coaxial flow. For the higher density ratio cases, the inner stream integrity was maintained better than for the homogeneous cases. The flow system was found to be one of combined wake-coaxial flow with possible backflow. Author

N69-31359*# National Aeronautics and Space Administration. Langley Research Center, Langley Station, Va.

DRAG REDUCTION DUE TO GAS INJECTION THROUGH VARIOUS DISCRETE SLOTS ON A THREE-DIMENSIONAL WING AT MACH 2.01

Russell B. Sorrells, III, K. R. Czarnecki, and Lorraine F. Satchell Washington Jul. 1969 45 p refs
(NASA-TN-D-5307) Avail: CFSTI CSCL 20D

Force measurements were made of the drag reduction due to the injection of gas into a turbulent boundary layer through discrete slots of various sizes and configurations on a three-dimensional semispan wing at a Mach number of 2.01. Air, helium, and Freon were injected, transition was fixed, and the tests were conducted at Reynolds numbers, based on the mean geometric chord, ranging up to 4.48×10^6. The theoretically estimated and measured skin-friction reductions are compared. It was found that for the supersonic transport and for the slot drags incurred in this investigation, engine bleed air does not provide sufficient mass flow to warrant the use of air injection for drag reduction over an entire wing span. However, if the engine bleed air is injected only over the nacelles, it appears possible at Mach 2.0 to achieve a drag reduction equivalent to from 9 to 35 percent of the nacelle skin friction, the percentage depending on the amount of bleed plenum pressure energy that is used for thrust. Greater drag reductions were obtained by injecting helium into the boundary layer than by injecting air or Freon. In the design of an ejection system, the slot drag and the available thrust rather than the skin-friction reduction should be optimized, and the possible lift interference effects of an injected gas should be considered in selecting the location of an ejection slot or nozzle. Author

N69-31887*# Applied Physics Lab., Johns Hopkins Univ., Silver Spring, Md.

UNIFIED ANALYSIS OF TURBULENT JET MIXING

Joseph A. Schetz Washington NASA Jul. 1969 32 p refs
Prepared jointly with Md. Univ., College Park
(NASA Order R-76; Contract NOw-62-0604-c) Avail: CFSTI CSCL 20D

A unified model for the eddy viscosity in jet mixing flows is presented. The successful boundary layer model due to Clauser is given a new interpretation that permits generalization to a wide variety of turbulent flows. The specific functional expression for a given flow problem is derived. Comparisons of experimental results and calculations using the unified model as well as models previously suggested are presented. The cases considered include planar and axi-symmetric flows, varying temperature, foreign gas injection, both subsonic and supersonic external flow, and a range of the mass flow parameter, $\rho_j u_j / \rho_e u_e$, from 0.04 to 4.0. The unified model provided results in better agreement with the data over this range of conditions than those for any previously suggested model. Author

N69-31888*# National Aeronautics and Space Administration. Lewis Research Center, Cleveland, Ohio.

SUMMARY OF RECENT GASEOUS REACTOR FLUID MECHANICS EXPERIMENTS

Robert G. Ragsdale and Chester D. Lanzo Washington Aug. 1969 16 p refs
(NASA-TM-X-1847) Avail: CFSTI CSCL 20D

Three recent gaseous-nuclear rocket related fluid mechanics experiments have shown ways of reducing the mixing of two coflowing streams. In a rocket engine, such a reduction would mean less uranium loss or a lower pressure reactor. Two of the experiments were conducted with room temperature gases. The third experiment used induction heating to simulate fission heating. In these experiments, no major flow recirculation and mixing was observed, as contrasted with previous studies. Author

N69-32217*# National Aeronautics and Space Administration. Lewis Research Center, Cleveland, Ohio.
A FLOW EXPERIMENT ON A CURVED-POROUS-WALL GAS-CORE REACTOR GEOMETRY
Chester D. Lanzo Washington Aug. 1969 14 p refs
(NASA-TM-X-1852) Avail: CFSTI CSCL 20B

An air-air fluid flow experiment was conducted to determine the merit of a curved, porous wall gas-core reactor concept. Photographs of the flow are shown, and fuel concentration profiles are presented. The fuel volume fraction varied from 0.51 to 0.28 as the propellant -to-fuel mass flow ration was increased from 25 up to 100. The concept looks useful and merits further research. Author

N69-32377*# National Aeronautics and Space Administration. Lewis Research Center, Cleveland, Ohio.
STABILITY OF TWO-FLUID WHEEL FLOWS WITH AN IMPOSED UNIFORM AXIAL MAGNETIC FIELD
Carl F. Monnin and John J. Reinmann Washington Aug. 1969 51 p refs
(NASA-TN-D-5372) Avail: CFSTI CSCL 20D

The stability of an incompressible two-fluid wheel flow to infinitesimal helical disturbances is studied. The inner fluid is heavy and has infinite electrical conductivity, while the outer fluid is light and is nonconducting. An axial magnetic field is externally imposed on both fluids. This configuration may be viewed as a Rayleigh-Taylor problem in the frame of the rotating fluid and is dynamically unstable. Growth rates increase with increasing axial wavelength and azimuthal mode numbers, but decrease with increasing axial magnetic field. By increasing the magnetic field sufficiently, the system can be made stable to short axial wavelength disturbances for any azimuthal mode. Author

N69-32480*# Applied Physics Lab., Johns Hopkins Univ., Silver Spring, Md.
THE INTERACTION AND PENETRATION OF GASEOUS JETS IN SUPERSONIC FLOW
R. C. Orth, J. A. Schetz, and F. S. Billig Washington NASA Jul. 1969 46 p refs
(NASA Order R-76; Contract NOw-62-0604-c)
(NASA-CR-1386) Avail: CFSTI CSCL 20D

Experiments and analysis of the penetration of a gaseous jet from a discrete orifice into a supersonic stream, and the associated interaction with the external flow, are discussed. Included in the interaction is the definition of the shape of the stand-off shock in the main flow. A governing parameter in this analysis is the degree of underexpansion of the jet which has been shown to be directly related to the ratio of jet static pressure to the pressure downstream of a strong disturbance in the main stream. For underexpanded jets the location of the Mach disk which is paramount to the definition of the penetration has been explicitly given. For matched pressure injection or for the region of flow downstream of the Mach disk, a solid body drag model has been revised and extended to describe the penetration into a supersonic stream. The study encompassed the effects of free stream Mach number, hole size and shape and the molecular weight, Mach number, and pressure of the injectant. An exemplary case of the design of the injectors for a typical supersonic combustor is given. Author

N69-33261*# National Aeronautics and Space Administration. Lewis Research Center, Cleveland, Ohio.
CAVITATION PERFORMANCE OF LINE-MOUNTED 80.6 DEG HELICAL INDUCER IN HYDROGEN
Royce D. Moore and Phillip R. Meng Washington Aug. 1969 20 p refs
(NASA-TM-X-1854) Avail: CFSTI CSCL 20D

The noncavitating and cavitating performance of a line-mounted 80.6° helical inducer was determined in hydrogen over a liquid temperature range of 34.1° to 42.2° R (18.9 to 23.4 K) and a flow coefficient range of 0.08 to 0.12 at rotative speeds of 25,000 and 30,000 rpm. The tank pressure requirement for this line-mounted inducer was compared with that for the same inducer closely coupled to the tank. The tank pressure requirement was determined to be greater for the line-mounted inducer. Inducer net positive suction head requirement increased with increasing flow coefficient and rotative speed and decreased with increasing temperature. Noncavitating head-rise coefficient, which decreased with increasing flow coefficient, was unaffected by temperature and rotative speed. Author

N69-33353*# National Aeronautics and Space Administration. Lewis Research Center, Cleveland, Ohio.
EXPERIMENTAL AND THEORETICAL TURBULENT BOUNDARY LAYER DEVELOPMENT IN A MACH 4.4 WATER-COOLED CONICAL NOZZLE
Donald R. Boldman, James F. Schmidt, and Robert C. Ehlers Washington Aug. 1969 43 p refs
(NASA-TN-D-5377) Avail: CFSTI CSCL 20D

Boundary layer temperature and velocity measurements were obtained at three stations in the supersonic portion of a 30°-50° C-D cooled nozzle operating with an adiabatic and a cooled inlet. Tests were performed with heated air at nominal Mach numbers 2.1 to 4.4. The ratio of wall-to-stagnation temperature was 0.8 at Mach 2.1 and 0.6 at Mach 4.4. The results indicated that the thermal boundary layer in supersonic flow was not described by a 1/7 power law. The experimental momentum and displacement thicknesses compared favorably to predictions based on the integral boundary layer theories. Author

N69-33421*# National Aeronautics and Space Administration. Ames Research Center, Moffett Field, Calif.
LINEARIZED THEORY OF STAGNATION POINT HEAT AND MASS TRANSFER AT HYPERSONIC SPEEDS
Kenneth K. Yoshikawa Washington Aug. 1969 35 p refs
(NASA-TN-D-5246) Avail: CFSTI CSCL 20D

An explicit closed-form solution has been obtained for the compressible, viscous shock-layer energy equation with mass addition or suction. The solution is applicable at very high speeds, when the interactions between the heated gas behind the shock wave and the layer of injected or ablated gases from the surface must be considered as well as the effect of heat conduction across the shock layer. The solution consists of the energy equation decoupled from the other conservation equations and then linearized by the introduction of constant values for the thermal and transport properties. Results of using the solution show explicitly that the effect of gas injection on convective heat transfer depends on the Stanton number without mass addition and on the relative molecular weights, and thermal and transport properties of the free-stream and injected gases. The solution is substantiated by comparisons with more exact solutions. Author

N69-34709*# Cornell Aeronautical Lab., Inc., Buffalo, N.Y.
NONEQUILIBRIUM GASDYNAMICS
William S. Watt Washington NASA Aug. 1969 39 p refs
(Contract NASr-109)
(NASA-CR-1411; CAL-AD-1689-A-10) Avail: CFSTI CSCL 20D

Theoretical and experimental studies of nonequilibrium phenomena pertinent to propulsion are reported. In particular, the emphasis was directed toward obtaining a better understanding of the chemistry, fluid mechanics and the coupling of these in hydrogen propulsion systems. Research has been concentrated in three areas: (1) development of a computer program for the numerical solution of nonequilibrium expansions of reacting gas mixtures and its application to recombination in rocket nozzles; (2) experimental studies of nonequilibrium phenomena in nozzle expansion flows;

and (3) experimental studies of dissociation kinetics behind shock waves. While this research program was initially concerned with dissociation and recombination in hydrogen and the effect of catalytic additives on these phenomena, the techniques developed have been extended to investigate other nonequilibrium systems of interest in the propulsion and aerospace fields. Author

N69-35365*# Israel Program for Scientific Translations, Ltd., Jerusalem.

HIGH-TEMPERATURE PROPERTIES OF GASES. PHYSICAL GAS DYNAMICS, THERMODYNAMICS, AND PHYSICS OF COMBUSTION

A. S. Predvoditelev, ed. 1969 214 p refs Transl. into ENGLISH of the Book "Svoistva Gazov Pri Vysokikh Temperaturakh: Fizicheskaya Gazodinamika, Termodinamika i Fizika Goreniya" Moskva, Izd. Nauka, 1967

(NASA-TT-F-558) Copyright. Avail: CFSTI CSCL 20D

Theoretical and experimental studies of gas flow properties at high tempratures, their thermodynamic functions and physicochemical processes are presented. Experimental results regarding the ionization and dissociation of gases and the properties of ionized gases in magnetic fields are included. For individual titles, see N69-35365 through N69-35395.

N69-35842*# National Aeronautics and Space Administration. Lewis Research Center, Cleveland, Ohio.

NATURAL FREQUENCY OF LIQUIDS IN ANNULAR CYLINDERS UNDER LOW GRAVITATIONAL CONDITIONS

Thomas L. Labus Washington Sep. 1969 30 p refs

(NASA-TN-D-5412) Avail: CFSTI CSCL 20D

As a part of the general study of liquid behavior in a low gravity environment, an experimental investigation was conducted to determine the natural frequency of liquid sloshing in annular cylinders. Static contact angles were restricted to near zero degrees. The experiments were conducted over a range of gravitational conditions, including normal gravity, such that the bond numbers ranged from approximately 200. The natural frequency for deep liquid depths was empirically correlated with known system parameters as a function of the Bond number. Author

N69-36805*# National Aeronautics and Space Administration. Langley Research Center, Langley Station, Va.

COMPARISON OF PREDICTION METHODS AND STUDIES OF RELAXATION IN HYPERSONIC TURBULENT NOZZLE-WALL BOUNDARY LAYERS

Dennis M. Bushnell, Charles B. Johnson, William D. Harvey, and William V. Feller Washington Sep. 1969 35 p refs

(NASA-TN-D-5433) Avail: CFSTI CSCL 20D

Recent turbulent boundary-layer measurements on axisymmetric nozzle walls at Mach numbers of 6, 8, and 19 are presented and compared with the predictions of two theoretical methods. One of the methods was of the integral type; the other was a finite-difference solution to the governing differential equations. The integral method gave good predictions of the data at Mach 6 and 8 and a reasonable prediction at Mach 19. Results for the finite-difference approach were available only at Mach 8, for which good agreement with data was obtained. A survey of boundary-layer data indicates that the variation of total temperature with velocity for flat-plate type of flows can be represented within the scatter of the data by the linear Crocco relation, whereas for nozzle-wall flows, this relation is generally more nearly quadratic. A finite-difference solution for the Mach 8 nozzle-wall boundary layer resulted in a quadratic-type temperature-velocity relation in the strong favorable pressure-gradient region downstream of the throat. However, near the nozzle exit the theoretical solution tended to approach the linear variation of Crocco. Apparently, the observed quadratic variation in nozzle boundary layers can be at least partly accounted for by the pressure-gradient history of the flow. Author

N69-36830*# National Aeronautics and Space Administration. Langley Research Center, Langley Station, Va.

A MODIFIED METHOD OF INTEGRAL RELATIONS APPROACH TO THE BLUNT-BODY EQUILIBRIUM AIR FLOW FIELD, INCLUDING COMPARISONS WITH INVERSE SOLUTIONS

L. Bernard Garrett, John T. Suttles, and John N. Perkins (N. C. State Univ.) Washington Sep. 1969 94 p refs

(NASA-TN-D-5434) Avail: CFSTI CSCL 01A

A modified approach to the first order approximation of the method of integral relations is presented for the numerical calculation of the inviscid, adiabatic flow field around a blunt nose body traveling at hypersonic speeds. Solutions have been obtained and computed flow field data are presented for the adiabatic steady flow of a perfect gas and air in chemical equilibrium. The results obtained by the present method of solution are compared with results obtained by using inverse methods, property derivative integral relations methods, and experiment. The results indicate that the present method provides an accurate, versatile solution of the blunt body flow field, and the relative simplicity of the method should allow extension to coupled radiating flow field analyses. Author

N69-36940*# National Aeronautics and Space Administration. Ames Research Center, Moffett Field, Calif.

POWER- AND CROSS-SPECTRA AND SPACE-TIME CORRELATIONS OF SURFACE FLUCTUATING PRESSURES AT MACH NUMBERS BETWEEN 1.6 and 2.5

Wei J. Chyu and Richard D. Hanly Sep. 1969 21 p refs

(NASA-TN-D-5440) Avail: CFSTI CSCL 20D

The statistical properties of pressure fluctuations that were measured on surfaces adjacent to attached and separated turbulent boundary layers developed on an ogive cylinder and on the cylinder ahead of a 45° cone frustum were studied. Power- and cross-spectra, space-time correlations, convection velocities embracing both broad and narrow frequency bands, and coherence of the pressure field are presented. The pressure field under the attached boundary layer exhibits properties similar to those at subsonic speeds. Correlations and coherence functions showed a strong dependence on Mach number. Convection velocities are nearly constant with frequency in attached flow, but they vary greatly with frequency in separated flow. Coherence functions are significantly lower in separated flow than under attached boundary layers. Under both attached and separated boundary layers the phase-shift relationship of cospectra and quadspectra is a function of wave number $f\xi_1/U_c(f)$, where f, ξ_1, and U_c represent frequency, spatial distance, and convection velocity, respectively. Author

N69-37271*# National Aeronautics and Space Administration. Lewis Research Center, Cleveland, Ohio.

EFFECT OF ANGLE OF ATTACK AND INJECTION PRESSURE ON JET PENETRATION AND SPREADING FROM A DELTA WING IN SUPERSONIC FLOW

Frederick P. Povinelli, Louis A. Povinelli, and Martin Hersch Washington Sep. 1969 23 p refs

(NASA-TM-X-1889) Avail: CFSTI CSCL 20D

Helium injection into the vortex flow generated over the lee side of a half-delta model was studied in a Mach 2 airstream. Concentration contours were obtained at two positions downstream of the injection orifice. Angle of attack and injection pressure were varied. Oil-streak photographic data were used to determine the location of the vortex on the delta surface. Penetration and spreading of the injectant were enhanced with increasing angle of attack. Increasing injection pressure increased the penetration but had little effect on spreading. Maximum penetration occurred at the highest angle of attack and injection pressure tested. Author

N69-37370*# National Aeronautics and Space Administration. Ames Research Center, Moffett Field, Calif.

UPWASH PATTERNS ON ABLATING AND NONABLATING CONES OF HYPERSONIC SPEEDS

John B. McDevitt and Jack A. Mellenthim Washington Jul. 1969 34 p refs

(NASA-TN-D-5346) Avail: CFSTI CSCL 20D

A study has been made of the upwash patterns on slender ablating and nonablating cones at angle of attack in the hypersonic flow regime. An oil-film technique was used to display the surface streamlines on the nonablating models and tests were conducted with both laminar and transitional boundary layers. The boundary-layer-edge Mach number and model wall temperature were found to have a strong influence on the magnitude of surface upwash angles. The measured surface upwash angles at small angles of attack agreed well with theoretical estimates in the laminar case. At transitional Reynolds numbers clear evidence was obtained that streamwise vortices are entrained within the boundary layer for cones at angle of attack. Tests of ablating cones at transitional Reynolds numbers resulted in upwash groove patterns eroded in the model surfaces. These grooves were interpreted to be the result of vortices intensifying local heating rates. The upward inclination of the grooves agreed closely with the inclination of the vortex paths measured on the nonablating cones under similar test conditions. Author

N69-37604*# National Aeronautics and Space Administration. Ames Research Center, Moffett Field, Calif.

EFFECTS OF ANGLE OF ATTACK AND BLUNTNESS ON LAMINAR HEATING-RATE DISTRIBUTIONS OF A 15 DEG CONE AT A MACH NUMBER OF 10.6

Joseph W. Cleary Washington Oct. 1969 56 p refs

(NASA-TN-D-5450) Avail: CFSTI CSCL 20D

Distributions of laminar heating rates are presented from wind-tunnel tests in air at a free-stream Mach number of 10.6 and unit Reynolds numbers from 0.4×10^6 to 1.8×10^6 per foot. Results shown are for angles of attack from 0° to 20° and bluntness ratios from 0 to 0.183. Measurements are included of surface streamlines made by an oil-streak technique. Heating-rate measurements are compared with predictions of similarity theory for $0 \leq \alpha \leq 20°$ and good agreement is indicated. Author

N69-37965*# National Aeronautics and Space Administration. Lewis Research Center, Cleveland, Ohio.

INJECTION OF AN INVISCID SEPARATED JET AT AN OBLIQUE ANGLE TO A MOVING STREAM

Marvin E. Goldstein and Willis Braun Washington Oct. 1969 72 p refs

(NASA-TN-D-5460) Avail: CFSTI CSCL 20D

An analytical solution has been obtained to the problem of a two-dimensional incompressible jet injected into a moving stream from an orifice set at an oblique angle to the stream. It is assumed that the jet separates from the downstream edge of the orifice. The solution is valid when the normalized difference between the total pressure in the jet and the total pressure in the main stream is not too large. Typical flow patterns are shown to illustrate the effects of varying both the jet offset ratio and the total pressure within the jet. Author

N69-38012*# National Aeronautics and Space Administration. Lewis Research Center, Cleveland, Ohio.

DISCHARGE COEFFICIENTS FOR THICK PLATE ORIFICES WITH APPROACH FLOW PERPENDICULAR AND INCLINED TO THE ORIFICE AXIS

John E. Rohde, Hadley T. Richards, and George W. Metger Washington Oct. 1969 30 p refs

(NASA-TN-D-5467) Avail: CFSTI CSCL 20D

Experimental discharge coefficients were obtained for thick plate orifices with the approaching flow perpendicular or inclined to the orifice axis. Parameters investigated were temperature and pressure levels; orifice pressure differential; approach Mach number; orifice diameter, thickness, and inlet edge condition; orifice surface finish; interference of multiple orifices; and approach passage geometry and length. The discharge coefficients were found to be dependent on approach Mach number, static pressure differential across the orifice, inlet edge radius on the orifice, angle between the main flow and the axis of the orifice, and the ratio of the orifice thickness to diameter. Author

N69-38032*# National Aeronautics and Space Administration. Lewis Research Center, Cleveland, Ohio.

MOTION OF SINGLE BUBBLES UNDER LOW GRAVITATIONAL CONDITIONS

John B. Haggard, Jr., and William J. Masica Washington Oct. 1969 32 p refs

(NASA-TN-D-5462) Avail: CFSTI CSCL 20D

An experimental study was undertaken to examine single, noncondensable bubble motion under low-gravity conditions. These data were compared with normal-gravity theory and empirical results. The M number (a characteristic dimensionless parameter containing gravity and the liquid properties) was found to be a significant parameter in correlating normal- and low-gravity data. This report, together with normal-gravity theory, predicts bubble shape and terminal velocity when the liquid properties, the bubble volume, and the applied gravity field are known. The results are applicable to a range of spherical and ellipsoidal bubbles with Reynolds numbers above 50. Author

N69-38156*# National Aeronautics and Space Administration. Langley Research Center, Langley Station, Va.

FLOW-FIELD AND DRAG CHARACTERISTICS OF SEVERAL BOUNDARY-LAYER TRIPPING ELEMENTS IN HYPERSONIC FLOW

Allen H. Whitehead, Jr. Washington Oct. 1969 40 p refs

(NASA-TN-D-5454) Avail: CFSTI CSCL 20D

Flow field and drag characteristics of several tripping-element shapes were examined under laminar boundary layer conditions at a free-stream Mach number of 6.8 to assess the contribution of the elements to the drag of wind tunnel models and to examine flow field characteristics around individual element shapes. The element drag coefficient based on local conditions depends primarily on element shape, the spacing between the elements, and the ratio of the element height to boundary layer height. Advantageously, certain element shapes have drag coefficients which are relatively independent of the ratio of element height to boundary layer height for values of this ratio that have practical application for hypersonic wind tunnel facilities. Author

N69-38782*# Applied Theory, Santa Monica, Calif.

NUMERICAL CALCULATION OF VISCOUS COMPRESSIBLE FLUID FLOW AROUND AN OSCILLATING RIGID CYLINDER

John G. Trulio and Leonard Walitt Washington NASA Oct. 1969 77 p refs

(Contract NAS8-18034)

(NASA-CR-1467) Avail: CFSTI CSCL 20D

A numerical investigation was conducted of viscous, compressible flow about a circular cylinder executing harmonic motion normal to the free stream flow direction. The oscillatory motion of the cylinder led to vortex shedding, and to a Karman vortex street. Calculations were made at a Mach number of .20, Reynolds numbers of 100 and 1000, a constant cylinder oscillation amplitude equal to 10% of the cylinder radius, and a range of cylinder oscillation frequencies. The variation with oscillation

frequency of the time-averaged-drag coefficient, root-mean-squared lift coefficient, and shedding frequency, are presented. In general, increasing the cylinder oscillation frequency decreased the time-averaged drag coefficient, increased the root-mean-squared lift coefficient, and had very little effect on the shedding frequency. Author

N69-39177*# National Aeronautics and Space Administration. Ames Research Center, Moffett Field, Calif.

A METHOD OF CHARACTERISTICS FOR STEADY THREE-DIMENSIONAL SUPERSONIC FLOW WITH APPLICATION TO INCLINED BODIES OF REVOLUTION

John V. Rakich Washington Oct. 1969 61 p refs
(NASA-TN-D-5341) Avail: CFSTI CSCL 20D

Characteristics theory for three-dimensional compressible flow is reviewed and the compatibility equations are derived in terms of pressure and stream angles as dependent variables. The relative merits of bicharacteristic and reference plane methods are discussed. A reference plane method is described which employs a uniformly spaced finite difference mesh between the body and shock surfaces. Numerical procedures for differentiation and interpolation ensure second-order accuracy in terms of mesh spacing. Results for the flow around inclined, circular cones, both blunted and pointed, are presented to demonstrate the method described. Predictions of surface and pitot pressures are in good agreement with available experimental results for a 15° sphere-cone at 10° angle of attack. Bluntness effects on shock-layer properties far from the nose are reasonably well predicted. Author

N69-39303*# National Aeronautics and Space Administration. Lewis Research Center, Cleveland, Ohio.

A PHOTOGRAPHIC STUDY OF A BROMINE JET IN A COAXIAL AIRSTREAM WITH HONEYCOMBS AT THE INJECTION PLANE

Charles C. Masser Washington Oct. 1969 25 p refs
(NASA-TM-X-1900; E-5190) Avail: CFSTI CSCL 20D

A photographic study was made of a bromine jet issuing into a coaxially flowing airstream. Honeycomb sections were placed into either or both the airstream and the bromine jet. The objective was to determine if the amount of bromine in the near jet region can be increased by the presence of a honeycomb at the jet injection plane. It was found there was no increase of bromine in the near jet region by the presence of honeycomb sections in either or both the bromine tube or airstream at the jet injection plane. However, the presence of honeycomb sections influences the transition from laminar to nonlaminar appearing jets. Author

N69-39916*# National Aeronautics and Space Administration. Lewis Research Center, Cleveland, Ohio.

INJECTION OF AN ATTACHED INVISCID JET AT AN OBLIQUE ANGLE TO A MOVING STREAM

Marvin E. Goldstein and Willis Braun Washington Oct. 1969 41 p refs
(NASA-TN-D-5501; E-5106) Avail: CFSTI CSCL 20D

An analytical solution was obtained to the problem of a two-dimensional inviscid, incompressible jet injected into a moving stream from an orifice set at an oblique angle to the stream for the case where the jet does not separate from the downstream edge of the orifice. The solution is valid when the difference between the total pressure in the jet and the total pressure in the main stream is not too large. Typical flow patterns are presented to illustrate the effects of varying both the orifice angle and the total pressure within the jet. Author

N69-40137*# National Aeronautics and Space Administration. Langley Research Center, Langley Station, Va.

FLUCTUATING PROPERTIES OF TURBULENT BOUNDARY LAYERS FOR MACH NUMBERS UP TO 9

William D. Harvey, Dennis M. Bushnell, and Ivan E. Beckwith Washington Oct. 1969 51 p refs
(NASA-TN-D-5496) Avail: CFSTI CSCL 20D

Estimates of the variation in intensity of the longitudinal velocity fluctuations across hypersonic turbulent boundary layers at Mach numbers from 8.2 to 8.9 were made. These estimates were based on experimental measurements of fluctuating density and pitot pressure in the nozzle-wall boundary layer of a shock tunnel. Also, it is shown that reasonable estimates of the root-mean-square values of the fluctuating velocity, density, and temperature for Mach numbers from 1.72 to 8.9 can be made by using a mixing-length approach. Comparison with previous experimental data indicate that the intensity of these fluctuating quantities, expressed in terms of suitable normalizing parameters, may be essentially independent of Mach number up to about Mach 9. Author

N69-40200*# Nielsen Engineering and Research, Inc., Palo Alto, Calif.

THEORETICAL STUDY OF VORTEX SHEDDING FROM BODIES OF REVOLUTION UNDERGOING CONING MOTION

Gary D. Kuhn, Selden B. Spangler, and Jack N. Nielsen Washington NASA Oct. 1969 61 p refs
(Contract NAS2-4765)
(NASA-CR-1448; NEAR-TR-14) Avail: CFSTI CSCL 20D

Based on experimental evidence of the existence of a steady asymmetric vortex system on a slender body in coning motion, a theoretical flow model for vortex shedding was developed using potential flow methods and slender-body theory. The model provides for the calculation of the strength and position of each of the two vortices representing the areas of concentrated vorticity in the crossflow plane and the resulting force distribution induced on the body. Initial vortex locations very close to the body must be prescribed to start the computation. The flow model developed is felt to describe reasonably accurately the nature of the vortex-like separated flow over the body and the vortex-induced force distribution. Author

N69-40824*# National Aeronautics and Space Administration, Washington, D.C.

SHOCK WAVES IN REAL GASES

T. V. Bazhenova et al Oct. 1969 187 p refs Transl. into ENGLISH of the book "Udarnyye Volny v Realnykh Gazakh" Moscow, Nauka Press, 1968 p 15–195
(NASA-TT-F-585) Avail: CFSTI CSCL 20D

The propagation of strong shock waves are considered in terms of the real properties of the gas media, since the temperature increase behind the shock wave produces excitation and ionization. Visualization and photographic techniques for studying shock wave propagation in shock tubes are described. Gas dynamic flow variables, and the reflection of shock waves in various gases are discussed. Results of the study are tabulated. F.O.S.

N69-41213*# National Aeronautics and Space Administration. Lewis Research Center, Cleveland, Ohio.

ANALYSIS OF THE MIXING REGION FOR A TWO-DIMENSIONAL JET INJECTED AT AN ANGLE TO A MOVING STREAM

Willis Braun and Marvin E. Goldstein Washington Nov. 1969 25 p refs
(NASA-TN-D-5531; E-5163) Avail: CFSTI CSCL 20D

An analysis was made of the laminar and turbulent mixing of a two-dimensional jet issuing from an orifice whose two walls are parallel to the free-stream velocity but not necessarily coplanar with each other. The difference of total pressure between the jet and the stream is assumed small compared with the dynamic pressure of the stream. The results of previous inviscid analyses are used to obtain the velocity profiles in the mixing region and the thickness of the region for jets which are separated from the

downstream wall and for those which are attached. Results show that, when the orifice walls are coplanar, the attached jet has higher velocities than the separated jet as it turns into the stream; therefore, the attached jet has a thinner mixing region. Author

13

GEOPHYSICS

Includes aeronomy; upper and lower atmosphere studies; oceanography; cartography; and geodesy. For related information see also: 20 Meteorology; 29 Space Radiation; and 30 Space Sciences.

A69-10491 *#
SPACECRAFT OCEANOGRAPHY - ITS SCIENTIFIC AND ECONOMIC IMPLICATIONS FOR THE NEXT DECADE.
John W. Sherman (NASA; U.S. Naval Oceanographic Office, Washington, D.C.) and Leroy Cheney (General Electric Co., Philadelphia, Pa.).
United Nations, Conference on the Exploration and Peaceful Uses of Outer Space, Vienna, Austria, Aug. 14-27, 1968, Paper 68-95878. 25 p. 7 refs.

Discussion of some of the contributions that spacecraft oceanography can make to man's increased knowledge and use of the sea. The development of remote sensors and oceanographic employment of research aircraft are considered in detail. Oceanographic achievements in connection with the determination of biological indices, sea state, and sea surface temperature are discussed, as well as the results of bathymetric and hydrographic studies and studies of coastal processes, sea ice, and the air-sea interaction. It is concluded that if a need for a daily global look at the world ocean is determined, orbiting satellites can provide all-weather oceanographic data for complementing the higher-resolution data gathered by the more conventional means of ships, buoys, and aircraft. Developments in spacecraft and allied satellite technologies offer promising results in these fields of operation. I.P.

A69-11125 *
OGO-2 MAGNETIC FIELD OBSERVATIONS DURING THE MAGNETIC STORM OF MARCH 13-15, 1966.
R. A. Langel and J. C. Cain (NASA, Goddard Space Flight Center, Greenbelt, Md.).
(International Association of Geomagnetism and Aeronomy, Symposium on Special Events, Saint-Gall, Switzerland, Oct. 2, 1967.) Annales de Géophysique, vol. 24, July-Sept. 1968, p. 857-869. 27 refs.

Analysis of magnetic field data from the OGO-2 spacecraft and from surface magnetic observatories for the period from Mar. 13 to 15, 1966. During this interval there occurred a magnetic storm with a Dst decrease of 122 γ. The results indicate a nonsymmetric inflation of the magnetosphere, with the field decrease in the dusk sector being a factor of about three more than that in the dawn sector. The evidence indicates that the sources of both Dst and Ds in low latitudes are external to the satellite altitudes (410 to 1510 km). Polar ionospheric currents were detected more than 1.5 hr before the main phase of the storm. These currents conform to the classical "2-celled" model, which includes a concentrated eastward current in the evening local time sector, and a concentrated westward current in the morning local time sector. F.R.L.

A69-11226 *
PROPAGATION OF THE SUDDEN COMMENCEMENT OF JULY 8, 1966, TO THE MAGNETOTAIL.
M. Sugiura, T. L. Skillman, B. G. Ledley, and J. P. Heppner (NASA, Goddard Space Flight Center, Greenbelt, Md.).
Journal of Geophysical Research, vol. 73, Nov. 1, 1968, p. 6699-6709. 17 refs.

A sudden magnetic field increase associated with the July 8, 1966, sudden commencement (SC) was observed by the OGO 3 satellite in the magnetotail. By use of the IMP 3 and Explorer 33 observations made by Ness and Taylor (1968) of the interplanetary shock that caused the SC, it is shown that the magnetospheric propagation of the field increase toward the tail is faster than the propagation of the interplanetary shock just outside the bow shock. Conclusions drawn include (1) that the observed magnetic field increase in the tail is unlikely to be due to an increased lateral pressure of the post-shock solar wind gas from the side of the tail, and (2) that the transfer of additional polar magnetic flux to the tail due to the increase in the solar wind pressure on the front side of the magnetosphere can account for the observed tail field increase. (Author)

A69-11234 *
PLASMA OBSERVATIONS ON EXPLORER 34.
K. W. Ogilvie (NASA, Goddard Space Flight Center, Greenbelt, Md.), T. D. Wilkerson (NASA, Goddard Space Flight Center, Greenbelt; Maryland, University, Institute for Fluid Dynamics and Applied Mathematics, College Park, Md.), and L. F. Burlaga.
Journal of Geophysical Research, vol. 73, Nov. 1, 1968, p. 6809-6824. 27 refs.
Grant No. NsG-283.

Description of the results of the observations of the Goddard Space Flight Center/University of Maryland plasma experiment on Explorer 34 during three magnetic storms, May 30, June 5, and June 25, 1967. Particular attention is given to the interaction of discontinuities with the earth and to changes in the abundance of helium in the plasma. Detailed comparisons with magnetic field observations on the same satellite are used to interpret the observations and to identify shocks and tangential discontinuities. The observations are consistent with the relationship derived by Siscoe (1966) between the magnitude of such sudden changes in the earth's magnetic field and the solar wind parameters. The local shock speeds are derived from data obtained at the time of the sudden commencements. An example of an si^+ si^- pair is discussed, and in this case the negative impulse is shown to be due to a tangential discontinuity rather than a shock, whereas the positive impulse is associated with a shock. Helium observations are described which show that during the main phase of some geomagnetic storms the abundance ratio n_a/n_p shows a marked increase. In the May 30 storm it attained a value of 0.15 ± 0.02, 5-1/2 hr after the SC, an increase of seven times over the value observed earlier. I.P

A69-11237 *
THE CISLUNAR GEOMAGNETIC TAIL GRADIENT IN 1967.
J. D. Mihalov and C. P. Sonett (NASA, Ames Research Center, Space Sciences Div., Moffett Field, Calif.).
Journal of Geophysical Research, vol. 73, Nov. 1, 1968, p. 6837-6841. 6 refs.

Examination of the geomagnetic tail field gradient during the summers of 1966 and 1967 for secular change. Data are used from Ames magnetometers on Explorers 33 and 35. The 1967 data are compared with the earlier published 1966 Explorer 33 results. Secular change of the tail field magnitude gradient is not found in the comparison. I.P.

A69-12299 *
EARTH'S BOW SHOCK - ELAPSED-TIME OBSERVATIONS BY TWO CLOSELY SPACED SATELLITES.
E. W. Greenstadt, I. M. Green (TRW Systems Group, Space Sciences Laboratory, Redondo Beach, Calif.), and D. S. Colburn (NASA, Ames Research Center, Space Sciences Div., Moffett Field, Calif.).
Science, vol. 162, Nov. 22, 1968, p. 898-901. 14 refs.

Coordinated observations of the earth's bow shock were made as Vela 3A and Explorer 33 passed within six earth radii of each other. Elapsed time measurements of shock motion give directly determined velocities in the range 1 to 10 km/sec and establish the existence of two regions, one of large amplitude magnetic "shock" oscillations and another of smaller, sunward, upstream oscillations. Each region is as thick as 1 earth radius, or more. (Author)

13 GEOPHYSICS

A69-12741 *
THE PLASMAPAUSE AND ITS RELATION TO THE ION COMPOSITION IN THE TOPSIDE IONOSPHERE.
H. G. Mayr (NASA, Goddard Space Flight Center, Aeronomy Branch, Greenbelt, Md.).
Planetary and Space Science, vol. 16, Nov. 1968, p. 1405-1414. 14 refs.

Investigation of the concept that the high O^+ - H^+ transition level at latitudes above 50° and the plasmapause with its characteristic density plateau may be strongly correlated. It is shown that plasma escape can produce sufficiently large fluxes at latitudes where the field lines are open, thus significantly decreasing the hydrogen-ion density. As a result, plasma diffusion across lines is induced - coupled with upward fluxes of ionization along field lines, which leads to the formation of a plateau that characterizes the transition region from the open to the closed magnetosphere. Collision-type perpendicular diffusion would produce an enormously rapid transition over a distance of a few meters, which is not observed. This suggests that a turbulent state is built up in the transition region; thus, Bohm's coefficient for turbulent diffusion is employed, and this leads to a quantitatively satisfying description of the plasmapause. M.M.

A69-13328 *
FRICTIONAL FORCES AND COLLISION FREQUENCIES BETWEEN MOVING ION AND NEUTRAL GASES.
Peter Stubbe (NASA, Goddard Space Flight Center, Laboratory for Space Sciences, Greenbelt, Md.).
Journal of Atmospheric and Terrestrial Physics, vol. 30, Dec. 1968, p. 1965-1985. 26 refs.

Study of the frictional force between moving ions and neutral gases, showing how the corresponding collision frequencies have to be defined in order to maintain the validity of the terms used. An expression is derived for the momentum transfer collision frequency ν_{in} between ions and neutral particles as a function of temperature and the relative flow velocity $|v_i - v_n|$. The result indicates that for most practical applications ν_{in} may be considered as independent of $|v_i - v_n|$. However, for very high velocities - i.e., a convection flow from the magnetosphere into the ionosphere, this dependence may be significant. Numerical values for ν_{in} are presented. P.v.T.

A69-14012 *
AVERAGE MAGNETIC FIELD CONFIGURATION OF THE OUTER MAGNETOSPHERE.
D. H. Fairfield (NASA, Goddard Space Flight Center, Laboratory for Space Sciences, Greenbelt, Md.).
Journal of Geophysical Research, vol. 73, Dec. 1, 1968, p. 7329-7338. 24 refs.

Over 1500 hours of data from the satellites IMP 1, 2, and 3 have been used to study the configuration of the magnetic field in the outer magnetosphere between 5 and 18 $R_\oplus$. Hourly average field vectors were projected in the solar magnetic equatorial plane and in 24 meridian sections corresponding to each hour of local time. The plots show the sweeping back of the field toward the tail and the dawn and dusk transition from compressed dayside field lines to extended nightside field lines. Constant B contours in the equatorial plane were constructed, and flux conservation was used to establish a quantitative relationship between the equatorial crossing point of an outer magnetosphere field line and the latitude of its earth intersection. A contour diagram in the equatorial plane designating the latitude of field line origin permits the mapping of low-altitude phenomena to the equatorial plane and vice versa. Auroral oval field lines are found to come from the region of the magnetopause in the daylight hemisphere but from well within the magnetosphere in the night hemisphere. The outermost closed field line is found to come from approximately 78° throughout the dayside hemisphere. (Author)

A69-14661 *
COMBINED SOLUTION FOR LOW DEGREE LONGITUDE HARMONICS OF GRAVITY FROM 12- AND 24-HOUR SATELLITES.
Carl A. Wagner (NASA, Goddard Space Flight Center, Special Projects Branch, Greenbelt, Md.).
Journal of Geophysical Research, vol. 73, Dec. 15, 1968, p. 7651-7660. 17 refs.

Examination of over 600 near-stationary orbits of five high-altitude communications satellites for the strong effects on them of low-degree earth-gravity harmonics. The accelerated drift of these 12- and 24-hr orbits due to the earth's anomalous potential has been measured at 50 longitude locations. From these accelerations five low-degree earth-gravity harmonics which resonate with these orbits have been calculated (10 gravity coefficients). The best-determined harmonic is felt to be H_{22}, which dominates the accelerated drift of the three 24-hr satellites (Syncoms 2 and 3, and Early Bird), and the two 12-hr satellites (Molniya 1 and Cosmos 41). The normalized constants found for this harmonic, the other four harmonics in decreasing order of their estimated strength of absolute determination, and their normalized coefficients are given. The measured drift accelerations themselves are compared with accelerations calculated from a number of recently published geoids derived from satellite data and a combination of satellite and surface-gravity data. The "best" geoid representing these accelerations is a 1967 Smithsonian Astrophysical Observatory determination of Köhnlein. F.R.L.

A69-14975 *
TEMPERATURES OF THE EARTH'S UPPER ATMOSPHERE.
J. C. G. Walker (Yale University, Dept. of Geology and Geophysics, New Haven, Conn.) and N. W. Spencer (NASA, Goddard Space Flight Center, Laboratory for Atmospheric and Biological Sciences, Greenbelt, Md.).
Science, vol. 162, Dec. 27, 1968, p. 1437-1442. 70 refs.
Grant No. NGR-07-004-100.

Study of the electron, ion, and neutral-particle temperatures of the earth's upper atmosphere. At most altitudes the electron temperature exceeds the ion temperature and the ion temperature, in turn, exceeds the neutral-particle temperature. Since energy is exchanged between the gases, the different temperatures are related, but the relationship is complex. It is quite common, for example, for the electron temperature to increase while the neutral-particle temperature is decreasing. A similar multiplicity of temperatures in the upper atmospheres of the planets is expected. P.v.T.

A69-16261 *
DIRECT IN SITU MEASUREMENTS OF WAVE PROPAGATION IN THE NEUTRAL THERMOSPHERE.
George P. Newton, David T. Pelz, and Hans Volland (NASA, Goddard Space Flight Center, Aeronomy Branch, Greenbelt, Md.).
Journal of Geophysical Research, vol. 74, Jan. 1, 1969, p. 183-196. 19 refs.

Evaluation of local variations in the atmospheric density, measured by the density gauges on the Explorer 32 satellite, confirming that waves propagate in the neutral atmosphere. The waves were observed in the Northern Hemisphere over the altitude range from 286 km (satellite perigee) to at least 510 km. Apparently, four integrally related wavelengths have been measured, a "fundamental" and the second, third, and fourth harmonics. These waves are interpreted as free internal gravity waves propagating predominantly north-south, or south-north, with maximum horizontal wavelengths between 130 and 520 km. The altitude dependence of the apparent vertical half-wavelengths results from the satellite moving with varying vertical velocity through a slowly propagating wave pattern with nearly vertical phase planes. This interpretation is consistent with observations of large-scale traveling ionospheric disturbances by Thome (1964) and Georges (1968). P.v.T.

A69-16267 *
MEASUREMENTS OF ELECTRON COOLING RATES IN THE MID-LATITUDE AND AURORAL-ZONE THERMOSPHERE.
L. H. Brace, H. G. Mayr (NASA, Goddard Space Flight Center, Aeronomy Branch, Greenbelt, Md.), and G. R. Carignan (Michigan, University, Dept. of Electrical Engineering, Ann Arbor, Mich.).
Journal of Geophysical Research, vol. 74, Jan. 1, 1969, p. 257-266. 18 refs.

Two day-night pairs of thermosphere probe rockets, launched at Wallops Island, Va., in March 1965 and at Churchill, Manitoba,

in November 1965 have provided altitude profiles of electron temperature and concentration at midday and midnight. Altitude profiles of N_2 measured on the same four flights have in addition provided neutral gas temperature profiles. These data are employed to calculate electron cooling rate profiles, and these in turn are interpreted in terms of ionospheric heat sources. The daytime electron heat source for the F region, at both middle latitudes (L = 2.9) and in the auroral zone (L ≈ 8), appears consistent with solar ultraviolet heating. The nighttime F-region, however, appears to be heated by downward conduction from the protonosphere at middle latitudes and by particle heating in the auroral zone. The source of electron heating for the E region both day and night and at both locations cannot be explained by direct solar heating. This may be produced by neutral winds, electric currents, an unknown chemical reaction or, as Walker has suggested, selective heating of the electrons by excited N_2 having lifetimes in the E region of the order of a day. (Author)

A69-16268 *

MIDLATITUDE NEUTRAL THERMOSPHERE DENSITY AND TEMPERATURE MEASUREMENTS.

David T. Pelz and George P. Newton (NASA, Goddard Space Flight Center, Greenbelt, Md.).

Journal of Geophysical Research, vol. 74, Jan. 1, 1969, p. 267-271. 16 refs.

Description of an ensemble of six independent aeronomy experiments which was launched from Wallops Island, Virginia, on Mar. 2, 1966, at 1300 EST. Two Bayard-Alpert ionization gauges, similar to those on the Explorer 17 satellite, were flown to measure neutral atmospheric density and temperature. However, the Bayard-Alpert gauges appear to have pumped or adsorbed virtually all of the atmospheric atomic oxygen (O) to which they were exposed, and thus measured only the molecular nitrogen (N_2), molecular oxygen (O_2), and helium (He) in the region from 150- to 450-km altitude. The deduced N_2 number densities agree with nearly simultaneous measurements obtained from a neutral mass spectrometer and a solar EUV extinction experiment. Previous N_2 measurements from thermosphere probes, obtained under similar solar and geomagnetic conditions, agree well with these data. M.M.

A69-16407 *

DIURNAL VARIATION OF THE ION TEMPERATURE.

K. K. Mahajan (Cornell-Sydney University Astronomy Center, Arecibo Ionospheric Observatory, Arecibo, Puerto Rico; NASA, Goddard Space Flight Center, Greenbelt, Md.).

Journal of Atmospheric and Terrestrial Physics, vol. 31, Jan. 1969, p. 93-101. 18 refs.

Results on the diurnal variation of the ion temperature, obtained from the Thomson scatter spectra at Arecibo, in the height range 250-475 km are presented. At 250 km where the ion temperature (T_i) is expected to be nearly equal to the neutral temperature (T_n), T_i is generally observed to show diurnal maximum at 16 hr LT and diurnal minimum at 4 hr LT with no appreciable change in these times with solar activity. The average day to night T_i ratio at 250 km is found to be 1.45. These results are in apparent conflict with the satellite drag analysis in which T_n is found to have a diurnal maximum at 14 hr LT and day to night temperature ratio around 1.30. At 475 km where T_i is significantly above T_n, the diurnal behavior of T_i is observed to be different on different days. The day-to-day and hour-to-hour variations in T_i at this height are found to be due to changes in the electron density and electron temperature and seem consistent in terms of an energy budget that includes heating of the ion gas by the hotter thermal electrons and cooling by the neutral atmosphere. (Author)

A69-16411 *

COORDINATED ROCKET MEASUREMENTS ON THE D-REGION WINTER ANOMALY. I - EXPERIMENTAL RESULTS.

C. F. Sechrist, Jr., E. A. Mechtly, J. S. Shirke (Illinois, University, Dept. of Electrical Engineering, Aeronomy Laboratory, Urbana, Ill.), and J. S. Theon (NASA, Goddard Space Flight Center, Greenbelt, Md.).

Journal of Atmospheric and Terrestrial Physics, vol. 31, Jan. 1969, p. 145-153. 11 refs.
Grant No. NsG-511.

Evaluation of nearly simultaneous rocket measurements of D-region temperatures and electron densities, conducted on Jan. 31, 1967, an anomalous winter day, at Wallops Island, Va. The electron density profile for Jan. 31, 1967, was generally similar to the one measured on the anomalous winter day of Jan. 10, 1966, the densities of 70 to 80 km height range being about five times greater than those on a normal winter day. The rocket grenade temperature profile for the anomalous day revealed a strong temperature inversion at 70 km and a warm layer extending from the inversion to 84 km; this temperature structure was significantly different from that at the same altitude on the normal day of Feb. 3, 1967. P. v. T.

A69-16417

WHISTLER MODE PROPAGATION IN THE PRESENCE OF A LONGITUDINAL ELECTROSTATIC FIELD.

L. Stenflo (Uppsala, University, Institute of Physics, Uppsala, Sweden).

Journal of Atmospheric and Terrestrial Physics, vol. 31, Jan. 1969, p. 197-200. 7 refs.

A dispersion relation for the whistler mode propagation in a homogeneous plasma, situated in parallel constant electric and magnetic fields, has been derived. Collisions have been considered by means of a Fokker-Planck model. It is shown that the amplification found in a previous work is not possible because of the collisional damping. (Author)

A69-18838 *

RAY TRACING STUDIES FOR THE TOPSIDE IONOSPHERE.

Lawrence Colin, Jerry Shmoys (NASA, Ames Research Center, Space Sciences Div., Moffett Field, Calif.), and Geraldine McCulley (Informatics, Inc., Palo Alto, Calif.).

Journal of Geophysical Research, vol. 74, Feb. 1, 1969, p. 809-814. 9 refs.

Investigation of the effects of nonvertical propagation on high-altitude topside sounder data reduction. Although the extraordinary, ordinary, and Z rays exhibit significant lateral deviation in a spherically stratified ionosphere, the resultant effects on analysis accuracy are generally tolerable; however, ionospheric tilts produce very large effects. The joint use of the three modes for future analyses is suggested. The use of ray tracing, along with the normal methods, may be an important required tool for the accurate reduction of topside sounder ionograms. G. R.

A69-18839 *

SOUNDING ROCKET MEASUREMENTS OF ION COMPOSITION AND CHARGED PARTICLE TEMPERATURES IN THE TOPSIDE IONOSPHERE.

E. J. R. Maier (NASA, Goddard Space Flight Center, Laboratory for Space Sciences, Greenbelt, Md.).

Journal of Geophysical Research, vol. 74, Feb. 1, 1969, p. 815-823. 19 refs.

Discussion of ion composition and charged-particle temperatures at altitudes from 300 to 600 km. The major ion constituent was found to be O^+ over the entire altitude range, decreasing from >99% of the total ion concentration at 300 km to 88% at 600 km. distinct populations. Both the local-time and magnetic latitude distribution of both classes of signals are investigated. When the magnetic latitude distributions are extrapolated downward to 1000-km altitudes, the results are consistent with previous satellite observations at these low altitudes. However, the equatorial distributions cannot be inferred by simply projecting the magnetic noise measured at low altitudes onto the equator along flux tubes. The in situ measurements cannot determine the exact location of the source of all the noise observed. However, it is found that steady noise is definitely generated near 45° magnetic latitude on the dayside of the magnetosphere for L values from 6 to 10, and that bursts are generated near the equator above L = 6 from 0400 to 1800 local time. (Author)

13 GEOPHYSICS

A69-19360 *
EXTERNAL AERODYNAMICS OF THE MAGNETOSPHERE.
John R. Spreiter, Alberta Y. Alksne, and Audrey L. Summers (NASA, Ames Research Center, Space Sciences Div., Moffett Field, Calif.).
IN: PHYSICS OF THE MAGNETOSPHERE; PROCEEDINGS OF THE CONFERENCE, BOSTON COLLEGE, CHESTNUT HILL, MASS., JUNE 19-28, 1967. [A69-19351 07-29]
Conference sponsored by the U.S. Air Force and Boston College.
Edited by R. L. Carovillano, J. F. McClay, and H. R. Radoski.
Dordrecht, D. Reidel Publishing Co. (Astrophysics and Space Science Library. Volume 10), 1968, p. 301-375. 106 refs.

Summary of some of the basic ideas, both theoretical and experimental, that support the correspondence between the flow of the solar wind past the earth and its magnetosphere, and the problem of the external aerodynamics of round-nosed bodies in a supersonic stream. A connected account of many of the principal quantitative results that have been obtained through application and extension of methods developed originally for the aerodynamics of reentry vehicles is presented. In addition, the basic concepts of the theory of the solar wind itself are outlined in some detail in order to illustrate the basic unity of the entire theoretical description of the solar wind and its interaction with the geomagnetic field. Extensive discussions of the internal consistency of the theory and the degree to which the results correspond to conditions observed in space are included to provide an understanding of the overall reliability of the theory. F.R.L.

A69-19364 *
REVIEW OF AMES RESEARCH CENTER PLASMA-PROBE RESULTS FROM PIONEERS 6 AND 7.
J. H. Wolfe and D. D. McKibbin (NASA, Ames Research Center, Space Sciences Div., Moffett Field, Calif.).
IN: PHYSICS OF THE MAGNETOSPHERE; PROCEEDINGS OF THE CONFERENCE, BOSTON COLLEGE, CHESTNUT HILL, MASS., JUNE 19-28, 1967. [A69-19351 07-29]
Conference sponsored by the U.S. Air Force and Boston College.
Edited by R. L. Carovillano, J. F. McClay, and H. R. Radoski.
Dordrecht, D. Reidel Publishing Co. (Astrophysics and Space Science Library. Volume 10), 1968, p. 435-460. 29 refs.

Description of the results of magnetospheric studies made with the aid of Pioneers 6 and 7. Two results obtained from the Pioneer missions are discussed. The first concerns the data obtained by Pioneer 6, revealing a density spike associated with the shock front and a density increase by a factor of approximately 3 as the flow crossed the shock. The second result discussed concerns plasma fluctuations noted by Pioneer 7 within the frequency range from 0.1 to 10 Hz, which continued intermittently for about six days. Z.W.

A69-19365 *
THE GEOMAGNETIC TAIL - TOPOLOGY, RECONNECTION AND INTERACTION WITH THE MOON.
C. P. Sonett, D. S. Colburn, R. G. Currie, and J. D. Mihalov (NASA, Ames Research Center, Space Sciences Div., Moffett Field, Calif.).
IN: PHYSICS OF THE MAGNETOSPHERE; PROCEEDINGS OF THE CONFERENCE, BOSTON COLLEGE, CHESTNUT HILL, MASS., JUNE 19-28, 1967. [A69-19351 07-29]
Conference sponsored by the U.S. Air Force and Boston College.
Edited by R. L. Carovillano, J. F. McClay, and H. R. Radoski.
Dordrecht, D. Reidel Publishing Co. (Astrophysics and Space Science Library. Volume 10), 1968, p. 461-484. 26 refs

A preliminary assessment of the geometry of the geomagnetic tail is made using data from the Ames magnetometer on the Explorer 33 satellite. The general shape corresponds to the earlier findings of Ness et al. The tail is regular to distances greater than 82 R_E. The field values vary for $K_p \leqslant 2+$ from a low of about 4 gamma to a high value of 40 gamma. Generally the values are in the neighborhood of 10-20 gamma. A distinct skewing of the field lines away from the solar-antisolar direction is observed, such that an added component of magnetic field in the direction of planetary motion is present on both sides of the null plane. The skewing appears to be greatest near the null plane. An increase in field magnitude with increasing K_p is observed. Little cross gradient is observed in the tail field. Strong evidence for reconnection of field lines is found, and statistics are presented for a dual effect regarding the residual Z field across the null plane. The interaction of the tail field with the moon is discussed in terms of the mechanism of Sonett and Colburn. (Author)

A69-20944 *
PARTITION COEFFICIENTS OF RARE-EARTH ELEMENTS AND BARIUM BETWEEN IGNEOUS MATRIX MATERIAL AND ROCK-FORMING-MINERAL PHENOCRYSTS. I.
C. C. Schnetzler and J. A. Philpotts (NASA, Goddard Space Flight Center, Laboratory for Theoretical Studies, Geochemistry Laboratory, Greenbelt, Md.).
IN: ORIGIN AND DISTRIBUTION OF THE ELEMENTS; PROCEEDINGS OF THE INTERNATIONAL SYMPOSIUM, PARIS, FRANCE, MAY 8-11, 1967. [A69-20892 08-30]
Symposium sponsored by UNESCO and the International Union of Geological Sciences.
Edited by L. H. Ahrens.
Oxford, Pergamon Press, Ltd. (International Series of Monographs in Earth Sciences. Volume 30), 1968, p. 929-937; Discussion, L. A. Haskin and H. D. Holland, p. 937, 938. 12 refs.

Determination of the partition coefficients between natural melts (represented by igneous matrix material) and amphibole, augite, olivine, and plagioclase phenocrysts for eight rare-earth elements and barium, by means of a mass-spectrometric stable-isotope-dilution technique. Peridotite nodules, crystallization of plagioclase, and relationships between basalts are discussed in terms of the partition coefficient data. B.H.

A69-20945 *
GENESIS OF CONTINENTAL DIABASES AND OCEANIC THOLEIITES CONSIDERED IN LIGHT OF RARE-EARTH AND BARIUM ABUNDANCES AND PARTITION COEFFICIENTS.
J. A. Philpotts and C. C. Schnetzler (NASA, Goddard Space Flight Center, Laboratory for Theoretical Studies, Geochemistry Laboratory, Greenbelt, Md.).
IN: ORIGIN AND DISTRIBUTION OF THE ELEMENTS; PROCEEDINGS OF THE INTERNATIONAL SYMPOSIUM, PARIS, FRANCE, MAY 8-11, 1967. [A69-20892 08-30]
Symposium sponsored by UNESCO and the International Union of Geological Sciences.
Edited by L. H. Ahrens.
Oxford, Pergamon Press, Ltd. (International Series of Monographs in Earth Sciences. Volume 30), 1968, p. 939-947. 19 refs.

Rare-earth and barium abundances in the chilled-contacts of four diabases and in the rock-standard W-1 have been determined by mass-spectrometric isotope dilution. The similarity of the abundances provides strong additional evidence of the compositional uniformity of diabases. This uniformity is interpreted to mean that diabase melts are probably the result of either very limited partial fusion or almost complete fusion of similar source materials. Application of rare-earth and barium partition-coefficients for clinopyroxene leads to the conclusion that diabases might be the result of very limited partial fusion of the same kind of source material from which oceanic tholeiites are derived by a process involving complete or almost complete fusion; a source material composed of clinopyroxene is implied in this model. The rare-earth and Ba data might also be compatible with the genesis of diabases by very limited partial fusion of hypersthene-achondrite-like material. (Author)

A69-21404 *#
ALBEDO MEASUREMENTS OVER THE ANTARCTIC.
W. E. McGovern (New York University, Dept. of Meteorology and Oceanography, New York, N.Y.) and S. I. Rasool (NASA, Goddard Space Flight Center, Goddard Institute for Space Studies; New York University, Dept. of Meteorology and Oceanography, New York, N.Y.).
IN: THE SCIENTIFIC REPORT OF THE ROCKWELL POLAR FLIGHT, NOVEMBER 14-17, 1965.
Compiled by S. A. Korff.
S. A. Korff, New York University, Physics Dept., Bronx, N.Y., 1968, p. 63-65.
Grant No. NsG-499.

Results of measurements of the solar radiation reflected by the surface and the atmosphere of the Antarctic, made by an Eppley radiometer. The main results are that (1) the average reflectivity of the surface atmosphere system over this region of Antarctica, under cloudless conditions, is 56 ± 6%, and (2) the reflectivity varies inversely as the solar zenith angle. This is mainly due to the increased atmospheric absorption for large zenith angles, about 15% per vertical thickness of the atmosphere. If the observed value of

the bubbles travel along their spiral paths more rapidly, the bubble velocity being directly proportional to the angular velocity of the liquid. M.M.

A69-21661 *

EFFECT OF NEUTRAL SHEET CURRENTS ON THE SHAPE AND MAGNETIC FIELD OF THE MAGNETOSPHERE TAIL.

John R. Spreiter and Alberta Y. Alksne (NASA, Ames Research Center, Space Sciences Div., Moffett Field, Calif.).

Planetary and Space Science, vol. 17, Feb. 1969, p. 233-246. 21 refs.

Modification of the usual first-order theory of the shape of the magnetosphere boundary that incorporates in a simple way the principal effects of the electrical currents in the neutral sheet of the extended geomagnetic tail. Numerical results presented for a variety of representative cases show that an additional flaring out of the magnetosphere tail ultimately of the order of a few earth radii occurs over a distance of several tens of earth radii, and that there is an associated decrease in the intensity of the magnetic field because of the need to approximately conserve the total magnetic flux in each half of the tail cross section. Comparisons with data obtained in space with Explorer 18 and 33 satellites and Pioneer 6 and 7 spacecraft show that this modification of the theory leads to a substantial improvement in the agreement between the calculated and observed dimensions of the magnetosphere tail and the strength of the magnetic field contained therein. (Author)

A69-23770 *

THE POLAR-CAP ABSORPTION ON 7-10 JULY 1966.

Y. Hakura (NASA, Goddard Space Flight Center, Greenbelt, Md.).

IN: THE PROTON FLARE PROJECT (THE JULY 1966 EVENT). [A69-23725 10-29]
Edited by A. C. Stickland.
Cambridge, Mass., MIT Press (Annals of the IQSY. Volume 3), 1969, p. 337-352. 24 refs.

The time history of a PCA event on July 7-10, 1966 was analyzed using 16 riometers in the northern polar region and concurrent satellite observations of solar cosmic radiations. The first onset of PCA was noticed at 0120 UT at Shepherd Bay, Canada, and the slight enhanced ionization of a few tenths of 1 dB covered the whole North Pole region before 0200 UT. On the other hand, auroral zone stations observed the PCA after 0200. The two-stepped onset of the PCA corresponds to the differential arrival of ionizing electrons and protons at the earth, detected by the satellites. The flux of 40-keV electron busts observed by the satellites Explorer 33 and IMP-3 can explain the first onset of a slight PCA near the geomagnetic pole. The PCA in the polar region marked a maximum of 2.5 dB on 30 MHz at 1300 on July 7, and then decayed gradually until it went down below 0.3 dB after 2345 on July 8. The lowest latitude of the PCA during the geomagnetically calm period was some 63° in corrected geomagnetic latitude. After the onset of geomagnetic disturbances, the PCA superposed upon it the auroral zone absorption that appeared even in the lower auroral zone. (Author)

A69-23777 *

EVIDENCE OF CONTRACTION OF THE EARTH'S THERMAL PLASMASPHERE SUBSEQUENT TO THE SOLAR FLARE EVENTS OF 7 AND 9 JULY 1966.

H. A. Taylor, Jr., H. C. Brinton, and M. W. Pharo, III (NASA, Goddard Space Flight Center, Aeronomy Branch, Greenbelt, Md.).

IN: THE PROTON FLARE PROJECT (THE JULY 1966 EVENT). [A69-23725 10-29]
Edited by A. C. Stickland.
Cambridge, Mass., MIT Press (Annals of the IQSY. Volume 3), 1969, p. 389-394. 12 refs.

Direct measurements of thermal H^+ and He^+ in the magnetosphere have been obtained from ion mass spectrometers on OGO 1 and 3 satellites. Typical H^+ profiles exhibit a gradual decrease in concentration with altitude within the plasmasphere, while the outer boundary of the plasmasphere is characterized by an abrupt decrease in concentration to 5 ions cm^{-3} or less. This boundary, the plasmapause, is observed to move inward and outward in an inverse correlation with the magnetic activity index Kp. The magnetosphere was disturbed during the solar flare period July 7-9, 1966, and on July 9, the plasmapause was observed to be unusually low, at L = 3.3. This observation contrasted with measurements of the plasmapause on both preceding and succeeding orbits, when in the absence of flares and magnetic disturbance the H^+ boundary was observed to expand to L values as high as 6. These measurements correlate well with "knee" whistler observations of the plasmapause. (Author)

A69-25150 *

FULL WAVE CALCULATIONS OF GRAVITY WAVE PROPAGATION THROUGH THE THERMOSPHERE.

H. Volland (NASA, Goddard Space Flight Center, Greenbelt, Md.).

Journal of Geophysical Research, vol. 74, Apr. 1, 1969, p. 1786-1795. 17 refs.

Results of full-wave calculations performed within the frequency range of gravity waves ($10^{-3} \leq \omega \leq 10^{-2}$ sec^{-1}) for a thermospheric model between 150 and 500 km in altitude. In this altitude range, gravity waves are coupled with heat conduction waves. Reflection, transmission, conversion, and coupling from one wave type into the other one are described by the elements of the scattering matrix. The dependence of these elements on height and angle of incidence is discussed. The transmission coefficients of gravity waves calculated by full-wave theory are compared with simple ray calculations, and the results show that ray treatment is a sufficient approximation for obliquely upward propagating gravity waves and that gravity waves predominate throughout the thermosphere. The thermosphere reacts like a selective filter with respect to upward propagating gravity waves. (Author)

A69-25153 *

MULTI-EXPERIMENT DETECTION OF THE PLASMAPAUSE FROM EOGO SATELLITES AND ANTARCTIC GROUND STATIONS.

D. L. Carpenter, C. G. Park (Stanford University, Stanford Radioscience Laboratory, Stanford, Calif.), H. A. Taylor, Jr., and H. C. Brinton (NASA, Goddard Space Flight Center, Laboratory for Atmospheric and Biological Sciences, Greenbelt, Md.).

Journal of Geophysical Research, vol. 74, Apr. 1, 1969, p. 1837-1847. 12 refs.
NSF-supported research; Contract No. NAS 5-2131.

Correlation study of plasmapause position measured by three independent experiments involving: (1) ion mass spectrometers on OGO 1 and OGO 3; (2) broadband vlf receivers (0.3-12.5 kHz) on OGO 1 and OGO 3; and (3) broadband vlf recordings at Antarctica, near the 90° meridian. In the satellite vlf data, the plasmapause crossings are identified by abrupt changes in observed whistler and vlf noise activity, and by noise bands of limited duration. In two cases of simultaneous vlf and ion data from the same satellite, plasmapause crossings were detected by both experiments within less than 0.1 R_E in L value. In eight cases of OGO 1 ion data and simultaneous ground whistler data spaced from 1 to 12 hours from OGO in local time, good agreement was found between the measured plasmapause positions. The comparisons provide new verification of the worldwide extent of the plasmapause. Previous indications that the radius of the plasmapause is frequently about constant, over large local-time sectors in the range 0-18 LT, are also verified. B.H.

A69-25157 *

AN INTERPRETATION OF OGO LIGHT ION ABUNDANCE MEASUREMENTS.

Lawrence Colin, Stuart W. Dufour, and Dora S. Willoughby (NASA, Ames Research Center, Space Sciences Div., Moffett Field, Calif.).

Journal of Geophysical Research, vol. 74, Apr. 1, 1969, p. 1863-1866. 12 refs.

Investigation of a diffusive equilibrium theory to account for the light-ion abundance measurements of the OGO satellites. It is shown that reasonable latitudinal distributions of temperature, temperature gradient, and composition can be found that are compatible (using field-aligned diffusive equilibrium with positive temperature gradients) with published OGO data. G.R.

A69-25284 *#
ION-EXOSPHERE WITH VARIABLE CONDITIONS AT THE BAROPAUSE.
R. E. Hartle (NASA, Goddard Space Flight Center, Laboratory for Space Sciences, Greenbelt, Md.).
Physics of Fluids, vol. 12, Feb. 1969, p. 455-462. 12 refs.

The model ion-exosphere of Eviatar et al. (1964) for a nonrotating planet with a static, centered-dipole magnetic field is generalized by permitting the density and temperature to vary over the baropause. In particular, the density and/or temperature are allowed to differ at the conjugate magnetic field points of the baropause. For this case, the ion and electron velocity-distribution functions, satisfying the Vlasov equations in the drift approximation, are constructed. Then, the species densities are determined from the distributions, and are compared with the corresponding results of Eviatar et al. for the case of uniform density and temperature at the baropause. In addition, the particle current densities, pressures, and temperatures are derived. (Author)

A69-26012 *#
ON THE SEMIANNUAL VARIATION OF THE UPPER ATMOSPHERE.
Isadore Harris (NASA, Goddard Space Flight Center, Greenbelt, Md.) and Wolfgang Priester (Bonn, Universität, Astronomisches Institut, Bonn, West Germany; NASA, Goddard Space Flight Center, Goddard Institute for Space Studies, New York, N.Y.).
Journal of the Atmospheric Sciences, vol. 26, Mar. 1969, p. 233-240. 36 refs.

Investigation of several possible mechanisms which could be invoked to explain the observed semiannual density variation in the thermosphere and exosphere. A variation of the height of the mixtopause leads to a large density variation for heights above 700 km. Below that height, however, the density is essentially invariant to this process. This invariance is to some degree caused by the neglect of downward heat transport by eddy diffusion at the bottom of the thermosphere. The limitations of using the simple mixtopause scheme in this context are discussed. A small permanent heat flux conducted into the lower exosphere from above can be ruled out on the grounds that it fails to explain the observed amplitude at a height of 200 km. A variation of this flux by 3×10^{-2} erg/cm^2-sec would yield a sufficiently large density variation only for heights above 300 km. The recent observations at heights below 200 km indicate that the temperature and density at the bottom of the thermosphere (90 to 120 km) vary with a semiannual period. (Author)

A69-26101 *
THE UPPER ATMOSPHERE AS A MULTIPLY REFRACTIVE MEDIUM FOR NEUTRAL AIR MOTIONS.
H. Volland (NASA, Goddard Space Flight Center, Greenbelt, Md.).
Journal of Atmospheric and Terrestrial Physics, vol. 31, Apr. 1969, p. 491-514. 13 refs.

Under the influence of gravity and heat conduction four plane characteristic waves obliquely incident on a horizontally stratified atmosphere can propagate, two of them upward and the two other downward. The two pairs of characteristic waves are the well-known acoustic gravity waves and the heat conduction waves. Molecular viscosity generates two more pairs of characteristic waves, the ordinary and the extraordinary viscosity waves. Ion drag and Coriolis force make the atmosphere anisotropic with respect to the characteristic waves. Their propagation characteristics for east to west and north to south propagation differ from each other. Some analytical solutions of the eigenvalues of these eight characteristic waves are given in this paper. Numerical calculations of the eigenvalues depending on the parameters of the thermosphere and on frequency, azimuth, and angle of incidence are presented and discussed in some detail. (Author)

A69-26333 *#
OCEAN CIRCULATION AND CLIMATIC CHANGES.
S. I. Rasool (NASA, Goddard Space Flight Center, Goddard Institute for Space Studies, New York, N.Y.) and J. S. Hogan (New York University, New York, N.Y.).
(Conference on Ocean Circulation and Climatic Changes, Goddard Institute for Space Studies, New York, N.Y., Mar. 7, 8, 1968.) American Meteorological Society, Bulletin, vol. 50, Mar. 1969, p. 130-134.
Grant No. NsG-499.

Discussion of the role of the ocean as a regulator of climate and a key to the solution of the problem of climatic change. It is pointed out that the causes of climatic change may be a variable energy input from solar radiation or lunar tidal friction. The problem reduces then to determining how fluctuations in an extraterrestrial source of energy are translated into variations in global temperature. A first step toward the eventual solution of the problem can be made by investigating the manner in which the input of the solar energy over the globe is redistributed by the oceans. Several investigations of the large-scale interaction between the atmosphere and ocean are discussed. G.R.

A69-26739 *
THE GEOMAGNETIC TAIL.
Norman F. Ness (NASA, Goddard Space Flight Center, Laboratory for Space Sciences, Greenbelt, Md.).
(U.S. National Academy of Sciences and NASA Goddard Space Flight Center, International Symposium on the Physics of the Magnetosphere, Washington, D.C., Sept. 3-13, 1968.)
Reviews of Geophysics, vol. 7, Feb.-May 1969, p. 97-127. 72 refs.

Review of past experimental and theoretical models of the geomagnetic tail in the magnetosphere. The geometry of the geomagnetic tail and the earth's bow shock in cislunar space and the orbits of the satellites that have studied the geomagnetic tail are illustrated. The magnetic field measurements of the geomagnetic tail near the midnight meridian plane made by the satellite IMP 1 in 1964 are discussed. Significant measurements (performed by IMP 2) of the outer geomagnetic field demonstrating the gradual formation of the geomagnetic tail in the dawn-to-midnight region of the magnetosphere are presented. Spectra of electron counting rates measured in the magnetosheath and the plasma sheet by the Vela satellites are presented. Measurements of the magnetic-field intensity and electron velocity and density by Pioneer 7 are also given. M.G.

A69-27821 *
FRICTION BETWEEN MANTLE AND CORE OF THE EARTH AS A CAUSE OF THE SECULAR CHANGE IN OBLIQUITY.
Shinko Aoki (NASA, Goddard Space Flight Center, Greenbelt, Md.).
Astronomical Journal, vol. 74, Mar. 1969, p. 284-291. 21 refs.

Investigation of the causes of the discrepancy between the observed and theoretical values of the secular change in the obliquity of the orbital motion of the earth. A suggestion that this difference might come from an interaction between the mantle and the core of the earth is investigated. A very simple model of two rigid components with friction between them is considered. It is found that a damping time for the friction of about 40 years is required. This solution implies a drift of the core relative to the mantle of the order of $0\overset{\circ}{.}3$ per year, which is almost the same as the observed "west drift." G.R.

A69-28493 *#
FEASIBILITY OF DETERMINING ATMOSPHERIC OZONE FROM OUTGOING INFRARED ENERGY.
C. Prabhakara (NASA, Goddard Space Flight Center, Greenbelt, Md.; NASA, Goddard Space Flight Center, Goddard Institute for Space Studies, New York, N.Y.).
Monthly Weather Review, vol. 97, Apr. 1969, p. 307-314. 19 refs.

The high-resolution (5 cm^{-1}) measurements of the outgoing IR energy in the region of the 9.6-μ ozone band offer a means of determining the vertical distribution and total amount of ozone in the earth's atmosphere. With the application of radiative transfer theory and perturbation technique, a method is developed to deduce such information. The method hinges on a two-parametric representation of the ozone distribution in the earth's atmosphere. An error analysis based on four case studies is presented to show how well the atmospheric ozone could be determined. It is found that a small error in radiance value is magnified considerably in the inferred atmospheric ozone. (Author)

A69-29116 *

D-REGION ELECTRON DENSITY MEASUREMENTS DURING THE SOLAR ECLIPSE OF MAY 20, 1966.

J. A. Kane (NASA, Goddard Space Flight Center, Laboratory for Space Sciences, Greenbelt, Md.).

Planetary and Space Science, vol. 17, Apr. 1969, p. 609-616. 9 refs.

Rocket (Underwood and Muney, 1967) and satellite observations of 2 to 8 Å X-ray emission indicate that the solar eclipse of May 20, 1966, occurred during a period in which the sun was moderately active. The Goddard Space Flight Center conducted a series of small sounding rocket experiments to measure the ionospheric D-region electron density profile during successive stages of the eclipse. Compared to the uneclipsed profile, an order of magnitude reduction is observed in the D-region profile obtained near totality. From the electron density measurements together with the X-ray spectral data of Underwood and Muney it is concluded that on May 20, 1966, 2 to 8 Å X rays were not the dominant source of D-region ionization below approximately 80 km. (Author)

A69-31351 *#

THE POLAR EXOSPHERE NEAR SOLAR MAXIMUM.

Gerald M. Keating, James A. Mullins, and Edwin J. Prior (NASA, Langley Research Center, Hampton, Va.).

COSPAR, Plenary Meeting, 12th, Prague, Czechoslovakia, May 11-24, 1969, Paper. 23 p. 17 refs.

Investigation of the neutral polar exosphere between 550 and 900 km near the period of maximum solar activity by the satellites Explorer 19 and Explorer 24. With the increased heating in the upper atmosphere, atomic oxygen concentrations have increased to the extent that the drag effects of constituents other than atomic oxygen were negligible near 550 km. Thus the global distribution of atomic oxygen could be determined from the drag measurements of Explorer 24. Nighttime atomic oxygen concentrations were much lower than expected, but daytime concentrations were close to predictions. The most significant result of the high-latitude measurements is that polar atomic oxygen concentrations are found to be 30% higher than expected, and inferred polar exospheric temperatures are higher by 60 K. G. R.

A69-31974 *

IMPLICATIONS FOR IONOSPHERIC CHEMISTRY AND DYNAMICS OF A DIRECT MEASUREMENT OF ION COMPOSITION IN THE F2 REGION.

H. C. Brinton, M. W. Pharo, III, H. G. Mayr, and H. A. Taylor, Jr. (NASA, Goddard Space Flight Center, Laboratory for Atmospheric and Biological Sciences, Greenbelt, Md.).

Journal of Geophysical Research, vol. 74, June 1, 1969, p. 2941-2951. 25 refs.

Description of spectrometric rocket measurements of the concentrations of O^+, N^+, H^+, He^+, NO^+, O_2^+, and N_2^+ between 200 k and peak altitude, 630 km, at 1300 EST on Mar. 2, 1966, above Wallops Island. The dominant ion throughout the altitude range was O^+, with a maximum concentration of 5×10^5 ions/cm^3 at 260 km. The first detection of H^+ occurred at 230 km, its concentration increasing to 7×10^3 ions/cm^3 at peak altitude. The H^+/He^+ ratio was never lower than 6.0, the value at 420 km. The molecular ions NO^+ and O_2^+ were important constituents at 200 km, the concentration of each being 5×10^4 ions/cm^3; the concentrations of these ions fell off rapidly above this altitude. M. M.

A69-31981 *

BANDED CHORUS - A NEW TYPE OF VLF RADIATION OBSERVED IN THE MAGNETOSPHERE BY OGO 1 AND OGO 3.

W. J. Burtis (Stanford University, Radioscience Laboratory, Stanford; NASA, Ames Research Center, Moffett Field, Calif.) and R. A. Helliwell (Stanford University, Radioscience Laboratory, Stanford, Calif.).

Journal of Geophysical Research, vol. 74, June 1, 1969, p. 3002-3010. 11 refs.
Contract No. NAS 5-2131; Grants No. NsG-174-05-020-008; No. NGR-05-020-288.

Satellites OGO 1 and OGO 3 observe vlf discrete emissions in the magnetosphere primarily in a single, variable frequency band. The frequency, f, of this "banded chorus" depends on the equatorial electron gyrofrequency, f_{H0}, for the field line passing through the satellite, typical ratios of f/f_{H0} being 0.2-0.5. Evidently the emissions are produced near the equator at a fraction of the electron gyrofrequency, as predicted by electron cyclotron resonance generation mechanisms. A secondary dependence of the banded chorus frequency on dipole latitude, such that the lower ratios of f/f_{H0} are found at higher latitudes, is interpreted to mean that the emissions are generated at about half the electron gyrofrequency, but deviate inward from the field line to lower L values as they propagate earthward. Theoretical support is given by ray tracings showing the inward deviation of nonducted whistler-mode radiation due to the curvature of the magnetic field. Banded chorus has been observed at all local times, but is most common in the morning magnetosphere, outside the plasmapause. (Author)

A69-32083 *

F-REGION IONIZATION AND HEATING DURING MAGNETIC STORMS.

S. Chandra and J. R. Herman (NASA, Goddard Space Flight Center, Laboratory for Space Sciences, Greenbelt, Md.).

Planetary and Space Science, vol. 17, May 1969, p. 841-851. 27 refs.

Solution of the continuity and heat conduction equations for electrons, ions, and neutral species simultaneously from the viewpoint of studying the F-region magnetic storm behavior. It is shown that many of the observed changes in the F region during the main phase of a magnetic storm can be successfully explained by assuming a decrease in oxygen concentration at the turbopause level. The specific changes in neutral composition, electron density, and electron, ion, and neutral temperatures during magnetic storms are discussed for different solar conditions. (Author)

A69-32099 *

TRANSMISSION OF ALFVEN WAVES THROUGH THE EARTH'S BOW SHOCK.

James F. McKenzie (California, University, Dept. of Applied Electrophysics, La Jolla, Calif.) and Karl O. Westphal (NASA, Ames Research Center, Theoretical Studies Branch, Moffett Field, Calif.).

Planetary and Space Science, vol. 17, May 1969, p. 1029-1037. 11 refs.
Grant No. NGR-05-009-081.

Calculation of the transmission of Alfvén waves through the earth's bow shock on the basis of the theory of hydromagnetic shocks. For conditions typical of the solar wind it is shown that the amplitude of the magnetic field of the transmitted Alfvén wave is about three times larger than that of the incident, and, in addition, another Alfvén wave is generated with amplitude roughly equal to the incident wave amplitude. Since longitudinal waves are greatly amplified on passage through strong shocks and, as shown in the paper, transverse Alfvén waves undergo only moderate amplification, the energy flux of long wavelength waves in the magnetosheath ought to be predominantly in acoustic-type waves rather than in transverse waves. (Author)

A69-32187 *

RESULTS OF ROCKET MEASUREMENTS IN THE LOWER AURORAL IONOSPHERE.

K. Folkestad, B. Landmark, G. Slovli (Forsvarets Forsknings-institutt, Kjeller, Norway), and J. A. Kane (NASA, Goddard Space Flight Center, Greenbelt, Md.).

Journal of Atmospheric and Terrestrial Physics, vol. 31, June 1969, p. 835-844. 12 refs.
Research supported by the Royal Norwegian Council for Scientific and Industrial Research.

Discussion of rocket measurements of electrons, positive ions, and particles with energies greater than 40 keV in the ionospheric D region. From the particle data the height variation of the production of ion pairs is derived. This in turn is combined with the electron and ion measurements in an attempt to estimate the numerical values of the ion-ion recombination coefficient α_i. The results indicate a variation of α_i from 10^{-6} to 10^{-7} cm/sec in the height range from 70 to 80 km. (Author)

13 GEOPHYSICS

A69-32314 *
THE ROLE OF ATOMIC OXYGEN IN THE IONOSPHERIC E- AND F-REGION BEHAVIOR.
J. R. Herman and S. Chandra (NASA, Goddard Space Flight Center, Laboratory for Space Sciences, Greenbelt, Md.).
Planetary and Space Science, vol. 17, June 1969, p. 1247-1256. 8 refs.

Simultaneous solution of the continuity and heat conduction equations for the electron, ion, and neutral gases to show the effect of using the heat loss arising from the excitation of the fine structure levels of atomic oxygen and the heat input from a height-dependent electron heating efficiency. The solutions are compared to Thomson backscatter data obtained under conditions similar to those used in the theoretical model. A family of solutions is presented for three different values of the atomic oxygen density at the turbopause level and compares favorably to certain widely observed features of the main phase of a magnetic storm. From the comparison, it is shown that the results of decreasing the atomic oxygen density at the turbopause level are consistent with the observed changes in both the neutral and ionized constituents relative to quiet magnetic conditions. (Author)

A69-33155 *#
THE ANELASTIC APPROXIMATION FOR THERMAL CONVECTION.
D. O. Gough (NASA, Goddard Space Flight Center, Goddard Institute for Space Studies; New York University, Courant Institute of Mathematical Sciences, New York, N.Y.).
Journal of the Atmospheric Sciences, vol. 26, May 1969, p. 448-456. 12 refs.

Formal scale analysis of the equations of motion in a plane parallel atmosphere, assuming conditions to be such that relative fluctuations in density and temperature are small. It is found that an energetically consistent set of approximate equations can be derived which preclude the existence of acoustic motions. Such equations can be used to describe subsonic convection or internal gravity waves. Under certain conditions the analysis can be generalized to include vertical pulsations of the atmosphere. (Author)

A69-33156 *#
APPLICATION OF A NONLINEAR LEAST-SQUARES METHOD TO ATMOSPHERIC TEMPERATURE SOUNDING.
Thomas L. Barnett (NASA, Manned Spacecraft Center, Atmospheric Physics Branch, Houston, Tex.).
Journal of the Atmospheric Sciences, vol. 26, May 1969, p. 457-461. 13 refs.

Application of an optimization program for least-squares estimation of nonlinear parameters to the problem of atmospheric temperature sounding. From simulated sets of intensity measurements at 12 frequencies in the 15-μ CO_2 atmospheric band, this program is used to solve for the temperatures at five altitudes throughout the troposphere. It is shown that both temperature and altitude can be treated as variables in order to obtain the best match to the real profile. (Author)

A69-34283 *
THEORETICAL SPECTRAL SCATTERING OF ICE CLOUDS IN THE NEAR INFRARED.
James E. Hansen and Howard Cheyney (NASA, Goddard Space Flight Center, Goddard Institute for Space Studies, New York, N.Y.).
Journal of Geophysical Research, vol. 74, June 20, 1969, p. 3337-3346. 19 refs.
Grants No. NsG-499; No. NsG-33-016-013.

Calculation of the spectral reflectivity of clouds of ice spheres for the near-infrared wavelength region ($1 \lesssim \lambda \lesssim 4\,\mu$) for comparison with laboratory observations of ice clouds. The laboratory cloud particles were highly nonspherical ice crystals; however, it is shown that the major feature of the theoretical spectrum is in close agreement with the observations when spheres of equal volume are employed in the radiative transfer problem. The results provide some support for the contention that randomly oriented nonspherical particles may be replaced by equivalent spheres for calculations of reflected intensities. The reflectivities are shown to be sensitive to the particle size, especially the reflectivity minima near 1.5 and 2.0 μ. Changes by a factor of 2 in the particle size cause significant variations in the major reflectivity features; this result verifies that spectral reflectivity measurements can be of considerable value for cloud identification. The agreement of the theoretical and experimental spectra also indicates that it should be possible to obtain meaningful conclusions from IR reflectivity measurements of planetary atmospheres, such as the observations that have been made on the atmosphere of Venus. (Author)

A69-34284 *
ON THE ESTIMATION OF RELATIVE HUMIDITY PROFILES FROM MEDIUM-RESOLUTION INFRARED SPECTRA OBTAINED FROM A SATELLITE.
Barney J. Conrath (NASA, Goddard Space Flight Center, Greenbelt, Md.).
Journal of Geophysical Research, vol. 74, June 20, 1969, p. 3347-3361. 17 refs.

Study of the problem of obtaining estimates of the vertical humidity distribution in the troposphere on the basis of IR spectra obtained by TIROS satellites. Measurements of radiation emitted by the atmosphere of the earth in the IR absorption band of water vapor, obtained with satellite-borne instrumentation, contain information on atmospheric relative humidity. Two methods are developed for estimating tropospheric relative humidity profiles from IR spectral measurements for which the spectral resolution elements are narrow in comparison with the total width of the absorption band but wide in comparison with a single absorption line. G.R.

A69-34365 *
GENERATION OF AN ARTIFICIAL AURORA.
Wilmont N. Hess (NASA, Manned Spacecraft Center, Science and Applications Directorate, Houston, Tex.).
Science, vol. 164, June 27, 1969, p. 1512, 1513.

On Jan. 26, 1969, an Aerobee 350 rocket was fired from Wallops Island, Virginia, carrying an electron accelerator. Above 230 km, the electron guns put out a 0.5-A beam of 10-keV electrons in pulses of 1-sec duration aimed downward along the earth's magnetic field lines. The interaction of the electron beam with the atmosphere at an altitude of about 100 km generated enough light so that the auroral rays produced could be photographed on the ground by television camera systems. (Author)

A69-34421 *#
MICROWAVE OBSERVATIONS OF SEA STATE FROM AIRCRAFT.
W. Nordberg, J. Conaway, and P. Thaddeus (NASA, Goddard Space Flight Center, Laboratory for Atmospheric and Biological Sciences, Greenbelt, Md.).
Royal Meteorological Society, Quarterly Journal, vol. 95, Apr. 1969, p. 408-413. 7 refs.

Measurement, from aircraft at up to 12-km altitude, of the thermal radiation emitted by natural water surfaces at a wavelength of 1.55 cm. The dependence of the radiation on surface roughness is studied in view of its possible importance to satellite observation of sea state. (Author)

A69-34935 *
ELECTRIC FIELDS IN THE VICINITY OF AURORAL FORMS FROM MOTIONS OF BARIUM VAPOR RELEASES.
Eugene M. Wescott, John D. Stolarik, and James P. Heppner (NASA, Goddard Space Flight Center, Laboratory for Space Sciences, Greenbelt, Md.).
Journal of Geophysical Research, vol. 74, July 1, 1969, p. 3469-3487. 15 refs.

Observations of the motions of eleven barium-vapor clouds released from three Nike-Tomahawk rockets during the fall of 1967 from the auroral-zone rocket range at Andøya, Norway. It is found that the magnitude of E driving ionospheric currents cannot be deduced solely from ground observations because of the variable ionospheric electrical conductivity. Large gradients and/or irregularities in the E field are found to exist most of the time. These are revealed on three different time-space scales: (1) from differences in velocity for parallel moving clouds, (2) from velocity changes along the path of a given cloud, and (3) in the form of rayed structure within a cloud. Z.W.

A69-34947 *
EXPLORER 12 MAGNETOPAUSE OBSERVATIONS - LARGE-SCALE NONUNIFORM MOTION.
Richard L. Kaufmann (New Hampshire, University, Dept. of Physics, Durham, N. H.) and Andrei Konradi (NASA, Goddard Space Flight Center, Greenbelt, Md.).
Journal of Geophysical Research, vol. 74, July 1, 1969, p. 3609-3627. 17 refs.
NSF Grants No. GP-5255; No. GA-1131.

Study of a number of events that provide evidence that relatively small portions of the magnetopause occasionally become severely distorted. The largest distortions are generally elongated in the north-south direction, and the magnetosheath magnetic field is usually either nearly parallel or antiparallel to the magnetospheric field. As a result, the distortions do not involve severe bending of any magnetic field lines. The distortion is frequently triggered by a change in the properties of the solar wind. A model involving propagation of a thin discontinuity past the earth is consistent with the observations. Observationally the severe distortions are distinct from the small-scale, more or less uniform radial excursions of the magnetopause that are seen on a large fraction of all magnetopause crossings. They are also distinct from the expansions and contractions of the entire magnetosphere in response to changing solar wind pressure. (Author)

A69-34954 *
IONOSPHERIC AND MAGNETIC OBSERVATIONS AT 1000 KILOMETERS DURING THE GEOMAGNETIC STORM AND AURORA OF MAY 25-26, 1967.
J. A. Findlay, P. L. Dyson, L. H. Brace (NASA, Goddard Space Flight Center, Greenbelt, Md.), A. J. Zmuda, and W. E. Radford (Johns Hopkins University, Applied Physics Laboratory, Silver Spring, Md.).
Journal of Geophysical Research, vol. 74, July 1, 1969, p. 3705-3712. 18 refs.
Contract No. NOw-62-0604-C.

Comparison of electron temperature and number density measurements and of transverse magnetic disturbances obtained at 1000 km before, during, and after the magnetic storm and aurora of May 25, 26, 1967, with visual observations of the aurora. A degree of correlation is apparent. Throughout the latitudinal region of visual aurora the electron temperature and its latitudinal variations were much greater than are observed under quiet conditions. Temperatures in excess of 6500°K and temperature variations of greater than 500°K within less than 4 km along the satellite path were measured. Temperatures this high suggest a heat source other than auroral electron bombardment. The electron number density was also extremely structured through the region of visual aurora. Horizontal gradients were observed in which the number density changed by greater than 50% in less than 100 m along the satellite path. The greatest number density measured was $\sim 6.5 \times 10^4$ cm^{-3} (at $\Lambda = 53°$). The magnetometer recorded a number of disturbances (as large as 306 γ) in the region of unusual concentration and temperature behavior. (Author)

A69-35274 *
GEOLOGIC ORBITAL PHOTOGRAPHY - EXPERIENCE FROM THE GEMINI PROGRAM.
P. D. Lowman, Jr. (NASA, Goddard Space Flight Center, Greenbelt, Md.).
Photogrammetria, vol. 24, June 1969, p. 77-106. 46 refs.

Discussion of the Gemini terrain photography experiment and of the advantages and disadvantages of geologic orbital photography. Equipment used for terrain photography in the Gemini program included Hasselblad 500-C and SWC cameras and the Maurer 70 mm Space Camera with 38, 80, and 250 mm lenses. Specific geologic applications of the Gemini photographs included the study and remapping of part of Northern Baja California and the study of the tectonics and geology of northern Chihuahua, Mexico. The major advantages of orbital photography, as shown by the Gemini pictures, appear to be large area per picture, global coverage, unlimited dissemination, and availability of color or multispectral coverage. G. R.

A69-35977 *
MANGANOAN ILMENITE FROM A SIERRAN ADAMELLITE.
Kenneth G. Snetsinger (NASA, Ames Research Center, Space Sciences Div., Moffett Field, Calif.).
American Mineralogist, vol. 54, Mar.-Apr. 1969, p. 431-436. 14 refs.

Study of manganoan ilmenite occurring as a late minor accessory constituent of an adamellite in the northwest part of the Bass Lake quadrangle, Mariposa County, Calif. The mineral is not zoned, but it does show appreciable grain-to-grain variation in manganese and iron. Electron microprobe analysis of a grain containing highest manganese gives manganous oxide 11.1, ferrous oxide 28.8, titanium dioxide 52.0, ferric oxide 4.5, manganese sesquioxide 3.3, aluminum oxide 0.3, and vanadium trioxide 0.06 wt %. Valence states of manganese and iron were estimated with the electron microprobe by comparing line intensity ratios of these elements with an analyzed ilmenite and a synthetic oxide. G.R.

A69-37490 *
PREDICTION OF GEOMAGNETIC SECULAR CHANGE CONFIRMED.
Anne B. Kahle, R. H. Ball (RAND Corp., Santa Monica, Calif.), and J. C. Cain (NASA, Goddard Space Flight Center, Greenbelt, Md.).
Nature, vol. 223, July 12, 1969, p. 165. 7 refs.

Study of the correlation between the eccentric dipole motion and the change in length of day. A new model of the geomagnetic field was recently derived from data recorded by the OGO-2 and OGO-4 spacecraft. Using this model the eccentric dipole motion is westward at 0.114 deg/year. This new value confirms the predicted decrease some time during this period to a level about equivalent to that forty years earlier. G.R.

A69-37855 *
OBJECTIVES, HISTORY, AND PRINCIPAL ACHIEVEMENTS OF THE TOPSIDE SOUNDER AND ISIS PROGRAMS.
John E. Jackson (NASA, Goddard Space Flight Center, Laboratory for Space Sciences, Greenbelt, Md.) and E. S. Warren (Communications Research Centre, Ottawa, Canada).
IEEE, Proceedings, vol. 57, June 1969, p. 861-865. 37 refs.

Discussion of the ionospheric satellites that have been developed and launched as a result of the topside sounder and ISIS programs. The mission objectives, the feasibility studies, the program coordination, and the more important scientific accomplishments are summarized. (Author)

A69-37864 *
THE REDUCTION OF TOPSIDE IONOGRAMS TO ELECTRON-DENSITY PROFILES.
John E. Jackson (NASA, Goddard Space Flight Center, Greenbelt, Md.).
IEEE, Proceedings, vol. 57, June 1969, p. 960-976. 26 refs.

Review of the basic principles of the ionosonde technique for ionospheric electron-density determination, with special emphasis on the satellite version. It is shown that the lamination method of data reduction, developed initially for the analysis of ionograms obtained with ground-based ionosondes, can be used to calculate the electron density N vs true height h in the topside ionosphere provided a number of refinements are introduced. These refinements are required because the extraordinary wave data have to be used to obtain N(h) profiles from topside ionograms, and because these data are very sensitive to the magnetic field variation over the great altitude range of topside soundings. A complete procedure for analyzing topside ionograms, based upon a parabolic-in-log N lamination method is presented which incorporates (1) the actual values of the earth's magnetic field at all heights, (2) a change in

variable which renders the group path integrand finite at the reflection point, and (3) iteration until successive calculations agree to within 0.01 km. A procedure was also developed to insure and accelerate the convergence of the iteration process. The importance of each refinement is discussed and illustrated quantitatively. It is shown that this new N(h) reduction technique can, in theory, yield topside electron-density profiles with an altitude accuracy of a few kilometers over a 3000 to 400 km altitude range. This theoretical accuracy can be achieved using typically ten to twenty data points per ionogram. In practice, the errors in the N(h) profiles arise primarily from the limited resolution of the ionograms, calibration inaccuracies, and deviations from vertical propagation. (Author)

A69-37867 *
GLOBAL ELECTRON DENSITY DISTRIBUTIONS FROM TOPSIDE SOUNDINGS.
K. L. Chan and Lawrence Colin (NASA, Ames Research Center, Space Sciences Div., Moffett Field, Calif.).
IEEE, Proceedings, vol. 57, June 1969, p. 990-1004. 62 refs.

Global morphology of electron density distributions in the topside ionosphere during sunspot minimum as deduced from Alouette 1 and 2 ionograms. Graphs are shown illustrating the variations of electron density with altitude (400 to 3000 km), dip latitude (plus or minus 90 deg), local time (24 hours), and season (December and June solstices; equinox) for both quiet and disturbed geomagnetic field conditions. Average daytime and nighttime electron density distributions, based on the analysis of large quantities of Alouette 1 quiet-time data, are presented for the lower altitudes (less than 1000 km) and for low and middle dip latitudes for each season. Large-scale anomalous features are summarized and discussed with respect to their bottomside counterparts where such exist. (Author)

A69-37882 *
COMPARISON OF RESULTS OF EXPLORER XXXI DIRECT MEASUREMENT PROBES.
J. L. Donley, L. H. Brace, J. A. Findlay (NASA, Goddard Space Flight Center, Greenbelt, Md.), John H. Hoffman (Southwest Center for Advanced Studies, Dallas, Tex.), and Gordon L. Wrenn (London, University, University College, Mullard Space Science Laboratory, London, England).
IEEE, Proceedings, vol. 57, June 1969, p. 1078-1084. 6 refs.

Comparison of measurements of the major ionospheric parameters of ion and electron density and temperature and ionic species made by direct measurement probes on the Explorer 31 satellite. Plasma density results are compared with simultaneous data from the Alouette 2 satellite. Probe results are from the following experiments: planar ion trap, planar electron trap, cylindrical electrostatic probes, high-resolution magnetic ion mass spectrometer, planar Langmuir plate, and spherical ion probe. The plasma densities measured by the various probes generally agree with simultaneous Alouette 2 sounder values to within 20 per cent. Electron temperatures measured by three different types of probes generally agree within 10 per cent. Ion composition measurements by the planar ion trap and spherical probe show good agreement with the high-resolution magnetic mass spectrometer. Ion temperature measurements from the ion trap are consistently higher than spherical ion probe results. (Author)

A69-37887 *
DIFFUSIVE EQUILIBRIUM IN THE TOPSIDE IONOSPHERE.
S. J. Bauer (NASA, Goddard Space Flight Center, Laboratory for Space Sciences, Greenbelt, Md.).
IEEE, Proceedings, vol. 57, June 1969, p. 1114-1118. 41 refs.

Discussion of the general features of a diffusive equilibrium model for the topside ionosphere. The question of the applicability and limitations of such a concept is debated. It is noted that, although diffusive equilibrium may not always be strictly applicable, the concept provides a readily available analytical model for the general features of the topside ionosphere. M.M.

A69-37888 *
A REVIEW OF THE THEORIES CONCERNING THE EQUATORIAL F2 REGION IONOSPHERE.
Richard A. Goldberg (NASA, Goddard Space Flight Center, Laboratory for Space Sciences, Greenbelt, Md.).
IEEE, Proceedings, vol. 57, June 1969, p. 1119-1126. 55 refs.

Review of the major theories dealing with the equatorial F region, as categorized into two basic groups, causal and semi-phenomenological. It is pointed out that the mechanisms postulated in the electrodynamic drift theory are consistent in that they produce agreement between observations and theoretical results, but are lacking in direct experimental verification. It is noted that the transequatorial neutral winds currently postulated as the basic cause of transhemispheric asymmetries during solstice conditions require further investigation. M.M.

A69-37893 *
MODEL STUDIES OF THE KINKED Z TRACE IN TOPSIDE IONOGRAMS.
Lawrence Colin and K. L. Chan (NASA, Ames Research Center, Moffett Field, Calif.).
IEEE, Proceedings, vol. 57, June 1969, p. 1143-1147.

Review of the propagation characteristics of the Z trace observed on topside ionograms, with special consideration of the "kinked" Z trace. It is shown that the kink can be explained by a simple magnetoionic theory. A confirmation of this contention is found by a ray propagation analysis. V.P.M.

A69-37896 *
TEMPERATURE AND ION ABUNDANCE PROFILES DEDUCED FROM SIMULTANEOUS EXPLORER XXXI AND ALOUETTE II DATA.
Lawrence Colin, Stuart W. Dufour, and Dora S. Willoughby (NASA, Ames Research Center, Space Sciences Div., Moffett Field, Calif.).
IEEE, Proceedings, vol. 57, June 1969, p. 1154-1158. 9 refs.

Combination of field-aligned electron concentration profiles from the Alouette 2 sounder with simultaneous measurements of ion and electron temperatures and relative ionic abundances measured by the Explorer 31 satellite at its orbit, to deduce plasma temperature and ion concentration profiles, using a diffusive equilibrium theory. Analysis of eleven Alouette 2-Explorer 31 passes during December 1965, and January 1966 indicates that regions of constant or slightly decreasing plasma temperature with height are common in the lower exosphere. These results imply the presence of regions of negative or zero ion temperature gradients since experiment and theory generally yield nonnegative electron temperature gradients over the altitude range considered. M.M.

A69-38084 *
AN IMPROVED MODEL EQUATORIAL ELECTROJET WITH A MERIDIONAL CURRENT SYSTEM.
M. Sugiura (NASA, Goddard Space Flight Center, Laboratory for Space Sciences, Greenbelt, Md.) and D. J. Poros (Vitro Corporation of America, Vitro Services; NASA, Goddard Space Flight Center, Laboratory for Space Sciences, Greenbelt, Md.).
Journal of Geophysical Research, vol. 74, Aug. 1, 1969, p. 4025-4034. 13 refs.

The effective-conductivity model for the equatorial electrojet presented earlier is revised by including a meridional current system, thus making the current density divergence-free. Using a spherical harmonic expansion for the geomagnetic field, a model electrojet is constructed for each of the east longitudes of 0, 40, 80, 180, and 280 deg. It is shown that the essential feature of the meridional current system is the existence of two current loops, one on each side of the dip equator, with an equatorward current in the lower E region, an upward current over the dip equator, and a return current flowing in the upper E region. The intensities of the electrojet and the associated meridional current are significantly dependent on longitude, being strongest over Peru and weakest over India. The new model predicts a reversed (westward) current in a thin, narrow layer

located at several degrees off the dip equator, which is due to a reversal of the vertical polarization field. The meridional current loop creates a toroidal magnetic field of an intensity comparable with that of the main electrojet. (Author)

A69-38087 *
DIURNAL AND SEASONAL VARIATION OF ATMOSPHERIC ION COMPOSITION; CORRELATION WITH SOLAR ZENITH ANGLE.
H. C. Brinton, R. A. Pickett, and H. A. Taylor, Jr. (NASA, Goddard Space Flight Center, Laboratory for Atmospheric and Biological Sciences, Greenbelt, Md.).
Journal of Geophysical Research, vol. 74, Aug. 1, 1969, p. 4064-4073. 23 refs.

Global measurement of the diurnal and seasonal variations of the primary atmospheric ions in the earth's topside ionosphere between 280 and 2700 km, using the ion mass spectrometer on Explorer 32. Evidence of direct correlation between solar zenith angle and the low and midlatitude distributions of thermal positive O, N, He, and H ions was obtained as the satellite orbit plane traversed one complete diurnal cycle between June 11 and Oct. 5, 1966. M.M.

A69-38088 *
TEMPERATURE SHAPE PARAMETER OF THE THERMOSPHERE DETERMINED FROM PROBE DATA.
Gary R. Swenson (NASA, Marshall Space Flight Center, Aerospace Environment Div., Aero-Astrodynamics Laboratory, Huntsville, Ala.).
Journal of Geophysical Research, vol. 74, Aug. 1, 1969, p. 4074-4078. 8 refs.

Analysis of temperature shape parameters deduced from 18 thermosphere probe flights. Findings show a dependence of the shape parameter on the hour angle, indicating the thermospheric temperature profile to be more dependent on the dynamics of heating and cooling than on the exospheric temperature. (Author)

A69-38100 *
LATITUDINAL VARIATIONS IN THE NEUTRAL ATMOSPHERIC DENSITY.
George P. Newton and David T. Pelz (NASA, Goddard Space Flight Center, Greenbelt, Md.).
Journal of Geophysical Research, vol. 74, Aug. 1, 1969, p. 4169-4174. 22 refs.

Summary of in-situ atmospheric density measurements from the Explorer 32 density gauges for the time period from May through October 1966 revealing a latitudinal density structure in the neutral thermosphere during geomagnetically undisturbed times. For altitudes between 300 and 700 km the summer northern latitude densities are greater than the equatorial densities. For latitudes greater than 55 deg N, the northern latitude to equatorial latitude density ratio is smallest during the day (near 1.3) and increases at night to values greater than 2. Large (greater than 3) high-latitude to equatorial density ratios are observed near or in the auroral zone. These large ratios are observed even on geomagnetically quiet days. These results suggest that auroral zone and high latitude heating is a permanent feature of the summer thermosphere. (Author)

A69-38261 *
INFRARED MEASUREMENTS OF VARIATIONS IN STRATOSPHERIC WATER VAPOUR.
P. M. Kuhn, M. S. Lojko (ESSA, Boulder, Colo.), and E. W. Petersen (NASA, Ames Research Center, Moffett Field, Calif.).
Nature, vol. 223, Aug. 2, 1969, p. 462-464. 10 refs.

Determination of water vapor profiles in the stratosphere over long aircraft traverses from infrared radiometric observations under cloudless conditions by an inverse solution of the radiative transfer equation of Wark and Fleming (1966). The measurements indicate frequent variations of stratospheric water vapor apparently associated with tropospheric meteorological features. F.R.L.

A69-38334
SPACE RESEARCH IX; COSPAR, PLENARY MEETING, 11TH, TOKYO, JAPAN, MAY 9-21, 1968, PROCEEDINGS.
Meeting co-sponsored by the Japanese Committee on Space Research.
Edited by K. S. W. Champion, P. A. Smith, and R. L. Smith-Rose.
Amsterdam, North-Holland Publishing Co., 1969. 786 p. In English and French.
$34.

CONTENTS:

FOREWORD. M. Roy, p. vii.

PREFACE. K. S. W. Champion, P. A. Smith, and R. L. Smith-Rose, p. ix, x.

TRACKING, TELEMETRY AND DYNAMICS OF SATELLITES.

A NEW METHOD FOR OPTICAL TRACKING OF SPACE PROBES. P. P. Dobronravin, V. M. Mozherin, V. K. Prokofiev, and N. S. Chernykh, p. 1-3. (For abstract see issue 15, page 2729, Accession no. A68-32001)

A NEW AUTOMATIC CAMERA FOR SATELLITE TRACKING. A. M. Lozinskii and G. A. Leikin, p. 4, 5. (For abstract see issue 15, page 2777, Accession no. A68-32000)

SIMULTANEOUS TRACKING OF THE PAGEOS SATELLITE WITH SMALL CAMERAS PLACED AT LARGE DISTANCES. A. G. Massevich, S. K. Tatevian, and N. N. Kovalenko, p. 6-14. (For abstract see issue 15, page 2729, Accession no. A68-31999)

A MULTI-COINCIDENCE METHOD OF PHOTON COUNTING FOR OPTICAL TRACKING. M. Nanjo (Ministry of International Trade and Industries, Osaka, Japan), Y. Izawa, and C. Yamanaka (Osaka University, Osaka, Japan), p. 15-22. (For abstract see issue 15, page 2729, Accession no. A68-31949)

EXPERIMENTS IN LASER ECHO PHOTOGRAPHY ON SATELLITES (EXPERIENCES DE PHOTOGRAPHIE D'ECHOS LASER SUR SATELLITES). P. Muller, R. Moreau, and C. Veret (Paris, Observatoire, Meudon, Hauts-de-Seine, France), p. 23-28. (See A69-38335 21-07)

INITIAL PROCESSING OF FRENCH D1A SATELLITE EXPERIENCE (PREMIERES REDUCTIONS DE L'EXPERIENCE FRANÇAISE SUR SATELLITE D1A). J. Kovalevsky, F. Barlier, and I. Stellmacher (Meudon, Observatoire, Meudon, Hauts-de-Seine; Bureau des Longitudes; Paris, Université, Paris, France), p. 29-36. (See A69-38336 21-13)

OUTLINE OF A GENERAL ORBIT DETERMINATION METHOD. M. Schneider (München, Technische Hochschule, Munich, West Germany), p. 37-40. 8 refs. (See A69-38337 21-30)

FIRST-ORDER THEORY OF ORBITAL TRANSFER FOR GEODETIC SATELLITE MISSIONS. F. M. Calabria and A. Vallone (Geonautics, Inc., Falls Church, Va.), p. 41-48. 7 refs. (See A69-38338 21-30)

DISPERSION OF THE POSITIONS OF GEOS FLASHES—STUDY OF THE CAUSES (DISPERSION DES POSITIONS DES ECLAIRS DE GEOS—ETUDE DES CAUSES). P. Muller (Paris, Observatoire, Meudon, Hauts-de-Seine, France), p. 49-52. (See A69-38339 21-30)

DIAGNOSIS OF SPACECRAFT SURFACE PROPERTIES AND DYNAMICAL MOTIONS BY OPTICAL PHOTOMETRY. K. E. Kissell (USAF, Aerospace Research Laboratories, Wright-Patterson AFB, Ohio), p. 53-75. 38 refs. (See A69-38340 21-07)

THE EFFECT OF SOLAR-RADIATION PRESSURE ON DETERMINATION OF THE SEMIMAJOR AXIS IN SATELLITE-ORBIT COMPUTATION. J. W. Slowey (Smithsonian Institution, Cambridge, Mass.), p. 76-82. (For abstract see issue 15, page 2857, Accession no. A68-31979)

COSMIC DUST.

SPACE CONTAMINATION DUE TO MANNED VEHICLES. N. S. Kovar (Houston, University, Houston, Tex.), R. P. Kovar (William Marsh Rice University, Houston, Tex.), and G. P. Bonner (NASA, Manned Spacecraft Center, Houston, Tex.), p. 85-94. 7 refs. (See A69-38341 21-30)

CONTAMINANT PARTICLE TRAJECTORIES NEAR A SPACECRAFT. R. Grenda, S. Neste, and R. K. Soberman (General Electric Co., Philadelphia, Pa.), p. 95-101. (For abstract see issue 15, page 2856, Accession no. A68-31916)

DIRECT OBSERVATION OF PARTICULATE AND IMPACT CONTAMINATION OF "OPTICAL" SURFACES IN SPACE. D. S. Hallgren (Union University, Albany, N.Y.) and C. L. Hemenway (Union University; New York, State University, Albany, N.Y.), p. 102-110. (For abstract see issue 15, page 2856, Accession no. A68-31919)

A POSSIBLE INTER-RELATION BETWEEN INTERSTELLAR AND INTERPLANETARY COSMIC DUST. J. M. Greenberg (Rensselaer Polytechnic Institute, Troy, N.Y.), p. 111-115. (For abstract see issue 15, page 2858, Accession no. A68-32002)

METEOR PHYSICS AND THE DENSITY OF PARTICLES AT SATELLITE AND BALLOON ALTITUDES. P. W. Hodge and D. E. Brownlee (Washington, University, Seattle, Wash.), p. 116-119. 13 refs. (See A69-38342 21-13)

TERMINAL VELOCITIES OF SMALL PARTICLES IN THE EARTH'S UPPER ATMOSPHERE. U. Shafrir (Tel-Aviv University, Ramat-Aviv, Israel) and G. J. Dittberner (Wisconsin, University, Madison, Wis.), p. 120-128. (For abstract see issue 15, page 2842, Accession no. A68-31974)

PARTICLE COLLECTION RESULTS FROM RECENT ROCKET AND SATELLITE EXPERIMENTS. R. A. Skrivanek, S. A. Chrest, and R. F. Carnevale (USAF, Cambridge Research Laboratories, Bedford, Mass.), p. 129-139. 9 refs. (See A69-38343 21-30)

COLLECTION OF METEORIC DUST AFTER THE LEONID METEOR SHOWER 1965. C. L. Hemenway (New York, State University; Union University, Albany, N.Y.) and D. S. Hallgren (Union University, Albany, N.Y.), p. 140-146. (For abstract see issue 15, page 2858, Accession no. A68-32003)

PENETRATION STUDIES OF IRON DUST PARTICLES IN THIN FOILS. E. Grün and P. Rauser (Max-Planck-Institut für Kernphysik, Heidelberg, West Germany), p. 147-154. 11 refs. (See A69-38344 21-14)

THE MEASUREMENT OF MICROMETEORITE IMPACT FLUXES. R. C. Jennison and J. A. M. McDonnell (Canterbury, University, Canterbury, Kent, England), p. 155, 156.

THE NATURE OF NOCTILUCENT CLOUDS. G. Witt (Stockholm, University, Stockholm, Sweden), p. 157-169. 20 refs. (See A69-38345 21-13)

NUCLEATION AND GROWTH OF NOCTILUCENT CLOUD PARTICLES. E. Hesstvedt (Oslo, University, Oslo, Norway), p. 170-174. (See A69-38346 21-13)

A CONDENSATION MODEL OF NOCTILUCENT CLOUD FORMATION. A. D. Christie (Meteorological Service of Canada, Toronto, Canada), p. 175-182. (For abstract see issue 15, page 2809, Accession no. A68-31954)

EXTRATERRESTRIAL ORIGIN OF NOCTILUCENT CLOUDS. R. K. Soberman (General Electric Co., Philadelphia, Pa.), p. 183-189. 16 refs. (See A69-38347 21-13)

MEASUREMENT OF MICROMETEORITE IMPACTS FROM A SOUNDING ROCKET DURING A NOCTILUCENT CLOUD DISPLAY. B. A. Lindblad (Royal University Observatory, Lund, Sweden), p. 190-197. 6 refs. (See A69-38348 21-30)

AN OPTICAL MODEL FOR THE DETECTION OF COSMIC DUST IN THE UPPER ATMOSPHERE. F. Link (Československá Akademie Věd, Prague, Czechoslovakia), p. 198-200. (See A69-38349 21-13)

RADIATIONS.

A STUDY OF SOLAR AND COSMIC RADIATION FROM THE VENUS 4 SPACE PROBE. S. N. Vernov, A. E. Chudakov, P. V. Vakulov, E. V. Gorchakov, P. P. Ignatiev, N. N. Kontor, S. N. Kuznetsov, Iu. I. Logachev, G. P. Liubimov, A. G. Nikolaev, and N. V. Pereslegina, p. 203-214. (For abstract see issue 15, page 2841, Accession no. A68-31962)

COMPOSITION OF COSMIC RAYS MEASURED IN GEMINI XI. F. W. O'Dell, M. M. Shapiro, R. Silberberg, B. Stiller, C. H. Tsao (U.S. Navy, Naval Research Laboratory, Washington, D.C.), N. Durgaprasad, C. E. Fichtel, D. E. Guss, and D. V. Reames (NASA, Goddard Space Flight Center, Greenbelt, Md.), p. 215-221. (See A69-38350 21-29)

A SPECTRAL MEASUREMENT OF THE COSMIC X-RAY BACKGROUND DOWN TO 2 KEV. D. W. Green, B. G. Wilson, and A. J. Baxter (Calgary, University, Calgary, Canada), p. 222-225. 5 refs. (See A69-38351 21-29)

OBSERVATIONS ON DISCRETE X-RAY SOURCES. G. Buselli, M. C. Clancy, P. J. N. Davison, P. J. Edwards, K. G. McCracken, and R. M. Thomas (Adelaide, University, Adelaide, Australia), p. 226, 227.

ON THE DETERMINATION OF NIGHT SKY BRIGHTNESS FROM A SPACE VEHICLE. N. A. Dimov and A. B. Severnyi, p. 228.

IONOSPHERE.

THE IONIZATION OF THE LOWER IONOSPHERE UNDER THE INFLUENCE OF CORPUSCULAR RADIATION. V. F. Tulinov, L. V. Shibaeva, and S. G. Iakovlev, p. 231-236. 11 refs. (See A69-38352 21-29)

A STUDY OF THE LOWER IONOSPHERE OVER THE GEOMAGNETIC EQUATOR AT THUMBA USING A LANGMUIR AND PLASMA NOISE PROBE. S. Prakash, B. H. Subbaraya, and S. P. Gupta (Physical Research Laboratory, Ahmedabad, India), p. 237-245. 12 refs. (See A69-38353 21-13)

THE ELECTRON DENSITY PROFILE OF AURORAL LAYERS AS OBSERVED WITH ESRO ROCKETS AT KIRUNA. K. G. Jacobs, R. Kist, and K. Rawer (Deutsche Bundespost, Breisach, West Germany), p. 246-255. (For abstract see issue 15, page 2764, Accession no. A68-31937)

MASS SPECTROMETER MEASUREMENTS OF POSITIVE IONS AND NEUTRAL GAS BETWEEN 100 AND 233 KM ABOVE ANDÖYA, NORWAY. F. Arnold, W. Berthold, B. Betz, P. Lämmerzahl, and J. Zähringer (Max-Planck-Institut für Kernphysik, Heidelberg, West Germany), p. 256-261. 9 refs. (See A69-38354 21-13)

ROCKET OBSERVATION OF THE IONOSPHERE IN TWILIGHT CONDITIONS. K. Hirao, T. Tohmatsu, T. Ogawa (Tokyo, University, Tokyo, Japan), and H. Oya (Kyoto University, Kyoto, Japan), p. 262-266. 8 refs. (See A69-38355 21-13)

THE EFFECTIVE ELECTRON-LOSS COEFFICIENT AT HEIGHTS OF 200 TO 400 KM DURING INCREASING SOLAR ACTIVITY (1965-1966). N. M. Shutte and I. A. Knorin, p. 267-272. (For abstract see issue 15, page 2842, Accession no. A68-31970)

IONOSPHERIC EFFECTS OF THE FASTER ROTATION OF THE UPPER ATMOSPHERE. N. Matuura (Ministry of Posts and Telecommunications, Tokyo, Japan), p. 273-278. (For abstract see issue 15, page 2764, Accession no. A68-31944)

A PRELIMINARY ROCKET INVESTIGATION OF VERY LOW FREQUENCY IONOSPHERIC RESONANCES. R. E. Barrington (Defence Research Board, Ottawa, Canada), p. 279-286. (See A69-38356 21-07)

IONOSPHERIC ELECTRON TEMPERATURE MEASURED BY A GYRO-PLASMA PROBE. H. Oya and T. Aso (Kyoto University, Kyoto, Japan), p. 287-296. (For abstract see issue 15, page 2765, Accession no. A68-31993)

THE STRUCTURE OF THE TOPSIDE IONOSPHERE OVER JAPAN. N. Matuura and T. Ondoh (Ministry of Posts and Telecommunications, Tokyo, Japan), p. 297-303. (For abstract see issue 15, page 2764, Accession no. A68-31945)

PARTICLE TRAPPING AND PLASMA OSCILLATIONS IN THE SATELLITE-DISTURBED IONOSPHERE. V. C. Liu (Michigan, University, Ann Arbor, Mich.), p. 304-308. 7 refs. (See A69-38357 21-29)

SOME REMARKS ON THE ORIGIN OF LOWER HYBRID RESONANCE NOISE IN THE IONOSPHERE. R. E. Horita and T. Watanabe (British Columbia, University, Vancouver, Canada), p.

309-314. 6 refs. (See A69-38358 21-13)

MAGNETOSPHERE.

RECENT RESULTS IN THE STUDY OF AURORAL X RADIATION (RESULTATS RECENTS SUR L'ETUDE DU RAYONNEMENT X AURORAL). F. Cambou, G. Maral, and J.P. Treilhou (Toulouse, Université, Toulouse, France), p. 317-326. 10 refs. (See A69-38359 21-29)

AERONOMY.

ATOMIC OXYGEN GLOW AT 6300 Å FROM 1967 ROCKET DATA. T. M. Tarasova, p. 329-335. (See A69-38360 21-13)

COORDINATED MEASUREMENTS FROM TWO MULTI-EXPERIMENT ROCKETS IN AN AURORA. J. C. Ulwick (USAF, Cambridge Research Laboratories, Bedford, Mass.), K. D. Baker (Utah, University, Salt Lake City, Utah), and E. R. Hegblom (American Science and Engineering, Inc., Cambridge, Mass.), p. 336-342. (See A69-38361 21-13)

UPPER ATMOSPHERE PARAMETERS OBTAINED FROM RECENT FALLING SPHERE MEASUREMENTS AT EGLIN, FLORIDA. A. C. Faire and K. S. W. Champion (USAF, Cambridge Research Laboratories, Bedford, Mass.), p. 343-353. (For abstract see issue 15, page 2766, Accession no. A68-32011)

LARGE-SCALE WIND MOTION AND TURBULENCE IN THE UPPER ATMOSPHERE FROM ROCKET EXPERIMENTS. M. S. Ahmad (Pakistan Space and Upper Atmosphere Research Committee, Karachi, Pakistan), p. 354-362. (See A69-38362 21-13)

E-REGION VERTICAL NEUTRAL WINDS. M. A. Macleod (USAF, Cambridge Research Laboratories, Bedford, Mass.), p. 363-373. 20 refs. (See A69-38363 21-13)

NEUTRAL ATMOSPHERE WINDS ABOVE 100 KM. P. D. Bhavsar, M. S. Narayanan, and K. R. Rao (Physical Research Laboratory, Ahmedabad, India), p. 374, 375.

CONSEQUENCES OF FINE STRUCTURE IN THE VERTICAL TEMPERATURE PROFILE ON RADIATIVE TRANSFER IN THE MESOSPHERE. S. R. Drayson and E. S. Epstein (Michigan, University, Ann Arbor, Mich.), p. 376-384. (For abstract see issue 15, page 2810, Accession no. A68-31995)

THE SPECTRAL BRIGHTNESS OF AN INHOMOGENEOUS SPHERICAL ATMOSPHERE. R. Bellman (Southern California, University, Los Angeles, Calif.), H. Hagiwada, R. Kalabra (RAND Corp., Santa Monica, Calif.), and S. Ueno (Kyoto University, Kyoto, Japan), p. 385-391. (For abstract see issue 15, page 2856, Accession no. A68-31955)

A COMPARISON OF CIRA 1965 TO SOUNDING ROCKET UPPER ATMOSPHERE DATA IN INDONESIA. Karjoto and M. H. Sunjata (Indonesian National Aeronautics and Space Institute, Java, Indonesia), p. 392-401. (For abstract see issue 15, page 2763, Accession no. A68-31932)

WINTER ATMOSPHERE–STRATOSPHERE TO THE TURBOPAUSE.

SIMILARITIES IN THE ANNUAL BEHAVIOUR OF THE STRATOSPHERE AND THE D- AND E-LAYER OF THE IONOSPHERE. H. Schwentek (Max-Planck-Institut für Aeronomie, Lindau über Northeim, West Germany), p. 405-417. (For abstract see issue 15, page 2762, Accession no. A68-31635)

NITRIC OXIDE IN THE MESOSPHERE AND ITS VARIATIONS. A. P. Mitra (NASA, Goddard Space Flight Center, Greenbelt, Md.), p. 418-432. 20 refs. (See A69-38364 21-13)

LOWER THERMOSPHERE IONS IN THE NIGHTTIME AURORAL ZONE. G. Horiuchi (Meteorological Agency, Tokyo, Japan), p. 433-441. 26 refs. (See A69-38365 21-13)

COMPOSITION CHANGES IN THE LOWER THERMOSPHERE. F. S. Johnson (Southwest Center for Advanced Studies, Dallas, Tex.) and B. Gottlieb (Bishop College, Dallas, Tex.), p. 442-446. 5 refs. (See A69-38366 21-13)

REVIEW OF UPPER ATMOSPHERE PROPERTIES.

REVIEW OF ATMOSPHERIC STRUCTURE IN THE REGION 30-100 KM. G. V. Groves (London, University, University College, London, England), p. 449-458. (For abstract see issue 15, page 2764, Accession no. A68-31942)

REVIEW OF THE PROPERTIES OF THE LOWER THERMOSPHERE. K. S. W. Champion (USAF, Cambridge Research Laboratories, Bedford, Mass.), p. 459-477. (For abstract see issue 15, page 3765, Accession no. A68-31994)

THE NEUTRAL ATMOSPHERE ABOVE 200 KM—A PROGRESS REPORT. L. G. Jacchia (Smithsonian Institution, Cambridge, Mass.), p. 478-486. (For abstract see issue 15, page 2764, Accession no. A68-31939)

TEMPERATURE AND DENSITY OF THE THERMOSPHERE IN 1966-1967. M. Ia. Marov and A. M. Alpherov (Akademiia Nauk SSSR, Moscow, USSR), p. 487-498. (For abstract see issue 15, page 2765, Accession no. A68-31946)

THERMOSPHERE AND EXOSPHERE.

MEASUREMENTS OF SOME NEUTRAL COMPONENTS OF THE ARCTIC THERMOSPHERE. E. D. Biuro, A. P. Zhukov, G. M. Martynkevich, and E. G. Shvidkovskii, p. 501-507. 12 refs. (See A69-38367 21-13)

MASS SPECTROMETER INVESTIGATION OF THE NEUTRAL ATMOSPHERIC COMPOSITION AT THUMBA EQUATORIAL ROCKET LAUNCHING STATION. G. I. Golishev, S. M. Poloskov, A. A. Pokhunkov, D. B. Rozhdestvenskii, B. I. Morozov (Glavnoe Upravlenie Gidrometeorologicheskoi Sluzhby SSSR, Moscow, USSR), J. S. Shirke, and J. N. Desai (Physical Research Laboratory, Ahmedabad, India), p. 508-511. (For abstract see issue 15, page 2764, Accession no. A68-31941)

NEUTRAL PARTICLE DENSITY RATIOS IN THE THERMOSPHERE AS DERIVED FROM MASS SPECTROMETRIC MEASUREMENTS ABOVE SARDINIA. D. Offermann, U. Von Zahn, W. Bitterberg, and K. Bruchhausen (Bonn, Universität, Bonn, West Germany), p. 512, 513. (See A69-38368 21-13)

THERMOSPHERIC TEMPERATURES IN THE CENTRAL ARCTIC. I. N. Ivanova, G. A. Kokin, and A. F. Chizhov, p. 514-518. (For abstract see issue 15, page 2764, Accession no. A68-31938)

THERMOSPHERIC DENSITIES AND TEMPERATURES FROM EUV ABSORPTION MEASUREMENTS BY OSO-III. H. E. Hinteregger and L. A. Hall (USAF, Cambridge Research Laboratories, Bedford, Mass.), p. 519-529. (For abstract see issue 15, page 2766, Accession no. A68-32012)

DIURNAL TEMPERATURE VARIATIONS AND VERTICAL PARTICLE FLUXES IN THE UPPER ATMOSPHERE. L. A. Antonova and G. S. Ivanov-Kholodnyi, p. 530-533. (For abstract see issue 15, page 2841, Accession no. A68-31957)

CHANGES IN THE LOWER EXOSPHERE SINCE SOLAR MINIMUM. G. M. Keating (NASA, Langley Research Center, Hampton, Va.), p. 534-546. (For abstract see issue 15, page 2763, Accession no. A68-31930)

EQUATORIAL ATMOSPHERIC DENSITY OBTAINED FROM SAN MARCO II SATELLITE BETWEEN 200 AND 350 KM. L. Broglio (Roma, Università, Rome, Italy), p. 547-554. (See A69-38369 21-13)

GLOBAL ATMOSPHERIC RESEARCH PROGRAMME (GARP).

PRESENT STATUS OF CLOUD VELOCITY COMPUTATIONS FROM THE ATS I AND ATS III SATELLITES. T. Fujita (Chicago, University, Chicago, Ill.), p. 557-570. (See A69-38370 21-20)

RELATIONSHIP BETWEEN OBSERVED WINDS AND CLOUD VELOCITIES DETERMINED FROM PICTURES OBTAINED BY THE ESSA III, ESSA V AND ATS I SATELLITES. T. Izawa (Ministry of Transportation, Tokyo, Japan) and T. Fujita (Chicago, University, Chicago, Ill.), p. 571-579. (See A69-38371 21-20)

ANGULAR CHARACTERISTICS OF THE REFLECTANCE OF THE EARTH-ATMOSPHERE SYSTEM AS OBTAINED FROM A SYNCHRONOUS SATELLITE. E. Raschke (Ruhr-Universität, Bochum, West Germany), p. 580-585. 5 refs. (See A69-38372 21-13)

EOLE CONSTANT LEVEL BALLOON FLIGHTS IN THE TROPOSPHERE. P. Morel (Centre National de la Recherche Scientifique, Verrières-le-Buisson, Essonne, France), p. 586-589. (See A69-38373 21-02)

SOME REMARKS ON METEOROLOGICAL MEASURE-

MENTS WITH OCCULTATION SATELLITES. A. Kliore (California Institute of Technology, Pasadena, Calif.), p. 590-602. 6 refs. (See A69-38374 21-13)

DENSITY MEASUREMENT WITH RADIO WAVE OCCULTATION TECHNIQUES. B. B. Lusignan (Stanford University, Stanford, Calif.), p. 603-609. (See A69-38375 21-13)

MICROWAVE REFRACTION AS A TECHNIQUE FOR SATELLITE METEOROLOGY—SOME PROBLEMS. F. F. Fischbach, M. E. Graves, and L. M. Jones (Michigan, University, Ann Arbor, Mich.), p. 610-616. (See A69-38376 21-07)

NATIONAL ACTIVITIES RELATIVE TO GARP OBSERVING SYSTEMS. S. Ruttenberg (COSPAR, Paris, France), p. 617-621.

MOON AND PLANETS.

THE LUNAR ORBITER PROGRAM. W. E. Brunk (NASA, Washington, D.C.), p. 625-656. (See A69-38377 21-30)

THE EROSION PROCESSES ON THE LUNAR SURFACE. Z. Kopal (Boeing Co., Seattle, Wash.), p. 657-677. (See A69-38378 21-30)

LUNAR EXPLORER 35. N. F. Ness (NASA, Goddard Space Flight Center, Greenbelt, Md.), p. 678-703. 29 refs. (See A69-38379 21-30)

THE ATMOSPHERE OF VENUS FROM RECENT INVESTIGATIONS. A. D. Kuzmin, p. 704-711. (For abstract see issue 15, page 2856, Accession no. A68-31921)

STRUCTURE OF THE ATMOSPHERE OF VENUS DERIVED FROM MARINER V S-BAND MEASUREMENTS. A. Kliore, D. L. Cain, G. S. Levy (California Institute of Technology, Pasadena, Calif.), G. Fjeldbo (Stanford University, Stanford, Calif.), and S. I. Rasool (NASA, Goddard Space Flight Center, New York, N.Y.), p. 712-729. 13 refs. (See A69-38380 21-30)

TEMPERATURE AND DENSITY OF THE VENUS ATMOSPHERE ACCORDING TO MEASUREMENTS OBTAINED BY VENERA 4. V. V. Mikhnevich and V. A. Sokolov, p. 730-744. (For abstract see issue 15, page 2856, Accession no. A68-31920)

THE ATMOSPHERE OF THE PLANET VENUS FROM DATA OF THE SOVIET SPACE PROBE VENERA 4. V. S. Avduevskii, M. Ia. Marov, and M. K. Rozhdestvenskii, p. 745-759. (For abstract see issue 15, page 2856, Accession no. A68-31917)

INDUCED MAGNETOSPHERE OF VENUS. F. S. Johnson and J. E. Midgley (Southwest Center for Advanced Studies, Dallas, Tex.), p. 760-763. 7 refs. (See A69-38381 21-30)

INDEX OF AUTHORS, p. 769, 770.

A69-38364 *

NITRIC OXIDE IN THE MESOSPHERE AND ITS VARIATIONS.

A. P. Mitra (NASA, Goddard Space Flight Center, Laboratory for Space Sciences, Greenbelt, Md.).

IN: SPACE RESEARCH IX; COSPAR, PLENARY MEETING, 11TH, TOKYO, JAPAN, MAY 9-21, 1968, PROCEEDINGS. (A69-38334 21-13)

Meeting co-sponsored by the Japanese Committee on Space Research.

Edited by K. S. W. Champion, P. A. Smith, and R. L. Smith-Rose.

Amsterdam, North-Holland Publishing Co., 1969, p. 418-432. 20 refs.

Discussion of the distributions, seasonal variations, and the resulting ionospheric implication of mesospheric nitric oxide. Attention is given to the principal features of an average distribution for this constituent that would be consistent with photochemical considerations, with the diurnal and solar cycle variations in D-region ionization, and with the relative abundances of the molecular nitric oxide and oxygen ions. The extent to which the average profile may vary seasonally in middle latitudes is examined. Large winter enhancements occur in NO concentrations at all D region heights above about 70 km due to the winter warming at these heights. The enhanced region is limited roughly between 70 and 90 km, the lower limit being controlled by the rapid loss of nitric oxide through reactions with ozone. Ionospheric implications of these NO distributions are also discussed. (Author)

A69-38482

ATMOSPHERIC EMISSIONS; PROCEEDINGS OF THE NATO ADVANCED STUDY INSTITUTE, AGRICULTURAL COLLEGE OF NORWAY, ÅS, NORWAY, JULY 29-AUGUST 9, 1968.

Institute supported by NATO, the U.S. Air Force, and the U.S. Navy.

Edited by B. M. McCormac (Lockheed Aircraft Corp., Research Laboratories, Palo Alto, Calif.) and Anders Omholt (Oslo, University, Oslo, Norway).

New York, Van Nostrand Reinhold Co., 1969. 573 p.

$25.95.

CONTENTS:

PREFACE. B. M. McCormac (Lockheed Aircraft Corp., Palo Alto, Calif.) and A. Omholt (Oslo, University, Oslo, Norway), p. vii, viii.

DEDICATION TO SYDNEY CHAPMAN.

SYDNEY CHAPMAN. F. Roach, p. 3-8.

AURORA—ORIENTATION.

AURORAL SCIENCE, 1600 TO 1965—TOWARDS ITS GOLDEN AGE? S. Chapman (National Center for Atmospheric Research, Boulder, Colo.; Alaska, University, College, Alaska), p. 11-25. 14 refs. (See A69-38483 21-13)

TELEVISION OBSERVATION OF AURORAS. T. N. Davis (Alaska, University, College, Alaska), p. 27-35. 12 refs. (See A69-38484 21-13)

FUNDAMENTAL ELECTROMAGNETIC PROCESSES IN THE OUTER MAGNETOSPHERE. C.-G. Fälthammar (Royal Institute of Technology, Stockholm, Sweden), p. 37-46. 60 refs. (See A69-38485 21-13)

AURORAL SPECTROSCOPY A. V. Jones (National Research Council, Ottawa, Canada), p. 47-62. 50 refs. (See A69-38486 21-13)

POLAR CAP EMISSIONS. K. Lassen (Dansk Meteorologisk Institut, Copenhagen, Denmark), p. 63-71. 17 refs. (See A69-38487 21-13)

AURORAL AND POLAR CAP ABSORPTION. B. Hultqvist (Kungl. Vetenskapsakademien, Kiruna, Sweden), p. 73-90. 79 refs. (See A69-38488 21-13)

AURORAL OBSERVATIONS—PARTICLES AND THEIR EFFECTS.

SUMMARY OF ROCKET MEASUREMENTS OF AURORAL PARTICLE PRECIPITATION. B. A. Whalen and I. B. McDiarmid (National Research Council, Ottawa, Canada), p. 93-106. 24 refs. (See A69-38489 21-13)

FINE STRUCTURE IN THE ENERGY SPECTRUM OF LOW ENERGY AURORAL ELECTRONS. D. S. Evans (NASA, Goddard Space Flight Center, Greenbelt, Md.), p. 107-118. 18 refs. (See A69-38490 21-13)

COORDINATED MEASUREMENTS OF PARTICLES, LUMINOSITY, AND ELECTRON CONCENTRATIONS. R. E. Meyerott and J. E. Evans (Lockheed Aircraft Corp., Palo Alto, Calif.), p. 119-130. 13 refs. (See A69-38491 21-13)

PULSATING AURORA. A. Omholt (Oslo, University, Oslo, Norway), G. J. Kvifte, and H. Pettersen (Auroral Observatory, Tromsø, Norway), p. 131-143. 35 refs. (See A69-38492 21-13)

OBSERVATIONS OF AURORAL PHENOMENA AT CONJUGATE POINTS. J. K. Hargreaves (ESSA, Boulder, Colo.), p. 145-152. 54 refs. (See A69-38493 21-13)

ELECTROMAGNETIC EMISSIONS IN THE kHz BAND DURING AURORA. L. Harang (Oslo, University, Oslo, Norway), p. 153-163. 9 refs. (See A69-38494 21-13)

VLF AND LF EMISSIONS IN AURORAL REGIONS OF THE IONOSPHERE. T. S. Jørgensen (Dansk Meteorologisk Institut, Copenhagen, Denmark), p. 165-174. 19 refs. (See A69-38495 21-13)

SIMULTANEOUS GROUND AND SATELLITE MEASUREMENTS OF THE ENHANCED ELECTROMAGNETIC BAND EMISSION BETWEEN 500 AND 1000 Hz. J. Holtet and A. Egeland (Norske Institutt for Kosmisk Fysikk, Oslo, Norway), p. 175-179. (See A69-38496 21-13)

SOME CHARACTERISTICS OF AURORAL ZONE X-RAYS. G. Kremser (Max-Planck-Institut für Aeronomie, Lindau über Northeim, West Germany), p. 181-191.

GEOMAGNETIC PULSATIONS IN THE AURORAL ZONE. K. Wilhelm (Max-Planck-Institut für Aeronomie, Lindau über Northeim, West Germany), p. 193-199. 24 refs. (See A69-38497 21-13)

RADIO OBSERVATIONS OF THE AURORA BY CONTINUOUS WAVE TRANSMISSIONS. G. Lange-Hesse (Max-Planck-Institut für Aeronomie, Lindau über Northeim, West Germany), p. 201-212. 17 refs. (See A69-38498 21-13)

MODULATION OF AURORAL ELECTRONS NEAR THE EQUATORIAL PLANE. G. M. Courtier, D. A. Bryant, and A. D. Johnstone (Science Research Council, Slough, Bucks., England), p. 213-217. 6 refs. (See A69-38499 21-13)

SATELLITE MEASUREMENTS ON AURORAL PARTICLE FLUXES. R. G. Johnson and R. D. Sharp (Lockheed Aircraft Corp., Palo Alto, Calif.), p. 219-231. 32 refs. (See A69-38500 21-13)

LATITUDINAL DISTRIBUTION OF AURORAL AND AIRGLOW EMISSIONS. R. H. Eather (William Marsh Rice University, Houston, Tex.), p. 233-239. 17 refs. (See A69-38501 21-13)

AURORA—FUNDAMENTAL CAUSES.

PENETRATION OF PARTICLES INTO THE ATMOSPHERE. M. Walt and C. R. Chappell (Lockheed Aircraft Corp., Palo Alto, Calif.), p. 243-249. 14 refs. (See A69-38502 21-13)

MAGNETOSPHERIC CONVECTION PATTERNS INFERRED FROM HIGH LATITUDE ACTIVITY. J. P. Heppner (NASA, Goddard Space Flight Center, Greenbelt, Md.), p. 251-266. 22 refs. (See A69-38503 21-13)

MAGNETOSPHERIC SUBSTORM. S.-I. Akasofu (Alaska, University, College, Alaska), p. 267-276. 23 refs. (See A69-38504 21-13)

AURORAL CURRENT SYSTEMS. R. Boström (Kungl. Tekniska Högskolan, Stockholm, Sweden), p. 277-284. 30 refs. (See A69-38505 21-13)

FIELD ALIGNED CURRENTS AND AURORAL PRECIPITATION. L. P. Block and C.-G. Fälthammar (Kungl. Tekniska Högskolan, Stockholm, Sweden), p. 285-292. 38 refs. (See A69-38506 21-13)

HIGHLY IRREGULAR ARTIFICIAL PLASMA CLOUDS IN THE AURORAL ZONE. G. Haerendel, R. Lüst, E. Rieger, and H. Völk (Max-Planck-Institut für Physik und Astrophysik, Garching, West Germany), p. 293-303. 6 refs. (See A69-38507 21-13)

PROBE MEASUREMENTS OF ELECTRIC FIELDS IN SPACE. T. L. Aggson (NASA, Goddard Space Flight Center, Greenbelt, Md.), p. 305-316. 13 refs. (See A69-38508 21-13)

HELIUM IN THE ATMOSPHERE, AURORA AND SOLAR WIND. W. I. Axford (California, University, La Jolla, Calif.), p. 317-325. 38 refs. (See A69-38509 21-13)

RELATION OF ENERGETIC PARTICLES IN THE PLASMA SHEET TO THE AURORAL ZONE. K. A. Anderson (California, University, Berkeley, Calif.), p. 327-336. 15 refs. (See A69-38510 21-13)

SOME RECENT RESULTS USING THE DUNGEY MODEL. T. W. Speiser (Colorado, University, Boulder, Colo.), p. 337-349. 35 refs. (See A69-38511 21-13)

OBSERVATIONS IN THE MAGNETOTAIL AND THEIR INTERPRETATION. E. W. Hones, Jr. (California, University, Los Alamos, N. Mex.), p. 351-363. 13 refs. (See A69-38512 21-13)

AIRGLOW—ORIENTATION.

UPPER ATMOSPHERIC EMISSION PROCESSES. W. Swider, Jr. (USAF, Cambridge Research Laboratories, Bedford, Mass.), p. 367-382. 79 refs. (See A69-38513 21-13)

NIGHT AIRGLOW PHENOMENOLOGY. S. M. Silverman (USAF, Cambridge Research Laboratories, Bedford, Mass.), p. 383-397. 89 refs. (See A69-38514 21-13)

TWILIGHT OBSERVATIONS. G. Kvifte (Agricultural College of Norway, Ås, Norway), p. 399-410. 56 refs. (See A69-38515 21-13)

AIRGLOW SPECTROSCOPIC TEMPERATURES. G. G. Shepherd (London, University, University College, London, England; Saskatchewan, University, Saskatoon, Saskatchewan, Canada), p. 411-422. 61 refs. (See A69-38516 21-13)

IONOSPHERIC PHENOMENA RELATED TO AIRGLOW. L. Thomas (Science Research Council, Slough, Bucks., England), p. 423-435. 100 refs. (See A69-38517 21-13)

AIRGLOW—OBSERVATIONS AND INTERPRETATIONS.

THE NIGHTGLOW AND THE F REGION IONOSPHERE. F. E. Roach, p. 439-447. 15 refs. (See A69-38518 21-13)

NI ($^4S-^2D$) RADIATION IN THE NIGHT AIRGLOW AND LOW LATITUDE AURORA. G. M. Weill (Centre National de la Recherche Scientifique, Paris, France), p. 449-470. 56 refs. (See A69-38519 21-13)

SUNSET TO SUNRISE VARIATIONS OF THE OH EMISSION OF THE NIGHT SKY. E. R. Huppi and A. T. Stair, Jr. (USAF, Cambridge Research Laboratories, Bedford, Mass.), p. 471-475. 11 refs. (See A69-38520 21-13)

LUMINOUS EFFICIENCY OF ELECTRON INDUCED EMISSION IN NITROGEN. R. O'Neil (USAF, Cambridge Research Laboratories, Bedford, Mass.) and G. Davidson (American Science and Engineering, Inc., Cambridge, Mass.), p. 477-483. 19 refs. (See A69-38521 21-24)

PREDAWN ENHANCEMENT OVER BRITAIN. R. W. Smith (Belfast, Queen's University, Belfast, Northern Ireland), p. 485-488.

SUMMARY ON SPECTROSCOPY OF ROCKET RELEASES. O. Harang (Auroral Observatory, Tromsø, Norway), p. 489-499. 50 refs. (See A69-38522 21-13)

AIRGLOW AND VERTICAL EDDY TRANSPORT. E. Hesstvedt (Oslo, University, Oslo, Norway), p. 501-505. 6 refs. (See A69-38523 21-13)

STRUCTURE OF THE TURBULENT FIELD FROM 90 TO 120 KM. J. Barat and J. Blamont (Centre National de la Recherche Scientifique, Verrières-le-Buisson, Essonne, France), p. 507-514. 7 refs. (See A69-38524 21-13)

ON NIGHTGLOW INTENSITY VARIATIONS CONNECTED WITH VERTICAL MOVEMENTS IN THE UPPER ATMOSPHERE. J. Dachs (Ruhr-Universität, Bochum, West Germany), p. 515-517. 5 refs. (See A69-38525 21-13)

NOTE ON THE MECHANISM OF THE 5577 Å OI NIGHT GLOW EMISSION AT 100 KM. C. P. Lagos (Massachusetts Institute of Technology, Cambridge, Mass.), p. 519-521. 10 refs. (See A69-38526 21-13)

SEMI-EMPIRICAL CROSS SECTIONS AND THE AIRGLOW AND AURORA. A. E. S. Green, L. R. Peterson, and S. S. Prasad (Florida, University, Gainesville, Fla.), p. 523-532. 31 refs. (See A69-38527 21-13)

THE POLAR WIND AND ITS IMPLICATIONS. P. M. Banks (California, University, La Jolla, Calif.), p. 533-538. 12 refs. (See A69-38528 21-13)

HYDROGEN AND HELIUM IN THE UPPER ATMOSPHERE. B. A. Tinsley (Southwest Center for Advanced Studies, Dallas, Tex.), p. 539-544. 33 refs. (See A69-38529 21-13)

CONFERENCE REVIEW AND CONCLUSIONS.

SUMMARY AND CONCLUSIONS. M. Walt (Lockheed Aircraft Corp., Palo Alto, Calif.), p. 547-558.

APPENDIX I—GLOSSARY, p. 559.

INDEX, p. 561-563.

A69-38490 *

FINE STRUCTURE IN THE ENERGY SPECTRUM OF LOW ENERGY AURORAL ELECTRONS.

D. S. Evans (NASA, Goddard Space Flight Center, Greenbelt, Md.). IN: ATMOSPHERIC EMISSIONS; PROCEEDINGS OF THE NATO ADVANCED STUDY INSTITUTE, AGRICULTURAL COLLEGE OF NORWAY, ÅS, NORWAY, JULY 29-AUGUST 9, 1968. (A69-38482 21-13)

Institute supported by NATO, the U.S. Air Force, and the U.S. Navy.

Edited by B. M. McCormac and Anders Omholt.

New York, Van Nostrand Reinhold Co., 1969, p. 107-118. 18 refs.

Study of the energy spectrum of primary auroral particles for the purpose of determining some unique characteristics which may be linked to specific acceleration or precipitation mechanisms. A review of a number of rocket investigations of the energy spectra of low-energy auroral electrons is presented. It is concluded that auroral energy spectra exhibiting structure, especially peaks, must now be viewed as a common, if not typical occurrence, indicating that electrostatic fields have played a role in the acceleration process. B.H.

A69-38503 *

MAGNETOSPHERIC CONVECTION PATTERNS INFERRED FROM HIGH LATITUDE ACTIVITY.

J. P. Heppner (NASA, Goddard Space Flight Center, Greenbelt, Md.).

IN: ATMOSPHERIC EMISSIONS; PROCEEDINGS OF THE NATO ADVANCED STUDY INSTITUTE, AGRICULTURAL COLLEGE OF NORWAY, ÅS, NORWAY, JULY 29-AUGUST 9, 1968. (A69-38482 21-13)

Institute supported by NATO, the U.S. Air Force, and the U.S. Navy.

Edited by B. M. McCormac and Anders Omholt.

New York, Van Nostrand Reinhold Co., 1969, p. 251-266. 22 refs.

Discussion of high-latitude magnetospheric convection in terms of the information provided and restrictions imposed by the distribution of ionospheric current. Models of magnetospheric convection are drawn after Axford and Hines (1961), Taylor and Hones (1965), Nishida (1966), and Brice (1967). A study is made of the current pattern from magnetic disturbance plots, the convective boundary from OV1-10, and the magnetospheric convection pattern. The convection implications of the disturbance pattern are discussed and are related to the plasmapause, the solar wind, Nishida's patterns, midday auroral belt convection, and dawn-to-dusk and noon-to-midnight asymmetries. V.P.M.

A69-38508 *

PROBE MEASUREMENTS OF ELECTRIC FIELDS IN SPACE.

T. L. Aggson (NASA, Goddard Space Flight Center, Greenbelt, Md.).

IN: ATMOSPHERIC EMISSIONS; PROCEEDINGS OF THE NATO ADVANCED STUDY INSTITUTE, AGRICULTURAL COLLEGE OF NORWAY, ÅS, NORWAY, JULY 29-AUGUST 9, 1968. (A69-38482 21-13)

Institute supported by NATO, the U.S. Air Force, and the U.S. Navy.

Edited by B. M. McCormac and Anders Omholt.

New York, Van Nostrand Reinhold Co., 1969, p. 305-316. 13 refs.

Review of direct measurements of dc electric fields from sounding rockets. Although the first attempts at these measurements were made almost a decade ago, it is only in the last several years that quantitative measurements of geophysical electric fields have been obtained. The magnitudes of several recent direct probe measurements of dc electric fields in the ionosphere are in essential agreement with measurements made with the cloud technique, and there is considerable agreement with the predictions of the magnitude of these fields based on theories of ionosphere Sq currents at lower latitudes. At auroral latitudes a strong anticorrelation of the measured electric fields with auroral luminosity has been observed. This anticorrelation effect is not completely understood, but it places several strong restrictions on the location, the impedance, and the direction of the auroral dynamo. (Author)

A69-39747 *

THE SIMULTANEOUS INVESTIGATION OF ATTENUATION AND EMISSION BY THE EARTH'S ATMOSPHERE AT WAVELENGTHS FROM 4 CENTIMETERS TO 8 MILLIMETERS.

George G. Haroules and Wilfred E. Brown, III (NASA, Electronics Research Center, Microwave Laboratory, Cambridge, Mass.).

Journal of Geophysical Research, vol. 74, Aug. 20, 1969, p. 4453-4471. 19 refs.

Daily solar measurements of atmospheric absorption and atmospheric emission were conducted simultaneously for a period of nine months during 1967 and 1968. Nighttime observations of emission followed daytime observations of absorption and emission. The month of June 1968 provided a fortuitous opportunity to observe absorption during rain since 23 out of 30 days had light to heavy rainfall. The brightness temperature of clouds was measured by the multifrequency instrument during the observation period. The observational frequencies of 8, 15, 19, and 35 GHz were used to determine the frequency correlation between meteorological phenomena and the atmospheric parameters associated with the fine structure characteristics of absorption and emission. (Author)

A69-39964 *

MEASUREMENTS IN THE IONOSPHERE OF THE ASPECT DEPENDENCE OF ANTENNA REACTANCE. I—VARIATIONS ARISING FROM THE INHOMOGENEOUS PLASMA DISTRIBUTION ABOUT THE VEHICLE.

Robert G. Stone, Joseph Fainberg, and J. K. Alexander (NASA, Goddard Space Flight Center, Laboratory for Space Sciences, Greenbelt, Md.).

Planetary and Space Science, vol. 17, Aug. 1969, p. 1437-1447. 9 refs.

Measurements of the antenna reactance from a sounding rocket traveling through the ionosphere, showing variations related to the rocket spin period. The observed variations can be resolved into components with periodic time structure equal to the spin period, half the spin period, or a mixture of these. The relative importance of these components depends on the experiment configuration and the flight trajectory, as well as on the magnetoionic parameters. To account for the observations, it is necessary to take into consideration the response of an antenna to the magnetoionic medium and to the disturbance produced in the ambient plasma by the rocket motion. Examples of the plasma distribution about the rocket, as inferred from the antenna reactance measurements, are shown and discussed. (Author)

A69-40515 *

DIURNAL VARIATIONS IN THE THERMOSPHERE FROM A SERIES OF MARSHALL-UNIVERSITY-OF-MICHIGAN PROBES.

Don K. Weidner and Gary R. Swenson (NASA, Marshall Space Flight Center, Aero-Astrodynamics Laboratory, Aerospace Environment Div., Huntsville, Ala.).

Journal of Geophysical Research, vol. 74, Sept. 1, 1969, p. 4755-4764. 23 refs.

Results of rocket measurements of the diurnal variation in the concentration and temperature of molecular nitrogen. Omegatron mass spectrometers measured the molecular nitrogen concentration from 150 to 320 km, and temperature was derived from the molecular nitrogen scale height. Under the assumption of diffusive equilibrium, molecular and atomic oxygen concentration profiles were calculated. The calculated concentration profiles of molecular oxygen and nitrogen are in excellent agreement with other direct observations but are in poor agreement with theoretical model atmospheres that are based on satellite-drag-determined densities. Diurnal variations in the constituent concentrations, temperature, and mass density are found to be completely reasonable with maximum values near 1400 hours and minimum values near 0400 hours. For rocket-borne mass spectrometer measurements, the wall loss coefficient is indicated to be near 1 for atomic oxygen. The well-known controversial factor-of-two difference between density determined from satellite-drag data and that obtained from mass spectrometers can be resolved when reasonable physical assumptions are made. (Author)

A69-41341 *
RUBIDIUM-STRONTIUM CORRELATION STUDY OF MOLDAVITES AND RIES CRATER MATERIAL.
C. C. Schnetzler, John A. Philpotts, and W. H. Pinson, Jr. (NASA, Goddard Space Flight Center, Planetology Branch, Greenbelt, Md.).
(Corning Glass Works and Smithsonian Institution, International Tektite Symposium, 3rd, Corning, N.Y., Apr. 16-18, 1969.)
Geochimica et Cosmochimica Acta, vol. 33, Sept. 1969, p. 1015-1021. 18 refs.

Study of moldavites and material from the Ries Crater carried out in order to ascertain whether a rubidium-strontium isochronal relationship, analogous to that between the Ivory Coast tektites and material from the Bosumtwi Crater, exists in this particular case. The results indicate that the Rb/Sr values of the Ries Crater material are different from those of the moldavites and that in contrast to the Ivory Coast tektite/Bosumtwi Crater relationship, no definite isochronal correlation or chemical similarity was detected between the moldavites and the Ries Crater material. Thus this work supports previous suggestions that the moldavites are not simply melted equivalents of the Ries materials. O.H.

A69-41342 *
Sr ISOTOPE PATTERNS WITHIN THE SOUTHEAST AUSTRALASIAN STREWN-FIELD.
W. Compston (Australian National University, Dept. of Geophysics and Geochemistry, Canberra, Australia) and Dean R. Chapman (NASA, Ames Research Center, Moffett Field, Calif.).
(Corning Glass Works and Smithsonian Institution, International Tektite Symposium, 3rd, Corning, N.Y., Apr. 16-18, 1969.)
Geochimica et Cosmochimica Acta, vol. 33, Sept. 1969, p. 1023-1036. 14 refs.

Study of the Rb-Sr isotope patterns within the tektites from the Southeast Australasian strewn-field. In an analysis of ten specimens of Southeast Australasian tektites, an attempt was made to define isochrones for particular chemical types, and to correlate the distribution of Rb and Sr within the types with that of the major elements of the types, in order to clarify the meaning of the isochrones. The results show that in the formation of these tektites, Rb volatization played only a negligible role. Instead, the separate isochrones found within the strewn-field characterize their different source rocks, and may contribute to their eventual identification. O.H.

A69-42428 *
THE LOCATION OF THE DIP EQUATOR AT E-LAYER ALTITUDE.
Joseph C. Cain (NASA, Goddard Space Flight Center, Greenbelt, Md.).
(International Symposium on Equatorial Aeronomy, 3rd, Ahmedabad, India, Feb. 3-10, 1969.)
Radio Science, vol. 4, Sept. 1969, p. 781-784. 7 refs.

Tabulation of the position of the magnetic dip equator at 100 km, and of the gradient of position with time and altitude, using the POGO (19/68), GSFC (12/66), and IGRF (10/68) geomagnetic field models. The positions agree within a few tenths of a degree with each other but differ up to 2 deg from older models and charts. The maximum gradients with time (0.2 deg /yr) and altitude (-0.3 deg /100 km) occur to the west of Africa. (Author)

A69-42438 *
RESPONSE OF THE 1000-KILOMETER IONOSPHERE TO MAGNETIC STORMS.
B. M. Reddy, D. R. Lakshmi (National Physical Laboratory of India, New Delhi, India), and L. H. Brace (NASA, Goddard Space Flight Center, Greenbelt, Md.).
(International Symposium on Equatorial Aeronomy, 3rd, Ahmedabad, India, Feb. 3-10, 1969.)
Radio Science, vol. 4, Sept. 1969, p. 851-857. 18 refs.

Use of measurements of electron concentration and electron temperatures by the Langmuir probe experiment of the Explorer 22 satellite during 1966 to study the response of the topside ionosphere, at 1000 km, to magnetic storms. The analysis was limited to the American longitudes (50 to 130 deg W) over a latitude range from 50 deg S to 70 deg N geomagnetic. The day-time response is characterized by various degrees of electron-density enhancements over the entire latitude range, with the winter high latitudes undergoing the highest enhancement. The electron-temperature changes are not so unique. An attempt is made to explain some of these features qualitatively, based on thermal expansion of the upper atmosphere during storms and the "viscous drag" of the solar plasma on the magnetosphere. (Author)

A69-42817 * #
SOME SYSTEMS POSSIBILITIES FOR GLOBAL ATMOSPHERIC RESEARCH PROGRAM.
Morris Tepper (NASA, Office of Space Science and Applications, Washington, D.C.) and Stanley Ruttenberg (National Center for Atmospheric Research, Boulder, Colo.).
American Astronautical Society and Operations Research Society of America, Joint National Meeting, Denver, Colo., June 17-20, 1969, AAS Paper 69-120. 22 p.

Discussion of a space-based observing system which, coupled with expanded surface and nonspace observational techniques now being actively developed as part of the World Weather Watch, could provide in the next years a substantial step toward actual realization of complete global atmospheric observations. Measurements of winds with the aid of balloons located by statellites are considered as well as wind tracing by clouds. Infrared and microwave sounding of the atmosphere for temperature and water vapor is discussed, and the suitability of measurements of the mass field as numerical inputs for a general circulation model is estimated. The proposed satellite-based system for the early Global Atmospheric Research Program experiment is described. P.G.

A69-42837 * #
POTENTIAL CONTRIBUTIONS OF ORBITAL EARTH RESOURCES DATA TO URBAN PLANNING.
Charles T. N. Paludan (NASA, Marshall Space Flight Center, Astrionics Laboratory, Huntsville, Ala.).
American Astronautical Society and Operations Research Society of America, Joint National Meeting, Denver, Colo., June 17-20, 1969, AAS Paper 69-483. 12 p. 10 refs.

Discussion of some possible applications of multispectral orbital photography to the urban planning problem. In order to overcome the major problem of maintaining up-to-date land-use data, a coverage of all major U.S. cities is suggested by multispectral photography. Orbital cameras yielding scales as small as 1:1,000,000, can efficiently answer the problem of frequent and low-cost acquisition of relevant data. Some potential contributions of such data are discussed. Several commercial aspects and consequences are described. As an example of the investigation of urban land-use patterns, simulated orbital data pertaining to portions of the city of Denver are examined. O.H.

A69-42905 *
HYDROMAGNETIC RADIATION FROM ELECTRIC AND MAGNETIC DIPOLES IN THE MAGNETOSPHERE.
A. K. Sundaram (NASA, Langley Research Center, Hampton, Va.).
Canadian Journal of Physics, vol. 47, Aug. 15, 1969, p. 1643-1656. 15 refs.

Investigation of the radiation characteristics of elementary electric and magnetic dipoles in a homogeneous, anisotropic, cold plasma of infinite extent with a uniform magnetostatic field. The cases treated include the electromagnetic sources taken parallel and perpendicular to the magnetostatic field. In all cases, expressions for the field components are obtained which are valid at frequencies well below the ion cyclotron frequency. It is found that electric and magnetic dipole sources when oriented perpendicularly to the

magnetic field excite both ordinary and extraordinary modes. For the ordinary mode, the waves are guided in both directions within cones of small apex angle aligned with the static field. When the dipole sources are aligned with the magnetic field, it is found that the electric dipole excites only the ordinary mode leading to guided wave propagation, while the magnetic dipole excites only the extra-ordinary mode. In all cases, the waves propagate at Alfvén speed. The radiation characteristics are isotropic for the extraordinary mode excited by the perpedicular electric dipole and are nearly isotropic for the aligned magnetic dipole. For other cases, the radiated power is concentrated in opposite directions along the static field. (Author)

A69-43181 *
LATITUDINAL OBSERVATIONS OF THE THERMAL BALANCE IN THE NIGHTTIME PROTONOSPHERE.
K. K. Mahajan and L. H. Brace (NASA, Goddard Space Flight Center, Greenbelt, Md.).
Journal of Geophysical Research, vol. 74, Oct. 1, 1969, p. 5099-5112. 20 refs.

Results of Alouette 2 electrostatic probe measurements of the nighttime electron temperature and concentration in the height range from 2000 to 3000 km on global basis. The major feature of the protonosphere at this altitude is a broad minimum in electron temperature at the low altitudes with values around 1800 deg K. The electron temperature increases sharply to over 3000 deg K at the middle latitudes. The electron concentration exhibits a pair of maxima at about 30 deg north and south with values ranging from 4000 per cu cm in fall to 8000 per cu cm in local summer. No definitive seasonal dependence is apparent in electron temperature. Comparison of the present Alouette 2 measurements with nearly simultaneous measurements on Explorer 22 during summer 1966 reveal positive temperature gradient of electron temperature along field lines. These gradients are consistent with the thermal energy stored in the nocturnal protonosphere, and therefore no external souce of heat is required to explain the observations. (Author)

N69-10492*# Rocketdyne, Canoga Park, Calif. Research Dept.
APPLICATION OF BIOGEOCHEMISTRY TO MINERAL PROSPECTING A Survey
Washington NASA 1968 135 p refs
(Contract NAS8-5604)
(NASA-SP-5056) Avail: CFSTI CSCL 08G

The application of a combination of disciplines into the hybrid science termed biogeochemistry has gained momentum in recent decades, bringing the benefit of research into the overlapping areas of geology, biology, and chemistry. This report coalesces these technologies in a coherent interrelationship for application to mineral prospecting. Theoretical concepts are presented, including the geochemical cycle through which chemical elements pass in the process of becoming plant nutrients, the physiological requirements necessary for plant growth, and the interrelationship of these two bodies of knowledge which are directly applicable to the solution for the problem of prospecting. Author

N69-12384*# Israel Program for Scientific Translations, Ltd., Jerusalem.
THE EARTH IN THE UNIVERSE
V. V. Fedynskii, ed. 1968 408 p refs Transl. into ENGLISH of the book "Zemlya vo Vselennoi" Moscow, Izd. Sotsial-Ekon. Lit, 1964 Publ. for NASA and NSE
(NASA-TT-F-345; TT-66-51025) Avail: CFSTI CSCL 23

A series of articles is presented covering a broad range of subjects by a group of Soviet scientists writing on some of the problems of modern science, such as the structure of matter, the nature of physical fields, the formation and evolution of the Earth and the universe, solar activity and the Earth, and the interaction between the Earth's biosphere and physical fields. Some facts from the history of science which are related to the emergence of science into the reaches of outer space are also presented. Many of the ideas expressed in the articles of this collection draw upon the works of great Russian scientists of the past whose topical interest has been revived with the onset of the space age. Author

N69-14290*# National Aeronautics and Space Administration. Goddard Space Flight Center, Greenbelt, Md.
A PRELIMINARY STUDY OF THE DETECTION OF GEOMORPHOLOGICAL FEATURES OVER NORTHEAST AFRICA BY SATELLITE RADIATION MEASUREMENTS IN THE VISIBLE AND INFRARED
Jean Pouquet and Ehrhard Raschke Washington Dec. 1968 20 p refs
(NASA-TN-D-4648) Avail: CFSTI CSCL 08F

Measurements from the meteorological satellite Nimbus 2 of reflected solar and emitted infrared radiations, day and night, over Northeast Africa were used to investigate some geomorphological features of the ground. It was found; (1) The daytime measurements of emitted longwave radiations are deceptive because of the differences in local solar times across a scan, (2) Nighttime measurements are closely related to solar reflectances over the same areas, (3) When nighttime infrared measurements depart from the general trend shown by the reflectance, this opposition helps in the detection of such geomorphological features as rock formation and soil moisture. It is pointed out that these investigations are no more than a tentative approach restricted chiefly because of the low resolution of the medium resolution infrared channels of Nimbus 2. Author

N69-14450*# National Aeronautics and Space Administration. Goddard Space Flight Center, Greenbelt, Md.
AN APPROACH TO THE REMOTE DETECTION OF EARTH RESOURCES IN SUB-ARID LANDS
Jean Pouquet Washington Dec. 1968 26 p refs
(NASA-TN-D-4647) Avail: CFSTI CSCL 08I

The purpose was to find a better geological tool utilizing the nighttime infrared radiations emitted by the ground, and thereby obtain a better knowledge of the agricultural possibilities of arid and sub-arid lands. The equivalent black body temperatures derived from Nimbus 2 high resolution infrared radiometer in the spectral range 3.5–4.2μ (atmospheric window) were analyzed for all available orbits from May until mid-November 1966. From this preliminary study certain predominant features emerged and were used as a basis for the interpretation of data. For the final interpretation only a few examples were selected: Death Valley and surroundings, and Salton Sea–Colorado River region. The principal results are: detection of tectonic accidents, already known, with emphasis upon the western branch of the San Andreas Fault system; reconstitution of the upper Pleistocene hydrographic patterns showing the link between Saline, Panamint, and Death Valleys, and the Colorado River, and the former courses of this river; the possibilities of humidity storage suggested by areas showing slightly higher nighttime temperatures than expected; close relationships between the agricultural possibilities involved in the preceding statement and the geomorphological stage reached by the different valleys and basins. Author

N69-16539*# Aztec School of Languages, Inc., Acton, Mass.
AURORAE AND AIRGLOW. RESULTS OF THE RESEARCH ON THE INTERNATIONAL GEOPHYSICAL PROJECTS. COLLECTION OF ARTICLES, NO. 13
V. I. Krasovskiy ed. Washington NASA Jan. 1969 148 p refs Transl. into ENGLISH of the publ. "Polyarnyye Siyaniya i Svecheniye Nochnogo Neba. Rezul'taty Issledovaniy Po Mezhdunarodnym Geofizicheskim Proyektam" Moscow, Nauka Press, 1967 p 1–118
(Contract NASw-1962)
(NASA-TT-F-530) Avail: CFSTI CSCL 04A

CONTENTS:

1. CHARACTERISTICS OF SPATIAL DISCONTINUITIES IN THE λ 5577 Å EMISSION OF ATOMIC OXYGEN IN AIRGLOW G. A. Nasyrov p 1–7 refs (See N69-16540 06-13)

2. SPATIAL VARIATIONS OF THE AIRGLOW IN THE AREA OF λ 5893 Å G. A. Nasyrov p 8–10 refs (See N69-16541 06-13)

3. AN EXAMINATION OF THE SPACE-TIME PROPERTIES OF HYDROXYL EMISSION O. G. Taranova p 11–21 refs (See N69-16542 06-13)

4. HYDROXYL EMISSION AT HIGH LATITUDES N. I. Fedorova p 22–41 refs (See N69-16543 06-13)

5. CERTAIN PROPERTIES OF HYDROXYL EMISSION N. N. Shefov p 42–49 refs (See N69-16544 06-13)

6. SOME RESULTS OF OBSERVATIONS OF HYDROXYL EMISSION FROM THE UPPER ATMOSPHERE IN ABASTUMANI L. M. Fishkova et al p 50–56 refs (See N69-16545 06-13)

7. DIURNAL VARIATIONS IN HELIUM EMISSION O. G. Taranova p 57–60 refs (See N69-16546 06-13)

8. TWILIGHT HELIUM EMISSION AT HIGH LATITUDES N. I. Fedorova p 61–72 refs (See N69-16547 06-13)

9. STATISTICAL PROPERTIES OF THE HELIUM EMISSION N. N. Shefov p 73–78 refs (See N69-16548 06-13)

10. VARIATIONS IN THE H_α EMISSION AND HYDROGEN DISTRIBUTION IN THE UPPER ATMOSPHERE AND THE GEOCORONA L. M. Fishkova et al p 79–83 refs (See N69-16549 06-13)

11. ANGULAR AND ENERGY DISTRIBUTION OF PROTONS IN AURORAE O. L. Vaysberg p 84–95 refs (See N69-16550 06-13)

12. RELATIVE POPULATIONS OF THE UPPER VIBRATIONAL LEVELS OF $2PGN_2$ BANDS IN AURORAE AT VARIOUS LATITUDES F. K. Shuyskaya p 96–100 refs (See N69-16551 06-13)

13. OBSERVATION OF THE AURORA ON FEBRUARY 11, 1958, AT THE ROSHCHINO STATION F. K. Shuyskaya p 101–119 refs (See N69-16552 06-13)

14. DISTRIBUTION OF AURORAE AND MAGNETIC DISTURBANCES AT HIGH LATITUDES IN RELATION TO THE ASYMMETRIC SHAPE OF THE MAGNETOSPHERE Y. I. Fel'dshteyn p 120–145 refs (See N69-16553 06-13)

N69-16545*# Aztec School of Languages, Inc., Acton, Mass.

SOME RESULTS OF OBSERVATIONS OF HYDROXYL EMISSION FROM THE UPPER ATMOSPHERE IN ABASTUMANI

L. M. Fishkova et al *In its* Aurorae and Airglow. Collection of Articles, no. 13 Jan. 1969 p 50–56 refs (See N69-16539 06-13)

Avail: CFSTI CSCL 04A

Variations in OH emission were obtained during a solar cycle. The minimum intensity for 1962–1963 had a greater amplitude than that for 1954–1955. The seasonal variations in rotational temperature have a greater amplitude for the bands from the upper vibrational levels. A study of the intensity variations in the OH bands, in relation to the zenith distance, shows that an increase in T (OH) corresponds to a lowering of the emitting layer. Author

N69-18126*# Utah Univ., Salt Lake City.

THEORETICAL COMPARISON OF BEADS, WIRES, AND FILMS AS ROCKETSONDE TEMPERATURE SENSORS IN THE MESOSPHERE

Forrest L. Staffanson Washington NASA Feb. 1969 52 p refs

(Grant NGR-45-003-025)

(NASA-CR-1286; UTEC-MR-67-055) Avail: CFSTI CSCL 04A

Parameters are compared for three basic sensor shapes: the small sphere, the thin circular cylinder in cross flow, and the thin flat plate in parallel flow. For quantitative comparisons arbitrary sensor specifications and environmental conditions are shosen. The thickness dimension is as thin as practical for the respective shape. The volume specific heat corresponds to a material commonly used for the respective shape. For uniformity in absorptivity and emissivity each of the three shapes is assumed to have a thin opaque coat of aluminum with solar absorptivity, long wave absorptivity, and emissivity. The air flow and radiation environment is approximately that encountered by a sensor mounted on a stable parachute sonde system having weight and dimension of the ARCAS system and falling in the altitude interval 90 to 50 km. From the theroetical comparison of the thermometric performance of the three basic shapes, it is found that the two dimensional or pianar shape appears generally the most promising for future immersion sensor designs. Its principal features are: small recovery factor associated with its larger aerodynamic characteristic length, small thermal mass associated with its thinness, etc. B.P.

N69-18700*# National Meteorological Center, Suitland, Md. Upper Air Branch.

METEOROLOGICAL ROCKET RESEARCH SINCE 1959 AND CURRENT REQUIREMENTS FOR OBSERVATIONS AND ANALYSIS ABOVE 60 KILOMETERS

Roderick S. Quiroz Washington NASA Feb. 1969 69 p refs

(NASA Order L-719)

(NASA-CR-1293) Avail: CFSTI CSCL 04A

A detailed survey is made of routine rocket soundings since 1959, yielding measurements of neutral parameters up to 60 km, and of special rocket soundings giving data to ca. 100 km. The distribution of soundings, of which only 21% have been taken in latitudes north of 40°N, is given by station and year for more than 30 rocket sites, including foreign locations. Observational accuracies are examined in sufficient depth to permit an evaluation of the broad validity of the measurements. The observational errors may be appreciable, depending on the conditions of measurement, yet the observations are considered to efficiently delineate the broad atmospheric structure and circulation above radiosonde levels. Error contamination, however, may be critical in small-scale analysis. Author

N69-19024*# National Aeronautics and Space Administration. Langley Research Center, Langley Station, Va.

A TECHNIQUE TO INFER ATMOSPHERIC TEMPERATURE FROM HORIZON RADIANCE PROFILES

Thomas B. McKee, Ruth I. Whitman, and Jules J. Lambiotte, Jr. Washington Feb. 1969 33 p refs

(NASA-TN-D-5068) Avail: CFSTI CSCL 04A

A technique is presented to infer atmospheric temperature structure from horizon radiance profiles. The technique was implemented for a spectral region of absorption due to the CO_2 molecule (615 cm^{-1} to 715 cm^{-1}). Inferred temperature accuracy is shown when input data are errorless and when input data have been perturbed with errors for the altitude range from 20.5 km to 55.5 km. Atmospheric temperatures were inferred from measured horizon radiance profiles and compared with estimated temperature structure as an example of the application of the technique to real data. Author

N69-23318*# National Aeronautics and Space Administration. Goddard Space Flight Center, Greenbelt, Md.

AN ATLAS OF TIROS 7 MONTHLY MAPS OF EMITTED RADIATION IN THE 8/12 MICRON ATMOSPHERIC WINDOW OVER THE INDIAN OCEAN AREA

Earl R. Kreins and Lewis J. Allison Washington Apr. 1969 28 p refs

(NASA-TN-D-5101) Avail: CFSTI CSCL 04B

The Tiros 7 meteorological satellite contained a five channel

medium resolution scanning radiometer. One of the channels responded to emitted radiation in the 8- to 12-micron portion of the electromagnetic spectrum, where gaseous absorption in the atmosphere is minimal and, therefore, the radiation detected at the satellite originates mainly from the earth's surface and/or clouds. Data from this channel have been compiled and mapped in a series of one 12-day mean map (June 1963) and 18 monthly mean maps (July 1963 through December 1964) of equivalent blackbody temperatures. The maps cover the area enclosed by 45 degrees north latidue, 50 degrees south latitude, 20 degrees east longitude, and 155 degrees east longitude. These satellite observations were originally analyzed in support of the International Indian Ocean Expedition. They are presented in a separate, compact form for users who are interested primarily in the radiation data and in details concerning the processing, display, analysis, and interpretation of these data. Author

N69-23557*# National Aeronautics and Space Administration. Ames Research Center, Moffett Field, Calif.

COMPUTATION OF TOPSIDE IONOGRAMS FROM N(h) PROFILES

Lawrence Colin, Kwok-Long Chan, and Jack G. K. Lee (Informa[illegible]s, Inc., Palo Alto, Calif.) Washington Apr. 1969 35 p refs

(NASA-TN-D-5052) Avail: CFSTI CSCL 04A

Model profiles of plasma frequency and gyrofrequency are chosen to simulate typical conditions observed in the topside ionosphere by the Alouette I sounder (1000 km) and the Alouette II sounder near apogee (3000 km). Examples of group refractive index profiles for these models are presented. By means of parabolic-in-log X lamination techniques applied to the plasma frequency profiles, cumulative delays are computed to illustrate the relative delays contributed by each lamination to the formation of topside ionograms. Complete ionograms (ordinary, extraordinary, and Z traces) are presented for all the models. Implications of the results to the inverse experimental problem of scaling ionogram data and computing electron concentration profiles are discussed. Author

N69-25013*# Aztec School of Languages, Inc., Acton, Mass. Research Transl. Div.

OBSERVATIONS OF NOCTILUCENT CLOUDS

Ch. I. Villman, ed. Washington NASA Apr. 1969 160 p refs Transl. into ENGLISH of the Book "Nablyudeniya Serebristykh Oblakov" Moscow, Nauka, 1967

(Contract NASw-1692)

(NASA-TT-F-546) Avail: CFSTI CSCL 04B

The principal advantages of time-lapse photography in examining the wave movements in the clouds and in determining the nature of the upper layer of the clouds and the lower layer, or the veil are presented. It is shown that the chemical composition of the condensed material in noctilucent clouds should be studied in greater detail, and that water vapor should not be considered the only possible substance comprising the condensed part of noctilucent clouds. Author

N69-26969*# National Aeronautics and Space Administration. Marshall Space Flight Center, Huntsville, Ala.

SURVEY AND COMPARATIVE ANALYSIS OF CURRENT GEOPHYSICAL MODELS

Jesco von Puttkamer Washington May 1969 66 p refs

(NASA-TN-D-5163) Avail: CFSTI CSCL 08E

By using currently accepted constants of geodesy, especially several different sets of oblateness coefficients, seven models of the geometry of the earth and its gravitational field are numerically derived and compared with each other and with a newly developed geopotential based on recent measurements of the secular and periodic perturbations of artificial satellite orbits. Conclusions are drawn which show, among other things, that the currently used NASA standard model deviates significantly from the best geoid, and that there are better analytical, as well as numerical, models by which improved approximation can be achieved. Also, it is shown that improvements in the numerical values of the used oblateness coefficients, rather than in their number, appear to have little influence on the values of the gravity, but that they affect the geometries significantly. Increasing the number of zonal harmonics coefficients, however, can lead to considerable improvements in the gravity model, at least in the range studied (up to and including J_{14}). Author

N69-27246*# National Aeronautics and Space Administration. Langley Research Center, Langley Station, Va.

A TECHNIQUE TO INFER ATMOSPHERIC WATER-VAPOR MIXING RATIO FROM MEASURED HORIZON RADIANCE PROFILES

Thomas B. Mc Kee, Ruth I. Whitman, and Jules J. Lambiotte, Jr. Washington Jun. 1969 36 p refs

(NASA-TN-D-5252) Avail: CFSTI CSCL 08H

A technique is presented to infer atmospheric water-vapor mixing-ratio structure from measured horizon radiance profiles when a method exists for calculating radiance profiles. The technique was implemented for the spectral interval, 315 cm^{-1} to 475 cm^{-1} of the rotational water-vapor band but the technique is not limited to that interval. Inferred mixing-ratio accuracy for the 10-km to 35-km altitude range is shown when the computer program input data contain no errors and when the computer program input is perturbed by errors normally found in measurements. Water-vapor mixing ratios were inferred from horizon radiance profiles measured in the summer in a latitude range from 17° North to 58° North from an NASA Project Scanner flight. No significant latitudinal variation existed above an altitude of 18 km. Below 18 km a latitudinal variation does exist that is consistent with the large variations that are known to exist in the troposphere. The mixing ratio decreases with altitude to a minimum at a point ranging from 3 km to 5 km above the tropopause altitude. Above an altitude of 20 km the mixing ratio shows a slight increase to 35 km. Author

N69-28019*# National Aeronautics and Space Administration. Goddard Space Flight Center, Greenbelt, Md.

GEOS I TRACKING STATION POSITIONS ON THE SAO STANDARD EARTH (C-5)

Francis J. Lerch, James G. Marsh, Maurice D. D'Aria (Wolf Res. and Develop. Corp.), and Ronald L. Brooks (Wolf Res. and Develop. Corp.) Washington Jun. 1969 38 p refs

(NASA-TN-D-5034) Avail: CFSTI CSCL 08E

For the purpose of long-arc satellite data reduction and intercomparison, all GEOS 1 participating tracking stations were transformed to a common datum. The common datum selected is the Smithsonian Astrophysical Observatory (SAO) Standard Earth C-5 model, in which the Baker–Nunn station positions are used as the controlling stations for all other stations to be transformed. Descriptions and formulation are presented to effect the transformations from major and isolated datums. An empirical transformation technique is explained in detail which may be employed advantageously when datum shifts are not known or when the control stations within a local datum are allowed to adjust independently on the world datum (SAO C-5). The transformation of local datum station coordinates is important to perform, since the datum shifts are quite large. Original and transformed station positions are presented in geodetic and Cartesian coordinates. Author

N69-28442*# National Aeronautics and Space Administration. Goddard Space Flight Center, Greenbelt, Md.

EVALUATION OF THE GODDARD RANGE AND RANGE RATE SYSTEM AT ROSMAN BY INTERCOMPARISON WITH GEOS I LONG-ARC ORBITAL SOLUTIONS

Francis J. Lerch, James G. Marsh, and Brian O'Neill (Wolf Res. and Develop. Corp., Bladensburg, Md.)
Washington Jun. 1969 52 p refs
(311-07-21-01-51)
(NASA-TN-D-5036) Avail: CFSTI CSCL 22C

The large volume of high precision optical observations of geos one provided the first opportunity to analyze the GRARR data recorded from the same satellite for systematic errors and biases. For this analysis, definitive long-arc optical orbital solutions determined from the GEOS one flashing lamp and passive data provided a very accurate standard for estimating these errors. The GRARR zero-set range bias and timing error estimates for the two satellite transponder channels, A and C, differed significantly. Twenty-six A channel passes analyzed had a mean zero-set range bias error of −7.8 meters with a standard deviation of 10.3 meters and a timing error of −2.1 milliseconds with a standard deviation of 4.0 milliseconds. Four C channel passes analyzed had a mean zero-set range bias error of 25.0 meters and a mean timing error of −0.6 milliseconds. This discrepancy can be explained in part by inaccuracies in the transponder delay curve. A timing error of up to 2 milliseconds can possibly be attributed to the orbital solution; however, the consistent results obtained from the shorter overlapping solutions indicate that these errors are due to other sources, either the GRARR system itself or station survey errors, etc. Further analysis and a possible expansion of the error model will be necessary before a complete explanation of these errors is possible.

Author

N69-28983*# Aztec School of Languages, Inc., Acton, Mass. Research Translation Div.

MOTIVE FORCES IN THE DEVELOPMENT OF THE EARTH AND PLANETS

V. V. Kesarev
Washington NASA Jun. 1969 136 p refs Transl. into ENGLISH of the Book "Dvizhushchiye Sily Razvitiya Zemli I Planet" Leningrad, Nedra Press, 1967
(Contract NASw-1692)
(NASA-TT-F-532) Avail: CFSTI CSCL 03B

An original concept is set forth concerning the nature of the earth and the planets. The hypothetical composition of primary planetary matter is developed on a wide physical and chemical basis. Changes in planetary characteristics are connected in the closest way with the evolution of planetary matter. It is shown that the proposed chemical model of the earth can be extended to other inner and outer planets. The book is intended for geologists, physicists, chemists, and for all those who are interested in modern problems of natural science.

Author

N69-29491*# National Aeronautics and Space Administration, Washington, D. C.

THE FACE OF THE EARTH AND ITS ORIGIN

G. N. Katterfeld Jun. 1969 134 p refs Transl. into ENGLISH of the book "Lik Zemli i ego Proiskhozhdeniye" Moscow, State Publishing House of Geograph. Lit., 1962
(NASA-TT-F-533) Avail: CFSTI CSCL 08E

The terrestrial deforming forces derived, from its rotation, and from alternate compression and expansion of the terrestrial body (pulsation), associated with the action of gravity and with that of internal physicochemical reactions are studied. It is shown that the net result of the interaction of these forces over the course of enormous periods of time has been the establishment of lines of maximal stress which have given rise to tectonic movements in the mantle. This has led to the well-known antipodal character of terrestrial relief: land masses (elevations) on one side of the globe are counterbalanced by water masses (depressions) on the other; and also to a number of other peculiarities, such as the wedge shape exhibited by the continents, and the distribution of volcanic activity. It is believed that the tidal action of the moon (which originated in nearby space at the same time as the earth) was an important factor leading to the imbalance in terrestrial relief.

Author

N69-31851*# Aztec School of Languages, Inc., Maynard, Mass.

TRANSFER OF MICROWAVE RADIATION IN THE ATMOSPHERE [PERENOS MIKROVOLNOVOGO IZLUCHENIYA V ATMOSFERE]

K. S. Shifrin, ed. Washington NASA Jul. 1969 194 p refs Transl. into ENGLISH from Tr. Gl. Geofiz. Observ. (Leningrad), no. 222, 1968
(Contract NASw-1692)
(NASA-TT-F-590) Avail: CFSTI CSCL 04A

CONTENTS:

1. INVESTIGATION OF THE FIELD OF MICROWAVE RADIATION IN THE ATMOSPHERE K. S. Shifrin et al p 1–18 refs (See N69-31852 18-20)

2. EXPERIMENTAL INVESTIGATIONS OF THE CHARACTERISTICS OF THERMAL RADIO EMISSION FROM THE SURFACE OF THE SEA A. M. Shutko p 19–21 refs (See N69-31853 18–13)

3. THERMAL RADIATION AND REFLECTION FROM A ROUGH SEA SURFACE IN THE MICROWAVE RANGE K. S. Shifrin et al p 22–50 refs (See N69-31854 18–13)

4. DETERMINING THE TEMPERATURE OF THE WATER SURFACE FROM RADIO EMISSION IN THE CENTIMETER BAND Yu. I. Rabinovich et al p 51–55 refs (See N69-31855 18-13)

5. THERMAL RADIATION FROM ICE IN THE CENTIMETER AND DECIMETER BANDS A. A. Kurskaya et al p 56–64 refs (See N69-31856 18-13)

6. DETERMINING THE WATER VAPOR CONTENT IN THE ATMOSPHERE FROM MEASUREMENTS OF MICROWAVE RADIATION Yu. I. Rabinovich et al p 65-78 refs (See N69-31857 18-20)

7. ABSORPTION AND SCATTERING OF MICROWAVES IN PRECIPITATION K. S. Shifrin et al p 79–89 refs (See N69-31858 18-23)

8. TRANSFER OF MICROWAVE RADIATION IN CLOUDS AND PRECIPITATION B. A. Volchok et al p 90–107 refs (See N69-31858 18-23)

9. INVESTIGATION OF RADIO EMISSION AND ABSORPTION OF A CLOUDY ATMOSPHERE IN THE MILLIMETER AND CENTIMETER WAVE BANDS A. Ye. Basharinov et al p 108–121 refs (See N69-31860 18-23)

10. EXPERIMENTAL INVESTIGATIONS OF ATTENUATION AND RADIO EMISSION FROM RAIN IN THE UHF-BAND B. G. Kutuza p 122–132 refs (See N69-31861 18-23)

11. CONTRASTS IN RADIOBRIGHTNESS TEMPERATURES DURING OBSERVATIONS OF CLOUDS AND PRECIPITATIONS V. D. Stepanenko p 133–147 refs (See N69-31862 18-20)

12. SEVERAL GEOMETRIC CHARACTERISTICS OF CLOUDS AND PRECIPITATIONS BASED ON RADAR OBSERVATIONS V. D. Stepanenko p 148–151 refs (See N69-31863 18-20)

13. THE STRUCTURE OF PRECIPITATION FIELDS IN THE UKRAINE Zh. D. Alibegova p 152–156 refs (See N69-31864 18-20)

14. POSSIBLE ERRORS IN ABSOLUTE MEASUREMENTS OF RADIO EMISSION Yu. I. Rabinovich et al p 156–169 refs (See N69-31865 18-23)

15. RADIO EMISSION FROM CLOUDS AND PRECIPITATIONS Yu. I. Rabinovich, G. G. Shchukin et al p 170–173 refs (See N69-31866 18-23)

16. FEATURES OF THE METHOD OF ULTRAHIGH FREQUENCY RADIOMETRIC PROBING OF THE ATMOSPHERE FROM AIRCRAFT A. Ye. Basharinov, S. T. Yegorov et al p 174–181 refs (See N69-31867 18-13)

17. THERMAL RADIO EMISSION FROM AN ICE COVER IN THE UHF-BAND L. T. Tuchkov et al p 182–185 refs (See N69-31868 18-13)

13 GEOPHYSICS

N69-31961*# General Dynamics Corp., San Diego, Calif.
STUDY OF AIR POLLUTANT DETECTION BY REMOTE SENSORS
C. B. Ludwig, R. Bartle, and M. Griggs Washington NASA Jul. 1969 160 p refs
(Contract NAS12-630)
(NASA-CR-1380; GDC-DBE68-011) Avail: CFSTI CSCL 04A

The feasibility of detecting the major air pollutants by earth-oriented, satellite-borne sensors is investigated. The major pollutants considered are carbon monoxide, sulfur dioxide, ozone, ammonia, nitrogen dioxide, typical hydrocarbons, and peroxyacetyl nitrate. The spectral region considered extends from the ultraviolet to the microwave region. The detection is to be accomplished by observing the change in radiation level due to the presence of air pollutants. In the ultraviolet and visible region, the reflected sunlight provides the radiation, while in the infrared and microwave region the thermal emission from the earth and its atmosphere is the source of radiation. In the first case, the detection is adversely affected by Rayleigh and Mie scattering of the sunlight in the atmosphere, which is not readily accounted for, particularly for satellite observations. In the second case, the detection is influenced by meteorological conditions, which must be obtained by independent measurements either from the satellite directly or from the global weather-station network. Considerations of the number of species accessible to optical detection, the matter of day and night detection, and of specificity indicate that the infrared region extending from 3.5μ to 13μ is the most useful one. Author

N69-33555*# National Aeronautics and Space Administration, Washington, D.C.
SYNOPTIC ANALYSIS OF THE SOUTHERN HEMISPHERE STRATOSPHERE
Alvin J. Miller (Natl. Meteorol. Center, Hillcrest Heights, Md.) and Frederick G. Finger (Natl. Meteorol. Center, Hillcrest Heights, Md.) Aug. 1969 24 p refs
(NASA-TM-X-1814) Avail: CFSTI CSCL 04B

Rawinsonde data from 84 stations in the Southern Hemisphere are combined with constant-level balloon information to construct weekly hemispheric analyses for the 30-mb level for the month of June, 1967. Rocket information from Chamical, Argentina; Natal, Brazil, and Ascension Island are employed to infer the circulation at higher levels. During the period of study, the lower stratosphere of the Southern Hemisphere was dominated by a polar low with a subtropical ridge present at about 20°S. The lateral extent of the westerlies increased with height with the result that westerly winds existed in the tropical region at upper levels. Author

N69-34891*# National Aeronautics and Space Administration. Electronics Research Center, Cambridge, Mass.
MAGNETOSPHERIC DUCT PROPAGATION RESEARCH USING ALOUETTE-2 TOPSIDE-SOUNDER OBSERVATIONS
Jayaram Ramasastry and Edward J. Walsh Washington Aug. 1969 75 p refs
(NASA-TN-D-5332) Avail: CFSTI CSCL 04A

This report presents a discussion of the intesne field-aligned propagation activity in the longitudes of Singapore observed by the Alouette-2 topside sounder. The frequency occurrence of sequences of ionograms containing conjugate echo traces is discussed in detail and attributed to the presence of field-aligned irregularities over a wide L-value range in the magnetosphere. Also described is the development of a unified model of field-aligned ducts in the magnetosphere from the analysis of the fine structure and diffuseness of the conjugate echo traces observed by the Alouette-2 sounder. The proposed model for the magnetospheric ducts is a large-scale, field-aligned, gaussian enhancement of electron density with a superimposed fine structure of small-scale gaussian ripples so that the large-scale variation has a ribbed rather than a smooth structure. Mathematical and digital ray-tracing analyses of the new model, along with illustrative ionograms which were used in postulating the model, are presented. Author

N69-35660*# Temple Univ. Research Inst., Philadelphia, Pa.
DEVELOPMENT OF A BARIUM CHEMICAL RELEASE SYSTEM
C. S. Stokes, E. W. Smith, and W. J. Murphy Washington NASA Aug. 1969 43 p refs
(Contracts NAS1-6199; NAS1-7070)
(NASA-CR-1415) Avail: CFSTI CSCL 04A

A method for producing Ba° and Ba^{+} in a gaseous medium was developed utilizing a liquid propulsion system. The fuel consisted of $BaCl^2$ and $Ba(NO^3)_2$ salts dissolved in hydrazine. The oxidizers tested were OF_2, ClF_3 and F_2. The Ba^{o} and Ba^{+} yield for all systems at varying oxidizer/fuel ratios was measured using spectroscopic techniques. The chemical system producing the highest yield of Ba^{o} and Ba^{+} consisted of a 17% $BaCl_2$-16% $Ba(NO^3)_2$-67% N_2H_4 fuel mixture tested with fluorine. Author

N69-40893*# National Aeronautics and Space Administration. Goddard Space Flight Center, Greenbelt, Md.
HYDRATION, OXIDATION, AND THE ORIGIN OF THE CALC-ALKALI SERIES
Robert F. Mueller Washington Nov. 1969 32 p refs
Grant NSF GA-307)
(NASA-TN-D-5400) Avail: CFSTI CSCL 08G

A physicochemical interpretation is given for the calc-alkali differentiation series of igneous rocks as distinguished particularly from gabbroic series such as the Skaergaard complex. It is found that, contrary to previous assumptions, the oxygen fugacity decreases markedly during calc-alkaline differentiation and in this way resembles the situation in gabbroic complexes. The affinity of water for the melt has the important consequence of increasing the solubilities of the quartzofeldspathic components more than those of the ferromagnesian components, so that the phase boundaries are shifted toward lower liquidus temperatures. The result is that the courses of the crystallization paths are directed into a region of quartzo-feldspathic rather than gabbroic liquids. Author

N69-40924*# National Aeronautics and Space Administration. Goddard Space Flight Center, Greenbelt, Md.
ATMOSPHERIC DENSITIES MEASURED BY THE EXPLORER 17 DENSITY GAUGES: ANALYSIS OF ERRORS AND THEIR EFFECTS UPON THE MEASUREMENTS
G. P. Newton and Richard Horowitz Washington Nov. 1969 36 p refs
(NASA-TN-D-5447) Avail: CFSTI CSCL 04A

The atmospheric total density data from the Explorer 17 Atmospheric Density Experiment are presented. The equations used for interpretation of the gauge output currents in terms of atmospheric density are derived. Possible systematic error due to gauge calibration, energetic gas beam-surface interaction, adsorption-desorption effects, chemical compound production, and gauge nonlinearity are evaluated; and it is concluded that the previously reported density values should be increased by 35 percent. The effects of variations in atmospheric composition on the density values are as follows: If an atmosphere of 100% atomic oxygen was assumed, but the atmosphere was really 100% helium, the density values should be increased by a factor of 1.6. Correspondingly, if the atmosphere was really 100% molecular nitrogen, the density values should be decreased by a factor of 0.72. Author

14

INSTRUMENTATION AND PHOTOGRAPHY

Includes design, installation, and testing of instrumentation systems; gyroscopes; measuring instruments and gages; recorders; transducers; aerial photography; and telescopes and cameras.

A69-10113 *#
ULTRASONIC DETECTION AND MEASUREMENT OF FATIGUE CRACKS IN NOTCHED SPECIMENS.
S. J. Klima and J. C. Freche (NASA, Lewis Research Center, Cleveland, Ohio).
Society for Experimental Stress Analysis, Fall Meeting, San Francisco, Calif., Oct. 28-Nov.1, 1968, Paper. 34 p. 9 refs.

Description of an ultrasonic technique used to observe the formation and growth of fatigue cracks in notched cylindrical specimens subjected to reversed axial cyclic loading. Fatigue curves of life-to-initial detectable cracks as well as life-to-fracture are obtained for an aluminum, a titanium, and a cobalt base alloy as well as a maraging steel. Depth of initially detectable cracks ranged approximately from 0.013 to 0.10 mm. Curves are also obtained relating ultrasonic system output-voltage to crack depth up to 0.76 mm for three materials. These curves are used to demonstrate the capability of the device for monitoring crack growth. Z.W.

A69-10890 *
X-RAY FLUORESCENCE OF ROCK SAMPLES AS APPLIED TO GEOLOGICAL PROBLEMS.
Richard A. Laidley (NASA, Manned Spacecraft Center, Houston, Tex.).
Applied Spectroscopy, vol. 22, Sept.-Oct. 1968, p. 420-422. 5 refs.

Three methods of sample preparation of rock specimens have been evaluated for precision and accuracy. A fusion technique was found to give the best precision. Standard deviations (1 σ) using this method and expressed as percent of the amount present for several elements are Al 0.83, Si 0.64, K 0.43, Ca 0.43, Mn 0.48, and Fe 0.24. Three recent studies of compositional variation were performed on volcanic rocks. Analyses of samples from the Hopi Buttes, Ariz., on obsidian flows from Newberry Caldera, Ore., and on igneous rocks collected from grids or linear traverses give data which, in each case, are useful in making significant interpretations about the geologic history of the rocks concerned. These examples illustrate the rapidity and high quality of quantitative chemical analyses which can be obtained by application of X-ray fluorescence analytical techniques. (Author)

A69-10927 *
VACUUM DISTILLATION TECHNIQUE FOR RECOVERY OF ALKALI-METAL REACTION PRODUCTS.
Randall F. Gahn (NASA, Lewis Research Center, Cleveland, Ohio).
Analytical Chemistry, vol. 40, May 1968, p. 996-998. 9 refs.

Description of the vacuum technique for the isolation and recovery of alkali-metal reaction products. The procedure described is designed to minimize reaction-product contamination by carrying out all operations in high-vacuum or inert-gas atmospheres. The separation of reaction products from excess alkali metal is accomplished by vacuum distillation to avoid the use of solvent or reactants. This procedure is applied to the recovery of products from the reactions of potassium and lithium with tantalum, niobium, vanadium, and oxygen. Two examples are cited as an indication of the application and reproducibility of the procedure - namely, the isolation of the reaction products from the potassium-tantalum-oxygen system, and the isolation of the reaction products from the potassium-oxygen system. Z.W.

A69-11468 *
PLANETARY ATMOSPHERE MASS SPECTROMETRY.
N. W. Spencer (NASA, Goddard Space Flight Center, Greenbelt, Md.).
American Astronautical Society, Conference on Advanced Space Experiments, Ann Arbor, Mich., Sept. 16-18, 1968, Paper 68-183. 27 p. 10 refs.

Description of the conceptual basis for and the details of two systems representative of the existing instrumental technology in planetary (chiefly Mars and Venus) atmospheric composition determination. One of these systems is the one which has been developed to optimize data systems capability. It employs the adaptive scan approach - i.e., it searches for a mass of sufficient concentration to provide a useful measurable output signal and then measures and stores the magnitude of the output signal using only a single digital word. It also records the identity of the mass of the gas measured. For the quantitative detection and measurement of the positive-ion constitution of planetary atmospheres, a system using a Bennett ion spectrometer sensor has been derived from systems in use in earth satellites, such as the OGO and the Atmosphere Explorer series. The planetary design also employs a data system optimization scheme. In contrast to a neutral spectrometer, however, flat-topped peaks are not possible, and thus the output signal maximum is measured by a "peak-detecting" device. P.v.T.

A69-12392 *#
THERMODIELECTRIC RADIOMETER.
Larry D. Russell (NASA, Ames Research Center, Moffett Field, Calif.) and Benjamin H. Beam (NASA, Ames Research Center, Radiations Research Branch, Moffett Field, Calif.).
(American Institute of Aeronautics and Astronautics, Aerodynamic Testing Conference, 3rd, San Francisco, Calif., Apr. 8-10, 1968, Paper 68-403.)
Journal of Spacecraft and Rockets, vol. 5, Dec. 1968, p. 1501-1503. 7 refs.

A new type of fast-response, thermal detector has been developed for measuring transient radiant flux. The detector operates on a mechanism of thermally induced depolarization of a polymer film dielectric. The film is charged to a voltage gradient of approximately 100 v/μ and, when it is heated by absorbed radiation, it produces a proportional open-circuit voltage increment. The detector is designed to measure the total energy or power of a transient, short-duration pulse of radiant flux. Polymer thermal-dielectric radiometers have been built and used for measuring the total power radiated by a high-speed shock wave. Sensitivities on the order of 20 v/joule/cm^2 and a time response on the order of microseconds have been achieved. (Author)

A69-12869 *
ADAPTIVE DATA COMPRESSION FOR VIDEO SIGNALS.
R. L. Kutz, J. A. Sciulli, and R. A. Stampfl (NASA, Goddard Space Flight Center, Greenbelt, Md.).
IN: ADVANCES IN COMMUNICATION SYSTEMS: THEORY AND APPLICATIONS. VOLUME 3.
Edited by A. V. Balakrishnan.
New York, Academic Press, Inc., 1968, p. 29-66. 11 refs.

Discussion of experiments with several prediction schemes to maximize the probability of prediction (p). The results show that

the average value of p attained was nearly the same for all methods considered. In pure prediction capability, the adaptive sample-conditioned mode predictor yielded the best performance of all methods. Its superiority is minimized, however, when its implementation requirements are compared with those of the nonadaptive Markov predictor. Since all prediction methods provided nearly the same prediction efficiency, a study was made of the effects of channel errors on one of the simplest of possible systems - namely, a system consisting of the Markov predictor and the word-pair encoder.
F.R.L.

A69-13104 *#
MICROSECOND RESPONSE SYSTEM FOR MEASURING SHOCK ARRIVAL BY CHANGES IN STREAM ELECTRICAL IMPEDANCE IN A SHOCK TUBE.
Robert E. Dannenberg and Donald E. Humphry (NASA, Ames Research Center, Moffett Field, Calif.).
Review of Scientific Instruments, vol. 39, Nov. 1968, p. 1692-1696. 6 refs.

An instrument is described that is suitable for measuring the position and velocity of high-speed compression waves, rarefaction waves, and gas interface regions in shock tubes. The sensor is a twin-electrode probe mounted in the wall of the tube with a small dc voltage impressed across the electrodes. A simple power supply amplifier, and gate pulse generator complete the instrument. The probe provides a sensitive microsecond reponse to changes in the electrical impedance of the gas stream flowing across the sensor. In addition, the probe is inexpensive, rugged, and easy to install. It has been possible to correlate the output signals from this instrument with the different regions of shock tube flow at shock speeds from 2.29 to 7.01 km/sec into air. (Author)

A69-13108 *#
APPARATUS FOR THE PRECISION MEASUREMENT OF INTERNAL FRICTION.
D. P. Detwiler, S. J. Holden, W. A. Sowa, T. J. Woronowicz, M. G. Hudick (Wilkes College, Wilkes-Barre, Pa.), and T. M. Heslin (Wilkes College, Wilkes-Barre, Pa.; NASA, Goddard Space Flight Center, Greenbelt, Md.).
Review of Scientific Instruments, vol. 39, Nov. 1968, p. 1727-1730. 11 refs.
USAF-supported research.

Description of an apparatus, which permits routine measurement of internal friction as low as 2×10^{-7} and Young's modulus as a function of temperature, frequency, and strain amplitude in extremely low-loss materials. The system described herein can be used to investigate a variety of materials and is not hampered by the limitations placed upon composite resonator systems. It has been successfully used to study internal friction in the amplitude-independent and amplitude-dependent regions in pure and $CaCl_2$-doped NaCl. (Author)

A69-13221 *
A LUNAR-SURFACE ELECTRIC-FIELD DETECTOR.
B. W. Sherman (Missouri, University, Dept. of Electrical Engineering, Columbia, Mo.), R. H. Manka (NASA, Manned Spacecraft Center, Space Physics Div., Houston, Tex.), H. R. Anderson (William Marsh Rice University, Dept. of Space Science, Houston, Tex.), M. C. Terry, and J. D. Droppleman (Lockheed Aircraft Corp., Lockheed Electronics Co., Houston, Tex.).
IN: EASCON '68; INSTITUTE OF ELECTRICAL AND ELECTRONICS ENGINEERS, ELECTRONICS AND AEROSPACE SYSTEMS CONVENTION, WASHINGTON, D.C., SEPTEMBER 9-11, 1968, RECORD. [A69-13176 03-07]
New York, Institute of Electrical and Electronics Engineers, Inc., 1968, p. 339-344.

Description of the electron-beam meter as an instrument to be used for monitoring the lunar-surface electric field. This instrument, currently being developed, performs its task by directing a beam of electrons over the lunar surface and measuring the deflection of the beam caused by the electric field. The theory of operation of the instrument is presented, and several factors affecting the performance of the instrument are discussed. Important factors are the alignment, cross section, and energy of the beam and environmental parameters, such as plasma-particle currents and the ambient magnetic field. The potential of the instrument is considered. A breadboard model of the instrument has been built, and its performance characteristics are given. P.v.T.

A69-13851 *#
AEROSPACE SENSOR SYSTEMS.
Gene G. Mannella (NASA, Electronics Research Center, Cambridge, Mass.).
Astronautics and Aeronautics, vol. 6, Dec. 1968, p. 26-35. 9 refs.

Discussion of aerospace sensor systems designed to meet the challenge of demanding modern tasks and increasing complexity. With the present emphasis on systems, there has rapidly developed a diverse spread of sensor-system requirements. The discussion depicts the state of affairs in several representative areas such as adaptive multimode sensors and multispectral sensing. The latter is a new approach assuming that some component in an image can be recognized by an electronic system through size, shape, feature, tone, texture, and pattern characteristics. In the spectrum-matching imaging system, each resolution element is simultaneously scanned in many spectral bands. In atmospheric probing by laser, "laser radar" closely parallels conventional microwave radar. Another technique that may prove important utilizes "Raman scattering" - a small amount of light scattered at a wavelength different from the wavelength of the laser beam. P.v.T.

A69-14360 *
PHOTOGRAPHIC CONTROL SYSTEM FOR PROJECT APOLLO LAUNCHES.
A. N. Greene (NASA, Kennedy Space Center, Cocoa Beach, Fla.).
Society of Motion Picture and Television Engineers, Technical Conference, 104th, Washington, D.C., Nov. 10-15, 1968, Paper 104-20. 10 p.
$0.50.

The engineering, documentary, and metric photography requirements for Project Apollo manned launches demand hundreds of cameras located in an environment of extreme heat, vibration, and sound pressure. Photographic measurements of engine ignition in millisecond steps, valve closures, mechanical arm retractions, umbilical disconnect, and vehicle trajectory are made from the launcher deck, umbilical tower, and perimeter camera sites. Emergency cameras are positioned to cover an explosive area in case of failure. Film speeds of 1000 frames/sec with magazine-size limitation require sequence timing of 1/10 sec resolution. Fifty programable sequences are available with interlocks consistent with the launch countdown computer. (Author)

A69-14916 *#
MEASUREMENT OF GAS TEMPERATURE AND THE RADIATION COMPENSATING THERMOCOUPLE.
Glenn E. Daniels (NASA, Marshall Space Flight Center, Huntsville, Ala.).
Journal of Applied Meteorology, vol. 7, Dec. 1968, p. 1026-1035. 21 refs.

The achievement of a high degree of accuracy in gas-temperature measurement has been a problem in many investigations. The theory of such measurement is presented together with an analysis of a device known as the radiation compensating thermocouple, which is designed to cancel out errors from the radiation environment inherent in other systems of measurement. The mathematical concepts and results of experimental work are included. Results of tests provided data on the errors of air-temperature measurement with single thermocouples used without shields, and proved that carefully fabricated radiation compensated thermocouples measure the true air temperature with very small errors. (Author)

A69-15028 *
LASER DISPLAY SYSTEMS. I - SCANNERS.
D. W. Kennedy, C. R. Grauling, A. J. Devaney, and R. D. Wright (NASA, Electronics Research Center, Cambridge, Mass.).
Instruments and Control Systems, vol. 41, Dec. 1968, p. 59-63. 21 refs.

Discussion of scanned laser-beam display techniques, which are adapted from CRT technology with lasers and appropriate controllers substituted for the CRT and its deflection apparatus. The laser beam can be deflected mechanically, refractively, or diffractively. Gas ion lasers are presently most attractive for display applications, because they produce continuous emission. The helium-neon laser seems inherently limited to less than 1 W of light output. Argon and krypton lasers, capable of higher power output, are four orders of magnitude less efficient in converting electric to optical power. One

watt of optical power is sufficient for a moderate-size display. An argon laser can illuminate a 1 m^2 screen with brightness of about 30 ft-lambert. A flying-spot scanner illuminates both an object and the display screen. The simultaneous scanning of the scene and the display screen provides automatic synchronization of the video signal with the scan pattern, and obviates the need for a sawtooth scanning device. P.v.T.

A69-15428 *

ENTRY VEHICLE INSTRUMENTATION FOR HEAT SHIELD ABLATION MEASUREMENTS.

Peter J. LeBel and James M. Russell (NASA, Langley Research Center, Hampton, Va.).

(Instrument Society of America, Annual Conference and Exhibit, 20th, Los Angeles, Calif., Oct. 4-7, 1965, Paper.)
ISA Transactions, vol. 7, no. 3, 1968. p. 187-193. 11 refs.

Calculation of expressions for the Zener tunneling current and optical-absorption coefficient in the presence of crossed and parallel electric and magnetic fields, using WKB solutions to the two-band model. The results obtained are supported by the photon-assisted tunneling experiments of a preceding paper and by other tunneling experiments. Apart from differences not resolved by these experiments, the results obtained for crossed fields are the same as those obtained by Aronov and Pikus, who used a quite different treatment of a model identical to the authors', except for the inclusion of spin effects, which do not appear to alter the results significantly. It is shown that the main features of electron tunneling in crossed and parallel fields can be adequately explained by using a semiclassical WKB treatment, which, in addition, provides a good physical picture of the tunneling process. M.F.

A69-15514 *#

HEAT-TRANSFER TELEMETRY FOR MODELS USING THERMOCOUPLE SENSORS.

Dean R. Harrison and William K. Lockman (NASA, Ames Research Center, Moffett Field, Calif.).

(American Institute of Aeronautics and Astronautics, Aerodynamic Testing Conference, 3rd, San Francisco, Calif., Apr. 8-10, 1968, Paper 68-407.)
Journal of Spacecraft and Rockets, vol. 6, Jan. 1968, p. 76-78. 16 refs.

A telemetry technique has been developed utilizing thermocouple sensors for determining low afterbody heating rates on free-flight blunt cone models under test in a high-enthalpy shock tunnel. Signals generated by a thermocouple calorimeter type of heat-transfer sensor were amplified and used to control the frequency of an rf transmitter. Electrical noise introduced by the flow of ionized air past the model was greatly reduced by electrostatic shielding of the electronics and the sensing thermocouple. Tests were conducted in a 1-ft shock tunnel to measure the base heating of blunt 15° half-angle cones in a high-enthalpy (11 mjoules/kg) flow. Under these conditions, an unshielded model produced SNRs of approximately 1. The addition of shielding reduced noise to the point where it was negligible. Heating rates determined from these tests were in the order of 1 to 4 watts/cm^2. (Author)

A69-16105 *#

A FLUIDIC PROPORTIONAL THRUSTER SYSTEM FOR SOUNDING ROCKET APPLICATIONS.

D. M. Chisel (NASA, Ames Research Center, Moffett Field, Calif.) and R. K. Rose (General Electric Co., Schenectady, N.Y.).

American Society of Mechanical Engineers, Winter Annual Meeting and Energy Systems Exposition, New York, N.Y., Dec. 1-5, 1968, Paper 68-WA/FE-32. 7 p.
Members, $0.75; nonmembers, $1.50.

Presentation of the description and development status of a new proportional fluidic thruster concept. The new control concept, originated at NASA-Ames, provides control torques by gas expulsion proportional to an electrical or fluidic command signal. The system is being developed for a sounding rocket control application. Compared to present bang-bang thruster systems, the concept eliminates the characteristic control limit cycle and provides significantly better pointing accuracy, as demonstrated by breadboard hardware tests of the concept. The studies also show that the control requires less power and has superior growth potential. (Author)

A69-16135 *#

VENTURI METER WITH SEPARABLE DIFFUSER.

T. J. Dudzinski, R. C. Johnson, L. N. Krause (NASA, Lewis Research Center, Cleveland, Ohio).

American Society of Mechanical Engineers, Winter Annual Meeting and Energy Systems Exposition, New York, N.Y., Dec. 1-5, 1968, Paper 68-WA/FM-2. 5 p. 18 refs.
Members, $0.75; nonmembers, $1.50.

The effects on venturi meter efficiency and discharge coefficient of a radial, outward step at the transition from throat to diffuser are reported over a Reynolds number range of 1 x 10^4 to 5 x 10^5 and over a Mach number range of 0.2 to 1.0. Step size was varied from 0 to 12.5% of the throat radius. The efficiency increases with increasing Reynolds number, decreases with increasing Mach number, and decreases as step size increases beyond 2%. The discharge coefficient was independent of Mach number, step size, and back-pressure variation at critical flow. (Author)

A69-16755 *#

ADVANCED AIR DATA SENSING TECHNIQUES.

Rodney K. Bogue and Lannie D. Webb (NASA, Flight Research Center, Edwards AFB, Calif.).

IN: INTERNATIONAL AEROSPACE INSTRUMENTATION SYMPOSIUM, 5TH, CRANFIELD, BEDS., ENGLAND, MARCH 25-28, 1968, PROCEEDINGS. [A69-16747 05-14]
Symposium sponsored by the College of Aeronautics and the Instrument Society of America.
London, Peter Peregrinus, Ltd., 1968, p. 66-75. 14 refs.

Determination of the feasibility of using a fluidic-type temperature sensor for measuring total temperature on an aircraft traveling at hypersonic speeds within the atmosphere. Problem areas that do not severely limit the application but do require further study to assess the total effect of each problem in the system operation were revealed. A partial total-temperature time history of X-15 flight 53 (Oct. 3, 1967) up to peak Mach number is shown, together with radar measurements of the X-15 Mach number and altitude, in addition to the data obtained from the shielded thermocouple sensor and the fluidic sensor. M.M.

A69-16932 *#

EFFECTS OF ENERGETIC PARTICLES ON PHOTOMULTIPLIERS IN EARTH ORBITS UP TO 1500 KM.

Walter B. Fowler, Edith I. Reed (NASA, Goddard Space Flight Center, Greenbelt, Md.), and Jacques E. Blamont (Centre Nationale de la Recherche Scientifique, Paris, France).

Optical Society of America, Annual Meeting, Pittsburgh, Pa., Oct. 9-11, 1968, Paper. 19 p. 7 refs.

Discussion of the response of several types of photomultipliers to energetic particles in terms of observed background current. Examples are drawn primarily from photometers for observation of the earth's airglow on OGO 2 and OGO 4; brief reference is made to other OGO photometers. The largest background current was observed on OGO 2 from an EMR 541E, a sapphire end-window tube with an S-20 photocathode. At a maximum of the inner electron belt, cathode current exceeded 10^{-9} A at about 1500 km. Several components are noted in the background current, with the most prominent due to the inner radiation belt and a component with the latitude distribution characteristic of cosmic rays. Estimated instantaneous proton and electron fluxes are compared with background current in order to obtain an approximate responsivity to energetic particles. P.v.T.

A69-18827 *

Δ-T CURVES FOR MEASURING MAGNETIC TAPE LINK JITTER.

J. Y. Sos (NASA, Goddard Space Flight Center, Advanced Equipment Design Section, Processor Development Branch, Greenbelt, Md.), J. M. Cole (U.S. Army, Electronics Command, Fort Monmouth, N.J.), W. B. Poland, Jr. (NASA, Goddard Space Flight Center, Greenbelt, Md.), and G. Weiss.

Telemetry Journal, vol. 3, Oct.-Nov. 1968, p. 43-46, 48-52. 5 refs.

A method for measuring the root-mean-square time delay error (Δ) between points on a record vs their separation in playback time (T) has been described in the literature. The present work derives the theoretical relationships between the Δ-T curve and the

autocorrelation function of a pure sine wave recorded on the tape, and uses this correspondence to establish a connection between jitter spectra and Δ-T curves. A simple instrument for measuring these curves with high accuracy is described, and results of measurements made on a number of intermediate-band tape units are presented. These measurements show that a low-mass tape unit may be superior to high-mass units by more than an order of magnitude. The utility of the Δ-T measurement technique is discussed on the basis of its direct relationship to PCM and coherent recording applications, and its value as a standard means for evaluating time delay error in magnetic tape links is described. (Author)

A69-19185 *

COMPUTER ANALYSIS OF TRACKS IN NUCLEAR EMULSION UTILIZING DIGITIZED VIDEO SCAN.

D. V. Reames (NASA, Goddard Space Flight Center, Greenbelt, Md.) and C. H. Ehrmann.

(Institute of Electrical and Electronics Engineers, Nuclear Science Symposium, 15th, Montreal, Canada, Oct. 23-25, 1968, Paper 2 A-7.)

IEEE Transactions on Nuclear Science, vol. NS-16, Feb. 1969, p. 127-131.

A system has been developed to make density measurements on particle tracks in nuclear emulsions. The output signal of a vidicon viewing the track through a microscope is digitized to detect developed grains in the emulsion. This digitized information is transferred in real time to a computer which selects grains falling in the track, sums their volumes, and computes parameters related to their spatial distribution. Analysis of tracks of arbitrary angles is accomplished by rotating the track image in the focal plane with a Pechan prism and by driving the focal plane through the emulsion while taking data. (Author)

A69-19192 *

A GAMMA RAY TELESCOPE UTILIZING LARGE AREA WIRE SPARK CHAMBERS.

H. B. Ögelman (NASA, Goddard Space Flight Center, Greenbelt, Md.), R. W. Ross, C. H. Ehrmann, C. E. Fichtel, and D. A. Kniffen.

(Institute of Electrical and Electronics Engineers, Nuclear Science Symposium, 15th, Montreal, Canada, Oct. 23-25, 1968, Paper 3 A-5.)

IEEE Transactions on Nuclear Science, vol. NS-16, Feb. 1969, p. 304-308. 5 refs.

Development of a second-generation gamma-ray telescope for further experiments in balloon-borne astronomy. This instrument is composed of 32 wire-grid spark chamber modules, each 50 x 50 cm^2, utilizing two-coordinate ferrite-core readout. The detector is flown on a 27,000-ft^3 research balloon, in a search for discrete gamma-ray sources and supernova explosions. B.H.

A69-19968 *

DISPLAY REQUIREMENTS FOR ADVANCED MANNED SPACECRAFT.

Robert C. Duncan (NASA, Electronics Research Center, Cambridge, Mass.).

(NASA, Symposium, Cambridge, Mass., Sept. 19, 20, 1967.)

Spaceflight, vol. 11, Mar. 1969, p. 95-101.

Discussion of displays and controls in manned space vehicles, a fundamental purpose of which is to integrate man into the vehicle system. Displays take the form of dials, attitude indicators, and computer-derived status and maneuver data. The unique capabilities of man as a controller of systems are the ability to perform an almost unlimited diversity of tasks. The instrumentation of the Mercury, Gemini, and Apollo spacecraft is described. The relative role of man and automated systems for control during the Apollo mission is considered. F.R.L.

A69-20165 *#

PICOSECOND PULSE MEASUREMENT BY TWO-PHOTON EXCITATION OF PHOTOGRAPHIC FILM.

David C. Burnham and Kenneth W. Billman (NASA, Electronics Research Center, Cambridge, Mass.).

Applied Physics Letters, vol. 13, Dec. 15, 1968, p. 419-421. 6 refs.

A simple technique for observing picosecond light pulses is demonstrated. The overlap between two light beams is measured by two-photon excitation of a photographic film which is below threshold for one-photon excitation. The resolution of the method is variable and limited only by the bandwidth of the photographic film. (Author)

A69-21087 *

OPTICAL DESIGN OF A GLANCING INCIDENCE X-RAY TELESCOPE.

J. D. Mangus and J. H. Underwood (NASA, Goddard Space Flight Center, Greenbelt, Md.).

Applied Optics, vol. 8, Jan. 1969, p. 95-102. 19 refs.

Description of the optical design of a Wolter type-1 glancing incidence X-ray telescope for the wavelength region from 6 to 100 Å. The theoretical performance of the instrument is evaluated by ray tracing. The results of laboratory and rocket flight tests on a prototype instrument are described. It is concluded that it is theoretically possible to obtain high resolution in the imaging of celestial objects in X rays through the use of the glancing incidence telescope. B.H.

A69-21394 *

LASER DISPLAY SYSTEMS. II.

D. W. Kennedy, C. R. Grauling, R. D. Wright (NASA, Electronics Research Center, Cambridge, Mass.), and A. J. Devaney.

Instruments and Control Systems, vol. 42, Feb. 1969, p. 109-112. 26 refs.

Discussion of holographic display and its applications. Ultrasonic vibrations can be used as the "illuminating" source to produce holograms. These waves have lengths two or three orders of magnitude greater than those of light, and produce correspondingly larger records. A conventional hologram can be made by reducing the original pattern to optical proportions. A similar effect has been noted using microwave radiation. Materials other than photographic emulsions respond to laser light. Alkali-halide crystals can be induced to form electron holes by displacing atoms. The holes respond to light in unique ways and give the potential for recording digital data. The applications mentioned include an aircraft landing display system and a movie system. The ability to generate holograms by computer offers a valuable potential interface between man and computer. G.R.

A69-21555 *

APPLICATION OF LASER DOPPLER VELOCITY INSTRUMENTATION TO THE MEASUREMENT OF JET TURBULENCE.

Robert M. Huffaker (NASA, Marshall Space Flight Center, Huntsville, Ala.), Charles E. Fuller (Hayes International Corp., Birmingham, Ala.), and T. R. Lawrence (Lockheed Aircraft Corp., Lockheed Missiles and Space Co., Huntsville, Ala.).

Society of Automotive Engineers, International Automotive Engineering Congress, Detroit, Mich., Jan. 13-17, 1969, Paper 690266. 50 p. 10 refs.

Members, $1.00; nonmembers, $1.50.

Design considerations and description of a three-dimensional laser Doppler velocity (LDV) instrument, capable of measuring the mean velocity and the velocity fluctuations of three components at a point in a flow. An application of the instrument to mean velocity and turbulence measurement in a subsonic jet shear layer is considered, and the appropriate data are presented. Comparison with the data obtained with the LDV instrument and a hot-wire anemometer indicates good agreement. From theoretical considerations and the data presented, it is concluded that the LDV instrument is a proven tool for the study of turbulent flow. P.v.T

A69-21642 *#

HIGH RESOLUTION BALLOONBORNE TEMPERATURE SENSOR.

Dennis W. Camp (NASA, Marshall Space Flight Center, Huntsville, Ala.) and Frank E. Caplan (GCA Corp., Bedford, Mass.).

Journal of Applied Meteorology, vol. 8, Feb. 1969, p. 159-166.

Description of a high-resolution lightweight temperature sensor

for use on the Jimsphere balloon. An error analysis of the temperature sensor is presented which shows the sensor to have an rms error of 0.44°C at the surface (ground level), and that the rms error increases to 0.89°C at 18 km. Three flight tests of the sensor are briefly discussed. The temperature data from these flight tests are compared with temperature data obtained from rawinsonde measurements made simultaneously with the Jimsphere temperature sensor tests. (Author)

A69-21651 *#
IMPROVED METHOD OF REMOVING PLASTIC BACKING FILMS FROM CARBON ELECTRON MICROSCOPE REPLICAS.
Gilbert H. Walker and Boyd L. Williams (NASA, Langley Research Center, Hampton, Va.).
Review of Scientific Instruments, vol. 39, Dec. 1968, p. 1968-1970.

Description of a modification of the Beals and Bigelow method of removing plastic backing films from carbon replicas. The main feature of the modification is provision for maintaining the specimens in a horizontal position, allowing the more effective removal of plastic backing films and producing less breakage of delicate replicas made from such materials as carbon. The modification is more effective and results in fewer losses of delicate replicas than when other removal methods are used. M.M.

A69-22434 *
GUIDANCE AND CONTROL COMPONENTS FOR SPACE APPLICATIONS.
Carl Janow (NASA, Washington, D.C.).
IN: NATIONAL ELECTRONICS CONFERENCE, 24TH, CHICAGO, ILL., DECEMBER 9-11, 1968, PROCEEDINGS. [A69-22433 09-09]
Conference sponsored by the Illinois Institute of Technology, the Institute of Electrical and Electronics Engineers, Northwestern University, and the University of Illinois.
Oak Brook, Ill., National Electronics Conference, Inc., 1968, p. 30-35. 14 refs.

Description of new guidance and control system components designed to meet the reliability, lifetime, and performance requirements of future space experiments and missions. The control components described include the control moment gyro, the microinch actuator, and the brushless dc motor; guidance components include the electrically supported gyro and the laser gyro. It is noted that the development of a component should not be considered complete unless a sufficient or satisfactory mathematical model has been developed. B.H.

A69-22522 *#
INSTRUMENTATION USED TO DEFINE PERFORMANCE OF SMALL SIZE, LOW POWER GAS TURBINES.
Samuel M. Futral, Milton Kofskey, and Harold E. Rohlik (NASA, Lewis Research Center, Cleveland, Ohio).
American Society of Mechanical Engineers, Annual Gas Turbine Conference and Products Show, 14th, Cleveland, Ohio, Mar. 9-13, 1969, Paper 69-GT-104. 8 p.
Members, $0.75; nonmembers, $1.50.

Discussion of problems encountered in testing a 6-in. radial-inflow turbine engine. The inlet pressure at design Reynolds number was 3.4 psia, and the actual torque was 13 in.-lb. The shaft rotated at 21,600 rpm and the turbine developed 4.5 horsepower. Weight flow was 0.28 lb/sec. Factors affecting measurement accuracy are discussed along with a description of the instruments, the recording systems, and calibration techniques - e.g., miniaturized probes, low-pressure level transducers, precise power absorbers. Precision of the measurements and resulting accuracy of the performance variables - namely, flow, torque, speed, and efficiency - are included. M.G.

A69-24838 *
ROCKET SPECTROHELIOGRAPH FOR THE Mg II LINE AT 2802.7 Å.
Kerstin Fredga (NASA, Goddard Space Flight Center, Greenbelt, Md.).
Applied Optics, vol. 8, Feb. 1969, p. 333-343. 21 refs.

Description of a rocket-borne spectroheliograph designed to take monochromatic pictures of the sun in the Mg II line at 2802.7 Å. The photographic system consists of a Questar telescope, a Solc type birefringent filter, and an automatic Robot camera. The double Solc filter has a spectral bandwidth of 3.5 Å. The two units in the double filter have been thoroughly tested and are compared with theoretically calculated transmission curves. Two new types of linear film polarizers for the UV region have been tested and used in the filter. A temperature control unit was developed which stabilized the filter temperature in flight to within ±0.2°C. The instrument has been tested in vacuum and to the Aerobee-150 vibration specifications. It has been flown and successfully recovered three times and performed excellently during each flight. (Author)

A69-25310 *#
AN INVESTIGATION OF THE DECOUPLING EFFECTS IN A MAGNETIC FORMING BERYLLIUM COIL ASSEMBLY.
M. E. Davis, Jerry W. Rogers, D. D. Wier (Mississippi State University, Dept. of Electrical Engineering, State College, Miss.), and J. D. Bennight (NASA, Marshall Space Flight Center, Huntsville, Ala.).
IN: INSTITUTE OF ELECTRICAL AND ELECTRONICS ENGINEERS, ANNUAL REGION III CONVENTION, 7TH, COCOA BEACH, FLA., NOVEMBER 18-20, 1968, RECORD. [A69-25288 11-07]
New York, Institute of Electrical and Electronics Engineers, Inc., 1968, p. S9-4p1 to S9-4p6. 8 refs.

A beryllium coil assembly was developed by NASA for the purpose of forming metallic materials by making use of intense magnetic fields. The work described was performed in order to determine the force exerted by the coil on a plate as it becomes decoupled from the coil. The mutual coupling between the coil and plate as a function of distance of separation was determined. Differential equations with time varying coefficients were derived which describe the currents in a two ring coil and plate circuit. The solution of these equations was accomplished by the analog computer. With the solution currents, the force of repulsion between the coil and plate was calculated. (Author)

A69-26546 *#
APPLICATION OF THE LASER DOPPLER FLOWMETER TO FLUID FLOW MEASUREMENTS.
J. W. Dunning, Jr. (NASA, Lewis Research Center, Cleveland, Ohio), J. C. Angus, and R. Edwards (Case-Western-Reserve University, Cleveland, Ohio).
American Institute of Chemical Engineers, National Meeting, 64th, New Orleans, La., Mar. 16-20, 1969, Paper. 19 p. 10 refs.

Discussion of a laser Doppler flowmeter for heterodyne detection of laser light scattered from a moving fluid. The flowmeter may be used to obtain the velocity of the fluid and the velocity distribution in the scattering volume (30 μ diam). The technique has a wide dynamic range (10^{-3} to 10^{5} cm/sec). An analysis of the scattering indicates that the velocity distribution is very closely related to the spectrum of the scattered light. The spatial resolution obtainable is on the order of 10 μ (4×10^{-4} in.), and is limited by optical considerations. M.G.

A69-26974
SYMPOSIUM ON REMOTE SENSING OF ENVIRONMENT, 5TH, UNIVERSITY OF MICHIGAN, ANN ARBOR, MICH., APRIL 16-18, 1968, PROCEEDINGS.
Symposium sponsored by the U.S. Navy, the U.S. Air Force, the U.S. Army, the U.S. Geological Survey, and the Department of Agriculture.
Ann Arbor, Michigan, University, Willow Run Laboratories, 1968. 991 p.
$10.00.

CONTENTS:

FOREWORD. D. C. Parker, p. vii-ix.

PHOTOGRAPHY - AN ELECTRONIC-IONIC MEDIUM FOR REMOTE SENSING APPLICATIONS. R. G. Tarkington (Eastman Kodak Co., Rochester, N.Y.), p. 3-7. 13 refs. [See A69-26975 12-14]

MICROWAVE RADIOMETRIC CAPABILITIES AND TECHNIQUES. H. I. Ewen (Ewen Knight Corp., East Natick, Mass.), F. Haneman (Cutler-Hammer, Inc., Melville, N.Y.), R. M.

14 INSTRUMENTATION AND PHOTOGRAPHY

Kalafus, R. Mailloux (NASA, Electronics Research Center, Cambridge, Mass.), M. E. Louapre (Aerojet-General Corp., El Monte, Calif.), and D. H. Steinbrecher (Massachusetts Institute of Technology, Cambridge, Mass.), p. 9-58. 121 refs. [See A69-26976 12-07]

PHASED ARRAYS FOR SPACEBORNE MICROWAVE SENSORS. M. E. Louapre (Aerojet-General Corp., El Monte, Calif.), p. 59-68. 20 refs. [See A69-26977 12-09]

CURRENT PROGRAM AND CONSIDERATIONS OF THE FUTURE FOR EARTH RESOURCES SURVEY. H. E. Newell (NASA, Washington, D.C.), p. 69-75. [See A69-26978 12-34]

LINE SCAN DEVICES AND WHY USE THEM. D. S. Lowe (Michigan, University, Ann Arbor, Mich.), p. 77-101. 11 refs. [See A69-26979 12-14]

INVITED COMMENTS - LINE SCAN AND WHY TO USE THEM. R. W. Stingelin (HRB-Singer, Inc., State College, Pa.), p. 103-105. [See A69-26980 12-14]

AN INTERPRETER'S PERSPECTIVE ON MODERN AIRBORNE-RADAR IMAGERY. R. B. Innes (Michigan, University, Ann Arbor, Mich.), p. 107-122.

SURVEILLANCE OF AIR POLLUTION FROM AIRBORNE AND SPACE PLATFORMS. A. R. Barringer, B. C. Newbury, and A. J. Moffat (Barringer Research, Ltd., Rexdale, Ontario, Canada), p. 123-155. 6 refs. [See A69-26981 12-14]

RADIOPHASE - A NEW SYSTEM OF CONDUCTIVITY MAPPING. A. R. Barringer and J. D. McNeill (Barringer Research, Ltd., Rexdale, Ontario, Canada), p. 157-167. 7 refs. [See A69-26982 12-13]

AIRCRAFT POLARIMETRIC AND PHOTOMETRIC OBSERVATIONS. W. G. Egan (Grumman Aircraft Engineering Corp., Bethpage, N.Y.), p. 169-189. 9 refs. [See A69-26983 12-14]

ADVANCES IN GEOGRAPHIC AND THEMATIC MAPPING APPLICATIONS OF REMOTE SENSOR DATA. A. C. Gerlach (U.S. Geological Survey, Washington, D.C.), p. 191-196. [See A69-26984 12-34]

LEGAL AND SOCIAL POLICY RAMIFICATIONS OF REMOTE SENSING TECHNIQUES. S. D. Estep (Michigan, University, Ann Arbor, Mich.), p. 197-217.

INTERACTION OF LIGHT WITH A PLANT CANOPY. W. A. Allen and A. J. Richardson (Department of Agriculture, Weslaco, Tex.), p. 219-232. [See A69-26985 12-14]

THE USE OF RADAR IN THE DISCRIMINATION AND IDENTIFICATION OF AGRICULTURAL LAND USE. D. E. Schwarz and F. Caspall (Kansas, University, Lawrence, Kan.), p. 233-247. 9 refs. [See A69-26986 12-14]

DETERMINING THE USEFULNESS OF SPACE PHOTOGRAPHY FOR NATURAL RESOURCE INVENTORY. R. N. Colwell (California, University, Berkeley, Calif.), p. 249-289. 72 refs. [See A69-26987 12-14]

EFFECT OF PUBESCENCE ON REFLECTANCE OF LIGHT. H. W. Gausman and R. Cardenas (Department of Agriculture, Weslaco, Tex.), p. 291-297.

APPLICATIONS OF ECONOMIC ANALYSIS TO PROBLEMS OF DATA COLLECTION BY REMOTE SENSING TECHNIQUES. W. Gensurowsky (Department of Agriculture, Natural Resource Economics Div.), p. 299-305. 5 refs. [See A69-26988 12-34]

USE OF REMOTE SENSING FOR LIVESTOCK INVENTORIES. H. F. Huddleston (Department of Agriculture, Washington, D.C.) and E. H. Roberts (California, University, Berkeley, Calif.), p. 307-323.

DETAILED PLANT AND SOIL THERMAL REGIME IN AGRONOMY. C. L. Wiegand, M. D. Heilman, and A. H. Gerbermann (Department of Agriculture, Weslaco, Tex.), p. 323-342. 29 refs. [See A69-26989 12-13]

ADAPTIVE PATTERN RECOGNITION OF AGRICULTURE IN WESTERN KANSAS BY USING A PREDICTIVE MODEL IN CONSTRUCTION OF SIMILARITY SETS. R. M. Haralick (Kansas, University; Center for Research, Inc., Lawrence, Kan.), p. 343-356. [See A69-26990 12-14]

REMOTE SENSING AND THE FOREST SURVEY...PRESENT APPLICATIONS, RESEARCH, AND A LOOK AT THE FUTURE. R. C. Aldrich (Department of Agriculture, Berkeley, Calif.), p. 357-372. 22 refs. [See A69-26991 12-14]

APPLYING REMOTE SENSING TECHNOLOGY FOR IMPROVING RANGE RESOURCE INVENTORIES. D. M. Carneggie (California, University, Berkeley, Calif.), p. 373-385. 8 refs. [See A69-26992 12-14]

PREVISUAL DETECTION OF PONDEROSA PINE TREES DYING FROM BARK BEETLE ATTACK. R. C. Heller (Department of Agriculture, Berkeley, Calif.), p. 387-434. 15 refs. [See A69-26993 12-14]

AN APPLICATION OF INFRARED REMOTE SENSING TO ECOLOGICAL STUDIES - BEAR MEADOWS BOG, PENNSYLVANIA. R. W. Stingelin (HRB-Singer, Inc., State College, Pa.), p. 435-440.

COLOR AERIAL PHOTOGRAPHY FOR AQUATIC VEGETATION SURVEYS. J. E. Lukens (HRB-Singer, Inc., State College, Pa.), p. 441-446.

PROJECT FIRE SCAN - SUMMARY OF 5 YEARS' PROGRESS IN AIRBORNE INFRARED FIRE DETECTION. S. N. Hirsch (U.S. Forest Service, Missoula, Mont.), p. 447-457. [See A69-26994 12-34]

INFRARED MAPPING OF LARGE FIRES. R. L. Bjornsen (U.S. Forest Service, Washington, D.C.), p. 459-464.

FIRE DETECTION FEASIBILITY TESTS AND SYSTEM DEVELOPMENT. R. A. Wilson (U.S. Forest Service, Missoula, Mont.), p. 465-477. [See A69-26995 12-14]

REMOTE SENSING OF THE POLAR REGIONS. J. C. Reed (Arctic Institute of North America, Washington, D.C.), p. 479-481.

MULTISPECTRAL SURVEY IN THE ALASKAN ARCTIC. R. Horvatch and D. S. Lowe (Michigan, University, Ann Arbor, Mich.), p. 483-496. [See A69-26996 12-13]

OCEANOGRAPHIC APPLICATIONS OF REMOTE SENSING. J. B. Zaitzeff and J. W. Sherman, III (U.S. Naval Oceanographic Office, Washington, D.C.), p. 497-527. 37 refs. [See A69-26997 12-13]

INVESTIGATING THE OCEAN BOTTOM WITH SIDE-SCANNING SONAR. J. E. Sanders and C. S. Clay (Columbia University, Dobbs Ferry, N.Y.), p. 529-547.

AN INFRARED TECHNIQUE FOR TRACKING THE GULF STREAM. R. L. Pickett (U.S. Navy, Naval Oceanographic Office, Washington, D.C.), p. 549-554.

OCEAN WAVE PROFILE AND SPECTRA MEASUREMENT USING AN AIRBORNE MAGNETOMETER. R. Baker and P. W. U. Graefe (National Research Council, Ottawa, Canada), p. 555-570. 8 refs. [See A69-26998 12-13]

COASTAL WATER PENETRATION USING MULTISPECTRAL PHOTOGRAPHIC TECHNIQUES. E. Yost and S. Wenderoth (Long Island University, Greenvale, N.Y.), p. 571-586.

EVALUATION OF AN INFRARED SPECTROMETER AS A CLEAR AIR TURBULENCE DETECTOR. I. M. Weiss (Barnes Engineering Co., Stamford, Conn.), p. 587-597. [See A69-26999 12-14]

EVALUATION OF AN INFRARED SPECTROMETER AS A CLEAR AIR TURBULENCE DETECTOR. II. G. K. Mather (National Research Council, Ottawa, Canada), p. 599-608. [See A69-27000 12-14]

OPTICAL RADAR STUDIES OF THE ATMOSPHERE. J. D. Lawrence, Jr., M. P. McCormick, S. H. Melfi (NASA, Langley Research Center, Hampton, Va.), and D. P. Woodman (College of William and Mary, Williamsburg, Va.), p. 609-616. 13 refs. [See A69-27001 12-07]

RADIOMETRIC OBSERVATIONS OF THUNDERSTORM CELLS. M. T. Decker and E. J. Dutton (ESSA, Boulder, Colo.), p. 617-629. [See A69-27002 12-20]

CIRRUS CLOUD INFLUENCE ON 6.4-6.9 μ OBSERVATIONS. E. S. Merritt, D. Chang, and D. Beran (Allied Research Associates, Inc., Concord, Mass.), p. 631-654. [See A69-27003 12-13]

RADAR AS A TOOL IN METEOROLOGY, ENTOMOLOGY AND ORNITHOLOGY. T. G. Konrad (Johns Hopkins University, Silver Spring, Md.), p. 655-665. 16 refs. [See A69-27004 12-07]

REMOTE SENSING FOR ENGINEERING INVESTIGATION OF TERRAIN - INTRODUCTION. R. D. Leighty (U.S. Army, Cold Regions Research and Engineering Laboratory, Hanover, N.H.), p. 667, 668.

REMOTE SENSING FOR ENGINEERING INVESTIGATION OF TERRAIN - RADAR SYSTEMS. R. D. Leighty (U.S. Army, Cold Regions Research and Engineering Laboratory, Hanover, N.H.), p. 669-685. 28 refs. [See A69-27005 12-14]

REMOTE SENSING FOR ENGINEERING INVESTIGATION OF TERRAIN - PHOTOGRAPHIC SYSTEMS. O. W. Mintzer (Ohio State University, Columbus, Ohio), p. 687-699. 57 refs. [See A69-27006 12-14]

REMOTE SENSING FOR ENGINEERING INVESTIGATION OF TERRAIN - INFRARED SYSTEMS. D. C. Parker (Michigan,

University, Ann Arbor, Mich.), p. 701-709. 9 refs. [See A69-27007 12-14]

ENGINEERING APPLICATIONS OF MICROWAVE RADIOMETRY. A. T. Edgerton (Aerojet-General Corp., El Monte, Calif.), p. 711-724. 8 refs. [See A69-27008 12-14]

REMOTE SENSING APPLICATIONS TO HIGHWAY ENGINEERING. H. T. Rib (Federal Highway Administration), p. 725-736.

GAMMA-RAY MEASUREMENTS TO EVALUATE SOIL PROPERTIES. A. N. Williamson (U.S. Army, Vicksburg, Miss.), p. 737-746.

THE POTENTIAL OF RADAR IN GEOLOGICAL EXPLORATION. L. F. Dellwig, H. C. MacDonald, and J. N. Kirk (Kansas, University, Lawrence, Kan.), p. 747-763. 9 refs. [See A69-27009 12-14]

RADAR SCATTEROMETER DATA ANALYSIS TECHNIQUES. R. K. Moore, W. P. Waite, J. R. Lundien, and H. W. Masenthin (Center for Research, Inc., Lawrence, Kan.), p. 765-780. 8 refs. [See A69-27010 12-14]

SIDELOOKING RADAR IMAGERY. A. N. Kover (U.S. Geological Survey, Silver Spring, Md.), p. 781-785.

INFRARED SENSING OF ACTIVE GEOLOGIC PROCESSES. J. D. Friedman (U.S. Geological Survey, Washington, D.C.) and R. S. Williams, Jr. (USAF, Cambridge Research Laboratories, Wright-Patterson AFB, Ohio), p. 787-815. [See A69-27011 12-13]

INVITED COMMENTS - INFRARED SENSING OF ACTIVE GEOLOGIC PROCESSES. G. Palmason (Gudmundur Pálmason Orkfustofnun, Iceland), p. 817-820.

THE METHODS OF APPLICATIONS OF INFRARED AERIAL PHOTOGRAPHY WHEN STUDYING THE VOLCANOES AND THERMAL ACTIVITIES OF KAMCHATKA PENINSULA (SUMMARY). V. B. Komarov, B. V. Shilin, M. M. Miroshnikov, and Iu. A. Feoktistov, p. 821.

EDITOR'S NOTE, p. 823-825.

THE STATUS OF REMOTE SENSING IN HYDROLOGY. C. J. Robinove (U.S. Geological Survey, Washington, D.C.), p. 827-831.

EVALUATION OF AIRBORNE GAMMA-RAY SPECTROMETRY IN THE BANCROFT AND ELLIOT LAKE AREAS OF ONTARIO, CANADA. A. G. Darnley and M. Fleet (Geological Survey of Canada, Ottawa, Canada), p. 833-853.

APPLICATION OF AIRBORNE GAMMA-RADIATION MEASUREMENTS TO PEDOLOGIC MAPPING. R. S. Foote (Texas Instruments, Inc., Dallas, Tex.), p. 855-875.

DETECTION, DELINEATION, AND MONITORING OF SUBSURFACE COAL FIRES BY AERIAL INFRARED SCANNING. W. M. Knuth, W. Fisher, Jr., and R. W. Stingelin (HRB-Singer, Inc., State College, Pa.), p. 877-881.

REMOTE SENSORS AND GEOGRAPHICAL SCIENCE. J. R. Borchert (Minnesota, University, Minneapolis, Minn.), p. 883-888.

REMOTE SENSING OF URBAN ENVIRONMENTS. R. H. Alexander (U.S. Geological Survey, Washington, D.C.), L. W. Bowden (California, University, Riverside, Calif.), D. F. Marble, and E. G. Moore (Northwestern University, Evanston, Ill.), p. 889-911. 19 refs. [See A69-27012 12-34]

UTILIZATION OF MULTIBAND AERIAL PHOTOGRAPHS IN URBAN HOUSING QUALITY STUDIES. B. S. Wellar (Northwestern University, Evanston, Ill.), p. 913-926.

METHODS OF FEASIBILITY AND ECONOMIC ANALYSIS OF REMOTE SENSING APPLICATIONS. A. H. Muir (Planning Research Corp., Washington, D.C.) and I. J. Sattinger (Michigan, University, Ann Arbor, Mich.), p. 927-939. [See A69-27013 12-34]

REMOTE SENSING ACTIVITIES OF COMMITTEES OF THE NATIONAL RESEARCH COUNCIL. E. M. Risley (National Research Council, Washington, D.C.), p. 941-944.

CLOSING COMMENTS AT THE 5TH SYMPOSIUM ON REMOTE SENSING OF ENVIRONMENT. G. J. Zissis (Michigan, University, Ann Arbor, Mich.), p. 945-948.

A69-27946 *

SPACE-BORNE OPTICAL TELESCOPES - AN INTRODUCTION.

Hector C. Ingrao (NASA, Electronics Research Center, Cambridge, Mass.).

IEEE Transactions on Aerospace and Electronic Systems, vol. AES-5, Mar. 1969, p. 240, 241.

Discussion of the requirements for a space-borne optical telescope and review of work concerning its development. Space telescopes of very large diameter, with resolution corresponding to an aperture of at least 120 in. and detecting radiation between 800 Å and 1 mm are becoming technically feasible and will be uniquely important. A series of papers is mentioned as representative of the work under way in some of the problem areas. G.R.

A69-27951 *

EVALUATION OF MULTIPOINT INTERACTION IN THE DESIGN OF A THIN DIFFRACTION-LIMITED ACTIVE MIRROR.

Jeremiah F. Creedon (NASA, Langley Research Center, Hampton, Va.) and Hugh J. Robertson (Perkin-Elmer Corp., Norwalk, Conn.).

IEEE Transactions on Aerospace and Electronic Systems, vol. AES-5, Mar. 1969, p. 287-293. 6 refs.

Active control of a thin, deformable mirror is one approach to obtaining diffraction-limited performance from large orbiting telescopes. The control system design requires knowledge of the mirror reaction to the multiple forces used to maintain the desired mirror figure. A structural analysis program is used to obtain estimates of the static deflections of a point-loaded, thin, shallow, spherical primary mirror. The calculated deflections are compared to experimentally measured deflections for a specific configuration. (Author)

A69-27952 *

PRECISE ATTITUDE STABILIZATION OF A LARGE ORBITING TELESCOPE COUPLED TO A CREW COMPARTMENT.

Frederick R. Morrell (NASA, Langley Research Center, Hampton, Va.).

IEEE Transactions on Aerospace and Electronic Systems, vol. AES-5, Mar. 1969, p. 294-299.

Description of computer simulation results for the planar equations of motion of an attitude-stabilized orbiting telescope passively coupled to a manned service module. This coupling is provided through a set of soft springs and a two-axis gimbal aligned with the telescope center of mass. Principal nonlinearities in the suspension system and the telescope control system are included. The simulation indicates preliminary feasibility of this operational mode. (Author)

A69-29561 *#

AN APPLICATION OF OPTICAL TELEMETRY TO SHOCK TUBE MEASUREMENTS.

Robert E. Dannenberg (NASA, Ames Research Center, Moffett Field, Calif.) and Howard Katzman (Dacom, Inc., Palo Alto, Calif.).

Review of Scientific Instruments, vol. 40, May 1969, p. 640-642.

Description of an optical carrier, single-channel telemetry system. The system provides complete electrical isolation between data acquisition instrumentation and data storage or recording facilities. It has a bandwidth from dc to 50 kHz and has been used successfully in a shock tube facility where high voltage isolation is required for protection of instrumentation. G.R.

A69-29564 *#

MEASUREMENT OF THE VELOCITY AND ATTENUATION OF ULTRASONIC PULSES IN THE PRESENCE OF NOISE.

R. C. Williamson (NASA, Electronics Research Center, Cambridge, Mass.).

Review of Scientific Instruments, vol. 40, May 1969, p. 666-670. 14 refs.

The well developed techniques of coherent detection and signal averaging may be used to extend the range and accuracy of measurements of ultrasonic velocity and attenuation. Significant improvements in SNR are obtained by averaging a coherently detected echo train in a signal averager such as a multichannel analyzer or boxcar integrator. A standard circuit of this type is described and analyzed. Comparison of coherent detection and rectification shows the inherent advantages of coherent detection for signal-to-noise enhancement. (Author)

A69-31868 *#

DETERMINATION OF THERMODYNAMIC PROPERTIES WITH OPTICAL CROSS-CORRELATION METHODS.

F. R. Krause (NASA, Marshall Space Flight Center, Huntsville, Ala.), W. O. Davies, and M. W. P. Cann (IIT Research Institute, Chicago, Ill.).

(American Institute of Aeronautics and Astronautics, Aerospace Sciences Meeting, 5th, New York, N.Y., Jan. 23-26, 1967, Paper 67-149.)
AIAA Journal, vol. 7, Apr. 1969, p. 587-592. 17 refs.

Results of an experimental study concerning the spectrum (and its variation with time) of the laser action from a $CaF_2:Sm^{2+}$ crystal when it is excitation by ruby-laser radiation at temperatures from ~65°K to >77°K. It is demonstrated that the laser action (beginning at a pure electron line of 708 μ) moves towards the long-wave direction with increasing temperature while the intensity of the long-wave components increases. The variation of lasing intensity with time is described. T.M.

A69-32324 *
BURIED COLLECTOR GAUGE FOR MEASUREMENTS IN THE 10^{-11} TORR PRESSURE RANGE.
Leonard T. Melfi, Jr. (NASA, Langley Research Center, Hampton, Va.).
Journal of Vacuum Science and Technology, vol. 6, Mar.-Apr. 1969, p. 322-325. 9 refs.

Description of a new ionization gauge in which a shielded collector is used to lower the X-ray current. Pressures as low as 4×10^{-12} torr have been indicated with an estimated X-ray current corresponding to a pressure below 2.6×10^{-12} torr. Calibration of the gauge on an orifice flowrate system in the pressure range between 10^{-6} and 10^{-9} torr with 4-mA emission and a collector to filament voltage of -300 V yielded a gauge constant of 20 $torr^{-1}$. For pressure below 10^{-9} torr the buried collector gauge was compared to the bent-beam Helmer gauge. Data from tests performed on the bent-beam Helmer gauge are also given. These include a calibration and a plot of gauge constant as a function of emission current in the range between 0.1 and 10 mA. (Author)

A69-32326 *
EXPERIMENTAL EVALUATION OF THE RATE-OF-RISE METHOD FOR MEASURING OUTGASSING RATES OF THREE GASES BETWEEN 10^{-6} AND 10^{-3} TORR.
Gerald L. Gregory (NASA, Langley Research Center, Hampton, Va.).
Journal of Vacuum Science and Technology, vol. 6, Mar.-Apr. 1969, p. 344-346.

Experimental determination of the accuracy to which known leak rates of three gases can be measured with the rate-of-rise technique. The study consists in measuring known leak rates of nitrogen, methane, and helium gases in the leak range from 5×10^{-6} to 5×10^{-4} torr-liter/sec, although only the results for a leak rate of 1×10^{-5} torr-liter/sec are discussed. M.G.

A69-32855 *#
IMPROVED METHOD OF INJECTING THE AUDIO SIGNAL IN AUTOMATIC LANGMUIR PROBE SECOND DERIVATIVE PLOTTERS.
Roman Krawec (NASA, Lewis Research Center, Cleveland, Ohio).
Review of Scientific Instruments, vol. 40, June 1969, p. 842, 843.

Description of an improved method of superimposing a small sinusoidal audio frequency signal on the dc probe voltage of an automatic plotting device. The new method eliminates the distortion of data which occurs with the procedure proposed by Branner et al. (1963) under certain specified conditions. G.R.

A69-32891 *
SCANNING ELECTRON MIRROR MICROSCOPY AND SCANNING ELECTRON MICROSCOPY OF INTEGRATED CIRCUITS.
James E. Cline, James M. Morris, and Seymour Schwartz (NASA, Electronics Research Center, Technology Assistance Div., Failure Mechanisms Branch, Cambridge, Mass.).
(Institute of Electrical and Electronics Engineers, Annual Reliability of Physics Symposium, 7th, Washington, D.C., Dec. 2-4, 1968.)
IEEE Transactions on Electron Devices, vol. ED-16, Apr. 1969, p. 371-375. 9 refs.

Comparison of the recently developed scanning electron mirror microscope (SEMM) with other types of electron microscopes, such as the electron mirror microscope (EMM) and the scanning electron microscope (SEM), for examining integrated circuits. Potential advantages of the SEMM include high resolution, elimination of electron bombardment damage, and high sensitivity of voltage gradients, magnetic fields, and topography. Preliminary observations of integrated circuits obtained with the feasibility SEMM at various specimen potentials are discussed. (Author)

A69-33107 *#
FLOW-DIRECTION MEASUREMENT WITH FIXED-POSITION PROBES IN SUBSONIC FLOW OVER A RANGE OF REYNOLDS NUMBERS.
Lloyd N. Krause and Thomas J. Dudzinski (NASA, Lewis Research Center, Cleveland, Ohio).
Instrument Society of America, National Aerospace Instrumentation Symposium, 15th, Las Vegas, Nev., May 5-7, 1969, Paper. 15 p. 7 refs.

Study of the correlations between measured fixed-probe pressures and flow direction over a range of Reynolds number, Mach number, and flow angle encountered in investigations of subsonic flow. Only a single type of probe design, consisting of clustered tubes, with the flow-direction tubes cut off at 45°, was checked experimentally. It was found that flow direction is measurable to within about 1° over most combinations of flow conditions in the range investigated. G.R.

A69-33264 *#
PORTABLE REFLECTOMETER.
Mitchell W. Finkel (NASA, Goddard Space Flight Center, Greenbelt, Md.).
American Institute of Aeronautics and Astronautics, Thermophysics Conference, 4th, San Francisco, Calif., June 16-18, 1969, Paper 69-599. 6 p. 6 refs.
Members, $1.00; nonmembers, $1.50.

Description of an integrating-sphere reflectometer. The optical system is enclosed in a 9 x 5 in. cylindrical housing upon which a 4.5-in. integrating sphere is centrally mounted. The system weights less than six pounds, so that it is decidedly portable. The spectral region is intended to extend from 0.35 to 2.4 μ, which can be scanned in 1 to 3 min. G.R.

A69-34334
AMERICAN SOCIETY OF PHOTOGRAMMETRY, ANNUAL MEETING, 35TH, WASHINGTON, D.C., MARCH 9-14, 1969, TECHNICAL PAPERS.
Falls Church, Va., American Society of Photogrammetry, 1969. 427 p.
$5.00.

CONTENTS:

USE OF RELATIVE CONTROL INFORMATION IN ANALYTICAL EXTRATERRESTRIAL PHOTOGRAPHY. E. M. Mikhail (Purdue University, Lafayette, Ind.), p. 202-220. 6 refs. [See A69-34335 18-14]

OUT-OF-THIS-WORLD PHOTOGRAMMETRY. P. E. Norman (NASA, Manned Spacecraft Center, Houston, Tex.), p. 269-285. 13 refs. [See A69-34336 18-14]

USING THE TIME DIMENSION FOR AUTOMATED CROP SURVEYS FROM SPACE. D. Steiner (Waterloo, University, Waterloo, Ontario, Canada), p. 286-300. 19 refs. [See A69-34337 18-13]

IMAGE-TONE ENHANCEMENT. D. S. Ross (Philco-Ford Corp., Palo Alto, Calif.), p. 301-319. 7 refs. [See A69-34338 18-14]

USE OF HIGH-ALTITUDE JET PHOTOGRAPHY FOR TOPOGRAPHIC MAPPING. R. E. Altenhofen (U.S. Geological Survey, Menlo Park, Calif.), p. 372-388. 9 refs. [See A69-34339 18-14]

A69-34336 *
OUT-OF-THIS-WORLD PHOTOGRAMMETRY.
Paul E. Norman (NASA, Manned Spacecraft Center, Mapping Sciences Laboratory, Houston, Tex.).
IN: AMERICAN SOCIETY OF PHOTOGRAMMETRY, ANNUAL MEETING, 35TH, WASHINGTON, D.C., MARCH 9-14, 1969,

TECHNICAL PAPERS. [A69-34334 18-14]
Falls Church, Va., American Society of Photogrammetry, 1969, p. 269-285. 13 refs.

Discussion of the NASA lunar surveying and mapping activities of special significance in the field of photogrammetry. The imagery and control data obtained by the Lunar Orbiter photographic satellite and the photogrammetric data reduction techniques used in preparation for the manned lunar landing are discussed as examples of the importance of this new branch of high-altitude photography. The potential of surveying and mapping from space is discussed. B. H.

A69-34442 *#
EQUATIONS FOR ERRORS IN TURBULENCE MEASUREMENTS WITH INCLINED HOT WIRES.
James C. Hill (Washington, University, Dept. of Chemical Engineering, Seattle, Wash.; NASA, Goddard Space Flight Center, Greenbelt, Md.) and Charles A. Sleicher (Washington, University, Dept. of Chemical Engineering, Seattle, Wash.).
Physics of Fluids, vol. 12, May 1969, pt. 1, p. 1126, 1127.
NSF-supported research.

Extension of the results of Champagne and Sleicher (1967, 1968) on the errors incurred in turbulence measurements by assuming normal-component cooling of hot wires to include greater tangential cooling. Results are also presented for errors in turbulence heat-flux measurements. (Author)

A69-34691 *
A FAMILY OF PORTABLE VERSATILE AEROSOL PARTICLE ANALYZERS.
E. Rosenblum, L. Long (NASA, Electronics Research Center, Cambridge, Mass.), W. Burgess, and P. Reist (Harvard University, School of Public Health, Boston, Mass.).
(Association for the Advancement of Medical Instrumentation, Annual Meeting, 3rd, Houston, Tex., July 1968.)
Association for the Advancement of Medical Instrumentation, Journal, vol. 3, Jan. 1969, p. 18-24. 5 refs.

Description of a family of instruments developed for the measurement of aerosols both during space flight and in the laboratory. The instruments can be used to measure the concentration and size distribution of aerosol particles in the size range of 0.5 to 100 μ. A self-contained, hand-held, battery-operated aerosol particle analyzer was designed, fabricated, and flight qualified. This instrument, whose principle of measurement is based on forward angle light scattering, weighs less than 5-1/2 lb, and has envelope dimensions of 3.75 x 5 x 7.2 in. It samples 1/60 ft^3 of air during a 1-min operating period, and sorts the information obtained on the light scattered from each particle into its appropriate size group. G.R.

A69-35101 *#
A REVIEW OF THE IMAGE DISSECTOR METEOROLOGICAL CAMERAS AND A VIEW OF THEIR FUTURE.
Edward W. Koenig (International Telephone and Telegraph Corp., Aerospace/Optical Div., Fort Wayne, Ind.) and Gilbert A. Branchflower (NASA, Goddard Space Flight Center, Greenbelt, Md.).
IN: SPACE, TECHNOLOGY, AND SOCIETY; CANAVERAL COUNCIL OF TECHNICAL SOCIETIES, SPACE CONGRESS, 6TH, COCOA BEACH, FLA., MARCH 17-19, 1969, PROCEEDINGS. VOLUME 1. [A69-35070 18-34]
Edited by L. E. Jones, III.
Cape Canaveral, Fla., Canaveral Council of Technical Societies, 1969, p. 16-23 to 16-41.
Contracts No. NAS 5-9619; No. NAS 5-9671; No. NAS 5-11617; No. NAS 5-11618.

Description of the operation and achievements of the ATS-III IDC (Applications Technology Satellite III Image Dissector Camera) and the NIMBUS IDCS (Image Dissector Camera System). The ATC III contains an image dissector, a sun sensor for the spin rate, and the electronics required to synchronize camera timing and operation with spacecraft spin, and to retain proper phasing for earth viewing once initial phase has been commanded from the ground. The camera generates one line of video with each spacecraft rotation and is unique in that the IDC output contains all the frame and line synchronization information necessary to display the video with a minimum of special ground support equipment. The NIMBUS IDCS is an 800 TV line system with a line rate of 4 Hz and a video bandwidth of 1800 Hz. The video will be transmitted to earth in real-time AM/FM with an AM subcarrier of 2400 Hz and will be simultaneously recorded on spacecraft recorders. Camera resolution is 25% at 800 TV lines, and the output video has a highlight SNR of 38 dB (p-p/rms). Some applications of the image dissector camera are discussed, the most important being its potential use as an earth resources sensor. B.H.

A69-35724 *
PHOTOMULTIPLIER AREA SENSITIVITY MEASUREMENTS USING A MULTICOLOR DISPLAY TECHNIQUE.
Otto Youngbluth, Jr. (NASA, Langley Research Center, Hampton, Va.).
IN: ICIASF '69; INTERNATIONAL CONGRESS ON INSTRUMENTATION IN AEROSPACE SIMULATION FACILITIES, 3RD, POLYTECHNIC INSTITUTE OF BROOKLYN, FARMINGDALE, N.Y., MAY 5-8, 1969, RECORD. (A69-35714 19-11)
New York, Institute of Electrical and Electronics Engineers, Inc. (IEEE Publication 69 C 19-AES), 1969, p. 86-91, 321-325.

Description of a method for rapidly obtaining color-coded area sensitivity maps of photomultiplier tubes (PMTs). The PMT area sensitivity can be recorded in color contour form, a mesa form, or in a combination of these forms and colors. The technique provides a fast simple means of obtaining important PMT input-output characteristics. The mapping technique is practical for studying fatigue and circuit design effects on photodetector output characteristics. The best uniformity is obtained when the focus-electrode voltage is adjusted between that of the cathode and the dynode voltage. B.H.

A69-35796 *#
RESULTS OF GROUND AND FLIGHT TESTS OF THE APOLLO OPTICS.
Charles E. Manry (NASA, Manned Spacecraft Center, Houston, Tex.).
IN: INSTITUTE OF NAVIGATION, ION NATIONAL SPACE MEETING ON SPACE NAVIGATION—PRESENT AND FUTURE, HOUSTON, TEX., APRIL 22-24, 1969, PROCEEDINGS. (A69-35789 19-21)
Washington, D.C., Institute of Navigation, 1969, p. 125-148.

Description of ground and flight tests of the Apollo optics system aimed at determining the performance of the instruments in simulated and actual sunlit space environments. The results of these tests are discussed, along with several design changes which might improve the performance of the instruments in sunlight. (Author)

A69-36259 *
SURVEYING EARTH RESOURCES WITH REMOTE SENSORS.
John D. Koutsandreas (NASA, Washington, D.C.).
IN: NTC 69; INSTITUTE OF ELECTRICAL AND ELECTRONICS ENGINEERS, NATIONAL TELEMETERING CONFERENCE, WASHINGTON, D.C., APRIL 22-24, 1969, RECORD. (A69-36237 19-07)
New York, Institute of Electrical and Electronics Engineers, Inc., 1969, p. 132-144. 15 refs.

Description of the progress of the NASA Earth Resources Survey Aircraft Program. From an initial Convair 240 aircraft with six elementary remote sensors, the program has progressed to where in 1969 nearly two dozen advanced sensors will be evaluated with additional NASA aircraft. These aircraft include the NASA MSC Electra P-3A, and Lockheed C-130B for sensor experimentation up to 35,000 ft. For flights above 50,000 ft, an agreement with the U.S. Air Force allows for remote sensor system testing on board and RB-57F aircraft of the Air Weather Service. With the increased payload, altitude, and range capabilities of these aircraft, electromagnetic sensors operating in the microwave, IR, visible, and UV parts of the spectrum are being evaluated. The remote sensors are evaluated for their application as a space system for the detection of oceanographic, geologic, geographic, hydrologic, and agricultural

phenomena. Federal user agencies and cooperating scientists participating in the program are being exposed to a new technology for conducting geoscience research from spaceborne platforms. Future sensor systems for the geoscientists are introduced. (Author)

A69-36375 *
A SIMPLE A. C. TECHNIQUE FOR GALVANOMAGNETIC AND SHUBNIKOV-DE HAAS MEASUREMENTS.
J. A. Woollam (NASA, Lewis Research Center, Cleveland, Ohio).
Cryogenics, Oct. 1968, p. 312, 313. 8 refs.

Description of a simple method for reducing joule heating and fields generated by sample currents and for nearly eliminating voltages induced by the magnetic field and thermoelectric emf's in galvanometric and Shubnikov-de Haas measurements. The technique uses ac currents in the sample and takes advantage of the high SNR of a commercial lock-in amplifier. M.M.

A69-36378 *
A DUAL-BEAM SOURCE OF ACTINIC LIGHT FOR PHOTOSYNTHESIS RESEARCH.
Angelo Paul Margozzi, Milton Henderson, and Ellen C. Weaver (NASA, Ames Research Center, Moffett Field, Calif.).
Photochemistry and Photobiology, vol. 9, 1969, p. 549-553.

Description of a dual-beam source of white or nearly monochromatic light for photosynthesis studies. The device provides programmed, repetitive sample illumination with variable intensity, pulse duration, and sequence. It utilizes a lamp with an integral heat rejecting reflector and contains a fiber optic bundle which efficiently transmits the light, diffusely and evenly illuminating the sample. (Author)

A69-36489 * #
AN IMPROVED COLLIMATOR FOR EXTREME ULTRAVIOLET AND X RAYS.
J. H. Underwood (NASA, Goddard Space Flight Center, Solar Physics Branch, Greenbelt, Md.).
Review of Scientific Instruments, vol. 40, July 1969, p. 894-896. 5 refs.

Description of a mechanical collimator using random arrays of apertures for the observation of the sun and other celestial objects at very short wavelengths. The instrument is an improvement over collimators using regular arrays of apertures. A technique is discussed for producing random arrays of apertures of various shapes on film. An alternative method of making the plates for the X-ray and UV regions is described in which the random coordinates generated by the computer are recorded on magnetic tape, and the tapes are used in conjunction with a tape-controlled drilling machine. The use of a random array of apertures in a spectrometer is described, and it is shown that with this scheme fewer plates are required to suppress off-axis radiation. B.H.

A69-36490 * #
TRACER DIFFUSION STUDIES ON METALS USING A MICROTOME.
D. Graham (NASA, Lewis Research Center, Cleveland, Ohio).
Review of Scientific Instruments, vol. 40, July 1969, p. 897-901.

A microtome has been used to remove Z-micron sections from metal specimens as part of a radiotracer diffusion study. The technique is described in detail and includes a design for an orientation stage to obtain sections parallel to the diffusion interface. The equipment has been used successfully on Zr, Ti, Fe, Pd, Ag, and Cu, and diffusion profiles for self-diffusion in Fe, Zr, and Ag are given. This instrument extends the sectioning method into the area of diffusion zone analysis previously occupied exclusively by abrasion techniques. (Author)

A69-36931 *
OUT-OF-THIS-WORLD PHOTOGRAMMETRY.
Paul E. Norman (NASA, Manned Spacecraft Center, Houston, Tex.).
Photogrammetric Engineering, vol. 35, July 1969, p. 693-701. 13 refs.

Summary of the NASA lunar survey and mapping activities, with particular emphasis on the generation of control by analytical photogrammetric methods. Analytical photogrammetry, camera-position data, and altitude data were used to obtain information concerning the topography of landing sites, as well as the position of lunar features required for the Apollo manned lunar landing. Data reduction for the Apollo missions is considered to demonstrate the potential of surveying and mapping from space, particularly for establishing control and for small-scale mapping. B.H.

A69-37227 * #
A NOVEL USE OF A TELESCOPE TO PHOTOGRAPH METAL DIAPHRAGM OPENINGS.
Dah Yu Cheng, Robert E. Dannenberg, and Walter E. Stephens (NASA, Ames Research Center, Moffett Field, Calif.).
AIAA Journal, vol. 7, June 1969, p. 1209-1211.

Description of a camera-telescope arrangement which makes it possible to view metal diaphragm openings within a shock tube. The diaphragm is observed through a window in the end wall of the shock tube with an astronomical telescope focused onto an image converter camera. The image of the diaphragm is reflected into the telescope by an optically flat mirror at the end of the shock tube. G.R.

A69-37876 *
CYLINDRICAL ELECTROSTATIC PROBES EMPLOYED ON ALOUETTE II AND EXPLORER XXXI SATELLITES.
James A. Findlay and L. H. Brace (NASA, Goddard Space Flight Center, Greenbelt, Md.).
IEEE, Proceedings, vol. 57, June 1969, p. 1054-1056. 8 refs.

Description of the cylindrical electrostatic probes flown on both Alouette 2 and Explorer 31, which make it possible to perform intersatellite comparisons of directly measured parameters. The sensors are identical, but differences between the two satellites resulted in differences of data format and probe potential. It is noted that interference from the topside sounder on Alouette 2 has made data processing difficult. P.G.

A69-37877 *
COMPARISON OF CYLINDRICAL ELECTROSTATIC PROBE MEASUREMENTS ON ALOUETTE II AND EXPLORER XXXI SATELLITES.
L. H. Brace and James A. Findlay (NASA, Goddard Space Flight Center, Greenbelt, Md.).
IEEE, Proceedings, vol. 57, June 1969, p. 1057-1060. 8 refs.

Comparisons of probe measurements obtained simultaneously on the Alouette 2 and Explorer 31 satellites. The results are discussed in terms of implications for future missions which combine both the sounder and direct measurements on a single spacecraft. M.M.

A69-37878 *
THE THERMAL ION AND ELECTRON TRAP EXPERIMENTS ON THE EXPLORER XXXI SATELLITE.
John L. Donley (NASA, Goddard Space Flight Center, Laboratory for Space Sciences, Greenbelt, Md.).
IEEE, Proceedings, vol. 57, June 1969, p. 1061-1063. 10 refs.

Description of the planar thermal ion and electron trap experiments on the Explorer 31 satellite. These are capable of measuring ion and electron density and temperature and ionic composition at the satellite. Instrumentation, principles of operation, data analysis procedures, and sources of error are discussed. (Author)

A69-40019 * #
X-RAY IMAGING WITH MULTIPLE-PINHOLE CAMERAS USING A POSTERIORI HOLOGRAPHIC IMAGE SYNTHESIS.
George W. Stroke, Gilbert S. Hayat (New York, State University, Electro-Optical Sciences Center, Stony Brook, N.Y.), Richard B. Hoover (NASA, Marshall Space Flight Center, Huntsville, Ala.), and

James H. Underwood (NASA, Goddard Space Flight Center, Greenbelt, Md.).
Optics Communications, vol. 1, July-Aug. 1969, p. 138-140. 10 refs.
Navy-supported research; Grant No. NGR-33-015-068.

Description of a new form of extended-source Fourier-transform holography used to synthetize into a single image the multiplicity of N identical images obtained by a multiple-pinhole camera in X-ray astronomy. This technique provides a holographic solution for achieving the considerable SNR gain conceived by Dicke (1968). Z.W.

A69-40989 *
A 2-¼- BY 2-¼-INCH PHOTOGRAMMETRIC CAMERA SYSTEM FOR THE MOON.
Richard E. Thompson (NASA, Manned Spacecraft Center, Houston, Tex.).
IN: NEW HORIZONS IN COLOR AERIAL PHOTOGRAPHY; PROCEEDINGS OF THE SEMINAR, NEW YORK, N.Y., JUNE 9-11, 1969. (A69-40985 22-14)
Seminar sponsored by the American Society of Photogrammetry and the Society of Photographic Scientists and Engineers.
Falls Church, Va., American Society of Photogrammetry, 1969, p. 175-183.

Description of a unique photogrammetric camera system developed from NASA requirements to document the lunar-surface environment during manned space-flight exploration. For this photographic situation (which is constrained by weight limitations, restricted manual ability of the photographer, safety considerations, and a harsh environment), NASA has modified its general-purpose Hasselblad camera system to enable the recording of photogrammetric data. Specially designed lenses are used on the NASA version of the Hasselblad 500 EL-camera body in which a precision glass-plate reseau grid system has been installed and calibrated. With this photogrammetric system, more meaningful photographic data will be returned from the lunar surface than has been possible before in the manned space-flight program. Furthermore, because of its general-purpose design, this camera system may have valuable applications on earth. (Author)

A69-41216 *
GAUGE COMPARISON STUDY OF THE MAGNETRON, BURIED COLLECTOR, BENT-BEAM, AND NUDE MODULATED BAYARD-ALPERT GAUGES.
William S. Lassiter (NASA, Langley Research Center, Hampton, Va.).
Journal of Vacuum Science and Technology, vol. 6, May-June 1969, p. 418, 419. 5 refs.

Investigation of the linearity of a bent-beam ionization gauge, using as a reference a calibrated, nude Modulated Bayard-Alpert (MBA) gauge. Also included in the study were a nude, single buried collector gauge, and a tubulated magnitron gauge. The linearity of the bent-beam gauge was determined by plotting the indicated pressure of the bent-beam gauge against equivalent nitrogen pressure as calculated from the results of the nude MBA gauge. Operating parameters for the nude MBA, buried collector, and bent-beam gauges are shown in a table. It is shown that the bent-beam gauge is linear down to 7 (10^{-12}) torr. B.H.

A69-41633 *
A COMPARISON OF INFRARED-EMITTANCE MEASUREMENTS AND MEASUREMENT TECHNIQUES.
John P. Millard and Elmer R. Streed (NASA, Ames Research Center, Moffett Field, Calif.).
Applied Optics, vol. 8, July 1969, p. 1485-1492. 12 refs.
Contracts No. NAS 2-2839; No. NAS 2-3769.

Values of directional and hemispherical emittance of twelve coatings were needed in support of a spacecraft experiment. Laboratory measurements were made by two calorimetric and four reflectance techniques and with two portable devices designed for field or laboratory operation. The measurement results are compared, primarily on the basis of hemispherical emittance values deduced from each. The limitations and uncertainties of each technique are summarized. (Author)

A69-42858 * #
A RADIOMETER FOR MEASURING SOLAR FLUX VARIATIONS.
Roger C. Linton (NASA, Marshall Space Flight Center, Space Sciences Laboratory, Huntsville, Ala.).
American Astronautical Society and Operations Research Society of America, Joint National Meeting, Denver, Colo., June 17-20, 1969, AAS Paper 69-254. 13 p. 10 refs.

The lack of sufficient radiometric precision and the inability to eliminate effects of atmospheric turbulence have prevented a satisfactory determination of the actual stability of the solar constant. If variations do exist, the magnitude is probably less than the sensitivity of most radiometers. A radiometer was developed to provide a plus or minus one-per cent accuracy and a precision of 0.01 per cent. The designed performance was verified using an evacuated hohlraum cavity as a standard. The novel features which give this instrument its extreme sensitivity are discussed, together with the advantages of using such a sensor for spacecraft measurements. The essential feature of this radiometer which distinguishes it from all others involves the utilization of alternating current circuitry to limit the controlling parameter to a frequency. The radiometer concept has been validated and a working unit is being tested. (Author)

A69-43192 *
THE USE OF ^{184}W AS A THERMAL FLUX MONITOR AT HIGH TEMPERATURES.
Lauren L. Ball, Paul J. Richardson, and Dean W. Sheibley (NASA, Lewis Research Center, Plum Brook Station, Sandusky, Ohio).
Nuclear Applications and Technology, vol. 7, Oct. 1969, p. 393-396. 7 refs.

Description of the use of naturally occurring W-184 as a dosimeter for thermal neutrons at temperatures up to 3000 deg K in short irradiations of 40 hr or less. The W-184 thermal-neutron capture cross section is found to be 1.94 plus or minus 0.08 b. The radiochemical separation methods and counting techniques for W-185 are described. Z.W.

N69-10933*# National Aeronautics and Space Administration. Langley Research Center, Langley Station, Va.
RESOLUTION CHANGES IN LITHIUM-DRIFTED SILICON SEMICONDUCTOR DETECTORS IRRADIATED WITH 0.5, 1.0, 2.0, AND 3.0 MeV ELECTRONS
Herbert D. Hendricks and Donald H. Phillips Washington Nov. 1968 32 p refs
(NASA-TN-D-4901) Avail: CFSTI CSCL 07E

Lithium-drifted silicon semiconductor detectors (2 mm deep and 80 mm^2 surface area) were irradiated with 0.5, 1.0, 2.0, and 3.0 MeV electrons. Fluence thresholds for damage were measured by monitoring resolution changes in the 0.972 MeV conversion electrons from ^{207}Bi. The fluence for 100-percent change in detector resolution was found to be approximately 10^{12} e/cm^2. Irradiations with 1 MeV electrons made at 10^7, 10^8, and 10^9 e/cm^2-sec gave no apparent flux dependence in the damage effects. Author

N69-13176*# National Aeronautics and Space Administration. Lewis Research Center, Cleveland, Ohio.
LIGHTING IN CRYOGENIC AND NONCRYOGENIC FLUIDS
Robert C. Hendricks and Kenneth H. Baumeister Washington Dec. 1968 12 p refs Film Supplement Number C-260 to this report is available on loan from NASA, Lewis Research Center
(NASA-TM-X-1654) Avail: CFSTI CSCL 13A

An experimental study provided conditions for operating standard light bulbs that were submerged in ordinary and cryogenic fluids. Successful operation occurred whenever the light source came to thermal equilibrium with its environment. Author

14 INSTRUMENTATION AND PHOTOGRAPHY

N69-13311*# National Aeronautics and Space Administration. Langley Research Center, Langley Station, Va.
A RADIOMETER FOR USE IN THERMAL STUDIES OF SPACECRAFT
George E. Sweet and Howard B. Miller Washington Dec. 1968 36 p refs
(NASA-TN-D-4925) Avail: CFSTI CSCL 14B

A new disk radiometer that is essentially a modification of a loss measuring slug transducer has been designed for space vacuum-thermal environmental studies. The device is operable in vacuums less than 1.3×10^{-3} N/m^2 at ambient temperature levels from 80° K to 450° K. Both steady state and time-varying total irradiances with magnitudes between 200 and 1500 W/m^2 can be measured with an error of about 10 percent. Once the radiometer is calibrated by using an extended black body reference source, it can be used in a variety of thermal study situations without recalibration. Because it is small in size (2.3-cm diameter by 0.5-cm height) and external cooling or constant temperature references are not required, it effects a minimal thermal disturbance to the test surface. The major feature of this radiometer is a shield which is located between the sensor and mounting surface. This shield is instrumented so that an empirical correction can be applied to the radiometer measurements to compensate for unwanted heat transfer between the sensor and mounting surface. Criteria are presented for designing the sensor so that it will remain in temperature equilibrium with relevant heat sources and thus simplify data reduction. Example applications of the radiometer to a thermal control balloon model are also presented. Author

N69-14351*# Raytheon Co., Sudbury, Mass.
LASER DOPPLER VELOCITY INSTRUMENT
E. Rolfe, J. K. Silk, S. Booth, K. Meister, and R. M. Young Washington NASA Dec. 1968 332 p refs
(Contract NAS8-20413)
(NASA-CR-1199; R67-4450) Avail: CFSTI CSCL 14B

Analytical and experimental data are presented on the development of a laser Doppler velocity instrument for measuring gas velocity. The instrument measures the Doppler shift of light scattered from particles moving with the gas, using Mie (Raleigh–Gans) scattering. The velocity thus measured is independent of particle temperature. An experimental comparison of the hot wire anemometer with the laser Doppler velocity instrument demonstrated excellent correspondence between the two. Measurements of velocity up to approximately Mach 2 in the seven inch wind tunnel compared well with simultaneous velocity measurements using the existing conventional tunnel instrumentation. Measurements were made with a one watt argon laser, and with a 50 milliwatt helium–neon laser. Several methods of signal processing were investigated and an optimum design concept established. This consisted of a wide range narrow band frequency tracker, whose output can be directly recorded on tape to give all necessary information on turbulence and velocity. Author

N69-15381*# National Aeronautics and Space Administration. Langley Research Center, Langley Station, Va.
AN OPTICAL SYSTEM FOR RECORDING SCHLIEREN IMAGES WITH A CONTINUOUS WRITING ULTRA HIGH SPEED FRAMING CAMERA
Lemuel E. Mauldin, III and E. Conrad Compton Washington Jan. 1969 33 p refs
(NASA-TN-D-4986) Avail: CFSTI CSCL 14E

The integrated system comprising the ultrahigh speed camera, the f/8 Z-light-path schlieren system, the focusing lenses, the square-wave-pulse light generator, and the two-beam knife-edge assembly affords up to 72 consecutive schlieren photographs at a recording rate up to 1,200,000 frames per second. The generator provides selectable pulse durations of 60, 250, and 1000 microseconds. This controlled-duration light source eliminates the need for an elaborate high speed shutter normally used with continuous light sources. A two-beam knife-edge assembly splits the Z-type schlieren beam into two separate and complete schlieren images of the test area and direct them into the camera. The system provides good quality pictures of supersonic particles and hypersonic gas flow. Author

N69-16097*# National Aeronautics and Space Administration. Langley Research Center, Langley Station, Va.
EXPERIMENTAL STUDY IN VACUUM OF THE RATE-OF-RISE OUTGASSING-MEASUREMENT TECHNIQUE
Gerald L. Gregory Washington Jan. 1969 45 p refs
(NASA-TN-D-4973) Avail: CFSTI CSCL 14B

A parametric study was conducted to determine the capabilities of the rate-of-rise outgassing-measurement technique. In the rate-or-rise technique the rate of pressure rise due to outgassing in a closed volume is a measure of the outgassing rate. The study consisted in experimentally measuring, at room temperature, with the rate-of-rise technique known leak rates of nitrogen, methane, and helium gases in the leak range of 5×10^{-6} to 5×10^{-4} torr-liter-second^{-1} and in the high vacuum range of 10^{-6} to 10^{-3} torr. Nitrogen and methane leak rates were measurable to within an experimental accuracy of ±20 percent of the known leak rate; whereas helium leak rates were measurable to within an accuracy of ±25 percent of the known leak rate. Errors as large as a factor of 10 in the measurement of leak rates were found to exist as the result of ionization-gage pumping. These errors were reduced by reducing gage pumping effects. Within the experimental uncertainty of the investigation for the gases considered, adsorption phenomena were not observed to influence rate-of-rise results. Author

N69-16099*# Denver Univ., Colo. Research Inst.
THE USE OF THERMODYNAMIC PROPERTIES OF METAL-GAS SYSTEMS AS REDUCED-PRESSURE STANDARDS
Charles E. Lundin Washington NASA Jan. 1969 34 p refs
(Contract NAS1-7391)
(NASA-CR-1271) Avail: CFSTI CSCL 14B

The erbium-hydrogen binary system was investigated by means of a Sievert's apparatus to determine the applicability of such a metal-gas system for a low-pressure standard. A thermodyanmic relationship was empirically determined for the two-phase region, erbium solid solution plus erbium dihydride, for the pressure range N69-15873 10^{-4} to 10 torr and the temperature range of 550 to 950°C. This relationship, the van't Hoff equation, is a first-order equation representing the dissociation of hydrogen gas from the dihydride phase to form the metal solid solution as a function of temperature. The coefficient of determination for the data presented was computed to be 0.999. Data is presented on the feasibility of using metal-oxygen and metal-nitrogen systems as secondary low-pressure standards. Author

N69-16100*# Boeing Co., Seattle, Wash.
SHEAR STRAIN PROPERTIES TO 10^{-10} OF SELECTED OPTICAL MATERIALS
William A. Eul and W. William Woods Washington NASA Jan. 1969 77 p refs
(Contract NAS1-7627)
(NASA-CR-1257) Avail: CFSTI CSCL 11F

The nonrecoverable (plastic) torsional strain of AISI 304L corrosion-resistant steel, CER-VIT 101, fused silica 7940, and fused silica 7971 was experimentally determined as a function of applied torsional stress. Stress and strain ranges of 200 to 10,000 psi and 0.0005 to 2 microinches per inch, respectively, were recorded. Significant differences between as-machined and annealed specimens were observed. Information obtained from this program is to be applied in the design and manufacture of large diffraction limited optics. Author

N69-16382*# National Aeronautics and Space Administration. Lewis Research Center, Cleveland, Ohio.
DESIGN AND PERFORMANCE OF FLUERIC SHOCK POSITION SENSOR FOR A MIXED-COMPRESSION SUPERSONIC INLET
William S. Griffin Washington Jan. 1969 57 p refs
(NASA-TM-X-1733) Avail: CFSTI CSCL 01C

A flueric sensor for normal shock position has been developed and tested on a Mach 2.5 mixed compression axisymmetric supersonic inlet. The sensor detects shock position by sensing the most rearward minimum in static wall pressure profile. Static and dynamic responses of the sensor were evaluated. Static response agreed relatively well with theory, but dynamic response indicated further improvements to the sensor as well as suggestions for improving the sensor's dynamic performance. Author

N69-17259*# National Aeronautics and Space Administration. Langley Research Center, Langley Station, Va.
AN ANALYTICAL PROCEDURE FOR OPTIMIZING TELEVISION SYSTEMS FOR PLANETARY DESCENT MISSIONS
Friedrich O. Huck Washington Feb. 1969 28 p refs
(NASA-TN-D-5061) Avail: CFSTI CSCL 17B

An analytical procedure is developed for optimizing spacecraft television systems to secure proper overlap between successive pictures and maximum surface resolution during planetary descent. The television characteristics of concern are optical field of view and number of scan lines. Results show how the optimum combination of these characteristics depends on target brightness, camera sensitivity, transmission rate, and spacecraft trajectory values. Author

N69-17702*# National Aeronautics and Space Administration. Lewis Research Center, Cleveland, Ohio.
DYNAMIC CALIBRATION OF TURBINE FLOWMETERS BY MEANS OF FREQUENCY RESPONSE TESTS
Grady H. Stevens Washington Feb. 1969 15 p refs
(NASA-TM-X-1736) Avail: CFSTI CSCL 14B

A technique for dynamic calibration of turbine flowmeters for small-amplitude sinusoidal perturbations was investigated. The investigation included a theoretical analysis and an experimental evaluation of a typical flowmeter for a range of frequencies and mean flow rates. The indicated flow was related to the actual flow by a first-order lag function. This lag function was completely defined by a breakpoint frequency which was directly proportional to mean flow rate. The proportional constant was determined experimentally for a typical flowmeter. This calibration constant was sufficient for completely specifying the flowmeter dynamics over the range of mean flows investigated. Author

N69-17944*# National Aeronautics and Space Administration. Langley Research Center, Langley Station, Va.
REQUIREMENTS OF MARTIAN TELEVISION EXPERIMENT FOR THREE POINT-MASS DESCENT TRAJECTORIES
Friedrich O. Huck, Leonard P. Kopia, and Robert B. Spiers, Jr. Washington Feb. 1969 37 p refs
(NASA-TN-D-5062) Avail: CFSTI CSCL 17B

An analytical approach is used to specify the transmission rate and field-of-view requirements of a television experiment on board a spacecraft as it descends through the Martian atmosphere to land a surface laboratory. The objectives of this experiment are to provide a chain of overlapping images between orbiter and surface-laboratory pictures and a 1-meter-resolution survey of the landing site before impact. Preliminary estimates of the requirements and prediction of the performance are based on three point-mass trajectories, which are the result of numerical integrations of the spacecraft motion through two different Martian atmospheric models. It is found that a single television system can achieve the experiment objectives. For a 200-line television system, the required transmission rates range from 1.4 ± 10^5 to 2.7 ± 10^5 bits per second, and the fields of view range from 12° to 22°, depending on the descent trajectory and the camera viewing direction. This required transmission rate may be halved by employing two television systems. Author

N69-18953*# Communication and Systems, Inc., Falls Church, Va.
ANALYSIS OF TWO ALTERNATE DAMPING SYSTEMS FOR GEOS GRAVITY GRADIENT STABILIZED SATELLITE
Washington NASA Feb. 1969 137 p refs
(Contract NASw-1503)
(NASA-CR-1282; R-4035-30-1) Avail: CFSTI CSCL 09E

Eddy current rod and magnetically anchored eddy current rod dampers were analyzed to derive the theoretical performance characteristics of each system and to determine which was the more suitable for GEOS satellites. Major operating conditions were simulated, and the two systems were compared as to space flight factors such as altitude and size limitations. It was found that the eddy current rod damper performs considerably better than the magnetically anchored one for polar orbits of 600 n. mi. altitude, but deteriorates more rapidly for non-polar orbits or at higher altitudes. Although this damper could be improved by adding more rods, a significant improvement would require more rods than could be carried on this satellite, but might be possible on other spacecraft. Magnetically anchored dampers are therefore better suited for GEOS; however two factors heretofore unexplored in the laboratory tests should be investigated. One is the fact that the axis of relative rotation between the two major components is generally not stationary with respect to either part. In addition, evidence that only a certain component of the damper generated torque is effective in damping satellite librations has also been found. A.C.R.

N69-20777*# Weston Instruments, Inc., College Park, Md.
DEGRADATION OF MULTIPLIER PHOTOTUBES EXPOSED TO SPATIAL RADIATIONS
M. John Brown, M. S. Bae, and S. Dark Washington NASA Mar. 1969 246 p refs
(CONTRACT NASI-7648)
(NASA-CR-1304) Avail: CFSTI CSCL 09A

The degradation of multiplier phototubes was determined from properties measured in situ during exposure to simulated spatial radiations. A complete analysis of the orbital environments for a specific spacecraft was accomplished to determine operational parameters of a phototube detector. The experimental apparatus was then arranged to provide the spatial environments at real time conditions. Exposure of four identical phototubes was conducted to evaluate the synergistic effect of combined radiations including solar, lunar, and earth irradiances and electron-proton accelerated particle radiations over a seven month period. The phototubes were fabricated for high stability using beryllium copper dynodes in each of fourteen stages and their spectral sensitivity was from 250 to 700 nanometers. Selection of the phototube was based on detector requirements in starmapping from an orbiting spacecraft. Laboratory test results indicate that the phototube is relatively stable when exposed to single radiation sources of solar and charged particles, but degrades when exposed to combined radiations, especially when the irradiation profile included lunar viewing. Author

N69-20874*# National Aeronautics and Space Administration. Lewis Research Center, Cleveland, Ohio.
ELECTRONIC POSITION INDICATOR FOR LATCHING SOLENOID VALVES
Robert J. Frye and Heinz L. Wimmer Washington Mar. 1969 9 p refs
(NASA-TM-X-1760) Avail: CFSTI CSCL 09A

14 INSTRUMENTATION AND PHOTOGRAPHY

The design and operation of an electronic position indicator for a double-latching solenoid valve are presented. Valve stem position in the solenoid coils is detected by sensing the resistive component of the coil impedance. Four units utilizing this principle have operated successfully for over 1400 hours in a test facility. Author

N69-20941*# National Aeronautics and Space Administration. Langley Research Center, Langley Station, Va.
THE DESIGN AND UNCERTAINTY ANALYSIS OF AN IMPROVED TOTAL HEMISPHERICAL EMITTANCE TRANSIENT CALORIMETER
William R. Wade and Donald J. Progar Washington Mar. 1969 21 p refs
(NASA-TN-D-5106) Avail: CFSTI CSCL 14B

This paper presents the design, the uncertainty analysis, and the test results for several selected materials of a transient calorimetric apparatus for measurement of the total hemispherical emittance of materials for a temperature range from 223° K to 523° K. The uncertainties of the system define the type and magnitude of systematic errors when the calorimetric method of measuring emittance is utilized. The design details which minimize or eliminate these errors are emphasized in the description of the system design. Maximum probable uncertainty has been determined for this system and the results of test runs on highly polished samples of copper and aluminum compare favorably with values of total emittance published by other investigators. Author

N69-21117*# Raytheon Co., Sudbury, Mass.
SPACE GEODESY ALTIMETRY STUDY
Myer Kolker and Ephraim Weiss Washington NASA Mar. 1969 350 p refs
(CONTRACT NASw-1709)
(NASA-CR-1298; R68-4459) Avail: CFSTI CSCL 17G

Performed was a tradeoff analysis of radar and laser space altimetry systems operating in the 1971-1972 time period over the sea surface for providing useful geodetic data. User requirements in the field of geodesy are translated into altimetry performance requirements. These are used as requirement specifications for the design of a candidate laser altimeter system and a candidate radar altimeter system. A tradeoff analysis comparing the two candidate systems results in the selection of the candidate radar altimeter system. Author

N69-21408*# National Aeronautics and Space Administration. Lewis Research Center, Cleveland, Ohio.
ON THE RESOLUTION AND IMAGE INTENSITY OF THE FIELD-ION MICROSCOPE
Victor G. Weizer and Americo F. Forestieri Washington Mar. 1969 15 p refs
(NASA-TN-D-5125) Avail: CFSTI CSCL 14B

The voltage required to produce blurring of a field-ion image spot was measured as a function of tip temperature. The results indicate that the ion current causing the blurring originates at an adsorbed phase on the surface, and a transit time blurring mechanism operates at low temperatures, whereas at higher temperatures an orbit time blurring mechanism best explains the data. The explanation of the failure of the plane in tungsten to image successfully above 5K is shown to lie in the imaging process itself, not in the action of the blurring mechanisms. Maximum resolution was obtained at 5 K, not at 21 K as generally believed. A method of image intensification is described that has advantages over other existing methods. Author

N69-23470*# National Aeronautics and Space Administration. Lewis Research Center, Cleveland, Ohio.
MEASUREMENT OF LIQUID AND TWO-PHASE HYDROGEN DENSITIES WITH A CAPACITANCE DENSITY METER
George E. Turney and Roger W. Snyder Washington Apr. 1969 42 p refs
(NASA-TN-D-5015) Avail: CFSTI CSCL 14C

A three-dimensional, wire matrix, capacitance density meter was used to measure the density of liquid and two-phase hydrogen flow. The measurements were made in a 4-inch (10.6-cm) nominal diameter propellant feedline of a full-scale, simulated, nuclear-rocket test system. An evaluation of this capicitance density meter was made by comparing the density meter measurements with corresponding calculated densities in the feedline. The local hydrogen densities measured with the density meter were in relatively close agreement with the calculated densities. For the most part, the calculated and measured densities differed by less than ±15 percent of the full-scale (liquid hydrogen) density. Author

N69-23895*# National Aeronautics and Space Administration. Lewis Research Center, Cleveland, Ohio.
SURFACE TEMPERATURE MAPPING WITH INFRARED PHOTOGRAPHIC PYROMETRY FOR TURBINE COOLING INVESTIGATIONS
Frank G. Pollack and Robert O. Hickel Washington May 1969 49 p refs
(NASA-TN-D-5179) Avail: CFSTI CSCL 14B

An infrared photographic pyrometry system was investigated to map surface temperature distribution in the range of 1000° to 2500°F. The system was designed to determine the surface temperature distribution of cooled turbine vanes installed in a static cascade facility. A relative energy measurement technique was used for calibrating film density to surface temperature. The calibration method was independent of surface emissivity and viewpath attenuation factor, and compensates for photographic variations. Experimental test targets in air and a hot gas stream were photographed. These thermal images of the targets are evaluated. Temperature information is reduced from each thermal image. The data are presented in the form of calibrated temperature contour maps. Temperature measurements with this method were within the 1-percent accuracy of the calibration point reference temperature over a considerable portion of the film response curve. Author

N69-24751*# IIT Research Inst., Chicago, Ill.
AIR POLLUTION MONITORING INSTRUMENTATION A Survey
Alvin Lieberman and Peter Schipma Washington NASA 1969 78 p refs
(Contract NASw-1716)
(NASA-SP-5072) Avail: CFSTI CSCL 14B

The purpose of this survey is to aid in transferring air-pollution-monitoring technology developed in aerospace research to the general industrial domain. Information from two sources is presented. First, a comprehensive literature search was made, resulting in the bibliography included. Second, NASA centers and industrial and research organizations were contacted. Thirty-two instruments and techniques, originally developed for aerospace needs, are covered in this survey. These items were found to be novel and/or improvements in the area of air pollution monitoring. A summary of the state of the art in this field precedes the discussion of the above items so that the aerospace-developed items can be compared to current practice. The state of the art articles cover gas and vapor analyses and control methods, while the NASA developed contributions cover spacecraft cabin atmosphere monitors, hazardous-gas and trace-gas analyses, welding gas analyzers, clean-assembly-area monitoring, contaminants in fluids, biosphere studies, air pollution monitors, and fuel cell applications in monitoring. Author

N69-27267*# National Aeronautics and Space Administration. Electronics Research Center, Cambridge, Mass.
COMPILATION OF DATA FROM RELATED

TECHNOLOGIES IN THE DEVELOPMENT OF AN OPTICAL PILOT WARNING INDICATOR SYSTEM
Roy Paananen, Keith Gunn, Sejfi Protopapa, Robert Ryan and Ann Story Washington May 1969 101 p refs
(NASA-TN-D-5174) Avail: CFSTI CSCL 01D

The results of analytical efforts on some of the major scientific and engineering aspects of a proposed optical pilot warning indicator are reported. No fundamental obstacles, including projections for its ultimate economic acceptance, appear to stand in the way of early synthesis of prototype xenon lamp silicon detector systems for field tests. Certain system variations look promising for future growth. Author

N69-28023*# Fairchild Camera and Instrument Corp., Syosset, N.Y.
PLANETARY FILM RECONNAISSANCE SYSTEM
Robert Bashe and Ira Schwartz Washington Jun. 1969 94 p ref
(Contract NASI-7688)
(NASA-CR-1358) Avail: CFSTI CSCL 14C

A planetary film system was designed and fabricated that incorporates film as the recording medium in conjunction with automatic film processing and a solid state electro-mechanical readout device. Initial performance evaluation tests are discussed and the direction of continuing effort in the devleopment of such future scientific reconnaissance film systems is indicated. The camera portion of the system incorporates a variable framing rate and a reversible film transport drive. The format is 3 inches by 1 inch, on 35mm film. The processing section utilizes a monobath impregnated web for complete processing and drying of exposed film. The web is encapsulated to prevent evaporation of the processing chemicals, a technique well suited for the processing of film on long duration reconnaissance missions. The conversion of developed scene images into equivalent time-varying video signals is accomplished by an electro-mechanical scanner which uses precision lead screw drives and a semiconductor source and detector for scanning. The use of a mechanical scanner results in high linearity for film readout. The selectable scan rate is compatible with projected unmanned interplanetary space craft data transmission rates. Author

N69-28402*# Midwest Research Inst., Kansas City, Mo.
STUDY OF LOW PRESSURE APPLICATION OF NEW ORBITRON AND IRON GAUGE DESIGNS
Charles M. Gosselin Washington NASA Jun. 1969 41 p refs
(Contract NAS1-7458)
(NASA-CR-1300) Avail: CFSTI CSCL 14B

Three experimental orbitron gauges were designed and fabricated. These gauges were designed so as to use the technique of reduced ion-collector area which was introduced by Bayard and Alpert, and the technique of suppression of photoemission from the ion collection introduced by Schuman. The basic concepts of UHV measurements and a basic model of orbitron gauge operation are reviewed. Also fabrication techniques are described. Pressure response curves are displayed. The combination of the suppressor grid with the orbitron gauge appear to offer significant promise for operation below 10^{-11} torr. A second type gauge was also studied viz. the buried collector gauge. A pressure response curve is also displayed for this device. Author

N69-28909*# National Aeronautics and Space Administration. Washington, D.C.
EARTH PHOTOGRAPHS FROM GEMINI 6 THROUGH 12
1968 335 p refs
(NASA-SP-171) Avail: SOD $8.00; CFSTI CSCL 14E

A representative sampling of color photographs of the earth's surface is presented, chosen from among hundreds taken by the Gemini astronauts in the course of scientific experiments, including synoptic terrain and weather photography. The pictures are grouped geographically and have accompanying explanatory notes. P.A.B.

N69-29153*# National Aeronautics and Space Administration. Langley Research Center, Langley Station, Va.
DESIGN OF AN ELECTRONICALLY SCANNED STAR SENSOR WITH DIGITAL OUTPUT
Aaron J. Ostroff and K. C. Romanczyk Washington Jun. 1969 37 p refs
(NASA-TN-D-5281) Avail: CFSTI CSCL 14B

A technique for detecting the change in position of a star on the focal plane of a telescope is described. In this technique an image dissector is used to scan the focal plane and to generate position information. Both theoretical and experimental data are presented. The theoretical analysis contains information on signal-to-noise ratio and relationships between star magnitude, system stability, and sweep frequency. Statistical methods are included for determining the standard deviation for detecting any signal pulse, and for calculating the error involved for one or for several measuring periods. The experimental data contain information on the variation of system stability with star magnitude as functions of sweep frequency, threshold level, and averaged data. All testing is for a simulated 3 meter diameter telescope operating at f/100. Results show that for a triangular sweep frequency of 100 hertz and a star magnitude of +10, the system is stable to within ±26.4 nanoradians. This represents a system signal-to-noise ratio of 370. Other results indicate that the system is linear within ±0.6 percent of best straight line over a total field of view of ±9.76 milliradians. Author

N69-29196*# National Aeronautics and Space Administration. Lewis Research Center, Cleveland, Ohio.
THERMAL ELECTROMOTIVE FORCE CHANGE FOR 87PT13Rh/PT THERMOCOUPLES IN 1530 K, 10 TO THE MINUS 8 TORR ENVIRONMENT FOR 3700 HOURS
Andrew J. Szaniszlo Washington Jun. 1969 24 p refs
(NASA-TN-D-5287) Avail: CFSTI CSCL 14B

The thermal-emf change for 87Pt13Rh/Pt thermocouples was determined by recalibrations in air after 3700 hours exposure to a low-impurity environment with a temperature of 1530°K and a nitrogen equivalent pressure of 3×10^{-8} torr. Wire size was 0.05 cm (0.020 in.), with two-hole, high-purity alumina (99.5 percent) as the insulator. The range of the thermal-emf changes was −2.0° to −3.6°K (average value, −2.8°K). Wire-impurity concentration along the wire was determined by emission spectrographic analysis, which showed iron to have the highest concentration increase at the junction and the largest concentration gradient near the junction. The change in the ratio of resistance at 300°K to the resistance at 4.2°K was determined for samples of the platinum-wire leg, and test-induced grain-structure changes determined with photomicrographs. Author

N69-29331*# National Aeronautics and Space Administration. Lewis Research Center, Cleveland, Ohio.
EMPIRICAL OBSERVATIONS ON THE SENSITIVITY OF HOT CATHODE IONIZATION TYPE VACUUM GAGES
Robert L. Summers Washington Jun. 1969 47 p refs
(NASA-TN-D-5285) Avail: CFSTI CSCL 14B

A study of empirical methods of predicting the relative sensitivities of hot cathode ionization gages is presented. Using previously published gage sensitivities, several rules for predicting relative sensitivity are tested. The relative sensitivity to different gases is shown to be invariant with gage type, in the linear range of gage operation. The total ionization cross section, molecular and molar polarizability, and refractive index are demonstrated to be useful parameters for predicting relative gage sensitivity. Using data from the literature, the probable error of predictions of relative gage sensitivity based on these molecular properties is found to be about 10 percent. A comprehensive table of predicted relative sensitivities, based on empirical methods, is presented. Author

14 INSTRUMENTATION AND PHOTOGRAPHY

N69-29553*# National Aeronautics and Space Administration. Lewis Research Center, Cleveland, Ohio.

A THERMOCOUPLE TECHNIQUE FOR MEASURING HOT-GAS-SIDE WALL TEMPERATURES IN ROCKET ENGINES

Ronald G. Huff Washington Jun. 1969 32 p refs
(NASA-TN-D-5291) Avail: CFSTI CSCL 14B

A technique is given for installing small-size, quartz-insulated, single-wire thermocouples on thin-wall rocket cooling tubes to measure the hot-gas-side wall temperatures. The lead and junction are protected from the hot gases by electroplating metal on the wall, which buries the lead and junction. The plating is faired to the wall to prevent disruption of the boundary layer. The upper temperature limit, which is due to the breakdown of the quartz electrical insulation, is 2060° R (1144°K). Calibrations are given. Author

N69-29730*# National Aeronautics and Space Administration. Flight Research Center, Edwards, Calif.

EVALUATION OF AN INDIRECT VIEWING SYSTEM FOR LIFTING-BODY TERMINAL-AREA NAVIGATION AND LANDING TASKS

Harold G. Gaidsick, William H. Dana, and Robert C. McCracken Washington Jul. 1969 29 p refs
(NASA-TN-D-5299) Avail: CFSTI CSCL 14B

A short-eye-relief optical system, consisting of two monocular periscopes with overlapping fields of view, was mounted in an F-104B airplane to evaluate the feasibility of using an indirect viewing system in place of normal vision for performing simulated lifting-body approaches and landings. Three approach techniques were used in the study. Performance was evaluated by measuring touchdown distance from a marked touchdown point and rate of sink and airspeed at touchdown. Results obtained with the optics system were compared with normal vision results. The ability of the pilots to perform simulated lifting-body tasks was not noticeably reduced with the optics system. The workload and other pilot acceptance factors, however, indicated that this particular system required improvement in design, even though the pilots could readily adapt to its use. Although the results of this flight evaluation are acceptable in terms of optics system evaluation, it was apparent that more effort is required in the development of local-area navigational techniques, specifically to include limited visibility conditions. Author

N69-30506*# National Aeronautics and Space Administration. Lewis Research Center, Cleveland, Ohio.

PERFORMANCE OF TWO MODELS OF COMMERCIAL UNBONDED STRAIN-GAGE-TYPE ABSOLUTE PRESSURE TRANSDUCER AT 260 DEG C

Ralph D. Lewis Washington Jul. 1969 23 p ref
(NASA-TN-D-5327) Avail: CFSTI CSCL 14B

Four transducers of each model were tested. Probable error for the sample transducers was 1 percent of span if each transducer was calibrated at 260°C and zero shifts were corrected for. Zeros shifted with time, storage at room temperature after initial testing for 650 hours at 260°C, and temperature cycling. Maximum rate of zero shift was about 0.01 percent of span per hour. Rate of zero shift usually decreased with time at 260°C. Mean sensitivity change in 650 hours at 260°C was 0.07 percent of initial value. Mean nonlinearity at 260°C was 40 and 0.51 percent of span, respectively, for the two models. Mean hysteresis at 260°C was 0.55 and 0.11 percent of span. Author

N69-31958*# American Optical Corp., Framingham Centre, Mass. Research Div.

HOLOGRAPHIC MICROSCOPY FOR THE DETERMINATION OF FAILURE MECHANISMS IN MONOLITHIC CIRCUITS

Raoul F. van Ligten Washington NASA Jul. 1969 54 p refs
(Contract NAS12-584)
(NASA-CR-1394) Avail: CFSTI CSCL 14B

Described is a holographic microscopic technique for testing integrated circuits through the various stages of design and production. Holographic interferometry is used in the various stages of metallization, shadowing, surface contamination, and inspection for over or under etching of integrated circuit wafers. The local phase variation of gold–aluminum bonds at the pads on the chips where gold leads are connected is measured by illuminating the wafer from the substrate side with infrared light to which silicon is transparent. Interferometry techniques yield from the refracted wavefront the optical path difference proportional to the refractive index change multiplied by diffusion depth. The refractive index in turn is related to the diffusion concentration. G.G.

N69-32286*# National Aeronautics and Space Administration. Langley Research Center, Langley Station, Va.

SIMULATION STUDIES OF SOME SUPERSONIC TRANSPORT INSTRUMENTATION REQUIREMENTS AND OPERATING PROBLEMS

Norman S. Silsby Washington Aug. 1968 40 p refs
(NASA-TN-D-5280) Avail: CFSTI CSCL 14B

Results pertinent to some supersonic transport (SST) flight instrumentation requirements and operating problems are presented. The results were obtained during departures and arrivals in simulated operations in air traffic control (ATC) environments representing both present-day systems and future concepts and in some special tests. An SST airplane flight simulator and the Federal Aviation Administration's ATC simulation facilities were used to create the real-time simulations. Airline crews operated the SST simulator and experienced air traffic controllers operated the ATC simulation facilities. The tests were conducted under instrument flight rules (IFR) with two design study configurations of the SST. Author

N69-32682*# National Aeronautics and Space Administration. Langley Research Center, Langley Station, Va.

EVALUATION OF A PARACHUTE LOAD DISTRIBUTION MEASURING SYSTEM DURING LOW ALTITUDE DROP TESTS

Ira S. Hoffman Washington Jul. 1969 22 p refs
(NASA-TM-X-1832) Avail: CFSTI CSCL 01C

In conjunction with the low-altitude preflight drop test phase of the NASA supersonic high altitude parachute experiments (SHAPE) program, canopy-load-distribution measurements were made on each of three types of parachute during deployment (by means of a mortar) from an aircraft-dropped payload. Loads were measured with miniature load cells at various locations on the canopies and in the suspension lines of 30- and 40-foot-diameter (9.14 and 12.19 meters) parachutes, with a total of seven measurements of this type being made on each of seven instrumented parachute drops. Out of a total of 49 such individual measurement attempts, there were six individual load-cell problems, which included one of lead-wire breakage during parachute deployment. Total parachute load measurements were also made during each test by means of a tensiometer in the main riser line. In addition, for the total parachute instrumentation program, data from approximately 40 percent of the channels were not obtained due apparently to onboard telemetry malfunction. A commercially available stretch cable was used in the hard wire data transmission link between all transducers and their corresponding telemetry channels in the payload. Author

N69-33322*# National Aeronautics and Space Administration, Washington, D.C.

EVALUATION OF MOTION-DEGRADED IMAGES

1969 178 p refs Presented at a seminar, Cambridge, Mass., 3–5 Dec. 1968
(NASA-SP-193) Avail: SOD $2.00; CFSTI CSCL 14E

Primarily discussed is the state-of-the-art and the progress made in the development of techniques for the removal of motion degradations from photographic imagery. Emphasis is placed on degradations induced by atmospheric turbulence. For individual titles, see N69-33322 through N69-33345.

N69-34628*# National Aeronautics and Space Administration. Langley Research Center, Langley Station, Va.
THE CALCULATED RESPONSE OF A THREE-CRYSTAL PAIR SPECTROMETER
Clemans A. Powell, Jr. Washington Aug. 1969 35 p refs
(NASA-TM-X-1857) Avail: CFSTI

A computer analysis was made to determine the response and efficiency of a three-crystal sodium iodide scintillation spectrometer. An iterative spectrum-unfolding method was modified to analyze experimental spectra taken with the spectrometer. The response and efficiency agree well with limited experimental data. The unfolding technique yields errors in response and efficiency much smaller than those anticipated. Author

N69-35265*# National Aeronautics and Space Administration. Lewis Research Center, Cleveland, Ohio.
EVALUATION OF A VOLUME-RATIO SYSTEM FOR VACUUM GAGE CALIBRATION FROM 10 TO THE MINUS 8 POWER TO 10 TORR
Raymond Holanda Washington Sep. 1969 23 p refs Avail: CFSTI
(NASA-TN-D-5406) Avail: CFSTI CSCL 14B

An evaluation was made of a volume-ratio calibration system in the range from 10^{-8} to 10 torr. An error analysis showed that the pressures could be produced with a limit of error of about $\pm 1\text{-}1/2$ percent at 10^{-6} torr to ± 4 percent at 10^{-8} torr. An analysis was made of the effects of volume-ratio and reference pressure-gage inaccuracies, temperature effects, ionization-gage pumping, ultimate pressure, transfer-volume-cycle gas generation, out-gassing, and adsorption. Sample calibrations of vacuum gages are provided. The upper and lower pressure limitations of this system are discussed. Author

N69-36985*# National Aeronautics and Space Administration. Marshall Space Flight Center, Huntsville, Ala.
CALIBRATION OF PEGASUS AND EXPLORER 23 DETECTOR PANELS
Robert J. Naumann, David W. Jex, and Clyde L. Johnson Washington Sep. 1969 40 p refs
(NASA-TR-R-321) Avail: CFSTI CSCL 14B

Several series of tests were conducted to establish the ballistic limit for the various detector panels. In these tests extremely small, carefully sized beads were launched in a velocity range that included the perforation threshold. By varying the size, a ballistic limit curve was established on a mass-velocity plot. Such curves were then extrapolated to average meteor velocity to obtain the characteristic mass for each sensor. Additional tests were conducted on the Pegasus panels using the Pegasus test tool, which contains the identical electronic circuitry used by the flight models. These tests included hot and cold tests, thermal cycling after impact, and oblique impacts. Several types of anomalous events noted in the operation of the spacecraft could be simulated in this manner. Some indication of the dependence of detection threshold upon size was obtained. Author

N69-37876*# Perkin-Elmer Corp., Pomona, Calif.
ANALYTICAL STUDY OF CONTAMINANT AND ATMOSPHERIC SENSOR, PHASE 1
Washington NASA Sep. 1969 137 p refs
(Contract NAS1-7260)
(NASA-CR-1375; SPO-20224) Avail: CFSTI CSCL 14B

Research was directed towards the modification of the previously designed two gas atmospheric sensor system (mass spectrometer) to measure the partial pressures of oxygen, nitrogen, carbon dioxide, and water vapor within a space vehicle environment. An analytical study of the necessary modifications which would allow the two gas sensor to monitor the atmospheric constituents, selected contaminants, and summation of contaminants has been performed for both helium-oxygen and nitrogen-oxygen atmospheres. Several approaches utilizing the two gas sensor as the basic component were analyzed. The accumulator cell approach offered the most feasible solution of the problems encounted. The results of the study lead to the definition of a contaminant and atmospheric sensor, utilizing the accumulator cell, meeting the performance goals while still having acceptable weight, power, and size specifications. Author

N69-38144*# National Aeronautics and Space Administration. Ames Research Center, Moffett Field, Calif.
ABSOLUTE RADIOMETERS FOR USE IN BALLISTIC-RANGE AND SHOCK-TUBE EXPERIMENTS
Roger A. Craig and William C. Davy Washington Oct. 1969 61 p refs
(NASA-TN-D-5360) Avail: CFSTI CSCL 14B

This report is a discussion of the design, calibration, and use of radiometers to measure absolute spectral emission in ballistic range and shock tube experiments. These radiometers are characterized by a frequency response and a dynamic range sufficient to span the widely different frequencies and intensities of calibration and experiment sources. Radiometers discussed consist of a filter (transmission filter or monochromator), a detector (multiplier phototube or infrared photodiode), and a close-coupled amplifier. Response equations are developed that relate the test data to emission from a calibration standard. The principal problems of use of these radiometers (e.g., multiplier phototube stability and saturation. Infrared photodiode rise time and linearity, limiting noise, filter side-band transmission and standard lamp operation) are discussed. Three currently operating ballistic range and shock tube applications are described in detail. Author

N69-38766*# National Aeronautics and Space Administration. Lewis Research Center, Cleveland, Ohio.
AN IMPROVED DELAYED NEUTRON FISSION PRODUCT MONITOR
James D. Heckelman and Konstanty Semenchuk Washington Oct. 1969 21 p refs
(NASA-TM-X-1886) Avail: CFSTI CSCL 18D

This fission product monitor (FPM) was developed at NASA's 60-megawatt (thermal) test reactor at the Plum Brook Station. Two neutron detectors are used to monitor the delayed neutrons at two different locations in the primary collant system. The ratio (detector 1 count rate)/(detector 2 count rate) is used to indicate the presence of fission products. During normal reactor operation when significant fission products are not present in the primary cooling water (PCW), the neutrons present at the detectors are from the decay of nitrogen 17. When fission products appear in the PCW, their half-lives are different from the half-life of N^{17} The ratio will thus change, and the change may be uniquely related to the fission product activity in the PCW. The activity of the fission product iodine 134 in the PCW of the Plum Brook Reactor is routinely determined. Calculations provided the theoretical FPM ratios for assumed I^{134} levels. The theoretical curve was then verified by actual measurements taken during many reactor operating hours. Calibration of the FPM system is easily accomplished by interchanging the detectors at one detector location and adjusting the electronics so that the counting rates of both detector channels are equal. The monitor is in operation and has demonstrated reliable results. Author

14 INSTRUMENTATION AND PHOTOGRAPHY

N69-40059*# National Aeronautics and Space Administration. Lewis Research Center, Cleveland, Ohio.

FLOW-DIRECTION MEASUREMENT WITH FIXED-POSITION PROBES

Thomas J. Dudzinski and Lloyd N. Krause Washington Oct. 1969 16 p refs

(NASA-TM-X-1904) Avail: CFSTI CSCL 14B

Because of space limitations and system complexity in many aeronautical applications, movable probes cannot be used to measure flow direction. This report presents correlations between measured fixed-probe pressures and airflow direction over a range of Reynolds number, Mach number, and flow angle. Flow direction is measurable to within about 1° over combinations of flow conditions in the range $1000 \leq Re \leq 40\,000$, $0.3 \leq M \leq 0.9$, $-30° \leq \text{angle} \leq +30°$. Author

N69-40812*# National Aeronautics and Space Administration. Manned Spacecraft Center, Houston, Tex.

THE EFFECT OF OBJECT MOTION IN FRAUNHOFER HOLOGRAPHY WITH APPLICATION TO VELOCITY MEASUREMENTS

William P. Dotson, Jr. Washington Nov. 1969 23 p refs

(NASA-TN-D-5515) Avail: CFSTI CSCL 14E

The in-line Fraunhofer hologram is analyzed with the assumption that the object moves a significant distance during the observation tiem. An equation is derived which predicts the effect that object motion has upon the recorded fringe pattern. An analysis of the fringe pattern recorded on the film consequently yields the total motion of the object during the observation time. It is also possible to reconstruct the resultant hologram so that the path the object traveled during the exposure time is reproduced. This knowledge, coupled with the exposure time, yields the desired measurement of the object velocity. Author

15

MACHINE ELEMENTS AND PROCESSES

Includes bearings, seals, pumps, and other mechanical equipment; lubrication, friction, and wear; manufacturing processes and quality control; reliability; drafting; and materials fabrication, handling, and inspection.

A69-10912 *

PRELIMINARY EVALUATION OF GREASES TO 600 F AND SOLID LUBRICANTS TO 1500 F IN BALL BEARINGS.

H. E. Sliney and R. L. Johnson (NASA, Lewis Research Center, Cleveland, Ohio).

(American Society of Lubrication Engineers, Annual Meeting, 23rd, Cleveland, Ohio, May 6-9, 1968, Preprint 68AM 7C-2.)

ASLE Transactions, vol. 11, Oct. 1968, p. 330-337. 17 refs.

A special apparatus designed for the evaluation of high-temperature lubricants in 20-mm-bore ball bearings is described. The results of bearing runs at temperatures up to 1500°F in air are reported. Of the greases evaluated, a fluorocarbon grease, provided bearing lubrication for longer times at 450 and 600°F than either polyphenyl ether or silicone greases thickened with dyes and/or MoS_2. Cobalt alloy ball bearings, lubricated either with barium fluoride-calcium fluoride coatings bonded to the cages, or with porous metal cages impregnated with these fluorides, ran successfully at 1200 and 1500°F under a thrust load of 30 lb and at a shaft speed of 5000 rpm.

(Author)

A69-11324 *

EHD LUBRICATION.

Erwin V. Zaretsky (NASA, Lewis Research Center, Bearing Materials and Fatigue Section, Cleveland, Ohio) and William J. Anderson (NASA, Lewis Research Center, Bearings Branch, Cleveland, Ohio).

Machine Design, vol. 40, Nov. 7, 1968, p. 167-173. 8 refs.

Discussion of the conditions necessary for the formation of elastohydrodynamic (EHD) films and their use in lubrication. The formation of EHD films is found to depend on two mutually dependent factors: the hydrodynamic properties of the fluid and the deformation of the contact zone. Surface topography is shown to be important in the EHD lubrication process. The fact that some measurements of EHD film thicknesses were less than half the value predicted by theory is attributed to the non-Newtonian behavior of the lubricant. On the basis of EHD theory, the basic design procedures for the use of EHD films in lubricating gears, roller bearings, and ball bearings are outlined.

P.G.M.

A69-16486 *

CRYOGENIC POSITIVE EXPULSION BLADDERS.

R. F. Lark (NASA, Lewis Research Center, Cleveland, Ohio).

IN: CRYOGENIC PROPERTIES OF POLYMERS; PROCEEDINGS OF THE NASA-CASE CONFERENCE ON THE PROPERTIES OF POLYMERS AT CRYOGENIC TEMPERATURES, NASA LEWIS RESEARCH CENTER AND CASE-WESTERN-RESERVE UNIVERSITY, CLEVELAND, OHIO, APRIL 25-27, 1967. [A69-16485 05-18]

Edited by T. T. Serafini and J. L. Koenig.

New York, Marcel Dekker, Inc., 1968, p. 1-15.

NASA-Lewis in-house and contractual experimental programs were conducted to determine the cryogenic flexibility of single and multiple plies of thin polymeric films at 77 and 20 K. Results of cryogenic flexibility or "twist-flex" testing showed that thin Mylar films are the most flexible of the films tested. The relation between cryogenic cycle life, film thickness, and the number of plies for Mylar film is reported at 77 and 20 K, and results of contractual testing of Mylar, Kapton, and polyethylene film bladders at 20 K are summarized. Bladder material combinations showing the lowest helium gas porosity after 25 liquid hydrogen cycles are Mylar and an organic filament-reinforced polyethylene film laminate and Kapton/Nomex-Nylon.

(Author)

A69-19308 *

DEPOSITION OF MoS_2 FILMS BY PHYSICAL SPUTTERING AND THEIR LUBRICATION PROPERTIES IN VACUUM.

T. Spalvins (NASA, Lewis Research Center, Cleveland, Ohio).

(American Society of Mechanical Engineers and American Society of Lubrication Engineers, Lubrication Conference, Atlantic City, N. J., Oct. 8-10, 1968, ASLE Paper 68 LC-15.)

ASLE Transactions, vol. 12, Jan. 1969, p. 36-41; Discussion, Mel Lavik (Midwest Research Institute, Kansas City, Mo.) and A. J. Haltner (General Electric Co., Philadelphia, Pa.), p. 41, 42; Author's Closure, p. 42, 43. 19 refs.

Physical dc sputtering of MoS_2 was used to apply MoS_2 films for use as a solid lubricant on rotating and sliding components. This method does not utilize binders or burnishing. Friction experiments in vacuum (10^{-11} torr) were conducted on these films (~2000 Å thick). The coefficient of friction for these films was similar to the reported values for resin bonded films. The long endurance life of these films in friction experiments indicates good adherence. The good adherence results from cleanliness of the surface (etched) and the relatively high energies of the sputtered material on arrival at the surface. These sputtered MoS_2 films were consistent in regard to stoichiometry, adherence, thickness, and uniformity when the sputtering conditions were accurately controlled from run to run.

(Author)

A69-19310 *

COOLING STUDIES WITH HIGH-SPEED BALL BEARINGS OPERATING IN COLD HYDROGEN GAS.

David E. Brewe, Harold H. Coe, and Herbert W. Scibbe (NASA, Lewis Research Center, Cleveland, Ohio).

(American Society of Mechanical Engineers and American Society of Lubrication Engineers, Lubrication Conference, Atlantic City, N. J., Oct. 8-10, 1968, ASLE Paper 68 LC-2.)

ASLE Transactions, vol. 12, Jan. 1969, p. 66-75; Discussion, J. B. Accinelli (Aerojet-General Corp., Sacramento, Calif.) and M. F. Butner (North American Rockwell Corp., Canoga Park, Calif.), p. 75, 76; Authors' Closure, p. 76. 8 refs.

Experiments and analyses were performed to determine the cooling requirements for 40-mm bore ball bearings using 60°R (-400°F) hydrogen gas. The bearings were run at shaft speeds to 35,000 rpm and thrust loads to 400 lb. A bronze-filled polytetrafluoroethylene (PTFE) retainer was used to lubricate the bearings. Bearing outer-race temperature varied as the inverse of hydrogen gas flow rate through the bearing. From this inverse relation, a minimum flow equation was developed for the range of bearing operating conditions. The minimum flow rate required for bearing cooling was more sensitive to speed than to load increases. Film transfer to the inner-race grooves and retainer wear is indicated and discussed.

(Author)

A69-19666 *

RECENT EXPERIENCE IN HIGH PRESSURE GASEOUS HYDROGEN EQUIPMENT OPERATED AT ROOM TEMPERATURE.

W. B. McPherson and C. E. Cataldo (NASA, Marshall Space Flight Center, Huntsville, Ala.).

American Society for Metals, Materials Engineering Exposition and Congress, Detroit, Mich., Oct. 14-17, 1968, Paper D 8-14.1. 14 p. 9 refs.

Members, $1.50; nonmembers, $3.00.

Study of the failures of pressure vessels storing gaseous hydro-

gen, and recommendations for the use of new materials. It is found that the A517-F steel vessels, as currently fabricated, are not satisfactory for hydrogen. More rigid manufacturing controls might produce an acceptable vessel. All large hydrogen pressure vessels should have an access for periodic internal inspection by magnetic-particle, dye-penetrant, or other nondestructive methods. Bourdon tubes in pressure gauges must be made from materials that are less susceptible to hydrogen deterioration. A 300 series stainless steel or a Be-copper alloy may be satisfactory. Z. W.

A69-20529 *#
THE USE OF A HEAT SHRINKABLE SLEEVE IN A LUBRICANT-FREE CONNECTOR FOR GLASS VACUUM SYSTEMS.
Betty S. Del Duca (NASA, Lewis Research Center, Cleveland, Ohio).
Journal of Physics, Part E - Journal of Scientific Instruments, vol. 2, Feb. 1969, p. 211.

Brief description of a technique for assembling glass systems in the purification of reagents and solvents in electrochemical studies, without using vacuum grease on the joints. In this technique shrinkable polyolefin tubing is used to compress standard O-ring joints instead of vacuum grease. V. Z.

A69-21392 *
ELASTIC CRACK-EDGE DISPLACEMENTS FOR THE COMPACT TENSION SPECIMEN.
Ernest Roberts, Jr. (NASA, Lewis Research Center, Cleveland, Ohio).
Materials Research and Standards, vol. 9, Feb. 1969, p. 27. 5 refs

Derivation of displacements and stress intensity factors as a function of crack length for the compact tension specimen of the proposed ASTM recommended proportions. Displacements are presented at both the load line and the crack edge. The data were generated by the method of boundary collocation. M. M.

A69-22301
ADVANCED TECHNIQUES FOR MATERIAL INVESTIGATION AND FABRICATION; SOCIETY OF AEROSPACE MATERIAL AND PROCESS ENGINEERS, NATIONAL SYMPOSIUM AND EXHIBIT, 14TH, COCOA BEACH, FLA., NOVEMBER 5-7, 1968, PROCEEDINGS. North Hollywood, Calif., Western Periodicals Co. (Science of Advanced Materials and Process Engineering Proceedings. Volume 14), 1968. 1223 p.
$35.

CONTENTS:

PREFACE. S. R. Locke, p. viii.

MICROSCOPY.
THE USE OF THE POLARIZED LIGHT MICROSCOPE FOR METALLIC CRYSTALLOGRAPHIC STUDIES. R. E. Reed-Hill (Florida, University, Gainesville, Fla.) and W. A. Slippy, Jr. (Sperry Rand Corp., Gainesville, Fla.), I-1-1 (26 p.). 8 refs. [See A69-22302 09-14]
DIRECT RECORDING ELECTRON DIFFRACTION FOR THIN FILM MATERIALS STUDIES. D. B. Dove and M. B. Heritage (Florida, University, Gainesville, Fla.), I-1-2 (8 p.). 11 refs. [See A69-22303 09-14]
DYNAMIC ELECTRON MICROSCOPY OF HIGH TEMPERATURE REACTIONS. S. J. Mayhan and J. L. Daniel (Battelle Memorial Institute, Richland, Wash.), I-1-3 (21 p.). 25 refs. [See A69-22304 09-14]
STUDY OF FAILURE MODES IN FIBER GLASS REINFORCED PLASTICS BY ELECTRON MICROSCOPY. C. K. Goberdhan (North American Rockwell Corp., Columbus, Ohio), I-1-4 (19 p.). [See A69-22305 09-18]
APPLICATION OF ELECTRON MICROSCOPY TO STUDIES OF TITANIUM AND TITANIUM ALLOYS. T. R. Cass (Martin Marietta Corp., St. Louis, Mo.), I-1-5 (1 p.).

SPECIAL TEST TECHNIQUES.
MICROWAVE STUDIES FOR DETERMINING RE-ENTRY HEAT SHIELD BOND INTEGRITY AND THICKNESS. H. F. Hansell and A. E. Oaks (General Electric Co., Philadelphia, Pa.), I-2-1 (14 p.). [See A69-22306 09-14]
DIELECTRIC RELAXATION IN MATERIALS ANALYSIS. L. L. Hench (Florida, University, Gainesville, Fla.), I-2-2 (12 p.). 29 refs. [See A69-22307 09-26]
EVALUATION TECHNIQUES FOR SIMPLE MECHANICAL PROPERTY TESTS ON COMPOSITE MATERIALS. C. A. Yamamoto (Lockheed Aircraft Corp., Sunnyvale, Calif.), I-2-3 (26 p.). [See A69-22308 09-14]
ON MEASURING THE PROPERTIES OF ADHESIVES IN BONDED JOINTS. J. L. Rutherford, F. C. Bossler, and E. J. Hughes (General Precision Systems, Inc., Little Falls, N.J.), I-2-4 (21 p.). 13 refs. [See A69-22309 09-14]
INVESTIGATION OF A LAMINATED SHIELDING MATERIAL FOR AUDIO AND MICROWAVE FREQUENCIES. F. J. Young and D. A. Colling (Westinghouse Electric Corp., Pittsburgh, Pa.), I-2-5 (13 p.). [See A69-22310 09-14]
HIGH-TEMPERATURE MAGNETIC TEST TECHNIQUES AND ANALYSES. R. J. Towner (Westinghouse Electric Corp., Lima, Ohio), J. J. Clark (Westinghouse Electric Corp., Pittsburgh, Pa.), R. A. Lindberg (NASA, Lewis Research Center, Cleveland, Ohio), and D. M. Pavlovic, I-2-6 (22 p.). 19 refs. [See A69-22375 09-15]

SPECTROSCOPY AND THERMAL ANALYSIS.
CHARACTERIZATION OF THERMOSETTING RESIN CURING BEHAVIOR BY THERMAL ANALYSIS UNDER PRESSURE. M. Ezrin and G. C. Claver (Monsanto Co., Springfield, Mass.), I-3-1 (14 p.). 6 refs. [See A69-22311 09-14]
THE USE OF TGA DATA IN THE SIMULATION OF THE DEGRADATION OF PLASTICS. D. Hender (Leesona Corp., Great Neck, N.Y.), I-3-2 (20 p.). [See A69-22312 09-18]
MASS SPECTROMETRIC ANALYSIS OF SILICON CARBIDE. J. A. Baker (Dow Corning Corp., Hemlock, Mich.), I-3-3 (11 p.). [See A69-22313 09-06]
MASS SPECTROMETRIC THERMAL ANALYSIS OF POLYMERS. H. W. Goldstein (General Electric Co., Philadelphia, Pa.), I-3-4 (18 p.). [See A69-22314 09-06]
IDENTIFICATION OF SIZES, FINISHES OR TREATMENTS ON GLASS FIBERS BY PYROLYSIS-ATTENUATED TOTAL REFLECTANCE INFRARED SPECTROSCOPY. L. R. Weiner (U.S. Army, Systems Command, Picatinny Arsenal, Dover, N.J.), I-3-5 (22 p.). 12 refs. [See A69-22315 09-06]
A RAPID, SENSITIVE MATERIALS CONTAMINATION SCREENING TECHNIQUE. D. W. Dunipace, K. S. Horr, R. W. Jackson, H. C. Poehlmann, and M. M. Reynolds (Ball Brothers Research Corp., Boulder, Colo.), I-3-6 (11 p.).
BONDING CHARACTERISTICS OF ALKYL CYANOACRYLATE ADHESIVES. W. F. Thomsen and P. T. von Bramer (Eastman Chemical Products, Inc.), I-4-1 (7 p.). [See A69-22316 09-18]
ADHEREND MECHANICAL PROPERTIES LIMIT ADHESIVE BOND STRENGTHS. R. F. Wegman and A. T. Devine (U.S. Army, Systems Command, Picatinny Arsenal, Dover, N.J.), I-4-2 (15 p.). [See A69-22317 09-18]
LAMINATED ADHESIVE BONDED STRUCTURES. T. J. Reinhart, Jr., G. Y. Young (U.S. Army, Materials Laboratory, Wright-Patterson AFB, Ohio), and J. A. Cherry (Dayton, University, Dayton, Ohio), I-4-3 (24 p.). [See A69-22318 09-17]
METHOD OF TESTING THE PLASTIC LAMINATE PHASE OF COMPOSITE ARMOR. R. M. Plumley (Atkins and Merrill, Inc., Marlboro, Mass.), I-4-4 (11 p.). [See A69-22319 09-15]
THERMOELASTIC PROPERTIES OF UNIDIRECTIONAL FILAMENTARY COMPOSITES BY A SEMIEMPIRICAL MICROMECHANICS THEORY. C. C. Chamis (Case-Western-Reserve University, Cleveland, Ohio), I-4-5 (32 p.). 28 refs. [See A69-22320 09-18]
MECHANICAL TESTING OF SILICA PHENOLIC COMPOSITES AT ELEVATED TEMPERATURES. R. D. Carnahan (Aerospace Corp., El Segundo, Calif.), I-4-6 (16 p.). [See A69-22321 09-18]

METALLURGY.
OXIDATION PROTECTION OF REFRACTORY METALS BY INORGANIC COMPOUNDS. G. Geschwind (Grumman Aircraft Engineering Corp., Bethpage, N.Y.), I-5-1 (33 p.). 21 refs. [See A69-22322 09-17]
AN INVESTIGATION OF THE FATIGUE BEHAVIOR OF A BORON-EPOXY-REINFORCED TITANIUM COMPRESSOR DISK.

J. A. Mangiapane, S. A. Sattar, and D. D. Profant (United Aircraft Corp., East Hartford, Conn.), I-5-2 (11 p.). [See A69-22323 09-32]

ELECTRON FRACTOGRAPHIC STUDY OF FATIGUE CRACKS IN WROUGHT BERYLLIUM SHEET. M. Russo, J. F. Krieg, and H. C. Tourkakis (McDonnell Douglas Corp., St. Louis, Mo.), I-5-3 (7 p.). [See A69-22324 09-14]

COMPATIBILITY OF REFRACTORY METALS, PRECIOUS METALS AND SEVERAL COATINGS. E. Benn (North American Rockwell Corp., Canoga Park, Calif.), I-5-4 (17 p.). [See A69-22325 09-11]

COATED REFRACTORY ALLOY FOR REUSABLE RE-ENTRY STRUCTURES. R. H. Witt (Grumman Aircraft Engineering Corp., Bethpage, N.Y.), I-5-5 (18 p.). 8 refs. [See A69-22326 09-17]

PLASTIC STRUCTURES.

"B" STAGED EPOXY-S GLASS PREPREGS. N. Chessin and T. Roche (Martin Marietta Corp., Orlando, Fla.), II-1A-1 (23 p.). [See A69-22327 09-18]

THE USE OF PLANAR RIBBON WINDING FOR CONTROL OF POLAR BUILD-UP IN FILAMENT-WOUND TANKAGE. D. A. Stang (Martin Marietta Corp., Friendship International Airport, Md.), II-1A-2 (14 p.). [See A69-22328 09-15]

AN AUTOMATIC FABRICATION PROCESS FOR COMPOSITE AIRCRAFT STRUCTURES. S. Yurenka and J. T. Parks (McDonnell Douglas Corp., St. Louis, Mo.), II-1A-3 (10 p.). [See A69-22329 09-15]

METHODS OF FABRICATING SUPER INSULATION BLANKETS. J. W. Maccalous (Martin Marietta Corp., Denver, Colo.), II-1A-4 (12 p.). [See A69-22330 09-15]

THE USE OF HIGH STRENGTH, ROOM TEMPERATURE VULCANIZING SILICONE RUBBER IN TOOLING AND FABRICATION OF AIRCRAFT AND MISSILE COMPONENTS. J. K. Wessel, E. W. Beck, and M. A. Maudlin (Dow Corning Corp., Midland, Mich.), II-1A-5 (12 p.). [See A69-22331 09-15]

ELECTRO PLATING, CHEMICAL MILLING.

CHEMICAL MILLING OF TITAN III TRANSTAGE TITANIUM TANK SEGMENTS. D. M. Shuford (Martin Marietta Corp., Denver, Colo.), II-1B-1 (1 p.).

THE CHARACTERISTICS OF THE MG-B COMPOSITE SYSTEM. A. L. Cunningham, L. G. Davies, and J. A. Alexander (General Technologies Corp., Reston, Va.), II-1B-2 (12 p.). [See A69-22332 09-15]

HIGH RELIABILITY IN FLUID TRANSMISSION SYSTEMS THROUGH BRAZED JOINTS. V. E. Padilla (McDonnell Douglas Corp., Cocoa Beach, Fla.), II-1B-3 (10 p.). [See A69-22333 09-15]

ADVANCED CONTROL OF THE FUSION WELDING PROCESSES. E. P. Vilkas and R. W. Reynolds (Sciaky Bros., Inc., Chicago, Ill.), II-1B-4 (15 p.). [See A69-22334 09-15]

FRICTION WELDING OF AEROSPACE MATERIALS. P. J. Gripshover, H. D. Hanes, and J. H. Peterson (Battelle Memorial Institute, Columbus, Ohio), II-1B-5 (12 p.). 6 refs. [See A69-22335 09-15]

MICROCIRCUIT FABRICATION TECHNOLOGY.

HYBRID CIRCUITS - WHY AND WHERE. J. M. Wbulbroun (Microtek Electronics, Inc., Cambridge, Mass.), II-1C-1 (10 p.). [See A69-22336 09-15]

THICK FILM HYBRID TECHNOLOGY. M. L. Topfer (Radio Corporation of America, Somerville, N.J.), II-1C-2 (25 p.). [See A69-22337 09-15]

ACTIVE DEVICE ASSEMBLY TECHNIQUES. T. J. Matcovich (Drexel Institute of Technology, Philadelphia, Pa.), II-1C-3 (7 p.). 15 refs. [See A69-22338 09-15]

PLASTIC STRUCTURES.

FABRICATION OF UNIAXIAL FILAMENT-REINFORCED EPOXY TUBES FOR STRUCTURAL APPLICATIONS. J. G. Davis, Jr. (NASA, Langley Research Center, Hampton, Va.), II-2A-1 (14 p.). 8 refs. [See A69-22339 09-15]

INVESTIGATION OF BORON FILAMENT WOUND AIRCRAFT LANDING GEARS. T. J. Reinhart (USAF, Materials Laboratory, Wright-Patterson AFB, Ohio) and S. Yurenka (McDonnell Douglas Corp., St. Louis, Mo.), II-2A-2 (14 p.). [See A69-22340 09-15]

"THORNEL" COMPOSITE FUSELAGE SECTION FABRICATION. A. A. Pallozzi and J. M. Criscione (Union Carbide Corp., Parma, Ohio), II-2A-3 (2 p.). [See A69-22341 09-15]

DIFFUSION BONDING - DIFFUSION WELDING.

JOINING TECHNIQUES FOR THORIA DISPERSION STRENGTHENED MATERIALS. R. E. Yount (General Electric Co., New York, N.Y.), II-2B-1 (24 p.). [See A69-22342 09-15]

VACUUM BRAZING - A JOINING MEDIA OF THE SIXTIES. M. M. Schwartz (Martin Marietta Corp., Friendship International Airport, Md.), II-2B-2 (17 p.). [See A69-22343 09-15]

FABRICATING SiC PARTS BY CHEMICAL VAPOR DEPOSITION. E. L. Kern, D. W. Hamill, and K. A. Jacobson (Dow Corning Corp., Hemlock, Mich.), II-2B-3 (26 p.). 14 refs. [See A69-22344 09-15]

DEVELOPMENT OF HOLLOW TURBINE DISKS. J. A. Mangiapane, J. J. O'Connor, and C. V. Sundt (United Aircraft Corp., East Hartford, Conn.), II-2B-4 (12 p.). [See A69-22345 09-15]

LOW TEMPERATURE MAGNESIUM DIP BRAZING. R. Ward, F. N. Atkin, and R. H. Oehme (General Electric Co., Utica, N.Y.), II-2B-5 (16 p.). [See A69-22346 09-15]

MICROJOINING TECHNOLOGY.

INFRARED IN-PROCESS MICRO-WELD EVALUATOR. R. G. Howard (Martin Marietta Corp., Orlando, Fla.), II-2C-1 (11 p.). [See A69-22347 09-15]

RELIABILITY ASPECTS OF MICROJOINTS. C. M. Ryerson (Hughes Aircraft Co., Culver City, Calif.), II-2C-2 (16 p.). [See A69-22348 09-15]

MICRO SOLDERING TECHNIQUES FOR HYBRID CIRCUIT ASSEMBLIES. M. C. Samuelson (Martin Marietta Corp., Orlando, Fla.), II-2C-3 (13 p.). [See A69-22349 09-15]

ADVANCED CHEMICAL MILLING. I. Custman (Radio Corporation of America, New York, N.Y.), II-2C-4 (1 p.).

MACHINING OF COMPOSITES AND REFRACTORIES.

NEW FINISHING PROCESSES FOR OXIDE CERAMICS. H. P. Kirchner (Ceramic Finishing Co., State College, Pa.), II-3A-1 (41 p.). 32 refs. [See A69-22350 09-15]

FABRICATION-TESTING-DESIGN OF Al-B COMPOSITE MATERIALS. J. F. Dolowy, Jr., H. Shimizu, R. J. Taylor, and B. A. Webb (Marquardt Corp., Van Nuys, Calif.), II-3A-2 (16 p.). [See A69-22351 09-15]

FERROMAGNETIC COMPOSITE MATERIALS FOR MICROWAVE SHIELDING. D. A. Colling (Westinghouse Electric Corp., Pittsburgh, Pa.), E. B. Littlefield (Purdue University, Ft. Wayne, Ind.), and L. Lesensky (Raytheon Co., Waltham, Mass.), II-3A-3 (20 p.). [See A69-22352 09-15]

FABRICATION OF COMPLICATED POWDER-METALLURGICAL SHAPES BY HYDROSTATIC PRESSING. P. J. Gripshover and H. D. Hanes (Battelle Memorial Institute, Columbus, Ohio), II-3A-4 (6 p.). 6 refs. [See A69-22353 09-15]

PRINTED CIRCUITS AND MULTILAYER BOARD FABRICATION.

APPLICATIONS OF POLYIMIDE MATERIALS IN ELECTRONIC CIRCUITRY. J. R. Cannizzaro (International Business Machines Corp., Owego, N.Y.), II-3B-1 (17 p.). [See A69-22354 09-15]

AN APPLICATION OF AUTOMATIC PLASMA NEEDLE ARC FUSION WELDING FOR MINIATURE ELECTRONIC DEVICES. C. E. Wirsing (International Business Machines Corp., Owego, N.Y.), II-3B-2 (13 p.). 10 refs. [See A69-22355 09-15]

FLEXIBLE PRINTED CIRCUITRY IN THE AWG-10 MISSILE CONTROL SYSTEM ON THE F-4J. W. S. Haug (Electro-Mechanisms, Inc.), II-3B-3 (15 p.). [See A69-22356 09-15]

ROTOGRAVURE PRINTING OF FLEXIBLE PRINTED CIRCUITS. G. A. Deighton and M. Edelstein (International Business Machines Corp., Burlington, Vt.), II-3B-4 (11 p.). [See A69-22357 09-15]

MANUFACTURING ASPECTS OF TECHNOLOGY FEASIBILITY SPACECRAFT STERILIZATION AND BIOASSAY PROGRAM. J. P. McDonald, R. McKinney, and D. M. Shuford (Martin Marietta Corp., Denver, Colo.), II-3B-5 (19 p.). [See A69-22358 09-05]

STRETCH FORMING - SPIN FORMING.

A STUDY OF CHEMICAL COMPATIBILITY BETWEEN CERAMIC WHISKERS AND METALLIC MATRICE MATERIALS. K. P. Staudhammer, A. Toy, and M. E. Kirkpatrick (TRW Systems Group, Redondo Beach, Calif.), II-4A-1 (16 p.). [See A69-22359 09-17]

15 MACHINE ELEMENTS AND PROCESSES

PROCESSING OF RESIN MATRIX COMPOSITES OF WHISKERIZED GRAPHITE FIBER. R. G. Shaver (General Technologies Corp., Reston, Va.) and J. V. Milewski (Thermokinetic Fibers, Inc., Nutley, N.J.), II-4A-2 (21 p.). 7 refs. [See A69-22360 09-15]

EXTRUSION AND HOT ROLLING - TWO ADVANCED FABRICATION TECHNIQUES FOR THE PREPARATION OF WHISKER-METAL COMPOSITES. W. Wolkowitz and T. S. Stanislaw (Grumman Aircraft Engineering Corp., Bethpage, N.Y.), II-4A-3 (16 p.). 5 refs. [See A69-22361 09-15]

FABRICATION AND PROPERTIES OF GRAPHITE-FIBER, NICKEL-MATRIX COMPOSITES. R. V. Sara (Union Carbide Corp., Parma, Ohio), II-4A-4 (21 p.). 5 refs. [See A69-22362 09-15]

ABLATIVES AND HIGH TEMPERATURES.

GLASS REINFORCED POLYIMIDE LAMINATE - A NEW HIGH PERFORMANCE MATERIAL. S. P. Florkoski and B. I. Halperin (International Business Machines Corp., Owego, N.Y.), II-4B-1 (5 p.). [See A69-22363 09-18]

DEVELOPMENT AND PROPERTIES OF PYROLYTIC CARBON FELT COMPOSITES. H. O. Pierson (Sandia Corp., Albuquerque, N. Mex.), II-4B-2 (20 p.). 8 refs. [See A69-22364 09-18]

THERMOPLASTIC ADHESIVES AND REINFORCED PLASTIC LAMINATES FOR STRUCTURAL USAGE. F. G. Dean and T. A. Rozanski, III (Boeing Co., Seattle, Wash.), II-4B-3 (17 p.). 8 refs. [See A69-22365 09-18]

DEVELOPMENT OF POLYIMIDE-GLASS FABRIC LAMINATES WITH NONFLAMMABLE CHARACTERISTICS IN HIGH OXYGEN CONCENTRATION SPACECRAFT ENVIRONMENTS. H. M. Clancy, R. A. Kaumeyer, and S. Y. Yoshino (North American Rockwell Corp., Downey, Calif.), II-4B-4 (23 p.). [See A69-22366 09-18]

3-D REINFORCEMENT. B. Stiff and R. Lurie (Avco Corp., New York, N.Y.), II-4B-5 (1 p.).

ADHESIVES - BONDING.

A NEW METHOD OF PRESSURE CONTROL FOR ADHESIVE BONDING. D. M. Shuford, J. F. Rudy, and J. J. Damico (Martin Marietta Corp., Denver, Colo.), II-5A-1 (17 p.). [See A69-22367 09-15]

ELECTRON BEAM RADIATION CURING OF LIQUID MERCAPTAN TERMINATED BUTADIENE-ACRYLONITRILE COPOLYMERS. W. Brenner, A. Adler, W. Kapfer (New York University, Bronx, N.Y.), W. Oliver (Radiation Dynamics, Inc., Westbury, N.Y.), and R. Drake (B. F. Goodrich Chemical Co., Cleveland, Ohio), II-5A-2 (13 p.). 7 refs. [See A69-22368 09-15]

FABRICATION OF A DISPENSER FOR AN EIGHT SATELLITE PAYLOAD. H. L. Hillesland and K. T. Fujimoto (Philco-Ford Corp., Palo Alto, Calif.), II-5A-3 (10 p.). [See A69-22369 09-15]

ATTACHMENT CONCEPTS FOR BRITTLE MATERIALS. T. P. Airhart, J. E. Burroughs, and V. J. Studer (General Dynamics Corp., Fort Worth, Tex.), II-5A-4 (15 p.). 5 refs. [See A69-22370 09-11]

HIGH ENERGY FORMING.

RECENT ADVANCES IN EXPLOSIVE FORMING. W. A. Beck (Martin Marietta Corp., Denver, Colo.), II-5B-1 (9 p.). [See A69-22371 09-15]

THE EFFECTS OF DISCONTINUITIES ON THE FATIGUE STRENGTH OF ALUMINUM WELDS. M. S. Hersh (General Dynamics Corp., San Diego, Calif.), II-5B-2 (20 p.). [See A69-22372 09-17]

ULTRASONICALLY ASSISTED INSTALLATION OF FASTENERS. W. H. Sproat and A. Kremheller (Lockheed Aircraft Corp., Marietta, Ga.), II-5B-3 (14 p.). 10 refs. [See A69-22373 09-11]

COMPOUND CONTOURING OF TITANIUM FUSELAGE SKINS. G. Pfanner (Fairchild Hiller Corp., Farmingdale, N.Y.), II-5B-4 (13 p.). 5 refs. [See A69-22374 09-15]

A69-22339 *#

FABRICATION OF UNIAXIAL FILAMENT-REINFORCED EPOXY TUBES FOR STRUCTURAL APPLICATIONS.

John G. Davis, Jr. (NASA, Langley Research Center, Hampton, Va.).

IN: ADVANCED TECHNIQUES FOR MATERIAL INVESTIGATION AND FABRICATION; SOCIETY OF AEROSPACE MATERIAL AND PROCESS ENGINEERS, NATIONAL SYMPOSIUM AND EXHIBIT, 14TH, COCOA BEACH, FLA., NOVEMBER 5-7, 1968, PROCEEDINGS. [A69-22301 09-15]

North Hollywood, Calif., Western Periodicals Co. (Science of Advanced Materials and Process Engineering Proceedings, Volume 14), 1968, II-2A-1 (14 p.). 8 refs.

Description of a process for fabricating uniaxial filament-reinforced epoxy tubes. The process utilizes hand layup techniques, a Teflon mandrel, and a heat-shrinkable Teflon sleeve. At the present, over 40 tubes of boron-epoxy and S-glass-epoxy have been fabricated using the process reported. The tubes are essentially void free, exhibit less dimensional variation than the tolerances set for commercially available extruded aluminum tubing, and display a smooth surface finish. Short sections of both types of tubing have been subjected to axial compression tests. The boron-epoxy and S-glass-epoxy tubes exhibited average strengths of 309 ksi and 207 ksi, respectively. (Author)

A69-23050 *#

ASSURING SATURN QUALITY THROUGH NONDESTRUCTIVE TESTING.

Robert W. Neuschaefer (NASA, Marshall Space Flight Center, Huntsville, Ala.).

American Society for Nondestructive Testing, Spring Conference, Los Angeles, Calif., Mar. 10-13, 1969, Paper. 27 p. 9 refs.

The Saturn V space vehicle is briefly described. The organizational responsibilities of NDT groups are discussed along with the approach to management of research and development activities. Applications of the various NDT methods employed to evaluate the materials and processes used in the manufacture of the various stages and major components are described. Emphasis is placed on a discussion of the special NDT methods and equipment developed to satisfy the unique requirements of the Apollo program. Advancements in the state-of-the-art, including a solid-state radiographic image amplifier and an rf device suitable for measuring the thickness of nonmetallics on metallic objects, are described. (Author)

A69-27231 *

VARIOUS MODES OF WEAR AND THEIR CONTROLLING FACTORS.

E. E. Bisson (NASA, Lewis Research Center, Fluid System Components Div., Cleveland, Ohio).

(American Society for Testing and Materials, Annual Meeting, 71st, San Francisco, Calif., June 23-28, 1968, Paper.)

IN: EVALUATION OF WEAR TESTING; AMERICAN SOCIETY FOR TESTING AND MATERIALS, ANNUAL MEETING, 71ST, SYMPOSIUM, SAN FRANCISCO, CALIF., JUNE 23-28, 1968, PROCEEDINGS. [A69-27230 13-15]

Symposium sponsored by the Committee on Simulated Service Testing.

Philadelphia, American Society for Testing and Materials (ASTM Special Technical Publication No. 446), 1969, p. 1-22. 23 refs.

Discussion of the various modes of wear, the mechanisms involved in each, and the mitigation of wear in some of the modes. The various modes of wear include adhesion, abrasion, corrosion and surface fatigue. Fretting (fretting corrosion or friction oxidation) is a special combination of adhesive, corrosive, and abrasive wear. Adhesive wear involves adhesive forces which are strong enough to form cold welds at the contacting asperities. During relative motion, shear takes place at the welds. The shear strength at these welds is strongly influenced by contamination, either deliberate or accidental. There is a marked influence of crystal structure on friction and adhesive wear. In general, the hexagonal structure gives lower friction and wear than the cubic structure. Experimental studies show that the lattice parameters in hexagonal crystals also affect friction. Abrasive wear involves damage to a soft surface by a hard surface, either one of the two surfaces, or a third body. Hardness, work hardness, crystallite orientation, and elastic modulus of the contacting surfaces can all influence wear. Corrosive wear involves corrosion, followed by wear of the corrosive film. Surface fatigue normally appears as local pitting or flaking. Wear damage of this type is a function of a number of stress cycles. All modes of wear lead to loss of dimen-

sional tolerances, high operating cost, and excessive expense (in time and money) for replacement of worn parts. A complete understanding of the basic mechanisms of wear permits alleviation and mitigation. P.v.T.

A69-27271 *#
EXPERIMENTAL STABILITY STUDIES OF THE HERRINGBONE-GROOVED GAS-LUBRICATED JOURNAL BEARING.
Robert E. Cunningham, David P. Fleming, and William J. Anderson (NASA, Lewis Research Center, Cleveland, Ohio).
(American Society of Mechanical Engineers, Lubrication Symposium, Las Vegas, Nev., June 17-20, 1968, Paper 68-LubS-25.)
ASME, Transactions, Series F - Journal of Lubrication Technology, vol. 91, Jan. 1969, p. 52-57; Discussion, A. W. Lawrence (Hamilton Standard Systems Center, Farmington, Conn.) and C. C. W. Ng (United Aircraft Corp., East Hartford, Conn.), p. 57, 58; Authors' Closure, p. 58, 59. 15 refs.

Experimental studies were conducted on six rotors, 1-1/2 in. diameter by 12-1/4 in. long operating in ambient air to high compressibility numbers. Herringbone-groove geometries and clearances were varied to determine their effect on half-frequency whirl (HFW). All rotors were operated vertically and without any applied radial load. Results show that half-frequency-whirl onset is very sensitive to radial clearance. Limited test results indicate that a fully grooved bearing is more stable than a partially grooved one, other parameters being equal. Generally fair agreement between theory and experiment was achieved for predicting HFW onset speeds. (Author)

A69-27366 *
CONFIGURATIONS FOR GAS TURBINE COMPRESSOR END SEALS.
J. W. Bjerklie, H. S. Cheng, D. F. Wilcock (Mechanical Technology, Inc., Latham, N.Y.), L. Ludwig, and D. Townsend (NASA, Lewis Research Center, Cleveland, Ohio).
(American Society of Lubrication Engineers, Annual Meeting, 23rd, Cleveland, Ohio, May 6-9, 1968, Preprint 68AM 4B-4.)
Lubrication Engineering, vol. 25, Apr. 1969, p. 169-175.
Contract No. NAS 3-7605.

Modern high performance multistage axial flow compressors have several air leakage paths which reduce compressor performance. The most significant leakage occurs past the labyrinth seal at the high pressure end of the compressor. Since it was estimated that this leakage reduced the compressor efficiency by 1%, a project was undertaken to develop low-leakage-rate noncontact seals which would reduce compressor end-seal leakage by an order of magnitude. A large number of seal concepts and ideas were examined for suitability. Each concept was evaluated on the basis of leakage rate, tracking capability, gas film stability, thermal and elastic distortion, wear, and reliability. Since the concepts involved combinations of the several types of primary seal and secondary seal, these are examined separately, followed by a screening analysis of the most viable concepts. The screening results in the selection of concepts for detailed design study. (Author)

A69-28854 *#
COMPUTER-GENERATED GRAPHICS IN AEROSPACE DESIGN AND ANALYSIS.
Frederic A. Hills (NASA, Electronics Research Center, Cambridge, Mass.).
American Society of Mechanical Engineers, Design Engineering Conference and Show, New York, N.Y., May 5-8, 1969, Paper 69-DE-65. 6 p. 13 refs.
Members, $0.75; nonmembers, $1.50.

Discussion of NASA's direct and indirect use of computer-driven graphical techniques. Though emphasis is placed upon NASA application of these techniques to the specific areas of design, analysis, and simulation, the paper attempts to synthesize a more extensive computer-graphics context within which the design usage may be assessed, correlated, and projected into the future. Examples of the use of graphics in space-related design are given, and relevant techniques are cited. (Author)

A69-29001 *#
ENERGETICS IN VACUUM DEPOSITION METHODS FOR DEPOSITING SOLID FILM LUBRICANTS.
T. Spalvins (NASA, Lewis Research Center, Cleveland, Ohio).
American Society of Lubrication Engineers, Annual Meeting, Philadelphia, Pa., May 5-8, 1969, Paper. 16 p. 6 refs.

High energy or plasma deposition methods (dc, RF sputtering, and ion plating) as new approaches to the application of solid film lubricants to components requiring lubrication. Films can be deposited under controlled operational conditions. The strength and durability of the film are related to adhesion, which depends on the interfacial and film characteristics. These are directly related to the kinetic energy of the impinging metal atoms. If the deposition conditions are standardized during the film application, composition, adherence thickness, and uniformity can be accurately repeated and controlled. B.H.

A69-30315 *
A SURVEY OF LEAK DETECTION FOR AEROSPACE HARDWARE.
Frederic E. Wells (NASA, Marshall Space Flight Center, Huntsville, Ala.).
(American Society for Nondestructive Testing, National Conference, 28th, Detroit, Mich., Oct. 14-17, 1968, Paper.)
Materials Evaluation, vol. 27, May 1969, p. 97-101.

Survey of leak detection equipment, practice, and philosophy applicable to external leak testing of aerospace hardware. The survey is based on experimentation and evaluation work performed at the Marshall Space Flight Center (MSFC), engineering analysis of work by others, and the experience gained at MSFC during extensive checkout work on three major vehicle programs. The three principal areas covered are (1) setting acceptance limits, (2) techniques currently available, and (3) selecting a technique for a particular job. Systems and components are leak checked because of danger from leaking fluids, possible depletion of system fluids, quality control of manufacturing processes and assembly techniques, and detection of degraded components. The techniques described are liquid leak detector agents, thermal detectors, halogen detectors, and helium mass spectrometers. F.R.L.

A69-30481 *
NUMERICAL SOLUTIONS FOR THE FLOW AND PRESSURE FIELDS IN AN IDEALIZED SPIRAL GROOVED PUMPING SEAL.
John Zuk and Harold E. Renkel (NASA, Lewis Research Center, Cleveland, Ohio).
American Society of Lubrication Engineers, British Hydromechanics Research Association, and American Society of Mechanical Engineers, International Conference on Fluid Sealing, 4th, Philadelphia, Pa., May 5-9, 1969, ASLE FICFS Preprint 30. 13 p. 20 refs.
Members, $0.75; nonmembers, $1.50.

Spiral-grooved pumping seal model formulated for laminar, incompressible flow for the limiting case of zero land clearance. The numerical solutions of the exact governing equations show a bidirectional (pumping and leakage) vortex flowfield. Results are compared to classical models of the groove axial flow (general Couette flow which is used in deriving Reynolds' lubrication equation and moving wall duct flow) which neglect the coupling of the groove crossflow. The solutions show that the crossflow shifts the pumping flow toward the land leading edge. For a Reynolds number of 100 and groove depth-to-width ratio less than or equal to 1/8, the classical models are shown to be good approximations for the relation of axial pressure gradient to net volume flow. The groove cross-section static pressure is nearly constant except near the moving surface region. A low pressure region suggests the possibility of degassing and cavitation, whereas a high pressure region near the land leading edge results in a lift force acting on the moving surface. (Author)

A69-30492 *
SHAFT FACE SEAL WITH SELF-ACTING LIFT AUGMENTATION FOR ADVANCED GAS TURBINE ENGINES.
Robert L. Johnson and Lawrence P. Ludwig (NASA, Lewis Research Center, Cleveland, Ohio).

American Society of Lubrication Engineers, British Hydromechanics Research Association, and American Society of Mechanical Engineers, International Conference on Fluid Sealing, 4th, Philadelphia, Pa., May 5-9, 1969, ASLE FICFS Preprint 27. 11 p. 9 refs.
Members, $0.75; nonmembers, $1.50.

Indication of the need to incorporate in advanced engines shaft seals with improved pressure, temperature, and speed capabilities. In particular, the high-speed requirement suggests that the seals must not have rubbing contact. Labyrinth seals have disadvantages in high leakage (efficiency loss) and debris entrainment, and conventional face seals are subject to high wear, because face deformation can increase seal closing force and thus cause heavy rubbing contact. It is shown that incorporation of self-acting lift pads to the conventional face seal prevents rubbing contact, even though face deformation occurs; feasibility was demonstrated in 560 hr of operation at 100-psi (69-N/cm^2) pressure differential, 600°F (589 K) gas temperature, and 380-ft/sec (116-m/sec) sliding speed. Positive separation of the sealing faces with acceptable leakage rates was obtained. Proposed advanced systems using seals with self-acting lift pads are described. P. v. T.

A69-30610 *
SLIDING FRICTION OF COPPER ALLOYS IN VACUUM.
Jane Jellison, Roamer Predmore, and C. L. Staugaitis (NASA, Goddard Space Flight Center, Greenbelt, Md.).
(American Society of Mechanical Engineers and American Society of Lubrication Engineers, Lubrication Conference, Atlantic City, N.J., Oct. 8-10, 1968, ASLE Paper 68 LC-5.)
ASLE Transactions, vol. 12, Apr. 1969, p. 171-180; Discussion Morton Antler (Burndy Corp., Norwalk, Conn.) and M. Cocks (SKF Industries, Inc., King of Prussia, Pa.), p. 181, 182. 15 refs.

Results of sliding friction experiments which involve copper and Cu-Be alloy plates in contact with copper, Cu-Be alloy, steel, and titanium alloy sliders and were performed in air and vacuum. Microhardness and metallographic examination of plate and slider interface suggests friction and wear by the adhesive friction mechanism with prow formation. Transfer of strain-hardened metal wear debris across the sliding interface was observed. The friction coefficient and the prow size generally increased in vacuum. (Author)

A69-30901 *#
CONTACT CONFORMITY EFFECTS ON SPINNING TORQUE AND FRICTION.
M. W. Dietrich, R. J. Parker, E. V. Zaretsky, and W. J. Anderson (NASA, Lewis Research Center, Cleveland, Ohio).
(American Society of Mechanical Engineers and American Society of Lubrication Engineers, Lubrication Conference, Atlantic City, N.J., Oct. 8-10, 1968, ASME Paper 68-Lub-10.)
ASME, Transactions, Series F - Journal of Lubrication Technology, vol. 91, Apr. 1969, p. 308-313. 5 refs.

Lubricated and unlubricated tests were conducted in the NASA spinning friction apparatus with SAE 52100 steel specimens with ball-race conformities of infinity (a ball on a flat), 60, 55, and 51%. For a constant conformity under lubricated conditions, the coefficient of spinning friction decreased from approximately 0.5 to 0.05 with increasing load and stress. At a constant stress, the coefficient of spinning friction increased with decreasing conformity (increasing percent conformity). Under unlubricated conditions, the coefficient of spinning friction remained relatively constant regardless of load, stress, or conformity, having values within a scatter band of 2.5 to 6.0. For a constant stress under both lubricated and unlubricated conditions, the greater the conformity (the smaller the percent conformity), the higher the torque. (Author)

A69-34378 *#
EFFECT OF THREE ADVANCED LUBRICANTS ON HIGH-TEMPERATURE BEARING LIFE.
E. N. Bamberger (General Electric Co., Cincinnati, Ohio), E. V. Zaretsky, and W. J. Anderson (NASA, Lewis Research Center, Cleveland, Ohio).
American Society of Mechanical Engineers, Lubrication Symposium, San Francisco, Calif., June 17-19, 1969, Paper 69-LubS-18. 9 p. 14 refs.
Members, $0.75; nonmembers, $1.50.

Rolling-element fatigue tests conducted with 120-mm bore angular-contact ball bearings made of AISI M-50 steel with a synthetic paraffinic oil, a fluorocarbon, and a 5P4E polyphenyl ether. At 600°F under a low-oxygen environment, the synthetic paraffinic oil and the fluorocarbon gave bearing lives approximately 14 and 3 times AFBMA-predicted (catalog) life, respectively. With the polyphenyl ether, bearing life was less than AFBMA-predicted (catalog) life in an air environment at 600°F. At temperatures of 400 and 500°F with the synthetic paraffinic oil, there was no statistical difference in life from those bearings tested with the same fluid at 600°F. For the synthetic paraffinic oil and the fluorocarbon, bearing fatigue was subsurface-initiated. For the polyphenyl ether, bearing failure was mainly from surface distress, wear, and superficial pitting. (Author)

A69-34381 *#
ELASTOHYDRODYNAMIC LUBRICATION OF A SPINNING BALL IN A NONCONFORMING GROOVE.
C. W. Allen (Chico State College, Chico, Calif.), D. P. Townsend, and E. V. Zaretsky (NASA, Lewis Research Center, Cleveland, Ohio).
American Society of Mechanical Engineers, Lubrication Symposium, San Francisco, Calif., June 17-19, 1969, Paper 69-LubS-11. 6 p. 12 refs.
Members, $0.75; nonmembers, $1.50.

Elastohydrodynamic solution for the spinning torque of a ball spinning without rolling in a nonconforming groove. The solution is compared with experimental results using a synthetic paraffinic oil as the lubricant. A modified pressure-viscosity relation is proposed. The theory predicts increase in torque with stress and spinning speed and decreasing conformity. Good agreement was obtained between theoretical predictions and experimental results. (Author)

A69-34415 *#
TRANSIENT PUMPING PERFORMANCE OF A TWO SPEED, HYDRAULIC TURBINE DRIVEN INDUCER SYSTEM.
J. Farquhar, B. K. Lindley (Aerojet-General Corp., Sacramento, Calif.), and W. A. Rostafinski (NASA, Lewis Research Center, Cleveland, Ohio).
American Institute of Aeronautics and Astronautics, Propulsion Joint Specialist Conference, 5th, U.S. Air Force Academy, Colorado Springs, Colo., June 9-13, 1969, Paper 69-551. 14 p. 14 refs.
Members, $1.00; nonmembers, $1.50.

Description of the analysis, design, and experimental evaluation of a two speed, hydraulic turbine driven pump inducer system. The system incorporates an inducer which is driven by a hydraulic turbine. The hydraulic turbine is in turn driven by a flow supplied by an axial flow rotor which is running at a higher speed and is mounted between the inducer and the hydraulic turbine. All three blade rows operate at essentially full system flow rate. The system is representative of a rocket engine liquid hydrogen boost pump where the rotor would be attached to the main stage pump. General expressions relating the significant design variables of such systems are presented together with expressions defining limits for stable (hydraulically locked) operation. Testing of the system in water is described together with comparisons of steady state and transient behavior with predictions. A digital computer model for the transient behavior of the system is described. (Author)

A69-34476
ANNUAL SYMPOSIUM ON RELIABILITY, CHICAGO, ILL., JANUARY 21-23, 1969, PROCEEDINGS.
Symposium sponsored by the Institute of Electrical and Electronics Engineers, the Institute of Environmental Sciences, the American Society for Nondestructive Testing, and the American Society for Quality Control.

New York, Institute of Electrical and Electronics Engineers, Inc. (Annals of Assurance Sciences. Volume 2, No. 1), 1969. 662 p. $8.00.

CONTENTS:

AUTHOR INDEX, p. vii.

ANALYTICAL TECHNIQUES.

READINESS OF DORMANT SYSTEMS SUBJECT TO PERIODIC CHECKOUT. I. Bazovsky (Genge Industries, Inc., Sherman Oaks, Calif.), p. 1-4. 5 refs. [See A69-34477 18-15]

MATHEMATICAL MODELING OF HUMAN PERFORMANCE RELIABILITY. T. L. Regulinski (USAF, Air University, Wright-Patterson AFB, Ohio) and W. B. Askren (USAF, Human Resources Laboratory, Wright-Patterson AFB, Ohio), p. 5-11. 16 refs. [See A69-34478 18-05]

FAULT TREE AND RELIABILITY ANALYSIS COMPARISON. K. H. Eagle (Boeing Co., Huntsville, Ala.), p. 12-17. 5 refs. [See A69-34479 18-15]

EVALUATING SYSTEM STATES IN THEIR MISSION PHASES. B. Tiger (Radio Corporation of America, Camden, N.J.), p. 18-26. 5 refs. [See A69-34480 18-15]

ENVIRONMENTAL TESTING.

ENVIRONMENTAL TESTING - THE KEY TO HIGH RELIABILITY. R. L. V. Hamm (Collins Radio Co., Cedar Rapids, Iowa), p. 27-33. [See A69-34481 18-15]

ENVIRONMENTAL AND RELIABILITY DEMONSTRATION TESTING. W. J. Barber Jr. (LTV Aerospace Corp., Dallas, Tex.), p. 34-39. [See A69-34482 18-15]

ANALYSIS OF FAILURES IN SPACECRAFT AND AIRCRAFT COMPONENTS. T. L. Pulliam (McDonnell Douglas Corp., St. Louis, Mo.), p. 40-47. [See A69-34483 18-15]

RELIABILITY MANAGEMENT.

RELIABILITY TASKS VS PRODUCT RELIABILITY. D. I. Troxel (Radio Corporation of America, Camden, N.J.), p. 48-53. [See A69-34484 18-15]

COST OF RELIABILITY IMPROVEMENT. A. H. Hevesh (Avco Corp., Wilmington, Mass.), p. 54-61. 7 refs. [See A69-34485 18-34]

RELIABILITY - WHAT HAPPENS IF ...? E. F. Taylor (General Electric Co., Philadelphia, Pa.), p. 62-67. [See A69-34486 18-15]

RELIABILITY MANAGEMENT SIMULATION EXERCISE. V. Rehg (USAF, Institute of Technology, Wright-Patterson AFB, Ohio), p. 68-72. [See A69-34487 18-11]

RELIABILITY PHYSICS.

PHYSICS OF CONTROL OF ELECTRONIC DEVICES. C. Y. Ang, P. H. Eisenberg, and H. C. Mattraw (North American Rockwell Corp., Anaheim, Calif.), p. 73-85. 5 refs. [See A69-34488 18-15]

A TECHNIQUE FOR DETERMINING THE LIFE CAPABILITY OF INDIVIDUAL SEMICONDUCTORS. T. M. Walsh (General Electric Co., Valley Forge, Pa.), p. 86-90. 5 refs. [See A69-34489 18-15]

CAUSAL APPROACH TO RELIABILITY. R. G. Stewart (Lockheed Aircraft Corp., Palo Alto, Calif.), p. 91-99. 8 refs. [See A69-34490 18-15]

SELECTION OF RELIABLE RADIATION HARD COMPONENTS. G. E. Schmitz (Sperry Rand Corp., St. Paul, Minn.), p. 100-107. 5 refs. [See A69-34491 18-15]

MARINE PRODUCTS RELIABILITY.

APPLYING RELIABILITY IN MARINE ENGINEERING DESIGN. R. E. Apple, H. M. Simpson, and J. E. Hogstad (Litton Industries, Inc., Culver City, Calif.), p. 108-117.

THE USE OF SIMULATION FOR MISSION RELIABILITY IN SCENARIO TYPE ENGAGEMENTS. P. Sgouros (U.S. Naval Material Command, Naval Applied Science Laboratory, Brooklyn, N.Y.), p. 118-126.

MECHANICAL FAILURE TECHNOLOGY - A COORDINATED GOVERNMENT PROGRAM. M. B. Peterson (Mechanical Technology, Inc., Latham, N.Y.) and D. Flage (U.S. Navy, Office of Naval Research, Washington, D.C.), p. 127-132. [See A69-34492 18-15]

STATE OF THE ART - ASSESSMENT OF RELIABILITY AND MAINTAINABILITY AS APPLIED TO SHIP SYSTEMS. B. L. Retterer (ARINC Research Corp., Washington, D.C.), p. 133-145.

AVAILABILITY.

APPROXIMATE SYSTEM AVAILABILITY MODELS. K. Grace Jr. (Bell Telephone Laboratories, Inc., Whippany, N.J.), p. 146-152. 6 refs. [See A69-34493 18-15]

SOLVING FOR THE MTTR OF COMPLEX SYSTEMS. L. R. Doyon (Northeastern University; Raytheon Co., Wayland, Mass.), p. 153-161. 5 refs. [See A69-34494 18-15]

WAITING LINE (QUEUEING) EFFECTS ON AVAILABILITY. E. P. Virene (Boeing Co., Seattle, Wash.), p. 162-167. 8 refs. [See A69-34495 18-15]

SPECIFICATIONS AND VERIFICATION OF AVAILABILITY IN TOTAL PACKAGE PROCUREMENT. G. F. Floyd (Bissett-Berman Corp., Santa Monica, Calif.), p. 168-172.

INCREASING HAZARD FUNCTIONS AND OVERHAUL POLICY. W. M. Bassin (Operations Research, Inc., Silver Spring, Md.), p. 173-180.

PARTS AND COMPONENTS.

ECONOMICAL RELIABILITY PROGRAM DESIGN. B. L. Bair and A. Fox (General Electric Co., Syracuse, N.Y.), p. 181-190. 9 refs. [See A69-34496 18-34]

RELIABILITY OF BEAM-LEAD SEALED-JUNCTION DEVICES. D. S. Peck (Bell Telephone Laboratories, Inc., Allentown, Pa.), p. 191-201. 7 refs. [See A69-34497 18-15]

RELIABILITY OF EPOXY TRANSISTORS. E. A. Herr and A. Fox (General Electric Co., Syracuse, N.Y.), p. 202-210. 6 refs. [See A69-34498 18-15]

FAILURE ANALYSIS - ITS ROLE IN SCREENING DECISIONS. E. A. Doyle, Jr. and V. C. Kapfer (USAF, Rome Air Development Center, Griffiss AFB, N.Y.), p. 211-234. [See A69-34499 18-09]

OPERATIONAL FAILURE ANALYSIS.

BALLISTIC MISSILE AND AIRCRAFT OPERATIONAL EFFECTIVENESS. F. J. Ruther (USAF, Logistics Command, Wright-Patterson AFB, Ohio), p. 235-237. [See A69-34500 18-15]

FLIGHT PERFORMANCE ANALYSIS OF SPACE SYSTEMS. B. B. Klawans and E. C. Thomas (General Electric Co., King of Prussia, Pa.), p. 238-243. [See A69-34501 18-31]

FLIGHT FAILURE ANALYSIS. W. R. Abbott and L. E. Jenkins (Lockheed Aircraft Corp., Sunnyvale, Calif.), p. 244-249. [See A69-34502 18-15]

SYSTEM/COST EFFECTIVENESS.

AN OPERATIONS RESEARCH APPROACH TO SYSTEM EFFECTIVENESS. A. Constantinides (Communications and Systems, Inc., Falls Church, Va.), p. 250-255. 15 refs. [See A69-34503 18-15]

COST EFFECTIVENESS VIA WEIGHTED FACTOR ANALYSIS. N. Salatino and M. Feistman (Radio Corporation of America, Camden, N.J.), p. 256-262. [See A69-34504 18-34]

OPERATIONAL SYSTEM EFFECTIVENESS STUDY - A LAYMAN'S APPROACH. H. Reiche (Department of National Defence, Ottawa, Canada), p. 263-269. [See A69-34505 18-34]

WARRANTY COST ESTIMATES FOR AVIONIC SUBSYSTEMS. P. O. Nerber (International Business Machines Corp., Owego, N.Y.), p. 270-275. [See A69-34506 18-34]

TEST AND DEMONSTRATION.

MILITARY VEHICLE RELIABILITY ASSESSMENT. A. L. Dillin (U.S. Army, Tank-Automotive Command, Warren, Mich.), p. 276-279.

WANTED - REALISTIC ALTERNATIVES TO MIL-STD-781. P. B. Brigham (Martin Marietta Corp., Orlando, Fla.), p. 280-287. [See A69-34507 18-15]

PREFAILURE ANALYSIS - ENHANCES PRODUCT RELIABILITY. R. E. Pederson (Honeywell, Inc., Hopkins, Minn.), p. 288-293. [See A69-34508 18-15]

THE ANALYSIS OF ACCELERATED TEMPERATURE-TESTS. R. A. Evans (Research Triangle Institute, Research Triangle Park, N.C.), p. 294-302. [See A69-34509 18-11]

RELIABILITY OF MEDICAL INSTRUMENTATION.

ELECTRICAL HAZARDS IN HOSPITAL INSTRUMENTATION.

J. A. Hopps (National Research Council, Ottawa, Canada), p. 303-307.

ELECTRICAL SHOCK & RELIABILITY CONSIDERATIONS IN CLINICAL INSTRUMENTS. J. G. Neuland (Beckman Instruments, Inc., Mountain View, Calif.), p. 308-313.

RELIABILITY OF ECG INSTRUMENTATION IN A HOSPITAL. J. B. Johnson (Veterans Administration, Little Rock, Ark.) and J. O. Wear (Veterans Administration; Arkansas, University, Little Rock, Ark.), p. 314-319.

SAFETY AND RELIABILITY IN MEDICAL ELECTRONICS. J. F. Crump (Brooklyn, Polytechnic Institute, Brooklyn, N.Y.), p. 320-322.

A69-35177 *#

EFFECT OF OXYGEN CONCENTRATION ON SYNTHETIC PARAFFINIC AND ADVANCED ESTER BASE LUBRICANTS IN BEARING TESTS AT 400° AND 450°F.

Richard J. Parker and Erwin V. Zaretsky (NASA, Lewis Research Center, Cleveland, Ohio).

American Society of Mechanical Engineers, Spring Lubrication Symposium, San Francisco, Calif., June 17-19, 1969, Paper. 26 p. 16 refs.

Determination of the effects of oxygen concentration on the oxidation of a synthetic paraffinic oil and an advanced Type II ester by means of bearing tests run at 400 and 450°F. The 20-mm bore ball bearings were run at 10,600 rpm and 70 lb thrust load. The oxygen content of the gas in the bearing chamber was varied from less than 0.1% to approximately 21% by volume. The increase in bearing torque, lubricant viscosity, and acid number were used as indicators of lubricant oxidation and degradation. The advanced ester exhibited less oxidation than did the synthetic paraffinic oil under similar test conditions. A time limitation on the effectiveness of oxidation inhibitors in both lubricants was indicated. Tests with the bearing not rotating produced relatively small increases in lubricant viscosity. (Author)

A69-35183 *#

THE INFLUENCE OF ORDERING ON THE FRICTION AND WEAR OF METALS IN VACUUM.

William A. Brainard and Donald H. Buckley (NASA, Lewis Research Center, Cleveland, Ohio).

American Vacuum Society and American Institute of Mining, Metallurgical, and Petroleum Engineers, Vacuum Metallurgical Conference, Pittsburgh, Pa., June 16-19, 1969, Paper. 20 p. 20 refs.

Determination of the effect of atomic ordering on the friction and wear of alloys in a vacuum environment. The classic copper-gold system and the iron-cobalt system were investigated. Alloys were prepared in the range Cu_3Au, CuAu, and FeCo. All of these solid solutions exhibit atomic ordering. Sliding friction experiments were conducted in vacuum (10^{-9} to 10^{-7} torr) utilizing a 0.476-cm radius rider specimen sliding on a 6.35-cm-diam disk. Friction and wear were examined at various temperatures, various loads, and various sliding velocities. It was found for all the solid solutions that friction is markedly lower in the ordered state than in the disordered state. Further wear is also significantly decreased by ordering. Sliding velocity and temperature were found to effect the friction of the ordered materials. The type of ordering and the friction coefficient as the critical temperature are compared. Initial investigation of a vanadium-iron cobalt alloy which has an ordered alpha phase shows this alloy to have promise as a potential bearing material. (Author)

A69-35501

MATERIALS AND PROCESSES FOR THE 70'S; SOCIETY OF AEROSPACE MATERIAL AND PROCESS ENGINEERS, NATIONAL SYMPOSIUM AND EXHIBITION, 15TH, LOS ANGELES, CALIF., APRIL 29-MAY 1, 1969, PROCEEDINGS.

North Hollywood, Western Periodicals Co.; Azusa, Calif., Society of Aerospace Material and Process Engineers (Science of Advanced Materials and Process Engineering Proceedings. Volume 15), 1969. 1161 p.
$37.50.

CONTENTS:

PREFACE. A. J. Tuckerman and R. A. Dunaetz. 1 p.

UNIQUE APPLICATIONS OF COMPOSITES IN AEROSPACE STRUCTURES.

ADVANCED COMPOSITE MATERIAL APPLICATIONS IN FUTURE BOOSTERS AND SPACECRAFT. L. J. Korb (North American Rockwell Corp., Downey, Calif.), p. 1-28. (See A69-35502 19-17)

THE DEVELOPMENT OF HEXAGONAL AND NON-HEXAGONAL CELL PHENOLIC HONEYCOMB AS AN ENERGY-DISSIPATING MATERIAL. A. C. Knoell (California Institute of Technology, Pasadena, Calif.) and W. M. Meyers (Honeycomb Products, Inc., Miami, Fla.), p. 29-36. 5 refs. (See A69-35503 19-18)

APPLICATION OF ADVANCED MATERIALS TO TRUSS STRUCTURES. J. G. Davis, Jr. and D. R. Rummler (NASA, Langley Research Center, Hampton, Va.), p. 37-57. 7 refs. (See A69-35504 19-17)

GLASS REINFORCED P13N POLYIMIDE LAMINATES HAVING IMPROVED PROCESSING CHARACTERISTICS. R. W. Vaughan, J. F. Jones, H. R. Lubowitz, and E. A. Burns (TRW Systems Group, Redondo Beach, Calif.), p. 59-65. (See A69-35505 19-18)

COMPARISON OF BORON-EPOXY AND BORON-ALUMINUM COMPOSITES. L. W. Davis (Harvey Aluminum, Inc., Torrance, Calif.), p. 67-74. (See A69-35506 19-17)

EVALUATION OF BORON-ALUMINUM COMPOSITE MATERIAL FOR SPACE STRUCTURES. R. A. Happe and A. J. Yeast (North American Rockwell Corp., Downey, Calif.), p. 75-89. (See A69-35507 19-15)

BERYLLIUM-REINFORCED ALUMINUM. J. N. Fleck and M. Goldstein (Battelle Memorial Institute, Columbus, Ohio), p. 91-99. (See A69-35508 19-17)

MECHANICAL PROPERTIES OF BRAZE-BONDED BORSIC-ALUMINUM COMPOSITES. C. E. Carlson, E. J. Delgrosso, and E. M. Varholak (United Aircraft Corp., Windsor Locks, Conn.), p. 101-115. 6 refs. (See A69-35509 19-17)

ELECTROFORMING OF ALUMINUM COMPOSITE STRUCTURES BY CODEPOSITION OF HIGH STRENGTH, HIGH MODULUS FIBERS. F. J. Schmidt, I. J. Hess, C. H. Esola, and A. G. Buschow (General Electric Co., Philadelphia, Pa.), p. 117-124. 7 refs. (See A69-35510 19-15)

CONTINUOUS CASTING AS A COMPOSITE FABRICATION PROCESS. J. A. Alexander and L. G. Davies (General Technologies Corp., Reston, Va.), p. 125-137. 22 refs. (See A69-35511 19-15)

SYNTACTIC FOAM PREPREGS--A NEW COMPOSITE CONSTRUCTION MATERIAL. F. E. Corse and R. C. Kausen (Whittaker Corp., Costa Mesa, Calif.), p. 139-150. (See A69-35512 19-18)

DESIGN APPLICATION OF HIGH-MODULUS FILAMENT-WOUND COMPOSITES TO AEROSPACE PROPELLANT AND PRESSURIZATION TANKS. A. Feldman, A. J. Giguere, and D. A. Stang (Martin Marietta Corp., Denver, Colo.), p. 151-161. (See A69-35513 19-18)

A NEW POLYIMIDE RESIN IN BORON REINFORCED COMPOSITES. J. F. Jones, R. W. Vaughan, and E. A. Burns (TRW Systems Group, Redondo Beach, Calif.), p. 163-169. (See A69-35514 19-18)

MIXED BORON COMPOSITES FOR SOLID ROCKET NOZZLES. J. J. Warga (Aerojet-General Corp., Sacramento, Calif.), p. 171-178. 8 refs. (See A69-35515 19-18)

BORON/EPOXY SUPPORT STRUT FOR NON-INTEGRAL CRYOGENIC TANTAGE. M. A. Nadler, S. Y. Yoshino, and F. J. Darms, Jr. (North American Rockwell Corp., Downey, Calif.), p. 179-207. 10 refs. (See A69-35516 19-18)

PREPARATION AND CHARACTERIZATION OF A NOVEL FORM OF Si_3N_4 FIBER. A. L. Cunningham and L. G. Davies (General Technologies Corp., Reston, Va.), p. 209-217. 10 refs. (See A69-35517 19-18)

GRAPHITE-EPOXY COMPOSITE MATERIAL PROPERTIES. J. E. Bell (Boeing Co., Seattle, Wash.), p. 219-228. 7 refs. (See A69-35518 19-18)

ADVANCES IN FIBER REINFORCED CARBON AND

GRAPHITE. A. P. Penton and W. M. Fassell (Philco-Ford Corp., Newport Beach, Calif.), p. 229-237. (See A69-35519 19-18)

MEASURING ELASTIC MODULUS AND TENSILE STRENGTH OF HIGH MODULUS GRAPHITE. H. J. Brown (HITCO, Gardena, Calif.), p. 239-247. (See A69-35520 19-18)

TENSILE AND CYCLIC FATIGUE PROPERTIES OF GRAPHITE FILAMENT-WOUND PRESSURE VESSELS AT AMBIENT AND CRYOGENIC TEMPERATURES. M. P. Hanson (NASA, Lewis Research Center, Cleveland, hio), p. 249-256. 7 refs. (See A69-35521 19-18)

CARBON MICROSPHERES—A NEW HIGH-PERFORMANCE FILLER MATERIAL FOR LOW-WEIGHT, HIGH-TEMPERATURE APPLICATION. R. G. Shaver and W. M. Powers (General Technologies Corp., Reston, Va.), p. 257-263. (See A69-35522 19-18)

MATERIALS AND PROCESSES FOR ENVIRONMENTAL EXTREMES.

INVESTIGATIONS OF THE UNIQUE MEMORY PROPERTIES OF 55-NITINOL ALLOY. J. E. Cooper, D. E. Bowker (NASA, Langley Research Center, Hampton, Va.), and W. B. Cross (Goodyear Aerospace Corp., Akron, Ohio), p. 265-274. 16 refs. (See A69-35523 19-17)

PREPARATION AND PROPERTIES OF CAST BERYLLIUM-ALUMINUM ALLOYS. L. B. Griffiths, W. J. Richmond, and R. H. Krock (P. R. Mallory and Co., Inc., Burlington, Mass.), p. 275-283. (See A69-35524 19-17)

CERAMIC ARMOR SYSTEMS TODAY. W. J. Carberry and K. H. Kohnken (Carborundum Co., Niagara Falls, N.Y.), p. 285-296. (See A69-35525 19-18)

DIBORIDE MATERIALS, CANDIDATES FOR AEROSPACE APPLICATIONS. E. V. Clougherty, E. T. Peters, and D. Kalish (ManLabs, Inc., Cambridge, Mass.), p. 297-308. 9 refs. (See A69-35526 19-18)

THERMOPLASTIC POLYARYLSULFONE FOR USE AT 500°F. G. A. Morneau (Minnesota Mining and Manufacturing Co., St. Paul, Minn.), p. 309-317. (See A69-35527 19-18)

PHOSPHORUS-CONTAINING RESINS AND COMPOSITES FOR ENVIRONMENTAL EXTREMES. R. M. Washburn, D. W. Karle, R. W. Hunter, and L. B. Marantz (McDonnell Douglas Corp., Santa Monica, Calif.), p. 319-334. 15 refs. (See A69-35528 19-18)

RADIATION STABILITY OF UNFILLED PYRRONE MOLDINGS. H. L. Price and V. L. Bell (NASA, Langley Research Center, Hampton, Va.), p. 335-347. 9 refs. (See A69-35529 19-18)

MATERIALS IN A NUCLEAR ENVIRONMENT. J. P. Hughes and F. J. Schmitz (Argonne National Laboratory, Argonne, Ill.), p. 349-360. 16 refs. (See A69-35530 19-18)

COMBINED ENVIRONMENT SPACE SIMULATION IN THE 1970'S. W. L. Tierney (Lockheed Aircraft Corp., Sunnyvale, Calif.), p. 361-371. 30 refs. (See A69-35531 19-11)

HIGH STRENGTH, SELF-BONDING RTV SILICONE RUBBER ADHESIVE SEALANTS. M. D. Beers (General Electric Co., Waterford, N.Y.), p. 373-381. (See A69-35532 19-18)

ADVANCES IN HYDROFLUOROCARBON INTEGRAL FUEL TANK SEALANT DEVELOPMENT. W. F. Anspach (USAF, Materials Laboratory, Wright-Patterson AFB, Ohio), p. 383-397. (See A69-35533 19-18)

EPICHLOROHYDRIN-ETHYLENE OXIDE RUBBER IN SEALS. F. W. Bickel (McDonnell Douglas Corp., Santa Monica, Calif.), p. 399-411. (See A69-35534 19-18)

POLY(2,4-PERFLUOROALKYLENE-6-PERFLUOROALKYL-TRIAZINE—SNEW HIGH TEMPERATURE ELASTOMERS. E. Dorfman, W. E. Emerson, R. J. Gruber, A. A. Lemper (Hooker Chemical Corp., Niagara Falls, N.Y.), and T. L. Graham (USAF, Wright-Patterson AFB, Ohio), p. 413-420. (See A69-35535 19-06)

ABLATIVE THERMAL PROTECTION AT LOW HEATING RATES. R. B. Pope, S. R. Riccitiello, H. E. Goldstein, and J. A. Parker (NASA, Ames Research Center, Moffett Field, Calif.), p. 421-434. 12 refs. (See A69-35536 19-18)

LOW COST ABLATIVE MATERIALS FOR SOLID ROCKET NOZZLES. J. J. Warga, H. O. Davis, and J. A. Lampman (Aerojet-General Corp., Sacramento, Calif.), p. 435-444. (See A69-35537 19-18)

DIELECTRIC PROCESSING FOR LOW-COST ABLATION HEAT SHIELDS. C. B. King (NASA, Langley Research Center, Hampton, Va.), p. 445-453. (See A69-35538 19-15)

PYROLYTIC GRAPHITE COATED COMPOSITE MATERIALS. E. L. Olcott (Atlantic Research Corp., Alexandria, Va.) and D. R. Zorich (USAF, Rocket Propulsion Laboratory, Edwards AFB, Calif.), p. 455-463. 11 refs. (See A69-35539 19-18)

MULTI-FOIL THERMAL INSULATION. M. L. Paquin (Thermo Electron Corp., Waltham, Mass.), p. 465-478. 5 refs. (See A69-35540 19-17)

MATERIALS AND PROCESSES FOR ELECTRONIC APPLICATIONS.

FABRICATION OF ULTRAHIGH-PURITY ALUMINUM STRIP FOR USE IN CRYOGENIC MAGNETS. D. L. Cheever, R. E. Monroe (Battelle Memorial Institute, Columbus, Ohio), and G. Campbell (USAF, Materials Laboratory, Wright-Patterson AFB, Ohio), p. 479-489. (See A69-35541 19-15)

UNIDIRECTIONALLY SOLIDIFIED COBALT-BASED ALLOYS FOR ELEVATED TEMPERATURE MAGNETIC APPLICATION. R. Kossowsky and D. A. Colling (Westinghouse Electric Corp., Pittsburgh, Pa.), p. 491-500. 26 refs. (See A69-35542 19-17)

SPECIAL CORE MATERIAL TECHNOLOGIES FOR SPACE POWER ELECTRONIC APPLICATIONS. D. M. Pavlovic (Westinghouse Electric Corp., Lima, Ohio), p. 501-508. 11 refs. (See A69-35543 19-15)

ERECTABLE STRUCTURES AND MESHES FOR SPACE APPLICATIONS. H. J. Sheetz, III (Radio Corporation of America, Princeton, N.J.), p. 509-519. 13 refs. (See A69-35544 19-32)

HYBRID POLYIMIDE/EPOXY GLASS MULTILAYER FABRICATION. R. A. Grueninger (International Business Machines Corp., Owego, N.Y.), p. 521-529. (See A69-35545 19-15)

PERFORMANCE OF EPOXY MOLDING COMPOUNDS ON DIP INTEGRATED CIRCUITS. G. Johnson and R. Benham (Dexter Corp., Olean, N.Y.), p. 531-537. (See A69-35546 19-09)

CONFORMAL COATING FOR GLASS ENCASED COMPONENTS. H. M. Gonzalez (TRW Systems Group, Redondo Beach, Calif.), p. 539-546. (See A69-35547 19-09)

PRESSURE APPLIED DIELECTRICS. J. Currie and J. Delmonte (Furane Plastics, Inc., Los Angeles, Calif.), p. 547-557. (See A69-35548 19-09)

A NEW ONE-PART SILICONE ENCAPSULANT. A. R. Knivila (Dow Corning Corp., Midland, Mich.), p. 559-565. (See A69-35549 19-09)

NEW JOINING TECHNIQUES.

ELECTROSTATIC CONTROL FOR PORTABLE CLEAN ROOMS. H. Heuring (International Business Machines Corp., New York, N.Y.), p. 567-572. (See A69-35550 19-31)

DEVELOPMENT AND USE OF MOLDED SHIM FOR AIRCRAFT STRUCTURE. H. P. Owen and R. J. Stout (General Dynamics Corp., Fort Worth, Tex.), p. 573-591. 6 refs. (See A69-35551 19-15)

WIDE INTEGRALLY STIFFENED TITANIUM EXTRUSIONS. G. W. Stacher (Lockheed Aircraft Corp., Marietta, Ga.), p. 593-600. (See A69-35552 19-15)

MACHINED FASTENED JOINTS—THEIR USE IN AEROSPACE STRUCTURES. D. L. Swartz (General-Electro Mechanical Corp., Buffalo, N.Y.) and D. K. Bazaj (New York, State University, Buffalo, N.Y.), p. 601-620. (See A69-35553 19-15)

THE FEASIBILITY OF RESISTANCE WELDING IN A HARD VACUUM. D. L. Cheever, D. G. Howden, and R. E. Monroe (Battelle Memorial Institute, Columbus, Ohio), p. 621-632. 7 refs. (See A69-35554 19-15)

PLASMA ELECTRON BEAM DEVELOPMENT FOR WELDING APPLICATIONS. R. M. Poorman (NASA, Marshall Space Flight Center, Huntsville, Ala.) and K. L. Boring (General Electric Co., Schenectady, N.Y.), p. 633-648. (See A69-35555 19-15)

LASER WELDING STRUCTURAL ALLOYS AND PARTS. H. H. Witt, W. Kaehler, and D. Kloepper (Grumman Aircraft Engineering Corp., Bethpage, N.Y.), p. 649-679. (See A69-35556 19-15)

HONEYCOMB PANEL FABRICATION BY SALT BATH

15 MACHINE ELEMENTS AND PROCESSES

BRAZING. F. J. Coffey, V. E. Padilla, and W. J. Nowak (McDonnell Douglas Corp., St. Louis, Mo.), p. 681-685. (See A69-35557 19-15)

DIFFUSION BONDED TITANIUM HONEYCOMB SANDWICH. J. W. Frazier (Tool Research and Engineering Corp., Santa Ana, Calif.), p. 687-696. (See A69-35558 19-15)

DIFFUSION BONDING OF SUPERALLOYS. T. F. Berry and G. S. Hoppin, III (General Electric Co., Evendale, Ohio), p. 697-714. 5 refs. (See A69-35559 19-15)

HIGH TEMPERATURE THERMOPLASTIC ADHESIVES. H. H. Levine and F. D. Trischler (Whittaker Corp., San Diego, Calif.), p. 715-718. (See A69-35560 19-18)

ADHESIVE BONDING OF BERYLLIUM. M. C. St. Cyr (McDonnell Douglas Corp., Santa Monica, Calif.), p. 719-731. (See A69-35561 19-15)

EFFECT OF OUTDOOR AGING ON UNSTRESSED, ADHESIVE-BONDED ALUMINUM TO ALUMINUM LAP SHEAR JOINTS. M. J. Bodnar and R. F. Wegman (U.S. Army, Materials Engineering Laboratory, Picatinny Arsenal, Dover, N.J.), p. 733-745. 20 refs. (See A69-35562 19-15)

EXTENDING THE THERMAL RANGE OF RTV ADHESIVE BONDS. J. F. Yurk (TRW Systems Group, Redondo Beach, Calif.), p. 747-754. (See A69-35563 19-15)

SPRAY DEOXIDIZING FOR ALUMINUM METALBONDING. H. R. Herrigel (Boeing Co., Renton, Wash.), p. 755-765. 6 refs. (See A69-35564 19-15)

ELECTRICAL CONDUCTIVITY AS AN INDEX OF CURE CYCLE IN ADHESIVE BONDING OF AGE HARDENING ALLOYS. R. T. Howard, p. 767-772. (See A69-35565 19-15)

MATERIALS AND PROCESSES FOR DETERIORATION PREVENTION.

REVERSION RESISTANT URETHANES. P. Meadows, S. Sheth, and J. Delmonte (Furane Plastics, Inc., Los Angeles, Calif.), p. 773-780. (See A69-35566 19-18)

THE EFFECTS OF MILITARY ENVIRONMENTS ON THE STRENGTH OF FILAMENT WOUND GLASS REINFORCED EPOXY COMPOSITES. J. Gnapp (U.S. Army, Materials Engineering Laboratory, Picatinny Arsenal, Dover, N.J.), p. 781-799. 10 refs. (See A69-35567 19-15)

A PROGRAM TO EVALUATE MATERIALS FOR UNDERGROUND EXPOSURE IN EXTREME ENVIRONMENTS. J. B. Nathan, Jr. (Honeywell, Inc., Hopkins, Minn.), p. 801-815. (See A69-35568 19-15)

MICROBIOLOGICAL DEGRADATION OF AIRCRAFT MATERIALS. H. G. Hedrick (General Dynamics Corp., Fort Worth, Tex.), p. 817-827. 21 refs. (See A69-35569 19-17)

EFFECT OF PROCESSING VARIABLES ON PROPERTIES OF CHROMATE TREATED ALUMINUM. S. R. Brown (U.S. Naval Material Command, Naval Air Development Center, Johnsville, Pa.), p. 829-840. 5 refs. (See A69-35570 19-15)

DEVELOPMENT OF IMPROVED CORROSION RESISTANT CLADDINGS FOR HIGH STRENGTH ALUMINUM ALLOYS. F. H. Meyer, Jr. (USAF, Materials Laboratory, Wright-Patterson AFB, Ohio) and T. A. Lowe (Kaiser Aluminum and Chemical Corp., Spokane, Wash.), p. 841-852. (See A69-35571 19-15)

THE STRESS CORROSION BEHAVIOR OF BERYLLIUM AND Be-38% Al ALLOY IN A SALT WATER ENVIRONMENT. H. D. Moore, Jr. (Lockheed Aircraft Corp., Marietta, Ga.). p. 853-859. 7 refs. (See A69-35572 19-17)

THE OXIDATION OF LiF-COATED REFRACTORY METALS. G. Geschwind and G. Padawer (Grumman Aircraft Engineering Corp., Bethpage, N.Y.), p. 861-873. 16 refs. (See A69-35573 19-17)

MATERIALS RELIABILITY AND TESTING TECHNIQUES.

SIGNATURE ANALYSIS—A MATERIAL RELIABILITY TESTING TECHNIQUE. R. B. Socky (General Electric Co., New York, N.Y.), p. 875-904. 25 refs. (See A69-35574 19-15)

RADIOACTIVE GAS PENETRANTS FOR NONDESTRUCTIVE TEST INSPECTIONS. W. C. Eddy, Jr. (Industrial Nucleonics Corp., Columbus, Ohio), p. 905-912. (See A69-35575 19-15)

HOLOGRAPHIC NONDESTRUCTIVE TESTING (HNDT) OF AIRCRAFT MATERIALS. W. A. McCaughey, R. M. Grant, and G. M. Brown (GC Optronics, Inc., Ann Arbor, Mich.), p. 913-922. (See A69-35576 19-15)

ULTRASONICS—A NONDESTRUCTIVE TECHNIQUE FOR PREDICTING THE RESIDUAL LIFE OF COMPRESSIVELY FATIGUED FILAMENT WOUND COMPOSITES. C. K. Cole (IIT Research Institute, Chicago, Ill.) and M. H. Zoiss (Barnes Drill Co., Elmhurst, Ill.), p. 923-942. (See A69-35577 19-15)

FLAW SIZE EVALUATION IN IMMERSED ULTRASONIC TESTING. J. D. Hislop (Rolls-Royce, Ltd., Derby, England), p. 943-979. 17 refs. (See A69-35578 19-15)

RELIABLE GLASS-FIBER-FILLED POLYTETRAFLUOROETHYLENE MATERIALS FOR PISTON SEALS IN HIGH-PRESSURE OIL-FREE AIR COMPRESSORS. G. L. Thomas (U.S. Naval Material Command, Ship Research and Development Laboratory, Annapolis, Md.), p. 981-1002. 9 refs. (See A69-35579 19-15)

A THEORY AND TESTER MEASUREMENT CORRELATION ABOUT MoS_2 DRY FILM LUBRICANT WEAR. J. W. McCain (North American Rockwell Corp., Canoga Park, Calif.), p. 1003-1019. 32 refs. (See A69-35580 19-15)

ADHESIVE SHEAR STRENGTH OF ICE TO BONDED SOLID LUBRICANTS. J. R. Jones and M. N. Gardos (Hughes Aircraft Co., Culver City, Calif.), p. 1021-1029. 6 refs. (See A69-35581 19-15)

DEVELOPMENT AND TESTING OF INTERMETALLIC COATED TITANIUM ALLOY GEARS. S. H. Cohen, E. J. Delgrosso, J. L. Mattavi, and J. F. McGivern (United Aircraft Corp., Windsor Locks, Conn.), p. 1031-1042. 13 refs. (See A69-35582 19-15)

DEGRADATION OF MAGNESIUM ALLOY MECHANICAL PROPERTIES BY CRYSTAL TWINNING AND THE INVESTIGATION OF METHODS FOR RECOVERY. G. G. Schimel (Boeing Co., Seattle, Wash.), p. 1043-1054. (See A69-35583 19-17)

MATERIALS AND PROCESSES PROJECTIONS FOR THE FUTURE.

ADVANCED COMPOSITE, HIGH-MODULUS TAPE PLACEMENT MACHINES: THE NEXT THREE GENERATIONS—DIGITAL SETTINGS TO FULL-TIME TAPE CONTROL. E. E. Hardesty (Goldsworthy Engineering, Inc., Los Angeles, Calif.), p. 1055-1071. (See A69-35584 19-15)

SPACE RIGIDIZATION TECHNIQUES FOR EXPANDABLE STRUCTURES. S. Schwartz (Hughes Aircraft Co., Culver City, Calif.), p. 1073-1088. 15 refs. (See A69-35585 19-32)

ELASTOMERS AND COATINGS FOR EXTREME ENVIRONMENTS—CURRENT AND FUTURE. W. P. Johnson (USAF, Materials Laboratory, Wright-Patterson AFB, Ohio), p. 1089-1100. 18 refs. (See A69-35586 19-18)

MATERIALS/PROCESSES PROJECTIONS BASED ON MCD CONSTRAINTS. L. Raymond and R. J. Usell, Jr. (Aerospace Corp., El Segundo, Calif.), p. 1101-1108. (See A69-35587 19-32)

PROCESSING OF MATERIALS IN SPACE. W. H. Steurer (General Dynamics Corp., San Diego, Calif.), p. 1109-1129. 15 refs. (See A69-35588 19-15)

MATERIALS PROCESSING IN SPACE. L. R. McCreight (General Electric Co., Philadelphia, Pa.), p. 1131-1140. (See A69-35589 19-15)

AUTHOR INDEX, p. 1141, 1142.

SUBJECT INDEX, p. 1143, 1144.

A69-35538 *

DIELECTRIC PROCESSING FOR LOW-COST ABLATION HEAT SHIELDS.

Charles B. King (NASA, Langley Research Center, Hampton, Va.).

IN: MATERIALS AND PROCESSES FOR THE 70'S; SOCIETY OF AEROSPACE MATERIAL AND PROCESS ENGINEERS, NATIONAL SYMPOSIUM AND EXHIBITION, 15TH, LOS ANGELES, CALIF., APRIL 29-MAY 1, 1969, PROCEEDINGS. (A69-35501 19-15)

North Hollywood, Western Periodicals Co.; Azusa, Calif., Society of Aerospace Material and Process Engineers (Science of Advanced Materials and Process Engineering Proceedings. Volume 15), 1969, p. 445-453.

A heat-shield concept which simplifies fabrication and application of ablative panels to entry vehicles is described. Results from an experimental program where typical panels were fabricated using dielectric heating are presented and discussed. The relative costs of this approach and state-of-the-art heat-shield fabrication are discussed. (Author)

A69-35555 *
PLASMA ELECTRON BEAM DEVELOPMENT FOR WELDING APPLICATIONS.
Richard M. Poorman (NASA, Marshall Space Flight Center, Manufacturing Engineering Laboratory, Huntsville, Ala.) and Kenneth L. Boring (General Electric Co., Research and Development Center, Schenectady, N.Y.).
IN: MATERIALS AND PROCESSES FOR THE 70'S; SOCIETY OF AEROSPACE MATERIAL AND PROCESS ENGINEERS, NATIONAL SYMPOSIUM AND EXHIBITION, 15TH, LOS ANGELES, CALIF., APRIL 29-MAY 1, 1969, PROCEEDINGS. (A69-35501 19-15)
North Hollywood, Western Periodicals Co.; Azusa, Calif., Society of Aerospace Material and Process Engineers (Science of Advanced Materials and Process Engineering Proceedings. Volume 15), 1969, p. 633-648.

A new electron source, called plasma electron beam, is described. This source derives its beam current from secondary emission by ion bombardment and gives long life and good performance under poor vacuum conditions. A brief summary is given of its characteristics and of recent developments in its design and control. Chamber designs for use with this electron source are shown, with emphasis on advantages in gas pressures higher than required for most electron beam welding. Descriptions of material welded and specific test results are presented for several materials of interest for large space vehicle construction. Predictions as to further development and application are discussed. (Author)

A69-35999
ANNALS OF ASSURANCE SCIENCES; PROCEEDINGS OF THE EIGHTH RELIABILITY AND MAINTAINABILITY CONFERENCE, DENVER, COLO., JULY 7-9, 1969.
Conference sponsored by the American Institute of Aeronautics and Astronautics, the Society of Automotive Engineers, and the American Society of Mechanical Engineers.
New York, Gordon and Breach, Science Publishers, Inc., 1969. 597 p.
$30.

CONTENTS:
PREFACE. F. A. Thompson, p. ix, x.

TRANSPORTATION SYSTEMS.
TRANSPORTATION SYSTEM SAFETY. C. S. Bartholomew (Boeing Co., Seattle, Wash.), p. 1, 2.
COMPUTERIZED CONTROL OF SURFACE TRAFFIC - A STATUS REPORT. L. I. Lann (U.S. Bureau of Public Roads, Washington, D.C.), p. 3-11.
RELIABILITY AND MAINTAINABILITY OF THE FAA'S ARTS-III TERMINAL AIR TRAFFIC CONTROL SYSTEM. J. C. Mercer (Federal Aviation Administration, Washington, D.C.), p. 12-21. (See A69-36000 19-21)
SATELLITE MAINTENANCE USING REMOTE MANIPULATOR SPACECRAFT. A. Interian (General Electric Co., Valley Forge, Pa.), D. A. Kugath (General Electric Co., Schenectady, N.Y.), and W. H. Allen (NASA, Moffett Field, Calif.), p. 22-32. 5 refs. (See A69-36001 19-31)

PREDICTION, ASSESSMENT AND DEMONSTRATION.
0.9999 VS. 0.9000: IT'S A MATTER OF VALUE—AN ESSAY. I. Nathan (Xerox Corp., Webster, N.Y.), p. 33-35.
RELIABILITY WITH ALLOWABLE DOWNTIME. M. Epstein and G. Weinstock (Communications and Systems, Inc., Paramus, N.J.), p. 36-39. (See A69-36002 19-15)
THE SYSTEM APPROACH TO RELIABILITY DEMONSTRATION. J. J. Bussolini and S. A. Weisberg (Grumman Aircraft Engineering Corp., Bethpage, N.Y.), p. 40-48. (See A69-36003 19-15)
"BAD-AS-OLD" ANALYSIS OF SYSTEM FAILURE DATA. H. Ascher and H. Feingold (U.S. Naval Material Command, Applied Science Laboratory, Brooklyn, N.Y.), p. 49-62.
MODIFICATION OF GAS TURBINE COMPONENT LIFE PREDICTIONS UTILIZING EXPERIENCE AND THE DISCRETE FORMULATION OF BAYES THEOREM. T. L. Salt and M. H. Monahan (General Electric Co., Lynn, Mass.), p. 63-68. (See A69-36004 19-28)

SYSTEMS ENGINEERING OPTIMIZED CONTRACTING.
OPTIMIZED SYSTEM ENGINEERING—INTRODUCTION. G. F. Keeling (USAF, Washington, D.C.) and J. L. Maybell (McDonnell Douglas Corp., Santa Monica, Calif.), p. 69.
INDUSTRY VIEWS ON OPTIMIZED CONTRACTING FOR SYSTEMS ENGINEERING MANAGEMENT, MIL-STD-XXX. O. A. Bernhoff (McDonnell Douglas Corp., Huntington Beach, Calif.), p. 70-76. (See A69-36005 19-34)
THE SYSTEMS EFFECTIVENESS FUNCTION—FROM A MANAGERIAL POINT OF VIEW. D. E. Hibsman and J. Meltzer (Aerospace Corp., El Segundo, Calif.), p. 77-84. (See A69-36006 19-34)
A COMPUTERIZED COST MODEL FOR SPACE SYSTEMS. T. L. Fagan (General Electric Co., Philadelphia, Pa.), p. 85-89. (See A69-36007 19-34)
THE DEVELOPMENT AND APPLICATION OF A METHODOLOGY OF PROGRAM RISK EVALUATION. E. L. Welker, G. E. Ingram, and C. R. Herrmann (General Electric Co., Santa Barbara, Calif.), p. 90-98. (See A69-36008 19-34)

SYSTEMS DESIGN FOR RELIABILITY, MAINTAINABILITY AND SAFETY.
SYSTEMS DESIGN FOR RELIABILITY, MAINTAINABILITY AND SAFETY—INTRODUCTION. L. P. Michaelis (General Dynamics Corp., Fort Worth, Tex.), p. 99.
PHYSICS OF FAILURE IN SPACECRAFT APPLICATION. H. S. Dodge (General Electric Co., Philadelphia, Pa.), p. 100-104. (See A69-36009 19-31)
IMPROVEMENT IN EFFECTIVENESS OF AN EARTH ORBITAL MISSION THROUGH UTILIZATION OF STANDBY SYSTEMS. S. S. Calderon and F. E. Senator (McDonnell Douglas Corp., Huntington Beach, Calif.), p. 105-114. 9 refs. (See A69-36010 19-31)
C-5A RELIABILITY PROGRAM. F. A. Stovall (Lockheed Aircraft Corp., Marietta, Ga.), p. 115-122. (See A69-36011 19-02)
SYSTEM COST EFFECTIVENESS ANALYSIS. G. A. Laureyns, R. E. Morris, and W. M. Rowell, Jr. (General Dynamics Corp., Fort Worth, Tex.), p. 123-134. (See A69-36012 19-03)
HUMAN AND DESIGN RELIABILITY MEASUREMENT. C. H. Veen (Bendix Corp., South Bend, Ind.), p. 135-142. (See A69-36013 19-15)

ASSURANCE VIA TESTING.
ASSURANCE VIA TEST. A. M. Smith (General Electric Co., Philadelphia, Pa.), p. 143, 144.
MISSION ASSURANCE THROUGH INTEGRATED TESTING. J. W. Carter (Martin Marietta Corp., Denver, Colo.), p. 145-152. 8 refs. (See A69-36014 19-15)
THE APOLLO SPACECRAFT QUALIFICATION PROGRAM. R. J. Westerheid (General Electric Co., Houston, Tex.), p. 153-159. (See A69-36015 19-31)
SURVEYOR—HARD TRAILS TO SOFT LANDINGS. M. E. Goble and D. O. Marriage (Hughes Aircraft Co., Culver City, Calif.), p. 160-173. (See A69-36016 19-31)
RELIABILITY/MAINTAINABILITY FIELD TEST EVALUATION OF FLYING CRANE HELICOPTER. C. D. Holbert (United Aircraft Corp., Stratford, Conn.) and R. E. Heitert (U.S. Army, Aviation Systems Command, St. Louis, Mo.), p. 174-180. (See

15 MACHINE ELEMENTS AND PROCESSES

A69-36017 19-02)

INCIPIENT FAILURE DETECTION—THE DETECTION OF INCIPIENT FAILURE IN CERTAIN HYDRAULIC COMPONENTS. H. L. Balderston (Boeing Co., Seattle, Wash.), p. 181-190. 6 refs. (See A69-36018 19-03)

MICROELECTRONICS.

RELIABILITY MODELING AND MICROCIRCUIT PREDICTION. C. M. Ryerson (Hughes Aircraft Co., Culver City, Calif.), p. 191-198. (See A69-36019 19-09)

MICROELECTRONIC PROCESS/QUALITY CONTROLS. W. B. Rossnagel (General Electric Co., Philadelphia, Pa.), p. 199-210. 13 refs. (See A69-36020 19-09)

THE IMPACT OF MICROELECTRONICS ON MAINTENANCE AND MAINTAINABILITY. C. E. Cunningham (Philco-Ford Corp., Palo Alto, Calif.), p. 211-217. 6 refs. (See A69-36021 19-09)

A SYSTEM FOR EFFECTIVE TRANSFERRAL OF MICROELECTRONIC RELIABILITY EXPERIENCE. H. A. Lauffenburger (IIT Research Institute, Chicago, Ill.) and J. L. Fuchs (USAF, Rome Air Development Center, Griffiss AFB, N.Y.), p. 218-227.

FIELD FAILURE RATES AS THEY RELATE TO GSE AND FACILITIES.

BRIEF COMMENTS ON ESTABLISHMENT OF FAILURE RATES—INTRODUCTION. O. H. Fedor, F. L. Christ (NASA, Kennedy Space Center, Cocoa Beach, Fla.), L. R. Webster, and L. B. Barrentine (Radiation, Inc., Melbourne, Fla.), p. 228.

THE CREDIBILITY OF RELIABILITY MEN AND NUMBERS. R. W. Burrows (Martin Marietta Corp., Denver, Colo.), p. 229-232.

IMPACT OF SPECIFICATIONS AND STANDARDS ON THE DEVELOPMENT AND USE OF FAILURE RATES. C. M. Ryerson (Hughes Aircraft Co., Culver City, Calif.), p. 233-237.

THE IMPACT OF FAILURE DATA ON MANAGEMENT OF A LAUNCH OPERATIONS RELIABILITY PROGRAM. R. E. Cato, Jr. (NASA, Kennedy Space Center, Cocoa Beach, Fla.) and W. C. Wheadon (General Electric Co., Cocoa Beach, Fla.), p. 238-243. (See A69-36022 19-11)

FIELD FAILURE RATES FOR SELECTED KSC GROUND SUPPORT EQUIPMENT. E. E. Bean and C. E. Bloomquist (Planning Research Corp., Los Angeles, Calif.) p. 244-250. (See A69-36023 19-11)

QUANTIFICATION OF HUMAN PERFORMANCE.

QUANTIFICATION OF HUMAN PERFORMANCE—INTRODUCTION. A. D. Swain (Sandia Corp., Albuquerque, N. Mex.), p. 251-254.

ERROR PATTERNS AMONG POSITIONS INVOLVED IN PREPARATION OF CODED MACHINE INPUTS. E. M. Jones and S. J. Munger (American Institutes for Research, Pittsburgh, Pa.), p. 255-262.

PERSONNEL SUBSYSTEMS IMPACT ON C-5 EQUIPMENT AND SYSTEM DESIGN. H. L. Parris and T. J. Hall (Lockheed Aircraft Corp., Marietta, Ga.), p. 263-271. 8 refs. (See A69-36024 19-05)

FIELD TEST OF A TECHNIQUE FOR ESTABLISHING PERSONNEL PERFORMANCE REQUIREMENTS. R. E. Blanchard and R. L. Smith (Integrated Sciences Corp., Santa Monica, Calif.), p. 272-277. 5 refs. (See A69-36025 19-05)

USE OF A HUMAN RELIABILITY TECHNIQUE TO SELECT DESIRABLE DESIGN CONFIGURATIONS. D. Meister (Bunker-Ramo Corp., Canoga Park, Calif.), p. 278-282. 7 refs. (See A69-36026 19-05)

COMMERCIAL AND CONSUMER PRODUCTS.

RELIABILITY, MAINTAINABILITY, AND DOLLARS—INDICES OF CUSTOMER SATISFACTION. A. R. Adler (General Electric Co., Schenectady, N.Y.), p. 283, 284.

XEROX SERVICING COST MODEL. R. DeSantis, I. Nathan, and R. Reddy (Xerox Corp., Webster, N.Y.), p. 285-293.

TEST AND EVALUATION TECHNIQUES ASSIST RELIABILITY ASSURANCE IN CONSUMER PRODUCTS. P. P. Bohlool (Whirlpool Corp., St. Joseph, Mich.), p. 294-297.

PREDICTING PRODUCT RELIABILITY FROM ACCELERATED TEST RESULTS. C. G. Plithides (General Electric Co., Louisville, Ky.), p. 298-303.

FAILURE ANALYSIS—A KEY ELEMENT IN COMMERCIAL PRODUCT RELIABILITY. S. J. Keene, Jr. (International Business Machines Corp., Boulder, Colo.), p. 304-308.

DC-10 RELIABILITY PROGRAM. H. A. Reesing (McDonnell Douglas Corp., Long Beach, Calif.), p. 309-314. (See A69-36027 19-02)

SYSTEM SAFETY.

RESULTS FOR SYSTEM SAFETY—INTRODUCTION. N. E. Classon (Boeing Co., Seattle, Wash.), p. 315.

DETECTION AND MINIMIZATION OF CHEMICALLY INDUCED IGNITION HAZARDS OF GLYCOL FLUIDS. W. R. Downs (NASA, Manned Spacecraft Center, Houston, Tex.) and D. B. Boies (IIT Research Institute, Chicago, Ill.), p. 316-324. 6 refs. (See A69-36028 19-18)

COMPUTERIZATION OF SYSTEM/PRODUCT FAULT TREES. K. Kanda (Boeing Co., Seattle, Wash.), p. 325-333. 6 refs. (See A69-36029 19-08)

OPTIMIZATION OF CONNECTOR-PIN ASSIGNMENTS IN ELECTRICAL/ELECTRONIC WIRING SYSTEMS. R. D. Craig (Boeing Co., Seattle, Wash.), p. 334-340. (See A69-36030 19-09)

STRUCTURAL AND MECHANICAL RELIABILITY TECHNOLOGY.

STRUCTURAL AND MECHANICAL RELIABILITY TECHNOLOGY—INTRODUCTION. G. Reethof (Pennsylvania State University, University Park, Pa.) and A. R. Townsend (General Motors Corp., Indianapolis, Ind.), p. 341, 342.

THE DETERMINATION OF DISTRIBUTIONS THAT DESCRIBE THE FAILURES OF MECHANICAL COMPONENTS. J. H. Bompas-Smith (Rolls-Royce, Ltd., Derby, England), p. 343-356. 14 refs. (See A69-36031 19-15)

DISTRIBUTIONS OF CYCLES-TO-FAILURE IN SIMPLE FATIGUE AND THE ASSOCIATED RELIABILITIES. D. Kececioglu, R. E. Smith, and E. A. Felsted (Arizona, University, Tucson, Ariz.), p. 357-374. 15 refs. (See A69-36032 19-32)

OPTIMUM STRUCTURAL DESIGN BASED ON RELIABILITY AND PROOF-LOAD TEST. M. Shinozuka (Columbia University, New York, N.Y.) and J.-N. Yang (California Institute of Technology, Pasadena, Calif.), p. 375-391. 13 refs. (See A69-36033 19-32)

THE STATUS OF THE INCORPORATION OF RELIABILITY TECHNIQUES INTO MECHANICAL ENGINEERING EDUCATION. C. Birnie, Jr. (Pennsylvania State University, University Park, Pa.), p. 392-402.

SYSTEMS ANALYSIS.

ANALYSIS OF SHIPBOARD ELECTRONICS USING SIMULATION TECHNIQUES. C. C. Eliot and R. Briggs (Raytheon Co., Bedford, Mass.), p. 403-416.

A COMPARISON OF STATIC AND DYNAMIC SYSTEM EFFECTIVENESS ANALYSIS. G. L. Seller (Honeywell, Inc., Minneapolis, Minn.), p. 417-425.

ANALYTICAL EVALUATION OF LAUNCH STRATEGY USING PAST COUNTDOWN HOLD DATA. W. B. Gevarter (Bellcomm, Inc., Washington, D.C.), p. 426-434. 13 refs. (See A69-36034 19-31)

MEASUREMENT OF THE LOGISTIC CONSEQUENCES OF R & M. I. Katz (USAF, Logistics Command, Wright-Patterson AFB, Ohio), p. 435-444.

ASSURANCE TECHNIQUES IN LOGISTICS MANAGEMENT.

LOGISTICS—AN ASSURANCE TECHNOLOGY. D. A. Barnes (McDonnell Douglas Corp., Santa Monica, Calif.), p. 445-451.

RELIABILITY INFLUENCE ON LIFE CYCLE COSTS. G. B. Cohen (Sylvania Electric Products, Inc., Buffalo, N.Y.), p. 452-459.

MANAGEMENT ASPECTS OF MAINTAINABILITY AND MAINTENANCE ANALYSIS. H. C. Slawson (Boeing Co., Seattle, Wash.), p. 460-465. (See A69-36035 19-34)

MAINTAINABILITY, THE MEASURE OF AVAILABILITY. T.

O. Wright (Boeing Co., Seattle, Wash.), p. 466-469. (See A69-36036 19-15)

A COST EFFECTIVE APPROACH TO INTEGRATED LOGISTIC SUPPORT. S. Duhan and P. Myslicki (Boeing Co., Philadelphia, Pa.), p. 470-475.

CASE HISTORIES OF MATERIALS AND PROCESSES.

CASE HISTORIES OF MATERIALS AND PROCESSES—INTRODUCTION. A. H. Hehn (IIT Research Institute, Chicago, Ill.), p. 476, 477.

THE SURVIVABILITY OF DELICATE COMPONENTS IN A SUSTAINED HIGH G LOAD ENVIRONMENT. M. J. Shumaker and W. L. Harvey (Martin Marietta Corp., Denver, Colo.), p. 478-485. (See A69-36037 19-31)

BAYESIAN APPLICATIONS.

MORE BAYESIAN RELIABILITY EVALUATION—INTRODUCTION. W. T. Weir (General Electric Co., Philadelphia, Pa.), p. 486, 487.

PARTIAL PRIOR INFORMATION AND SHORTER CONFIDENCE INTERVALS. J. J. Deely and W. J. Zimmer (Sandia Corp., Albuquerque, N. Mex.), p. 488-496. (See A69-36038 19-19)

A BAYESIAN APPROACH TO RELIABILITY DEMONSTRATION. H. Balaban (ARINC Research Corp., Annapolis, Md.), p. 497-506. 7 refs. (See A69-36039 19-15)

A SEQUENTIAL BAYES PROCEDURE FOR RELIABILITY DEMONSTRATION. R. E. Schafer and N. D. Singpurwalla (Hughes Aircraft Co., Fullerton, Calif.), p. 507-514. 6 refs. (See A69-36040 19-15)

BAYESIAN CONFIDENCE LIMITS FOR SYSTEM RELIABILITY. M. D. Springer (Arkansas, University, Fayetteville, Ark.) and W. E. Thompson (General Research Corp., Santa Barbara, Calif.), p. 515-523. 17 refs. (See A69-36041 19-15)

SIMULATION METHOD APPLIED TO RELIABILITY ANALYSIS OF TURBOJET ENGINE COMPONENTS OPERATING IN AIRLINE SERVICE. R. S. Dorsey and H. A. Truscott (General Electric Co., Cincinnati, Ohio), p. 524-529. (See A69-36042 19-28)

AN INTRODUCTION TO MIL-STD-883 TEST METHODS AND PROCEDURES FOR MICROELECTRONICS. E. P. O'Connell (USAF, Rome Air Development Center, Griffiss AFB, N.Y.), p. 530-542. 9 refs. (See A69-36043 19-09)

THE REAL WORLD OF SYSTEM EFFECTIVENESS. J. A. Harkins (Center for Naval Analyses, Arlington, Va.), p. 543-557. 26 refs. (See A69-36044 19-34)

CUMULATIVE INDEX, p. 558-578.

AUTHOR INDEX, p. 579, 580.

A69-38567 *

THE RELEASE OF HYDROGEN ON BALL MILLING CHROMIUM IN WATER.

Alan Arias (NASA, Lewis Research Center, Cleveland, Ohio).

International Journal of Powder Metallurgy, vol. 4, Oct. 1968, p. 7-15. 5 refs.

Study of the reaction which occurs on ball milling chromium in water in gas tight ball mills. The pressure of the hydrogen released was determined as a function of ball milling time. The amount of oxygen reacted with the chromium was calculated, and the nature of the oxide formed by the reaction was determined. From the data so obtained, the thickness of the chromium oxide layer was calculated. G.R.

A69-38950 *

A FEASIBILITY STUDY OF A TECHNIQUE FOR SORTING PARTICLES BY SHAPE.

Norman S. Land (NASA, Langley Research Center, Environmental Systems Section, Hampton, Va.).

Materials Research and Standards, vol. 9, June 1969, p. 26-29, 77. 6 refs.

Description of a possible sieving method, which, with further research, could be used for sorting particles by shape. A consideration of the basic process involved in sieving indicates that the elongated particle should pass through a sieve at a slower rate than short particles with the same minimum dimension. This basic premise suggests a convenient technique for sorting by shape utilizing standard sieving equipment. Results of experiments with specially prepared particles and with randomly crushed gravel are reported. V.P.M.

A69-39367 * #

EXPERIMENTS IN HYDRODYNAMIC GREASE BEARINGS.

John L. Burch and Peter H. Broussard (NASA, Marshall Space Flight Center, Astrionics Laboratory, Huntsville, Ala.).

American Institute of Aeronautics and Astronautics, Guidance, Control, and Flight Mechanics Conference, Princeton, N.J., Aug. 18-20, 1969, Paper 69-836. 11 p. 8 refs.

Members, $1.00; nonmembers, $1.50.

NASA-supported research.

Investigation of the suitability of using hydrodynamic conical- and spherical-shaped spiral-grooved grease bearings as a replacement for gyro ball bearings. It is noted that gyro bearings used in extended space missions should have low friction, be relatively stiff, be capable of multiple starts and stops, and operate in a smooth stable manner without attention for a year or longer. Grease bearings have been built and tested for rotors which vary in diameter from a few centimeters to 30.5 cm and vary in weight from a few grams to 22.7 kg. Speeds ranging from 12,000 to 50,000 rpm have been maintained for hundreds of hours in both air and vacuum environments. Generally, these bearings have operated satisfactorily and retained their lubricant. P.G.

A69-42802 * #

SPACE TOOL STATE-OF-THE-ART, AND CONSIDERATIONS FOR FUTURE SPACE TOOL-EQUIPMENT DESIGN.

Charles C. Kubokawa (NASA, Ames Research Center, Moffett Field, Calif.).

American Astronautical Society and Operations Research Society of America, Joint National Meeting, Denver, Colo., June 17-20, 1969, AAS Paper 69-438. 21 p. 11 refs.

Results of a study to catalog tools and equipment specifically designed for extravehicular and intravehicular activities in space and on the lunar surface. The present state of development of space tools is described. Details of existing equipment and tool designs, their development status, evaluation tests, and specifications are outlined. A total of 97 space tools have been identified and are qualified as new space tools expressly designed and fabricated for space operations. The problems encountered in designing new space tools are discussed, citing a recently developed latch system as an example. It is stressed that consideration should be given to the idea of keeping reusable tools, unused life-support supplies, parts, fuel, and similar materials either in lunar or planetary orbits or on planetary surfaces for future use as logistics-support and safety backup, and to help reduce the payload of future space flights. P.G.

A69-43126 * #

SPUTTERING OF SOLID LUBRICANTS.

T. Spalvins (NASA, Lewis Research Center, Cleveland, Ohio).

University of Rochester and Bendix Corp., Symposium on the Deposition of Thin Films, 3rd, Rochester, N.Y., Sept. 9, 10, 1969, Paper. 13 p. 5 refs.

Solid film lubricants (Au, molybdenum disulfide, and tungsten disulfide) were deposited by dc triode sputtering on Ni, Ni-Cr, and Nb surfaces. These thin (2000 Å) sputtered films were tested in friction experiments under ultrahigh vacuum conditions to determine their effectiveness as a lubricant. It was found that these films had a low coefficient of friction and displayed exceptionally long endurance lives. The structure and characteristics of the films were

investigated using electron transmission microscopy and electron diffraction techniques. The sputtered Au films were crystalline and the particle size could be measured. The particle sizes for molybdenum disulfide, and tungsten disulfide were smaller than the limit of resolution by the above methods. Accordingly, they would be considered amorphous. (Author)

A69-43416

AIRCRAFT STRUCTURES AND MATERIALS APPLICATION; SOCIETY OF AEROSPACE MATERIAL AND PROCESS ENGINEERS, NATIONAL TECHNICAL CONFERENCE, SEATTLE, WASH., SEPTEMBER 9-11, 1969, PROCEEDINGS.

North Hollywood, Calif., Western Periodicals Co. (National SAMPE Technical Conference. Volume 1), 1969. 555 p.
$25.

CONTENTS:

PREFACE, p. V.
PREFACE. M. W. Heimerdinger, p. IX.

MANUFACTURING CONCEPTS.
DEVELOPMENT OF MAGNESIUM-LITHIUM ALLOY HONEYCOMB CORE. H. E. Pattee and R. E. Keith (Battelle Memorial Institute, Columbus, Ohio), p. 1-15. (See A69-43417 24-15)
DESIGN, FABRICATION AND TEST OF A BORON WING STRUCTURE. A. August, A. London, and W. Ludwig (Grumman Aerospace Corp., Bethpage, N.Y.), p. 17-27. (See A69-43418 24-15)
A PRACTICAL METHOD OF FABRICATING EFFICIENT AERO-STRUCTURES, UTILIZING UNIDIRECTIONAL BORON COMPOSITE WITH METAL. J. Henshaw, P. J. Roy, and M. D. Russell (Avco Corp., Lowell, Mass.), p. 29-40. (See A69-43419 24-15)
EVALUATION OF METHODS FOR REPAIR OF POLYIMIDE AND POLYIMIDE/TITANIUM SANDWICH COMPOSITES. G. E. Wintermute (Goodyear Aerospace Corp., Litchfield Park, Ariz.), p. 41-48. (See A69-43420 24-15)
ADVANCES IN THE CORROSION RESISTANCE OF BONDED STRUCTURES. R. B. Krieger, Jr. (American Cyanamid Co., Havre de Grace, Md.), p. 49-60. (See A69-43421 24-17)

ENVIRONMENTAL CONCEPTS IN DESIGN.
A SYSTEMS APPROACH TO FLAMMABILITY CONTROL FOR AEROSPACE SAFETY APPLICATION. F. Y. Hayashi and N. R. Kiehlo (North American Rockwell Corp., Anaheim, Calif.), p. 61-70. (See A69-43422 24-18)
A SYSTEM FOR RATING OXYGEN FLAMMABILITY OF AEROSPACE MATERIALS. J. W. McCain (North American Rockwell Corp., Canoga Park, Calif.), p. 71-81. 8 refs. (See A69-43423 24-18)
AEROSPACE APPLICATIONS FOR "KYNOL" FIBERS. L. C. Wohrer, F. J. Frechette, and J. Economy (Carborundum Co., Niagara Falls, N.Y.), p. 83-89. (See A69-43424 24-18)

MATERIALS APPLICATION.
ADHESIVE JOINTS FOR PRESTRESSING WOOD BEAMS. J. Peterson (Oregon State University, Corvallis, Ore.), p. 91-97. (See A69-43425 24-15)
JOINT CONCEPTS FOR CARBON COMPOSITE STRUCTURES. R. F. Zabora and J. T. Hoggatt (Boeing Co., Seattle, Wash.), p. 99-109. (See A69-43426 24-15)
COBALT-BASE ALLOYS IN AEROSPACE. F. R. Morral (Battelle Memorial Institute, Columbus, Ohio), p. 111-121. 24 refs. (See A69-43427 24-17)
FAILURE ANALYSIS AND CORROSION CONTROL. R. H. Williams (USAF, Materials Laboratory, Wright-Patterson AFB, Ohio), p. 123-139. (See A69-43428 24-15)
CONCORDE ELEVONS—AN EXERCISE IN EUTECTONY. R. L. Mordellet (Sud-Aviation, Suresnes, Hauts-de-Seine, France), p. 141-150. (See A69-43429 24-32)
MATERIALS SELECTION CRITERIA FOR AEROSPACE PRESSURE VESSEL CONSTRUCTION. T. J. Bosworth (Boeing Co., Seattle, Wash.), p. 151-170. 11 refs. (See A69-43430 24-15)

TITANIUM.
MANUFACTURING TECHNOLOGY IN TITANIUM. L. G. Orr (Boeing Co., Seattle, Wash.), p. 171-175. (See A69-43431 24-15)
THE CARE AND TREATMENT OF TITANIUM FROM INGOT TO FINISHED PRODUCT. R. H. Shoemaker (Kolene Corp., Detroit, Mich.), p. 177-200. (See A69-43432 24-15)
TITANIUM INVESTMENT CASTINGS. F. L. Parkinson (Boeing Co., Seattle, Wash.), p. 201-218. 5 refs. (See A69-43433 24-15)
METALLURGICAL AND STRUCTURAL ASPECTS OF DIFFUSION BONDED TITANIUM HONEYCOMB SANDWICH. D. H. Emero and M. J. Mejia (Stresskin Products Co., Santa Ana, Calif.), p. 219-229. 7 refs. (See A69-43434 24-15)
BRAZED TITANIUM HONEYCOMB SANDWICH. B. E. Kramer (Aeronca, Inc., Middletown, Ohio), p. 231-241. (See A69-43435 24-15)
STRUCTURAL MATERIALS FOR THE SST. L. J. Fielder (Boeing Co., Seattle, Wash.), p. 242-252. (See A69-43436 24-15)

FASTENERS.
RECENT DEVELOPMENTS IN STRUCTURAL AIRFRAME FASTENERS. F. L. Gill (Hi-Shear Corp., Torrance, Calif.), p. 253-260. (See A69-43437 24-15)
FATIGUE RESISTANT FASTENER. H. M. Wittmeyer and F. E. Smode (Huck Manufacturing Co., Detroit, Mich.), p. 261-269. 17 refs. (See A69-43438 24-15)
AEROSPACE FASTENER SYSTEMS—A PROPOSAL FOR STANDARDIZATION. M. J. Church (United Air Lines, Inc., San Francisco, Calif.), p. 271-276. 5 refs. (See A69-43439 24-15)
IMPROVING FASTENED STRUCTURAL FATIGUE. R. B. Whiteside (Standard Pressed Steel Co., Jenkintown, Pa.), p. 277-280. (See A69-43440 24-15)
MECHANICAL FASTENERS FOR HIGH TEMPERATURE STRUCTURE. J. N. Howell (Boeing Co., Seattle, Wash.), p. 281-283. (See A69-43441 24-15)
THE MOD LOOK IN AIRCRAFT FASTENER CORROSION CONTROL. E. Taylor (Standard Pressed Steel Co., Jenkintown, Pa.), p. 285-292. 18 refs. (See A69-43442 24-17)

COMPOSITE STRUCTURES.
OFF-AXIS COMPRESSIVE PROPERTIES OF FIBERGLASS/EPOXY FACED HONEYCOMB SANDWICH STRUCTURE. R. B. Lantz (Avco Corp., Nashville, Tenn.), p. 293-306. 13 refs. (See A69-43443 24-32)
COMPOSITE STRUCTURAL ELEMENTS FOR MISSILE INTERSTAGE APPLICATION. P. B. Kennedy (Boeing Co., Seattle, Wash.), p. 307-320. 9 refs. (See A69-43444 24-15)
FABRICATION AND EVALUATION OF MODMOR II CARBON FIBER REINFORCED P13N POLYIMIDE LAMINATES. E. A. Burns, R. W. Vaughan, and A. Toy (TRW Systems Group, Redondo Beach, Calif.), p. 321-330. 7 refs. (See A69-43445 24-15)
CHARACTERISTICS OF GRAPHITE FIBER/POLYIMIDE RESIN COMPOSITES. R. A. Pike and C. P. Maynard (United Aircraft Corp., East Hartford, Conn.), p. 331-349. 7 refs. (See A69-43446 24-18)
DEVELOPMENT OF HIGH MODULUS GRAPHITE/ASBESTOS REINFORCED LAMINATES. M. Varlas (General Dynamics Corp., San Diego, Calif.), p. 351-360. 5 refs. (See A69-43447 24-18)
MANUFACTURING CONCEPTS IN APPLICATION OF MOLDED ADVANCED COMPOSITES TO AEROSPACE COMPONENTS. L. W. Toth and T. J. Boller (Goodyear Aerospace Corp., Akron, Ohio), p. 361-368. (See A69-43448 24-15)
THERMAL/MECHANICAL STRENGTHENING OF 6061 Al-B COMPOSITES. J. F. Dolowy, Jr. and R. J. Taylor (Marquardt Corp., Van Nuys, Calif.), p. 369-377. (See A69-43449 24-17)
METALLOGRAPHIC STUDY OF FATIGUED UNIAXIAL BORON EPOXY COMPOSITES. J. G. Faller and R. B. Freeman

(Boeing Co., Philadelphia, Pa.), p. 379-390. 11 refs. (See A69-43450 24-18)

FRACTURE TOUGHNESS OF ALUMINUM-BORON COMPOSITES. N. R. Adsit and W. E. Witzell (General Dynamics Corp., San Diego, Calif.), p. 391-398. 7 refs. (See A69-43451 24-17)

EXPLOSIVE BONDING OF METAL MATRIX COMPOSITES. O. Y. Reece (NASA, Marshall Space Flight Center, Huntsville, Ala.), p. 399-415. (See A69-43452 24-15)

ELASTOMERS AND FOAMS.

SPRAYABLE POLYURETHANE FOAM INSULATION—SATURN S-II BOOSTER. C. Cerquettini (North American Rockwell Corp., Downey, Calif.), p. 417-419. (See A69-43453 24-18)

LOW DENSITY RTV SILICONE RUBBER SEALANTS. R. A. Smith (General Electric Co., Waterford, N.Y.), p. 421-426. (See A69-43454 24-18)

ELASTOMERS FOR THE SUPERSONIC TRANSPORT. R. A. Vickers and W. G. Joyce (Boeing Co., Seattle, Wash.), p. 427-437. (See A69-43455 24-18)

POLYURETHANE PROTECTIVE COATINGS FOR RADOME COVERS. R. J. Adler (Bendix Corp., North Hollywood, Calif.), p. 439-446. 8 refs. (See A69-43456 24-18)

RTV SILICONE RUBBER APPLICATIONS IN AIRCRAFT STRUCTURES. E. W. Beck (Dow Corning Corp., Costa Mesa, Calif.), p. 447-451. (See A69-43457 24-18)

ADHESIVES.

A NEW THEORY OF DYNAMIC ADHESION. E. P. Plueddemann (Dow Corning Corp., Midland, Mich.), p. 453-465. 41 refs. (See A69-43458 24-15)

THERMOPLASTIC BONDING IN NEW AIRCRAFT DESIGNS. A. B. Kerr (Furane Plastics, Inc., Los Angeles, Calif.), p. 467-472. (See A69-43459 24-15)

DYNAMIC MECHANICAL PROPERTIES OF ADHESIVES. D. K. Klapprott (Shell Chemical Co., Pittsburg, Calif.), p. 473-492. 9 refs. (See A69-43460 24-18)

THICKNESS OF ADHESIVE JOINTS IN SANDWICH STRUCTURES—THE MEASUREMENT AND ACCEPTANCE CRITERIA OF. H. Sanders and S. Westerback (Grumman Aerospace Corp., Bethpage, N.Y.), p. 493-521. (See A69-43461 24-32)

DEVELOPMENT OF ADHESIVE-BONDED JOINTS FOR GLASS RESIN COMPOSITE SANDWICH STRUCTURES. R. F. Wegman, M. J. Bodnar (U.S. Army, Picatinny Arsenal, Dover, N.J.), and S. F. Lutters (United Aircraft Corp., Stratford, Conn.), p. 523-539. (See A69-43462 24-32)

THE ANALYSIS OF ADHESIVE RESINS IN AEROSPACE APPLICATIONS. J. G. Hendrickson (Boeing Co., Renton, Wash.), p. 541-549. 13 refs. (See A69-43463 24-18)

ANAEROBIC ADHESIVES FOR STRUCTURAL AIRCRAFT BONDING. R. F. Barnes (Boeing Co., Renton, Wash.), p. 551-554. (See A69-43464 24-18)

MOUNTING OPTICAL COMPONENTS WITH ADHESIVES. C. V. Cagle and H. L. Lee (Epoxylite Corp., South El Monte, Calif.), p. 555-563. 7 refs. (See A69-43465 24-15)

A69-43452 *
EXPLOSIVE BONDING OF METAL MATRIX COMPOSITES.
Orvil Y. Reece (NASA, Marshall Space Flight Center, Astronautics Laboratory, Huntsville, Ala.).
IN: AIRCRAFT STRUCTURES AND MATERIALS APPLICATION; SOCIETY OF AEROSPACE MATERIAL AND PROCESS ENGINEERS, NATIONAL TECHNICAL CONFERENCE, SEATTLE, WASH., SEPTEMBER 9-11, 1969, PROCEEDINGS. (A69-43416 24-15)
North Hollywood, Calif., Western Periodicals Co. (National SAMPE Technical Conference. Volume 1), 1969, p. 399-415.

High-strength steel wire filaments and modular filament sheets were explosively bonded in metal matrices to form unidirectional filament reinforced composites. The lay-up procedures, explosives used, and problem areas are discussed. Tensile data and photomicrographs of the explosively bonded interfaces are presented.
(Author)

N69-10055*# National Aeronautics and Space Administration. Lewis Research Center, Cleveland, Ohio.
PERFORMANCE AND ANALYSIS OF SEALS FOR INERTED LUBRICATION SYSTEMS OF TURBINE ENGINES
Robert L. Johnson, William R. Loomis, and Lawrence P. Ludwig Washington Aug. 1968 24 p refs
(NASA-TN-D-4761) Avail: CFSTI CSCL 11A

An inerted lubricating system incorporating a 125-millimeter ball bearing and 6.33-inch(161-mm-) diameter face contact seals was operated for short duration screening runs in a simulated turbine engine sump at speeds to 14,000 rpm and bulk oil temperatures to 500°F. The ball bearings operated satisfactorily to 600°F outer race temperature under a 3280-pound (14,590 N) thrust load with four of the five lubricants evaluated in these short time runs. A peristent problem encountered was wear and leakage of the shaft seals. Additional experimental studies and analysis identified seal thermal deformation as a major factor in seal wear and leakage. New seals, revised to mitigate thermal deformations, were designed, analyzed, and subjected to preliminary experimental studies.
Author

N69-10228*# National Aeronautics and Space Administration. Lewis Research Center, Cleveland, Ohio.
EXPERIMENTS ON THE STABILITY OF WATER LUBRICATED HERRINGBONE-GROOVE JOURNAL BEARINGS. 1: THEORETICAL CONSIDERATIONS AND CLEARANCE EFFECTS
Frederick T. Schuller, David P. Fleming, and William J. Anderson Washington Nov. 1968 30 p refs
(NASA-TN-D-4883) Avail: CFSTI CSCL 13I

Hydrodynamic journal bearing stability tests were conducted with three different herringbone journal configurations. The bearings had a 1.5-inch (3.8-cm) diameter and were tested in water at 80°F (300°K) at speeds to 12,000 rpm, with unit loads to 36.9 psi (25.4×10^4 N/m^2). The stability of herringbone-groove journal bearings was far superior to that of a 100° partial-arc bearing, especially at zero load. No significant differences in the zero load threshold of stability were observed among the three different configurations of herringbone journal bearings tested. Theoretical analysis for herringbone-groove journal bearings predicts a larger range of stable operation than was observed experimentally.
Author

N69-10231*# National Aeronautics and Space Administration. Lewis Research Center, Cleveland, Ohio.
INCOMPRESSIBLY LUBRICATED RAYLEIGH STEP JOURNAL BEARING. 2: INFINITE-LENGTH SOLUTION
Bernard J. Hamrock and William J. Anderson Washington Nov. 1968 28 p refs
(NASA-TN-D-4873) Avail: CFSTI CSCL 13I

A theoretical analysis of pressure distribution, load capacity, attitude angle, and friction force was performed for an eccentric Rayleigh step journal bearing with varying numbers of steps and infinite length. The results indicated that one step placed around the journal was optimal. For small eccentricity ratios the optimal film thickness ratio was 1.7, while there were three optimal ratios of the angle subtended by the ridge to the angle subtended by the pad of 0.4, 0.45, and 0.5. These ratios depend on whether load capacity, or stability, or both load capacity and stability is more important in the application being considered.
Author

N69-10249*# National Aeronautics and Space Administration. Lewis Research Center, Cleveland, Ohio.
INFLUENCE OF SURFACE FILMS ON FRICTION AND DEFORMATION OF SINGLE CRYSTAL AND POLYCRYSTALLINE GOLD
Donald H. Buckley Washington Nov. 1968 23 p refs
(NASA-TN-D-4875) Avail: CFSTI CSCL 11F

Sliding friction experiments were conducted with single crystal and polycrystalline gold with various media present. These

included air, water, hexadecane, and hexadecane with 0.02 weight percent stearic acid; experiments were also conducted with various gold halide films formed on the surface. The alloying of copper with gold was also employed to improve the adsorbability of various media to gold. Results of the investigation indicate that ordinary atmospheric contaminants influenced the friction and deformation of gold. Water will not wet clean gold and thus provides the same friction and deformation behavior as that observed in air. The halides of gold all reduced friction and deformation of gold; the most effective halides were the chlorides for friction and iodides for deformation. The addition of a small concentration of copper to gold improved the ability of an organic acid to lubricate gold. Author

N69-10298*# Franklin Inst., Philadelphia, Pa. Research Labs.
STUDY OF PRETESTING EFFECTS ON ELECTROEXPLOSIVE DEVICES
M. G. Kelly and R. G. Amicone Washington NASA Nov. 1968 70 p refs
(Contract NAS1-6281)
(NASA-CR-1203; F-C1859) Avail: CFSTI CSCL 19A

The answers to a questionnaire sent to various NASA installations and suppliers dealing with the currently used pretesting practices are discussed. The currents used for bridge resistance and continuity checks vary from 20 μ amps to 20 mamps. No-fire and/or "1 amp, 1 watt" pretests are applied by almost all users and suppliers. Voltage breakdown and dielectric strength tests use voltages ranging from 50 to 1400 volts. Electrostatic tests involve voltages of from 9 to 25 KV applied to the EED from a 500 pf capacitor. The no-fire test was judged to be one of the most severe pretests if applied to EEDs intended for actual use. Experiments were performed on EEDs using the results of the questionnaire as a guide. A severe version of the voltage breakdown test was used to condition COMMAND squibs, FOX squibs and MASSEY-1000 igniters. Subsequent tests showed no significant changes in the constant current sensitivity, functioning time, electrostatic sensitivity, and bridgewire power sensitivity due to the conditioning. A technique for the theoretical analysis of pretest effects is presented. Some knowledge of the EED thermal parameters is required for this approach. Author

N69-10370*# National Aeronautics and Space Administration. Lewis Research Center, Cleveland, Ohio.
INFLUENCE OF NUMBER OF OPERABLE SLIP SYSTEMS ON FRICTION CHARACTERISTICS OF SINGLE-CRYSTAL AND POLYCRYSTALLINE MAGNESIUM
Donald H. Buckley Washington Jan. 1968 14 p refs
(NASA-TN-D-4351) Avail: CFSTI CSCL 11F

An investigation was conducted to determine the influences of a change in the number of operable slip systems in magnesium on its friction behavior. Friction experiments were conducted with a hemisphere sliding on a flat disk surface. The load was 50 grams and the sliding velocity was 0.001 centimeter per second. Single crystals of basal and prismatic orientations and polycrystalline magnesium were examined over the temperature range of $-195°$ to 90°C. The results of this investigation indicate that the friction properties of magnesium, like other hexagonal metals, are anisotropic. Friction is lower on the basal than on the prismatic plane by a factor of 2. Multiple slip introduces greater ductility in polycrystalline magnesium and increases the friction. Friction is the lowest for polycrystalline magnesium at those temperatures where basal is the primary deformation slip mechanism. Author

N69-10757*# National Aeronautics and Space Administration. Goddard Space Flight Center, Greenbelt, Md.
SLIDING FRICTION OF COPPER ALLOYS IN VACUUM
Jane Jellison, Roamer Predmore, and C. L. Staugaitis Washington Nov. 1968 20 p refs
(NASA-TN-D-4824) Avail: CFSTI CSCL 11F

Sliding friction experiments involving copper and Cu-Be alloy plates in contact with copper, Cu-Be alloy, steel and titanium alloy sliders were performed in air and vacuum. Microhardness and metallographic examination of plate and slider interface suggests friction and wear by the adhesive friction mechanism with prow formation. Transfer of strain hardened metal wear debris across the sliding interface was observed. The friction coefficient and the prow size generally increased in vacuum. Author

N69-13256*# National Aeronautics and Space Administration. Lewis Research Center, Cleveland, Ohio.
STABILITY ANALYSIS FOR UNLOADED EXTERNALLY PRESSURIZED GAS-LUBRICATED BEARINGS WITH JOURNAL ROTATION
David P. Fleming, Robert E. Cunningham, and William J. Anderson Washington Dec. 1968 35 p refs
(NASA-TN-D-4934) Avail: CFSTI CSCL 13I

A small eccentricity analysis was performed for a bearing with two feeding planes, each of which is assumed to be a line source. Numerical results were obtained for a range of bearing number, pressure ratio, feeding parameter, and orifice recess volume A digital computer program was written to obtain these results and is included. Steady-state load and attitude angle were obtained, as well as stability data. Stability decreased markedly with increasing recess volume; moreover, for large recess volume and low bearing number, an increase in pressure ratio decreased stability. There was no correlation between stability and steady-state attitude angle for any of the cases studied. Fair agreement was obtained with available experimental data. Author

N69-14082*# National Aeronautics and Space Administration. Lewis Research Center, Cleveland, Ohio.
AN ANALYTICAL METHOD FOR PREDICTING THE PERFORMANCE OF CENTRIFUGAL PUMPS DURING PRESSURIZED STARTUP
Wojciech Rostafinski Washington Jan. 1969 40 p refs
(NASA-TN-D-4967) Avail: CFSTI CSCL 13K

The pressure drop characteristics of centrifugal pumps during pressurized startup were studied analytically. Mathematical expressions for negative head characteristics were developed and applied to the prediction of pressure drop characteristics for three pumps. Comparison of calculated and experimental performance points verified the analytical method developed. Author

N69-14214*# Ampex Corp., Redwood City, Calif.
STUDY, FABRICATION AND TESTING OF A FOIL-BEARING ROTOR SUPPORT SYSTEM
L. Licht and A. Eshel Washington NASA Nov. 1968 233 p refs
(Contract NASw-1456)
(NASA-CR-1157; RR-68-2) Avail: CFSTI CSCL 13I

Tests are conducted in both the vertical and horizontal attitudes, in excess of rated speed, 60,000 rpm, with the foil bearing stable and free from "half-frequency whirl" encountered in conventional gas-lubricated journal bearings. External pressurization is applied briefly to separate the foil surfaces from the journal during the initial and final stages of rotation only, with adequate self-acting support and foil separation established at approximately 6000 rpm. The response of the foil-rotor system to residual unbalance and to impact is studied. The foil-rotor assembly housing is mounted on a vibrator and subjected to excitation normal to the axis of rotation. Measured gap widths and results predicted by theory are compared, and an attempt is made to account for the effects of inertia and compressibility of the fluid, of extensibility and temperature increase of the foil, and of friction of the foil supports. The potential and practicality of gas-lubricated foil bearings for high-speed turbomachines is demonstrated, with the following advantages: (1) Stability (freedom from "half-frequency whirl); (2)

Tolerance of distortion and misalignment, coupled with excellent wipe-wear characteristics; and (3) Ability to accommodate excursions of journals exceeding by an order of magnitude the clearance of rigid-surface gas bearings. Author

N69-14241*# National Aeronautics and Space Administration, Washington, D. C.
JOINING CERAMICS AND GRAPHITE TO OTHER MATERIALS
H. E. Pattee, R. M. Evans, and R. E. Monroe 1968 89 p refs
(NASA-SP-5052) Avail: SOD $1.00 CSCL 13H

In discussing the joining of bulk ceramics to metals and other materials, this report emphasized ceramic-to-metal joining as applied in the electronics industry. However, the techniques developed for joining ceramics to the metals of interest to the electronics industry can usually be applied to other materials as well. Data are summarized on joining ceramics to other materials available from Government and industrial research. Much of the research was prompted by a need to develop joining or sealing techniques for specific applications which are related throughout the report in hope that the information can be applied to applications that are similar or involve unusual materials or service conditions. The sections include: a review of ceramics, metals, and brazing filler metals; joint configurations and surface preparation; the theory of ceramic-to-metal joining; fusion, solid phase, gas-pressure, and solid liquid phase joining; and fusion and nonfusion joining of graphite. B.P.

N69-14383*# National Aeronautics and Space Administration. Lewis Research Center, Cleveland, Ohio.
ROLLING-ELEMENT FATIGUE LIFE OF AUSFORMED M-50 STEEL BALLS
Richard J. Parker and Erwin V. Zaretsky Washington Dec. 1968 17 p refs
(NASA-TN-D-4954) Avail: CFSTI CSCL 13I

Rolling element fatigue lives of a group of ausformed consumable electrode vacuum melted steel balls were compared with two groups of conventionally processed balls in the NASA five-ball fatigue tester. Results indicate an inprovement in fatigue life with the ausformed balls at least three times that of the conventionally processed balls. Author

N69-16104*# Kaman Aircraft Corp., Bloomfield, Conn.
THE BOSSLER COUPLING
R. J. Mayerjak and R. B. Bossler, Jr. Washington NASA Jan. 1969 119 p refs
(Contract NASw-1554)
(NASA-CR-1241; KAMAN-R-741) Avail: CFSTI CSCL 13I

A flexible drive-shaft coupling which is suitable for any level of power transmission is reported. This report presents the results of an investigation of the mechanical characteristics of the couplings. The investigation included analyses and tests. Simplified coupling analysis methods, parameter studies, and design guidelines were developed. The test areas include torsion, stiffness, strain, fatigue, constancy of velocity, critical speed, and balancing. The tests substantiated the analyses for predicting internal forces and moments, steady and alternating stress, bending and change-of-length stiffness, critical speeds, and the effects of unbalance. The coupling has unusual capability for accommodating combined axial motion, misalignment, and torque. The coupling can survive shock-torque greatly in excess of ultimate continuous torque and transient misalignments over three times the design continuous operating angle. Author

N69-16197*# National Aeronautics and Space Administration. Lewis Research Center, Cleveland, Ohio.
THE EFFECT OF ORIENTATION AND THE PRESENCE OF SURFACE ACTIVE MATERIALS ON THE FRICTION, DEFORMATION AND WEAR OF ALUMINUM
Donald A. Buckley Washington Jan. 1969 25 p refs
(NASA-TN-D-4994) Avail: CFSTI CSCL 20K

Sliding friction experiments were conducted on single crystal and polycrystalline aluminum surfaces. The influence of the following on friction, deformation and wear were determined: (1) orientation of single crystals and textured polycrystalline sheet, (2) liquid metal embrittlement, (3) surface active organics, and (4) alloying with silver. Results indicate that friction and wear of aluminum is highly anisotropic. With single crystals, friction and wear are sensitive both to atomic plane and crystallographic direction of sliding. The presence of embrittling liquid metals on the surface of aluminum was found to reduce surface deformation during sliding. The presence of organic acids and alcohols were found to increase the deformability of oxidized aluminum surfaces. Author

N69-16367*# National Aeronautics and Space Administration. Lewis Research Center, Cleveland Ohio.
ROLLING-ELEMENT BEARING LIFE FROM 400° TO 600°F
Edwin V. Zaretsky, William J. Anderson, and Eric N. Bamberger (GE, Cincinnati) Washington Jan. 1969 23 p refs
(NASA-TN-D-5002) Avail: CFSTI CSCL 13I

Rolling-element fatigue tests were conducted with 120-mm bore angular-contact ball bearings made of AISI M-50 steel using a synthetic paraffinic oil at temperatures of 400° to 600°F. Bearing life in this temperature range exceeded AFBMA-predicted (catalog) life by a factor greater than 13. Failure was by classical subsurface rolling-element fatigue. Under simulated conditions EHD minimum film thicknesses ranged from 10 to 5 microinches for temperatures from 400° to 600°F, respectively. Author

N69-16463*# United Aircraft Corp., East Hartford, Conn.
BRAYTON-CYCLE TURBOMACHINERY ROLLING-ELEMENT BEARINGS
R. Cohen, H. Means, and P. Heyl Washington NASA Jan. 1969 288 p refs
(Contract NAS3-7635)
(NASA-CR-1229) Avail: CFSTI CSCL 13I

Evaluated were candidate Brayton-cycle turbomachinery configurations incorporating gas bearings. Pratt and Whitney Aircraft has conducted a development effect on a flight-type rolling element rotor support system to provide a backup to the gas bearing approach. This program included the design of two-shaft results of welded specimens. The first two proofmass assemblies to be welded by the laser method were experimental vehicles in the effort to isolate the source of null bias shifts observed on a standard Model 7 instrument after exposure to sterilization temperature. Modifications of the design will be necessary to reduce the constrainment current from approximately 100 ma. Author

N69-17988*# National Aeronautics and Space Administration. Electronics Research Center, Cambridge, Mass.
INTRODUCTION TO COMPUTER AIDED RELIABILITY DATA ANALYSIS
Charles R. Toye Washington Feb. 1969 80 p refs
(NASA-TN-D-5009) Avail: CFSTI CSCL 14D

This report describes the significant features required for the collection, coding, and documentation of hi-rel test data. It also contains a user's manual for the CARDA program, a third-generation computer program designed to fulfill the data reduction, analysis, and presentation requirements found in high reliability component specifications. Author

N69-19775*# Franklin Inst., Philadelphia, Pa. Research Labs.
HIGH PERFORMANCE TURBOALTERNATOR AND ASSOCIATED HARDWARE. 3. DESIGN OF BACKUP GAS BEARINGS

15 MACHINE ELEMENTS AND PROCESSES

W. Shapiro, J. T. McCabe, T. W. Chu, and V. Castelli Washington NASA Feb. 1969 150 p refs Prepared for Pratt and Whitney Aircraft
(Contract NAS3-6013)
(NASA-CR-1292; F-B2263; PWA-3070-Vol-3) Avail: CFSTI CSCL 13I

A detailed description of a program is presented for the analysis and design of a gas (argon) bearing system for a Brayton cycle turbo-alternator that produces electric power in a space vehicle. Because of the complex nature of the lubrication problem, the analysis was accomplished by numerical methods programmed on a digital computer. For both the thrust and journal bearings, steady-state and dynamic analyses were accomplished. The steady-state results provided parametric performance over a wide range of operating conditions. The more complicated and lengthy dynamic analysis was used to establish the stability of the bearings and bearing-rotor system using geometric variables selected on the basis of steady-state results. Steady-state performance of both the journal and thrust bearings is considered excellent and stability characteristics of the journal bearings are marginal. Author

N69-19786*# Hydronautics, Inc., Laurel, Md.
EXPERIMENTAL AND ANALYTICAL INVESTIGATIONS ON MULTIPLE LIQUID IMPACT EROSION
A. Thiruvengadam and S. L. Rudy Washington NASA Mar. 1969 102 p refs
(Contract NASw-1608)
(NASA-CR-1288; TR-719-1) Avail: CFSTI CSCL 11F

Results are summarized concerning the erosion of 1100-O aluminum and 316 stainless steel. A rotating-disk facility was used to test six specimens simultaneously at three different velocities. High speed and conventional motion pictures with stroboscopic illumination were taken to show the qualitative phenomenon of liquid jet impact. The threshold impact velocity at which erosion was observed after ten million impacts was determined. The threshold water hammer stress on the material corresponding to this threshold velocity was correlated with the high frequency endurance limit corresponding to ten million fatigue cycles using the magnetostriction vibratory apparatus. The ratio between the fatigue endurance limit and the water hammer stress is 1.7 for the aluminum and 3.0 for the stainless steel. A mathematical theory to predict the rate of cavitation erosion as a function of exposure time was extended to multiple liquid impact erosion. The results indicate that the peak rate of erosion varies as the fifth power of the velocity of impact; the observed time of the peak rate varies as the one-fifth power of the impact velocity. Scanning electron microphotographs of specimens eroded both by cavitation and by liquid impingement were compared, and an apparent similarity in the material removal processes further justifies the use of a common theory. K.W.

N69-19800*# National Aeronautics and Space Administration. Lewis Research Center, Cleveland Ohio.
FRICTION AND WEAR OF NINE SELECTED POLYMERS WITH VARIOUS FILLERS IN LIQUID HYDROGEN
Donald W. Wisander and Robert L. Johnson Washington Mar. 1969 20 p refs
(NASA-TN-D-5073) Avail: CFSTI CSCL 11I

Experiments were conducted with a 0.1875-inch- (0.476-cm-) radius hemisphere of nine polymers in sliding contact with a rotating 17-4 PH disk in liquid hydrogen. Sliding velocity was 2300 feet per minute (701 m/min) at a load of 1 kilogram. Results indicate that several filled polymers show promise. Graphite-filled polyamide (nylon), graphite filled and glass-fiber-filled polytrifluorochlorethylene (PTFCE), and a 50-percent polytetrafluoroethylene (PTFE)–50-percent polyparaphenyl have friction and wear similar to filled-PTFE composites commonly used in cryogenic applications. Author

N69-20938*# National Aeronautics amd Space Administration. Lewis Research Center, Cleveland, Ohio.
LUBRICATION WITH SOME POLYPHENYL ETHERS AND SUPERREFINED MINERAL OILS IN A 600° F (316° C) INERTED VANE PUMP LOOP
William R. Jones, Jr., William F. Hady, and Max A. Swikert Washington Mar. 1969 18 p refs
(NASA-TN-D-5096) Avail: CFSTI CSCL 11H

A vane pump loop was used to determine the lubricating ability as well as thermal and shear degradation of some polyphenyl ethers and superrefined mineral oils. Experimental conditions included 250 psig pump pressure, 425° F (219° C) fluid temperature at the pump inlet, 600° F (316° C) fluid temperature at the heater outlet, 1.73×10^4 m/hr surface velocity and an inert cover gas (nitrogen). Low vane wear was obtained with a 77 centistoke (100° F) (38° C) napthenic mineral oil and two naphthenic-paraffinic blends. Higher wear was obtained with a 15 centistoke (100° F) (38° C) paraffinic mineral oil, a four and a five ring polyphenyl ether, and a modified polyphenyl ether (C-ether). Author

N69-20939*# National Aeronautics and Space Administration. Lewis Research Center, Cleveland, Ohio.
PRELIMINARY INVESTIGATION OF GRAPHITE FLUORIDE $(CF_x)_n$ AS A SOLID LUBRICANT
Robert L. Fusaro and Harold E. Sliney Washington Mar. 1969 20 p refs
(NASA-TN-D-5097) Avail: CFSTI CSCL 11H

Friction and wear life studies were conducted on burnished (rubbed on) films of a potential, new, solid lubricant $(CF_x)_n$. Results were compared with those of similar tests for graphite and MoS_2. The comparisons showed that, at any one specific temperature, the wear lives of $(CF_x)_n$ films exceeded those of graphite or MoS_2. Also, the friction coefficient of $(CF_x)_n$ was less than that of graphite and approximately equal to that of MoS_2. The upper temperature limitation of the $(CF_x)_n$ burnished films is about 400° C. The influence of the fluorine-to-carbon ratio in the compound was investigated and did not seem to be of importance in the range considered (1.12 to 0.7). Author

N69-21772*# Mechanical Technology, Inc., Latham, N. Y.
HIGH-PERFORMANCE TURBOALTERNATOR AND ASSOCIATED HARDWARE. 2: DESIGN OF GAS BEARINGS
A. Frost, J. W. Lund, and P. W. Curwen Washington NASA Mar. 1969 349 p refs Prepared for Pratt and Whitney Aircraft, East Hartford, Conn.
(Contract NAS3-6013)
(NASA-CR-1291; MTI-67TR29; PWA-3070-Vol-2) Avail: CFSTI CSCL 13I

The National Aeronautics and Space Administration is conducting an evaluation of Brayton cycle turbomachinery configurations. As part of this program, a turboalternator incorporating a two stage axial-flow turbine driving an inductor alternator supported on gas bearings has been designed. The gas bearings were designed and successfully tested in a gas bearing dynamic simulator. Testing of the simulator under full electrical load and under certain electrical fault conditions indicated satisfactory operation of the rotor system. Author

N69-22970*# National Aeronautics and Space Administration. Lewis Research Center, Cleveland, Ohio.
PERFORMANCE AND EVALUATION OF TWO LIQUID-METAL PUMPS FOR SODIUM-POTASSIUM SERVICE
Sol H. Gorland, Thomas P. Hecker, and Roy A. Lottig Washington Apr. 1969 16 p refs
(NASA-TM-X-1765) Avail: CFSTI CSCL 13L

Two identical hermetically-sealed motor-driven centrifugal pumps operated for 1483 hours in NaK loops, one at 1150° F

(895 K) and the other at 450° F (505 K). The pumps incorporate NaK-lubricated tilting-pad journal and thrust bearings, and were designed to withstand a nuclear radiation environment. The induction motors were "canned" inside the pump housings to eliminate the need for absolute seals between the pump and the motor. Both pumps operated successfully for the 1483 hours without maintenance. There were no parametric excursions outside the envelopes considered safe for 10,000 or more hours of operation. Author

N69-22992*# National Aeronautics and Space Administration. Lewis Research Center, Cleveland, Ohio.

THE THERMAL STABILITY AND FRICTION OF THE DISULFIDES, DISELENIDES, AND DITELLURIDES OF MOLYBDENUM AND TUNGSTEN IN VACUUM

William A. Brainard Washington Apr. 1969 24 p refs

(NASA-TN-D-5141) Avail: CFSTI CSCL 11F

Thermal stability and friction experiments were conducted with the disulfides, diselenides, and ditellurides of molybdenum and tungsten in ultrahigh vacuum. Weight loss rates were plotted as a function of temperature: thermal dissociation temperatures were observed by mass spectrometry. Friction experiments showed the materials were limited as high temperature lubricants by evaporation, dissociation, and wear. Generally, as lubricants, the diselenides provided the best performance up to 1400° F, whereas the ditellurides provided the poorest because of a low thermal dissociation temperature. Author

N69-23232*# National Aeronautics and Space Administration. Lewis Research Center, Cleveland, Ohio.

SHAFT FACE SEAL WITH SELF-ACTING LIFT AUGMENTATION FOR ADVANCED GAS TURBINE ENGINES

Robert L. Johnson and Lawrence P. Ludwig Washington Apr. 1969 23 p refs

(NASA-TN-D-5170) Avail: CFSTI CSCL 11A

The need in advanced engines for shaft seals with improved pressure, temperature, and speed capabilities is pointed out. In particular, the high speed requirement suggests that the seals must not have rubbing contact. Labyrinth seals have disadvantages in high leakage (efficiency loss) and debris entrainment, and conventional face seals are subject to high wear because face deformation can increase seal closing force and thus cause heavy rubbing contact. It is shown that incorporation of self-acting lift pads to the conventional face seal prevents rubbing contact even though face deformation occurs; feasibility was demonstrated in 560 hours of operation at 100-pound-per-square-inch pressure differential, 600° F gas temperature, and 380-feet-per-second sliding speed. Positive separation of the sealing faces with acceptable leakage rates was obtained. Proposed advanced systems using seals with self-acting lift pads are described. Author

N69-23466*# National Aeronautics and Space Administration. Lewis Research Center, Cleveland, Ohio.

VIBRATION OF SHAFT FACE SEALS AND STABILIZING EFFECT OF VISCOUS AND FRICTION DAMPING

Thomas N. Strom, Lawrence P. Ludwig, and John C. Hudelson Washington Apr. 1969 20 p refs

(NASA-TN-D-5161) Avail: CFSTI CSCL 13I

In inert and reducing environments both at room and elevated temperatures, undamped seals operated with severe vibration which caused early bellows fatigue and high leakage rates of a 1.57 inch (3.99 cm) mean diameter seal operating to speeds of 165 feet per second (50.3 m/sec) at 24 000 rpm. Friction damping by mechanical dampers and the viscous damping by oil in the bellows were both effective in maintaining seal stability. Nosepiece temperatures caused by the sliding contact were high enough to reduce hardness of the mating seal seats. Author

N69-23768*# National Aeronautics and Space Administration. Lewis Research Center, Cleveland, Ohio.

PERFORMANCE AND EVALUATION OF A LIQUID-METAL PUMP FOR MERCURY SERVICE

Sol H. Gorland, Roy A. Lottig, and Thomas P. Hecker Washington May 1969 14 p refs

(NASA-TM-X-1766) Avail: CFSTI CSCL 13I

An induction-motor-powered centrifugal pump operated successfully for 1455 hr at a mercury loop at 350° to 400°F (450 to 480 K) without maintenance. Approximately 1325 hr were at the steady-state condition of 11 570 lb/hr (5250 kg/hr) flow with a head of 83.2 ft (249 J/kg). Polyphenyl-ether-lubricated ball bearings were used in the pump. Author

N69-24791*# National Aeronautics and Space Administration. Lewis Research Center, Cleveland, Ohio.

EXPERIMENTAL STUDY OF PUMP AND SEAL CHARACTERISTICS OF HELICAL GROOVE GEOMETRY INCORPORATED IN A COMBINED BEARING AND PUMP

Lawrence P. Ludwig, Thomas N. Strom, and Robert L. Johnson Washington May 1969 27 p refs

(NASA-TN-D-5225) Avail: CFSTI CSCL 13I

Combined bearing and pump rotors with 14.5° and 20° helix grooves were evaluated in a hermetically sealed pump. Oil, water, freon, and mercury were used in the studies at Reynolds numbers (based on clearance) between 2 and 2800. As predicted by theory, the pump pressure rise was linearly related to rotor peripheral velocity at low Reynolds numbers (2 to 12); however, between the investigated Reynolds numbers of 300 to 2800, the pump pressure rise varied with velocity raised to a power between 1.76 and 1.85. Above a Reynolds number of 1000, experimental friction factors were greater than those of other published experimental data. Maximum pump efficiencies were in the range of 2 to 3 percent for operation with water and freon. Torque data indicate that full fluid film lubrication was obtained with oil, water, freon, and mercury. Author

N69-24932*# National Aeronautics and Space Administration. Lewis Research Center, Cleveland, Ohio.

EXPERIMENTS ON POWER LOSS IN HERRINGBONE GROOVED, GAS-LUBRICATED JOURNAL BEARINGS

David P. Fleming, Robert E. Cunningham and William J. Anderson Washington May 1969 22 p refs

(NASA-TN-D-5224) Avail: CFSTI CSCL 13I

Power loss was determined for herringbone journal bearings operating in air to speeds of 60,000 rpm. Power loss (relative to that calculated for a plain bearing of the same dimensions) did not vary widely for the range of geometric variables used. Relative power loss increased with speed and was generally higher than for a plain bearing. The dimensional value of power loss was higher than that in a reference tilting pad bearing at a speed of 38,500 rpm. Author

N69-26311*# National Aeronautics and Space Administration. Lewis Research Center, Cleveland, Ohio.

EFFECT OF OXYGEN CONCENTRATION ON AN ADVANCED ESTER LUBRICANT IN BEARING TESTS AT 400° AND 450°F

Richard J. Parker and Erwin V. Zaretsky Washington Jun. 1969 14 p refs

(NASA-TN-D-5262) Avail: CFSTI CSCL 13I

Tests were run with 20-mm bore angular-contact ball bearings at 400° and 450°F (477 and 505 K) to determine the effects of oxygen concentration on the oxidation of an advanced Type II ester. The bearings were run at 10 600 rpm and 70-pound thrust load. Oxygen content of the gas in the bearing chamber was varied from less than 0.1 percent to approximately 21 percent by volume. Increases in bearing torque, lubricant viscosity, and acid number

were used as indicators of lubricant oxidation and degradation. The advanced ester exhibited less oxidation than did a synthetic paraffinic oil under similar test conditions. A time limitation (induction period) on the effectiveness of the oxidation inhibitor in the ester was indicated. Author

N69-26314*# National Aeronautics and Space Administration. Lewis Research Center, Cleveland, Ohio.
EFFECT OF OXYGEN CONCENTRATION ON THE PERFORMANCE OF SYNTHETIC PARAFFINIC OILS IN SHORT TERM BEARING TESTS FROM 400° TO 500°F
Richard J. Parker and Erwin V. Zaretsky Washington May 1969 18 p refs
(NASA-TN-D-5152) Avail: CFSTI CSCL 13I

The effect of ambient oxygen concentration on the performance of a synthetic parafinic oil with and without an oxidation inhibitor was studied in bearing tests at 400° to 500°F. Bearing torque increase was correlated with increases in lubricant viscosity due to lubricant oxidation. The viscosity and total acid number of the uninhibited oil increased as oxygen concentration increased. The viscosity increases were attributed to bearing operation in the presence of oxygen. Tests with the bearing not rotating produced relatively small increases in viscosity. The oxidation inhibitor significantly reduced oxidation of the oil at 400°F for oxygen concentrations up to 21 percent. Longer term bearing tests at 400°F show a limitation on the effective life (induction period) of the lubricant with the oxidation inhibitor. Author

N69-27078*# National Aeronautics and Space Administration. Lewis Research Center, Cleveland, Ohio.
EXPERIMENTS ON ROTATING EXTERNALLY PRESSURIZED, AIR JOURNAL BEARINGS. PART 1: LOAD CAPACITY AND STIFFNESS
Robert E. Cunningham, David P. Fleming, and William J. Anderson Washington Jun. 1969 17 p refs
(NASA-TND-5191) Avail: CFSTI CSCL 13I

A series of tests was conducted to determine the load and stiffness characteristics of a pair of orifice-compensated, externally pressurized journal bearings. The diameters were a nominal 6.3 cm and the length 9.5 cm. Each bearing was equipped with 12, 0.56-mm diameter orifices. The orifices were arranged in two circumferential planes, six equally spaced in each plane. Results were obtained at an average radial clearance of 0.034 mm over a speed range of 0 to 25,000 rpm. Radial loads were varied up to 189 pounds per bearing or 20.2 psi unit load and air supply pressure ratios from 1.7 to 6. The results of these tests show that load capacity is generally less than that predicted by linearized PH theory or by pressure perturbation theory. Agreement is fair at eccentricity ratios up to 0.1 and at higher supply pressures. A comparison of test results with the two perturbation theories shows that the observed load capacity data agree better with the pressure perturbation theory. Overall load capacity is increased by shaft rotation (self-acting effects). The increase is greatest at the higher eccentricity ratios and lower supply pressures. Experimental data of stiffness as a function of compressibility number are in close agreement with theory at the higher supply pressures. Author

N69-27955*# National Aeronautics and Space Administration. Lewis Research Center, Cleveland, Ohio.
EXPERIMENTS ON THE STABILITY OF WATER LUBRICATED HERRINGBONE-GROOVE JOURNAL BEARINGS. 2: EFFECTS OF CONFIGURATION AND GROOVE TO RIDGE CLEARANCE RATIO
Frederick T. Schuller, David P. Fleming, and William J. Anderson Washington Jun. 1969 24 p refs
(NASA-TN-D-5264) Avail: CFSTI CSCL 13I

Hydrodynamic stability tests in water were performed on six 1.5-in.-(3.8-cm-) diameter herringbone-grooved journals having 10, 20, or 40 full or partial grooves. A maximum speed of 11,500 rpm with stable operation at zero load was attained. The number and length of grooves did not appreciably affect the zero load stability limits of the herringbone-grooved journal bearings. Generally, the herringbone-grooved journals had maximum stability (a maximum fractional frequency whirl onset speed) when the groove to ridge clearance ratio was closest to 2.1 as predicted by incompressible flow theory. Author

N69-27956*# National Aeronautics and Space Administration. Lewis Research Center, Cleveland, Ohio.
EXPERIMENTS ON ROTATING EXTERNALLY PRESSURIZED AIR JOURNAL BEARINGS. 2: ATTITUDE ANGLE AND AIR FLOW
Robert E. Cunningham, David P. Fleming, and William J. Anderson Washington Jun. 1969 15 p refs
(NASA-TN-D-5192) Avail: CFSTI CSCL 13I

Experimental attitude angles and airflow are compared with theory for a pair of 2-1/2-inch (6.3-cm) diameter by 3-3/4-inch (9.5-cm) long externally pressurized air bearings. Attitude angles vary with shaft speed as predicted by small-eccentricity pressure perturbation theory but are generally larger in magnitude. The attitude-eccentricity locus of the journal center for a supply pressure ratio of 1.7 is similar to that of a plain selfacting bearing. Measured airflows were in excellent agreement with calculated values. Shaft speeds varied from 0 to 25,000 rpm, and radial loads varied up to 20.2 psi (139 kN/m^2). The supply pressure range covered was approximately 24 to 88 psia (169 to 610 kN/m^2). Author

N69-28592*# Franklin Inst., Philadelphia, Pa. Research Labs.
NASA CONTRIBUTIONS TO FLUID-FILM LUBRICATION: A SURVEY
1969 202 p refs
(Contract NSR-39-005-015)
(NASA-SP-5058) Avail: SOD $2.00 CSCL 11H

A comprehensive review is presented of fluid-film lubrication technology which benefitted from research and development in the aerospace field. The contents include chapters on: space age bearing and lubrication requirements; principles of full fluid-film lubrication; state of the art at the onset of the space age; incompressible hydrostatic lubrication; compressible hydrostatic lubrication; incompressible hydrodynamic lubrication; compressible hydrodynamic lubrication; squeeze-film lubrication; and the impact of NASA generated contributions. B.P.

N69-28862*# National Aeronautics and Space Administration. Lewis Research Center, Cleveland, Ohio.
A PROCEDURE FOR FURNACE BRAZING BUTT JOINTS IN TUNGSTEN-URANIUM DIOXIDE CERMET CYLINDERS AT 3000°C
Thomas J. Moore and Donald W. Adams Washington Jun. 1969 22 p refs
(NASA-TM-X-1815) Avail: CFSTI CSCL 13H

A procedure was developed to successfully join the longitudinal

seam of a tungsten–uranium dioxide cermet cylinder by furnace brazing. Brazing was done in helium at 3000°C with a tungsten – 25-weight-percent osmium braze alloy. A moderate loss of tensile strength of the cermet parent material at 2500°C occurred due to the brazing cycle. The loss in strength was attributed to increased grain size of the tungsten matrix and possibly to migration of UO_2 along the grain boundaries of the tungsten matrix. Author

N69-29165*# National Aeronautics and Space Administration. Lewis Research Center, Cleveland, Ohio.

METHOD FOR PREDICTION OF PUMP CAVITATION PERFORMANCE FOR VARIOUS LIQUIDS, LIQUID TEMPERATURES, AND ROTATIVE SPEEDS

Robert S. Ruggeri and Royce D. Moore Washington Jun. 1969 33 p refs

(NASA-TN-D-5292) Avail: CFSTI CSCL 13K

A method for predicting the cavitation performance of pumps with various liquids, liquid temperatures, and rotative speeds is presented. Both theoretical and experimental studies used in formulating the method are discussed. Good agreement was obtained in comparisons between experimental and predicted results of cavitation performance for several pumps operated in liquids that exhibit a wide range of physical properties. Use of the method requires that two sets of test data be available for the pump and operating conditions of interest, but these data need not be for the same liquid, temperature, or pump speed. Numerical examples are presented. Author

N69-29476*# National Aeronautics and Space Administration. Lewis Research Center, Cleveland, Ohio.

INVESTIGATION OF TWO-PHASE HYDROGEN FLOW IN PUMP INLET LINE

Donald C. Urasek, Phillip R. Meng, and Robert E. Connelly Washington Jul. 1969 17 p refs

(NASA-TN-D-5258) Avail: CFSTI CSCL 13K

An investigation was conducted to evaluate the vapor- to mixture-volume ratio present in the inlet line of a pump when liquid hydrogen is pumped in a boiling condition from a sealed tank. Both an experimental and an analytical approach were used. The good agreement obtained between the experimental and analytical results indicated that the vapor- to mixture-volume ratio can be predicted with reasonable accuracy. These estimated values of vapor- to mixture-volume ratio, when used with previously reported results, may be useful in predicting pump inducer performance with two-phase flow. Author

N69-29568*# National Aeronautics and Space Administration. Lewis Research Center, Cleveland, Ohio.

RARE EARTH FLUORIDES AND OXIDES: AN EXPLORATORY STUDY OF THEIR USE AS SOLID LUBRICANTS AT TEMPERATURES TO 1800 DEG F (1000 DEG C)

Harold E. Sliney Washington Jul. 1969 25 p refs

(NASA-TN-D-5301) Avail: CFSTI CSCL 11H

Powdered lanthanide trifluorides such as LaF_3 and CeF_3, used as solid lubricants, significantly reduced the wear of Inconel 600 riders in sliding contact with Inconel 750 during lubrication experiments in air and in argon at temperatures up to 1800°F (1000°C). Rare earth oxides were poor lubricants compared to the fluorides. Fluoride powders were good film-formers; they were smeared into adherent film on the wear track by the stresses in the zone of sliding contact. The oxides were not film-formers. It was also shown that fusion-bonded LaF_3 and CeF_3 coatings, containing CaF_2–BaF_2 eutectic or LiF as melting point depressants, have possibilities as solid lubricant coatings. Author

N69-30062*# National Aeronautics and Space Administration. Lewis Research Center, Cleveland, Ohio.

A FABRICATION PROCESS FOR GLASS COATED ELECTRON-BOMBARDMENT ION THRUSTER GRIDS

Bruce A. Banks Washington Jul. 1969 40 p refs

(NASA-TN-D-5320) Avail: CFSTI CSCL 13H

A method was developed for producing nearly bubble-free glass coatings for molybdenum ion thruster accelerator grids. The method involves a helium diffusion process. Grids for 5-, 15-, and 30-cm-diameter thrusters were fabricated and tested. Pertinent grid design criteria and test results are presented. Author

N69-30069*# National Aeronautics and Space Administration. Lewis Research Center, Cleveland, Ohio.

EFFECT OF FLUID TEMPERATURE ON THE CAVITATION PERFORMANCE OF A HIGH HUB-TIP RATIO AXIAL FLOW PUMP IN WATER TO 250 DEGREES F (394 K)

Walter S. Cunnan, George Kovich, and Dean C. Reemsnyder Washington Jul. 1969 32 p refs

(NASA-TN-D-5318) Avail: CFSTI CSCL 13K

An axial flow pump was tested in deaerated water at temperatures to 250°F. Noncavitation performance is independent of fluid temperature in this range. A reduction in the required net positive suction head of 2.0 to 6.0 feet was measured in 250°F water under that in 80°F water at similar operating conditions. This improvement in cavitation performance increases with increasing flow coefficient and decreasing head-rise coefficient ratios. Cavitation formations in the rotor were visually observed and photographed in 80°F water. Slight suction surface cavitation damage occurred near the tip leading edges during the 162 hours of operation. Author

N69-30401*# National Aeronautics and Space Administration, Washington, D.C.

INTERDISCIPLINARY APPROACH TO FRICTION AND WEAR Conference Proceedings

P. M. Ku, ed. (Southwest Res. Inst.) GPO 1968 489 p refs NASA-sponsored Symp. held in San Antonio, Tex., 28–30 Nov. 1967

(NASA-SP-181) Avail: SOD $2.25; CFSTI CSCL 11H

CONTENTS:

1. STRUCTURE OF SURFACES AND THEIR INTERACTIONS H. C. Gatos (MIT, Cambridge) p 7–84 refs (See N69-30402 17-26)
2. TOPOGRAPHY OF SOLID SURFACES J. B. P. Williamson (Burndy Corp.) p 85–142 refs (See N69-30403 17-26)
3. SURFACE INTERACTIONS IN SLIDING F. F. Ling (Rensselaer Polytech. Inst.) p 143–179 refs (See N69-30404 17-15)
4. FRICTION AND ADHESION M. E. Merchant (Cincinnati Milling Machine Co.) p 181–265 refs (See N69-30405 17-15)
5. WEAR J. F. Archard (Leicester Univ.) p 267–333 refs (See N69-30406 17-15)
6. BOUNDARY LUBRICATION D. Godfrey (Chevron Res. Co.) p 335–384 refs (See N69-30407 17-15)
7. CRITICAL APPRAISAL AND RESEARCH OPPORTUNITIES: THE LUBRICATION RESEARCH VIEWPOINT D. Tabor (Cambridge Univ.) p 385–472 refs (See N69-30408 17-15)
8. CRITICAL APPRAISAL AND RESEARCH OPPORTUNITIES: THE MATERIALS RESEARCH VIEWPOINT K. R. Lawless (Va. Univ.) p 433–478 refs (See N69-30409 17-15)

N69-31884*# National Aeronautics and Administration. Lewis Research Center, Cleveland, Ohio.

FRICTION AND CONTACT RESISTANCE DURING SLIDING IN VACUUM OF SOME LOW-RESISTIVITY METALS

15 MACHINE ELEMENTS AND PROCESSES

LUBRICATED WITH SPUTTERED MOLYBDENUM DISULFIDE FILMS

John S. Przybyszewski and Talivadis Spaluins Washington Jul. 1969 22 p refs

(NASA-TN-D-5349) Avail: CFSTI CSCL 13I

Thin films of MoS_2 were applied by direct-current sputtering to copper, silver, and beryllium disk specimens and to copper disk specimens ion plated with gold, rhodium, or palladium. Low-speed sliding friction tests in ultrahigh vacuum showed that adherent, low-friction ($0.01 < f < 0.1$) films were obtained on all specimens except oxygen-free high conductivity copper. However, the average dynamic contact resistance was high (> 1 ohm) for all specimens except silver. High resistance peaks were a feature of all specimens throughout the duration of all tests. Author

N69-33011*# National Aeronautics and Space Administration. Marshall Space Flight Center, Huntsville, Ala.

SPACE MANUFACTURING MACHINE

Hans F. Wuenscher, inventor (to NASA) Filed 28 Apr. 1969 28 p (NASA-Case-MFS-20410; US-Patent-Appl-SN-819599) Avail: CFSTI CSCL 13I

An apparatus or machine for use in the low and zero gravity environment of orbital space flight for various manufacturing operations is described. The apparatus includes a cylindrical tank-like capsule in which manufacturing operations are carried out. An environmental control system is provided for controlling the atmosphere and pressure. High and low frequency coils along with electrostatic field coils are mounted in the capsule for positioning, spinning, transporting, and agitating materials being processed. Heating means are included for the melting of materials, and various probes are provided for adding liquid or gaseous materials to the materials or workpieces being processed. A mixing apparatus is included for preparing and placing mixtures of materials in the capsule for processing. Various equipment is provided for alloying, casting, molding, drawing, blowing, and other manufacturing and processing operations. NASA

N69-33258*# National Aeronautics and Space Administration. Lewis Research Center, Cleveland, Ohio.

EXPERIMENTS ON THE STEADY STATE CHARACTERISTICS OF HERRINGBONE-GROOVED AIR-LUBRICATED JOURNAL BEARINGS

Robert E. Cunningham, David P. Fleming, and William J. Anderson Washington Aug. 1969 28 p refs

(NASA-TN-D-5386) Avail: CFSTI CSCL 13I

Experiments were conducted with five rotors 3.81 cm in diameter and equipped with two herringbone-grooved patterns. Results showed that a range of groove-to ridge-clearance ratios of 2.0 to 2.4 has greater load capacities than do ratios greater or less than this optimum range. Load capacity increases with eccentricity ratio at a rate greater than linear. Agreement with a small-eccentricity pressure perturbation theory was good for groove-to ridge-clearance ratios in this optimum range but only at eccentricity ratios less an 0.3. These rotors were operated under unidirectional loading to a maximum compressibility number of 45. Author

N69-33281*# National Aeronautics and Space Administration. Lewis Research Center, Cleveland, Ohio.

COMPUTER PROGRAM FOR VISCOUS, ISOTHERMAL COMPRESSIBLE FLOW ACROSS A SEALING DAM WITH SMALL TILT ANGLE

John Zuk and Patricia J. Smith Washington Aug. 1969 89 p refs

(NASA-TN-D-5373) Avail: CFSTI CSCL 13I

An analysis of the flow across a sealing dam of the type that appears in gas turbine seals was developed for steady, laminar, subsonic, isothermal compressible flow. The analysis is valid for both parallel sealing dam surfaces and surfaces separated by a small tilt angle. The computer program determines mass flow rate, pressure and velocity distributions, Mach number, force, center of pressure, axial film stiffness rotational flow and pressure flow Reynolds numbers, power loss, and approximate temperature rise resulting from viscous shearing. The output is in both English units and the International System of Units. Some of the results can be automatically plotted. Author

N69-33450*# Pratt and Whitney Aircraft, East Hartford, Conn.

DESIGN OF BRAYTON ROTATING UNIT ON ROLLING-ELEMENT BEARINGS

R. Cohen and J. Clausi Washington NASA Aug. 1969 98 p (Contract NAS3-10949)

(NASA-CR-1401; PWA-3549) Avail: CFSTI CSCL 13I

The National Aeronautics and Space Administration is developing a Brayton-cycle space power system as part of its evaluation of potential long-life nuclear and solar electrical power sources. The candidate Brayton-cycle system under active investigation incorporates a single-shaft rotating unit consisting of a compressor, turbine and alternator rotating on gas bearings. This study was conducted to design such a Brayton rotating unit operating on oil-lubricated rolling-element bearings. Design of the bearing system was based on the technology demonstrated in two 2500-hour endurance tests successfully conducted in previous programs. Therefore, the bearing system design should be capable of development for mission lifetimes in excess of 10,000 hours with no significant oil contamination of the power system. Author

N69-33800*# National Aeronautics and Space Administration. Goddard Space Flight Center, Greenbelt, Md.

DEVELOPMENT OF A WELD QUALITY MONITOR

J. G. Etzel and J. A. Munford Washington Aug. 1969 11 p refs

(NASA-TN-D-5304) Avail: CFSTI CSCL 13I

Development of a nondestructive method of evaluating crosswire resistance welded joints used in electronic packaging is discussed. Mechanical strength and reproducibility of strength were determined for several alloy combinations. Data indicated that an optimum degree of embedment exists for each combination of materials. This report describes the development of an electromechanical device that automatically measures and displays the embedment of each welded joint and locks out the welding machine if the embedment value is not within preset upper and lower limits. Author

N69-34707*# National Aeronautics and Space Administration. Langley Research Center, Langley Station, Va.

INFLUENCE OF VARIOUS FABRICATION METHODS ON THE COMPRESSIVE STRENGTH OF TITANIUM SKIN-STRINGER PANELS

Richard A. Pride, Dick M. Royster, and James E. Gardner Washington Aug. 1969 44 p refs

(NASA-TN-D-5389) Avail: CFSTI CSCL 20K

Thirty-seven skin stringer panels were fabricated from Ti-8Al-1Mo-1V titanium alloy by riveting, resistance and arc spotwelding, tungsten inert gas and electron beam fusion welding, and diffusion bonding in order to investigate the effect of the various fabrication methods on the compressive strength. Also included in the investigation were two integrally stiffened panels machined from thick plate. The panels were representative of airplane wing or fuselage surfaces. Experimental buckling and maximum loads were determined for each panel. Results of strength tests for

the various joining techniques were compared with each other and with compressive strength calculations. The quality of the joining methods was generally good as evidenced by the behavior of the skin stringer panels in end compression. The joining methods maintained the integrity of the joint through buckling up to the maximum compressive strength of the panels. The maximum strengths of the panels showed good conformity with calculated results obtained from existing compressive strength analyses. Author

N69-35769*# National Aeronautics and Space Administration. Lewis Research Center, Cleveland, Ohio.

TORQUE AND LEAKAGE RATES OF VARIOUS LUBRICATED LIP SEAL DESIGNS AT A PERIPHERAL VELOCITY OF 120 FEET PER SECOND

Lawrence P. Ludwig, Thomas N. Strom, and Robert L. Johnson Washington Sep. 1969 16 p refs

(NASA-TN-D-5411) Avail: CFSTI CSCL 11A

Lip-type shaft seals were run at peripheral velocities representative of requirements in mechanical components for rocket engines. The seals with butyl rubber lips had prominent wear-in torque peaks that were attributed to lip temperature rise and subsequent lip shrinkage (Gow-Joule effect). This effect could cause sudden failure; gradual wear-in, however, reduced failure probability. The seals with glass-filled polytetrafluoroethylene lips also exhibited wear-in torque peaks. The seals with graphite-filled polytetrafluoroethylene lips exhibited low leakage and good wear characteristics. Running torques of the various lip seal types were similar to that of a segmented-carbon shaft seal. For butyl and graphite-filled polytetrafluoroethylene lip seals, the dynamic gas leakage rates were similar to the static leakage rates. Author

N69-35788*# National Aeronautics and Space Administration. Lewis Research Center, Cleveland, Ohio.

LUBRICANTS FOR INERTED LUBRICATION SYSTEMS IN ENGINES FOR ADVANCED AIRCRAFT

William R. Loomis, Dennis P. Townsend, and Robert L. Johnson Washington Sep. 1969 22 p refs

(NASA-TN-D-5420) Avail: CFSTI CSCL 11H

The feasibility of using presently available liquid lubricants in advanced high-speed aircraft engines was studied with both nitrogen inerted recirculating and once-through mist lubrication systems. Three fluids (a mixed ester, a synthetic paraffinic hydrocarbon, and a perfluorinated polymeric fluid) performed satisfactorily with the recirculating system in 3- to 10-hour runs in a full-scale simulated aircraft bearing and seal assembly at outer race bearing temperatures to 700° F (644K) and with a bulk fluid temperature of 500° F (533K). The principal problem was excessive leakage of the oil-side bellows face seal. Only one lubricant (synthetic paraffinic hydrocarbon) performed satisfactorily with the once-through mist system at a bearing temperature of 600° F (589K). Author

N69-35799*# National Aeronautics and Space Administration. Lewis Research Center, Cleveland, Ohio.

INVESTIGATION OF ISOTHERMAL, COMPRESSIBLE FLOW ACROSS A ROTATING SEALING DAM. 1: ANALYSIS

John Zuk and Lawrence P. Ludwig Washington Sep. 1969 36 p refs

(NASA-TN-D-5344) Avail: CFSTI CSCL 11A

The flow across a parallel sealing dam of the type that appears in gas turbine seals is analyzed for steady, laminar, subsonic, isothermal compressible flow with relative rotation of the sealing dam surfaces. Rational effects in velocity profiles pressure profiles, and other physical quantities of interest are found. Conditions are given under which a hydrostatic analysis of the radial pressure flow is a valid approximation. The error in estimating the mass leakage by using the hydrostatic radial flow formula is given. Author

N69-35859*# National Aeronautics and Space Administration, Washington, D.C.

MECHANISMS WITH ELASTIC COUPLINGS: DYNAMICS AND STABILITY

A. Ye. Kobrinskiy Washington NASA Jun. 1969 315 p refs Transl. into ENGLISH of the book "Mekhanizmy s Uprugimi Svyazyami. Dinamika i Ustoychivost" Moscow, Nauka Press, 1964 (Contract NASw-1695)

(NASA-TT-F-534) Avail: CFSTI CSCL 13E

Elastic couplings, as contrasted to elastic links are not actually a part of a mechanism's kinematic linkage. These couplings are analyzed under conditions of vibrating support or pulsating external forces. Vibrating and vibroimpact mechanisms are analyzed. A brief outline of the elements of the theory of differential and difference equations is included. The effects of friction and of clearances on kinematic pairs are analyzed. Author

N69-36349*# Virginia Univ., Charlottesville. Dept. of Mechanical Engineering.

RIGID ROTOR DYNAMICS

Edgar J. Gunter, Jr. and P. De Choudhury Washington NASA Aug. 1969 173 p refs

(Grant NGR-47-005-050)

(NASA-CR-1391) Avail: CFSTI CSCL 13I

The dynamic motion of an unbalanced rigid body rotor in general linearized bearings is analyzed and is applicable to fluid film as well as rolling elements bearings for small bearing displacements. The complete nonlinear dynamical equations of motion, including motor acceleration, are derived by Lagrange's equations to include the influence of damped, flexibly mounted bearing supports. The dynamical equations of motion are linearized by assuming constant angular shaft velocity and shaft displacements, which are small in comparison to the rotor characteristic length. Computer programs to analyze the rotor steady state motion due to unbalance and the stability and complete transient response are presented. As an example, these computer programs are applied to evaluate the characteristics of a NASA experimental hybrid gas bearing rotor system. Author

N69-38641*# National Aeronautics and Space Administration. Lewis Research Center, Cleveland, Ohio.

CAVITATION DAMAGE AND THE EFFECT OF FLUID TEMPERATURE ON THE PERFORMANCE OF AN AXIAL-FLOW PUMP IN LIQUID SODIUM

Walter S. Cunnan and Dean C. Reemsnyder Washington Oct. 1969 25 p refs

(NASA-TN-D-5484) Avail: CFSTI CSCL 13L

An axial flow pump with three different blade materials was tested for 232 hours in liquid sodium at temperatures of 1000° and 1500° F (811° and 1089°K). Noncavitation performance is essentially independent of fluid temperature in this range. A maximum reduction in required net positive suction head of 13 feet (4 m) under that at 1000° F (811°K) was obtained in 1500° F (1089°K) sodium. The reduction increased with increasing flow coefficient, increasing rotative speed, and decreasing head rise coefficient ratio. Severe suction surface cavitation damage occurred near the blade tip leading edges after a 32-hour cavitation damage test. Rene 41 is more resistant to cavitation damage from sodium than either the 316 or 318 stainless steel blades. Cavitation damage increases significantly with rotative speed at constant suction specific speed. Author

N69-41210*# National Aeronautics and Space Administration. Lewis Research Center, Cleveland, Ohio.

15 MACHINE ELEMENTS AND PROCESSES

SPEED EFFECTS ON BALL SPINNING TORQUE

Dennis P. Townsend, Marshall W. Dietrich, and Erwin V. Zaretsky
Washington Nov. 1969 18 p refs
(NASA-TN-D-5527) Avail: CFSTI CSCL 13H

Tests were conducted in the NASA spinning friction apparatus to determine the effect of ball spinning speed on torque and coefficient of spinning friction. Reasonably good agreement was obtained between experimental torque values and theoretical torque predictions using an elastohydrodynamic analysis with a modified pressure-viscosity relation. Spinning torque increased with spinning speed, but the rate of increase was less than predicted from theory. This difference in the rate of increase in torque with speed was attributed to shearing of the lubricant which reduced the lubricant viscosity in the contact ellipse. No correlation was found between experimental and theoretical coefficients of spinning friction using a dry contact friction model. Author

16

MASERS

Includes applications of masers and lasers. For basic research see: 26 Physics, Solid-State.

A69-12617 *

TEMPERATURE TUNING OF AN ORGANIC DYE LASER.

Gottfried T. Schappert, Kenneth W. Billman, and David C. Burnham (NASA, Electronics Research Center, Cambridge, Mass.).

Applied Physics Letters, vol. 13, Aug. 15, 1968, p. 124-126.

Measurement of the wavelength spectrum of an organic dye laser (DTTC in ethanol) pumped by a Q-switched ruby laser. The measurement is made as a function of temperature (-117°C to +78°C) for several dye concentrations. Absorption and fluorescence spectra are also obtained. The results are in qualitative agreement with the model of vibrationally broadened two-level system, each of which is separately thermalized. M.G.

A69-14189 *#

EVIDENCE FOR SINUSOIDAL PHASE MODULATION IN SMALL SELF-TRAPPED FILAMENTS.

J. R. Lifsitz (NASA, Electronics Research Center, Cambridge, Mass.) and H. P. H. Grieneisen.

Applied Physics Letters, vol. 13, Oct. 1, 1968, p. 245, 246. 10 refs. NASA-supported research.

Description of evidence indicating that, in some cases at least, a sinusoidal phase modulation is responsible for the spectral broadening observed in trapped filaments of laser and Raman light. This type of modulation has been recently suggested by Cheung et al. (1968). M.M.

A69-14290 *

MIE TOTAL AND DIFFERENTIAL BACKSCATTERING CROSS SECTIONS AT LASER WAVELENGTHS FOR JUNGE AEROSOL MODELS.

M. P. McCormick, J. D. Lawrence, Jr. (NASA, Langley Research Center, Hampton, Va.), and F. R. Crownfield, Jr. (College of William and Mary, Williamsburg, Va.).

Applied Optics, vol. 7, Dec. 1968, p. 2424, 2425. 5 refs.

Calculation of backscattering and total cross sections for a Junge size distribution of spherical aerosol particles with a refractive index of 1.5. The calculations have been performed at the laser wavelengths and second harmonics of ruby and neodymium. The average differential cross section for a particular backscatter, and average total cross section per particle are tabulated. M.M.

A69-17901 *#

TIME DEPENDENT SPECTROSCOPY OF FLASHLAMP PUMPED DYE LASERS.

H. Furumoto and H. Ceccon (NASA, Electronics Research Center, Cambridge, Mass.).

Applied Physics Letters, vol. 13, Nov. 15, 1968, p. 335-337. 6 refs.

Time-resolved emission spectra from flashlamp-pumped organic dye lasers were recorded with an image converter camera. The characteristics of several dyes are examined and compared. The rhodamine dyes show a uniform spectral output, but other dyes show an irregular time-dependent spectral output. (Author)

A69-18482 *

METHODS FOR THE MEASUREMENT OF FREQUENCY AND STABILITY OF LASER GENERATORS IN THE INFRARED.

L. Frenkel (NASA, Electronics Research Center, Cambridge, Mass.) and M. A. Pollack (Bell Telephone Laboratories, Inc., Holmdel, N. J.).

IN: MOGA 68; INTERNATIONAL CONFERENCE ON MICROWAVE AND OPTICAL GENERATION AND AMPLIFICATION, 7TH, HAMBURG, WEST GERMANY, SEPTEMBER 16-20, 1968, PROCEEDINGS [MOGA 68; INTERNATIONALE TAGUNG ÜBER ERZEUGUNG UND VERSTÄRKUNG VON SCHWINGUNGEN IM OPTISCHEN UND MIKROWELLENBEREICH, 7TH, HAMBURG, WEST GERMANY, SEPTEMBER 16-20, 1968, PROCEEDINGS]. [A69-18420 07-09]
Berlin, VDE-Verlag GmbH (Nachrichtentechnische Fachberichte. Volume 35), 1968, p. 757-763. 12 refs.

The frequencies of several laser lines in the far-infrared region have recently been measured. These measurements consist of the mixing of the laser radiation with radiation from either a second precisely known laser line or with the high-order harmonics of a millimeter wave source in a special point-contact mixer. The specific example of the very accurate measurement of the 118.6 μ line is given in detail, and the stability of the beats between the sources is discussed. The extension of these techniques to even higher frequencies is considered. (Author)

A69-19082 *

IODINE INFRARED LASER.

Hongsuk H. Kim, Roy A. Paananen, Philip L. Hanst (NASA, Electronics Research Center, Cambridge, Mass.), and Thomas F. Deutsch (Raytheon Co., Research Div., Waltham, Mass.).

(Institute of Electrical and Electronics Engineers, International Quantum Electronics Conference, Miami, Fla., May 14-17, 1968, Paper T-5.)
IEEE Journal of Quantum Electronics, vol. QE-4, Nov. 1968, p. 908-911. 7 refs.

CW laser emission, attributed to electronic transitions in the iodine atom, has been obtained at 8 wavelengths between 3.0 and 9.0 μ. The strongest CW lines are at 3.429 and 4.862 μ. One of the weaker CW lines, 5.497 μ, becomes relatively strong when the laser is operated in a pulsed mode. The laser self-pulses under certain operating conditions. The gain on the strong lines is high, and oscillation can be obtained with very little optical feedback. A maximum power output of 325 mW from all the lines has been obtained to date. The power is shifted from line to line by placing a prism or a selective absorber within the cavity. (Author)

A69-19641 *#

WAVELENGTH DEPENDENCE OF LASER-BEAM SCINTILLATION.

Michael W. Fitzmaurice, Jack L. Bufton, and Peter O. Minott (NASA, Goddard Space Flight Center, Greenbelt, Md.).

(Optical Society of America, Spring Meeting, Washington, D.C., Mar. 13-16, 1968.)
Optical Society of America, Journal, vol. 59, Jan. 1969, p. 7-10. 7 refs.

An experiment has been performed to confirm the proportionality between log-amplitude variance and the 7/6 power of wavenumber predicted by Tatarski for horizontal propagation from a spherical-wave transmitter to a point detector. The validity of this proportionality was tested for two wavelengths: 0.632 and 10.6 μ. Beams from a helium-neon and a CO_2 laser were simultaneously transmitted over a folded 1.2-km horizontal path and were detected with a photomultiplier and a gold-doped germanium detector. The primary scintillation statistic (log-amplitude variance) was evaluated for each wavelength with a digital computer, and the ratio of variances at 0.632 and 10.6 μ was found to be in close agreement with predic-

tions. Power spectral density, autocorrelation, and cumulative probability density were also evaluated for each wavelength. Scintillation statistics at 10.6 μ were found to be log normal, as in the visible. (Author)

A69-21088 *
A WAVELENGTH-SELECTIVE, REPETITIVELY PULSED CO_2 LASER.
Philip L. Hanst and John A. Morreal (NASA, Electronics Research Center, Cambridge, Mass.).
Applied Optics, vol. 8, Jan. 1969, p. 109-115. 7 refs.

A CO_2 laser has been constructed and operated with two gas absorption cells built into the cavity. One of the cells contains a gas that controls the wavelength of emission. The other cell contains a gas that forces the laser into a high-frequency pulsed mode of operation. Details of the laser construction are given. The pulsing and wavelength shifting are accounted for by the spectroscopic and kinetic properties of the gases. The proper choice of absorbing gases has produced high-power pulsed operation at various wavelengths between 9.08 and 10.6 μ at repetition rates of up to 100 kHz. Applications and advantages of the wavelength-selective, repetitively pulsed laser are discussed. (Author)

A69-24005 *#
SULFUR DIOXIDE SUBMILLIMETER LASER.
Thomas M. Hard (NASA, Electronics Research Center, Cambridge, Mass.).
Applied Physics Letters, vol. 14, Feb. 15, 1969, p. 130.

A mixture of 0.4-torr SO_2 with 0.4-torr He lases at 70.98, 66.14, 51.89, and 46.44 cm^{-1} when excited by a pulsed discharge. The previous report of CW oscillation on the first and the third of these lines is confirmed. (Author)

A69-26330 *
SIMULTANEOUS HCN AND H_2O LASER EMISSION IN MIXTURES CONTAINING H, C, N, AND O.
T. M. Hard, F. A. Haak (NASA, Electronics Research Center, Cambridge, Mass.), and O. M. Stafsudd (California, University, Los Angeles, Calif.).
IEEE Journal of Quantum Electronics, vol. QE-5, Feb. 1969, p. 132.

Observation of simultaneous laser emission at 337 and 118 μ in a pulsed discharge through a mixture of N_2, O_2, and either CH_4 or $(C_2H_5)_2O$. A search for the 469-μ line in $(C_2H_5)_2O$ plus N_2 was unsuccessful. The line is regarded as spurious, in view of air leaks and the observation of simultaneous HCN and H_2O laser emission. F.R.L.

A69-42187 *
OPTICAL PUMPS FOR ORGANIC DYE LASERS.
H. W. Furumoto and H. L. Ceccon (NASA, Electronics Research Center, Cambridge, Mass.).
Applied Optics, vol. 8, Aug. 1969, p. 1613-1623. 28 refs.

Several types of low energy, ultrafast flashlamp systems have been investigated as optical pumps for lasers using fast decaying fluorescent materials, in particular, organic dyes. Of the various systems examined, the coaxial lamp with a spark gap switch proved to be the most useful for pumping the organic dyes. Parameters optimized were the gas type, gas pressure, discharge volume, and electrical circuitry. At optimum operation, the annular volume of the coaxial lamp is completely filled with the discharge and the current rise time is determined mainly by the external circuit inductance. The rapidity and uniformity of the discharge is attributed to photoionization of the gas fill. Current rise times are typically 140 nsec for energies up to 100 J. Because of the photoionization process, these coaxial lamps are considered to be a different class of flashlamps from the standard capillary discharge lamp, the sliding spark lamp, and the ablating wall lamp. Less useful systems that were investigated are described, and the reasons for their deficiencies are analyzed. (Author)

A69-42192 *
HYDROCARBON GAS ABSORPTION BY A HeNe LASER BEAM AT A 3.39-μ WAVELENGTH.
Dean N. Jaynes and Benjamin H. Beam (NASA, Ames Research Center, Moffett Field, Calif.).
Applied Optics, vol. 8, Aug. 1969, p. 1741, 1742. 6 refs.

Measurement of the absorption coefficients of a number of hydrocarbon gases for a laser beam at 3.39 microns. The tabulated results show rather wide variations in absorption coefficient from spectroscopic data. For example, spectroscopic data at low resolution (Pierson et al., 1956) show that ethane absorbs more strongly than methane, while the reverse is shown by the present measurements. M.M.

N69-25357*# National Aeronautics and Space Administration. Electronics Research Center, Cambridge, Mass.
THE INTERACTION OF INTENSE LASER BEAMS WITH FREE ELECTRONS
Edward S. Sarachik Washington May 1969 30 p refs
(NASA-TN-D-5205) Avail: CFSTI CSCL 20E

The field of high intensity electrodynamics is introduced and surveyed. Various aspects of the interactions of intense laser beams with free electrons are considered, including harmonic generation, refraction, the Kapitza–Dirac effect, and quantum phenomena. A complete bibliography is included. Author

N69-29934*# Raytheon Co., Waltham, Mass.
A PROGRAM TO EVALUATE DYE LASERS AS HIGH POWER, PULSED, VISIBLE LIGHT SOURCES
Michael Bass, Thomas Deutsch, and Marvin Weber Washington NASA 11Jul. 1969 81 p refs
(Contract NAS12-635)
(NASA-CR-1374; S-1112) Avail: CFSTI CSCL 20E

Experimental and theoretical efforts to understand dye laser operation are discussed. The approach used by McCumber for treating phonon-terminated lasers was applied to investigate the gain properties of dye lasers and was extended to include effects arising from population buildup in the triplet-level system and associated triplet–triplet absorptive losses. The gain is expressed in terms of time-dependent excited-state populations, spectral emission, and/or absorption functions. For a given optical-pump pulse, a computer program was used to solve rate equations for the populations up to threshold and to calculate the gain as a function of time and frequency. The gain varies with frequency over the broad fluorescence bands characteristic of dye molecules and with time until the threshold for laser action is reached. Experiments using rhodamine 6G verify the predicted dependence of the laser frequency and time of threshold on cavity Q and demonstrate laser frequency tuning by adjusting the opening time of an intracavity Q switch. Author

17

MATERIALS, METALLIC

Includes cermets; corrosion; physical and mechanical properties of materials; metallurgy; and applications as structural materials. For basic research see: 06 Chemistry. For related information see also: 18 Materials, Nonmetallic; and 32 Structural Mechanics.

A69-10612 *

COMMENTS ON SLOW CRACK GROWTH OF STEELS IN HYDROGEN AND WATER ENVIRONMENTS.

Dell P. Williams (NASA, Ames Research Center, Moffett Field, Calif.).

Scripta Metallurgica, vol. 2, July 1968, p. 385-391. 12 refs.

Results of a study of the pressure- and temperature-dependence of slow cracking of fully hardened AISI-SAE 4130 steel in gaseous hydrogen. A comparison of the data with the previously reported growth kinetics in water and water vapor appears to clarify the seemingly anomalous behavior noted in the latter two environments. M.G.

A69-17872 *

THE COMPATIBILITY OF MATERIALS.

Walter H. Kohl (NASA, Electronics Research Center, Cambridge, Mass.).

IEEE Spectrum, vol. 6, Jan. 1969, p. 67-74. 40 refs.

The success of space-age endeavors depends greatly upon the materials used to construct a certain module, part, or subsystem, and on the interaction between these materials and their immediate environment. A metal, for example, must retain its physical integrity in shape, ductility, and tensile strength over stringent stress and temperature ranges; it must be able to withstand proximity with other materials, metallic and nonmetallic, while maintaining chemical stability. Nonmetallic materials must be compounded to prevent such reactions as outgassing or decomposition at high altitudes; others, such as ablative ceramics, must disintegrate in a certain manner. The demand for more specialized, more durable substances has created a new materials technology. (Author)

A69-18154 *#

SOLAR ABSORPTANCE AND HEMISPHERICAL EMITTANCE OF VARIOUS METALS AT SPACE CONDITIONS.

John R. Jack (NASA, Lewis Research Center, Environmental Physics Section, Cleveland, Ohio) and Ernie W. Spisz (NASA, Lewis Research Center, Cleveland, Ohio).

American Institute of Aeronautics and Astronautics, Aerospace Sciences Meeting, 7th, New York, N.Y., Jan. 20-22, 1969, Paper 69-60. 8 p. 12 refs.

Members, $1.00; nonmembers, $1.50.

A cyclic incident radiation technique has been used to determine the thermal radiation properties (total hemispherical emittance and normal solar absorptance) of twelve metals over the temperature range from 200 to 560 K. The thermal radiation data for the metals were obtained using the "as received" surface of one-mil-thick foil material with only an alcohol bath to clean the surface. For the temperature range covered, the total hemispherical emittance of the metals increased with increasing temperature, the normal solar absorptance was approximately constant, and the absorptance-emittance ratio decreased with increasing temperature due to the increase in emittance. A comparison is made between the experimental emittance data and the emittance values calculated from electromagnetic relationships to establish whether these theories can be used to predict thermal radiative property data for real metals. (Author)

A69-18790 *

REFRACTORY METAL ALLOYS: METALLURGY AND TECHNOLOGY; PROCEEDINGS OF A SYMPOSIUM ON METALLURGY AND TECHNOLOGY OF REFRACTORY METALS, WASHINGTON, D.C., APRIL 25, 26, 1968.

Symposium sponsored by the American Institute of Mining, Metallurgical and Petroleum Engineers and NASA.

Edited by I. Machlin (U.S. Naval Air Systems Command, Materials and Processes Branch, Washington, D.C.), R. T. Begley (Westinghouse Electric Corp., Astronuclear Laboratory, Pittsburgh, Pa.) and E. D. Weisert (North American Rockwell Corp., Rocketdyne Div., Canoga Park, Calif.).

New York, Plenum Press, 1968. 499 p.

$22.50.

CONTENTS:

PREFACE. I. Machlin (U.S. Naval Air Systems Command, Washington, D.C.), R. T. Begley (Westinghouse Electric Corp., Pittsburgh, Pa.), and E. D. Weisert (North American Rockwell Corp., Canoga Park, Calif.), p. v, vi.

BASIC STRENGTHENING MECHANISMS IN REFRACTORY METALS. B. A. Wilcox, p. 1-39. [For abstract see issue 11, page 2040, Accession no. A68-25857]

HIGH TEMPERATURE CREEP AND FRACTURE BEHAVIOR OF THE REFRACTORY METALS. R. T. Begley, D. L. Harrod, and R. E. Gold (Westinghouse Electric Corp., Pittsburgh, Pa.), p. 41-83. [For abstract see issue 19, page 3610, Accession no. A68-36888]

THE EFFECT OF THERMAL-MECHANICAL TREATMENTS ON THE STRUCTURE AND PROPERTIES OF REFRACTORY METALS. R. A. Perkins (Lockheed Aircraft Corp., Palo Alto, Calif.), p. 85-120. [For abstract see issue 15, page 2800, Accession no. A68-32100]

INTERACTIONS IN COATED REFRACTORY METAL SYSTEMS. A. G. Metcalfe and A. R. Stetson (International Harvester Co., San Diego, Calif.), p. 121-163. [For abstract see issue 19, page 3610, Accession no. A68-36889]

INTERACTIONS OF REFRACTORY METALS WITH ACTIVE GASES IN VACUA AND INERT GAS ENVIRONMENTS. H. Inouye (Oak Ridge National Laboratory, Oak Ridge, Tenn.), p. 165-195. [For abstract see issue 01, page 99, Accession no. A69-11042]

HYDROGEN EFFECTS IN REFRACTORY METALS. W. T. Chandler and R. J. Walter (North American Rockwell Corp., Canoga Park, Calif.), p. 197-249. [For abstract see issue 15, page 2800, Accession no. A68-32158]

THE COMPATIBILITY OF REFRACTORY METALS WITH LIQUID METALS. E. E. Hoffman and R. W. Harrison (General Electric Co., Cincinnati, Ohio), p. 251-287. [For abstract see issue 15, page 2798, Accession no. A68-31555]

REFRACTORY METALS IN SPACE ELECTRIC POWER CONVERSION SYSTEMS. J. W. Semmel, Jr. (General Electric Co., Cincinnati, Ohio), p. 289-324. [For abstract see issue 12, page 2241, Accession no. A68-27066]

RECENT ADVANCES IN COLUMBIUM ALLOYS. R. G. Frank (General Electric Co., Cincinnati, Ohio), p. 325-372. 144 refs. [See A69-18791 07-17]

CONSIDERATIONS IN THE DEVELOPMENT OF TANTALUM BASE ALLOYS. R. W. Buckman, Jr. and R. C. Goodspeed (Westinghouse Electric Corp., Pittsburgh, Pa.), p. 373-394. [For abstract see issue 19, page 3613, Accession no. A68-37521]

ADVANCED PROCESSING TECHNOLOGY AND HIGH TEMPERATURE MECHANICAL PROPERTIES OF TUNGSTEN BASE ALLOYS (A REVIEW). H. G. Sell (Westinghouse Electric Corp., Bloomfield, N.J.), p. 395-450. 100 refs. [See A69-18792 07-17]

THE LESS COMMON REFRACTORY METALS (RHENIUM, TECHNETIUM, HAFNIUM, NOBLE METALS). J. Maltz (NASA, Washington, D.C.), p. 451-488. 78 refs. [See A69-18793 07-17]

INDEX, p. 489-491.

A69-18791
RECENT ADVANCES IN COLUMBIUM ALLOYS.
R. G. Frank (General Electric Co., Cincinnati, Ohio).
IN: REFRACTORY METAL ALLOYS: METALLURGY AND TECHNOLOGY; PROCEEDINGS OF A SYMPOSIUM ON METALLURGY AND TECHNOLOGY OF REFRACTORY METALS, WASHINGTON, D.C., APRIL 25, 26, 1968. [A69-18790 07-17]
Symposium sponsored by the American Institute of Mining, Metallurgical and Petroleum Engineers and NASA.
Edited by I. Machlin, R. T. Begley, and E. D. Weisert.
New York, Plenum Press, 1968, p. 325-372. 144 refs.

The status of columbium alloys is reviewed with respect to major applications, production, cost, and selected properties. Alloys with low to moderate strength and good ductility, and that are readily fabricated and weldable, are commercially available. These alloys were the first of the columbium base alloys to receive serious consideration for use in components on actual flight systems. Emphasis in the development of new columbium alloys over the past several years has been directed toward the achievement of greater creep strength in the 2000 to 2400°F temperature range and more recently, toward improved oxidation resistance in combination with varying levels of strength and ductility. (Author)

A69-18792
ADVANCED PROCESSING TECHNOLOGY AND HIGH TEMPERATURE MECHANICAL PROPERTIES OF TUNGSTEN BASE ALLOYS (A REVIEW).
H. G. Sell (Westinghouse Electric Corp., Lamp Div., Metals Research Section, Bloomfield, N.J.).
IN: REFRACTORY METAL ALLOYS: METALLURGY AND TECHNOLOGY; PROCEEDINGS OF A SYMPOSIUM ON METALLURGY AND TECHNOLOGY OF REFRACTORY METALS, WASHINGTON, D.C., APRIL 25, 26, 1968. [A69-18790 07-17]
Symposium sponsored by the American Institute of Mining, Metallurgical and Petroleum Engineers and NASA.
Edited by I. Machlin, R. T. Begley, and E. D. Weisert.
New York, Plenum Press, 1968, p. 395-450. 100 refs.

Review of advances in the manufacturing of tungsten-base alloys by powder metallurgy, fusion, and chemical-vapor deposition techniques. The mechanical properties of many alloys are discussed in terms of the effect of alloying on the ductile-brittle transition temperature and on the high-temperature tensile and creep strength. An attempt is made to assess the state of the tungsten-alloy technology, and to determine how successful numerous development efforts have been in achieving high-temperature strength and in improving low-temperature ductility. M.M.

A69-18793 *
THE LESS COMMON REFRACTORY METALS (RHENIUM, TECHNETIUM, HAFNIUM, NOBLE METALS).
Joseph Maltz (NASA, Washington, D.C.).
IN: REFRACTORY METAL ALLOYS: METALLURGY AND TECHNOLOGY; PROCEEDINGS OF A SYMPOSIUM ON METALLURGY AND TECHNOLOGY OF REFRACTORY METALS, WASHINGTON, D.C., APRIL 25, 26, 1968. [A69-18790 07-17]
Symposium sponsored by the American Institute of Mining, Metallurgical and Petroleum Engineers and NASA.
Edited by I. Machlin, R. T. Begley, and E. D. Weisert.
New York, Plenum Press, 1968, p. 451-488. 78 refs.

Previous reviews of the status of the less-common refractory metals are cited and supplemented with discussions of newer developments. The physical metallurgy of rhenium and of technetium, an artificial element which has only recently become available in sufficient amount for metallurgical studies to be possible, are surveyed. New data on phase equilibria, mechanical and physical properties, and availability are included. Special attention is also given to the roles of hafnium-tantalum alloys and of iridium as oxidation-resistant coatings suitable for special situations. Insofar as the potential usage of the less-common refractory metals in applications which depend upon their high melting point is concerned, high cost and low availability preclude any radical changes in the near future. (Author)

A69-20190 *
YIELDING AND FRACTURE IN TUNGSTEN AND TUNGSTEN-RHENIUM ALLOYS.
P. L. Raffo (NASA, Lewis Research Center, Cleveland, Ohio).
Journal of the Less-Common Metals, vol. 17, Feb. 1969, p. 133-149. 44 refs.

A study was made of the mechanical properties of vacuum arc-melted tungsten and tungsten-rhenium alloys in the temperature range 77 to 810 K in order to elucidate the mechanism by which rhenium additions lower the ductile-brittle transition temperature of tungsten. The temperature and strain rate dependency of the yield stress of tungsten are reduced by alloying with rhenium, inferring a reduction in the Peierls stress. The reduction in the transition temperature is attributed to the reduced Peierls stress through its effect on the mobility and rate of multiplication of dislocations. (Author)

A69-20204 *
FIBER-METAL MATRIX COMPOSITES.
John W. Weeton (NASA, Lewis Research Center, Composite Materials Branch, Cleveland, Ohio).
Machine Design, vol. 41, Feb. 20, 1969, p. 142-156. 9 refs.

Discussion of the state of the art of fiber-reinforced metal-matrix materials. The importance of fiber-reinforced metals is based upon using to advantage the high strength of fiber materials by imbedding them into a metallic matrix. Today's fibers have fantastically high strengths. Strength of whiskers of some materials ranges from 3 to 5 x 10^6 psi. Most fiber-metal matrix composites produced thus far have been used for R&D work. The composites are being seriously considered for many of the hot components in gas-turbine engines. Total use of fiber-metal matrix composites in the U.S. in 1968 is estimated at 1000 lb; use in 1969 is expected to be about 10,000 lb; and by 1973, the total will probably approach 500,000 lb. G.R.

A69-20557 *
A DISLOCATION MODEL PERTAINING TO THE STRENGTH OF ELASTICALLY INHOMOGENEOUS MATERIALS.
Dhanjoo N. Ghista (NASA, Ames Research Center, Moffett Field, Calif.) and William D. Nix (Stanford University, Dept. of Materials Science, Stanford, Calif.).
Materials Science and Engineering, vol. 3, Jan. 1969, p. 293-298. 10 refs.
ARPA-supported research.

Description of a dislocation model of the strength of elastically inhomogeneous crystalline materials which is based on the elastic interactions between dislocations and periodic fluctuations of the shear modulus. The model rests on the assumption that the elastic energy of a dislocation in an inhomogeneous material can be treated as if the shear modulus varies radially from the axis of the dislocation. For simplicity, the shear modulus is assumed to vary according to a Bessel function of the first kind of order either 0 or 1. The variation in the elastic energy of a dislocation with position in an inhomogeneous material is accounted for by a variable phase factor which is included in the argument of the Bessel functions. The model suggests that the critical stress required to initiate plastic flow increases linearly with the amplitude of the shear modulus variation and inversely with the wavelength. The predictions of the model are consistent with some of the findings on the strength of alloys strengthened by spinodal decomposition. (Author)

A69-22990 *
SUPERPLASTICITY IN TUNGSTEN-RHENIUM ALLOYS.
M. Garfinkle, W. R. Witzke, and W. D. Klopp (NASA, Lewis Research Center, Refractory Metals Section, Cleveland, Ohio).
Metallurgical Society of AIME, Transactions, vol. 245, Feb. 1969, p. 303-308. 21 refs.

The tensile properties of binary W-Re alloys containing up to 33 at. % Re were determined at temperatures from 78 to 3630°F. Elongations as high as 260% were observed in electron-beam-melted

tungsten containing 23 at. % Re when tensile-tested at 3630°F after a 1-hr anneal at 3090°F. All alloys tested under these conditions with rhenium contents between 20 and 28 at. % exhibited elongations of at least 200%. These alloys also showed enhanced grain growth rates. The values of strain-rate sensitivity ranged between 0.2 and 0.3 for the alloys exhibiting high elongations. However, for swaged alloys tested just above the recrystallization temperature, strain-rate sensitivities as high as 0.8 were observed. The high-temperature strengths of the high-rhenium-content alloys were also less than those of alloys with intermediate rhenium contents. (Author)

A69-26495 * #
PROTECTIVE COATINGS FOR CHROMIUM ALLOYS.
Salvatore J. Grisaffe and Robert E. Oldrieve (NASA, Lewis Research Center, Cleveland, Ohio).
American Society for Metals and American Society of Tool and Manufacturing Engineers, Western Metal and Tool Conference and Exposition, Los Angeles, Calif., Mar. 10-14, 1969, Paper. 23 p. 15 refs.

Summary of studies aimed at providing combined protection of chromium alloys against nitrogen embrittlement and air oxidation. Both ductile metal clads and coatings of silicides, aluminides, and noble metals were investigated. The results of furnace air exposures at temperatures to 2400°F show that most systems greatly reduce nitrogen contamination and oxidation attack as compared to the unprotected chromium alloy substrates. However, most systems cause at least partial enbrittlement in themselves by harmful interdiffusion with the substrates. Of the systems studied, iron silicide coatings appeared to cause the least embrittlement while still providing adequate furnace oxidation resistance. At this time, no protection systems appear ready for engine applications. Z. W.

A69-26496 * #
PLANE STRAIN FRACTURE TOUGHNESS TESTS ON TWO-INCH-THICK MARAGING STEEL PLATE AT VARIOUS STRENGTH LEVELS.
J. E. Srawley (NASA, Lewis Research Center, Cleveland, Ohio).
International Conference on Fracture, 2nd, Brighton, Sussex, England, Apr. 13-18, 1969, Paper. 28 p. 19 refs.

Results of tests of 1.8-in.-thick three-point bend and compact (tension) specimens substantiate the current ASTM recommended practice for plane strain fracture toughness (K_{Ic}) testing. Erroneously low results were obtained with 0.5-in. thick bend specimens when the ratio of K_{Ic} to yield strength exceeded 0.45 $in.^{1/2}$, thus emphasizing the importance of requiring minimum specimen dimensions proportional to the square of this ratio. Shallow face grooves in 0.5-in.-thick specimens had no useful effect. The maraging temperatures ranged from 700 to 1100°F, yield strength from 173 to 260 ksi, and K_{Ic} from 67 to 147 ksi-$in.^{1/2}$. The K_{Ic} values were approximately proportional to the reciprocal of the square of yield strength, and also to a strain hardening index derived from the ratio of yield to ultimate tensile strength. (Author)

A69-28682 *
STAGE-I INTERSTITIALS IN ELECTRON-IRRADIATED TUNGSTEN.
J. A. DiCarlo (Brookhaven National Laboratory, Upton, N.Y.; NASA, Lewis Research Center, Cleveland, Ohio), C. L. Snead, Jr., and A. N. Goland (Brookhaven National Laboratory, Upton, N.Y.).
Physical Review, 2nd Series, vol. 178, Feb. 15, 1969, p. 1059-1072. 40 refs.
AEC-NASA-supported research.

Single crystals and polycrystalline 5-mil tungsten wires of high purity were irradiated at 20 K with 2.5-MeV electrons. Stage-I defect behavior was studied by internal friction, dynamic Young's modulus, and resistivity measurements. The friction and modulus samples were electrostatically driven at their fundamental flexural mode (~600 Hz). After irradiation, a prominent but transient internal-friction peak was observed at 30 K. Simultaneous resistivity and mechanical-property measurements during isochronal annealing indicate that the friction peak recovers during a major close-pair recovery substage and that long-range interstitial motion occurs between 45 and 100 K. Arguments are presented which identify the stress-induced ordering of the interstitial members of close Frenkel pairs as the source of the 30 K relaxation peak. Single crystal results on relaxation strength vs stress direction suggest that the interstitials are not ⟨111⟩ but most probably are ⟨110⟩ split interstitials. Defect asymmetry and activation energies for reorientation (E_r = 0.066 ± 0.01 eV) and annealing (E_a = 0.11 ± 0.01 eV) are determined for the 30 K process. Internal-friction background increase with heavy irradiation is discussed. (Author)

A69-29010 * #
TUNGSTEN ALLOY FIBER REINFORCED NICKEL BASE ALLOY COMPOSITES FOR HIGH TEMPERATURE TURBOJET ENGINE APPLICATIONS.
D. W. Petrasek and R. A. Signorelli (NASA, Lewis Research Center, Cleveland, Ohio).
American Society for Testing and Materials, Symposium on Composite Testing and Design, New Orleans, La., Feb. 10-14, 1969, Paper. 16 p. 7 refs.

The potential of tungsten-2% thoria, 218 tungsten, and tungsten-1% thoria wire reinforced nickel-base superalloy composites for turbine bucket applications was evaluated based on stress-rupture strength and oxidation and impact resistance. The results indicate that refractory metal alloy fiber-superalloy composites have potential for turbine bucket use based on the properties measured. Composites were produced having stress-rupture properties superior to conventional cast superalloys at use temperatures of 2000 and 2200°F. The 100- and 1000-hr stress-rupture strength of the composite at 2000°F was 49,000 and 37,000 psi, respectively. A few thousands of an inch of matrix or cladding material was found to be sufficient to protect the fibers from oxidation at 2000°F for times up to 300 hr. At 300°F and above the impact resistance of the composite compares favorably with that of superalloys. (Author)

A69-33564
FRACTURE: AN ADVANCED TREATISE. VOLUME 4 - ENGINEERING FRACTURE DESIGN.
Edited by Harold Liebowitz (George Washington University, School of Engineering and Applied Science, Washington, D.C.).
New York, Academic Press, Inc., 1969. 469 p.
$23.

CONTENTS:

PREFACE. H. Liebowitz (George Washington University, Washington, D.C.), p. vii-xii.

EVALUATION OF FRACTURE TESTS AND SPECIMEN PREPARATION. W. J. Hall (Illinois, University, Urbana, Ill.), p. 1-44. 40 refs. [See A69-33565 17-17]

PLANE STRAIN FRACTURE TOUGHNESS. J. E. Srawley (NASA, Lewis Research Center, Cleveland, Ohio), p. 45-68. 26 refs. [See A69-33566 17-17]

TEMPERATURE EFFECTS ON FRACTURE. W. E. Witzell and N. R. Adsit (General Dynamics Corp., San Diego, Calif.), p. 69-112. 40 refs. [A69-33567 17-17]

FRACTURE AND CARRYING CAPACITY OF NOTCHED COLUMNS. H. Liebowitz (George Washington University, Washington, D.C.), p. 113-171.

PRESTRESSED BRITTLE STRUCTURES. R. L. Barnett (Felt Products Manufacturing Co., Skokie, Ill.) and P. C. Hermann (Chicago Bridge and Iron Co., Plainfield, Ill.), p. 173-274. 30 refs. [See A69-33568 17-32]

DESIGN OF ATTACHMENTS AND CONNECTIONS WITH BRITTLE MATERIALS. W. H. Dukes and F. M. Anthony (Bell Aerospace Corp., Buffalo, N.Y.), p. 275-335. 21 refs.

EFFECTS OF RESIDUAL STRESS ON BRITTLE FRACTURE. A. A. Wells (Belfast, Queen's University, Belfast, Northern Ireland), p. 337-370.

BRITTLE FRACTURE IN WELDMENTS. W. H. Munse (Illinois, University, Urbana, Ill.), p. 371-438.

AUTHOR INDEX, p. 439-443.

SUBJECT INDEX, p. 444-455.

A69-33566 *
PLANE STRAIN FRACTURE TOUGHNESS.
John E. Srawley (NASA, Lewis Research Center, Cleveland, Ohio).
IN: FRACTURE: AN ADVANCED TREATISE. VOLUME 4 -

ENGINEERING FRACTURE DESIGN. [A69-33564 17-17]
Edited by Harold Liebowitz.
New York, Academic Press, Inc., 1969, p. 45-68. 26 refs.

The general concept of the K_{Ic} plane strain fracture toughness is reviewed, and the current (tentative) standard procedure for determination of K_{Ic} with crack-notched bend specimens is discussed in detail. The standard procedure constitutes an operational definition of K_{Ic} which is somewhat arbitrary, but no more so than is the definition of offset yield strength. Experimental data for high-strength steels, titanium, and aluminum alloys validate the standard procedure for determination of K_{Ic}, and confirm that it is reasonable to regard K_{Ic} as an inherent material property which controls fracture under conditions of sufficiently high constraint. However, the required specimen dimensions increase in proportion to the square of the ratio of K_{Ic} to yield strength, and impractically large specimens may be required for tough, low-strength materials. The standard test procedure for bend specimens can be adapted to other types of specimens with the aid of information given in an appendix. (Author)

A69-34186 *
CREEP OF POWDER METALLURGY RHENIUM AT 0.43 TO 0.72 T_m.
Peter L. Raffo and Walter R. Witzke (NASA, Lewis Research Center, Cleveland, Ohio).
Metallurgical Society of AIME, Transactions, vol. 245, Apr. 1969, p. 889, 890. 6 refs.

Description of some exploratory experiments designed to study the creep rate/stress/temperature relation and other facets of the creep of rhenium. The tests were carried out in vacuum in the temperature range from 2200 to 4000°F at stresses ranging from 4 to 20 ksi. The variation of minimum creep rate with stress and temperature is shown for recrystallized unalloyed rhenium, and the stress dependence of the temperature-compensated minimum creep rate for recrystallized unalloyed rhenium is given. G.R.

A69-35182 *#
A STUDY OF ADHESION TO A RHENIUM SURFACE WITH LEED.
Donald H. Buckley (NASA, Lewis Research Center, Cleveland, Ohio).
American Vacuum Society and American Institute of Mining, Metallurgical, and Petroleum Engineers, Vacuum Metallurgy Conference, Pittsburgh, Pa., June 16-19, 1969, Paper. 27 p. 12 refs.

Study, in a LEED apparatus, of the adhesion of a quartz fiber to a rhenium (10$\bar{1}$0) plane. Forces applied to the fiber in contact with the surface as well as those required to separate the solid surfaces were measured. LEED patterns were obtained before and after adhesive contact for both clean surfaces and surfaces with an oxygen layer. Two adsorption structures were seen to develop with the admission of oxygen to the (10$\bar{1}$0) surface of rhenium, a near (2 x 2) structure and also a (1 x 3) structure. Adhesion of the quartz to rhenium occurred in the presence and in the absence of the oxygen layers. On surface separation, brittle fracture of quartz was observed to occur. (Author)

A69-35184 *#
EFFECT OF TEMPERATURE AND PRESSURE ON CAVITATION DAMAGE TO A COBALT BASE ALLOY IN SODIUM.
Stanley G. Young and James R. Johnston (NASA, Lewis Research Center, Cleveland, Ohio).
American Society for Testing and Materials, Annual Meeting, 72nd, Atlantic City, N. J., June 22-26, 1969, Paper. 25 p. 15 refs.

A vibratory apparatus was used to subject the cobalt-base alloy, L-605, to cavitation damage in sodium at 400, 800, and 1200°F. Cover gas pressures were varied from 1 to 4 atm (1 to 4 x 10^5 N/m^2) at each temperature. Increasing pressure increased the cavitation damage at each test temperature. Damage was greatest at the 800°F test temperature for all pressures. A volume loss rate contour diagram was constructed to show cavitation damage in terms of the combined temperature and pressure of the sodium. (Author)

A69-35504 *
APPLICATION OF ADVANCED MATERIALS TO TRUSS STRUCTURES.
John G. Davis, Jr. and Donald R. Rummler (NASA, Langley Research Center, Hampton, Va.).
IN: MATERIALS AND PROCESSES FOR THE 70'S; SOCIETY OF AEROSPACE MATERIAL AND PROCESS ENGINEERS, NATIONAL SYMPOSIUM AND EXHIBITION, 15TH, LOS ANGELES, CALIF., APRIL 29-MAY 1, 1969, PROCEEDINGS. (A69-35501 19-15)
North Hollywood, Western Periodicals Co.; Azusa, Calif., Society of Aerospace Material and Process Engineers (Science of Advanced Materials and Process Engineering Proceedings. Volume 15), 1969, p. 37-57. 7 refs.

Lightly loaded truss-type structures applicable to unmanned spacecraft have been fabricated using beryllium, Be-38% Al alloy, and uniaxial boron filament-reinforced epoxy tubing with adhesively bonded joints. The trusses were subjected to both dynamic and static loading conditions. Weight savings in excess of 50%, compared to an aluminum truss, have been demonstrated. (Author)

A69-35523 *
INVESTIGATIONS OF THE UNIQUE MEMORY PROPERTIES OF 55-NITINOL ALLOY.
John E. Cooper, David E. Bowker (NASA, Langley Research Center, Applied Materials and Physics Div., Hampton, Va.), and William B. Cross (Goodyear Aerospace Corp., Akron, Ohio).
IN: MATERIALS AND PROCESSES FOR THE 70'S; SOCIETY OF AEROSPACE MATERIAL AND PROCESS ENGINEERS, NATIONAL SYMPOSIUM AND EXHIBITION, 15TH, LOS ANGELES, CALIF., APRIL 29-MAY 1, 1969, PROCEEDINGS. (A69-35501 19-15)
North Hollywood, Western Periodicals Co.; Azusa, Calif., Society of Aerospace Material and Process Engineers (Science of Advanced Materials and Process Engineering Proceedings. Volume 15), 1969, p. 265-274. 16 refs.

An analysis is presented of experimental investigations conducted to evaluate certain mechanical properties associated with the unique memory effect of 55-Nitinol alloy. Tests were conducted on 100-, 20-, 15-, and 10-mil-diam wires and 6- and 3-mil-thick foil specimens. The analysis included determination of degree of shape recovery, restoring force, and mechanical work capability as a function of temperature and initial strain levels. Stress-strain and electrical resistivity measurements as a function of temperature are also presented. (Author)

A69-36435 *
EFFECT OF STRESS RATIO ON FATIGUE-CRACK GROWTH IN 7075-T6 ALUMINUM-ALLOY SHEET.
C. Michael Hudson and Joseph T. Scardina (NASA, Langley Research Center, Hampton, Va.).
(National Symposium on Fracture Mechanics, Lehigh University, Bethlehem, Pa., June 19-21, 1967.)
Engineering Fracture Mechanics, vol. 1, Apr. 1969, p. 429-446. 14 refs.

Results of axial-load fatigue-crack-propagation tests conducted on 12-in.-wide sheet specimens made of 7075-T6 aluminum alloy. These tests were made at stress ratios R (ratio of the minimum stress to the maximum stress) ranging from -1.0 to 0.8 and at maximum stress levels ranging from 5 to 50 ksi to study the effects of stress ratio on fatigue-crack growth. The fatigue-crack-propagation data were analyzed using Paris' stress-intensity analysis (1964). The data from tests at negative R values fell into a relatively narrow scatter band, along with the results from the R equals 0 tests on a plot of rate against stress-intensity range. Apparently, the compression portion of the loading cycle did not significantly affect crack-growth in these tests. The data from tests at different positive stress ratios fell into discrete bands on these plots. These bands varied systematically with R—i.e., the higher the stress ratio at a given range of the stress-intensity factor, the higher the rate of fatigue-crack growth. This spread in rates was small at the lower stress-intensity range, but became progressively larger as the stress-intensity range was increased. Semiempirical equations developed by Forman et al.,

(1966), by Broek and Schijve (1963), and by Paris were fitted to the data from this investigation, using a least-squares fit. Forman's equation gave the best fit to the data. The fracture surfaces of the specimens changed from the normal mode to a shear mode within a reasonably narrow range of crack growth rates for all R values.The stress-intensity range at transition was approximately a constant for tests at negative stress ratios. Forman's equation adequately represented the variation between the stress ratio and the stress-intensity range at positive stress ratios. A.B.K.

A69-36440 * #
MASS DEPENDENCE OF SELF-DIFFUSION IN IRON.
D. Graham (NASA, Lewis Research Center, Cleveland, Ohio).
Journal of Applied Physics, vol. 40, May 1969, p. 2386-2390. 12 refs.

Study of the mass dependence of self-diffusion in iron by serial sectioning in the alpha, gamma, and delta phases of iron. Values for the isotope effect, assuming a single vacancy exchange, are 0.71 ± 0.06 at 1452 C (bcc), 0.79 ± 0.05 at 1338 C (fcc), and 0.69 ± 0.14 at 869 C (bcc). Thus, in each case the isotope effect equals the correlation factor within experimental error. Measurements at 720 and 770 C appear to be influenced by diffusion along grain boundaries, producing a marked reduction in the apparent isotope effect. Z.W.

A69-39434 *
HOT SALT STRESS CORROSION OF A TITANIUM ALLOY—GENERATION OF HYDROGEN AND ITS EMBRITTLING EFFECT.
H. R. Gray (NASA, Lewis Research Center, Cleveland, Ohio).
Corrosion, vol. 25, Aug. 1969, p. 337-341. 18 refs.

Alloy specimens of Ti-8Al-1Mo-1V were salt-coated and exposed to conditions conducive to hot salt stress corrosion. Subsequent tensile tests revealed that ductility was strain-rate and temperature sensitive. Embrittlement was more pronounced at slow crosshead speeds in the vicinity of ambient temperature. After salt exposure, ductility was restored by vacuum annealing. Substantial increases in hydrogen content were measured in embrittled specimens. These results demonstrate that hydrogen can be generated during elevated temperature exposure to salt, and that the subsequent embrittlement is a manifestation of "slow strain rate" hydrogen embrittlement. (Author)

A69-43718 * #
NASA PROGRAMS FOR DEVELOPMENT OF HIGH-TEMPERATURE ALLOYS FOR ADVANCED ENGINES.
John C. Freche and Robert W. Hall (NASA, Lewis Research Center, Cleveland, Ohio).
(International Council of the Aeronautical Sciences, Congress, 6th, Munich, West Germany, Sept. 9-13, 1968, Paper 68-26.)
Journal of Aircraft, vol. 6, Sept.-Oct. 1969, p. 424-431. 34 refs.

Description of an extensive program to develop improved materials for advanced air-breathing engines. Considerable progress has been made in several areas. Of most immediate importance is the development of an advanced cast nickel-base alloy, NASA-TRW VI-A. This alloy shows approximately a 50°F (28°C) improvement in temperature over the strongest superalloys currently in use. Even larger improvements over the strengths of currently used superalloys have been achieved in chromium alloys and metal-matrix composite materials. However, many problems remain to be solved before the opportunities indicated by these latter developments can be used in aircraft engines. Foremost among the needs at this time is that for improved oxidation, nitridation, and erosion-resistant coatings to permit use of these stronger materials at temperatures consistent with their strength potential. M. M.

N69-10262# Joint Publications Research Service, Washington, D. C.
USE OF LASER RADAR FOR INVESTIGATING ATMOSPHERIC PROPERTIES
O. K. Kostko *In its* Collection of Articles on Instr. for Studying Upper Atmosphere 22 Oct. 1968 p 88-110 refs (See N69-10251 01-14)
Avail: CFSTI

The possibility of using lasers for atmospheric studies is examined on the basis of some foreign investigations. Author

N69-10764*# National Aeronautics and Space Administration. Langley Research Center, Langley Station, Va.
AN EVALUATION OF COATED MOLYBDENUM AND COLUMBIUM ALLOYS IN HIGH-TEMPERATURE SUPERSONIC AIRSTREAMS
Irvin M. Miller Washington Nov. 1968 32 p refs
(NASA-TN-D-4877) Avail: CFSTI CSCL 11F

An experimental study was made to investigate the oxidation behavior of four commercially coated refractory metal systems in supersonic airstreams: Durak B and Vought IX coated TZM, and Cr-Ti-Si and Cr-$MoSi_2$ coated Cb-752. Cyclic coating life and temperature data were obtained on 0.375-inch-diameter (0.953 cm) blunt-nose models at surface temperatures from 2600° to 3000°F (1700° to 1920°K) and at air stagnation pressures behind the shock wave of 0.03, 0.10, and 5.5 atmospheres. The oxidation behavior of uncoated molybdenum- and columbium-alloy models of the same size and shape was also studied in the same test environments. Coating life of the TZM/Durak B, Cb-752/Cr-Ti-Si, and Cb-752/Cr-$MoSi_2$ systems was significantly lower at air stagnation pressures of 0.10 and 0.03 atmosphere than at 5.5 atmospheres. At these low-pressure conditions, the coating life of these three coating systems did not exceed 32 minutes. The uncoated columbium alloys oxidized catastrophically at air stagnation pressures of 0.10 and 0.03 atmosphere in less than 20 seconds at temperatures well below the melting points of the alloys. Author

N69-10827*# National Aeronautics and Space Administration. Lewis Research Center, Cleveland, Ohio.
FEASIBILITY OF PRODUCING DISPERSION STRENGTHENED CHROMIUM BY BALL-MILLING IN HYDROGEN HALIDES
Alan Arias Washington Nov. 1968 39 p refs
(NASA-TN-D-4912) Avail: CFSTI CSCL 11F

Chromium, with and without 4 volume percent thoria, and nickel powders were ground to fine powder sizes by ball milling in gaseous hydrogen halides. After reducing the milled chromium in flowing hydrogen under pulsating pressure at about 680°C, submicron size powders with 4 to 500 ppm residual halogens were obtained. The compacted chromium-thoria alloys had interparticle spacings ranging from 2.1 to 6.5 micrometers. After 100 hours at 1318° C the interparticle spacing of the 2.1-micrometer alloy increased to 5.2 micrometers. Submicron size chromium and nickel powders were also obtained by pulsating hydrogen reduction of their chlorides. Author

N69-10931*# National Aeronautics and Space Administration. Lewis Research Center, Cleveland, Ohio.
ABSORPTION RATE STICKING PROBABILITIES FOR OXYGEN ON COLUMBIUM AND DILUTE COLUMBIUM-ZIRCONIUM ALLOYS
Charles A. Barrett Washington Nov. 1968 41 p refs
(NASA-TN-D-4885) Avail: CFSTI CSCL 11F

Sticking probabilities for oxygen on columbium and dilute columbium–zirconium alloys were derived from ratios of oxygen absorption rates to their corresponding oxygen fluxes. Oxygen test pressures were varied from 10^{-7} to 10^{-5} torr over temperatures between 1158 and 1373 K. The absorption rates were derived from a pressure-drop technique and fluxes from constant pressure measurements. The kinetics of the reaction are discussed as well as characteristics of the test method. Author

N69-11012*# National Aeronautics and Space Administration. Langley Research Center, Langley Station, Va.

COMPRESSIVE PROPERTIES AND COLUMN EFFICIENCY OF METALS REINFORCED ON THE SURFACE WITH BONDED FILAMENTS

George W. Zender and H. Benson Dexter Washington Nov. 1968 47 p refs

(NASA-TN-D-4878) Avail: CFSTI CSCL 11D

Compressive tests were performed on metal tubes axially reinforced with filaments bonded to the tube outer surface. Sixty-eight magnesium, aluminum, and titanium tubes reinforced with boron or S-glass filaments were tested. The specimens consisted, by volume, of approximately 50 percent metal, 25 percent filament, and 25 percent epoxy resin. Remarkable mechanical properties indicating substantial weight-saving potential for aerospace structures were obtained. Mass-strength comparisons using the experimental results showed the boron-reinforced metals to weigh from 25 to 40 percent of the weight ot titanium for compressive crushing strength and from 40 to 60 percent for column instability. Magnesium or aluminum reinforced with S-glass filaments weighs less than 50 percent of the weight titanium for compressive crushing strength and about 70 percent for column instability. The concept of bonding high-performance filaments to metal structures builds upon the large existing background of fabrication technology for aerospace structures. This advantage along with the potential weight saving indicated by test data suggests important practical application in structural design. Author

N69-11420*# Astro Research Corp., Santa Barbara, Calif.

CERTAIN PHYSICAL PROPERTIES AND APPLICATIONS OF NITINOL

H. U. Schuerch Washington NASA Nov. 1968 67 p refs

(Contract NAS7-426)

(NASA-CR-1232; ARC-R-280) Avail: CFSTI CSCL 11F

Experimental investigations have been performed on a number of physical properties of the nickel-titanium alloy known as Nitinol. The program was limited to wires and tapes of two specific compositions. Four types of tests were undertaken to characterize some of the thermomechanical memory effects observed in this alloy: (1) Stress-strain, for repeated load applications at constant temperature; (2) Temperature-elongation, for repeated temperature cycles at constant stress level; (3) Temperature-elongation for repeated temperature cycles at discontinuously variable stress levels simulating a thermodynamic power generation cycle; and (4) Differential thermal analysis of unstressed samples for the complete transition temperature range during repeated cooling and heating cycles. Several engineering models demonstrating different applications of Nitinol were designed, fabricated, and tested. Descriptions of the physical properties characterized in the tests and of the various models and devices are presented in the report. Author

N69-14193*# National Aeronautics and Space Administration, Washington, D. C.

THE METALLURGY, BEHAVIOR, AND APPLICATION OF THE 18-PERCENT NICKEL MARAGING STEELS A Survey

A. M. Hall and C. J. Slunder 1968 143 p refs Prepared by Battelle Mem. Inst., Columbus, Ohio

(NASA-SP-5051) Avail: SOD $1.50; CFSTI CSCL 11F

A comprehensive view is presented on the technical status of 18% nickel maraging steels and on the outlook for the future of these materials. Research and development efforts are reviewed in production, mechanical and physical properties, corrosion behavior, physical metallurgy, as well as in forming, joining, and heat treating. Patterns of usage, methods of producing a broad range of mill products, and other applications and uses are also discussed. The purpose of the survey was to provide the research worker, the materials engineer, the process engineer, the designer, and other interested persons information to assist in the selection of these steels for appropriate application and to serve as a point of departure for further study and evaluation of the maraging steels. The majority of the steels reviewed contained additions of cobalt, molybdenum, and titanium. B.P.

N69-14403*# National Aeronautics and Space Administration. Lewis Research Center, Cleveland, Ohio.

REVIEW OF DUCTILIZING OF GROUP VIA ELEMENTS BY RHENIUM AND OTHER SOLUTES

William D. Klopp Washington Dec. 1968 36 p refs

(NASA-TN-D-4955) Avail: CFSTI CSCL 11F

The ductility of Group 6A alloys containing rhenium and other solutes from Groups 7A and 8A was reviewed. The rhenium ductilizing effect, found in Group 6A alloys containing 25 to 35 at. %Re, is promoted by other solutes from Group 7A and the early portions of Group 8A. The hardness minimums and lowered ductile-brittle transition temperatures observed in dilute Mo-Re and W-Re alloys are attributed to solution softening. This phenomenon occurs at low temperatures and is common to many dilute body-centered-cubic alloys containing substitutional solutes. Author

N69-14873*# National Aeronautics and Space Administration. Langley Research Center, Langley Station, Va.

STRAIN RATE SENSITIVITY OF THREE TITANIUM ALLOY SHEET MATERIALS AFTER PROLONGED EXPOSURE AT 550°F (561°K)

Robert M. Baucom Washington Jan. 1969 33 p refs

(NASA-TN-D-4981) Avail: CFSTI CSCL 11F

Results are presented of an investigation of the effects of strain rate on three titanium-alloy sheet materials before and after prolonged exposure without stress at 550°F (561°K). The strain-rate sensitivity of the three alloys, Ti–8Al–1Mo–1V, Ti–4Al–3Mo–1V, and Ti–6Al–4V, was determined from the results of tensile tests performed at three strain rates on smooth and V-notched specimens. Little change in the tensile properties of smooth and V-notched specimens was observed at any given strain rate during accumulated exposure times up to 22,000 hours. This result indicates that the alloys under investigation are apparently stable for the exposures noted. The effect of an increase in strain rate on the tensile properties was generally a moderate increase in strength for each of the alloys. The sensitivity of Ti–8Al–1Mo–1V and Ti–4Al–3Mo–1V to sharp notches tended to decrease with an increase in strain rate. Author

N69-16380*# National Aeronautics and Space Administration. Lewis Research Center, Cleveland, Ohio.

HIGH TEMPERATURE MECHANICAL PROPERTIES OF POLYCRYSTALLINE HAFNIUM CARBIDE AND HAFNIUM CARBIDE CONTAINING 13-VOLUME-PERCENT HAFNIUM DIBORIDE

William A. Sanders and Hubert B. Probst Washington Jan. 1969 23 p refs

(NASA-TN-D-5008) Avail: CFSTI CSCL 11F

Hot pressed, single phase HfC and HfC containing 13-vol % HfB_2 were tested in three point transverse rupture to temperatures as high as 4755°F. Hot hardness tests were also run to 3200°F. Separate effects on the transverse rupture behavior of HfC due to the HfB_2 second phase and due to a grain size difference are discussed on the basis of strength, deformation, and metallographic results. The probable mechanisms responsible for deformation are also discussed. In hot hardness tests of HfC containing 13 vol % HfB_2 second phase, a change in the temperature dependency of hot hardness at 2600°F is discussed and related to the degree of cracking around indentations. Author

N69-16383*# National Aeronautics and Space Administration. Lewis Research Center, Cleveland, Ohio.
ANALYTICAL STUDY OF FLOW REDUCTION DUE TO OXIDATION OF WIRE-FORM POROUS SHEET FOR TRANSPIRATION COOLED TURBINE BLADES
Albert Kaufman Washington Jan. 1969 23 p refs
(NASA-TN-D-5001) Avail: CFSTI CSCL 11F

Cyclic and static oxidation data for wires of N155, Driver-Harris 242, TD nickel-chromium, and Hastelloy X from 1400°F to 2000°F were used to determine flow reduction effects for pore diameters from 10 to 100 micrometers and exposure times up to 600 hours. Analytical results were compared with experimental flow reduction data for oxidized wire-form porous sheets from other investigators. Conclusions were drawn as to the suitability of these materials for transpiration cooling with a metal temperature of 1800°F. Author

N69-16465*# National Aeronautics and Space Administration. Lewis Research Center, Cleveland, Ohio.
HOT-SALT STRESS-CORROSION OF TITANIUM ALLOYS: GENERATION OF HYDROGEN AND ITS EMBRITTLING EFFECT
Hugh R. Gary Washington Jan. 1969 20 p refs
(NASA-TN-D-5000) Avail: CFSTI CSCL 11F

Alloy specimens of Ti-8Al-1Mo-1V were salt coated and exposed to conditions conducive to hot salt stress corrosion. Subsequent tensile tests revealed that ductility was strain-rate and temperature sensitive. Embrittlement was more pronounced at slow crosshead speeds in the vicinity of ambient temperature. After salt exposure, ductility was restored by vacuum annealing. Substantial increases in hydrogen content were measured in embrittled specimens. These results demonstrate that hydrogen can be generated during elevated temperature exposure to salt and that the subsequent embrittlement is a manifestation of the phenomenon of slow-strain-rate hydrogen embrittlement. Author

N69-17277*# National Aeronautics and Space Administration. Lewis Research Center, Cleveland, Ohio.
EXAMINATION OF OXIDE SCALES ON HEAT RESISTING ALLOYS
Salvatore J. Grisaffe and Carl E. Lowell Washington Feb. 1969 44 p refs
(NASA-TN-D-5019) Avail: CFSTI

Twelve iron, nickel, and cobalt heat resisting alloys were cyclic furnace oxidation tested at from 1400° to 2200°F (1033 to 1478 K) for from 4 to 600 hours. Retained oxide scales and spall were identified using X-ray diffraction combined with X-ray fluorescence analyses. Metallography clarified scale growth sequences. After 600 hours at 2000°F (1366 K), the condition most studied, the best oxidation resistance, as reflected by weight change and spall weight, was exhibited by alloys forming single oxide scales of Al_2O_3 or Cr_2O_3. For alloys that developed multioxide scales, spinel constituent composition or lattice parameter did not correlate with oxidation resistance. Author

N69-18952*# United Aircraft Corp., East Hartford, Conn.
PROPERTIES OF HIGH EMITTANCE MATERIALS
R. E. Cleary, R. Emanuelson, W. Luoma, and C. Ammann Washington NASA Feb. 1969 139 p refs
(Contract NAS3-4174)
(NASA-CR-1278) Avail: CFSTI CSCL 11F

Results of a four year program to determine the suitability of selected high emittance materials for use as coatings on beryllium, Nb–1Zr, and AISI-310 stainless steels used in space power plant radiators are presented. Materials coated on beryllium included calcium, iron, and zirconium titanate, anodized beryllium, and aluminum oxide–aluminum titanate. Specimens were aged in vacuum at 800°, 1200°, and 1400°F for periods up to 1000 hours. The first three titanates were found to be compatible with beryllium for at least 1000 hours up to 1200°F, but the latter two coatings did not perform well. Long term emittance tests were conducted on calcium and iron titanate coated AISA-310 stainless steel, iron titanate coated Nb–1Zr, and Nb–1Zr coated with aluminum oxide–aluminum titanate. The stainless steel specimens were heated in vacuum to 1350°F for 20,000 hours, and the Nb–1Zr specimens were vacuum tested at 1700°F for 10,000 hours; all were thermally cycled to room temperature once a week. Varying degrees of stable emittance, bond strength, coating structure, and diffusion of coating constituents were found in the specimens as a function of hours tested, temperatures used, and thermal cycling. A.C.R

N69-19200*# National Aeronautics and Space Administration. Lewis Research Center, Cleveland, Ohio.
EXPLORATORY STUDY OF MECHANICAL PROPERTIES AND HEAT TREATMENT OF MOLYBDENUM-HAFNIUM-CARBON ALLOYS
Peter L. Raffo Washington Feb. 1969 44 p refs
(NASA-TN-D-5025) Avail: CFSTI CSCL 11F

A preliminary study was made of the structure and properties of Mo – Hf – C alloys. The compositions of the alloys ranged from 0.09 to 1.83 atomic percent Hf and 0.29 to 1.07 atomic percent C. The mechanical properties of these alloys were measured in the as-swaged, recrystallized, solution-treated, and aged conditions at room temperature and 1500° to 3000°F (1088 to 1922°K). The mechanical properties were compared with data on other molybdenum alloys the literature, and two commercial molybdenum alloys that were evaluated during this program. The Mo – Hf – C alloys show a strength advantage over the other alloys in creep-rupture tests at 2400°F (1588°K) and short-time tensile tests at 3000°F (1922°K). Author

N69-19203*# National Aeronautics and Space Administration. Langley Research Center, Langley Station, Va.
TENSILE PROPERTIES AND CREEP STRENGTH OF THREE ALUMINUM ALLOYS EXPOSED UP TO 25000 HOURS AT 200 DEG TO 400 DEG F (370 DEG TO 480 DEG K)
Dick M. Royster Washington Jan. 1969 44 p refs
(NASA-TN-D-5010) Avail: CFSTI CSCL 11F

The tensile properties and creep strength of three aluminum-alloy sheet materials exposed up to 25000 hours at 200° to 400° F were investigated. The materials investigated were clad 2024–T81, X2020–T6, and clad RR–58 aluminum alloys. These alloys are representative of the types considered for a supersonic transport operating in the Mach 2 speed range. The effect of longtime, elevated-temperature exposures was determined from changes in tensile and notch properties at room temperature. The short-time, elevated-temperature tensile properties as well as the tensile stress required to produce 0.1-percent creep were determined. Metallurgical studies were made to determine micro-structural changes in the alloys due to exposure. With the exception of the X2020–T6 alloy, the material tensile properties were not severely affected by longtime unstressed exposure. The X2020–T6 alloy also exhibited poor notch toughness. Low creep strength in the aluminum alloys at temperatures above 300° F may limit their use for longtime exposures. Author

N69-19827*# National Aeronautics and Space Administration. Langley Research Center, Langley Station, Va.
A METHOD FOR CHARACTERIZING THE SURFACE CLEANLINESS DURING ADHESION TESTING
James H. Bradford, Jr. Washington Mar. 1969 45 p refs
(NASA-TN-D-5055) Avail: CFSTI CSCL 11F

It has been shown that the degree of adhesion of metals depends upon the surface cleanliness. The paper presents a method

that was used to characterize the surface cleanliness of nickel during an adhesion experiment. The change in the work function of the surface as the metal was cleaned was used to indicate the degree of cleanliness. The point at which the work function was stable with additional cleaning was used as the cleanest surface. The cleaning technique was an argon-ion bombardment and heating process. Measurements showed that the maximum adhesion forces occurred when the surfaces were the cleanest. The cleaned surfaces were recontaminated with oxygen and the adhesion force decreased to zero. Author

N69-19831*# Aerojet-General Corp., Sacramento, Calif.
HYDROGEN GAS PRESSURE VESSEL PROBLEMS IN THE M-1 FACILITIES
J. S. Laws, V. Frick, and J. McConnell Washington NASA Mar. 1969 65 p refs
(Contract NAS3-2555)
(NASA-CR-1305; Rept-8800-67) Avail: CFSTI CSCL 13D

Pertinent data and information are given relating to a series of failures, or structural defects, experienced with high pressure, gaseous hydrogen storage receivers procured for, installed, and used as part of the M–1 Engine Development Program. Author

N69-19886*# Varian Associates, San Carlos, Calif.
SOLUBILITY AND DIFFUSION OF OXYGEN IN TANTALUM
M. Parkman, R. Pape, R. McRae, D. Brayton, and L. Reed Washington NASA Feb. 1969 155 p refs
(Contract NAS3-7626)
(NASA-CR-1276; APO-68-1101) Avail: CFSTI CSCL 11F

The solubility of oxygen in tantalum between 600° and 900°C was determined by using a resistivity technique. Carefully reproduced pulses of oxygen were admitted to a high vacuum quartz tube furnace containing a tantalum wire. During each pulse, oxygen was maintained in contact with the specimen for a standard reproduced time after which the oxygen was pumped out and the resistance measured. A plot of change in resistance from the starting value versus number of oxygen charges resulted in a linear curve followed by one or more parabolic curves. The end of the linear section was interpreted to be the phase boundary. Specimens were analyzed by neutron activation to relate change in resistance to oxygen content. Changes in slope of the resistance versus temperature curve for Ta containing between 0.007% and 0.12% oxygen were found at about 450° and 750°C. An anomoly in the curve of resistance versus temperature for oxygen-doped Ta was found at about 900°C. Both of these effects were found in the 2-phase region and appear to be associated with the oxides. Preliminary solubility data were obtained with columbium and Ta–10W alloy. A trial run was made to test a proposed method of measuring diffusion of oxygen in refractory metals. Author

N69-19930*# National Aeronautics and Space Administration. Lewis Research Center, Cleveland, Ohio.
COMPATIBILITY TESTS OF MOLTEN URANIUM WITH TUNGSTEN AND TUNGSTEN—1.5 PERCENT HAFNIUM
Philip D. Takkunen Washington Mar. 1969 32 p refs
(NASA-TN-D-5076) Avail: CFSTI CSCL 11F

Isothermal compatibility tests were conducted on sealed tungsten (W) and tungsten–1.5-weight-percent hafnium (W–1.5Hf) capsules containing uranium (U) for 10 to 200 hours at 1200° and 1500° C. Extensive intergranular attack was observed in wrought W rod and in vapor deposited W. Hafnium appeared to offer some promise in reducing intergranular attack on W. Single crystal W appeared to be compatible with molten U although some evidence of mass transfer attack was found. In addition, U climbed up the sides of the single crystal capsules and attacked grain boundaries in the closure weld. Cracks were formed in all the capsule walls during cooling after U had solidified. Author

N69-20789*# National Aeronautics and Space Administration. Lewis Research Center, Cleveland, Ohio.
SOLUBILITIES OF VANADIUM, TITANIUM, AND ZIRCONIUM IN LIQUID POTASSIUM
Stephan Stecura Washington Mar. 1969 21 p refs
(NASA-TN-D-5093) Avail: CFSTI CSCL 07D

The solubility of vanadium in liquid potassium containing less than 20 wt ppm of oxygen between 1012 and 1341 K is about 6 to 70 wt ppm, respectively. The heat of solution for the vanadium solubility is 21 ± 4 kilocalories per mole (87.9 kJ/mole). Titanium and zirconium solubilities in liquid potassium between 1020 and 1341 K are less than 4 and 10 wt ppm, respectively. Vanadium, titanium, and zirconium solubilities were studied in potassium doped with potassium nitrate (KNO_3). The data suggest that KNO_3 is not a good doping agent for determining the effect of oxygen on the solubilities of transition metals in liquid potassium. Author

N69-21404*# National Aeronautics and Space Administration. Lewis Reserrch Center, Cleveland, Ohio.
FABRICATION OF CERMETS OF URANIUM NITRIDE AND TUNGSTEN OR MOLYBDENUM FROM MIXED POWDERS AND FROM COATED PARTICLES
Philip D. Takkunen Washington Apr. 1969 35 p refs
(NASA-TN-D-5136) Avail: CFSTI CSCL 11B

Cermets containing uranium nitride particles dispersed in a matrix of tungsten or molybdenum were fabricated by cold-pressing and sintering mixed powders and by hot isostatic compaction of metal-coated UN particles. The effects of powder particle size and sintering conditions (time, temperature, and atmosphere) on the microstructure and density of cermets containing 50 volume percent UN were studied. Some sintered cermets were further densified by hot pneumatic impaction. Spherical UN particles coated with W or Mo were consolidated by hot isostatic compaction to produce dense cermets containing from 50 to 70 volume percent UN. Author

N69-22993*# National Aeronautics and Space Administration. Lewis Research Center, Cleveland, Ohio.
DYNAMIC STRAIN AGING DURING THE CREEP AND TENSILE TESTING OF A MOLYBDENUM-TITANIUM-CARBON ALLOY
Peter L. Raffo Washington Apr. 1969 26 p refs
(NASA-TN-D-5169) Avail: CFSTI CSCL 11F

A study was made of the creep and tensile properties of a Mo–0.82 Ti–0.20 C (at. %) alloy in the temperature range 1800° to 3200°F. A peak in the flow stress–temperature curve was noted for this alloy at 1800°F. The strain rate sensitivity of the flow stress was negative in the temperature range 1500° to 2200°F. The creep rate of this alloy above 2400°F has a stress and temperature dependence equal to that of unalloyed molybdenum. At temperatures below about 2400°F, the creep rate at a given stress depends not only on the stress and temperature, but on the entire preloading history. Precipitation occurs on dislocations in specimens crept at 1800°F. It was deduced that the strengthening effects noted during the creep and short time tests are directly related to carbide precipitation during plastic deformation. Precipitation during deformation has two main effects. The first is associated with the decrease in the mobile dislocation density which leads to a greatly decreased creep rate in a constant stress creep test and an increased work hardening rate in a constant strain rate tensile test. Secondly, precipitation during deformation may decrease the rate of recovery. Author

N69-23004*# National Aeronautics and Space Administration. Langley Research Center, Langley Station, Va.
MECHANICAL PROPERTIES AND COLUMN BEHAVIOR OF

THIN WALL Be–38Al ALLOY TUBING
Donald R. Rummler Washington Apr. 1969 48 p refs
(NASA-TN-D-5145) Avail: CFSTI CSCL 11F

The results of an experimental investigation to determine the mechanical properties at room temperature and column behavior of commercially produced Be–38Al alloy tubing are presented. The investigation included tubing in both the as-extruded and annealed conditions. Microhardness measurements and metallurgical studies were also performed. Column-buckling loads were predicted by using the tangent modulus, derived from compressive stress-strain curves, in the inelastic column-buckling equation. Author

N69-23084*# National Aeronautics and Space Administration. Lewis Research Center, Cleveland, Ohio.
EXPLORATORY STUDY OF SILICIDE, ALUMINIDE, AND BORIDE COATINGS FOR NITRIDATION–OXIDATION PROTECTION OF CHROMIUM ALLOYS
Joseph R. Stephens and William D. Klopp Washington Apr. 1969 28 p refs
(NASA-TN-D-5157) Avail: CFSTI CSCL 11F

Chromium alloys were coated with silicon, aluminum, and boron by pack cementation. None of these simple coatings provided adequate nitridation-oxidation protection for a chromium +0.17 wt % yttrium alloy substrate as shown by a substantial increase in the ductile-brittle transition temperature after air exposure for 100 hr at 2100°F (1420°K). Iron modified silicide coatings afforded good protection, holding the transition temperature of air exposed specimens to 350°F (450°K) compared to 200°F (370°K) for recrystallized uncoated specimens. Additional attractive modifying elements included iron-molybdenum, iron-molybdenum-tungsten, iron-molybdenum-tungsten-titanium, and vanadium-molybdenum-tungsten-titanium. Author

N69-23465*# National Aeronautics and Space Administration. Lewis Research Center, Cleveland, Ohio.
SIGMA PHASE FORMATION AND ITS EFFECT ON STRESS-RUPTURE PROPERTIES OF IN-100
Robert L. Dreshfield and Richard L. Ashbrook Washington Apr. 1969 26 p refs
(NASA-TN-D-5185) Avail: CFSTI CSCL 11F

Three IN-100 compositions, sigma free to very sigma prone, were made by adding aluminum and titanium to one master heat. At 1550°F (843°C), the sigma free alloy had no sigma after 5000 hours; the very sigma prone alloy formed sigma in less than 24 hours. Sigma prone alloys had rupture lives as low as 10 percent of that expected for sigma free alloys in sigma forming, temperature–time realms. Sigma phase had no discernible effect on rupture ductility. The use of time–temperature parameters in sigma forming alloys was analyzed. Author

N69-23731*# National Aeronautics and Space Administration. Lewis Research Center, Cleveland, Ohio.
CREEP-RUPTURE DATA FOR WELDED N-155 TUBES
Richard E. Morris Washington May 1969 31 p refs
(NASA-TN-D-5195) Avail: CFSTI CSCL 11F

Creep rupture pressure tests were conducted to obtain creep deformation and lifetime data for use in the design of a helium-to-air heat exchanger with a 10,000 hour life for nuclear airplane application. Design curves are presented for 2 percent strain, 5 percent strain, and rupture in a graph of stress against Larson-Miller parameter. Creep strength of the tubes was about 2/3 of the sheet strengths given in handbooks. Tube strength was limited by the strength of the weld. Thermally cycled specimens had approximately 10 percent lower strength and higher average equivalent bore strains than specimens tested at constant temperature. Author

N69-25243*# National Aeronautics and Space Administration. Lewis Research Center, Cleveland, Ohio.
CORROSION OF METALS IN DEIONIZED WATER AT 30°C (100°F)
Barbara A. Johnson Washington May 1969 11 p refs
(NASA-TM-X-1791) Avail: CFSTI CSCL 11F

The corrosion of copper, cadmium, tungsten, and Mallory-1000 is discussed. Mention is made of 304 stainless steel, 1100 aluminum, titanium, tantalum, silver, and boron steel, all of which showed no corrosion. The importance of corrosion in nuclear reactor cooling water is discussed. Data were obtained by chemical analyses of the water rather than from physical measurement of the test specimen. Author

N69-25363*# National Aeronautics and Space Administration. Lewis Research Center, Cleveland, Ohio.
LEED STUDIES OF ADHESION TO A RHENIUM SURFACE
Donald H. Buckley Washington May 1969 19 p refs
(NASA-TN-D-5229) Avail: CFSTI CSCL 11A

Adhesion studies were conducted in a LEED apparatus with a quartz fiber contacting a rhenium $(10\bar{1}0)$ plane. Forces applied to the fiber in contact with the surface as well as those required to separate the solid surfaces were measured. LEED patterns were obtained before and after adhesive contact for both clean surfaces and surfaces with an oxygen layer. Adhesion of the quartz to rhenium occurred in the presence of, as well as the absence of, the oxygen layer. On surface separation, brittle fracture of quartz was observed to occur. Two structures were seen to develop with the admission of oxygen to the $(10\bar{1}0)$ surface of rhenium, a near (2×2) structure and also a (1×3) structure. Author

N69-26192*# National Aeronautics and Space Administration. Lewis Research Center, Cleveland, Ohio.
EVALUATION OF TWO NICKEL-BASE ALLOYS, ALLOY 713C AND NASA TAZ-8A, PRODUCED BY EXTRUSION OF PREALLOYED POWDERS
John C. Freche, William J. Waters, and Richard L. Ashbrook Washington May 1969 33 p refs
(NASA-TN-D-5248) Avail: CFSTI CSCL 11F

Prealloyed powders of Alloy 713C and TAZ-8A were made by inert gas atomization and extruded. The powder products were evaluated by tensile and stress rupture tests in the as-extruded and heat-treated conditions. Significant improvements in room temperature and 1200°F (649°C) strength were obtained over the as-cast condition, but lower strengths and superplastic behavior were observed for the extruded powder alloys in the 1800° to 2000°F (982° to 1094°C) temperature range. It was possible to hot form the TAZ-8A powder product at low strain rates and low applied loads. Heat treatments eliminated superplasticity. Author

N69-26258*# National Aeronautics and Space Administration. Lewis Research Center, Cleveland, Ohio.
LEED STUDY OF THE ADHESION OF VARIOUS MATERIALS TO THE (111) SURFACE OF NICKEL
Donald H. Buckley Washington May 1969 23 p refs
(NASA-TN-D-5247) Avail: CFSTI CSCL 11F

Adhesion studies were made with copper, tungsten, oxidized tungsten, and quartz contacting a nickel (111) surface. The copper, tungsten, oxidized tungsten, and quartz were in the form of 1 mm diameter flat ended fibers. Loads of 20 to 150 mg were employed with surface contact times of 10 to 300 sec. The nickel (111) surface was examined before and after adhesion contact with LEED. With clean metals, fracture in tension occurred in the lower cohesive strength material. When copper contacted nickel, a surface alloy formed. The contacting of clean nickel with an oxidized

tungsten surface resulted in oxygen transfer from tungsten to nickel with surface rearrangement. Quartz adhered to nickel with fracture occurring in the quartz on separation of the surfaces. Author

N69-26952*# National Aeronautics and Space Administration. Lewis Research Center, Cleveland, Ohio.

CONTROLLED OXYGEN ADDITIONS TO REFRACTORY METALS

Charles A. Barrett Washington May 1969 16 p refs

(NASA-TM-X-1799) Avail: CFSTI CSCL 11F

Controlled oxygen additions (doping) to refractory metals were carried out by a pressure-drop technique involving the use of an oxygen leak into a vacuum system at elevated temperatures. The method and apparatus are described, as well as the variability, precision, and accuracy of the method. Author

N69-26959# Air Force Systems Command, Wright-Patterson AFB, Ohio. Foreign Technology Div.

FATIGUE STRENGTH OF ELECTROLYTICALLY BORATED STEEL IN RELATION TO THE CHARACTER OF DISTRIBUTION OF INTERNAL STRESSES

B. G. Gurevich et al 29 Oct. 1968 10 p refs Transl. into ENGLISH from Fiz.-Khim. Mekhan. Materialov, Akad. Nauk Ukr. SSF (Kiev), v. 3, no. 6, 1967 p 693–699

(AD-683990; FTD-MT-24-380-68) Avail: CFSTI CSCL 11/6

Electrolytic coating of steel with boron, which is accompanied by the formation of high-hardness borides in the surface layer of steel, is employed to enhance the wear resistance of machine parts performing under conditions of abrasive wear. Since such machine parts often are exposed to cyclic loads, it was of interest to elucidate the effect of electrolytic boronizing on the fatigue strength of steels. Accordingly, the results of fatigue tests of electrolytically boronized specimens of 38KhS steel are presented. The decrease in fatigue strength after boronizing is due to the boronizing-induced compressive stresses in the boronized layer; these are balanced by high tensile stresses which are chiefly located in an extremely thin layer directly underneath the boronized layer. TAB

N69-27061*# National Aeronautics and Space Administration. Lewis Research Center, Cleveland, Ohio.

A PROPOSED MODEL FOR THE EFFECT OF OXIDATION ON THE HIGH-TEMPERATURE DEFORMATION OF NICKEL

James S. Wolf Washington Jun. 1969 71 p refs

(NASA-TN-D-5266) Avail: CFSTI CSCL 11F

The high-temperature deformation of unalloyed nickel is strongly affected by the presence of surface scale layers formed when creep tests are conducted in oxygen. Under applied stresses of 6.90 to 13.79 MN/m^2 (1000 to 2000 psi), the deformation rate of specimens at 1000°C is initially enhanced and later retarded upon their contact with oxygen gas. A phenomenological model of the transient creep process is proposed which accounts for these observations in terms of the self-pressurization and barrier qualities of the scale. A generalization of this model to other materials and to other environments is considered. Author

N69-27300*# Israel Program for Scientific Translations, Ltd., Jerusalem.

HIGH TEMPERATURE STRENGTH OF MATERIALS

G. S. Pisarenko, ed., et al, 1969 639 p refs Transl. into ENGLISH of the Book "Prochnost' Materialov Pri Vysokikh Temperaturakh" Kiev, Izd. Naukova Dumka, 1966 Published for NASA and NSF /ts IPST Cat. No. 5141

(NASA-TT-F-508; TT-68-50308) Copyright. Avail: CFSTI CSCL 11F

The results of investigations of the high temperature strength of materials and machine parts are presented. Emphasis is placed on the methods of investigating the physical and mechanical strength and ductility characteristics of a large class of heat resistant materials (mostly high melting) in a wide temperature range (up to 3500°k), under the action of constant and variable thermal and mechanical loads, inducing simple and compound states of stress. The apparatus, machines, stands, and instruments designed for this purpose are also described. The strength characteristics of different materials subjected to static (short and long time), as well as to vibrational loads, are discussed, together with thermal fatigue and thermal shock, including the cyclic action of high temperature gas flow. Elasticity characteristics and the load carrying capacity of machine parts are examined. The problem of measurement accuracy and reiability and the methods of processing test results with the aid of statistical mathematics are considered. Author

N69-28863*# National Aeronautics and Space Administration. Lewis Research Center, Cleveland, Ohio.

EFFECT OF TEMPERATURE AND PRESSURE ON CAVITATION DAMAGE TO A COBALT BASE ALLOY IN SODIUM

Stanley G. Young and James R. Johnston Washington Jun. 1969 22 p refs

(NASA-TN-D-5273) Avail: CFSTI CSCL 11F

A vibratory apparatus was used to subject the cobalt base alloy, L-605, to cavitation damage in sodium at 400°, 800°, and 1200°F. Cover gas pressures were varied from 1 to 4 atmospheres (10 to 40 N/cm^2) at each temperature. Increasing pressure increased the cavitation damage at each test temperature. Damage was greatest at the 800°F test temperature for all pressures. A volume-loss-rate contour diagram was constructed to show cavitation damage in terms of the combined temperature and pressure of the sodium. Author

N69-31065*# National Aeronautics and Space Administration. Lewis Research Center, Cleveland, Ohio.

CORROSION IN A COBALT ALLOY, TWO-PHASE MERCURY LOOP

Alex Vary, Coulson M. Scheuermann, Louis Rosenblum, and Warren H. Lowdermilk Washington Jul. 1969 36 p refs

(NASA-TN-D-5326) Avail: CFSTI CSCL 11F

A two-phase mercury corrosion loop was operated for 1147 hr at a peak liquid temperature of 1075° F (858 K). The loop was constructed of the cobalt-base alloy HS-25 (L-605). The maximum corrosion occurred in the boiler inlet near the point where two-phase flow began and the liquid temperature peaked. The loop results were compared with corrosion capsule tests and other loops of the same alloy. The corrosion markedly exceeded that found in either the reflux capsules or flow-velocity loops operated at the same temperature. Author

N69-31873*# National Aeronautics and Space Administration. Lewis Research Center, Cleveland, Ohio.

A NICKEL BASE ALLOY, WAZ-20, WITH IMPROVED STRENGTH IN THE 2000 DEG TO 2200 DEG F RANGE

William J. Waters and John C. Freche Washington Aug. 1969 23 p refs

(NASA-TN-D-5352) Avail: CFSTI CSCL 11F

A nickel-base alloy based on the nickel–aluminum–tungsten system was developed with high strength in the 2000° to 2200°F (1094° to 1205°C) range. It has a tensile strength of 20,000 psi (137.9 MN/m^2) at 2200°F (1205°C). Application of directional solidification techniques increased intermediate temperature tensile strength and generally increased ductility and stress rupture life. The combination of properties of the alloy suggest that it may have potential for application to stator vanes of advanced gas turbine engines. Author

N69-31883*# National Aeronautics and Space Administration. Lewis Research Center, Cleveland, Ohio.
DYNAMIC STRAIN AGING IN CARBIDE STRENGTHENED MOLYBDENUM ALLOYS
Peter L. Raffo Washington Jul. 1969 19 p refs
(NASA-TN-D-5355) Avail: CFSTI CSCL 11F

A study was made of the dynamic strain aging processes in carbide strengthened molybdenum alloys. Strengthening due to dynamic strain aging was observed in the temperature range 1500° to 2400°F (1088 to 1588 K). The strengthening is believed to arise from the pinning of mobile dislocations by metal-carbon pairs or clusters and/or carbide precipitates. This immobilization of the dislocations led to a high work-hardening rate and the observed strengthening. Author

N69-31889*# National Aeronautics and Space Administration. Lewis Research Center Cleveland, Ohio.
BURST TESTING OF TUNGSTEN TUBING AT TEMPERATURES FROM 3000 DEG TO 4500 DEG F (1650 DEG TO 2480 DEG C)
Charles A. Gyorgak Washington Jul. 1969 20 p refs
(NASA-TM-X-1843) Avail: CFSTI CSCL 11F

Thin-walled tungsten tubing, 3/8 inch (9.5 mm) or 1/2 inch (12.7 mm) in diameter, produced by three extrusion techniques, by two vapor-deposition processes, or by electroforming in a molten fluoride bath were internally pressurized to failure at temperatures from 3000° to 4500° F (1650° to 2480°C). The burst strength of the majority of the tungsten tubes was equal to or greater than the ultimate tensile strength of wrought tungsten. Test results showed that the tungsten hexachloride vapor-deposition process is capable of producing tubing as strong as wrought tungsten tubing. The failure propagation was intergranular in all tungsten tubes tested. Author

N69-31895*# National Aeronautics and Space Administration. Lewis Research Center, Cleveland, Ohio.
SOLAR ABSORPTANCES AND SPECTRAL REFLECTANCES OF 12 METALS FOR TEMPERATURES RANGING FROM 300 to 500 K
Ernie W. Spisz, Albert J. Weigand, Robert L. Bowman, and John R. Jack Washington Aug. 1969 22 p refs
(NASA-TN-D-5353) Avail: CFSTI CSCL 11F

The solar absorptance of 12 metals (Al, Cu, Au, Mo, Ni, Pt, Ag, stainless steel 304, Ta, Sn, Ti, and V) were determined over the temperature range from 250 to 550 K by two different experimental methods. Direct measurements of solar absorptance were made with a cyclic radiation method using a high intensity carbon arc solar simulator. Indirect measurements of solar absorptance were obtained from spectral reflectance measurements obtained from an integrating sphere reflectometer over the wavelength range from 0.33 to 2.16 μm. The solar absorptance data as obtained from the two different methods as well as the spectral reflectance data are presented for the 12 metals. Author

N69-31977*# National Aeronautics and Space Administration. Lewis Research Center, Cleveland, Ohio.
MECHANICAL PROPERTIES OF ARC-MELTED TUNGSTEN-RHENIUM-HAFNIUM-CARBON ALLOYS
William D. Klopp and Walter R. Witzke Washington Jul. 1969 38 p refs
(NASA-TN-D-5348) Avail: CFSTI CSCL 11F

A study was conducted on the effect of 4 atomic percent rhenium on the mechanical properties of hafnium carbide strengthened tungsten-base alloys. The high temperature strengthening from HfC and improved low temperature bend ductility from the rhenium addition could be combined without detrimental interaction. Maximum strength alloys contained 0.3 to 0.4 mol percent hafnium carbide. The highest tensile strength observed at 3500°F (1927°C) was 75.4 ksi (520 MN/m^2) in the solution annealed and aged condition, while the mean 4t bend transition temperature noted was 200°F (93°C) for as-rolled sheet. Author

N69-32558*# National Aeronautics and Space Administration. Langley Research Center, Langley Station, Va.
EFFECT OF OUTDOOR EXPOSURE AT ELEVATED TEMPERATURE ON THE FATIGUE LIFE OF Ti-8Al-1Mo-1V TITANIUM ALLOY AND AM 350 STAINLESS STEEL SHEET
Edward P. Phillips Washington Jul. 1969 27 p refs
(NASA-TN-D-5362) Avail: CFSTI CSCL 11F

Constant-amplitude bending fatigue tests were conducted outdoors on central-hole (stress concentration factor of 1.6) and fusion-welded sheet specimens of duplex-annealed Ti-8Al-1Mo-1V titanium alloy and cold-rolled and tempered AM 350 stainless steel. The specimens were maintained at 550°F (561°K) during most of the exposure period to approximate the operating environment of a Mach 3 transport aircraft. The heating was interrupted when cyclic loads were applied, any time rain or snow was falling, and for a 4-hour period each night to allow dew to form. A static load was applied continuously for the duration of the tests. For comparison, tests were also conducted indoors at room temperature at the same stress levels. The results indicate that the outdoor test environment reduced the fatigue life of all materials tested. Based on the number of load cycles to produce the first failures, outdoor life was never reduced to less than 1/2 the indoor life; but the median outdoor life of the central-hole AM 350 specimen was reduced to 1/5 the median indoor life. Author

N69-33307*# National Aeronautics and Space Administration. Lewis Research Center, Cleveland, Ohio.
OXIDATION AND THERMAL FATIGUE CRACKING OF NICKEL- AND COBALT-BASE ALLOYS IN A HIGH VELOCITY GAS STREAM
James R. Johnston and Richard L. Ashbrook Washington Aug. 1969 50 p refs
(NASA-TN-D-5376) Avail: CFSTI CSCL 11F

The superalloys IN-100, B-1900, Mar M-200, TAZ8A, Hastelloy X, TD-NiCr, L-605, X-40, Mar M-509A, and WI-52 were cyclically tested for resistance to oxidation in high velocity gas streams for 100 cycles between room temperature and temperatures up to 2000°F. Conventionally cast nickel base alloys were more resistant to weight loss than cast cobalt base alloys, but cast cobalt base alloys were more resistant to thermal fatigue cracking. However, Hastelloy X and directionally solidified and single grain Mar M-200 did not crack even after 100 cycles to 2000°F. Simulated steady state conditions reduced weight loss and incidence of cracking of the six alloys so tested. Author

N69-34704*# National Aeronautics and Space Administration. Langley Research Center, Langley Station , Va.
EFFECT OF STRESS RATIO ON FATIGUE-CRACK GROWTH IN 7075-T6 AND 2024-T3 ALUMINUM-ALLOY SPECIMENS
C. Michael Hudson Washington Aug. 1969 31 p refs
(NASA-TN-D-5390) Avail: CFSTI CSCL 11F

Axial load fatigue crack growth tests were conducted on 12 inch-wide sheet specimens made of 7075-T6 and 2024-T3 aluminum alloy. These tests were made at stress ratios R (ratio of the minimum stress to the maximum stress) ranging from -1.0 to 0.8 and at maximum stress levels ranging from 5 to 50 ksi to study the effects of stress ratio on fatigue crack growth. The experimental results were analyzed by using the stress intensity method. For a given positive stress ratio, the fatigue crack growth rate was a single valued function of the stress intensity range for both 7075-R6 and 2024-T3 aluminum alloys. For $R \geq 0$ the crack growth rates varied systematically with R for both materials; the

higher stress ratios produced higher rates of fatigue crack growth for a given stress intensity range. Fatigue cracks in the 7075-T6 aluminum alloy grew at the same rates in all tests with $R \leq 0$ when the same maximum stress intensity factor was applied. In contrast, fatigue cracks in the 2024-T3 aluminum alloy grew faster in the tests with $R = -1$ than in the tests with $R = 0$ when the same maximum stress intensity factor was applied. Empirical equations previously developed by various investigators were fitted to the experimental data. In general, good correlation was obtained. Author

N69-34916*# National Aeronautics and Space Administration. Lewis Research Center, Cleveland, Ohio.

THE INFLUENCE OF CRACK LENGTH AND THICKNESS IN PLANE STRAIN FRACTURE TOUGHNESS TESTS

Melvin H. Jones and William F. Brown, Jr. Washington Aug. 1969 30 p refs

(NASA-TM-X-1860) Avail: CFSTI CSCL 11F

It is shown that K_{Ic} values determined in accordance with the present ASTM E-24 proposed test method for plane strain fracture toughness of metallic materials can vary moderately within the specimen size and geometric limitations imposed by the test method. The magnitude of these variations will depend on the material properties and would be increased by relaxation of the size requirements. The possibility of employing subsized specimens for screening materials regarding their plane strain fracture toughness was explored as well as several methods for relating these values to unaxial tensile data. Author

N69-35514*# Pratt and Whitney Aircraft, East Hartford, Conn.

TESTING OF HIGH-EMITTANCE COATINGS

R. E. Cleary and C. Ammann Washington NASA Aug. 1969 113 p refs

(Contract NAS3-10609)

(NASA-CR-1413) Avail: CFSTI CSCL 11F

Three coatings were applied to the platinum -20 wt.% rhodium alloy substrate by plasma spraying at a temperature of 1000±50° F. These coatings were hafnium oxide, cerium oxide, and iron titanate. The hafnium oxide was also applied chemically by the vapor deposition process. Initially, emittance testing of the plasma-sprayed coatings for 200 hours at 2100° F in a vacuum of 1×10^{7} torr or better disclosed these values for total hemispherical emittance:hafnium oxide, 0.51 to 0.64, cerium oxide, 0.87 to 0.91; iron titanate, 0.94. The emittance of the chemically vapor deposited hafnia was 0.63 to 0.71. The coatings were aged in air for 1500 hours at 1100°F. They were subsequently tested in vacuum at temperature of about 2100°F. The emittance was cerium oxide, 0.86 to 0.91; iron titanate, 0.90; hafnium oxide, 0.74 to 0.75. The cerium oxide coating was also tested for 2000 hours at 2100° F in a vacuum of 1×10^{-7} torr or better with an emittance of 0.85 to 0.93. Author

N69-35688*# National Aeronautics and Space Administration. Lewis Research Center, Cleveland, Ohio.

CRYOGENIC FRACTURE PROPERTIES OF THIN AISI 301 60-PERCENT COLD-REDUCED SHEET AT VARIOUS ANGLES TO THE ROLLING DIRECTION

Frederick D. Calfo Washington Sep. 1969 25 p refs

(NASA-TN-D-5413) Avail: CFSTI CSCL 11F

Fracture properties at various angles to the rolling direction in 0.022-in (0.056-cm-) thick AISI 301 60-percent cold-reduced stainless-steel sheet were determined. Specimens 3, 6, and 12 in. (7, 6, 15, 2, and 30.5 cm) wide were tested at -423° -320°, and 70°F. A gradual increase in yield and ultimate strengths was noted at all test temperatures as specimen orientation approached the transverse direction. Net fracture strength reductions of as much as 34 percent of the room temperature values were noted at cryogenic temperatures as the orientation of the cracked specimens approached the transverse direction. Author

N69-35764*# National Aeronautics and Space Administration. Lewis Research Center, Cleveland, Ohio.

RECENT DEVELOPMENTS IN CHROMIUM AND CHROMIUM ALLOYS

William D. Klopp Washington Sep. 1969 28 p refs

(NASA-TM-X-1867) Avail: CFSTI CSCL 11F

Recent developments in chromium pertinent to its potential use in advanced jet engines are reviewed. Although chromium has a strength-to-density advantage over nickel, its inherent brittleness and furthe embrittlement by nitrogen during high temperature exposure are serious limitations to its use. Twelve chromium alloys are currently under development, the strongest showing a potential 150° F (83 K) service temperature advantage over nickel-base superalloys. However, a better balance between solution strengthening and precipitate strengthening must be achieved in order to improve the low temperature ductility of these alloys. Improved coatings for protection against nitrogen embrittlement must be developed. Author

N69-35836*# Aztec School of Languages, Inc., Maynard, Mass.

HIGH TEMPERATURE OXIDATION PROTECTION OF TUNGSTEN

V. Ye. Ivanov et al Washington NASA Aug. 1969 132 p refs Transl. into ENGLISH of the book "Zashchita Volframa ot Okisleniya pri Vysokikh Temperaturakh" Moscow, "Atom" Press, 1968

(Contract NASw-1692)

(NASA-TT-F-583) Avail: CFSTI CSCL 11F

This book is intended for specialists in the field of high-temperature materials and protective coatings. The book reviews achievements in the field of protection of tungsten and its alloys from high-temperature gaseous corrosion. Particular attention is paid to corrosion- and heat-resisting coatings. The behavior of various coatings, the materials and methods used for their production, as well as the physicochemical mechanism of their formation and protective action are examined. The authors also analyze the possible utilization of tungsten as a high-temperature structural material, the oxidation of tungsten at high temperatures, and recent achievements in the development of refractory and corrosion-resistant tungsten-base alloys. Author

N69-36221*# National Aeronautics and Space Administration. Langley Research Center, Langley Station, Va.

HOT-SALT-STRESS-CORROSION CRACKING AND ITS EFFECT ON TENSILE AND STRESS-RUPTURE PROPERTIES OF Ti-6Al-4V TITANIUM-ALLOY SHEET

Dick M. Royster Washington Sep. 1969 36 p refs

(NASA-TN-D-5417) Avail: CFSTI CSCL 11F

Self-stressed, tensile, and stress-rupture specimens were made from 0.040-inch-thick (1.0 mm) annealed sheet. The self-stressed specimens, with stresses of 25 and 50 ksi (170 and 340 MN/m^2), were sprayed with a 3.4-percent sodium chloride solution and exposed at temperatures from 500° F to 600° F (530 K to 590 K) up to 10,000 hours. Cracking was obtained after approximately 20 hours at 600° F for the 50 ksi stress, but no cracking was noted at 500° F for up to 10,000 hours at either stress. The tensile specimens were salt coated in the same manner as the self-stressed specimens and exposed up to 1600 hours at temperatures from 550° F to 650° F (560 K to 620 K) and 50 ksi stress to develop and grow hot-salt-stress-corrosion cracks. When tested at room temperature, the presence of stress-corrosion cracks resulted in a large reduction in elongation. There was also a large decrease in tensile strength for the specimens exposed at 650° F. The salt-coated stress-rupture specimens were exposed at temperatures from 600° F to 700° F (590 K to 650 K) for stresses of 50 to 100 ksi (340 to 690 MN/m^2) until rupture occurred. A time-temperature parameter analysis was made of both the crack-initiation and stress-rupture data. A difference between the time for crack initiation and the time for stress rupture by a factor on the order of 300 was indicated. Author

N69-36367*# Goodyear Aerospace Corp., Akron, Ohio.
NITINOL CHARACTERIZATION STUDY
William B. Cross, Anthony H. Kariotis, and Frederick J. Stimler Washington NASA Sep. 1969 69 p refs
(Contract NAS1-7522)
(NASA-CR-1433; GER-14188) Avail: CFSTI CSCL 11F

Nickel--titanium alloys were tested for its suitability for potential applications in space. Materials from several melts were fabricated into rods, wires, and foils for the investigation. The alloy shows remarkable recovery behavior after being molded into other shapes. Results indicate that improved processing techniques could produce even greater mechanical work from 55-Nitinol. Indications are that the substance can be used in space applications for expandable and erectable structures. E.H.W.

N69-36653*# National Aeronautics and Space Administration. Lewis Research Center, Cleveland, Ohio.
STATISTICAL ANALYSIS OF HIGH-TEMPERATURE CREEP-RATE DATA FOR ALLOYS OF TANTALUM, MOLYBDENUM, AND COLUMBIUM
William L. Maag and William F. Mattson Washington Sep. 1969 23 p refs
(NASA-TN-D-5424) Avail: CFSTI CSCL 11F

Empirical creep-rate equations are presented for the refractory-metal alloys T-111, T-222, TZM, TZC, D-43, and Cb-1Zr. These metals are considered potential structural materials for space power systems. The method of least suqares was used to statistically analyze experimental creep data reported by other investigators. The form of the correlating equations is based on the theory that creep rate is a function of material temperature, stress, and structure. The equations cover a temperature range of 1256 to 1922 K (1800° to 3000° F) and a stress range of 3.4×10^6 to 5.5×10^8 Nm^{-2} (500 to 80,000 psi). The variability associated with each correlating equation is expressed in terms of its standard deviation. Author

N69-36697*# National Aeronautics and Space Administration. Goddard Space Flight Center, Greenbelt, Md.
EVALUATION OF META-BENZENEDISULFONIC ACID AS A STRESS-REDUCING ADDITIVE IN A WATTS NICKEL ELECTROPLATING BATH
J. A. Munford and C. E. Whitfield Washington Sep. 1969 9 p refs
(NASA-TN-D-5188) Avail: CFSTI CSCL 11F

The determination of the internal stress level and deposit hardness of nickel electrodeposited for a Watts-type bath containing controlled quantities of meta-benzenedisulfonic acid are described. The internal stress level was found to be highly sensitive to current density at low concentrations of the additive. As the additive concentration was increased, the stress level increased substantially, passed through a maximum, and then decreased at high concentrations. Deposit hardness was found to be more sensitive to current density than to stress level; no predictable relationship between stress and deposit hardness was observed. Author

N69-36723*# Lockheed Aircraft Corp., Sunnyvale, Calif.
EMISSIVITY COATINGS FOR LOW-TEMPERATURE SPACE RADIATORS
G. R. Cunnington, J. R. Grammer, and F. J. Smith Washington NASA Sep. 1969 refs
(Contract NAS3-7630)
(NASA-CR-1420) Avail: CFSTI CSCL 11C

Studies were made on the effects of simulated solar ultraviolet radiation, temperature, and vacuum on the stability of solar absorptance and total hemispherical emittance of seven potential low temperature space power system radiator coatings. A calorimetric in situ technique was used to measure broadband spectral and total absorptance and total hemispherical emittance as a function of time of exposure to an ultraviolet source (xenon lamp) at a 1-sun level. Exposures were for durations varying from 500 to 10,000 hr and a temperatures from 300°K to 533°K. The coatings investigated were titanium dioxide and zinc oxide pigments in methyl silicone binders; zinc oxide, zirconium silicate, and aluminum silicate in potassium silicate binders; and the optical solar relfector. The optical solar reflector was the most stable coating at 150°F; no change in its solar absorptance or total hemispherical emittance was observed during testing. Zinc oxide in potassium silicate showed the greatest stability for the paint type coatings; total hemispherical emittance remained constant and solar absorptance increased 0.06 during 10,000 hr of exposure at 422°K. Author

N69-36831*# TRW, Inc., Cleveland, Ohio. Equipment Labs.
MECHANICAL BEHAVIOR OF TANTALUM-BASE T-111 ALLOY AT ELEVATED TEMPERATURE
K. D. Sheffler, J. C. Sawyer, and E. A. Steigerwald Washington NASA Sep. 1969 27 p refs
(Contract NAS3-9439)
(NASA-CR-1436; ER-7365) Avail: CFSTI CSCL 11F

The tantalum-base alloy T-111 has been creep tested in an ultrahigh vacuum environment at temperatures and stresses chosen to provide approximately 1 percent creep in times up to 15,000 hours. Design data from five different heats are presented in the form of a Larson Miller plot for 1 percent creep life. Elevated temperature tension test data show a strain aging reaction in the 1400° to 2200° F range which produces unusual transient creep behavior. Values of activation energy and stress exponent suggest that steady state creep of T-111 is governed by a diffusion controlled microcreep mechanism rather than by nonconservative dislocation motion. Author

N69-37436*# National Aeronautics and Space Administration. Lewis Research Center, Cleveland, Ohio.
EFFECT OF NUCLEAR RADIATION AT CRYOGENIC TEMPERATURES ON THE TENSILE PROPERTIES OF TITANIUM AND TITANIUM-BASE ALLOYS
Charles L. Younger and Fred A. Haley Washington Sep. 1969 53 p refs
(NASA-TN-D-5442) Avail: CFSTI CSCL 11F

An experimental investigation of the effects of reactor irradiation at 17 K on tensile properties of titanium and titanium-base alloys has been conducted in special test loops at the Plum Brook Reactor Facility. Commercially pure titanium, titanium – 5 aluminum – 2.5 tin, titanium – 6 aluminum – 4 vanadium, and titanium – 8 aluminum – 1 molybdenum – 1 vanadium alloys showed significant increases in tensile strength and probable decreases in ductility following reactor exposures up to 10×10^{17} fast neutrons per square centimeter. The influences of impurities, preirradiation heat treatment, and postirradiation heat treatment on radiation damage were also evaluated. Author

N69-38074*# National Aeronautics and Space Administration. Lewis Research Center, Cleveland, Ohio.
DISPERSION-STRENGTHENED NICKEL PRODUCED FROM ULTRAFINE COMMINUTED POWDERS
Max Quantinetz and John W. Weeton Washington Oct. 1969 28 p refs
(NASA-TN-D-5421) Avail: CFSTI CSCL 11F

An investigation conducted to produce dispersion strengthened products by a mechanical comminution and blending approach was combined with a study of the effect of varying degrees of thermomechanical processing on the strength of the materials produced. Dispersion strengthened nickel products comparable or better in strength to the best available commercial products were produced. While the products generally increased in strength with

increased amounts of thermomechanical processing, changes in composition of the composite were shown to affect the response of the material to the working process. Author

N69-38794*# National Aeronautics and Space Administration. Lewis Research Center, Cleveland, Ohio.
AN EVALUATION OF THREE OXIDATION-RESISTANT ALLOY CLADDINGS FOR IN 100 AND WI 52 SUPERALLOYS
Michael A. Gedwill Washington Oct. 1969
(NASA-TN-D-5483; E-5011) Avail: CFSTI CSCL 11F

This study demonstrated the feasibility of protecting typical turbine alloys from cyclic furnace oxidation by cladding them with oxidation resistant alloy foils. Foils of Ni-30Cr-1.4Si, Ni-20Cr-4Al-1.2Si, and Fe-25Cr-4Al-1Y were bonded to IN 100 (Ni base) and WI 52 (Co base). Cyclic oxidation exposure to 200 hours was conducted at 1900° and 2000° F (1310 and 1360 K). At 1900° F (1310 K), gravimetric, metallographic, and inter-diffusion analyses showed all three claddings capable of providing excellent protection for both substrates. At 2000°F (1360 K), Ni-30Cr-1.4Si and Fe-25Cr-4Al-1Y provided excellent protection for WI 52, while Ni-20Cr-4Al-1.2Si afforded good protection for IN 100. Author

N69-39182*# National Aeronautics and Space Administration. Lewis Research Center, Cleveland, Ohio.
DISLOCATION STRUCTURES IN SINGLE CRYSTAL TUNGSTEN AND TUNGSTEN ALLOYS
Joseph R. Stevens Washington Oct. 1969 Washington Oct. 1969 21 p refs
(NASA-TN-D-5493; E-5098) Avail: CFSTI CSCL 11F

Deformation of tungsten single crystals as a function of strain, temperature, and alloying was studied by transmission electron microscopy. Unalloyed tungsten, W-1 and 3 percent Re, and W-1 and 3 percent Ta single crystals oriented for (101) [111] slip were deformed in compression at 150°, 300°, and 590°K. Transmission microscopy revealed that the substructure in unalloyed tungsten is similar to substructures in other refractory metals when compared on the basis of homologous temperature. The primary effect of rhenium additions is to produce edge dipolskl homologous temperature. The primary effect of rhenium additions is to produce edge dipoles in the wake of screw dislocations. Tantalum has a lesser effect on dislocation substructure. Author

N69-40053*# National Aeronautics and Space Administration. Lewis Research Center, Cleveland, Ohio.
SOLUBILITIES OF MOLYBDENUM AND TUNGSTEN IN LIQUID POTASSIUM
Stephan Stecura Washington Oct. 1969 14 p refs
(NASA-TN-D-5504) Avail: CFSTI CSCL 11F

A study was made of the solubilities of molybdenum and tungsten in liquid potassium containing less than 15 ppm by weight of oxygen. The solubility of molybdenum at 1040° and 1316°K is about 6 and 13 ppm by weight and that of tungsten at 1055° and 1328°K is about 20 and 130 ppm by weight, respectively. The apparent heats of solutions for molybdenum and tungsten solubilities in liquid potassium are 6.7 ±0.8 and 17.6 ±1.2 kcal/mole (28.0 and 73.7 kJ/mole), respectively. The solubility data for molybdenum are either the true solubility data, or relatively close to the true solubility data, for molybdenum in liquid potassium between 1040° and 1316°K. The solubility data for tungsten in liquid potassium between 1055° and 1328°K suggest that the solubility values might have been influenced by interstitial impurities, particularly by oxygen. Author

N69-40057*# Battelle Memorial Inst., Columbus, Ohio.
RESEARCH ON METALLURGICAL CHARACTERISTICS AND PERFORMANCE OF MATERIALS USED FOR SLIDING ELECTRICAL CONTACTS Summary Report, 1 May 1968 – 30 Apr. 1969
W. H. Abbott and E. S. Bartlett Washington NASA Oct. 1969 61 p refs
(Contract NAS12-657)
(NASA-CR-1447) Avail: CFSTI CSCL 11F

Studies of the friction, wear, and contact resistance stability of nine wrought gold alloys and three electroplated gold systems were made in both N_2-20 O_2 and high vacuum. Sliding durations were 100 cycles in N_2-20 O_2 and 500 cycles in vacuum. Environmental tests were made on each materials system. These consisted of exposure to flowers of sulfur at 30°C, and 1000-hour storage in N_2-20 O_2 at 200°C. Wear test and control specimens exposed in this manner were analyzed by contact resistance measurements and analysis of surface films. All of the wrought gold alloys showed high friction (μ_k = 1.2-2.0) and wear rates in both air and vacuum. No correlation was apparent between wear rates, wear mechanism, and mechanical properties. Differences in wear and friction were attributed almost entirely to differences in surface chemistry or surface energy of the alloy. Contact resistance stability was shown to be closely related to wear mechanism and resistivity. High resistivity and fine wear particles always produced static contact resistance instability and high noise levels. Author

N69-40242*# National Aeronautics and Space Administration. Lewis Research Center, Cleveland, Ohio.
HOT-SALT STRESS-CORROSION OF A TITANIUM ALLOY UNDER A SIMULATED TURBINE-ENGINE COMPRESSOR ENVIRONMENT
Hugh R. Gray and James R. Johnston Washington Oct. 1969 35 p refs
(NASA-TN-D-5510) Avail: CFSTI CSCL 11F

Threshold curves for hot-salt stress-corrosion of the Ti-8Al-1Mo-1V alloy were determined for a variety of exposure conditions that simulated the environment found in a compressor of a gas turbine engine. Specimen surface condition was the most influential variable. Specimens in the as-machined condition exhibited higher threshold stresses than did stress-relieved specimens. High velocity airflow and high air pressure raised the threshold curves for embrittlement slightly, but did not eliminate embrittlement entirely. Salt concentration, air dewpoint, and salt deposition temperature did not significantly shift threshold curves. Longer exposure times lowered threshold stresses. Author

18

MATERIALS, NONMETALLIC

Includes corrosion; physical and mechanical properties of materials (e.g., plastics); and elastomers, hydraulic fluids, etc. For basic research see: 06 Chemistry. For related information see also: 17 Materials, Metallic; 27 Propellants; and 32 Structural Mechanics.

A69-10861 *

A SURVEY OF THE PHOTODEGRADATION OF ORGANIC POLYMERS EXPOSED TO ULTRAVIOLET RADIATION.

Ronald F. Reinisch and Hermilo R. Gloria (NASA, Ames Research Center, Moffett Field, Calif.).

Solar Energy, vol. 12, Sept. 1968, p. 75-84. 17 refs.

Examination of some of the variables involved in the photodegradation of organic polymers, with special emphasis given to research on the photochemistry of polyvinyl chloride. Attention is focused on those variables that are critical to the successful UV stabilization of polymers, and on a discussion of the nature of the UV absorbing grouping, the wavelength dependence of the photochemical reaction, and the rate-enhancing effect of polychromatic radiation. M.G.

A69-16160 *#

EFFECT OF GAMMA RADIATION IN VACUUM ON THE TENSILE PROPERTIES OF POLYMER FILMS.

H. L. Price (NASA, Langley Research Center, Hampton, Va.). American Society of Mechanical Engineers, Winter Annual Meeting and Energy Systems Exposition, New York, N. Y., Dec. 1-5, 1968, Paper 68-WA/RP-6. 8 p. 15 refs.

Members, $0.75; nonmembers, $1.50.

The tensile properties of polymer films have been measured in air after the films were exposed to gamma radiation in vacuum. The dose rate was approximately 1.6 Mrads per hour for doses to 2000 Mrads at a pressure of 10^{-6} torr. Four 0.001-in.-thick films were tested: poly(ethylene terephthalate) or PETP; poly(cyclohexylenedimethylene terephthalate) or PCTP; poly(vinylidene fluoride) or PVF_2; and a polyimide or PI. The yield strength, tangent modulus, tensile and elongation at break were obtained from the tensile tests. The average value and standard deviation of each property are given, based on the results of 25 tests at each dose. The data show the effect on the tensile properties of chain scission and cross linking and indicate the useful dose range of the films subjected to ionizing radiation. (Author)

A69-16485 *

CRYOGENIC PROPERTIES OF POLYMERS; PROCEEDINGS OF THE NASA-CASE CONFERENCE ON THE PROPERTIES OF POLYMERS AT CRYOGENIC TEMPERATURES, NASA LEWIS RESEARCH CENTER AND CASE-WESTERN-RESERVE UNIVERSITY, CLEVELAND, OHIO, APRIL 25-27, 1967.

Edited by T. T. Serafini (NASA, Lewis Research Center, Polymers Research Section, Cleveland, Ohio) and J. L. Koenig (Case-Western-Reserve University, School of Engineering, Polymer Science Div., Cleveland, Ohio).

New York, Marcel Dekker, Inc., 1968. 310 p.

$13.75.

CONTENTS:

PREFACE. T. T. Serafini (NASA, Lewis Research Center, Cleveland, Ohio) and J. L. Koenig (Case-Western-Reserve University, Cleveland, Ohio), p. v.

CRYOGENIC POSITIVE EXPULSION BLADDERS. R. F. Lark (NASA, Lewis Research Center, Cleveland, Ohio), p. 1-15. [See A69-16486 05-15]

ADHESIVES FOR CRYOGENIC APPLICATIONS. L. M. Roseland (McDonnell Douglas Corp., Huntington Beach, Calif.), p. 17-28. 5 refs. [See A69-16487 05-18]

GLASS-, BORON-, AND GRAPHITE-FILAMENT-WOUND RESIN COMPOSITES AND LINERS FOR CRYOGENIC PRESSURE VESSELS. M. P. Hanson (NASA, Lewis Research Center, Cleveland, Ohio), p. 29-43. 8 refs. [See A69-16488 05-18]

THE MECHANICAL BEHAVIOR OF POLY(ETHYLENE TEREPHTHALATE). I. M. Ward (Bristol, University, Bristol, England), p. 45-72. 27 refs. [See A69-16489 05-18]

EFFECT OF FILM PROCESSING ON CRYOGENIC PROPERTIES OF POLY(ETHYLENE TEREPHTHALATE). R. E. Eckert (Purdue University, West Lafayette, Ind.) and T. T. Serafini (NASA, Lewis Research Center, Cleveland, Ohio), p. 73-86. 10 refs. [See A69-16490 05-18]

MECHANICAL PROPERTIES OF EPOXY RESINS AND GLASS/EPOXY COMPOSITES AT CRYOGENIC TEMPERATURES. L. M. Soffer and R. Molho (Aerojet-General Corp., Azusa, Calif.), p. 87-117. 8 refs. [See A69-16491 05-18]

MECHANICAL RELAXATION OF POLY-4-METHYL-PENTENE-1 AT CRYOGENIC TEMPERATURES. M. Takayanagi and N. Kawasaki (Kyushu University, Fukuoka, Japan), p. 119-136. 12 refs. [See A69-16492 05-18]

TRANSITIONS IN GLASSES AT LOW TEMPERATURES. R. A. Haldon, W. J. Schell, and R. Simha (Southern California, University, Los Angeles, Calif.), p. 137-153. 31 refs. [See A69-16493 05-06]

MECHANICAL BEHAVIOR OF POLY(ETHYLENE TEREPHTHALATE) AT CRYOGENIC TEMPERATURES. C. D. Armeniades, I. Kuriyama, J. M. Roe, and E. Baer (Case-Western-Reserve University, Cleveland, Ohio), p. 155-169. 32 refs. [See A69-16494 05-18]

INFRARED STUDIES OF CHAIN FOLDING IN POLYMERS. II - POLYETHYLENE TEREPHTHALATE. J. L. Koenig and M. J. Hannon (Case-Western-Reserve University, Cleveland, Ohio), p. 171-197.

CRYSTALLIZATION OF POLYETHYLENE TEREPHTHALATE FROM THE GLASSY AMORPHOUS STATE. G. S. Y. Yeh and P. H. Geil (Case-Western-Reserve University, Cleveland, Ohio), p. 199-213.

STRAIN-INDUCED CRYSTALLIZATION OF POLYETHYLENE TEREPHTHALATE. G. S. Y. Yeh and P. H. Geil (Case-Western-Reserve University, Cleveland, Ohio), p. 215-241.

MOLECULAR MOTION IN POLYTETRAFLUOROETHYLENE AT CRYOGENIC TEMPERATURES. E. S. Clark (Du Pont de Nemours and Co., Inc., Wilmington, Del.), p. 243-248. 6 refs. [See A69-16495 05-24]

SYNTHESIS OF ULTRAHIGH MOLECULAR WEIGHT POLY(ETHYLENE TEREPHTHALATE). L.-C. Hsu (NASA, Lewis Research Center, Cleveland, Ohio), p. 249-261. 17 refs. [See A69-16496 05-24]

DEVELOPMENT OF VULCANIZABLE ELASTOMERS SUITABLE FOR USE IN CONTACT WITH LIQUID OXYGEN. P. D. Schuman, E. C. Stump, and G. Westmoreland (Peninsula ChemResearch, Inc., Gainesville, Fla.), p. 263-278. 37 refs. [See A69-16497 05-06]

SYNTHESIS OF FLUORINATED POLYURETHANES. R. Gosnell and J. Hollander (Whittaker Corp., San Diego, Calif.), p. 279-298. [See A69-16498 05-06]

INDEX, p. 299-302.

A69-16487 *

ADHESIVES FOR CRYOGENIC APPLICATIONS.

L. M. Roseland (McDonnell Douglas Corp., Douglas Aircraft Co., Missile and Space Systems Group, Huntington Beach, Calif.).

IN: CRYOGENIC PROPERTIES OF POLYMERS; PROCEEDINGS OF THE NASA-CASE CONFERENCE ON THE PROPERTIES OF POLYMERS AT CRYOGENIC TEMPERATURES, NASA LEWIS RESEARCH CENTER AND CASE-WESTERN-RESERVE UNIVERSITY, CLEVELAND, OHIO, APRIL 25-27, 1967. [A69-16485 05-18]

Edited by T. T. Serafini and J. L. Koenig.
New York, Marcel Dekker, Inc., 1968, p. 17-28. 5 *refs.*
NASA-sponsored research.

The paper includes a review of the cryogenic behavior on several adhesive materials encountered in the fabrication of NASA's liquid hydrogen-liquid oxygen powered Saturn S-IVB stage built by Douglas. It describes some of the materials and techniques known to improve joint strength in cryogenic applications. The results of a recent Douglas cryogenic structural adhesive evaluation program are presented. The ability of the resin system to absorb energy, the inclusion of a selected glass mat in the cured bond line, and the use of ambifunctional silane primers for the improvement of cryogenic joint strengths are discussed. (Author)

A69-16488 *

GLASS-, BORON-, AND GRAPHITE-FILAMENT-WOUND RESIN COMPOSITES AND LINERS FOR CRYOGENIC PRESSURE VESSELS.
Morgan P. Hanson (NASA, Lewis Research Center, Cleveland, Ohio).
IN: CRYOGENIC PROPERTIES OF POLYMERS; PROCEEDINGS OF THE NASA-CASE CONFERENCE ON THE PROPERTIES OF POLYMERS AT CRYOGENIC TEMPERATURES, NASA LEWIS RESEARCH CENTER AND CASE-WESTERN-RESERVE UNIVERSITY, CLEVELAND, OHIO, APRIL 25-27, 1967. [A69-16485 05-18]
Edited by T. T. Serafini and J. L. Koenig.
New York, Marcel Dekker, Inc., 1968, p. 29-43. 8 refs.

Preliminary results of an evaluation of boron and graphite filaments as possible reinforcements for cryogenic propellant tanks. The composite tensile strength characteristics of glass, boron, and graphite at 297, 77, and 20 K are determined. The composite interlaminar shear strength of these materials and the single-filament strengths of boron are determined at 297 and 77 K. Cyclic tests are performed at 77 and 20 K on cylinders having aluminum foil liners to determine the cyclic life and mode of linear failure of these cylinders. Z.W.

A69-16489

THE MECHANICAL BEHAVIOR OF POLY(ETHYLENE TEREPHTHALATE).
I. M. Ward (Bristol, University, H. H. Wills Physics Laboratory, Bristol, England).
IN: CRYOGENIC PROPERTIES OF POLYMERS; PROCEEDINGS OF THE NASA-CASE CONFERENCE ON THE PROPERTIES OF POLYMERS AT CRYOGENIC TEMPERATURES, NASA LEWIS RESEARCH CENTER AND CASE-WESTERN-RESERVE UNIVERSITY, CLEVELAND, OHIO, APRIL 25-27, 1967. [A69-16485 05-18]
Edited by T. T. Serafini and J. L. Koenig.
New York, Marcel Dekker, Inc., 1968, p. 45-72. 27 refs.

Study of the mechanical anisotropy of poly(ethylene terephthalate) and its relation to molecular structure and the cold-drawing process. It is found that the molecular orientation is the predominant factor in determining the mechanical anisotropy below the glass transition temperature. The cold-drawing behavior of this polymer is studied over a wide range of test conditions and polymer constitution with respect to its preorientation, crystallinity, and chemical cross-linking. Z.W.

A69-16490 *

EFFECT OF FILM PRO ESSING ON CRYOGENIC PROPERTIES OF POLY(ETHYLENE TEREPHTHALATE).
Roger E. Eckert (Purdue University, School of Chemical Engineering, West Lafayette, Ind.) and Tito T. Serafini (NASA, Lewis Research Center, Polymers Research Section, Cleveland, Ohio).
IN: CRYOGENIC PROPERTIES OF POLYMERS; PROCEEDINGS OF THE NASA-CASE CONFERENCE ON THE PROPERTIES OF POLYMERS AT CRYOGENIC TEMPERATURES, NASA LEWIS RESEARCH CENTER AND CASE-WESTERN-RESERVE UNIVERSITY, CLEVELAND, OHIO, APRIL 25-27, 1967. [A69-16485 05-18]
Edited by T. T. Serafini and J. L. Koenig.
New York, Marcel Dekker, Inc., 1968, p. 73-86. 10 refs.

The effects of stretch temperature, heat-set temperature, and heat-set time on the cryogenic mechanical properties of PET film were studied by using a two-level factorial experiment. Squares of amorphous PET sheet were given a simultaneous biaxial 3X stretch in a laboratory film stretcher at either 85 or 95°C. The levels of heat-set temperature and time investigated were 190 and 210°C and 15 and 120 sec, respectively. Crystallinities of the films were determined by the density-gradient technique. Tensile properties were measured in liquid nitrogen (77 K) and liquid hydrogen (20 K). Biaxial burst properties were obtained in liquid nitrogen. It was found that processing variables significantly affect the stress-strain properties of PET film at cryogenic temperatures. These results and encouraging values of flexibility offer leads for possible use of specially processed PET films for cryogenic space applications. (Author)

A69-16491 *

MECHANICAL PROPERTIES OF EPOXY RESINS AND GLASS/EPOXY COMPOSITES AT CRYOGENIC TEMPERATURES.
L. M. Soffer and R. Molho (Aerojet-General Corp., Von Karman Center, Azusa, Calif.).
IN: CRYOGENIC PROPERTIES OF POLYMERS; PROCEEDINGS OF THE NASA-CASE CONFERENCE ON THE PROPERTIES OF POLYMERS AT CRYOGENIC TEMPERATURES, NASA LEWIS RESEARCH CENTER AND CASE-WESTERN-RESERVE UNIVERSITY, CLEVELAND, OHIO, APRIL 25-27, 1967. [A69-16485 05-18]
Edited by T. T. Serafini and J. L. Koenig.
New York, Marcel Dekker, Inc., 1968, p. 87-117. 8 refs.
Contract No. NAS 3-6287.

The mechanical properties of four modified-epoxy resin systems were investigated. Tensile properties (including strength, modulus, and elongation), notch toughness, impact strength, the coefficient of linear thermal contraction, and thermal-shock resistance were determined for cast-resin specimens at 75, -320, and -423°F. Interlaminar shear strengths (Naval Ordnance Laboratory horizontal shear and short-span shear) were obtained for glass-filament-wound-composite specimens at the three temperatures. The two systems with the best cryogenic properties were a hybrid-epoxy/polyurethane (resin 4A) and a highly modified bisphenol-A epoxy (resin 2). In choosing the optimum system, the same tests (except for notch toughness, impact strength, and short-span shear) were performed on filament-wound-composite specimens at the three temperatures. In these tests the performance of resin 4A was better than, or at least comparable to, that of resin 2. (Author)

A69-16492

MECHANICAL RELAXATION OF POLY-4-METHYL-PENTENE-1 AT CRYOGENIC TEMPERATURES.
Motowo Takayanagi and Nobuhiro Kawasaki (Kyushu University, Faculty of Engineering, Fukuoka, Japan).
IN: CRYOGENIC PROPERTIES OF POLYMERS; PROCEEDINGS OF THE NASA-CASE CONFERENCE ON THE PROPERTIES OF POLYMERS AT CRYOGENIC TEMPERATURES, NASA LEWIS RESEARCH CENTER AND CASE-WESTERN-RESERVE UNIVERSITY, CLEVELAND, OHIO, APRIL 25-27, 1967. [A69-16485 05-18]
Edited by T. T. Serafini and J. L. Koenig.
New York, Marcel Dekker, Inc., 1968, p. 119-136. 12 refs.

Observation, in the temperature dispersion curve of poly-4-methyl-pentene-1 (P4MP1), of the secondary absorption associated with thermal motion of side chains (β_{sc}). The absorption can be observed as a doublet at about -150 to -160°C (110 cps). By inspecting the absorptions of the various kinds of samples with different crystallinity, including bulk-crystallized and solution-grown crystals, the low-temperature secondary absorption can be separated into the β_{sc}-A absorption associated with the frozen amorphous chains and the β_{sc}-C absorption associated with the defect region within the crystal phase. The effect of crystal transformation, γ-ray irradiation, and annealing of single crystals upon the β absorption was also considered. F.R.L.

A69-16494

MECHANICAL BEHAVIOR OF POLY(ETHYLENE TEREPHTHALATE) AT CRYOGENIC TEMPERATURES.

C. D. Armeniades, I. Kuriyama, J. M. Roe, and Eric Baer (Case-Western-Reserve University, Div. of Polymer Science, Cleveland, Ohio).
IN: CRYOGENIC PROPERTIES OF POLYMERS; PROCEEDINGS OF THE NASA-CASE CONFERENCE ON THE PROPERTIES OF POLYMERS AT CRYOGENIC TEMPERATURES, NASA LEWIS RESEARCH CENTER AND CASE-WESTERN-RESERVE UNIVERSITY, CLEVELAND, OHIO, APRIL 25-27, 1967. [A69-16485 05-18]
Edited by T. T. Serafini and J. L. Koenig.
New York, Marcel Dekker, Inc., 1968, p. 155-169. 32 refs.

The mechanical behavior of poly(ethylene terephthalate) (PET) was studied at temperatures from 4 to 300 K with a free oscillating torsion pendulum and an Instron tester. Torsion pendulum data show the presence of relaxation maxima below 80 K. Noncrystalline specimens show a small peak at 48 K (δ) and a shoulder at 8 to 12 K (ϵ). A peak at 20 K is observed in crystalline samples, both oriented and unoriented. In addition drawn specimens show a pronounced peak at 48 K and the asymmetric maximum in the 100 to 240-K region is split into two peaks. The logarithmic decrement in the β-loss region decreases with increasing crystallinity and orientation, while the cryogenic loss peaks increase in intensity. Tensile tests with biaxially oriented and heat-set films show a twofold increase in elastic modulus and a tenfold increase in toughness at cryogenic temperatures when compared with "amorphous" PET. (Author)

A69-26813 *
ABLATIVE CHARACTERIZATION OF SEVEN HEAT SHIELD MATERIALS - A REVIEW OF THE NASA-SRI ROUND-ROBIN PROGRAM.
N. K. Hiester, C. F. Clark (Stanford Research Institute, Physical Sciences Div., Menlo Park, Calif.), and N. S. Vojvodich (NASA, Ames Research Center, Thermo- and Gas-Dynamics Div., Moffett Field, Calif.).
IN: AMERICAN INSTITUTE OF AERONAUTICS AND ASTRONAUTICS AND AMERICAN SOCIETY OF MECHANICAL ENGINEERS, STRUCTURES, STRUCTURAL DYNAMICS AND MATERIALS CONFERENCE, 10TH, NEW ORLEANS, LA., APRIL 14-16, 1969, PROCEEDINGS. [A69-26807 12-32]
New York, American Society of Mechanical Engineers, 1969, p. 57-68. 13 refs.
Contract No. NASr-49(15).

The results of a comprehensive NASA-sponsored ablation test program, which was managed by Stanford Research Institute and monitored by Ames Research Center, NASA, are presented. Detailed measurements of mass loss rates (total and pyrolysis) and temperature (surface and internal) were obtained for a number of ablation materials in twelve arc-heated wind tunnels over a wide range in convective heating rate (50 to 3300 Btu/ft^2 sec), stagnation point pressure (0.004 to 30 atm), and stream enthalpy (1700 to 34,000 Btu/lb). The materials evaluated, which are considered to be representative of current heat shield formulations, included Teflon, phenolic-nylon (one high-density and two low-density versions), two formulations of silicone elastomer, and an epoxy-novolac in a fiberglass honeycomb. Test stream centerline calibration data are compared for the participating facilities, and some radial profiles of heating rate are shown to illustrate the uniformity of the air environments. Correlations of the mass loss and temperature measurements, in terms of measured environmental parameters, are suggested by dimensional analysis and evaluated by a regression program. The influence of model scale, heating rate, and pressure level are considered and comparisons are made with existing data. Delineation and discussion of the differences in the ablative response of the various materials are emphasized. (Author)

A69-29411
SOCIETY OF PLASTICS ENGINEERS, ANNUAL TECHNICAL CONFERENCE, 27TH, CHICAGO, ILL., MAY 5-8, 1969, PROCEEDINGS.
Greenwich, Conn., Society of Plastics Engineers, Inc. (Technical Papers. Volume 15), 1969. 646 p.
Members, $15.; nonmembers, $20.

CONTENTS:

UNIAXIAL COMPRESSIVE CREEP OF POLYTETRAFLUOROETHYLENE. D. A. Thomas (Imperial Chemical Industries, Ltd., Welwyn Garden City, Herts., England), p. 148-153. 6 refs. [See A69-29412 14-18]

PROCESSING TECHNIQUES FOR BORON FILAMENT WOUND COMPOSITE STRUCTURES. P. W. Juneau, Jr., V. N. Saffire (General Electric Co., Philadelphia, Pa.), D. P. Hug, and D. Golladay (Hercules, Inc., Cumberland, Md.), p. 218-226. 5 refs. [See A69-29413 14-15]

FILL-TO-WARP RATIO EFFECTS IN WOVEN ROVING LAMINATES. D. M. Boles and J. A. Rolston (Owens-Corning Fiberglas Corp., Granville, Ohio), p. 416-423. [See A69-29414 14-18]

PREPARATION AND COMPRESSION MOLDING OF SALT-LIKE INTERMEDIATE PYRRONE (BIDA-EG-DAB). H. L. Price and V. L. Bell (NASA, Langley Research Center, Hampton, Va.), p. 617-623. 13 refs. [See A69-29415 14-18]

A69-29415 *#
PREPARATION AND COMPRESSION MOLDING OF SALT-LIKE INTERMEDIATE PYRRONE (BTDA-EG-DAB).
Howard L. Price and Vernon L. Bell (NASA, Langley Research Center, Hampton, Va.).
IN: SOCIETY OF PLASTICS ENGINEERS, ANNUAL TECHNICAL CONFERENCE, 27TH, CHICAGO, ILL., MAY 5-8, 1969, PROCEEDINGS. [A69-29411 14-18]
Greenwich, Conn., Society of Plastics Engineers, Inc. (Technical Papers. Volume 15), 1969, p. 617-623. 13 refs.

Compression molding processes for three molecular forms of Pyrrone salt-like intermediate molding powders. Three different procedures were investigated to compression mold the Pyrrones. The one-pressure procedure, in which a pressure of 6,500 psi was applied at room temperature and a 450°F curve temperature was used, was not satisfactory. A modified one-pressure procedure, in which the die was charged with previously heated powder and the pressure was applied at 500°F, permitted small moldings to be made at 700°F. A two-pressure molding procedure was used successfully to mold both small and large disks. The results of this investigation show that the critical factor in molding the Pyrrones is the elimination of volatiles. G.R.

A69-33288 *#
STUDIES OF ULTRAVIOLET IRRADIATION EFFECTS IN ZnO-TYPE THERMAL CONTROL COATING PIGMENTS.
R. L. Kroes, Arun P. Kulshreshtha (NASA, Marshall Space Flight Center, Space Sciences Laboratory, Huntsville, Ala.), T. Mookherji, and J. D. Hayes (Brown Engineering Co., Inc., Huntsville, Ala.).
American Institute of Aeronautics and Astronautics, Thermophysics Conference, 4th, San Francisco, Calif., June 16-18, 1969, Paper 69-639. 9 p.
Members, $1.00; nonmembers, $1.50.
Contracts No. NAS 8-30148; No. NAS 8-20166.

Study of the UV-induced degradation process in zinc oxide, consisting of photo-Hall, luminescence, and EPR measurements on single-crystal, powder, and thin-film samples. Optical, magnetic, and electrical measurements were made under reduced and elevated pressures of dry oxygen, in situ, and in atmospheres of sulfur, tellurium, selenium, and carbon monoxide. The results are found to be in good agreement with a proposed degradation model. B.H.

A69-33762 *#
TEST PARAMETERS, MATERIAL CHARACTERIZATION, AND THE WHITE THERMAL CONTROL COATING STABILITY PROBLEM.
Dennis Farnsworth (Martin Marietta Corp., Thermophysics Laboratory, Baltimore, Md.) and John Buckley (NASA, Langley Research Center, Hampton, Va.).
American Institute of Aeronautics and Astronautics, Thermophysics Conference, 4th, San Francisco, Calif., June 16-18, 1969, Paper 69-641. 12 p. 29 refs.
Members, $1.00; nonmembers, $1.50.
Contracts No. NAS 2-4963; No. NAS 1-7043.

Description of a program initiated to evaluate the high-melting-point, high-density, ceramic oxides as white thermal control coating pigments. A new testing facility was available for the program, and

efforts were made concurrent with coating studies to identify better methods of conducting environmental tests. In the coating studies, a major effort was undertaken to characterize the pigments in terms of purity, particle size, and microstructure. During the early ultraviolet exposure test, new information was obtained that indicated important influence of impurities lower than 20 ppm. The activity in environmental testing was to more nearly simulate the solar wind outside the earth's magnetosphere. To this end, thermal electrons were added to the proton beam, thereby evaluating equal number and combinations of protons and electrons. The paper documents the material characterization, environmental influence of neutral beams, measurement of UV damage using X-ray diffraction, theoretical influences of impurities in UV stability, and the results of synthesis and evaluation activities. (Author)

A69-35521 *
TENSILE AND CYCLIC FATIGUE PROPERTIES OF GRAPHITE FILAMENT-WOUND PRESSURE VESSELS AT AMBIENT AND CRYOGENIC TEMPERATURES.
Morgan P. Hanson (NASA, Lewis Research Center, Cleveland, Ohio).
IN: MATERIALS AND PROCESSES FOR THE 70'S; SOCIETY OF AEROSPACE MATERIAL AND PROCESS ENGINEERS, NATIONAL SYMPOSIUM AND EXHIBITION, 15TH, LOS ANGELES, CALIF., APRIL 29-MAY 1, 1969, PROCEEDINGS. (A69-35501 19-15)
North Hollywood, Western Periodicals Co.; Azusa, Calif., Society of Aerospace Material and Process Engineers (Science of Advanced Materials and Process Engineering Proceedings. Volume 15), 1969, p. 249-256. 7 refs.

Graphite fibers were fabricated into NOL rings and biaxial-wound cylinders. Filament tensile strengths of NOL rings were determined at 75, -320, and -423 deg F. Comparisons were made of ambient temperature fiber tensile strengths as obtained from NOL rings, strand tests, and biaxially wound cylinders. Fatigue characteristics of internally pressurized cylinders were determined at 75 and -320 deg F. Fatigue comparisons are made of graphite and glass filament-wound cylinders on the basis of specific strength. (Author)

A69-35529 *
RADIATION STABILITY OF UNFILLED PYRRONE MOLDINGS.
Howard L. Price and Vernon L. Bell (NASA, Langley Research Center, Hampton, Va.).
IN: MATERIALS AND PROCESSES FOR THE 70'S; SOCIETY OF AEROSPACE MATERIAL AND PROCESS ENGINEERS, NATIONAL SYMPOSIUM AND EXHIBITION, 15TH, LOS ANGELES, CALIF., APRIL 29-MAY 1, 1969, PROCEEDINGS. (A69-35501 19-15)
North Hollywood, Western Periodicals Co.; Azusa, Calif., Society of Aerospace Material and Process Engineers (Science of Advanced Materials and Process Engineering Proceedings. Volume 15), 1969, p. 335-347. 9 refs.

An investigation has been made of the stability of unfilled pyrrone moldings to electron irradiation in air. Previous radiation data have shown that pyrrone films made with pyromellitic dianhydride retained their mechanical properties after doses up to 50,000 Mrads. The present investigation included preparing the molding powder from benzophenone tetracarboxylic acid dianhydride and diaminobenzidine in either dimethylacetamide or ethylene glycol. A workable (but not necessarily optimum) molding procedure was developed to form the powder into parts suitable for mechanical testing. The molded parts were cut into test specimens for flexural tests at elevated temperatures to 600 deg F (582 deg K) and, after exposure to electron radiation in air, to doses of 50,000 Mrads (5×10^{10} rad). (Author)

A69-35536 *
ABLATIVE THERMAL PROTECTION AT LOW HEATING RATES.
Ronald B. Pope, Salvatore R. Riccitiello, Howard E. Goldstein, and John A. Parker (NASA, Ames Research Center, Moffett Field, Calif.).
IN: MATERIALS AND PROCESSES FOR THE 70'S; SOCIETY OF AEROSPACE MATERIAL AND PROCESS ENGINEERS, NATIONAL SYMPOSIUM AND EXHIBITION, 15TH, LOS ANGELES, CALIF., APRIL 29-MAY 1, 1969, PROCEEDINGS. (A69-35501 19-15)
North Hollywood, Western Periodicals Co.; Azusa, Calif., Society of Aerospace Material and Process Engineers (Science of Advanced Materials and Process Engineering Proceedings. Volume 15), 1969, p. 421-434. 12 refs.

Evaluation of ablative materials for thermal protection at low heating rates is discussed. Initially, 21 different materials with densities between 225 and 2200 kg/cu m were evaluated by performing convective heating tests in arc-heated nitrogen streams and observing the backface temperature rise and surface recession. Modified polyurethane foam composite with a density of 54 kg/cu m, which has characteristics desirable for ablative thermal protection, was developed. The ablative performance of the foam was evaluated, and excellent insulative performance was demonstrated. Ablative performance of the foam materials is compared with the performance of state-of-the-art materials and with analytical predictions. (Author)

A69-36028 *
DETECTION AND MINIMIZATION OF CHEMICALLY INDUCED IGNITION HAZARDS OF GLYCOL FLUIDS.
W. R. Downs (NASA, Manned Spacecraft Center, Houston, Tex.) and David B. Boies (IIT Research Institute, Chicago, Ill.).
IN: ANNALS OF ASSURANCE SCIENCES; PROCEEDINGS OF THE EIGHTH RELIABILITY AND MAINTAINABILITY CONFERENCE, DENVER, COLO., JULY 7-9, 1969. (A69-35999 19-15)
Conference sponsored by the American Institute of Aeronautics and Astronautics, the Society of Automotive Engineers, and the American Society of Mechanical Engineers.
New York, Gordon and Breach, Science Publishers, Inc., 1969, p. 316-324. 6 refs.

Electrical circuits of spacecraft, military aircraft, and naval vessels generally contain silver or silver-clad conductors. A spillage or seepage of a glycol/water solution on silver-clad wires or defectively insulated components carrying direct current creates a flammability hazard by the reaction of the silver anode in contact with glycol solution. The effects of the chemical reactions leading to ignition produce radio-frequency disturbances (detectable on an AM receiver) and induce rapid fluctuations of current as a function of contact time. When spillages of glycol/water occur on electrical equipment, the circuit elements must be washed and the parts tested for freedom from contamination before the system can be qualified as hazard-free. Techniques for flushing electrical circuitry as a part of quality assurance procedures are described. The results of a study of pinhole leaks in aluminum tubing of a glycol loop system disclosed that pinhole leaks do not develop rapidly from corrosion and that confidence in a tubing system is verified if no leakages develop as a result of hydrostatic pressure qualification tests. (Author)

A69-36208 *
STATIC OXIDATION AND COMPATIBILITY OF BORON NITRIDE AND BORON NITRIDE COMPOSITE TO 2000°C.
John D. Buckley (NASA, Langley Research Center, Flight Vehicles and Systems Div., Spacecraft Equipment Section; George Washington University, Hampton, Va.).
(American Ceramic Society, Annual Meeting, 70th, Chicago, Ill., Apr. 20-25, 1968.)
American Ceramic Society Bulletin, vol. 48, July 1969, p. 711-715. 13 refs.

Two grades of boron nitride and a boron nitride composite were subjected to temperatures up to 1500 deg C in air and up to 2000

deg C in a vacuum for various periods of time. The results showed that composition influences thermal shock and oxidation resistance of boron nitride bodies. Compatibility tests were made with four refractory oxides, JTA graphite composite, and five refractory metals at temperatures up to 1800 deg C. Little or no reaction occurred between the boron nitride compositions and the refractory ceramics up to 1500 deg C and the refractory metals up to 1000 deg C.
(Author)

A69-38533 *
PLASTICS IN SPACE FLIGHT PROGRAMS.
James Kingsbury (NASA, Marshall Space Flight Center, Propulsion and Vehicle Engineering Laboratory, Materials Div., Huntsville, Ala.).
IN: SOCIETY OF THE PLASTICS INDUSTRY, NATIONAL PLASTICS CONFERENCE, CHICAGO, ILL., NOVEMBER 12-15, 1968, PROCEEDINGS.
Stamford, Conn., Technomic Publishing Co., Inc., 1969, p. 108-113.

Discussion of the use of plastics in the Apollo-Saturn V Program. While on a weight basis their use represents a small percentage of the total materials used, the criticality of the plastic components equals, and in some cases exceeds that of other materials. The following categories of plastic application are covered: foam, honeycomb, conformal coatings, embedment compounds, dielectrics, damping compounds, adhesives, sealants, and gaskets.B.H.

A69-39236 * #
EXPERIMENTAL EVALUATION OF POLYURETHANE FOAM COMPOSITES FOR LOW-HEATING-RATE THERMAL PROTECTION.
Ronald B. Pope, Salvatore R. Riccitiello, and John A. Parker (NASA, Ames Research Center, Moffett Field, Calif.).
Journal of Spacecraft and Rockets, vol. 6, Apr. 1969, p. 506-509. 9 refs.

Experimental evaluation of polyurethane foam composites for thermal protection at heating rates between 170 and 1020 kW per sq m in oxidizing environments. It is found that a polyurethane foam (51) modified with astroquartz fiber exhibits the highest surface temperature and low surface erosion. Z.W.

A69-41715 *
THE DEVELOPMENT OF POLYBENZIMIDAZOLE COMPOSITES AS ABLATIVE HEAT SHIELDS.
Robert R. Dickey, John H. Lundell, and John A. Parker (NASA, Ames Research Center, Moffett Field, Calif.).
Journal of Macromolecular Science, Series A—Chemistry, vol. 3, July 1969, p. 573-584. 16 refs.
Contract No. NAS 7-340.

Description of the formulation of several new low-density polybenzimidazole (PBI) composites. The proposed structure of the basic linear PBI prepolymer and of several highly cross-linked PBI polymers are presented. The cross-linked PBI's were obtained either thermally (by postcuring to a high temperature) or chemically (by the use of either preoxidized polyfunctional amines or triphenyl trimeasate as a comonomer in the polymerization). Both the linear and the cross-linked PBI composite materials were tested in an arc-heated wind tunnel at a stagnation-point heating rate of 800 W per sq cm and a surface pressure of 2.5 atm. For comparison, a standard phenolic-nylon material of approximately the same density was also tested. The test results show that the linear PBI composite had a lower mass-loss rate than the phenolic-nylon material. The results also indicate that the ablation performance of PBI composites can be substantially improved by cross-linking. The improvement is particularly noticeable in regions of high surface shear. (Author)

N69-10005 Illinois Univ., Urbana.
SINTERING KINETICS OF ULTRA FINE CALCIA STABILIZED ZIRCONIA
David Griffith Wirth, Jr. (Ph.D. Thesis) 1967 104 p
Avail: Univ. Microfilms: HC $5.20/Microfilm $3.00 Order No. 68-1887

Kinetics for the initial, intermediate, and final stages of sintering of ultrafine calcia stabilized zirconia were determined. Initial stage kinetics as determined by isothermal shrinkage measurements indicated a grain boundary mechanism of material transport was operative. The activation energy for sintering in this stage agreed quite closely with that for oxygen ion diffusion indicating that this species was rate controlling. This indicated that overall cation diffusion was enhanced. The results of intermediate stage kinetics as determined by isothermal porosity determination also indicated that oxygen ion was still the rate controlling diffusing species. The material transport mechanism was postulated to still be grain boundary diffusion based on the high grain boundary volume to bulk volume ratio as indicated by the small crystallite size and high activation energy for crystallite growth. Final stage kinetics as determined by isothermal grain growth studies indicated that rate control had been transferred to the cation species in the bulk. Dissert. Abstr.

N69-10066*# National Aeronautics and Space Administration. Langley Research Center, Langley Station, Va.
A STUDY TO DETERMINE THE PRESENCE OF VOLTAGE BREAKDOWN DUE TO PROTON IRRADIATION IN POLYMERIC MATERIALS
Herbert D. Hendricks and William E. Miller Washington Nov. 1968 21 p refs
(NASA-TM-X-1688) Avail: CFSTI CSCL 11I

A study was made to determine proton induced voltage breakdowns in a series of polymeric materials: Kapton (H-film), Teflon (TFE), Pyrrone, Mylar, and polyethylene. Proton energy was varied from 0.40 to 3.25 MeV with a flux of 10^9, 10^{10}, 10^{11}, or 2×10^{11} protons/cm^2-sec. Samples were irradiated to a fluence of 10^{13} to 5×10^{14} protons/cm^2 for each test. Sample temperatures were 27°C and -134°C. No charge storage or induced voltage breakdown effects were observed. This observation is in sharp contrast to the numerous induced voltage breakdowns observed for electron irradiation of similar types of polymeric samples. A theory developed by Nichols and van Lint predicts that a behavior of this type should be less prevalent because of proton rather than electron irradiation. Author

N69-10754*# National Aeronautics and Space Administration. Langley Research Center, Langley Station, Va.
CRYSTALLOGRAPHIC DATA ON SELECTED ARTIFICIAL GRAPHITES WITH COMMENTS ON THE ROLE OF THE DEGREE OF CRYSTAL DEVELOPMENT IN OXIDATION
Howard G. Maahs Washington Nov. 1968 18 p refs
(NASA-TN-D-4888) Avail: CFSTI CSCL 11I

Crystallographic parameters have been measured by X ray diffraction on 40 grades of commercially available, nonpyrolytic, artificial graphite (that is, industrially manufactured graphite consisting of filler and binder). The parameters measured are the lattice dimensions (a and d_c), and the crystallite diameter and height. Since artificial graphite is composed of a mixture of two or more graphite carbons, the measured crystallographic parameters are apparent only and are truly representative of neither the filler nor the binder. However, the measured interlayer spacing of artificial graphite is a good approximation of that of the filler. A survey of the literature indicates that the less graphitic a carbon, the less resistant the carbon is to oxidation. For this reason the binder in artificial graphite should be locally more reactive than the filler. Therefore, the aerodynamic erosion resistance of artificial graphite may be largely dependent on the binder, particularly in high-shear environments in which filler particles may be mechanically removed because of preferential oxidation of the binder matrix. Author

18 MATERIALS, NONMETALLIC

N69-14400*# Westinghouse Electric Corp., Lima, Ohio.
MAGNETIC AND ELECTRICAL MATERIALS CAPABLE OF OPERATING IN THE 800° TO 1600°F TEMPERATURE RANGE
R. E. Stapleton Washington NASA Dec. 1968 129 p refs
(Contract NAS3-6465)
(NASA-CR-1213; WAED-67-24E) Avail: CFSTI CSCL 09A

Four candidate high-purity dielectric materials were fabricated into thin wafer, test capacitors and their electrical properties were measured in vacuum at temperatures up to 1100°F. These materials included: pyrolytic boron nitride, single crystal Al_2O_3, hot-pressed BeO, and polycrystalline Al_2O_3. The data shows that pyrolytic boron nitride (PBN) has superior electrical properties over the temperature range and can be fabricated into very thin (<0.001 inch) large area capacitor wafers. A number of multi-layer capacitors (pyrolytic boron nitride dielectric) have been designed and evaluated at temperatures up to 1100°F. Sputtered, thin film electrodes were used on all devices. The feasibility of interconnecting these electrodes without supplementary metal foil tabs has been demonstrated. An extended life test was successfully completed on a five wafer pyrolytic boron nitride (PBN) capacitor at 1100°F in vacuum. Author

N69-14764*# Texas Univ., Austin.
FORCE-PENETRATION CHARACTERISTICS OF A SAND HORIZONTALLY PENETRATED BY PLATES, CONES, AND SPHERICAL SEGMENTS
Paul A. Hustad and William R. Cox Washington NASA Jan. 1969 217 p refs
(Grant NsG-604)
(NASA-CR-1252) Avail: CFSTI CSCL 08M

The influence of time upon the force-penetration characteristics of sand was determined by varying the velocity at which the models penetrated into the backfills. Three separate phases of laboratory testing were included. The first consisted of designing a test setup and performing pilot tests that simulated the classical plane-strain earth-pressure problem. The second phase utilized much the same type of loading apparatus as that used in Phase I. Two heights of walls, 1 ft and 1.5 ft, were penetrated at various constant velocities into loose and dense backfills. For the range of velocities that were utilized, the observations showed that the time effects were negligible. The third phase utilized two sizes of right-circular cones and spherical segments which were penetrated into backfills horizontally supported by polyethylene membranes. The rate and vertical depth below the soil surface at which the models penetrated the loose and dense backfills were varied. The same general range of velocities as in Phase II were utilized, and it was found that the time effects were negligible. Equations are presented that provide a means of predicting the maximum horizontal and vertical soil reactions. Author

N69-19825*# National Aeronautics and Space Administration. Langley Research Center, Langley Station, Va.
MECHANICAL BEHAVIOR OF BORON-EPOXY AND GLASS-EPOXY FILAMENT-WOUND CYLINDERS UNDER VARIOUS LOADS
Harvey W. Herring, Robert M. Baucom, and Richard A. Pride Washington Mar. 1969 66 p refs
(NASA-TN-D-5050) Avail: CFSTI CSCL 11D

A study was made to determine the mechanical behavior of boron-epoxy and S-glass–epoxy filament-wound cylinders under tensile, compressive, torsional, and pressure loads. These cylinders were fabricted in either an orthotropic winding pattern or an isotropic pattern. Conventional theory used to predict the elastic behavior of glass-epoxy filament-wound cylinders was discovered to be equally adequate for the boron-epoxy cylinders. Since Young's modulus for a boron filament is much greater than that for a glass filament, the boron-epoxy cylinders were considerably stiffer than those of glass-epoxy. Attempts to correlate cylinder failure strengths calculated from existing state-of-the-art theories with experimental failure strengths met with varying success. Thus, additional research is necessary before failure characteristics of filament-wound composite cylinders, either glass- or boron-reinforced, can be accurately predicted. Author

N69-19918*# National Aeronautics and Space Administration. Langley Research Center, Langley Station, Va.
TENSILE BEHAVIOR OF BORON FILAMENT REINFORCED EPOXY RINGS AND BELTS
Robert M. Baucom Washington Mar. 1969 31 p refs
(NASA-TN-D-5053) Avail: CFSTI CSCL 11D

The room-temperature tensile characteristics of boron-filament epoxy-resin composites have been determined. The effect of low to elevated temperatures on rings and cyclic loading on belts was also investigated. An analysis of the tensile strength of the monofilaments used for the fabrication of the composite specimens is included. In addition, a theoretical analysis of the bending stresses inherent in ring tensile testing is presented. The average strength of the boron monofilaments before winding into the rings and belts was about 406 ksi (2800 MN/m^2). The average room temperature strength of the composites ranged from 90 ksi (620 MN/m^2) for the rings to 66 ksi (455 MN/m^2) for the belts. These low composite strengths are the result of two principal factors: low filament-volume fraction in the composite, and bending stresses induced by the ring test fixtures. With these two factors considered, the filament strength in the composite ring was 85% of the average monofilament strength. Author

N69-20790*# National Aeronautics and Space Administration. Lewis Research Center, Cleveland, Ohio.
LOW-DENSITY FOAM FOR INSULATING LIQUID–HYDROGEN TANKS
Irving E. Summer Washington Mar. 1969 52 p refs
(NASA-TN-D-5114) Avail: CFSTI CSCL 11I

A lightweight polyurethane foam insulation for liquid hydrogen tanks of space vehicles was developed that (1) could be foamed in place, (2) did not crack when chilled to liquid hydrogen temperature, and (3) had a thermal conductivity of 0.0137 W/(m)(K) (0.0079 Btu/(hr)(ft)(°R) at a mean temperature of 136 K (243° R). The foaming-in-place technique in which the foam constituents were poured directly on the tank, coupled with the specific foam formulation, produced a 34.4-kg/m^3–(2.14-lb/ft^3) density foam that remained structurally intact during all simulated ground-hold, vibration, and space-hold tests conducted. Thermophysical properties of the foam were determined, and thermal stress profiles throughout a layer of insulation were calculated. Author

N69-21384*# National Aeronautics and Space Administration. Lewis Research Center, Cleveland, Ohio.
MATHEMATICAL ANALYSIS OF THE FITZGERALD APPARATUS
Donald R. Behrendt and James P. Cusick Washington Mar. 1969 19 p refs
(NASA-TN-D-5116) Avail: CFSTI CSCL 11J

The machine developed by E. R. Fitzgerald to investigate the dynamic mechanical properties of solids is reanalyzed to take account of effects due to a shorted turn on the drive tube. The shorted turn arises from an extension of the aluminum portion of the drive tube into the radial magnetic field. The new analysis predicts the anomalous calibration data of the machine as well as the asymmetry and negative values of loss compliance associated with resonant phenomena. Author

N69-23843*# National Aeronautics and Space Administration. Electronics Research Center, Cambridge, Mass.
A BONDING MATERIAL FOR OPTICALLY IMMERSING INFRARED DETECTORS FROM 2 TO 14 MICROMETERS
Richard D. Packard Washington May 1969 15 p refs
(NASA-TM-X-1776) Avail: CFSTI CSCL 11A

The visible and infrared transmitting properties of a specific epoxy resin are analyzed and shown to be suitable for bonding infrared detectors, operating in the 2–14 μm spectral region, to an optically transmitting substrate for immersed applications. Additionally, this resin permits preliminary system alignment using visible radiation. The resin also has desirable physical properties for such bonding applications. Author

N69-26448*# Hughes Aircraft Co., Culver City, Calif.
DEVELOPMENT AND PROCESSING OF PYRONNE POLYMERS
L. E. Karre, L. B. Keller, and L. J. Miller Washington NASA May 1969 105 p refs
(Contract NAS1-6287)
(NASA-CR-1310; P68-148) Avail: CFSTI CSCL 07C

This report describes the development and processing of polymers formed from the condensation reaction of aromatic dianhydrides with aromatic tetraamines in various solvents. In Phase I, the primary efforts involved the synthesis and characterization of the polymer formed from the condensation of pyromellitic dianhydride (PMDA) with diaminobenzidine (DAB) in polar solvents and the subsequent preparation and testing of fabricated articles. In Phase II, primary efforts included the synthesis, characterization, and subsequent fabrication of the polymer formed from the condensation of benzophenone tetracarboxylic dianhydride (BTDA) with diaminobenzidine (DAB) in the esterifying solvent ethylene glycol (EG). Phase III of the program was directed toward laminates fabricated from the polymer formed from the condensation of BTDA with DAB in the esterifying solvent ethanol (EtOH) had flexural strength above 70,000 psi and moduli above 3×10^6 psi, but more important, the thermal stability was greatly improved. The most promising resin system of the three investigated, from the standpoint of both mechanical strength and thermal stability, is the polymer formed from BTDA and DAB in ethanol. Author

N69-28203*# National Aeronautics and Space Administration. Lewis Research Center, Cleveland, Ohio.
OUTGASSING CHARACTERISTICS OF AN EXPOXY-IMPREGNATED MAGNET COIL
Ronald J. Schertler Washington Jun. 1969 12 p refs
(NASA-TM-X-1813) Avail: CFSTI CSCL 11I

Outgassing tests a function of temperature were conducted using an epoxy-impregnated magnet coil. Glass tape impregnated with epoxy resin provided the electrical insulation between the conductors. Outgassing data were taken by measuring the rate of pressure rise due to the magnet coil heating in a closed vacuum system. The outgassing rate increased exponentially from 3.05×10^{-8} torr-liter per square centimeter-second at an epoxy temperature of 24° C to 9.0×10^{-7} torr-liter per square centimeter-second at 53°C. The coil assembly had a higher outgassing rate at temperatures above 30°C than small disk-shaped samples of the same epoxy. Author

N69-29559*# Franklin Inst., Philadelphia, Pa. Research Labs.
ELECTRICAL CHARACTERISTICS OF PYRRONE POLYMERS
P. J. Reucroft, H. Scott, P. L. Kronick, and F. L. Serafin Washington Publ NASA Jun. 1969 58 p refs
(Contract NASI-7408)
(NASA-CR-1367) Avail: CFSTI

Polyimidazopyrrolone or Pyrrone polymers, a new class of aromatic-heterocyclic polymers which have outstanding thermal and radiolytic stability, are studied. A detailed determination of the alternating current and direct current electrical properties of Pyrrone polymers and the effect of high energy radiation on these properties are described. Author

N69-33321*# National Aeronautics and Space Administration. Lewis Research Center, Cleveland, Ohio.
FAILURE CRITERIA FOR FILAMENTARY COMPOSITES
Christos C. Chamis Washington Aug. 1969 32 p refs
(NASA-TN-D-5367) Avail: CFSTI CSCL 11D

A two level, linear, semiempirical theory for a failure criterion is described. The theory predicts the strength behavior of unidirectional filamentary composites under uniaxial and combined stress from basic constituent material properties and fabrication process considerations. Applications of the theory to several filament nonmetallic matrix composites are presented and comparisons are made with experimental data. These results show good agreement between theory and experiment. Simple and combined strength envelopes are generated to illustrate the versatility of the theory and to point out problem areas in experimental work and design. Author

N69-34134*# National Aeronautics and Space Administration. Lewis Research Center, Cleveland, Ohio.
SURFACE TENSION, VISCOSITY, AND DENSITY MEASUREMENTS OF TWO FLUOROCARBON SOLVENTS, FC-43 AND FC-78
Thom A. Coney Washington Aug. 1969 11 p refs
(NASA-TM-X-1862) Avail: CFSTI CSCL 20D

The surface tension, viscosity, and density of fluorocarbon solvents FC-43 and FC-78 were measured as functions of temperature. A Du Noüy tensiometer, a falling ball viscometer, and a specific gravity chainomatic balance were used in the measurements. Liquid temperatures were varied from 5° to 30° C. Property values at 20° C were 16.7 dynes per centimeter, 6.49 centipoise and 1.9053 grams per cubic centimeter, for FC-43 and 13.2 dynes per centimeter, 0.62 centipoise, and 1.7290 grams per cubic centimeter, for FC-78. Author

N69-34547*# National Aeronautics and Space Administration. Langley Research Center, Langley Station, Va.
EFFECTS OF CYCLIC HEATING AND THERMAL SHOCK ON HAFNIA STABILIZED WITH CALCIA, MAGNESIA, and YTTRIA
John D. Buckley and David R. Wilder (Iowa State Univ., Ames) Washington Aug. 1969 43 p refs
(NASA-TN-D-5279) Avail: CFSTI CSCL 1/C

Solid solutions of HfO_2-CaO, HfO_2-Y_2O_3, and HfO_2-MgO were studied for: (1) temperature effects on stabilization (the process of eliminating or limiting the monoclinictatragonal crystallographic inversion common in hafnia at ≈1700°C); (2) effects of cyclic heating on the crystal lattice stability; and (3) thermal shock effects on partially and fully stabilized hafnia. Calcia-stabilized hafnia exhibited similar solubility when sintered at 2000° and at 1800°C. Yttria-stabilized hafnia indicated that sintering at 2000°C and at times over 9 were necessary to obtain near-maximum solution. The high vapor pressure of magnesia limits sintering temperatures for magnesia-stabilized specimens to 1800°C. Yttria-stabilized hafnia maintains its stability whereas magnesia- and calcia-stabilized specimens destabilize when subjected to a single heat cycle (25° to 1750°C). Reheating to 1925° C for 30 min under 10^{-5} torr did not produce restabilization. Hafnia stabilized with calcia or yttria maintained original stability when subjected to 25 cycles between 1040° and 1730°C in air at ambient pressure. Magnesia-stabilized hafnia was stable when removed from the furnace at 1730°C and cooled in ambient air, but was unstable

when removed at 1040°C and cooled under the same conditions. Overall thermal-shock resistance yttria-stabilized hafnia quickly cooled in ambient air from temperatures up to 2000°C was superior to the others. K.W.

N69-34708*# National Aeronautics and Space Administration. Langley Research Center, Langley Station, Va.

MOLECULAR ORIENTATION AND MECHANICAL ANISOTROPY IN POLYETHYLENE, POLYPROPYLENE, AND POLY(ETHYLENE TEREPHTHALATE) FILMS

Howard L. Price Washington Aug. 1969 21 p refs Presented at Silver Anniv. Tech. Conf. of the Soc. of Plastics Engr., Detroit, May 1967 Submitted for publication

(NASA-TN-D-5380) Avail: CFSTI CSCL 11I

Sonic pulse velocity measurement of the molecular orientation in polyethylene, polypropylene, and poly(ethylene terephthalate) films are presented. The orientation is correlated with the tensile properties which were measured at several angles in the plane of the film. The mechanical anisotropy is shown by the variation of the tensile properties and the stress relaxation modulus with direction in the plane of the film. Author

N69-36762*# RAI Research Corp., Long Island City, N.Y.

AN INVESTIGATION OF THE BASIC PROPERTIES OF IRRADIATED POLYETHYLENE MEMORY MATERIALS

Preston Keusch, Donald Greer, and John Rozembersky Washington NASA Sep. 1969 122 p refs

(Contract NAS1-7335)

(NASA-CR-1384; RAI-397) Avail: CFSTI CSCL 11H

Described are the properties, work, and conclusions reached on irradiated polyethylene memory materials. The properties affecting crosslinking, the main memory factor which determines the memory in the materials were investigated using different commercial polyethylene materials. These properties include: molecular weight, molecular weight distribution, and the degree of branching. It was found that the molecular weight distribution was the main factor that influenced the crosslinking efficiency. The conditions at which crosslinking occurs- temperature, oxygen environment, and the radiation dose were investigated. Memory studies were performed on the commercial materials to see if they completely restored after being deformed. The mechanical properties of the superior memory material tested, Poly-Eth 5555 film, were also presented. Low temperature tests, tensile tests, and modulus of elasticity were determined for all of the materials. It was concluded that the material with the best crosslinking properties had the best memory characteristics. Author

N69-40339*# National Aeronautics and Space Administration. Lewis Research Center, Cleveland, Ohio.

TRANSMISSION EFFECTS ON PLASTIC FILMS IRRADIATED WITH ULTRAVIOLET LIGHT, ELECTRONS, AND PROTONS

Evelyn Anagnostou and Adolph E. Spakowski Washington Oct. 1969 12 p refs

(NASA-TM-X-1905) Avail: CFSTI CSCL 11C

Several plastic films, suitable as covers for thin film CdS solar cells, were irradiated by ultraviolet light in vacuum. The films were bombarded by 1-MeV electrons at fluences up to 1×10^{17} electrons/cm^2, and one of the films was bombarded by 800-keV protons at fluences up to 1×10^{14} protons/cm^2. The effect of these environments on the transmission of the plastics in the wavelength range 0.350 to 1.200 μm was measured. The most promising cover material was Teflon -FEP. Author

19

MATHEMATICS

Includes calculation methods and theory; and numerical analysis. For applications see: 08 Computers.

A69-13370 *

NUMERICAL SOLUTION OF SYMMETRIC POSITIVE DIFFERENTIAL EQUATIONS.

Theodore Katsanis (NASA, Lewis Research Center, Cleveland, Ohio).

Mathematics of Computation, vol. 22, Oct. 1968, p. 763-783. 8 refs.

A finite-difference method for the solution of symmetric positive linear differential equations is developed. The method is applicable to any region with piecewise smooth boundaries. Methods for solution of the finite-difference equations are discussed. The finite-difference solutions are shown to converge at essentially the rate $O(h^{1/2})$ as $h \to 0$, h being the maximum distance between adjacent mesh-points. An alternate finite-difference method is given with the advantage that the finite-difference equations can be solved iteratively. However, there are strong limitations on the mesh arrangements which can be used with this method. (Author)

A69-13375 *

HIGH ACCURACY GAMMA FUNCTION VALUES FOR SOME RATIONAL ARGUMENTS.

D. C. Galant and P. F. Byrd (NASA, Ames Research Center, Moffett Field, Calif.).

Mathematics of Computation, vol. 22, Oct. 1968, p. 885-887.

Tabulation of high-accuracy gamma-function values for some rational arguments. During the course of determining accurate Gaussian quadrature formulas for certain nonclassical weight functions, it was necessary to compute $\Gamma(p/q)$ to 60D to obtain moments to high accuracy. In particular, $\Gamma(p/q)$ was needed for $p = 1, 2, \ldots, q - 1$, $2p \neq q$, and $q = 3, 4, 5, 8, 10$. The quantities $\Gamma(p/q)$, which for special cases also arise in the computation of Bessel functions of fractional order or of the Airy functions, were calculated using an interpretive routine that treated floating-point numbers of 70 significant figures. F.R.L.

A69-17250 *

RECURSIVE FORMULAS FOR THE EVALUATION OF THE CONVOLUTION INTEGRAL.

H. H. Trauboth (NASA, Marshall Space Flight Center, Huntsville, Ala.).

Association for Computing Machinery, Journal, vol. 16, Jan. 1969, p. 63-72.

Derivation of recursive formulas for the numerical evaluation of the real convolution integral which is a valuable mathematical tool for simulating control systems and electrical networks on a digital computer. The formulas are derived for the case where the impulse response is given analytically. These formulas require considerably less computation time and memory space than the general time series formulas, and can be effectively applied for digital simulation of continuous physical systems. M.G.

A69-26605 *#

ANALYTIC CONTINUATION OF APPELL'S HYPERGEOMETRIC SERIES F_2 TO THE VICINITY OF THE SINGULAR POINT x = 1, y = 1.

G. E. Hahne (NASA, Ames Research Center, Moffett Field, Calif.)

Journal of Mathematical Physics, vol. 10, Mar. 1969, p. 524-531. 18 refs.

The infinite series, absolutely convergent if $|x| + |y| < 1$, for Appell's $F_2(\alpha, \beta, \beta', \gamma, \gamma'; x, y)$ is analytically continued into a linear combination of four infinite series in powers of $(x - 1)$ and $(y - 1)$; each of the latter four series is absolutely convergent if $|x - 1| + |y - 1| < 1$. The analytic continuation is carried out by manipulation of the Mellin-Barnes integral representations for the hypergeometric functions appearing in the course of the calculation. (Author)

A69-40333 *#

A COMPARISON OF GRADIENT DEPENDENT TECHNIQUES FOR THE MINIMIZATION OF AN UNCONSTRAINED FUNCTION OF SEVERAL VARIABLES.

Terry A. Straeter (NASA, Langley Research Center, Hampton, Va.).

American Institute of Aeronautics and Astronautics, Aerospace Computer Systems Conference, Los Angeles, Calif., Sept. 8-10, 1969, Paper 69-951. 6 p. 14 refs.

Members, $1.00; nonmembers, $1.50.

Use of a simplified aerospace problem and Rosenbrock's parabolic valley function as a basis for comparison with respect to ease of implementation and speed of convergence in terms of number of function evaluations. The problem is a two-dimensional minimum time-to-intercept problem with constant thrust in free space. The Armstrong-Marquardt method, a minimization algorithm for a sum-of-squares-type function arising in boundary-value problems in optimal control, is applied. Tables summarizing the results are given. F.R.L.

A69-40573 *

A SPECIAL CLASS OF DYNAMICAL POLYSYSTEMS.

J. A. Lovingood (NASA, Marshall Space Flight Center, Aero-Astrodynamics Laboratory, Huntsville, Ala.).

Journal of Differential Equations, vol. 6, Sept. 1969, p. 326-336. 9 refs.

Study of a metric state-time dynamical polysystem of a special type $(X \times T, \Omega, \lambda, \tau)$ where X is a metric space and Ω is a sequentially compact topological space. It is found that metric state-time dynamical polysystems with the space Ω sequentially compact have no sliding-state trajectories. M.M.

A69-41260 *#

PERIODIC SMALL-AMPLITUDE SOLUTIONS TO VOLTERRA'S PROBLEM OF TWO CONFLICTING POPULATIONS AND THEIR APPLICATION TO THE PLASMA CONTINUITY EQUATIONS.

J. Reece Roth (NASA, Lewis Research Center, Cleveland, Ohio).

Journal of Mathematical Physics, vol. 10, Aug. 1969, p. 1412-1414. 15 refs.

Solution of the coupled set of first-order nonlinear differential equations describing a generalized form of Volterra's problem of two conflicting populations, using an approximate method. The solutions obtained in this analysis are relevant to special cases of the classical problem of predator and prey, and also to certain low-frequency oscillations in partially ionized plasmas that arise from periodic solutions to the neutral and charged-particle continuity equations. (Author)

A69-42792 *

NUMERICAL SOLUTION OF TRICOMI EQUATION USING THEORY OF SYMMETRIC POSITIVE DIFFERENTIAL EQUATIONS.

Theodore Katsanis (NASA, Lewis Research Center, Cleveland, Ohio).

SIAM Journal on Numerical Analysis, vol. 6, June 1969, p. 236-253. 9 refs.

The Tricomi equation can be expressed in symmetric positive form. Admissible boundary conditions assure existence and uniqueness of solutions. It is shown that boundary conditions are admissible for the Tricomi equation for any region with piecewise smooth boundaries. A wide choice of boundary conditions is possible. A Tricomi equation with a known analytical solution is solved by a finite difference scheme for symmetric positive equations as an illustration of the numerical results which can be obtained. There is

strong convergence to the analytical solutions, but pointwise divergence. Smoothing of the solution reduces the divergence, however, and satisfactory numerical results are obtained. (Author)

N69-11419*# North American Rockwell Corp., Canoga Park, Calif.
VARIABLE MESH METHODS FOR DIFFERENTIAL EQUATIONS
R. Van Wyk Washington NASA Nov. 1968 40 p refs
(Contract NAS7-470)
(NASA-CR-1247; REPT-R-7491) Avail: CFSTI CSCL 12A

A multistep predictor-corrector method for the numerical solution of ordinary differential equations is developed. The difference equations employed are generalizations, for the case of variable mesh spacing, of previous formulas requiring fixed step size. In addition to retaining the high local accuracy and convergence properties of the earlier methods, the variable mesh method is developed in a form conductive to the generation of effective criteria for the selection of subsequent step sizes in the step by step solution of differential equations. These criteria are based on considerations of truncation error, convergence of corrector iterations, and an extensive treatment of relative numerical stability. The algorithm has been tested extensively and compared with other methods. The results of the comparison favor the new method. Also discussed are an extension of the variable mesh multistep method for the case of stiff equations and application of the variable mesh approach to partial differential equations. Author

N69-13368*# National Aeronautics and Space Administration, Washington, D. C.
COMPUTERIZED ARRHENIUS RELIABILITY EXTRAPOLATION TECHNIQUES
Charles R. Toye (Elec. Res. Center) Dec. 1968 16 p refs
(NASA-TN-D-4902) Avail: CFSTI CSCL 12A

Computerized mathematical techniques and algorithms useful in obtaining extrapolated component failure rates derived from the Arrhenius equation are presented. The mathematics of the Arrhenius equation is reviewed. A computer program for the calculation of an important constant in the equation is given, and a computerized extrapolation procedure is illustrated. Author

N69-14002*# National Aeronautics and Space Administration. Lewis Research Center, Cleveland, Ohio.
FORTRAN PROGRAM FOR SPLINE FIT CURVE
Theodore Katsanis Washington Dec. 1968 12 p refs
(NASA-TM-X-1707) Avail: CFSTI CSCL 12A

The spline fit curve is a convenient method for fitting a curve through a given set of points. This report describes a FORTRAN IV computer program which will calculate the spline fit curve, with function values, first and second derivatives, and curvature at any desired interpolated points. Author

N69-14476*# National Aeronautics and Space Administration. Marshall Space Flight Center, Huntsville, Ala.
REGRESSION ANALYSIS PROCEDURES FOR THE EVALUATION OF TRACKING SYSTEM MEASUREMENT ERRORS
Bobby G. Junkin Washington Dec. 1968 141 p refs
(NASA-TN-D-4826) Avail: CFSTI CSCL 17I

A regression analysis method for Tracking System Error Model Studies (TEMS) is presented for evaluating systematic errors in measurements obtained from various tracking systems. The mathematical procedures include a rigorous least squares adjustment of error model parameters with constraints, using a priori values for these parameters and their variances. Truncated tracker error models for representing the systematic errors are established using the TEMS method in conjunction with a stepwise regression procedure. This procedure involves examining at every step the variables incorporated in the error model in previous steps. A specific variable is deleted from or entered into the model by using the Gaussian Elimination Method for solving the linear system of normal equations in the regression. Although C-band radar error models are used, the procedures can be adapted to other types of tracking systems. Results from application to the Apollo-Saturn 501 (AS-501) flight test data are presented and indicate generally acceptable truncated C-band radar error models. Author

N69-17249*# Clemson Coll., S. C.
A FAMILY OF SOLUTIONS OF CERTAIN NONAUTONOMOUS DIFFERENTIAL EQUATIONS BY SERIES OF EXPONENTIAL FUNCTIONS
T. G. Proctor and H. H. Suber Washington NASA Feb. 1969 26 p refs
(Grant NGR-41-001-016)
(NASA-CR-1294) Avail: CFSTI CSCL 12A

Construction theorems are presented for the solutions of certain nonautonomous differential equations. Exponential series solutions are given for a family of periodic solutions of a Ricatti equation with odd periodic coefficients and finite Fourier series expansion. This result is generalized to the existence of a first order quasi-periodic vector differential equation which is odd in the independent variable. Applications are included. Author

N69-20940*# National Aeronautics and Space Administration. Electronics Research Center, Cambridge, Mass.
FOURIER ANALYSIS BY THE METHOD OF SELECTED ORDINATES
James N. Hallock Washington Mar. 1969 28 p ref
(NASA-TN-D-5083) Avail: CFSTI CSCL 12A

The selected ordinate method for determining the Fourier coefficients of a periodic curve is of great use when an approximate value is desired in a very short ime. Tables of the ordinates are given. Evaluation of a coefficient is reduced to a simple summation. Author

N69-21143*# Mathematics and Biology Corp., Benton, Kans.
BOUNDEDNESS THEOREMS AND OTHER MATHEMATICAL STUDIES OF A HODGKIN–HUXLEY TYPE SYSTEM OF DIFFERENTIAL EQUATIONS: NUMERICAL TREATMENT OF THRESHOLDS AND STATIONARY VALUES
Stephen W. Brady Washington NASA Mar. 1969 130 p refs
(Contract NSR-38-080-001)
(NASA-CR-1272) Avail: CFSTI CSCL 12A

Constructed is a mathematical model for the flow of electric current through the surface membrane of membranous cells such as skeletal muscle fibers, pacemakers, receptors, and heart cells with plateau type behavior. The gross behavior of the electrical properties of these cells is simulated by parameterization and by varying the sustained constant membrane current density. The model exhibits the threshold "on–off" aspects of nerves as required depending on the numerical justification for using the steady state approximately to treat the local stimulation effects together with three subsidiary first order differential equations taken from the Hodgkin–Huxley model. G.G.

N69-22988*# National Aeronautics and Space Administration. Ames Research Center, Moffett Field, Calif.
A GENERALIZED AVERAGING METHOD FOR LINEAR DIFFERENTIAL EQUATIONS WITH ALMOST PERIODIC COEFFICIENTS
Thomas J. Coakley Washington Apr. 1969 17 p refs
(NASA-TN-D-5167) Avail: CFSTI CSCL 12A

A new method for analyzing linear differential equations with almost periodic coefficients is described and discussed. The

method is essentially a generalization of the classical Floquet theory developed for linear periodic systems. By use of the method, it is shown that an almost periodic system with rapidly varying coefficients can always be reduced or transformed to a corresponding system with either constant or slowly varying coefficients. An example is discussed which illustrates the method and indicates how the reduced system is frequently more easily analyzed than the original system. Author

N69-23355*# National Aeronautics and Space Administration. Ames Research Center, Moffett Field, Calif.
ON SOME NUMERICAL DIFFICULTIES IN INTEGRATING THE EQUATIONS FOR ONE-DIMENSIONAL NONEQUILIBRIUM NOZZLE FLOW
Harvard Lomax, Harry E. Bailey, and Franklyn B. Fuller Washington Apr. 1969 38 p refs
(NASA-TN-D-5176) Avail: CFSTI CSCL 12A

Several numerical difficulties arise in the problem of integrating the ordinary differential equations that represent the flow of a gas in chemical nonequilibrium through a nozzle. These difficulties are identified with parasitic eigenvalues, saddle-point behavior, and indeterminate forms. The numerical difficulties and the methods that successfully overcame them for the particular examples analyzed are discussed in this report. Author

N69-23788*# National Aeronautics and Space Administration. Ames Research Center, Moffett Field, Calif.
THE USE OF INTEGRAL TRANSFORMS IN THE ESTIMATION OF TIME VARIABLE PARAMETERS
Henry C. Lessing and D. Francis Crane Washington May 1969 47 p refs
(NASA-TN-D-5194) Avail: CFSTI CSCL 12A

A study was made of the concept of integral transformations applied to the differential form of the system equations and the use of these equations in parameter estimation. The two principal results of the study are given: the extension of the transformation equations to explicitly account for time variability of the system parameters, and an extension of the application of the concept to the output error formulation of the parameter estimation problem. It is shown that, as a result, the output error formulation acquires stability properties that were impossible previously. Experimental results are presented to illustrate the theoretical developments. These results show the ability of the new formulations to estimate parameters that are highly variable with time. Author

N69-25311*# National Aeronautics and Space Administration. Lewis Research Center, Cleveland, Ohio.
A SYSTEMATIC APPROACH TO MODEL DEVELOPMENT BY COMPARISON OF EXPERIMENTAL AND ANALYTICAL REGRESSION COEFFICIENTS
John H. Lynch Washington May 1969 25 p refs
(NASA-TM-X-1797) Avail: CFSTI CSCL 12A

The substance of the approach consists of reducing specific results obtained from a model and from experiments to orthogonal response surfaces and comparing the regression coefficients. This polynomial representation displays the behavior of the model in a form that is much more easily analyzed than simultaneous differential or integral equations, especially when the model is numerical. A sample application to a reactor physics problem is included. Author

N69-26248*# Stanford Univ., Calif.
APPROXIMATING PROPERTIES OF LINEAR MODELS FOR INPUT–OUTPUT DESCRIPTIONS
Ernest Gunther Holzmann Washington NASA May 1969 153 p refs
(Grant NGR-020-073)
(NASA-CR-1319) Avail: CFSTI CSCL 12A

B. L. Ho's existence theorem states necessary and sufficient conditions for strict realizability that are satisfied only in ideal situations. Mathematical proof is given that good dynamical simulation is possible with linear models which represent partial, rather than minimal, realizations. The restrictions of B.L. Ho's theorem do not apply to partial realizations, and the class of partially realizable input–output descriptions is large enough for practical purposes. For any normal sequence of scalar Markov parameters, the transfer function of each partial realization is shown to lie on the diagonal of the E-array corresponding to the given sequence. The proof is based on the classical theory of the Padé approximation. Relevant parts of this theory are reviewed and developed in the report, including a new, stronger form of Padé's representation theorem. As a by-product of this research, a sharpened, computationally more efficient version of B. L. Ho's minimal realization algorithm was derived. Author

N69-28196*# Arizona Univ., Tucson.
COMPUTATION OF REGIONS OF CONSTRAINED STABILITY FOR NONLINEAR CONTROL SYSTEMS
Demosthenes P. Gelopulos and Donald R. Schultz Washington NASA Jun. 1969 143 p refs
(Grant NsG-490)
(NASA-CR-1328) Avail: CFSTI CSCL 12A

The classical control system stability criterion is revised, and methods are devised for determining the region of stability. Excursion stability is defined in such a way that the practical constraints on the system are incorporated into the stability measure. Computational algorithms are devised which are used to determine the region of excursion stability. Two distinct algorithms evolve which are compared on the basis of computational efficiency. The revision of the stability criterion ties stability analysis to the physical system and thereby makes stability analysis useful for engineering purposes. A key feature of the algorithms, which may be used for evaluating the stability of nonlinear systems, is the fact that it is not necessary to select any state functions on any intuitive or semi-intuitive bases. Therefore, the algorithms are not inherently limited to low order systems. Author

N69-28256*# Pittsburgh Univ., Pa.
STABILITY THEORY OF NONLINEAR OPERATIONAL DIFFERENTIAL EQUATIONS IN HILBERT SPACE
Chia-Ven Pao Washington NASA. May 1969 177 p refs
(Grant NGR-39-011-039)
(NASA-CR-1356) Avail: CFSTI CSCL 12A

The object of this research is to establish some criteria for the existence, uniqueness, stability, asymptotic stability and stability region of a solution of the linear or nonlinear, time-invariant or time-varying operational differential equations (i.e., equations of evolution) in Banach spaces and in Hilbert spaces, from which criteria for the same results regarding a solution of the corresponding type of partial or ordinary differential equations can be deduced. In the linear case, semi-scalar product on a Banach space and linear semi-group theory are used; in the nonlinear case, equivalent inner product on a Hilbert space and the concept of nonlinear semi-group are introduced. Author

N69-29141*# National Aeronautics and Space Administration. Electronics Research Center, Cambridge, Mass.
A FORMALIZATION OF MEASUREMENT SCALE FORMS
Wayne A. Lea Washington Jun. 1969 44 p refs
(NASA-TN-D-5277) Avail: CFSTI CSCL 12A

A mathematical model of measurement and specific scale forms is developed, using the minimum mathematical structure

necessary to define each scale type. Measurement is defined, and a series of restrictions are applied to measurements to yield a precisely specified hierarchy of measurement scale forms including nominal, ordinal, interval, and ratio scales, as well as several others. Equivalences are mathematically defined for each scale form, and theorems are presented specifying the sets of transformations under which equivalence is preserved, thus yielding the scale form invariances. The hiearchy of measurement scale forms is summarized in a pictorial 'spectrum' diagram. Author

N69-29268*# Arizona Univ., Tucson.
THE DESIGN OF LINEAR MULTIVARIABLE CONTROL SYSTEMS USING MODERN CONTROL THEORY (WITH APPLICATIONS TO COUPLED CORE REACTOR CONTROL)
Charles R. Slivinsky, Donald G. Schultz, and Lynn E. Weaver Washington NASA Jun. 1969 184 p refs
(Grant NGL-03-002-006)
(NASA-CR-1345) Avail: CFSTI CSCL 12A

Both conventional, frequency-domain techniques and modern, combined frequency-domain, time-domain procedures are considered. Two basic design requirements are noninteraction and that specified subsystem transfer functions be achieved. Conventional methods are shown to have the disadvantage of complexity, both in carrying out the design calculations and in the physical implementation of the compensation. The attention centers on the state variable feedback design of multivariable systems, including procedures for identifying the fixed zeroes of the subsystems and the number of subsystem poles controlled by state variable feedback. By treating each subsystem individually, previously developed knowledge of state variable feedback design of single-input, single-output systems can be applied. Three methods for adding dynamics to the multivariable system before state variable feedback is applied are proposed for improving the system response. A coupled-core nuclear reactor with a three-core linear model is examined as an example of the application of state variable feedback design. K. W.

N69-29648*# National Aeronautics and Space Administration. Manned Spacecraft Center, Houston, Tex.
APPLICATIONS OF QUASILINEARIZATION THEORY TO SYSTEM IDENTIFICATION
George A. Zupp, Jr. and S. Bart Childs (Houston Univ.) Washington Jul. 1969 32 p refs
(NASA-TN-D-5300) Avail: CFSTI CSCL 12A

The theoretical development and application of quasi-linearization techniques to problems of system identification are presented. A one-degree-of-freedom system is used for the examples for the identification problems. Several numerical experiments are presented that relate the effects of noisy input data to the accuracy obtained in computing unknown parameters of the governing differential equations. Also presented are the application of quasi-linearization to the identification problems of automobile coasting and parachute dynamics. Conclusions from these experiments are included. Author

N69-30610*# National Aeronautics and Space Administration. Goddard Space Flight Center, Greenbelt, Md.
THE X^2 STATISTIC AND THE GOODNESS OF FIT TEST
Peter D. Argentiero, Robert A. Morris, (Md. Univ., College Park) and Robert H. Tolson (NASA. Langley Res. Center, Langley, Va.) Washington Jun. 1969 134 p refs
(NASA-TR-R-313) Avail: CFSTI CSCL 12A

The probability density function of the X^2 statistic is derived. The applicability of the X^2 statistic to goodness of fit tests and its approximation by the chi-square variable are discussed in some detail. Tables of critical values of the X^2 statistic are provided for a range of sample sizes N and equiprobable categories K which prove useful in goodness of fit tests. An example is given to demonstrate that the proper application of tables of critical values of X^2 can add considerable precision to a goodness of fit test when small samples are involved. Author

N69-30753*# National Aeronautics and Space Administration. Marshall Space Flight Center, Huntsville, Ala.
LOW-ORDER CLASSICAL RUNGE-KUTTA FORMULAS WITH STEPSIZE CONTROL AND THEIR APPLICATION TO SOME HEAT TRANSFER PROBLEMS
Erwin Fehlberg Washington Jul. 1969 46 p refs
(NASA-TR-R-315) Avail: CFSTI CSCL 12A

In an earlier report, the author derived fifth-to eighth-order Runge–Kutta formulas with stepsize control. In this paper, similar first- to fourth-order formulas are developed. Such low-order formulas are of interest in some heat transfer problems. It is well-known that the parabolic partial differential equations of such problems can be reduced to ordinary differential equations. However, it is also well-known that the application of Runge–Kutta methods to such problems is often very time-consuming. Higher-order formulas do not offer advantages in this respect, since stability considerations, resulting from the exponential character of the solution, exclude an increase of the integration stepsize that would make such high-order formulas meaningful. Therefore, low-order Runge–Kutta formulas can be expected to solve such problems more efficiently than any high-order formula. For the efficiency of Runge–Kutta formulas, it is essential that their truncation errors be as small as possible. Author

N69-31303*# National Aeronautics and Space Administration. Goddard Space Flight Center, Greenbelt, Md.
ON THE SHAPE PRESERVING EXPANSION AND CONTRACTION OF OBJECTS IN E^3
P. D. Argentiero Washington Jul. 1969 41 p refs
(NASA-TN-D-5240) Avail: CFSTI CSCL 12A

Several theorems are given relating the geometric structure of X to the fashion in which S(X) is topologically and algebraically imbedded in C(X). It is shown that an arc in E^N is a regular Euler set if, and only if, it is a generalized logarithmic spiral. This is a generalization of a classical result obtained by Euler. Also, a proof is given that a subset of E^3 is a regular Euler set if, and only if, it can be represented as the union of a family of logarithmic spirals. Author

N69-32319*# National Aeronautics and Space Administration. Lewis Research Center, Cleveland, Ohio.
DESIGN OF EXPERIMENTS AS DOUBLY TELESCOPING SEQUENCES OF BLOCKS WITH APPLICATION TO A NUCLEAR REACTOR EXPERIMENT
Arthur G. Holms and Steven M. Sidik Washington Aug. 1969 41 p refs
(NASA-TN-D-5369) Avail: CFSTI CSCL 12A

A blocked two-level factorial experiment was designed to measure the radiolysis of water. Effects of controlled variables are biased by changes in radiation with time and by equipment changes between fuel cycles; the experiment is therefore doubly confounded. Experimenting is subject to unplanned curtailments with respect to the first bias, and might be expanded with respect to the second. So that the more important parameters can be estimated free of biases ordinarily resulting from the indefinite size of the experiment, the rationale is given for arranging the blocks of the experiment in a doubly telescoping (orthogonally blocked) sequence. Author

N69-34360*# Philco-Ford Corp., Palo Alto, Calif.
MANIPULATION ERRORS IN FINITE ELEMENT ANALYSIS OF STRUCTURES

R. J. Melosh and E. L. Palacol Washington NASA Aug. 1969 145 p refs
(Contract NAS5-10369)
(NASA-CR-1385) Avail: CFSTI CSCL 12A

These errors for the displacement and force methods of structural analysis for systems of finite elements in series and in parallel are examined. The principal manipulation error involves distortion of the mantissa of the floating decimal representation of the number. This error depends upon the selection of number base, number of places carried, arithmetic mode, and manipulation mode. These characteristics are fixed by the selection of computer hardware and software. The manipulation error is also influenced by problem scale, structural idealization, the sequencing of joints and elements, selection of coordinate axes, element representations used, choice between the force or displacement method, and the algorithm selected for solving the load-deflection relationships for the structure. Errors are studied in the input–output, generation, and elimination phases of calculation. The input–output phase involves that part of the problem in which the data is introduced into the computer and results are output for analyst interpretation. Input errors are not significant. Author

N69-36923*# National Aeronautics and Space Administration. Ames Research Enter, Moffett Field, Calif.

CHEBYSHEV SERIES SOLUTION OF NONLINEAR ORDINARY DIFFERENTIAL EQUATIONS: INITIAL-VALUE PROBLEMS

Kin L. Lee and Paul F. Byrd Washington Sep. 1969 77 p refs
(NASA-TM-X-1882 Avail: CFSTI CSCL 12A

The approximate Chebyshev series solution of nonlinear ordinary differential equations based on Picard iteration is discussed. Detailed algorithms are provided for the numerical solution of initial-value problems involving (a) a system of n first-order nonlinear differential equations, and (b) an nth-order nonlinear differential equation. Methods to accelerate the convergence of the iterative procedures are also proposed. FORTRAN 4 subroutines for the algorithms with options for accelerating convergency are given. Author

N69-37033*# California Univ., Berkeley. Electronics Research Lab.

TOWARD A THEORY OF FUZZY SYSTEMS

L. A. Zadeh Washington NASA Sep. 1969 40 p refs
(Grant NGL-05-002-016)
(NASA-CR-1432; ERL-69-2) Avail: CFSTI CSCL 12A

The systems encountered in the real world which are too complex and/or too ill-defined to be susceptible of exact analysis are investigated. The concept of a fuzzy set, that is, a class which admits of intermediate grades of membership in it, opens the possibility of analyzing such systems both qualitatively and quantitatively by allowing the input and/or the output and/or the state of the system to range over fuzzy sets. Several basic concepts relating to the characterization of discrete-time fuzzy systems are introduced, and input-output-state equations for such systems are developed. Author

N69-38178*# National Aeronautics and Space Administration. Langley Research Center, Langley Station, Va.

ESTIMATION OF VARIANCE BY A RECURSIVE EQUATION

M. Melvin Bruce Washington Oct. 1969 29 p refs
(NASA-TN-D-5465) Avail: CFSTI CSCL 12A

A recursive equation is presented for the purpose of estimation of the variance of a sequence of independent random numbers. The use of this recursive equation makes it possible to perform a running estimate of the variance as the samples are received sequentially. An analysis of the recursive equation is included to show that it gives an asymptotically unbiased estimate of the variance. The variance of the estimated variance is derived for the special case of random numbers with a Gaussian probability distribution. Author

N69-38655*# National Aeronautics and Space Administration. Langley Research Center, Langley Station, Va.

A NEW MATRIX THEOREM AND ITS APPLICATION FOR ESTABLISHING INDEPENDENT COORDINATES FOR COMPLEX DYNAMICAL SYSTEMS WITH CONSTRAINTS

William C. Walton, Jr. and Earl C. Steeves Washington Oct. 1969 28 p refs
(NASA-TR-R-326; L-6052) Avail: CFSTI CSCL 12A

A method is presented by which equations of motion of a linear mechanical system can be derived in terms of independent coordinates when the system is described in terms of coordinates which are not independent but instead are governed by linear homogeneous equations of constraint. There is a discussion of the origin in practical vibrations analysis of dynamical systems involving equations of constraint. Methods previously used for handling such systems are discussed and the method is demonstrated to have the following advantages: (1) For the most general constraint equations, solution of the equations is reduced in substance to computing the eigenvalues and eigenvectors of a symmetric matrix. (2) The method is applicable when there are redundancies in the equations of constraint. Author

N69-40088*# National Aeronautics and Space Administration. Lewis Research Center, Cleveland, Ohio.

APPLICATION OF MODERN NETWORK THEORY TO ANALYSIS OF COMPLEX SYSTEMS

John C. Faken Washington Oct. 1969 46 p refs
(NASA-TN-D-5511) Avail: CFSTI CSCL 12A

Present day systems have grown to exceed the intuitive grasp of systems analysts, thus negating the value of techniques which depend upon intuition as a substitute for mathematical rigor. A methodology based on the Modern Network Theory of electrical engineering is presented which, when considered in the light of digital computer technology, shows up as a capable and powerful tool for the analysis of complex systems. The examples presented to demonstrate the various techniques show that Modern Network Theory is not limited to electrical systems but appears to be applicable to systems in general. Author

20

METEOROLOGY

Includes climatology; weather forecasting; and visibility studies. For related information see also: 13 Geophysics; and 30 Space Sciences.

A69-10463 *#
ATMOSPHERIC STRUCTURE RESEARCH FOR LONG-TERM FORECASTING.
William Nordberg (NASA, Goddard Space Flight Center, Laboratory for Atmospheric and Biological Sciences, Greenbelt, Md.).
United Nations, Conference on the Exploration and Peaceful Uses of Outer Space, Vienna, Austria, Aug. 14-27, 1968, Paper 68-95397. 21 p. 14 refs.

Discussion of the feasibility of deriving meteorological parameters relating to the temperature, density, moisture, and energy structure of the atmosphere using satellite observations. The development of mathematical models that simulate the planetary and cyclone scale structure of the atmosphere is seen as important in long-term forecasting by satellite. The need for global atmospheric observations, for a period of a few months to a year, which will provide adequate data input for such models, is stressed. The various methods of making and interpreting satellite observations of atmospheric structure are described. Since the major spacecraft and onboard remote sensing devices for the required observations are so complex and expensive, international cooperation in the launching and operation of such weather satellites is considered imperative. P.G.M.

A69-10474 *#
INTERNATIONAL EXPERIMENTATION WITH COMMUNICATIONS SATELLITES.
Leonard Jaffe (NASA, Office of Space Science and Applications, Washington, D.C.).
United Nations, Conference on the Exploration and Peaceful Uses of Outer Space, Vienna, Austria, Aug. 14-27, 1968, Paper 68-95421. 22 p.

Summary of the international experimentation with U.S. satellites during the last ten years. Fourteen experimental communications satellites have been launched by the U.S. since December 1958. Two of these were passive reflecting satellites, Echo 1 and Echo 2; seven were medium-altitude active satellites: Score, Courier, Telstar 1 and 2, Relay 1 and 2, and ATS 2. Five satellites were synchronous altitude satellites, and three of these five were geostationary satellites. The UK and France participated in experiments with the first passive satellite, Echo 1. As the program went on, additional countries became involved, including the Federal Republic of Germany, Brazil, Italy, the USSR, Japan, Canada, the Scandinavian countries, Spain, and India. Still other countries were involved from time to time. Each participating nation followed its own theories in the mechanical and electrical design, and all participants exchanged technical information with other participants without restraint. P.v.T.

A69-10483 *#
WEATHER RESEARCH SATELLITES.
Morris Tepper (NASA, Office of Space Science and Applications, Washington, D.C.).
United Nations, Conference on the Exploration and Peaceful Uses of Outer Space, Vienna, Austria, Aug. 14-27, 1968, Paper 68-95350. 19 p.

Description of a broad program of meteorological satellite research, including specific plans for unmanned satellites, and of future possibilities with a meteorologist on board a manned spacecraft. An outline is given of the program, starting with the first satellite efforts concerned with observation systems designed to provide global cloud cover information, and improvements introduced into the satellites, instruments, and techniques. A discussion is given of the extrapolation of observational data to provide information on the future positions of such atmospheric phenomena as fronts, hurricanes, jet streams, and cloud complexes. The current program is reviewed. It has three objectives: (1) to provide global and local observations of cloud cover both day and night, (2) to provide "continuous" observation of the earth's cloud cover, and (3) to provide measurements of the vertical structure of the atmosphere. The possible contributions to meteorology by a man in space are considered. I.P.

A69-10695 *#
CHARACTERISTICS OF TURBULENCE OBSERVED AT THE NASA 150-M METEOROLOGICAL TOWER.
George H. Fichtl (NASA, Marshall Space Flight Center, Huntsville, Ala.).
Journal of Applied Meteorology, vol. 7, Oct. 1968, p. 838-844. 12 refs.

Recent observations of turbulence obtained at the NASA 150-m meteorological tower located at Kennedy Space Center, Fla., are presented. The wind data were obtained at the 18-, 30-, 60-, 90-, 120-, and 150-m levels, while temperature data were obtained at the 3-, 18-, 60-, 120-, and 150-m levels. Most of the tests were made during the daylight hours, and the duration time of each test ranged between 30 and 60 min. A survey of the surface roughness length associated with the tower site is presented. Estimates of the roughness length were calculated with wind profile laws consistent with the Monin-Obukhov similarity hypothesis. In the case of those wind directions θ in the ranges $0^\circ \leqq \theta < 150^\circ$, $180^\circ \leqq \theta < 240^\circ$, and $300^\circ \leqq \theta < 360^\circ$ the roughness length is 0.23 m, while for those wind directions in the ranges $150^\circ \leqq \theta < 180^\circ$ and $240^\circ \leqq \theta < 300^\circ$, the roughness length has the values 0.51 and 0.65 m, respectively. Longitudinal turbulence spectra calculated from recent observations are also presented. It is shown that the nondimensional frequency nz/u, associated with the peak of the logarithmic spectrum, is proportional to $z^{4/5}$, where u is the wind speed at height z and n is the frequency. Based on an analysis of the logarithmic spectrum in the inertial subrange, it is implied that the local mechanical production of turbulent energy is balanced by the local viscous dissipation at the 18-m level. (Author)

A69-13852 *#
NEW WIND-MONITORING SYSTEM PROTECTS R&D LAUNCHES.
William W. Vaughan (NASA, Marshall Space Flight Center, Aerospace Environment Div., Huntsville, Ala.).
Astronautics and Aeronautics, vol. 6, Dec. 1968, p. 41-43. 5 refs.

Evaluation of all-weather, accurate and detailed wind-profile measurements to protect space vehicle and missile launches and to substantiate analytical studies. Recent development and operational deployments of the FPS-16 Radar/Jimsphere System significantly minimizes vehicle failure risks when properly integrated into a flight-simulation program. P.v.T.

A69-18038 *#
ATMOSPHERIC MEASUREMENTS FROM SATELLITES.
Robert M. Rados (NASA, Goddard Space Flight Center, Greenbelt, Md.).
American Institute of Aeronautics and Astronautics, Aerospace Sciences Meeting, 7th, New York, N.Y., Jan. 20-22, 1969, Paper 69-158. 10 p.
Members, $1.00; nonmembers, $1.50.

Brief survey of atmospheric measurements from satellites. A chronology of satellites which have provided atmospheric measurements and the specific sensors which were flown, a listing of planned satellites with their atmospheric sensors, and some vital statistics on the sensors which have been flown or which are under development, are tabulated. It is noted that recent exploration of the ATS-1 images of cloud cover on an hourly basis has demonstrated the potential of defining winds in the tropical areas and the movement of vorticity patterns from the Southern to the Northern Hemisphere. The use of WEFAX through the ATS 1 and 2 satellites has demonstrated the practicality of transmitting data collected

and analyzed to a central location to users in remote or distant locations which either cannot provide facilities of their own or cannot obtain these analyses more efficiently. Satellites can also be used to measure sferics and sea state through the use of microwave radiometers, lasers, etc. M.M.

A69-28466 *

WIND MEASUREMENTS IN NOCTILUCENT CLOUDS.
J. S. Theon, W. S. Smith, and W. E. McGovern (NASA, Goddard Space Flight Center, Aeronomy Branch, Greenbelt, Md.).
Science, vol. 164, May 9, 1969, p. 715, 716. 5 refs.

The results of eight soundings conducted from sites at high latitude during the summers of 1963 through 1965 suggest that a relation exists between the winds at the mesopause and the occurrence of noctilucent clouds. These measurements indicate that situations in which noctilucent clouds are present are associated with lower wind speeds than is the case where there are no clouds. (Author)

A69-33001 *#

SATELLITE MAPPING OF THE PACIFIC TROPICAL CLOUDINESS.
Jacob Bjerknes (California, University, Los Angeles, Calif.), Lewis J. Allison, Guenter Warnecke (NASA, Goddard Space Flight Center, Greenbelt, Md.), Earl R. Kreins (USAF, Environmental Technical Applications Center, Washington, D.C.), and Frederic A. Godshall (ESSA, Silver Spring, Md.).
American Meteorological Society, Bulletin, vol. 50, May 1969, p. 313-322. 17 refs.

Sampling survey of a six-year period of satellite-observed tropical Pacific cloudiness. The variable position of the boundary between the west Pacific equatorial rain clouds over warm water and the east Pacific aridity along the equator over cool upwelling water is considered. Features of the geographic cloudiness distribution not generally observable are discussed, and the generally held assumption that the bulk of tropical rain over the oceans is generated when the sea is warmer than the air is verified. B.H.

A69-33732

CLEAR AIR TURBULENCE AND ITS DETECTION; BOEING COMPANY, SYMPOSIUM, SEATTLE, WASH., AUGUST 14-16, 1968, PROCEEDINGS.
Edited by Yih-Ho Pao and Arnold Goldburg (Boeing Co., Boeing Scientific Research Laboratories, Seattle, Wash.).
New York, Plenum Press, 1969. 555 p.
$22.50.

CONTENTS:

PREFACE. G. S. Schairer and G. L. Hollingsworth (Boeing Co., Seattle, Wash.), p. v.

FOREWORD. Y.-H. Pao and A. Goldburg (Boeing Co., Seattle, Wash.), p. vi-ix.

THE SIGNIFICANCE OF CLEAR AIR TURBULENCE IN LARGE SCALE METEOROLOGY. R. G. Fleagle (Washington, University, Seattle, Wash.), p. 1-3.

THE ORIGIN AND NATURE OF CLEAR AIR TURBULENCE.

THE NATURE OF CLEAR AIR TURBULENCE (A REVIEW). E. R. Reiter, p. 7-33. [For abstract see issue 24, page 4628, Accession no. A68-45278]

MECHANISMS OF CLEAR AIR TURBULENCE. R. S. Scorer, p. 34-50. [For abstract see issue 24, page 4628, Accession no. A68-45279]

A THEORY OF CLEAR AIR TURBULENCE. R. R. Long (Johns Hopkins University, Baltimore, Md.), p. 51-62. 7 refs. [See A69-33733 17-20]

INSTABILITY OF THE THERMAL WIND. A. J. Faller and R. Kaylor (Maryland, University, College Park, Md.), p. 63-72. 5 refs. [See A69-33734 17-20]

ORIGIN AND STRUCTURE OF TURBULENCE IN STABLY STRATIFIED MEDIA. Y.-H. Pao (Boeing Co., Seattle, Wash.), p. 73-99. 30 refs. [See A69-33735 17-20]

ON THE ENERGY SUPPLY OF CLEAR AIR TURBULENCE. J. A. Businger, p. 100-108. [For abstract see issue 24, page 4626, Accession no. A68-45265]

LARGE SCALE PROCESSES CONTRIBUTING ENERGY TO CLEAR AIR TURBULENCE. F. I. Badgley, p. 109-123. [For abstract see issue 24, page 4626, Accession no. A68-45262]

THE OBSERVATIONAL RESULTS OF CLEAR AIR TURBULENCE.

TECHNICAL AND METEOROLOGICAL PLANNING TO MEET THE ALLCAT PROGRAM OBJECTIVES. N. V. Loving, p. 127-143. [For abstract see issue 24, page 4627, Accession no. A68-45274]

METEOROLOGICAL ANALYSIS OF CLEAR AIR TURBULENCE IN THE STRATOSPHERE. F. A. Mitchell and D. T. Prophet (Lockheed Aircraft Corp., Burbank, Calif.), p. 144-182. [See A69-33736 17-20]

THE PROBABILISTIC STRUCTURE OF CLEAR AIR TURBULENCE - SOME OBSERVATIONAL RESULTS AND IMPLICATIONS. J. A. Dutton, G. J. Thompson, and D. G. Deaven, p. 183-206. [For abstract see issue 24, page 4627, Accession no. A68-45268]

TURBULENCE AT LOW ALTITUDES - SUMMARY OF THE RESULTS OF LO-LOCAT PHASES I AND II. F. K. Atnip (Boeing Co., Wichita, Kan.), p. 228-231. [See A69-33737 17-20]

THE COLORADO LEE WAVE PROGRAM. D. K. Lilly and W. Toutenhoofd (National Center for Atmospheric Research, Boulder, Colo.), p. 232-245. [See A69-33738 17-20]

RECENT INVESTIGATIONS OF CLEAR-AIR TURBULENCE IN THE U.S.S.R. N. K. Vinnichenko, p. 246-270. [For abstract see issue 24, page 4628, Accession no. A68-45280]

CLEAR AIR TURBULENCE RESEARCH ACTIVITIES AT THE NATIONAL AERONAUTICAL ESTABLISHMENT. G. K. Mather, p. 271-287. [For abstract see issue 24, page 4627, Accession no. A68-45275]

A STUDY OF THE RELATION OF CLEAR AIR TURBULENCE TO THE MESOSCALE STRUCTURE OF THE JET STREAM REGION. R. J. Reed, p. 288-307. [For abstract see issue 24, page 4627, Accession no. A68-45277]

DETAILED WIND AND TEMPERATURE PROFILES. G. H. Fichtl, D. W. Camp, and W. W. Vaughan (NASA, Marshall Space Flight Center, Huntsville, Ala.), p. 308-333. 19 refs. [See A69-33739 17-20]

THE FORECASTING OF CLEAR AIR TURBULENCE.

CLEAR AIR TURBULENCE AND UPPER LEVEL METEOROLOGICAL PATTERNS. D. Colson, p. 337-360. [For abstract see issue 24, page 4626, Accession no. A68-45267]

RECENT STUDIES RELATED TO CLEAR AIR TURBULENCE. R. T. H. Collis, R. M. Endlich, and R. L. Mancuso, p. 361-377. [For abstract see issue 24, page 4626, Accession no. A68-45266]

THE DETECTION OF CLEAR AIR TURBULENCE.

CLEAR AIR TURBULENCE DETECTION METHODS (A REVIEW) D. Atlas, p. 381-401. [For abstract see issue 24, page 4626, Accession no. A68-45261]

RADAR INVESTIGATIONS OF ATMOSPHERIC STRUCTURE AND CAT IN THE 3 TO 20-KM REGION. K. R. Hardy, K. M. Glover, and H. Ottersten (USAF, Cambridge Research Laboratories, Bedford, Mass.), p. 402-416. 14 refs. [See A69-33740 17-20]

PROBING THE OPTICALLY CLEAR ATMOSPHERE WITH RADAR. I. Katz, p. 417-424. [For abstract see issue 24, page 4627, Accession no. A68-45271]

RADAR ECHOES FROM CLEAR AIR INHOMOGENEITIES. W. E. Buehler, C. H. King, and C. D. Lunden, p. 425-435. [For abstract see issue 24, page 4626, Accession no. A68-45264]

THE REMOTE DETECTION OF CLEAR AIR TURBULENCE BY INFRARED RADIATION. R. W. Astheimer, p. 436-448. [For abstract see issue 24, page 4625, Accession no. A68-45260]

INFRARED CLEAR AIR TURBULENCE DETECTION AND WARNING SYSTEM. E. F. Flint, p. 449-475. [For abstract see issue 24, page 4586, Accession no. A68-45269]

MICROWAVE AND INFRARED SCATTERING AND ABSORPTION RELATED TO ATMOSPHERIC INHOMOGENEITIES. C. I. Beard, W. T. Kreiss, and W. G. Tank, p. 476-480. [For abstract see issue 24, page 4626, Accession no. A68-45263]

LASER BACKSCATTER CORRELATION WITH TURBULENT REGIONS OF THE ATMOSPHERE. J. D. Lawrence, Jr., M. P. McCormick, S. H. Melfi, and D. P. Woodman, p. 481-497. [For abstract see issue 24, page 4600, Accession no. A68-45272]

PANEL DISCUSSION AND CONCLUSION.

PANEL DISCUSSION, p. 501-518.

FLOOR DISCUSSION, p. 519-523.

CONCLUSION, p. 523-525.
CONTRIBUTING AUTHORS, p. 526-529.
AUTHOR INDEX, p. 531-535.
SUBJECT INDEX, p. 536-542.

A69-33739 *
DETAILED WIND AND TEMPERATURE PROFILES.
G. H. Fichtl, D. W. Camp, and W. W. Vaughan (NASA, Marshall Space Flight Center, Huntsville, Ala.).
IN: CLEAR AIR TURBULENCE AND ITS DETECTION; BOEING COMPANY, SYMPOSIUM, SEATTLE, WASH., AUGUST 14-16, 1968, PROCEEDINGS. [A69-33732 17-20]
Edited by Yih-Ho Pao and Arnold Goldburg.
New York, Plenum Press, 1969, p. 308-333. 19 refs.
NASA-supported research.

Analysis of three detailed temperature profiles and the associated wind profiles obtained with the aid of the Jimsphere/FPS-16 radar wind sensing system during October 1967 at Cape Kennedy. The analysis is based on a consideration of structure functions, which represent the vertical mean square difference in the temperature and wind spread fluctuations about the mean profiles over the vertical length scale. It is shown that the wind-temperature sensing data thus obtained could be of considerable importance in assessing the output from remote clear air turbulence detectors, whether ground-based or mounted on board aircraft. B.H.

A69-36405 * #
ON A STEADY STATE THEORY OF GLOBAL MONSOONS.
M. Sankar-Rao (NASA, Goddard Space Flight Center, Goddard Institute for Space Studies, New York, N.Y.) and Barry Saltzman (Travelers Research Center, Inc., Hartford, Conn.).
Tellus, vol. 21, no. 3, 1969, p. 308-330. 30 refs.
ESSA Contract No. E 22-137-67N.

Steady-state solution of the quasi-geostrophic perturbation equations for the forced response of the atmosphere to a parametized form of heating which is proportional to the difference between the mean low-level air temperature and the prescribed ground surface temperature. The solutions, obtained as a sum of spherical harmonic components, are shown to be sensitive to the form of the vertical variation of the heating, as well as to the horizontal scale. This is due to the possibility of a "matching" of the vertical variation of the internal forcing with the vertical variation of the solution for the "quasi-resonant" horizontal mode. For a particular vertical variation of the heating which is removed from this point of magnified quasi-resonance, the composite solutions up to the fifteenth degree, for January and July conditions in the Northern Hemisphere, show a fair amount of agreement with observed normal maps. The main errors are a tendency for the computed features to be displaced to the east of the observations at both upper and lower levels, and an overly weak response over Asia and the Pacific. Some possibilities for improving the model are discussed. (Author)

A69-36926 * #
CLOUD HEIGHT CONTOURING FROM APOLLO 6 PHOTOGRAPHY.
Victor S. Whitehead, Ivan D. Browne, and Joe G. Garcia (NASA, Manned Spacecraft Center, Houston, Tex.).
American Meteorological Society, Bulletin, vol. 50, July 1969, p. 522-528.

Analysis of selected photographs taken during the unmanned Apollo 6 mission in which they were subjected to stereoscopic photogrammetry to determine the heights of cloud bases and the tops of convective clouds. Examples of how these calculated heights may be used to infer the physical characteristics of the ambient atmosphere are shown. The detail within the photographs permits contouring of cloud-top heights within mesoscale systems. Accuracies of height determination are estimated to be plus or minus 250 m. (Author)

A69-38120 * #
A CLOUD-COVER SIMULATION PROCEDURE.
S. Clark Brown (NASA, Marshall Space Flight Center, Aerospace Environment Div., Huntsville, Ala.).
Astronautics and Aeronautics, vol. 7, Aug. 1969, p. 86-88.

Description of a simulation procedure for providing realistic worldwide cloud-cover data in a format amenable to computer simulation of earth-oriented space missions. A computer program using a Monte-Carlo mission-simulation procedure for processing the cloud-cover data is described, and the results are evaluated. B.H.

A69-42896 * #
STATISTICAL SPECIFICATION OF THE 500-MB HEIGHT FIELDS USING SMOOTHED MEDIUM-RESOLUTION RADIOMETRIC FIELDS OF NIMBUS II.
Frank L. Martin (NASA, Goddard Space Flight Center, Greenbelt, Md.; U.S. Naval Postgraduate School, Monterey, Calif.).
Journal of Applied Meteorology, vol. 8, Aug. 1969, p. 668-686. 13 refs.
Navy-supported research.

Over an area spanning the North American Continent from tropical to polar latitudes, and between 40 and 135 deg W longitude, four consecutive days of the Nimbus 2 Medium Resolution Infrared five-channel equivalent blackbody temperatures and of 1000-mb geopotential fields were used to specify the 500-mb field of geopotential. Three of the four days were reserved for dependent data, the fourth day being reserved for independent test-case data. The data samples were stratified into "extratropical" and subtropical-tropical areas, and then pooled three-day stepwise, with screening regression equations being developed by areas. In the lower latitude stratifications, the 500-mb regression equations were only of marginal significance, but in the extratropical zone (latitudes 32-64 deg N), the regressions have 500-mb height specifications with multiple correlation coefficients of 0.95. Moreover, in the independent-data test case, no shrinkage of explained variances occurred in these extratropical latitudes. Here the most important predictors for $Z_5(I, J)$ were the equivalent blackbody temperatures in the 14-16 micron and 10-11 micron channels, the 1000-mb geopotential, and finally an effective blackbody temperature associated with the solar-reflectance channel. (Author)

A69-43066 * #
TESTS OF THE EFFECT OF GRID RESOLUTION IN A GLOBAL PREDICTION MODEL.
M. Sankar Rao (NASA, Goddard Space Flight Center, Goddard Institute for Space Studies, New York, N.Y.) and Ludwig Umscheid, Jr. (Computer Applications, Inc., New York, N.Y.).
Monthly Weather Review, vol. 97, Sept. 1969, p. 659-664. 7 refs.

Assessment of the results of tests of an integration scheme proposed by Kurihara and Holloway (1967) which has a variable angular grid spacing and offers advantages in problems of geophysical fluid dynamics by rigorously conserving mass and energy. In order to examine the errors produced by the expanded angular grid spacing near the poles, an attempt was made to investigate the accuracy of this scheme by numerical experiments involving various grid resolutions. The results show that, in order to achieve a solution with acceptable accuracy, the grid spacing near the pole has to be decreased by a factor of 9. O.H.

A69-43154 *
OBSERVATIONS OF THE REFLECTION PROPERTIES OF THE EARTH-ATMOSPHERE SYSTEM AND THE CLOUD FORMATION ABOVE THE EQUATORIAL PACIFIC FROM A SYNCHRONOUS SATELLITE (BEOBACHTUNGEN DER REFLEXIONSEIGEN-

SCHAFTEN DES SYSTEMS ERDE-ATMOSPHÄRE UND DER BEWÖLKUNG ÜBER DEM ÄQUATORIALEN PAZIFIK VON EINEM SYNCHRONEN SATELLITEN AUS).

Ehrhard Raschke (Ruhr-Universität, Bochum, West Germany) and William R. Bandeen (NASA, Goddard Space Flight Center, Laboratory for Atmospherical and Biological Sciences, Greenbelt, Md.).

(Verband Deutscher Meteorologischer Gesellschaften, Deutsche Geophysikalische Gesellschaft, American Meteorological Society, and Royal Meteorological Society, Meteorologen-Geophysiker-Tagung, Hamburg, West Germany, Apr. 1-6, 1968.)

Annalen der Meteorologie, no. 4, 1969, p. 200-205. 13 refs. In German.

Study of the dependence of the bidirectional reflectances of the earth-atmosphere system on the zenith and the relative azimuth angle of observation and on the zenith angle of the sun. Digitized camera signals of the satellite ATS-1 were used in the investigation. Conditions were studied for cloudless and overcast atmospheres. The results, which, in part, show a strong angular dependence, are used to obtain an objective estimate of the effective cloudiness. G.R.

N69-12934*# National Aeronautics and Space Administration. Lewis Research Center, Cleveland, Ohio.

ATMOSPHERIC LIMITS ON THE OBSERVATIONAL CAPABILITIES OF AEROSPACECRAFT

John C. Evvard Washington Dec. 1968 23 p refs

(NASA-TN-D-4940) Avail: CFSTI CSCL 04B

Atmospheric turbulence decreases the ground observational capability of an aerospacecraft. Most of the effect arises from transient distortions of the light path near the surface (up to 15 or 20 km) where the air density is high. Hence, the viewing accuracy of a satellite observer looking at the ground is generally much higher than for a ground observer viewing a satellite. Estimates of the atmospheric resolving power error for both the ground and the aerospacecraft observer have been made. The estimated uncertainty of viewing a point on the ground directly beneath an aerospacecraft need be no larger than 12 centimeters. Expressions are derived for the altitude and angular dependency of the uncertainty. Author

N69-13629*# Lockheed-California Co., Burbank.

A STUDY OF JIMSPHERE WIND PROFILES AS RELATED TO SPACE VEHICLE DESIGN AND OPERATIONS

S. I. Adelfang, E. V. Ashburn, and A. Court Washington NASA Nov. 1968 116 p refs

(Contract NAS8-20747)

(NASA-CR-1204; LR-21588) Avail: CFSTI CSCL 04B

During the period December 1964 through April 1967, Jimsphere wind sensors were used to obtain 1194 profiles in the altitude range 1 km to 20 km over Cape Kennedy. This report consists of an analysis of the winds and wind shears derived from the Jimsphere data. The zonal and meridional components of the wind were found to have a distribution that is significantly closer to a normal distribution that the distribution of the components determined for the winds measured by conventional radiosonde methods. Extreme ($\geq$ 95%) Jimsphere wind speeds at 7 km through 15 km are not independent of the extreme wind speeds at 12 km altitude. Mean shears at 8, 12, and 16 km are a function of a power of the shear layer thickness, Δz for $\Delta z \leq 1$ km. The power is 1 for mean zonal and scalar shears, not clearly defined for mean meridional shears, and 2/3 for mean vector shears. The standard deviation and the 95% scalar, vector, zonal, and meridional shears are also a function of the altitude interval Δz to the 2/3 power. Given that the shear is extreme at 12 km altitude the simultaneous occurrence of non-overlapping extreme vector and zonal shears measured over altitude layers of 50 to 1000 meters, is a low probability event. Definitions of steady state wind and gusts are discussed in terms of filtering the wind data for the relevant frequency ranges and in terms of space vehicle characteristics. Author

N69-14505*# National Aeronautics and Space Administration. Langley Research Center, Langley Station, Va.

WIND VELOCITY PROFILES MEASURED BY THE SMOKE-TRAIL METHOD AT THE EASTERN TEST RANGE, 1963

Robert W. Miller, James C. Manning, and Robert M. Henry Washington Dec. 1968 129 p refs

(NASA-TN-D-4880) Avail: CFSTI CSCL 04B

Fifty-four detailed wind velocity profiles measured by the smoke-trail technique at the Eastern Test Range during 1963 are presented. The altitude range covered is from approximately 2 to 22 kilometers and the maximum velocity measured exceeds the 99-percent highest value. The persistence of the wind profile shape, under some conditions, for periods up to 2 hours is demonstrated and illustrations are given of the accuracy of the smoke-trail method. Author

N69-16214*# Texas Western Coll., El Paso Shellenger Research Labs.

EXAMETNET DATA REPORT SERIES Annual Report, 1966

Washington NASA 1968 190 p Sponsored by NASA, Comision Nacl. de Invest. Espacial., and Comissao Nacl. de Atividades Espaciais

(NASA-SP-175) Avail: CFSTI CSCL 04B

This annual publication contains, for the year 1966, the meteorological rocket observational wind and temperature data acquired by each participant of the network. Appendixes concerning related activities of the EXAMETNET are also included in the annual reports. The appendix for this report contains the special 1965 firing series from Wallops Island, Virginia, for the months of September through November. Author

N69-17772*# National Aeronautics and Space Administration, Washington, D. C.

A COMPARISON OF DATA OBTAINED BY THE MT-135 AND ARCAS METEOROLOGICAL ROCKET SYSTEMS

A. J. Miller (ESSA, Washington), H. M. Woolf (ESSA, Washington), and F. G. Finger (ESSA, Washington) Feb. 1969 23 p refs

(NASA-TM-X-1726) Avail: CFSTI CSCL 04B

Results of comparisons of wind and temperature data obtained by closely spaced launchings of Japanese MT-135 and American ARCAS meteorological rocket systems are presented. In general, smoothed temperature profiles show a certain disagreement that is unexplained at this time. Perturbation profiles of wind and temperature, on the other hand, indicate a high degree of correlation that tends to substantiate the existence of small-scale features. Author

N69-22570*# National Aeronautics and Space Administration. Wallops Station, Wallops Island, Va.

EXAMETNET DATA REPORT SERIES: ANNUAL REPORT, 1967

Washington 1969 188 p refs Prepared by Texas Univ., Shellenger Research Labs., El Paso

(NASA-SP-176) Avail: CFSTI CSCL 04B

Exametnet meteorological rocket launchings and data dissemination are conducted synoptically from launch sites at Chamical, Argentina; Natal, Brazil; and Wallops Island, Virginia, U.S.A. The reduced data from the launchings for each quarter are checked, further reduced, compiled, and published in the Exametnet Data Report Series. These network data reports, after being reviewed and edited by all participants of the Exametnet, are then compiled into the annual publication for broad dissemination. This annual publication contains, for the year 1967, the meteorological rocket observational data acquired by each participant. Appendixes concerning related activities of the Exametnet are also included in the annual reports. The appendixes for this report describe the data

and some of the technical and scientific activities of Exametnet participants and in addition, list all Exametnet and related publications. Author

N69-35523*# National Aeronautics and Space Administration, Washington, D.C.
RESPONSE CHARACTERISTICS OF METEOROLOGICAL ROCKET WIND REDUCTION TECHNIQUES
Alvin J. Miller (ESSA, Hillcrest Heights, Md.) Aug. 1969 14 p refs
(NASA-TM-X-1850) Avail: CFSTI CSCL 04B

By use of analytical expressions for position and time as functions of height the response characteristics of the height-based and time-based manual wind reduction techniques for meteorological rocketsondes are deduced. It is shown that the height-based method is more consistent in depicting medium-scale perturbations than is the time-based method. This is accomplished, however, at the expense of the simplicity of the time-based system. Author

N69-35528*# GCA Corp., Bedford, Mass.
INFERENCE OF STRATOSPHERIC TEMPERATURE AND MOISTURE PROFILES FROM OBSERVATIONS OF THE INFRARED HORIZON Final Report
Frederick B. House and George Ohring Washington NASA Aug. 1969 62 p refs
(Contract NAS1-7572)
(NASA-CR-1419; GCA-TR-69-5-N) Avail: CFSTI CSCL 04B

The feasibility of inferring temperature and moisture profiles in the stratosphere from horizon radiances in the 15 micron CO_2 band and the H_2O rotational band was studied. Investigations are performed of inversion techniques, absorption band structures, error analyses and problems related to instrument design. A relatively simple inference method termed the instant inversion technique is developed and applied successfully to both theoretical radiance profiles and observed orison radiances from Project Scanner. A detailed analysis of these inversion results leads to a recommended measurement and data reduction technique to determine both temperature and moisture profiles in the stratosphere and lower mesosphere. Author

N69-35570*# Pennsylvania State Univ., University Park.
INVESTIGATION OF THE TURBULENT WIND FIELD BELOW 150-METER ALTITUDE AT THE EASTERN TEST RANGE
Alfred K. Blackadar, John A. Dutton, H. A. Panofsky, and Anton Chaplin Washington NASA Aug. 1969 105 p refs
(Contract NAS8-21140)
(NASA-CR-1410) Avail: CFSTI CSCL 04B

The development of suitable analytical and empirical models for studying the characteristics of wind near the ground as a source of aerodynamic loads imposed on vehicles during launch operations is discussed. Factors affecting the structure of the wind, wind shear, and associated turbulence so as to permit predictions about the statistical effects of wind on space vehicles, both on the launch pad and during the first few moments of flight are also investigated. Statistical models of the turbulent environment constructed on the basis of the climatology of the relevant parameters are presented. Author

N69-36622 Hydrometeorological Service of the USSR
PERIODICITY IN ATMOSPHERIC CIRCULATION AND STRATOSPHERIC WARMINGS OVER ANTARCTICA
L. A. Zhdanov *In* World Meteorol. Organ. Polar Meteorol. 1967 p 345–363 refs (See N69-36601 21-20)
Copyright. Avail: Issuing Activity

500-mb geopotential data over Antarctica, averaged for a five-year period (1958–1962), revealed one climatic cyclone with the center located inside the triangle formed by stations Vostok, Amundsen-Scott and McMurdo. Periodicities in the atmospheric circulation are described. Stratospheric warmings occur during periods of increased cyclonic activity, and appear to be preceded by a small temperature increase in the troposphere and the lower stratosphere up to the 100-mb and 50-mb levels. In the lower stratosphere the circumpolar vortex over Antarctica does not break down into two centers during stratospheric warming periods as is usually observed over the Arctic, where the powerful cyclonic systems in the northern hemisphere can reach central Arctic areas. Author (ESRO)

N69-36976*# National Aeronautics and Space Administration. Lewis Research Center, Cleveland, Ohio.
QUADRATURE VARIATIONS IN DISCRETE-ORDINATES CALCULATIONS
Robert E. Sullivan Washington Sep. 1969 19 p refs
(NASA-TM-X-1887) Avail: CFSTI CSCL 12A

Techniques to reduce computer time required to solve the Boltzmann transport equation in the discrete ordinates (S_n) approximation were studied. These techniques are based on initial use of low-order angular quadrature or spatial mesh to generate preliminary neutron flux distributions which are then converged in the high-order detail required of the final calculation. Results indicate that these modifications to the standard S_n method can decrease problem execution times and yield results which are as accurate as those obtained with the standard method. Author

N69-39526*# National Aeronautics and Space Administration, Washington, D.C.
PROGRESS OF NASA RESEARCH ON WARM FOG PROPERTIES AND MODIFICATION CONCEPTS Symposium Proceedings
1969 127 p refs NASA Conf. held in Washington, D.C., 6 Feb. 1969
(NASA-SP-212) Avail: CFSTI CSCL 04B

CONTENTS:

1. A REVIEW OF PROJECT FOG DROPS R. J. Pilie (Cornell Aeron. Lab., Inc.) p 1–23 refs (See N69-39527 23-20)
2. SOME PRINCIPLES OF FOG MODIFICATION WITH HYGROSCOPIC NUCLEI J. E. Jiusto (New York State Univ.) p 24–39 refs (See N69-39528 23-20)
3. VERIFICATION IN LABORATORY SEEDING EXPERIMENTS R. J. Pilie (Cornell Aeron. Lab., Inc.) p 40–56 (See N69-39529 23-20)
4. DISSIPATION OF NATURAL FOG IN THE ATMOSPHERE W. G. Kocmond (Cornell Aeron. Lab., Inc.) p 57–74 ref (See N69-39530 23-20)
5. COMPUTER SIMULATION OF FOG SEEDING EXPERIMENTS W. J. Eadie (Cornell Aeron. Lab., Inc.) p 75–85 refs (See N69-39531 23-20)
6. LABORATORY EXPERIMENTS WITH SEEDING AGENTS OTHER THAN NaCl W. C. Kocmond (Cornell Aeron. Lab., Inc.) p 86–96 (See N69-39532 23-20)

21

NAVIGATION

Includes guidance; autopilots; star and planet tracking; inertial platforms; and air traffic control. For related information see also: 07 Communications.

A69-10479 *#
THE GENERAL UTILITY AND CHARACTER OF PROSPECTIVE NAVIGATION SERVICES SATELLITE SYSTEMS.
Eugene Ehrlich (NASA, Office of Space Science and Applications, Washington, D.C.).
United Nations, Conference on the Exploration and Peaceful Uses of Outer Space, Vienna, Austria, Aug. 14-27, 1968, Paper 68-95363. 18 p.

Discussion of a navigation satellite - a spacecraft system whose mission is to provide "useful" services during movements of manned terrestrial-based vehicles from one point to another. These services are those that will make travel more economical, safer, and more comfortable, and include position determination service, communications service, and telemetry service for ships, aircraft, etc. Three satellite concepts, two conceived by Westinghouse Corporation and by Philco Corporation, and the TRW navigation satellite concept are discussed. The character of the satellite, orbits, and user equipment are considered in detail. I.P.

A69-11005 *
AN APPROACH TO AUTONOMOUS ORBITAL NAVIGATION.
Saul Moskowitz (NASA, Electronics Research Center, Guidance Laboratory, Cambridge, Mass.).
(International Federation of Automatic Control, Symposium on Automatic Control in Space, 2nd, Vienna, Austria, Sept. 4-8, 1967, Paper.)
IEEE Transactions on Aerospace and Electronic Systems, vol. AES-4, Sept. 1968, p. 736-751. 6 refs.

Suggestion of a particular autonomous solution to the orbital navigation problem. The solution, although probably nonoptimal, is practical, and many aspects of it have been proven feasible through both analysis and actual spaceflight evaluation. The formulation of the orbital parameters problem in terms of geometric and orientation plays a significant role in the realization of the proposed approach. The scheme yields a direct measure of orbital parameters through several alternate approaches, rather than one which measures and corrects for deviations from a reference trajectory. M.M.

A69-13214 *
APPROACH GUIDANCE PLANET TRACKER.
Murray K. Cohen (Kollsman Instrument Corp., Elmhurst, N.Y.) and Mark Gorstein (NASA, Electronics Research Center, Cambridge, Mass.).
IN: EASCON '68; INSTITUTE OF ELECTRICAL AND ELECTRONICS ENGINEERS, ELECTRONICS AND AEROSPACE SYSTEMS CONVENTION, WASHINGTON, D.C., SEPTEMBER 9-11, 1968, RECORD. [A69-13176 03-07]
New York, Institute of Electrical and Electronics Engineers, Inc., 1968, p. 279-289.

Demonstration of a working breadboard model of a planet tracker which can acquire and track over a wide range of planet size and phase illumination. The approach taken is that of a no-moving-part tracker using an image dissector as the sensor. An image of the planet is focused on the dissector cathode. A circular scan with a superimposed radial dither scans the outline of the electron image. Error signals are generated when there is lack of coincidence between the planet and scan centers. A hardware description and the results of a preliminary test evaluation are given. A closed-loop tracking-error analysis which accounts for signal-to-noise effects derived from planet photometric data is also presented. I.P.

A69-15501 *#
ITERATIVE GUIDANCE APPLIED TO GENERALIZED MISSIONS.
Helmut J. Horn (NASA, Marshall Space Flight Center, Dynamics and Flight Mechanics Div., Aero-Astrodynamics Laboratory, Huntsville, Ala.), Doris C. Chandler (NASA, Marshall Space Flight Center, Dynamics and Flight Mechanics Div., Guidance Branch, Huntsville, Ala.), and Volis L. Buckelew (NASA, Marshall Space Flight Center, Dynamics and Flight Mechanics Div., Guidance Branch, Guidance Application Section, Huntsville, Ala.).
(American Institute of Aeronautics and Astronautics, Guidance, Control and Flight Dynamics Conference, Huntsville, Ala., Aug. 14-16, 1967, Paper 67-620.)
Journal of Spacecraft and Rockets, vol. 6, Jan. 1969, p. 4-8. 7 refs.

The iterative guidance mode (IGM) was developed to satisfy the launch vehicle requirements of the Saturn-Apollo flights. Improvements in the formulation of the guidance equations extend the application of the IGM to more general missions: (1) a more sophisticated prediction of the "effective" gravity vector which permits use of the guidance scheme for extended trajectory arcs without deterioration of the optimization characteristics; (2) development of equations which permit the use of total energy as an additional end constraint, reducing or entirely eliminating the need of precomputation and curve fitting for a major group of missions; and (3) the reduction of sensitivity to noise in the acceleration measurement, which is achieved by computing and filtering a fictitious thrust, the product of measure acceleration, and computed mass. The effectiveness of these modifications, which are presented against the background of a short derivation of the basic equations, is numerically evaluated for selected trajectories. (Author)

A69-16716
RADIO TECHNICAL COMMISSION FOR AERONAUTICS, ANNUAL ASSEMBLY MEETING, WASHINGTON, D.C., SEPTEMBER 25, 26, 1968, PROCEEDINGS.
Washington, D.C., Radio Technical Commission for Aeronautics, 1968. 156 p.
$2.00.

CONTENTS:

OPENING REMARKS. A. W. Wuerker. 1 p.

KEYNOTE ADDRESS - POLICY ASPECTS OF AERONAUTICAL R&D. F. W. Lehan (U.S. Department of Transportation, Washington, D.C.). 9 p.

THE R&D EFFORT.

INDUSTRY R&D. C. F. Horne (General Dynamics Corp., Pomona, Calif.). 9 p.

THE R&D EFFORT. J. A. Weber (Federal Aviation Administration, Washington, D.C.). 7 p. [See A69-16717 05-34]

NASA AVIATION ELECTRONICS RESEARCH. R. J. Hayes (NASA, Electronics Research Center, Cambridge, Mass.). 13 p. [See A69-16718 05-34]

POLICY ASPECTS OF MILITARY R&D. F. J. Larsen (Department of Defense, Washington, D.C.). 6 p.

AIR TRAFFIC CONTROL.

ATC AUTOMATION. F. J. Howland (Federal Aviation Administration, Washington, D.C.). 8 p. [See A69-16719 05-21]

AREA NAVIGATION. R. W. Martin (Federal Aviation Administration, Washington, D.C.). 8 p. [See A69-16720 05-21]

CONTROLLER MANPOWER AND TRAINING. F. L. Bailey. 13 p.

COMMUNICATIONS.

AERONAUTICAL SATELLITE COMMUNICATIONS - A PROGRESS REVIEW. W. W. Buchanan (Aeronautical Radio, Inc., Annapolis, Md.). 10 p. [See A69-16721 05-21]

DIGITAL COMMUNICATIONS. B. F. McLeod (Pan American World Airways, Inc., New York, N.Y.). 11 p. [See A69-16722 05-07]

PUBLIC AIR-GROUND COMMUNICATIONS. C. H. Elmendorf (American Telephone and Telegraph Co.). 7 p.

NEWSREEL REPORT - 1968. W. W. Parrish. 9 p.

AIRCRAFT OPERATIONS - V/STOL. G. P. Bates, Jr. (Federal Aviation Administration, Washington, D.C.). 14 p. [See A69-16723 05-02]

AN AIRPORT SURFACE TRAFFIC CONTROL SYSTEM (STRACS). V. E. Bonaventura (Port of New York Authority, New York, N.Y.). 11 p. [See A69-16724 05-21]

COLLISION AVOIDANCE SYSTEM. F. C. White (Air Transport Association of America, Washington, D.C.). 7 p. [See A69-16725 05-21]

PROGRESS IN PILOT WARNING INDICATORS. H. L. Anderton (NASA, Microwaves and Optics Branch, Washington, D.C.). 7 p. [See A69-16726 05-21]

CLOSING REMARKS. T. H. Taylor (Aeronautical Radio, Inc., Annapolis, Md.). 3 p.

A69-16726 *#
PROGRESS IN PILOT WARNING INDICATORS.
Henry L. Anderton (NASA, Microwaves and Optics Branch, Washington, D.C.).
IN: RADIO TECHNICAL COMMISSION FOR AERONAUTICS, ANNUAL ASSEMBLY MEETING, WASHINGTON, D.C., SEPTEMBER 25, 26, 1968, PROCEEDINGS. [A69-16716 05-21]
Washington, D.C., Radio Technical Commission for Aeronautics, 1968. 7 p.

Discussion of the problems to be expected in developing a useful pilot warning indicator at a price which will generate sufficient sales to equip all aircraft. It is suggested that installation of these devices may have to be compulsory, as was the case with seat belts for automobiles. The cooperative Doppler pilot warning indicator being developed at the Langley Research Center is discussed. F.R.L.

A69-17580 *
UTILIZATION OF GROUND-BASED GUIDANCE SYSTEMS TO SUPPLEMENT ONBOARD GUIDANCE OF SPACE VEHICLES.
J. P. Mayer (NASA, Manned Spacecraft Center, Mission Planning and Analysis Div., Houston, Tex.), R. P. Parten, and R. E. Ernull (NASA, Manned Spacecraft Center, Flight Operations Directorate, Houston, Tex.).
IN: INTERNATIONAL ASTRONAUTICAL FEDERATION, INTERNATIONAL ASTRONAUTICAL CONGRESS, 18TH, BELGRADE, YUGOSLAVIA, SEPTEMBER 24-30, 1967, PROCEEDINGS. VOLUME 1 - ASTRODYNAMICS, GUIDANCE AND CONTROL, MISCELLANEA. [A69-17560 06-30]
Edited by Michał Łunc.
Oxford, Pergamon Press, Ltd.; Warsaw, Państwowe Wydawnictwo Naukowe, 1968, p. 393-404.

Discussion of the guidance systems used for U.S. manned space flights, involving a combination of onboard and ground-based systems. Because of the greater storage capacity and speed of the ground computers and the greater ground display capacity, more precise solutions to complicated guidance problems, such as in-flight mission planning, can be achieved. Onboard systems, on the other hand, are better suited for such guidance functions as terminal phase guidance and closed-loop, powered-flight steering. Both the Gemini and Apollo programs utilize guidance systems which rely heavily on both onboard and ground functions. The best qualities of both systems are combined to optimize the safety and success of the mission. P.v.T.

A69-17589 *
THE DESIGN OF A LARGE ANGLE THREE-AXIS ATTITUDE SERVOMECHANISM FOR SPACECRAFT.
G. Meyer (NASA, Ames Research Center, Moffett Field, Calif.).
IN: INTERNATIONAL ASTRONAUTICAL FEDERATION, INTERNATIONAL ASTRONAUTICAL CONGRESS, 18TH, BELGRADE, YUGOSLAVIA, SEPTEMBER 24-30, 1967, PROCEEDINGS. VOLUME 1 - ASTRODYNAMICS, GUIDANCE AND CONTROL, MISCELLANEA. [A69-17560 06-30]
Edited by Michał Łunc.
Oxford, Pergamon Press, Ltd.; Warsaw, Państwowe Wydawnictwo Naukowe, 1968, p. 499-505.

Definition of an attitude servo as a control system which adjusts the attitude and angular velocity of the spacecraft so as to follow the reference which may be varying in time. Such systems are multidimensional, multivariable, nonlinear, and nonautonomous with infinite sets of forcing functions and initial conditions. A procedure for designing such systems for spacecraft which are controlled by means of an arbitrary angular momentum exchange and storage device is presented. The discussion is restricted neither to small-angle motion nor to single-axis motion of the spacecraft. Indeed, the nonlinear effects arising from kinematics and gyroscopic action, the presence of bounds on angular momentum exchange rate and storage capacity of the controlling device, and variations in system parameters are taken into account. The proposed control scheme forces the spacecraft into the desired attitude by generating torque about all three axes simultaneously. P.v.T.

A69-19135 *
PRELIMINARY EXPERIMENT RESULTS FROM THE OMEGA POSITION LOCATION EQUIPMENT (OPLE).
H. S. Horiuchi (NASA, Goddard Space Flight Center, Greenbelt, Md.).
IN: INTERNATIONAL TELEMETERING CONFERENCE, LOS ANGELES, CALIF., OCTOBER 8-11, 1968, PROCEEDINGS. [A69-19092 07-07]
Conference sponsored by the International Foundation for Telemetering.
Tarzana, Calif., International Foundation for Telemetering (ITC Proceedings. Volume 4), 1968, p. 631-638.

Results of analysis of data taken during fixed platform, road, and aircraft tests of the OPLE system, which indicate that a fixed or moving platform can be located with reasonable accuracy. The purpose of the experiment was to demonstrate the feasibility of using the Omega navigational system in conjunction with synchronous satellites to establish a global tracking and data collection system. OPLE consists of an OPLE Control Center (OCC), located at Goddard Space Flight Center (GSFC), a synchronous satellite (ATS-3), platform electronic packages (PEP), and the Omega navigational network. F.R.L.

A69-19208 *
IRRADIATION AND MANUAL NAVIGATION.
Richard F. Haines and William H. Allen (NASA, Ames Research Center, Moffett Field, Calif.).
(Institute of Navigation, Annual Meeting, 24th, Monterey, Calif., June 19-21, 1968.)
Navigation, vol. 15, Winter 1968-1969, p. 355-365. 45 refs.

Description of the results of a series of investigations of the minimal angle of resolution (MAR) between a point and an extended circular source and between a point source and a simulated horizon. A total of 11 highly trained male observers took part in the experiments. All had 20:20 distance acuity. Each observer moved a point source along various frontal plane meridians behind an extended source in order to determine at what position it became invisible due to the effects of irradiation. The results indicate that: (1) the apparent edge of high-luminance targets can be displaced as much as 15' from the target's actual edge under some viewing conditions; (2) the MAR is a function of both the contrast ratio between the target and background and the luminance of the point source; and (3) the detrimental effects of irradiation are not reduced by using optical filters across the entire field of view to reduce the luminance of the extended source. The findings are related to certain aspects of manual navigation currently in use. M.M.

A69-19212 *
RECENT PROGRESS IN NAVIGATION SATELLITES.
L. M. Keane (NASA, Electronics Research Center, Cambridge, Mass.).
(INSTITUTE OF NAVIGATION, NATIONAL AIR MEETING ON SUPERSONIC NAVIGATION, SEATTLE, WASH., NOVEMBER 15, 16, 1967, PROCEEDINGS, p. 226-241.)
Navigation, vol. 15, Winter 1968-1969, p. 415-423.

Examination of studies of navigation by satellite which emphasize designing the satellite system so that a user may navigate without the requirement for an onboard transmitter. Compared to a totally active or transponding system, this approach offers the advantages of increased numbers of potential users and increased resistance to interference. Independent measurements of position for North Atlantic ATC can be made simultaneously by incorporating transmitters into aircraft and relaying the position-measurement data on ground command. The results of recent studies of hyperbolic ranging systems and long-baseline interferometer approaches are presented. Spectrum occupancy, satellite power, lane ambiguities, and computational procedures are discussed. Modes of operation which show promise for improving SST operation are described. F. R. L.

A69-25724 *
GUIDANCE AND CONTROL FOR ATMOSPHERIC ENTRY.
R. C. Duncan (NASA, Electronics Research Center, Cambridge, Mass.).
IN: RE-ENTRY AND PLANETARY ENTRY PHYSICS AND TECHNOLOGY. II - ADVANCED CONCEPTS, EXPERIMENTS, GUIDANCE-CONTROL AND TECHNOLOGY. [A69-25718 11-31]
Edited by W. H. T. Loh.
New York, Springer-Verlag New York, Inc. (Applied Physics and Engineering Series. Volume 3), 1968, p. 205-256.

Examination of the concepts and hardware for guidance and control of the Mercury, Gemini, and Apollo spacecraft. The accuracy requirements of the Apollo guidance and control systems are largely based upon the reentry phase of the mission which is the most stringent from the standpoint of guidance system performance. The guidance system requirements for reentry are a function of the following: (1) initial condition errors at the reentry interface, (2) initial stable member alignment accuracy, (3) inertial component accuracy, (4) guidance equation mechanization, (5) reentry range requirements, and (6) allowable reentry dispersion. P. v. T.

A69-34843
AVIONICS NAVIGATION SYSTEMS.
Edited by Myron Kayton (TRW Systems Group, Redondo Beach, Calif.) and W. R. Fried (North American Rockwell Corp., Autonetics Div., Anaheim, Calif.).
New York, John Wiley and Sons, Inc., 1969. 688 p.
$24.95.

CONTENTS:

PREFACE. M. Kayton (TRW Systems Group, Redondo Beach, Calif.) and W. R. Fried (North American Rockwell Corp., Anaheim, Calif.), p. vii-ix.

INTRODUCTION TO AIRCRAFT NAVIGATION. A. B. Moody (Federal Aviation Administration, Washington, D.C.), p. 1-12. 12 refs. [See A69-34844 18-21]

THE NAVIGATION EQUATIONS. M. Kayton (TRW Systems Group, Redondo Beach, Calif.), p. 13-57. 30 refs. [See A69-34845 18-21]

AIRBORNE DIGITAL COMPUTERS. S. Schoen (Litton Industries, Inc., Beverly Hills, Calif.), p. 58-93. 63 refs. [See A69-34846 18-08]

AIRBORNE ANALOG COMPUTERS. T. J. Thomas (Singer-General Precision, Inc., Little Falls, N.J.), p. 94-122. 33 refs. [See A69-34847 18-08]

RADIO NAVIGATION. S. H. Dodington (International Telephone and Telegraph Corp., Nutley, N.J.), p. 123-206. 78 refs. [See A69-34848 18-21]

DOPPLER NAVIGATION. W. R. Fried (North American Rockwell Corp., Anaheim, Calif.), p. 207-280. 79 refs. [See A69-34849 18-21]

INERTIAL NAVIGATION. M. Kayton (TRW Systems Group, Redondo Beach, Calif.), p. 281-341. 47 refs. [See A69-34850 18-21]

AIRBORNE RADAR NAVIGATION. C. A. Wiley, p. 342-382. 27 refs. [See A69-34851 18-21]

CELESTIAL NAVIGATION. G. Quasius (General Electric Co., Valley Forge, Pa.), p. 383-420. 23 refs. [See A69-34852 18-21]

ATTITUDE AND HEADING REFERENCES. W. G. Wing (Sperry Rand Corp., Great Neck, N.Y.), p. 421-443. 7 refs. [See A69-34853 18-21]

AIR-DATA SYSTEMS. J. H. Andresen, Jr. (Intercontinental Dynamics Corp., Englewood, N.J.) and M. Kayton (TRW Systems Group, Redondo Beach, Calif.), p. 444-463. 20 refs. [See A69-34854 18-21]

SATELLITE NAVIGATION AIDS. R. C. Duncan (NASA, Electronics Research Center, Cambridge, Mass.), p. 464-491. 23 refs. [See A69-34855 18-21]

AUTOMATIC FLIGHT CONTROL. R. E. Andeen (Sperry Rand Corp., Phoenix, Ariz.), p. 492-519. 44 refs. [See A69-34856 18-21]

LANDING GUIDANCE. M. Kayton (TRW Systems Group, Redondo Beach, Calif.), p. 520-554. 67 refs. [See A69-34857 18-21]

DISPLAYS. F. B. Brady (Singer-General Precision, Inc., Washington, D.C.), p. 555-578. 28 refs. [See A69-34858 18-21]

AIR TRAFFIC CONTROL. P. T. Astholz (Federal Aviation Administration, Washington, D.C.), p. 579-611. 94 refs. [See A69-34859 18-21]

INDEX, p. 645-666.

A69-34855 *
SATELLITE NAVIGATION AIDS.
Robert C. Duncan (NASA, Electronics Research Center, Cambridge, Mass.).
IN: AVIONICS NAVIGATION SYSTEMS. [A69-34843 18-21]
Edited by Myron Kayton and W. R. Fried.
New York, John Wiley and Sons, Inc., 1969, p. 464-491. 23 refs.

Discussion of the artificial earth satellite as an aid to navigation. Whereas navigation with the help of natural heavenly bodies is an angle-only system, artificial satellite navigation can be of three kinds: (1) angle-measuring systems, (2) range- or range-rate measuring systems, and (3) range-and-angle systems. The salient features of all three are treated in terms of orbital mechanics, ground coverage, and atmospheric-refraction errors in communication. V. P. M.

A69-35789
INSTITUTE OF NAVIGATION, ION NATIONAL SPACE MEETING ON SPACE NAVIGATION—PRESENT AND FUTURE, HOUSTON, TEX., APRIL 22-24, 1969, PROCEEDINGS.
Washington, D.C., Institute of Navigation, 1969. 337 p.
Members, $10.00; nonmembers, $15.

CONTENTS:

PREFACE. R. H. Battin (Massachusetts Institute of Technology, Cambridge, Mass.), p. i-iii.

NAVIGATION CONCEPTS.

AUTONOMOUS NAVIGATION FOR MARS ENTRY. H. C. Von Struve, III and P. S. Stafford (Martin Marietta Corp., Denver, Colo.), p. 1-15. 5 refs. (See A69-35790 19-21)

INVESTIGATION OF PLANETARY NAVIGATION USING SPACECRAFT-BASED MEASUREMENTS. W. G. Breckenridge and T. C. Duxbury (California Institute of Technology, Pasadena, Calif.), p. 17-30. (See A69-35791 19-21)

A CONCEPT OF MIDCOURSE AND TERMINAL GUIDANCE WITH SINGLE POSITION FIXES OBTAINED FROM ONBOARD OPTICAL MEASUREMENTS. H. A. Hamer (NASA, Langley Research Center, Hampton, Va.), p. 31-55. (See A69-35792 19-21)

ORBIT ESTIMATION USING MANUAL SPACE NAVIGA-

TION SENSORS. J. F. Kasper, Jr. and S. A. Levine (Analytic Sciences Corp., Reading, Mass.), p. 57-88. 5 refs. (See A69-35793 19-21)

AN OPTIMUM FILTER FOR DETERMINING THE TRAJECTORY OF MANEUVERABLE OBJECTS. L. Bonin (Lockheed Aircraft Corp., Houston, Tex.), p. 89-105. 5 refs. (See A69-35794 19-14)

COMPUTERS AND NAVIGATION SENSORS.

THE INDUCED-EMISSION OSCILLATOR NAVIGATION SENSOR. W. L. Zingery (North American Rockwell Corp., Anaheim, Calif.), p. 107-124. 19 refs. (See A69-35795 19-21)

RESULTS OF GROUND AND FLIGHT TESTS OF THE APOLLO OPTICS. C. E. Manry (NASA, Manned Spacecraft Center, Houston, Tex.), p. 125-148. (See A69-35796 19-14)

THE APOLLO LUNAR MODULE LANDING RADAR. L. S. Reel and V. J. Poehls (Ryan Aeronautical Co., San Diego, Calif.), p. 149-170. (See A69-35797 19-07)

DESIGN METHODS FOR FAULT-TOLERANT NAVIGATION COMPUTERS. A. Avizienis (California Institute of Technology, Pasadena; California, University, Los Angeles, Calif.), p. 171-185. 6 refs. (See A69-35798 19-08)

NAVIGATION SYSTEMS TECHNOLOGY.

APOLLO NAVIGATION, GUIDANCE, AND CONTROL SYSTEMS—A PROGRESS REPORT. D. G. Hoag (Massachusetts Institute of Technology, Cambridge, Mass.), p. 187-217. 15 refs. (See A69-35799 19-21)

STAR/HORIZON MEASUREMENTS FOR ONBOARD SPACECRAFT NAVIGATION. J. A. Hand (Massachusetts Institute of Technology, Cambridge, Mass.), p. 219-242. 15 refs. (See A69-35800 19-21)

GUIDANCE AND CONTROL CONSIDERATIONS FOR ADVANCED MANNED SPACE MISSIONS. R. A. Gardiner and G. Xenakis (NASA, Manned Spacecraft Center, Houston, Tex.), p. 243-262. 19 refs. (See A69-35801 19-21)

SEAN—A STRAPDOWN ELECTROSTATIC GYRO AEROSPACE NAVIGATOR. B. M. Dobrotin (California Institute of Technology, Pasadena, Calif.), p. 263-278. (See A69-35802 19-21)

SIRU—A NEW INERTIAL SYSTEM CONCEPT FOR IN-FLIGHT RELIABILITY AND MAINTAINABILITY. R. Crisp, J. P. Gilmore, and A. L. Hopkins, Jr. (Massachusetts Institute of Technology, Cambridge, Mass.), p. 279-305. 5 refs. (See A69-35803 19-21)

PANEL DISCUSSION—FUTURE SPACE NAVIGATION, p. 307-336.

A69-35792 * #

A CONCEPT OF MIDCOURSE AND TERMINAL GUIDANCE WITH SINGLE POSITION FIXES OBTAINED FROM ONBOARD OPTICAL MEASUREMENTS.

Harold A. Hamer (NASA, Langley Research Center, Hampton, Va.).

IN: INSTITUTE OF NAVIGATION, ION NATIONAL SPACE MEETING ON SPACE NAVIGATION—PRESENT AND FUTURE, HOUSTON, TEX., APRIL 22-24, 1969, PROCEEDINGS. (A69-35789 19-21)

Washington, D.C., Institute of Navigation, 1969, p. 31-55.

Description of manual procedures developed for midcourse and terminal guidance. Requiring only simple onboard calculations, these procedures lead to guidance predictions sufficiently accurate for emergency backup guidance, rapid onboard navigation and guidance checks, and so forth. The methods have been studied in detail for earth-to-moon trajectories, and are being studied further for application to interplanetary trajectories. They are being considered also with regard to controlling entry angle on moon-to-earth trajectories. The terminal procedure appears to be especially promising for interplanetary missions because the target-planet ephemeris error limits the reliability of earth-based radar measurements. (Author)

A69-35801 * #

GUIDANCE AND CONTROL CONSIDERATIONS FOR ADVANCED MANNED SPACE MISSIONS.

R. A. Gardiner and G. Xenakis (NASA, Manned Spacecraft Center, Houston, Tex.).

IN: INSTITUTE OF NAVIGATION, ION NATIONAL SPACE MEETING ON SPACE NAVIGATION—PRESENT AND FUTURE, HOUSTON, TEX., APRIL 22-24, 1969, PROCEEDINGS. (A69-35789 19-21)

Washington, D.C., Institute of Navigation, 1969, p. 243-262. 19 refs.

Discussion of the directions that future manned navigation, guidance, and control developments are likely to take. The scope of these future developments is shown to be encompassed by the types of space transportation systems to be used and the objectives of the exploration bases to be developed. The requirements for an earth orbital exploration base and its supporting logistics shuttle are considered in the context of past experience and the unique requirements of the future. It is shown that there will be a transition from programs that are principally developmental in nature, to programs which are more operationally conditioned. This fact, coupled with the resulting longer duration missions, indicates a need for a reconsideration of the manned navigation, guidance, and control system approaches. The mechanization challenge for the future will not be in meeting discrete performance requirements. It will result from the need to meet stringent reliability goals that will, more than ever before, be intimately associated with program costs. (Author)

A69-35953 * #

EVALUATION OF STRAPDOWN GUIDANCE SYSTEMS ON INTERPLANETARY MISSIONS.

Ellis F. Hitt (Battelle Memorial Institute, Columbus Laboratories, Systems and Electronics Dept., Columbus, Ohio) and Edmund J. Koenke (NASA, Electronics Research Center, Guidance Laboratory, Cambridge, Mass.).

(American Institute of Aeronautics and Astronautics, Guidance, Control, and Flight Dynamics Conference, Pasadena, Calif., Aug. 12-14, 1968, Paper 68-828.)

Journal of Spacecraft and Rockets, vol. 6, May 1969, p. 623-626.

Contract No. NAS 12-550.

Techniques developed for evaluation of strapdown guidance systems designed for automated interplanetary missions are discussed. Cost effectiveness is defined with cost equal to the guidance system weight and effectiveness equal to the probability that the guidance system operates correctly. System weight is the sum of the inertial sensing unit, computer, midcourse correction system, and energy source weights. The effectiveness probability is the appropriate combination of the probabilities related to failures due to component unreliability, insufficient midcourse fuel, and excessive target miss. Using this model, penalty functions relating parameters describing weight, accuracy, reliability, and power requirements of candidate systems are presented. Techniques for estimating these parameters and features of the computer programs implementing the work are discussed. Results for an interplanetary trajectory to Jupiter are presented and point to areas requiring development to improve strapdown guidance systems for automated interplanetary missions. (Author)

A69-39386 * #

A PRECISION AUTOCOLLIMATING SOLAR SENSOR.

R. K. Melugin (NASA, Ames Research Center, Moffett Field, Calif.), J. M. Hall, and D. F. Johnson (Exotech, Inc., Rockville, Md.).

American Institute of Aeronautics and Astronautics, Guidance, Control, and Flight Mechanics Conference, Princeton, N.J., Aug. 18-20, 1969, Paper 69-858. 6 p.

Members, $1.00; nonmembers, $1.50.

Contract No. NAS 2-4050.

Alignment changes in attitude sensors and spacecraft structure

that usually occur during launch and space environments cause degradation in attitude control accuracy. A new sensor concept is described which utilizes a miniature, integral electronic autocollimator to measure arc second alignment changes of a high-accuracy solar attitude sensor relative to a reference surface. Although the concept is implemented in a solar sensor, it is applicable to other instruments where high angular measurement accuracy is required. Design features include solid quartz optics to minimize thermal deformation, an optical bandpass filter to minimize detector thermal drift, and signal processing electronics to permit arc second telemetry resolution. Flight data described include an in-flight solar cell detector calibration and a summary of sensor performance on a sounding rocket flight. The sensor solar attitude measurement uncertainty was less than 2.0 arc seconds root sum square. (Author)

A69-39390 * #
GROUND-BASED GUIDANCE FOR LAND-LANDING MANNED SPACECRAFT EQUIPPED WITH LOW-VELOCITY DESCENT SYSTEMS.
Donald J. Bourque (NASA, Manned Spacecraft Center, Houston, Tex.).
American Institute of Aeronautics and Astronautics, Guidance, Control, and Flight Mechanics Conference, Princeton, N.J., Aug. 18-20, 1969, Paper 69-864. 7 p.
Members, $1.00; nonmembers, $1.50.

Results of an extensive series of flight tests of a 400-lb spacecraft model, equipped with a 20-ft single-keel parawing in conjunction with an experimental ground-based guidance system called the terminal landing system. The tests were conducted to identify flight-operations requirements and to support test and development of low-velocity descent systems. Three basic approach and landing procedures were designed, tested, and analyzed: (1) high-altitude glide path intercept, (2) low-altitude glide path intercept, and (3) spiral. Analyses of test data indicate that the high-altitude glide path intercept approach is usually best under normal landing conditions but that the low-altitude glide path intercept approach provides the best chance of correcting contingency situations brought about by changes in system performance or predicted winds. It is concluded that the terminal landing system concept is workable as an operational ground-based guidance system. (Author)

A69-39396 * #
AN ADVANCED LASER TRACKING TECHNIQUE FOR FUTURE SPACE GUIDANCE SYSTEMS.
Charles L. Wyman (NASA, Marshall Space Flight Center, Astrionics Laboratory, Huntsville, Ala.).
American Institute of Aeronautics and Astronautics, Guidance, Control, and Flight Mechanics Conference, Princeton, N.J., Aug. 18-20, 1969, Paper 69-870. 8 p. 7 refs.
Members, $1.00; nonmembers, $1.50.

Description of an advanced laser tracking technique for future space guidance systems utilizing single mode diffraction limited GaAs lasers, precision laser beam deflectors, and an ultralinear image dissector. A 0.1-deg laser beam and a 0.1-deg instantaneous field of view are scanned synchronously over a 30 by 30-deg acquisition field. Once acquired, a target will be illuminated and tracked anywhere within the 30 by 30-deg field. The particular setup described is directed toward cooperative rendezvous, docking, and stationkeeping applications. Z.W.

A69-39405 * #
GUIDANCE AND CONTROL PARAMETERS OF A PLANETARY CARTOGRAPHIC PROBE.
Saul Moskowitz (NASA, Electronics Research Center, Computer and Guidance Technology Div., Cambridge, Mass.).
American Institute of Aeronautics and Astronautics, Guidance, Control, and Flight Mechanics Conference, Princeton, N.J., Aug. 18-20, 1969, Paper 69-879. 15 p. 10 refs.
Members, $1.00; nonmembers, $1.50.

Study of the guidance and control requirements for a planetary orbiting cartographic spacecraft. Mapping scales of $1:10^6$ and $1:5(10^6)$ were selected for the parametric study of lunar, Martian, and Jovian cartography. Relations are derived connecting camera pointing angle, field of view, and imaging resolution in terms of planetary physical characteristics and mapping scale. From these, orbit selection rules are formulated. The choice of an image overlap of 10 per cent leads to spacecraft attitude control requirements. The resulting overall guidance and control parameters are described in terms of possible instrumentation subsystems. (Author)

A69-39406 * #
AUTONOMOUS NAVIGATION IN LONG-DURATION, HIGHLY ECCENTRIC ORBITS ABOUT MARS.
Flora Byars Lowes (NASA, Manned Spacecraft Center, Houston, Tex.).
American Institute of Aeronautics and Astronautics, Guidance, Control, and Flight Mechanics Conference, Princeton, N.J., Aug. 18-20, 1969, Paper 69-880. 9 p. 8 refs.
Members, $1.00; nonmembers, $1.50.

Study of the problem of effective autonomous navigation for a manned spacecraft in long-duration, highly eccentric orbits. A statistical error analysis using star-horizon, unknown-landmark, and surface-beacon measurements is presented for a 300-day orbital stay time about Mars. The data are processed with a Kalman filter, and the methods are evaluated for their applicability and effectiveness in minimizing estimated state errors and in producing reasonable measurement schedules. Results of the study indicate that the two optical angle-measurement methods, although constrained by the orbital geometry, can be optimally combined and used for only 4 hours during each day to produce an accuracy of less than 1 n mi. The estimated error in the spacecraft position obtained by continuous onboard-radar tracking of surface beacons is larger than that obtained with the optical navigation techniques. However, this result is dependent on the beacon location errors and was found to improve as knowledge of the locations increased. (Author)

A69-39409 * #
SATURN V NAVIGATION UPDATE.
R. M. O'Brien (Boeing Co., Southeast Div., Huntsville, Ala.) and J. P. Sheats (NASA, Marshall Space Flight Center, Aero-Astrodynamics Laboratory, Huntsville, Ala.).
American Institute of Aeronautics and Astronautics, Guidance, Control, and Flight Mechanics Conference, Princeton, N.J., Aug. 18-20, 1969, Paper 69-883. 6 p. 5 refs.
Members, $1.00; nonmembers, $1.50.

Investigation of the influence of navigation state-vector update on lunar mission completion capability for Saturn V. Midcourse correction budget exceedance rates are compared for unupdated and updated navigation with the expected navigation hardware and scheme errors. Accelerometer failure cases produce large navigation errors and are therefore analyzed extensively. The amount of midcourse correction budget strongly affects the number of exceedances due to navigation hardware, but influences accelerometer failure cases only slightly. The same is true of the effect of launch date, flight azimuth, and opportunity. Vehicle performance dispersions have a large influence on accelerometer-failure cases but do not affect navigation error cases. The expected navigation update accuracy is adequate. For the severe portion of the launch window, the number of times per million flights that mission objectives are compromised through proposed budget exceedance is reduced from 15,400 to 3,360 by navigation update. (Author)

21 NAVIGATION

A69-39410 * #
A NEW MODEL PERFORMANCE INDEX FOR THE ENGINEERING DESIGN OF FLIGHT CONTROL SYSTEMS.
Herman A. Rediess (NASA, Flight Research Center, Edwards, Calif.) and H. Philip Whitaker (Massachusetts Institute of Technology, Cambridge, Mass.).
American Institute of Aeronautics and Astronautics, Guidance, Control, and Flight Mechanics Conference, Princeton, N.J., Aug. 18-20, 1969, Paper 69-885. 12 p. 12 refs.
Members, $1.00; nonmembers, $1.50.
Grant No. NGR-22-009-229.

Description of the theory and application of a new performance index, the Model PI, that brings engineering design specifications into the analytical design process. A parameter optimization design procedure is established that starts with practical engineering specifications and uses the Model PI as a synthesis tool to obtain a satisfactory design. The Model PI represents a new criterion for approximating one dynamical system by another, based on a novel geometrical representation of linear autonomous systems. It is shown to be an effective performance index in designing practical systems and to be substantially more efficient than a comparable model-referenced integral squared error performance index. The design procedure is demonstrated by designing a lateral-directional stability augmentation system for the X-15 aircraft. (Author)

A69-39429 * #
FLIGHT TEST REPORT OF EXPERIMENTS IN INERTIAL NAVIGATION SYSTEM UPDATING.
R. J. Madigan and J. Canniff (NASA, Electronics Research Center, Cambridge, Mass.).
American Institute of Aeronautics and Astronautics, Guidance, Control, and Flight Mechanics Conference, Princeton, N.J., Aug. 18-20, 1969, Paper 69-842. 8 p.
Members, $1.00; nonmembers, $1.50.

Results of guidance and navigation flight tests, demonstrating some of the improvements that may be achieved in navigation system performance by having an onboard inertial system in communication with an external navigation aid. Aided-inertial system performance and the determination of inertial system flight readiness are discussed. Attention is given to system configuration, aided system performance as a function of controlled degradation of the inertial measurement unit, aided system performance in the position/velocity update mode, and stationary (fixed position) navigation as a technique for evaluating system performance prior to flight commitment. B.H.

A69-39644
GUIDANCE AND CONTROL IN SPACE; INTERNATIONAL FEDERATION OF AUTOMATIC CONTROL, CONGRESS, 4TH, WARSAW, POLAND, JUNE 16-21, 1969, PROCEEDINGS.
Warsaw, Wydawnictwa Czasopism Technicznych NOT (Technical Session 43), 1969. 130 p. In English and Russian.

CONTENTS:

CERTAIN PROBLEMS OF STRUCTURAL SYNTHESIS OF SPATIAL MOTION CONTROL SYSTEMS FOR AN ORBITAL AIRCRAFT IN THE EARTH'S ATMOSPHERE (NEKOTORYE VOPROSY SINTEZA STRUKTUR SISTEM UPRAVLENIIA PROSTRANSTVENNYM DVIZHENIEM ORBITAL'NOGO SAMOLETA V ATMOSFERE ZEMLI). B. N. Petrov, N. P. Kolpakova, V. A. Vasil'ev, and A. I. Pavlenko (Moskovskii Aviatsionnyi Institut, Moscow, USSR), p. 3-18. 6 refs. (See A69-39645 21-21)

OPTIMUM INTERPLANETARY MIDCOURSE VELOCITY-CORRECTION SCHEDULES. T. B. Murtagh (NASA, Manned Spacecraft Center, Houston, Tex.), p. 19-38. 11 refs. (See A69-39646 21-21)

OPTIMUM PARAMETRIC LAWS OF SPACE VEHICLE DESCENT CONTROL (OPTIMAL'NYE PARAMETRICHESKIE ZAKONY UPRAVLENIIA SNIZHENIEM KOSMICHESKOGO APPARATA). V. M. Ponomarev and V. I. Gorodetskii (Leningradskii Gosudarstvennyi Universitet, Leningrad, USSR), p. 39-51. 7 refs. (See A69-39647 21-21)

STOCHASTIC OPTIMIZATION OF SPACECRAFT DESCENT CONTROL IN THE ATMOSPHERE (STOKHASTICHESKAIA OPTIMIZATSIIA UPRAVLENIIA SPUSKOM KOSMICHESKOGO APPARATA V ATMOSFERE). A. G. Vlasov, E. I. Mitroshin, and I. S. Ukolov (Moskovskii Aviatsionnyi Institut, Moscow, USSR), p. 52-66. (See A69-39648 21-21)

MOTION CONTROL DURING ENTRY INTO THE ATMOSPHERE (UPRAVLENIE DVIZHENIEM PRI VKHODE V ATMOSFERU). D. E. Okhotsimskii, A. P. Bukharkina, and Iu. F. Golubev (Akademiia Nauk SSSR, Institut Prikladnoi Matematiki, Moscow, USSR), p. 67-83. (See A69-39649 21-21)

STOCHASTIC PROBLEMS OF ROCKET DYNAMICS (STOKHASTICHESKIE ZADACHI RAKETODINAMIKI). Iu. P. Plotnikov (Moskovskii Aviatsionnyi Institut, Moscow, USSR), p. 84-100. 10 refs. (See A69-39650 21-21)

STATISTICAL SYNTHESIS OF OPTIMAL PULSED CONTROL SYSTEMS FOR SPACE VEHICLES WITH ALLOWANCE FOR CONSTRAINTS IMPOSED ON THE SYSTEM STRUCTURE (STATISTICHESKII SINTEZ OPTIMAL'NYKH IMPUL'SNYKH SISTEM UPRAVLENIIA KOSMICHESKIKH OB'EKTOV S UCHETOM OGRANICHENII PO STRUKTURE SISTEMY). A. Ia. Andrienko (Akademiia Nauk SSSR, Institut Avtomatiki i Telemekhaniki, Moscow, USSR), p. 101-114. (See A69-39651 21-21)

SYNTHESIS OF AN OPTIMAL ORBIT CONTROL SYSTEM FOR A STABLE ARTIFICIAL EARTH SATELLITE (SINTEZ OPTIMAL'NOI SISTEMY UPRAVLENIIA ORBITOI STATSIONARNOGO ISKUSSTVENNOGO SPUTNIKA ZEMLI). A. A. Lebedev, M. N. Krasil'shchikov, and V. V. Malyshev (Moskovskii Aviatsionnyi Institut, Moscow, USSR), p. 115-130. 7 refs. (See A69-39652 21-21)

A69-39646 * #
OPTIMUM INTERPLANETARY MIDCOURSE VELOCITY-CORRECTION SCHEDULES.
Thomas B. Murtagh (NASA, Manned Spacecraft Center, Houston, Tex.).
IN: GUIDANCE AND CONTROL IN SPACE; INTERNATIONAL FEDERATION OF AUTOMATIC CONTROL, CONGRESS, 4TH, WARSAW, POLAND, JUNE 16-21, 1969, PROCEEDINGS. (A69-39644 21-21)
Warsaw, Wydawnictwa Czasopism Technicznych NOT (Technical Session 43), 1969, p. 19-38. 11 refs.

Analysis of a theoretical basis for the optimization of interplanetary midcourse velocity-correction schedules as set forth in published literature. Cicolani's results (1966) are discussed, and suggestions are made as to how the limitations involved could be eliminated by reforming his optimal timing equations. Another set of equations is developed for predicting the optimal timing of a sequence of variable-time-of-arrival velocity corrections, using Cicolani's assumptions with regard to the accuracy of the navigation system and the statistical model of the guidance system. The analytical results for individual and combined optimal velocity correction strategies are compared with the results of a simulation program using an earth-based radar and an onboard sextant with a Kalman filter tracking data for two typical interplanetary missions. Good agreement is obtained between the theoretical results and the simulation results, especially when the amount of earth-based radar is increased. V.Z.

A69-39764 * #
A PASSIVE METHOD FOR SCANNING THE CELESTIAL SPHERE.
Albert J. Fleig, Jr. (NASA, Goddard Space Flight Center, Stabilization and Control Branch, Greenbelt, Md.).
(American Institute of Aeronautics and Astronautics, Guidance, Control and Flight Dynamics Conference, Pasadena, Calif., Aug.

12-14, 1968, Paper 68-854.)
Journal of Spacecraft and Rockets, vol. 7, July 1969, p. 846, 847.

A passive method for scanning the celestial sphere which is applicable to missions requiring long lifetime and moderate pointing accuracies is described. The spacecraft is spin-stabilized, and it is the spin axis which is caused to follow the scan pattern. The scan is obtained by combining the gravity gradient-induced precession of the spacecraft's spin axis about its orbit pole with the oblateness-induced precession of the orbit pole. The parameters directly affecting a particular mission are the orbit altitude, inclination, and eccentricity and the body spin rate, cone angle, and inertia difference. Design curves which can be used for parameter tradeoff studies of these factors are included. (Author)

A69-40327 * #
A SIMPLIFIED KALMAN ESTIMATOR FOR AN AIRCRAFT LANDING DISPLAY.
Robert B. Merrick (NASA, Ames Research Center, Theoretical Guidance and Control Branch, Moffett Field, Calif.).
American Institute of Aeronautics and Astronautics, Aerospace Computer Systems Conference, Los Angeles, Calif., Sept. 8-10, 1969, Paper 69-944. 9 p.
Members, $1.00; nonmembers, $1.50.

Description of the application of Kalman filter simulation for estimating the position and velocity of an aircraft from data given by an airborne digital computer in a zero-zero landing system. The on-board estimator must operate within very limited allowances of computation time (70 milliseconds) and computer storage (600 words). The pertinent observation equations are linearized around the current estimated trajectory. The first mechanization of the Kalman filter approach drastically exceeded the on-board computer constraints. Several substantial simplifications were made to meet these constraints, and the results show that equivalent performance is obtainable with a much simpler system. Z.W.

A69-43245 * #
SATELLITE ATTITUDE CONTROL USING A TORQUED, 2-AXIS-GIMBALED BOOM AS THE ACTUATOR.
James A. Gatlin (NASA, Goddard Space Flight Center, Greenbelt, Md.), A. G. Buckingham, and W. H. Pleasants (Westinghouse Electric Corp., Defense and Space Center, Baltimore, Md.).
(American Institute of Aeronautics and Astronautics, Guidance, Control, and Flight Dynamics Conference, Pasadena, Calif., Aug. 12-14, 1968, Paper 68-857.)
Journal of Spacecraft and Rockets, vol. 6, Sept. 1969, p. 1013-1018.

Description of a commandable gravity-gradient boom for satellite precision attitude control. Each of the two boom gimbal axes is equipped with a torquer and a shaft encoder. Satellite attitude control is maintained, using an active attitude reference and torquing against the inertia of the boom. Gravity-gradient torques keep the boom "anchored" in the gravity field, and small momentum wheels damp the boom librations. Yaw-axis momentum control utilizes the orbital coupling of the roll/yaw axes. Results of linear analyses, computer simulations, and some hardware tests exemplify the performance of this commandable gravity gradient system and demonstrate its feasibility. The system can be expected to statically point to any spot on the earth to within $\pm 0.1^{\circ}$ and to track low-altitude satellites to within $\pm 0.5^{\circ}$. P.v.T.

N69-10056*# National Aeronautics and Space Administration. Langley Research Center, Langley Station, Va.
INFLUENCE OF ANGLE OF GLIDE SLOPE ON THE ACCURACY OF PERFORMING INSTRUMENT APPROACHES IN A SIMULATOR
Lindsay J. Lina and George C. Canavos Washington Nov. 1968 44 p refs
(NASA-TN-D-4835) Avail: CFSTI CSCL 17G

A simulator study was made to determine the effect of glide slope angle on the accuracy of performing a landing approach and a go around. Statistical evaluation of the data indicates that the angle of glide slope had no appreciable effect on the accuracy of approach but had an influence on the minimum altitude in the missed approach maneuver. The probability of completing a landing without excessive maneuvering in the last few seconds of flare is reduced by a varying cross wind. Author

N69-10069*# National Aeronautics and Space Administration. Langley Research Center, Langley Station, Va.
COMPARISON OF INFORMATION DISPLAY CONCEPTS FOR LANDING OF VTOL AIRCRAFT
William Gracey Washington Nov. 1968 44 p refs
(NASA-TN-D-4861) Avail: CFSTI CSCL 17G

A variety of instrument displays for the landing of VTOL aircraft are described. The displays are classified in terms of basic concepts for the presentation of attitude and guidance information. The concepts range from the simple display of vertical- and horizontal-situation information to the more complex combination of attitude and guidance information in perspective form. The information elements of the displays are presented either in abstract form or with varying degrees of realism. Guidance information is combined as flight-director commands in some displays and as pictorial presentations in others. Tests of those displays that have been evaluated either in simulators or in flight are discussed. The review of these tests shows that the only display with which VTOL landings have been achieved in flight (under simulated zero–zero conditions) is the real-world display of a closed circuit television system. A televised display of a simulated real-world landing site is therefore suggested as a possible form of display for achieving VTOL landings under zero–zero conditions. Author

N69-10372*# National Aeronautics and Space Administration. Langley Research Center, Langley Station, Va.
ANALYTIC APPROXIMATIONS FOR APPLICATION TO SPACECRAFT OPTICAL NAVIGATION ON SHORT DATA ARCS
Alton P. Mayo and William M. Adams, Jr. Washington Nov. 1968 32 p refs
(NASA-TN-D-4863) Avail: CFSTI CSCL 17G

The standard least squares orbit determination procedures are simplified for application to a navigation system where position fixes are taken over a short trajectory arc. Basic assumptions used are as follows: (1) for small perturbations in spacecraft state, velocity deviations remain constant and position deviations increase linearly with time and (2) the sensitivity of the measurements to small spacecraft position changes remains constant over the trajectory arc. Simple analytic expressions are then derived for estimating the accuracy of the spacecraft position and velocity as a function of the number of fixes and the time span over which the fixes are made, or inversely the number of fixes and the time span over which they must be made for a prescribed position and velocity accuracy. For a large number of measurements the standard deviation of the position error was shown to vary inversely as the square root of the number of measurements, as expected, and the standard deviation of the velocity error was shown to vary inversely as the product of the square root of the number of measurements and the time span over which the measurements are made. Simplified equations are also derived for determining the orbit (state) of the spacecraft. Author

N69-14332*# National Aeronautics and Space Administration. Ames Research Center, Moffett Field, Calif.
SEXTANT SIGHTING MEASUREMENTS FROM ON BOARD THE GEMINI 12 SPACECRAFT
Donald W. Smith and Bedford A. Lampkin Washington Dec. 1968 30 p refs
(NASA-TN-D-4952) Avail: CFSTI CSCL 17G

21 NAVIGATION

The capability of a spacecraft navigator to make in-flight navigation measurements from on board the spacecraft using a hand-held sextant has been studied extensively. Tests on board the orbiting Gemini 12 spacecraft were designed to determine the effect of the actual spaceflight environment on navigator performance. The results show that: (1) hand-held sextant measurement performance is excellent providing a standard deviation of measurement error less than 10 arc seconds; (2) spacecraft rotational motion and the actual spacecraft environment had little effect on the navigator performance; and (3) window-induced measurement errors in the Gemini 12 spacecraft were small and predictable. The optical hand-held sextant appears to have application to on-board navigation for future manned space flights. Author

N69-14346*# National Aeronautics and Space Administration. Langley Research Center, Langley Station, Va.

INFRARED HORIZON PROFILES FOR WINTER CONDITIONS FROM PROJECT SCANNER

Ruth I. Whitman, Thomas B. Mc Kee and Richard E. Davis Washington Dec. 1968 127 p refs

(NASA-TN-D-4905) Avail: CFSTI CSCL 17G

Measured horizon radiance profiles in spectral bands of 615 cm^{-1} to 715 cm^{-1} (carbon dioxide) and 315 cm^{-1} to 475 cm^{-1} (rotational water vapor) from the Project Scanner flight of December 10, 1966 are shown. Data cover a latitude range from 13° North to 61° North. Excellent agreement between the measured and independently predicted radiance profiles in the CO_2 band where horizontal temperature gradients are small verifies the analytical technique. When the horizontal temperature gradients are large, the computational model used is inadequate for predicting radiance profiles. Seasonal and latitudinal variations in radiance profiles are shown to be primarily a function of the variations in temperature structures. In the 315 cm^{-1} to 475 cm^{-1} (H_2O) region, mixing ratios of water vapor were deduced at low latitudes from the radiance measurements. Under both summer and winter meteorological conditions, the same trends in the mixing ratio above the tropopause are evident, that is, a region of relatively constant mixing ratio followed by a region of increasing mixing ratio. Author

N69-14382*# National Aeronautics and Space Administration. Lewis Research Center, Cleveland, Ohio.

SIMULATION STUDIES OF THE SUPERSONIC TRANSPORT IN FUTURE AIR TRAFFIC CONTROL SYSTEMS

Richard H. Sawyer, Norman S. Silsby, and Milton D. Mc Laughlin Washington Dec. 1968 90 p refs

(NASA-TN-D-4944) Avail: CFSTI CSCL 17G

The problems anticipated for the supersonic transport (SST) in operations in simulated Air Traffic Control (ATC) systems were studied in real time by using an SST aircraft flight simulator and the Federal Aviation Administration ATC simulation facilities. Airline crews operated the SST flight simulator, and experienced air-traffic controllers operated at ATC simulation facilities. Design-study configurations of the SST were used in the tests. The test program consisted of departures and arrivals under weather conditions which required operations by FAA Instrument Flight Rules in the New York, Los Angeles, San Francisco, and London terminal areas. For the future ATC system concepts investigated, substantial changes in course (up to nearly 50°) at supersonic speeds were required in many instances on the airway routes and to effect transition to and from the high-altitude track systems. Such changes were detrimental to SST performance and increased the workload for the crew. Further, substantial amounts of maneuver fuel were required for complying with ATC flight-path restrictions and for following indirect routings along the airways and to and from the high-altitude track systems. Author

N69-14399*# National Aeronautics and Space Administration. Ames Research Center, Moffett Field, Calif.

MINIMUM THRUST FOR CORRECTING KEPLERIAN ORBITS WITH APPLICATION TO INTERPLANETARY GUIDANCE

Frederick W. Boltz Washington Dec. 1968 69 p refs

(NASA-TN-D-4945) Avail: CFSTI CSCL 22C

The first-order thrust requirements obtained in the analysis are presented in terms of the optimum thrust angle and the minimum derivative of thrust-produced velocity impulse with respect to the particular orbital parameter to be corrected. Minimum thrust requirements are found for correction at a given point along an orbit of the semimajor axis, the eccentricity, and the true anomaly or orientation of the line of apsides (argument of pericenter) within the orbital plane. Minimum thrust requirements are also found for correcting the orbital radius at an arbitrary point and the elapsed flight time to arrive at that point. In addition, thrust requirements are obtained for correction at a given point along an orbit of the elapsed flight time to a second arbitrary point having a fixed value of orbital radius. A general formulation of the thrust requirements for simultaneous correction of any pair of the orbital parameters that define the in-plane motion is presented in terms of the minimum thrust requirements for correction of each of the parameters separately. Author

N69-16503*# National Aeronautics and Space Administration. Manned Spacecraft Center, Houston, Tex.

PLANETARY PROBE GUIDANCE ACCURACY INFLUENCE FACTORS FOR CONJUNCTION-CLASS MISSIONS

Thomas B. Murtagh Washington Jan. 1969 42 p refs

(NASA-TN-D-4852) Avail: CFSTI CSCL 22C

The influence of spacecraft onboard radar data type and accuracy, of nominal entry trajectory parameters, and of planet radius uncertainty for unmanned planetary probe guidance is presented for a typical conjunction-class mission. The results of the analysis indicate that a probe guidance corridor on the order of 24 nautical miles can be obtained for a total midcourse velocity requirement less than 100 fps. The corridor results were more sensitive to variations in the nominal entry trajectory parameters than to variations in the assumed error in the radius of the target planet. Author

N69-17780*# National Aeronautics and Space Administration. Ames Research Center, Moffett Field, Calif.

SECOND ORDER ERRORS IN LINEARIZED VELOCITY CORRECTIONS AND THEIR EFFECTS ON THE RATE OF CONVERGENCE OF ITERATIVE SOLUTIONS

John D. McLean Washington Feb. 1969 37 p refs

(NASA-TN-D-5037) Avail: CFSTI CSCL 17G

Two methods of computing linearized corrections are considered. The first, referred to as the linear method, computes the velocity correction as a linear function of position and velocity deviations at the time of the correction. The second method, referred to as the half-linear method, computes the trajectory ahead to the terminal time and then determines velocity correction as a linear function of the actual terminal error. The linear and half-linear guidance laws are presented together with formulas for predicting the errors in them caused by nonlinearity. These formulas are based on the assumption that the errors are adequately represented by second-order terms. Second-order errors are presented for both guidance methods on conic trajectories with eccentricities of 0.2, 0.98, and 2.0, and the errors for the two guidance methods are compared. A simulated lunar mission is used as an example to show how the data from the conic trajectories can be used to give a qualitative idea of the relative performance of the linear and half-linear methods on an n-body trajectory. The relative advantage of using the linear or half-linear method to compute the first velocity correction when iteration is used to reduce the residual error is investigated. Also, the effect of neglecting perturbing forces in calculating the state transition matrix is considered. Author

N69-17788*# National Aeronautics and Space Administration, Washington, D. C.
AIRCRAFT NAVIGATION
S. S. Fedchin et al Feb. 1969 570 p Transl. into ENGLISH of the book "Samoletovozhdeniye" Moscow, Transp., 1966
(NASA-TT-F-524) Avail: CFSTI CSCL 17G

The theory and practice of aircraft navigation at the modern level of aviation technology are summarized in this book; the most important practical problems of the utilization of general, radio engineering, and astronomical means of aircraft navigation are set forth; the procedure of the pilot's preparation for flight, the means of calculating the distance and duration of a flight, and the carrying out of prelanding maneuvering and landing of the aircraft under complex meteorological conditions during the day or at night are elucidated. The basic material of the book, sufficient for the practical mastery of the means and methods of aircraft navigation, is presented with the application of mathematics within the limits of a secondary school course. The problems which are necessary for a deeper study of the material are discussed in terms of principles of higher mathematics. The book is intended for pilots and navigators. It can be used as a textbook for students of civil aviation educational institutions. Author

N69-19518*# National Aeronautics and Space Administration, Washington, D. C.
GUIDANCE AND NAVIGATION FOR ENTRY VEHICLES
Nov. 1968 47 p refs
(NASA-SP-8015) Avail: CFSTI CSCL 17G

The scope of this document is limited to the atmospheric entry phase of flight for vehicles with maximum L/D ratios less than 1.5. The end of entry is assumed to occur at 100,000 feet for horizontal landing vehicles, and at deployment of the terminal landing system (parachute, paraglider, etc.) for low L/D vehicles. Some discussion of the deorbit maneuver as it affects the entry G&N function is included, but detailed aspects of retrofire for deorbit will be covered in a separate monograph dealing with thrusting maneuvers in space. The entry G&N system is primarily concerned with the motion of the vehicle center of mass along a desired flightpath. It is closely coupled with the entry stabilization and control (S&C) system which is concerned with vehicle attitude motions about the center of mass. The S&C problem for Earth entry is the subject of another monograph. Author

N69-20936*# National Aeronautics and Space Administration. Langley Research Center, Langley Station, Va.
FIXED-BASE VISUAL SIMULATION OF PILOT CONTROLLED DESCENTS OF AN ADVANCED APOLLO SPACECRAFT WITH AN ALL-FLEXIBLE PARAWING
G. Kimball Miller, Jr., Byron M. Jaquet, and Douglas B. Price Washington Mar. 1969 61 p refs
(NASA-TN-D-5049) Avail: CFSTI CSCL 17G

A fixed-base visual simulation study has been conducted to determine the ability of an onboard pilot to control an all-flexible parawing and an advanced Apollo capsule combination to preselected landing sites. The investigation employed a closed-circuit television system in conjunction with an earth-terrain model for image generation and permitted six rigid-body degrees of freedom of the vehicle. The pilot controlled the vehicle through the use of a hand controller which activated simulated constant-rate reels to induce rear keel-line changes for pitch control and differential wing-tip line changes for lateral control. The simulated viewing system provided the pilot with a field of view of 34.6° by 48.3°. The optical axis of the viewing system could be controlled in pitch to permit viewing anywhere between the local vertical and the local horizontal. The pilot's task was to assume command of the vehicle at altitudes up to 18000 feet (5486.4 meters) and control the vehicle to the center of a specified landing site under the influence of various wind profiles with maximum velocities up to 27 ft/sec (8.2 m/sec). The results of the investigation showed that the pilots could consistently land within about 1400 feet (426.7 meters) of the center of the desired site regardless of the wind conditions or instrumentation employed. Author

N69-21402*# National Aeronautics and Space Administration. Electronics Research Center, Cambridge, Mass.
DIRECTION COSINE COMPUTATIONAL ERROR
John W. Jordan Washington Mar. 1969 104 p refs
(NASA-TR-R-304) Avail: CFSTI CSCL 17G

Strapdown inertial systems possess a potential advantage over more conventional inertial systems since they do not require a mechanical gimbal structure to maintain a stable coordinate reference. Instead, strapdown systems replace the gimbal structure by a direction cosine matrix which is contained in and updated by the system computer. To assess the performance of a strapdown system or to determine the computer requirements, a detailed study of the computational error introduced by the computer is necessary. This report is concerned with the techniques which may be employed to estimate the computational error and its effects on system performance. Although focused upon a particular problem of practical importance, many of the techniques have a wider applicability to aerospace software in general. Author

N69-21502*# Bendix Corp., Teterboro, N.J.
DESIGN AND DEVELOPMENT OF A MULTIPURPOSE, BORESIGHTED STAR TRACKER
George V. Zito and E. A. Chilton Washington NASA Mar. 1969 117 p refs
(Contract NAS5-3780)
(NASA-CR-976) Avail: CFSTI CSCL 17G

The multipurpose star tracker contains several novel features: (1) the Channeltron ® image dissector which replaces the plurality of dynodes required by conventional photomultipliers with a single continuous strip electron multiplier; (2) a scanning system in which a multi-lobed scan serves for both acquisition and tracking in a single mode, automatically generating proportional and saturated zones; (3) the use of magneto-resistive bridge multipliers as modulators; and (4) microcircuited timing and demodulator circuits. It will track navigational stars and the center of illumination of the planets Mars, Venus, and Mercury. It will track the brighter of two stars within its 8 degree field of view provided the star is brighter than one visual magnitude and separated from other stars by at least 50 minutes of arc. The completed tracker weighs only 5 lbs and requires 4.65 watts of power. The prototype unit and the flight unit have been supplied with alternate mounting configurations to satisfy a wide range of applications.

N69-22936*# National Aeronautics and Space Administration. Ames Research Center, Moffett Field, Calif.
SIMULATION STUDIES FOR PLANNING AN IN-FLIGHT EXPERIMENT TO DEFINE MANUAL GUIDANCE AND CONTROL TECHNIQUES FOR LARGE LAUNCH VEHICLES
De Lamar M. Watson, Gordon H. Hardy, and Glenn W. Stinnett Washington Apr. 1969 32 p refs
(NASA-TN-D-5150) Avail: CFSTI CSCL 17G

The simulator program described was undertaken to define an in-flight experiment to evaluate manual control system concepts for Saturn class launch vehicles. The techniques and manual control system configurations developed in earlier studies were adapted to the uprated Saturn I, which was the vehicle chosen for the experiment. Discussions of the vehicle and manual control system configuration, the handling qualities, and two manual guidance display schemes are presented. An assessment is made of the impact of the proposed experiment on mission reliability. Author

21 NAVIGATION

N69-22969*# National Aeronautics and Space Administration. Langley Research Center, Langley Station, Va.

NIGHT SKY BACKGROUND CONDITIONS AND LAUNCH WINDOWS FOR RESEARCH EXPERIMENTS

Jean C. Keating Washington Apr. 1969 32 p refs

(NASA-TM-X-1772) Avail: CFSTI CSCL 17G

Darkness of the night sky background is required by many research experiments during various portions of their flight. A method was originally developed for the Trailblazer series to define launch windows that coincide with periods during which the brightness of the night sky background results solely from the illumination produced by the myriad of stars. Since this same method has proved useful to many other experiments as well, a general description of the method and the computer program developed to determine such launch windows are discussed. For any location between latitudes 60°N and 60°S, such times of launch may be determined to an accuracy of 2 minutes. Author

N69-22996*# National Aeronautics and Space Administration. Ames Research Center, Moffett Field, Calif.

EVALUATION OF A PILOT DESCRIBING FUNCTION METHOD APPLIED TO THE MANUAL CONTROL ANALYSIS OF A LARGE FLEXIBLE BOOSTER

Dallas G. Denery and Brent Y. Creer Washington Apr. 1969 26 p refs

(NASA-TN-D-5149) Avail: CFSTI CSCL 17G

In the pilot describing function technique of manual control analysis, the pilot is represented by a linear describing function and a statistically described remnant. The remnant accounts for that part of the pilot output not linearly correlated with the input. The technique was pioneered in work on manual control of rigid vehicles and has resulted in a catalog of pilot describing functions and remnant data applicable to certain pilot tasks. In this report, the method is evaluated for use in analyzing the pilot control of a large flexible booster. There are two phases in the present investigation. In the first, the pilot describing function method is evaluated when applied to the analysis of pilot control of an uncompensated booster. A piloted flight simulator is used and the pilot describing function, remnant and performance opinion ratings are measured. In the second phase, the pilot describing function method is evaluated when used to define a compensation system for the flexible booster. Pilot opinion ratings measured for this compensating system, using a flight simulator, are compared with ratings estimated using the pilot describing function method. Author

N69-26195*# National Aeronautics and Space Administration. Langley Research Center, Langley Station, Va.

AN ANALYSIS OF TERRAIN BIAS ERROR IN PLANETARY RADAR ALTIMETERS

Richard F. Harrington and William D. Stanley Washington May 1969 39 p refs

(NASA-TN-D-5220) Avail: CFSTI

Terrain bias error in a pulse modulated radar altimeter with an omnidirectional antenna and a leading-edge range tracker was analyzed for planetary applications. The backscatter function of Muhleman was used as the radar cross section model. An impulse response was first derived as a basis for determining arbitrary pulse returns by linear systems techniques. An ideal square pulse was assumed for the transmitted pulse, and a computer program was developed for generating pulse returns. An ideal bandwidth-limited receiver was then simulated on the computer and used to filter the pulse returns. The position of the received pulse leading edge was defined as the time of the 50 percent amplitude point of the pulse. In order to assess the measurable error resulting from the pulse returns, an ideal square pulse was used as an input to the receiver simulation program. The position of the leading edge of the ideal square pulse after filtering was compared with that calculated from the pulse return. Results indicated that terrain bias error varies only slightly with filter type and number of poles, is approximately constant for bandwidths greater than one-half the reciprocal of the pulsewidth, but increases significantly as the bandwidth is decreased, and is directly proportional to pulsewidth. Author

N69-26232*# Michigan Univ., Ann Arbor.

COMPUTER MECHANIZATION OF SIX-DEGREE OF FREEDOM FLIGHT EQUATIONS

L. E. Fogarty and R. M. Howe Washington NASA May 1969 27 p refs

(Contract NASr-54(06))

(NASA-CR-1344) Avail: CFSTI CSCL 17G

Solution of the six degree of freedom flight equations for aircraft and missiles continues to represent one of the most important application areas for analog, hybrid, and digital computer systems. Important computer requirements such as accuracy and speed are dependent very much on the choice of axis system for the translation equations of motion. In this connection it is well known that the flight-path axis system makes much lower accuracy and speed demands on the computer than does the body-axis system. Despite this a number of current computer mechanizations continue to use body axes for solving the translational equations of motion. Because of this, unnecessary demands of accuracy or frequency response are placed on the computer and many mechanizations which could be all analog or all digital have shifted to hybrid implementation. The advantages of flight path axes are pointed out and the overall equation requirements for solving the six-degree of freedom flight equations are summarized. Author

N69-27268*# National Aeronautics and Space Administration. Goddard Space Flight Center, Greenbelt, Md.

EXPLORER 35 ATTITUDE CONTROL SYSTEM

J. V. Fedor, T. W. Flatley, M. F. Federline, and J. R. Metzger Washington Jun. 1969 28 p

(NASA-TN-D-5187) Avail: CFSTI CSCL 17G

This report deals with background history, system description, system operation, maneuvering concept and theory, gas bearing testing, and preliminary flight performance of the attitude control system used on the AIMP E spacecraft (Explorer 35), launched July 19, 1967. Author

N69-28018*# National Aeronautics and Space Administration. Ames Research Center, Moffett Field, Calif.

A DETAILED STUDY OF MANUAL BACKUP CONTROL SYSTEMS FOR THE SATURN V LAUNCH VEHICLE

Gordon H. Hardy, Richard L. Kurrowski, Ronald M. Gerdes, Glen W. Stinnett, and Glen D. Ritter (NASA. Marshall Space Flight Center)

Washington Jun. 1969 58 p refs

(NASA-TN-D-5261) Avail: CFSTI CSCL 17G

A detailed study was made of manual backup control systems suitable for the first stage of the Saturn 5 launch vehicle. A technique to measure the manual control system reliability with a piloted simulator was developed. Two manual backup control systems were considered: a load relief and a no load relief system. Both systems allowed the pilot to close an adaptive control loop that is parallel to the primary automatic control system. The system failure modes associated with the primary system, as well as those associated with the additional hardware for the piloted backup system, were considered. An analog piloted simulation was used and included rigid-body, engine-actuator, vehicle-bending, propellant-sloshing, and control-system dynamics. Over a thousand simulated flights with randomly selected failures were made with three research pilots. The results indicate that for the failure modes and automatic system considered, the piloted manual backup system can reduce the probability of mission failure by a factor of 2. Trajectory dispersions at first-stage cutoff were significantly reduced. The hand-controller and pressure-suit configurations had little effect on system performance. Author

N69-29595*# National Aeronautics and Space Administration. Langley Research Center, Langley Station, Va.
LOW-SPEED DEPLOYMENT, INFLATION, AND STEADY-DESCENT CHARACTERISTICS OF RAM-AIR-INFLATED BALLOON RECOVERY SYSTEMS WITH PERIPHERAL AIRSCOOP
Sanger M. Burk, Jr. Washington Jun. 1969 24 p refs Film supplement number L-1048 to this report is available on loan from NASA. Langley Research Center, Langley Station, Va.
(NASA-TN-D-5186) Avail: CFSTI CSCL 01A

A free-flight investigation at low subsonic speeds has been conducted in a 20-foot vertical tunnel on several 6.0-foot-diameter ram-air-inflated balloons with various numbers and locations of peripheral airscoops to determine the deployment, inflation, and steady-descent characteristics of this type of recovery system. The configurations consisted of balloons constructed with 6, 12, and 24 gores with airscoops in each gore. Some of the balloons also were equipped with an open throat to provide additional inlet area. The results of the investigation indicated that the altitude loss during deployment and inflation, and the inflation time of the balloon decreased as the total airscoop area of the balloons increased. The balloons however reached their final drag coefficient and rate of descent considerably before they became completely inflated; and in some instances, balloons with a smaller airscoop area achieved their final drag coefficient and finaly steady-state rate of descent with less altitude loss than balloons with a greater airscoop area. Location of the airscoops higher on the balloon, up to a point somewhat above the maximum diameter, produced a more rapid inflation and less altitude loss. Also, the use of an open throat together with peripheral airscoops increased the balloon inflation rate somewhat and reduced the altitude loss. Author

N69-29967*# Stanford Univ., Calif.
ANALYSIS OF OSCILLATIONS IN PULSE-MODULATED SATELLITE ATTITUDE CONTROL SYSTEMS
Robert Newhall Clark Washington NASA Jul. 1969 108 p refs
(Grant NGR-05-020-007)
(NASA-CR-1369; SUDAAR-361) Avail: CFSTI CSCL 22B

This study reveals the relationship between the physical parameters and the principal limit cycle oscillation of a pulse-modulated feedback system of the type used for attitude control in satellites. The pulse actuation used in this sytem implies there will be a limit cycle oscillation about the equilibrium point. A two-pulse limit cycle is the most efficient and most accurate one possible. Tn integral-pulse-frequency modulator is established as having the requisite steady-state dynamic characteristics for the existence of the two-pulse limit cycle. The stability of the limit cycle is then determined from a transient analysis of the system, using a method based on the geometrical properties of the state transition equations. Previously, stability analysis of this nature has been approached using Lyapunov-like methods or conventional frequency domain techniques. The conditions under which four-pulse, six-pulse, and higher order limit cycle oscillations can occur are also determined, and their existence is verified experimentally, using digital simulation. Author

N69-30946*# National Aeronautics and Space Administration. Flight Research Center, Edwards, Calif.
FLIGHT INVESTIGATION OF A FLUIDIC AUTOPILOT SYSTEM
Wilton P. Lock and Shu W. Gee Washington Jul. 1969 32 p refs
(NASA-TN-D-5298) Avail: CFSTI CSCL 17G

A flight investigation was made of an experimental fluidic flight control system capable of various modes of operation, including altitude hold, heading hold, wings leveler, and turn control. The fluidic control system was tested in each mode at two flight conditions: cruise at 5000 feet, and cruise at 10,000 feet. Although stability problems were encountered early in the program, stable performance was achieved in each control mode for the flight conditions tested. High reliability was demonstrated, in that there were no failures with the fluidic elements themselves. Failures were experienced, however, with the mechanical portion of the mechanical fluidic components. Flight investigation revealed a number of areas in which improvement is needed before the system can be considered operational. Aircraft altitude changes caused noticeable changes in the null of the fluidic components, and gain reduction with increased altitude was experienced with sensors and amplifiers. Author

N69-31227*# National Aeronautics and Space Administration. Ames Research Center, Moffett Field, Calif.
METHODS FOR PREDICTING SPACECRAFT-WINDOW-INDUCED LINE-OF-SIGHT DEVIATIONS
Kenneth C. White and Burnett L. Gadeberg Washington Jul. 1969 34 p refs
(NASA-TN-D-5238) Avail: CFSTI CSCL 17G

Methods have been developed for predicting angular line-of-sight deviations induced by spacecraft windows. The description of the window surface shape requires an accurate knowledge of the flatness distribution over the whole window surface, the parallelism between the surfaces of the window, and the surface deformation due to pressure loading. The window surface flatness distribution and the parallelism between surfaces are determined from interference photographs of the window. Pressure deformations of windows with known edge support conditions are computed by means of known analytical solutions or a finite element structural analysis computer program. Pressure deformations of windows with unknown edge conditions are determined experimentally from interference photographs of the window surfaces. The prediction methods were used to compute the line-of-sight (LOS) deviations for a Gemini spacecraft window. The computed LOS deviations were compared with experimentally measured LOS deviations to assess the validity of the methods developed. A detailed statistical analysis of the differences between computed and experimentally measured data indicated that the results agreed to within 2 arcsec mean difference and 4 arcsec standard deviation. Author

N69-34672*# Analytic Sciences Corp., Reading, Mass.
DESIGN OF STRAPDOWN GYROSCOPES FOR A DYNAMIC ENVIRONMENT Interim Scientific Report
Arthur A. Sutherland, Jr. and William S. Beebee Washington NASA Aug. 1969 186 p refs
(Contract NAS12-508)
(NASA-CR-1396; TR-101-4; ISR-2) Avail: CFSTI CSCL 17G

Some aspects of the analysis of vibration-induced attitude errors in strapdown inertial navigators are discussed. Three common pulse torquing techniques for strapdown gyros are described. The important considerations in choosing a rebalance scheme are reviewed and relative advantages of the three approaches are discussed. Binary and ternary pulse rebalanced gyros are analyzed using describing functions. Closed loop sinusoidal transfer characteristics are obtained analytically and compared with the results of detailed gyro simulations. The effects of compliance between the gyro wheel and gimbal are also illustrated by analysis and simulation. Compensation of limit cycling binary torqued gyros is treated with the goal of providing a better closed loop response. A discussion of the dithered binary gyro is presented, illustrating limit cycle determination and closed loop characteristics. The appendices provide details in support of the report body and also treat diverse subjects such as dynamic errors in single-degree-of-freedom pendulous accelerometers, gyro misalignment caused by angular rates about the output axis and the recovery of angular rate information from pulse torqued gyros. Author

N69-36997*# National Aeronautics and Space Administration. Electronics Research Center, Cambridge, Mass.

21 NAVIGATION

AN ACCURATE STRAPDOWN DIRECTION COSINE ALGORITHM

John W. Jordan Washington Sep. 1969 16 p refs
(NASA-TM-D-5384) Avail: CFSTI CSCL 17G

This report presents an efficient algorithm for calculating the direction cosines of a strapdown inertial system. It is suitable for calculation on a general purpose digital computer; it includes a correction for commutativity error, and has no truncation error. Simulation results are included. Author

N69-38041*# Ohio State Univ., Columbus, Ohio.
TECHNIQUES FOR GENERATION OF CONTROL AND GUIDANCE SIGNALS DERIVED FROM OPTICAL FIELDS

H. Hemami, M. B. Kuhner, and L. T. Bashark Washington NASA Oct. 1969 72 p refs
(Grant NGR-36-008-076)
(NASA-CR-1443; RF-2421) Avail: CFSTI CSCL 17G

A general transfer functional is derived for optical systems that relates the image intensity to the spatial autocorrelation of the aperture and temporal autocorrelation of the received signals. A simple method of detection of star images by cross-correlation techniques is developed. This cross-correlation requires certain image density characteristics that can be constructed by appropriate prefiltering of the signals. Synthesis of a class of such filters is carried out in a sequence of experiments, and the feasibility and performance of the filters are discussed. Two methods of estimating the position of the star image are developed and their implications discussed. One method is based on generalized mean square error criterion and requires prefiltering and full knowledge of the star image intensity. For the second method partial knowledge about the star image is sufficient. Author

N69-40055*# National Aeronautics and Space Administration. Langley Research Center, Langley Station, Va.
A LIMB RADIANCE CALCULATION APPROACH FOR MODEL ATMOSPHERES CONTAINING HORIZONTAL GRADIENTS OF TEMPERATURE AND PRESSURE

Richard E. Davis Washington. Oct. 1969 37 p refs
(NASA-TN-D-5495) Avail: CFSTI CSCL 17G

A method is developed, using a numerical limb radiance computational model for the 14- to 16-micron CO_2 band, that accounts for the fact that real atmospheres strictly never show the spherically symmetric temperature and pressure stratification that is normally assumed in the calculations of limb radiance. Equations incorporating the effects of horizontal gradients are given, and tests performed with a modified numerical radiance computational program are described. Some examples of the application of the method are given. An improvement in the computational accuracy is achieved by the new method. This result is significant under winter conditions when strong latitudinal temperature gradients exist in the middle and polar latitudes. Author

N69-41036*# Stanford Univ., Calif.
MINIMUM FUEL ATTITUDE CONTROL OF A NONLINEAR SATELLITE SYSTEM WITH BOUNDED CONTROL BY A METHOD BASED ON LINEAR PROGRAMMING

Gary D. Wolske and I. Fluegge-Lotz Washington NASA Oct. 1969 108 p refs
(Grant NGR-05-020-007)
(NASA-CR-1450; SUDAAR 374) Avail: CFSTI CSCL 17G

Fuel optimal controls are computed for the large angle attitude motions of a satellite system in which the control is obtained by three sets of gas jets with bounded thrusts, each generating torques about one of the principal axes of inertia. Using a result from optimal control theory, an algorithm is developed that iteratively improves on an initial guess (nominal) for the control history which does not meet terminal constraints and/or does not minimize the fuel cost. In using the algorithm, which is based on linear programming, it is necessary to express the variation of the fuel cost and variations of the components of the terminal state constraint vector as linear functions of variations in the control. The algorithm is tested on two sets of satellite differential equations. In one case, all dynamical effects are considered. In the other case, because control torque bounds are large enough, it is possible to neglect gravity gradient torque effects and orbital motion effects. A method to recursively approach minimum time control solutions by using this minimum fuel algorithm is described and illustrated. Author

22

NUCLEAR ENGINEERING

Includes nuclear reactors and nuclear heat sources used for propulsion and auxiliary power. For basic research see: 24 Physics, Atomic, Molecular, and Nuclear. For related information see also: 03 Auxiliary Systems; and 28 Propulsion Systems.

A69-13128 *#
SIGNIFICANT EXPERIENCES OF THE NASA PLUM BROOK REACTOR FACILITY.
H. B. Barkley, Jr. (NASA, Lewis Research Center, Cleveland, Ohio).
American Nuclear Society, Winter Meeting, Washington, D.C., Nov. 11-16, 1968, Paper. 34 p. 5 refs.

Description of the purposes and experimental programs of the NASA Plum Brook Reactor Facility (PBRF) at Sandusky, Ohio. The purposes of the reactor facilities are to determine the tolerance of specimens to radiation in a nuclear radiation environment, the nature and the cause of radiation-induced changes in the specimens, and methods of increasing their radiation tolerance. The experiments support the application of nuclear power to space for power and propulsion. The experimental program conducted at PBRF is outlined, the represented facilities and experiment-oriented accomplishments are summarized, and several significant problems which have been encountered and solved are discussed. P.v.T.

A69-13131 *#
EXPERIENCES WITH BERYLLIUM SWELLING AND REPLACEMENT IN THE PLUM BROOK REACTOR.
William Fecych (NASA, Lewis Research Center, Sandusky, Ohio).
American Nuclear Society, Winter Meeting, Washington, D.C., Nov. 11-16, 1968, Paper. 22 p.

A description is given of problems encountered from distortion and failure of major reactor core components in the high neutron fluence regions of the Plum Brook Reactor. Reactor material surveillance programs, the failure mode of the components, component replacement methods, associated health hazards, and the distortion of components against neutron fluence are described. (Author)

A69-14799 *
A NUCLEAR THERMIONIC SPACE POWER CONCEPT USING ROD CONTROL AND HEAT PIPES.
John L. Anderson and Edward Lantz (NASA, Lewis Research Center, Cleveland, Ohio).
Nuclear Applications, vol. 5, Dec. 1968, p. 424-436. 17 refs.

A nuclear reactor space power system using out-of-pile thermionic diodes, heat pipes, and a dual central absorber rod type of reactivity control has been studied. Emphasis is placed on the neutronic aspects and general feasibility of the concept. Comparison is made between uranium-233 and -235 nitride and plutonium-239 nitride fuels. From a neutronic standpoint, plutonium-239 nitride is found to be a slightly better fuel than uranium-233 nitride for this fast-spectrum reactor. In this concept, heat is transferred from the reactor core to the thermionic diodes by layers of radial heat pipes stacked alternately with slabs of fuel. For this out-of-pile concept, which would supply ~130 kW(e), the reactor can be considerably smaller than the equivalent reactor with in-pile diodes. (Author)

A69-18825 *
GAMMA HEATING IN THIN HEAVY-ELEMENT ABSORBERS.
John H. Lynch, Richard J. Crum, and Harry J. Reilly (NASA, Lewis Research Center, Cleveland, Ohio).
Nuclear Applications, vol. 5, Dec. 1968, p. 456-463. 12 refs.

The ratio of gamma heating in tungsten to that in an equal volume of water is calculated for the case of a thin tungsten detector in a water shield. One-dimensional transport-theory calculations yielded response polynomials that predict this ratio as a function of source energy, shield thickness, and detector thickness. Electron transport effects and useful results are presented in the form of graphs. (Author)

A69-18954 *
CAVITY REACTOR CRITICAL EXPERIMENTS.
J. F. Kunze, G. D. Pincock (General Electric Co., Idaho Falls, Idaho), and R. E. Hyland (NASA, Lewis Research Center, Cleveland, Ohio).
Nuclear Applications, vol. 6, Feb. 1969, p. 104-115. 18 refs.
NASA-sponsored research.

The cavity reactor concept consists of a core, generally of dilute fuel, surrounded by a moderating reflector. This concept has long been considered as a means of attaining very high temperatures in a gaseous core, since the fuel need not be in contact with structural material. A number of critical experiments have been performed on configurations of different core size and shape, different structural material thicknesses between the cavity and reflector, different coolant densities surrounding the core, and with various other alterations. The principal purpose was to evaluate the effects of engineering design variables for a cavity propulsion reactor concept. Experiments reveal that a power reactor with the required structure and a cavity size of 182.9 cm in diameter by 121.9 cm long can be expected to have a critical core loading of between 20 and 30 kg of ^{235}U. (Author)

A69-21249 *#
A METHOD FOR OBTAINING PERFORMANCE BOUNDARIES OF COMPLETE SPACE PROPULSION SYSTEMS CONTAINING NUCLEAR-ELECTRIC STAGES.
Federico G. Casal (NASA, Ames Research Center and Office of Advanced Research and Technology, Mission Analysis Div., Moffett Field, Calif.).
American Institute of Aeronautics and Astronautics, Electric Propulsion Conference, 7th, Williamsburg, Va., Mar. 3-5, 1969, Paper 69-249. 6 p. 8 refs.
Members, $1.00; nonmembers, $1.50.

Discussion of a method for comparing the performances of space propulsion systems of widely differing characteristics. Biased comparisons can be avoided by systematically arranging and selecting the ground rules of the comparison before they are fed into the analysis. Meaningful results can be obtained in spite of the large range of uncertainties attached to some of the performance parameters by adopting the use of scaling laws which reflect major trends or other relationships of interest rather than scattered performance estimates. The method is not intended as a tool for economic analysis, although, under certain conditions, it is capable of furnishing insight into some first-order economic effects. G.R.

A69-31522 *
ADVANTAGES OF USING A COMBINATION ELECTROMAGNETIC AND MATERIAL SHIELD.
R. D. Shelton, H. E. Stern, and J. W. Watts (NASA, Marshall Space Flight Center, Huntsville, Ala.).
Nuclear Science and Engineering, vol. 36, June 1969, p. 304-308. 5 refs.

Method for calculation of the proton dose in a receiver behind a combination electromagnetic and material shield. Dose calculations for a typical Van Allen proton spectrum and three solar-proton-event spectra are presented. In general, the electromagnetic shield stops protons below a certain threshold energy and reduces the number and

energy of protons above this energy, and material shielding is more effective against these protons of reduced energy since proton stopping power increases with decreasing energy. (Author)

A69-32660 *#
APPLICATION OF NUCLEAR SOLID-CORE ROCKETS TO INTERPLANETARY ORBITAL LAUNCH BY MULTIORBIT INJECTION.
Jack Funk and Stewart F. McAdoo, Jr. (NASA, Manned Spacecraft Center, Houston, Tex.).
American Institute of Aeronautics and Astronautics, Propulsion Joint Specialist Conference, 5th, U.S. Air Force Academy, Colorado Springs, Colo., June 9-13, 1969, Paper 69-535. 6 p. 6 refs.
Members, $1.00; nonmembers, $1.50.

Evaluation of the performance of nuclear solid-core engines for orbital launch of spacecraft. An injection technique is presented that uses several thrusting subarcs near the perigee of intermediate orbits to accelerate the spacecraft to escape earth orbit. The performance of nuclear engines of different sizes is evaluated for orbital launch by multiorbit injection of spacecraft of initial gross weights of 1.5 to 2.25 million pounds. The effects of engine clustering and the number of intermediate orbits are considered. The results indicate that the 75,000-pound-thrust engine will outperform clustered or high-thrust engines, if more than four intermediate orbits are used. P.G.

A69-32728 *#
SOME RECENT GASEOUS REACTOR FLUID MECHANICS EXPERIMENTS.
Robert G. Ragsdale and Chester D. Lanzo (NASA, Lewis Research Center, Cleveland, Ohio).
American Institute of Aeronautics and Astronautics, Propulsion Joint Specialist Conference, 5th, U.S. Air Force Academy, Colorado Springs, Colo., June 9-13, 1969, Paper 69-477. 8 p. 7 refs.
Members, $1.00; nonmembers, $1.50.

Results of experiments performed on geometries that would be used in an open-cycle engine, indicating that it may be possible to reduce the uranium loss rate by a factor of 2 to 10 below that indicated by previous experiments. One of the experiments employed induction heating to simulate fission heating. A central stream of argon simulated the uranium of an engine, and hydrogen was flowed around it. Concentration measurements made with a probe show that heat addition eliminated a recirculation flow pattern that was present with cold flow. The new flow pattern had much less mixing or interaction between the two streams. The second experiment described used straight coaxial flow of two gas streams through a cylindrical test section. These tests used iodine-colored air to simulate the central uranium stream and clear air to simulate the outer hydrogen propellant. These tests were conducted at high, engine-simulating Reynolds numbers. Flow visualization has disclosed that injection of the two gas streams through a very porous, foamlike material eliminates a recirculation cell that previously occurred. The third experiment discussed examined the flow characteristics of a curved, porous wall cavity. In a two-dimensional mock-up of this concept, clear, propellant-simulating air was injected through the porous wall, and smoky, uranium-simulating air was injected through a shower-head injector at one end of the cavity. Both gases exited through a nozzle opening that opposed the fuel injection port. These tests show the existence of a large, relatively stagnant fuel region in the center of the cavity. Each of the experiments has disclosed a favorable flow characteristic. Enough information is now available to incorporate these three features into one test to evaluate their combined effect on projected gaseous reactor engine loss rates. (Author)

A69-32761 *#
STATUS OF THE NUCLEAR POWERED AIRPLANE.
Frank E. Rom (NASA, Lewis Research Center, Cleveland, Ohio).
American Institute of Aeronautics and Astronautics, Propulsion Joint Specialist Conference, 5th, U.S. Air Force Academy, Colorado Springs, Colo., June 9-13, 1969, Paper 69-554. 13 p. 10 refs.
Members, $1.00; nonmembers, $1.50.

Determination of the major obstacles to practical, safe, and economical nuclear power plants for aircraft, and summary of the results of limited analytical and experimental efforts made to assess the possibility of overcoming these obstacles. Some of the reasons why it is believed that nuclear aircraft are worth investigating, what the major obstacles are, the steps taken to overcome them, and the progress made to date are discussed. Some typical nuclear systems are described, and performance estimates are made. P.v.T.

A69-33483 *#
AN EXPERIMENT ON THE MHD-DRIVEN FLOW FOR A GAS CORE NUCLEAR ROCKET.
Wendell L. Love and Chul Park (NASA, Ames Research Center, Moffett Field, Calif.).
American Institute of Aeronautics and Astronautics, Fluid and Plasma Dynamics Conference, San Francisco, Calif., June 16-18, 1969, Paper 69-727. 14 p. 19 refs.
Members, $1.00; nonmembers, $1.50.

A fluid-dynamic simulation of a gas core nuclear rocket chamber has been made with the objective of separating a light and heavy gas by means of the centrifugal force produced by MHD-driven rotation. The test apparatus, a closed cylinder filled with a mixture of xenon and helium, uses a radial magnetic field configuration with an axial electric current passing between 16 pairs of electrodes. By observing the behavior of the discharge and the luminosity of the gas at different locations, the mode of discharge was found to be stable and suitable for effective separation. A rotating flow with transonic Mach number was produced, as evidenced by the ratio (greater than 2) of the pressure at the wall of the cylinder to that at the center. Spectroscopic measurements of the plasma condition show an appreciable degree of separation of the two species. The Hall parameter was found to be less than one. (Author)

A69-35178 *#
MONTE CARLO CALCULATIONS OF A HEMISPHERICAL DUCT NEUTRON STREAMING EXPERIMENT.
L. Clemons, G. N. Wrights, and D. Shook (NASA, Lewis Research Center, Cleveland, Ohio).
American Nuclear Society, Annual Meeting, 15th, Seattle, Wash., June 15-19, 1969, Paper. 11 p. 7 refs.

Investigation of the applicability of Monte Carlo calculations to neutron streaming problems. Two hemispherical air-filled-duct experiments were set up in a water tank. PuBe neutron sources of 5 and 10 curies, respectively, were positioned at the bottom of the duct. A 5 x 5 cm NE-213 liquid organic scintillator was used to measure the intensity and spectra of neutrons leaking from the top of the ducts. The Oak Ridge National Laboratory unfolding technique was used to obtain the neutron spectra. The experimental geometry was set up on the COHORT-II Monte Carlo shielding code, and the intensity and spectra of neutrons leaking from the ducts was calculated at point detectors. It is concluded that the application of the Monte Carlo method can provide valuable insight into the intensity of neutrons streaming through ducts in shields. The COHORT-II program has calculated neutron streaming for two hemispherical ducts that agree well with experimental measurements. P.G.

A69-35180 *#
PARAMETRIC STUDY OF LARGE NUCLEAR SURFACE EFFECTS MACHINES.
Albert F. Kascak (NASA, Lewis Research Center, Cleveland, Ohio).
American Nuclear Society, Annual Meeting, 15th, Seattle, Wash., June 15-19, 1969, Paper. 23 p.

Description of some performance estimates of a high-speed peripheral-jet nuclear-powered surface-effects machine. The calculations incorporate a recently proposed nuclear aircraft reactor concept; this high-temperature reactor reduces shield weight and eliminates the need for a heavy preheater. Payload fraction and reactor power are calculated for vehicle gross weights from 1000 to 5000 tons, forward velocities from 0 to 250 knots, and clearance heights from 10 to 50 feet. For these ranges, the payload varied from 0 to 60% of the gross weight, and the total reactor power varied from 400 to 10,000 MW. (Author)

A69-35181 *#
A FLOW EXPERIMENT ON A CURVED-POROUS-WALL GAS-CORE REACTOR GEOMETRY.
Chester D. Lanzo (NASA, Lewis Research Center, Cleveland, Ohio).
American Nuclear Society, Annual Meeting, 15th, Seattle, Wash., June 15-19, 1969, Paper. 12 p.

Results of an air-to-air experiment carried out to evaluate a new gas-core reactor flow pattern. The objective was to determine

the general character of the flow and to obtain some overall quantitative measurements of its potential for gas-core reactor application. The geometry tested was made up of a curved porous wall, through which the propellant (clear air) was introduced. The fuel (smoky air) was injected at one end of the cavity. Both gases exited through a subsonic port at the opposite end of the cavity. It is concluded that a relatively large, stagnant fuel volume forms in the reactor cavity for propellant-to-fuel flow-rate ratios as high as 100. Specifically, at this mass-flow-ratio, the effective fuel volume is about 28% of the total cavity volume. F. R. L.

A69-38274 *
MEASURED THERMAL-NEUTRON-FLUX PERTURBATIONS IN CYLINDERS IN A TEST REACTOR.
John H. Lynch and Lawrence E. Peters, Jr. (NASA, Lewis Research Center, Sandusky, Ohio).
Nuclear Applications and Technology, vol. 7, Aug. 1969, p. 128-138. 7 refs.

Description of a model for calculating the perturbation of the thermal-neutron flux by the test specimens in the design of irradiation experiments. A cylindrical shape was selected as being most representative of irradiation test specimens, and measurements of perturbation effects were made for several cylinders of different dimensions and materials. Regression analysis was used to obtain polynomials from these measurements, which can be used to predict the flux perturbation, depression, and self-shielding factors as functions of cylinder materials and dimensions, and control-rod position. B.H.

A69-39219 * #
THE NUCLEAR ROCKET PROGRAM—ITS STATUS AND PLANS.
L. C. Corrington (AEC-NASA, Space Nuclear Propulsion Office, Cleveland, Ohio).
(American Institute of Aeronautics and Astronautics, Propulsion Joint Specialist Conference, 4th, Cleveland, Ohio, June 10-14, 1968, Paper 68-610.)
Journal of Spacecraft and Rockets, vol. 6, Apr. 1969, p. 465-470. 12 refs.
(For abstract see issue 17, page 3211, Accession no. A68-33801)

A69-42266 *
STUDY OF A 300 kWe RANKINE CYCLE ADVANCED NUCLEAR-ELECTRIC SPACE POWER SYSTEM.
J. A. Heller, T. A. Moss, and G. J. Barna (NASA, Lewis Research Center, Cleveland, Ohio).
IN: AMERICAN INSTITUTE OF CHEMICAL ENGINEERS, INTERSOCIETY ENERGY CONVERSION ENGINEERING CONFERENCE, 4TH, WASHINGTON, D.C., SEPTEMBER 22-26, 1969, PROCEEDINGS. (A69-42236 23-03)
Conference co-sponsored by the American Institute of Aeronautics and Astronautics, the American Nuclear Society, the American Society of Mechanical Engineers, the American Chemical Society, the Institute of Electrical and Electronics Engineers, and the Society of Automotive Engineers.
New York, American Institute of Chemical Engineers, 1969, p. 465-483. 19 refs.

System analysis of a nominal 300 kWe potassium system employing a lithium cooled fast reactor and 2100 deg F turbine inlet. Trends in performance and weight are discussed for variations in design parameters. Performance and design of major components are reviewed, including material considerations. A typical conceptual system layout is shown. (Author)

N69-10067*# National Aeronautics and Space Administration. Lewis Research Center, Cleveland, Ohio.
NUCLEAR-ROCKET PROPULSION
Frank E. Rom Washington Nov. 1968 40 p refs
(NASA-TM-X-1685) Avail: CFSTI CSCL 21F

The three basic types of nuclear rocket powerplants (solid, liquid, and gas core) are compared. Solid core systems are expected to have specific impulses of 850 seconds with negligible fuel loss. The liquid core nuclear rocket will have a uranium loss rate of 0.01 to 0.1 mass unit per mass unit of hydrogen if specific impulses in the range of 1200 to 1500 seconds are desired. The gas core system will have similar loss rates of uranium but will produce specific impulses in the range of 1500 to 2500 seconds. Author

N69-10099*# National Aeronautics and Space Administration. Lewis Research Center, Cleveland, Ohio.
URANIUM DIOXIDE VENT LOSS IN AN EXTERNALLY FUELED THERMIONIC REACTOR CONCEPT
James J. Ward and Robert B. Ruch Washington Nov. 1968 21 p refs
(NASA-TN-D-4922) Avail: CFSTI CSCL 18J

An analysis of fuel losses through a fission gas vent in a nuclear thermionic reactor concept is presented. The converters are externally fueled with ceramic uranium dioxide (UO_2), and fuel losses during both steady-state operation and temperature excursions are estimated. Calculations were performed for element fuel-volume fractions of 0.275 and 0.55 with converter heat fluxes of 50 and 100 W/cm^2 at an emitter temperature of 2000°K. The absolute UO_2 loss during a temperature excursion and the ratio of UO_2 loss during an excursion to the yearly steady-state loss are presented as functions of time for each case. Author

N69-10216*# National Aeronautics and Space Administration. Lewis Research Center, Cleveland, Ohio.
ESTIMATION OF FISSION-PRODUCT GAS PRESSURE IN URANIUM DIOXIDE CERAMIC FUEL ELEMENTS
Walter A. Paulson and Roy H. Springborn Washington Nov. 1968 32 p refs
(NASA-TN-D-4823) Avail: CFSTI CSCL 18J

Fission-product gas pressure in macroscopic voids was calculated over the temperature range of 1000° to 2500°K for clad uranium dioxide fuel elements operating in a fast neutron spectrum. The calculated fission-product yields for uranium-233 and uranium-235 used in the pressure calculations were based on experimental data compiled from various sources. The contributions of cesium, rubidium, and other condensible fission products are included with those of the gases xenon and krypton. At low temperatures, xenon and krypton are the major contributors to the total pressure. At high temperatures, however, cesium and rubidium can make a considerable contribution to the total pressure. Author

N69-10734*# National Aeronautics and Space Administration. Lewis Research Center, Cleveland, Ohio.
CALCULATION OF FUEL LOSS FROM VENTED NUCLEAR FUEL ELEMENTS FOR SPACE POWER REACTORS
Richard E. Gluyas Washington Nov. 1968 40 p refs
(NASA-TN-D-4913) Avail: CFSTI CSCL 18L

The rate of loss of uranium dioxide (UO_2) or of uranium mononitride (UN) from cylindrical nuclear fuel elements which are vented to prevent buildup of high fission gas pressures has been calculated for various conditions. For 10,000 hr operation at a cladding temperature of 1400°C and venting to a vacuum, the maximum fuel temperature allowable for UO_2 is about 2000°C and for UN about 1800°C. These temperatures may be increased to about 2500° and 2600°C, respectively, by venting to an argon atmosphere containing enough oxygen or nitrogen to prevent decomposition of the fuels. Author

N69-13309*# National Aeronautics and Space Administration. Lewis Research Center, Cleveland, Ohio.
POINT DEFECT CALCULATIONS IN TUNGSTEN
Ronald L. Danilowicz Washington Dec. 1968 14 p refs
(NASA-TN-D-4918) Avail: CFSTI CSCL 20B

Calculations were made with a computer code developed for making point defect calculations in body centered cubic metals. A semi-empirical cubic potential based on experimental data was also developed for tungsten for these calculations. The vacancy

migration energy for tungsten was calculated. The calculated value of 1.73 electron volts, together with experimental data, suggests that vacancies migrate in stage 3 recovery in tungsten. The formation energies for six possible equilibrium interstitial configurations were also calculated. The ⟨110⟩ split interstitial was the most stable configuration for tungsten with a formation energy of 9.73 electron volts. Author

N69-14481*# National Aeronautics and Space Administration. Lewis Research Center, Cleveland, Ohio.
PREDICTIVE EQUATIONS FOR THERMAL NEUTRON FLUX PERTURBATION EFFECTS IN CYLINDERS
John H. Lynch and Lawrence E. Peters, Jr. Washington Dec. 1968 24 p refs
(NASA-TN-D-4949) Avail: CFSTI CSCL 18K

The thermal neutron flux perturbation, depression, and self-shielding factors were measured for several cylinders having different materials and dimensions. The measurements were done for the high-flux test positions of the Plum Brook Reactor. Results of these measurements were fitted to polynomials that can be used by designers of irradiation experiments to predict flux perturbation effects in test specimens. The experiment design, results, and uncertainty are discussed. The behavior of the perturbation factor around the experiment design center is also examined. Author

N69-14503*# National Aeronautics and Space Administration. Lewis Research Center, Cleveland, Ohio.
TRANSFER FUNCTIONS FOR RADIATOR DYNAMICS IN THE SNAP-8 SYSTEM
Robert W. Leko and Kent S. Jefferies Washington Dec. 1967 22 p refs
(NASA-TN-D-4946) Avail: CFSTI CSCL 18N

An analytical study was conducted to determine approximate radiator transfer functions for use in SNAP-8 ground test facilities. Theoretical equations for transient heat transfer and flow processes in the radiator were programmed on a digital computer. With this computer simulation, the frequency response of the radiator-outlet temperature was determined. Approximate transfer functions were determined from the frequency-response information. The transfer function determined for outlet temperature to inlet temperature was a single lag of third order cascaded with a dead-time function. The time constant and dead time were inversely proportional to flow rate. The simplified transfer function chosen to describe the response of outlet temperature to inlet flow rate was a first-order lag. The first-order lag time constant was in inverse proportion to the flow rate. Author

N69-16381*# National Aeronautics and Space Administration. Lewis Research Center, Cleveland, Ohio.
REACTIVITY CHANGES OF A FAST REACTOR CORE DUE TO ELASTIC-PLASTIC STRAIN AND CREEP
Richard L. Puthoff Washington Jan. 1969 39 p refs
(NASA-TN-D-5012) Avail: CFSTI CSCL 18J

An elastic–plastic and creep analysis which predicts the actual core movement during the reactor operation and determines corresponding reactivity change is presented. A transport code was used for determining core reactivity. A reference design is included to aid in applying the analysis. The design consists of a 12-inch (30.48-cm) core containing uranium dioxide fuel surrounded by a 4-inch thick tungsten reflector. A reactivity decrease of –$3.85 resulted during the heating period with further reactivity decreases of –$0.06 during the first 90 hours and –$0.05 between 90 and 2000 hours. Author

N69-17313*# National Aeronautics and Space Administration. Lewis Research Center, Cleveland, Ohio.
A 1-MEGAWATT REACTOR DESIGN FOR BRAYTON-CYCLE SPACE POWER APPLICATION. PART 1: THERMAL ANALYSIS AND CORE DESIGN
Charles L. Whitmarsh, Jr. and Paul T. Kerwin Washington Feb. 1969 45 p refs
(NASA-TN-D-5013) Avail: CFSTI CSCL 18L

Thermal–hydraulic calculations were performed for a 1-Mw gas-cooled reactor designed to retain all fission gases and to operate for 25,000 hours with a coolant outlet temperature of 1650°K. These data were combined with neutronics data in an effort to minimize core size. Parameters investigated were fuel-element configuration, fuel-cladding temperature, radial and axial power distributions, coolant inlet temperature, coolant pressure, and reactor pressure drop. Author

N69-17314*# National Aeronautics and Space Administration Lewis Research Center, Cleveland, Ohio.
A 1-MEGAWATT REACTOR DESIGN FOR BRAYTON-CYCLE SPACE POWER APPLICATION. PART 2: NEUTRONICS DESIGN
Charles L. Whitmarsh, Jr. and Paul T. Kerwin Washington Feb. 1969 33 p refs
(NASA-TN-D-5014) Avail: CFSTI CSCL 18L

General characteristics were determined for a gas-cooled reactor designed to operate at 1 Mw for 25,000 hours, with a coolant outlet temperature of 1650 K. Design curves relating core size to fuel concentration are presented as a function of radial power flattening. Author

N69-17701*# National Aeronautics and Space Administration. Lewis Research Center, Cleveland, Ohio.
EXPERIENCE WITH AND IMPROVEMENTS IN CONTAINMENT VESSEL PENETRATIONS
Charles W. Conant Washington Feb. 1969 19 p refs
(NASA-TM-X-1735) Avail: CFSTI CSCL 18J

Early containment vessel leak rate tests showed that potted electrical penetrations were a major contributor to the containment vessel leakage. This type of penetration was largely replaced with hermetic penetrations. Leak rate testing of the hermetic penetrations is done by the pressure decay method having a sensitivity better than 0.001 ft^3/day (2.8×10^{-5} m^3/day). The tests show that the average penetration leak rate is less than 0.003 ft^3/day (8.5×10^{-5} m^3/day). The use of hermetic penetrations has significantly reduced leakage through electrical penetrations, reduced maintenance, and reduced effort required to change cables penetrating the containment vessel. Author

N69-20795*# National Aeronautics and Space Administration. Lewis Research Center, Cleveland, Ohio.
USE OF TUNGSTEN-184 AS A THERMAL FLUX MONITOR AT HIGH TEMPERATURES
Lauren L. Ball, Paul J. Richardson, and Dean W. Sheibley Washington Mar. 1969 9 p refs
(NASA-TN-D-5113) Avail: CFSTI CSCL 18D

Tungsten-184 has been found to be a useful dosimeter for thermal neutrons, particularly for high-temperature applications. Correlation of neutron flux with cobalt-59 activation and uranium-235 fission density for short-term irradiations is shown. The tungsten-184, thermal neutron capture cross section in the Plum Brook Reactor was found to be 1.94 ± 0.08 barns. Cadmium ratios for tungsten-184 are about one-fifth of the value found for cobalt-59. The radiochemistry and counting techniques for tungsten-185 are described. Author

N69-20854*# National Aeronautics and Space Administration. Lewis Research Center, Cleveland, Ohio.
OPEX 2: A RADIATION SHIELD OPTIMIZATION CODE
Gerald P. Lahti Washington Mar. 1969 26 p refs
(NASA-TM-X-1769) Avail: CFSTI CSCL 18F

A radiation shield optimization procedure based on the

computer code, OPEX-II, is described. The OPEX-II code, based on an earlier, steepest-descent-method code OPEX, has been recoded to improve coding, simplify data input, use spherical geometry, and alter the dose-thickness relation when a layer has been removed. A complete description of how to obtain the necessary input data for OPEX-II from other transport calculations is given. Data input instructions, FORTRAN IV code listing, and a sample problem optimizing a seven-layer shield of tungsten and lithium hydride for a space power reactor are given. Author

N69-22555*# National Aeronautics and Space Administration. Lewis Research Center, Cleveland, Ohio.
NONDESTRUCTIVE DETERMINATION OF URANIUM 235 DISTRIBUTION BY FIXED POSITION GAMMA SCANNING
Paul J. Richardson and Dale C. Berner Washington Apr. 1969 8 p refs
(NASA-TM-X-1779) Avail: CFSTI CSCL 18I

A nondestructive method for determining fuel density variation in small, unirradiated, clad UO_2 plates is described. A plate is scanned at fixed positions instead of scanning a plate moving past a detecting system. Variations are calculated by a statistical sampling where it is not possible to analyze the whole plate. Author

N69-22946# Atomics International, Canoga Park, Calif.
PREPARATION OF UC AND UC-W- SPECIMENS FOR AN IRRADIATION TEST OF THE VALUE OF A FINE-PARTICLE DISPERSION IN THE CONTROL OF FISSION GAS SWELLING (EXP-NRX-9-101 EXPERIMENT)
A. C. Hott 31 May 1968 41 p refs
(Contract AT(04-3)-701)
(NAA-SR-12629) Avail: CFSTI

The preparation and characterization of fuel samples for an irradiation test of fission gas swelling in tungsten-doped uranium monocarbide are described. Details are given on the arc melting and casting and the zone melting processes used to prepare the 0.33-in. diameter fuel slugs. Electron micrographs are presented which show the presence of fine particles. The fuel samples have been further characterized by chemical analysis, optical metallography, length measurement, and density determination. Density change is the chief measure of the swelling which occurs during irradiation, and the comparison of the swelling of the tungsten-containing samples with that of the control samples is the chief indication of the value of tungsten additions for the reduction of fuel swelling. The density and other properties of the 114 fuel slugs for use as reference data during the postirradiation examination are given. Author (NSA)

N69-23450*# United Aircraft Corp., East Hartford, Conn.
INITIAL RADIO-FREQUENCY GAS HEATING EXPERIMENTS TO SIMULATE THE THERMAL ENVIRONMENT IN A NUCLEAR LIGHT BULB REACTOR
John S. Kendall, Ward C. Roman, and Paul G. Vogt Washington NASA Apr. 1969 105 p refs
(Contract NASw-847)
(NASA-CR-1311; G-910091-17) Avail: CFSTI CSCL 18K

Initial experiments were conducted to develop an intense radiant energy source which would eventually be capable of producing radiant energy fluxes equal to those expected in a full scale nuclear light bulb engine. The test program was conducted using the UARL 1.2- megw r-f induction heater at dc input power levels up to approximately 250 kw to supply energy to the simulated fuel containment region of a vortex. The primary objective of the experimental program was to determine the effect of various parameters on the power radiated from the vortex, the power deposited in the peripheral wall of the vortex tube, and the power carried away by convection from the vortex. Both argon discharges with no seed and argon discharges seeded with submicron carbon and tungsten particles were employed. Tests were conducted at discharge pressures up to 6.0 atm abs and with up to 85 kw of power deposited in the discharge; of this, 35 kw was radiated through a water cooled transparent wall surrounding the discharge. The 35 kw of radiant energy represents a radiant energy flux of about 12.0 kw/in.^{2} (1.86 kw/cm^2), which corresponds to an equivalent black body radiating temperature of 7600 R. Author

N69-24055*# Humphreys Corp., Concord, N. H. TAFA Div.
INDUCTION PLASMA HEATING: HIGH POWER, LOW FREQUENCY OPERATION AND PURE HYDROGEN HEATING
M. L. Thorpe and L. W. Scammon Washington NASA May 1969 59 p refs
(Contract NAS3-9375)
(NASA-CR-1343) Avail: CFSTI CSCL 20I

Induction plasma heating systems were developed and tested to powers up to 1000 kW. Operation on diatomic gases such as air at frequencies as low as 220 KHz was achieved with continuous operation at exit gas enthalpies over 40,000 Btu/lb. Pure hydrogen heating was demonstrated at 4 MHz and 100 kW producing exit gas enthalpies over one million Btu/lb. High power sheath mode operation was also achieved. Author

N69-24802*# National Aeronautics and Space Administration. Lewis Research Center, Cleveland, Ohio.
ANALYSIS OF CYLINDRICAL REACTOR FUEL PIN FOR CLAD STRESS CAUSED BY FISSION GASES
Louis Gedeon and Armin F. Lietzke Washington Apr. 1969 22 p refs
(NASA-TN-D-5178) Avail: CFSTI CSCL 18J

An analysis of a reactor fuel pin with a central void is presented which considers stresses in the clad caused by fission gas pressure. It is shown that, for a given fuel volume, the clad and void volumes may be optimized to give a minimum stress in the clad. Stress and strain in the clad may be calculated from equations and graphs of a stress parameter as a function of a heat generation parameter and the fuel to pin volume ratio. An illustrative example is presented showing how the analysis and creep properties of the clad may be used in conjunction with reactor criticality calculations. Author

N69-25305*# National Aeronautics and Space Administration. Lewis Research Center, Cleveland, Ohio.
RADIAL POWER TAILORING FOR A URANIUM DIOXIDE T-111 CLAD REACTOR WITH CONTAINED FISSION PRODUCT GASES
Wendell Mayo and Robert M. Westfall Washington May 1969 21 p refs
(NASA-TM-X-1795) Avail: CFSTI CSCL 18J

A method is presented to evaluate the power capability of a nonvented reactor design which meets required excess reactivity and control requirements without undergoing more than 1 percent diametric creep in the T-111 fuel pin cladding. Optimized 3 fuel zone power tailoring allows a power level of 2.83 megawatts thermal compared to 2.42 for the unzoned reactor. An extension of the method is used to change core size while meeting all other requirements to obtain 3-megawatts-thermal power. The unzoned reactor size is 50.1 centimeters in length and equivalent circular diameter compared to 47.8 for the zoned reactor for 3-megawatts-thermal power. Author

N69-26231*# National Aeronautics and Space Administration. Lewis Research Center, Cleveland, Ohio.
A NEW METHOD FOR TREATMENT OF UNCERTAINTIES IN NUCLEAR REACTOR HEAT TRANSFER CALCULATIONS
Harry J. Reilly, John D. Hansell (Toledo Univ.), and George L. Heath (Toledo Univ.) Washington May 1969 18 p ref
(NASA-TM-X-1802) Avail: CFSTI CSCL 18I

A method for performing probability calculations for fuel clad surface temperatures of nuclear reactors is presented. The method properly treats factors which vary systematically over the whole core, factors which vary over a plate, and those that vary at a spot. One method of choosing spot size for plate-type reactors is shown and a more general method is discussed. The method is not restricted to normal distributions. The calculated value for probability of success, that is, surface temperature not exceeding coolant saturation temperature, is identified as strictly applicable only to the instant of reactor startup. Also the effect of continued operation is discussed. It is observed that the probability of success may be more nearly equal to values obtained by the deterministic method than to those obtained by the statistical method. Author

N69-26233*# National Aeronautics and Space Administration. Lewis Research Center, Cleveland, Ohio.

EXPERIENCES WITH BERRYLLIUM SWELLING AND REPLACEMENT IN THE PLUM BROOK REACTOR

William Fecych Washington May 1969 15 p refs Presented at Am. Nucl. Soc. Meeting, Washington, D.C., 11–16 Nov. 1968

(NASA-TM-X-1794) Avail: CFSTI CSCL 09I

A description is given of problems encountered from distortion and failure of major reactor core components in the high neutron fluence regions of the Plum Brook Reactor. Reactor material surveillance programs, the failure mode of the components, component replacement methods, associated health hazards, and the distortion of components against neutron fluence are described. Author

N69-26270*# National Aeronautics and Space Administration. Lewis Research Center, Cleveland, Ohio.

A NUCLEAR THERMIONIC SPACE POWER CONCEPT USING ROD CONTROL AND HEAT PIPES

John L. Anderson and Edward Lantz Washington May 1969 32 p refs

(NASA-TN-D-5250) Avail: CFSTI CSCL 18K

A space power system using a fast spectrum nuclear reactor, out-of-pile thermionic diodes, heat pipes, and a dual central absorber rod type of reactivity control has been studied. Emphasis is placed on the neutronic aspects and general feasibility of the concept.

N69-28212*# National Aeronautics and Space Administration. Lewis Research Center, Cleveland Ohio.

THE FUEL-EMITTER SEPARATION PROBLEM IN EXTERNALLY FUELED THERMIONIC DIODES

Harry W. Davison Washington Jun. 1969 32 p refs

(NASA-TM-X-1812) Avail: CFSTI CSCL 18J

The fuel temperature and reactor power responses following fuel-emitter separation were calculated using a one-dimensional, linearized, time-dependent-heat-transfer model. The time-dependent power density in the fuel is calculated using space-independent, monoenergetic neutron diffusion theory. Six neutron delay groups and temperature coefficients of reactivity for all diode components are included in the analysis. Fuel melting is predicted in the reference diode design, and radial cooling fins are recommended as a design modification to avoiding fuel melting. Author

N69-29593*# National Aeronautics and Space Administration. Lewis Research Center, Cleveland, Ohio.

NEUTRONIC COMPARISON OF BERYLLIUM OXIDE AND MOLYBDENUM FOR MOVABLE REFLECTOR CONTROL OF A FAST-SPECTRUM REACTOR

Charles L. Whitmarsh, Jr. and Wendell Mayo Washington Jun. 1969 26 p refs

(NASA-TM-X-1822) Avail: CFSTI CSCL 18K

A neutronic comparison of beryllium oxide and molybdenum as the major constituents of axially translating radial reflectors for the reactivity control of a fast-spectrum reactor is made. Both one- and two-dimensional transport calculations are used. The analysis indicates that the multiplication factors, power distributions, and reactivity control worth are nearly the same for both types of reflector materials. The normally higher worth of the beryllium oxide reflector is reduced because of (1) the presence of molybdenum canning material in the reflector and a tantalum alloy pressure vessel between the core and the reflector, and (2) the need to provide cooling and helium containment. Author

N69-29671*# National Aeronautics and Space Administration Lewis Research Center, Cleveland, Ohio.

USE OF "FASTER" CODE FOR SIGNIFICANTLY REDUCING DUCTED REACTOR SHIELD COMPUTATION TIME

Millard L. Wohl and Thomas M. Jordan (ART Res. Corp., Los Angeles) Washington Jul. 1969 8 p refs

(NASA-TM-X-1828) Avail: CFSTI CSCL 18I

The neutron number spectrum computed by the FASTER code at point detectors in a ducted water slab configuration is compared with similar results generated by the 05R code. Excellent agreement is found, verifying the quick-running FASTER code for this type of shielding analysis. Author

N69-30070*# National Aeronautics and Space Administration. Lewis Research Center, Cleveland, Ohio.

AN ANALOG COMPUTER STUDY OF THE LOW-FREQUENCY FLOW DYNAMICS OF TWO NUCLEAR ROCKET COLD-FLOW ENGINE SYSTEMS

Harry W. Fox, Jr. and Ronald J. Blaha Washington Jul. 1969 85 p refs

(NASA-TN-D-5312) Avail: CFSTI CSCL 21F

An analog computer study is made of the low-frequency flow dynamics observed with liquid hydrogen flowing in two different nuclear-rocket cold-flow (unfueled) engine systems. The prediction of the low-frequency response depends largely upon the generation of the proper mass-flow storage in the system. This is achieved by relating, in the model lumping, the average values of

N69-31870*# National Aeronautics and Space Administration. Lewis Research Center, Cleveland, Ohio.

NERVA CONTROL DRUM ACTUATOR IRRADIATION TEST PROGRAM

David J. Robinson, John T. Mayer, and Richard R. Wyer Washington Jul. 1969 46 p refs

(NASA-TN-D-5347) Avail: CFSTI CSCL 18K

A test program was conducted to evaluate the NERVA control drum actuator in the environments of cryogenic temperature, nuclear radiation, and vacuum. The actuator was irradiated for 21.8 hours with a total gamma dose of 1.3×10^{11} ergs per gram (1.3×10^{9} rads) and a neutron fluence of 2×10^{16} neutrons per square centimeter without any degradation in performance. Further irradiation testing was attempted but the actuator malfunctioned. A postirradiation examination revealed extensive radiation damage to the feedback potentiometer. Other actuator components showed no significant radiation damage that would produce detectable changes in actuator performance. Author

N69-31986*# National Aeronautics and Space Administration. Lewis Research Center, Cleveland, Ohio.

HELICAL DUCT GEOMETRY ROUTINE FOR THE SHIELDING COMPUTER PROGRAM "FASTER"

Thomas M. Jordan (ART Res. Corp., Los Angeles), and Millard L.

Wohl Washington Aug. 1969 20 p ref
(NASA-TM-X-1838) Avail: CFSTI CSCL 18I

A method for tracking neutrons through a slab penetrated by a helical voided duct is presented and verified. The FORTRAN listings of computer subroutines that perform the numerical analysis are included; these subroutines are designed to be used with FASTER, a high efficiency Monte Carlo code. Neutron number spectra were calculated at several points in and near the emergent end of a duct through a 20- and a 100-centimeter thick water slab having a point source at the center of the inlet. Author

N69-32317*# National Aeronautics and Space Administration. Lewis Research Center, Cleveland, Ohio.
CAUSES, MEASUREMENT, AND ELIMINATION OF FUEL ELEMENT FISSION PRODUCT LEAKAGE AT THE NASA PLUM BROOK REACTOR
A. Bert Davis and Richard H. Brickley Washington Aug. 1969 28 p refs
(NASA-TN-D-5374) Avail: CFSTI CSCL 18I

Fission product leakage from the fuel elements of the Plum Brook Reactor (PBR) Facility resulted from corrosion and physical damage of the elements. The causes of the corrosion and physical damage are discussed. A method of measuring fission product release from irradiated elements and a method of remote disassembly and examination of leaking elements in the PBR Hot Laboratory Facility are described. The use of the iodine-133 to iodine-131 ration and a nitrogen-17 fission product monitor in detecting the injection and source of fission products in the reactor cooling water system are discussed. Author

N69-33132*# National Aeronautics and Space Administration. Lewis Research Center, Cleveland, Ohio.
SIGNIFICANT EXPERIENCES OF THE NASA PLUM BROOK REACTOR FACILITY
H. B. Barkley, Jr. Washington Aug. 1969 16 p refs Presented at Am. Nucl. Soc. Conf., Washington, D.C., 11–16 Nov. 1968
(NASA-TM-X-1853) Avail: CFSTI CSCL 18K

Representative facility oriented and experiment oriented accomplishments of the NASA Plum Brook Reactor Facility at Sandusky, Ohio, are presented. Several significant problems solved are descriped. To provide a context for understanding the information in the report, a brief description of the facility, its purposes, and the experimental program and environments are included. Author

N69-33273*# National Aeronautics and Space Administration. Lewis Research Center, Cleveland, Ohio.
THERMIONIC FUEL IRRADIATION EXPERIMENT DESCRIPTION
Robert P. Migra, Leonard J. Kaszubinski, and Robert L. Brown Washington Aug. 1969 48 p refs
(NASA-TM-X-1858) Avail: CFSTI CSCL 18J

An instrumented lead-type experiment for the irradiation of encapsulated fuel and insulator specimens at temperatures and fast neutron fluxes that simulate thermionic reactor conditions is described. Fast neutron fluxes are obtained by use of a dadmium and boron carbide shield to remove the thermal neutrons and a portion of the epithermal neutrons. Automatic temperature control of the fuel is obtained by varying a mixture of argon and helium gas in a thin annulus between the primary and secondary containment secondary containment barriers of the fuel capsule. Author

N69-35723*# National Aeronautics and Space Administration. Lewis Research Center, Cleveland, Ohio.
THE POTENTIAL OF NUCLEAR POWER FOR HIGH-SPEED OCEAN-GOING AIR-CUSHION VEHICLES
Frank E. Rom and Albert F. Kascak Washington Sep. 1969 34 p refs
(NASA-TM-X-1871) Avail: CFSTI CSCL 21F

The use of nuclear powerplants based on nuclear aircraft technology to power ocean-going air-cushion vehicles has been investigated. Because aircraft nuclear powerplants might be an order of magnitude lighter than current nuclear marine plants, the performance of nuclear air-cushion vehicles is dramatically altered. Instead of vehicles limited to short ranges and speeds of about 80 knots, they become vehicles with virtually unlimited range and speeds in the range of 100 to 200 knots. The study considers vehicles with gross weights of 1000 to 10,000 tons and clearance heights from 10 to 40 feet, which are sufficient to clear ocean waves 80 to over 90 percent of the time. The cargo capacity ranges from 20 to 50 percent of the gross weight. Direct operating costs are 2 to 5 cents per ton-mile and are independent of the distance travelled. Author

N69-35817*# National Aeronautics and Space Administration. Lewis Research Center, Cleveland, Ohio.
COMPARISON OF TUNGSTEN AND DEPLETED URANIUM IN MINIMUM-WEIGHT, LAYERED SHIELDS FOR A SPACE POWER REACTOR
Gerald P. Lahti and Paul F. Herrmann Washington Sep. 1969 17 p refs
(NASA-TM-X-1874; E-5079) Avail: CFSTI CSCL 18J

The weights of layered spherical shields for a fast spectrum 2.2-megawatt-thermal nuclear space power reactor have been calculated for two candidate gamma shield materials, tungsten and depleted uranium, using natural lithium hydride as the material for neutron smelding. Each shield configuration was optimized to a dose rate constraint of 2 millirem per hour at 20 meters. A one-dimensional discrete ordinates transport program and a steepest-descent method optimization program were used. Author

N69-35848*# National Aeronautics and Space Administration. Lewis Research Center, Cleveland, Ohio.
EVALUATION OF THE ICOHORT 2 MONTE CARLO SHIELDING CODE: GAMMA RAY TRANSPORT USING SOURCE DIRECTION BIASING
Harvey S. Bloomfield and Lester Clemons, Jr. Washington Sep. 1969 9 p refs
(NASA-TM-X-1877) Avail: CFSTI CSCL 18F

An evaluation of the gamma ray transport portion of the COHORT II Monte Carlo shielding code is presented. This evaluation was accomplished by solving the point source, infinite medium, scattering problem and comparing COHORT II output spectra with the widely accepted moments method solution of the same problem. In addition, the COHORT II source angular biasing option was shown to be a valid technique for reduction of variance. Author

N69-36756*# National Aeronautics and Space Administration. Lewis Research Center, Cleveland, Ohio.
REFLECTOR-BASED POISON-DRUM CONTROL ON EQUAL-SIZE REACTOR CORES FUELED WITH URANIUM-233 AND WITH URANIUM-235
Wendell Mayo and Robert M. Westfall Washington Sep. 1969 18 p refs
(NASA-TM-X-1883) Avail: CFSTI CSCL 18J

Reflector based poison drum control was marginal for a heavily loaded, long life, high temperature, fast spectrum reactor core with a length to diameter ratio of about one and using uranium-235 or uranium-233 in the nitride form. A tantalum based alloy and tungsten were used as fuel pin cladding and internal core support. Beryllium oxide and molybdenum reflectors were considered as were the number of control drums, the drum spacings, and the poison sector thickness for both reactors. A one dimensional

transport theory program was used for all reactivity control calculations. Author

N69-36757*# National Aeronautics and Space Administration. Lewis Research Center, Cleveland, Ohio.
PARAMETRIC STUDY OF LARGE NUCLEAR SURFACE EFFECTS MACHINES
Albert F. Kascak Washington NASA Sep. 1969 41 p refs
(NASA-TM-X-1888; E-4919) Avail: CFSTI CSCL 18K

Some performance estimates of a high speed peripheral jet nuclear powered surface effects machine are described. The calculations incorporate a recently proposed nuclear airplane reactor concept; this high temperature reactor reduces shield weight and eliminates a need for a heavy preheater. Payload fraction and reactor power are calculated for vehicle gross weights from 1000 to 5000 tons, forward velocities from 0 to 250 knots, and clearance heights from 10 to 50 ft. For these ranges, the payload varied from 0 to 60 percent of the gross weight, and the total reactor power varied from 400 to 10,000 NW. Author

N69-37225*# National Aeronautics and Space Administration. Lewis Research Center, Cleveland, Ohio.
A SIMPLE METHOD FOR DETERMINATION OF FISSION GASES TRAPPED IN IRRADIATED FUEL FORMS
Dean W. Sheibley Washington Oct. 1969 9 p refs
(NASA-TM-X-1893) Avail: CFSTI CSCL 18J

A simple, rapid, safe, quantitative method for determining fission gases trapped in Mo-UO_2 and W-UO_2 cermets is described. The method uses electrolytic dissolution of the cladding and matrix, and acid dissolution of the fuel. The gaseous activity is collected in charcoal collection vials at liquid-nitrogen temperature. Recovery is greater than 99 percent. Fission gas activity is determined by gamma counting the gas-collection vials. The explosion hazard due to the electrolytic production of hydrogen and oxygen is eliminated. The accuracy of the method is ±2.5 percent (standard deviation) at 10^8 disintegrations per minute. Author

N69-39186*# National Aeronautics and Space Administration. Lewis Research Center, Cleveland, Ohio.
ANALYSIS AND EXPERIMENTS WITH A PULSED NEUTRON SOURCE FOR AN UNREFLECTED SOLUTION REACTOR UP TO 50 DOLLARS SHUTDOWN
Daniel Fieno, Thomas A. Fox, Robert A. Mueller, and C. Hubbard Ford Washington Oct. 1969 59 p refs
(NASA-TN-D-5487) Avail: CFSTI CSCL 18K

Pulsed-source experiments have been performed for an unreflected, cylindrical solution reactor for heights varying from delayed critical to highly subcritical systems. The fuel solution consists of enriched (93.2 percent U^{235}) uranyl fluoride salt (UO_2F_2) dissolved in water. For these experiments a hydrogen to U^{235} atom ratio of 975 is used, thus giving highly thermal reactor spectra. Multigroup-transport-theory-calculated values of the fundamental prompt-mode decay constant are compared with experimental values. Also, calculated values for the subcritical reactivity are compared with values obtained from the experiments by using the inhour method, the method of Simmons and King, and the three well-known "area-ratio" methods – those of Garelis and Russell, Sjöstrand, and Gozani. Author

N69-40060*# National Aeronautics and Space Administration. Lewis Research Center, Cleveland, Ohio.
A STEAM CYCLE FOR AIRCRAFT NUCLEAR PROPULSION
Lawrence H. Fishback Washington Oct. 1969 21 p refs
(NASA-TM-X-1907) Avail: CFSTI CSCL 18E

A preliminary cycle analysis of a steam-driven, nuclear-powered turbofan engine is presented. It is found that maximum efficiency and minimum thrust per unit airflow both occur for a bypass ratio of zero. (This corresponds to minimum heat-exchanger-outlet air temperature.) Parametric numerical results are presented which can be used for selecting the proper engine operating conditions for a given airplane. Author

N69-40061*# National Aeronautics and Space Administration. Lewis Research Center, Cleveland, Ohio.
CHARACTERISTICS OF A 2.17-MEGAWATT FAST-SPECTRUM REACTOR CONCEPT USING AN AXIALLY MOVING REFLECTOR CONTROL SYSTEM
Wendell Mayo, Charles L. Whitmarsh, Jr., John V. Miller, and Hubert W. Allen Washington Oct. 1969 28 p refs
(NASA-TM-X-1911) Avail: CFSTI CSCL 18I

Neutronic, fluid flow, and heat-transfer calculations were performed for a reactor concept which makes extensive use of refractory metals for structure, cladding the uranium nitride fuel, and reflectors. Lithium-7 is the coolant. A design objective of operation for 50,000 hours at 2.17 MW is achieved by fuel zoning to shape the power and the temperature distributions in the core and equalize fuel cladding stresses. Calculations show that reactivity control requirements can be met with an axially moving reflector outside of the pressure vessel. Author

23

PHYSICS, GENERAL

Includes acoustics, cryogenics, mechanics, and optics. For astrophysics see: 30 Space Sciences. For geophysics and related information see also: 13 Geophysics, 20 Meteorology, and 29 Space Radiation.

A69-10012 *

ANTI-STOKES GENERATION IN TRAPPED FILAMENTS OF LIGHT.

C. A. Sacchi, C. H. Townes (Massachusetts Institute of Technology, Cambridge, Mass.), and J. R. Lifsitz (NASA, Electronics Research Center, Cambridge, Mass.).

Physical Review, 2nd Series, vol. 174, Oct. 10, 1968, p. 439-447. 19 refs.

NASA-USAF-supported research.

The angles of emission and frequency shifts of anti-Stokes radiation from small-scale trapped filaments of intense laser light in a number of liquids are examined and interpreted theoretically. For a given order of vibrational anti-Stokes radiation, a plot of angle of emission vs frequency resembles sections of nested parabolas which open toward higher frequencies, with apices a few tens of wave numbers below the unshifted anti-Stokes frequency, and very little intensity extending above this unshifted frequency. Various modulation mechanisms which smear out the Stokes and anti-Stokes frequencies are discussed, as well as the wave-vector matching conditions which appear to produce the angular distribution of radiation. Relatively simple approximations predict that the maximum extent toward lower frequencies of parabolas associated with the first anti-Stokes is one-half the vibrational frequency. The second and third anti-Stokes can extend twice and three times as far, respectively. (Author)

A69-11288 *

RELATIVITY, HEAT AND "FICTITIOUS" FORCES.

F. C. Jones (NASA, Goddard Space Flight Center, Laboratory for Theoretical Studies, Greenbelt, Md.).

Nuovo Cimento, vol. 57B, Oct. 11, 1968, p. 307-314. 15 refs.

Examination of the conventional formulation of the transformation laws for certain thermodynamic quantities which has been questioned by several authors. Their objection is based on a particular force that arises in the conventional picture whenever a heat transfer is observed in a frame other than the rest frame. The claim is made that this force is fictitious and hence should be disregarded when computing the mechanical work. It is shown that, if a suitable mechanical model of heat is adopted, this force becomes quite understandable in mechanical terms and thus perhaps not so fictitious after all. M. M.

A69-12179 *

DIPOLE SHIELDING FACTOR IN HARTREE-FOCK THEORY.

Edward S. Chang (NASA, Goddard Space Flight Center, Laboratory for Theoretical Studies, Greenbelt, Md.).

Journal of Chemical Physics, vol. 49, Oct. 1, 1968, p. 2904-2906. 9 refs.

Demonstration that the dipole shielding factor in the coupled Hartree-Fock approximation is identically N/Z for any atomic S state. This suggests that variational-perturbation methods which yield poor values of the shielding factor may give unreliable Hartree-Fock values for other atomic properties such as the polarizability. M. M.

A69-14295 *

DAMPING FACTOR FOR THE LEAST-SQUARES METHOD OF OPTICAL DESIGN.

Donald R. Buchele (NASA, Lewis Research Center, Cleveland, Ohio).

Applied Optics, vol. 7, Dec. 1968, p. 2433-2435. 6 refs.

Discussion of the possibility of automatic determination of the damping factor in the damped least-squares method of optical design, by using second derivatives of the residuals. This provides at least a first approximation about the degree of nonlinearity of the system of equations and the size of the residuals. It was tested with algebraic equations and with integral equations of three variables with good results. M. M.

A69-19649 *#

LUMINANCE REQUIREMENTS FOR HUE IDENTIFICATION IN SMALL TARGETS.

Mary M. Connors (NASA, Ames Research Center, Moffett Field, Calif.).

Optical Society of America, Journal, vol. 59, Jan. 1969, p. 91-97. 29 refs.

Foveal luminance thresholds for the identification of red (642 nm), yellow (584 nm), green (521 nm), and blue (468 nm) were determined by the method of constant stimuli for a range of small stimulus sizes and for two exposure durations. The luminances necessary for chromatic and absolute thresholds were also specified. The luminance required for chromatic threshold was found to be lowest for the 642-nm stimulus and highest for the 468-nm stimulus; the threshold for correct hue identification was found to be inversely related to wavelength. The ratios of the luminance necessary for hue perception to the absolute threshold ranged from 1.14 for the 642-nm stimulus to 1.51 for the 584-nm stimulus. The ratio of the luminance required for correct hue identification to the absolute threshold ranged from 1.32 for the 642-nm stimulus to 3.33 for the 521-nm stimulus. More reliable responses and fewer confusions in the hue identification were associated with the 642-nm stimulus than with the other wavelengths. The identification thresholds of this study are compared with the detection thresholds for similar targets. (Author)

A69-20745 *

SELF-MODULATION, SELF-STEEPENING, AND SPECTRAL DEVELOPMENT OF LIGHT IN SMALL-SCALE TRAPPED FILAMENTS.

T. K. Gustafson, J. P. Taran (Massachusetts Institute of Technology, Research Laboratory of Electronics, Cambridge, Mass.), H. A. Haus (Massachusetts Institute of Technology, Dept. of Electrical Engineering and the Research Laboratory of Electronics, Cambridge, Mass.), J. R. Lifsitz (NASA, Electronics Research Center, Cambridge, Mass.), and P. L. Kelley (Massachusetts Institute of Technology, Lincoln Laboratory, Lexington, Mass.).

Physical Review, 2nd Series, vol. 177, Jan. 5, 1969, p. 306-313. 18 refs.

Research supported by the Office National d'Etudes et de Recherches Aérospatiales and the Délégation Générale à la Recherche Scientifique et Technique; Contract No. DA-28-043-AMC-02536(E).

Study of the spectral broadening associated with light propagating in self-trapped filaments through liquids with large optical Kerr constants. The influence of a nonzero orientational relaxation time and of linear dispersion on the phase (and amplitude) development of the light as it interacts with the optically nonlinear medium is treated. The effect of dispersion is apparently much less important, particularly in the case where propagation distances are short compared with the shock distance. However, dispersion, combined with a finite relaxation time, does introduce an exponential gain in the forward direction. For a small nonlinearity, the peak gain is equal to the stimulated Rayleigh gain in the backward direction, but it falls off with increasing nonlinearity, because of the Stokes-anti-

Stokes interaction. Spectra computed for a picosecond pulse and for a 100% sinusoidally modulated light beam of infinite extent are compared. Because of its periodicity, the latter possesses a fine structure and is influenced differently by the orientational relaxation. M.G.

A69-21751 *#
FOUR-PHOTON OPTICAL PARAMETRIC NOISE IN WATER.
Donald L. Weinberg (NASA, Electronics Research Center, Cambridge, Mass.).
Applied Physics Letters, vol. 14, Jan. 1, 1969, p. 32-34. 7 refs.

Optical parametric noise has been produced in a centrosymmetric medium, water, by a 9-MW ruby laser beam. The wavelengths (in the visible) and the angles of emission agree with the tuning curve calculated for a phase-matched four-photon process. A power of $\approx 1/2\mu$W emitted into a 38-Å band is observed in the low-loss wavelength range, in approximate agreement with theory. Very strong idler absorption has little apparent effect on the signal power or bandwidth. (Author)

A69-23647 *#
OPTICAL CONSTANTS OF SOME PUMP OILS IN THE VACUUM ULTRAVIOLET.
Fred W. Paul (NASA, Goddard Space Flight Center, Test and Evaluation Div., Greenbelt, Md.).
Optical Society of America, Spring Meeting, San Diego, Calif., Mar. 11-14, 1969, Paper. 20 p.

Results of measurements of the reflectance and absorption coefficients of three diffusion pump oils; (1) DC 704, (2) DC 705, and (3) Octoil. The methods and equipment used are illustrated including the configuration of the light source, monochromator, and detector for the measurement of the absorption coefficient down to Lyman alpha. The pump oils were measured at three thicknesses in the wavelength range from 1215 to 4000 Å. Results are tabulated in terms of the absorption coefficient vs wavelength for the three diffusion pump oils. B.H.

A69-24836 *
GEOMETRIC OPTICAL IMAGE ABERRATIONS OF SINGLE AND DOUBLE MIRRORS.
Hubert F. A. Tschunko (NASA, Electronics Research Center, Optics Laboratory, Cambridge, Mass.) and Martin G. Hurwitz (Itek Corp., Lexington, Mass.).
Applied Optics, vol. 8, Feb. 1969, p. 283-287. 5 refs.

Examination of the advantages and disadvantages of single and double mirror systems. Geometrical image aberrations of spherical and paraboloidal single mirrors are given as functions of the focal number and angle of field. Geometrical image aberrations of paraboloidal-hyperboloidal double mirror systems are given as functions of primary focal number, secondary magnification, angle of field, and mutual position tolerances. The image aberrations for present and future diameter ranges are discussed in relation to wave optical limits. Optimal sizes of uncorrected fields of view are derived for different focal numbers. (Author)

A69-25323 *#
MULTIPLE SCATTERING IN THE KAPITZA-DIRAC EFFECT.
G. T. Schappert (NASA, Electronics Research Center, Cambridge, Mass.).
Physics Letters, vol. 29A, Mar. 24, 1969, p. 6, 7. 7 refs.

Discussion of a simple multiple-scattering approach to the Kapitza-Dirac effect describing the scattering of electrons by a standing electromagnetic wave. It is shown that this approach leads to two coupled rate equations and results in a transition probability less than unity. M.G.

A69-29587 *#
STRENGTHS OF THE FUNDAMENTAL BANDS OF ICE AND SOLID HYDROGEN IN COMPOSITE GRAINS.
K. S. Krishna Swamy (NASA, Goddard Space Flight Center, Greenbelt, Md.) and N. C. Wickramasinghe (Cambridge University, Institute of Theoretical Astronomy, Cambridge, England; Arizona, University, Steward Observatory, Tucson, Ariz.).
The Observatory, vol. 89, Apr. 1969, p. 57-59. 15 refs.

Investigation of suitable theoretical models for the interstellar grains. Considered are graphite core-ice mantle grains with mantle radii of various values. The extinction efficiency is calculated from the usual Güttler theory. Graphite particles covered with solid hydrogen mantles are also discussed. G.R.

A69-32053 *
EXACT FIELDS OF CHARGE AND MASS DISTRIBUTIONS IN GENERAL RELATIVITY.
J. M. Cohen (NASA, Goddard Space Flight Center, Goddard Institute for Space Studies, New York, N.Y.) and M. D. Cohen (Newark College of Engineering, Mathematics Dept., Newark, N.J.).
Nuovo Cimento, vol. 60B, Apr. 11, 1969, p. 241-248. 9 refs.

Exact solutions to Einstein's field equations generated via static, spherically symmetric mass and charge distributions. In the limit in which the mass density vanishes but the charge density does not, the mass seen by an observer at infinity does not vanish and the metric exterior to the source can be the Reisner-Nordstrom or Schwarzschild solution depending on the charge distribution. This mass, generated by the energy density of the electromagnetic field, cannot be set equal to zero for a body of finite size. If the charge is concentrated in a thin shell, and the charge and mass as seen by an observer at infinity are set equal to those of an electron, the radius of the shell is half the classical electron radius. Finally, we exhibit a class of solutions in which the redshift (from a point in the body to infinity) is maximum at the surface rather than at the center. (Author)

A69-33674 *
FREQUENCY MEASUREMENTS IN THE FAR INFRARED - LIMITATIONS IMPOSED BY THE NOISE SPECTRUM IN HARMONIC MIXING.
L. Frenkel and T. Sullivan (NASA, Electronics Research Center, Cambridge, Mass.).
IEEE Transactions on Microwave Theory and Techniques, vol. MTT-17, May 1969, p. 281, 282.

Study, on a spectrum analyzer, of beat frequencies resulting from several orders of mixing of the power of two klystrons. The fifth-order beat note of klystrons operating at 130 and 65 GHz, respectively, has been counted directly. It is found that higher order beats are generally buried in the noise but that the frequency average can be accurately determined. (Author)

A69-39582 * #
VISCOSITY MEASUREMENTS OF DILUTE SOLUTIONS OF HELIUM-3 IN SUPERFLUID HELIUM-4 BETWEEN 0.1 and 1.2°K.
R. W. H. Webeler and G. Allen (NASA, Lewis Research Center, Cleveland, Ohio).
Physics Letters, vol. 29A, Apr. 7, 1969, p. 93, 94. 7 refs.

Viscosity measurements of three dilute solutions of He 3 in superfluid He 4 have been made between 0.1 and 1.2 deg K for 1.09, 1.57, and 4.67 per cent molar concentrations of He 3. A torsional crystal technique with low rim velocity was employed. (Author)

A69-41357 *
SOLUTION OF THE DIRAC EQUATION IN ORTHOGONAL ELECTRIC AND MAGNETIC FIELDS.
V. Canuto and C. Chiuderi (NASA, Goddard Space Flight Center, Goddard Institute for Space Studies, New York, N.Y.).
Nuovo Cimento, Lettere, vol. 2, Aug. 21, 1969, p. 223-227. 10 refs.

Investigation of the solution of the Dirac equation in external electromagnetic fields, using a number of configurations which give rise to an exact solution. A further exact solution is derived for the case of constant electric and magnetic fields orthogonal to each other. Such a field configuration is often encountered in physical problems—e.g., the computation of the transverse transport properties of a plasma in a magnetic field. This process is important in neutron stars or white dwarf stars with intense magnetic fields. F.R.L.

A69-42149 * #
PRODUCTION OF AN INTENSE HELIUM CONTINUUM BELOW 230 Å.
A. J. Caruso and Shardanand (NASA, Electronics Research Center, Cambridge, Mass.).
Optical Society of America, Journal, vol. 59, Aug. 1969, p. 960-962. 8 refs.

A capillary spark in helium was used to produce the He II line spectrum between 308.8 and 230.7 Å, as well as an intense helium continuum between 228.8 Å and approximately 120 Å. Three autoionized resonance transitions of helium between 206.2 and 192.2 Å were studied by use of the helium continuum. (Author)

A69-42150 * #
INTERFEROMETRICALLY MEASURED THORIUM LINES BETWEEN 2747 AND 4572 Å.
David Goorvitch, Francisco P. J. Valero (NASA, Ames Research Center, Moffett Field, Calif.), and Alicia L. Clúa (La Plata, Universidad Nacional, Departamento de Física, La Plata, Argentina). *Optical Society of America, Journal*, vol. 59, Aug. 1969, p. 971-975. 12 refs.

Tabulation of interferometrically measured wavelengths for 278 thorium lines in the range from 2747 to 4572 Å. The light source was a liquid-nitrogen-cooled hollow-cathode lamp with 1 torr of argon as the carrier gas. Each line was measured from interferograms taken with a Fabry-Pérot interferometer having 20-, 40-, and 50-mm spacers, and the results were averaged after making the correction for dispersion of optical path. The combination principle was used as a test of the accuracy of the measurements. The results are compared with those of different investigators. A relative shift of plus .0004 Å is obtained when the electrodeless discharge tube is compared with the hollow-cathode lamp. The origin of this shift is discussed and attributed partly to differences in the standards used to calibrate the interferometer and partly to differences in the light sources. (Author)

A69-43119 * #
THEORY OF PHASE TRANSITIONS IN SOLID HYDROGEN.
Lawrence Flax (NASA, Lewis Research Center, Cleveland, Ohio). *American Physical Society, Quantum Theory of Solids Meeting, Aspen, Colo., Sept. 1-5, 1969, Paper.* 12 p. 6 refs.

Description of a scheme which attempts to account for some of the fluctuations of the angular momentum operator as a possible basis for a better theoretical understanding of phase transitions in solid hydrogen. The decoupling scheme used is similar to the Callen (1963) decoupling approximation used in magnetism. This constitutes an improvement over the random-phase approximation employed by Raich and Etters (1967, 1968). The model described undergoes a first-order orientational transition to the disordered phase at a certain temperature. G.R.

N69-10889*# National Aeronautics and Space Administration. Lewis Research Center, Cleveland, Ohio.
HIGH-FIELD ELECTROMAGNETS AT NASA LEWIS RESEARCH CENTER
James C. Laurence Washington Nov. 1968 49 p refs
(NASA-TN-D-4910) Avail: CFSTI CSCL 20C

The design, construction details, and performances are described of conventional, water cooled copper magnets and cryogenically cooled (superconductive and nonsuperconductive) magnets with field strengths of 3 to 20 teslas. The devices which are used to power and control the magnets are also described. They include a homopolar generator, transformer–rectifier system, and flux pump. Author

N69-20870*# National Aeronautics and Space Administration. Lewis Research Center, Cleveland, Ohio.
A FORTRAN CODE FOR COMPUTING THE PRINCIPLE MASS MOVEMENTS OF INERTIA OF COMPOSITE BODIES
James E. Cake Washington Mar. 1969 38 p refs
(NASA-TM-X-1754) Avail: CFSTI CSCL 20K

A mathematical model of the mass characteristics of composite bodies has been programmed for digital computer processing. The description and equation development of the mathematical model are presented. The technique is of particular interest for spacecraft whose size or mass prohibits the use of experimental measurement in an inertia laboratory. The computer program is written in the FORTRAN IV (version 13) language and is operational on the IBM 7094 Direct Couple System. A sample problem illustrates the input data requirements and the output format of the program. The use options of the program and program limitations are fully described. Author

N69-20905*# National Aeronautics and Space Administration. Langley Research Center, Langley Station, Va.
TABLES OF MIE SCATTERING FUNCTIONS FOR PARTICLES WITH REFRACTIVE INDEX 1.5
M. P. McCormick and J. D. Lawrence, Jr. Washington Mar. 1969 55 p
(NASA-TN-D-5110) Avail: CFSTI CSCL 04A

Single-particle backscatter intensity functions and efficiency factors for spherical particles of refractive index 1.5 have been calculated by using rigorous Mie theory. The single-particle results have been integrated over a Junge size distribution of four laser wavelengths for a range of parameters representative of the atmospheric aerosol. The laser wavelengths are 1.0600 μm, 0.6943 μm, 0.5300 μm, and 0.3472 μm, corresponding to the output of a neodymium laser and ruby laser and their second harmonics, respectively. The Junge size-distribution parameters 2.50, 3.00, 3.50, and 4.00 and particle radii limits of approximately 0.04 to 3.00 μm, 0.04 to 10.00 μm, 0.08 to 3.00 μm, and 0.08 to 10.00 μm were used. Author

N69-22545*# Kaman Nuclear, Colorado Springs, Colo.
VARIABILITY OF SOUND PROPAGATION PREDICTION DUE TO ATMOSPHERIC VARIABILITY
C. Eugene Buell Washington NASA Apr. 1969 85 p refs
(Contract NAS8-11348)
(NASA-CR-1338; KN-68-698-4) Avail: CFSTI CSCL 20A

It covers topics related to estimating sound intensity from a stationary source in the natural atmosphere; it also covers some of the problems of estimating sound intensity from a moving sound source. In both cases the far field of sound propagation is of primary interest (1. to 40. km). The major results in the first part deal with the estimation of intensity by calculating a single ray and associated parameters and the method of locating caustics above the ground. To estimate sound intensity at a point the rate of change of distance to the returning ray with respect to initial inclination angle is required. This may be obtained numerically from the distance of the returning ray when they were calculated for several rays. It seems desirable to differentiate the integrals for distance with respect to inclination formally and compute these derivatives as part of the ray tracing procedure. Author

N69-22769*# National Aeronautics and Space Administration. Lewis Research Center, Cleveland, Ohio.
ABSORPTION OF INFRARED RADIATION BY ICE CRYODEPOSITS
Stephen V. Pepper Washington Apr. 1969 22 p refs
(NASA-TN-D-5181) Avail: CFSTI CSCL 20M

The absorption of isotropic 300 K black-body radiation by ice cryodeposits is analyzed theoretically. The analysis is based on the hypothesis that the cryodeposit reflects infrared radiation specularly. The effects of interfering and noninterfering multiply reflected waves are investigated. The main results of the analysis are predictions of the absorptance as a function of cryodeposit thickness. The effect of interference is to lower the cryodeposit absorptance for thicknesses less than 2 micrometers. Reasonably good agreement with available experimental data has been achieved over a wide range of thicknesses. Author

N69-23199*# Kaman Sciences Corp., Colorado Springs, Colo.
THE EFFECTS OF ATMOSPHERIC FLUCTUATIONS AND REPRESENTATION UPON PROPAGATED SOUND

R. C. Bundgaard Washington NASA Apr. 1969 108 p refs
(Contract NAS8-11348)
(NASA-CR-1337; KN-67-698-2) Avail: CFSTI CSCL 20A

The diagnosed strength of noise fields was obtained by the conventional ray tracing method. When this method is applied to the general problem of estimating expected variations in sound intensity level, the procedure suffers from two disadvantages: the procedure does not always give an estimate; in several instances, its application may be physically unsound. Whenever the ray method does give an estimate, however, it was found that the estimated field strength depends upon the observed atmosphere and the way in which the observed atmosphere is to be represented. The Monte Carlo method is used for estimating short period fluctuations in the noise fields, by means of an artificial experiment for sampling small scale changes in the atmosphere. A nonlinear technique is introduced for representing the aerological observations. The two methods are compared as well as the results obtained by them. It is concluded that the linear method introduces big errors into the diagnosed strength of noise fields. It is recommended that nonlinear methods be used instead of the straight stepped representation of aerological parameters. Author

N69-25344*# Rochester Applied Science Associates, Inc., N. Y.
A THEORY FOR PREDICTING THE ROTATIONAL AND VORTEX NOISE OF LIFTING ROTORS IN HOVER AND FORWARD FLIGHT
S. Gene Sadler and Robert G. Loewy Washington NASA May 1969 75 p refs
(Contract NAS1-7618)
(NASA-CR-1333) Avail: CFSTI CSCL 01C

This method allows either near or far field noise to be calculated, including all effects other than blade thickness and random turbulence in the boundary layer or the wake. The effects of both impulsive changes in load around the azimuth and that of vortex noise were investigated for various flight conditions for the H-34 helicopter and for the HU-1A helicopter in hover. The predicted noise is presented both as plots of sound pressure level versus harmonic number and by plots of pressure time history. Comparisons of predicted results with appropriate measurements obtained for the HU-1A and H-34 were made for selected cases. It was concluded that the inclusion of vortex shedding effects, in addition to the rotational effects, significantly improved the prediction of the measured noise levels as compared to that obtained by considering only rotational effects. In addition, blade slap characteristics are most readily observed and thus investigated through the use of pressure time history plots. Author

N69-26307*# Bolt, Beranek, and Newman, Inc., Cambridge, Mass.
CORRELATION OF FLUCTUATING FORCES WITH THE SOUND RADIATION FROM RIGID FLOW SPOILERS
Hanno H. Heller, Sheila E. Widnall, and Colin G. Gordon Washington NASA May 1969 118 p refs
(Contract NAS1-7552)
(NASA-CR-1340; BBN-1734) Avail: CFSTI CSCL 20A

Results of a theoretical and experimental study of the correlation of fluctuating forces on rigid flow spoilers and the resulting sound radiation are presented. For this experiment, we developed a system of force transducers to measure simultaneously, yet independently, the drag and lift components of the fluctuating forces on flow spoilers within an experimental jet pipe system. The results of the study suggest strongly that spoiler-generated noise is of dipole character, since a direct correlation of fluctuating forces with the radiated sound was found. For evaluation of the data, a theory was developed to predict the sound power radiated from pipe-immersed flow spoilers. This theory considered the effect of the enclosure upon the sources and the effect of pipe end reflection. Both monopole and dipole sources were treated. An increase of the dipole sound power output by a factor of 3 for frequencies below the pipe cut-off frequency was predicted and experimentally confirmed. Author

N69-29477*# National Aeronautics and Space Administration. Goddard Space Flight Center, Greenbelt, Md.
EXPERIMENTAL DETERMINATION OF EDDY-CURRENT TORQUES ON BODIES ROTATING RELATIVE TO A UNIFORM MAGNETIC FIELD
J. C. Boyle, E. J. Mosher, and J. M. Greyerbiehl Washington Jul. 1969 31 p refs
(NASA-TN-D-5086) Avail: CFSTI CSCL 20C

This report presents eddy-current torque measurements made on conducting bodies of various shapes. The results obtained are compared with available theory as well as with the findings of other experimenters. A novel feature of this program is that the test specimens were held stationary while the magnetic field was rotated. This not only eliminated problems of windage and bearing friction, but permitted extension of the tests into higher frequency ranges than had previously been investigated. Also included is a brief discussion of the implications to present and future spacecraft. Author

N69-31984*# National Aeronautics and Space Administration. Lewis Research Center, Cleveland, Ohio.
A LEED STUDY OF THE ADHESION OF GOLD TO COPPER AND COPPER-ALUMINUM ALLOYS
Donald H. Buckley Washington Aug. 1969 18 p refs
(NASA-TN-D-5351) Avail: CFSTI CSCL 20B

The adhesion of the (111) surface of gold to clean (111) surfaces of copper, aluminum, and copper–aluminum alloys was studied with the aid of LEED. Concentrations in copper as low as 1.0 at. % are sufficient to increase the adhesive bonding of gold to copper fivefold. This adhesion is characteristic of what is observed for gold contacting aluminum. The gold also transferred epitaxially to the copper–aluminum alloys, taking on the lattice characteristics of the alloy. Increases in contact load resulted in increases in the amount of gold adhering to the alloy surface. Author

N69-35286*# Southampton Univ. (England).
THE TRANSIENT RESPONSE OF COUPLED ACOUSTO-MECHANICAL SYSTEMS
A. Craggs Washington NASA Aug. 1969 82 p refs
(Grant NGR-52-025-003)
(NASA-CR-1421) Avail: CFSTI CSCL 20A

The behavior of a coupled plate acoustic cavity system is studied using a computer orientated technique. Some simplifying assumptions are made about the nature of the cavity pressure; it is assumed to be uniform and a function of the volume displacement of the boundary. The plate system is represented by an assemblage of rectangular finite elements and the equations of motion are expressed in terms of displacements; the effect of the cavity is simply to introduce an extra stiffness matrix term. The simplifying assumptions are removed and both the plate and acoustic systems are idealized using finite elements, the acoustic system being formulated in terms of pressures. The results show that where the window is large and flexible, and the cavity small, the in vacuo normal modes become coupled and there is a change in the natural frequencies of the system, and consequently a considerable modification to the in vacuo response. The acoustic finite element results show that in the frequency range excited by sonic booms the acoustic responses of a room with one flexible window are dominated by the lower plane wave depth modes. Author

N69-36974*# Pratt and Whitney Aircraft, East Hartford, Conn.
ANALYTICAL AND EXPERIMENTAL STUDIES FOR PREDICTING NOISE ATTENUATION IN ACOUSTICALLY

TREATED DUCTS FOR TURBOFAN ENGINES
Ernest Feder and Lee Wallace Dean, III Washington NASA Sep. 1969 112 p refs
(Contract NAS1-7129)
(NASA-CR-1373; PWA-3486) Avail: CFSTI CSCL 20A

Analytical and experimental studies were performed along with measuring acoustic properties of duct lining materials. The system developed for this program measured the impedance of acoustic materials in the presence of grazing airflow velocities from 0 to 700 fps. The specimens included perforated plates, resistive materials, and perforated plates with a resistive backing material. The rate of change of these acoustic properties was determined for each type of specimen, and it was noted that the resistance of the acoustic specimens increased and the reactance generally decreased with increasing flow velocity and sound pressure level. The analytical studies obtained solutions for sound wave propagation in terms of modes in a rectangular duct lined on parallel sides with identical acoustic treatments, and the noise attenuation in the duct was determined by means of linear theory from the pressure decay coefficients of the modes. The effect of changing distances between treatments from 2-1/2 to 20 inches was examined. Results indicate that maximum attenuation occurs at low frequencies. Comparison were made of the two methods with good agreements. Author

N69-37028*# National Aeronautics and Space Administration. Lewis Research Center, Cleveland, Ohio.
PHENOMENOLOGICAL THEORY OF LOUDNESS
Walton L. Howes Washington Sep. 1969 51 p refs
(NASA-TN-D-5422) Avail: CFSTI CSCL 20A

Alternative time- and frequency-domain equations are presented for predicting the loudness of a wide variety of statistically stationary and nonstationary sounds, either continuous or discontinuous. Zwislocki's theory of temporal summation and S. S. Stevens' psychoacoustic conversion law are incorporated in the present mathematical theory. Frequency domain formulas of Zepler and Harel for impulsive sonic booms and Jones for steady noise represent specializations of the present formulas. For sinusoidal inputs, modified Fletcher – Munson auditory response curves are predicted. For an impulsive input the measured response is also predicted. Author

N69-38180*# National Aeronautics and Space Administration Marshall Space Flight Center, Huntsville, Ala.
PRESSURE EFFECT OF A SOUND WAVE ON A CRYOGENIC FLUID
Fritz Kramer Washington Jul. 1967 23 p refs
(NASA-TN-D-4024) Avail: CFSTI CSCL 20A

It has been observed that a sound wave incident upon the surface of a liquid in an open container can produce a positive pressure differential between the liquid and the ambient atmosphere. This pressure is noticeable only when the liquid is close to its boiling point. The proposal has been made to utilize such a pressure differential for keeping a cryogenic propellant settled at the bottom of its tank during gravity-free flight in space. The report shows that this pressure can be explained as an effect of cavitation of the liquid during the negative half-cycle of the acoustic pressure wave. Author

N69-39178*# National Aeronautics and Space Administration. Goddard Space Flight Center, Greenbelt, Md.
DIGITAL SIMULATION OF ROTATIONAL KINEMATICS
Ai Chun Fang and Benjamin G. Zimmerman Washington Oct. 1969 26 p refs
(NASA-TN-D-5302) Avail: CFSTI CSCL 12A

This report documents a comparative study of the problems encountered in implementing the kinematic equations of rigid-body rotation. Comparing the efficiency and accuracy of the Euler angles and quaternions, the study indicates that quarternions are far superior to Euler angles for a large-angle simulation. The report explores the mechanization of the quaternion-constrained equations in order to obtain improved accuracy and simulation speed. It also describes the development of a new constraining technique (called derivative constraint) for the quaternions and stability criteria for stable solution of the constrained equations. By use of these stability criteria, the optimum feedback gain constant for the constrained kinematic equations can be selected. Author

24

PHYSICS, ATOMIC, MOLECULAR, AND NUCLEAR

Includes atomic, molecular and nuclear physics. For applications see: 22 Nuclear Engineering. For related information see also: 29 Space Radiation.

A69-10100 *
DECAY OF ^{136}La AND ^{134}La.
Glenn M. Julian and Theodore E. Fessler (NASA, Lewis Research Center, Cleveland, Ohio).
Physical Review, 2nd Series, vol. 172, Aug. 20, 1968, p. 1208-1213.

Experimental study of the β decay of ^{136}La and ^{134}La in order to clarify the nature of the low-lying excited states of the near-spherical daughter nuclei $^{136}Ba_{80}$ and $^{134}Ba_{78}$. The energies and relative intensities of the γ rays emitted were measured using a γ-ray spectrometer. Exactly one excited state of ^{136}Ba was discovered at about twice the energy of the first excited state. No evidence of a hypothesized 0^+ vibrational triplet member in ^{134}Ba was found. P.G.M.

A69-10901 *
TABLES FOR THE CALCULATION OF RADIAL MULTIPOLE MATRIX ELEMENTS BY THE COULOMB APPROXIMATION.
G. K. Oertel (NASA, Washington, D.C.) and L. P. Shomo (NASA, Langley Research Center, Hampton, Va.).
Astrophysical Journal Supplement Series, vol. 16, Aug. 1968, p. 175-218. 18 refs.

Generalization of the Coulomb approximation formalism developed by Bates and Damgaard (1949) to the multipole case in order to compute extended tables of Coulomb approximation radial matrix elements for particular dipole and quadrupole transitions. A generalized formula for multipole hydrogen transition integrals is also given. P. G. M.

A69-10960 *
SPECTRAL LINE INTENSITIES IN A NONEQUILIBRIUM NITROGEN PLASMA.
C. Park (NASA, Ames Research Center, Moffett Field, Calif.).
Journal of Quantitative Spectroscopy and Radiative Transfer, vol. 8, Oct. 1968, p. 1633-1653. 31 refs.

For given ratios of nonequilibrium ground state number density to equilibrium ground state number density, and given electron temperatures, the relative populations of excited states of atomic nitrogen in a collision-dominated nonequilibrium plasma, consisting of atoms, singly charged ions, and electrons, are calculated by the method of Bates, Kingston, and McWhirter (1962 - two papers). This method uses Gryzinski's semiclassical cross sections for the collisional excitation of electronic states of an atom. From the resulting populations, the spectral intensities of two prominant visible lines are calculated assuming the plasma to be optically thin for these lines. It is shown that, with the exception of a decaying plasma at temperatures greater than 8000 K, the calculated nonequilibrium intensities disagree with the equilibrium spectral line intensities that would be conventionally employed to determine the temperature of a plasma in equilibrium. (Author)

A69-12551 *
ATTENUATION CROSS SECTIONS OF Xe AND Xe_2 NEAR RESONANCE LINE 1469.6 Å.
Shardanand (NASA, Electronics Research Center, Measurement and Instrumentation Techniques Laboratory, Cambridge, Mass.).
Journal of Quantitative Spectroscopy and Radiative Transfer, vol. 8, Aug. 1968, p. 1533-1536. 6 refs.

Measurement of the total attenuation of radiation near the resonance line 1469.6 Å for xenon gas, using the absorption-measurement technique. The photo-attenuation cross sections of Xe and Xe_2 are derived from total attenuation measurements by means of a method previously used (Shardanand, 1967) for determining the concentration of the diatomic species. M. M.

A69-12833 *
A SHOCK TUBE DETERMINATION OF THE ELECTRONIC TRANSITION MOMENT OF THE C_2 (SWAN) BANDS.
J. O. Arnold (NASA, Ames Research Center, Moffett Field, Calif.).
Journal of Quantitative Spectroscopy and Radiative Transfer, vol. 8, Nov. 1968, p. 1781-1794. 28 refs.

Measurements of the electronic transition moment for the C_2 (Swan) $A^3\Pi_g - X^3\Pi_\mu$ bands have been made in emission behind incident shock waves in CO_2-Argon gas mixtures. The value obtained at the (0, 0) head for the square of the dimensionless transition moment is $3.5_6 \pm 0.5_0$, corresponding to an absorption electronic f-number of 0.035 ± 0.005. The electronic transition moment variation with internuclear separation is also discussed. (Author)

A69-12924 *
ELASTIC SCATTERING OF SLOW ELECTRONS BY TWO-ELECTRON IONS.
M. R. C. McDowell (NASA, Goddard Space Flight Center, Greenbelt, Md.).
Physical Review, 2nd Series, vol. 175, Nov. 5, 1968, p. 189-196. 24 refs.

A one-channel model, previously used for He, is extended to allow calculation of elastic scattering by H^- and Li^+ at energies up to 3 rydbergs. Nonseparable ground-state wave functions are used, allowance being made for exchange, and dipole and quadrupole polarization potentials. Results for Li^+ are in good agreement with quantum-defect-method values. Calculated differential cross sections for elastic scattering by H^- at energies of 1/2 and 1 rydberg are presented. Deviations from Coulomb scattering are marked. Phase shifts ($\ell = 0, 1$) for higher members of the isoelectronic sequence ($4 \leqslant Z \leqslant 10$) are given at threshold and at 1 rydberg. (Author)

A69-13098 *#
ALPHA-GAMMA ANGULAR CORRELATIONS IN ^{120}Sn.
William M. Stewart, Regis F. Leonard, and Norton Baron (NASA, Lewis Research Center, Cleveland, Ohio).
American Physical Society, Meeting, Miami Beach, Fla., Nov. 25-27, 1968, Paper. 21 p.

Measurement of the angular correlation between inelastically scattered alpha particles and gamma rays emitted from the first 2^+ state of ^{120}Sn. The experiment was performed using the 42-MeV alpha-particle beam of the Lewis 152-cm cyclotron. A typical gated and ungated alpha spectrum is shown. The elastic peaks have been normalized, and the enhancement of the 2^+ state in the gated spectrum can be seen. The number of counts in the gated elastic spectrum, multiplied by the ratio of the cross sections, makes it possible to correct for random counts. The random counts subtracted from the number of gated inelastic counts give the true coincidence counts. The total reaction cross section is of the order of two barns, only a small fraction of which is inelastically scattered. This is quite evident by the fact that no peak could be seen in the gamma-ray spectrum for the 2^+ state of ^{120}Sn. As a result of this, typical true-to-chance ratios were of the order of one to six. M. M.

A69-13099 *#
ANOTHER STUDY OF THE DECAY OF I^{123}.
James W. Blue (NASA, Lewis Research Center, Cleveland, Ohio) and Vincent J. Sodd (U.S. Public Health Service, National Center for Radiological Health, Cincinnati, Ohio).
American Physical Society, Meeting, Miami Beach, Fla., Nov.

25-27, 1968, Paper. 9 p.

Investigation of the possibility of producing I^{123} for use in medical diagnoses. The production method used has fewer contaminating activities than any other method. Two new gamma rays were observed at about 200 keV, together with previously unreported gamma rays at 330, 454, 554, 562, 837, 877 and 894 keV, which are attributed to the decay of I^{123}. The region between 180 and 250 keV is plotted, and an error made by Ragaini (1968) is pointed out. M. M.

A69-13100 *#

ALPHA-GAMMA ANGULAR CORRELATIONS ON ^{58}Ni.

Norton Baron, Regis F. Leonard, and William M. Stewart (NASA, Lewis Research Center, Cleveland, Ohio).

American Physical Society, Meeting, Miami Beach, Fla., Nov. 25-27, 1968, Paper. 15 p. 11 refs.

Investigation of the angular correlations between 42-MeV alpha particles inelastically scattered from the 1.452-MeV, 2^+ level of ^{58}Ni, and the subsequently emitted decay gammas. Three optical model potentials having real well depths of 64, 102, and 157 MeV were found to predict similar elastic cross sections. However, the back angle inelastic cross sections calculated using the optical potential having a real well depth of 157 MeV agreed with the measured back angle 2^+ cross sections somewhat better. The deformation parameters β_2 predicted by all three calculations agreed reasonably well with the quoted experimental value of $.214 \pm .021$ obtained from Coulomb-excitation measurements (Stelson and McGowan, 1962, and Owen and Satchler, 1964). M. M.

A69-13321 *

DOUBLET ELECTRONIC STATES OF THE BENZYL RADICAL.

John C. Schug and Donald H. Phillips (Virginia Polytechnic Institute, Dept. of Chemistry and Dept. of Physics, Blacksburg; NASA, Langley Research Center, Hampton, Va.).

Journal of Chemical Physics, vol. 49, Oct. 15, 1968, p. 3734, 3735. 13 refs.

Description of the results of recent configuration-interaction calculations of the doublet electronic state of the benzyl radical which are in better agreement with the experimental facts than previous findings. Symmetries, excitation energies, and oscillator strengths for the benzyl radical are tabulated in three approximations All three approximations gave the correct symmetries and energies for the lowest excited state, and all predicted an unobserved weakly allowed transition in the neighborhood of 3.1 eV. M. M.

A69-13464 *#

ELASTIC SCATTERING OF 600 MEV PROTONS FROM He^3.

E. T. Boschitz, W. K. Roberts, J. S. Vincent (NASA, Lewis Research Center, Cleveland, Ohio), M. Blocher, K. Gotow, (NASA, Lewis Research Center, Cleveland, Ohio; Virginia Polytechnic Institute, Blacksburg, Va.), P. C. Gugelot (NASA, Lewis Research Center, Cleveland, Ohio; Virginia, University, Charlottesville, Va.), and C. F. Perdrisat (NASA, Lewis Research Center, Cleveland, Ohio; College of William and Mary, Williamsburg, Va.).

American Physical Society, Meeting, Miami Beach, Fla., Nov. 25-27, 1968, Paper. 4 p.

The differential cross section of 600 MeV protons elastically scattered from He^3 has been measured between 19 and 45° in the laboratory. The protons scattered from a gas target were detected in a range telescope. They were recorded in coincidence with the recoiling He^3 particles in order to discriminate against nonelastic events. The differential cross section displays a shallow minimum near 29°. The depth of this minimum appears to be intermediate between the minimum 26.5° which we observed in the p-He^4 scattering, and the lack of a diffraction structure in the p-D cross section at the same energy. The data are compared with calculations based on the Glauber high energy approximation. (Author)

A69-13469 *

DEUTERON BREAK-UP BY 42 MEV ALPHA PARTICLES.

Robert E. Warner (Oberlin College, Oberlin, Ohio) and Robert W. Bercaw (NASA, Lewis Research Center, Cleveland, Ohio).

Nuclear Physics, vol. A109, 1968, p. 205-217. 16 refs.
NSF-supported research.

Deuteron breakup by 42-MeV alpha particles was studied by measuring absolute cross sections for coincidence detection of the proton and scattered alpha particle. Prominent peaks due to ^5He and ^5Li final-state interactions as well as broad spectator peaks appear in the energy spectra. Only moderate success was achieved in using single-level R-matrix theory to fit the line shape of the final-state interaction peaks. (Author)

A69-14966 *

POLARIZATION IN PROTON-^4He SCATTERING AT 540 MEV.

K. Gotow (Virginia Polytechnic Institute, Blacksburg, Va.), E. T. Boschitz, W. K. Roberts, J. S. Vincent (NASA, Lewis Research Center, Cleveland, Ohio), P. C. Gugelot (Virginia, University, Charlottesville, Va.), C. F. Perdrisat, and L. W. Swenson (College of William and Mary, Williamsburg, Va.).

Physical Review Letters, vol. 21, Dec. 30, 1968, p. 1816-1819. 13 refs.
Grant No. NGL-47-004-033.

Evaluation of measurements of the asymmetry of polarized protons scattered from ^4He for laboratory angles between 4° and 42° at the proton energy of 540 MeV. The results are compared with the elastic p-^4He scattering cross section at 588 MeV. P.v.T.

A69-16428 *

ON THE NATURE OF ION-MOLECULE COLLISIONS.

J. V. Dugan, Jr., J. H. Rice (NASA, Lewis Research Center, Cleveland, Ohio), and J. L. Magee (Notre Dame, University, Radiation Laboratory, Notre Dame, Ind.).

Chemical Physics Letters, vol. 2, Aug. 1968, p. 219-222. 5 refs.

Study of randomly generated ion-molecule collisions of $Ar^+ + CO$ and $N^+ + NO$ pairs by means of computer plots. The results of the present work are discussed on the basis of the results on charge exchange due to Böhme et al. (1967). It is shown that the collisions are not of the spiraling variety. M. G.

A69-16495

MOLECULAR MOTION IN POLYTETRAFLUOROETHYLENE AT CRYOGENIC TEMPERATURES.

E. S. Clark (Du Pont de Nemours and Co., Inc., Plastics Dept., Wilmington, Del.).

IN: CRYOGENIC PROPERTIES OF POLYMERS; PROCEEDINGS OF THE NASA-CASE CONFERENCE ON THE PROPERTIES OF POLYMERS AT CRYOGENIC TEMPERATURES, NASA LEWIS RESEARCH CENTER AND CASE-WESTERN-RESERVE UNIVERSITY, CLEVELAND, OHIO, APRIL 25-27, 1967. [A69-16485 05-18]
Edited by T. T. Serafini and J. L. Koenig.
New York, Marcel Dekker, Inc., 1968, p. 243-248. 6 refs.

Speculation is offered on the nature of the molecular motion in crystals of polytetraflubroethylene at temperatures well below the $19^\circ C$ transition. It is proposed that a specific type of defect in the chain, a helix reversal point, creates a mechanism whereby large dynamic angular displacements of chain segments about their long axes can occur without significantly affecting the X-ray diffraction data. (Author)

A69-16496 *

SYNTHESIS OF ULTRAHIGH MOLECULAR WEIGHT POLY(ETHYLENE TEREPHTHALATE).

Li-Chen Hsu (NASA, Lewis Research Center, Cleveland, Ohio).

IN: CRYOGENIC PROPERTIES OF POLYMERS; PROCEEDINGS OF THE NASA-CASE CONFERENCE ON THE PROPERTIES OF POLYMERS AT CRYOGENIC TEMPERATURES, NASA LEWIS RESEARCH CENTER AND CASE-WESTERN-RESERVE UNIVERSITY, CLEVELAND, OHIO, APRIL 25-27, 1967. [A69-16485 05-18]
Edited by T. T. Serafini and J. L. Koenig.
New York, Marcel Dekker, Inc., 1968, p. 249-261. 17 refs.

Poly(ethylene terephthalate) of number-average molecular weight on the order of 120,000 was prepared from commercial-grade material in the solid state with a gas chromatograph apparatus. Parameters studied were the catalyst, particle size, the molecular weight of the starting material, the reaction temperature and time, and the nature and flow rate of the carrier gas. (Author)

A69-17027 *
EXCITATION OF THE n^1S STATES OF HELIUM BY PROTON IMPACT.
William J. B. Oldham, Jr. (NASA, Manned Spacecraft Center, Houston, Tex.).
Physical Review, 2nd Series, vol. 174, Oct. 5, 1968, p. 145-148. 14 refs.

The first Born-approximation cross sections for proton excitation of helium from the ground state to the n^1S (n = 4 to 7) states are calculated using a 53-term correlated ground-state wave function and 40-term correlated wave functions for the excited states. Generalized oscillator strengths for the respective transitions are also given. The results are compared with the only previous theoretical calculation and with existing experimental values. The agreement between theory and experiment is poor for absolute values, but the curves obtained from log σ vs log E plots have the same slope at large impact energies. (Author)

A69-17134 *
PHOTO-IONIZATION OF LITHIUM - A MANY-BODY CALCULATION.
Edward S. Chang and M. R. C. McDowell (NASA, Goddard Space Flight Center, Laboratory for Theoretical Studies, Greenbelt, Md.).
Physical Review, 2nd Series, vol. 176, Dec. 5, 1968, p. 126-136. 27 refs.

The photoionization cross section a_ν of lithium has been calculated to second order in Brueckner-Goldstone perturbation theory with the Hartree-Fock model as the zero-order approximation, for ejected electron energies in the range $0 \leq k^2 \leq 0.36$ Ry. Other Hartree-Fock calculations of a_ν are analyzed using certain new theorems relating alternative forms of the matrix element. The final second-order perturbed values of a_ν in the length and velocity formulations are in good agreement with experiment throughout the energy range studied. (Author)

A69-17138 *
ELECTRON-IMPACT IONIZATION OF H(2s) AND H(2p).
H. Lee Kyle and K. Omidvar (NASA, Goddard Space Flight Center, Laboratory for Theoretical Studies, Greenbelt, Md.).
Physical Review, 2nd Series, vol. 176, Dec. 5, 1968, p. 164-172. 25 refs.

Calculation of the impact-ionization cross sections for the second quantum level of atomic hydrogen. The Born-exchange approximation developed by Peterkop (1960) is used in the calculation, as well as the original binary-collision approximation of Vainshtein et al. (1963) and the modified form developed by Omidvar (1967) and Crothers (1967). The results obtained are compared with the Born and Born-Ochkur calculations. M. G.

A69-17817 *
MOLECULAR MOTION AND RAMAN BAND SHAPES IN LIQUID NITROGEN AND OXYGEN.
Michael Scotto (NASA, Electronics Research Center, Cambridge, Mass.).
Journal of Chemical Physics, vol. 49, Dec. 15, 1968, p. 5362-5366. 17 refs.

Spontaneous Raman band shapes have been measured in liquid nitrogen and oxygen. Depolarization ratios have also been measured and compared with those in the gas. Correlation functions are obtained from Q-branch spectra, and the time dependence of rotational motion is discussed. Motional narrowing and rotational quenching are considered as possible mechanisms which could give rise to the observed spectra. (Author)

A69-19165 *
ABSORPTION COEFFICIENTS FOR HYDROGEN. I.
R. W. Patch (NASA, Lewis Research Center, Cleveland, Ohio).
Journal of Quantitative Spectroscopy and Radiative Transfer, vol. 9, Jan. 1969, p. 63-87. 66 refs.

Tables and graphs of the number densities of H, H^+, e^-, H_2, H^-, H_2^+, and H_3^+ in a hydrogen gas or plasma in thermodynamic equilibrium were computed for temperatures from 300 to 40,000 K and pressure from 1 to 1000 atm except for a small, high-density region. For temperatures above 2000 K, the Debye-Hückel approximation was employed. The ion H_3^+ had not been included in previous calculations and was found to cause large increases in e^- and H^- number densities at small degrees of ionization. In computing the H_2^+ and H_2 partition functions, use was made of complete tables of rotational-term values for the ground electronic states. The rotational-term value table for H_2 is included. The relative positions of H_2 singlet and triplet states were redetermined. Morse potentials are given for all singly excited attractive states of H_2 with principal quantum number up to 17. The results are believed to be the most accurate available. (Author)

A69-19782 *
QUANTUM THEORY OF AN ELECTRON GAS WITH ANOMALOUS MAGNETIC MOMENTS IN INTENSE MAGNETIC FIELDS.
Hong-Yee Chiu (NASA, Goddard Space Flight Center, Goddard Institute for Space Studies, New York; New York, State University, Physics Dept. and Earth and Space Sciences Dept., Stony Brook, N.Y.), Vittorio Canuto (NASA, Goddard Space Flight Center, Goddard Institute for Space Studies, New York, N.Y.), and Laura Fassio-Canuto (National Polytechnic Institute, Dept. of Physics, Mexico City, Mexico).
Physical Review, 2nd Series, vol. 176, Dec. 25, 1968, p. 1438-1442. 10 refs.

Investigation of the properties of an electron gas in intense magnetic fields. Expressions are obtained for the thermodynamic energy density, particle density, the magnetic moment, and pair density (created in equilibrium with the system) for a gas of electrons with an anomalous magnetic moment, using the exact eigenvalues of the Dirac-Pauli equation for an electron with an anomalous magnetic moment, obtained by Ternov et al. According to the solution of Ternov et al., the lowest energy states of the electrons can be zero at certain field strengths. It is shown that pair creation does not occur spontaneously at the expense of the magnetic-field energy, but only at the expense of the thermodynamic energy of other particles of the system. Exact expressions for the pair density are given. (Author)

A69-19788 *
MAXIMUM NUMBER OF BINARY COLLISIONS FOR THREE RELATIVISTIC POINT PARTICLES.
G. Doolen (NASA, Goddard Space Flight Center, Greenbelt, Md.).
Physical Review, 2nd Series, vol. 176, Dec. 25, 1968, p. 1541-1543.

As a step toward understanding relativistic rescattering singularities, attention is given to n_{max}, the maximum number of binary collisions allowed by special relativity among three particles with zero-range forces. It is found that for three equal-mass particles $n_{max} = 3$. However, for three particles with masses $m_1 = m_3 = 1$ and $m_2 < 1$, n_{max} decreases with increasing total energy W from its nonrelativistic value, which is between ∞ and 4, to its final value of 4, when $W > 1/m_2$. (Author)

A69-20153 *
RATIONAL APPROXIMATIONS TO GAUNT FACTORS.
R. D. Chapman (NASA, Goddard Space Flight Center, Laboratory for Space Sciences, Solar Physics Branch, Greenbelt, Md.).
Journal of Quantitative Spectroscopy and Radiative Transfer, vol. 9, Feb. 1969, p. 315, 316.

Derivation of coefficients for calculating hydrogenic photoionization Gaunt factors by a rational approximation. The photoionization factors from the first twenty-one orbitals, 1s, 2s, 2p, ..., 6h, are fitted with a rational quadratic of the form $[(a + bx + x^2)/(d + ex + x^2)]C$ (x = wavelength in microns). Fitting coefficients for the wavelength range $0.0036\ \mu < \lambda < 0.0911\ \mu$ and $0.0911\ \mu \leq \lambda$ are tabulated. M. G.

A69-20206 *
ON A PEAKING APPROXIMATION IN SCATTERING THEORY.
H. L. Kyle and M. R. C. McDowell (NASA, Goddard Space Flight Center, Greenbelt, Md.).
Journal of Physics, Part B - Atomic and Molecular Physics, vol. 2, Jan. 1969, p. 15-18. 13 refs.

Evaluation of a scheme, due to Kang and Foland (1967), for calculating cross sections for the excitation and ionization of atoms and ions by electrons. A particular peaking approximation in the

scheme which is used to evaluate a Coulomb-Born matrix element is shown to badly misrepresent their total and differential cross sections for the 1s → 2s transition in atomic hydrogen at low impact energies. M.G.

A69-20736 *

DOUBLET SUPPRESSION IN THE PRINCIPAL SERIES OF CESIUM.
Reginald J. Exton (NASA, Langley Research Center, Hampton, Va.)
Physical Review, 2nd Series, vol. 177, Jan. 5, 1969, p. 114-121. 24 refs.

Study of the suppression of the doublet structure in mixtures of cesium and foreign gases with increasing foreign-gas concentration. The observations are made in absorption with the foreign gases helium, neon, argon, xenon, and neopentane. The foreign gases which demonstrate complete suppression (xenon and neopentane) also produce satellites on both doublet components. The growth of the satellites with increasing foreign gas concentration is shown to produce anomalously broadened lines, considering that the satellite and its parent line together constitute the same transition. The anomalous broadening of the components results in excessive loss of measured absorption as the center of the lines is depressed, and the absorption in the wings predominates. Assuming a minimum detectable absorptivity of 0.03, the absorption of the weaker components ($^2P_{1/2}$) is seen to be undetectable for many of the higher doublets, while the strong components ($^2P_{3/2}$) remain detectable, although considerably broadened. (Author)

A69-20738 *

BEHAVIOR OF THE IONIZATION CROSS SECTION IN COLLISIONS OF HIGH-ENERGY ELECTRONS WITH HYDROGENIC ATOMS.
K. Omidvar (NASA, Goddard Space Flight Center, Laboratory for Theoretical Studies, Greenbelt, Md.).
Physical Review, 2nd Series, vol. 177, Jan. 5, 1969, p. 212-218. 18 refs.

Derivation of the cross section per unit range of the energy of the ejected electron and of the total cross section for the ionization of a hydrogenic atom of nuclear charge Z by an electron with nonrelativistic high energy. A relationship for the average energy of the ejected electrons is given. Different features of the high-energy impact ionization, and a certain connection between the ionization and the discrete level excitation are discussed. M.G.

A69-22249 *

MOLECULAR HYDROGEN INELASTIC ELECTRON IMPACT CROSS SECTIONS - A SEMICLASSICAL METHOD.
G. M. Prok, C. F. Monnin, and H. J. Hettel (NASA, Lewis Research Center, Cleveland, Ohio).
Journal of Quantitative Spectroscopy and Radiative Transfer, vol. 9, Mar. 1969, p. 361-369. 15 refs.

Calculation of the cross sections for ionization and excitation of diatomic molecules by electron impact using a modification of Gryzinski's semiclassical theory. The theoretical model is described. Specific results are given for molecular hydrogen from the ground state to $E(2s\sigma\,^1\Sigma_g^+)$, $B(2p\sigma\,^1\Sigma_u^+)$, $C(2p\pi\,^1\Pi_u)$, and $D(3p\pi\,^1\Pi_u)$ states, and for ionization. Calculations were carried out to 360 eV. In addition, some results for the nitrogen molecule are presented. The excitation calculations are compared to Born and Born-Ochkur approximations. This comparison shows that the molecular model gives acceptable estimates of cross sections for excitation of ground-state molecular hydrogen. The ionization results for both molecular hydrogen and molecular nitrogen are in good agreement with experimentally obtained cross sections. (Author)

A69-26097 *#

MOLECULAR VIBRATION SPECTRA FROM FIELD EMISSION ENERGY DISTRIBUTIONS.
D. J. Flood (NASA, Lewis Research Center, Cleveland, Ohio).
Physics Letters, vol. 29A, Apr. 7, 1969, p. 100, 101.

A calculation is presented which predicts a change in the energy distribution of field-emitted electrons due to inelastic electron-molecule interactions near the metal-vacuum interface. The derivative of the energy distribution of electrons which undergo such an interaction should yield information on the IR adsorption spectra of such molecules. (Author)

A69-29007 *#

CORE POLARIZATION EFFECTS IN INELASTIC SCATTERING.
William F. Ford and Richard C. Braley (NASA, Lewis Research Center, Cleveland, Ohio).
American Physical Society, Spring Meeting, Washington, D.C., Apr. 28-May 1, 1969, Paper. 12 p. 6 refs.

The effect of including core states in inelastic scattering calculations, in addition to the usual valence nucleon states, is investigated for several nuclei in the 2s-1d shell. The initial and final nuclear states are represented by projected Hartree-Fock wave functions, and cross sections are calculated in the distorted-wave Born approximation. Results are compared to those obtained using nuclear states with inert, spherical cores and to experiment. When the same spherical core is present in both initial and final nuclear states, it makes no contribution to the inelastic cross section. When the core is deformed, its effect on the angular distribution is still negligible, but the magnitude of the cross section is brought into better agreement with experiment. (Author)

A69-29008 *#

A LARGE-ANGLE APPROXIMATION FOR HIGH-ENERGY SCATTERING.
William F. Ford and Norman E. Pentz (NASA, Lewis Research Center, Cleveland, Ohio).
American Physical Society, Spring Meeting, Washington, D.C., Apr. 28-May 1, 1969, Paper. 9 p. 9 refs.

Proposal of a new method of performing high-energy scattering calculations based on the Watson multiple-scattering formalism. It is shown that an approximation similar to Glauber theory can be developed which is valid from small to moderately large angles. A detailed study of the error is presented for the double-scattering term, and it is demonstrated that for p-He^4 scattering at 1 BeV, the suggested approximation predicts the correct phase and magnitude to within 5% for scattering angles from 0 to 80° in the CM system. (Author)

A69-29337 *

RELATION BETWEEN NUCLEAR LEVEL DENSITY PARAMETERS AND MASS SHELL.
P. J. Brancazio (New York, City University, Brooklyn College, Brooklyn, N.Y.; Yeshiva University, Belfer Graduate School of Science, New York, N.Y.) and A. G. W. Cameron (Yeshiva University, Belfer Graduate School of Science; NASA, Goddard Space Flight Center, Goddard Institute for Space Studies, New York, N.Y.).
Canadian Journal of Physics, vol. 47, May 1, 1969, p. 1029-1035. 15 refs.
AEC-supported research.

Previous work by Gilbert and Cameron has demonstrated a linear relation between the nuclear level density parameter a and the mass shell correction S. However, different relations were obtained for deformed and undeformed nuclei. A single relation can be obtained if a deformation energy is added to the reference mass formula. This deformation energy is proportional to the number of neutrons or protons to the nearest closed shell. (Author)

A69-29923 *#

APPROXIMATE HIGHER IONIZATION POTENTIALS FOR THE HEAVIER ELEMENTS.
S. O. Kastner (NASA, Goddard Space Flight Center, Solar Physics Branch, Greenbelt, Md.).
Journal of Chemical Physics, vol. 50, Apr. 1, 1969, p. 2896-2901. 7 refs.

Approximate ionization potentials for the high ionization stages of elements with an atomic number Z = 31-92, obtained by simply calculating binding energies in the hydrogenlike approximation from a table of limiting screening constants given by Froese (1963). The ionization potentials are compared with available values for lower Z. G.R.

A69-32201 *

UNIFORMITY OF PROTON BEAMS AVAILABLE AT THE NASA SYNCHROCYCLOTRON (SREL).
Gerald F. Hill, William C. Honaker, and K. H. Kim (NASA, Langley Research Center, Hampton, Va.).

(Radiological Society of North America, Scientific Assembly and Annual Meeting, 53rd, Chicago, Ill., Nov. 26-Dec. 1, 1967.)
Radiology, vol. 91, Sept. 1968, p. 562-567. 6 refs.

Description of a 600-MeV proton synchrocyclotron capable of simulating the space radiation environment. The synchrocyclotron is part of NASA's facilities at the Space Radiation Effects Laboratory. Space radiation simulation is achieved by degrading either of the two primary extracted proton beams having measured energies of 595 and 325 MeV. The primary extracted beams are degraded to lower energies by using copper absorbers located in the magnet hall of the facility. Proton beams having energies from 595 to approximately 30 MeV can be obtained at the target position. M.G.

A69-33118 *

EXCITATION SPECTRUM FOR A BOSE GAS WITH REPULSIVE CORE AND ATTRACTIVE WELL.

Gerald V. Brown (NASA, Lewis Research Center, Cleveland, Ohio) and Michael H. Coopersmith (Case-Western-Reserve University, Cleveland, Ohio).

Physical Review, 2nd Series, vol. 178, Feb. 5, 1969, p. 327-344. 39 refs.

Microscopic derivation of the correct qualitative features of the He II elementary excitation spectrum for a realistic interparticle potential using a form of pair Hamiltonian. The strong repulsive core is included by using reaction matrix elements in the Hamiltonian, and the attractive well is successfully included by assuming a generalized Bose-Einstein condensation. The pair Hamiltonian is diagonalized by the thermodynamically equivalent Hamiltonian method of Wentzel (1960). Numerical solution of the equations yields spectra with phonon and roton regions. Since the energies in the spectrum are too high when the Yntema-Schneider (1950) potential is used, another potential is constructed which still fits the second-virial-coefficient data and gives better results. Spectra calculated for a series of attractive well strengths show the effect of weaker wells. (Author)

A69-33753 *

MEASUREMENT OF THE $^{10}B(n, \alpha)^{7}Li$, $^{7}Li^{*}$ RELATIVE CROSS SECTIONS IN THE KEV REGION.

Donald Bogart (NASA, Lewis Research Center, Cleveland, Ohio) and Lowell L. Nichols (Battelle Memorial Institute, Pacific Northwest Laboratories, Richland, Wash.).

Nuclear Physics, vol. A125, no. 2, 1969, p. 463-476. 15 refs.

Derivation of relative cross sections for $^{10}B(n, \alpha)^{7}Li$, $^{7}Li^{*}$ from measurements of the counting ratios of a $^{10}BF_3$ proportional counter and a precision long counter used to monitor relative neutron fluxes. Monoenergetic neutrons were produced by a Van de Graaff accelerator in the energy region from 30 to 800 keV. When the relative cross sections are normalized to a 1/v variation below 80 keV, the data lie above a 1/v line from 80 to 550 keV indicating departures of 15% at 140 keV and 20% at 220 keV. M.M.

A69-35166 *

E2 TRANSITION RATES FOR ^{20}Ne.

William F. Ford and Richard C. Braley (NASA Lewis Research Center, Cleveland, Ohio).

Nuclear Physics, vol. A126, 1969, p. 671-674. 11 refs.

Calculation of E2 transition rates in ^{20}Ne, using projected Hartree-Fock wave functions. Some of the calculations are made with enlarged basis function spaces or with states with Wood-Saxon radial dependence. Results are compared to upper limits predicted by SU (Satpathy and Nair, 1968). (Author)

A69-35179 *#

RESONANCE NEUTRON CAPTURE IN A THICK SLAB OF DEPLETED URANIUM.

Gerald P. Lahti (NASA, Lewis Research Center, Cleveland, Ohio).

American Nuclear Society, Annual Meeting, 15th, Seattle, Wash., June 15-19, 1969, Paper. 25 p. 7 refs.

Calculation of capture rates, using various widely used group cross section generating techniques, for the case of 3 to 11-eV neutrons in a 3.14-cm-thick slab of depleted uranium sandwiched between polyethylene slabs. An experimentally verified fine group cross section generating procedure, GAROL, and multigroup neutron transport calculations for the 3 to 11-eV region provided the standard spatial capture distribution for comparison. Although the one group cross section calculated by GAROL preserves the total neutron capture rate, it did not reproduce the correct multigroup spatial distribution. This incorrect spatial capture rate resulted in a 19% underestimate in capture gamma leakage. Other one-group formulations, such as those obtained with GAM-II, are inappropriate for use in a transport calculation in a resonance absorber and can result in a factor of 2 underestimate in neutron capture rate with no reproduction of the correct spatial distribution. (Author)

A69-35239 *

LINE BY LINE CALCULATION OF SPECTRA FROM DIATOMIC MOLECULES AND ATOMS ASSUMING A VOIGT LINE PROFILE.

J. O. Arnold, E. E. Whiting, and G. C. Lyle (NASA, Ames Research Center, Moffett Field, Calif.).

Journal of Quantitative Spectroscopy and Radiative Transfer, vol. 9, June 1969, p. 775-798. 25 refs.

Computer program that predicts the spectra resulting from electronic transitions of diatomic molecules and atoms. The program produces a spectrum by accounting for the contributions from all the individual rotational and atomic lines considered in the calculations. The integrated intensity of each line is distributed in the spectrum by an approximate Voigt profile. The program can produce spectra for either optically thin gases or for cases where simultaneous emission and absorption occur. The method allows calculations ranging from the absorption of incident radiation by a column of cold gas to the high temperature self-absorbed emission spectrum from a nonisothermal gas. The computed spectrum can be output directly and, if desired, the predicted output of a grating spectrograph or a fixed wavelength radiometer can be generated, including instrumental broadening and sensitivity. Several examples illustrating the versatility of the program are presented. (Author)

A69-35489 *

ELASTIC SCATTERING OF 21-MEV PROTONS FROM NITROGEN-14, OXYGEN-16, ARGON-40, NICKEL-58, AND TIN-116.

Norton Baron, Regis F. Leonard (NASA, Lewis Research Center, Cleveland, Ohio), and David A. Lind (Colorado, University, Boulder, Colo.).

Physical Review, 2nd Series, vol. 180, Apr. 20, 1969, p. 978-986. 12 refs.
AEC Contract No. AT (11-1)-535.

Measurement of differential cross sections for 21-MeV incident protons elastically scattered from ^{14}N, ^{16}O, ^{40}Ar, ^{58}Ni, and ^{116}Sn. An optical-model analysis was performed on these data and on previously measured elastic polarizations of 21-MeV incident protons scattered from the same nuclei. The optical potential used in the analysis included a real central term, a surface absorption term, and a real spin-orbit term. Good fits to both the cross sections and polarizations for all nuclei except ^{16}O were obtained by allowing the nine parameters of the optical potential to vary from nucleus to nucleus. The diffuseness parameters derived to fit the ^{14}N and ^{16}O data in general differ considerably from those derived to fit the scattering from the heavier nuclei. These results are compared with those of two other calculations in which two different sets of non-unique constant geometrical optical-model parameters were assumed and only the three potential strengths were obtained by searching. As expected, these constant-geometry calculations gave poorer agreement with the data. The disagreement with the polarizations of ^{14}N and ^{16}O was very pronounced. (Author)

A69-36171

INTERNATIONAL SYMPOSIUM ON HIGH- AND MEDIUM-ENERGY MOLECULAR BEAMS, 2ND, CANNES, FRANCE, JULY 1-4, 1969, PROCEEDINGS (SYMPOSIUM INTERNATIONAL SUR LES JETS MOLECULAIRES DE HAUTE ET DE MOYENNE ENERGIE, 2ND, CANNES, FRANCE, JULY 1-4, 1969, PROCEEDINGS.

Paris, Direction des Recherches et Moyens d'Essais, 1969. 219 p. In French and English.

CONTENTS:

SKIMMER INTERACTION--TRANSITION FROM A "SHOCK BEAM" TO A SUPERSONIC NOZZLE BEAM. U. Bossel (Syracuse University, Syracuse, N.Y.), p. 1-9. (See A69-36172 19-01)

PERTURBATION OF THE VELOCITY DISTRIBUTION IN THE SCATTERING OF MOLECULAR BEAMS—A THERMAL BEAM EFFECT. I. Amdur, G. Starkschall, A. M. Falick, and R. R. Bertrand (Massachusetts Institute of Technology, Cambridge, Mass.), p. 25-32. 7 refs. (See A69-36173 19-24)

DEVELOPMENT AND STUDY OF A CESIUM JET (REALISATION ET ETUDE D'UN JET DE CESIUM). Ch. Millet and J. Millet (Aix-Marseille, Université, Marseille, France), p. 42-53. 5 refs. (See A69-36174 19-24)

CHARACTERIZATION OF MULTICHANNEL SOURCES AND THEIR UTILIZATION IN MOLECULAR BEAM SYSTEMS. R. H. Jones, V. R. Kruger, and D. R. Olander (California, University, Berkeley, Calif.), p. 54-60. (See A69-36175 19-24)

A 4-200 EV NEUTRAL MOLECULAR BEAM. R. O. Doughty (General Dynamics Corp., Fort Worth, Tex.) and W. J. Schaetzle (Alabama, University, Tuscaloosa, Ala.), p. 61-67. (See A69-36176 19-24)

APPLICATION OF MOLECULAR BEAMS TO THE STUDY OF GAS SURFACE INTERACTIONS AT LOW AND MODERATE ENERGIES. L. Trilling (Massachusetts Institute of Technology, Cambridge, Mass.), p. 81-90. (See A69-36177 19-24)

REACTIVE SCATTERING FROM SOLID SURFACES—ATOM BEAM REACTIONS OF OXYGEN WITH HEATED GERMANIUM AND SILICON SINGLE-CRYSTALS. R. J. Madix and A. Susu (Stanford University, Stanford, Calif.), p. 91-97. (See A69-36178 19-24)

APPLICATION OF AN IMPROVED MODEL OF THE WALL BOUNDARY CONDITION TO MOLECULAR BEAM SCATTERING FROM A SOLID SURFACE. M. Epstein (Aerospace Corp., El Segundo, Calif.), p. 98-104. (See A69-36179 19-24)

STUDY OF THE INFLUENCE OF THE ROUGHNESS OF A SOLID SURFACE ON THE REFLECTION OF MOLECULAR JETS (ETUDES SUR L'INFLUENCE DE LA RUGOSITE D'UNE SURFACE SOLIDE SUR LA REFLEXION DE JETS MOLECULAIRES). P. Bark and A. Nikuradse (Institut für Elektronen- und Ionenforschung, Munich, West Germany), p. 108-113. 6 refs. (See A69-36180 19-24)

STUDIES ON THE BEHAVIOUR OF GAS MOLECULES SCATTERED BY A SOLID SURFACE—ANALYSES FOR MONOENERGETIC AND MAXWELLIAN BEAMS. M. G. C. Piat (Torino, Politecnico, Turin, Italy), p. 118-126. 8 refs. (See A69-36181 19-24)

IN-SITU MOLECULAR BEAM EXPERIMENTS IN EARTH ORBIT. J. O. Ballance (NASA, Marshall Space Flight Center, Huntsville, Ala.) and R. L. Chuan (Atlantic Research Corp., Costa Mesa, Calif.), p. 136-140. 5 refs. (See A69-36182 19-24)

HEATED SUPERSONIC BEAM STUDY OF THE HELIUM-ARGON INTERMOLECULAR POTENTIAL. R. M. Yealland, T. R. Govers, and J. M. Deckers (Toronto, University, Toronto, Canada), p. 148-153. 6 refs. (See A69-36183 19-24)

ROTATIONAL TEMPERATURE DEPENDENCE OF THE TOTAL SCATTERING CROSS SECTION OF N_2 ON RARE GASES. J. A. Phipps and J. E. Scott, Jr. (Virginia, University, Charlottesville, Va.), p. 154-157. (See A69-36184 19-24)

MEASUREMENT OF Ar-Kr INTEGRAL CROSS SECTIONS AT INTERMEDIATE ENERGIES WITH AN ARC-HEATED AERODYNAMICALLY ACCELERATED ATOM BEAM. D. H. Winicur, E. L. Knuth, and W. E. Rodgers (California, University, Los Angeles, Calif.), p. 158-163. 6 refs. (See A69-36185 19-24)

ENERGY DEPENDENCE OF THE ELASTIC TOTAL COLLISION CROSS SECTION OF IDENTICAL MOLECULES—^{4}He. H. Pauly (Bonn, Universität, Bonn, West Germany), M. G. Dondi, G. Scoles, and F. Torello (Consiglio Nazionale delle Ricerche; Genova, Università, Genoa, Italy), p. 168-176. 13 refs. (See A69-36186 19-24)

IONIZATION CROSS SECTIONS OF ALKALIS ON DIATOMIC HALOGENS IN THE EV-REGION. A. P. M. Baede, A. Moutinho, A. E. de Vries, and J. Los (Stichting voor Fundamenteel Onderzoek der Materie, Amsterdam, Netherlands), p. 177-181. 5 refs. (See A69-36187 19-24)

SHOCK IONIZATION BY IMPACT AGAINST A GAS TARGET OF TRIATOMIC HYDROGEN MOLECULES (IONISATION PAR CHOCS SUR UNE CIBLE GAZEUSE DES MOLECULES TRIATOMIQUES D'HYDROGENE). F. M. Devienne (Laboratoire de Physique Moléculaire des Hautes Energies, Peymeinade, Alpes-Maritimes, France), p. 182-191. 5 refs. (See A69-36188 19-24)

INVERSE PROBLEM IN ATOM-ATOM SCATTERING IN WKB-APPROACH. G. Vollmer (Freiburg, Universität, Freiburg im Breisgau, West Germany), p. 192-194. (See A69-36189 19-24)

MEASUREMENT OF EFFECTIVE CHARGE-EXCHANGE AND STRIPPING CROSS SECTIONS OF INCIDENT IONS AND ATOMS (MASSES OF 1, 2, AND 3) ENCOUNTERING A VAPOR TARGET AT ENERGIES RANGING FROM 1 TO 50 KEV (MESURE DES SECTIONS EFFICACES D'ECHANGE DE CHARGE ET DE "STRIPPING" POUR DES IONS ET DES ATOMES INCIDENTS (MASSES 1, 2, ET 3) D'ENERGIE COMPRISE ENTRE 1 ET 50 KEV RENCONTRANT UNE CIBLE DE VAPEUR D'EAU). R. Dagnac, D. Blanc, and D. Molina (Toulouse, Université, Toulouse, France), p. 201-211. 5 refs. (See A69-36190 19-24)

A69-36182 * #

IN-SITU MOLECULAR BEAM EXPERIMENTS IN EARTH ORBIT.

James O. Ballance (NASA, Marshall Space Flight Center, Huntsville, Ala.) and Raymond L. Chuan (Atlantic Research Corp., Missile Systems Div., Costa Mesa, Calif.).

IN: INTERNATIONAL SYMPOSIUM ON HIGH- AND MEDIUM-ENERGY MOLECULAR BEAMS, 2ND, CANNES, FRANCE, JULY 1-4, 1969, PROCEEDINGS (SYMPOSIUM INTERNATIONAL SUR LES JETS MOLECULAIRES DE HAUTE ET DE MOYENNE ENERGIE, 2ND, CANNES, FRANCE, JULY 1-4, 1969, PROCEEDINGS). (A69-36171 19-24)

Paris, Direction des Recherches et Moyens d'Essais, 1969, p. 136-140. 5 refs.

Description of experiments for studying the interaction between neutral molecules or atoms and a solid surface on large satellites. A Molsink type of experimental chamber is described which contains a target plate of some specified material to be studied. A densitometer is considered for accurate determination of the pertinent atmospheric property-mass density. Satellites in the form of a sphere and a paddle wheel are proposed to provide drag coefficient data as basis for the determination of pertinent parameters. G.R.

A69-36424 * #

QUENCHING OF $N_2(A\ ^3\Sigma_u^+)$ IN HIGH VIBRATIONAL LEVELS BY NITROGEN ATOMS.

Michael P. Weinreb and Gene G. Mannella (NASA, Electronics Research Center, Cambridge, Mass.).

Journal of Chemical Physics, vol. 50, Apr. 1, 1969, p. 3129-3131. 8 refs.

Determination of the rate coefficient for the primary process involved in removing nitrogen in high vibrational levels from active nitrogen. The investigation is based on measurements of the intensity of the glow which appears in the gas when a mixed stream of nitrogen atoms and discharged oxygen passes over a nickel, cobalt, or copper surface. G.R.

A69-39467 *

ONE-BOSON-EXCHANGE CONTRIBUTIONS TO HIGH-ENERGY $p\bar{p}$ ELASTIC SCATTERING IN A NONLOCAL FIELD THEORY.

L. Fassio-Canuto (NASA, Goddard Space Flight Center, Goddard Institute for Space Studies, New York, N.Y.).

Physical Review, 2nd Series, vol. 181, May 25, 1969, p. 1980-1984. 15 refs.

Research supported by the State University of New York.

The proton-antiproton elastic scattering in the GeV region is studied through the exchange of heavy bosons. Within the framework of a local field theory, the experimental results cannot be reproduced satisfactorily. Better agreement is obtained when suitable vertex functions representing a nonlocal Lagrangian are introduced. The fundamental length contained in the vertex function is found to be the nucleon Compton wavelength. (Author)

A69-39665 *
ROTATIONAL EXCITATION OF DIATOMIC MOLECULES BY ELECTRON IMPACT.
Edward S. Chang and A. Temkin (NASA, Goddard Space Flight Center, Greenbelt, Md.).
Physical Review Letters, vol. 23, Aug. 25, 1969, p. 399-403. 18 refs.

Rotational excitation of homonuclear diatomic molecules can be simply yet accurately calculated from the scattering parameters of elastic electron-molecule scattering in the fixed-nuclei approximation. The total scattering cross sections for Δj not equal to 0 transitions are independent of s-wave parameters, and ratios of Δj equal to plus or minus 2 cross sections agree with experimental results in diatomic hydrogen and with rotational close-coupling calculations. Absolute total and differential cross sections can be explained. (Author)

A69-40186 *
EQUATIONS OF STATE AT HIGH PRESSURE FROM THE THOMAS-FERMI ATOM MODEL.
J. J. Gilvarry (NASA, Ames Research Center, Space Sciences Div., Moffett Field, Calif.).
IN: THE APPLICATION OF MODERN PHYSICS TO THE EARTH AND PLANETARY INTERIORS; PROCEEDINGS OF THE NATO ADVANCED STUDY INSTITUTE, UNIVERSITY OF NEWCASTLE-UPON-TYNE, NEWCASTLE-UPON-TYNE, ENGLAND, MARCH 29-APRIL 4, 1967. (A69-40172 22-30)
Edited by S. K. Runcorn.
London and New York, Wiley-Interscience, 1969, p. 313-403. 100 refs.

Application of the Thomas-Fermi approximation, conceived originally as a semiclassical method of calculating the electron distribution in a heavy atom, to the calculation of equations of state and thermodynamic functions at high pressure. The principal interest is in the problem of extracting the actual equation of state and the pertinent thermodynamic functions from the relevant differential equations of the statistical atom model. A brief description of the theoretical basis is given. The physical assumptions peculiar to the application of the statistical atom model at high pressure are stated explicitly. It is emphasized that the physical terms corresponding to a Thomas-Fermi computation for zero-temperature and first-order temperature perturbation represent merely the first two terms in an asymptotic series expansion. Practical applications lie in the study of lunar craters, meteorite impacts, the structure of the earth, and in various other fields. F.R.L.

A69-40759 *
EXPERIMENTAL OBSERVATION OF CONTINUITY-EQUATION OSCILLATIONS IN SLIGHTLY IONIZED DEUTERIUM, NEON AND HELIUM GAS.
J. Reece Roth (NASA, Lewis Research Center, Cleveland, Ohio).
Plasma Physics, vol. 11, Sept. 1969, p. 763-777. 13 refs.

Low-frequency oscillations in the electron number density of slightly ionized deuterium, neon, and helium have been systematically observed over the frequency range from 100 Hz to 80 kHz. These oscillations can be identified with periodic solutions to the neutral and charged particle continuity equations. The frequency of the oscillation was observed to be independent of magnetic field strength and to have the predicted square-root dependence on the product of electron and neutral number density. The continuity-equation oscillation mechanism has been observed over more than five orders of magnitude in the product of electron and neutral number density. (Author)

A69-41044 *
STUDY OF THE $Sc^{45}(\alpha, t)Ti^{46}$ REACTION AT 41 MEV.
Joseph R. Priest and John S. Vincent (NASA, Lewis Research Center, Cleveland; Miami University, Physics Dept., Oxford, Ohio).
Physical Review, 2nd Series, vol. 182, June 20, 1969, p. 1121-1130. 27 refs.

Measurement of thirteen angular distributions from 8 to 70 deg for the Sc^{45}(alpha, t)Ti^{46} reaction at 41 Mev. Very selective population of the states of Ti^{46} was observed, and the populated states correlate well with states of the $Sc^{45}(He^3, d)Ti^{46}$ reaction which have large $l_p = 3$ spectroscopic strengths. M.M.

A69-41045 *
INELASTIC SCATTERING CALCULATIONS WITH PROJECTED HARTREE-FOCK WAVE FUNCTIONS.
Richard C. Braley and William F. Ford (NASA, Lewis Research Center, Cleveland, Ohio).
Physical Review, 2nd Series, vol. 182, June 20, 1969, p. 1174-1185. 22 refs.

Calculation of inelastic proton scattering cross sections for several target nuclei in the 2s-1d shell. Inelastic cross sections are calculated in the distorted-wave Born approximation. Hartree-Fock wave functions projected onto states of good angular momentum represent the initial and final states of the nucleus. The cross sections are generally correct in shape, but too small in magnitude; it is suggested that the latter feature results from the assumption of an inert core. To test this hypothesis, the Ne-20 cross section is recalculated using a 20-particle wave function. The result compares more favorably with experiment. (Author)

A69-43123 * #
THE INTERACTION OF INTERMEDIATE ENERGY PROTONS WITH LIGHT NUCLEI.
E. T. Boschitz (NASA, Lewis Research Center, Cleveland, Ohio).
Symposium on Nuclear Reaction Mechanisms and Polarization Phenomena, Quebec, Canada, Sept. 1, 2, 1969, Paper. 35 p. 36 refs.

Study of the elastic and quasi-elastic scattering of 600-MeV protons with deuterium, He 3, and He 4 at the NASA-SREL synchrocyclotron. Differential cross sections have been obtained for the scattering of protons from the light nuclei. The p-p data are in excellent agreement with the predictions from the Livermore phase shifts. The p-d, p-He-3, and p-He-4 scattering data are compared with calculations which are based on multiple scattering theories by Watson, and by Glauber (1959). The large angle p-d data are compared with the predictions of a model recently proposed by Kerman and Kisslinger. The D(p,2p)n and He^4(p,2p)t cross sections have been measured in symmetric geometry for laboratory angles varying from 28 to 56 deg. From these data the Fermi momentum distribution is calculated, assuming the plane wave impulse approximation. G.R.

A69-43124 * #
COMPUTER-MADE MOVIES AND PLOTTING DESCRIPTIONS OF ION-MOLECULE COLLISIONS WITH POLAR TARGETS.
John V. Dugan, Jr., R. Bruce Canright, Jr., Raymond W. Palmer (NASA, Lewis Research Center, Cleveland, Ohio), and John L. Magee (Notre Dame, University, Notre Dame, Ind.).
International Union of Pure and Applied Physics, International Conference on Physics of Electronics and Atomic Collisions, 6th, Cambridge, Mass., July 28-Aug. 2, 1969, Paper. 20 p. 8 refs.

Movies and time history plots of ion-dipole collisions involving the polar molecules (CO, HCl, and acetonitrile) have been made using a computer-plotter. The three polar molecules studied cover a range of dipole moments and moments of inertia of interest in ion-molecule collisions. The results of numerical integration are stored on magnetic tape and processed by the IBM 360/67, using calls to subroutines of the CDC DD 280 plotter system. These plot results on 35-mm film are made into black-on-white prints, whereas the movies are converted to 16-mm white-on-black. The collision movies provide instantaneous correlation of (ion) translational and (dipole) rotational motion during interaction. The movie results and time history plots complement each other in providing qualitative and quantitative results of collision behavior. All three polar rotators are hindered by the incident ion; the nature and chemical aspects of this hindered rotation are discussed. (Author)

A69-43125 * #
ELASTIC SCATTERING OF 600 MEV PROTONS FROM LIGHT NUCLEI.

Edmund T. Boschitz (NASA, Lewis Research Center, Cleveland, Ohio).
International Union of Pure and Applied Physics, International Conference on High Energy Physics and Nuclear Structure, 3rd, New York, N.Y., Sept. 8-12, 1969, Paper. 9 p. 14 refs.

Study of differential cross section and polarization in elastic p-p, p-d, p-^{3}He, and p-^{4}He scatterings. The experiments were performed at the proton synchrocyclotron of the NASA Space Radiation Effects Laboratory in Virginia. The data obtained are presented in a number of graphs. An interesting feature concerning the proton/helium 4 differential cross section and polarization is the diffraction type pattern in both data with the minima coinciding. The curves presented are based on preliminary calculations by Pentz and Ford (1969). G.R.

A69-43700 * #
COLLISIONAL IONIZATION AND RECOMBINATION RATES OF ATOMIC NITROGEN.
Chul Park (NASA, Ames Research Center, Moffett Field, Calif.).
AIAA Journal, vol. 7, Aug. 1969, p. 1653, 1654. 6 refs.

Discussion of an analysis showing that, under the assumption of a quasi-steady nonequilibrium distribution of electronic state populations, the collisional ionization-rate equation reduces to a simple form even when the energy-level structure and inelastic collision cross sections involved are fairly complex. The rate of change of electron density in a collision-dominated simple plasma consisting of electrons, singly charged ions, and atoms is obtained by summing the rates of all bound-free and free-bound transitions by a collisional process. G.R.

N69-12778*# National Aeronautics and Space Administration. Lewis Research Center, Cleveland, Ohio.
EXCITED STATES OF BARIUM 136 AND BARIUM 134
Glenn M. Julian and Theodore E. Fessler Washington Dec. 1968 26 p refs
(NASA-TN-D-4933) Avail: CFSTI CSCL 20H

Sources of 9.87-minute lanthanum 136 and 6.82-minute lanthanum 134 were made by bombarding enriched barium 136 and barium 134 with 10-MeV protons. A 20-cubic-centimeter lithium-drifted germanium detector was used to observe the gamma rays emitted by lanthanum 136 and lanthanum 134. The energies and relative intensities of these gamma rays were measured. The results suggest the existence of excited states of barium 136 at 818.5, 1578.9, 2080.2, 2128.5, 2141.0, and 2315.6 keV, and excited states of barium 134 at 604.7, 1168.2, 2159.7, 2336.4, 2489.3, 2565.1, 2599.9, and 2693.3 keV. Author

N69-12840*# National Aeronautics and Space Administration. Lewis Research Center, Cleveland, Ohio.
ELASTIC SCATTERING OF 21-MeV PROTONS FROM NITROGEN 14, OXYGEN 16, ARGON 40, NICKEL 58, AND TIN 116
Norton Baron, Regis F. Leonard, and David A. Lind (Colo. Univ., Boulder) Washington Dec. 1968 26 p refs
(NASA-TN-D-4932) Avail: CFSTI CSCL 20H

Differential cross section angular distributions were measured for 21 MeV incident protons elastically scattered from ^{14}N, ^{16}O, ^{40}A, ^{58}Ni, and ^{116}Sn. An optical model analysis was performed on these data and on previously measured elastic polarizations of 21 MeV incident protons scattered from the same nuclei. The optical potential used in this analysis included a real central term, a surface absorption term, and a real spin orbit term. Good fits to both the cross sections and polarizations for all nuclei except ^{16}O were obtained by allowing the nine parameters of the optical potential to vary from nucleus to nucleus. Author

N69-13152*# National Aeronautics and Space Administration. Lewis Research Center, Cleveland, Ohio.
RESONANCE INTEGRALS OF RHENIUM FOR A WIDE RANGE OF SAMPLE SIZES
Clarence R. Pierce, Donald F. Shook, and Donald Bogart Washington Dec. 1968 22 p refs
(NASA-TN-D-4938) Avail: CFSTI CSCL 11F

Resonance integrals were measured for ^{185}Re, ^{187}Re, and natural rhenium for foil and film thicknesses from 0.12 to about 10^{-6} centimeter using both activation and reactivity methods The thinnest samples yielded dilute resonance integral values of 1790±60, 323±20, and 866±35 barns for ^{185}Re, ^{187}Re, and natural rhenium, respectively. Resonance integrals calculated for the range of sample size using recently measured resonance parameters to 100 electron volts were found to be lower than the measured values by about 10 percent. Author

N69-13210*# National Aeronautics and Space Administration. Lewis Research Center, Cleveland, Ohio.
MINIMIZATION OF OPTICAL SCATTERING EFFECTS THROUGH USE OF OPTIMAL MONOCHROMATOR SLIT GEOMETRY
Richard Lee Ponting Washington Dec. 1968 12 p refs
(NASA-TM-X-1702) Avail: CFSTI CSCL 20F

The object of this calculation was to determine whether the effects of the scattering of resonance radiation on the data taken from an excitation cross section chamber could be minimized by adjusting the monochromator slit geometry. The study was done on a high speed digital computer, using random numbers to pick the scattering parameters. This method is shown to give an average number of scatters per photon in agreement with previous studies of the integral equation for the scattering process. Further results of the calculation show that adjustment of the nomochromator slit geometry can minimize the effect of scattering and indicate the form this geometry should take. Author

N69-14288*# National Aeronautics and Space Administration. Lewis Research Center, Cleveland, Ohio.
QUANTUM THEORY OF A PARTICLE OSCILLATOR COLLISION APPLIED TO GAS-SURFACE INTERACTIONS AT CRYOGENIC TEMPERATURES
Jerry D. Smith Washington Dec. 1968 40 p refs
(NASA-TN-D-4982) Avail: CFSTI CSCL 20J

The Schroedinger equation was solved numerically for a one-dimensional collision between a harmonic oscillator and a particle, with a rectangular trapping potential. General solutions were sums of states, each a product of a particle wave function and an oscilator wave function. A correlation was suggested between probability current densities for states within the well and sticking of gas atoms on surfaces, where sticking is regarded as arising from multiple collisions. Energy accommodation coefficients were formulated and compared with helium–tungsten experiments for the temperature range 20° to 120°K. The theory underestimates the accommodation coefficient at lower temperatures and overestimates it at higher temperatures. Results indicate that only approximate qualitative predictions of the coefficient are possible with this simplified model. Author

N69-14448*# National Aeronautics and Space Administration. Goddard Space Flight Center, Greenbelt, Md.
THEORETICAL MOLECULAR LINE ABSORPTION OF CO IN LATE SPECTRAL TYPE ATMOSPHERES
Virgil G. Kunde Washington Dec. 1968 37 p refs
(NASA-TN-D-4798) Avail: CFSTI CSCL 07D

The line positions, line intensities, and collisional line half-widths were calculated for the fundamental, first-overtone, and second-overtone vibration–rotation bands of $C^{12}O^{16}$ and $C^{13}O^{16}$. The $C^{12}O^{16}$ and $C^{13}O^{16}$ line intensities were computed for temperatures ranging from 175° to 3500°K and were weighted in accordance with a terrestrial C^{12}/C^{13} abundance ratio. All lines within 5 to 6 orders of magnitude of the maximum line intensity of a band were considered (≈4500 lines at 35°K). Author

N69-14482*# National Aeronautics and Space Administration. Lewis Research Center, Cleveland, Ohio.

SCATTERING OF 42 MeV (6.7pJ) ALPHA PARTICLES FROM EVEN ISOTOPES OF CADMIUM. SUPPLEMENT 1: ABSOLUTE CROSS SECTIONS

Norton Baron, Regis F. Leonard, and William M. Stewart Washington Dec. 1968 14 p ref

(NASA-TN-D-4948) Avail: CFSTI CSCL 20H

Measurements were performed to permit the determination of absolute cross sections for elastic and inelastic scattering of 42 MeV alpha particles from the even isotopes of cadmium. Previously reported measurements could not be converted to absolute cross sections because of the presence on the targets of a gold backing of unknown thickness. The thickness of the backing has been determined by measuring the yield of elastically scattered alpha particles from a gold foil of known thickness and comparing this yield with that observed from the gold backing during the cadmium experiment. Optical model and distorted-wave Born approximation calculations are carried out and compared with the absolute cross sections. Author

N69-15375*# National Aeronautics and Space Administration. Lewis Research Center, Cleveland, Ohio.

TRANSPORT STUDY OF NEUTRON AND PHOTON ATTENUATION THROUGH LITHIUM HYDRIDE AND TUNGSTEN SPHERICAL MEDIA

John A. Peoples and Daniel Fieno Washington Jan. 1969 33 p refs

(NASA-TN-D-4989) Avail: CFSTI CSCL 20H

The S_n transport theory and a point kernel method were used to study the attenuation of point fission neutrons in LiH and Li^6H; point 8.00 MeV photons in tungsten, and neutrons and secondary protons from a fast reactor through a laminated W–Li^6H shield. The results show that the two methods calculate in agreement neutron and photon doses through these media provided (1) at least a P_3S_{16} transport calculation is used, and (2) for neutron attenuation, the point kernel method uses a distributed neutron removal cross section for Li and Li^6 of 0.1000 cm^2/g and 0.1156 cm^2/g. Secondary photon source strength and distributions in the tungsten shells of the laminated tungsten-Li^6H shield were also determined using a P_3S_{16} transport calculation. Author

N69-17976*# National Aeronautics and Space Administration. Lewis Research Center, Cleveland, Ohio.

HARTREE-FOCK CALCULATIONS WITH WOOD-SAXON BASIS FUNCTIONS

William F. Ford and Richard C. Braley Washington Feb. 1969 25 p

(NASA-TN-D-5066) Avail: CFSTI CSCL 20H

Hartree–Fock method is used to study the even–even N = Z nuclei in the 2s-1d shell. Basis functions with correct asymptotic behavior are generated by use of a Wood–Saxon well. The results are compared with calculations using the conventional harmonic oscillator basis. It is found that most of the Wood–Saxon results may be obtained with a harmonic oscillator basis if the oscillator parameter is carefully chosen. Author

N69-19113*# National Aeronautics and Space Administration. Langley Research Center, Langley Station, Va.

TRANSMISSION OF 2.43 MeV ELECTRONS THROUGH THICK SILICON TARGETS

Jag J. Singh Washington Feb. 1969 41 p refs

(NASA-TN-D-5075) Avail: CFSTI CSCL 20H

The energy and angular distribution of electrons transmitted through silicon targets of various thicknesses have been measured for perpendicularly incident electrons of energy 2.43 MeV. The transmitted electron spectra were measured with 5 mm deep lithium drifted silicon detectors. The experimental results have been compared with the Monte Carlo results obtained by Berger and Seltzer. The Monte Carol program includes the effects of secondary electrons and photons and also the effects of ionization energy-loss fluctuations. The inclusion of these effects in the theoretical calculations has reduced the discrepancy between the theory and the experiment considerably. The target thickness at which the average cosine of the deflection angles reaches its asymptotic value is measured to be 2.5 ± 0.1 millimeters for 2.43 MeV electrons normally incident on plane parallel silicon targets. Author

N69-19828*# National Aeronautics and Space Administration. Langley Research Center, Langley Station, Va.

LITHIUM-DRIFTED SILICON DETECTORS AS LOW-ENERGY PHOTON SPECTROMETERS

Sherwin M. Beck Washington Mar. 1969 23 p refs

(NASA-TN-D-5056) Avail: CFSTI CSCL 20H

Lithium-drifted silicon detectors were fabricated from 10,000 ohm-centimeter, p-type silicon and were tested for use as low-energy photon spectrometers. Three X-ray and gamma ray sources (Am^{241}, Co^{57}, Cd^{109}) were used to determine the energy resolution. At 77° K and less than 10^{-5} torr (1.33 mN/m^2) the detector resolution varied from 0.82 keV (full width half maximum (FWHM)) at a photon energy of 22.10 keV to 1.04 keV (FWHM) at 122.05 keV with detector-amplifier noise (measured with a pulse generator) almost constant at 0.75 keV (FWHM). From these measurements an intrinsic detector resolution corresponding to a Fano factor of 0.205 was calculated. Author

N69-21462*# National Aeronautics and Space Administration. Ames Research Center, Moffett Field, Calif.

A COMPUTER PROGRAM FOR A LINE BY LINE CALCULATION OF SPECTRA FROM DIATOMIC MOLECULES AND ATOMS ASSUMING A VOIGT LINE PROFILE

Ellis E. Whiting, James O. Arnold, and Gilbert C. Lyle Washington Mar. 1969 116 p refs

(NASA-TN-D-5088) Avail: CFSTI CSCL 20F

A Fortran IV computer program for predicting the spectra resulting from electronic transitions of diatomic molecules and atoms local thermodynamic equilibrium is described in detail. Included are instructions for preparing the input data, a program listing, and complete flow charts. The program produces a spectrum by accounting for the contribution of each rotational and atomic line considered. The integrated intensity of each line is distributed in the spectrum by an approximate Voigt profile. The program can produce spectra for optically thin gases or for cases where simultaneous emission and absorption occurs. In addition, the program can compute the spectrum resulting from the absorption of incident radiation by a column of cold gas or the high temperature, self-absorbed emission spectrum from a nonisothermal gas. The computed spectrum can be output directly or combined with a slit function and sensitivity calibration to predict the output of a grating spectrograph or a fixed wavelength radiometer. Author

N69-22934*# National Aeronautics and Space Administration. Lewis Research Center, Cleveland, Ohio.

OPTICAL MODEL ANALYSIS OF PROTON SCATTERING IN THE RANGE 16 TO 22 MeV

Edmund T. Boschitz Washington Apr. 1969 37 p refs

(NASA-TN-D-5067) Avail: CFSTI CSCL 20H

Polarization, differential cross section, and total reaction cross section data for the scattering of 16- to 22-MeV protons from complex nuclei were analyzed with the optical model. An average potential was obtained which describes most of the data. Deviations from the average spin orbit potential were observed for nuclei with doubly closed shells. The analysis of the energy dependence of proton scattering from O^{16} showed that a smooth

variation of the optical model parameters results in satisfactory fits to the data between 30 and 50 MeV. The parameters cannot be extrapolated into the 20-MeV range. Author

N69-24826*# National Aeronautics and Space Administration. Lewis Research Center, Cleveland, Ohio.

ANALYSIS OF GOLD SPHERE TRANSMISSION EXPERIMENTS AT 24-keV NEUTRON ENERGY USING SPIN-DEPENDENT s-WAVE STATISTICS

Thor T. Semler Washington May 1969 23 p refs

(NASA-TN-D-5211) Avail: CFSTI CSCL 20H

The average capture cross section for gold at a neutron energy of 24 keV was obtained by analysis of published sphere transmission experiments that use Sb–Be source neutrons. The analysis compares results using merged s-wave spin-state statistical data and separated spin-state statistical data. Values of 725 ± 30 mb are obtained using separated spin-state data, and 660 ± 30 mb using merged spin-state data. The value of 725 ± 30 mb is in agreement with the larger of recent gold activation cross section measurements at 24 keV, which have a range of from 640 ± 25 mb to 713 ± 40 mb for the average capture cross section. Author

N69-24919*# National Aeronautics and Space Administration. Lewis Research Center, Cleveland, Ohio.

STUDY OF THE (α,t) REACTION ON SCANDIUM-45 AT 41 MeV

Joseph R. Priest (Miami Univ., Oxford, Ohio) and John S. Vincent Washington May 1969 28 p refs

(NASA-TN-D-5216) Avail: CFSTI CSCL 20H

Thirteen angular distributions were measured from 8° to 70° for the Sc^{45} (α,t)Ti^{46} reaction at 41 MeV. All exhibit the same basic shape, which is consistent with a distorted wave calculation where three units of angular momentum are transferred. Relative spectroscopic strengths for these transitions agree well with experimental values obtained by others for the (He^3,d) reaction. Good overall agreement is obtained in a comparison with spectroscopic factors calculated from the McMullen, Bayman, and Zamick model for Sc^{45} and Ti^{46}. Author

N69-25848*# Israel Program for Scientific Translations. Ltd., Jerusalem.

SCATTERING REACTIONS AND DECAY IN NONRELATIVISTIC QUANTUM MECHANICS [RASSEYANIE, REAKTSII I RASPADY v NERELYATIVISTSKOI KUANTOVOI MEKHANIKE]

A. I. Baz et al 1969 245 p refs Transl. into ENGLISH from RUSSIAN Sponsored in part by NASA and NSF *Its* IPST Cat. No. 5149

(NASA-TT-F-510; TT-68-50309) Avail: CSCL 20J

With the aim of filling the gap between standard quantum mechanics textbooks and advanced level works in the theory of quantized fields, a detailed presentation of particular problems is given, based on the premise that renormalization and creation problems can be studied in the nonrelativistic approximation. The theory of scattering and the S-matrix and the theory of unstable particles are discussed. Among the subjects covered are the following: properties of the solutions of the Schroedinger equation which have a discrete spectrum of eigenvalues, states which form a continuum, analytical properties of the wave function, Green's function and perturbation theory, quasi-stationary states, fundamental properties of multichannel systems, threshold effects, and a new formulation of the Lee model. Original research is included on the problem of scattering amplitude singularities when new channels are opened, the lifetime of intermediate states in scattering, and a nonrelativistic approach to particle creation and nonconservation of parity. P.A.B.

N69-28911*# National Aeronautics and Space Administration. Goddard Space Flight Center, Greenbelt, Md.

MODELS OF THE TRAPPED RADIATION ENVIRONMENT. VOLUME 5: INNER BELT PROTONS

James P. Lavine (Wolf Res. and Develop. Corp.) and James I. Vette Washington 1969 61 p refs

(NASA-SP-3024-Vol-5) Avail: CFSTI CSCL 20H

This report is the fifth in a series describing model environments of the charged particles trapped in the geomagnetic field. The preceding volumes gave mode environments for protons and electrons in the inner zone, electrons in the inner and outer zones, electrons at synchronous altitudes, and low energy protons. The omnidirectional, integral fluxes for the five previous proton environments were presented in the form: $J(>E;B,L) = J(>E_1; B,L)e^{-(E-E_1)/E_0(B,L)}$ where E_1 is the reference energy for the environment and E_0 (B,L) is the spectral parameter. The energy ranges for the environments were determined by the existence of an E_0 that represented the data within the desired accuracy. The previous proton environments were for the energy ranges <0.1 to <4 MeV, <4 to <15 MeV, <15 to <30 MeV, <30 to <50 MeV, and <50 Mev. The environment, AP6, combines the data of the previous models for <4 to <15 MeV and <15 to <30 MeV with newer data to form a single model for <4 to <30 MeV and L = 1.2 to 4.0. Both power law and exponential spectral functions were investigated. It was found that a power law provided a more accurate representation of the data over the region of B-L space of interest. The results of the power law spectrum only are presented. Author

N69-30073*# National Aeronautics and Space Administration. Lewis Research Center, Cleveland, Ohio.

A COMPARISON OF ROTATIONAL COLLISION NUMBERS OBTAINED FROM DIFFERENT DEFINITIONS

Frank J. Zeleznik Washington Jul. 1969 47 p refs

(NASA-TN-D-5321) Avail: CFSTI CSCL 20H

Two different definitions of rotational relaxation times were used to calculate rotational collision numbers for pure polar gases. One definition was based on the relaxation equation for rotational energy while the other was based on the connection between relaxation time and volume viscosity. For the purposes of the calculation, a polar molecule was taken to be a point dipole imbedded in a hard core and the interaction between molecules was confined to a plane. A classical calculation showed that the two definitions are equivalent, at least through the third order of a perturbation calculation. Both definitions predicted that increasing the temperature and decreasing the dipole moment and moment of inertia should increase the rotational collision number. The results are in qualitative agreement with experiment insofar as the dipole moment and moment of inertia dependence are concerned. No conclusion can be made concerning the correctness of the theoretical temperature dependence since the experimental temperature dependence is somewhat in doubt. Author

N69-30074*# National Aeronautics and Space Administration. Lewis Research Center, Cleveland, Ohio.

EXCITED STATES OF XENON-130 POPULATED BY BETA DECAY

Theodore E. Fessler, Glenn M. Julian, and S. Jha Washington Jul. 1969 19 p refs

(NASA-TN-D-5329) Avail: CFSTI CSCL 20H

Gamma rays emitted in the beta decay of 5^- ^{130}I and 1^+ ^{130}Cs have been studied with Ge(Li) and NaI(Tl) spectrometers. Twenty-four transitions were observed in the decay of ^{130}I, and 16 were observed in the decay of ^{130}Cs. From the gamma-ray singles spectra and from coincidence studies, the following excited levels of ^{130}Xe have been deduced: 536.1 (2^+), 1122.1 (2^+), 1204.5 (4^+), 1785.9, 1793.5, 1800.1, 1808.1,

1943.9 (5+), 2016.1, 2150.6 2171.3, 2223.3, 2242.8, 2361.8 (6+), 2427.0, 2532.3, 2608.6, and 2752.3 keV. No evidence has been found for the population of a possible 0^+ vibrational triplet member at about twice the energy of the first excited state. Author

N69-31338*# National Aeronautics and Space Administration. Langley Research Center, Langley Station, Va.

ANALYSIS OF A MOLECULAR BEAM SYSTEM UTILIZING A KNOWN PRESSURE SOURCE

Alphonsa Smith Washington Jul. 1969 28 p refs

(NASA-TN-D-5308) Avail: CFSTI CSCL 20H

An analysis is presented of a molecular beam system which utilizes the combined techniques of pressure attenuation, molecular beaming, and cryopumping to produce accurately known pressures in the ultrahigh vaccum region. The system is shown to have a known molecular density with a maximum uncertainty of 6 percent over a variable range of pressures from 6.65×10^{-11} to 1.33×10^{-5} newton/meter^2 (5×10^{-13} to 10^{-7} torr). The kinetic behavior of gas flow in each component of the system is analyzed to determine the important system parameters and to establish their optimum values so that a maximum range of beam density is obtained. Author

N69-33416*# Ling-Temco-Vought, Inc., Dallas, Tex.

INVESTIGATION OF BREMSSTRAHLUNG PRODUCTION IN SPACECRAFT MATERIALS

W. E. Dance and W. J. Rainwater Washington NASA Jul. 1969 215 p refs

(Contract NAS1-7772)

(NASA-CR-1377; Rept-0-71100/8R-18) Avail: CFSTI CSCL 20H

Bremsstrahlung spectra resulting from bombardment of typical spacecraft materials by monoenergetic electrons were experimentally determined in the electron energy range 0.5 to 2.5 MeV. Spectral measurements were made for five angles of electron incidence using a NaI(T1) spectrometer. Integration of the spectra over all possible angles of incidence, with subsequent conversion of the result to dose, yielded for the case of a spherical shell, the bremsstrahlung dose spectra at each electron energy due to a unit omnidirectional flux of electrons. Types of target materials investigated are: 1) solid alloy slabs, 2) laminated alloys, and 3) ablative materials backed by alloyed honeycomb structures. Slab thicknesses of the alloys Ti 6A1 4V, A1 7075-T6, and Stainless 321 were chosen so as to stop 2.5 MeV electrons. Bremsstrahlung dose values inside spherical shells of the target materials were determined, assuming the omnidirectional electron environment found in synchronous orbits. Author

N69-34541*# Ling-Tempo-Vought, Inc., Dallas, Tex.

AN EXPERIMENTAL STUDY OF ELECTRON TRANSMISSION AND BREMSSTRAHLUNG PRODUCTION

D. H. Rester Washington NASA Aug. 1969 143 p refs

(Contract NAS8-21055)

(NASA-CR-1383; Rept-0-71100/9R-1) Avail: CFSTI CSCL 08H

Measurements of electron bremsstrahlung cross sections at an incident electron energy of 50 KeV with a Ge (Li) spectrometer are included in this report. A determination of electron electron bremsstrahlung yields from cross section measurements on Be, for which the electron electron component of the total bremsstrahlung yield is large is also reported. Measurements of electron transmission of Al and Au targets for normal incidence of the electron beam at a bombarding energy of 2.5 MeV are described, and studies of electron transmission for a cosine law source and measurements electron bremsstrahlung production for non normal incidence. Collectively, these experiments adequately describe the electron interactions in matter in the low to intermediate energy range considered to be of importance for comparison to computations of electron transport and bremsstrahlung production. Author

N69-35508*# National Aeronautics and Space Administration. Lewis Research Center, Cleveland, Ohio.

A COMPUTER PLOTTING DESCRIPTION OF ION-MOLECULE COLLISIONS WITH LONG-LIVED CAPTURE COMPLEXES

John V. Dugan, Jr. and James H. Rice Washington Sep. 1969 30 p refs

(NASA-TN-D-5407) Avail: CFSTI CSCL 20H

Spiraling in ion molecule collisions with polarizable and/or polar targets is investigated numerically using computer plotting techniques.Collision orbits and interaction behavior are studied for a range of collision parameters on the IBM 360/67 and 7094 computers with the CDC DD280 plotter. Multiple reflections off a hard core barrier at small ion molecule separations occur only in collisions with permanent dipoles. Multiple reflection times for 2 to 2000 reflections are 10 to 10^3 times longer than times for single reflections. Long multiple reflection collision times, however, do no mean large capture cross sections; the capture cross section values are much less than those predicted by the adiabatic theory. Author

N69-36901*# National Aeronautics and Space Administration. Lewis Research Center, Cleveland, Ohio.

MULTIGROUP CALCULATIONS OF RESONANCE NEUTRON CAPTURE IN A THICK SLAB OF DEPLETED URANIUM

Gerald P. Lahti Washington Sep. 1969 16 p refs

(NASA-TM-X-1878) Avail: CFSTI CSCL 20H

Capture rates were calculated, using various widely used group cross section generating techniques, for the case of 3 to 11 eV neutrons in a 3.14-cm thick slab of depeleted uranium sandwiched between polyethylene slabs. An experimentally verified fine group cross section generating procedure, GAROL, and multigroup neutron transport calculations for the 3- to 11-eV region provided the standard spatial capture distribution for comparison. The one group cross section calculated by GAROL preserves the total neutron capture rate. Other one group formulations such as obtained with GAM-2 are inappropriate for use in a transport calculation in a resonance absorber and can result in a factor of 2 underestimate in neutron capture rate. Author

N69-36924*# National Aeronautics and Space Administration. Lewis Research Center, Cleveland, Ohio.

MOLECULAR VIBRATION SPECTRA FROM FIELD EMISSION ENERGY DISTRIBUTIONS

Dennis J. Flood Washington Sep. 1969 23 p refs

(NASA-TN-D-5423) Avail: CFSTI CSCL 20H

A calculation is presented which predicts a change in the energy distribution of field emitted electrons due to electron–molecule interactions at the metal–vacuum interface. The derivative of the energy distribution of electrons which undergo such an interaction should yield information on the infrared absorption spectra of the absorbed molecules. Author

N69-36929*# National Aeronautics and Space Administration. Langley Research Center, Langley Station, Va.

EVALUATION OF A TECHNIQUE FOR MEASURING ION ENERGY LOSS IN VAPOR-DEPOSITED MATERIALS

Joseph S. Heyman Washington Sep. 1969 18 p refs
(NASA-TN-D-5430) Avail: CFSTI CSCL 20H

A technique for measuring ion energy loss values for vapor-deposited materials has been investigated. The technique employed vapor-depositing the desired thickness of material on a floated gold substrate target. The target was then placed in a proton beam while silicon semiconductor detectors monitored simultaneously the initial and exit beam energy. The investigation covered a wide range of target thicknesses (2 to 25 μm) and energies (0.5 to 3.4 MeV). A computer program was developed to reduce the data and correct for the gold substrate and the finite sample thickness. A comparison of these data with values reported in the literature indicates agreement to within ± 1.6 percent over the tested ranges. Although the technique has been evaluated for protons in aluminum it is expected to yield accurate results for other ions and/or materials. Author

N69-36931*# National Aeronautics and Space Administration. Langley Research Center, Langley Station, Va.

ANALYSIS OF THE GAMMA-RAY-BACKSCATTER TECHNIQUE FOR DIRECT MEASUREMENT OF THE DENSITY OF THE MARTIAN ATMOSPHERE

Peter J. Le Bel Washington Sep. 1969 28 p refs
(NASA-TN-D-5431) Avail: CFSTI CSCL 20H

Studies have been conducted of a technique that uses the backscattering of gamma radiation emitted by a radiosotope source to measure the ambient density of the Martian atmosphere during entry of a spacecraft into the atmosphere. The results show the feasibility of the measurement up to an altitude of about 100,000 feet (30.5 km) in the least dense of the Voyager-Mars model atmospheres. No probes or special windows through the spacecraft skin or heat shield are required because of the penetrating ability of the radiation. A source strength at Mars of 20 curies (1 curie = 3.7×10^{10} disintegrations per second) of gamma radiation is required. The measurement is essentially unaffected by the composition of the atmosphere by the shock layer, and by motions of the vehicle. An engineering-model density sensor, which has been fabricated and tested, has a mass of 5 pounds a volume of 90 inches^3 and required 5 watts of power for operation. Further miniaturization of the device appears practical. Sterilization of the sensor is not expected to present major problems. Author

N69-38564*# Ali (Dolores E.), Berkeley, Calif.

MEASUREMENTS OF NEGATIVE ION PRODUCTION IN ATMOSPHERIC GASES

Dolores E. Ali Washington NASA Oct. 1969 42 p refs
(Contract NAS2-5209)
(NASA-CR-1406) Avail: CFSTI CSCL 20H

Two electron capture by H^+ and He^+ in collisions with various gases was investigated. The method used to measure effective cross sections for the charge changing reactions allows direct determination of the energy defects. Preliminary cross sections were obtained for two electron capture by H^+ at 0.28 keV and for H^+ and He^+ at 2 keV. In addition, negative ions formed by electron bombardment of gases in the ion source were mass analyzed. The charge exchange gases used in the cross section measurements were H_2, N_2, O_2, Kr, and Xe for H^+ at 2 keV; Kr, He, H_2, N_2, and O_2 for He^+ at 2 keV; and H_2, O_2, and Xe for H^+ at 0.28 keV. The corresponding cross sections range from 10^{-19} to 10^{-17} cm^2 for H^+ at 2 keV; 10^{-23} to 10^{-21} cm^2 for He^+ at 2 keV; and 10^{-21} to 10^{-19} cm^2 for H^+ at 0.28 keV. Finally, an attempt was made to observe two electron capture by N^+ at 2 keV; the results were inconclusive. Author

N69-38773*# National Aeronautics and Space Administration. Lewis Research Center, Cleveland, Ohio.

SURVEY OF ELECTRON-CESIUM COLLISION PROBABILITIES: MOMENTUM TRANSFER COLLISIONS

James A. Dayton, Jr. Washington Oct. 1969 20 p refs
(NASA-TM-X-1897; E-5154) Avail: CFSTI CSCL 20H

This report contains a comprehensive collection of the experimental and theoretical values of the electron-cesium atom probability of collision for momentum transfer at electron energies up to 2.0 eV. It was found that a considerable lack of agreement exists, with regard not only to the magnitude of the collision probability at a given energy, but also to the position (even the existence) of minima and maxima. Qualified recommendations of the correct values are offered. Author

N69-39184*# National Aeronautics and Space Administration. Lewis Research Center, Cleveland, Ohio.

CALCULATED INTERACTION ENERGY AND DIPOLE MOMENT IN COLLISIONS OF TWO HYDROGEN MOLECULES

R. W. Patch Washington Oct. 1969 44 p refs
(NASA-TN-D-5486; E-5075) Avail: CFSTI CSCL 20H

Calculations were carried out using orthogonalized valence-bond theory. Methods of calculating accurate values of integrals are given. Linear, planar perpendicular, quadrilateral, and nonplanar perpendicular configurations were included with intermolecular distances from 2.5 to 5.5 bohrs (0.13 to 0.29 nm) and two internuclear distances. The interaction energies obtained appear to be valid for intermolecular distances less than 4.5 bohr (0.24 nm) but are too large at appreciably greater intermolecular distances due to insufficient allowance for electron correlation in the wave function. A simple average interaction energy (Morse potential) for practical applications is cited which correlates calculations in this report and experiments. Author

N69-39187*# National Aeronautics and Space Administration. Lewis Research Center, Cleveland, Ohio.

INTERIM ABSORPTION COEFFICIENTS AND OPACITIES FOR HYDROGEN PLASMA AT HIGH PRESSURE

R. W. Patch Washington Oct. 1969 88 p refs
(NASA-TM-X-1902; E-5147) Avail: CFSTI CSCL 20H

The spectral absorption coefficient was calculated for hydrogen for photons with wave numbers from 500 to 400 000 cm^{-1} (infrared, visible, and ultraviolet). The plasma was assumed to be in local thermodynamic equilibrium at temperatures from 3000° to 90 000°R (1667 to 50 000 K) and pressures from 100 to 1000 atm (1.013×10^7 to 1.013×10^8 N/m^2). Fifteen absorption processes were included. The calculation included the hydrogen triatomic molecular ion H^+_3 in the composition as well as deviations of the real index of refraction from one near the plasma wave number. Both caused significant effects on the spectral absorption coefficient. The Planck and Rosseland mean opacities were derived and calculated. Author

N69-40979*# National Aeronautics and Space Administration. Lewis Research Center, Cleveland, Ohio.

INTERACTION OF 42-MeV ALPHA PARTICLES WITH HELIUM-3

John S. Vincent and Edmund T. Boschitz Washington Nov. 1969 20 p refs
(NASA-TN-D-5530) Avail: CFSTI CSCL 20H

The center-of-mass differential cross section for the elastic scattering of 42-MeV alpha particles from ^{3}He was measured between 20° and 160°. Nonelastic events were integrated to estimate the total reaction cross section. Differential cross sections for ^{3}He(α,p)^6 Li to the ground and first excited states were measured between 20° and 160°. An optical model description of the elastic data gives a satisfactory description if the absorptive potential is radially extended beyond the real potential. The reaction cross sections are qualitatively described by the distorted-wave Born approximation theory. Author

25

PHYSICS, PLASMA

Includes magnetohydrodynamics. For applications see: 28 Propulsion Systems.

A69-12349 *

A TECHNIQUE FOR MEASURING THE ELECTRON DENSITY OF DENSE, THICK, STEADY-STATE PLASMAS.

Paul R. Caron and Frank Russo (NASA, Electronics Research Center, Cambridge, Mass.).

IEEE Transactions on Antennas and Propagation, vol. AP-16, Sept. 1968, p. 611, 612.

A technique for measuring the electron density of dense, thick, steady-state plasmas using a swept microwave interferometer is described. An expression is developed relating the average electron density to a phase shift less than 180° when the phase change introduced by the plasma is large. (Author)

A69-12399 *#

NOTE ON THE TIMES CHARACTERISTIC ON THE MOTION OF MAGNETIC LINES OF FORCE.

Kunitomo Sakurai (Kyoto University, Ionosphere Research Laboratory, Kyoto, Japan; NASA, Goddard Space Flight Center, Greenbelt, Md.).

Journal of Geomagnetism and Geoelectricity, vol. 20, no. 3, 1968, p. 281-283. 7 refs.

Demonstration that the moving velocity of magnetic lines of force always becomes stationary for a relaxation time of the current in a cold electron-proton plasma longer than τ_2. In a medium where the Hall effect cannot be neglected, the time τ_2 must be, therefore, adopted as a characteristic time on the motion of magnetic lines of force. M.M.

A69-13113 *#

FURTHER EXPERIMENTS ON ION-CYCLOTRON-WAVE GENERATION IN THE RF SELF-SUSTAINED MODE.

Clyde C. Swett, Henry J. Hettel, and Roman Krawec (NASA, Lewis Research Center, Cleveland, Ohio).

American Physical Society, Annual Meeting, 10th, Miami, Fla., Nov. 13-16, 1968, Paper. 15 p.

Installation of grid structures in the plasma near the magnetic mirrors has improved the performance of the apparatus used to generate ion cyclotron waves. The range of magnetic fields over which the plasma can be sustained by the rf power alone has been widened, power absorption has been increased, and electron density and degree of ionization have been somewhat increased. Oxygen impurity content produced by bombardment of the alumina tube inside of the rf coil has also increased. From 30 to 50% of the plasma power appeared directly as heat in this tube. Variation of plasma wavelength with magnetic field is presented and difficulties encountered in trying to match the plasma wavelength to the coil wavelength are noted. Wall heat-balance measurements determined the energy flux distribution to the wall. (Author)

A69-13114 *#

POWER COUPLING AND WAVE FIELDS OF ION-CYCLOTRON WAVES IN A FINITE LENGTH SYSTEM.

Donald R. Sigman and John J. Reinmann (NASA, Lewis Research Center, Cleveland, Ohio).

American Physical Society, Annual Meeting, 10th, Miami, Fla., Nov. 13-16, 1968, Paper. 19 p. 5 refs.

Development of a Fourier series approach to calculate wave fields of and power transfer to a plasma column of finite length, surrounded by a radio-frequency coil. The plasma model contains thermal and collisional effects. Calculations show that wave fields to be measured in the laboratory and power transfer as a function of magnetic field are strongly dependent on the strength of the damping mechanism. In strongly damped situations power transfer efficiency can be far below that predicted for a cold collisionless plasma model. In lightly damped cases wave reflections from the ends of the system are responsible for standing-wave patterns and considerable structure in the power transfer against magnetic field curves. B.H.

A69-13115 *#

SOME OBSERVATIONS ON THE RELATIONSHIP BETWEEN INSTABILITIES AND TURBULENCE IN PLASMA.

John S. Serafini (NASA, Lewis Research Center, Cleveland, Ohio).

American Physical Society, Annual Meeting, 10th, Miami, Fla., Nov. 13-16, 1968, Paper. 16 p. 20 refs.

The relation between plasma turbulence and plasma instability was examined experimentally using the spectrum of plasma fluctuations. The experimental data were obtained on a crossed-field plasma device (axial electric and radial magnetic fields) with a slightly-ionized, low-current and low-pressure argon discharge. The fluctuations were measured using ion-collecting and floating Langmuir probes. The effect of the external electric and magnetic fields on the rms amplitude and spectra of the fluctuations is presented and discussed. The role of coherent oscillations (instability) as a driving source for the plasma turbulence is indicated. Comparison of the situation in plasma turbulence with that in fluid dynamic turbulence is made where appropriate. (Author)

A69-14456 *#

FREQUENCY CONVERSION IN THE SHEATH CAPACITANCE OF A GLOW DISCHARGE PLASMA.

R. T. Hilbish (Purdue University, Dept. of Electrical Engineering, Plasma Research Laboratory, Lafayette, Ind.; NASA, Flight Research Center, Edwards, Calif.), R. M. Montgomery, and R. A. Holmes (Purdue University, Dept. of Electrical Engineering, Plasma Research Laboratory, Lafayette, Ind.).

Journal of Applied Physics, vol. 39, Nov. 1968, p. 5782-5791. 7 refs. Army-Navy-USAF-supported research.

Study of large-signal, high-frequency phenomena occurring in a slightly ionized plasma contained within a pair of metallic coaxial cylinders. An rf equivalent circuit is developed wherein the sheath is represented by a voltage-dependent capacitor in parallel with a voltage-dependent resistor, the presheath by a series resistor, and the plasma region by a series resistor and inductor. It is found that when the sheath is thin compared to the radius of the inner cylinder, the voltage dependence of the sheath capacitor reduces to a form identical with that of an abrupt junction varactor diode, so that the plasma capacitor is properly called a plasma varactor. As an application of the plasma varactor, frequency doubling using standard semiconductor varactor techniques is attempted. The resultant peak conversion efficiency is found to be 31.6% at a drive frequency of 142 MHz and input power of 0.42 W. It is shown that the sheath conductance is responsible for this low conversion efficiency relative to that obtainable from a semiconductor varactor. (Author)

A69-18145 *#

THEORETICAL POPULATION INVERSION IN A DECAYING NITROGEN PLASMA COLUMN.

Chul Park (NASA, Ames Research Center, Moffett Field, Calif.).

American Institute of Aeronautics and Astronautics, Aerospace Sciences Meeting, 7th, New York, N.Y., Jan. 20-22, 1969, Paper 69-48. 13 p. 22 refs.
Members, $1.00; nonmembers, $1.50.

Theoretical analysis of a decaying plasma column of atomic nitrogen, free from external fields and confined motionless in a circular cylinder. Starting from equilibrium, the temporal changes in the plasma properties and the population of bound electronic states as a result of the energy losses by radiation and conduction are cal-

culated on the axis of the plasma column. The radial distribution of electron temperature is assumed to be parabolic, and the plasma is assumed to be optically thin. The collisional excitation rates are derived from the Born-Ochkur approximation. The results show that a strong population inversion occurs between $2p^3\ ^2P$ and $3s^4P$ states, giving rise to 1837-Å line radiation for about 10 nsec under the following conditions: (1) the initial electron temperature is over 14,000 K; (2) the initial electron density is on the order of 10^{16} cm^{-3}; and (3) the radius of the containing cylinder is on the order of 0.1 cm. (Author)

A69-18171 *#
DOPPLER-SHIFT MEASUREMENTS OF AXIAL AND ROTATIONAL VELOCITIES IN AN MPD ARC.
Ulrich Kogelschatz (NASA, Langley Research Center, Hampton, Va.).
American Institute of Aeronautics and Astronautics, Aerospace Sciences Meeting, 7th, New York, N.Y., Jan. 20-22, 1969, Paper 69-110. 8 p. 11 refs.
Members, $1.00; nonmembers, $1.50.

Study of an MPD arc using a bariated tungsten cathode with NH_3 as a propellant (current: 100 to 700 A; magnetic field: 600 to 5000 G; mass flow: 10 and 17.5 mg/sec). A 3.4-m spectrograph (Ebert mounting) was used. Reference lines from an iron arc were used rather than lines from the plasma beam. The advantages are: (1) the reference lines are close to the plasma lines but do not overlap; (2) the reference lines are narrow so that their center is better defined. The shifts were obtained from microdensitometer traces of photographic plates. All ion lines are noticeably slanted with respect to the reference lines, indicating strong rotation of the plasma beam. Rotational and axial velocities of nitrogen ions were obtained at different axial positions. Neutral species (nitrogen, hydrogen) show much smaller axial velocities and no rotation. Clear evidence of ion acceleration in the magnetic nozzle downstream of the electrode gap could be established. (Author)

A69-19988 *#
MAGNETOHYDRODYNAMIC SHOCK WAVES IN NON-ALIGNED FLOW.
Shigeki Morioka and John R. Spreiter (NASA, Ames Research Center, Space Sciences Div., Moffett Field, Calif.).
Journal of Plasma Physics, vol. 3, Feb. 1969, p. 81-96. 7 refs.

The steady shock discontinuity in the flow of a perfectly conducting gas with an arbitrarily oriented magnetic field is considered by taking as the parameters the Mach number, the Alfvén Mach number, the magnetic field direction, and the shock angle. The shock solutions satisfying the conservation laws as well as the entropy and evolutionary conditions are given by the roots of a simple cubic equation and the associated formulas. Several special cases are discussed analytically and numerically. The possible types of MHD shock waves are shown on the speed-deflection phase plane, and the possible shock configurations in the physical space are discussed on the basis of them. (Author)

A69-20521 *
ANALYSIS OF INTEGRATED CHARGED PARTICLE ENERGY SPECTRA FROM GRIDDED ELECTROSTATIC ANALYZERS.
J. Reece Roth (NASA, Lewis Research Center, Cleveland, Ohio) and Marion Clark (Cornell University, Ithaca, N.Y.).
Plasma Physics, vol. 11, Feb. 1969, p. 131-143. 23 refs.

The work relates the shape of the retarding potential curve produced by gridded electrostatic analyzers to the floating potential, the kinetic temperature, and the half-angle subtended in velocity space by the particles. Special emphasis is placed on the case in which the particles are Maxwellianized but restricted within a "loss cone" in velocity space of half-angle θ_0. The cases of pulsed and steady-state supply of particles are both considered. By using an appropriate computer program to compare the analytical expressions derived herein with experimental retarding potential curves, it is possible to obtain significantly more information about the velocity distribution than is possible with conventional methods of data reduction. (Author)

A69-20795 *
WAVE COUPLING ACROSS A DENSITY DISCONTINUITY IN A MAGNETIZED PLASMA.
Stephen Morin and David Kahn (NASA, Electronics Research Center, Cambridge, Mass.).
Physics of Fluids, vol. 11, Dec. 1968, p. 2627-2634. 15 refs.

The plane-wave solutions of the linearized hydrodynamic equations and Maxwell's equations for a fully ionized plasma are used to investigate the properties of plasma oscillation modes which propagate perpendicularly to an external magnetic field. Energy conversion among these modes at a density discontinuity separating two semiinfinite plasmas is investigated. Numerical results illustrate the variations of various energy coupling eificiencies with angle of incidence, propagation frequency, and magnetic field intensity. In contrast to the field-free case previously considered, it is found that energy conversion occurs among all of the plasma modes for normally incident waves. Very high efficiencies of energy conversion between field-modified electron and transverse waves are found for propagation frequencies below the hybrid frequency $(\omega_e^2 + \omega_B^2)^{1/2}$ where ω_e and ω_B are, respectively, the electron plasma frequency and the electron cyclotron frequency. (Author)

A69-20796 *
LONGITUDINAL WAVE PROPAGATION IN VISCOUS FULLY IONIZED PLASMAS.
David Kahn (NASA, Electronics Research Center, Cambridge, Mass.).
Physics of Fluids, vol. 11, Dec. 1968, p. 2635-2643. 18 refs.

A collisional theory of wave propagation in two-fluid fully ionized gases is formulated from the coupled set of Maxwell and Boltzmann equations for an investigation of the collisional damping and dispersion of electron and ion waves. The electron and ion velocity distribution functions of the Boltzmann equations are expanded in Sonine polynomials to an order that gives the collision integrals for the electron and ion self-interactions as well as for the electron-ion interactions. This approximation permits the determination of viscous as well as friction-caused electron and ion wave attenuation and dispersion. It is found that the inclusion of the self-interaction integrals (viscous terms) lead to values of the attenuation and dispersion functions which are substantially different quantitatively (and in some frequency regimes, also qualitatively) from the values obtained previously without these terms. (Major ion wave damping, for example, occurs when the wave and ion-ion collision frequencies are comparable, a result not obtainable from the inviscid theory.) The attenuation and dispersion functions are numerically (and in several limiting cases of interest, analytically) evaluated as functions of the self- and interparticle collision to wave frequency ratios and as functions of the plasma to wave frequency ratios for several different plasmas. (Author)

A69-20797 *
QUASILINEAR THEORY OF HYDROMAGNETIC WAVES IN COLLISIONLESS PLASMA.
Aaron Barnes (NASA, Ames Research Center, Space Sciences Div., Moffett Field, Calif.).
Physics of Fluids, vol. 11, Dec. 1968, p. 2644-2654. 32 refs.

A quasi-linear theory of hydromagnetic waves in a nonrelativistic collisionless plasma (with no superthermal "tail") is derived. It is shown that the time evolution of the space-averaged velocity distribution function of each species is described by a diffusion equation in velocity space, and that this "diffusion" can be split into resonant and nonresonant parts. The resonant diffusion determines the heating of the (finite-β) plasma by damping hydromagnetic waves; such heating enhances electron and ion kinetic temperature parallel to the average magnetic field, and does not affect transverse temperatures. Quasi-linear quenching of the hose instability is discussed as an example. (Author)

A69-20807 *
DIFFUSION OF FAST ELECTRONS IN STOCHASTIC MAGNETIC FIELDS.

G. A. Massel (NASA, Langley Research Center, Hampton, Va.) and M. R. Feix (NASA, Langley Research Center, Hampton; College of William and Mary, Williamsburg, Va.).
Physics of Fluids, vol. 11, Dec. 1968, p. 2738-2740. 6 refs.

Study of the diffusion of fast electrons in a stochastic magnetic field, for the simple case of the fluctuating field parallel to the steady field. It is shown that, in the limit of observation times greater than both the Larmor period and the correlation time of the stochastic field, the diffusion coefficient can be obtained explicitly as a function of the ratio of the correlation time to the Larmor period. The result holds for all values of the ratio of these characteristic times. M. G.

A69-20809 *
GUIDING CENTER DRIFTS IN TIME-DEPENDENT MERIDIONAL MAGNETIC FIELDS.
Thomas J. Birmingham (NASA, Goddard Space Flight Center, Laboratory for Theoretical Studies, Greenbelt, Md.).
Physics of Fluids, vol. 11, Dec. 1968, p. 2749-2752.

The problem of a particle trapped in a time-dependent meridional magnetic mirror field and at the same time subjected to a time-dependent perpendicular electric field is considered. Bounce-averaged guiding-center theory is used to derive expressions for the drift velocity components. These drift expressions depend in a straightforward fashion on the structures of the magnetic and electric fields and on the particle charge, kinetic energy, longitudinal invariant, and bounce period. In the special case of a static magnetic field, no electric field, and J = 0 particles, the drift equations are integrated and the bounce-averaged guiding-center trajectory is obtained. (Author)

A69-21919 *#
ELECTROTHERMAL INSTABILITIES IN THE ENTRANCE REGION OF AN MHD GENERATOR.
J. Marlin Smith (NASA, Lewis Research Center, Cleveland, Ohio).
American Physical Society, Annual Meeting, 10th, Miami Beach, Fla., Nov. 13-16, 1968, Paper. 22 p.

Study of the stability of the subregion of abrupt electron density rise in the entrance region of a nonequilibrium MHD generator. The steady-state solution is one of uniform gasdynamic properties and electron temperature, but with an electron density gradient which is solely a function of the ionization rate. This rate is evaluated at an electron temperature obtained by equating the Joule heating to the elastic collisional and ionization energy loss. The governing equations upon which the perturbation is taken are those of Kerrebrock (1964), with the exception that recombination is neglected in the electron continuity equation. A solution is found in the limit that the ambipolar diffusion field is small compared to the transverse applied electric field. The solution is found to be stable in the limit of zero magnetic field, but to be unstable in the presence of a magnetic field. M. G.

A69-22045 *
STUDY OF THE STRUCTURE OF SWITCH-ON IONIZING SHOCK WAVES.
John Tendys (NASA, Goddard Space Flight Center, Laboratory for Theoretical Studies, Greenbelt, Md.).
Plasma Physics, vol. 11, Mar. 1969, p. 223-235. 12 refs.

Study of the structure of switch-on ionizing shock waves, using a conductivity proportional to the degree of ionization. The Navier-Stokes equations with constant viscosity and heat conductivity coefficients were used. It is found that the condition proposed by Kulikovskii and Liubimov on the structure of the shock can be used to choose a unique downstream state for a given upstream state which agrees with experimental results for a suitable choice of conductivity. It is found that this is equivalent to choosing the minimum shock thickness keeping the transverse magnetic field component always the same sign. In the weak shock limit, the condition that the downstream velocity is equal to the slow hydromagnetic wave speed is also found to hold. (Author)

A69-23660 *#
ELECTRIC-FIELD DISTRIBUTION IN PULSED HIGH-CURRENT-DENSITY DISCHARGES IN HELIUM AND HELIUM-HYDROGEN MIXTURES.
Frank Allario (Brooklyn, Polytechnic Institute, Brooklyn, N.Y.; NASA, Langley Research Center, Hampton, Va.) and Nathan Wainfar (Brooklyn, Polytechnic Institute, Brooklyn, N.Y.).
Journal of Applied Physics, vol. 40, Feb. 1969, p. 675-681. 12 refs.
Army-Navy-USAF-supported research.

The results of a study on high-current-density, pulsed glow discharges in He and He-H_2 mixtures are presented. These results trace the temporal development of the electric-field and wall-potential distribution appearing between the electrodes of a discharge tube as the discharges approach dynamic equilibrium. These discharges, of 1.3 μsec duration, are sustained in 2.5-cm-diam pyrex tubes with interelectrode gaps variable between 10 and 40 cm. The pressure range runs from 0.50 to 5.0 torr. As the discharge approaches dynamic equilibrium late in the discharge pulse, current densities of the order of 15 A/cm^2 are maintained. The buildup of the electric field in the vicinity of the cathode is determined by time-resolved measurements of the Stark splitting of lines in the helium and hydrogen spectrum. The axial component of the electric-field and wall-potential distribution in the rest of the discharge are obtained from signals induced on a series of externally placed electrostatic ring probes. Fields as high as 78 kV/cm were detected at the cathode face, while uniform fields of the order of 10 V/cm torr were found in most of the rest of the discharge. Comments are made on the transition region between high- and low-field regions in the discharge. (Author)

A69-24305 *#
MINIMUM ENERGY PROPERTY OF A BOUNDED ONE-DIMENSIONAL PLASMA.
Frank Hohl (NASA, Langley Research Center, Hampton, Va.).
Physics of Fluids, vol. 12, Jan. 1969, p. 230-233. 11 refs.

Analytic and numerical methods are used to investigate the dynamics, stability, and approach to equilibrium of a bounded, collisionless one-dimensional plasma with a fixed neutralizing ion background. A class of stationary solutions of the nonlinear Vlasov equation is found which represents minimum energy states. It is found that the quasi-equilibrium state which is reached after several plasma periods is close to the Fermi distribution predicted by Lynden-Bell (1967). (Author)

A69-24315 *#
EXPERIMENTAL OBSERVATION OF LOW-FREQUENCY OSCILLATIONS DESCRIBED BY THE PLASMA CONTINUITY EQUATIONS.
J. Reece Roth (NASA, Lewis Research Center, Cleveland, Ohio).
Physics of Fluids, vol. 12, Jan. 1969, p. 260-262. 6 refs.

Low-frequency oscillations in the electron number density of a slightly ionized gas have been experimentally observed over the range 10^2-10^5 Hz. The oscillations are identified with periodic solutions to the neutral- and charged-particle continuity equations. (Author)

A69-28232 *#
COAXIAL-FLOW STABILIZATION OF AN ALTERNATING-CURRENT PLASMA ARC.
Chester D. Lanzo (NASA, Lewis Research Center, Nuclear Systems Div., Cleveland, Ohio).
(American Institute of Aeronautics and Astronautics, Fluid and Plasma Dynamics Conference, Los Angeles, Calif., June 24-26, 1968, Paper 68-706.)
AIAA Journal, vol. 7, Mar. 1969, p. 538-540.

Experimental results are presented for a coaxial-flow-stabilized, ac, 12- to 22-cps (12- to 22-Hz) electric arc. The arc is maintained along the centerline of an argon jet. Coflowing streams of either helium or nitrogen surround the central argon jet. The arc is stabilized by the flow field of the two gases. General characteristics of arc behavior are described for various operating conditions. Arc voltage-current curves are shown. Arc length is varied from 1 to

12 in. (2.54 to 30.5 cm). Photographs of the arc at maximum intensity are shown. (Author)

A69-28364
SPATIAL HARMONICS OF THE HARMONIC-FREQUENCY INSTABILITIES OF THE ELECTRON CYCLOTRON HALF-FREQUENCY [HARMONIQUES SPATIAUX DES INSTABILITES AUX FREQUENCES HARMONIQUES DE LA DEMI-FREQUENCE CYCLOTRONIQUE ELECTRONIQUE].
Jack Olivain, Françoise Perceval, and Mariano Perulli (EURATOM and Commissariat à l'Energie Atomique, Groupe de Recherches sur la Fusion, Fontenay-aux-Roses, Hauts-de-Seine, France).
Académie des Sciences (Paris), Comptes Rendus, Série B - Sciences Physiques, vol. 268, no. 15, Apr. 14, 1969, p. 1005-1008. 5 refs. In French.

Study of a system of two symmetrical electron beams confined by a uniform magnetic field. The "spatial harmonics" of the harmonic-frequency instabilities of the cyclotron half-frequency are observed, as well as the doubling of the cyclotron modes. M.G.

A69-30913 *#
KINETIC THEORY OF INHOMOGENEOUS SYSTEMS.
John C. Price (NASA, Goddard Space Flight Center, Laboratory for Theoretical Studies, Greenbelt, Md.).
Physics of Fluids, vol. 12, Mar. 1969, p. 593-606. 12 refs.

A theory is developed which treats the coupled equations of the various hierarchies in inhomogeneous systems as simultaneous equations in time. This scheme proceeds by successive approximations rather than a power series expansion. The theory is suitable for the derivation of equations for nonuniform and force-driven systems. Examples are given for a plasma and a Boltzmann gas. (Author)

A69-34439 *#
COLLISION DAMPING OF LONGITUDINAL PLASMA WAVES.
Kyoko Matsuda (NASA, Goddard Space Flight Center, Laboratory for Theoretical Studies, Greenbelt, Md.).
Physics of Fluids, vol. 12, May 1969, pt. 1, p. 1081-1083. 9 refs.

Calculation of the collision damping of longitudinal plasma waves using Rostoker's (1964) test particle method. The dispersion relation including collision effects is obtained, and the damping factor is calculated for the case of large wavelength. The result presents a correction to the previous calculations by other authors. G.R.

A69-38242 * #
INTERACTION OF MAGNETOACOUSTIC AND ENTROPY WAVES WITH NORMAL MAGNETOHYDRODYNAMIC SHOCK WAVES.
K. O. Westphal (NASA, Ames Research Center, Moffett Field, Calif.) and J. F. McKenzie (California, University, Dept. of Applied Electrophysics, La Jolla, Calif.).
Physics of Fluids, vol. 12, June 1969, p. 1228-1236. 14 refs.

Derivation of equations for the amplitudes of magnetoacoustic and entropy waves diverging from a normal MHD shock as a result of an incident disturbance of the same kind, assuming that the magnetic field is parallel to the flow. The solutions of these equations are then used to construct the ratios of the amplitudes of the transmitted to the incident waves. The ratios of energy fluxes associated with the incident and transmitted waves are obtained in terms of the solutions of the governing equations. The formulas are applied to an example. (Author)

A69-38713 * #
TEMPORAL PLASMA ECHOES.
John C. Baker and William J. B. Oldham, Jr. (NASA, Manned Spacecraft Center, Houston, Tex.).
Physics of Fluids, vol. 12, July 1969, p. 1525, 1526.

Results of a computer experiment conducted on a 9000-particle plasma to test the theoretical prediction of temporal echoes. The second-order echo is found at the time and wave number predicted by the theory. (Author)

A69-43122 * #
A THEORY OF MOVING STRIATIONS BASED ON THE CONTINUITY-EQUATION PLASMA OSCILLATION.
J. Reece Roth (NASA, Lewis Research Center, Cleveland, Ohio).
International Union of Pure and Applied Physics, International Conference on Phenomena in Ionized Gases, 9th, Bucharest, Rumania, Sept. 1-6, 1969, Paper. 13 p. 10 refs.

Study of oscillations arising as a consequence of the transit time delays of neutral and charged particles as they move through an ionized gas. Since the time delays prevent a detailed balance between the production and loss terms of the continuity equations and lead to a relaxation oscillation of the neutral and charged particle member densities, the previous spatially independent theory of these oscillations was extended to traveling wave solutions of the space-dependent continuity equations. These travelling waves are identified with moving striations. O.H.

N69-10471*# National Aeronautics and Space Administration. Langley Research Center, Langley Station Va.
COMPUTER EXPERIMENTS ON THE MICROSCOPIC BEHAVIOR OF ONE-DIMENSIONAL PLASMAS
Richard H. Weinstein and Belinda H. Adams Washington Nov. 1968 59 p refs
(NASA-TN-D-4831) Avail: CFSTI CSCL 20I

The detailed motions of a system of 1000 particles simulating a one dimensional electrostatic plasma have been followed by using the IBM 7040/7094 Direct Coupled System at the Langley Research Center. The particle interactions are collective and as the calculation proceeds stepwise through time, the position-velocity histories of all the particles completely specify the successive states of the system. These data constitute an experiment, upon which measurements can be made. The velocity distribution function, the Fourier harmonics of the potential energy, the spatial correlations of the electric field, and the drag and velocity diffusion of test particles are measured for the Maxwellian and uniform velocity distributions. Comparison of the present work with both earlier experiments and the predictions of zeroeth and first-order plasma kinetic theory have yielded generally good agreement for all measurements in both equilibrium and nonequilibrium plasmas. The detailed behavior of the long wavelength harmonics of the potential energy is, however, unresolved for regions where the assumptions of the zeroeth-order theory are not satisfied. Author

N69-14525*# National Aeronautics and Space Administration. Lewis Research Center, Cleveland, Ohio.
EXPERIMENTAL OBSERVATION OF OSCILLATIONS DESCRIBED BY THE CONTINUITY EQUATIONS OF SLIGHTLY IONIZED DEUTERIUM, NEON, AND HELIUM GAS
J. Reece Roth Washington Dec. 1968 58 p refs
(NASA-TN-D-4950) Avail: CFSTI CSCL 20I

Low-frequency oscillations in the electron number density of a slightly ionized gas have been observed in deuterium, neon, and helium over the frequency range from 10^2 to 8×10^4 Hz. These oscillations can be identified with periodic solutions to the neutral- and charged-particle continuity equations. The observed functional dependence of the waveform and of the peak-to-peak amplitude of the oscillation are qualitatively consistent with this

mechanism. The frequency of the oscillation was independent of magnetic field strength and had the predicted square-root dependence on the product of electron and neutral number density. Author

N69-16466*# National Aeronautics and Space Administration. Lewis Research Center, Cleveland, Ohio.
COMPONENTS OF A HYDROGEN PLASMA INCLUDING MINOR SPECIES
R. W. Patch Washington Jan. 1969 97 p refs
(NASA-TN-D-4993) Avail: CFSTI CSCL 20I

Tables and graphs of the number densities of hydrogen atoms (H), protons (H^+), free electrons (e^-), hydrogen molecules (H_2), negative hydrogen ions (H^-), hydrogen diatomic molecular ions (H^+_2), and hydrogen triatomic molecular ions (H^+_3) in a hydrogen gas or plasma in thermodynamic equilibrium were computed for temperatures from 300 to 40,000 K and pressures from 1.01325×10^5 to 1.01325×10^8 N/m^2 (1 to 1000 atm) except for a small, high density region. For temperatures above 2000 K, the Debye–Huckel approximation was employed. Morse potentials are given for all singly excited attractive states of H_2 with principal quantum numbers to 17. A FORTRAN IV computer program for computing number densities and other properties of a hydrogen plasma is included. Author

N69-17212*# General Dynamics Corp., San Diego, Calif.
EXPERIMENTS ON A HIGH POWER, PULSED, CONSTRICTED ARC HEATER
Rolf Dethlefsen Washington NASA Feb. 1969 53 p refs
(Contract NAS2-4665)
(NASA-CR-1246; GDC-DBE68-008) Avail: CFSTI CSCL 20I

Pulsed experiments on a high power constricted arc with axial flow were performed by discharging a lumped parameter transmission line composed of a number of capacitors and inductors. The arc current ranged from 1.8 to 3.6 KA with a flow rate of nitrogen from 5 to 40 g/sec. High speed photographs revealed flow instabilities. Under certain circumstances, the arc did not fill the tube; instead a relatively concentrated arc filament fluctuated about the tube. A swirling gas inlet was effective in reducing arc instabilities. Evidence for strong Maecker cathode jets was also found. Impinging on the constrictor walls, these jets could lead to increased erosion, or shorting of segments in a continuous facility. Cathode jets could be eliminated by using a cathode with simultaneous arc attachment on four parallel tungsten rods. This four-pin cathode also showed lower cathode erosion than a cathode with a single tungsten rod. In addition, a cascading circuit for gas breakdown triggering of the long tube was developed which is superior to wire explosion triggering. Author

N69-18041*# Michigan Univ., Ann Arbor.
AN EXPERIMENTAL AND THEORETICAL ANALYSIS OF THE CONVECTED BALANCED ARC
Leland Malcolm Nicolai (Ph.D. Thesis) Washington NASA Feb. 1969 194 p refs
(Grant NGR-23-005-128)
(NASA-CR-1267) Avail: CFSTI CSCL 20I

The behavior of direct current electric arcs in cross-flow and transverse magnetic fields was studied by observing interaction and energy exchange processes between the arc, the velocity field, and the magnetic field. Experiments with high current arcs immersed in supersonic airstreams proved that with cone cylinder electrodes the arc always slanted with the anode spot upstream of the cathode spot. The peak temperature was located forward of the arc axis. Slant angle at constant Mach number increased slightly with increasing current. A theoretical continuum fluid model was formed based on the experimental observation that the convected balanced arc is impervious to free stream. Analysis of the arc core, based upon this model, showed that one dimensional equations gave a satisfactory approximation for the temperature distribution along the x axis; as the joule heating term coefficient decreased to its constant value, the calculated peak temperature shifted to a more forward position and finally distorted around the periphery of the front half of the arc. G.G.

N69-19131*# National Aeronautics and Space Administration. Lewis Research Center, Cleveland, Ohio.
LABORATORY SIMULATION OF SOLAR WIND–EARTH INTERACTION
Donald L. Chubb Washington Feb. 1969 12 p refs
(NASA-TM-X-1738) Avail: CFSTI CSCL 04A

A laboratory simulation experiment of the interaction of the solar wind and the earth's magnetic field is being conducted. The plasma flow is produced by an MPD arc and a magnetic dipole is used to simulate the earth's magnetic field. The initial investigations of the stagnation region of the flow show a rapid rise in the plasma potential. The magnetic field in this region is also altered from the dipole type behavior it exhibits when no flow exists. This region of change is plasma potential and magnetic field has a thickness characterized by the electron cyclotron radius. It appears to be a merging together of a collisionless deceleration and stagnation of the flow. However, whether or not a collisionless shock wave exists has not been conclusively demonstrated. Author

N69-19783*# National Aeronautics and Space Administration. Lewis Research Center, Cleveland, Ohio.
POSSIBLE APPLICATIONS OF THE CONTINUITY-EQUATION PLASMA OSCILLATION TO PULSARS AND OTHER PERIODIC ASTROPHYSICAL PHENOMENA
J. Reece Roth Washington Mar. 1969 60 p refs
(NASA-TN-D-5078) Avail: CFSTI CSCL 03B

The continuity equations for neutral and charged particles in a partly ionized gas may possess periodic solutions. These oscillations are suggested as a possible clock mechanism for periodic astrophysical phenomena such as geomagnetic micropulsations, pulsars, and of long-period fluctuatins in the charged particle density of the interstellar medium. A mathematical model of these oscillations is derived and applied to two cases of astrophysical interest; an isolated, virtually uniform region of partially ionized gas; and a slightly ionized stellar or planetary atmosphere, the characteristics of which vary with position. The theoretical analysis is supplemented by an experimental investigation of the pulsed production and loss of electrons from a magnetically confined laboratory plasma which was subject to the continuity-equation oscillation. Some pulsar like characteristics were observed and measured in this plasma. Author

N69-20875*# National Aeronautics and Space Administration. Lewis Research Center, Cleveland, Ohio.
ELECTROTHERMAL INSTABILITIES IN THE ENTRANCE REGION OF AN MHD GENERATOR
J. Marlin Smith Washington Mar. 1969 23 p refs
(NASA-TM-X-1761) Avail: CFSTI CSCL 20I

In the entrance region of a nonequilibrium MHD generator one finds an abrupt rise in electron temperature followed by a four- or five-decade increase in electron density. We consider the stability of this region of abrupt electron density rise. A solution is found in the limit that the ambipolar diffusion field is small compared to the transverse applied electric field. The solution is found to be stable in the limit of zero magnetic field but to be unstable in the presence of a magnetic field. Author

N69-20997*# National Aeronautics and Space Administration. Langley Research Center, Langley Station, Va.
CAUSES OF MAGNETIC-FIELD NONUNIFORMITY AND ITS EFFECT ON STABILITY OF THETA-PINCH PLASMA
Joseph Norwood, Jr. Washington Mar. 1969 65 p refs
(NASA-TR-R-303) Avail: CFSTI CSCL 20I

Sources of the field nonuniformity are delineated and discussed. These include the collector-plate geometry, the nonlinear effect of the plasma, end effects in the coil, discontinuity in gap spacing as the current flows into the coil, and effects of the alteration in axial current distribution due to skin effect. Next the various methods for stabilizing the plasma by eliminating field gradients are described, and a new method involving the use of a flux concentrator is proposed. The advantages of this method are compared with advantages of other techniques that have been used. Also, results of quantitative measurements of the field uniformity in an exact 1/2-scale model of the Langley theta pinch are presented. These results include flux concentrator and collector-plate-extension effects as well as the effect of the volume of the collector-plate structure which excludes high frequency flux due to skin effect. Finally, experiments which suggest that full scale theta pinches without extensions are capable of being stabilized by flux-concentrator techniques are described. Author

N69-21124*# United Aircraft Corp., East Hartford, Conn.
THEORETICAL INVESTIGATION OF THE COMPOSITION AND LINE EMISSION CHARACTERISTICS OF ARGON–TUNGSTEN AND ARGON–URANIUM PLASMAS
N. L. Krascella Washington NASA Mar. 1969 76 p refs
(Contract NASw-847)
(NASA-CR-1313; G-910092-10) Avail: CFSTI CSCL 20I

A theoretical investigation was conducted to determine the composition and integrated line emission characteristics of various ionization species of tungsten, uranium, and argon. The study was made to facilitate radiant heat transfer analysis in the seeded propellant and nuclear fuel regions of gaseous-core nuclear rocket engines and to provide a basis of comparison for a concurrent experimental program designed to examine line emission

N69-22638*# United Aircraft Corp., East Hartford, Conn.
THEORETICAL INVESTIGATIONS OF r-f INDUCTION HEATED PLASMAS
Arthur E. Mensing and Laurence Boedeker Washington NASA Apr. 1969 79 p refs
(Contract NASw-847)
(NASA-CR-1312; G-910091-18) Avail: CFSTI CSCL 20I

Theoretical analyses were made to investigate the power deposition and energy removal in radio frequency induction heated plasmas. These investigations were directed toward the high power, high pressure, radiating r-f plasmas that are being used to simulate the thermal environment of the nuclear light bulb reactor. Two related investigations are described in this report. In one, the power deposition and energy dissipation characteristics of infinite-cylinder r-f heated argon plasmas at pressures of 1.0 and 10 atm were studied. The electromagnetic field equations, energy equation, and heat conduction equation were integrated numerically starting with specified values of temperature and axial magnetic field at the centerline. In the second investigation, the coupling between the plasma discharge and the r-f generator was studied using an infinite-cylinder, constant-conductivity model. The analysis was used to investigate the effects of discharge power, reactive power, and discharge size on the surface radiation heat flux and to examine the effect of r-f frequency shifts on matching. Author

N69-22920*# United Aircraft Corp., East Hartford, Conn.
EXPERIMENTAL INVESTIGATION OF THE SPECTRAL EMISSION CHARACTERISTICS OF ARGON-TUNGSTEN AND ARGON-URANIUM INDUCTION HEATED PLASMAS
Pierre J. Marteney, A. E. Mensing, and N. L. Krascella Washington NASA Apr. 1969 48 p refs
(Contract NASw-847)
(NASA-CR-1314; G-910092-00) Avail: CFSTI CSCL 20I

An experimental study was conducted to determine the emission characteristics of gaseous tungsten and uranium located in an rf induction heated, vortex stabilized argon discharge. The tungsten and uranium were introduced into the discharge in the form of tungsten and hexafluoride or uranium hexafluoride at heavy atom to argon mass ratios and a total pressure of one atmosphere. Temperatures in the heavy atom seeded discharges were determined to be approximately 8500 deg K, and were ascertained by measuring neutral argon atom relative line intensity ratios by the Boltzmann method. Temperatures determined by this method were confirmed by measurements of absolute neutral argon atom line intensities and absolute argon ion continuum intensities. Spectra were obtained for pure argon, tungsten hexafluoride–argon, and uranium hexafluoride–argon systems in the wavelength region from 125 A (0.125 micron) to 100,000 A (10 micron). The experimental data were reduced to obtain integrated continuum and line intensities over intervals of 100 A for pure argon. Integrated line intensities were obtained over wavelength intervals of 100 A for tungsten and uranium after correcting the experimental results for the contribution to total intensity due to argon continuum and lines. Author

N69-22942*# National Aeronautics and Space Administration. Langley Research Center, Langley Station, Va.
INVESTIGATION OF A PLASMA ACCELERATOR WITH MAGNETIC FIELD ARRANGED TO PRODUCE A DIVERGENT-NOZZLE EFFECT
Joseph D. Brooks and William D. Beasley Washington Apr. 1969 32 p refs
(NASA-TN-D-5122) Avail: CFSTI CSCL 20I

The results of an experimental investigation of a plasma accelerator at static pressures from 0.765 mm Hg to 2.60 mm Hg are presented. The continuous flow device used a dc arc to provide the plasma and a dc magnetic field that is shaped to provide both the constriction of the plasma and the pressure gradient that produces the flow. Pressure measurements within a certain range of parameters were obtained. Effects of increased magnetic field strength, arc current, and pressure upon the Mach number are given. Author

N69-23451*# United Aircraft Corp., East Hartford, Conn.
NUCLEAR STUDIES OF THE NUCLEAR LIGHT BULB ROCKET ENGINE
Thomas S. Latham Washington NASA Apr. 1969 81 p refs
(Contract NASw-847)
(NASA-CR-1315; G-910375-3) Avail: CFSTI CSCL 20I

Analytical studies were conducted to determine U-233 critical mass requirements, neutron kinetic behavior, and neutron and gamma ray heating rates for the nuclear light bulb rocket engine. The nuclear light bulb is a multiple-cavity gaseous nuclear rocket engine in which energy is transferred by thermal radiation from gaseous nuclear fuel through internally cooled transparent walls to seeded hydrogen propellant. The engine considered in this report employs seven separate cavities, each having a length of 6 ft and an average diameter of 2.3 ft. Beryllium oxide is employed between the unit cavities, and layers of BeO and graphite surround the seven units to provide neutron reflection. The criticality analysis allowed the effects of engine design changes on critical mass to be investigated. Among the factors that were varied were the total moderator mass, the amount of BeO between unit cavities, the distribution of moderator mass, the amount of tungsten seed in the hydrogen propellant, and the amount of hafnium required to shield the fuel injection and recirculation system ducts. The analysis also

considered factors affecting the kinetic behavior of a nuclear light bulb engine. Author

N69-23787*# National Aeronautics and Space Administration. Langley Research Center, Langley Station, Va.
A SEMIEMPIRICAL COLLISION MODEL FOR PLASMAS
Willard E. Meador Washington May 1969 35 p refs
(NASA-TR-R-310) Avail: CFSTI CSCL 20I

A collision model similar in many respects to that of a Lorentz gas is developed for plasmas. Two assumptions are made: (1) the totality of interparticle force laws (including electron–electron) can be replaced with a single parameter determined by the unique ratio of generalized electric field to temperature gradient that can exist in a bounded, nonmagnetic, and currentless plasma of given composition; (2) the electron dynamics governed by such an average potential are Lorentz-like in the sense that the effective electron collision partners behave as heavy scattering centers. With the collision model thus specified and held fixed, the first order kinetic equation is solved exactly for a succession of more complex plasma conditions; the corresponding distribution functions are used to predict such diverse properties as entropy, entropy and diffusion relaxation times, electromagnetic tensor conductivities, thermal conductivity, and thermal diffusion. The method apparently provides an adequate scheme for utilizing experimental data when microscopic collision parameters are scarcely known and for directly extending previous calculations to more complex conditions. Author

N69-24920*# National Aeronautics and Space Administration. Lewis Research Center, Cleveland, Ohio.
A NEW MOMENTUM INTEGRAL METHOD FOR TREATING MAGNETOHYDRODYNAMIC AND SIMPLE HYDRODYNAMIC ENTRANCE FLOWS
Richard E. Schwirian Washington May 1969 30 p refs
(NASA-TN-D-5215) Avail: CFSTI CSCL 20I

A new momentum-integral method has been devised for describing the incompressible flow of a conducting fluid in the entrance of a magnetohydrodynamic channel. The method is distinctive in that an edge stress is permitted to exist at the point of intersection of the boundary layer and the free stream. A prudent choice of the edge stress variation forces the governing differential equation to yield an asymptotic solution with the correct wall stress. Accurate analytical solutions are obtained for laminar flow with and without a magnetic field. Nonmagnetic turbulent flow is also well described by this method. Author

N69-25394*# National Aeronautics and Space Administration. Lewis Research Center, Cleveland, Ohio.
ANALYSIS OF ELECTRON ANALOG SIMULATION OF ION CONTAINMENT IN MAGNETIC FIELDS
Nelson L. Milder and Harold R. Kaufman Washington May 1969 33 p refs
(NASA-TN-D-5217) Avail: CFSTI CSCL 20I

The π-theorem of dimensional analysis has been used to obtain similarity parameters characterizing the interaction of a charged-particle gas with a magnetic field. These parameters are used to derive scaling relations for simulating ion-containment systems with electron-containment systems (electron analogs). The scaling conditions are used to correlate the results of an electron-containment experiment to a similar ion-containment experiment, both reported in the literature. The analysis is extended to include a discussion of the possibility of collisionless plasma simulation. Plasma-containment simulation is considered from the viewpoint of the stability of static systems. The theoretical possibility of flute instability simulation is discussed. Author

N69-26313*# National Aeronautics and Space Administration. Ames Research Center, Moffett Field, Calif.
CIRCULATING CURRENTS IN LINEAR CROSSED-FIELD GENERATORS AND ACCELERATORS
Gustav A. Carlson Washington May 1969 14 p refs
(129-02-08-01-00-21)
(NASA-TN-D-5244) Avail: CFSTI CSCL 20I

Boundary layers on the walls of linear crossed-field plasma generators and accelerators cause circulating electrical currents that can greatly affect the operation of these devices. Expressions are derived for the velocity and current distributions in the open circuit device from the analysis for fully developed incompressible magnetohydrodynamic (MHD) flow in a square duct with nonconducting walls. From these distributions the viscous and ohmic heat generation rates in the working fluid were calculated for Hartmann numbers up to 24, where the magnetic force is dominant. Measured heat-transfer rates to the walls of an open circuit J × B plasma accelerator were found to increase with applied magnetic field strength at the insulator walls but to remain nearly constant at the electrode walls. A comparison of theory and experiment indicates that the calculated heat generation has both the magnitude and spatial distribution to explain the observed heat-transfer rates. The circulating currents significantly decelerate the flow near the center of the duct, and will exist in any MHD duct in which there is an appreciable boundary layer and a large conductivity extending to near the walls. Author

N69-29140*# National Aeronautics and Space Administration. Electronics Research Center, Cambridge, Mass.
PLASMA GENERATION USING A LARGE V-GROOVE CATHODE DISCHARGE
Paul R. Caron Washington Jun. 1969 37 p refs
(NASA-TN-D-5269) Avail: CFSTI CSCL 20I

The results of an investigation of the plasma parameters generated by a large V-groove cathode discharge are presented. The cathode consists of a 12-inch aluminum plate into which V-grooves of 1/8-inch spacing and 60-deg angle are milled. With this cathode, a negative glow discharge is produced which yields a stable, steady-state plasma. Electron densities up to 2×10^{12} cm^{-3} have been obtained in the 12-inch diameter chamber. The electron temperature is about 1200°K and is independent of discharge current and gas pressure over the range 0.3 to 1.0 torr. The discharge operates in much the same fashion as a conventional brush cathode discharge but with lower operating voltage for equal current densities. The lower operating voltage, which reduces the arcing problems at the cathode-glass junction, and the relative ease in fabricating the V-groove cathode make it an attractive alternative to the brush cathode for many applications. Author

N69-29600*# National Aeronautics and Space Administration. Electronics Research Center, Cambridge, Mass.
A LABORATORY STUDY OF MICROWAVE RADIOMETRIC TECHNIQUES FOR RE-ENTRY PLASMA MEASUREMENTS
P. R. Caron, G. Haroules, W. Brown, III, and F. Russo Washington Jul. 1969 35 p refs
(NASA-TN-D-5274) Avail: CFSTI CSCL 20I

The results of a laboratory study of plasma radiometric techniques applicable to reentry plasma measurements are presented. The laboratory plasma is generated by a glow discharge in helium using a large V-groove cathode. The operating characteristics of the discharge are quite similar to those of the brush cathode discharge. The electron density and temperature are determined as a function of position, discharge current, and gas pressure using Langmuir probes and microwave reflectometers, and the collision frequency is calculated using these measured values. The plasma noise radiation is measured as a function of discharge current using a microwave radiometer operating in the absolute mode. It is shown that numerical values of electron density, collision frequency, and electron

temperature can be derived from curves of plasma noise as a function of discharge current. Author

N69-29905*# National Aeronautics and Space Administration. Lewis Research Center, Cleveland, Ohio.
ENERGY TRANSFER AND ION COST IN A HYDROGEN PLASMA
Carl F. Monnin and George M. Prok Washington Jul. 1969 19 p refs
(NASA-TN-D-5319) Avail: CFSTI CSCL 20I

A Maxwellian electron gas interacts with a cold neutral hydrogen gas with various degrees of dissociation. The electron temperature range is 3 to 100 eV. The plasma is assumed to be tenuous and in the steady state. The power is assumed to be lost by radiation, ionization, and kinetic energy carried to the walls per second by the charged particles. The wall loss term used is calculated from sheath theory. The cost of producing a proton in various mixtures of neutral atomic and molecular hydrogen is also presented. Author

N69-30622*# National Aeronautics and Space Administration. Lewis Research Center, Clevelend, Ohio.
REFRACTIVE INDEX: PARTICLE DENSITY NONEQUILIBRIUM CESIUM PLASMAS PROBED BY A MULTIFREQUENCY HELIUM-NEON LASER
Richard B. Lancashire Washington Jul. 1969 24 p refs
(NASA-TN-D-5328) Avail: CFSTI CSCL 20I

The refractive index of a nonequilibrium cesium plasma is computed for the free electrons and neutral atoms ($6S_{1/2}$ to $7P_{3/2}$ levels) at laser wavelengths of 0.6328, 1.1523. and 3.3914 μm. Densities of the neutrals were computed using quasi-steady-state solutions to the various level rate equations for typical thermionic diode conditions (initial cesium atom densities from 10^{15} to 10^{17} cm^{-3} and electron temperatures from 1500° to 3000°K). The dominant contributors to the refractive index are the ground-state neutrals and the free electrons. The results indicate the usefulness of the technique to measure local cesium atom densities accurately. Author

N69-34897*# Northwestern Univ., Evanston, Ill.
EXPERIMENTAL INVESTIGATION OF MAGNETOAERODYNAMIC FLOW AROUND BLUNT BODIES
S. Kranc, M. C. Yuen, and A. B. Cambel Washington NASA Aug. 1969 158 p refs
(Grant NsG-547)
(NASA-CR-1393) Avail: CFSTI CSCL 20I

The drag on a blunt body with a self-contained electromagnet was measured with the body placed in a low density argon plasma stream. Tests were conducted in a steady flow of plasma produced in a direct current arc and expanded to supersonic speeds. Measurements were restricted to one flow condition and the influence of viscosity and the Hall effect were both considered. From experimental measurements of the total drag on the body, the Lorentz force on the magnet and the pressure force on the body, the viscous forces on the body were deduced and empirical relations for the data were generated. The flow field around the body was investigated spectroscopically, and the predicted increase in shock stand-off distance observed photographically. Spectroscopic measurements showed that the electrons in the plasma were out of thermal equilibrium in the plasma and that the flow was essentially nonreacting. Author

N69-35732*# National Aeronautics and Space Administration. Lewis Research Center, Cleveland, Ohio.
ANALYTICAL AND EXPERIMENTAL STUDIES OF MHD GENERATORS CATHODES EMITTING IN A "SPOT" MODE
Lester D. Nichols and Maris A. Mantenieks Washington Sep. 1969 refs
(NASA-TN-D-5414) Avail: CFSTI CSCL 20I

The sheath current-voltage characteristics for a plane cathode emitting current from a thermionic arc spot are derived. The derivation is based upon the requirement of energy conservation at the cathode spot and also in an ionization region adjacent to the spot. The results for given gas conditions and electrode work function predict a sheath voltage which decreases with both increasing current for a fixed undisturbed (i.e., far from the spot) cathode temperature, and increasing disturbed cathode temperature at a fixed current. Experimental data is shown which supports the conclusions predicted by the model. Author

N69-36755*# National Aeronautics and Space Administration. Electronic Research Center, Cambridge, Mass.
SPECTROSCOPIC STUDY OF A HELIUM ARC
Victor E. Scherrer Washington Sep. 1969 13 p refs
(NASA-TN-D-5396) Avail: CFSTI CSCL 20I

A plasma source which has the characteristics desired for astrophysical spectral measurements is described. A high frequency (1 MHz) capacitor discharge through an arc tube containing needle electrodes heated helium to kinetic electron temperatures varying from 10 eV to over 100 eV. Diagnostic measurements included time resolved spectroscopy and high speed photography. Author

N69-36939*# National Aeronautics and Space Administration. Electronics Research Center, Cambridge, Mass.
FEASIBILITY OF DETECTING RADIATION SCATTERED FROM A PLASMA
Melville Clark, Jr. Washington Sep. 1969 56 p refs
(NASA-TN-D-5311) Avail: CFSTI CSCL 20I

It is shown that it is possible to detect radiation scattered from a plasma in doppler-shifted lines. The method provides a way of measuring the fluctuation in plasma charge density. Author

N69-38010*# National Aeronautics and Space Administration. Flight Research Center, Edwards, Calif.
SUMMARY OF XB-70 AIRPLANE COCKPIT ENVIRONMENTAL DATA
Kirk S. Irwin and William H. Andrews Washington Oct. 1969 24 p refs
(NASA-TN-D-5449) Avail: CFSTI

Thermal, acoustical, and acceleration environmental data were obtained for the crew compartment of the XB-70 airplane during the 186-flight-hour airworthiness test program. Temperature levels, gradients, and time histories are presented for the cockpit walls, floor, and windshields. Heat transfer through the walls and along the floor produced no crew discomfort. Thermal radiation from the hot inner windshield would have been objectionable to the crew if they had not been protected by insulated flight suits and helmets with faceplates. The acoustical environment of the crew compartment was similar to that of other military turbojet bomber aircraft. At Mach 3 the sound-pressure level in the XB-70 cockpit, primarily generated by onboard electrical and environmental equipment, was 96 decibels, which is about 10 decibels higher than that measured on a present subsonic jet transport. Subsonically the cockpit noise levels exceeded military specification limits by as much as 10 decibels at frequencies above 400 hertz. At cruise conditions the cockpit noise levels exceeded the supersonic transport internal-noise-level design criteria in the frequency range above 300 hertz. Acceleration data for the XB-70 crew compartment and center of gravity are presented for taxi, takeoff, subsonic buffet, and atmospheric-turbulence conditions. Author

N69-38227*# Lockheed Missles and Space Co., Palo Alto, Calif.
RADIANT ENERGY TRANSFER MEASUREMENTS IN AIR
Allen D. Wood and Kenneth H. Wilson Washington NASA Oct. 1969 89 p refs
(Contract NAS7-579)
(NASA-CR-1390; LMSC-681796) Avail: CFSTI CSCL 20I

Temperatures and total radiant intensities were measured in air plasmas created in the reflected shock region of a 12-inch diameter, arc-driven shock tube. The temperatures were used to explore the difference between the total intensity measurements and theoretical predictions which were evaluated at the gasdynamic property values. The temperature measurements utilized the following spectroscopic techniques: (1) measuring the integrated intensity of certain atomic lines and multiplets; (2) fitting profiles to measured line shapes; and (3) measuring the spectral intensity of the continuum at 4935 Å. Temperatures between 10,750° and 13,000°K were measured with a typical precision of ± 4%. This precision could not be maintained at higher temperatures. The results indicate that, on the average, the measured temperatures were 4% below the gasdynamic values, which could account for the difference between the total intensity measurements and the predictions in this temperature range. Further, the erratic shot to shot deviations of 0 to 8% between the measured and gasdynamic temperatures suggest that the actual plasma temperatures were not adequately predictable from the incident shock velocity. Author

N69-39302*# National Aeronautics and Space Administration. Langley Research Center, Langley Station, Va.
FREE-STREAM ELECTRON CONCENTRATION IN AN ARC-HEATED WIND TUNNEL AND CORRELATION OF LANGMUIR PROBE AND MICROWAVE INTERFEROMETER MEASUREMENTS
Roy J. Duckett and W. Linwood Jones, Jr. Washington Oct. 1969 40 p refs
(NASA-TN-D-5500; L-6679) Avail: CFSTI CSCL 20I

Langmuir probes and microwave interferometer studies were made in the free stream of a Mach 10 arc-heated wind tunnel using air and nitrogen as test media. Electron concentrations were measured from 1×10^{10} electrons per cubic centimeter. The measured electron concentrations were measured from 1×10^{9} to 6×10^{10} electrons per cubic centimeter. The measured electron concentrations were compared with the finite-rate nonequilibrium calculations and were found to be about 1 order of magnitude greater for the case of air and several orders of magnitude for nitrogen. Several mechanisms are examined for the increased electron concentration. Correlation of the microwave interferometer and conical Langmuir probe measurements yielded results which agreed within a factor of 2. The mean electron temperature measured by the Langmuir probe was equal to the gas temperature at the throat of the nozzle. Author

26

PHYSICS, SOLID-STATE

Includes semiconductor theory; and superconductivity. For applications see: 16 Masers. For related information see also: 10 Electronics.

A69-10009 •
TEMPERATURE-DEPENDENT ISOMER SHIFT AND ANHARMONIC BINDING OF Sn^{119} IN Nb_3Sn FROM MÖSSBAUER-EFFECT MEASUREMENTS.
J. S. Shier (California, University, Los Alamos Laboratory, Los Alamos, N. Mex.; NASA, Electronics Research Center, Cambridge, Mass.) and R. D. Taylor (California, University, Los Alamos Scientific Laboratory, Los Alamos, N. Mex.).
Physical Review, 2nd Series, vol. 174, Oct. 10, 1968, p. 346-350. 25 refs.
AEC-sponsored research.
Study of the temperature dependence of the Mössbauer recoil-free fraction, and examination of the line shift of Sn^{119} in several Nb_3Sn absorbers between 4 and 375 K. The recoil-free fraction measurements show that the forces on the tin atoms are highly anharmonic. The line-shift measurements are interpreted in terms of a temperature-dependent electron density at the tin nucleus, which is shown to support previous suggestions of a very narrow d band near the Fermi level. (Author)

A69-10557 *
CURRENT CONTROLLED NEGATIVE RESISTANCE IN N-TYPE GALLIUM ARSENIDE.
Wayne E. Hughes (NASA, Goddard Space Flight Center, Advanced Development Div., Greenbelt, Md.).
IEEE, Proceedings, vol. 56, Oct. 1968, p. 1715. 6 refs.
Observation of a negative differential resistance effect that can produce relaxation-type oscillations at frequencies in the 10^4 to 10^5-Hz range in n-type gallium arsenide. The frequency of the oscillations is found to be dependent upon the sample current. M. G.

A69-10934 *
OPTICAL ABSORPTION IN TRIPHENYLMETHYLARSONIUM TETRACYANOQUINODIMETHAN SINGLE CRYSTALS.
T. Mookherji (NASA, Marshall Space Flight Center, Huntsville, Ala.).
Solid-State Communications, vol. 5, 1967, p. 981-984. 7 refs.
Optical constants of triphenylmethylarsonium-TCNQ are evaluated by the reflectance technique between 0.4 and 2.4 μ. The Cauchy-type dispersion relation satisfactorily describes the reflection coefficients in the region of 1.0 to 1.25 μ. The absorption mechanism beyond 1.50 eV has been explained on the basis of indirect transitions. (Author)

A69-12408 *#
GaSb-ZnTe HETEROJUNCTION.
H. Serreze, S. Fischler, and D. Sawyer (NASA, Electronics Research Center, Cambridge, Mass.).
Journal of Applied Physics, vol. 39, Oct. 1968, p. 5330. 5 refs.
Description of a method for successfully fabricating a heterojunction formed between the III-V compound GaSb and the II-VI compound ZnTe. The degree of lattice mismatch for these semiconductor materials with the same zinc blende structure is ~0.1%. The difference in bandgaps is about 1.6 eV, while the difference in melting points is about 590°C. M. G.

A69-16357 *#
THERMOMAGNETIC EFFECTS AND FERMI SURFACE TOPOLOGY - RESULTS IN METALLIC TIN AT LOW TEMPERATURES.
John A. Woollam (NASA, Lewis Research Center, Cleveland, Ohio).
American Physical Society, Winter Meeting, San Diego, Calif., Dec. 18-20, 1968, Paper. 15 p. 8 refs.
The adiabatic Nernst-Ettingshausen thermoelectric, and thermal transverse-even coefficients are measured in magnetic fields to 3.3 tesla (33 kG), and at temperatures between 1.2 and 4.2 K in metallic tin. The results demonstrate the effects of Fermi surface topology on the Nernst-Ettingshausen coefficient. Quantum oscillations in the thermopower had amplitudes in good agreement with theory. (Author)

A69-16358 *#
EFFECT OF BIAS LIGHT ON THE SPECTRAL RESPONSE OF Cu_2S-CdS CELLS.
A. E. Potter, Jr., R. L. Schalla, H. W. Brandhorst, Jr., and L. Rosenblum (NASA, Lewis Research Center, Cleveland, Ohio).
Institute of Electrical and Electronics Engineers, Photovoltaic Specialists Conference, Pasadena, Calif., Nov. 19-21, 1968, Paper. 5 p.
The effects of red, blue, and no bias light on the spectral response of the Cu_2S-CdS cell have been studied. These bias-light effects are qualitatively explained by a model incorporating a photoconductive layer formed by diffusion of copper into the CdS. The spectral response of the cell under any bias-light condition appears to be the normal response due to photon absorption as modified by the energy gate characteristics of the photoconductive layer. (Author)

A69-16529 *
VACANCY RELAXATIONS IN B.C.C. CRYSTALS.
H. H. Grimes and J. H. Rice (NASA, Lewis Research Center, Cleveland, Ohio).
Journal of Physics and Chemistry of Solids, vol. 29, 1968, p. 1481-1484.
Determination of the vacancy relaxations in bcc crystals by calculating the energy of the crystal as a function of the radial displacements from the defect of the first nearest neighbor sets, and subsequently minimizing this function using Davidon's (1963) method. It is found that a crystal of about 2000 or more atoms is sufficient to obtain the desired accuracy. Below this size, the atoms relax more toward the vacancy because of the absence of attractive forces beyond the crystal surface. Above this size, additional interactions make only a negligible contribution to the relaxation energy. Z. W.

A69-16877 *
INVESTIGATION OF RADIATION DAMAGE IN MOSFETS USING BIAS-TEMPERATURE TREATMENTS.
Vitaly Danchenko (NASA, Goddard Space Flight Center, Spacecraft Technology Div., Flight Data Systems Branch, Greenbelt, Md.) and Sidney S. Brashears (Electro-Mechanical Research, Inc., College Park, Md.).
(Institute of Electrical and Electronics Engineers, Annual Conference on Nuclear and Space Radiation Effects, University of Montana, Missoula, Mont., July 15-18, 1968.)
IEEE Transactions on Nuclear Science, vol. NS-15, Dec. 1968, p. 182-186. 8 refs.
Radiation damage in thermally-grown p-channel enhancement mode MOS devices irradiated with 1.5 MeV electrons at various doses and gate potentials was investigated by applying bias-temperature (B-T) treatments. It was found that at negative and small positive gate biases applied during irradiation, electrons are trapped in weakly bound states in the oxide. These trapped electrons may readily be removed from the oxide by B-T treatment. The ratio of electrons trapped in the oxide to the radiation-induced net positive charge has a maximum at about -3 V bombardment bias. This region of gate

bias also corresponds to the minimum of radiation damage commonly observed in this type of device. At zero bombardment bias a saturation of shallow electron trapping is observed at a dose of 3 - 6 x 10^{13} e/cm^2. (Author)

A69-17772 *#
HIGH PHOTOVOLTAGES IN CADMIUM SULFIDE FILMS.
Henry W. Brandhorst, Jr., Ferdinand L. Acampora, and Andrew E. Potter, Jr. (NASA, Lewis Research Center, Cleveland, Ohio).
Journal of Applied Physics, vol. 39, Dec. 1968, p. 6071-6077. 34 refs.

Photovoltages larger than the band gap were observed in thin films of CdS which had high resistances and were not uniformly thick. The decay of the photovoltage after removal of light and the effects of temperature and light intensity on the photovoltage were studied and compared to a theoretical model. The results conform with the concept that the photovoltage is due to a space charge produced by a nonuniform distribution of trapped carriers in a multitude of series-connected elements. Analysis of the decay of the photovoltage showed the presence of at least four trapping levels at 0.08, 0.14, 0.26, and 0.41 eV. (Author)

A69-21350 *#
REACTIVE DEPOSITION OF CUBIC SILICON CARBIDE.
Arthur J. Learn and K. E. Haq (NASA, Electronics Research Center, Cambridge, Mass.).
Journal of Applied Physics, vol. 40, Jan. 1969, p. 430.

Description of the formation of cubic (beta) silicon carbide films, which was achieved by a new procedure involving the volatilization of silicon in the presence of acetylene. Silicon vapor was provided both by dc sputtering and by evaporation. The silicon vapor was directed toward a heated substrate and allowed to react with acetylene. The experimental conditions under which silicon carbide films could be synthesized are discussed. P.v.T.

A69-21351 *#
CHEMICAL PROCESSES IN SiC FORMATION BY REACTIVE DEPOSITION AND CHEMICAL CONVERSION.
K. E. Haq and Arthur J. Learn (NASA, Electronics Research Center, Cambridge, Mass.).
Journal of Applied Physics, vol. 40, Jan. 1969, p. 431.

Study of the chemical processes occurring in SiC formation due to reactive deposition and chemical conversion, under conditions where pyrolysis is prevented. Experiments are described which exclude the pyrolysis of hydrocarbon by chemical conversion at the heated Si surface and lead to a growth mechanism of Si involving its outward diffusion. The implications connected with this reactive deposition are discussed. Z.W.

A69-21652 *
BERYLLIUM AS AN ACCEPTOR IN SILICON.
J. B. Robertson and R. K. Franks (NASA, Langley Research Center, Hampton, Va.).
Solid-State Communications, vol. 6, no. 11, 1968, p. 825, 826. 6 refs.

Description of an experiment in which silicon was doped with beryllium by thermal diffusion. Electrical and optical measurements are given, showing the resulting silicon to be p-type, with two neutral acceptor levels. The strong p-type conductivity of beryllium-doped silicon implies that beryllium occupies predominantly a substitutional site in the silicon lattice. It is thought that the center responsible for one of the acceptor spectra is an isolated substitutional beryllium atom, and that the center responsible for the other spectrum, or perhaps both centers, are complexes containing at least one substitutional beryllium atom. The beryllium could be complexed with other impurities, with defects, or possibly with itself. B.H.

A69-21753 *#
CURRENT OSCILLATIONS IN PHOTOEXCITED GALLIUM-ARSENIDE.
Walter Viehmann (NASA, Goddard Space Flight Center, Materials Research and Development Branch, Greenbelt, Md.).
Applied Physics Letters, vol. 14, Jan. 1, 1969, p. 39-41. 12 refs.

Observation of current oscillations in two types of semiinsulating, strongly photoconducting GaAs at room temperature. The GaAs sample is oxygen-compensated and chromium-compensated. The relation of the oscillations to deep acceptor levels inferred from photoconductivity excitation spectra is discussed. M.G.

A69-21808 *
MEASUREMENTS OF THE WORK FUNCTION AND DESORPTION ENERGY OF CESIUM AND POTASSIUM ON (100) TUNGSTEN.
D. L. Fehrs (NASA, Electronics Research Center, Cambridge, Mass.), T. J. Lee (Massachusetts Institute of Technology, Research Laboratory of Electronics, Cambridge, Mass.), and R. E. Stickney (Massachusetts Institute of Technology, Dept. of Mechanical Engineering, Cambridge, Mass.).
IN: INSTITUTE OF ELECTRICAL AND ELECTRONICS ENGINEERS, ANNUAL THERMIONIC CONVERSION SPECIALIST CONFERENCE, 7TH, FRAMINGHAM, MASS., OCTOBER 21-23, 1968, CONFERENCE RECORD. [A69-21806 09-03]
New York, Institute of Electrical and Electronics Engineers, Inc., 1968, p. 10-17. 14 refs.
Research supported by the Massachusetts Institute of Technology; Grant No. NGR-22-009-091; Contract No. DA-28-043-AMC-02636(E).

Evaluation of measurements of the desorption of alkali metals from metallic substrates made with the aid of a modulated molecular-beam apparatus. A principal feature of the apparatus is that ultra-high-vacuum conditions (~10^{-10} torr) are attained, so as to reduce the rate of contamination of the surface. Assuming the adsorption residence time τ to be of the form $\tau = \tau_0 \exp(e^+/kT)$, $\tau_0 = (1.24 \pm 0.14) \times 10^{-13}$ sec and $e^+ = 2.06 \pm 0.01$ eV are obtained for Cs on W(100) in the limit of zero coverage. These values are compared with similar results obtained by Koenig and Pigford (1966) and by Scheer and Fine (1962). P.v.T.

A69-23989 *
BERYLLIUM AS AN ACCEPTOR IN SILICON.
J. B. Robertson and R. K. Franks (NASA, Langley Research Center, Hampton, Va.).
Solid-State Communications, vol. 6, no. 11, 1968, p. 825, 826. 6 refs.

Description of an experimental study in which beryllium is thermally diffused into silicon. The electronic properties of the doped silicon are studied with IR absorption spectroscopy and electrical measurements. Infrared absorption spectra show two distinct acceptor centers with ground states at $E_v + 0.145$ eV and at $E_v + 0.191$ eV. M.G.

A69-24006 *#
IMPURITY EFFECTS ON ANNEALING OF RADIATION DEFECTS IN SILICON.
P. H. Fang (NASA, Electronics Research Center, Cambridge, Mass.) and P. Iles (Globe-Union, Inc., Centralab Semiconductors, El Monte, Calif.).
Applied Physics Letters, vol. 14, Feb. 15, 1969, p. 131, 132. 7 refs.

Observation of an anomalously low annealing temperature of a radiation-induced defect in silicon, heavily doped with a phosphorous impurity. A shift of about 100°C is observed in the isochronal annealing temperature of the dominant annealing stage in p-on-n silicon solar cells with a heavy donor concentration of 10^{17} cm^{-3} in the n region and low oxygen concentration in the crystal. Isochronal recovery characteristics of solar cells with different donor and oxygen concentrations are shown. M.G.

A69-26500 *#
SPIN WAVE APPROXIMATION FOR ANISOTROPIC HEISENBERG ANTIFERROMAGNET.
Lawrence Flax (NASA, Lewis Research Center, Cleveland, Ohio) and John C. Raich (Colorado State University, Fort Collins, Colo.).
American Physical Society, Annual Meeting, Philadelphia, Pa., Mar. 24-27, 1969, Paper. 9 p.
NSF Grant No. GP-9042.

Description of a method of evaluating certain temperature-dependent sums that occur in the theory of magnetism. The method is illustrated by applying the anisotropic model of Dalton and Wood (1967) to treat the case of an antiferromagnet in the spin-wave approximation. It is shown that the thermodynamic quantities of interest can be calculated explicitly in terms of elliptic integrals over the entire temperature range of interest. The case of a bcc lattice is examined as an illustration of the proposed method. M.G.

A69-27400 *

EFFECTIVE MASSES IN Zr-DOPED SUPERCONDUCTING CERAMIC $SrTiO_3$.

D. M. Eagles (NASA, Electronics Research Center, Cambridge, Mass.).

Physical Review, 2nd Series, vol. 178, Feb. 10, 1969, p. 668-677. 29 refs.

Analysis of published experimental results on superconducting transition temperature as a function of carrier concentration and on magnetic field penetration depths in Zr-doped ceramic $SrTiO_3$. From the penetration-depth results it is deduced that the ratio of effective masses m_3 and m_1 for 3% and 1% of Ti ions replaced by Zr satisfies $(m_3/m_1) \simeq 1.48$ if Zr ions are the main scattering centers. Using a model involving screened electron-electron interaction via intervalley phonons of energy 0.0497 eV modified by intervalley Coulomb repulsion and by intravalley effects, it is shown that the transition-temperature data can be fitted fairly well with mass changes of the above magnitude, provided that the ratio of phonon-induced to Coulomb intervalley interactions is postulated to increase by about 5% for each percent of Zr doping. It is argued that the large mass increases may imply that a crossing of levels associated with small and large mass states is taking place as Zr is added. The possibility of superconductivity at very low carrier concentrations in specimens with 3% Zr content is discussed. (Author)

A69-28007 *

ADHESION MECHANISM OF GOLD-UNDERLAYER FILM COMBINATIONS TO OXIDE SUBSTRATES.

K. E. Haq, K. H. Behrndt, and Ilse Kobin (NASA, Electronics Research Center, Cambridge, Mass.).

(American Vacuum Society, National Vacuum Symposium, 15th, and Thin-Film Symposium, Pittsburgh, Pa., Oct. 28-Nov. 1, 1968.) Journal of Vacuum Science and Technology, vol. 6, Jan.-Feb. 1969, p. 148-152. 9 refs.

Investigation of the adhesion between glass or oxidized Si substrates and evaporated gold films in combination with an adherent intermediate layer of Ta, Si, Ge, or Cr. Experimental results are described in detail regarding changes of adhesion as a function of the relative thickness of the Au and underlayer films, time, environment, and treatment after deposition. They can be explained in terms of the thermodynamic properties of the respective Au-underlayer systems. In the case of Au-Si and Au-Ge, alloying and diffusion processes play the dominant role while, for Au-Ta, oxidation of Ta is responsible for adhesion changes. Most importantly, in the Au-Cr system, none of the above processes are effective, at least up to 450°C. Consequently, no loss of adhesion was observed for periods of one month and thicknesses of the Cr layer of only about 10 Å. (Author)

A69-29005 *#

MAGNETOTHERMAL OSCILLATIONS IN PRESSURE-ANNEALED PYROLYTIC GRAPHITE.

Dennis J. Flood (NASA, Lewis Research Center, Cleveland, Ohio).

American Physical Society, Meeting, Kent, Ohio, Apr. 18, 19, 1969, Paper. 17 p. 16 refs.

Observation of magnetothermal oscillations in pressure-annealed, pyrolytic graphite. Two experimental techniques for observing the oscillatory temperature changes as a function of field are discussed, field modulation and the use of a low frequency ac bridge to detect changes in thermometer resistance. The method used most extensively was that of field modulation. The periodicity of the oscillatory variations in temperature of the sample of pressure-annealed, pyrolytic graphite used in the experiments agrees well with that obtained for hole carriers. A long period oscillation tentatively ascribed to the minority electron pocket occurring at the corners of the Brillouin zone was observed. The period of this oscillation was estimated to be $(0.85 \pm 0.05) \times 10^{-4}$ gauss^{-1} (0.85 ± 0.05 tesla^{-1}), and is not in good agreement with other published values for these carriers. B.H.

A69-29006 *#

INELASTIC SCATTERING CALCULATIONS WITH WOOD-SAXON HARTREE-FOCK WAVE FUNCTIONS.

Richard C. Braley, William F. Ford (NASA, Lewis Research Center, Cleveland, Ohio), and Jacob Bar-Touv (Case-Western-Reserve University, Cleveland, Ohio).

American Physical Society, Spring Meeting, Washington, D.C., Apr. 28-May 1, 1969, Paper. 14 p. 8 refs.

Discussion of the results of inelastic cross section calculations for several 2s-1d shell nuclei, in which the nuclear form factors are constructed from projected HF wave functions, using a Wood-Saxon basis. A comparison is made to similar calculations using a harmonic oscillator basis. B.H.

A69-29009 *#

SELF-CONSISTENT MANY-ELECTRON THEORY OF ELECTRON WORK FUNCTIONS AND SURFACE POTENTIAL CHARACTERISTICS FOR SELECTED METALS.

John R. Smith (NASA, Lewis Research Center, Cleveland, Ohio).

American Vacuum Society, Vacuum Science Symposium, Los Alamos, N. Mex., Apr. 28-30, 1969, Paper. 35 p. 57 refs.

Electron work functions, surface potentials, and electron number density distributions and electric fields in the surface region of 26 metals, calculated from first principles within a free electron model. The number of "free" electrons per atom is taken as the group number as listed in the periodic table. Grain orientation effects are not considered. The calculation proceeds from an expression of the total energy as a functional of the electron number density, including exchange and correlation energies as well as a first inhomogeneity term. The self-consistent solution is then obtained by a variational procedure related to the Ritz method. Surface barriers are found to be due in most cases to many-body effects, but dipole barriers are small only for a number of alkali metals, and become quite large for the transition metals. Surface energies are found to be inadequately described in this model, which neglects atomistic effects. Considering the simplicity of the model, reasonable results are obtained for electron work functions and surface potential characteristics for all metals studied, maximum electron densities varying by a factor of over 60. B.H.

A69-32262 *

PHONONS, ELECTRONS, AND PROTONS IN FERROELECTRIC MATERIALS.

B. D. Silverman (NASA, Electronics Research Center, Cambridge, Mass.).

IN: AMPERE CONFERENCE, 15TH, GRENOBLE, FRANCE, SEPTEMBER 16-21, 1968, PROCEEDINGS [COLLOQUE AMPERE, 15TH, GRENOBLE, FRANCE, SEPTEMBER 16-21, 1968, PROCEEDINGS]. Amsterdam, North-Holland Publishing Co., 1969, p. 168-186. 82 refs.

General review of recent theoretical and experimental results concerning the displacive ferro-paraelectrics; $BaTiO_3$, $SrTiO_3$, and $KTaO_3$, and the hydrogen bonded ferroelectrics; and KH_2PO_4 and its deuterated isomorphs. The connection of the more recent results with earlier theories is discussed, and the relationship between the higher frequency optical properties and lower frequency dielectric properties is examined. For the displacive ferroelectrics, emphasis is placed on the role played by electronic polarization in lowering one transverse optical frequency and in driving the ferroelectric instability. The recent Raman scattering results of Kaminow and Damen (1968) are qualitatively discussed in terms of a proton tunneling model for KH_2PO_4. (Author)

A69-32792 *#

LUMINESCENCE FROM AROMATIC POLYMERS, MONOMERS, AND DIMERS UNDER HIGH-ENERGY ELECTRON EXCITATION.

Donald H. Phillips (NASA, Langley Research Center, Hampton,

Va.) and John C. Schug (Virginia Polytechnic Institute, Dept. of Chemistry, Blacksburg, Va.).
Journal of Chemical Physics, vol. 50, Apr. 15, 1969, p. 3297-3306. 34 refs.
NSF-supported research.

Luminescence spectra of various polymers and solid-model compounds induced by 1-MeV electrons. The presence of enhanced triplet emission and absence of singlet emission from poly(p-xylene), poly(monochloro-p-xylene), and the model compound dibenzyl are interpreted on the basis of a molecular resonance model. Some triplet excimer and other long-wavelength (450 to 550 mμ) emissions were also observed in these spectra. The spectra of the monomers p-xylene and 2-chloro-p-xylene consisted primarily of long-wavelength emission (400 to 600 mμ), while the spectra of frozen toluene and durene exhibited both neutral molecule singlet and the long-wavelength emission. Benzene exhibited only singlet, singlet excimer, triplet, and triplet excimer emission. The polymers poly(ethylene-2,6-naphthalene-dicarboxylate), poly(ethyleneterephthalate), and polysulfone emitted primarily from singlet and singlet excimer states. The model compounds for these polymers, dimethyl-2,6-naphthalenedicarboxylate, dimethylterephthalate, and methyl-p-toluenesulfonate exhibited varying amounts of singlet, triplet, excimer, and neutral or ionic radical emission. (Author)

A69-32824 *
DIFFERENTIAL PHOTO EFFECTS IN GALLIUM ARSENIDE-METAL JUNCTIONS.
Walter Viehmann (NASA, Goddard Space Flight Center, Materials Research and Development Branch, Greenbelt, Md.).
Infrared Physics, vol. 9, May 1969, p. 21-29. 5 refs.

Results of alloying pairs of low-melting metal pellets to n-type and p-type semiinsulating GaAs. The I-V characteristics of the resulting n-i-n or p-i-p devices under intense illumination were generally symmetrical about the origin and showed pronounced double saturation. In the spectral dependence of the photocurrent under geometrical and electrical bias, wideband photoresponse, narrow-band response, and sign-reversal of the photocurrent as a function of wavelength were observed. These response functions are explained as the differential output of two diodes connected back to back. (Author)

A69-33754 *
FLUX FLOW IN MATERIALS WHERE $\chi \sim 1$.
W. R. Hudson and R. J. Jirberg (NASA, Lewis Research Center, Cleveland, Ohio).
Solid-State Communications, vol. 7, no. 4, 1969, p. 429-431. 6 refs.

Investigation of the Kim-Anderson flux theory for materials with $\chi \sim 1$. The analysis yields the spectrum of the number of pinning sites with a particular pinning force. M.M.

A69-35477 *#
OPTICAL ABSORPTION IN TETRACYANOQUINODIMETHAN.
T. Mookherji and G. M. Arnett (NASA, Marshall Space Flight Center, Space Sciences Laboratory, Huntsville, Ala.).
Journal of Chemical Physics, vol. 50, May 1, 1969, p. 4090-4092. 13 refs.

Description of reflection and transmission measurements (in the range 0.29-2.5 μ) on "as grown" surfaces of tetracyanoquinodimethan. The data are analyzed by the Kramers-Kronig method to yield the optical constants. Optical constants were also calculated from the reflectance measurements at different angles of incidence using Fresnel's equations. The absorption coefficients thus obtained are interpreted in terms of an allowed direct transition which was further verified by transmission measurements. (Author)

A69-35788 *#
CURRENT STATUS OF SCANNING ELECTRON MICROSCOPY IN SEMICONDUCTOR DEVICE RELIABILITY PHYSICS.
Robert J. Anstead and Samuel R. Floyd (NASA, Goddard Space Flight Center, Greenbelt, Md.).
IN: INSTITUTE OF ELECTRICAL AND ELECTRONICS ENGINEERS, ANNUAL SEMINAR ON FAILURE ANALYSIS, 2ND, UNIVERSITY OF PENNSYLVANIA, PHILADELPHIA, PA., MAY 22, 1969, PROCEEDINGS. (A69-35781 19-09)
Philadelphia, Institute of Electrical and Electronics Engineers, Inc., 1969, p. 45-55.

The scanning electron microscope has proven to be a versatile instrument in studying reliability problems in semiconductor devices. The use of this instrument in a number of modes to evaluate or perform failure analyses on these devices is described. Micrographs presenting views having great depth of field at magnifications up to 40,000x and resolutions of less than 400 Å have been produced and are included. This has been invaluable in detecting topological defects not observable with optical microscopes. Further verification of these anomalies has been possible with voltage contrast micrographs. In addition, a beam-induced current mode has been used to examine subsurface properties. Dynamic observations of electromigration phenomena and physical discontinuities are currently being investigated. In particular, the thermally induced diffusion of gold from a gold ball-bond into an aluminum interconnection of a microelectronic circuit is described. A series of photographs depicting the progressive diffusion steps of the gold along the aluminum stripe are shown. (Author)

A69-36045 *
SELF-CONSISTENT MANY-ELECTRON THEORY OF ELECTRON WORK FUNCTIONS AND SURFACE POTENTIAL CHARACTERISTICS FOR SELECTED METALS.
John R. Smith (NASA, Lewis Research Center, Cleveland, Ohio).
Physical Review, 2nd Series, vol. 181, May 10, 1969, p. 522-529. 52 refs.

Electron work functions, surface potentials, and electron number density distributions and electric fields in the surface region of 26 metals are calculated from first principles within the free-electron model. The number of free electrons per atom is taken as the group number as listed in the Periodic Table. Grain orientation effects are not considered. The calculation proceeds from an expression of the total energy as a functional of the electron number density including exchange and correlation energies as well as a first inhomogeneity term. The self-consistent solution is then obtained by a variational procedure akin to the Ritz method. Surface barriers are found, in most cases, to be due principally to many-body effects, but dipole barriers are small only for a number of alkali metals, becoming quite large for the transition metals. Surface energies are found to be inadequately described by this model which neglects atomistic effects. Considering the simplicity of the model, reasonable results are obtained for electron work functions and surface potential characteristics for all metals studied, maximum electron densities varying by a factor of over 60. (Author)

A69-36445 * #
NUCLEAR MAGNETIC RESONANCE STUDY OF THE NIOBIUM-NITROGEN SYSTEM NbN_x.
Robert A. Bennett, H. O. Hooper (Wayne State University, Dept. of Physics, Detroit, Mich.), and U. Roy (NASA, Marshall Space Flight Center, Materials Div., Metallic Materials Branch, Huntsville, Ala.).
Journal of Applied Physics, vol. 40, May 1969, p. 2441-2444. 11 refs.
AEC-supported research; Grant No. AF AFOSR 68-1494.

Nuclear magnetic resonance study of the phases of the system NbN_x in several samples of niobium nitride with mole fractions of nitrogen ranging from 0.884 to 0.95. The epsilon phase was identified by a characteristic second-order quadrupolar broadened central position transition with two sets of satellite lines also being observed. The quadrupole coupling constant was determined for the epsilon phase and for the delta phase. The relative amounts of each phase were determined in two samples. Z.W.

A69-37280 *
THEORY OF TRANSITIONS FROM LARGE TO NEARLY-SMALL POLARONS, WITH APPLICATION TO Zr-DOPED SUPERCONDUCTING $SrTiO_3$.
D. M. Eagles (NASA, Electronics Research Center, Cambridge, Mass.).
Physical Review, 2nd Series, vol. 181, May 15, 1969, p. 1278-1290. 47 refs.

Derivation of expressions for the matrix elements of the Hamiltonian and overlap integrals between large-polaron and nearly-small-polaron states in terms of various large- and nearly-small-polaron parameters. The dependence of the mass of the ground state on the bare-electron mass in a region of transition between large- and nearly-small-polaron states is found. Parameters of the theory are evaluated using the continuum-polarization model of electron-phonon interactions. Modifications due to anisotropy and the presence of many longitudinal polar modes of lattice vibration are briefly discussed. M.M.

A69-40730 •
COMPTON PROFILE OF LiH.
Walter C. Phillips (NASA, Electronics Research Center, Cambridge, Mass.) and R. J. Weiss (U.S. Army, Materials Research Laboratory, Watertown, Mass.).
Physical Review, 2nd Series, vol. 182, June 15, 1969, p. 923-925. 7 refs.

The Compton profile from a single crystal of LiH has been measured with the X-ray scattering vector along the (100), (110), and (210) directions. The valence-electron contribution to the measured profile is in marked disagreement with that calculated from the crystal-field wave functions of Hurst. The observations indicate that the valence-electron momentum distribution is broader in momentum space than the distribution obtained from a superposition of the negative H ion and positive Li ion wave functions for either the free ions or the negative H ion in a positive Li point-lattice crystalline field. It appears that a more extensive calculation is required to get agreement with both the X-ray scattering factor and Compton-profile measurements. For the three crystal orientations studied, the Compton profiles show only a small anisotropy.(Author)

A69-43121 * #
THICKNESS OPTIMIZATION FOR DYNAMICALLY STABLE SUPERCONDUCTING TAPES.
Gerald V. Brown (NASA, Lewis Research Center, Cleveland, Ohio).
Institute of Physics and Physical Society, International Conference on High Magnetic Fields and Their Applications, Nottingham, England, Sept. 17-19, 1969, Paper. 8 p. 6 refs.

Study of optimum thicknesses of dynamically stable composite superconducting tapes. By assuming dynamic stability, the optimum thicknesses of superconductor and normal stabilizing metal were calculated for any value of substrate (structure) thickness. It is concluded that the total current density obtained for the optimum thicknesses increases as the substrate thickness decreases, and that the total current density would increase if the superconductor critical current could be increased, but cannot be larger than the critical value for self-supporting turns. The effect on maximum current density of "wasted" space such as insulation, cooling channels, etc., is indicated for the stability-limited region and for the mechanical force-limited region. O.H.

A69-43344 *
FORMATION AND STRUCTURE-SENSITIVE PROPERTIES—AN INTRODUCTION.
Robert F. Behrndt (NASA, Electronics Research Center, Cambridge, Mass.).
Journal of Vacuum Science and Technology, vol. 6, July-Aug. 1969, p. 439-442. 37 refs.

Outline of the areas in thin-film deposition in which additional information is needed to provide more than a qualitative picture of the processes. Topics discussed include film formation, methods of film deposition, and the relation between film formation, structure, and properties. Z.W.

A69-43345 *
EFFECT OF OXYGEN ON THE FORMATION OF GERMANIUM FILMS.
Robert F. Adamsky, Klaus H. Behrndt, and William T. Brogan (NASA, Electronics Research Center, Cambridge, Mass.).
Journal of Vacuum Science and Technology, vol. 6, July-Aug. 1969, p. 542-545. 8 refs.

Investigation of the influence of background oxygen pressure at levels between 10^{-10} and 10^{-6} torr on the crystallographic order of Ge films evaporated on (111) Ge. The substrates were chemically cleaned and/or subjected to thermal in situ cleaning. Oxygen partial pressures down to about 5×10^{-9} torr were found to increase the epitaxial temperature by 50 to 75 deg C, and the amorphous-polycrystalline transition by 125 to 150 deg C for substrate temperatures in the range from 150 to 310 deg C. At partial pressures of about 5×10^{-8} torr, the oxygen effect increases with decreasing substrate temperature and increasing deposition rate, while preannealing of the substrates at 600 deg C eliminates subsequent oxygen effects. The observations are interpreted in terms of oxide formation; they offer an explanation for the appreciable decrease in epitaxial temperature for films deposited in ultrahigh vacuum compared to conventional vacuum. (Author)

A69-43666 * #
MERCURY CADMIUM TELLURIDE AS A 1-20 μM WAVELENGTH INFRARED DETECTOR FOR SPACE APPLICATIONS.
Richard D. Packard (NASA, Electronics Research Center, Cambridge, Mass.).
AIAA Journal, vol. 7, Aug. 1969, p. 1570-1573. 9 refs.

Discussion of the applicability of mercury cadmium telluride (HgCdTe) as an IR detector in satellites for terrestrial, atmospheric, and ocean mapping, IR astronomy, and optical communications. The alloy under study was developed for fast elevated-temperature IR detection at wavelengths ranging from 1 to 20 microns, particularly for operation in the region between 8 and 14 microns. Available experimental data indicate that the chemical stability of the alloy is marginally adequate for operation in the space environment. Attention is given to the possibility of operation using (passive) space radiative cooling, which would eliminate the need for cryogens, increase service life, and reduce size and weight of the detector system. V.P.

N69-10125*# National Aeronautics and Space Administration. Electronics Research Center, Cambridge, Mass.
MERCURY CADMIUM TELLURIDE AS A 1- TO 20-MICROMETER WAVELENGTH INFRARED DETECTOR FOR SPACE APPLICATIONS
Richard D. Packard Washington Nov. 1968 17 p refs
(NASA-TN-D-4904) Avail: CFSTI CSCL 20L

Mercury cadmium telluride (HgCdTe) offers attractive possibilities for fast, elevated operating temperature infrared detection from 1- to 20-micrometer (μm) wavelengths, particularly in the 8- to 14-μm wavelength region for which it was developed. HgCdTe is considered for use in satellites for terrestrial, atmospheric, and ocean mapping; infrared astronomy; and optical communications. Its chemical stability in the space environment is open to some question; however, experimental data so far accumulated indicate that it is marginally adequate for such purposes. Some attention is given to the possibility of operation using (passive) space radiative cooling; this would eliminate the need for cryogens and provide a much longer operating lifetime as well as reductions in size and weight of the detector system. Author

26 PHYSICS, SOLID-STATE

N69-10817*# General Technology Corp., Lawrenceville, N. J.
COMPATIBILITY CONDITIONS OF THE THEORY OF MICROMORPHIC ELASTIC SOLIDS
A. Cemal Eringen Washington NASA Nov. 1968 19 p refs
(Contract NASw-1589)
(NASA-CR-1236; TR-8-5) Avail: CFSTI CSCL 20L

The compatibility conditions for the strain measures of the theory of micromorphic elastic solids are presented. Specific forms are given for the linear theory and for the linear micropolar elasticity. Author

N69-14086*# National Aeronautics and Space Administration. Lewis Research Center, Cleveland, Ohio.
A SUMMARY OF THE MEASUREMENT AND INTERPRETATION OF THE HALL COEFFICIENT AND RESISTIVITY OF SEMICONDUCTORS
D. Michael Stretchberry Washington Dec. 1968 51 p refs
(NASA-TM-X-1711) Avail: CFSTI CSCL 20L

Previously published methods of measuring and interpreting the Hall coefficient and resistivity of semiconductors are summarized. The conventional and van der Pauw methods of measurement are briefly discussed. Mobility is shown to be a function of carrier scattering in a specific semiconductor. The equations for charge carrier concentration are developed for both extrinsic and intrinsic conduction. These equations are then used as the basis for interpreting the measured experimental data. The analysis of the data near the intrinsic range and the temperature range over which the experimental measurements must be made are specified. Author

N69-14565*# National Aeronautics and Space Administration. Lewis Research Center, Cleveland, Ohio.
ELECTRICAL RESISTIVITY AS A FUNCTION OF DEUTERIUM CONCENTRATION IN PALLADIUM
Gust Bambakidis, Robert J. Smith, and Dumas A. Otterson Washington Dec. 1968 17 p refs
(NASA-TN-D-4970) Avail: CFSTI CSCL 20L

The electrical resistivity of the palladium-deuterium system was measured to a deuterium- to palladium-atom ratio of 0.9 at temperatures of 273, 77, and 4.2 K. The resistivity ratio $\rho(x)/\rho(0)$ was plotted as a function of the atom ratio x at 273 and 4.2 K. A modification of Mott's model for the resistivity of transition-metal alloys was used to calculate the structural resistivity. A good fit to the data at 4.2 K was obtained by assuming that the number of d-holes per palladium atom takes on the value of 0.55 to 0.60 on addition of deuterium. Author

N69-18897*# National Aeronautics and Space Administration. Langley Research Center, Langley Station, Va.
CHANGES IN MINORITY-CARRIER LIFETIME IN SILICON AND GALLIUM ARSENIDE RESULTING FROM IRRADIATION WITH 22- AND 40-MeV PROTONS
Marvin E. Beatty Washington Feb. 1969 26 p refs
(NASA-TN-D-5028) Avail: CFSTI CSCL 20L

Experiments were performed to examine the differences in the damage produced in n-type and p-type silicon and n-type gallium arsenide by irradiation with 22-MeV and 40-MeV protons. The parameter used to examine these differences was the minority-carrier lifetime in the base region of a photovoltaic p-n junction. From the data obtained, the relative merits of the three types of semiconductor material are compared in regard to their performance in a space radiation environment. Results of the experiments indicate gross differences in reduction of minority carrier lifetime between the three materials. Gallium arsenide was least affected by radiation; p-type silicon was next. Curves and tables are presented to depict some differences between the materials. It is concluded that gallium arsenide might be preferable to silicon in some devices to be subjected to a radiation environment. It was also found that 22-MeV protons produced a much higher degree of damage in silicon than 40-MeV protons did. The differences in damage produced were not so pronounced for gallium arsenide irradiated with protons of these two energies. Author

N69-19781*# National Aeronautics and Space Administration. Lewis Research Center, Cleveland, Ohio.
IMPURITY PROFILE AND ENERGY BAND DIAGRAM FOR THE CUPROUS SULFIDE-CADMIUM SULFIDE HETEROJUNCTION
Henry W. Brandhorst, Jr. Washington Mar. 1969 19 p refs
(NASA-TN-D-5079) Avail: CFSTI CSCL 20L

Capacitance measurements were used to determine the impurity profile for a Cu_2S–CdS heterojunction formed by acid etching a polycrystalline, evaporated layer of CdS, and dipping it into a cuprous ion solution. Capacitance–voltage measurements were made both in the dark and under illumination. The barrier height of the junction was determined to be 0.85 V. The impurity profile is unaffected by red light, but blue light reduces the compensation of a copper-diffused CdS layer. The capacitance measurements, Hall measurements, and an electron microprobe analysis were used to assemble a band structure for the heterojunction which shows four distinct regions. Author

N69-20798*# National Aeronautics and Space Administration. Lewis Research Center, Cleveland, Ohio.
RESONANT MODE ANALYSIS OF THE FITZGERALD APPARATUS
James P. Cusick and Donald R. Behrendt Washington Mar. 1969 22 p refs
(NASA-TN-D-5103) Avail: CFSTI CSCL 14B

Mechanical models are given to represent several nonideal machine modes; the effect of these modes upon drive tube motion is calculated. Fitzgerald's procedure for data analysis is used to calculate the effect of nonideal modes upon the dynamic compliance. The calculations show resonances in the calculated compliance which are indistinguishable from those reported by Fitzgerald. Author

N69-21500*# National Aeronautics and Space Administration. Lewis Research Center, Cleveland, Ohio.
SUPERCONDUCTIVE DUST CORES FOR INDUCTIVE ELEMENTS
Russell J. Jirberg Washington Apr. 1969 38 p refs
(NASA-TN-D-5137) Avail: CFSTI CSCL 20C

The use of superconductive dust as a core filler for inductive coils was investigated as a means of producing magnetically variable inductive elements. Both lead and niobium-filled cores were studied in static background magnetic fields. The observed inductance variations and the origin of alternating-current losses are discussed in relation to their superconducting properties. Author

N69-22552*# National Aeronautics and Space Administration. Langley Research Center, Langley Station, Va.
ANNEALING OF 22–, 40–, and 158–MeV PROTON DAMAGE IN n– AND p–TYPE SILICON
Marvin E. Beatty, III and Gerald F. Hill Washington Apr. 1969 26 p refs
(NASA-TN-D-5119) Avail: CFSTI CSCL 20L

Studies on n– and p-type silicon irradiated with 22–, 40 and 158-MeV protons and annealed at 100°C, 200°C, and 300° are reported. A fluence dependence was found for protons i which the annealing decreased as the fluence increased and wa compared with results previously reported for electrons. Alternate increases and decreases in minority-carrier lifetime during isotherma annealing is discussed. Author

N69-22573*# National Aeronautics and Space Administration. Electronics Research Center, Cambridge, Mass.
SIMPLIFIED THEORY AND TRANSDUCER POTENTIALITIES OF THE "PINCH EFFECT" IN SEMICONDUCTORS
Ernest E. Pittelli and Wilhelm Rindner Washington Apr. 1969 22 p refs
(NASA-TN-D-5130) Avail: CFSTI CSCL 20L

The recently reported electric pinch effect in anisotropic semiconductors is analyzed theoretically with emphasis on the underlying physical phenomena. The theory is generalized to apply to extrinsic semiconductors and to encompass effects in the direction transverse to stress and electric field. In extrinsic material the magnitude of the pinch effect is reduced by the ratio of minority to majority carriers. In the transverse direction a potential difference is generated by two essentially independent mechanisms: a highly surface-dependent diffusion caused by a stress-dependent concentration gradient of free carriers, and a surface-independent transverse piezoresistance. The potential and limitations in the utilization of the pinch effect for electromechanical transducers are examined. Author

N69-22965*# National Aeronautics and Space Administration. Lewis Research Center, Cleveland, Ohio.
PUMPED HELIUM TESTS OF A 51-CENTIMETER BORE NIOBIUM-TIN MAGNET
Willard D. Coles, Gerald V. Brown, Erwin H. Meyn, and E. R. Schrader (RCA) Washington Apr. 1969 12 p refs
(NASA-TN-D-5158) Avail: CFSTI CSCL 20L

Performance data are presented for tests of 51-cm bore solenoids operated at temperatures below 2°K. The magnet coils are wound of vapor-deposited Nb_3Sn ribbon which was copper-clad for one of the magnets and silver-plated for the others. Coil protection was provided by cross-layer shorting strips which also provide very limited stabilization. Each coil was designed to produce a 4.0-T center field. Results obtained at the low temperature are compared with those obtained at 4.2°K. System description and charging characteristics are included in the discussion. Author

N69-24916*# National Aeronautics and Space Administration. Lewis Research Center, Cleveland, Ohio.
NONLINEAR FLUX FLOW IN SINGLE CRYSTAL NIOBIUM
Wayne R. Hudson and Russel J. Jirberg Washington May 1969 14 p refs
(NASA-TN-D-5198) Avail: CFSTI CSCL 20B

The consequences of a low Ginzburg–Landau κ are noted in the behavior of a high purity single crystal of niobium. The flux flow voltages are not explained by the Kim Anderson theory. A modification to the theory is proposed, and its implications are discussed. Author

N69-25412*# National Aeronautics and Space Administration. Lewis Research Center, Cleveland, Ohio.
GALVANOMAGNETIC AND THERMOMAGNETIC EFFECTS IN WHITE TIN IN FIELDS TO 3.3 TESLA AND AT TEMPERATURES BETWEEN 1.2 AND 4.2 K
John A. Woollam Washington May 1969 30 p refs
(NASA-TN-D-5227) Avail: CFSTI CSCL 20L

The Nernst–Ettingshausen, thermoelectric power, thermal transverse-even, magnetoresistance, and Hall coefficients are measured in metallic tin. The results show that the Nernst–Ettingshausen coefficient is large, and anisotropic with respect to angle between field and crystal axes. The Nernst–Ettingshausen anistropy closely resembles that of the magnetoresistance coefficient. The temperature and field dependencies of the adiabatic coefficients are predicted from a theory for the isothermal coefficients, and these predictions are compared with experiment. Quantum oscillations in thermoelectric power are discussed; amplitudes are in reasonably good agreement with theory. Author

N69-27840*# National Aeronautics and Space Administration. Lewis Research Center, Cleveland, Ohio.
QUIESCENT-AIR PERFORMANCE OF A TRUNCATED TURBOJET PLUG NOZZLE WITH SHROUD AND PLUG BASE FLOWS FROM A COMMON SOURCE
Albert L. Johns Washington Jun. 1969 29 p refs
(NASA-TM-X-1807) Avail: CFSTI CSCL 21H

A 10° half-angle conical plug nozzle with a design pressure ratio of 26.3 and a 50-percent plug trunctation was tested in configurations simulating afterburner on and off. A 40-percent increase in primary throat area was provided by either a simulated primary iris flap or by relative translation between the primary shroud and plug. Thrust efficiency was maintained at values between 97 and 99 percent over a range of pressure ratios by proper location of the cylindrical outer shroud. These peak efficiencies were generally obtained with the sum of shroud and plug base flows from 5 to 7 percent of the primary flow. Author

N69-28096*# Virginia Univ., Charlottesville.
THE THIN FILM IRIS
R. L. Ramey, H. S. Landes, and E. A. Manus Washington NASA Jun. 1969 36 p refs
(Grant NGR-47-005-001)
(NASA-CR-1364; EE-4012-111-69U) Avail: CFSTI CSCL 20L

Because of the ability of a thin metallic film to support a tangential component of electric field at its surface, it is possible to construct microwave irises with these films which display a capacitive reactance, where their exact counterparts constructed with a metal foil appear as an inductive reactance. A theoretical analysis of this effect is made, and the results compared to experimental observations. Author

N69-29407*# National Aeronautics and Space Administration. Lewis Research Center, Cleveland, Ohio.
ADHESION OF GOLD TO VARIOUS PLANES OF COPPER STUDIED WITH LEED
Donald H. Buckley Washington Jun. 1969 20 p refs
(NASA-TN-D-5290) Avail: CFSTI CSCL 20L

An investigation was conducted with the aid of LEED, to determine the influence of crystallographic orientation on adhesion of gold to copper. A single gold orientation contacted three planes of copper, the (111), (100), and (110) planes. Adhesion under light loads resulted in adherence of gold to all three planes of copper. This result could be correlated with theoretical considerations of adhesive and cohesive bonding forces. The gold bonded epitaxially to all three planes of copper, with the weakest force of adhesion occurring to the (111) plane of copper. While lattice strains were observed to occur in gold as a result of such adhesive contacts, no such strain was noted in the copper. Author

N69-29588*# National Aeronautics and Space Administration. Lewis Research Center, Cleveland, Ohio.
RANDOM PHASE APPROXIMATION FOR THE ANISOTROPIC HEISENBERG FERROMAGNET
Lawrence Flax and John C. Raich (Colo. State Univ.) Washington Jun. 1969 21 p refs
(NASA-TN-D-5286) Avail: CFSTI CSCL 20L

The theory of anisotropic Heisenberg ferromagnets is developed in the random phase and spin wave approximation. It is shown that thermodynamic quantities such as magnetization can be expressed in analytic form for all temperatures. To demonstrate the applicability of this technique the magnetization for body-centered, face-centered, and simple-cubic lattices was calculated. Author

N69-29724*# Research Triangle Inst., Durham, N.C.
A FEASIBILITY STUDY OF A MINIATURE SOLID-STATE PRESSURE TRANSDUCER
C. D. Parker Washington NASA Jul. 1969 67 p refs
(Contract NAS1-7489)
(NASA-CR-1366) Avail: CFSTI CSCL 14B

The piezojunction effect, i.e., the sensitivity of the electrical characteristics of a p–n junction to mechanical strain, is summarized and its potential as a stress transducing mechanism discussed. Several configurations are described which provide for using the piezojunction effect as the sensory phenomenon in a pressure transducer, including a unique silicon needle sensor with a p–n junction in the needle apex. Needle sensors with excellent electrical characteristics were fabricated and demonstrated to be extremely sensitive to stress. These were fabricated into pressure transducers which detected pressure differentials of less than 100 μHg. Author

N69-30072*# National Aeronautics and Space Administration. Lewis Research Center, Cleveland, Ohio.
GROWTH OF 2-H SILICON CARBIDE CRYSTALS
J. Anthony Powell Washington Jul. 1969 15 p refs
(NASA-TN-D-5313) Avail: CFSTI CSCL 20B

Crystals of one of the rarer crystalline modifications of silicon, 2H SiC, were grown. These crystals with dimensions up to 3.3 mm in the c-direction and 0.3 mm in the a-directions were usually transparent and either colorless or amber colored. Growth was by the reduction of methyltrichlorosilane (CH_3SiCl_3) in a H_2 atmosphere in the temperature range 1300° to 1400°C. The vapor-liquid-solid (VLS) mechanism, which has been suggested for previous 2H SiC growth, was not involved in this growth. Factors affecting the crystal growth were the susceptor temperature profile and the CH_3SiCl_3 concentration in H_2. Author

N69-37272*# National Aeronautics and Space Administration. Lewis Research Center, Cleveland, Ohio.
ABSORPTION OF HYDROGEN BY PALLADIUM AND ELECTRICAL RESISTIVITY UP TO HYDROGEN-PALLADIUM ATOM RATIOS OF 0.97
Dumas A. Otterson and Robert J. Smith Washington Sep. 1969 17 p refs
(NASA-TN-D-5441) Avail: CFSTI CSCL 20L

The electrical resistivity of the palladium-hydrogen system (PdH_x) was measured to a H/Pd atom ration x of 0.97 at 4.2° and 273°K. The Bambakidis, Smith, and Otterson model proposed for the palladium-deuterium system (PdD_x) is applied to PdH. The model is used to explain the concentration dependence of the peak in resistivity as a function of temperature near 50°K and the concentration dependence in the resistivity scatter due to quench rate observed at 4.2°K. The present results are virtually independent of hydrogen isotope effects. Techniques used to attain values of x up to 0.97 are given. Hydrogen retention by these specimens is discussed. Author

N69-39239*# National Aeronautics and Space Administration. Lewis Research Center, Cleveland, Ohio.
MAGNETOTHERMAL OSCILLATIONS IN PRESSURE ANNEALED, PYROLYTIC GRAPHITE
Dennis J. Flood Washington Oct. 1969 23 p refs
(NASA-TN-D-5488; E-5032) Avail: CFSTI CSCL 20L

Magnetothermal oscillations arising from the majority hole carriers have been observed in pressure-annealed, pyrolytic graphite. The period of the oscillations was measured as a function of angle between the magnetic field H and the c-axis of the crystal. The period for H along the c-axis is 0.151 ± 0.005 tesla^{-1}. The sample had a resistance ratio of 1/2 from room temperature to 4.2 K. Data were obtained at 1.3 K in fields ranging from 0.35 to 10 tesla. Author

N69-40056*# National Aeronautics and Space Administration. Lewis Research Center, Cleveland, Ohio.
IONIC CONDUCTIVITY OF LANTHANUM FLUORIDE
William L. Fielder Washington Oct. 1969 16 p refs
(NASA-TN-D-5505) Avail: CFSTI CSCL 20B

The electrical conductivities of lanthanum fluoride single crystals containing from 0.02 to 0.15 mole percent calcium ion impurities were measured between 25° and 740° C. The activation energies for the formation of Schottky defects and for the migration of fluoride ion vacancies are 46 and 7.6 kcal/mole (192 and 32 kJ/mole) respectively. Mechanisms are proposed for the fluoride ion conduction process in lanthanum fluoride. Author

27

PROPELLANTS

Includes fuels; igniters; and oxidizers. For basic research see: 06 Chemistry; and 33 Thermodynamics and Combustion. For related information see also: 28 Propulsion Systems.

A69-14468 *

SAFETY PLANNING FOR THE USE OF REACTIVE CRYOGENS IN LARGE VOLUME.

Erskine E. Harton, Jr. (NASA, Safety Office, Washington, D.C.).
(New York Academy of Sciences, Conference on Prevention of and Protection Against Accidental Explosion of Munitions, Fuels and Other Hazardous Mixtures, New York, N.Y., Oct. 10-13, 1966.)
New York Academy of Sciences, Annals, vol. 152, Oct. 28, 1968, p. 51-60. 21 refs.

Review of current research being conducted to determine safety criteria for FLOX and LF_2 in order to establish before-the-fact launch criteria for a FLOXed Atlas booster. At the start of the program, it was surmised that all existing exposure limits were unrealistic, since they were developed to show permissible limits for industrial employees who would be expected to encounter the materials repeatedly. The current programs as they relate to fluorine and HF are to determine and/or develop: (1) detection and analytical instrumentation, (2) evaporation-rate/source-strength data, (3) short-term emergency exposure levels, (4) toxic vapor suppression and neutralization techniques, (5) protective clothing and equipment, (6) conversion rate of GF_2 to HF in the presence of moisture, (7) effects on ecology, (8) fire control, (9) dynamic impacting of FLOX- and LF_2-fuel mixtures, and (10) compatibility of materials. Tabular data from these and other studies are presented, showing the currently established human emergency exposure limits for rocket operations, nontoxic, no-lung-damage levels and LC_{50} values for animals exposed to GF_2, results of LF_2, FLOX, and LO_2 spill tests, and NASA-prescribed toxic limits for FLOX engine test firing. On the basis of hitherto completed studies, it is postulated that the launch of an Atlas booster using FLOX as the oxidizer is feasible, but the launch window would be severely restricted at existing facilities, due to limited favorable meteorological conditions.
G.V.

A69-14474 *

CHARACTERISTICS OF LIQUID PROPELLANT EXPLOSIONS.

R. F. Fletcher (NASA, Manned Spacecraft Center, Houston, Tex.).
(New York Academy of Sciences, Conference on Prevention of and Protection Against Accidental Explosion of Munitions, Fuels and Other Hazardous Mixtures, New York, N.Y., Oct. 10-13, 1966.)
New York Academy of Sciences, Annals, vol. 152, Oct. 28, 1968, p. 432-440. 9 refs.

Description of the factors which influence the reaction processes of liquid propellant explosions (often considered to be low-order detonations followed by deflagration) and the nature of the energy released. It is determined that, proportionally, the amount of propellant which detonates is generally small, except when the propellant is ideally mixed with an oxidizer, and that the detonation is almost instantly followed by deflagration, which continues until the propellant mass is expended. The major hazard of liquid propellant explosions is, therefore, the fire and/or fireball. The size, duration, and expansion rate of the fireball are dependent upon the rates of propellant combustion and air addition, and the diameter and duration are functions of the cube root of the propellant weight. The combustion rate governs the rate of air addition, but the two rates are not concurrent. The air addition increases with fireball size, first serving as an oxidizer keeping the temperature high, then as a diluent cooling the fireball. It is emphasized that the explosion hazard as compared to equivalent quantities of TNT is not applicable in close proximity to the explosion, since in most cases the thermal hazard is primary in these regions, and the TNT equivalency applies at great distances from the event.
G.V.

A69-14475 *

THE SATURN FIREBALL.

Richard W. High (NASA, Manned Spacecraft Center, Houston, Tex.).
(New York Academy of Sciences, Conference on Prevention of and Protection Against Accidental Explosion of Munitions, Fuels and Other Hazardous Mixtures, New York, N.Y., Oct. 10-13, 1966.)
New York Academy of Sciences, Annals, vol. 152, Oct. 28, 1968, p. 441-451. 6 refs.

Description of the thermal environment associated with liquid propellant explosions derived from empirical data, and correlation of these data with predictions made with the use of an analytical model. In the empirical study of some experimental tests and missile failures, equations were derived by a least-squares regression analysis of the data to describe the maximum diameter and duration of fireballs as a function of the propellant weight. Tabular data are presented to show the reasonable agreement between the empirical data and those predicted using optimum conditions for the analytical model for the case of a Saturn V fireball with a total propellant weight of 5.5 million pounds. It is concluded that the analytical study, in addition to supplying confirmatory information on the general characteristics of fireball hazards, supplied refined information on the dynamic behavior of a fireball and the shape of the thermal radiation pulse, thereby permitting evaluation of the heating rate as a function of time.
G.V.

A69-14477 *

A SYSTEMATIC APPROACH FOR THE ANALYTICAL ANALYSIS AND PREDICTION OF THE YIELD FROM LIQUID PROPELLANT EXPLOSIONS.

E. A. Farber (Florida, University, College of Engineering, Gainesville, Fla.) and J. H. Deese (NASA, Kennedy Space Center, Facilities Technology Office, Cocoa Beach, Fla.).
(THE CHALLENGE OF SPACE; PROCEEDINGS OF THE THIRD SPACE CONGRESS, COCOA BEACH, FLA., MARCH 7-10, 1966, p. 520-532; New York Academy of Sciences, Conference on Prevention of and Protection Against Accidental Explosion of Munitions, Fuels and Other Hazardous Mixtures, New York, N.Y., Oct. 10-13, 1966.)
New York Academy of Sciences, Annals, vol. 152, Oct. 28, 1968, p. 654-665. 20 refs.
Contract No. NAS 10-1255.

Consideration of mathematical difficulties arising in studies of collisions between high-energy particles. The difficulties are associated with the physical complexities of such collisions. Future advances in the field are believed to depend on the development of effective techniques for determining changes in the properties of a target nucleus being filled with nucleons of a colliding nucleus, the contribution of the interference between the cascades produced by these nucleons, and the probability of various types of splitting of the residual portion of a colliding nucleus during the peripheral impact.
V.Z.

A69-23003

USE OF PYROTECHNIC AND EXPLOSIVE ELEMENTS IN SPACE SYSTEMS; CENTRE NATIONAL D'ETUDES SPATIALES, INTERNATIONAL CONFERENCE, TARBES, HAUTES-PYRENEES, FRANCE, JULY 9-12, 1968, PROCEEDINGS [UTILISATION DES ELEMENTS PYROTECHNIQUES ET EXPLOSIFS DANS LES SYSTEMES SPATIAUX; CENTRE NATIONAL D'ETUDES SPATIALES,

27 PROPELLANTS

COLLOQUE INTERNATIONAL, TARBES, HAUTES-PYRENEES, FRANCE, JULY 9-12, 1968, PROCEEDINGS].
Paris, Dunod Editeur, 1969. 478 p. In French and English.

CONTENTS:
FOREWORD [AVANT-PROPOS], p. VII.

QUALIFICATION FOR SPACE ENVIRONMENT [QUALIFICATION POUR AMBIANCE SPATIALE].

USE OF STATISTICAL RELIABILITY METHODS IN PYROTECHNICS - APPLICATION TO DETONATING CUTTING FUSES [EMPLOI DES METHODES STATISTIQUES FIABILISTES EN PYROTECHNIE - APPLICATION AUX CORDEAUX DETONANTS DE DECOUPAGE]. R. Amiable and H. Carabin (Direction des Poudres, Sevran, France), p. 1-24. [See A69-23004 10-27]

QUALIFICATION OF SPACE STAGE SEPARATIONS [QUALIFICATION DES SEPARATIONS D'ETAGES SPATIAUX]. R. Marguet and J. Trichard (ONERA, Châtillon-sous-Bagneux, Hauts-de-Seine, France), p. 25-40. [See A69-23005 10-11]

ELECTRICAL DEVICES FOR SPACE APPLICATIONS - PROBLEMS OF DESIGN AND INITIATION [LES ARTIFICES ELECTRIQUES A APPLICATIONS SPATIALES - PROBLEMES DE CONCEPTION ET D'INITIATION]. G. Bouguyon (Direction Technique des Armements Terrestres, Tarbes, Hautes-Pyrénées, France), p. 41-55. [See A69-23006 10-27]

IMPROVEMENT IN THE RESISTANCE TO SEVERE ENVIRONMENTS OF SHOCK-IGNITION PYROTECHNIC DEVICES [AMELIORATION A LA TENUE AUX ENVIRONNEMENTS SEVERES DES ARTIFICES PYROTECHNIQUES PAR ALLUMAGE PAR CHOC]. R. Gencey (Direction Technique des Armements Terrestres, Bourges, Cher, France), p. 57-67. [See A69-23007 10-27]

QUALIFICATION OF EXPLOSIVE COMPONENTS FOR USE IN A SEVERE ENVIRONMENT [QUALIFICATION DES COMPOSANTS EXPLOSIFS POUR EMPLOI EN AMBIANCE SEVERE]. M. Thevenin (Direction Technique des Armements Terrestres, Bourges, Cher, France), p. 69-77. [See A69-23008 10-27]

EXPLOSIVES AND PYROTECHNIC COMPOSITION [EXPLOSIFS ET COMPOSITION PYROTECHNIQUE].

CHARACTERISTICS OF IGNITER FORMULATIONS. J. E. Sinclair (U.S. Naval Postgraduate School, Monterey, Calif.), p. 79-84. [See A69-23009 10-27]

THE EXPLOSIVE CHARACTERISTICS OF PRIMER EXPLOSIVES [LES CARACTERISTIQUES EXPLOSIVES DES EXPLOSIFS D'AMORCAGE]. M. Lenotre (Direction Technique des Armements Terrestres, Tarbes, Hautes-Pyrénées, France), p. 85-98. [See A69-23010 10-27]

NEW PRIMING EXPLOSIVES AND THEIR SPACE APPLICATIONS [LES EXPLOSIFS D'AMORCAGE NOUVEAUX ET LEURS APPLICATIONS SPATIALES]. T. Piechowicz (Direction Technique des Armements Terrestres, Tarbes, Hautes-Pyrénées, France), p. 99-104. 17 refs. [See A69-23011 10-27]

PROBLEMS OF ANALYZING PRIMING EXPLOSIVES [LES PROBLEMES D'ANALYSE DES EXPLOSIFS D'AMORCAGE]. J. L. Cazaux (Direction Technique des Armements Terrestres, Tarbes, Hautes-Pyrénées, France), p. 105-109. [See A69-23012 10-27]

CHEMISTRY OF TETRAZOLE-BASED EXPLOSIVES [CHIMIE DES DERIVES EXPLOSIFS DES TETRAZOLES]. H. Morisson (Direction Technique des Armements Terrestres, Tarbes, Hautes-Pyrénées, France), p. 111-120. 34 refs. [See A69-23013 10-06]

APPLICATION OF HEAT RESISTANT EXPLOSIVES TO SPACE SYSTEMS. E. E. Kilmer (U.S. Navy, Ordnance Systems Command, Silver Spring, Md.), p. 121-137. 6 refs. [See A69-23014 10-27]

DEVELOPMENT OF INITIATING AND IGNIFEROUS MATERIALS FOR USE IN EXTREME CONDITIONS. C. H. Miller (Ministry of Technology, Explosives Research and Development Establishment, Waltham Abbey, Essex, England), p. 139-149. [See A69-23015 10-27]

BASIC STUDIES OF THE MECHANISM OF SHOCK INITIATION IN GRANULAR EXPLOSIVES. L. B. Seely, B. O. Reese, and M. Evans (Stanford Research Institute, Menlo Park, Calif.), p. 151-169. 6 refs. [See A69-23016 10-27]

INITIATION OF PRIMING EXPLOSIVES BY ELECTRONS AND PHOTONS [INITIATION DES EXPLOSIFS D'AMORCAGE PAR ELECTRONS ET PAR PHOTONS]. L. D'Ast (Direction Technique des Armements Terrestres, Tarbes, Hautes-Pyrénées, France), p. 171-182. 10 refs. [See A69-23017 10-27]

THE DEVELOPMENT OF A NON-CONDUCTIVE IGNITION COMPOSITION FOR RFI PROTECTION OF SPACECRAFT ELECTRO-EXPLOSIVE DEVICES. J. T. Greenslade (Space Ordnance Systems, Inc., El Segundo, Calif.), p. 183-193. [See A69-23018 10-27]

RF-HAZARDS TO ELECTRO EXPLOSIVE DEVICES. G. Schroer (Junkers Flugzeug- und Motorenwerke GmbH, Munich, West Germany), p. 195-219. [See A69-23019 10-27]

EXAMPLES OF APPLICATIONS [EXEMPLES D'APPLICATIONS].

CRITERIA GOVERNING THE DESIGN OF ELECTRO-EXPLOSIVE DEVICES FOR EXTREME CONDITIONS. L. E. Medlock (Imperial Chemical Industries, Ltd., Stevenston, Ayr., Scotla ..), p. 221-228. [See A69-23020 10-27]

PRIMERS AND OTHER EXPLOSIVE WIRE DEVICES - CONDITIONS FOR USING THEM ON MISSILES [LES AMORCES ET AUTRES ARTIFICES A FIL EXPLOSE - LEURS CONDITIONS D'EMPLOI SUR MISSILES]. P. Y. Hervé (Direction Technique des Armements Terrestres, Bourges, Cher, France), p. 229-264. 11 refs. [See A69-23021 10-27]

DESIGNING ELECTRO-EXPLOSIVE DEVICES FOR SPACE. D. E. Davenport, L. D. Pitts (General Precision Systems, Inc., Sunnyvale, Calif.), and H. D. Peckham (Gavilan College, Gilroy, Calif.), p. 265-321. 11 refs. [See A69-23022 10-27]

STAGE SEPARATION BY DETONATING FUSES [LE DECOUPAGE INTER-ETAGE PAR CORDEAUX DETONANTS]. H. Carabin (Direction des Poudres, Sevran, France) and B. Ceyrat (Direction Technique des Armements Terrestres, Bourges, Cher, France), p. 323-342. [See A69-23023 10-27]

USE OF PYROTECHNICAL DEVICES ON A BALLISTIC ROCKET [EMPLOI DE DISPOSITIFS PYROTECHNIQUES SUR UN ENGIN BALISTIQUE]. J. Doute (Société pour l'Etude et la Réalisation d'Engins Balistiques, S.A., Courbevoie, Hauts-de-Seine, France), p. 343-356. [See A69-23024 10-27]

IGNITION SYSTEMS FOR PROPELLANT UNITS [SYSTEMES D'ALLUMAGE DE BLOCS DE PROPERGOL]. F. Chanut (Société pour l'Etude et la Réalisation d'Engins Balistiques, S.A., Courbevoie, Hauts-de-Seine, France), p. 357-367. [See A69-23025 10-27]

A PYROTECHNIC-ACTIVATED CALORIMETER FOR FLIGHT RESEARCH AT LUNAR RETURN VELOCITY. D. D. Davis, Jr. and C. Wood (NASA, Langley Research Center, Hampton, Va.), p. 369-378. [See A69-23026 10-11]

NOSE FAIRINGS SEPARATION SYSTEM EXPLOSIVE DEVICES OF THE ELDO EUROPA I LAUNCHER. M. Porru (Fiat S.p.A., Turin, Italy), p. 379-402. 6 refs. [See A69-23027 10-03]

USE OF EXPLOSIVE AND PYROTECHNICAL ELEMENTS IN THE TECHNOLOGY OF HOT-WATER ROCKETS. G. Partel (Centro Studi Trasporti Missilistici, Rome, Italy), p. 403-418. [See A69-23028 10-28]

THE SCIENTIFIC AND ENGINEERING APPLICATIONS OF PYROTECHNICS IN THE SKYLARK UPPER ATMOSPHERE SOUNDING ROCKET. G. G. E. Lewis (British Aircraft Corp. /Guided Weapons/, Ltd., Filton, Bristol, England), p. 419-428. [See A69-23029 10-31]

DESCRIPTION OF A "HOLLOW CHARGE" PYROTECHNIC CIRCUIT CLOSER [DESCRIPTION D'UN CONJONCTEUR PYROTECHNIQUE A "CHARGE-CREUSE"]. A. Winaver (Compagnie Française Thomson Houston-Hotchkiss Brandt, Paris, France), p. 429-439. [See A69-23030 10-03]

PYROTECHNIC CIRCUIT CLOSER USING THE CONDUCTIVITY OF A HOLLOW CHARGE JET [CONJONCTEUR PYROTECHNIQUE UTILISANT LA CONDUCTIVITE DU JET D'UNE CHARGE CREUSE]. B. Ceyrat (Direction Technique des Armements Terrestres, Bourges, Cher, France), p. 441-448. [See A69-23031 10-03]

THE EJECTION OF INSTRUMENTS FROM SOUNDING ROCKET PAYLOADS. W. T. Fisher and D. J. Brown (Bristol Aerojet, Ltd., Banwell, Somerset, England), p. 449-457. [See A69-23032 10-03]

TWO-WAY PYROTECHNIC VALVE FOR HIGH-PRESSURE GAS [VANNE DOUBLE A FONCTIONNEMENT PYROTECHNIQUE POUR GAZ HAUTE PRESSION]. F. Gandillot (Nord-Aviation, Châtillon-sous-Bagneux, Hauts-de-Seine, France), p. 459-466. [See A69-23033 10-03]

NOSECONE EJECTION SYSTEM WITH PYROTECHNIC DEVICES USED IN CENTAURE ROCKET FOR RFMS EXPERIMENT. A. P. J. A. Kalam (Thumba Equatorial Rocket Launching Station, Trivandrum, Kerala, India), p. 467-472. [See A69-23034 10-03]

A69-32345 *#
VAPOR-PHASE COMBUSTION PHENOMENA WHEN Zr DROPLETS BURN IN OXYGEN.
R. L. Marshall and G. L. Pellett (NASA, Langley Research Center, Propulsion Branch, Hampton, Va.).
Combustion Institute, Spring Meeting, China Lake, Calif., Apr. 28, 29, 1969, Paper WSCI 69-4. 32 p. 14 refs.

Study, by spectroscopic and photographic techniques, of the combustion of laser-ignited, 365-μ Zr droplets, falling in ultrapure O_2 at pressures from 30 to 760 torr. The droplet flame structure exhibited several phenomena involving vapor-phase transport of zirconium-containing species exterior to the parent droplet. After a short "autoignition" period, characterized by surface oxidation and rapid temperature rise, a spatially distinct condensation zone, comprised of small "circulating" liquid ZrO_2 droplets, was observed to form. Its sharp outer boundary decreased substantially in size with increasing O_2 pressure. At pressures $\geq$380 torr, large satellite or follower droplets of ZrO_2 grew in the wake region and eventually contacted and coalesced with the parent droplet. Measured growth rates of satellite droplets at $\geq$380 torr indicated that, up to the time of first coalescence, most of the O_2 consumed ended up as ZrO_2 in the condensation zone. A spatially distinct zone of radiation emission was observed within the outer condensation zone close to the parent droplet surface; its radial position was nearly independent of O_2 pressure. This "inner-flame" zone was tentatively identified with spectroscopically observed ZrO emission that was postulated to result from vapor-phase reactions between Zr and oxygen species. (Author)

N69-16153*# National Aeronautics and Space Administration. Lewis Research Center, Cleveland, Ohio.
NONEQUILIBRIUM CALCULATIONS OF METHANE FLUORINE OXYGEN AND BUTENE-1-FLUORINE OXYGEN ROCKET PERFORMANCE
David A. Bittker Washington Jan. 1969 39 p refs
(NASA-TN-D-4991) Avail: CFSTI CSCL 21I

Equilibrium and kinetically limited performance, calculated using a one-dimensional model, are presented for methane and butene-1 rocket fuels combined with fluorine-oxygen mixtures for chamber pressures of 100 and 300 psia (6.895×10^5 and 2.069×10^6 N/m^2) and the oxidant-fuel ratio range of 2.5 to 6. Rate-controlling chemical reactions in the recombination process are identified and quantitatively rated in importance. Performance sensitivity to rate-constant uncertainty is studied in detail. It is shown that a one-dimensional kinetic flow model can be used to calculate performance in satisfactory agreement with the available experimental data and that no more than three reactions are rate controlling on the entire process. Author

N69-16195*# National Aeronautics and Space Administration. Lewis Research Center, Cleveland, Ohio.
THEORETICAL NONEQUILIBRIUM PERFORMANCE OF OXYGEN DIFLUORIDE-DIBORANE ROCKET PROPELLANT
David A. Bittker Washington Jan. 1969 28 p refs
(NASA-TN-D-4992) Avail: CFSTI CSCL 21I

Theoretical performance, both equilibrium and rate-limited, is presented for the oxygen difluoride-diborane propellant system. A one-dimensional kinetic flow model was used. The work also includes identification of the rate controlling chemical reactions in the recombination process. Reactions are quantitatively rated in importance and the sensitivity of performance to the uncertainty of individual rate constants is studied in detail. Results indicate that the hydrogen-atom recombination is the predominant reaction in the entire process as far as performance is concerned and that no reaction involving boron species has a significant effect on performance. The theoretical performance level of oxygen difluoride-diborane is significantly higher than that for the methane-fluorine/oxygen propellant, the most energetic of the hydrocarbon-fluorine/oxygen systems. Author

N69-19026*# National Aeronautics and Space Administration. Lewis Research Center, Cleveland, Ohio.
DYNAMIC RESPONSE OF HYDRAZINE-NITROGEN TETROXIDE COMBUSTION TO TRANSVERSE GAS FLOW
Marshall C. Burrows Washington Feb. 1969 25 p refs
(NASA-TN-D-4984) Avail: CFSTI CSCL 21B

Combustion stability of a hypergolic system was studied for several variations of triplet element design. Tangential nitrogen flow induced the traveling transverse mode of instability within the chamber. Two types of unstable combustion were initiated by the nitrogen flow. In one type, the amplitude of the transverse wave was coupled to the tangential flow of nitrogen in that the oscillatory amplitude was proportional to the nitrogen flow. The second type of unstable combustion was induced by the nitrogen flow but continued with undiminished amplitude when nitrogen flow decreased making it a self-coupled response. The self-coupled response could be eliminated when center jet stability was increased sufficiently by increasing center jet velocity, diameter, or extending tube length downstream from the injector face. Observed jet breakup was correlated with an atomization model based on the progressive spreading of the liquid jets prior to impingement. The effect of transverse gas flow on jet breakup is evaluated. The breakup of jets prior to impingement can produce nonaxial flow sufficient to initiate combustion instability in a combustor. Sustained oscillations can also be driven by in-phase fuel decomposition and interfacial reactions. Proper shielding, alinement, and impingement of the jets within each injector element will minimize the generation of nonaxial flows which are conducive to unstable combustion. Author

N69-35321*# National Aeronautics and Space Administration. Manned Spacecraft Center, Houston, Tex.
SOME LIQUID OXYGEN/LIQUID HYDROGEN EXPLOSIVE EFFECTS IN CONTROLLED FAILURE-MODE TESTS
Richard W. High Washington Sep. 1969 33 p refs
(NASA-TN-D-5382) Avail: CFSTI CSCL 21I

The explosive yield data from three launch vehicle propellants are analyzed and compared. These data from controlled failure mode tests are found to be proportional to the interface area of contact between the fuel and oxidizer. The comparison of the data at short delay times suggests that, when the interface area of contact is equal, the potential hazard of liquid oxygen/liquid hydrogen is similar to that of liquid oxyben/kerosene and to nitrogen tetroxide/Aerozine-50. Author

N69-36225*# National Aeronautics and Space Administration. Langley Research Center, Langley Station, Va.
EXPERIMENTAL INVESTIGATION OF THE EFFECT OF ALUMINUM SIZE AND LOADING ON THE BURNING RATE OF SOLID PROPELLANTS UNDER ACCELERATION
G. Burton Northam and Wayne P. Jessee Washington Sep. 1969 26 p refs
(NASA-TN-D-5397) Avail: CFSTI CSCL 21I

Composite polybutadiene acrylic acid (PBAA) propellants were tested under centrifugal acceleration forces directed normal into the burning surface to determine the effect of aluminum particle size and aluminum mass loading on the burning rate. The weight-median diameters of the aluminum powders used in the propellants were 6, 14, and 29 μm; propellants with aluminum mass loadings of 0, 8, and 16 percent were used. The various propellant compositions were tested in a slab motor configuration with a unidirectional burning propellant grain with a 0.5-inch (12.7-mm) web thickness. Centrifuge firings were made at three pressure levels for each of six acceleration levels from static to 280g. Increasing the aluminum particle size from 6 to 29 μm resulted in increased burning rates under acceleration loads directed normal into the propellant surface. Decreasing the aluminum mass loading of the propellant decreased the acceleration sensitivity of the burning rate in the region below 150 and increased the sensitivity in the region above 150g. Author

28

PROPULSION SYSTEMS

Includes air breathing, electric, liquid, solid, and magnetohydrodynamic propulsion. For nuclear propulsion see: 22 Nuclear Engineering. For basic research see: 23 Physics, General; and 33 Thermodynamics and Combustion. For applications see: 31 Space Vehicles. For related information see also: 27 Propellants.

A69-12375 *#
OPTIMAL CONTROL APPLICATION FOR ELECTROTHERMAL MULTIJET SYSTEMS ON SYNCHRONOUS EARTH SPACECRAFT.
William C. Isley (NASA, Goddard Space Flight Center, Systems Div., Auxiliary Propulsion Branch, Systems Analysis and Electric Propulsion Section, Greenbelt, Md.).
(American Institute of Aeronautics and Astronautics, Electric Propulsion and Plasmadynamics Conference, Colorado Springs, Colo., Sept. 11-13, 1967, Paper 67-723.)
Journal of Spacecraft and Rockets, vol. 5, Dec. 1968, p. 1444-1451. 5 refs.
Contract No. NAS 5-10349.

Study of high-temperature fast flows which are involved in space vehicle reentry and in the flight of certain missiles where ionization phenomena appear. A magnetic blast shock tube developed by the aerothermodynamic laboratory of the CNRS is described, and its application to the study of high temperature flows is discussed. F. R. L.

A69-15000 *
PROPULSION ASSISTED BY MICROWAVE POWER.
J. M. Bonneville (NASA, Electronics Research Center, Cambridge, Mass.).
(Symposium on Microwave Power, Boston, Mass., Mar. 22, 1968, Paper D 2.)
Journal of Microwave Power, vol. 3, Dec. 1968, p. 187-193. 12 refs.

Study of practical applications of microwaves to various propulsion requirements including spacecraft launching, power transmission in space, and ground takeoff assist (for aircraft) for fuel economy. Power requirements are presented for some specific cases, and problems associated with the use of microwaves as part of the power system are outlined, as are some means of solution. B.H.

A69-15622 *
JET ENGINE INLET NOISE CONTROL.
D. Chestnutt (NASA, Langley Research Center, Hampton, Va.).
Sound and Vibration, vol. 2, Dec. 1968, p. 10-14. 8 refs.

Discussion of the influence of inlet guide vanes on the radiation of noise from the inlet of a compressor. Suppression of this noise during an aircraft landing approach is particularly desirable. An aircraft turbofan engine is illustrated which emits noise from three major sources. They are the primary jet, the fan discharge, and the inlet. The inlet noise is made up of broadband noise and discrete tones from the rotating machinery. Inlet guide vanes may be located in such a manner as to minimize the noise due to wake interactions. They may also be used effectively for local choking of the inlet flow. Both the wake interaction and the choked-flow phenomena are discussed. It is found that choked flow through the guide vanes is effective for noise control, but practical problems have limited its application to hardware now in service. P. v. T.

A69-16136 *#
ADVANCED CONCEPTS TO INCREASE TURBINE BLADE LOADING.
W. L. Stewart and A. J. Glassman (NASA, Lewis Research Center, Cleveland, Ohio).
American Society of Mechanical Engineers, Winter Annual Meeting and Energy Systems Exposition, New York, N.Y., Dec. 1-5, 1968, Paper 68-WA/GT-11. 5 p. 5 refs.
Members, $0.75; nonmembers, $1.50.

Investigation of turbine-blade loading in terms of surface diffusion and loading-effectiveness parameters. These parameters serve to define the level of loading, with higher values of each representing higher loading on the blade. Advanced blading concepts designed for efficient use of high values for each of these factors are discussed. Experimental results demonstrating these design concepts are described. M. M.

A69-16233 *
AN EXPERIMENTAL INVESTIGATION OF A HIGH-VOLTAGE ELECTRON-BOMBARDMENT ION THRUSTER.
David C. Byers (NASA, Lewis Research Center, Cleveland, Ohio).
(Electrochemical Society, Meeting, Boston, Mass., May 5-9, 1968, Paper 170D.)
Electrochemical Society, Journal, vol. 116, Jan. 1969, p. 9-17. 27 refs.

Description of the performance of a mercury electron-bombardment thruster at large values of net accelerating potential. A 20-cm thruster is tested at values of ion beam current and net accelerating potential up to 0.165 A and 70 kV, respectively. A maximum beam power of about 10 kW is obtained. The maximum supportable electric field strength between accelerator grids is approximately constant at 2×10^6 V/m for spacings between 0.5 and 3.0 cm. The ion chamber performance is qualitatively similar to that at low accelerating voltages. The power efficiency is measured and found to be consistent with data taken with low-voltage thrusters operated at similar conditions. Z. W.

A69-21212 *#
AMMONIA RESISTOJET STATION KEEPING SUBSYSTEM ABOARD APPLICATIONS TECHNOLOGY SATELLITE (ATS) IV.
R. Shaw, T. K. Pugmire (Avco Corp., Avco Space Systems Div., Auxiliary Propulsion Dept., Lowell, Mass.), and R. A. Callens (NASA, Goddard Space Flight Center, Auxiliary Propulsion Branch, Greenbelt, Md.).
American Institute of Aeronautics and Astronautics, Electric Propulsion Conference, 7th, Williamsburg, Va., Mar. 3-5, 1969, Paper 69-296. 10 p
Members, $1.00; nonmembers, $1.50.
Contract No. NAS 5-10394.

A 50-μ-lb thrust, ammonia fueled Resistojet system was on board the ATS-4 which was launched Aug. 10, 1968, into a decaying eliptical orbit. The Resistojet system was designed to provide 400 lb-sec total impulse for east-west station keeping and station changing in the planned geosynchronous orbit. The system weighed 16 lb, including 3 lb of ammonia, and used 11 w. During the two month satellite lifetime, the system operated 825 hr consuming 35% of its fuel, equivalent to one year maximum or two years minimum use rate if the spacecraft had been placed into a synchronous orbit. Flight test data, notably calibration measurements, leakage measurements, plenum depletion flow rates, and plenum pressure compared excellently with ground tests. Attention paid during design and ground test to valve selection, orifice sizing, porous plug flow techniques, ammonia-material compatibility, and contamination control contributed significantly to the flight success. (Author)

A69-21216 *#
REVIEW OF THE NASA PROGRAM IN ELECTRIC PROPULSION.

James Lazar (NASA, Office of Advanced Research and Technology, Washington, D.C.).
American Institute of Aeronautics and Astronautics, Electric Propulsion Conference, 7th, Williamsburg, Va., Mar. 3-5, 1969, Paper 69-248. 10 p. 23 refs.
Members, $1.00; nonmembers, $1.50.

The early application of electric propulsion for spacecraft position control and for small, automated interplanetary spacecraft continues to be a major goal of the electric propulsion program. The NASA-supported flight programs and laboratory efforts directed toward this goal are presented. The technology program aimed at auxiliary propulsion for application satellites and manned space stations, and prime propulsion for solar powered automated spacecraft is reviewed. The results from the Application Technology Satellite flights and the progress of the SERT 2 flight project are also summarized. (Author)

A69-21218 *#
CESIUM CONTACT ION MICROTHRUSTER EXPERIMENT ABOARD APPLICATIONS TECHNOLOGY SATELLITE (ATS) IV.
Robert E. Hunter, Robert O. Bartlett (NASA, Goddard Space Flight Center, Greenbelt, Md.), Robert M. Worlock, and Edmund L. James (Electro-Optical Systems, Inc., Pasadena, Calif.).
American Institute of Aeronautics and Astronautics, Electric Propulsion Conference, 7th, Williamsburg, Va., Mar. 3-5, 1969, Paper 69-297. 5 p.
Members, $1.00; nonmembers, $1.50.

On Aug. 10, 1968, ATS 4 was launched into a low-altitude parking orbit, remaining attached to the Centaur stage which failed to achieve a second burn. On board were two ion microthruster systems, and a spacecraft potential monitor which employed one of the gravity gradient booms as a Langmuir probe. The booms were deployed just prior to the last of five ion engine test periods. The large ram ion currents available from the relatively dense ambient plasma precluded the achievement of appreciable neutralizer emission current except for a few brief periods. During the last test, emission currents up to roughly half the beam current were obtained and spacecraft potentials as great as -133 volts were measured. Notable achievements, in addition to providing the first successful orbital test of an ion engine, include demonstration of the absence of detectable EMI and the satisfactory operation of the zero-g feed system. (Author)

A69-21221 *#
INVESTIGATION OF A HOLLOW CATHODE DISCHARGE PLASMA.
George A. Csiky (NASA, Lewis Research Center, Cleveland, Ohio).
American Institute of Aeronautics and Astronautics, Electric Propulsion Conference, 7th, Williamsburg, Va., Mar. 3-5, 1969, Paper 69-258. 11 p. 7 refs.
Members, $1.00; nonmembers, $1.50.

A mercury-vapor-fed hollow cathode of the type used in SERT II thrustors was operated in a bell jar. Voltage-current characteristics and ranges of mercury flow rate were determined for the principal observed discharge modes of "spot" and "plume." Discharge currents ranged up to 3 A and voltages to 60 V. Plasma potential, electron density, and electron temperature in the external discharge region were measured by Langmuir probe techniques. The atom density profile for a neutral efflux was estimated and compared with measured electron densities in the plasma. Also the attenuation of the primary electron current with distance was calculated. Based on the results, it is suggested that the 11 V equipotential plateau, found between the cathode and anode in both operational modes, penetrates into the orifice region in the spot mode but not in the plume mode. (Author)

A69-21224 *#
DURABILITY OF THE SERT II HOLLOW CATHODE AND FUTURE APPLICATIONS OF HOLLOW CATHODES.
Vincent K. Rawlin and William R. Kerslake (NASA, Lewis Research Center, Cleveland, Ohio).
American Institute of Aeronautics and Astronautics, Electric Propulsion Conference, 7th, Williamsburg, Va., Mar. 3-5, 1969, Paper 69-304. 16 p. 12 refs.
Members, $1.00; nonmembers, $1.50.

The SERT II thrustor uses a mercury fed hollow cathode for both the main discharge chamber and for the neutralizer cathode. The design of these two nearly identical cathodes was determined by a previous development program. The work presents the results of life testing seven main and six neutralizer cathodes in experimental thrustor systems for periods up to 3438 hr. The main cathode emits 2 A to the discharge chamber and has at this current level a maximum projected lifetime of 15,000 hr. When emission currents greater than 2.5 A were drawn, the projected lifetime was sharply reduced. The neutralizer cathode injects 0.25 A of electrons into the ion exhaust beam and has a maximum projected lifetime of 33,000 hr. A hollow cathode has been tested in a bell jar as a simulated neutralizer for more than 10,000 hr. Larger hollow cathodes developed for use in large thrustors emitted 10 to 30 A and showed no wear after 234 hr. (Author)

A69-21225 *#
ONSET OF ROTATING DISTURBANCE IN THE INTERELECTRODE REGION AND EXHAUST JET OF AN MPD ARC.
Frank Allario, Olin Jarrett, Jr., and Robert V. Hess (NASA, Langley Research Center, Aero-Physics Div., Plasma Physics Section, Hampton, Va.).
American Institute of Aeronautics and Astronautics, Electric Propulsion Conference, 7th, Williamsburg, Va., Mar. 3-5, 1969, Paper 69-232. 9 p. 11 refs.
Members, $1.00; nonmembers, $1.50.

Experimental results of a parametric study of the onset of rotating disturbances ($f \leq 500$ kHz) in the plasma of a 15 to 40 kW MPD arc. Measurements were taken in the exhaust and interelectrode regions, using optical and electrostatic probes. The dependence of critical magnetic field (B_c) on mass flow, background pressure, and propellant are given. In argon, B_c varied from 800 to 1800 gauss for a mass flow change of 14 to 100 mg/sec. Considerably higher values of B_c were obtained in xenon. Little dependence on background pressure was found. Diagnostics were performed on the quiet preonset and the postonset plasma states. The latter evolved from a coherent disturbance at low B to an apparent turbulent state at high B. Thrust measurements in these different plasma states are discussed. (Author)

A69-21233 *#
A COLLISIONLESS MODEL FOR HIGH SPECIFIC IMPULSE ACCELERATORS.
Velvin R. Watson (NASA, Ames Research Center, Moffett Field, Calif.).
American Institute of Aeronautics and Astronautics, Electric Propulsion Conference, 7th, Williamsburg, Va., Mar. 3-5, 1969, Paper 69-278. 8 p. 8 refs.
Members, $1.00; nonmembers, $1.50.

Estimates of particle free paths within axisymmetric plasma accelerators that produce specific impulses of about 10^5 sec suggest that the ions receive most of their energy directly from the electromagnetic fields rather than from collisions. A computer is used to simulate such a collisionless plasma with constant applied accelerating voltage and without applied magnetic field. Movies of the simulation illustrate how the particles are accelerated by the fields, how the particle motions in turn modify the fields, and how this interaction causes a net acceleration of the particles out of the accelerator exhaust. A theory developed from the qualitative plasma motion observed with the computer simulation is used to derive accelerator performance characteristics. The theory predicts optimum performance with no applied magnetic field and with a mass flow proportional to current. The resulting specific impulse is proportional to the current, and the voltage and thrust are proportional to the current squared. (Author)

A69-21236 *#
SEGMENTED ANODE, CO_2-H_2 PERFORMANCE AND HOLLOW CATHODE EROSION TESTS ON A LOW POWER MPD ARC THRUSTER.
James A. Burkhart (NASA, Lewis Research Center, Cleveland, Ohio).

American Institute of Aeronautics and Astronautics, Electric Propulsion Conference, 7th, Williamsburg, Va., Mar. 3-5, 1969, Paper 69-242. 15 p. 12 refs.
Members, $1.00; nonmembers, $1.50.

Current measurements on a thrustor segmented into 4 circular sectors showed that there was a rotating current spoke unless a large capacitor was across the discharge. Measurements on a thrustor segmented into cylindrical bands showed that the discharge always had an ac ripple but no axial motion of the current attachment on the anode. The ac impedance of the discharge circuit affected both the amplitude and frequency spectrum of the ac. The ability of the small MPD arc thrustor to run on CO_2-H_2 was demonstrated. Thrust to power ratios of 21.8 mN/kW were obtained at specific impulses of 100 sec. At higher specific impulses performance was poorer than with Ar or Xe. Results of a 638 hr life test on an argon hollow cathode are reported. Erosion was found to be position sensitive. Use of an automatic current control lowered the cathode erosion rate by a factor of four from that previously reported. (Author)

A69-21239 *#

THE EFFECT OF BACKGROUND PRESSURE AND MAGNETIC FIELD SHAPE ON MPD THRUSTER PERFORMANCE.

D. J. Connolly and R. J. Sovie (NASA, Lewis Research Center, Cleveland, Ohio).

American Institute of Aeronautics and Astronautics, Electric Propulsion Conference, 7th, Williamsburg, Va., Mar. 3-5, 1969, Paper 69-243. 9 p. 9 refs.
Members, $1.00; nonmembers, $1.50.

The effects of background pressure and magnetic field shape on MPD thrustor performance were experimentally studied. High background pressure was found to influence thrustor performance in two ways. Doppler shift spectroscopic measurements showed that as the pressure was raised, the axial velocity of the propellant decreased thereby degrading performance. At the same time the performance was augmented, however, by entrainment and acceleration of background gas. The relative importance of the two effects depended on the pressure and mass flow rate. The shape of the magnetic field at the cathode was varied from converging to rapidly diverging in the downstream direction. There was no degradation in performance until the field diverged quite rapidly. Performance measurements were made on two MacDonnell radiation cooled thrustors. Results obtained agree with those of MacDonnell. (Author)

A69-21246 *#

SYSTEMS CHARACTERISTICS OF LIQUID MERCURY CATHODE THRUSTERS.

P. D. Reader (NASA, Lewis Research Center, Cleveland, Ohio) and H. J. King (Hughes Aircraft Co., Research Laboratories, Malibu, Calif.).

American Institute of Aeronautics and Astronautics, Electric Propulsion Conference, 7th, Williamsburg, Va., Mar. 3-5, 1969, Paper 69-237. 7 p. 7 refs.
Members, $1.00; nonmembers, $1.50.
NASA-sponsored research.

The use of solar photovoltaic power sources for unmanned electrically propelled interplanetary missions imposes power-matching, "throttling," and sequenced shutdown requirements on the spacecraft propulsion subsystem as the solar flux varies with solar distance. The thrustors are required to operate over at least a 2 to 1 current density range if the contemplated mission ends with a single thrustor in operation. The paper describes the characteristics of a propulsion system employing a liquid mercury cathode thrustor which satisfies the above constraints. The physical and operational characteristics of the liquid mercury cathode, feed system, and thrustor are discussed along with their power conditioning requirements. It is concluded that the liquid mercury cathode offers easily controlled, time invariant thrustor performance. The control characteristics of the thrustor indicate that relatively modest power supply regulation requirements should be adequate. (Author)

A69-21251 *#

PROBLEMS IN PLANNING FOR THE INTRODUCTION OF PRIMARY ELECTRIC PROPULSION.

J. W. Haughey (NASA, Office of Space Science and Applications, Washington, D.C.) and D. S. Edgecombe (Battelle Memorial Institute, Columbus Laboratories, Columbus, Ohio).

American Institute of Aeronautics and Astronautics, Electric Propulsion Conference, 7th, Williamsburg, Va., Mar. 3-5, 1969, Paper 69-247. 11 p. 33 refs.
Members, $1.00; nonmembers, $1.50.
Contract No. NASw-1146.

NASA has a continuing need for rational long range planning of objectives, programs, and investments. The orderly identification of the requirements for new propulsion systems for the automated space program is one of the responsibilities of Launch Vehicle and Propulsion Programs in the NASA Office of Space Science and Applications. A number of unique problems have been encountered in attempting to carry out this responsibility relative to the introduction of primary electric propulsion. Owing primarily to the complexity of the required calculations, the performance-data base is incomplete. Credible cost estimates, always difficult to obtain even for conventional propulsion systems, are scarce. Consequently, only rudimentary cost-effectiveness studies have been accomplished to date. Management questions exist concerning organizational control and responsibility for development of electric propulsion. Current NASA efforts promise to alleviate some of these problems, however, and allow rational planning for electric propulsion. (Author)

A69-21252 *#

PROPELLANT CONDENSATION ON SURFACES NEAR AN ELECTRIC ROCKET EXHAUST.

Thaine W. Reynolds and Edward A. Richley (NASA, Lewis Research Center, Cleveland, Ohio).

American Institute of Aeronautics and Astronautics, Electric Propulsion Conference, 7th, Williamsburg, Va., Mar. 3-5, 1969, Paper 69-270. 11 p. 15 refs.
Members, $1.00; nonmembers, $1.50.

The problem of neutral propellant atom fluxes arriving at surfaces situated near the exhaust of ion thrustors is considered. The problem is of interest because, for interplanetary missions, the combination of long thrusting times and low surface temperatures may allow ample opportunity for the build-up of an adsorbed layer of propellant. Both the thermal and electrical behavior of solar panel arrays, for example, could be affected by such a layer. Even spacecraft component surfaces outside a line-of-sight to the thrustor exhaust may receive propellant impingement through reflection or reevaporation from primary surfaces. Some simplified calculations of arrival rates are presented that allow accurate estimates to be made of the possible problem for a given spacecraft design. A specific case of a Jupiter fly-by mission is evaluated in more detail. It is shown that condensation could occur on panels during the latter third of the thrusting period. (Author)

A69-21254 *#

ELECTROTHERMAL INSTABILITY - AN EXPLANATION OF THE MPD ARC THRUSTER ROTATING SPOKE PHENOMENON.

J. Marlin Smith (NASA, Lewis Research Center, Cleveland, Ohio).

American Institute of Aeronautics and Astronautics, Electric Propulsion Conference, 7th, Williamsburg, Va., Mar. 3-5, 1969, Paper 69-231. 11 p. 9 refs.
Members, $1.00; nonmembers, $1.50.

Electrothermal instabilities have been investigated as a possible explanation of the rotating spoke phenomenon observed in recent arc thrustor experiments. A mode that exists in the limit of full ionization or at low ionization rates is compared to experimental results. In order to relate the local properties of electron density, temperature, and electric field (needed to evaluate the theory) to the gross properties measured in the experiments, the thrustor is treated as a constant area duct with heat addition sufficient to drive the working fluid to Mach 1 at the throat. This results in a set of equations which give the local properties in terms of the mass flow, local electric field, and heat addition. The mass flow is a measured quantity. The local electric field and heat addition are functions of the thermal

efficiency of the thrustor. Insufficient knowledge of this efficiency for the experimental data analyzed necessitated approximating the local electric field by taking it to be the critical electric field. The heat addition was then assumed to be given by the product of the measured total current and a voltage given by the product of the critical electric field and the interelectrode gap width. The calculated frequencies agree reasonably well with the experimental results. (Author)

A69-21255 *#
SERT II FLIGHT-TYPE THRUSTER SYSTEM PERFORMANCE.
David C. Byers and John F. Staggs (NASA, Lewis Research Center, Cleveland, Ohio).
American Institute of Aeronautics and Astronautics, Electric Propulsion Conference, 7th, Williamsburg, Va., Mar. 3-5, 1969, Paper 69-235. 13 p. 15 refs.
Members, $1.00; nonmembers, $1.50.

The performance of the SERT II thrustor system over the range of operating parameters expected on the SERT II mission is described. The major parameters varied were the extraction voltages (over a range of 1000 V) and the thrust level (over a three to one range). The overall thrustor efficiency was found (at the rated value of 0.25 A beam current) to decrease from about 71% at 4770 sec specific impulse to about 68% at 4300 sec specific impulse. The required neutralizer equivalent neutral flow rate increased by about 0.007 A when the neutralizer anode voltage was decreased from 30 to 22 V. The neutralizer flow rate more than doubled when the beam current was decreased from the rated value of 0.250 A to 0.075 A. Various life tests indicate that the operational lifetime of all thrustor components is in excess of mission requirements. (Author)

A69-21256 *#
PERFORMANCE AND CONTROL OF A 30-CENTIMETER DIAMETER, LOW IMPULSE KAUFMAN THRUSTER.
Robert T. Bechtel (NASA, Lewis Research Center, Cleveland, Ohio).
American Institute of Aeronautics and Astronautics, Electric Propulsion Conference, 7th, Williamsburg, Va., Mar. 3-5, 1969, Paper 69-238. 14 p. 8 refs.
Members, $1.00; nonmembers, $1.50.

An experimental investigation was conducted to develop a 30-cm diameter, mercury bombardment thrustor for potential space applications. Thrustor operating efficiencies were improved by variation of the discharge chamber geometry and magnetic field shape. A single, glass-coated grid system was used to achieve efficient thrustor operation at lower specific impulse than previous bombardment thrustors. Propellant utilization efficiencies greater than 90% and discharge losses less than 200 eV/ion were attained. Estimated overall thrustor efficiency was about 58% at a specific impulse of 2200 sec. The investigation included a control system which afforded enough flexibility to throttle the ion beam current over a range of 2 to 1. This was accomplished without compromising expected lifetime of thrustor components. (Author)

A69-21257 *#
DESIGN AND DEVELOPMENT OF AN ANNULAR SLIT COLLOID THRUSTER.
Kenneth W. Stark (NASA, Goddard Space Flight Center, Greenbelt, Md.).
American Institute of Aeronautics and Astronautics, Electric Propulsion Conference, 7th, Williamsburg, Va., Mar. 3-5, 1969, Paper 69-287. 6 p.
Members, $1.00; nonmembers, $1.50.

A research and development program was conducted in annular slit colloid thrustor technology. Performance testing has proven the feasibility of this thrustor in meeting the design goals of 150 micropounds thrust, a charge to mass ratio of 3000 coulombs/kg and a specific impulse of 900 sec. Tests were conducted to determine a practical screen voltage for all thrustor operating conditions. Duration and thrustor voltage variation tests were conducted proving the feasibility and practicality of the annular slit design. (Author)

A69-21261 *#
ION ACCELERATOR DESIGNS FOR KAUFMAN THRUSTERS.
Walter C. Lathem (NASA, Lewis Research Center, Cleveland, Ohio).
American Institute of Aeronautics and Astronautics, Electric Propulsion Conference, 7th, Williamsburg, Va., Mar. 3-5, 1969, Paper 69-261. 12 p. 11 refs.
Members, $1.00; nonmembers, $1.50.

Effects of varying the geometric parameters of a two-grid ion accelerator system for Kaufman thrustors are presented in terms of ion beam optics and accelerator grid lifetime. Results were obtained using a digital computer program and an electrolytic tank analog. The geometrical parameters investigated include the grid thicknesses, grid hole diameters and spacings, and grid separation distances. Other variables which affect the optics and the lifetime are then discussed. These variables include, fraction open area of the screen, geometrical scaling, total voltage, net-to-total voltage ratio, propellant utilization efficiency, overall grid diameter, and total number of grid holes. The results presented can serve as guidelines for designing future two-grid accelerator systems. Also included are new techniques for obtaining the shape and location of the downstream plasma boundary, and for predicting the minimum accelerator potential needed to prevent electron backstreaming. (Author)

A69-21731 *#
ONSET OF ROTATING DISTURBANCE IN LINEAR HALL CURRENT ACCELERATOR.
Barry D. Sidney, Frank Allario, and Robert V. Hess (NASA, Langley Research Center, Plasma Physics Section, Hampton, Va.).
American Institute of Aeronautics and Astronautics, Electric Propulsion Conference, 7th, Williamsburg, Va., Mar. 3-5, 1969, Paper 69-381. 7 p. 15 refs.
Members, $1.00; nonmembers, $1.50.

Study of the effect of a magnetic field near the cathode on the instability in linear Hall current accelerators, using a geometry with uniformity of the radial magnetic field extending over the entire anode to cathode region. In this geometry an onset of the instability for a critical value of the radial magnetic field is observed. The cathode region is shown to be the area of origin of the instability, and the instability can be suppressed throughout the region between the electrodes by controlling the radial magnetic field near the cathode only. P.v.T.

A69-26787 *#
BOMBARDMENT THRUSTER INVESTIGATIONS AT THE LEWIS RESEARCH CENTER.
Edward A. Richley and William R. Kerslake (NASA, Lewis Research Center, Cleveland, Ohio).
(American Institute of Aeronautics and Astronautics, Propulsion Joint Specialist Conference, 4th, Cleveland, Ohio, June 10-14, 1968, Paper 68-542.)
Journal of Spacecraft and Rockets, vol. 6, Mar. 1969, p. 289-295. 36 refs.

The current status of various research programs on mercury electron-bombardment thrusters is reviewed. Future thruster requirements as predicted from mission analysis are briefly discussed to establish the relationship with present programs. Thrusters ranging in size from 5 to 150 cm in diameter are described. These thrusters have possible near- to far-term applications extending from station keeping to primary propulsion, respectively. Included is a 5-cm thruster having a power-to-thrust ratio of 220 kW/lb, the 15-cm diameter SERT II thruster, and a 30-cm thruster designed to produce a 1.5-amp beam at 2,700 sec specific impulse. Research activities on thruster components are reported in the context of the various thruster programs. These include glass-coated, single accelerator grids that have accumulated more than 500 hr operating time, high-current hollow cathodes of 10 amp emission, and a minimum-B discharge chamber. (Author)

A69-29433 *
SHORTER COMBUSTORS FOR HIGH-TEMPERATURE JET ENGINES.
William H. Roudebush (NASA, Lewis Research Center, Combustor Branch, Cleveland, Ohio).
Space/Aeronautics, vol. 51, Apr. 1969, p. 74-77.

Survey of problems affecting the design of combustors for high-temperature jet engines, and discussion of ways to solve them. The subjects considered include the challenges of longer lifetime, the design of a central shroud of scoops, problems of overheating and warpage, and combustion efficiency. G. R.

A69-31890 *#
A STUDY OF THE AXIAL VELOCITIES IN AN AMMONIA MPD THRUSTER.
R. J. Sovie and D. J. Connolly (NASA, Lewis Research Center, Cleveland, Ohio).
AIAA Journal, vol. 7, Apr. 1969, p. 723-725.

Study of the measurement of the exit velocities of individual species in a plasma exhaust. The axial velocities were obtained by measuring the Doppler shifts of the various spectral lines emitted by the plasma constituents. Typical results for the velocity of the various exhaust species are illustrated. The variation of ion velocity with magnetic field shape was also investigated. M. M.

A69-32676 *#
SUPERSONIC WIND TUNNEL INVESTIGATION OF INLET-ENGINE COMPATIBILITY.
Robert E. Coltrin and James E. Calogeras (NASA, Lewis Research Center, Cleveland, Ohio).
American Institute of Aeronautics and Astronautics, Propulsion Joint Specialist Conference, 5th, U.S. Air Force Academy, Colorado Springs, Colo., June 9-13, 1969, Paper 69-487. 11 p.
Members, $1.00; nonmembers, $1.50.

Results from an experimental investigation in a 10 x 10-ft supersonic wind tunnel of inlet-produced dynamic distortion and its effects on the stall margin of a J-85 turbojet engine. Compressor face total pressure fluctuations were surveyed by a rotating rake, and resultant recordings were analyzed as to both amplitude and frequency content. The magnitude of dynamic distortion was generally found to vary with terminal shock strength, but was favorably influenced by vortex generator placement in the subsonic diffuser. Results of spectral analysis indicate a flat power spectrum to 300 Hz which then decreased by 75% at 1000 Hz. In most cases, a bypass cavity resonance was superimposed on this spectrum at about 270 Hz. Cross-spectra information indicated that the low-frequency coherence between two probes was high for close probe spacing but fell off rapidly with increased distance. Rms pressure fluctuations of 5% of the steady-state total pressure were found to cause complete stall margin degradation at certain engine speeds. (Author)

A69-32678 *#
AERODYNAMIC STUDIES OF SCALE MODEL TURBINES FOR THE M-1 ENGINE.
Roy G. Stabe and John F. Kline (NASA, Lewis Research Center, Cleveland, Ohio).
American Institute of Aeronautics and Astronautics, Propulsion Joint Specialist Conference, 5th, U.S. Air Force Academy, Colorado Springs, Colo., June 9-13, 1969, Paper 69-553. 10 p. 11 refs.
Members, $1.00; nonmembers, $1.50.

Results of the experimental investigation of two turbines that were scale-model versions of the M-1 rocket engine oxygen and hydrogen pump-drive turbines. Both turbines were two-stage velocity compounded units utilizing toroidal inlet manifolds with radial feedpipes. The principal objectives of the investigation were to determine the performance of the turbines and to identify the problems associated with the compact inlet manifolds. The results of these investigations showed that the overall static efficiency was approximately as designed for both turbines. However, high fluid velocities in the compact toroidal inlet manifolds resulted in substantial variations in static and total pressure around the circumference of the manifold and large total pressure losses. The manifold total pressure loss was correlated with the velocity of the fluid in the manifold feedpipe. This loss was about the equivalent of the feedpipe dynamic pressure. (Author)

A69-32686 *#
PERFORMANCE OF A SINGLE-STAGE TURBINE AS AFFECTED BY VARIABLE STATOR AREA.
Thomas P. Moffitt, Warren J. Whitney, and Harold J. Schum (NASA, Lewis Research Center, Cleveland, Ohio).
American Institute of Aeronautics and Astronautics, Propulsion Joint Specialist Conference, 5th, U.S. Air Force Academy, Colorado Springs, Colo., June 9-13, 1969, Paper 69-525. 10 p. 10 refs.
Members, $1.00; nonmembers, $1.50.

Single-stage turbine investigated at various stator setting angles. The turbine tested included stator assemblies set at 70, 100, and 130% of design. Included is a description of the turbine; the performance of the stator over the range of settings, considering both blade loss and surface velocity distribution; and the overall performance of the turbine, including both efficiency and weight flow as affected by the stator setting. Factors contributing to the observed variation in efficiency are discussed. (Author)

A69-32706 *#
THE FLIGHT INVESTIGATION OF PRESSURE PHENOMENA IN THE AIR INTAKE OF AN F-111A AIRPLANE.
Donald R. Bellman and Donald L. Hughes (NASA, Flight Research Center, Edwards, Calif.).
American Institute of Aeronautics and Astronautics, Propulsion Joint Specialist Conference, 5th, U.S. Air Force Academy, Colorado Springs, Colo., June 9-13, 1969, Paper 69-488. 12 p.
Members, $1.00; nonmembers, $1.50.

Jet-engine compressor stalls appear to be the result of inlet flow conditions and the tolerance of the engine to these conditions. To obtain parameters that might permit the relative assessment of the inlet and engine in regard to compressor stall, flight tests were conducted on a F-111A number 6 aircraft. The left inlet was instrumented with both steady-state and dynamic-type pressure sensors, and flights were made at Mach numbers up to 2. Many compressor stalls were encountered as a result of increasing the angle of attack and of operating with the compression-cone position and angle offset from the normal position. The data show a generally low level of duct turbulence and that steady-state distortion is the most prominent cause of the compressor stalls. However, at Mach numbers above 1.8, the excitation of the duct resonant frequency of about 27 Hz could have a significant effect on the engine. At the compressor face, high turbulence levels are associated with areas of low pressure recovery. With increasing angle of attack above a certain baseline, there is a corresponding increase in distortion, but not necessarily in level of turbulence. The maximum static pressure at the compressor face at the time of a compressor stall is primarily dependent on the compressor discharge pressure and is about 13% of this pressure. (Author)

A69-32711 *#
A METHOD FOR PREDICTING THE PERFORMANCE OF HIGH REACTION SUPERSONIC COMPRESSOR BLADE SECTIONS.
Emanuel Boxer (NASA, Langley Research Center, Hampton, Va.).
American Institute of Aeronautics and Astronautics, Propulsion Joint Specialist Conference, 5th, U.S. Air Force Academy, Colorado Springs, Colo., June 9-13, 1969, Paper 69-522. 15 p. 21 refs.
Members, $1.00; nonmembers, $1.50.

The flow process within supersonic blading is rationalized as a means of predicting the performance near the point of maximum pressure ratio and efficiency. The basic premise is that the flow which separates from the suction surface due to the influence of the terminal shock does not reattach to the surface. As a result, downstream of the trailing edge of the blade, the flow undergoes a sudden-area-enlargement type of dump diffusion process with a consequent increase in both total pressure loss and static pressure ratio. A method of predicting blade section performance is developed in which the parameters that govern the dump diffusion process are obtained by assuming normal shock total pressure recovery and a static pressure rise within the passage equal to the empirical peak separated turbulent boundary-layer value for a flat plate. Comparison of predicted performance with experimental data indicates good agreement over a wide range of inlet Mach number and blade geometry, provided that the flow convergence due to sidewall separation in stationary two-dimensional cascades and the radial mass flow distribution behind three-dimensional rotating supersonic cascades are taken into consideration. (Author)

A69-32714 *#
MEPSIS - MINIMAL ELECTRIC PROPULSION SYSTEMS FOR INTERPLANETARY SPACECRAFT.
Kenneth I. Duck and William C. Isley (NASA, Goddard Space Flight Center, Greenbelt, Md.).
American Institute of Aeronautics and Astronautics, Propulsion Joint Specialist Conference, 5th, U.S. Air Force Academy, Colorado Springs, Colo., June 9-13, 1969, Paper 69-499. 10 p. 14 refs.
Members, $1.00; nonmembers, $1.50.

The MEPSIS concept is explored as a means to obtain near-term interplanetary flight applications for electric propulsion systems. The advantages associated with incorporating a low-thrust upper stage into a conventional all-chemical mission are assessed in terms of payload and/or reduced trip time. Existing and near-term, low-thrust systems are examined for a mid-1970 Jupiter flyby. Results show that the MEPSIS approach can increase net payload by as much as 8% or reduce flight time by approximately 20 days using current power and propulsion system technology. Payload improvements can be higher than 20% or flight time can be reduced in excess of three months using only reasonable advances in power system technology. In addition, the high initial velocity increment imparted by the chemical stage provides a degree of mission utility in that failure of the low thrust stage will not cause a complete failure of the outer probe capability. (Author)

A69-32732 *#
A TWO-DIMENSIONAL, MIXED-COMPRESSION INLET SYSTEM DESIGNED TO SELF-RESTART AT A MACH NUMBER OF 3.5.
Warren E. Anderson and Norman D. Wong (NASA, Ames Research Center, Moffett Field, Calif.).
American Institute of Aeronautics and Astronautics, Propulsion Joint Specialist Conference, 5th, U.S. Air Force Academy, Colorado Springs, Colo., June 9-13, 1969, Paper 69-447. 8 p. 5 refs.
Members, $1.00; nonmembers, $1.50.

Methodology leading to the design of a Mach 3.5 high-performance, two-dimensional, mixed-compression inlet system with self-restart capability. The principal feature of the design is a variable ramp system employing a flexible isentropic surface to provide efficient external compression on-design and engine airflow matching with low spillage drag off-design. An engine-face variable bypass system was also provided. Pertinent experimental results are presented for a range of Mach numbers from 1.55 to 3.5. Results show high overall performance with moderate penalties associated with self-restart at Mach numbers of about 3.0 and above. Further bleed system optimization promises a means to eliminate these penalties and extend the self-restart capability to inlet systems of higher contraction ratios and thus potentially higher performance. (Author)

A69-32735 *#
A SURVEY AND EVALUATION OF RESEARCH ON THE DISCHARGE CHAMBER PLASMA OF A KAUFMAN THRUSTER.
Nelson L. Milder (NASA, Lewis Research Center, Cleveland, Ohio).
American Institute of Aeronautics and Astronautics, Propulsion Joint Specialist Conference, 5th, U.S. Air Force Academy, Colorado Springs, Colo., June 9-13, 1969, Paper 69-494. 14 p. 41 refs.
Members, $1.00; nonmembers, $1.50.

Review of proposed theoretical models of the discharge process occurring in electron bombardment thrustors, in terms of the analytical approaches to the problem, the results obtained, and the model limitations incurred. To facilitate evaluation, five areas affecting thrustor performance are considered - the electron distribution, excitation and ionization processes, discharge energy per beam ion, propellant utilization, and ion chamber geometry and magnetic field. The most successful model of the discharge to date is based on a semiempirical approach. Measured values of plasma parameters are used to calculate ion production rates, ion current to chamber walls, and discharge energy cost per exhaust beam ion. The method appears to yield good agreement with experiment. The ratio of primary to Maxwellian electrons in the discharge chamber plasma generally is found to be less than 0.1. The major loss process appears to be wall recombination; attempts to analyze this loss mechanism are discussed. Existing problem areas are tabulated. (Author)

A69-32737 *#
PRESSURANT GAS REQUIREMENTS FOR THE PRESSURIZED DISCHARGE OF LIQUID HYDROGEN FROM PROPELLANT TANKS.
Robert J. Stochl and Richard L. DeWitt (NASA, Lewis Research Center, Cleveland, Ohio).
American Institute of Aeronautics and Astronautics, Propulsion Joint Specialist Conference, 5th, U.S. Air Force Academy, Colorado Springs, Colo., June 9-13, 1969, Paper 69-526. 11 p. 5 refs.
Members, $1.00; nonmembers, $1.50.

Evaluation of certain major experimental results obtained with large vehicle-type spherical tanks (5- and 13-ft diam) in tests of pressurant gas requirements for the pressurized discharge of liquid hydrogen. The information obtained can be used to aid in the design of optimum pressurization systems for particular missions. The results were also used to determine the capability of an analytical program to predict the pressurant gas requirements. In general, the analytical program was able to predict the pressurant requirements within ±10% for all no-slosh test conditions, with the exception of the straight injector data which were accurate within ±30%. P.v.T.

A69-32762 *#
SPACE STORABLE PROPELLANT PERFORMANCE DEMONSTRATION.
B. J. Waldman, J. Friedman (North American Rockwell Corp., Rocketdyne Div., Canoga Park, Calif.), and P. N. Herr (NASA, Lewis Research Center, Cleveland, Ohio).
American Institute of Aeronautics and Astronautics, Propulsion Joint Specialist Conference, 5th, U.S. Air Force Academy, Colorado Springs, Colo., June 9-13, 1969, Paper 69-505. 7 p. 6 refs.
Members, $1.00; nonmembers, $1.50.

Description of a closely controlled experimental program conducted to establish maximum deliverable specific impulse performance of F_2-O_2/CH_4 and OF_2/B_2H_6 and to provide a basis for setting realistic development performance goals. Identical hardware and instrumentation were used for both propellants to make the results completely compatible. The fuels were injected in gaseous form to ensure near complete combustion. Three different nozzle geometries were used to establish the effect of contour on delivered performance at a chamber pressure of 100 psia and a thrust of 2500 lbf. The nozzles consisted of a 15° cone and a 70% bell each of 60:1 area ratio, and a 15° cone of 4:1 area ratio. The compound OF_2 achieved more performance than the equivalent F_2-O_2 combination for both fuels by an amount that agrees with the recently adopted NBS heat of formation for OF_2. (Author)

A69-34018 *#
STUDY OF A FAMILY OF SUPERSONIC INLET SYSTEMS.
Norman E. Sorensen, Donald B. Smeltzer (NASA, Ames Research Center, Moffett Field, Calif.), and Robert W. Cubbison (NASA, Lewis Research Center, Cleveland, Ohio).
(American Institute of Aeronautics and Astronautics, Propulsion Joint Specialist Conference, 4th, Cleveland, Ohio, June 10-14, 1968, Paper 68-580.)
Journal of Aircraft, vol. 6, May-June 1969, p. 184-188. 5 refs.

A theoretical and experimental program is reviewed showing the performance capabilities of a family of three large-scale axisymmetric inlet systems. The major objective of the program was to investigate relatively short inlet systems capable of high performance over the complete Mach number range. The trade-off of important performance parameters such as engine-face pressure recovery and distortion for boundary-layer bleed was determined. The three inlets were designed for Mach numbers 2.5, 3.0, and 3.5. Vortex generators were used just downstream of the throats to control the flow distortion at the engine face. The Mach-number 2.5 and 3.5 designs had engine airflow bypass systems. The results have shown that high performance was more difficult to achieve as the design Mach number increased because the boundary layer occupied an increasing percentage of the flow in the throat. The bypass systems have not presented serious performance problems. (Author)

A69-35108 *

ELECTRIC SPACE PROPULSION.

Ernst Stuhlinger (NASA, Marshall Space Flight Center, Huntsville, Ala.).

Science Journal, vol. 5A, July 1969, p. 61-67.

Discussion of various types of electric propulsion systems and their use for manned planetary-exploration flights. A description is given of the arc jet engine, the ion engine, and the plasma engine. The initial mass in orbit required for a manned Mars round trip is considered as a function of travel time for various propulsion systems (all chemical, all electric, all nuclear, and an electric spacecraft with a nuclear escape booster). The efficiency of an ion thrustor as a function of the exhaust velocity is shown. G.R.

A69-35175 *#

STALL AND DISTORTION INVESTIGATION OF A YTF30-P-1 TURBOFAN ENGINE.

John H. Povolny (NASA, Lewis Research Center, Cleveland, Ohio).

U.S. Air Force Aero Propulsion Laboratory, Airframe-Propulsion Compatibility Symposium, Miami Beach, Fla., June 24-26, 1969, Paper. 17 p.

Assessment of preliminary results on a YTF30-P-1 engine obtained from a program set up to evaluate and understand the effect of both steady-state and dynamic distortions on the performance and stall characteristics of advanced turbine engines. The high-response compressor interstage instrumentation and specialized testing techniques that were required for the conduct of this program are described, and some of the data thus obtained are presented. The preliminary results indicate that the instrumentation and specialized techniques do provide invaluable information that will help immeasurably in formulating engine dynamic simulations. (Author)

A69-38118 * #

PROPULSION SYSTEMS FOR MANNED EXPLORATION OF THE SOLAR SYSTEM.

Wolfgang E. Moeckel (NASA, Lewis Research Center, Electromagnetic Propulsion Div., Cleveland, Ohio).

Astronautics and Aeronautics, vol. 7, Aug. 1969, p. 66-77. 42 refs.

Examination of the relationship between propulsion-system performance and planetary mission capability. The anticipated preformance for the chief advanced propulsion concepts, ranging from fairly well-defined systems such as solid-core, nuclear-fission rockets to speculative systems such as the thermonuclear fusion rocket is considered. Missions and systems are matched to indicate the extent and rate of progress with regard to each system in the foreseeable future. Two types of propulsion systems are considered: specific-impulse-limited, or high-thrust systems, and specific mass-limited, or low-thrust, power-limited systems. B.H.

A69-39217 * #

EFFECTS OF ACCELERATION UPON SOLID-ROCKET PERFORMANCE.

G. B. Northam and M. H. Lucy (NASA, Langley Research Center, Applied Materials and Physics Div., Hampton, Va.).

(Interagency Chemical Rocket Propulsion Group and American Institute of Aeronautics and Astronautics, Solid Propulsion Conference, 3rd, Atlantic City, N.J., June 4-6, 1968, AIAA Paper 68-530.)

Journal of Spacecraft and Rockets, vol. 6, Apr. 1969, p. 456-459. 6 refs.

NASA-Langley is currently engaged in a research program to determine the parameters that affect the combustion characteristics of solid-propellant rocket motors in acceleration environments. Tests conducted to date indicate that solid-propellant burning rates in an acceleration environment are strongly dependent upon propellant composition, combustion pressure, acceleration level, and orientation of the acceleration vector with respect to the burning surface. The paper presents results obtained from testing double-base, polyurethane, and polybutadiene propellants at acceleration levels to 300 g at various orientations of the acceleration vector with respect to the burning surface. The tests were conducted using a unidirectional-burning propellant slab (4 in. x 6 in. x 0.5 in. web) mounted on a ballistic centrifuge. Extinguishment or interrupted-burning tests using this motor were also performed under various acceleration levels, orientations, and burn times to determine the characteristics of the burning surface under these test conditions. (Author)

A69-39373 * #

NEW FUNCTIONAL APPROACHES FOR REDUNDANT INERT GAS THRUSTER SYSTEMS.

C. E. Hallum, W. F. Kaufman (Philco-Ford Corp., Aeronutronic Div., Newport Beach, Calif.), and D. M. Chisel (NASA, Ames Research Center, Moffett Field, Calif.).

American Institute of Aeronautics and Astronautics, Guidance, Control, and Flight Mechanics Conference, Princeton, N.J., Aug. 18-20, 1969, Paper 69-843. 12 p. 5 refs.

Members, $1.00; nonmembers, $1.50.

Contract No. NAS 2-3664.

Discussion of valving concepts and new functional approaches for inert gas thrustor systems providing redundancy safeguards at minimum costs of weight, volume, and power. Only inert gas thrustor systems with reaction forces in the range of 0.02 to 0.5 lb are considered. The preliminary design of a new functional approach for a spin stabilized satellite is described. Test results of the capabilities of critical elements of the new system are summarized, showing that any single failure can be tolerated with negligible effect on system efficiency. B.H.

A69-39754 * #

ATS-III RESISTOJET THRUSTER SYSTEM PERFORMANCE.

T. Kent Pugmire, W. S. Davis (Avco Corp., Auxiliary Propulsion Dept., Lowell, Mass.), and William Lund (NASA, Goddard Space Flight Center, Greenbelt, Md.).

(American Institute of Aeronautics and Astronautics, Propulsion Joint Specialist Conference, 4th, Cleveland, Ohio, June 10-14, 1968, Paper 68-553.)

Journal of Spacecraft and Rockets, vol. 7, July 1969, p. 790-794. 5 refs.

Contract No. NAS 5-10342.

Description of an ammonia-fueled resistojet engine, and the results of its testing on the ATS-III spacecraft. The 8-lb 10-W engine consists of a self-pressurized ammonia storage with a feed system; two thrustors with nominal thrust levels of 10×10^{-6} lb; and an electronic package for command control, power conditioning, and telemetry conditioning of the system's performance monitoring equipment. The flight tests were designed to demonstrate the operation and function of the resistojet in a space environment and to obtain millipound thrust measurements in space. Except for problems encountered with the solenoid valves, both objectives were successfully met. Space measurements for both cold flow and electrically heated flow compared well with ground measurements. V.Z.

A69-42865 * #

APPLICATIONS AND DEVELOPMENT OF SPACE NUCLEAR ELECTRIC POWER SYSTEMS.

Joseph D. Lafleur, Jr. (U.S. Atomic Energy Commission, Washington, D.C.) and Fred Schulman (NASA, Washington, D.C.).

American Astronautical Society and Operations Research Society of America, Joint National Meeting, Denver, Colo., June 17-20, 1969, AAS Paper 69-305. 56 p. 9 refs.

Review of the applications and development of space nuclear electric power systems, summarizing the current status of these applications and citing nuclear power technology and system development programs. A general description of nuclear power applications is given, including systems already launched, those ready for launch, those being developed for launch, and those likely to be developed. The present and expected future considerations underlying the selection of a power system for particular space environ-

ments are analyzed. Earth satellites, lunar planetary vehicles, and landers are reviewed, and isotope generator development, reactor system technology, and power conversion technology are discussed and summarized. It is concluded that the program to provide technology for space nuclear power is today furnishing generators for earth satellite missions and for experiments on the surface of the moon. In the second decade of this program, there are strong trends toward planetary probes and landers, additional automated lunar surface experiments, military satellites, and manned space missions that will benefit greatly from the use of on-board nuclear power. It is predicted that the program will enable important missions free from the environment and attitude restraints common in nonnuclear power systems in use today to be realized. O.H.

A69-43238 * #
CESIUM CONTACT ION MICROTHRUSTER EXPERIMENT ABOARD APPLICATIONS TECHNOLOGY SATELLITE (ATS)-IV.
Robert E. Hunter, Robert O. Bartlett (NASA, Goddard Space Flight Center, Greenbelt, Md.), Robert M. Worlock, and Edmund L. James (Electro-Optical Systems, Inc., Pasadena, Calif.).
(American Institute of Aeronautics and Astronautics, Electric Propulsion Conference, 7th, Williamsburg, Va., Mar. 3-5, 1969, Paper 69-297.)
Journal of Spacecraft and Rockets, vol. 6, Sept. 1969, p. 968-970.

Description of a method for presenting the results of stress calculations for cases with two load systems in a design chart for stationary creep. The chart yields a dimensionless number by which standard maximum stress is multiplied in order to give the maximum stress for the nonlinear creep states. B. B.

N69-10296*# National Aeronautics and Space Administration. Lewis Research Center, Cleveland, Ohio.
EFFECT OF VARIABLE STATOR AREA ON PERFORMANCE OF A SINGLE-STAGE TURBINE SUITABLE FOR AIR COOLING. 5: STATOR DETAILED LOSSES WITH 70 PERCENT DESIGN AREA
Herman W. Prust, Thomas P. Moffitt, and Bernard Bider Washington Nov. 1968 26 p refs
(NASA-TM-X-1696) Avail: CFSTI CSCL 21E

The turbine is being investigated at stator area settings of 70, 100, and 130 percent of design. This report presents the experimental and analytically predicted results for the stator having a closed (70 percent) area setting and compares these results with similar results obtained for the design (100 percent) area and open (130 percent) area settings. The final results are presented in terms of kinetic energy loss coefficients as a function of velocity level. The experimental losses were close to those predicted analytically and indicate a stator efficiency of about 96 percent. Author

N69-12831*# National Aeronautics and Space Administration. Lewis Research Center, Cleveland, Ohio.
FOULING CHARACTERISTICS OF ASTM JET A FUEL WHEN HEATED TO 700°F IN A SIMULATED HEAT EXCHANGER TUBE
James J. Watt, Albert Evans, Jr. and Robert R. Hibbard Washington Dec. 1968 29 p refs
(NASA-TN-D-4958) Avail: CFSTI CSCL 21D

Supersonic aircraft might profitably utilize the greater heat sink that would be made available if fuels could be heated to higher temperatures than is current practice. Therefore, the ASTM Jet A fuels were heated to 700°F (644 K) under simulated heat exchanger conditions. Tests were made with air-saturated and deoxygenated fuels at pressures ranging from 2.5 to 615 psia (1.72×10^4 to 424×10^4 N/m^2 abs) for periods of 20 hours, and the amounts of tube surface fouling were determined. Very small amounts of solids collected on the surface in all cases; the accumulated solids represented from 0.05 to 2.5 ppm of the fuel. The deposits decreased markedly when the dissolved oxygen was removed from the fuel and, in general, decreased with increasing pressure. Author

N69-13237*# National Aeronautics and Space Administration. Lewis Research Center, Cleveland, Ohio.
PERFORMANCE INVESTIGATION OF BIPROPELLANT FRACTIONAL-POUND THRUSTERS
R. J. Rollbuhler Washington Dec. 1968 24 p refs
(NASA-TM-X-1699) Avail: CFSTI CSCL 21H

The performance capabilities of four fractional-pound-thrust chemical bipropellant rocket thrusters were investigated experimentally. The thrusters were tested with hydrazine-type fuels and nitrogen tetroxide oxidizer in a vacuum of 0.5 to 3.0 torr. Data were obtained to calculate the performance parameters as functions of propellant mixture ratio. Maximum characteristic exhaust velocity ranged from 3400 to 3700 ft/sec (1038 to 1130 m/sec). Peak values of specific impulses varied from 155 to 245 sec. Operational difficulties increased with decreasing propellant injection orifice size (blockage). Hypergolic ignition did not present any problems. Instrumentation limitations prevented the obtaining of pulsing operation data. Author

N69-13275*# National Aeronautics and Space Administration. Lewis Research Center, Cleveland, Ohio.
TEST OF IMPROVED IGNITER FOR FIRST STAGE SEPARATION ROCKETS FOR THE ATLAS-CENTAUR LAUNCH VEHICLE
Richard W. Heath, Henry Synor, and Ralph F. Schmiedlin Washington Dec. 1968 12 p refs
(NASA-TM-X-1676) Avail: CFSTI CSCL 21H

During the course of the Atlas-Centaur separation tests, conducted at the Lewis Research Center, anomalies were discovered in the performance of the igniters that fire the Atlas retarding rockets. A new igniter was developed and tested to assess its marginality. The test results indicated that the new igniter possessed a sufficient margin of performance for flight operations. Author

N69-14210*# General Electric Co., Lynn, Mass. Aircraft Engine Group.
PERFORMANCE COMPARISONS OF HIGH MACH NUMBER COMPRESSOR ROTOR BLADING
J. P. Gostelow, K. W. Krabacher, and L. H. Smith, Jr. Washington NASA Dec. 1968 81 p refs
(Contract NAS3-7617)
(NASA-CR-1256) Avail: CFSTI CSCL 21E

Results of testing of four 1400 ft/sec tip speed single stage compressor rotors are presented. All rotors exceeded design efficiency and flow at conditions corresponding to design point operation. Operating range, from peak efficiency to stall, is highest in rotors designed for a low tip diffusion factor and which have the minimum amount of supersonic camber. Author

N69-14313*# National Aeronautics and Space Administration. Lewis Research Center, Cleveland, Ohio.
EXPERIMENTAL INVESTIGATION OF A 10° CONICAL TURBOJET PLUG NOZZLE WITH IRIS PRIMARY AND TRANSLATING SHROUD AT MACH NUMBERS FROM 0 TO 2.0
Donald L. Bresnahan Washington Dec. 1968 44 p refs
(NASA-TM-X-1709) Avail: CFSTI CSCL 21E

The efficiency of a full-length plug nozzle with a simulated iris primary throat remained above 96.5 percent at all flight conditions except subsonic cruise where external flow effects were significant. Nozzle efficiency was also sensitive to subsonic cruise pressure ratio, varying from 0.918 to 0.942 for pressure ratios from 3.25 to 4.0. Plug truncations to 30 percent of full length at supersonic cruise resulted in a 1 percent loss in efficiency. At subsonic cruise, the effects of truncation were greater, resulting in approximately 1/2 percent efficiency loss with a 65 percent plug and more than 3 percent loss with the 30 percent plug length. Author

N69-14384*# National Aeronautics and Space Administration. Lewis Research Center, Cleveland, Ohio.
LIQUID ROCKET ACOUSTIC-MODE-INSTABILITY STUDIES AT A NOMINAL THRUST OF 2000 POUNDS
E. William Conrad, Harry E. Bloomer, John P. Wanhainen, and David W. Vincent Washington Dec. 1968 95 p refs
(NASA-TN-D-4968) Avail: CFSTI CSCL 21H

Acoustic stability data for both hydrogen-oxygen and earth-storable propellant combinations were collected and correlated as far as possible. Several injector variables that presumably affect the oscillatory energy generation process provided significant stability improvements. Complete stabilization of hydrogen-oxygen rockets was achieved by proper selection of injection areas, element size, and oxidizer tube extension. Several injector variables influenced the stability of earth-storable propellants; however, dynamic stability was not achieved through injector modification. Energy absorbers were effective in suppressing acoustic-mode instability with both propellant combinations. Preliminary design guides for acoustic liners are also given. Author

N69-14386*# National Aeronautics and Space Administration. Lewis Research Center, Cleveland, Ohio.
INFLUENCE OF HIGH-TURBINE INLET TEMPERATURE ENGINES IN A METHANE-FUELED SST WHEN TAKEOFF JET NOISE LIMITS ARE CONSIDERED
Robert W. Koenig and Gerald A. Kraft Washington Dec. 1968 60 p refs
(NASA-TN-D-4965) Avail: CFSTI CSCL 21E

Afterburning turbojet, nonafterburning turbojet, and duct-burning turbofan engine designs were optimized with respect to payload and direct operating cost for a Mach 3.0 cruise SST both with and without takeoff noise constraints. Only jet noise was considered, and none of the engines had noise suppressors. Design turbine-inlet temperature was varied from 2200° to 3100°F (1204° to 1704°C). Without noise restrictions, improvements occurred as the turbine-inlet temperature was raised. The duct-burning turbofan was best at low turbine temperatures, but the nonafterburning turbojet was superior at the upper temperatures. When jet exhaust noise restrictions are imposed, the duct-burning turbofan cycle was superior to the other cycles, with high-turbine-inlet temperature offering little benefit. High-turbine-inlet temperatures offer no benefits to turbojet cycles with noise restrictions. Author

N69-15475*# National Aeronautics and Space Administration. Lewis Research Center, Cleveland, Ohio.
ROCKET ENGINE EVALUATION OF EROSION AND CHAR AS FUNCTIONS OF FABRIC ORIENTATION FOR SILICA-REINFORCED NOZZLE MATERIALS
Donald A. Peterson, Jerry M. Winter, and Arthur M. Shinn, Jr. Washington Jan. 1969 43 p refs
(NASA-TM-X-1721) Avail: CFSTI CSCL 21H

Thirty-five silica reinforced ablative specimens were evaluated. Quartz reinforcement was determined to have the greatest resistance to erosion, but a low cost silica powder-filled material was also high in erosion resistance. A fabric orientation of 60° to the nozzle centerline resulted in low char depth and high erosion resistance. The fabric layup angle to the gas stream should be minimized to minimize char depth and reduce engine weight. A 0° helix angle used for rosette layups resulted in delaminations and severe erosion. Author

N69-16122*# National Aeronautics and Space Administration. Goddard Space Flight Center, Greenbelt, Md.
PRECISION FLOW MEASUREMENT TECHNIQUES FOR LOW-THRUST AUXILIARY-PROPULSION LIQUID ROCKETS
Daniel J. Grant Washington Jan. 1969 22 p refs
(NASA-TN-D-4785) Avail: CFSTI CSCL 21H

This paper concerns techniques for improving precision in measuring propellant consumption of small (0.5 to 5.0-lbf thrust) rocket engines. By proper use of impeller wheel meters for steady flow and a photometric device for pulsed flow, propellant flow and consumption data accuracies of better than 1% can be achieved. Flow-measurement requirements are considered for both steady and pulsed firing modes, for specific impulses of 150 to 350 seconds, and for oxidizer/fuel ratios from 1 to 2. Frequency standards are used to correlate test-stand data with laboratory calibrations of impeller flowmeters. Fluid dynamic simulation is obtained by selecting inert fluids with kinematic viscosities approximately equal to those of the propellants. Anomalous behavior during calibrations indicates that normal turbine meter frequency-viscosity characteristics are not applicable to impeller-wheel units. The accuracy of the photometric device for pulsed-mode flow measurements depends on fluid meniscus displacement and can provide 99.7% probable range accuracy of $-0.423 \pm 3(0.999)\%$ for a 1.75-inch displacement. The initial models are applicable to a thrust range of 1/2 to 25 lbf. Author

N69-16152*# National Aeronautics and Space Administration. Lewis Research Center, Cleveland, Ohio.
ON THE DESIGN OF ACOUSTIC LINERS FOR ROCKET ENGINES: MAXIMUM DAMPING AS A DESIGN OBJECTIVE
Bert Phillips Washington Jan. 1969 16 p refs
(NASA-TM-X-1720) Avail: CFSTI CSCL 21H

A study was conducted to determine what the parameters of an acoustic liner should be to maximize liner damping. This was accomplished by solving the wave equation exactly for the frequency and damping of low order tangential and radial modes in a lined cylindrical cavity. The results, presented as dimensionless frequency and damping for each mode plotted in the impedance plane, indicate that α, the acoustic absorption coefficient, can be used to design a liner provided that the liner real impedance is larger than unity. Author

N69-16154*# National Aeronautics and Space Administration. Lewis Research Center, Cleveland, Ohio.
PERFORMANCE OF SWIRL-CAN TURBOJET COMBUSTORS AT SIMULATED SUPERSONIC COMBUSTOR-INLET CONDITIONS
Helmut F. Butze, Arthur M. Trout, and Harry M. Moyer Washington Jan. 1969 28 p refs
(NASA-TN-D-4996) Avail: CFSTI CSCL 21H

A turbojet combustor comprising an array of swirl cans was evaluated in a rectangular duct at conditions simulating supersonic flight. Tests were conducted at a pressure of 3 atmospheres, inlet-air temperatures of 540° and 1140°F (556 and 889 K), and combustor reference velocities up to 190 feet per second (57.9 m/sec). At combustor-outlet temperatures near 2200°F (1478 K) combustion efficiencies were near 100 percent. At a diffuser-inlet Mach number of 0.3 and an outlet- to inlet-temperature ratio of 2.5, the overall pressure loss was 4.6 percent. At an inlet-air temperature of 1140°F (889 K), temperature rise variation ratios ΔTVR below 1.25 were obtained. Author

N69-16213*# National Aeronautics and Space Administration. Lewis Research Center, Cleveland, Ohio.
INVESTIGATION OF FLOW RANGE AND STABILITY OF THREE INDUCER-IMPELLER PUMP COMBINATIONS OPERATING IN LIQUID HYDROGEN
Donald C. Urasek Washington Jan. 1969 26 p refs
(NASA-TM-X-1729) Avail: CFSTI CSCL 21H

The effect of inducer-impeller matching on flow range and stability was studied by running three variable lead inducers in combination with a centrifugal impeller. The three inducers were designed for flows of 0.80, 1.00, and 1.20 of impeller design flow.

The low flow limit imposed by unstable flow was essentially independent of inducer-impeller matching, whereas the high flow limit imposed by cavitation was improved when the inducer was designed for a higher flow rate than that of the impeller. Author

N69-17276*# National Aeronautics and Space Administration. Lewis Research Center, Cleveland, Ohio.

A SURVEY OF SALT DEPOSITS IN COMPRESSORS OF FLIGHT GAS TURBINE ENGINES

Richard L. Ashbrook Washington Jan. 1969 26 p refs

(NASA-TN-D-4999) Avail: CFSTI CSCL 21E

Salt concentrations on airfoils of compressors of commercial and military gas turbine engines removed from aircraft for overhaul were measured and compared to concentrations reported to cause stress-corrosion damage in laboratory tests. Concentrations in small local areas were determined, as well as the average concentrations for entire airfoils or for the concave or convex sides alone. Qualitative distributions of salt on airfoils were obtained with contact prints. Average salt concentrations from engines used for long transoceanic flights (a relatively mild exposure) exceeded 0.1 mg/in. (0.015 mg/cm^2). Local concentrations more than 10 times as great were found on some blades. Author

N69-17781*# National Aeronautics and Space Administration. Lewis Research Center, Cleveland, Ohio.

STEADY-STATE AIRFLOW AND AFTERBURNING PERFORMANCE CHARACTERISTICS OF FOUR J85-GE-13 TURBOJET ENGINES

Robert J. Antl and Richard R. Burley Washington Feb. 1969 27 p refs

(NASA-TM-X-1742) Avail: CFSTI CSCL 21E

Tests to calibrate four J85-GE-13 afterburning turbojet engines in support of a flight test program were conducted in an altitude facility. Data were obtained over a simulated altitude range of 15,000 to 55,000 feet and a simulated flight Mach number range of 0.8 to 1.7. Included are data on compressor airflow and interstage bleed characteristics, afterburner temperature rise and total pressure drop, and engine net thrust. The engines were calibrated with the manufacturer's variable area convergent nozzle and four, fixed area, water cooled convergent–divergent nozzles having an expansion ratio of 1.3. Comparisons are shown between the engines tested and with the engine manufacturer's predicted results. Author

N69-17847*# National Aeronautics and Space Administration. Lewis Research Center, Cleveland, Ohio.

MEASUREMENTS OF SOME PROPERTIES OF A DISCHARGE FROM A HOLLOW CATHODE

George A. Csiky Washington Feb. 1969 36 p refs

(NASA-TN-D-4966) Avail: CFSTI CSCL 21C

A mercury vapor fed hollow cathode of the type used in SERT II Kaufman thrusters was operated in a bell jar. Voltage current characteristics and ranges of mercury flow rate and anode distance were determined for the principal observed discharge modes of spot and plume with discharge currents ranging up to 3 amperes. Plasma potential, electron density, and electron temperature in the uniform potential external discharge were measured by Langmuir probe techniques. Tentative theoretical models of potential distribution are suggested and discussed for the two modes. Author

N69-19017*# National Aeronautics and Space Administration. Lewis Research Center, Cleveland, Ohio.

EXPERIMENTAL PERFORMANCE OF A WATER-ELECTROLYSIS ROCKET

R. James Rollbuhler Washington Feb. 1969 28 p refs

(NASA-TM-X-1737) Avail: CFSTI CSCL 21H

An experimental investigation was conducted to evaluate the performance characteristics of nominal 1-pound- (4.4-N-) thrust water-electrolysis rocket engine system. The system was tested over a range of propellant flow rates and for various run durations in a vacuum pressure environment. The test results indicated a system specific impulse of 338 ± 17 seconds obtainable at a combustion-chamber pressure of 15 psia. Combustion efficiency was greater than 90 percent of theoretical, and combustion instability was not detected in any of the tests. Author

N69-19782*# National Aeronautics and Space Administration. Lewis Research Center, Cleveland, Ohio.

EVALUATION OF 7.8-INCH-THROAT-DIAMETER INSERTS AND A UNIQUE COOLING CONCEPT IN A STORABLE-PROPELLANT ROCKET ENGINE

Jerry M. Winter and Donald A. Peterson Washington Mar. 1969 33 p refs

(NASA-TM-X-1756) Avail: CFSTI CSCL 20H

Nominal test conditions were 100 psia (689 kN/m^2) chamber pressure, an oxidant to fuel ratio of 2.0, and an initial throat diameter of 7.82 in. (19.8 cm). The propellants were nitrogen tetroxide and a blend of 50 percent hydrazine with 50 percent unsymmetrical dimethyl hydrazine. Magnesium oxide reinforced with metallic honeycomb failed structurally after 60 sec firing duration. AJT0992 (hafnium carbide, silicon carbide, graphite composite) provided nominal erosion protection for 140 sec. A unique active cooling concept was also evaluated. A perforated nozzle wall (linear) was used in conjunction with graphite ribs to conduct heat into an ammonium fluoroborate reservoir surrounding the liner. Three versions of the concept failed either structurally or by excessive throat erosion. These large-size inserts demonstrated less durability than the same materials in a smaller size. Author

N69-19980*# National Aeronautics and Space Administration. Lewis Research Center, Cleveland, Ohio.

PERFORMANCE OF VARIOUS OXIDE-MAGAZINE CATHODES IN KAUFMAN THRUSTERS

David C. Byers Washington Mar. 1969 29 p refs

(NASA-TN-D-5074) Avail: CFSTI CSCL 20H

The performance of various oxide magazine cathodes in the mercury-discharge of a Kaufman thruster is presented. Emission current of the final design was 2.0 amperes at a cathode heater input power between about 70 and 80 watts during thruster operation. The emission current was found to follow a thermionic characteristic up to some level of emission, above which other limitations dominate the emission current. The emission current also appeared to be limited at high values of propellant utilization efficiency. Tests with a large variety of chemical constituents led to no fundamental improvements over the initial chemical block type. Author

N69-20876*# National Aeronautics and Space Administration. Goddard Space Flight Center, Greenbelt, Md.

FLIGHT PERFORMANCE OF FW-4D SOLID-PROPELLANT ROCKET MOTOR ON DELTA 50 (AIMP-E)

Daniel Dembrow Washington Mar. 1969 47 p refs

(NASA-TN-D-4987) Avail: CFSTI CSCL 21H

The in-flight performance is summarized of the FW-4D solid-propellant rocket motor used as the third stage of the Delta 50 launch vehicle for the first Anchored Interplanetary Monitoring Platform (AIMP-E), Lunar Explorer. This was the first Delta to use a digital integrating accelerometer for accurately determining third-stage velocity. The instrumentation included a rocket-chamber pressure transducer, a longitudinal accelerometer, and a counter and encoder for converting the digital accelerometer output into two forms: integrated acceleration × time (i.e., velocity) pulses and accumulated pulse count. The correlation between predicted and observed third-stage performance was excellent. Author

N69-21463*# National Aeronautics and Space Administration. Langley Research Center, Langley Station, Va.
EFFECT OF PLUG AND SHROUD GEOMETRY VARIABLES ON PLUG-NOZZLE PERFORMANCE AT TRANSONIC SPEEDS
Bobby L. Berrier Washington Mar. 1969 196 p refs
(NASA-TN-D-5098) Avail: CFSTI CSCL 21E

Geometry variables were plug truncation (0, 30, 72.5, and 100 percent of full length from annular throat), shroud boattail angle (8°, 20°, and 30°), and truncated plug base shape (flat and semitoroidal). All nozzle configurations were designed to operate at a jet total pressure ratio of 16.5. The ratio of annular throat area to maximum cross sectional area was 0.25. The wind tunnel Mach number was varied from 0 to 1.30. The jet total pressure ratio was varied from 1.0 to approximately 8.0 depending on the external airstream Mach number. Model angle of attack was 0° for all tests. A comparison of experimental plug pressures and theoretical plug pressures obtained by the method of characteristics is made. The performance of the 15° cone plug nozzle was shown to be higher than the performance of a comparable isentropic plug nozzle. The results also show that plug truncation decreases cone plug nozzle performance although the 15° cone plug was truncated 30 percent with a loss of generally less than 1 percent. The 72.5 and 100 percent truncated, plug nozzle configurations show severe losses in nozzle performance. Increasing boattail angle generally decreased cone plug nozzle performance except for the 100 percent truncated, plug nozzle configurations. Author

N69-21476*# Wyle Labs., Inc., Huntsville, Ala.
THEORETICAL STUDIES OF COMPRESSOR NOISE
M. V. Lowson Washington NASA Mar. 1969 109 p refs
(Contract NAS1-6885)
(NASA-CR-1287; WR-68-15) Avail: CFSTI CSCL 20A

Analytical results for both sound pressure and sound power are given for four separate source mechanisms in the compressor, including rotating and stationary force and mass fluctuations. Each mechanism is modeled by a cascade of point sources, one on each blade, with appropriate phase relations between them. The results demonstrate that the rotor and stator are equally significant in the noise generation process. The leading features are the demonstration of equivalent cutoff effects without a duct, the particularly unfavorable acoustic power and directivity characteristics near to cutoff, and the favorable effects of low order modes on the sound. The principal problem in the prediction of noise is in predicting the aerodynamic characteristics of the wake flows in the compressor. A crude model for the wake flow is used to derive results which give acceptable comparison with the experiment. The effects of increasing rotor-stator and stator-rotor separation are discussed. In general it appears that the theory is in fairly good agreement with the experiment, and can therefore be used for design studies. Author

N69-21648*# National Aeronautics and Space Administration. Lewis Research Center, Cleveland, Ohio.
EXPERIMENTAL INVESTIGATION OF A 10 DEG CONICAL TURBOJET PLUG NOZZLE WITH TRANSLATING PRIMARY AND SECONDARY SHROUDS AT MACH NUMBERS FROM 0 TO 2.0
Donald L. Bresnahan Washington Apr. 1969 34 p refs
(NASA-TM-X-1777) Avail: CFSTI CSCL 21E

Nozzle efficiencies and pumping characteristics were measured with and without external flow for a configuration employing a translating primary shroud for throat area variation. Efficiencies are compared with those of an alternate configuration employing an iris-type primary shroud. Both configurations were appropriate for an afterburning turbojet engine cycle. At subsonic speeds with the cylindrical secondary shroud retracted, the nozzles performed about the same. However, with the secondary shroud extended for operation at supersonic speeds, the translating primary provided a lower efficiency at the full-afterburning position. The pumping characteristics of the translating primary shroud were such that secondary flow could be provided to cool the primary nozzle and the shroud at all flight conditions except takeoff. Author

N69-23519*# National Aeronautics and Space Administration. Lewis Research Center, Cleveland, Ohio.
STEADY-STATE INTERACTIONS FROM MACH 1.98 TO 2.58 BETWEEN A TURBOJET ENGINE AND AN AXISYMMETRIC INLET WITH 60-PERCENT INTERNAL AREA CONTRACTION
Robert E. Coltrin and David A. Choby Washington Apr. 1969 28 p refs
(NASA-TM-X-1780) Avail: CFSTI CSCL 21E

An investigation of the steady-state interactions between a Mach 2.5 axisymmetric mixed-compression inlet and a turbojet engine was conducted. Engine installation did not grossly alter the magnitude or distribution of total pressure at the inlet diffuser exit from the values obtained with a choked plug installed. However, when a large circumferential total-pressure distortion was present at the compressor face, the engine altered the flow field by inducing a circumferential distortion in the static pressure without significantly affecting the total-pressure profile. Limited data at a constant speed showed that large radial distortions caused a slight loss in compressor pressure ratio. Author

N69-24223*# General Motors Corp., Indianapolis, Ind. Allison Div.
EXPERIMENTAL INVESTIGATION OF ADVANCED CONCEPTS TO INCREASE TURBINE BLADE LOADING. 4: PERFORMANCE EVALUATION OF PLAIN ROTOR BLADE WITH PLOW TYPE VORTEX GENERATORS
H. G. Lueders Washington NASA Apr. 1969 45 p refs
(Contract NAS3-7902)
(NASA-CR-1342; EDR-4909-Vol-4) Avail: CFSTI CSCL 21E

The overall performance of a single stage turbine designed with a rotor blade suction surface diffusion factor of 0.3 and negative hub reaction was investigated over a range of equivalent speeds and expansion ratios. Plow type vortex generators were attached to the forward portion of the blade suction surface to prevent flow separation. Rotor exit surveys were taken of total pressure, flow angle, temperature, and hot wire data. A number of rotor blades had static pressure orifices located at the mean line section to record blade surface static pressures during rotation. The results of this investigation are compared with the performance of the same blade without the vortex generators attached. The overall performance characteristics of the turbine with vortex generators were very similar to the turbine without vortex generators. The total efficiencies at design equivalent speed and expansion ratio were 88.6 and 88.4 percent for the vortex generator and plain blade turbine, respectively. The turbine loss patterns, as determined from exit surveys, were very similar for the two tests. Author

N69-24922*# National Aeronautics and Space Administration. Lewis Research Center, Cleveland, Ohio.
CONCEPTUAL STUDY OF ROCKET-SCRAMJET HYBRID ENGINES IN A LIFTING REUSABLE SECOND STAGE
Andrzej Dobrowolski and John L. Allen Washington May 1969 55 p refs
(NASA-TM-D-5218) Avail: CFSTI CSCL 21H

A simplified analysis of a prismatic-delta configuration flying a near minimum fuel consumption path from staging to orbit showed relative advantages for air-augmented propulsion systems. The trajectory had a constant product of pressure and Mach number during powered flight which extended to speeds slightly greater than orbital so that a zoom maneuver could be used to obtain final orbital altitude. For staging at Mach 10, the estimated payload fraction (payload to staging weight) for the best air-augmented case (3:1 ratio of air to rocket flow) was 1-1/2 times

better than that using pure rocket power and 7-1/2 times better than that using pure scramjet power. Author

N69-24938*# National Aeronautics and Space Administration. Lewis Research Center, Cleveland, Ohio.
RESTART AND HIGH RESPONSE TERMINAL SHOCK CONTROL FOR AN AXISYMMETRIC MIXED-COMPRESSION INLET WITH 60-PERCENT INTERNAL CONTRACTION
Michael J. Crosby, George H. Neiner, and Gary L. Cole Washington May 1969 16 p refs
(NASA-TM-X-1792) Avail: CFSTI CSCL 21E

Results from investigations include analysis followed by experimental results obtained from an axisymmetric, mixed-compression inlet tested at Mach 2.5. The inlet was terminated successively with a large volume, a choked orifice at the engine face station, and a turbojet engine. The normal shock control systems were subjected to downstream (0 to 140 Hz) and upstream (0 to 20 Hz) flow disturbances. The normal shock controllers investigated indicated increased performance with electronic compensation and multiple feedback. The restart controllers maintained closed-loop bypass door control throughout the restart cycle, minimizing distortion while maximizing pressure recovery. Author

N69-26224*# National Aeronautics and Space Administration. Marshall Space Flight Center, Huntsville, Ala.
INVESTIGATION OF SA-501 S-IVB AUXILIARY
K. Coates and E. Donald
Washington May 1969 46 p
(NASA-TN-D-5207) Avail: CFSTI CSCL 21E

Several anomalies which occurred on the S-IVB auxiliary propulsion system during the SA-501 flight are reported. The anomalies of primary significance were low chamber pressure for several engines beginning at the start of the S-IVB powered flight and high propellant temperatures experienced late in flight. An investigation of possible causes by theoretical analysis and hardware testing was conducted by MSFC. The analyses indicated that the high propellant temperature was caused by a degradation of the Auxiliary Propulsion System (APS) module surface paint thermal properties, which in turn was caused by S-II stage retro-rocket exhaust gas plume impingement. The cause of the anomalous chamber pressures of several engines at the beginning of S-IVB powered flight was verified by testing to be contamination of the engine injector because of burp firing at ambient conditions at KSC. The investigation resulted in the deletion of the burp firing requirement prior to launch at KSC and in modification to the APS hardware to prevent the temperature rise of the propellant. Author

N69-27019*# National Aeronautics and Space Administration. Lewis Research Center, Cleveland, Ohio.
PERFORMANCE AND STALL LIMITS OF A YTF30-P-1 TURBOFAN ENGINE WITH UNIFORM INLET FLOW
Willis M. Braithwaite and William R. Vollmar
Washington Jun. 1969 38 p refs
(NASA-TM-X-1803) Avail: CFSTI CSCL 21H

Performance and operating limits with uniform compressor inlet flow at a Reynolds number index of 0.5 are presented for a YTF30-P-1 (serial number P-647218) two-spool turbofan engine. A description is also included of the high frequency pressure measurement system developed and the techniques used in this investigation. Results are presented in the form of compressor maps, stall lines, bypass ratio, rotor speed match, and typical time histories. Author

N69-29321*# National Aeronautics and Space Administration. Lewis Research Center, Cleveland, Ohio.
STEADY-STATE STRESS RELAXATION ANALYSIS OF TURBINE BLADE COOLING DESIGNS
Albert Kaufman Washington Jun. 1969 47 p refs
(NASA-TN-D-5282) Avail: CFSTI CSCL 21H

An analytical evaluation was made of five turbine blade cooling configurations for advanced airbreathing engines on the basis of the time to a local creep strain of 1% for cast IN 100. The longest life was shown by the transpiration design followed by the multiple small hole design. Curves were established to predict the multiple small hole blade life under various combinations of turbine inlet and coolant temperatures and coolant to total gas flow ratios. Author

N69-29405*# National Aeronautics and Space Administration. Lewis Research Center, Cleveland, Ohio.
APPLICATION OF A DOUBLE-DEAD-TIME MODEL DESCRIBING CHUGGING TO LIQUID PROPELLANT ROCKET ENGINES HAVING MULTIELEMENT INJECTORS
John R. Szuch Washington Jul. 1969 40 p refs
(NASA-TN-D-5303) Avail: CFSTI CSCL 21H

Stability limits were determined experimentally for a 1.4-inch-(3.56-cm-) diameter rocket engine. Liquid oxygen and gaseous hydrogen were the propellants. A chamber pressure of 250 psia (172 N/cm^2) and a mixture ratio of 5.0 were maintained for contraction ratios of about 1.9 and 3.0. A seven-element injector was run with both concentric-tube and transpiration-cooled faceplate methods of fuel injection. Data were also obtained with a 421-element 10.8-inch diameter engine. For comparison with experimental data, stability boundaries were generated on the analog computer. Results indicated that accurate predictions of stability limits can be made using the double-dead-time model and existing vaporization and drop-size correlations. Large engine instabilities were prevented because of feed system coupling effects, as predicted by the analysis. Author

N69-30560*# National Aeronautics and Space Administration. Lewis Research Center, Cleveland, Ohio.
DESIGN OF INJECTORS AND ABLATIVE THRUST CHAMBERS FOR A FLOX-PROPANE ROCKET ENGINE WITH A 1.2-INCH THROAT DIAMETER
Jerry M. Winter, Donald A. Peterson, and Albert J. Pavli Washington Jul. 1969 38 p refs
(NASA-TN-D-5324) Avail: CFSTI CSCL 21H

An in-house study was conducted for the design and testing of liquid FLOX-propane 1.2-inch (3.05-cm-) throat-diameter rocket engines. Experimental characteristic velocity efficiency as a function of oxidant-to-fuel ratio was determined for four different injector types. An erosion-free 300-second continuous firing capability was demonstrated using a graphite cloth phenolic chamber and nozzle operating at 100-psia (689-kN/m^2) chamber pressure and at an oxidant-to-fuel ratio of 4.5 with a delivered characteristic velocity efficiency level of 95.4 percent (97.5 percent corrected). Erosion-free operation at 200-psia (1378 kN/m^2) chamber pressure required use of a graphite throat insert. Author

N69-30980*# National Aeronautics and Space Administration. Lewis Research Center, Cleveland, Ohio.
ANALYSIS OF THE DYNAMIC RESPONSE OF LIQUID JET ATOMIZATION TO ACOUSTIC OSCILLATIONS
Marcus F. Heidmann and John F. Groeneweg Washington Jul. 1969 44 p refs
(NASA-TN-D-5339) Avail: CFSTI CSCL 21E

An atomization model prescribing jet breakup when jet distortion caused by aerodynamic forces attains a critical value is used to analytically and numerically evaluate the atomization rate perturbations caused by acoustic oscillations. The varied dynamic response within traveling, standing, and radial transverse acoustic modes is presented. An amplifying effect of a steady tangential velocity on dynamic response is also examined and compared with

experimental evidence. The results generally imply that jet atomization dynamics can significantly affect the stability of a rocket engine combustor. Author

N69-31336# National Aeronautics and Space Administration Lewis Research Center, Cleveland, Ohio.

DYNAMIC RESPONSE OF A MACH 2.5 AXISYMMETRIC INLET WITH ENGINE OR COLD PIPE AND UTILIZING 60 PERCENT SUPERSONIC INTERNAL AREA CONTRACTION

Joseph F. Wasserbauer Washington Jul. 1969 61 p refs
(NASA-TN-D-5338) Avail: CFSTI CSCL 21H

The inlet was subjected to sinusoidal bypass area disturbances with frequencies up to 240 hertz and to sinusoidal external disturbances with frequencies up to 15 hertz. Dynamic response data are presented for terminal shock position and selected static pressures throughout the inlet. These results were obtained for the inlet coupled to either an engine or to a cold-pipe configuration. The effect of varying the cold-pipe length and throat bleed configuration are also presented. The dynamic response of the inlet to bypass area disturbances exhibited resonant conditions. The effect of an engine could be simulated with a cold pipe of appropriate length. Author

N69-32318*# National Aeronautics and Space Administration. Lewis Research Center, Cleveland, Ohio.

GASEOUS HYDROGEN REQUIREMENTS FOR THE DISCHARGE OF LIQUID HYDROGEN FROM A 1.52 METER (5 FT) DIAMETER SPHERICAL TANK

Robert J. Stochl, Philip A. Masters, Richard L. De Witt, and Joseph E. Malon Washington Aug. 1969 64 p refs
(NASA-TN-D-5336) Avail: CFSTI CSCL 21I

An experimental investigation was conducted to determine the effect of various physical parameters on the pressurant gas requirements during the pressurization and explusion of liquid hydrogen from a 1.52-m-diameter spherical tank. The experimental results were compared with results predicted by an analytical program. Tests were conducted for a range of outflow rates at a nominal operating pressure level of $34.47 \times 10^4 N/m^2$ using inlet gas temperatures of 167°, 298°, and 355°K. Data were obtained using three pressurant injector geometries (hemisphere, radial, and straight pipe) and two tank wall thicknesses (0.762 and 0.409 cm). The experimental results indicate that the inlet gas temperature has the strongest influence on the pressurant gas requirements followed closely by the influence of injector geometry. Fair agreement existed between the analysis and experimental data when using a diffuser-type (hemisphere and radial) injector. The agreement between the experimental data and the analysis was not good when using the straight pipe injector. Author

N69-33211*# National Aeronautics and Space Administration. Lewis Research Center, Cleveland, Ohio.

GASEOUS-HYDROGEN PRESSURANT REQUIREMENTS FOR THE DISCHARGE OF LIQUID HYDROGEN FROM A 3.96 METER (13 FT) DIAMETER SPHERICAL TANK

Robert J. Stochl, Phillip A. Masters, Richard L. De Witt, and Joseph E. Malloy Washington Aug. 1969 62 p refs
(NASA-TN-D-5387) Avail: CFSTI CSCL 21E

The effects of various physical parameters on the pressurant gas requirements during the pressurization and expulsion of liquid hydrogen from a 3.96 meter diameter spherical tank. The experimental results were also compared with results predicted by a previously developed analytical program. The experimental results show that injector geometry, inlet gas temperature, and tank pressure level have a strong influence on the actual pressurant gas requirements. There was fair agreement between the analysis and experimental data when using the hemisphere injector. However, the analysis in its present form does not adequately predict pressurant requirements when using the straight pipe injector. Author

N69-33319*# National Aeronautics and Space Administration. Lewis Research Center, Cleveland, Ohio.

SIMPLIFIED ANALYTICAL MODEL FOR USE IN DESIGN OF PUMP-INLET ACCUMULATORS FOR THE PREVENTION OF LIQUID-ROCKET LONGITUDINAL OSCILLATION (POGO)

William Lewis Washington Aug. 1969 38 p refs
(NASA-TN-D-5394) Avail: CFSTI CSCL 21H

Prevention of pogo by means of an accumulator at the pump inlet is facilitated by a simplified analytical model that expresses the net in-phase force feedback in terms of the admittance of the accumulator, thereby providing a frame of reference for the use of judgment in the design. Treating the effects of the fuel and oxidizer systems as independent and additive and reckoning force feedback at the structure modal frequency only permit a simple description of the primary mechanism. A novel feature of the model is that the effect of outflow perturbations on tank-bottom pressure is included in the net-thrust function. Author

N69-33354*# Israel Program for Scientific Translations, Ltd., Jerusalem.

MECHANICS OF SPACEFLIGHT LOW-THRUST

G. L. Grodzovskii, Yu. N. Ivanov, and V. V. Tokarev 1969 578 p refs Transl. into ENGLISH of the book "Mekhanika Kosmicheskogo Poleta S Maloi Tyagoy" Moscow, Izd. *An SSSR, 1966 578 p Published for NASA and NSF*
(NASA-TT-F-502; TT-68-50301) Avail: CFSTI CSCL 21H

CONTENTS:

1. BASIC PARAMETERS AND LAYOUT OF SPACE PROPULSION SYSTEMS p 1–13 (See N69-33355 19-28)
2. PHYSICAL PRINCIPLES OF THE ELEMENTS OF SPACE PROPULSION SYSTEMS p 14–81 (See N69-33356 19-28)
3. GENERALIZED PARAMETERS OF SPACE PROPULSION SYSTEMS p 82–88 (See N69-33357 19-28)
4. IDEAL POWER-LIMITED ENGINE. SEPARATION OF THE VARIATIONAL PROBLEM. OPTIMUM WEIGHT RATIOS p 89–117 (See N69-33358 19-28)
5. IDEAL POWER-LIMITED ENGINE. OPTIMUM PROGRAMS OF THRUST ACCELERATION p 118–166 (See N69-33359 19-28)
6. UNTHROTTLED ENGINES. SEPARATION OF THE VARIATIONAL PROBLEM. OPTIMUM PROGRAMS OF THE THRUST VECTOR p 167–201 (See N69-33360 19-28)
7. REAL POWER-LIMITED ENGINES p 202–238 (See N69-33361 19-28)
8. ENGINES WITH LIMITED EXHAUST VELOCITY. OPTIMUM COMBINATION OF ENGINES WITH LIMITED EXHAUST VELOCITY AND LIMITED POWER p 239–264 (See N69-33362 19-28)
9. PROPULSION SYSTEMS WITH ENERGY AND MASS ACCUMULATION. ENGINES WHOSE THRUST AND POWER ARE FUNCTIONS OF THE COORDINATES AND TIME p 265–336 (See N69-33363 19-28)
10. MODIFICATIONS OF THE OPTIMUM CRITERION p 337–364 (See N69-33364 19-28)
11. RELIABILITY CONSIDERATIONS IN OPTIMIZATION PROBLEMS p 365–402 (See N69-33365 19-28)
12. EXTRA WEIGHT REQUIRED FOR TRAJECTORY CORRECTION p 403–410 (See 69-33366 19-31)
13. ANALYTIC SOLUTIONS OF THE EQUATIONS OF DYNAMICS p 411–433 (See N69-33367 19-31)
14. FUNCTIONAL NUMERICAL METHODS FOR ESTABLISHING OPTIMUM SOLUTIONS p 434–462 (See N69-33368 19-19)
15. FINITE-DIMENSIONAL NUMERICAL OF ESTABLISHING OPTIMUM SOLUTIONS p 463–475 (See N69-33369 19-19)
16. DESCRIPTION OF THE DYNAMIC MANEUVERS p 476–496 (See N69-33370 19-19)

28 PROPULSION SYSTEMS

N69-33806*# National Aeronautics and Space Administration. Lewis Research Center, Cleveland, Ohio.
EXPERIMENTAL STUDY OF LOW-SPEED OPERATING CHARACTERISTICS OF A LIQUID HYDROGEN CENTRIFUGAL TURBOPUMP
Guy H. Ribble, Jr., and George E. Turney Washington Aug. 1969 22 p refs
(NASA-TM-X-1861) Avail: CFSTI CSCL 21H

The low speed operating characteristics of a liquid hydrogen centrifugal turbopump are discussed. The turbopump was operated at several speeds, ranging from 6.7 to 49 percent of the rated speed. The rated operating speed is 22,500 rpm. At the rated flow parameter of 0.346 gallon per minute per rpm, the pump isentropic efficiencies were 9, 32, and 63 percent for speeds of 1500, 3000, and 6000 rpm, respectively. The isentropic efficiency was nearly constant for speeds above 6000 rpm. The head characteristics of the turbopump follow the affinity laws for the range of operating conditions investigated. At the pump rated flow parameter, an average total head parameter of 65×10^{-6} ft(rpm)^2 was obtained. Author

N69-34575*# National Aeronautics and Space Administration. Langley Research Center, Langley Station, Va.
SUBSONIC AERODYNAMIC CHARACTERISTICS OF A LARGE-SCALE 1.075-PRESSURE-RATIO TIP-TURBINE CRUISE-FAN PROPULSION SYSTEM AT ANGLE OF ATTACK
Francis J. Capone Washington Aug. 1969 64 p refs
(NASA-TN-D-5316) Avail: CFSTI

Aerodynamic characteristics and pressure distributions of a large-scale 1.075-pressure-ratio tip-turbine cruise fan at angle of attack were studied in the 16-foot transonic tunnel. The purpose was to determine trends rather than absolute levels in performance since the fan was originally designed as a low-pressure-ratio lift fan. The gas generator was closely coupled to the fan so that the gas-generator nacelle extended forward and below the fan nacelle. The investigation was conducted at Mach numbers of 0.30, 0.50, and 0.70 and at angles of attack from $-2°$ to $8°$. The test Reynolds number based on the fan diameter (91.44 cm) varied from 3.90×10^6 to 11.25×10^6. Angle-of-attack variation affected only the external pressure distributions at the fan-cowl leading edge. Premature supercritical flow occurred on the fairing between the fan and gas-generator nacelles at angles of attack of $2°$ and $5°$ at a Mach number of 0.70, well below the fan-nacelle design Mach number of 0.81. Nacelle minimum drag occurred at an angle of attack of $2°$, and both the lift and pitching-moment curves were linear over an angle-of-attack range of $-2°$ to $5°$ throughout the Mach number range of the test. Author

N69-34674*# National Aeronautics and Space Administration. Lewis Research Center, Cleveland, Ohio.
PROPULSION SYSTEMS FOR MANNED EXPLORATION OF THE SOLAR SYSTEM
W. E. Moeckel Washington Aug. 1969 37 p refs
(NASA-TM-X-1864) Avail: CFSTI CSCL 21H

The first portion of this report relates planetary round-trip times to the performance parameters of two types of propulsion systems: type I is specific-impulse limited (with high thrust), and type II is specific-mass limited (with low thrust). The second part of the report discusses advanced propulsion concepts of both types and evaluates their limitations. The discussion includes nuclear-fission rockets (solid, liquid, and gaseous core), nuclear-pulse propulsion, nuclear -electric rockets, and thermonuclear-fusion rockets. Particular attention is given to the last of these, because it is less familiar than the others. A general conclusion is that the more advanced systems, if they prove feasible, will reduce trip time to the near planets by factors of 3 to 5, and will make several outer planets accessible to manned exploration. Author

N69-35526*# National Aeronautics and Space Administration. Langley Research Center, Langley Station, Va.
SUBSONIC PERFORMANCE CHARACTERISTICS OF A LARGE-SCALE 1.075-PRESSURE-RATIO TIP-TURBINE CRUISE-FAN PROPULSION SYSTEM
Francis J. Capone and Harry T. Norton, Jr. Washington Aug. 1969 278 p refs
(NASA-TN-D-5314) Avail: CFSTI CSCL 21E

An investigation has been conducted in the Langley 16-foot transonic tunnel to determine internal and external performance characteristics of a large-scale 1.075-pressure-ratio tip-turbine cruise fan. The intent of this investigation was to determine trends rather than absolute levels in performance since the fan was originally designed as a low-pressure-ratio lift fan. The effects of geometry change and exit-area variation on performance were determined with three fan cowls, afterbodies, and nozzle-exit plugs. The gas generator was closely coupled to the fan and resulted in a gas-generator nacelle that extended forward and below the fan nacelle. Eight configurations were investigated at Mach numbers from 0 to 0.05 and at an angle attack of $0°$. The test Reynolds number based on the fan diameter (36.00 inches (91.44 cm)) varied from 3.90×10^6 to 11.25×10^6. The results showed that the fan operated at the design pressure ratio or near design fan rotational speeds for all configurations. Only changes in exit area affected internal performance. Because the net thrust decreased rapidly with increasing free-stream Mach number (due to low-pressure-ratio fan), the drag-minus-thrust coefficients became positive for all the configurations tested above a Mach number of 0.50. Author

N69-35712*# National Aeronautics and Space Administration. Lewis Research Center, Cleveland, Ohio.
A COMPARISON OF EXPERIMENTAL AND CALCULATED HELIUM REQUIREMENTS FOR THE PRESSURIZATION OF A CENTAUR LIQUID HYDROGEN TANK
Raymond Lacovic Washington Sep. 1969 15 p refs
(NASA-TM-X-1870) Avail: CFSTI CSCL 21I

Ramp pressurization tests were conducted with gaseous helium in a thick-walled liquid hydrogen tank with the shape and approximate volume of a Centaur liquid hydrogen flight vehicle tank. The helium requirements were obtained at two pressure levels above liquid hydrogen saturation pressure, at four tank ullages, and for various ramp times. For all except small ullages there was good agreement between the experimentally determined helium requirements and the requirements predicted by an analytical program developed at the Lewis Research Center. Author

N69-35847*# National Aeronautics and Space Administration. Lewis Research Center, Cleveland, Ohio.
DESIGN, DEVELOPMENT, AND TESTING OF A 1000 POUND (4450 N) THRUST FLOX-PROPANE ABLATIVE ROCKET ENGINE
Donald A. Peterson, Jerry M. Winter, and Albert J. Pavli Washington Sep. 1969 21 p refs
(NASA-TM-X-1873) Avail: CFSTI CSCL 21H

A pressure-fed liquid FLOX-liquid propane rocket engine was designed and test fired at 100 psia (690 kN/m^2) chamber pressure and 1000 pounds (4450 N) thrust. A 137 element oxidant-fuel-oxidant triplet injector produced a characteristic exhaust velocity efficiency of 95.2 percent (96.1 percent corrected) at an O/F of 4.5. The injector was successfully scaled from a 150-pound thrust design. A long run capability was demonstrated by firing an ablative graphite cloth/phenolic thrust chamber for about 200 seconds total time with a throat area change less than ± 4 percent. Author

N69-36680*# General Motors Corp., Indianapolis, Ind.
EXPERIMENTAL INVESTIGATION IN AN ANGULAR CASCADE SECTOR OF HIGHLY LOADED TURBINE STATOR BLADING. VOLUME 4: PERFORMANCE OF A JET-FLAPPED BLADE
James L. Bettner Washington NASA Sep. 1969 144 p refs
(Contract NAS3-9404)
(NASA-CR-1423; EDR-5315-Vol-4) Avail: CFSTI CSCL 21E

A jet-flapped blade has been tested in a six-blade annular cascade, and three jet slot sizes of 0.022, 0.031, and 0.040 in. with three secondary flow rates for each slot have been investigated. The combinations of jet slot height and secondary flow rates produced a range of mean section jet momentum coefficient, C_{jm}, values of up to 0.08. The momentum coefficient is the ratio of jet-to-total momentum that exists at the blade trailing edge. Experimental results are compared with those for a plain blade designed to the same loading level as the jet-flapped blade but with greater solidity. The axial chord solidity, C_x/s, for the plain blade was 1.29, whereas it was only 1.18 for the jet-flapped blade. Flow visualization results revealed that flow separation was essentially prevented all the way to the trailing edge region of the center blades of the cascade. Author

N69-36844*# National Aeronautics and Space Administration. Lewis Research Center, Cleveland, Ohio.
AN ELECTRON BOMBARDMENT THRUSTER OPERATED WITH A CUSPED MAGNETIC FIELD
Allen J. Cohen Washington Sep. 1969 21 p refs
(NASA-TN-D-5448) Avail: CFSTI CSCL 21C

The performance of two 20-centimeter-diameter electron bombardment thrusters with an axial magnetic field and a superimposed cusp magnetic field was experimentally determined. The thruster lengths were 20 and 10 centimeters, respectively. The cusp field was added to suppress the anomalous diffusion phenomenon found in the discharge chamber of the thruster. Discharge performance and discharge noise measurements were obtained. Anomalous diffusion appeared to be suppressed by the addition of the cusp field; however, thruster performance was not enhanced. Author

N69-36882*# National Aeronautics and Space Administration. Lewis Research Center, Cleveland, Ohio.
A COMPUTER PROGRAM FOR COMPOSING COMPRESSOR BLADING FROM SIMULATED CIRCULAR-ARC ELEMENTS ON CONICAL SURFACES
James E. Crouse, David C. Janetzke, and Richard E. Schwirian Washington Sep. 1969 84 p refs
(NASA-TN-D-5437) Avail: CFSTI CSCL 01A

A blade element layout method is developed and combined with a stacking procedure in a computer program to compose a complete compressor blade. The layout method simulates the circular arc type blade element on a cone with the preservation of the constant rate of angle change. The computer program is capable of handling a multiple circular arc blade element. It calculates blade corss section coordinates and geometric properties for mechanical design and stress analysis. Author

N69-36932*# National Aeronautics and Space Administration. Langley Research Center, Langley Station, Va.
EFFECT OF JET VELOCITY AND AXIAL LOCATION OF NOZZLE EXIT ON THE PERFORMANCE OF A TWIN-JET AFTERBODY MODEL AT MACH NUMBERS UP TO 2.2
Bobby Lee Berrier and Frederick H. Wood, Jr. Washington Sep. 1969 80 p refs
(NASA-TN-D-5393) Avail: CFSTI CSCL 21E

The twin-jet afterbody model using two balances to measure thrust-minus-afterbody drag, and afterbody drag separately at static conditions and at Mach numbers up to 2.20 at a constant angle of attack of 0° was studied. A high pressure air system was used to simulate the nozzle flow at jet total-pressure ratios up to 22.0. All configurations had identical nondimensional area distributions. The results indicate that performance was generally increased by moving the jet exits to the extreme aft end of the afterbody for Mach numbers up to 1.30. The configurations utilizing nozzles with low exit velocity (convergent nozzles) had lower afterbody drag than configurations utilizing nozzles with higher exit velocity (convergent-divergent nozzles) at most test conditions. Author

N69-36998*# National Aeronautics and Space Administration. Lewis Research Center, Cleveland, Ohio.
MULTISTAGE COMPRESSOR SIMULATION APPLIED TO THE PREDICTION OF AXIAL FLOW INSTABILITIES
Ross G. Willoh and Kurt Seldner Washington Sep. 1969 27 p refs
(NASA-TM-X-1880) Avail: CFSTI CSCL 21H

A simulation model for the one-dimensional steady state and dynamic performance of an axial flow compressor is presented. The modeling technique is applied to the eight stage J 85-13 compressor. It is shown that the simulation stability boundary coincides with the compressor stall line. Analytical and experimental results are presented and compared. Author

N69-38599*# National Aeronautics and Space Administration. Lewis Research Center, Cleveland, Ohio.
EXPERIMENTAL INVESTIGATION OF DYNAMIC DISTORTION IN A MACH 2.50 INLET WITH 60 PERCENT INTERNAL CONTRACTION AND ITS EFFECT ON TURBOJET STALL MARGIN
James E. Calogeras Washington Oct. 1969 45 p refs
(NASA-TM-X-1842; E-5102) Avail: CFSTI CSCL 21H

The Lewis 10- by 10-foot supersonic wind tunnel of dynamic distortion within an inlet and of its effect on the stall margin of a J85-GE-13 turbojet engine was studied. Results indicate that average rms pressure fluctuations of 5 percent of the steady-state total pressure can completely degrade stall margin at certain engine speeds. Vortex generators were much more effective than throat bleed in suppressing dynamic distortion at off-design operating conditions. The presence of the engine appeared to have no effect on either the magnitude or the spatial distribution of dynamic distortion. Author

N69-39185*# National Aeronautics and Space Administration. Lewis Research Center, Cleveland, Ohio.
AIRBREATHING PROPULSION SYSTEM TESTING USING SWEEP FREQUENCY TECHNIQUES
Daniel I. Drain, William M. Burton, and Francis J. Paulovich Washington Oct. 1969 34 p refs
(NASA-TN-D-5485; E-5144) Avail: CFSTI CSCL 21E

The use of sweep frequency input in lieu of constant frequency input for determining system characteristics is discussed. Methods are furnished to determine the magnitude of errors that result from using a sweep frequency into a time delay, a first order system, and a second order system with various averaging techniques. The ability of the analysis method to reject noise is indicated for signal-to-noise ratios as low as one. Experience using the system for jet engine - inlet tests indicates a time saving factor of 10 to 1 with results which are as accurate and more complete than constant frequency testing. On-line data processing can be accomplished by components usually found in portable analog computers. Author

28 PROPULSION SYSTEMS

N69-40058*# National Aeronautics and Space Administration. Lewis Research Center, Cleveland, Ohio.
PERFORMANCE OF RADIATION-COOLED MAGNETOPLASMADYNAMIC ARC THRUSTERS
Dennis J. Connolly and Ronald J. Sovie Washington Oct. 1969 12 p refs
(NASA-TM-X-1908) Avail: CFSTI CSCL 21E

Results are given for performance tests on three different radiation-cooled MPD arc thrusters. These are the Avco X-7CR and the McDonnell-Douglas X-4A and X-7. The results are compared to those obtained by the contractors. Author

N69-40078*# National Aeronautics and Space Administration. Lewis Research Center, Cleveland, Ohio.
EFFECTS OF THREE OUTLET-ANNULUS AREA BLOCKAGE CONFIGURATIONS ON THE PERFORMANCE OF A 20-INCH (50.8-CM) AXIAL-FLOW COMPRESSOR ROTOR
Walter M. Osborn and George W. Lewis, Jr. Washington Oct. 1969 24 p refs
(NASA-TN-D-5506) Avail: CFSTI CSCL 01A

An inlet-stage axial-flow rotor was tested with tip annulus flow blockages of 22, 55, and 75 percent inserted downstream of the rotor. All three blockages eliminated rotating stall at speeds as high as 0.7 design and enabled the rotor to be operated under stable conditions to much lower flows than that of the unblocked rotor. Torque values of 83, 64, and 52 percent of the unblocked rotor resulted from blocking 22, 55 and 75 percent of the air flow, respectively, at 0.7 of design speed. The rotor efficiency was adversely affected by the blockages with losses of 22, 38, and 44 percemtage points, respectively, at 0.7 of design speed. Blade temperatures and stresses remained within operational limits. Author

N69-40080*# National Aeronautics and Space Administration. Lewis Research Center, Cleveland, Ohio.
COMBUSTION STABILITY OF SINGLE SWIRL-CAN COMBUSTOR MODULES USING ASTM-A1 LIQUID FUEL
Richard W. Niedzwiecki and Robert E. Jones Washington Oct. 1969 28 p refs
(NASA-TN-D-5436) Avail: CFSTI CSCL 21B

Swirl-can combustor modules were evaluated in a 6-inch-(15.24-cm-) diameter duct at a pressure of 1 atmosphere, at inlet air temperatures of 100° to 700° F (311 to 644 K), and at airflow rates of 1.0 to 4.8 pounds per second (0.454 to 2.18 kg/sec). Swirl-can combustor modules consisted of a carburetor incorporating a low pressure fuel entry system, a swirler assembly, and a combustor can. Effects of combustor can diameter, module length, swirler assembly type and flow area, and inlet air temperature were determined on combustion stability, combustion efficiency, and flame length. A correlation of combustion stability with swirl-can module parameters was obtained. Author

N69-40329*# National Aeronautics and Space Administration. Lewis Research Center, Cleveland, Ohio.
HELIUM PRESSURIZATION SYSTEMS FOR LIQUID-METHANE FUEL IN SUPERSONIC TRANSPORTS
Joseph D. Eisenberg Washington Oct. 1969 44 p refs
(NASA-TN-D-5519) Avail: CFSTI CSCL 21I

An analytical study was made to determine the possibility of using helium pressurization systems to pressurize the fuel on a methane-fueled supersonic aircraft. Three systems were proposed and investigated, all characterized by zero or minimum loss of helium. These systems are the helium circulation system, the helium rebottled system, and the minimum helium loss system. The effect on payload of the three systems were determined analytically. Results indicate that these systems offer potential solutions to the tankage problem but are exceedingly complex and involve the use of a great number of mechanical devices. Author

N69-40776*# Bell Aerosystems Co., Buffalo, N.Y.
EMPIRICALLY DETERMINED WIND AND SCALE EFFECTS ON HOT GAS RECIRCULATION CHARACTERISTICS OF JET V/STOL AIRCRAFT
Patrick E. Ryan and Wayne J. Cosgrove Washington NASA Oct. 1969 128 p refs
(Contract NAS1-7463)
(NASA-CR-1445; BAC-2099-956005) Avail: CFSTI CSCL 21H

Small scale tests were conducted to investigate the inlet temperature rise (ITR) and hot gas recirculation of three basic configurations representative of jet V/STOL aircraft. Small scale lift jet engine models (approximately 1/16) and a small scale model (0.24) of a NASA jet V/STOL aircraft model were operated at full scale exhaust conditions (1200°F, and exhaust total pressure ratio from 1.7 to 2.0) so as to maintain exhaust momentum similitude. The major test parameters included wind speed and direction, model height above ground, exhaust deflection angle, angle of attack, wing planform to jet exhaust area ratio, and model geometry. Ground winds were found to distort the recirculation of hot gases such as to result in maximum ingestion at approximately 30 fps. Wind direction attenuated ITR as did the presence of wings and exhaust deflection angles. Insight was gained into the structure and distortion of the flow field as affected by wind. Small scale ITR data based on full scale exhaust conditions may be used to reliably assess full scale gross design effects on ITR. Author

29

SPACE RADIATION

Includes cosmic radiation; solar flares; solar radiation; and Van Allen radiation belts. For related information see also: 13 Geophysics; and 24 Physics, Atomic, Molecular, and Nuclear.

A69-11227 *

RING CURRENT PARTICLE DISTRIBUTIONS DERIVED FROM RING CURRENT MAGNETIC FIELD MEASUREMENTS.

R. A. Hoffman (NASA, Goddard Space Flight Center, Greenbelt, Md.) and L. J. Cahill, Jr. (New Hampshire, University, Durham, N.H.).

Journal of Geophysical Research, vol. 73, Nov. 1, 1968, p. 6711-6722. 17 refs.

Grant No. NsG-624.

The particle energy density distribution for the symmetric portion of the Apr. 17, 1965, magnetic storm has been deduced from the measured ring current magnetic field profile. This distribution contains a basic spatial distribution and a time decay term that is a function of distance in order to accomplish the fit between the calculated magnetic effects of the particles and the measured ring current field over a period of a day. With various assumptions as to the particle loss, the time decay yields the average energy of the particles as a function of distance and thence the total integral omnidirectional proton flux. (Author)

A69-12092 *

ISOTROPIC GAMMA RADIATION AND THE METAGALACTIC COSMIC RAY INTENSITY.

F. W. Stecker (NASA, Goddard Space Flight Center, Greenbelt, Md.).

Nature, vol. 220, Nov. 16, 1968, p. 675, 676. 15 refs.

Discussion of the possible source of metagalactic gamma rays. Decay of neutral pi-mesons generated in metagalactic cosmic-ray interactions is suggested as a possible source of high-energy gamma rays. The upper limits on the present metagalactic cosmic-ray intensity are calculated on the basis of data obtained from the OSO 3 experiment, assuming the time dependence of the metagalactic cosmic-ray flux, and a proper cosmological model describing the universe. Z. W.

A69-12714 *

COLLISIONLESS HEATING OF THE SOLAR-WIND PLASMA. I.

Aaron Barnes (NASA, Ames Research Center, Space Sciences Div., Moffett Field, Calif.).

Astrophysical Journal, vol. 154, Nov. 1968, pt. 1, p. 751-759. 16 refs.

Derivation of the general theory of heating of collisionless plasma by hydromagnetic waves. It is shown that damping of fast-mode hydromagnetic waves can heat both protons and electrons, enhancing the "component" of kinetic (ion or electron) temperature parallel to the mean magnetic field, but not affecting the transverse temperatures. A numerical calculation of the heating associated with fast-mode waves as a function of propagation direction is given, and a qualitative summary of the ways in which the heating depends on plasma conditions is presented. (Author)

A69-12928

INTERNATIONAL CONFERENCE ON COSMIC RAYS, 10TH, CALGARY, CANADA, JUNE 19-30, 1967, PROCEEDINGS. PART A - INVITED AND RAPPORTEUR PAPERS.

Conference sponsored by the International Union of Pure and Applied Physics, the University of Calgary, and the National Research Council of Canada.

Edited by J. R. Prescott, B. G. Wilson, M. D. Wilson, and D. C. Rose.

Calgary, Canada, University of Calgary, 1967. 579 p. $5.00.

CONTENTS:

PREFACE. B. G. Wilson, p. III, IV.

ON THE ORIGIN OF COSMIC RAYS. V. L. Ginzburg and S. I. Syrovatskii (Akademiia Nauk SSSR, Moscow, USSR), p. 48-81. 51 refs. [See A69-12929 03-29]

GALACTIC X-RAY SOURCES. S. Hayakawa (Nagoya University, Nagoya, Japan), p. 82-105. 37 refs. [See A69-12930 03-29]

GAMMA RAY ASTRONOMY. J. G. Duthie (Rochester, University, Rochester, N.Y.), p. 106-133. 20 refs. [See A69-12931 03-29]

THE ORIGIN OF COSMIC RAYS. G. Burbidge (California, University, San Diego, Calif.), p. 134-145. [See A69-12932 03-29]

THE MODULATION OF GALACTIC COSMIC RAYS BY INTERPLANETARY MAGNETIC FIELDS. W. R. Webber (Minnesota, University, Minneapolis, Minn.), p. 146-193. 58 refs. [See A69-12933 03-29]

ENERGETIC SOLAR PARTICLES. C. E. Fichtel (NASA, Goddard Space Flight Center, Greenbelt, Md.), p. 194-234. 57 refs. [See A69-12934 03-29]

THE EARTH'S MAGNETIC FIELD. J. A. Jacobs (British Columbia, University, Vancouver, Canada), p. 235-268. 23 refs. [See A69-12935 03-13]

ATMOSPHERIC EFFECTS ON COSMIC RAY MONITORS. M. Bercovitch (Atomic Energy of Canada, Ltd., Chalk River, Ontario, Canada), p. 269-344. 27 refs. [See A69-12936 03-29]

THE INVESTIGATION OF THE EXTENSIVE AIR SHOWERS AT SEA LEVEL. S. N. Vernov and G. B. Khristiansen (Moskovskii Gosudarstvennyi Universitet, Moscow, USSR), p. 345-396. 34 refs. [See A69-12937 03-29]

RAPPORTEUR PAPER ON EXTENSIVE AIR SHOWERS. C. B. A. McCusker (Sydney, University, Sydney, Australia), p. 397-415. 12 refs. [See A69-12938 03-29]

STRONG INTERACTIONS AT ENERGIES > 10^{11} EV. N. A. Dobrotin and S. A. Slavatinskii (Akademiia Nauk SSSR, Moscow, USSR), p. 416-434. 11 refs. [See A69-12939 03-29]

THEORETICAL ASPECTS OF HIGH ENERGY STRONG INTERACTIONS. E. L. Feinberg (Akademiia Nauk SSSR, Moscow, USSR), p. 435-473. 47 refs. [See A69-12940 03-24]

INTERACTIONS AT VERY HIGH ENERGIES. P. H. Fowler (Bristol, University, Bristol, England), p. 474-479. [See A69-12941 03-29]

A COSMIC RAY PROGRAM FOR THE STUDY OF STRONG INTERACTION PHYSICS IN THE RANGE OF 100-1000 GEV. L. W. Jones (Michigan, University, Ann Arbor, Mich.), p. 480-505. 16 refs. [See A69-12942 03-29]

REPORT ON THE HIGH ALTITUDE PARTICLE PHYSICS FACILITY. L. H. Smith (California, University, Berkeley, Calif.), p. 506-511. [See A69-12943 03-29]

THE STUDY OF THE HIGH ENERGY COSMIC RAY PARTICLES WITH THE "PROTON" SATELLITES. N. L. Grigorov, V. E. Nesterov, I. D. Rapoport, I. A. Savenko, and G. A. Skuridin (Akademiia Nauk SSSR; Moskovskii Gosudarstvennyi Universitet, Moscow, USSR), p. 512-524. 9 refs. [See A69-12944 03-29]

ULTRA-HIGH ENERGY INTERACTIONS. M. Koshiba (Denver, University, Denver, Colo.; Tokyo, University, Tokyo, Japan), p. 525-557. 17 refs. [See A69-12945 03-29]

MUONS AND NEUTRINOS. A. W. Wolfendale (Durham, University, Durham, England), p. 558-572. [See A69-12946 03-29]

29 SPACE RADIATION

A69-12934 *#
ENERGETIC SOLAR PARTICLES.
Carl E. Fichtel (NASA, Goddard Space Flight Center, Greenbelt, Md.).
IN: INTERNATIONAL CONFERENCE ON COSMIC RAYS, 10TH, CALGARY, CANADA, JUNE 19-30, 1967, PROCEEDINGS. PART A - INVITED AND RAPPORTEUR PAPERS. [A69-12928 03-29]
Conference sponsored by the International Union of Pure and Applied Physics, the University of Calgary, and the National Research Council of Canada.
Edited by J. R. Prescott, B. G. Wilson, M. D. Wilson, and D. C. Rose.
Calgary, Canada, University of Calgary, 1967, p. 194-234. 57 refs.

Review of the fundamental aspects of solar cosmic radiation - i.e., the acceleration of particles, energetic particles as a sample of the sun, and the propagation of the particles from the sun to the earth. A brief historical sketch and a short summary of the present experimental information related to these particles are given. This data summary is weighted toward that experimental evidence which seems now to be most closely related to the problems under discussion. P.v.T.

A69-14008 *
LANGMUIR PROBE EVIDENCE FOR A NOCTURNAL IONIZATION SOURCE AT FORT CHURCHILL.
James C. G. Walker (Yale University, Dept. of Geology and Geophysics, New Haven, Conn.), L. H. Brace (NASA, Goddard Space Flight Center, Aeronomy Branch, Greenbelt, Md.), and M. H. Rees (Colorado, University, Laboratory for Atmospheric and Space Physics, Boulder, Colo.).
Journal of Geophysical Research, vol. 73, Dec. 1, 1968, p. 7285-7290. 34 refs.
NSF Grant No. GA-1238; Grant No. NGR-07-004-100.

Electron concentrations and temperatures measured in a nocturnal rocket flight at Fort Churchill, Manitoba, were considerably higher than nocturnal values measured at lower latitudes, particularly in the F1 region. We attribute this to a high-latitude energy source provided by bombardment of the atmosphere by energetic auroral electrons. By calculating the ionospheric electron concentrations and temperatures that result from auroral bombardment, we can deduce the flux and energy spectrum of the incident particles. The ionospheric data correspond to a bombarding flux of 1.25×10^8 electrons/cm^2-sec with a mean energy of 1.2 keV. Other data indicate that weak auroral bombardment and enhanced electron concentrations in the E and F1 regions are permanent features of the nocturnal auroral oval. (Author)

A69-14015 *
DYNAMICS OF A CHARGED PARTICLE IN A SPIRAL FIELD.
Joseph A. Burns and Gerald Halpern (NASA, Goddard Space Flight Center, Laboratory for Theoretical Studies, Greenbelt, Md.).
Journal of Geophysical Research, vol. 73, Dec. 1, 1968, p. 7377-7384. 7 refs.

The adiabatic guiding center motion of an energetic charged particle in an idealized representation of the interplanetary magnetic field is discussed. Expressions are presented for all drift velocity components. A comparison of these drifts establishes that, for the cases of physical interest, the electric drift velocity is by far the dominant drift velocity. Considering only the electric drift velocity, an expression is derived for the time of flight of a particle leaving the sun. Similarly, it is shown analytically that the particles remain attached to the same field line on which they left the sun, thus indicating their point of origin. High-energy unscattered particles are shown to be rapidly channeled down the field lines, which results in a highly anisotropic particle distribution in the vicinity of the earth. These analytic results are in excellent agreement with numerical integration of the complete drift equation and compare favorably with the experimental data. (Author)

A69-15528 *
RELATIVISTIC ELECTRONS FROM SOLAR FLARES.
T. L. Cline and F. B. McDonald (NASA, Goddard Space Flight Center, Greenbelt, Md.).
Solar Physics, vol. 5, Dec. 1968, p. 507-530. 16 refs.

Discussion of observations of interplanetary relativistic electrons from several solar-flare events monitored through 1964 to mid-1967. These are the first direct spectral measurements and time histories, made outside the magnetosphere, of solar-flare electrons having relativistic velocities. The 3- to 12-MeV electrons detected have kinetic energies about two orders of magnitude higher than those solar electrons previously studied in space, and measurements of both the time histories and energy spectra for a number of events in the present solar cycle were carried out. These measurements are compared with solar X-ray data and with measurements of related interplanetary solar protons. Energy spectra and total numbers of the interplanetary electrons, compared with those of the flare-site electrons calculated from X-ray and microwave measurements, indicate that probably a small fraction of flare electrons escapes into interplanetary space. M.G.

A69-16361 *
COSMIC-RAY PROPAGATION.
C. E. Fichtel and D. V. Reames (NASA, Goddard Space Flight Center, Greenbelt, Md.).
Physical Review, 2nd Series, vol. 175, Nov. 25, 1968, p. 1564-1576. 34 refs.

The general problem of the propagation of cosmic rays from their source until they are observed in the vicinity of the earth is reviewed. The effect of matter on the cosmic-ray composition is considered in detail, and the effect of diffusion is treated in the depth necessary to study some models of the cosmic radiation not previously considered in this manner. The results of these calculations show that there are some aspects of the experimental observations, such as the ratio of light to medium nuclei as a function of energy, which are not consistent with any equilibrium model of the cosmic radiation which does not include a rigidity dependence in the mean free path. This conclusion is independent of the source spectrum assumed and is valid for a large class of source distributions. A series of possible explanations for the discrepancy between the observed experimental data and the theoretical predictions of the equilibrium picture are considered, and shown to be unlikely. Faced with this dilemma, attention is turned to a simple nonequilibrium model, consisting of one fairly close single source superimposed on a general background. This picture was chosen because it seemed the simplest first step from equilibrium. The calculations show that this picture leads to considerably better agreement with the experimental data, especially on the ratio of light to medium nuclei as a function of energy/nucleon. At least one irreconcilable experimental datum remains, namely, the one measurement of the fluorine-to-oxygen ratio. (Author)

A69-17268
DEPARTMENT OF ATOMIC ENERGY, SYMPOSIUM ON COSMIC RAYS, ELEMENTARY PARTICLE PHYSICS AND ASTROPHYSICS, 10TH, ALIGARH MUSLIM UNIVERSITY, ALIGARH, INDIA, DECEMBER 12-16, 1967, PROCEEDINGS.
Bombay, Department of Atomic Energy, 1968. 725 p.

CONTENTS:

PRIMARY COSMIC RADIATION.

PROPAGATION OF COSMIC RADIATION IN THE INTERSTELLAR SPACE (INVITED TALK). M. V. K. Apparao (Tata Institute of Fundamental Research, Bombay, India), p. 1-13. 13 refs. [See A69-17269 06-29]

INTERSTELLAR HELIUM SPECTRUM, H^2/He^4 AND He^3/He RATIOS IN COSMIC RAYS AND THE AMOUNT OF MATTER TRAVERSED AT LOW ENERGIES. S. Biswas and S. Ramadurai (Tata Institute of Fundamental Research, Bombay, India), p. 14-18. [See A69-17270 06-29]

LITHIUM, BERYLLIUM, BORON AND FLUORINE NUCLEI IN COSMIC RADIATION. R. Cowsik, Y. Pal, S. N. Tandon, and R. P. Verma (Tata Institute of Fundamental Research, Bombay, India), p. 19-23. 11 refs. [See A69-17271 06-29]

STEADY STATE SPECTRA OF PROTON AND HELIUM NUCLEI AND THEIR MODULATION. Y. Pal, S. N. Tandon, and R. P. Verma (Tata Institute of Fundamental Research, Bombay, India), p. 24-27. 10 refs. [See A69-17272 06-29]

SPECTRA OF HEAVY AND SUPER HEAVY NUCLEI IN STEADY

STATE. R. Cowsik, Y. Pal, S. N. Tandon, and R. P. Verma (Tata Institute of Fundamental Research, Bombay, India), p. 28-32. 12 refs. [See A69-17273 06-29]

CHARGE COMPOSITION AND ENERGY SPECTRA OF COSMIC RAY NUCLEI WITH Z = 10 - 28. V. S. Bhatia, V. S. Chohan, S. D. Pabbi, P. S. Kainth (Punjab University, Chandigarh, India), and S. Biswas (Tata Institute of Fundamental Research, Bombay, India), p. 33-37. [See A69-17274 06-29]

THE FLUX OF PRIMARY HELIUM NUCLEI NEAR HYDERABAD DURING 1965. R. K. Puri and P. K. Aditya (Indian Institute of Technology, Delhi, India), p. 38-41. 14 refs. [See A69-17275 06-29]

RIGIDITY SPECTRUM OF COSMIC RAY HELIUM NUCLEI $\geq$ 12 BV. K. C. Anand, R. R. Daniel, S. A. Stephens, B. Bhowmik, P. K. Aditya, R. K. Puri (Tata Institute of Fundamental Research, Bombay; Delhi, University; Indian Institute of Technology, Delhi, India), and C. S. Krishna, p. 42, 43. [See A69-17276 06-29]

RIGIDITY SPECTRUM OF COSMIC RAY HELIUM NUCLEI USING A MAGNETIC SPECTROGRAPH. R. Cowsik, Y. Pal, S. N. Tandon, and R. P. Verma (Tata Institute of Fundamental Research, Bombay, India), p. 44-47A. [See A69-17277 06-29]

SPLASH ALBEDO MEASUREMENTS OVER HYDERABAD (λ = 8°N. GEO. MAG.). P. K. Kunte, R. Sunderrajan, and G. S. Gokhale (Tata Institute of Fundamental Research, Bombay, India), p. 48-51. [See A69-17278 06-29]

ON THE RIGIDITY SPECTRA OF TOTAL PRIMARY COSMIC RADIATION. K. Kasturirangan and N. W. Nerurkar (Physical Research Laboratory, Ahmedabad, India), p. 52-56. [See A69-17279 06-29]

COMPOSITION OF THE 2ND SEPTEMBER 1966 SOLAR PARTICLE EVENT. N. Durgaprasad (Tata Institute of Fundamental Research, Bombay, India), C. E. Fichtel, D. E. Guss, and D. V. Reames (NASA, Goddard Space Flight Center, Greenbelt, Md.) p. 57-60. [See A69-17280 06-29]

SOLAR NEUTRONS. G. Joseph (Tata Institute of Fundamental Research, Bombay, India), p. 61-69. [See A69-17281 06-29]

NUCLEAR EFFECTS DUE TO SOLAR COSMIC RAYS IN METEORITES. D. Lal, R. S. Rajan, and V. S. Venkatavardan (Tata Institute of Fundamental Research, Bombay, India), p. 70-75. [See A69-17282 06-29]

THE DISTRIBUTION OF ELEMENTS OF Z > 24 IN COSMIC RADIATION AS DEDUCED FROM STUDIES OF METEORITIC MINERALS (REVIEW). D. Lal (Tata Institute of Fundamental Research, Bombay, India), p. 76, 77.

PRODUCTION RATES OF NUCLIDES IN THICK TARGETS AND STONE METEORITES. P. S. Goel and B. M. P. Trivedi (Institute of Higher Technology, Kanpur, India), p. 78, 79. [See A69-17283 06-29]

EXPERIMENT TO DETERMINE THE CHARGE COMPOSITION OF HEAVY NUCLEI OF PRIMARY COSMIC RADIATION NEAR GEOMAGNETIC EQUATOR. P. C. Agrawal, M. V. K. Appa Rao, S. V. Damle, G. S. Gokhale, and P. K. Kunte (Tata Institute of Fundamental Research, Bombay, India), p. 80-83.

TRANSISTORISED MULTICHANNEL PULSE HEIGHT ANALYSER AND RECORDING SYSTEM FOR BALLOON BORNE COSMIC RAY TELESCOPE. S. V. Damle, M. F. D'Cunha, G. Joseph, A. P. Kamat, S. B. Patankar, S. R. Ramachandra, and K. V. Srinivasan (Tata Institute of Fundamental Research, Bombay, India), p. 84-86. [See A69-17284 06-14]

SPARK CHAMBERS FOR STUDY OF COSMIC RAYS AT BALLOON ALTITUDES. P. C. Agrawal (Tata Institute of Fundamental Research, Bombay, India), p. 87-91. [See A69-17285 06-14]

ATTEMPTS TO DETECT RELATIVISTIC HEAVY NUCLEI WITH PLASTICS. R. R. Sunderrajan and A. S. Tamhane (Tata Institute of Fundamental Research, Bombay, India), p. 92-95. [See A69-17286 06-14]

PHASE TRANSITION DETECTORS AND LIQUID STRUCTURE. N. C. Varshneya (Roorkee, University, Roorkee, India), p. 96-100.

COSMIC RAYS AS PROBES TO STUDY INTERPLANETARY CONDITIONS.

MODULATION OF GALACTIC COSMIC RAYS (REVIEW). R. P. Kane (Physical Research Laboratory, Ahmedabad, India), p. 101-108. [See A69-17287 06-29]

SOLAR COSMIC RAYS AS PROBES TO STUDY THE INTERPLANETARY CONDITIONS (REVIEW). U. R. Rao (Physical Research Laboratory, Ahmedabad, India), p. 109-127. [See A69-17288 06-29]

INTERRELATIONSHIP BETWEEN SOLAR COSMIC RAY ANISOTROPY AND INTERPLANETARY MAGNETIC FIELD. U. R. Rao (Physical Research Laboratory, Ahmedabad, India), K. G. McCracken (Adelaide, University, Adelaide, Australia), and N. F. Ness (NASA, Greenbelt, Md.), p. 128.

DIURNAL VARIATION OF LOW ENERGY COSMIC RADIATION. U. R. Rao (Physical Research Laboratory, Ahmedabad, India) and K. G. McCracken (Adelaide, University, Adelaide, Australia), p. 129.

ANISOTROPIES OF GALACTIC COSMIC RAYS. D. Patel, V. Sarabhai, and G. Subramanian (Physical Research Laboratory, Ahmedabad, India), p. 130-132. [See A69-17289 06-29]

ANISOTROPIES IN FORBUSH DECREASES. V. S. Iyengar, A. S. Prakasarao, and U. R. Rao (Physical Research Laboratory, Ahmedabad, India), p. 133-137. [See A69-17290 06-29]

DAILY VARIATION OF COSMIC RAY INTENSITY - SOLAR AND TERRESTRIAL RELATIONSHIP. R. P. Kane (Physical Research Laboratory, Ahmedabad, India), p. 138-145. [See A69-17291 06-29]

27-DAY VARIATIONS IN COSMIC RAY INTENSITY AND ITS RELATION TO LONGITUDINAL DISTRIBUTION OF ACTIVE REGIONS IN SOLAR CORONA. P. N. Pathak (Physical Research Laboratory, Ahmedabad, India), p. 146-148. [See A69-17292 06-29]

VARIATIONAL COEFFICIENTS FOR VERTICAL AND INCLINED MESON TELESCOPES WITH APPLICATION TO THE DAILY VARIATION FOR TRIVANDRUM. K. N. Nair (Physical Research Laboratory, Ahmedabad, India), p. 149-151. [See A69-17293 06-14]

EXPERIMENTAL DETERMINATION OF TEMPERATURE EFFECT ON μ MESONS RECORDED AT TRIVANDRUM. K. N. Nair and V. Sarabhai (Physical Research Laboratory, Ahmedabad, India), p. 152-154. [See A69-17294 06-14]

AZIMUTH EFFECT OF COSMIC RAY MESON INTENSITY AT AHMEDABAD. V. S. Iyengar (Physical Research Laboratory, Ahmedabad, India), p. 155-158. [See A69-17295 06-14]

LARGE AREA SCINTILLATION TELESCOPES. L. V. Kargathra (Physical Research Laboratory, Ahmedabad, India), p. 159-161. [See A69-17296 06-14]

MULTIPLICITY SPECTRUM OF A IGY NEUTRON MONITOR AT GULMARG. M. M. Bimal Khedkar, N. W. Nerurkar, and H. Razdan (Physical Research Laboratory, Ahmedabad, India), p. 162-164. [See A69-17297 06-14]

EXTENSIVE AIR SHOWERS AND MUONS.

CURRENT AIR SHOWER INVESTIGATIONS (INVITED TALK). G. T. Murthy (Tata Institute of Fundamental Research, Bombay, India), p. 165-180. [See A69-17298 06-29]

STUDIES IN EXTENSIVE AIR SHOWERS AT OOTACAMUND. B. K. Chatterjee, N. V. Gopalakrishnan, G. T. Murthy, B. V. Sreekantan, M. V. Srinivasa Rao, S. C. Tonwar, and R. H. Vatcha (Tata Institute of Fundamental Research, Bombay, India), p. 181-187. [See A69-17299 06-29]

THE KOLAR GOLD FIELDS EXTENSIVE AIR SHOWER EXPERIMENT. B. K. Chatterjee, G. T. Murthy, S. Naranan, K. Sivaprasad, B. V. Sreekantan, A. Suri, and P. R. Viswanath (Tata Institute of Fundamental Research, Bombay, India), p. 188-193. [See A69-17300 06-29]

CALCULATION OF SOME CHARACTERISTICS OF EXTENSIVE AIR SHOWERS USING DIFFERENT MODELS OF HIGH ENERGY NUCLEAR INTERACTIONS. G. T. Murthy, K. Sivaprasad, M. V. S. Rao, S. C. Tonwar, R. H. Vatcha, and P. R. Viswanath (Tata Institute of Fundamental Research, Bombay, India), p. 194-201. 12 refs. [See A69-17301 06-29]

DURGAPUR COSMIC RAY MAGNETIC SPECTROGRAPH. B. C. Nandi and M. S. Sinha (Regional Engineering College, Durgapur, India), p. 202-207. [See A69-17302 06-14]

DEVELOPMENT OF A BIG CLOUD CHAMBER FOR MEASURING THE SPECIFIC IONISATION OF MUONS. A. K. Das and M. S. Sinha (Regional Engineering College, Durgapur, India), p. 208-211. [See A69-17303 06-14]

MUON-BUNDLES OBSERVED AT SEALEVEL. A. K. Das and M. S. Sinha (Regional Engineering College, Durgapur, India), p. 212-215. [See A69-17304 06-29]

ENERGY SPECTRUM OF MUONS FROM THEIR KNOCK-ON ELECTRONS. A. K. Das and M. S. Sinha (Regional Engineering College, Durgapur, India), p. 216-219. [See A69-17305 06-29]

CERENKOV RADIATION OF HIGH ENERGY MUONS. K. M.

Pathak (Cotton College, Gauhati, India) and M. G. Thompson (Durham, University, Durham, England), p. 220-223. [See A69-17306 06-29]

ELECTRONS, X-RAYS AND GAMMA-RAYS.

X-RAY ASTRONOMY - A REVIEW. B. V. Sreekantan (Tata Institute of Fundamental Research, Bombay, India), p. 224-250. 18 refs. [See A69-17307 06-29]

COSMIC ELECTRONS (INVITED TALK). S. A. Stephens (Tata Institute of Fundamental Research, Bombay, India), p. 251-267. [See A69-17308 06-29]

COSMIC RAY ELECTRONS IN THE GALAXY. K. C. Anand, R. R. Daniel, and S. A. Stephens (Tata Institute of Fundamental Research, Bombay, India), p. 268-270. [See A69-17309 06-29]

ELECTRONS IN METAGALAXY AND THEIR IMPLICATIONS. K. C. Anand, R. R. Daniel, and S. A. Stephens (Tata Institute of Fundamental Research, Bombay, India), p. 271-273. [See A69-17310 06-29]

ISOTROPIC BACKGROUND COSMIC X-RAYS AND UPPER LIMITS FOR SOLAR X-RAY FLUX. U. R. Rao, E. V. Chitnis, and A. S. Prakasarao (Physical Research Laboratory, Ahmedabad, India), p. 274-278. [See A69-17311 06-29]

PROPOSED EXPERIMENTS TO MEASURE THE SPECTRA AND TIME VARIATION OF X-RAY SOURCES. P. C. Agrawal, M. V. K. Appa Rao, S. Biswas, G. S. Gokhale, P. K. Kunte, R. K. Manchanda, and B. V. Sreekantan (Tata Institute of Fundamental Research, Bombay, India), p. 279-282. [See A69-17312 06-29]

THE 0.5 MEV GAMMA RAY FLUX AT BALLOON ALTITUDES OVER 7.6°N GEOMAGNETIC LATITUDE. U. R. Rao, V. S. Iyengar, and A. S. Prakasarao (Physical Research Laboratory, Ahmedabad, India), p. 283-286. [See A69-17313 06-29]

STELLAR PHYSICS.

RADIO EMISSION FROM SUPERNOVA REMNANTS (REVIEW). M. R. Kundu (Tata Institute of Fundamental Research, Bombay, India), p. 287-306. [See A69-17314 06-30]

RELATIVISTIC ASTROPHYSICS AND GRAVITATIONAL COLLAPSE (REVIEW). S. M. Chitre (Tata Institute of Fundamental Research, Bombay, India), p. 307-324. [See A69-17315 06-30]

MAGNETOSTATIC STELLAR CORONA. S. P. Tarafdar (Tata Institute of Fundamental Research, Bombay, India), p. 325-328. [See A69-17316 06-30]

ON THE POSSIBLE EXISTENCE OF SH IN SOLAR ATMOSPHERE. M. C. Pande, V. P. Gaur, and B. M. Tripathi (Uttar Pradesh State Observatory, Naini Tal, India), p. 329-332. [See A69-17317 06-30]

SOME PROPERTIES OF THE SOURCES OF SLOWLY VARYING COMPONENT AND OF BURSTS AT 612 MC/S. M. R. Kundu, G. Swarup, V. K. Kapahi, and J. D. Isloor (Tata Institute of Fundamental Research, Bombay, India), p. 333.

DECAMETER RADIO EMISSION FROM JUPITER AND SOLAR ACTIVITY. C. H. V. Sastry (Astrophysical Observatory, Kodaikanal, India), p. 334.

SOLAR RADIO SPECTROSCOPE (FREQUENCY RANGE 40-240 MHZ) AT AHMEDABAD (LAT. 23°01'N; LONG. 72°36'E), INDIA. R. V. Bhonsle and S. K. Alurkar (Physical Research Laboratory, Ahmedabad, India), p. 335-339. [See A69-17318 06-14]

RAYLEIGH SCATTERING CROSS-SECTIONS OF He, C, N AND O. S. P. Tarafdar and M. S. Vardya (Tata Institute of Fundamental Research, Bombay, India), p. 340-343. [See A69-17319 06-30]

THREE COLOUR PHOTOELECTRIC PHOTOMETRY OF KP PERSEI. S. C. Joshi (Uttar Pradesh State Observatory, Naini Tal, India), p. 344-346.

MOLECULAR RATIOS AS INDICATORS OF ELEMENTAL ABUNDANCE RATIOS. P. Giannone, N. Virgopia (Roma, Osservatorio Astronomico, Rome, Italy), and M. S. Vardya (Tata Institute of Fundamental Research, Bombay, India), p. 347-349. [See A69-17320 06-30]

ON CONVECTIVE PROCESSES IN LATE-TYPE STARS. S. M. Chitre and M. S. Vardya (Tata Institute of Fundamental Research, Bombay, India), p. 350-352. [See A69-17321 06-30]

ON NOVA DELPHINI 1967. A. Bhatnagar and A. T. Doss (Astrophysical Observatory, Kodaikanal, India), p. 353-355.

ON THE SPECTRA OF RADIO SOURCES CYGNUS LOOP AND IC443. M. R. Kundu and T. Velusamy (Tata Institute of Fundamental Research, Bombay, India), p. 356-361. [See A69-17322 06-30]

VARIATION OF ELECTRONIC CHARGE WITH COSMIC TIME. S. M. Chitre and Y. Pal (Tata Institute of Fundamental Research, Bombay, India), p. 362-364. [See A69-17323 06-30]

SYNCHROTRON RADIATION FROM TRAPPED ELECTRONS IN THE VAN ALLEN BELT. R. N. Singh and R. P. Singh (Banaras Hindu University, Varanasi, India), p. 365-369. [See A69-17324 06-29]

A69-17280 *#

COMPOSITION OF THE 2ND SEPTEMBER 1966 SOLAR PARTICLE EVENT.

N. Durgaprasad (Tata Institute of Fundamental Research, Bombay, India), C. E. Fichtel, D. E. Guss, and D. V. Reames (NASA, Goddard Space Flight Center, Greenbelt, Md.).

IN: DEPARTMENT OF ATOMIC ENERGY, SYMPOSIUM ON COSMIC RAYS, ELEMENTARY PARTICLE PHYSICS AND ASTROPHYSICS, 10TH, ALIGARH MUSLIM UNIVERSITY, ALIGARH, INDIA, DECEMBER 12-16, 1967, PROCEEDINGS. [A69-17268 06-29] Bombay, Department of Atomic Energy, 1968, p. 57-60.

Description of the charge composition of the 3^+ solar flare of Sept. 2, 1966, that occurred at 0538 UT at Fort Churchill, Canada. The charge and energy spectra of all the components are tabulated. The results obtained show that the rigidity spectra of singly and multiply charged nuclei are similar, in agreement with the results obtained by other investigators. M.M.

A69-18113 *#

RADIATION PLAN FOR THE APOLLO LUNAR MISSION.

Jerry L. Modisette, Manuel D. Lopez, and Joseph W. Snyder (NASA, Manned Spacecraft Center, Space Physics Div., Houston, Tex.).

American Institute of Aeronautics and Astronautics, Aerospace Sciences Meeting, 7th, New York, N.Y., Jan. 20-22, 1969, Paper 69-19. 5 p.

Members, $1.00; nonmembers, $1.50.

The radiation protection plan for the Apollo Program is based on real-time monitoring of solar activity and radiation in the spacecraft to provide data on which to base estimates of the radiation to be expected. The major radiation hazard is from solar flare particle events, which are unlikely to occur during any given mission. The monitoring system, consisting of onboard dosimeters and the Solar Particle Alert Network, provides early warning through observation of solar flares and the associated radio bursts and a continual updating of the radiation picture as particles arrive at the spacecraft. Prediction criteria have been developed which are progressively revised as more data are received, with a corresponding reduction in the error limits on the prediction of radiation dose. (Author)

A69-19351

PHYSICS OF THE MAGNETOSPHERE; PROCEEDINGS OF THE CONFERENCE, BOSTON COLLEGE, CHESTNUT HILL, MASS., JUNE 19-28, 1967.

Conference sponsored by the U.S. Air Force and Boston College. Edited by R. L. Carovillano (Boston College, Chestnut Hill, Mass.), J. F. McClay (USAF, Office of Aerospace Research, Cambridge Research Laboratories, Space Physics Laboratory, Bedford, Mass.), and H. R. Radoski (Boston College, Weston Observatory, Weston, Mass.).

Dordrecht, D. Reidel Publishing Co. (Astrophysics and Space Science Library. Volume 10), 1968. 686 p.

$35.10.

CONTENTS:

PREFACE. R. L. Carovillano (Boston College, Chestnut Hill, Mass.), p. v, vi.

TUTORIAL LECTURES.

DYNAMICAL PROPERTIES OF THE MAGNETOSPHERE. E. N. Parker (Chicago, University, Chicago, Ill.), p. 3-64. 9 refs. [See A69-19352 07-13]

SOLAR WIND INTERACTIONS AND THE MAGNETOSPHERE. A. J. Dessler (William Marsh Rice University, Houston, Tex.),

p. 65-105. 57 refs. [See A69-19353 07-29]
WHISTLERS AND VLF EMISSIONS. R. A. Helliwell (Stanford University, Stanford, Calif.), p. 106-146. 12 refs. [See A69-19354 07-13]
PARTICLE DESCRIPTION OF THE MAGNETOSPHERE. J. A. Van Allen (Iowa, University, Iowa City, Iowa), p. 147-217. 10 refs. [See A69-19355 07-29]
WAVES AND PARTICLES IN THE MAGNETOSPHERE. J. W. Dungey (London, University, Imperial College of Science and Technology, London, England), p. 218-259. 19 refs. [See A69-19356 07-29]

INVITED RESEARCH PAPERS.
INFLATION OF THE INNER MAGNETOSPHERE. L. J. Cahill, Jr. (Minnesota, University, Minneapolis, Minn.), p. 263-270. 9 refs. [See A69-19357 07-13]
RECENT OBSERVATIONS OF LOW-ENERGY CHARGED PARTICLES IN THE EARTH'S MAGNETOSPHERE. L. A. Frank (Iowa, University, Iowa City, Iowa), p. 271-289. 41 refs. [See A69-19358 07-29]
MAGNETIC ENERGY RELATIONSHIPS IN THE MAGNETOSPHERE. R. L. Carovillano (Boston College, Chestnut Hill, Mass.) and J. J. Maguire (William Marsh Rice University, Houston, Tex.), p. 290-300. 17 refs. [See A69-19359 07-13]
EXTERNAL AERODYNAMICS OF THE MAGNETOSPHERE. J. R. Spreiter, A. Y. Alksne, and A. L. Summers (NASA, Ames Research Center, Moffett Field, Calif.), p. 301-375. 106 refs. [See A69-19360 07-13]
OBSERVATIONS OF THE SOLAR WIND, BOW SHOCK AND MAGNETOSHEATH BY THE VELA SATELLITES. I. B. Strong (California, University, Los Alamos, N. Mex.), p. 376-391. 21 refs. [See A69-19361 07-29]
REVIEW AND INTERPRETATION OF PARTICLE MEASUREMENTS MADE BY THE VELA SATELLITES IN THE MAGNETOTAIL. E. W. Hones, Jr. (California, University, Los Alamos, N. Mex.), p. 392-408. 14 refs. [See A69-19362 07-29]
SATELLITE STUDIES OF THE EARTH'S MAGNETIC TAIL. K. W. Behannon and N. F. Ness (NASA, Goddard Space Flight Center, Greenbelt, Md.), p. 409-434. 39 refs. [See A69-19363 07-29]
REVIEW OF AMES RESEARCH CENTER PLASMA-PROBE RESULTS FROM PIONEERS 6 AND 7. J. H. Wolfe and D. D. McKibbin (NASA, Ames Research Center, Moffett Field, Calif.), p. 435-460. 29 refs. [See A69-19364 07-13]
THE GEOMAGNETIC TAIL - TOPOLOGY, RECONNECTION AND INTERACTION WITH THE MOON. C. P. Sonett, D. S. Colburn, R. G. Currie, and J. D. Mihalov (NASA, Ames Research Center, Moffett Field, Calif.), p. 461-484. 26 refs. [See A69-19365 07-13]
MAGNETIC TURBULENCE IN SHOCKS. C. F. Kennel (California, University, Los Angeles, Calif.) and H. E. Petschek (Avco Corp., Everett, Mass.), p. 485-513. 36 refs. [See A69-19366 07-25]
CYCLOTRON- AND BOUNCE-RESONANCE SCATTERING OF ELECTRONS TRAPPED IN THE EARTH'S MAGNETIC FIELD. C. S. Roberts (Bell Telephone Laboratories, Inc., Murray Hill, N.J.), p. 514-533. 28 refs. [See A69-19367 07-29]
PENETRATION OF AURORAL ELECTRONS INTO THE ATMOSPHERE. M. Walt, W. M. MacDonald (Lockheed Aircraft Corp., Palo Alto, Calif.; Maryland, University, College Park, Md.), and W. E. Francis (Lockheed Aircraft Corp., Palo Alto, Calif.), p. 534-555. 11 refs. [See A69-19368 07-13]
ENERGY TRANSFER TO AND THROUGH IONOSPHERIC ELECTRONS. N. P. Carleton (Smithsonian Institution; Harvard University, Cambridge, Mass.), p. 556-562. [See A69-19369 07-13]
MAGNETOSPHERIC AND HIGH LATITUDE IONOSPHERIC DISTURBANCE PHENOMENA. N. Brice (Cornell University, Ithaca, N.Y.), p. 563-585. 26 refs. [See A69-19370 07-13]
PARTICLE DYNAMICS AT THE SYNCHRONOUS ORBIT. J. W. Freeman, Jr. and J. J. Maguire (William Marsh Rice University, Houston, Tex.), p. 586-604. [See A69-19371 07-29]
SHOCK AND MAGNETOPAUSE BOUNDARY OBSERVATIONS WITH IMP-2. J. H. Binsack (Massachusetts Institute of Technology, Cambridge, Mass.), p. 605-621. 7 refs. [See A69-19372 07-13]
LOW-ENERGY ELECTRONS IN THE MAGNETOSPHERE AS OBSERVED BY OGO-1 AND OGO-3. V. M. Vasyliunas (Massachusetts Institute of Technology, Cambridge, Mass.), p. 622-640. 20 refs. [See A69-19373 07-29]
SUMMARY OF EXPERIMENTAL RESULTS FROM M.I.T. DETECTOR ON IMP-1. S. Olbert (Massachusetts Institute of Technology, Cambridge, Mass.), p. 641-659. [See A69-19374 07-13]
CHARGED PARTICLE DIFFUSION BY VIOLATION OF THE THIRD ADIABATIC INVARIANT. T. J. Birmingham, T. G. Northrop (NASA, Goddard Space Flight Center, Greenbelt, Md.), and C.-G. Fälthammar (Kungl. Tekniska Högskola, Stockholm, Sweden), p. 660-677. 23 refs. [See A69-19375 07-29]
INDEX OF NAMES, p. 679-683.
INDEX OF SUBJECTS, p. 684-686.

A69-19363 *

SATELLITE STUDIES OF THE EARTH'S MAGNETIC TAIL.
Kenneth W. Behannon and Norman F. Ness (NASA, Goddard Space Flight Center, Laboratory for Space Sciences, Greenbelt, Md.).
IN: PHYSICS OF THE MAGNETOSPHERE; PROCEEDINGS OF THE *CONFERENCE, BOSTON COLLEGE, CHESTNUT HILL, MASS.*, JUNE 19-28, 1967. [A69-19351 07-29]
Conference sponsored by the U.S. Air Force and Boston College. Edited by R. L. Carovillano, J. F. McClay, and H. R. Radoski. Dordrecht, D. Reidel Publishing Co. (Astrophysics and Space Science Library. Volume 10), 1968, p. 409-434. 39 refs.

Review of satellite experiments which have extensively mapped the earth's magnetic tail, thus contributing to current knowledge of the structure, temporal behavior, shape, and length of the magnetic tail. The tail is a permanent extension of the magnetosphere with magnetic lines of force pointing directly away from the sun south of the plane of the magnetospheric equator and toward the sun above this plane. The oppositely directed bundles of field lines are separated by a "neutral sheet," which is a weak magnetic-field reaction between 0.1 and 1 R_E thick, and which is generally in motion. Impulsive field magnitude decreases have been observed in the magnetic tail in association with transient electron events. The occurrence of these electron bursts decreases with distance from the neutral sheet. Magnetic storms have been observed in the tail in correlation with worldwide terrestrial disturbances. F.R.L.

A69-19375 *

CHARGED PARTICLE DIFFUSION BY VIOLATION OF THE THIRD ADIABATIC INVARIANT.
T. J. Birmingham, T. G. Northrop (NASA, Goddard Space Flight Center, Laboratory for Theoretical Studies, Greenbelt, Md.), and C.-G. Fälthammar (Kungl. Tekniska Högskola, Stockholm, Sweden).
(Physics of Fluids, vol. 10, Nov. 1967, p. 2389-2398.)
IN: PHYSICS OF THE MAGNETOSPHERE; PROCEEDINGS OF THE CONFERENCE, BOSTON COLLEGE, CHESTNUT HILL, MASS., JUNE 19-28, 1967. [A69-19351 07-29]
Conference sponsored by the U.S. Air Force and Boston College. Edited by R. L. Carovillano, J. F. McClay, and H. R. Radoski. Dordrecht, D. Reidel Publishing Co. (Astrophysics and Space Science Library. Volume 10), 1968, p. 660-677. 23 refs.

An equation which describes statistically the motion of charged particles in response to fluctuating electric and magnetic fields is derived. The particles are assumed to be moving in a mirror-type magnetic geometry. In addition to a static magnetic field there are small superposed fields fluctuating randomly on such a time scale that the first and second adiabatic invariants, M and J, are conserved, but the third or flux invariant Φ is violated. By using second adiabatic theory a two-dimensional diffusion equation is obtained valid on a much longer time scale than that of the fluctuations. Elements of the diffusion tensor are time-space correlations of fluctuation-induced perturbations in the guiding center drifts. These drift perturbations are systematically derived and shown to reduce simply in various special cases. (Author)

A69-20066 *

COSMIC-RAY DEUTERIUM AND HELIUM-3 OF SECONDARY ORIGIN AND THE RESIDUAL MODULATION OF COSMIC RAYS.
Reuven Ramaty (NASA, Goddard Space Flight Center, Greenbelt, Md.) and Richard E. Lingenfelter (California, University, Institute

of Geophysics and Planetary Physics, Los Angeles, Calif.).
Astrophysical Journal, vol. 155, Feb. 1969, pt. 1, p. 587-608. 74 refs.
NSF Grant No. GP-849.

Assuming that cosmic-ray deuterons and helium-3 nuclei are of secondary origin, it is shown that a unique determination of both the cosmic-ray path length and the residual interplanetary field modulation at solar minimum may be made from a comparison of the calculated and measured intensities of these two nuclei. This determination does not depend on any assumptions regarding either the source spectra or the unmodulated proton-to-alpha particle ratio of the primary cosmic rays. The production of deuterium and helium-3 by cosmic-ray interactions in the Galaxy is calculated by considering energy-dependent cross sections, interaction kinematics, and demodulated cosmic-ray spectra. The resulting flux at the earth is obtained by taking into account leakage from the Galaxy, ionization losses, nuclear breakup, and modulation. From a comparison of these calculations with the measured deuterium and helium-3 intensities at the earth, it is concluded that within the experimental uncertainties all the data can be understood in terms of an energy-independent, cosmic-ray path length of 4 ± 1 g cm^{-2} and a residual interplanetary field modulation at solar minimum. (Author)

A69-20632 *
THE RELATIVE ENERGY SPECTRA OF CARBON AND OXYGEN NUCLEI IN THE PRIMARY COSMIC RADIATION.
T. T. Von Rosenvinge, W. R. Webber (Minnesota, University, Minneapolis, Minn.), and J. F. Ormes (NASA, Goddard Space Flight Center, Greenbelt, Md.).
Astrophysics and Space Science, vol. 3, Jan. 1969, p. 4-13. 20 refs.
Grant No. NsG-281-62.

Results of measurements of the energy spectra of carbon and oxygen nuclei in the primary cosmic radiation over the energy range from 140 MeV/n to 30 BeV/n. An average C/O ratio of 1.11 ± 0.02 is obtained at the top of the atmosphere. This ratio is found to be constant to within ~ 5% over the entire energy range. The energy spectra of these two nuclei are presented and compared with earlier measurements and with satellite observations at low energies. After correction for propagational effects in 4 g/cm^2 of interstellar hydrogen, the "source" C/O ratio is found to be ~ 0.9. The astrophysical implications of this C/O ratio are discussed. (Author)

A69-20645 *
CORONAE AROUND HELIUM STARS AND X-RAY SOURCES.
Kyoji Nariai (NASA, Goddard Space Flight Center, Greenbelt, Md.).
(International Astronomical Union, Colloquium on Mass Loss from Stars, Trieste, Italy, Sept 12-16, 1968.).
Astrophysics and Space Science, vol. 3, Jan. 1969, p. 160-162.

Calculation of the acoustic energy generation for helium-rich composition, showing that the maximum acoustic energy generation is located around 12,000 K at log g = 4 and 15,000 K at log g = 6. The author's suggestion in his last paper that a helium star, ν Sgr, may have a corona seems to be justified. The X-ray radiation from a corona around a helium star is strongest when the physical parameters of the star are log g ~ 6 and T_e ~ 15,000 K, but the total energy flux is too small to account for the observed X-ray sources. (Author)

A69-20699 *
DISCRETE SOURCE INTERPRETATION OF RECENT HIGH ENERGY COSMIC GAMMA RAY MEASUREMENTS.
H. Ögelman (NASA, Goddard Space Flight Center, Greenbelt, Md.).
Nature, vol. 221, Feb. 22, 1969, p. 753, 754. 26 refs.

Interpretation of the recent high-energy cosmic gamma-ray measurements obtained by gamma-ray detector on the OSO-3 spacecraft, assuming that most of this flux is caused by unresolved discrete sources. From the total measured fluxes in the X-ray and gamma-ray region the spectral index is established and compared with the measurements of the power-law index in the soft and hard X-ray region. The gamma-ray fluxes are compared with balloon experiments in the 100-MeV region. The predicted -2.0 spectra fit quite well with experimental measurements up to 0.5 MeV. Z. W.

A69-21459 *
COSMIC GAMMA RAYS FROM METAGALACTIC PROTON-ANTIPROTON ANNIHILATION.
F. W. Stecker (NASA, Goddard Space Flight Center, Greenbelt, Md.).
Nature, vol. 221, Feb. 1, 1969, p. 425-428. 15 refs.

Discussion of annihilation gamma radiation spectra. Annihilation gamma radiation has a characteristic spectrum which distinguishes it from other types of cosmic gamma radiation. Such spectra, based on the results of recent accelerator experiments on antiproton annihilation and including cosmological distortions of local annihilation gamma ray spectra, are presented. Some differences between gamma rays from metagalactic cosmic-ray collisions and annihilation spectra are pointed out. G. R.

A69-21645 *
THE SOLAR ELECTROMAGNETIC RADIATION ENVIRONMENT.
Harriet H. Malitson (NASA, Goddard Space Flight Center, Laboratory for Space Sciences, Greenbelt, Md.).
(Solar Energy Society, Annual Meeting, 3rd, Tempe, Ariz., Mar. 20-22, 1967.)
Solar Energy, vol. 12, Dec. 1968, p. 197-203. 17 refs.

Discussion of observations of the spectral distribution of solar electromagnetic radiation from wavelengths shorter than 1 Å to wavelengths longer than 100 m using many different techniques, each of which is applicable only over a small part of the total range. Most of the energy emitted by the sun (98%) lies between 3000 and 40,000 Å. A large fraction of the solar radiation falling between these wavelength limits manages to penetrate the earth's atmosphere, so that it can be studied from ground level. By observing the amount of solar energy reaching the ground at many times during the day, an extrapolation can be made that gives a reasonably accurate value of the energy received at the top of the atmosphere - the solar constant. No radiation from the sun at wavelengths below approximately 2900 Å has been detected at ground level, and very little radiation in the IR at wavelengths greater than 30-40,000 Å can come through the atmosphere. Observations must therefore be made in these spectral regions from rockets or satellites. B. H.

A69-21646 *
SOLAR IRRADIANCE CURVES AND ABSORPTANCE OF SATELLITE COATINGS.
M. P. Thekaekara (NASA, Goddard Space Flight Center, Greenbelt, Md.).
Solar Energy, vol. 12, Dec. 1968, p. 205-215. 18 refs.

Comparison of data published by Johnson (1954) for the spectral distribution of solar irradiance at the mean sun-earth distance (in the absence of the earth's atmosphere) with recently published data by other authors. All data have been normalized to those of Johnson so as to bring out the differences in spectral distribution. The results are displayed as histograms of the energy over a 0.01 μ bandwidth. Data on the spectral absorptance of 18 typical satellite surface coatings and the relative efficiency of silicon solar cells have been combined with solar spectral irradiance data to determine the energy absorbed over small bandwidths of 0.01 or 0.02 μ. Numerical integration has been performed to find the energy absorbed over the entire spectral range. It is seen that the efficiency of the solar cell is lower and the absorptances of practically all surface coatings are greater on the assumption of the Johnson curve than on the assumptions of any of the other compared curves. B. H.

A69-21699 *
135-1650 KEV SOLAR PROTONS AFTER THE FLARE OF JULY 7, 1966, OBSERVED IN THE MAGNETOTAIL AND MAGNETOSHEATH.
Andrei Konradi (NASA, Goddard Space Flight Center, Greenbelt, Md.).
Journal of Geophysical Research, vol. 74, Mar. 1, 1969, p. 1158-1163. 20 refs.

Protons with energies E >135 keV were observed in the tail of the magnetosphere after the flare of July 7, 1966. These protons have an isotropic pitch-angle distribution. The maximum intensity

of the protons reached ~1.2 x 10^4 (cm^2 sec ster)$^{-1}$ for particles with E > 120 keV between 1000 and 1100 UT and 1400 and 1500 UT July 8, 1966. The energy spectrum of the protons expressed as an exponential in rigidity indicates a monotonic softening: the characteristic rigidity, P_0, changing from about 50 to 10 MV. An hour-long excursion of the satellite into the magnetosheath during the peak of the proton flux showed that the proton intensity is lower in the magnetosheath than in the magnetosphere by a factor of 2. The observed pitch-angle distribution is flat in both regions. (Author)

A69-22167 *
OSO-III - PRELIMINARY SCIENTIFIC RESULTS.
John C. Brandt (NASA, Goddard Space Flight Center, Laboratory for Space Sciences, Solar Physics Branch, Greenbelt, Md.).
Solar Physics, vol. 6, Feb. 1969, p. 171-174. 12 refs.

Discussion of preliminary results related to seven scientific experiments carried out by the satellite OSO-3. Observations were made of the solar extreme ultraviolet, soft and hard solar X rays, cosmic X rays and γ rays, cosmic-ray particles, and the near-earth optical-wavelength radiation environment. G.R.

A69-22169 *
X-RAY AND EXTREME ULTRAVIOLET (1-400 Å) SPECTROSCOPY OF THE SUN, FROM OSO-III.
W. M. Neupert, W. A. White, W. J. Gates, M. Swartz, and R. M. Young (NASA, Goddard Space Flight Center, Laboratory for Space Sciences, Solar Physics Branch, Greenbelt, Md.).
Solar Physics, vol. 6, Feb. 1969, p. 183-192. 12 refs.

X-ray spectra of the sun have been obtained during solar flares. New emission lines are observed in the spectral range from 1.3 to 3 Å, and 8 to 20 Å. The most intense of the new emission features are tentatively attributed to optical transitions in high stages of ionization of iron (Fe XXV through Fe XX). Studies of the variability of these lines during flares provide new information for the development of a hot plasma in the initial stages of the flare event. (Author)

A69-22203 *
ON THE GENERATION OF SYNCHROTRON AND X-RAY EMISSION FROM ELECTRONS WITH ENERGY BELOW mc^2 IN SOLAR FLARES.
Stephen S. Holt and Thomas L. Cline (NASA, Goddard Space Flight Center, Greenbelt, Md.).
Astrophysical Journal, vol. 154, Dec. 1968, pt. 1, p. 1027-1038. 17 refs.

An attempt is made to reconcile a single source of electrons with both the hard X-ray and microwave radio emission observed at the peak of the solar flare of July 7, 1966. The spectral and temporal characteristics of the X-ray emission are used to determine the total number of electrons involved in the emission, as well as the shape of the generating electron spectrum. This is the first instance in which a generating electron spectrum has been directly inferred from experimental data. The spectrum is found to be $J(\gamma)d\gamma = A(\gamma - 1)^{-3}\, d\gamma$ or steeper, so that the bulk of the microwave emission originates from electrons with energies below mc^2. Both the observed X-radiation and synchrotron radiation can be explained in terms of the same electron source if the source region is high in the chromosphere, where the maximum field may be as high as 1000 G. (Author)

A69-22231 *
IRON LINE EMISSION FROM X-RAY SOURCES.
S. S. Holt, E. A. Boldt, and P. J. Serlemitsos (NASA, Goddard Space Flight Center, Greenbelt, Md.).
Astrophysical Journal, vol. 154, Dec. 1968, pt. 2, p. L137-L140. 8 refs.

Estimation of the response, as a function of temperature, of an X-ray detector with energy resolution of about 15% to a 1-keV window centered at 6.9 keV in the emission spectrum of a thermal source, using the results of Tucker (1967). It is pointed out that X-ray sources for which thermal models have been proposed should exhibit line structure for energies below 10 keV. The $(1s)^2$-1s2p transition in Fe XXV at 6.64 keV is the emission line that is characteristically the most easily observable, and its absence in experimentally observed spectra is shown to constrain proposed thermal models severely. M.M.

A69-23753 *
VERY HIGH ENERGY SOLAR X-RAYS OBSERVED DURING THE PROTON EVENT OF 7 JULY 1966.
T. L. Cline, S. S. Holt (NASA, Goddard Space Flight Center, Greenbelt, Md.), and E. W. Hones, Jr. (California, University, Los Alamos Scientific Laboratory, Los Alamos, N. Mex.).
IN: THE PROTON FLARE PROJECT (THE JULY 1966 EVENT). [A69-23725 10-29]
Edited by A. C. Stickland.
Cambridge, Mass., MIT Press (Annals of the IQSY. Volume 3), 1969, p. 193-197.

The time history and spectral intensity of solar X rays of energies from 80 keV to more than 500 keV were observed during the flare event of July 7, 1966. These measurements, made with the satellite OGO 3, cover the highest energy range available thus far and show this event to have the greatest measured hard X-ray intensity of any solar event studied in detail to date. Three intensity peaks at about 0027, 0029, and 0037 UT coincide with the times of microwave intensity maxima. A study of the spectral and temporal features of the X-ray emission, and comparison with the radio data, indicate a nonthermal bremsstrahlung origin for the X rays. (Author)

A69-23766 *
RELATIVISTIC SOLAR ELECTRONS DETECTED DURING THE 7 JULY 1966 PROTON FLARE EVENT.
T. L. Cline and F. B. McDonald (NASA, Goddard Space Flight Center, Greenbelt, Md.).
IN: THE PROTON FLARE PROJECT (THE JULY 1966 EVENT). [A69-23725 10-29]
Edited by A. C. Stickland.
Cambridge, Mass., MIT Press (Annals of the IQSY. Volume 3), 1969, p. 295-298. 6 refs.

The July 7, 1966, flare event provided the first opportunity to detect relativistic solar electrons in interplanetary space. The solar electrons, observed with the satellite IMP 3, have energies between 3 and 12 MeV, nearly two orders of magnitudes higher than any previously studied in space. Since they are relativistic electrons, they therefore provide a new parameter in the study of solar particle events. The electrons were separable from low-energy solar protons for several hours following the flare of 0027 UT and were, in fact, the only detectable low-energy particles between 0100 and 0200 UT. The electron energy spectrum and complete time history were measured from a position outside geomagnetic influence and show a compatibility with the general diffusion picture, having a delayed onset and profile similar to the high-velocity proton histories of other events. Other features of the event are also outlined. (Author)

A69-24466 *
PREDICTIONS OF EXTRAGALACTIC GAMMA RAY FLUXES BETWEEN 1 AND 100 MEV.
F. W. Stecker (NASA, Goddard Space Flight Center, Theoretical Studies Branch, Greenbelt, Md.) and Joseph Silk (Cambridge University, Institute of Theoretical Astronomy, Cambridge, England).
Nature, vol. 221, Mar. 29, 1969, p. 1229-1231. 17 refs.

Discussion of the implications which four processes producing gamma rays would have for extragalactic gamma ray fluxes between 1 and 100 MeV. Considered are three collisional processes and a fourth process involving matter-antimatter annihilation. Observational studies of isotropic gamma radiation in the indicated range are critical for determining the dominant processes producing gamma rays in the metagalaxy and their cosmological implications. G.R.

A69-25144 *
PHOTOELECTRON FLUX IN THE TOPSIDE IONOSPHERE MEASURED BY RETARDING POTENTIAL ANALYZERS.
B. C. Narasinga Rao and J. L. Donley (NASA, Goddard Space Flight Center, Laboratory for Space Sciences, Greenbelt, Md.).

Journal of Geophysical Research, vol. 74, Apr. 1, 1969, p. 1715-1719. 6 refs.

Satellite measurements of suprathermal electrons made at the time of conjugate sunrise indicate that they represent photoelectrons escaping from the production level of about 300 km and moving along the geomagnetic field lines into the conjugate ionosphere. The daytime maximum value of the flux is about 2.5×10^8 electrons cm^{-2} sec^{-1}. The spectral distribution of the flux shows a maximum around 5-10 eV. (Author)

A69-25162 *

RADAR BACKSCATTER AND ROCKET PROBE MEASUREMENTS OF ELECTRON TEMPERATURE ABOVE ARECIBO.

L. H. Brace, K. K. Mahajan (NASA, Goddard Space Flight Center, Greenbelt, Md.), and H. C. Carlson (Cornell-Sydney University Astronomy Center, Arecibo Ionospheric Observatory, Arecibo, Puerto Rico).

Journal of Geophysical Research, vol. 74, Apr. 1, 1969, p. 1883-1885. 11 refs.

Results of a comparison of the rocket profiles of the electron temperature obtained at 0330 T and 1530 LT on Mar. 19, 1968, with temperatures derived nearly simultaneously by the radar method at Arecibo Observatory. The resulting backscatter profiles and rocket profiles are given and discussed. The agreement between these two measurement techniques is remarkably good in the daytime flight; at altitudes below 180 km and above 240 km, the agreement between these two measurement techniques is remarkably good in the daytime flight; at altitudes below 180 km and above 240 km, the agreement is within 5%. For nighttime, above 286 km, there is a difference of 10%. M.G.

A69-26736 *

PLASMA FLOW AROUND THE MAGNETOSPHERE.

John R. Spreiter and Alberta Y. Alksne (NASA, Ames Research Center, Space Sciences Div., Moffett Field, Calif.).

(U.S. National Academy of Sciences and NASA Goddard Space Flight Center, International Symposium on the Physics of the Magnetosphere, Washington, D.C., Sept. 3-13, 1968.)

Reviews of Geophysics, vol. 7, Feb.-May 1969, p. 11-50. 82 refs.

Review of the salient features of the flow of solar plasma past the magnetosphere, including the velocity, density, temperature, and temperature anisotropies of the solar wind, and the variations in space and time of the magnetic field. Theoretical aspects of the steady-state interaction of the solar wind and the geomagnetic field are examined, using the continuum description provided by the equations of magnetohydrodynamics of a perfect dissipationless gas. An outline is provided of the series of approximations, and their observational and theoretical justifications, used to reduce the complex free-boundary magnetohydrodynamic flow problem to a series of tractable problems. A set of results is provided for representative conditions in the solar wind. The irregular or fluctuating character of the flow downstream of the bow wave, and the nature of the magnetosphere tail and surrounding flow at great distances for the earth are also treated. M.G.

A69-26943 *

PRELIMINARY COMPARISON OF SOLAR WIND PLASMA OBSERVATIONS IN THE GEOMAGNETOSPHERIC WAKE AT 1000 AND 500 EARTH RADII.

Devrie S. Intriligator, John H. Wolfe, Darrell D. McKibbin, and Harold R. Collard (NASA, Ames Research Center, Space Sciences Div., Moffett Field, Calif.).

Planetary and Space Science, vol. 17, Mar. 1969, p. 321-331. 14 refs.

Preliminary comparison of observations in the expected region of the geomagnetic tail at 1000 earth radii and 500 earth radii indicates that the measured plasma characteristics in these regions are similar. In each case, intervals of quiescent plasma ion energy spectra are interrupted by abrupt changes in the magnitude and shape of the ion spectra or by complete absence of measurable plasma. Each of these regions is highly disturbed and is most appropriately described by the term "geomagnetospheric wake." A comparison with measurements in the near-earth region of the geomagnetic tail indicates that the characteristics of the geomagnetic tail apparently undergo significant changes between 80 R_E and 500 R_E. (Author)

A69-27144 *

INNER-BELT VAN ALLEN RADIATION.

Stanley C. Freden (Aerospace Corp., El Segundo, Calif.; NASA, Manned Spacecraft Center, Houston, Tex.).

Space Science Reviews, vol. 9, Mar. 1969, p. 198-242. 121 refs.

Survey of the present state of knowledge about the inner radiation zone. This includes a historical review of empirical data and theoretical considerations concerning electrons, protons, and heavier particles. Included are results obtained from the various high-altitude nuclear tests. Recent experimental results are presented, and some newer theoretical ideas, such as pitch-angle scattering and radial diffusion, are discussed as applied to the data. Comparisons of the measured fluxes, spectra, and time variations with the theoretical calculations are made where possible. Some conclusions are drawn pertaining to the sources and loss processes for the trapped particles, and some comments are made regarding future measurements in the inner zone. (Author)

A69-27554 *

OSCILLATOR STRENGTHS AND WAVELENGTHS OF SOME X-RAY AND EXTREME-ULTRAVIOLET SPECTRUM LINES OF HIGHLY IONIZED IRON.

Robert D. Chapman (NASA, Goddard Space Flight Center, Solar Physics Branch, Greenbelt, Md.).

Astrophysical Journal, vol. 156, Apr. 1969, pt. 1, p. 87-91. 6 refs.

Determination of the oscillator strengths for X-ray and EUV transitions between configurations with principal quantum numbers $n \leq 4$, in the spectra Fe XXV, Fe XXIV, Fe XXIII, and Fe XXII. The report deals with the spectra of the helium-like, lithium-like, beryllium-like, and boron-like ions of iron. These ions all have simple energy-level diagrams. G.R.

A69-27593 *#

INFRARED RADIATION ASSOCIATED WITH PROTOSTARS.

A. G. W. Cameron (Yeshiva University, Belfer Graduate School of Science; NASA, Goddard Space Flight Center, Goddard Institute for Space Studies, New York, N.Y.).

Royal Society (London), Philosophical Transactions, Series A, vol. 264, Apr. 24, 1969, p. 227-233. 10 refs.

NASA-supported research.

Discussion of various stages in the collapse of an interstellar gas cloud into a cluster of protostars. The residual gas of the cloud which does not go into the protostars should form an opaque envelope which will thermalize the energy output of the protostars and will be detectable as a high-luminosity IR object. The IR object in Orion newly discovered by Low is interpreted to be one of these objects. (Author)

A69-28936 *

CONVECTION ELECTRIC FIELDS AND THE DIFFUSION OF TRAPPED MAGNETOSPHERIC RADIATION.

Thomas J. Birmingham (NASA, Goddard Space Flight Center, Laboratory for Theoretical Studies, Greenbelt, Md.).

Journal of Geophysical Research, vol. 74, May 1, 1969, p. 2169-2181. 40 refs.

Possible importance of time-dependent convection electric fields as an agent for diffusing trapped magnetospheric radiation inward toward the earth. By using a formalism (Birmingham, Northrop, and Fälthammar, 1967) based on first principles, and by adopting a simple model for the magnetosphere and its electric field, we succeed in deriving a one-dimensional diffusion equation to describe statistically the loss-free motion of mirroring particles with arbitrary but conserved values of the first two adiabatic invariants M and J. Solution of this equation bears out the fact that reasonable electric field strengths, correlated in time for no longer than the azimuthal drift period of an average particle, move particles toward the earth at a rate at least an order of magnitude faster than electric fields whose source is a fluctuating current on the magnetopause. (Author)

A69-28938 *
MORPHOLOGY OF ELECTRON CONCENTRATION ENHANCEMENT AT A HEIGHT OF 1000 KILOMETERS AT POLAR LATITUDES.
Teruo Sato and Lawrence Colin (NASA, Ames Research Center, Space Sciences Div., Moffett Field, Calif.).
Journal of Geophysical Research, vol. 74, May 1, 1969, p. 2193-2207. 40 refs.

A study based on Alouette 1 data of electron concentration enhancement at a height of 1000 km at polar latitudes during 1962-1964. The major features are: (1) enhancement occurs in three apparently independent concentric zones, zones 1, 2, and 3. Zone 1 includes the area with invariant latitudes higher than about 80°. The upper boundaries of zones 2 and 3 are, respectively, at approximately 80° and 73° at magnetic noon and at somewhat lower latitudes at magnetic midnight. The extent of width of each zone varies with season and magnetic activity, and within each zone enhancement occurs sporadically in space and time. (2) Enhancement occurs with maximum frequency at different magnetic local times in each zone. Occurrence frequencies and amplitudes are subject to magnetic local time, seasonal and magnetic activity effects. The latter two effects on occurrence frequency are especially notable in zones 1 and 3. It is suggested that the enhancement is caused by particle ionization due to precipitation of low-energy electrons (E < keV). (Author)

A69-28939 *
STORM-TIME VARIATIONS OF THE ELECTRON CONCENTRATION IN THE POLAR TOPSIDE IONOSPHERE.
Teruo Sato and K. L. Chan (NASA, Ames Research Center, Space Sciences Div., Moffett Field, Calif.).
Journal of Geophysical Research, vol. 74, May 1, 1969, p. 2208-2216. 16 refs.

Storm-time (Kp > 4) variations of electron concentration in the polar topside ionosphere are studied. Variation profiles at invariant latitudes higher than 60° were derived for 24 Alouette 1 satellite passes directly over or near the north geomagnetic pole. The results show that storm-time variations depend on magnetic local time, invariant latitude, and altitude. The cause of the variations is discussed. (Author)

A69-28950 *
HIGH-LATITUDE IONIZATION SPIKES OBSERVED BY THE POGO ION CHAMBER EXPERIMENT.
J. E. McCoy (William Marsh Rice University, Dept. of Space Science; NASA, Manned Spacecraft Center, Houston, Tex.).
Journal of Geophysical Research, vol. 74, May 1, 1969, p. 2309-2318. 39 refs.
Contract No. NAS 5-9317.

Study of ionization "spikes" observed by the POGO spacecraft which was launched into a low polar orbit on Oct. 14, 1965, and carried an ion chamber experiment sensitive to electrons with energies greater than 1 MeV and protons greater than 10 MeV. These spikes were found to be present near the high-latitude boundary of stably trapped radiation on at least 30% of the satellite passes through this region. Their frequency of occurrence increases markedly with increased magnetic disturbance. Occurrence of those spikes lying just inside the observed boundary of trapping appears to be evenly distributed with respect to local time, but the occurrence of spikes at latitudes outside the region of stable trapping is predominantly in the dawn hemisphere. It is argued that these spikes are the result of injection of high-energy electrons (E ~ 1 MeV) onto field lines near the boundary of trapping and are associated with the electron "islands" reported in the magnetospheric tail by Anderson et al. (1965, 1967, 1968). It is shown that the spatial distribution of spikes as observed by POGO should be expected as a consequence of electron drift, in the postmidnight quadrant, into a region of pseudotrapping. P.v.T.

A69-28963 *
SUPRATHERMAL ELECTRONS IN THE POLAR IONOSPHERE.
E. J. R. Maier (NASA, Goddard Space Flight Center, Laboratory for Space Sciences, Greenbelt, Md.).
Journal of Geophysical Research, vol. 74, May 1, 1969, p. 2421-2424. 10 refs.

Discussion of some observations of the energy distributions of the suprathermal (5 < E < 200 eV) electrons in the polar ionosphere. The data were obtained from a transit of Explorer 31 through the polar region on Dec. 16, 1965. The fluxes of electrons of energy greater than 15 eV and greater than 68 eV are plotted as a function of the magnetic latitude. Integral electron spectra and differential electron spectra are also shown. G.R.

A69-28964 *
LOW-ENERGY ELECTRON PRECIPITATION AT HIGH LATITUDES.
R. A. Hoffman (NASA, Goddard Space Flight Center, Greenbelt, Md.).
Journal of Geophysical Research, vol. 74, May 1, 1969, p. 2425-2432. 6 refs.

Discussion of data for low-energy electron fluxes at high latitudes, obtained from two detectors in a satellite launched on July 28, 1967, into a low-altitude polar orbit. The responses of the 0.7-keV and 7.3-keV detectors to precipitating electrons in the Northern Hemisphere during a number of orbits are discussed. G.R.

A69-29948 *
EQUILIBRIUM SPECTRA OF SECONDARY COSMIC-RAY POSITRONS IN THE GALAXY AND THE SPECTRUM OF COSMIC GAMMA-RAYS RESULTING FROM THEIR ANNIHILATION.
F. W. Stecker (NASA, Goddard Space Flight Center, Greenbelt, Md.).
Astrophysics and Space Science, vol. 3, Apr. 1969, p. 579-599. 36 refs.

Derivation of a general formula for calculating the gamma ray spectrum resulting from the annihilation of cosmic-ray positrons. This formula is used to calculate the annihilation gamma ray spectra from various equilibrium spectra of secondary galactic positrons, which are then compared with the gamma ray spectra produced by other astrophysical processes. B.H.

A69-29967 *
SOLAR ACTIVITY AND THE 11-YEAR MODULATION OF COSMIC RAYS.
V. K. Balasubrahmanyan (NASA, Goddard Space Flight Center, Greenbelt, Md.).
Solar Physics, vol. 7, Apr. 1969, p. 39-45. 21 refs.

The cosmic-ray intensity during the 18th and 19th solar cycles is examined in the light of Gnevyshev's suggestion of the presence of two maxima in each solar cycle. The 18th solar cycle (1944-1954) has two prominent and widely separated cosmic-ray minima corresponding in phase with the two maxima in Bartel's A_p index. For the 19th solar cycle the existence of two minima is less prominent than for the 18th solar cycle. The maximum at higher solar latitudes is more effective in reducing cosmic-ray intensity than the maximum at the lower latitudes. A_p, however, has a larger maximum during the lower latitude solar maximum. A relation between A_p and cosmic-ray intensity is obtained. This relationship is shown to be consistent with Parker's solar-wind theory of the modulation of cosmic rays. (Author)

A69-29971 *
LARGE VELOCITY DISCONTINUITIES IN THE SOLAR WIND.
Leonard F. Burlaga (NASA, Goddard Space Flight Center, Laboratory for Space Sciences, Greenbelt, Md.).
Solar Physics, vol. 7, Apr. 1969, p. 72-86. 12 refs.

Analysis of the results of interplanetary plasma observations made by Explorer 34, in which 11 discontinuous solar-wind speed changes (not associated with shocks) of more than 60 km/sec in less than 3 min were detected. These events called uD's may show a velocity change of either sign, but the plasma density and temperature do not change appreciably across them. The existence of these uD's is shown to be consistent with the theory of the Helmholtz instability. G.P.

29 SPACE RADIATION

A69-30005
SOLAR-TERRESTRIAL PHYSICS: SOLAR ASPECTS; INTERNATIONAL YEARS OF THE QUIET SUN AND COSPAR, JOINT SYMPOSIUM, LONDON, ENGLAND, JULY 17-22, 1967, PROCEEDINGS. PART 1.
Edited by A. C. Stickland.
Cambridge, Mass., MIT Press (Annals of the IQSY. Volume 4), 1969. 422 p.
$19.50.

CONTENTS:
FOREWORD. W. J. G. Beynon, p. v.

THE ACTIVITY OF THE QUIET SUN.
THE HISTORY AND MORPHOLOGY OF SOLAR ACTIVITY, 1964-1965. H. W. Dodson and E. R. Hedeman (Michigan, University, Lake Angelus, Mich.), p. 3-35. 14 refs. [See A69-30006 15-30]
ENERGETIC SOLAR RADIATIONS. H. Friedman (U.S. Navy, Naval Research Laboratory, Washington, D.C.), p. 36-56. 28 refs. [See A69-30007 15-29]
ENERGETIC SOLAR PARTICLES. E. N. Parker (Chicago, University, Chicago, Ill.), p. 57-61. [For abstract see issue 19, page 3315, Accession no. A67-35492]
THE MAGNETOSPHERIC SUBSTORM. K. A. Anderson (California, University, Berkeley, Calif.), p. 62-64. 10 refs. [See A69-30008 15-13]

INTERPLANETARY SPACE.
ORIGIN OF THE SOLAR WIND AND ITS ASTROPHYSICAL ASPECTS. E. R. Mustel (Akademiia Nauk SSSR, Astronomicheskii Sovet, Moscow, USSR), p. 67-87. 65 refs. [See A69-30009 15-29]
DIRECT MEASUREMENTS OF INTERPLANETARY MAGNETIC FIELDS AND PLASMAS. N. F. Ness (NASA, Goddard Space Flight Center, Greenbelt, Md.), p. 88-109. 48 refs. [See A69-30010 15-30]
COMETS, INTERPLANETARY SPACE, AND THE PROBLEMS OF THE SOLAR SYSTEM. S. K. Vsekhsviatskii (Kievskii Gosudarstvennyi Universitet, Kiev, Ukrainian SSR), p. 110-118. 22 refs. [See A69-30011 15-30]
STUDIES OF MAGNETIC INHOMOGENEITIES IN INTERPLANETARY SPACE USING SOLAR AND GALACTIC COSMIC-RAY MEASUREMENTS. A. N. Charakhchian (Akademiia Nauk SSSR, Moscow, USSR) and T. N. Charakhchian (Moskovskii Gosudarstvennyi Universitet, Moscow, USSR), p. 119-130. [For abstract see issue 19, page 3325, Accession no. A67-35493]
SOME COMMENTS ON THE EXISTENCE OF A DENSITY GRADIENT OF THE COSMIC RADIATION PERPENDICULAR TO THE PLANE OF THE ECLIPTIC. P. L. Marsden (Leeds University, Leeds, England), p. 131-137. [For abstract see issue 19, page 3315, Accession no. A67-35490]

THE COSMIC RADIATION.
GROUND-BASED SYNOPTIC OBSERVATIONS OF COSMIC RAYS. H. Carmichael (Atomic Energy of Canada, Ltd., Chalk River, Ontario, Canada), p. 141-174. 33 refs. [See A69-30012 15-29]
UNDERGROUND COSMIC-RAY MEASUREMENTS. H. Elliot (London, University, Imperial College of Science and Technology, London, England), p. 175-180. 10 refs. [See A69-30013 15-29]
SOME OBSERVATIONS ON THE 11-YEAR MODULATION OF GALACTIC COSMIC RAYS. W. R. Webber (Minnesota, University, Minneapolis, Minn.), p. 181-186. [For abstract see issue 19, page 3315, Accession no. A67-35487]
IQSY OBSERVATIONS OF LOW-ENERGY GALACTIC AND SOLAR COSMIC RAYS. F. B. McDonald (NASA, Goddard Space Flight Center, Greenbelt, Md.), p. 187-216. 63 refs. [See A69-30014 15-29]
COSMIC RAY VARIATIONS - THEORY. L. I. Dorman (Akademiia Nauk SSSR, Institut Zemnogo Magnetizma, Ionosfery i Rasprostraneniia Radiovoln, Krasnaya Pakhra, USSR), p. 217-268. 85 refs. [See A69-30015 15-29]
SOME PROBLEMS OF DETECTING GALACTIC ANISOTROPIES. A. J. Somogyi (Magyar Tudományos Akadémia, Budapest, Hungary), p. 269-273. [For abstract see issue 19, page 3315, Accession no. A67-35484]
MODULATION OF COSMIC-RAY ELECTRONS. S. Hayakawa (Nagoya University, Nagoya, Japan), p. 274-278. [For abstract see issue 19, page 3315, Accession no. A67-35496]

THE EARTH'S RADIATION BELTS.
THE EARTH'S RADIATION BELTS. S. N. Vernov (Moskovskii Gosudarstvennyi Universitet, Moscow, USSR), p. 281-301. 66 refs. [See A69-30016 15-29]
COMMENTS AND SPECULATIONS CONCERNING THE RADIATION BELTS. C. E. McIlwain (California, University, La Jolla, Calif.), p. 302-306. [For abstract see issue 19, page 3315, Accession no. A67-35485]
SOME QUANTITATIVE ASPECTS OF ELECTRON PRECIPITATION IN AND NEAR THE AURORAL ZONE. D. K. Bailey (ESSA, Boulder, Colo.), p. 307, 308.

AURORA AND AIRGLOW.
THE PHENOMENOLOGY AND MORPHOLOGY OF AURORAE. Ia. I. Feldstein (Akademiia Nauk SSSR, Institut Zemnogo Magnetizma, Ionosfery i Rasprostraneniia Radiovoln, Krasnaya Pakhra, USSR), S. I. Isaev (Akademiia Nauk SSSR, Kol'skii Filial, Poliarnyi Geofizicheskii Institut, Murmansk, USSR), and A. I. Lebedinskii, p. 311-348. [For abstract see issue 19, page 3224, Accession no. A67-35495]
SPECTROSCOPIC MORPHOLOGY OF AURORA. A. V. Jones (Saskatchewan, University, Saskatoon, Saskatchewan, Canada), p. 349-363. 46 refs. [See A69-30017 15-13]
INCOMING LOWER ENERGY PARTICLES AND THEIR ASSOCIATION WITH AIRGLOW AND AURORAE. B. J. O'Brien (William Marsh Rice University, Houston, Tex.), p. 364-374. 30 refs. [See A69-30018 15-13]
NIGHT AIRGLOW OBSERVATIONS DURING THE IQSY. F. E. Roach, L. L. Smith, and J. R. McKennan (ESSA, Boulder, Colo.), p. 375-387. 7 refs. [See A69-30019 15-13]
AIRGLOW RESEARCH DURING AND SINCE THE IQSY. G. Weill (Centre National de la Recherche Scientifique, Paris, France), p. 388-399. 40 refs. [See A69-30020 15-13]
HYDROGEN AND HYDROXYL EMISSIONS IN THE NIGHTGLOW. N. N. Shefov and Iu. L. Truttse (Akademiia Nauk SSSR, Institut Fiziki Atmosfery, Moscow, USSR), p. 400-406. [For abstract see issue 19, page 3223, Accession no. A67-35483]
AUTHOR INDEX, p. 407.
SUBJECT INDEX, p. 409-414.

A69-30014 *
IQSY OBSERVATIONS OF LOW-ENERGY GALACTIC AND SOLAR COSMIC RAYS.
F. B. McDonald (NASA, Goddard Space Flight Center, Greenbelt, Md.).
IN: SOLAR-TERRESTRIAL PHYSICS: SOLAR ASPECTS; INTERNATIONAL YEARS OF THE QUIET SUN AND COSPAR, JOINT SYMPOSIUM, LONDON, ENGLAND, JULY 17-22, 1967, PROCEEDINGS. PART 1. [A69-30005 15-29]
Edited by A. C. Stickland.
Cambridge, Mass., MIT Press (Annals of the IQSY. Volume 4), 1969, p. 187-216. 63 refs.

Summary of the more important developments in the evaluation of the IQSY cosmic-ray observations made by the spacecraft of the Zond, Luna, Proton, Pioneer, Mariner, OGO, and IMP series. The hydrogen and helium energy spectra have been determined with great precision over the range from 10 to 1000 MeV/nucleon. The relative modulation over this interval is well described by either a $1/R$ (where R is the particle rigidity) dependence or the equivalent $1/\beta$ (β = particle velocity relative to c, the velocity of light) dependence at low energies changing to a $1/\beta R$ dependence as 1 GeV is approached. Observations of the cosmic-ray gradient out to 1.5 AU have proven to be a valuable addition to the spectral observations. Solar cosmic-ray studies with detectors of greatly increased sensitivity combined with lower energy thresholds have revealed a great variety of observed events. P.v.T.

A69-30759 *
2-20 KEV SPECTRUM OF X-RAYS FROM THE CRAB NEBULA AND THE DIFFUSE BACKGROUND NEAR GALACTIC ANTICENTER.
Elihu A. Boldt, Upendra D. Desai, and Stephen S. Holt (NASA, Goddard Space Flight Center, Greenbelt, Md.).

Astrophysical Journal, vol. 156, May 1969, pt. 1, p. 427-436. 15 refs.

Description of X-ray data from the Crab Nebula and its apparently source-free neighborhood on the celestial sphere near galactic anti-center. With ~2 keV resolution, the Crab Nebula is found to have a structureless spectrum which is consistent with a power law of index -1.93 ± .05 in the differential photon flux between 2 and 20 keV. The diffuse X-ray background is found to exhibit a harder spectrum than the Crab Nebula in the same energy range. The 2-20 keV background spectrum, with index -1.3 ± .1, is significantly flatter than that reported at higher energies. (Author)

A69-31963 *
CAUSES OF SUDDEN COMMENCEMENTS AND SUDDEN IMPULSES.
L. F. Burlaga and K. W. Ogilvie (NASA, Goddard Space Flight Center, Laboratory for Space Sciences, Extraterrestrial Physics Branch, Greenbelt, Md.).
Journal of Geophysical Research, vol. 74, June 1, 1969, p. 2815-2825. 18 refs.

The causes of 19 worldwide changes in the earth's magnetic field, occurring between June and December 1967, were determined by examining magnetic field and plasma data for the solar wind near the earth. Seven of the events were classified as storm sudden commencements (ssc) and four as sudden impulses (si) by most stations reporting them. All of the ssc's were caused by hydromagnetic shocks. Two of the si's were negative impulses (si⁻) and were caused by tangential discontinuities across which the density decreased. The other two si's were distinct pulses in the magnetograms, and were caused by dense spots in the solar wind with dimensions ≈0.005 AU. There was no consensus among the reporting magnetic observatories as to whether the remaining eight events should be called si's or ssc's. Five of these events were caused by shocks and the other three by tangential discontinuities in the solar wind, but there seems to be no sure way to predict the type of structure from the shape of the magnetogram pulse. The rise time of the impulse in th H component of the magnetogram is apparently determined by something other than the type, the speed, or the thickness of an interplanetary discontinuity that caused the event. (Author)

A69-31975 *
ELECTRON MEASUREMENTS BEARING ON THE ENERGY AND PARTICLE BALANCE OF THE UPPER F REGION.
L. H. Brace, H. G. Mayr, and J. A. Findlay (NASA, Goddard Space Flight Center, Greenbelt, Md.).
Journal of Geophysical Research, vol. 74, June 1, 1969, p. 2952-2961. 10 refs.

Interpretation of electron temperature and density profiles measured between 120 and 630 km at midday at Wallops Island on Mar. 2, 1966. The temperature profile exhibits a strong positive gradient (24°/km) below 150 km followed by a smooth transition to a much smaller positive gradient (1.5°/km) above 300 km. Between 300 and 400 km, the electron concentration decreases with a scale height of about 100 km, which is significantly lower than the diffusive equilibrium scale height for the observed temperatures. Furthermore, the scale height more than doubles between 400 and 500 km. This change in scale height in a region where the mean ion mass and the electron temperature are nearly constant is also inconsistent with diffusive equilibrium and suggests that some dynamic process was occurring at the time of the flight. A simultaneous solution of the particle and energy continuity equations for the F region is carried out with the aid of inputs and boundary conditions from measurements of neutral composition, neutral gas temperature, and ion composition from the same vehicle. This analysis makes it possible to conclude that the upper F region was not in diffusive equilibrium between 300 and 500 km and that the low plasma scale height at these altitudes was consistent with either a neutral atmospheric wind or a rapid temporal variation on O^+. (Author)

A69-31984 *
PROTON ENTRY INTO THE MAGNETOSPHERE ON MAY 26, 1967.
D. J. Williams (NASA, Goddard Space Flight Center, Greenbelt, Md.) and C. O. Bostrom (Johns Hopkins University, Applied Physics Laboratory, Silver Spring, Md.).
Journal of Geophysical Research, vol. 74, June 1, 1969, p. 3019-3026. 22 refs.
NASA-supported research; Contract No. NOw-62-0604-c.

Comparison of low-energy proton observations over the polar cap and in the interplanetary and magnetosheath regions for May 26, 1967. The results indicate that at this time the entry of low-energy solar protons into the magnetosphere was controlled by a diffusion process. It also appears that the protons had access to the entire figure-8 current pattern in the geomagnetic tail and diffused into the two approximately circular cylinders containing the field lines from the northern and southern polar caps. A first approximation value of 10^{15}-10^{16} cm^2 sec^{-1} is obtained for the radial diffusion coefficient, D_{rr}, in the tail. No value can be derived for the diffusion coefficient along the field line, D_{zz}, with the present data. Consequently, in the present case, only a rough upper limit of $L \leq (420\text{-}2400) R_E$ is obtained for the distance to the region where low-energy protons are diffused into the tail. (Author)

A69-31990 *
ION, ELECTRON, AND NEUTRAL TEMPERATURES DERIVED FROM ION COMPOSITION DISTRIBUTION.
B. C. Narasinga Rao (NASA, Goddard Space Flight Center, Laboratory for Space Sciences, Greenbelt, Md.).
Journal of Geophysical Research, vol. 74, June 1, 1969, p. 3054-3057. 10 refs.

Demonstration of the possibility of deriving the ion, electron, and neutral temperatures from the ion composition distribution, using the appropriate expressions. It is assumed that the vertical distribution, which is mainly controlled by temperature, does not change within the horizontal distance between upleg and downleg measurements. Therefore, it is appropriate to use the average of the two scale heights derived from upleg and downleg distributions to represent the true vertical scale height. M. M.

A69-32082 *
THE INFLUENCE OF VARYING SOLAR FLUX ON IONOSPHERIC TEMPERATURES AND DENSITIES - A THEORETICAL STUDY.
J. R. Herman and S. Chandra (NASA, Goddard Space Flight Center, Laboratory for Space Sciences, Greenbelt, Md.).
Planetary and Space Science, vol. 17, May 1969, p. 815-840. 36 refs.

Solution of the electron continuity equation and the heat conduction equations for electrons, ions, and neutral species simultaneously for specified boundary conditions and values of the solar flux. These solutions have yielded a set of self-consistent steady-state profiles for a variety of midday solar conditions that are in agreement with observational data. To produce these profiles, only the boundary conditions and solar flux are used as variable parameters of the problem. It is shown that the neutral temperature and the resulting neutral gas composition play a dominant role in determining the charged-particle density and temperature profiles. This leads to a picture of the solar-cycle variation where composition changes in the neutral gas (introduced at the lower boundary) must be combined with the solar-flux variation to produce physically reasonable results. Of the five neutral gases used, (N_2, O_2, O, He, H) the atomic oxygen density variations are shown to be most effective in producing the observed trends for all the temperatures and densities in the E and F regions. (Author)

A69-32315 *
ENERGY SPECTRUM OF THE SECONDARY ELECTRONS AND THE FLUORESCENT EFFICIENCY OF ELECTRONS IN THE 3914-Å BAND.
S. P. Khare (Indian Institute of Technology, Dept. of Physics, Bombay, India; NASA, Goddard Space Flight Center, Laboratory for Theoretical Studies, Greenbelt, Md.).
Planetary and Space Science, vol. 17, June 1969, p. 1257-1268. 32 refs.

Use of the relation given by Vriens (1965) for the total ionization cross sections to obtain ionization cross section per unit energy range. For slow secondary electrons, the cross sections are in

fair agreement with the first Born cross sections. It is further shown that for the production of fast secondary electrons, Møller cross section satisfactorily approximates the Born cross section. The expressions are employed to calculate the efficiency with which the kinetic energy of an electron, absorbed in air of uniform density, is converted into photon energy in the 3914-Å band. The results are compared with available theoretical and experimental investigations. (Author)

A69-32321 *

RIOMETER MEASUREMENTS, SOLAR PROTON INTENSITIES AND RADIATION DOSE RATES.

Richard D. Juday (NASA, Manned Spacecraft Center, Space Physics Div., Houston, Tex.) and G. W. Adams (ESSA, Research Laboratories, Boulder, Colo.).

Planetary and Space Science, vol. 17, June 1969, p. 1313-1319.

In the course of the development of a solar-proton monitoring system utilizing ground-based equipment, we have found several numerical relationships which minimize the need to know the spectral forms in relating daytime polar-cap riometer measurements, particle intensities, and dose rates. We show that, to a good approximation, one can start with riometer absorption as a function of time, calculate the intensity of protons with energies greater than 11 MeV vs time, calculate hard- and soft-spectrum limits to the proton energy spectrum vs time, and finally, determine upper and lower limits to the radiation dosage for the event. (Author)

A69-32806 *

ORIGIN OF GALACTIC GAMMA-RAYS.

F. W. Stecker (NASA, Goddard Space Flight Center, Theoretical Studies Branch, Greenbelt, Md.).

Nature, vol. 222, May 31, 1969, p. 865. 10 refs.

Interpretation of the gamma-ray observations by Clark et al. (1968) as further evidence in support of an interstellar gas in the galactic disk with a mean density of 5 cm^{-3}. Production of neutral pions and bremsstrahlung in interstellar cosmic-ray collisions would then account for the observed gamma rays. P. G.

A69-34168 *

CORRECTIONS TO TWO PREVIOUS ARTICLES ON EXTRAGALACTIC GAMMA RAYS AND IMPLICATIONS OF THE CORRECTED RESULTS.

F. W. Stecker (NASA, Goddard Space Flight Center, Theoretical Studies Branch, Greenbelt, Md.).

Nature, vol. 222, June 21, 1969, p. 1157, 1158.

Correction of an error which affects two articles by Stecker (1968, 1969) on extragalactic radiation. Equation (1) of the 1968 article should contain a different factor in the denominator. This correction, applied to equation (12) of the 1969 article, affects the index α of equation (15). This index then becomes 2 for a low-density model and 1.5 for an Einstein-de Sitter model universe. F. R. L.

A69-34301 *

INTERPLANETARY GAS. XVI.

John C. Brandt, Charles Wolff (NASA, Goddard Space Flight Center, Laboratory for Space Sciences, Solar Physics Branch, Greenbelt, Md.), and Joseph P. Cassinelli (Washington, University, Dept. of Astronomy, Seattle, Wash.).

Astrophysical Journal, vol. 156, June 1969, pt. 1, p. 1117-1124. 24 refs.

Numerical calculation of a model of the quiet solar wind with magnetic field, using the momentum equations developed by Weber and Davis (1967), but with energy transport governed by the first law of thermodynamics with heat conduction. The model is close to observed densities of coronal electrons for $r \gtrsim 2\ R_\odot$. Near the earth, the model has $N_e = 6\ cm^{-3}$, $w = 315$ km/sec, $T = 325,000°K$, and a garden-hose angle of 55°; the Alfvén point is at $r = 31.4\ R_\odot$, and the angular momentum per unit mass in the solar equator is $L = 1.4 \times 10^{19}\ cm^2/sec$, a value which gives an e-folding time for solar rotational braking of 5×10^9 yr. The azimuthal velocity (w_ϕ) of the plasma near the earth is 2.5 km/sec, a value consistent with the determination for quiet times from type I comet tails. (Author)

A69-34939 *

ION DEPLETION IN THE HIGH-LATITUDE EXOSPHERE - SIMULTANEOUS OGO 2 OBSERVATIONS OF THE LIGHT ION TROUGH AND THE VLF CUTOFF.

H. A. Taylor, Jr., H. C. Brinton (NASA, Goddard Space Flight Center, Greenbelt, Md.), D. L. Carpenter (Stanford University, Radioscience Laboratory, Stanford, Calif.), F. M. Bonner (Aero Geo Astro Co., College Park, Md.), and R. L. Heyborne (Utah State University, Dept. of Electrical Engineering, Logan, Utah).

Journal of Geophysical Research, vol. 74, July 1, 1969, p. 3517-3528. 25 refs.
NSF-supported research; Contract No. NAS 5-3093; Grant No. NGR-05-020-288.

Description of the simultaneous observations of positive-ion composition, vlf earth-to-satellite transmission, and whistlers obtained from the OGO 2 satellite during October 1965 in a polar, dawn-dusk orbit. It is found that as the satellite moves poleward above about 55° invariant latitude, sudden depletions of the light ion components of the topside ionosphere are observed, wherein the concentrations of H^+ and He^+ decrease by as much as an order of magnitude within 3° Λ. The possible mechanisms for this depletion are discussed. Z. W.

A69-35006 *

PHOTODISINTEGRATION OF ULTRAHIGH-ENERGY COSMIC RAYS BY THE UNIVERSAL RADIATION FIELD.

F. W. Stecker (NASA, Goddard Space Flight Center, Theoretical Studies Branch, Greenbelt, Md.).

Physical Review, 2nd Series, vol. 180, Apr. 25, 1969, p. 1264-1266. 15 refs.

Detailed calculation of the effectiveness of the universal radiation field in disintegrating ultrahigh-energy cosmic-ray nuclei. It is concluded that this process cannot lead to a pure proton interpretation of the air-shower observations above 10^8 GeV. Photodisintegration by universal radiation is shown to be insignificant on time scales of 10^{10} yr or less for helium nuclei below 10^{10} GeV, or for iron nuclei below 10^{11} GeV total energy. Photodisintegration by dilute starlight photons in intergalactic space is considered insignificant on time scales of 10^{10} or less at all energies. B. H.

A69-35204 *

A SCHEMATIC MODEL FOR CERTAIN X-RAY SOURCES.

A. G. W. Cameron (Yeshiva University, Belfer Graduate School of Science; NASA, Goddard Space Flight Center, Goddard Institute for Space Studies, New York, N.Y.).

Astrophysical Letters, vol. 3, June 1969, p. 171-173. 7 refs.
NASA-NSF-supported research.

Description of a possible evolutionary pathway for a star near the end of its active evolution, which may create a mass reservoir. It is demonstrated that the thin-source bremsstrahlung temperatures of some X-ray sources are in the range expected for mass accretion onto a white dwarf. It is suggested that a variation of the proces which produces planetary nebulae may produce a ring of material orbiting close to the surface of a white dwarf star, and that it is mass accretion from this ring which is responsible for the X-ray emission. P. G.

A69-35415 *#

MAGNETIC STRUCTURE OF SUNSPOT GROUPS WHICH PRODUCE SOLAR PROTON FLARES.

Kunitomo Sakurai (NASA, Goddard Space Flight Center, Laboratory for Space Sciences, Greenbelt, Md.).

Journal of Geomagnetism and Geoelectricity, vol. 21, no. 1, 1969, p. 463-470. 42 refs.

Solar proton flares take place due to the release of magnetic energy accumulated within the sunspot magnetic flux tube of force lying in the chromosphere and the lower corona. The rotational motion of sunspot groups on the photospheric surface causes twisting of the magnetic lines of force. This rotational motion is counterclockwise (clockwise) in the northern (southern) hemisphere when viewed from the earth. The accumulation of magnetic energy within the flux tube due to this twisting continues to proceed until some

instability is induced along the flux tube. It is further shown that the magnetic configuration of sunspot groups is important for the triggering of a solar proton flare. (Author)

A69-36218 * #
TWO-PHOTON PROCESSES IN THE SOLAR X-RAY SPECTRUM.
T. Scott Smith (NASA, Goddard Space Flight Center, Laboratory for Space Sciences, Solar Physics Branch, Greenbelt, Md.).
(Colloque International d'Astrophysique, 15th, Liège, Belgium, June 24-26, 1968.)
Société Royale des Sciences de Liège, Mémoires, vol. 17, 1969, p. 243, 244.

Study of two-photon decay of metastable levels of hydrogenic and helium-like ions in the solar corona. It is shown that at coronal densities the metastable levels in hydrogen and helium are depopulated via proton collisional excitation to the 2p level. In lower density cases, such as planetary nebulae, the levels are apparently radiatively depopulated and are an important source of continuum emission. It is concluded that two-photon continua of elements heavier than carbon will provide an important source of solar X-ray continuum. This must be taken into account in the interpretation of line-to-continuum ratios in the region from 20 to 50 angstroms. Two-photon continua provide an additional source of radiative energy loss, thus increasing the total radiation loss of the corona by 5 to 10%. B.H.

A69-37551 *
MICROWAVE AND HARD X-RAY BURSTS FROM SOLAR FLARES.
Stephen S. Holt and Reuven Ramaty (NASA, Goddard Space Flight Center, Greenbelt, Md.).
Solar Physics, vol. 8, July 1969, p. 119-141. 34 refs.

Application of detailed theories of (1) gyrosynchrotron emission and absorption in a magnetoactive plasma, (2) X-ray production by the bremsstrahlung of nonthermal electrons on ambient hydrogen, and (3) electron relaxation in a partially ionized and magnetized gas, to the solar flare burst phenomenon. The hard X-ray and microwave bursts are shown to be consistent with a single source of nonthermal electrons, where both emissions arise from electrons with energies smaller than mass times the speed of light squared. Furthermore, the experimental X-ray and microwave data make it possible to deduce the properties of the electron distribution, the values of the ambient magnetic field, the hydrogen density, and the size of the emitting region. The proposed model, although derived mostly from observations of the July 7, 1966 flare, is shown to be representative of this type of event. (Author)

A69-37558 *
ENHANCEMENT OF IONIZING RADIATION DURING A SOLAR FLARE.
O. K. Garriott (Stanford University, Radioscience Laboratory, Stanford, Calif.; NASA, Manned Spacecraft Center, Houston, Tex.), A. V. Da Rosa, M. J. Davis (Stanford University, Radioscience Laboratory, Stanford, Calif.), L. S. Wagner, and G. D. Thome (Cornell-Sydney University Astronomy Center, Arecibo Ionospheric Observatory, Arecibo, Puerto Rico).
Solar Physics, vol. 8, July 1969, p. 226-239. 12 refs.
Grant No. NGR-05-020-001.

Measurements of electron concentrations in the ionosphere, between 100 and 250 km altitude, were used to compute the increase in solar ionizing radiation during two flares on May 21 and 23, 1967. Since the altitude of maximum absorption of the solar energy (approximately unit optical depth) depends on the wavelength of the radiation, it is possible to estimate separately the energy enhancement in different portions of the spectrum. An ionizing energy flux increase of nearly 5 erg per sq cm per sec was observed on May 21, while on the 23rd, the increase was over 7 erg per sq cm per sec. In both flares, most of the absolute increase occurred in the 20-205 Å region of the spectrum, although the relative increase was much larger at the shorter wavelengths. (Author)

A69-37574 *
PULSED X-RAY EMISSION OF NP 0532 IN MARCH 1968.
E. A. Boldt, U. D. Desai, S. S. Holt, P. J. Serlemitsos, and R. F. Silverberg (NASA, Goddard Space Flight Center, Greenbelt, Md.).
Nature, vol. 223, July 19, 1969, p. 280, 281. 5 refs.

Measurement of the pulsed X-ray emission associated with the pulsar NP 0532 in the Crab Nebula. The investigation was conducted with a six-element detector flown on an Aerobee 150 rocket from White Sands, N. M. It is estimated that the pulsed X-ray emission is about 15 per cent of the total X-ray flux from the nebula. G.R.

A69-37880 *
EXPLORER XXXI TOTAL CURRENT MONITOR EXPERIMENTS.
E. J. R. Maier (NASA, Goddard Space Flight Center, Laboratory for Space Sciences, Greenbelt, Md.).
IEEE, Proceedings, vol. 57, June 1969, p. 1068-1071.

Results of measurements of the suprathermal electron flux by means of retarding potential analyzers on Explorer 31. Samples of various types of data are presented, and some of the analysis procedures are discussed. Detailed analyses of particle flux measurements obtained in the energy range of 7 to 200 eV are presented for the data from three spacecraft transits of the polar region. The integral flux and derived differential velocity distributions yield the result that in the polar trough region there is an enhanced energy density of the suprathermal particles, with a value comparable to that of the ambient thermal plasma. At lower latitudes, the pressure of suprathermal particles is significantly less than that of the thermal plasma. (Author)

A69-38098 *
DIRECTION OF THE NEARBY GALACTIC MAGNETIC FIELD INFERRED FROM A COSMIC-RAY DIURNAL ANISOTROPY.
Kenneth H. Schatten (California, University, Space Sciences Laboratory, Berkeley, Calif.; NASA, Goddard Space Flight Center, Greenbelt, Md.) and John M. Wilcox (California, University, Space Sciences Laboratory, Berkeley, Calif.).
Journal of Geophysical Research, vol. 74, Aug. 1, 1969, p. 4157-4161. 19 refs.
NSF Grant No. GA-1319; Contract No. Nonr-3656(26); Grant No. NGR-05-003-230.

A twenty-year wave in the diurnal anisotropy component of galactic cosmic rays arriving at the earth from the asymptotic direction 128 deg E of the sun has been found by Forbush. This wave is interpreted in terms of enhanced magnetic reconnection between the nearby galactic field and the field lines in the polar regions of the heliosphere during one-half of the twenty-year solar magnetic cycle. This interpretation leads to the result that the component parallel to the solar rotation axis of the nearby galactic field is directed northward. (Author)

A69-38350 *
COMPOSITION OF COSMIC RAYS MEASURED IN GEMINI XI.
F. W. O'Dell, M. M. Shapiro, R. Silberberg, B. Stiller, C. H. Tsao (U.S. Navy, Naval Research Laboratory, Washington, D.C.), N. Durgaprasad, C. E. Fichtel, D. E. Guss, and D. V. Reames (NASA, Goddard Space Flight Center, Greenbelt, Md.).
IN: SPACE RESEARCH IX; COSPAR, PLENARY MEETING, 11TH, TOKYO, JAPAN, MAY 9-21, 1968, PROCEEDINGS. (A69-38334 21-13)
Meeting co-sponsored by the Japanese Committee on Space Research.
Edited by K. S. W. Champion, P. A. Smith, and R. L. Smith-Rose.
Amsterdam, North-Holland Publishing Co., 1969, p. 215-221.
NASA-supported research.

Use of an oriented research nuclear emulsion detector capable of time resolution in the Gemini 11 flight to investigate the primary cosmic-ray nuclei above the earth's atmosphere. This was the first satellite exposure of an emulsion apparatus designed to collect high-quality tracks of heavy nuclei under a negligible thickness of

matter (0.07 g/sq cm). Time resolution was obtained by moving a lower stack, consisting of emulsions of various sensitivities, with respect to a sensitive upper stack at the rate of 25 microns/min. It is thus possible to separate the "useful" tracks—formed during the oriented portion of the flight—from those formed at other times. It is also possible to correlate tracks with the varying geomagnetic rigidity cutoff. Data are presented on the relative abundances of individual chemical elements in the high-energy cosmic radiation above the earth's atmosphere. Problems involved in relating the data to the geomagnetic field are described. (Author)

A69-38811

COSMIC RAY STUDIES IN RELATION TO RECENT DEVELOPMENTS IN ASTRONOMY AND ASTROPHYSICS; TATA INSTITUTE OF FUNDAMENTAL RESEARCH, COLLOQUIUM, BOMBAY, INDIA, NOVEMBER 11-16, 1968, PROCEEDINGS.

Edited by R. R. Daniel (Tata Institute of Fundamental Research, Bombay, India), P. J. Lavakare, and S. Ramadurai.

Bombay, Tata Institute of Fundamental Research, 1969. 382 p. $7.00.

CONTENTS:

FOREWORD. M. G. K. Menon (Tata Institute of Fundamental Research, Bombay, India), p. I-III.

ABUNDANCES OF THE ELEMENTS. A. G. W. Cameron (Yeshiva University; NASA, Goddard Space Flight Center, New York, N.Y.), p. 1-24. 18 refs. (See A69-38812 21-29)

NUCLEOSYNTHESIS. W. A. Fowler (California Institute of Technology, Pasadena, Calif.), p. 25-44. 27 refs. (See A69-38813 21-30)

COMPOSITION OF COMSIC RAYS. S. Biswas (Tata Institute of Fundamental Research, Bombay, India), p. 45-65. 48 refs. (See A69-38814 21-29)

COMPOSITION AND ENERGY SPECTRUM OF PRE-HISTORIC COSMIC RADIATION. D. Lal (Tata Institute of Fundamental Research, Bombay, India), p. 65-72. 19 refs. (See A69-38815 21-29)

ON THE PROPAGATION OF COSMIC RAYS. Y. Pal (Tata Institute of Fundamental Research, Bombay, India), p. 73-83. 21 refs. (See A69-38816 21-29)

X-RAY AND GAMMA RAY ASTRONOMY. B. Rossi (Massachusetts Institute of Technology, Cambridge, Mass.), p. 84-104. 47 refs. (See A69-38817 21-29)

INTERPRETATIONS OF THE BACKGROUND COMPONENT OF X-RAYS AND GAMMA RAYS. S. Hayakawa (Nagoya University, Nagoya, Japan), p. 105-121. 17 refs. (See A69-38818 21-29)

INTERSTELLAR MATTER. H. C. van de Hulst (Leiden, Rijksuniversiteit, Sterrewacht, Leiden, Netherlands), p. 122-130. (See A69-38819 21-30)

CONTINUUM RADIO EMISSION AND MAGNETIC FIELDS IN THE GALAXY. J. R. Shakeshaft (Cambridge University, Cambridge, England), p. 131-141. 20 refs. (See A69-38820 21-29)

THE MICROWAVE BACKGROUND RADIATION. W. H. McCrea (Sussex, University, Brighton, England), p. 142-150. 9 refs. (See A69-38821 21-29)

COSMIC RAYS AT ENERGIES BEYOND 10^{12} EV. B. V. Sreekantan (Tata Institute of Fundamental Research, Bombay, India), p. 151-180. 50 refs. (See A69-38822 21-29)

COSMIC RAY ELECTRONS. R. R. Daniel (Tata Institute of Fundamental Research, Bombay, India), p. 181-201. 36 refs. (See A69-38823 21-29)

THE DYNAMICAL BEHAVIOR OF THE GASEOUS DISK OF THE GALAXY. E. N. Parker (Chicago, University, Chicago, Ill.), p. 202-216. 57 refs. (See A69-38824 21-30)

QUASARS—INTERPRETATIVE. W. H. McCrea (Sussex, University, Brighton, England), p. 218-230. 9 refs. (See A69-38825 21-30)

OBSERVATIONS OF PULSARS. J. R. Shakeshaft (Cambridge University, Cambridge, England), p. 231-244. 39 refs. (See A69-38826 21-30)

SOLAR NEUTRINOS. W. A. Fowler (California Institute of Technology, Pasadena, Calif.), p. 245-258. 28 refs. (See A69-38827 21-29)

RADIO SOURCE COUNTS. J. R. Shakeshaft (Cambridge University, Cambridge, England), p. 259-263. 10 refs. (See A69-38828 21-30)

A69-38812 * #

ABUNDANCES OF THE ELEMENTS.

A. G. W. Cameron (Yeshiva University, Belfer Graduate School of Science; NASA, Goddard Space Flight Center, Goddard Institute for Space Studies, New York, N.Y.).

IN: COSMIC RAY STUDIES IN RELATION TO RECENT DEVELOPMENTS IN ASTRONOMY AND ASTROPHYSICS; TATA INSTITUTE OF FUNDAMENTAL RESEARCH, COLLOQUIUM, BOMBAY, INDIA, NOVEMBER 11-16, 1968, PROCEEDINGS. (A69-38811 21-29)

Edited by R. R. Daniel, P. J. Lavakare, and S. Ramadurai.

Bombay, Tata Institute of Fundamental Research, 1969, p. 1-23; Discussion, p. 23, 24. 18 refs.

Review of some of the history of the development of abundance compilations of the elements made by Suess and Urey (1956) and by Cameron (1957, 1959, 1963). On the basis of Suess and Urey's findings, it was possible to determine that a number of different nuclear processes had been responsible for cooking the elements. Cameron's 1963 abundance table was based primarily upon meteoritic abundance measurements. The basic character of carbonaceous chondrites is reviewed. The problem of the abundance which should be chosen for iron is discussed, as well as some of the abundance anomalies which are observed in stars. It is considered that results of work by Brancazio and Cameron (1967) may have some significance for some cosmic ray studies, particularly with reference to the acceleration of solar cosmic rays. F.R.L.

A69-39506 *

X RAYS FROM THE SUN.

W. M. Neupert (NASA, Goddard Space Flight Center, Laboratory for Space Sciences, Solar Physics Branch, Greenbelt, Md.).

IN: ANNUAL REVIEW OF ASTRONOMY AND ASTROPHYSICS. VOLUME 7. (A69-39501 21-30)

Edited by Leo Goldberg, David Layzer, and J. G. Phillips.

Palo Alto, Calif., Annual Reviews, Inc., 1969, p. 121-148. 145 refs.

Brief description of the techniques of observation of the solar X-ray spectrum, emphasizing those aspects which influence the interpretation of data. Recent results, particularly on the X-ray emission associated with flares, are considered. The advantages and disadvantages of crystal and grating spectrometers for wavelengths below 100 Å are summarized. Estimates of coronal electron temperature and emission measure associated with solar active regions are tabulated. It is noted that current observations attest to the basic correctness of de Jager's classification of X-ray emission into nonthermal and quasi-thermal components. M.M.

A69-40090 *

THE CHEMICAL COMPOSITION OF GALACTIC AND SOLAR COSMIC RAYS.

Frank B. McDonald (NASA, Goddard Space Flight Center, Greenbelt, Md.).

IN: EXTRA-TERRESTRIAL MATTER; CENTRAL STATES UNIVERSITIES AND ARGONNE NATIONAL LABORATORY, CONFERENCE, ARGONNE, ILL., MARCH 7, 8, 1968, PROCEEDINGS. (A69-40083 22-30)

Conference co-sponsored by the U.S. Atomic Energy Commission and the Associated Midwest Universities.

Edited by C. A. Randall, Jr.

De Kalb, Ill., Northern Illinois University Press, 1969, p. 179-199; Discussion, p. 199-201.

Recent developments in balloonborne and spaceborne detectors, Cerenkov counters, emulsions, laboratory fossil track studies, and

measurements of fragmentation parameters, have yielded new data on stripped cosmic ray nuclei with atomic numbers from 1 to 92. Relative nuclear abundances seem to differ significantly from the universal cosmic abundances. It is now possible to separate solar cosmic rays from galactic cosmic rays. There appears to be no unique accelerating mechanism, but instead several mechanisms seem to make significant contributions. Although the details are not yet understood, these mechanisms must account for a total cosmic ray energy of 10^{56} ergs and a supply rate of some 10^{42} ergs per sec. (Author)

A69-40300 *
TYPE III RADIO BURSTS IN THE OUTER CORONA.
J. K. Alexander, H. H. Malitson, and R. G. Stone (NASA, Goddard Space Flight Center, Greenbelt, Md.).
Solar Physics, vol. 8, Aug. 1969, p. 388-397. 23 refs.

Type III solar radio bursts observed from 3.0 to 0.45 MHz with the ATS 2 satellite over the period April-October 1967 have been analyzed to derive two alternative models of active region streamers in the outer solar corona. Assuming that the bursts correspond to radiation near the electron plasma frequency, "pressure equilibrium" arguments lead to streamer model one in which the streamer electron temperature derived from collision damping time falls off much more rapidly than in the "average" corona and the electron density is as much as 25 times the average coronal density at heights of 10 to 50 solar radii. In model two, the streamer electron temperature is assumed to equal the average coronal temperature, giving a density enhancement which decreases from a factor of 10 close to the sun to less than a factor of two at large distances. When the burst frequency drift is interpreted as resulting from the outward motion of a disturbance that stimulates the radio emission, model one gives a constant velocity of about 0.35c for the exciting disturbance as it moves to large distances, while with model two there is a decrease in the velocity to less than 0.2c beyond 10 solar radii. (Author)

A69-40305 *
HELIUM ABUNDANCE IN THE SOLAR WIND.
K. W. Ogilvie (NASA, Goddard Space Flight Center, Laboratory for Space Sciences, Greenbelt, Md.) and T. D. Wilkerson (Maryland, University, Institute for Fluid Dynamics and Applied Mathematics, College Park, Md.).
Solar Physics, vol. 8, Aug. 1969, p. 435-449. 25 refs.
Grant No. NsG-283.

Results of observations of hydrogen and helium ions in the solar wind, carried out on board Explorer 34. These ions are completely separated by means of electrostatic and magnetic fields. The average value of the ratio of number densities is 0.051 plus or minus .02, derived from over 3000 hr of measurement. Variations about this value from about 0.01 up to greater than 0.15 occur, and there are more high values than can be explained by random variation. A tentative association with some geomagnetic storms is suggested. The above value of abundance, assuming that plasma emitted in the ecliptic plane is a fair sample of the output of the sun, combined with other recent work by other methods, indicates that the solar abundance may be about half the previously quoted estimate of approximately 0.1. (Author)

A69-40504 *
CORRELATION OF SOLAR MICROWAVE AND SOFT X-RAY RADIATION. I—THE SOLAR CYCLE AND SLOWLY VARYING COMPONENTS.
Charles D. Wende (Iowa, University, Dept. of Physics and Astronomy, Iowa City, Iowa; NASA, Goddard Space Flight Center, National Space Science Data Center, Greenbelt, Md.).
Journal of Geophysical Research, vol. 74, Sept. 1, 1969, p. 4649-4660. 16 refs.
Contracts No. JPL-951563; No. NAS 5-9076; No. Nonr-1509(06); Grant No. NsG-233-62.

The integral solar X-ray flux between 2 and 12 Å was measured by the spacecraft Injun 1, Injun 3, Explorer 33, and Explorer 35. The integral flux between 2 and 9 Å was observed by the Mariner 5 spacecraft. The data from Injuns 1 and 3 and Explorers 33 and 35, when averaged in monthly intervals, show a long-term variation in activity of at least a factor of 5 between 1961 and 1969. A slowly varying component that tracks the 10-cm radio flux is observed in the X-ray flux. This X-ray flux variation, about a factor of 10, correlates with the appearance of major active regions on the solar disk. This slowly varying component correlates well with radio fluxes at frequencies greater than about 1 GHz and less well with radio fluxes at lower frequencies. The X-ray spectrum, obtained by comparing the 2 and 9 Å flux with the 2 and 12 Å flux, hardens during periods of high solar activity and may harden during flares, but it does not soften. (Author)

A69-40577 *
ON THE NATURE OF THE HIGH-FREQUENCY CUTOFFS OF TYPE IV SOLAR RADIO BURSTS.
R. Ramaty (NASA, Goddard Space Flight Center, Greenbelt, Md.).
Astrophysical Letters, vol. 4, Aug. 1969, p. 43-45. 14 refs.

Investigation of the high-frequency cutoff of synchrotron radiation resulting from electrons with an anisotropic pitch-angle distribution. It is shown that this effect could be responsible for the high-frequency cutoffs of type IV bursts at decimeter, meter, and decameter wavelengths. (Author)

A69-40641 *
THE COSMIC GAMMA-RAY SPECTRUM FROM SECONDARY-PARTICLE PRODUCTION IN THE METAGALAXY.
F. W. Stecker (NASA, Goddard Space Flight Center, Greenbelt, Md.).
Astrophysical Journal, vol. 157, Aug. 1969, pt. 1, p. 507-514. 22 refs.

Discussion of the form and intensity of the spectrum of cosmic gamma rays resulting from the production and decay of neutral pions produced in metagalactic cosmic-ray p-p collisions. It is assumed that intergalactic space contains ionized hydrogen gas at a density of .0001 per cu cm, as is consistent with recent X-ray observations at 0.25 keV. The Friedmann solution to the Einstein field equations of general relativity is used as a description of our expanding Universe, and a discussion is presented of the effects of redshift and spatial curvature on the generation and distortion of the local gamma-ray spectrum from the decay of neutral pions. Numerical calculations are presented for the Einstein-de Sitter solution, which is found to be an adequate model for these calculations. Two models are presented to represent the possible flux of metagalactic cosmic rays. In calculating metagalactic gamma-ray spectra, the effect of gamma-ray absorption at large redshifts is taken into account. A discussion of the results is given. The results indicate that future gamma-ray experiments in the region of 1-100 MeV may yield valuable information relating to cosmology, cosmogony, and the metagalactic cosmic-ray flux. (Author)

A69-40643 *
COSMIC X-RAY BREMSSTRAHLUNG ASSOCIATED WITH SUPRATHERMAL PROTONS.
Elihu Boldt and Peter Serlemitsos (NASA, Goddard Space Flight Center, Greenbelt, Md.).
Astrophysical Journal, vol. 157, Aug. 1969, pt. 1, p. 557-562. 23 refs.

Demonstration that copious X-ray production attends the collisions of suprathermal protons with ambient electrons. Such suprathermal protons have been detected in association with solar-flare events and cosmic rays. The X-ray emission to be expected for the well-observed solar-proton event of Sept. 28, 1961, agrees with measurements. It is demonstrated that suprathermal cosmic-ray protons propagating through the interstellar gas could be responsible

for a detectable component of the diffuse sky background of X rays. The possible role of suprathermal protons in producing the X rays emitted by the Crab Nebula is examined and found to be inconclusive. F.R.L.

A69-42667 *
OBSERVATIONS OF COSMIC-RAY ELECTRONS BETWEEN 2.7 AND 21.5 MEV.
G. M. Simnett and F. B. McDonald (NASA, Goddard Space Flight Center, Greenbelt, Md.).
Astrophysical Journal, vol. 157, Sept. 1969, pt. 1, p. 1435-1447. 17 refs.

Results of IMP 4 satellite measurements of the intensity of electrons with energies of 2.7 to 21.5 MeV in interplanetary space during the period from July 3 through Aug. 27, 1967. The measured electron intensity is believed to be uncontaminated by solar electrons. The analysis procedure for background subtraction and the subsequent derivation of the electron spectrum are described in detail. The results of electron-accelerator calibrations are used extensively. The origin of the electrons is discussed, and the results are compared with the predicted intensity of knock-on electrons from proton-electron collisions in interstellar space. The measured electron spectrum is shown to be compatible with a sole origin in the galactic knock-on component if solar modulation of low-energy electrons is insignificant. (Author)

A69-43003 *
A THEORY OF THERMOSPHERE DYNAMICS. I—DIURNAL AND SOLAR CYCLE VARIATIONS.
H. Volland (NASA, Goddard Space Flight Center, Greenbelt, Md.).
Planetary and Space Science, vol. 17, Sept. 1969, p. 1581-1597. 20 refs.

It is shown that the diurnal density and temperature variation within the thermosphere is generated not only by solar EUV heat input but also by a tidal wave from the lower atmosphere which penetrates into the thermosphere and predominates the diurnal variations below an altitude of 250 km. Assuming a tidal wave from below which is not dependent on solar activity and assuming solar EUV heat input to be proportional to the solar activity, the observed diurnal density variation and its dependence on solar activity can be explained and reproduced quantitatively with help of a two-dimensional model between 100 and 400 km. The calculated density agrees with the Jacchia model above 300 km and with observations made by Priester, May, King-Hele, Taeusch, and Marov below 250 km. (Author)

A69-43169 *
SOLAR MODULATION OF GALACTIC COSMIC RAYS. I.
L. A. Fisk (California, University, Institute for Pure and Applied Physical Sciences, Dept. of Applied Physics and Information Science, La Jolla, Calif.; NASA, Goddard Space Flight Center, Laboratory for Space Science, Greenbelt, Md.) and W. I. Axford (California, University, Dept. of Physics and Institute for Pure and Applied Physical Sciences, Dept. of Applied Physics and Information Science, La Jolla, Calif.).
Journal of Geophysical Research, vol. 74, Oct. 1, 1969, p. 4973-4986. 21 refs.
Contract No. DA-31-124-ARO(D)-257; Grant No. NGR-05-009-081.

Approximation of the equations governing cosmic-ray modulation (allowing for convection, diffusion, and energy changes) by means of simpler, more manageable equations describing the particle behavior in a limited energy range. The equations governing the behavior of cosmic rays according to the model assumed are presented, together with the sets of approximate equations valid at high and low energies. Some exact analytic solutions are obtained and are used to discuss the accuracy of the approximate equations. The possible uses of these approximate equations in treating the modulation problem are described. Z.W.

A69-43603
SOLAR FLARES AND SPACE RESEARCH; COSPAR, PLENARY MEETING, 11TH, SYMPOSIUM, TOKYO, JAPAN, MAY 9-11, 1968, PROCEEDINGS.
Symposium co-sponsored by the International Astronomical Union, the International Union of Geodesy and Geophysics, and the International Scientific Radio Union.
Edited by C. de Jager (Astronomical Institute, Utrecht, Netherlands) and Z. Švestka (Československá Akademie Věd, Astronomický Ústav, Ondřejov, Czechoslovakia).
Amsterdam, North-Holland Publishing Co., 1969. 421 p.
$20.

CONTENTS:

PREFACE. C. de Jager (Astronomical Institute, Utrecht, Netherlands) and Z. Švestka (Československá Akademie Věd, Ondřejov, Czechoslovakia), p. v.

INTRODUCTION—THE OPTICAL FLARE.

SOLAR FLARES—PROPERTIES AND PROBLEMS. C. de Jager (Astronomical Institute, Utrecht, Netherlands), p. 1-15. 34 refs. (See A69-43604 24-29)

THE OPTICAL FLARE. Z. Švestka (Československá Akademie Věd, Ondřejov, Czechoslovakia), p. 16-37. 31 refs. (See A69-43605 24-29)

SOLAR FLARES AND MAGNETIC FIELDS. A. B. Severnyi (Akademiia Nauk SSSR, Krymskaia Astrofizicheskaia Observatoriia, Partizanskoye, Ukrainian SSR), p. 38-60. 23 refs. (See A69-43606 24-29)

FLARE ASSOCIATED OPTICAL PHENOMENA. A. Bruzek (Fraunhofer Institut, Freiburg im Breisgau, West Germany), p. 61-77.

69 refs. (See A69-43607 24-29)

EUV, X- AND GAMMA-RAY OBSERVATION.

SOLAR EUV ENHANCEMENTS ASSOCIATED WITH FLARES. L. A. Hall and H. E. Hinteregger (USAF, Cambridge Research Laboratories, Bedford, Mass.), p. 81-86. (For abstract see issue 15, page 2842, Accession no. A68-32005)

X-RAY OBSERVATIONS OF SOLAR FLARES (Invited Review Paper). H. Friedman (U.S. Navy, Naval Research Laboratory, Washington, D.C.), p. 87-94. 14 refs. (See A69-43608 24-29)

OBSERVATIONS OF THE SOLAR FLARE SOFT X-RAY SPECTRUM AND COMPARISON WITH CENTIMETRIC RADIO BURSTS. W. M. Neupert, M. Swartz, W. A. White, and R. M. Young (NASA, Goddard Space Flight Center, Greenbelt, Md.), p. 95-101. 5 refs. (See A69-43609 24-29)

ENHANCEMENT OF THE SOLAR X-RAY SPECTRUM BELOW 25 Å DURING SOLAR FLARES. A. B. C. Walker, Jr. and H. R. Rugge (Aerospace Corp., El Segundo, Calif.), p. 102-112. (For abstract see issue 15, page 2841, Accession no. A68-31963)

THE TIME STRUCTURE OF SOLAR X-RAY BURSTS ABOVE 7.7 KEV. H. S. Hudson, L. E. Peterson, and D. A. Schwartz (California, University, La Jolla, Calif.), p. 113-120. 10 refs. (See A69-43610 24-29)

MEASUREMENTS OF SOLAR X-RAY EMISSION FROM THE OGO-IV SPACECRAFT. R. W. Kreplin, D. M. Horan, T. A. Chubb, and H. Friedman (U.S. Navy, Naval Research Laboratory, Washington, D.C.), p. 121-130. 6 refs. (See A69-43611 24-29)

OBSERVATIONS OF SOLAR X-RAY ACTIVITY WITH A PROPORTIONAL COUNTER SPECTROMETER ON OSO-IV. J. L. Culhane, P. W. Sanford, M. L. Shaw (London, University, University College, London, England), K. A. Pounds, and D. G. Smith (Leicester, University, Leicester, England), p. 131-133.

SUDDEN INCREASE IN HIGH ENERGY GAMMA-RAY INTENSITY OBSERVED AT BALLOON ALTITUDE. I. Kondo and F. Nagase (Nagoya University, Nagoya, Japan), p. 134-143. 8 refs. (See A69-43612 24-29)

INTERPRETATION OF TIME CHARACTERISTICS OF SOLAR X-RAY BURSTS. T. Takakura (Tokyo, University, Tokyo, Japan), p. 144-150. 10 refs. (See A69-43613 24-29)

THEORY OF HARD X-RAY BURSTS. R. Snijders (Utrecht,

Rijksuniversiteit, Utrecht, Netherlands), p. 151-154.

SOLAR COSMIC-RAY FLARES DEDUCED FROM THE DEVELOPING PATTERNS OF SID'S. K. Sakurai (Kyoto University, Kyoto, Japan), p. 155-162. (For abstract see issue 15, page 2842, Accession no. A68-31971)

FLARE ASSOCIATED RADIO AND PARTICLE EVENTS.

FLARE-ASSOCIATED RADIO BURSTS. T. Takakura (Tokyo, University, Tokyo, Japan), p. 165-180. 29 refs. (See A69-43614 24-29)

AN INVESTIGATION OF SOLAR X-RAY AND RADIO EMISSIONS AND THEIR RELATIONSHIP TO IONOSPHERIC PHENOMENA. A. Krüger, J. Taubenheim, and G. Entzian (Deutsche Akademie der Wissenschaften, Berlin, East Germany), p. 181-193. 6 refs. (See A69-43615 24-29)

SPECTRAL CONSIDERATIONS OF MICROWAVE SOLAR BURSTS. J. P. Castelli, J. Aarons (USAF, Cambridge Research Laboratories, Bedford, Mass.), G. A. Michael (USAF, Ent AFB, Colo.), C. Jones (Boston University, Boston, Mass.), and H. C. Ko (Ohio State University, Columbus, Ohio), p. 194-201. 13 refs. (See A69-43616 24-29)

HIGH ENERGY PARTICLE EVENTS ASSOCIATED WITH SOLAR FLARES. K. G. McCracken (Adelaide, University, Adelaide, Australia), p. 202-214. 6 refs. (See A69-43617 24-29)

POLAR CAP ABSORPTION AND GROUND LEVEL EFFECTS (Invited Review Paper). B. Hultqvist (Kungl. Vetenskapsakademien, Kiruna, Sweden), p. 215-257. 177 refs. (See A69-43618 24-29)

OBSERVATIONS OF SOLAR PROTONS ABOARD OV3-3 AND ATS-1. J. B. Blake, G. A. Paulikas, and S. C. Freden (Aerospace Corp., El Segundo, Calif.), p. 258-266. (For abstract see issue 15, page 2840, Accession no. A68-31922)

MEASUREMENT OF COSMIC RAY ANISOTROPY OF SOLAR ORIGIN BY EXPLORER 34 SATELLITE. U. R. Rao (Physical Research Laboratory, Ahmedabad, India), F. R. Allum, W. C. Bartley, R. A. R. Palmeira (Southwest Center for Advanced Studies, Dallas, Tex.), J. A. Harries, and K. G. McCracken (Adelaide, University, Adelaide, Australia), p. 267-276. 5 refs. (See A69-43619 24-29)

THE CHARGE COMPOSITION OF SOLAR COSMIC RAYS AND SOLAR ABUNDANCES. D. V. Reames and C. E. Fichtel (NASA, Goddard Space Flight Center, Greenbelt, Md.), p. 277, 278.

THE 28 JANUARY 1967 SOLAR COSMIC RAY EVENT AND RELATED COMPLICATIONS. A. J. Masley (McDonnell Douglas Corp., Santa Monica, Calif.), p. 279-283. (For abstract see issue 15, page 2840, Accession no. A68-31926)

THE 23 AND 28 MAY 1967 SOLAR COSMIC RAY EVENTS. A. D. Goedeke and A. J. Masley (McDonnell Douglas Corp., Santa Monica, Calif.), p. 284-293. (For abstract see issue 15, page 2840, Accession no. A68-31924)

SOLAR WIND DISTURBANCES ASSOCIATED WITH FLARES (Invited Review Paper). J. M. Wilcox (California, University, Berkeley, Calif.), p. 294-309. 16 refs. (See A69-43620 24-29)

POLAR CAP IONOSPHERIC RESPONSE TO SOLAR COSMIC RAY EVENTS OBSERVED BY MARINERS 2 AND 4. H. L. Stolov (New York, City University; NASA, Goddard Space Flight Center, New York, N.Y.), p. 310-318. 11 refs. (See A69-43621 24-29)

EFFECTS ASSOCIATED WITH THE SECTOR BOUNDARY CROSSING ON 8 JULY 1966. Z. Švestka (Československá Akademie Věd, Ondřejov, Czechoslovakia), p. 319-326. (For abstract see issue 15, page 2842, Accession no. A68-31967)

A LARGE SCALE PATTERN IN THE SOLAR MAGNETIC FIELD. J. M. Wilcox (California, University, Berkeley, Calif.) and R. Howard (Carnegie Institution of Washington and California Institute of Technology, Pasadena, Calif.), p. 327, 328.

THEORIES AND LABORATORY EXPERIMENTS ON SOLAR FLARES.

THEORETICAL ASPECTS OF THE FLARE PHENOMENON (Invited Review Paper). H. U. Schmidt (Max-Planck-Institut für Physik und Astrophysik, Munich, West Germany), p. 331-345. 33 refs. (See A69-43622 24-29)

ON THE MECHANISM OF SOLAR FLARES. S. I. Syrovatskii (Akademiia Nauk SSSR, Fizicheskii Institut, Moscow, USSR), p. 346-355.

A POSSIBLE MECHANISM FOR SOLAR FLARES. H. Elliot (London, University, Imperial College of Science and Technology, London, England), p. 356-362. 10 refs. (See A69-43623 24-29)

THE NATURE OF SOLAR FLARES. D. H. Menzel (Smithsonian Institution and Harvard University, Cambridge, Mass.), p. 363-367. (For abstract see issue 15, page 2841, Accession no. A68-31927)

FAST CHANGES OF SUNSPOT EQUILIBRIUM CONDITIONS AND SOLAR FLARES. Y. D. Žugžda (Akademiia Nauk SSSR, Institut Zemnogo Magnetizma, Ionosfery i Rasprostraneniia Radiovoln, Akademgorodok, USSR), p. 368-373. 5 refs. (See A69-43624 24-29)

LABORATORY EXPERIMENTS ON SOLAR FLARE MODEL BY LASER. C. Yamanaka, T. Yamanaka, Y. Izawa, T. Sasaki, N. Tsuchimori, and M. Onishi (Osaka University, Osaka, Japan), p. 374-383. (For abstract see issue 15, page 2792, Accession no. A68-31965)

FORECASTING OF SOLAR ACTIVITY.

ON LONG-TERM FORECASTS OF SOLAR ACTIVITY. V. Bumba and R. Howard (Československá Akademie Věd, Ondřejov, Czechoslovakia), p. 387-396. 30 refs. (See A69-43625 24-29)

ON FORECASTS OF INTERPLANETARY AND GEOPHYSICAL CONDITIONS. R. Howard and V. Bumba (Československá Akademie Věd, Ondřejov, Czechoslovakia), p. 397-404. 6 refs. (See A69-43626 24-30)

FLARE FORECASTING. P. Simon, M. J. Martres, and J.-P. Legrand (Meudon, Observatoire, Meudon, Hauts-de-Seine, France), p. 405-411. (For abstract see issue 15, page 2842, Accession no. A68-31975)

SUMMARY OF SYMPOSIUM. E. N. Parker (Chicago, University, Chicago, Ill.), p. 412-418.

AUTHOR INDEX, p. 419.

A69-43609 *

OBSERVATIONS OF THE SOLAR FLARE SOFT X-RAY SPECTRUM AND COMPARISON WITH CENTIMETRIC RADIO BURSTS.

W. M. Neupert, M. Swartz, W. A. White, and R. M. Young (NASA, Goddard Space Flight Center, Greenbelt, Md.).

IN: SOLAR FLARES AND SPACE RESEARCH; COSPAR, PLENARY MEETING, 11TH, SYMPOSIUM, TOKYO, JAPAN, MAY 9-11, 1968, PROCEEDINGS. (A69-43603 24-29)

Symposium co-sponsored by the International Astronomical Union, the International Union of Geodesy and Geophysics, and the International Scientific Radio Union.

Edited by C. de Jager and Z. Švestka.

Amsterdam, North-Holland Publishing Co., 1969, p. 95-101. 5 refs.

Solar X-ray and EUV emission spectra between 1 and 400 Å have been obtained over a period of greater than ten months by the OSO 3 satellite. Data were taken by two uncollimated single crystal spectrometers (1-3 Å and 6-25 Å), a grazing incidence grating spectrometer (20-400 Å), and an ion chamber integrating the solar flux between 2 and 8 Å mounted in the pointed section of the satellite. Comparison of 1-3 Å crystal spectrometer data with ion chamber data during a 3B flare indicates that the ion chamber current corresponds most closely to the continuum flux near 3 Å. Maximum soft X-ray emission occurs after peak impulsive microwave emission suggesting a build-up of hot X-ray emitting plasma in the initial stage of the flare event. (Author)

A69-43621 *

POLAR CAP IONOSPHERIC RESPONSE TO SOLAR COSMIC RAY EVENTS OBSERVED BY MARINERS 2 AND 4.

Harold L. Stolov (New York, City University, City College; NASA, Goddard Space Flight Center, Goddard Institute for Space Studies, New York, N.Y.).

IN: SOLAR FLARES AND SPACE RESEARCH; COSPAR, PLENARY MEETING, 11TH, SYMPOSIUM, TOKYO, JAPAN, MAY

9-11, 1968, PROCEEDINGS. (A69-43603 24-29)
Symposium co-sponsored by the International Astronomical Union, the International Union of Geodesy and Geophysics, and the International Scientific Radio Union.
Edited by C. de Jager and Z. Švestka.
Amsterdam, North-Holland Publishing Co., 1969, p. 310-318. 11 refs.

Examination of the f_{min} observations from all available high-latitude ionosonde stations in the Northern and Southern Hemispheres in conjunction with the solar proton measurements taken by Mariners 2 and 4 during the October 1962 and February 1965 events, respectively. The time profiles of polar cap absorption indicate that the asymmetrical magnetosphere model of Reid and Sauer (1967) is not tenable during these periods. The presence of high energy protons (greater than 10 MeV) in ionospherically detectable intensities early in the events makes it impossible to distinguish between the Dessler (1964) and Dungey (1961, 1963) models. (Author)

N69-24924*# Techtran Corp., Glen Burnie, Md.
SOME PROBLEMS OF THE PHYSICS OF HIGH ENERGIES AND COSMIC RAYS
S. A. Azimov, ed. Washington NASA Apr. 1969 136 p refs Transl. into ENGLISH of the book "Nekotoryye Voprosy Fiziki Vysokikh Energiy i Kosmicheskikh Luchey" Tashkent, Fan, 1967
(Contract NASw-1695)
(NASA-TT-F-535) Avail: CFSTI CSCL 04A

The diffraction dissociation of protons on complex nuclei of a photoemulsion at an energy of 24 BeV, as well as a detailed analysis of the coherent interactions of π-mesons with an energy of 17 BeV are presented. An analysis of the experimental data is made by means of original methods which are based on the utilization of mathematical statistics and relativistic kinematics. Inelastic proton–nucleon collisions are examined for a wide range of energies. Author

N69-28111*# National Aeronautics and Space Administration. Goddard Space Flight Center, Greenbelt, Md.
INFRARED SPECTRAL IRRADIANCE MEASUREMENTS IN A SPACE ENVIRONMENT SIMULATOR
John F. Rogers Washington Jun. 1969 30 p refs
(NASA-TN-D-5166) Avail: CFSTI CSCL 04A

An experimental program for measuring the infrared spectral irradiance from 2.9 to 29.3μ in the space environment simulator was completed. During the series of measurements, the chamber was operated at full environmental conditions: solar simulation, liquid nitrogen conditioned walls, and a vacuum of 10^{-7} torr. Measurements were made with and without a spacecraft model in the chamber. Data are presented for the spectral irradiance and total irradiance as a function of instrument aspect angle, position in the chamber, solar simulator power variations, and spacecraft aspect angle. Results of the experiment indicate a collimated and a diffuse component of the radiation in the spectral range measured. Author

N69-29652*# National Aeronautics and Space Administration. Goddard Space Flight Center, Greenbelt, Md.
LECTURES IN HIGH ENERGY ASTROPHYSICS
H. Oegelman, ed. and J. R. Wayland, Jr., ed. (Md. Univ., College Park) Washington 1969 170 p refs
(NASA-SP-199) Avail: CFSTI CSCL 04A

CONTENTS:

1. CURRENT PROBLEMS OF HIGH-ENERGY ASTROPHYSICS H. Oegelman p 1–21 refs (See N69-29653 16-29)

2. ORIGIN, COMPOSITION, AND PROPAGATION OF THE NUCLEAR COMPONENT OF COSMIC RAYS C. Fichtel p 23–34 refs (See N69-29654 16-29)

3. COSMIC-RAY ELECTRONS AND RELATED ASTROPHYSICAL PROBLEMS R. Ramaty p 35–48 refs (See N69-29655 16-29)

4. COSMIC RAY PHOTONS E. Boldt p 49–83 refs (See N69-29656 16-29)

5. PLASMA ASPECTS OF COSMIC RAYS D. Wentzel (Md. Univ., College Park) p 85–91 refs (See N69-29657 16-29)

6. RELATIVISTIC STOCHASTIC PROCESSES J. R. Wayland (Md. Univ., College Park) p 93–109 refs (See N69-29658 16-29)

7. PROPAGATION OF SOLAR COSMIC RAYS IN THE INTERPLANETARY MAGNETIC FIELD E. C. Roelof p 111–135 refs (See N69-29659 16-29)

8. INTERPLANETARY DUST L. W. Bandermann (Hawaii Univ.) p 137–165 refs (See N69-29660 16-29)

N69-33401*# Aztec School of Languages, Inc., Maynard, Mass. Research Translation Div.
SOLAR ACTIVITY, NO. 3 Collection of Articles
E. R. Mustel, ed. et al Washington NASA Jul. 1969 193 p refs Transl. into ENGLISH of the publ. "Solnechnaya Aktivnost. Sbornik Statey. No. 3" Moscow, Nauka Press, 1968 p 5–147
(Contract NASw-1692)
(NASA-TT-F-581) Avail: CFSTI CSCL 04A

CONTENTS:

1. FORCELESS STRUCTURE OF MAGNETIC FIELDS IN THE ATMOSPHERE OF ACTIVE SOLAR REGIONS AND PROBLEMS OF THE GENERATION OF GEOEFFECTIVE CORPUSCULAR STREAMS E. I. Mogilevskiy p 1–38 refs (See N69-33402 19-29)

2. SIMULTANEOUS MEASUREMENT OF MAGNETIC FIELDS AT TWO LEVELS IN THE SOLAR ATMOSPHERE I. A. Zhulin et al p 39–50 refs (See N69-33403 19-29)

3. MEASUREMENT OF MAGNETIC FIELDS IN PROMINENCES AND THE STRUCTURE OF THE MAGNETIC FIELD IN THE REGION OF CHROMOSPHERIC FILAMENTS B. A. Ioshpa p 51–76 refs (See N69-33404 19-29)

4. MAGNETIC-FIELD RADIATION-SCATTERING MATRIX DERIVED WITH ALLOWANCE FOR THE PHASE COUPLINGS OF THE UPPER-LEVEL WAVE FUNCTION V. N. Obridko p 77–85 refs (See N69-33405 19-29)

5. APPLICABILITY OF THE EXISTING THEORIES OF THE FORMATION OF SPECTRAL LINES IN A MAGNETIC FIELD FOR QUANTITATIVE INTERPRETATION OF SOLAR MAGNETOGRAPH READINGS V. N. Obridko p 86–94 refs (See N69-33406 19-29)

6. FACULA STRUCTURE M. A. Livshits p 95–106 refs (See N69-33407 19-29)

7. THE AREA VARIATION CURVE AND THE LIFETIME OF CHROMOSPHERIC FLARES S. O. Obashev p 107–117 refs (See N69-33408 19-29)

8. TOTAL ENERGY OF CHROMOSPHERIC FLARES S. O. Obashev p 118–121 refs (See N69-33409 19-29)

9. ENERGY CLASSIFICATION OF CHROMOSPHERIC FLARES C. O. Obashev p 122–124 refs (See N69-33410 19-29)

10. CONTOURS OF THE Mg I b_1–b_4 AND Sr II 4216 AND 4078 Å LINES IN THE CHROMOSPHERE N. S. Shilova p 125–129 refs (See N69-33411 19-29)

11. HELIUM IONIZATION AND THE EXCITATION OF ORTHOHELIUM IN THE SOLAR ATMOSPHERE R. A. Gulyayev p 130–146 refs (See N69-33412 19-29)

12. SHAPE OF THE CONTOURS OF THE Hα LINE IN PROMINENCES M. Yu. Zel'dina p 147–156 refs (See N69-33413 19-29)

13. SPECTRAL PHOTOMETRY OF THE CHROMOSPHERIC FLARE OF JULY 12, 1961 P. N. Polupan p 157–172 refs (See N69-33414 19-29)

14. THE SYNCHRONISM OF ACTIVE FLUCTUATIONS OF THE OLD AND NEW CYCLES IN THE INTERMEDIATE EPOCH V. S. Chistyakov p 173–182 refs (See N69-33415 19-29)

30

SPACE SCIENCES

Includes astronomy and astrophysics; cosmology; lunar and planetary flight and exploration; and theoretical analysis of orbits and trajectories. For related information see also: 11 Facilities, Research and Support; and 31 Space Vehicles.

A69-10498 *#
CONTRIBUTIONS AND RESULTS OF SPACE SCIENCE PROGRAMS.
Homer E. Newell (NASA, Washington, D.C.).
United Nations, Conference on the Exploration and Peaceful Uses of Outer Space, Vienna, Austria, Aug. 14-27, 1968, Paper. 13 p.

Discussion of the rapid and remarkable advances in science and related fields which have come about through space research. Major examples presented outline the advances in electricity and electronics, the air transportation industry, and nuclear power. The advantages of space sciences and their unique contributions are noted. Atmospheric sciences, communications, planetary sciences, and astronomy are selected as some of the areas which have gained from space research. Future benefits which may be derived for mankind are considered. I.P.

A69-11228 *
MEASUREMENTS OF THE PERTURBED-INTERPLANETARY MAGNETIC FIELD IN THE LUNAR WAKE.
Harold E. Taylor, K. W. Behannon, and N. F. Ness (NASA, Goddard Space Flight Center, Greenbelt, Md.).
Journal of Geophysical Research, vol. 73, Nov. 1, 1968, p. 6723-6735. 13 refs.

Measurements of the interplanetary magnetic field in the vicinity of the moon have been made from lunar orbit on Explorer 35. No shocks are observed in the vicinity of the moon, either in front of the moon or within 5.4 R_M behind the moon. The interplanetary magnetic field appears to be convected past the lunar body without much distortion. A regular pattern of magnetic perturbations is observed when passing through the lunar wake. The perturbation amplitude is small and variable, typically less than 30% of the ambient interplanetary magnetic field. Simultaneous measurements made by Explorer 33 while in the interplanetary medium but not in the lunar wake show that even sharp changes in the interplanetary magnetic field are found essentially undistorted in the lunar wake. These simultaneous measurements also help to identify the magnetic perturbation pattern in the wake region. (Author)

A69-11292 *
COMMENTS ON THE PAPER BY D. G. REA AND B. T. O'LEARY, "ON THE COMPOSITION OF THE VENUS CLOUDS."
James E. Hansen and Howard Cheyney (NASA, Goddard Space Flight Center, Institute for Space Studies, New York, N.Y.).
Journal of Geophysical Research, vol. 73, Sept. 15, 1968, p. 6136, 6137. 8 refs.
Grants No. NsG-399; No. NsG-33-016-013.

Brief critique of a paper by Rea and O'Leary (1968) that concluded: "there is no direct evidence for H_2O ice crystals, and furthermore, if they do exist on Venus and dominate the near-infrared scattering process, they must be submicron in diameter." Arguments are presented against the existence of clouds of micron-sized ice crystals. M.G.

A69-11475 *
AN INTEGRATED EXPERIMENT FOR COMPOSITIONAL ANALYSIS FROM AN ORBITER.
Isadore Adler and Jacob Trombka (NASA, Goddard Space Flight Center, Greenbelt, Md.).
American Astronautical Society, Conference on Advanced Space Experiments, Ann Arbor, Mich., Sept. 16-18, 1968, Paper 68-197. 27 p. 7 refs.

Study of the atomic and nuclear radiation which is naturally emitted from the moon and is characteristic of the elements that make up the lunar surface. The direction and analysis of this radiation can be used to determine chemical composition. Accordingly, an integrated experimental package for measuring gamma rays (natural and induced), secondary X rays, alpha particle emission, and neutron albedo is described. The advantages of this approach are an economy in technology and more comprehensive data collection, leading to improved interpretation of lunar processes. P.v.T.

A69-11481 *
MAGNETOMETER EXPERIMENT.
P. Dyal and C. P. Sonett (NASA, Ames Research Center, Space Sciences Div., Moffett Field, Calif.).
American Astronautical Society, Conference on Advanced Space Experiments, Ann Arbor, Mich., Sept. 16-18, 1968, Paper 68-206. 25 p. 18 refs.

Description of a magnetometer experiment the purpose of which is to measure the magnetic field on the lunar surface and from these measurements determine some of the deep electrical properties of the moon. The experiment will also elucidate the solar plasma/lunar surface interaction. The moon is considered a spherical body with a conductivity σ, permeability μ, and dielectric constant ε, immersed in a moving conducting plasma with a "frozen in" magnetic field. Recent magnetic field measurements indicate a permanent magnetic dipole moment for the whole moon to be essentially zero (less than 10^{20} G-cm^3). Radar measurements indicate a surface relative ε of 2.6 and σ of 10^{-4} mhos/m at 10^8 Hz. The results of the magnet experiment on Surveyor suggest a surface relative μ of 1.04. Electromagnetic properties of the moon will be studied by measuring the vector magnetic field at two points on the lunar surface for a period of one year. The magnetometers are part of the Apollo Lunar Surface Experiments Package that will be emplaced by a team of astronauts during the first and second landed missions. These instruments measure the vector magnetic field from 0 to ±400 gamma with a resolution of 0.2 gamma and a time response from dc to 1 Hz. The magnetometer has a site survey capability, thus making it an automatic magnetic observatory on the lunar surface. I.P.

A69-12104 *#
THE LOWER ATMOSPHERE OF MARS - A PROGRESS REPORT.
John C. Brandt (NASA, Goddard Space Flight Center, Greenbelt, Md.) and H. Spinrad (California, University, Berkeley, Calif.).
IN: THE ATMOSPHERES OF VENUS AND MARS.
Edited by J. C. Brandt and M. B. McElroy.
New York, Gordon and Breach, Science Publishers, Inc., 1968, p. 21-33. 43 refs.

The current status of our knowledge of the pressure, temperature, and composition of the Martian lower atmosphere is reviewed. Photometric, spectroscopic, and occultation techniques appear to produce consistent results. A surface pressure of 10 ± 4 mb and a characteristic temperature of about 200 K are found; the atmosphere is roughly 50% or more CO_2 and the remaining major constituent(s), if any, are unidentified. These values appear to have considerable support, but the history of the study of the Martian atmosphere indicates that undue reliance should not be placed on the current consensus. (Author)

A69-12105 *#
MULTIPLE LIGHT SCATTERING IN PLANETARY ATMOSPHERES.
H. C. van de Hulst (Leiden, State University, Observatory, Leiden, Netherlands) and K. Grossman (NASA, Goddard Institute for Space Studies, New York, N.Y.).
IN: THE ATMOSPHERES OF VENUS AND MARS.

Edited by J. C. Brandt and M. B. McElroy.
New York, Gordon and Breach, Science Publishers, Inc., 1968, p. 35-55. 18 refs.
Grant No. NsG-499.

Discussion of the diffuse reflection and transmission by plane, homogeneous atmospheres consisting of particles with an anisotropic scattering pattern. The doubling method, in which the properties of a layer of double thickness are found by putting two layers of single thickness together, is found to be the most convenient. It can be pursued with great accuracy from very thin to very thick layers. The accuracy obtained with various integration schemes in depth and in angle is discussed. It is shown that the results thus obtained for thick layers can be numerically fitted to the asymptotic theory for very thick layers. This also provides results for semiinfinite layers with 4- to 5-figure accuracy. Examples computed for the Henyey-Greenstein function with asymmetry factors ranging from -0.75 to +0.875, and optical thickness from 1/16 to 64, are given. Attention is drawn to similarity relations whereby results with variously peaked phase function can be compared. M.M.

A69-12108 *#
THE DRY MASSIVE MODEL OF THE ATMOSPHERE OF VENUS AND THE MICROWAVE PHASE EFFECT.
Patrick Thaddeus (NASA, Goddard Space Flight Center, Goddard Institute for Space Studies, New York, N.Y.).
IN: THE ATMOSPHERES OF VENUS AND MARS.
Edited by J. C. Brandt and M. B. McElroy.
New York, Gordon and Breach, Science Publishers, Inc., 1968, p. 99-102. 6 refs.

Analysis of the mechanism responsible for the microwave phase effect of Venus assuming a dry massive model of the Venusian atmosphere. The microwave phase effect observed at 10 cm, and the distribution of microwave emission over the planet's surface at the same wavelength indicate the following sequence of brightness temperatures at the subsolar and antisolar points and at the poles: T_B (subsolar) > T_B (antisolar) > T_B (polar). It is natural to suppose that this sequence is a consequence of diurnal thermal changes over the lowest atmospheric scale height, but it is noteworthy that the same sequence can be produced by a convective boundary layer and surface thermal wave in an atmosphere too massive to show significant diurnal thermal change. As long as the convective boundary layer is optically thin in the infrared, radiative transfer confines the three brightness temperatures to an interval of at most 30 K, which is several times smaller than the spread indicated by radio observations. T.M.

A69-12109 *#
ON THE EXOSPHERIC TEMPERATURE OF VENUS.
S. H. Gross (Brooklyn, Polytechnic Institute, Farmingdale, N.Y.), W. E. McGovern (New York University, Dept. of Meteorology and Oceanography, New York, N.Y.), and S. I. Rasool (NASA, Goddard Space Flight Center, Goddard Institute for Space Studies; New York University, Dept. of Meteorology and Oceanography, New York, N.Y.).
IN: THE ATMOSPHERES OF VENUS AND MARS.
Edited by J. C. Brandt and M. B. McElroy.
New York, Gordon and Breach, Science Publishers, Inc., 1968, p. 103-107. 11 refs.

A calculation of the exospheric temperature of Venus for a variety of composition models of the atmosphere indicates that if CO_2 is present in relatively large proportions (>20% by volume) T_{ex} is in the range of 600 to 800 K. However, for CO_2 concentrations <5%, T_{ex} could be as high as 3000 K. It is suggested that a measurement of the exospheric temperature, already planned for the Mariner 1967 flyby mission to Venus, could help resolve the controversy on the concentration of CO_2 in Venus atmosphere. (Author)

A69-12224 *
PRINCIPAL SCIENCE RESULTS FROM SURVEYOR 5.
L. D. Jaffe, W. E. Brown, Jr., E. M. Christensen, J. W. Lucas, R. H. Norton (California Institute of Technology, Jet Propulsion Laboratory, Pasadena, Calif.), S. A. Batterson (NASA, Langley Research Center, Dynamic Loads Div., Hampton, Va.), S. E. Dwornik (NASA, Washington, D.C.), D. E. Gault (NASA, Ames Research Center, Planetology Branch, Moffett Field, Calif.), R. F. Scott (California Institute of Technology, Div. of Engineering and Applied Science, Pasadena, Calif.), E. M. Shoemaker (U.S. Geological Survey, Astrogeology Branch, Flagstaff, Ariz.), G. H. Sutton (Hawaii, University, Hawaii Institute of Geophysics, Honolulu, Hawaii), and A. L. Turkevich (Chicago, University, Enrico Fermi Institute for Nuclear Studies and Dept. of Chemistry, Chicago, Ill.).
Journal of Geophysical Research, vol. 73, Nov. 15, 1968, p. 7165-7167.

The area of Mare Tranquillitatis in which Surveyor 5 landed appears to be similar to sites in Oceanus Procellarum. The gross elemental composition of the surface material and its response to a magnet are similar to those of a basalt. The debris layer appears to consist of aggregates of the order of 1 cm in diameter consisting of the grains and set in a matrix of less-coherent fine grains (most of them 2 to 60 μ in diameter) mixed with some rocky fragments 1 mm and larger. The static bearing strength is less than 10^4 dynes/cm^2 for the upper few millimeters and averages approximately 3×10^5 dynes/cm^2 for the upper few centimeters. The evidence suggests that chemical differentiation has occurred in the moon, probably owing to internal heat sources; this is consistent with the hypothesis that the maria are basaltic volcanic flows. (Author)

A69-12225 *
LUNAR SURFACE MECHANICAL PROPERTIES.
E. M. Christensen, R. Choate, L. D. Jaffe, R. L. Spencer (California Institute of Technology, Jet Propulsion Laboratory, Pasadena, Calif.), S. A. Batterson (NASA, Langley Research Center, Dynamic Loads Div., Hampton, Va.), H. E. Benson (NASA, Manned Spacecraft Center, Houston, Tex.), R. E. Hutton (TRW Systems Group, Redondo Beach, Calif.), R. H. Jones (Hughes Aircraft Co., El Segundo, Calif.), H. Y. Ko (Colorado, University, Boulder, Colo.), F. N. Schmidt (Bellcomm, Inc., Washington, D.C.), R. F. Scott (California Institute of Technology, Pasadena, Calif.), and G. H. Sutton (Hawaii, University, Hawaii Institute of Geophysics, Honolulu, Hawaii).
Journal of Geophysical Research, vol. 73, Nov. 15, 1968, p. 7169-7192. 14 refs.

The surface material at the Surveyor 5 site is granular and slightly cohesive. Spacecraft footpads plowed trenches in this material as the spacecraft slid during landing. For a compressible soil model, a static bearing capacity of 2.7 newtons/cm^2 gave best agreement with the observations. Static firing of the vernier engines against the surface moved surface particles; a crater 20 cm in diameter and about 1 cm deep was produced, apparently at engine shutdown. The permeability of the soil to gases, to a depth of about 25 cm, is 1×10^{-8} cm^2, corresponding to soil particles mostly 2 to 60 μ in diameter. (Author)

A69-12271 *
GRAVITATIONAL EXPERIMENTS WITH A CYLINDRICAL GALAXY.
R. W. Hockney (Stanford University, Institute for Plasma Research, Stanford, Calif.; NASA, Langley Research Center, Hampton, Va.).
(Colloque sur le Probleme Gravitationnel des N Corps, Paris, France, Aug. 16-18, 1967.)
Bulletin Astronomique, vol. 3, no. 2, 1968, p. 199-207. 5 refs.

A collisionless computer model is used to perform gravitational experiments with a two-dimensional galaxy. The motion of 2000 mass rods is computed step-wise in time as they move according to Newton's laws of motion in their mutual gravitation field. The results are displayed as a motion picture and show the types of galactic structure that can arise from purely gravitational effects. A galaxy with insufficient rotation to balance gravitational attraction is seen to collapse and form filamentary condensations, then to change through structures similar to the "spirals" and "barred spirals," and finally to settle down to a cylindrical form reminiscent of an "elliptical" galaxy. (Author)

A69-12272 *
COMPUTER SOLUTIONS OF THE GRAVITATIONAL N-BODY PROBLEM.
Frank Hohl (NASA, Langley Research Center, Hampton, Va.).
(Colloque sur le Problème Gravitationnel des N Corps, Paris, France, Aug. 16-18, 1967.)
Bulletin Astronomique, vol. 3, no. 2, 1968, p. 227-239; Discussion, M. Henon (Centre National de la Recherche Scientifique, Paris, France), Von Hoerner, and King, p. 240. 8 refs.

Computer study of a collisionless self-gravitating system using a two-dimensional model. The model consists of a large number of rods of equal mass that are of infinite extent in the z-direction.

These rods move in the x-y plane under the action of their mutual gravitational attraction. The gravitational field is obtained by solving the Poisson equation and the system is advanced stepwise in time. Results of some simple experiments containing up to 4000 particles or mass rods are given. The calculations indicate that filamentary and other irregular structures similar to those of some actual stellar systems can be obtained by purely gravitational effects. M.G.

A69-12301
VOYAGE TO THE PLANETS; AMERICAN ASTRONAUTICAL SOCIETY AND THE NATIONAL SPACE CLUB, GODDARD MEMORIAL SYMPOSIUM, 5TH, WASHINGTON, D.C., MARCH 14, 15, 1967, PROCEEDINGS.
Tarzana, Calif., American Astronautical Society (AAS Science and Technology Series. Volume 16), 1968. 182 p.
Members, $8.45; nonmembers, $11.25.

CONTENTS:

FOREWORD. E. Burgess, p. ix.
DOORWAY TO THE UNIVERSE. G. T. Seaborg (U.S. Atomic Energy Commission, Washington, D.C.), p. 1-8.
MAN AND SPACE. A. C. Clarke, p. 9-21.
NATIONAL PRESTIGE. G. P. Miller, p. 23-30.
THE MARINERS. W. H. Pickering (California Institute of Technology, Pasadena, Calif.), p. 31-49. [See A69-12302 02-31]
GALACTIC JUPITER PROBES. J. F. Clarke, E. W. Hymowitz, and J. H. Trainor (NASA, Goddard Space Flight Center, Greenbelt, Md.), p. 51-64. 6 refs. [See A69-12303 02-30]
THE VOYAGER PROGRAM. E. M. Cortright (NASA, Washington, D.C.), p. 65-92. [For abstract see issue 12, page 2002, Accession no. A67-25232]
PAVING THE WAY FOR MANNED PLANETARY EXPLORATION. C. W. Mathews (NASA, Office of Manned Space Flight, Washington, D.C.), p. 93-106. [For abstract see issue 12, page 2002, Accession no. A67-25233]
MANNED EXPEDITIONS TO MARS AND VENUS. E. Z. Gray and F. P. Dixon (NASA, Office of Manned Space Flight, Washington, D.C.), p. 107-135. [See A69-12304 02-30]
MEANWHILE, BACK ON EARTH... C. S. Sheldon, II (U.S. Library of Congress, Washington, D.C.), p. 137-156. [For abstract see issue 12, page 2040, Accession no. A67-25234]
THE ROLE OF THE DIPLOMAT. R. F. Packard (U.S. Department of State, Washington, D.C.), p. 157-164. [For abstract see issue 12, page 2040, Accession no. A67-25235]
PLANETARY EXPLORATION STRATEGY. J. W. Findlay (National Radio Astronomy Observatory, Green Bank, W. Va.), p. 165-171. [See A69-12305 02-30]
THE PATH TO VOYAGER. C. S. Pittendrigh (Princeton University, Princeton, N.J.), p. 173.

A69-12303 *
GALACTIC JUPITER PROBES.
J. F. Clarke, E. W. Hymowitz, and J. H. Trainor (NASA, Goddard Space Flight Center, Greenbelt, Md.).
IN: VOYAGE TO THE PLANETS; AMERICAN ASTRONAUTICAL SOCIETY AND THE NATIONAL SPACE CLUB, GODDARD MEMORIAL SYMPOSIUM, 5TH, WASHINGTON, D.C., MARCH 14, 15, 1967, PROCEEDINGS. [A69-12301 02-30]
Tarzana, Calif., American Astronautical Society (AAS Science and Technology Series. Volume 16), 1968, p. 51-64. 6 refs.

Discussion of the Galactic Jupiter Probe program and of its scientific goals. The broad and basic scientific goal of the U.S. space program is to understand the origin of the solar system, its evolution, and its present status. Among the most interesting Jovian phenomena observed in the past decade have been the non-thermal radio emissions in the decimetric and decametric wavelength regions, leading to the hypothesis of a strong Jovian magnetic field, similar to the earth's Van Allen radiation belt. A Jupiter probe could investigate these radio emissions. A direct measurement of the helium to hydrogen ratio of the Jovian atmosphere represents an important item in understanding the evolution and structure of the planet. P.v.T.

A69-12304 *
MANNED EXPEDITIONS TO MARS AND VENUS.
Edward Z. Gray and Franklin P. Dixon (NASA, Office of Manned Space Flight, Washington, D.C.).
IN: VOYAGE TO THE PLANETS; AMERICAN ASTRONAUTICAL SOCIETY AND THE NATIONAL SPACE CLUB, GODDARD MEMORIAL SYMPOSIUM, 5TH, WASHINGTON, D.C., MARCH 14, 15, 1967, PROCEEDINGS. [A69-12301 02-30]
Tarzana, Calif., American Astronautical Society (AAS Science and Technology Series. Volume 16), 1968, p. 107-135.

Identification of the role of manned Mars and Venus missions in an overall planetary exploration program. Growth from present Mariner and Voyager capabilities to manned spacecraft with advanced probe and sensor systems and sample return capability is discussed. Phasing of this evolution with Apollo activities and system capabilities to give a logical program leading to manned reconnaissance, sample retrieval, and surface exploration of Mars is presented. A broad capability to support and focus the future national space activity is associated with the goals of planetary exploration. P.v.T.

A69-12390 *#
DIRECT ENTRY LONGITUDINAL RANGE DISPERSION OF UNMANNED MARS LANDERS.
E. Brian (NASA, Langley Research Center, Aerophysics Div., Missions Section, Hampton, Va.) and Edwin F. Harrison (NASA, Langley Research Center, Aerophysics Div., Hampton, Va.).
Journal of Spacecraft and Rockets, vol. 5, Dec. 1968, p. 1497, 1498.

Discussion of the longitudinal range dispersion of unmanned Mars landers, defined as the difference between the ranges traversed during the atmospheric ranging phase on the overshoot boundary using the VM-8 model atmosphere and the undershoot boundary using the VM-9 atmosphere. Syrtis Major, with a maximum dimension of about 900 km, is used as an example of a possible landing site. I.P.

A69-12545 *#
UPPER LIMIT ON THE SPATIAL DENSITY OF ASTEROIDAL DEBRIS.
Donald J. Kessler (NASA, Manned Spacecraft Center, Meteoroid Sciences Branch, Houston, Tex.).
AIAA Journal, vol. 6, Dec. 1968, p. 2450.

Determination of an upper limit on the spatial density of asteroidal debris by means of measurements of the gegenschein. The gegenschein can be explained as a backscattering peak in the phase function of the interplanetary dust-particle distribution determined by the zodiacal light. However, regardless of the source of the gegenschein, the amount of asteroidal debris cannot reflect more light than is observed. This is the basis of an upper limit on the asteroidal spatial density. F.R.L.

A69-12680 *
MANNED SPACE FLIGHT - THE FUTURE.
George E. Mueller (NASA, Washington, D.C.).
(British Interplanetary Society, Special Meeting, University College, London, England, Aug. 10, 1968.)
Spaceflight, vol. 10, Dec. 1968, p. 406-414.

Discussion of the future space programs as governed by the limitations of space exploitation due to the high cost of putting payload into orbit, and the inaccessibility of objects after they have been launched. It is suggested that the next major thrust in space will be the development of an economical launch vehicle for shuttling between earth and such installations as the orbiting space stations, which will soon be in operation. The Orbital Workshop, now under development, is described in extensive detail. B.H.

A69-12801
SPACE PROJECTIONS FROM THE ROCKY MOUNTAIN REGION; PROCEEDINGS OF THE SYMPOSIUM, DENVER, COLO., JULY 15, 16, 1968. VOLUME 1.
Symposium sponsored by the American Astronautical Society and the American Institute of Aeronautics and Astronautics.
Tarzana, Calif., American Astronautical Society, 1968. 477 p.
Price of three volumes, $10.00.

CONTENTS:

PLANETARY EXPLORATION.
UPPER ATMOSPHERE OF VENUS. C. A. Barth (Colorado,

University, Boulder, Colo.). 7 p. 11 refs. [See A69-12802 02-30]

THE ATMOSPHERE OF VENUS - A REVIEW OF RECENT OBSERVATIONS AND THEORIES. A. R. Barger (Martin Marietta Corp., Denver, Colo.). 25 p. 62 refs. [See A69-12803 02-30]

THE SEARCH FOR LIFE - PLANETARY EVOLUTION. R. S. Young (NASA, Washington, D.C.). 19 p. [See A69-12804 02-04]

ICE CAPS ON VENUS? W. F. Libby (Colorado, University, Boulder, Colo.; California, University, Los Angeles, Calif.). 26 p.

RADIOPHYSICS OF JUPITER. J. W. Warwick (Colorado, University, Boulder, Colo.). 17 p. 9 refs. [See A69-12805 02-30]

PLANETARY ATMOSPHERE DETERMINATION ERROR ANALYSIS USING KALMAN FILTER. A. C. Serold (Martin Marietta Corp., Denver, Colo.). 23 p. [See A69-12806 02-30]

GEOLOGICAL AND ATMOSPHERIC PHYSICS.

SATELLITE SYSTEM FOR DETERMINING THE GEOPOTENTIAL. C. B. Winn (Colorado State University, Fort Collins, Colo.). 17 p. 12 refs. [See A69-12807 02-30]

LINEAMENT TREND ANALYSIS OF GEMINI RED SEA PHOTOGRAPHY. R. J. Bridwell (Colorado School of Mines, Golden, Colo.). 15 p. 11 refs. [See A69-12808 02-13]

MEASUREMENT OF AIR DENSITY. C. D. Westlund and O. C. Haycock (Utah, University, Salt Lake City, Utah). 15 p. [See A69-12809 02-14]

STUDIES OF EARTH AIRGLOW. A. M. Despain and D. J. Baker (Utah State University, Logan, Utah). 32 p. 10 refs. [See A69-12810 02-13]

ELECTRONICS.

ANTICIPATED ANTENNA PROBLEMS ON MARS AND VENUS PROBES. C. H. Brockmeyer (Martin Marietta Corp., Denver, Colo.). 19 p. 13 refs. [See A69-12811 02-09]

ELECTRICAL MEASUREMENTS OF AN ERECTABLE PARABOLA FOR SPACE MISSIONS. D. Holst (Martin Marietta Corp., Denver, Colo.). 18 p. [See A69-12812 02-09]

RETRODIRECTIVE ANTENNA ARRAY SYSTEM. G. E. Johnson (Martin Marietta Corp., Denver, Colo.). 15 p. [See A69-12813 02-09]

MULTICHANNEL DATA COMPRESSION SIMULATION. W. A. Stevens (Martin Marietta Corp., Denver, Colo.). 19 p. 5 refs. [See A69-12814 02-08]

PROPER DIGITAL FILTERS. C. A. Halijak (Denver, University, Denver, Colo.). 8 p. 12 refs. [See A69-12815 02-08]

INVESTIGATION OF SYNCHRONOUS-WAVE R-F TO D-C CONVERSION. D. C. Watson, R. W. Grow, and C. C. Johnson (Utah, University, Salt Lake City, Utah). 17 p. [See A69-12816 02-07]

ADAPTIVE MULTIPLEX TELEMETRY - ITS USE IN DATA MANAGEMENT. N. R. Sheppard (Ball Brothers Research Corp., Boulder, Colo.). 24 p. 5 refs. [See A69-12817 02-07]

MISSION ANALYSIS.

THE MECHANICS AND APPLICATIONS OF THE PLANETARY SWINGBY TECHNIQUE FOR OPTIMIZATION OF INTERPLANETARY TRAJECTORIES. G. A. Flandro (Utah, University, Salt Lake City, Utah). 23 p. 15 refs. [See A69-12818 02-30]

STABILITY OF HIGHLY ELLIPTIC VENUS ORBITS UNDER THE INFLUENCE OF SOLAR GRAVITATIONAL PERTURBATIONS. D. G. Roos (Martin Marietta Corp., Friendship International Airport, Md.). 21 p. [See A69-12819 02-30]

TWO-DIMENSIONAL REPRESENTATION OF PLANETARY PROBE TARGETING CONSIDERATIONS. S. G. Homic (Martin Marietta Corp., Denver, Colo.). 13 p. [See A69-12820 02-30]

LAUNCH PERIOD, TARGETING AND ERROR ANALYSIS FOR MARS DIRECT AND ORBITAL MISSIONS. D. W. Marquet (Martin Marietta Corp., Friendship International Airport, Md.). 42 p. [See A69-12821 02-30]

PAYLOAD MAXIMIZATION AND MISSION MODE COMPARISON FOR HARD AND SOFT MARTIAN LANDERS. G. R. Knowles and D. A. Howard (Martin Marietta Corp., Friendship International Airport, Md.). 23 p. [See A69-12822 02-31]

MISSION INFLUENCE ON THE AEROTHERMODYNAMIC ENVIRONMENT FOR A VENUS ENTRY VEHICLE. H. C. Norman and P. M. Hart (Martin Marietta Corp., Friendship International Airport, Md.). 28 p. [See A69-12823 02-30]

A69-13427 *

NASA'S DEVELOPING STRATEGY OF SPACE APPLICATIONS.

Donald P. Rogers (NASA, Office of Space Science and Applications, Washington, D.C.).

TRW Space Log, vol. 8, Fall 1968, p. 3-11.

Discussion of the Space Application Program of NASA, emphasizing the need for various teams of experts to develop specific objectives of applications missions. Following the successful single-purpose Echo, Relay, Telstar, and Syncom Programs, the communications R&D program broadened its base in the Applications Technology Satellite (ATS) Program. The trend of the NASA R&D program has obviously been toward more complexity and more versatility, and toward multidisciplinary use of the larger spacecraft classes that an increased launch vehicle capability has made possible. The sequential technology development stages from Relay through Syncom to Early Bird and from Tiros to ESSA satellites have established a possible pattern for future evolution from R&D to operational systems. P.v.T.

A69-13699 *#

AN EXPERIMENT TO DETERMINE THE STRUCTURE OF A PLANETARY ATMOSPHERE.

Simon C. Sommer and Layton Yee (NASA, Ames Research Center, Moffett Field, Calif.).

American Institute of Aeronautics and Astronautics, Annual Meeting and Technical Display, 5th, Philadelphia, Pa., Oct. 21-24, 1968, Paper 68-1054. 10 p. 10 refs.

Members, $1.00; nonmembers, $1.50.

Assessment of the validity of a method of measuring the structure and mean molecular weight of an unknown atmosphere on the basis of high-altitude tests in the earth's atmosphere. Instruments were carried as an auxiliary experiment on a large parachute research vehicle, the fourth flight in the NASA Planetary Entry Parachute Program. The vehicle, a 60° half-angle cone with a diameter of 4.57 m, was balloon-launched to an altitude of 39.6 km and then propelled to a Mach number of 1.7 by onboard rockets. The trajectory history was deduced from onboard instruments which measured pressure, temperature, and acceleration in a velocity-density regime similar to that expected during the terminal phase of a Mars entry. An analysis developed for determining ambient conditions and atmosphere structure from onboard measurements is reviewed. Atmosphere-structure data agree well with ground-based observations and meteorological measurements. G.V.

A69-13775 *

GRAPHITE PARTICLE MODEL FOR NML CYGNUS.

K. S. Krishna Swamy (NASA, Goddard Space Flight Center, Greenbelt, Md.) and N. C. Wickramasinghe (Arizona, University, Steward Observatory, Tucson, Ariz.).

Nature, vol. 220, Nov. 30, 1968, p. 896, 897. 9 refs.

Discussion of the possibility that the IR radiation from NML Cygnus comes from a circumstellar shell of graphite particles. The formation of such particles seems likely, because NML Cygnus probably has an O/C ratio close to unity. It is pointed out that graphite particles are sufficiently refractory to withstand the temperatures of 600 to 900 K which seem to be involved. F.R.L.

A69-13781 *

INVESTIGATIONS IN HANSEN'S PLANETARY THEORY.

Peter Musen (NASA, Goddard Space Flight Center, Greenbelt, Md.).

Bulletin Astronomique, vol. 3, no. 3, 1968, p. 361-376. 6 refs.

Investigation of the nature of the basic function W of Hansen's theory. Following von Zeipel, dW/dt is obtained here as the projection of the perturbations in the acceleration vector on a variable vector $\vec{N}$, which is selected in such a way that dW/dt is totally integrable. The geometric characteristics of Hansen's theory favor the expansion of the perturbations into trigonometric series with the disturbed mean anomalies of planets as arguments. Such a form of expansion eliminates the need to develop $\vec{W}$ and the disturbing force in powers of the perturbations of the mean anomalies. The integration of the differential equations of the problem is accomplished by the method of successive approximation using the expansion of the integrating operator into series. (Author)

A69-14005 *
INTRINSIC MAGNETIC PROPERTIES OF THE LUNAR BODY.
Kenneth W. Behannon (NASA, Goddard Space Flight Center, Laboratory for Space Sciences, Greenbelt, Md.).
Journal of Geophysical Research, vol. 73, Dec. 1, 1968, p. 7257-7268. 15 refs.

Reversal of the ambient tail field by 180° when the moon and Explorer 35 in lunar orbit traverse the neutral sheet permits a separation of permanent and induced field contributions to the total field observed near the moon. When compared with calculated permanent and induced field effects, the results of this analysis lead to new upper limits of 10^{20} gauss cm^3 on the lunar magnetic moment and 4 γ on the lunar surface field. Limiting the moment induced in the moon by the magnetotail field permits an upper limit of 1.8 to be set on the bulk relative magnetic permeability of the moon.
(Author)

A69-14126 *
ON THE RELATION BETWEEN THE AMPLITUDE OF LIGHT AND RADIAL VELOCITY VARIATIONS OF β CANIS MAJORIS STARS.
Kam-Ching Leung (NASA, Goddard Space Flight Center, Goddard Institute for Space Studies, New York, N.Y.).
Astrophysics and Space Science, vol. 2, Nov. 1968, p. 302-306. 32 refs.

Investigation of the relation between the amplitude of light and the amplitude of the radial velocity for β Canis Majoris stars. This relation is found to be linear. However, the two stars BW Vul and σ Sco, which have the largest radial-velocity variations, do not seem to share this relationship. Separate listings are made of all the observations derived from simultaneous observations, and of those known to have very small variation in the amplitude of the light and radial-velocity curves, on the one hand, and of the stars which have no simultaneous observations and are known to have appreciable variation in the amplitudes of their light and radial-velocity curves, on the other.
B.H.

A69-14519 *
SPACE MISSION ANALYSIS.
John S. Mackay (NASA, Office of Advanced Research and Technology, Mission Analysis Div., Moffett Field, Calif.).
IN: ENGINEERING APPLICATIONS OF DIGITAL COMPUTERS.
Edited by T. R. Bashkow.
New York, Academic Press, Inc., 1968, p. 235-263. 19 refs.

Discussion of the use of digital computers in space flight simulation and for optimization of vehicle performance. The mission analysis problem is examined. Aspects of space vehicle trajectory simulation are studied with reference to differential equations of motion, space vehicle propulsion systems, and the minimizing of mission propellant. Computer solutions involving methods of numerical integration and the two-point boundary-value problem are considered. The effects of payload as a criterion, and vehicle mass allocation on mission payload estimation are discussed. Attention is given to optimizing total vehicle design.
F.R.L.

A69-14626 *
LINE BLANKETING IN STARS.
K. S. Krishna Swamy (NASA, Goddard Space Flight Center, Greenbelt, Md.).
Astronomical Society of the Pacific, Publications, vol. 80, Aug. 1968, p. 406-409. 10 refs.

Comparison of scaled solar models and those based on the gray-body temperature distribution in order to determine which of the models is a better representation of stellar atmospheres. It is shown that the scaled solar models are a better representation. The nongray and the gray-body temperature distribution of the sun, ϵ Eridani, and 45 Tauri are tabulated.
M.G.

A69-14631 *
ISOSTASY ON THE MOON.
John A. O'Keefe (NASA, Goddard Space Flight Center, Greenbelt, Md.).
Science, vol. 162, Dec. 20, 1968, p. 1405, 1406. 14 refs.

Discussion of lunar gravitational anomalies from the viewpoint of internal density variations. The excess mass in the maria over what would be called for by isostasy may be connected with the fact that the maria are filled with some sort of material, which has arrived there after the formation of most of the highland topography. It appears that there are internal stress differences, at depth of the order of a few hundred kilometers, which amount to 30 to 50 bars. It should be pointed out that the material which flooded the circular maria must have come from points which were hundreds of kilometers away, either downward or sidewise. The most likely guess is that it came from depth of 500 km or more inside the moon.
P.v.T.

A69-14979 *
POTASSIUM FELDSPAR IN WEEKEROO STATION, KODAIKANAL, AND COLOMERA IRON METEORITES.
T. E. Bunch (NASA, Ames Research Center, Space Sciences Div., Moffett Field, Calif.) and Edward Olsen (Field Museum of Natural History, Dept. of Geology, Chicago, Ill.).
Science, vol. 162, Dec. 27, 1968, p. 1507, 1508.

Electron-microprobe analysis of the feldspar contained in the Weekeroo Station meteorite. The K_2O content ranges, in analyses made on each of ten very small grains, from 0.90 to 11.5 wt %, with a corresponding reciprocal Na_2O content of 9.8 to 3.1 wt %; the average is 4.9% K_2O and 7.6% Na_2O. X-ray diffraction studies indicate a possible antiperthitic intergrowth of sodic plagioclase and potassium feldspar.
P.v.T.

A69-15503 *#
LUNAR ORBITER MISSION DESIGN.
Norman L. Crabill and Wilbur L. Mayo (NASA, Langley Research Center, Hampton, Va.).
(American Institute of Aeronautics and Astronautics, Aerospace Sciences Meeting, 6th, New York, N.Y., Jan. 22-24, 1968, Paper 68-47.)
Journal of Spacecraft and Rockets, vol. 6, Jan. 1969, p. 18-24. 5 refs.
[For abstract see issue 06, page 1088, Accession no. A68-17470]

A69-15589 *#
COLLAPSE THEORY OF DIMPLE CRATERS.
John A. O'Keefe (NASA, Goddard Space Flight Center, Laboratory for Theoretical Studies, Greenbelt, Md.).
Irish Astronomical Journal, vol. 8, June-Sept. 1968, p. 209-211.

Critical discussion of Urey's (1965) proposal that the dimple craters on the surface of the moon represent flows of a granular surface material through a fissure into the interior of the moon. Analogies between terrestrial sink holes and the dimple craters are discussed. It is suggested that the dimple craters represent the channels through which gases from the lunar interior reach the surface.
M.G.

A69-15834
HIGHLIGHTS OF ASTRONOMY; INTERNATIONAL ASTRONOMICAL UNION, GENERAL ASSEMBLY, 13TH, PRAGUE, CZECHOSLOVAKIA, AUGUST 22-31, 1967, PROCEEDINGS.
Edited by Luboš Perek.
Dordrecht, D. Reidel Publishing Co., 1968. 556 p. In English and French.
$26.

CONTENTS:

PREFACE. L. Perek. 1 p.
EXPLORING THE MOON. A. A. Mikhailov (Akademiia Nauk SSSR, Leningrad, USSR), p. 3-11. [See A69-15835 05-30]
RADIO GALAXIES AND QUASARS. I. M. Ryle (Cambridge University, Cambridge, England), p. 33-44. [See A69-15836 05-30]
RADIO GALAXIES AND QUASARS. II. A. Sandage (Carnegie Institution of Washington and California Institute of Technology, Pasadena, Calif.), p. 45-70. 33 refs. [See A69-15837 05-30]
RECENT TECHNIQUES IN SOLAR OPTICAL ASTRONOMY FROM SPACE. E. M. Reeves (Harvard University, Cambridge, Mass.), p. 75-93. 31 refs. [See A69-15838 05-14]
ULTRAVIOLET ASTRONOMY. R. Wilson (United Kingdom Atomic Energy Authority, Culham, Berks., England), p. 94-107. 55 refs. [See A69-15839 05-30]
NEW TECHNIQUES IN X-RAY ASTRONOMY. C. de Jager (Utrecht, State University, Utrecht, Netherlands), p. 108-123. 17 refs. [See A69-15840 05-14]
SOLAR AND INTERPLANETARY MAGNETIC FIELDS AND

PLASMAS. J. M. Wilcox (California, University, Berkeley, Calif.), p. 124-135. 23 refs. [See A69-15841 05-30]

INFRARED ASTRONOMY. F. J. Low (William Marsh Rice University, Houston, Tex.; Arizona, University, Tucson, Ariz.), p. 136-147. 33 refs. [See A69-15842 05-30]

SOME PROBLEMS AND INSTRUMENTAL FEATURES OF SUBMILLIMETER ASTRONOMY. A. E. Salomonovich (Akademiia Nauk SSSR, Moscow, USSR), p. 148-163. 38 refs. [See A69-15843 05-30]

NEW TECHNIQUES IN SPACE RADIO-ASTRONOMY. J.-L. Steinberg (Meudon, Observatoire, Meudon, Hauts-de-Seine; Paris, Observatoire, Paris, France), p. 164-175. 25 refs. [See A69-15844 05-30]

RESULTS FROM DETAILED STUDIES OF X-RAY SOURCES. R. Giacconi (American Science and Engineering, Inc., Cambridge, Mass.), p. 192-201. 14 refs. [See A69-15845 05-29]

THE X-RAY SPECTRA OF CYGNUS XR-1 AND THE CRAB NEBULA. L. E. Peterson (California, University, La Jolla, Calif.), p. 202-205. 6 refs. [See A69-15846 05-29]

X-RAYS RADIATION OF A NEUTRON STAR AS A RESULT OF GAS ACCRETION. Ja. B. Zel'dovič, p. 216-219. 10 refs. [See A69-15847 05-29]

THE COSMIC X-RAY BACKGROUND. R. J. Weymann (Arizona, University, Tucson, Ariz.), p. 220-227. 9 refs. [See A69-15848 05-29]

LITHIUM OBSERVATIONS IN THE SUN. E. A. Müller, p. 243-246. 14 refs. [See A69-15849 05-30]

ON THE LITHIUM ABUNDANCE IN SUNSPOTS AND THE UNDISTURBED SOLAR ATMOSPHERE. E. Dubov, E. Prokof'ev, and A. Severnyi, p. 247-250. 8 refs. [See A69-15850 05-30]

THEORIES PROPOSED TO EXPLAIN QUASI-STELLAR OBJECTS AND RADIO GALAXIES. G. Burbidge (California, University, San Diego, Calif.), p. 376-378. [See A69-15851 05-30]

THE EVOLUTION OF QUASI-STELLAR SOURCES AND RADIO GALAXIES. M. Ryle (Cambridge University, Cambridge, England), p. 380-383. 12 refs. [See A69-15852 05-30]

THE MAGNETODYNAMIC MODEL OF QUASARS. L. M. Ozernoi (Akademiia Nauk SSSR, Moscow, USSR), p. 384-388. 23 refs. [See A69-15853 05-30]

INVESTIGATION OF POSSIBLE ABUNDANCE ANOMALIES IN CLOSE BINARIES OF SPECTRAL TYPES A0-A2 AND F5-F6. Y. Kondo (NASA, Goddard Space Flight Center, Greenbelt, Md.), p. 432-436. 7 refs. [See A69-15854 05-30]

THE EVOLUTION OF CLOSE BINARIES AND THE Am STARS. P. S. Conti (California, University, Santa Cruz, Calif.), p. 437-442. 20 refs. [See A69-15855 05-30]

ORIGIN OF BINARIES FROM A CONSIDERATION OF ANGULAR MOMENTUM. S.-S. Huang (Northwestern University, Evanston, Ill.), p. 443-450. 17 refs. [See A69-15856 05-30]

A DESCRIPTION OF THE LUNAR ORBITER SPACECRAFT. I. Taback, p. 462-470. [See A69-15857 05-31]

PHOTOGRAPHIC RESULTS OF THE LUNAR ORBITER PROGRAM. W. E. Brunk (NASA, Washington, D.C.), p. 471-523. [See A69-15858 05-30]

SPACE OBSERVATIONS NEEDED FOR IMPROVING OUR KNOWLEDGE OF SOLAR FLARES. A. B. Severnyi (Akademiia Nauk SSSR, Partizanskoye, Ukrainian SSR), p. 530-532. [See A69-15859 05-29]

SPACE OBSERVATIONS OF FLARE SPRAYS AND RELATED SURGE PHENOMENA. Y. Öhman (Kungl. Vetenskapsakademien, Saltsjöbaden, Sweden), p. 533-537. 11 refs. [See A69-15860 05-29]

THE NEEDS AND REQUIREMENTS FROM THE STANDPOINT OF THE ULTRAVIOLET SOLAR OBSERVATIONS. E. M. Reeves (Harvard University, Cambridge, Mass.), p. 538-540. [See A69-15861 05-30]

HARD SOLAR X-RAY BURSTS. C. de Jager (Utrecht, State University, Utrecht, Netherlands), p. 541-543. [See A69-15862 05-29]

SOLAR GAMMA RAYS AND THEIR CORRELATION WITH SPACE AND GROUND-BASED OBSERVATIONS. G. G. Fazio (Smithsonian Institution and Harvard University, Cambridge, Mass.), p. 544-546. [See A69-15863 05-29]

A69-15854 *

INVESTIGATION OF POSSIBLE ABUNDANCE ANOMALIES IN CLOSE BINARIES OF SPECTRAL TYPES A0-A2 AND F5-F6.

Yoji Kondo (NASA, Goddard Space Flight Center, Greenbelt, Md.).

IN: HIGHLIGHTS OF ASTRONOMY; INTERNATIONAL ASTRONOMICAL UNION, GENERAL ASSEMBLY, 13TH, PRAGUE, CZECHOSLOVAKIA, AUGUST 22-31, 1967, PROCEEDINGS. [A69-15834 05-30]
Edited by Luboš Perek.
Dordrecht, D. Reidel Publishing Co., 1968, p. 432-435; Discussion, p. 435, 436. 7 refs.

Investigation of the spectra of 11 close binary systems with periods of about 1 to 100 days and with spectral types of about A4 to F2 (IV-V). The work was undertaken as a follow-up on an investigation by Abt (1965), who found that such binaries are all Am stars. Preliminary results on metallicity in close binaries are given. G.R.

A69-15858 *

PHOTOGRAPHIC RESULTS OF THE LUNAR ORBITER PROGRAM.

William E. Brunk (NASA, Washington, D.C.).

IN: HIGHLIGHTS OF ASTRONOMY; INTERNATIONAL ASTRONOMICAL UNION, GENERAL ASSEMBLY, 13TH, PRAGUE, CZECHOSLOVAKIA, AUGUST 22-31, 1967, PROCEEDINGS. [A69-15834 05-30]
Edited by Luboš Perek.
Dordrecht, D. Reidel Publishing Co., 1968, p. 471-523.

Discussion of the goals and photographic results of the Lunar Orbiter Program. A selection of photographs obtained from five missions, and showing interesting and previously unobserved features, is presented. Representative samples of high-resolution photography of possible Apollo sites are shown, together with an earth-based photograph of the Copernicus region. A series of vertical and oblique photographs taken in the Lunar Orbiter-3 mission with a change in orbital inclination from 12 to 21° show additional regions of scientific interest. Other photographs show the front-side coverage of Lunar Orbiters 1, 2, 3, and 4, sections of the high-resolution regions containing well-known lunar features, craters, and a chart of the lunar far-side. M.M.

A69-16252 *

PARTICLE SHADOWING BY THE MOON.

J. A. Van Allen (Iowa, University, Dept. of Physics and Astronomy, Iowa City, Iowa) and N. F. Ness (NASA, Goddard Space Flight Center, Greenbelt, Md.).

Journal of Geophysical Research, vol. 74, Jan. 1, 1969, p. 71-93. 13 refs.
Contract No. NAS 5-9076.

Evaluation of observations made by Explorer 33 and Explorer 35 during the period from Nov. 10 to 22, 1967, when the earth-moon system was bathed in an isotropic, homogeneous beam of solar electrons and protons whose intensities were slowly varying functions of time. During this period, the moon and Explorer 35 passed from interplanetary space through the magnetotail. The angular distributions of the intensity of both electrons and protons were accurately isotropic within the magnetotail as well as in interplanetary space. Study of 33 cases of clear electron shadowing and two cases of less clear shadowing suggests the following principal conclusions: (1) magnetic lines of force from external sources thread through the moon in a rectilinear manner, as though it did not exist, and (2) electron shadowing data provide no direct information on the region of access of interplanetary electrons into the magnetotail, but do provide an upper limit on the trans-B diffusion velocity of electrons due to all causes. P.v.T.

A69-16264 *

ANALYSIS OF FLUCTUATIONS IN THE INTERPLANETARY MAGNETIC FIELD OBTAINED BY IMP 2.

Nobuki Kawashima (NASA, Goddard Space Flight Center, Greenbelt, Md.).

Journal of Geophysical Research, vol. 74, Jan. 1, 1969, p. 225-230. 13 refs.

Data from the IMP 2 magnetic experiment obtained in interplanetary space are analyzed to study the character of the fluctuations in the magnetic field from the MHD point of view. The fluctuation in interplanetary space is quite anisotropic relative to the steady magnetic field, with the fluctuations transverse to the magnetic line of force much larger than the longitudinal component of fluctuations. This anisotropy gradually decays as the amplitude of the fluctuation increases and tends to become rather isotropic. These fluctuations may be related to the thermal anisotropy of solar

radio emission value. The relations on which this procedure is based are derived and analyzed. These relations determine the variations in the spatial density of radio galaxies, regardless of whether these variations are of an evolutionary nature or are due to the inapplicability of the cosmological models used. V.Z.

A69-16278 *

EXPLORER 35 MEASUREMENTS OF LOW-ENERGY PLASMA IN LUNAR ORBIT.

G. P. Serbu (NASA, Goddard Space Flight Center, Laboratory for Space Sciences, Greenbelt, Md.).

Journal of Geophysical Research, vol. 74, Jan. 1, 1969, p. 372-376. 9 refs.

Discussion of some preliminary observations of low-energy plasma $E < 500$ eV, taken during lunar orbits of Explorer 35. The plasma measurements reported were made by means of a planar multigrid sensor programmed as a retarding potential analyzer. The integral spectrum for both electrons and ions is obtained in the energy range from 0 to 500 eV. Some descriptive characteristics of the lunar void, based on the observations from the Explorer 35 integral electron spectra, are given. P.v.T.

A69-16476 *

DYNAMICS OF A ROTATING SPACE STATION.

Walter Krause Polstorff (NASA, Marshall Space Flight Center, Research and Development Applications Div., Computation Laboratory, Huntsville, Ala.).

IN: SIMULATION: THE DYNAMIC MODELING OF IDEAS AND SYSTEMS WITH COMPUTERS.

Edited by John McLeod.

New York, McGraw-Hill Book Co., 1968, p. 144-159. 7 refs.

Formulation of equations describing the reaction of a space vehicle to rotating machinery and to mass motion inside the vehicle. These equations include the angular impulse introduced by the moving mass. The dynamics of a cylindrical space station rotating about its major axis once every ten seconds is evaluated numerically. The long cylinder provides the large distance between the axis of rotation and the crew compartment needed to generate comfortable artificial gravity. But the rotating cylinder is known to have little dynamic stability around its longitudinal axis. Nevertheless, the stability characteristics of this configuration are found to be acceptable, provided that there is as little as 0.2% asymmetry between the major and intermediate moments of inertia. Detailed investigations were performed on an analog computer, showing the effect of path and timing on the magnitude of the disturbance caused by a mass relocation. M.M.

A69-16931 *

AN INTERPRETATION OF THE PECULIAR HELIUM STAR HZ 29.

Richard Stothers (NASA, Goddard Space Flight Center, Goddard Institute for Space Studies, New York, N.Y.).

Astrophysical Journal, vol. 154, Nov. 1968, pt. 2, p. L91-L94. 34 refs.

Discussion of the characteristics of HZ29, a faint high-latitude star that shows only lines of He I, which are unusually wide and shallow, while undergoing a photometric variation with a period of 9 and/or 18 min. It is suggested that HZ29 is a luminous star of high mass and heavy composition, and that its variability is due to nuclear-energized radial pulsations. A number of reasons are given why HZ29 should not be a white dwarf in a close-binary system as it had been first proposed. G.R.

A69-17006 *

COMPOSITION OF THE LUNAR HIGHLANDS - POSSIBLE IMPLICATIONS FOR EVOLUTION OF THE EARTH'S CRUST.

Paul D. Lowman, Jr. (NASA, Goddard Space Flight Center, Planetology Branch, Greenbelt, Md.).

Journal of Geophysical Research, vol. 74, Jan. 15, 1969, p. 495-504. 66 refs.

Theoretical investigation of the implications posed for the origin of the earth's continents and ocean basins by three possible chemical compositions of the lunar highlands: ultrabasic, basic, and intermediate to acidic. Ultrabasic or basic lunar highlands would imply that the existence of sialic crust on earth is due to some major difference between the earth and the moon; the three most likely differences are presence of an atmosphere, presence of a core, and size. The theory that continents are essentially geosynclinal accretions is shown by recent geological investigations to have numerous weaknesses and may imply an age for the earth of over 5 billion years. A proposed alternative is that large, thick primordial continents were formed by high-pressure magmatic processes caused by early segregation of the core, with later continental evolution being essentially subordinate accretion to and reworking of these protocontinents. P.v.T.

A69-17074 *#

CONTRIBUTIONS AND RESULTS OF MANNED SPACE FLIGHT PROGRAMS.

George E. Mueller (NASA, Office of Manned Space Flight, Washington, D.C.).

United Nations, Conference on the Exploration and Peaceful Uses of Outer Space, Vienna, Austria, Aug. 14-27, 1968, Paper. 14 p.

Discussion of the technological, scientific, and practical contributions resulting from the manned space flight programs of the U.S. to date. The accumulation of medical data on the ability of body organs to function without consistent gravitational forces, and under the combined effects of acceleration, weightlessness, and rapid deceleration during atmospheric reentry is reviewed, and tests to determine man's ability to perform, command, and make decisions outside the earth's atmosphere are reported. Psychological data on man's ability to endure in an isolated void are discussed. The contribution of space photography to oceanography, agriculture, weather prediction, and social engineering is cited, and the technological by-products of space research, such as the integrated circuit, are discussed in terms of their contribution to technological advances in nonspace activities. B.H.

A69-17560

INTERNATIONAL ASTRONAUTICAL FEDERATION, INTERNATIONAL ASTRONAUTICAL CONGRESS, 18TH, BELGRADE, YUGOSLAVIA, SEPTEMBER 24-30, 1967, PROCEEDINGS. VOLUME 1 - ASTRODYNAMICS, GUIDANCE AND CONTROL, MISCELLANEA.

Edited by Michał Łunc.

Oxford, Pergamon Press, Ltd.; Warsaw, Państwowe Wydawnictwo Naukowe, 1968. 640 p. In English, Russian, and French.

Price of four volumes, $90.

CONTENTS:

CONTRIBUTORS, p. v, vi.

TEN YEARS OF SPACE EXPLORATION BY THE SOVIET UNION. L. I. Sedov (Akademiia Nauk SSSR, Moscow, USSR), p. 1-17. [See A69-17561 06-30]

THE OPENING DECADE OF SPACE EXPLORATION - THE UNITED STATES PROGRAM. W. H. Pickering (California Institute of Technology, Pasadena, Calif.), p. 19-40. [See A69-17562 06-30]

FREE MOTION.

SATELLITE MOTION AROUND AN AXISYMMETRIC PLANET [DVIZHENIE SPUTNIKA OKOLO OSESIMMETRICHNOI PLANETY]. B. Popovich (Niš, Univerzitet, Niš, Yugoslavia), p. 43-55. [See A69-17563 06-30]

ON PROPERTIES OF TRAJECTORIES OF BALLISTIC REENTRY. E. A. Bockemüller (Deutsche Forschungsanstalt für Luft- und Raumfahrt, Braunschweig, West Germany), p. 57-60. [See A69-17564 06-30]

PERTURBATIONS OF STATIONARY ORBITAL SPACECRAFT AT AN ARBITRARY LATITUDE, DUE TO THE EARTH'S TRIAXIALITY [SUR LES PERTURBATIONS DES VAISSEAUX ORBITAUX STATIONNAIRES A UNE LATITUDE ARBITRAIRE, DUES A LA TRIAXIALITE DE LA TERRE]. M. M. Niță (Académie des Sciences, Bucharest, Rumania), p. 61-72. 9 refs. [See A69-17565 06-30]

VARIATIONS OF PARAMETERS FOR TRAJECTORY INTEGRATIONS BY MODERN PERTURBED-VARIATION METHODS. S. Herrick (California, University, Los Angeles, Calif.), p. 73-85. [For abstract see issue 03, page 560, Accession no. A68-14525]

A NEW METHOD OF SOLVING THE EQUATIONS OF CELESTIAL MECHANICS. N. St. Kalitzin (B'lgarska Akademiia na Naukite, Sofia, Bulgaria), p. 87, 88. [See A69-17566 06-30]

MOTION AROUND THE CENTER OF GRAVITY.

LIAPUNOV STABILITY ANALYSIS OF FREELY SPINNING SYSTEMS. P. W. Likins (California, University, Los Angeles, Calif.) and D. L. Mingori (Aerospace Corp., El Segundo, Calif.), p. 89-102. 16 refs. [See A69-17567 06-31]

ON STABILITY OF STATIONARY MOTIONS OF THE GYROSTAT-SATELLITE. V. V. Rumiantsev (Akademiia Nauk SSSR, Moscow, USSR), p. 103-108. [For abstract see issue 24, page 4241, Accession no. A67-42400]

THE STABILITY ANALYSIS OF COUPLED LIBRATIONAL MOTION OF AN AXI-SYMMETRIC SATELLITE IN A CIRCULAR ORBIT. V. J. Modi and R. C. Brereton (British Columbia, University, Vancouver, Canada), p. 109-120. [For abstract see issue 24, page 4231, Accession no. A67-42384]

ASSESSMENT OF THE ATTITUDE PERTURBATIONS OF A SPINNING SATELLITE ON AN ORBIT OF LARGE ECCENTRICITY. M. L. Renard (Carnegie-Mellon University, Pittsburgh, Pa.), p. 121-139. 32 refs. [See A69-17568 06-31]

MOTION OF AN ARTIFICIAL SATELLITE RELATIVE TO CENTER OF MASS IN A RESONANCE REGIME [DVIZHENIE ISKUSSTVENNOGO SPUTNIKA OTNOSITEL'NO TSENTRA MASS V REZONANSNOM REZHIME]. A. P. Torzhevskii (Akademiia Nauk SSSR, Moscow, USSR), p. 141-149. [For abstract see issue 17, page 3267, Accession no. A68-35193]

ROTATION AND ORIENTATION ANALYSIS OF THE PROTON 2 SATELLITE [ANALIZ VRASHCHENIIA I ORIENTATSII SPUTNIKA "PROTON-2"]. V. V. Beletskii, V. V. Golubkov, and N. G. Khatskevich (Akademiia Nauk SSSR, Moscow, USSR), p. 151-161. [For abstract see issue 17, page 3270, Accession no. A68-34411]

OPTIMIZATION. I.

SYNTHESIS OF THE ANALYTICAL RESULTS ON OPTIMAL TRANSFERS BETWEEN KEPLERIAN ORBITS [SYNTHESE DES RESULTATS ANALYTIQUES SUR LES TRANSFERTS ET LES RENDEZ-VOUS OPTIMAUX ENTRE ORBITES KEPLERIENNES]. C. Marchal, J.-P. Marec (ONERA, Châtillon-sous-Bagneux, Hauts-de-Seine, France), and C. B. Winn (Colorado State University, Fort Collins, Colo.), p. 163-198. [For abstract see issue 03, page 557, Accession no. A68-13984]

SOME RECENT RESULTS IN AEROSPACE VEHICLE TRAJECTORY OPTIMIZATION TECHNIQUES. E. J. Bauman (U.S. Air Force Academy, Colorado Springs, Colo.), C. T. Leondes (California, University, Los Angeles, Calif.), G. Paine (California Institute of Technology, Pasadena, Calif.), and R. A. Niemann, p. 199-231. 17 refs. [See A69-17569 06-30]

TRAJECTORY OPTIMIZATION BY A DIRECT DESCENT PROCESS. L. E. Fogarty and R. M. Howe (Michigan, University, Ann Arbor, Mich.), p. 233-254. 8 refs. [See A69-17570 06-30]

OPTIMAL MANEUVER FOR VEHICLE RENDEZVOUS IN MINIMUM-FUEL CIRCULAR ORBITS, TAKING INTO ACCOUNT NONLINEAR EQUATIONS OF MOTION FOR THE PURSUING VEHICLE [SUR LA MANOEUVRE OPTIMALE POUR LE RENDEZ-VOUS DES ENGINS SUR DES ORBITES CIRCULAIRES A MINIMUM DE COMBUSTIBLE, COMPTE TENU DES EQUATIONS NON LINEAIRES DU MOUVEMENT DE L'ENGIN POURSUIVANT]. A. Marinescu (Academia Română, Bucharest, Rumania), p. 255-266. 6 refs. [See A69-17571 06-31]

OPTIMIZATION. II.

CONJUGATE DIRECTION METHODS FOR PARAMETER OPTIMIZATION. H. J. Kelley and G. E. Myers (Analytical Mechanics Associates, Inc., Westbury, N.Y.), p. 267, 268.

LOW THRUST SWINGBY TRAJECTORIES. H. E. Rauch (Lockheed Aircraft Corp., Palo Alto, Calif.), p. 269-284. 13 refs. [See A69-17572 06-30]

A SUCCESSIVE APPROXIMATION TECHNIQUE FOR CONSTRUCTING A NEAR-OPTIMUM GUIDANCE LAW. C. Pfeiffer (TRW Systems Group, Redondo Beach, Calif.), p. 285-291. 6 refs. [See A69-17573 06-21]

THE HAMILTON-JACOBI METHOD APPLIED TO THE LOW-THRUST TRAJECTORY PROBLEM. W. E. Miner (NASA, Electronics Research Center, Cambridge, Mass.), B. D. Tapley, and W. F. Powers (Texas, University, Austin, Tex.), p. 293-305. 17 refs. [See A69-17574 06-30]

SUFFICIENT CONDITIONS FOR OPTIMUM FIXED TIME IMPULSIVE TRAJECTORIES. P. M. Lion (Princeton University, Princeton, N.J.), p. 307-317. 7 refs. [See A69-17575 06-30]

OPTIMUM SPACECRAFT GUIDANCE WITH MEASUREMENT UNCERTAINTY. J. J. Deyst, Jr. (Massachusetts Institute of Technology, Cambridge, Mass.), p. 319-326. 5 refs. [See A69-17576 06-21]

AN INDIRECT NUMERICAL METHOD BASED ON OFFSET VECTORS FOR OBTAINING SOLUTIONS TO OPTIMUM CONTROL PROBLEMS. C. F. Price (Massachusetts Institute of Technology, Cambridge, Mass.), p. 327-339. 11 refs. [See A69-17577 06-10]

ORBITAL TRANSFERS [CHANGEMENT D'ORBITES]. M. J. Dispés-Marcó (Productos Pirelli, S.A., Manresa, Spain), p. 341-349. [See A69-17578 06-30]

TRAJECTORY CONTROL.

A DECOUPLED SHIFTING MEMORY FILTER METHOD FOR RADIO TRACKING OF SPACE VEHICLES. R. Cosaert (European Space Vehicle Launcher Development Organization, Paris, France) and E. Gottzein (Bölkow GmbH, Ottobrunn, West Germany), p. 353-360. [For abstract see issue 24, page 4122, Accession no. A67-42385]

OPTIMUM CONTROL OF SPACE-VEHICLE ORBITAL ELEMENTS. Y. Nishikawa (California, University, Los Angeles, Calif.) and N. Sannomiya (Kyoto University, Kyoto, Japan), p. 361-378. 9 refs. [See A69-17579 06-21]

SLOSHING STABILITY INVESTIGATIONS RELATING TO THE ELDO A LAUNCH VEHICLE DURING FIRST STAGE FLIGHT. D. G. Ewart and K. F. R. Lofthouse (Hawker Siddeley Dynamics, Ltd., Stevenage, Herts., England), p. 379-392. [For abstract see issue 24, page 4241, Accession no. A67-42396]

UTILIZATION OF GROUND-BASED GUIDANCE SYSTEMS TO SUPPLEMENT ONBOARD GUIDANCE OF SPACE VEHICLES. J. P. Mayer, R. P. Parten, and R. E. Ernull (NASA, Manned Spacecraft Center, Houston, Tex.), p. 393-404. [See A69-17580 06-21]

DETERMINATION OF SPACECRAFT CONDITIONS DURING REENTRY INTO THE ATMOSPHERE [OPREDELENIE USLOVII VKHODA KOSMICHESKOGO APPARATA PRI SPUSKE V ATMOSFERE]. Iu. F. Golubev (Akademiia Nauk SSSR, Moscow, USSR), p. 405-412. [See A69-17581 06-31]

COMMENTS ON THE PROBLEM OF CONTROLLING A PILOTED SPACE VEHICLE [ZAMECHANIIA O PROBLEME UPRAVLENIIA PILOTIRUEMOGO KOSMICHESKOGO APPARATA]. N. N. Moiseev (Akademiia Nauk SSSR, Moscow, USSR), p. 413, 414.

USE OF ELECTRONIC COMPUTERS FOR DETERMINING THE AERODYNAMIC CHARACTERISTICS OF AIRCRAFT [ISPOL'ZOVANIE ELEKTRONNO-SCHETNYKH MASHIN DLIA OPREDELENIIA AERODINAMICHESKIKH KHARAKTERISTIK LETATEL'NYKH APPARATOV]. O. M. Belotserkovskii (Akademiia Nauk SSSR, Moscow, USSR), p. 415-420. [See A69-17582 06-01]

ATTITUDE CONTROL.

A SEPARABLE PAYLOAD CONTROL SYSTEM FOR ORIENTATION OF SCIENTIFIC RESEARCH INSTRUMENTS. E. E. Shaw and G. R. Strevey (Ball Brothers Research Corp., Boulder, Colo.), p. 421-435. [See A69-17583 06-31]

SIMULATION OF THE ATTITUDE STABILIZATION OF THE DODGE SPACECRAFT WITH TIME-LAG MAGNETIC DAMPING. V. L. Pisacane, P. P. Pardoe, and J. M. Whisnant (Johns Hopkins University, Silver Spring, Md.), p. 437-445. 8 refs. [See A69-17584 06-31]

NUTATIONAL STABILITY OF MULTI-BODY SPIN-STABILIZED SATELLITES. W. G. Hughes (Ministry of Technology, Royal Aircraft Establishment, Farnborough, Hants., England), p. 447-454. [See A69-17585 06-31]

ATTITUDE CONTROL PROBLEMS IN EARTH-ORIENTED SPACECRAFT - AN ILLUSTRATIVE EXAMPLE. S. D. Dorfman (Hughes Aircraft Co., El Segundo, Calif.), p. 455-466. [See A69-17586 06-31]

ATTITUDE CONTROL OF A HIGHLY ACCURATE SPACE STABILIZED PLATFORM AND EXPERIMENTAL PACKAGE. G. J. N. Smith, C. Wearmouth, and R. D. McQueen (Hawker Siddeley Dynamics, Ltd., Stevenage, Herts., England), p. 467-486. [See A69-17587 06-21]

STABILIZATION CONCEPTS FOR ASTRONOMICAL SATELLITES. W. Göschel (Bölkow GmbH, Ottobrunn, West Germany), p. 487-498. [See A69-17588 06-31]

THE DESIGN OF A LARGE ANGLE THREE-AXIS ATTITUDE SERVOMECHANISM FOR SPACECRAFT. G. Meyer (NASA, Ames Research Center, Moffett Field, Calif.), p. 499-505. [See A69-

17589 06-21]

SPACECRAFT SYSTEMS.
COMPARATIVE EVALUATION OF MECHANICALLY AND ELECTRONICALLY DESPUN ANTENNAS FOR SPACECRAFT. A. R. Giddis (Raytheon Co., Sudbury, Mass.) and T. P. Jordan (Sylvania Electric Products, Inc., Waltham, Mass.), p. 509-517. [See A69-17590 06-09]
THE HELIOGYRO, AN INTERPLANETARY FLYING MACHINE. R. H. MacNeal (Astro Research Corp., Santa Barbara, Calif.), p. 519-528. 6 refs. [See A69-17591 06-31]

PROPULSION AND REENTRY.
LIQUID ROCKET COMBUSTION - AN AERODYNAMICALLY CONTROLLED PROCESS. R. J. Priem (NASA, Lewis Research Center, Cleveland, Ohio), p. 529-537. [For abstract see issue 24, page 4256, Accession no. A67-42720]
LAMINAR BOUNDARY LAYER SEPARATION AND REATTACHMENT NEAR A CONCAVE CORNER. M. Holt (California, University, Berkeley, Calif.), p. 539-544. [See A69-17592 06-12]
A MULTI-MISSION INTERPLANETARY PROBE USING 3-KW SOLAR ELECTRIC PROPULSION. L. A. Gore, H. M. Hunter, H. F. Meissinger, and R. A. Park (TRW Systems Group, Redondo Beach, Calif.), p. 545-562. [See A69-17593 06-28]
EVALUATION OF THE EFFECTS OF SIMULATED SPACE STORAGE ON SOLID PROPELLANT ROCKET MOTORS. J. S. Hrivnak (Thiokol Chemical Corp., Elkton, Md.), p. 563-581. [See A69-17594 06-27]

LIFE IN SPACECRAFT.
PROBLEMS RELATING TO THE OBJECTIVE EVALUATION OF THE REACTIVITY OF THE ORGANISM. L. Novák (Československá Akademie Věd, Brno, Czechoslovakia), p. 583-587. 7 refs. [See A69-17595 06-04]

A69-17574 *
THE HAMILTON-JACOBI METHOD APPLIED TO THE LOW-THRUST TRAJECTORY PROBLEM.
W. E. Miner (NASA, Electronics Research Center, Guidance and Navigation Theory Branch, Cambridge, Mass.), B. D. Tapley (Texas, University, Dept. of Aerospace Engineering, Austin, Tex.), and W. F. Powers (Texas, University, Dept. of Engineering Mechanics, Austin, Tex.).
IN: INTERNATIONAL ASTRONAUTICAL FEDERATION, INTERNATIONAL ASTRONAUTICAL CONGRESS, 18TH, BELGRADE, YUGOSLAVIA, SEPTEMBER 24-30, 1967, PROCEEDINGS. VOLUME 1 - ASTRODYNAMICS, GUIDANCE AND CONTROL, MISCELLANEA. [A69-17560 06-30]
Edited by Michał Łunc.
Oxford, Pergamon Press, Ltd.; Warsaw, Państwowe Wydawnictwo Naukowe, 1968, p. 293-305. 17 refs.
Grant No. NGR-44-012-046.
The optimum motion of a continuously thrusting space vehicle is studied using Hamilton-Jacobi perturbation theory. The canonic constants of motion are obtained for a base solution in which only the inverse square gravitational force field components are considered. A procedure is shown for developing the analytical expressions for the rates of change of the canonic constants due to the effects of the engine thrust. (Author)

A69-18042 *#
MODEL ATMOSPHERES OF MERCURY.
Otha H. Vaughan, Jr. (NASA, Marshall Space Flight Center, Aerospace Environment Div., Aero-Astrodynamics Laboratory, Huntsville, Ala.).
American Institute of Aeronautics and Astronautics, Aerospace Sciences Meeting, 7th, New York, N.Y., Jan. 20-22, 1969, Paper 69-54. 16 p. 32 refs.
Members, $1.00; nonmembers, $1.50.
Model atmospheres for the planet Mercury have been developed to provide preliminary environmental criteria for use in spacecraft design and engineering trade-off studies. These models were developed by using the "most realistic" atmospheric compositions, and temperature and pressure data obtained from a survey of the literature. Atmospheric parameters are computed by using hydrostatic equations. These models were developed by considering variable molecular weight and nonisothermal temperature profiles and by assuming that the atmosphere is not dynamic. Minimum density, mean density, and maximum density models for both the dark and sunlit sides of Mercury are discussed. (Author)

A69-18090 *#
THE ASTRODYNAMICIST'S ROLE VIS-A-VIS THE SYSTEMS ENGINEER.
J. Reynolds Duncan, Jr. (NASA, Marshall Space Flight Center, Huntsville, Ala.).
American Institute of Aeronautics and Astronautics, Aerospace Sciences Meeting, 7th, New York, N.Y., Jan. 20-22, 1969, Paper 69-124. 12 p.
Members, $1.00; nonmembers, $1.50.
Discussion of the problem of effective two-way communications, with emphasis placed upon the compilation of astrodynamical data for use by the system engineer in the preliminary phases of mission planning. Such data should be presented in a form which is easily understood and which cannot be easily misinterpreted by persons with little or no knowledge of astrodynamics. Wherever astrodynamical parameters may impose constraints upon a mission, a clear indication should be given of the possible consequences for violation of these constraints. When alternatives are available, they should be indicated, along with any penalties associated with their use. The results of the astrodynamicist's effort should be a well-informed system engineer who has the overall picture of the effects of astrodynamical parameters upon a mission and thus will be able to perform meaningful tradeoff studies with regards to system design and performance. P.v.T.

A69-18601 *
THE OPPOSITION EFFECT OF MARS AND ITS IMPLICATIONS.
B. T. O'Leary (NASA, Manned Spacecraft Center, Houston, Tex.) and D. G. Rea (California, University, Space Sciences Laboratory, Berkeley, Calif.; NASA, Washington, D.C.).
Icarus, vol. 9, Nov. 1968, p. 405-428. 41 refs.
Grant No. NsG-101-61; Contract No. NASr-220.
An extensive analysis of photometric and spectrophotometric measurements of Mars is performed. Included are details of the Martian opposition effect reported earlier by O'Leary and their relationship with corresponding measurements of various samples in the laboratory. It is found that the ferric oxides - limonite, goethite, and hematite - all show a greater opposition effect than does Mars. These samples showed very small limb-darkening, again in disagreement with the Martian case. There is finally the 0.87-μ ferric oxide band which is missing in the Martian spectrum. These three points argue strongly against limonites, goethites, or hematites as the predominant covering for the Martian surface. This interpretation does not contradict previous polarimetric data, since the polarimetric results are sufficiently uncertain as to encompass many possible substances. (Author)

A69-18604 *
GENETIC IMPLICATIONS OF LUNAR REGOLITH THICKNESS VARIATIONS.
Verne R. Oberbeck and William L. Quaide (NASA, Ames Research Center, Moffett Field, Calif.).
Icarus, vol. 9, Nov. 1968, p. 446-465. 25 refs.
Analysis of the distribution of the thickness of the regolith in 12 Lunar Orbiter sites. Each of the sites analyzed has one of four types of thickness distribution characterized by approximate median values of 3.3, 4.6, 7.5, and 16 m. The regolith thickness correlates directly with cratering density, and the average regolith thickness computed from volumes of all craters in an area is in excellent agreement with the measured average thickness determined through use of normal and concentric craters. The forms of the distributions of thickness determined from crater ejecta distribution maps are also in excellent agreement with the forms of measured distributions. The results indicate that most of the craters considered and the regolith must be of impact origin. Evidence is presented which supports the view that the substrate rocks are of volcanic flow origin, and that flow activity occurred repeatedly in any one place

but came to a close at different times in different regions of the moon. P. v. T.

A69-18607 *

THE LOWER IONOSPHERE OF MARS.

A. C. Aikin (NASA, Goddard Space Flight Center, Laboratory for Space Sciences, Greenbelt, Md.).

Icarus, vol. 9, Nov. 1968, p. 487-497. 61 refs.

Study of the ionization of the Martian atmosphere below 100 km in the context of recent data on the atmosphere and ionosphere of the planet. Suggested sources of ionization include: solar ultraviolet and X-radiation, cosmic rays, meteors, radioactive material within the atmosphere, radioactivity of the surface, the solar wind, and protons originating from solar flares. Loss processes, including charge rearrangement, dissociative recombination of ions and electrons, and negative ion formation are detailed. Possible importance of the negative ion CO_4^- is discussed. Its distribution will depend on the O_2 content of the atmosphere as well as the distribution of O and CO. CO^- and CO_3^- may also be present in the ionosphere. It is shown that combination of the solar photoionization rate with that due to cosmic radiation will lead to an ion density minimum. The magnitude of the ion density and location of the minimum will depend on the atmospheric model chosen, solar activity, and solar zenith angle as well as such factors as the presence of particulate matter and meteor ionization. (Author)

A69-19262 *

WATER ON THE MOON AND A NEW NONDIMENSIONAL NUMBER.

John A. O'Keefe (NASA, Goddard Space Flight Center, Greenbelt, Md.).

Science, vol. 163, Feb. 14, 1969, p. 669, 670. 8 refs.

A nondimensional number called the Jeffreys number, which represents the ratio of the Reynolds number to the Froude number, is useful in geophysical problems related to the motion of viscous masses under gravity. The Jeffreys number is used to show that it is impossible for the lunar maria to be underlain by a layer of material 1 km thick and having the plastic properties of ice. (Author)

A69-19404 *

UPPER LIMITS TO THE INTENSITY OF BACKGROUND RADIATION AT $\lambda = 1.32$, 0.559, AND 0.359 MM.

V. J. Bortolot, Jr., J. F. Clauser (Columbia University, Physics Dept., New York, N. Y.), and P. Thaddeus (NASA, Goddard Space Flight Center, Goddard Institute for Space Studies; Columbia University, Physics Dept., New York, N. Y.).

Physical Review Letters, vol. 22, Feb. 17, 1969, p. 307-310. 14 refs.

From observations of interstellar optical absorption lines of CN, CH, and CH^+, it is possible to impose upper limits, at three wavelengths, on the intensity of background radiation in the interstellar medium. These limits are consistent with the existence of thermal background radiation at a temperature of ~3 K, but can be reconciled with the results of a recent rocket observation by Shivanandan, Houck, and Harwit only if the intense flux which they report is concentrated into a sharp line which happens to avoid the molecular resonances, or if this flux is of local origin. (Author)

A69-19715 *

COSMIC RADIO NOISE INTENSITY FROM 0.45 TO 3.0 MHz OBSERVED BY THE ATS II SATELLITE.

Richard R. Weber, Robert G. Stone, and C. Raymond Somerlock (NASA, Goddard Space Flight Center, Greenbelt, Md.).

Astronomy and Astrophysics, vol. 1, Jan. 1969, p. 44-47. 18 refs.

Discussion of cosmic radio-noise measurements conducted by a satellite-borne Ryle-Vonberg radiometer with a 76-m wide angle V antenna. The measurements were obtained from 0.45 to 3.0 MHz for an altitude range of 180 to 11,000 km. The existence of some spacecraft radio interference allows establishment only of upper limits to the continuum spectrum, which shows a substantial decrease at the lower frequencies. Using this data and other low frequency observations in a two-component Galactic model, an emission measure of 1.2 cm^{-6} pc toward the Galactic poles is computed. G. R.

A69-19874 *#

PERIODIC ORBITS IN THE RESTRICTED THREE-BODY PROBLEM IN THE NEIGHBORHOOD OF RESONANCES OF TYPE (k + 1)/k [ÜBER PERIODISCHE BAHNEN IM EINGESCHRÄNKTEN DREIKÖRPERPROBLEM UND IN DER NÄHE DER KOMMENSURABILITÄTEN VOM TYPUS (k + 1)/k].

Lloyd H. Carpenter (NASA, Goddard Space Flight Center, Greenbelt, Md.) and Karl Stumpff.

Astronomische Nachrichten, vol. 291, no. 1, 1968, p. 25-35. In German.

Numerical investigations of the form and character of periodic solutions of the restricted three-body problem in the sun-Jupiter system and in the neighborhood of resonances of type (k+1)/k. The results obtained give new insight into the genealogy of periodic orbits in the regions which do not contain Poincare solutions of the first kind. Z. W.

A69-20051 *

THE GALAXY M82. I - ANALYSIS OF THE OBSERVATIONS.

Alan B. Solinger (Michigan, University, Dept. of Physics, Ann Arbor, Mich.; NASA, Goddard Space Flight Center, Goddard Institute for Space Studies, New York, N. Y.).

Astrophysical Journal, vol. 155, Feb. 1969, pt. 1, p. 403-415. 29 refs.

AEC-supported research.

Analysis of the relevant radio and optical data shows that a synchrotron interpretation of the polarized optical continuum observed at large distances from the center of M82 should be ruled out. It is shown that the $H\alpha$ emission from the filaments is collisionally excited, and that a blast-wave interpretation of the explosion provides a suitable heating mechanism. The observed circular orientation of the electric vectors of the polarized light can be produced by scattering of light from a proposed Seyfert-like nucleus (located at the center of the explosion) by free electrons behind the shock front. The optical luminosity of the nucleus is estimated to be of order 10^{43} ergs/sec (just about that of a Seyfert nucleus). It is probably obscured by dust. On the basis of the extant data, it is concluded that M82 should be regarded as a Seyfert-like galaxy, seen edge-on. This eliminates two incongruities associated with the galaxy: those of its being the only radio irregular, and only exploding irregular. (Author)

A69-20624 *

NATURE OF RADIO AND OPTICAL EMISSIONS FROM PULSARS.

Hong-Yee Chiu, Vittorio Canuto (NASA, Goddard Space Flight Center, Goddard Institute for Space Studies, New York, N. Y.), and Laura Fassio-Canuto (New York, State University, Dept. of Earth and Space Sciences, Stony Brook, N. Y.).

Nature, vol. 221, Feb. 8, 1969, p. 529-531. 9 refs.

Consideration of how rotating and oscillating magnetic neutron stars can account for the radio and optical signals from pulsars. It is shown that the theory for ultraviolet line emissions already advanced by the authors can also account for the optical pulses observed by Cocke et al. (1969). Several predictions concerning the nature of the signals are put forward. F. R. L.

A69-20644 *

MASS LOSS FROM CORONAE AND ITS EFFECT UPON STELLAR ROTATION.

Kyoji Nariai (NASA, Goddard Space Flight Center, Greenbelt, Md.).

(International Astronomical Union, Colloquium on Mass Loss from Stars, Trieste, Italy, Sept. 12-16, 1968.)

Astrophysics and Space Science, vol. 3, Jan. 1969, p. 150-159. 36 refs.

Calculation of the acoustic energy-generation rate from the convective zone for various models. Results show that a chromosphere and a corona can be expected around stars with temperatures lower than 8000 K at the main sequence, and lower than 6500 K at $\log g = 2$. When a star is rotating rapidly, mass loss from its corona is large and can be an effective mechanism of braking the stellar rotation. If this mechanism is effective, the slow rotation of stars later than F2 may be attributed to a loss of angular momentum through a stellar wind that is effective in their main-sequence phase. Stars with mass $M > 1.5$ $M_\odot$ lose mass through a stellar wind during their contraction phase. The mass-loss rate is larger than the solar value because of the larger energy input into the chromosphere-corona system and be-

cause of the smaller gravitational potential at the surface. T Tauri stars may be the observational counterparts for such stars. Since the duration of the contraction phase is very short (less than 10^7 years), the braking mechanism works only in the presence of a strong magnetic field (Ap) or in the presence of a companion (Am). (Author)

A69-20686 *

METEORITE FALL AT PUEBLITO DE ALLENDE, CHIHUAHUA, MEXICO - PRELIMINARY INFORMATION.

E. A. King, Jr., E. Schonfeld, K. A. Richardson (NASA, Manned Spacecraft Center, Lunar Receiving Laboratory, Houston, Tex.), and J. S. Eldridge (Oak Ridge National Laboratory, Oak Ridge, Tenn.).

Science, vol. 163, Feb. 28, 1969, p. 928, 929.

Description of the properties specimens from the meteorite fall in 1969 at Chihuahua, Mexico. The meteorite is a chondrite (C3 and C4) with both opaque and microcrystalline matrices. Specimens were brought to a low background gamma counter less than four and a half days after the fall, and gamma rays from short-lived isotopes have been observed. B. H.

A69-20729 *

RADIO EMISSION FROM MAGNETIC NEUTRON STARS - A POSSIBLE MODEL FOR PULSARS.

Hong-Yee Chiu and Vittorio Canuto (NASA, Goddard Space Flight Center, Goddard Institute for Space Studies, New York, N.Y.).

Physical Review Letters, vol. 22, Mar. 3, 1969, p. 415-419. 22 refs.

Demonstration that the radio emission from a neutron star with a magnetic field of 10^9 G or more can account for the radio emission of pulsars. It is suggested that pulsars also emit two bands, one in the UV or optical, and the other in the IR in the decamicron wavelength range. M. G.

A69-20770 *

THE INSTABILITY OF STELLAR STRUCTURES INTERMEDIATE BETWEEN WHITE DWARFS AND NEUTRON STARS.

A. G. W. Cameron (Yeshiva University, Belfer Graduate School of Science; NASA, Goddard Space Flight Center, Goddard Institute for Space Studies, New York, N.Y.) and J. M. Cohen (NASA, Goddard Space Flight Center, Goddard Institute for Space Studies, New York, N.Y.).

Astrophysical Letters, vol. 3, Jan. 1969, p. 3-5. 6 refs.
AEC-NSF-NASA-supported research.

Discussion of Drake's suggestion (1968) that apparent multimillisecond periodicities in pulsar signals may correspond to vibrations of neutron stars. In the present work, stellar models are reexamined in the appropriate density range (of the order of 10^{13} gm/cm^3) with an improved equation of state. It is concluded that suitable structures, intermediate between white dwarfs and neutron stars, are unlikely. M. G.

A69-20892

ORIGIN AND DISTRIBUTION OF THE ELEMENTS; PROCEEDINGS OF THE INTERNATIONAL SYMPOSIUM, PARIS, FRANCE, MAY 8-11, 1967.

Symposium sponsored by UNESCO and the International Union of Geological Sciences.
Edited by L. H. Ahrens (Cape Town, University, Cape Town, Republic of South Africa).
Oxford, Pergamon Press, Ltd. (International Series of Monographs in Earth Sciences. Volume 30), 1968. 1192 p. In English and French. $48.

CONTENTS:

PREFACE. L. H. Ahrens (Cape Town, University, Cape Town, Republic of South Africa), p. ix, x.

INTRODUCTORY REMARKS. E. Ingerson (Texas, University, Austin, Tex.), p. xi-xvii.

THEORIES OF ORIGIN.

THE EMPIRICAL FOUNDATIONS OF NUCLEOSYNTHESIS. W. A. Fowler (California Institute of Technology, Pasadena, Calif.), p. 3-29. 61 refs. [See A69-20893 08-24]

PRIMEVAL ELEMENT ABUNDANCES. P. J. E. Peebles (Princeton University, Princeton, N.J.), p. 31-37. 21 refs. [See A69-20894 08-30]

VIBRATIONAL INSTABILITY OF MASSIVE STARS AND HELIUM FORMATION [INSTABILITE VIBRATIONNELLE DES ETOILES MASSIVES ET FORMATION D'HELIUM]. A. Boury and P. Ledoux (Liège, Université, Liège, Belgium), p. 39-41. 10 refs. [See A69-20895 08-30]

NEUTRON CAPTURE CROSS-SECTIONS AND THE S-PROCESS. J. H. Gibbons and R. L. Macklin (Oak Ridge National Laboratory, Oak Ridge, Tenn.), p. 43-62. 15 refs. [See A69-20896 08-24]

NUCLEOSYNTHESIS OF THE ISOTOPES OF LEAD. D. D. Clayton, p. 63-76. 11 refs. [See A69-20897 08-24]

NUCLEOSYNTHESIS IN SUPERNOVA EXPLOSIONS. J. W. Truran, W. D. Arnett (NASA, Goddard Space Flight Center, New York, N.Y.), S. Tsuruta (Smithsonian Institution, Cambridge, Mass.), and A. G. W. Cameron (Yeshiva University; NASA, Goddard Space Flight Center, New York, N.Y.), p. 77-89. 17 refs. [See A69-20898 08-30]

THE UTILIZATION OF NUCLEAR PARTICLE TRACKS IN SOLIDS TO STUDY THE DISTRIBUTION OF CERTAIN ELEMENTS IN NATURE AND IN THE COSMIC RADIATION. P. B. Price, R. L. Fleischer (General Electric Co., Schenectady, N.Y.), and R. M. Walker (Washington University, St. Louis, Mo.), p. 91-100. 19 refs. [See A69-20899 08-30]

ON THE EXISTENCE OF PLUTONIUM-244 IN THE EARLY SOLAR SYSTEM. P. K. Kuroda and R. Ganapathy (Arkansas, University, Fayetteville, Ark.), p. 101-109. 22 refs. [See A69-20900 08-30]

NUCLEOSYNTHESIS OF LITHIUM, BERYLLIUM, AND BORON, AND THE FORMATION OF THE SOLAR SYSTEM [SUR LA NUCLEOSYNTHESE DU LITHIUM, DU BERYLLIUM ET DU BORE ET LA FORMATION DU SYSTEME SOLAIRE]. R. Bernas, E. Gradsztajn, H. Reeves, F. Yiou (Centre National de la Recherche Scientifique, Orsay, Essonne, France), and E. Schatzman (Centre National de la Recherche Scientifique, Paris, France), p. 111-116. 11 refs. [See A69-20901 08-30]

ASTROPHYSICAL IMPLICATIONS OF THE STELLAR ABUNDANCES OF Li, Be AND B. H. Reeves (Centre National de la Recherche Scientifique, Orsay, Essonne; Centre National de la Recherche Scientifique, Paris, France), p. 117-123. 7 refs. [See A69-20902 08-30]

A NEW TABLE OF ABUNDANCES OF THE ELEMENTS IN THE SOLAR SYSTEM. A. G. W. Cameron (Yeshiva University; NASA, Goddard Space Flight Center, New York, N.Y.), p. 125-143. 15 refs. [See A69-20903 08-30]

SOLAR, STELLAR AND INTERSTELLAR ABUNDANCES.

THE CHEMICAL COMPOSITION OF NORMAL STELLAR ATMOSPHERES. L. H. Aller (California, University, Los Angeles, Calif.), p. 147-153. 7 refs. [See A69-20904 08-30]

THE SOLAR ABUNDANCES. E. A. Müller (Observatoire, Geneva, Switzerland), p. 155-176. 82 refs. [See A69-20905 08-30]

SOLAR ABUNDANCES OF SOME REPRESENTATIVE ELEMENTS FROM THE STANDPOINT OF NUCLEOSYNTHESIS [ABONDANCES SOLAIRES DE QUELQUES ELEMENTS REPRESENTATIFS AU POINT DE VUE DE LA NUCLEOSYNTHESE]. N. Grevesse, G. Blanquet, and A. Boury (Liège, Université, Liège, Belgium), p. 177-182. 16 refs. [See A69-20906 08-30]

ON THE ABUNDANCES IN THE SOLAR CORONA. S. R. Pottasch (Groningen, Rijksuniversiteit, Groningen, Netherlands), p. 183-190. 6 refs. [See A69-20907 08-30]

CHEMICAL COMPOSITIONS OF DIFFUSE NEBULAE. L. H. Aller (California, University, Los Angeles, Calif.), p. 191-193. 8 refs. [See A69-20908 08-30]

CHEMICAL COMPOSITION OF OLD STARS. B. E. J. Pagel (Royal Greenwich Observatory, Herstmonceux, Sussex, England), p. 195-204. 28 refs. [See A69-20909 08-30]

THE COMPOSITION OF LATE-TYPE PECULIAR STARS. B. Warner (Oxford University, Oxford, England), p. 205-223. 126 refs. [See A69-20910 08-30]

ABUNDANCES IN THE MAGNETIC STARS. W. P. Bidelman (Michigan, University, Ann Arbor, Mich.), p. 225-231. 26 refs. [See A69-20911 08-30]

THE PROBLEM OF LITHIUM AND THE OTHER LIGHT ELEMENTS DEUTERIUM, BERYLLIUM AND BORON. M. Hack (Trieste, Osservatorio Astronomico, Trieste, Italy), p. 233-238.

18 refs. [See A69-20912 08-30]

DETAILED ANALYSIS OF THE STAR ϕ AURIGAE. G. Cayrel de Strobel (NASA, Goddard Space Flight Center, New York, N.Y.), p. 239-243. 5 refs. [See A69-20913 08-30]

METEORITES.

THE PROBLEM OF ELEMENTAL ABUNDANCES. H. C. Urey (California, University, La Jolla, Calif.), p. 247-253. 23 refs. [See A69-20914 08-30]

SOLAR ELEMENT ABUNDANCES AND THE COMPOSITION OF METEORITES. H. E. Suess (California, University, La Jolla, Calif.), p. 255, 256.

FRACTIONATION OF SOME ABUNDANT LITHOPHILE ELEMENT RATIOS IN CHONDRITES. L. H. Ahrens and H. von Michaëlis (Cape Town, University, Cape Town, Republic of South Africa), p. 257-272. 31 refs. [See A69-20915 08-30]

RARE EARTH ABUNDANCES IN METEORITIC CHONDRULES. R. A. Schmitt, R. H. Smith, and D. A. Olehy (Gulf General Atomic, Inc., San Diego, Calif.; Oregon State University, Corvallis, Ore.), p. 273-282. 21 refs. [See A69-20916 08-30]

INDIUM ABUNDANCES IN CHONDRITIC AND ACHONDRITIC METEORITES AND IN TERRESTRIAL ROCKS. R. A. Schmitt (Gulf General Atomic, Inc., San Diego, Calif.) and R. H. Smith (Oregon State University, Corvallis, Ore.), p. 283-300. 44 refs. [See A69-20917 08-30]

THE DISTRIBUTION OF GOLD AND IRIDIUM IN METEORITIC AND TERRESTRIAL MATERIALS. W. D. Ehmann and P. A. Baedecker (Kentucky, University, Lexington, Ky.), p. 301-311. 12 refs. [See A69-20918 08-30]

ABUNDANCES OF SOME VOLATILE ELEMENTS IN METEORITES. W. D. Ehmann, K. W. Lieberman, J. T. Tanner (Kentucky, University, Lexington, Ky.), and J. F. Lovering (Australian National University, Canberra, Australia), p. 313-319. 23 refs. [See A69-20919 08-30]

MERCURY ABUNDANCES AND THERMAL HISTORY OF METEORITES. G. W. Reed and S. Jovanovic (Argonne National Laboratory, Argonne, Ill.), p. 321-328. 11 refs. [See A69-20920 08-30]

A COMPARISON OF TRACE ELEMENT DISTRIBUTION IN THE METAL PHASE OF CHONDRITES AND IN IRON METEORITES. A. A. Smales, D. Mapper, and K. F. Fouché (United Kingdom Atomic Energy Authority, Harwell, Berks., England), p. 329-344. 31 refs. [See A69-20921 08-30]

DISTRIBUTION OF TRACE ELEMENTS IN SMITHONIA IRON METEORITE BY SPARK SOURCE MASS SPECTROMETRY. E. Berkey and G. H. Morrison (Cornell University, Ithaca, N.Y.), p. 345-357. 9 refs. [See A69-20922 08-30]

CHLORINE AS AN INDICATOR OF TERRESTRIAL CONTAMINATION IN IRON METEORITES. E. Berkey and D. E. Fisher (Cornell University, Ithaca, N.Y.), p. 359-366. 10 refs. [See A69-20923 08-30]

EXTINCT RADIOACTIVITIES AND THE HISTORY OF THE ELEMENTS AND THE SOLAR SYSTEM. J. H. Reynolds (California, University, Berkeley, Calif.), p. 367-377. 23 refs. [See A69-20924 08-30]

NEON AND XENON IN CARBONACEOUS CHONDRITES. R. O. Pepin (Minnesota, University, Minneapolis, Minn.), p. 379-386. 22 refs. [See A69-20925 08-30]

THE DISTRIBUTION OF POTASSIUM AND ARGON IN CHONDRITES. G. Turner (Sheffield, University, Sheffield, England), p. 387-398. 7 refs. [See A69-20926 08-30]

AGES OF SILICATE INCLUSIONS IN IRON METEORITES. D. S. Burnett, G. J. Wasserburg, D. D. Bogard, and P. Eberhardt (California Institute of Technology, Pasadena, Calif.), p. 399-409. 16 refs. [See A69-20927 08-30]

RADIOGENIC AND COSMIC-RAY EXPOSURE AGES OF METEORITES, THEIR ORBITS AND PARENT BODIES. H. Wänke (Max-Planck-Institut für Chemie, Mainz, West Germany), p. 411-421. 25 refs. [See A69-20928 08-30]

DYNAMICAL STUDIES OF ASTEROIDAL AND COMETARY ORBITS AND THEIR RELATION TO THE ORIGIN OF METEORITES. G. W. Wetherill (California, University, Los Angeles, Calif.), p. 423-443. 37 refs. [See A69-20929 08-30]

THE COMETARY ORIGIN OF METEORS DEDUCED FROM THE EFFECT OF SOLAR COSMIC RADIATION ON METEORITES AND THE SIGNIFICANCE OF THIS ORIGIN [ORIGINE COMETAIRE DES METEORITES DEDUITE DE L'EFFET DU RAYONNEMENT COSMIQUE SOLAIRE DANS LES METEORITES ET LA CONSEQUENCE DE CETTE ORIGINE]. Y. Yokoyama, H. Mabuchi, and J. Labeyrie (Commissariat à l'Energie Atomique; Centre Nationale de la Recherche Scientifique, Gif-sur-Yvette, Essonne, France), p. 445-456. 23 refs. [See A69-20930 08-30]

THE LL-GROUP CHONDRITES. K. Fredriksson, J. Nelen, and B. J. Fredriksson (Smithsonian Institution, Washington, D.C.), p. 457-466. 27 refs. [See A69-20931 08-30]

MORPHOLOGICAL VARIATIONS OF THE MAGNETITE OF CARBONACEOUS METEORITES OF ALAIS, IVUNA AND ORGUEIL [VARIATIONS MORPHOLOGIQUES DE LA MAGNETITE DES METEORITES CARBONEES D'ALAIS, IVUNA ET ORGUEIL]. J. Jedwab (Bruxelles, Université Libre, Brussels, Belgium), p. 467-478. 25 refs. [See A69-20932 08-30]

EVALUATION OF THE ABLATION RATE OF SAINT-SEVERIN AMPHOTERITE ON THE BASIS OF A STUDY OF THE TRACKS OF HEAVY IONS IN THE PRIMARY FLUX OF COSMIC RADIATION [EVALUATION DU TAUX D'ABLATION DE L'AMPHOTERITE DE SAINT-SEVERIN PAR L'ETUDE DES TRACES D'IONS LOURDS DU FLUX PRIMAIRE DU RAYONNEMENT COSMIQUE]. Y. Cantelaube and P. Pellas (Ministère de l'Education, Paris, France), p. 479-491. 12 refs. [See A69-20933 08-30]

PLANETS, ASTEROIDS, COMETS, TEKTITES.

CHEMICAL ABUNDANCES IN PLANETARY ATMOSPHERES. T. Owen (IIT Research Institute, Chicago, Ill.), p. 495-508. 44 refs. [See A69-20934 08-30]

THE SURFACE GEOCHEMISTRY OF SOLID BODIES IN SPACE. E. J. Zeller (Kansas, University, Lawrence, Kan.) and L. B. Ronca (USAF, Cambridge Research Laboratories, Bedford, Mass.), p. 509-519. 24 refs. [See A69-20935 08-30]

BORON IN TEKTITES. A. A. Mills (United Kingdom Atomic Energy Authority, Atomic Energy Research Establishment, Harwell, Berks., England), p. 521-531. 50 refs. [See A69-20936 08-30]

GEOCHEMISTRY OF AUSTRALIAN IMPACT GLASSES AND TEKTITES (AUSTRALITES). S. R. Taylor (Australian National University, Canberra, Australia; California, University, La Jolla, Calif.), p. 533-541. 34 refs. [See A69-20937 08-30]

DENSITY OF ZODIACAL DUST IN INTERPLANETARY SPACE. J. W. Rhee (Maryland, University, College Park, Md.), p. 543-546. 8 refs. [See A69-20938 08-30]

TERRESTRIAL ABUNDANCES.

THE COMPOSITION OF THE CRUST. K. K. Turekian (Yale University, New Haven, Conn.), p. 549-557. 16 refs. [See A69-20939 08-13]

GEOCHEMISTRY OF ANDESITES. S. R. Taylor (Australian National University, Canberra, Australia; California, University, La Jolla, Calif.), p. 559-583. 35 refs. [See A69-20940 08-13]

BRIEF NOTES ON ELEMENTAL ABUNDANCES IN ULTRAMAFIC ROCKS. L. H. Ahrens (Cape Town, University, Cape Town, Republic of South Africa), p. 585, 586.

THE GEOCHEMICAL EVOLUTION OF CONTINENTAL ROCKS - A MODEL. T. F. W. Barth (Mineralogisk-Geologisk Museum, Oslo, Norway), p. 587-597.

ABUNDANCES OF THE CHEMICAL ELEMENTS IN THE MAIN ROCK TYPES OF THE LITHOSPHERE IN RELATION TO A SYSTEM OF CORRELATIONS. E. Schroll (Bundesministerium für Handel und Wiederaufbau, Vienna, Austria), p. 599-617.

EQUILIBRIUM DISTRIBUTION OF ELEMENTS BETWEEN COEXISTING SOLID-SOLUTION PHASES. A. Muan (Pennsylvania State University, University Park, Pa.), p. 619-627.

DISTRIBUTION REGULARITIES OF TRACE ELEMENTS IN GRANITOID INTRUSIONS OF THE BATHOLITH AND HYPABYSSAL TYPES. L. V. Tauson (Akademiia Nauk SSSR, Institut Geokhimii, Irkutsk, USSR), p. 629-639.

THE FUNCTION OF THE RARE ELEMENT DISTRIBUTION IN GRANITOIDS AND THEIR PARAMETERS. M. I. Kuzmin (Akademiia Nauk SSSR, Institut Geokhimii, Irkutsk, USSR), p. 641-648.

DISTRIBUTION REGULARITIES OF TRACE ELEMENTS IN MINERALS OF GRANITOIDS. V. D. Kozlov (Akademiia Nauk SSSR, Institut Geokhimii, Irkutsk, USSR), p. 649-661.

DISTRIBUTION OF RARE-EARTH ELEMENTS (RE), YTTRIUM, BERYLLIUM AND TIN IN ALKALINE GRANITOIDS AND THEIR METASOMATITES. L. V. Tauson, V. I. Kovalenko, A. S. Znamenskaia, L. L. Petrov, V. A. Legeido, E. I. Popolitov, and S. R. Prokopenko (Akademiia Nauk SSSR, Institut Geokhimii, Irkutsk, USSR), p. 663-677.

ON STATISTICAL DISTRIBUTION OF THE AVERAGE ABUNDANCES OF CHEMICAL ELEMENTS IN THE EARTH'S CRUST AND METEORITES. A. A. Beus (All-Union Polytechnical Institute, Moscow, USSR), p. 679-685. 5 refs. [See A69-20941 08-13]

DISTRIBUTION OF Pb-ISOTOPES, Sn, Nb, Ta, Zr AND Hf IN GRANITOIDS OF NIGERIA. A. I. Tugarinov, V. I. Kovalenko, E. B. Znamenskii, V. A. Legeido, E. V. Sobatovich, S. B. Brandt, and V. D. Tsykhanskii (Akademiia Nauk SSSR, Institut Geokhimii i Analiticheskoi Khimii, Moscow, USSR), p. 687-699.

GEOCHEMISTRY OF ALKALIS IN GRANITOID ROCKS - ENDOMORPHISM OR HYDROTHERMAL METASOMATISM IN THE DIORITES AND QUARTZ GABBROS IN THE PYRENEES [SUR LA GEOCHIMIE DES ALCALINS DANS LES ROCHES DE GRANITISATION - ENDOMORPHISME OU METASOMATOSE HYDROTHERMALE DANS LES DIORITES ET GABBROS QUARTZIQUES DES PYRENEES]. M. Roubault and H. de la Roche (Centre de Recherches Pétrographiques et Géochimiques, Nancy, France), p. 701-719.

GEOCHEMISTRY OF THE PEGMATITES IN YUGOSLAVIA [LA GEOCHIMIE DES PEGMATITES EN YOUGOSLAVIE]. S. Pavlović and D. Nikolić (Beograd, Univerzitet, Belgrade, Yugoslavia), p. 721-737.

LEAD CONTENTS IN K-FELDSPARS OF YOUNG IGNEOUS ROCKS OF THE DINARIDES AND NEIGHBOURING AREAS. N. Cuturic, N. Kafol (Institute of Geological and Geophysical Research, Belgrade, Yugoslavia), and S. Karamata (Beograd, Univerzitet, Belgrade, Yugoslavia), p. 739-747.

DISTRIBUTION OF Be IN GRANITIC ROCKS OF THE SWISS ALPS. T. Hügi, J.-P. Saheurs, and E. Spycher (Bern, Universität, Berne, Switzerland), p. 749-760.

LITHIUM, SODIUM AND POTASSIUM IN ALPINE ULTRAMAFIC ROCKS. Z. Maksimović and S. Maksimović (Beograd, Univerzitet, Belgrade, Yugoslavia), p. 761-775.

GEOCHEMICAL INVESTIGATION ON DIFFERENTIATED GRANITE PLUTONS IN THE BLACK FOREST. P. Hahn-Weinheimer and H. Johanning (München, Technische Hochschule, Munich, West Germany), p. 777-793.

MAGMATIC DIFFERENTIATION AND AUTOMETASOMATISM IN A ZONED GRANITIC BATHOLITH FROM CENTRAL TEXAS, U.S.A. P. C. Ragland, G. K. Billings, and J. A. S. Adams (North Carolina, University, Chapel Hill, N.C.; Louisiana State University, Baton Rouge, La.; William Marsh Rice University, Houston, Tex.), p. 795-823.

ON THE DISTRIBUTION AND ROLE OF OXYGEN IN THE GEOCHEMISTRY OF THE EARTH'S CRUST. A. Volborth (Nevada, University, Reno, Nev.), p. 825-854.

RADIOACTIVE ELEMENTS IN THE CANADIAN PRECAMBRIAN SHIELD AND THE INTERIOR OF THE EARTH. D. M. Shaw (McMaster University, Hamilton, Ontario, Canada), p. 855-870.

THE TERRESTRIAL ABUNDANCE RELATIONSHIP BETWEEN POTASSIUM AND RUBIDIUM. A. J. Erlank (Cape Town, University, Cape Town, Republic of South Africa), p. 871-888.

RELATIVE AND ABSOLUTE TERRESTRIAL ABUNDANCES OF THE RARE EARTHS. L. A. Haskin, F. A. Frey, T. R. Wildeman (Wisconsin, University, Madison, Wis.), and M. A. Haskin (Max-Planck-Institut für Kernphysik, Heidelberg, West Germany), p. 889-912. 17 refs. [See A69-20942 08-13]

STUDY OF THE DISTRIBUTION AND ABUNDANCE OF TRANSITION ELEMENTS IN THE EARTH'S CRUST COMPARED TO THE RARE EARTHS [ETUDE DE LA DISTRIBUTION ET DE L'ABONDANCE DES ELEMENTS DE TRANSITION DANS L'ECORCE TERRESTRE, COMPAREE A CELLES DES TERRES RARES]. C. J. Allègre, M. Javoy, and G. Michard (Paris, Université, Saint-Maur, Val-de-Marne, France), p. 913-928. 12 refs. [See A69-20943 08-13]

PARTITION COEFFICIENTS OF RARE-EARTH ELEMENTS AND BARIUM BETWEEN IGNEOUS MATRIX MATERIAL AND ROCK-FORMING-MINERAL PHENOCRYSTS. I. C. C. Schnetzler and J. A. Philpotts (NASA, Goddard Space Flight Center, Greenbelt, Md.), p. 929-938. 12 refs. [See A69-20944 08-13]

GENESIS OF CONTINENTAL DIABASES AND OCEANIC THOLEIITES CONSIDERED IN LIGHT OF RARE-EARTH AND BARIUM ABUNDANCES AND PARTITION COEFFICIENTS. J. A. Philpotts and C. C. Schnetzler (NASA, Goddard Space Flight Center, Greenbelt, Md.), p. 939-947. 19 refs. [See A69-20945 08-13]

THE ABUNDANCE OF CO_2 IN THE EARTH'S ATMOSPHERE THROUGH GEOLOGIC TIME. H. D. Holland (Princeton University, Princeton, N.J.), p. 949-954. [See A69-20946 08-13]

THE DISTRIBUTION OF RADIOGENIC GASES IN THE REGIONS OF EXOCONTACTS OF INTRUSIONS AND IN CONTACT ZONES OF SOME MINERALS BEING IN PARAGENETIC EQUILIBRIUM. S. B. Brandt, V. I. Kovalenko, I. L. Lapides, V. N. Smirnoff, and N. V. Volkova (Akademiia Nauk SSSR, Institut Geokhimii, Irkutsk, USSR), p. 955-965.

SOURCE OF HELIUM IN NATURAL GAS. A. N. Chowdhury and S. Banerjee (Geological Survey of India, Calcutta, India), p. 967-970. 9 refs. [See A69-20947 08-13]

RELATIVE ABUNDANCE OF GAS INCLUSIONS IN SEVERAL DEEP-LEVEL MAGMATIC MINERALS [ABONDANCE RELATIVE DES GAZ INCLUS DANS QUELQUES MINERAUX MAGMATIQUES D'ORIGINE PROFONDE]. M. Chemla, R. Brousse, C. Causse (Paris, Université, Orsay, Essonne, France), and J. C. Touray (Paris, Université, Paris, France), p. 971-979.

FACTORS AFFECTING ELEMENT DISTRIBUTIONS IN SEDIMENTS. D.W. Spencer, E. T. Degens (Woods Hole Oceanographic Institution, Woods Hole, Mass.), and G. Kulbicki (Société Nationale des Pétroles d'Aquitaine, Pau, France), p. 981-998.

CHEMICAL FRACTIONATION IN THE SEDIMENTARY ENVIRONMENT. K. H. Wedepohl (Göttingen, Universität, Göttingen, West Germany), p. 999-1016.

SECULAR CHANGE OF THE CHEMICAL COMPOSITION OF SEA WATER. K. Sugawara (Nagoya University, Nagoya, Japan), p. 1017-1021.

RELATIONSHIP BETWEEN THE DISTRIBUTION OF ELEMENTS IN ARGILLACEOUS MINERALS AND THE TRIASSIC PALEOGEOGRAPHY OF THE JURA [RELATION ENTRE LA REPARTITION DES ELEMENTS DANS LES MINERAUX ARGILEUX ET LA PALEOGEOGRAPHIQUE TRIASIQUE DU JURA]. G. Ataman and J. Lucas (Centre National de la Recherche Scientifique, Strasbourg, France), p. 1023-1037.

ABUNDANCE AND DISTRIBUTION OF CERTAIN ELEMENTS IN THE SEDIMENTARY FORMATION OF THE PARIS BASIN [ABONDANCE ET REPARTITION DE CERTAINS ELEMENTS DANS LES FORMATIONS SEDIMENTAIRES DU BASSIN DE PARIS]. F. Bienner, B. de Jekhowsky, R. Pelet, and B. Tissot (Institut Français du Pétrole, Rueil-Malmaison, Hauts-de-Seine, France), p. 1039-1063.

THE ABUNDANCE OF MERCURY IN 300 NATURAL WATER SAMPLES FROM TUSCANY AND LATIUM (CENTRAL ITALY). M. Dall'Aglio (Comitato Nazionale per l'Energia Nucleare, Rome, Italy), p. 1065-1081.

INFLUENCE OF STRUCTURAL FACTORS ON THE STATISTICAL LAWS OF THE DISTRIBUTION OF AN ELEMENT [INFLUENCE DES FACTEURS STRUCTURAUX SUR LES LOIS STATISTIQUES DE DISTRIBUTION D'UN ELEMENT]. P. Leymarie (Centre National de la Recherche Scientifique, Nancy, France), p. 1083-1091.

THE GEOCHEMICAL IMPORTANCE OF FISSION ELEMENTS IN THE STUDY OF THE BALANCE AND MOBILITY OF TRACE ELEMENTS [L'IMPORTANCE GEOCHIMIQUE DES ELEMENTS FISSURAUX DANS L'ETUDE DU BILAN ET DE LA MOBILITE DES ELEMENTS EN TRACES]. J. Goni and C. Guillemin (BRGM, Orléans, Loiret, France), p. 1093-1112.

THE FLUOR IN THE ROCKS - ANALYSIS ERROR, STANDARD SPECIMENS, ABUNDANCE - DISTRIBUTION IN THE GRANODIORITE OF MOUNT CAPANNE (ISLAND OF ELBA, TUSCANY) [LE FLUOR DANS LES ROCHES - ERREUR D'ANALYSE, ECHANTILLONS-STANDARDS, ABONDANCE - DISTRIBUTION DANS LA GRANODIORITE DU MTE CAPANNE (ILE D'ELBE, TOSCANE)]. M. Martini and F. Tonani (Istituto di Mineralogia, Petrografia e Geochimica, Florence, Italy), p. 1113-1126.

GERMANIUM AND INDIUM - A COMPARISON BETWEEN THE REGIONAL MEAN CONTENTS AND THE CLARKE VALUES [GERMANIUM UND INDIUM - EIN VERGLEICH ZWISCHEN REGIONALEN DURCHSCHNITTSGEHALTEN UND DEN CLARKE-WERTEN]. H. J. Rösler, W. Schrön, and B. Voland (Freiberg, Bergakademie, Freiberg, East Germany), p. 1127-1138.

DISTRIBUTION OF ECONOMICALLY EXPLOITABLE COPPER IN THE EARTH [SUR LA DISTRIBUTION DU CUIVRE ECONOMIQUEMENT EXPLOITABLE SUR LA TERRE]. H. Pélissonnier (Paris, Université, Paris, France), p. 1139-1149.

ENRICHMENTS OF TRANSITION-METAL IONS IN SILICATE CRYSTAL STRUCTURES. R. G. Burns (Oxford University, Oxford, England), p. 1151-1164.

AUTHOR INDEX, p. 1165-1178.

A69-20898 *
NUCLEOSYNTHESIS IN SUPERNOVA EXPLOSIONS.
J. W. Truran, W. D. Arnett (NASA, Goddard Space Flight Center, Goddard Institute for Space Studies, New York, N.Y.), S. Tsuruta (Smithsonian Institution, Smithsonian Astrophysical Laboratory, Cambridge, Mass.), and A. G. W. Cameron (Yeshiva University, Belfer Graduate School of Science; NASA, Goddard Space Flight Center, Goddard Institute for Space Studies, New York, N.Y.).
IN: ORIGIN AND DISTRIBUTION OF THE ELEMENTS; PROCEEDINGS OF THE INTERNATIONAL SYMPOSIUM, PARIS, FRANCE, MAY 8-11, 1967. [A69-20892 08-30]
Symposium sponsored by UNESCO and the International Union of Geological Sciences.
Edited by L. H. Ahrens.
Oxford, Pergamon Press, Ltd. (International Series of Monographs in Earth Sciences. Volume 30), 1968, p. 77-89. 17 refs.
NASA-AEC-supported research.
The implications of recent studies of the dynamics of the cores of highly evolved massive stars are considered with regard to the general problems of nucleosynthesis. The typical conditions estimated for these models are shown to be very promising for the process of element synthesis by neutron capture on a fast time scale (the r-process of Burbidge et al., 1957). (Author)

A69-20903 *
A NEW TABLE OF ABUNDANCES OF THE ELEMENTS IN THE SOLAR SYSTEM.
A. G. W. Cameron (Yeshiva University, Belfer Graduate School of Science; NASA, Goddard Space Flight Center, Goddard Institute for Space Studies, New York, N.Y.).
IN: ORIGIN AND DISTRIBUTION OF THE ELEMENTS; PROCEEDINGS OF THE INTERNATIONAL SYMPOSIUM, PARIS, FRANCE, MAY 8-11, 1967. [A69-20892 08-30]
Symposium sponsored by UNESCO and the International Union of Geological Sciences.
Edited by L. H. Ahrens.
Oxford, Pergamon Press, Ltd. (International Series of Monographs in Earth Sciences. Volume 30), 1968, p. 125-143. 15 refs.
AEC-NASA-supported research.
Compilation of a new table of the abundances of the elements, presumably characteristic of primitive solar matter. The table is based as much as possible on abundances in Type I carbonaceous chondrites. Other sources, used where necessary, are ordinary chondrites, solar atmospheric abundances, and solar cosmic-ray abundances. Eight elements were interpolated using criteria based on the theory of nucleosynthesis in stars. A discussion is given of some features of the abundance table which should be taken into account in theories of nucleosynthetic processes. (Author)

A69-20913 *
DETAILED ANALYSIS OF THE STAR ϕ AURIGAE.
G. Cayrel de Strobel (NASA, Goddard Space Flight Center, Goddard Institute for Space Studies, New York, N.Y.).
IN: ORIGIN AND DISTRIBUTION OF THE ELEMENTS; PROCEEDINGS OF THE INTERNATIONAL SYMPOSIUM, PARIS, FRANCE, MAY 8-11, 1967. [A69-20892 08-30]
Symposium sponsored by UNESCO and the International Union of Geological Sciences.
Edited by L. H. Ahrens.
Oxford, Pergamon Press, Ltd. (International Series of Monographs in Earth Sciences. Volume 30), 1968, p. 239-243. 5 refs.
Study of ϕ Aurigae (HD 35620) by means of a differential model-atmosphere analysis with respect to ϵ Virginis, assuming the LTE approximation, hydrostatic equilibrium, and a temperature distribution homologous to the solar one. The detailed analysis leads to an effective temperature of 4200 K, a surface gravity log g = 1.0, and a microturbulent velocity of 3.5 km/sec. Using these parameters, the star formerly qualitatively classified as having strong metallic lines, becomes slightly metal-deficient. The discrepancy between the calcium abundance of ϕ Aurigae found in the present analysis and that found by Spinrad comes essentially from a difference in the effective temperatures attributed to the star. G.R.

A69-21204 *#
LOW-THRUST MISSION SIMULATION - FEEDBACK TO HARDWARE DEFINITION.
Alfred C. Mascy (NASA, Office of Advanced Research and Technology, Mission Analysis Div., Moffett Field, Calif.).
IN: AMERICAN INSTITUTE OF AERONAUTICS AND ASTRONAUTICS, ELECTRIC PROPULSION CONFERENCE, 7TH, WILLIAMSBURG, VA., MARCH 3-5, 1969, PROCEEDINGS. [A69-21201 09-30]
New York, American Institute of Aeronautics and Astronautics, Inc., 1969, p. 16-21. 9 refs.
The major functional elements of low-thrust mission feasibility studies are outlined, and their dependence on hardware definition is discussed. A suggested approach is offered to integration of realistic power plant characteristics into an overall mission simulation tool. Discrete levels of sophistication are possible which allow the analyst the flexibility of trading quantity with quality of cases. An example mission is analyzed using various definitions of several functional elements. The performance using a parametric approach to cover the uncertainty in power plant specific mass is compared to absolute performance using assumed technology levels. The actual performance of a projected propulsion system is then studied by assuming specific characteristics of a power plant. As another example, the importance of thrustor technology definition is depicted by analyzing the nominal mission under the assumption of various functional relationships between jet velocity and thrustor efficiency. The differing results point up the necessity of increased awareness of technology growth, hardware definition, and realistic system constraints. (Author)

A69-21206 *#
INTERPLANETARY LOW-THRUST MISSION ANALYSIS.
William C. Strack (NASA, Lewis Research Center, Cleveland, Ohio).
IN: AMERICAN INSTITUTE OF AERONAUTICS AND ASTRONAUTICS, ELECTRIC PROPULSION CONFERENCE, 7TH, WILLIAMSBURG, VA., MARCH 3-5, 1969, PROCEEDINGS. [A69-21201 09-30]
New York, American Institute of Aeronautics and Astronautics, Inc., 1969, p. 28-36. 9 refs.
General description of the past experience and current status of low-thrust interplanetary mission analysis at the Lewis Research Center. The overall mission model is defined, and the interactions between its major elements are discussed. A computer program philosophy is recommended that permits mission analyses at different levels of simulation accuracy, and the Lewis N-Body Code is described by way of example. The first level determines overall mission effectiveness and selects the optimum operating values of the primary variables. Succeeding levels refine the results of the first level by including higher-order effects and secondary variables. (Author)

A69-21244 *#
THE VERSATILITY OF ELECTRICALLY PROPELLED SPACECRAFT FOR PLANETARY MISSIONS.
E. Stuhlinger, D. P. Hale, C. C. Dailey, and L. Katz (NASA, Marshall Space Flight Center, Space Sciences Laboratory, Huntsville, Ala.).
American Institute of Aeronautics and Astronautics, Electric Propulsion Conference, 7th, Williamsburg, Va., Mar. 3-5, 1969, Paper 69-253. 16 p. 15 refs.
Members, $1.00; nonmembers, $1.50.
A solar-electric propulsion spacecraft concept called AREPS (Advanced Reconnaissance Electric Planetary Spacecraft) with 20 kW of electric power at the target planet can perform repeated coverage of the Mars or the Venus surface with good resolution. At Mars, AREPS is captured in a circular orbit of 10,000 km altitude. It then descends to approximately 820 km through a set of discrete intermediate orbits which allow essentially total photographic coverage of the planet at each altitude. At Venus, also with 20 kW of electric power at the planet, the spacecraft descends from a capture altitude of 3900 km to 1000 km for a complete mapping of the surface of Venus. A comparison of AREPS with a spacecraft that uses only chemical propulsion shows that electric propulsion provides an eightfold advantage in scientific payload. A comparison with a nuclear-electric spacecraft with the same mass in planetary orbit shows that the nuclear-electric system would have at least three times the electric power. (Author)

A69-21454 *
POSSIBLE CONVERSION OF ROTATIONAL ENERGY OF THE NEUTRON STAR IN THE CRAB NEBULA INTO ENERGY OF RELATIVISTIC ELECTRONS.
A. Finzi (NASA, Goddard Space Flight Center, Goddard Institute for Space Studies, New York, N.Y.) and R. A. Wolf (William Marsh Rice University, Dept. of Space Science, Houston, Tex.).
Astrophysical Journal, vol. 155, Feb. 1969, pt. 2, p. L107, L108. 5 refs.
NASA-supported research; NSF Grant No. GA-3922.

Discussion of the implications of the observation of an increasing period of the pulsating radio source in the Crab Nebula. The observation that this period is increasing at a rate of 1 part in 2×10^3 per year suggests that a neutron star is releasing rotational energy at a rate of about 10^{38} ergs sec^{-1}, which is approximately the rate of energy release needed to account for the observed production of relativistic electrons at the center of the nebula. M.M.

A69-21843 *#
INVERSION OF DENSITY IN THE CONVECTIVE ZONE.
K. S. Krishna Swamy (NASA, Goddard Space Flight Center, Greenbelt, Md.).
The Observatory, vol. 89, Feb. 1969, p. 26, 27.

Remark on the density inversion in the convective zone of stellar photospheres, indicating that this phenomenon should not necessarily occur in all cases. Curves of density vs temperature are plotted, showing that density inversion occurs only under certain conditions in the ε Eridani atmosphere model and does not occur at all in the Groombridge 1830 atmosphere model. V.Z.

A69-21937 *#
EXPLICIT UPPER BOUNDS FOR ERROR PROPAGATION IN THE N-BODY FIELD.
Albert Rosen (NASA, Goddard Space Flight Center, Laboratory for Space Sciences, High Energy Astrophysics Branch, Greenbelt, Md.)
AIAA Journal, vol. 7, Feb. 1969, p. 211-215. 6 refs.

Description of a simple means for bounding the propagated trajectory error induced by an impulsive initial error in the n-body field. Formulas are derived for the maximum acceptable initial error, given the mission tolerances, and for the maximum time of negligible propagated error, given the initial impulses and mission tolerances. An example illustrates the use of the results within the solar system. (Author)

A69-22047 *
COSMOGENIC RARE GASES AND THE ^{40}K-^{40}Ar AGE OF THE KODAIKANAL IRON METEORITE.
D. D. Bogard (California Institute of Technology, Charles Arms Laboratory of the Geological Sciences, Pasadena, Calif.; NASA, Manned Spacecraft Center, Houston, Tex.), D. S. Burnett, and G. J. Wasserburg (California Institute of Technology, Charles Arms Laboratory of the Geological Sciences, Pasadena, Calif.).
Earth and Planetary Science Letters, vol. 5, Jan. 1969, p. 273-281. 18 refs.
NSF Grants No. GP-7976; No. GA-1073; Grant No. NGR-05-002-044; Contract No. Nonr-220(47).

Discussion of measurements of cosmogenic He, Ne, and Ar in the metal phase and of the K-Ar ages of two glass inclusions in the Kodaikanal iron meteorite. The small amounts of cosmogenic rare gas are best interpreted as due to a low cosmic ray exposure age. From empirical production rates, ages of 12, 15, and 15 m.y. were obtained from the ^3He, ^{21}Ne, and ^{38}Ar concentrations, respectively. The $^3He/^{21}Ne$, $^3He/^4He$, and $^4He/^{38}Ar$ ratios are all consistent with low shielding during the exposure. The feldspar and glass have approximately equal K-Ar ages of 3.5 ± 0.1 and $3.3 \pm 0.1 \times 10^9$ yr, respectively. These results place constraints on possible origins for the glass and feldspar. G.R.

A69-22055 *
ATMOSPHERES OF METAL-DEFICIENT STARS - MAIN SEQUENCE STARS.
K. S. Krishna Swamy (NASA, Goddard Space Flight Center, Laboratory for Space Sciences, Greenbelt, Md.).
Astronomy and Astrophysics, vol. 1, Mar. 1969, p. 297-304. 16 refs.

Systematic study of the atmospheres of metal-deficient stars of spectral type K and G. Model atmospheres are constructed for effective temperatures of 4500, 5000, 5500, and 6000 K, and for hydrogen-to-metal ratios of 1, 5, 10, 40, and 100 times the solar value. The effect of reduced metal abundance on the atmospheric structure of these stars is studied. The relation of this work to the study of subdwarfs is emphasized. M.G.

A69-22183 *
SUDDEN COMMENCEMENT ASSOCIATED DISCONTINUITIES IN THE INTERPLANETARY MAGNETIC FIELD OBSERVED BY IMP 3.
Harold E. Taylor (NASA, Goddard Space Flight Center, Laboratory for Space Sciences, Greenbelt, Md.).
Solar Physics, vol. 6, Feb. 1969, p. 320-334. 19 refs.

Examination of the magnetic field measurements made by the magnetic field experiment on the IMP 3 spacecraft at the time of geomagnetic SSC events. Thirty-six such events occured while IMP 3 was in the interplanetary medium during 1965, 1966, and 1967 and have been analyzed. Of these events eight must have been tangential discontinuities, two are either tangential discontinuities or rotational discontinuities, and 26 are possible shock waves. These 26 possible shocks have similar magnetic signatures. The larger SSC events were more likely to be caused by possible shocks, while the smaller events were often associated with tangential discontinuities. The orientation of the discontinuity surfaces of the 26 possible shocks shows a preference to be aligned somewhere between a direction perpendicular to the sun-earth line and a direction tangent to the local spiral angle of the magnetic field. It was possible to associate solar flares with 14 of the 26 possible shock events. M.M.

A69-22189 *
ON THE FLOW OF GAS FROM THE GALACTIC CENTER.
D. W. Moore (NASA, Goddard Space Flight Center, Goddard Institute for Space Studies, New York, N.Y.) and E. A. Spiegel (New York University, Dept. of Physics, New York, N.Y.).
Astrophysical Journal, vol. 154, Dec. 1968, pt. 1, p. 863-874. 13 refs.

Analysis of a steady axisymmetric flow out of the galactic center, neglecting magnetic and turbulent stresses and the self-gravitation of the gas. The flow is in a disk and possesses angular momentum, but otherwise the problem is like solar-wind theory, and it is assumed that initial conditions are specified at the edge of the nuclear disk. The equations of motion are then quite simple, and their solution indicates that the flow must contain a nearly discontinuous transition from supersonic to subsonic conditions. This transition must be a compressible hydraulic jump, or bore, which generates intense turbulence and gives rise to H II on the downstream edge of the bore. The bore causes radial deceleration of the gas and hence density enhancement, and it is suggested that this phenomenon is associated with the expanding arm. (Author)

A69-22199 *
ANALYSIS OF SUBDWARF HD 25329.
K. S. Krishna Swamy (NASA, Goddard Space Flight Center, Greenbelt, Md.).
Astrophysical Journal, vol. 154, Dec. 1968, pt. 1, p. 983-986. 7 refs.

Study of the subdwarf HD 25329 through the model-atmosphere approach. From an analysis of the profiles of $H\alpha$, λλ5896 and 5890 of Na I, and λ5183 of Mg I, T_e for this subdwarf was found to equal 4800 K, and a hydrogen-to-metal ratio of 20 times the solar value was obtained. This is in good agreement with the curve-of-growth study of Pagel and Powell (1966). The profiles used in the study were based on tracings of spectrograms from the Mount Wilson and Palomar Observatories. G.R.

A69-22211 *
PRIMORDIAL HELIUM AND THE LUMINOSITY OF HORIZONTAL-BRANCH STARS.
Naruyoshi Asano (Nagoya University, Nagoya, Japan) and Daiichiro Sugimoto (NASA, Goddard Space Flight Center, Greenbelt, Md.).
Astrophysical Journal, vol. 154, Dec. 1968, pt. 1, p. 1127-1133. 23 refs.

It is shown that the absolute magnitudes of the horizontal-branch stars and of the field RR Lyrae stars are observationally well correlated with their metal abundances. Theoretically, these stars are in the helium-burning phase. By studying models involving helium flash, theoretical luminosities of the stars in the helium-burning phase are determined for different abundances of helium and of metals. Comparison of the models with observation indicates that the helium concentration is as high as the value predicted by the theory of its origin by primordial synthesis. (Author)

A69-22216 *

FILTER PHOTOMETRY OF SATURN IN THE SPECTRAL REGION λλ2950-2450.

Robert C. Bless (Wisconsin, University, Space Astronomy Laboratory and Washburn Observatory, Madison, Wis.; NASA, Goddard Space Flight Center, Greenbelt, Md.), Arthur D. Code, and Donald J. Taylor (Wisconsin, University, Space Astronomy Laboratory and Washburn Observatory, Madison, Wis.).

Astrophysical Journal, vol. 154, Dec. 1968, pt. 1, p. 1151-1153. 9 refs.
Grant No. NsG-618.

Discussion of ultraviolet observations of Saturn obtained with three rocket-borne photoelectric photometers. The photometer band passes of about 300 Å were isolated by interference filters with peak transmissions at λλ2800, 2500, and 2100. The fluxes, albedos, and thickness of the H_2 layer of Saturn are presented. It is suggested that the cloud top lies at a greater optical depth in the infrared than in the ultraviolet. G.R.

A69-22264 *

FAR-INFRARED OBSERVATION OF THE GALACTIC-CENTER REGION AT 100 MICRONS.

William F. Hoffmann (NASA, Goddard Space Flight Center, Goddard Institute for Space Studies, New York, N.Y.) and Carl L. Frederick (Yeshiva University, Physics Dept., New York, N.Y.).

Astrophysical Journal, vol. 155, Jan. 1969, pt. 2, p. L9-L13. 8 refs.
Grant No. NGR-33-008-012.

An intense far-infrared source has been detected at 100 μ in the direction of the galactic center. The source has an extension along the galactic plane of at least 6°5, a flux density of $1.8 \pm 0.8 \times 10^{-19}$ W m^{-2} Hz^{-1}, and a brightness temperature averaged over a 2°3 beamwidth of 16 K. If the source is at the distance of the Galactic center, its luminosity is 2.7×10^{42} ergs sec^{-1}. A possible mechanism is thermal emission of interstellar dust grains. The intensity is 30 times that anticipated for this process. (Author)

A69-22421 *

PULSATIONAL INSTABILITIES IN HYDROGEN-POOR MASSIVE BLUE STARS. I.

Norman R. Simon and Richard Stothers (NASA, Goddard Space Flight Center, Goddard Institute for Space Studies, New York, N.Y.).

Astrophysical Journal, vol. 155, Jan. 1969, pt. 1, p. 247-255. 31 refs.

Investigation of the structure and pulsational properties of massive stars with helium cores and thin, hydrogen-poor envelopes. The core structures are very insensitive to modifications of the hydrogen envelope. However, it is found that the total stellar radius and luminosity are modified by the integrated hydrogen content and by the hydrogen gradient, respectively. The models are pulsationally stable under modest conditions of central condensation (due to a hydrogen-burning shell and/or high hydrogen content). The unstable models are energized almost entirely by the helium reactions in the core, while most of the damping occurs in the thin hydrogen envelope. For each mass, the period is remarkably insensitive to the envelope modifications. The critical models dividing stable from unstable models are determined by (1) a pulsational eigenfrequency $\omega^2 \sim 3$, and (2) the size of the hydrogen gradient. (Author)

A69-22426 *

COLLISIONLESS HEATING OF THE SOLAR-WIND PLASMA. II.

Aaron Barnes (NASA, Ames Research Center, Space Sciences Div., Moffett Field, Calif.).

Astrophysical Journal, vol. 155, Jan. 1969, pt. 1, p. 311-321. 28 refs.

The theory of heating of collisionless plasma by damping hydromagnetic waves is applied in a qualitative model of solar-wind heating. It is proposed that an efflux of 5×10^{26} ergs sec^{-1}, in the form of fast-mode magnetoacoustic waves, propagates outward into the outer corona. Most of this wave energy is transformed into electron and ion thermal energy through damping, within a few solar radii, and is expected to enhance the velocity of the wind at the orbit of earth. A smaller amount of this wave energy will not be absorbed until it has propagated far from the sun; the absorption of this part of the wave energy will enhance the temperature of the solar-wind ions, and because the ion-ion mean free path is long in this region, the ion temperature will remain high even at the orbit of earth. The proposed heating model qualitatively accounts for the discrepancy between the observed solar-wind velocities and ion temperatures, and those predicted by the Sturrock-Hartle two-fluid model of the solar wind. (Author)

A69-23183 *

PLANETARY PROBE - ORIGIN OF ATMOSPHERE OF VENUS.

Robert F. Mueller (NASA, Goddard Space Flight Center, Greenbelt, Md.).

Science, vol. 163, Mar. 21, 1969, p. 1322-1324. 24 refs.

The high temperatures and chemical composition, as determined by space probe and terrestrial observation, suggest that the present atmosphere of Venus has formed by chemical interaction with the lithosphere. Although the precise reactions have not been identified, good theoretical approximations to the molecular abundance may be obtained from reactions applicable to terrestrial rocks. The high temperatures and chemical reactivity create conditions on Venus which are fundamentally different from those on the cooler terrestrial planets where the attainment of equilibrium is prevented by kinetic barriers. (Author)

A69-23679 *

EXTINCTION BY INTERSTELLAR GRAINS, MIE PARTICLES AND POLYCYCLIC AROMATIC MOLECULES.

B. Donn (NASA, Goddard Space Flight Center, Laboratory for Space Sciences, Greenbelt, Md.) and K. S. Krishna Swamy.

(Netherlands Physical Society, International Conference on Laboratory Astrophysics, Lunteren, Netherlands, Sept. 2-6, 1968.)
Physica, vol. 41, Feb. 21, 1969, p. 144-150. 22 refs.

Comparison of observed interstellar extinction with proposed grain models. It is shown that the theoretical extinction curves for pure iron, ice-coated iron, Oort-van de Hulst size distribution of dirty ice, or pure graphite particles do not seem to be able to reproduce the observed reddening curve over the entire wavelength region of the spectrum. Composite particles of graphite core with dirty ice mantle seemed to satisfy the observed reddening curves within the present accuracy of the observations. This discrepancy is not considered to be a definitive criterion for the interstellar grain composition due to the lack of observations in the far ultraviolet region of the spectrum, and the large uncertainties in the present observations. The importance of refining the UV extinction curve to the short wave limit to determine the UV extinction curve in different regions of the Galaxy or in different regions of space is emphasized as being of major value for the study of interstellar grains. B. H.

A69-23773 *

OBSERVATIONS OF THE INTERPLANETARY MAGNETIC FIELD, 4-12 JULY 1966.

N. F. Ness (NASA, Goddard Space Flight Center, Laboratory for Space Sciences, Greenbelt, Md.) and H. E. Taylor.

IN: THE PROTON FLARE PROJECT (THE JULY 1966 EVENT). [A69-23725 10-29]
Edited by A. C. Stickland.
Cambridge, Mass., MIT Press (Annals of the IQSY. Volume 3), 1969, p. 366-374. 9 refs.

Simultaneous interplanetary magnetic field measurements by geocentric satellites Explorer 33 and IMP-3 have been made of the MHD shock wave associated with the sudden commencement storm

on July 8, 1966. Detailed analyses of the arrival time and orientation of the shock surface and shock normals show that the surface was not perpendicular to the sun-earth line. Velocity had decreased so that at 1 AU it was less than 710 km/sec compared with the average velocity of 950 km/sec computed from the transit time from the parent solar flare class 2B on July 7, 1966. (Author)

A69-24100 *
MICROSCALE FLUCTUATIONS IN THE INTERPLANETARY MAGNETIC FIELD.
L. F. Burlaga, K. W. Ogilvie, and D. H. Fairfield (NASA, Goddard Space Flight Center, Laboratory for Space Sciences, Greenbelt, Md.).
Astrophysical Journal, vol. 155, Mar. 1969, pt. 2, p. L171-L175. 10 refs.

Results of simultaneous measurements of the interplanetary plasma and magnetic field, obtained during 1967 by the Explorer 34 satellite. The results show that microscale magnetic-field fluctuations are governed by the local balance between the proton thermal energy density and the magnetic-field energy density. M.G.

A69-24103 *
ON THE COMPOSITION OF CIRCUMSTELLAR GRAINS.
Robert C. Gilman (NASA, Goddard Space Flight Center, Goddard Institute for Space Studies, New York, N.Y.).
Astrophysical Journal, vol. 155, Mar. 1969, pt. 2, p. L185-L187. 18 refs.
Grant No. NGR-33-008-012.

Calculation of the molecular equilibrium of both condensates and gaseous compounds in stellar atmospheres in order to determine the composition of circumstellar grains. It is considered likely that circumstellar grains of oxygen-rich cool stars will be composed mainly of refractory silicates such as Mg_2SiO_4 and Al_2SiO_5. For carbon-rich stars the grains are mainly carbon, while for the transition stars silicon carbide predominates. B.H.

A69-24125 *
RED SUPERGIANTS AND NEUTRINO EMISSION.
Richard Stothers (NASA, Goddard Space Flight Center, Goddard Institute for Space Studies, New York, N.Y.).
Astrophysical Journal, vol. 155, Mar. 1969, pt. 1, p. 935-956. 151 refs.

Collection and analysis of data on the supergiants in all early-type clusters and associations of the Galaxy and Magellanic Clouds which contain known red-supergiant members, in the light of current theory. No major differences seem to exist between the Galaxy and the Magellanic Clouds in this study. Dating of the clusters from the luminosities of their blue supergiants indicates decreasing and increasing numbers of blue and red supergiants, respectively, with age. Luminosity functions show that the blue/red ratio is >5 at high masses and ~1 at lower masses. While a one-to-one correspondence exists between luminosity and mass for the core helium-burning supergiants, it is lacking for the red supergiants because of a funneling effect, in analogy with the K giants. On the basis of the large blue-red ratio among the most massive supergiants and the independent theoretical and observational evidence that early core helium burning occurs in the red-supergiant region, it is concluded that some effect must take massive stars rapidly through, or away from, the red-supergiant region after core helium burning. Mixing and mass loss are shown to be inadequate mechanisms. M.M.

A69-24429 *
A MODEL OF INTERPLANETARY AND CORONAL MAGNETIC FIELDS.
Kenneth H. Schatten, John M. Wilcox (California, University, Space Sciences Laboratory, Berkeley, Calif.), and Norman F. Ness (NASA, Goddard Space Flight Center, Greenbelt, Md.).
Solar Physics, vol. 6, Mar. 1969, p. 442-455. 11 refs.
NSF Grant No. GA-1319; Contract No. Nonr-3656(26); Grants No. NsG-243; No. NGR-05-003-230.

A model of the large-scale magnetic field structure above the photosphere uses a Green's function solution to Maxwell's equations. Sources for the magnetic field are related to the observed photospheric field and to the field computed at a "source" surface about 0.6 $R_\odot$ above the photosphere. The large-scale interplanetary magnetic field sector pattern is related to the field pattern at this "source" surface. The model generates magnetic field patterns on the "source" surface that compare well with interplanetary observations. Comparisons are shown with observations of the interplanetary magnetic field obtained by the IMP 3 satellite. (Author)

A69-25107 *
THERMODYNAMIC APPROACH TO THE EQUATION OF STATE OF A MAGNETIZED FERMI GAS.
V. Canuto (NASA, Goddard Space Flight Center, Goddard Institute for Space Studies, New York, N.Y.), H. Y. Chiu (NASA, Goddard Space Flight Center, Goddard Institute for Space Studies, New York; New York, State University, Physics Dept. and Earth and Space Sciences Dept., Stony Brook, N.Y.), and L. Fassio-Canuto (Instituto Politécnico Nacional, Centro de Investigación y de Estudios Avanzados, Mexico City, Mexico).
Astrophysics and Space Science, vol. 3, Feb. 1969, p. 258-267. 14 refs.

The equations of state for a magnetized Fermi gas are re-derived by generalizing the physical definition of the pressure. A simplified derivation is given of the energy eigenvalues of a free electron in a magnetic field, based on the use of simple harmonic oscillators. Physical interpretations of the results are presented. Possible astrophysical applications are also discussed. (Author)

A69-25644 *#
MANNED SPACE MISSIONS - GATEWAY TO OUR FUTURE IN SPACE.
Robert R. Gilruth (NASA, Manned Spacecraft Center, Houston, Tex.).
Challenge, vol. 8, Spring 1969, p. 19-23.

Discussion of the need for manned space stations and their role in future space exploration. The advantages of space stations with crews of more than 10 to 12 people are discussed. The space station should provide an earth-like environment including the use of artificial gravity. The primary objective of the post-Apollo program is the establishment of man's capability to function in space for significantly long periods of time. Investigations will be conducted in an orbital workshop. Activities to be conducted on board the space station of the future can be classified under two general headings: (1) observational experiments which include astronomy and earth sensing, and (2) onboard experiments involving bioscience, biomedicine, and high-energy physics. Details of a space station are described which could be launched in three parts by three Saturn-V rockets. G.R.

A69-25812 *
ULTRAVIOLET SPECTROPHOTOMETRY OF EARLY-TYPE STARS.
Theodore P. Stecher (NASA, Goddard Space Flight Center, Greenbelt, Md.).
Astronomical Journal, vol. 74, Feb. 1969, p. 98-102. 15 refs.

Stellar energy distribution in the ultraviolet were obtained by objective-grating spectrometers mounted in spinning rockets. The resolution was 100 Å and the data were corrected for interstellar extinction. The resulting spectra of stars ranging in spectral type F5IV to O5f and WC7 are presented and discussed. (Author)

A69-25813 *
SURVEY OF THE REGION OF LACERTA OB1.
George Coyne (Woodstock College, Woodstock, Md.), Jaylee Burley-Mead (NASA, Goddard Space Flight Center, Laboratory for Theoretical Studies, Greenbelt, Md.), and Michele Kaufman (Harvard University, Harvard College Observatory, Cambridge, Mass.).
Astronomical Journal, vol. 74, Feb. 1969, p. 103-107. 15 refs.
Grant No. NsG-670.

Determination of the spectral classes and photographic magnitudes for a total of 3621 stars in the region of the association Lac OB1. Astrophotometer measures of images on glass reproductions of the Palomar Sky Survey plates have been used for the photometry, and spectral classes have been determined by using color equivalents according to the Tikhoff method. The star counts indicate that there s an excess of early A stars on the main sequence in the concentrated egion of the association as compared to the dispersed region. Also,

the total area of the survey shows a deficiency of stars later than F5 when comparison is made to counts in nearby selected areas. It is recommended that membership determinations be made for the A stars which constitute the clustering in the concentrated region of the association. (Author)

A69-26019 *#
EMPIRICAL DETERMINATION OF HEATING EFFICIENCIES IN THE MARS AND VENUS ATMOSPHERES.
Richard W. Stewart and Joseph S. Hogan (NASA, Goddard Space Flight Center, Goddard Institute for Space Studies, New York, N.Y.).
Journal of the Atmospheric Sciences, vol. 26, Mar. 1969, p. 330-332. 11 refs.
Grant No. NsG-499.

Description of an empirical method for determining the heating efficiency of extreme solar ultraviolet radiation interacting with a carbon dioxide atmosphere. The method is based on a theoretical analysis of Mariner data on the ionospheres of Mars and Venus. M.G.

A69-26020 *#
EXOSPHERIC TEMPERATURES ON MARS AND VENUS.
Joseph S. Hogan and Richard W. Stewart (NASA, Goddard Space Flight Center, Goddard Institute for Space Studies, New York, N.Y.).
Journal of the Atmospheric Sciences, vol. 26, Mar. 1969, p. 332, 333.
Grant No. NsG-499.

Calculation of the exospheric temperatures of Mars and Venus, based on previously derived empirical values of the photoionization heating efficiency. Atmospheric models are computed for conditions appropriate to the occultations of Mariner 4 on Mars and Mariner 5 on Venus. The distributions of temperature obtained for Mars and Venus are illustrated. M.G.

A69-26129 *#
THE PLANET VENUS, AFTER MARINER-5.
S. Ichtiaque Rasool (Centre National de la Recherche Scientifique, Institut d'Astrophysique, Paris, France; NASA, Goddard Space Flight Center, Goddard Institute for Space Studies, New York, N.Y.).
Sciences et Industries Spatiales, vol. 4, no. 11, 12, 1968, p. 39-43.

Analysis of the extensive information on the atmosphere of Venus obtained by two space probes, Venera 4 (USSR) and Mariner 5 (USA). By combining the results from the two spacecraft, it has been possible to obtain more information on the upper atmosphere of Venus than was available on the upper atmosphere of the earth only 30 years ago. The Venusian atmosphere has been found to be mainly CO_2 with only 1% water. The surface temperature ranges from 300 to 400°C, and the total pressure is about 100 atm. F.R.L.

A69-26341 *
MICROMETEOROID INTERACTION WITH THE ATMOSPHERE.
Joseph J. Kornblum (NASA, Ames Research Center, Space Sciences Div., Moffett Field, Calif.).
Journal of Geophysical Research, vol. 74, Apr. 15, 1969, p. 1893-1907. 23 refs.

Calculation of the size and velocity of stony meteoric particles during their passage through the earth's atmosphere. The particles are assumed to be nonrotating spheres with a density of 3.4 g/cm^3. The analysis is restricted to particles of radius less than 50 μ, and thus problems of shielding by the ablated vapor molecules, fragmentation, and heat storage are avoided. To determine the size changes of the particles due to vaporization, the ablation model of Allen, Baldwin, and James (1965) is adopted. Entering velocities of 12, 15, 20, 30, 40, 50, 60, and 70 km/sec are considered. The meteoric vapor pressure law proposed for stone by Öpik (1958) is adopted. The particles are followed down to an altitude of 55 km except when completely vaporized at higher altitudes. This involves determining the velocity as it changes from its entering velocity to terminal velocity. It is assumed that in the transition flow region between free molecular flow and continuum flow, the drag force on the particle is described by the modified Stokes law experimentally determined by Millikan (1923). It is shown that the applicable terminal velocity is the kinetic terminal velocity and not the free molecular flow terminal velocity. (Author)

A69-26342 *
CONCENTRATION AND COLLECTION OF METEORIC DUST IN THE ATMOSPHERE.
Joseph J. Kornblum (NASA, Ames Research Center, Space Sciences Div., Moffett Field, Calif.).
Journal of Geophysical Research, vol. 74, Apr. 15, 1969, p. 1908-1919. 41 refs.

Discussion of an approximate method of predicting particle collections from balloon-borne, ground-based, or rocket-borne collectors. Previous results concerning the size and velocity histories of stony micrometeoroids are used to predict, for various entry fluxes, the meteoric dust to be expected from various collectors. The collection results of the Luster sounding rocket experiments and the balloon collections of Bhandari et al. (1968) are in agreement with the predictions for low entry fluxes but not with the collection results to be expected from high entry fluxes computed from Venus Flytrap and the early satellite data. G.R.

A69-26371 •
PARTICLE SIZE DISTRIBUTION OF LUNAR SURFACE MATERIAL.
Curtis C. Mason (NASA, Manned Spacecraft Center, Houston, Tex.).
Geological Society of America, Bulletin, vol. 80, Apr. 1969, p. 587-594. 10 refs.

Critical examination of previous analyses of the particle size distribution of lunar surface material, which assumed a log-log particle size distribution. It is shown that a distribution of this type would mean that, with no bounds set on particle size, the total volume of particles would go to infinity. If bounds are set, the mode would be the size interval at one of the extremes. This is considered to be a highly improbable size distribution by the author, who believes that a Guassian size distribution is more realistic. Using a Gaussian particle size distribution and 50% porosity, plus a surface irregularity correction, the mean particle size at the Surveyor 1 site is 9.6 μ, and the mean particle size at the Surveyor 3 site is 54 μ. B.H.

A69-27158 *
THERMAL EMISSION BY GRAINS AND THE FREE-FREE EMISSION FROM PLANETARY NEBULAE.
K. S. Krishna Swamy (NASA, Goddard Space Flight Center, Greenbelt, Md.).
Astronomical Society of the Pacific, Publications, vol. 81, Apr. 1969, p. 154-167. 12 refs.

Calculation of the expected thermal emission for each of 49 planetary nebulae on the basis of a graphite grain model. The free-free emission from each of these planetaries is also calculated. The results of these calculations show that the infrared emission from grains of several planetary nebulae should be detectable. It is believed that this study should be of considerable help to observers who are interested in the measurement of these infrared fluxes. More observations of the type done for NGC 7027 are recommended for other planetaries, as they will be of considerable help in knowing not only more about the grains but also about their effect on the planetaries themselves. (Author)

A69-27172 *
STARS THAT DO NOT TWINKLE OUTSIDE THE EARTH'S ATMOSPHERE.
W. Cunningham (NASA, Manned Space Flight Center, Houston, Tex.) and L. Marshall Libby (Colorado, University, Boulder, Colo.; RAND Corp., Santa Monica, Calif.).
Nature, vol. 222, Apr. 19, 1969, p. 253, 254.

Discussion of two factors emerging from observations by Apollo 7 and Apollo 8 that stars observed by the human eye outside the earth's atmosphere show no obvious time variations of their visible light intensity for time lapses from tenths of a second up to several minutes. First, the absence of star twinkling is of great importance to the lunar observation laboratory. A search for and study of twinkling from the advantageous position of a moon-based astronomical laboratory will offer a new method to determine the distances to stars. Second, absence of visible star twinkling excludes random laser action in stellar atmospheres and gaseous nebulosities for time variations from tenths of seconds up to several minutes. F.R.L.

A69-27555 *
ROCKET SPECTROGRAPHIC OBSERVATIONS OF α VIRGINIS.
Andrew M. Smith (NASA, Goddard Space Flight Center, Greenbelt, Md.).
Astrophysical Journal, vol. 156, Apr. 1969, pt. 1, p. 93-105. 23 refs.

Two spectrograms of α Vir (Bl V) in the wavelength interval $928 < \lambda < 1350$ Å and with 0.8 Å resolution were successfully recorded on a rocket flight June 1, 1967. The data revealed hydrogen Lyman absorption lines through Ly-ζ and, in addition, evidence for 128 absorption lines arising from the ground and low-lying states in ions of C, N, Si, S, Cl, Ti, V, Cr, and Fe. The results imply that strong line blanketing occurs at $\lambda < 1350$ Å. No interstellar absorption lines due to H_2 were observed; an upper limit for the mean number density of this molecule between the earth and α Vir is 3.1×10^{-4} cm^{-3}. (Author)

A69-27576 *
A CRITERION FOR NUCLEAR-ENERGIZED PULSATIONAL INSTABILITY.
Norman R. Simon and Richard Stothers (NASA, Goddard Space Flight Center, Goddard Institute for Space Studies, New York, N.Y.).
Astrophysical Journal, vol. 156, Apr. 1969, pt. 1, p. 377-380. 6 refs.

Discussion of some general properties of nuclear-energized pulsations of stars. These are treated within the framework of the linear quasi-adiabatic theory. Results are derived from a number of detailed calculations of stellar models. The plotted models represent a fairly wide range of stellar configurations with differing compositions, nuclear temperature exponents, and energy sources, including models with hydrogen-burning shells, and can be considered to represent a general characteristic of the linear pulsation theory. First-overtone pulsations are calculated for three extreme models, two of which are models with helium-burning cores and hydrogen-burning shells. The third is a homogeneous hydrogen-burning model, constructed to produce a highly unstable fundamental mode. Model and pulsation characteristics are shown in tabulated form. B.H.

A69-27599 *#
A FAR INFRARED SKY SURVEY.
N. J. Woolf (NASA, Goddard Space Flight Center, Goddard Institute for Space Studies; Columbia University, Astronomy Dept., New York, N.Y.), W. F. Hoffmann (NASA, Goddard Space Flight Center, Goddard Institute for Space Studies, New York, N.Y.), C. L. Frederick (Yeshiva University, Belfer Graduate School, New York, N.Y.), and F. J. Low (Arizona, University, Lunar and Planetary Laboratory, Tucson, Ariz.).
Royal Society (London), Philosophical Transactions, Series A, vol. 264, Apr. 24, 1969, p. 267-271. 9 refs.
NASA-supported research.

Description of a balloon-borne instrument for making far infrared sky surveys with 2° angular resolution. In two initial flights at a wavelength of 320 μ approximately half of the celestial sphere including most of the northern Milky Way was surveyed. The thermal emission of the moon was determined. The upper limit to the flux from other sources was 3×10^{-12} W cm^{-2} in the 300 to 360 μ band. A blackbody (optically thick) source 2° or greater in diameter yielding this flux would have a temperature of 10°K. A warmer, small or optically thin source providing this much radiation in the Rayleigh-Jeans tail of the Planck distribution would have a temperature averaged over the 2° beam of 0.6°K. These observations can be used to set upper limits to the opacity and temperature of interstellar grains. (Author)

A69-27817 *
IONIZATION AND RAY FORMATION IN COMETS.
Jurgen Rahe and Bertram Donn (NASA, Goddard Space Flight Center, Laboratory for Space Sciences, Greenbelt, Md.).
Astronomical Journal, vol. 74, Mar. 1969, p. 256-258. 29 refs.

An observational approach is used as a test for theories of the interaction of comets with the solar wind. Attention is directed to the fact that ionization of cometary matter as well as ray formation take place within a distance of a few hundred kilometers from the "photometric" nucleus. A theory of these observations has to deal simultaneously with both phenomena in a distance from the nucleus that is an order-of-magnitude smaller than generally assumed in theories of the interaction between solar plasma and cometary material. It is emphasized that observed fluctuations and oscillations of the initial outflow of ionized tail material from its source near the nucleus might have an effect on the direction and structure of individual tail rays and the tail axis. (Author)

A69-27907 *
THE MOON'S RESOURCES.
P. D. Lowman, Jr. (NASA, Goddard Space Flight Center, Greenbelt, Md.).
Science Journal, vol. 5, May 1969, p. 90-95.

Study of the possibility of using lunar resources for supplying the needs of a lunar colony. The use of lunar soil as building material and the extraction of water, oxygen, and rocket propellants from lunar materials is discussed. Recovery methods not competitive with earth-supplied materials for a small base may become quite feasible for a large lunar colony, which could possibly obtain a considerable part of its raw material needs from lunar resources. G.R.

A69-27908 *
EXPLORATION OF THE MOON.
A. J. Meyer (NASA, Manned Spacecraft Center, Houston, Tex.).
Science Journal, vol. 5, May 1969, p. 97-102.

Description of a number of vehicles for the exploration of the lunar surface. General problems of lunar exploration are discussed, such as varying degrees of accessibility of different parts of the lunar surface. Different types of vehicles for lunar local transportation are described, including flying machines and wheeled vehicles. A special approach is also considered in which an automated roving vehicle could be delivered anywhere on the moon's front face. G.R.

A69-28504 *
MULTIPLE MIDCOURSE MANEUVERS IN INTERPLANETARY GUIDANCE.
Abolghassem Ghaffari (NASA, Goddard Space Flight Center, Greenbelt, Md.).
Astronautica Acta, vol. 14, Mar. 1969, p. 267-273. 8 refs.

An attempt has been made to investigate the number and location of midcourse maneuvers in an interplanetary mission. The case of a flyby Jovian mission with a spin stabilized spacecraft is considered. The mission objectives are a flyby within 10^6 km of the planet Jupiter and a flight time from earth to Jupiter of 500 days. The spacing-ratio method has been applied, and it is shown that a constant spacing-ratio of 2.5 for the velocity sensitivity leads to a near optimum spacing of correction times. (Author)

A69-28869 *
SILICATE SPHERULES FROM TUNGUSKA IMPACT AREA - ELECTRON MICROPROBE ANALYSIS.
Billy P. Glass (NASA, Goddard Space Flight Center, Planetology Branch, Greenbelt, Md.).
Science, vol. 164, May 2, 1969, p. 547-549. 17 refs.

The major oxide composition of four silicate spherules from the area of forest devastated by the explosion of the Tunguska meteorite has been determined by electron microprobe analysis. In general, the spherules have compositions similar to that of igneous glass except for the low iron and the high calcium oxide content of the three spherules that have a low content of silicon dioxide. None of the spherules seem to have compositions similar to the silicate portion of any major meteorite group. (Author)

A69-28957 *
INTERPLANETARY SECTOR STRUCTURE IN THE RISING PORTION OF THE SUNSPOT CYCLE.
John M. Wilcox (California, University, Space Sciences Laboratory, Berkeley, Calif.) and David S. Colburn (NASA, Ames Research Center, Moffett Field, Calif.).
Journal of Geophysical Research, vol. 74, May 1, 1969, p. 2388-2392. 9 refs.
NSF Grant No. GA-1319; Grants No. NsG-243; No. NGR-05-003-230; Contract No. Nonr-3656(26).

The interplanetary sector structure during the rising portion of the sunspot cycle in 1966 and 1967 has been investigated. The sector pattern is often quasi-stationary for a few rotations, followed by an appreciable change in the next rotation. When a sector boundary passes the earth, geomagnetic activity tends to increase, an effect rather similar to that observed near sunspot minimum. The recurrence period of the interplanetary field during the interval investigated was 27.5 ± 0.1 days. (Author)

A69-29878 *
CALCULATIONS ON THE COMPOSITION OF THE TERRESTRIAL PLANETS.
Ray T. Reynolds and Audrey L. Summers (NASA, Ames Research Center, Space Sciences Div., Moffett Field, Calif.).
Journal of Geophysical Research, vol. 74, May 15, 1969, p. 2494-2511. 60 refs.

Improved estimates of the major element chemical abundances within the earth, Venus, Mars, Mercury, and the moon. The calculations are based on mathematical models. Approximate equations of state at high pressure for the important constituents of the terrestrial planets are constructed from experimental data and theoretical relations. Bounds on the amounts of these materials present within detailed self-consistent models of the terrestrial planets are calculated, subject to the assumption of additive partial molar volumes, and the sensitivity of the abundance calculations to variations in the primary assumptions is indicated. Representative models give calculated total iron mass fractions of 0.38 for the earth, 0.35 for Venus, 0.26 for Mars, 0.68 for Mercury, and 0.13 for the moon. (Author)

A69-29882 *
ORIGIN OF THE MOON.
John A. O'Keefe (NASA, Goddard Space Flight Center, Laboratory for Theoretical Studies, Greenbelt, Md.).
Journal of Geophysical Research, vol. 74, May 15, 1969, p. 2758-2767. 21 refs.

Examination of various theories concerning the origin of the moon in the light of recent data. The theories can be classified into three categories which involve (1) the development of the moon as separate body in the earth's vicinity; (2) its development in some other part of the solar system, followed by capture; and (3) development by fission of the earth. The implications of the theories are examined, and explanations are offered for the small mass of the moon relative to the mass of the earth, the deficiency of the total angular momentum of the present earth-moon system, and the evidence of differential volatilization in the early history of the earth. G.R.

A69-29946 *
CONVECTION IN NORMAL STARS AND METAL-DEFICIENT STARS.
K. S. Krishna Swamy (NASA, Goddard Space Flight Center, Greenbelt, Md.).
Astrophysics and Space Science, vol. 3, Apr. 1969, p. 552-563. 24 refs.

The depths at which convection starts have been calculated for main sequence stars and giant stars of various effective temperatures and hydrogen-to-metal ratios. It is found that for late-type stars of $T_e \gtrsim 4400$ K convection starts at $\tau \gtrsim 0.1$. In metal-deficient stars, convection starts at shallower optical depths compared to normal stars of the same spectral type. The larger the metal deficiency, the shallower is the depth at which convection starts. The importance of convection in the study of metal-deficient stars and late type stars are also discussed. (Author)

A69-29970 *
DIRECTIONAL DISCONTINUITIES IN THE INTERPLANETARY MAGNETIC FIELD.
Leonard F. Burlaga (NASA, Goddard Space Flight Center, Laboratory for Space Sciences, Greenbelt, Md.).
Solar Physics, vol. 7, Apr. 1969, p. 54-71. 10 refs.

The interplanetary magnetic field has different characteristics on different scales, and a given physical theory may not be applicable or relevant on all scales. Four scales are defined in terms of time intervals on which the data may be viewed. Many discontinuities in the magnetic-field direction are seen on the mesoscale (≈4 days, ≈1 AU). The characteristics of such directional discontinuities which were observed by Pioneer 6 during the period Dec. 16, 1965-Jan. 4, 1966 are presented, with special emphasis on their distribution in time. Previously, it was suggested that such discontinuities are simply boundaries of spaghetti-like filaments extending from the sun to the earth. Here it is shown that on the mesoscale unique filaments with sharp boundaries containing well-ordered magnetic fields are not always seen although discontinuities are always present at ≈1 AU. Thus, the interplanetary medium appears to be discontinuous rather than filamentary. The filamentary model implies that discontinuities originate at the sun and are convected with the solar wind. The discontinuous model allows the additional possibility that the discontinuities form in the interplanetary medium far from the sun. (Author)

A69-30010 *
DIRECT MEASUREMENTS OF INTERPLANETARY MAGNETIC FIELDS AND PLASMAS.
N. F. Ness (NASA, Goddard Space Flight Center, Laboratory for Space Sciences, Greenbelt, Md.).
IN: SOLAR-TERRESTRIAL PHYSICS: SOLAR ASPECTS; INTERNATIONAL YEARS OF THE QUIET SUN AND COSPAR, JOINT SYMPOSIUM, LONDON, ENGLAND, JULY 17-22, 1967, PROCEEDINGS. PART 1. [A69-30005 15-29]
Edited by A. C. Stickland.
Cambridge, Mass., MIT Press (Annals of the IQSY. Volume 4), 1969, p. 88-109. 48 refs.

Review of the synoptic picture which has emerged from the extended solar corona as observed from 0.7 to 1.5 AU during the last six years by the Mariner, IMP, Pioneer, and Vela spacecraft. The direct measurement of the interplanetary plasma and its embedded magnetic field during the past several years has verified the theoretical model developed principally by Parker (1963). Detailed measurements reveal a morphology in which the permanent longitudinal structure of the solar plasma and magnetic field at the solar surface is reflected in an apparent corotation of spatial structure observed between 0.7 and 1.5 AU. The interplanetary magnetic field is identified to be of solar origin and to result from the extension of photospheric fields into interplanetary space by the solar plasma. Gradients and interplanetary plasma and magnetic field have been observed in good agreement with the classic solar wind model. Microscale structure of the interplanetary medium shows the alignment of plasma thermal anisotropies with the instantaneous magnetic field and the mesoscale feature of collimation of solar cosmic rays along the interplanetary magnetic field immediately after injection. The macroscale sector structure of the interplanetary magnetic field reveals longitudinal variations of the corona which persist over several solar rotations. P.v.T.

A69-30188 *#
FUTURE MISSIONS FOR LIBRATION-POINT SATELLITES.
Robert W. Farquhar (NASA, Electronics Research Center, Cambridge, Mass.).
Astronautics and Aeronautics, vol. 7, May 1969, p. 52-56. 10 refs.

Consideration of the establishment of a continuous communication link between the earth and the far side of the moon by forcing a single relay satellite to follow a trajectory about the earth-moon L_2 point, where it could be visible from both spots. The average stationkeeping cost of this "halo orbit" would be about 500 fps per year and could be reduced by an order of magnitude if some occultation were permitted. By enlarging the halo orbit so that the satellite has a line-of-sight contact with a second relay satellite stationed at the L_1 point, a point-to-point communications network covering most of the lunar surface could be established. This libration-point network could serve as a navigation and control center for extensive lunar exploration. It is pointed out that this communications capability could be used by cosmonauts as well as astronauts, and should receive serious consideration as a possible joint Soviet-American space venture. B.H.

A69-30376 *
SOME ASPECTS OF INTERPLANETARY EARTH-ENTRY SIMULATION.
Edward M. Sullivan, Wayne D. Erickson, G. Louis Smith, and John T. Suttles (NASA, Langley Research Center, Hampton, Va.).
IN: MAN IN HIS ENVIRONMENT; INSTITUTE OF ENVIRONMENTAL SCIENCES, ANNUAL TECHNICAL MEETING AND EQUIPMENT EXPOSITION, 15TH, ANAHEIM, CALIF., APRIL 20-24, 1969, PROCEEDINGS. [A69-30356 15-11]
Mt. Prospect, Ill., Institute of Environmental Sciences, 1969, p. 269-275. 15 refs.

Study of problems of entry at speeds near 15 km/sec. The investigations had a threefold purpose: (1) to define and obtain quantitative analyses of the aerothermochemical and fluid-mechanical effects associated with each of the geometries of the vehicle shape in question; (2) to define the significant parameters in the problem so that a test program can be established based on adequate simulation of these parameters; and (3) define, if possible, a test program which will validate the analyses and give a firmer basis for geometry selection. The subjects considered include the blunt body, the slender body, and a coordinated analytical, ground experimental, and flight test program for evaluating blunt bodies. G. R.

A69-30766 *
ON THE PULSATION HYPOTHESIS FOR MASSIVE RED SUPERGIANTS.
Richard Stothers (NASA, Goddard Space Flight Center, Goddard Institute for Space Studies, New York, N.Y.).
Astrophysical Journal, vol. 156, May 1969, pt. 1, p. 541-547. 17 refs.

The fundamental mode of radial pulsation has been calculated for convective envelopes in adiabatic equilibrium including radiation pressure. The theoretical Q-values are compared with the observational Q-values of variable M supergiants in galactic associations. The variability of these massive red supergiants can be explained on the pulsation hypothesis if a suitable readjustment of some of the observed periods is made. Pulsation seems to be suggested by (1) the cyclical variations in magnitude, spectrum, and radius in individual stars, (2) a period-luminosity relation, and (3) a period-spectrum relation for the group of stars. (Author)

A69-30769 *
DYNAMICAL MODELS OF NOVAE.
Warren M. Sparks (Indiana University, Astronomy Dept., Bloomington, Ind.; NASA, Goddard Space Flight Center, Greenbelt, Md.).
Astrophysical Journal, vol. 156, May 1969, pt. 1, p. 569-595. 58 refs.
Research supported by Indiana University, the University of California, the Goethe Link Fund, the Zaccheus Daniel Foundation for Astronomical Science, and NASA.

Study of the dynamics of a nova outburst by means of a time-dependent hydrodynamics computer program which includes transport of energy by radiation and convection. Two distinct types of ejections which could give rise to novae are identified. The "flash" nova (e.g., T CrB) has a very rapidly rising and falling light curve and a rapidly decreasing velocity curve. A strong shock wave which imparts a velocity greater than the escape velocity to the outer layers of the star will produce this behavior. A less rapidly rising and falling light curve and a nearly constant velocity are characteristic of the "ordinary" nova (e.g., GK Per). These features will result when the stellar material is forced outward by a pressure front which is not a shock wave. The premaximum halt, which is characteristic of the latter type of nova, results from the temperature dependence of the opacity of neutral hydrogen. (Author)

A69-30883 *
MESSIER 87 - THE GALAXY OF GREATEST KNOWN MASS.
John C. Brandt and Robert G. Roosen (NASA, Goddard Space Flight Center, Laboratory for Space Sciences, Solar Physics Branch, Greenbelt, Md.).
Astrophysical Journal, vol. 156, May 1969, pt. 2, p. L59-L61. 16 refs.

Determination of the velocity dispersion of the nucleus of Messier 87 by the method of Burbidge, Burbidge, and Fish (1961). A mass of 2.7×10^{12} $M_\odot$ was calculated from the virial theorem, yielding a mass-to-light (photographic) ratio of 85. P.v.T.

A69-31405 *#
RESULTS ON THE MASS AND THE GRAVITATIONAL FIELD OF THE MOON AS DETERMINED FROM DYNAMICS OF LUNAR SATELLITES.
William H. Michael, Jr., W. Thomas Blackshear, and John P. Gapcynski (NASA, Langley Research Center, Hampton, Va.).
COSPAR, Plenary Meeting, 12th, Prague, Czechoslovakia, May 11-24, 1969, Paper. 23 p. 20 refs.

Review of procedures and a summary of recent results on the mass and gravitational field of the moon. Gravitational field solutions, as represented by spherical harmonic expansions of the potential through various degrees and order are available, and typical solutions obtained by the different procedures are presented. The relative and absolute precisions of the solutions in fitting the data are illustrated by residual plots and other considerations. Lunar surface elevation plots, based on the gravitational coefficients (assuming homogeneity), illustrate the distribution and magnitude of mass anomalies over the lunar sphere. For a 13-th order field, the contour plots show considerable correlation with published mascon results in regions where such results are available. The recently obtained gravitational field results are applied to determination of the moments of inertia of the moon, which correspond very closely to overall homogeneous density distribution in the moon, and to determination of other properties related to mass distribution. (Author)

A69-31442 *#
THE ELECTRICAL CONDUCTIVITY AND INTERNAL TEMPERATURE OF THE MOON.
Norman F. Ness (NASA, Goddard Space Flight Center, Laboratory for Space Sciences, Greenbelt, Md.).
COSPAR, Plenary Meeting, 12th, Prague, Czechoslovakia, May 11-24, 1969, Paper. 15 p. 8 refs.

Determination of the internal electrical conductivity of the moon, based on a study of its dynamic response to discontinuities in the interplanetary magnetic field. The decay of the eddy currents induced in the lunar interior by such transients can be used to determine the characteristic diffusion time of the magnetic field in the interior, and hence its electrical conductivity. The induction of electric currents in the lunar interior indicates an effective time constant for eddy current decay of less than 20 sec. This means an electrical conductivity of less than 10^{-4} mho/meter in the lunar interior. The electrical conductivity of silicate rocks depends mainly upon temperature. Thus limitations on possible thermal models of the moon, consistent with the electrical conductivity measurements, can be obtained. These results are compared with various models of the thermal history, to obtain a class of allowed lunar interiors. It is concluded that the moon must be a relatively young body (1×10^9 yr) if it possesses a homogeneous heat source composition similar to chondritic meteorites. If differentiation of radiogenic heat sources near the surface has taken place, the moon can be as old as 4×10^9 yr. M.G.

A69-32154 *#
ROCKET TRAJECTORY OPTIMIZATION BY A SECOND-ORDER NUMERICAL TECHNIQUE.
H. J. Kelley (Analytical Mechanics Associates, Inc., Westbury, N.Y.), B. R. Uzzell, and S. S. McKay, II (NASA, Manned Spacecraft Center, Mission Planning and Analysis Div., Mathematical Physics Branch, Houston, Tex.).
AIAA Journal, vol. 7, May 1969, p. 879-884. 7 refs.
Contract No. NAS 9-4036.

Mathematical technique and digital computer program for optimizing multistage rocket trajectories. The system model is that for three-dimensional vacuum flight in a central gravitational field, with coasts represented as conic arcs and times of transition between thrusting and coasting treated as parameters to be optimized simultaneously with the steering-angle histories. The optimization process is a second-order scheme. In a first computational phase, terminal constraints are handled in penalty-function approximation,

and a step-size restriction is imposed, with the intention of insuring that the Euler solution approached corresponds to a minimum. In a second phase, the approximate solution is refined, and terminal conditions are satisfied in the limit as the iterations converge. The evolution of the computer program is described, including the development of improved step-size controls, auxiliary diagnostic tests, and features favoring numerical accuracy. Some applications to shaping maneuver sequences for the Apollo-Saturn spacecraft are presented. (Author)

A69-32177 *#
OPTIMAL CONTINUOUS LOW-THRUST TRAJECTORIES FOR CO-ALTITUDE RENDEZVOUS.
Roger R. Burrows and Gordon A. Wood (NASA, Marshall Space Flight Center, Aero-Astrodynamics Laboratory, Huntsville, Ala.).
AIAA Journal, vol. 7, May 1969, p. 983-985.

Analysis of the problem of minimum-time rendezvous between a continually thrusting interceptor vehicle and a passive target vehicle on the basis of a calculus-of-variations (COV) treatment. It is assumed that both vehicles are in the same orbit and have an initial angular separation. The problem had been solved by Hahn and Itzen (1965) by a steepest-ascent method. From the results of the more exact COV method it is found that Hahn and Itzen's control synthesis was quite good, but that their vertical velocity results seem to be at variance with the COV results for small initial angular separations. G.R.

A69-32240 *
A FIRST-ORDER THEORY FOR THE ROTATIONAL MOTION OF A TRIAXIAL RIGID BODY ORBITING AN OBLATE PRIMARY.
Robert L. Holland (NASA, Marshall Space Flight Center, Space Sciences Laboratory, Huntsville, Ala.) and Hans J. Sperling (NASA, Marshall Space Flight Center, Aero-Astrodynamics Laboratory, Huntsville, Ala.).
Astronomical Journal, vol. 74, Apr. 1969, p. 490-496. 8 refs.

Description of new results which predict the principal effect of the gravitational and magnetic torques on the rotational motion of an asymmetrical rigid body in a regressing orbit about an oblate primary mass. Using the method of averages, a first-order theory is developed and three integrals, which determine the motion of the angular-momentum vector, are derived. The solutions are periodic in a rotating coordinate system defined by the orbit plane and line of nodes. The results may be applied to astronomical problems of precession and the astronautical problem of artificial satellites. (Author)

A69-32261 *#
SOLAR SPECTRAL IRRADIANCE MEASURED FROM 38,000 FEET WITH A LEISS MONOCHROMATOR AND A PHOTOELECTRIC FILTER RADIOMETER.
James J. Webb (NASA, Goddard Space Flight Center, Greenbelt, Md.).
Optical Society of America, Spring Meeting, San Diego, Calif., Mar. 11-14, 1969, Paper. 11 p. 9 refs.

Solar spectral irradiance measurements made from NASA's Convair 990 research aircraft using a Leiss double-prism monochromator and a photoelectric filter radiometer. Six flights were made over the Pacific and western U.S. at an altitude of 38,000 ft. Excellent agreement is noted between the two instruments through a wavelength range of 0.3 to 1.1 μ, even though they are optically and electronically dissimilar. Instrument calibrations were performed in flight using an NBS-type quartz-iodine standard of spectral irradiance. Extrapolation to zero air mass was facilitated by the fact that at 38,000 ft the aircraft was above 80% of the permanent gases of the atmosphere and, more importantly, above 99.9% of the water vapor and all the atmospheric pollutants. The resulting solar spectral curves differ significantly from Johnson's (1954) in several regions. The solar constant obtained was 0.135 W/cm^2, which is about 3.3% less than Johnson's, but is in good agreement with recently published values of Drummond (1968) and others. (Author)

A69-32300 *
THE ASHEN LIGHT - AN AURORAL PHENOMENON ON VENUS.
Joel S. Levine (NASA, Goddard Space Flight Center, Goddard Institute for Space Studies; New York University, Geophysical Sciences Laboratory, New York, N.Y.).
Planetary and Space Science, vol. 17, June 1969, p. 1081-1087. 18 refs.
Grant No. NsG-499.

Analysis of 129 visual observations of the "ashen light," the luminous glow on the dark side of Venus, made between 1954 and 1962. Spectroscopic and photometric studies attempting to detect dark-side emission on Venus are reviewed and discussed in light of the visual occurrence of the glow. A general increase in the geomagnetic index, coinciding with the occurrence of the ashen light at times of inferior conjunction of Venus, suggests that the ashen light is an auroral phenomena due to solar particle bombardment on the dark-side of Venus. This possibility is explored in terms of the nature and characteristics of the visual ashen light observations and in terms of the recent Mariner 5 and Venera 4 data on the upper atmosphere of Venus. (Author)

A69-32309 *
INTERPLANETARY FIELD AND GEOMAGNETIC VARIATIONS - A UNIFIED VIEW.
J. Hirshberg and D. S. Colburn (NASA, Ames Research Center, Space Sciences Div., Moffett Field, Calif.).
Planetary and Space Science, vol. 17, June 1969, p. 1183-1206. 44 refs.

Study of the relationship between interplanetary magnetic fields, seen by a magnetometer on board Explorer 33, and surface magnetic variations. Emphasis is placed on achieving a unified view of all experimental results. The sun was considerably disturbed during the period covered by this study, giving an excellent opportunity to observe the magnetic configuration of flare-induced interplanetary storms and their relation to geomagnetic storms. It was also found that high-velocity plasma and intense, highly disturbed interplanetary fields are also typical of interplanetary storms. F. R. L.

A69-32803 *
SPIN DOWN EFFECTS IN NEUTRON STARS.
George S. Greenstein (Yeshiva University, Belfer Graduate School of Science, New York, N.Y.) and A. G. W. Cameron (Yeshiva University, Belfer Graduate School of Science; NASA, Goddard Space Flight Center, Goddard Institute for Space Studies, New York, N.Y.).
Nature, vol. 222, May 31, 1969, p. 862, 863. 10 refs.
NSF-NASA-supported research.

Theoretical discussion of the sudden decrease of the period of PSR 0833-45 during the week of Feb. 24 to Mar. 3, 1969. It is proposed, that this decrease arose as a result of a sudden onset of an instability of differential rotation within PSR 0833-45. P. G.

A69-32811 *
UNUSUAL 1 TO 5 GHz SOLAR RADIO EMISSION OF 29 OCTOBER 1968.
R. A. Mennella and J. H. Reid (NASA, Manned Spacecraft Center, Houston, Tex.).
Astrophysical Letters, vol. 3, May 1969, p. 129-132.

On Oct. 29, 1968, solar activity produced possibly the largest burst of solar microwave radiation ever measured - 1.420 GHz. The activity occurred between 1515-1652 UT and provided peaks of 379,000 x 10^{-22} W/m^2-Hz, 5370 x 10^{-22} W/m^2-Hz, and 570 W/m^2-Hz at 1.420 GHz, 2.695 GHz, and 4.995 GHz, respectively. The solar radio emission appears to have originated from an active region just behind the west limb. (Author)

A69-33059 *
A STUDY OF THE COMPOSITION OF THE LOWER SOLAR CORONA.
M. P. Nakada (NASA, Goddard Space Flight Center, Greenbelt, Md.).
Solar Physics, vol. 7, May 1969, p. 302-320. 37 refs.

Examination of some trends in the composition of the lower solar corona due to mixing and diffusion. Mixing has been treated through plausible inference from the thermal gradient and through

analogy with the neutral atmosphere of the earth. These indicate that diffusion may be important in the lower corona. Changes in composition due to pressure and thermal gradients have been calculated with multicomponent diffusion equations. Results indicate that (1) large enhancements of heavy elements are possible and (2) the composition of the corona can show large variations with values of the thermal gradient in the lower corona. (Author)

A69-33159 *#
EXACT AND APPROXIMATE SOLUTIONS FOR MULTIPLE SCATTERING BY CLOUDY AND HAZY PLANETARY ATMOSPHERES.
James E. Hansen (NASA, Goddard Space Flight Center, Goddard Institute for Space Studies, New York, N.Y.).
Journal of the Atmospheric Sciences, vol. 26, May 1969, p. 478-487. 18 refs.

Determination of the accuracy of the multiple scattering solutions obtained by omitting the diffraction peak from cloud phase functions. Exact multiple scattering solutions for phase functions typical of both clouds and hazes are compared to solutions obtained with analytic phase functions. Calculations for all the phase functions are made for optically thin and optically thick atmospheres. B.H.

A69-33161 *#
EFFECT OF CLOUD SCATTERING ON LINE FORMATION IN THE ATMOSPHERE OF VENUS.
John F. Potter (NASA, Goddard Space Flight Center, Goddard Institute for Space Studies, New York, N.Y.).
Journal of the Atmospheric Sciences, vol. 26, May 1969, p. 511-517. 18 refs.
Contract No. NAS 9-5191.

Analysis in which corrections for anisotropic scattering in a cloudy medium are added to a synthetic spectrum analysis by Belton, Hunten, and Goody (1968) of CO_2 bands and a water vapor line in the spectrum of Venus. It is found that to a good approximation the introduction of anisotropic scattering merely renormalizes the theoretical curves, so that the corrections can be applied without recalculating the synthetic spectra. Since the line shapes and relative intensities are unaltered, derived pressures and temperatures remain the same. The corrected results indicate that the scattering mean free path in the Cytherian clouds resembles that for terrestrial cirrus clouds and that there is at least 20 times too little water vapor present to be in equilibrium with a water or ice cloud. (Author)

A69-33664 *
AIRGLOW AND STAR PHOTOGRAPHS IN THE DAYTIME FROM A ROCKET.
D. C. Evans and L. Dunkelman (NASA, Goddard Space Flight Center, Greenbelt, Md.).
Science, vol. 164, June 20, 1969, p. 1391-1393. 11 refs.

Comparison of the day sky brightness at altitudes above 100 km with the night sky viewed from the ground. Photographs of the constellation Cygnus taken in the daytime during a rocket flight indicate that the day sky brightness in the wavelength region from 3600 to 7000 Å is only slightly brighter than the night sky viewed from the ground. No diffuse cloud of particles was apparent in the vicinity of the rocket payload, but discrete particles must be considered in the design of instruments for rockets and satellites. G.R.

A69-34043
COMMERCIAL UTILIZATION OF SPACE; AMERICAN ASTRONAUTICAL SOCIETY, ANNUAL MEETING, 13TH, DALLAS, TEX., MAY 1-3, 1967, PROCEEDINGS.
Edited by J. R. Gilmer, A. M. Mayo, and R. C. Peavey.
Tarzana, Calif., American Astronautical Society (Advances in the Astronautical Sciences. Volume 23. Lloyd V. Berkner Memorial Volume), 1968. 508 p.
$23.50.

CONTENTS:

FOREWORD. J. R. Gilmer, A. M. Mayo, and R. C. Peavey, p. vii-x.

INTRODUCTION - OVERVIEW. A. M. Mayo, p. 5-27.

THE OPPORTUNITY.

KEYNOTE ADDRESS. G. H. Stoner (Boeing Co., Patrick AFB, Fla.), p. 31-38.

THE CHALLENGE OF THE COMMERCIAL UTILIZATION OF SPACE. L. V. Berkner (Southwest Center for Advanced Studies, Dallas, Tex.), p. 39-46.

DEPARTURES FROM PRESENT TECHNOLOGY.

NASA APPLICATIONS TECHNOLOGY. L. Jaffe, p. 49-55. [For abstract see issue 15, page 2557, Accession no. A67-29944]

SATELLITE COMMUNICATIONS - A RENEWED CHALLENGE IN RESOURCE UTILIZATION. R. C. Kirby and T. deHaas, p. 57, 58. [For abstract see issue 15, page 2437, Accession no. A67-29945]

MICROELECTRONICS. C. L. Hogan and S. L. Levy, p. 59-63. [For abstract see issue 15, page 2452, Accession no. A67-29946]

THE MAN-MACHINE-ENVIRONMENTAL INTERFACE. A. H. Schwichtenberg, p. 64. [For abstract see issue 15, page 2432, Accession no. A67-29947]

DEPARTURES - STRUCTURES AND MATERIALS. L. A. Riedinger, p. 65-68. [For abstract see issue 15, page 2575, Accession no. A67-29948]

VEHICLES AND PROPULSION - AN OVERVIEW. A. B. Greenberg, p. 69-73. [For abstract see issue 15, page 2570, Accession no. A67-29949]

COMMERCIAL UTILIZATION OF SPACE - PANEL.

COMMERCIAL UTILIZATION OF SPACE - AN INTRODUCTION. W. von Braun (NASA, Marshall Space Flight Center, Huntsville, Ala.), p. 77-82.

FUTURE TRENDS IN EARTH ORBITAL TRANSPORTATION. R. E. Fisher, p. 83-87. [For abstract see issue 15, page 2546, Accession no. A67-29950]

ESTIMATION OF FUTURE PROGRESS. J. M. West (NASA, Manned Spacecraft Center, Houston, Tex.), p. 88, 89.

SPACE COMMUNICATIONS - A MAJOR CANDIDATE FOR COMMERCIAL UTILIZATION OF SPACE. H. K. Ziegler (U.S. Army, Electronics Command, Fort Monmouth, N.J.), p. 90-92.

PANEL DISCUSSION, p. 95-106.

SPACE COMMERCE - AN ECONOMIC FOUNDATION FOR THE FUTURE - PANEL, p. 109-124.

EARTH-SPACE APPLICATIONS.

NASA SPACE APPLICATIONS - AN OVERVIEW. R. C. Seamans, Jr., p. 127-139. [For abstract see issue 15, page 2583, Accession no. A67-29951]

EARTH APPLICATIONS - AN OVERVIEW. C. F. Luce (U.S. Department of the Interior, Washington, D.C.), p. 140-146.

COMMUNICATIONS IN THE SPACE AGE - HOTLINE TO THE WORLD. D. W. Coyle (International Television, Inc.), p. 148-152.

COMMUNICATION AND BROADCASTING.

SATELLITES AND FUTURE COMMUNICATIONS, INCLUDING BROADCAST. J. L. Hult, p. 155-157. [For abstract see issue 15, page 2437, Accession no. A67-29952]

SPACE COMMUNICATIONS IN THE 21ST CENTURY. F. A. Gicca (Raytheon Co., Lexington, Mass.), p. 158.

PROPAGATION LIMITATIONS TO EARTH-SPACE RADIO COMMUNICATIONS FOR FREQUENCIES BELOW 10 GHz. C. G. Little, p. 159. [For abstract see issue 15, page 2437, Accession no. A67-29953]

WINDOWS TO SPACE (FROM 10^{10} Hz UP). R. Kompfner, p. 160. [For abstract see issue 15, page 2478, Accession no. A67-29954]

DIRECT SATELLITE BROADCAST. S. Gubin, p. 161, 162. [For abstract see issue 15, page 2570, Accession no. A67-29955]

INFORMATION HANDLING AND LIBRARIES.

INTRODUCTORY REMARKS. E. Miller (Documentation, Inc., College Park, Md.), p. 165, 166.

DEVELOPING A NATIONAL INFORMATION NETWORK FOR THE SPACE AGE. R. W. Hodgers, Jr. (Western Union Telegraph Co., Inc., New York, N.Y.), p. 167, 168.

INFORMATION CENTERS IN THE SPACE AGE. C. W. Sherwin (U.S. Department of Commerce, Washington, D.C.), p. 169.

INFORMATION HANDLING. P. C. Goldmark (Columbia Broadcasting System, Inc., Stamford, Conn.), p. 170.

RETENTION AND DATA DISPLAY. M. S. Day (NASA, Office of Technology Utilization, Washington, D.C.), p. 171.
REMOTE ACCESS TO INFORMATION. J. Becker (EDUCOM), p. 172.

WEATHER AND NAVIGATION.
THE FUTURE POTENTIALS OF NAVIGATION SATELLITES. E. Ehrlich, p. 175-181. [For abstract see issue 15, page 2570, Accession no. A67-29956]
SATELLITE NAVIGATIONAL AIDS FOR TRANSPORTATION OF THE 1970's. D. W. Roese, p. 182, 183. [For abstract see issue 15, page 2515, Accession no. A67-29957]
THE USE OF SATELLITES TO TRACK GHOST BALLOONS. V. E. Lally, p. 184, 185. [For abstract see issue 15, page 2420, Accession no. A67-29958]
ENVIRONMENTAL PREDICTION USING ORBITAL SENSORS. W. O. Davis and J. P. Kuettner, p. 186-190. [For abstract see issue 15, page 2478, Accession no. A67-29959]
METEOROLOGICAL SATELLITES AND THE WORLD WEATHER WATCH. C. A. Spohn (ESSA, Rockville, Md.), p. 191.

OCEANOGRAPHY AND TERRESTRIAL RESOURCES.
MAPPING OF THE LAND FROM SPACE. F. J. Doyle, p. 195. [For abstract see issue 15, page 2478, Accession no. A67-29960]
THE OCEANS - AN OVERVIEW REGARDING THE COMMERCIAL UTILIZATION OF SPACE. R. E. Stevenson (Bureau of Commercial Fisheries, Galveston, Tex.), p. 196-201.
REMOTE SENSING IN AGRICULTURE/FORESTRY. A. B. Park (U.S. Department of Agriculture, Washington, D.C.), p. 202, 203.
APPLICATIONS OF SPACE DATA TO WATER RESOURCES. P. Bock, p. 204.
MINERAL AND LAND RESOURCES. W. T. Pecora (U.S. Department of the Interior, Washington, D.C.), p. 205, 206.
TOOLS FOR THE FUTURE - REMOTE SENSING. M. R. Holter (Michigan, University, Ann Arbor, Mich.), p. 207, 208.

INDUSTRIAL RESEARCH AND MANUFACTURING.
NEW TOOLS FOR THE INQUISITIVE MIND - THE INDUSTRIAL RESEARCH LABORATORY IN SPACE. T. S. Burkhalter and S. S. White (Texas Instruments, Inc., Dallas, Tex.), p. 211-219.
DESIGN OF A COMMERCIAL SPACE STATION. V. D. Kirkland and R. L. Gervais, p. 220-222. [For abstract see issue 15, page 2557, Accession no. A67-29961]
NEW USES FOR NUCLEAR ENERGY IN OUTER SPACE. P. Harteck and S. Dondes, p. 223. [For abstract see issue 15, page 2558, Accession no. A67-29962]
LOCAL TRANSPORTATION IN COMMERCIAL SPACE OPERATIONS. H. M. Graham, p. 224-233. [For abstract see issue 15, page 2432, Accession no. A67-29963]
SPACE OPTICS AND ASTRONOMY. D. N. Buell and M. L. Scott (Chrysler Corp., New Orleans, La.), p. 234, 235.
THE USES OF ORBITING REFLECTOR SATELLITES. A. G. Buckingham and H. M. Watson, p. 236, 237. [For abstract see issue 15, page 2570, Accession no. A67-29964]

MEDICAL RESEARCH AND APPLICATIONS.
WORLD HEALTH MAINTENANCE. E. B. Konecci (Texas, University, Austin, Tex), p. 241.
BIOLOGICAL "FUEL CELLS" FROM THE ELECTRIC FISH TO MAN. H. Strughold (USAF, Aerospace Medical Div., Brooks AFB, Tex.), p. 242, 243.
THE USE OF SPACE AS A RESEARCH TOOL. J. D. Gatts (Fairchild Hiller Corp., Farmingdale, N.Y.), p. 244.
THE UTILIZATION AND ENGINEERING OF AN ORBITAL HOSPITAL. O. H. Minney (VARO, Inc., Garland, Tex.), p. 245.
COMMERCIAL UTILIZATION OF OUR SPACE PROGRAM IN ITS APPLICATION OF SPACE MEDICAL RESEARCH. L. D. Proctor (Henry Ford Hospital), p. 246, 247.

TOURISM.
HOTELS IN SPACE. B. Hilton (Hilton Hotels Corp.), p. 251-257.
SPACE TOURISM. K. A. Ehricke, p. 259-291. [For abstract see issue 15, page 2558, Accession no. A67-29965]
SPACE MANUFACTURING. R. F. Mettler (TRW Systems Group, Redondo Beach, Calif.), p. 295-306.

TRANSPORTATION.
FUTURE SPACEPORT FACILITIES - TECHNOLOGY AND ECONOMICS. K. H. Debus, p. 309-325. [For abstract see issue 15, page 2467, Accession no. A67-29943]
IMPACT OF PERFORMANCE IMPROVEMENTS AND REUSE ON THE COST OF SPACE TRANSPORTATION. C. J. Dorrenbacher and R. J. Gunkel, p. 327, 328. [For abstract see issue 15, page 2570, Accession no. A67-29967]
UNCONVENTIONAL PROPULSION SYSTEMS. R. J. Rosa (Avco Corp., Everett, Mass.), p. 329.
CONSIDERATIONS OF NUCLEAR POWER AND PROPULSION. J. D. Lafleur, Jr. and F. C. Schwenk, p. 330, 331. [For abstract see issue 15, page 2516, Accession no. A67-29967]
AN ECONOMICAL APPROACH TO SPACE TRANSPORTATION. E. N. Hall (United Aircraft Corp., Windsor Locks, Conn.), p. 332, 333.
COMMERCIAL SPACE TRANSPORTATION POSSIBILITIES. M. W. Hunter, II, p. 334, 335. [For abstract see issue 15, page 2571, Accession no. A67-29968]

SOCIAL IMPLICATIONS.
THE FIRST 2,000 YEARS OF THE SPACE AGE. P. A. Campbell, p. 339.
PRESENT VALUES AND FUTURE ASPIRATIONS. J. E. Coppage and J. R. Tabibian (TRW Systems Group, Redondo Beach, Calif.), p. 340, 341.
A CRITIQUE ON THE APPLICATION OF SYSTEMS ANALYSIS TO SOCIAL PROBLEMS. I. R. Hoos (California, University, Berkeley, Calif.), p. 342.
COMMERCIAL UTILIZATION OF SPACE - SOME ASPECTS OF A POSSIBLE FUTURE. K. B. Bley (Hughes Aircraft Co., Culver City, Calif.) and R. D. Shaver (RAND Corp., Santa Monica, Calif.), p. 343.
COMMERCIAL UTILIZATION OF SPACE - THE ECONOMIC, POLITICAL, AND CULTURAL IMPACT ON THE WORLD OF TOMORROW. J. C. Casey and E. Gardner (USAF, Systems Command, Washington, D.C.), p. 344, 345.
EDUCATIONAL IMPLICATIONS OF COMMERCIAL UTILIZATION OF SPACE. H. G. Stever (Carnegie-Mellon University, Pittsburgh, Pa.), p. 349-355.

EDUCATION.
MAN AND HIS ENVIRONMENT - A CHALLENGE TO EDUCATION. S. F. Singer (U.S. Department of the Interior, Washington, D.C.), p. 359-372.
MAN-RATING THE EDUCATIONAL SYSTEM. R. C. Flothow (Lockheed Aircraft Corp., Sunnyvale, Calif.), p. 373.
IMPACT OF COMMERCE IN SPACE ON EDUCATION - TECHNOLOGY IN EDUCATION. N. Hackerman (Texas, University, Austin, Tex.), p. 374.
SPACE SCIENCE AND THE UNIVERSITIES. J. C. Allred (Houston, University, Houston, Tex.), p. 375.
A WORLD FEDERATION OF LEARNING. D. A. Cowan (Dallas, University, Dallas, Tex.), p. 376.

INTERNATIONAL COOPERATION.
PATTERNS OF INTERNATIONAL SPACE APPLICATIONS AND THEIR EXTENSION. A. W. Frutkin (NASA, Washington D.C.), p. 379-389.
INTERNATIONAL CO-OPERATION FROM THE U. N. VIEWPOINT. K. Waldheim, p. 391, 392.
INTERNATIONAL COOPERATION FROM THE BUSINESS VIEWPOINT. R. W. Porter, p. 393.
INTERNATIONAL COOPERATION IN SATELLITE COMMUNICATIONS. J. A. Johnson (Communications Satellite Corp., Washington, D.C.), p. 394.
SPACE COMMERCE - AN OPPORTUNITY FOR THE FUTURE - PANEL, p. 397.

THE SPACE ENTREPRENEUR - OVERVIEW.
INTRODUCTORY REMARKS. C. Skeen (Ling-Temco-Vought, Inc., Dallas, Tex.), p. 401.
THE CHALLENGE TO PRIVATE ENTERPRISE. G. M. Bunker (Martin Marietta Corp., Friendship International Airport, Md.), p. 403-417.

THE SPACE ENTREPRENEUR - MANAGEMENT.

REQUIREMENTS FOR MANAGEMENT OF SPACE ENTERPRISES. G. W. Hoover, p. 421.
MANAGEMENT OF SPACE ENTERPRISES. G. Kozmetsky, p. 422. [For abstract see issue 15, page 2583, Accession no. A67-29969]

THE SPACE ENTREPRENEUR - FINANCE.
THE IMPACT OF COMMUNICATIONS SATELLITES ON THE TELEVISION INDUSTRY. L. L. Johnson (RAND Corp., Santa Monica, Calif.), p. 425.
FINANCING SPACE VENTURES. A. H. Frady, Jr. (Merrill Lynch, Pierce, Fenner and Smith, Inc., New York, N.Y.), p. 426, 427.
INSURANCE FOR COMMERCIAL VENTURES IN OUTER SPACE. C. C. Pell, Jr. (Marine Office of America; Associated Aviation Underwriters, New York, N.Y.), p. 428.

THE SPACE ENTREPRENEUR - LAW.
COMMERCIAL UTILIZATION OF SPACE AND THE LAW. P. G. Dembling (NASA, Washington, D.C.), p. 431.
LAW AND THE UTILIZATION OF SPACE. R. F. Packard (U.S. Department of State, Office of Outer Space Affairs, Washington, D.C.), p. 432-433.

REALIZING THE OPPORTUNITY.
INTRODUCTORY REMARKS. E. C. Welsh (National Aeronautics and Space Council, Washington, D.C.), p. 437, 438.
ECONOMIC NEED AND PAYOFF. D. A. Hicks (Northrop Corp., Hawthorne, Calif.), p. 439-449.
COMMERCIAL EXPLOITATION OF SPACE TECHNOLOGY. G. E. Mueller (NASA, Washington, D.C.), p. 451-457.
DEVELOPMENT OF NEEDED TECHNOLOGY. R. L. Bisplinghoff (Massachusetts Institute of Technology, Cambridge, Mass.) and J. L. Sloop (NASA, Washington, D.C.), p. 459-476.
REALIZING THE INDUSTRIAL OPPORTUNITY. A. N. Stanton (VARO, Inc., Garland, Tex.), p. 477-483.
SUMMARY OF MEETING. L. V. Berkner, p. 485-488.

A69-34044 *
COMMERCIAL EXPLOITATION OF SPACE TECHNOLOGY.
George E. Mueller (NASA, Washington, D.C.).
IN: COMMERCIAL UTILIZATION OF SPACE; AMERICAN ASTRONAUTICAL SOCIETY, ANNUAL MEETING, 13TH, DALLAS, TEX., MAY 1-3, 1967, PROCEEDINGS. [A69-34043 17-30]
Edited by J. R. Gilmer, A. M. Mayo, and R. C. Peavey.
Tarzana, Calif., American Astronautical Society (Advances in the Astronautical Sciences. Volume 23. Lloyd V. Berkner Memorial Volume), 1968, p. 451-457.

General discussion of the progress achieved in space exploration with some indication of the potential it represents. The first commercial utilization of space by the communication satellite is cited as an example of the possibilities that could open in this field. The various aspects of the problem of reducing costs to make commercial utilization feasible and practicable are surveyed. The base upon which all these future capabilities rest is the Apollo Program which is discussed in terms of NASA's role in working with the industrial and academic communities in developing commercial uses for space. V.P.M.

A69-34297 *
CURVE-OF-GROWTH ANALYSIS FOR THE CLOSE BINARY HR 5317
Yoji Kondo (NASA, Manned Spacecraft Center, Astronomy Branch, Houston, Tex.) and George E. McCluskey, Jr. (Lehigh University, Math-Astronomy Dept., Bethlehem, Pa.).
Astrophysical Journal, vol. 156, June 1969, pt. 1, p. 1007-1012. 14 refs.

The single-lined spectroscopic binary HR 5317 was observed with a dispersion of 13.5 Å mm^{-1} at the coudé focus of the 84-in. reflector of the Kitt Peak National Observatory. The strength of the Balmer lines indicates a spectral type no later than F6, while the metallic lines give a spectral type of F8 or later. A curve-of-growth analysis was carried out. The results indicate that the elements Mg, Mn, Ca, and Sr are overabundant with respect to the standard star 110 Her. The results are somewhat dependent on the adopted luminosity class for HR 5317. (Author)

A69-34359
ADVANCED SPACE EXPERIMENTS; AMERICAN ASTRONAUTICAL SOCIETY, CONFERENCE, ANN ARBOR, MICH., SEPTEMBER 16-18, 1968, PROCEEDINGS.
Edited by O. L. Tiffany and E. M. Zaitzeff (Bendix Corp., Ann Arbor, Mich.).
Tarzana, Calif., American Astronautical Society (Advances in the Astronautical Sciences. Volume 25), 1969. 530 p.
Members, $12.60; nonmembers, $16.75.

CONTENTS:
FOREWORD. O. L. Tiffany and E. M. Zaitzeff (Bendix Corp., Ann Arbor, Mich.), p. vii, viii.

INTRODUCTION.
REALISM ABOUT SPACE. E. M. Cortright (NASA, Langley Research Center, Hampton, Va.), p. 3-10.
OUR FUTURE IN SPACE. G. V. Jagt, p. 11-19.
SCIENTIFIC SPACE RESEARCH - THE NEXT 10 YEARS. J. W. Findlay (National Radio Astronomy Observatory, Green Bank, W. Va.), p. 21-28. [See A69-34360 18-30]

PLANETARY ORBITAL, ENTRY, AND FLYBY EXPERIMENTS.
INTRODUCTION. R. F. Fellows (NASA, Washington, D.C.), p. 31-34.
BISTATIC RADAR ASTRONOMY. V. R. Eshleman, p. 35-43. [For abstract see issue 02, page 311, Accession no. A69-11467]
PLANETARY ATMOSPHERE MASS SPECTROMETRY. N. W. Spencer, p. 45-68. [For abstract see issue 02, page 311, Accession no. A69-11468]
PLANETARY ULTRAVIOLET EXPERIMENTS. C. A. Barth, p. 69-77. [For abstract see issue 02, page 311, Accession no. A69-11469]
S-BAND OCCULTATION EXPERIMENTS. A. J. Kliore and B. Seidel, p. 79-101. [For abstract see issue 02, page 311, Accession no. A69-11470]
PLANETARY MAGNETIC FIELD EXPERIMENTS. E. J. Smith, p. 103-130. [For abstract see issue 02, page 311, Accession no. A69-11471]
DIRECT MEASUREMENTS OF PLANETARY AMOSPHERES BY ENTRY PROBES. A. Seiff, p. 131-158. [For abstract see issue 02, page 311, Accession no. A69-11472]

PLANETARY SURFACE EXPERIMENTS.
INTRODUCTION. R. V. Meghreblian (California Institute of Technology, Pasadena, Calif.), p. 161-163.
BIOLOGICAL STUDIES OF MARS - THEORETICAL CONSIDERATIONS AND A PRACTICAL EXPERIMENT. F. Fanale, C. Stembridge, and N. H. Horowitz, p. 165-177.
PLANETARY ATMOSPHERES - COMPOSITIONAL AND OTHER CHANGES ASSOCIATED WITH THE PRESENCE OF LIFE. J. E. Lovelock and C. E. Giffin, p. 179-193. 8 refs. [See A69-34361 18-30]
RELEVANCE OF FUTURE SPACE MISSIONS TO THE ORIGIN OF THE SOLAR SYSTEM. J. Witting, p. 195-236. [For abstract see issue 01, page 153, Accession no. A69-10823]
A PLANETARY STUDY AND ITS IMPLEMENTATION. D. G. Rea, p. 237-255. [For abstract see issue 02, page 311, Accession no. A69-11473]

LUNAR ORBITAL EXPERIMENTS.
LUNAR ORBITAL MISSION PLANS. R. J. Allenby (NASA, Apollo Lunar Exploration Office, Washington, D.C.), p. 259-262. [See A69-34362 18-30]
ORBITAL INFRARED EXPERIMENTS. J. W. Salisbury and G. R. Hunt, p. 263-278. [For abstract see issue 02, page 312, Accession no. A69-11474]
AN INTEGRATED EXPERIMENT FOR COMPOSITIONAL ANALYSIS FROM AN ORBITER. I. Adler and J. Trombka, p. 279-302. [For abstract see issue 02, page 312, Accession no. A69-11475]
EXPLORATION OF GRAVITATIONAL ANOMALIES OF PLANETS FROM ORBITING VEHICLES. P. H. Savet, p. 303-331. [For abstract see issue 02, page 312, Accession no. A69-11476]
DETERMINATION OF ELECTRICAL PARAMETERS OF THE MOON. S. H. Ward, p. 333-346. [For abstract see issue 02, page 312, Accession no. A69-11477]

LUNAR SURFACE EXPERIMENTS.
INTRODUCTION. A. H. Chidester (U.S. Geological Survey,

Flagstaff, Ariz.), p. 349, 350.

SURVEYOR RESULTS. A. R. Hibbs, p. 351-353. [For abstract see issue 06, page 1001, Accession no. A69-17162]

LUNAR GEOLOGICAL FIELD INVESTIGATIONS. G. A. Swann, p. 355-362. [For abstract see issue 02, page 312, Accession no. A69-11478]

LUNAR GEOPHYSICS. G. Simmons (Massachusetts Institute of Technology, Cambridge, Mass.), p. 363-380. 26 refs. [See A69-34363 18-30]

POST-APOLLO - PASSIVE SEISMIC EXPERIMENT. G. V. Latham, p. 381-390. [For abstract see issue 02, page 312, Accession no. A69-11479]

THE VELOCITY STRUCTURE OF THE MOON. R. L. Kovach, p. 391-400. [For abstract see issue 02, page 312, Accession no. A69-11480]

MAGNETOMETER EXPERIMENT. P. Dyal and C. P. Sonett, p. 401-420. [For abstract see issue 02, page 312, Accession no. A69-11481]

THE LUNAR HEAT FLOW EXPERIMENT. M. G. Langseth, p. 421-440. [For abstract see issue 02, page 313, Accession no. A69-11482]

THE FUTURE OF LUNAR EXPLORATION. W. N. Hess (NASA, Manned Spacecraft Center, Houston, Tex.), p. 441-461.

PARTICLES AND FIELDS EXPERIMENTS.

INTRODUCTION. G. H. Ludwig (NASA, Goddard Space Flight Center, Greenbelt, Md.), p. 465, 466.

THE INTERPLANETARY MAGNETIC FIELD - SOLAR ORIGIN AND TERRESTRIAL EFFECTS. J. M. Wilcox (California, University, Berkeley, Calif.), p. 467.

LOW FREQUENCY WAVES IN THE MAGNETOSPHERE. R. A. Helliwell (Stanford University, Stanford, Calif.), p. 469, 470.

THE STRUCTURE OF THE MAGNETOSPHERE. L. J. Cahill, Jr. (Minnesota, University, Minneapolis, Minn.), p. 471, 472.

AURORAL PHENOMENA. B. J. O'Brien (William Marsh Rice University, Houston, Tex.), p. 473.

LOW ENERGY CHARGED PARTICLES IN THE EARTH'S MAGNETOSPHERE. L. A. Frank (Iowa, University, Iowa City, Iowa), p. 475-478.

ASTRONOMY IN SPACE.

INTRODUCTION. O. C. Mohler (Michigan, University, Ann Arbor, Mich.), p. 481, 482.

X-RAY SOURCES. W. A. Hiltner (Chicago, University, Chicago, Ill.), p. 483-502. 30 refs. [See A69-34364 18-30]

SPACE OBSERVATIONS OF THE SOLAR CORONA. R. M. MacQueen, p. 503-519. [For abstract see issue 02, page 313, Accession no. A69-11483]

OPTICAL SPACE ASTRONOMY. W. G. Tifft, p. 521-530. [For abstract see issue 02, page 313, Accession no. A69-11484]

THE RESULTS AND INTERPRETATION OF SOME OF THE HARVARD OSO-IV OBSERVATIONS. L. Goldberg, R. W. Noyes, W. H. Parkinson, E. M. Reeves, and G. L. Withbroe, p. 531, 532. [For abstract see issue 02, page 313, Accession no. A69-11485]

INTERPRETATION OF VENUS LYMAN-α EMISSION AS OBSERVED FROM MARINER V. M. B. McElroy and L. Wallace, p. 533-539. [For abstract see issue 02, page 313, Accession no. A69-11486]

A69-34362 *

LUNAR ORBITAL MISSION PLANS.

Richard J. Allenby (NASA, Apollo Lunar Exploration Office, Washington, D.C.).

IN: ADVANCED SPACE EXPERIMENTS; AMERICAN ASTRONAUTICAL SOCIETY, CONFERENCE, ANN ARBOR, MICH., SEPTEMBER 16-18, 1968, PROCEEDINGS. [A69-34359 18-30]

Edited by O. L. Tiffany and E. M. Zaitzeff.

Tarzana, Calif., American Astronautical Society (Advances in the Astronautical Sciences. Volume 25), 1969, p. 259-262.

Summary of a series of lunar orbital mission plans intended to optimize spacecraft procurement, flight schedules, science objectives, and available funds. It is suggested that the greatest opportunity for orbital science is provided by the presently empty Sector I of the Service Module. Consideration is also given to employing a subsatellite that can be ejected into lunar orbit from Sector I of the Service Module, and which could remain in lunar orbit as an independent spacecraft. V.P.M.

A69-34374 *

PREDICTING LUNAR TEMPERATURES.

Billy P. Jones (NASA, Marshall Space Flight Center, Space Sciences Laboratory, Theoretical Thermophysics Branch, Huntsville, Ala.).

IN: THERMAL DESIGN PRINCIPLES OF SPACECRAFT AND ENTRY BODIES. [A69-34372 18-33]

Edited by J. T. Bevans.

New York, Academic Press, Inc. (Progress in Astronautics and Aeronautics. Volume 21), 1969, p. 469-487. 52 refs.

Review of the chain of developments in constructing theoretical models for predicting lunar temperatures. The thread that runs through this survey is the point of view that the essential differences in the various models and the means of their progressive evolvement have been the manner in which the physical properties have entered. Consequently, the models are characterized and discussed through the assumptions about the physical properties which appear in the heat conduction equation. Taken up, in order, are the homogeneous models, the quasi-homogeneous or two-layer models, and the variable property models. More attention is devoted to the variable property models, since the other types are more widely known. The paper includes a specific proposal of a model type which is the next logical step in the evolution and which seems to meet the known requirements and incorporates the experience represented by the reviewed works. (Author)

A69-34941 *

BOW SHOCK ASSOCIATED WAVES OBSERVED IN THE FAR UPSTREAM INTERPLANETARY MEDIUM.

D. H. Fairfield (NASA, Goddard Space Flight Center, Laboratory for Space Sciences, Greenbelt, Md.).

Journal of Geophysical Research, vol. 74, July 1, 1969, p. 3541-3553. 15 refs.

Analysis of the magnetic data of the Explorer 34 satellite with a view to studying the .01-.05 Hz transverse magnetic field waves in the region between the bow shock and 34 earth radii. It is concluded that the waves are associated with the earth's bow shock since they only occur when projection of the interplanetary field observed at the spacecraft intersects the shock. Whistler propagation and local generation by a two-stream instability are discussed as alternate theoretical explanations for the presence of the waves. V.P.M.

A69-34952 *

A NEW CRITERION FOR THE IDENTIFICATION OF MICROMETEOR IMPACT SITES ON ALUMINIZED GLASS.

Luc Secretan and Otto E. Berg (NASA, Goddard Space Flight Center, Greenbelt, Md.).

Journal of Geophysical Research, vol. 74, July 1, 1969, p. 3681-3692. 9 refs.

New criterion for the identification of true impact sites by hypervelocity space particles on aluminized glass specimens. The basic method of detection of these impact sites lies in the examination of postflight specimens for new perforations in the aluminum covering and more specifically for damage or fracture of the glass substrate beneath the aluminum coating. It is shown that micron size iron particles impacting at 2 to 5 km/sec will fracture aluminum-coated glass in a typically conchoidal pattern. This effect can serve as a criterion in the analysis of suspected hypervelocity space impacts. Absence of this fracture betrays the fact that the impacting particle lacked the structural strength, mass, or velocity needed to fracture the glass. (Author)

A69-34994 *

SEARCH FOR ULTRA-SHORT LIGHT PULSES FROM PULSARS.

H. Ögelman and S. Sobieski (NASA, Goddard Space Flight Center, Greenbelt, Md.).

Nature, vol. 223, July 5, 1969, p. 47, 48.

Interpretation of the results obtained in using Cerenkov light detectors in observations of pulsar CP 1133 and of the pulsars NP 0532 and NP 0527. The results of the tests argue strongly against optical pulses of nanosecond duration originating in the

pulsars observed. However, atmospheric Cerenkov light bursts initiated by gamma rays from the pulsars would go undetected by the instrumentation, due to the restricted angular aperture deliberately chosen for this search. Because of the instrumental technique pulsar light sharply peaked in wavelength would also go undetected. G. R.

A69-35348 * #
INFRARED PHOTOMETRY OF A HELIUM STAR, HD 30353.
Thomas A. Lee (NASA, Goddard Space Flight Center, Goddard Institute for Space Studies, New York, N. Y.) and Kyoji Nariai (NASA, Goddard Space Flight Center, Greenbelt, Md.).
Astronomical Society of Japan, Publications, vol. 21, no. 1, 1969, p. 67-70. 10 refs.

Consideration of IR data for HD 30353, a helium-rich, single-lined spectroscopic binary. The IR colors suggest that the invisible component may be a KO-type supergiant. The large K-L index implies additional IR radiation, possibly arising in a circumstellar envelope like that found for υ Sgr. B. H.

A69-35934 * #
AN APPROXIMATE SOLUTION FOR THE SHORT-TERM MOTION OF A LUNAR SATELLITE.
George H. Born (NASA, Manned Spacecraft Center, Computation and Analysis Div., Houston, Tex.) and Byron D. Tapley (Texas, University, Dept. of Aerospace Engineering and Engineering Mechanics, Austin, Tex.).
(American Astronautical Society and American Institute of Aeronautics and Astronautics, Astrodynamics Specialist Conference, Jackson, Wyo., Sept. 3-5, 1968, AAS Paper 68-096.)
Journal of Spacecraft and Rockets, vol. 6, May 1969, p. 513-519. 13 refs.
Contract No. NAS 9-6963.
(For abstract see issue 20, page 3853, Accession no. A68-38688)

An approximation for earth-based Doppler and range tracking data as a function of time is derived. The Doppler formula is used to transform a pass of tracking data into the equivalent observation of six quantities whose observational noise is a function of the original Doppler hardware model only and not of the spacecraft geometry. This transformation succeeds in making clear the relationships and geometrical factors that determine navigational accuracies during the heliocentric phase of a mission. The increased insight made possible is exploited in charting (1) navigational accuracy vs spacecraft geometry, (2) the effects of augmenting the basic Doppler data with range data, and (3) the influence of station location errors on the estimates of spacecraft position and velocity. (Author)

A69-35956 * #
IMPULSIVE ORBIT TRANSFER OPTIMIZATION BY AN ACCELERATED GRADIENT METHOD.
Ivan L. Johnson, Jr. (NASA, Manned Spacecraft Center, Mission Planning and Analysis Div., Mathematical Physics Branch, Houston, Tex.).
(Astrodynamics Conference, Houston, Tex., Dec. 12-14, 1967.)
Journal of Spacecraft and Rockets, vol. 6, May 1969, p. 630-632. 11 refs.

Description of the accelerated gradient program, a digital computer program developed for analyzing impulsive orbit transfer optimization using the Pines (1965) and Nakashima (1966) universal-variable formulation. The formulation, programming, and accumulation of data for a three-impulse orbit transfer problem are presented as examples of the application of this method. The accelerated gradient program is applied with the universal-variable, two-body formulation to obtain an optimal solution featuring both an intermediate trajectory constraint and an inequality constraint. The accelerated gradient program consists of two phases; the first treats the optimization problem in an approximate form, and the second refines the solution using an algorithm obtained by Newton's method. B.H.

A69-35966 *
DYNAMICAL STUDY OF AN H II REGION.
Sabatino Sofia (NASA, Goddard Space Flight Center, Goddard Institute for Space Studies, New York, N.Y.; South Florida, University, Dept. of Astronomy, Tampa, Fla.).
Astronomical Society of the Pacific, Publications, vol. 81, June 1969, p. 265-269. 6 refs.

A study of the "equilibrium region" left behind the expanding ionization front in an H II region is performed in order to investigate the influence of the usually neglected dynamical effects in the structure of the region. Attention is given to a 40,000 deg K star surrounded by an H II region with an initial electron temperature of 10,000 deg K and an initial electron density of 100. The gas is allowed to heat up, cool down, and move according to general hydrodynamic equations. It is found that after about 15,000 years, the gas has relaxed to the same temperature found by the static treatment and that while small velocities (due to the gravitational attraction of the star) and density differences have developed, they are not significant. In consequence, a static treatment for the "equilibrium region" is perfectly adequate, unless transient effects of a time scale below about 15,000 years are concerned. (Author)

A69-36072
METEORITE RESEARCH; PROCEEDINGS OF THE SYMPOSIUM, VIENNA, AUSTRIA, AUGUST 7-13, 1968.
Symposium sponsored by UNESCO, the International Council of Scientific Unions, the International Astronomical Union, the International Union of Geological Sciences, the International Association of Geochemistry and Cosmochemistry, and the Meteoritical Society. Edited by P. M. Millman (National Research Council, Ottawa, Canada).
New York, Springer-Verlag New York, Inc.; Dordrecht, D. Reidel Publishing Co. (Astrophysics and Space Science Library. Volume 12), 1969. 955 p. In English, Russian, and French.
$48.
CONTENTS:

INTRODUCTION. P. M. Millman (National Research Council, Ottawa, Canada), p. V-IX.

EARLY HISTORY OF METEORITES.
NUCLEAR ABUNDANCE RULES AND THE COMPOSITION OF METEORITES. H. E. Suess (California, University, La Jolla, Calif.), p. 3-6. (See A69-36073 19-30)
PHYSICAL CONDITIONS IN THE PRIMITIVE SOLAR NEBULA. A. G. W. Cameron (Yeshiva University; NASA, Goddard Space Flight Center, New York, N.Y.), p. 7-15. 12 refs. (See A69-36074 19-30)
ORIGIN OF METEORITES AND PLANETARY COSMOGONY. B. Iu. Levin (Akademiia Nauk SSSR, Institut Fiziki Zemli, Moscow, USSR), p. 16-30. 72 refs. (See A69-36075 19-30)
SOME PROBLEMS OF CONSOLIDATION AND DIFFERENTIATION OF THE MATTER OF THE SOLAR SYSTEM IN RELATION TO THE TIME STAGES OF ITS FORMATION (O NEKOTORYKH VOPROSAKH KONSOLIDATSII I DIFFERENTSIATSII VESHCHESTVA SOLNECHNOI SISTEMY V SVIAZI S VREMENNYMI ETAPAMI EE STANOVLENIIA). V. I. Baranov and K. G. Knorre (Akademiia Nauk SSSR, Institut Geokhimii i Analiticheskoi Khimii, Moscow, USSR), p. 31-40. 10 refs. (See A69-36076 19-30)
RECENT FOSSIL TRACK STUDIES BEARING ON EXTINCT Pu^{244} IN METEORITES. J. Shirck, M. Hoppe, M. Maurette, and R. Walker (Washington University, St. Louis, Mo.), p. 41-50. 15 refs. (See A69-36077 19-30)
PRIOR'S DIAGRAM FOR CHONDRITES (DIAGRAMMA PRAIORA DLIA KHONDRITOV). A. A. Iavnel' (Akademiia Nauk SSSR, Komitet po Meteoritam, Moscow, USSR), p. 51-59. 38 refs. (See A69-36078 19-30)
DISCUSSIONS OF SESSION I, p. 60-63.

COMPOSITION AND STRUCTURE.
METEORITES AND THE HIGH-TEMPERATURE ORIGIN OF TERRESTRIAL PLANETS. W. Kiesl and F. Hecht (Wien,

Universität, Vienna, Austria), p. 67-74. 24 refs. (See A69-36079 19-30)

STUDY OF TRACE ELEMENT ABUNDANCE IN METEORITES BY NEUTRON ACTIVATION. R. Rieder and H. Wänke (Max-Planck-Institut für Chemie, Mainz, West Germany), p. 75-86. 41 refs. (See A69-36080 19-30)

CONTENT AND ISOTOPIC COMPOSITION OF CARBON IN THE LIGHT AND DARK PORTIONS OF GAS-RICH CHONDRITES. F. Begemann and K. Heinzinger (Max-Planck-Institut für Chemie, Mainz, West Germany, p. 87-92. 19 refs. (See A69-36081 19-30)

MÖSSBAUER INVESTIGATION OF THE UNEQUILIBRATED ORDINARY CHONDRITES. E. L. Sprenkel-Segel (Illinois Institute of Technology, Chicago; Argonne National Laboratory, Argonne, Ill.), p. 93-105. 33 refs. (See A69-36082 19-30)

MÖSSBAUER SPECTROSCOPY APPLIED TO THE CLASSIFICATION OF STONE METEORITES. W. Herr and B. Skerra (Köln, Universität, Cologne, West Germany), p. 106-122. 24 refs. (See A69-36083 19-30)

ISOTOPIC COMPOSITION OF LITHIUM IN SOME METEORITES AND THE ROLE OF NEUTRONS IN THE NUCLEOSYNTHESIS OF THE LIGHT ELEMENTS IN THE SOLAR SYSTEM. R. Bernas, E. Gradsztajn, and A. Yaniv (Centre National de la Recherche Scientifique, Orsay, Essonne, France), p. 123-131. 8 refs. (See A69-36084 19-30)

DETERMINATION OF BORON, LITHIUM, AND CHLORINE IN METEORITES. M. Quijano-Rico and H. Wänke (Max-Planck-Institut für Chemie, Mainz, West Germany), p. 132-145. 58 refs. (See A69-36085 19-30)

DISCUSSIONS OF SESSION II, p. 146-152.

COMPOSITION AND STRUCTURE.

THE SHARPS CHONDRITE—NEW EVIDENCE ON THE ORIGIN OF CHONDRULES AND CHONDRITES. K. Fredriksson (Smithsonian Institution, Washington, D.C.), p. 155-165. 29 refs. (See A69-36086 19-30)

FRACTIONATION OF SOME ABUNDANT LITHOPHILE ELEMENT RATIOS IN CHONDRITES. L. H. Ahrens, H. v. Michaelis, A. J. Erlank, and J. P. Willis (Cape Town, University, Cape Town, Republic of South Africa), p. 166-173. 6 refs. (See A69-36087 19-30)

ON THE FORMATION OF CHONDRULES AND METAL PARTICLES BY "SHOCK MELTING." F. Wlotzka (Max-Planck-Institut für Chemie, Mainz, West Germany), p. 174-184. 49 refs. (See A69-36088 19-30)

THE FORMATION OF CHONDRULES AND CHONDRITES AND SOME OBSERVATIONS ON CHONDRULES FROM THE TIESCHITZ METEORITE. G. Kurat (Naturhistorisches Museum, Vienna, Austria), p. 185-190. 18 refs. (See A69-36089 19-30)

THE MAJOR-ELEMENT COMPOSITION OF INDIVIDUAL CHONDRULES OF THE BJURBÖLE METEORITE. L. S. Walter (NASA, Goddard Space Flight Center, Greenbelt, Md.), p. 191-205. 32 refs. (See A69-36090 19-30)

GENESIS OF THE CALCIUM-RICH ACHONDRITES IN LIGHT OF RARE-EARTH AND BARIUM CONCENTRATIONS. C. C. Schnetzler and J. A. Philpotts (NASA, Goddard Space Flight Center, Greenbelt, Md.), p. 206-216. 27 refs. (See A69-36091 19-30)

THE LEOVILLE, KANSAS, METEORITE—A POLYMICT BRECCIA OF CARBONACEOUS CHONDRITES AND ACHONDRITE. K. Keil (New Mexico, University, Albuquerque, N. Mex.; American Meteorite Laboratory, Denver, Colo.), G. I. Huss, and H. B. Wiik (Geologinen Tutkimuslaitos, Helsinki, Finland), p. 217.

DISCUSSIONS OF SESSION III, p. 218-223.

ISOTOPE STUDIES AND CHRONOLOGY.

COSMIC-RADIATION-INDUCED RADIOACTIVITY OF THE MOON AND METEORITES AND THE ORIGIN OF METEORITES (RADIOAKTIVNOST' LUNY I METEORITOV, VYZVANNAIA KOSMICHESKIMI LUCHAMI, I PROISKHOZHDENIE METEORITOV). A. K. Lavrukhina, G. K. Ustinova, T. A. Ibraev, and R. I. Kuznetsova (Akademiia Nauk SSSR, Institut Geokhimii i Analiticheskoi Khimii, Moscow, USSR), p. 227-245. 33 refs. (See A69-36092 19-30)

COSMIC-RAY PRODUCED RADIONUCLIDES AND RARE GASES NEAR THE SURFACE OF SAINT-SEVERIN METEORITE. K. Marti, R. M. Lindstrom, J. R. Arnold, N. G. Bhandari (California, University, La Jolla, Calif.), and J. P. Shedlovsky (California, University, La Jolla, Calif.; National Center for Atmospheric Research, Boulder, Colo.), p. 246-266. 57 refs. (See A69-36093 19-30)

COSMIC-RAY PRODUCED RADIONUCLIDES IN THE BARWELL AND SAINT-SEVERIN METEORITES. F. Begemann, R. Rieder, E. Vilcsek, and H. Wänke (Max-Planck-Institut für Chemie, Mainz, West Germany), p. 267-274. 16 refs. (See A69-36094 19-30)

ON THE ENERGY SPECTRUM OF IRON-GROUP NUCLEI AS DEDUCED FROM FOSSIL-TRACK STUDIES IN METEORITIC MINERALS. D. Lal, R. S. Rajan, A. S. Tamhane (Tata Institute of Fundamental Research, Bombay, India), J. C. Lorin, and P. Pellas (Ministère de l'Education, Paris, France), p. 275-285. 17 refs. (See A69-36095 19-30)

FOSSIL TRACKS IN METEORITES AND THE CHEMICAL ABUNDANCE AND ENERGY SPECTRUM OF EXTREMELY HEAVY COSMIC RAYS. M. Maurette, P. Thro, R. Walker, and R. Webbink (Washington University, St. Louis, Mo.), p. 286-315. 18 refs. (See A69-36096 19-30)

ON THE FLUX OF LOW-ENERGY PARTICLES IN THE SOLAR SYSTEM DURING THE LAST 10 MILLION YEARS. B. S. Amin, D. Lal, R. S. Rajan, A. S. Tamhane, V. S. Venkatavaradan (Tata Institute of Fundamental Research, Bombay, India), J. C. Lorin, and P. Pellas (Ministère de l'Education, Paris, France), p. 316-327. 27 refs. (See A69-36097 19-30)

HEAT GENERATION IN METEORITES DURING THE EARLY STAGE OF THE SOLAR SYSTEM. H. Reeves and J. Audouze (Commissariat à l'Energie Atomique, Gif-sur-Yvette, Essonne; Centre National de la Recherche Scientifique, Paris, France), p. 328-334. 22 refs. (See A69-36098 19-30)

SOME STABLE AND LONG-LIVED NUCLIDES PRODUCED BY SPALLATION IN METEORITIC IRON. M. Shima, M. Imamura, H. Matsuda, and M. Honda (Tokyo, University, Tokyo, Japan), p. 335-347. 30 refs. (See A69-36099 19-30)

DISCUSSIONS OF SESSION IV, p. 348-351.

ISOTOPIC STUDIES AND CHRONOLOGY.

CHLORINE-36 AND ARGON-39 PRODUCTION RATES IN THE METAL OF STONE AND STONY-IRON METEORITES. F. Begemann and E. Vilcsek (Max-Planck-Institut für Chemie, Mainz, West Germany), p. 355-362. 28 refs. (See A69-36100 19-30)

^{39}K(n, p)-PRODUCED ^{39}Ar IN CHONDRITES—NEW DATA AND THEIR INTERPRETATION IN TERMS OF SIZE, EXPOSURE AGE AND ORBITAL ELEMENTS. F. Begemann and H. Wänke (Max-Planck-Institut für Chemie, Mainz, West Germany), p. 363-371. 36 refs. (See A69-36101 19-30)

RADIATION AGES OF CHONDRITES. G. Spannagel and G. Heusser (Max-Planck-Institut für Kernphysik, Heidelberg, West Germany), p. 372-386. 46 refs. (See A69-36102 19-30)

EVALUATION OF ^{53}Mn BY (n, γ) ACTIVATION, ^{26}Al AND SPECIAL TRACE ELEMENTS IN METEORITES BY γ-COINCIDENCE TECHNIQUES. U. Herpers, W. Herr (Köln, Universität, Cologne, West Germany), and R. Wölfle (Kernforschungsanlage, Jülich, West Germany), p. 387-396. 37 refs. (See A69-36103 19-30)

BERYLLIUM-10 IN IRON METEORITES, THEIR COSMIC-RAY EXPOSURE AND TERRESTRIAL AGES. C. Chang and H. Wänke (Max-Planck-Institut für Chemie, Mainz, West Germany), p. 397-406. 12 refs. (See A69-36104 19-30)

THERMAL HISTORIES OF METEORITES BY THE ^{39}Ar-^{40}Ar METHOD. G. Turner (Sheffield, University, Sheffield, England), p. 407-417. 28 refs. (See A69-36105 19-30)

THE STONY METEORITE KRÄHENBERG. W. Kempe and O. Müller (Max-Planck-Institut für Kernphysik, Heidelberg, West Germany), p. 418-428.

K/Ar-AGE DETERMINATIONS OF IRON METEORITES. V. W. Kaiser and J. Zähringer (Max-Planck-Institut für Kernphysik,

Heidelberg, West Germany), p. 429-443. 16 refs. (See A69-36106 19-30)

AGES OF THE Ca-RICH ACHONDRITES. D. Heymann (William Marsh Rice University, Houston, Tex.), E. Mazor (Weizmann Institute of Science, Rehovot, Israel), and E. Anders (Chicago, University, Chicago, Ill.), p. 444-457. 37 refs. (See A69-36107 19-30)

DISCUSSIONS OF SESSION V, p. 458-463.

COMPOSITION AND STRUCTURE.

THE STATUS OF ISOTOPIC AGE DETERMINATIONS ON IRON AND STONE METEORITES. G. J. Wasserburg and D. S. Burnett (California Institute of Technology, Pasadena, Calif.), p. 467-479. 31 refs. (See A69-36108 19-30)

MINERALOGY, PETROLOGY, AND CLASSIFICATION OF TYPES 3 AND 4 CARBONACEOUS CHONDRITES. W. R. Van Schmus (Kansas, University, Lawrence, Kan.), p. 480-491. 26 refs. (See A69-36109 19-30)

MINERALOGICAL STUDY OF THE LANCE CHONDRITE C III (ETUDE MINERALOGIQUE DE LA CHONDRITE C III DE LANCE). M. C. Michel-Lévy (Paris, Université; Centre National de la Recherche Scientifique, Paris, France), p. 492-499. 16 refs. (See A69-36110 19-30)

THE USE OF SELECTED-AREA ELECTRON DIFFRACTION IN METEORITE MINERALOGY. J. F. Kerridge (London, University, Birkbeck College, London, England), p. 500-504. 12 refs. (See A69-36111 19-14)

GENETICAL INTERRELATIONS BETWEEN UREILITES AND CARBONACEOUS CHONDRITES. G. Mueller (Miami, University, Coral Gables, Fla.; Concepción, Universidad, Concepción, Chile), p. 505-517. 16 refs. (See A69-36112 19-30)

GAS-CHROMATOGRAPHIC MASS-SPECTROMETRIC STUDIES ON THE ISOPRENOIDS AND OTHER ISOMERIC ALKANES IN METEORITES. J. Oró and E. Gelpi (Houston, University, Houston, Tex.), p. 518-523. 22 refs. (See A69-36113 19-30)

FORMATION OF ORGANIC COMPOUNDS IN SOLID BODIES BY SOLAR AND COSMIC PROTON BOMBARDMENT. E. J. Zeller and G. Dreschhoff (Kansas, University, Lawrence, Kan.), p. 524-533. 15 refs. (See A69-36114 19-30)

DISCUSSIONS OF SESSION VI, p. 534-538.

ORBITS.

ASTRONOMICAL INFORMATION ON METEORITE ORBITS. P. M. Millman (National Research Council, Ottawa, Canada), p. 541-551. 36 refs. (See A69-36115 19-30)

METEORITE RADIANTS AND ORBITS. B. Iu. Levin and A. N. Simonenko (Akademiia Nauk SSSR, Institut Fiziki Zemli, Moscow, USSR), p. 552-558. 33 refs. (See A69-36116 19-30)

ORBITAL CLUES TO THE NATURE OF METEORITE PARENT BODIES. E. Anders and P. J. Mellick (Chicago, University, Chicago, Ill.), p. 559-572. 35 refs. (See A69-36117 19-30)

RELATIONSHIPS BETWEEN ORBITS AND SOURCES OF CHONDRITIC METEORITES. G. W. Wetherill (California, University, Los Angeles, Calif.), p. 573-589. 17 refs. (See A69-36118 19-30)

INTERPLANETARY DUST. S. F. Singer (U.S. Department of the Interior, Washington, D.C.), p. 590-599. 11 refs. (See A69-36119 19-30)

PHOTOGRAPHIC NETWORKS FOR FIREBALLS. R. E. McCrosky (Smithsonian Institution, Cambridge, Mass.) and Z. Ceplecha (Československá Akademie Věd, Ondřejov, Czechoslovakia), p. 600-612. 8 refs. (See A69-36120 19-30)

A NETWORK FOR RAPID ANALYSIS OF FIREBALL TRAJECTORIES. V. D. Chamberlain (Michigan State University, East Lansing, Mich.), p. 613-622. 14 refs. (See A69-36121 19-11)

DISCUSSIONS OF SESSION VII, p. 623-629.

COMPOSITION AND STRUCTURE.

MAGNETIC PROPERTIES OF METEORITES IN THE SOVIET COLLECTION (MAGNITNYE SVOISTVA METEORITOV KOLLEKTSII SOVETSKOGO SOIUZA). E. G. Gus'kova and V. I. Pochtarev (Akademiia Nauk SSSR, Institut Zemnogo Magnetizma, Ionosfery i Rasprostraneniia Radiovoln, Leningrad, USSR), p. 633-637. (See A69-36122 19-30)

PHASE RELATIONS IN THE SYSTEM Cr-Fe-S. A. El Goresy and G. Kullerud (Carnegie Institution of Washington, Washington, D.C.), p. 638-656. 28 refs. (See A69-36123 19-18)

METALLIC PHASE OF STONE METEORITES (PHASE METALLIQUE DES METEORITES PIERREUSES). R. Cayé, R. Giraud (Bureau de Recherche Géologique et Minières, Orléans, France), and A. Sandrea (Paris, Université, Paris, France), p. 657-668. 5 refs. (See A69-36124 19-30)

INVESTIGATIONS ON A QUANTITATIVE MINERALOGICAL CHARACTERIZATION OF METEORITES BY MODAL ANALYSIS. G. Dörfler and H. G. Hiesböck (Wien, Universität, Vienna, Austria), p. 669-682. 32 refs. (See A69-36125 19-30)

THE PHOSPHATE MINERALOGY OF METEORITES. L. H. Fuchs (Argonne National Laboratory, Argonne, Ill.), p. 683-695. 38 refs. (See A69-36126 19-30)

A CHONDRITIC INCLUSION OF UNIQUE TYPE IN THE CUMBERLAND FALLS METEORITE. R. A. Binns (New England, University, Armidale, New South Wales, Australia), p. 696-704. 20 refs. (See A69-36127 19-30)

RECONSTRUCTION OF THE SAINT-SEVERIN METEORITE IN SPACE (RECONSTRUCTION DE LA METEORITE SAINT-SEVERIN DANS L'ESPACE). Y. Cantelaube, P. Pellas (Ministère de l'Education, Paris, France), D. Nordemann, and J. Tobailem (Commissariat à l'Energie Atomique, Gif-sur-Yvette, Essonne, France), p. 705-713. 8 refs. (See A69-36128 19-30)

DISCUSSIONS OF SESSION VIII, p. 714-717.

COMPOSITION AND STRUCTURE.

THE CLASSIFICATION OF IRON METEORITES. J. I. Goldstein (NASA, Goddard Space Flight Center, Greenbelt, Md.), p. 721-737. 21 refs. (See A69-36129 19-30)

SUPERIOR ANALYSES OF IRON METEORITES. C. B. Moore, C. F. Lewis, and D. Nava (Arizona State University, Tempe, Ariz.), p. 738-748. 14 refs. (See A69-36130 19-30)

PHOSPHORUS IN METEORITIC NICKEL-IRON. S. J. B. Reed (British Museum /Natural History/, London, England), p. 749-762. 35 refs. (See A69-36131 19-30)

THE FORMATION OF PHOSPHIDES IN IRON METEORITES. A. S. Doan, Jr. and J. I. Goldstein (NASA, Goddard Space Flight Center, Greenbelt, Md.), p. 763-779. 26 refs. (See A69-36132 19-30)

PHOSPHIDE AND CARBIDE INCLUSIONS IN IRON METEORITES. M. F. Comerford (Smithsonian Institution, Cambridge, Mass.), p. 780-795. 31 refs. (See A69-36133 19-30)

PRE-TERRESTRIAL DEFORMATION EFFECTS IN IRON METEORITES. H. J. Axon (Manchester, University, Manchester, England), p. 796-805. 13 refs. (See A69-36134 19-30)

DYNAMICALLY DEFORMED STRUCTURES IN SOME METEORITES. B. Baldanza and G. Pialli (Perugia, Università, Perugia, Italy), p. 806-825. 20 refs. (See A69-36135 19-30)

SHOCK HISTORIES OF HEXAHEDRITES AND Ga-Ge GROUP III OCTAHEDRITES. A. V. Jain and M. E. Lipschutz (Purdue University, Lafayette, Ind.), p. 826-837. 24 refs. (See A69-36136 19-30)

DISCUSSIONS OF SESSION IX, p. 838-842.

ISOTOPE STUDIES AND CHRONOLOGY.

RARE GASES IN STONY METEORITES. H. W. Müller and J. Zähringer (Max-Planck-Institut für Kernphysik, Heidelberg, West Germany), p. 845-856.

RARE-GAS MEASUREMENTS IN SEPARATE MINERAL PHASES OF THE OTIS AND ELENOVKA CHONDRITES. P. Bochsler, P. Eberhardt, J. Geiss, and N. Grögler (Bern, Universität, Berne, Switzerland), p. 857-874. 40 refs. (See A69-36137 19-30)

SHORT EXPOSURE AGES OF METEORITES DETERMINED FROM THE SPALLOGENIC $^{36}Ar/^{38}Ar$ RATIOS. J. C. Huneke, P. Signer (Eidgenössische Technische Hochschule, Zurich, Switzerland), F. Begemann (Eidgenössische Technische Hochschule, Zurich, Switzerland; Max-Planck-Institut für Chemie, Mainz, West Germany), and L. E. Nyquist, p. 875-886. 38 refs. (See A69-36138 19-30)

SPALLOGENIC RARE GASES IN TAENITE SEPARATED

FROM IRON METEORITES. L. Schultz (Eidgenössische Technische Hochschule, Zurich, Switzerland; Max-Planck-Institut für Chemie, Mainz, West Germany), J. C. Huneke, P. Singer (Eidgenössische Technische Hochschule, Zurich, Switzerland), and L. E. Nyquist, p. 887-894. 19 refs. (See A69-36139 19-30)

RARE GASES IN THE IRON AND IN THE INCLUSIONS OF THE CAMPO DEL CIELO METEORITE, EL TACO. H. Hintenberger, H. Weber (Max-Planck-Institut für Chemie, Mainz, West Germany), and L. Schultz (Eidgenössische Technische Hochschule, Zurich, Switzerland; Max-Planck-Institut für Chemie, Mainz, West Germany), p. 895-900. 8 refs. (See A69-36140 19-30)

THE THERMAL RELEASE OF RARE GASES FROM SEPARATED MINERALS OF THE MOCS METEORITE. J. C. Huneke, H. Funk, V. Köppel, P. Signer (Eidgenössische Technische Hochschule, Zurich, Switzerland), and L. E. Nyquist, p. 901-921. 22 refs. (See A69-36141 19-30)

DISTRIBUTION AND ORIGIN OF PRIMORDIAL HELIUM, NEON, AND ARGON IN THE FAYETTEVILLE AND KAPOETA METEORITES. G. H. Megrue (Smithsonian Institution, Cambridge, Mass.), p. 922-930. 18 refs. (See A69-36142 19-30)

DISCUSSIONS OF SESSION X, p. 931-935.

LIST OF PARTICIPANTS, p. 937-940.

A69-36074 •

PHYSICAL CONDITIONS IN THE PRIMITIVE SOLAR NEBULA.

A. G. W. Cameron (Yeshiva University, Belfer Graduate School of Science; NASA, Goddard Space Flight Center, Goddard Institute for Space Studies, New York, N.Y.).

IN: METEORITE RESEARCH; PROCEEDINGS OF THE SYMPOSIUM, VIENNA, AUSTRIA, AUGUST 7-13, 1968. (A69-36072 19-30)

Symposium sponsored by UNESCO, the International Council of Scientific Unions, the International Astronomical Union, the International Union of Geological Sciences, the International Association of Geochemistry and Cosmochemistry, and the Meteoritical Society. Edited by P. M. Millman.

New York, Springer-Verlag New York, Inc.; Dordrecht, D. Reidel Publishing Co. (Astrophysics and Space Science Library. Volume 12), 1969, p. 7-15. 12 refs.

NSF-NASA-supported research.

Discussion of a physical model of the primitive solar nebula. Two solutions of the distribution of the angular momentum per unit mass are demonstrated. It is assumed that the nebula cools at constant central pressure. In the range of 2000 to 5000 deg K the opacity is small and the nebula is in radiative equilibrium. At lower temperatures the opacity is greatly increased, due to molecules (for example, water molecules) and to condensed particles (mainly iron and silicate grains). This produces thermally driven convection out to a nebular radius of a few astronomical units. In this region there is renewed turbulent viscosity, which leads to outward transport of angular momentum and inward net transport of mass to form the sun. It is assumed that the accumulation of small particles into larger bodies always takes place in the presence of gas and is assisted by turbulence and acceleration by electric fields. Lightning flashes may play a role in the formation of chondrites. It is shown that continued convective transport through a range of temperatures must be important for the chemistry of the accumulating material. P.G.

A69-36090 •

THE MAJOR-ELEMENT COMPOSITION OF INDIVIDUAL CHONDRULES OF THE BJURBÖLE METEORITE.

Louis S. Walter (NASA, Goddard Space Flight Center, Planetology Branch, Greenbelt, Md.).

IN: METEORITE RESEARCH; PROCEEDINGS OF THE SYMPOSIUM, VIENNA, AUSTRIA, AUGUST 7-13, 1968. (A69-36072 19-30)

Symposium sponsored by UNESCO, the International Council of Scientific Unions, the International Astronomical Union, the International Union of Geological Sciences, the International Association of Geochemistry and Cosmochemistry, and the Meteoritical Society. Edited by P. M. Millman.

New York, Springer-Verlag New York, Inc.; Dordrecht, D. Reidel Publishing Co. (Astrophysics and Space Science Library. Volume 12), 1969, p. 191-205. 32 refs.

Analysis of 82 chondrules of the Bjurböle meteorite for Si, Al, Fe, Ca, Mg, K, Na, and Ni content. Fifty-three of these have been analyzed for sulfur. There are no relationships between silicon dioxide, aluminum oxide, and CaO content and the sizes of chondrules. Thus, within the mass range of chondrules studied, there appears to have been no effect of selective vapor fractionation which might have resulted from a flash-melting process during the formation of chondrules. M.M.

A69-36091 •

GENESIS OF THE CALCIUM-RICH ACHONDRITES IN LIGHT OF RARE-EARTH AND BARIUM CONCENTRATIONS.

Charles C. Schnetzler and John A. Philpotts (NASA, Goddard Space Flight Center, Planetology Branch, Greenbelt, Md.).

IN: METEORITE RESEARCH; PROCEEDINGS OF THE SYMPOSIUM, VIENNA, AUSTRIA, AUGUST 7-13, 1968. (A69-36072 19-30)

Symposium sponsored by UNESCO, the International Council of Scientific Unions, the International Astronomical Union, the International Union of Geological Sciences, the International Association of Geochemistry and Cosmochemistry, and the Meteoritical Society. Edited by P. M. Millman.

New York, Springer-Verlag New York, Inc.; Dordrecht, D. Reidel Publishing Co. (Astrophysics and Space Science Library. Volume 12), 1969, p. 206-216. 27 refs.

Discussion of the implications of rare-earth and barium concentrations found in nine calcium-rich achondrites, two plagioclase separates, two pyroxene separates, and a chondrite composite for the genesis of the calcium-rich achondrites. The brecciated basaltic achondrites have higher absolute rare-earth and barium concentrations than those in the average chondrite, but similar relative concentrations. Rare-earth and barium data, petrography, and chemistry indicate that the brecciated achondrites cannot be cumulates of pigeonite or plagioclase, which have fractionated relative rare-earth and barium concentrations. G.R.

A69-36129 •

THE CLASSIFICATION OF IRON METEORITES.

J. I. Goldstein (NASA, Goddard Space Flight Center, Planetology Branch, Greenbelt, Md.).

IN: METEORITE RESEARCH; PROCEEDINGS OF THE SYMPOSIUM, VIENNA, AUSTRIA, AUGUST 7-13, 1968. (A69-36072 19-30)

Symposium sponsored by UNESCO, the International Council of Scientific Unions, the International Astronomical Union, the International Union of Geological Sciences, the International Association of Geochemistry and Cosmochemistry, and the Meteoritical Society. Edited by P. M. Millman.

New York, Springer-Verlag New York, Inc.; Dordrecht, D. Reidel Publishing Co. (Astrophysics and Space Science Library. Volume 12), 1969, p. 721-737. 21 refs.

Description of a genetic classification system that attempts to group iron meteorites which form in the same parent body. This system uses a comparison of two independent parameters, which have been used to group iron meteorites in the past. One of these is the cooling rate of the parent body during the formation of the Widmanstätten pattern, and the other is the Ga-Ge trace element content. Cooling rate groups have been defined by using measurements of both bandwidth and Ni content of over 250 irons. With the addition of a large amount of bandwidth data, the more commonly used structural classification system for irons has also been refined. All the pertinent meteorite data used in this study are included in an appendix for further use. It was found that the cooling rate groups and Ga-Ge groups are correlated. This indicates that meteorites

common to both groups come from the same parent body. Such a genetic classification system will indicate important samples to be studied in the future. (Author)

A69-36132 *
THE FORMATION OF PHOSPHIDES IN IRON METEORITES.
A. S. Doan, Jr. and J. I. Goldstein (NASA, Goddard Space Flight Center, Planetology Branch, Greenbelt, Md.).
IN: METEORITE RESEARCH; PROCEEDINGS OF THE SYMPOSIUM, VIENNA, AUSTRIA, AUGUST 7-13, 1968. (A69-36072 19-30)
Symposium sponsored by UNESCO, the International Council of Scientific Unions, the International Astronomical Union, the International Union of Geological Sciences, the International Association of Geochemistry and Cosmochemistry, and the Meteoritical Society. Edited by P. M. Millman.
New York, Springer-Verlag New York, Inc.; Dordrecht, D. Reidel Publishing Co. (Astrophysics and Space Science Library. Volume 12), 1969, p. 763-779. 26 refs.

The iron-rich corner of the Fe-Ni-P phase diagram has been redetermined between 1100 and 650 deg C in order to determine the necessary conditions for the formation of the phosphide minerals observed in iron meteorites. The heat-treated alloys were examined, and the phase boundaries were established by the use of the electron microprobe. The results are applied to the various types of iron meteorites to describe the necessary conditions to yield the diversity of shape and Ni composition of schreibersite and rhabdite. As a result of the phase diagram studies, it can be inferred that thermal equilibrium is maintained in iron meteorites to cooling temperatures of 650 deg C. Macroscopic phosphides (hieroglyphic or star-shaped and Brezina lamellae) form from the liquid if the meteorites contain less than 8.5 wt % Ni and more than 2.5 wt % P, or more than 10 wt % Ni and more than 1.3 wt % P; they can form from the gamma phase above 900 deg C. Microscopic schreibersite nucleates primarily at alpha/gamma interfaces as meteorites enter the alpha-gamma-phosphide phase field at low temperatures. Rhabdites form from kamacite at low temperatures when Ni and P diffusion is severely limited. The diversity of phosphide structures and Ni contents can be explained in terms of meteorite compositions, the Fe-Ni-P phase stability relations, and the diffusion of Ni and P in the solid state. Phosphorus contents determined chemically for meteorites containing macroscopic phosphides are grossly underestimated. Data on the P content of 11 octahedrites and one ataxite were obtained by a point count method. (Author)

A69-36209 *
FUNDAMENTAL PROBLEMS OF THE SOLAR SYSTEM.
A. G. W. Cameron (Yeshiva University, Belfer Graduate School, New York, N.Y.).
(American Geophysical Union, National Fall Meeting, San Francisco, Calif., Dec. 2-4, 1968.)
EOS, vol. 50, June 1969, p. 424-427.
NASA-supported research.

Discussion of new studies in solar system physics and chemistry which should lead to the establishment of new boundary conditions to satisfy a successful theory of the origin of the solar system. The properties of planetary atmospheres, planetary surfaces, planetary magnetic fields, and planetary composition are reexamined in light of recent research by new techniques and a new depth of understanding of solar system objects gained from space probes. The early history of the solar wind is discussed on the basis of recent knowledge of the properties of newly formed stars obtained by astrophysical spectroscopy. B.H.

A69-36219 * #
ON THE INTERPRETATION OF INTENSITY RATIOS OF FORBIDDEN IRON AND CALCIUM TRANSITIONS IN THE SOLAR CORONA.
T. Scott Smith (NASA, Goddard Space Flight Center, Laboratory for Space Sciences, Solar Physics Branch, Greenbelt, Md.).
(Colloque International d'Astrophysique, 15th, Liège, Belgium, June 24-26, 1968.)
Société Royale des Sciences de Liège, Mémoires, vol. 17, 1969, p. 245. 6 refs.

Reexamination of the effect of intensity ratios of forbidden iron and calcium transitions in the solar corona on the Fe/Ca ratio. Transitions of the electron configurations from which dominant cascade populations in Fe XIV and Ca XV populations are derived are given, showing two cascading configurations in Fe but only one in Ca. The effects of this situation are worked out using and extrapolating oscillator strengths from Garstang (1962). B.H.

A69-36337 *
A RELAXATION METHOD FOR THE COMPUTATION OF MODEL STELLAR ATMOSPHERES.
Michael J. Price (Kitt Peak National Observatory, Tucson, Ariz.; NASA, Goddard Space Flight Center, Goddard Institute for Space Studies, New York, N.Y.).
Astrophysics and Space Science, vol. 4, June 1969, p. 182-212. 20 refs.

Formulation of a general Monte Carlo relaxation method for the computation of physically self-consistent model stellar atmospheres. The local physical state is obtained by solving simultaneously the equations of statistical equilibrium for the atomic and ionic level populations, the kinetic energy balance equation for the electron gas to obtain the electron temperature, and the equation of radiative transfer. Anisotropic Thomson scattering is included in the equation of transfer, and radiation pressure effects are included in the hydrostatic equation. The constraints of hydrostatic and radiative equilibrium are enforced. Local thermodynamic equilibrium (LTE) is assumed as a boundary condition deep in the atmosphere. Elsewhere in the atmosphere LTE is not assumed. The statistical equilibrium equations are solved with no assumptions made concerning detailed balance for the bound-bound radiative processes. The source function is formulated in microscopic detail. All atomic processes contributing to the absorption and emission of radiation are included. The kinetic energy balance equation for the electron gas is formulated in detail. All atomic processes by which kinetic energy is gained and lost by the electron gas are included. The method has been applied to the computation of a model atmosphere for a pure hydrogen early-type star. An idealized model of the hydrogen atom with five bound levels and the continuum was adopted. The results of the trial calculation are discussed with reference to stability, accuracy, and convergence of the solution. (Author)

A69-36338 *
ATMOSPHERES OF EXTREME METAL-DEFICIENT STARS.
K. S. Krishna Swamy (NASA, Goddard Space Flight Center, Greenbelt, Md.).
Astrophysics and Space Science, vol. 4, June 1969, p. 218-232. 18 refs.

Construction of atmospheric models for effective temperatures of 4000, 4500, and 5000 K, for hydrogen-to-metal ratios of 1, 100, 1000, and 10,000 times the solar values, and for surface gravities of 20,000 and 200. The effect of metal deficiency on the atmospheric structure of these stars is studied. M.M.

A69-37136 *
SOLAR CYCLE VARIATION OF EXOSPHERIC TEMPERATURES ON MARS AND VENUS—A PREDICTION FOR MARINER 6 AND 7.
Richard W. Stewart and Joseph S. Hogan (NASA, Goddard Space Flight Center, Goddard Institute for Space Studies, New York, N.Y.).
Science, vol. 165, July 25, 1969, p. 386-388. 6 refs.

Study of the effects of variations in the extreme ultraviolet solar radiation on the upper atmospheres of Mars and Venus. The results indicate that the exospheric temperature on Mars varies from 300 to 600 deg K during the solar cycle, with a corresponding range on Venus of 450 to 850 deg K. At the present time, the temperature of the Martian exosphere should be approximately 500 deg K. G.R.

A69-37334 *
PHYSICAL PROPERTIES OF THE RADIO-EMITTING REGION IN SCO XR-1.
G. R. Riegler (Maryland, University, Dept. of Physics and Astronomy, College Park, Md.) and R. Ramaty (NASA, Goddard Space Flight Center, Greenbelt, Md.).
Astrophysical Letters, vol. 4, July 1969, p. 27-31. 19 refs.
Grant No. NGL-21-002-033.

Analysis, on recent observations, showing that the radio emission from Sco XR-1 is synchrotron radiation of relativistic electrons in an extended low-density region surrounding a denser core which produces the X-ray and optical continua. The linear dimensions of the radio-emitting region are larger than about 10 million kilometers, the ambient density is less than about 10^9 per cu cm, and the radiation could typically be produced by electrons of about 15 MeV in a magnetic field of a few gauss. (Author)

A69-37492 * #
SOLID HYDROGEN COATED GRAPHITE PARTICLES IN THE INTERSTELLAR MEDIUM. I.
N. C. Wickramasinghe (Cambridge University, Institute of Theoretical Astronomy, Cambridge, England) and K. S. Krishna Swamy (NASA, Goddard Space Flight Center, Greenbelt, Md.).
Royal Astronomical Society, Monthly Notices, vol. 144, no. 1, 1969, p. 41-54. 40 refs.

Solid hydrogen coated graphite particles may be expelled from regions of star-formation into the general interstellar medium. The solid para-hydrogen mantles, which contain a small proportion of ortho-hydrogen, could be stable against evaporation in the general interstellar radiation field. They are also stable against physical and chemical sputtering in H I regions. Extinction efficiencies are calculated for solid hydrogen particles and for graphite particles with solid hydrogen mantles. Graphite core-solid hydrogen grains are capable of producing excellent agreement with the interstellar extinction observations from 20,000 to 1100 Å. The graphite core radius may be in the range of .04 to .06 microns and the solid hydrogen mantle radius in the range of .15 to .25 microns. The albedo and phase function of these particles are consistent with the requirements imposed by the diffuse galactic light. (Author)

A69-37529 *
APPLICATION OF HANSEN'S METHOD TO THE Xth SATELLITE OF JUPITER.
Milton Charnow (Computer Sciences Corp., Washington, D.C.), Peter Musen, and Jesse L. Maury (NASA, Goddard Space Flight Center, Greenbelt, Md.).
Journal of the Astronautical Sciences, vol. 15, Nov.-Dec. 1968, p. 303-312. 15 refs.

Summary of the new elements and of the general perturbations of the tenth satellite of Jupiter. A modification of Hansen's theory, as suggested by Musen (1963), was used as the theoretical foundation for the programming and for the expansion of Hansen's coordinates of the satellite into trigonometric series in four basic arguments. The complete collection of formulas is given in the exposition. Also described are the program and the operations for handling the expansions and for integrating the differential equations of the theory by means of iteration. The new set of the elements represents the observations in the interval 1938 to 1967 better than the previous sets. The residuals are now of the order of only a few seconds of arc. (Author)

A69-37554 *
POWER SPECTRA OF THE INTERPLANETARY MAGNETIC FIELD.
James W. Sari (Maryland, University, Dept. of Physics, College Park, Md.) and Norman F. Ness (NASA, Goddard Space Flight Center, Laboratory for Space Sciences, Greenbelt, Md.).
Solar Physics, vol. 8, July 1969, p. 155-165. 17 refs.
Grant No. NsG-695.

Results of computations of the power spectra of interplanetary magnetic field fluctuations which have been performed with data from the Pioneer 6 satellite. The power spectra exhibit an inverse square frequency dependence in the range from 0.00028 to 0.016 cps for periods of both quiet and disturbed field conditions. Both the shape and power levels of these spectra are found to be due to the presence of directional discontinuities in the microstructure (less than 0.01 AU) of the interplanetary magnetic field. Power spectra at lower frequencies, in the range of 0.0000023 to 0.00014 cps, reflect the field macrostructure (greater than 0.1 AU) and exhibit a frequency dependence roughly between 1/f and f to the minus 1.5 power. The results are related to theories of galactic cosmic-ray modulation and are found to be consistent with recent observations of the modulation. G.R.

A69-37573 *
MASS LOSS FROM PULSATING NEUTRON STARS.
Richard Stothers (NASA, Goddard Space Flight Center, Goddard Institute for Space Studies, New York, N.Y.).
Nature, vol. 223, July 19, 1969, p. 279, 280. 25 refs.

Discussion of a new mechanism, involving radial pulsations of a neutron star which is losing mass, for interpreting the observed period and the secular increase of the period of the Crab Nebula pulsar. It is pointed out that the cause of the decrease of the rate of mass loss with time is connected with the change in structure of the pulsar. V.P.M.

A69-38095 *
DEPENDENCE OF THE LUNAR WAKE ON SOLAR WIND PLASMA CHARACTERISTICS.
K. W. Ogilvie and N. F. Ness (NASA, Goddard Space Flight Center, Laboratory for Space Sciences, Greenbelt, Md.).
Journal of Geophysical Research, vol. 74, Aug. 1, 1969, p. 4123-4128. 17 refs.

Simultaneous measurement, in cislunar space, of the characteristics of the solar wind plasma, as observed by Explorer 34, and the perturbed magnetic field in the lunar wake, as detected by Explorer 35, performed during the period from July to October 1967. The plasma parameter for the ions is found to be more important in determining the magnitude of the umbral positive and penumbral negative anomalies than the direction of the interplanetary magnetic field. A quantitative comparison of these observations with the lunar wake theory of Whang indicates that the solar wind electrons must contribute even more significantly than the ions to the effective beta for the plasma. (Author)

A69-38173 *
WHY THE TEMPERATURE RISE DOES NOT OCCUR IN RADIATIVE EQUILIBRIUM IN STELLAR CHROMOSPHERES OF DOMINANT H^{-2} OPACITY.
S. D. Jordan (NASA, Goddard Space Flight Center, Greenbelt, Md.).
Astrophysical Journal, vol. 157, July 1969, pt. 1, p. 465-467. 7 refs.

Study showing that the temperature inversion in the lower solar chromosphere is very unlikely to result from the influence of the photospheric radiation field on the low-density gas. Dissipation of mechanical energy is therefore necessary to produce the rise. It is shown that, since this effect follows directly from the dominance of the continuum opacity by the negative hydrogen ion, the same conclusion follows for all stellar chromospheres where the negative hydrogen ion dominates the continuum opacity. B.H.

A69-38255 *
THE THERMAL RADIATION FIELD EMITTED BY ANISOTROPICALLY SCATTERING CLOUDY PLANETARY ATMOSPHERES.
R. E. Samuelson (NASA, Goddard Space Flight Center, Greenbelt, Md.).
Icarus, vol. 10, Mar. 1969, p. 258-273. 9 refs.

The Mie theory is used to compute particle albedos phase functions, and extinction cross sections for a variety of particle-size distribution functions and complex indexes of refraction. It is found that the particle albedos and the extinction cross sections are quite dependent on the index of refraction, but that the shape of the phase function is not. It is concluded that because of the way in which these parameters enter the equation of radiative transfer, it is impossible to deduce uniquely the complex index of refraction of cloud materials by observing cloudy atmospheres over a single wavelength interval in the thermal infrared. Next, two methods—the method of discrete ordinates and an exact method—are used to investigate the outgoing thermal radiation field at the top of cloudy atmospheres as a function of the scattering and thermal properties of the atmosphere. Both isothermal and uniformly mixed convective atmospheres are considered in some detail. For limb-darkening observations over a single wavelength interval it is concluded that (1) the optical thickness can be fairly well determined except for the special set of cases of optical thicknesses between 1.5 and infinity and albedos greater than 0.4; (2) the particle albedo can be determined only for the cases of optical thicknesses between 1.5 and 4 and only for albedos less than 0.4; and (3) no information is available regarding either the particle sizes of the shape of the phase functions under any circumstances. On the other hand, it is found that the outgoing flux at the top of the atmosphere is sensitive to almost all the relevant single-scattering parameters, implying that observations of the limb function at several independent wavelengths would be extremely useful. (Author)

A69-38377 *
THE LUNAR ORBITER PROGRAM.
William E. Brunk (NASA, Washington, D.C.).
IN: SPACE RESEARCH IX; COSPAR, PLENARY MEETING, 11TH, TOKYO, JAPAN, MAY 9-21, 1968, PROCEEDINGS. (A69-38334 21-13)
Meeting co-sponsored by the Japanese Committee on Space Research.
Edited by K. S. W. Champion, P. A. Smith, and R. L. Smith-Rose.
Amsterdam, North-Holland Publishing Co., 1969, p. 625-656.

Summary of NASA's Lunar Orbiter Program of lunar photography from an orbiting spacecraft. A total of more than 1600 high-quality photographs of the lunar surface yielded a coverage of the entire lunar earthside at a resolution of 100 m or better. Selected portions of this surface were photographed with resolutions up to 1 m. Also, photographs of over 95 per cent of the lunar farside were obtained with a medium-resolution camera. These photographs, with a resolution of 1 km or better, have been used to produce a chart of the lunar farside. High-resolution photographs of some regions containing features of great scientific interest are presented. V.P.M.

A69-38379 *
LUNAR EXPLORER 35.
Norman F. Ness (NASA, Goddard Space Flight Center, Greenbelt, Md.).
IN: SPACE RESEARCH IX; COSPAR, PLENARY MEETING, 11TH, TOKYO, JAPAN, MAY 9-21, 1968, PROCEEDINGS. (A69-38334 21-13)
Meeting co-sponsored by the Japanese Committee on Space Research.
Edited by K. S. W. Champion, P. A. Smith, and R. L. Smith-Rose.
Amsterdam, North-Holland Publishing Co., 1969, p. 678-703. 29 refs.

Results of measurements obtained from the launch of the mission satellite Lunar Explorer 35. Bistatic radar measurements of the electromagnetic properties of the lunar surface have been studied by monitoring the transmitted and reflected rf signal. The spacecraft has operated continuously since launch and has provided new data. During its orbit about the earth, the moon is immersed in either interplanetary space or the geomagnetosheath-geomagnetotail formed by the solar wind interaction with the earth. In the geomagnetotail, no evidence is found for a lunar magnetic field limiting the magnetic moment to less than one-millionth of the earth's. In the interplanetary medium no evidence is found for a bow shock wave due to supersonic solar wind flow. The moon does not accrete interplanetary magnetic field lines as theorized by Golf (1966) and Tozer (1967). Small magnetic field perturbations consisting of penumbral increases and decreases, but only umbral increases, are observed due to the diamagnetic properties of the plasma which develops on the antisolar side of the moon. Diffusion of interplanetary field lines through the lunar body indicates a low electrical conductivity for the outer layer of the moon. V.P.M.

A69-38479 *
AN ANALYSIS OF THE SOLAR SODIUM D LINES.
A. M. Wilson (Cambridge University, Observatories, Cambridge, England; NASA, Goddard Space Flight Center, Solar Physics Div., Greenbelt, Md.) and G. Worrall (Cambridge University, Observatories, Cambridge, England).
Astronomy and Astrophysics, vol. 2, Aug. 1969, p. 469-476. 5 refs.

Analysis, by a direct inversion of the line profiles, of Waddell's (1962) observations of the D lines in the solar spectrum. The principal conclusion is that the line source function in the Doppler core is significantly dependent on frequency. (Author)

A69-38546 * #
COORDINATE SYSTEM INFLUENCE ON THE REGULARIZED TRAJECTORY OPTIMIZATION PROBLEM.
J. M. Lewallen (NASA, Manned Spacecraft Center, Computation and Analysis Div., Houston, Tex.), O. A. Schwausch (Lockheed Aircraft Corp., Lockheed Electronics Co., Houston, Tex.), and B. D. Tapley (Texas, University, Dept. of Aerospace Engineering, Austin, Tex.).
American Institute of Aeronautics and Astronautics and American Astronautical Society, Astrodynamics Conference, Princeton, N.J., Aug. 20-22, 1969, AIAA Paper 69-903. 11 p. 10 refs.
Members, $1.00; nonmembers, $1.50.

Investigation of the effect of using regularized variables to enhance the numerical integration process associated with the optimal trajectory of a continuously thrusting space vehicle. The integration characteristics of both the rectangular Cartesian and the polar cylindrical coordinates are considered for an optimal low-thrust earth-escape spiral trajectory and an optimal low-thrust earth-Jupiter transfer trajectory. The numerical accuracy achieved and the computer time required are compared for various numerical integration-error bounds by using both the regularized and the unregularized equations. The results obtained indicate that (for space vehicles which experience wide variations in the gravitational force magnitude) significant reductions in computing time can be obtained by using the regularized trajectory optimization equations. More favorable computer times for the problems considered are obtained when the polar coordinates are used. Also, if the numerically evaluated Hamiltonian is used as an indication of integration error generation, the tradeoff between integration time and integration error becomes apparent. Finally, it is shown that the polar coordinates are less sensitive to errors in the initial Lagrange multipliers than the rectangular coordinates. V.P.M.

A69-38600 *
NEW STATE OF FERROMAGNETISM IN DEGENERATE ELECTRON GAS AND MAGNETIC FIELDS IN COLLAPSED BODIES.
Hyung Joon Lee (Brookhaven National Laboratory, Upton, N.Y.), Vittorio Canuto, Claudio Chiuderi (NASA, Goddard Space Flight

Center, Goddard Institute for Space Studies, New York, N.Y.), and Hong-Yee Chiu (NASA, Goddard Space Flight Center, Goddard Institute for Space Studies; New York, City University, City College, Physics Dept., New York; New York, State University, Dept. of Earth and Space Sciences and Dept. of Physics, Stony Brook, N.Y.). *Physical Review Letters*, vol. 23, Aug. 18, 1969, p. 390-393. 15 refs. AEC-sponsored research.

A new state of ferromagnetism in a degenerate electron gas is found and shown to be stable. This magnetism is the sum of all microscopic magnetic moments associated with electrons in their respective Landau levels, while the Landau levels of the system are in turn maintained by this macroscopic magnetization. The maximum field in the Landau orbital ferromagnetism state is 10 MG for white-dwarf densities and 10^{12} G for neutron-star densities. (Author)

A69-38973 *
NON-DIFFUSE INFRARED EMISSION FROM THE LUNAR SURFACE.
James K. Harrison (NASA, Marshall Space Flight Center, Space Sciences Laboratory, Huntsville, Ala.).
International Journal of Heat and Mass Transfer, vol. 12, June 1969, p. 689-697. 9 refs.

Results of calculations of the thermal radiation from the lunar surface incident onto a flat surface of unit area located a small distance above the moon. The orientation and height of the flat surface vary. The thermal radiation from the moon's surface is assumed to be nondiffuse. The calculations show that the thermal energy flux incident onto the flat surface can differ significantly for

binding energy of each dust particle exactly offsets its rest mass so that its active mass remains constant during an unlimited growth of a

A69-39215 • #
A SUBSATELLITE CONCEPT FOR MARTIAN FIELDS AND PARTICLES MEASUREMENTS.
Carle A. Privette (NASA, Ames Research Center, Space Science Div., Moffett Field, Calif.) and Samuel Urcis (North American Rockwell Corp., Space Div., Downey, Calif.).
Journal of Spacecraft and Rockets, vol. 6, Apr. 1969, p. 443-447. 8 refs.

Summary of the results of a feasibility study of the Orbital Experimental Capsule (OEC) as a subsatellite concept for measurements of Martian fields and particles. The OEC would be a subsatellite system for proposed Mars-exploring vehicles such as Voyager. The simplest form of the OEC would weigh about 75 lb and would remain coorbital with the Voyager, relaying data to it continuously. More complex versions weighing up to 160 lb and capable of changing orbit would perform a wider variety of experiments. Z.W.

A69-39221 • #
UNMANNED OUTER PLANET CAPTURE MISSIONS.
Susan M. Norman (NASA, Ames Research Center, Moffett Field, Calif.).
(American Astronautical Society and American Institute of Aeronautics and Astronautics, Astrodynamics Specialist Conference, Jackson, Wyo., Sept. 3-5, 1968, AAS Paper 68-105.)
Journal of Spacecraft and Rockets, vol. 6, Apr. 1969, p. 473-475.

The performance advantages of employing elliptic capture orbits for unmanned missions to Jupiter, Saturn, Uranus, and Neptune are investigated. As part of this investigation, the relative merits of the direct flight mode and the Jupiter swingby mode of heliocentric transfers are compared. A method of presentation is shown that permits the effects of trip time, capture orbit eccentricity, and transfer mode to be evaluated. It is shown that, depending on the weight to be placed in planetary orbit, definite trip time-orbit eccentricity regions exist within which either transfer mode is superior. (Author)

A69-39337 * #
A CLOSED-FORM SOLUTION FOR MINIMUM-FUEL, CONSTANT THRUST TRAJECTORIES.
Donald J. Jezewski (NASA, Manned Spacecraft Center, Mission Planning and Analysis Div., Houston, Tex.) and Judith M. Stoolz.
American Institute of Aeronautics and Astronautics and American Astronautical Society, Astrodynamics Conference, Princeton, N.J., Aug. 20-22, 1969, AIAA Paper 69-905. 10 p. 7 refs.
Members, $1.00; nonmembers, $1.50.

Investigation of the transfer of a vehicle in a vacuum between arbitrary boundary conditions with minimum fuel consumption for the case where two external accelerations (thrust and gravity) are considered. In a previous study, Cherry (1964) assumed that these accelerations could be replaced by a linear function of time. A less severe assumption can be imposed by replacing only the gravity-acceleration terms with polynomials in time. The necessary condition for optimal thrusting for this assumption requires that the primer be a linear function of time. The resulting equations can be integrated completely to yield sufficient equations in terms of the boundary conditions on the state, the five independent constants of the primer vector, and the solution time. Example problems are solved for transfers between (1) fixed states, (2) free terminal argument of periapsis, and (3) free terminal true anomaly and argument of periapsis. (Author)

A69-39339 • #
OPTIMAL TRAJECTORY COORDINATE-MULTIPLIER SYSTEMS WITH CONSTANT OF THE MOTION COMPONENTS.
William E. Miner (NASA, Electronics Research Center, Computational Theory and Techniques Branch, Cambridge, Mass.) and William F. Powers (Michigan, University, Dept. of Aerospace Engineering, Ann Arbor, Mich.).
American Institute of Aeronautics and Astronautics and American Astronautical Society, Astrodynamics Conference, Princeton, N.J., Aug. 20-22, 1969, AIAA Paper 69-907. 8 p. 6 refs.
Members, $1.00; nonmembers, $1.50.
Contract No. NASr-54(06); Grant No. NGR-23-005-329.

Attempt to extend the range of applicability of the known vector integral for the optimal trajectory problem. The range of applicability is extended in two ways. First, it is shown that there exists a large class of coordinate systems such that a conjugate Lagrange multiplier is a constant of the motion. For generating systems with this property, a method is presented which can be applied to the problem of defining nonstandard state variables for which a conjugate multiplier is a constant of the motion. Second, a nontrivial canonical transformation is used to generate a new system of canonical variables such that three of the variables are strictly functions of the components of the vector integral. Thus, the three variables are constants of the motion for the optimal trajectory problem. In addition the canonical transformation is effected in such a way that all the new canonical variables are constants of the motion for the coast-arc problem. V.P.M.

A69-39340 * #
AN ENCKE-TYPE SPECIAL PERTURBATION METHOD.
George H. Born (NASA, Manned Spacecraft Center, Computation and Analysis Div., Houston, Tex.).
American Institute of Aeronautics and Astronautics and American Astronautical Society, Astrodynamics Conference, Princeton, N.J., Aug. 20-22, 1969, AIAA Paper 69-908. 8 p.
Members, $1.00; nonmembers, $1.50.

Description of a combination analytical-numerical integration method for solving the differential equations of a modified set of Lagrange's planetary equations. The integration method is an Encke-type method because it involves integrating the deviations between the actual trajectory and a reference trajectory. The reference trajectory is obtained from an analytical solution containing the dominant secular and periodic effects of the gravitational

field of the primary body. A set of nonsingular elements is used so that the method will be valid for all circular and elliptical motions. It is shown that the method is an accurate and efficient means of satellite ephemeris generation. (Author)

A69-39346 * #
BRANCHED TRAJECTORY OPTIMIZATION BY THE PROJECTED GRADIENT TECHNIQUE.
Joseph Gera (NASA, Langley Research Center, Hampton, Va.).
American Institute of Aeronautics and Astronautics and American Astronautical Society, Astrodynamics Conference, Princeton, N.J., Aug. 20-22, 1969, AIAA Paper 69-917. 11 p. 6 refs.
Members, $1.00; nonmembers, $1.50.

A numerical procedure based on the projected gradient technique is developed for the optimization of branched trajectories. A dynamical system is said to have a branched trajectory whenever the state and the control of the system are multiple-valued functions over a portion of the flight path. For example, the flight path of a rocket vehicle which breaks into two or more parts each with a separate mission, is a branched trajectory. It is shown that only minor modifications to the standard projected gradient technique are needed in order to obtain optimal branched solutions. No numerical difficulties were encountered in the computations, and the convergence properties of the method are encouraging from the standpoint of the use of the method for more complex problems. (Author)

A69-39361 * #
THE EFFECTS OF THE GALILEAN MOONS ON JUPITER FLYBY TRAJECTORIES.
Bernard Kaufman (NASA, Goddard Space Flight Center, Greenbelt, Md.).
American Institute of Aeronautics and Astronautics and American Astronautical Society, Astrodynamics Conference, Princeton, N.J., Aug. 20-22, 1969, AIAA Paper 69-932. 9 p. 21 refs.
Members, $1.00; nonmembers, $1.50.

Investigation of the perturbative effects of the four largest moons of Jupiter on a spacecraft that passes close to Jupiter, using a total of 20 different transfer trajectories. An accurate model for the moons is utilized in the equations of motion which are numerically integrated over the time that the probe spends within Jupiter's sphere of influence. The effects of the moons' perturbations on the postencounter heliocentric trajectories are shown to be large enough to warrant their inclusion in detailed mission simulations, particularly when precision targeting is required (Jupiter swingby to an outer planet). (Author)

A69-39362 * #
ON THE NORMALIZED HODOGRAPHIC MAPPING FOR CONSTRAINED TRAJECTORY FAMILIES.
Fang Toh Sun (NASA, Electronics Research Center, Cambridge, Mass.).
American Institute of Aeronautics and Astronautics and American Astronautical Society, Astrodynamics Conference, Princeton, N.J., Aug. 20-22, 1969, AIAA Paper 69-924. 20 p. 11 refs.
Members, $1.00; nonmembers, $1.50.
Grant No. NsG-558.

Description of a special method of hodographic mapping for families of constrained trajectories. A nondimensional velocity space is introduced, and the complexity of a family of infinite Keplerian trajectories under given constraints is reduced by such a mapping to the simple geometry of a unit circle and a characteristic curve or surface in this vector space. The latter plays the dual role of being the locus of hodograph origins on one hand, and the eccentricity indicatrix of the family on the other hand. It, together with the unit circle, constitutes the normalized hodograph image of the entire family. The fundamental concepts and principles underlying this mapping are outlined. A set of rules is developed which makes it possible to observe the global characteristics of the family and those of its particular trajectories from its normalized hodograph image. A number of Keplerian trajectory families under typical constraints are mapped. Applications of such a mapping to the solution of trajectory problems are illustrated with examples. To facilitate the analytic treatment, and to provide quick graphic solutions, a set of normalized hodographic maps is presented. (Author)

A69-39521 *
MASS LOSS FROM CORONAE AND ITS EFFECT UPON STELLAR ROTATION.
Kyoji Nariai (NASA, Goddard Space Flight Center, Greenbelt, Md.).
IN: MASS LOSS FROM STARS; ASTRONOMICAL OBSERVATORY OF TRIESTE, COLLOQUIUM ON ASTROPHYSICS, 2ND, TRIESTE, ITALY, SEPTEMBER 12-17, 1968, PROCEEDINGS. (A69-39520 21-30)
Colloquium co-sponsored by the International Astronomical Union. Edited by Margherita Hack.
Dordrecht, Netherlands, D. Reidel Publishing Co. (Astrophysics and Space Science Library. Volume 13), 1969, p. 122-131. 36 refs.

The acoustic energy-generation rate from the convective zone was calculated for various models. Results show that a chromosphere and a corona can be expected around stars with temperature lower than 8000 deg K at the main sequence, and lower than 6500 deg K at log g equals 2. When a star is rotating rapidly, mass loss from its corona is large, and can be an effective mechanism of braking the stellar rotation. If this mechanism is effective, the slow rotation of stars later than F2 is the result of the loss of the angular momentum through a stellar wind that is effective in their main sequence phase. Stars with mass greater than 1.5 solar mass lose mass through a stellar wind during their contraction phase. The mass-loss rate is larger than the solar value because of the larger energy input into the chromosphere-corona system and because of the smaller gravitational potential at the surface. T Tauri stars may be the observational counterparts for such stars. As the duration of the contraction phase is very short, the braking mechanism works only in the presence of a strong magnetic field or in the presence of a companion. (Author)

A69-39568 *
RESONANT SPIN STATES AND THE ANOMALOUS ROTATION OF MERCURY.
C. P. Sonett (NASA, Ames Research Center, Moffett Field, Calif.).
Comments on Astrophysics and Space Physics, vol. 1, July-Aug. 1969, p. 122-127. 9 refs.

Review of theoretical examinations of the resonant spin states and anomalous rotation of Mercury. The theories of Peale and Gold (1965) and Pettengill and Dyce (1965) are considered as the basis of an extensive reexamination of the mechanism of tidally degraded spins. It is concluded that the theory of tidal despin is in accord with the theory of a hot interior. A large metal fraction is indicated by the high average planetary density, making it likely that the interior is strongly differentiated chemically and requires a substantial input of heat from tides, primordial sources, radioactivity, or electromagnetic effects. This heat is not considered likely to be lost through radiation, in which event tidal distortion can be accounted for easily. B.H.

A69-39584 *
ROTATIONAL BURSTING OF SMALL CELESTIAL BODIES—EFFECTS OF RADIATION PRESSURE.
Stephen J. Paddack (NASA, Goddard Space Flight Center, Greenbelt, Md.).
Journal of Geophysical Research, vol. 74, Aug. 15, 1969, p. 4379-4381. 11 refs.

Study showing that solar radiation pressure can cause rotational bursting and eventual elimination from the solar system of small magnetic bodies in space by a "windmill" effect. A time to bursting of about 60 years is calculated for an idealized body. On the basis of a simple experiment, it is estimated that actual bodies, such as nonmagnetic meteorites and tektites, will reach bursting speed in about 60,000 years. B.H.

A69-39889 *
PORPHYRINS IN METEORITES—METAL COMPLEXES IN ORGUEIL, MURRAY, COLD BOKKEVELD, AND MOKOIA CARBONACEOUS CHONDRITES.
G. W. Hodgson (NASA, Ames Research Center, Exobiology Div., Moffett Field, Calif.) and B. L. Baker (Research Council of Alberta, Edmonton, Alberta, Canada).
Geochimica et Cosmochimica Acta, vol. 33, Aug. 1969, p. 943-958. 41 refs.

Investigation carried out to obtain more definitive data to test the identification of pigments found in certain meteorites as porphyrins. Results obtained by absorption spectrophotometry in earlier studies were extended by excitation spectrofluorometry based on analytical demetallation of the porphyrin complexes using methanesulfonic acid. In several instances, the liberated free-base porphyrins were sufficiently abundant to be recovered and transferred to neutral solution for spectral characterization. Soret peak positions ranging from 390 to 413 nm were observed; non-Soret peaks occurred in the range from 490 to 615 nm. Fluorescence emission was observed at about 625 and 685 nm, with the peaks at the longer wavelength predominating, in contrast to the reverse pattern for common terrestrial geochemical porphyrins. Extensive evaluations were made of the possibilities of contamination for the origin of the meteorite pigments involving terrestrial soils, dusts, and microorganisms. Porphyrins from fungi and bacteria seemed the most serious potential contaminants, but no evidence of such contamination was found. Since the specific biogenic attributes previously assigned to extraterrestrial porphyrins can no longer be accepted, the meteorite porphyrins may be interpreted as representing either prebiotic chemical evolution, or forms of life or diagenesis appreciably different from those responsible for terrestrial porphyrins. (Author)

A69-39965 *
RADIATION FIELDS OF ENERGETIC ELECTRONS IN HELICAL ORBITS WITHIN A MAGNETOACTIVE PLASMA.
K. Sakurai (NASA, Goddard Space Flight Center, Greenbelt, Md.) and T. Ogawa (Kyoto University, Ionosphere Research Laboratory, Kyoto, Japan).
Planetary and Space Science, vol. 17, Aug. 1969, p. 1449-1458. 18 refs.

Derivation of the radiation fields produced by an energetic electron moving in a helical orbit in a magnetoactive plasma by solving Maxwell's equations exactly. These fields consist of three components which are characterized by different wave frequencies related to the anisotropic nature of the medium. The results obtained appear to be useful in investigating the suppression of low frequencies of type IV solar radio bursts and galactic emission, and suggest that the explanation for the influence of ambient plasmas on the gyrosynchrotron radiation from energetic electrons must be modified. (Author)

A69-40083
EXTRA-TERRESTRIAL MATTER; CENTRAL STATES UNIVERSITIES AND ARGONNE NATIONAL LABORATORY, CONFERENCE, ARGONNE, ILL., MARCH 7, 8, 1968, PROCEEDINGS.
Conference co-sponsored by the U.S. Atomic Energy Commission and the Associated Midwest Universities.
Edited by C. A. Randall, Jr. (Ohio University, Athens, Ohio).
De Kalb, Ill., Northern Illinois University Press, 1969. 341 p. $12.50.

CONTENTS:

FOREWORD. A. F. Foster (Toledo, University, Toledo, Ohio), p. v.
WELCOMING REMARKS. R. Duffield (Argonne National Laboratory, Argonne, Ill.), p. vii, viii.
EDITOR'S PREFACE. C. A. Randall, Jr. (Ohio University, Athens, Ohio), p. ix, x.
PRESIDENT'S PREFACE. H. F. Henry, p. xi, xii.

METEORITES AND TEKTITES.
COMPOSITION OF STONY METEORITES. B. Mason (Smithsonian Institution, Washington, D.C.), p. 3-24. (See A69-40084 22-30)
ORIGIN OF ORGANIC MATTER IN METEORITES. M. Studier (Argonne National Laboratory, Argonne, Ill.), p. 25-56. (See A69-40085 22-30)
ORIGIN OF TEKTITES. J. A. O'Keefe (NASA, Goddard Space Flight Center, Greenbelt, Md.), p. 57-90. (See A69-40086 22-30)

LUNAR SCIENCE.
THE LUNAR REGOLITH. E. Shoemaker (U.S. Geological Survey, Flagstaff, Ariz.), p. 93-136. (See A69-40087 22-30)
CHEMICAL ANALYSIS OF THE LUNAR SURFACE. J. H. Patterson (Argonne National Laboratory, Argonne, Ill.), p. 137-161. (See A69-40088 22-30)
LUMINESCENCE AND CHEMICAL EFFECTS OF SOLAR PROTONS INCIDENT UPON THE LUNAR SURFACE. E. Zeller (Kansas, University, Lawrence, Kan.), p. 162-176. (See A69-40089 22-30)

COSMIC RAYS.
THE CHEMICAL COMPOSITION OF GALACTIC AND SOLAR COSMIC RAYS. F. B. McDonald (NASA, Goddard Space Flight Center, Greenbelt, Md.), p. 179-201. (See A69-40090 22-29)

COSMIC RAYS AND ATMOSPHERIC NEUTRONS.
THE ELECTRON COMPONENT OF COSMIC RAYS. P. Meyer (Chicago, University, Chicago, Ill.), p. 205-216. (See A69-40091 22-29)
COSMIC RAY NEUTRON STUDIES. S. Korff (New York University, New York, N.Y.), p. 217-237. (See A69-40092 22-29)
NEUTRON EXPOSURE IN SUPERSONIC TRANSPORT. R. Wallace (California, University, Berkeley, Calif.), p. 238-264. (See A69-40093 22-29)
EFFECT OF SOIL AND WATER ON COSMIC RAY NEUTRONS. J. Kastner (Argonne National Laboratory, Argonne, Ill.), p. 265-274. (See A69-40094 22-29)
COSMIC RAY NEUTRONS AND CARBON-14 PRODUCTION. R. Gold (Argonne National Laboratory, Argonne, Ill.), p. 275-287. (See A69-40095 22-29)

COMETS AND DUST.
INTERSTELLAR DUST. A. N. Witt (Toledo, University, Toledo, Ohio), p. 291-303. (See A69-40096 22-30)
COMETARY NUCLEI. A. H. Delsemme (Toledo, University, Toledo, Ohio), p. 304-316. (See A69-40097 22-30)

CONFERENCE SUMMARY.
PANEL DISCUSSION, p. 319-325.
BIOGRAPHICAL SKETCHES OF AUTHORS, p. 326-329.
INDEX, p. 330, 331.

A69-40086 *
ORIGIN OF TEKTITES.
John A. O'Keefe (NASA, Goddard Space Flight Center, Laboratory for Theoretical Studies, Greenbelt, Md.).
IN: EXTRA-TERRESTRIAL MATTER; CENTRAL STATES UNIVERSITIES AND ARGONNE NATIONAL LABORATORY, CONFERENCE, ARGONNE, ILL., MARCH 7, 8, 1968, PROCEEDINGS. (A69-40083 22-30)
Conference co-sponsored by the U.S. Atomic Energy Commission and the Associated Midwest Universities.
Edited by C. A. Randall, Jr.
De Kalb, Ill., Northern Illinois University Press, 1969, p. 57-85; Discussion, p. 85-90.

Tektites are small green to black siliceous glass bodies which resemble obsidian but differ in chemical composition from terrestrial glasses. Although tektites appear in many different shapes, two facts are significant: their size is of the order of centimeters, and their

surfaces are always pitted, grooved, or moulded. Prior to the Surveyor experiments, opinion on the origin of tektites was fairly evenly divided between the proponents of a lunar origin and the proponents of a terrestrial origin. The successful series of experiments conducted by Professor Turkevich on the Surveyors in September and November 1967 and January 1968 have had a great impact upon the problems of lunar geology and thus upon the possible origin of tektites. The current thinking about their origin is discussed. (Author)

A69-40172

THE APPLICATION OF MODERN PHYSICS TO THE EARTH AND PLANETARY INTERIORS; PROCEEDINGS OF THE NATO ADVANCED STUDY INSTITUTE, UNIVERSITY OF NEWCASTLE-UPON-TYNE, NEWCASTLE-UPON-TYNE, ENGLAND, MARCH 29-APRIL 4, 1967.

Edited by S. K. Runcorn (Newcastle-upon-Tyne, University, School of Physics, Newcastle-upon-Tyne, England).
London and New York, Wiley-Interscience, 1969. 666 p.
$35.

CONTENTS:

CONTRIBUTORS, p. v-vii.

PREFACE. S. K. Runcorn (Newcastle-upon-Tyne, University, Newcastle-upon-Tyne, England), p. ix.

CELESTIAL AND TERRESTRIAL PHYSICS IN HISTORICAL PERSPECTIVE. L. Rosenfeld, p. 1-6.

COSMOLOGY AND GEOPHYSICS.

CONSIDERATIONS FROM COSMOLOGY AND GALACTIC STRUCTURE WHICH SUGGEST A SECULAR CHANGE IN G. C. Gilbert (Newcastle-upon-Tyne, University, Newcastle-upon-Tyne, England), p. 9-18. 20 refs. (See A69-40173 22-30)

A COSMOLOGIST LOOKS AT THE HYPOTHESIS OF A CHANGE IN THE GRAVITATIONAL CONSTANT. G. C. McVittie (Illinois, University, Urbana, Ill.), p. 19-28. 14 refs. (See A69-40174 22-30)

THE OBLATENESS OF THE SUN. I. W. Roxburgh (Sussex, University, Brighton, England), p. 29-31. (See A69-40175 22-30)

DIRAC'S PRINCIPLE OF COSMOLOGY AND RADIOACTIVE DATING. E. R. Kanasewich (Alberta, University, Edmonton, Alberta, Canada) and J. C. Savage (Toronto, University, Toronto, Canada), p. 35-46. 49 refs. (See A69-40176 22-30)

A PALAEONTOLOGICAL METHOD OF TESTING THE HYPOTHESIS OF A VARYING GRAVITATIONAL CONSTANT. S. K. Runcorn (Newcastle-upon-Tyne, University, Newcastle-upon-Tyne, England), p. 47-51. 15 refs. (See A69-40177 22-30)

ON THE POSSIBILITY OF AVOIDING RAMSEY'S HYPOTHESIS IN FORMULATING A THEORY OF EARTH EXPANSION. P. Jordan (Hamburg, Universität, Hamburg, West Germany), p. 55-63. 19 refs. (See A69-40178 22-30)

THE SLOW EXPANSION HYPOTHESIS. L. Egyed (Eötvös Lóránd Egyetem, Budapest, Hungary), p. 65-75. 16 refs. (See A69-40179 22-30)

ENERGY CHANGES IN AN EXPANDING EARTH. A. E. Beck (Western Ontario, University, London, Ontario, Canada), p. 77-83. 7 refs. (See A69-40180 22-13)

GLOBAL PALAEOGEOGRAPHY AND EARTH EXPANSION. H. Termier and G. Termier (Paris, Université, Paris, France), p. 87-101. 14 refs. (See A69-40181 22-13)

CRUSTAL TECTONIC EVIDENCE FOR EARTH EXPANSION. R. Dearnley (Institute of Geological Sciences, London, England), p. 103-110. 32 refs. (See A69-40182 22-13)

OUTLINE OF THE PALAEOMAGNETIC METHOD OF DETERMINING ANCIENT EARTH RADII. E. Irving (Leeds University, Leeds, England), p. 111.

NEW DETERMINATIONS OF ANCIENT EARTH RADII FROM PALAEOMAGNETIC DATA. S. I. Van Andel and J. Hospers (Amsterdam, University, Amsterdam, Netherlands), p. 113-121. 15 refs. (See A69-40183 22-13)

SOLID STATE PHYSICS AND GEOPHYSICS.

CONDUCTIVITY ANOMALIES WITH SPECIAL REFERENCE TO THE ANDES. U. Schmucker, p. 125-138.

MAGNETIC DEEP SOUNDING AND LOCAL CONDUCTIVITY ANOMALIES. D. I. Gough (Alberta, University, Edmonton, Alberta, Canada) and J. S. Reitzel (Southwest Center for Advanced Studies, Dallas, Tex.), p. 139-153.

ELECTRICAL CONDUCTIVITY ANOMALIES IN THE MANTLE AND CRUST IN CANADA. E. R. Niblett, K. Witham (Dominion Observatory, Ottawa, Canada), and B. Caner (Victoria Magnetic Observatory; Dominion Astrophysical Observatory, Victoria; British Columbia, University, Vancouver, British Columbia, Canada), p. 155-172.

TRANSPORT PROPERTIES OF OLIVINES. T. J. Shankland (Newcastle-upon-Tyne, University, Newcastle-upon-Tyne, England), p. 175-190.

OPTICAL ABSORPTION IN SILICATES. R. G. Burns (Oxford, University, Oxford, England), p. 191-211.

THE NATURE AND GEOPHYSICAL IMPORTANCE OF SPIN PAIRING IN MINERALS OF ION (II). R. G. J. Strens (Leeds University, Leeds, England), p. 213-220.

CONVECTION AND STRESS PROPAGATION IN THE UPPER MANTLE. W. M. Elsasser (Princeton University, Princeton, N.J.), p. 223-246. 51 refs. (See A69-40184 22-13)

DIAMONDS AND DEEP FLUIDS IN THE UPPER MANTLE. F. C. Frank (Bristol, University, Bristol, England), p. 247-250.

STEADY-STATE DIFFUSIONAL CREEP. F. R. Nabarro (Cambridge University, Cambridge, England), p. 251.

THE DIFFUSION OF BOUNDARY DISTURBANCES THROUGH A NON-NEWTONIAN MANTLE. C. A. Berg (Massachusetts Institute of Technology, Cambridge, Mass.), p. 253-272.

THE FORMATION OF OCEANIC TRENCHES AND THE MECHANISM OF PERMANENT DEFORMATION IN THE MANTLE. C. A. Berg (Massachusetts Institute of Technology, Cambridge, Mass.), p. 273-283.

HIGH-PRESSURE PHYSICS AND THE EARTH'S INTERIOR.

SEISMIC AND RELATED EVIDENCE ON COMPRESSIBILITY IN THE EARTH. K. E. Bullen (Sydney, University, Sydney, Australia), p. 287-297.

COMPOSITION AND STATE OF THE EARTH'S INTERIOR. F. Birch (Harvard University, Cambridge, Mass.), p. 299.

COSMOLOGICAL ASPECTS IN THE THEORY OF PLANETARY INTERIORS. T. Herczeg (Hamburg, Universität, Hamburg, West Germany), p. 301-309. 21 refs. (See A69-40185 22-30)

EQUATIONS OF STATE AT HIGH PRESSURE FROM THE THOMAS-FERMI ATOM MODEL. J. J. Gilvarry (NASA, Ames Research Center, Moffett Field, Calif.), p. 313-403. 100 refs. (See A69-40186 22-24)

HIGH-PRESSURE BEHAVIOUR OF SOLIDS. N. H. March (Sheffield, University, Sheffield, England), p. 405-422. 21 refs. (See A69-40187 22-23)

ELASTIC CONSTANTS OF OXIDE COMPONENTS USED TO ESTIMATE THE PROPERTIES OF THE EARTH'S INTERIOR. O. L. Anderson and R. C. Lieberman (Columbia University, Palisades, N.Y.), p. 425-448.

SHOCK WAVE DATA AND THE STUDY OF THE EARTH. T. J. Ahrens (California Institute of Technology, Pasadena, Calif.) and C. F. Petersen (Stanford Research Institute, Menlo Park, Calif.), p. 449-461. 42 refs. (See A69-40188 22-13)

DEVELOPMENTS IN TECHNIQUES.

BRILLOUIN SCATTERING—A NEW GEOPHYSICAL TOOL. D. L. Anderson, C. G. Sammis (California Institute of Technology, Pasadena, Calif.), and R. A. Phinney (Princeton University, Princeton, N.J.), p. 465-477.

APPLICATION OF NEUTRON DIFFRACTION AND MÖSSBAUER STUDIES TO ROCK MAGNETISM. W. O'Reilly (Newcastle-upon-Tyne, University, Newcastle-upon-Tyne, England), p. 479-484.

MÖSSBAUER EFFECT STUDIES OF MAGNETIC MINERALS. C. E. Johnson (United Kingdom Atomic Energy Authority, Harwell, Berks., England), p. 485-496.

FISSION TRACK DATING AND PROCESSES IN THE EARTH'S INTERIOR. R. L. Fleischer, P. B. Price (General Electric Co., Schenectady, N.Y.), and R. M. Walker (Washington University, St. Louis, Mo.), p. 499-503.

GAS LASERS AND THE MEASUREMENT OF LONG PERIOD AND SECULAR CHANGES OF STRAIN. A. H. Cook (Ministry of Technology, National Physical Laboratory, Teddington, Middx., England), p. 505-512. (See A69-40189 22-16)

A LASER SEISMOMETER. G. C. P. King and D. Davies (Cambridge University, Cambridge, England), p. 513-522.

SOME IMPLICATIONS FOR PHYSICS AND GEOPHYSICS OF LASER RANGE MEASUREMENTS FROM EARTH TO A LUNAR RETRO-REFLECTOR. C. O. Alley, D. G. Currie (Maryland, University, College Park, Md.), J. E. Faller (Wesleyan University, Middletown, Conn.), P. L. Bender (National Bureau of Standards and Colorado, University, Boulder, Colo.), and R. H. Dicke (Princeton University, Princeton, N.J.), p. 523-530. 19 refs. (See A69-40190 22-16)

APOLLO LUNAR SAMPLE ANALYSIS PROGRAM—A PROGRESS REPORT. V. R. Wilmarth (NASA, Washington, D.C.), p. 533-546. (See A69-40191 22-11)

MAGNETOHYDRODYNAMICS.

THE JARAMILLO EVENT AS DETECTED IN OCEANIC CORES. N. D. Opdyke (Columbia University, Palisades, N.Y.), p. 549-552.

THE BRAGINSKII DYNAMO. J. G. Tough and R. D. Gibson (Newcastle-upon-Tyne, University, Newcastle-upon-Tyne, England), p. 555-569. 5 refs. (See A69-40192 22-25)

THE HERZENBERG DYNAMO. R. D. Gibson (Newcastle-upon-Tyne, University, Newcastle-upon-Tyne, England), p. 571-576. (See A69-40193 22-25)

THE BULLARD-GELLMAN DYNAMO. R. D. Gibson, P. H. Roberts (Newcastle-upon-Tyne, University, Newcastle-upon-Tyne, England), and S. Scott (Rutherford College of Technology, Newcastle-upon-Tyne, England), p. 577-602. 13 refs. (See A69-40194 22-30)

DYNAMO WAVES. G. O. Roberts (Newcastle-upon-Tyne, University, Newcastle-upon-Tyne, England), p. 603-628. 7 refs. (See A69-40195 22-25)

A CLASS OF SOLUTIONS OF THE MAGNETOHYDRODYNAMIC DYNAMO PROBLEM. S. Childress (New York University, New York, N.Y.), p. 629-648. 8 refs. (See A69-40196 22-25)

ON THE DYNAMICS OF THE EARTH'S DEEP INTERIOR. R. Hide (Massachusetts Institute of Technology, Cambridge, Mass.), p. 651, 652.

PLANETARY MAGNETOHYDRODYNAMIC WAVES AS A PERTURBATION OF DYNAMO SOLUTIONS. G. Suffolk and D. W. Allan (London, University, King's College, London, England), p. 653-656.

SECOND-CLASS MAGNETO-ROSSBY WAVES. K. Stewartson (London, University, University College, London, England), p. 657.

THE EARTH AS A FUNDAMENTAL PHYSICS LABORATORY.

SEARCH FOR MAGNETIC MONOPOLES. H. H. Kolm (Massachusetts Institute of Technology, Cambridge, Mass.), p. 661-672. 24 refs. (See A69-40197 22-23)

AUTHOR INDEX, p. 673-682.

SUBJECT INDEX, p. 683-692.

A69-40304 *

HYDROMAGNETIC SHOCKS IN THE SOLAR WIND.

K. W. Ogilvie and L. F. Burlaga (NASA, Goddard Space Flight Center, Laboratory for Space Sciences, Greenbelt, Md.).

Solar Physics, vol. 8, Aug. 1969, p. 422-434. 16 refs.

Application of the Rankine-Hugoniot relations to shock-like discontinuities measured by both magnetic field and plasma instruments on the satellite Explorer 34 between May 30, 1967 and Jan. 11, 1968. Shock normals were either determined from the magnetic field observations, or from the times of occurrence of the discontinuity at Explorers 33, 34, and 35. The Rankine-Hugoniot relations are obeyed to the accuracy of the observations, and the values of shock velocities, density ratios, and Mach numbers indicate that at 1 AU the typical interplanetary shock is not strong, although all the events studied caused geomagnetic impulses. (Author)

A69-40524 * #

SIMPLE MODEL FOR A ROTATING NEUTRAL PLANETARY EXOSPHERE.

K. M. Hagenbuch and R. E. Hartle (NASA, Goddard Space Flight Center, Laboratory for Space Sciences, Greenbelt, Md.).

Physics of Fluids, vol. 12, Aug. 1969, p. 1551-1559. 7 refs.

Generalization of the model neutral exosphere of Öpik and Singer for a nonrotating planet by permitting the corresponding barosphere to rotate uniformly at an angular velocity which may or may not be equal to that of the planet. For this case, the velocity-distribution function satisfying the collisionless Boltzmann equation is constructed. Then the density is determined from the distribution and is compared with the corresponding result for a nonrotating planet obtained by Öpik and Singer. In addition, the radial and azimuthal fluxes are derived. Based on the result for the azimuthal flux, the point at which exospheric corotation can be said to have broken down is indicated for several conditions. It is shown that in all cases, for a given radius, the density at the equator exceeds the density at the pole. For example, a model terrestrial neutral exosphere of hydrogen, helium, and oxygen has density ratios between the pole and the equator of 0.984, 0.869, and 0.530, respectively, when r equals $2R$. (Author)

A69-40650 *

AN EXPLANATION FOR THE BLUE SEQUENCE OF VARIABLE STARS.

Richard Stothers and Norman R. Simon (NASA, Goddard Institute for Space Studies, New York, N.Y.).

Astrophysical Journal, vol. 157, Aug. 1969, pt. 1, p. 673-681. 38 refs.

Nuclear energy of the stellar core is found to be the direct source of energy fed into radial pulsations in two classes of blue variable stars. The mu-mechanism (reversal of the gradient of mean molecular weight, which reduces the central condensation) or the beta-mechanism (high radiation pressure) can explain the basic variability of beta Cephei stars if they are burning hydrogen in their cores, have accreted a helium-rich envelope, and are the luminous secondaries of close binary systems. If the composition reversal does not lead to significant mixing in the envelope, the mu-mechanism will operate in inhomogeneous stars of 6-95 solar masses. If rapid mixing takes place, the beta-mechanism will operate in completely homogeneous stars of 12-60 solar masses. The beta-mechanism can also explain the variability of many Wolf-Rayet stars if they are burning helium in their cores, have masses in excess of about 8 solar masses with a thin or absent hydrogen envelope, and are the luminous primaries of close binary systems. (Author)

A69-40652 *

THE ATMOSPHERE OF THE HELIUM-CARBON STAR BD+10°2179.

Kurt Hunger and Daniel Klinglesmith (NASA, Goddard Space Flight Center, Greenbelt, Md.).

Astrophysical Journal, vol. 157, Aug. 1969, pt. 1, p. 721-735. 31 refs.

Grant No. NsG-503.

Analysis of the helium-carbon star BD+10°2179 by using a grid of constant flux models with the parameter Y. The model that best represents the observed data gives an effective temperature of 16,000

deg K, log g equal to 2.8, Y equal to 0.45, X mass fraction of hydrogen equal to 0.0001, a mass fraction of carbon equal to 0.55, and a zero turbulent velocity. The mass of the star is estimated to be equal to or greater than 0.5 solar mass. On the basis of the high carbon content, the helium stars BD+10°3179 and HD 124448 are considered to be hot carbon stars. P.G.

A69-40772 *
INTERSTELLAR EXTINCTION IN THE ULTRAVIOLET. II.
Theodore P. Stecher (NASA, Goddard Space Flight Center, Greenbelt, Md.).
Astrophysical Journal, vol. 157, Aug. 1969, pt. 2, p. L125, L126. 5 refs.

Study of interstellar extinction in the UV from the spectra of zeta and epsilon Persei. Two spectrophotometric scans of both stars have been obtained with a three-channel scanner attached to a 32-cm telescope mounted in a pointed Aerobee rocket. The stars were observed sequentially near the peak of the flight. Each scan on each star was of 20 sec duration and covered a wavelength range from 1150 to 4000 Å. The interstellar extinction in magnitudes is presented as a function of inverse wavelength. It is noted that the curve obtained is very similar to that reported previously by Stecher (1965). Its features are briefly discussed. P.G.

A69-41058 • #
THE ROYAL ASTRONOMICAL SOCIETY OF CANADA 1968.
Malcolm M. Thomson (Pittsburgh, University, Dept. of Physics and Allegheny Observatory, Pittsburgh, Pa.; NASA, Goddard Space Flight Center, Astrophysics Branch, Greenbelt, Md.).
Royal Astronomical Society of Canada, Journal, vol. 63, Aug. 1969, p. 189-192.
NSF-supported research.

Description of a high-resolution visual observation of a meteor, showing the microstructure of the train. The observation was obtained by means of a large refractor at a magnification of about 600. Four distinct phases of the observation are described in detail. B.H.

A69-41351 *
CHEMICAL COMPOSITION OF IVORY COAST MICROTEKTITES.
Billy P. Glass (NASA, Goddard Space Flight Center, Planetology Branch, Greenbelt, Md.).
(Corning Glass Works and Smithsonian Institution, International Tektite Symposium, 3rd, Corning, N.Y., Apr. 16-18, 1969.)
Geochimica et Cosmochimica Acta, vol. 33, Sept. 1969, p. 1135-1147. 14 refs.

Electron microprobe analysis of the chemical composition of 28 microscopic glassy objects, found in a deep-sea sediment core taken near the Ivory Coast. It is shown that, while one group of these glassy objects has a chemical composition similar to normal microtektites, the other group is characterized by a bottle-green color and has a low silica and a high MgO content. Both these groups are discussed in detail and are compared with other microtektites. The chemical data presented are interpreted as confirming a previous suggestion that these glassy objects are microtektites and that they represent a portion of the Ivory Coast tektite strewn-field. O.H.

A69-41388 *
AN EMPIRICALLY DERIVED EROSION LAW AND ITS APPLICATION TO LUNAR MODULE LANDING.
Curtis C. Mason and Edward F. Nordmeyer (NASA, Manned Spacecraft Center, Houston, Tex.).
Geological Society of America, Bulletin, vol. 80, Sept. 1969, p. 1783-1787.

Erosion tests performed on a particulate material in a .0001-torr vacuum indicate that the volume of material eroded is directly proportional to the thrust level, and inversely proportional to the square root of the height above the surface. By assuming that the volume eroded is also directly proportional to the thrust duration and applying this law to the size of the crater formed during the Surveyor 5 vernier engine firing, indications are that during Lunar Module landing a crater would be eroded which would be 60 in. in diameter and from 1.6 to 2.5 in. deep. (Author)

A69-41477 *
APOLLO AND BEYOND.
George E. Mueller (NASA, Washington, D.C.).
Spaceflight, vol. 11, Sept. 1969, p. 298-303.

Outline of the Apollo 11 mission, and survey of future prospects in space exploration. The first step in future space exploration will be a geological survey of the moon and the creation of a moon base. The moon base may be used for installing scientific instruments (such as large optical, radio, X-ray and gamma-ray telescopes, and radio interferometers), for monitoring the solar system (especially particles and fields), for laser communication with spacecraft, and as a refueling and launch platform. The second step is the establishment of a large and versatile manned space station in earth orbit, constructed of specialized modules with a minimum operational life of ten years. This station would be used for observations of the earth, studies of the effect of environment on man, animals, and plants, and investigations of cosmic radiation and the possibilities of manufacturing unique items in space. The third step is the construction of reusable economic space vehicles (shuttles) which would shuttle cargo and passengers from earth to earth orbit or to lunar bases, deploying wings after entering the atmosphere and landing with turbofan engines. The fourth step is the introduction of radically new concepts in the areas of checkout and control in all newly designed space vehicles. O.H.

A69-41611 *
EXOBIOLOGY AND THE EXPLORATION OF MARS.
D. G. Rea (NASA, Washington, D.C.).
Applied Optics, vol. 8, July 1969, p. 1267-1269.

Survey of experiments and techniques conducted to study the possible existence of a Martian biota. Rapid advances have been made by the Mariner 4 flyby and will be made by the Mariner 1969 flybys and the Mariner 1971 orbiters. *In situ* measurements, including some aimed at detecting manifestations of life, will be carried out on the Viking landers in 1973. The results should make it possible to discuss more quantitatively than at present the various questions related to indigenous Martian life forms. (Author)

A69-41617 *
MEASUREMENTS IN THE ATMOSPHERE OF MARS.
Alvin Seiff (NASA, Ames Research Center, Vehicle Environment Div., Moffett Field, Calif.).
Applied Optics, vol. 8, July 1969, p. 1305-1314. 16 refs.

The detailed definition of the key features of Mars' atmosphere from one or a few entries and landings is a challenging task involving a variety of measurements (taken during entry and after landing) correlated with observations from orbiters and flyby missions. The properties of interest include profiles to high altitudes of the atmospheric state properties, composition (abundant gases and minor constituents related to life processes), and meteorological factors such as winds, clouds, and variations in pressure and temperature. Profiles of the atmosphere are best measured during entry, by techniques which are described. The lander, if designed for lifetimes of days to weeks, can contribute information on diurnal variability of the atmosphere, and possibly on clouds and winds. Landings at several latitudes and in different seasonal regions will probably be required to complete a first-order description of the atmosphere. (Author)

A69-41623 *
EXTRATERRESTRIAL LIFE DETECTION.

R. S. Young (NASA, Office of Space Science and Applications, Washington, D.C.).
Applied Optics, vol. 8, July 1969, p. 1355-1360. 13 refs.

Survey of experiments designed to test the potential of another planet to give rise to and subsequently to sustain an indigenous biota. Experiments must be designed to seek out the fundamental attributes of life. They must be capable of being interpreted in an unambiguous fashion and of being integrated into an experimental package which can deal with a planetary surface so that the evidence required can be obtained through organized sequential analyses of a relatively small sample of the surface. The basic life attributes discussed are chemistry, morphology, growth, and metabolism. Included are experimental approaches to the acquisition of such data. (Author)

A69-41896 • #
RECURRENT NATURE OF LAGRANGE MULTIPLIERS FOR OPTIMAL LOW-THRUST EARTH-JUPITER TRANSFERS.
J. D. Hart, W. T. Fowler (Texas, University, Austin, Tex.), and J. M. Lewallen (NASA, Manned Spacecraft Center, Computation and Analysis Div., Houston, Tex.).
AIAA Journal, vol. 7, July 1969, p. 1357, 1358.
Grant No. NsG-551.

Study of repetitive behavior in the initial Lagrange multipliers and mission durations for a series of low-thrust Earth-Jupiter transfers. A three-dimensional solar system model is used, and the equations of motion are stated in terms of a heliocentric, inertial set of rectangular Cartesian coordinates. The xy-plane lies in the ecliptic plane, and the x-axis coincides with the ascending node of Jupiter's orbit. It is seen that the initial Lagrange multipliers associated with the variables in the xy-plane do exhibit a recurrent type of behavior. The fact that the solar system model is three-dimensional and assumes an elliptic orbit for Jupiter keeps the recurrent behavior from being periodic. G.R.

A69-42191 *
SOLAR IRRADIANCE MEASUREMENTS FROM A RESEARCH AIRCRAFT.
M. P. Thekaekara, R. Kruger, and C. H. Duncan (NASA, Goddard Space Flight Center, Greenbelt, Md.).
Applied Optics, vol. 8, Aug. 1969, p. 1713-1732. 30 refs.

Results of measurements of the solar constant and solar spectrum, made from a research aircraft flying at 11.58 km, above almost all of the highly variable and absorbing constituents of the atmosphere. A wide range of solar zenith angles was covered during six flights for over 14 hr of observation. Results are presented from nine different instruments which complemented each other in measuring techniques and wavelength range and were calibrated and operated by different experimenters. A new value of the solar constant, 135.1 mW per sq cm, has been derived, as well as a revised solar spectral irradiance curve for zero air mass. (Author)

A69-42375 *
THE SPECTRUM OF THE COSMIC RADIO BACKGROUND BETWEEN 0.4 AND 6.5 MHz.
J. K. Alexander, L. W. Brown, T. A. Clark, R. G. Stone, and R. R. Weber (NASA, Goddard Space Flight Center, Laboratory for Space Sciences, Greenbelt, Md.).
Astrophysical Journal, vol. 157, Sept. 1969, pt. 2, p. L163-L165. 7 refs.

Results of measurements of the average spectrum of the radio background for a broad region near the north galactic pole. Data were obtained over the range 0.4-6.5 MHz on the basis of experiments on the Radio Astronomy Explorer satellite. The spectrum turns over below 4 MHz in a manner that supports the concept of a uniform admixture of galactic emission regions having a spectral index of 0.43 (plus or minus .05) and absorbing ionized-hydrogen regions having a mean electron density of about 0.03 per cu cm in the galactic disk. (Author)

A69-42377 *
INFRARED EXCESS OF RY SGR.
T. A. Lee (NASA, Goddard Space Flight Center, Goddard Institute for Space Studies, New York, N.Y.) and M. W. Feast (Radcliffe Observatory, Pretoria, Republic of South Africa).
Astrophysical Journal, vol. 157, Sept. 1969, pt. 2, p. L173-L176. 12 refs.

A large IR excess has been found for RY Sgr, an R CrB-type variable star. During a recent eight-month interval, the visual brightness increased, while the radiation in the 2 to 3.4 micron region decreased. These observations support the general model for R CrB proposed by Stein et al., in which the IR flux is ascribed to blackbody radiation from a circumstellar cloud of particles ejected at the time of deep minimum. (Author)

A69-42394 *
INTERPLANETARY SHOCK WAVES. I—GROSS STRUCTURE.
C. P. Sonett (NASA, Ames Research Center, Moffett Field, Calif.).
Comments on Astrophysics and Space Physics, vol. 1, Sept.-Oct. 1969, p. 178-185. 19 refs.

Preliminary study of the large-scale structure and evolution of interplanetary shock waves. It is indicated that collision-free shock waves are probably a common feature of interplanetary space, both in connection with the interaction of the solar wind and certain classes of planets and with the free propagation of a field of disturbances in the solar wind itself. It is also shown that shock waves can propagate in collision-free media probably through mechanisms connected with wave-particle interactions leading to enhanced resistivity and possibly also to enhanced viscosity due to ions. To establish the overall structure of shock waves, the aerodynamic theory is successfully applied. O.H.

A69-42404 * #
CARROLL'S METHOD APPLIED TO SMALL STELLAR ROTATIONS.
Alistair Wilson (NASA, Goddard Space Flight Center, Solar Physics Branch, Greenbelt, Md.).
Royal Astronomical Society, Monthly Notices, vol. 144, no. 3, 1969, p. 325-332. 7 refs.

Application of Carroll's Fourier transform method to the determination of small stellar rotation velocities. The method was tested, using the sodium D line profiles generated by the sun rotating at speeds up to 30 km/sec, and was found to be accurate to 2 km/sec. The method was then applied to lines in the spectrum of Arcturus. An upper limit of 3.5 km/sec for the rotation velocity of this star can be established by this method. G.R.

A69-42417 * #
MHD RANKINE-HUGONIOT EQUATIONS APPLIED TO EARTH'S BOW SHOCK.
J. D. Mihalov, C. P. Sonett, and J. H. Wolfe (NASA, Ames Research Center, Space Sciences Div., Moffett Field, Calif.).
Journal of Plasma Physics, vol. 3, Sept. 1969, p. 449-463. 33 refs.

Comparison of computed results with upstream and downstream thermal pressures, the downstream ion density, and vector flow velocity measured by the Ames plasma probe on the Pioneer 6 spacecraft as earth's bow shock was traversed. The upstream ion density and vector flow velocity measured on Pioneer 6 by this experiment are used as independent variables, together with Pioneer 6 magnetic field measurements. MHD Rankine-Hugoniot equations for an isotropic plasma are used for these computations. Reasonable agreement is obtained between the measured and computed downstream ion density, thermal pressure, and convective velocity magnitude and orientation, only when a change is made to a downstream magnetic field value used in the calculation. There is disagreement between several determinations of shock orientation and that deduced from coplanarity of the reported magnetic fields; the shock orientation provides the coordinate system for solving the

Rankine-Hugoniot equations. If a shock orientation determined by velocity coplanarity is used in the calculations, all computed quantities agree well with the experimental results. Other results suggest that a disagreement between computed and measured upstream thermal pressures may not be negligible in comparison with experimental uncertainties in upstream velocity and density. If the computations included anisotropic pressure terms and/or other factors such as plasma turbulence, better agreement might be obtained between computed and measured upstream thermal pressures. (Author)

A69-42556 *
PROGRESS REPORT ON PULSARS.
Stephen P. Maran (NASA, Goddard Space Flight Center, Greenbelt, Md.; Kitt Peak National Observatory, Tucson, Ariz.) and A. G. W. Cameron (Yeshiva University, Belfer Graduate School of Science; NASA, Goddard Space Flight Center, Goddard Institute for Space Studies, New York, N.Y.).
Earth and Extraterrestrial Sciences, vol. 1, Aug. 1969, p. 3-25. 286 refs.

Review of new advances in the study of pulsars made mainly during the last two years. New observations made regarding the Crab Nebula include the discovery of optical flashes by Cocke et al. (1969). Several lines of evidence in support of the identification of pulsars as neutron stars are discussed. A number of recent investigations concerning the radio properties of pulsars are described. The importance of pulsars for the study of interstellar gas and magnetic fields is considered, and the positions of pulsars are listed. The present status of pulsar theory is reviewed. G.R.

A69-42610 *
THE INTERSTELLAR H_2 MOLECULE.
T. P. Stecher (NASA, Goddard Space Flight Center, Greenbelt, Md.) and D. A. Williams (Manchester, University, Institute of Science and Technology, Manchester, England).
Astrophysical Letters, vol. 4, Sept. 1969, p. 99-101. 14 refs.

Interstellar extinction observations and the photodissociation cross section for positively charged diatomic hydrogen give an upper limit of .0003 per cu cm to its mean number density in interstellar space. Consideration of formation mechanisms suggests that sufficient positively charged diatomic hydrogen may be present to contribute to interstellar extinction especially around young hot stars. The wavelength dependence of the extinction produced by positively charged diatomic hydrogen is similar to that produced by grains, except in the far ultraviolet where the extinction due to positively charged diatomic hydrogen is relatively larger. (Author)

A69-42681
PLASMA INSTABILITIES IN ASTROPHYSICS; PROCEEDINGS OF THE CONFERENCE, MONTEREY, CALIF., OCTOBER 14-17, 1968.
Conference sponsored by the American Astronomical Society, the America. Physical Society, Stanford University, and the U.S. Atomic Energy Commission.
Edited by D. G. Wentzel and D. A. Tidman (Maryland, University, College Park, Md.).
New York, Gordon and Breach, Science Publishers, Inc., 1969. 426 p.
$25.

CONTENTS:

PREFACE. D. G. Wentzel and D. A. Tidman (Maryland, University, College Park, Md.), p. v.

LIST OF CONTRIBUTORS, p. vii.

NONTHERMAL PHENOMENA OF ASTROPHYSICS AND THEIR RELATION TO PLASMA PHYSICS. A. G. W. Cameron (Yeshiva University; NASA, Goddard Space Flight Center, New York, N.Y.), p. 1-16. 25 refs. (See A69-42682 24-30)

PLASMA INSTABILITIES.

MHD INSTABILITIES. E. A. Frieman (Princeton University, Princeton, N.J.), p. 17-32. 16 refs. (See A69-42683 24-25)

THE TEARING MODE. H. P. Furth (Princeton University, Princeton, N.J.), p. 33-47. 10 refs. (See A69-42684 24-25)

TWO-STREAM INSTABILITIES. A. Simon (Rochester, University, Rochester, N.Y.), p. 49-58. (See A69-42685 24-25)

VELOCITY-ANISOTROPY INSTABILITIES. E. G. Harris (Tennessee, University, Knoxville; Oak Ridge National Laboratory, Oak Ridge, Tenn.), p. 59-70. 7 refs. (See A69-42686 24-25)

SOLAR ACTIVITY.

SOLAR FLARES. A. Bruzek (Fraunhofer-Gesellschaft zur Förderung der angewandten Forschung, Freiburg im Breisgau, West Germany), p. 71-90. 106 refs. (See A69-42687 24-29)

OBSERVATION OF AN X-RAY FLARE—SPATIAL DISTRIBUTION AND PHYSICAL PARAMETERS. G. S. Vaiana and R. Giacconi (American Science and Engineering, Inc., Cambridge, Mass.), p. 91-118. 7 refs. (See A69-42688 24-29)

RADIO EVIDENCE OF INSTABILITIES AND SHOCK WAVES IN THE SOLAR CORONA. J. P. Wild (Commonwealth Scientific and Industrial Research Organization, Epping, New South Wales, Australia), p. 119-138. 18 refs. (See A69-42689 24-30)

THE MICROSTRUCTURE OF SUNSPOTS. J. M. Beckers (USAF, Cambridge Research Laboratories, Sunspot, N. Mex.), p. 139-152. 28 refs. (See A69-42690 24-30)

SUNSPOTS AND PHOTOSPHERIC CONVECTION. N. O. Weiss (Cambridge University, Cambridge, England), p. 153-169. 59 refs. (See A69-42691 24-30)

EARTH ENVIRONMENT.

INSTABILITY PHENOMENA OF THE MAGNETOSPHERE. C. F. Kennel (California, University, Los Angeles, Calif.), p. 171-198. 21 refs. (See A69-42692 24-13)

OBSERVATIONS OF THE MICROSTRUCTURE OF THE EARTH'S BOW SHOCK. R. W. Fredricks (TRW Systems Group, Redondo Beach, Calif.) and P. J. Coleman, Jr. (California, University, Los Angeles, Calif.), p. 199-228. 7 refs. (See A69-42693 24-13)

SHOCK WAVES IN COLLISIONLESS PLASMAS. D. A. Tidman (Maryland, University, College Park, Md.), p. 229-235. 31 refs. (See A69-42694 24-25)

COSMIC RADIATION.

DYNAMICAL PROPERTIES AND EFFECTS OF COSMIC RAYS IN THE GALAXY. E. N. Parker (Chicago, University, Chicago, Ill.), p. 237-252. 58 refs. (See A69-42695 24-29)

PARTICLE DYNAMICS IN STOCHASTIC ELECTROMAGNETIC FIELDS. D. E. Hall (Walla Walla College, Walla Walla, Wash.), p. 253.

PARTICLE ACCELERATION IN ASTROPHYSICS. D. G. Wentzel (Maryland, University, College Park, Md.), p. 271-281. 35 refs. (See A69-42696 24-25)

THE STRUCTURE AND EVOLUTION OF EXTRAGALACTIC SOURCES. K. I. Kellermann (National Radio Astronomy Observatory, Green Bank, W. Va.), p. 283-296. 18 refs. (See A69-42697 24-30)

EXPLOSIONS IN GALAXIES AND QUASARS. P. A. Sturrock (Stanford University, Stanford, Calif.), p. 297-328. 53 refs. (See A69-42698 24-30)

THE ROLE OF THE MAGNETIC FIELD IN STAR FORMATION. L. Mestel (Manchester, University, Manchester, England), p. 329-352. 38 refs. (See A69-42699 24-30)

CONCLUDING REMARKS. L. Woltjer (Columbia University, New York, N.Y.), p. 353-355.
ABSTRACTS OF CONTRIBUTED PAPERS, p. 357-411.
INDEX, p. 413-417.

A69-42682 * #
NONTHERMAL PHENOMENA OF ASTROPHYSICS AND THEIR RELATION TO PLASMA PHYSICS.
A. G. W. Cameron (Yeshiva University, Belfer Graduate School of Science; NASA, Goddard Space Flight Center, Goddard Institute for Space Studies, New York, N.Y.).
IN: PLASMA INSTABILITIES IN ASTROPHYSICS; PROCEEDINGS OF THE CONFERENCE, MONTEREY, CALIF., OCTOBER 14-17, 1968. (A69-42681 24-30)
Conference sponsored by the American Astronomical Society, the American Physical Society, Stanford University, and the U.S. Atomic Energy Commission.
Edited by D. G. Wentzel and D. A. Tidman.
New York, Gordon and Breach, Science Publishers, Inc., 1969, p. 1-16. 25 refs.
NSF-NASA-supported research.

Survey of various fields of astrophysics which are in close relation to plasma physics. The characteristics of the outer boundaries of solid bodies, especially the planets, are discussed with regard to their magnetic fields, acceleration of particles, and solar wind interaction. Stellar phenomena are treated from the standpoint of plasma physics with particular emphasis on solar processes. The propagating in a turbulent medium such as the Galaxy. With regard to the electron number density and the magnetic field as homogeneous random functions (with nonzero mean), the results are given in terms of the mean values and two-point correlation functions of these quantities. Application to a simple, statistically homogeneous, disk model of the Galaxy and its turbulence is then considered. The predictions of the model for the means and variances are consistent with the observed Faraday rotations and dispersions in pulsar signals, although the observations are not yet sufficient to provide a definitive test of the theory. The mean values are much as those discussed by previous authors who did not consider the fluctuations. The variances of the Faraday rotations and dispersions in pulsar signals are used to estimate statistical parameters such as the correlation length and rms fluctuations associated with turbulence in the Galaxy. The correlation length is approximately equal to the 250-pc thickness of the galactic disk. (Author)

A69-42810 * #
THE CHALLENGE OF PLANETARY EXPLORATION.
Pitt G. Thome (NASA, Office of Space Science and Applications, Washington, D.C.).
American Astronautical Society and Operations Research Society of America, Joint National Meeting, Denver, Colo., June 17-20, 1969, AAS Paper 69-286. 14 p.

Discussion of the objectives of planetary exploration and of a flight program to achieve them. The present status of planetary exploration is briefly reviewed. Items of information to be obtained concerning the physical characteristics are listed for each planet, the comets, and asteroids. Another objective of planetary exploration is to determine whether life exists elsewhere in the solar system. A third objective is to make comparisons of the characteristics of the various objects in the solar system. Other objectives are concerned with the determination of the true extent of our solar system and with the utilization of the unique capabilities of man for in situ exploration of the planet Mars. A table is presented with a tentative schedule of solar system space missions during the period from 1971 to 1979. G.R.

A69-42825 * #
FUTURE MANNED AND AUTOMATED EARTH ORBITAL SCIENCE MISSIONS.
Henry J. Smith (NASA, Washington, D.C.).
American Astronautical Society and Operations Research Society of America, Joint National Meeting, Denver, Colo., June 17-20, 1969, AAS Paper 69-036. 9 p.

Review of past achievements in space research, and discussion of the expected scientific knowledge from future manned and automated earth orbital science missions. A general outline is given of the achievements in space research up to the present day, and the future modes of conducting space science research are reviewed. The scientific progress to be expected from the planned orbiting physics and chemistry laboratory is discussed, along with the future space astronomy and earth observations. The possible advances of future aerospace medicine and space biology, offering vital links for understanding the nature of life, are considered. O.H.

A69-42844 * #
SPACE MANUFACTURING UNIQUE TO ZERO GRAVITY ENVIRONMENT.
Hans F. Wuenscher (NASA, Marshall Space Flight Center, Huntsville, Ala.).
American Astronautical Society and Operations Research Society of America, Joint National Meeting, Denver, Colo., June 17-20, 1969, AAS Paper 69-486. 30 p. 11 refs.

Discussion of space manufacturing processes which work only in orbit due to the low and zero gravity environment. Two unique process groups are discussed: buoyancy and thermal convection sensitive processes, and molecular forces controlled processes. Some basic physical data are shown and seven basic processes are described. Examples of unique products are given for each of the process groups. The range of recommended products includes heterogeneous radiation shieldings, isotope fuels, high strength fittings, high purity reactor casings, hollow precision balls, ultrathin membranes for "solid state chemistry," optical components, multilayer curved components, and controlled density materials for armor plates, turbine blades, high temperature structures, and sonar components. All these products have unique new features and can be made only in an extended zero "g" environment; this means these are not cost tradeoff cases of terrestrial vs orbital processing. (Author)

A69-42852 * #
A HISTORICAL NOTE ON THE GENESIS OF MANNED INTERPLANETARY FLIGHT.
Robert B. Merrifield (NASA, Manned Spacecraft Center, Houston, Tex.).
American Astronautical Society and Operations Research Society of America, Joint National Meeting, Denver, Colo., June 17-20, 1969, AAS Paper 69-501. 21 p. 46 refs.

Outline of the history of manned space flight and the development of spacecraft. Nineteenth century speculations about the possibilities of space flight are cited, and the formation of space flight societies between the two World Wars is described. Scientific and technical literature about space flight as well as frictional accounts, are reviewed. The development of rockets during World War Two is interpreted. The beginnings of manned space flights are illustrated in their chronological, logical, and political aspects. The possibilities of future interplanetary flights are discussed. P.G.

A69-42860 * #
INVESTIGATION OF AN EARLY FLYBY SEQUENCE FOR IMAGING OF THE PLANET MERCURY.
Larry A. Manning (NASA, Office of Advanced Research and Technology, Mission Analysis Div., Moffett Field, Calif.).
American Astronautical Society and Operations Research Society of America, Joint National Meeting, Denver, Colo., June 17-20, 1969, AAS Paper 69-258. 22 p. 17 refs.

Analysis of direct and Venus-swingby trajectories to Mercury with regard to optical imaging of the planet from flyby missions. The interplanetary trajectories are coupled with Mercury's rotational

characteristics defining the planetocentric geometry at arrival. The locations of the flyby periapsis and their relationship to the regions of solar illumination are assessed in terms of optical imaging objectives. A representative vidicon type imager is hypothesized for use in mapping the planet at resolutions of 700 to 2000 meters. Three missions are then selected to provide nearly complete mapping of the surface of Mercury, and the resulting coverage is studied in detail. These missions are the 1973 Venus swingby, the low-energy 1974 direct, and the 1975 Venus swingby. The 1973 Venus swingby is the critical opportunity from the surface coverage standpoint. If it is missed, coverage of the same planetocentric longitudes cannot be obtained until the 1980's. The payload capability of representative launch vehicles for these opportunities is determined to be in the range of 1000 to 6000 lb. (Author)

A69-42863 * #
THE PIONEER MISSION TO JUPITER.
H. F. Matthews and C. F. Hall (NASA, Ames Research Center, Moffett Field, Calif.).
American Astronautical Society and Operations Research Society of America, Joint National Meeting, Denver, Colo., June 17-20, 1969, AAS Paper 69-290. 24 p.

Brief review of some broader aspects of the Pioneer F/G mission for flights to Jupiter in 1972 and 1973 initiated recently by NASA for the purpose of exploring the interplanetary medium, the planet and its environment, and the nature of the asteroid belt both scientifically and as a hazard to space flight. The topics covered include the 1972 launch opportunity, the interplanetary trajectory, the scientific experiment program, and the proposed spacecraft design. Also considered are the communication and data control system of the spacecraft. V.Z.

A69-42883 * #
THE PIONEER SPACECRAFT PROGRAM.
Glenn A. Reiff (NASA, Washington, D.C.).
American Astronautical Society and Operations Research Society of America, Joint National Meeting, Denver, Colo., June 17-20, 1969, AAS Paper 69-066. 52 p. 46 refs.

Summary of the origins of the Pioneer program, and description of the configuration of the current spacecraft. The positions of the interplanetary Pioneers, operating in orbits around the sun, enable them to provide unique data needed to forecast the arrival of space disturbances near the earth. The first Pioneers helped pave the way to the moon; the next was a trailblazer into deep space, and the following four established a network of outposts for monitoring the interplanetary medium. A broad morphology of interplanetary phenomena is beginning to emerge. Additional Pioneers are planned for the early 1970's as pathfinders past the orbit of Mars, through the asteroidal belt, and into the vicinity of Jupiter. They are to be joined by the German-developed Helios spacecraft exploring inwards toward the sun. F.R.L.

A69-42887 *
A COMMENT ON THE NEBULOSITY ABOUT FG SAGITTAE.
Karl G. Henize (NASA, Manned Spacecraft Center, Astronaut Office, Houston, Tex.).
Astronomical Society of the Pacific, Publications, vol. 81, June 1969, p. 274, 275. 5 refs.

Discussion of the nebulosity around FG Sagittae, first observed and photographed by Henize (1961). Herbig and Boyarchuk (1968) made a detailed astrophysical study of this object, and point out its probable significance to the study and origin of planetary nebulae. They conclude that the characteristics of the nebulosity indicate that it was ejected from the star approximately 3000 years ago, and that the evolution of the spectrum of the star from 1955 to 1967 strongly suggests that the star is currently ejecting a second nebular shell. F.R.L.

A69-42890 *
ILMENITE IN ORDINARY CHONDRITES.
Kenneth G. Snetsinger (NASA, Ames Research Center, Space Sciences Div., Moffett Field, Calif.) and Klaus Keil (New Mexico, University, Dept. of Geology and Institute of Meteoritics, Albuquerque, N. Mex.).
American Mineralogist, vol. 54, May-June 1969, p. 780-786. 11 refs.

Discussion of the average composition of ilmenite for "equilibrated" ordinary chondrites. The iron content of ilmenite tends to increase when passing from H- to L- to LL-group chondrites, whereas magnesium and manganese have the reverse tendency. Because the iron and magnesium variation is the same as observed in pyroxene, olivine, and chromite of equilibrated chondrites, it is suggested that ilmenite is in equilibrium with these minerals. F.R.L.

A69-43197 *
LASER BEAM DIRECTED AT THE LUNAR RETRO-REFLECTOR ARRAY—OBSERVATIONS OF THE FIRST RETURNS.
James Faller, Irvin Winer (Wesleyan University, Middletown, Conn.), Walter Carrion, Thomas S. Johnson, Paul Spadin (NASA, Goddard Space Flight Center, Greenbelt, Md.), Lloyd Robinson, E. Joseph Wampler, and Donald Wieber (California, University, Lick Observatory, Santa Cruz, Calif.).
Science, vol. 166, Oct. 3, 1969, p. 99-102.
NSF Grant No. GP-6310; Contract No. NAS 5-10752; Grant No. NGR-07-006-005.

Detection of return signals from an optical retroreflector array placed on the moon by the Apollo 11 astronauts. After the return signal was first detected it continued to appear with the expected time delay for the remainder of the night. The observed range is in excellent agreement with the predicted ephemeris. Transmitting between 7 and 8 joules per pulse, it was found that each return signal averaged more than one photoelectron. This is in good agreement with calculations of the expected signal strength. (Author)

A69-43254 * #
EFFECT OF THE MOON'S INFRARED EMISSION ON THERMAL CALCULATIONS.
James K. Harrison (NASA, Marshall Space Flight Center, Space Sciences Laboratory, Huntsville, Ala.).
Journal of Spacecraft and Rockets, vol. 6, Sept. 1969, p. 1059-1061. 5 refs.

Use of the expression developed by Ashby and Burkhard (1967) for predicting the directional IR emission from the lunar surface in order to calculate the temperature of an object near the surface. This result is then compared to a similar calculation, taking the surface emission to be diffuse. When making thermal calculations of objects on the moon's surface, the directional characteristics should be taken into account to obtain the greatest amount of accuracy. F.R.L.

N69-10470*# National Aeronautics and Space Administration. Electronics Research Center, Cambridge, Mass.
A COMPARISON OF A CLASS OF EARTH-MOON ORBITS WITH A CLASS OF ROTATING KEPLER ORBITS
R. F. Hoelker and B. P. Winston Washington Nov. 1968 65 p refs
(NASA-TN-D-4903) Avail: CFSTI CSCL 22C

In two concurrent series of graphs, a class of orbits in the Earth-Moon (E-M) field and a class of Kepler orbits in rotating coordinates are depicted and compared. A general discussion of characteristics of rotating Kepler orbits is included. The model used for the E-M orbits is that of the restricted problem of three bodies. The orbits of the class depicted originate at the E-M line, half of the E-M distance beyond the moon with velocity orthogonal to the E-M line within the E-M plane. Author

N69-10756*# National Aeronautics and Space Administration. Ames Research Center, Moffett Field, Calif.
RESPONSE ENVELOPE: A GLOBAL DESCRIPTION OF THREE-AXIS LARGE ANGLE SPACECRAFT ATTITUDE CONTROL SYSTEMS
George Meyer Washington Nov. 1968 34 p refs
(NASA-TN-D-4896) Avail: CFSTI CSCL 22B

Arbitrary three axis, large angle attitude control systems of highly maneuverable spacecraft capable of tracking time-varying target attitudes are considered. Such systems are inherently

multivariable, multidimensional, nonlinear, and nonautonomous with infinite sets of forcing functions and initial conditions. The concept of a response envelope is introduced. It provides an analytical procedure for judging whether a proposed attitude control system of this type is fast enough for the mission of the spacecraft. It is defined as a scalar function of time which at each instant is the maximum possible three-dimensional attitude error between spacecraft and target for any admissible initial condition, time variation of target attitude, and disturbance. A simple procedure is presented for computing the response envelope approximately. The approximation is conservative and may be used as a basis for accepting a proposed system. The procedure is based on the Liapunov theory and a prototype of general attitude control systems. The proposed procedure is illustrated by a numerical example based on an Orbiting Astronomical Observatory. Author

N69-13274*# Michigan Univ., Ann Arbor.
ON THE GENERATION OF IDEAL COORDINATE SYSTEMS FOR THE ANALYSIS OF OPTIMAL TRAJECTORIES
William F. Powers Washington NASA Dec. 1968 24 p refs
(Contract NASr-54(06))
(NASA-CR-1250) Avail: CFSTI CSCL 22C

A relatively well-known property of continuously thrusting optimal trajectories is that there exists a vector constant of the motion which is linear in the Lagrange multipliers. Since the relationship between the corresponding Lagrange multipliers for different sets of state variables is linear, the possibility exists that there is an ideal coordinate system such that three of the associated Lagrange multipliers are constants of the motion. It is shown that such a situation is impossible for more than one of the three constants of the motion. However, a method due to Whittaker is applicable to the problem of generating sets of state variables such that one of the corresponding Lagrange multipliers is a constant of the motion. It is shown that the system of variables generated by cylindrical coordinates possesses this property and, for a large class of problems, the remaining constants of the motion are used effectively to reduce from twelve to nine the number of differential equations which define three-dimensional, optimal trajectories. Author

N69-13300*# Michigan Univ., Ann Arbor.
COMPUTER MECHANIZATION OF REENTRY EQUATIONS WITH FOUR DEGREES OF FREEDOM
R. M. Howe Washington NASA Dec. 1968 14 p refs
(Contract NASr-54(06))
(NASA-CR-1249) Avail: CFSTI CSCL 22C

An effective method for controlling the flight path of a vehicle during reentry into the atmosphere is to utilize aerodynamic lift forces. By controlling the bank angle of the vehicle the lift force vector can be directed upwards or downwards to effect the down-range impact point, or sidewards to effect the cross-range impact point. In computing trajectories for such vehicles there are fundamentally four degrees of freedom which must be represented. These are the three translational degrees of freedom and one rotational, namely the roll motion. In solving the translational equations for reentry there are sizable computing advantages in using a modified flight-path axis system called the H-frame. The purpose of this report is to add the fourth degree of freedom to these equations in order to allow the trajectory computation for lifting reentry vehicles with controlled bank angle. Author

N69-13844*# National Aeronautics and Space Administration, Washington, D. C.
OBJECTIVES AND GOALS IN SPACE SCIENCE AND APPLICATIONS 1968
John E. Naugle 1968 97 p refs
(NASA-SP-162) Avail: SOD $1.50; CFSTI CSCL 22

The objectives, current programs, and future mission options developed during planning efforts to integrate program activities on a NASA-wide basis are presented in synoptic, nontechnical form. The main areas considered pertain to space physics, astronomy, lunar exploration, planetary exploration, bioscience, and space applications. Several viewpoints are included on the relative emphasis which should be placed on future program options. M.G.J.

N69-14392*# Michigan Univ., Ann Arbor. Radio Astronomy Observatory.
INSTRUMENTATION FOR RADIO ASTRONOMY MEASUREMENTS ABOARD THE OGO-5 SPACECRAFT
B. D. MacRae 20 Sep. 1968 142 p refs
(Contract NAS5-9099)
(NASA-CR-98670) Avail: CFSTI CSCL 22A

This report describes the design considerations and performance characteristics of a satellite-borne instrumentation system designed and constructed at the University of Michigan Radio Astronomy Observatory. The system is designed to make radio astronomy measurements at eight discrete frequencies from 50 kHz to 3.5 MHz. These measurements are to detect Solar and Jovian radio frequency bursts and to determine the relative average level of cosmic background radiation down to 50 kHz. Procedures used for preflight and in-flight noise calibrations are discussed. A description of the ground support equipment used for preflight testing is given. The instrument was successfully launched aboard the OGO-V(E) spacecraft on 4 March 1968 into an elliptical orbit having the following approximate parameters: perigee, 292 kilometers; apogee, 147,000 kilometers; inclination to the equator, 31°; period, 63 hours, 25 minutes. The initial data from the instrument looks excellent and the instrument should successfully fulfill its missions. The scientific aspects and results of this program will be published separately. Author

N69-14428*# National Aeronautics and Space Administration. Manned Spacecraft Center, Houston, Tex.
A COMPUTER PROGRAM FOR CALCULATING EXTERNAL THERMAL-RADIATION HEAT LOADS AND TEMPERATURES OF SPACECRAFT ORBITING THE PLANETS OR THE MOON
Harold L. Finch (Midwest Res. Inst.), Duncan Sommerville (Midwest Res. Inst.), Robert Vogt, and Davis Bland Washington Dec. 1968 195 p refs
(NASA-TR-R-278) Avail: CFSTI CSCL 22A

A versatile computer program to predict the thermal history of a spacecraft orbiting a celestial body is documented. With this program, all external thermal-radiation heat loads, thin-skin temperatures, or both, are computed for a spinning or oriented spacecraft as a function of orbit position and time. The generalized program applies to any spacecraft configuration. A major feature of the program is its applicability to effects resulting from the extreme surface temperature of the Moon. Author

N69-14479*# National Aeronautics and Space Administration. Goddard Space Flight Center, Greenbelt, Md.
APPLICATION OF HANSEN'S METHOD TO THE Xth SATELLITE OF JUPITER
Peter Musen, Jesse L. Maury, and Milton Charnow (Computer Sci. Corp.) Washington Dec. 1968 26 p refs
(NASA-TN-D-4979) Avail: CFSTI CSCL 03C

New orbital elements and the table of the general perturbations of the Xth satellite of Jupiter are presented. A modification of Hansen's theory was the theoretical foundation for the programming and for the expansion of Hansen's coordinates of the satellite into trigonometric series in four basic arguments. The complete collection of formulas is given, and the program and operations for handling the expansions and for integrating the differential equations of the theory by means of iteration are described. The new set of elements represents the observations in the interval 1938–1967 better than the previous sets. The residuals are now of the order of only a few seconds of arc. Author

N69-14861*# National Aeronautics and Space Administration. Manned Spacecraft Center, Houston, Tex.

MATCHED CONIC SOLUTIONS TO ROUND TRIP INTERPLANETARY TRAJECTORY PROBLEMS THAT INSURE STATE-VECTOR CONTINUITY AT ALL BOUNDARIES

Victor R. Bond Washington Jan. 1969 36 p refs
(NASA-TN-D-4942) Avail: CFSTI CSCL 22C

A technique is presented for computing the matched-conic solutions of interplanetary trajectories for use as reference trajectories in guidance and navigation simulations. Continuity in position, velocity, and time at the sphere of influence is insured. The chief advantage of the matching technique is its capability of being adapted to several mission types. Examples are presented of the types of missions considered: the free-flyby mission, the powered-flyby mission, and the stopover mission with a parking orbit about the target planet. Author

N69-14943*# International Information, Inc., Philadelphia, Pa.

THEORY OF MOTION OF THE PLANET PLUTO. PART 2: PLUTONIAN PERTURBATION OF THE SECOND ORDER WITH RESPECT TO PERTURBING MASSES. PART 3: RECALCULATION OF FIRST-ORDER PLUTONIAN PERTURBATIONS WITH RESPECT TO PERTURBING MASSES. PART 4: NEW ELEMENTS OF PLUTO [TEORIYA DVIZHENIYA PLUTONA. CHAST' VTORAYA. VOZMUSHCHENIYA PLUTONA VTOROGO PORYADKA OTNOSITEL'NO VOZMUSHCHAYUSHCHIKH MASS. CHAST'TREY'YA. PEREVYCHISLENIYE VOZMUSHCHENIY PLUTONA PERVOGO PORYADKA OTNOSITEL'NO VOZMUSHCHAYUSHCHIKH MASS. CHAST'CHETVERTAYA. NOVYYE ELEMENTY PLUTONA]

Sh. G. Sharaf et al Washington NASA Jan. 1969 180 p refs *Transl. into ENGLISH from Tr. Inst. Teor. Astron. (Moscow)*, v. 10, 1964
(Contract NASw-1499)
(NASA-TT-F-491) Avail: CFSTI CSCL 03C

The Plutonian perturbations of the second order are determined in relation to the masses of Jupiter, Saturn, and Uranus. The Laplace–Newcomb method is utilized for the calculations. Newcomb operators, as related to mean anomalies, are employed in the calculation of the perturbation function. The equations of motion are obtained, the second members evaluated, and formulas presented for the determination of long-period terms by a more convenient method. Then the Plutonian perturbations of the first order are determined once again in relation to the masses of the large planets, using the new elements of Pluto, while increasing the accuracy of the development of the perturbing function, and while using formulas transformed by the long-period perturbations of Pluto due to Uranus. Tables of coefficients of Newcomb operators are presented. The Plutonian elements are corrected according to observations made between 1914 and 1958. Author

N69-14944*# International Information, Inc., Philadelphia, Pa.

THEORY OF MOTION OF THE PLANET PLUTO. PART 1: PLUTONIAN PERTURBATIONS OF THE FIRST ORDER WITH RESPECT TO PERTURBING MASSES [TEORIYA DVIZHENIYA PLUTONA. CHAST'PERVAYA. VOZMUSHCHENIYA PLUTONA PERVOGO PORYADKA OTNOSITEL'NO VOZMUSHCHAYUSHCHIKH MASS]

Sh. G. Sharaf Washington NASA Jan. 1969 148 p refs Transl. into ENGLISH from Tr. Inst. Teor. Astron. (Moscow), v. 4, 1955
(Contract NASw-1499)
(NASA-TT-F-490) Avail: CFSTI CSCL 03C

Perturbations of the first order by the four large planets were determined. A preliminary improvement of Bauer's elements was performed, based on observations made between 1914 and 1951. Newcomb's method of expanding the perturbation function, the methods of controlling the operator coefficients, and the technique for calculating the expansion coefficients of the perturbation function on analytic computers are outlined. Methods for determining the perturbations of the logarithm of the radius vector, length of the orbit; length of the node and inclination, and the constants of integration are given as well as the perturbations by Neptune between 1912 and 1955. A summary of the Plutonian observations and of the normal positions is presented as well as a method for correcting the elements applied to Pluto and the new Plutonian elements. The symbolic expansion of the perturbation function, a table of operator coefficients, the partial values of the operators for computing corrections for the second term, and some errors in the expressions for Newcomb's operators are included. Author

N69-16210*# National Aeronautics and Space Administration. Langley Research Center, Langley Station, Va.

A COMPUTATIONAL METHOD FOR TIME-OPTIMAL SPACE RENDEZVOUS

Ernest S. Armstrong and Athena T. Markos Washington Jan. 1969 58 p refs
(NASA-TN-D-5017) Avail: CFSTI CSCL 22C

A method is presented for obtaining space rendezvous trajectories between a one stage rocket vehicle and a target in a circular Keplerian orbit. The trajectories satisfy the necessary conditions of the Pontryagin maximum principle for time optimal rendezvous in which no terminal mass constraint is placed on the rocket. The use of Pontryagin's theory leads to a two point boundary value problem. A digital program is given for the iterative solution of this problem. The method is successfully applied for the determination of time optimal rendezvous trajectories between a vehicle launched from the surface of the moon and a target in an 80 nautical mile circular orbit. Author

N69-16571*# *National Aeronautics and Space Administration*, Washington, D. C.

THE BOOK OF MARS

Samuel Glasstone 1968 315 p refs
(NASA-SP-179) Avail: SOD $5.25 CSCL 03

This book contains information about Mars, gained over a period of years by many scientists throughout the world, from the use of sensitive instruments and theoretical evaluation. The possibility of life on Mars is analyzed and guidelines for avoidance of Mars contamination during spacecraft exploration of the planet are included. G.G.

N69-17305*# National Aeronautics and Space Administration. Lewis Research Center, Cleveland, Ohio.

TWO-BURN ESCAPE MANEUVERS WITH AN INTERMEDIATE COASTING ELLIPSE

Edward A. Willis, Jr. Washington Feb. 1969 31 p refs
(NASA-TN-D-5011) Avail: CFSTI CSCL 22C

Escape maneuvers having two burns separated by a coasting ellipse are compared with conventional single-burn maneuvers for low circular initial orbits and a wide range of launch energies. One- and two-stage vehicles with nuclear and chemical propulsion are considered. This two-burn escape mode yields significantly lower initial mass and engine size, and improved launch window capability. Author

N69-17815*# National Aeronautics and Space Administration. Marshall Space Flight Center, Huntsville, Ala.

THERMAL AND DIELECTRIC PROPERTIES OF A HOMOGENEOUS MOON BASED ON MICROWAVE AND INFRARED TEMPERATURE OBSERVATIONS

Ted A. Calvert Washington Feb. 1969 43 p refs
(NASA-TM-X-1734) Avail: CFSTI CSCL 03B

A homogeneous lunar model was used to establish theoretically the relationship of the thermal properties of the moon to its dielectric properties. This was accomplished using lunar observational data obtained in the microwave and infrared wavelengths. Measured values of loss tangent, dielectric constant, and thermal diffusivity for postulated lunar materials are compared to values calculated from microwave and infrared observations. Lunar microwave brightness temperatures are compared to subsurface temperatures based on

selection of a thermal parameter and a depth into the lunar interior. The measured values of loss tangent and dielectric constant for the postulated materials agree with the values based on lunar observations; however, it is not possible to establish which sample offers the best comparison. The microwave brightness temperature curves do not offer good agreement with the calculated subsurface temperatures since the phase lag and amplitudes could not be made to agree simultaneously. As a result, it may be possible to use the homogeneous model to relate the electrical properties of the lunar material to its thermal properties. Author

N69-20810*# National Aeronautics and Space Administration. Lewis Research Center, Cleveland, Ohio.

OPTIMAL THREE DIMENSIONAL LAUNCH VEHICLE TRAJECTORIES WITH ATTITUDE AND ATTITUDE RATE CONSTRAINTS

Fred Teren and Omer F. Spurlock Washington Mar. 1969 49 p refs

(NASA-TN-D-5117) Avail: CFSTI CSCL 22C

Equations are derived for maximizing payload capability for nonplaner boost trajectories arising from range safety considerations. The assumed range safety constraints are satisfied by requiring a fixed vehicle azimuth heading during the initial part of the trajectory. This azimuth (attitude) constraint is removed as soon as certain land areas have been avoided. An attitude rate limit is also imposed to prevent discontinuous attitude changes. The calculus of variations is used to formulate and solve the mathematical problem. A simplified method is also presented for obtaining the auxiliary variational terminal conditions associated with free end conditions. Sample results are presented for sun-synchronous and planetary missions. Author

N69-20916*# National Aeronautics and Space Administration, Washington, D. C.

MODELS OF VENUS ATMOSPHERE, 1968

Robert A. Schiffer (JPL) and Andrew J. Beck (JPL) Dec. 1968 32 p refs

(NASA-SP-8011) Avail: CFSTI CSCL 03B

This monograph provides a set of engineering models of the Venus atmosphere, based on theory and data. In preparing these models, an assessment was made of the effects which planetary atmospheric characteristics might have on the performance of the space vehicle and its major subsystems. These characteristics include the structure, composition, and dynamics of the atmosphere, which can have both aerodynamic and thermal effects on the space vehicle. Of these atmospheric variables, the vertical distribution of mass density is regarded as the most critical parameter for design functions which involve aerodynamic effects. However, chemical composition and temperature structure also require definition because they affect density and thermal calculations. In addition, the viscosity, specific heats, and speed of sound influence vehicle aerothermodynamic analyses; and atmospheric winds affect entry dynamics for terminal descent. Finally, the atmospheric aerosol content and opacity constrain the design of landed solar power systems and influence performance of communications equipment. Author

N69-21018*# National Aeronautics and Space Administration. Langley Research Center, Langley Station, Va.

EFFECT OF GRAVITATIONAL-MODEL SELECTION ON ACCURACY OF LUNAR ORBIT DETERMINATION FROM SHORT DATA ARCS

Harold A. Hamer and Katherine G. Johnson Washington Mar. 1969 40 p refs

(NASA-TN-D-5105) Avail: CFSTI CSCL 22C

The purpose of the present report is to give an insight into the accuracy of lunar orbit determination which may be expected with gravitational models having relatively few coefficients. The gravitational models investigated included the spherical harmonics through the fourth order. The results of the analysis were obtained by fitting tracking data from Lunar Orbiter Missions I and III. Relatively short data arcs of a few orbital periods were used in determining the orbit. For the most part, the JPL program was used for the data fits; additional results are presented in which up to 21 coefficients were determined from the Lungfish (lunar gravitational field in spherical harmonics) orbit-determination program. The orbit-determination accuracy was analyzed by studying the effects of varying the gravitational model and the length of the data arc. In certain cases the gravitational coefficients were solved for and in others the coefficients were held fixed at predetermined values. Various criteria used to compare the cases included results from the fitted data arc as well as data predicted ahead of this arc. Author

N69-21506*# California Inst. of Tech., Pasadena.

STABLE CRACK PROPAGATION IN A VISCOELASTIC STRIP

Hans-Karl Mueller (Ph.D. Thesis) Washington NASA Mar. 1969 145 p refs

(Grant NsG-172-60)

(NASA-CR-1279) Avail: CFSTI CSCL 20K

A crack of given length propagating with small, constant speed through a viscoelastic strip is considered. The strip is strained by displacing its shearfree edges. Linear theory is applied. The stress on the line of crack advancement and the shape of the crack surface are calculated for a state of plane stress. The energy which is released when the crack extends a small distance is calculated. This crack energy depends on the crack speed and involves the creep function of the material. A characteristic length enters in the course of its derivation. This length does not appear in the case of an elastic material and is considered as an additional material property necessary to describe visco-elastic crack propagation. The energy conservation equation is established by considering a small control volume surrounding the crack tip. The relevant material properties are discussed and presented for a polyurethane rubber (Solithane 113–50/50). The results of the material characterization are used to calculate the crack speed as a function of applied strain and temperature. Author

N69-21526*# National Aeronautics and Space Administration. Marshall Space Flight Center, Huntsville, Ala.

SCIENTIFIC EXPERIMENTS FOR THE APOLLO TELESCOPE MOUNT

Washington Mar. 1969 60 p refs

(NASA-TN-D-5020) Avail: CFSTI CSCL 17H

The Apollo Telescope Mount is to be a manned solar observatory to make measurements of the sun by placing telescopes and instruments above the earth's atmosphere. These instruments will obtain data on the transitions occurring in elements ionized in the vicinity of the sun's surface. These data are contained in the ultraviolet and x-ray spectrum that is almost completely absorbed by the earth's atmosphere. Orbiting telescopes would also observe flares and regions of the corona that are either hidden to telescopes on earth or are covered with scattered light. The white light coronagraph experiment will therefore be operated outside the light scattering effects of the earth's atmosphere. Two ultraviolet experiments will obtain spectral line intensity and high spectral resolution measurements. Two x-ray experiments will be used to study solar flares and the dynamics of the solar atmosphere. Descriptions of these five experiments and the associated equipment are presented in this report. Author

N69-22226*# National Aerounautics and Space Administration, Washington, D. C.

SIXTH ANNUAL MEETING OF THE WORKING GROUP ON EXTRATERRESTRIAL RESOURCES

1968 247 p refs Meeting held at Brooks AFB, Tex., 19–21 Feb. 1968

(NASA-SP-177) Avail: CFSTI CSCL 22A

In the conference papers presented, attention was focused on various aspects of environment and resources; mining and

processing; biotechnology and human factors; facility design, construction, and operation; and logistic requirements. For individual titles, see N69-22227 through N69-22246.

N69-22571*# National Aeronautics and Space Administration. Langley Research Center, Langley Station, Va.
INVESTIGATION OF OCCULTATION AND IMAGERY PROBLEMS FOR ORBITAL MISSIONS TO VENUS AND MARS
Richard N. Green Washington Apr. 1969 64 p refs
(NASA-TN-D-5104) Avail: CFSTI CSCL 22B

A computer program for the purpose of providing mission design data for planetocentric elliptical orbits about either Mars or Venus was developed. The times at which the satellite enters into and exits from the shadows of the Sun, Earth, and Canopus are computed. In addition, the positions in orbit that correspond to desirable lighting conditions on the surface for vertical photography are computed. A program option allows for these conditions to be examined at various times by permitting the planet to proceed in its orbit about the Sun. The mean heliocentric position of the planet, the angles in the Earth-Sun-planet triangle, and the associated distances are also included in the list of output parameters. The program is written in Fortran IV language for a digital computer and contains 27 subroutines of general use. A description of the program input and output, a complete Fortran listing of the program, and samples of the input and output are included. Author

N69-22939*# National Aeronautics and Space Administration. Langley Research Center, Langley Station, Va.
EFFECTS OF CLOUD COVER ON SELECTION OF RECOVERY SITES FOR FUTURE EARTH ORBITAL MISSIONS
Paul F. Holloway Washington Apr. 1969 20 p refs
(NASA-TN-D-5120) Avail: CFSTI CSCL 04B

Climatological summaries are shown to be very useful as a site-selection constraint. A possible global recovery network has been proposed which can be considered as a nucleus for most future earth orbital recovery operations. This analysis has been based on climatological summaries of the probability of 3/10 or less cloud cover. A cursory analysis of other weather conditions at the sites, such as surface winds, ceiling height, gusts, and air turbulence, has indicated that no particular conditions might be expected which would rule out any of the recommended recovery sites from future consideration. Author

N69-23708*# National Aeronautics and Space Administration. Langley Research Center, Langley Station, Va.
COMPUTER SIMULATION OF A CYLINDRICAL GALAXY
Frank Hohl Washington May 1969 51 p refs
(NASA-TN-D-5200) Avail: CFSTI CSCL 03B

A two-dimensional computer model is used to investigate the evolution of a self-gravitating cylindrical galaxy. The evolution of systems containing up to 100,000 mass rods is investigated by following the self-consistent motion of the mass rods. As the system evolves in time, it displays the various shapes observed in actual galaxies; however, any spiral structure which appears during the initial stages of the evolution disappears after about 10 rotations, and the final state of the system is that of a rotating bar or a circular cluster with a high central condensation. It is found that violent relaxation of phase mixing causes any unstable system quickly to build up large random velocities. The rate of buildup of random motions in stable systems was found to be described by a Chandrasekhar-type relaxation time. Author

N69-23782*# National Aeronautics and Space Administration. Goddard Space Flight Center, Greenbelt, Md.
A GRAPHIC METHOD FOR DETERMINING THE ABSOLUTE ATTITUDE OF SOUNDING ROCKET VEHICLES
Charles F. Miller, Jr. Washington May 1969 20 p refs
(NASA-TN-D-5172) Avail: CFSTI CSCL 22C

Measurements show that a rocket axis may trace out a complex attitude sequence. Using measurable parameters, a method is outlined which plots these three dimensional phenomena in two dimensions. The sun and its position, and the magnetic flux vector and its position, are used in combination with the solar and magnetic aspect angles at the rocket to determine attitude. When the time sequence of rocket attitudes is plotted, the momentum vector can be accurately determined. With any known rocket position, any other portion of the sky can, by coordinate transformation, be mapped from that orientation. The method was corroborated by a FORTRAN program. Author

N69-24170*# National Aeronautics and Space Administration. Goddard Space Flight Center, Greenbelt, Md.
A SEARCH FOR GAMMA-RAYS FROM THE CRAB NEBULA USING A DIGITIZED SPARK CHAMBER
Donald Avery Kniffen Washington May 1969 73 p refs
(NASA-TR-R-308) Avail: CFSTI CSCL 03B

Gamma ray astronomy provides an opportunity to obtain information directly related to the physical processes taking place within celestial objects; processes that may also give rise to the energetic charged particle cosmic rays. The detection of celestial gamma ray point sources may shed some light on the origin of cosmic rays. One of the most likely sources, the Crab nebula, was chosen for investigation in this experiment. The detector developed for this investigation is a digitized spark chamber, mounted in an oriented gondola and flown by balloon above all but a small amount of the earth's atmosphere. The detector is triggered by a scintillation counter Cerenkov detector charged particle telescope, in the event that no charged particle has passed through the anticoincidence scintillator that surrounds the entire detector. Analysis of the data consists of examining each event recorded during the flight for the pair-production events. The celestial arrival direction of each gamma ray is estimated by the bisector of the pair. The construction of the chamber with many thin plates alternated with the spark modules allows a determination of the gamma ray energy in the 30- to 250-Mev energy range by the multiple scattering technique. Author

N69-24206*# Scientific Translation Service, La Canada, Calif.
ATLAS OF THE REVERSE SIDE OF THE MOON, PART 2
Yu. N. Lipskiy et al Washington NASA. Apr. 1969 92 p refs Transl. into ENGLISH of the Publ. "Atlas Obratnoy Storony Luny. Chast' 2" Moscow, Nauka Press, 1967
(Contract NASw-1496)
(NASA-TT-F-514) Avail: CFSTI CSCL 03A

An atlas has been compiled of photographs and data derived from Zond-3 observations of the reverse side of the moon. Discussed in the report are: (1) a description of the satellite and its flight to the moon; (2) details of the on-board phototelevision system; (3) extension of a single system of selenographic coordinates to the eastern section of the reverse side of the moon; (4) analysis of photographs, compilation of a map, and catalog of formations discovered; (5) object identification in overlapping region of photographs obtained by Luna-3 and Zond-3; (6) distribution density, size, and shape of craters; (7) topographic features of selected objects; (8) photometric characteristics of selected objects and (9) a brief global survey of the lunar surface. Also included are lists of names proposed for formations discovered on the reverse side of the moon. A.L.

N69-24950*# TRW Systems, Redondo Beach, Calif.
SOME OPTIMAL BRANCHED TRAJECTORIES
Joseph D. Mason Washington NASA May 1969 72 p refs
(Contract NAS1-8011)
(NASA-CR-1331) Avail: CFSTI CSCL 22C

Branched trajectories are a class of trajectories that includes the motion of several vehicles which travel united for some time and then break apart in order to proceed individually to separate end conditions. The problem is transformed to the classical variational problem of Bolza by several linear transformations of time. At this point the established necessary minimizing conditions of optimal

control theory may be applied. A number of applications are considered and numerical solutions are obtained in two cases. -Author

N69-25460*# National Aeronautics and Space Administration, Washington, D. C.
SIGNIFICANT ACHIEVEMENTS IN SPACE SCIENCE 1967
1968 548 p refs
(NASA-SP-167) Avail: SOD $2.50; CFSTI CSCL 03B

CONTENTS:

1. STELLAR ASTRONOMY L. W. Frederick, D. D. Meizel, and A. C. Miller (Va. Univ.) p 1–39 refs (See N69-25461 13-30)

2. SPACE BIOSCIENCE B. Berman (George Washington Univ.) and D. W. Jenkins p 41–137 refs (See N69-25462 13-04)

3. IONOSPHERES AND RADIO PHYSICS S. J. Bauer (NASA. Goddard Space Flight Center) and E. R. Schmerling p 139–161 refs (See N69-25463 13-13)

4. PARTICLES AND FIELDS E. C. Roelof (NASA. Goddard Space Flight Center), L. D. Kavanagh, Jr., and A. W. Schardt p 163–265 refs (See N69-25464 13-24)

5. PLANETARY ATMOSPHERES F. S. Johnson, F. D. Colegrove, W. B. Hanson, R. R. Hodges, Jr., J. E. Midgeley et al p 267–301 refs (See N69-25465 13-30)

6. PLANETOLOGY L. S. Walter, B. M. French, and P. D. Lowman (NASA. Goddard Space Flight Center) p 303–437 refs (See N69-25466 13-30)

7. SOLAR PHYSICS R. G. Teske (Michigan Univ.), G. K. Oertel, H. Glaser p 439–558 refs (See N69-25467 13-30)

N69-26235*# National Aeronautics and Space Administration. Goddard Space Flight Center, Greenbelt, Md.
STATISTICS OF THE REGION OF LACERTA OB1
George Coyne, Jaylee Burley Mead, and Michele Kaufman Washington May 1969 21 p refs
(NASA-TN-D-5060) Avail: CFSTI CSCL 03A

Spectral classes and photographic magnitudes have been determined for 3621 stars in the region of the association Lacerta OB1. Astrophotometer measures of images on glass reproductions of the Palomar Sky Survey plates have been used for the photometry, and spectral classes have been determined by using color equivalents according to the Tikhoff method. The star counts indicate that there is an excess of early A stars on the main sequence in the concentrated region of the association as compared with the dispersed region. Also, the total area of our survey shows deficiency of stars later than F5 as compared with counts in nearby Selected Areas. It is recommended that membership determinations be made for the A stars that constitute the clustering in the concentrated region of the association. Author

N69-26239*# National Aeronautics and Space Administration. Lewis Research Center, Cleveland, Ohio.
UNACCELERATED GEOCENTRIC VELOCITIES AND INFLUX RATES OF SPORADIC PHOTOGRAPHIC METEORS
C. D. Miller Washington NASA May 1969 61 p refs
(NASA-TN-D-5245) Avail: CFSTI CSCL 03B

A weighting factor to correct photographic bias due to mass and velocity was applied to Smithsonian data for over 2000 sporadic meteors. The factor was supported by confirmation of predicted agreement between a velocity histogram for meteors of all masses obtained with its use and a raw distribution for large masses. An equation was found for geocentric velocity distribution unaccelerated by earth gravity. Exponent of mass of 1.34 was obtained in equation for cumulative mass distribution using mass scale of McCrosky and Posen. An average velocity of 13.8 km/sec was obtained, virtually independent of mass. Author

N69-26252*# National Aeronautics and Space Administration. Goddard Spaceflight Center, Greenbelt, Md.
AN ACCURACY AND SPEED COMPARISON OF THE VINTI AND BROUWER ORBIT PREDICTION METHODS
M. L. Bonavito, Stan Watson, and Harvey Walden Washington May 1969 13 p refs
(NASA-TN-D-5203) Avail: CFSTI CSCL 22C

The Viniti orbit prediction method, developed as part of the tracking and prediction program for artificial earth satellites, was compared with the Brouwer orbit prediction method using versions of both methods which consider the first four zonal harmonics of the earth's gravitational field. Several sets of inertial coordinates and velocities for both real and hypothetical satellites were used to produce 100 revolutions of each orbit. Prediction accuracy was investigated by comparing the in-track position error accumulated by each of the two methods every 10 revolutions. In every case it was found that the Vinti method produced considerably less in-track error, while operating at a computational speed comparable to that of the Brouwer method. Furthermore, it was observed that when one attempts to augment the Brouwer method so that its accuracy will be of the same order as that of the Vinti theory, the computational speeds of the two methods are no longer comparable; rather, the Vinti program is estimated to be faster by at least a factor of eight. Author

N69-27169*# Israel Program for Scientific Translations, LTD., Jerusalem.
RR LYRAE STARS
V. P. Tsesevich 1969 365 p refs Transl. into ENGLISH of the book "Zvezdy Tipa RR Liry" Kiev, Izd. Naukova Dumka, 1966 Published for NASA and NSF *Its* Cat. No. 5443
(NASA-TT-F-562; TT-69-55025) Copyright. Avail: CFSTI CSCL 03A

Extensive observations on the individual properties of RR Lyrae stars are discussed, emphasizing problems of the stability and regularity of the oscillations. Topics covered include: stable and nonstable oscillations, regular and irregular variation of periods, and extreme and strange stars. A bibliography and an index to the stars discussed are included. E.C.

N69-27412*# National Aeronautics and Space Administration. Goddard Space Flight Center, Greenbelt, Md.
GRAVITY MODEL COMPARISON USING GEOS 1 LONG-ARC ORBITAL SOLUTIONS
Francis J. Lerch, James G. Marsh, and Brian O'Neill (Wolf Res. and Develop. Corp., Bladensburg, Md.) Washington Jun. 1969 47 p refs
(NASA-TN-D-5035) Avail: CFSTI CSCL 22C

Satellite tracking data have been analyzed using three different sets of coefficients in the mathematical model that describes the earth's gravitational field. The results were intended to be used not as a definitive evaluation of the different coefficients but as an assessment of the effects that different published sets of coefficients, station coordinates, and earth parameters have on orbital geodetic results. Orbital solutions were estimated from optical tracking data from the GEOS I satellite, taken by five major geodetic optical tracking networks. The residual differences between the observed and computed ranges were analyzed for zero-set range bias errors, timing errors, and random errors. These comparisons serve to reinforce what was intuitively obvious–that for long-arc geodetic work, the most complete set of gravity coefficients, together with consistent station coordinates, should be used. Author

N69-28050*# National Aeronautics and Space Administration. Goddard Space Flight Center, Greenbelt, Md.
A SEMI-ANALYTIC THEORY FOR THE MOTION OF A LUNAR SATELLITE
Giorgio E. O. Giacaglia, (Yale Univ.), James P. Murphy, and Theodore L. Felsentreger Washington Jun. 1969 94 p refs
(NASA-TN-D-5043) Avail: CFSTI CSCL 22A

The theory is developed to third order, where first order

is 10^{-2}. Perturbative effects which are considered include those due to the attraction of the moon, earth, and sun, the nonsphericity of the moon's gravitational field, the oblateness of the earth, coupling of lower-order terms, solar radiation pressure, and physical libration. Short-period terms and those with the period of the moon's longitude are produced by means of von Zeipel's method; it is proposed to obtain the secular perturbations, and those depending only on the argument of perilune, by numerical integration of the equations of motion. Author

N69-28441*# National Aeronautics and Space Administration. Ames Research Center, Moffett Field, Calif.

JUPITER SWINGBY MISSIONS TO NONSPECIFIC LOCATIONS IN INTERPLANETARY SPACE

Jerry M. Deerwester Washington Jun. 1969 38 p refs (NASA-TN-D-5271) Avail: CFSTI CSCL 22C

Trajectories based on the Jupiter swingby flight mode that may be appropriate for exploration of interplanetary space are described. Interplanetary space refers to regions of the solar system that can be characterized by perihelion or aphelion distances, heliocentric inclinition, and the like. Trajectories to particular targets (planets, asteroids, or comets) are not considered. The results for seven values of earth departure velocity are summarized as a series of contour charts that depict the features of the post-Jupiter encounter trajectories. The coordinate system employed on these charts is inclination of the passage hyperbola at Jupiter and the pericenter distance. The following post encounter trajectory parameters are illustrated: perihelion and aphelion distances; heliocentric inclinations; and flight times to perihelion, maximum heliocentric latitude, 10 AU, and 50 AU. It is shown that, within this class of Jupiter swingbys, greater trajectory flexibility in terms of reduced flight times, higher inclinations, etc., is achieved with increasing earth departure speed. Author

N69-29115*# National Aeronautics and Space Administration. Langley Research Center, Langley Station, Va.

DETERMINATION OF LUNAR EQUATORIAL RADIUS USING IMAGE-MOTION COMPENSATION SENSOR DATA FROM LUNAR ORBITER I

Harold R. Compton and William R. Wells Washington Jun. 1969 21 p refs (NASA-TN-D-5231) Avail: CFSTI CSCL 03B

The telemetry data from the image-motion compensation sensor (V/H sensor) on the Lunar Orbiter 1 spacecraft were analyzed to determine the radius of the moon in the equatorial region from about 50° west to about 40° east selenographic longitude. The results indicate that over this region the lunar radii determined from these data vary from a minimum of 1734.6 km to a maximum of 1738.6 km. The arithmetic mean of these radii is 1736.5 km or about 1.5 km smaller than the mission planning value of 1738.09 km prior to the Ranger and Lunar Orbiter series of spacecraft. An asymmetrical bulge toward the earth was noted in the general area of Sinus Medii. The values of the lunar radii were compared with those determined from a harmonic analysis, Ranger 8 impact analysis, radar measurements, and photogrammetric techniques. Except for the harmonic analysis, these radii are in good agreement with the Lunar Orbiter values. Author

N69-29557*# National Aeronautics and Space Administration. Ames Research Center, Moffett Field, Calif.

TRIM ATTITUDE, LIFT AND DRAG OF THE APOLLO COMMAND MODULE WITH OFFSET CENTER-OF-GRAVITY POSITIONS AT MACH NUMBERS TO 29

Charles E. De Rose Washington (NASA-TN-D-5276) Avail: CFSTI CSCL 22A

Measurements have been made with free-flight test models of the drag, lift, and trim attitude of a shortened version of the Apollo Command Module for Mach numbers 10 to 29 and free-stream Reynolds numbers 20,000 to 300,000. The tests were performed in a hypervelocity free-flight aerodynamic facility, using models launched from a 1.27-cm bore light-gas gun. Two center-of-gravity positions (offset from the model centerline by 0.046 and 0.028 diameter) were investigated. Resulting trim angles were 151° and 162°, respectively. Lift/drag ratios for the two trim angles were 0.435 and 0.255. Both trim angle and lift/drag ratio showed no variation with Mach number or Reynolds number within the limits investigated. Lift and drag data obtained from this investigation compare quite closely to those obtained from previous wind-tunnel tests and from Apollo flight results. Good agreement of the trim angles was obtained when, in each case, the location of the center of gravity was referenced to the axis of symmetry of the primary pressure supporting surface, the blunt face. Author

N69-29569*# National Aeronautics and Space Administration. Manned Spacecraft Center, Houston, Tex.

TRANSLUNAR ABORT TECHNIQUES FOR NONFREE-RETURN MISSIONS

Gus R. Babb, Jr. Washington Jul. 1969 26 p ref (NASA-TM-X-1806) Avail: CFSTI CSCL 22A

A method of translunar abort for nonfree-return missions is considered in which the service module is jettisoned (more than doubling the abort propulsion capability of the lunar-module descent propulsion system) before the transearth maneuver is performed. During the transearth flight, the lunar module provides the life-support and power requirements for the crew. Author

N69-29738*# National Aeronautics and Space Administration. Lewis Research Center, Cleveland, Ohio.

INTERPLANETARY PROBE MISSIONS WITH SOLAR-ELECTRIC PROPULSION SYSTEMS

Charles L. Zola Washington Jul. 1969 41 p refs (NASA-TN-D-5293) Avail: CFSTI CSCL 22A

A preliminary study is made of trajectories and propulsion system design parameters for solar electric propulsion spacecraft for several interplanetary missions. Using the Atlas–Centaur as a common launch vehicle, payload capability comparisons are also made for each mission between the solar electric propulsion system and an alternative high performance chemical propulsion upper stage. Payload capability of the solar electric system is at least 300 kilograms for flyby missions to Jupiter, Saturn, Uranus, and Neptune, with trip times competitive with or shorter than those of ballistic systems. Loose elliptic capture missions to these four planets, as well as Mars and Mercury, can be accomplished with at least 200 kilograms of payload. Author

N69-30611*# National Aeronautics and Space Administration Goddard Space Flight Center, Greenbelt, Md.

AN ANALYSIS OF SATELLITE POSITIONAL UNCERTAINTY BY STATISTICAL MECHANICS

N. L. Bonavito Washington Jul. 1969 15 p refs (NASA-TN-D-5259) Avail: CFSTI CSCL 22C

This paper treats, from a statistical mechanics viewpoint, the justification for acknowledging satellite positional uncertainty through in-track error buildup. In addition, by relating the angular momentum to a quantity defined as the virial parameter, through a derived quantity defined as the vector density function, it is shown that for any conservative system, the periodic variations, and hence the cross track error, will time average to zero. This is a direct consequence of the conservation of angular momentum. Author

N69-31058*# National Aeronautics and Space Administration. Goddard Space Flight Center, Greenbelt, Md.

THE PIONEER 8 COSMIC DUST EXPERIMENT

Otto E. Berg and F. Frank Richardson Washington Jul. 1969 14 p (NASA-TN-D-5267) Avail: CFSTI CSCL 14B

A cosmic dust sensor comprising a unique array of sensor, sensor controls, and in-flight calibrations was placed in a heliocentric orbit (0.99 to 1.088 a.u.) on December 13, 1967, on board the

Pioneer 8 satellite. The ionization and momentum imparted by the impact of a cosmic dust particle upon a surface are measured by the sensor to determine the particle's direction, speed, and mass. Prelaunch calibration studies using the Goddard Space Flight Center electrostatic accelerator have shown that the sensors can measure kinetic energies of impacting particles as low as 0.6 erg and momenta as low as 2×10^{-5} dyne-sec. Author

N69-31362*# Michigan Univ., Ann Arbor.
ANALYTICAL SOLUTIONS OF A CLASS OF OPTIMUM ORBIT MODIFICATIONS
Nguyen X. Vinh and Christian Marchal Washington NASA Jul. 1969 37 p refs
(Contract NASr-54(06))
(NASA-CR-1379) Avail: CFSTI CSCL 22C

A complete analytical solution of several fundamental problems in orbital corrections is presented. The initial orbit is represented by a given point in the phase space while the final oribit is constrained to stay in a given curve which can be bounded, unbounded, or is composed of a finite number of segments of different curves. The inclusion of atmospheric maneuver as part of the optimum process is discussed, and its analytical treatment can be carried out by modifying the final state to include the set of orbits having their perigees at the boundary of the atmosphere. The selection of the apogee and perigee distances as state variables gives a symmetric form to the problem and results in a linear differential equation of the first order for the ratio of the adjoint variables. The introduction of a curve of comparison, called the separatrix, facilitates the discussion of the existence of a corner on an optimal trajectory. Author

N69-31960*# TRW Systems Group, Redondo Beach, Calif.
AN EXPERIMENTAL FEASIBILITY STUDY FOR THE PREPARATION OF THERMO-OXIDATIVELY STABLE PYRRONE LAMINATES
H. R. Lubowitz, R. J. Jones, H. N. Cassey, R. W. Vaughan, and E. A. Burns Washington NASA Jul. 1969 37 p refs
(Contract NAS1-8384)
(NASA-CR-1404; TRW-11433-6005-R0-00) Avail: CFSTI CSCL 11G

This report describes the preparation of Pyrrone laminates, from a sulfone dianhydride, which would be suitable for long-term exposure to extreme thermal and oxidative environments. The work was divided into three principal tasks: (1) monomer synthesis; (2) polymer synthesis and characterization, and (3) laminate processing and evaluation. Pyrrone resins were prepared from bis (3,4-dicarboxyphenoxyphenyl) sulfone dianhydride and 3,3'-diaminobenzidine. Suitable conditions were determined for preparing laminates from completely soluble Pyrrone precursors. The laminates, which were made under relatively mild processing conditions, had medium void content and had mechanical properties similar to other state of the art condensation polymers. The experimental feasibility study has given results that demonstrate several interesting features of the Pyrrone films and laminates prepared from (3,4-dicarboxyphenoxyphenyl) sulfone dianhydride and 3,3'-diaminobenzidine. This resin gave neat resin and composite properties similar to or exceeding those published for state of the art Pyrrone polymer systems. Author

N69-31989*# Scripta Technica, Inc., Washington, D.C.
PHYSICS OF THE MOON AND PLANETS
I. K. Koval ed. NASA Jun. 1969 116 p refs Transl. into ENGLISH of the book "Fizika Luny i Planet" Kiev, Naukova Dumka Press, 1966
(Contract NASw-1694)
(NASA-TT-F-502) Avail: CFSTI CSCL 03B

CONTENTS:

1. SPECTRAL REFLECTIVE PROPERTIES OF THE LUNAR SURFACE M. N. Mironova p 1–5 refs (See N69-31990 18-30)
2. BRIGHTNESS DISTRIBUTION ALONG THE EQUATOR OF INTENSITY OF VENUS IN THE SPECTRAL INTERVAL 3300 –6700 Å Ye. I. Didychenko p 6–10 refs (See N69-31991 18-30)
3. ELECTROPHOTOMETRIC SECTIONS OF THE DISK OF MARS IN PORTIONS OF THE SPECTRAL INTERVAL 355-600 nm L. A. Bugayenko et al p 11–32 refs (See N69-31992 18-30)
4. THE POSITION OF THE BRIGHTNESS MAXIMUM ON THE DISK OF MARS I. K. Koval p 33–45 refs (See N69-31993 18-30)
5. POLARIZATIONAL PROPERTIES OF THE ATMOSPHERE AND SURFACE OF MARS A. V. Morozhenko p 45–66 refs (See N69-31994 18-30)
6. AN INVESTIGATION OF THE POLARIZATIONAL PROPERTIES OF LIGHT REFLECTED FROM VARIOUS SAMPLES OF TERRESTRIAL ROCKS A. V. Morozhenko p 67–90 refs (See N69-31995 18-30)
7. ULTRAVIOLET ABOSRPTION IN DIFFERENT ZONES OF JUPITER V. V. Avramchuk p 91–97 refs (See N69-31996 18-30)
8. A NEW TYPE OF INTENSITY MICROPHOTOMETER L. A. Bugayenko et al p 98–100 refs (See N69-31997 18-14)
9. AN INVESTIGATION OF THE RELIEF OF THE LUNAR SURFACE IN THE REGION OF THE CRATER KEPLER BY A PHOTOMETRIC METHOD L. R. Lisina p 101–112 refs (See N69-31998 18-30)

N69-32316*# National Aeronautics and Space Administration. Goddard Space Flight Center, Greenbelt, Md.
PARAMETRIC ANGLES OF TRAJECTORY DETERMINED FIELD LINE INTERSECTS PREDICTING THE LOCATION OF ARTIFICIAL AURORAS
E. G. Stassinopoulos Washington Aug. 1969 33 p refs
(NASA-TN-D-5189) CSCL 22C

Geomagnetic field lines are traced from points on a ballistic trajectory to the points where they cross a given altitude shell. The intersects thus obtained are called trajectory determined intersects. Three parametric angles identify and describe their positions: the look-angles ψ and ϵ, azimuth and elevation respectively, which relate an intersect to a fixed location on the earth; and the line angle $\alpha_\odot$. The locus of all trajectory-determined intersects is the intersect trace at the specified altitude level. The intersect trace of a sample rocket trajectory is obtained for the 100 kilometer level. The variations of the parametric angles with time and altitude are calculated for 19 ground locations distributed symmetrically around the launch site. For the specific flight path considered, there exists an area on the earth where optimum parametric angle conditions prevail, i.e., minimum changes in ψ and ϵ, and smallest values of $\alpha_\odot$. Finally, the observer-intersect distance is calculated for all stations. Author

N69-33490*# General Dynamics/Fort Worth, Tex.
SPACE FLIGHT HANDBOOKS, VOLUME 3. PLANETARY FLIGHT HANDBOOK, PART 7: DIRECT TRAJECTORIES TO JUPITER, SATURN, URANUS, AND NEPTUNE. GENERAL DISCUSSION, CONTOUR CHARTS AND RELATED GRAPHICAL INFORMATION
Washington NASA 1969 105 p refs
(Contract NAS2-4982)
NASA-SP-35-Vol-3-Pt-7) Avail: SOD $1.25; CFSTI CSCL 22A

This handbook contains trajectory data and a related series of charts and tables for one-way direct trajectories to Jupiter, Saturn, Uranus, and Neptune. The time period covered is for launch opportunities from 1976–1986 with the exception of trajectories to Jupiter, which span the launch opportunities from 1981 to 1986. Tables of the planetary constants used in the trajectory computations, tables of nodal crossing dates, and auxiliary charts for determining the incremental velocity requirements for departure from earth and entry into orbit at the target planets are included. Along with planetary ephemerides for the years 1970 to 2000.

Hyperbolic excess speed contour charts are presented. The charts display contours of constant excess speeds at earth departure and target planet arrival on a grid of earth departure date and target planet arrival date. The appendix contains a description of a data tape which contains a complete record of the tabular trajectory data. Author

N69-33560*# Techtran Corp., Glen Burnie, Md.
MOTION OF ARTIFICIAL SATELLITES IN THE EARTH'S GRAVITATIONAL FIELD
Yu. G. Yevtushenko, I. A. Krylov, R. F. Merzhanova, and G. V. Samoylovich Washington NASA Jun. 1969 310 p refs Transl. into ENGLISH of the book "Dvizheniye Iskusstvennykh Sputnikov v Gravitatisionnom Pole Zemli" Moscow, Acad. of Sci. Computer Center, 1967
(Contract NASw-1695)
(NASA-TT-F-539) Avail: CFSTI CSCL 22C

Quantitative and qualitative analyses are used to describe the disturbing factors in the motion of artificial earth satellites due to the eccentricity of the earth's gravitational field. Pertinent equations are presented for special forms of disturbing functions in a specially selected coordinate system. Some methods for describing the motion of artificial satellites in an eccentric field of terrestrial attraction are considered. Brief consideration is given to various forces which disturb the Keplerian orbits of artificial earth satellites. J.M.C.

N69-33595*# National Aeronautics and Space Administration. Ames Research Center, Moffett Field, Calif.
CONFERENCE ON ELECTROMAGNETIC EXPLORATION OF THE MOON, 11-13 JUNE 1968 REPORT OF THE PROGRAM EVALUATION COMMITTEE
Washington 1969 27 p refs
(NASA-SP-174) Avail: CFSTI CSCL 22A

Recommendations are made to enhance the contribution that electromagnetic methods might make to lunar exploration. Topics discussed include the purpose and goals of electromagnetic lunar work, the criteria used to evaluate proposed experiments or methods, and the role of budgetary constraints in the recommendations. Three types of experiments are proposed and include the magnetometer experiment, the radio frequency probe, and the pulsed radar probe. A description is given of these experiments together with an analysis of the necessary supporting research and technology. D.L.G.

N69-34850*# General Dynamics Fort Worth, Tex.
PLANETARY FLIGHT HANDBOOK. PART 8: JUPITER SWINGBY MISSIONS TO SATURN, URANUS, NEPTUNE, AND PLUTO
Washington NASA Jan. 1969 131 p refs *Its* Space Flight Handbooks Vol. 3
(Contract NAS2-4982)
(NASA-SP-35; Pt. 8) Avail: SOD $1.50; CFSTI CSCL 22A

Trajectory data and related information for outer-planet swingby missions available during the launch periods 1976 through 1983 are presented. Data for two types of missions are included: single-planet (Jupiter) swingbys to Saturn, Uranus, Neptune, and Pluto and multiplanet swingbys composed of sequential encounters with Jupiter, Saturn, Uranus, and Neptune (referred to as grand tour mission). Author

N69-34884*# National Aeronautics and Space Administration. Langley Research Center, Langley Station, Va.
THE RED-SHIFT MAGNITUDE RELATION AND OBSERVATIONAL DATA
Windsor L. Sherman Washington Aug. 1969 26 p refs
(NASA-TN-D-5398) Avail: CFSTI CSCL 03A

The red-shift – magnitude relation for uniform, zero-pressure models of the universe is one of the stronger relationships connecting theory and observation is cosmology. This relationship has been used to determine models for the universe from the observed apparent magnitudes and red shifts of galaxies. The problems associated with the use of the red-shift – magnitude relation to determine a model universe are discussed. In particular, the effects of evolution and selection on the use of the red-shift – magnitude relation are considered. Selection is the tendency of observers to select intrinsically brighter sources for observation as the distance to the sources increases. The results indicate that the red-shift – magnitude relation should be used with caution when determining a model for the universe because the variation of the intrinsic luminosity of sources must be taken into account. Author

N69-35513*# Control Data Corp., Minneapolis, Minn.
METHOD OF DERIVING ORBITAL PERTURBING PARAMETERS FROM ONBOARD OPTICAL MEASUREMENTS OF AN EJECTED PROBE OR A NATURAL SATELLITE
C. B. Grosch and H. R. Paetznick Washington NASA Aug. 1969 98 p refs
(Contract NAS1-7540; Proj-9580)
(NASA-CR-1412) Avail: CFSTI CSCL 03A

An analytical investigation has been made to evaluate a method of determining perturbing forces by sightings taken from an orbiting spacecraft to a secondary satellite. The sightings, which are angular measurements between the satellite and certain stars, were assumed to be made intermittently over periods ranging from a fraction of one orbit to many days. In the investigation, the accuracy of determining the orbit of the spacecraft and of deriving the forces which perturb the orbit was studied. The study was conducted for spacecraft orbits about Mars, Venus, Moon, and Earth. The perturbing forces due to the gravitation potential of Mars, Venus, and the Moon were considered, as were the forces due to radiation pressure and drag for Earth. Author

N69-36143*# National Aeronautics and Space Administration. Langley Research Center, Langley Station, Va.
APPROXIMATION TO THE STATISTICS OF MIDCOURSE VELOCITY CORRECTIONS
Lawrence H. Hoffman and George R. Young Washington Sep. 1969 40 p refs
(NASA-TN-D-5381) Avail: CFSTI CSCL 22A

A simple approximation for the mean and standard deviation of the magnitude of a statistical velocity correction vector is derived. Approximate methods are presented for making probability statements about the velocity correction vector. These methods are shown to be adequate for calculating the fuel budget for a velocity correction. Comparisons are made with exact results obtained by numerical integration. Results obtained by the root-sum-square method of determining a fuel budget are also compared with the exact numerically integrated results. The data presented indicate that the probability density function of the magnitude of a velocity correction vector can be fitted accurately with a gamma distribution having an integer shape parameter, and thus probability statements about the magnitude can be made. The accuracy of the gamma distribution fit is examined for a number of representative covariance matrices. Author

N69-36439*# International Business Machines Corp., Cambridge, Mass. Federal Systems Div.
RAPID OPTIMIZATION OF MULTIPLE-BURN ROCKET FLIGHTS, 8 MARCH 1968 – 8 MARCH 1969
K. R. Brown, E. F. Harrold, And G. W. Johnson Washington NASA Sep. 1969 55 p refs
(Contract NAS8-21315)
(NASA-CR-1430; IBM-150) Avail: CFSTI CSCL 22C

An indirect (shooting) method was developed for optimization of multiple-burn rocket flights. The method is fast enough to warrant consideration as a real-time guidance scheme, yet it is free of special-purpose approximations or artificial mission restrictions. The

algorithm and the analysis on which it was based are described, and test results indicative of the power of the method are given. Author

N69-36451*# National Aeronautics and Space Administration, Washington, D.C.
SURVEYOR PROGRAM RESULTS Final Report
1969 432 p refs
(NASA-SP-184) Avail: SOD $4.75; CFSTI CSCL 03B

CONTENTS:

1. SURVEYOR PROGRAM RESULTS: INTRODUCTION L. D. Jaffe and R. H. Steinbacher p 1 – 12 refs (See N69-36452 21-31)

2. PRINCIPAL SCIENTIFIC RESULTS FROM THE SURVEYOR PROGRAM L. D. Jaffe, C. O. Alley, S. A. Batterson, E. M. Christensen, S. E. Dwornik et al p 13 – 17 (See N69-36453 21-30)

3. TELEVISION OBSERVATIONS FROM SURVEYOR E. M. Shoemaker, E. C. Morris, R. M. Batson, H. E. Holt, K. B. Larson et al p 19 – 128 refs (See N69-36454 21-30)

4. LUNAR SURFACE MECHANICAL PROPERTIES R. Choate, S. A. Batterson, E. M. Christensen, R. E. Hutton, L. D. Jaffe et al p 129 – 169 refs (See N69-36455 21-30)

5. SOIL MECHANICS SURFACE SAMPLER R. F. Scott and F. I. Roberson p 171 – 179 refs (See N69-36456 21-30)

6. LUNAR SURFACE TEMPERATURES AND THERMAL CHARACTERISTICS J. W. Lucas, W. A. Hagemeyer, J. M. Saari, L. D. Stimpson, and J. M. F. Vickers p 181 – 202 refs (See N69-36457 21-30)

7. LUNAR SURFACE ELECTROMAGNETIC PROPERTIES D. O. Muhleman, W. E. Brown, Jr., L. Davis, J. Negus de Wys, and W. H. Peake p 203 – 269 refs (See N69-36458 21-30)

8. THE ALPHA-SCATTERING CHEMICAL ANALYSIS EXPERIMENT ON THE SURVEYOR LUNAR MISSIONS A. L. Turkevich, W. A. Anderson, T. E. Economou, E. J. Franzgrote, H. E. Griffin et al p 271 – 350 refs (See N69-36459 21-30)

9. LUNAR THEORY AND PROCESSES D. E. Gault, J. B. Adams, R. J. Collins, T. Gold, G. P. Kuiper et al p 351 – 367 refs (See N69-36460 21-30)

10. SURVEYOR POSTTOUCHDOWN ANALYSES OF TRACKING DATA F. B. Winn p 369 – 395 refs (See N69-36461 21-30)

11. LASER BEAM POINTING TESTS C. O. Alley and D. G. Currie p 397 – 403 refs (See N69-36462 21-16)

12. ASTRONOMY: SOLAR CORONA OBSERVATIONS R. H. Norton p 405 refs (See N69-36463 21-30)

13. EFFECTS OF LUNAR PARTICLES ON SPACECRAFT MIRROR SURFACES L. D. Jaffe and J. J. Rennilson p 407 – 412 refs (See N69-36464 21-31)

14. THE LUNAR SUNSET PHENOMENON L. H. Allen p 413 – 418 ref (See N69-36465 21-30)

N69-36892*# National Aeronautics and Space Administration. Goddard Space Flight Center, Greenbelt, Md.
OPTICAL SIMULATION OF A RADIO-ASTRONOMY INTERFEROMETER EXPERIMENT
James P. Strong, III Washington Sep. 1969 15 p
(NASA-TN-D-5357) Avail: CFSTI CSCL 03B

A laser technique has been used to simualte processed output from a proposed spaceborne radio-astronomy interferometer experiment comprising two satellites separated by a controlled distance. The experiment effectively transmits the Fourier transform of the radio stars over the celestial sphere. The Fourier transform is a function of the distance between the two satellites and of the direction of the line connecting them. The existence of upper and lower bounds on the distance between the satellites creates voids in the Fourier transform space, causing resolution problems in the reconstruction of the star pattern on the ground from the Fourier transform. Because coherent optical techniques can obtain the two-dimensional Fourier transform, they can be used to simulate the proposed experiment. Optical filters can be made which represent the voids in the Fourier transform of the star pattern. An inverse transform shows the effects of the filtering, simulating the effects of the voids. Optical filtering in general and the particular optical system used are discussed. Results are shown for 1-MHz and 10-MHz RF sources, representing the worst and the best resolution expected. Author

N69-36930*# National Aeronautics and Space Administration. Goddard Space Flight Center, Greenbelt, Md.
A UNIFIED FORM OF LAMBERT'S THEOREM
E. R.Lancaster and R. C. Blanchard Washington Sep. 1969 15 p refs
(NASA-TN-D-5368) Avail: CFSTI CSCL 12A

A unified form of Lambert's theorem is presented which is valid for elliptic, hyperbolic, and parabolic orbits. The key idea involves the selection of an independent variable x and a parameter q such that the normalized time of flight T is a single-valued function of x for each value of q. The parameter q depends only upon known quantities. For less than one revolution, T is a monotonic function of x for each q, making possible the construction of a simple algorithm for finding x, given T and Q. Detailed sketches are given for T(x, q) and formulas developed for the velocity vectors at the initial and final times. Also included is a careful derivation of the classical form of Lambert's equations, including the multirevolution cases. Author

N69-37777*# National Aeronautics and Space Administration. Lewis Research Center, Cleveland, Ohio.
TABULATIONS OF CONFIGURATION FACTORS BETWEEN ANY TWO SPHERES AND THEIR PARTS
Norman T. Grier Washington 1969 424 p refs
(NASA-SP-3050) Avail: CFSTI CSCL 12A

Tables of values of the configuration factors between two spheres, between parts of one sphere and parts of another sphere, and between a point on one sphere and parts of another sphere are presented. The parts are areas that subtend angles that are multiples of 15° in both the colatitudinal and longitudinal directions. The equations are derived in the bispherical coordinate system. Values are presented for the ratio of radii r_2/r_1 of the spheres from 0.01 to 1.00. The distance between centers of spheres was varied from $(1.001 + r_2/r_1)r_1$ to $100r_1$, where r_1 is the radius of the larger sphere. Conditions corresponding to the earth – moon situation are also included in the calculations. Author

N69-37893*# National Aeronautics and Space Administration. Goddard Space Flight Center, Greenbelt, Md.
PLANETARY EFFECTS IN THE MOTION OF NATURAL SATELLITES
Peter Musen Washington Oct. 1969 28 p refs
(NASA-TN-D-5284) Avail: CFSTI CSCL 03C

Addition of the direct and indirect planetary perturbations to the author's 1963 modification of Hansen's theory is proposed. The method described can determine the Saturnian effects upon the motion of the outer Jovian satellites. The expansion of the disturbing function and of its derivatives is reduced to a form convenient for programming. Author

N69-37993*# California Inst. of Tech., Pasadena. Div. of Physics, Mathematics and Astronomy.
TWO-MICRON SKY SURVEY: A PRELIMINARY CATALOG
G. Neugebauer and R. B. Leighton Washington NASA Aug. 1969 316 p refs Revised
(Grant NGL-05-002-007)
(NASA-SP-3047-Rev) Avail: CFSTI CSCL 03B

In 1965 an infrared sky survey was imitiated. The purpose of the survey was to obtain an unbiased sample of celestial objects that emit in the infrared region and to study their characteristics. Such properties as apparent intensities, colors, variability, and spatial distributions were of primary interest. In addition, it was expected that objects having extreme redness might be found and,

if so, would be of great interest. This catalog contains a complete listing of all objects detected on the survey that had a flux density at 2.2μ exceeding approximately 4 $\times$ 10^{-25} $Wm^{-2}Hz^{-1}$. The data were obtained from January 30, 1965, through April 7, 1968. Because of the limitations in the telescope mounting, the northern limit of the survey was set at plus 81°. The southern limit of minus 33° was set to include the region of the galactic center at minus 30°. Objects at minus 33° are observed through an air mass of 2.58; the extinction effects on observations further to the south become prohibitive. Author

N69-38145*# National Aeronautics and Space Administration, Ames Research Center, Moffett Field, Calif.

A UNIFIED TREATMENT OF LUNAR THEORY AND ARTIFICIAL SATELLITE THEORY

William A. Mersman Washington Oct. 1969 38 p refs

(NASA-TN-D-5459) Avail: CFSTI CSCL 12A

Lunar theory and artificial satellite theory are treated by a unified method that is a generalization of the von Zeipel procedure. The technique of separation of variables is used to generate a single canonical transformation that eliminates the time and all the angle variables from the Hamiltonian. The validity of the method is established and the calculations are carried far enough to illustrate the techniques involved. Author

N69-38643*# Techtran Corp., Glen Burnie, Md.

RADIOPHYSICS: RADIOPHYSICAL INVESTIGATIONS OF VENUS, 1965–1966 [RADIOFIZIKA: RADIOFIZICHESKIYE ISSLEDOVANIYA VENERY, 1965–1966]

A. D. Kuzmin Washington NASA Sep. 1969 158 p refs Transl. into ENGLISH of the Book "Radiofizika. 1965–1966. Radiofizicheskiye Issledovaniya Venery" Moscow, 1967 p 1–151 (Contract NASw-1695)

(NASA-TT-F-536) Avail: CFSTI CSCL 03B

An attempt is made to sum up radio astronomical and radar observations of Venus for a period of 10 years, including information obtained concerning the physical conditions on this planet based upon these observations. The status of research on physical conditions on Venus, based upon data obtained through optical observations and radiophysical investigations are presented. The theory of radio emanation of a planet with a radiation absorbent atmosphere is examined. The relationship between parameters measured in radio astronomic and radar observations, and the physical characteristics of the planet has been determined. A survey of the results of radio astronomic and radar measurements of Venus at the mid-1966 stage is given, and available experimental data defining the physical conditions on Venus are summarized. The direction of further investigations of Venus is projected. Author

N69-38658*# National Aeronautics and Space Administration, Langley Research Center, Langley Station, Va.

A FEASIBILITY STUDY OF DETERMINING PHYSICAL PROPERTIES OF THE MARTIAN ATMOSPHERE BY USE OF SOLAR OCCULTATION AS SEEN FROM AN ARTIFICIAL SATELLITE

H. Andrew Wallio and James R. Williams Washington Oct. 1969 64 p refs

(NASA-TN-D-5443) Avail: CFSTI CSCL 03B

The occultation of sunlight through five model Martian atmospheres as seen from an artificial satellite is examined. The mathematical model of the atmospheres includes effects of refraction, Rayleigh scattering, limb darkening, and finite sun size. The study further shows that it is feasible to use the occultation of the sun as a method of determining scale height and surface pressure provided the shorter visible light wavelengths (3500 angstroms) are used. Author

N69-38769*# National Aeronautics and Space Administration, Marshall Space Flight Center, Huntsville, Ala.

NUMERICAL INTEGRATION IN A RIGID-BODY TRAJECTORY PROGRAM

John Edd Moore Washington Sep. 1969 111 p refs

(NASA-TN-D-5425) Avail: CFSTI CSCL 22C

A comparison is made of the fourth order Runge–Kutta numerical integration technique with two numerical integration formulas in a mathematical model used for computing rigid body, first-stage trajectories of a Saturn space vehicle. The scope of the problem is to describe the mathematical model and to present a derivation of the differential equations of motion which it comprises; to establish a basis for comparing the integration techniques; and to generate sufficient comparison data to establish which integration technique is the most practical to use in this model from a standpoint of computer run time and accuracy. An analysis of the data showed a fourth-order formula to be the most practical integration technique to use in computer programs of this type from a standpoint of computation time, accuracy, and stability of the solution. Author

N69-39213*# National Aeronautics and Space Administration, Langley Research Center, Langley Station, Va.

LUNAR ORBITER 1, PRELIMINARY RESULTS: LUNAR TERRAIN ASSESSMENT AND SELENODESY, MICROMETEOROID, AND RADIATION MEASUREMENTS

J. Kenrick Hughes and Gerald W. Brewer Washington 1969 147 p refs

(NASA-SP-197) Avail: CFSTI CSCL 03B

This mission was designed to examine selected areas along the equator on the lunar near side in preparation for the Apollo manned landing. The preliminary information in this report consists of photographs of the lunar terrain taken from the orbiting spacecraft as well as results of secondary experiments. Terrain selection and photographic evaluation techniques are discussed. The photographs of lunar terrain features are accompanied by commentary and geological interpretations. The secondary studies cover the lunar gravitational field, tracking data, ranging data, lunar radius determination by means of the image-motion compensator (V/H sensor), meteoroid detection, and radiation measurements obtained with the two scintillation dosimeters. K.W.

N69-39336*# National Aeronautics and Space Administration, Marshall Space Flight Center, Huntsville, Ala.

DETERMINATION OF METEOROID ENVIRONMENTS FROM PHOTOGRAPHIC METEOR DATA

Charles C. Dalton Washington Oct. 1969 134 p refs

(NASA-TR-R-322; M-146) Avail: CFSTI CSCL 03B

A mathematical model is used to represent Opik's 1958 physical theory of meteors in a form convenient for programming the computation of meteoroid photometric mass values. Sub-samples of 333 photographic meteors from McCrosky and Posen's sample are selected with respect to magnitude scaled for minimum velocity. A statistical comparison between the 1958 Opik result and the 1933 Opik provisional result, the Harvard-Meteor project basis for mass values, is given. Meteor and orbit parameter distributions and mean cumulative flux in absolute units for mass, momentum and energy are given separately for the terrestrial influx and for the lunar and interplanetary vehicle onfluxes. Author

N69-40062*# Michigan Univ., Ann Arbor.

NON-LINEAR LONGITUDINAL DYNAMICS OF AN ORBITAL LIFTING VEHICLE

Nguyen X. Vinh and Arthur J. Dobrzelecki Washington NASA Oct. 1969 38 p refs

(Contract NASr-54(06))

NASA-CR-1449) Avail: CFSTI CSCL 22C

This paper presents an analytical study of the longitudinal dynamics of a thrusting, lifting, orbital vehicle in a nearly circular orbit. The translation motion is composed of a non-linear oscillation, or phugoid, and a spiral mode which results in either decay or dilatation of the orbit depending on the perturbed initial conditions. The non-linear effects on the phugoid period and damping are small in the altitude range considered. Elements of the orbit such as radial distance, velocity, and flight path angle were

obtained explicitly as functions of time. The behavior of the variations of these elements is correctly predicted. Explicit expressions for period and damping of the angle-of-attack mode were derived. It is shown that a critical altitude may exist at which the phugoid mode and the angle-of-attack mode have nearly equal periods. Near this resonance altitude linearized solutions are no longer valid and a study of the non-linear equations shows that there is a strong interaction between the translational and the rotational modes resulting in a switching of the two frequencies of oscillations. Author

N69-40325*# TRW Systems Group, Redondo Beach, Calif.
SEQUENTIAL PROCESSING TECHNIQUES FOR TRAJECTORY ESTIMATION
C. G. Pfeiffer, D. D. Morrison, R. E. Mortensen, J. V. Breakwell, W. H. Berry et al Washington NASA Oct. 1969 135 p refs
(Contract NAS2-4553)
(NASA-CR-1360) Avail:CFSTI CSCL 22C

This report describes the state of the art in sequential processing techniques for trajectory estimation. A major topic discussed is the effect of nonlinearities, with the aim of developing and justifying practical algorithms for treating the problem. Since nonlinear, maximum likelihood estimation theory has been successfully used in orbit determination for some years, this approach has been emphasized over the more recently suggested nonlinear minimum variance technique. Author

N69-40326*# National Aeronautics and Space Administration, Washington, D.C.
NASA SPACE VEHICLE DESIGN CRITERIA-ENVIRONMENT. METEOROID ENVIRONMENT MODEL—1969 (NEAR EARTH TO LUNAR SURFACE)
B. G. Cour-Palais Mar. 1969 35 p refs
(NASA-SP-8013) Avail: CFSTI CSCL 03C

This monograph treats only the meteoroid environment of cometary origin in the mass range between 10^{-12} and 1 gram at one astronomical unit (1 A.U.) from the Sun near the ecliptic plane. Also included are the lunar ejecta created by the impact of cometary particles on the lunar surface. In this region (1 A.U.) the contribution of asteroidal particles to the total meteoroid population is considered to be negligible. The meteoroid and the lunar surface ejecta flux-mass models and the associated density and velocity characteristics presented herein are for engineering application in the design of space vehicles for near-Earth orbit, cislunar, lunar orbit, and lunar surface missions. Author

N69-40592*# Techtran Corp., Glen Burnie, Md.
OPTIMAL TRANSFERS BETWEEN CLOSE ELLIPTICAL ORBITS [TRANSFERTS OPTIMAUX ENTRE ORBITES ELLIPITIQUES PROCHES]
J. P. Marec Washington NASA Sep. 1969 272 p refs Transl. into ENGLISH from ONERA Publ. no. 121, 1967 p 5-235
(Contract NASw-1695)
(NASA-TT-F-554) Avail: CFSTI CSCL 22C

The optimal rendezvous and transfers (minimum mass consumption for a given duration) between close elliptical orbits are analyzed in the case of propulsion systems characterized by a constant ejection velocity and a limited thrust; the performance obtained is compared to the performance of propulsion systems characterized by a modulable thrust and a limited power. The choice of the orbital elements as state components, added to the linearization hypothesis, leads to important simplifications (the adjoint vector is constant, in particular). This gives some general results concerning, among others things, the number of maximum thrust arcs per revolution, the singular cases when the linearized solution is not unique but degenerates into a large number of solutions and the induction phenomena (nonimposed variations of some orbital elements, induced by the imposed variations of the other orbital elements). Author

N69-41150*# National Aeronautics and Space Administration, Washington, D.C.
A LONG-RANGE PROGRAM IN SPACE ASTRONOMY: POSITION PAPER OF THE ASTRONOMY MISSIONS BOARD
Robert O. Doyle (Harvard College Obs.), ed. Jul. 1969 316 p refs
(NASA-SP-213) Avail: SOD $1.50; CFSTI CSCL 03A

The potential for advancement of astronomy by the space program is considered. Astronomical instruments located in space can reach regions of the electromagnetic spectrum which do not penetrate the earth's atmosphere. This multiwavelength approach is shown to be a multidisciplinary activity. One of the major unresolved problems in astronomy is considered to be the Crab Nebula which consists of an enormous cloud of glowing gas resulting from the explosion of a star in A.D. 1054. Close to the center is a pulsar which may be a neutron star, in which matter is compressed to a density of 10 billion tons per cubic inch. The energy radiated is more than 100 times greater than that of the sun, despite the fact that the pulsar is only six miles in diameter. The long range program developed is considered to be well balanced, worthwhile, and imaginative. F.O.S.

31

SPACE VEHICLES

Includes launch vehicles; manned space capsules; clustered and multistage rockets; satellites; sounding rockets and probes; and operating problems. For basic research see: 30 Space Sciences. For related information see also: 28 Propulsion Systems; and 32 Structural Mechanics.

A69-11395 *#
WHY SPACE STATIONS?
Robert R. Gilruth (NASA, Manned Spacecraft Center, Houston, Tex.).
Astronautics and Aeronautics, vol. 6, Nov. 1968, p. 54-60.

Review of current basic space-station design requirements, including a brief discussion of NASA earth-orbital plans for the Apollo Applications Program and a projection of this program to large space stations of the future. An experiment program involving a space-station configuration is outlined. Visualized as the components of this program concept are an earth-like environment with a 10 to 14-psi air life-support system and 1/2 to 1-g artificial-gravity adjustment, a counterrotating zero-g laboratory, a 50-man crew expandable to 100 through supply missions, a high inclination of $\geq 50^{\circ}$, and attached and stationkeeping experiment modules. It is pointed out that an orbital station should represent a base for developments and operations equivalent in function to terrestrial bases for space exploration. V.Z.

A69-12373 *#
A DYNAMIC STABILITY STUDY OF A CENTRIFUGE-EQUIPPED SPACE STATION.
R. K. Sleeper and H. C. Lester (NASA, Langley Research Center, Hampton, Va.).
(American Institute of Aeronautics and Astronautics, Aerospace Sciences Meeting, 6th, New York, N.Y., Jan. 22-24, 1968, Paper 68-142.)
Journal of Spacecraft and Rockets, vol. 5, Dec. 1968, p. 1432-1437. 6 refs.

A linear stability investigation has been conducted on a mathematical model which may be representative of a space-station-centrifuge configuration. The configurations exhibited two basic types of instability. The first consisted of a region, bounded by the upper and lower critical speeds, in which a self-excited pure divergence occurs similar to that exhibited by rotating shafts with elliptical cross sections. All configurations studied exhibited this type of instability which occurs at lower centrifuge rotational speeds. The second type of instability, occurring at higher rotational speeds, is a self-excited mechanical instability of an oscillatory divergent nature similar to that experienced by helicopter pylon-rotor systems. Careful analysis and design of space-station-centrifuge configurations may preclude these types of instabilities from occurring within the operational speed ranges of the system. (Author)

A69-12384 *#
INTEGRATION OF A ROCKET MOTOR INTO THE SCOUT VEHICLE.
Veryl Dean Crowder (NASA, Langley Research Center, Hampton, Va.).
(American Institute of Aeronautics and Astronautics, Propulsion Joint Specialist Conference, 4th, Cleveland, Ohio, June 10-14, 1968.)
Journal of Spacecraft and Rockets, vol. 5, Dec. 1968, p. 1482, 1483.

Discussion of some of the problems that have been solved in the course of integrating various rocket motors into the Scout vehicle to improve performance. The motors discussed include the BE3-A9, the XSR57-UT-1 (FW4), the X-258, and the X-254. I.P.

A69-13556 *#
STATUS OF THE AERODYNAMIC CHARACTERISTICS OF THE APOLLO ENTRY CONFIGURATION.
E. R. Hillje (NASA, Manned Spacecraft Center, Houston, Tex.) and R. Savage (Boeing Co., Houston, Tex.).
American Institute of Aeronautics and Astronautics, Entry Vehicle Systems and Technology Meeting, Williamsburg, Va., Dec. 3-5, 1968, Paper 68-1143. 12 p. 15 refs.
Members, $1.00; nonmembers, $1.50.

Discussion of the current status of analyses of aerodynamics data obtained from wind-tunnel and flight tests on Apollo command module configurations. Flight data obtained during the entry phase of Missions AS-202, Apollo 4, and Apollo 6 are presented. Typical results of an accuracy analysis of the flight data are included. Flight data are in reasonably good agreement with wind-tunnel results, but at speeds above about Mach 10, where little ground-test data were obtained, surprisingly large variations in trim lift-to-drag ratio and angle of attack occurred. These variations, which were almost linear in time, are believed to be a result of real gas effects. (Author)

A69-13558 *#
APOLLO THERMAL-PROTECTION SYSTEM DEVELOPMENT.
R. Bryan Erb, L. T. Chauvin (NASA, Manned Spacecraft Center, Structures and Mechanics Div., Houston, Tex.), D. H. Greenshields (NASA, Manned Spacecraft Center, Structures and Mechanics Div., Thermal Technology Branch, Houston, Tex.), J. E. Pavlosky (NASA, Manned Spacecraft Center, Houston, Tex.), and C. L. Statham (North American Rockwell Corp., Space Div., Thermal Protection Unit, Downey, Calif.).
American Institute of Aeronautics and Astronautics, Entry Vehicle Systems and Technology Meeting, Williamsburg, Va., Dec. 3-5, 1968, Paper 68-1142. 14 p. 37 refs.
Members, $1.00; nonmembers, $1.50.

The development of the Apollo thermal-protection system is presented chronologically and includes a discussion of the avenues explored, the problems encountered, and the rationale which resulted in a blunt vehicle protected by a low-density ablator in a honeycomb matrix bonded to a steel sandwich structure. Extensive ground and flight tests and analytical studies were performed to support this development. A flight test program was designed to provide data at extreme conditions within the flight corridor, and the results of these flights were used to verify system performance and to refine prediction capability. It is concluded that structural and manufacturing considerations often outweigh thermal-performance considerations in system design, that many important-appearing problems are not significant, and that the technology gained in the Apollo Program forms a reliable base for the development of future thermal-protection systems. (Author)

A69-13564 *#
DECELERATION-CONTROL SYSTEM FOR AEROBRAKING AND SKIPOUT TO ORBIT AT MARS.
Albert A. Schy and Jack A. White (NASA, Langley Research Center, Hampton, Va.).
American Institute of Aeronautics and Astronautics, Entry Vehicle Systems and Technology Meeting, Williamsburg, Va., Dec. 3-5, 1968, Paper 68-1146. 6 p. 7 refs.
Members, $1.00; nonmembers, $1.50.

Aerobraking into a planetary atmosphere generally involves less weight penalty than thrust deceleration. An investigation is carried out to determine whether a deceleration-command roll-control system on a lifting body can provide entry corridors for the aerobraking maneuver at Mars consistent with achievable approach guidance accuracy. Results are presented varying the Mars atmosphere, L/D, m_e/C_DA, control system parameters, and entry speed. If the atmosphere is unknown a priori (within presently accepted limits) minimum L/D somewhat greater than 0.3 is required. Thus, for lifting capsules the control system provides corridors requiring onboard guidance, while for lifting bodies ($L/D \geq 1$) earth-based guidance might be adequate. System effectiveness is relatively insensitive to control parameter variation. (Author)

A69-13565 *#
ATMOSPHERIC ENTRY INTO THE MAJOR PLANETS WITH EMPHASIS ON JUPITER.
Michael E. Tauber (NASA, Ames Research Center, Moffett Field, Calif.).
American Institute of Aeronautics and Astronautics, Entry Vehicle Systems and Technology Meeting, Williamsburg, Va., Dec. 3-5, 1968, Paper 68-1150. 9 p. 18 refs.
Members, $1.00; nonmembers, $1.50.

The objectives of this study are to define a near minimum heating shape for a probe designed to enter the atmosphere of Jupiter at 50 km/sec. Four atmospheric compositions, pure H_2, 0.6 H_2 - 0.4 He, 0.4 H_2 - 0.6 He (by volume), and pure He, were considered. Equations for radiative heating, including lines and continua, and convective heating, including effects of mass-addition blockage, were derived. Heating calculations were made for blunt and conical bodies, for lifting and ballistic entry. It is concluded that entries should be made in the direction of planetary rotation, near the equator, at shallow flight-path angles so that heating rates will remain tolerable; advanced heat-shield materials are required; blunt-body heat-shield fractions become very large and conical bodies must probably be used. (Author)

A69-13670 *#
EVALUATION OF ENTRY AND TERMINAL DECELERATION SYSTEMS FOR UNMANNED MARTIAN LANDERS.
Edwin F. Harrison and Travis H. Slocumb, Jr. (NASA, Langley Research Center, Hampton, Va.).
American Institute of Aeronautics and Astronautics, Entry Vehicle Systems and Technology Meeting, Williamsburg, Va., Dec. 3-5, 1968, Paper 68-1147. 8 p. 12 refs.
Members, $1.00; nonmembers, $1.50.

Early unmanned Mars lander vehicles will be severely payload limited due to the low entry vehicle ballistic coefficient, and small launch vehicle (Titan III class) requirements. Since the deceleration systems comprise a major portion of the vehicle weight, a comprehensive study has been performed to minimize the decelerator weights in order to provide a maximum payload capability. Various terminal descent systems were considered with primary emphasis on the parachute-propulsion soft lander, and the parachute-impact attenuator rough lander for out-of-orbit and direct entry with ballistic and lifting entry vehicles. An important phase of the study was the comparison of recent contractual specific design results with the present parametric analysis. The results indicate that the soft lander deceleration systems are lighter than those of the rough lander when conditions of minimum surface density, maximum winds, and surface irregularities are considered. (Author)

A69-13673 *#
DEFINITION OF ENTRY CORRIDOR THERMAL LIMITS FOR APOLLO SPACECRAFT.
George Strouhal (NASA, Manned Spacecraft Center, Structures and Mechanics Div., Thermal Protection Section, Houston, Tex.), Donald M. Curry (NASA, Manned Spacecraft Center, Structures and Mechanics Div., Houston, Tex.), and Raymond G. Posgay (TRW Systems Group, Thermodynamics Dept., Aerothermodynamics Section, Houston, Tex.).
American Institute of Aeronautics and Astronautics, Entry Vehicle Systems and Technology Meeting, Williamsburg, Va., Dec. 3-5, 1968, Paper 68-1144. 7 p. 10 refs.
Members, $1.00; nonmembers, $1.50.

The design of a thermal protection system is normally accomplished very early in the development stages of a program. Several design trajectories which represent extreme points in the operational corridor are used to design the thermal protection system. The use of this "as built" heat shield is required at other than design conditions within the entry corridor and may result in excessive bondline temperatures. An analysis is presented to define the operational capabilities of the Apollo thermal protection system. Various spacecraft and trajectory parameters are considered to determine if a design heat-shield bondline-temperature thermal limit can be established for the Apollo command module. An Apollo entry corridor is presented with the heat shield bondline temperature limit lines. These limits are used by the flight controller for mission planning activities and real-time control decisions. (Author)

A69-13777 *
RESONANT PERTURBATIONS OF EXISTING SATELLITES.
Carl A. Wagner (NASA, Goddard Space Flight Center, Greenbelt, Md.) and Bruce C. Douglas (Wolf Research and Development Corp., Bladensburg, Md.).
Nature, vol. 220, Nov. 30, 1968, p. 898, 899.

Study of the geopotential resonant perturbations on the orbits of 83 existing satellites. The resonances are with high-order terms in the geopotential and are of definite concern to investigators studying the variations of the along-track positions of these satellites. It is usually true that orbits with high inclination are the most likely to suffer large perturbations due to resonance. F.R.L.

A69-15298 *
LOX PREVALVE TO PREVENT POGO EFFECT ON SATURN 5.
Erich E. Goerner (NASA, Marshall Space Flight Center, Pogo Working Group, Huntsville, Ala.).
Space/Aeronautics, vol. 50, Dec. 1968, p. 72-74.

Analysis of tests conducted before the third Saturn V launch to correct unpredicted longitudinal oscillations in the two previous Saturn V launches. The mathematical model and verification procedures are outlined. Early tests showed that the pressurant for the prevalve accumulator would have to be helium rather than gaseous oxygen. Other tests showed that helium ingested by the engine system would not have an adverse effect on engine performance. A criticality analysis of the prevalve accumulator system, which was found to be at the center of the longitudinal oscillation problem, indicated no risk of single-point failures, in which the failure of a single component would render the entire system inoperable. The prevalve accumulator system also has a built-in fail-safety feature: once the accumulators are fully charged with helium it seems probable that some of the gas will remain trapped in each of them throughout the flight. B.H.

A69-16380 *#
OPTIMUM PACKAGING DESIGN AND SPARING LEVELS FOR EXTENDED MANNED SPACE MISSIONS.
Donald E. Wagner (NASA, Manned Spacecraft Center, Houston, Tex.).
Operations Research Society of America, National Meeting, 34th, Philadelphia, Pa., Nov. 6-9, 1968, Paper. 41 p. 5 refs.

Investigation of the problem of optimizing the design of manned spacecraft systems with respect to the modular level at which onboard replacement of failed modules should be carried out. Failed items are assumed to be nonrepairable. The optimum design is considered to be the minimum weight (cost) for which a required reliability can be attained. A specific set of design alternatives, in the form of a hierarchy of candidate replacement modules, is used as the framework from which an optimum design is determined. A solution is obtained by a specialized version of a branch-and-bound integer programming algorithm. It is assumed that there is no degradation of the reliability of spares and that the time to failure of each component follows a negative exponential probability law. Provision is made for considering any number of common components for each replacement module. It is assumed that each penalty for sparing a given module, such as the fault isolation or replacement time, can be expressed in terms of a common parameter. An example problem is presented as a basis for discussion. M.M.

A69-17596
INTERNATIONAL ASTRONAUTICAL FEDERATION, INTERNATIONAL ASTRONAUTICAL CONGRESS, 18TH, BELGRADE, YUGO-

SLAVIA, SEPTEMBER 24-30, 1967, PROCEEDINGS. VOLUME 2 - SPACECRAFT SYSTEMS, EDUCATION.
Edited by Michał Łunc.
Oxford, Pergamon Press, Ltd.; Warsaw, Państwowe Wydawnictwo Naukowe, 1968. 521 p.
Price of four volumes, $90.

CONTENTS:
CONTRIBUTORS, p. v, vi.

PROJECT REVIEWS.
PROJECT REVIEW - SCOUT LAUNCH VEHICLE. M. Green (LTV Aerospace Corp., Dallas, Tex.), p. 3-15. [See A69-17597 06-31]
TRAJECTORY AND MISSION ANALYSIS ASPECTS OF JUPITER FLYBY PROBES. V. A. Lee, D. W. Jones, and M. C. Poteet (General Dynamics Corp., Fort Worth, Tex.), p. 17-31. [See A69-17598 06-30]
ECONOMICS OF COMMERCIAL SPACE STATIONS. T. J. Gordon, L. M. Dicke, and J. S. Nieroski (McDonnell Douglas Corp., Huntington Beach, Calif.), p. 33-55. 13 refs. [See A69-17599 06-30]
POLITICAL AND TECHNICAL ALTERNATIVES FOR INTERNATIONAL SPACE PROJECTS. H. H. Koelle (Berlin, Technische Universität, Berlin, West Germany), p. 57-74. [For abstract see issue 08, page 1489, Accession no. A68-20722]
SIGNIFICANT STAGES OF SPACE RESEARCH IN FRANCE SINCE THE SEVENTEENTH INTERNATIONAL CONGRESS OF ASTRONAUTICS (OCTOBER 1966 TO SEPTEMBER 1967) [ETAPES MARQUANTES DE LA RECHERCHE SPATIALE EN FRANCE DEPUIS DE XVIIEME CONGRES INTERNATIONAL D'ASTRONAUTIQUE (OCTOBRE 1966-SEPTEMBER 1967)]. L. Blosset (Centre National d'Etudes Spatiales, Paris, France), p. 75-82.

SYSTEMS ENGINEERING. I - MANNED.
OPTIMAL SYSTEMS FOR HEAT REMOVAL BY RADIATION (A REVIEW) [OPTIMAL'NYE SISTEMY OTVODA TEPLA IZLUCHENIEM (OBZOR)]. G. L. Grodzovskii and Iu. G. Zhulev (Akademiia Nauk SSSR, Moscow, USSR), p. 83-92. 24 refs. [See A69-17600 06-33]
CRITICAL ENGINEERING PROBLEMS OF SPACE STATIONS. T. J. Gordon and R. L. Gervais (McDonnell Douglas Corp., Huntington Beach, Calif.), p. 93-118. [See A69-17601 06-30]
SYSTEMS ENGINEERING, MANNED SPACE FLIGHT. C. W. Mathews (NASA, Washington, D.C.), p. 119-138. [See A69-17602 06-31]
STUDY OF A RADIATING SYSTEM WITH CONICAL HEAT REMOVING PROJECTIONS [ISSLEDOVANIE IZLUCHATEL'NOI SISTEMY S KONICHESKIMI TEPLOOTVODIASHCHIMI SHIPAMI]. Iu. G. Zhulev and Iu. F. Potapov (Akademiia Nauk SSSR, Moscow, USSR), p. 139-145. [See A69-17603 06-33]
STUDY OF HEAT STORAGE CELLS FOR SPACE SOLAR POWER PLANTS [ISSLEDOVANIE TEPLOVYKH AKKUMULIATOROV DLIA KOSMICHESKIKH SOLNECHNYKH ENERGOUSTANOVOK]. V. M. Matveev (Akademiia Nauk SSSR, Moscow, USSR), p. 147-151. [See A69-17604 06-03]

SYSTEMS ENGINEERING. II - UNMANNED.
THE ESRO II SATELLITE PROJECT. A. Kutzer (European Space Research Organization, Noordwijk-Binnen, Netherlands), p. 153-162. [For abstract see issue 24, page 4241, Accession no. A67-42402]
THE LUNAR ORBITER - AN INTEGRATED DESIGN. R. J. Helberg and C. H. Nelson (NASA, Langley Research Center, Hampton, Va.), p. 163-172. [For abstract see issue 24, page 4241, Accession no. A67-42404]
DEVELOPMENT AND MANAGEMENT OF THE INTERPLANETARY PIONEER SPACECRAFT. C. F. Hall (NASA, Ames Research Center, Moffett Field, Calif.), p. 173-186. [See A69-17605 06-31]
THE EVOLUTION OF THE MARINER SPACECRAFT. J. N. James (California Institute of Technology, Pasadena, Calif.), p. 187-198. [For abstract see issue 24, page 4241, Accession no. A67-42399]

STRUCTURES. I - EXPANDABLE, FOLDABLE, AND INFLATED SPACE STRUCTURES.
DEPLOYABLE ELEMENTS OF THE ORBITING GEOPHYSICAL OBSERVATORIES. W. E. Scull and T. W. Beard (NASA, Goddard Space Flight Center, Greenbelt, Md.), p. 199-208. [See A69-17606 06-31]
EFFECT OF SMALL BENDING STIFFNESS ON DEFORMATION OF INFLATED STRUCTURES. P. F. Jordan and P. E. Shelley (Martin Marietta Corp., Baltimore, Md.), p. 209-217. 8 refs. [See A69-17607 06-32]
A FOLDABLE TUBULAR CONNECTION AND ITS APPLICATION TO AN EXPANDABLE LATTICE COLUMN. J. Fernandez-Sintes (Instituto Nacional de Técnica Aeroespacial, Madrid, Spain), p. 219-227. 5 refs. [See A69-17608 06-32]
INFLATABLE SOLAR SHIELDS FOR CRYOGENIC SPACE VEHICLES. J. E. Marshall and L. R. Jones (General Dynamics Corp., Fort Worth, Tex.), p. 229-235. [See A69-17609 06-31]
DYNAMICS OF LARGE FLEXIBLE SPACE VEHICLE SYSTEMS SUBJECTED TO ARBITRARY FORCE AND MOTION INPUTS. Yi-Yuan Yu (General Electric Co., Valley Forge, Pa.), p. 237-247. [For abstract see issue 24, page 4240, Accession no. A67-42395]

STRUCTURES. II - THERMO-ELASTICITY AND RADIATION EFFECTS ON STRUCTURES.
TEMPERATURE DISTRIBUTIONS AND THERMAL STRESSES IN BIMETALLIC I-BEAM STRUCTURES. D. J. Johns, J. A. Gibson, G. Marriott, A. Syed, and G. Sims (Loughborough University of Technology, Loughborough, Leics., England), p. 249-262. 8 refs. [See A69-17610 06-32]
THE CHANGES IN THE (TWO-DIMENSIONAL) STRESS DISTRIBUTION ROUND A RECTANGULAR HOLE WITH ROUNDED CORNERS, CAUSED BY A VARYING INTERNAL PRESSURE AND TEMPERATURE. J. B. Spooner, E. O. Brönlund, I. Fried, and J. H. Argyris (Stuttgart, Technische Universität, Stuttgart, West Germany), p. 263-278. 5 refs. [See A69-17611 06-32]
SIMULATION OF THE RADIATION EFFECT OF A SPACE MEDIUM ON SPACECRAFT ELEMENTS [MODELIROVANIE RADIATSIONNOGO VOZDEISTVIIA KOSMICHESKOI SREDY NA ELEMENTY KOSMICHESKIKH APPARATOV]. A. I. Akishin, Iu. V. Bulgakov, S. S. Vasil'ev, S. N. Vernov, V. S. Nikolaev, and I. B. Teplov (Akademiia Nauk SSSR, Moscow, USSR), p. 279-291. 6 refs. [See A69-17612 06-11]
THERMOELASTIC EFFECTS ON GRAVITY GRADIENT STABILIZATION OF ARTIFICIAL SATELLITES. C. Arduini and G. Quozzo (Roma, Università, Rome, Italy), p. 293-306. 9 refs. [See A69-17613 06-32]
NUMERICAL SOLUTION AND EXPERIMENTAL EVALUATION OF ELASTOPLASTIC PROBLEMS FOR MULTIPLY CONNECTED SHELLS OF REVOLUTION. M. Durand and E. Jankovich (Sud Aviation, Paris, France), p. 307-316. 7 refs. [See A69-17614 06-32]
GENERAL THEORY OF THREE-LAYER STRUCTURES AND ITS APPLICATIONS [OBSHCHAIA TEORIIA TREKHSLOINYKH KONSTRUKTSII I EE PRILOZHENIIA]. E. I. Grigoliuk (Akademiia Nauk SSSR, Moscow, USSR), p. 317-322. 26 refs. [See A69-17615 06-32]

INVERSE PROBLEMS OF SATELLITE METEOROLOGY.
APPLICATION OF REGULARIZATION METHODS IN INVERSE PROBLEMS OF ATMOSPHERIC OPTICS. A. N. Tikhonov, K. Ia. Kondratev, V. B. Glasko, and Y. M. Timofeev (Leningradskii Gosudarstvennyi Universitet, Leningrad, USSR), p. 325-338. 13 refs. [See A69-17616 06-13]
INVERSE PROBLEMS IN RADIATIVE TRANSFER - A REVIEW. B. J. Conrath (NASA, Goddard Space Flight Center, Greenbelt, Md.), p. 339-360. 10 refs. [See A69-17617 06-13]
INVERSION TECHNIQUES AND THEIR PROBLEMS. R. Zirkind (Brooklyn, Polytechnic Institute, Farmingdale, N.Y.), p. 361-367. 16 refs. [See A69-17618 06-23]
CLOUD PRODUCTION IN LOW-PRESSURE AREAS OVER EUROPE, AS OBSERVED BY METEOROLOGICAL SATELLITES [DIE WOLKENPRODUKTION VON TIEFDRUCKGEBIETEN ÜBER EUROPA, BEOBACHTET MIT METEOROLOGISCHEN SATELLITEN]. L. Kletter (Zentralanstalt für Meteorologie und Geodynamik, Vienna, Austria), p. 369-386. 7 refs. [See A69-17619 06-20]
SOME TOPICS ON RADIATION MEASUREMENTS FROM SATELLITE. Kyo Sekihara (Ministry of Transportation, Tokyo, Japan), p. 387-389.

MULTI-PURPOSE APPLICATION SATELLITES.
ADVANCED METEOROLOGICAL SATELLITE. A. Adelman (International Business Machines Corp., Bethesda, Md.), p. 391-

406. [For abstract see issue 24, page 4240, Accession no. A67-42392]

THE CALIBRATION OF MULTICHANNEL RADIOMETERS FOR APPLICATION IN SPACECRAFT AND SPACE SIMULATION PROGRAMS. A. J. Drummond, J. R. Hickey, W. J. Scholes (Eppley Foundation for Research, Newport, R.I.), and E. G. Laue (California Institute of Technology, Pasadena, Calif.), p. 407-422. 9 refs. [See A69-17620 06-14]

THE CALIBRATION OF A SATELLITE INFRARED SPECTROMETER. D. T. Hilleary, S. P. Anderson (ESSA, Suitland, Md.), A. R. Karoli, and J. R. Hickey (Eppley Foundation for Research, Newport, R.I.), p. 423-437. 9 refs. [See A69-17621 06-14]

DEEP-SPACE COMMUNICATIONS.

CONTROLLABILITY OF DEEP SPACE ELECTROMAGNETIC WAVE PROPAGATION IN NON-VACUUM. M. Z. v. Krzywoblocki (Michigan State University, East Lansing, Mich.), p. 439-444. [See A69-17622 06-07]

A COMMUNICATIONS SYSTEM FOR INTERPLANETARY SPACECRAFT [SISTEMA SVIAZI S MEZHPLANETNYMI KOSMICHESKIMI APPARATAMI]. Iu. K. Khodarev (Akademiia Nauk SSSR, Moscow, USSR), p. 445-449. [See A69-17623 06-07]

THE ASCEND STUDY - ADVANCED SYSTEM FOR COMMUNICATIONS AND EDUCATION IN NATIONAL DEVELOPMENT. B. B. Lusignan (Stanford University, Stanford, Calif.), p. 453-465.

ASTRONAUTICS INSTRUCTION AT ALL LEVELS OF EDUCATION. I - SECONDARY SCHOOLS. J. G. Meitner (Stanford Research Institute, Menlo Park, Calif.), p. 467-477.

PROPOSAL TO ESTABLISH AN INTERNATIONAL ASTRONAUTICS INSTITUTE. J. Indrikis, p. 479-488.

COMMUNICATION SATELLITES FOR EDUCATIONAL TELEVISION. J. Jansen (TRW Systems Group, Redondo Beach, Calif.), p. 489-497. [See A69-17624 06-31]

COMMUNICATION SATELLITE TECHNOLOGY AND INTERNATIONAL EDUCATION AND INFORMATION EXCHANGE. A. L. Horley (Stanford University, Stanford, Calif.), p. 499-507.

SOME THOUGHTS CONCERNING EDUCATION IN ASTRONAUTICS. V. J. Modi and R. C. Brereton (British Columbia, University, Vancouver, Canada), p. 509-513.

A69-17602 *

SYSTEMS ENGINEERING, MANNED SPACE FLIGHT.

C. W. Mathews (NASA, Washington, D.C.).

IN: INTERNATIONAL ASTRONAUTICAL FEDERATION, INTERNATIONAL ASTRONAUTICAL CONGRESS, 18TH, BELGRADE, YUGOSLAVIA, SEPTEMBER 24-30, 1967, PROCEEDINGS. VOLUME 2 - SPACECRAFT SYSTEMS, EDUCATION. [A69-17596 06-31]

Edited by Michał Łunc.

Oxford, Pergamon Press, Ltd.; Warsaw, Państwowe Wydawnictwo Naukowe, 1968, p. 119-137.

Description of some of the major concepts utilized in the U.S. to provide for a logical development of flight hardware, for the successful conduct of flight operations, and for the achievement of maximum benefits from each mission. Objectives of the Mercury, Gemini, and Apollo programs are outlined. Mission modes considered were the direct launch mode, earth orbit rendezvous, and lunar orbit rendezvous. Operational features of lunar orbit rendezvous are discussed. Attention is given to systems selection and configuration, redundancy and crew integration, related systems engineering factors, systems engineering of special projects, and in-flight and postflight considerations. F.R.L.

A69-17605 *

DEVELOPMENT AND MANAGEMENT OF THE INTERPLANETARY PIONEER SPACECRAFT.

C. F. Hall (NASA, Ames Research Center, Moffett Field, Calif.) and A. B. Mickelwait (TRW Systems Group, Redondo Beach, Calif.).

IN: INTERNATIONAL ASTRONAUTICAL FEDERATION, INTERNATIONAL ASTRONAUTICAL CONGRESS, 18TH, BELGRADE, YUGOSLAVIA, SEPTEMBER 24-30, 1967, PROCEEDINGS. VOLUME 2 - SPACECRAFT SYSTEMS, EDUCATION. [A69-17596 06-31]

Edited by Michał Łunc.

Oxford, Pergamon Press, Ltd.; Warsaw, Panstwowe Wydawnictwo Naukowe, 1968, p. 173-186.

Description of the tools, techniques, and procedures applied in the development of the Pioneer program for scientific exploration of space, and of the systems engineering aspects of this program. The Pioneer mission objectives are the systematic measurement of magnetic fields, plasma, high-energy particles, and dust in interplanetary space within the range of minimum and maximum solar activity, at large azimuthal distances from the earth (between 0.8 and 1.2 AU from the sun). Methods of launching five Pioneer spacecraft are described. F.R.L.

A69-17606 *

DEPLOYABLE ELEMENTS OF THE ORBITING GEOPHYSICAL OBSERVATORIES.

W. E. Scull and T. W. Beard (NASA, Goddard Space Flight Center, Greenbelt, Md.).

IN: INTERNATIONAL ASTRONAUTICAL FEDERATION, INTERNATIONAL ASTRONAUTICAL CONGRESS, 18TH, BELGRADE, YUGOSLAVIA, SEPTEMBER 24-30, 1967, PROCEEDINGS. VOLUME 2 - SPACECRAFT SYSTEMS, EDUCATION. [A69-17596 06-31]

Edited by Michał Łunc.

Oxford, Pergamon Press, Ltd.; Warsaw, Państwowe Wydawnictwo Naukowe, 1968, p. 199-208.

Description of the twelve or thirteen deployable appendages of the Orbiting Geophysical Observatory (OGO), an attitude-controlled spacecraft. Their purpose is to conduct large numbers of geophysical scientific experiments within the earth's atmosphere, the magnetosphere, and cislunar space. The various types of deployment, hold-down and release, and latch devices are described. Details of the design and deployment testing of appendages are given. To assure positive torque at all angular positions of appendages during deployment, the torque output at each angle θ is determined. Deployments in orbit and the oscillations of appendages in orbit are considered. F.R.L.

A69-17672 *

PROGRESS REPORT ON APOLLO PROGRAM.

Michael Collins (NASA, Manned Spacecraft Center, Houston, Tex.).

(Society of Experimental Test Pilots, Symposium, 12th, Beverly Hills, Calif., Sept. 26-28, 1968.)

Society of Experimental Test Pilots, Technical Review, vol. 9, no. 2, 1968, p. 231-240.

Description of the Apollo 4, 5, and 6 space missions with a preview concerning the program for the Apollo 7, 8, and 9 missions. Apollo 4, the first Saturn V flight, was launched in November 1967. The second Saturn V flight, called Apollo 6, was launched in April 1968. Both flights carried Command and Service Modules into earth orbit. A number of anomalies occurred during the Apollo 6 mission. The first and only Lunar Module flight, called Apollo 5, took place on Jan. 22, 1968. It was a systems test with emphasis on firing the two Lunar Module engines. G.R.

A69-18204 *#

A STUDY OF SATURN AS-502 COUPLING LONGITUDINAL STRUCTURAL VIBRATION AND LATERAL BENDING RESPONSE DURING BOOST.

R. S. Ryan (NASA, Marshall Space Flight Center, Dynamics Analysis Branch, Huntsville, Ala.), J. G. Papadopoulos, L. A. Kiefling (NASA, Marshall Space Flight Center, Aero-Astrodynamics Laboratory, Huntsville, Ala.), R. Odum, W. Jarvinen, and J. Kennoy (Northrop Corp., Northrop Nortronics, Huntsville, Ala.).

American Institute of Aeronautics and Astronautics, Aerospace Sciences Meeting, 7th, New York, N.Y., Jan. 20-22, 1969, Paper 69-58. 10 p.

Members, $1.00; nonmembers, $1.50.

Analysis of the Saturn AS-502 space vehicle for both mass and spring coupling with the "pogo" phenomenon acting as the longitudinal excitation force. Although the mass coupling influence was small, a large lateral acceleration resulted from a spring-type coupling between the ascent and descent stages of the LEM during the latter part of S-IC burn. A response analysis of the vehicle using time-varying coefficients was made and compared with observed flight conditions. The results of the study confirm the necessity of including dynamic cross-coupling mechanisms for adequate prediction of vehicle response. The resulting simulation closely duplicated flight results. The important vehicle parameters involved in creating the lateral/longitudinal coupling phenomenon were studied. M.M.

A69-18210 *#
DYNAMIC STABILITY CHARACTERISTICS OF LARGE-SIZE 120° BLUNTED CONICAL SPACECRAFT IN A SIMULATED MARTIAN ENVIRONMENT.
Charles H. Whitlock, Richard J. Bendura, and Allen B. Henning (NASA, Langley Research Center, Hampton, Va.).
American Institute of Aeronautics and Astronautics, Aerospace Sciences Meeting, 7th, New York, N.Y., Jan. 20-22, 1969, Paper 69-104. 7 p. 17 refs.
Members, $1.00; nonmembers, $1.50.

Dynamic stability derivatives were obtained from three flight tests of a 4.8-m diameter spacecraft at Mach numbers between 0.48 and 1.5. Results from different flights show positive dynamic stability for Mach numbers 1.15 or below. At higher velocities, dynamic instability was indicated over a wide range of angles of attack. Correlation of the large-scale flight data with a limited number of ballistics range results suggests that the excessive transonic instability may be associated with low angle-of-attack oscillations. (Author)

A69-18328 *#
DESIGN, SIMULATION AND FLIGHT PERFORMANCE OF THE RADIO ASTRONOMY EXPLORER-A SATELLITE.
D. L. Blanchard (NASA, Goddard Space Flight Center, Greenbelt, Md.), R. M. Davis, E. A. Lawlor, and L. Beltracchi (Avco Corp., Avco Space Systems Div., Lowell, Mass.).
U.S. Air Force Systems Command and Aerospace Corp., Symposium on Gravity Gradient Attitude Stabilization, El Segundo, Calif., Dec. 3-5, 1968, Paper. 22 p.

Status report of the accuracy and flight performance of the RAE-A satellite. Several conclusions, which can be of use to other large gravity-gradient stabilized spacecraft, are drawn. In the region where boom deflections are small, the deadbeat deployment scheme is a very effective method for reducing the initial transient librational motions and quickly achieving gravity-gradient capture. The three-dimensional behavior of this deadbeat deployment has been accurately predicted with a flexible-body simulation. The boom parameters obtained from ground measurements appear to be quite accurate for use in the simulation model during the deployment and acquisition phase. The double deadbeat deployment is very effective in minimizing transient motions when antenna-boom deflections are large due to the extreme flexibility associated with very long booms. The articulated damper torsion wire suspended with hysteresis damping seems to perform as theory predicts. M.M.

A69-18334 *#
IMPLEMENTATION OF A SEMI-ACTIVE GRAVITY GRADIENT CONTROLLER.
P. S. Hui (NASA, Goddard Space Flight Center, Greenbelt, Md.) and J. G. Zaremba (TRW Systems Group, Electronic Systems Div., Control Systems Laboratory, Redondo Beach, Calif.).
U.S. Air Force Systems Command and Aerospace Corp., Symposium on Gravity Gradient Attitude Stabilization, El Segundo, Calif., Dec. 3-5, 1968, Paper. 27 p.
Contracts No. NAS 5-10253; No. NAS 5-10453.

Description of the hardware design which implements a semi-active gravity-gradient stabilization system (SAGS) for controlling the attitude of a low-altitude earth-oriented spacecraft. Briefly, the SAGS control scheme employs an active-reaction wheel scanner for pitch-attitude control. The roll/yaw control is achieved by operating the pitch wheel with a momentum bias, and by gimbaling the wheel and coupling it to the vehicle through an energy-removal mechanism. Long-term momentum buildup is prevented by gravity-gradient restoring torques. The SAGS controller, which yields a single mechanical unit that provides the entire attitude-control function, is described together with the component units implementing the SAGS. M.M.

A69-18338 *#
APPLICATION OF GRAVITY GRADIENT STABILIZATION TO LARGE MANNED SPACE VEHICLES.
G. S. Nurre (NASA, Marshall Space Flight Center, Huntsville, Ala.) and P. C. Weygandt (General Electric Co., Missile and Space Div., King of Prussia, Pa.).
U.S. Air Force Systems Command and Aerospace Corp., Symposium on Gravity Gradient Attitude Stabilization, El Segundo, Calif., Dec. 3-5, 1968, Paper. 14 p.
Contract No. NAS 8-2117.

Study of system designs (with performance predictions) for gravity gradient stabilization of the S-IVB stage at 400 km altitude and the lunar module at synchronous altitude. Linearized equations of motion are used to develop parametric design curves from which weight, damping time, and accuracy tradeoffs are made. System designs are selected from tradeoff results and performance predictions made using a nonlinear digital computer simulation. Requirements for a new class of gravity stabilization components are derived from the selected system designs. P.v.T.

A69-19126 *
THE SMALL ASTRONOMY SATELLITE (SAS) PROGRAM.
Marjorie R. Townsend (NASA, Goddard Space Flight Center, Greenbelt, Md.).
IN: INTERNATIONAL TELEMETERING CONFERENCE, LOS ANGELES, CALIF., OCTOBER 8-11, 1968, PROCEEDINGS. [A69-19092 07-07]
Conference sponsored by the International Foundation for Telemetering.
Tarzana, Calif., International Foundation for Telemetering (ITC Proceedings. Volume 4), 1968, p. 481-502.

Description of the basic spacecraft functions of the Small Astronomy Satellite. The emphasis is put on its key feature, the control system, as proposed for early sky surveys, and the changes needed in it for later flights which will require a pointing capability of one arc minute or better. Its flexibility and versatility for application to many types of astronomy experiments are examined. Z.W.

A69-19195 *
THE SMALL SCIENTIFIC SATELLITE (S^3) PROGRAM AND ITS FIRST PAYLOAD.
Donald J. Williams (NASA, Goddard Space Flight Center, Greenbelt, Md.).
(Institute of Electrical and Electronics Engineers, Nuclear Science Symposium, 15th, Montreal, Canada, Oct. 23-25, 1968, Paper 3 C-1.)
IEEE Transactions on Nuclear Science, vol. NS-16, Feb. 1969, p. 322-335. 6 refs.

Description of the Small Scientific Satellite (S^3) program, which provides a scientific "bench" for use by experimenters, for a wide variety of investigations in the magnetosphere and near interplanetary space, employing the Scout launch vehicle. In the conduct of these scientific missions, the S^3 program affords the experimenter control over parameters affecting the investigation - e.g., orbit, attitude control, and orientation. In addition, complete in-flight control of the data format is available through the use of an onboard set of stored program instructions which govern the collection of the data, and which are reprogrammable via ground command. Many of the spacecraft subsystems are modular, and are used according to the experimenter's needs. The research capabilities of the program are discussed, the characteristics of the various subsystems are described, and the first payload is examined as a space nuclear instrumentation system. B.H.

A69-22866 *#
THE NEW FUTURE FOR MANNED SPACECRAFT DEVELOPMENTS.
George E. Mueller (NASA, Office of Manned Space Flight, Washington, D.C.).
Astronautics and Aeronautics, vol. 7, Mar. 1969, p. 24-32.

Discussion of new developments for manned spacecraft either currently under way or planned for the future. A confluence of design concepts, technological advance, and operational experience now makes possible a space transport that will cut the cost to deliver a payload to orbit by an order of magnitude and so open the space station to extensive commercial, scientific, and engineering exploitation. The Apollo applications program, making maximum use of the knowledge and the equipment from the Apollo program, takes a step toward the establishment of a space station. Space-shuttle basic operational concepts are discussed. Trends in the cost of orbiting a payload are considered. G.R.

A69-25498 *#
THE USE OF HELIUM BUBBLES AS A POGO FIX IN LAUNCH VEHICLE PROPELLANT LINES.
Brantley R. Hanks and David G. Stephens (NASA, Langley Research Center, Hampton, Va.).

IN: AMERICAN INSTITUTE OF AERONAUTICS AND ASTRONAUTICS, STRUCTURAL DYNAMICS AND AEROELASTICITY SPECIALIST CONFERENCE, NEW ORLEANS, LA., APRIL 16, 17, 1969, PROCEEDINGS. [A69-25492 11-32]
New York, American Institute of Aeronautics and Astronautics, Inc., 1969, p. 42-46.

A technique for lowering the natural frequencies of launch vehicle propellant lines was investigated as a possible means for alleviating pogo oscillations. Gaseous helium injected into a line during flow increases the compressibility of the propellant and thus lowers the natural frequency of the propellant feed system. This phenomenon was studied in the laboratory using a water flow line which was mounted on a whirl table to simulate flight-acceleration conditions. The acoustic resonances of the line were measured for controlled amounts of helium injected into the water ranging from 0 to 2.5 vol %. Results indicate that substantial reductions in both the resonant frequency and the pressure response at resonance can be achieved with the helium bubble injection technique. The experimental frequency data are successfully predicted by an analysis based on a theory for the sound velocity in liquid-gas mixtures. (Author)

A69-25500 *#
MINIMIZING SPACECRAFT STRUCTURE/CONTROL-SYSTEM INTERACTION.
Richard B. Noll (Kaman Corp., Kaman AviDyne, Burlington, Mass.) and Curtis H. Spenny (NASA, Electronics Research Center, Cambridge, Mass.).
IN: AMERICAN INSTITUTE OF AERONAUTICS AND ASTRONAUTICS, STRUCTURAL DYNAMICS AND AEROELASTICITY SPECIALIST CONFERENCE, NEW ORLEANS, LA., APRIL 16, 17, 1969, PROCEEDINGS. [A69-25492 11-32]
New York, American Institute of Aeronautics and Astronautics, Inc., 1969, p. 58-65. 20 refs.
Contract No. NAS 12-613.

Spacecraft structure/control-system interaction problems and their minimization are reviewed. Interaction problems are identified with three basic structural configurations. Representative spacecraft examples in each category are discussed to illustrate various methods which have been used to minimize interactions. Examples include Explorer 3, ATS, Apollo CSM/LM, ISIS 1, OSO, 1963 49B, DODGE, and Radio Astronomy Explorer. Design improvements based on flight experience are emphasized. While interaction problems of manned spacecraft have required greater-in-depth studies, in-flight difficulties are shown to be most numerous on spacecraft equipped with extendible booms. The majority of these interactions are attributed to the susceptibility of the booms to the solar environment. Interaction effects on spacecraft which are spin stabilized about the principal axis of minimum moment of inertia are included. (Author)

A69-25501 *#
A METHOD FOR DIGITAL COMPUTATION OF SPACECRAFT RESPONSE IN THE DOCKING MANEUVER.
C. Bodley, G. Morosow (Martin Marietta Corp., Dynamics and Loads Section, Denver, Colo.), and W. Holland (NASA, Marshall Space Flight Center, Huntsville, Ala.).
IN: AMERICAN INSTITUTE OF AERONAUTICS AND ASTRONAUTICS, STRUCTURAL DYNAMICS AND AEROELASTICITY SPECIALIST CONFERENCE, NEW ORLEANS, LA., APRIL 16, 17, 1969, PROCEEDINGS. [A69-25492 11-32]
New York, American Institute of Aeronautics and Astronautics, Inc., 1969, p. 66-74.

Analytical study of the docking dynamics of two space vehicles, and development of equations of motion cast in matrix form and amenable to numerical solution. The use of Hamilton's principle with constraint equations and Lagrange multipliers is made in the formulation. The equations of motion considering both a massless and a finite-mass docking mechanism are defined. Graphical results are presented for an illustrative example. Results of the analysis as applied to a typical Apollo Applications Program cluster are also shown. (Author)

A69-25718
RE-ENTRY AND PLANETARY ENTRY PHYSICS AND TECHNOLOGY. II - ADVANCED CONCEPTS, EXPERIMENTS, GUIDANCE-CONTROL AND TECHNOLOGY.
Edited by W. H. T. Loh (North American Rockwell Corp., Space Div., Downey, Calif.).
New York, Springer-Verlag New York, Inc. (Applied Physics and Engineering Series. Volume 3), 1968. 300 p.
$12.40.

CONTENTS:

PREFACE. W. H. T. Loh (North American Rockwell Corp., Downey, Calif.), p. vii.

ENTRY EXPERIMENTATION.

ENTRY FLIGHT RESEARCH AND EXPERIMENTATION. D. G. Stone (NASA, Langley Research Center, Hampton, Va.), p. 3-26. [See A69-25719 11-31]

ENTRY CONCEPTS AND TECHNOLOGY.

LIFTING ENTRY CONCEPTS. J. G. Logan, Jr. (Aerospace Corp., Pasadena, Calif.), p. 29-76. 41 refs. [See A69-25720 11-31]

ENTRY FROM LUNAR AND PLANETARY MISSIONS. J. F. McCarthy, Jr. (North American Rockwell Corp., Downey, Calif.), p. 77-143. 18 refs. [See A69-25721 11-31]

ATMOSPHERIC BRAKING ENTRY AND ASSOCIATED TECHNOLOGIES. K. A. Ehricke (North American Rockwell Corp., Anaheim, Calif.), p. 144-181. 5 refs. [See A69-25722 11-31]

ENTRY PROPULSION AND LOWER SYSTEMS TECHNOLOGY. R. W. Bussard (Electro-Optical Systems, Inc., Pasadena, Calif.), p. 182-204. 5 refs. [See A69-25723 11-28]

GUIDANCE AND CONTROL FOR ATMOSPHERIC ENTRY. R. C. Duncan (NASA, Electronics Research Center, Cambridge, Mass.), p. 205-256. [See A69-25724 11-21]

DYNAMICS OF PLANETARY APPROACH. W. T. Thomson (California, University, Santa Barbara, Calif.), p. 257-280. [See A69-25725 11-31]

ADVANCED ENTRY PROGRAMS.

ENTRY RESEARCH AND DEVELOPMENT PROGRAM MANAGEMENT. J. F. Shea (NASA, Manned Spacecraft Center, Washington, D.C.), p. 283-293. [See A69-25726 11-34]

A69-25719 *
ENTRY FLIGHT RESEARCH AND EXPERIMENTATION.
David G. Stone (NASA, Langley Research Center, Hampton, Va.).
IN: RE-ENTRY AND PLANETARY ENTRY PHYSICS AND TECHNOLOGY. II - ADVANCED CONCEPTS, EXPERIMENTS, GUIDANCE-CONTROL AND TECHNOLOGY. [A69-25718 11-31]
Edited by W. H. T. Loh.
New York, Springer-Verlag New York, Inc. (Applied Physics and Engineering Series. Volume 3), 1968, p. 3-26.

Discussion of certain aspects of the problem of entering planetary atmospheres, such as configuration, trajectory planning, instrumentation, calorimetry, aerodynamic heating, and the development of rocket-vehicle techniques for ranges from low supersonic speeds to earth-escape speeds. Typical early rocket models and vehicles are illustrated, leading up to a discussion of the trajectory technique now used for simulating reentry conditions for earth environment and for simulating entry into planetary atmospheres. The problems of developing suitable instrumentation and calorimetry techniques are examined, and examples of rocket vehicle heating investigations are given. The nature of hypervelocity heating and problems of measurement are discussed, and a description is given of Project Fire undertaken by NASA to investigate the heating environment of vehicles entering the earth's atmosphere at velocities slightly higher than return velocities from a lunar mission. P.v.T.

A69-26874 *
DEVELOPMENT OF THE BALLISTIC ROCKET CONCEPT FOR ROCKET CLIMATOLOGY [ENTWICKLUNG RAKETEN-BALLISTISCHER KONZEPTE FÜR DIE RAKETEN-KLIMATOLOGIE].
G. H. R. Reisig (NASA, Marshall Space Flight Center, Huntsville, Ala.).
(Deutsche Gesellschaft für Luft- und Raumfahrt, Symposium, Cologne, West Germany, May 16, 1968.)
Raumfahrtforschung, vol. 13, Mar.-Apr. 1969, p. 62-71. 16 refs.
In German.

Study of the ballistic effects of the atmosphere for the benefit of rocket vehicle engineers. The characteristic features of rocket mechanics require the application of climatological concepts of meteorology. Because of the inherent stability criteria of rocket ballistics, the atmospheric parameters must be standardized in terms of coherent altitude-dependent profiles. These coherent profiles can, at present, be established only for atmospheric density and velocity of sound (in connection with rocket noise) in a form applicable to rocket vehicle technology. It is recommended that appropriate analytical models of profiles for the parameters of the wind field (speed, direction, shear, and turbulence) be developed.
F.R.L.

A69-31849 *#
NUCLEAR ROCKET APPLICATIONS - MISSION AND LAUNCH-VEHICLE VERSATILITY.
Paul Johnson (U.S. Atomic Energy Commission and NASA, Space Nuclear Propulsion Office, Washington, D.C.).
American Institute of Aeronautics and Astronautics, Propulsion Joint Specialist Conference, 5th, U.S. Air Force Academy, Colorado Springs, Colo., June 9-13, 1969, Paper 69-555. 19 p. 19 refs.
Members, $1.00; nonmembers, $1.50.

Discussion of several mission areas for nuclear rockets used as Saturn V third stages. Emphasis is placed on the utility of increased payload or velocity, and on the resulting engine and stage requirements. Performance comparisons are shown for nuclear upper stages on a number of possible launch vehicles. The sensitivity of the system to various engine and stage parameters, including cost, and the corresponding impact on nuclear-rocket planning are discussed.
M.M.

A69-32658 *#
SATURN V LONGITUDINAL OSCILLATION (POGO) SOLUTION.
A. L. Worlund (NASA, Marshall Space Flight Center, Huntsville, Ala.), R. D. Hill, and G. L. Murphy (Brown Engineering Co., Inc., Huntsville, Ala.).
American Institute of Aeronautics and Astronautics, Propulsion Joint Specialist Conference, 5th, U.S. Air Force Academy, Colorado Springs, Colo., June 9-13, 1969, Paper 69-548. 8 p. 5 refs.
Members, $1.00; nonmembers, $1.50.

Analysis of a longitudinal vehicle instability encountered during the second flight of the Saturn V. These oscillations resulted from closed-loop coupling of the oxidizer feed system and the first vehicle longitudinal mode. Recurrence of this instability was to be precluded by detuning the structural/propulsion subsystems - i.e., lowering the S-IC stage propulsion system resonance below the structural frequency. Techniques for adding compressibility were evaluated by criteria designed to (1) assure solution adequacy by analysis and test demonstration prior to implementation, (2) provide vehicle retrofit capability, (3) preclude launch schedule impact, and (4) minimize performance degradation. Analyses encompassing the limits of pertinent parameters, experimental verification of propulsion system dynamics and stage/engine performance and compatibility tests demonstrated that the oxidizer prevalves, converted to accumulators by filling the housing cavities with helium, would prevent POGO oscillations on subsequent Saturn V vehicles. The Apollo 8 flight demonstrated that the POGO solution was effective.
P.G.

A69-32755 *#
EVALUATION OF EXPERIMENTAL AND ANALYTICAL DATA FOR ORBITAL REFUELING SYSTEMS.
C. C. Wood (NASA, Marshall Space Flight Center, Astronautics Laboratory, Propulsion and Thermodynamics Div., Huntsville, Ala.).
American Institute of Aeronautics and Astronautics, Propulsion Joint Specialist Conference, 5th, U.S. Air Force Academy, Colorado Springs, Colo., June 9-13, 1969, Paper 69-566. 12 p. 28 refs.
Members, $1.00; nonmembers, $1.50.

Discussion of study limitations and the validity of excessive extrapolation to apply transient data to low-gravity fluid behavior. An orbital fluid transfer experiment is presented that removes restrictions imposed by earth-based tests.
(Author)

A69-34519 *
SPACECRAFT FAILURE RATES - WHERE ARE WE?
Abraham Leventhal (NASA, Goddard Space Flight Center, Greenbelt, Md.), Charles E. Bloomquist (Planning Research Corp., Los Angeles, Calif.), and Jerome A. Joseph (TRW Systems Group, Redondo Beach, Calif.).
IN: ANNUAL SYMPOSIUM ON RELIABILITY, CHICAGO, ILL., JANUARY 21-23, 1969, PROCEEDINGS. [A69-34476 18-15]
Symposium sponsored by the Institute of Electrical and Electronics Engineers, the Institute of Environmental Sciences, the American Society for Nondestructive Testing, and the American Society for Quality Control.
New York, Institute of Electrical and Electronics Engineers, Inc. (Annals of Assurance Sciences. Volume 2, No. 1), 1969, p. 444-452. 11 refs.

Detailed analysis of the failure-rate aspects of the Orbiting Geophysical Observatories (OGO) program with respect to cost, schedule, and performance tradeoffs. The parts program, component and systems design review procedures, design modifications to improve reliability, and the prelaunch failure reporting and feedback system are considered, and the compromises required by the program to meet cost and schedule constraints are discussed. The impact of these efforts on the observed in-orbit performance of the spacecraft is summarized. The results of the study are compared with results from more general surveys of spacecraft reliability.
B.H.

A69-34864 *
A TOTAL PERSPECTIVE WEIGHT TECHNIQUE FOR ADVANCED MANNED SPACECRAFT.
W. Heineman, Jr. (NASA, Manned Spacecraft Center, Houston, Tex.).
Society of Aeronautical Weight Engineers, Annual Conference, 28th, San Francisco, Calif., May 5-8, 1969, Paper 793. 13 p.
Members, $1.00; nonmembers, $1.50.

Discussion of the fundamental engineering principles involved in estimating and forecasting weight in manned spacecraft designs. It is shown that the relationship between manned spacecraft size and weight is a primary parameter for estimating from a technological and engineering standpoint. A compatible weight growth forecast, based on the weight estimate, is dependent on the primary parameter of program maturity, which is obtained from a combination of time-oriented parameters and the historically reported weight status. The described technique is considered to be applicable to all manned spacecraft, including space stations.
B.H.

A69-35067 *#
SPACE MANUFACTURING MODULES.
James R. Williams (NASA, Marshall Space Flight Center, Huntsville, Ala.).
IN: SPACE, TECHNOLOGY, AND SOCIETY; CANAVERAL COUNCIL OF TECHNICAL SOCIETIES, SPACE CONGRESS, 6TH, COCOA BEACH, FLA., MARCH 17-19, 1969, PROCEEDINGS. VOLUME 2. [A69-35055 18-34]
Edited by L. E. Jones, III.
Cape Canaveral, Fla., Canaveral Council of Technical Societies, 1969, p. 11-31 to 11-48.

Description of a proposed program which would provide a capability for manufacturing operations in space. The initial phase of the program will initiate an investigation of the effect of zero gravity on manufacturing processes during earth orbit flight. A work package is described which is currently being prepared to fly with Apollo Applications Program Orbital Workshop Flight No. 2. As a second phase, an improved space manufacturing process chamber is being planned. A third phase proposes the development of a room size manufacturing module which would be designed to dock to an earth orbiting space station proposed for launch in the mid-1970s. This module would contain work area for at least two of the problems associated with achieving a balanced spin stabilized rocket are discussed.
(Author)

A69-35094 *#
THE IMPACT OF BIOSCIENCES REQUIREMENTS ON BIOSATELLITE ATTITUDE CONTROL.
J. D. Carpenter, E. T. Thomas (General Electric Co., Philadelphia, Pa.), and J. C. Van Ess (NASA, Ames Research Center, Moffett Field, Calif.).
IN: SPACE, TECHNOLOGY, AND SOCIETY; CANAVERAL COUNCIL OF TECHNICAL SOCIETIES, SPACE CONGRESS, 6TH, COCOA BEACH, FLA., MARCH 17-19, 1969, PROCEEDINGS. VOLUME 1. [A69-35070 18-34]

31 SPACE VEHICLES

Edited by L. E. Jones, III.
Cape Canaveral, Fla., Canaveral Council of Technical Societies, 1969, p. 10-31 to 10-52. 8 refs.

Discussion of the design, development, and flight-test results of the Biosatellite attitude control system. Results of analyses of payload perturbing effects to determine the forces and moments to which the payload is sensitive are given. The role of simulation activity in the development of the attitude control system is discussed, with particular emphasis on the importance of these simulation studies in the analysis and evaluation of control system performance in the deorbit phase of the mission. The effects of geophysical phenomena on sensors, and the incorporation of the sensors in the simulation program to enhance its validity are discussed. The control system configuration is defined, and its special features, such as the versatility of recovery time and location, are discussed.
B. H.

A69-36329 *
ASSURING SATURN QUALITY THROUGH NONDESTRUCTIVE TESTING.
Robert W. Neuschaefer (NASA, Marshall Space Flight Center, Huntsville, Ala.).
(American Society for Nondestructive Testing, Spring Conference, Los Angeles, Calif., Mar. 10-13, 1969, Paper.)
Materials Evaluation, vol. 27, July 1969, p. 145-152. 9 refs.

The Saturn V space vehicle is briefly described. The organizational responsibilities of NDT groups are discussed along with the approach to management of research and development activities. Applications of the various NDT methods employed to evaluate the materials and processes used in the manufacture of the various stages and major components are described. Emphasis is placed on a discussion of the special NDT methods and equipment developed to satisfy the unique requirements of the Apollo program. Advancements in the state-of-the-art, including a solid-state radiographic image amplifier and an rf device suitable for measuring the thickness of nonmetallics on metallic objects, are described. (Author)

A69-36464 *
MANNED SPACE STATIONS.
R. R. Gilruth (NASA, Manned Spacecraft Center, Houston, Tex.).
(International Astronautical Congress, 19th, Orbital Laboratory Symposium, New York, N.Y., Oct. 13-19, 1968.)
Spaceflight, vol. 11, Aug. 1969, p. 258-263.

Discussion of the advantages and characteristics of earth-orbiting space stations. A station that merges space technology with elements of pure and applied science into a single facility which can be logistically operated at a single place in space is described. Its purpose will be to thrust basic research into a new and stimulating environment. Permanency and vastness will be the station's predominant assets, and it will provide a stately reservoir of energy and utilizable volume. M.M.

A69-36674 *
THE ORBITING GEOPHYSICAL OBSERVATORIES.
Wilfred E. Scull (NASA, Goddard Space Flight Center, Greenbelt, Md.).
IEEE Transactions on Geoscience Electronics, vol. GE-7, Apr. 1969, p. 55-60.

The OGO systems are designed to fulfill a primary objective of conducting large numbers of significant, diversified experiments for making scientific and technological measurements within the earth's atmosphere, the magnetosphere, and cislunar space to obtain a better understanding of earth-sun relationships and the earth as a planet. The observatories include six appendages of different lengths for experiments requiring locations at a distance from the main body. Five degrees of freedom allow the capability of continuously orienting solar and antisolar, geocentric and antigeocentric, and orbital experiments within relatively close limits. Designed to include five basic subsystems of structure, stabilization and control, power, communications and data handling, and thermal control, the observatories have well defined interfaces for experiments. Five of the six observatories in the program have already been launched and have returned significant scientific information. Weights of the observatories range from 1073 to 1400 lb, including as many as 390 lb of experiments. One hundred six experiments have already been orbited on the five spacecraft, with 26 experiments scheduled for the last mission. Orbits have included three highly eccentric orbits inclined initially approximately 31 deg, and two low-altitude nearly circular polar orbits. The orbit for the last mission, OGO-F, is of the latter type. (Author)

A69-37156 * #
APPLICATION OF DIFFERENTIAL SYNTHESIS TO DESIGN OF MULTIAXIS STABILITY AUGMENTATION SYSTEMS.
Raymond C. Montgomery and Howard G. Hatch, Jr. (NASA, Langley Research Center, Hampton, Va.).
(American Institute of Aeronautics and Astronautics, Guidance, Control, and Flight Dynamics Conference, Pasadena, Calif., Aug. 12-14, 1968, Paper 68-834.)
Journal of Aircraft, vol. 6, July-Aug. 1969, p. 336-343. 9 refs.

A differential synthesis technique is developed for multiple input linear feedback systems that allows direct calculation of the set of feedback gains and control interconnects that yield arbitrarily selected flying-qualities parameters. This is accomplished by parametrically relating differential gain and interconnect changes to differential changes in flying-qualities parameters. The procedure is illustrated by synthesizing a linear feedback control for the linearized lateral dynamics of a lifting-body entry vehicle whose flying qualities were unacceptable in the unaugmented conditon. The differential synthesis method developed is suitable for digital computer formulation and is easily adapted to systems of high order.
(Author)

A69-37287 *
LAUNCH CONSTRAINTS.
Harold Zweigbaum (NASA, Kennedy Space Center, Cocoa Beach, Fla.).
Space/Aeronautics, vol. 51, Feb. 1969, p. 55-62.

Discussion of launch constraints for space missions which require launching within certain well defined time periods to place the spacecraft within some definite relative position to certain celestial bodies. Launch constraints for Mariner spacecraft are described. The "business end" of an interplanetary trajectory constrains the entire flight and therefore ultimately bounds the launch opportunity as well. A table is presented listing launch opportunity constraints and launch window constraints. Injection energy, injection precision, occultation of reference bodies, communications range, probability of impact on target, and experiment requirements are considered. G.R.

A69-38117 * #
A COMMENTARY ON LOW-COST SPACE TRANSPORTATION.
A. O. Tischler (NASA, Office of Advanced Research and Technology, Chemical Propulsion Div., Washington, D.C.).
Astronautics and Aeronautics, vol. 7, Aug. 1969, p. 50-64. 5 refs.

Discussion of the problems involved in achieving low-cost-rate transportation as a mandatory goal for the future space program. These problems include development of the concept of recovery and reuse; traffic studies related to payloads in each mass class of vehicle, to vehicle orbits or trajectory paths, and to vehicle rate of launch; an assurance of adequate resources of funds and facilities, and a realistic appraisal of the technological and managerial resources required to meet program goals. A study of launch system costs is presented, and

a chart is included showing comparative costs of a combination of reusable spacecraft and expendable launch vehicle, a combination of fully reusable launch vehicle and spacecraft, and an expendable one-way cargo carrier. It is concluded that the chief expenditure of money at the present time should be directed toward hardware advanced development and experimental model testing. B.H.

A69-39376 * #
ATTITUDE CONTROL OF A MANNED EARTH ORBITING SPACE STATION.
R. S. Ryan, H. E. Worley, D. D. Nixon, F. R. Grissett, and C. W. Billups (NASA, Marshall Space Flight Center, Aero-Astrodynamics Laboratory, Huntsville, Ala.).
American Institute of Aeronautics and Astronautics, Guidance, Control, and Flight Mechanics Conference, Princeton, N.J., Aug. 18-20, 1969, Paper 69-846. 9 p.
Members, $1.00; nonmembers, $1.50.

Evaluation of mass expulsion and momentum control systems, optimized from the standpoint of thermal inputs to the station, solar power, pointing accuracies, and control system torque requirements. The sensitivity of the system to variations in inertia data, aerodynamics, and control system characteristics is determined. The basic mission and its requirements are outlined, and simulation models are discussed. Attention is given to basic trends for mass expulsion vs momentum devices. Specific results for the orbital workshop mission using reaction jets for control are presented. The final decision of whether reaction jet control or control moment gyros are best is made on the basis of cost, reliability, propellant capacity, weight, control accuracy, and other factors. For the orbital workshop phases of the AAP Cluster I mission, it is considered that the reaction jet type system met these conditions better. The ATM phase of the mission was controlled better using control moment gyros due to the fine pointing-accuracy requirements. F.R.L.

A69-39384 • #
AIR BEARING TABLE MECHANIZATION AND VERIFICATION OF A SPACECRAFT WIDE ANGLE ATTITUDE CONTROL SYSTEM.
Bruce H. Dishman and Francis J. Moran (NASA, Ames Research Center, Moffett Field, Calif.).
American Institute of Aeronautics and Astronautics, Guidance, Control, and Flight Mechanics Conference, Princeton, N.J., Aug. 18-20, 1969, Paper 69-856. 9 p.
Members, $1.00; nonmembers, $1.50.

Experimental study of the problem of controlling the attitude of a space vehicle slewing through large angles in three dimensions. The investigation is based on a control system synthesized from Euler's theorem on rotation which states that any attitude change of a rigid body may be accomplished by a single rotation about a properly chosen axis. A theoretical analysis showed that a system using the control law has global stability. The investigation was carried out using an air bearing table to simulate the spacecraft, two gimbaled star trackers as position sensors, rate gyroscopes to provide damping information, and reaction wheels as control torques. An on-line digital computer acts as a real-time controller which determines the control axis orientation from star tracker gimbal outputs, and generates simultaneous commands to the three torques. The experimental results show that the control system was stable while slewing through large angles and had excellent pointing accuracy. (Author)

A69-39402 * #
MAN'S ROLE IN LAUNCH VEHICLE GUIDANCE AND CONTROL.
Gordon H. Hardy (NASA, Ames Research Center, Moffett Field, Calif.).
American Institute of Aeronautics and Astronautics, Guidance, Control, and Flight Mechanics Conference, Princeton, N.J., Aug. 18-20, 1969, Paper 69-876. 17 p. 22 refs.
Members, $1.00; nonmembers, $1.50.

Survey of studies associated with manual guidance and control of large launch vehicles. Using the Saturn launch vehicles, the scope of the studies included control feasibility, guidance feasibility, control reliability, and guidance and control hardware implementation considerations. While these studies have already led to the incorporation of a backup manual guidance system for the later Apollo-Saturn V flights, attempts are made to extract results and conclusions that will be applicable to the next generation launch vehicles. It is concluded that the pilot is an effective adaptive element and, when used in conjunction with properly tailored guidance and control systems, should effectively contribute to the mission success and reliability of future launch vehicles. Piloted systems should be considered early in the vehicle design phase. V.P.M.

A69-39403 * #
STABILITY ANALYSIS OF APOLLO-SATURN V PROPULSION AND STRUCTURE FEEDBACK LOOP.
George L. von Pragenau (NASA, Marshall Space Flight Center, Astrionics Laboratory, Huntsville, Ala.).
American Institute of Aeronautics and Astronautics, Guidance, Control, and Flight Mechanics Conference, Princeton, N.J., Aug. 18-20, 1969, Paper 69-877. 16 p. 17 refs.
Members, $1.00; nonmembers, $1.50.

Study of multiforce feedback, first experienced in the Saturn V space vehicle, from the general viewpoint of multivariable feedback systems. The application of the Nyquist plot is demonstrated. Pogo loop components, such as the propulsion system and especially the eigenvalue problem of the structural model, are discussed. A comparison is made between the linearly unstable first flight stage of the AS-502 vehicle and one of the later vehicles, the AS-504, which was successfully stabilized by the addition of a helium gas accumulator to cushion the propellant. P.G.

A69-39691 *
TRANSPORTATION TO EARTH ORBIT—1975-1985.
Leonard Roberts (NASA, Office of Advanced Research and Technology, Mission Analysis Div., Moffett Field, Calif.).
IN: REDUCING THE COST OF SPACE TRANSPORTATION; AMERICAN ASTRONAUTICAL SOCIETY, GODDARD MEMORIAL SYMPOSIUM, 7TH, WASHINGTON, D.C., MARCH 4, 5, 1969, PROCEEDINGS. (A69-39686 21-34)
Edited by G. K. Chacko.
Tarzana, Calif., American Astronautical Society (AAS Science and Technology Series. Volume 21), 1969, p. 89, 91-107.

Discussion of the costs involved in the transportation of crew and passengers to and from orbit to future space stations. It is shown that cost reductions to the order of a factor of 10 appear feasible with current technology, providing the transportation system evolves from present systems, based on the acceptance of low-cost operating modes. Further reductions, based on concepts that depart from past systems, depend on the development of combined launch vehicle-spacecraft configurations in which a major part of the propulsion is recovered and reused. The extent of these cost reductions is shown to depend on both technical advances and new operational philosophies. B.H.,

A69-39695 *
TOWARD EFFICIENT SHUTTLE SERVICE TO EARTH ORBIT.
Eugene S. Love (NASA, Langley Research Center, Aero-Physics Div., Hampton, Va.).
IN: REDUCING THE COST OF SPACE TRANSPORTATION; AMERICAN ASTRONAUTICAL SOCIETY, GODDARD MEMORIAL SYMPOSIUM, 7TH, WASHINGTON, D.C., MARCH 4, 5, 1969, PROCEEDINGS. (A69-39686 21-34)
Edited by G. K. Chacko.
Tarzana, Calif., American Astronautical Society (AAS Science and Technology Series. Volume 21), 1969, p. 201-220.

Consideration of the long-life shuttle system, the desirable goals of which are low cost, efficient transportation of personnel and cargo, and safety. An essential requirement is the ability to serve a major segment of both NASA and DOD needs. The concepts and availability of three basic systems are discussed. The first two are partially reusable systems, featuring either vertical takeoff and horizontal landing, or vertical takeoff and vertical landing. The third

system, fully reusable, is two-stage and utilizes the horizontal takeoff and horizontal landing concept. Recovery systems such as parawing-type devices, runway landers, and deployable rotors receive attention. Aspects of advanced shuttle operation and the sequence of development are considered. F.R.L.

A69-39753 * #
AN ADVANCED CRYOGENIC CORE CONCEPT FOR A FLEXIBLE AND ECONOMICAL DELIVERY SYSTEM.
Edward W. Gomersall and Robert E. Slye (NASA, Office of Advanced Research and Technology, Mission Analysis Div., Moffett Field, Calif.).
(American Institute of Aeronautics and Astronautics, Propulsion Joint Specialist Conference, 4th, Cleveland, Ohio, June 10-14, 1968, Paper 68-812.)
Journal of Spacecraft and Rockets, vol. 7, July 1969, p. 785-789. 8 refs.

Studies of a launch-vehicle concept, employing an advanced, cryogenic, single-stage-to-orbit core, are described. The paper provides some propulsion-oriented parametric performance and design trade information derived in these studies. The concept offers a base-delivered payload range twice that of the Saturn V but with the same takeoff weight. Payloads of up to 2 million pounds can be delivered to orbit by thrust augmentation. The cost of this delivery system is anticipated to be low, primarily because a single stage is involved and, even with thrust augmentation, the entire system is started on the ground; thus, the problem of staging and altitude ignition is avoided. (Author)

A69-39760 * #
REAL-TIME TARGETING FOR THE APOLLO LUNAR ORBIT INSERTION MANEUVER.
Ronald L. Berry and Robert F. Wiley (NASA, Manned Spacecraft Center, Mission Planning and Analysis Div., Houston, Tex.).
(American Institute of Aeronautics and Astronautics, Guidance, Control, and Flight Dynamics Conference, Pasadena, Calif., Aug. 12-14, 1968, Paper 68-848.)
Journal of Spacecraft and Rockets, vol. 7, July 1969, p. 824-830.

Real-time targeting for the Apollo program lunar orbit insertion (LOI) burn is difficult because of the expected approach trajectory dispersions and the constraints on the burn. For certain situations, some of the orbit shape and landing-site target objectives cannot be achieved. Therefore, several impulsive LOI maneuvers are computed, each violating only one target objective. To do this, a series of states along the approach trajectory is generated. At each state, an impulsive maneuver is computed, violating only one target objective. Violations of the objectives are determined at the impulse point from plane geometry and simple orbital mechanics. The maneuver missing the objective the least is retained and displayed to the flight controller. The flight controller selects a best solution based on the mission status at that time. The guidance constants are then determined by computing a finite burn which matches the orbital parameters of the impulsive maneuver. (Author)

A69-39968 *
PERTURBATIONS OF EXISTING RESONANT SATELLITES.
Carl A. Wagner (NASA, Goddard Space Flight Center, Laboratory for Theoretical Studies, Greenbelt, Md.) and Bruce C. Douglas (Wolf Research and Development Corp., Applied Sciences Dept., College Park, Md.).
Planetary and Space Science, vol. 17, Aug. 1969, p. 1505-1517. 11 refs.

Analysis of the resonant perturbations to the 20th degree and order on 83 existing satellites. This analysis reveals that terms of order (m) 2 and 12 to 14 are well represented by existing resonant satellites. Only a few resonances for the other orders are available. The phenomenon of shallow resonance has also been studied. It is shown that, to accurately analyze resonant orbits, considerable attention to calculation of mean mean motion is necessary. Highly accurate formulas for calculating mean mean motion have been derived. The study also shows that, for resonant orbits with beat periods less than about 15 days, the frequencies contributed by the terms resonant with an orbit are all nearly the same, making such orbits of limited value for geodesy if considered individually. This situation is aggravated for orbits at or near the critical inclination. (Author)

A69-40542 * #
DEPLOYABLE AERODYNAMIC DECELERATORS FOR SPACE MISSIONS.
C. L. Gillis (NASA, Langley Research Center, Applied Materials and Physics Div., Hampton, Va.).
(American Institute of Aeronautics and Astronautics, Annual Meeting and Technical Display, 5th, Philadelphia, Pa., Oct. 21-24, 1968, Paper 68-1081.)
Journal of Spacecraft and Rockets, vol. 6, Aug. 1969, p. 885-890. 15 refs.

Discussion of the status of technology on items of importance in the selection of deployable aerodynamic decelerators for space missions. The operational mode considered is decelerator deployment following entry into planetary atmospheres. Summaries of drag and estimated weight information are presented for several types of decelerators, and it is concluded that two of the most efficient decelerators are the subsonic-type parachute and an attached inflatable configuration. Some alternate mission possibilities utilizing these two decelerators are reviewed. Large-scale flight experience indicates that satisfactory supersonic speed deployments of subsonic parachutes are attainable, although dynamic problems exist at Mach numbers above 2. The inflatable device should provide satisfactory deployments at higher Mach numbers although no large-scale experience exists. Good low-speed stability during steady descent is attainable for both types of decelerators. P.v.T.

A69-40550 * #
DAMPING DERIVATIVES OF 120° CONICAL SPACECRAFT FROM FLIGHTS IN A LOW-DENSITY ENVIRONMENT.
Charles H. Whitlock, Richard J. Bendura, and Allen B. Henning (NASA, Langley Research Center, Hampton, Va.).
(American Institute of Aeronautics and Astronautics, Aerospace Sciences Meeting, 7th, New York, N.Y., Jan. 20-22, 1969, Paper 69-104.)
Journal of Spacecraft and Rockets, vol. 6, Aug. 1969, p. 937-939. 11 refs.

Dynamic stability derivatives were obtained from three flight tests of a 4.8-m diameter spacecraft at Mach numbers between 0.48 and 1.5. Results from different flights show positive dynamic stability for Mach numbers 1.15 or below. At higher velocities, dynamic instability was indicated over a wide range of angles of attack. Correlation of the large-scale flight data with a limited number of ballistics range results suggests that the excessive transonic instability may be associated with low angle-of-attack oscillations. (Author)

A69-42835 * #
METEOROLOGICAL SATELLITES—BEYOND THE FIRST NINE YEARS.
R. L. Haley (NASA, Washington, D.C.).
American Astronautical Society and Operations Research Society of America, Joint National Meeting, Denver, Colo., June 17-20, 1969, AAS Paper 69-421. 16 p. 12 refs.

Survey of the major characteristics of the individual missions in the NIMBUS Program, with emphasis on results of NIMBUS 3 launched Apr. 14,1969. Developments that are now underway in future satellite programs to improve both short and long-term weather forecasting are also discussed. (Author)

A69-42838 * #
THE IMPACT OF APOLLO APPLICATION ON SPACE STATION ENGINEERING.
William D. Green, Jr. (NASA, Washington, D.C.).

American Astronautical Society and Operations Research Society of America, Joint National Meeting, Denver, Colo., June 17-20, 1969, AAS Paper 69-491. 20 p.

Discussion of the Apollo Applications Program spacecraft (AAP 1 and AAP 2), as a major step in the transition of manned space flight from the pioneering missions of the first decade to a future period in which men will operate in space for purposes of exploitation. Particular attention is given to the aspects of the AAP that are directly associated with and are most important for future space station engineering. The four principal areas of AAP impact on space station technology are examined. They are (1) equipment technology—basic phenomena, device tests, operational use and evaluation, and definition of validation of requirements, (2) system technology—architecture, orientation management, thermal behavior, communications and data management, and checkout and maintainability, (3) program technology—test policy for long duration systems, interface control and verification for orbital "first mate," and development and in-flight configuration control, and (4) operations. V.P.

A69-42842 * #
SAFETY FOR LARGE SPACE STATIONS.
Jack W. Wild (NASA, Office of Manned Space Flight, Washington, D.C.).
American Astronautical Society and Operations Research Society of America, Joint National Meeting, Denver, Colo., June 17-20, 1969, AAS Paper 69-518. 25 p.

Review of the NASA safety studies which have been accomplished over the past several years. Some of the foreseeable safety problems associated with 12-man and 50-man space stations are discussed, and the applicability of current space safety practices is considered. The approaches discussed include damage containment and control techniques, escape concepts, earth based rescue, and possible combinations of the foregoing. Specific areas in which additional information should be developed are highlighted. (Author)

A69-43120 * #
AN APPROACH TO COST ANALYSIS IN LOW COST LAUNCH VEHICLE STUDIES.
Thomas Campbell (NASA, Washington, D.C.) and Robert A. Schneider (NASA, Lewis Research Center, Cleveland, Ohio).
Interagency Chemical Rocket Propulsion Group, Liquid Propulsion Meeting, 11th, Miami, Fla., Sept. 16-18, 1969, Paper. 12 p.

Review of historical costs revealing specific shortcomings of current low-cost studies, and outline of a method by which valid studies of low-cost approaches may be conducted to make possible the eventual selection of a total approach to low-cost transportation that is really cost-effective. Emphasis is placed on the need to consider all factors in examining "low-cost" vehicle proposals. Two major cost areas in current programs, sustaining engineering and plant economics, are discussed. The main features of the proposed approach are: clear definition of program objectives and common ground rules, development and interpretation of cost and program baselines, thorough and complete treatment of all candidates, and comparative analysis of the total program cost estimates for all candidates to select the most cost-effective program. P.G.

N69-10295*# National Aeronautics and Space Administration. Lewis Research Center, Cleveland, Ohio.
ATLAS-CENTAUR AC-12 FLIGHT PERFORMANCE FOR SURVEYOR 3
Washington Nov. 1968 171 p refs
(NASA-TM-X-1678) Avail: CFSTI CSCL 22D

Atlas-Centaur vehicle AC-12, launched on April 17, 1967, was the third operational flight in the Centaur program. The vehicle carried Surveyor 3, which was boosted into a lunar intercept trajectory by the parking orbit mode of ascent. This mode of ascent included placing the Centaur in a circular orbit, coasting under low gravity conditions, and restarting the Centaur main engines to supply energy to attain the proper lunar-intercept trajectory. This report includes a flight performance evaluation of the Atlas-Centaur launch vehicle system from lift-off through Centaur retromaneuver. Author

N69-10775*# National Aeronautics and Space Administration. Langley Research Center, Langley Station, Va.
EXPERIMENTAL VIBRATION CHARACTERISTICS OF A 1/40-SCALE DYNAMIC MODEL OF THE SATURN 5 LAUNCH UMBILICAL TOWER CONFIGURATION
John J. Catherines Washington Nov. 1968 75 p refs
(NASA-TN-D-4870) Avail: CFSTI CSCL 22D

The results of bending vibration tests on 1/40-scale dynamic models of the Saturn V launch vehicle and its umbilical tower are presented herein. The lateral vibratory response characteristics of these structures, considered separately and as an integral configuration mounted on the launch platform, are presented. Mode shapes, resonant frequencies, and damping values were determined over a frequency range of 10 to 300 hertz (0.25 to 7.5 hertz, full-scale equivalent). The resuls include data for two simulated mass conditions corresponding to a fueled and an unfueled launch vehicle. A description of the models is presented and the scaling concepts employed in their design are discussed. The first four cantilever modes and frequencies of the 1/40-scale models of the vehicle and tower are presented. At its first resonance, the tower responds in planes which are not coincident with its planes of symmetry. The test results for the complete configuration indicate considerable coupling between the launch vehicle and the tower at the higher frequencies, but little coupling at the lower frequencies (below 60 hertz) even though the first cantilever modes of the vehicle and tower were included in this low-frequency range. Author

N69-10934*# National Aeronautics and Space Administration. Langley Research Center, Langley Station, Va.
VIBRATION ANALYSIS OF A 1/40-SCALE DYNAMIC MODEL OF SATURN 5 LAUNCH PLATFORM-UMBILICAL TOWER CONFIGURATION
Howard M. Adelman and Earl C. Steeves Washington Nov. 1968 61 p refs
(NASA-TN-D-4871) Avail: CFSTI CSCL 22D

An analysis was performed to determine the lateral-vibrational characteristics of a 1/40-scale dynamic model of the Apollo-Saturn 5 vehicle–umbilical tower configuration. The direct stiffness method was employed for the calculations. The analysis treats the vibration of the complete configuration confined to the plane of the tower and vehicle center lines, although the tower itself was analyzed in two directions. Results are presented for the umbilical tower alone, the vehicle alone, the umbilical tower mounted on the launch platform and the complete vehicle–umbilical tower configuration. The flexible connection between the vehicle and launch platform had to be represented by a rotational spring to obtain good agreement with experiment. All the analytical results were compared with experimental results and the good agreement indicates that the direct stiffness method provides an effective technique for computing the vibrational characteristics of complex structures. Author

N69-11007*# National Aeronautics and Space Administration. Langley Research Center, Langley Station, Va.
LATERAL VIBRATION CHARACTERISTICS OF A 1/40-SCALE DYNAMIC MODEL OF APOLLO-SATURN 5 LAUNCH VEHICLE
Earl C. Steeves and John J. Catherines Washington Nov. 1968 45 p refs
(NASA-TN-D-4872) Avail: CFSTI CSCL 22D

Analytical and experimental investigations of the lateral vibration characteristics of a dynamically similar 1/40-scale model

of the Apollo-Saturn 5 launch vehicle have been performed. A brief description of the model is given and the procedures used in the tests and reduction of the data are discussed. The idealization of the model and method of analysis are presented. The free-free natural frequencies and corresponding mode shapes are presented for weights corresponding to several flight times including staged configurations. In addition, cantilever results and experimental modal damping values are presented. Good agreement was found between analytical and experimental results; thus the idealization is validated and the beam idealization adequately represents the motion of the model over the frequency range of the investigation. On comparing the frequency of the 1/40-scale model with those of a 1/10-scale replica model, good agreement is found for the first three modes. This comparison indicates that the degree of relaxation of replica scaling used in the design of the 1/40-scale model is acceptable for determining the first three launch-vehicle bending modes. The importance of proper representation of the tie-down condition and the importance of the inclusion of shear deformation are demonstrated. Author

N69-13232*# National Aeronautics and Space Administration. Manned Spacecraft Center, Houston, Tex.
POSTFLIGHT OPTICAL EVALUATION OF THE RIGHT-HAND AND LEFT-HAND WINDOWS OF GEMINI MISSIONS 4, 5, 6, AND 7
George P. Bonner, Michael F. Heidt, Carl L. Kotila, John A. Lintott, John E. Novotny et al Washington Dec. 1968 50 p
(NASA-TN-D-4916) Avail: CFSTI CSCL 22B

Transmission and relative resolution measurements were made before cleaning, and transmission, schlieren, relative resolution, and interferometric measurements were made after cleaning, on the right-hand and left-hand windows of Gemini spacecraft G-IV to G-VII. Chemical analyses of the contamination cleaned from the windows show that the primary constituent is amorphous silica. Author

N69-14010*# National Aeronautics and Space Administration. Goddard Space Flight Center, Greenbelt, Md.
TIME REQUIRED FOR AN ADEQUATE THERMAL-VACUUM TEST OF FLIGHT MODEL SPACECRAFT
A. R. Timmins Washington Dec. 1968 23 p refs
(NASA-TN-D-4908) Avail: CFSTI CSCL 22B

This report presents data from the thermal-vacuum tests of 11 flight spacecraft. The data show that total test time is not as important as the time required at four kinds of thermal stress levels. The data base was chosen to include three programs of differing complexity and differing test emphasis, prior to the system test. The individual and collective data indicate a minimum thermal-vacuum system test time of 13 days regardless of the prior test program. The 13 days need to be distributed as follows: 1, 4, 4, and 4 for ambient, transient, cold, and hot thermal-vacuum environments, respectively. Author

N69-14033*# National Aeronautics and Space Administration. Lewis Research Center, Cleveland, Ohio.
A WIND PROFILE FOR GENERATING CONTROL REQUIREMENTS FOR ROCKET VEHICLES USING LIQUID-INJECTION CONTROL SYSTEMS
Carl J. Daniele and Fred Teren NASA Dec. 1968 31 p refs
(NASA-TM-X-1708) Avail: CFSTI CSCL 22B

A synthetic wind profile with a plateau 5700 meters in width and which drops linearly from this plateau to zero wind velocity at zero altitude and to zero wind velocity at 20-km altitude was found to be the best fit of the type investigated to ten real winds with 90 to 95 percent peak wind velocities measured at the Eastern Test Range. Deflection-impulse requirements were obtained by using this new profile. These requirements were compared to those obtained for the ten real winds for five typical solid launch vehicles, and good agreement was obtained. To illustrate the use of the new synthetic profile, thrust-vector control (TVC) injectant requirements were then calculated for the five launch vehicles for 99 percent winds. Author

N69-15374*# National Aeronautics and Space Administration. Langley Research Center, Langley Station, Va.
AN INVESTIGATION OF THE OPTIMUM DESIGN AND FLIGHT OF ROCKETS
John D. Bird Washington Jan. 1969 35 p refs
(NASA-TR-R-297) Avail: CFSTI CSCL 22D

An analysis using classical variational methods was made whereby significant physical characteristics of rockets were determined in an optimal sense. A two-point boundary value problem was formulated which, when solved, provided the significant physical parameters and flight path for a two-stage rocket which would deliver a given payload to orbit with minimum total initial mass. Numerical solutions were carried out for nine cases by an iterative method. The results show how the stage masses and thrusts should be proportioned for various structural efficiencies in the fuel tanks and rocket motors. Analyses of the type carried out for this investigation should be useful in the sizing and, generally, in the design of rockets. Author

N69-15634*# National Aeronautics and Space Administration. Ames Research Center, Moffett Field, Calif.
RESEARCH PROBLEMS IN ATMOSPHERE ENTRY AND LANDING FOR MANNED PLANETARY MISSIONS
C. A. Syvertson Washington Jan. 1969 34 p refs Presented at the AIAA Technol. for Manned Planetary Missions Meeting, New Orleans, 4–6 Mar. 1968
(NASA-TN-D-4977) Avail: CFSTI CSCL 22A

Some of the research problems associated with atmosphere entry for manned planetary missions are assessed with primary emphasis on the problems related to missions to Mars and Venus. The assessment is divided into two parts: First, the requirements associated with entering the Earth's atmosphere are defined, and second, those associated with atmosphere entry and landing at the target planet are considered. The assessment of the problems of entering the Earth's atmosphere has shown that maximum entry speeds can be expected to range from about 15 to 18 km/sec. The problems of entry at these hyperbolic speeds are then compared with the problems of entering at Apollo's speed of about 11 km/sec. These comparisons include corridor depths, acceleration histories, and convective and radiative heating. It is also shown that for missions to Mars and Venus the entry speeds are relatively modest, being about 6 to 10 km/sec at Mars and about 11 to 13 km/sec at Venus. With the low surface pressures estimated for Mars, very large parachutes deployed at conditions well beyond current experience will be required. Author

N69-16155*# Measurement Analysis Corp., Los Angeles, Calif.
A METHOD FOR PREDICTING LAUNCH VEHICLE VIBRATION LEVELS IN THE REGION OF THE SPACECRAFT ADAPTOR
A. G. Piersol and W. F. Van Der Laan Washington NASA Jan. 1969 115 p refs
(Contract NAS1-7490)
(NASA-CR-1227; MAC-709-10) Avail: CFSTI CSCL 22D

This report derives and presents a set of prediction curves for launch vehicle vibration levels in the region of the spacecraft adaptor structure. The prediction curves are developed by a regression analysis of previous data collected for various different launch vehicle configurations, and are based upon six rudimentary

parameters describing the launch vehicle flight and propulsion conditions. The intent is to provide a basis for making preliminary vibration predictions early in the conceptual design of a new launch vehicle configuration so that test specifications and design criteria can be established for the procurement of long lead time equipment items. The predictions are presented in terms of average power spectral densities in octave band frequency intervals for liftoff transonic flight, and maximum dynamic pressure flight. All data used to arrive at the prediction curves are presented, and the efficiency of the curves is fully evaluated. Author

N69-16221 *# Ling-Temco-Vought, Inc., Dallas, Tex.
ROLL AND YAW COMPENSATION FEASIBILITY STUDY
P. D. Fremming Washington NASA Jan. 1969 113 p refs
(Contract NAS1-5592)
(NASA-CR-1209; REPT-3-32000/7R-36) Avail: CFSTI CSCL 22D

The feasibility of using roll and yaw compensation to reduce the inclination error of the Scout launch vehicle was investigated. The recommended circuit configuration, a discussion of the recommended checkout method and equipment, and a description of the installation requirements are included. From the analyses, it was concluded that a pre-programmed type of multiplier is the only system currently known to have sufficient accuracy to meet the requirements of roll and yaw compensation. Analysis showed that a gyro drift rate caused by the compensation unit of greater than 0.5 degrees per hour degrades the inclination accuracy improvements realized by the addition of the roll and yaw compensation. Since a steady voltage across the gyro torquer produces a drift rate, it is concluded that the null uncertainty of the compensation unit must be less than 0.0002 volts to meet the drift requirements. Only the pre-programmed multiplier can meet this null requirement. This device achieves the required multiplication by changing the gain of the compensator as a function of the pitch program rate on command from the Intervalometer. Author

N69-17801 *# National Aeronautics and Space Administration. Langley Research Center, Langley Station, Va.
THE DETERMINATION OF A STABILITY INDICATIVE FUNCTION FOR LINEAR SYSTEMS WITH MULTIPLE DELAYS
John D. Shaughnessy and Yasutada Kashiwagi (Stanford Res. Inst., Menlo Park, Calif.) Washington Feb. 1969 35 p refs
(NASA-TR-R-301) Avail: CFSTI CSCL 12A

A theoretical study is made of the stability of a class of linear differential-difference equations with multiple delays. A direct method for determining the exact stability boundaries for homogeneous, linear differential-difference equations with constant coefficients and constant delays is formulated. This formulation results in a stability indicative function, depending on a single parameter, which determines the number of roots of the transcendental characteristic equation that have positive real parts. It is proved that the system is stable if and only if this function has a value of zero. A second-order system with delays in the velocity and position feedback terms is considered as an example, the stability regions for this system are determined for a range of delays and coefficients. It is observed that introduction of a delay has a definite destabilizing effect on the system, and introduction of a second delay has a compounding effect to further reduce stability. However, this example clearly illustrates that certain combinations of delays can stabilize an unstable system. This phenomenon is discussed from a theoretical point of view. Author

N69-17851 *# National Aeronautics and Space Administration. Goddard Space Flight Center, Greenbelt, Md.
NIMBUS 2 FLIGHT EVALUATION AND ENGINEERING REPORT, LAUNCH THROUGH ORBIT 5275
Joseph J. McNaney (GE), Bennie A. Palmer (GE), and Ralph Shapiro Washington Feb. 1969 197 p refs
(NASA-TN-D-4881) Avail: CFSTI CSCL 22A

This report covers the flight history of Nimbus 2 from its launch on May 15, 1966, through orbit 5275 on June 15, 1967, providing an engineering evaluation of the performance during this period. The mission successfully met all technological and scientific objectives, the only failures being the tape recorders, PCM, MRIR, AVCS, and HRIR; these failures occurred during orbits 949, 985, 1443, and 2455, respectively. As of March 15, 1968 (22 months, orbit 9020), the spacecraft was performing satisfactorily with little change in performance since June 15, 1967, except for the solar array drive. After October 1967, the drive system evidenced occasional erratic behavior and since then has been operated in the high-torque mode. The real time data systems are still being used. Author

N69-20965*# National Aeronautics and Space Administration. Langley Research Center, Langley Station, Va.
FULL-SCALE DYNAMIC LANDING-IMPACT INVESTIGATION OF A PROTOTYPE LUNAR MODULE LANDING GEAR
Ulysse J. Blanchard Washington Mar. 1969 43 p refs Film supplement number L-1011 to this report is available on loan from NASA. Langley Research Center, Langley Station, Va.
(NASA-TN-D-5029) Avail: CFSTI CSCL 22B

The full-scale tests were conducted with a planar (three degrees of freedom) lunar gravity simulator and a full scale test vehicle. Structural integrity of a prototype landing gear system (struts and deployment trusses) was substantiated. Dynamic performance of the landing gear struts was good for all landing conditions tested including those which produced near maximum strokes and loads. Theoretical results were in agreement with experimental results obtained for landing accelerations, gear forces and strokes, and vehicle pitch motions. Author

N69-21017*# National Aeronautics and Space Administration. Goddard Space Flight Center, Greenbelt, Md.
THE SMALL ASTRONOMY SATELLITE (SAS) PROGRAM
Majorie R. Townsend Washington Mar. 1969 23 p
(NASA-TN-D-5099) Avail: CFSTI CSCL 22B

The Small Astronomy Satellite (SAS), one of NASA'S newest Explorer-class programs, can provide at relatively low cost much previously unavailable basic information on low and high energy radiation from sources both inside and outside the galaxy. This report gives sufficient information concerning the SAS volume and weight, and the power, command, telemetry, and control systems to permit the reader to ascertain its suitability for specific astronomy experiments. Project reliability requirements and environmental test conditions are included in the appendixes. Author

N69-21065*# National Aeronautics and Space Administration. Goddard Space Flight Center, Greenbelt, Md.
RELAY PROGRAM Final Report
Washington 1968 368 p refs
(NASA-SP-151) Avail: SOD $3.25; CFSTI CSCL 22B

The operations of Relay 1 and 2 are summarized for the period July through December 1964. The performance of the two spacecraft is compared and certain design modifications incorporated in Relay 2 as a result of experience with Relay 1 are described. The results of the Relay 2 communication experiments conducted by the Mojave Station from 1 January through 1 July 1965 are presented. In describing the Relay 2 performance, the format of the Project Relay Communication Experiments Plan R1-0521 is generally followed. Similar experiments, conducted by ground stations

in other countries, are also reported. The station included: Raisting, Germany; Fucino, Italy; Kashima and Ibaraki, Japan; Rao, Sweden; Grinon, Spain; and Goonhilly Downs, England. B.P.

N69-21111*# National Aeronautics and Space Administration. Langley Research Center, Langley Station, Va.
ON LATERAL CABLE OSCILLATIONS OF CABLE-CONNECTED SPACE STATIONS
Willard W. Anderson Washington Mar. 1968 85 p refs
(NASA-TN-D-5107) Avail: CFSTI CSCL 22B

The influence of lateral cable oscillations on a spinning cable-connected space station is defined in terms of steady-state and transient response to torques acting on the space station. The system is defined by using linear rigid-body equations and a dual formulation of the cable modes. Damping is included in the dual formulation and estimates of this damping are provided. The analysis allows a determination of the required depth of modeling for a given system in terms of the system parameters and the expected disturbances. Energy flow within the system is discussed by using a system bond graph. Author

N69-21399*# National Aeronautics and Space Administration. Lewis Research Center, Cleveland, Ohio.
ATLAS-CENTAUR AC-11 FLIGHT PERFORMANCE FOR SURVEYOR 4
Washington 14 Apr. 1969 157 p
(NASA-TM-X-1768) Avail: CFSTI CSCL 22B

The final evaluation of the Atlas-Centaur AC-11 vehicle systems performance for the Surveyor 4 mission is given, from lift-off through the Centaur retromaneuver. Successful launching and achievement of mission objectives are described. A detailed systems analysis is presented for the propulsion, pneumatic, hydraulic, propellant loading and utilization, separation and jettison, electrical, guidance, and control systems, and for the vehicle structures. Supplemental flight, trajectory, and performance data are included, along with performance calculation techniques for the Centaur engine. P.A.B.

N69-22630*# National Aeronautics and Space Administration. Langley Research Center, Langley Station, Va.
SCALED LUNAR MODULE JET EROSION EXPERIMENTS
Norman S. Land and Harland F. Scholl Washington Apr. 1969 42 p refs Supplement Number L-1043 to this report is available on loan from Langley Research Center
(NASA-TN-D-5051) Avail: CFSTI CSCL 22B

An experimental research program was conducted on the erosion of particulate surfaces by a jet exhaust. These experiments were scaled to represent the lunar module during landing. A conical gold-gas nozzle simulating the lunar module nozzle was utilized. The investigation was conducted within a large vacuum chamber by using gravel or glass beads as a simulated soil. The effects of thrust, descent speed, nozzle terminal height, particle size on crater size, and visibility during jet erosion were determined. Results indicate that, from an erosion and visibility standpoint, the best landing mode for a lunar module type of vehicle would involve: site inspection and selection above the incipient erosion height, and a fast descent to the highest drop-in altitude that the vehicle structure could withstand. A slow and cautious descent with hovering just above the lunar surface would greatly increase crater size and impair visibility. Author

N69-22937*# National Aeronautics and Space Administration, Lewis Research Center, Cleveland, Ohio.
EXPERIMENTAL BENDING STRENGTH OF AN ATLAS LV-3C BOOSTER BEYOND COMPRESSIVE SKIN WRINKLING
Robert P. Miller Washington Apr. 1969 57 p refs
(NASA-TN-D-5156) Avail: CFSTI CSCL 22B

Three bending-strength tests were performed at Lewis Research Center, on a full-scale Atlas LV-3C booster to determine the bending strength available after the start of compressive wrinkling of the vehicle tank skin. Experimental data are compared with analytical predictions and show a good correlation. A description of these tests, the test results, and a method of analytically evaluating postwrinkling bending of thin-walled pressure-stabilized cylinders are presented. Author

N69-24038*# National Aeronautics and Space Administration. Lewis Research Center, Cleveland, Ohio.
ATLAS-AGENA FLIGHT PERFORMANCE FOR THE APPLICATIONS TECHNOLOGY SATELLITE ATS-1 MISSION
Washington May 1969 97 p refs
(NASA-TM-X-1784) Avail: CFSTI CSCL 22B

Flight performance is discussed from liftoff through the final attitude maneuver. The Atlas–Agena vehicle systems performed satisfactorily throughout the flight, including the standard Agena clamshell shroud which was used for the first time to provide aerodynamic shielding for the spacecraft during ascent through the atmosphere. Aerospace ground equipment operated properly during the countdown and launch, except that the 2-inch motion switch failed at liftoff, and the time of first motion had to be derived from the 8-inch motion switch. Detailed discussions are included on the following aspects of the flight: (1) trajectory and performance; (2) Atlas vehicle system performance; (3) Agena spacecraft system performance; and (4) launch operations. In addition, evaluation of the final Agena transfer orbit parameters demonstrated,that these were within the requirements established for the ATS-1 mission. A.C R.

N69-24760*# Israel Program for Scientific Translations, Ltd., Jerusalem.
HANDBOOK OF ASTRONAUTICS
N. Ya. Kondrat'ev, ed. et al 1968 230 p Transl. into ENGLISH of the book "Spravochnik Po Kosmonavtike" Moscow, Voennoe Izd., Min. Oborony SSSR, 1966 Published for NASA and NSF
(NASA-TT-F-500; TT-68-50304) Copyright. Avail: CFSTI CSCL 05B

Material taken from Soviet and non-Soviet sources was used to compile this handbook. The structure of the universe is considered, and descriptions of the stars and the solar system are given, followed by a review of systems of celestial coordinates. The physical characteristics of the upper atmosphere and the exosphere are considered. Data on the dynamics of injection, orbiting, and descent and on the orbits and trajectories of spacecraft are given. Spacecraft navigation is covered, together with some problems of maneuvering and positioning. The basic phenomena affecting the human organism during space flight, space cabin environmental control, and life support systems are described. A classification of spacecraft and of their engine systems is given as well as an account of the milestones of space exploration and scientific and other uses of spacecraft. Most of the book deals with near-Earth space flight, but some problems of lunar and interplanetary flight are also covered. K.W.

N69-24942*# National Aeronautics and Space Administration. Lewis Research Center, Cleveland, Ohio.
ANALYTICAL EVALUATION OF SPACE STORABLE PROPELLANTS FOR UNMANNED JUPITER AND SATURN ORBITER MISSIONS
John C. Oglebay, Gary D. Sagerman, and Harold H. Valentine Washington May 1969 60 p refs
(NASA-TM-X-1793) Avail: CFSTI CSCL 22D

An analytical study was performed to evaluate the potential

application of space storable propellants to unmanned planetary orbit missions. The study concentrated on retrostages for Jupiter and Saturn orbiter missions. The performance capabilities and space storage characteristics of Earth storable, space storable, and deep cryogenic stages are compared. Mission times up to 1500 days were considered, and all results shown are based on nonvented propellant storage over the entire mission time. Author

N69-26458*# National Aeronautics and Space Administration. Langley Research Center, Langley Station, Va.

FLIGHT-TEST RESULTS FROM SUPERSONIC DEPLOYMENT OF AN 18-FOOT-DIAMETER (5.49 METER) TOWED BALLUTE DECELERATOR

John J. Mayhue and Clinton V. Eckstrom Washington May 1969 26 p refs Film Supplement Number L-1045 to this report is available on loan from NASA. Langley Research Center, Langley Station, Va.

(NASA-TM-X-1773) Avail: CFSTI CSCL 22B

A ram-air-inflated, towed ballute decelerator having a maximum frontal diameter of 18 feet (5.49 meters) was deployed during free flight at a Mach number of 3.15 and a dynamic pressure of 38.5 lb/ft^2 (1843.4 N/m^2). Deployment and extraction of the test ballute were normal but inflation stopped about 1 second after mortar firing and produced an average plateau drag force of 1500 pounds (6.7 kN) for about 1 second. Approximately 30 percent of expected total frontal area was obtained. Examination of a motion-picture film showed no unusual events during initial filling of the ballute; however, shortly after ballute growth stopped, failure of the fabric at one inlet leading edge was observed. A large aft-end rip also became evident after decay of the plateau drag forces later in the flight. It is postulated that incomplete filling of the test ballute may have been caused by prolonged whipping action of the envelope fabric which prevented sufficient inlet exposure, eventually led to inlet failure, and may have contributed to an aft-end rip during the initial inflation process. Author

N69-26570*# National Aeronautics and Space Administration. Langley Research Center, Langley Station, Va.

STATIC LONGITUDINAL AERODYNAMIC CHARACTERISTICS OF SOME SUPERSONIC DECELERATOR MODELS AT MACH NUMBERS OF 2.30 AND 4.63

Edwin E. Davenport Washington May 1969 36 p refs

(NASA-TN-D-5219) Avail: CFSTI CSCL 01A

An experimental investigation of spherically blunted 120° cones, tension shell models, and a model representative of an attached inflatable decelerator (AID) has been conducted at Mach numbers of 2.30 and 4.63 through an angle-of-attack range from about −5° to about 20°. The results show a reduction in axial force with an increase in shoulder radius for the cone models. Good agreement between theoretical and experimental values of standoff distance and bow-wave shape was obtained for the 120° cone models at Mach 4.63. The tension shell models produced a higher level of axial-force coefficients than did the cone models. After inflation the attached inflatable decelerator model produced about twice the axial-force coefficient of the cone models. Author

N69-26993*# Bendix Corp., Mishawaka, Ind.

STUDY OF A MODULAR EXTRAVEHICULAR ACTIVITY WORK PLATFORM

Washington NASA May 1969 67 p refs

(Contract NASw-1820)

(NASA-CR-1361; BMSD-6182) Avail: CFSTI CSCL 22B

Results of studies to establish conceptual configurations for extravehicular activity (EVA) work platforms to be used by suited astronauts in orbital operations are presented. The concept chosen consisted of a 1500 pound self-propelled EVA work platform made up of five modules which are removable and interchangeable to an extent permitting the orbital assembly of a mission oriented work platform. The scope of the study included a preliminary design of major subsystems and construction of a full scale mockup. Author

N69-27260*# National Aeronautics and Space Administration. Lewis Research Center, Cleveland, Ohio.

ATLAS-AGENA FLIGHT PERFORMANCE FOR THE APPLICATIONS TECHNOLOGY SATELLITE ATS-2 MISSION

Washington May 1969 105 p refs

(NASA-TM-X-1800) Avail: CFSTI CSCL 22C

The Atlas–Agena launch vehicle boosted the Applications Technology Satellite ATS-2 into a transfer orbit with a perigee of 100 nautical miles (185 km) and an apogee of 6000 nautical miles (11 112 km). However, the Agena second burn did not occur, and the final circular orbit was not achieved. The Agena engine failed to restart for second burn because a propellant isolation valve malfunctioned. This report discusses the flight performance of the Atlas–Agena launch vehicle from lift-off through the Agena vehicle retromaneuver. A discussion of the propellant isolation valve failure is also included. Author

N69-27299*# General Dynamics/Convair, San Diego, Calif.

ANALYSIS AND DESIGN OF SPACE VEHICLE FLIGHT CONTROL SYSTEMS. VOLUME 16: ABORT

Arthur L. Greensite Washington NASA May 1969 209 p refs

(Contract NAS8-21383)

(NASA-CR-835; GDC-DDE-68-001) Avail: CFSTI CSCL 22C

The state of the art of abort procedures is discussed in terms of defining the problem areas and indicating the trends of current research. Abort methodology differs in each of five regions: (1) on the pad, (2) atmospheric, (3) exoatmospheric, (4) orbital, and (5) lunar. Recommended procedures are examined for each of these abort conditions. Unclassified details relating to the complete Gemini and Apollo abort systems are presented, and some of the more sophisticated rescue and recovery systems are briefly surveyed, including satellite life jackets, rafts, and boats, EGRESS (emergency global rescue escape and survival system), and the paracone system. Emphasis is placed on control system requirements for abort problems; hardware implementations are discussed in general terms where appropriate. P.A.B.

N69-28166*# National Aeronautics and Space Administration. Manned Spacecraft Center, Houston, Tex.

AERODYNAMIC LOADS ON DEPLOYED CANARD SURFACES AND ROCKET NOSE SECTION OF THE APOLLO LAUNCH ESCAPE VEHICLE

William C. Moseley, Jr. and Branch S. Phillips Washington Jun. 1969 89 p refs

(NASA-TN-D-5260) Avail: CFSTI CSCL 22B

Wind-tunnel tests were conducted using a 0.150-scale model of the forward section of the Apollo launch escape rocket. Pressure data were obtained for the body section of the model. Aerodynamic and pressure data were obtained on the canard surfaces of the model. Three removable canards were used; two were instrumented for pressure data and one was instrumented for force and moment data. Tests were conducted at Mach numbers of 0.68, 1.06, 1.50, and 2.00 and at canard deployment angles of 30°, 60°, 90°, and 115° with full deployment at the 115° angle. Results of these tests are presented in tabular and graphic forms. Author

N69-28861*# Astro Research Corp., Santa Barbara, Calif.

HELIOGYRO SOLAR SAILER Summary Report

Richard H. Mac Neal, John M. Hedgedeth, and Hans U. Schuerch Washington NASA Jun. 1969 84 p refs

(Contract NAS7-427)

(NASA-CR-1329; ARC-R-297) Avail: CFSTI CSCL 22B

Studies have been performed on the feasibility of a large solar-sail vehicle using long, narrow blades and operating in the manner of a helicopter rotor. This vehicle, the Heliogyro, is superior to other propulsion and attitude-control systems for many missions requiring large total impluse and long flight times. A conceptual configuration has been evolved in which the thin aluminized film blades are unrolled from spools during deployment. Centrifugal forces are used for stiffening the long, narrow solar sails. Control of the attitude of the sail with respect to the solar rays is accomplished by pivoting the deployment spools and thus rotating

the long blades about their lengthwise axes. Combinations of collective and cyclic blade pitch can provide all of the required control responses. Results of the various theoretical analyses which have led to this Heliogyro solar-sail concept are summarized. Evaluations of a number of missions are presented. The desirability of an experimental program to develop technology and establish feasibility is indicated. Author

N69-29594*# National Aeronautics and Space Administration. Lewis Research Center, Cleveland, Ohio.

ATLAS-AGENA PERFORMANCE FOR THE 1967 MARINER VENUS MISSION

Washington Jun. 1969 109 p

(NASA-TM-X-1826) Avail: CFSTI CSCL 22B

The Atlas–Agena successfully launched a Mariner unmanned deep space probe during 1967 to fly by the planet Venus. This report discusses the performance of the Atlas–Agena from lift-off through the Agena posigrade maneuver. The objective of the mission was to extend scientific knowledge about the size and mass of Venus and the density and composition of the planet's atmosphere. Author

N69-30339*# National Aeronautics and Space Administration. Electronics Research Center, Cambridge, Mass.

SPACECRAFT MAGNETIC TORQUES

Mar. 1969 55 p refs

(NASA-SP-8018) Avail: CFSTI CSCL 22B

The magnetic torque resulting from the interaction between the magnetic properties of a spacecraft and the ambient magnetic field is studied in the light of magnetic disturbance torque considered in the determination of spacecraft attitude motion, control actuator sizing, expendable fuel requirements, and spin decay. The two design criteria associated with magnetic disturbance torques are: (1) assessment of the magnitude of the torque; and (2) control over the spacecraft magnetic characteristics during design and development to assure achievement of an acceptably low magnetic disturbance torque. F.O.S.

N69-30631*# National Aeronautics and Space Administration. Lewis Research Center, Cleveland, Ohio.

EXPERIMENTAL LATERAL BENDING DYNAMICS OF THE ATLAS-CENTAUR-SURVEYOR LAUNCH VEHICLE

Robert P. Miller and Theodore F. Gerus Washington Jul. 1969 24 p refs

(NASA-TM-X-1837) Avail: CFSTI CSCL 22B

A series of full-scale dynamic tests was conducted to determine the lateral bending dynamics of the launch vehicle. The tests were made at several simulated flight times to obtain a good experimental definition of the vehicle dynamic response in the bending mode frequency range. Parameters measured were bending mode frequencies, damping, mode shapes, and linearity. The bending mode frequencies measured ranged from 2.59 to 31.9 Hz. Damping measured averaged about 2.0 percent of critical. Mode shapes were well defined and continuous in the lower-frequency modes but indicated discontinuities in the higher modes. The modal response was very linear over the excitation range chosen, and only small differences between pitch and yaw axes were seen. Phase relations of various response points for three modes were also measured. Author

N69-32021*# National Aeronautics and Space Administration, Washington, D.C.

THE APOLLO SPACECRAFT. VOLUME 1: A CHRONOLOGY

Ivan D. Ertel and Mary Louise Morse 1969 275 p

(NASA-SP-4009) Avail: SOD $2.50; CFSTI CSCL 22B

A chronology of the Apollo spacecraft program up to November 7, 1962 provides specific documented information of a wide range of events both directly and indirectly related to this program. References to the Mercury and Gemini programs are included. During this period of time, the Apollo project was basically involved in mission definition, contractor selection, and final selection of mode and module for lunar orbit. The abbreviations, committees, major spacecraft contractors, funding, organizational charts, Apollo launch vehicles, and the flight summary are appended. J.A.M.

N69-32298*# National Aeronautics and Space Administration. Goddard Space Flight Center, Greenbelt, Md.

ATTITUDE STABILITY OF A CLASS OF PARTIALLY FLEXIBLE SPINNING SATELLITES

Thomas W. Flatley Washington Aug. 1968 18 p refs

(NASA-TN-D-5268) Avail: CFSTI CSCL 22B

A stability criterion is presented for spinning satellites, which consist of a rigid, symmetric, central body and four radial booms of arbitrary flexibility. Author

N69-32713*# National Aeronautics and Space Administration. Langley Research Center, Langley Station, Va.

AN EVALUATION TEST OF A FULL SCALE REPLICA OF THE RAM-CA FLIGHT HEAT SHIELD IN A ROCKET ENGINE EXHAUST

Kenneth Sutton, Ernest V. Zoby, and David H. Butler Washington Jul. 1969 49 p refs

(NASA-TM-X-1841) Avail: CFSTI CSCL 22B

An evaluation test of the RAM-CA heat shield was conducted in a rocket engine exhaust using a full-scale replica of the flight heat shield. The primary purpose of the test was to study some possible problems that would affect the heat-shield design and that could not be completely simulated on small models in the materials research test facilities. Of special concern in the present evaluation were the effects on the heat-shield performance of the hole patterns in the phenolic-carbon material at the nose region and of the junction between the phenolic-carbon material and teflon used along the afterbody. The present test evaluation did not show any problems that would disqualify the RAM-CA heat-shield design for flight application. Author

N69-33380*# National Aeronautics and Space Administration. Langley Research Center, Langley Station, Va.

TRANSONIC AERODYNAMIC CHARACTERISTICS OF A SATURN IB MANNED ORBITING RESEARCH LABORATORY LAUNCH VEHICLE

Stuart G. Flechner and Richard A. Langhans Washington Aug. 1969 44 p refs

(NASA-TM-X-1848) Avail: CFSTI CSCL 22B

A wind-tunnel investigation was conducted at Mach numbers from 0.40 to 1.20, angles of attack from -6° to 20°, and model roll angles of 0°, 45°, and 90° to determine the transonic aerodynamic characteristics of the Saturn 1B launch vehicle with a proposed manned orbiting research laboratory (MORL). The model was tested with natural and fixed boundary-layer transition, and with and without four thrust-augmentation rockets attached to the booster. Author

N69-36501*# National Aeronautics and Space Administration, Washington, D.C.

PROJECT GEMINI TECHNOLOGY AND OPERATIONS: A CHRONOLOGY

James M. Grimwood, Barton C. Hacker, and Peter J. Vorzimer 1969 324 p refs

(NASA-SP-4002) Avail: SOD $2.75; CFSTI CSCL 22A

A chronological study of the Gemini project is presented. Historical and background information from the inception of the project is given. Included also are the qualifications set forth for the NASA contractors in the development of the Gemini spacecraft, along with subsequent flight tests. Appendixes covering flight summary data, the program and the mission objectives, vehicle manufacturing and testing histories, and the worldwide tracking network are included. J.M.C.

N69-37030*# National Aeronautics and Space Administration, Washington, D.C.

EFFECTS OF STRUCTURAL FLEXIBILITY ON SPACECRAFT CONTROL SYSTEMS

Apr. 1969 47 p refs
(NASA-SP-8016) Avail: CFSTI CSCL 22B

Selection, design, and evaluation of a spacecraft control system for operation in the presence of a flexible structure are outlined. Design and flight experiences of four structural configuration categories are reviewed: (1) the compact, near-rigid spin-stabilized body; (2) the compact body with flexibly connected rigid appendages; (3) the compact body with flexible appendages; and (4) the large flexible body with active control during thrust maneuvers. Potential problems are pointed out in design and operation of dual-spin-stabilized spacecraft with flexibility, spin-stabilized spacecraft encountering spin resonance, spacecraft with flexibility in the control loop, spacecraft with multiple controllers, and large vehicles with increased flexibility. Stability and control criteria as well as recommended practices are stated for application in analytical studies, simulation studies, and tests. A listing of space vehicle design criteria documents issued by NASA is included. K.W.

N69-37281*# National Aeronautics and Space Administration. Lewis Research Center, Cleveland, Ohio.

FLIGHT PERFORMANCE OF ATLAS-AGENA LAUNCH VEHICLES IN SUPPORT OF THE LUNAR ORBITER MISSIONS 3, 4, AND 5

Washington Aug. 1969 140 p refs
(NASA-TM-X-1859) Avail: CFSTI CSCL 22B

Performance evaluations are presented for the last three of five successful Atlas-Agena vehicles, launched from the Eastern Test Range in support of the Lunar Orbiter series of photographic and selenographic missions. These flights were so similar that results are combined into a single report. Lunar Orbiter III was launched February 5, 1967 (referenced to GMT), followed by Lunar Orbiter IV on May 4, 1967, and Lunar Orbiter V on August 1, 1967. All three flights used a similar mode of ascent wherein the Atlas boosted the Agena-Lunar Orbiter into a proper suborbital coast ellipse. After separation of the Agena-spacecraft from the Atlas, the Agena engine was started and the Agena-spacecraft was injected into the desired approximate 185-kilometer circular parking orbit. After an orbital coast period, the Agena engine was restarted, and the spacecraft was injected into the lunar transfer trajectory. Insertion of the spacecraft into the translunar trajectories was very accurate. Out of the allocated 75-meter-per-second spacecraft midcourse correction capability, only 3.3 meters-per-second would have been required for Lunar Orbiter III, 10.8 for Lunar Orbiter IV, and 19.5 for Lunar Orbiter V to place the spacecraft onto the proper trajectory for the spacecraft deboost into its initial orbit around the moon. All three Lunar Orbiters successfully achieved the desired lunar orbits. For individual titles see N69-37281 – N69-37286. Author

N69-37840*# National Aeronautics and Space Administration. Lewis Research Center, Cleveland, Ohio.

FLIGHT PERFORMANCE OF THE ATLAS-AGENA LAUNCH VEHICLE IN SUPPORT OF THE APPLICATIONS TECHNOLOGY SATELLITE ATS-3

Sep. 1969 114 p
(NASA-TM-X-1879) Avail: CFSTI CSCL 22B

Three Applications Technology Satellites were launched by Atlas – Agena vehicles for experimentation in communications, cloud cover photography, and spacecraft environment. The flight performance of the Atlas – Agena vehicle (for ATS-3) from lift-off through the Agena reorientation maneuver is discussed. This flight in November 1967 concluded the Applications Technology Satellite missions launched by the Atlas – Agena vehicle. Author

N69-38820*# National Aeronautics and Space Administration. Manned Spacecraft Center, Houston, Tex.

ENTRY AERODYNAMICS AT LUNAR RETURN CONDITIONS OBTAINED FROM THE FLIGHT OF APOLLO 4 (AS-501)

Ernest R. Hillje Washington Oct. 1969 79 p refs
(NASA-TN-D-5399) Avail: CFSTI CSCL 22B

The flight aerodynamic characteristics of the Apollo 4 entry configuration (Command Module 017) were calculated from onboard-recorded inertial-platform accelerations and attitudes and from reconstructed trajectory data. Modified trim wind-tunnel data and hybrid data (modified wind-tunnel data adjusted to the flight-derived angle of attack) were compared to the flight-derived aerodynamics. Comparison of the modified trim wind-tunnel data to flight-derived data showed the initial trim angle of attack to be lower by approximately 1.5° and the resultant lift-to-drag ratio to be higher by approximately 10 percent. The flight-derived lift-to-drag ratio and the angles of attack in the hypersonic region 6.0, at which point comparison of the modified trim wind-tunnel data to flight-derived data showed much better agreement. Author

N69-40269*# National Aeronautics and Space Administration. Goddard Space Flight Center, Greenbelt, Md.

NASA SPACE VEHICLE DESIGN CRITERIA-ENVIRONMENT. MAGNETIC FIELDS: EARTH AND TERRESTRIAL

Mark Harris (Exotech, Inc., Washington) and Robert Lyle (Exotech, Inc., Washington) Washington Mar. 1969 70 p refs
(NASA-SP-8017) Avail: CFSTI CSCL 22B

Information on the strength and direction of the natural magnetic fields is presented for use as a guide in vehicle design. Covered are the geomagnetic field (the volume of space about the Earth i.e., the magnetosphere), the interplanetary field (Sun's field), and the fields of the planets and their natural satellites. Concerning the geomagnetic field, the present state of knowledge limits the availability of a definitive analytical model to about 6.6 Earth radii (synchronous altitude). For the regions beyond this altitude, the available information has been reviewed to determine both quantitative and qualitative data useful for design purposes. The information includes data on variations, disturbances, the various magnetic currents, regions, and effects in the magnetosphere. The analytical models of the geomagnetic field that are discussed include the spherical harmonic expansion model, the quadrupole model, the spin-axis dipole model, and the tilted dipole model. The geocentric, geodetic, geomagnetic, local geomagnetic, solar ecliptic, and solar magnetospheric coordinate systems are briefly defined. Dimensions, units of measurement, and conversion factors are given. K.W.

N69-40781*# National Aeronautics and Space Administration. Ames Research Center, Moffett Field, Calif.

THE INFLUENCE OF THERMAL DISTORTION ON THE PERFORMANCE OF GRAVITY-STABILIZED SATELLITES

Gerd Kanning Washington Nov. 1969 15 p refs
(NASA-TN-D-5435) Avail: CFSTI CSCL 22B

An analysis is made of the effect of thermal distortion of booms on the attitude of a gravity-stabilized satellite. The attitude computed when only the effects of thermal distortion on the solar pressure torques were considered is compared with the attitude computed when the interdependent effects of changing geometry and mass distribution were considered as well. The calculations were made for several satellites having either symmetrical or asymmetrical boom arrangements. Calculations for all arrangements were made for low orbits inclined 45° to the sunline. In addition, calculations were made for one symmetric configuration for synchronous attitude. The results indicated that including the effects of changing geometry and mass distribution is not important for symmetrical arrangements, but is important for asymmetrical boom arrangements. Furthermore, for asymmetrical boom arrangements, it was found that the thermal distortion can provide some compensation for the unbalanced solar pressure torques attributable to asymmetry. Thus, the best pointing accuracy might be achieved with booms designed to have a specific thermal distortion. Author

N69-40813*# National Aeronautics and Space Administration. Manned Spacecraft Center, Houston, Tex.

PREFLIGHT OPTICAL EVALUATION OF THE RIGHT-HAND

31 SPACE VEHICLES

HATCH WINDOWS OF GEMINI MISSIONS 7, 8, 9, AND 12
George P. Bonner, Michael F. Heidt, Carl L. Kotila, John A. Lintott, John E. Novotny et al Washington Nov. 1969 19 p
(NASA-TN-D-5471) Avail: CFSTI CSCL 22B

Preflight studies of the transmission, schlieren, and resolution qualities of the Gemini spacecraft G-7, G-8, G-9, and G-12 right-hand hatch windows were conducted. Transmission measurements were made for angles of incidence of 0°, 15°, 30°, and 45°. All windows were comparable in transmission qualities, and the schlieren studies indicated that all windows were excellent in optical quality. Relative resolution was tested by resolution-chart photography. The G-12 window proved superior in resolution.
Author

32

STRUCTURAL MECHANICS

Includes structural element design and weight analysis; fatigue; thermal stress; impact phenomena; vibration; flutter; inflatable structures; and structural tests. For related information see also: 17 Materials, Metallic; and 18 Materials, Nonmetallic.

A69-12516 *#
SOME RECENT ADVANCES IN THE INVESTIGATION OF SHELL BUCKLING.
Manuel Stein (NASA, Langley Research Center, Hampton, Va.).
(American Institute of Aeronautics and Astronautics, Aerospace Sciences Meeting, 6th, New York, N.Y., Jan. 22-24, 1968, Paper 68-103.)
AIAA Journal, vol. 6, Dec. 1968, p. 2339-2345. 35 refs.

Presentation of a survey which includes the buckling of shells under loads for which the shell is sensitive to initial imperfections. Results for such cases show that improvements in experiment and theory have produced previously unobtainable agreement. The necessity of the correct (and consistent) theoretical specification of boundary conditions is demonstrated. Recent stiffened cylinder results are surveyed to expose the large effects on the buckling strength of internal or external stiffening, axial load applied eccentric to the wall neutral surface, and the addition of small meridional curvature. (Author)

A69-15507 *#
STRUCTURAL AND DECELERATOR DESIGN OPTIONS FOR MARS ENTRY.
L. D. Guy (NASA, Langley Research Center, Structures Research Div., Structural Mechanics Branch, Hampton, Va.).
(American Institute of Aeronautics and Astronautics, and American Society of Mechanical Engineers, Structures, Structural Dynamics and Materials Conference, 9th, Palm Springs, Calif., Apr. 1-3, 1968, AIAA Paper 68-344.)
Journal of Spacecraft and Rockets, vol. 6, Jan. 1969, p. 44-49. 15 refs.

Influence of structural considerations on system configuration and selection for unmanned planetary exploration. Studies which have considered entry into the atmosphere of Mars show that each phase of deceleration within the atmosphere can benefit from advances in structural technology. The capsule aeroshell provides the major portion of the velocity reduction, and the influence of structural design options on the evolution of aeroshell configurations is discussed. In the transition phase, some form of aerodynamic decelerator is employed to augment the drag of the aeroshell. The relative efficiencies of various decelerators are examined and the potential of an advanced configuration to enhance mission capability is determined. Finally, system requirements of the landing phase, in which retroengines and/or an impact attenuation system are employed, are discussed. P.v.T.

A69-16433 *
ELASTIC DISPLACEMENTS FOR VARIOUS EDGE-CRACKED PLATE SPECIMENS.
Bernard Gross, Ernest Roberts, Jr., and John E. Srawley (NASA, Lewis Research Center, Cleveland, Ohio).
International Journal of Fracture Mechanics, vol. 4, Sept. 1968, p. 267-276. 16 refs.

The relative displacement per unit load of two conjugate points is used as a quantitative indicator of crack extension in plane strain fracture toughness measurements. The necessary displacement data are presented in dimensionless form for five types of single-edge-crack specimens: three-point bending, pure bending, remote axial tension, eccentric tension of compact rectangular specimens, and eccentric tension of tapered varieties. The results were obtained by a boundary collocation method of elastic analysis, and are highly precise. (Author)

A69-16742 *
SOME GENERAL PRINCIPLES OF DYNAMIC INSTABILITY OF SOLID BODIES.
Rong C. Shieh (Illinois, University, Chicago, Ill.; NASA, Langley Research Center, Hampton, Va.) and Ernest F. Masur (Illinois, University, Chicago, Ill.).
Zeitschrift für angewandte Mathematik und Physik, vol. 19, Nov. 25, 1968, p. 927-941. 24 refs.
NSF Grant No. GK-368.

The stability of the equilibrium of solid bodies (with emphasis on elastic and Voigt-Kelvin bodies) is investigated. It is assumed that the applied loads may have nonconservative and gyroscopic components although explicit time-dependence is excluded. As is well known, classical static or energy methods may fail to settle the question of stability for so broad a class of problems. The present paper aims to be reasonably comprehensive. Through the use of the modal vibration method, general stability criteria are established on the basis of "equivalent energy" conditions. These criteria are sufficiently general to contain previously published criteria as special cases; in addition, some new features are developed. A numerical example is included for demonstration purposes. (Author)

A69-18133 *#
AXISYMMETRIC STATIC AND DYNAMIC BUCKLING OF SPHERICAL CAPS DUE TO CENTRALLY DISTRIBUTED PRESSURES.
Wendell B. Stephens and Robert E. Fulton (NASA, Langley Research Center, Hampton, Va.).
American Institute of Aeronautics and Astronautics, Aerospace Sciences Meeting, 7th, New York, N.Y., Jan. 20-22, 1969, Paper 69-89. 15 p. 19 refs.
Members, $1.00; nonmembers, $1.50.

Approximation of Sanders' axisymmetric nonlinear elastic shell theory, including provision for general orthotropy along the shell meridian, by finite-difference equations including the Houbolt backward-difference formulation in time. The equations are then applied to the nonlinear response of an isotropic shallow spherical cap subjected to static and dynamic loads. Axisymmetric static buckling is determined by investigating the convergence characteristics of the static numerical solution as the "top of the knee" buckling point is reached. Dynamic buckling is defined as the threshold load at which large increases in the peak amplitude of the average dynamic displacement occur. Axisymmetric buckling loads are given for a spherical cap subjected to a constant static pressure or step pulse of infinite duration distributed axisymmetrically over a portion of the center of the shell. The influence of the size of the loaded area and of moment and in-plane boundary conditions on both static and dynamic buckling is studied, as well as the use of various criteria to define the threshold load for dynamic buckling. (Author)

A69-18193 *#
A GEOMETRICALLY EXACT FINITE ELEMENT FOR THIN SHELLS OF REVOLUTION.
Howard M. Adelman, Donnell S. Catherines, and William C. Walton,

Jr. (NASA, Langley Research Center, Hampton, Va.).
American Institute of Aeronautics and Astronautics, Aerospace Sciences Meeting, 7th, New York, N.Y., Jan. 20-22, 1969, Paper 69-56. 10 p.
Members, $1.00; nonmembers, $1.50.

Description of a study for determining a preferred representation of a shell for the purpose of predicting the complicated boundary-layer stress distributions occurring near clampled edges during vibration in a normal mode. The study is made using a finite-element method developed by Adelman et al. (1959). The finite element is precisely congruent to the portion of the shell it represents. The finite-element method is applied to the computation of the stresses in a mode exhibiting complicated boundary-layer stresses for a cylindrical shell clamped at each end. The distributions of various kinds of stresses and stress resultants calculated by the finite-element method are compared to calculations by exact theory.
M.G.

A69-18331 *#
THERMOELASTIC INSTABILITY OF OPEN SECTION BOOMS.
James H. Donohue and Harold P. Frisch (NASA, Goddard Space Flight Center, Greenbelt, Md.).
U.S. Air Force Systems Command and Aerospace Corp., Symposium on Gravity Gradient Attitude Stabilization, El Segundo, Calif., Dec. 3-5, 1968, Paper. 35 p.

Description of theoretical and experimental results which support the contention that the anomalous motion of the OGO 4 spacecraft can be explained by the thermally induced oscillation theory. It is shown from the results of the simple lumped-parameter model and from Frisch's complex thermoelastic model that the possibility of preventing thermal oscillations, or at least reducing the flutter amplitude, can be achieved in many ways such as perforating the boom, decreasing the absorptivity, increasing the thermal lag, and increasing bending damping. However, all of these approaches are felt to be of questionable value. The most reasonable approach is to significantly stiffen the boom in torsion.
M.M.

A69-21479 *#
FAILURE CRITERIA FOR FILAMENTARY COMPOSITES.
Christos C. Chamis (NASA, Lewis Research Center, Cleveland, Ohio).
American Society for Testing and Materials, Conference on Composite Materials: Testing and Design, New Orleans, La., Feb. 11-13, 1969, Paper. 46 p. 33 refs.
Contract No. AF 33(615)-3110.

Description of a two-level, linear, semiempirical theory for a failure criterion. The theory predicts the strength behavior of unidirectional filamentary composites under uniaxial and combined stress from basic constituent material properties and fabrication process considerations. Application of the theory to several filament/nonmetallic-matrix composites are presented, and comparisons are made with experimental data. These results show good agreement between theory and experiment. Simple and combined strength envelopes are generated to illustrate the versatility of the theory and to point out problem areas in experimental work and design.
(Author)

A69-23057 *#
PLANE STRAIN FRACTURE TOUGHNESS TESTS ON TWO-INCH-THICK MARAGING STEEL PLATE AT VARIOUS STRENGTH LEVELS.
J. E. Srawley (NASA, Lewis Research Center, Cleveland, Ohio).
International Congress on Fracture, International Conference on Fracture, 2nd, Brighton, England, Apr. 13-18, 1969, Paper. 16 p. 19 refs.

Results of tests of 1.8-in. thick three-point bend and compact (tension) specimens substantiate the current proposed ASTM recommended practice for plane strain fracture toughness (K_{Ic}) testing. Erroneously low results were obtained with 0.5-in. thick bend specimens when the ratio of K_{Ic} to yield strength exceeded 0.45 $in.^{1/2}$ thus emphasizing the importance of requiring minimum specimen dimensions proportional to the square of this ratio. Shallow face grooves in 0.5-in. thick specimens had no useful effect. The maraging temperatures ranged from 700 to 1100°F, yield strength from 173 to 260 ksi, and K_{Ic} from 67 to 147 $ksi\text{-}in.^{1/2}$ The K_{Ic} values were approximately proportional to the reciprocal of the square of yield strength, and also to a strain hardening index derived from the ratio of yield to ultimate tensile strength.
(Author)

A69-24184 *#
COMPARISON OF FLEXIBLE- AND FIRM-FOUNDATION ROTOR CRITICAL-SPEED ANALYSES.
R. H. Cavicchi (NASA, Lewis Research Center, Cleveland, Ohio).
American Society of Mechanical Engineers, Vibrations Conference, Philadelphia, Pa., Mar. 30-Apr. 2, 1969, Paper 69-Vibr-49. 15 p. 8 refs.
Members, $0.75; nonmembers, $1.50.

Critical analysis of undamped rigid rotors on flexible foundations. The analysis predicts four unique solutions, two more than predicted by a firm-foundation model, which is treated as a special case. Approximate agreement exists, however, between the corresponding solutions obtained from the two models. For the firm-foundation model, when the center of gravity is located away from the bearing-centerline midpoint, two additional solutions appear. As the center of gravity is moved progressively outward, critical speeds of the hf set increase and those of the lf set decrease. Pencil shapes are more sensitive to center-of-gravity location than disks. The same simple solution that approximates flexible-foundation results is also good for firm-foundation geometries whose centers of gravity lie between the bearing-centerline quarter points.
M.M.

A69-25492
AMERICAN INSTITUTE OF AERONAUTICS AND ASTRONAUTICS, STRUCTURAL DYNAMICS AND AEROELASTICITY SPECIALIST CONFERENCE, NEW ORLEANS, LA., APRIL 16, 17, 1969 AND AMERICAN SOCIETY OF MECHANICAL ENGINEERS AND AMERICAN INSTITUTE OF AERONAUTICS AND ASTRONAUTICS, STRUCTURES, STRUCTURAL DYNAMICS, AND MATERIALS CONFERENCE, 10TH, NEW ORLEANS, LA., APRIL 14-16, 1969, PROCEEDINGS.
New York, American Institute of Aeronautics and Astronautics, Inc., 1969. 425 p.
Members, $15; nonmembers, $22.

CONTENTS:

OPTIMIZATION OF STRUCTURES TO SATISFY FLUTTER REQUIREMENTS. M. J. Turner (Boeing Co., Seattle, Wash.), p. 1-8. 9 refs. [See A69-25493 11-32]

DYNAMIC OPTIMIZATION OF COMPLEX STRUCTURES. C. P. Rubin (Hughes Aircraft Co., El Segundo, Calif.), p. 9-14. 9 refs. [See A69-25494 11-32]

STRUCTURAL OPTIMIZATION IN THE DYNAMICS RESPONSE REGIME - A COMPUTATIONAL APPROACH. R. L. Fox (Case-Western-Reserve University, Cleveland, Ohio) and M. P. Kapoor (Institute of Higher Technology, Kanpur, India), p. 15-22. 9 refs. [See A69-25495 11-32]

OPTIMAL DESIGN OF STRUCTURES WITH CONSTRAINTS ON NATURAL FREQUENCY. B. R. McCart (Augustana College, Rock Island, Ill.), E. J. Haug, and T. D. Streeter (U.S. Army, Weapons Command, Rock Island, Ill.), p. 23-31. 8 refs. [See A69-25496 11-32]

SATURN V POGO AND A SOLUTION. R. L. Rich (Boeing Co., New Orleans, La.), p. 32-41. [See A69-25497 11-31]

THE USE OF HELIUM BUBBLES AS A POGO FIX IN LAUNCH VEHICLE PROPELLANT LINES. B. R. Hanks and D. G. Stephens (NASA, Langley Research Center, Hampton, Va.), p. 42-46. [See A69-25498 11-31]

DYNAMIC STABILITY OF CYLINDRICAL PROPELLANT TANKS. D. D. Kana and W.-H. Chu (Southwest Research Institute, San Antonio, Tex.), p. 47-57. 9 refs. [See A69-25499 11-32]

MINIMIZING SPACECRAFT STRUCTURE/CONTROL-SYSTEM INTERACTION. R. B. Noll (Kaman Corp., Burlington, Mass.) and C. H. Spenny (NASA, Electronics Research Center, Cambridge, Mass.), p. 58-65. 20 refs. [See A69-25500 11-31]

A METHOD FOR DIGITAL COMPUTATION OF SPACECRAFT RESPONSE IN THE DOCKING MANEUVER. C. Bodley, G. Morosow (Martin Marietta Corp., Denver, Colo.), and W. Holland (NASA, Marshall Space Flight Center, Huntsville, Ala.), p. 66-74. [See A69-25501 11-31]

DYNAMICS OF A LIBRATION-DAMPED DISCRETIZED CRUCIFORM STRUCTURE. J. L. Farrell, J. K. Newton, and D. A. Hedland (Westinghouse Electric Corp., Baltimore, Md.), p. 75-83. 21 refs. [See A69-25502 11-32]

A NEW METHOD FOR COMPUTING THE DYNAMIC RESPONSE OF AIRCRAFT TO THREE-DIMENSIONAL TURBULENCE. F. D. Eichenbaum (Lockheed Aircraft Corp., Marietta, Ga.), p. 84-94. 8 refs. [See A69-25503 11-02]

PROBLEMS IN THE USE OF THE EXPECTED NUMBER OF EXCEEDANCES IN ESTABLISHING DESIGN GUST LOADS. C. S. O'Hearne (Martin Marietta Corp., Orlando, Fla.), p. 95-101. 10 refs. [See A69-25504 11-02]

ON FIRST-EXCURSION FAILURE OF RANDOMLY EXCITED STRUCTURES. Y. K. Lin (Illinois, University, Urbana, Ill.), p. 102-111. 14 refs. [See A69-25505 11-32]

RANDOM ACOUSTIC RESPONSE OF A CYLINDRICAL SHELL. C. Hwang and W. S. Pi (Northrop Corp., Hawthorne, Calif.), p. 112-120. 6 refs. [See A69-25506 11-32]

DYNAMIC STABILITY OF THIN CIRCULAR PLATES SUBJECTED TO PURELY STOCHASTIC RADIAL EXCITATION. J. A. Lepore (Pennsylvania, University, Philadelphia, Pa.) and H. C. Shah (Stanford University, Stanford, Calif.), p. 121-130. 12 refs. [See A69-25507 11-32]

THE APPLICATION OF FILAMENT COMPOSITES TO AEROELASTIC MODELS. H. F. Hunter and J. B. Bailey (Lockheed Aircraft Corp., Marietta, Ga.), p. 131-143. 6 refs. [See A69-25508 11-32]

MODAL COUPLING IN THERMALLY STRESSED PLATES. C. D. Bailey (Ohio State University, Columbus, Ohio), p. 144-152. [See A69-25509 11-32]

THE STABILITY OF DYNAMIC SYSTEMS WITH PERIODICALLY VARYING PARAMETERS. P. Crimi (Rochester Applied Science Associates, Inc., Rochester, N.Y.), p. 153-161. 11 refs. [See A69-25510 11-32]

TWO-DIMENSIONAL STRESS WAVE PROPAGATION IN THICK MULTILAYERED CYLINDRICAL SHELLS. B. P. Shafer (California, University, Los Alamos, N. Mex.), p. 162-173. [See A69-25511 11-32]

ON THE DYNAMIC PLASTIC RESPONSE OF FINITE BARS. E. R. Wood (Georgia Institute of Technology, Atlanta, Ga.) and T. H. Liu, p. 174-184. 6 refs. [See A69-25512 11-32]

THE CLASSIFICATION OF PARTIAL DIFFERENTIAL EQUATIONS IN STRUCTURAL DYNAMICS. P. C. Chou and R. F. Perry (Drexel Institute of Technology, Philadelphia, Pa.), p. 185-194. 25 refs. [See A69-25513 11-32]

COMPRESSIBILITY EFFECTS ON OSCILLATING ROTOR BLADES IN HOVERING FLIGHT. W. P. Jones and B. M. Rao (Texas Agricultural and Mechanical University, College Station, Tex.), p. 195-204. 8 refs. [See A69-25514 11-01]

VISCOUS FLOW-INDUCED VIBRATIONS OF A FLAT PLATE SUSPENDED IN A NARROW CHANNEL. F. T. Dodge and A. F. Muller (Southwest Research Institute, San Antonio, Tex.), p. 205-209. 5 refs. [See A69-25515 11-32]

SOME FLUTTER SOLUTIONS USING FINITE ELEMENTS. M. D. Olson (National Research Council, Ottawa, Canada), p. 210-218. 11 refs. [See A69-25516 11-32]

FLUTTER INDUCED BY AERODYNAMIC INTERFERENCE BETWEEN WIND AND TAIL. O. Sensburg (Entwicklungsring Süd GmbH, Munich, West Germany) and B. Laschka (Vereinigte Flugtechnische Werke GmbH, Munich, West Germany), p. 219-227. 11 refs. [See A69-25517 11-32]

SERVO CONTROL OF FLUTTER. J. G. Theisen (Lockheed Aircraft Corp., Marietta, Ga.) and W. C. Robinette, p. 228-240. 17 refs. [See A69-25518 11-32]

AXISYMMETRIC VIBRATION OF CONICAL SHELLS. R. F. Hartung and W. A. Loden (Lockheed Aircraft Corp., Palo Alto, Calif.), p. 241-252. 6 refs. [See A69-25519 11-32]

EFFECTS OF INPLANE AND ROTARY INERTIA ON THE FREQUENCIES OF ECCENTRICALLY STIFFENED CYLINDRICAL SHELLS. S. Parthan and D. J. Johns (Loughborough University of Technology, Loughborough, Leics., England), p. 253-261. 9 refs. [See A69-25520 11-32]

A THEORETICAL ANALYSIS OF THE FREE VIBRATION OF DISCRETELY STIFFENED CYLINDRICAL SHELLS WITH ARBITRARY END CONDITIONS. D. M. Egle (Oklahoma, University, Norman, Okla.) and K. E. Soder, Jr. (Atlantic Research Corp., Costa Mesa, Calif.), p. 262-274. 51 refs. [See A69-25521 11-32]

A SURVEY OF MODERN NONSENSE AS APPLIED TO MATRIX COMPUTATIONS. R. A. Rosanoff (North American Rockwell Corp., Downey, Calif.), p. 275-284. 15 refs. [See A69-25522 11-19]

INFLUENCE OF IN-PLANE EDGE SUPPORT FLEXIBILITY ON THE NONLINEAR FLUTTER OF LOADED PLATES. C. S. Ventres and E. H. Dowell (Princeton University, Princeton, N.J.), p. 285-295. 15 refs. [See A69-25523 11-32]

FLUTTER DESIGN CHARTS FOR STRESSED ISOTROPIC PANELS. C. P. Shore (NASA, Langley Research Center, Hampton, Va.), p. 296-301. 21 refs. [See A69-25524 11-32]

A METHOD FOR COMPUTING THE RESPONSE OF A GENERAL AXISYMMETRIC SHELL WITH AN ATTACHED ASYMMETRIC STRUCTURE. E. C. Steeves, B. J. Durling, and W. C. Walton, Jr. (NASA, Langley Research Center, Hampton, Va.), p. 302-328. 8 refs. [See A69-25525 11-32]

PREDICTION OF NONLINEAR TRANSIENT RESPONSE OF STRUCTURES. R. J. Melosh and D. M. Kelley (Philco-Ford Corp., Palo Alto, Calif.), p. 329-335. 14 refs. [See A69-25526 11-32]

STRESS WAVE PROPAGATION USING THE EXTENDED RITZ METHOD. E. B. Becker (Texas, University, Austin, Tex.) and R. E. Nickell (Bell Telephone Laboratories, Inc., Whippany, N.J.), p. 336-348. 17 refs. [See A69-25527 11-32]

TRANSIENT DYNAMIC RESPONSE OF LINEARLY VISCOELASTIC STRUCTURES AND CONTINUA. D. W. Malone (Purdue University, Lafayette, Ind.) and J. J. Connor (Massachusetts Institute of Technology, Cambridge, Mass.), p. 349-356. 13 refs. [See A69-25528 11-32]

TRANSFORMATION OF VARIABLES FOR REDUNDANCY OPTIMIZATION IN THE RANK FORCE METHOD. J. Robinson and G. W. Haggenmacher (Lockheed Aircraft Corp., Burbank, Calif.), p. 357-363. 6 refs. [See A69-25529 11-32]

DYNAMICS OF SPIN-STIFFENED DEPLOYABLE SPACE STRUCTURES. J. M. Hedgepeth (Astro Research Corp., Santa Barbara, Calif.), p. 364-374. 5 refs. [See A69-25530 11-32]

OBSERVATIONS ON THE MECHANISM OF THERMAL TORQUE INSTABILITY. P. F. Jordan (Martin Marietta Corp., Baltimore, Md.), p. 375-382. 5 refs. [See A69-25531 11-32]

FREQUENCIES AND MODE SHAPES OF A 100-FOOT SPACE ERECTABLE PARABOLIC ANTENNA. R. K. Gieseke (General Dynamics Corp., San Diego, Calif.), p. 383-396. 8 refs. [See A69-25532 11-32]

ON THE SPIN-STABILITY OF A FLEXIBLE BODY. J. M. Talcott (Fairchild Hiller Corp., Germantown, Md.), p. 397-404. 8 refs. [See A69-25533 11-32]

THERMALLY INDUCED VIBRATIONS OF LONG THIN-WALLED CYLINDERS OF OPEN SECTION. H. P. Frisch (NASA, Goddard Space Flight Center, Greenbelt, Md.), p. 405-420. 9 refs. [See A69-25534 11-32]

A69-25524 *#

FLUTTER DESIGN CHARTS FOR STRESSED ISOTROPIC PANELS. Charles P. Shore (NASA, Langley Research Center, Hampton, Va.). IN: AMERICAN INSTITUTE OF AERONAUTICS AND ASTRONAUTICS, STRUCTURAL DYNAMICS AND AEROELASTICITY SPECIALIST CONFERENCE, NEW ORLEANS, LA., APRIL 16, 17, 1969, PROCEEDINGS. [A69-25492 11-32]
New York, American Institute of Aeronautics and Astronautics, Inc., 1969, p. 296-301. 21 refs.

Until recently, correlation between theory and experiment for the flutter of panels stressed to the verge of buckling has not been achieved because of the theoretical prediction of anomalous zero dynamic pressure flutter points. However, a recent linear flutter analysis which includes hysteretic structural damping on the bending terms of the flutter equation eliminates the anomalous zero dynamic pressure flutter points and yields good agreement with experiment. Thus, it appears that empirical flutter envelopes now used in design can be replaced by design procedures with a more rigorous analytical basis. This work develops and presents design charts for isotropic panels on the verge of buckling for typical values of structural

damping. Use of these charts permits conservative panel design for wide ranges of panel length-width ratio, in-plane stress ratio, and edge rotational restraint. (Author)

A69-25525 *#
A METHOD FOR COMPUTING THE RESPONSE OF A GENERAL AXISYMMETRIC SHELL WITH AN ATTACHED ASYMMETRIC STRUCTURE.
Earl C. Steeves, Barbara J. Durling, and William C. Walton, Jr. (NASA, Langley Research Center, Hampton, Va.).
IN: AMERICAN INSTITUTE OF AERONAUTICS AND ASTRONAUTICS, STRUCTURAL DYNAMICS AND AEROELASTICITY SPECIALIST CONFERENCE, NEW ORLEANS, LA., APRIL 16, 17, 1969, PROCEEDINGS. [A69-25492 11-32]
New York, American Institute of Aeronautics and Astronautics, Inc., 1969, p. 302-328. 8 refs.

Description of a method for the analysis of axisymmetric ring stiffened shells with an attached asymmetric structure. The components making up the system are idealized separately leading to a Lagrangian and virtual work statement for each component. The components are assumed to be joined by either axisymmetric line connections or by point connections; equations of constraint describing these connections among the components are written. The solution of these equations enables the transformation of the component Lagrangians into the coupled Lagrangian for the system from which the equations of motion are derived. A discussion of the nature of the idealization of shell and ring components is given. Results of an application of the method to compute the natural vibration modes of a planetary landing vehicle model suspended in a conical adapter are presented. A normal mode expansion is used for both the conical adapter and vehicle model, and the nature of the convergence with respect to the number of modes used is discussed. (Author)

A69-25534 *#
THERMALLY INDUCED VIBRATIONS OF LONG THIN-WALLED CYLINDERS OF OPEN SECTION.
Harold P. Frisch (NASA, Goddard Space Flight Center, Greenbelt, Md.).
IN: AMERICAN SOCIETY OF MECHANICAL ENGINEERS AND AMERICAN INSTITUTE OF AERONAUTICS AND ASTRONAUTICS, STRUCTURES, STRUCTURAL DYNAMICS, AND MATERIALS CONFERENCE, 10TH, NEW ORLEANS, LA., APRIL 14-16, 1969, PROCEEDINGS. [A69-25492 11-32]
New York, American Institute of Aeronautics and Astronautics, Inc., 1969, p. 405-420. 9 refs.

Recent satellites have carried long extendable appendages of the type classified as thin-walled cylinders of open section for such diverse purposes as dipole antennas, gravity-gradient stabilization booms, and electric-field probes. This document presents the equations which describe the coupled nonplanar transverse and torsional vibrations of such an antenna when it is exposed to a directional solar thermal field (sunlight). To obtain a numerical solution, the equations are specialized to the case of a clamped-free cylinder of open section having the nominal characteristics of the antennas in orbit. Comparison of results with actual flight data shows that the hypothesis leads to conclusions consistent with the observed phenomena. The numerical examples show that the thermally induced vibration problem can be eliminated by literally zippering the antenna's open section, in various fashions, so as to effectively increase its torsional rigidity. (Author)

A69-25958 *
NOTE ON INCLINATION OF FATIGUE CRACKS IN PLANE STRAIN FRACTURE TOUGHNESS TEST SPECIMENS.
D. M. Fisher and A. J. Repko (NASA, Lewis Research Center, Cleveland, Ohio).
Materials Research and Standards, vol. 9, May 1969, p. 28, 29. 5 refs.

Determination of the effect of angular deviation of a fatigue crack from a plane perpendicular to the longitudinal specimen axis on the results of plane strain fracture toughness (K_{Ic}) testing of high-strength metallic materials. It is found that the K_{Ic} test results of 7075-T651 aluminum alloy bend test specimens are higher than the plane strain fracture toughness when the deviation of the fatigue crack plane from the plane of symmetry of the crack starter notch exceeds 15°. Three-point bending fatigue permits much greater control of fatigue crack development than does cantilever bending. The fatigue crack rate across the thickness of the specimen can be varied by adjusting the point of loading with respect to that direction. Z.W.

A69-26807
AMERICAN INSTITUTE OF AERONAUTICS AND ASTRONAUTICS AND AMERICAN SOCIETY OF MECHANICAL ENGINEERS, STRUCTURES, STRUCTURAL DYNAMICS AND MATERIALS CONFERENCE, 10TH, NEW ORLEANS, LA., APRIL 14-16, 1969, PROCEEDINGS.
New York, American Society of Mechanical Engineers, 1969. 477 p. Members, $15.; nonmembers, $22.

CONTENTS:

ANALYSIS OF A SIMPLY-SUPPORTED LAMINATED ANISOTROPIC RECTANGULAR PLATE. J. M. Whitney (USAF, Materials Laboratory, Dayton, Ohio) and A. W. Leissa (Ohio State University, Columbus, Ohio), p. 1-8. 8 refs. [See A69-26808 12-32]

A STUDY OF VARIOUS IDEALISATIONS FOR WING STRUCTURES AND NUMERICAL PROCEDURES INVOLVED USING MATRIX METHODS. R. A. Tinawi (Canadair, Ltd., Montreal, Canada), p. 9-17. 12 refs. [See A69-26809 12-32]

EXACT SOLUTION FOR NATURAL FREQUENCIES OF RING-STIFFENED CYLINDERS. K. Forsberg (Lockheed Aircraft Corp., Palo Alto, Calif.), p. 18-30. 8 refs. [See A69-26810 12-32]

STRUCTURAL ANALYSIS AND EXPERIMENTAL CORRELATION OF A COMPLEX SHELL UNDER ASYMMETRIC LOADS. S. Klein (Aerospace Corp., San Bernardino, Calif.), p. 31-39. 9 refs. [See A69-26811 12-32]

ANALYSIS OF A RING-STRUT STRUCTURE ON AN ELASTIC FOUNDATION. A. J. Dennis (United Aircraft Corp., East Hartford, Conn.), p. 40-47. 6 refs. [See A69-26812 12-32]

EFFECT OF ABLATION ON THERMAL CONDUCTIVITY TO 5000 R IN PHENOLIC-CARBON AND PHENOLIC-GRAPHITE. W. A. Clayton (Boeing Co., Seattle, Wash.), T. J. Fabish (Battelle Memorial Institute, Columbus, Ohio), and G. L. Denman (USAF, Materials Laboratory, Dayton, Ohio), p. 48-56.

ABLATIVE CHARACTERIZATION OF SEVEN HEAT SHIELD MATERIALS - A REVIEW OF THE NASA-SRI ROUND-ROBIN PROGRAM. N. K. Hiester, C. F. Clark (Stanford Research Institute, Menlo Park, Calif.), and N. S. Vojvodich (NASA, Ames Research Center, Moffett Field, Calif.), p. 57-68. 13 refs. [See A69-26813 12-18]

COMPARISON OF THE ABLATION PERFORMANCE OF ASBESTOS PHENOLIC WITH SILICA PHENOLIC IN THE CAL WAVE SUPERHEATER. P. B. Brandt (TRW Systems Group, Redondo Beach, Calif.), p. 69-77. [See A69-26814 12-18]

ABLATION TEST SPECIMEN ENVIRONMENT AT HIGH TEMPERATURE. S. G. Babcock (General Motors Corp., Warren, Mich.), R. N. Groves, Jr. (Midwest Applied Science Corp., West Lafayette, Ind.), and R. F. Hoglund, p. 78-88. 5 refs. [See A69-26815 12-33]

DESIGN AND TESTING OF ABLATION MODELS WITH CONTROLLED PRESSURE GRADIENTS. W. T. Barry (Aerospace Corp., El Segundo, Calif.) and E. B. Fisher (Cornell Aeronautical Laboratory, Inc., Buffalo, N.Y.), p. 89-95. 8 refs. [See A69-26816 12-11]

SUPER INSULATION - THIN, LIGHTWEIGHT PROTECTION AGAINST RE-ENTRY HEAT. F. Notaro and W. E. Grunert (Union Carbide Corp., Tonawanda, N.Y.), p. 96-103. 5 refs. [See A69-26817 12-11]

NONLINEAR ANALYSIS FOR AXISYMMETRIC ELASTIC STRESSES IN RING-STIFFENED, SEGMENTED SHELLS OF REVOLUTION. D. Bushnell (Lockheed Aircraft Corp., Palo Alto, Calif.), p. 104-113. 16 refs. [See A69-26818 12-32]

COMPUTATIONAL STABILITY IN NONLINEAR DISCRETE STRUCTURAL SYSTEMS. H. A. Kamel (Arizona, University, Tucson, Ariz.) and R. L. Sack (Boeing Co., Renton, Wash.), p. 114-124. 13 refs. [See A69-26819 12-32]

SHALLOW SHELLS WITH LARGE DEFLECTIONS - INTEGRAL

EQUATIONS TECHNIQUE. D. Krajcinovic (Ingersoll-Rand Co., Princeton, N.J.), p. 125-134. 5 refs. [See A69-26820 12-32]

FINITE DEFLECTION DISCRETE ELEMENT ANALYSIS OF SANDWICH PLATES AND CYLINDRICAL SHELLS WITH LAMINATED FACES. L. A. Schmit, Jr. and G. R. Monforton (Case-Western-Reserve University, Cleveland, Ohio), p. 135-150. 15 refs. [See A69-26821 12-32]

ON THE IMPROVEMENT OF APPROXIMATE SOLUTIONS FOR LARGE DEFLECTIONS OF PLATES. D. L. Sikarskie and C.-L. Lou (Michigan, University, Ann Arbor, Mich.), p. 151-157. 6 refs. [See A69-26822 12-32]

NONLINEAR STRUCTURE ANALYSIS BY FORCE METHOD AND SUBORDINATED STEP PROCEDURE. J. Sobieszczanski (St. Louis University, St. Louis, Mo.), p. 158-171. 28 refs. [See A69-26823 12-32]

AVERAGE ELASTIC PROPERTIES AND STRESS FIELDS FOR COMPOSITE CONTINUA. G. H. Gaonkar (Washington, University, St. Louis, Mo.), p. 172-182. 16 refs. [See A69-26824 12-32]

EFFECT OF TIME AT TEMPERATURE ON THE MECHANICAL PROPERTIES OF A FABRIC REINFORCED PHENOLIC HEAT SHIELD MATERIAL. L. L. Lander, Jr., J. Atkinson, and C. C. Theberge (Avco Corp., Wilmington, Mass.), p. 183-192. 8 refs. [See A69-26825 12-18]

CARBON-CARBON MATERIALS FOR AEROSPACE APPLICATIONS. H. M. Stoller and E. R. Frye (Sandia Corp., Albuquerque, N. Mex.), p. 193-212.

DEVELOPMENT OF AN F-5 BORON-EPOXY CONTOURED LANDING GEAR DOOR. F. St. Germain and R. Helm (Northrop Corp., Hawthorne, Calif.), p. 213-222. [See A69-26826 12-15]

STATE-OF-THE-ART CRYOGENIC THERMAL PROTECTION FOR SPACE APPLICATION. A. C. Rogers, Jr. (North American Rockwell Corp., Downey, Calif.), p. 223-234. 16 refs. [See A69-26827 12-31]

STRUCTURAL EFFICIENCY OF DIFFUSION BONDED TITANIUM HONEYCOMB SANDWICH. D. H. Emero and R. M. Ault (Stresskin Products Co., Santa Ana, Calif.), p. 235-243. 13 refs. [See A69-26828 12-17]

WHY CAN'T ENGINEERING COLLEGES PRODUCE GOOD ENGINEERS? A. G. Hansen (Georgia Institute of Technology, Atlanta, Ga.), p. 244-247.

INDUSTRY NEEDS FOR DESIGN ORIENTED ENGINEERING GRADUATES. I. G. Hedrick (Grumman Aircraft Engineering Corp., Bethpage, N.Y.), p. 248, 249.

ENGINEERING EDUCATION VERSUS NEEDS OF AEROSPACE COMPANIES. J. F. McCarthy, Jr. (North American Rockwell Corp., El Segundo, Calif.), p. 250-255.

HIGH STRENGTH STEELS - PRESENT STATUS AND FUTURE PROSPECTS. E. R. Parker and V. F. Zackay (California, University, Berkeley, Calif.), p. 256-260. 9 refs. [See A69-26829 12-17]

MECHANICAL PROPERTIES OF BRITTLE MATRIX COMPOSITES. M. A. Stett and R. M. Fulrath (California, University, Berkeley, Calif.), p. 261-268. 18 refs. [See A69-26830 12-17]

SOME UNIQUE MECHANICAL PROPERTIES OF GLASS. J. D. Mackenzie (Rensselaer Polytechnic Institute, Troy, N.Y.), p. 269-273. 12 refs. [See A69-26831 12-18]

FINE-GRAINED CERAMICS - THE ROLE OF PRESSURE CALCINTERING. E. Scala, S. K. Dutta, and G. E. Gazza (U.S. Army, Army Materials and Mechanics Research Center, Watertown, Mass.), p. 274-284. 33 refs. [See A69-26832 12-18]

THE MATERIALS-STRUCTURES INTERFACE - A SYSTEMS APPROACH TO AIRFRAME STRUCTURAL DESIGN. W. J. Crichlow (Lockheed Aircraft Corp., Burbank, Calif.), p. 285-318. 25 refs. [See A69-26833 12-32]

LAUNCH AND MISSION INFLUENCES ON SPACE PROPULSION SYSTEM DESIGN. D. S. Garcia, T. Fahrner, and K. P. Johnson (McDonnell Douglas Corp., Huntington Beach, Calif.), p. 319-329. 8 refs. [See A69-26834 12-28]

AN INVESTIGATION ON FATIGUE CRACK PROPAGATION AND FAILSAFE DESIGN OF STIFFENED LARGE ALUMINUM ALLOY PANELS WITH VARIOUS CRACK STOPPERS. D. Y. Wang (McDonnell Douglas Corp., Long Beach, Calif.), p. 330-343. 9 refs. [See A69-26835 12-32]

THERMOSTRUCTURAL SIMULATION OF LIFTING VEHICLE STRUCTURES. T. E. Hess (General Electric Co., Philadelphia, Pa.), J. R. Vinson (Delaware, University, Newark, Del.), S. Shore (Pennsylvania, University, Philadelphia, Pa.), and J. M. Rizzo (Meridian Engineering Co., Philadelphia, Pa.), p. 344-352. [See A69-26836 12-11]

TEST EVALUATION OF A 2500°F STRUCTURAL COMPONENT. M. G. Childers, K. A. Wilhelm (Lockheed Aircraft Corp., Burbank, Calif.), and P. P. Plank (Lockheed Aircraft Corp., Sunnyvale, Calif.), p. 353-361. 5 refs. [See A69-26837 12-15]

A THEORETICAL EXAMINATION OF THE VALIDITY OF "ACCELERATED" STRUCTURAL TESTS UNDER CREEP CONDITIONS. K. H. Sayers (Bell Aerospace Corp., Buffalo, N.Y.), p. 362-368. 10 refs. [See A69-26838 12-32]

LARGE DEFLECTION ANALYSIS OF ELASTIC-PLASTIC SHELLS OF REVOLUTION. P. V. Marcal (Brown University, Providence, R.I.), p. 369-379. 30 refs. [See A69-26839 12-32]

AN EXPERIMENTAL STUDY OF THE BUCKLING OF ANISOTROPIC PLATES. T. P. Kicher (Case-Western-Reserve University, Cleveland, Ohio) and J. F. Mandell (Massachusetts Institute of Technology, Cambridge, Mass.), p. 380-385. 7 refs. [See A69-26840 12-32]

ON THE APPLICATION OF INVERSE DIFFERENTIAL OPERATORS TO THE SOLUTION OF CYLINDER BUCKLING AND OTHER PROBLEMS. S. B. Batdorf (Aerospace Corp., San Bernardino, Calif.), p. 386-391. 18 refs. [See A69-26841 12-32]

THE BUCKLING AND POST-BUCKLING BEHAVIOR OF SPHERICAL CAPS UNDER AXISYMMETRIC LOAD. J. R. Fitch (General Electric Co., Schenectady, N.Y.) and B. Budiansky (Harvard University, Cambridge, Mass.), p. 392-403. 15 refs. [See A69-26842 12-32]

BUCKLING AND POSTBUCKLING BEHAVIOR OF COMPOSITE CYLINDRICAL SHELLS UNDER AXIAL COMPRESSION. N. S. Khot (USAF, Flight Dynamics Laboratory, Wright-Patterson AFB, Ohio), p. 404-412. 12 refs. [See A69-26843 12-32]

MATERIALS FOR A MINIMUM COST SPACE LAUNCH VEHICLE. E. G. Kendall, L. Raymond, H. M. Blaes (Aerospace Corp., El Segundo, Calif.), and J. Hintz (USAF, Rocket Propulsion Laboratory, Edwards AFB, Calif.), p. 413-421. 7 refs. [See A69-26844 12-31]

RELIABILITY OF ANALYSIS TECHNIQUES AND SENSITIVITY TO MATERIAL PROPERTIES. J. C. Schutzler and H. W. Babel (McDonnell Douglas Corp., Santa Monica, Calif.), p. 422-428. 14 refs. [See A69-26845 12-17]

PROPAGATION LAWS OF FATIGUE CRACKS. S. Yusuff (West Virginia University, Morgantown, W. Va.), p. 429-437. 13 refs. [See A69-26846 12-32]

SOME DYNAMIC MECHANICAL PROPERTIES OF DISTENDED CARBONS. L. M. Lee, R. P. May, and T. R. Guess (Sandia Corp., Albuquerque, N. Mex.), p. 438-452. 27 refs. [See A69-26847 12-18]

A CUMULATIVE DAMAGE CONCEPT IN RAIN EROSION STUDY. C.-H. Mok (General Electric Co., Philadelphia, Pa.), p. 453-455. 10 refs. [See A69-26848 12-32]

THE FRACTURE OF POLYMERS AND FIBER REINFORCED POLYMER COMPOSITES. F. J. McGarry (Massachusetts Institute of Technology, Cambridge, Mass.), p. 456-471. [See A69-26849 12-18]

A69-28252 *#

THE CALCULATION OF THERMAL-FATIGUE LIFE BASED ON ACCUMULATED CREEP DAMAGE.

David A. Spera (NASA, Lewis Research Center, Cleveland, Ohio). American Society of Mechanical Engineers, Gas Turbine Conference and Products Show, Cleveland, Ohio, Mar. 9-13, 1969, Paper. 64 p. 16 refs.

Description of a method for predicting crack initiation in high-temperature components subjected to arbitrary thermal-mechanical cycling. Thermal-fatigue tests of the Glenny type are analyzed using a modification of the Robinson-Taira cumulative damage theory and the empirical method of universal slopes to calculate the number of cycles required to initiate cracks. It is found that considering both creep and fatigue damage, cyclic creep-rupture is the dominant failure mode in the Glenny-type thermal-fatigue tests. The assumptions of (1) the invariance of total strain with plastic flow and creep, and (2) the inverse proportionality of the creep strain rate and rupture time lead to the calculation of thermal stresses in a greatly simplified manner with adequate accuracy. Z.W.

A69-28288 *#
THE EFFECT OF VISCOSITY IN HYPERVELOCITY IMPACT CRATERING.
Robert W. MacCormack (NASA, Ames Research Center, Moffett Field, Calif.).
American Institute of Aeronautics and Astronautics, Hypervelocity Impact Conference, Cincinnati, Ohio, Apr. 30-May 2, 1969, Paper 69-354. 8 p. 17 refs.
Members, $1.00; nonmembers, $1.50.

A numerical method, of second order in both time and space, for the solution of the time-dependent compressible Navier-Stokes equations is presented. Conditions for stability are discussed. The method has been applied to calculate an axisymmetric flowfield produced by hypervelocity impact. Results are given for impacts of aluminum cylinders (having diameters of 0.16, 0.32, and 0.64 cm) into aluminum targets. Viscosities of zero and 10^4 poise were assumed. Both plates and semiinfinite targets are considered at an impact speed of 10 km/sec. It is concluded that viscous effects become increasingly important as projectile size diminishes, and cannot be neglected during the initial stages of crater formation for projectiles smaller than 0.5 cm in diameter. (Author)

A69-28299 *#
IMPACT CHARACTERISTICS IN FUSED SILICA.
Robert E. Flaherty (NASA, Manned Spacecraft Center, Space Physics Div., Meteoroid Sciences Branch, Houston, Tex.).
American Institute of Aeronautics and Astronautics, Hypervelocity Impact Conference, Cincinnati, Ohio, Apr. 30-May 2, 1969, Paper 69-367. 18 p.
Members, $1.00; nonmembers, $1.50.

A special technique was developed for detailed microscopic examination of crater cross sections in fused-silica targets. Photomicrographs of targets have been studied using this technique, and basic differences that distinguish hypervelocity impacts from low-energy-impact damage were discovered. It was also discovered that low-velocity-impact craters, when viewed with bottom lighting, have approximately 75% of the crater area blacked out because of fractures that totally reflect the light, whereas, with respect to hypervelocity impacts (5 km/sec and more), this blacked-out area approximates 10%. The ratio of the crater diameter to crater depth (deepest fissure) for low-velocity and hypervelocity impacts averages 2 and 7, respectively. The hypervelocity impacts exhibit a well-defined central region of pulverized glass surrounded by a large smooth conchoidal chip-out; at velocities above 10 km/sec, this central area shows signs of hydrodynamic flow. (Author)

A69-28304 *#
METEOROID PROTECTION BY MULTIWALL STRUCTURES.
Burton G. Cour-Palais (NASA, Manned Spacecraft Center, Space Physics Div., Meteoroid Sciences Branch, Houston, Tex.).
American Institute of Aeronautics and Astronautics, Hypervelocity Impact Conference, Cincinnati, Ohio, Apr. 30-May 2, 1969, Paper 69-372. 12 p.
Members, $1.00; nonmembers, $1.50.

Investigation of the design principles of spaced, multiwall meteoroid protection in the light of experimental data generated during the Apollo Program. The outer wall or shield is shown to be the most important element in the meteoroid-spacecraft interaction. The condition of the debris is primarily a function of the shock pressure, the melting points of the meteoroid and the shield, the length of the meteoroid, and the thickness of the shield. Spacing between the walls is effective up to approximately 25 to 30 times the length of the meteoroid. The effects of placing additional elements (insulation or honeycomb cells) between the two walls are discussed, and the efficiency of various protective configurations is presented. (Author)

A69-28305 *#
AN EXPERIMENTAL IMPACT INVESTIGATION OF ALUMINUM DOUBLE-SHEET STRUCTURES.
C. Robert Nysmith (NASA, Ames Research Center, Moffett Field, Calif.).
American Institute of Aeronautics and Astronautics, Hypervelocity Impact Conference, Cincinnati, Ohio, Apr. 30-May 2, 1969, Paper 69-375. 6 p.
Members, $1.00; nonmembers, $1.50.

Evaluation of an experiment wherein small pyrex-glass spheres were fired into aluminum double-sheet targets at velocities up to 8.8 km/sec to determine the individual effects of front- and rear-sheet thickness and sheet spacing upon penetration resistance for conditions under which a considerable portion of the front-sheet spray material is melted. It was observed that the ballistic limit of a structure varies with the 1.9 power of the front-sheet thickness, the 3.6 power of the rear-sheet thickness, and with at least the fifth power of sheet spacing. The data were also correlated on the basis of total-sheet thickness, and an optimum thickness distribution for these tests was determined on the basis of an optimization analysis. It was observed that, within the velocity limits of these tests, structures with front sheet to projectile diameter ratios equal to or greater than 0.5 or rear sheet to projectile diameter ratios equal to or greater than 0.1 deviated from the high-speed correlation and failed in a manner more representative of low-speed impact. P.v.T.

A69-33559
FRACTURE: AN ADVANCED TREATISE. VOLUME 5 - FRACTURE DESIGN OF STRUCTURES.
Edited by Harold Liebowitz (George Washington University, School of Engineering and Applied Science, Washington, D.C.).
New York, Academic Press, Inc., 1969. 539 p.
$25.

CONTENTS:

PREFACE. H. Liebowitz (George Washington University, Washington, D.C.), p. vii-xii.
FRACTURE ARREST. J. I. Bluhm (U.S. Army, Army Materials and Mechanics Research Center, Watertown, Mass.), p. 1-63. 82 refs. [See A69-33560 17-32]
FRACTURE DESIGN PRACTICES FOR ROTATING EQUIPMENT. S. Yukawa, D. P. Timo (General Electric Co., Schenectady, N.Y.), and A. Rubio (General Electric Co., Fitchburg, Mass.), p. 65-157. 51 refs. [See A69-33561 17-32]
FRACTURE DESIGN PRACTICES FOR PRESSURE PIPING. A. R. Duffy, G. M. McClure, R. J. Eiber, and W. A. Maxey (Battelle Memorial Institute, Columbus, Ohio), p. 159-232. 38 refs. [See A69-33562 17-32]
SELECTION OF MATERIAL AND OTHER ASPECTS OF DESIGN AGAINST BRITTLE FRACTURE IN LARGE STEEL STRUCTURES. R. W. Nichols and A. Cowan (United Kingdom Atomic Energy Authority, Culcheth, Warrington, England), p. 233-284.
FRACTURE DESIGN PRACTICES FOR ORDNANCE STRUCTURES. J. Adachi (U.S. Army, Materiel Command, Watertown, Mass.), p. 285-381.
FRACTURE DESIGN PRACTICES FOR SHIP STRUCTURES. G. Murray Boyd, p. 383-470.
FRACTURE DESIGN ANALYSIS FOR AIRFLIGHT VEHICLES. P. Kuhn (NASA, Langley Research Center, Hampton, Va.), p. 471-500. 17 refs. [See A69-33563 17-32]
AUTHOR INDEX, p. 501-506.
SUBJECT INDEX, p. 507-525.

A69-33563 *
FRACTURE DESIGN ANALYSIS FOR AIRFLIGHT VEHICLES.
Paul Kuhn (NASA, Langley Research Center, Structures Research Div., Hampton, Va.).
IN: FRACTURE: AN ADVANCED TREATISE. VOLUME 5 - FRACTURE DESIGN OF STRUCTURES. [A69-33559 17-32]
Edited by Harold Liebowitz.
New York, Academic Press, Inc., 1969, p. 471-500. 17 refs.

Brief discussion of experiences which led to the conclusion that the design procedure for flight vehicles should include adequate consideration of the effect which service-induced cracks would have on the strength of the structure. Pertinent design requirements are discussed. A method is presented which, in its current state of development, explains how the crack strength of a material can

be defined and how the crack strength of a simple part can be predicted. Desirable extensions of the method are outlined.
(Author)

A69-35657 * #
A SIMPLIFIED METHOD OF ESTIMATING THE RESPONSE OF LIGHT AIRCRAFT TO CONTINUOUS ATMOSPHERIC TURBULENCE.
E. L. Peele and Roy Steiner (NASA, Langley Research Center, Hampton, Va.).
American Institute of Aeronautics and Astronautics, Aircraft Design and Operations Meeting, Los Angeles, Calif., July 14-16, 1969, Paper 69-766. 12 p. 12 refs.
Members, $1.00; nonmembers, $1.50.

Power spectral density techniques employed in the design of large flexible civil aircraft for atmospheric turbulence are rather complex. For the small rigid aircraft, this degree of complexity may be unwarranted. Consequently, a procedure for determining the gust response based on two rigid-body degrees of freedom was investigated. Using certain simplifying assumptions, formulas are derived and presented for calculating the vertical and lateral gust response to independently applied vertical and lateral gusts. The formulas utilize parametric charts of "response integrals" which are functions of the aircraft reduced frequency, the damping ratio, and a gust scale parameter. The response quantities for a given set of aircraft parameters can be obtained by substituting into appropriate formulas values of two response integrals read from the charts. Sample numerical calculations are included which illustrate the use of the simplified procedure. (Author)

A69-41914 * #
FLUTTER BOUNDARY FOR SIMPLY SUPPORTED UNSTIFFENED CYLINDERS.
Sidney C. Dixon and M. Latrelle Hudson (NASA, Langley Research Center, Structures Research Div., Aerothermoelasticity Section, Hampton, Va.).
AIAA Journal, vol. 7, July 1969, p. 1390, 1391. 11 refs.

Description of a single semiempirical stability boundary for the flutter of simply supported cylinders that is applicable for wide ranges of the length-radius ratio and the radius-thickness ratio. The results given were obtained from a flutter analysis of conical shells which was specialized for a cylinder. O.H.

A69-42133 *
ROSMAN I DYNAMIC ANALYSIS.
T. G. Butler (NASA, Goddard Space Flight Center, Greenbelt, Md.).
IN: STRUCTURES TECHNOLOGY FOR LARGE RADIO AND RADAR TELESCOPE SYSTEMS; PROCEEDINGS OF THE INTERNATIONAL SYMPOSIUM, MASSACHUSETTS INSTITUTE OF TECHNOLOGY, CAMBRIDGE, MASS., OCTOBER 18-20, 1967. (A69-42120 23-11)
Symposium sponsored by the U.S. Navy and the Massachusetts Institute of Technology.
Edited by J. W. Mar and Harold Liebowitz.
Cambridge, MIT Press, 1969, p. 201-217.

Dynamic analysis of the Rosman I antenna which possesses an 85-ft-diam reflector and is used in collecting data from earth-orbiting satellites. The purpose of the analysis was to determine the response of the structure to natural frequencies over the control system band from 0 to 30 Hz. Special attention is given to the analysis of the transfer function spectra between the drive gears and the feedbox. The analysis includes six individual static solutions of the particular segments and a combination of these segments into a single large influence coefficient matrix for the entire structure. An eigenvalue solution is given for the reduced model, as well as a transfer-function solution of this model. Z.W.

A69-42991 * #
CLOSING MATERIALS RESEARCH STRUCTURAL DESIGN CYCLE.
Christos C. Chamis (NASA, Lewis Research Center, Cleveland, Ohio).
(American Society of Civil Engineers, Specialty Conference on Optimization and Nonlinear Problems, Chicago, Ill., Apr. 18-20, 1968.)
American Society of Civil Engineers, Engineering Mechanics Division, Journal, vol. 95, Oct. 1969, p. 1255-1268. 8 refs.
Contract No. AF 33(615)-3110.

Study of the efficient material utilization by simultaneous optimization of structural and material designs as a result of the combined efforts of the structural designer and materials researcher. An effective approach is presented in which several optimum designs from materials with known combinations of constituent-materials and fabrication-processing variables are obtained, and, subsequently, a materials evaluation function is fitted through the several optimum designs in the constituent-materials processing-variables space and, finally, the optimum point of this space is then sought. It is demonstrated that a capability for the simultaneous optimization of structural and material designs can be developed. Capabilities of this type provide the missing link in the materials-research structural-design cycle, which is vital for efficient overall design in complex loading conditions. Such capabilities are very fruitful where no direct functional relationships exist between the structural performance of the material and the properties of its constituents, such as optimum proportioning of concrete constituents, metal alloying, and crop growing. O.H.

A69-43671 * #
MINIMUM-WEIGHT STIFFENED SHELLS WITH SLIGHT MERIDIONAL CURVATURE DESIGNED TO SUPPORT AXIAL COMPRESSIVE LOADS.
W. Jefferson Stroud and Nancy P. Sykes (NASA, Langley Research Center, Structures Research Div., Hampton, Va.).
AIAA Journal, vol. 7, Aug. 1969, p. 1599-1601. 5 refs.

Application of a computer program proposed by Morrow and Kicher (1968) to the determination of the effect of "barreling" (slight meridional curvature) on the strength of ring and stringer stiffened shells designed to support axial compressive loads. It is shown that barreling of such shells can lead to appreciable weight savings. For a cylindrical shell 200 in. long and 400 in. in diameter, the maximum weight saving is on the order of 30 per cent. V.P.

N69-10057*# National Aeronautics and Space Administration. Langley Research Center, Langley Station, Va.
SHOCK-WAVE PRESSURE DECAY IN POLYCARBONATE TARGETS IMPACTED BY CYLINDRICAL POLYCARBONATE PROJECTILES
John D. Di Battista Washington Nov. 1968 21 p refs
(NASA-TN-D-4864) Avail: CFSTI CSCL 20K

The shock wave pressure decay along the impact axis has been obtained as a function of the shock wave depth in polycarbonate targets, impacted at 6.4 and 7.4 km/sec, with cylindrical polycarbonate projectiles having fineness ratios of 0.715. The shock wave pressure as a function of the shock wave depth was obtained by impacting various thickness targets with similar projectiles. Either the projectile velocity or the maximum spray velocity emanating from the target rear surface was used to obtain the compressed target material particle velocity at the target rear surface just prior to the shock wave reflection. The shock wave pressure associated with the compressed material particle velocity was computed by using the second Rankine–Hugoniot jump condition across a shock and a quadratic relation between compressed material particle velocity and shock wave velocity. Experimental data on the transient shock wave phenomena were taken in low sound speed targets which could be impacted at hypervelocities with cylinders of like material using conventional light gas guns. The data presented herein are useful for comparison with results of hydrodynamic

numerical calculations. The projectile launching, detecting, and photographing techniques along with target placement used to obtain unskewed cylindrical projectile impacts are fully described. Author

N69-10225*# General Electric Co., Philadelphia, Pa.
THEORETICAL PREDICTION OF CRATER SIZE FOR HYPERVELOCITY IMPACT BY REDUCED-DENSITY PARTICLES, 18 MAY 1966–17 AUGUST 1967
T. D. Riney and J. F. Heyda Washington NASA Nov. 1968 109 p refs
(Contract NAS3-8512)
(NASA-CR-1196) Avail: CFSTI CSCL 20K

A theoretical study is presented which predicts the depth of craters produced in a thick aluminum alloy target, AL-2024 T6, when impacted by low density heterogeneous and homogeneous projectiles at velocities of 7.35, 20, and 50 km/sec. The prediction is based on a hydrodynamic model for computing the flow field and a comparison of the computed dynamic pressure with the yield stress of the target for terminating the crater. This indirect method for including the strength effect is first shown to give an accurate prediction of the final crater produced by a normal density aluminum projectile at an impact velocity for which experimental data are available. The criterion is then applied for heterogeneous porous projectiles and homogeneous projectiles of reduced density for velocities in the meteoroid range. Also included is the development of an improved equation of state for homogeneous reduced density projectiles and the numerical technique, involving linked particle-in-cell and Eulerian finite difference schemes, that was employed for the calculations. Author

N69-10297*# National Aeronautics and Space Administration. Langley Research Center, Langley Station, Va.
ANALYSIS OF THE AEROELASTIC DIVERGENCE OF TWO EXPERIMENTAL UNGUIDED LAUNCH VEHICLES
Clarence P. Young, Jr. Washington Nov. 1968 30 p refs
(NASA-TN-D-4846) Avail: CFSTI CSCL 20K

A theoretical analysis of two experimental launch vehicles which are known to have failed because of aeroelastic divergence is presented. Data for the analysis and the calculated aeroelastic divergence characteristics are provided. The analytical results and the flight results of the two divergent vehicles are compared. The correlation of the analytical predictions with the actual flight behavior is used for evaluating the method of analysis and to explore further the aeroelastic divergence phenomenon in unguided launch vehicles. Author

N69-11008*# Southampton Univ. (England).
TRANSIENT VIBRATION ANALYSIS OF LINEAR SYSTEMS USING TRANSITION MATRICES
Anthony Craggs Washington NASA Nov. 1968 26 p refs
(Grant NGR-52-025-003)
(NASA-CR-1237) Avail: CFSTI CSCL 20K

A step by step transition matrix method is presented for solving a set of equations of motion. The stability criteria which govern the choice of step size are given in the first part of the report: these are related to the highest eigenvalue of the system under consideration. The use of the technique for evaluating the response to a set of forces and prescribed motions is given in a theoretical discussion. Using the finite element displacement procedure to idealise the structure the method has been applied to several rectangular plate problems and good agreement is obtained between theoretical and experimental results. The results for the transient motion of a simply supported plate are compared with similar results obtained by using a standard 4th order Runge–Kutta procedure and it is shown that the transition matrix solutions are more accurate, and there is also a substantial decrease in the computation time per step. Author

N69-11010*# California Univ., Los Angeles.
GEOMETRIC PROPERTIES OF A PRESTRESSED SEGMENTED SPHERICAL SHELL
R. L. Brackett, F. R. Shanley, and L. P. Felton Washington NASA Nov. 1968 32 p refs
(Grant NSG-423)
(NASA-CR-1231; Rept.-68-23) Avail: CFSTI CSCL 20K

Ceramics are potentially excellent structural materials because of their high moduli of elasticity and great compressive strengths. However, their brittleness, coupled with fabrication difficulties, has been a major drawback to their increased use. The problems might be overcome if structures were to be constructed of small segments with the assemblage being prestressed. This report discusses the design and construction of a plastic model of a prestressed dome constructed of 180 triangular plate segments. Prestressing is accomplished by cables running between segments, parallel to segment edges. Prestressing forces are adjusted by special fittings located around the perimeter of the dome. Author

N69-13034*# National Aeronautics and Space Administration. Langley Research Center, Langley Station, Va.
BUCKLING OF AN EQUATORIAL SEGMENT OF A SPHERICAL SHELL LOADED BY ITS OWN WEIGHT
Robert E. Blum and Harvey G. Mc Comb, Jr. Washington Dec. 1968 29 p refs
(NASA-TN-D-4921) Avail: CFSTI CSCL 20K

Buckling equations are solved for a simply supported equatorial segment of a spherical shell loaded in the axial direction by its own weight. The Galerkin method is used to obtain a critical-thickness parameter for buckling as a function of the shell material and geometric properties and of the relative proportions of the shell weight supported at the upper and lower edges. Results of the present method are compared with those of a simplified approach in which the spherical shell segment is assumed to buckle if the maximum compressive stress is greater than the critical compressive stress for a complete spherical shell loaded by uniform external pressure. This comparison indicates that the simplified approach yields larger thicknesses than the method presented here. The particular proportions of the shell weight which should be supported at the upper and lower edges to minimize the tendency to buckle are also determined. Results have been used in the design of a large rectangular reinforced-plastic shell segment which simulates the lunar surface in the lunar orbit and landing approach simulator. Author

N69-14169*# National Aeronautics and Space Administration. Marshall Space Flight Center, Huntsville, Ala.
A STUDY OF STIFFNESS MATRICES FOR THE ANALYSIS OF FLAT PLATES
Dennis A. Kross Washington Dec. 1968 47 p refs
(NASA-TN-D-4927) Avail: CFSTI CSCL 20K

The analysis of thin plates in bending is considered with four different rectangular finite element representations. The first representation approximates the transverse displacement by a sixth-order two-dimensional generalization of a Hermitian interpolation polynomial. This representation requires that the Kirchhoff hypothesis be satisfied throughout the element. Therefore the transverse shear strains vanish, and the element exhibits no shear stiffness. The second representation uses a simple bilinear approximation for the transverse displacements and rotations without the Kirchhoff hypothesis. In the latter case both shear-stiffness and bending-stiffness matrices are obtained. The third approximation use a discrete Kirchhoff hypothesis which introduces a constraint between the transverse nodal displacements and nodal rotations.

This case also contains both bending and shear stiffness. The fourth representation uses only the bending stiffness developed in the previous case. This is a logical approximation since the discrete Kirchhoff hypothesis causes the transverse shears to vanish in the limit. Numerical examples are presented to demonstrate the relative accuracy of the finite elements investigated. Author

N69-14254*# Case Western Reserve Univ., Cleveland, Ohio.
STRUCTURAL SYNTHESIS OF A STIFFENED CYLINDER
William M. Morrow, II and Lucien A. Schmit, Jr. Washington NASA Dec. 1968 169 p refs
(Grant NsG-110-61)
(NASA-CR-1217) Avail: CFSTI CSCL 20K

The problem of structural synthesis of a cylindrical shell stiffened in the longitudinal and circumferential directions with rectangular cross-section stiffeners is treated. The design variables are the dimensions and spacings of the stiffeners and the thickness of the skin, seven in all. The synthesis method uses the penalty function method of Fiacco and McCormick to transform the basic inequality constrained minimization problem into a sequence of unconstrained minimization problems. The stability analysis of the cylinder is a linear analysis including the effects of stiffener eccentricity. Numerical results are presented which illustrate the effectiveness of the penalty function approach, the importance of multiple load conditions, the influence of internal versus external stiffening, the effect of minimum gage limitations on the optimum design, and the advantage that stiffening in both directions exhibits compared with stiffening in only one direction. Author

N69-14306*# National Aeronautics and Space Administration. Langley Research Center, Langley Station, Va.
EFFECT OF THE CHEMICAL STATE OF PYROLYSIS GASES ON HEAT-SHIELD MASS
William D. Brewer, C. W. Stroud, and Ronald K. Clark Washington Dec. 1968 27 p refs
(NASA-TN-D-4975) Avail: CFSTI CSCL 20M

Results are presented from an analytical investigation to determine the effect of the chemical state of the pyrolysis gases on the heat-shield mass required for a reentry vehicle in a given environment. Mass per unit area of ablative material required is calculated for a number of constant-heating-rate environments and the total mass is calculated for a lifting-body vehicle in a typical reentry trajectory. The required mass of ablative material is calculated for three different assumptions: (1) The pyrolysis gases are in chemical equilibrium at all times. (2) The gases are chemically frozen at 500°K. (3) The gases change from the frozen state to equilibrium over some temperature range. The results show that in all calculations considerably more material is required if the gases remain chemically frozen as initially formed than if the gases are in equilibrium at all times. For the lifting-body vehicle, 28 percent more material is required if the gases are chemically frozen than if the gases are in chemical equilibrium. Some experimental data are given which indicate that the transition from the frozen state to equilibrium may take place above 1400°K and over a temperature range of about 200°K. Author

N69-14315*# National Aeronautics and Space Administration. Ames Research Center, Moffett Field, Calif.
PROJECTILE SHAPE EFFECTS ON HYPERVELOCITY IMPACT CRATERS IN ALUMINUM
B. Pat Denardo Washington Dec. 1968 16 p refs
(NASA-TN-D-4953) Avail: CFSTI CSCL 20K

Linear high density polyethylene cylinders, with fineness ratios of 1/6, 1/3, 2/3, 1, and 3, and spheres were launched into thick targets of hard aluminum at velocities up to 11.3 km/sec. The effects of projectile shape on the various crater parameters were determined quantitatively from the basic crater dimensions: depth, diameter, and volume. In the hypervelocity regime, the dimensionless penetration, P/d, varied with the projectile fineness ratio, l/d, to the 1/4 power for fineness ratios between 1/6 and 1. For fineness ratios greater than 1, the power increased and approached unity, as would be expected from shaped-charge jet theory. For engineering purposes, in the hypervelocity regime, a sphere produces the same crater as a cylinder of equal diameter and l/d of 2/3. Author

N69-14477*# Wichita State Univ., Kans.
SOME EQUILIBRIUM AND FREE VIBRATION PROBLEMS ASSOCIATED WITH CENTRIFUGALLY STABILIZED DISK AND SHELL STRUCTURES
Walter Eversman Washington NASA Dec. 1968 237 p refs
(Grant NGR-17-003-004)
(NASA-CR-1178) Avail: CFSTI CSCL 20K

Equations for shallow, isotropic, spherical shells spinning about their polar axis are derived from a variational principle and specialized to the case of a spinning flat membrane disk. The problem of transverse vibrations is solved for a fully clamped hub and a loosely clamped hub on an annular disk. Vibrational analysis of shallow shells indicates that the spinning shell equilibrium problem must be solved first to provide the necessary stress and displacement distributions for the vibration equations of motion. The equilibrium problem is treated by linear theory for a freely spinning shell and by both linear and nonlinear theory for the spinning shell with a fully clamped hub. It is found that bending effects are important, particularly for shells with a small ratio of rise to thickness, and that a continuous transition from the shell solution to that for a spinning flat disk requires that bending be included. The nonlinear effect of finite rotations of shell elements is found to be strong and increases as the ratio of shell rise to shell thickness increases. It is concluded that a nonlinear theory which includes both membrane and bending effects should be employed for the general analysis of the equilibrium configuration. Author

N69-14480*# National Aeronautics and Space Administration. Lewis Research Center, Cleveland, Ohio.
EFFECT OF RADIUS ON BULGING AND FRACTURE OF THROUGH-CRACKED CYLINDRICAL PRESSURE VESSELS AT CRYOGENIC TEMPERATURES
Timothy L. Sullivan and William S. Pierce Washington Dec. 1968 28 p refs
(NASA-TN-D-4951) Avail: CFSTI CSCL 20K

Burst tests of through-cracked, thin-walled cylinders fabricated from Ti-5Al-2.5Sn, extra low interstitial grade, and 2014-T6 Al were conducted at −320° and −423° F (77 and 20 K). The diameters of the cylinders tested were approximately 6 and 18 in. (15 and 46 cm). The titanium alloy test results showed the pressure bulge coefficient was essentially constant for these two diameters. Comparison of the experimental results with an expression for predicting hoop fracture stress proposed by Eiber showed a good fit with the aluminum alloy data but a poor fit with the titanium alloy data. Author

N69-14506*# National Aeronautics and Space Administration. Ames Research Center, Moffett Field, Calif.
AN IMPACT ENERGY-ABSORBING STRUT EMPLOYING TUBE CUTTING
Robert W. Warner and Arthur G. Kaskey Washington Dec. 1968 38 p refs
(NASA-TN-D-4941) Avail: CFSTI CSCL 20K

An experimental evaluation is described for a tubular, nontelescoping, pin-ended strut that absorbs impact energy by tube cutting. Since this strut is shorter than a two-part telescoping strut, it offers a means for reducing the wieght of any energy-absorbing truss (or other structure) in which a short strut is appropriate. The

cutting load is reasonably constant over the stroke and repeatable for the impact velocities tested, which ranged from 3.0 to 11.9 feet per second, and for variations in impact weight, stroke length, and precutting. The lower and more meaningful of the two specific energy absorptions evaluated herein (5893 ft-lb per lbm) is obtained by dividing the product of the mean cutting load and the maximum possible stroke by the total strut weight (including end fittings). When modified in overall strut length, material, and number of cutters, as a check on adaptability, the system continued to function successfully. Author

N69-14553*# National Aeronautics and Space Administration. Washington, D. C.
NASA SPACE VEHICLE DESIGN CRITERIA (STRUCTURES): PROPELLANT SLOSH LOADS
Aug. 1968 188 p refs
(NASA-SP-8009) Avail: CFSTI CSCL 20K

Sloshing of propellants may adversely affect the stability of a space vehicle and the integrity of the tank structure. Sloshing describes the free-surface oscillations of a fluid in a partially filled tank. These oscillations result from lateral and longitudinal displacements or angular motions of the vehicle. This undesirable sloshing phenomenon may be controlled by the proper geometrical design of the tank and by the addition of baffles. Tank geometry influences the natural sloshing frequencies and sloshing modes, forced response, and resultant pressure forces and moments acting on the tank. Baffles increase the effective fluid damping and thereby reduce the duration of free oscillations and the magnitude of forced oscillations. Dynamic coupling between the sloshing propellant and the elastic structure may have a large influence on the vibration frequencies and mode shapes of the elastic tank. This coupled propellant/elastic-tank system may also exhibit dynamic instabilities, either as an independent system or coupled with some other system component. This monograph is concerned primarily with the loads on the tank during lateral and longitudinal sloshing and with baffle pressure loads due to sloshing. Author

N69-15378*# Brown Engineering Co., Inc., Huntsville, Ala.
THE GENERAL INSTABILITY OF ECCENTRICALLY STIFFENED CYLINDRICAL SHELLS UNDER AXIAL COMPRESSION AND LATERAL PRESSURE
John N. Dickson and Richard H. Brolliar Washington NASA Jan. 1969 120 p refs
(Contract NAS8-20073)
(NASA-CR-1280) Avail: CFSTI CSCL 20K

A method of determining the general instability load of an orthogonally stiffened cylindrical shell under axial compression and lateral pressure is presented. The governing equations were derived using small deflection theory; and, consequently, the validity of the method must be restricted to moderately or heavily stiffened cylinders. All the stiffnesses occurring in stiffened shells of this type were incorporated, and the rings and stringers were considered eccentric with respect to the skin middle surface. Local buckling of the skin between adjacent stringers before general instability was allowed, and the resulting reductions in stiffness properties of the skin were determined as a function of the two principal strains. Analytical and experimental results are compared for twenty-nine stiffened cylinders loaded in compression and for six stiffened cylinders loaded in bending. The method has been programmed for use with an IBM 7094 computer. The computer program and detailed instructions for its use are included. Author

N69-15632*# National Aeronautics and Space Administration. Marshall Space Flight Center, Huntsville, Ala.
THE INFLUENTIAL ASPECTS OF ATMOSPHERIC DISTURBANCES ON SPACE VEHICLE DESIGN USING STATISTICAL APPROACHES FOR ANALYSIS
Robert S. Ryan and Alberta W. King Washington Jan. 1969 112 p refs
(NASA-TN-D-4963) Avail: CFSTI CSCL 22B

The influential aspects of various wind profile disturbances on the dynamic response of the vehicle are considered. Particular emphasis is given to separating the influence of wind shears, turbulence and quasi-steady wind speed on the dynamic response during the boost phase of flight. Four hundred and seven individual detailed (Jimsphere) wind profiles are the primary wind inputs, although the MSFC synthetic profile is also discussed. The time response to each profile is run and a statistical analysis made. Severe profiles are ranked in terms of the bending moment at two vehicle stations for the Saturn 5 vehicle. The influence of results on vehicle design and flight operational procedures is determined. Author

N69-16091*# National Aeronautics and Space Administration. Langley Research Center, Langley Station, Va.
EFFECTS OF STRUCTURAL DAMPING ON FLUTTER OF STRESSED PANELS
Charles P. Shore (M.S. Thesis—Va. Polytech. Inst.) Washington Jan. 1969 35 p refs
(NASA-TN-D-4990) Avail: CFSTI CSCL 20K

The flutter of stressed orthotropic panels with edge rotational restraint is investigated theoretically. A modal solution which utilizes two-dimensional quasi-steady aerodynamic theory and includes both structural and aerodynamic damping is presented. The investigation was conducted in an attempt to explain the existing discrepancies between theoretical and experimental results for stressed panels, in particular for panels stressed near buckling, the most critical flutter condition. Structural damping is represented in the present analysis in a manner consistent with the representation for a Kelvin-Voigt viscoelastic body. Numerical results are presented to indicate that such a representation of structural damping eliminates the physically untenable results that have been obtained for certain values of the input parameters in previous analyses. Additionally, representation of structural damping in this manner results in a reasonable correlation between theory and experiment over the entire range of stress from zero to buckling. Author

N69-16114*# Case Western Reserve Univ., Cleveland, Ohio.
THE STRUCTURAL SYNTHESIS OF AN ABLATING THERMOSTRUCTURAL PANEL
William A. Thornton and Lucien A. Schmit, Jr. Washington NASA Dec. 1968 205 p refs
(Grant NsG-110-61)
(NASA-CR-1215) Avail: CFSTI CSCL 22B

The development of a structural synthesis capability for ablating thermostructural panels in a planetary entry environment is reported. The synthesis utilizes a penalty function technique in conjunction with integrated behavior constraints. The thermal analysis includes the effects of surface recession and pyrolysis gas transpiration. The ablator layer is structural. Design variables are the layer thicknesses and panel size. Behavior constraints are the temperature at the ablator-structure interface and at the backwall, panel deflection, ablator stress, structural layer stress, intercell face buckling, and char strain. The synthesis will minimize panel weight or panel thickness. The results of 12 test cases are presented. It is found that the usual a priori assumptions about the panel thermal profiles required for minimum weight designs are not justified. Author

N69-16115*# National Aeronautics and Space Administration. Lewis Research Center, Cleveland, Ohio.
A DIGITAL COMPUTER PROGRAM FOR DETERMINING

THE ELASTIC-PLASTIC DEFORMATION AND CREEP STRAINS IN CYLINDRICAL RODS, TUBES AND VESSELS
Richard L. Puthoff Washington Jan. 1969 49 p refs
(NASA-TM-X-1723) Avail: CFSTI CSCL 20K

A generalized plane-strain elastic–plastic analysis and a creep analysis of a long hollow (or solid) cylinder are presented. These analyses use the method of successive approximations for solution. The equations are converted into finite difference formulation and programmed on an IBM 7094 Mod 2 digital computer. The cylinder is subjected to thermal gradients and pressure loads. The resulting stresses and strains calculated are printed as the output. A sample problem is included, along with program operation instructions and listings. Examples of components for which the analysis can be used are reactor pressure shells, fuel elements, and heat-exchanger tubes with symmetrical temperature gradients and constant pressure loads. Author

N69-16156 *# Michigan Univ., Ann Arbor.
SENSITIVITY OF THE CREEP-RUPTURE PROPERTIES OF NICKEL-BASE SUPERALLOY SHEET TO SHARP EDGE-NOTCHES IN THE TEMPERATURE RANGE OF 1000 °F–1400 °F
David J. Wilson, James W. Freeman, and Paul D. Goodell Washington NASA Jan. 1969 45 p refs
(Grant NsG-124)
(NASA-CR-1263) Avail: CFSTI CSLC 20K

Investigations to evaluate the severe time-dependent, edge-notch sensitivity known to occur in thin sheet nickel-base superalloys exposed under stress at 1000° and 1200°F are presented. Studies over a wide range of heat-treated conditions, has served to define the scope of this problem in 0.026-inch thick sheet. In addition, exploratory data have been obtained on the influence of notch acuity and sheet thickness on the notch sensitivity. Both smooth and edge-notched specimens fractured by the initiation and growth of intergranular cracks, followed by abrupt transgranular fracture due to the increase in stress caused by creep cracking. Analysis of these processes showed that the degree of notch sensitivity was strongly dependent upon the effect of the notches on the time required for the initiation of the creep crack and the early stages of its growth. There were some differences among alloys and within an alloy with heat treatment and test temperature. Author

N69-16211 *# National Aeronautics and Space Administration. Langley Research Center, Langley Station, Va.
WIND-TUNNEL STUDY OF DEFLECTED-ELEVATOR FLUTTER ENCOUNTERED ON A T-TAIL AIRPLANE
Maynard C. Sandford and Charles L. Ruhlin Washington Feb. 1969 23 p refs
(NASA-TN-D-5024) Avail: CFSTI CSCL 20K

An exploratory study of a horizontal tail flutter encountered on the T-tail of a large multijet cargo airplane was conducted in the transonic dynamics tunnel at Mach numbers up to 0.93. The airplane flutter, consisting primarily of a coupled elevator rotation and stabilizer torsion oscillation at about 24 cps, occurred at a Mach number near 0.8 at several altitudes and was initiated only when the elevators were deflected about 8° or greater. The wind tunnel study employed a 1/8.5 size flutter model which consisted of a geometrically, dynamically, and elastically scaled empennage and aft fuselage, and dynamically and elastically, but not geometrically, simulated wings, nacelles, and forward fuselage. The basic flutter phenomenon experienced on the airplane was reproduced by the model in the wind tunnel although the model predicted considerably higher flutter speeds than those of the airplane at Mach number 0.8. The model flutter speed boundary was nearly flat from a Mach number of 0.41 to 0.89 and rose sharply and curved inward tending to form a closed flutter region at the extreme Mach numbers. In order to initiate model flutter, an elevator deflection angle of 8° in the trailing-edge-down attitude was required, whereas on the airplane, flutter occurred for an elevator deflection of 8° in either an up or down direction. Author

N69-16469 *# National Aeronautics and Space Administration. Langley Research Center, Langley Station, Va.
A METHOD FOR COMPUTATION OF VIBRATION MODES AND FREQUENCIES OF ORTHOTROPIC THIN SHELLS OF REVOLUTION HAVING GENERAL MERIDIONAL CURVATURE
Howard M. Adelman, Donnell S. Catherines, and William C. Walton, Jr. Washington Jan. 1969 88 p refs
(NASA-TN-D-4972) Avail: CFSTI CSCL 20K

A procedure is described for computing the vibration modes and frequencies of thin shells of revolution having general meridional curvature and orthotropic elastic properties. The procedure is based on the finite element method in which the direct stiffness approach is used. A geometrically exact finite element is employed. A computer program based on this procedure has been written and details of the program are described. The geometric characteristics of the shell are used as inputs to the program in the form of functions of the meridional coordinate. The stiffness and mass matrices are computed by numerical integration by use of the trapezoidal rule. The computer program is applied to several shell configurations including two cylinders, two conical frustums, shells of both positive and negative Gaussian curvature, and an annular plate. Frequencies are correlated with frequencies from previous investigations for these shells. The agreement between results of the present analysis and results from the previous investigations is generally excellent. Author

N69-17258 *# National Aeronautics and Space Administration. Langley Research Center, Langley Station, Va.
RATIOS OF STEADY-STATE RESPONSES TO VARIOUS TRANSIENT RESPONSES, BOTH HAVING EQUAL MAXIMUM EXCITATION LEVELS
Richard W. Faison Washington Feb. 1969 35 p refs
(NASA-TN-D-5070) Avail: CFSTI CSCL 20K

Presented are acceleration response ratios as determined by a single-degree-of-freedom system analysis for three types of commonly encountered transient excitations. The transient excitations were (1) a modulated sine wave of half-modulation-period duration, (2) a modulated cosine wave of a quarter-modulation-period duration, and (3) a damped sinusoid. Closed-form solutions for the acceleration responses were obtained by Laplace transform techniques. The ratio of maximum absolute acceleration response for the transient sinusoid to the maximum absolute acceleration response of a steady-state sinusoid having the same frequency is given. Numerical results are presented as the response ratios for various nondimensional parameters. Author

N69-17275 *# National Aeronautics and Space Administration. Lewis Research Center, Cleveland, Ohio.
CRACK TOUGHNESS CHARACTERISTICS OF SEVERAL ALLOYS FOR USE IN HEAVY SECTIONS OF HIGH SPEED AIRCRAFT
Raymond T. Bubsey and William F. Brown, Jr. Washington Jan. 1969 38 p refs
(NASA-TN-D-4998) Avail: CFSTI CSCL 11F

Plane strain crack toughness K_{Ic} tests were made on four heavy section candidate alloys for high speed aircraft. The data are analyzed by using the plane strain crack-size factor $(K_{Ic}/\sigma_{YS})^2$, where σ_{YS} is the 0.2-percent yield strength. The alloys investigated were maraging 250 grade steel, 9Ni–4Co–30 steel, 300M steel, PH 13-8Mo stainless steel, and titanium 6Al–6V–2Sn. These alloys were supplied in fabricated section sizes which ranged from

1/2-inch (13-mm) plate to 13- by 13-inch (330- by 330-mm) forgings. Single-edge-crack tension specimens were used to study the influence of crack orientation in respect to the fibers and to establish the general influence of section size. Double-edge-crack tension specimens were used to determine the effect of test temperature which varied from −110°F to 650°F. The influence of melting practice on the plane strain crack toughness on maraging 250 grade steel was also investigated. Author

N69-17737*# National Aeronautics and Space Administration. Langley Research Center, Langley Station, Va.
IDENTIFICATION OF STRUCTURAL SYSTEMS BY USE OF NEAR-RESONANCE TESTING
John P. Raney and James T. Howlett Washington Feb. 1969 40 p refs
(NASA-TN-D-5069) Avail: CFSTI CSCL 20K

A recent innovation for determining the governing differential equations of motion of a complex structure is described. Numerical values for the mass, stiffness, and damping coefficients of the dynamical equations associated with a particular input response or transmission path are computed from the data usually obtained in conventional vibration tests of a structure. The theory is based on the dynamic properties of multidegree-of-freedom linear systems. The method requires the steady state response (acceleration, velocity, or displacement) and the driving sinusoidal force input for transmission paths of interest to be determined experimentally for a few frequencies near each major structural resonance. Application of the method is illustrated by determining from experimental data the equations of motion of the 1/10 scale and 1/40 scale models of the Apollo–Saturn V launch vehicle with cantilevered–free and free–free boundary conditions, respectively. Transient responses computed by using the identified equations for the 1/40 scale model are shown to agree favorably with experimental results and to be slightly superior to the results produced by conventional structural analysis. Author

N69-17766*# Barry Wright Corp., Watertown, Mass.
LOSS FACTOR AND RESONANT FREQUENCY OF VISCOELASTIC SHEAR-DAMPED STRUCTURAL COMPOSITES
Thomas F. Derby and Jerome E. Ruzicka Washington NASA Feb. 1969 20 p refs
(Contract NAS1-7580)
(NASA-CR-1269) Avail: CFSTI CSCL 20K

An investigation is conducted to evaluate the loss factor, resonant frequency and thermal conductivity characteristics of structural composites with viscoelastic shear damping mechanisms. Theoretical solutions and graphical design data for damping and resonant frequency are developed for four types of viscoelastic shear damped structural composites: two elastic-element, symmetrical three elastic element unsymmetrical three elastic-element; and N identical elastic laminate configurations. The equations and design procedures for predicting loss factor and resonant frequency are verified by the results of experimental measurements made on laboratory beam specimens. Thermal conductivity characteristics of laminated viscoelastic shear-damped plates are investigated theoretically and experimentally, with consideration given to methods for increasing thermal conductivity and the subsequent effect on structural damping. Author

N69-17770*# Washington Univ., Seattle.
PHOTOVISCOELASTIC MODEL TESTING
Charles W. Fowlkes Washington NASA Feb. 1969 97 p refs
(Grant NsG-401)
(NASA-CR-1289; REPT-68-2) Avail: CFSTI CSCL 20K

The experimental procedures necessary to perform a complete, two-dimensional viscoelastic stress analysis using the photoviscoelastic method are outlined. These procedures are illustrated in the solution of several example problems. The example problems cover the range of variables encountered in photoviscoelastic model testing. A description of the necessary laboratory apparatus is included. Author

N69-19030*# Iowa Univ., Iowa City.
IMPROVEMENT OF AN INTEGRAL EQUATION METHOD IN PLANE ELASTICITY THROUGH MODIFICATION OF SOURCE DENSITY REPRESENTATION
Kwan Rim and Allen S. Henry Washington NASA Feb. 1969 47 p refs
(Contract NsG-576)
(NASA-CR-1273) Avail: CFSTI CSCL 20K

The research reported herein shows that greater accuracy in calculated boundary stress components can be obtained if the numerically-determined, piece-wise constant source density functions are replaced by functions which, with their first derivatives, are continuous on the boundary. In contrast to other reported results, this modification permits one to compute unknown boundary stress components directly from the approximate stress function without recourse to such indirect techniques as extrapolation, numerical differentiation, and others. As the result, a direct comparison between the specified boundary stresses and those boundary stresses consistent with the approximate biharmonic stress function is now made possible; and thereby the usefulness of the integral equation method in plane elasticity is considerably enhanced. Author

N69-21042*# National Aeronautics and Space Administration Langley Research Center, Langley Station, Va.
EFFECTS OF BOTTOM-STRUCTURE FLEXIBILITY ON WATER LANDING LOADS OF APOLLO SPACECRAFT MODELS
Sandy M. Stubbs and Melvin E. Hathaway Washington Mar. 1969 31 p refs
(NASA-TN-D-5108) Avail: CFSTI CSCL 20K

A landing investigation has been made to determine the effects of heat-shield flexibility on pressures and accelerations for water landings of Apollo spacecraft models. An additional purpose was to obtain accurate acceleration data on the landing impact of a spherical body in water for use in refinements of rigid-body analytical calculations. Two solid models and one flexible-bottom model were tested to determine impact pressures and accelerations. The flexible bottom was scaled in stiffness from an early Apollo heat-shield structural design. The test conditions were limited to symmetrical landing attitudes (0°) without horizontal velocity in order to obtain pressure profiles and loads on the bottom surfaces of the models from a limited number of data channels. Two vertical velocities were used to determine the effect of velocity on the forces applied to the flexible bottom. Good agreement was obtained between computed and experimental acceleration results for the solid models. Results from this investigation indicate that a virtual water mass factor of 0.9 should be used in computing impact forces for rigid spherical surfaces shaped like the Apollo aft heat shield. Pressure profiles were obtained from which forces and accelerations could be derived. The pressures, forces, and accelerations on the solid models vary approximately as the square of the velocity. Author

N69-21392*# National Aeronautics and Space Administration. Lewis Research Center, Cleveland, Ohio.
FACTORS INFLUENCING LOW CYCLE CRACK GROWTH IN 2014-T6 ALUMINUM SHEET AT −320°F (77K)

William S. Pierce and Timothy L. Sullivan Washington Apr. 1969 43 p refs
(NASA-TN-D-5140) Avail: CFSTI CSCL 20L

An investigation was conducted to determine the low-cycle (under 10,000 cycles) crack growth characteristics of through-center-cracked specimens 0.060 in. thick subjected to tension–tension cyclic loading. The following factors were studied: minimum to maximum initial stress intensity ratio R_i; the maximum gross stress applied, as percentage of critical fracture stress; and cyclic rate. The crack growth rate was found to be a function of stress level expressed as percentage of critical fracture stress for specimens tested at the same R_i value. A crack growth relation was developed which takes into account changes in R_i in the low-cycle region. When the cycle rate was decreased from 0.5 to 0.05 Hz, the cyclic life was reduced, but only for high initial stress intensities. Author

N69-21401*# General Technology Corp., Lawrenceville, N. J.
A CONTINUUM THEORY FOR AN ELASTIC SOLID WITH ELASTIC MICRO-INCLUSIONS
L. M. Habip Washington NASA Mar. 1969 24 p refs
(Contract NASw-1589)
(NASA-CR-1321; TR-8-7) Avail: CFSTI CSCL 20K

By analogy with the results of a higher order continuum theory, explicit dispersion relations governing the lowest and next higher modes of propagation of plane, longitudinal waves in an unbounded, elastic particulate composite solid are obtained in terms of the relative properties of the constituent materials. The corresponding ratio of group velocity to phase velocity is likewise evaluated. These and further relationships valid for a special case are exhibited graphically. Author

N69-21403*# City Coll. of the City of New York.
DYNAMIC RESPONSE OF STRUCTURAL ELEMENTS EXPOSED TO SONIC BOOMS
David H. Cheng and Jacques E. Benveniste Washington NASA Mar. 1969 47 p refs
(Grant NGR-33-013-011)
(NASA-CR-1281) Avail: CFSTI CSCL 20K

The structural elements of interest are uniform beams and plates with various boundary conditions. The disturbances are represented by a variety of boom signatures which approximate those obtained from field measurements. Responses of structural elements to a unit impulse and to a unit force moving at a constant velocity are first obtained. This enables a comparison to be made of the relative dynamic effects of an N-shaped pressure pulse and an N-shaped traveling wave on a simple structure. It is followed by a study on the effects of boundary restraints using an N-shaped pressure pulse. Based on the results due to such idealized boom signatures as sine pulse, half-cosine pulse, triangular pulse, N-shaped pulse, and N-shaped pulse with spikes, two simplified methods in evaluating the boom effects on structural elements are proposed: One requires only the knowledge of the peak pressure and the other, the positive impulse. Neither requires the specification of the exact shape of the boom signature. Author

N69-21569*# General Technology Corp., Lawrenceville, N. J.
ON THE DETERMINATION OF MICROMORPHIC MATERIAL CONSTANTS FROM PROPERTIES OF THE CONSTITUENTS
Richard F. Maye Washington NASA Mar. 1969 24 p refs
(Contract NASw-1589)
(NASA-CR-1320; TR-8-6) Avail: CFSTI CSCL 20K

Using relationships given by Eringen and Suhubi on the general theory of micro-elasticity, this report studies the relationship of a linear micromorphic material to linear classically elastic constituents and also investigates the possibility of obtaining the material constants from the properties of the constituents. The special case of a two constituent isotropic micromorphic material is considered in detail. For this case, all constituent properties except three are easily evaluated. Determination of the eighteen micromorphic material moduli and the micromorphic interia constant is therefore reduced to the experimental determination of the three unknowns. A.L.

N69-21814*# National Aeronautics and Space Administration. Lewis Research Center, Cleveland, Ohio.
EFFECT OF ULTRASONIC VIBRATION ON PRECIPITATION HARDENING OF STEELS AND SUPERALLOYS
Stanley G. Young and L. Leonard (Case Western Reserve Univ., Cleveland) Washington Mar. 1969 38 p refs
(NASA-TN-D-5131) Avail: CFSTI CSCL 11F

Specimens of a 300 grade maraging steel, 17-4PH steel, A-286, Rene 41, and L-605 were subjected to ultrasonic vibration during aging. Ultrasonic vibration increased the hardening rate but did not increase the maximum hardness above that of statically aged specimens. The heat treating environment (which included sodium, chloride salts, and air) was found to influence the observed hardening rates of vibrated aged specimens. Author

N69-22773# National Aeronautics and Space Administration. Langley Research Center, Langley Station, Va.
NATURAL VIBRATION MODAL ANALYSIS
J. S. Archer (TRW Systems) Sep. 1968 35 p refs
(NASA-SP-8012) Avail: CFSTI CSCL 20K

Resulting from the need for uniform criteria in space vehicle design, a discussion is presented on the state of the art, basic criteria, and recommended practices for obtaining natural vibration modal data and its subsequent analysis. The results of such analyses provide a description of the linear dynamic characteristics of the space vehicle structure and are basic to understanding the dynamic transient accelerations, velocities, and displacements experienced by the vehicle under any kind of excitation. A.C.R.

N69-22821*# National Aeronautics and Space Administration. Langley Research Center, Langley Station, Va.
EFFECT OF SHALLOW MERIDIONAL CURVATURE ON THE VIBRATION OF NEARLY CYLINDRICAL SHELLS
Paul A. Cooper Washington Apr. 1969 41 p refs
(NASA-TN-D-5143) Avail: CFSTI CSCL 20K

Curvature effects on minimum natural frequencies of nearly cylindrical shells with either positive or negative Gaussian curvature were investigated. The positive Gaussian curvature shells have minimum natural frequencies well above those of corresponding cylindrical shells. The minimum natural frequencies of the negative Gaussian curvature shells generally are below those of the corresponding cylinders, and evidence wide variations in value and large reductions in magnitude occurring at certain critical values of curvature. The large reductions in magnitude result from a condition of essentially inextensional vibration. It is shown that membrane theory affords a simple method of determining the modal wavelength ratio and curvature combinations at which these reductions occur, whereas pure bending theory gives a good estimate of the magnitudes of the associated frequencies. Author

N69-22823*# National Aeronautics and Space Administration. Lewis Research Center, Cleveland, Ohio.
STRESS-RUPTURE AND TENSILE PROPERTIES OF REFRACTORY-METAL WIRES AT 2000° AND 2200°F (1093° AND 1204°C)
Donald W. Petrasek and Robert A. Signorelli Washington Apr. 1969 41 p refs

(NASA-TN-D-5139) Avail: CFSTI CSCL 20K

Tungsten, molybdenum, and columbium base alloy wires were tested at room temperature, 2000°F (1093°C) and 2200°F (1204°C). Metallographic examinations were also made of the wire microstructure after testing. Ultimate tensile strength values of up to 240,000 psi for W – 5%, Re – 2% ThO_2 wire tested at 2000°F and up to 160,000 psi for W – 3% Re wire tested at 2200°F were obtained. The best strength values obtained for a 100 hour rupture life were 96,000 psi at 2000°F and 69,000 psi at 2200°F for W – 2% ThO_2 wire. These properties suggested that the wires showed promise as potential fiber reinforcements in the 2000° to 2200°F temperature range. Author

N69-22932*# National Aeronautics and Space Administration. Langley Research Center, Langley Station, Va.

LONGITUDINAL VIBRATION CHARACTERISTICS OF 1/10–SCALE APOLLO/SATURN 5 REPLICA MODEL

Larry D. Pinson and H. Wayne Leonard Washington Apr. 1969 97 p refs

(NASA-TN-D-5159) Avail: CFSTI 20L

A lumped parameter analysis was employed to assess the applicability of such an analysis to a complex Saturn V type of launch vehicle and to investigate the effects of tank orthotropy and the method of representing the mass of contained liquids on the calculated natural modes and frequencies of the system. An approximate theory which accounts for tank wall orthotropy is developed for the calculation of springs associated with liquid tank systems. A simple analysis is presented which shows that the actual value of the mass of the contained liquid may not be the correct value for incorporation into a lumped parameter analysis. Model test results are presented for first stage propellant loading conditions corresponding to several time points during first stage burn. The experiment and analysis show generally good correlation in both frequency and deflection shape for structural modes; however, discrepancies are found when the system responds in either propellant modes or in coupled structural propellant modes. Also, use of an analytical equivalent liquid mass value for contained liquids produces better agreement with experiment for the liquid tank modes whereas actual liquid mass values produced better agreement for structural modes. Author

N69-22982*# General Technology Corp., Lawrenceville, N. J.

A LATTICE MODEL FOR COMPOSITE MATERIALS

T. R. Tauchert, T. Y. Chang, and A. C. Eringen Washington NASA Apr. 1969 24 p refs

(Contract NASw-1589)

(NASA-CR-1322; TR-8-8) Avail: CFSTI CSCL 20K

A lattice theory is developed for composite materials in which the matrix and inclusions of the composite are idealized as a gridwork of thermoelastic bars attached to small rigid masses. This model generalizes the spring and mass model prominent in the classical lattice theory of solids. Replacement of the springs by elastic bars provides extra internal degrees of freedom beyond the central force model of the lattice theory. The lattice representation leads to a system of finite difference equations of motion which can be used to solve dynamic and thermal stress problems numerically. Equations for stress and couple stress are obtained, which are identical in form to those of the linear theory of micropolar thermoelasticity. Author

N69-22983*# Drexel Inst. of Tech., Philadelphia, Pa.

MCDIT 21: A COMPUTER CODE FOR ONE-DIMENSIONAL ELASTIC WAVE PROBLEMS

Richard W. Mortimer and James F. Hoburg Washington NASA Apr. 1969 33 p refs

(Grant NGR-39-004-13)

(NASA-CR-1306; Rept-340-2) Avail: CFSTI CSCL 20K

The code involves the application of the method of characteristics to the displacement governing differential equations of motion of the structures. Some of the structures which can be analyzed by this program include shells, Mindlin plates, bars, and Timoshenko beams; subroutines for these structures have been prewritten for the user. The code is capable of handling boundary conditions which may be specified as step, ramp, exponential, and sinusoidal time functions; these have also been prewritten for the user. Detailed instructions for the use of the program, its computational procedure, and its limitations are given. An example involving the impacting of a conical shell is included. Author

N69-22994*# National Aeronautics and Space Administration. Lewis Research Center, Cleveland, Ohio.

CRATER CHARACTERISTICS OF 11 METAL ALLOYS UNDER HYPER-VELOCITY IMPACT INCLUDING EFFECTS OF PROJECTILE DENSITY AND TARGET TEMPERATURE

Nestor Clough, Seymour Lieblein, and A. R. McMillan (General Motors Corp., Santa Barbara, Calif.) Washington Apr. 1969 28 p refs

(NASA-TN-D-5135) Avail: CFSTI CSCL 20K

Spherical Pyrex, aluminum, steel, nylon, and Inlyte projectiles were accelerated to velocities from 4.88 to 8.35 kilometers per second and impacted against thick flat plate targets at room and elevated temperatures. Targets impacted were aluminum alloys 2024-T6, 7075–T6, and 356–T51; columbium – 1 percent zirconium; tantalum; vanadium; molybdenum–TZM, A–286; Inconel–718; 316 stainless steel; and L–605. Correlations were determined for the effects of projectile density and target temperature on the cratering characteristics of these materials. Author

N69-23096*# Measurement Analysis Corp., Los Angeles, Calif.

SUMMARY OF RANDOM VIBRATION PREDICTION PROCEDURES

R. L. Barnoski, A. G. Piersol, W. F. Van Der Laan, P. H. White and E. F. Winter Washington NASA Apr. 1969 147 p refs

(Contract NAS8-20020)

(NASA-CR-1302) Avail: CFSTI CSCL 20K

Various procedures suggested in recent years for the prediction of random vibration environments in modern flight vehicles are summarized and discussed. A total of fifteen individual techniques are included. The basic principles of the procedures are outlined, and known experiences in their use are reviewed. Special attention is given to the assumptions inherent in their use as well as the information required for their application. The relative advantages and limitations of the procedures are detailed. Author

N69-23320*# National Aeronautics and Space Administration. Langley Research Center, Langley Station, Va.

BUCKLING OF THIN-WALLED CIRCULAR CYLINDERS

V. I. Weingarten (Univ. of Southern Calif.), P. Seide (Univ. of Southern Calif.), and J. P. Peterson Aug. 1968 58 p refs Revised

(NASA-SP-8007) Avail: CFSTI CSCL 20K

Current practices for predicting buckling of uniform stiffened and unstiffened circular cylindrical shells under various types of static loading, and suggested procedures that yield estimates of static buckling loads are presented. Details are given on recommended practices for isotropic unstiffened cylinders, orthotropic cylinders, isotropic sandwich cylinders, and cylinders with an elastic core. These discussions include axial compression, bending, external or lateral pressure, torsion, and combined loads. The important problems and the limitations of the procedures are indicated. N.E.N.

N69-23448*# National Aeronautics and Space Administration. Langley Research Center, Langley Station, Va.

RESPONSE OF AN INFINITE ELASTIC PLATE TO AXISYMMETRIC INITIAL VELOCITY DISTRIBUTIONS WITH APPLICATION TO HYPERVELOCITY IMPACT

Robert J. Hayduk Washington Apr. 1969 29 p refs

(NASA-TN-D-5118) Avail: CFSTI CSCL 20K

Classical plate theory is used to study the response of an infinite plate to an axisymmetric initial velocity distribution over a central region. The expression for the bending stress is reduced to a single definite integral which depends upon the initial velocity distribution. The deflection is reduced to the Hankel inversion integral for three example distributions: conical, cylindrical, and spherical. The analysis indicates that the conical distribution causes larger stresses at the origin and deflections of the plate at short times after initiation than either the spherical or cylindrical distribution. A simple relationship is derived for the failure thickness of an elastic plate responding to an axisymmetric initial momentum, monotonically decreasing in the radial direction. The failure-thickness relationship is shown to correlate with available experimental hypervelocity impact data where the initial momentum was induced by disk projectiles of various diameters. Author

N69-23697*# National Aeronautics and Space Administration. Manned Spacecraft Center, Houston, Tex.

FORCES ON A FLEXIBLE SHELL DURING WATER IMPACT

David A. Hamilton Washington May 1969 30 p refs

(NASA-TM-X-1781) Avail: CFSTI CSCL 20K

Water impact tests were conducted with a 1/4-scale model of the Apollo command module. The tests were made to observe loads on the heat shield and at the center of gravity of the model. Results showed the nature of the loading on the center of gravity and related the loading to the heat-shield accelerations and the water pressure force. Author

N69-24056*# Oklahoma Univ., Norman. School of Aerospace and Mechanical Engineering.

AN APPROXIMATE THEORY FOR TRANSVERSE SHEAR DEFORMATION AND ROTATORY INERTIA EFFECTS IN VIBRATING BEAMS

D. M. Egle Washington NASA May 1969 19 p refs

(Grant NGR-37-003-035)

(NASA-CR-1317) Avail: CFSTI CSCL 20K

A beam theory, which includes the effects of transverse shear deformation and rotatory inertia, and whose kinetic and potential energy may be written in terms of a single dependent variable, is developed in this paper. This simplification will reduce the computational effort required in the analysis of complex beams or structures composed of a number of beams. This is accomplished by neglecting the coupling between the transverse shear deformation and the rotatory inertia. Comparisons of natural frequencies calculated by this theory with those of the Timoshenko theory show that this coupling is indeed negligible. Author

N69-24131*# National Aeronautics and Space Administration. Langley Research Center, Langley Station, Va.

BUCKLING OF THIN-WALLED TRUNCATED CONES

V. I. Weingarten (Univ. of Southern Calif.), and P. Seide (Univ. of Southern Calif.) Sep. 1968 32 p refs

(NASA-SP-8019) Avail: CFSTI CSCL 20K

Practices are recommended for predicting buckling of uniform stiffened and unstiffened circular conical shells under various types of static loading, and procedures are suggested that yield estimates of static buckling loads which are considered to be conservative. Isotropic and orthotropic shells are discussed with respect to axial compression, bending, hydrostatic pressure, torsion, and combined loads. Sandwich shells with isotropic and orthotropic face sheets are investigated, and expressions are given for failures due to core crushing, intracell buckling, and face wrinkling. N.E.N.

N69-24765*# National Aeronautics and Space Administration. Langley Research Center, Langley Station, Va.

HYPERVELOCITY IMPACT ANALYSIS BY THE METHOD OF CHARACTERISTICS

Richard Madden Washington Jan. 1969 45 p refs

(NASA-TR-R-298) Avail: CFSTI CSCL 20K

A computer method has been developed to analyze the initial hydrodynamic phase of hypervelocity impact. The method is based on solving the inviscid, non heat-conducting, unsteady fluid dynamic equations in cylindrical coordinates by utilizing an approach based on the method of characteristics. The method generated an operational computer program applicable to the impact of an infinitely long right circular cylinder striking a semi-infinite target of the same material. The projectile is assumed to be traveling parallel to its axis of symmetry, and the target is initially at rest. Results are presented for the pressure and velocity fields at various times following the impact. The pressure fields are compared with the pressure fields calculated from an existing hydrodynamic analysis. Author

N69-24876*# General Electric Co., Philadelphia, Pa.

ZERO THERMAL EXPANSION COMPOSITES OF HIGH STRENGTH AND STIFFNESS

Norris F. Dow and B. Walter Rosen Washington NASA May 1969 88 p refs

(Contract NAS1-7659)

(NASA-CR-1324) Avail: CFSTI CSCL 11D

The results of a program to study the analysis and design of filamentary composites of zero coefficient of thermal expansion in one direction are reported. Guidelines are given for the selection of filamentary and binder materials and reinforcement configurations to achieve the desired thermal stability. Three dimensional reinforcement configurations are shown to be substantially stronger, stiffer, and more capable of achieving zero thermal expansion with a wider variety of material combinations than two dimensional configurations. Author

N69-25001*# National Aeronautics and Space Administration. Ames Research Center, Moffett Field, Calif.

DEVELOPMENT OF MICHELL MINIMUM WEIGHT STRUCTURES

Dhanjoo N. Ghista and Meyer M. Resnikoff Jan. 1968 32 p refs

(NASA-TN-D-4345) Avail: CFSTI CSCL 13M

The Michell strain criterion is used to develop minimum weight structures to equilibrate some interesting force systems of significance to aeronautics and the space technology. Michell prescribed a strain criterion for the members of a minimum volume structure (i.e., a structure having the minimum amount of material) to equilibrate a given force system. The research work contributory to this paper is divided into three independent sections. In the first section, a theorem is presented on the superposition of Michell structures and applied to develop optimum structures for two basic force systems. In the second section a solution is obtained to the governing equations developed by Hemp for the form of an optimum structure satisfying the Michell strain criterion condition in two dimensions. In the third section two well-known orthogonal systems of curves— the dipolar and the spherical—are selected for member layout of Michell structures. Author

N69-25301*# National 'Aeronautics and Space Administration. Lewis Research Center, Cleveland, Ohio.

CLEVIS DESIGN FOR COMPACT TENSION SPECIMENS USED IN PLANE-STRAIN FRACTURE TOUGHNESS TESTING

Raymond T. Bubsey, Melvin H. Jones, and William F. Brown, Jr. Washington May 1969 19 p refs

(NASA-TM-X-1796) Avail: CFSTI CSCL 20K

Friction effects in a conventional roundhole clevis used for testing compact tension fracture toughness specimens was presented. The results showed measured plane-strain fracture toughness K_{Ic} values could be too high by about 10 percent when

the loading-pin-to-hole clearances are only a few thousandths of an inch. Lubrication was found to have only a small effect. Increasing the pin clearance reduces the friction effects, but uncertainties in the initial position of the load axis with respect to the slot tip (equivalent to variation in crack length to width ratio a/W) result in a possible spread in K_{Ic} values of nearly 5 percent. A new clevis design is described which greatly minimizes the errors caused by friction and variations in effective a/W. This design is proportioned to permit testing of materials having a wide range of toughness and yield strength. Author

N69-26223*# National Aeronautics and Space Administration. Langley Research Center, Langley Station, Va.
ANALYTICAL INVESTIGATION OF AN INFLATABLE LANDING SYSTEM HAVING OMNIDIRECTIONAL AND MULTIPLE IMPACT CAPABILITIES
John R. McGehee, Melvin E. Hathaway, and Cornelia B. Dexter Washington May 1969 58 p refs
(NASA-TN-D-5236) Avail: CFSTI CSCL 01C

The landing characteristics of a 20-compartment spherical-gas-bag landing system have been investigated for an impact normal to a smooth surface. An analysis was derived and programmed for machine computation. Calculations were made to indicate the omnidirectional, multiple-impact, and kinetic-energy-dissipating capabilities over a wide range of ambient pressures. The results of the computations are presented and show that this landing system has omnidirectional and multiple-impact capabilities. With proper design the system can dissipate 80 to 90 percent of the touchdown kinetic energy during the first impact. The computed results also indicate that this system may be designed to dissipate substantially the entire landing kinetic energy after two impacts. The ability of this landing system to perform satisfactorily over a wide range of ambient pressures has also been demonstrated through computations for landings of a selected vehicle. Author

N69-26234*# Astro Research Corp., Santa Barbara, Calif.
INVESTIGATION OF A COILABLE LATTICE COLUMN
R. F. Crawford Washington NASA May 1969 31 p ref
(Contract NAS7-427)
(NASA-CR-1301; ARC-R-310) Avail: CFSTI

A lattice column consisting of six longerons interconnected by crossed helical braces was fabricated and tested to determine the feasibility of its concept and to verify analysis of its structural performance. Its helical braces from a cross-sectional shape which can be elastically flattened. This flattened column can then be coiled longitudinally into a relatively small cylindrical volume. The test segment of the column was fabricated of 0.035 inch diameter steel wires joined together with coins into which the intersection of the wires was soldered. Tests were performed on the segment to determine its torsional stiffness, axial buckling strength, and its capability to be flattened and coiled. Author

N69-26315*# Bolt, Beranek, and Newman, Inc., Van Nuys, Calif.
DEVELOPMENT OF IMPEDANCE SIMULATION FIXTURES FOR SPACECRAFT VIBRATION TESTS
Terry D. Scharton Washington NASA May 1969 62 p refs
(Contract NAS1-7600)
(NASA-CR-1351; BBN-1703) Avail: CFSTI CSCL 20K

An experimental program to develop vibration test fixtures which simulate the mount impedance of aerospace structures is conducted. Three fixtures designed to simulate the impedance of a launch vehicle are fabricated and evaluated in research vibration tests of a 1/2-scale mode Nimbus spacecraft. The results of the research tests indicate that impedance simulation fixtures eliminate some of the problems associated with conventional rigid fixtures at high frequencies. Guidelines for designing impedance simulation fixtures are presented. Author

N69-26559*# Illinois Univ., Urbana. Dept. of Theoretical and Applied Mechanics.
THE CONFORMAL MAPPING OF THE INTERIOR OF THE UNIT CIRCLE ONTO THE INTERIOR OF A CLASS OF SMOOTH CURVES
Thomas F. Moriarty and Will J. Worley Washington NASA May 1969 50 p refs
(Grant NGR-14-005-010)
(NASA-CR-1357) Avail: CFSTI CSCL 12A

The coefficients of the series representing the conformal mapping of the interior of the unit circle onto the interior of a class of smooth curves are tabulated for various parameters. Precise graphical comparisons of several cases have been included to graphically illustrate the nature and accuracy of the conformal mappings. A Fortran IV computer program has been listed to aid those interested in cases not included in the report. Author

N69-28038*# National Aeronautics and Space Administration. Langley Research Center, Langley Station, Va.
ELASTOPLASTIC STRESS-STRAIN BEHAVIOR AT NOTCH ROOTS IN SHEET SPECIMENS UNDER CONSTANT-AMPLITUDE LOADING
John H. Crews, Jr. Washington Jun. 1969 34 p refs
(NASA-TN-D-5253) Avail: CFSTI CSCL 20K

Edge-notched sheet specimens with elastic stress-concentration factors of 2, 4, and 6 were investigated for several levels of constant-amplitude reversed loading. These specimens were fabricated from 2024-T3 aluminum alloy, SAE 4130 (normalized and stress relieved) steel, and AISI 4130 (normalized) steel. Cyclic stresses and strains were determined experimentally at the notch roots by a companion-specimen method and were compared with notch-root stresses and strains calculated by using both the modified Stowell and the Neuber equations. Close correlation was found between calculated and experimental results. Author

N69-28164*# Oklahoma Univ., Norman.
A THEORETICAL ANALYSIS OF THE FREE VIBRATION OF DISCRETELY STIFFENED CYLINDRICAL SHELLS WITH ARBITRARY END CONDITIONS
D. M. Egle and K. E. Soder, Jr. Washington NASA Jun. 1969 87 p refs
(Grant NGR-37-003-035)
(NASA-CR-1316) Avail: CFSTI CSCL 20K

A theoretical analysis for the free vibration of ring and stringer stiffened cylindrical shells, with the stiffeners treated as discrete elements, was developed and programmed for digital computer solution. The analysis is capable of handling arbitrary end conditions and arbitrary distributions of stiffeners. The theory includes flexure and extension of the shell; and flexure (about two perpendicular axes), extension and torsion of the stiffeners, including the possibility of nonsymmetric stiffener cross sections. Stiffener flexural cross stiffening is also included in an approximate manner. The three translational shell inertia components and all six of the stiffener inertia components are considered. The problem is formulated with the energy method and the Rayleigh-Ritz technique is employed to obtain an approximate solution. The assumed axial displacement functions are kept in a general form allowing the use of any set of functions needed to satisfy the end conditions. Both the symmetric and antisymmetric circumferential modes are used in the analysis. Author

N69-28624*# California Univ., Berkeley.
INCREMENTAL ANALYSIS OF LARGE DEFORMATIONS IN MECHANICS OF SOLIDS WITH APPLICATIONS TO AXISYMMETRIC SHELLS OF REVOLUTION
Saeed Yaghmai Washington NASA Jun. 1969 181 p refs
(Grants NGR-05-003-014; NSF GK-750)

(NASA-CR-1350) Avail: CFSTI CSCL 20K

A general incremental variational method for the analysis of geometrically and physically nonlinear problems in continuum mechanics is developed. This variational method is applicable to any type of material properties. In particular, nonlinear constitutive laws for elastic, and elastic–plastic materials are considered. Starting from the basic principles in continuum mechanics, such as the invariance requirements and the thermodynamic laws, general incremental constitutive equations were derived for nonlinear elastic materials. For the elastic–plastic materials an incremental constitutive law is considered where deformations are infinitesimal but rotations are finite. The method was specialized and applied to the analysis of large deflections of elastic–plastic axisymmetrically deformed shells of revolution. The displacement formulation of the finite element method was exploited for this problem and a digital computer program was written for the numerical analysis. Author

N69-28658*# National Aeronautics and Space Administration. Langley Research Center, Langley Station, Va.

DESIGN, FABRICATION, AND TESTS OF TUBULAR BERYLLIUM AND Be-38-Al ALLOY TRUSS-TYPE STRUCTURES

Donald R. Rummler and Gregory R. Wichorek Washington Jun. 1969 74 p refs

(NASA-TN-D-5254) Avail: CFSTI CSCL 20K

Four lightly loaded, tubular, truss-type structures with the same configuration have been designed, fabricated, and tested. Adhesively bonded joints were used to fabricate a beryllium truss, a Be-38Al alloy truss, and an aluminum truss. The fourth truss was aluminum with welded joints. The bonded trusses were designed for the same loading condition. The beryllium and Be38Al trusses had a mass of 1.42 and 1.51 lbm respectively, whereas the bonded aluminum truss had a mass of 3.0 lbm. The trusses were subjected to both dynamic and static tests. The trusses successfully survived the dynamic tests which subjected the trusses to the maximum design loading conditions. For the dynamic tests, comparisons between measured and calculated first-bending-mode frequencies and mode shapes also show satisfactory agreement. All four trusses exhibited a nonlinear response to dynamic loads. For the static tests, comparisons between measured and calculated truss member strains and joint deflections show satisfactory agreement. Viscoelastic joint deflections were observed during static tests on all the bonded trusses. Joint failures observed during static tests on the bonded aluminum truss were attributed to the viscoelastic properties of the adhesive. Author

N69-29159*# National Aeronautics and Space Administration. Lewis Research Center, Cleveland, Ohio.

CRITICAL-SPEED ANALYSIS OF RIGID ROTORS ON FLEXIBLE FOUNDATIONS

Richard H. Cavicchi Washington Jun. 1969 48 p refs

(NASA-TN-D-4858) Avail: CFSTI CSCL 01A

A critical-speed analysis of undamped rigid rotors on flexible foundations reveals four conical-mode solutions comprising forward and backward precession. There is also a two-solution bouncing-mode set dependent only on foundation-to-rotor mass and spring-constant ratios. Although analysis of a firm foundation model omits two of the four conical-mode solutions, good agreement exists between the two corresponding solutions. The flexible-foundation analysis can be approximated by a simple firm-foundation result when the foundation-to-rotor spring-constant ratio is zero or infinite. Only three calculations are needed in this range to cover all intermediate values. Author

N69-29558*# Dynatech Corp., Cambridge, Mass.

ASYMMETRIC NONLINEAR DYNAMIC RESPONSE AND BUCKLING OF SHALLOW SPHERICAL SHELLS

Atis A. Liepins Washington NASA Jun. 1969 83 p refs (Contract NAS1-6586)

(NASA-CR-1376) Avail: CFSTI CSCL 20K

A numerical method and computer program are developed for the computation of the large deflection dynamic response of simply supported shallow spherical shells subjected to a class of spatially asymmetric and timewise step loadings. The numerical method employs two dimensional spatial finite differences, timewise finite differences together with Houbolt's method, and solution by Newton's procedure together with an extension of Potters method. Response histories and asymmetric dynamic buckling loads for several geometries and load durations are presented. Author

N69-29589*# National Aeronautics and Space Administration. Ames Research Center, Moffett Field, Calif.

ON THE PHENOMENON OF THERMOELASTIC INSTABILITY (THERMAL FLUTTER) OF BOOMS WITH OPEN CROSS SECTION

Richard M. Beam Washington Jun. 1969 19 p refs

(NASA-TN-D-5222) Avail: CFSTI CSCL 13M

Laboratory experiments performed to demonstrate the phenomenon of thermoelastic flutter of booms with open cross section are described. The problem of torsional instability is chosen for theoretical treatment and comparison with quantitative experimental results. The theoretical and experimental models show: (1) One-degree-of-freedom torsional thermoelastic flutter is possible and predictable. (2) Thermoelastic coupling can stabilize as well as destabilize a system. (3) Small amplitude linear theory can predict thermoelastic instability. Author

N69-29607*# National Aeronautics and Space Administration. Langley Research Station, Langley Station, Va.

FATIGUE OF NOTCHED Ti-8Al-1Mo-1V TITANIUM ALLOY AT ROOM TEMPERATURE AND 550 DEG F (560 DEG K) WITH FLIGHT-BY-FLIGHT LOADING REPRESENTATIVE OF A SUPERSONIC TRANSPORT

L. A. Imig and Walter IIIg Washington Jul. 1969 44 p refs

(NASA-TN-D-5294) Avail: CFSTI CSCL 20K

Fatigue studies were conducted on notched sheet specimens of Ti–8Al–1Mo–1V titanium alloy. The effects of loading parameters and elevated temperature on fatigue life were investigated in variable-amplitude tests that simulated flight loading of a supersonic transport operating at a Mach number of 3. Test stresses were applied flight by flight either at room temperature or at 550°F (560°K). Test results indicated a strong influence of design mean stress, the ground-air-ground cycle, and elevated temperature. Effects due to simulated taxi stresses and thermal stresses were observed to be small. A series of constant-amplitude tests on the same type of specimen that was used in the variable-amplitude tests was conducted to provide data for a linear cumulative-damage analysis. Author

N69-29672*# National Aeronautics and Space Administration. Lewis Research Center, Cleveland, Ohio.

THE CALCULATION OF ELEVATED TEMPERATURE CYCLIC LIFE CONSIDERING LOW CYCLE FATIGUE AND CREEP

David A. Spera Washington Jul. 1969 25 p refs

(NASA-TN-D-5317) Avail: CFSTI CSCL 20K

A general method is presented for calculating the cyclic life of a material subjected to isothermal stress- or strain-cycling at temperatures which may be in the creep range. Failure is assumed to be caused either by the accumulation of creep damage or by conventional, time-independent fatigue. A modification of the life-fraction rule and the method of universal slopes are used to

calculate creep and fatigue lives, respectively. The method of cyclic life analysis is evaluated by using data on four high temperature alloys. Calculated and observed lives are in good agreement. Author

N69-29734*# National Aeronautics and Space Administration. Lewis Research Center, Cleveland, Ohio.
ANALYSIS OF DYNAMIC JETTISON HINGE FORCES FOR CENTAUR NOSE FAIRING
Hsin Ming Tang Washington Jul. 1969 30 p refs
(NASA-TM-X-1821) Avail: CFSTI CSCL 20K

Dynamic loads on nose fairing hinges are determined by a combination of tests and analyses. Transfer-function techniques are used. Hinge-force evaluations are determined according to normal mode theory for three-directional motion making use of data from tests of a fairing in a free–free end condition. A parametric study is presented of the hinge forces due tc rigid body motion alone and combined motions of the rigid body and elastic modes. Author

N69-30754*# National Aeronautics and Space Administration, Washington, D.C.
THE DESIGN OF CONICAL SHELLS SUBJECTED TO ANTISYMMETRIC LOADINGS
A. D. Kovalenko et al Jun. 1969 100 p refs Transl. into ENGLISH of the book "Raschet Konicheskikh Obolochek pri Antisimmetrichnykh Nagruzkakh" Kiev, Naukova Dumka Press, 1966 p 1–494
(NASA-TT-F-518) Avail: CFSTI CSCL 20K

This book presents a method of design of antisymmetrically stressed conical shells, and also of elastic systems consisting of rings, circular plates, cylindrical and conical shells used as construction elements in turboengineering and other branches of mechanical engineering. Formulas and tables for the design of these elastic elements are given. The tables were compiled on the basis of analytical solutions derived on the BESM-2M digital computer. The book is intended for engineers and technicians, as well as research scientists working with the design and strength calculations of thin-walled elements of machines. Author

N69-31056*# National Aeronautics and Space Administration. Lewis Research Center, Cleveland, Ohio.
A SEMIEMPIRICAL FRACTURE ANALYSIS FOR SMALL SURFACE CRACKS
Thomas W. Orange Washington Jul. 1969 34 p refs
(NASA-TN-D-5340) Avail: CFSTI

A semiempirical modification of Irwin's fracture analysis for a semielliptical surface crack in a plate is proposed. When it is applied to surface crack test data from the literature, a single toughness parameter is obtained which relates fracture stress to crack size with reasonable accuracy. The method appears usable when crack size and material thickness are too small to allow a valid analysis using conventional fracture mechanics principles. It is even effective when fracture stresses are above yield. A similar analysis for through-the-thickness cracks is discussed but not evaluated. Application to low-cycle fatigue crack propagation studies is proposed. Author

N69-31300*# National Aeronautics and Space Administration. Lewis Research Center, Cleveland, Ohio.
TENSILE AND CYCLIC FATIGUE PROPERTIES OF GRAPHITE FILAMENT-WOUND PRESSURE VESSELS AT AMBIENT AND CRYOGENIC TEMPERATURES
Morgan P. Hanson Washington Jul. 1969 13 p refs
(NASA-TN-D-5354) Avail: CFSTI CSCL 20K

Graphite fibers were fabricated into NOL rings and biaxial-wound cylinders. Filament tensile strengths of NOL rings were determined at 75°, −320°, and −423° F (297°, 77° and 20°K). Comparisons were made of ambient-temperature fiber tensile strengths as obtained from NOL rings, strand tests, and biaxially wound cylinders. Fatigue characteristics of internally pressurized cylinders were determined at 75° and −320°F (297 and 77 K). Fatigue comparisons are made of graphite and glass-filament wound cylinders on the basis of specific strength. Author

N69-33232*# National Aeronautics and Space Administration. Goddard Space Flight Center, Greenbelt, Md.
DESIGN TECHNIQUES FOR SMALL SCIENTIFIC SATELLITE STRUCTURES
J. M. Madey and R. C. Baumann Washington Jul. 1969 106 p refs
(NASA-TN-D-4988) Avail: CFSTI CSCL 22B

A description of the design, development, integration, and testing of small scientific satellite structures in sufficient detail to serve as a design guide for the apprentice designer. It describes the many considerations and procedures involved from the initial concept phase through launch and post-flight analysis. To relate the general considerations and procedures to actual programs, data in the form of illustrations, specifications, checkoff lists, and other reference documents are provided for specific satellites. Author

N69-33420*# National Aeronautics and Space Administration. Langley Research Center, Langley Station, Va.
AN ANALYTICAL EVALUATION OF THE DENTING OF AIRPLANE SURFACES BY HAIL
Robert G. Thomson and Robert J. Hayduk Washington Aug. 1969 35 p refs
(NASA-TN-D-5363) Avail: CFSTI CSCL 20K

Hailstone damage to aircraft is exhibited as denting or complete penetration. An analytical evaluation of such denting characteristics of aircraft surfaces is idealized by having a crushable spherical projectile impact normal to a flat plate. Separate elastic and rigid-plastic analyses have been developed previously by using the classical thin-plate bending approach. As applied in this paper, the elastic analysis determines the area of the sheet around the center of impact, which has become plastic. The rigid-plastic analysis applied to this central plastic region determines the resulting permanent deformation (dent). Numerical results are presented in detail for the permanent deformations of two specific sheet thicknesses. Author

N69-33481*# National Aeronautics and Space Administration. Lewis Research Center, Cleveland, Ohio.
DEVELOPMENT OF IMPROVED THROAT INSERTS FOR ABLATIVE ROCKET ENGINES
Jerry M. Winter and Donald A. Peterson Washington Jul. 1969 166 p refs Film Supplement Number C-261 to this report is available on loan from NASA. Lewis Research Center, Cleveland, Ohio
(NASA-TN-D-4964) Avail: CFSTI CSCL 20K

Seventy-five throat inserts and nine complete nozzle designs were evaluated in a storable propellant (nitrogen tetroxide and a 50-percent blend of unsymmetrical dimethyl hydrazine with hydrazine) rocket engine. An insert of iridium-rhenium on a tungsten substrate ran successfully until gas diffusion through the porous iridium caused substrate oxidation. Composites of hypereutectic carbides; anion deficient zirconium oxide; mixed oxides of hafnium, titanium, and zirconium; wire reinforced zirconium oxide; and a refractory macrolaminate were all run through a varied and extended duty cycle. Rocket-engine testing, in the combustion environment

of interest, for the intended duty cycle, was the most efficient method of advanced material evaluation. A motion-picture film supplement is avaiable on request. Author

N69-34744*# Rochester Applied Science Associates, Inc., N.Y.
A METHOD FOR ANALYZING THE AEROELASTIC STABILITY OF A HELICOPTER ROTOR IN FORWARD FLIGHT
Peter Crimi Washington NASA Aug. 1969 110 p refs
(Contract NAS1-74-11)
(NASA-CR-1332; RASA-68-10) Avail: CFSTI CSCL 01A

The exact solution to the perturbation equations of motion of a rotor in forward flight is studied. Effects of compressibility, stall, and reversed flow are taken into account, and there is no restriction on the number of degrees of freedom which can be analyzed. The equations of motion of a rotor blade in forward flight were derived in terms of the normal modes of free vibration of the blade. Aerodynamic forces were expressed on the basis of quasi-steady flow, using strip theory. Perturbation equations were generated by expanding all aerodynamic forces in the perturbation variables about their steady-state values. The equations are of the form of a coupled set of linear, second-order differential equations with periodically varying coefficients. A method was then developed for analyzing the stability of linear dynamic systems with periodically varying parameters. Stability is determined by calculation of all the characteristic values of the system. Author

N69-34970*# National Aeronautics and Space Administration. Marshall Space Flight Center, Huntsville, Ala.
LONGITUDINAL MASS-SPRING MODELING OF LAUNCH VEHICLES
Rudolf F. Glaser Washington Aug. 1969 37 p refs
(NASA-TN-D-5371) Avail: CFSTI CSCL 22B

To determine longitudinal axisymmetric vibration modes of launch vehicles, simplified models must be established. Application of Galerkin's method to the equations of motion of the above simplified system is proposed, using the container-liquid modes with special normalization factors as coordinate functions. The resulting model is based on the energy law. The use of the container-liquid modes, results in accurate representation of significant structural and inertial characteristics of the container-liquid system. The special normalization of the coordinate functions converts the container-liquid systems directly in lumped parameter systems, having a number of degrees of freedom equal to the number of coordinate functions used. The containers are assumed cylindrical membranes with flat, rigid bottoms. For simplicity, typical tandem parts of vehicles, consisting of only one or two solid masses and springs and one liquid-filled container, are examined. Because of the rapid decrease of the equivalent modal masses (with increasing mode number), restriction to one-term approaches does not mean considerable loss of accuracy. Comparison of analytical results with experiments provides satisfactory agreement. Author

N69-35515*# Philco-Ford Corp., Newport Beach, Calif. Space and Re-entry Systems Div.
STRUCTURAL OPTIMIZATION OF SANDWICH AND RING-STIFFENED 120 DEGREE CONICAL SHELLS SUBJECTED TO EXTERNAL PRESSURE
Gerald A. Cohen Washington NASA Aug. 1969 70 p refs
(Contract NAS1-5554-6)
(NASA-CR-1424) Avail: CFSTI CSCL 20K

A practical optimum design procedure is developed for lightly loaded shells of revolution of both sandwich and ring-stiffened construction. For ring-stiffened shells, this procedure employs a design computer program as well as shell prebuckling and buckling analysis programs. Specific point designs for 120° truncated cones are obtained over a wide range of critical pressure for two base radii. The results show that for low loading, ring-stiffened construction is more efficient than sandwich construction.
Author

N69-36220*# National Aeronautics and Space Administration. Langley Research Center, Langley Station, Va.
THE DYNAMIC RESPONSE OF A FLEXIBLE ROTOR BLADE TO A CONCENTRATED FORCE MOVING FROM TIP TO ROOT
John F. Ward Washington Sep. 1969 43 p refs
(NASA-TN-D-5410) Avail: CFSTI CSCL 20K

An approximate analytical solution is presented of the dynamic response of a flexible rotor blade to a radially moving force. The results are interpreted specifically in terms of helicopter rotor-blade vibration chracteristics associated with tip-vortex impingement. These results indicate that low-frequency-mode resonant amplification of repetitive-impulse loadings may be encountered at moderate to high forward speeds on lifting rotor systems. The resonant conditions are encountered in sequence with increasing forward speed. For blades of conventional design, the resonant frequencies are encountered at noninteger multiples of rotor rotational speed. Author

N69-36357*# Philco-Ford Corp., Newport Beach, Calif.
SYNTHESIS OF OPTIMUM STRUCTURAL DESIGNS FOR CONICAL AND TENSION SHELL MARS ENTRY CAPSULES
Gerald A. Cohen, Richard M. Foster, and James R. Dowty Washington NASA Aug. 1969 101 p refs
(Contract NAS1-5554-4)
(NASA-CR-1365) Avail: CFSTI CSCL 20K

Optimum design procedures are developed for lightweight, low ballistic coefficient entry capsules of both sandwich and ring-stiffened construction. These procedures are used to obtain specific point designs for 120° blunted cone and 0A.833 tension shell capsule configurations. Aeroshell and base ring weight correlations are presented for the 120° sandwich cones. The effects of variation in structural temperature, ballistic coefficient, peak dynamic pressure, capsule size, and structural material are considered. Author

N69-38642*# National Aeronautics and Space Administration. Langley Research Center, Langley Station, Va.
STRESS CONCENTRATION AROUND BROKEN FILAMENTS IN A FILAMENT-STIFFENED SHEET
W. B. Fichter Washington Oct. 1969 33 p refs
(NASA-TN-D-5453) Avail: CFSTI CSCL 20L

Stress distributions around single and double cuts (groups of adjacent broken filaments) in an idealized composite sheet consisting of parallel tension-carrying filaments embedded in a shear-carrying matrix are analyzed by an influence-function technique. Static-load concentration factors for two equal collinear cuts are obtained and are compared with some related results for a single cut. Dynamic-load concentration factors, corresponding to sudden breaking of filaments, also are obtained for two of the simplest double-cut cases. In addition, matrix shear forces are investigated for some single-cut and double-cut cases. Finally, loads in broken filaments are calculated for some single-cut cases, and their implications in some current failure analyses of composite materials are briefly discussed. The interaction between two collinear cuts is essentially local and is roughly confined to separation distances on the order of the cut length. For closely spaced cuts, however, the interaction between cuts is seen to be pronounced. For a single cut, an expression analogous to the filament load concentration factor is obtained for the maximum shear force in the matrix as a function of the cut length. The results suggest that for some combinations of constituent mechanical properties, the composite might be more susceptible to filament tensile failure at some cut lengths, but more susceptible to matrix shear failure at others. Author

32 STRUCTURAL MECHANICS

N69-38781*# Astro Research Corp., Santa Barbara, Calif.
AXISYMMETRIC AND CYLINDRICAL ISOSTABILOIDS
Peter R. Preiswerk, John M. Hedgepeth, and Hans U. Schuerch Washington NASA Oct. 1969 50 p refs
(Contract-NAS 7-427)
(NASA-CR-1444; ARC-R-299) Avail: CFSTI CSCL 20K

The differential equations for the geometric layout of compression-loaded axisymmetric and cylindrical two-family filamentary structures are established. The analytical formulation is based upon the requirement that failure due to local instability occurs simultaneously in the whole structure. Solutions are obtained for the particular case where the body force due to the structure's own weight is the only load. For this special case, the shapes of the meridian and the cross section, respectively, have been determined, as well as the pattern of the filaments. In addition, the weight per area covered by the structure is formulated and discussed. Minimum-weight configurations are defined. Examples for large earth-based and moon-based structures are presented. Author

N69-38808*# National Aeronautics and Space Administration. Marshall Space Flight Center, Huntsville, Ala.
SATURN 5, S-4B PANEL FLUTTER QUALIFICATION TEST Final Report
J. J. Nichols Washington Oct. 1969 32 p refs
(NASA-TN-D-5439) Avail: CFSTI CSCL 20K

A fullscale segment of the S-4B stage forward skirt was tested to determine the flutter characteristics of the thin skin panels bounded by internal rings and external stiffeners. The wind tunnel tests were conducted over a Mach number range of 1.3 through 1.6 and dynamic pressures to 950 psf. Test runs were made by setting tunnel conditions shown in Table I and varying the compressive load on the specimen from 0 to 60 kips. Runs were also made at zero load while holding a constant Mach number and differential pressure across the specimen and varying the dynamic pressure. No flutter was noted during the dynamic pressure sweeps at zero axial load. Limited amplitude flutter was observed during most of the load sweeps. However, an inspection of the skirt segment did not reveal any noticeable damage such as cracks near the rivet lines resulting from the stresses induced by the flutter motion. The test was terminated after a stringer located on the side of the test segment buckled under the applied compressive load. The stringer buckle originated across a permanent buckle in the adjacent skin that was built-in during fabrication of the specimen. Author

N69-38809*# National Aeronautics and Space Administration. Ames Research Center, Moffett Field, Calif.
EXPERIMENTAL INVESTIGATION OF THE MOMENTUM TRANSFER ASSOCIATED WITH IMPACT INTO THIN ALUMINUM TARGETS
C. Robert Nysmith and B. Pat Denardo Washington Oct. 1969 17 p refs
(NASA-TN-D-5492; A-3252) Avail: CFSTI CSCL 20K

Aluminum spheres of 3.2-mm diameter were fired into thin 2024-T3 aluminum targets at velocities to 8.1 km/sec, and the axial components of the ejecta and target momenta were measured. It was observed that the momentun transfer associated with impacts into thin targets can be classified into four different impact phases; these phases reflect differing physical processes in the targets, and are determined by the impact velocity and the target thickness. The physical processes are described and the momentum data within each impact phase are correlated. Measurements of target mass loss, minimum hole diameter, and threshold-spallaton velocity are also reported. Author

N69-39393*# National Aeronautics and Space Administration. Lewis Research Center, Cleveland, Ohio.
CALCULATION OF THERMAL-FATIGUE LIFE BASED ON ACCUMULATED CREEP DAMAGE
David A. Spera Washington Oct. 1969 39 p refs
(NASA-TN-D-5489; E-4950) Avail: CFSTI CSCL 20K

A method is presented for predicting the onset of thermal-fatigue cracking in high-temperature components under service conditions. Starting from basic material properties, life is calculated by considering two distinct failure modes: (1) cyclic creep-rupture, using a modification of the well-known life-fraction rule proposed by Robinson and Taira, and (2) conventional, time-independent, low-cycle fatigue, using empirical equations of the Method of Universal Slopes developed by Manson. The method is illustrated by using Glenny-type thermal-fatigue test data on the nickel-base alloy Nimonic 90. In 24 of the 28 cases analyzed, cyclic creep-rupture was the dominant failure mode. Author

N69-40087*# National Aeronautics and Space Administration. Langley Research Center, Langley Station, Va.
EXPERIMENTAL INVESTIGATION OF FLUTTER AT MACH 3 OF ROTATIONALLY RESTRAINED PANELS AND COMPARISON WITH THEORY
Charles P. Shore Washington Oct. 1969 33 p refs
(NASA-TN-D-5508) Avail: CFSTI CSCL 20K

An experimental investigation was conducted at a Mach number of 3 in the Langley 9- by 6-foot thermal structures tunnel to study the effects of damping and edge rotational restraint on the flutter characteristics of thermally stressed, flat, isotropic panels with length-width ratios of 3.3 and 3.7. Measured panel natural vibration frequencies were compared with calculated frequencies in order to estimate the panel edge rotational restraints. Comparisons of experimental and theoretical flutter results show that small-deflection theory can adequately predict the flutter of stressed panels up to the point of buckling if edge rotational restraint is accounted for and aerodynamic damping and frequency-independent hysteretic structural damping are included. Furthermore, the region, where the theoretical transition-point value of the flutter parameter is very sensitive to variations in panel length-width ratio and edge rotational restraint when structural damping is zero, becomes insensitive to these variations when the appropriate value of structural damping is used. Author

N69-40359*# United Aircraft Corp., East Hartford, Conn. Research Labs.
SIMPLIFIED PROCEDURES FOR ESTIMATING FLAPWISE BENDING MOMENTS ON HELICOPTER ROTOR BLADES. PART 2: TABLES
Anton J. Landgrebe Washington NASA Oct. 1969 92 p ref
(Contract NAS1-7880)
(NASA-CR-1441) Avail: CFSTI CSCL 20K

Tables are presented of the bending moment transfer coefficients as a supplement to previously published procedures and charts for estimating flapwise bending moments on helicopter rotor blades. These transfer coefficients are for each independent parameter of blade bending moment for nine combinations of mass and frequency parameters and six advance ratios (0.25 to 1.4). In addition, coefficients for the fourth and fifth harmonics for the low advance ratios (0.25 to 0.5) and six blade stations for the hingeless blade coefficients are given. Author

N69-40935*# North Carolina State Univ., Raleigh.
THE RADIATION RESISTANCE OF CYLINDRICAL SHELLS
Charles J. Runkle and Franklin D. Hart Washington NASA Oct. 1969 128 p refs
(Grant NGR-34-002-035)
(NASA-CR-1437) Avail: CFSTI CSCL 20K

A study is made of the radiation resistance of long cylindrical

shells in contact with an ideal compressible acoustic medium of infinite extent. The goal of the study is the development of useful engineering results in graphical form which are valid over a wide frequency range for broad types of shell materials and for various acoustic media. The problem is formulated mathematically in terms of two descriptive differential equations: one for the cylindrical shell, and the other for the acoustic medium. The equation of motion for the shell which is excited by a source in the interior is developed in terms of the radial displacement of the surface subject to the hypotheses that the shell, composed of isotropic elastic material, obeys thin shell equations of deformation. The equation of motion of the acoustic medium is the well known wave equation. The solution to these equations is obtained by imposition of a boundary condition establishing velocity compatibility at the shell-fluid interface and by the requirement that the results satisfy the radiation condition in the limit at large distances from the surface of the shell. Author

N69-41141*# National Aeronautics and Space Administration. Langley Research Center, Langley Center, Va.

ANALYTICAL AND EXPERIMENTAL INVESTIGATION OF END-PLANE ROTATIONS OF TRUNCATED CONES UNDER BENDING LOADS

Richard W. Faison, John L. Gilbert, and William H. Richards Washington Nov. 1969 30 p refs

(NASA-TN-D-5536; L-6019) Avail: CFSTI CSCL 20K

An analytical and experimental investigation of the bending characteristics of truncated conical beams subjected to constant moment loading was made. It has been determined that elementary beam theory becomes inadequate for determining the stiffness of truncated conical sections as the cone half-angle increases. A correction coefficient which accounts for the degeneration of stiffness from that computed by use of the elementary beam theory is presented to be applied to the stiffness parameter of thin wall truncated cone sections. The correction coefficient was determined by membrane theory analysis of a truncated cone subjected to end-plane rotations, and corroborative experimental results were obtained from small scale tests. Author

N69-41229*# National Aeronautics and Space Administration. Langley Research Center, Langley Station, Va.

CALCULATION OF THE PENETRATION FLUX FOR A MULTIWALL STRUCTURE ON THE LUNAR ORBITER SPACECRAFT

Donald H. Humes Washington Nov. 1969 25 p refs

(NASA-TN-D-5455) Avail: CFSTI CSCL 20K

The method used to calculate the penetration flux for the Lunar Orbiter multiwall structure consisting of the thermal barrier and the photo-subsystem container is presented. The calculation of the efficiency factor showed that the multiwall structure provided better protection against meteoroids than a single aluminum wall with the same mass per unit area. The calculated efficiency factor was 5.9. The flight data from the five Lunar Orbiter missions verified that the multiwall structure was more effective than a single aluminum wall of the same mass per unit area, but the data were not adequate to determine the value of the multiwall efficiency factor. Author

33

THERMODYNAMICS AND COMBUSTION

Includes ablation, cooling, heating, heat transfer, thermal balance, and other thermal effects; and combustion theory. For related information see also: 12 Fluid Mechanics; and 27 Propellants.

A69-10110 *#
STATISTICAL MECHANICAL THEORIES OF TRANSPORT PROPERTIES.
Richard S. Brokaw (NASA, Lewis Research Center, Cleveland, Ohio).
International Conference on the Properties of Steam, Tokyo, Japan, Sept. 9-13, 1968, Paper. 65 p. 111 refs.

Study of the selection, correlation, and prediction of the transport properties of steam. Dwelling principally on results which have some bearing on the properties of steam, rather than theoretical developments per se, theories are considered as they relate to the following regimes: (1) the dilute gas; (2) the dissociating gas (in the case of steam, temperatures in excess of 1700°C at atmospheric pressure); (3) the moderately dense gas; (4) the gas in the critical region; and (5) the liquid state. It is found that statistical mechanical theories of transport properties can help in correlating and selecting properties of steam under many conditions where experimental data are available, and that theory can be used to make reasonable predictions for some regimes for which there are no data. P.v.T.

A69-10112 *#
HYDRAZINE-NITROGEN TETROXIDE COMBUSTION RESPONSE TO TRANSVERSE GAS FLOWS.
Marshall C. Burrows (NASA, Lewis Research Center, Cleveland, Ohio).
Interagency Chemical Rocket Propulsion Group, Combustion Conference, 5th, Howard County, Md., Oct. 1-3, 1968, Paper. 12 p. 5 refs.

The dynamic response of hypergolic triplet elements to transverse gas flow was evaluated. Coupled response was noted when the oscillation was damped upon cessation of tangential nitrogen flow. Uncoupled response resulted when the oscillation became self-sustaining. Response characteristics were greatly affected by physical changes in the injection element. Photographs of the jet breakup within the windowed chamber showed different atomization rates for the two response regions. Calculated breakup lengths were somewhat longer than observed lengths. Hydrazine decomposition and reaction between propellant interfaces could have aided the high atomization rates in providing sufficient in-phase energy to sustain the transverse oscillations. (Author)

A69-10847 *
EXPERIMENTAL MEASUREMENTS OF THERMAL RADIATION PROPERTIES BY CYCLIC INCIDENT RADIATION.
Ernie W. Spisz and John R. Jack (NASA, Lewis Research Center, Cleveland, Ohio).
Applied Optics, vol. 7, Nov. 1968, p. 2259-2263. 5 refs.

A new experimental technique is developed to determine simultaneously the total hemispherical emittance, solar absorptance, and absorptance-emittance ratio for metals at cryogenic temperatures. The method compares the temperature response of thin metal samples to a sinusoidal perturbation of an imposed radiant intensity. Emittance data are presented for aluminum, copper, and 304 stainless steel over the temperature range from 150 to 500 K. From the data, the applicability of the cyclic radiant intensity method is evaluated, and the problems associated with extending the method to temperatures below 150 K are discussed. (Author)

A69-12547 *#
DOWNSTREAM RADIATION FLUX TO BLUNT ENTRY VEHICLES.
Raymond K. Burns (NASA, Lewis Research Center, Cleveland, Ohio) and Calvin C. Oliver (Purdue University, Lafayette, Ind.).
AIAA Journal, vol. 6, Dec. 1968, p. 2452, 2453. 6 refs.

Results of radiative flux calculations for a wide-angle blunted conical body. They show that the downstream flux distributions are more severe for very blunt bodies than for hemispheres with the same nose radius. Because of the upstream influence, the stagnation-region heat flux for a very blunt body is different from that for a hemisphere. It is indicated that self-absorption of radiation has a significant effect on the downstream flux distribution for wide-angle blunted cones. The results were obtained by using a modification of the integral method developed by Hoshizaki and Wilson (1965). F.R.L.

A69-14736 *#
CORRELATIONS FOR STAGNATION-POINT RADIATIVE HEAT TRANSFER.
Walter B. Olstad (NASA, Langley Research Center, Gas Physics Section, Hampton, Va.).
AIAA Journal, vol. 7, Jan. 1969, p. 170-172. 13 refs.

Discussion of correlations of calculations by several investigators of the stagnation-point radiative heating rates for earth reentry. It is pointed out that the good agreement among the nongray-gas results of the various investigators, when presented in terms of the cooling factors, indicates the effectiveness of the correlations. It appears that the effects of radiation cooling can be adequately accounted for through the use of simple nongray absorption-coefficient models. Reasonable estimates of the stagnation-point radiation heating rates can then be obtained by multiplying adiabatic heating rates by the cooling factors shown in correlation curves. M.M.

A69-16122 *#
SUBJECT CLASSIFICATION BIBLIOGRAPHY FOR THERMAL CONTACT RESISTANCE STUDIES.
C. J. Moore, Jr. (North Carolina State University, Raleigh, N.C.), Harry Atkins (NASA, Marshall Space Flight Center, Research Projects Laboratory, Huntsville, Ala.), and H. A. Blum (Southern Methodist University, Dallas, Tex.).
American Society of Mechanical Engineers, Winter Annual Meeting and Energy Systems Exposition, New York, N.Y., Dec. 1-5, 1968, Paper 68-WA/HT-18. 12 p. 244 refs.
Members, $0.75; nonmembers, $1.50.

Listing of technical literature concerned with thermal contact resistance studies. Three tables are provided which contain index numbers arranged in groups corresponding to certain subject titles. A list follows in which the index numbers are correlated to literature citations. Table 1 deals with experimental results for contacts in the presence of conducting fluids, Table 2 with experimental results for contacts at low ambient gas pressures, and Table 3 with special topics and topics closely related to thermal contacts. G.R.

A69-17804 *#
EXPERIMENTAL TRANSMITTANCE AND ABSORPTION CROSS SECTIONS OF CARBON PARTICLES SUSPENDED IN A JET.
Chester D. Lanzo (NASA, Lewis Research Center, Cleveland, Ohio).
Optical Society of America, Journal, vol. 58, Dec. 1968, p. 1630-

1633.

Measurement of the transmittance of a flowing stream of nitrogen gas seeded with nominal 0.009-μ carbon particles. All measurements were made at 1-atm pressure and room temperature. The measurements were made by passing a beam of light from an external source through the seeded gas stream, and then determining the transmittance with a spectrophotometer. The experimental results show that the absorption cross section decreases as the seed density increases. This is attributed to particle agglomeration. The measurements also show that the transmittance is almost independent of wavelength for wavelengths from 200 to 3500 nm. At a seed density of 10^{-5} g/cm^3, the absorption cross section lies between 17,000 and 19,600 cm^2/g. At a seed density of 10^{-4} g/cm^3, the absorption cross section lies between 10,800 and 13,000 cm^2/g. (Author)

A69-18055 *#
COMPARISON OF THE PERFORMANCE OF A CHARRING ABLATOR UNDER TRANSIENT AND CONSTANT COMBINED CONVECTIVE AND RADIATIVE HEATING.
Roy M. Wakefield and John H. Lundell (NASA, Ames Research Center, Moffett Field, Calif.).
American Institute of Aeronautics and Astronautics, Aerospace Sciences Meeting, 7th, New York, N.Y., Jan. 20-22, 1969, Paper 69-151. 10 p. 6 refs.
Members, $1.00; nonmembers, $1.50.

The behavior of phenolic nylon in stepwise varied heating cycles was investigated experimentally. The transient heating conditions were arbitrary, and were obtained by major variations in radiative heating and minor variations in enthalpy and pressure. Three rates of change of heating were provided by varying cycle times. The mass of material pyrolyzed and surface recession were determined over partial and complete cycles. For comparison, calculations of ablator performance in time-varying heating were made using pyrolysis rates and surface recession rates determined for each level of heating in constant heating tests. Differences between measured and calculated results are attributed to transients in material response due to changes in heating levels. (Author)

A69-18083 *#
BALLISTIC RANGE TESTS OF ABLATING AND NONABLATING SLENDER CONES.
Peter F. Intrieri, Donn B. Kirk, and Gary T. Chapman (NASA, Ames Research Center, Moffett Field, Calif.).
American Institute of Aeronautics and Astronautics, Aerospace Sciences Meeting, 7th, New York, N.Y., Jan. 20-22, 1969, Paper 69-179. 10 p. 26 refs.
Members, $1.00; nonmembers, $1.50.

The feasilibity of using a ballistic range to study effects of ablation on the aerodynamic characteristics of slender cones is discussed. Calculations indicate that with the proper choice of test conditions, models made of realistic heat-shield-type materials can achieve near steady-state ablation over their entire conical surface early in the flight. A series of ballistic range tests of ablating and nonablating 10° cones is described, and experimental data consisting of drag, static and dynamic stability, and lift are presented. The experimental data show that ablation significantly reduces the drag and static stability but has little effect on dynamic stability and lift. Calculations show that the measured reduction in drag coefficient can be attributed to the loss in skin friction due to ablation, but that this loss in skin friction accounts for only about one-third of the measured reduction in static stability. Similar conclusions are obtained when the same calculations are applied to wind-tunnel ablation data (paradichlorobenzene models). Finally, it is shown that the angular motions of the ablating models are markedly different from and less regular than those of the nonablating models. (Author)

A69-18126 *#
MICROSCOPIC OBSERVATION OF INTERFACIAL PHENOMENA.
T. C. Bannister and B. E. Richard (NASA, Marshall Space Flight Center, Huntsville, Ala.).
American Institute of Aeronautics and Astronautics, Aerospace Sciences Meeting, 7th, New York, N.Y., Jan. 20-22, 1969, Paper 69-95. 6 p. 6 refs.
Members, $1.00; nonmembers, $1.50.

Microscopic time lapse movies were made in the profile of the solid/liquid interface during melting and freezing of several materials. These studies evolved from the requirement to understand phase change processes being developed for use in thermal control of spacecraft as a reversible heat sink. Among the test materials used were hexadecane, octadecane, and water. Most of the interfaces were polycrystalline with the individual grains on the order of 1×10^{-3} mm^3. The interfacial topology was clearly defined and was found to vary with the growth rate. The interfacial growth was interesting as the propagation of the crystal grains was influenced by several factors - i.e., thermal gradients, anisotropic crystal properties, bubble formation, and impurities. (Author)

A69-18303 *
COMBINED RADIATION AND CONDUCTION HEAT TRANSFER - APPLICATION IN DESIGN.
Dudley G. McConnell (NASA, Lewis Research Center, Cleveland, Ohio).
Society of Automotive Engineers, International Automotive Engineering Congress, Detroit, Mich., Jan. 13-17, 1969, Paper 690197. 10 p. 20 refs.
Members, $1.00; nonmembers, $1.50.

Description of the heat equation for combined radiation and conduction transfer as applied to a plane stratified absorbing-emitting medium. Two special cases are discussed. In the first case, the solution for the temperature profile around an opaque hollow sphere is presented. The sphere is subject to external radiation; it has arbitrary conductance and variable surface optical properties. This case shows the individual and combined effects of the conductance parameter, and the surface radiative properties (absorptance and emittance). The second case concerns the temperature profile and heat transfer through a layer of solid condensed gas. Here the temperature profile shows that the effect of volume absorption is much like that of a distributed heat source. (Author)

A69-18305 *
GENERALIZED APPROACH TO THE THERMAL ANALYSIS OF ORBITING SPACECRAFT.
Robert F. Greene, Jr., Richard E. Turner, and Nathan D. Watson (NASA, Langley Research Center, Hampton, Va.).
Society of Automotive Engineers, International Automotive Engineering Congress, Detroit, Mich., Jan. 13-17, 1969, Paper 690202. 7 p. 13 refs.
Members, $1.00; nonmembers, $1.50.

Description of a generalized approach used in the thermal analysis of complex orbiting spacecraft. The approach, consisting of the development of a mathematical model and its refinement, using verification testing, has allowed close predictions of actual spacecraft temperatures during flight. The application of this approach in the analysis of the Injun 5 (Explorer 40) spacecraft is discussed as an example. M.M.

A69-20064 *
RADIATIVE TRANSFER BY DOUBLING VERY THIN LAYERS.
James E. Hansen (NASA, Goddard Space Flight Center, Goddard Institute for Space Studies, New York, N.Y.).
Astrophysical Journal, vol. 155, Feb. 1969, pt. 1, p. 565-573. 10 refs.

A doubling principle first used by van de Hulst has been developed to provide rapid and accurate results for the problem of diffuse reflection from a plane-parallel atmosphere. The method described eliminates the need for numerically solving an equation of radiative transfer by beginning with a layer of such small optical thickness that the initial scattering and transmission functions are given by the phase function. An application is made to spectral scattering by clouds in the visual and near infrared, where the phase function is strongly peaked in the forward direction. (Author)

A69-21982 *#
EFFECTS OF PYROLYSIS-GAS CHEMICAL REACTIONS ON SURFACE RECESSION OF CHARRING ABLATORS.
Roy M. Wakefield, John H. Lundell, and Robert R. Dickey (NASA, Ames Research Center, Moffett Field, Calif.).
(American Institute of Aeronautics and Astronautics and American Society of Mechanical Engineers, Structures, Structural Dynamics and Materials Conference, 9th, Palm Springs, Calif., Apr. 1-3, 1968, AIAA Paper 68-302.)
Journal of Spacecraft and Rockets, vol. 6, Feb. 1969, p. 122-128. 11 refs.

Theoretical and experimental investigation of the effects of reactions between the pyrolysis gases and an air stream. Results show that for conditions comparable to atmospheric entry from manned space flight, surface removal can range from less than 20 to more than 80% of the value for diffusion-controlled oxidization of graphite. Assumptions in the theoretical analysis are Lewis and Prandtl numbers of unity, equilibrium in reactions between the stream, pyrolysis gases, and surface and equal diffusion coefficients for all gaseous species. Cases considered include both ablation with equal velocities of the surface and interface between the char and virgin material (true steady state) and ablation with surface velocity less than the interface velocity (quasi-steady state). Comparison of theoretical and experimental results for phenolic nylon materials is made, using both quasi-steady-state and true steady-state data. Reasonable quantitative agreement is found over a wide range of test conditions. It is concluded that the decreased surface recession, under quasi-steady-state ablation, is the result of mass transfer blockage and consumption of oxygen in gas-phase chemical reactions. (Author)

A69-24283 *#
STATISTICAL THEORY OF THERMAL CONVECTION AT LARGE PRANDTL NUMBER.
J. R. Herring (NASA, Goddard Space Flight Center, Greenbelt, Md.).
Physics of Fluids, vol. 12, Jan. 1969, p. 39-52. 16 refs.

Three statistical theories of turbulence are applied to thermal convection between infinite slippery plates in the limit of infinite Prandtl number. The range of Rayleigh number R investigated is $657 \leq R \leq 1.25 \times 10^4$. The theories, which are compared in a series of numerical calculations, are the direct interaction approximation, the quasi-linear approximation, and the quasi-normal approximation. The direct interaction approximation gives results for the evolution Nusselt number in good agreement with some simple exact solutions to the problem. The flow predicted by this method is very persistent. Turbulence first appears just at critical R, and its intensity gradually increases with increasing R. The quasi-normal approximation gives satisfactory results for $R \lesssim 2000$, but some of the initial value problems lead to an unphysical negative temperature autocorrelation spectrum for larger R. In none of the initial value problems for $R > 2 \times 10^3$ did the quasi-normal procedure yield a sensible stationary state. The quasi-linear approximation appears to limit the maximum heat transport given by both the other approximations predicting about 8% larger heat transport than the direct interaction approximation. (Author)

A69-24456
ADVANCES IN HEAT TRANSFER. VOLUME 5.
Edited by T. F. Irvine, Jr. (New York, State University, Stony Brook, N.Y.) and J. P. Hartnett (Illinois, University, Dept. of Energy Engineering, Chicago, Ill.).
New York, Academic Press, Inc., 1968. 548 p.
$22.50.

CONTENTS:

PREFACE. T. F. Irvine, Jr. (New York, State University, Stony Brook, N.Y.) and J. P. Hartnett (Illinois, University, Chicago, Ill.), p. vii.
APPLICATION OF MONTE CARLO TO HEAT TRANSFER PROBLEMS. J. R. Howell (NASA, Lewis Research Center, Cleveland, Ohio), p. 1-54. 80 refs. [See A69-24457 11-33]
FILM AND TRANSITION BOILING. D. P. Jordan (Texas Technological College, Lubbock, Tex.), p. 55-128. 76 refs. [See A69-24458 11-33]
CONVECTION HEAT TRANSFER IN ROTATING SYSTEMS. F. Kreith (Colorado, University, Boulder, Colo.), p. 129-151. 205 refs. [See A69-24459 11-33]
THERMAL RADIATION PROPERTIES OF GASES. C. L. Tien (California, University, Berkeley, Calif.), p. 253-324. 95 refs. [See A69-24460 11-33]
CRYOGENIC HEAT TRANSFER. J. A. Clark (Michigan, University, Ann Arbor, Mich.), p. 325-517. 279 refs. [See A69-24461 11-33]
AUTHOR INDEX, p. 519-529.
SUBJECT INDEX, p. 531-538.

A69-24457 *
APPLICATION OF MONTE CARLO TO HEAT TRANSFER PROBLEMS.
John R. Howell (NASA, Lewis Research Center, Cleveland, Ohio).
IN: ADVANCES IN HEAT TRANSFER. VOLUME 5. [A69-24456 11-33]
Edited by T. F. Irvine, Jr. and J. P. Hartnett.
New York, Academic Press, Inc., 1968, p. 1-54. 80 refs.

Discussion of the application of the Monte Carlo method to problems of heat-transfer analysis including radiation, rarefied-gas energy transfer, and conduction. The present work is intended to help programmers decide whether to use the Monte Carlo method or finite-difference techniques for the solution of integral equations. The details of the method are briefly outlined, and the problem of choosing from probability distributions is discussed. Random numbers and evaluation of error are also treated. The application of the method to surface interaction problems in thermal radiative transfer and to radiation in absorbing-emitting media is examined. Molecular flow problems with collisions in rarefied-gas dynamics and free-molecule flow are also discussed. The use of the Monte Carlo method in the solution of heat conduction problems and the derivation of the Laplace equation are noted. The evaluation of integrals with the method is also treated. M.G.

A69-26781 *#
HEAT-TRANSFER AND PRESSURE ANALYSIS OF ROCKET EXHAUST IMPINGEMENT ON FLAT PLATES AND CURVED PANELS.
William C. Rochelle (NASA, Marshall Space Flight Center, Huntsville, Ala.) and Douglas E. Kooker (Lockheed Aircraft Corp., Lockheed Missiles and Space Co., Aero-Mechanics Dept., Huntsville, Ala.).
Journal of Spacecraft and Rockets, vol. 6, Mar. 1969, p. 248-256. 42 refs.

Experimental and theoretical correlations of pressure and heating rate were obtained under a wide variety of test conditions for rocket exhausts impinging on flat plates and curved panels. Axisymmetric real-gas exhaust plumes were generated using the method of characteristics and equilibrium chemistry to provide input to the heating and pressure analysis. Impingement pressures were calculated using both a relieved-boundary approach and the Newtonian impact theory for strong- and weak-shock interaction regions. Heating rates in the weak-shock region were obtained using various methods, including a turbulent iteration method and the Spalding and Chi (1964) turbulent skin-friction method. A modification of an equation given by Fay and Riddell (1958) was used in the strong-shock region. The results showed that pressures and heating rates can be predicted satisfactorily. (Author)

A69-27784 *#
EFFECTIVE SLIP COEFFICIENTS FOR COUPLED CONDUCTION-RADIATION PROBLEMS.
J. R. Howell and M. E. Goldstein (NASA, Lewis Research Center, Cleveland, Ohio).
ASME, Transactions, Series C - Journal of Heat Transfer, vol. 91, Feb. 1969, p. 165, 166. 7 refs.

Derivation of a solution to the linearized exact equations of combined conduction and radiation transfer, valid near the boundary, for the case of an absorbing-emitting gas in arbitrary geometry.

This solution is then matched asymptotically to the diffusion solution far from the wall. The slip coefficient which gives the correct boundary condition for the diffusion solution of the coupled problem is thus derived. M. G.

A69-28462 *
LUMINOUS FOG LAYER SURROUNDING A ZIRCONIUM DROPLET BURNING IN AN OXYGEN-CONTAINING ATMOSPHERE.
R. L. Marshall (NASA, Langley Research Center, Hampton, Va.), L. S. Nelson, and N. L. Richardson (Sandia Corp., Sandia Laboratory, Albuquerque, N. Mex.).
Combustion and Flame, vol. 13, Apr. 1969, p. 216-219.
NASA-AEC-supported research.

Discussion of the observation by high magnification photography of a luminous spherical layer that surrounds a zirconium droplet as it burns during free fall through an oxygen-containing atmosphere. It is conjectured that the presence of this luminous region can exert a significant influence on the heat and mass transfer processes that occur in the combustion. G. R.

A69-32780 *#
HEAT TRANSFER AND THERMAL BOUNDARY LAYER IN A CONICAL NOZZLE.
Donald R. Boldman and Robert W. Graham (NASA, Lewis Research Center, Cleveland, Ohio).
American Institute of Aeronautics and Astronautics, Propulsion Joint Specialist Conference, 5th, U.S. Air Force Academy, Colorado Springs, Colo., June 9-13, 1969, Paper 69-474. 7 p. 7 refs.
Members, $1.00; nonmembers, $1.50.

Heat transfer and thermal boundary-layer measurements were obtained in a 30° half-angle of convergence by 15° half-angle of divergence nozzle operating with air. The effects of inlet thermal boundary-layer thickness on the nozzle heat transfer and boundary layer were determined by operating the nozzle with an uncooled and a cooled inlet. All of the measurements were obtained at a nominal stagnation temperature of 970°R and at stagnation pressures up to 300 psia. These conditions produced throat Reynolds numbers in the range of 6×10^5 to 5×10^6. The turbulent boundary-layer temperature profiles in the nozzle generally were not described by a 1/7 power law. When "laminarization" occurred, the temperature profiles did not correspond to a laminar 1/2 power profile. At high Reynolds numbers, the Bartz integral energy calculation provided good predictions of the experimental values of energy thickness in the nozzle. Subsequent calculations of throat heat transfer were within about 20% of the experimental values. (Author)

A69-33258 *#
THEORETICAL PREDICTIONS OF NONGRAY RADIANT HEAT TRANSFER IN HIGH-TEMPERATURE NONISOTHERMAL CO_2-N_2 MIXTURES.
Robert E. Boughner (Purdue University, Lafayette, Ind.; NASA, Langley Research Center, Hampton, Va.) and Calvin C. Oliver (Purdue University, Lafayette, Ind.).
American Institute of Aeronautics and Astronautics, Thermophysics Conference, 4th, San Francisco, Calif., June 16-18, 1969, Paper 69-636. 12 p. 30 refs.
Members, $1.00; nonmembers, $1.50.

Theoretical analysis of equilibrium radiative heat transfer in the stagnation region of a viscous, conducting, radiating shock layer formed around a blunt body entering a CO_2-N_2 atmosphere. The nongray nature of the gas is accounted for by a spectral evaluation of the radiant heat flux, employing simple spectral absorption coefficients for the transport processes due to photoionization, free-free electron interactions, and molecular band transitions. For molecular band systems, a simplified absorption model which smooths out the detailed vibrational-rotational structure but retains the general band shape is developed, and its accuracy and range of applicability are established. The simplified absorption models are utilized to assess the contribution of the CN and CO(4+) band systems to the total radiative emission and to evaluate the effect of self-absorption by the CO(4+) system on the radiative flux to the surface. Stagnation-point spectral and integrated radiative heat-transfer results are presented for several flight conditions, body sizes, and CO_2-N_2 mixtures. (Author)

A69-33269 *#
THERMAL TESTS OF AN IMPROVED LOUVER SYSTEM FOR SPACECRAFT THERMAL CONTROL.
O. W. Clausen (TRW Systems Group, Redondo Beach, Calif.) and J. P. Kirkpatrick (NASA, Ames Research Center, Mountain View, Calif.).
American Institute of Aeronautics and Astronautics, Thermophysics Conference, 4th, San Francisco, Calif., June 16-18, 1969, Paper 69-627. 7 p. 10 refs.
Members, $1.00; nonmembers, $1.50.
Contract No. NAS 2-4266.

Results of an analytical and experimental design study directed toward improving the thermal performance of an existing spacecraft thermally actuated louver system. An experimental program was conducted to quantitatively assess the heat losses of the present unit in a closed condition. Based on the results of these tests and on analytical studies of the characteristics of an open system, an improved configuration was designed, fabricated, and tested. The results indicated an increase in the dynamic range (open-to-closed emittance ratio) of over 200%. The thermal performance of this improved louver system is compared with data available in the literature for other louver systems. (Author)

A69-33270 *#
RESULTS FROM THE ATS-3 REFLECTOMETER EXPERIMENT.
James B. Heaney (NASA, Goddard Space Flight Center, Greenbelt, Md.).
American Institute of Aeronautics and Astronautics, Thermophysics Conference, 4th, San Francisco, Calif., June 16-18, 1969, Paper 69-644. 12 p. 21 refs.
Members, $1.00; nonmembers, $1.50.

A reflectometer experiment, capable of measuring relative specular reflectance in five wavelength bands, was placed in a synchronous orbit aboard the ATS 3 satellite. Eighteen test samples and two reference surfaces were carried on the experiment, and eight of these samples were protected from sources of environmental damage by fused silica shields. All of the test samples are highly reflecting specular materials having Al or Ag surfaces either uncoated or coated with SiO, SiO_2, Al_2O_3, or MgF_2. The results have shown a noticeable difference between shielded and unshielded samples. The loss of reflectance is generally restricted to wavelengths less than 1200 nm and is most evident in the 300 to 400 nm region. This observed decrease in reflectance has been converted to a change in solar absorptance for some samples. The change is more severe than that observed in other experiments, either flight or laboratory, from which comparable data are available. (Author)

A69-33299 *#
THERMAL CONTACT RESISTANCE MEASUREMENTS AT AMBIENT PRESSURES OF ONE ATMOSPHERE TO 3×10^{-12} MM Hg AND COMPARISON WITH THEORETICAL PREDICTIONS.
John F. Cassidy and Herman Mark (NASA, Lewis Research Center, Cleveland, Ohio).
American Institute of Aeronautics and Astronautics, Thermophysics Conference, 4th, San Francisco, Calif., June 16-18, 1969, Paper 69-629. 11 p. 9 refs.
Members, $1.00; nonmembers, $1.50.

Comparison of the results of thermal contact resistance measurements made at ambient pressures of 1 atm to 3×10^{-12} mm Hg with two theoretical predictions which include the effects of thermal conductivity of the interface void gas and of surface texture parameters. Theoretical predictions did not agree with experimental results over the complete range of ambient pressures, but agreement between the Mikic theory and experiment occurred at vacuum conditions since the theory includes surface texture parameters of waviness and roughness. The experimental procedure included surface texture measurements of waviness, roughness, and profile. Each parameter was analyzed over the interface surface by a digital computer program which resulted in values of number of contact points, real to apparent area ratio, void volume, average asperity slope, and average roughness height for various applied loadings. (Author)

A69-34372
THERMAL DESIGN PRINCIPLES OF SPACECRAFT AND ENTRY BODIES.

Edited by J. T. Bevans (TRW Systems Group, Redondo Beach, Calif.).
New York, Academic Press, Inc. (Progress in Astronautics and Aeronautics. Volume 21), 1969. 846 p.
$17.50.

CONTENTS:

PREFACE. J. T. Bevans (TRW Systems Group, Redondo Beach, Calif.), p. ix-xii.

THERMAL ANALYSIS.

HIGHER-ORDER APPROXIMATIONS FOR LUMPED SYSTEM ANALYSIS OF EVACUATED ENCLOSURES. T. J. Love and W. D. Turner, p. 3-19. [For abstract see issue 17, page 3288, Accession no. A68-34059]

OPTICAL MEASUREMENTS OF THE RADIATION CONFIGURATION FACTOR. J. W. Baughn and G. A. Monroe, p. 21-30. [For abstract see issue 17, page 3288, Accession no. A68-34060]

OPTICAL SHAPE FACTOR DATA PROCESSING THROUGH COMPUTER GRAPHICS. T. Ishimoto and J. A. Moses (TRW Systems Group, Redondo Beach, Calif.), p. 31-34. [See A69-34373 18-14]

AN EXPERIMENTAL TECHNIQUE FOR MEASURING LOCAL SOLAR IRRADIATION WITH A MODEL SPACECRAFT. R. P. Bobco, p. 35-57. [For abstract see issue 17, page 3288, Accession no. A68-34061]

AN APPROXIMATE ANALYTIC SOLUTION OF THE STEADY-STATE THERMAL DESIGN PROBLEM OF SPACE RADIATORS. L. Lopez and A. J. Chapman, p. 59-72. [For abstract see issue 17, page 3288, Accession no. A68-34062]

ENTRY HEATING - CONVECTION, RADIATION, AND ABLATION.

RADIATIVE TRANSPORT IN INVISCID NONADIABATIC STAGNATION-REGION SHOCK LAYERS. W. A. Page, D. L. Compton, W. J. Borucki, D. L. Ciffone, and D. M. Cooper, p. 73-111. [For abstract see issue 17, page 3079, Accession no. A68-34074]

RADIATION TRANSFER THROUGH HIGH-TEMPERATURE SHOCK LAYERS. M. Thomas, p. 113-140. [For abstract see issue 17, page 3289, Accession no. A68-34078]

REMOTE SENSING OF RAREFIED GAS FLOWS THROUGH A FLUORESCENCE TECHNIQUE. C. B. Ludwig and J. A. L. Thomson, p. 141-167. [For abstract see issue 17, page 3163, Accession no. A68-34079]

THERMODYNAMIC PERFORMANCE OF CARBON IN HYPERTHERMAL ENVIRONMENTS. T. A. Dolton, H. E. Goldstein, and R. E. Maurer, p. 169-201. [For abstract see issue 17, page 3286, Accession no. A68-34046]

A RAPID TECHNIQUE FOR ESTIMATING ABLATIVE HEAT SHIELD WEIGHTS FROM PLASMA JET TEST DATA. S. A. Mezines, p. 203-223. [For abstract see issue 17, page 3285, Accession no. A68-34042]

SURFACE OXIDATION WITH STREAMWISE VARIATION OF WALL REACTIVITY. L. F. Hearne, L. W. Gallagher, and L. W. Woodruff, p. 225-248. [For abstract see issue 17, page 3143, Accession no. A68-34047]

HYPERSONIC, DIFFUSION-CONTROLLED OXIDATION OF TUNGSTEN. L. M. Gilbert, p. 249-271. [For abstract see issue 17, page 3188, Accession no. A68-34048]

ROCKET EXHAUST EFFECTS.

SPECTRAL RADIANCE OF MODEL ROCKET EXHAUST PLUMES AT HIGH ALTITUDES. J. Llinas and D. J. McCaa, p. 275-304. [For abstract see issue 17, page 3287, Accession no. A68-34058]

EFFECTS OF THE LM DESCENT ENGINE EXHAUST ON LUNAR SURFACE TEMPERATURES. A. E. Wechsler, p. 305-317. [For abstract see issue 17, page 3255, Accession no. A68-34035]

LUNAR AND PLANETARY VEHICLES DESIGN.

A STUDY OF THE THERMAL KILL OF VIABLE ORGANISMS DURING MARS ATMOSPHERIC ENTRY. C. H. Bursey, Jr., W. Dobley, Jr., and J. Parker, p. 321-337. [For abstract see issue 17, page 3090, Accession no. A68-34043]

PREDICTION OF THE MARTIAN THERMAL ENVIRONMENT. F. B. Tatom, P. B. Deshpande, F. T. Hung, and O. H. Vaughan, p. 339-364. [For abstract see issue 17, page 3256, Accession no. A68-34039]

THERMAL CONTROL ASPECTS OF A STATIONARY MARTIAN SURFACE LABORATORY. R. G. Nagel, p. 365-389. [For abstract see issue 17, page 3285, Accession no. A68-34041]

THERMAL TESTING UNDER SIMULATED MARTIAN ENVIRONMENT. T. Buna, p. 391-417. [For abstract see issue 17, page 3285, Accession no. A68-34040]

LM PASSIVE THERMAL DESIGN AND TEST. A. Bartilucci, E. Lee, and M. N. Tawil, p. 419-444. [For abstract see issue 17, page 3268, Accession no. A68-34038]

REMOTE MEASUREMENTS.

DETERMINATION OF OPTICAL AND PHYSICAL PROPERTIES OF ARTIFICIAL SATELLITES BY PASSIVE GROUND-BASED PHOTOMETRY. R. J. Preski, p. 447-468. [For abstract see issue 17, page 3100, Accession no. A68-34034]

PREDICTING LUNAR TEMPERATURES. B. P. Jones (NASA, Marshall Space Flight Center, Huntsville, Ala.), p. 469-487. 52 refs. [See A69-34374 18-30]

LUNAR SURFACE THERMAL CHARACTERISTICS DURING ECLIPSE FROM SURVEYORS III, V AND AFTER SUNSET FROM SURVEYOR V. G. Vitkus, J. W. Lucas, and J. M. Saari, p. 489-505. [For abstract see issue 17, page 3256, Accession no. A68-34037]

THERMAL RADIATION PROPERTIES.

EMISSION, TOTAL INTERNAL REFLECTION, AND TUNNELING OF THERMAL RADIATION IN METALS. R. P. Caren and C. K. Liu, p. 509-530. [For abstract see issue 17, page 3288, Accession no. A68-34064]

MEASUREMENTS OF THERMAL RADIATION OF SOLIDS AT LIQUID-HELIUM TEMPERATURES. E. G. Cravalho, G. A. Domoto, and C. L. Tien, p. 531-542. [For abstract see issue 17, page 3288, Accession no. A68-34065]

A TECHNIQUE FOR THE MEASUREMENT OF SPECTRAL REFLECTANCES AT LOW TEMPERATURES IN THE INFRARED AND FAR INFRARED. M. C. Jones and D. C. Palmer, p. 543-557. [For abstract see issue 17, page 3163, Accession no. A68-34066]

DEVELOPMENT OF PHASE-CHANGE COATINGS. R. N. Griffin and B. Linder, p. 559-574. [For abstract see issue 17, page 3195, Accession no. A68-34067]

JOINT CONDUCTANCE.

SIMULTANEOUS RADIATION AND CONDUCTION BETWEEN ROUGH SURFACES. D. H. Timmons and J. O. Mingle, p. 577-589. [For abstract see issue 17, page 3287, Accession no. A68-34054]

THERMAL CONDUCTANCE OF TWO-DIMENSIONAL CONSTRICTIONS. T. N. Veziroglu and S. Chandra, p. 591-615. [For abstract see issue 17, page 3286, Accession no. A68-34052]

AN EXACT SOLUTION FOR THERMAL CONDUCTION THROUGH A TWO-DIMENSIONAL ECCENTRIC CONSTRICTION. R. U. Sexl and D. G. Burkhard (Georgia, University, Athens, Ga.), p. 617-620. [See A69-34375 18-33]

EFFECTS OF TRANSIENT PRESSURE ENVIRONMENTS ON HEAT TRANSFER IN ONE-DIMENSIONAL COMPOSITE SLABS WITH CONTACT RESISTANCE. C. J. Morre, Jr. and H. A. Blum, p. 621-636. [For abstract see issue 17, page 3286, Accession no. A68-34051]

THEORY OF RADIATIVE DEGRADATION.

AN ANALYTICAL STUDY OF A SOLAR DEGRADATION MODEL FOR THERMAL CONTROL MATERIALS AND SOME RAMIFICATIONS FOR ACCELERATED SOLAR RADIATION TESTING. A. M. Smith and A. Y. Lee, p. 639-663. [For abstract see issue 17, page 3289, Accession no. A68-34071]

LABORATORY MEASUREMENTS.

EFFECTS OF EXTREME ULTRAVIOLET ON THE OPTICAL PROPERTIES OF THERMAL CONTROL COATINGS. D. D. Swofford, V. L. Mangold, and S. W. Johnson, p. 667-695. [For abstract see issue 17, page 3213, Accession no. A68-34073]

ELECTRON-ULTRAVIOLET RADIATION EFFECTS ON THERMAL CONTROL COATINGS. R. R. Brown, L. B. Fogdall, and S. S. Cannaday, p. 697-724. [For abstract see issue 17, page 3289, Accession no. A68-34070]

EFFECTS OF COMBINED ELECTRON-ULTRAVIOLET IRRADIATION ON THERMAL CONTROL COATINGS IN VACUO AT 77°K. J. K. Miles, P. R. Cheever, and J. Romanko, p. 725-740. [For

abstract see issue 17, page 3286, Accession no. A68-34044]

THE DEVELOPMENT OF S-13G-TYPE THERMAL-CONTROL COATINGS. G. A. Zerlaut, F. O. Rogers, and G. Noble, p. 741-766. [For abstract see issue 17, page 3195, Accession no. A68-34080]

FLIGHT EXPERIMENTS.

RESULTS FROM THE THERMAL CONTROL COATINGS EXPERIMENT ON OSO-III. J. P. Millard, p. 769-795. [For abstract see issue 17, page 3290, Accession no. A68-34084]

ENVIRONMENTAL STUDIES OF THERMAL CONTROL COATINGS FOR LUNAR ORBITER. W. S. Slemp and T. W. E. Hankinson, p. 797-817. [For abstract see issue 17, page 3290, Accession no. A68-34082]

THERMAL CONTROL EXPERIMENTS ON THE LUNAR ORBITER SPACECRAFT. C. R. Caldwell and P. A. Nelson, p. 819-852. [For abstract see issue 17, page 3269, Accession no. A68-34083]

CONTRIBUTION TO VOLUME 21, p. 853-855.

A69-37188 * #
EXPANSION OF SIMULATED STORABLE PROPELLANTS IN A SUPERSONIC NOZZLE.
Robert Friedman, Raymond E. Gaugler, and Erwin A. Lezberg (NASA, Lewis Research Center, Hypersonic Propulsion Section, Cleveland, Ohio).
(American Institute of Aeronautics and Astronautics, Propulsion Joint Specialist Conference, 4th, Cleveland, Ohio, June 10-14, 1968, Paper 68-635.)
AIAA Journal, vol. 7, June 1969, p. 1115-1118. 13 refs.

An experimental investigation of exhaust-nozzle temperatures for the storable system, 50% UDMH (unsymmetrical dimethylhydrazine) and 50% hydrazine/nitrogen tetroxide, was conducted using hydrogen and methane fuel burned in oxygen-enriched air to provide the same atomic constituents as the storable propellants. Oxidant-fuel mass ratios of 1.6 to 2.5 at 3.7 atm combustion-chamber pressure were simulated by control of the fuel, oxygen, and air flows; inlet enthalpies were duplicated by preheating the oxidant in a pebble-bed storage heater. Static temperatures, measured by a spectral line reversal pyrometer at 5 stations in the expanding portion of 5.5 area-ratio, Mach 3 nozzle were found to be nearly insensitive to oxidant-fuel ratio and close to temperatures calculated for a frozen expansion. The study demonstrated the feasibility of the simulation technique for exhaust-nozzle kinetic studies. Results agreed well with a simplified kinetic analysis based on a "sudden freezing" of the nozzle recombination reactions at an area ratio of 1.04 upstream of the throat. (Author)

A69-37198 * #
STAGNATION-POINT HEAT TRANSFER IN ARC-HEATED HELIUM AND ARGON.
Ronald B. Pope (NASA, Ames Research Center, Moffett Field, Calif.).
AIAA Journal, vol. 7, June 1969, p. 1159-1161. 13 refs.

Discussion of arc-heated flows of helium and argon discharged into a reservoir and then expanded to low pressures and high velocities in converging-diverging supersonic nozzles. The effect of flow nonequilibrium on heat transfer is evaluated, and flow enthalpy is determined. It is shown that arc-heated flows of helium are superior to those of argon for studying ablative mechanisms in a chemically inert environment, because high heating rates and high flow enthalpies can be obtained without encountering the problem of nonequilibrium. P.G.

A69-37290 *
PASSIVE THERMAL CONTROL BY SECOND-SURFACE MIRROR.
E. R. Streed (NASA, Ames Research Center, Vehicle Systems Design Branch, Moffett Field, Calif.).
Space/Aeronautics, vol. 51, Feb. 1969, p. 82, 84, 86, 87, 88.

Description of an intermediate solution to the problem posed by changes in solar absorptance for present spacecraft coatings. A second-surface mirror, which in effect is a highly reflective outer skin is proposed for spacecraft that will have to fly before new stable coatings are developed. In its most radiation-resistant form, the second-surface mirror consists of vacuum-deposited silver on a fused-silica substrate with a thickness of about 0.008 in. G.R.

A69-38951 *
PREDICTING TRANSPORT PROPERTIES OF DILUTE GASES.
Richard S. Brokaw (NASA, Lewis Research Center, Cleveland, Ohio).
(American Chemical Society, Meeting, 155th, San Francisco, Calif., Apr. 1968.)
I & EC—Industrial and Engineering Chemistry, Process Design and Development, vol. 8, Apr. 1969, p. 240-253. 69 refs.

Description of methods for predicting viscosity, thermal conductivity, and diffusion of nonpolar and polar gases and their mixtures. Calculations are based on a modified Stockmayer potential for polar molecules, which reduces to the Lennard-Jones potential for interactions between nonpolar molecules. Methods are developed for estimating the force constants characterizing these potentials from boiling point, liquid density, and dipole moment, if any. The thermal conductivity of polyatomic gases is computed using the theory of Mason (1968) and Monchick (1961). Techniques are presented for calculating the resonant correction and for estimating collision numbers for rotational relaxation. Finally, methods of calculating diffusion coefficients, viscosity, and thermal conductivity for gas mixtures are considered. Numerical examples are included. Z.W.

A69-39433 *
AN ANALYTICAL SOLUTION FOR SOLIDIFICATION OF A MOVING WARM LIQUID ONTO AN ISOTHERMAL COLD WALL.
Joseph M. Savino and Robert Siegel (NASA, Lewis Research Center, Cleveland, Ohio).
International Journal of Heat and Mass Transfer, vol. 12, July 1969, p. 803-809. 7 refs.

Generation of successive solutions for the instantaneous frozen layer thickness and temperature profile in the solidified layer by an analytical iteration technique. Each iteration was more accurate than the preceding one, and the succession of solutions converged rapidly. Analytical expressions obtained were of a simple form and agreed with numerical and approximate solutions of other investigators. (Author)

A69-40359 * #
THE SELECTION OF SPACECRAFT OPTICAL COATINGS FOR TEMPERATURE CONTROL.
F. A. Costello (Delaware, University, Newark, Del.), T. P. Harper (General Electric Co., Philadelphia, Pa.), R. Kidwell (NASA, Goddard Space Flight Center, Thermophysics Branch, Greenbelt, Md.), and G. L. Schrenk (Pennsylvania, University, Philadelphia, Pa.).
American Institute of Aeronautics and Astronautics, Aerospace Computer Systems Conference, Los Angeles, Calif., Sept. 8-10, 1969, Paper 69-979. 11 p. 6 refs.
Members, $1.00; nonmembers, $1.50.

Description of a FORTRAN computer program and its mathematical development. The program optimizes the coating pattern on the basis of the time-averaged temperatures of each of the critical elements in the vehicle. To start the optimization process, the designer selects, or has the computer select, an initial guess at the optimum coating pattern. The temperatures are then predicted from a finite-element analysis that uses a matrix-inversion, iterative solution to the heat-balance equations. Each temperature thus calculated is compared to its prescribed limits. A modified "maximum-rate-of-descent" method of optimization is then used to select a new coating pattern based on the one temperature that is

farthest from the midrange of its prescribed limits. The new pattern is then used to restart the optimization cycle. The method is demonstrated on one hypothetical satellite and on the Explorer 26 space probe. (Author)

A69-43511 * #
PRESSURE WAVE PROPAGATION IN TWO-PHASE MIXTURES.
Robert E. Henry (NASA, Lewis Research Center, Cleveland, Ohio).
American Institute of Chemical Engineers and American Society of Mechanical Engineers, National Heat Conference, 11th, Minneapolis, Minn., Aug. 3-6, 1969, Paper. 26 p. 14 refs.

Investigation of the mechanism for interphase momentum transfer during the propagation of an infinitesimal pressure pulse through a bubbly two-phase mixture. The result indicates that the effects of heat and momentum transfer may be correlated as a function of void fraction. A correlation for the propagation velocity is developed from air-water data, which had a system pressure of 25 psia, and it is compared with air-water and steam-water results for pressure levels ranging from 10 to 285 psia. The good agreement substantiates the analytical development. The importance of the mixing technique with regards to the temporal and spatial uniformity of the flow is discussed, and the experimental data are shown to be in agreement with the expected trends. A short discussion of the essential differences between the two-phase propagation velocities of an infinitesimal pulse and that of a sound wave is also included. (Author)

A69-43540 * #
STABILITY OF CYLINDRICAL BUBBLES IN A VERTICAL PIPE.
Y. Y. Hsu and F. F. Simon (NASA, Lewis Research Center, Cleveland, Ohio).
American Society of Mechanical Engineers and American Institute of Chemical Engineers, Heat Transfer Conference, Minneapolis, Minn., Aug. 3-6, 1969, ASME Paper 69-HT-28. 10 p. 23 refs.
Members, $0.75; nonmembers, $1.50.

Photographic study of the stability of cylindrical bubbles rising in vertical pipes of various diameters (1.27 to 30 cm). Single cylindrical bubbles remain stable in pipes of all sizes for durations up to 10 to 20 sec, provided that the flowfield is quiescent. Bubble-splitting occurs when the bubble is in the presence of disturbances such as pressure pulsation, convection cells, or the wake of a leading bubble. The wake effect is studied in detail. The critical bubble spacing for instability increases with the square of the diameter. (Author)

A69-43541 * #
INLET EFFECTS ON BOILING AND NEAR CRITICAL HYDROGEN HEAT TRANSFER.
S. S. Papell (NASA, Lewis Research Center, Cleveland, Ohio) and D. D. Brown (Babcox and Wilcox Co., Lynchburg, Va.).
American Society of Mechanical Engineers and American Institute of Chemical Engineers, Heat Transfer Conference, Minneapolis, Minn., Aug. 3-6, 1969, ASME Paper 69-HT-27. 11 p. 9 refs.
Members, $0.75; nonmembers, $1.50.

Investigation of the influence of hydrodynamic entrance conditions on boiling and near-critical hydrogen heat transfer with the aid of electrically heated test sections designed with different inlet geometries. Boiling data comparisons at a system pressure of 50 psia over a range of inlet velocities from about 11 to 68 ft/sec showed that vigorous "film" boiling is not influenced by the difference in hydrodynamic entrance conditions. The opposite is true in the heat flux region usually referred to as "minimum" film boiling, where the inlet geometry was found to dictate the type of boiling regime. In direct contrast to the trends in the boiling data, it was found that the near-critical data at system pressures of 200 and 300 psia were influenced by inlet conditions at the higher heat fluxes but not at the lower heat fluxes. At the higher heat fluxes, the heat transfer rates for the developing flow system (plenum) were significantly higher than those of the fully developed flow system (straight inlet). These results persisted over the entire test section length. P.G.

A69-43542 * #
TRANSITION FROM FILM TO NUCLEATE BOILING IN VERTICAL FORCED FLOW.
F. F. Simon and R. J. Simoneau (NASA, Lewis Research Center, Cleveland, Ohio).
American Society of Mechanical Engineers and American Institute of Chemical Engineers, Heat Transfer Conference, Minneapolis, Minn., Aug. 3-6, 1969, ASME Paper 69-HT-26. 16 p. 18 refs.
Members, $0.75; nonmembers, $1.50.

Study of the transition from film boiling to nucleate boiling for liquid nitrogen flowing in an electrically heated tube. For this type of heating, wall conduction is believed to govern the boiling transition. A conduction analysis was combined with a film boiling analysis for an analytical prediction of the transition heat flux. A visual experiment of film boiling aided the film boiling analysis. The analytical results are in good agreement with the experimental data. (Author)

A69-43550 * #
THE ROTATING HEAT PIPE--A WICKLESS, HOLLOW SHAFT FOR TRANSFERRING HIGH HEAT FLUXES.
Vernon H. Gray (NASA, Lewis Research Center, Applied Heat Transfer Branch, Cleveland, Ohio).
American Society of Mechanical Engineers and American Institute of Chemical Engineers, Heat Transfer Conference, Minneapolis, Minn., Aug. 3-6, 1969, ASME Paper 69-HT-19. 6 p. 5 refs.
Members, $0.75; nonmembers, $1.50.

Description of a new type of heat pipe that rotates about its longitudinal centerline and utilizes centrifugal acceleration instead of capillaries for return-pumping of condensate. Several alternative design configurations are presented. Advantages cited include the ability to overcome effects of gravity and vehicular accelerations, and heat fluxes up to an order of magnitude higher than comparable capillary-type heat pipes. Research tests and analyses on various component parts of the rotating heat pipe are reviewed. Specifically, these tests include the effects of centrifugal accelerations in a rotating boiler, the condensation of vapors on rotating surfaces, the behavior of high velocity vapor in tubes, and the pumping of liquids by rotation of their containers. Finally, the overall performances of the rotating and conventional heat pipes are compared. Three of the many attractive applications of rotating heat pipes are illustrated and described. These examples involve cooling of motor rotors, cooling of jet engine turbine rotor blades, and air conditioning with a compact unit having one moving part. (Author)

A69-43564 * #
HYPERBOLIC HEAT-CONDUCTION EQUATION--A SOLUTION FOR THE SEMI-INFINITE BODY PROBLEM.
K. J. Baumeister (NASA, Lewis Research Center, Cleveland, Ohio) and T. D. Hamill (McDonnell Douglas Corp., McDonnell Douglas Astronautics Co., Huntington Beach, Calif.).
American Society of Mechanical Engineers and American Institute of Chemical Engineers, Heat Transfer Conference, Minneapolis, Minn., Aug. 3-6, 1969, ASME Paper 69-HT-1. 6 p. 10 refs.
Members, $0.75; nonmembers, $1.50.

Determination of the effect of the propagation velocity of heat on the temperature and heat-flux distribution in a semiinfinite body due to a step change in temperature at the surface. The solution yields a maximum but finite heat flux under the conditions of a step change. This is contrary to the infinite value predicted by the error function solution to the Fourier transient conduction equation. In addition, assuming convection is conduction-limited, an upper limit for convective heat transfer coefficients is postulated. (Author)

33 THERMODYNAMICS AND COMBUSTION

A69-43680 * #
ABLATION EFFECTS ON THE APOLLO AFTERBODY HEAT TRANSFER.
George Lee (NASA, Ames Research Center, Moffett Field, Calif.).
AIAA Journal, vol. 7, Aug. 1969, p. 1616-1618.

Study of the effects of ablation on the Apollo afterbody heat transfer for the angle-of-attack range over which the Apollo vehicle normally reenters the earth's atmosphere. Both effects of ablation from the nose cap (a simulation of front heat shield ablation in the flight vehicle), and the combined effects of ablation from the nose cap and afterbody, were determined in simulated tests conducted in an arc-heated air wind tunnel. It is concluded that ablation has the effect of reducing the afterbody heat transfer by as much as 40 per cent. Moreover, it is shown that the heat transfer data can be correlated in terms of parameters obtained from simplified boundary-layer theories. O.H.

N69-10227*# National Aeronautics and Space Administration. Lewis Research Center, Cleveland, Ohio.
TRANSIENT SOLIDIFICATION OUTSIDE A COOLED PIPE WITH APPLICATION TO A SOLAR BRAYTON HEAT RECEIVER
Wellington W. Hu Washington Nov. 1968 33 p refs
(NASA-TN-D-4897) Avail: CFSTI CSCL 20M

The analysis involves time-variant heat conduction with the liquid-solid boundary moving radially through the axisymmetric heat-storage material as heat is transferred to the flowing cooling medium. Solutions were obtained by simultaneously solving the integrated nonlinear differential equations through numerical means. Quasi-steady radial heat conduction is utilized at an instant of time. Solutions for wall temperature, gas temperature, and solidification thickness along the tube for a 35-minute shadow portion of an Earth orbit are obtained for a solar Brayton heat receiver. A simplified solution neglecting the wall-temperature variation is also derived to compare with the numerical method. Author

N69-10420*# National Aeronautics and Space Administration. Lewis Research Center, Cleveland, Ohio.
EXPERIMENTAL STUDIES ON SHADOW SHIELDS FOR THERMAL PROTECTION OF CRYOGENIC TANKS IN SPACE
Richard H. Knoll and Edward R. Bartoo Washington Nov. 1968 73 p refs
(NASA-TN-D-4887) Avail: CFSTI CSCL 20M

Experiments were performed on multiple flat-disk shadow shields to determine the effects of shield spacing, number, emissivity, lateral conductance, and targeting (high-emissivity coatings on annular rings of shields) on thermal performance. The experimental data, in general, agreed closely with an analytical model which assumed diffuse surfaces with nonuniform radiosity. A shadow-shield system for a hypothetical space vehicle was designed, scaled down, and tested. Results demonstrated: (1) a lightweight method of shield construction; (2) shield-support interactions; and (3) reduction of support heat leaks by shield location, attachment methods, and the use of high-emissivity coatings. Author

N69-10473*# National Aeronautics and Space Administration. Lewis Research Center, Cleveland, Ohio.
THERMAL ANALYSIS OF SHADOW SHIELDS AND STRUCTURAL MEMBERS IN A VACUUM
Robert J. Boyle and Richard H. Knoll Washington Nov. 1968 125 p refs
(NASA-TN-D-4876) Avail: CFSTI CSCL 20M

An analysis considering nonuniform radiosity and assuming diffusely emitting and reflecting surfaces is presented. The shields are planar and circular, while the sources may be surfaces of revolution. The effects of source geometry, number of shields, spacing, and surface properties are discussed. Shield conductivity and selective coatings are investigated. Specularly and diffusely reflecting surfaces are discussed under the simplifying assumption of uniform radiosity. Also, the effects of thermal radiation on the temperatures of a conducting structural member are analyzed. Results are presented showing the effects of significant parameters on the temperature profiles and heat transfer rates. The computer program for the shield analysis is listed. Author

N69-10932*# National Aeronautics and Space Administration. Langley Research Center, Langley Station, Va.
ROTATIONAL AND VIBRATIONAL TEMPERATURE MEASUREMENTS IN THE 12-INCH HYPERSONIC CERAMIC-HEATED TUNNEL
John C. Hoppe Washington Nov. 1968 37 p refs
(NASA-TN-D-4892) Avail: CFSTI CSCL 20M

An electron beam fluorescence technique has been employed to measure free-stream nitrogen rotational and vibrational temperatures in air at the Langley 12-inch hypersonic ceramic-heated tunnel. This work included establishing the sources of measurement uncertainty and minimizing their effect on the temperature measurements. An extensive laboratory study to determine the accuracy of the instrument system preceded tests made at the facility. Measurements obtained at the facility included a rotational temperature range from 39°K to 72°K and a corresponding vibrational temperature range from 850°K to 1320°K. In addition, static translational temperatures were determined as well as the condition of nonequilibrium existing in the gas expansion. Uncertainties in these measured temperatures are estimated to be ±5 to ±7 percent for the rotational temperatures, and ±15 percent for the vibrational temperatures. During the preliminary laboratory investigation of the technique for vibrational temperature measurement, experimental evidence indicated that at least one reported transition probability needed correction. In addition, some deviation from the expected linear analysis for rotational temperature was experienced. Finally, the measured temperatures generally agree with aerodynamic predictions and fall between the extreme frozen flow and equilibrium flow cases. A first-order nonequilibrium theory fits the observations approximately. Author

N69-12739*# National Aeronautics and Space Administration. Lewis Research Center, Cleveland, Ohio.
DESIGN-POINT PERFORMANCE OF A DOUBLE CONTAINMENT TANTALUM AND STAINLESS STEEL MERCURY BOILER FOR SNAP-8
James A. Albers, Ronald H. Soeder, and Pierre A. Thollot Washington Dec. 1968 56 p refs
(NASA-TN-D-4926) Avail: CFSTI CSCL 20M

Experimental data were obtained on the performance of a SNAP-8 tantalum and stainless-steel double-containment boiler. The boiler was a counterflow heat exchanger consisting of seven tubes coiled with a 2-1/2-turn helical shell. The experimental results are presented for a total operating time of 1445 hours. The range of mercury flow rates was from 7,500 to 11,800 lb mass/hr (3400 to 5350 kg/hr), and the primary NaK flow was varied from 29,000 to 49,000 lb mass/hr (13,000 to 22,200 kg/hr). The NaK temperature into the boiler was varied from 1272 to 1318°F (962 to 988°K). Author

N69-13231*# National Aeronautics and Space Administration. Langley Research Center, Langley Station, Va.
EFFECTS OF STEADY-STATE ACCELERATION ON COMBUSTION CHARACTERISTICS OF AN ALUMINIZED COMPOSITE SOLID PROPELLANT
G. Burton Northam Washington Dec. 1968 43 p refs
(NASA-TN-D-4914) Avail: CFSTI CSCL 21I

The objective was to determine the effect of acceleration level, and acceleration field orientation on the combustion of

aluminized composite solid propellant. Unidirectional burning slab motors were fired on a ballistics centrifuge at acceleration levels from 0g to 300g. Tests were conducted with the acceleration loads directed normal into the burning surface, normal out of the burning surface, and at orientations of 0°, 30°, 60°, and 75° into the burning surface. The resulting surface condition of the propellant was examined under the various test conditions by extinguishing a limited number of propellant samples. As the normal acceleration load into the burning surface increased, the average propellant burning rate, the pitting of the propellant surface, and the amount of metallic-like residue retained within the test motor increased. At orientations other than normal and into the burning surface, neither the burning rate, the pitting, nor the metallic-like residue were much increased at acceleration levels as high as 300g. At an average chamber pressure of 500 psia (3.45 MN/m^2) the propellant burning rate increased approximately 21 percent as the normal acceleration level was raised from 0g to 300g. Author

N69-14171*# Stanford Research Inst., Menlo Park, Calif.
COMPARATIVE EVALUATION OF ABLATING MATERIALS IN ARC PLASMA JETS
Nevin K. Hiester and Carroll F. Clark Washington NASA Dec. 1968 197 p refs
(Contract NASr-49(15))
(NASA-CR-1207) Avail: CFSTI CSCL 20M

In a round-robin ablation study, Teflon and high-density phenolic-nylon models were evaluated at various enthalpies and heating rates under supersonic conditions. These two high-density materials were evaluated at stagnation pressures up to 10 atmospheres for the former and 30 atmospheres for the latter. The effect of model size was also evaluated using both hemispherical and flat-faced Teflon models having effective radii varying from one-quarter to four times the radius used previously. The mass loss rates again correlated with the results from the earlier study, except that high-density phenolic-nylon models showed a rapid increase in ablation above a stagnation pressure of about 2.5 atmospheres. These higher rates were also correlated, and found to agree, with literature data for these same pressure regime. Five new low-density materials—Langley phenolic-nylon, Hughes phenolic-nylon, Avcoat epoxy-novalac-filled honeycomb, Langley silicone elastomer, and General Electric silicone elastomer—were also studied at enthalpies from 2500 to 34,000 Btu/lb and stagnation pressures from 0.004 to 2 atmospheres. Mass loss rates, front surface, and internal temperatures were measured for these materials. Author

N69-14501*# National Aeronautics and Space Administration. Langley Research Center, Langley Station, Va.
A FLIGHT MEASUREMENT OF OPTICAL RADIATION FROM SHOCK-HEATED AIR BY USING A TRAILBLAZER 2 VEHICLE
Lloyd S. Keafer, Jr. and Ernest F. Burcher Washington Dec. 1968 46 p refs
(NASA-TN-D-4937) Avail: CFSTI CSCL 22C

A flight measurement of optical radiation from shock-heated air was obtained by using a Trailblazer II vehicle. Observations in two spectral bands were made near the stagnation point of a high-velocity (6 km/sec) body at extremely high altitudes (80 to 55 km). The reentry body configuration and the reentry velocity allowed observations of nonequilibrium radiation effects not previously measured in flight. Severe truncation and collision limiting were experienced. The measurement results were compared to analytical predictions and previous experiments. The experiment results complemented those from Project Fire and those from ground-based investigations and can be applied to the problem of reentry heating and to the evaluation of the concept of optically detecting and tracking noncooperative reentry vehicles. The measurement technique used in this experiment, because of its simplicity, may be applicable to other reentry experiments. Author

N69-14588*# National Aeronautics and Space Administration. Lewis Research Center, Cleveland, Ohio.
HEAT-TRANSFER COEFFICIENTS FOR HYDROGEN FLOWING THROUGH PARALLEL HEXAGONAL PASSAGES AT SURFACE TEMPERATURES TO 2275 K
Jack G. Slaby and William F. Mattson Washington Dec. 1968 25 p refs
(NASA-TN-D-4959) Avail: CFSTI CSCL 20M

Local forced-convection heat-transfer data are presented for hydrogen flowing through an electrically heated test section composed of 19 hexagonal parallel passages with a length- to equivalent-diameter ratio of 63.5. The data cover ranges of surface-to hydrogen-temperature ratios from 1.43 to 3.38, bulk Reynolds numbers from 12,950 to 21,960, surface temperatures to 2275 K, and outlet hydrogen temperatures to 747 K. The results are correlated in terms of Nusselt, Prandtl, and modified Reynolds numbers. The data fell within about ±20 percent of the correlating equations. The heat-transfer results agreed with those obtained from a parallel flat-plate test section with similar dimensions. Author

N69-16181*# National Aeronautics and Space Administration. Langley Research Center, Langley Station, Va.
MULTIDIMENSIONAL GAS FLOW THROUGH PERMEABLE CHAR LAYERS AND ITS EFFECTS ON ABLATION
Harold G. Bush and Marvin B. Dow Washington Jan. 1969 39 p refs
(124-07-01-34-23)
(NASA-TR-R-296) Avail: CFSTI CSCL 20M

A theoretical analysis of the pressure fields within the char layers of cylindrical and hemispherical ablation models is presented. The distribution over the surface of mass flow from the char layer is given for both geometries. These multidimensional mass-flow distributions show that gas flow through the char layer can be significantly different from the one-dimensional assumption previously used by ablation analysts. Further, the theoretical results show that it is possible for the external pressure field to cause gas flow into the char layer, in which case the diffusion of energy and oxygen through the boundary layer to the material surface is increased. The appropriate analytical results were used to modify an existing one-dimensional ablation computer program to make convective blocking at the ablator surface responsive to the major parameters governing mass flow through permeable char layers. A comparison of analytical and experimental results shows that ablation performance can be significantly affected by multidimensional mass flow through the char layer. Author

N69-16268*# National Aeronautics and Space Administration. Langley Research Center, Langley Station, Va.
SOLUTIONS OF BLUNT-BODY STAGNATION-REGION FLOWS WITH NONGRAY EMISSION AND ABSORPTION OF RADIATION BY A TIME-ASYMPTOTIC TIME-ASYMPTOTIC
Linwood B. Callis Washington Jan. 1969 55 p refs
(129-01-03-09-23)
(NASA-TR-R-299) Avail: CFSTI CSCL 20M

A second-order time-asymptotic solution to radiation-coupled stagnation-region flows is presented. The solution is applied to the hypervelocity flow over blunt vehicles of inviscid, nonconcucting, equilibrium air, emitting and absorbing nongray radiation. Velocities, nose radii, and altitudes covered by the analysis are sufficient to bracket reentry trajectories of current interest. Radiative heat-transfer rates for the range of interest and typical profiles of pressure, density, enthalpy, temperature, and velocity are shown. The nature of the time-asymptotic solution is discussed and it is shown to be a feasible means of achieving second-order accurate solutions to radiation-coupled shock-layer flows. Step-function models of the absorption coefficient are used in order to evaluate the divergence of the radiation flux vector. An analysis is carried out to determine what effect variations in the spectral complexity of the step model

absorption coefficients used in the analysis will have on the thermodynamic and flow profiles of interest and on the nongray radiative heat-transfer rates. An existing correlation for the cooling factor, the ratio of the radiation heat-transfer rate to the adiabatic radiation heeat-transfer rate, is extended to larger velocities than heretofore considered. Author

N69-17438*# Lockheed Missiles and Space Co., Palo Alto, Calif.
EFFECT OF SHOCK PRECURSOR HEATING ON RADIATIVE FLUX TO BLUNT BODIES
L. E. Lasher and K. H. Wilson Washington NASA Feb. 1969 23 p refs
(Contract NAS7-509)
(NASA-CR-1265) Avail: CFSTI CSCL 22C

A solution using a one dimensional heating representation is used to determine the precursor heating correction to the surface flux. Based on these results, one can judge when a fully coupled radiative–gasdynamic flow analysis is needed. The conservative absorption model predicts only a 10% effect at U_∞ = 65,000 fps on the surface radiative heat flux. A correction of this order is not considered to be sufficiently important to justify a detailed coupled solution. When the cold air is preheated substantially, the absorption resulting from this model may be underestimated. A liberal absorption model is considered and indicates that at a velocity of 60,000 fps the correction to surface radiative flux would amount to 25%. The true coupling effect of the precursor heating probably lies somewhere between the results produced by the two absorption models. The conclusion is reached that for velocities less than 60,000 fps precursor heating effects are relatively unimportant in determining the radiative flux reaching the body surface. At velocities greater than 60,000 fps the amount of energy loss from the shock layer and a resultant precursor heating correction is felt to be sufficiently large to justify a more detailed analysis. Author

N69-18125*# Lockheed Missiles and Space Co., Palo Alto, Calif.
SERIES SOLUTION FOR HYPERSONIC FLOW ABOUT BLUNT BODIES
Y. S. Chou Washington NASA Feb. 1969 88 p refs
(Contract NAS7-509)
(NASA-CR-1266) Avail: CFSTI CSCL 20D

The Blasius type series formulation for hypersonic perfect gas flow over an axisymmetric blunt body was made. A three term series solution, based on the thin layer equations and a two term iterative solution based on the three term thin layer solution were obtained. Some of the conclusions reached were: (1) The present series solution seems most effective for a sphere; the convergence of the series is fast. The first two terms of the thin layer series are sufficient to describe the flow field accurately up to the sonic line and no iterative solution will be necessary. The concentric shock will be a good first approximation for a sphere. (2) For paraboloids, and for those body shapes will produce hyperboloidal shock waves, the present series solution is found to converge rather slowly, especially for the pressure field. The proposed iterative solution shows improvement over thin layer solution. (3) The thin layer equation is found to be applicable to ellipsoids with moderate bluntness such as the ones discussed in the examples. (4) The solution is not applicable at low free stream Mach numbers due to the hypersonic assumption made in the analysis as well as due to the fact that we have neglected the terms of order ϵ^2. Author

N69-18898*# National Aeronautics and Space Administration. Lewis Research Center, Cleveland, Ohio.
CORRELATION OF GAS-SIDE HEAT TRANSFER FOR AXISYMMETRIC ROCKET ENGINE NOZZLES
Uwe H. von Glahn Washington Feb. 1969 25 p refs
(NASA-TM-X-1748) Avail: CFSTI CSCL 20M

Empirical correlating equations were developed to predict gas-side transfer for nozzles without a wall temperature step change near the nozzle entrance (such as regeneratively cooled rocket engines) over a wide range of conditions and configurations. The use of the reference enthalpy method for predicting fluid properties in these equations facilitated the correlation of heated air and rocket firing data. Author

N69-19117*# Lockheed Missiles and Space Co., Palo Alto, Calif.
EFFECT OF ABLATION PRODUCT ABSORPTION AND LINE TRANSITIONS ON SHOCK LAYER RADIATIVE TRANSPORT
K. H. Wilson and H. Hoshizaki Washington NASA Feb. 1969 101 p refs
(Contract NAS7-509)
(NASA-CR-1264) Avail: CFSTI CSCL 20D

The effects of ablation product absorption and atomic line transitions on radiative transport within the shock layer enveloping an ablating blunt body were studied by a gas-dynamic analysis modified to handle large mass injection rates. The large mass injection rate problem was approached by two separate analyses. One approach considered a fully viscous flow but treated the velocity field solution in two separate layers. The other approach considered the total shock layer to consist of a distinct inviscid ablation product layer and distinct air layer. An approximate treatment of radiation transport in lines was devised. This approximate treatment uses the concept of "equivalent line" parameters to reduce the numerical calculations to a tractable level. Within the equivalent line approximation a mixture of C, N, and O atomic transitions is included. Two major conclusions are reached. Firstly, that energy transported in atomic lines is responsible for roughly 50% of the radiative transport within shock layers at conditions typical of superorbital entry. Secondly, ablation product species significantly absorb continuum radiative flux from the high-temperature portion of the shock layer at mass injection levels the order of 5% of the free-stream mass flux. Author

N69-20008*# National Aeronautics and Space Administration. Marshall Space Flight Center, Huntsville, Ala.
THERMAL CONDUCTION THROUGH AN EVACUATED IDEALIZED POWDER OVER THE TEMPERATURE RANGE OF 100 DEG K TO 500 DEG K
Ronald B. Merrill Washington Mar. 1969 82 p refs
(NASA-TN-D-5063) Avail: CFSTI CSCL 20M

Measurement of the radiative thermal conduction of an ideal powder as a function of temperature was conducted to find a suitable experimental method. Three classes of techniques were investigated: steady state, probe, and pulse. A hybrid type, the differential line heat source method, was selected and applied to spherical barium silicate glass beads with sample sizes of 10μ to 20μ, 38μ to 53μ, and 125μ to 243μ, in a vacuum of at least 2×10^{-6} torr. Various statistical treatments of the data as well as the raw data itself are discussed and compared as to probable accuracy. Previous work in this area is reviewed and an equation to describe the conductivity–temperature relationship of the form $K = AT^3 + B$ proposed. K.R.G.

N69-20882*# National Aeronautics and Space Administration. Lewis Research Center, Cleveland, Ohio.
MEASURED EFFECTS OF GASEOUS FLOW SYSTEM DYNAMICS ON ACOUSTIC-MODE COMBUSTION INSTABILITY
John F. Groeneweg Washington Mar. 1969 17 p refs
(NASA-TN-D-5080) Avail: CFSTI CSCL 21B

Experiments in which hydrogen injection geometry was changed in a T-burner combustor demonstrated that hydrogen flow system dynamics can influence acoustic-mode instability. Stability boundaries for the combustor were shifted by changing the hydrogen manifold volume and by changing the amount of propellant stream

interaction. The results were compatible with stability boundaries calculated from a combustor response model if the time delay, which was assumed to exist between injection and combustion of the hydrogen, varied with propellant flow rates. Author

N69-22931*# National Aeronautics and Space Administration. Lewis Research Center, Cleveland, Ohio.
VARIATION OF CONVECTIVE HEAT-TRANSFER COEFFICIENT AROUND A SIMULATED ROCKET COOLING TUBE SECTION
Ronald G. Huff Washington Apr. 1969 30 p refs
(NASA-TN-D-5168) Avail: CFSTI CSCL 20M

An experiment was performed using an insulated pipe through which hot air flowed. The pipe wall was made of tubes having a semicircular cross section which simulates the geometry found in many rocket engines. The peripheral variation of the convective heat transfer coefficient between the gas and the tubes was measured for one of the tubes. It was found that the coefficient is equal to the coefficient at the creast of the tube times the cosine of the angle measured from the crest. Author

N69-22933*# National Aeronautics and Space Administration. Langley Research Center, Langley Station, Va.
AN INVESTIGATION OF ABLATION BEHAVIOR OF AVCOAT 5026/39M OVER A WIDE RANGE OF THERMAL ENVIRONMENTS
Roger K. Crouch and Gerald D. Walberg Washington Apr. 1969 36 p refs
(NASA-TM-X-1778) Avail: CFSTI CSCL 20M

The ablation behavior of the material was found to be strongly dependent on the level of heat-transfer coefficient. At values of heat transfer coefficient less than 0.17 lbm/ft^2-sec (0.83 kg/m^2-sec), measured char recession rates were comparable to those predicted for diffusion-controlled char oxidation. At high values of heat transfer coefficient, the ablation rate increased rapidly with increasing heat transfer coefficient and severe mechanical char failure was observed. The structure, composition, and removal rate of the char were significantly influenced by stream oxygen content at low heat transfer coefficients but not at high heat transfer coefficients. Empirical correlations were found between the mass loss rate and the heat transfer coefficient and between the mass loss rate and a parameter related to the product of oxygen flow to the surface and a reference shear. Author

N69-22997*# National Aeronautics and Space Administration. Langley Research Center, Langley Station, Va.
LAMINAR HEAT-TRANSFER DISTRIBUTIONS FOR A BLUNTED-CONE, CONE-FRUSTUM REENTRY CONFIGURATION AT MACH 10
J. David Dearing Washington Apr. 1969 21 p refs
(NASA-TN-D-5146) Avail: CFSTI CSCL 20M

The aerodynamic heating characteristics of a spherically blunted cone, cone-frustum reentry configuration with a hypersonic lift–drag ratio of about 1.5 were determined at a nominal free stream Mach number of 10 and at Reynolds numbers based on free stream conditions and model length of 0.56×10^6, 1.47×10^6, and 2.67×10^6. The measured longitudinal distributions exhibit a small dip, or minimum, in the heating just aft of the blunted nose similar to that exhibited by the pressure distributions of blunted cones. On the windward ray, the heating was unaffected by Reynolds number and increased with angle of attack. The measured heat transfer distributions indicate a narrow band of locally higher heating associated with the reattachment of vortices near the leeward ray for all angles of attack greater than or equal to the forecone half angle. This phenomenon appears to be dependent upon Reynolds number as well as angle of attack. The measured base heating rate was less than 0.2 percent of the stagnation point heating rate. Author

N69-23351*# National Aeronautics and Space Administration. Lewis Research Center, Cleveland, Ohio.
ON THE DESIGN OF ACOUSTIC LINERS FOR ROCKET ENGINES: HELMHOLTZ RESONATORS EVALUATED WITH A ROCKET COMBUSTOR
Bert Phillips, Ned P. Hannum, and Louis M. Russell Washington Apr. 1969 28 p refs
(NASA-TN-D-5171) Avail: CFSTI CSCL 21B

A study was made to improve the design of rocket engine acoustic liners.Helmholtz resonators with variable cavity depths were tested with an unstable rocket combustor. Combustor pressure oscillations inside the resonators and in the combustor and the phase angles between them were measured. From these measurements resonator aperture effective lengths were calculated. A new correlation for the effective lengths at high mean gas velocities is presented. A nonlinear resonator model is evaluated and used to calculate the aperture resistance. The calculated resistances were correlated by an empirical function of the mean and oscillatory flows. Author

N69-23471*# National Aeronautics and Space Administration. Lewis Research Center, Cleveland, Ohio.
VIEW FACTORS FOR TOROIDS AND THEIR PARTS
Norman T. Grier and Ralph D. Sommers Washington Apr. 1969 88 p refs
(NASA-TN-D-5006) Avail: CFSTI CSCL 20M

Various radiation view factors for a toroid have been calculated using a high-speed digital computer. The results are presented in graphs and tables. The view factors included are: (1) between differential elements and bands on a toroid, (2) between differential- and finite-sized elements, (3) between finite-sized elements and the whole toroid, and (4) between a toroid and itself. The range of toroidal parameters used was such that all possible toroids are included in the calculations. Orthogonal toroidal coordinates were used in the computer calculation. Toroidal coordinates and their use in writing the view factor equations are discussed. Author

N69-23707*# National Aeronautics and Space Administration. Lewis Research Center, Cleveland, Ohio.
DESIGN AND FABRICATION OF A COUNTERFLOW DOUBLE-CONTAINMENT TANTALUM-STAINLESS STEEL MERCURY BOILER
Laurence W. Gertsma and David W. Medwid Washington May 1969 38 p refs
(NASA-TN-D-5092) Avail: CFSTI CSCL 20M

A boiler was designed using 7 tantalum (Ta) tubes for containment of the mercury with each Ta tube placed inside a flattened stainless steel tube. These tubes were coiled, bundled, and inserted into a coiled, large diameter stainless steel tube which contains the primary NaK. The large difference in thermal expansion between the Ta and the stainless steel tubes was accommodated by the flattened stainless steel tube allowing the Ta tube to radially move with respect to the stainless steel tube. All tubes were equalized in length by uniformly twisting the tube bundle 360° Author

N69-24168*# National Aeronautics and Space Administration. Lewis Research Center, Cleveland, Ohio.
EFFECT OF SIZE ON NORMAL-GRAVITY SELF-PRESSURIZATION OF SPHERICAL LIQUID HYDROGEN TANKAGE
John C. Aydelott and Charles M. Spuckler Washington, May 1969 42 p refs
(NASA-TN-D-5196) Avail: CFSTI CSCL 20M

A study was conducted to obtain a correlating parameter which would relate the rate of pressure rise to the volume of spherical liquid hydrogen tankage. A nonventing 22 inch diameter spherical tank partially filled with liquid hydrogen was subjected to

four uniformly heated self-pressurization tests with various combinations of percent filling and heat transfer rate. These data were compared with data from a similar study on a 9 inch diameter, uniformly heated, spherical tank. The two sets of data verified the analysis which predicted the same change in pressure in each tank for equal values of heat added per unit volume. Author

N69-24824*# National Aeronautics and Space Administration. Lewis Research Center, Cleveland, Ohio.

CHARACTERIZATION OF PRESSURE PERTURBATIONS INDUCED IN A ROCKET COMBUSTOR BY A MACHINE GUN

Daniel E. Sokolowski, David W. Vincent and E. William Conrad Washington May 1969 46 p refs

(NASA-TN-D-5214) Avail: CFSTI 21B

The purpose of this experimental study was to develop a new explosive device for use in rocket combustor stability rating tests and to evaluate the performance of the device over a wide range of operating conditions. Evaluation tests were conducted with two different liquid propellant combinations at a chamber pressures up to 300 psia (2070 kN/m^2 abs) and thrusts up to 20,000 pounds (89 kN). Results proved that a 30 caliber machine gun was successful in perturbing the combustion environment and in many cases initiated high frequency combustion instability. Characteristics of explosively induced pressure perturbations were related to operating conditions of the gun and combustor. It was concluded that inducing a perturbation through a single port, as compared with a multiport bomb ring, enhanced the ability to interpret the measured perturbation characteristics. Author

N69-25312*# National Aeronautics and Space Administration. Lewis Research Center, Cleveland, Ohio.

SIMPLE EQUATIONS FOR CALCULATING TEMPERATURE DISTRIBUTIONS IN RADIATING GRAY GASES

Robert G. Ragsdale and Albert F. Kascak Washington May 1969 41 p refs

(NASA-TN-D-5226) Avail: CFSTI CSCL 20M

Algebraic equations are presented for the temperature distribution in a radiating gray gas. The equations are in good agreement with exact solutions for the entire range of opacities for a constant absorption coefficient and uniformly distributed heat sources, for spherical, cylindrical, or slab geometries. It is shown numerically how to include a variable absorption coefficient and a nonuniform heat source distribution. Author

N69-26236*# National Aeronautics and Space Administration. Lewis Research Center, Cleveland, Ohio.

IMPULSIVE MOTION ON A FLAT PLATE PULSED WITH UNIFORM HEAT FLUX

Thomas H. Cochran and Eva T. Jun Washington May 1969 39 p refs

(NASA-TN-D-5249) Avail: CFSTI CSCL 20M

An analytical study was conducted for a semi-infinite flat plate that had fluid impulsively moved on its surface and at the same time pulsed with uniform heat flux over a prescribed length. The numerical solution, which was obtained by an implicit finite-difference method with nonuniform lattice dimensions, was compared with a solution for transient conduction in a slab and with a solution of the complete energy equation from the integral method of Karman-Pohlhausen. The solutions were confined to positions on the plate over which the flow is strictly transient and to fluids with Prandtl numbers greater than 1. Author

N69-26247*# National Aeronautics and Space Administration. Electronics Research Center, Cambridge, Mass.

THERMODYNAMIC PROPERTIES OF LIQUID H_2O AND D_2O AND THEIR MIXTURES

Mark Solomon Washington May 1969 14 p refs

(120-34-02-01)

(NASA-TN-D-5223) Avail: CFSTI CSCL 20M

The liquid and gas phase equilibria $H_2O + D_2O = 2HDO$ have been reinvestigated. By combining spectroscopic and vapor pressure data, fairly good agreement is found between the experimental and calculated enthalpy for the liquid phase reaction. It is found that the value of the equilibrium constant for the liquid phase reaction is very close to the geometric mean value of 4.0. Author

N69-26975*# National Aeronautics and Space Administration. Marshall Space Flight Center, Huntsville, Ala.

TABLES AND GRAPHS OF FUNCTIONS NECESSARY FOR SOLVING NONLINEAR HEAT TRANSFER CONSTANT AREA FIN PROBLEMS WITH EXAMPLES ON THEIR USE

A. R. Shouman and J. W. Price Washington May 1969 490 p refs

(NASA-TN-D-5173) Avail: CFSTI CSCL 20M

The two functions describing the solution to the nonlinear constant area fin one-dimensional heat transfer problem are evaluated and presented by tables and graphs. The use of the tables and graphs is demonstrated by considering several sample problems. Author

N69-27620*# National Aeronautics and Space Administration. Lewis Research Center, Cleveland, Ohio.

VENTING OF LIQUID HYDROGEN TANKAGE

John C. Aydelott and Charles M. Spuckler Washington Jun. 1969 36 p refs

(NASA-TN-D-5263) Avail: CFSTI CSCL 07D

A 22-in. diameter spherical tank partially filled with liquid hydrogen was subjected to three venting tests. Two of the tests were conducted with uniform heating of the tank and the third with top heating only. The experimentally determined venting rates were compared with theoretically predicted venting rates equal to the energy input divided by the heat of vaporization. Each experimental venting rate was much less than the corresponding theoretically predicted venting rate. The difference between the theoretical and experimental results was concluded to be primarily caused by the super-heating of the venting vapor, an effect that is commonly neglected in the analysis of venting cryogenic tanks. Author

N69-28209*# National Aeronautics and Space Administration. Langley Research Center, Langley Station, Va.

AN EXPERIMENTAL AND ANALYTICAL INVESTIGATION OF BALLOON-TYPE ENCLOSURES FOR THERMAL CONTROL OF SATELLITES

George E. Sweet Washington Jun. 1969 55 p refs

(NASA-TN-D-5230) Avail: CFSTI CSCL 20M

An experimental and analytical investigation of balloon-type thermal-control enclosures for satellites indicates that payload temperature uniformity is 1 to 2 orders of magnitude better than that for an unprotected satellite. Both analytical and measured results indicate that low-mittance interior and exterior enclosure surfaces provide the most uniform temperatures for an enclosed payload. High-emittance interior surfaces, on the other hand, would result in the most uniform temperatures for the enclosure walls. Model tests indicate that temperature uniformities of 5°K to 10°K are feasible for a small, solid, nonconducting payload located near the center of the enclosure. Tests of a telescope-balloon model indicated that the temperature uniformity of the uninsulated telescope cylindrical shell was about 0.5°K. Experimental results also indicated that the temperature uniformity of surfaces near the center of the enclosure are insensitive to satellite orientation and changes in simulated payload heat dissipation. Calculated results indicate that a double-wall balloon with closely spaced walls would provide appreciably better temperature uniformity than a single-wall balloon. A method for constructing a double-wall icosahedron enclosure is described. Author

N69-28318*# National Aeronautics and Space Administration. Lewis Research Center, Cleveland, Ohio.

FILM BOILING FROM SUBMERGED SPHERES

Robert C. Hendricks and Kenneth J. Baumeister Washington Jun. 1969 68 p refs

(NASA-TN-D-5124) Avail: CFSTI CSCL 20M

The energy and momentum equations are solved analytically to predict the heat transfer coefficient of small submerged spheres in film boiling. The analysis is based on the postulate that the rate of entropy production is maximized. In addition, the small sphere theory is matched with the film-boiling correlation for flat plates to give a heat transfer correlation which applies for large, as well as small, spheres. Author

N69-28440*# National Aeronautics and Space Administration. Langley Research Center, Langley Station, Va.

A STUDY OF THE PERFORMANCE OF LOW-DENSITY PHENOLIC-NYLON ABLATORS

James N. Moss and William E. Howell Washington Jun. 1969 44 p refs

(NASA-TN-D-5257) Avail: CFSTI CSCL 20M

The ablative effectiveness of some of the low density (160 to 320 kg/m^3) materials was about 1.5 times that of a 580 kg/m^3 phenolic–nylon ablator. Furthermore, it was found that a 220 kg/m^3 ablator provided high ablative effectiveness while maintaining good structural char integrity when exposed to a range of test conditions that included most environmental conditions experienced by a manned lifting-body entry vehicle. In addition, an analysis was made of the mass requirements for an ablative heat shield of a blunted half-cone entry vehicle (one-half of a 13° half-angle cone). The analysis shows that the mass of ablative heat shield required is strongly dependent on the entry attitude, decreasing with increasing angle of attack. A 34-percent reduction in the total mass of the ablative heat shield may be obtained by using a phenolic–nylon ablator with a density of 220 kg/m^3 rather than one with a density of 580 kg/m kg/m^3. Author

N69-29598*# National Aeronautics and Space Administration. Lewis Research Center, Cleveland, Ohio.

THREE-PHASE HEAT TRANSFER: TRANSIENT CONDENSING WITH FREEZING ON A NONISOTHERMAL INCLINED PLANE

William A. Olsen, Jr. and Frank B. Molls Jun. 1969 55 p refs

(NASA-TN-D-5289) Avail: CFSTI CSCL 20M

The transient phase change process that occurs when a vapor contacts a very cold inclined plate is analyzed. The vapor condenses to form a growing liquid layer that flows down the plate. Below this two phase region there is a three phase region where the thickening condensate layer flows over a growing frozen layer. Heat and mass are transferred across moving phase boundaries. The solution involves the Karmen–Pohlhausen method which results in quasi-linear partial differential equations for the phase thicknesses that are solved by characteristic and finite difference methods. Numerous two phase special cases are also discussed. Author

N69-29599*# National Aeronautics and Space Administration. Langley Research Center, Langley Station, Va.

EXPLORATORY STUDY OF OPEN-FACE HONEYCOMB TO REDUCE TEMPERATURE OF HYPERSONIC AIRCRAFT STRUCTURE

L. Roane Hunt and R. R. Howell Washington Jul. 1969 24 p refs

(NASA-TN-D-5278; L-6383) Avail: CFSTI CSCL 20M

An exploratory study was conducted in the Mach 7 pilot tunnel to determine the effectiveness of open-face honeycomb structure as a means of reducing the temperature of a hypersonic aircraft structure. The wind tunnel tests were conducted at a unit Reynolds number of 9 × 10^5 per foot (3 × 10^6 per meter), a Mach number of 7.0, a stagnation temperature of 3400°R (1890°K), and angles of attack from 0° to 10°. The results indicate that for zero angle of attack the steady state temperatures of the surfaces beneath open-face honeycomb structure were 0.82 to 0.88 of a smooth reference surface under the same conditions. Author

N69-30064*# National Aeronautics and Space Administration. Lewis Research Center, Cleveland, Ohio.

TEST OF SODIUM BOILING IN A SINGLE TUBE-IN-SHELL HEAT EXCHANGER OVER THE RANGE 1720° TO 1980° F (1211 to 1355 K)

James P. Lewis, Donald E. Groesbeck, and Harold H. Christenson Washington Jul. 1969 129 p refs

(NASA-TN-D-5323) Avail: CFSTI CSCL 20M

Sodium was boiled in a vertical 1/2-inch inside diameter by 4-foot long tube. The columbium alloy boiler operated at flow rates of 75 to 380 lbm/hr and up to 0.93 quality. Boiling performance depended on whether the inlet flow was two-phase or liquid. Two phase momentum pressure drops were 1-1/2 times frictional drops. Qualities over 0.9 were obtained at some critical (burnout) boilimg conditions. Liquid superheats up to 250°F existed before initiation of boiling. Author

N69-30245*# Scripta Technica, Inc., Washington, D.C.

TRANSIENT TEMPERATURE FIELDS IN SHELLS

M. D. Mikhaylov NASA Jun. 1969 98 p refs Transl. into ENGLISH of the book "Nestationarnyye Temperaturnyye Polya V Obolochkakh" Moscow, Energiya Press, 1967

(Contract NASw-1694)

(NASA-TT-F-552) Avail: CFSTI CSCL 20M

The monograph discusses the theory of transient one-dimensional heat conduction processes occurring in plane one- and two-layer plates at various boundary conditions on the skin and the heat-resistant coating. Solutions are given for transient temperature fields in porous walls cooled by a forced flow of a cooling medium. Formulas for determining thermal stresses are also given. Detailed tables of the roots of characteristic equations and initial temperature amplitudes facilitate the use of these equations in practical computation. The solutions may be applied to designing heat shields in aircraft and rockets, or to other branches of engineering. Author

N69-30317*# National Aeronautics and Space Administration. Lewis Research Center, Cleveland, Ohio.

THERMAL RADIATION HEAT TRANSFER. VOLUME 2: RADIATION EXCHANGE BETWEEN SURFACES AND IN EXCLOSURES

John R. Howell and Robert Siegel Washington 290 p refs

(NASA-SP-164-Vol-2) Avail: SOD $1.50; CFSTI CSCL 20M

A theory was developed for computing thermal radiation within enclosures. An enclosure is defined as an envelope of solid surfaces or open areas which completely surround a surface. By considering the radiation going from the surface to all parts of the enclosure, and the radiation arriving at the surface from all parts of the enclosure, it is assured that all the radiative contributions are accounted for. It is assumed that the medium in the space between the surfaces is perfectly transparent and does not participate in the radiative interchange. The main topics of discussion are: (1) exchange of radiant energy between black isothermal surfaces, (2) radiation exchange in an enclosure composed of diffuse-gray surfaces, (3) radiation in enclosures having some specularly reflecting surfaces, (4) the exchange of thermal radiation between nondiffuse nongray surfaces, (5) the Monte Carlo approach to radiant interchange problems, and (6) radiation in the presence of other modes of energy transfer. For Volume 1, see N68-28530. E.C.

33 THERMODYNAMICS AND COMBUSTION

N69-30507*# Scripta Technica, Inc., Washington, D.C.
LIQUID METALS
P. L. Kirillov, ed., et al NASA May 1969 474 p refs Transl. into ENGLISH of the book "Zhidkiye Metally" Moscow, at Atomizdat., 1967 p 1–446
(Contract NASw-1694)
(NASA-TT-F-522) Avail: CFSTI CSCL 20M

Problems pertaining to the development of fast neutron reactors are discussed in terms of heat transfer in round, annular, and square channels; heat transfer and fluid dynamics of intricately-shaped passages; boiling and condensation of metals; and techniques of working with liquid metals. For individual titles, see N69-30508 through N69-30548. M.G.J.

N69-30726*# National Aeronautics and Space Administration. Langley Research Center, Langley Station, Va.
DATA-REDUCTION TECHNIQUE FOR DETERMINING RAPIDLY RISING HEATING RATES TO THERMALLY THICK WALLS
James L. Dillon, Robert L. Wright, and G. Louis Smith Washington Jul. 1969 28 p refs
(NASA-TN-D-5309) Avail: CFSTI CSCL 20M

The integral method of determining aerodynamic heat flux from temperatures measured at four locations within a thermally thick wall was analyzed for rapidly rising heating rates and large thermal as well as physical thicknesses. A restricted-exponential function was developed for curve fitting the four values of $c_w(T)\frac{\partial T}{\partial t}$ through the wall (where c_w denotes specific heat of wall material; T, temperature; and t, time). The restricted-exponential function more accurately describes the variation of $c_w(T)\frac{\partial T}{\partial t}$ through the wall than the previously used polynomial curve fit and improves the accuracy of the integral heating method for determining rapidly rising heating rates to walls of large thermal thickness (large temperature gradients through the wall). Results are presented for simulated flight measurements for both smooth temperature data and scattered temperature data (standard deviation of 150° R_n or 8.3°K) for two arrangements of sensor locations through the wall. Author

N69-31869*# National Aeronautics and Space Administration. Lewis Research Center, Cleveland, Ohio.
THE USE OF ENERGY THICKNESS IN PREDICTION OF THROAT HEAT TRANSFER IN ROCKET NOZZLES
Robert W. Graham and Donald R. Boldman Washington Jul. 1969 31 p refs
(NASA-TN-D-5356) Avail: CFSTI CSCL 20M

Boundary layer profile measurements in the convergent portion of a convergent–divergent nozzle have verified that the thermal layer is much thicker than the velocity layer. This observation supports the use of the integral energy boundary layer analysis in estimating heat transfer at the throat of a nozzle. An approximate integral-energy method is proposed which will enable gas-side, throat heat transfer predictions to be made without the aid of a large computer. The method was tested over a range of nozzle geometries (area contraction ratios, 4 to 19) and temperature ratios (wall to gas ratios from 0.25 to 0.85). Author

N69-31947*# Aztec School of Languages, Inc., Acton, Mass. Research Translation Div.
BOUNDARY LAYER AND CHEMICAL REACTIONS
B. V. Alekseyev Washington NASA Jul. 1969 123 p refs Transl. into ENGLISH of the book "Pogranichnyy Sloy S Khimicheskimi Reaktsiyami" Moscow, Acad. of Sci. Computer Center, 1967
(Contract NASw-1692)
(NASA-TT-F-549) Avail: CFSTI CSCL 20M

Problem formulation and the numerical solution to equations of a chemically nonequilibrium boundary layer are presented. All the numerical calculations have been made from a sample of heatprotective carbon. The numerical results obtained by calculating the frozen and equilibrium boundary layer are also compared with the results of calculating the chemically nonequilibrium boundary layer. The effect from a model of molecular reactions on the parameters of the boundary layer and the discrepancies in the experimental data with respect to the pressure of saturated carbon vapors are studied. In the calculations the final reaction rate on the surface of the covering and in the pores of the material have been considered. In making the numerical calculations, formulas and numerical values for the transfer coefficients, and the chemical reaction constant were used. Author

N69-32340*# National Aeronautics and Space Administration. Lewis Research Center, Cleveland, Ohio.
EFFECT OF INJECTION ELEMENT RADIAL DISTRIBUTION AND CHAMBER GEOMETRY ON ACOUSTIC MODE INSTABILITY IN A HYDROGEN OXYGEN ROCKET
John P. Wanhainen and C. Joe Morgan Washington Aug. 1969 45 p refs
(NASA-TN-D-5375) Avail: CFSTI CSCL 20M

An experimental investigation of both 20,000- and 50,000-pound- (89- and 222-kN) thrust engines with concentric tube injectors was conducted to determine the effect of variations in injection element radial distribution, thrust chamber diameter and thrust chamber axial flow area on tangential-acoustic-mode stability characteristics. These characteristics were evaluated by determining the hydrogen injection temperature below which combustion was unstable. An annulus, void of injection elements, at the perimeter of the injector, was found to be detrimental to stability. A generalized response factor model was used in the analysis of the experimental results. Author

N69-32468*# National Aeronautics and Space Administration. Lewis Research Center, Cleveland, Ohio.
STABILITY AND PERFORMANCE CHARACTERISTICS OF SEVERAL HYDRAZINE AND NITROGEN TETROXIDE HOT GAS GENERATORS FOR LARGE SCALE SUPERSONIC COMBUSTOR TESTING
John P. Wanhainin and David W. Vincent Washington Aug. 1969 36 p refs
(NASA-TM-X-1845) Avail: CFSTI CSCL 21E

Performance and stability characteristics of seven different injectors utilizing injection types of like-on-like doublet elements, a combination of like-on-like doublet and showerhead elements, oxidant-fuel-oxidant triplet elements, and a combination of pentad and triplet elements were investigated in 20,000-lb (89-kN) thrust engines. A baffle configuration and two different liner configurations were employed to provide additional stability margin to the basic combustors. The like-on-like doublet or the like-on-like doublet and shower-head element injectors were the only configurations that were statically stable. Acoustic liners provided some dynamic stability. Author

N69-32683*# National Aeronautics and Space Administration. Lewis Research Center, Cleveland, Ohio.
DESIGN STUDIES ON THE EFFECT OF ORIENTATION, LUNATION, AND LOCATION OF THE PERFORMANCE OF LUNAR RADIATORS
Thomas Dallas, Anthony J. Diaguila, and James F. Saltsman Washington Aug. 1969 40 p refs
(NASA-TM-X-1846) Avail: CFSTI CSCL 20M

Calculations were made to study the performance of a vertical and horizontal positioned radiator on the moon's surface. The effects of orientation, lunation, and location of the heat-rejection rate of the radiator were observed. Author

N69-33314*# National Aeronautics and Space Administration. Lewis Research Center, Cleveland, Ohio.
ANALYSIS OF TOTAL-PRESSURE LOSS AND AIRFLOW DISTRIBUTION FOR ANNULAR GAS TURBINE COMBUSTORS
Robert R. Tacina and Jack Grobman Washington Aug. 1969 44 p refs
(NASA-TN-D-5385) Avail: CFSTI CSCL 21H

A computer program was used for the analysis of the annular gas turbine combustor, and the effects of a number of geometric and flow variables on the total pressure loss and airflow distribution. The results, where comparable, agree very well with previously calculated tubular combustor data. The following are significant extensions to the previously available data: (1) an increased range of open hole area in the dome, (2) combined effect of reference Mach number and heat release, (3) the use of a liner hole with a scoop and, (4) the use of a liner in which the cross sectional area varies with length. Author

N69-34892*# National Aeronautics and Space Administration. Lewis Research Center, Cleveland, Ohio.
SOLID-PROPELLANT COMBUSTION INSTABILITY AND THE ROLE OF VELOCITY COUPLING
Louis A. Povinelli Washington Aug. 1969 50 p refs
(NASA-TN-D-5395) Avail: CFSTI CSCL 21B

This report is concerned with the role of pressure and velocity coupling in solid propellant combustion instability. The status of knowledge is reviewed, including current efforts directed toward improving propellant response theory. Recent work on driving mechanisms indicates the importance of velocity on the coupling process. The advantages and disadvantages of using the vortex burner and the T-burner for making response measurements are discussed. New results from the vortex burner are presented, regarding the effect of burning rate catalyst and aluminum oxide on the occurrence and severity of combustion instability. The relevance of the research results to rocket motors is discussed. Author

N69-34966*# National Aeronautics and Space Administration. Langley Research Center, Langley Station, Va.
CHEMICAL EQUILIBRIUM OF ABLATION MATERIALS INCLUDING CONDENSED SPECIES
C. W. Stroud and Kay L. Brinkley Washington Aug. 1969 41 p refs
(NASA-TN-D-5391) Avail: CFSTI CSCL 20M

A computer program for calculating the multiphase chemical equilibrium of an arbitrary system is described and the complete program is included as an appendix. This program was used to calculate the chemical equilibrium of low-density phenolic nylon over a wide range of conditions. The effects of including carbon in the condensed phase on equilibrium composition and ablative performance are discussed. Methods for incorporating the improtant effects of chemical equilibrium into ablation analyses are described. Author

N69-35508*# National Aeronautics and Space Administration. Lewis Research Center, Cleveland, Ohio.
EXPERIMENTAL MEASUREMENTS OF EXPANDING STORABLE-PROPELLANT PRODUCTS SIMULATED BY COMBUSTION OF GASEOUS REACTANTS
Robert Friedman, Raymond E. Gaugler, and Erwin A. Lezberg Washington Sep. 1969 26 p refs
(NASA-TN-D-5404) Avail: CFSTI CSCL 21B

The storable system, 50-weight-percent unsymmetrical dimethylhydrazine and 50-percent hydrazine fuel with nitrogen tetroxide oxidizer, was simulated by combustion of hydrogen and methane with oxygen-enriched air in order to focus attention on the non-equilibirium expansion process. Static temperatures and pressures for the expanding combustion products, simulating a storable propellant equivalence ratio range of 0.9 to 1.4, were measured in a 5.6-area-ratio conical nozzle. Temperatures were nearly independent of oxidant-fuel ratio and were close to those calculated for frozen-expansion and kinetic analyses. Author

N69-35516*# Philco-Ford Corp., Newport Beach, Calif.
EVALUATION OF CONFIGURATION CHANGES ON OPTIMUM STRUCTURAL DESIGNS FOR A MARS ENTRY CAPSULE
Gerald A. Cohen Washington NASA Aug. 1969 51 p refs
(Contract NAS1-5554-5)
(NASA-CR-1414) Avail: CFSTI CSCL 20K

Optimum structural designs for Martian entry capsules are obtained for 140° blunted cone, 60° spherical dish, and 0A.65 tension shell configurations. These designs have 19 foot base diameters and are based on theoretical pressure and convective heat transfer distributions for orbit mode entry with a ballistic coefficient of 0.32 slug/Ft $^{.2}$ Author

N69-35949*# National Aeronautics and Space Administration. Flight Research Center, Edwards, Calif.
EVALUATION OF AN INFRARED HEATING SIMULATION OF A MACH 4.63 FLIGHT ON AN X-15 HORIZONTAL STABILIZER
Rodger A. Fields and Andrew Vano Washington Sep. 1969 35 p refs
(NASA-TN-D-5403) Avail: CFSTI CSCL 20M

Temperatures recorded on the X-15 horizontal stabilizer during a Mach 4.63 flight were simulated in the laboratory. A liquid-nitrogen evaporative cooler was used to cool the structure to a prelaunch condition; the heating was provided by an infrared heating system with closed-loop control. The simulated flight produced temperatures from approximately -05° F (228° K) to 750° F (672° K). The simulation was evaluated by comparing flight-measured temperatures with those measured during the simulation. Author

N69-36299*# National Aeronautics and Space Administration. Langley Research Center, Langley Station, Va.
A PROCEDURE FOR RAPID COMPUTATION OF EQUILIBRIUM CHEMICAL COMPOSITION AND THERMODYNAMIC PROPERTIES OF THE GENERALIZED ARGON-NITROGEN-OXYGEN-HYDROGEN GAS SYSTEM
Vincent R. Mascitti Washington Sep. 1969 32 p refs
(NASA-TN-D-5416) Avail: CFSTI CSCL 20M

A procedure is described for the rapid computation of the equilibrium chemical composition and thermodynamic properties of the generalized argon-nitrogen-oxygen-hydrogen gas mixture system for non ionized conditions. The procedure employs a variation of the Newton iteration scheme to solve for chemical composition. The generalized model reduces to the hydrogen-air, hydrogen-oxygen, pure hydrogen, and equilibrium air systems. A computer program listing of the calculation procedure for this gas model is presented. Author

N69-36701*# National Aeronautics and Space Administration. Lewis Research Center, Cleveland, Ohio.
HEAT-TRANSFER CHARACTERISTICS OF A WATER-TO-CRYOGENIC-HYDROGEN HEAT EXCHANGER
Walter F. Weiland, Jr. and Donald W. Adams Washington Sep. 1969 32 p refs
(NASA-TN-D-5429) Avail: CFSTI CSCL 20M

Heat-transfer and pressure drop measurements were obtained for a heat exchanger suitable for regeneratively cooling the water in a water-moderated nuclear rocket reactor. The heat exchanger was of shell-and-tube design having parallel fluid flow with cryogenic hydrogen inside the tubes. The ranges of conditions investigated for steady-state operation are inlet water temperature from 600°

to 660° R, inlet hydrogen temperature from 100° to 180° R, inlet fluid pressure of approximately 700 psia, and flow in the turbulent region. The investigation included conditions where ice is expected to be formed on the tubes. The results are compared with predicted values. The transient conditions investigated simulated expected conditions during reactor startup. Author

N69-36806*# National Aeronautics and Space Administration. Lewis Research Center, Cleveland, Ohio.

COMPARISON OF PREDICTED NOZZLE COLLANT SIDE HEAT TRANSFER AND FLUID FLOW WITH EXPERIMENTAL VALUES FROM PHOEBUS-2A NUCLEAR TESTS

Maynard F. Taylor Washington Sep. 1969 18 p refs
(NASA-TM-X-1881) Avail: CFSTI CSCL 20M

A recently reported method of predicting heat-transfer coefficients for the extreme conditions encountered in the cooling passages of regeneratively cooled nuclear rocket nozzles is used to predict pressures and temperatures at 34 stations in the Phoebus 2A nozzle. The predicted pressure and temperatures at the exit of the cooling passages are compared with the measured values of EP-IV nuclear tests and found to be in very good agreement. Incremental values of coolant temperatures and pressures, coolant passage wall temperatures, and heat flux to the coolant are calculated and shown. It is shown that a constant C_g of 0.026 yields values for coolant exit pressure and temperature that are in very good agreement with measured values. Author

N69-37936*# National Aeronautics and Space Administration. Lewis Research Center, Cleveland, Ohio.

THERMODYNAMIC AND TRANSPORT PROPERTIES OF AIR AND THE COMBUSTION PRODUCTS OF NATURAL GAS AND OF ASTM-A-1 FUEL WITH AIR

David J. Poferl, Roger A. Svehla, and Kenneth Lewandowski Washington Oct. 1969 52 p refs
(NASA-TN-D-5452) Avail: CFSTI CSCL 20M

The ratio of specific heats, molecular weight, viscosity, specific heat at constant pressure, thermal conductivity, and Prandtl number were calculated for air, the combustion products of natural gas and air, and the combustion products of ASTM-A-1 jet fuel and air. These properties were calculated for temperatures from 300 to 2500 K, pressures of 3 and 10 atm (3.04×10^5 and 10.03×10^5 N/m^2), and fuel-air ratios from zero to stoichiometric. Adiabatic combustion temperatures were also determined. The theoretical data for thermal conductivity and Prandtl number were compared with experimental values of these properties available in the literature. Agreement between the theoretical and experimental data was within 5 percent. Author

N69-38271*# National Aeronautics and Space Administration. Langley Research Center, Langley Station, Va.

SIMULATION OF PYROLYSIS-GAS FLOW THROUGH A CHAR LAYER DURING ABLATION

Ronald K. Clark Washington Oct. 1969 38 p refs
(NASA-TN-D-5464) Avail: CFSTI CSCL 20M

An experimental study was made to provide some insight into the complex thermochemical phenomena occurring during the flow of pyrolysis gases through an ablator char layer. Resistance-heated porous carbon slabs were used to simulate ablator char layers, and mixtures of methane and helium, simulating pyrolysis gases, were passed through the heated carbon. Tests were made with carbon temperatures up to approximately 3800°R (2100 K) with various mass flow rates, methane concentrations, and carbon thicknesses for two different porosities. Temperatures of the entrance and exit surfaces of the carbon were measured, and gas temperatures and temperature profiles through the carbon were calculated by a simplified analysis. Gas samples were taken at the exit surface of the carbon and analyzed to determine the hydrogen mole fraction which was used as an index to the extent of gas-phase reactions. Postexposure metallographic analyses of the carbon specimens were made to investigate the deposition of carbon in the specimen voids. Principal conclusions from this study are (1) the methane reacts to form hydrogen, solid carbon, and traces of ethylene and acetylene; (2) a transition region of small temperature range exists below which the gas composition is frozen and above which the composition is in chemical equilibrium; (3) the transition region occurs at lower temperatures with greater carbon internal areas; (4) significant amounts of laminar-type carbon, not resulting from gas-phase reactions, were deposited in the specimen voids; and (5) the gas and solid temperatures apparently did not equilibrate until the gases approached the exit surface of the carbon. Author

N69-40356*# National Aeronautics and Space Administration. Langley Research Center, Langley Station, Va.

A METHOD OF INTEGRAL RELATIONS SOLUTION FOR RADIATING, NONADIABATIC, INVISCID FLOW OVER A BLUNT BODY

John T. Suttles Washington Oct. 1969 60 p refs
(NASA-TN-D-5480) Avail: CFSTI CSCL 20D

An approximate computational scheme was developed in which a method of integral relations is used to calculate the radiating, nonadiabatic, inviscid flow field for a blunt body reentering the earth's atmosphere. The method was applied for a one-strip approximation with an equilibrium-air gas model. A radiation model was used which takes into account the frequency dependence of the radiation, self-absorption by the gas, and atomic-line radiation as well as the important continuum radiation processes. Results calculated by the method are presented for a sphere at conditions representative of an earth reentry of a manned vehicle from an interplanetary mission. These results show general features for a radiating, nonadiabatic flow which are in agreement with other reported results. It is also shown that the radiative heat fluxes on the surface of a sphere, nondimensionalized with the stagnation-point value, are relatively insensitive to both nonadiabatic effects and body size. In addition, adiabatic results are presented which show that the large overpredictions of stagnation-point tangential-velocity gradient, which have been found in solutions by other methods of integral relations, have been avoided. Author

N69-40437*# National Aeronautics and Space Administration. Lewis Research Center, Cleveland, Ohio.

PENETRATION MODEL EXPLANATION FOR TURBULENT FORCED-CONVECTION HEAT TRANSFER OBSERVED IN NEAR-CRITICAL FLUIDS

Robert W. Graham Washington Oct. 1969 31 p refs
(NASA-TN-D-5522) Avail: CFSTI CSCL 20M

The traditional steady-state model of turbulent convection in a thermal boundary layer has been modified to include a nonsteady penetration component of heat transfer. The penetration mechanism is assumed to result from appreciable changes in the specific volume of local agglomerates of fluid near the wall under heating conditions. In some respects the penetration mechanism is similar to boiling. The overall model has been applied to forced convection of several fluids near their critical thermodynamic state. Some success has been achieved in using the model to account for the differences between the experimental data and conventional turbulent flow heat-transfer correlations for variable property fluids. Author

N69-40455*# Purdue Univ., Lafayette, Ind. Thermophysical Properties Research Center.

A COMPREHENSIVE PROGRAM FOR THE COMPILATION AND ANALYSIS OF THERMAL RADIATIVE PROPERTIES DATA

D. P. De Witt, M. C. Muinzer, and R. S. Hernicz Washington NASA Sep. 1969 126 p refs
(Contract NSR-15-005-037)

(NASA-CR-1431) Avail: CFSTI CSCL 11B

The program's objectives are to identify, collect, extract and analyze data on the thermal radiative properties for general dissemination. Effort is being concentrated on the technological materials of special interest to aerospace requirements under environmental conditions likely to occur in space application. Data are presented in tabular and graphical forms with accompanying tables giving specifications for the test specimens. For each material four prime properties are identified — emittance, reflectance, absorptance and transmittance — and further grouped according to geometric conditions (hemispherical, normal and angular) and wavelength conditions (spectral, total, solar, and integrated). When sufficient evidence exists, the data was analyzed and figures of "recommended" values for specific surface and/or environmental conditions are presented. The first part of the program is nearing completion (metallic elements and alloys) and the second and third parts are now well under way. Author

N69-40780*# National Aeronautics and Space Administration. Ames Research Center, Moffett Field, Calif.

CONVECTIVE HEAT-TRANSFER RATES ON LARGE-ANGLE CONICAL BODIES AT HYPERSONIC SPEEDS

David A. Stewart and Joseph G. Marvin Washington Nov. 1969 16 p refs

(NASA-TN-D-5526) Avail: CFSTI CSCL 20M

Heat-transfer rates were measured on large-angle conical bodies with large half-angles (δ) between 50° and 90°, at angles of attack from 0° to 30°. The results at 0° angle of attack were predicted with Lees' similarity theory, using calculated flow properties at the boundary-layer edge. The calculated flow properties were obtained from Newtonian theory for the 50° cone and from a one- or two-strip solution using the method of integral relations for the other cones. At 0° angle of attack, an increase in cone angle resulted in a decrease in the heating rate over much of the body. However, high heating rates occurred at the shoulder of both the δ = 80° and δ = 90° shapes because of local pressure gradients. On the windward side of the cones, the heating rate increased with angle of attack. Author

N69-40789*# National Aeronautics and Space Administration. Lewis Research Center, Cleveland, Ohio.

CONVECTIVE HEAT-TRANSFER COEFFICIENTS FROM A SOLUTION OF THE CONDUCTION EQUATION FOR A WALL SEPARATING TWO FLUIDS, ONE HAVING AN OSCILLATING TEMPERATURE

Ronald G. Huff Washington Oct. 1969 84 p refs

(NASA-TN-D-5520) Avail: CFSTI CSCL 20M

The temperature response of a wall which separates two fluids, one having a sinusoidally oscillating temperature, has been analytically determined. The solutions show that the convective heat-transfer coefficients on both sides of the wall can be determined experimentally if a single wall temperature along with the hot fluid and coolant temperatures are known as functions of time. From traces of these temperatures, the frequency of oscillation and either the amplitude ratio or the phase lag angle between the forced fluid and wall temperatures are measured. These are used in the solutions for the coefficients. The method is particularly applicable to rocket engines. Author

34

GENERAL

Includes reports of a broad nature related to industrial applications and technology, and to basic research; defense aspects; law and related legal matters; and legislative hearings and documents.

A69-10467 *#
THE AEROSPACE STIMULUS TO TECHNOLOGICAL ADVANCE.
John L. Sloop and Mac C. Adams (NASA, Washington, D.C.).
United Nations, Conference on the Exploration and Peaceful Uses of Outer Space, Vienna, Austria, Aug. 14-27, 1968, Paper 68-95321.
20 p.

Survey of some areas in which science and technology play a vital role in the economic and social benefits of people. Particular attention is given to the accomplishments of aerospace technology. The benefits which arise from aerospace technology and the stimulus which it provides for advancing technology useful in other fields are examined. V.P.

A69-10472 *#
OVERVIEW OF SPACE APPLICATIONS PROGRAMS.
Leonard Jaffe (NASA, Office of Space Science and Applications, Washington, D.C.).
United Nations, Conference on the Exploration and Peaceful Uses of Outer Space, Vienna, Austria, Aug. 14-27, 1968, Paper 68-95437.
21 p.

Discussion of aspects of the Space Applications program - including communications and navigation, meteorology, earth resources survey, and geodesy. The objective of the U.S. Navigation and Traffic/Control program is to develop the needed space technology to provide (1) more accurate position-finding for ships and aircraft, (2) a basis for an improved means of traffic control, and (3) emergency aids. The daytime meteorological requirements are currently fulfilled by the TIROS Operational Satellite (TOS) System. Two versions of the same spacecraft are used, one to carry the Automatic Picture Transmission system and the other to carry the global cloud cover storage system called the Advanced Vidicon Camera System (AVCS). The TIROS-M, now under development, will combine the APT and AVCS systems in one single spacecraft. At the moment, there are no satellites specifically devoted to Earth Resources Survey. Current efforts are devoted to analyzing imagery and other data obtained from other spacecraft for the purpose of surveying. In geodesy, the objects of the Program are: (1) to establish a unified world datum which will permit connecting existing local datum systems within ±10 m to a common geocentric reference frame; and (2) to provide refined description of the world-wide variations of the earth's gravitational field. P.v.T.

A69-10506 *#
THE NASA UNIVERSITY PROGRAM.
Francis B. Smith (NASA, Washington, D.C.).
United Nations, Conference on the Exploration and Peaceful Uses of Outer Space, Vienna, Austria, Aug. 14-27, 1968, Paper 68-95413.
15 p.

Discussion of the major role the universities have played in developing the U.S. Aerospace programs and of their essential part in future aeronautical and space research. It is believed that mission-oriented government agencies must have a close and direct relationship with universities and that universities are dependent on this relationship to maintain a viable link with the rapidly advancing world of science and technology. Neither project-oriented nor institution-oriented research alone provides an adequate basis for productive relationships between governmental agencies and universities. The innovative approaches used by NASA through the Sustaining University Program are making possible important advancements, both in aerospace research and in the universities themselves. It is believed that the principles underlying NASA's total university program offer a sound approach to government-university relationships in a wide variety of social-political environments. P.v.T.

A69-10512 *#
THE GOVERNMENT ROLE IN TECHNOLOGY UTILIZATION PROGRAMS.
Richard L. Lesher (NASA, Washington, D.C.).
United Nations, Conference on the Exploration and Peaceful Uses of Outer Space, Vienna, Austria, Aug. 14-27, 1968, Paper 68-95313.
21 p.

Discussion of the NASA Technology Utilization Program, its goals, operation, and degree of success. This program was initiated to provide for the widest practicable and appropriate dissemination of information concerning the activities of NASA and their results. This is accomplished through numerous publications, six Regional Dissemination Centers operated by universities and research institutions, conferences cosponsored with the Small Business Administration, and other efforts. Well thought-out flexible, evolutionary technology transfer programs have proven to be the best as measured by the returns of national investment in the form of new technology. P.G.M.

A69-10515 *#
EDUCATION AND TRAINING.
Robert Jastrow (NASA, Goddard Space Flight Center, Goddard Institute for Space Studies, New York, N.Y.).
United Nations, Conference on the Exploration and Peaceful Uses of Outer Space, Vienna, Austria, Aug. 14-27, 1968, Paper 68-95809.
15 p.

Discussion of education and training in the sciences and of factors motivating students in these fields. In the U.S., according to an illuminating study by Margaret Mead and Rhoda Metraux, the general high school student has a strongly negative attitude toward science and scientists, as science involves things, not people. The same attitude has been found to exist in the UK. The typical student begins school with a lively, fresh interest in all aspects of his physical environment. But in some way, in the interval between the beginning of elementary school and the completion of secondary school, the natural scientific curiosity is extinguished. It is believed that the reason lies partly in the organization of the material. Introductory science is usually presented in separate compartments, in a watered-down version of techniques and laws useful to the research scientist. It was found that a reorganization of the traditional scientific topics under the title of "Space Science" is an excellent way to overcome this particular problem in introductory science teaching. This enables the student to see the separate fields of science as a mosaic which, viewed from a distance, forms an image of the student himself in relationship to his environment. P.v.T.

A69-10516 *#
NASA PROGRAMS AND OPPORTUNITIES FOR INTERNATIONAL COOPERATION IN SPACE.
Arnold W. Frutkin (NASA, Washington, D.C.).
United Nations, Conference on the Exploration and Peaceful Uses of Outer Space, Vienna, Austria, Aug. 14-27, 1968, Paper 68-95367.
14 p.

Discussion of the specific and substantial international programs of space cooperation which were made possible by the U.S. It is estimated that, during fiscal 1968, a total of almost $30,000,000 is being expended by cooperating nations in their portion of such activities. These programs have been extraordinarily successful and rewarding for all concerned. In virtually all cases, each start has been followed by other and growing efforts. Important scientific gains are evident. Opportunities for further cooperation exist and are being encouraged. P.v.T.

A69-10519 *#
EDUCATIONAL MATERIALS PRODUCED BY THE SPACE PROGRAM.
James V. Bernardo (NASA, Office of Public Affairs, Washington, D.C.).
United Nations, Conference on the Exploration and Peaceful Uses of Outer Space, Vienna, Austria, Aug. 14-27, 1968, Paper 68-95291. 15 p.

Study of the question of whether a sustained and long-lasting stimulus to education in the U.S. has developed in response to the space program. It is believed that scientific research and technological developments associated with space exploration have already had, and will continue to have, major effects on course content and the learning process. Unfolding developments of the space program provide a well-informed and skillful teacher many opportunities to lead pupils into the exhilarating and satisfying experience of critical thinking. The student can be led to sense and define problems for study; to state the hypotheses concerning these problems; to gather, sort, and weigh evidence available to him; to learn to distinguish assumptions from facts; and to arrive at conclusions. The teacher can present techniques and skills used by NASA scientists in interpreting data and in stating their findings on the basis of tested evidence. P.v.T.

A69-10525 *#
INTERNATIONAL LIABILITY FOR DAMAGES CAUSED BY THE LAUNCHING OF OBJECTS INTO OUTER SPACE - THEORY AND APPLICATIONS.
Paul G. Dembling (NASA, Washington, D.C.).
United Nations, Conference on the Exploration and Peaceful Uses of Outer Space, Vienna, Austria, Aug. 14-27, 1968, Paper 68-95337. 22 p.

Discussion of the necessity for developing a broad multinational consensus on criteria governing international liability for damages caused by the launching of objects into outer space. Precedents for such liability are found in existing laws, particularly those involving collisions of ships at sea. Three theoretical bases for liability are proposed: (1) the claimant state would at least be required to prove that the launching state was guilty of negligence, (2) the launching state would have the right to rebut the presumption of negligence, and (3) the claimant must persuade the appropriate court, claims commission, or adjudicating entity that the acts or omissions of the launching state were unreasonable under all of the circumstances. In determining the international obligation of a launching state to provide compensation for damages, it is felt that no duty should be owed to nationals of the launching state. P.G.M.

A69-15576 *
THE VARIOUS STAGES OF DEVELOPMENT OF ASTRONAUTICS IN THE U.S. - TECHNOLOGICAL AND ECONOMIC ASPECTS [DIE VERSCHIEDENEN ENTWICKLUNGSNIVEAUS DER RAUMFAHRT IN DEN USA - TECHNISCHE UND WIRTSCHAFTLICHE GESICHTSPUNKTE].
Wilhelm A. Mrazek (NASA, Marshall Space Flight Center, Huntsville, Ala.).
VDI Zeitschrift, vol. 110, no. 35, 1968, p. 1537-1542. In German.

Analysis of the high level of preparatory technology of American space programs. It is stressed that the hardware development for manned space travel, with its components and techniques, provides the technological level from which future space activities can be planned. A requirement for future missions is a space rescue system, but it is found that there is no economic advantage in developing recoverable individual booster stages. Low-cost, throw-away booster systems, large electrical power generators, and electrical and nuclear propulsion systems are indicated as the main areas of further development of the space program. B.H.

A69-15987 *
FEDERAL GOVERNMENT CONTRACTING - THE LEGAL DEBATE REGARDING NASA SERVICE CONTRACTS.
James M. Hollis (NASA, Manned Spacecraft Center, Houston, Tex.).
National Contract Management Journal, vol. 2, Fall 1968, p. 91-115.

Detailed exploratory analysis of complex problems engendered by the rulings of the U.S. Civil Service Commission's General Counsel and the Comptroller General in 1965 and 1968, in which they questioned the legality of certain federal support service contracts, and explanation of the government's position, insofar as the situation permits, regarding contracting out for services. In part, because the studying, bargaining, compromising, and decision making are still in process, the methodology used in the presentation is mixed - i.e., the analysis is based on research of written data, observations from participating directly in government procurement and contracting, and interviews with several individuals who are currently involved in, and concerned with the legal debate. It is considered that the general trend is toward a degree of curtailment in the federal practice of contracting out for some services, but that the situation, which is still fluid, could change drastically as a result of action by the courts, the Congress, and/or the Chief Executive. G.V.

A69-16718 *#
NASA AVIATION ELECTRONICS RESEARCH.
Richard J. Hayes (NASA, Electronics Research Center, Cambridge, Mass.).
IN: RADIO TECHNICAL COMMISSION FOR AERONAUTICS, ANNUAL ASSEMBLY MEETING, WASHINGTON, D.C., SEPTEMBER 25, 26, 1968, PROCEEDINGS. [A69-16716 05-21]
Washington, D.C., Radio Technical Commission for Aeronautics, 1968. 13 p.

Discussion of the NASA research program in electronics as it relates to civil aviation. The work carried on at various facilities is outlined. At Ames Research Center studies of all-weather landing, airborne radar zero-zero landing, and inertial navigation data correction are under way. The Electronics Research Center has undertaken a research program aimed at developing and demonstrating the key avionic system technologies that would make V/STOL aircraft all-weather operations both technically and economically feasible. Some related avionics research activities are discussed. Brief attention is given to the work of the Flight Research Center and the Langley Research Center. F.R.L.

A69-16836 *
IDEAL SAFETY SYSTEM FOR ACCIDENT PREVENTION.
Jerome Lederer (NASA, Washington, D.C.).
(Symposium on Air Safety, Southern Methodist University, Dallas, Tex., Apr. 22-24, 1968.)
Journal of Air Law and Commerce, vol. 34, Summer 1968, p. 336-342.

Consideration of the foreseeable and unforeseeable aspects of accident prevention. Practical ideals demand that the inevitable safety tradeoffs and compromises in design or operation be fully rationalized and documented on the basis of trying to prevent the more probable undesired events. Special factors cited as operating to prevent "incidents" from assuming disastrous proportions are foresight, alertness, structural integrity, training, redundancy, and organization. An ideal system for accident prevention would eliminate human error, whether it is caused individually or collectively. F.R.L.

A69-17059 *#
INTERNATIONAL BENEFITS OF COOPERATIVE TRACKING AND DATA ACQUISITION AGREEMENTS.
Gerald M. Truszynski (NASA, Washington, D.C.).
United Nations, Conference on the Exploration and Peaceful Uses of Outer Space, Vienna, Austria, Aug. 14-27, 1968, Paper 68-95912. 16 p.

Description of a 28-station global instrumentation network to provide support for a variety of international flight projects. Located in the U.S. and 14 other countries and territories, they are operated by approximately 4000 highly trained U.S. and host country personnel. These stations are linked together by a network of ground communications which provide real-time information necessary for critical decisions. Computer facilities are also provided both at the stations and at intermediate points in the communications system, as well as at the main control center, where the large amounts of data collected from flight projects are processed into usable form. Techniques for choosing station sites and personnel are reviewed, and the technical and operational criteria surrounding the location of a space tracking and data acquisition station are discussed, especially

in relation to minimizing electromagnetic interference. The design and construction of the stations is discussed, and their technical operation reviewed. The training of personnel is dealt with and the use of station equipment by host country scientists is reported. B.H.

A69-17068 *#
COOPERATION THROUGH THE EXCHANGE OF SCIENTIFIC AND TECHNICAL INFORMATION.
Melvin S. Day (NASA, Washington, D.C.).
United Nations, Conference on the Exploration and Peaceful Uses of Outer Space, Vienna, Austria, Aug. 14-27, 1968, Paper 68-95317. 9 p.

Review of the NASA scientific and technical information program for building a repository of technical data and literature to support the work of scientists, engineers, and technical managers, and for exchanging this information with other countries. The activities and

A69-22863 *#
ADAPTING SPACE PLANS TO CHANGING TIMES.
H. S. Becker (NASA, Marshall Space Flight Center, Huntsville, Ala.).
Astronautics and Aeronautics, vol. 7, Mar. 1969, p. 16, 17.

Discussion of a flexible approach to space exploration planning. It is stressed that the relationships between design features and program requirements which determine costs and schedules should be quantized. The design of new spacecraft, manned or unmanned, to exploit larger launch vehicles is recommended. It is pointed out that the time has come to take greater advantage of past experience to shorten development times, to reduce costs through fewer tests and to apply program controls truly suited to the design of the new systems. By considering only one-of-a-kind exploration-type missions, the emergence of a design technology that will make space much more significant commercially and industrially may be delayed. G.R.

A69-26978 *#
CURRENT PROGRAM AND CONSIDERATIONS OF THE FUTURE FOR EARTH RESOURCES SURVEY.
H. E. Newell (NASA, Washington, D.C.).
IN: SYMPOSIUM ON REMOTE SENSING OF ENVIRONMENT, 5TH, UNIVERSITY OF MICHIGAN, ANN ARBOR, MICH., APRIL 16-18, 1968, PROCEEDINGS. [A69-26974 12-14]
Symposium sponsored by the U.S. Navy, the U.S. Air Force, the U.S. Army, the U.S. Geological Survey, and the Department of Agriculture.
Ann Arbor, Michigan, University, Willow Run Laboratories, 1968, p. 69-75.

Summary of the progress made in using spacecraft for earth resources sensing purposes, with an assessment of current needs and problem areas. In meteorology, progress in establishing an operational satellite program has been rapid. Automatic picture transmission systems were initiated with Tiros 8 in 1963. High resolution IR imagery allowing nighttime cloud cover mapping was introduced with Nimbus 1 in 1964, and spin stabilization in sun-synchronous orbit was achieved with Tiros 10 in 1965. These advances led to the operational ESSA satellites, which are now routinely supplying meteorological data in the weather forecasting system. The oceanographic features studied and developed to the point of satellite applicability are sea surface temperature, sea state, sea ice, and marine life detection. In forestry and agriculture, seasonable and even diurnal changes in spectral signatures introduce complications. Besides, the identification of individual forest species or different crops requires different types of sensors. But there is now considerable evidence that IR photography permits early detection of diseased crop and trees. Aircraft sensing in hydrology has been used to trace fresh water discharge in salt water and pollution discharge into fresh water, largely on the basis of temperature differences identifiable by IR imagery. Similarly, IR imagery has been used to identify hot springs. Additional needs and future plans are discussed. P.v.T.

A69-30426 *
COST PLUS AWARD FEE CONTRACTING.
Gordon W. Rule (U.S. Naval Material Command, Procurement Control and Clearance Div.) and James E. Cravens (NASA, Washington, D.C.).
Defense Management Journal, vol. 5, Winter 1968-1969, p. 27-29.

Discussion of cost plus award fee (CPAF) contracting, a subjective incentive system based upon after-the-fact evaluation of overall performance effectiveness. The system was first explored in the early sixties. Various aspects of the system are discussed including the concept of the CPAF contract, practices of the defense department and NASA, efficiencies, and some isolated deficiencies found in procurement and in contract administration. G.R.

A69-32430 *
RATIONALE OF THE NASA BIOMEDICAL APPLICATIONS PROGRAM.
Melvin S. Day (NASA, Office of Technology Utilization, Houston, Tex.).
(Association for the Advancement of Medical Instrumentation, Annual Meeting, 3rd, Houston, Tex., July 1968.)
Association for the Advancement of Medical Instrumentation, Journal, vol. 3, Mar. 1969, p. 91-93.

Application of techniques developed in aeromedical research by the Biomedical Applications Team of NASA to other branches of medicine. These techniques include space miniaturization techniques applied to transmitters for cardiac sensors, methods developed originally for sterilizing spacecraft components and then applied to the sterilization of surgical rooms and instruments, and a NASA design for air bearings in rocket guidance systems, adapted for use in a large ballistocardiograph that floats a man, free of stray vibrations, while his heartbeat is measured. B.H.

A69-32654 *#
COST DATA FOR ECONOMICAL ORBITAL TRANSPORTATION SYSTEM DESIGN.
D. Grim, R. Hardy (Boeing Co., Huntsville, Ala.), and C. Rutland (NASA, Manned Space Flight Center, Huntsville, Ala.).
American Institute of Aeronautics and Astronautics, Propulsion Joint Specialist Conference, 5th, U.S. Air Force Academy, Colorado Springs, Colo., June 9-13, 1969, Paper 69-439. 9 p.
Members, $1.00; nonmembers, $1.50.

Initial results of a study to investigate the feasibility of reducing recurring cost of future space transportation systems. To realize cost reductions on future space systems, design philosophy must be oriented to emphasize cost optimization in the same way that performance optimization has been used as systems criteria in the past. The total problem of space-cost-minimization is described, and historical and extrapolated cost trends are presented. A sample cost study applied to a booster system for earth orbital logistics is discussed. Cost data are presented as a function of design configuration and operational variables. High cost elements and cost drivers are identified and related to current practices. Guidelines are derived which lead toward the goal of reducing space transportation costs with emphasis on new approaches to propulsion systems. (Author)

A69-34552 *
AERONAUTICS, ROCKETRY, AND ASTRONAUTICS.
Eugene M. Emme (NASA, Washington, D.C.).
Technology and Culture, vol. 9, July 1968, p. 436-455. 13 refs.

Review of professional programs held during the past two years dealing with developments in aeronautics, rocketry, and astronautics. These programs demonstrate the awakening of some scholarly interest in dynamic engineering areas which are still deficient in historical memoirs, and which have heretofore been left mainly to literary exploitation by commercial interests. F.R.L.

A69-35055
SPACE, TECHNOLOGY, AND SOCIETY; CANAVERAL COUNCIL OF TECHNICAL SOCIETIES, SPACE CONGRESS, 6TH, COCOA

34 GENERAL

BEACH, FLA., MARCH 17-19, 1969, PROCEEDINGS. VOLUME 2. Edited by L. E. Jones, III (Florida, University, Gainesville, Fla.). Cape Canaveral, Fla., Canaveral Council of Technical Societies, 1969. 311 p.
Price of two volumes, $20.

CONTENTS:

ADVANCED TECHNOLOGY APPLICATIONS.
PROCESS FOR THERMAL FIXATION OF ATMOSPHERIC NITROGEN. F. Maslan (Sanders Associates, Inc., Nashua, N. H.), p. 1-1 to 1-13.

POWER SYSTEMS.
LARGE SOLAR ARRAYS - THE EMERGING SPACE POWER WORKHORSE. J. E. Boretz, Sr. (TRW Systems Group, Redondo Beach, Calif.), p. 2-1 to 2-18. 16 refs. [See A69-35056 18-03]

EDUCATION.
INNOVATION AND CREATIVITY IN AVIATION AND SPACE EDUCATION. J. A. Lauderbaugh (Aerospace Technical Institute, Melbourne, Fla.), p. 3-1 to 3-4.

REMOTE SENSING OF EARTH RESOURCES.
REMOTE SENSING OF SEA SURFACE TEMPERATURE. P. K. Rao, W. R. Curtis, A. E. Strong, and E. P. McClain (ESSA, Washington, D.C.), p. 5-1 to 5-10. [See A69-35057 18-13].
A REAL-TIME FISHERIES SATELLITE SYSTEM. R. E. Stevenson (U.S. Department of the Interior, Galveston, Tex.), p. 5-11 to 5-14.
REMOTE SENSING OF EARTH RESOURCES USING MANNED SPACECRAFT. W. A. Spindell (TRW Systems Group, Redondo Beach, Calif.), p. 5-15 to 5-34. 12 refs. [See A69-35058 18-31]

MANAGEMENT.
MICROMATION AND MICROGRAPHICS. J. E. Babcock (NASA, Washington, D.C.), p. 6-1 to 6-37. [See A69-35059 18-34]

COMMUNICATIONS.
GENCOM - A GENERALIZED COMMUNICATION MODEL CONCEPT. W. V. Neisius (TRW Systems Group, Redondo Beach, Calif.), p. 7-1 to 7-10.
DATA COMPRESSION USING ORTHOGONAL FUNCTIONS. J. A. Lebo (North American Rockwell Corp., Anaheim, Calif.), p. 7-11 to 7-15. [See A69-35060 18-07]

GROUND SUPPORT SYSTEMS.
CLINICAL TOXICOLOGIC STUDIES ON FREON R FE 1301. C. H. Hine, H. W. Elliott, J. W. Kaufman, and S. Leung (Hine Laboratories, Inc.; California, University, San Francisco, Calif.), p. 8-1 to 8-4. [See A69-35061 18-05]
THE DESIGN, TESTING AND IMPLEMENTATION OF A HALON 1301 FIRE EXTINGUISHMENT SYSTEM FOR USE IN THE APOLLO/SATURN LUNAR MODULE ADAPTER AT KENNEDY SPACE CENTER LAUNCH COMPLEX 39. D. C. Weaver (Catalytic-Dow, Titusville, Fla.), p. 8-5 to 8-9. [See A69-35062 18-03]
A NEW DOCUMENTATION SYSTEM FOR THE MISSISSIPPI TEST FACILITY. R. D. Harlow (General Electric Co., Bay St. Louis, Miss.), p. 8-11 to 8-43. [See A69-35063 18-11]
CONCEPTS AND ADVANTAGES OF ADAPTABLE, INTEGRATED SPACE VEHICLE GROUND SUPPORT EQUIPMENT. F. R. Radcliffe and J. M. Ray (General Electric Co., Cape Canaveral, Fla.), p. 8-45 to 8-52. [See A69-35064 18-11]

OCEANOGRAPHY.
FISHERY OCEANOGRAPHY FROM SPACE. K. L. Drennan (U. S. Department of the Interior, Pascagoula, Miss.), p. 9-1 to 9-6.
AN OVERVIEW OF THE NAVY'S PROGRAM IN OCEAN ENGINEERING. N. T. Monney (U.S. Naval Material Command, Washington, D.C.), p. 9-7 to 9-11.

SATELLITE APPLICATIONS.
TRANSOCEANIC TRAFFIC CONTROL AND OPERATIONAL SUPPORT USING SATELLITE SYSTEMS. J. H. Craigie (TRW Systems Group, Redondo Beach, Calif.), p. 11-1 to 11-5. 7 refs. [See A69-35065 18-21]
SATELLITE COMMUNICATIONS IN THE NAVY - A LOOK BACK AND A LOOK FORWARD. L. E. Johnson (U.S. Navy, Washington, D.C.), p. 11-7 to 11-11.
ANALYSIS OF SELECTED OPPORTUNITIES FOR MANUFACTURING IN SPACE. B. W. Wahl (McDonnell Douglas Corp., Huntington Beach, Calif.), p. 11-13 to 11-29. 21 refs. [See A69-35066 18-34]
SPACE MANUFACTURING MODULES. J. R. Williams (NASA, Marshall Space Flight Center, Huntsville, Ala.), p. 11-31 to 11-48. [See A69-35067 18-31]

PANEL SESSION.
SYNOPSIS - THE APPLICATION OF SPACE AGE TECHNOLOGY TO SOCIETY'S NEEDS. L. E. Jones, III (Florida, University, Cape Canaveral, Fla.), p. 13-1 to 13-6.

PANEL SESSION.
SYNOPSIS - MANNED VS UNMANNED SPACE EXPLORATION. S. Steuer (General Electric Co., Cape Canaveral, Fla.), p. 14-1 to 14-5.

ADVANCED TECHNOLOGY APPLICATIONS. II.
A SYSTEM OF COMPUTER PROGRAMS TO CALCULATE AERODYNAMIC CHARACTERISTICS FOR MISSILES, REENTRY VEHICLES AND SPACECRAFT AT ANGLES OF ATTACK. A. J. Schwalb and H. D. Francisco (Martin Marietta Corp., Orlando, Fla.), p. 15-1 to 15-8. 7 refs. [See A69-35068 18-08]
SONOBUOY MILS (SMILS). G. R. Hamilton and M. E. Drake (U.S. Navy, Solar Station, New York, N.Y.), p. 15-9 to 15-16.

TRANSPORTATION.
THE CRISIS IN SPACE - TRANSPORTATION IN MEGALOPOLIS. R. A. Nelson (U.S. Department of Transportation, Washington, D.C.), p. 17-1 to 17-4.
AN APPLICATION OF AEROSPACE TECHNOLOGY AND SYSTEMS TO COMMERCIAL AVIATION. A. A. Paris (Radio Corporation of America, Moorestown, N.J.), p. 17-5 to 17-22. [See A69-35069 18-09]

SPIN-OFFS FROM SPACE.
NASA CONTRIBUTIONS TO MATHEMATICAL MODELING AND SIMULATION WITH APPLICATIONS OUTSIDE OF THE AEROSPACE INDUSTRY. R. H. Rea (Abt Associates, Inc., Cambridge, Mass.), p. 18-1 to 18-8.

A69-35059 * #
MICROMATION AND MICROGRAPHICS.
Jack E. Babcock (NASA, Washington, D.C.).
IN: SPACE, TECHNOLOGY, AND SOCIETY; CANAVERAL COUNCIL OF TECHNICAL SOCIETIES, SPACE CONGRESS, 6TH, COCOA BEACH, FLA., MARCH 17-19, 1969, PROCEEDINGS. VOLUME 2. [A69-35055 18-34]
Edited by L. E. Jones, III.
Cape Canaveral, Fla., Canaveral Council of Technical Societies, 1969, p. 6-1 to 6-37.

Analytical study of the use of nonimpact printing in a computer and discussion of the advantages it could offer over the conventional method. The bottleneck at the output end of the ordinary computer creates a speed imbalance which could best be avoided by microfilming with a high-speed microfilm recorder. A comparison is made with the printout method, and it is shown that a very considerable saving can result by switching to the new system.

V. P. M.

A69-35070
SPACE, TECHNOLOGY, AND SOCIETY; CANAVERAL COUNCIL OF TECHNICAL SOCIETIES, SPACE CONGRESS, 6TH, COCOA BEACH, FLA., MARCH 17-19, 1969, PROCEEDINGS. VOLUME 1.
Edited by L. E. Jones, III (Florida, University, Gainesville, Fla.).
Cape Canaveral, Fla., Canaveral Council of Technical Societies, 1969. 466 p.
Price of two volumes, $20.

CONTENTS:

FOREWORD. M. Ross (NASA, Kennedy Space Center, Fla.), p. iii.

ADVANCED TECHNOLOGY APPLICATIONS. I.
METHODS FOR DETERMINING THERMAL ACCOMMODATION COEFFICIENTS FROM FREE MOLECULE FLOW HEAT TRANSFER DATA. D. E. Klett and R. K. Irey (Florida, University, Gainesville, Fla.), p. 1-1 to 1-8. 6 refs. [See A69-35071 18-33]
THE UNFORESEEN BACKGROUND OF SPACE ACHIEVEMENTS. G. E. Lundquist (ARO, Inc., Arnold Air Force Station, Tenn.), p. 1-9 to 1-12.
COMPARISON OF MEASURED AND THEORETICAL VALUES OF ELECTRICAL CONDUCTIVITY IN A LOW DENSITY PLASMA. R. M. Boatman (Tennessee, University, Tullahoma, Tenn.), p. 1-13 to 1-19. 14 refs. [See A69-35072 18-25]
ABSORPTION OF ULTRAVIOLET RADIATION IN THE REFLECTED REGION OF A SHOCK TUBE. R. D. Evans (Florida Technological University, Orlando, Fla.), p. 1-21 to 1-25. 19 refs. [See A69-35073 18-33]

POWER SYSTEMS.
THE FUTURE OF DC BRUSHLESS MOTORS IN AEROSPACE APPLICATIONS. F. O. Simons, Jr. (Florida, University, Orlando, Fla.), p. 2-1 to 2-6. 12 refs. [See A69-35074 18-03]
NERVA - CONTRIBUTING TODAY AND TOMORROW. D. L. Ledbetter, D. C. Eaton, and L. A. Habas (Aerojet-General Corp., Sacramento, Calif.), p. 2-7 to 2-14. 17 refs. [See A69-35075 18-22]

EDUCATION.
EDUSAT - AN EDUCATIONAL TELEVISION SATELLITE SYSTEM FOR THE UNITED STATES. E. Steinhardt (Old Dominion College, Norfolk, Va.; West Virginia University, Morgantown, W. Va.), p. 3-1 to 3-8. 9 refs. [See A69-35076 18-34]
THE INFLUENCE OF SPACE EXPLORATION ON SCIENCE EDUCATION. J. V. Bernardo (NASA, Office of Public Affairs, Washington, D.C.), p. 3-9 to 3-14. [See A69-35077 18-34]
EVALUATION OF INSTRUCTIONAL MONOGRAPHS IN UNIVERSITY AND INDUSTRIAL USE. K. A. McCollom (Oklahoma State University, Stillwater, Okla.), p. 3-15 to 3-19. [See A69-35078 18-34]
THE USE OF TECHNOLOGY IN REVOLUTIONIZING ACADEMIA. P. D. Arthur (California, University, Irvine, Calif.), p. 3-21 to 3-25.
THE ROLE OF TECHNICAL SOCIETIES IN EDUCATION. R. L. Young (Tennessee, University, Tullahoma, Tenn.) and E. K. Latvala (ARO, Inc., Arnold Air Force Station, Tenn.), p. 3-27 to 3-34.
GRADUATE EDUCATION IN FLORIDA IN 1980. L. E. Grinter (Florida, University, Gainesville, Fla.), p. 3-35 to 3-37.

RELIABILITY.
STOCHASTIC FAILURE MODELS BASED UPON DISTRIBUTIONS OF STRESS PEAKS. R. L. Patterson (Florida, University, Gainesville, Fla.), p. 4-1 to 4-5. [See A69-35079 18-15]
STRESS WAVE EMISSION - AN IMPORTANT NEW TOOL FOR THE TECHNICAL COMMUNITY. A. T. Green (Aerojet-General Corp., Sacramento, Calif.), p. 4-7 to 4-17. 7 refs. [See A69-35080 18-32]
OPTIMAL RESOURCE ALLOCATION FOR MAXIMUM RELIABILITY. P. M. Ghare and R. E. Taylor (Virginia Polytechnic Institute, Blacksburg, Va.), p. 4-19 to 4-23. 12 refs. [See A69-35081 18-15]
A COST-EFFECTIVE LOOK AT SPACECRAFT COMPONENT TESTING. L. Gomberg (Radio Corporation of America, Princeton, N.J.), p. 4-25 to 4-27. [See A69-35082 18-11]
PLANNING FOR FLIGHT SYSTEM AVAILABILITY UNDER UNCERTAINTY. C. L. Proctor and R. S. Leavenworth (Florida, University, Gainesville, Fla.), p. 4-29 to 4-35. 5 refs. [See A69-35083 18-31]

REMOTE SENSING OF EARTH RESOURCES.
SATELLITE SNOW SURVEILLANCE - A DOWN-TO-EARTH USE OF SPACE TECHNOLOGY. J. C. Barnes and C. J. Bowley (Allied Research Associates, Inc., Concord, Mass.), p. 5-1 to 5-12. 11 refs. [See A69-35084 18-20]

MANAGEMENT.
THE STRUCTURE OF COMPLEX PHYSICAL PERFORMANCE. E. W. Karnes (Martin Marietta Corp., Denver, Colo.), D. Hilsendager, and T. Spiritoso (Temple University, Philadelphia, Pa.), p. 6-1 to 6-8. 8 refs. [See A69-35085 18-05]
MANAGEMENT CONTRIBUTIONS OF SPACE TECHNOLOGY - AN ANALYTICAL REPORT. J. G. Milliken (Denver, University, Denver, Colo.), p. 6-9 to 6-16. 31 refs. [See A69-35086 18-34]
THE LAUNCH-COST BOTTLENECK. R. A. Lynch (General Dynamics Corp., San Diego, Calif.), p. 6-17 to 6-25. [See A69-35087 18-31]

COMMUNICATIONS.
OPTIMUM PRE-EMPHASIS FOR FREQUENCY MODULATION APPLICATIONS. K. W. Merz (Boeing Co., Cocoa Beach, Fla.), p. 7-1 to 7-7. 12 refs. [See A69-35088 18-07]
SATELLITE COMMUNICATIONS TO MOBILE TERMINALS - A FORECAST OF NEEDS AND TECHNIQUES. Q. C. Wilson (Acton Laboratories, Inc., Acton, Mass.), p. 7-9 to 7-16. 11 refs. [See A69-35089 18-07]

GROUND SUPPORT SYSTEMS.
APPLICATION OF HALON 1301 TO THE PREVENTION OF OR EXTINGUISHMENT OF AEROZINE-50 FIRES. R. W. Van Dolah and D. Burgess (Bureau of Mines, Pittsburgh, Pa.), p. 8-1 to 8-14. [See A69-35090 18-03]

OCEANOGRAPHY.
WHY AN OCEANOGRAPHER OF THE NAVY? F. J. Ruder (U.S. Navy, Alexandria, Va.), p. 9-1 to 9-4.
SPACE OCEANOGRAPHY - APPLICATIONS AND BENEFITS. E. E. Ludwick, Jr. (General Electric Co., Bay St. Louis, Miss.), p. 9-5 to 9-35. 5 refs. [See A69-35091 18-31]

CONTROL SYSTEMS.
SENSITIVITY AND OPTIMIZATION THEORY FOR LAUNCH VEHICLE ATTITUDE CONTROL SYSTEM SYNTHESIS. W. A. Walter and F. O. Simons, Jr. (Florida, University, Gainesville, Fla.), p. 10-1 to 10-8. 5 refs. [See A69-35092 18-31]
LEARNING CONTROL SYSTEMS - REVIEW AND OUTLOOK. K. S. Fu (Purdue University, Lafayette, Ind.), p. 10-9 to 10-23. 50 refs. [See A69-35093 18-10]
ON SEPARATE COMPUTATION OF ARCS FOR OPTIMAL CONTROL PROBLEMS WITH STATE VARIABLE INEQUALITY CONSTRAINTS. W. E. Hamilton, Jr. and A. J. Koivo (Purdue University, Lafayette, Ind.), p. 10-25 to 10-29.
THE IMPACT OF BIOSCIENCES REQUIREMENTS ON BIOSATELLITE ATTITUDE CONTROL. J. D. Carpenter, E. T. Thomas (General Electric Co., Philadelphia, Pa.), and J. C. Van Ess (NASA, Ames Research Center, Moffett Field, Calif.), p. 10-31 to 10-52. 8 refs. [See A69-35094 18-31]

INFORMATION SYSTEMS.
INTERDISCIPLINARY DISSEMINATION OF AEROSPACE TECHNOLOGY - A HOLISTIC APPROACH. L. S. Berger (Southwest Research Institute, San Antonio, Tex.), p. 12-1 to 12-3.
NATIONAL CLEARINGHOUSE URBAN INFORMATION SYSTEM. H. L. Olesen (General Electric Co., Philadelphia, Pa.), p. 12-5 to 12-20.
AN ON-LINE CONVERSATIONAL INFORMATION STORAGE AND RETRIEVAL SYSTEM. A. L. Scheidegger (General Electric Co., Cape Canaveral, Fla.), p. 12-21 to 12-30. [See A69-35095 18-08]
SPACECRAFT DATA STORAGE IN THE 1970's. R. J. Treadwell (Radio Corporation of America, Princeton, N.J.), p. 12-31 to 12-35. 7 refs. [See A69-35096 18-08]

ADVANCED TECHNOLOGY APPLICATIONS. II.
AN AUTOMATED APPROACH TO PREDICTING RF SIGNAL MARGINS FOR MISSILE FLIGHT TESTS. R. H. Moody (TRW Systems Group, Cape Canaveral, Fla.), p. 15-1 to 15-9. [See A69-35097 18-07]
A SATELLITE ASSOCIATION PROCEDURE. A. G. Lubowe (Bell Telephone Laboratories, Inc., Whippany, N.J.), p. 15-11 to 15-18. [See A69-35098 18-07]
THE IMPACT OF SPEECH COMMUNICATION WITH COMPUTER. W. A. Lea (NASA, Electronics Research Center, Cambridge, Mass.), p. 15-19 to 15-31. 47 refs. [See A69-35099 18-08]

METEOROLOGY.

METEOROLOGICAL SUPPORT TO THE AIR FORCE EASTERN TEST RANGE. H. D. Turner, W. J. Czagas (USAF, Washington, D.C.), and O. H. Daniel (Pan American World Airways, Inc., New York, N.Y.), p. 16-1 to 16-4.

FREQUENCY AND DURATION OF THUNDERSTORMS IN THE CAPE KENNEDY AREA. C. J. Neumann (ESSA, Miami, Fla.), p. 16-5 to 16-21. 7 refs. [See A69-35100 18-20]

A REVIEW OF THE IMAGE DISSECTOR METEOROLOGICAL CAMERAS AND A VIEW OF THEIR FUTURE. E. W. Koenig (International Telephone and Telegraph Corp., Fort Wayne, Ind.) and G. A. Branchflower (NASA, Goddard Space Flight Center, Greenbelt, Md.), p. 16-23 to 16-41. [See A69-35101 18-14]

THE ADVANCED METEOROLOGICAL SOUNDING SYSTEM. K. Wood (Motorola, Inc., Scottsdale, Ariz.), p. 16-43 to 16-62. 7 refs. [See A69-35102 18-09]

ELECTRICAL STRUCTURE OF THE STRATOSPHERE AND MESOSPHERE. W. L. Webb (U.S. Army, Electronics Command, White Sands Missile Range, N. Mex.), p. 16-63 to 16-74. 33 refs. [See A69-35103 18-13]

TRANSPORTATION.

PLANNING FLORIDA'S TRANSPORTATION FOR THE SPACE AGE. J. Hunter (Florida Department of Transportation), p. 17-1 to 17-4.

AN OPTIMAL CONTROL ALGORITHM FOR RAMP METERING OF URBAN FREEWAYS. L. S. Yuan and J. B. Kreer (Michigan State University, East Lansing, Mich.), p. 17-5 to 17-8.

SURVEY DATA COLLECTION FOR URBAN SYSTEMS ANALYSIS. A. N. Sommers (Vitro Corporation of America, Silver Spring, Md.), p. 17-9 to 17-15.

SPIN-OFFS FROM SPACE.

SECONDARY USES OF AEROSPACE BIOMEDICAL TECHNOLOGY. T. D. Browne (Denver, University, Denver, Colo.), p. 18-1 to 18-4. 7 refs. [See A69-35104 18-34]

NASA TECHNOLOGY UTILIZATION PROGRAM. L. DuGoff (NASA, Kennedy Space Center, Cocoa Beach, Fla.), p. 18-5 to 18-30. [A69-35105 18-34]

SPACE TECHNOLOGY UTILIZATION IN AN INDUSTRIAL COMPANY - A CASE STUDY. R. A. Gaiser (Ball Brothers Co., Muncie, Ind.), p. 18-31 to 18-33.

A69-35077 *#

THE INFLUENCE OF SPACE EXPLORATION ON SCIENCE EDUCATION.

James V. Bernardo (NASA, Office of Public Affairs, Washington, D.C.).

IN: SPACE, TECHNOLOGY, AND SOCIETY; CANAVERAL COUNCIL OF TECHNICAL SOCIETIES, SPACE CONGRESS, 6TH, COCOA BEACH, FLA., MARCH 17-19, 1969, PROCEEDINGS. VOLUME 1. [A69-35070 18-34]

Edited by L. E. Jones, III.

Cape Canaveral, Fla., Canaveral Council of Technical Societies, 1969, p. 3-9 to 3-14.

Discussion of NASA efforts in striving to relate developments in space science and technology to classroom education. NASA prepares space-related instructional materials for teachers. These materials contain suggested classroom and laboratory activities and lists of selected references. They include space-related curriculum supplements for secondary schools in biology, chemistry, physics, mathematics, industrial arts, physical sciences, astronomy, and general science. Concepts, principles, and topics are chosen from standard course outlines, and from material developed from NASA's scientific and technical achievements, for use as the teacher desires.

G. R.

A69-35105 *#

NASA TECHNOLOGY UTILIZATION PROGRAM.

Lee DuGoff (NASA, Kennedy Space Center, Cocoa Beach, Fla.).

IN: SPACE, TECHNOLOGY, AND SOCIETY; CANAVERAL COUNCIL OF TECHNICAL SOCIETIES, SPACE CONGRESS, 6TH, COCOA BEACH, FLA., MARCH 17-19, 1969, PROCEEDINGS. VOLUME 1. [A69-35070 18-34]

Edited by L. E. Jones, III.

Cape Canaveral, Fla., Canaveral Council of Technical Societies, 1969, p. 18-5 to 18-30.

Survey of the program and purposes of the NASA Technology Utilization Program. It is noted that NASA has been conducting a vigorous experimental program to bring about the multiple use of the new knowledge gained as a result of activities under NASA contracts. By encouraging additional uses of this new knowledge, an additional return on the national investment is derived for the civilian economy. It is concluded that the NASA Technology Utilization Program provides a mechanism through which the rewards of aerospace technology can be shared for the benefit of all mankind.

P. G.

A69-35624 • #

MISSION ANALYSIS OF GENERAL AVIATION IN THE 1970'S.

Hubert M. Drake, George C. Kenyon, and Thomas L. Galloway (NASA, Office of Advanced Research and Technology, Mission Analysis Div., Moffett Field, Calif.).

American Institute of Aeronautics and Astronautics, Aircraft Design and Operations Meeting, Los Angeles, Calif., July 14-16, 1969, Paper 69-818. 21 p.

Members, $1.00; nonmembers, $1.50.

General aviation is expected to perform an increasingly important role in the national transportation system. The possible character of this role, as to missions, types of general aviation aircraft, and competition with other transportation modes, is examined. Assessment is made of the relative attractiveness of individual transportation modes by use of a simplified economic descriptor, time-value. The transportation system is considered for the years 1968, 1975, and 1980. The impact of advancing technology is considered, along with such economic factors as fuel taxes. General aviation is shown to be perhaps the dominant economic mode for short-haul transportation of multiple business travelers in the coming decade. Achieving and maintaining this competitive position relative to other transportation modes will require intensive research and development particularly in short field performance, overall system economics, and ease of piloting. Provision of adequate and convenient ground facilities is crucial to realizing the potential of short field aircraft. (Author)

A69-36460 *

STATUS REPORT ON SPACE MEDICINE IN THE UNITED STATES.

Charles A. Berry (NASA, Manned Spacecraft Center, Houston, Tex.). *(International Congress on Aviation and Space Medicine, 17th, Oslo, Norway, Aug. 7, 1968.)*

Aerospace Medicine, vol. 40, July 1969, p. 762-769. 8 refs.

The major challenge to the discipline of space medicine is a characterization of the nature and degree of the major changes in man's functional capabilities resulting from prolonged exposure to the space-flight environment. Project Mercury proved that man could survive brief exposures to space flight. The Gemini flights investigated man's body systems in more detail and demonstrated changes involving the red blood cell mass, cardiovascular conditioning, bone density, exercise capacity, and muscle nitrogen. None of these changes were limiting, and nature had indicated further investigation. The Apollo series has conducted some detailed pre- and postflight evaluations to further define the magnitude of these changes. The Apollo Applications Program will give the first opportunity to determine why and how some of these changes occur by providing a laboratory in space. Medical experiments programmed for the 38- and 56-day flights involve the cardiovascular system, respiratory and energy expenditure, the musculoskeletal system, neurophysiology of the vestibular system, and sleep. (Author)

A69-37102

INTERNATIONAL ASTRONAUTICAL FEDERATION, COLLOQUIUM ON THE LAW OF OUTER SPACE, 11TH, NEW YORK, N.Y., OCTOBER 17, 18, 1968, PROCEEDINGS.

Edited by M. D. Schwartz (California, University, Davis, Calif.).

South Hackensack, N.J., Fred B. Rothman and Co.; Davis, California, University, 1969. 399 p. In English, French, and Spanish.

$15.

CONTENTS:

PREFACE. M. D. Schwartz (California, University, Davis, Calif.), p. iii.

INTRODUCTION.
OPENING REMARKS. E. Pépin, p. 1.
INTRODUCTION. P. G. Dembling, p. 2-4.

INTERPRETATION OF THE SPACE TREATY.
INTRODUCTORY REPORT. E. Galloway (U.S. Library of Congress, Washington, D.C.), p. 8-23. (See A69-37103 20-34)
INTERPRETATION OF THE TERM "PEACEFUL" IN THE LIGHT OF THE SPACE TREATY. A. Meyer (Köln, Universität, Cologne, West Germany), p. 24-29. 11 refs. (See A69-37104 20-34)
THE JURIDICAL MEANING OF THE TERM "PEACEFUL" IN THE 1967 SPACE TREATY. M. G. Markov (Fribourg, Université, Fribourg, Switzerland), p. 30-35. 9 refs. (See A69-37105 20-34)
ON THE QUESTION OF INTERPRETATION OF THE TERM "PEACEFUL USE OF OUTER SPACE" CONTAINED IN THE SPACE TREATY. G. P. Zhukov, p. 36-39. (See A69-37106 20-34)
INTERPRETING ARTICLE II OF THE OUTER SPACE TREATY. S. Gorove (Mississippi, University, University, Miss.), p. 40-44. (See A69-37107 20-34)
ASPECTS OF INTERNATIONAL RESPONSIBILITY OF INTERNATIONAL SPACE ORGANIZATIONS (ASPECT DE LA RESPONSABILITE INTERNATIONALE DES ORGANISATIONS INTERNATIONALES DE L'ESPACE). H. Kaltenecker and J. Arets (Organisation Européenne de Recherches Spatiales, Paris, France), p. 45-49. (See A69-37108 20-34)
THE OUTER SPACE TREATY OF JANUARY 27, 1967, AND ITS AFTERMATH. N. M. Poulantzas (Utrecht, State University, Utrecht, Netherlands), p. 50-56. (See A69-37109 20-34)
EFFORTS TOWARD A COMPROMISE WITH RESPECT TO THE CONVENTION ON THE LIABILITY FOR DAMAGE CAUSED BY SPACE OBJECTS (LA RECHERCHE D'UN COMPROMIS EN MATIERE DE CONVENTION SUR LA RESPONSABILITE POUR LES DOMMAGES CAUSES PAR DES OBJETS SPATIAUX). J.-L. Vencatassin (Centre National de la Recherche Scientifique, Paris, France), p. 57-62. (See A69-37110 20-34)
INTERNATIONAL CONSULTATION AND THE SPACE LAW TREATIES. J. G. Verplaetse, p. 63-68. (See A69-37111 20-34)
SUMMARY OF DISCUSSIONS, p. 69-72.
AGAINST THE SO-CALLED "BROADER" INTERPRETATION OF THE TERM "PEACEFUL" IN INTERNATIONAL SPACE LAW. M. G. Markov (Fribourg, Université, Fribourg, Switzerland), p. 73-81. 16 refs. (See A69-37112 20-34)
INTERPRETATION OF THE TREATY ON OUTER SPACE. R. Mankiewicz (McGill University, Montreal, Canada), p. 82-84.

INTERPRETATION OF THE RESCUE AGREEMENT.
INTRODUCTORY REPORT, p. 85-92.
INTERPRETING SALIENT PROVISIONS OF THE AGREEMENT ON THE RESCUE OF ASTRONAUTS, THE RETURN OF ASTRONAUTS, AND THE RETURN OF OBJECTS LAUNCHED INTO OUTER SPACE. S. Gorove (Mississippi, University, University, Miss.), p. 93-97. (See A69-37113 20-34)
PROBLEMS ARISING FROM INTERPRETATION OF AGREEMENT ON RESCUE OF ASTRONAUTS, RETURN OF ASTRONAUTS AND RETURN OF OBJECTS LAUNCHED INTO OUTER SPACE. V. Kopal (Czechoslovak Academy of Sciences, Prague, Czechoslovakia), p. 98-105. (See A69-37114 20-34)
COMMENTS ON RESCUE AND RETURN OF ASTRONAUTS ON EARTH AND IN OUTER SPACE. R. C. Hall, p. 106-123. 30 refs. (See A69-37115 20-34)
INTERNATIONAL COOPERATION ON THE RESCUE OF ASTRONAUTS. G. P. Zhukov, p. 124-132. 8 refs. (See A69-37116 20-34)
SOME OBSERVATIONS ON REGISTRATION OF SPACECRAFT. I. H. Ph. Diederiks-Verschoor, p. 133-136. 7 refs. (See A69-37117 20-34)
THE NOTION OF SPACE ACTIVITY AND SOME PROBLEMS OF REGISTRATION. I. Herczeg, p. 137-139. (See A69-37118 20-34)
SUMMARY OF DISCUSSIONS, p. 140-142.

LEGAL STATUS OF STATIONS ON CELESTIAL BODIES.
INTRODUCTORY REPORT, p. 143, 144.
THE JURIDICAL PROBLEM OF A LUNAR STATION (LA PROBLEMATICA JURIDICA DE UNA ESTACION LUNAR). M. A. Ferrer, p. 145-157. (See A69-37119 20-34)
LEGAL STATUS OF NATIONAL STATIONS ON CELESTIAL BODIES. J. R. Tamm, p. 158-162.
INTERVENTIONS WITH RESPECT TO PERMANENT STATIONS ON THE MOON. R. Mankiewicz (McGill University, Montreal, Canada), p. 163-165.

TELECOMMUNICATIONS BY SATELLITES.
INTRODUCTORY REPORT, p. 166-175. (See A69-37120 20-34)
THE DEFINITIVE ARRANGEMENTS FOR INTELSAT. T. E. Donahue, Jr. (Communications Satellite Corp., Washington, D.C.), p. 176-185. (See A69-37121 20-34)
THE INTERNATIONAL TELECOMMUNICATIONS SATELLITE CONSORTIUM AND ESTABLISHED PRINCIPLES GOVERNING ACTIVITIES IN SPACE—AN ANALYSIS OF CONSISTENCY. S. E. Doyle (U.S. Department of State, Washington, D.C.), p. 186-198. (See A69-37122 20-34)
JURIDICAL STANDARDS APPLICABLE TO THE LEGAL AND COMMERCIAL EXPLOITATION OF COMMUNICATIONS SATELLITES (NORMAS JURIDICAS APLICABLES A LA EXPLOTACION LEGAL Y COMERCIAL DE SATELITES DE COMUNICACIONES). S. Estradé, p. 199-206. (See A69-37123 20-34)
SOME SUGGESTIONS CONCERNING AN ORGANIZATION FOR OUTER SPACE. T. Tabanera, p. 207-209.
REMARKS ON CERTAIN LEGAL PRINCIPLES OF BUILDING SPACE TELECOMMUNICATION SYSTEMS. V. S. Vereshchetin (Akademiia Nauk SSSR, Moscow, USSR), p. 210-213. (See A69-37124 20-34)
INTERNATIONAL COORDINATION OF DIFFERENT SPACE TELECOMMUNICATIONS SYSTEMS. R. K. Woetzel, p. 214-218. (See A69-37125 20-34)
SUMMARY OF DISCUSSIONS, p. 219-225.
INTERVENTION WITH RESPECT TO SATELLITE-TELECOMMUNICATION. R. Mankiewicz (McGill University, Montreal, Canada), p. 226, 227.

NEXT STEPS IN SPACE LAW AND OTHER SUBJECTS.
NEXT STEPS IN SPACE LAW. E. Pépin, p. 228-235. (See A69-37126 20-34)
INTERNATIONAL LIABILITY FOR DAMAGES CAUSED BY THE LAUNCHING OF OBJECTS INTO OUTER SPACE. P. B. Dembling (NASA, Washington, D.C.), p. 236-245. (See A69-37127 20-34)
SEVEN STAGES IN THE DEVELOPMENT OF SPACE LAW. C. W. Jenks, p. 246-263. 28 refs. (See A69-37128 20-34)
SURVEY AND PROSPECTS OF THE LAW OF OUTER SPACE—1968. F. W. von Rauchhaupt, p. 264-270. 6 refs. (See A69-37129 20-34)
FIELD OF APPLICATION OF SPACE LAW (LE CHAMP D'APPLICATION DU DROIT DE L'ESPACE). J.-L. Vencatassin (Centre National de la Recherche Scientifique, Paris, France), p. 271-274. (See A69-37130 20-34)
TENDENCIES AND PROSPECTS OF THE DEVELOPMENT OF SPACE LAW. G. P. Zhukov, p. 275-288. (See A69-37131 20-34)
THE LEGAL FRONTIER IN THE UNITED STATES SPACE PROGRAM. G. J. Alexander, p. 289-315. 110 refs. (See A69-37132 20-34)
lat, THE EUROPEAN SPACE CONFERENCE. M. G. Bourély, p. 316, 317.
SPACE LAW ANALOGIES FOR THE SEA-BED AND OCEAN

FLOOR. C. Q. Christol (Southern California, University, Los Angeles, Calif.), p. 318-325.

THE ROLE OF NATIONS NOT DIRECTLY ENGAGED IN SPACE ACTIVITIES IN THE CREATION OF THE PRINCIPLES OF THE NEW SPACE LAW. D. Krstic (Beograd, Univerzitet, Belgrade, Yugoslavia), p. 326, 327.

MULTIPLE USE DOCTRINES AS SPACE LAW. H. A. Shiffer (Pacific Institute of International and Space Law, Los Angeles, Calif.) and P. W. Snyders, p. 328-335. 8 refs. (See A69-37133 20-34)

A REEXAMINATION OF THE APPROACH TO SPACE LAW. S. Thomas, p. 336-338.

CONTROL AND USE OF PLANETARY RESOURCES. E. Brooks, p. 339-350. 29 refs. (See A69-37134 20-34)

CODE OF SPACE LAW (CODE DE DROIT SPATIAL). E. Monnerat, p. 351-354. (See A69-37135 20-34)

THE WORLD'S SPACE DAY. E. B. Moine, p. 355, 356.

ADDENDUM TO THE PROCEEDINGS OF THE XITH COLLOQUIUM.

VLADIMIR MANDL—FOUNDER OF SPACE LAW. V. Kopal (Československá Akademie Věd, Prague, Czechoslovakia), p. 357-361.

VLADIMIR MANDL—THE FATHER OF SPACE LAW. G. Reintanz (Halle, Universität, Halle, East Germany), p. 362-365.

OTHER INFORMATION, p. 366-370.

ROUND TABLE ON THE DETERMINATION OF THE SCIENTIFIC FACTORS FOR DEFINING OUTER SPACE, p. 371-395.

A69-37127 * #
INTERNATIONAL LIABILITY FOR DAMAGES CAUSED BY THE LAUNCHING OF OBJECTS INTO OUTER SPACE.
Paul B. Dembling (NASA, Washington, D.C.).
IN: INTERNATIONAL ASTRONAUTICAL FEDERATION, COLLOQUIUM ON THE LAW OF OUTER SPACE, 11TH, NEW YORK, N.Y., OCTOBER 17, 18, 1968, PROCEEDINGS. (A69-37102 20-34)
Edited by M. D. Schwartz.
South Hackensack, N.J., Fred B. Rothman and Co.; Davis, California, University, 1969, p. 236-245.

Examination of the criteria and procedures necessary for governing international liability for personal injury or property damage caused by the space activities of a state other than that in which the injury or damage occurred. Major problems are explored, which make it obvious that the subject is extremely complex. A large measure of international agreement has been achieved on solutions to many of the issues that have been raised. It is considered that progress in outer space depends upon the lawyers and policymakers no less than upon the scientists and engineers. F.R.L.

A69-38022 *
IN-HOUSE RESEARCH ON THE MANAGEMENT OF R&D IN GOVERNMENT AGENCIES.
William L. Williams (NASA, Langley Research Center, Hampton, Va.; George Washington University, Washington, D.C.) and Michael Radnor (Northwestern University, Evanston, Ill.).
(Institute of Management Sciences, International Meeting, 17th, Mexico City, Mexico, Aug. 22-25, 1967.)
IEEE Transactions on Engineering Management, vol. EM-16, May 1969, p. 67-71. 5 refs.
Grant No. NsG-495.

Discussion of the need for in-house R&D management research activities in government agencies. Problems of manning and training of personnel to conduct such research programs are described. Case studies of new and on-going activities are presented. The work summarizes a workshop, devoted to the subject of in-house management research activities, that was held at Northwestern University, Dec. 12, 13, 1966. Participating were representatives from a dozen governmental organizations and Northwestern. The first day explored the methods of organizing and conducting in-house studies within the various governmental organizations represented. The second day was devoted to a meeting on in-house research programs within NASA. (Author)

A69-39133 *
THE DESIGN OF A HIGHLY PARALLEL COMPUTER ORGANIZATION.
Louis J. Koczela (North American Rockwell Corp., Autonetics Div., Anaheim, Calif.) and Gary Y. Wang (NASA, Electronics Research Center, Aerospace Computer Branch, Cambridge, Mass.).
IEEE Transactions on Computers, vol. C-18, June 1969, p. 520-529. 17 refs.
Contract No. NAS 12-108.

Description of the design of a computer organization for general-purpose computing with a very high tolerance of failure while taking advantage of future large-scale integration techniques. A high degree of parallel computations may be executed. The organization distributes processing logic along with memory to form "cells." The architecture and operation of the cells are developed. Design aspects of the cells are presented along with software considerations of the organization. (Author)

A69-39581 *
OPERATING EXPERIENCE WITH NASA/SCAN—A LARGE SCALE SELECTIVE ANNOUNCEMENT SERVICE.
Van A. Wente and Gifford A. Young (NASA, Washington, D.C.).
IN: AMERICAN SOCIETY FOR INFORMATION SCIENCE, ANNUAL MEETING, COLUMBUS, OHIO, OCTOBER 20-24, 1968, PROCEEDINGS. VOLUME 5—INFORMATION TRANSFER.
New York, Greenwood Publishing Corp., 1968, p. 217-222.

Description of a new NASA current-awareness service known as SCAN (Selected Current Aerospace Notices) to promote selectivity in the transfer of information to the secondary media such as abstract journals, accession lists, and bibliographies. It is shown that an effective system would increase the selectiveness of documents offered to the individual user and cut down the time required to review the selected announcements. The characteristics of SCAN are outlined, and a typical SCAN notification listing is illustrated. A table of comparative costs at three levels of SCAN participation is presented, showing that, for a large community of users, the SCAN type of service would constitute one of the least expensive methods of information transfer now available. B.H.

A69-39686
REDUCING THE COST OF SPACE TRANSPORTATION; AMERICAN ASTRONAUTICAL SOCIETY, GODDARD MEMORIAL SYMPOSIUM, 7TH, WASHINGTON, D.C., MARCH 4, 5, 1969, PROCEEDINGS.
Edited by G. K. Chacko (TRW Systems Group, Washington, D.C.).
Tarzana, Calif., American Astronautical Society (AAS Science and Technology Series. Volume 21), 1969. 252 p.
$9.75.

CONTENTS:

PREFACE. G. K. Chacko (TRW Systems Group, Washington, D.C.), p. v, vi.

GREETINGS. G. P. Miller (U.S. Congress, Washington, D.C.), p. 1.

MESSAGE. A. D. Schnyer (NASA, Washington, D.C.), p. 3.

KEYNOTE ADDRESS. C. W. Mathews (NASA, Washington, D.C.), p. 5, 7-10.

SESSION I CHAIRMAN'S REMARKS. W. R. Hedrick, Jr. (USAF, Washington, D.C.), p. 11, 13, 14.

ECONOMIC FACTORS OF SPACE TRANSPORTATION. D. S. LeVine and R. H. Lea (Martin Marietta Corp., Denver, Colo.), p. 15-26. (See A69-39687 21-34)

LOW COST BOOSTER PROPULSION—TECHNOLOGY AND MANAGEMENT. D. M. Ross (USAF, Rocket Propulsion Laboratory, Edwards AFB, Calif.), p. 27-42. (See A69-39688 21-34)

AIRCRAFT DESIGN AND DEVELOPMENT EXPERIENCE RELATED TO REUSABLE LAUNCH VEHICLES. F. J. Dore (General Dynamics Corp., San Diego, Calif.), p. 43-69. 13 refs. (See A69-39689 21-31)

AN APPROACH TO LOW COST SPACE TRANSPORTATION.

R. R. Kearton (Lockheed Aircraft Corp., Sunnyvale, Calif.), p. 71, 73-81. (See A69-39690 21-34)

SESSION II CHAIRMAN'S REMARKS. D. R. Lord (NASA, Washington, D.C.), p. 83, 85-87.

TRANSPORTATION TO EARTH ORBIT—1975-1985. L. Roberts (NASA, Office of Advanced Research and Technology, Moffett Field, Calif.), p. 89, 91-107. (See A69-39691 21-31)

PROGRESS REPORT ON A LAUNCH VEHICLE COST BREAKTHROUGH. H. J. McClellan (Boeing Co., Houston, Tex.), p. 109-128. (See A69-39692 21-34)

REUSABLE SPACE TRANSPORTATION SYSTEMS: 1970-1980—AN EVOLUTIONARY VIEW. F. Raymes and J. I. Dodds (North American Rockwell Corp., Downey, Calif.), p. 129-131, 133-165. (See A69-39693 21-31)

COMPARISON OF SIX DESIGNS OF LOW COST LAUNCH VEHICLES. P. Dergarabedian and J. B. Kendrick (TRW Systems Group, Redondo Beach, Calif.), p. 169-200. (See A69-39694 21-31)

TOWARD EFFICIENT SHUTTLE SERVICE TO EARTH ORBIT. E. S. Love (NASA, Langley Research Center, Hampton, Va.), p. 201-220. (See A69-39695 21-31)

LOW COST ORBITAL TRANSPORTATION—HOW BIG A STEP! C. D. Marks and R. G. Quest (McDonnell Douglas Corp., St. Louis, Mo.), p. 221-241. (See A69-39696 21-34)

CONCLUDING LUNCHEON ADDRESS. W. von Braun (NASA, Marshall Space Flight Center, Huntsville, Ala.), p. 243-257.

A69-42812 * #
NEW APPROACH TO LOGISTICS MANAGEMENT.
Clifford J. Hall and Hiland Gardner (NASA, Manned Spacecraft Center, Apollo Applications Program Office, Houston, Tex.).
American Astronautical Society and Operations Research Society of America, Joint National Meeting, Denver, Colo., June 17-20, 1969, AAS Paper 69-204. 17 p.

Description of a revised logistics management system developed for the Apollo Applications Program of the NASA Manned Spacecraft Center. The management problems and constraints resulting from the interprogram activities and from common or concurrent use of equipment are discussed. Also presented are the logistics techniques evolving from system analyses, the methods derived for the application of requirements, and techniques for controlling the logistics management process. V.Z.

A69-42820 * #
PLANNING FUTURE SPACE PROGRAMS—ARE WE ON THE RIGHT TRACK?
Harold S. Becker (NASA, Marshall Space Flight Center, Advanced Projects Office, Huntsville, Ala.).
American Astronautical Society and Operations Research Society of America, Joint National Meeting, Denver, Colo., June 17-20, 1969, AAS Paper 69-083. 8 p.

Consideration of those aspects of space programs which are of particular interest to the customers—i.e., Congress, the Administration, and the general public. It must be asked whether a proposed program provides the ability to accomplish a high-value mission (one for which a high price must be paid) and whether it exploits new technical or scientific approaches providing (1) greater performance at the same cost, (2) reduced cost for the same performance, or (3) both reduced cost and increased performance. The differences between an "explorational-emotional interest" program and an "evolutionary-utilitarian" project should be better understood in each case. The maturity of the space program indicates that the time has come to apply newly designed thinking to new technological capabilities, to shorten development times, to reduce costs through fewer tests and less documentation, and to apply program controls truly suited to the designs of the new systems. F.R.L.

A69-42828 • #
NASA SPACE PROGRAM POSSIBILITIES AND UPPER STAGE IMPLICATIONS.
Bernard Maggin and Alfred Nelson (NASA, Office of Program Plans and Analysis, Washington, D.C.).
American Astronautical Society and Operations Research Society of America, Joint National Meeting, Denver, Colo., June 17-20, 1969, AAS Paper 69-359. 22 p.

The space flight missions being considered for the 1970's are reviewed to provide a basis for consideration of future launch vehicle upper stage requirements. Based on a broad examination of possible missions, it is concluded that the present stable of upper stages plus the full development of several systems under study should satisfy the missions being considered for this coming decade. It is noted that an area of interest is the "space engine" designed for the unique long term, intermittent operations in space for lunar, planetary, and interplanetary exploration, and flexible manned operations. (Author)

A69-42851 * #
SYSTEM SAFETY—A MANAGEMENT SYSTEM FOR SAFETY USED IN MANNED SPACE FLIGHT.
P. H. Bolger (NASA, Manned Space Flight Safety Office, Washington, D.C.).
American Astronautical Society and Operations Research Society of America, Joint National Meeting, Denver, Colo., June 17-20, 1969, AAS Paper 69-522. 13 p. 6 refs.

Description of the management system for safety as presently employed in NASA's Manned Space Flight Program. This system has evolved as a result of experience and lessons learned in the evolution of manned space flight over the past eight years and as the most effective way to assure the best degree of risk management or control while meeting space program objectives within cost and schedule constraints. It is used to provide for a comprehensive safety review of all phases of such programs including their flight system and manufacturing tests, and the launch and control facility activities. It further provided an accounting or reporting method to assure that hazards once identified are eliminated or controlled. The need for this management system has evolved as a result of rapid technology advances, greatly increased complexity of systems, and the vastly expanded objectives of today's programs. The conditions required for successful implementation of this system are enumerated. O.H.

A69-42930 *
ORGANIZATIONAL COMMUNICATION.
Walter Wiesman (NASA, Marshall Space Flight Center, Huntsville, Ala.).
Defense Management Journal, vol. 5, Summer 1969, p. 33-37.

Discussion of communication in governmental, industrial, and business organizations, with emphasis on the development of an internal communication program. Internal (organizational) communication is defined as the total influence of any number of diverse factors on any or all members of a workforce. Conclusions drawn from previous experience with internal communication programs are summarized. The key factors which are essential to effective communication are presented and explained. Methods of improving the internal communication system ("special interest" approaches) are discussed in detail. O.H.

N69-10662*# National Aeronautics and Space Administration, Washington, D. C.
APPLICATIONS OF SYSTEMS ANALYSIS MODELS: A SURVEY
1968 73 p Prepared for NASA by ABT Assoc. Inc.
(NASA-SP-5048) Avail: SOD $0.50 CFSTI CSCL 05A

This publication discusses the adaptation and application of know-how and methods that NASA has used to problems that continually confront management, for example, long-range planning, cost effectiveness and control, and market development. It also deals with the use of these modern techniques in urban and regional planning, and points out their potential helpfulness to city officials

and the administrators of public health, educational, and other programs. It emphasizes NASA-funded work that may be as meaningful outside the aerospace field as it has been within it. Author

N69-13159*# Texas Univ., Austin.
AN APPLICATION OF SIMILITUDE TO MODEL DESIGN OF A SOIL-PROJECTILE SYSTEM
Katsuyuki Awoshika and William R. Cox Washington NASA Nov. 1968 121 p refs
(Grant NsG-604)
(NASA-CR-1210) Avail: CFSTI CSCL 20K

A model design by means of similitude, or dimensional analysis, was made for the simulation of a space capsule landing on soils. In order to examine the validity of the model design for sands, a series of cone model tests was carried out on Ottawa Sand and Colorado River Sand. The weights of cone models were 43.0 and 129.5 pounds. The impact velocity of models was in the relatively low range of 10 to 23 fps. The validity was checked by examining the agreement of the measured variables from one of the models with the prediction of variables from the other model. The results were satisfactory. A model design law is discussed for clayey soils impacted with projectiles consisting of a circular plate, a wedge, and a sphere. The application of this model design law to vertical impact tests of a circular plate, a cone and a sphere on a clay was examined. Author

N69-18057*# University of Southern Calif., Los Angeles.
EVALUATION OF THE GODDARD RESEARCH AND ENGINEERING MANAGEMENT EXERCISE SIMULATION
A. J. Rowe, P. Gruendeman, and D. McConaughy Washington NASA Feb. 1968 97 p refs
(Grant NSR-05-018-089)
(NASA-CR-1275) Avail: CFSTI CSCL 05A

Evaluated is a computer program designed to simulate the environment of a project manager involved in research and development activities of spacecraft management. The program uses a hypothetical spacecraft project—an orbiting optical observatory—which is described in a series of technical and administrative documents. The player-participant assumes the role of a project manager and is allowed to make decisions on schedules, costs, and hardware G.G.

N69-22510*# National Aeronautics and Space Administration, Washington, D. C.
NASA SCIENCE AND TECHNOLOGY ADVISORY COMMITTEE FOR MANNED SPACE FLIGHT. WINTER STUDY ON USES OF MANNED SPACE FLIGHT, 1975–1985. VOLUME 1: PROCEEDINGS
1969 45 p Conf. held at La Jolla, Calif., 6–9 Dec. 1968
(NASA-SP-196-Vol-1) Avail: CFSTI CSCL 05A

Considered are various applications of manned space flight to scientific and technological objectives in future research. Emphasis is placed on: (1) exploration and initial colonization of the Moon; (2) exploration of Mars and other planets by manned landings; and (3) use of orbiting stations for Earth applications, astronomy, and research in the natural and life sciences. Achievement of a manned low cost transportation system and the use of a long duration manned space station develop as the most important step in the evolution of manned space flight capability. G.G.

N69-26112*# Techtran Corp., Glen Burnie, Md.
FROM A SCIENTIFIC HERITAGE
F. A. Tsander Washington NASA May 1969 101 p refs Transl. into ENGLISH of the book "Iz Nauchnogo Naslediya" Moscow, Nauka, 1967
(Contract NASw-1695)
(NASA-TT-F-541) Avail: CFSTI CSCL 03B

This collection was made up on the basis of materials from the personal archives of F.A. Tsander, which the author of this article has kept to the present day. A considerable portion of this collection consists of certain materials from the lectures and reports of Tsander in the area on interplanetary voyages. In this bibliography, the works are arranged in chronological order of their publication. In those cases when the archives of F.A. Tsander contain manuscript copies of published works, this is indicated with the date of the manuscript. B.P.

N69-28868*# Denver Univ., Colo.
TECHNOLOGY TRANSFER: A SELECTED BIBLIOGRAPHY
M. Terry Sovel Washington NASA Jun. 1969 103 p refs
(Contract NSR-06-004-063)
(NASA-CR-1355) Avail: CFSTI CSCL 05B

This is a comprehensive compilation of 428 works on the subject of technology transfer. Technology is considered here to be technical information, including scientific knowledge, making possible the conception, development, design, production, and distribution of goods and services. Transfer here means the effective communication of such information from one person or source to a recipient who accepts it for consideration and possible application. The bibliography contains chiefly primary sources, and outdated information has been eliminated. K.W.

N69-29492*# National Aeronautics and Space Administration, Washington, D.C.
NASA SCIENTIFIC AND TECHNICAL REPORTS FOR 1968. A SELECTED LISTING
May 1969 453 p refs
(NASA-SP-7033) Avail: CFSTI CSCL 05B

This publication contains a combined selective listing of NASA reports that were announced during 1968 in *Scientific and Technical Aerospace Reports (STAR)*, NASA's semimonthly announcement journal for the aerospace sciences. The documents listed were issued as part of the following NASA report series: *Special Publications* (NASA SP). *Technical Reports* (NASA TR-), *Technical Notes* (NASA TN D-), *Technical Memorandums* (NASA TM X-), *Technical Translations* (NASA TT F-), and *Contractor Reports* (NASA CR-). The listing does not include references to journal articles that were published as a result of NASA-sponsored activities. The volume has been limited to reports which were printed and widely distributed. Access to material thus omitted from this listing continues to be available through STAR and its indexes. The arrangement of this publication is the same as that of STAR. The first section contains the bibliographic citations and abstracts arranged by STAR subject categories. The second section contains five indexes (subject, personal author, corporate source, report/accession number, and accession/report number.) Author

N69-31333*# National Aeronautics and Space Administration. Goddard Spaceflight Center, Greenbelt, Md.
TEST PLAN OPTIMIZATION FOR AN EXPLORER-SIZE SPACECRAFT
J. H. Boeckel and A. R. Timmins Washington Jul. 1969 18 p refs
(NASA-TN-D-5283) Avail: CFSTI CSCL 22B

Although GSFC policy has required both a prototype (qualification model) and a flight (acceptance model) spacecraft, rising costs have caused a reexamination of this approach. In both the Interplanetary Monitoring Platform (IMP) and the Radio Astronomy Explorer (RAE) projects, a single spacecraft (termed proto-flight) was qualified and then successfully launched. The analysis discussed herein was conducted, using Monte Carlo techniques, to estimate whether this concept is truly cost-effective. The results of the study show a savings of approximately $1

million, using the proto-flight approach. It also shows that rigorous subsystem testing is effective in reducing costs if initial hardware quality is poor. The analysis assumes that each test approach treated produces equivalent spacecraft launch-readiness. Whether this assumption is true has not been determined; however, it could be expected to have some limitations. Author

N69-31836*# Aztec School of Languages, Inc., Maynard, Mass.
TRANSACTIONS OF THE NINTH SCIENTIFIC CONFERENCE OF GRADUATE STUDENTS AND JUNIOR SCIENTIFIC ASSOCIATES OF THE INSTITUTE FOR THE HISTORY OF NATURAL SCIENCE AND TECHNOLOGY, SECTION ON THE HISTORY OF AVIATION AND COSMONAUTICS
Yu. V. Biryukov Washington NASA Jun. 1969 58 p refs Transl. into ENGLISH of the book "Trudy IX Nauchnoy Konferentsii Aspirantov i Mladshikh Nauchnykh Sotrudnikov Instituta Istorii Yestestvoznaniya i Tekhniki, Sektsii Istorii Aviatsii i Kosmonavtiki" Moscow, Izd. AN SSSR, 1966
(Contract NASw-1692)
(NASA-TT-F-540) Avail: CFSTI CSCL 05B

CONTENTS:

1. THE HISTORY OF THE DESIGNING OF LIQUID-PROPELLANT ROCKET ENGINES AS A NEW TYPE OF ROCKET ENGINE Yu. V. Biryukov p 1–10 refs (See N69-31837 18-28)
2. THE HISTORY OF THE DEVELOPMENT OF ELECTRIC ROCKET ENGINE SYSTEMS V. I. Belolipetskiy p 11–18 refs (See N69-37838 18-28)
3. THE DEVELOPMENT OF LARGE-SCALE ROCKET DESIGNING IN THE USA IN 1944–48 I. N. Bubnov p 19–25 refs (See N69-31839 18-28)
4. THE DEVELOPMENT AND USE OF LIQUID-PROPELLANT ROCKET ENGINES IN AVIATION IN THE USA (1940–1958) G. V. Skvortsov p 26–34 refs (See N69-31840 18-28)
5. AN ANALYSIS OF THE MOMENT OF TRANSITION IN AVIATION FROM PISTON ENGINES TO JETS Yu. S. Voronkov p 35–44 refs (See N69-31841 18-28)
6. THE HISTORY OF THE HYPOTHESIS ON THE RADIATION BELTS OF THE EARTH R. G. Bazurin p 45–50 refs (See N69-31842 18-29)
7. SOME NOTES TO THE APPEARANCE AND DEVELOPMENT OF INERTIAL NAVIGATIONAL SYSTEMS P. N. Polokhin p 51–55 refs (See N69-31843 18-21)

N69-31946*# National Aeronautics and Space Administration, Washington, D.C.
AEROSPACE RELATED TECHNOLOGY FOR INDUSTRY
1969 177 p refs Presented at the Technol. Util. Conf., Langley Res. Center, Hampton, Va. 22 May 1969
(NASA-SP-5075) Avail: CFSTI CSCL 05B

The purpose of the Technology Utilization Program is to speed up the transfer of technology across regions, across disciplines, across industries, across medicine, and across education. As generators of new technology, NASA began in 1964 to sponsor regional conferences for the purpose of acquainting commerce and industry with the results of aerospace related research and development that could have practical application in the marketplace. Author

N69-32430*# National Aeronautics and Space Administration, Washington, D.C.
MANAGEMENT: A CONTINUING LITERATURE SURVEY WITH INDEXES
Jun. 1969 58 p refs
(NASA-SP-7500(03)) Avail: CFSTI CSCL 05B

This is a compilation of references to unclassified reports and periodical articles on the subject of management that may be found in the NASA scientific and technical information system. The publication assembles groups of citations formerly announced in separate journals, *Scientific and Technical Aerospace Reports (STAR)* and *International Aerospace Abstracts (IAA)*, together with other reports included in the system but not previously announced. This issue covers references to material from both NASA and non-NASA sources that entered the system in 1968. The items are grouped in nine categories. Subject, personal author, and corporate source indexes are provided. Author

N69-34917*# National Aeronautics and Space Administration, Washington, D.C.
THE SYSTEMS APPROACH TO MANAGEMENT. AN ANNOTATED BIBLIOGRAPHY. WITH INDEXES
Jul. 1969 69 p refs
(NASA-SP-7501) Avail: CFSTI CSCL 05B

The announcements of the systems approach to management appear by accession number and are grouped under the following categories: the systems concept, recent developments, specific functions, multi-national organization, manpower management, public administration, impact on management, and practical applications. F.O.S.

N69-36314*# Aztec School of Languages, Inc., Acton, Mass. Research Translation Div.
TRANSACTIONS OF THE TENTH SCIENTIFIC CONFERENCE OF THE INSTITUTE OF HISTORY OF NATURAL SCIENCE AND TECHNOLOGY [TRUDY X NAUCHNOY KONFERENTSII ASPIRANTOV I MLADSHIKH NAUCHNYKH SOTRUDNIKOV INSTITUTA]
Yu. V. Biryukov et al Washington NASA Sep. 1969 66 p refs Transl. into ENGLISH from RUSSIAN Conf. Conf. held at Moscow, 1967
(Contract NASw-1692)
(NASA-TT-F-537) Avail: CFSTI CSCL 05A

CONTENTS:

1. THE ROLE OF S. P. KOROLEV IN THE DEVELOPMENT OF SOVIET ROCKET TECHNOLOGY DURING THE PERIOD OF ITS ORIGIN AND ESTABLISHMENT (1930–1941) Yu. V. Biryukov p 1–12 refs (See N69-36315 21-31)
2. THE PRINCIPLE CHARACTERISTICS AND DESIGN FEATURES OF R. GODDARD'S ROCKETS I. N. Bubnov p 13–23 refs (See N69-36316 21-28)
3. THE CONSTRUCTION OF AN ELECTRIC ROCKET ENGINE IN THE GAS DYNAMICS LABORATORY L. M. Aleksandrova p 24–30 refs (See N69-36317 21-28)
4. AN ANALYSIS OF THE DEVELOPMENT OF AVIATION MODELING IN THE 19th CENTURY Yu. I. Novokshonov p 31–39 refs (See N69-36318 21-02)
5. FORMATION OF THE PRINCIPAL TYPES OF GAS-TURBINE ENGINES Yu. S. Voronkov p 40–48 refs (See N69-36319 21-08)
6. THE DEVELOPMENT AND USE OF LIQUID-PROPELLANT ROCKET ENGINES IN EXPERIMENTAL AIRCRAFT IN THE USA (1944–1953) G. V. Skvortsov p 49–57 refs (See N69-36320 21-28)
7. THE HISTORY OF THE DEVELOPMENT OF THE PRINCIPLES FOR DETERMINING THE POSITION OF AN AIRCRAFT IN SPACE, BASED ON THE USE OF A PENDULUM P. N. Polozhin p 58–62 refs (See N69-36321 21-14)

N69-38951*# National Aeronautics and Space Administration. Goddard Space Flight Center, Greenbelt, Md.
SIGNIFICANT ACCOMPLISHMENTS IN SCIENCE, 1968
Washington 1969 196 p Proc. of a Symp. held at Greenbelt, Md., 10 Jan. 1969

(NASA-SP-195) Avail: CFSTI CSCL 03B

Satellite experiment and astronomical observation data are presented on the atmospheric composition of the earth, geomagnetism, extraterrestrial radiation, solar activity, and planetary atmospheres. For individual titles, see N69-38952 through N69-38994.

N69-39957*# National Aeronautics and Space Administration. Electronics Research Center, Cambridge, Mass.

FUTURE FIELDS OF CONTROL APPLICATION

Washington 1969 144 p refs Proc. of Conf. Held in Cambridge, Mass. 10-11 Feb. 1969

(NASA-SP-211) Avail: CFSTI CSCL 05A

CONTENTS:

1. WELCOMING ADDRESS J. C. Elms p 1 – 2

2. POSSIBLE AREAS OF CONTROL THEORY IN PRINT COMMUNICATION J. L. Hallenbeck (Time, Inc.) p 3 – 13 (See N69-39958 23-07)

3. DISCUSSION OF HALLENBECK PAPER H. M. Paynter (Mass. Inst. of Tech., Cambridge) p 15 – 22 (See N69-39959 23-07)

4. BIOLOGICAL CYBERNETICS L. Stark (Calif. Univ., Berkeley) p 23 – 38 (See N69-39960 23-05)

5. AIR TRANSPORTATION R. F. Lambert (American Airlines, Inc., N.Y.) p 39 – 53 (See N69-39961 23-02)

6. URBAN STUDIES: AN OPPORTUNITY FOR SYSTEMS ENGINEERING J. E. Gibson (Oakland Univ.) p 55 – 65 refs (See N69-39962 23-02)

7. WORLD BANK OPERATIONS IN THE LESS-DEVELOPED COUNTRIES I. S. Friedman (Intern. Bank for Reconst. and Develop.) p 67 – 86 (See N69-39963 23-34)

8. DISCUSSION OF FRIEDMAN PAPER Yu-Chi Ho (Harvard Univ., Cambridge) p 87 – 97 ref (See N69-39964 23-34)

9. CONTROL TECHNOLOGY APPLIED TO PRODUCTION PROBLEMS C. V. Foster (Continental Oil Co.) p 99 – 110 refs (See N69-39965 23-15)

10. DISCUSSION OF FOSTER PAPER T. J. Williams (Purdue Univ.) p 111 – 119 (See N69-39966 23-08)

11. BIOLOGICAL OCEANOGRAPHY G. C. Ewing (Woods Hole Oceanog. Inst.) p 121 – 133 (See N69-39967 23-13)

12. REFLECTIONS ON GIFFORD EWING'S PAPER J. V. Breakwell (Stanford Univ.) p 135 – 136 (See N69-39968 23-13)

13. HOW DO WE MEET FUTURE CONTROL CHALLENGES ? L. A. Zadeh (Calif. Univ., Berkeley) p 137 – 146 (See N69-39969 23-10)

SUBJECT INDEX

NASA SCIENTIFIC AND TECHNICAL REPORTS AND PUBLICATIONS FOR 1969

A Selected Listing

Typical Subject Index Listing

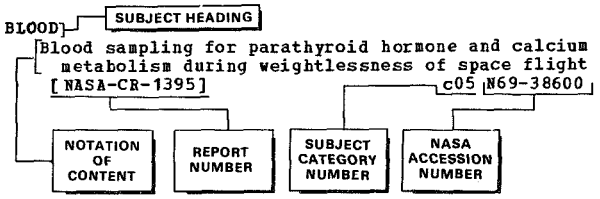

The subject heading is a key to the subject content of the document. The Notation of Content (NOC), rather than the title of the document, is used to provide a more exact description of the subject matter. The report number helps to indicate the type of document cited (e.g., NASA report, translation, NASA contractor report). The subject category number indicates the subject category in the abstract section in which the citation is located. The accession number denotes the number by which the citation is identified within the subject category. The NOC's are arranged under each subject heading in ascending accession number order. "A" items precede "N" items in this index.

A

A STARS
Spectral classes and photographic magnitudes determined for region Lacerta OB1
[NASA-TN-D-5060] c30 N69-26235

ABERRATION
Single and double mirror systems geometrical optical image aberrations noting focal number, angle of field, secondary magnification and mutual position tolerances
c23 A69-24836

ABIOGENESIS
NASA Planetary Exploration Program to gather data on origin of solar system and life, discussing planetary evolution and extraterrestrial life
c04 A69-12804

ABLATION
Charring phenolic nylon ablator material pyrolysis and surface recession for cyclic and constant combined convective and radiative heating
[AIAA PAPER 69-151] c33 A69-18055
Oxygen depletion effect in chemical reactions between pyrolysis gases and air stream on surface recession of charring ablators
[AIAA PAPER 68-302] c33 A69-21982
Subliming ablation effects on boundary layer transition for cones in hypersonic flow, discussing Reynolds numbers measured in wind tunnel tests
[AIAA PAPER 68-40] c01 A69-31881
Apollo afterbody heat transfer, studying ablation effects for various reentry angles of attack
c33 A69-43680
Pressure fields and multidimensional gas flow in permeable char layers and effects on ablation
[NASA-TR-R-296] c33 N69-16181
Ablation product absorption and line transitions effects on shock layer radiative transport around blunt body
[NASA-CR-1264] c33 N69-19117
Ablation behavior of heat shield of Apollo command module over wide range of thermal environments
[NASA-TM-X-1778] c33 N69-22933

ABLATIVE MATERIALS
Apollo thermal protection system, noting low density ablation, flight and ground tests
[AIAA PAPER 68-1142] c31 A69-13558
Make wire, light pipe and spring wire ablation sensors development for measuring parameters of heat shield materials for reentry vehicles
c14 A69-15428
Ballistic range tests to study ablation effects on aerodynamic characteristics of ablating and nonablating slender cones
[AIAA PAPER 69-179] c33 A69-18083
Ablation characteristics of heat shield materials measured in arc heated wind tunnels, considering influence of model scale, heating rate and pressure level
c18 A69-26813
Heating facility for testing ablative heat shield material models in combined convective and radiative heating environment with constant or transient heating conditions
[AIAA PAPER 69-342] c11 A69-28278
Ablative materials thermal protection characteristics at low heating rates evaluated by convective heating tests, stressing polyurethane foam composite
c18 A69-35536
Ablation heat shields, emphasizing dielectric low cost fabrication and application to entry vehicles
c15 A69-35538
Flash X ray unit with special film transport devices to obtain sequenced dynamic radiographs of ablating models during reentry simulation tests
c11 A69-35720
Line source technique for ablative heat shield materials thermal conductivity measurements, comparing vacuum and atmospheric test results
[AIAA PAPER 69-1013] c11 A69-40386
Low density polybenzimidazole composites as ablative heat shields, discussing arc-heated wind tunnel tests of linear and crosslinked structures
c18 A69-41715
Transmission loss and effects on antenna radiation patterns and impedance produced by thermally degraded ablation materials
[NASA-TN-D-4879] c07 N69-10885
Radio frequency transmission characteristics of ablation materials for planetary entry vehicle heat shields
[NASA-TN-D-4920] c07 N69-13158
Comparative evaluation of ablative materials in arc plasma jets
[NASA-CR-1207] c33 N69-14171
Rocket engine evaluation of erosion and char as functions of fabric orientation for silica reinforced nozzle materials
[NASA-TM-X-1721] c28 N69-15475
Transient thermal analysis and structural analysis for synthesis of ablating thermostructural panels in planetary entry environment
[NASA-CR-1215] c32 N69-16114
Ablative effectiveness of low density phenolic nylon materials
[NASA-TN-D-5257] c33 N69-28440
Throat and nozzle insert design for ablative rocket engine using storable propellants
[NASA-TN-D-4964] c32 N69-33481
Chemical equilibrium of ablation materials including condensed species
[NASA-TN-D-5391] c33 N69-34966

ABLATIVE NOSE CONES
Charring phenolic nylon ablator material pyrolysis and surface recession for cyclic and constant combined convective and radiative heating
[AIAA PAPER 69-151] c33 A69-18055
Aerodynamic characteristics of large-angle cones in supersonic lifting capabilities
[NASA-TN-D-5499] c01 N69-40026

ABORT APPARATUS
Manned spacecraft control system requirements for

abort problems
[NASA-CR-835] c31 N69-27299
ABORT TRAJECTORIES
Translunar abort technique for nonfree-return missions
[NASA-TM-X-1806] c30 N69-29569
ABSORBERS (MATERIALS)
Conference on NASA research in noise reduction of subsonic jet aircraft - nacelle acoustic linings, sound generation in jet engines, and operational noise effects on humans
[NASA-SP-189] c02 N69-11542
ABSORPTANCE
Solar absorptance, total hemispherical emittance and absorptance/emittance ratio for metals at cryogenic temperatures measured simultaneously with sinusoidally perturbed incident radiation
c33 A69-10847
Solar absorptance and hemispherical emmitance of metals at space conditions determined with cyclic incident radiation technique
[AIAA PAPER 69-60] c17 A69-18154
ABSORPTION
Absorption of hydrogen by palladium and electrical resistivity of hydrogen-palladium system
[NASA-TN-D-5441] c26 N69-37272
ABSORPTION CROSS SECTIONS
Radiation attenuation cross sections of monatomic and diatomic xenon gas from UV absorption measurements near resonance line
c24 A69-12551
Transmittance and absorption cross sections of carbon particles suspended in flowing stream of nitrogen gas
c33 A69-17804
Boron 10 absorption cross sections from counting ratios measurements of boron trifluoride proportional counter used to monitor neutron fluxes
c24 A69-33753
ABSORPTION SPECTRA
Doublet structure suppression in mixtures of cesium and foreign gases, discussing absorption observations
c24 A69-20736
Rocket spectrographic observations of Alpha Virginis noting hydrogen Lyman absorption lines
c30 A69-27555
Absorption coefficient measurement for hydrocarbon gases for He-Ne laser beam at 3.39 microns, tabulating coefficients, noting variations from spectroscopic data
c16 A69-42192
ABSORPTIVITY
Optical absorption coefficients for triphenylmethylarsonium tetracyanoquinodimethan complex single crystal, evaluating reflectance
c26 A69-10934
Hydrogen absorption coefficients, giving number densities in hydrogen gas or plasma for wide range of temperature and pressure
c24 A69-19165
Rational approximation for coefficients used in calculating hydrogenic photoionization Gaunt factors
c24 A69-20153
Diffusion pump oil reflectance and absorption coefficients measured in three thicknesses using light source, monochromator and detector
c23 A69-23647
Absorption coefficient measurement for hydrocarbon gases for He-Ne laser beam at 3.39 microns, tabulating coefficients, noting variations from spectroscopic data
c16 A69-42192
Absorption rate sticking probabilities for oxygen on niobium and dilute niobium-zirconium alloys
[NASA-TN-D-4885] c17 N69-10931
Interim absorption coefficients and opacities for hydrogen plasma at high pressure
[NASA-TM-X-1902] c24 N69-39187
ABSTRACTS
NASA scientific and technical information program for building technical data and literature repository for scientists, engineers and technical managers, describing IAA and STAR
[UN PAPER 68-95317] c34 A69-17068
Annotated bibliography and indexes on aerospace medicine and biological effects - Feb. 1969
[NASA-SP-7011/60/] c04 N69-19714
Combined selective listing of NASA scientific and technical reports announced during 1968
[NASA-SP-7033] c34 N69-29492
ABUNDANCE
Spectra of close binary systems, analyzing abundance anomalies, noting metallicity results
c30 A69-15854
Origin and distribution of elements - Conference, Paris, May 1967
c30 A69-20892
Solar system elements abundance compilation based on carbonaceous chondrites and nucleosynthesis in stars
c30 A69-20903
Continental diabases and oceanic tholeiites in light of rare earth and barium abundances and partition coefficients indicating fusion process
c13 A69-20945
Atmospheric models for metal deficient stars of K and G spectral type, studying reduced metal abundance effect on atmospheric structure
c30 A69-22055
Primordial helium and horizontal branch star luminosity, obtaining luminosities in He burning phase for different He and metal abundances from models
c30 A69-22211
Curve of growth analysis for close binary HR 5317 indicating Mg, Mn, Ca and Sr overabundance respecting standard star 110 Her
c30 A69-34297
Atmospheric models for specified effective temperatures, hydrogen-to-metal ratios and surface gravities in studying metal deficiency effect on stellar atmosphere
c30 A69-36338
Abundance compilations of elements due to nuclear processes, discussing carbonaceous chondrites character
c29 A69-38812
Chemical composition of galactic and solar cosmic rays, discussing differences from universal cosmic abundances, using Cerenkov counters, emulsions, etc
c29 A69-40090
AC GENERATORS
Argon turboalternator design and testing for Brayton cycle space power system, discussing inlet operating temperature and shaft bearings and rotation
c03 A69-42279
Design, fabrication, and testing of 12-kilowatt inductor alternator, voltage regulator-exciter, and parasitic loading speed controller - summary
[NASA-TN-D-4874] c03 N69-10088
Turboalternator gas bearing system for spacecraft electric power production
[NASA-CR-1292] c15 N69-19775
Digital computer program for homopolar inductor alternator electromagnetic design analysis
[NASA-TN-D-5072] c03 N69-19799
Performance of two stage axial flow turbogenerator with gas bearing rotor support system
[NASA-CR-1290] c03 N69-21771
Design and performance of gas bearing system for turboalternators
[NASA-CR-1291] c15 N69-21772
Performance characteristics of 14.3 kVA modified Lundell alternator for 1200 Hz Brayton cycle space power system
[NASA-TN-D-5405] c03 N69-35537
Motor starting characteristics of two inductor alternators
[NASA-TM-X-1912] c03 N69-40440
ACCELERATION (PHYSICS)
Acceleration effects on forced convection in turbulent boundary layer, noting heat transfer history and rates prediction
c12 A69-21480
Accelerated boundary layers classified in terms of integral balance of pressure, inertia, wall friction forces and entrainment momenta
[AIAA PAPER 69-666] c12 A69-33462
Acceleration effects on solid propellant rocket motors combustion characteristics
[AIAA PAPER 68-530] c28 A69-39217
Human responses to aerospace environment related to acceleration, vibration, sound, and noise

[NASA-CR-1205-VOL-2] c04 N69-12588
Steady state acceleration effects on combustion characteristics of aluminized composite solid propellant
[NASA-TN-D-4914] c33 N69-13231
Object motion effect in Fraunhofer holography with application to velocity measurements
[NASA-TN-D-5515] c14 N69-40812

ACCELERATION STRESSES (PHYSIOLOGY)
Human body dynamic response to vibration combined with linear acceleration, noting changes in body mechanical impedance and resonance
c05 A69-11335
Neutral buoyancy microelectrode for prolonged recording from single nerve units
c05 A69-11865
Human angular acceleration sensitivity using rotation and oculogyral illusion perception as indicators, relating to spatial orientation and flight control task precision
c05 A69-41674

ACCELERATION TOLERANCE
Thermal, acoustical, and acceleration environments of XB-70 airplane crew compartment in airworthiness tests
[NASA-TN-D-5449] c25 N69-38010

ACCELEROMETERS
FM/AM telemetry circuits with three axis piezoelectric accelerometer for measurements during impact tests of soft landing models
c07 A69-23279
Navigation state vector update effect on lunar mission completion capability for Saturn 5, emphasizing hardware and scheme errors and accelerometer failure
[AIAA PAPER 69-883] c21 A69-39409

ACCEPTABILITY
Tone and duration effects on perceived noisiness
[NASA-CR-1283] c04 N69-18722

ACCEPTOR MATERIALS
Strong p-type conductivity of silicon doped with beryllium by thermal diffusion, giving electrical and optical measurements
c26 A69-21652

ACCIDENT PREVENTION
Ideal safety system for accident prevention, considering foreseeable and unforeseeable aspects to eliminate individual or collective human error
c34 A69-16836

ACCLIMATIZATION
Artificial heat acclimatization effect on orthostatic tolerance in man exposed to stresses of heat, exercise and dehydration
c05 A69-32810

ACCOMMODATION COEFFICIENT
Measurement of thermal accommodation coefficients between liquids and high temperature gases in low pressure reentry communications blackout intervals
[NASA-CR-1330] c07 N69-32721

ACCUMULATORS
Analytical model for use in design of pump inlet accumulators for prevention of liquid rocket longitudinal oscillation
[NASA-TN-D-5394] c28 N69-33319

ACETATES
Acetate carbon 14 utilization in centrifuged rats, analyzing metabolism by measuring plasma glucose, FFA and lipids synthesis
c04 A69-19429
Acetate-2-C 14 conversion to C 14 carbon dioxide and C 14 fatty acids in rats with 2/3 of liver removed
c04 A69-35976

ACHONDRITES
Ca-rich achondrites genesis implied from rare earth and Ba absolute and relative concentrations
c30 A69-36091

ACOUSTIC ATTENUATION
Ultrasonic pulse velocity and attenuation measurement in presence of noise, using coherent detection and signal averaging
c14 A69-29564

ACOUSTIC DUCTS
Conference on NASA research in noise reduction of subsonic jet aircraft - nacelle acoustic linings, sound generation in jet engines, and operational noise effects on humans
[NASA-SP-189] c02 N69-11542

ACOUSTIC INSTABILITY
Liquid rocket acoustic instability for hydrogen-oxygen and earth storable propellant combinations
[NASA-TN-D-4968] c28 N69-14384
Injector radial distribution and thrust chamber geometry effect on acoustic mode instability in hydrogen oxygen engines
[NASA-TN-D-5375] c33 N69-32340

ACOUSTIC MEASUREMENTS
Temperature effects on turbofan and turbojet noise radiation
[NASA-CR-1472] c02 N69-40439

ACOUSTIC PROPERTIES
Transient response of coupled acoustic cavity resonators
[NASA-CR-1421] c23 N69-35286
Radiation resistance of cylindrical shells in ideal compressible acoustic medium
[NASA-CR-1437] c32 N69-40935

ACOUSTIC VELOCITY
Velocity of 1 MHz sound waves in He 4 along isotherms just above critical temperature, noting specific heat ratio for 4.5 and 5 K isotherms
c23 A69-17142

ACOUSTICS
Human responses to aerospace environment related to acceleration, vibration, sound, and noise
[NASA-CR-1205-VOL-2] c04 N69-12588
Harmonic content of pressure wave shapes in strong traveling transverse acoustic modes
[NASA-TM-X-1716] c12 N69-15371
Parameters of acoustic liner for maximum liner damping for rocket engines
[NASA-TM-X-1720] c28 N69-16152

ACTIVATION ENERGY
Reaction rate constants of ion-molecule interchange reaction as function of temperature, flow velocity, activation energy and constant part of steric factor P
c06 A69-32312
Chemical reactions activation energy at high temperature, noting cross section shape role for deducing activation energy from rate data
c06 A69-34443

ACTUATORS
Fluidic integrated circuits for control of pneumatic stepping-motor actuator system
[NASA-TN-D-5155] c03 N69-22896
NERVA control drum actuator tests in cryogenic temperature, nuclear radiation, and vacuum environments
[NASA-TN-D-5347] c22 N69-31870

ADAPTERS
Prediction curves for launch vehicle vibration levels in region of spacecraft adaptor
[NASA-CR-1227] c31 N69-16155

ADAPTIVE CONTROL
Adaptive compression system for predicting and encoding video data for transmission in noiseless channel
c14 A69-12869
Adaptive simulation using modal clustering and method of potential functions
[NASA-CR-1179] c08 N69-10316

ADDITIVES
Controlled oxygen additions to refractory metal alloys
[NASA-TM-X-1799] c17 N69-26952

ADENOSINE TRIPHOSPHATE (ATP)
NADH stimulation of ATP dependent carbon dioxide fixation in crude extracts of Hydrogenomonas facilis, considering allosteric regulation of phosphoribulokinase activity
c04 A69-30036
Adenosine triphosphate /ATP/ content of terrestrial soils, based on firefly bioluminescent reaction, for Mars soil problems
c04 A69-37567

ADHESION
Gold-underlayer film combinations adhesion to oxide substrates, describing adhesion changes as function of Au and underlayer film thickness, time, environment, etc
c26 A69-28007

Quartz fiber adhesion to Re measured in LEED /low energy electron diffraction/ apparatus for clean and O layer surfaces, noting brittle fracture
c17 A69-35182
Low energy electron diffraction analysis of quartz fiber adhesion to rhenium crystal surface
[NASA-TN-D-5229] c17 N69-25363
Low energy electron diffraction study of adhesion of various materials to nickel surface
[NASA-TN-D-5247] c17 N69-26258
Adhesion of gold on copper planes studied with low energy electron diffraction
[NASA-TN-D-5290] c26 N69-29407
Adhesion of gold to copper and to copper aluminum alloys
[NASA-TN-D-5351] c23 N69-31984

ADHESION TESTS
Theory and method for characterizing surface cleanliness of nickel during adhesion testing
[NASA-TN-D-5055] c17 N69-19827

ADHESIVES
Cryogenic behavior of adhesive materials used in fabrication of liquid hydrogen/liquid oxygen powered Saturn S-4B stage
c18 A69-16487

ADIABATIC EQUATIONS
Equation describing statistically trapped particle motion under influence of fields varying in time and space
c29 A69-19375

ADIABATIC FLOW
Numerical calculation of inviscid adiabatic flow field around blunt bodies at hypersonic speeds
[NASA-TN-D-5434] c12 N69-36830

ADRENAL METABOLISM
Adrenal epinephrine and phenylethanolamine n-methyl transferase /PNMT/ activity in rat bearing transplantable pituitary tumor
c04 A69-20374
Rats adrenal corticosterone concentrations changes in response to ACTH, determining response sensitivity dependence on time after hypophysectomy
c04 A69-39871
Compensatory hypertrophy effects on adrenal phenylethanolamine n-methyl transferase /PNMT/ activity in rats
c04 A69-41404

ADRENOCORTICOTROPIN (ACTH)
Rats adrenal corticosterone concentrations changes in response to ACTH, determining response sensitivity dependence on time after hypophysectomy
c04 A69-39871

ADSORPTION
Heats of adsorption of carbon dioxide on silver /I/ oxide and copper /II/ oxide by gas chromatography
c06 A69-38277

AERIAL PHOTOGRAPHY
Conference on motion degraded images and correcting procedures - optical filters and digital methods for blurring removal from photographic imagery
[NASA-SP-193] c14 N69-33322

AERIAL RUDDERS
Transonic wind tunnel evaluation of variable stabilizer configuration effects on hypersonic elliptical lifting body dynamics
[NASA-TM-X-1789] c01 N69-25244

AEROBEE ROCKET VEHICLE
Artificial aurora generated at 100 km altitude by electron beam fired downward from Aerobee 350 rocket above 230 km along earth magnetic field lines
c13 A69-34365

AEROBES
Cellular localization of acetyl-coenzyme A synthetase in yeast, noting enzyme distribution during aerobic growth on glucose
c04 A69-15333

AERODYNAMIC BRAKES
Deceleration control system for aerobraking and skipcut to orbit at Mars
[AIAA PAPER 68-1146] c31 A69-13564
Structural and aerodynamic developments in attached inflatable decelerators for deployment of payload at supersonic speeds
[AIAA PAPER 68-929] c02 A69-39015
Aerodynamic deceleration systems for space missions, considering deployment of subsonic parachute and inflatable configuration following atmospheric entry
[AIAA PAPER 68-1081] c31 A69-40542
Flexible parawing lifting decelerator research data from wind tunnel and flight tests, noting manned space vehicle recovery and aircraft escape systems
[AIAA PAPER 68-967] c02 A69-43715
Aerodynamic characteristics of blunted cones, tension shell, and attached inflatable decelerator models
[NASA-TN-D-5219] c31 N69-26570

AERODYNAMIC CHARACTERISTICS
V/STOL aircraft characteristics, emphasizing propeller, ducted fan and turbojet types
c02 A69-15563
NASA research on flexible and stiffened flexible wings, discussing range of applicability, aerodynamic characteristics and wind tunnel results
c02 A69-15568
Factors influencing development of both wind tunnel and flight test technology for determining aerodynamic derivatives of aircraft motions
c11 A69-15572
Ballistic range tests to study ablation effects on aerodynamic characteristics of ablating and nonablating slender cones
[AIAA PAPER 69-179] c33 A69-18083
Subsonic lifting surface theory including leading edge, discussing singularities in solution of integral equation for determination of aerodynamic properties
[AIAA PAPER 69-37] c01 A69-18167
Flow simulation on wind tunnel test models for aerodynamic characteristics of aircraft design, discussing boundary layer and external flow coupling
[AIAA PAPER 69-660] c11 A69-33471
Aerodynamic and flight characteristics of variable geometry entry spacecraft during subsonic wing deployment and landing
[AIAA PAPER 69-742] c01 A69-34407
Aerodynamic performance tests of autorotative unpowered rotor entry vehicle model at various Mach numbers and angles of attack
[AIAA PAPER 68-950] c01 A69-37155
Aerostatic and aerodynamic characteristics of Dart Vee tethered balloon system
c02 A69-40813
Aerodynamic characteristics of COIN aircraft model with boundary layer control on inverted V-tail
[NASA-TN-D-4856] c02 N69-10935
Hypersonic aerodynamic characteristics of low fineness ratio variable geometry logistics spacecraft model
[NASA-TM-X-1701] c01 N69-13218
Inflation, drag, and stability characteristics of towed inflatable ballute decelerator at free flight
[NASA-TN-D-4943] c01 N69-17398
Effects of cone angle, base flare angle, and corner radius on Mach 3 aerodynamic characteristics of large angle cones
[NASA-TN-D-5048] c01 N69-19926
Wind tunnel tests for V/STOL aircraft having direct-lift and lift-cruise jet nozzles
[NASA-TM-X-1758] c01 N69-20016
Aerodynamic characteristics and ground effects of supersonic transport with double Delta wing
[NASA-TN-D-5102] c02 N69-21020
Antenna effects on aerodynamic characteristics of 0.410 scale model Cajun rocket at Mach numbers from 2.30 to 4.63
[NASA-TM-X-1771] c01 N69-21106
Wind tunnel investigation of twin keel parawing aerodynamic characteristics
[NASA-TN-D-5199] c01 N69-23781
Transonic wind tunnel evaluation of variable stabilizer configuration effects on hypersonic elliptical lifting body dynamics
[NASA-TM-X-1789] c01 N69-25244
Aerodynamic characteristics of annular cascade of blades
[NASA-CR-1323] c01 N69-25327

Aerodynamic characteristics of blunted cones, tension shell, and attached inflatable decelerator models
[NASA-TN-D-5219] c31 N69-26570
Aerodynamic characteristics determined during development of Apollo launch escape vehicle configuration in wind tunnel tests
[NASA-TN-D-5208] c01 N69-29027
Aerodynamic investigation of sharp cone-cylinder spikes on 120 degree blunted cones at Mach numbers of 3, 4.5, and 6
[NASA-TN-D-5201] c01 N69-29154
Transonic aerodynamic characteristics of two hypersonic cruise configurations
[NASA-TM-X-1816] c01 N69-29231
Jet exhaust location effects on longitudinal aerodynamic characteristics of jet V/STOL model
[NASA-TN-D-5333] c01 N69-33210
Supersonic aerodynamic characteristics and shock standoff distances for large angle cones with and without cylindrical afterbodies
[NASA-TN-D-5334] c01 N69-33237
Aerodynamic characteristics effected by parallel-staged simple aerodynamic configuratıcns at Mach numbers of 3 and 6
[NASA-TN-D-5379] c01 N69-33302
Wind tunnel investigation for determination of subsonic and transonic aerodynamic characteristics of Saturn 1B launch vehicle
[NASA-TM-X-1848] c31 N69-33380
Wind tunnel tests of subsonic aerodynamic characteristics of large scale tip turbine cruise fan with 1.075 pressure ratic at angle of attack
[NASA-TN-D-5316] c28 N69-34575
Aerodynamic characteristics of blunt space capsules and slender reentry bodies with bulbous bases
[NASA-CR-1339] c01 N69-35521
Aerodynamics and flight dynamics of turbojet aircraft
[NASA-TT-F-542] c01 N69-38670
Aerodynamic characteristics of large-angle cones in supersonic lifting capabilities
[NASA-TN-D-5499] c01 N69-40026

AERODYNAMIC COEFFICIENTS
Wind tunnel wall constraints effects at extreme force coefficients during V/STOL testing shown different from effects in conventional aircraft testing
c11 A69-15574
Aerodynamic coefficients from observed motion of body in flight, eliminating need for closed form solutions by employing numerical solutions to equations of motion
[AIAA PAPER 69-134] c01 A69-18161
Wind tunnel tests of opening characteristics of all flexible parawing
[NASA-TN-D-5031] c02 N69-17700
Aerodynamic characteristics in pitch of scale model of two and three stage rocket configuration at Mach numbers of 0.4 to 4.63
[NASA-TN-D-5378] c01 N69-34986
Entry aerodynamics at lunar return conditions from command module of Apollo 4 flight
[NASA-TN-D-5399] c31 N69-38820
Wind tunnel study of aerodynamic pressures on Apollo command module configuration
[NASA-TN-D-5514] c01 N69-40345

AERODYNAMIC CONFIGURATIONS
Hypersonic body shaping for minimum drag and improved performance from view of flight regimes, discussing implications of pressure laws
[AIAA PAPER 69-181] c01 A69-18052
Wind tunnel test of aerodynamic characteristics of scale model of Tomahawk launch vehicle at Mach speeds
[NASA-TM-X-1684] c01 N69-10732
Aerodynamic characteristics of full scale model sailwing with aspect ratio 5.9
[NASA-TN-D-5047] c01 N69-19243
Laminar heat transfer distributions for blunted-cone, cone frustum reentry configuration at hypersonic speed using Reynolds number
[NASA-TN-D-5146] c33 N69-22997
Design method for far field sonic boom shock strength and impulse independent of body length and volume
[NASA-TN-D-5148] c01 N69-23927
Transonic aerodynamic characteristics of two hypersonic cruise configurations
[NASA-TM-X-1816] c01 N69-29231
Aerodynamic characteristics effected by parallel-staged simple aerodynamic configurations at Mach numbers of 3 and 6
[NASA-TN-D-5379] c01 N69-33302

AERODYNAMIC DRAG
Drag influence on mission performance of hypersonic aircraft during climb and cruise, noting payload capacity
c02 A69-37154
Structural and aerodynamic developments in attached inflatable decelerators for deployment of payload at supersonic speeds
[AIAA PAPER 68-929] c02 A69-39015
Numerical solution for minimum induced drag, and associated loading, of nonplanar wings
[NASA-CR-1218] c01 N69-10343
User manual for computer program 55VD for computatıcn of minimum induced drag and load distribution of nonplanar wings
[NASA-CR-1218-SUPPL] c01 N69-12286
Predicting lift and drag for slender sharp-edge Delta wings in ground proximity
[NASA-TN-D-4891] c01 N69-16180
Transonic wind tunnel tests of aerodynamic drag and lift forces on circular cylinder in two dimensional flow at high Reynolds number
[NASA-TR-R-300] c01 N69-17304
Wind tunnel magnetic support and balance system for measuring sphere drag
[NASA-CR-1353] c11 N69-25343
Free flight test model measurement of drag, lift, and trim in wind tunnel for Apollo command module
[NASA-TN-D-5276] c30 N69-29557
Aerodynamic drag effects of hypersonic magnetohydrodynamic plasma flow around blunt bodies
[NASA-CR-1393] c25 N69-34897
Aerodynamic drag of external fuel tanks attached to X-15-2 airplane at Mach numbers of 1.6 to 2.3
[NASA-TM-X-1895] c01 N69-38065

AERODYNAMIC FORCES
Wind tunnel wall constraints effects at extreme force coefficients during V/STOL testing shown different from effects in conventional aircraft testing
c11 A69-15574
Skin friction measurement in aerodynamic tests using thin liquid crystal coatings with changes in maximum light scattering wavelength in response to shearing forces
c11 A69-29029
Numerical solution of coupled, nonlinear, equation of motion for rigid blade to simulate response sensitivity and blade-motion stability of fully articulated rotor
[NASA-TN-D-5032] c01 N69-17289
Aerodynamic characteristics of large semi-span V/STOL tilt-wing with single propeller tested for modes of propeller rotation
[NASA-TN-D-5016] c01 N69-17312
Effects of aerodynamic forces on jet engine noise from rigid flow spoilers
[NASA-CR-1340] c23 N69-26307

AERODYNAMIC HEAT TRANSFER
Surface pressure and heat transfer over blunt conical body in hypersonic flow with uniform mass addition of various gases
[AIAA PAPER 69-716] c01 A69-33463
Apollo afterbody heat transfer, studying ablation effects for various reentry angles of attack
c33 A69-43680

AERODYNAMIC HEATING
Configuration, trajectory planning, instrumentation, calorimetry and aerodynamic heating for planetary atmosphere entry
c31 A69-25719
Spacecraft sterilization by destructive heating with thermite or high velocity entry friction before entering planet atmosphere
c05 A69-31472
Leading edge effects on laminar flat plate boundary layer and aerodynamic heating at Mach 10.4
[NASA-TN-D-5160] c12 N69-23467

Measurements of mutual interference heating for probe antenna mounted on Apollo reentry configuration
[NASA-TM-X-1787] c01 N69-29318
High enthalpy arc tunnel at Langley Research Center for simulating aerodynamic heating and forces during spacecraft reentry
[NASA-TN-D-5295] c11 N69-29981

AERODYNAMIC LOADS
Numerical solution for minimum induced drag, and associated loading, of nonplanar wings
[NASA-CR-1218] c01 N69-10343
Aerodynamic loads on deployed canard surfaces and rocket nose section of Apollo launch escape vehicle
[NASA-TN-D-5260] c31 N69-28166
Load and temperature effects on fatigue strength of notched titanium alloy sheet for supersonic transport operation
[NASA-TN-D-5294] c32 N69-29607

AERODYNAMIC NOISE
Theoretical study of discrete frequency noise generated by turbocompressors and blades
[NASA-CR-1287] c28 N69-21476

AERODYNAMIC STABILITY
Dynamic stability derivatives of large angle blunted conical spacecraft near transonic speed in simulated Mars environment for various angles of attack
[AIAA PAPER 69-104] c31 A69-18210
Dynamic stability derivatives of large angle blunted conical spacecraft near transonic speed in simulated Mars environment for various angles of attack
c31 A69-40550
Computing span loads and stability derivatives due to sideslip, yawing, and rolling for wings in compressible flow
[NASA-TN-D-4929] c01 N69-14001
Aerodynamic stability of helicopter rotor in forward flight
[NASA-CR-1332] c32 N69-34744

AERODYNAMIC STALLING
Inlet produced dynamic distortion and effects on stall margin of J-85 turbojet engine from supersonic wind tunnel tests
[AIAA PAPER 69-487] c28 A69-32676
Steady state and dynamic distortion influence on performance and stall of turbofan engine, discussing compressor instrumentation, tests and simulation data
c28 A69-35175
Conditions for supersonic aircraft entering critical stall and spin regimes
[NASA-TT-F-526] c02 N69-31917

AERODYNAMICS
Entry phase flight data of Missions AS-202, Apollo 4 and 6 compared with wind tunnel aerodynamics data
[AIAA PAPER 68-1143] c31 A69-13556
Aerodynamics of bodies of revolution in nonplanar motion using nonlinear functional analysis of moments for motion about center of gravity
[AIAA PAPER 68-20] c01 A69-14714
Solar wind flow past earth and magnetosphere correspondence to external aerodynamics of round nosed bodies in supersonic stream
c13 A69-19360
Aerodynamics of rotary wing and V/STOL aircraft- Conference, Buffalo, June 1969, Volume 2, Wind tunnel testing, new concepts in rotor control
c01 A69-35226
Aerodynamics of rotary wing and V/STOL aircraft - Conference, Buffalo, June 1969, Volume 3
c01 A69-41369
Aerodynamic and thermodynamic calibration of nonequilibrium air flow in Ames 1-foot shock tunnel
[NASA-TN-D-4985] c11 N69-15633
Computer program for aerodynamic analysis of turbomachine blades
[NASA-TM-X-1764] c01 N69-22553

AEROELASTICITY
Analysis of aeroelastic divergence phenomena in unguided launch vehicles
[NASA-TN-D-4846] c32 N69-10297

AERONAUTICAL ENGINEERING
Historical development of liquid propellant rocket engines and aviation models
[NASA-TT-F-537] c34 N69-36314

AERONAUTICS
Aeronautic electronics - Conference, Washington, D.C., September 1968
c21 A69-16716
Aviation and astronautics - Conference, Tel-Aviv and Haifa, March 1969
c12 A69-29011
Professional programs for aeronautics, rocketry and astronautics development
c34 A69-34552
NASA computer language CLASP coordinated with evolution of SPL /Space Programming Language/ for aeronautics and space programming
[AIAA PAPER 69-957] c08 A69-40339

AEROSOLS
Mie total and differential backscattering cross sections at laser wavelengths for Junge size distribution aerosol models
c16 A69-14290
Self contained hand held battery operated aerosol particle analyzer, measuring aerosol concentration and size distribution for laboratory and space flight applications
c14 A69-34691
Mie scattering calculations on laser wavelengths and atmospheric aerosols
[NASA-TN-D-5110] c23 N69-20905

AEROSPACE ENGINEERING
Aerospace technology role in economic and social benefits
[UN PAPER 68-95321] c34 A69-10467
Rocket motor integration into Scout vehicle to improve performance
c31 A69-12384
Materials compatibility for space requirements, discussing shape retention, ductility, tensile strength, dissimilar materials stability, etc
c17 A69-17872
Electrochemical generators for space application - Conference, Paris, December 1967
c03 A69-21034
Aerospace material investigation and fabrication techniques - Conference, Cocoa Beach, November 1968
c15 A69-22301
Compressive behavior of uniaxial filament reinforced epoxy tubes for aerospace structures, using hand layup method with Teflon mandrel and sleeve
c15 A69-22339
Ballistically effective atmospheric parameters for rocket vehicle design manuals involving application of climatological concepts of meteorology
c31 A69-26874
NASA manned aerospace simulation techniques and equipment as used at Ames Research Center, noting applications to various types of manned vehicles
[ASME PAPER 69-DE-56] c11 A69-28844
Computer driven graphical techniques for aerospace design and analysis
[ASME PAPER 69-DE-27] c15 A69-28854
Leak detection for aerospace hardware, discussing equipment, operations, checkout, etc
c15 A69-30315
Design philosophy for cost reductions on future space transportation systems, exemplifying application to booster system for earth orbital logistics
[AIAA PAPER 69-439] c34 A69-32654
Space, technology and society - Conference, Cocoa Beach, Florida, March 1969, Volume 1
c34 A69-35070
Materials and processes for aerospace applications in 1970s - Conference, Los Angeles, April- May 1969
c15 A69-35501
Differential synthesis technique application to design of multiaxis stability augmentation systems for aerospace vehicles
[AIAA PAPER 68-834] c31 A69-37156
Hydrodynamic conical and spherical spiral grooved grease bearings replacement of gyro ball bearings for extended space missions
[AIAA PAPER 69-836] c15 A69-39367
Aerodynamic deceleration systems for space missions, considering deployment of subsonic

parachute and inflatable configuration following atmospheric entry
[AIAA PAPER 68-1081] c31 A69-40542
Apollo Applications Program /AAP/ spacecraft, describing contributions to space station engineering
[AAS PAPER 69-491] c31 A69-42838
Space nuclear electric power systems applications and development, summarizing current status and near future programs
[AAS PAPER 69-305] c28 A69-42865
Cost analysis in low cost launch vehicle studies emphasizing sustaining engineering and plant economics
c31 A69-43120
Aircraft Structures and Materials Application - Conference, Seattle, September 1969
c15 A69-43416
NASA development work on high efficiency batteries for space electric power systems
[NASA-SP-172] c03 N69-18042
Computer program for research and engineering management of spacecraft projects
[NASA-CR-1275] c34 N69-18057
Soviet handbook of astronautics covering spacecraft and operating problems of near-earth spaceflight
[NASA-TT-F-500] c31 N69-24760
Upgrading of electronic power supply for greater reliability in aerospace use
[NASA-TM-X-1875] c03 N69-35763

AEROSPACE ENVIRONMENTS
Vacuum integrating sphere for measuring solar absorptance in space environment to determine thermal control coatings qualifications
[AIAA PAPER 69-1021] c11 A69-40392
Thermal analysis of shadow shields and structural members in space environment
[NASA-TN-D-4876] c33 N69-10473
Human responses to aerospace environment in relation to microwave, light, thermal, and ionizing radiation
[NASA-CR-1205-VOL-1] c04 N69-12434
Human responses to aerospace environment related to acceleration, vibration, sound, and noise
[NASA-CR-1205-VOL-2] c04 N69-12588
Conversion tables for studies of human responses to aerospace environment
[NASA-CR-1205-VOL-4] c04 N69-12600
Disk radiometer for use in space vacuum-thermal environmental studies
[NASA-TN-D-4925] c14 N69-13311
Summary of potential adverse effects of artificial gravity and weightlessness on astronaut physiological processes and performance in aerospace environment
[NASA-TN-D-4980] c05 N69-15629
Aerospace Medicine and Biology bibliography on biological, physiological, psychological, and environmental effects on man during aerospace flight
[NASA-SP-7011/57/] c04 N69-16537
Hydrogenomonas cultures investigated for metabolic waste utilization in aerospace life support systems
[NASA-CR-1296] c05 N69-22766
Adaptation to hypoxia, acclimatization, and conditioning in human and animal subjects from Space Biology collection
[NASA-TT-F-580] c04 N69-32131

AEROSPACE INDUSTRY
Instrumentation in the aerospace industry - Conference, Boston, June 1968, Volume 14
c11 A69-23245

AEROSPACE MEDICINE
Aeromedical developments by NASA biomedical applications program applied to general medical equipment including cardiac sensors, surgical sterilization, ballistocardiograph, etc
c34 A69-32430
Space medicine to characterize nature and degree of changes in human functional capabilities due to space flight environment prolonged exposure
c34 A69-36460
Aviation and space medicine - Conference, Oslo, August 1968
c05 A69-41783
Aerospace medicine - Conference, Amsterdam, September 1969
c04 A69-43369
Annotated bibliography and indexes on aerospace medicine and biological effects - September 1968
[NASA-SP-7011/55/] c04 N69-11695
Annotated bibliography and indexes on aerospace medicine and biological effects - October 1968
[NASA-SP-7011/56/] c04 N69-14387
NASA contributions to bioinstrumentation system - survey
[NASA-SP-5054] c04 N69-14860
Aerospace Medicine and Biology bibliography on biological, physiological, psychological, and environmental effects on man during aerospace flight
[NASA-SP-7011/57/] c04 N69-16537
Annotated bibliography and indexes on aerospace medicine and biological effects - Dec. 1968
[NASA-SP-7011/58/] c04 N69-19023
Annotated bibliography and indexes on aerospace medicine and biological effects - Feb. 1969
[NASA-SP-7011/60/] c04 N69-19714
Annotated bibliography and indexes on aerospace medicine and biological effects - Mar. 1969
[NASA-SP-7011/61/] c04 N69-23126
Cumulative index to continuing bibliography on aerospace medicine and biological effects - 1968
[NASA-SP-7011/59/] c04 N69-24752
Annotated bibliography and indexes on aerospace medicine and biological effects - Apr. 1969
[NASA-SP-7011/62/] c04 N69-24822
Annotated bibliography and indexes on aerospace medicine and biological effects - Apr. 1969
[NASA-SP-7011/65/] c04 N69-31923
Annotated bibliography and indexes on Aerospace Medicine and Biology - Aug. 1969
[NASA-SP-7011/67/] c04 N69-37887
Bibliography on aerospace medicine and related biological research
[NASA-SP-7011/66/] c04 N69-37909
Annotated bibliography and indexes on aerospace medicine and biological effects - Apr. 1969
[NASA-SP-7011/63/] c04 N69-38235
Annotated bibliography and indexes on aerospace medicine and biological effects - May 1969
[NASA-SP-7011/64/] c04 N69-38242
Gravitational and acceleration effects on man and organisms, and biological effects of radiation
[NASA-TT-F-528] c05 N69-38701

AEROSPACE SCIENCES
Scientific advances from space research in communications astronomy, electronics, transportation, etc
c30 A69-10498
Science education and training, discussing student motivation
[UN PAPER 68-95809] c34 A69-10515
Space projections - AIAA-AAS Conference, Denver, July 1968, Volume 3
c11 A69-11755
Space projections - Conference, Denver, July 1968, Volume 1
c30 A69-12801
Space exploration influence on science education, showing NASA instructional materials for teachers in biology, chemistry, physics, mathematics, industrial arts, etc
c34 A69-35077
Life sciences and space research on biological effects of radiation in space - COSPAR Conference, Tokyo, May 1968
c04 A69-37612
Space research - COSPAR Conference, Tokyo, May 1968
c13 A69-38334
Manned space flight history and spacecraft development
[AAS PAPER 69-501] c30 A69-42852
Solar flare and space research - COSPAR Conference, Tokyo, May 1968
c29 A69-43603
Objectives, current programs, and future mission options in space sciences and applications
[NASA-SP-162] c30 N69-13844
Combined selective listing of NASA scientific and technical reports announced during 1968
[NASA-SP-7033] c34 N69-29492

AEROSPACE SYSTEMS
Electronics and aerospace systems - IEEE Conference, Washington, D.C., September 1968

c07 A69-13176
Aerospace sensor systems, discussing adaptive multimode sensors and multispectral sensing, electronic recognition of image components, laser radar and Raman scattering technique
c14 A69-13851
Spacecraft systems, education - Conference, Belgrade, September 1967
c31 A69-17596
Weightless simulators effectiveness for obtaining space systems maintainability criteria, using nonparametric experimental design for performance data
c05 A69-17648
Spaceborne optical telescopes requirements and development including mirror material and construction, optical design, servocontrol, etc
c14 A69-27946
Leak detection for aerospace hardware, discussing equipment, operations, checkout, etc
c15 A69-30315
Technology utilization by industries of aerospace sciences and systems - conferences
[NASA-SP-5075] c34 N69-31946

AEROSPACE VEHICLES
Turboalternator gas bearing system for spacecraft electric power production
[NASA-CR-1292] c15 N69-19775
Lightweight polyurethane insulation for liquid hydrogen tanks of space vehicles
[NASA-TN-D-5114] c18 N69-20790
Summary of random vibration prediction procedures for aerospace vehicles, with bibliography
[NASA-CR-1302] c32 N69-23096

AEROSPACEPLANES
Lifting body type M2-F1 and M2-F2 aircraft enabling astronauts to make own landings at choice airport
c02 A69-13367

AEROTHERMODYNAMICS
Finite difference techniques used in numerical solutions for inviscid radiating shock layers around spheres at hyperbolic speed in air
[NASA-TR-R-311] c12 N69-26504

AFRICA
Detecting geomorphological features over northeast Africa by Nimbus 2 visible and infrared radiation measurements
[NASA-TN-D-4648] c13 N69-14290

AFTERBODIES
Apollo afterbody heat transfer, studying ablation effects for various reentry angles of attack
c33 A69-43680
Supersonic aerodynamic characteristics and shock standoff distances for large angle cones with and without cylindrical afterbodies
[NASA-TN-D-5334] c01 N69-33237
Large scale wind tunnel investigation of lifting body with inflatable and rigid afterbody
[NASA-TN-D-5468] c01 N69-38775

AFTERBURNING
Steady state airflow and afterburning performance characteristics of four J85-GE-13 turbojet engines
[NASA-TM-X-1742] c28 N69-17781
Performance characteristics of truncated, conical plug nozzle with cylindrical outer shroud
[NASA-TM-X-1807] c26 N69-27840

AGING (BIOLOGY)
Mortality kinetics of Drosophila melanogaster, comparing effects of gamma radiation-induced life shortening and natural aging
c04 A69-30444

AGING (METALLURGY)
Dynamic strain aging in carbide strengthened molybdenum alloys
[NASA-TN-D-5355] c17 N69-31883

AILERONS
Flight tests of modified aileron direct lift control system during approach and landing of F8-C aircraft
[NASA-TN-D-4854] c02 N69-10371

AIR
Stagnation point boundary layer with suction and injection in equilibrium dissociating air
[NASA-TN-D-3889] c12 N69-14314
Creep rupture data on welded tubes for helium to air heat exchanger design
[NASA-TN-D-5195] c17 N69-23731
Thermodynamic and transport properties of air, and combustion products of natural gas and air, and jet engine fuel and air
[NASA-TN-D-5452] c33 N69-37936

AIR BREATHING ENGINES
Technology trends in airbreathing propulsion, discussing noise control for subsonic jet transports, turbine blade cooling, etc
[AIAA PAPER 69-774] c02 A69-35648
NASA programs for development of high temperature alloys for advanced air breathing engines emphasizing cast Ni-base alloy
[ICAS PAPER 68-26] c17 A69-43718
Steady state stress relaxation analysis of turbine blade cooling designs
[NASA-TN-D-5282] c28 N69-29321
Dynamic performance analysis of fast-response fuel control valve for air breathing engine research
[NASA-TN-D-5331] c03 N69-29977
Dynamic tests for air breathing engines using sweep frequency techniques
[NASA-TN-D-5485] c28 N69-39185

AIR COOLING
Stator performance with cooling by air ejection from trailing edges of blades
[NASA-TM-X-1901] c03 N69-39335

AIR DUCTS
Monte Carlo method application to neutron streaming in hemispherical air-filled ducts in water tank to determine leakage through nuclear reactor shields
c22 A69-35178

AIR FLOW
Parasitic eigenvalue in integration of equations governing one dimensional flow of chemically reactive gas
c12 A69-18317
Multiple function combination probe design for compressor and turbine air flow research
c11 A69-31917
Oxidation behavior of coated molybdenum and niobium alloys in high temperature supersonic air streams
[NASA-TN-D-4877] c17 N69-10764
Momentum diffusion between two supersonic airstreams passing through oblique shock waves
[NASA-TN-D-4974] c12 N69-15631
Aerodynamic and thermodynamic calibration of nonequilibrium air flow in Ames 1-foot shock tunnel
[NASA-TN-D-4985] c11 N69-15633
Steady state airflow and afterburning performance characteristics of four J85-GE-13 turbojet engines
[NASA-TM-X-1742] c28 N69-17781
Air flow and attitude angle compared with theory for rotating externally pressurized air journal bearings
[NASA-TN-D-5192] c15 N69-27956
Computer analysis of total pressure loss and air flow distribution in annular flow gas turbine combustion chambers
[NASA-TN-D-5385] c33 N69-33314

AIR INTAKES
Performance test from Mach 2.58 to 1.98 of axisymmetric mixed-compression inlet system with 60 percent internal contraction
[NASA-TM-X-1739] c01 N69-19130

AIR JETS
Turbulent mixing of compressible air in supersonic and subsonic coaxial jet flows
[NASA-TN-D-5315] c02 N69-30727

AIR MASSES
Solar constant and spectral irradiance curve for zero air mass obtained from aircraft measurements
c30 A69-42191

AIR NAVIGATION
Collection of articles on avionics navigation systems covering navigation equations, airborne digital and analog computers, radio, Doppler and inertial navigation, etc
c21 A69-34843
Guidance and navigation flight tests, demonstrating system performance improvements by onboard inertial system communicating with external navigation aid
[AIAA PAPER 69-842] c21 A69-39429

Indirect optical viewing system in F-104B for simulated lifting-body approach and landing tasks
[NASA-TN-D-5299] c14 N69-29730
Navigation-aids identification decoder and display device for general aviation aircraft
[NASA-TN-D-5445] c09 N69-38852

AIR POLLUTION
Air pollution monitoring instrumentation developed for aerospace uses surveyed for industrial applications
[NASA-SP-5072] c14 N69-24751
Air pollution detection using satellite observation
[GDC-DBE-68-011] c13 N69-31961

AIR SAMPLING
Air pollution monitoring instrumentation developed for aerospace uses surveyed for industrial applications
[NASA-SP-5072] c14 N69-24751

AIR TRAFFIC
Aeronautic electronics - Conference, Washington, D.C., September 1968
c21 A69-16716

AIR TRAFFIC CONTROL
Navigation satellites system designed for ATC without requirement for onboard transmitter, discussing spectrum occupancy, satellite power, lane ambiguities and computational procedures
c21 A69-19212
Simulation studies of supersonic transports in future air traffic control systems
[NASA-TN-D-4944] c21 N69-14382
Supersonic transport performance during real time simulated operations in future air traffic control system environments
[NASA-TN-D-5018] c02 N69-17257

AIR TRANSPORTATION
General aviation missions in national transportation system /1968, 1975, 1980/, considering fuel taxes, overall system economics, ground facilities, etc
[AIAA PAPER 69-818] c34 A69-35624

AIRBORNE EQUIPMENT
Pilot warning indicators to equip all aircraft at low cost, discussing Doppler system
c21 A69-16726
Double sideband suppressed carrier FM telemetry system as airborne data recorder, discussing noise, environmental conditions, laboratory and flight tests
c07 A69-19132
Error analysis of high resolution balloon-borne temperature sensor and comparison of temperature data with simultaneous rawinsonde measurements
c14 A69-21642
Solar spectral irradiance measured by airborne instruments, discussing construction, calibration, etc, of photoelectric filter radiometer and Leiss monochromator
c30 A69-32261
Laboratory and flight tests of airborne solid state UHF telemetry transmitter, discussing miniaturized coaxial hardware from RF power conservation viewpoint
c07 A69-35996
NASA Earth Resources Survey Aircraft Program, describing aircraft and remote sensors characteristics
c14 A69-36259
Tools and equipment for extravehicular and intravehicular activities in space and on lunar surface
[AAS PAPER 69-438] c15 A69-42802

AIRBORNE/SPACEBORNE COMPUTERS
Onboard SDP-3 computer data system core for IMP spacecraft, considering payload
c08 A69-13243
Stored program computer for small scientific spacecraft, noting program and data memory capacities
c08 A69-15472
Apollo mission simulation, discussing Command Module Simulator /CMS/, onboard computer system and dynamic visual presentation via infinity-optics display
[SMPTE PAPER 105-74] c11 A69-25768
IMP-1 experiment, describing design and applications of SDP-3 computer
c08 A69-36265
Onboard computers on rockets and satellites - Conference, Paris, December 1968
c08 A69-37377
Onboard spacecraft computer design, programming and operation based on dual bussing system
c08 A69-37384
SDP-3-A general purpose stored program computer designed for small scientific spacecraft onboard data system, noting computerized simulation
c08 A69-37385
Onboard processor servicing spacecraft sensors, programmable from ground, discussing functions and applications
c08 A69-39921
Kalman filter simulation for estimating aircraft position and velocity from airborne digital computer data in zero-zero landing system
[AIAA PAPER 69-944] c21 A69-40327
Programmable data handling and telemetry systems for scientific satellites, noting system checkout, spacecraft integration, software and ground data processing
c08 A69-41735
Spaceborne stored program computer design for OAO-C, noting auxiliary command storage, spacecraft monitoring and malfunction reporting, etc
c08 A69-41736
SDP-3 small serial computer for engineering experiment on IMP spacecraft, discussing design modifications to improve performance
c08 A69-41737
Spacecraft onboard data handling system with MSI complementary MOS arrays, describing various components
c08 A69-41739
Spacecraft central data system for deep space solar probe data management
c08 A69-42621

AIRCRAFT
Theory and practice of aircraft navigation - textbook
[NASA-TT-F-524] c21 N69-17788

AIRCRAFT ACCIDENTS
Ideal safety system for accident prevention, considering foreseeable and unforeseeable aspects to eliminate individual or collective human error
c34 A69-16836
Human survival in flight emergencies involving commercial and general aviation aircraft
[NASA-CR-1262] c02 N69-14763

AIRCRAFT COMPARTMENTS
Thermal, acoustical, and acceleration environments of XB-70 airplane crew compartment in airworthiness tests
[NASA-TN-D-5449] c25 N69-38010

AIRCRAFT CONFIGURATIONS
Computer program for calculating wall interference factors of V/STOL aircraft and conventional airplanes
[NASA-TR-R-302] c01 N69-19028

AIRCRAFT CONTROL
Flight simulation requirements for reducing aircraft training flight time, discussing control system and instrument motion characteristics, visual simulation and critical maneuvers motion
c11 A69-41139
Full scale wind tunnel investigation of lateral and longitudinal stability and control characteristics of light twin engine airplane
[NASA-TN-D-4983] c02 N69-17303
Direct side-force maneuvering system on deflected X-14A jet VTOL aircraft without changing bank angle
[NASA-TN-D-5175] c02 N69-22572
Flight tests of fluidic flight control system for aircraft
[NASA-TN-D-5298] c21 N69-30946
Pilot ratings of lateral directional handling for wide range of aircraft characteristics - graphs
[NASA-TN-D-5358] c02 N69-35762

AIRCRAFT DESIGN
Flow simulation on wind tunnel test models for aerodynamic characteristics of aircraft design, discussing boundary layer and external flow coupling

[AIAA PAPER 69-660] c11 A69-33471
Potential structural materials and design concepts for light aircraft
[NASA-CR-1285] c02 N69-20848

AIRCRAFT DETECTION
Clear air turbulence detection in troposphere by multifrequency radiometric sensor, noting multibeam system for supersonic aircraft
c09 A69-42536
Development of optical pilot warning indicator system for aircraft detection
[NASA-TN-D-5174] c14 N69-27267

AIRCRAFT ENGINES
Location effect of power plants on aft-mounted supersonic cruise exhaust nozzles at transonic speeds in flight and wind tunnel
[AIAA PAPER 69-427] c01 A69-32769
Historical developments in aviation and astronautics including liquid propellant rocket engine design, electric rocket engines, aircraft engines, and inertial guidance
[NASA-TT-F-540] c34 N69-31836
Feasibility tests on liquid lubricants for inerted lubrication systems of advanced aircraft engines
[NASA-TN-D-5420] c15 N69-35788

AIRCRAFT INSTRUMENTS
Orbiting satellite global all-weather oceanographic data acquisition to complement higher resolution data from ships, buoys and aircraft remote sensors
[UN PAPER 68-95878] c13 A69-10491
Fluidic type temperature sensor for total temperature measurement for hypersonic aircraft in atmosphere
c14 A69-16755
Solar constant and spectral irradiance curve for zero air mass obtained from aircraft measurements
c30 A69-42191
Instrument display devices for landing VTOL aircraft
[NASA-TN-D-4861] c21 N69-10069
Peripheral vision displays for presenting dynamic control information
[NASA-CR-1239] c05 N69-14478
Evaluation of contact analog display in landing approaches with helicopters
[NASA-TN-D-5241] c02 N69-27177
Transfer of microwave radiation in atmosphere and underlying surfaces measured by aircraft instruments
[NASA-TT-F-590] c13 N69-31851
Supersonic transport instrumentation and flight simulation
[NASA-TN-D-5280] c14 N69-32286

AIRCRAFT LANDING
Landing performance in T-33A aircraft with loss of binocular vision compared to perfcrmance with both eyes
c05 A69-41675
Instrument display devices for landing VTOL aircraft
[NASA-TN-D-4861] c21 N69-10069
Flight tests of modified aileron direct lift control system during approach and landing of F8-C aircraft
[NASA-TN-D-4854] c02 N69-10371

AIRCRAFT MODELS
Exhaust gas reingestion and inlet flow distortion in V/STOL lift engines, discussing static and wind tunnel testing using fighter configuration models
[AIAA PAPER 68-78] c01 A69-26762
C-5A aircraft model high subsonic speed tests, correlating data from three transonic wind tunnels
[AIAA PAPER 69-794] c01 A69-35636
Analysis of two dimensional inviscid model jet impingement under verticle takeoff airplane
[NASA-TN-D-5288] c01 N69-29479
Wind tunnel studies of scaled model of multijet cargo airplane
[NASA-TN-D-5538] c02 N69-40937

AIRCRAFT NOISE
Aircraft created pressure patterns responsible for sonic boom, discussing design techniques for noise reduction
c02 A69-30369
Theory for predicting rotational and vortex noise of lifting rotors in hovering and forward flight
[NASA-CR-1333] c23 N69-25344

AIRCRAFT PERFORMANCE
Factors influencing development of both wind tunnel and flight test technology for determining aerodynamic derivatives of aircraft motions
c11 A69-15572
Test facilities and techniques for low speed flight prcblems of aircraft handling qualities, stability, control and performance
c11 A69-15575
X-15 research aircraft program piloting problems, ground facilities, heat transfer, space flight and steep reentry
c02 A69-26872
Drag influence on mission performance of hypersonic aircraft during climb and cruise, noting payload capacity
c02 A69-37154
Kalman filter simulation for estimating aircraft position and velocity from airborne digital computer data in zero-zero landing system
[AIAA PAPER 69-944] c21 A69-40327
IFR flight tests of Breguet 941 STOL transport
[NASA-TN-D-4939] c02 N69-13252
Supersonic transport performance during real time simulated operations in future air traffic control system environments
[NASA-TN-D-5018] c02 N69-17257
Pilot rating scales and their use in assessing aircraft handling qualities
[NASA-TN-D-5153] c02 N69-22539

AIRCRAFT PILOTS
Exercise prescription for hypokinetic airline pilots to prevent physiological deterioration and maintain performance, discussing predictive tests, tolerance evaluation, training regimens, etc
c05 A69-41800

AIRCRAFT SAFETY
Ideal safety system for accident prevention, considering foreseeable and unforeseeable aspects to eliminate individual or collective human error
c34 A69-16836
NASA flight safety research, discussing size effects on aircraft handling and built-in response to failure modes
c02 A69-19764
Nuclear aircraft power plant, discussing safety, economy and obstacles
[AIAA PAPER 69-554] c22 A69-32761
Air safety - Conference, Anaheim, October 1968
c02 A69-41127
XB-70 aircraft test data as applied to SST safety, describing aircraft design, flight characteristics, instrumentation, takeoff and landing, etc
c02 A69-41143

AIRCRAFT STABILITY
Newton-Raphson technique development for determining stability derivatives from flight data, noting use of a priori wind tunnel information
[AIAA PAPER 69-315] c02 A69-22379
Differential synthesis technique application to design of multiaxis stability augmentation systems for aerospace vehicles
[AIAA PAPER 68-834] c31 A69-37156
Motion stabilization criteria for aircraft during spatial maneuvers
[NASA-TT-F-555] c02 N69-24761
Spin and recovery characteristics of 1/30 scale subsonic attack aircraft model determined in wind tunnel tests
[NASA-TM-X-1788] c02 N69-37976

AIRCRAFT STRUCTURES
Aircraft Structures and Materials Application - Conference, Seattle, September 1969
c15 A69-43416
Potential structural materials and design concepts for light aircraft
[NASA-CR-1285] c02 N69-20848
Jet exhaust location effects on longitudinal aerodynamic characteristics of jet V/STOL model
[NASA-TN-D-5333] c01 N69-33210

Elastic and plastic analyses of hail damage to aircraft surfaces
[NASA-TN-D-5363] c32 N69-33420

AIRCRAFT TIRES
Runway grooving to improve aircraft tire traction in adverse weather tested by F-4D and Convair 990A under wet conditions
[AIAA PAPER 69-773] c02 A69-35649
Reverted rubber during skidding of aircraft tires
[NASA-CR-1398] c02 N69-34915

AIRCRAFT WAKES
Path and shape of jet directed at large angles to subsonic free stream
[NASA-TN-D-4919] c01 N69-11634

AIRFIELD SURFACE MOVEMENTS
Airplane response to ground roughness from three-track runway and taxiway profiles by elevation angle measurements
[NASA-TN-D-5444] c02 N69-38770

AIRFOILS
Transonic wind tunnel studies on airfoil to determine effects of Reynolds number and boundary layer transition location on shock induced separated flow
[NASA-TN-D-5003] c01 N69-16121
Measured static aerodynamic forces for hypersonic flutter analysis on airfoil models in helium flow
[NASA-TN-D-5233] c01 N69-26271

AIRGLOW
Spectral and electrophotometric studies of upper atmosphere - airglows, atomic oxygen, hydroxyl emission, helium line spectra, auroras, and solar cycle effects on magnetosphere
[NASA-TT-F-530] c13 N69-16539

AIRLINE OPERATIONS
Airplane response to ground roughness from three-track runway and taxiway profiles by elevation angle measurements
[NASA-TN-D-5444] c02 N69-38770

ALBEDO
Particle albedos and extinction cross sections computed by Mie theory showing dependence on refractivity, considering thermal radiation from cloudy planetary atmospheres
c30 A69-38255

ALGORITHMS
Algorithm for Navier-Stokes and continuity equations used to derive curvilinear coordinate system
c08 A69-14858
Adaptive random search algorithm utilizing boundary cost-function hypersurfaces measurement to implement Pontryagin maximum principle, discussing hybrid computer use, iterative solution and convergence properties
c08 A69-33745
Impulsive orbit transfer optimization using accelerated gradient program based on Newtonian algorithm for digital computer method
c30 A69-35956
N-terminal parent networks with symmetry constraints derived for nonredundant one port configurations through combinatorial functions test patterns, using computer algorithm
c08 A69-42524
Algorithm for computing direction cosine matrix of strapdown inertial system
[NASA-TN-D-5384] c21 N69-36997

ALIPHATIC COMPOUNDS
Geochemical synthesis of branched chain acyclic polymers from irradiated isoprene
c04 A69-43750

ALKALI METALS
Vacuum distillation technique for isolation and recovery of alkali metal reaction products with Ta, Ni, V and oxygen
c14 A69-10927

ALKENES
Mechanical relaxation of poly 4 methyl pentene 1 at cryogenic temperatures, discussing temperature dispersion curve and secondary absorption associated with thermal motion of side chains
c18 A69-16492

ALL-WEATHER AIR NAVIGATION
All weather wing profile monitoring system using FPS-16 radar/jimsphere system and flight simulation for protection of space vehicle and missile launches
c20 A69-13852

ALLOYS
Alloying pairs of metal pellets to n and p type semiinsulating GaAs, discussing photo effects
c26 A69-32824

ALOUETTE 2 SATELLITE
Conjugate echoes in Alouette 2 topside sounder ionograms explained by multiple reflections between conjugate points of field line, noting magnetospheric waveguides role
c07 A69-20045
Cylindrical electrostatic probes on Alouette 2 and Explorer 31 satellites used in intersatellite comparison of directly measured ionospheric electron temperature and density
c14 A69-37876
Cylindrical electrostatic probe measurements on Alouette 2 and Explorer 31, considering implications for future missions
c14 A69-37877
Plasma temperature and ion concentration profiles determined from simultaneous measurements by Alouette 2 and Explorer 31 satellites of electron density, temperature and ion abundance
c13 A69-37896
Alouette 2 sounding data for magnetospheric field aligned propagation duct model
[NASA-TN-D-5332] c13 N69-34891

ALPHA PARTICLES
Angular correlation of inelastically scattered alpha particles and gamma rays emitted from 2-plus state of Sn 120
c24 A69-13098
Angular correlation between inelastically scattered 42 MeV alpha particles and emitted gammas from 2-plus Ni 58
c24 A69-13100
Absolute cross sections for coincidence detection of deuteron breakup by 42 MeV alpha particles, showing He 5 and Li 5 final state interaction peaks
c24 A69-13469
Asymmetry of polarized protons scattered from He 4 at 540 MeV for laboratory angles between 4 and 42 degrees
c24 A69-14966
Angular distributions for Sc 45 Ti 46 nuclear reactions involving 41 MeV alpha particles bombardment described by Born approximation
c24 A69-41044
Absolute cross sections for scattering of 42 MeV alpha particles from even isotopes of cadmium
[NASA-TN-D-4948] c24 N69-14482
Alpha particle-triton reaction on scandium 45 at 41 MeV
[NASA-TN-D-5216] c24 N69-24919
Elastic and nonelastic scattering cross sections from 42 MeV alpha particles interacting with helium isotopes
[NASA-TN-D-5530] c24 N69-40979

ALPHANUMERIC CHARACTERS
Alphanumeric listing and digital data x-y plotting by high speed printer, describing equipment modifications and control software
c08 A69-33108
High speed printer for hard copy alphanumeric listings and digital data plots
[NASA-TN-D-5474] c08 N69-38654

ALTERNATING CURRENT
Ac technique using lock-in power amplifier SNR for measuring galvanomagnetic and Shubnikov-de-Haas effects, noting error reduction
c14 A69-36375

ALTIMETERS
Tradeoff analysis on radar and laser space altimeter systems for sea surface geodesy
[NASA-CR-1298] c14 N69-21117

ALUMINUM
Cryogenic solenoids with pure Al conductor for production of strong magnetic fields, discussing softness and strain resistivity problems
c03 A69-26497
Aluminum double sheet target penetration resistance determined by studying high velocity pyrex glass impact effects on front/rear sheets and spacing
[AIAA PAPER 69-375] c32 A69-28305

Calorimetric, optical, and vibration investigation of stretch-formed aluminum solar concentrators for thermionic converters
[NASA-TN-D-4889] c03 N69-10708
Projectile shape effects on hypervelocity impact craters in aluminum
[NASA-TN-D-4953] c32 N69-14315
Effect of orientation and presence of surface active materials on friction and wear of aluminum
[NASA-TN-D-4994] c15 N69-16197
Electrochemical behavior of the aluminum electrode in molten salt electrolytes
[NASA-TN-D-5503] c06 N69-40240

ALUMINUM ALLOYS
Inclination effect of fatigue cracks on plane strain fracture toughness of 7075-T651 Al alloy, discussing cantilever bending
c32 A69-25958
Lightly loaded truss structures fabricated from Be, Be-Al alloy and uniaxial B filament reinforced epoxy tubing for unmanned spacecraft applications
c17 A69-35504
Axial load fatigue crack propagation tests on Al alloy sheets for stress ratio effects
c17 A69-36435
Theoretical prediction of crater size in Al alloy for hypervelocity impact by reduced density particles
[NASA-CR-1196] c32 N69-10225
Tensile properties and creep strength of aluminum alloys
[NASA-TN-D-5010] c17 N69-19203
Experimental and analytical studies of multiple liquid impact erosion of aluminum and stainless steel
[NASA-CR-1288] c15 N69-19786
Factors influencing low cycle crack growth of aluminum sheet specimens
[NASA-TN-D-5140] c32 N69-21392
Mechanical properties and column behavior of thin wall beryllium-aluminum alloy tubing
[NASA-TN-D-5145] c17 N69-23004
Adhesion of gold to copper and to copper aluminum alloys
[NASA-TN-D-5351] c23 N69-31984
Outdoor high temperature corrosion tests for aluminum alloys and titanium alloys, and stainless steels
[NASA-TN-D-5362] c17 N69-32558
Stress ratio effects on fatigue crack growth in sheet aluminum alloys
[NASA-TN-D-5390] c17 N69-34704
Momentum transfer from impact into thin aluminum meteor bumper targets
[NASA-TN-D-5492] c32 N69-38809

ALUMINUM COATINGS
Dielectric overcoating effects on electromigration Al interconnections, showing dependence on thickness and surface passivation
c09 A69-32889
Al interconnections discontinuities at integrated circuit contact windows observed by scanning electron microscope, noting catastrophic failure and Si presence
c09 A69-32893
Hypervelocity micrometeor impact sites identification on aluminized glass, using conchoidal pattern as criterion in analysis
c30 A69-34952
Steady state acceleration effects on combustion characteristics of aluminized composite solid propellant
[NASA-TN-D-4914] c33 N69-13231

AMBIENT TEMPERATURE
Tensile and cyclic fatigue properties of graphite filament-wound pressure vessels at ambient and cryogenic temperatures
[NASA-TN-D-5354] c32 N69-31300
Removal of acid gases and oxides of nitrogen from spacecraft cabin atmospheres at ambient temperatures
[NASA-CR-1388] c05 N69-37517
Pressurized liquid nitrogen inside parametric amplifier structures for input, noise, and temperature improvements
[NASA-TN-D-5509] c09 N69-40079

AMINES
Electron transport chain of monovalent and divalent cations and of polyamines, studying effects on menadione reductase activity to determine salt dependence
c04 A69-41077

AMMONIA
Radiation induced reduction of ammoniacal nickel /2/ sulfate to metallic nickel
[NASA-TN-D-5213] c06 N69-24940

AMMONIUM PERCHLORATES
Ammonium perchlorate high temperature decomposition by using carbon dioxide laser pyrolysis/mass spectrometry
[AIAA PAPER 69-143] c06 A69-18111

AMPLIFICATION
Logarithmic variation criteria for stability of feedback systems with time varying gains
c10 A69-13073

AMPLIFIER DESIGN
Hybrid integrated parametric amplifier design considerations for fabrication in microstrip transmission line
c09 A69-10193
Four terminal silicon planar p-n-p-n model operating as semiconductor small signal linear tetrode amplifier, discussing properties and mathematical models
c09 A69-35293

ANALOG SIMULATION
Analog simulation of closed loop Brayton cycle test facility
[NASA-TM-X-1715] c03 N69-14312
Physical model for plasma containment simulation in magnetic fields
[NASA-TN-D-5217] c25 N69-25394

ANALOG TO DIGITAL CONVERTERS
Spacecraft analog to digital conversion system employing metal oxide semiconductor field effect transistors
[NASA-TN-D-5228] c08 N69-29478

ANALYSIS (MATHEMATICS)
Equations for pressure signature of supersonic projectile in stratified atmosphere
[NASA-TN-D-4890] c02 N69-10087
Theoretical analysis of pressure distribution, load capacity, attitude angle, and friction force for eccentric Rayleigh step journal bearing - infinite length solution
[NASA-TN-D-4873] c15 N69-10231
Small eccentricity stability analysis for externally pressurized gas lubricated bearings with journal rotation
[NASA-TN-D-4934] c15 N69-13256
Approximate mathematical analysis of supersonic inlet dynamics
[NASA-TN-D-4969] c01 N69-14289
Operational analysis of mass measuring system in orbiting spacecraft
[NASA-TN-D-5039] c04 N69-19115
Mathematical analysis of Fitzgerald apparatus measuring solids dynamic mechanical properties
[NASA-TN-D-5116] c18 N69-21384
Thermal flutter analysis of booms with open cross section
[NASA-TN-D-5222] c32 N69-29589
Model analysis for viscosity in jet mixing flows
[NASA-CR-1382] c12 N69-31887
Aviation pilot reactions and opinions on grooved runways
[NASA-CR-1428] c02 N69-35861
Mathematical analysis of wave structure in supersonic flow
[NASA-CR-1438] c04 N69-37062
Analytic function theory applications to analysis of single-sideband angle modulated systems
[NASA-TN-D-5446] c07 N69-37602
Modern network theory applications to analysis of complex systems
[NASA-TN-D-5511] c19 N69-40088

ANALYTIC FUNCTIONS
Analytic continuation of Appell hypergeometric series into linear combination of four infinite series
c19 A69-26605
Analytic time function models of stochastic processes of noise and modulation
[NASA-TR-R-314] c07 N69-29230

Analytical solutions of optimum orbit modifications
[NASA-CR-1379] c30 N69-31362
Analytic function theory applications to analysis of single-sideband angle modulated systems
[NASA-TN-D-5446] c07 N69-37602

ANALYZERS
Energy conversion and distribution of spiraling electron beam using retarding field analyzer
[NASA-TN-D-5490] c09 N69-41208

ANCHORS (FASTENERS)
Magnetically anchored eddy current and eddy current rod dampers for GEOS gravity gradient stabilized satellite
[NASA-CR-1282] c14 N69-18953

ANGLE OF ATTACK
Three dimensional hypersonic steady flow around blunt and pointed cones at nonzero angles of attack calculated by method of characteristics
[AIAA PAPER 69-187] c01 A69-18176
Effects of angle of attack and bluntness on shock layer properties of cones at supersonic speeds
[NASA-TN-D-4909] c01 N69-10789
Effect of unit Reynolds number, nose bluntness, angle of attack, and roughness on transition on 5 degree half-angle cone at Mach 8
[NASA-TN-D-4961] c01 N69-14872
Surface pressure distribution on spherical blunted cones, and correlation of Mach numbers, cone angle, and angle of attack
[NASA-TN-D-5204] c01 N69-24764
Turbulent boundary layer of subsonic transport fuselage with pressure gradient, Reynolds number, and angle of attack
[NASA-TN-D-5242] c01 N69-28112
Conditions for supersonic aircraft entering critical stall and spin regimes
[NASA-TT-F-526] c02 N69-31917
Jet fighter aircraft lateral directional stability at high angles of attack
[NASA-TN-D-5361] c02 N69-32337
Jet velocity and axial location of nozzle exit on performance of twin-jet afterbody model
[NASA-TN-D-5393] c28 N69-36932
Effect of angle of attack and injection pressure on jet penetration and spreading from Delta wing in supersonic flow
[NASA-TM-X-1889] c12 N69-37271
Laminar heating rate from wind tunnel tests using angle of attack and Reynolds number
[NASA-TN-D-5450] c12 N69-37604

ANGLES (GEOMETRY)
Fourth angle driving law for different four gimbal systems used for simulation display and inertial platform isolation
c11 A69-26265
X-15 research aircraft program piloting problems, ground facilities, heat transfer, space flight and steep reentry
c02 A69-26872
Photomultiplier tubes performance enhancement by light incidence on photocathode at oblique angles explained by reflection
c23 A69-42194
Effects of cone angle, base flare angle, and corner radius on Mach 3 aerodynamic characteristics of large angle cones
[NASA-TN-D-5048] c01 N69-19926
Cryogenic fracture properties of thin AISI 301 cold reduced sheet at different angles to rolling direction
[NASA-TN-D-5413] c17 N69-35688
Aerodynamic characteristics of large-angle cones in supersonic lifting capabilities
[NASA-TN-D-5499] c01 N69-40026

ANGULAR ACCELERATION
Rotational velocity estimates by observers during angular acceleration, noting vestibular function interpretation
c04 A69-15332
Psychophysical methods for determining perception threshold of angular acceleration in man during vertical rotation
c04 A69-15969
Human angular acceleration sensitivity using rotation and oculogyral illusion perception as indicators, relating to spatial orientation and flight control task precision
c05 A69-41674
Human physiological responses to angular acceleration during breath holding, Mi, Valsalva and Meuller respiratory maneuvers in hollow spherical simulator
c05 A69-41679
Aluminum size and loading effects on burning rate of centrifugal accelerated solid propellants
[NASA-TN-D-5397] c27 N69-36225

ANGULAR CORRELATION
Angular correlation of inelastically scattered alpha particles and gamma rays emitted from 2-plus state of Sn 120
c24 A69-13098
Angular correlation between inelastically scattered 42 MeV alpha particles and emitted gammas from 2-plus Ni 58
c24 A69-13100

ANGULAR DISTRIBUTION
Emission and frequency shift angles of anti-Stokes radiation from trapped filaments of laser light in liquids
c23 A69-10012
Angular distributions for Sc 45 Ti 46 nuclear reactions involving 41 MeV alpha particles bombardment described by Born approximation
c24 A69-41044
Energy and angular distribution of electrons transmitted through silicon targets
[NASA-TN-D-5075] c24 N69-19113

ANGULAR MOMENTUM
Stellar rotation braking due to mass loss from coronae through stellar wind based on calculation of acoustic energy generation from convective zone
c30 A69-20644
Lunar origin theories, considering moon/earth mass ratio, earth-moon system angular momentum deficiency and differential volatilization in earth
c30 A69-29882
Quiet solar wind model with magnetic field numerically calculated, obtaining coronal electron densities and angular momentum near earth
c29 A69-34301
Primitive solar nebula physical model considered under angular momentum conservation in collapsing fragment
c30 A69-36074
Order-disorder transitions in solid hydrogen, discussing model to explain molecular rotation angular momentum operator fluctuations
c23 A69-43119
Generation of ideal coordinate systems for analysis of optimal trajectories
[NASA-CR-1250] c30 N69-13274

ANGULAR VELOCITY
Relation between amplitude of light and radial velocity variations of beta Canis Majoris stars
c30 A69-14126
Rotational velocity estimates by observers during angular acceleration, noting vestibular function interpretation
c04 A69-15332
Three axis attitude servomechanism design to adjust attitude and angular velocity of spacecraft
c21 A69-17589
Elastohydrodynamic solution for ball torque spinning without rolling in nonconforming groove, showing increase in torque with stress and spinning and decreasing conformity
[ASME PAPER 69-LUBS-11] c15 A69-34381
Neutral exosphere model for nonrotating planet permitting barosphere uniform rotation at certain angular velocity, determining velocity distribution and density
c30 A69-40524
Carroll Fourier transform method applied to stellar spectra lines to determine small rotational velocities
c30 A69-42404
Conditions for supersonic aircraft entering critical stall and spin regimes
[NASA-TT-F-526] c02 N69-31917

ANIMALS
Respiratory system and oxygen metabolism regulation in man and animals
[NASA-TT-F-501] c04 N69-31401

Gravitational and acceleration effects on man and organisms, and biological effects of radiation
[NASA-TT-F-528] c05 N69-38701
ANISOTROPIC MEDIA
Anisotropic Heisenberg ferromagnets in random phase and spin wave approximation
[NASA-TN-D-5286] c26 N69-29588
ANISOTROPY
Twenty year wave in diurnal anisotropy component of galactic cosmic rays arriving at earth from asymptotic direction east of sun interpreted as magnetic reconnection
c29 A69-38098
Molecular orientation and mechanical isotropy in polyethylene, polypropylene, and polyethylene terephthalate films
[NASA-TN-D-5380] c18 N69-34708
ANNEALING
Electric field effects on thermal annealing of electron irradiation damage in p-channel MOSFET device
c09 A69-16562
Annealing temperature of radiation defects in phosphorus doped silicon, discussing isochronal recovery characteristics of solar cells with different donor and oxygen concentrations
c26 A69-24006
Analysis of annealed and proton irradiated silicon
[NASA-TN-D-5119] c26 N69-22552
Diffusion lengths of silicon solar cells after radiation damage and annealing by X ray method
[NASA-TM-X-1894] c03 N69-37827
Magnetothermal oscillations in pressure annealed pyrolytic graphite
[NASA-TN-D-5488] c26 N69-39239
ANNIHILATION REACTIONS
Cosmic gamma ray spectra from metagalactic proton-antiproton annihilation
c29 A69-21459
Extragalactic gamma ray fluxes predicted, discussing collisions, matter-antimatter annihilation and cosmological implications
c29 A69-24466
Annihilation gamma ray spectra from equilibrium spectra of secondary galactic positrons
c29 A69-29948
ANNUAL VARIATIONS
Semiannual density variations in thermosphere and exosphere as function of mixtopause height variations
c13 A69-26012
Diurnal and seasonal variations of primary atmospheric ions in topside ionosphere correlated with solar zenith angle, using ion mass spectrometer on Explorer 32
c13 A69-38087
Distributions, seasonal variations and ionospheric implications of mesospheric nitric oxide concentration
c13 A69-38364
ANNULAR FLOW
Reduction of noise from underexpanded axisymmetric jet flows using radial jet flow impingement
[AIAA PAPER 68-81] c12 A69-28212
Flow characteristics and wall heat transfer in separated flow region of annular cavity at free stream hypersonic speed and high gas temperature
[AIAA PAPER 68-672] c01 A69-37185
Application of boundary layer control concepts to highly loaded turbine stator blades in annular cascades
[NASA-CR-1219] c01 N69-14211
Computer analysis of total pressure loss and air flow distribution in annular flow gas turbine combustion chambers
[NASA-TN-D-5385] c33 N69-33314
Natural frequency of liquids in annular cylinders under low gravity conditions
[NASA-TN-D-5412] c12 N69-35842
ANNULI
Properties and uses of liquid metal reactor fuels, including heat transfer processes in variously shaped channels, boiling and condensation of metals, and reactor control equipment
[NASA-TT-F-522] c33 N69-30507
ANTARCTIC REGIONS
Albedo over Antarctic, measuring solar radiation reflected by surface and atmosphere by Eppley radiometer
c13 A69-21404
ANTENNA ARRAYS
Radiating collinear open ended waveguides and near field coupling analyzed using simultaneous integral equations and Fourier series expansion of aperture field
c09 A69-24984
Backfire antenna radiation characteristics and physical dimensions for tracking and telemetry applications, including five element array model
c07 A69-36251
Gain measurement of two element phased array aperture antenna during ATS-C tracking
c07 A69-36254
ANTENNA FEEDS
Multiplicative feed system for monopulse angle tracking antennas, discussing influence of sidelobe and backlobe responses on control function slope determining antenna bearing angle
c11 A69-37704
Waveguide fed rectangular aperture antenna with dielectric plug load, describing admittance/ resonant perturbation due to excited TE mode
c09 A69-41589
Parabolic antenna properties generated by dual band circularly polarized focused two channel monopulse feed system, discussing tracking data from helicopter, Apollo 8 and Cassiopeia A
c07 A69-41752
ANTENNA RADIATION PATTERNS
Radiation pattern of axial slot on circular conducting cylinder based on wedge diffraction and creeping wave theory
c07 A69-24993
Backfire antenna radiation characteristics and physical dimensions for tracking and telemetry applications, including five element array model
c07 A69-36251
VHF cavity backed cylindrical gap antenna input tuning impedance and equatorial radiation patterns controlled by cavity adjustments
c09 A69-40698
Equatorial radiation pattern of parallel plate TEM mode axial slot on elliptical conducting cylinders, using wedge diffraction and creeping wave theory
c09 A69-40703
Edge diffraction effects in TEM axially slotted finite ground plane on radiation pattern in waveguides of different geometries
c07 A69-41588
Simple antenna with good circular polarization over wide space sector, showing geometry, normalized orthogonal field distributions and beamwidth range, considering slot combinations
c09 A69-41590
Transmission loss and effects on antenna radiation patterns and impedance produced by thermally degraded ablation materials
[NASA-TN-D-4879] c07 N69-10885
Apollo astronaut, backpack monopole antenna and its radiation patterns
[NASA-TN-D-5081] c07 N69-23882
Slope diffraction analysis of TEM parallel plate guide patterns
[NASA-CR-1326] c07 N69-26273
ANTENNAS
Waveguide fed rectangular aperture antenna with dielectric plug load, describing admittance resonant perturbation due to excited TE mode
c09 A69-41589
Antenna effects on aerodynamic characteristics of 0.410 scale model Cajun rocket at Mach numbers from 2.30 to 4.63
[NASA-TM-X-1771] c01 N69-21106
ANTHROPOMETRY
Human responses to spacecraft cabin atmosphere, pressure, and contamination, and water supply, diet, and anthropometry
[NASA-CR-1205-VOL-3] c04 N69-12592
ANTIFERROMAGNETISM
Anisotropic Heisenberg antiferromagnetism in spin wave approximation, calculating thermodynamic quantities in terms of elliptic integrals
c26 A69-26500
ANTIFRICTION BEARINGS
Hydrodynamic conical and spherical spiral grooved grease bearings replacement of gyro ball bearings for extended space missions

[AIAA PAPER 69-836] c15 A69-39367
Magnetic air bearings for use as low friction overhead support fixtures in vertical lunar gravity simulator
[NASA-CR-1235] c05 N69-14213
Performance evaluation of oil lubrication system for antifriction bearing rotor system of Brayton cycle turbomachinery
[NASA-CR-1229] c15 N69-16463
Pump and seal parameters for helical groove, hermetically sealed pump and bearing rotor
[NASA-TN-D-5225] c15 N69-24791

ANTIPROTONS
Cosmic gamma ray spectra from metagalactic proton-antiproton annihilation
c29 A69-21459
Proton-antiproton high energy elastic scattering by bosons exchange, introducing vertex functions for nonlocal Lagrangian
c24 A69-39467

AORTA
Elastic behavior of large blood vessels in canine aorta by measuring dispersion and attenuation of artificially induced pressure waves
c04 A69-14692

APERTURES
Admittance of parallel plate waveguide aperture with infinite flange illuminating metal sheet, using wedge diffraction theory and integral transform method
c09 A69-12328
Radiating collinear open ended waveguides and near field coupling analyzed using simultaneous integral equations and Fourier series expansion of aperture field
c09 A69-24984
Air gap tolerances effect on admittance of TEM mode dielectric and plasma coated slot antennas determined by variational method
c09 A69-24986
Mechanical collimator using random aperture arrays for celestial observation at extreme UV and X rays
c14 A69-36489
Admittance of parallel plate aperture illuminating displaced dielectric-dielectric boundary
[NASA-TN-D-5038] c07 N69-19114

APOLLO APPLICATIONS PROGRAM
Space station design requirements, Apollo applications program and various experimental programs
c31 A69-11395
Communications for Apollo Applications Program, considering extended duration manned missions in low earth orbit and Gemini, Saturn and Apollo hardware
c07 A69-19124
Manned spacecraft developments, considering Apollo Applications Program, space station establishment, space shuttle operations and payload cost
c31 A69-22866
Stored program data processor used as PCM telemetry data acquisition system for postApollo applications, considering format and bit rate changes
c07 A69-36280
Fuel cell /battery and solar array/ battery systems for manned Apollo Applications Program /AAP/ space vehicles, considering mission and power requirements
c03 A69-42244
Logistics management developed for Apollo Applications Program of NASA Manned Spacecraft Center
[AAS PAPER 69-204] c34 A69-42812
Apollo Applications Program /AAP/ spacecraft, describing contributions to space station engineering
[AAS PAPER 69-491] c31 A69-42838

APOLLO FLIGHTS
Entry phase flight data of Missions AS-202, Apollo 4 and 6 compared with wind tunnel aerodynamics data
[AIAA PAPER 68-1143] c31 A69-13556
Apollo 4, 5 and 6 space missions, with preview of Apollo 7, 8 and 9 missions
c31 A69-17672

APOLLO LUNAR SURFACE EXPERIMENTS PACKAGE
Lunar laser beam retroreflection observations, showing agreement with predicted ephemeris and signal strength
c30 A69-43197

APOLLO PROJECT
Magnetometer experiment for Apollo project to measure lunar surface magnetic field, describing mission requirements and instrumentation
[AAS PAPER 68-206] c30 A69-11481
Photographic control system requirements for Project Apollo manned launches, considering extreme heat, vibration and sound pressure environment
[SMPTE PAPER 104-20] c14 A69-14360
Systems engineering activities in manned space flight involving design, development, manufacture, test and operation of Mercury, Gemini and Apollo flight systems
c31 A69-17602
Radiation protection plan for Apollo lunar mission based on real time monitoring of solar activity and radiation in spacecraft
[AIAA PAPER 69-19] c29 A69-18113
Nondestructive testing methods for Saturn 5 space vehicle with emphasis on NDT equipment for Apollo program
c15 A69-23050
Apollo mission simulation, discussing Command Module Simulator /CMS/, onboard computer system and dynamic visual presentation via infinity-optics display
[SMPTE PAPER 105-74] c11 A69-25768
Thermal Vacuum /TV/ manned test operations related to Apollo lunar module in simulated space environment
c05 A69-30394
NASA lunar survey and mapping for generating Apollo satellite landing navigation control, using analytic photogrammetry, camera position and altitude data of lunar topography
c14 A69-36931
Plastics applications in Apollo-Saturn 5 program, considering foam, honeycomb, conformal coatings, embedment compounds, dielectrics, damping compounds, adhesives, sealants and gaskets
c18 A69-38533
Real time targeting for Apollo lunar orbit insertion maneuver burn, discussing impulsive maneuvers for flight control
[AIAA PAPER 68-848] c31 A69-39760
Apollo lunar sample collection and analysis, discussing astronauts activity and equipment, sample types, laboratories for radioactive counting and gas analysis, etc
c11 A69-40191
Direct stiffness method of computing vibrational characteristics of dynamic model of Apollo-Saturn 5 vehicle - umbilical tower configuration
[NASA-TN-D-4871] c31 N69-10934
Lateral vibration characteristics of dynamic model of Apollo-Saturn 5 launch vehicle
[NASA-TN-D-4872] c31 N69-11007
Apollo astronaut, backpack monopole antenna and its radiation patterns
[NASA-TN-D-5081] c07 N69-23882
Chronology of Apollo spacecraft program to 7 Nov. 1962
[NASA-SP-4009] c31 N69-32021

APOLLO SPACECRAFT
Apollo thermal protection system, noting low density ablation, flight and ground tests
[AIAA PAPER 68-1142] c31 A69-13558
Entry corridor thermal entry limits for Apollo spacecraft defined for design of thermal protection system
[AIAA PAPER 68-1144] c31 A69-13673
Apollo 4, 5 and 6 space missions, with preview of Apollo 7, 8 and 9 missions
c31 A69-17672
Radiation measurements inside Apollo 4 and 6 command modules during passage through trapped radiation belts
[AIAA PAPER 69-17] c05 A69-18202
Guidance and control concepts and hardware for atmospheric entry of Mercury, Gemini and Apollo spacecraft
c21 A69-25724

Manned spacecraft fuel cell selection and design, discussing Gemini ion exchange membrane and Apollo Bacon cell systems
c03 A69-32406
Apollo optics system ground and flight performance tests results, suggesting possible design changes for sunlit space environments
c14 A69-35796
Apollo-Saturn 5 propulsion and structure feedback loop, analyzing POGO components and Nyquist plot application
[AIAA PAPER 69-877] c31 A69-39403
Telecommunications performance of two lunar relay satellite system /LRSS/, determining operation capabilities with Apollo communications system
c07 A69-42508
Apollo afterbody heat transfer, studying ablation effects for various reentry angles of attack
c33 A69-43680
Identification of structural systems using near resonance testing
[NASA-TN-D-5069] c32 N69-17737
Optical simulation landing system for evaluating pilot controlled flexible parawing and Apollo capsule combination performance during landing
[NASA-TN-D-5049] c21 N69-20936
Effect of heat shield flexibility on water landing loads of Apollo spacecraft models
[NASA-TN-D-5108] c32 N69-21042
Ablation behavior of heat shield of Apollo command module over wide ranges of thermal environments
[NASA-TM-X-1778] c33 N69-22933
Relationship between binocular depth perception and optical distortion in Apollo pressure suit helmets and visors
[NASA-TN-D-5162] c05 N69-22990
Aerodynamic loads on deployed canard surfaces and rocket nose section of Apollo launch escape vehicle
[NASA-TN-D-5260] c31 N69-28166
Aerodynamic characteristics determined during development of Apollo launch escape vehicle configuration in wind tunnel tests
[NASA-TN-D-5208] c01 N69-29027
Measurements of mutual interference heating for probe antenna mounted on Apollo reentry configuration
[NASA-TM-X-1787] c01 N69-29318
Free flight test model measurement of drag, lift, and trim in wind tunnel for Apollo command module
[NASA-TN-D-5276] c30 N69-29557
Entry aerodynamics at lunar return conditions from command module of Apollo 4 flight
[NASA-TN-D-5399] c31 N69-38820
Wind tunnel study of aerodynamic pressures on Apollo command module configuration
[NASA-TN-D-5514] c01 N69-40345

APOLLO TELESCOPE MOUNT
Real time digital computer hardware simulation of Apollo Telescope Mount /ATM/ mission
[AIAA PAPER 69-940] c11 A69-40323
Objectives and experiment designs for Apollo telescope mount
[NASA-TN-D-5020] c30 N69-21526

APOLLO 11 FLIGHT
Apollo 11 mission and future space exploration prospects including moon base, manned space station, reusable shuttle vehicles, etc
c30 A69-41477

APOLLO 7 FLIGHT
Clinical report on Apollo 7 and 8 mission medical data, discussing preflight preventive medical activities, inflight treatment, radiation levels, etc
c05 A69-22542

APOLLO 8 FLIGHT
Clinical report on Apollo 7 and 8 mission medical data, discussing preflight preventive medical activities, inflight treatment, radiation levels, etc
c05 A69-22542
Rate of loss of uranium dioxide or uranium mononitride from vented nuclear fuel element
[NASA-TN-D-4913] c22 N69-10734

APPENDAGES
Deployable appendages of OGO attitude controlled spacecraft design
c31 A69-17606

APPLICATIONS OF MATHEMATICS
Computerized Arrhenius equation component reliability extrapolation techniques
[NASA-TN-D-4902] c19 N69-13368

APPLICATIONS TECHNOLOGY SATELLITES
Space applications program including communications and navigation meteorology, earth resources survey and geodesy
[UN PAPER 68-95437] c34 A69-10472
NASA Space Application Program strategy, discussing research and development trend toward complexity, versatility and multidisciplinary use of larger spacecraft
c30 A69-13427
Cosmic radio noise intensity measurements by ATS 2 satellite-borne radiometer
c30 A69-19715
Ammonia resistojet stationkeeping subsystem onboard ATS 4 satellite, noting flight test data agreement with ground tests
[AIAA PAPER 69-296] c28 A69-21212
Cesium contact ion microthrustor experiment onboard ATS 4, measuring emission currents and spacecraft potentials
[AIAA PAPER 69-297] c28 A69-21218
ATS 3 satellite reflectometer experiment carrying test samples to measure specular reflectance, noting silica shield effects
[AIAA PAPER 69-644] c33 A69-33270
Solar cell radiation damage during 416.8 days in synchronous orbit on satellite ATS 1, discussing radiation shields
c03 A69-35704
Gain measurement of two element phased array aperture antenna during ATS-C tracking
c07 A69-36254
ATS 3 spacecraft ammonia-fueled resistojet engine test performance
[AIAA PAPER 68-553] c28 A69-39754
Intersatellite microwave laser communication system for ATS-F and ATS-G, discussing experiment, functional design and parameters
c07 A69-41758
Atlas-Agena flight performance for Applications Technology Satellite-1 mission
[NASA-TM-X-1784] c31 N69-24038
Postflight analysis of flight performance of Atlas Agena launch vehicle for Applications Technology Satellite ATS-2 mission
[NASA-TM-X-1800] c31 N69-27260
Flight performance of Atlas Agena launch vehicle in support of Applications Technology Satellite-3
[NASA-TM-X-1879] c31 N69-37840

APPROACH CONTROL
V/STOL aircraft radar inertial navigation system, describing approach and landing phase flight test results
[AAS PAPER 69-401] c02 A69-42831
Flight tests of modified aileron direct lift control system during approach and landing of F8-C aircraft
[NASA-TN-D-4854] c02 N69-10371
Operational limitations in flying noise abatement approaches
[NASA-TN-D-5497] c02 N69-39188

APPROXIMATION
Coulomb approximation for dipole and quadrupole transitions, calculating tables for radial matrix elements
c24 A69-10901
Equations governing cosmic ray modulation and approximate equations valid at high and low energies
c29 A69-43169
Approximate mathematical analysis of supersonic inlet dynamics
[NASA-TN-D-4969] c01 N69-14289
Nonlinear compressible flow problems - half-space of ideal compressible fluid motion due to arbitrary pressure front
[NASA-TT-F-560] c12 N69-27168
Complete approximation in Euclidean space of new boundary value problem
[NASA-TT-F-577] c12 N69-29235
Approximation for mean and standard deviation of magnitude of statistical velocity correction vector
[NASA-TN-D-5381] c30 N69-36143

Concepts of theory of fuzzy systems
[NASA-CR-1432] c19 N69-37033
ARC CHAMBERS
High enthalpy arc tunnel at Langley Research Center for simulating aerodynamic heating and forces during spacecraft reentry
[NASA-TN-D-5295] c11 N69-29981
ARC DISCHARGES
Segmented anode, carbon dioxide-hydrogen performance and hollow cathode erosion tests on low power MPD arc thrustor, noting current measurements
[AIAA PAPER 69-242] c28 A69-21236
Pulsed experiments on high powered constricted electric arc with axial flow performed by discharging transmission line
[GDC-DBE-68-008] c25 N69-17212
Performance of radiation cooled magnetoplasmadynamic arc thrustors
[NASA-TM-X-1908] c28 N69-40058
ARC HEATING
He and Ar arc-heated flows into reservoir and expansion in converging-diverging supersonic nozzles, considering flow equilibrium effect on heat transfer and enthalpy
c33 A69-37198
Exploding wire initiation and electrical operation of 40 kV system for arc heated drivers up to 10 feet long
[NASA-TN-D-5126] c11 N69-22989
Physical model for behavior of thermionic arc spots on MHD generator cathode
[NASA-TN-D-5414] c25 N69-35732
Langmuir and interferometric measurements on electron concentration in arc heated wind tunnel using air and nitrogen
[NASA-TN-D-5500] c25 N69-39302
ARC JET ENGINES
Electric propulsion systems for manned planetary exploration flights, discussing arc jet, ion and plasma engines
c28 A69-35108
ARC MELTING
Vacuum arc melted W and W-Re alloys mechanical properties, noting Re additions effects
c17 A69-20190
ARCAS ROCKET VEHICLES
Comparisons of wind and temperature data obtained by Japanese MT-135 and American ARCAS meteorological rocket systems in closely spaced launchings
[NASA-TM-X-1726] c20 N69-17772
ARGON
Composition and line emission characteristics of ionized tungsten, uranium, and argon
[NASA-CR-1313] c25 N69-21124
Rapid computation of equilibrium, chemical composition, and thermodynamic properties of argon-oxygen-hydrogen gas system
[NASA-TN-D-5416] c33 N69-36299
ARGON PLASMA
Spectral emission characteristics of gaseous tungsten and uranium in induction heated argon plasmas
[NASA-CR-1314] c25 N69-22920
ARITHMETIC
Tagged arithmetic system for use with FORTRAN programs
[NASA-TN-D-5370] c08 N69-32556
ARMED FORCES (UNITED STATES)
Balloon flights with space available for secondary experiments, discussing launching agencies and experiment design restrictions
c02 A69-40807
AROMATIC COMPOUNDS
Interstellar extinction models of classical Mie particles and quantum mechanical polycyclic aromatic molecules
c30 A69-23679
Syntheses and properties of pyrrone polymers
[NASA-CR-1310] c18 N69-26448
ARSENIC
Backward diodes in indium arsenide for microwave mixing
[NASA-TN-D-5401] c09 N69-36706
ARTERIES
Axial waves in blood vessels, determining phase velocities and damping, noting anisotropic behavior of artery wall
[SESA PAPER 1350] c04 A69-19726
ARTIFICIAL GRAVITY
Manned space stations for future space exploration, discussing earth-like environment, artificial gravity, human factors and time dependence
c30 A69-25644
Summary of potential adverse effects of artificial gravity and weightlessness on astronaut physiological processes and performance in aerospace environment
[NASA-TN-D-4980] c05 N69-15629
Operational and structural design criteria for artificial gravity stabilization of rotating space station
[NASA-TN-D-5426] c05 N69-39210
ARTIFICIAL SATELLITES
Evaluation of double wall balloon enclosure for thermal control of inertial satellites
[NASA-TN-D-5230] c33 N69-28209
Disturbing factors in motion of artificial earth satellites due eccentricity of earth gravitational field
[NASA-TT-F-539] c30 N69-33560
Lunar and artificial satellite theories treated by generalization of Von Zeipel procedure
[NASA-TN-D-5459] c30 N69-38145
Physical properties of Martian atmosphere using solar occultation seen from artificial satellite
[NASA-TN-D-5443] c30 N69-38658
Longitudinal dynamics of lifting vehicle in orbital flight
[NASA-CR-1449] c30 N69-40062
ASPECT RATIO
Aerodynamic characteristics of full scale model sailwing with aspect ratio 5.9
[NASA-TN-D-5047] c01 N69-19243
ASTEROIDS
Gegenschein measurements for determining upper limit on asteroidal debris spatial density
c30 A69-12545
ASTRIONICS
Spacecraft electronics - Conference, Chicago, December 1968
c09 A69-22433
ASTRODYNAMICS
Astrodynamics, guidance and control - Conference, Belgrade, September 1967, Volume 1
c30 A69-17560
Astrodynamical data compilation for use by system engineer for mission planning
[AIAA PAPER 69-124] c30 A69-18090
ASTRONAUT LOCOMOTION
Unstabilized astronaut, hand-held and integrated life support EVA maneuvering units tested in gimbaled six degree of freedom servo driven moving base simulator
[AAS PAPER 69-516] c05 A69-42850
Astronaut capability to maintain life support systems and cabin habitability in weightlessness
[NASA-CR-1405] c05 N69-36709
Simulation of astronaut locomotion on lunar surface to determine metabolic costs
[NASA-CR-1402] c05 N69-37964
ASTRONAUT PERFORMANCE
Space travel and lunar exploration medical problems
c04 A69-27909
Real time metabolic rate analysis of suited astronaut using heart rate and O methods during thermal vacuum and extravehicular mobility tests
[AIAA PAPER 69-993] c05 A69-40371
Human responses to spacecraft cabin atmosphere, pressure, and contamination, and water supply, diet, and anthropometry
[NASA-CR-1205-VOL-3] c04 N69-12592
Summary of potential adverse effects of artificial gravity and weightlessness on astronaut physiological processes and performance in aerospace environment
[NASA-TN-D-4980] c05 N69-15629
Astronaut extravehicular work performance under simulated weightlessness conditions
[NASA-CR-1334] c05 N69-27266
Predicting human performance in space environments
[NASA-CR-1370] c05 N69-30168
Physiological and psychological responses of man to space flight problems
[NASA-TT-F-529] c05 N69-32044

ASTRONAUTICS
Aviation and astronautics - Conference, Tel-Aviv and Haifa, March 1969
c12 A69-29011
Professional programs for aeronautics, rocketry and astronautics development
c34 A69-34552
ASTRONAUTS
Preflight and postflight leukocyte chromosome aberration analyses of Gemini astronauts
c04 A69-33173
Configurations for extravehicular activity work platforms for astronaut use in orbital assembly
[NASA-CR-1361] c31 N69-26993
ASTRONAVIGATION
Sextant sighting performance concerned with training and monochromatic stars
[NASA-TN-D-5190] c05 N69-35024
ASTRONOMICAL MODELS
IR radiation of NML Cygnus with O/C ratio close to unity ascribed to circumstellar shell of graphite particles
c30 A69-13775
Scaled solar and gray-body temperature distribution models compared to determine stellar atmosphere
c30 A69-14626
Instability of stellar structures intermediate between white dwarfs and neutron stars shown by stellar models, discussing pulsar signals periodicities
c30 A69-20770
Subdwarf HD 25329 studied with model atmosphere approach, using H alpha, Na I and Mg I profiles for effective temperature
c30 A69-22199
Structure and pulsational properties of massive stars with helium cores and thin hydrogen poor envelopes
c30 A69-22421
Collisionless plasma heating by damping hydromagnetic waves applied to solar wind qualitative model, discussing magnetoacoustic wave energy
c30 A69-22426
Interstellar extinction models of classical Mie particles and quantum mechanical polycyclic aromatic molecules
c30 A69-23679
Green function solution to Maxwell equations for interplanetary and coronal magnetic fields above photosphere, considering field at source surface
c30 A69-24429
Extinction efficiency of graphite core interstellar grains with solid hydrogen and ice mantles, using theoretical models
c23 A69-29587
Nova outburst dynamics investigation by time dependent hydrodynamics computer program including energy transport by radiation and convection
c30 A69-30769
Corrections to previous papers on extragalactic gamma rays, discussing effects on various cosmological models
c29 A69-34168
Quiet solar wind model with magnetic field numerically calculated, obtaining coronal electron densities and angular momentum near earth
c29 A69-34301
Lunar temperature prediction with emphasis on variable property models, noting assumptions about physical properties appearing in heat conduction equations
c30 A69-34374
X ray sources model, describing possible ring of matter around white dwarf near end of active evolution
c29 A69-35204
Primitive solar nebula physical model considered under angular momentum conservation in collapsing fragment
c30 A69-36074
Monte Carlo relaxation method for physically self consistent model stellar atmospheres, discussing stability, accuracy and convergence of solution
c30 A69-36337
Atmospheric models for specified effective temperatures, hydrogen-to-metal ratios and surface gravities in studying metal deficiency effect on stellar atmosphere
c30 A69-36338
Type 3 solar radio bursts observed during April - October 1967 for two alternative models of active region streamers in outer corona
c29 A69-40300
Red shift-magnitude relation for universe model and observational data
[NASA-TN-D-5398] c30 N69-34884
Meteoroid environment model for cometary origin near earth to lunar surface
[NASA-SP-8013] c30 N69-40326
ASTRONOMICAL PHOTOGRAPHY
Rocket-borne spectroheliograph for monochromatic solar photography in Mg II 2802.7 A line noting filter bandwidth, film polarizers and temperature control
c14 A69-24838
Day sky brightness at altitude above 100 km obtained during rocket flight compared to night sky viewed from ground
c30 A69-33664
ASTRONOMICAL PHOTOMETRY
Mars surface photometric and spectrophotometric measurements, relating opposition effect details with corresponding laboratory sample measurements
c30 A69-18601
Rocket-borne photoelectric photometers for UV observations of Saturn, using interference filters
c30 A69-22216
Spectral reflectance of planetary atmospheres, lunar topography, and planetary surface analyses
[NASA-TT-F-502] c30 N69-31989
ASTRONOMICAL TELESCOPES
Spaceborne optical telescopes requirements and development including mirror material and construction, optical design, servocontrol, etc
c14 A69-27946
Control system for thin diffraction limited orbiting astronomical telescope mirror based on structural analysis of static deflections
c14 A69-27951
Image converter camera and astronomical telescope arrangement for photographing metal diaphragm openings in shock tube
c14 A69-37227
Objectives and experiment designs for Apollo telescope mount
[NASA-TN-D-5020] c30 N69-21526
ASTRONOMY
Astronomy - Conference, Prague, August 1967
c30 A69-15834
Earth orbital manned space astronomy, discussing long range program, instruments, facilities and data processing
c11 A69-27947
Significant achievements in space sciences for 1967, including stellar astronomy, bioscience, ionospheres, planetology, particles and fields, solar physics, and planetary atmospheres
[NASA-SP-167] c30 N69-25460
Potential for advancement of astronomy by space programs
[NASA-SP-213] c30 N69-41150
ASTROPHYSICS
Cosmic rays, elementary particle physics and astrophysics - Conference, Aligarh, India, December 1967
c29 A69-17268
M-2 galaxy as Seyfert-like galaxy seem edge-on, using radio and optical data showing H alpha emission collisionally excited, discussing circular polarization
c30 A69-20051
Nucleosynthesis in dynamics of massive star cores, noting element synthesis by neutron capture in supernova explosions
c30 A69-20898
Plasma instabilities in astrophysics - Conference, Monterey, October 1968
c30 A69-42681
Nonthermal phenomena of astrophysics in relation to plasma physics, considering planetary and stellar regions, supernova envelopes,

interstellar medium, cosmic rays, radio galaxies, etc
c30 A69-42682
Observations and theoretical studies on Mars properties
[NASA-SP-179] c30 N69-16571
High energy cosmic radiation problems
[NASA-SP-199] c29 N69-29652

ATLAS AGENA LAUNCH VEHICLES
Atlas-Agena flight performance for Applications Technology Satellite-1 mission
[NASA-TM-X-1784] c31 N69-24038
Postflight analysis of flight performance of Atlas Agena launch vehicle for Applications Technology Satellite ATS-2 mission
[NASA-TM-X-1800] c31 N69-27260
Performance of Atlas-Agena vehicle frcm lift off through Agena posigrade maneuver
[NASA-TM-X-1826] c31 N69-29594
Flight performance of Atlas Agena launch vehicles in support of Lunar Orbiter missions 3, 4, and 5
[NASA-TM-X-1859] c31 N69-37281
Flight performance of Atlas Agena laurch vehicle in support of Applications Technology Satellite-3
[NASA-TM-X-1879] c31 N69-37840

ATLAS CENTAUR LAUNCH VEHICLE
Flight performance evaluation of Atlas Centaur launch vehicle AC-12 carrying Surveyor 3 lunar probe
[NASA-TM-X-1678] c31 N69-10295
Development and test firing of improved igniter for first stage retrorockets of Atlas Centaur launch vehicle
[NASA-TM-X-1676] c28 N69-13275
Systems analysis of Atlas-Centaur AC-11 flight performance for Surveyor 4
[NASA-TM-X-1768] c31 N69-21399
Lateral bending dynamic tests of Atlas Centaur Surveyor launch vehicle
[NASA-TM-X-1837] c31 N69-30631

ATLAS SLV-3 LAUNCH VEHICLE
Tests of bending strength on full scale model of Atlas LV-3C booster
[NASA-TN-D-5156] c31 N69-22937

ATMOSPHERIC ATTENUATION
Albedo over Antarctic, measuring solar radiation reflected by surface and atmosphere by Eppley radiometer
c13 A69-21404
Daily simultaneous solar measurements of microwave atmospheric absorption and emission to determine frequency correlation between meteorological phenomena and atmospheric parameters
c13 A69-39747
Variability in sonic boom signatures measured along 8000 foot linear microphone array
[NASA-TN-D-5040] c02 N69-17279
Radiometric measurements of atmospheric attenuation in electromagnetic spectrum
[NASA-TN-D-5087] c07 N69-22949
Radiometric techniques applicable to measurement of solar activity and atmospheric attenuation at millimeter wavelengths
[NASA-TR-R-306] c07 N69-22951

ATMOSPHERIC CIRCULATION
Mesopause wind measurements at high latitude locations by sounding rockets noting relation to noctilucent clouds
c20 A69-28466
Subsonic thermal convection or internal gravity waves from formal scale analysis of equations of motion in plane parallel atmosphere
c13 A69-33155
Comparison of ray trace methods for estimating sound intensity variations due to atmospheric variability as determined by Monte Carlo methods
[NASA-CR-1337] c23 N69-23199
Noctilucent clouds with wave movement, chemical composition, and water vapor
[NASA-TT-F-546] c13 N69-25013

ATMOSPHERIC COMPOSITION
Planetary atmosphere composition determination using mass spectrometry for neutral components, ion spectrometry for ionic components and data system optimization
[AAS PAPER 68-183] c14 A69-11468
Mars lower atmospheric pressure, temperature and composition, noting consistency between photometric, spectroscopic and occultation techniques
c30 A69-12104
Mars lower ionosphere ionization from spectroscopic and Mariner 4 occultation data, discussing various ionization sources
c30 A69-18607
Ion composition and charged particle temperatures at 300-600 km from sounding rocket and topside sounder Alouette 2 measurements
c13 A69-18839
Meteoritic dust particles collections prediction in atmosphere for low and high entry fluxes
c30 A69-26342
Atmospheric ozone vertical distribution and total amount determined by radiative transfer and perturbation theory, presenting error analysis
c13 A69-28493
Polar exosphere near solar maximum investigation by Explorer 19 and Explorer 24 drag satellites, considering density and atomic oxygen concentration measurements
c13 A69-31351
Helium-carbon star BD plus 10 degrees 2179 reanalyzed by grid of constant flux models containing right amount of C
c30 A69-40652
Mars atmospheric features from measurements during entry and after landing, discussing atmospheric state properties, diurnal variability, clouds and winds
c30 A69-41617
Atmospheric density measured by Explorer 17 density gages, and error analysis
[NASA-TN-D-5447] c13 N69-40924

ATMOSPHERIC DENSITY
Atmospheric density variation measurements by density gages on Explorer 32 satellite confirm wave propagation in neutral thermosphere as free internal gravity waves
c13 A69-16261
Midlatitude neutral thermosphere density and temperature measurements, noting effect of atomic oxygen adsorption by instruments
c13 A69-16268
Semiannual density variations in thermosphere and exosphere as function of mixtopause height variations
c13 A69-26012
Polar exosphere near solar maximum investigation by Explorer 19 and Explorer 24 drag satellites, considering density and atomic oxygen concentration measurements
c13 A69-31351
Explorer 32 atmospheric density measurements revealing neutral thermosphere latitudinal variations during geomagnetically undisturbed times
c13 A69-38100
Neutral exosphere model for nonrotating planet permitting barosphere uniform rotation at certain angular velocity, determining velocity distribution and density
c30 A69-40524
Gamma ray backscattering of radioisotope for measuring Martian atmospheric density
[NASA-TN-D-5431] c24 N69-36931
Atmospheric density measured by Explorer 17 density gages, and error analysis
[NASA-TN-D-5447] c13 N69-40924

ATMOSPHERIC ENTRY
Downstream radiation flux distribution calculated for blunt entry bodies, considering self absorption effects
c33 A69-12547
Entry phase flight data of Missions AS-202, Apollo 4 and 6 compared with wind tunnel aerodynamics data
[AIAA PAPER 68-1143] c31 A69-13556
Blunt and conical body optimum heat shield shapes for Jupiter atmospheric entry, noting shallow flight path
[AIAA PAPER 68-1150] c31 A69-13565
Entry and terminal deceleration systems for unmanned Martian landers, discussing parachute landing and lifting entry vehicles
[AIAA PAPER 68-1147] c31 A69-13670
Entry corridor thermal entry limits for Apollo spacecraft defined for design of thermal

protection system
[AIAA PAPER 68-1144] c31 A69-13673
Correlations of stagnation point radiative heat transfer for earth reentry, noting use of nongray absorption coefficient models
c33 A69-14736
Structural design options for decelerative aeroshell configurations for atmospheric entry on unmanned planetary explorations
[AIAA PAPER 68-344] c32 A69-15507
Reentry and planetary entry physics and technology 2, advanced concepts, experiments, guidance-control and technology
c31 A69-25718
Configuration, trajectory planning, instrumentation, calorimetry and aerodynamic heating for planetary atmosphere entry
c31 A69-25719
Guidance and control concepts and hardware for atmospheric entry of Mercury, Gemini and Apollo spacecraft
c21 A69-25724
Stony meteoric particles size and velocity during passage through atmosphere
c30 A69-26341
Spacecraft sterilization by destructive heating with thermite or high velocity entry friction before entering planet atmosphere
c05 A69-31472
Collection of papers on thermal design principles of spacecraft and entry bodies
c33 A69-34372
Aerodynamic deceleration systems for space missions, considering deployment of subsonic parachute and inflatable configuration following atmospheric entry
[AIAA PAPER 68-1081] c31 A69-40542
Radio frequency transmission characteristics of ablation materials for planetary entry vehicle heat shields
[NASA-TN-D-4920] c07 N69-13158
Research problems in atmospheric entry and landing of manned planetary space flights to Mars and Venus
[NASA-TN-D-4977] c31 N69-15634
Transient thermal analysis and structural analysis for synthesis of ablating thermostructural panels in planetary entry environment
[NASA-CR-1215] c32 N69-16114
Guidance and navigation for atmospheric entry phase of vehicles
[NASA-SP-8015] c21 N69-19518
Aerodynamic characteristics of blunted cones, tension shell, and attached inflatable decelerator models
[NASA-TN-D-5219] c31 N69-26570
Optimum structural design for Martian entry capsule configurations
[NASA-CR-1414] c33 N69-35516

ATMOSPHERIC ENTRY SIMULATION
Hypervelocity reentry simulation problems for slender and blunt bodies, defining significant parameters
c30 A69-30376

ATMOSPHERIC HEATING
Empirical determination of heating efficiency of extreme solar UV radiation interacting with carbon dioxide atmosphere of Mars and Venus
c30 A69-26019
Steady state solution of quasi-geostrophic perturbation equations for atmospheric forced response to parametized heating as global monsoon theory
c20 A69-36405

ATMOSPHERIC IONIZATION
Nocturnal electron concentrations and temperature at Manitoba measured by rocket-borne Langmuir probe, compared with F 1 region
c29 A69-14008
Mars lower ionosphere ionization from spectroscopic and Mariner 4 occultation data, discussing various ionization sources
c30 A69-18607
High latitude ionization spikes observed by POGO spacecraft, noting frequency correlation with magnetic disturbances and development by high energy electron injections
c29 A69-28950

ATMOSPHERIC MODELS
Atmospheric model development relating temperature, density, moisture and energy measurements from satellite observations for long term weather forecasting
[UN PAPER 68-95397] c20 A69-10463
Venus microwave phase effect analyzed assuming dry massive Venus atmospheric model, discussing heat transfer processes
c30 A69-12108
Venus exospheric temperature for various composition models, discussing carbon dioxide concentration effects
c30 A69-12109
Mercury atmospheric models for preliminary environmental criteria to be used in spacecraft design and engineering trade-off studies
[AIAA PAPER 69-54] c30 A69-18042
Aurigae star HD 35620 with respect to epsilon Virginis using model atmosphere and high dispersion spectra
c30 A69-20913
Density inversion in convective zone of stellar photospheres occurring in Eridani atmospheric model under certain conditions
c30 A69-21843
Atmospheric models for metal deficient stars of K and G spectral type, studying reduced metal abundance effect on atmospheric structure
c30 A69-22055
Subdwarf HD 25329 studied with model atmosphere approach, using H alpha, Na I and Mg I profiles for effective temperature
c30 A69-22199
Full wave calculation of gravity waves for thermospheric model, describing wave type reflection, transmission, conversion and coupling by scattering matrix elements
c13 A69-25150
Model ion-exosphere for nonrotating planet with static dipole magnetic field generalized by permitting density and temperature variations over baropause
c13 A69-25284
Satellite observations of geomagnetic tail in magnetosphere near midnight meridian plane, discussing formation, shape, plasma sheet and models
c13 A69-26739
Monte Carlo relaxation method for physically self consistent model stellar atmospheres, discussing stability, accuracy and convergence of solution
c30 A69-36337
Atmospheric models for specified effective temperatures, hydrogen-to-metal ratios and surface gravities in studying metal deficiency effect on stellar atmosphere
c30 A69-36338
Thermosphere temperature shape parameters from probe flights, showing dependence on hour angle
c13 A69-38088
Type 3 solar radio bursts observed during April - October 1967 for two alternative models of active region streamers in outer corona
c29 A69-40300
Neutral exosphere model for nonrotating planet permitting barosphere uniform rotation at certain angular velocity, determining velocity distribution and density
c30 A69-40524
Helium-carbon star BD plus 10 degrees 2179 reanalyzed by grid of constant flux models containing right amount of C
c30 A69-40652
Angular grid spacing resolution near poles effect tests in global prediction model for geophysical fluid dynamics, investigating forecast height and wind fields
c20 A69-43066
Polar cap ionospheric response to solar cosmic ray events observed by Mariners 2 and 4 solar proton measurements used to test magnetosphere models
c29 A69-43621
Model environment of inner belt proton fluxes
[NASA-SP-3024-VOL-5] c24 N69-28911
Alouette 2 sounding data for magnetospheric field aligned propagation duct model
[NASA-TN-D-5332] c13 N69-34891

Limb radiance calculation model for atmospheric carbon dioxide bands with pressure and temperature gradients
[NASA-TN-D-5495] c21 N69-40055
ATMOSPHERIC MOISTURE
Vertical tropospheric humidity distribution estimation from IR spectra obtained by TIROS satellites
c13 A69-34284
Computer program used to infer atmospheric water-vapor mixing ratio from measured horizon radiance profiles
[NASA-TN-D-5252] c13 N69-27246
Stratospheric and mesospheric temperature and moisture profiles determined from infrared horizon observations
[NASA-CR-1419] c20 N69-35528
ATMOSPHERIC PHYSICS
Structure and mean molecular weight measurement of unknown atmosphere assessed from high altitude tests in earth atmosphere
[AIAA PAPER 68-1054] c30 A69-13699
Radiative transfer by doubling very thin layers in problem of diffuse reflection from plane-parallel atmosphere eliminates numerically solving transfer equation
c33 A69-20064
Semiannual density variations in thermosphere and exosphere as function of mixtopause height variations
c13 A69-26012
Ballistically effective atmospheric parameters for rocket vehicle design manuals involving application of climatological concepts of meteorology
c31 A69-26874
Atomic oxygen density role in ionospheric E and F region magnetic stability, noting heat loss effect of atomic excitation
c13 A69-32314
Steady state solution of quasi-geostrophic perturbation equations for atmospheric forced response to parametized heating as global monsoon theory
c20 A69-36405
Satellite-based meteorological observation system for global atmospheric research program, discussing wind measurement, IR and microwave sounding possibilities, etc
[AAS PAPER 69-120] c13 A69-42817
ATMOSPHERIC PRESSURE
Mars lower atmospheric pressure, temperature and composition, noting consistency between photometric, spectroscopic and occultation techniques
c30 A69-12104
Venus atmosphere chemical composition, surface temperature and pressure obtained by Venera 4 and Mariner 5
c30 A69-26129
ATMOSPHERIC RADIATION
Inverse problems in radiative transfer applied to remote measurements of IR radiation from planetary atmospheres, noting temperature and water vapor inversions
c13 A69-17617
Particle albedos and extinction cross sections computed by Mie theory showing dependence on refractivity, considering thermal radiation from cloudy planetary atmospheres
c30 A69-38255
Atmospheric emissions - NATO Conference, Norway, July-August 1968
c13 A69-38482
Daily simultaneous solar measurements of microwave atmospheric absorption and emission to determine frequency correlation between meteorological phenomena and atmospheric parameters
c13 A69-39747
Transfer of microwave radiation in atmosphere and underlying surfaces measured by aircraft instruments
[NASA-TT-F-590] c13 N69-31851
ATMOSPHERIC SCATTERING
Multiple light scattering solutions accuracy by diffraction peak omission from cloud and haze analytic phase functions compared for optically thick and thin planetary atmospheres
c30 A69-33159
Cloud scattering corrections added to synthetic spectrum analysis of carbon dioxide bands and water vapor line in Venus spectrum
c30 A69-33161
ATMOSPHERIC STRATIFICATION
Characteristic plane harmonic free internal neutral atmospheric wave oblique propagation through horizontally stratified quiet atmosphere for various thermospheric parameters
c13 A69-26101
Centrifugation effects on body composition and growth of mice
c04 A69-33746
Equations for pressure signature of supersonic projectile in stratified atmosphere
[NASA-TN-D-4890] c02 N69-10087
Sonic boom propagation in stratified atmosphere using FORTRAN computer program with integral and differential equations
[NASA-CR-1299] c02 N69-22546
ATMOSPHERIC TEMPERATURE
Mars lower atmospheric pressure, temperature and composition, noting consistency between photometric, spectroscopic and occultation techniques
c30 A69-12104
Venus exospheric temperature for various composition models, discussing carbon dioxide concentration effects
c30 A69-12109
Electron, ion and neutral particle temperatures of upper atmosphere
c13 A69-14975
Midlatitude neutral thermosphere density and temperature measurements, noting effect of atomic oxygen adsorption by instruments
c13 A69-16268
Nonlinear least squares optimization program applied to atmospheric temperature sounding, solving for temperatures at various altitudes from simulated carbon dioxide intensity measurements
c13 A69-33156
UV solar radiation variation effects on Mars and Venus upper atmosphere temperatures
c30 A69-37136
Rocket sounding meteorological data of Exametnet for 1966
[NASA-SP-175] c20 N69-16214
Horizon radiance profile analysis for determining atmospheric temperature
[NASA-TN-D-5068] c13 N69-19024
Stratospheric and mesospheric temperature and moisture profiles determined from infrared horizon observations
[NASA-CR-1419] c20 N69-35528
ATMOSPHERIC TIDES
Diurnal and solar cycle variations of thermosphere density and temperature generated by solar EUV input and tidal wave, using two dimensional model
c29 A69-43003
ATMOSPHERIC TURBULENCE
Turbulence characteristics up to 150 m above ground, noting surface roughness length directional dependence, longitudinal turbulence spectra and turbulent energy budget
c20 A69-10695
Light rigid civil aircraft response to continuous atmospheric turbulence estimated using two rigid body degrees of freedom method for vertical and lateral gusts
[AIAA PAPER 69-766] c32 A69-35657
Atmospheric turbulence limits on resolution of manned aerospace observations of ground
[NASA-TN-D-4940] c20 N69-12934
Conference on motion degraded images and correcting procedures - optical filters and digital methods for blurring removal from photographic imagery
[NASA-SP-193] c14 N69-33322
Statistical effects of wind and atmospheric turbulence on launch vehicles
[NASA-CR-1410] c20 N69-35570
ATOM CONCENTRATION
Deuterium concentration effect on electrical resistivity of palladium-deuterium system
[NASA-TN-D-4970] c26 N69-14565

ATOMIC COLLISIONS
Ionizing shock front structure in monatomic gas, considering atom-atom and electron-atom collisional ionization rates
c12 A69-13138
Atomic nitrogen collisional ionization and recombination rates under assumed quasi-steady nonequilibrium distribution of electron state populations
c24 A69-43700
ATOMIC ENERGY LEVELS
Electron impact ionization cross sections for second quantum level of atomic H, using Born exchange approximation and Vainshtein approximation
c24 A69-17138
Nuclear level density and mass shell corrections relationship for deformed and undeformed nuclei
c24 A69-29337
Upper bounds for electromagnetic transition rates for Ne 20 determined using Hartree-Fock wave functions
c24 A69-35166
Two photon decay of metastable levels of hydrogenic and He-like ions in solar corona, depopulating via proton collisional excitation to 2p level
c29 A69-36218
Barium 134 and barium 136 excitation by proton irradiation
[NASA-TN-D-4933] c24 N69-12778
Excited states of xenon nuclei formed in beta decay of iodine and cesium isotopes
[NASA-TN-D-5329] c24 N69-30074
ATOMIC EXCITATIONS
First Born approximation cross sections for He excitation from ground state by proton impact calculated, using wave functions
c24 A69-17027
Electron impact ionization cross sections for second quantum level of atomic H, using Born exchange approximation and Vainshtein approximation
c24 A69-17138
Cross sections computed for excitation and ionization of atoms and ions by electrons, using peaking approximation to evaluate Coulomb-Born matrix approximation
c24 A69-20206
Atomic oxygen density role in ionospheric E and F region magnetic stability, noting heat loss effect of atomic excitation
c13 A69-32314
He 2 excitation spectrum for interparticle potential using pair Hamiltonian with repulsive core and attractive well
c24 A69-33118
Barium 134 and barium 136 excitation by proton irradiation
[NASA-TN-D-4933] c24 N69-12778
ATOMIC STRUCTURE
Dipole shielding factor in coupled Hartree-Fock approximation for atomic S state
c23 A69-12179
Solid solutions atomic ordering effect on friction and wear in vacuum, using CuAu and FeCo systems
c15 A69-35183
Inelastic proton scattering cross sections for target nuclei in 2s-1d shell calculated in distorted wave Born approximation with projected Hartree-Fock wave functions
c24 A69-41045
ATOMIC THEORY
Thomas-Fermi approximation applied to calculation of equations of state and thermodynamic functions at high pressure from differential equations of statistical atom model
c24 A69-40186
ATOMIZING
Dynamic response of liquid jet atomization to acoustic oscillations
[NASA-TN-D-5339] c28 N69-30980
ATTACK AIRCRAFT
Spin and recovery characteristics of 1/30 scale subsonic attack aircraft model determined in wind tunnel tests
[NASA-TM-X-1788] c02 N69-37976
ATTENUATION
Transport study of neutron and photon attenuation through lithium hydride and tungsten spheres
[NASA-TN-D-4989] c24 N69-15375
ATTITUDE (INCLINATION)
Graphic method determining sounding rocket vehicle attitude
[NASA-TN-D-5172] c30 N69-23782
Vibration induced attitude errors in strapdown inertial navigators
[NASA-CR-1396] c21 N69-34672
ATTITUDE CONTROL
Three axis attitude servomechanism design to adjust attitude and angular velocity of spacecraft
c21 A69-17589
Stochastic saturating systems optimal control computation, considering attitude control and tracking system design by elliptical differential equation of dynamic programming
c10 A69-30601
Precision autocollimating solar sensor design for attitude alignment changes, including detector calibration and sounding rocket flight test results
[AIAA PAPER 69-858] c21 A69-39386
Responsiveness of three axis, large angle attitude control systems of highly maneuverable spacecraft capable of tracking time-varying target attitudes
[NASA-TN-D-4896] c30 N69-10756
Flight performance of Explorer 35 attitude control system
[NASA-TN-D-5187] c21 N69-27268
Photoelectronic commutation by dc torquer-driven reaction wheel for spacecraft attitude control
[NASA-TN-D-5265] c03 N69-30945
In-flight simulation to evaluate simultaneous use of attitude control for jet VTOL maneuvering
[NASA-TN-D-5342] c02 N69-32110
ATTITUDE GYROS
Large solar sail vehicle to operate in manner of helicopter rotor
[NASA-CR-1329] c31 N69-28861
ATTITUDE INDICATORS
Radar attitude sensing system for determining vehicle roll, pitch, yaw, altitude and velocity of earth and lunar orbital vehicles
c07 A69-13183
Precision autocollimating solar sensor design for attitude alignment changes, including detector calibration and sounding rocket flight test results
[AIAA PAPER 69-858] c21 A69-39386
ATTITUDE STABILITY
Equations of motion computerized simulation for attitude stabilization of orbiting telescope coupled to crew compartment
c14 A69-27952
Spinning satellite attitude stability
[NASA-TN-D-5268] c31 N69-32298
AUDIO FREQUENCIES
Data distortion elimination by improved superimposing of sinusoidal audio frequency signal on dc voltage of automatic Langmuir probe second derivative plotters
c14 A69-32855
Prediction of loudness from frequency characteristics of sound
[NASA-TN-D-5422] c23 N69-37028
AUDITORY PERCEPTION
Auditory temporal masking of tonal signal by narrow band noise and perception of temporal order noting effects of intensity, frequency and time
c05 A69-24795
Prediction of loudness from frequency characteristics of sound
[NASA-TN-D-5422] c23 N69-37028
AUDITORY TASKS
Human information processing rates during one and two axis compensatory tracking tasks with secondary auditory task
c05 A69-23880
AUGER EFFECT
Auger and photoelectron spectroscopy for chemical analysis, noting effects of sample thickness, sample potential, surface contamination and X ray incident angle
c06 A69-19775

AURIGA CONSTELLATION
Aurigae star HD 35620 with respect to epsilon Virginis using model atmosphere and high dispersion spectra
c30 A69-20913
AURORAL ARCS
Visual ashen light observation on Venus possibly attributable to solar particle bombardment from dark side emission detection by spectroscopic and photometric studies
c30 A69-32300
AURORAL IONIZATION
Lower auroral ionosphere rocket measurements of electrons, positive ions and energy particles, deriving height variation of ion pair production and ion-ion recombination
c13 A69-32187
AURORAL ZONES
Electron cooling rates in midlatitude and auroral zone thermosphere measured by probe rockets
c13 A69-16267
Electric field variations in vicinity of auroral forms from motions of Ba vapor clouds released from Nike-Tomahawk rockets
c13 A69-34935
AURORAS
Artificial aurora generated at 100 km altitude by electron beam fired downward from Aerobee 350 rocket above 230 km along earth magnetic field lines
c13 A69-34365
Electron temperature, density and magnetic disturbances measurements at 1000 km compared with visual observations during 25-26 May 1967 magnetic storm and aurora
c13 A69-34954
Rocket measurements of primary auroral particles energy spectra indicating spectral structure acceleration peaks associated with electrostatic fields
c13 A69-38490
Ionospheric currents geophysical dc electric field measurement from sounding rockets, indicating anticorrelation with auroral luminosity
c13 A69-38508
Spectral and electrophotometric studies of upper atmosphere - airglows, atomic oxygen, hydroxyl emission, helium line spectra, auroras, and solar cycle effects on magnetosphere
[NASA-TT-F-530] c13 N69-16539
Parametric angles of trajectory-determined field line intersects predicting location of artificial auroras in magnetosphere
[NASA-TN-D-5189] c30 N69-32316
AUSFORMING
Rolling element fatigue life of ausformed steel balls
[NASA-TN-D-4954] c15 N69-14383
AUSTENITIC STAINLESS STEELS
Rolling element fatigue life of ausformed steel balls
[NASA-TN-D-4954] c15 N69-14383
AUTOCORRELATION
Root mean square time delay error with respect to playback time and autocorrelation function of tape recorded sine wave for studying jitter spectra
c14 A69-18827
Derivation of transfer function for optical system relating image intensity to spatial autocorrelation
[NASA-CR-1443] c21 N69-38041
AUTOMATIC CONTROL
Autonomous solution to orbital navigation problem yielding direct measure of orbital parameters
c21 A69-11005
Mercury ion thrusters and facilities automatic controls durability testing, discussing vacuum chamber systems, unattended operation and control
[AIAA PAPER 68-576] c11 A69-12385
Stochastic problems in control - Conference, Ann Arbor, June 1968
c10 A69-14693
Evaluation method for strapdown spacecraft guidance systems on automated interplanetary missions, using cost and system performance efficiency probability model
[AIAA PAPER 68-828] c21 A69-35953
Automatic control - Conference, Boulder, August 1969
c10 A69-43267
Measurement of pilot describing functions in single controller multiloop tasks
[NASA-CR-1238] c05 N69-15372
Shaft face seal with self acting lift augmentation for advanced gas turbine engines
[NASA-TN-D-5170] c15 N69-23232
Linear multivariable control system design using modern control theory, and application to coupled core reactor control
[NASA-CR-1345] c19 N69-29268
Development of automatic quality control device for measuring welded joints
[NASA-TN-D-5304] c15 N69-33800
Application of control theory to production engineering, transportation systems, urban development, biological oceanography, mass communications, and socio-economic problems
[NASA-SP-211] c34 N69-39957
AUTOMATIC CONTROL VALVES
Electronic position indicator for latching solenoid valves in SNAP 8 ground test facility
[NASA-TM-X-1760] c14 N69-20874
AUTOMATIC PICTURE TRANSMISSION
Computer programming of satellite orbit tracking angles for automatic picture transmission receiving stations
c07 A69-14917
Procurement and construction of automatic picture transmission ground station equipment for ESSA and Nimbus transmission
[NASA-SP-5080] c07 N69-31985
AUTOMATION
Automatic equipment for sampling and preparing gases by dual column gas chromatography for subsequent mass spectral analysis of carbon isotopes during methane metabolism
c06 A69-12603
AUTOROTATION
Flight investigation of lightweight helicopter to study feasibility of fixed collective pitch autorotations
[NASA-TN-D-5270] c02 N69-29232
AUTOTROPHS
Ribulose diphosphate carboxylase and phosphoribulokinase activity in chemosynthetic autotrophs Thiobacillus thioparus and Thiobacillus neapolitanus, noting sedimentation and gel filtration characteristics
c04 A69-11866
AUXILIARY POWER SOURCES
Electrochemical generators for space applications - Conference, Paris, December 1967
c03 A69-32405
Single shaft Brayton rotating unit for 2 to 10 kilowatt space power generation system
[NASA-TM-X-1869] c03 N69-39238
AVALANCHE DIODES
Effects of neutron irradiation on silicon voltage regulator Zener diodes
[NASA-TN-D-4923] c09 N69-10250
AVERAGE
Generalized averaging method for linear differential equations with almost periodic coefficients
[NASA-TN-D-5167] c19 N69-22988
AVIONICS
NASA civil aviation electronics research program, discussing feasibility of V/STOL aircraft all-weather operations
c34 A69-16718
Collection of articles on avionics navigation systems covering navigation equations, airborne digital and analog computers, radio, Doppler and inertial navigation, etc
c21 A69-34843
AXIAL COMPRESSION LOADS
Computer program determination of barreling effect on strength of ring and stringer stiffened shells designed to support axial compression loads
c32 A69-43671
Instability of eccentrically stiffened cylindrical shells under axial compression and lateral pressure
[NASA-CR-1280] c32 N69-15378

AXIAL FLOW
Performance comparisons of supersonic compressor rotor blades
[NASA-CR-1256] c28 N69-14210
Pulsed experiments on high powered constricted electric arc with axial flow performed by discharging transmission line
[GDC-DBE-68-008] c25 N69-17212
Performance of two stage axial flow turbogenerator with gas bearing rotor support system
[NASA-CR-1290] c03 N69-21771
Multistage turbocompressor simulation applied to performance prediction of axial flow instabilities
[NASA-TM-X-1880] c28 N69-36998
Outlet annulus area blockage configuration effects on performance of axial flow compressor rotor
[NASA-TN-D-5506] c28 N69-40078
AXIAL FLOW PUMPS
Performance and cavitation damage to axial flow pump rotor blades in high temperature liquid sodium
[NASA-TN-D-5138] c15 N69-21773
Fluid temperature effect on cavitation performance of axial flow pump
[NASA-TN-D-5318] c15 N69-30069
Cavitation damage and effect of fluid temperature on performance of axial flow pumps in liquid sodium
[NASA-TN-D-5484] c15 N69-38641
AXIAL FLOW TURBINES
Effect of rotor tip clearance on performance of 5-inch single-stage axial flow turbine
[NASA-TM-X-1757] c03 N69-20883
AXIAL LOADS
Axial load fatigue crack propagation tests on Al alloy sheets for stress ratio effects
c17 A69-36435
Buckling equations solved for equatorial segment of spherical shell loaded in axial direction by own weight
[NASA-TN-D-4921] c32 N69-13034
Stress ratio effects on fatigue crack growth in sheet aluminum alloys
[NASA-TN-D-5390] c17 N69-34704
AXIAL STRESS
Failure criteria for predicting filamentary composite strength under uniaxial and combined stresses from properties and fabrication process considerations
c32 A69-21479
Linear prediction of structural failure criteria for uniaxial fiber composites
[NASA-TN-D-5367] c18 N69-33321
AXISYMMETRIC BODIES
Cone-conical-frustrum configurations meeting center of gravity requirements for higher hypersonic lift-drag ratios in axisymmetric manned spacecraft
c01 A69-39237
Estimated supersonic flow field shock waves and sonic boom effects for cones and axisymmetric bodies
[NASA-TN-D-4935] c01 N69-13238
Stagnation pressure and heat transfer measurements of blunt axisymmetric bodies
[NASA-TN-D-5121] c01 N69-22554
Incremental analysis of large deformations in continuum mechanics with applications to axisymmetric shells of revolution
[NASA-CR-1350] c32 N69-28624
Differential equations for compression loaded axisymmetric cylindrical structures
[NASA-CR-1444] c32 N69-38781
AXISYMMETRIC FLOW
Steady axisymmetric gas flow from galactic center, determining supersonic to subsonic transition by equations of motion
c30 A69-22189
Finite difference method computer programs for calculation of velocities and streamlines on blade to blade surface of revolution of turbomachine
[ASME PAPER 69-GT-48] c01 A69-22495
Reduction of noise from underexpanded axisymmetric jet flows using radial jet flow impingement
[AIAA PAPER 68-81] c12 A69-28212
Theoretical analysis of axisymmetric flow in VTOL lift fan inlets without crossflow
[NASA-TN-D-5065] c01 N69-17831

B

B STARS
Rocket spectrographic observations of Alpha Virginis noting hydrogen Lyman absorption lines
c30 A69-27555
B-70 AIRCRAFT
XB-70 aircraft test data as applied to SST safety, describing aircraft design, flight characteristics, instrumentation, takeoff and landing, etc
c02 A69-41143
XB-70 aircraft flight tests of canard configurations
[NASA-TN-D-5359] c02 N69-32284
Thermal, acoustical, and acceleration environments of XB-70 airplane crew compartment in airworthiness tests
[NASA-TN-D-5449] c25 N69-38010
BACILLUS
Ribulose diphosphate carboxylase and phosphoribulokinase activity in chemosynthetic autotrophs Thiobacillus thioparus and Thiobacillus neapolitanus, noting sedimentation and gel filtration characteristics
c04 A69-11866
BACKFIRE
Backfire antenna radiation characteristics and physical dimensions for tracking and telemetry applications, including five element array model
c07 A69-36251
BACKGROUND RADIATION
Photomultipliers response to energetic particles in terms of background current using data from OGO experiments
c14 A69-16932
Background radiation intensity upper limits for mm and submillimeter wavelengths in interstellar medium, noting intense flux in far IR
c30 A69-19404
X ray energy spectrum from Crab Nebula and diffuse background on celestial sphere near galactic anticenter, noting spectral index
c29 A69-30759
Cosmic radio background noise spectrum near north galactic pole based on Radio Astronomy Explorer satellite experiments
c30 A69-42375
BACKLOBES
Multiplicative feed system for monopulse angle tracking antennas, discussing influence of sidelobe and backlobe responses on control function slope determining antenna bearing angle
c11 A69-37704
BACKSCATTERING
Mie total and differential backscattering cross sections at laser wavelengths for Junge size distribution aerosol models
c16 A69-14290
Backscattering due to collisions for electrons from emitter accelerated through positive ion sheath into plasma in thermionic diodes
c09 A69-17773
Radar backscatter and rocket profiles of ionospheric electron temperature, noting agreement in daytime flight measurements
c29 A69-25162
Optical radar studies of lower atmosphere, giving Mie theory calculations of clear atmosphere volume backscattering cross sections for four laser wavelengths
c07 A69-27001
Gamma ray backscattering of radioisotope for measuring Martian atmospheric density
[NASA-TN-D-5431] c24 N69-36931
BACKUPS
Multiwall meteoroid protection design in Apollo program, discussing bumper, backup sheet and honeycomb cells insulation
[AIAA PAPER 69-372] c32 A69-28304
BACKWARD WAVE TUBES
High performance silicon carbide backward diode, discussing device design and operational characteristics
c09 A69-22787
BACTERIA
Electron transport of Halobacterium cutirubrum,

discussing spectrophotometric identification of cytochromes
c04 A69-19481
Salts and organic solvents effect on halophile Halobacterium cutirubrum catalase, noting enzyme activity inhibition by cation and anion
c04 A69-35291

BALL BEARINGS
Ball bearings lubrication and wear in cryogenic hydrogen turbopumps by transfer films provided from self lubricating cage
c15 A69-10109
Ball bearing test apparatus for evaluation of greases and solid lubricants at high temperatures
[ASLE PREPRINT 68AM 7C-2] c15 A69-10912
Cooling requirements for high speed polytetrafluorethylene lubricated ball bearings operating in cold hydrogen gas, developing minimum gas flow rate equation
[ASLE PAPER 68-LC-2] c15 A69-19310
Contact conformity effects on spinning torque and friction coefficient in angular contact ball bearings from lubricated and unlubricated tests
[ASME PAPER 68-LUB-10] c15 A69-30901
Steel ball bearing high temperature fatigue life tested with synthetic paraffinic oil, fluorocarbon and polyphenyl ether
[ASME PAPER 69-LUBS-18] c15 A69-34378
Elastohydrodynamic solution for ball torque spinning without rolling in nonconforming groove, showing increase in torque with stress and spinning and decreasing conformity
[ASME PAPER 69-LUBS-11] c15 A69-34381
Oxygen concentration effects on oxidation of synthetic paraffinic and type II ester lubricants determined from ball bearing tests at 400 and 450 degrees F
c15 A69-35177
Rolling element fatigue life of ausformed steel balls
[NASA-TN-D-4954] c15 N69-14383
High temperature fatigue tests conducted to determine bearing life of angular contact ball bearing elements
[NASA-TN-D-5002] c15 N69-16367
Oxygen concentration effects on ester lubricant degradation during high temperature bearing test
[NASA-TN-D-5262] c15 N69-26311
Oxygen concentration effects on synthetic paraffinic oil lubricant performance in high temperature bearing tests
[NASA-TN-D-5152] c15 N69-26314

BALLISTIC RANGES
Ballistic range tests to study ablation effects on aerodynamic characteristics of ablating and nonablating slender cones
[AIAA PAPER 69-179] c33 A69-18083
Design, calibration, and use of radiometers to measure spectral emission in ballistic range and shock tube experiments
[NASA-TN-D-5360] c14 N69-38144

BALLISTIC TRAJECTORIES
Parametric angles of trajectory-determined field line intersects predicting location of artificial auroras in magnetosphere
[NASA-TN-D-5189] c30 N69-32316

BALLISTICS
Ballistically effective atmospheric parameters for rocket vehicle design manuals involving application of climatological concepts of meteorology
c31 A69-26874

BALLOON FLIGHT
Balloon-borne instrumentation for detection of far IR extended emission regions and bright point sources, describing results of initial flights
c30 A69-27599
Earth observations from balloons - Conference, Washington, D.C., February 1969
c02 A69-40803
Balloon flights with space available for secondary experiments, discussing launching agencies and experiment design restrictions
c02 A69-40807
Aerostatic and aerodynamic characteristics of Dart Vee tethered balloon system
c02 A69-40813

BALLOON SOUNDING
Gamma ray telescope development for balloon-borne astronomy in search for discrete gamma sources and supernova explosions
[IEEE PAPER 3A-5] c14 A69-19192
Earth observations from balloons - Conference, Washington, D.C., February 1969
c02 A69-40803
Winds aloft and wind shear analysis from jimsphere wind sensor balloon-radar data
[NASA-CR-1204] c20 N69-13629

BALLOONS
Evaluation of double wall balloon enclosure for thermal control of inertial satellites
[NASA-TN-D-5230] c33 N69-28209
Free flight performance characteristics of ram air inflated recovery balloons with peripheral airscoops
[NASA-TN-D-5186] c21 N69-29595

BALLS
Elastohydrodynamic analysis and experimental speed effects or ball spinning friction coefficients and torque
[NASA-TN-D-5527] c15 N69-41210

BALLUTES
Inflation, drag, and stability characteristics of towed inflatable ballute decelerator at free flight
[NASA-TN-D-4943] c01 N69-17398
Supersonic deployment and extraction of inflatable towed ballute decelerator
[NASA-TM-X-1773] c31 N69-26458

BAND STRUCTURE OF SOLIDS
Impurity profiles and energy band diagram for cuprous sulfide-CdS heterojunction based on capacitance, Hall and electron microprobe measurements
c03 A69-13075

BARIUM
Lanthanum isotopes beta decay, analyzing excitation of near spherical daughter nuclei of barium isotopes
c24 A69-10100
Continental diabases and oceanic tholeiites in light of rare earth and barium abundances and partition coefficients indicating fusion process
c13 A69-20945
Electric field variations in vicinity of auroral forms from motions of Ba vapor clouds released from Nike-Tomahawk rockets
c13 A69-34935
Ca-rich achondrites genesis implied from rare earth and Ba absolute and relative concentrations
c30 A69-36091
Barium 134 and barium 136 excitation by proton irradiation
[NASA-TN-D-4933] c24 N69-12778
Development of barium chemical release system
[NASA-CR-1415] c13 N69-35660

BARIUM TITANATES
Observation of photocurrents generated in Schottky barrier diodes on barium titanate, suggesting practical utility of photon-to-electron conversion efficiencies
c09 A69-18905

BASE FLOW
Performance characteristics of truncated, conical plug nozzle with cylindrical outer shroud
[NASA-TM-X-1807] c26 N69-27840

BASE HEATING
Telemetry technique utilizing thermocouple sensors for base heating determinations on free flight blunt cone in shock tunnels, noting electrical noise reduction
[AIAA PAPER 68-407] c14 A69-15514
Short duration tube wind tunnel supersonic testing, noting Saturn S-1C base heating and solid propellant rocket base burning tests
[AIAA PAPER 69-335] c11 A69-28271

BAYARD-ALPERT IONIZATION GAGES
Bent beam ionization gage linearity from calibrated nude Modulated Bayard-Alpert /MBA/ gage, discussing buried collector and tabulated magnetron gages
c14 A69-41216

BEAM CURRENTS
High voltage mercury electron bombardment ion thruster power efficiency

[ECS PAPER 170D] c28 A69-16233
Plasma electron beam for welding, deriving beam current from secondary emission by ion bombardment, discussing gas pressure, equipment and applications c15 A69-35555

BEAM WAVEGUIDES
First-order solutions for mutual coupling between waveguides which propagate two orthogonal modes
[NASA-TN-D-5180] c07 N69-24051

BEAMS (SUPPORTS)
Dynamic response of uniform beams and plates exposed to sonic booms
[NASA-CR-1281] c32 N69-21403

BEARINGS
Equations of motion for rigid body rotor in linearized bearings
[NASA-CR-1391] c15 N69-36349

BEAT FREQUENCIES
Beat frequency measurements in far IR due to harmonic mixing of klystrons, discussing noise role c23 A69-33674

BENDING
Stiffness matrices analysis of thin flat plates
[NASA-TN-D-4927] c32 N69-14169

BENDING MOMENTS
Tests of bending strength on full scale model of Atlas LV-3C booster
[NASA-TN-D-5156] c31 N69-22937
Approximative solution for dynamic response of flexible rotor blade to radially moving force
[NASA-TN-D-5410] c32 N69-36220
Tabulated bending moment transfer coefficients for helicopter rotor blades
[NASA-CR-1441] c32 N69-40359
Beam stiffness determined for thin walled truncated cones under bending loads
[NASA-TN-D-5536] c32 N69-41141

BENDING VIBRATION
Longitudinal structural vibration and lateral bending response mass and spring coupling in Saturn AS-502 during boost with longitudinal excitation by POGO effect
[AIAA PAPER 69-58] c31 A69-18204
Anomalous spacecraft OGO-D motion explained by open section boom thermally induced oscillations, discussing corrective measures c32 A69-18331
Vibration characteristics of 1/40 scale model of Saturn 5 launch vehicle and umbilical tower configuration
[NASA-TN-D-4870] c31 N69-10775

BERYLLIUM
Beryllium reflector distortion in Plum Brook Reactor due to neutron embrittlement and gas formation, noting material surveillance, replacement, etc c22 A69-13131
Strong p-type conductivity of silicon doped with beryllium by thermal diffusion, giving electrical and optical measurements c26 A69-21652
Refractory cone models made of copper and Co coated Be for force tests in high enthalpy hypersonic arc tunnels at high simulated attitudes c11 A69-26796
High emittance coating materials for beryllium, niobium-zirconium compounds, and stainless steel used in spacecraft radiators
[NASA-CR-1278] c17 N69-18952
Beryllium swelling and replacement in Plum Brook reactor
[NASA-TM-X-1794] c22 N69-26233
Structural response of tubular beryllium and beryllium aluminum alloy truss-type structures to dynamic and static loads
[NASA-TN-D-5254] c32 N69-28658

BERYLLIUM ALLOYS
Lightly loaded truss structures fabricated from Be, Be-Al alloy and uniaxial B filament reinforced epoxy tubing for unmanned spacecraft applications c17 A69-35504
Mechanical properties and column behavior of thin wall beryllium-aluminum alloy tubing
[NASA-TN-D-5145] c17 N69-23004
Structural response of tubular beryllium and beryllium aluminum alloy truss-type structures to dynamic and static loads
[NASA-TN-D-5254] c32 N69-28658

BERYLLIUM OXIDES
Neutron interaction behavior of beryllium oxide and molybdenum reflectors for nuclear reactors
[NASA-TM-X-1822] c22 N69-29593

BIAS
Red, blue and no bias light effects on spectral response of copper sulfide-cadmium sulfide cell, using model incorporating photoconductive layer c26 A69-16358
Terrain bias error analysis in pulse modulated planetary radar altimeters
[NASA-TN-D-5220] c21 N69-26195

BIBLIOGRAPHIES
Subject classification bibliography for thermal contact resistance
[ASME PAPER 68-WA/HT-18] c33 A69-16122
Annotated bibliography and indexes on aerospace medicine and biological effects - September 1968
[NASA-SP-7011/55/] c04 N69-11695
Annotated bibliography and indexes on aerospace medicine and biological effects - October 1968
[NASA-SP-7011/56/] c04 N69-14387
Aerospace Medicine and Biology bibliography on biological, physiological, psychological, and environmental effects on man during aerospace flight
[NASA-SP-7011/57/] c04 N69-16537
Annotated bibliography and indexes on aerospace medicine and biological effects - Dec. 1968
[NASA-SP-7011/58/] c04 N69-19023
Annotated bibliography and indexes on aerospace medicine and biological effects - Feb. 1969
[NASA-SP-7011/60/] c04 N69-19714
Summary of random vibration prediction procedures for aerospace vehicles, with bibliography
[NASA-CR-1302] c32 N69-23096
Annotated bibliography and indexes on aerospace medicine and biological effects - Mar. 1969
[NASA-SP-7011/61/] c04 N69-23126
Cumulative index to continuing bibliography on aerospace medicine and biological effects - 1968
[NASA-SP-7011/59/] c04 N69-24752
Annotated bibliography and indexes on aerospace medicine and biological effects - Apr. 1969
[NASA-SP-7011/62/] c04 N69-24822
Bibliography of works of Soviet engineer F. A. Tsander
[NASA-TT-F-541] c34 N69-26112
Technology transfer and utilization - bibliography
[NASA-CR-1355] c34 N69-28868
Structure, interactions, and topography of solid surfaces, sliding friction, adhesion, wear, and boundary lubrication conference topics
[NASA-SP-181] c15 N69-30401
Annotated bibliography and indexes on aerospace medicine and biological effects - Apr. 1969
[NASA-SP-7011/65/] c04 N69-31923
Bibliography of systems approach to management
[NASA-SP-7501] c34 N69-34917
Annotated bibliography and indexes on Aerospace Medicine and Biology - Aug. 1969
[NASA-SP-7011/67/] c04 N69-37887
Bibliography on aerospace medicine and related biological research
[NASA-SP-7011/66/] c04 N69-37909
Annotated bibliography and indexes on aerospace medicine and biological effects - Apr. 1969
[NASA-SP-7011/63/] c04 N69-38235
Annotated bibliography and indexes on aerospace medicine and biological effects - May 1969
[NASA-SP-7011/64/] c04 N69-38242

BINARY STARS
Spectra of close binary systems, analyzing abundance anomalies, noting metallicity results c30 A69-15854
Curve of growth analysis for close binary HR 5317 indicating Mg, Mn, Ca and Sr overabundance respecting standard star 110 Her c30 A69-34297
HD 30353 He binary star invisible component suggested as KO type supergiant from IR photometric data c30 A69-35348

BINARY SYSTEMS (MATERIALS)
Thermodynamic properties of erbium hydrogen binary

system evaluated for use as low pressure standard
[NASA-CR-1271] c14 N69-16099
BINOCULAR VISION
Relationship between binocular depth perception and optical distortion in Apollo pressure suit helmets and visors
[NASA-TN-D-5162] c05 N69-22990
BIOASSAY
Preflight and postflight leukocyte chromosome aberration analyses of Gemini astronauts
c04 A69-33173
Statistical method for automatic computer editing of biological data
[NASA-TN-D-5275] c08 N69-29592
BIOASTRONAUTICS
Gemini and Mercury space flights medical results, summarizing physiological effects noted on body systems
c04 A69-11074
Clinical report on Apollo 7 and 8 mission medical data, discussing preflight preventive medical activities, inflight treatment, radiation levels, etc
c05 A69-22542
Space travel and lunar exploration medical problems
c04 A69-27909
NASA Lunar Receiving Laboratory functional areas and physical, chemical, biological and quarantine activities for crew and lunar samples
c11 A69-38896
Physiological and psychological responses of man to space flight problems
[NASA-TT-F-529] c05 N69-32044
BIOCHEMISTRY
Dynamic differential thermal analysis with He flow performed on biological specimens, proteins and starches, showing discrete decomposition peaks monitoring pyrolysis process
c06 A69-31807
Biogeochemistry applications in mineral prospecting
[NASA-SP-5056] c13 N69-10492
Biochemical and metabolic effects of exposure of mice to helium-oxygen atmosphere
[NASA-CR-1372] c04 N69-40955
BIOENGINEERING
Hard space suit for use on planetary surfaces and extravehicular activity, discussing design, fabrication and mobility
c05 A69-12993
BIOGENY
Physical density and enzyme activity in coacervate biogenic molecular compounds
[NASA-TT-F-525] c04 N69-40324
BIOINSTRUMENTATION
Aeromedical developments by NASA biomedical applications program applied to general medical equipment including cardiac sensors, surgical sterilization, ballistocardiograph, etc
c34 A69-32430
NASA contributions to bioinstrumentation system - survey
[NASA-SP-5054] c04 N69-14860
Engineering problems survey on teleoperator control systems
[NASA-SP-5070] c05 N69-21478
Soviet handbook on operation principles, use, and installation of electrocardiographs and electromedical apparatus for therapeutics
[NASA-TT-F-523] c05 N69-27577
BIOLOGICAL EFFECTS
Biological effects on rhesus monkeys of high energy protons compared to effects of cobalt 60 gamma radiation
c04 A69-13498
Annotated bibliography and indexes on aerospace medicine and biological effects - September 1968
[NASA-SP-7011/55/] c04 N69-11695
Annotated biblicgraphy and indexes on aerospace medicine and biological effects - October 1968
[NASA-SP-7011/56/] c04 N69-14387
Aerospace Medicine and Biology bibliography on biological, physiological, psychological, and environmental effects on man during aerospace flight
[NASA-SP-7011/57/] c04 N69-16537
Annotated bibliography and indexes on aerospace medicine and biological effects - Dec. 1968
[NASA-SP-7011/58/] c04 N69-19023
Annotated bibliography and indexes on aerospace medicine and biological effects - Feb. 1969
[NASA-SP-7011/60/] c04 N69-19714
Annotated bibliography and indexes on aercspace medicine and biological effects - Mar. 1969
[NASA-SP-7011/61/] c04 N69-23126
Cumulative index to continuing bibliography on aerospace medicine and biological effects - 1968
[NASA-SP-7011/59/] c04 N69-24752
Annotated bibliography and indexes on aerospace medicine and biological effects - Apr. 1969
[NASA-SP-7011/62/] c04 N69-24822
Annotated bibliography and indexes on aerospace medicine and biological effects - Apr. 1969
[NASA-SP-7011/65/] c04 N69-31923
Annotated bibliography and indexes on Aerospace Medicine and Biology - Aug. 1969
[NASA-SP-7011/67/] c04 N69-37887
Annotated bibliography and indexes on aerospace medicine and biological effects - Apr. 1969
[NASA-SP-7011/63/] c04 N69-38235
Annotated bibliography and indexes on aerospace medicine and biological effects - May 1969
[NASA-SP-7011/64/] c04 N69-38242
BIOLUMINESCENCE
Adenosine triphosphate /ATP/ content of terrestrial soils, based on firefly bioluminescent reaction, for Mars soil problems
c04 A69-37567
BIOMETRICS
Neutral buoyancy microelectrode for prolonged recording from single nerve units
c05 A69-11865
BIONICS
Analytic model resembling thick walled ellipsoid of revolution incorporating three dimensional shape of human left ventricle and ventricular wall thickness effects
c05 A69-26235
BIOPAKS
Toxicity of plastic hardware containing biological space flight experiment
[NASA-TM-X-1818] c04 N69-29723
BIOSATELLITES
Biosatellite attitude control systems design development and flight test results for payload perturbing effects, discussing simulation activity
c31 A69-35094
BIOTECHNOLOGY
Experiment requirements for manned earth orbiting biotechnology laboratory
[NASA-CR-1409] c05 N69-35540
Design and equipment requirements for manned earth orbiting biotechnology laboratory
[NASA-CR-1408] c05 N69-35541
BIOTELEMETRY
EEG monitor helmet for aircraft or flight simulator programs, discussing sensing and transmitting system
c05 A69-26553
Real time metabolic rate analysis of suited astronaut using heart rate and O methods during thermal vacuum and extravehicular motility tests
[AIAA PAPER 69-993] c05 A69-40371
BIT SYNCHRONIZATION
PCM bit synchronizer/signal conditioners performance characteristics and specification
c09 A69-19120
BLACK BODY RADIATION
Solution to radiation-coupled stagnating flow with nongray emission over hypervelocity blunt body
[NASA-TR-R-299] c33 N69-16268
Absorption of black-body radiation by ice cryodeposits on metal substrates
[NASA-TN-D-5181] c23 N69-22769
BLACKOUT (PROPAGATION)
Measurement of thermal accommodation ccefficients between liquids and high temperature gases in low pressure reentry communications blackout intervals
[NASA-CR-1330] c07 N69-32721
BLADE TIPS
Effect of rotor tip clearance on performance of 5-inch single-stage axial flow turbine
[NASA-TM-X-1757] c03 N69-20883

BLAST DEFLECTORS
Blast shields testing
[NASA-TN-D-4894] c11 N69-10888
BLIND LANDING
Kalman filter simulation for estimating aircraft position and velocity from airborne digital computer data in zero-zero landing system
[AIAA PAPER 69-944] c21 A69-40327
BLOCKING
Blocked polyimide precursor resistance to thermal imidization compared to polyamic acid
[NASA-TN-D-5184] c06 N69-23353
Blocked two level factorial experiment to measure radiolysis of water in water cooled reactors
[NASA-TN-D-5369] c19 N69-32319
Outlet annulus area blockage configuration effects on performance of axial flow compressor rotor
[NASA-TN-D-5506] c28 N69-40078
BLOOD
Blood sampling for parathyroid hormone and calcium metabolism during weightlessness of space flight
[NASA-CR-1395] c05 N69-38600
BLOOD PLASMA
Identity between growth hormone degrading activity of pituitary gland and plasmin
c04 A69-17105
Acetate carbon 14 utilization in centrifuged rats, analyzing metabolism by measuring plasma glucose, FFA and lipids synthesis
c04 A69-19429
Repeated blood sampling effect on plasma cholinesterase, acid phosphatase, alkaline phosphatase and hematocrit ratios in domestic chickens
c04 A69-23158
BLOOD PRESSURE
Single channel pressure telemetry unit for chronic implantation into cardiac chambers or major blood vessels in unrestrained animals for measuring ventricular pressure
c05 A69-25642
Static pressure-diameter measurements on small pulmonary blood vessels of frogs, analyzing capillary septal area as function of intravascular pressures noting high compliance
c04 A69-40974
BLUNT BODIES
Downstream radiation flux distribution calculated for blunt entry bodies, considering self absorption effects
c33 A69-12547
Blunt and conical body optimum heat shield shapes for Jupiter atmospheric entry, noting shallow flight path
[AIAA PAPER 68-1150] c31 A69-13565
Telemetry technique utilizing thermocouple sensors for base heating determinations on free flight blunt cone in shock tunnels, noting electrical noise reduction
[AIAA PAPER 68-407] c14 A69-15514
Dynamic stability derivatives of large angle blunted conical spacecraft near transonic speed in simulated Mars environment for various angles of attack
[AIAA PAPER 69-104] c31 A69-18210
Solar wind flow past earth and magnetosphere correspondence to external aerodynamics of round nosed bodies in supersonic stream
c13 A69-19360
One strip method of integral relations applied to inviscid supersonic blunt body problem
c01 A69-21972
Hypervelocity reentry simulation problems for slender and blunt bodies, defining significant parameters
c30 A69-30376
Mach number, cone angle, bluntness and wall to recovery temperature ratio effects on slender cones boundary layer transition measurements at hypersonic speeds
c01 A69-33250
Nongray equilibrium radiative heat transfer in viscous radiating shock layer around blunt body entering high temperature nonisothermal carbon dioxide-nitrogen atmosphere
[AIAA PAPER 69-636] c33 A69-33258
Nongray absorption and radiation cooling on smooth symmetric blunt bodies included in modified Maslen flow field method for radiation and large blowing
[AIAA PAPER 69-637] c01 A69-33290
Surface pressure and heat transfer over blunt conical body in hypersonic flow with uniform mass addition of various gases
[AIAA PAPER 69-716] c01 A69-33463
Cone boundary layer transition location and Reynolds number as function of nose bluntness combined effect with Ar, air and He mass injection
[AIAA PAPER 67-706] c12 A69-33476
Dynamic stability derivatives of large angle blunted conical spacecraft near transonic speed in simulated Mars environment for various angles of attack
c31 A69-40550
Computational method for surface pressures on blunt bodies of revolution at small angles of attack in supersonic flow
[NASA-TN-D-4865] c01 N69-10215
Perturbation solution to blunt body stagnation region flow of radiating gas with radiation heat transfer
[NASA-TR-R-295] c12 N69-10788
Effect of unit Reynolds number, nose bluntness, angle of attack, and roughness on transition on 5 degree half-angle cone at Mach 8
[NASA-TN-D-4961] c01 N69-14872
Experimental surface pressure distributions on spherically blunted cone at Mach numbers from 1.50 to 4.63
[NASA-TM-X-1730] c01 N69-16209
Solution to radiation-coupled stagnating flow with nongray emission over hypervelocity blunt body
[NASA-TR-R-299] c33 N69-16268
Effect of shock precursor heating on radiative flux to blunt bodies
[NASA-CR-1265] c33 N69-17438
Series solution for hypersonic flow about blunt bodies
[NASA-CR-1266] c33 N69-18125
Ablation product absorption and line transitions effects on shock layer radiative transport around blunt body
[NASA-CR-1264] c33 N69-19117
Experimental pressure distributions on 120 deg cone at Mach 2.96 to 4.63 and angles of attack from 0 deg to 20 deg
[NASA-TN-D-5054] c01 N69-19826
Stagnation pressure and heat transfer measurements of blunt axisymmetric bodies
[NASA-TN-D-5121] c01 N69-22554
Finite difference techniques used in numerical solutions for inviscid radiating shock layers around spheres at hyperbolic speed in air
[NASA-TR-R-311] c12 N69-26504
Flow field predictions for radio attenuation measurements on blunt reentry cone
[NASA-CR-1308] c07 N69-28223
Aerodynamic investigation of sharp cone-cylinder spikes on 120 degree blunted cones at Mach numbers of 3, 4.5, and 6
[NASA-TN-D-5201] c01 N69-29154
Real gas effects on hypersonic aerodynamics of blunt vehicles simulated with tetrafluoromethane
[NASA-TR-R-312] c01 N69-29270
Supersonic flow characteristics in wake of blunt cones
[NASA-TN-D-5365] c01 N69-32299
Aerodynamic drag effects of hypersonic magnetohydrodynamic plasma flow around blunt bodies
[NASA-CR-1393] c25 N69-34897
Pressure distributions for blunt body wind tunnel models at supersonic speeds and angles of attack from 0 to 15 degrees
[NASA-TN-D-5392] c01 N69-35300
Aerodynamic characteristics of blunt space capsules and slender reentry bodies with bulbous bases
[NASA-CR-1339] c01 N69-35521
Numerical calculation of inviscid adiabatic flow field around blunt bodies at hypersonic speeds
[NASA-TN-D-5434] c12 N69-36830
Integral relations solution for radiating, nonadiabatic, inviscid flow over blunt body
[NASA-TN-D-5480] c33 N69-40356
BLURRING
Conference on motion degraded images and

correcting procedures - optical filters and digital methods for blurring removal from photographic imagery
[NASA-SP-193] c14 N69-33322
BOATTAILS
Jet effects on boattail pressure drag of isolated ejector nozzles at Mach 0.60 to 1.47
[NASA-TM-X-1785] c01 N69-26976
BODIES OF REVOLUTION
Aerodynamics of bodies of revolution in nonplanar motion using nonlinear functional analysis of moments for motion about center of gravity
[AIAA PAPER 68-20] c01 A69-14714
Geometrically exact finite element for thin shells of revolution, using approximation to predict boundary layer stress distribution during vibration
[AIAA PAPER 69-56] c32 A69-18193
Finite difference method computer programs for calculation of velocities and streamlines on blade to blade surface of revolution of turbomachine
[ASME PAPER 69-GT-48] c01 A69-22495
Analytic model resembling thick walled ellipsoid of revolution incorporating three dimensional shape of human left ventricle and ventricular wall thickness effects
c05 A69-26235
Computational method for surface pressures on blunt bodies of revolution at small angles of attack in supersonic flow
[NASA-TN-D-4865] c01 N69-10215
Finite element method for computing natural frequencies and mode shapes of thin shells of revolution
[NASA-TN-D-4972] c32 N69-16469
Mathematical model for determining total drag of pointed body of revolution in supersonic flow with turbulent boundary layer
[NASA-TN-D-5046] c01 N69-19925
Incremental analysis of large deformations in continuum mechanics with applications to axisymmetric shells of revolution
[NASA-CR-1350] c32 N69-28624
Characteristics method for determining three dimensional supersonic flow around inclined body of revolution
[NASA-TN-D-5341] c12 N69-39177
BODY CENTERED CUBIC LATTICES
Vacancy relaxations in bcc crystals using energy dependence on radial displacements from defect of nearest neighbor sets, discussing crystal size and shape
c26 A69-16529
BODY COMPOSITION (BIOLOGY)
Transensor implantation, sham implantation, no implantation and lighting effects on rat body composition, noting fat and water content
c04 A69-26557
Centrifugation effects on body composition and growth of mice
c04 A69-33746
BODY KINEMATICS
Mathematical simulation model for rigid body rotational kinematics
[NASA-TN-D-5302] c23 N69-39178
BODY MEASUREMENT (BIOLOGY)
Centrifugation effects on body composition and growth of mice
c04 A69-33746
BODY TEMPERATURE
Critical body temperature for intracranial self stimulation in white rats
c04 A69-13897
Light effects on circadian rhythms in monkeys, describing changes in deep body temperature and locomotor activity phase relationships
c04 A69-31336
Circadian rhythm phase relationships between photoperiodism and heart rate, locomotor activity and deep body temperature /DBT/ in unrestrained monkeys
c04 A69-42706
BOILERS
Water flow and cavitation in convergent-divergent boiler inlet nozzles
[NASA-TM-X-1689] c12 N69-10293
Design point performance of double containment tantalum and stainless steel mercury boiler for SNAP 8
[NASA-TN-D-4926] c33 N69-12739
Experimental and analytical study of dynamics of single tube counterflow boiler
[NASA-CR-1230] c12 N69-17751
Frequency response of forced flow single tube boiler with inserts and exit restriction
[NASA-TN-D-5023] c12 N69-17779
Fabrication of counterflow double wall tantalum-stainless steel mercury boiler
[NASA-TN-D-5092] c33 N69-23707
BOILING
Bimetallic heat exchanger tube performance in sodium boiling facility
[NASA-TN-D-5323] c33 N69-30064
Properties and uses of liquid metal reactor fuels, including heat transfer processes in variously shaped channels, boiling and condensation of metals, and reactor control equipment
[NASA-TT-F-522] c33 N69-30507
BOLZA PROBLEMS
Computation of optimal branched trajectories using classical variational problem of Bolza
[NASA-CR-1331] c30 N69-24950
BONES
Conference on bone diseases and regeneration, cellular differentiation, and homeostasis of calcium
[NASA-SP-161] c04 N69-10444
BOOMS (EQUIPMENT)
Thermal flutter analysis of booms with open cross section
[NASA-TN-D-5222] c32 N69-29589
BOOSTER ROCKET ENGINES
Evaluation of pilot describing function method applied to manual control analysis of large flexible booster in Saturn 5 launch vehicle simulator
[NASA-TN-D-5149] c21 N69-22996
BORESIGHTS
Design and development of boresighted star tracker
[NASA-CR-976] c21 N69-21502
BORIDES
High temperature mechanical properties of polycrystalline hafnium carbide containing 13-volume-percent hafnium diboride
[NASA-TN-D-5008] c17 N69-16380
BORN APPROXIMATION
First Born approximation cross sections for He excitation from ground state by proton impact calculated, using wave functions
c24 A69-17027
Elastic and nonelastic scattering cross sections from 42 MeV alpha particles interacting with helium isotopes
[NASA-TN-D-5530] c24 N69-40979
BORON
Lightly loaded truss structures fabricated from Be, Be-Al alloy and uniaxial B filament reinforced epoxy tubing for unmanned spacecraft applications
c17 A69-35504
Mechanical behavior of boron-epoxy and glass-epoxy filament-wound cylinders under various loads
[NASA-TN-D-5050] c18 N69-19825
Theory and test results of tensile strength of epoxy rings and belts reinforced by boron filaments
[NASA-TN-D-5053] c18 N69-19918
BORON FLUORIDES
Boron 10 absorption cross sections from counting ratios measurements of boron trifluoride proportional counter used to monitor neutron fluxes
c24 A69-33753
BORON NITRIDES
High temperature capacitor consisting of thin wafers of pyrolytic boron nitride noting fabrication, dissipation factor and capacitance
c03 A69-15299
Boron nitride and boron nitride composite under high temperatures in air and vacuum for various time periods, discussing thermal shock and oxidation resistance
c18 A69-36208
BORON 10
Boron 10 absorption cross sections from counting ratios measurements of boron trifluoride proportional counter used to monitor neutron

fluxes
c24 A69-33753
BOSONS
He 2 excitation spectrum for interparticle potential using pair Hamiltonian with repulsive core and attractive well
c24 A69-33118
Proton-antiproton high energy elastic scattering by bosons exchange, introducing vertex functions for nonlocal Lagrangian
c24 A69-39467
BOUGUER LAW
Unified form of Lambert theorem valid for orbits
[NASA-TN-D-5368] c30 N69-36930
BOUNDARY LAYER CONTROL
Effects of boundary layer bleed rate and location on performance of axisymmetric inlet designed for Mach 2.5
[NASA-TM-X-1692] c01 N69-10294
Aerodynamic characteristics of COIN aircraft model with boundary layer control on inverted V-tail
[NASA-TN-D-4856] c02 N69-10935
Application of boundary layer control concepts to highly loaded turbine stator blades in annular cascades
[NASA-CR-1219] c01 N69-14211
Trailing-edge flap system with boundary layer control and external jet augmentation for subsonic jet transport
[NASA-TN-D-5129] c01 N69-30722
BOUNDARY LAYER FLOW
Nonsimilar laminar boundary layer solutions with negative pressure gradient compared to experimental boundary layer velocity profiles, momentum and displacement thicknesses
[AIAA PAPER 69-35] c12 A69-18094
Pressure and temperature surveys of Mach 27-47 nozzle boundary layer at Ames M-50 He tunnel, determining velocity profiles, wall friction coefficient, etc
[AIAA PAPER 69-686] c12 A69-33441
BOUNDARY LAYER SEPARATION
Hypersonic flow distribution and separation types over highly swept Delta wing with trailing edge flaps at Mach 6
[AIAA PAPER 68-97] c01 A69-12522
Performance of tandem turbine blade and its influence on flow separation and visualization
[NASA-CR-1341] c01 N69-23892
Numerical analysis of laminar and turbulent mixing region for two dimensional jet injected at angle to moving stream
[NASA-TN-D-5531] c12 N69-41213
BOUNDARY LAYER STABILITY
Geometrically exact finite element for thin shells of revolution, using approximation to predict boundary layer stress distribution during vibration
[AIAA PAPER 69-56] c32 A69-18193
BOUNDARY LAYER TRANSITION
Subliming ablation effects on boundary layer transition for cones in hypersonic flow, discussing Reynolds numbers measured in wind tunnel tests
[AIAA PAPER 68-40] c01 A69-31881
Boundary layer trip geometry, size and location effects on position of transition at hypersonic speeds
c12 A69-33249
Mach number, cone angle, bluntness and wall to recovery temperature ratio effects on slender cones boundary layer transition measurements at hypersonic speeds
c01 A69-33250
Amplified boundary layer oscillations and transition at swept flat nosed wing attachment line with/without boundary layer suction analyzed by wind tunnel tests
c01 A69-33251
Free stream disturbances influence on hypersonic boundary layer transition Reynolds number in heated and unheated flows
[AIAA PAPER 69-704] c12 A69-33453
Cone boundary layer transition location and Reynolds number as function of nose bluntness combined effect with Ar, air and He mass injection
[AIAA PAPER 67-706] c12 A69-33476
Transonic wind tunnel studies on airfoil to determine effects of Reynolds number and boundary layer transition location on shock induced separated flow
[NASA-TN-D-5003] c01 N69-16121
BOUNDARY LAYERS
Cross hatching on various body surfaces due to periodic surface pressure fluctuations, discussing origin from counter-rotating longitudinal vortices in boundary layer
[AIAA PAPER 69-11] c12 A69-18213
Modified first order theory of magnetosphere boundary shape incorporating effects of neutral sheet currents of extended geomagnetic tail
c13 A69-21661
Plasma-pause position measurements by ion mass spectrometers and broadband VLF receivers on OGO 1 and OGO 3 and by broadband recordings at Antarctica
c13 A69-25153
Conducting fluid incompressible flow in entrance of MHD channel by momentum integral method, permitting edge stress existence at boundary layer free stream interface
[AIAA PAPER 69-724] c12 A69-33436
Accelerated boundary layers classified in terms of integral balance of pressure, inertia, wall friction forces and entrainment momenta
[AIAA PAPER 69-666] c12 A69-33462
Instantaneous frozen layer thickness and temperature profile in solidified layer obtained by iteration technique
c33 A69-39433
Stagnation point boundary layer with suction and injection in equilibrium dissociating air
[NASA-TN-D-3889] c12 N69-14314
Boundary layer interaction in cooling tubes of rocket engines tends to lower convective heat transfer
[NASA-TN-D-5168] c33 N69-22931
Nature of outside boundary layer on liquid sphere in steady, uniform stream
[NASA-CR-1362] c12 N69-24877
Boundary layer and chemical reactions in hypersonic gas flow
[NASA-TT-F-549] c33 N69-31947
Boundary layer control and trailing edge flaps for direct-lift control
[NASA-CR-1426] c02 N69-38819
BOUNDARY LUBRICATION
Structure, interactions, and topography of solid surfaces, sliding friction, adhesion, wear, and boundary lubrication conference topics
[NASA-SP-181] c15 N69-30401
BOUNDARY VALUE PROBLEMS
Adaptive random search algorithm utilizing boundary cost-function hypersurfaces measurement to implement Pontryagin maximum principle, discussing hybrid computer use, iterative solution and convergence properties
c08 A69-33745
Closed form solution for minimum fuel constant thrust trajectories for vehicle transfer in vacuum between arbitrary boundary conditions
[AIAA PAPER 69-905] c30 A69-39337
Minimization of unconstrained function of several variables by gradient dependent techniques, discussing applications to boundary value problems in optimal control
[AIAA PAPER 69-951] c19 A69-40333
Boundary conditions for Tricomi equation in symmetric positive form, showing analytical and finite difference solutions
c19 A69-42792
Integral equation method with continuous functions for calculating boundary stress components in plane elasticity
[NASA-CR-1273] c32 N69-19030
Complete approximation in Euclidean space of new boundary value problem
[NASA-TT-F-577] c12 N69-29235
Iterative solution of boundary value problem for rapid optimization of multiple-burn rocket flights
[NASA-CR-1430] c30 N69-36439
Chebyshev series solution of nonlinear ordinary differential equations - initial value problems
[NASA-TM-X-1882] c19 N69-36923

BOUSSINESQ APPROXIMATION
Boussinesq approximation for compressible fluids, discussing perturbation pressure and velocities and vertical scale motions
c12 A69-26013

BOW WAVES
Vela 3A and Explorer 33 elapsed time observations of earth bow shock
c13 A69-12299
Satellite observations of geomagnetic tail in magnetosphere near midnight meridian plane, discussing formation, shape, plasma sheet and models
c13 A69-26739
Transmission of Alfven waves through earth bow shock based on hydromagnetic shocks theory, discussing amplitude amplification
c13 A69-32099
Earth bow shock waves in far upstream interplanetary medium observed from magnetic data of Explorer 34 satellite
c30 A69-34941
MHD Rankine-Hugoniot equations for ion density, thermal pressure and convective velocity magnitude and orientation during Pioneer 6 traversal of earth bow shock
c30 A69-42417

BRAIN CIRCULATION
Centrifugation for removal of bullet fragment floating freely in ventricular system of human brain to fixed safe position in left lateral ventricle wall
c04 A69-43372

BRANCHING (PHYSICS)
Computation of optimal branched trajectories using classical variational problem of Bolza
[NASA-CR-1331] c30 N69-24950

BRAYTON CYCLE
Brayton-B generator for 2-10 kWe production, describing design, heat source/rejection, efficiencies and preliminary test data analysis
c03 A69-42278
Argon turboalternator design and testing for Brayton cycle space power system, discussing inlet operating temperature and shaft bearings and rotation
c03 A69-42279
Design, fabrication, and testing of 12-kilowatt inductor alternator, voltage regulator-exciter, and parasitic loading speed controller - summary
[NASA-TN-D-4874] c03 N69-10088
Transient solidification outside cooled pipe with application to solar Brayton heat receiver
[NASA-TN-D-4897] c33 N69-10227
Analog simulation of closed loop Brayton cycle test facility
[NASA-TM-X-1715] c03 N69-14312
One megawatt reactor design for Brayton cycle space power application - thermal analysis and core design
[NASA-TN-D-5013] c22 N69-17313
One megawatt reactor design for Brayton cycle space power application - neutronics design
[NASA-TN-D-5014] c22 N69-17314
Comparison of Brayton and Rankine cycle magnetogasdynamic space power generation systems for use with nuclear heat source
[NASA-TN-D-5085] c03 N69-20852
Test performance of radial inflow turbine for Brayton cycle space power system
[NASA-TN-D-5090] c03 N69-20937
Performance of gas bearing Brayton cycle turboalternator
[NASA-TM-X-1820] c03 N69-29707
Design of Brayton rotating unit with roller bearings for space power system
[NASA-CR-1401] c15 N69-33450
Performance characteristics of 14.3 kVA modified Lundell alternator for 1200 Hz Brayton cycle space power system
[NASA-TN-D-5405] c03 N69-35537
Electrothermal instabilities effects on Brayton and Rankine cycle magnetohydrodynamic space power generation systems
[NASA-TN-D-5461] c03 N69-37883

BRAZING
Furnace brazing butt joints in tungsten-uranium dioxide cermet cylinders at 3000 deg C
[NASA-TM-X-1815] c15 N69-28862

BREADBOARD MODELS
Electron beam meter application as lunar surface electric field detector, discussing breadboard model and performance characteristics
c14 A69-13221

BREATHING APPARATUS
High oxygen concentration breathing effect on foveal thresholds, using sea level tests on trained observers
c05 A69-12216

BREGUET 941 AIRCRAFT
IFR flight tests of Breguet 941 STOL transport
[NASA-TN-D-4939] c02 N69-13252

BREMSSTRAHLUNG
Origin of galactic gamma rays, discussing evidence in support of interstellar gas in galactic disk and production of neutral pions and bremsstrahlung
c29 A69-32806
Cosmic X ray bremsstrahlung due to collisions of suprathermal protons with ambient electron, giving clue about diffuse sky background of X rays
c29 A69-40643
Bremsstrahlung spectra from bombardment of typical spacecraft materials by monoenergetic electrons
[NASA-CR-1377] c24 N69-33416
Bremsstrahlung production due to electron beam bombardment
[NASA-CR-1383] c24 N69-34541

BRIGHTNESS
Luminous spherical fog layer surrounding burning zirconium droplet during free fall through oxygen containing atmosphere, noting effect on mass and heat transfer processes
c33 A69-28462

BRITTLENESS
Hot salt stress corrosion of Ti alloy, discussing hydrogen generation during elevated temperature exposure and embrittlement as manifestation of strain rate
c17 A69-39434

BROADCASTING
Technological and cost factors of voice broadcasts from satellites to earth
[NASA-TM-X-1747] c07 N69-19025

BROMINE
Photographic study of bromine jet flowing in coaxial airstream and impinging on stagnation surface
[NASA-TN-D-5209] c12 N69-24800

BUBBLES
Cylindrical bubbles stability in vertical pipes from photographs, describing wake, spacing, pressure pulsations and convection cells effects
[ASME PAPER 69-HT-28] c33 A69-43540
Reynolds number relation to single noncondensable bubble motion under low gravity conditions
[NASA-TN-D-5462] c12 N69-38032

BUCKLING
Recent advances in shell buckling, discussing imperfection sensitivity, boundary conditions and wall configuration
[AIAA PAPER 68-103] c32 A69-12516
Flutter design charts for isotropic panels stressed to verge of buckling for typical values of structural damping
c32 A69-25524
Buckling equations solved for equatorial segment of spherical shell loaded in axial direction by own weight
[NASA-TN-D-4921] c32 N69-13034
Predicting buckling of thin walled, uniform stiffened and unstiffened circular cylindrical shells under static loading
[NASA-SP-8007] c32 N69-23320
Buckling of thin walled truncated conical shells under static loads
[NASA-SP-8019] c32 N69-24131

BULBS
Aerodynamic characteristics of blunt space capsules and slender reentry bodies with bulbous bases
[NASA-CR-1339] c01 N69-35521

BULGING
Radius effect on bulging and fracture of through-cracked cylindrical pressure vessels at cryogenic temperatures
[NASA-TN-D-4951] c32 N69-14480

BUMPERS
Multiwall meteoroid protection design in Apollo program, discussing bumper, backup sheet and honeycomb cells insulation
[AIAA PAPER 69-372] c32 A69-28304
Momentum transfer from impact into thin aluminum meteor bumper targets
[NASA-TN-D-5492] c32 N69-38809
BUNCHING
Photon bunching effect in spatially coherent noise field enhanced by superposing monochromatic coherent signal and/or shaping incident noise spectra
c07 A69-31694
BURNING RATE
Acceleration effects on solid propellant rocket motors combustion characteristics
[AIAA PAPER 68-530] c28 A69-39217
Pressure and velocity coupling effects on combustion stability in solid propellant burning
[NASA-TN-D-5395] c33 N69-34892
Aluminum size and loading effects on burning rate of centrifugal accelerated solid propellants
[NASA-TN-D-5397] c27 N69-36225
BURNING TIME
Two burn spacecraft trajectories for escaping earth parking orbit
[NASA-TN-D-5011] c30 N69-17305
Parameters affecting firing time of simultaneously triggered trigatron spark gap switches
[NASA-TN-D-5077] c09 N69-20888
BUTT JOINTS
Furnace brazing butt joints in tungsten-uranium dioxide cermet cylinders at 3000 deg C
[NASA-TM-X-1815] c15 N69-28862

C

C-5 AIRCRAFT
C-5A aircraft model high subsonic speed tests, correlating data from three transonic wind tunnels
[AIAA PAPER 69-794] c01 A69-35636
CABLES
Flat conductor cable technology, discussing design, manufacture, specifications, etc
[ASME PAPER 69-DE-8] c03 A69-28855
CABLES (ROPES)
Effects of lateral cable oscillations on dynamic response of cable-connected space station
[NASA-TN-D-5107] c31 N69-21111
CADMIUM ISOTOPES
Absolute cross sections for scattering of 42 MeV alpha particles from even isotopes of cadmium
[NASA-TN-D-4948] c24 N69-14482
CADMIUM SELENIDES
Simulated space environmental effects on full and fractional size cadmium sulfide thin film solar cells
[NASA-TM-X-1884] c03 N69-36758
CADMIUM SULFIDES
Thermal cycling tests showing improvement in cadmium sulfide solar cell stability, noting effect of thermal cycling stresses
c03 A69-13074
Impurity profiles and energy band diagram for cuprous sulfide-CdS heterojunction based on capacitance, Hall and electron microprobe measurements
c03 A69-13075
Photovoltaic properties of CdS thin film solar cells and silicon cells at Jupiter temperature and solar intensity
c03 A69-13076
Cadmium sulfide films with larger than bandgap photovoltages, analyzing photovoltage decay and temperature and light intensity effects
c26 A69-17772
Effects of preparation techniques on thin film CdS solar cells
[NASA-TM-X-1722] c03 N69-15397
Impurity profile and energy band diagram for cuprous sulfide-cadmium sulfide heterojunction
[NASA-TN-D-5079] c26 N69-19781
Simulated micrometeoroid impact effect on silicon and cadmium sulfide solar cell performances
[NASA-TN-D-5133] c03 N69-21016
Thermal shock cycling of Kapton, copper, and molybdenum thin film cadmium sulfide solar cell
[NASA-TM-X-1819] c03 N69-29555
Large thin film cadmium sulfide solar cell electrical characteristics over ranging temperatures and radiant intensities
[NASA-TM-X-1899] c03 N69-38767
CADMIUM TELLURIDES
HgCdTe as IR satellite detector for terrestrial, atmospheric and ocean mapping, IR astronomy and optical communication
c26 A69-43666
Mercury cadmium telluride as 1 to 20 micrometer wavelength infrared detector for space applications
[NASA-TN-D-4904] c26 N69-10125
CAJUN ROCKET VEHICLE
Antenna effects on aerodynamic characteristics of 0.410 scale model Cajun rocket at Mach numbers from 2.30 to 4.63
[NASA-TM-X-1771] c01 N69-21106
CALCIUM
Intensity ratios effect of forbidden Fe and Ca transitions in solar corona on Fe/Ca ratio, noting cascading configurations
c30 A69-36219
Conference on bone diseases and regeneration, cellular differentiation, and homeostasis of calcium
[NASA-SP-161] c04 N69-10444
Cyclic heating and thermal shock effects on hafnia stabilized with calcia, magnesia, and yttria
[NASA-TN-D-5279] c18 N69-34547
CALCULATORS
COMPUTE time sharing calculator program for numerical calculations
[NASA-TN-D-5350] c08 N69-32685
CALCULUS OF VARIATIONS
Low thrust trajectories for minimum time rendezvous between continuous thrust interceptor and passive target vehicle, comparing calculus of variations and steepest ascent analyses
c30 A69-32177
Variational methods for determining optimum design and flight of rockets
[NASA-TR-R-297] c31 N69-15374
Incremental analysis of large deformations in continuum mechanics with applications to axisymmetric shells of revolution
[NASA-CR-1350] c32 N69-28624
Minimum drag bodies in hypersonic flow using calculus of variations
[NASA-TN-D-5438] c01 N69-36699
CALIBRATING
Aerodynamic and thermodynamic calibration of nonequilibrium air flow in Ames 1-foot shock tunnel
[NASA-TN-D-4985] c11 N69-15633
Design and operation of high temperature loads calibration laboratory
[NASA-TM-X-1868] c11 N69-36224
CALORIMETERS
Pyrotechnic activated calorimeter for reentry package design of vehicles entering earth atmosphere at lunar return velocities
c11 A69-23026
Design and performance prediction of calorimetric apparatus for measuring total hemispherical emittance of materials
[NASA-TN-D-5106] c14 N69-20941
CAMBERED WINGS
Experimental and theoretical study of symmetrical and cambered Delta wing configuration between Mach 2.0 and 10.7
[NASA-TN-D-5272] c01 N69-29269
CAMERAS
Gemini program for geologic orbital photography, discussing equipment used
c13 A69-35274
Extended source Fourier transform holography for single image synthesis of multiple identical images produced by multiple pinhole camera in X ray astronomy
c14 A69-40019
Photogrammetric camera system developed from NASA requirements to document lunar surface environment during manned space flight exploration
c14 A69-40989
Design, fabrication, assembly of planetary film reconnaissance system

[NASA-CR-1358] c14 N69-28023
CANARD CONFIGURATIONS
Aerodynamic loads on deployed canard surfaces and rocket nose section of Apollo launch escape vehicle
[NASA-TN-D-5260] c31 N69-28166
XB-70 aircraft flight tests of canard configurations
[NASA-TN-D-5359] c02 N69-32284
CANCER
Osmotically induced coalescence of sarcoma cells through intercellular bridges in vitro
[NASA-TN-D-5022] c04 N69-17782
CANTILEVER BEAMS
Transverse shear deformation and rotary inertia effects in vibrating beams
[NASA-CR-1317] c32 N69-24056
Beam stiffness determined for thin walled truncated cones under bending loads
[NASA-TN-D-5536] c32 N69-41141
CAPACITANCE
Frequency conversion in sheath capacitance of glow discharge plasma contained within metallic coaxial cylinders
c25 A69-14456
Time varying resistance wire to arrest oscillations in pulsed capacitor discharge circuit, deriving over, under and critical damping conditions
c09 A69-41228
Measurement of liquid and two phase hydrogen densities with capacitance density meter
[NASA-TN-D-5015] c14 N69-23470
Thin film microwave irises with capacitive reactance
[NASA-CR-1364] c26 N69-28096
CAPACITORS
High temperature capacitor consisting of thin wafers of pyrolytic boron nitride noting fabrication, dissipation factor and capacitance
c03 A69-15299
High purity dielectric materials tested in capacitors at high temperatures
[NASA-CR-1213] c18 N69-14400
CAPILLARIES (ANATOMY)
Static pressure-diameter measurements on small pulmonary blood vessels of frogs, analyzing capillary septal area as function of intravascular pressures noting high compliance
c04 A69-40974
CAPILLARY TUBES
Transient electro-osmosis of water in capillary tubes for pumping and generation modes, analyzing response to step change in pressure or voltage change under external loading
c06 A69-14862
CAPSULES
Vacuum ultraviolet detector-spectroscopy systems for capsule reentry measurements
[NASA-CR-1268] c09 N69-18761
CAPTURE EFFECT
Group cross section generating techniques to calculate neutron capture rates and spatial capture distribution in depleted thick U slab, using GAROL program
c24 A69-35179
Direct flight and Jupiter swingby heliocentric trajectory modes of elliptic capture orbits compared for unmanned missions to outer planets
[AAS PAPER 68-105] c30 A69-39221
CARBIDES
Dynamic strain aging in carbide strengthened molybdenum alloys
[NASA-TN-D-5355] c17 N69-31883
CARBON
Transmittance and absorption cross sections of carbon particles suspended in flowing stream of nitrogen gas
c33 A69-17804
RAM-CA carbon-phenolic heat shield test in rocket engine exhaust
[NASA-TM-X-1841] c31 N69-32713
CARBON ARCS
Spectral and operational characteristics of high intensity carbon arc solar simulator
[NASA-TM-X-1825] c11 N69-29737
CARBON COMPOUNDS
Composite carbon resistor characteristics used for accelerator terminal voltage measurement
[NASA-TM-X-1718] c24 N69-14398
Mechanical properties of alloys molybdenum hafnium carbon compounds
[NASA-TN-D-5025] c17 N69-19200
CARBON DIOXIDE
Carbon dioxide laser with two gas absorption cells in cavity for emission wavelength control and HF pulsed mode of operation
c16 A69-21088
Segmented anode, carbon dioxide-hydrogen performance and hollow cathode erosion tests on low power MPD arc thrustor, noting current measurements
[AIAA PAPER 69-242] c28 A69-21236
NADH stimulation of ATP dependent carbon dioxide fixation in crude extracts of Hydrogenomonas facilis, considering allosteric regulation of phosphoribulokinase activity
c04 A69-30036
Acetate-2-C 14 conversion to C 14 carbon dioxide and C 14 fatty acids in rats with 2/3 of liver removed
c04 A69-35976
Heats of adsorption of carbon dioxide on silver /I/ oxide and copper /II/ oxide by gas chromatography
c06 A69-38277
Solid electrolyte electrolysis of carbon dioxide and water as oxygen regeneration system for long manned space flights
[NASA-CR-1359] c05 N69-28099
Limb radiance calculation model for atmospheric carbon dioxide bands with pressure and temperature gradients
[NASA-TN-D-5495] c21 N69-40055
CARBON DIOXIDE CONCENTRATION
Venus exospheric temperature for various composition models, discussing carbon dioxide concentration effects
c30 A69-12109
Electronic transition moment for C /Swan/ bands measured in shock tube in carbon dioxide and argon mixtures
c24 A69-12833
Carbon dioxide levels monitoring in spacesuit research including limits of physiological acceptability
c05 A69-39170
CARBON DIOXIDE REMOVAL
Lithium peroxide utilization feasibility for oxygen supply and carbon dioxide control in extravehicular portable life support systems
[AIAA PAPER 69-620] c05 A69-33303
CARBON ISOTOPES
Automatic equipment for sampling and preparing gases by dual column gas chromatography for subsequent mass spectral analysis of carbon isotopes during methane metabolism
c06 A69-12603
CARBON MONOXIDE
Theoretical molecular line absorption of carbon monoxide in late spectral type stellar atmospheres
[NASA-TN-D-4798] c24 N69-14448
CARBON 14
Acetate carbon 14 utilization in centrifuged rats, analyzing metabolism by measuring plasma glucose, FFA and lipids synthesis
c04 A69-19429
Acetate-2-C 14 conversion to C 14 carbon dioxide and C 14 fatty acids in rats with 2/3 of liver removed
c04 A69-35976
CARBONACEOUS METEORITES
Solar system elements abundance compilation based on carbonaceous chondrites and nucleosynthesis in stars
c30 A69-20903
Meteorites pigments identification as porphyrins for extraterrestrial life evidence, noting sample analyses of Orgueil, Murray, Cold Bokkeveld and Mokoia carbonaceous chondrites
c30 A69-39889
CARDIAC VENTRICLES
Single channel pressure telemetry unit for chronic implantation into cardiac chambers or major blood vessels in unrestrained animals for measuring ventricular pressure
c05 A69-25642

Pneumatic driving system for heart assist or total replacement pumps, discussing design features and performance characteristics
c05 A69-42983

CARDIOVASCULAR SYSTEM
Axial waves in blood vessels, determining phase velocities and damping, noting anisotropic behavior of artery wall
[SESA PAPER 1350] c04 A69-19726
Single channel pressure telemetry unit for chronic implantation into cardiac chambers or major blood vessels in unrestrained animals for measuring ventricular pressure
c05 A69-25642
Cardiovascular conditioning suit to provide transmural pressure gradient in circulatory system during weightlessness
[NASA-CR-1206] c05 N69-13202

CARGO AIRCRAFT
Wind tunnel studies of scaled model of multijet cargo airplane
[NASA-TN-D-5538] c02 N69-40937

CARGO SPACECRAFT
Low cost efficient shuttle system for personnel and cargo transport to earth orbit for NASA and DOD needs
c31 A69-39695

CARRIER WAVES
Subcarrier phase modulated single sideband sinusoidal carrier synthesis, discussing signal power ratios, signal efficiency, design sensitivity, etc
c07 A69-29489

CARTESIAN COORDINATES
Numerical integration for continuously thrusting spacecraft optimal trajectory, considering rectangular Cartesian and polar cylindrical coordinates characteristics
[AIAA PAPER 69-903] c30 A69-38546

CASCADE FLOW
Application of boundary layer control concepts to highly loaded turbine stator blades in annular cascades
[NASA-CR-1219] c01 N69-14211
Aerodynamic characteristics of annular cascade of blades
[NASA-CR-1323] c01 N69-25327
Performance tests of jet flapped blade in six blade annular cascade
[NASA-CR-1423] c28 N69-36680

CATALASE
Salts and organic solvents effect on halophile Halobacterium cutirubrum catalase, noting enzyme activity inhibition by cation and anion
c04 A69-35291

CATALOGS (PUBLICATIONS)
Two-micron sky survey catalog of celestial objects
[NASA-SP-3047-REV] c30 N69-37993

CATHODE RAY TUBES
Superlinear and sublinear phosphors combined for producing single gun color cathode ray tubes
[NASA-CR-1228] c09 N69-14256

CATHODES
SERT 2 thrustor hollow cathode durability tested in bell jar
[AIAA PAPER 69-304] c28 A69-21224
Study of discharge from mercury vapor fed hollow cathode
[NASA-TN-D-4966] c28 N69-17847
Performance of various oxide magazine cathodes in Kaufman thrusters
[NASA-TN-D-5074] c28 N69-19980
Plasma generation using large V-groove cathode discharge
[NASA-TN-D-5269] c25 N69-29140

CATIONS
Cation concentration requirement of halophilic NADH dehydrogenase for stability and maximum activity
c06 A69-23127
Electron transport chain of monovalent and divalent cations and of polyamines, studying effects on menadione reductase activity to determine salt dependence
c04 A69-41077

CAVES
Collapse theory of dimple craters, analogies with terrestrial sink holes and dimple craters as channels for gas escape from interior
c30 A69-15589

CAVITATION CORROSION
Temperature and pressure effect on cobalt base alloy cavitation in liquid sodium, using vibratory apparatus and loss rate contour diagram
c17 A69-35184
Performance and cavitation damage to axial flow pump rotor blades in high temperature liquid sodium
[NASA-TN-D-5138] c15 N69-21773
Tandem bladed inducer tested in water for cavitation corrosion
[NASA-TN-D-5134] c01 N69-23769
Effect of temperature and pressure on cavitation damage to cobalt base alloy in sodium
[NASA-TN-D-5273] c17 N69-28863
Cavitation damage and effect of fluid temperature on performance of axial flow pumps in liquid sodium
[NASA-TN-D-5484] c15 N69-38641

CAVITATION FLOW
Jet pump head rise deterioration parameter for prediction of cavitation
c12 A69-15791
Noncavitating and cavitating performance of low area ratio water jet pumps, analyzing efficiency, area ratio, throat length, nozzle spacing and diffuser geometry
c03 A69-35176
Flow characteristics and wall heat transfer in separated flow region of annular cavity at free stream hypersonic speed and high gas temperature
[AIAA PAPER 68-672] c01 A69-37185
Prediction of thermodynamic effects of developed cavitation based on liquid hydrogen and Freon-114 data in scaled venturis
[NASA-TN-D-4899] c12 N69-10070
Water flow and cavitation in convergent-divergent boiler inlet nozzles
[NASA-TM-X-1689] c12 N69-10293
Noncavitating and cavitating performance of low area ratio water jet pumps having throat lengths of 3.54 diameters
[NASA-TN-D-5095] c03 N69-20797
Net positive suction head requirements for helical inducer in liquid hydrogen under varied flow and temperature conditions
[NASA-TM-X-1808] c09 N69-27841
Prediction of cavitation performance of centrifugal pumps
[NASA-TN-D-5292] c15 N69-29165
Fluid temperature effect on cavitation performance of axial flow pump
[NASA-TN-D-5318] c15 N69-30069
Noncavitating and cavitating performance of inducer in liquid hydrogen
[NASA-TM-X-1854] c12 N69-33261

CAVITIES
Unsteady two dimensional flow in square cavity with fluid initially at rest and constant velocity upper surface of cavity, noting vortex center
[AICHE PAPER 25C] c12 A69-14510
Flow characteristics in two dimensional channel with rectangular cavity
[NASA-CR-1245] c12 N69-14095

CAVITY RESONATORS
Helmholtz resonators with variable cavity depths tested with unstable rocket combustor
[NASA-TN-D-5171] c33 N69-23351
Transient response of coupled acoustic cavity resonators
[NASA-CR-1421] c23 N69-35286

CELESTIAL BODIES
Solar radiation pressure windmill effect in rotational bursting and elimination from solar system of small magnetic celestial bodies
c30 A69-39584
Two-micron sky survey catalog of celestial objects
[NASA-SP-3047-REV] c30 N69-37993

CELESTIAL SPHERE
Celestial sphere scanning by passive method applicable to space missions requiring long lifetime and moderate pointing accuracies
[AIAA PAPER 68-854] c21 A69-39764

CELL DIVISION
Weightlessness effects on fertilized frog egg development onboard Gemini 8 and 12 manned

orbital flights, discussing cell division, differentiation and embryogeneis
c04 A69-11084
CELLS (BIOLOGY)
Cellular localization of acetyl-coenzyme A synthetase in yeast, noting enzyme distribution during aerobic growth on glucose
c04 A69-15333
Viruslike particles in fat body cells and oenocytes of Drosophila melanogasters imagoes, in glial cells of cephalic ganglionic center of flies and in gamma radiated cells
c04 A69-42021
Conference on bone diseases and regeneration, cellular differentiation, and homeostasis of calcium
[NASA-SP-161] c04 N69-10444
Micro lagoon technique for culture and observation of isolated mammalian cells
[NASA-TN-D-4906] c04 N69-11056
Osmotically induced coalescence of sarcoma cells through intercellular bridges in vitro
[NASA-TN-D-5022] c04 N69-17782
Boundedness theorem, thresholds, and stationary values in modified Huxley-Hodgkin model for electric current flow through cell membrane
[NASA-CR-1272] c19 N69-21143
CENTAUR LAUNCH VEHICLE
Performance tests on dynamic jettison hinge loads of Centaur nose fairing
[NASA-TM-X-1821] c32 N69-29734
CENTER OF GRAVITY
Cone-conical-frustrum configurations meeting center of gravity requirements for higher hypersonic lift-drag ratios in axisymmetric manned spacecraft
c01 A69-39237
CENTRIFUGAL FORCE
Centrifugation for removal of bullet fragment floating freely in ventricular system of human brain to fixed safe position in left lateral ventricle wall
c04 A69-43372
Rotating wickless hollow shaft heat pipe utilizing centrifugal acceleration for return pumping of condensate and transferring high heat fluxes
[ASME PAPER 69-HT-19] c33 A69-43550
CENTRIFUGAL PUMPS
Analytical method for predicting performance of centrifugal pumps during pressurized startup
[NASA-TN-D-4967] c15 N69-14082
Performance tests on liquid metal pumps for sodium potassium loops
[NASA-TM-X-1765] c15 N69-22970
Liquid-metal centrifugal pump at mercury loop
[NASA-TM-X-1766] c15 N69-23768
Prediction of cavitation performance of centrifugal pumps
[NASA-TN-D-5292] c15 N69-29165
Low speed characteristics of liquid hydrogen centrifugal turbopumps
[NASA-TM-X-1861] c28 N69-33806
CENTRIFUGES
Space-station-centrifuge configuration dynamic stability exhibiting instabilities at lower and higher centrifuge rotational speeds
[AIAA PAPER 68-142] c31 A69-12373
CENTRIFUGING STRESS
Acetate carbon 14 utilization in centrifuged rats, analyzing metabolism by measuring plasma glucose, FFA and lipids synthesis
c04 A69-19429
Centrifugation effects on body composition and growth of mice
c04 A69-33746
Equilibrium and free vibration problems of centrifugally stabilized disk and shell structures
[NASA-CR-1178] c32 N69-14477
CEPHEID VARIABLES
Individual properties of RR Lyrae stars
[NASA-TT-F-562] c30 N69-27169
CERAMIC BONDING
Joining ceramics and graphite to other materials
[NASA-SP-5052] c15 N69-14241
CERAMIC COATINGS
Test program simulating solar wind outside magnetosphere to evaluate high melting point high density ceramic oxides as white thermal control coating pigments
[AIAA PAPER 69-641] c18 A69-33762
CERAMIC NUCLEAR FUELS
Fission product gas pressure calculated for uranium dioxide ceramic fuel elements
[NASA-TN-D-4823] c22 N69-10216
CERENKOV COUNTERS
Night sky Cerenkov light detectors observations of pulsars CP 1133, NP 0532 and NP 0527, noting instrumental limitation in detecting ultrashort light pulses
c30 A69-34994
CERMETS
Fabrication of cermets of uranium nitride and tungsten or molybdenum from mixed powders and from coated particles for nuclear fuel elements
[NASA-TN-D-5136] c17 N69-21404
Furnace brazing butt joints in tungsten-uranium dioxide cermet cylinders at 3000 deg C
[NASA-TM-X-1815] c15 N69-28862
CESIUM
Work function and desorption energy measurements of alkali metals from metallic substrates with modulated molecular beam, noting surface contamination
c26 A69-21808
Electron-cesium atom collision probability for momentum transfer
[NASA-TM-X-1897] c24 N69-38773
CESIUM DIODES
Backscattering due to collisions for electrons from emitter accelerated through positive ion sheath into plasma in thermionic diodes
c09 A69-17773
CESIUM ISOTOPES
Excited states of xenon nuclei formed in beta decay of iodine and cesium isotopes
[NASA-TN-D-5329] c24 N69-30074
CESIUM PLASMA
Refractive index computation for free electrons and neutral atoms in cesium plasma at helium neon laser wavelengths
[NASA-TN-D-5328] c25 N69-30622
CESIUM VAPOR
Doublet structure suppression in mixtures of cesium and foreign gases, discussing absorption observations
c24 A69-20736
Gas breakdown model for analyzing breakdown of Ce vapor filled crack in thermionic trilayer insulator
c03 A69-21840
Modified structural design of high temperature cesium vapor thyratrons
[NASA-CR-1417] c03 N69-36411
Development and inverter circuit tests of high temperature cesium vapor thyratrons
[NASA-CR-1435] c03 N69-36843
CHANNEL CAPACITY
Waveform distortion resulting from adjacent channel crosstalk and from amplitude and phase nonlinearity in channel filters in DSB/SC telemetry link
c07 A69-19130
CHARACTER RECOGNITION
Recognition program for handwritten information in real time computer operation
[NASA-CR-1284] c08 N69-21527
CHARGE CARRIERS
Performance tests of silicon and germanium transistors in intense magnetic fields
[NASA-TN-D-5428] c09 N69-36710
CHARGE DISTRIBUTION
Charge and energy composition of particles in solar flare, discussing rigidity spectra of singly and multiply charged nuclei
c29 A69-17280
Einstein field equations solutions generated via static spherically symmetric mass and charge distributions
c23 A69-32053
Computerized design parameters for realizable overdriven bimode varactor frequency doubler based on charge-voltage relationship at break point
c09 A69-37299
CHARGE EXCHANGE
Ion-molecule collisions of Ar-Co and N-No pairs, discussing charge exchange reaction rates and

spiraling nature
c24 A69-16428
Experimental measurements of two electron capture for negative ion production in atmospheric gases
[NASA-CR-1406] c24 N69-38564
CHARGE TRANSFER
Reaction rate constants of ion-molecule interchange reaction as function of temperature, flow velocity, activation energy and constant part of steric factor P
c06 A69-32312
CHARGED PARTICLES
Charged particle dynamics in spiral interplanetary magnetic field model, discussing electric drift velocity, point of origin and distribution
c29 A69-14015
Photomultipliers response to energetic particles in terms of background current using data from OGO experiments
c14 A69-16932
Ion composition and charged particle temperatures at 300-600 km from sounding rocket and topside sounder Alouette 2 measurements
c13 A69-18839
Equation describing statistically trapped particle motion under influence of fields varying in time and space
c29 A69-19375
Integrated charged particle energy spectra from gridded electrostatic analyzers, relating retarding potential curve to particle floating potential, kinetic temperature, etc
c25 A69-20521
Comet interaction with solar wind, assuming field tail coupling of ionized comet material to solar wind ions
c30 A69-27817
CHARRING
Charring phenolic nylon ablator material pyrolysis and surface recession for cyclic and constant combined convective and radiative heating
[AIAA PAPER 69-151] c33 A69-18055
Pressure fields and multidimensional gas flow in permeable char layers and effects on ablation
[NASA-TR-R-296] c33 N69-16181
Thermochemical data from simulated pyrolysis gas flow through ablating char layer
[NASA-TN-D-5464] c33 N69-38271
CHEBYSHEV APPROXIMATION
Chebyshev series solution of nonlinear ordinary differential equations - initial value problems
[NASA-TM-X-1882] c19 N69-36923
CHECKOUT
Debugging computer programs in terms of localization and correction of errors
[NASA-CR-1397] c08 N69-35613
CHEMICAL ANALYSIS
Auger and photoelectron spectroscopy for chemical analysis, noting effects of sample thickness, sample potential, surface contamination and X ray incident angle
c06 A69-19775
Sugars identification as trifluoethylacetyl polyol derivatives by gas-liquid chromatography
c04 A69-31539
Extraterrestrial life detection experiments integrated into single multipurpose space laboratory, including chemical analyses, metabolism identification, observation for molecular and/or cellular growth and replication
c05 A69-32970
Free lysine and dinitrophenyl /DNP/ derivatives determined quantitatively by ion exchange chromatography
c06 A69-33651
Chemical analysis and paragenesis of manganoan ilmenite from Sierran adamellite using electron microprobe
c13 A69-35977
Optical properties and chemical analysis of contaminants on Gemini spacecraft windows
[NASA-TN-D-4916] c31 N69-13232
Evaluation of various laboratory determination of oxygen in potassium and sodium
[NASA-TN-D-4971] c06 N69-14180
Analysis of sodium chloride deposits on compressor blades of flight gas turbine engines
[NASA-TN-D-4999] c28 N69-17276
CHEMICAL BONDS
Temperature dependent isomer shift and anharmonic binding of Sn 119 in niobium stannide, measuring Mossbauer recoil free fraction
c26 A69-10009
Rotational spectrum of ethylene episulfoxide to determine molecular structure, particularly orientation of C sub 2 S ring
c06 A69-20535
CHEMICAL COMPOSITION
Lunar composition analysis by measuring atomic and nuclear radiation emission from orbiter
[AAS PAPER 68-197] c30 A69-11475
Circumstellar grain compositions of stars with various O to C abundance ratios, calculating molecular equilibrium of condensates and gaseous compounds in stellar atmospheres
c30 A69-24103
Venus atmosphere chemical composition, surface temperature and pressure obtained by Venera 4 and Mariner 5
c30 A69-26129
Transensor implantation, sham implantation, no implantation and lighting effects on rat body composition, noting fat and water content
c04 A69-26557
Lower solar corona composition changes due to pressure and thermal gradients calculated with multicomponent diffusion equations
c30 A69-33059
Curve of growth analysis for close binary HR 5317 indicating Mg, Mn, Ca and Sr overabundance respecting standard star 110 Her
c30 A69-34297
Chemical composition of galactic and solar cosmic rays, discussing differences from universal cosmic abundances, using Cerenkov counters, emulsions, etc
c29 A69-40090
Ivory Coast microtektites chemical composition from electron microprobe analysis
c30 A69-41351
Noctilucent clouds with wave movement, chemical composition, and water vapor
[NASA-TT-F-546] c13 N69-25013
Rapid computation of equilibrium, chemical composition, and thermodynamic properties of argon-oxygen-hydrogen gas system
[NASA-TN-D-5416] c33 N69-36299
CHEMICAL ELEMENTS
Origin and distribution of elements - Conference, Paris, May 1967
c30 A69-20892
Solar system elements abundance compilation based on carbonaceous chondrites and nucleosynthesis in stars
c30 A69-20903
Approximate ionization potentials for high ionization stages of elements with atomic numbers 31 to 92 obtained by binding energy calculations
c24 A69-29923
CHEMICAL EQUILIBRIUM
Complex chemical equilibrium calculation, analyzing thermodynamic principles and solution to nonlinear equations
c06 A69-10588
Calculating equilibrium and kinetically limited performance using one dimensional model
[NASA-TN-D-4991] c27 N69-16153
Thermodynamic properties of liquid and gas phase equilibria of water plus heavy water
[NASA-TN-D-5223] c33 N69-26247
Chemical equilibrium of ablation materials including condensed species
[NASA-TN-D-5391] c33 N69-34966
CHEMICAL INDICATORS
Comparison of extraction procedures using 1-nitroso 2-naphthol and dimethylglyoxime for spectrophotometric determination of palladium in titanium alloys
[NASA-TM-X-1767] c06 N69-20801
CHEMICAL PROPERTIES
Effect of chemical properties of pyrolysis gases on heat shield mass required for lifting reentry vehicle in typical reentry trajectory
[NASA-TN-D-4975] c32 N69-14306
Properties of irradiated polyethylene memory materials

[NASA-CR-1384] c18 N69-36762
CHEMICAL REACTIONS
Vacuum distillation technique for isolation and recovery of alkali metal reaction products with Ta, Ni, V and oxygen c14 A69-10927
Reaction rate and mechanism for low temperature reaction between lithium hydride and liquid ammonia, noting chemisorbed ammonia dissociation at interface c06 A69-11285
Ultrahigh molecular weight polyethylene terephthalate synthesis from commercial solid state materials, noting effects of several parameters c24 A69-16496
Fluorinated polyurethanes synthesis for liquid oxygen environments and cryogenic structural utility, noting structural effects on LOX compatibility c06 A69-16498
Parasitic eigenvalue in integration of equations governing one dimensional flow of chemically reactive gas c12 A69-18317
Chemical processes in silicon carbide due to reactive deposition and chemical conversion, noting silicon growth mechanism involving outward diffusion c26 A69-21351
Oxygen depletion effect in chemical reactions between pyrolysis gases and air stream on surface recession of charring ablators
[AIAA PAPER 68-302] c33 A69-21982
Venus atmosphere origin, discussing high temperature effects and chemical composition via space probe and terrestrial observations c30 A69-23183
Ductile metal powder chemical reactions during comminution in pure or oxygenated water c06 A69-27762
Isothiocyanates and phenyl isocyanate reaction with hydrazinoethanol and hydrazincethyl hydrogen sulfate c06 A69-31808
Chemical reactions activation energy at high temperature, noting cross section shape role for deducing activation energy from rate data c06 A69-34443
H release, pressure and oxide layer formed by reaction during ball milling Cr in water c15 A69-38567
Boundary layer and chemical reactions in hypersonic gas flow
[NASA-TT-F-549] c33 N69-31947
Development of barium chemical release system
[NASA-CR-1415] c13 N69-35660
CHICKENS
Repeated blood sampling effect on plasma cholinesterase, acid phosphatase, alkaline phosphatase and hematocrit ratios in domestic chickens c04 A69-23158
CHOLESTEROL
Direct measurement of skin friction in wind tunnel testing by using cholesteric liquid crystals
[NASA-TM-X-1774] c12 N69-26956
CHONDRITES
Electron microprobe analysis of vanadium in presence of titanium by compositional measurement of chromite in chondritic meteorites c06 A69-18419
Chondrite meteorite fall /1969/ in Mexico, noting opaque and microcrystalline matrices and gamma rays from short lived isotopes c30 A69-20686
Meteorites pigments identification as porphyrins for extraterrestrial life evidence, noting sample analyses of Orgueil, Murray, Cold Bokkeveld and Mokoia carbonaceous chondrites c30 A69-39889
Ilmenite composition in equilibrated ordinary chondrites, analyzing Fe, Mg, Ti and Cr content c30 A69-42890
CHONDRULE
Bjurbole chrondrules composition and density, discussing formation of homogeneous olivines and pyroxenes c30 A69-36090
CHROMATOGRAPHY
Free lysine and dinitrophenyl /DNP/ derivatives determined quantitatively by ion exchange chromatography c06 A69-33651
CHROMITES
Electron microprobe analysis of vanadium in presence of titanium by compositional measurement of chromite in chondritic meteorites c06 A69-18419
CHROMIUM
H release, pressure and oxide layer formed by reaction during ball milling Cr in water c15 A69-38567
Feasibility of producing dispersion strengthened chromium by ball milling in hydrogen halides
[NASA-TN-D-4912] c17 N69-10827
CHROMIUM ALLOYS
Ductile metal clads and coatings of silicides, aluminides and noble metals to protect Cr alloys against nitrogen embrittlement and air oxidation c17 A69-26495
Ductilizing of Group 6A elements by rhenium and other solutes
[NASA-TN-D-4955] c17 N69-14403
Protective coatings for chromium alloys for use in advanced air breathing applications
[NASA-TN-D-5157] c17 N69-23084
Chromium base alloys for high temperature application in jet engines
[NASA-TM-X-1867] c17 N69-35764
CHROMOSOMES
Preflight and postflight leukocyte chromosome aberration analyses of Gemini astronauts c04 A69-33173
CHROMOSPHERE
Photospheric radiation field role in temperature inversion of stellar chromospheres with dominant H ion opacity, postulating mechanical energy dissipation c30 A69-38173
Spectral analysis of solar activity, including solar electromagnetic phenomena, facula structure, and periodic variations in chromospheric flares and solar cycles
[NASA-TT-F-581] c29 N69-33401
CHRONOLOGY
Kodaikanal iron meteorite measurements for cosmogenic rare gases and K-Ar isotopes ages for glass inclusions c30 A69-22047
Chronology of Apollo spacecraft program to 7 Nov. 1962
[NASA-SP-4009] c31 N69-32021
Chronological study of design and development of Gemini project
[NASA-SP-4002] c31 N69-36501
CHRONOPHOTOGRAPHY
Mitotic synchronization of fibroblasts with metabolic retardants by chronophotography
[NASA-TN-D-5021] c04 N69-17248
CIRCADIAN RHYTHMS
Light effects on circadian rhythms in monkeys, describing changes in deep body temperature and locomotor activity phase relationships c04 A69-31336
Circadian rhythms in nonhuman primates - Conference, Atlanta, July 1968 c04 A69-42701
Circadian rhythm phase relationships between photoperiodism and heart rate, locomotor activity and deep body temperature /DBT/ in unrestrained monkeys c04 A69-42706
CIRCUIT DIAGRAMS
Computer program for generation of test patterns for multiterminal devices and networks c08 A69-39604
CIRCUIT PROTECTION
Ignition hazards in electrical circuits contaminated by glycol fluids, describing hazard detection by RF methods, decontamination procedures, safety checks, etc c18 A69-36028
CIRCUIT RELIABILITY
Metal oxide semiconductor integrated circuits, showing failure rates and degradation causes c09 A69-31851

Scanning electron mirror microscope advantages over electron mirror and scanning electron microscopes for examining integrated circuits
c14 A69-32891
Al interconnections discontinuities at integrated circuit contact windows observed by scanning electron microscope, noting catastrophic failure and Si presence
c09 A69-32893
Reliability handbook for silicon monolithic microcircuits - applications
[NASA-CR-1346] c09 N69-23225
Reliability handbook for silicon monolithic microcircuits - failure mechanisms
[NASA-CR-1347] c09 N69-23226

CIRCUITS
Electric control and protection circuits for parallel operation of inverter-converter
[NASA-CR-1225] c10 N69-19003
Computer oriented error analysis of electrical circuits and nonlinear system performance
[NASA-TN-D-5112] c10 N69-22919
Development and inverter circuit tests of high temperature cesium vapor thyratrons
[NASA-CR-1435] c03 N69-36843

CIRCULAR CONES
Force penetration characteristics of sand horizontally penetrated by various geometrically shaped models
[NASA-CR-1252] c18 N69-14764
Effect of unit Reynolds number, nose bluntness, angle of attack, and roughness on transition on 5 degree half-angle cone at Mach 8
[NASA-TN-D-4961] c01 N69-14872
Newtonian aerodynamics for circular cones modified to produce lift at zero angle of attack
[NASA-TN-D-5193] c01 N69-23926

CIRCULAR CYLINDERS
Radiation pattern of axial slot on circular conducting cylinder based on wedge diffraction and creeping wave theory
c07 A69-24993
Semiempirical stability boundary for flutter of simply supported cylinders for various length-radius and radius-thickness ratios
c32 A69-41914
Transonic wind tunnel tests of aerodynamic drag and lift forces on circular cylinder in two dimensional flow at high Reynolds number
[NASA-TR-R-300] c01 N69-17304
Numerical calculation of viscous compressible flow around harmonic oscillating rigid cylinder
[NASA-CR-1467] c12 N69-38782

CIRCULAR ORBITS
Computational method for time optimal space rendezvous between rocket vehicle and circular orbit target
[NASA-TN-D-5017] c30 N69-16210

CIRCULAR POLARIZATION
Simple antenna with good circular polarization over wide space sector, showing geometry, normalized orthogonal field distributions and beamwidth range, considering slot combinations
c09 A69-41590
Parabolic antenna properties generated by dual band circularly polarized focused two channel monopulse feed system, discussing tracking data from helicopter, Apollo 8 and Cassiopeia A
c07 A69-41752

CIRCULAR SHELLS
Predicting buckling of thin walled, uniform stiffened and unstiffened circular cylindrical shells under static loading
[NASA-SP-8007] c32 N69-23320

CIRCULATION
Exhaust recirculation effects produced by two heated jets impinging on ground plane
[NASA-CR-1307] c01 N69-34703
Empirically determined wind and scale effects on hot gas recirculation characteristics of jet V/STOL aircraft
[NASA-CR-1445] c28 N69-40776

CISLUNAR SPACE
Secular change examination in cislunar geomagnetic tail field gradient during summers of 1966 and 1967, using Explorer 33 and 35 results
c13 A69-11237

CIVIL AVIATION
NASA civil aviation electronics research program, discussing feasibility of V/STOL aircraft all-weather operations
c34 A69-16718
General aviation missions in national transportation system /1968, 1975, 1980/, considering fuel taxes, overall system economics, ground facilities, etc
[AIAA PAPER 69-818] c34 A69-35624
Light rigid civil aircraft response to continuous atmospheric turbulence estimated using two rigid body degrees of freedom method for vertical and lateral gusts
[AIAA PAPER 69-766] c32 A69-35657

CLADDING
Analysis of cylindrical reactor fuel pin for clad stress caused by fission gases
[NASA-TN-D-5178] c22 N69-24802
Radial power tailoring for uranium dioxide-T-111 clad reactor with contained fission product gases
[NASA-TM-X-1795] c22 N69-25305
Three oxidation-resistant alloy foil claddings for protecting typical gas turbine engine alloys of nickel and cobalt
[NASA-TN-D-5483] c17 N69-38794

CLASSIFICATIONS
Subject classification bibliography for thermal contact resistance
[ASME PAPER 68-WA/HT-18] c33 A69-16122
Iron meteorites genetic classification based on parent body cooling rate and Ga-Ge trace element content
c30 A69-36129

CLEAN ROOMS
Clean room technologies for control of contaminants for component reliability
[NASA-SP-5074] c05 N69-33775

CLEANLINESS
Theory and method for characterizing surface cleanliness of nickel during adhesion testing
[NASA-TN-D-5055] c17 N69-19827

CLEAR AIR TURBULENCE
Clear air turbulence and detection - Conference, Seattle, August 1968
c20 A69-33732
Temperature profiles and associated wind profiles obtained with Jimsphere/FPS-16 radar system at Cape Kennedy, discussing remote CAT detector assessment
c20 A69-33739
Clear air turbulence detection in troposphere by multifrequency radiometric sensor, noting multibeam system for supersonic aircraft
c09 A69-42536

CLEARANCES
Effect of rotor tip clearance on performance of 5-inch single-stage axial flow turbine
[NASA-TM-X-1757] c03 N69-20883

CLIMATOLOGY
Ocean circulation as climate regulator, discussing role in redistributing climate-changing energy input from solar radiation or lunar tidal friction into atmosphere
c13 A69-26333
Ballistically effective atmospheric parameters for rocket vehicle design manuals involving application of climatological concepts of meteorology
c31 A69-26874
Cloud cover effects on selection of recovery sites for future earth orbital missions
[NASA-TN-D-5120] c30 N69-22939

CLIMBING FLIGHT
Optimum takeoff and climbout trajectory calculation technique for jet aircraft noise abatement
[NASA-TN-D-5182] c02 N69-26194

CLINICAL MEDICINE
Clinical report on Apollo 7 and 8 mission medical data, discussing preflight preventive medical activities, inflight treatment, radiation levels, etc
c05 A69-22542

CLOSED CYCLES
Analog simulation of closed loop Braytcn cycle test facility
[NASA-TM-X-1715] c03 N69-14312

CLOSED ECOLOGICAL SYSTEMS
Microbiology of water management subsystem for

manned space flight, discussing sterilization by heat and tests inside Integrated Life Support System /ILSS/
[SAE PAPER 680718] c05 A69-13441
Life in spacecraft - Conference, Belgrade, September 1967
c05 A69-17642

CLOUD COVER
Atmospheric measurements from satellites, discussing ATS-1 cloud images for definition of wind and use of WEFAX through ATS 2 satellites for data transmission
[AIAA PAPER 69-158] c20 A69-18038
Multiple light scattering solutions accuracy by diffraction peak omission from cloud and haze analytic phase functions compared for optically thick and thin planetary atmospheres
c30 A69-33159
Worldwide cloud cover simulation procedure providing data for computer simulation of earth oriented space missions, describing computer program using Monte Carlo mission simulation
c20 A69-38120
Cloud cover effects on selection of recovery sites for future earth orbital missions
[NASA-TN-D-5120] c30 N69-22939

CLOUD GLACIATION
Critique of paper on water crystal existence on Venus, presenting arguments against existence of clouds of micron sized ice crystals
c30 A69-11292

CLOUD HEIGHT INDICATORS
Heights of cloud bases and convective cloud tops determined by stereoscopic photogrammetry of Apollo 6 mission
c20 A69-36926

CLOUD PHOTOGRAPHS
Heights of cloud bases and convective cloud tops determined by stereoscopic photogrammetry of Apollo 6 mission
c20 A69-36926

CLOUD SEEDING
Research on warm fog properties, and dispersal concepts
[NASA-SP-212] c20 N69-39526

CLOUDS
Cloud scattering corrections added to synthetic spectrum analysis of carbon dioxide bands and water vapor line in Venus spectrum
c30 A69-33161
Ice clouds near IR spectral reflectivity dependence on particle size, acting application to planetary atmospheres
c13 A69-34283

CLOUDS (METEOROLOGY)
Survey of six year period of satellite observed tropical Pacific cloud mapping
c20 A69-33001
Bidirectional reflectance of earth atmosphere and cloud formation above equatorial Pacific observed by synchronous satellite as function of angular dependence
c20 A69-43154

CLUMPS
Adaptive simulation using modal clustering and method of potential functions
[NASA-CR-1179] c08 N69-10316

COALESCING
Osmotically induced coalescence of sarcoma cells through intercellular bridges in vitro
[NASA-TN-D-5022] c04 N69-17782

COASTING FLIGHT
Vector integral extension to optimal trajectory coordinate multiplier systems with constant of motion demonstrated for coast-arc problem
[AIAA PAPER 69-907] c30 A69-39339

COATINGS
Thermal control coatings, windows and mirrors for 1973 Mars Viking Lander vehicles under simulated Martian surface conditions
[AIAA PAPER 69-1023] c11 A69-40393
Emissivity coatings for low temperature space radiators
[NASA-CR-1420] c17 N69-36723

COAXIAL FLOW
Alternating current plasma arc coaxial flow stabilization
[AIAA PAPER 68-706] c25 A69-28232
Turbulent mixing of compressible air in supersonic and subsonic coaxial jet flows
[NASA-TN-D-5315] c02 N69-30727
Turbulence in mixing region of ducted coaxial flow of air-air and air-Freon 12 combination
[NASA-CR-1335] c12 N69-30728
Photographic study on bromine jet boundary shape in coaxial airstream with honeycombs at injection plane
[NASA-TM-X-1900] c12 N69-39303

COAXIAL PLASMA ACCELERATORS
Hydrodynamic stability of inviscid rotating coaxial jets
[NASA-CR-1363] c12 N69-24926

COBALT ALLOYS
Temperature and pressure effect on cobalt base alloy cavitation in liquid sodium, using vibratory apparatus and loss rate contour diagram
c17 A69-35184
Spectrochemical analysis of cobalt-base superalloys by liquid-layer solid-sample spark technique
[NASA-TM-X-1753] c06 N69-20853
Effect of temperature and pressure on cavitation damage to cobalt base alloy in sodium
[NASA-TN-D-5273] c17 N69-28863
Corrosion in cobalt alloy two phase mercury loop
[NASA-TN-D-5326] c17 N69-31065
Oxidation resistance and thermal fatigue cracking of nickel and cobalt base alloys in transonic gas streams
[NASA-TN-D-5376] c17 N69-33307

COBALT COMPOUNDS
Three oxidation-resistant alloy foil claddings for protecting typical gas turbine engine alloys of nickel and cobalt
[NASA-TN-D-5483] c17 N69-38794

CODING
Digital telemetry link coding as English language analogy, developing block code scheme combining bit, word and block error detection and correction methods
c07 A69-41745
Pioneer 9 deep space probe with telemetry link operated in coded mode with sequential decoding, discussing ground and flight test data
c07 A69-42522
Variable length codes for alphabets containing messages with assigned weighted information content
[NASA-TN-D-4962] c07 N69-15373
FASTER code for significantly reducing ducted reactor shield computation time for neutron number spectrum
[NASA-TM-X-1828] c22 N69-29671

COEFFICIENT OF FRICTION
Contact conformity effects on spinning torque and friction coefficient in angular contact ball bearings from lubricated and unlubricated tests
[ASME PAPER 68-LUB-10] c15 A69-30901

COEFFICIENTS
Partition coefficients between natural melts and plagioclase phenocrysts determined for rare earth elements and barium by mass spectrometry
c13 A69-20944
Generalized averaging method for linear differential equations with almost periodic coefficients
[NASA-TN-D-5167] c19 N69-22988
Elastohydrodynamic analysis and experimental speed effects on ball spinning friction coefficients and torque
[NASA-TN-D-5527] c15 N69-41210

COENZYMES
Cellular localization of acetyl-coenzyme A synthetase in yeast, noting enzyme distribution during aerobic growth on glucose
c04 A69-15333

COHERENT ACOUSTIC RADIATION
Ultrasonic pulse velocity and attenuation measurement in presence of noise, using coherent detection and signal averaging
c14 A69-29564

COHERENT LIGHT
Helium-neon laser discharge with striation oscillations in relation to pressure and current
[NASA-CR-1387] c08 N69-32350

COIN AIRCRAFT
Aerodynamic characteristics of COIN aircraft model with boundary layer control on inverted V-tail
[NASA-TN-D-4856] c02 N69-10935
COLD DRAWING
Mechanical anisotropy of polyethylene terephthalate and relation to molecular structure and cold drawing
c18 A69-16489
COLD PLASMAS
Explorer 35 measurements of low energy plasma in lunar orbit made by planar multigrid sensor programmed as retarding potential analyzer
c30 A69-16278
Hydromagnetic radiation characteristics of electric and magnetic dipoles in homogeneous anisotropic cold plasma, obtaining field components and wave propagation modes
c13 A69-42905
COLLIMATORS
Mechanical collimator using random aperture arrays for celestial observation at extreme UV and X rays
c14 A69-36489
COLLISION AVOIDANCE
Pilot warning indicators to equip all aircraft at low cost, discussing Doppler system
c21 A69-16726
Advanced electronic applications to navigation, data transmission, and airborne collision avoidance in general aviation aircraft and to simulated displays for low visibility landing
[NASA-CR-1240] c02 N69-14729
COLLISION PARAMETERS
Ion-molecule collisions of Ar-Co and N-No pairs, discussing charge exchange reaction rates and spiraling nature
c24 A69-16428
Numerical analysis of spiraling in ion molecule collisions with polar targets using computer plotting techniques
[NASA-TN-D-5407] c24 N69-35508
COLLISION RATES
Frictional forces and collision frequencies for ions moving in neutral gases
c13 A69-13328
Maximum number of binary collisions for three particles with zero range forces in relativistic rescattering singularities studies
c24 A69-19788
Rotational relaxation times for calculating rotational collision numbers in polar gases
[NASA-TN-D-5321] c24 N69-30073
COLLISIONLESS PLASMAS
Collisionless plasma heating by hydromagnetic waves in solar wind
c29 A69-12714
Quasi-linear theory of hydromagnetic waves in nonrelativistic collisionless plasma, noting resonant diffusion effect on plasma heating mode
c25 A69-20797
Particle free path estimates for axisymmetric high specific impulse plasma accelerators, discussing collisionless plasma simulated by computer
[AIAA PAPER 69-278] c28 A69-21233
Collisionless plasma heating by damping hydromagnetic waves applied to solar wind qualitative model, discussing magnetoacoustic wave energy
c30 A69-22426
Dynamics, stability and approach to equilibrium of bounded one dimensional collisionless plasma representing minimum energy states with nonlinear Vlasov equation solutions
c25 A69-24305
COLOR
Color coded area sensitivity maps of photomultiplier tubes by multicolor display technique, noting focus electrode voltage
c14 A69-35724
COLOR TELEVISION
Superlinear and sublinear phosphors combined for producing single gun color cathode ray tubes
[NASA-CR-1228] c09 N69-14256
COLOR VISION
Foveal luminances for chromatic and absolute thresholds for hue identification in case of small targets
c23 A69-19649
COLUMNS (SUPPORTS)
Mechanical properties and column behavior of thin wall beryllium-aluminum alloy tubing
[NASA-TN-D-5145] c17 N69-23004
Structural stability of lattice column of longerons and helical braces
[NASA-CR-1301] c32 N69-26234
COMBINATIONS (MATHEMATICS)
Impeller matching effects on flow range and stability operating in liquid hydrogen
[NASA-TM-X-1727] c28 N69-16213
COMBUSTION CHAMBERS
Shorter combustors for high temperature jet engines of high speed aircraft, considering lifetime, shroud scoops, overheating, warpage, etc
c28 A69-29433
Evaluating performance of swirl can turbojet combustor at simulated supersonic inlet conditions
[NASA-TN-D-4996] c28 N69-16154
Helmholtz resonators with variable cavity depths tested with unstable rocket combustor
[NASA-TN-D-5171] c33 N69-23351
Characterization of pressure perturbations induced in rocket combustor by machine gun
[NASA-TN-D-5214] c33 N69-24824
Dynamic stability and performance of injectors, rocket liners, and supersonic combustors
[NASA-TM-X-1845] c33 N69-32468
Computer analysis of total pressure loss and air flow distribution in annular flow gas turbine combustion chambers
[NASA-TN-D-5385] c33 N69-33314
Development of barium chemical release system
[NASA-CR-1415] c13 N69-35660
Combustion stability of single swirl can combustor modules using ASTM-A1 liquid fuel
[NASA-TN-D-5436] c28 N69-40080
COMBUSTION PHYSICS
Combustion response of hydrazine-nitrogen tetroxide hypergolic rocket propellants to transverse gas flows, noting coupled and uncoupled oscillations
c33 A69-10112
Luminous spherical fog layer surrounding burning zirconium droplet during free fall through oxygen containing atmosphere, noting effect on mass and heat transfer processes
c33 A69-28462
Laser ignited combustion of 365 micron Zr droplets falling in ultrapure oxygen using spectroscopic and photographic techniques, discussing vapor phase transport phenomena
[WSCI PAPER 69-4] c27 A69-32345
High temperature properties of gases - gas dynamics, thermodynamics, and combustion physics
[NASA-TT-F-558] c12 N69-35365
COMBUSTION PRODUCTS
Steady state acceleration effects on combustion characteristics of aluminized composite solid propellant
[NASA-TN-D-4914] c33 N69-13231
Thermodynamic and transport properties of air, and combustion products of natural gas and air, and jet engine fuel and air
[NASA-TN-D-5452] c33 N69-37936
COMBUSTION STABILITY
Measured effects of gaseous flow system dynamics on acoustic mode combustion instability
[NASA-TN-D-5080] c33 N69-20882
Double-dead-time model describing chugging to liquid propellant rocket engines having multielement injectors
[NASA-TN-D-5303] c28 N69-29405
COMBUSTION VIBRATION
Unstable combustion of hydrazine-nitrogen tetroxide caused by transverse gas flow
[NASA-TN-D-4984] c27 N69-19026
COMETS
Comet interaction with solar wind, assuming field tail coupling of ionized comet material to solar wind ions
c30 A69-27817
Meteoroid environment model for cometary origin near earth to lunar surface
[NASA-SP-8013] c30 N69-40326
COMMAND GUIDANCE
Tracking and data acquisition systems for

spacecraft and ground link through command, telemetry and tracking, noting data relay satellites, etc
c07 A69-33371

COMMAND MODULES
Radiation measurements inside Apollo 4 and 6 command modules during passage through trapped radiation belts
[AIAA PAPER 69-17] c05 A69-18202
Apollo mission simulation, discussing Command Module Simulator /CMS/, onboard computer system and dynamic visual presentation via infinity-optics display
[SMPTE PAPER 105-74] c11 A69-25768
Ablation behavior of heat shield of Apollo command module over wide range of thermal environments
[NASA-TM-X-1778] c33 N69-22933
Forces on flexible shells of Apollo command module during water impact
[NASA-TM-X-1781] c32 N69-23697
Entry aerodynamics at lunar return conditions from command module of Apollo 4 flight
[NASA-TN-D-5399] c31 N69-38820
Wind tunnel study of aerodynamic pressures on Apollo command module configuration
[NASA-TN-D-5514] c01 N69-40345

COMMERCIAL AIRCRAFT
Human survival in flight emergencies involving commercial and general aviation aircraft
[NASA-CR-1262] c02 N69-14763

COMMINUTION
Ductile metal powder chemical reactions during comminution in pure or oxygenated water
c06 A69-27762

COMMUNICATING
Communication in large organizations, describing internal communication model
c34 A69-42930

COMMUNICATION EQUIPMENT
Communications for Apollo Applications Program, considering extended duration manned missions in low earth orbit and Gemini, Saturn and Apollo hardware
c07 A69-19124

COMMUNICATION SATELLITES
Space applications program including communications and navigation meteorology, earth resources survey and geodesy
[UN PAPER 68-95437] c34 A69-10472
International experimentation with U.S. communications satellites, noting design variations with participants and restraintless information exchange
[UN PAPER 68-95421] c20 A69-10474
Multijet electrothermal systems for attitude control and stationkeeping of synchronous communications satellite
[AIAA PAPER 67-723] c28 A69-12375
Mutual RF interference between satellite and terrestrial telecommunications microwave relay system at shared frequencies
c07 A69-13242
Low degree earth gravity harmonics effect on 12 and 24 hour orbits of high altitude communications satellites
c13 A69-14661
RFI effects of earth based emitters on operation of geosynchronous satellites for data relay from near earth orbiting satellites, noting frequency assignments
c07 A69-41757
Technological and cost factors of voice broadcasts from satellites to earth
[NASA-TM-X-1747] c07 N69-19025
Experiment design for measuring radio frequency interference between communication satellite and terrestrial microwave relay system
[NASA-TN-D-5041] c07 N69-26272

COMMUNICATION THEORY
Man-computer speech communication, discussing model and aspects of acoustics, phonetics, linguistics, language training, physiology, psychology, bionics, etc
c08 A69-35099
Communication and information theories for digital and analog systems design
[NASA-TN-D-5472] c07 N69-39176

COMMUTATION
Feedback systems analysis, considering single phase and polyphase coupled and uncoupled commutation networks in forward loop and linear transfer function feedback loop
c10 A69-19853
Analysis of commutated networks employing feedback circuits
[NASA-TN-D-4893] c10 N69-10755

COMMUTATORS
Photoelectronic commutation by dc torquer-driven reaction wheel for spacecraft attitude control
[NASA-TN-D-5265] c03 N69-30945

COMPARISON
Systematic investigation of mathematical models by comparison of experimental and analytical regression coefficients
[NASA-TM-X-1797] c19 N69-25311
Flutter investigation at Mach 3 of rotationally restrained panels and comparison with theory
[NASA-TN-D-5508] c32 N69-40087

COMPATIBILITY
Compatibility conditions for strain measures of theory of micromorphic elastic solids
[NASA-CR-1236] c26 N69-10817
Compatibility tests of molten uranium with tungsten and tungsten-1.5 percent hafnium
[NASA-TN-D-5076] c17 N69-19930

COMPENSATORS
Feasibility of using roll and yaw compensation to reduce inclination error of Scout launch vehicle
[NASA-CR-1209] c31 N69-16221

COMPENSATORY TRACKING
Roll-motion cues for man-vehicle control in compensatory tracking task with disturbance input
c05 A69-23879
Human information processing rates during one and two axis compensatory tracking tasks with secondary auditory task
c05 A69-23880
Aspects of human operator performance in low order compensatory control tasks studied with regression analysis
[NASA-CR-1259] c05 N69-16212

COMPLEXITY
Concepts of theory of fuzzy systems
[NASA-CR-1432] c19 N69-37033

COMPONENT RELIABILITY
Beryllium reflector distortion in Plum Brook Reactor due to neutron embrittlement and gas formation, noting material surveillance, replacement, etc
c22 A69-13131
Space guidance and control system components, noting control moment gyro, actuator, brushless dc motor, electrically supported gyro and laser gyro
c14 A69-22434
Crack initiation prediction in high temperature components subjected to arbitrary thermal-mechanical cycling
c32 A69-28252
OGO program failure rate analysis with respect to cost, schedule and performance tradeoffs, considering component and systems design and reliability, prelaunch feedback, etc
c31 A69-34519
Computerized Arrhenius equation component reliability extrapolation techniques
[NASA-TN-D-4902] c19 N69-13368
Computer program for component quality control and reliability data analysis
[NASA-TN-D-5009] c15 N69-17988
Clean room technologies for control of contaminants for component reliability
[NASA-SP-5074] c05 N69-33775

COMPOSITE MATERIALS
Glass, boron and graphite filament wound resin composites and liners for cryogenic pressure vessels
c18 A69-16488
Cryogenic mechanical properties of epoxy resins and glass/epoxy composites
c18 A69-16491
Fiber-metal matrix composites fabrication, applications, mechanical properties and powder metallurgy
c17 A69-20204
Failure criteria for predicting filamentary composite strength under uniaxial and combined

stresses from properties and fabrication process considerations c32 A69-21479
Tungsten alloy fiber reinforced nickel base alloy composites stress-rupture strength, oxidation and impact resistance for high temperature turbojet engine buckets c17 A69-29010
Boron nitride and boron nitride composite under high temperatures in air and vacuum for various time periods, discussing thermal shock and oxidation resistance c18 A69-36208
Polyurethane foam composites for low heating rate thermal protection, noting astroquartz fiber additive effect on performance c18 A69-39236
Low density polybenzimidazole composites as ablative heat shields, discussing arc-heated wind tunnel tests of linear and crosslinked structures c18 A69-41715
Continuum theory for wave propagation in elastic composite solid with elastic microinclusions [NASA-CR-1321] c32 N69-21401
Development of lattice model for composite materials [NASA-CR-1322] c32 N69-22982
Zero thermal expansion composites of high strength and stiffness [NASA-CR-1324] c32 N69-24876
Linear prediction of structural failure criteria for uniaxial fiber composites [NASA-TN-D-5367] c18 N69-33321
Stress concentration around broken filaments in filament stiffened sheet [NASA-TN-D-5453] c32 N69-38642

COMPOSITE PROPELLANTS
Steady state acceleration effects on combustion characteristics of aluminized composite solid propellant [NASA-TN-D-4914] c33 N69-13231

COMPOSITE STRUCTURES
Loss factor and resonant frequency of viscoelastic shear damped structural composites [NASA-CR-1269] c32 N69-17766
FORTRAN program for computing principal mass moments of inertia of spacecraft treated as composite bodies [NASA-TM-X-1754] c23 N69-20870

COMPRESSED AIR
Magnetic air bearings for use as low friction overhead support fixtures in vertical lunar gravity simulator [NASA-CR-1235] c05 N69-14213

COMPRESSIBLE BOUNDARY LAYER
Nonsimilar laminar boundary layer solutions with negative pressure gradient compared to experimental boundary layer velocity profiles, momentum and displacement thicknesses [AIAA PAPER 69-35] c12 A69-18094
Compressible hypersonic turbulent boundary layers solution by finite difference method, relating mixing length to velocity profile shape factor [AIAA PAPER 69-684] c12 A69-33474
Calculation of compressible turbulent boundary layers with pressure gradients and heat transfer [NASA-CR-1303] c12 N69-21653
Graphical interpolation charts of local skin friction from compressible velocity profiles [NASA-SP-3048] c01 N69-25391

COMPRESSIBLE FLOW
Computing span loads and stability derivatives due to sideslip, yawing, and rolling for wings in compressible flow [NASA-TN-D-4929] c01 N69-14001
FORTRAN computer program for detailed solution of compressible, subsonic, nonviscous flow at leading or trailing edges of blade surface [NASA-TN-D-5091] c01 N69-22938
High pressure compressible flow systems in space vehicle ground support equipment [NASA-SP-3045] c12 N69-26987
Nonlinear compressible flow problems - half-space of ideal compressible fluid motion due to arbitrary pressure front [NASA-TT-F-560] c12 N69-27168
Turbulent mixing of compressible air in supersonic and subsonic coaxial jet flows [NASA-TN-D-5315] c02 N69-30727
Rotational effects on isothermal compressible flow across gas turbine sealing dam [NASA-TN-D-5344] c15 N69-35799
Numerical calculation of viscous compressible flow around harmonic oscillating rigid cylinder [NASA-CR-1467] c12 N69-38782

COMPRESSIBLE FLUIDS
Boussinesq approximation for compressible fluids, discussing perturbation pressure and velocities and vertical scale motions c12 A69-26013
Survey of incompressible and compressible fluid film hydrostatic and hydrodynamic lubrication [NASA-SP-5058] c15 N69-28592

COMPRESSING
Compression molding of molecular salt-like intermediate Pyrrone powders by two pressure method, noting volatiles elimination c18 A69-29415
Characteristics study of bicone mixed compression inlet for Mach 1.80 to 2.50 [NASA-TN-D-5084] c01 N69-20914

COMPRESSION LOADS
Differential equations for compression loaded axisymmetric cylindrical structures [NASA-CR-1444] c32 N69-38781

COMPRESSION TESTS
Compressive properties and weight saving of metals reinforced on surface with resin bonded fibers [NASA-TN-D-4878] c17 N69-11012

COMPRESSION WAVES
High speed compression waves, rarefaction waves and gas interface regions position and velocity measurement in shock tube by sensing electrical impedance c14 A69-13104

COMPRESSIVE STRENGTH
Failure criteria for predicting filamentary composite strength under uniaxial and combined stresses from properties and fabrication process considerations c32 A69-21479
Compressive behavior of uniaxial filament reinforced epoxy tubes for aerospace structures, using hand layup method with Teflon mandrel and sleeve c15 A69-22339
Influence of fabrication methods on compressive strength of titanium alloy skin stringer panels [NASA-TN-D-5389] c15 N69-34707

COMPRESSOR BLADES
Supersonic compressor blade sections performance prediction near maximum pressure ratio and efficiency by analyzing flow processes [AIAA PAPER 69-522] c28 A69-32711
Analysis of sodium chloride deposits on compressor blades of flight gas turbine engines [NASA-TN-D-4999] c28 N69-17276
Computer program for designing compressor blades [NASA-TN-D-5437] c28 N69-36882

COMPRESSOR EFFICIENCY
Jet engine compressor stalls in-flight investigation up to Mach 2 on F-111A by pressure sensors, noting steady state distortion role [AIAA PAPER 69-488] c28 A69-32706
Supersonic compressor blade sections performance prediction near maximum pressure ratio and efficiency by analyzing flow processes [AIAA PAPER 69-522] c28 A69-32711

COMPRESSOR ROTORS
Performance comparisons of supersonic compressor rotor blades [NASA-CR-1256] c28 N69-14210
Performance data for high tip speed compressor rotor operated with radial and inlet airflow distortions [NASA-TM-X-1798] c01 N69-26312
Outlet annulus area blockage configuration effects on performance of axial flow compressor rotor [NASA-TN-D-5506] c28 N69-40078

COMPRESSORS
Multiple function combination probe design for compressor and turbine air flow research c11 A69-31917
Performance and stall limits of YTF30-P-1 turbofan engine with uniform compressor inlet flow [NASA-TM-X-1803] c28 N69-27019

COMPTON EFFECT
Compton profile from single crystal of LiH measured with X ray scattering, noting valence-electron momentum distribution role
c26 A69-40730
COMPUTATION
Computation of regions of constrained stability for nonlinear control systems
[NASA-CR-1328] c19 N69-28196
FORTRAN program for computation of finite group tables
[NASA-TN-D-5402] c08 N69-35569
COMPUTER COMPONENTS
Onboard spacecraft computer design, programming and operation based on dual bussing system
c08 A69-37384
COMPUTER DESIGN
Onboard SDP-3 computer data system core for IMP spacecraft, considering payload
c08 A69-13243
IMP-1 experiment, describing design and applications of SDP-3 computer
c08 A69-36265
Onboard spacecraft computer design, programming and operation based on dual bussing system
c08 A69-37384
SDP-3-A general purpose stored program computer designed for small scientific spacecraft onboard data system, noting computerized simulation
c08 A69-37385
Computer organization design employing distributed processor to provide general purpose computing while taking advantage of large scale integration
c34 A69-39133
Interactive experimenter computer system software and hardware design considerations based on astronaut-machine/experimenter question-answer interactions
[AIAA PAPER 69-953] c08 A69-40335
Spaceborne stored program computer design for OAO-C, noting auxiliary command storage, spacecraft monitoring and malfunction reporting, etc
c08 A69-41736
SDP-3 small serial computer for engineering experiment on IMP spacecraft, discussing design modifications to improve performance
c08 A69-41737
Quadrature variations in discrete-ordinates calculation
[NASA-TM-X-1887] c20 N69-36976
COMPUTER GRAPHICS
Micromation and micrographics, discussing nonimpact printing in computer avoiding output imbalance by high speed microfilm recorder
c34 A69-35059
COMPUTER PROGRAMMING
Computer programming of satellite orbit tracking angles for automatic picture transmission receiving stations
c07 A69-14917
Onboard spacecraft computer design, programming and operation based on dual bussing system
c08 A69-37384
Programmable data handling and telemetry systems for scientific satellites, noting system checkout, spacecraft integration, software and ground data processing
c08 A69-41735
Synthesis methods for manual aerospace control systems using digital programming and man machine performance data with application to supersonic transport design
[NASA-CR-1208] c02 N69-13185
Variable length codes for alphabets containing messages with assigned weighted information content
[NASA-TN-D-4962] c07 N69-15373
Computer-generated computational errors in direction cosine matrix for strapdown inertial system
[NASA-TR-R-304] c21 N69-21402
Recognition program for handwritten information in real time computer operation
[NASA-CR-1284] c08 N69-21527
FORTRAN program for computation of finite group tables
[NASA-TN-D-5402] c08 N69-35569
COMPUTER PROGRAMS
Collisionless computer model performing gravitational experiments with two dimensional galaxy
c30 A69-12271
Computer study of collisionless self gravitating system using two dimensional model, obtaining gravitational field by solving Poisson equation
c30 A69-12272
Stored program computer for small scientific spacecraft, noting program and data memory capacities
c08 A69-15472
Finite difference method computer programs for calculation of velocities and streamlines on blade to blade surface of revolution of turbomachine
[ASME PAPER 69-GT-48] c01 A69-22495
COHORT-2 Monte Carlo computer program written in FORTRAN 4 to model radiation shielding problems
c08 A69-29004
Nova outburst dynamics investigation by time dependent hydrodynamics computer program including energy transport by radiation and convection
c30 A69-30769
Multistage rocket trajectories optimized by second order numerical technique and digital computer program, considering coasting, vacuum flight and transition times
c30 A69-32154
Thermal contact resistance measurement at various ambient pressures compared with theoretical predictions with each parameter analyzed over interface by computer program
[AIAA PAPER 69-629] c33 A69-33299
Man-computer speech communication, discussing model and aspects of acoustics, phonetics, linguistics, language training, physiology, psychology, bionics, etc
c08 A69-35099
Computer program to predict spectra from electronic transitions of diatomic molecules and atoms, noting line intensity distribution by Voigt profile
c24 A69-35239
Impulsive orbit transfer optimization using accelerated gradient program based on Newtonian algorithm for digital computer method
c30 A69-35956
Worldwide cloud cover simulation procedure providing data for computer simulation of earth oriented space missions, describing computer program using Monte Carlo mission simulation
c20 A69-38120
Computer experiment on 9000 particle plasma to test temporal echo theoretical prediction
c25 A69-38713
Computer program for generation of test patterns for multiterminal devices and networks
c08 A69-39604
NASA computer language CLASP coordinated with evolution of SPL /Space Programming Language/ for aeronautics and space programming
[AIAA PAPER 69-957] c08 A69-40339
Computer optimization of spacecraft optical coatings for temperature control, using finite element analysis and matrix inversion
[AIAA PAPER 69-979] c33 A69-40359
Space power systems analysis, using computer program to correlate systems characteristics with mission parameters for automated satellite repair vehicle and space stations
c03 A69-42240
N-terminal parent networks with symmetry constraints derived for nonredundant one port configurations through combinatorial functions test patterns, using computer algorithm
c08 A69-42524
Computer program determination of barreling effect on strength of ring and stringer stiffened shells designed to support axial compression loads
c32 A69-43671
Computer experiments on the microscopic behavior of one dimensional electrostatic plasma
[NASA-TN-D-4831] c25 N69-10471
User manual for computer program 55VD for computation of minimum induced drag and load

distribution of nonplanar wings
[NASA-CR-1218-SUPPL] c01 N69-12286
Point defect calculations for tungsten
[NASA-TN-D-4918] c22 N69-13309
Computerized Arrhenius equation component reliability extrapolation techniques
[NASA-TN-D-4902] c19 N69-13368
FORTRAN computer program for spline fit curve with function valves
[NASA-TM-X-1707] c19 N69-14002
Computer program for computation of thermal radiation heat loads and temperatures of spacecraft orbiting planets or moon
[NASA-TR-R-278] c30 N69-14428
FORTRAN computer program for designing supersonic inlets by characteristic theory
[NASA-TN-D-4960] c01 N69-14566
Digital computer program for analyzing elastic and plastic deformations and creep strains in solid and hollow cylindrical bodies
[NASA-TM-X-1723] c32 N69-16115
Finite element method for computing natural frequencies and mode shapes of thin shells of revolution
[NASA-TN-D-4972] c32 N69-16469
FORTRAN programs for calculating wind tunnel boundary interference factors
[NASA-TM-X-1740] c01 N69-17818
Computer program for component quality control and reliability data analysis
[NASA-TN-D-5009] c15 N69-17988
Conversational approach to matrix calculations on computers
[NASA-TM-X-1749] c08 N69-18954
Digital computer program for homopolar inductor alternator electromagnetic design analysis
[NASA-TN-D-5072] c03 N69-19799
FORTRAN 4 program for estimating off-design performance of radial inflow turbines
[NASA-TN-D-5059] c03 N69-19829
Modified Fourier transform for calculating human operator describing functions
[NASA-TM-X-1762] c08 N69-21119
Computer program for line-by-line calculation of spectra from diatomic molecules and atoms assuming Voigt line profile
[NASA-TN-D-5088] c24 N69-21462
Calculation of compressible turbulent boundary layers with pressure gradients and heat transfer
[NASA-CR-1303] c12 N69-21653
FORTRAN program for calculating velocities and streamlines on blade to blade stream surfaces of turbomachinery
[NASA-TN-D-5044] c01 N69-21811
Sonic boom propagation in stratified atmosphere using FORTRAN computer program with integral and differential equations
[NASA-CR-1299] c02 N69-22546
Computer program for aerodynamic analysis of turbomachine blades
[NASA-TM-X-1764] c01 N69-22553
Computer oriented error analysis of electrical circuits and nonlinear system performance
[NASA-TN-D-5112] c10 N69-22919
Computer program for dimensional analysis using FORTRAN 4 programming
[NASA-TN-D-5165] c08 N69-22935
FORTRAN computer program for detailed sclution of compressible, subsonic, nonviscous flow at leading or trailing edges of blade surface
[NASA-TN-D-5091] c01 N69-22938
Computer program for launch window determination from star illumination of night sky background
[NASA-TM-X-1772] c21 N69-22969
Computer program for one dimensional elastic wave problems connected with structural members
[NASA-CR-1306] c32 N69-22983
Computer analysis of light scattering data from polymer solutions
[NASA-TN-D-5177] c06 N69-22991
Accuracy and speed comparison between drag-free and numerical satellite orbit prediction methods
[NASA-TN-D-5203] c30 N69-26252
Computer program used to infer atmospheric water-vapor mixing ratio from measured horizon radiance profiles
[NASA-TN-D-5252] c13 N69-27246
Numerical method and computer program for computing deflection response of thin shells
[NASA-CR-1376] c32 N69-29558
Statistical method for automatic computer editing of biological data
[NASA-TN-D-5275] c08 N69-29592
FASTER code for significantly reducing ducted reactor shield computation time for neutron number spectrum
[NASA-TM-X-1828] c22 N69-29671
Current computer programs for low thrust trajectory analysis using flyby and rendezvous trajectories
[NASA-TM-X-1824] c08 N69-30014
Tagged arithmetic system for use with FORTRAN programs
[NASA-TN-D-5370] c08 N69-32556
COMPUTE time sharing calculator program for numerical calculations
[NASA-TN-D-5350] c08 N69-32685
Computer program for steady laminar, subsonic, and isothermal compressible flow across sealing dam
[NASA-TN-D-5373] c15 N69-33281
Computer analysis of total pressure loss and air flow distribution in annular flow gas turbine combustion chambers
[NASA-TN-D-5385] c33 N69-33314
Numerical analysis of spiraling in ion molecule collisions with polar targets using computer plotting techniques
[NASA-TN-D-5407] c24 N69-35508
Debugging computer programs in terms of localization and correction of errors
[NASA-CR-1397] c08 N69-35613
Computer program for designing compressor blades
[NASA-TN-D-5437] c28 N69-36882
Hardware-software provisions for multiple precision floating point arithmetic
[NASA-TM-X-1885] c08 N69-36918

COMPUTER STORAGE DEVICES

Stored program computer for small scientific spacecraft, noting program and data memory capacities
c08 A69-15472
Computer memory reduction through FORTRAN higher level language, discussing tradeoff between costs saved and additional logic hardware
[AIAA PAPER 69-963] c08 A69-40344

COMPUTERIZED DESIGN

Damping factor automatic determination by use of second derivatives of residuals for damped least squares method of optical design
c23 A69-14295
Computer driven graphical techniques for aerospace design and analysis
[ASME PAPER 69-DE-27] c15 A69-28854
Computerized design parameters for realizable overdriven bimode varactor frequency doubler based on charge-voltage relationship at break point
c09 A69-37299
Computer program for generation of test patterns for multiterminal devices and networks
c08 A69-39604
Germanium microwave backward diodes optimum design and performance prediction through computer calculation for important parameters
c09 A69-41224
FORTRAN computer program for designing supersonic inlets by characteristic theory
[NASA-TN-D-4960] c01 N69-14566
Evaluation of computer aids to augment human intellectual capability
[NASA-CR-1270] c08 N69-16140
Computerized telemetry filter design
[NASA-SP-3049] c08 N69-35816

COMPUTERIZED SIMULATION

Digital computers in space flight simulation and vehicle performance optimization, examining mission analysis
c30 A69-14519
Recursive formulas for numerical evaluation of real convolution integral for simulation of control systems and electrical networks on digital computer
c19 A69-17250
Particle free path estimates for axisymmetric high specific impulse plasma accelerators, discussing collisionless plasma simulated by computer
[AIAA PAPER 69-278] c28 A69-21233

NASA manned aerospace simulation techniques and equipment as used at Ames Research Center, noting applications to various types of manned vehicles
[ASME PAPER 69-DE-56] c11 A69-28844
Worldwide cloud cover simulation procedure providing data for computer simulation of earth oriented space missions, describing computer program using Monte Carlo mission simulation
c20 A69-38120
Real time digital computer hardware simulation of Apollo Telescope Mount /ATM/ mission
[AIAA PAPER 69-940] c11 A69-40323
Computer made movies and time history plots for ion-dipole collisions involving polar molecules /CO, HCL and acetonitrile/
c24 A69-43124
Adaptive simulation using modal clustering and method of potential functions
[NASA-CR-1179] c08 N69-10316
Advanced electronic applications to navigation, data transmission, and airborne collision avoidance in general aviation aircraft and to simulated displays for low visibility landing
[NASA-CR-1240] c02 N69-14729
Matched conic solutions to round trip interplanetary trajectory problems for use in guidance and navigation simulation
[NASA-TN-D-4942] c30 N69-14861
Determining sequential decoding performance and metric sensitivity by computer simulation
[NASA-TR-R-294] c07 N69-16196
Computer program for research and engineering management of spacecraft projects
[NASA-CR-1275] c34 N69-18057
Computer simulation of six degrees of freedom flight equations
[NASA-CR-1344] c21 N69-26232
Computerized simulation of low frequency dynamics of liquid hydrogen flow in nuclear rocket engine
[NASA-TN-D-5312] c22 N69-30070
Experimental verification of surface vehicle dynamics
[NASA-CR-1399] c11 N69-37022

CONCENTRATION (COMPOSITION)
Effects of temperature and electrolyte concentration on performance of fuel cell
[NASA-TN-D-5154] c03 N69-22940

CONCENTRATORS
Parametric analysis of surface temperatures and distortions of paraboloidal solar concentrators
[NASA-TN-D-5144] c03 N69-23356

CONDENSATES
Propellant condensation on surfaces near electric rocket exhaust, calculating particle arrival rates, backflow and desorption energies
[AIAA PAPER 69-270] c28 A69-21252
Circumstellar grain compositions of stars with various O to C abundance ratios, calculating molecular equilibrium of condensates and gaseous compounds in stellar atmospheres
c30 A69-24103
Absorption of black-body radiation by ice cryodeposits on metal substrates
[NASA-TN-D-5181] c23 N69-22769

CONDENSATION
Chemical equilibrium of ablation materials including condensed species
[NASA-TN-D-5391] c33 N69-34966

CONDENSING
Transient condensing with freezing on nonisothermal inclined plate
[NASA-TN-D-5289] c33 N69-29598
Properties and uses of liquid metal reactor fuels, including heat transfer processes in variously shaped channels, boiling and condensation of metals, and reactor control equipment
[NASA-TT-F-522] c33 N69-30507

CONDUCTING FLUIDS
Conducting fluid incompressible flow in entrance of MHD channel by momentum integral method, permitting edge stress existence at boundary layer free stream interface
[AIAA PAPER 69-724] c12 A69-33436

CONDUCTIVE HEAT TRANSFER
Combined radiation and conduction heat transfer equation applied to temperature profile around opaque hollow sphere and in solid condensed gas layer
[SAE PAPER 690197] c33 A69-18303
Combined conduction and radiation transfer equations solutions for absorbing-emitting gas, obtaining slip coefficient for diffusion solution correct boundary condition
c33 A69-27784
Simultaneous solution of continuity and heat conduction equations for ionospheric plasma consisting of electrons, atomic O ions and neutral gas species, discussing varying solar flux effects
c29 A69-32082
Simultaneous solution of continuity and heat conduction equations for ionospheric electrons, ions and neutral species for studying F region magnetic storm behavior
c13 A69-32083
Lunar temperature prediction with emphasis on variable property models, noting assumptions about physical properties appearing in heat conduction equations
c30 A69-34374
Film-nucleate boiling transition for liquid nitrogen in vertical forced flow in electrically heated tube, discussing conduction model and agreement with visual experiment
[ASME PAPER 69-HT-26] c33 A69-43542
Transient solidification outside cooled pipe with application to solar Brayton heat receiver
[NASA-TN-D-4897] c33 N69-10227
Heat transfer characteristics of water/cryogenic hydrogen heat exchanger for nuclear rocket reactor
[NASA-TN-D-5429] c33 N69-36701

CONDUCTIVITY
Measurement of radiative thermal conduction of ideal powder as function of temperature
[NASA-TN-D-5063] c33 N69-20008

CONDUCTORS
Flat conductor cable technology, discussing design, manufacture, specifications, etc
[ASME PAPER 69-DE-8] c03 A69-28855

CONES
Refractory cone models made of copper and Co coated Be for force tests in high enthalpy hypersonic arc tunnels at high simulated attitudes
c11 A69-26796
Subliming ablation effects on boundary layer transition for cones in hypersonic flow, discussing Reynolds numbers measured in wind tunnel tests
[AIAA PAPER 68-40] c01 A69-31881
Estimated supersonic flow field shock waves and sonic boom effects for cones and axisymmetric bodies
[NASA-TN-D-4935] c01 N69-13238
Laminar heat transfer distributions for blunted-cone, cone frustum reentry configuration at hypersonic speed using Reynolds number
[NASA-TN-D-5146] c33 N69-22997
Skin friction and heat transfer data for hypersonic turbulent layer on flat plates, wind tunnel wall, and cones
[NASA-TN-D-5089] c12 N69-29144
Supersonic aerodynamic characteristics and shock standoff distances for large angle cones with and without cylindrical afterbodies
[NASA-TN-D-5334] c01 N69-33237
Beam stiffness determined for thin walled truncated cones under bending loads
[NASA-TN-D-5536] c32 N69-41141

CONFERENCES
Life sciences and space research - COSPAR Conference, London, July 1967
c04 A69-11073
Space projections - AIAA-AAS Conference, Denver, July 1968, Volume 3
c11 A69-11755
Voyage to planets - Conference, Washington, D.C., March 1967
c30 A69-12301
Space projections - Conference, Denver, July 1968, Volume 1
c30 A69-12801
Cosmic rays - Conference, Calgary, Canada, June 1967
c29 A69-12928

Electronics and aerospace systems - IEEE Conference, Washington, D.C., September 1968
c07 A69-13176
Stochastic problems in control - Conference, Ann Arbor, June 1968
c10 A69-14693
Astronomy - Conference, Prague, August 1967
c30 A69-15834
Sterilization techniques for instruments and materials as applied to space research - COSPAR Conference, London, July 1967
c05 A69-15934
Cryogenic properties of polymers - NASA/Case Conference, Cleveland, April 1967
c18 A69-16485
Aeronautic electronics - Conference, Washington, D.C., September 1968
c21 A69-16716
Cosmic rays, elementary particle physics and astrophysics - Conference, Aligarh, India, December 1967
c29 A69-17268
Astrodynamics, guidance and control - Conference, Belgrade, September 1967, Volume 1
c30 A69-17560
Spacecraft systems, education - Conference, Belgrade, September 1967
c31 A69-17596
Life in spacecraft - Conference, Belgrade, September 1967
c05 A69-17642
Microwave and optical generation and amplification - Conference, Hamburg, September 1968
c09 A69-18420
Refractory metal alloys metallurgy and technology - Conference, Washington, D. C., April 1968
c17 A69-18790
Telemetering - Conference, Los Angeles, October 1968
c07 A69-19092
Magnetosphere - Conference, Boston College, June 1967
c29 A69-19351
Origin and distribution of elements - Conference, Paris, May 1967
c30 A69-20892
Electrochemical generators for space application - Conference, Paris, December 1967
c03 A69-21034
Thermionic conversion - Conference, Framingham, Mass., October 1968
c03 A69-21806
Aerospace material investigation and fabrication techniques - Conference, Cocoa Beach, November 1968
c15 A69-22301
Spacecraft electronics - Conference, Chicago, December 1968
c09 A69-22433
Pyrotechnic and explosive elements in space systems - Conference, Tarbes, France, July 1968
c27 A69-23003
Instrumentation in the aerospace industry - Conference, Boston, June 1968, Volume 14
c11 A69-23245
Tube techniques - IEEE Conference, New York, September 1968
c09 A69-24740
Space electronics, telemetry, antennas, computers - IEEE Conference, Cocoa Beach, Florida, November 1968
c07 A69-25288
Structures, structural dynamics, materials and aeroelasticity - ASME-AIAA Conference, New Orleans, April 1969
c32 A69-25492
Structures, structural dynamics and materials - AIAA-ASME Conference, New Orleans, April 1969
c32 A69-26807
Remote sensing of environment - Conference, University of Michigan, Ann Arbor, April 1968
c14 A69-26974
Relays - Conference, Oklahoma State University, April 1969
c09 A69-28042
Aviation and astronautics - Conference, Tel-Aviv and Haifa, March 1969
c12 A69-29011
Plastics engineering - Conference, Chicago, May 1969
c18 A69-29411
Solar-terrestrial physics, Solar aspects - IQSY/COSPAR Conference, London, July 1967, Part 1
c29 A69-30005
Man and environment - Conference, Anaheim, California, April 1969
c11 A69-30356
Electrochemical generators for space applications - Conference, Paris, December 1967
c03 A69-32405
Exobiology, Search for extraterrestrial life - AAS-AAAS Conference, New York, December 1967
c04 A69-32967
Viscous drag reduction - Conference, Dallas, September 1968
c12 A69-33247
Clear air turbulence and detection - Conference, Seattle, August 1968
c20 A69-33732
Commercial utilization of space - Conference, Dallas, May 1967
c30 A69-34043
Photogrammetry - Conference, Washington, D.C., March 1969
c14 A69-34334
Advanced space experiments - AAS Conference, Ann Arbor, September 1968
c30 A69-34359
Reliability - Conference, Chicago, January 1969
c15 A69-34476
Circuits and systems - Conference, Pacific Grove, California, October-November 1968
c10 A69-34671
Space, technology and society - Conference, Cocoa Beach, Florida, March 1969, Volume 2
c34 A69-35055
Space, technology and society - Conference, Cocoa Beach, Florida, March 1969, Volume 1
c34 A69-35070
Aerodynamics of rotary wing and V/STOL aircraft-Conference, Buffalo, June 1969, Volume 2, Wind tunnel testing, new concepts in rotor control
c01 A69-35226
Materials and processes for aerospace applications in 1970s - Conference, Los Angeles, April- May 1969
c15 A69-35501
Photovoltaics - IEEE Conference, Pasadena, November 1968
c03 A69-35678
Instrumentation in aerospace simulation facilities - Conference, Farmingdale, New York, May 1969
c11 A69-35714
Failure analysis - IEEE Conference, Philadelphia, May 1969
c09 A69-35781
Space navigation - Conference, Houston, April 1969
c21 A69-35789
Reliability and maintainability - Conference, Denver, July 1969
c15 A69-35999
Meteorite research - Conference, Vienna, August 1968
c30 A69-36072
High and medium energy molecular beams - Conference, Cannes, July 1969
c24 A69-36171
Telemetering - IEEE Conference, Washington, D.C., April 1969
c07 A69-36237
Space law - Conference, New York, October 1968
c34 A69-37102
Onboard computers on rockets and satellites - Conference, Paris, December 1968
c08 A69-37377
Life sciences and space research on biological effects of radiation in space - COSPAR Conference, Tokyo, May 1968
c04 A69-37612
Space research - COSPAR Conference, Tokyo, May 1968
c13 A69-38334
Atmospheric emissions - NATO Conference, Norway, July-August 1968
c13 A69-38482

Cosmic ray studies - Conference, Bombay, November 1968
c29 A69-38811
IEEE Conference - San Antonio, April 1969
c07 A69-39437
Guidance and control in space - Conference, Warsaw, June 1969
c21 A69-39644
Reducing cost of space transportation - AAS Conference, Washington, D.C., March 1969
c34 A69-39686
Extraterrestrial matter - Conference, Argonne, Illinois, March 1968
c30 A69-40083
Physics applications to earth and planetary interiors - NATO Conference, Newcastle-upon-Tyne, England, March-April 1967
c30 A69-40172
Earth observations from balloons - Conference, Washington, D.C., February 1969
c02 A69-40803
Air safety - Conference, Anaheim, October 1968
c02 A69-41127
Aerodynamics of rotary wing and V/STOL aircraft - Conference, Buffalo, June 1969, Volume 3
c01 A69-41369
Telemetering - Conference, Washington, D.C., September 1969
c07 A69-41734
Aviation and space medicine - Conference, Oslo, August 1968
c05 A69-41783
Structural technology for large radio and radar telescope systems - Conference, Cambridge, Mass., October 1967
c11 A69-42120
Electromagnetic compatibility, - IEEE Conference, Asbury Park, New Jersey, June 1969
c09 A69-42215
Energy conversion - Conference, Washington, D.C., September 1969
c03 A69-42236
Communications - IEEE Conference, Boulder, June 1969
c07 A69-42500
Plasma instabilities in astrophysics - Conference, Monterey, October 1968
c30 A69-42681
Circadian rhythms in nonhuman primates - Conference, Atlanta, July 1968
c04 A69-42701
Automatic control - Conference, Boulder, August 1969
c10 A69-43267
Aerospace medicine - Conference, Amsterdam, September 1969
c04 A69-43369
Aircraft Structures and Materials Application - Conference, Seattle, September 1969
c15 A69-43416
Solar flare and space research - COSPAR Conference, Tokyo, May 1968
c29 A69-43603
Conference on bone diseases and regeneration, cellular differentiation, and homeostasis of calcium
[NASA-SP-161] c04 N69-10444
Conference on NASA research in noise reduction of subsonic jet aircraft - nacelle acoustic linings, sound generation in jet engines, and operational noise effects on humans
[NASA-SP-189] c02 N69-11542
Runway and highway pavement grooving and traction studies
[NASA-SP-5073] c11 N69-20451
Lunar environment, bases, exploration, and extraterrestrial resources
[NASA-SP-177] c30 N69-22226
Structure, interactions, and topography of solid surfaces, sliding friction, adhesion, wear, and boundary lubrication conference topics
[NASA-SP-181] c15 N69-30401
Respiratory system and oxygen metabolism regulation in man and animals
[NASA-TT-F-501] c04 N69-31401
Technology utilization by industries of aerospace sciences and systems - conferences
[NASA-SP-5075] c34 N69-31946
Conference on motion degraded images and correcting procedures - optical filters and digital methods for blurring removal from photographic imagery
[NASA-SP-193] c14 N69-33322
Proposed electromagnetic exploration of moon
[NASA-SP-174] c30 N69-33595
Investigation of earth atmospheric composition, geomagnetism, extraterrestrial radiation, solar activity, and planetary atmospheres by satellite experiment and astronomical observations
[NASA-SP-195] c34 N69-38951
Application of control theory to production engineering, transportation systems, urban development, biological oceanography, mass communications, and socio-economic problems
[NASA-SP-211] c34 N69-39957

CONFORMAL MAPPING

Inviscid flow of two parallel slot jets impinging normally on surface
[NASA-TN-D-4957] c12 N69-14316
Conformal mapping of two dimensional jet flow from two nozzles striking plane surfaces
[NASA-TN-D-5064] c01 N69-17816
Outer and inner curved plates and shell shapes optimized by conformal mapping
[NASA-CR-1357] c32 N69-26559

CONICAL BODIES

Blunt and conical body optimum heat shield shapes for Jupiter atmospheric entry, noting shallow flight path
[AIAA PAPER 68-1150] c31 A69-13565
Three dimensional hypersonic steady flow around blunt and pointed cones at nonzero angles of attack calculated by method of characteristics
[AIAA PAPER 69-187] c01 A69-18176
Dynamic stability derivatives of large angle blunted conical spacecraft near transonic speed in simulated Mars environment for various angles of attack
[AIAA PAPER 69-104] c31 A69-18210
Surface pressure and heat transfer over blunt conical body in hypersonic flow with uniform mass addition of various gases
[AIAA PAPER 69-716] c01 A69-33463
Dynamic stability derivatives of large angle blunted conical spacecraft near transonic speed in simulated Mars environment for various angles of attack
c31 A69-40550
Effects of angle of attack and bluntness on shock layer properties of cones at supersonic speeds
[NASA-TN-D-4909] c01 N69-10789
Experimental surface pressure distributions on spherically blunted cone at Mach numbers from 1.50 to 4.63
[NASA-TM-X-1730] c01 N69-16209
Effects of cone angle, base flare angle, and corner radius on Mach 3 aerodynamic characteristics of large angle cones
[NASA-TN-D-5048] c01 N69-19926
Calorimetric efficiency of cone and column solar energy concentrator
[NASA-TN-D-5109] c03 N69-21088
Shock shape and surface pressure measurements on hypersonic pointed cones in helium
[NASA-TN-D-5343] c01 N69-31228
Supersonic flow characteristics in wake of blunt cones
[NASA-TN-D-5365] c01 N69-32299
Convective heat transfer rates on large angle conical bodies at hypersonic speeds
[NASA-TN-D-5526] c33 N69-40780

CONICAL NOZZLES

Inlet thermal boundary layer thickness effect on conical nozzle heat transfer and boundary layer determined by operating nozzle with cooled/uncooled inlet
[AIAA PAPER 69-474] c33 A69-32780
Performance of 10 deg conical turbojet plug nozzle with iris primary and translating shroud for supersonic cruise applications
[NASA-TM-X-1709] c28 N69-14313
Static tests of nozzle efficiency and pumping characteristics of conical turbojet plug nozzle with translating primary and secondary shrouds at Mach 0 to 2.0
[NASA-TM-X-1777] c28 N69-21648

Impingement forces, moments, and centers of pressure due to air jets in vacuum sphere
[NASA-TN-D-5147] c12 N69-23085
Turbulent boundary layer temperature and velocity measurements in supersonic water-cooled conical nozzle
[NASA-TN-D-5377] c12 N69-33353

CONICAL SHELLS
Buckling of thin walled truncated conical shells under static loads
[NASA-SP-8019] c32 N69-24131
Design calculations for conical shells and elastic systems subject to antisymmetric loads
[NASA-TT-F-518] c32 N69-30754
Structural design of conical and tension shells using sandwich structures
[NASA-CR-1365] c32 N69-36357

CONJUGATION
Conjugate echoes in Alouette 2 topside sounder ionograms explained by multiple reflections between conjugate points of field line, noting magnetospheric waveguides role
c07 A69-20045

CONNECTORS
Glass vacuum systems grease free assembly method using heat shrinkable polyolefin sleeve tubing connector for compression of O ring joints
c15 A69-20529

CONSTRAINTS
Normalized hodographic mapping for constrained trajectory families, discussing mapping concepts, information content and applications
[AIAA PAPER 69-924] c30 A69-39362
N-terminal parent networks with symmetry constraints derived for nonredundant one port configurations through combinatorial functions test patterns, using computer algorithm
c08 A69-42524
Ionization rate limiting processes behind strong shock waves in pure N, plotting electron density profile diagrams
c12 A69-43367
Computation of regions of constrained stability for nonlinear control systems
[NASA-CR-1328] c19 N69-28196
Matrix theorem and application to establishing independent coordinates for complex dynamical systems with constraints
[NASA-TR-R-326] c19 N69-38655

CONSTRUCTION MATERIALS
Lunar soil as building material and extraction of water, oxygen and rocket propellants from lunar materials for lunar colony needs
c30 A69-27907
Aircraft Structures and Materials Application - Conference, Seattle, September 1969
c15 A69-43416

CONTACT RESISTANCE
Subject classification bibliography for thermal contact resistance
[ASME PAPER 68-WA/HT-18] c33 A69-16122
Thermal contact resistance measurement at various ambient pressures compared with theoretical predictions with each parameter analyzed over interface by computer program
[AIAA PAPER 69-629] c33 A69-33299
Friction and contact resistance during sliding in vacuum of low resistivity metals lubricated with sputtered molybdenum disulfide
[NASA-TN-D-5349] c15 N69-31884
Friction, wear, and contact resistance of gold alloys and electroplated electric gold contacts
[NASA-CR-1447] c17 N69-40057

CONTAMINANTS
Optical properties and chemical analysis of contaminants on Gemini spacecraft windows
[NASA-TN-D-4916] c31 N69-13232
Contaminant and atmospheric sensor for spacecraft cabin environments
[NASA-CR-1375] c14 N69-37876

CONTAMINATION
Tritium contamination reduction in small ion accelerators for neutron production, discussing pumping problems and vacuum systems
c11 A69-26499

CONTINENTS
Origin and terrestrial relief of continents and oceans
[NASA-TT-F-533] c13 N69-29491

CONTINUITY EQUATION
Algorithm for Navier-Stokes and continuity equations used to derive curvilinear coordinate system
c08 A69-14858
Electron number density LF oscillations for ionized gas identified with periodic solutions to neutral and charged particle plasma continuity equations
c25 A69-24315
Simultaneous solution of continuity and heat conduction equations for ionospheric plasma consisting of electrons, atomic O ions and neutral gas species, discussing varying solar flux effects
c29 A69-32082
Simultaneous solution of continuity and heat conduction equations for ionospheric electrons, ions and neutral species for studying F region magnetic storm behavior
c13 A69-32083
LF oscillations in electron number density of ionized deuterium, Ne and He identified from particle continuity equation
c24 A69-40759
Electron density oscillations in ionized neon, helium, and deuterium gases
[NASA-TN-D-4950] c25 N69-14525
Possible applications of continuity equation plasma oscillations to other periodic astrophysical phenomena
[NASA-TN-D-5078] c25 N69-19783

CONTINUOUS RADIATION
Iodine IR laser, discussing CW emission obtained at various wavelengths and attributed to electronic transitions in atom
[IEEE PAPER T-5] c16 A69-19082

CONTINUUM MECHANICS
Continuum theory for wave propagation in elastic composite solid with elastic microinclusions
[NASA-CR-1321] c32 N69-21401
Incremental analysis of large deformations in continuum mechanics with applications to axisymmetric shells of revolution
[NASA-CR-1350] c32 N69-28624

CONTRACT NEGOTIATION
Cost plus award fee contracting incentive system based on after fact evaluation of performance effectiveness
c34 A69-30426

CONTRACTION
Shape preserving expansion and contraction of objects in E 3
[NASA-TN-D-5240] c19 N69-31303

CONTRACTS
Federal government contracting, discussing legality of NASA service contracts
c34 A69-15987

CONTROL
Matrix Riccati and matrix quadratic equations in problems of stochastic control and filtering
c10 A69-16601

CONTROL BOARDS
Displays and controls requirements in manned spacecraft to integrate man into vehicle system, noting man capability for task diversity
c14 A69-19968

CONTROL EQUIPMENT
Modular three dimensional mockup technique for economizing and facilitating design of control and display equipment
c05 A69-11953
Space guidance and control system components, noting control moment gyro, actuator, brushless dc motor, electrically supported gyro and laser gyro
c14 A69-22434
Microelectronic data and remote control function transmission system for wind tunnel testing of aircraft dynamic response to gusts and turbulence
c11 A69-23283
Spacecraft design for minimization of structure interaction with control system, noting susceptibility of extendible booms to solar environment
c31 A69-25500
Control system for thin diffraction limited orbiting astronomical telescope mirror based on

structural analysis of static deflections
c14 A69-27951
Design and analysis of modular servoamplifier for fast response electrohydraulic control systems
[NASA-TN-D-4898] c03 N69-10068
Computation of regions of constrained stability for nonlinear control systems
[NASA-CR-1328] c19 N69-28196
CONTROL RODS
Nuclear thermionic space power system using rod control and heat pipes
[NASA-TN-D-5250] c22 N69-26270
CONTROL SIMULATION
Biosatellite attitude control systems design development and flight test results for payload perturbing effects, discussing simulation activity
c31 A69-35094
Real time digital computer hardware simulation of Apollo Telescope Mount /ATM/ mission
[AIAA PAPER 69-940] c11 A69-40323
Human transfer characteristics in flight and ground simulation for roll tracking task
[NASA-TN-D-5007] c05 N69-17814
Indirect optical viewing system in F-104B for simulated lifting-body approach and landing tasks
[NASA-TN-D-5299] c14 N69-29730
In-flight simulation to evaluate simultaneous use of attitude control for jet VTOL maneuvering
[NASA-TN-D-5342] c02 N69-32110
CONTROL STABILITY
Spacecraft wide angle attitude control system stability analysis, using air bearing table simulation
[AIAA PAPER 69-856] c31 A69-39384
Space suit design with pressure stabilizer for force assisted elbow joint
[NASA-TN-D-5221] c05 N69-26259
Design and test criteria regarding structural flexibility effects on spacecraft stability and control systems
[NASA-SP-8016] c31 N69-37030
CONTROL VALVES
Dynamic performance analysis of fast-response fuel control valve for air breathing engine research
[NASA-TN-D-5331] c03 N69-29977
CONTROLLABILITY
Lifting body entry vehicles in low speed flight test program for determining handling qualities, discussing M2-F2 glide flights
c02 A69-15571
Calculated and flight measured handling quality factors of three subsonic jet transports
[NASA-TN-D-4832] c02 N69-10495
CONTROLLED ATMOSPHERES
Biochemical and metabolic effects of exposure of mice to helium-oxygen atmosphere
[NASA-CR-1372] c04 N69-40955
CONTROLLERS
Measurement of pilot describing functions in single controller multiloop tasks
[NASA-CR-1238] c05 N69-15372
CONVECTION
Optical depths of convection related to metal deficiency for main sequence and giant stars
c30 A69-29946
CONVECTION CURRENTS
High latitude magnetospheric convection patterns determined from ionospheric current distribution using magnetic disturbance plots
c13 A69-38503
Convected balanced electric arcs in transverse magnetic fields
[NASA-CR-1267] c25 N69-18041
CONVECTIVE FLOW
Stellar rotation braking due to mass loss from coronae through stellar wind based on calculation of acoustic energy generation from convective zone
c30 A69-20644
CONVECTIVE HEAT TRANSFER
Statistical theories of turbulence applied to thermal convection between infinite slippery plates at large Prandtl number
c33 A69-24283
Ablative materials thermal protection characteristics at low heating rates evaluated by convective heating tests, stressing polyurethane foam composite
c18 A69-35536
Forced convection heat-transfer data for hydrogen flow through heated parallel hexagonal passages
[NASA-TN-D-4959] c33 N69-14588
Boundary layer interaction in cooling tubes of rocket engines tends to lower convective heat transfer
[NASA-TN-D-5168] c33 N69-22931
Solution for shock layer energy equation with mass and convective heat transfer at hypersonic speed
[NASA-TN-D-5246] c12 N69-33421
Penetration model explanation for turbulent forced convection heat transfer in near-critical fluids
[NASA-TN-D-5522] c33 N69-40437
Convective heat transfer rates on large angle conical bodies at hypersonic speeds
[NASA-TN-D-5526] c33 N69-40780
Temperature response of wall separating two fluids one with oscillating temperature
[NASA-TN-D-5520] c33 N69-40789
CONVERGENCE
Second order errors in linearized velocity corrections and their effects on rate of convergence of iterative solutions
[NASA-TN-D-5037] c21 N69-17780
Noise in axisymmetric convergent electron beams
[NASA-TN-D-5212] c10 N69-24918
CONVERGENT-DIVERGENT NOZZLES
He and Ar arc-heated flows into reservoir and expansion in converging-diverging supersonic nozzles, considering flow equilibrium effect on heat transfer and enthalpy
c33 A69-37198
Water flow and cavitation in convergent-divergent boiler inlet nozzles
[NASA-TM-X-1689] c12 N69-10293
CONVERSATION
Conversational approach to matrix calculations on computers
[NASA-TM-X-1749] c08 N69-18954
CONVERSION TABLES
Conversion tables for studies of human responses to aerospace environment
[NASA-CR-1205-VOL-4] c04 N69-12600
CONVERTERS
Modularized static ac and dc inverters and converters for aerospace electrical power conditioning systems, discussing circuit functions and performance tests
c03 A69-42292
Thermionic converter with fluorine vapor deposited tungsten emitter etched to expose crystal planes
[NASA-CR-1381] c03 N69-35689
CONVOLUTION INTEGRALS
Recursive formulas for numerical evaluation of real convolution integral for simulation of control systems and electrical networks on digital computer
c19 A69-17250
COOLANTS
Comparison of predicted nozzle coolant side heat transfer and fluid flow with experimental values from Phoebus 2A nuclear tests
[NASA-TM-X-1881] c33 N69-36806
COOLING
Electron emitter cooling and plasma heating of thermionic converters noting effects of plasma density, diode spacing, etc
c03 A69-13127
Cooling requirements for high speed polytetrafluorethylene lubricated ball bearings operating in cold hydrogen gas, developing minimum gas flow rate equation
[ASLE PAPER 68-LC-2] c15 A69-19310
COOLING SYSTEMS
High power TWT tube cooling in space vehicle, discussing thermal control system based on heat pipe radiator
c09 A69-24747
Technology trends in airbreathing propulsion, discussing noise control for subsonic jet transports, turbine blade cooling, etc
[AIAA PAPER 69-774] c02 A69-35648
Performance tests of SNAP 8 lubrication and cooling subsystem
[NASA-TM-X-1731] c03 N69-20828
COORDINATE TRANSFORMATIONS
Algorithm for Navier-Stokes and continuity

equations used to derive curvilinear coordinate system
c08 A69-14858
Computer programming of satellite orbit tracking angles for automatic picture transmission receiving stations
c07 A69-14917
COORDINATES
Generation of ideal coordinate systems for analysis of optimal trajectories
[NASA-CR-1250] c30 N69-13274
Selected ordinates for Fourier analysis on periodic curve
[NASA-TN-D-5083] c19 N69-20940
Quadrature variations in discrete-ordinates calculation
[NASA-TM-X-1887] c20 N69-36976
Tabulated values of configuration factors between two spheres and parts of two spheres
[NASA-SP-3050] c30 N69-37777
Matrix theorem and application to establishing independent coordinates for complex dynamical systems with constraints
[NASA-TR-R-326] c19 N69-38655
COORDINATION
Coordination of voluntary movements of man in zero gravitational fields
[NASA-TT-F-578] c04 N69-31356
COORDINATION POLYMERS
Friction and wear of polymers with various fillers in liquid hydrogen
[NASA-TN-D-5073] c15 N69-19800
COPPER
Adhesion of gold on copper planes studied with low energy electron diffraction
[NASA-TN-D-5290] c26 N69-29407
COPPER ALLOYS
Sliding friction tests of Cu and Cu-Be alloy plates in contact with various alloy sliders in air and vacuum
[ASLE PAPER 68-LC-5] c15 A69-30610
Sliding friction and wear behavior of copper alloys in air and vacuum
[NASA-TN-D-4824] c15 N69-10757
Adhesion of gold to copper and to copper aluminum alloys
[NASA-TN-D-5351] c23 N69-31984
COPPER SULFIDES
Impurity profiles and energy band diagram for cuprous sulfide-CdS heterojunction based on capacitance, Hall and electron microprobe measurements
c03 A69-13075
Impurity profile and energy band diagram for cuprous sulfide-cadmium sulfide heterojunction
[NASA-TN-D-5079] c26 N69-19781
CORE FLOW
Fluid dynamic simulation of gas core nuclear rocket chamber for separating light and heavy gas via centrifugal force produced by MHD-driven rotational flow
[AIAA PAPER 69-727] c22 A69-33483
CORONAS
Stellar rotation braking due to mass loss from coronae through stellar wind based on calculation of acoustic energy generation from convective zone
c30 A69-20644
Acoustic energy generation for helium rich stars, discussing X ray radiation from helium star corona
c29 A69-20645
Stellar atmospheres acoustic energy generation rate calculations, studying corona mass ejection effects on stellar rotation
c30 A69-39521
CORRELATION
Surface pressure distribution on spherical blunted cones, and correlation of Mach numbers, cone angle, and angle of attack
[NASA-TN-D-5204] c01 N69-24764
CORRIDORS
Effect of spacecraft onboard radar range and range rate data and accuracy on unmanned probe entry guidance corridor
[NASA-TN-D-4852] c21 N69-16503
CORROSION
Corrosion in cobalt alloy two phase mercury loop
[NASA-TN-D-5326] c17 N69-31065
CORROSION PREVENTION
Corrosion and heat resistant coatings for oxidation protection of tungsten
[NASA-TT-F-583] c17 N69-35836
CORROSION RESISTANCE
Calorimetric analyses of metal corrosions in deionized heated water
[NASA-TM-X-1791] c17 N69-25243
Properties and uses of liquid metal reactor fuels, including heat transfer processes in variously shaped channels, boiling and condensation of metals, and reactor control equipment
[NASA-TT-F-522] c33 N69-30507
CORROSION TESTS
Outdoor high temperature corrosion tests for aluminum alloys and titanium alloys, and stainless steels
[NASA-TN-D-5362] c17 N69-32558
COSMIC DUST
Far IR source in galactic center detected at 100 microns, noting thermal emission of interstellar dust grains as possible mechanism
c30 A69-22264
Cosmic dust sensor experiment on Pioneer 8 space probe
[NASA-TN-D-5267] c30 N69-31058
COSMIC GASES
Kodaikanal iron meteorite measurements for cosmogenic rare gases and K-Ar isotopes ages for glass inclusions
c30 A69-22047
COSMIC NOISE
Cosmic radio noise intensity measurements by ATS 2 satellite-borne radiometer
c30 A69-19715
Cosmic radic background noise spectrum near north galactic pole based on Radio Astronomy Explorer satellite experiments
c30 A69-42375
COSMIC RAYS
Radioactive decay of neutral pions generated in metagalactic cosmic ray interactions as source of high energy isotropic gamma rays observed by OSO-3
c29 A69-12092
Galactic Jupiter Probes investigating Jupiter atmosphere and emissions and deep space cosmic radiation
c30 A69-12303
Cosmic rays - Conference, Calgary, Canada, June 1967
c29 A69-12928
Cosmic ray propagation, discussing interstellar matter effect on composition and diffusion effect necessary to study radiation models
c29 A69-16361
Cosmic rays, elementary particle physics and astrophysics - Conference, Aligarh, India, December 1967
c29 A69-17268
Cosmic ray deuteron and He 3 secondary origin and determination of cosmic ray path length and residual interplanetary field modulation
c29 A69-20066
Discrete source hypothesis for interpreting high energy cosmic gamma ray measurements obtained by OSO-3 spacecraft
c29 A69-20699
Cosmic gamma ray spectra from metagalactic proton-antiproton annihilation
c29 A69-21459
Solar extreme UV, soft and hard solar X rays, cosmic X rays and gamma rays, cosmic ray particles and near earth visible radiation observed by OSO-3
c29 A69-22167
Annihilation gamma ray spectra from equilibrium spectra of secondary galactic positrons
c29 A69-29948
Cosmic ray intensity during solar cycles, considering minima relationship to Bartel index maxima and solar wind modulation theory
c29 A69-29967
IQSY low energy galactic and solar cosmic ray observations made by various satellites and space probes, including hydrogen and helium energy spectra
c29 A69-30014

Photodisintegration of ultrahigh energy cosmic rays by universal radiation field, analyzing implications on origin and propagation time
c29 A69-35006
Twenty year wave in diurnal anisotropy component of galactic cosmic rays arriving at earth from asymptotic direction east of sun interpreted as magnetic reconnection
c29 A69-38098
Cosmic ray studies - Conference, Bombay, November 1968
c29 A69-38811
Chemical composition of galactic and solar cosmic rays, discussing differences from universal cosmic abundances, using Cerenkov counters, emulsions, etc
c29 A69-40090
Cosmic gamma rays spectrum from neutral pions production and decay in metagalactic cosmic ray p-p collisions, deriving models based on Einstein general relativity theory
c29 A69-40641
Cosmic X ray bremsstrahlung due to collisions of suprathermal protons with ambient electron, giving clue about diffuse sky background of X rays
c29 A69-40643
Cosmic ray detectors design for medium, low and very low energy events on IMP-1 spacecraft, noting PCM format
c07 A69-41738
IMP 4 satellite measurements of cosmic ray electrons in interplanetary space compared to predictions of electron intensity from interstellar proton-electron collisions
c29 A69-42667
Equations governing cosmic ray modulation and approximate equations valid at high and low energies
c29 A69-43169
High energy cosmic radiation problems
[NASA-SP-199] c29 N69-29652

COSMOLOGY
Origin and distribution of elements - Conference, Paris, May 1967
c30 A69-20892
Lunar origin theories, considering moon/earth mass ratio, earth-moon system angular momentum deficiency and differential volatilization in earth
c30 A69-29882
Corrections to previous papers on extragalactic gamma rays, discussing effects on various cosmological models
c29 A69-34168
Primitive solar nebula physical model considered under angular momentum conservation in collapsing fragment
c30 A69-36074
Boundary conditions for theory of solar system origin, discussing planetary atmospheres, surfaces, magnetic fields, composition and early solar wind
c30 A69-36209
Cosmological forces in planetary evolution
[NASA-TT-F-532] c13 N69-28983

COST ANALYSIS
General aviation missions in national transportation system /1968, 1975, 1980/, considering fuel taxes, overall system economics, ground facilities, etc
[AIAA PAPER 69-818] c34 A69-35624
Computer memory reduction through FORTRAN higher level language, discussing tradeoff between costs saved and additional logic hardware
[AIAA PAPER 69-963] c08 A69-40344
Cost analysis in low cost launch vehicle studies emphasizing sustaining engineering and plant economics
c31 A69-43120

COST ESTIMATES
Computing optimum flight profiles by Balakrishnan epsilon method, including equations of motion constraint in cost function to be minimized
[AIAA PAPER 69-75] c02 A69-18058
Cost plus award fee contracting incentive system based on after fact evaluation of performance effectiveness
c34 A69-30426
Valving concepts and functional approaches for inert gas attitude control thrustor systems providing redundancy safeguards at minimum weight, volume and power costs
[AIAA PAPER 69-843] c28 A69-39373
Monte Carlo method for estimating costs and optimal testing of Explorer size spacecraft
[NASA-TN-D-5283] c34 N69-31333

COST REDUCTION
Design philosophy for cost reductions on future space transportation systems, exemplifying application to booster system for earth orbital logistics
[AIAA PAPER 69-439] c34 A69-32654
Commercial utilization of space technology, discussing cost reduction and role of NASA Apollo Program
c30 A69-34044
Lunar orbital mission plans intended to optimize spacecraft procurement, flight schedules, science objectives and available funds
c30 A69-34362
Low cost rate transportation as mandatory goal for future space program, discussing recovery and reuse, launch system costs, hardware development, etc
c31 A69-38117
Reducing cost of space transportation - AAS Conference, Washington, D.C., March 1969
c34 A69-39686
Crew and passenger transportation to and from space station orbits, discussing cost reduction possibilities with current or future technology
c31 A69-39691
Cost analysis in low cost launch vehicle studies emphasizing sustaining engineering and plant economics
c31 A69-43120

COULOMB COLLISIONS
Cross sections computed for excitation and ionization of atoms and ions by electrons, using peaking approximation to evaluate Coulomb-Born matrix approximation
c24 A69-20206

COULOMB POTENTIAL
Coulomb approximation for dipole and quadrupole transitions, calculating tables for radial matrix elements
c24 A69-10901

COUPLED MODES
Radiating collinear open ended waveguides and near field coupling analyzed using simultaneous integral equations and Fourier series expansion of aperture field
c09 A69-24984
Transient response of coupled acoustic cavity resonators
[NASA-CR-1421] c23 N69-35286

COUPLING
Mechanical characteristics of flexible drive shaft coupling
[NASA-CR-1241] c15 N69-16104

COUPLINGS
Equations of motion computerized simulation for attitude stabilization of orbiting telescope coupled to crew compartment
c14 A69-27952
Dynamic stability of mechanisms with elastic couplings under vibratory impact
[NASA-TT-F-534] c15 N69-35859

COVARIANCE
Relationship between complex covariance and covariances of envelopes of Rician fading communication channels
[NASA-TN-D-4825] c07 N69-11011

COVERINGS
Optimum solar cell cover glass systems selected by studying interplanetary space environment effects of proton impact, temperature and concurrent illumination on radiation damage
c03 A69-35702
Aluminized plastic covers to reduce radiator sink temperatures on lunar surface
[NASA-TM-X-1729] c03 N69-17225

COWLINGS
Design effects on performance of two dimensional mixed-compression supersonic inlets with low angle cowls
[NASA-TN-D-5330] c01 N69-30060

CRAB NEBULA
X ray energy spectrum from Crab Nebula and diffuse background on celestial sphere near galactic anticenter, noting spectral index
c29 A69-30759
Pulsed X ray emission associated with pulsar NP 0532 in Crab Nebula measured by six element detector on Aerobee 150 rocket
c29 A69-37574
Crab Nebula pulsars radio properties, possible neutron star origin, interstellar gas and magnetic fields, etc
c30 A69-42556
Gamma ray detection from Crab Nebula using digitized spark chamber
[NASA-TR-R-308] c30 N69-24170

CRACK INITIATION
Displacements and stress intensity as function of crack length for compact tension specimen, considering load line and crack edge
c15 A69-21392
Inclination effect of fatigue cracks cn plane strain fracture toughness of 7075-T651 Al alloy, discussing cantilever bending
c32 A69-25958
Crack initiation prediction in high temperature components subjected to arbitrary thermal-mechanical cycling
c32 A69-28252
Semiempirical fracture analysis for semielliptical surface crack in plate
[NASA-TN-D-5340] c32 N69-31056

CRACK PROPAGATION
Ultrasonic detection and measurement of fatigue cracks in notched cylinders subjected to reversed axial cyclic loading
c14 A69-10113
Pressure and temperature dependence of slow crack growth in hardened steel in gaseous hydrogen environment
c17 A69-10612
Elastic displacements for edge cracked plate specimens used as crack extension indicator in plane strain fracture toughness measurements
c32 A69-16433
Axial load fatigue crack propagation tests on Al alloy sheets for stress ratio effects
c17 A69-36435
Crack toughness characteristics of high strength alloys for use in heavy sections of supersonic aircraft
[NASA-TN-D-4998] c32 N69-17275
Factors influencing low cycle crack growth of aluminum sheet specimens
[NASA-TN-D-5140] c32 N69-21392
Stable crack propagation in viscoelastic strip of polyurethane rubber
[NASA-CR-1279] c30 N69-21506
Stress ratio effects on fatigue crack growth in sheet aluminum alloys
[NASA-TN-D-5390] c17 N69-34704
Crack length and thickness influence in plane strain fracture toughness tests
[NASA-TM-X-1860] c17 N69-34916

CRACKING (FRACTURING)
Fracture design for airflight vehicles, discussing crack strength requirements and method for serviceability prediction
c32 A69-33563
Oxidation resistance and thermal fatigue cracking of nickel and cobalt base alloys in transonic gas streams
[NASA-TN-D-5376] c17 N69-33307

CRATERING
Collapse theory of dimple craters, analogies with terrestrial sink holes and dimple craters as channels for gas escape from interior
c30 A69-15589

CREEP ANALYSIS
Digital computer program for analyzing elastic and plastic deformations and creep strains in solid and hollow cylindrical bodies
[NASA-TM-X-1723] c32 N69-16115
Elastic-plastic and creep analysis predictions of core movement during operation of fast nuclear reactor
[NASA-TN-D-5012] c22 N69-16381
Dynamic creep model to determine oxidation effects on high temperature deformation of nickel
[NASA-TN-D-5266] c17 N69-27061
Creep rate equations for refractory metal alloys of tantalum molybdenum, and columbium
[NASA-TN-D-5424] c17 N69-36653

CREEP RUPTURE STRENGTH
Stress rupture and tensile properties of refractory metal wires at 2000 and 2200 deg F
[NASA-TN-D-5139] c32 N69-22823
Sigma phase formation and its effect on stress rupture properties of nickel base alloy IN-100
[NASA-TN-D-5185] c17 N69-23465
Creep rupture data on welded tubes for helium to air heat exchanger design
[NASA-TN-D-5195] c17 N69-23731
Cyclic life calculations of materials subjected to isothermal stress considering fatigue and creep
[NASA-TN-D-5317] c32 N69-29672
Creep rupture data for predicting thermal fatigue cracking of turbine blades or disks
[NASA-TN-D-5489] c32 N69-39393

CREEP STRENGTH
Columbium alloys properties, discussing creep strength, oxidation resistance, costs, production, etc
c17 A69-18791

CREEP TESTS
Creep rate-stress-temperature relations fcr powder metallurgy rhenium, discussing activation energy
c17 A69-34186
Dynamic strain aging during creep and tensile tests of molybdenum-titanium-carbon alloys
[NASA-TN-D-5169] c17 N69-22993

CRITERIA
Natural vibration modal analysis as related to space vehicle design criteria
[NASA-SP-8012] c32 N69-22773
Motion stabilization criteria for aircraft during spatial maneuvers
[NASA-TT-F-555] c02 N69-24761
Linear prediction of structural failure criteria for uniaxial fiber composites
[NASA-TN-D-5367] c18 N69-33321

CRITICAL FLOW
FORTRAN 4 subroutines for calculating critical flow factcr to determine mass flow rate of gaseous helium and nitrogen through critical flow nozzles
[NASA-SP-3046] c12 N69-16098

CRITICAL MASS
Uranium 233 critical mass requirements, neutron kinetic behavior, and neutron and gamma ray heating rates for nuclear light bulb rocket engine
[NASA-CR-1315] c25 N69-23451

CRITICAL POINT
Velocity of 1 MHz sound waves in He 4 along isotherms just above critical temperature, noting specific heat ratio for 4.5 and 5 K isotherms
c23 A69-17142

CRITICAL TEMPERATURE
Critical body temperature for intracranial self stimulatien in white rats
c04 A69-13897
Velocity of 1 MHz sound waves in He 4 along isotherms just above critical temperature, noting specific heat ratio for 4.5 and 5 K isotherms
c23 A69-17142
Penetration model explanation for turbulent forced convection heat transfer in near-critical fluids
[NASA-TN-D-5522] c33 N69-40437

CRITICAL VELOCITY
Undamped rigid rotor critical speed analysis for firm and flexible foundations, discussing effect of center of gravity and rotor shapes
[ASME PAPER 69-VIBR-49] c32 A69-24184

CROSS CORRELATION
Remote sensing cross-beam cross correlation methods of determining spatially resolved average thermodynamic properties
[AIAA PAPER 67-149] c14 A69-31868

CROSS COUPLING
Longitudinal structural vibration and lateral bending response mass and spring coupling in Saturn AS-502 during boost with longitudinal excitation by POGO effect
[AIAA PAPER 69-58] c31 A69-18204

CROSSED FIELD GUNS
Heat generation calculations and heat transfer measurements in circulating currents of linear crossed field generators and accelerators
[NASA-TN-D-5244] c25 N69-26313
CROSSLINKING
Low density polybenzimidazole composites as ablative heat shields, discussing arc-heated wind tunnel tests of linear and crosslinked structures
c18 A69-41715
Properties of irradiated polyethylene memory materials
[NASA-CR-1384] c18 N69-36762
CROSSTALK
Waveform distortion resulting from adjacent channel crosstalk and from amplitude and phase nonlinearity in channel filters in DSB/SC telemetry link
c07 A69-19130
CRUCIFORM WINGS
Wind tunnel tests to determine static aerodynamic characteristics of cruciform wing-body missiles at transonic and supersonic speeds
[NASA-TM-X-1839] c01 N69-31875
CRUISING FLIGHT
Performance of 10 deg conical turbojet plug nozzle with iris primary and translating shroud for supersonic cruise applications
[NASA-TM-X-1709] c28 N69-14313
CRYOGENIC FLUID STORAGE
Safety planning for use of reactive cryogens in large volume, noting FLOX and liquid fluorine
c27 A69-14468
Cryogenic flexibility of thin polymeric film plies for use as spacecraft positive expulsion bladders
c15 A69-16486
Glass, boron and graphite filament wound resin composites and liners for cryogenic pressure vessels
c18 A69-16488
Shadow shields for thermal protection of cryogenic tanks in space
[NASA-TN-D-4887] c33 N69-10420
CRYOGENIC FLUIDS
Ball bearings lubrication and wear in cryogenic hydrogen turbopumps by transfer films provided from self lubricating cage
c15 A69-10109
Illumination in cryogenic or noncryogenic fluids by standard light bulbs
[NASA-TM-X-1654] c14 N69-13176
CRYOGENIC MAGNETS
Cryogenic solenoids with pure Al conductor for production of strong magnetic fields, discussing softness and strain resistivity problems
c03 A69-26497
Variable voltage dc power supplies for energizing cryogenically cooled and superconductive electromagnets
c03 A69-26498
Design, construction, testing, and control devices for high-field electromagnets
[NASA-TN-D-4910] c23 N69-10889
CRYOGENIC ROCKET PROPELLANTS
Safety planning for use of reactive cryogens in large volume, noting FLOX and liquid fluorine
c27 A69-14468
Cryogenic core concept for flexible and economical delivery system
[AIAA PAPER 68-812] c31 A69-39753
Unstable combustion of hydrazine-nitrogen tetroxide caused by transverse gas flow
[NASA-TN-D-4984] c27 N69-19026
CRYOGENICS
Cryogenic properties of polymers - NASA/Case Conference, Cleveland, April 1967
c18 A69-16485
Quantum theory of particle-harmonic oscillator collision applied to gas-surface interactions at cryogenic temperatures
[NASA-TN-D-4982] c24 N69-14288
Absorption of black-body radiation by ice cryodeposits on metal substrates
[NASA-TN-D-5181] c23 N69-22769
NERVA control drum actuator tests in cryogenic temperature, nuclear radiation, and vacuum environments
[NASA-TN-D-5347] c22 N69-31870
Cryogenic fracture properties of thin AISI 301 cold reduced sheet at different angles to rolling direction
[NASA-TN-D-5413] c17 N69-35688
Effects of reactor irradiation at cryogenic temperatures on tensile properties of titanium and titanium-base alloys
[NASA-TN-D-5442] c17 N69-37436
CRYOPUMPING
Cryogenic molecular beam system with pressure attenuation
[NASA-TN-D-5308] c24 N69-31338
CRYSTAL DEFECTS
Vacancy relaxations in bcc crystals using energy dependence on radial displacements from defect of nearest neighbor sets, discussing crystal size and shape
c26 A69-16529
CRYSTAL DISLOCATIONS
Dislocation model of strength of elastically inhomogeneous crystalline materials based on elastic interactions between dislocations and periodic fluctuations of shear modulus
c17 A69-20557
Tungsten and tungsten alloy single crystal deformations determined as function of alloying, strain, and temperature
[NASA-TN-D-5493] c17 N69-39182
CRYSTAL GROWTH
Chemical processes in silicon carbide due to reactive deposition and chemical conversion, noting silicon growth mechanism involving outward diffusion
c26 A69-21351
Single crystal growth by controlled diffusion in silica gel using metathetical and decomplexation reactions
c06 A69-23371
Optimal growths of silicon carbide polytype crystals by methyltrichlorosilane reduction
[NASA-TN-D-5313] c26 N69-30072
CRYSTAL STRUCTURE
Influence of number of slip systems operating in magnesium on friction and effect of orientation of crystals on friction behavior
[NASA-TN-D-4351] c15 N69-10370
Physical properties of near stoichiometric nickel-titanium alloy Nitinol and some structural-mechanical applications employing these properties
[NASA-CR-1232] c17 N69-11420
CRYSTAL SURFACES
Low energy electron diffraction analysis of quartz fiber adhesion to rhenium crystal surface
[NASA-TN-D-5229] c17 N69-25363
CRYSTALLOGRAPHY
X ray crystallographic measurements of selected grades of commercial nonpyrolitic artificial graphite
[NASA-TN-D-4888] c18 N69-10754
CRYSTALS
Thermionic converter with fluorine vapor deposited tungsten emitter etched to expose crystal planes
[NASA-CR-1381] c03 N69-35689
CUBIC LATTICES
Cubic /beta/ silicon carbide films deposition by volatilization in presence of acetylene
c26 A69-21350
CULTURE TECHNIQUES
Micro lagoon technique for culture and observation of isolated mammalian cells
[NASA-TN-D-4906] c04 N69-11056
Hydrogenomonas cultures investigated for metabolic waste utilization in aerospace life support systems
[NASA-CR-1296] c05 N69-22766
Dies for imprinting microscopic lagoon fields in plastic surfaces for use in cell and tissue culture
[NASA-TN-D-5255] c04 N69-29195
CURRENT DENSITY
Optimum thickness of dynamically stable composite superconducting tapes determined for substrate thickness as function of current density
c26 A69-43121
CURRENT DISTRIBUTION
High latitude magnetospheric convection patterns determined from ionospheric current distribution

using magnetic disturbance plots
c13 A69-38503
Performance tests of silicon and germanium transistors in intense magnetic fields
[NASA-TN-D-5428] c09 N69-36710

CURRENT SHEETS
Modified first order theory of magnetosphere boundary shape incorporating effects of neutral sheet currents of extended geomagnetic tail
c13 A69-21661

CURVATURE
Effect of shallow meridional curvature on vibration of nearly cylindrical shells
[NASA-TN-D-5143] c32 N69-22821

CURVED PANELS
Pressure and heating rate correlations for rocket exhausts impinging on flat plates and curved panels, generating axisymmetric real gas exhaust plumes
c33 A69-26781
Outer and inner curved plates and shell shapes optimized by conformal mapping
[NASA-CR-1357] c32 N69-26559

CURVES (GEOMETRY)
Outer and inner curved plates and shell shapes optimized by conformal mapping
[NASA-CR-1357] c32 N69-26559

CUSHIONCRAFT GROUND EFFECT MACHINE
Cushioncraft ground effect machine with heave response and control concepts
[NASA-TN-D-5202] c02 N69-23449

CYANO COMPOUNDS
Reflection and transmission measurements on as grown surfaces of tetracyanoquinodimethan, obtaining optical constants by Kramer-Kronig method
c26 A69-35477

CYCLIC HYDROCARBONS
Interstellar extinction models of classical Mie particles and quantum mechanical polycyclic aromatic molecules
c30 A69-23679
Gas chromatographic and mass spectrometric analyses of alicyclic hydrocarbons from Carboniferous organic materials, noting alkane distribution and evolutionary histories
c06 A69-34184

CYCLIC LOADS
Ultrasonic detection and measurement of fatigue cracks in notched cylinders subjected to reversed axial cyclic loading
c14 A69-10113
Factors influencing low cycle crack growth of aluminum sheet specimens
[NASA-TN-D-5140] c32 N69-21392
Elastoplastic stress-strain behavior at notch roots in sheet specimens under constant amplitude loading
[NASA-TN-D-5253] c32 N69-28038

CYCLOTRON RESONANCE
Small signal and saturation characteristics for X band cyclotron resonance oscillator, discussing device design and configuration
c09 A69-22786
Frequency shifts observed in Alouette 2 cyclotron harmonic plasma resonances, noting antenna length and direction
c07 A69-37892
Cyclotron resonance oscillators as sources of millimeter waves
[NASA-TN-D-5237] c10 N69-28121

CYGNUS CONSTELLATION
IR radiation of NML Cygnus with O/C ratio close to unity ascribed to circumstellar shell of graphite particles
c30 A69-13775
Day sky brightness at altitude above 100 km obtained during rocket flight compared to night sky viewed from ground
c30 A69-33664

CYLINDERS
Furnace brazing butt joints in tungsten-uranium dioxide cermet cylinders at 3000 deg C
[NASA-TM-X-1815] c15 N69-28862

CYLINDRICAL ANTENNAS
Radiation pattern of axial slot on circular conducting cylinder based on wedge diffraction and creeping wave theory
c07 A69-24993
Directional solar thermal field /sunlight/ effect on coupled nonplanar transverse and torsional vibrations of satellite cylindrical antennas in orbit
c32 A69-25534
VHF cavity backed cylindrical gap antenna input tuning impedance and equatorial radiation patterns controlled by cavity adjustments
c09 A69-40698
Equatorial radiation pattern of parallel plate TEM mode axial slot on elliptical conducting cylinders, using wedge diffraction and creeping wave theory
c09 A69-40703

CYLINDRICAL BODIES
Prediction of thermal neutron flux perturbation effects in cylinders during irradiation tests
[NASA-TN-D-4949] c22 N69-14481
Observations of interface behavior during inflow to elliptical ended cylinder in weightlessness
[NASA-TM-X-1719] c12 N69-15473
Digital computer program for analyzing elastic and plastic deformations and creep strains in solid and hollow cylindrical bodies
[NASA-TM-X-1723] c32 N69-16115
Flow field from forward facing nozzles exhausting near large cylindrical body at free-stream Mach numbers of 3.0 and 6.0
[NASA-TN-D-5030] c01 N69-21000
Heat transfer to windward side of scale model for graphite lunar module fuel cylinder
[NASA-TN-D-5251] c12 N69-29608
Natural frequency of liquids in annular cylinders under low gravity conditions
[NASA-TN-D-5412] c12 N69-35842
Differential equations for compression loaded axisymmetric cylindrical structures
[NASA-CR-1444] c32 N69-38781

CYLINDRICAL CHAMBERS
Laminar incompressible viscous flow in short cylindrical vortex chamber with finite swirl ratio
[NASA-TN-D-5132] c12 N69-21400

CYLINDRICAL SHELLS
Structural synthesis of cylindrical shell reinforced with rectangular cross section stiffeners
[NASA-CR-1217] c32 N69-14254
Instability of eccentrically stiffened cylindrical shells under axial compression and lateral pressure
[NASA-CR-1280] c32 N69-15378
Effect of shallow meridional curvature on vibration of nearly cylindrical shells
[NASA-TN-D-5143] c32 N69-22821
Predicting buckling of thin walled, uniform stiffened and unstiffened circular cylindrical shells under static loading
[NASA-SP-8007] c32 N69-23320
Theoretical analysis of free vibration of discretely stiffened cylindrical shells with arbitrary end conditions
[NASA-CR-1316] c32 N69-28164
Radiation resistance of cylindrical shells in ideal compressible acoustic medium
[NASA-CR-1437] c32 N69-40935

CYLINDRICAL TANKS
Lateral sloshing in cylinders under low gravity conditions
[NASA-TN-D-5058] c12 N69-19112

CYTOCHROMES
Electron transport of Halobacterium cutirubrum, discussing spectrophotometric identification of cytochromes
c04 A69-19481
Flavoprotein/cytochrome b/559/ role as branch of Halobacterium electron transport in DPNH oxidase determined by salt dependence of reduced DPNH
c06 A69-37101

CYTOLOGY
Micro lagoon technique for culture and observation of isolated mammalian cells
[NASA-TN-D-4906] c04 N69-11056

D

D LINES
Solar Na D lines analysis by direct inversion of line source function, finding Doppler core

dependence on frequency
c30 A69-38479

D REGION
Simultaneous rocket measurements of D region temperatures and electron densities on anomalous winter day
c13 A69-16411
Rocket sounding measurements of ionospheric D region electron density profile during 20 May 1966 solar eclipse, discussing D region ionization source
c13 A69-29116
Lower auroral ionosphere rocket measurements of electrons, positive ions and energy particles, deriving height variation of ion pair production and ion-ion recombination
c13 A69-32187

DACRON (TRADEMARK)
Mission sequential environment effects on Dacron parachute material mechanical properties
[AIAA PAPER 69-1018] c11 A69-40390

DAMPING
Damping factor automatic determination by use of second derivatives of residuals for damped least squares method of optical design
c23 A69-14295
Parameters of acoustic liner for maximum liner damping for rocket engines
[NASA-TM-X-1720] c28 N69-16152
Magnetically anchored eddy current and eddy current rod dampers for GEOS gravity gradient stabilized satellite
[NASA-CR-1282] c14 N69-18953

DARK ADAPTATION
Detection time to light point source noting response to dark, star field and glare source backgrounds
c05 A69-17215

DATA ACQUISITION
Orbiting satellite global all-weather oceanographic data acquisition to complement higher resolution data from ships, buoys and aircraft remote sensors
[UN PAPER 68-95878] c13 A69-10491
International 28-station global instrumentation ground support network for space tracking and data acquisition
[UN PAPER 68-95912] c34 A69-17059
Multifunction Receiver System rationale, concepts, background requirements and technical justifications for tracking, telemetry and ranging data acquisition by Goddard Center
c07 A69-19101
Clinical report on Apollo 7 and 8 mission medical data, discussing preflight preventive medical activities, inflight treatment, radiation levels, etc
c05 A69-22542
Meteoritic dust particles collections prediction in atmosphere for low and high entry fluxes
c30 A69-26342
EEG monitor helmet for aircraft or flight simulator programs, discussing sensing and transmitting system
c05 A69-26553
Tracking and data acquisition systems for spacecraft and ground link through command, telemetry and tracking, noting data relay satellites, etc
c07 A69-33371
Digital data acquisition system with ultrahigh sampling rate for Ames electric arc shock tunnel, describing analog to digital conversion, data storage, system performance, etc
c11 A69-35744
PCM data handling system for NASA Space Tracking and Data Acquisition Network with explanation for output capabilities, noting BIOSAT project
c07 A69-36242
Stored program data processor used as PCM telemetry data acquisition system for postApollo applications, considering format and bit rate changes
c07 A69-36280
Tracking and Data Relay Satellite System with synchronous orbit satellites to relay data between low altitude earth orbital spacecraft and mission control centers
c07 A69-41755
Rosman I reflector antenna for collecting data from earth orbiting satellites, discussing dynamic analysis of structural response to natural frequencies
c32 A69-42133
Summary of lunar data and scientific observations generated by Surveyor landings on Moon
[NASA-SP-184] c30 N69-36451

DATA CORRELATION
Entry phase flight data of Missions AS-202, Apollo 4 and 6 compared with wind tunnel aerodynamics data
[AIAA PAPER 68-1143] c31 A69-13556
C-5A aircraft model high subsonic speed tests, correlating data from three transonic wind tunnels
[AIAA PAPER 69-794] c01 A69-35636
Daily simultaneous solar measurements of microwave atmospheric absorption and emission to determine frequency correlation between meteorological phenomena and atmospheric parameters
c13 A69-39747
Meaningful comparisons between single stimulus EEG records and average evoked potential
c05 A69-40163
Rotor aerodynamics research in terms of theoretical and experimental data comparison, rotor blade flow visualization and blade section camber
c01 A69-41372
Correlation study of simulation of Gemini extravehicular activity with flight results
[NASA-CR-1146] c05 N69-19902

DATA LINKS
Data relay satellite systems for support of NASA R and D missions, discussing communications between satellites and to mission control
c07 A69-25296
Optical carrier single channel telemetry system providing complete electrical isolation between shock tube data acquisition and data recording instrumentation
c14 A69-29561
Libration point relay satellites for continuous communication link between earth and lunar far side, discussing trajectories and halo orbit stationkeeping
c30 A69-30188
Ground data handling equipment characteristics for PCM telemetry link utilizing convolutional coding
c07 A69-36267
Digital telemetry link coding as English language analogy, developing block code scheme combining bit, word and block error detection and correction methods
c07 A69-41745
Real time telemetry, tracking and command links by synchronous satellite relay, describing ATS-Nimbus E S band experiment
c07 A69-41759
Pioneer 9 deep space probe with telemetry link operated in coded mode with sequential decoding, discussing ground and flight test data
c07 A69-42522
Optimum design of binary phase shift keyed communication links with noisy phase reference
[NASA-TN-D-4895] c07 N69-13155

DATA PROCESSING
Human information processing rates during one and two axis compensatory tracking tasks with secondary auditory task
c05 A69-23880
On-line central data processing system connected to time shared computer for recording data from test facilities, discussing hardware configuration, software considerations and advantages
c08 A69-33106
Ground data handling equipment characteristics for PCM telemetry link utilizing convolutional coding
c07 A69-36267
NASA current awareness service SCAN /selected current aerospace notices/, promoting selectivity in information transfer to abstract journals, accession lists and bibliographies
c34 A69-39581

Telemetry data processing, describing designation, tasks and possibilities of data reduction laboratory attached to NASA Goddard Space Flight Center
c11 A69-40352
Spacecraft central data system for deep space solar probe data management
c08 A69-42621

DATA RECORDING
On-line central data processing system connected to time shared computer for recording data from test facilities, discussing hardware configuration, software considerations and advantages
c08 A69-33106

DATA REDUCTION
Adaptive compression system for predicting and encoding video data for transmission in noiseless channel
c14 A69-12869
Nonvertical propagation effects on high altitude topside ionosphere sounder data reduction, using ray tracing
c13 A69-18838
NASA photogrammetric lunar activities, discussing imagery and control data by Lunar Orbiter and photogrammetric data reduction for preparing manned lunar landing
c14 A69-34336
Huffman minimum redundancy coding extension to run-length information based on Poisson distribution, including optimization and data compression applications
c07 A69-36262
Topside ionogram reduction for ionospheric electron density determination, using geomagnetic strength at all heights, iteration and change of variables
c13 A69-37864
Brayton-B generator for 2-10 kWe production, describing design, heat source/rejection, efficiencies and preliminary test data analysis
c03 A69-42278
Preprocessing procedures for reduction of electronic data from geodetic satellites
[NASA-CR-1183] c08 N69-11470
Computer program for component quality control and reliability data analysis
[NASA-TN-D-5009] c15 N69-17988
Minitrack data reduction procedures, with IBM 360 computer program description
[NASA-TN-D-5042] c08 N69-26193
Statistical method for automatic computer editing of biological data
[NASA-TN-D-5275] c08 N69-29592
Evaluation of height and time based meteorological rocket wind reduction techniques
[NASA-TM-X-1850] c20 N69-35523

DATA RETRIEVAL
NASA scientific and technical information program for building technical data and literature repository for scientists, engineers and technical managers, describing IAA and STAR
[UN PAPER 68-95317] c34 A69-17068

DATA SAMPLING
Digital data acquisition system with ultrahigh sampling rate for Ames electric arc shock tunnel, describing analog to digital conversion, data storage, system performance, etc
c11 A69-35744

DATA STORAGE
Stored program computer for small scientific spacecraft, noting program and data memory capacities
c08 A69-15472

DATA SYSTEMS
Onboard SDP-3 computer data system core for IMP spacecraft, considering payload
c08 A69-13243
PCM data handling system for NASA Space Tracking and Data Acquisition Network with explanation for output capabilities, noting BIOSAT project
c07 A69-36242
Programmable data handling and telemetry systems for scientific satellites, noting system checkout, spacecraft integration, software and ground data processing
c08 A69-41735
Spacecraft onboard data handling system with MSI complementary MOS arrays, describing various components
c08 A69-41739
Data systems coordinating standards developed from experience with STADAN, discussing operating environment and administrative decisions influence on implementation
c08 A69-41769
Spacecraft central data system for deep space solar probe data management
c08 A69-42621

DATA TRANSMISSION
International experimentation with U.S. communications satellites, noting design variations with participants and restraintless information exchange
[UN PAPER 68-95421] c20 A69-10474
NASA Technology Utilization Program, discussing information dissemination
[UN PAPER 68-95313] c34 A69-10512
WEFAX /Weather Facsimile/ experiment to explore operational feasibility of direct meteorological data transmission via satellite relay from central station to remote stations
c11 A69-13240
Microelectronic data and remote control function transmission system for wind tunnel testing of aircraft dynamic response to gusts and turbulence
c11 A69-23283
Variable length codes for alphabets containing messages with assigned weighted information content
[NASA-TN-D-4962] c07 N69-15373

DAWN CHORUS
Banded chorus, VLF discrete emissions in magnetosphere in single variable frequency band with frequency depending on equatorial electron gyrofrequency
c13 A69-31981

DAYGLOW
Day sky brightness at altitude above 100 km obtained during rocket flight compared to night sky viewed from ground
c30 A69-33664

DECAY
Nonlinear disturbance decay in unbounded viscous fluid
[NASA-TN-D-4947] c12 N69-14483
Scattering, reactions, and decay in nonrelativistic quantum mechanics
[NASA-TT-F-510] c24 N69-25848

DECELERATION
Deceleration control system for aerobraking and skipout to orbit at Mars
[AIAA PAPER 68-1146] c31 A69-13564
Entry and terminal deceleration systems for unmanned Martian landers, discussing parachute landing and lifting entry vehicles
[AIAA PAPER 68-1147] c31 A69-13670
NASA planetary entry parachute program for rocket launched and ballcon deployment tests
[AIAA PAPER 68-934] c02 A69-35952
Aerodynamic deceleration systems for space missions, considering deployment of subsonic parachute and inflatable configuration following atmospheric entry
[AIAA PAPER 68-1081] c31 A69-40542
Inflatable landing system investigated for impact normal to smooth surface
[NASA-TN-D-5236] c32 N69-26223

DECISION MAKING
Data systems coordinating standards developed from experience with STADAN, discussing operating environment and administrative decisions influence on implementation
c08 A69-41769

DECODING
Determining sequential decoding performance and metric sensitivity by computer simulation
[NASA-TR-R-294] c07 N69-16196
Log-a-posteriori probability metric for use in sequential decoding
[NASA-TN-D-4930] c07 N69-23163

DECONTAMINATION
Clean room technologies for control of contaminants for component reliability
[NASA-SP-5074] c05 N69-33775

DECOUPLING
Decoupling force exerted by magnetic forming Be coil assembly on metallic plate during forming
c14 A69-25310

DEEP SPACE
Galactic Jupiter Probes investigating Jupiter atmosphere and emissions and deep space cosmic radiation
c30 A69-12303
Manned spacecraft systems design optimization for extended space missions replacement modules
c31 A69-16380
Spacecraft central data system for deep space solar probe data management
c08 A69-42621

DEFORMATION
Influence of surface films on friction and deformation of single crystal and polycrystalline gold
[NASA-TN-D-4875] c15 N69-10249
Effect of orientation and presence of surface active materials on friction and wear of aluminum
[NASA-TN-D-4994] c15 N69-16197
Incremental analysis of large deformations in continuum mechanics with applications to axisymmetric shells of revolution
[NASA-CR-1350] c32 N69-28624

DEGREES OF FREEDOM
Light rigid civil aircraft response to continuous atmospheric turbulence estimated using two rigid body degrees of freedom method for vertical and lateral gusts
[AIAA PAPER 69-766] c32 A69-35657
Design and dynamic characteristics of vertical lunar gravity simulator with six degrees of freedom torso harness
[NASA-CR-1234] c05 N69-14979
Computer simulation of six degrees of freedom flight equations
[NASA-CR-1344] c21 N69-26232
Evaluation of six degrees of freedom motion simulator for Bell X-14A aircraft hovering characteristics
[NASA-TN-D-5383] c11 N69-35359

DEHYDRATION
Hypohydration effects on isometric muscular strength, noting decreasing trends in maximal strength
c04 A69-15983

DEIONIZATION
Calorimetric analyses of metal corrosions in deionized heated water
[NASA-TM-X-1791] c17 N69-25243

DELTA FUNCTION
Delta functions spectrum in reciprocal time domain for LC and RC structures due to impulse response in distributed parameters
c10 A69-21327

DELTA LAUNCH VEHICLE
Flight performance of FW-4D solid propellant rocket motor on third stage of Delta 50 launch vehicle
[NASA-TN-D-4987] c28 N69-20876

DELTA WINGS
Hypersonic flow distribution and separation types over highly swept Delta wing with trailing edge flaps at Mach 6
[AIAA PAPER 68-97] c01 A69-12522
Calculated and experimental hinge moments on trailing-edge flaps of swept Delta wings at hypersonic speeds and positive deflection angles
[NASA-TN-D-4268] c01 N69-10054
Predicting lift and drag for slender sharp-edge Delta wings in ground proximity
[NASA-TN-D-4891] c01 N69-16180
Tuft-grid photographic survey of flow field about low speed Delta wings
[NASA-TN-D-5045] c01 N69-19027
Aerodynamic characteristics and ground effects of supersonic transport with double Delta wing
[NASA-TN-D-5102] c02 N69-21020
Experimental and theoretical study of symmetrical and cambered Delta wing configuration between Mach 2.0 and 10.7
[NASA-TN-D-5272] c01 N69-29269
Helium penetration and spreading in Mach 2 airstream using Delta wing injector
[NASA-TN-D-5322] c01 N69-30878
Pressure and heat transfer on swept Delta wing with trailing-edge flap
[NASA-TN-D-5418] c01 N69-35855

DEMODULATORS
Design and performance of traveling wave phototube for coherent light demodulation
[NASA-TT-F-430] c09 N69-15441

DENSITOMETERS
Satellite-borne experiments of neutral molecular beam-solid surface interactions, describing Molsink chamber, densitometer, sphere and paddlewheel satellites
c24 A69-36182
Measurement of liquid and two phase hydrogen densities with capacitance density meter
[NASA-TN-D-5015] c14 N69-23470

DENSITY (MASS/VOLUME)
Hydrogen absorption coefficients, giving number densities in hydrogen gas or plasma for wide range of temperature and pressure
c24 A69-19165
Physical properties of near stoichiometric nickel-titanium alloy Nitinol and some structural-mechanical applications employing these properties
[NASA-CR-1232] c17 N69-11420
Nondestructive methods for fuel density determination in uranium dioxide
[NASA-TM-X-1779] c22 N69-22555
Surface tension, viscosity, and density of fluorocarbon solvents as function of temperature
[NASA-TM-X-1862] c18 N69-34134

DENSITY (NUMBER/VOLUME)
Number densities of hydrogen species in hydrogen plasma - tables
[NASA-TN-D-4993] c25 N69-16466

DENSITY DISTRIBUTION
Ring current particle energy density distribution for symmetric portion of magnetic storm derived from current magnetic field profile measurements
c29 A69-11227
Lunar gravitational anomalies from internal density variation viewpoint, discussing isostasy in maria
c30 A69-14631
Density inversion in convective zone of stellar photospheres occurring in Eridani atmospheric model under certain conditions
c30 A69-21843
Density and velocity fluctuations in hypersonic turbulent boundary layer based on Wallace data
c12 A69-31908

DENSITY MEASUREMENT
Midlatitude neutral thermosphere density and temperature measurements, noting effect of atomic oxygen adsorption by instruments
c13 A69-16268
Density measurements of particle tracks in nuclear emulsions utilizing digitized video scan, discussing operation and instrumentation
[IEEE PAPER 2A-7] c14 A69-19185
Explorer 32 atmospheric density measurements revealing neutral thermosphere latitudinal variations during geomagnetically undisturbed times
c13 A69-38100

DEPLETION
Tungsten and depleted uranium in minimum weight, layered shield comparisons for space power reactor
[NASA-TM-X-1874] c22 N69-35817

DEPLOYMENT
Deployable appendages of OGO attitude controlled spacecraft design
c31 A69-17606

DEPOLARIZATION
Spontaneous Raman band shapes and depolarization ratios in liquid nitrogen and oxygen measured and compared to gas, discussing time dependence of rotational motion
c24 A69-17817

DESCENT TRAJECTORIES
Requirement estimates and performance predictions for Martian television experiment onboard spacecraft in three point-mass descent trajectories
[NASA-TN-D-5062] c14 N69-17944

DESIGN
Design, development, and testing of 1000 pound

thrust FLOX-propane ablative rocket engine
[NASA-TM-X-1873] c28 N69-35847
DESORPTION
Work function and desorption energy measurements of alkali metals from metallic substrates with modulated molecular beam, noting surface contamination
c26 A69-21808
DESTRUCTION
Spacecraft sterilization by destructive heating with thermite or high velocity entry friction before entering planet atmosphere
c05 A69-31472
DETECTION
Gamma ray detection from Crab Nebula using digitized spark chamber
[NASA-TR-R-308] c30 N69-24170
DEUTERIUM
Deuterium concentration effect on electrical resistivity of palladium-deuterium system
[NASA-TN-D-4970] c26 N69-14565
DEUTERONS
Absolute cross sections for coincidence detection of deuteron breakup by 42 MeV alpha particles, showing He 5 and Li 5 final state interaction peaks
c24 A69-13469
Cosmic ray deuteron and He 3 secondary origin and determination of cosmic ray path length and residual interplanetary field modulation
c29 A69-20066
DIAPHRAGMS (MECHANICS)
Image converter camera and astronomical telescope arrangement for photographing metal diaphragm openings in shock tube
c14 A69-37227
DIATOMIC GASES
Radiation attenuation cross sections of monatomic and diatomic xenon gas from UV absorption measurements near resonance line
c24 A69-12551
Computer program for line-by-line calculation of spectra from diatomic molecules and atoms assuming Voigt line profile
[NASA-TN-D-5088] c24 N69-21462
DIATOMIC MOLECULES
Electron impact cross sections for diatomic molecule ionization and excitation from modified Gryzinski theory, discussing results from molecular models
c24 A69-22249
Computer program to predict spectra from electronic transitions of diatomic molecules and atoms, noting line intensity distribution by Voigt profile
c24 A69-35239
Diatomic molecules rotational excitation calculated from electron molecule elastic scattering parameters in fixed nuclei approximation
c24 A69-39665
Positively charged diatomic hydrogen molecules interstellar extinction and photodissociation cross section in terms of formation mechanisms
c30 A69-42610
Computer program for line-by-line calculation of spectra from diatomic molecules and atoms assuming Voigt line profile
[NASA-TN-D-5088] c24 N69-21462
DIBORANE
Specific impulse deliverable performance of space storable propellant combination flucrine-oxygen/methane and oxygen difluoride/diborane
[AIAA PAPER 69-505] c28 A69-32762
DIELECTRIC PROPERTIES
Ablation heat shields, emphasizing dielectric low cost fabrication and application to entry vehicles
c15 A69-35538
Thermal and dielectric properties of homogeneous moon based on microwave and infrared temperature observations
[NASA-TM-X-1734] c30 N69-17815
DIELECTRICS
Thermodielectric radiometer for transient radiant flux short duration pulse measurement, using thermally induced depolarization of polymer film dielectric
[AIAA PAPER 68-403] c14 A69-12392
Air gap tolerances effect on admittance of TEM mode dielectric and plasma coated slot antennas determined by variational method
c09 A69-24986
Reflection coefficient of symmetric parallel plate waveguide operating in TEM mode illuminating lossless dielectric layer, using wedge diffraction and geometrical optics methods
c09 A69-34802
Waveguide fed rectangular aperture antenna with dielectric plug load, describing admittance resonant perturbation due to excited TE mode
c09 A69-41589
High purity dielectric materials tested in capacitors at high temperatures
[NASA-CR-1213] c18 N69-14400
Admittance of parallel plate aperture illuminating displaced dielectric-dielectric boundary
[NASA-TN-D-5038] c07 N69-19114
DIES
Dies for imprinting microscopic lagoon fields in plastic surfaces for use in cell and tissue culture
[NASA-TN-D-5255] c04 N69-29195
DIFFERENCE EQUATIONS
Finite difference method for symmetric positive linear differential equations, discussing methods to solve finite difference equations generated
c19 A69-13370
DIFFERENTIAL EQUATIONS
Finite difference method for symmetric positive linear differential equations, discussing methods to solve finite difference equations generated
c19 A69-13370
Optimal stochastic control, discussing dynamic mathematical models described by differential equations
c10 A69-22567
Quasi-linear ordinary differential equations solutions for steady two dimensional stagnation point flows of nonNewtonian power law fluids
c12 A69-39674
Thomas-Fermi approximation applied to calculation of equations of state and thermodynamic functions at high pressure from differential equations of statistical atom model
c24 A69-40186
Coupled set of differential equations describing generalized Volterra problem of conflicting populations and application to plasma oscillations
c19 A69-41260
Variable mesh multistep methods for numerical solution of nonlinear differential equations
[NASA-CR-1247] c19 N69-11419
Solution of differential equations by series of exponential functions
[NASA-CR-1294] c19 N69-17249
Boundedness theorem, thresholds, and stationary values in modified Huxley-Hodgkin model for electric current flow through cell membrane
[NASA-CR-1272] c19 N69-21143
Sonic boom propagation in stratified atmosphere using FORTRAN computer program with integral and differential equations
[NASA-CR-1299] c02 N69-22546
Vinti dynamic problem relevance to prediction of satellite orbits using differential and integral equations
[NASA-TR-R-307] c30 N69-22948
Generalized averaging method for linear differential equations with almost periodic coefficients
[NASA-TN-D-5167] c19 N69-22988
Numerical difficulties in integrating equations for one dimensional nonequilibrium nozzle flow of gas
[NASA-TN-D-5176] c19 N69-23355
Existence, uniqueness, and stability criteria for linear and nonlinear operational differential equations in Banach and Hilbert spaces
[NASA-CR-1356] c19 N69-28256
Chebyshev series solution of nonlinear ordinary differential equations - initial value problems
[NASA-TM-X-1882] c19 N69-36923
DIFFERENTIAL INTERFEROMETRY
Holographic microscopy for performance prediction

and quality control of semiconductor devices and integrated circuits
[NASA-CR-1394] c14 N69-31958
DIFFERENTIAL THERMAL ANALYSIS
Dynamic differential thermal analysis with He flow performed on biological specimens, proteins and starches, showing discrete decomposition peaks monitoring pyrolysis process
c06 A69-31807
DIFFERENTIATION (BIOLOGY)
Differential thresholds for rotary and linear motion in the periphery
[NASA-CR-1439] c05 N69-36925
DIFFERENTIATORS
Alloying pairs of metal pellets to n and p type semiinsulating GaAs, discussing photo effects
c26 A69-32824
DIFFRACTION
Equatorial radiation pattern of parallel plate TEM mode axial slot on elliptical conducting cylinders, using wedge diffraction and creeping wave theory
c09 A69-40703
Diffraction dissociation of protons on complex nuclei of photoemulsion
[NASA-TT-F-535] c29 N69-24924
DIFFRACTION PATTERNS
Slope diffraction analysis of TEM parallel plate guide patterns
[NASA-CR-1326] c07 N69-26273
DIFFRACTION PROPAGATION
Edge diffraction effects in TEM axially slotted finite ground plane on radiation pattern in waveguides of different geometries
c07 A69-41588
DIFFUSE RADIATION
Multiple light scattering in planetary atmospheres, discussing diffuse reflection and transmission by atmosphere of particles with anisotropic scattering pattern
c30 A69-12105
X ray energy spectrum from Crab Nebula and diffuse background on celestial sphere near galactic anticenter, noting spectral index
c29 A69-30759
DIFFUSERS
Venturi meter with separable diffuser and radial outward step at transition from throat to diffuser, noting effect of step on efficiency
[ASME PAPER 68-WA/FM-2] c14 A69-16135
DIFFUSION
Single crystal growth by controlled diffusion in silica gel using metathetical and decomplexation reactions
c06 A69-23371
Mass dependence of self diffusion in Fe by serial sectioning in alpha, gamma and delta phases, determining isotope effect with Fe radioactive isotopes
c17 A69-36440
Ventilation-perfusion inequality increase effects on lung overall gas exchange, using digital model
c05 A69-38388
Momentum diffusion between two supersonic airstreams passing through oblique shock waves
[NASA-TN-D-4974] c12 N69-15631
DIFFUSION THEORY
Combined conduction and radiation transfer equations solutions for absorbing-emitting gas, obtaining slip coefficient for diffusion solution correct boundary condition
c33 A69-27784
Time dependent convection electric fields as agents for diffusing trapped magnetospheric radiation inward toward earth, discussing one dimensional diffusion equation
c29 A69-28936
Lower solar corona composition changes due to pressure and thermal gradients calculated with multicomponent diffusion equations
c30 A69-33059
Diffusion lengths of silicon solar cells after radiation damage and annealing by X ray method
[NASA-TM-X-1894] c03 N69-37827
DIGITAL COMPUTERS
On-line central data processing system connected to time shared computer for recording data from test facilities, discussing hardware configuration, software considerations and advantages
c08 A69-33106
Stored program data processor used as PCM telemetry data acquisition system for postApollo applications, considering format and bit rate changes
c07 A69-36280
Computer organization design employing distributed processor to provide general purpose computing while taking advantage of large scale integration
c34 A69-39133
Digital computer program for homopolar inductor alternator electromagnetic design analysis
[NASA-TN-D-5072] c03 N69-19799
Radiation view factors for toroid calculated by digital computer
[NASA-TN-D-5006] c33 N69-23471
DIGITAL DATA
Stochastic saturating systems optimal control computation, considering attitude control and tracking system design by elliptical differential equation of dynamic programming
c10 A69-30601
Alphanumeric listing and digital data x-y plotting by high speed printer, describing equipment modifications and control software
c08 A69-33108
Electronically scanned star sensor with digital output for orbiting astronomical telescope
[NASA-TN-D-5281] c14 N69-29153
High speed printer for hard copy alphanumeric listings and digital data plots
[NASA-TN-D-5474] c08 N69-38654
DIGITAL FILTERS
Filtering optimization prior to limiting digital signals in strong noise, detailing bandwidth choice of single pole low pass filter
c07 A69-39450
Cataloged pulse response curves for different types of conventional low pass filters
[NASA-TN-D-5494] c07 N69-40099
DIGITAL SIMULATION
Space vehicle docking dynamics and matrix equations of motion amenable to numerical solution on digital computer, using Hamilton principle and Lagrange multipliers
c31 A69-25501
Digital simulation computer stability analysis scheme premised on use of perturbed transient responses
c10 A69-32899
Ventilation-perfusion inequality increase effects on lung overall gas exchange, using digital model
c05 A69-38388
Numerical integration techniques for real time digital flight simulation
[NASA-TN-D-4900] c11 N69-11371
Mathematical simulation model for rigid body rotational kinematics
[NASA-TN-D-5302] c23 N69-39178
DIGITAL SYSTEMS
Digital data acquisition system with ultrahigh sampling rate for Ames electric arc shock tunnel, describing analog to digital conversion, data storage, system performance, etc
c11 A69-35744
Gamma ray detection from Crab Nebula using digitized spark chamber
[NASA-TR-R-308] c30 N69-24170
DIGITAL TECHNIQUES
Digital telemetry link coding as English language analogy, developing block code scheme combining bit, word and block error detection and correction methods
c07 A69-41745
Synthesis methods for manual aerospace control systems using digital programming and man machine performance data with application to supersonic transport design
[NASA-CR-1208] c02 N69-13185
DIMENSIONAL ANALYSIS
Computer program for dimensional analysis using FORTRAN 4 programming
[NASA-TN-D-5165] c08 N69-22935
DIMERS
Luminescence spectra of aromatic polymers,

monomers and dimers under high energy electron excitation using molecular resonance model c26 A69-32792

DIMETHYLHYDRAZINES
Liquid rocket acoustic instability for hydrogen-oxygen and earth storable propellant combinations
[NASA-TN-D-4968] c28 N69-14384
Gaseous reactant combustion simulation of dimethylhydrazine and hydrazine fuel system for nonequilibrium expansion studies
[NASA-TN-D-5404] c33 N69-35506

DIODES
Isothermal diode as study basis for internal complex controlling thermionic energy conversion c03 A69-21827
Figures of merit for experimental silicon carbide backward diode operable to 1000 degrees K
[NASA-TN-D-5183] c09 N69-23556

DIPOLE MOMENTS
Rotational spectrum of ethylene episulfoxide to determine molecular structure, particularly orientation of C sub 2 S ring c06 A69-20535
Computer made movies and time history plots for ion-dipole collisions involving polar molecules /CO, HCL and acetonitrile/ c24 A69-43124
Interaction energy and dipole moment in collisions of two hydrogen molecules
[NASA-TN-D-5486] c24 N69-39184

DIRAC EQUATION
Dirac equation in external electromagnetic fields, deriving solution for constant orthogonal electric and magnetic fields encountered in plasma transport c23 A69-41357

DIRECT CURRENT
Evaluation of magnetic materials for static inverters and converters, tested under square wave excitation and direct current excitation
[NASA-CR-1226] c03 N69-17765

DIRECT POWER GENERATORS
Variable voltage dc power supplies for energizing cryogenically cooled and superconductive electromagnets c03 A69-26498

DIRECTIONAL ANTENNAS
Backfire antenna radiation characteristics and physical dimensions for tracking and telemetry applications, including five element array model c07 A69-36251
Multiplicative feed system for monopulse angle tracking antennas, discussing influence of sidelobe and backlobe responses on control function slope determining antenna bearing angle c11 A69-37704

DIRECTIONAL CONTROL
Computer mechanization of reentry equations with four degrees of freedom
[NASA-CR-1249] c30 N69-13300
Algorithm for computing direction cosine matrix of strapdown inertial system
[NASA-TN-D-5384] c21 N69-36997

DIRECTIONAL STABILITY
Directional solar thermal field /sunlight/ effect on coupled nonplanar transverse and torsional vibrations of satellite cylindrical antennas in orbit c32 A69-25534
Jet fighter aircraft lateral directional stability at high angles of attack
[NASA-TN-D-5361] c02 N69-32337
Electro-optical instrument for measuring pointing direction of human eye
[NASA-CR-1422] c05 N69-39212

DIRECTIVITY
Thermal calculations of objects near lunar surface, considering IR emission directivity effects c30 A69-43254

DISCHARGE COEFFICIENT
Discharge nozzle coefficients for thick plate orifices with approach flow perpendicular and inclined to orifice axis
[NASA-TN-D-5467] c12 N69-38012

DISCONTINUITY
Discontinuities in interplanetary magnetic field direction presented on mesoscale from Pioneer 6 observation, emphasizing distribution in time c30 A69-29970
Al interconnections discontinuities at integrated circuit contact windows observed by scanning electron microscope, noting catastrophic failure and Si presence c09 A69-32893

DISCRETE FUNCTIONS
Theoretical study of discrete frequency noise generated by turbocompressors and blades
[NASA-CR-1287] c28 N69-21476

DISEASES
Conference on bone diseases and regeneration, cellular differentiation, and homeostasis of calcium
[NASA-SP-161] c04 N69-10444

DISINTEGRATION
Absolute cross sections for coincidence detection of deuteron breakup by 42 MeV alpha particles, showing He 5 and Li 5 final state interaction peaks c24 A69-13469

DISKS (SHAPES)
Equilibrium and free vibration problems of centrifugally stabilized disk and shell structures
[NASA-CR-1178] c32 N69-14477

DISPERSING
Feasibility of producing dispersion strengthened chromium by ball milling in hydrogen halides
[NASA-TN-D-4912] c17 N69-10827

DISPLAY DEVICES
Modular three dimensional mockup technique for economizing and facilitating design of control and display equipment c05 A69-11953
Scanned laser beam display techniques based on cathode ray tube technology, noting flying spot scanner and beam deflection c14 A69-15028
Displays and controls requirements in manned spacecraft to integrate man into vehicle system, noting man capability for task diversity c14 A69-19968
Holographic displays using ultrasonic vibrations or laser outputs as optical sources, discussing recording materials, responses and computer applications c14 A69-21394
Apollo mission simulation, discussing Command Module Simulator /CMS/, onboard computer system and dynamic visual presentation via infinity-optics display
[SMPTE PAPER 105-74] c11 A69-25768
Fourth angle driving law for different four gimbal systems used for simulation display and inertial platform isolation c11 A69-26265
Instrument display devices for landing VTOL aircraft
[NASA-TN-D-4861] c21 N69-10069
Superlinear and sublinear phosphors combined for producing single gun color cathode ray tubes
[NASA-CR-1228] c09 N69-14256
Peripheral vision displays for presenting dynamic control information
[NASA-CR-1239] c05 N69-14478
Advanced electronic applications to navigation, data transmission, and airborne collision avoidance in general aviation aircraft and to simulated displays for low visibility landing
[NASA-CR-1240] c02 N69-14729
Predictive display systems using repetitive, fast time, on-line computation
[NASA-CR-1274] c05 N69-17738
Rendezvous and station keeping simulator with fly around capability and virtual image viewing
[NASA-TN-D-5123] c11 N69-22629
Navigation-aids identification decoder and display device for general aviation aircraft
[NASA-TN-D-5445] c09 N69-38852

DISSOCIATION
Dissociation energy of gaseous titanium nitride
[NASA-TN-D-5027] c06 N69-19129

DISTILLATION
Vacuum distillation determination of O in Li, evaluating accuracy through O additions and recoveries, method blank and residue identification

c06 A69-40932
Vacuum distillation determination of oxygen in lithium
[NASA-TN-D-5197] c06 N69-23706
DISTILLATION EQUIPMENT
Vacuum distillation technique for isolation and recovery of alkali metal reaction products with Ta, Ni, V and oxygen
c14 A69-10927
DISTORTION
Relationship between binocular depth perception and optical distortion in Apollo pressure suit helmets and visors
[NASA-TN-D-5162] c05 N69-22990
Dynamic distortion of supersonic wind tunnel for turbojet engines
[NASA-TM-X-1842] c28 N69-38599
DISTRIBUTED AMPLIFIERS
Multiloop feedback in active distributed RC networks for low parameter sensitivity with low amplifier gain compared to single loop circuits
c10 A69-34679
DISTRIBUTION FUNCTIONS
Constitutive equation variation effect on near wall flow pattern of dilute polymer solutions
c12 A69-33257
Relation between ellipsoidal velocity distribution function and macroscopic flow equations
[NASA-TN-D-5026] c12 N69-17827
DISTURBING FUNCTIONS
Short term motion of lunar satellite, discussing third body disturbing functions and perturbation solution of nonsingular orbit elements
c30 A69-35934
Disturbing factors in motion of artificial earth satellites due eccentricity of earth gravitational field
[NASA-TT-F-539] c30 N69-33560
DISULFIDES
Thermal stability and friction of disulfides, diselenides, and ditellurides of molybdenum and tungsten in ultrahigh vacuum
[NASA-TN-D-5141] c15 N69-22992
DIURNAL VARIATIONS
Diurnal variations of low latitude VLF emissions observed at Hiraiso, Japan
c07 A69-13900
Electron cooling rates in midlatitude and auroral zone thermosphere measured by probe rockets
c13 A69-16267
Ion temperature diurnal variations at 250-475 km obtained from Thomson scatter spectra
c13 A69-16407
Diurnal and seasonal variations of primary atmospheric ions in topside ionosphere correlated with solar zenith angle, using ion mass spectrometer on Explorer 32
c13 A69-38087
Daily simultaneous solar measurements of microwave atmospheric absorption and emission to determine frequency correlation between metecrological phenomena and atmospheric parameters
c13 A69-39747
Rocket measurements of diurnal variations of F region concentrations and temperature of molecular N and O, showing disagreement with satellite drag data
c13 A69-40515
Diurnal and solar cycle variations of thermosphere density and temperature generated by solar EUV input and tidal wave, using two dimensional model
c29 A69-43003
DIVERGENCE
Analysis of aeroelastic divergence phenomena in unguided launch vehicles
[NASA-TN-D-4846] c32 N69-10297
DIVERGENT NOZZLES
Plasma accelerator with magnetic field producing divergent-nozzle effect
[NASA-TN-D-5122] c25 N69-22942
DOCUMENT STORAGE
Remote information retrieval facility description
[NASA-CR-1318] c08 N69-23381
DOPPLER EFFECT
Doppler shift measurements of axial and rotational velocities in MPD arc, using reference lines from iron arc
[AIAA PAPER 69-110] c25 A69-18171
Three dimensional laser Doppler velocity instrument for mean velocity and turbulence measurements in subsonic jet shear layer
[SAE PAPER 690266] c14 A69-21555
Laser Doppler flowmeter for heterodyne detection of laser light scattered from moving fluid applied to fluid velocity and velocity distribution measurements
c14 A69-26546
Axial velocities in ammonia MPD thrustor exhaust by measuring Doppler shifts of spectral lines emitted by plasma constituents
c28 A69-31890
Solar Na D lines analysis by direct inversion of line source function, finding Doppler core dependence on frequency
c30 A69-38479
Laser Doppler velocity instrument for measuring turbulence and mean velocity in subsonic and supersonic gas flows
[R-67-4450] c14 N69-14351
DOSIMETERS
Tungsten-184 used as thermal flux monitor at high temperatures in Plum Brook reactor
[NASA-TN-D-5113] c22 N69-20795
DOUBLE SIDEBAND TRANSMISSION
Waveform distortion resulting from adjacent channel crosstalk and from amplitude and phase nonlinearity in channel filters in DSB/SC telemetry link
c07 A69-19130
Double sideband suppressed carrier FM telemetry system as airborne data recorder, discussing noise, environmental conditions, laboratory and flight tests
c07 A69-19132
DRAG
Mathematical model for determining total drag of pointed body of revolution in supersonic flow with turbulent boundary layer
[NASA-TN-D-5046] c01 N69-19925
Subsonic expansion tube evaluation as device for studying particle drag in subsonic compressible slip flow
[NASA-CR-1354] c11 N69-28095
Minimum drag bodies in hypersonic flow using calculus of variations
[NASA-TN-D-5438] c01 N69-36699
Drag and stability characteristics of towed, conical decelerator
[NASA-TM-X-1833] c02 N69-38598
DRAG MEASUREMENT
Drag coefficients for spheres and sharp cones in rarefied hypersonic air flow obtained in shock tunnel using free flight technique
[AIAA PAPER 69-140] c01 A69-18184
Wind tunnel drag measurements on subsonic sphere
[NASA-CR-1392] c01 N69-30609
DRAG REDUCTION
Viscous drag reduction - Conference, Dallas, September 1968
c12 A69-33247
Turbulence measurements and roughness effects on viscous drag reduction with polymer solution in pipe flow, discussing friction factor, wall velocity profile, etc
c12 A69-33252
Concentration, flow rate and tube diameter effects on viscous drag reduction in nonpolar soap solutions, using pressure drop measurements to observe turbulent flow behavior
c12 A69-33253
Skin friction drag reducing high polymer solution injected into turbulent boundary layer to test effectiveness on marine vehicles
c12 A69-33254
Normal stress effects in viscoelastic fluid theories applied to one dimensional Burgers model of weak turbulence predicting drag reduction
c12 A69-33256
Constitutive equation variation effect on near wall flow pattern of dilute polymer solutions
c12 A69-33257
Numerical method for evaluation and utilization of supersonic nacelle-wing interference
[NASA-TN-D-5057] c01 N69-19641
Force measurements in drag reduction by gas injection into turbulent boundary layer through

supersonic wing slots
[NASA-TN-D-5307] c12 N69-31359
DRAINAGE
Vapor ingestion phenomenon during draining in weightlessness
[NASA-TN-D-5210] c12 N69-24917
DRIFT RATE
Charged particle dynamics in spiral interplanetary magnetic field model, discussing electric drift velocity, point of origin and distribution
c29 A69-14015
Trapped particles drift velocity in time dependent meridional magnetic and perpendicular electric field
c25 A69-20809
DROP SIZE
Mean drop size generated in vapor pressure regime of liquid water jet, noting effect of water temperature and orifice diameter
c12 A69-21995
Research on warm fog properties, and dispersal concepts
[NASA-SP-212] c20 N69-39526
DROP TESTS
Experimental verification of scale factors for parawing opening characteristics with dimensional ratios from 1/1.3 to 1/3
[NASA-TN-D-5071] c02 N69-19950
Parachute load distribution measurements with tensiometer during low altitude drop tests
[NASA-TM-X-1832] c14 N69-32682
DROPS (LIQUIDS)
Laser ignited combustion of 365 micron Zr droplets falling in ultrapure oxygen using spectroscopic and photographic techniques, discussing vapor phase transport phenomena
[WSCI PAPER 69-4] c27 A69-32345
Nature of outside boundary layer on liquid sphere in steady, uniform stream
[NASA-CR-1362] c12 N69-24877
Droplet wake minimization by surface tension changes
[NASA-CR-1368] c12 N69-24958
DROSOPHILA
Mortality kinetics of Drosophila melanogaster, comparing effects of gamma radiation-induced life shortening and natural aging
c04 A69-30444
DRUMS (CONTAINERS)
Reflector based poison drum control on equal size reactor cores fueled with U-233 and U-235
[NASA-TM-X-1883] c22 N69-36756
DRY CELLS
Signal electrode charge control of sealed Ni-Cd batteries, discussing signal voltage for overcharge control
c03 A69-23993
DRY HEAT
Spacecraft sterilization by destructive heating with thermite or high velocity entry friction before entering planet atmosphere
c05 A69-31472
DUCTED FANS
Performance of turbine driven V/STOL cruise fan propulsion system at subsonic Mach numbers
[NASA-TN-D-5314] c28 N69-35526
DUCTED FLOW
Monte Carlo method application to neutron streaming in hemispherical air-filled ducts in water tank to determine leakage through nuclear reactor shields
c22 A69-35178
Turbulence in mixing region of ducted coaxial flow of air-air and air-Freon 12 combination
[NASA-CR-1335] c12 N69-30728
FASTER computer program modified for tracking neutrons through reactor slabs penetrated by helical voided ducts
[NASA-TM-X-1838] c22 N69-31986
DUCTILITY
Ductile metal powder chemical reactions during comminution in pure or oxygenated water
c06 A69-27762
Ductilizing of Group 6A elements by rhenium and other solutes
[NASA-TN-D-4955] c17 N69-14403
DUCTS
Analytical and experimental studies for predicting noise attenuation in acoustically treated ducts for turbofan engines
[NASA-CR-1373] c23 N69-36974
DURABILITY
Results of endurance tests of SNAP 8 turbine alternator
[NASA-TM-X-1741] c03 N69-20913
DUST COLLECTORS
Meteoritic dust particles collections prediction in atmosphere for low and high entry fluxes
c30 A69-26342
DWARF STARS
Subdwarf HD 25329 studied with model atmosphere approach, using H alpha, Na I and Mg I profiles for effective temperature
c30 A69-22199
DYES
Organic dye laser frequency variation with temperature, noting absorption and fluorescence spectra
c16 A69-12617
Low energy ultrafast flashlamp systems as optical pumps for lasers using fast decaying fluorescent materials /organic dyes/
c16 A69-42187
Spectral emission of visible from Q switched dye lasers
[NASA-CR-1374] c16 N69-29934
DYNAMIC CHARACTERISTICS
Dynamical effects in structure of H II equilibrium region left behind expanding ionization front, showing temperature as function of distance from star
c30 A69-35966
Metric state-time dynamical polysystem with sequentially compact topological space, noting sliding state trajectories
c19 A69-40573
Approximate mathematical analysis of supersonic inlet dynamics
[NASA-TN-D-4969] c01 N69-14289
Design and dynamic characteristics of vertical lunar gravity simulator with six degrees of freedom torso harness
[NASA-CR-1234] c05 N69-14979
One megawatt reactor design for Brayton cycle space power application - neutronics design
[NASA-TN-D-5014] c22 N69-17314
Dynamic analysis and maximum stepping rate prediction for permanent magnet motor
[NASA-TN-D-5094] c03 N69-20780
Dynamic performance analysis of fast-response fuel control valve for air breathing engine research
[NASA-TN-D-5331] c03 N69-29977
Steady-state characteristics of herringbone grooved air lubricated journal bearings
[NASA-TN-D-5386] c15 N69-33258
Experimental verification of surface vehicle dynamics
[NASA-CR-1399] c11 N69-37022
Longitudinal dynamics of lifting vehicle in orbital flight
[NASA-CR-1449] c30 N69-40062
DYNAMIC CONTROL
Model performance index /PI/ providing criterion for approximating one dynamic flight control system by another based on geometrical representation of linear autonomous systems
[AIAA PAPER 69-885] c21 A69-39410
Peripheral vision displays for presenting dynamic control information
[NASA-CR-1239] c05 N69-14478
DYNAMIC MODELS
Transformation laws for thermodynamic quantities confirming conventional formulation by mechanical model of heat
c23 A69-11288
Kinetic theory model of plasma sheath transition applied to sheath structure in unignited mode of thermionic converter
c03 A69-21828
Optimal stochastic control, discussing dynamic mathematical models described by differential equations
c10 A69-22567
FM/AM telemetry circuits with three axis piezoelectric accelerometer for measurements during impact tests of soft landing models
c07 A69-23279

Nova outburst dynamics investigation by time dependent hydrodynamics computer program including energy transport by radiation and convection
c30 A69-30769
Flash X ray unit with special film transport devices to obtain sequenced dynamic radiographs of ablating models during reentry simulation tests
c11 A69-35720
Direct stiffness method of computing vibrational characteristics of dynamic model of Apollo-Saturn 5 vehicle - umbilical tower configuration
[NASA-TN-D-4871] c31 N69-10934
Lateral vibration characteristics of dynamic model of Apollo-Saturn 5 launch vehicle
[NASA-TN-D-4872] c31 N69-11007

DYNAMIC MODULUS OF ELASTICITY
Mathematical analysis of Fitzgerald apparatus measuring solids dynamic mechanical properties
[NASA-TN-D-5116] c18 N69-21384

DYNAMIC PROGRAMMING
Optimal stochastic control of small dynamic systems described by random differential equations, noting selective bibliography on several subjects
c10 A69-14697

DYNAMIC RESPONSE
Combustion response of hydrazine-nitrogen tetroxide hypergolic rocket propellants to transverse gas flows, noting coupled and uncoupled oscillations
c33 A69-10112
Human body dynamic response to vibration combined with linear acceleration, noting changes in body mechanical impedance and resonance
c05 A69-11335
Longitudinal structural vibration and lateral bending response mass and spring coupling in Saturn AS-502 during boost with longitudinal excitation by POGO effect
[AIAA PAPER 69-58] c31 A69-18204
Flexible rotor blade dynamic response to radially moving force, emphasizing helicopter rotor vibration characteristics associated with tip-vortex impingement
[AIAA PAPER 69-203] c02 A69-19546
Dynamic analysis of axisymmetric ring stiffened shells with attached asymmetric elastic structures, noting vibration modes
c32 A69-25525
Lunar dynamic response to discontinuities in interplanetary magnetic field to determine electrical conductivity and internal temperature
c30 A69-31442
Light rigid civil aircraft response to continuous atmospheric turbulence estimated using two rigid body degrees of freedom method for vertical and lateral gusts
[AIAA PAPER 69-766] c32 A69-35657
Rosman I reflector antenna for collecting data from earth orbiting satellites, discussing dynamic analysis of structural response to natural frequencies
c32 A69-42133
Statistical analysis on influential aspects of wind profile disturbance design and dynamic response of space vehicles
[NASA-TN-D-4963] c32 N69-15632
Experimental and analytical study of dynamics of single tube counterflow boiler
[NASA-CR-1230] c12 N69-17751
Frequency response of forced flow single tube boiler with inserts and exit restriction
[NASA-TN-D-5023] c12 N69-17779
Effects of lateral cable oscillations on dynamic response of cable-connected space station
[NASA-TN-D-5107] c31 N69-21111
Dynamic response of uniform beams and plates exposed to sonic booms
[NASA-CR-1281] c32 N69-21403
Wind tunnel tests of inflatable disk-gap-band and modified ringsail parachutes at low dynamic pressure
[NASA-TM-X-1786] c01 N69-23538
Numerical method and computer program for computing deflection response of thin shells
[NASA-CR-1376] c32 N69-29558
Lateral bending dynamic tests of Atlas Centaur Surveyor launch vehicle
[NASA-TM-X-1837] c31 N69-30631
Dynamic response of liquid jet atomization to acoustic oscillations
[NASA-TN-D-5339] c28 N69-30980
Dynamic response of supersonic mixed compression inlet coupled to cold pipe or turbojet engine
[NASA-TN-D-5338] c28 N69-31336
Approximative solution for dynamic response of flexible rotor blade to radially moving force
[NASA-TN-D-5410] c32 N69-36220

DYNAMIC STABILITY
Space-station-centrifuge configuration dynamic stability exhibiting instabilities at lower and higher centrifuge rotational speeds
[AIAA PAPER 68-142] c31 A69-12373
Logarithmic variation criteria for stability of feedback systems with time varying gains
c10 A69-13073
Dynamic instability of solid bodies, using modal vibration method to establish criteria on basis of equivalent energy conditions
c32 A69-16742
Linear state variable feedback to obtain asymptotic stabilization of linear dynamic systems
c10 A69-17947
Spherical caps axisymmetric static and dynamic buckling under load, using axisymmetric nonlinear elastic shell theory approximation and finite difference equations
[AIAA PAPER 69-89] c32 A69-18133
Stability of systems with sector nonlinearities determined by converting feedback equation into positive operators equation and by introducing appropriate multiplier
c10 A69-25450
Semiempirical stability boundary for flutter of simply supported cylinders for various length-radius and radius-thickness ratios
c32 A69-41914
Optimum thickness of dynamically stable composite superconducting tapes determined for substrate thickness as function of current density
c26 A69-43121
Dynamic stability and performance of injectors, rocket liners, and supersonic combustors
[NASA-TM-X-1845] c33 N69-32468
Dynamic stability of mechanisms with elastic couplings under vibratory impact
[NASA-TT-F-534] c15 N69-35859
Static and dynamic stability derivatives of model jet transport equipped with external flow jet augmented flaps
[NASA-TN-D-5408] c02 N69-36258

DYNAMIC STRUCTURAL ANALYSIS
Structures, structural dynamics, materials and aeroelasticity - ASME-AIAA Conference, New Orleans, April 1969
c32 A69-25492
Dynamic analysis of axisymmetric ring stiffened shells with attached asymmetric elastic structures, noting vibration modes
c32 A69-25525
Structures, structural dynamics and materials - AIAA-ASME Conference, New Orleans, April 1969
c32 A69-26807
Identification of structural systems using near resonance testing
[NASA-TN-D-5069] c32 N69-17737
Structural response of tubular beryllium and beryllium aluminum alloy truss-type structures to dynamic and static loads
[NASA-TN-D-5254] c32 N69-28658

DYNAMIC TESTS
Dynamic tests for air breathing engines using sweep frequency techniques
[NASA-TN-D-5485] c28 N69-39185

E

E REGION
Atomic oxygen density role in ionospheric E and F region magnetic stability, noting heat loss effect of atomic excitation
c13 A69-32314
Magnetic dip equator position at E layer and gradient with time and altitude, using

geomagnetic field models
c13 A69-42428
EAR
Prediction of loudness from frequency characteristics of sound
[NASA-TN-D-5422] c23 N69-37028
EARLY STARS
Spinning rockets UV spectrophotometry of early type stars, discussing instrumentation, calibration, data recording and stellar spectra
c30 A69-25812
EARTH (PLANET)
Earth bow shock waves in far upstream interplanetary medium observed from magnetic data of Explorer 34 satellite
c30 A69-34941
Recurrent Lagrange multipliers for optimal low thrust earth-Jupiter transfers, using three dimensional solar system model
c30 A69-41896
Structure of matter, physical fields, evolution of earth and universe, solar activity and earth, and interaction of earth biosphere with physical fields
[NASA-TT-F-345] c13 N69-12384
Space communications system for earth moon radio link
[NASA-TT-F-527] c07 N69-14973
EARTH ALBEDO
Albedo over Antarctic, measuring solar radiation reflected by surface and atmosphere by Eppley radiometer
c13 A69-21404
EARTH ATMOSPHERE
Atmospheric density variation measurements by density gages on Explorer 32 satellite confirm wave propagation in neutral thermosphere as free internal gravity waves
c13 A69-16261
Inverse problems in radiative transfer applied to remote measurements of IR radiation from planetary atmospheres, noting temperature and water vapor inversions
c13 A69-17617
Transmission of Alfven waves through earth bow shock based on hydromagnetic shocks theory, discussing amplitude amplification
c13 A69-32099
Bidirectional reflectance of earth atmosphere and cloud formation above equatorial Pacific observed by synchronous satellite as function of angular dependence
c20 A69-43154
Investigation of earth atmospheric composition, geomagnetism, extraterrestrial radiation, solar activity, and planetary atmospheres by satellite experiment and astronomical observations
[NASA-SP-195] c34 N69-38951
EARTH CORE
Earth mantle and core friction interaction suggested as cause of secular change in orbital motion obliquity
c13 A69-27821
EARTH CRUST
Possible evolution of earth continents and ocean basin, considering ultrabasic, basic, and intermediate to acidic lunar highlands chemical composition
c30 A69-17006
EARTH MANTLE
Earth mantle and core friction interaction suggested as cause of secular change in orbital motion obliquity
c13 A69-27821
EARTH ORBITAL RENDEZVOUS
Rendezvous and station keeping simulator with fly around capability and virtual image viewing
[NASA-TN-D-5123] c11 N69-22629
EARTH ORBITS
Communications for Apollo Applications Program, considering extended duration manned missions in low earth orbit and Gemini, Saturn and Apollo hardware
c07 A69-19124
Earth mantle and core friction interaction suggested as cause of secular change in orbital motion obliquity
c13 A69-27821
Visual acuity and visibility of markings on ground in long duration earth orbital space flight
[NASA-CR-1134] c05 N69-10813
Visual sensing and spacecraft guidance for earth orbit rendezvous maneuvers
[NASA-CR-1214] c05 N69-13161
Two burn spacecraft trajectories for escaping earth parking orbit
[NASA-TN-D-5011] c30 N69-17305
Nimbus 2 flight evaluation and engineering report covering launch through orbit 5275
[NASA-TN-D-4881] c31 N69-17851
EARTH PLANETARY STRUCTURE
Chemical composition of Earth, Venus, Mars, Mercury and Moon calculated from mathematical models, constructing approximate equations of state at high pressure
c30 A69-29878
Cosmological forces in planetary evolution
[NASA-TT-F-532] c13 N69-28983
Origin and terrestrial relief of continents and oceans
[NASA-TT-F-533] c13 N69-29491
EARTH RESOURCES PROGRAM
NASA Earth Resources Survey Aircraft Program, describing aircraft and remote sensors characteristics
c14 A69-36259
Nimbus 2 high resolution infrared radiometer data on earth resources of arid and subarid lands
[NASA-TN-D-4647] c13 N69-14450
EARTH RESOURCES TECHNOLOGY SATELLITES
Earth resources remote sensing from spacecraft noting meteorology, oceanography, forestry, agriculture and IR detection of plant diseases and pollution
c34 A69-26978
EARTH SATELLITES
Geopotential resonant orbital perturbations of existing satellites, noting high inclination role
c31 A69-13777
Disturbing factors in motion of artificial earth satellites due eccentricity of earth gravitational field
[NASA-TT-F-539] c30 N69-33560
EARTH SURFACE
Color photographs of earth surface taken during Gemini flights 6 through 12
[NASA-SP-171] c14 N69-28909
EARTH-MOON SYSTEM
Moon effect on intensity and angular distribution of energetic electron and proton shadowing as observed by Explorer satellites
c30 A69-16252
Lunar origin theories, considering moon/earth mass ratio, earth-moon system angular momentum deficiency and differential volatilization in earth
c30 A69-29882
EARTH-MOON TRAJECTORIES
Libration point relay satellites for continuous communication link between earth and lunar far side, discussing trajectories and halo orbit stationkeeping
c30 A69-30188
Comparison of class of orbits in Earth-Moon field and class of Kepler orbits in rotating coordinates by use of concurrent series of graphs
[NASA-TN-D-4903] c30 N69-10470
ECCENTRICITY
Theoretical analysis of pressure distribution, load capacity, attitude angle, and friction force for eccentric Rayleigh step journal bearing - infinite length solution
[NASA-TN-D-4873] c15 N69-10231
Disturbing factors in motion of artificial earth satellites due eccentricity of earth gravitational field
[NASA-TT-F-539] c30 N69-33560
ECHOES
Computer experiment on 9000 particle plasma to test temporal echo theoretical prediction
c25 A69-38713
ECONOMICS
Aerospace technology role in economic and social benefits
[UN PAPER 68-95321] c34 A69-10467

EDDY CURRENTS
Magnetically anchored eddy current and eddy current rod dampers for GEOS gravity gradient stabilized satellite
[NASA-CR-1282] c14 N69-18953
Eddy current torques on bodies rotating relative to uniform magnetic field
[NASA-TN-D-5086] c23 N69-29477
EDDY VISCOSITY
Incompressible turbulent boundary layer analysis by two region characterization for eddy viscosity, using Spalding generalized function and Prandtl free shear flow model
c12 A69-33255
EDITING ROUTINES (COMPUTERS)
Statistical method for automatic computer editing of biological data
[NASA-TN-D-5275] c08 N69-29592
EDUCATION
Science education and training, discussing student motivation
[UN PAPER 68-95809] c34 A69-10515
NASA programs impact on U.S. education
[UN PAPER 68-95291] c34 A69-10519
Spacecraft systems, education - Conference, Belgrade, September 1967
c31 A69-17596
Space exploration influence on science education, showing NASA instructional materials for teachers in biology, chemistry, physics, mathematics, industrial arts, etc
c34 A69-35077
Sextant sighting performance concerned with training and monochromatic stars
[NASA-TN-D-5190] c05 N69-35024
EFFICIENCY
Quantum communication systems performance evaluated by communication efficiency parameter
[NASA-TR-R-320] c07 N69-39264
EGGS
Weightlessness effects on fertilized frog egg development onboard Gemini 8 and 12 manned orbital flights, discussing cell division, differentiation and embryogeneis
c04 A69-11084
EIGENVALUES
Characteristic plane harmonic free internal neutral atmospheric wave oblique propagation through horizontally stratified quiet atmosphere for various thermospheric parameters
c13 A69-26101
EIGENVECTORS
Characteristic plane harmonic free internal neutral atmospheric wave oblique propagation through horizontally stratified quiet atmosphere for various thermospheric parameters
c13 A69-26101
Initial hydrodynamic phase of hypervelocity impact analyzed by computer program using eigenvector approach
[NASA-TR-R-298] c32 N69-24765
EINSTEIN EQUATIONS
Einstein field equations solutions generated via static spherically symmetric mass and charge distributions
c23 A69-32053
EJECTORS
Jet effects on boattail pressure drag of isolated ejector nozzles at Mach 0.60 to 1.47
[NASA-TM-X-1785] c01 N69-26976
ELASTIC BARS
Development of lattice model for composite materials
[NASA-CR-1322] c32 N69-22982
ELASTIC BODIES
Dynamic instability of solid bodies, using modal vibration method to establish criteria on basis of equivalent energy conditions
c32 A69-16742
Continuum theory for wave propagation in elastic composite solid with elastic microinclusions
[NASA-CR-1321] c32 N69-21401
ELASTIC DAMPING
Loss factor and resonant frequency of viscoelastic shear damped structural composites
[NASA-CR-1269] c32 N69-17766
Dynamic stability of mechanisms with elastic couplings under vibratory impact
[NASA-TT-F-534] c15 N69-35859
ELASTIC DEFORMATION
Elastic displacements for edge cracked plate specimens used as crack extension indicator in plane strain fracture toughness measurements
c32 A69-16433
Digital computer program for analyzing elastic and plastic deformations and creep strains in solid and hollow cylindrical bodies
[NASA-TM-X-1723] c32 N69-16115
Elastic and plastic analyses of hail damage to aircraft surfaces
[NASA-TN-D-5363] c32 N69-33420
ELASTIC PLATES
Response of infinite elastic plates to axisymmetric initial velocity distributions with application to hypervelocity impact
[NASA-TN-D-5118] c32 N69-23448
ELASTIC PROPERTIES
Mechanical anisotropy of polyethylene terephthalate and relation to molecular structure and cold drawing
c18 A69-16489
Dislocation model of strength of elastically inhomogeneous crystalline materials based on elastic interactions between dislocations and periodic fluctuations of shear modulus
c17 A69-20557
Compatibility conditions for strain measures of theory of micromorphic elastic solids
[NASA-CR-1236] c26 N69-10817
Integral equation method with continuous functions for calculating boundary stress components in plane elasticity
[NASA-CR-1273] c32 N69-19030
Determination of micromorphic material constants from elastic properties of constituents
[NASA-CR-1320] c32 N69-21569
Vibrations of turbomachine rotors and methods for determining optimal hydraulic damping mounts, vibrations of systems with friction, and self induced vibrations of compressor blades
[NASA-TT-F-547] c02 N69-36326
ELASTIC SCATTERING
Elastic scattering of slow electrons by negative H and positive Li ions, calculating differential cross sections and phase shifts
c24 A69-12924
Differential cross sections for elastic scattering of 600 Mev protons from He 3 between 19 and 45 degrees
c24 A69-13464
Elastic scattering cross sections for 21-MeV incident protons measured for nuclei differing in mass, determining optical model potential
c24 A69-35489
Proton-antiproton high energy elastic scattering by bosons exchange, introducing vertex functions for nonlocal Lagrangian
c24 A69-39467
Diatomic molecules rotational excitation calculated from electron molecule elastic scattering parameters in fixed nuclei approximation
c24 A69-39665
Intermediate energy protons elastic and quasi-elastic scattering from light nuclei, correlating p-D, p-He-3, p-p and p-He-4 data with various scattering models
c24 A69-43123
Differential cross section and polarization measurements for elastic scattering of high energy protons from light nuclei
c24 A69-43125
Elastic scattering of 21 MeV protons from nitrogen 14, oxygen 16, argon 40, nickel 58, and tin 116
[NASA-TN-D-4932] c24 N69-12840
Elastic and nonelastic scattering cross sections from 42 MeV alpha particles interacting with helium isotopes
[NASA-TN-D-5530] c24 N69-40979
ELASTIC WAVES
Harmonic content of pressure wave shapes in strong traveling transverse acoustic modes
[NASA-TM-X-1716] c12 N69-15371
Computer program for one dimensional elastic wave problems connected with structural members
[NASA-CR-1306] c32 N69-22983
ELASTOHYDRODYNAMICS
Elastohydrodynamic lubrication, discussing film

thickness and dependence on fluid hydrodynamics and contact zone deformation
c15 A69-11324
Elastohydrodynamic solution for ball torque spinning without rolling in nonconforming groove, showing increase in torque with stress and spinning and decreasing conformity
[ASME PAPER 69-LUBS-11] c15 A69-34381
Theory and clearance effects on stability of water lubricated herringbone-groove journal bearings
[NASA-TN-D-4883] c15 N69-10228
Elastohydrodynamic analysis and experimental speed effects on ball spinning friction coefficients and torque
[NASA-TN-D-5527] c15 N69-41210

ELASTOMERS
In situ vacuum testing requirement for valid measurement of vacuum induced changes in mechanical and thermal properties of various filled elastomers
c11 A69-22008

ELASTOPLASTICITY
Elastic-plastic and creep analysis predictions of core movement during operation of fast nuclear reactor
[NASA-TN-D-5012] c22 N69-16381
Elastoplastic stress-strain behavior at notch roots in sheet specimens under constant amplitude loading
[NASA-TN-D-5253] c32 N69-28038

ELECTRIC ARCS
Pulsed experiments on high powered constricted electric arc with axial flow performed by discharging transmission line
[GDC-DBE-68-008] c25 N69-17212
Convected balanced electric arcs in transverse magnetic fields
[NASA-CR-1267] c25 N69-18041
Exploding wire initiation and electrical operation of 40 kV system for arc heated drivers up to 10 feet long
[NASA-TN-D-5126] c11 N69-22989
Spectroscopic study of helium arc
[NASA-TN-D-5396] c25 N69-36755

ELECTRIC BATTERIES
Fuel cell /battery and solar array/ battery systems for manned Apollo Applications Program /AAP/ space vehicles, considering mission and power requirements
c03 A69-42244
NASA development work on high efficiency batteries for space electric power systems
[NASA-SP-172] c03 N69-18042

ELECTRIC BRIDGES
Analysis and design of inductors for protecting power transistors against current surges in inverter bridge circuits
[NASA-TN-D-4995] c10 N69-16198

ELECTRIC CHARGE
Signal electrode charge control of sealed Ni-Cd batteries, discussing signal voltage for overcharge control
c03 A69-23993

ELECTRIC CONTROL
Design and analysis of modular servoamplifier for fast response electrohydraulic control systems
[NASA-TN-D-4898] c03 N69-10068
Electric control and protection circuits for parallel operation of inverter-converter
[NASA-CR-1225] c10 N69-19003

ELECTRIC CURRENT
Backscattering due to collisions for electrons from emitter accelerated through positive ion sheath into plasma in thermionic diodes
c09 A69-17773
Modified first order theory of magnetosphere boundary shape incorporating effects of neutral sheet currents of extended geomagnetic tail
c13 A69-21661
Near cathode magnetic field effect on instability in linear Hall current accelerators, using geometry of field extending from anode to cathode region
[AIAA PAPER 69-381] c28 A69-21731
Current oscillations in semiinsulating O and Cr doped GaAs samples at room temperature, noting photoconductivity excitation spectra
c26 A69-21753
Boundedness theorem, thresholds, and stationary values in modified Huxley-Hodgkin model for electric current flow through cell membrane
[NASA-CR-1272] c19 N69-21143

ELECTRIC DIPOLES
Dipole shielding factor in coupled Hartree-Fock approximation for atomic S state
c23 A69-12179
Hydromagnetic radiation characteristics of electric and magnetic dipoles in homogeneous anisotropic cold plasma, obtaining field components and wave propagation modes
c13 A69-42905

ELECTRIC DISCHARGES
Sulfur dioxide-helium laser pulsed and CW submillimeter outputs
c16 A69-24005
Plasma generation using large V-groove cathode discharge
[NASA-TN-D-5269] c25 N69-29140

ELECTRIC EQUIPMENT TESTS
Design, fabrication, and testing of 12-kilowatt inductor alternator, voltage regulator-exciter, and parasitic loading speed controller - summary
[NASA-TN-D-4874] c03 N69-10088
Pretesting techniques of suppliers and users and effects on electroexplosive devices
[NASA-CR-1203] c15 N69-10298

ELECTRIC FIELDS
Dipole shielding factor in coupled Hartree-Fock approximation for atomic S state
c23 A69-12179
Electron beam meter application as lunar surface electric field detector, discussing breadboard model and performance characteristics
c14 A69-13221
Electric field effects on thermal annealing of electron irradiation damage in p-channel MOSFET device
c09 A69-16562
Trapped particles drift velocity in time dependent meridional magnetic and perpendicular electric field
c25 A69-20809
Electrothermal instabilities for explanation of MPD arc thrustor rotating spoke phenomenon, noting agreement with experimental results
[AIAA PAPER 69-231] c28 A69-21254
Pulsed glow discharges in He and He-H mixtures for high current density, noting electric field and wall potential distributions
c25 A69-23660
Time dependent convection electric fields as agents for diffusing trapped magnetospheric radiation inward toward earth, discussing one dimensional diffusion equation
c29 A69-28936
Electric fields and electron work functions, surface potentials and number density distributions in selected metals surfaces determined using free electron model
c26 A69-36045
Ionospheric currents geophysical dc electric field measurement from sounding rockets, indicating anticorrelation with auroral luminosity
c13 A69-38508
Dirac equation in external electromagnetic fields, deriving solution for constant orthogonal electric and magnetic fields encountered in plasma transport
c23 A69-41357

ELECTRIC GENERATORS
Design, construction, testing, and control devices for high-field electromagnets
[NASA-TN-D-4910] c23 N69-10889
Development of static inverters or converters operating electrically in parallel for space vehicle applications
[NASA-CR-1224] c03 N69-16379
Pump and seal parameters for helical groove, hermetically sealed pump and bearing rotor
[NASA-TN-D-5225] c15 N69-24791
Upgrading of electronic power supply for greater reliability in aerospace use
[NASA-TM-X-1875] c03 N69-35763
Single shaft Brayton rotating unit for 2 to 10 kilowatt space power generation system
[NASA-TM-X-1869] c03 N69-39238

ELECTRIC MOTORS
Magnetic core logic circuit system for bidirectional stepping motor drive voltage power supply control in proper phase and time sequence
c09 A69-11000
ELECTRIC NETWORKS
Analysis of commutated networks employing feedback circuits
[NASA-TN-D-4893] c10 N69-10755
Modern network theory applications to analysis of complex systems
[NASA-TN-D-5511] c19 N69-40088
ELECTRIC POTENTIAL
Transient electro-osmosis of water in capillary tubes for pumping and generation modes, analyzing response to step change in pressure or voltage change under external loading
c06 A69-14862
Voltage divider network board composed of composite carbon resistors for measurement of terminal voltage of 3 MeV Dynamitron electron accelerator recalibration
c11 A69-17705
Computerized design parameters for realizable overdriven bimode varactor frequency doubler based on charge-voltage relationship at break point
c09 A69-37299
Potential electrical response of p-n junction to mechanical strain
[NASA-CR-1366] c26 N69-29724
ELECTRIC POWER PLANTS
Selected conference papers on NASA technology utilization for electric power industry
[NASA-SP-5057] c03 N69-12575
Turboalternator gas bearing system for spacecraft electric power production
[NASA-CR-1292] c15 N69-19775
ELECTRIC PROPULSION
NASA program in electric propulsion, noting applications for spacecraft position control and for small automated interplanetary spacecraft
[AIAA PAPER 69-248] c28 A69-21216
Advanced reconnaissance electric planetary spacecraft /AREPS/ concept for repeated coverage of Mars or Venus surface, using solar-photovoltaic system
[AIAA PAPER 69-253] c30 A69-21244
Liquid mercury cathode thrustors characteristics satisfying constraints imposed by solar flux variations with distance from sun
[AIAA PAPER 69-237] c28 A69-21246
NASA long range planning of primary electric propulsion for automated space program
[AIAA PAPER 69-247] c28 A69-21251
Propellant condensation on surfaces near electric rocket exhaust, calculating particle arrival rates, backflow and desorption energies
[AIAA PAPER 69-270] c28 A69-21252
Solar and nuclear electric power technology for electric propulsion
[AIAA PAPER 69-826] c03 A69-32709
Minimal electric propulsion systems for interplanetary spacecraft, discussing payload, reduced trip time and low thrust systems for Jupiter flyby
[AIAA PAPER 69-499] c28 A69-32714
Electric propulsion systems for manned planetary exploration flights, discussing arc jet, ion and plasma engines
c28 A69-35108
Interplanetary probe missions with solar electric propulsion systems
[NASA-TN-D-5293] c30 N69-29738
ELECTRIC PULSES
Passive circuit to transform voltage of indefinitely repeated positive or negative pulses using transistors, diodes and magnetic cores
c09 A69-10564
Pulsed experiments on high powered constricted electric arc with axial flow performed by discharging transmission line
[GDC-DBE-68-008] c25 N69-17212
Transformer of closely spaced pulsed waveforms having nonzero average value
[NASA-TN-D-5473] c09 N69-38776
ELECTRIC RELAYS
Relays - Conference, Oklahoma State University, April 1969
c09 A69-28042
Electric relays requirements for spacecraft with magnetic field constraints
c09 A69-28046
Sealed and unsealed relay coils temperature rise at simulated outer space air pressure levels
c09 A69-28048
ELECTRIC ROCKET ENGINES
SERT 2 thrustor hollow cathode durability tested in bell jar
[AIAA PAPER 69-304] c28 A69-21224
Mercury electron bombardment thrusters, discussing mission, design, ground tests, components and thrust vectoring
c28 A69-26787
Historical developments in aviation and astronautics including liquid propellant rocket engine design, electric rocket engines, aircraft engines, and inertial guidance
[NASA-TT-F-540] c34 N69-31836
ELECTRIC SPARKS
Spectrochemical analysis of cobalt-base superalloys by liquid-layer solid-sample spark technique
[NASA-TM-X-1753] c06 N69-20853
ELECTRIC TERMINALS
Computer program for generation of test patterns for multiterminal devices and networks
c08 A69-39604
ELECTRIC WIRE
Flat conductor cable technology, discussing design, manufacture, specifications, etc
[ASME PAPER 69-DE-8] c03 A69-28855
ELECTRICAL FAULTS
Gas breakdown model for analyzing breakdown of Ce vapor filled crack in thermionic trilayer insulator
c03 A69-21840
Second breakdown and other thermal instabilities analyzed by heat flow equation, obtaining stability criteria predicting reduced power dissipation for transistor at low currents
c09 A69-31618
Proton induced voltage breakdowns in polymeric materials
[NASA-TM-X-1688] c18 N69-10066
ELECTRICAL IMPEDANCE
Admittance of parallel plate waveguide aperture with infinite flange illuminating metal sheet, using wedge diffraction theory and integral transform method
c09 A69-12328
Air gap tolerances effect on admittance of TEM mode dielectric and plasma coated slot antennas determined by variational method
c09 A69-24986
Multiplexer network synthesis based on arbitrary divisibility of frequency range and obtainability of input impedance at all frequencies
c09 A69-38530
VHF cavity backed cylindrical gap antenna input tuning impedance and equatorial radiation patterns controlled by cavity adjustments
c09 A69-40698
Waveguide fed rectangular aperture antenna with dielectric plug load, describing admittance resonant perturbation due to excited TE mode
c09 A69-41589
Admittance of parallel plate aperture illuminating displaced dielectric-dielectric boundary
[NASA-TN-D-5038] c07 N69-19114
ELECTRICAL MEASUREMENT
Voltage divider network board composed of composite carbon resistors for measurement of terminal voltage of 3 MeV Dynamitron electron accelerator recalibration
c11 A69-17705
Thermal contact resistance measurement at various ambient pressures compared with theoretical predictions with each parameter analyzed over interface by computer program
[AIAA PAPER 69-629] c33 A69-33299
ELECTRICAL PROPERTIES
Electrical properties and high energy radiation effect on Pyrrone polymers
[NASA-CR-1367] c18 N69-29559

Physical, mechanical, and electrical properties of 55-Nitincl - nickel-titanium alloy
[NASA-CR-1433] c17 N69-36367
Large thin film cadmium sulfide solar cell electrical characteristics over ranging temperatures and radiant intensities
[NASA-TM-X-1899] c03 N69-38767

ELECTRICAL RESISTANCE
Voltage divider network board composed of composite carbon resistors for measurement of terminal voltage of 3 MeV Dynamitron electron accelerator recalibration
c11 A69-17705
Time varying resistance wire to arrest oscillations in pulsed capacitor discharge circuit, deriving over, under and critical damping conditions
c09 A69-41228

ELECTRICAL RESISTIVITY
Coaxial three coil probe measuring local electrical conductivity and velocity in plasma streams, discussing operations in electrolytes and axisymmetric plasma stream
[AIAA PAPER 69-327] c25 A69-28264
Lunar dynamic response to discontinuities in interplanetary magnetic field to determine electrical conductivity and internal temperature
c30 A69-31442
Measurement and interpretation of Hall coefficient and resistivity of semiconductors
[NASA-TM-X-1711] c26 N69-14086
Deuterium concentration effect on electrical resistivity of palladium-deuterium system
[NASA-TN-D-4970] c26 N69-14565
Solubility of oxygen in tantalum determined by resistivity technique
[NASA-CR-1276] c17 N69-19886
Absorption of hydrogen by palladium and electrical resistivity of hydrogen-palladium system
[NASA-TN-D-5441] c26 N69-37272
Electrical conductivity of lanthanum fluoride single crystal with calcium impurities
[NASA-TN-D-5505] c26 N69-40056
Friction, wear, and contact resistance of gold alloys and electroplated electric gold contacts
[NASA-CR-1447] c17 N69-40057

ELECTROCARDIOGRAPHY
Soviet handbook on operation principles, use, and installation of electrocardiographs and electromedical apparatus for therapeutics
[NASA-TT-F-523] c05 N69-27577

ELECTROCHEMICAL CELLS
Electrochemical generators for space application - Conference, Paris, December 1967
c03 A69-21034
Electrochemical generators for space applications - Conference, Paris, December 1967
c03 A69-32405
NASA development work on high efficiency batteries for space electric power systems
[NASA-SP-172] c03 N69-18042
Electrochemical evaluation of electrode organic electrolyte combinations for rechargeable battery systems
[NASA-CR-1434] c03 N69-36829

ELECTROCHEMISTRY
Electrochemical behavior of the aluminum electrode in molten salt electrolytes
[NASA-TN-D-5503] c06 N69-40240

ELECTRODEPOSITION
Internal stress and deposit hardness of nickel electrodeposited containing controlled quantities of meta-benzenedisulfonic acid
[NASA-TN-D-5188] c17 N69-36697

ELECTRODES
Neutral buoyancy microelectrode for prolonged recording from single nerve units
c05 A69-11865
Signal electrode charge control of sealed Ni-Cd batteries, discussing signal voltage for overcharge control
c03 A69-23993
High performance light weight electrodes for hydrogen oxygen fuel cells
[NASA-CR-1216] c03 N69-14397
Electrochemical evaluation of electrode organic electrolyte combinations for rechargeable battery systems
[NASA-CR-1434] c03 N69-36829
Electrochemical behavior of the aluminum electrode in molten salt electrolytes
[NASA-TN-D-5503] c06 N69-40240

ELECTRODYNAMICS
Laser beam interactions with free electrons
[NASA-TN-D-5205] c16 N69-25357

ELECTROENCEPHALOGRAPHY
EEG monitor helmet for aircraft or flight simulator programs, discussing sensing and transmitting system
c05 A69-26553
Meaningful comparisons between single stimulus EEG records and average evoked potential
c05 A69-40163

ELECTROHYDRAULIC FORMING
Fast response electrohydraulic valve-controlled piston servo systems
[NASA-TN-D-5388] c03 N69-34652

ELECTROLYSIS
Water electrolysis, discussing oxygen generators for spacecraft prototype cells and testing
c05 A69-12987
Water electrolysis rocket engine performance tests
[NASA-TM-X-1737] c28 N69-19017
Solid electrolyte electrolysis of carbon dioxide and water as oxygen regeneration system for long manned space flights
[NASA-CR-1359] c05 N69-28099

ELECTROLYTES
Effects of temperature and electrolyte concentration on performance of fuel cell
[NASA-TN-D-5154] c03 N69-22940
Nuclear magnetic resonance and electron paramagnetic resonance techniques for aprotic electrolytes
[NASA-CR-1425] c06 N69-36413

ELECTROMAGNETIC ABSORPTION
Optical absorption coefficients for triphenylmethylarsonium tetracyanoquinodimethan complex single crystal, evaluating reflectance
c26 A69-10934
Picosecond light pulse measurement by two photon excitation of photographic film
c14 A69-20165
Reflection and transmission measurements on as grown surfaces of tetracyanoquinodimethan, obtaining optical constants by Kramer-Kronig method
c26 A69-35477
Absorption coefficient measurement for hydrocarbon gases for He-Ne laser beam at 3.39 microns, tabulating coefficients, noting variations from spectroscopic data
c16 A69-42192

ELECTROMAGNETIC COMPATIBILITY
Electromagnetic compatibility, - IEEE Conference, Asbury Park, New Jersey, June 1969
c09 A69-42215

ELECTROMAGNETIC FIELDS
Wave fields and coupling of RF power to ion cyclotron waves in finite length thermal collisional plasma column
c25 A69-13114
Dirac equation in external electromagnetic fields, deriving solution for constant orthogonal electric and magnetic fields encountered in plasma transport
c23 A69-41357

ELECTROMAGNETIC INTERACTIONS
Magnetic torque resulting from interaction between magnetic properties of spacecraft and ambient magnetic field
[NASA-SP-8018] c31 N69-30339

ELECTROMAGNETIC INTERFERENCE
Electromagnetic interference /EMI/ created by noise coupling through conductive paths, discussing responsibility for control within systems management
c07 A69-18944
Phase-lock loop demodulator ability to acquire and remain locked on signal under noise and pulse interference
c10 A69-42230

ELECTROMAGNETIC NOISE
Electromagnetic interference /EMI/ created by noise coupling through conductive paths, discussing responsibility for control within systems management
c07 A69-18944

Optical parametric noise in water by ruby laser beam for phase matched four photon process
c23 A69-21751
ELECTROMAGNETIC PROPERTIES
Lunar Explorer 35 measurements of lunar surface electromagnetic properties, magnetic fields and solar wind-moon interactions
c30 A69-38379
ELECTROMAGNETIC PUMPS
Cb-1Zr pumped sodium loop tests to evaluate loop components, EM pump, pressure transducers, and instrumentation techniques
[NASA-CR-1135] c03 N69-11373
Properties and uses of liquid metal reactor fuels, including heat transfer processes in variously shaped channels, boiling and condensation of metals, and reactor control equipment
[NASA-TT-F-522] c33 N69-30507
ELECTROMAGNETIC RADIATION
Solar electromagnetic radiation spectral distribution from ground level, rocket and satellite observations to obtain value of energy received at top of atmosphere
c29 A69-21645
Multiple scattering in Kapitza-Dirac effect describing electron scattering by standing electromagnetic wave, noting transition probability less than unity
c23 A69-25323
Reflection coefficient of symmetric parallel plate waveguide operating in TEM mode illuminating lossless dielectric layer, using wedge diffraction and geometrical optics methods
c09 A69-34802
ELECTROMAGNETIC SHIELDING
Proton dose in receiver behind combination electromagnetic and material shield, calculating dose for Van Allen and solar proton event spectra
c22 A69-31522
ELECTROMAGNETIC SPECTRA
Radiometric measurements of atmospheric attenuation in electromagnetic spectrum
[NASA-TN-D-5087] c07 N69-22949
ELECTROMAGNETIC WAVE FILTERS
Waveform distortion resulting from adjacent channel crosstalk and from amplitude and phase nonlinearity in channel filters in DSB/SC telemetry link
c07 A69-19130
Computerized telemetry filter design
[NASA-SP-3049] c08 N69-35816
ELECTROMAGNETIC WAVE TRANSMISSION
Proportionality between log-amplitude variance and 7/6 power of wavenumber for horizontal propagation from spherical wave transmitter to point detector
c16 A69-19641
ELECTROMAGNETISM
Proposed electromagnetic exploration of moon
[NASA-SP-174] c30 N69-33595
ELECTROMECHANICAL DEVICES
Development of automatic quality control device for measuring welded joints
[NASA-TN-D-5304] c15 N69-33800
ELECTROMIGRATION
Dielectric overcoating effects on electromigration Al interconnections, showing dependence on thickness and surface passivation
c09 A69-32889
ELECTROMOTIVE FORCES
Thermal electromotive force change for thermocouples in high temperature, low pressure environments for 3700 hours
[NASA-TN-D-5287] c14 N69-29196
ELECTRON ACCELERATORS
Voltage divider network board composed of composite carbon resistors for measurement of terminal voltage of 3 MeV Dynamitron electron accelerator recalibration
c11 A69-17705
Mercury electron bombardment thrusters, discussing mission, design, ground tests, components and thrust vectoring
c28 A69-26787
Artificial aurora generated at 100 km altitude by electron beam fired downward from Aerobee 350 rocket above 230 km along earth magnetic field lines
c13 A69-34365
Composite carbon resistor characteristics used for accelerator terminal voltage measurement
[NASA-TM-X-1718] c24 N69-14398
ELECTRON BEAM WELDING
Plasma electron beam for welding, deriving beam current from secondary emission by ion bombardment, discussing gas pressure, equipment and applications
c15 A69-35555
ELECTRON BEAMS
Electron beam meter application as lunar surface electric field detector, discussing breadboard model and performance characteristics
c14 A69-13221
Artificial aurora generated at 100 km altitude by electron beam fired downward from Aerobee 350 rocket above 230 km along earth magnetic field lines
c13 A69-34365
Electron beam fluorescence probe and afterglow investigation for hypersonic He flow visualization, observing qualitative structure
c11 A69-35722
Electron beam technique of measuring molecular rotational and vibrational temperatures of nitrogen in hypersonic tunnel using air as test gas
[NASA-TN-D-4892] c33 N69-10932
Noise in axisymmetric convergent electron beams
[NASA-TN-D-5212] c10 N69-24918
Bremsstrahlung production due to electron beam bombardment
[NASA-CR-1383] c24 N69-34541
Energy conversion and distribution of spiraling electron beam using retarding field analyzer
[NASA-TN-D-5490] c09 N69-41208
ELECTRON BOMBARDMENT
Bremsstrahlung production due to electron beam bombardment
[NASA-CR-1383] c24 N69-34541
Performance of two electron bombardment thrusters with axial magnetic field and superimposed cusp magnetic field
[NASA-TN-D-5448] c28 N69-36844
ELECTRON CAPTURE
Experimental measurements of two electron capture for negative ion production in atmospheric gases
[NASA-CR-1406] c24 N69-38564
ELECTRON COUNTERS
Solid state detector for electron spatial distribution measurements on OGO-F satellite, discussing design emphasizing reliability
c09 A69-36676
Planar thermal ion and electron trap experiments on Explorer 31 satellite, measuring ion and electron density and temperature and ionic composition
c14 A69-37878
ELECTRON DENSITY (CONCENTRATION)
Electron density measurement technique for dense thick steady state plasmas using swept microwave interferometer
c25 A69-12349
Electron number density LF oscillations for ionized gas identified with periodic solutions to neutral and charged particle plasma continuity equations
c25 A69-24315
Electron concentration enhancement in upper atmosphere at polar latitudes, noting three independent zones and relation to magnetic local time
c29 A69-28938
Free electron model for electron work functions and number density distributions and surface potentials in metals
c26 A69-29009
Quiet solar wind model with magnetic field numerically calculated, obtaining coronal electron densities and angular momentum near earth
c29 A69-34301
Electron temperature, density and magnetic disturbances measurements at 1000 km compared with visual observations during 25-26 May 1967 magnetic storm and aurora
c13 A69-34954

Electric fields and electron work functions, surface potentials and number density distributions in selected metals surfaces determined using free electron model
c26 A69-36045
Atomic nitrogen collisional ionization and recombination rates under assumed quasi-steady nonequilibrium distribution of electron state populations
c24 A69-43700
Electron density oscillations in ionized neon, helium, and deuterium gases
[NASA-TN-D-4950] c25 N69-14525
Computation of topside ionograms from electron concentration profiles
[NASA-TN-D-5052] c13 N69-23557
Electrothermal instabilities effects on Brayton and Rankine cycle magnetohydrodynamic space power generation systems
[NASA-TN-D-5461] c03 N69-37883
Langmuir and interferometric measurements on electron concentration in arc heated wind tunnel using air and nitrogen
[NASA-TN-D-5500] c25 N69-39302

ELECTRON DENSITY PROFILES
Electrothermal instabilities of ionization region of nonequilibrium MHD generator in presence of magnetic field
c25 A69-21919
Solid state detector for electron spatial distribution measurements on OGO-F satellite, discussing design emphasizing reliability
c09 A69-36676
Topside ionogram reduction for ionospheric electron density determination, using geomagnetic strength at all heights, iteration and change of variables
c13 A69-37864
Electron density profiles from topside ionograms compared to ground based sounding results, discussing error corrections
c07 A69-37865
Global electron density distribution morphology in topside ionosphere during sunspot minimum from Alouette 1 and 2 ionograms
c13 A69-37867
LF oscillations in electron number density of ionized deuterium, Ne and He identified from particle continuity equation
c24 A69-40759
Ionization rate limiting processes behind strong shock waves in pure N, plotting electron density profile diagrams
c12 A69-43367

ELECTRON DIFFRACTION
Low energy electron diffraction analysis of quartz fiber adhesion to rhenium crystal surface
[NASA-TN-D-5229] c17 N69-25363
Low energy electron diffraction study of adhesion of various materials to nickel surface
[NASA-TN-D-5247] c17 N69-26258
Adhesion of gold on copper planes studied with low energy electron diffraction
[NASA-TN-D-5290] c26 N69-29407

ELECTRON DIFFUSION
Fast electron diffusion in stochastic magnetic field, obtaining diffusion coefficient as function of ratio of correlation time to Larmor period
c25 A69-20807
Relativistic solar electron detection in interplanetary space during July 7, 1966 proton flare event, noting energy spectrum and time history
c29 A69-23766

ELECTRON EMISSION
Electron emitter cooling and plasma heating of thermionic converters noting effects of plasma density, diode spacing, etc
c03 A69-13127
Study of discharge from mercury vapor fed hollow cathode
[NASA-TN-D-4966] c28 N69-17847
Physical model for behavior of thermionic arc spots on MHD generator cathode
[NASA-TN-D-5414] c25 N69-35732

ELECTRON ENERGY
Nocturnal electron concentrations and temperature at Manitoba measured by rocket-borne Langmuir probe, compared with F 1 region
c29 A69-14008
Electron, ion and neutral particle temperatures of upper atmosphere
c13 A69-14975
Electron cooling rates in midlatitude and auroral zone thermosphere measured by probe rockets
c13 A69-16267
Rotational energy conversion of neutron star into relativistic electrons energy suggested by increasing period of pulsating radio source in Crab Nebula
c30 A69-21454
Synchrotron and X ray emission generation from upper chromosphere electrons during solar flares
c29 A69-22203
Radar backscatter and rocket profiles of ionospheric electron temperature, noting agreement in daytime flight measurements
c29 A69-25162
Molecular vibration absorption spectra from variation of field emitted electron energy distribution due to inelastic electron-molecule interaction at metal-vacuum interface
c24 A69-26097
Suprathermal electrons energy distributions as function of magnetic latitude in polar ionosphere obtained by Explorer 31 satellite observation
c29 A69-28963
Low energy electron precipitation data at northern high latitudes obtained from satellite low altitude polar orbit
c29 A69-28964
Rocket measurements of upper F region electron temperature and density profiles, for particle and energy balance of ionosphere topside, noting diffusive equilibrium
c29 A69-31975
Ion, electron and neutral temperatures from ion composition distribution, assuming no change in vertical distribution within horizontal distance between upleg and downleg measurements
c29 A69-31990
Energy spectrum of secondary electrons and fluorescent efficiency in 3914 A band, obtaining ionization cross section
c29 A69-32315
Electron temperature, density and magnetic disturbances measurements at 1000 km compared with visual observations during 25-26 May 1967 magnetic storm and aurora
c13 A69-34954
Cylindrical electrostatic probes on Alouette 2 and Explorer 31 satellites used in intersatellite comparison of directly measured ionospheric electron temperature and density
c14 A69-37876
Ionospheric parameters of ion and electron density and temperature and ionic species compared by direct measurement probes on Explorer 31 satellite
c13 A69-37882
Topside ionosphere response to magnetic storms, using Explorer 22 satellite electron concentration and temperature measurements
c13 A69-42438
Nighttime protonosphere thermal balance from Alouette 2 electrostatic probe measurements of electron temperature and concentration in magnetosphere
c13 A69-43181
Electron temperature instabilities in entrance region of magnetohydrodynamic generator
[NASA-TM-X-1761] c25 N69-20875
Bremsstrahlung spectra from bombardment of typical spacecraft materials by monoenergetic electrons
[NASA-CR-1377] c24 N69-33416

ELECTRON FLUX DENSITY
Satellite measurements of suprathermal electrons at conjugate sunrise, indicating photoelectron escape from production level and movement along geomagnetic lines into conjugate ionosphere
c29 A69-25144
Inner radiation zone including data on electrons, protons and heavier particles and results from high altitude nuclear tests
c29 A69-27144

Low energy electron precipitation data at northern high latitudes obtained from satellite low altitude polar orbit
c29 A69-28964
Suprathermal electron flux in lower latitudes and polar region analyzed from measurements by retarding potential analyzers on Explorer 31 satellite
c29 A69-37880
IMP 4 satellite measurements of cosmic ray electrons in interplanetary space compared to predictions of electron intensity from interstellar proton-electron collisions
c29 A69-42667

ELECTRON GAS
Quantum theory of electron gas with anomalous magnetic moments in intense magnetic fields, noting pair creation from thermodynamic energy in system
c24 A69-19782
Thermodynamic approach to equation of state of magnetized Fermi gas, deriving energy eigenvalues of free electron in magnetic field
c30 A69-25107
Ferromagnetism stable state in degenerate electron gas and magnetic fields in gravitationally collapsed bodies based on total microscopic magnetic moments associated with Landau level electrons
c30 A69-38600

ELECTRON IMPACT
Electron impact ionization cross sections for second quantum level of atomic H, using Born exchange approximation and Vainshtein approximation
c24 A69-17138
Hydrogenic atoms ionization by high energy electrons, discussing cross sections for ejected electrons and total energy
c24 A69-20738
Electron impact cross sections for diatomic molecule ionization and excitation from modified Gryzinski theory, discussing results from molecular models
c24 A69-22249

ELECTRON IRRADIATION
High voltage mercury electron bombardment ion thruster power efficiency
[ECS PAPER 170D] c28 A69-16233
Electric field effects on thermal annealing of electron irradiation damage in p-channel MOSFET device
c09 A69-16562
Electron radiation damage in MOSFET devices using bias temperature treatments
c26 A69-16877
Cross sections computed for excitation and ionization of atoms and ions by electrons, using peaking approximation to evaluate Coulomb-Born matrix approximation
c24 A69-20206
Internal friction, Young modulus and resistivity measurements for stage I interstitials in electron irradiated tungsten
c17 A69-28682
Discharge chamber plasma processes in electron bombardment ion thrustors, considering factors affecting thrustor performance
[AIAA PAPER 69-494] c28 A69-32735
Luminescence spectra of aromatic polymers, monomers and dimers under high energy electron excitation using molecular resonance model
c26 A69-32792
Unfilled Pyrrone prepared from powder into molded parts for flexural tests at elevated temperatures observed for stability to electron irradiation in air
c18 A69-35529
Electron irradiation effect on resolution of lithium-drifted silicon semiconductor detectors
[NASA-TN-D-4901] c14 N69-10933
Energy and angular distribution of electrons transmitted through silicon targets
[NASA-TN-D-5075] c24 N69-19113
Performance of various oxide magazine cathodes in Kaufman thrusters
[NASA-TN-D-5074] c28 N69-19980

ELECTRON MASS
Zr doped superconducting ceramic strontium titanate, noting effective electron mass variations and transition temperature
c26 A69-27400
Polarons large to nearly small transitions, studying ground state mass dependence on bare electron mass, electron-phonon interactions model, superconducting strontium titanate, etc
c26 A69-37280

ELECTRON MICROSCOPES
X ray fluorescence and electron microprobe for determining thin film thickness
c09 A69-19582
Plastic backing films removal from carbon electron microscope replicas by maintaining specimens in horizontal position
c14 A69-21651
Scanning electron mirror microscope advantages over electron mirror and scanning electron microscopes for examining integrated circuits
c14 A69-32891
Scanning electron microscopy for reliability studies in semiconductor devices
c26 A69-35788

ELECTRON MOBILITY
Radiation fields from energetic electron moving in helical orbit in magnetoactive plasma, using Maxwell equations
c30 A69-39965
Electron transport chain of monovalent and divalent cations and of polyamines, studying effects on menadione reductase activity to determine salt dependence
c04 A69-41077

ELECTRON PARAMAGNETIC RESONANCE
Nuclear magnetic resonance and electron paramagnetic resonance techniques for aprotic electrolytes
[NASA-CR-1425] c06 N69-36413

ELECTRON PHONON INTERACTIONS
Polarons large to nearly small transitions, studying ground state mass dependence on bare electron mass, electron-phonon interactions model, superconducting strontium titanate, etc
c26 A69-37280

ELECTRON PLASMA
Electron density oscillations in ionized neon, helium, and deuterium gases
[NASA-TN-D-4950] c25 N69-14525

ELECTRON PRECIPITATION
Low energy electron precipitation data at northern high latitudes obtained from satellite low altitude polar orbit
c29 A69-28964

ELECTRON PROBES
Electron microprobe analysis of potassium feldspar in Weekerco Station meteorite
c30 A69-14979
Electron microprobe analysis of vanadium in presence of titanium by compositional measurement of chromite in chondritic meteorites
c06 A69-18419
Electron beam fluorescence probe and afterglow investigation for hypersonic He flow visualization, observing qualitative structure
c11 A69-35722

ELECTRON SCATTERING
Elastic scattering of slow electrons by negative H and positive Li ions, calculating differential cross sections and phase shifts
c24 A69-12924
Ionizing shock front structure in monatomic gas, considering atom-atom and electron-atom collisional ionization rates
c12 A69-13138
Backscattering due to collisions for electrons from emitter accelerated through positive ion sheath into plasma in thermionic diodes
c09 A69-17773
Multiple scattering in Kapitza-Dirac effect describing electron scattering by standing electromagnetic wave, noting transition probability less than unity
c23 A69-25323
Diatomic molecules rotational excitation calculated from electron molecule elastic scattering parameters in fixed nuclei approximation
c24 A69-39665

Semiempirical collision model for plasmas
[NASA-TR-R-310] c25 N69-23787
Bremsstrahlung production due to electron beam bombardment
[NASA-CR-1383] c24 N69-34541
ELECTRON TRANSFER
Electron transport of Halobacterium cutirubrum, discussing spectrophotometric identification of cytochromes
c04 A69-19481
Flavoprotein/cytochrome b/559/ role as branch of Halobacterium electron transport in DPNH oxidase determined by salt dependence of reduced DPNH
c06 A69-37101
ELECTRON TRANSITIONS
Coulomb approximation for dipole and quadrupole transitions, calculating tables for radial matrix elements
c24 A69-10901
Electronic transition moment for C /Swan/ bands measured in shock tube in carbon dioxide and argon mixtures
c24 A69-12833
Doublet electronic states of benzyl radical, discussing configuration-interaction calculations and transition predictions
c24 A69-13321
Multiple scattering in Kapitza-Dirac effect describing electron scattering by standing electromagnetic wave, noting transition probability less than unity
c23 A69-25323
Oscillator strengths and wavelengths of X ray and EUV transitions in highly ionized iron line spectra
c29 A69-27554
Computer program to predict spectra from electronic transitions of diatomic molecules and atoms, noting line intensity distribution by Voigt profile
c24 A69-35239
Autoionized resonance transitions of He at 206.2-192.2 A using He continuum produced by capillary spark, also producing He II line spectra
c23 A69-42149
Excited states of xenon nuclei formed in beta decay of iodine and cesium isotopes
[NASA-TN-D-5329] c24 N69-30074
ELECTRONIC EQUIPMENT
Electronics and aerospace systems - IEEE Conference, Washington, D.C., September 1968
c07 A69-13176
IEEE Conference - San Antonio, April 1969
c07 A69-39437
Electronic position indicator for latching solenoid valves in SNAP 8 ground test facility
[NASA-TM-X-1760] c14 N69-20874
Upgrading of electronic power supply for greater reliability in aerospace use
[NASA-TM-X-1875] c03 N69-35763
ELECTRONIC EQUIPMENT TESTS
Metal oxide semiconductor integrated circuits, showing failure rates and degradation causes
c09 A69-31851
ELECTRONIC MODULES
Modularized static ac and dc inverters and converters for aerospace electrical power conditioning systems, discussing circuit functions and performance tests
c03 A69-42292
ELECTRONICS
NASA civil aviation electronics research program, discussing feasibility of V/STOL aircraft all-weather operations
c34 A69-16718
Space electronics, telemetry, antennas, computers - IEEE Conference, Cocoa Beach, Florida, November 1968
c07 A69-25288
ELECTRONS
Phonons, electrons and protons in ferro-paraelectrics and hydrogen bonded ferroelectrics, examining higher frequency optical and lower frequency dielectric properties
c26 A69-32262
Electron-cesium atom collision probability for momentum transfer
[NASA-TM-X-1897] c24 N69-38773
ELECTROPHOTOMETERS
Rocket-borne photoelectric photometers for UV observations of Saturn, using interference filters
c30 A69-22216
ELECTROPHOTOMETRY
Spectral and electrophotometric studies of upper atmosphere - airglows, atomic oxygen, hydroxyl emission, helium line spectra, auroras, and solar cycle effects on magnetosphere
[NASA-TT-F-530] c13 N69-16539
ELECTROSTATIC PRECIPITATORS
Rocket measurements of primary auroral particles energy spectra indicating spectral structure acceleration peaks associated with electrostatic fields
c13 A69-38490
ELECTROSTATIC PROBES
Nocturnal electron concentrations and temperature at Manitoba measured by rocket-borne Langmuir probe, compared with F 1 region
c29 A69-14008
Integrated charged particle energy spectra from gridded electrostatic analyzers, relating retarding potential curve to particle floating potential, kinetic temperature, etc
c25 A69-20521
Data distortion elimination by improved superimposing of sinusoidal audio frequency signal on dc voltage of automatic Langmuir probe second derivative plotters
c14 A69-32855
Cylindrical electrostatic probes on Alouette 2 and Explorer 31 satellites used in intersatellite comparison of directly measured ionospheric electron temperature and density
c14 A69-37876
Cylindrical electrostatic probe measurements on Alouette 2 and Explorer 31, considering implications for future missions
c14 A69-37877
Study of discharge from mercury vapor fed hollow cathode
[NASA-TN-D-4966] c28 N69-17847
ELECTROSTATIC PROPULSION
Research and development program in annular slit colloid thrustor technology, proving thrustor feasibility by performance tests
[AIAA PAPER 69-287] c28 A69-21257
ELECTROSTATIC SHIELDING
Dipole shielding factor in coupled Hartree-Fock approximation for atomic S state
c23 A69-12179
ELECTROTHERMAL ENGINES
Multijet electrothermal systems for attitude control and stationkeeping of synchronous communications satellite
[AIAA PAPER 67-723] c28 A69-12375
ELEMENTARY PARTICLES
Cosmic rays, elementary particle physics and astrophysics - Conference, Aligarh, India, December 1967
c29 A69-17268
ELEMENTS
Abundance compilations of elements due to nuclear processes, discussing carbonaceous chondrites character
c29 A69-38812
ELEVATION ANGLE
Airplane response to ground roughness from three-track runway and taxiway profiles by elevation angle measurements
[NASA-TN-D-5444] c02 N69-38770
ELLIPSOIDS
Analytic model resembling thick walled ellipsoid of revolution incorporating three dimensional shape of human left ventricle and ventricular wall thickness effects
c05 A69-26235
Relation between ellipsoidal velocity distribution function and macroscopic flow equations
[NASA-TN-D-5026] c12 N69-17827
ELLIPTICAL ORBITS
FORTRAN computer program for providing mission design data for elliptical orbits around Mars and Venus
[NASA-TN-D-5104] c30 N69-22571
Optimal rendezvous and transfers between close elliptical orbits

[NASA-TT-F-554] c30 N69-40592
ELLIPTICITY
Effects of angle of attack and bluntness on shock layer properties of cones at supersonic speeds
[NASA-TN-D-4909] c01 N69-10789
ELONGATION
Physical properties of near stoichiometric nickel-titanium alloy Nitinol and some structural-mechanical applications employing these properties
[NASA-CR-1232] c17 N69-11420
EMBRITTLEMENT
Ductile metal clads and coatings of silicides, aluminides and noble metals to protect Cr alloys against nitrogen embrittlement and air oxidation
c17 A69-26495
Hot salt stress corrosion of titanium alloys - generation of hydrogen and its embrittling effect
[NASA-TN-D-5000] c17 N69-16465
EMBRYOLOGY
Weightlessness effects on fertilized frog egg development onboard Gemini 8 and 12 manned orbital flights, discussing cell division, differentiation and embryogeneis
c04 A69-11084
EMISSION SPECTRA
Europium complexes high resolution emission spectra in relation to molecular configuration
c06 A69-10893
Diurnal variations of low latitude VLF emissions observed at Hiraiso, Japan
c07 A69-13900
Time dependent emission spectra from flashlamp pumped organic dye lasers recorded with image converter, comparing dyes characteristics
c16 A69-17901
Solar X ray and extreme UV spectra during flares, attributing intense emissions to optical transitions
c29 A69-22169
Iron line absence in emission spectrum of thermal X ray sources, constraining proposed thermal models
c29 A69-22231
Simultaneous HCN and HOH laser emission in pulsed discharge through mixture containing H, C, N, and O
c16 A69-26330
Thermal and free-free emission from planetary nebulae based on graphite grain model, discussing IR fluxes
c30 A69-27158
Spectral and electrophotometric studies of upper atmosphere - airglows, atomic oxygen, hydroxyl emission, helium line spectra, auroras, and solar cycle effects on magnetosphere
[NASA-TT-F-530] c13 N69-16539
EMISSIVITY
Emissivity coatings for low temperature space radiators
[NASA-CR-1420] c17 N69-36723
EMITTANCE
Solar absorptance, total hemispherical emittance and absorptance/emittance ratio for metals at cryogenic temperatures measured simultaneously with sinusoidally perturbed incident radiation
c33 A69-10847
Solar absorptance and hemispherical emmitance of metals at space conditions determined with cyclic incident radiation technique
[AIAA PAPER 69-60] c17 A69-18154
IR directional and hemispherical emittance of spacecraft thermal control coatings, comparing values determined by various measurement techniques
c14 A69-41633
High emittance coating materials for beryllium, niobium-zirconium compounds, and stainless steel used in spacecraft radiators
[NASA-CR-1278] c17 N69-18952
Emittance properties of hafnium oxide, cerium oxide, and iron titanate coatings on platinum rhodium alloy substrates
[NASA-CR-1413] c17 N69-35514
EMITTERS
Thermionic converter with chloride vapor deposited tungsten emitter and nickel collector
[NASA-CR-1416] c03 N69-32553
Thermionic converter with fluorine vapor deposited tungsten emitter etched to expose crystal planes
[NASA-CR-1381] c03 N69-35689
ENCAPSULATING
Irradiation of encapsulated fuel and fast neutron fluxes that simulate thermionic reactor conditions
[NASA-TM-X-1858] c22 N69-33273
ENCKE METHOD
Encke type analytical-numerical integration for solving differential equations of modified set of Lagrange planetary equations, obtaining satellite ephemeris for orbit prediction
[AIAA PAPER 69-908] c30 A69-39340
ENCLOSURES
Thermal radiation exchange between surfaces and enclosures
[NASA-SP-164-VOL-2] c33 N69-30317
ENDOCRINE SECRETIONS
Rats adrenal corticosterone concentrations changes in response to ACTH, determining response sensitivity dependence on time after hypophysectomy
c04 A69-39871
ENERGY ABSORPTION FILMS
Solar irradiance spectral distribution data normalized and combined with spectral absorptance of satellite surface coatings, obtaining absorbed energy for spectral range
c29 A69-21646
ENERGY BANDS
Impurity profiles and energy band diagram for cuprous sulfide-CdS heterojunction based on capacitance, Hall and electron microprobe measurements
c03 A69-13075
Impurity profile and energy band diagram for cuprous sulfide-cadmium sulfide heterojunction
[NASA-TN-D-5079] c26 N69-19781
ENERGY BUDGETS
Turbulence characteristics up to 150 m above ground, noting surface roughness length directional dependence, longitudinal turbulence spectra and turbulent energy budget
c20 A69-10695
Rocket measurements of upper F region electron temperature and density profiles, for particle and energy balance of ionosphere topside, noting diffusive equilibrium
c29 A69-31975
ENERGY CONVERSION
Plasma oscillation modes perpendicular to magnetic field used to study energy conversion by wave coupling across density discontinuity
c25 A69-20795
Rotational energy conversion of neutron star into relativistic electrons energy suggested by increasing period of pulsating radio source in Crab Nebula
c30 A69-21454
Isothermal diode as study basis for internal complex controlling thermionic energy conversion
c03 A69-21827
Solar simulator with xenon and krypton lamps designed for thermal balance tests, power conversion and material degradation experiments
c11 A69-30383
Energy conversion - Conference, Washington, D.C., September 1969
c03 A69-42236
ENERGY CONVERSION EFFICIENCY
Brayton-B generator for 2-10 kWe production, describing design, heat source/rejection, efficiencies and preliminary test data analysis
c03 A69-42278
Spacecraft solar cell near-maximum power operation by tracking optimum value with array temperature sensor
c03 A69-42303
ENERGY DISSIPATION
Nova outburst dynamics investigation by time dependent hydrodynamics computer program including energy transport by radiation and convection
c30 A69-30769
Second breakdown and other thermal instabilities analyzed by heat flow equation, obtaining stability criteria predicting reduced power dissipation for transistor at low currents

c09 A69-31618
Photospheric radiation field role in temperature inversion of stellar chromospheres with dominant H ion opacity, postulating mechanical energy dissipation
c30 A69-38173
Radio frequency induction heated plasmas with power deposition and energy removal
[NASA-CR-1312] c25 N69-22638
Inflatable landing system investigated for impact normal to smooth surface
[NASA-TN-D-5236] c32 N69-26223
Technique for measuring ion energy loss in vapor deposited materials
[NASA-TN-D-5430] c24 N69-36929

ENERGY DISTRIBUTION
Microscale fluctuations in interplanetary magnetic field, considering proton thermal energy and magnetic field energy densities
c30 A69-24100
Molecular vibration absorption spectra from variation of field emitted electron energy distribution due to inelastic electron-molecule interaction at metal-vacuum interface
c24 A69-26097
Suprathermal electrons energy distributions as function of magnetic latitude in polar ionosphere obtained by Explorer 31 satellite observation
c29 A69-28963
Energy and angular distribution of electrons transmitted through silicon targets
[NASA-TN-D-5075] c24 N69-19113
Molecular vibration spectra from field emission energy distributions
[NASA-TN-D-5423] c24 N69-36924
Energy conversion and distribution of spiraling electron beam using retarding field analyzer
[NASA-TN-D-5490] c09 N69-41208

ENERGY SOURCES
Oxygen supply inert diluent impurities effect on hydrogen-oxygen fuel cell performance
c03 A69-15310
Gamma heating rate measured by aqueous dosimeter converted to rate in thin tungsten detector in water shield through transport theory calculations, obtaining correction factors
c22 A69-18825

ENERGY SPECTRA
Absolute cross sections for coincidence detection of deuteron breakup by 42 MeV alpha particles, showing He 5 and Li 5 final state interaction peaks
c24 A69-13469
Charge and energy composition of particles in solar flare, discussing rigidity spectra of singly and multiply charged nuclei
c29 A69-17280
Integrated charged particle energy spectra from gridded electrostatic analyzers, relating retarding potential curve to particle floating potential, kinetic temperature, etc
c25 A69-20521
Energy spectra of carbon and oxygen nuclei in primary cosmic radiation, comparing results to earlier measurements and satellite observation
c29 A69-20632
Solar protons in magnetospheric tail after flare of July 7, 1966 with isotropic pitch angle distribution, expressing energy spectrum as exponential in rigidity
c29 A69-21699
Solar wind plasma observations in geomagnetospheric wake compared at 1000 and 500 earth radii, considering ion energy spectra and geomagnetic tail
c29 A69-26943
IQSY low energy galactic and solar cosmic ray observations made by various satellites and space probes, including hydrogen and helium energy spectra
c29 A69-30014
X ray energy spectrum from Crab Nebula and diffuse background on celestial sphere near galactic anticenter, noting spectral index
c29 A69-30759
Energy spectrum of secondary electrons and fluorescent efficiency in 3914 A band, obtaining ionization cross section
c29 A69-32315
He 2 excitation spectrum for interparticle potential using pair Hamiltonian with repulsive core and attractive well
c24 A69-33118
Rocket measurements of primary auroral particles energy spectra indicating spectral structure acceleration peaks associated with electrostatic fields
c13 A69-38490
Energy and angular distribution of electrons transmitted through silicon targets
[NASA-TN-D-5075] c24 N69-19113

ENERGY TRANSFER
Wave fields and coupling of RF power to ion cyclotron waves in finite length thermal collisional plasma column
c25 A69-13114
Radiative transfer by doubling very thin layers in problem of diffuse reflection from plane-parallel atmosphere eliminates numerically solving transfer equation
c33 A69-20064
Monte Carlo method application to heat transfer analysis including radiation, rarefied gas energy transfer and conduction
c33 A69-24457
Transformer for unilateral energy transfer using single domain uniaxial Permalloy film
c09 A69-39454
Impulsive fluid motion on flat plates pulsed with uniform heat flux
[NASA-TN-D-5249] c33 N69-26236
Energy transfer and ion cost in hydrogen plasma
[NASA-TN-D-5319] c25 N69-29905
Radiant energy transfer measurements in air plasma in reflected region of arc-driven shock tube
[NASA-CR-1390] c25 N69-38227

ENGINE CONTROL
30 cm diameter mercury bombardment low impulse thrustor development for potential space applications, discussing performance and control
[AIAA PAPER 69-238] c28 A69-21256

ENGINE DESIGN
Gas turbine compressor end seals, discussing air leakage paths, primary and secondary seals, design and efficiency
[ASLE PREPRINT 68AM 4B-4] c15 A69-27366
Shorter combustors for high temperature jet engines of high speed aircraft, considering lifetime, shroud scoops, overheating, warpage, etc
c28 A69-29433
M 3.5 two dimensional mixed compression inlet system with self restart using flexible variable ramp system
[AIAA PAPER 69-447] c28 A69-32732
Historical developments in aviation and astronautics including liquid propellant rocket engine design, electric rocket engines, aircraft engines, and inertial guidance
[NASA-TT-F-540] c34 N69-31836

ENGINE FAILURE
Steady state and dynamic distortion influence on performance and stall of turbofan engine, discussing compressor instrumentation, tests and simulation data
c28 A69-35175

ENGINE INLETS
Jet engine inlet noise control by modification of inlet guide vanes
c28 A69-15622
Inlet produced dynamic distortion and effects on stall margin of J-85 turbojet engine from supersonic wind tunnel tests
[AIAA PAPER 69-487] c28 A69-32676

ENGINE NOISE
Variation in engine noise for two landing approach configurations of jet transport aircraft
[NASA-TM-X-1896] c02 N69-38104

ENGINE STARTERS
M 3.5 two dimensional mixed compression inlet system with self restart using flexible variable ramp system
[AIAA PAPER 69-447] c28 A69-32732

ENGINE TESTS
Radial inflow gas turbine engine performance testing, discussing instrumentation, recording systems and calibration techniques

[ASME PAPER 69-GT-104] c14 A69-22522
Stator setting effect on single stage turbine performance, considering blade loss and surface velocity distribution
[AIAA PAPER 69-525] c28 A69-32686
Steady state airflow and afterburning performance characteristics of four J85-GE-13 turbojet engines
[NASA-TM-X-1742] c28 N69-17781
Flight performance of FW-4D solid propellant rocket motor on third stage of Delta 50 launch vehicle
[NASA-TN-D-4987] c28 N69-20876

ENGINEERING
IEEE Conference - San Antonio, April 1969 c07 A69-39437

ENGINEERING DRAWINGS
Steady state stress relaxation analysis of turbine blade cooling designs
[NASA-TN-D-5282] c28 N69-29321
Design of injectors and ablative thrust chambers for FLOX propane rocket engine with 1.2 inch throat diameter
[NASA-TN-D-5324] c28 N69-30560
Analytical model for use in design of pump inlet accumulators for prevention of liquid rocket longitudinal oscillation
[NASA-TN-D-5394] c28 N69-33319
Single shaft Brayton rotating unit for 2 to 10 kilowatt space power generation system
[NASA-TM-X-1869] c03 N69-39238

ENTHALPY
High enthalpy arc tunnel at Langley Research Center for simulating aerodynamic heating and forces during spacecraft reentry
[NASA-TN-D-5295] c11 N69-29981

ENTRANCES
Momentum integral method treating magnetohydrodynamic and simple hydrodynamic entrance flows
[NASA-TN-D-5215] c25 N69-24920

ENTROPY
Amplitude equations for magnetoacoustic and entropy waves diverging from normal MHD shock, obtaining energy flux ratios associated with incident and transmitted waves c25 A69-38242

ENVIRONMENT SIMULATION
Thermal control coatings, windows and mirrors for 1973 Mars Viking Lander vehicles under simulated Martian surface conditions
[AIAA PAPER 69-1023] c11 A69-40393
Hot-salt stress-corrosion of titanium alloy under simulated turbine engine compressor environment
[NASA-TN-D-5510] c17 N69-40242

ENVIRONMENT SIMULATORS
Magnetic air bearings for use as low friction overhead support fixtures in vertical lunar gravity simulator
[NASA-CR-1235] c05 N69-14213
Design and dynamic characteristics of vertical lunar gravity simulator with six degrees of freedom torso harness
[NASA-CR-1234] c05 N69-14979
Infrared radiation measurements in space environment simulator using integral equations
[NASA-TN-D-5166] c29 N69-28111

ENVIRONMENTAL CONTROL
Manned space stations for future space exploration, discussing earth-like environment, artificial gravity, human factors and time dependence c30 A69-25644
Remote sensing of environment - Conference, University of Michigan, Ann Arbor, April 1968 c14 A69-26974
Optimal design for improving thermal performance of existing spacecraft thermally actuated louver system by increasing open-to-closed emittance ratio
[AIAA PAPER 69-627] c33 A69-33269

ENVIRONMENTAL ENGINEERING
Mercury atmospheric models for preliminary environmental criteria to be used in spacecraft design and engineering trade-off studies
[AIAA PAPER 69-54] c30 A69-18042
Man and environment - Conference, Anaheim, California, April 1969 c11 A69-30356

ENVIRONMENTAL TESTS
Pressure and temperature dependence of slow crack growth in hardened steel in gaseous hydrogen environment c17 A69-10612
Solar simulator with xenon and krypton lamps designed for thermal balance tests, power conversion and material degradation experiments c11 A69-30383
Test program simulating solar wind outside magnetosphere to evaluate high melting point high density ceramic oxides as white thermal control coating pigments
[AIAA PAPER 69-641] c18 A69-33762
Handbook of solar simulation for thermal vacuum testing, discussing space environment, thermal control coatings, radiation sources, optical components, etc c11 A69-38894
Manned testing of EVA equipment in thermal-vacuum environment for qualification of Apollo extravehicular mobility unit, using lunar surface thermal simulator
[AIAA PAPER 69-992] c05 A69-40370
Orbiting Astronomical Observatory thermal test and evaluation program, discussing equipment and role in experimental design
[AIAA PAPER 69-995] c11 A69-40373
Mission sequential environment effects on Dacron parachute material mechanical properties
[AIAA PAPER 69-1018] c11 A69-40390
Solid film lubricants deposited by DC triode sputtering on Ni, Ni-Cr and Nb surfaces friction tested under ultrahigh vacuum conditions c15 A69-43126
Data from thermal vacuum tests of flight model spacecraft
[NASA-TN-D-4908] c31 N69-14010
Comparative evaluation of ablative materials in arc plasma jets
[NASA-CR-1207] c33 N69-14171
Liquid-vapor interface during outflow in weightlessness
[NASA-TM-X-1811] c12 N69-27954
NERVA control drum actuator tests in cryogenic temperature, nuclear radiation, and vacuum environments
[NASA-TN-D-5347] c22 N69-31870

ENZYME ACTIVITY
Ribulose diphosphate carboxylase and phosphoribulokinase activity in chemosynthetic autotrophs Thiobacillus thioparus and Thiobacillus neapolitanus, noting sedimentation and gel filtration characteristics c04 A69-11866
Cellular localization of acetyl-coenzyme A synthetase in yeast, noting enzyme distribution during aerobic growth on glucose c04 A69-15333
Identity between growth hormone degrading activity of pituitary gland and plasmin c04 A69-17105
Adrenal epinephrine and phenylethanolamine n-methyl transferase /PNMT/ activity in rat bearing transplantable pituitary tumor c04 A69-20374
Cation concentration requirement of halophilic NADH dehydrogenase for stability and maximum activity c06 A69-23127
Repeated blood sampling effect on plasma cholinesterase, acid phosphatase, alkaline phosphatase and hematocrit ratios in domestic chickens c04 A69-23158
NADH stimulation of ATP dependent carbon dioxide fixation in crude extracts of Hydrogenomonas facilis, considering allosteric regulation of phosphoribulokinase activity c04 A69-30036
Salts and organic solvents effect on halophile Halobacterium cutirubrum catalase, noting enzyme activity inhibition by cation and anion c04 A69-35291
Flavoprotein/cytochrome b/559/ role as branch of Halobacterium electron transport in DPNH oxidase determined by salt dependence of reduced DPNH c06 A69-37101

Substrate specificity of cathepsin C derived from rat liver, describing polymeric structure and behavior as acidic protein
c04 A69-37577
Electron transport chain of monovalent and divalent cations and of polyamines, studying effects on menadione reductase activity to determine salt dependence
c04 A69-41077
Compensatory hypertrophy effects on adrenal phenylethanolamine n-methyl transferase /PNMT/ activity in rats
c04 A69-41404
Respiratory system and oxygen metabolism regulation in man and animals
[NASA-TT-F-501] c04 N69-31401
Physical density and enzyme activity in coacervate biogenic molecular compounds
[NASA-TT-F-525] c04 N69-40324

ENZYMOLOGY
Ribulose diphosphate carboxylase and phosphoribulokinase activity in chemosynthetic autotrophs Thiobacillus thioparus and Thiobacillus neapolitanus, noting sedimentation and gel filtration characteristics
c04 A69-11866

EPHEMERIDES
Encke type analytical-numerical integration for solving differential equations of modified set of Lagrange planetary equations, obtaining satellite ephemeris for orbit prediction
[AIAA PAPER 69-908] c30 A69-39340

EPINEPHRINE
Adrenal epinephrine and phenylethanolamine n-methyl transferase /PNMT/ activity in rat bearing transplantable pituitary tumor
c04 A69-20374

EPOXY COMPOUNDS
Rotational spectrum of ethylene episulfoxide to determine molecular structure, particularly orientation of C sub 2 S ring
c06 A69-20535

EPOXY RESINS
Cryogenic mechanical properties of epoxy resins and glass/epoxy composites
c18 A69-16491
Compressive behavior of uniaxial filament reinforced epoxy tubes for aerospace structures, using hand layup method with Teflon mandrel and sleeve
c15 A69-22339
Compressive properties and weight saving of metals reinforced on surface with resin bonded fibers
[NASA-TN-D-4878] c17 N69-11012
Mechanical behavior of boron-epoxy and glass-epoxy filament-wound cylinders under various loads
[NASA-TN-D-5050] c18 N69-19825
Theory and test results of tensile strength of epoxy rings and belts reinforced by boron filaments
[NASA-TN-D-5053] c18 N69-19918
Visible and infrared transmitting properties of epoxy resin suitable for infrared detectors
[NASA-TM-X-1776] c18 N69-23843
Thermal outgassing tests on epoxy impregnated magnet coil
[NASA-TM-X-1813] c18 N69-28203

EQUATIONS OF MOTION
Equations formulated for space vehicle reaction to rotating machinery and internal mass motion, evaluating dynamics of cylindrical space station rotating about major axis
c30 A69-16476
Computing optimum flight profiles by Balakrishnan epsilon method, including equations of motion constraint in cost function to be minimized
[AIAA PAPER 69-75] c02 A69-18058
Aerodynamic coefficients from observed motion of body in flight, eliminating need for closed form solutions by employing numerical solutions to equations of motion
[AIAA PAPER 69-134] c01 A69-18161
Space vehicle docking dynamics and matrix equations of motion amenable to numerical solution on digital computer, using Hamilton principle and Lagrange multipliers
c31 A69-25501
Boussinesq approximation for compressible fluids, discussing perturbation pressure and velocities and vertical scale motions
c12 A69-26013
Equations of motion computerized simulation for attitude stabilization of orbiting telescope coupled to crew compartment
c14 A69-27952
Subsonic thermal convection or internal gravity waves from formal scale analysis of equations of motion in plane parallel atmosphere
c13 A69-33155
Vector integral extension to optimal trajectory coordinate multiplier systems with constant of motion demonstrated for coast-arc problem
[AIAA PAPER 69-907] c30 A69-39339
Transient vibration analysis of liner systems using transition matrices
[NASA-CR-1237] c32 N69-11008
Computer mechanization of reentry equations with four degrees of freedom
[NASA-CR-1249] c30 N69-13300
Equation of motion for predicting dynamic behavior of parachute payload system
[NASA-TN-D-4859] c02 N69-14504
Statistical analysis on influential aspects of wind profile disturbance design and dynamic response of space vehicles
[NASA-TN-D-4963] c32 N69-15632
Cushioncraft ground effect machine with heave response and control concepts
[NASA-TN-D-5202] c02 N69-23449
Computer simulation of six degrees of freedom flight equations
[NASA-CR-1344] c21 N69-26232
Equations of motion for rigid body rotor in linearized bearings
[NASA-CR-1391] c15 N69-36349
Matrix theorem and application to establishing independent coordinates for complex dynamical systems with constraints
[NASA-TR-R-326] c19 N69-38655

EQUATIONS OF STATE
Continuous time nonlinear dynamical system states variables estimated suboptimally from discrete noisy measurements with second order nonlinear filter, deriving dynamical equations
c10 A69-17939
Thermodynamic approach to equation of state of magnetized Fermi gas, deriving energy eigenvalues of free electron in magnetic field
c30 A69-25107
Thomas-Fermi approximation applied to calculation of equations of state and thermodynamic functions at high pressure from differential equations of statistical atom model
c24 A69-40186
Real helium hypersonic flow parameters for pressures to 3600 atmospheres and temperatures to 15,000 deg K applicable to hotshot type wind tunnels
[NASA-TN-D-4869] c12 N69-10443

EQUATORIAL ELECTROJET
Model equatorial electrojet with meridional current system constructed by spherical harmonic expansion for geomagnetic field, noting current loops
c13 A69-38084

EQUILIBRIUM
Ratio of equilibrium responses to transient responses both having equal excitation levels
[NASA-TN-D-5070] c32 N69-17258
Steady state stress relaxation analysis of turbine blade cooling designs
[NASA-TN-D-5282] c28 N69-29321
Rapid computation of equilibrium, chemical composition, and thermodynamic properties of argon-oxygen-hydrogen gas system
[NASA-TN-D-5416] c33 N69-36299

EQUILIBRIUM FLOW
Flow characteristics in two dimensional channel with rectangular cavity
[NASA-CR-1245] c12 N69-14095
Convected balanced electric arcs in transverse magnetic fields
[NASA-CR-1267] c25 N69-18041
Measured static aerodynamic forces for hypersonic flutter analysis on airfoil models in helium flow
[NASA-TN-D-5233] c01 N69-26271

EQUILIBRIUM METHODS
Equilibrium and free vibration problems of centrifugally stabilized disk and shell structures
[NASA-CR-1178] c32 N69-14477
EQUIPMENT SPECIFICATIONS
Design, fabrication, and testing of 12-kilowatt inductor alternator, voltage regulator-exciter, and parasitic loading speed controller - summary
[NASA-TN-D-4874] c03 N69-10088
ERBIUM
Thermodynamic properties of erbium hydrogen binary system evaluated for use as low pressure standard
[NASA-CR-1271] c14 N69-16099
EROSION
Module landing effects on lunar surface, deriving erosion law from Surveyor 5 engine firing test and vacuum test data
c30 A69-41388
Rocket engine evaluation of erosion and char as functions of fabric orientation for silica reinforced nozzle materials
[NASA-TM-X-1721] c28 N69-15475
Experimental and analytical studies of multiple liquid impact erosion of aluminum and stainless steel
[NASA-CR-1288] c15 N69-19786
Scaled lunar landing module jet erosion of simulated moon surfaces
[NASA-TN-D-5051] c31 N69-22630
ERROR ANALYSIS
Working breadboard model of planet tracker under various illuminating conditions, discussing hardware and closed loop tracking error analysis accounting for signal to noise effects
c21 A69-13214
Waveform distortion resulting from adjacent channel crosstalk and from amplitude and phase nonlinearity in channel filters in DSB/SC telemetry link
c07 A69-19130
Error analysis of high resolution balloon-borne temperature sensor and comparison of temperature data with simultaneous rawinsonde measurements
c14 A69-21642
Trajectory error propagation upper bounds in many body field for impulsive initial error, relating error to mission tolerances
c30 A69-21937
High energy scattering approximation valid from small to large angles, discussing errors and proton scattering by He
c24 A69-29008
Turbulence measurement errors with inclined hot wires described by equations, assuming normal component cooling includes greater tangential cooling
c14 A69-34442
Ac technique using lock-in power amplifier SNR for measuring galvanomagnetic and Shubnikov-de-Haas effects, noting error reduction
c14 A69-36375
Statistical error analysis of autonomous manned spacecraft navigation in long duration eccentric Mars orbits
[AIAA PAPER 69-880] c21 A69-39406
Regression analysis procedures for evaluating tracking system measurement errors
[NASA-TN-D-4826] c19 N69-14476
Error analysis of input noise temperature measurements of low noise amplifiers
[NASA-TN-D-4997] c07 N69-16162
Computer-generated computational errors in direction cosine matrix for strapdown inertial system
[NASA-TR-R-304] c21 N69-21402
Computer oriented error analysis of electrical circuits and nonlinear system performance
[NASA-TN-D-5112] c10 N69-22919
Terrain bias error analysis in pulse modulated planetary radar altimeters
[NASA-TN-D-5220] c21 N69-26195
Statistical analysis of satellite position with tracking error inclusion
[NASA-TN-D-5259] c30 N69-30611
Manipulation errors in finite element analysis of structures
[NASA-CR-1385] c19 N69-34360
Vibration induced attitude errors in strapdown inertial navigators
[NASA-CR-1396] c21 N69-34672
Volume-ratio system for vacuum gage calibration from 10 tc minus 8 to 10 torr
[NASA-TN-D-5406] c14 N69-35265
Atmospheric density measured by Explorer 17 density gages, and error analysis
[NASA-TN-D-5447] c13 N69-40924
ERROR CORRECTING DEVICES
Data distortion elimination by improved superimposing of sinusoidal audio frequency signal on dc voltage of automatic Langmuir probe second derivative plotters
c14 A69-32855
ERROR DETECTION CODES
Debugging computer programs in terms of localization and correction of errors
[NASA-CR-1397] c08 N69-35613
ERROR FUNCTIONS
Error reduction in identifying pilot describing function from flight test data by shifting input signal by pilot delay time in simulated computer model
c05 A69-11950
ERROR SIGNALS
Error reduction in identifying pilot describing function from flight test data by shifting input signal by pilot delay time in simulated computer model
c05 A69-11950
ESCAPE SYSTEMS
Flexible parawing lifting decelerator research data from wind tunnel and flight tests, noting manned space vehicle recovery and aircraft escape systems
[AIAA PAPER 68-967] c02 A69-43715
ESCAPE VELOCITY
Two burn spacecraft trajectories for escaping earth parking orbit
[NASA-TN-D-5011] c30 N69-17305
ESSA SATELLITES
Procurement and construction of automatic picture transmission ground station equipment for ESSA and Nimbus transmission
[NASA-SP-5080] c07 N69-31985
ESTERS
Oxygen concentration effects on oxidation of synthetic paraffinic and type II ester lubricants determined from ball bearing tests at 400 and 450 degrees F
c15 A69-35177
Oxygen concentration effects on ester lubricant degradation during high temperature bearing test
[NASA-TN-D-5262] c15 N69-26311
ESTIMATES
Continuous time nonlinear dynamical system states variables estimated suboptimally from discrete noisy measurements with second order nonlinear filter, deriving dynamical equations
c10 A69-17939
Recursive equation for estimating variance of sequential random numbers
[NASA-TN-D-5465] c19 N69-38178
ESTIMATING
Suboptimal estimator to Kalman filter containing scalar weighting factors
[NASA-TN-D-5082] c10 N69-21123
Integral transformations used in time variable parameter estimation
[NASA-TN-D-5194] c19 N69-23788
Sequential stochastic techniques for trajectory estimation
[NASA-CR-1360] c30 N69-40325
ETCHING
Thermionic converter with fluorine vapor deposited tungsten emitter etched to expose crystal planes
[NASA-CR-1381] c03 N69-35689
ETHYL ALCOHOL
Isothiocyanates and phenyl isocyanate reaction with hydrazinoethanol and hydrazinoethyl hydrogen sulfate
c06 A69-31808
EUCLIDEAN GEOMETRY
Complete approximation in Euclidean space of new boundary value problem
[NASA-TT-F-577] c12 N69-29235
EULER-CAUCHY EQUATIONS
Shape preserving expansion and contraction of

objects in E 3
[NASA-TN-D-5240] c19 N69-31303
EULER-LAGRANGE EQUATION
Encke type analytical-numerical integration for solving differential equations of modified set of Lagrange planetary equations, obtaining satellite ephemeris for orbit prediction
[AIAA PAPER 69-908] c30 A69-39340
EUROPIUM COMPOUNDS
Europium complexes high resolution emission spectra in relation to molecular configuration
c06 A69-10893
EVALUATION
Evaluation of contact analog display in landing approaches with helicopters
[NASA-TN-D-5241] c02 N69-27177
EVEN-EVEN NUCLEI
Absolute cross sections for scattering of 42 MeV alpha particles from even isotopes of cadmium
[NASA-TN-D-4948] c24 N69-14482
Hartree-Fock method used to study even-even nuclei in 2s-1d shell
[NASA-TN-D-5066] c24 N69-17976
EXCITATION
Lanthanum isotopes beta decay, analyzing excitation of near spherical daughter nuclei of barium isotopes
c24 A69-10100
Doublet electronic states of benzyl radical, discussing configuration-interaction calculations and transition predictions
c24 A69-13321
Diatomic molecules rotational excitation calculated from electron molecule elastic scattering parameters in fixed nuclei approximation
c24 A69-39665
EXHAUST FLOW SIMULATION
Hydrogen and methane combustion to simulate expansion of storable propellants
[AIAA PAPER 68-635] c33 A69-37188
EXHAUST NOZZLES
Location effect of power plants on aft-mounted supersonic cruise exhaust nozzles at transonic speeds in flight and wind tunnel
[AIAA PAPER 69-427] c01 A69-32769
Wind tunnel force and pressure tests of rocket engine nozzle extensions on X-15-2 model at supersonic and hypersonic speeds
[NASA-TM-X-1759] c01 N69-20873
EXHAUST SYSTEMS
Exhaust gas reingestion and inlet flow distortion in V/STOL lift engines, discussing static and wind tunnel testing using fighter configuration models
[AIAA PAPER 68-78] c01 A69-26762
EXHAUST VELOCITY
Axial velocities in ammonia MPD thrustor exhaust by measuring Doppler shifts of spectral lines emitted by plasma constituents
c28 A69-31890
EXHAUSTING
Liquid-vapor interface during outflow in weightlessness
[NASA-TM-X-1811] c12 N69-27954
EXISTENCE THEOREMS
Existence theorem using Pade approximation and matrices
[NASA-CR-1319] c19 N69-26248
EXOBIOLOGY
Extraterrestrial life possibility in solar system, noting Martian atmosphere and terrestrial life adaption to Mars simulations
c04 A69-11770
Mars biological exploration, discussing life detection, chemical and biological experimental strategy
[AIAA PAPER 68-1122] c04 A69-13700
Exobiology, Search for extraterrestrial life - AAS-AAAS Conference, New York, December 1967
c04 A69-32967
Mars exploration for life by Mariner flybys and orbiters and 1973 Viking landers
c30 A69-41611
Adaptation to hypoxia, acclimatization, and conditioning in human and animal subjects from Space Biology collection
[NASA-TT-F-580] c04 N69-32131
Bibliography on aerospace medicine and related biological research
[NASA-SP-7011/66/] c04 N69-37909
Gravitational and acceleration effects on man and organisms, and biological effects of radiation
[NASA-TT-F-528] c05 N69-38701
EXOSPHERE
Venus exospheric temperature for various composition models, discussing carbon dioxide concentration effects
c30 A69-12109
Model ion-exosphere for nonrotating planet with static dipole magnetic field generalized by permitting density and temperature variations over baropause
c13 A69-25284
Atmospheric models for exospheric temperatures of Mars and Venus based on photoionization heating efficiency
c30 A69-26020
Polar exosphere near solar maximum investigation by Explorer 19 and Explorer 24 drag satellites, considering density and atomic oxygen concentration measurements
c13 A69-31351
Ion depletion in high latitude exosphere, considering OGO 2 simultaneous observations of positive ion concentration, VLF signal propagation and whistlers
c29 A69-34939
Neutral exosphere model for nonrotating planet permitting barosphere uniform rotation at certain angular velocity, determining velocity distribution and density
c30 A69-40524
EXPANSION
Shape preserving expansion and contraction of objects in E 3
[NASA-TN-D-5240] c19 N69-31303
EXPERIMENTAL DESIGN
Solar simulator with xenon and krypton lamps designed for thermal balance tests, power conversion and material degradation experiments
c11 A69-30383
Interactive experimenter computer system software and hardware design considerations based on astronaut-machine/experimenter question-answer interactions
[AIAA PAPER 69-953] c08 A69-40335
Model design for simulation of space capsule landing on soils using similitude law
[NASA-CR-1210] c34 N69-13159
Objectives and experiment designs for Apollo telescope mount
[NASA-TN-D-5020] c30 N69-21526
Experiment design for measuring radio frequency interference between communication satellite and terrestrial microwave relay system
[NASA-TN-D-5041] c07 N69-26272
Design, calibration, and use of radiometers to measure spectral emission in ballistic range and shock tube experiments
[NASA-TN-D-5360] c14 N69-38144
EXPERIMENTATION
NASA Plum Brook Reactor Facility experimental program
[NASA-TM-X-1853] c22 N69-33132
Experiment requirements for manned earth orbiting biotechnology laboratory
[NASA-CR-1409] c05 N69-35540
EXPLODING WIRES
Exploding wire initiation and electrical operation of 40 kV system for arc heated drivers up to 10 feet long
[NASA-TN-D-5126] c11 N69-22989
EXPLORATION
Biogeochemistry applications in mineral prospecting
[NASA-SP-5056] c13 N69-10492
EXPLORER SATELLITES
NASA Small Astronomy Satellite /SAS/ program for radiation source detection
[NASA-TN-D-5099] c31 N69-21017
EXPLORER 17 SATELLITE
Atmospheric density measured by Explorer 17 density gages, and error analysis
[NASA-TN-D-5447] c13 N69-40924
EXPLORER 18 SATELLITE
IMP-1 experiment, describing design and

applications of SDP-3 computer
c08 A69-36265
EXPLORER 23 SATELLITE
Pegasus and Explorer 23 detector panels calibrated by determining particle perforation mass and velocity
[NASA-TR-R-321] c14 N69-36985
EXPLORER 29 SATELLITE
Evaluation of Goddard range and range rate system at Rosman by intercomparison with GEOS 1 long-arc orbital solutions
[NASA-TN-D-5036] c13 N69-28442
EXPLORER 31 SATELLITE
Cylindrical electrostatic probes on Alouette 2 and Explorer 31 satellites used in intersatellite comparison of directly measured ionospheric electron temperature and density
c14 A69-37876
Cylindrical electrostatic probe measurements on Alouette 2 and Explorer 31, considering implications for future missions
c14 A69-37877
Planar thermal ion and electron trap experiments on Explorer 31 satellite, measuring ion and electron density and temperature and ionic composition
c14 A69-37878
Plasma temperature and ion concentration profiles determined from simultaneous measurements by Alouette 2 and Explorer 31 satellites of electron density, temperature and ion abundance
c13 A69-37896
EXPLORER 35 SATELLITE
Lunar magnetic moment and surface field, discussing Explorer 35 field measurements
c30 A69-14005
Lunar Explorer 35 measurements of lunar surface electromagnetic properties, magnetic fields and solar wind-moon interactions
c30 A69-38379
Flight performance of Explorer 35 attitude control system
[NASA-TN-D-5187] c21 N69-27268
EXPLORER 40 SATELLITE
Explorer 40 satellite mathematical model and verification testing for close spacecraft flight temperature predictions
[SAE PAPER 690202] c33 A69-18305
EXPLOSIONS
Characteristics of liquid propellant explosions, analyzing detonation, shock wave formation and deflagration
c27 A69-14474
Saturn fireball thermal environment associated with liquid propellant explosions, using analytical model
c27 A69-14475
Blast shields testing
[NASA-TN-D-4894] c11 N69-10888
Nonlinear compressible flow problems - half-space of ideal compressible fluid motion due to arbitrary pressure front
[NASA-TT-F-560] c12 N69-27168
Explosive hazard evaluation of liquid oxygen liquid hydrogen propellants
[NASA-TN-D-5382] c27 N69-35321
EXPLOSIVE DECOMPRESSION
Biomechanical factors determining lung damage following explosive decompression of space suits in vacuum test chambers
[NASA-CR-1223] c05 N69-13969
EXPLOSIVE DEVICES
Pyrotechnic and explosive elements in space systems - Conference, Tarbes, France, July 1968
c27 A69-23003
EXPLOSIVE WELDING
Tensile data and photomicrographs of explosively bonded metal matrix composites interfaces
c15 A69-43452
EXPONENTIAL FUNCTIONS
Solution of differential equations by series of exponential functions
[NASA-CR-1294] c19 N69-17249
EXTERNAL STORES
Aerodynamic drag of external fuel tanks attached to X-15-2 airplane at Mach numbers of 1.6 to 2.3
[NASA-TM-X-1895] c01 N69-38065
EXTINCTION
Interstellar extinction models of classical Mie particles and quantum mechanical polycyclic aromatic molecules
c30 A69-23679
Extinction efficiency of graphite core interstellar grains with solid hydrogen and ice mantles, using theoretical models
c23 A69-29587
Positively charged diatomic hydrogen molecules interstellar extinction and photodissociation cross section in terms of formation mechanisms
c30 A69-42610
EXTRACTION
Comparison of extraction procedures using 1-nitroso 2-naphthol and dimethylglyoxime for spectrophotometric determination of palladium in titanium alloys
[NASA-TM-X-1767] c06 N69-20801
EXTRAPOLATION
Computerized Arrhenius equation component reliability extrapolation techniques
[NASA-TN-D-4902] c19 N69-13368
EXTRATERRESTRIAL ENVIRONMENTS
Soviet handbook of astronautics covering spacecraft and operating problems of near-earth spaceflight
[NASA-TT-F-500] c31 N69-24760
EXTRATERRESTRIAL LIFE
Extraterrestrial life possibility in solar system, noting Martian atmosphere and terrestrial life adaption to Mars simulations
c04 A69-11770
NASA Planetary Exploration Program to gather data on origin of solar system and life, discussing planetary evolution and extraterrestrial life
c04 A69-12804
Mars biological exploration, discussing life detection, chemical and biological experimental strategy
[AIAA PAPER 68-1122] c04 A69-13700
Exobiology, Search for extraterrestrial life - AAS-AAAS Conference, New York, December 1967
c04 A69-32967
Extraterrestrial life detection experiments integrated into single multipurpose space laboratory, including chemical analyses, metabolism identification, observation for molecular and/or cellular growth and replication
c05 A69-32970
Meteorites pigments identification as porphyrins for extraterrestrial life evidence, noting sample analyses of Orgueil, Murray, Cold Bokkeveld and Mokoia carbonaceous chondrites
c30 A69-39889
Mars exploration for life by Mariner flybys and orbiters and 1973 Viking landers
c30 A69-41611
Sequential analyses of planetary surface sample for extraterrestrial life detection, discussing chemistry, morphology, growth and metabolism for life attributes
c30 A69-41623
Observations and theoretical studies on Mars properties
[NASA-SP-179] c30 N69-16571
EXTRATERRESTRIAL MATTER
Extraterrestrial matter - Conference, Argonne, Illinois, March 1968
c30 A69-40083
Tektite origin theories, discussing Surveyor experiments effects on lunar geology and Tektite origin
c30 A69-40086
EXTRATERRESTRIAL RADIATION
Proton beams uniformity available at NASA synchrocyclotron designed for radiation biology research by simulating space radiation environment
c11 A69-15992
Extragalactic gamma ray fluxes predicted, discussing collisions, matter-antimatter annihilation and cosmological implications
c29 A69-24466
Corrections to previous papers on extragalactic gamma rays, discussing effects on various cosmological models
c29 A69-34168
Photodisintegration of ultrahigh energy cosmic rays by universal radiation field, analyzing implications on origin and propagation time

c29 A69-35006
Investigation of earth atmospheric composition, geomagnetism, extraterrestrial radiation, solar activity, and planetary atmospheres by satellite experiment and astronomical observations
[NASA-SP-195] c34 N69-38951
EXTRATERRESTRIAL RESOURCES
Lunar environment, bases, exploration, and extraterrestrial resources
[NASA-SP-177] c30 N69-22226
EXTRAVEHICULAR ACTIVITY
Hard space suit for use on planetary surfaces and extravehicular activity, discussing design, fabrication and mobility
c05 A69-12993
Space suit meteoroid protection for extravehicular activity, discussing Gemini and lunar surface EVA suits and bumper concept
[AIAA-PAPER-69-366] c05 A69-28298
Lithium peroxide utilization feasibility for oxygen supply and carbon dioxide control in extravehicular portable life support systems
[AIAA PAPER 69-620] c05 A69-33303
Manned testing of EVA equipment in thermal-vacuum environment for qualification of Apollo extravehicular mobility unit, using lunar surface thermal simulator
[AIAA PAPER 69-992] c05 A69-40370
Unstabilized astronaut, hand-held and integrated life support EVA maneuvering units tested in gimbaled six degree of freedom servo driven moving base simulator
[AAS PAPER 69-516] c05 A69-42850
Correlation study of simulation of Gemini extravehicular activity with flight results
[NASA-CR-1146] c05 N69-19902
Configurations for extravehicular activity work platforms for astronaut use in orbital assembly
[NASA-CR-1361] c31 N69-26993
Astronaut extravehicular work performance under simulated weightlessness conditions
[NASA-CR-1334] c05 N69-27266
Weightlessness simulation of Gemini extravehicular tasks using neutral-buoyancy underwater techniques
[NASA-TN-D-5235] c05 N69-28024
EXTREMUM VALUES
Trajectory error propagation upper bounds in many body field for impulsive initial error, relating error to mission tolerances
c30 A69-21937
EXTRUDING
Extruded prealloyed powder evaluation for two nickel-base alloys
[NASA-TN-D-5248] c17 N69-26192
EYE EXAMINATIONS
Electro-optical instrument for measuring pointing direction of human eye
[NASA-CR-1422] c05 N69-39212

G

F REGION
Rocket measurements of upper F region electron temperature and density profiles, for particle and energy balance of ionosphere topside, noting diffusive equilibrium
c29 A69-31975
Simultaneous solution of continuity and heat conduction equations for ionospheric electrons, ions and neutral species for studying F region magnetic storm behavior
c13 A69-32083
Atomic oxygen density role in ionospheric E and F region magnetic stability, noting heat loss effect of atomic excitation
c13 A69-32314
F 2 REGION
Spectrometric rocket measurements of ion concentrations between 200 and 630 km
c13 A69-31974
Causal and semiphenomenological theories concerning equatorial F 2 region, discussing electrodynamic drift theory and transequatorial winds
c13 A69-37888
F-111 AIRCRAFT
Jet engine compressor stalls in-flight investigation up to Mach 2 on F-111A by pressure sensors, noting steady state distortion role
[AIAA PAPER 69-488] c28 A69-32706
F-2 AIRCRAFT
Lifting body type M2-F1 and M2-F2 aircraft enabling astronauts to make own landings at choice airport
c02 A69-13367
F-8 AIRCRAFT
Flight tests of modified aileron direct lift control system during approach and landing of F8-C aircraft
[NASA-TN-D-4854] c02 N69-10371
FABRICATION
Compressive behavior of uniaxial filament reinforced epoxy tubes for aerospace structures, using hand layup method with Teflon mandrel and sleeve
c15 A69-22339
Materials research structural design cycle, discussing simultaneous optimization, constituent materials, fabrication process, load environment and mission constraints
c32 A69-42991
Determination of drag of fabrication-type surface roughness in turbulent boundary layer at transonic speeds
[NASA-TN-D-5004] c01 N69-16460
Development of air bearing lift pads
[NASA-TM-X-1724] c01 N69-16467
Fabrication of counterflow double wall tantalum-stainless steel mercury boiler
[NASA-TN-D-5092] c33 N69-23707
Influence of fabrication methods on compressive strength of titanium alloy skin stringer panels
[NASA-TN-D-5389] c15 N69-34707
Design, development, and testing of 1000 pound thrust FLOX-propane ablative rocket engine
[NASA-TM-X-1873] c28 N69-35847
FACTORIAL DESIGN
Blocked two level factorial experiment to measure radiolysis of water in water cooled reactors
[NASA-TN-D-5369] c19 N69-32319
FAIL-SAFE SYSTEMS
NASA flight safety research, discussing size effects on aircraft handling and built-in response to failure modes
c02 A69-19764
FAILURE
Reliability handbook for silicon monolithic microcircuits - failure mechanisms
[NASA-CR-1347] c09 N69-23226
Reliability handbook for failure analysis of silicon integrated microcircuits
[NASA-CR-1348] c09 N69-25328
FAILURE ANALYSIS
OGO program failure rate analysis with respect to cost, schedule and performance tradeoffs, considering component and systems design and reliability, prelaunch feedback, etc
c31 A69-34519
Failure analysis - IEEE Conference, Philadelphia, May 1969
c09 A69-35781
Linear prediction of structural failure criteria for uniaxial fiber composites
[NASA-TN-D-5367] c18 N69-33321
FAR FIELDS
Design method for far field sonic boom shock strength and impulse independent of body length and volume
[NASA-TN-D-5148] c01 N69-23927
FAR INFRARED RADIATION
Frequency and stability measurements in far IR laser region
c16 A69-18482
Far IR source in galactic center detected at 100 microns, noting thermal emission of interstellar dust grains as possible mechanism
c30 A69-22264
Balloon-borne instrumentation for detection of far IR extended emission regions and bright point sources, describing results of initial flights
c30 A69-27599
FAR ULTRAVIOLET RADIATION
Solar X ray and extreme UV spectra during flares, attributing intense emissions to optical transitions
c29 A69-22169

Diffusion pump oil reflectance and absorption coefficients measured in three thicknesses using light source, monochromator and detector
c23 A69-23647
Oscillator strengths and wavelengths of X ray and EUV transitions in highly ionized iron line spectra
c29 A69-27554
Diurnal and solar cycle variations of thermosphere density and temperature generated by solar EUV input and tidal wave, using two dimensional model
c29 A69-43003
Solar flare soft X ray and EUV emission spectra data obtained on OSO-3 satellite compared with centimetric radio bursts
c29 A69-43609

FAST NUCLEAR REACTORS
Elastic-plastic and creep analysis predictions of core movement during operation of fast nuclear reactor
[NASA-TN-D-5012] c22 N69-16381
Performance prediction for fast reactor with axially moving reflector control system
[NASA-TM-X-1911] c22 N69-40061

FATIGUE (MATERIALS)
Tensile and cyclic fatigue properties of graphite filament-wound pressure vessels at ambient and cryogenic temperatures
[NASA-TN-D-5354] c32 N69-31300

FATIGUE LIFE
Crack initiation prediction in high temperature components subjected to arbitrary thermal-mechanical cycling
c32 A69-28252
Rolling element fatigue life of ausformed steel balls
[NASA-TN-D-4954] c15 N69-14383
Cyclic life calculations of materials subjected to isothermal stress considering fatigue and creep
[NASA-TN-D-5317] c32 N69-29672
Creep rupture data for predicting thermal fatigue cracking of turbine blades or disks
[NASA-TN-D-5489] c32 N69-39393

FATIGUE TESTS
Ultrasonic detection and measurement of fatigue cracks in notched cylinders subjected to reversed axial cyclic loading
c14 A69-10113
Inclination effect of fatigue cracks on plane strain fracture toughness of 7075-T651 Al alloy, discussing cantilever bending
c32 A69-25958
Graphite fiber NOL rings and biaxial wound pressurized cylinders tested at ambient and cryogenic temperatures for tensile and cyclic fatigue properties
c18 A69-35521
Axial load fatigue crack propagation tests on Al alloy sheets for stress ratio effects
c17 A69-36435
Mechanical characteristics of flexible drive shaft coupling
[NASA-CR-1241] c15 N69-16104
High temperature fatigue tests conducted to determine bearing life of angular contact ball bearing elements
[NASA-TN-D-5002] c15 N69-16367
Crack toughness characteristics of high strength alloys for use in heavy sections of supersonic aircraft
[NASA-TN-D-4998] c32 N69-17275
Burst testing of tungsten tubing at high temperatures
[NASA-TM-X-1843] c17 N69-31889
Stress ratio effects on fatigue crack growth in sheet aluminum alloys
[NASA-TN-D-5390] c17 N69-34704

FATTY ACIDS
Acetate-2-C 14 conversion to C 14 carbon dioxide and C 14 fatty acids in rats with 2/3 of liver removed
c04 A69-35976

FEASIBILITY
Feasibility tests on liquid lubricants for inerted lubrication systems of advanced aircraft engines
[NASA-TN-D-5420] c15 N69-35788

FEED SYSTEMS
LOX prevalve accummulator system with He pressurant for prevention of POGO effect on Saturn 5
c31 A69-15298
Parabolic antenna properties generated by dual band circularly polarized focused two channel monopulse feed system, discussing tracking data from helicopter, Apollo 8 and Cassiopeia A
c07 A69-41752

FEEDBACK
Apollo-Saturn 5 propulsion and structure feedback loop, analyzing POGO components and Nyquist plot application
[AIAA PAPER 69-877] c31 A69-39403

FEEDBACK CIRCUITS
Feedback systems analysis, considering single phase and polyphase coupled and uncoupled commutation networks in forward loop and linear transfer function feedback loop
c10 A69-19853
Multiloop feedback in active distributed RC networks for low parameter sensitivity with low amplifier gain compared to single loop circuits
c10 A69-34679
Analysis of commutated networks employing feedback circuits
[NASA-TN-D-4893] c10 N69-10755

FEEDBACK CONTROL
Logarithmic variation criteria for stability of feedback systems with time varying gains
c10 A69-13073
Automatic closed loop distortionless control of magnetic field modulation using light sensitive resistor as one leg of attenuator
c09 A69-17708
Linear state variable feedback to obtain asymptotic stabilization of linear dynamic systems
c10 A69-17947
Feedback systems analysis, considering single phase and polyphase coupled and uncoupled commutation networks in forward loop and linear transfer function feedback loop
c10 A69-19853
Stability of systems with sector nonlinearities determined by converting feedback equation into positive operators equation and by introducing appropriate multiplier
c10 A69-25450
Differential synthesis technique application to design of multiaxis stability augmentation systems for aerospace vehicles
[AIAA PAPER 68-834] c31 A69-37156
Lifting body stability augmentation systems design, development, ground tests and flight data including frequency response, limit cycle and structural resonance
[AIAA PAPER 69-887] c02 A69-39413
Quadratic optimization applied to helicopter flight control design, assuming constant feedback gains and command step input with zero steady state error
c02 A69-43279
Problem of identifying input-output of pilot by measuring data from flight tests with pilot providing feedback control
[NASA-TN-D-5127] c05 N69-23842
Linear multivariable control system design using modern control theory, and application to coupled core reactor control
[NASA-CR-1345] c19 N69-29268

FELDSPARS
Electron microprobe analysis of potassium feldspar in Weekeroo Station meteorite
c30 A69-14979

FERMI SURFACES
Fermi surface topology effects on Nernst-Ettingshausen coefficient from measurements in magnetic fields to 3.3 tesla and 1.2-4.2 K temperatures in metallic tin
c26 A69-16357

FERRITES
Effects of lithium and oxygen losses on magnetic and crystallographic properties of spinel lithium ferrite
[NASA-TR-R-305] c06 N69-20775

FERROELECTRICITY
Phonons, electrons and protons in ferro-paraelectrics and hydrogen bonded ferroelectrics, examining higher frequency

optical and lower frequency dielectric properties
c26 A69-32262

FERROMAGNETISM
Ferromagnetism stable state in degenerate electron gas and magnetic fields in gravitationally collapsed bodies based on total microscopic magnetic moments associated with Landau level electrons
c30 A69-38600
Anisotropic Heisenberg ferromagnets in random phase and spin wave approximation
[NASA-TN-D-5286] c26 N69-29588
Physical properties of magnetic base ferrofluids
[NASA-CR-1407] c06 N69-33493

FERRY SPACECRAFT
Vehicles for lunar surface exploration and transportation including flying machines and wheeled vehicles
c30 A69-27908
Crew and passenger transportation to and from space station orbits, discussing cost reduction possibilities with current or future technology
c31 A69-39691
Low cost efficient shuttle system for personnel and cargo transport to earth orbit for NASA and DOD needs
c31 A69-39695

FIBER STRENGTH
Graphite fiber NOL rings and biaxial wound pressurized cylinders tested at ambient and cryogenic temperatures for tensile and cyclic fatigue properties
c18 A69-35521
Linear prediction of structural failure criteria for uniaxial fiber composites
[NASA-TN-D-5367] c18 N69-33321

FIBERS
Tensile and cyclic fatigue properties of graphite filament-wound pressure vessels at ambient and cryogenic temperatures
[NASA-TN-D-5354] c32 N69-31300

FIBROBLASTS
Mitotic synchronization of fibroblasts with metabolic retardants by chronophotography
[NASA-TN-D-5021] c04 N69-17248

FIELD COILS
Decoupling force exerted by magnetic forming Be coil assembly on metallic plate during forming
c14 A69-25310

FIELD EFFECT TRANSISTORS
Electric field effects on thermal annealing of electron irradiation damage in p-channel MOSFET device
c09 A69-16562
Electron radiation damage in MOSFET devices using bias temperature treatments
c26 A69-16877
Spacecraft analog to digital conversion system employing metal oxide semiconductor field effect transistors
[NASA-TN-D-5228] c08 N69-29478

FIELD EMISSION
Molecular vibration absorption spectra from variation of field emitted electron energy distribution due to inelastic electron-molecule interaction at metal-vacuum interface
c24 A69-26097
Molecular vibration spectra from field emission energy distributions
[NASA-TN-D-5423] c24 N69-36924

FIELD THEORY (PHYSICS)
Discontinuities in interplanetary magnetic field direction presented on mesoscale from Pioneer 6 observation, emphasizing distribution in time
c30 A69-29970
Einstein field equations solutions generated via static spherically symmetric mass and charge distributions
c23 A69-32053
Structure of matter, physical fields, evolution of earth and universe, solar activity and earth, and interaction of earth biosphere with physical fields
[NASA-TT-F-345] c13 N69-12384

FIGHTER AIRCRAFT
Jet fighter aircraft lateral directional stability at high angles of attack
[NASA-TN-D-5361] c02 N69-32337
Factors affecting flat spin characteristics of fighter aircraft with horizontal tail surfaces
[NASA-TN-D-5409] c02 N69-36807

FIGURE OF MERIT
Figures of merit for experimental silicon carbide backward diode operable to 1000 degrees K
[NASA-TN-D-5183] c09 N69-23556

FILAMENT WINDING
Glass, boron and graphite filament wound resin composites and liners for cryogenic pressure vessels
c18 A69-16488
Compressive behavior of uniaxial filament reinforced epoxy tubes for aerospace structures, using hand layup method with Teflon mandrel and sleeve
c15 A69-22339

FILAMENTS
Stress concentration around broken filaments in filament stiffened sheet
[NASA-TN-D-5453] c32 N69-38642

FILM BOILING
Hydrodynamic inlet conditions effect on film boiling and near critical hydrogen heat transfer, using data from electrically heated various geometry test sections
[ASME PAPER 69-HT-27] c33 A69-43541
Film-nucleate boiling transition for liquid nitrogen in vertical forced flow in electrically heated tube, discussing conduction model and agreement with visual experiment
[ASME PAPER 69-HT-26] c33 A69-43542
Heat transfer coefficients for film boiling from submerged spheres
[NASA-TN-D-5124] c33 N69-28318

FILM THICKNESS
Elastohydrodynamic lubrication, discussing film thickness and dependence on fluid hydrodynamics and contact zone deformation
c15 A69-11324
X ray fluorescence and electron microprobe for determining thin film thickness
c09 A69-19582
Dielectric overcoating effects on electromigration Al interconnections, showing dependence on thickness and surface passivation
c09 A69-32889
Analysis of flow stability of thin liquid film adjacent to high speed gas stream
[NASA-TN-D-4976] c12 N69-15630

FINENESS RATIO
Hypersonic aerodynamic characteristics of low fineness ratio variable geometry logistics spacecraft model
[NASA-TM-X-1701] c01 N69-13218

FINITE DIFFERENCE THEORY
Finite difference method for symmetric positive linear differential equations, discussing methods to solve finite difference equations generated
c19 A69-13370
Spherical caps axisymmetric static and dynamic buckling under load, using axisymmetric nonlinear elastic shell theory approximation and finite difference equations
[AIAA PAPER 69-89] c32 A69-18133
Boundary conditions for Tricomi equation in symmetric positive form, showing analytical and finite difference solutions
c19 A69-42792
Finite difference theory for transonic velocity calculations on blade-to-blade stream surface of turbomachine
[NASA-TN-D-5427] c01 N69-37521

FINS
Tables and graphs of functions for solving nonlinear constant area fin one dimensional heat transfer problem
[NASA-TN-D-5173] c33 N69-26975

FIRE PREVENTION
Ignition hazards in electrical circuits contaminated by glycol fluids, describing hazard detection by RF methods, decontamination procedures, safety checks, etc
c18 A69-36028

FISSION
Uranium carbides irradiation tests for control of nuclear fuels fission gas swelling
[NAA-SR-12629] c22 N69-22946

FISSION PRODUCTS
Fission product gas pressure calculated for uranium dioxide ceramic fuel elements
[NASA-TN-D-4823] c22 N69-10216
Analysis of cylindrical reactor fuel pin for clad stress caused by fission gases
[NASA-TN-D-5178] c22 N69-24802
Radial power tailoring for uranium dicxide-T-111 clad reactor with contained fission product gases
[NASA-TM-X-1795] c22 N69-25305
Source and cause of fuel element fission product leakage in reactor cooling water system at Plum Brook Reactor
[NASA-TN-D-5374] c22 N69-32317
Improved delayed neutron fission product monitor for operation in reactor coolant system
[NASA-TM-X-1886] c14 N69-38766

FIXED WINGS
Wind tunnel investigation of steady state aerodynamics of composite lift VTOL aircraft model combining rotary and fixed wings
[NASA-TN-D-5232] c02 N69-28097

FLAPS (CONTROL SURFACES)
Heat transfer and pressure distributions inside hinge line gap of wedge-flap combination at hypersonic speeds
[NASA-TN-D-4911] c01 N69-11009
Wind tunnel tests of large jet transport aircraft model with external flow jet flap
[NASA-TN-D-4928] c01 N69-14000
Auxiliary flap system tests using Boeing 367-80 transport aircraft and wind tunnels
[NASA-TN-D-5128-REV] c02 N69-31962

FLAT PLATES
Pressure and heating rate correlations for rocket exhausts impinging on flat plates and curved panels, generating axisymmetric real gas exhaust plumes
c33 A69-26781
Heat transfer and pressure distribution due to two-dimensional repetitive sine wave distortions on flat plate at Mach 20 in helium
[NASA-TN-D-4907] c12 N69-10804
Leading edge effects on laminar flat plate boundary layer and aerodynamic heating at Mach 10.4
[NASA-TN-D-5160] c12 N69-23467
Impulsive fluid motion on flat plates pulsed with uniform heat flux
[NASA-TN-D-5249] c33 N69-26236
Skin friction and heat transfer data for hypersonic turbulent layer on flat plates, wind tunnel wall, and cones
[NASA-TN-D-5089] c12 N69-29144
Transient condensing with freezing on nonisothermal inclined plate
[NASA-TN-D-5289] c33 N69-29598
Flow field measurements on flat plate with attached protuberances in supersonic turbulent boundary layer
[NASA-TN-D-5297] c12 N69-30071

FLAT SURFACES
Inviscid flow of two parallel slot jets impinging normally on surface
[NASA-TN-D-4957] c12 N69-14316
Exhaust recirculation effects produced by two heated jets impinging on ground plane
[NASA-CR-1307] c01 N69-34703

FLATTENING
Droplet wake minimization by surface tension changes
[NASA-CR-1368] c12 N69-24958

FLEXIBILITY
Unfilled Pyrrone prepared from powder into molded parts for flexural tests at elevated temperatures observed for stability to electron irradiation in air
c18 A69-35529
Frequency and critical speed analysis of rigid rotors on flexible foundations
[NASA-TN-D-4858] c32 N69-29159

FLEXIBLE BODIES
Mechanical characteristics of flexible drive shaft coupling
[NASA-CR-1241] c15 N69-16104
Design and test criteria regarding structural flexibility effects on spacecraft stability and control systems
[NASA-SP-8016] c31 N69-37030

FLEXIBLE WINGS
NASA research on flexible and stiffened flexible wings, discussing range of applicability, aerodynamic characteristics and wind tunnel results
c02 A69-15568

FLIGHT CHARACTERISTICS
Aerodynamic and flight characteristics of variable geometry entry spacecraft during subsonic wing deployment and landing
[AIAA PAPER 69-742] c01 A69-34407
Flight performance evaluation of Atlas Centaur launch vehicle AC-12 carrying Surveyor 3 lunar probe
[NASA-TM-X-1678] c31 N69-10295
Pilot rating scales and their use in assessing aircraft handling qualities
[NASA-TN-D-5153] c02 N69-22539
Postflight analysis of flight performance of Atlas Agena launch vehicle for Applications Technology Satellite ATS-2 mission
[NASA-TM-X-1800] c31 N69-27260
Flight performance of Explorer 35 attitude control system
[NASA-TN-D-5187] c21 N69-27268
Flight performance of Atlas Agena launch vehicles in support of Lunar Orbiter missions 3, 4, and 5
[NASA-TM-X-1859] c31 N69-37281
Flight performance of Atlas Agena launch vehicle in support of Applications Technology Satellite-3
[NASA-TM-X-1879] c31 N69-37840

FLIGHT CONTROL
Model performance index /PI/ providing criterion for approximating one dynamic flight control system by another based on geometrical representation of linear autonomous systems
[AIAA PAPER 69-885] c21 A69-39410
Quadratic optimization applied to helicopter flight control design, assuming constant feedback gains and command step input with zero steady state error
c02 A69-43279
Synthesis methods for manual aerospace control systems using digital programming and man machine performance data with application to supersonic transport design
[NASA-CR-1208] c02 N69-13185
Computer mechanization of reentry equations with four degrees of freedom
[NASA-CR-1249] c30 N69-13300
Flight tests of fluidic flight control system for aircraft
[NASA-TN-D-5298] c21 N69-30946
In-flight simulation to evaluate simultaneous use of attitude control for jet VTOL maneuvering
[NASA-TN-D-5342] c02 N69-32110
Iterative solution of boundary value problem for rapid optimization of multiple-burn rocket flights
[NASA-CR-1430] c30 N69-36439

FLIGHT HAZARDS
Light aircraft hazards due to trailing vortex generated by heavy transport aircraft, suggesting specific procedures for takeoff, landing and flight phase
[SAE PAPER 680220] c02 A69-14930

FLIGHT MECHANICS
Mechanics of low thrust space flight
[NASA-TT-F-507] c28 N69-33354

FLIGHT OPTIMIZATION
Computing optimum flight profiles by Balakrishnan epsilon method, including equations of motion constraint in cost function to be minimized
[AIAA PAPER 69-75] c02 A69-18058
Interplanetary midcourse velocity correction schedules optimization, discussing timing equations modifications, mission simulation and role of earth based radar
c21 A69-39646

FLIGHT PATHS
Computing optimum flight profiles by Balakrishnan epsilon method, including equations of motion constraint in cost function to be minimized
[AIAA PAPER 69-75] c02 A69-18058
Variational methods for determining optimum design and flight of rockets
[NASA-TR-R-297] c31 N69-15374

Computer simulation of six degrees of freedom flight equations
[NASA-CR-1344] c21 N69-26232

FLIGHT SAFETY
NASA flight safety research, discussing size effects on aircraft handling and built-in response to failure modes
c02 A69-19764
Air safety - Conference, Anaheim, October 1968
c02 A69-41127
Space station safety, discussing damage containment and control, escape and rescue, etc
[AAS PAPER 69-518] c31 A69-42842
Management system for safety in NASA Manned Space Flight Program, discussing hazard analyses and reduction precedence sequence
[AAS PAPER 69-522] c34 A69-42851

FLIGHT SIMULATION
Digital computers in space flight simulation and vehicle performance optimization, examining mission analysis
c30 A69-14519
Test facilities and techniques for low speed flight problems of aircraft handling qualities, stability, control and performance
c11 A69-15575
Low thrust mission simulation dependence on hardware definition, discussing power plant characteristics, jet velocity and thrustor efficiency
c30 A69-21204
Interplanetary low thrust mission analysis model, discussing major elements interactions
c30 A69-21206
Flight simulation requirements for reducing aircraft training flight time, discussing control system and instrument motion characteristics, visual simulation and critical maneuvers motion
c11 A69-41139
Numerical integration techniques for real time digital flight simulation
[NASA-TN-D-4900] c11 N69-11371
Pilots and flight simulator used in study of human visual sampling study
[NASA-CR-1258] c05 N69-14145
Simulation studies of supersonic transports in future air traffic control systems
[NASA-TN-D-4944] c21 N69-14382
Supersonic transport performance during real time simulated operations in future air traffic control system environments
[NASA-TN-D-5018] c02 N69-17257
Visual simulation image generation using flying spot scanner
[NASA-TN-D-5151] c11 N69-23194
In-flight simulation to evaluate simultaneous use of attitude control for jet VTOL maneuvering
[NASA-TN-D-5342] c02 N69-32110
Supersonic transport instrumentation and flight simulation
[NASA-TN-D-5280] c14 N69-32286
Infrared heating simulation of Mach 4.63 flight on X-15 horizontal stabilizer
[NASA-TN-D-5403] c33 N69-35949

FLIGHT SIMULATORS
NASA manned aerospace simulation techniques and equipment as used at Ames Research Center, noting applications to various types of manned vehicles
[ASME PAPER 69-DE-56] c11 A69-28844
Spacecraft wide angle attitude control system stability analysis, using air bearing table simulation
[AIAA PAPER 69-856] c31 A69-39384
Flight simulator with large lateral motion for large and supersonic transport aircraft, emphasizing reproduction of cockpit accelerations due to supersonic engine thrust loss
c11 A69-43044
Influence of angle of glide slope on accuracy of performing instrument approaches in simulator tests
[NASA-TN-D-4835] c21 N69-10056
Human transfer characteristics in flight and ground simulation for roll tracking task
[NASA-TN-D-5007] c05 N69-17814
Saturn 5 launch vehicle scale model tests for free vibration during first stage burn
[NASA-TN-D-5159] c32 N69-22932
Simulator program for defining in-flight experiment to evaluate manual control system for Saturn 1
[NASA-TN-D-5150] c21 N69-22936
Multimodality pilot model for visual and motion feedbacks derived from simulator program
[NASA-CR-1325] c05 N69-28071
Evaluation of six degrees of freedom motion simulator for Bell X-14A aircraft hovering characteristics
[NASA-TN-D-5383] c11 N69-35359

FLIGHT TEST VEHICLES
Flight test evaluation of small one man lunar flying device /POGO/, discussing vehicle control, pressure suit factors and piloting differences
[AIAA PAPER 68-240] c11 A69-12379

FLIGHT TESTS
Error reduction in identifying pilot describing function from flight test data by shifting input signal by pilot delay time in simulated computer model
c05 A69-11950
Lifting body entry vehicles in low speed flight test program for determining handling qualities, discussing M2-F2 glide flights
c02 A69-15571
Factors influencing development of both wind tunnel and flight test technology for determining aerodynamic derivatives of aircraft motions
c11 A69-15572
Optical design of Wolter type 1 glancing incidence X ray telescope for 6-100 A wavelength region, describing results of laboratory and rocket flight tests of prototype
c14 A69-21087
Ammonia resistojet stationkeeping subsystem onboard ATS 4 satellite, noting flight test data agreement with ground tests
[AIAA PAPER 69-296] c28 A69-21212
Newton-Raphson technique development for determining stability derivatives from flight data, noting use of a priori wind tunnel information
[AIAA PAPER 69-315] c02 A69-22379
Location effect of power plants on aft-mounted supersonic cruise exhaust nozzles at transonic speeds in flight and wind tunnel
[AIAA PAPER 69-427] c01 A69-32769
Biosatellite attitude control systems design development and flight test results for payload perturbing effects, discussing simulation activity
c31 A69-35094
Laboratory and flight tests of airborne solid state UHF telemetry transmitter, discussing miniaturized coaxial hardware from RF power conservation viewpoint
c07 A69-35996
Lifting body stability augmentation systems design, development, ground tests and flight data including frequency response, limit cycle and structural resonance
[AIAA PAPER 69-887] c02 A69-39413
Guidance and navigation flight tests, demonstrating system performance improvements by onboard inertial system communicating with external navigation aid
[AIAA PAPER 69-842] c21 A69-39429
Pioneer 9 deep space probe with telemetry link operated in coded mode with sequential decoding, discussing ground and flight test data
c07 A69-42522
V/STOL aircraft radar inertial navigation system, describing approach and landing phase flight test results
[AAS PAPER 69-401] c02 A69-42831
Flight tests of modified aileron direct lift control system during approach and landing of F8-C aircraft
[NASA-TN-D-4854] c02 N69-10371
Calculated and flight measured handling quality factors of three subsonic jet transports
[NASA-TN-D-4832] c02 N69-10495

IFR flight tests of Breguet 941 STOL transport
[NASA-TN-D-4939] c02 N69-13252
Flight tests with helicopters for studying manueverability
[NASA-TN-D-4931] c02 N69-14008
Flight performance of FW-4D solid propellant rocket motor on third stage of Delta 50 launch vehicle
[NASA-TN-D-4987] c28 N69-20876
Problem of identifying input-output of pilot by measuring data from flight tests with pilot providing feedback control
[NASA-TN-D-5127] c05 N69-23842
Atlas-Agena flight performance for Applications Technology Satellite-1 mission
[NASA-TM-X-1784] c31 N69-24038
Supersonic deployment and extraction of inflatable towed ballute decelerator
[NASA-TM-X-1773] c31 N69-26458
Flight investigation of lightweight helicopter to study feasibility of fixed collective pitch autorotations
[NASA-TN-D-5270] c02 N69-29232
Flight test performance of supersonic parachutes in low density environment
[NASA-TN-D-5296] c01 N69-30063
Flight tests of fluidic flight control system for aircraft
[NASA-TN-D-5298] c21 N69-30946
XB-70 aircraft flight tests of canard configurations
[NASA-TN-D-5359] c02 N69-32284
Systems developed for reducing pilot workload and tracking accuracy improvements during noise abatement landing approaches
[NASA-CR-1427] c02 N69-38657
Flight evaluation of tip turbine driven fans for lateral control in hovering VTOL aircraft
[NASA-TN-D-5491] c02 N69-38807
Boundary layer control and trailing edge flaps for direct-lift control
[NASA-CR-1426] c02 N69-38819

FLIGHT TIME
Flight simulation requirements for reducing aircraft training flight time, discussing control system and instrument motion characteristics, visual simulation and critical maneuvers motion
c11 A69-41139

FLIGHT TRAINING
Flight simulation requirements for reducing aircraft training flight time, discussing control system and instrument motion characteristics, visual simulation and critical maneuvers motion
c11 A69-41139

FLIGHT VEHICLES
Fracture design for airflight vehicles, discussing crack strength requirements and method for serviceability prediction
c32 A69-33563

FLOATING POINT ARITHMETIC
Hardware-software provisions for multiple precision floating point arithmetic
[NASA-TM-X-1885] c08 N69-36918

FLOW CHARACTERISTICS
Supersonic compressor blade sections performance prediction near maximum pressure ratio and efficiency by analyzing flow processes
[AIAA PAPER 69-522] c28 A69-32711
Flow simulation on wind tunnel test models for aerodynamic characteristics of aircraft design, discussing boundary layer and external flow coupling
[AIAA PAPER 69-660] c11 A69-33471
Flow characteristics and wall heat transfer in separated flow region of annular cavity at free stream hypersonic speed and high gas temperature
[AIAA PAPER 68-672] c01 A69-37185
Flow characteristics in two dimensional channel with rectangular cavity
[NASA-CR-1245] c12 N69-14095
Flow analysis to determine turbine efficiency as function of inlet temperature for two stage turbine
[NASA-TM-X-1728] c01 N69-17392
Surface pressure distribution on spherical blunted cones, and correlation of Mach numbers, cone angle, and angle of attack
[NASA-TN-D-5204] c01 N69-24764
Nonlinear flux flow in single crystal niobium
[NASA-TN-D-5198] c26 N69-24916
Flow and wake characteristics on turbine tandem blades in two dimensional cascade tunnel
[NASA-TM-X-1836] c01 N69-30632

FLOW DEFLECTION
Oblique shock wave properties with free stream Mach number and flow deflection angle as independent variables, noting explicit solution
c01 A69-25378

FLOW DIRECTION INDICATORS
Fixed position pressure probe for measuring subsonic flow direction over range of Reynolds number, Mach number and flow angle
c14 A69-33107
Tuft-grid photographic survey of flow field about low speed Delta wings
[NASA-TN-D-5045] c01 N69-19027
Flow direction measurement with fixed-position probes
[NASA-TM-X-1904] c14 N69-40059

FLOW DISTORTION
Inlet produced dynamic distortion and effects on stall margin of J-85 turbojet engine from supersonic wind tunnel tests
[AIAA PAPER 69-487] c28 A69-32676
Free stream disturbances influence on hypersonic boundary layer transition Reynolds number in heated and unheated flows
[AIAA PAPER 69-704] c12 A69-33453
Wind tunnel tests of distortion dynamics in Mach three mixed compression inlet
[NASA-TM-X-1706] c01 N69-13154
Steady-state interactions between turbojet engine and axisymmetric inlet with induced distortions
[NASA-TM-X-1780] c28 N69-23519
Performance data for high tip speed compressor rotor operated with radial and inlet airflow distortions
[NASA-TM-X-1798] c01 N69-26312

FLOW DISTRIBUTION
Hypersonic surface measurements and flowfield properties about slender cones in hypersonic viscous interaction regime
[AIAA PAPER 68-2] c01 A69-12520
Hypersonic flow distribution and separation types over highly swept Delta wing with trailing edge flaps at Mach 6
[AIAA PAPER 68-97] c01 A69-12522
Finite difference method computer programs for calculation of velocities and streamlines on blade to blade surface of revolution of turbomachine
[ASME PAPER 69-GT-48] c01 A69-22495
Numerical method for time dependent compressible Navier-Stckes equations applied to axisymmetric flow field produced by hypervelocity impact, examining viscous effects
[AIAA PAPER 69-354] c32 A69-28288
Flow and pressure fields for spiral grooved pumping seal with specified groove dimensions and Reynolds number
[ASLE FICFS PREPRINT 30] c15 A69-30481
Constitutive equation variation effect on near wall flow pattern of dilute polymer solutions
c12 A69-33257
Nongray absorption and radiation cooling on smooth symmetric blunt bodies included in modified Maslen flow field method for radiation and large blowing
[AIAA PAPER 69-637] c01 A69-33290
Gas core reactor curved porous walls geometry tested with clear and smoky air injection, noting mass flow ratio in reactor cavity
c22 A69-35181
Flow field throughout wind tunnel containing rotor with sharply defected blades, noting reversed flow effect in front of wake
c11 A69-35228
Tuft-grid photographic survey of flow field about low speed Delta wings
[NASA-TN-D-5045] c01 N69-19027
Flow field from forward facing nozzles exhausting near large cylindrical body at free-stream Mach numbers of 3.0 and 6.0
[NASA-TN-D-5030] c01 N69-21000
Base flow field at high altitude for four-engine clustered nozzle configuration

[NASA-TN-D-5164] c12 N69-24935
Net positive suction head requirements for helical inducer in liquid hydrogen under varied flow and temperature conditions
[NASA-TM-X-1808] c09 N69-27841
Flow field predictions for radio attenuation measurements on blunt reentry cone
[NASA-CR-1308] c07 N69-28223
Flow field measurements on flat plate with attached protuberances in supersonic turbulent boundary layer
[NASA-TN-D-5297] c12 N69-30071
Curved porous wall gas core reactor flow distribution experiment
[NASA-TM-X-1852] c12 N69-32217
Computer analysis of total pressure loss and air flow distribution in annular flow gas turbine combustion chambers
[NASA-TN-D-5385] c33 N69-33314
Analytical solution for inviscid separated jet injection at oblique angle into moving stream
[NASA-TN-D-5460] c12 N69-37965
Discharge nozzle coefficients for thick plate orifices with approach flow perpendicular and inclined to orifice axis
[NASA-TN-D-5467] c12 N69-38012
Flow field and drag characteristics of several laminar boundary layer tripping element in hypersonic flow
[NASA-TN-D-5454] c12 N69-38156

FLOW EQUATIONS
Parasitic eigenvalue in integration of equations governing one dimensional flow of chemically reactive gas
c12 A69-18317
Incompressible two dimensional turbulent boundary layer equations with arbitrary pressure distribution solved by weighted residual method
[AIAA PAPER 69-397] c12 A69-30478

FLOW MEASUREMENT
Venturi meter with separable diffuser and radial outward step at transition from throat to diffuser, noting effect of step on efficiency
[ASME PAPER 68-WA/FM-2] c14 A69-16135
Laser Doppler flowmeter for heterodyne detection of laser light scattered from moving fluid applied to fluid velocity and velocity distribution measurements
c14 A69-26546
Leak rate measurement accuracy of rate-of-rise technique for nitrogen, methane and He between millionth and thousandth torr
c14 A69-32326
Precision flow measurement techniques for low thrust auxiliary propulsion liquid rockets
[NASA-TN-D-4785] c28 N69-16122
Flow reduction due to oxidation of wire-form porous materials for transpiration cooled turbine blades
[NASA-TN-D-5001] c17 N69-16383
Flow direction measurement with fixed-position probes
[NASA-TM-X-1904] c14 N69-40059

FLOW RESISTANCE
Flow reduction due to oxidation of wire-form porous materials for transpiration cooled turbine blades
[NASA-TN-D-5001] c17 N69-16383

FLOW STABILITY
Linear amplification, nonlinear limiting and secondary instability induced by unsteady effects illustrated for various transitional flows, including roughness and streamwise vorticity
c12 A69-33248
Analysis of flow stability of thin liquid film adjacent to high speed gas stream
[NASA-TN-D-4976] c12 N69-15630
Impeller matching effects on flow range and stability operating in liquid hydrogen
[NASA-TM-X-1727] c28 N69-16213
Stability of water lubricated herringbone groove journal bearings
[NASA-TN-D-5264] c15 N69-27955
Hydrodynamic stability and vortex containment of two fluid wheel flow to helical disturbances contained by axial magnetic field
[NASA-TN-D-5372] c12 N69-32377
Multistage turbocompressor simulation applied to performance prediction of axial flow instabilities
[NASA-TM-X-1880] c28 N69-36998

FLOW THEORY
Incompressible turbulent boundary layer analysis by two region characterization for eddy viscosity, using Spalding generalized function and Prandtl free shear flow model
c12 A69-33255
Normal stress effects in viscoelastic fluid theories applied to one dimensional Burgers model of weak turbulence predicting drag reduction
c12 A69-33256
Constitutive equation variation effect on near wall flow pattern of dilute polymer solutions
c12 A69-33257
Kim-Anderson flux flow theory for materials with kappa nearly equal to 1, discussing pinning forces and sites
c26 A69-33754
Conformal mapping of two dimensional jet flow from two nozzles striking plane surfaces
[NASA-TN-D-5064] c01 N69-17816

FLOW VELOCITY
Finite difference method computer programs for calculation of velocities and streamlines on blade to blade surface of revolution of turbomachine
[ASME PAPER 69-GT-48] c01 A69-22495
Density and velocity fluctuations in hypersonic turbulent boundary layer based on Wallace data
c12 A69-31908
Reaction rate constants of ion-molecule interchange reaction as function of temperature, flow velocity, activation energy and constant part of steric factor P
c06 A69-32312
Technique for dynamically calibrating turbine flowmeters for small perturbations by means of frequency response tests
[NASA-TM-X-1736] c14 N69-17702
Frequency response of forced flow single tube boiler with inserts and exit restriction
[NASA-TN-D-5023] c12 N69-17779
Relation between ellipsoidal velocity distribution function and macroscopic flow equations
[NASA-TN-D-5026] c12 N69-17827
Flow rate effect on dynamic contact angle for wetting liquids in weightless environment
[NASA-TN-D-5115] c12 N69-20794
Gaseous reactant combustion simulation of dimethylhydrazine and hydrazine fuel system for nonequilibrium expansion studies
[NASA-TN-D-5404] c33 N69-35506

FLOW VISUALIZATION
Electron beam fluorescence probe and afterglow investigation for hypersonic He flow visualization, observing qualitative structure
c11 A69-35722
Rotor aerodynamics research in terms of theoretical and experimental data comparison, rotor blade flow visualization and blade section camber
c01 A69-41372
Performance of tandem turbine blade and its influence on flow separation and visualization
[NASA-CR-1341] c01 N69-23892

FLOWMETERS
Venturi meter with separable diffuser and radial outward step at transition from throat to diffuser, noting effect of step on efficiency
[ASME PAPER 68-WA/FM-2] c14 A69-16135
Laser Doppler flowmeter for heterodyne detection of laser light scattered from moving fluid applied to fluid velocity and velocity distribution measurements
c14 A69-26546
Technique for dynamically calibrating turbine flowmeters for small perturbations by means of frequency response tests
[NASA-TM-X-1736] c14 N69-17702
Flow direction measurement with fixed-position probes
[NASA-TM-X-1904] c14 N69-40059

FLOX
Safety planning for use of reactive cryogens in large volume, noting FLOX and liquid fluorine

c27 A69-14468
Design of injectors and ablative thrust chambers for FLOX propane rocket engine with 1.2 inch throat diameter
[NASA-TN-D-5324] c28 N69-30560
Design, development, and testing of 1000 pound thrust FLOX-propane ablative rocket engine
[NASA-TM-X-1873] c28 N69-35847

FLUID DYNAMICS
Fluid dynamic simulation of gas core nuclear rocket chamber for separating light and heavy gas via centrifugal force produced by MHD-driven rotational flow
[AIAA PAPER 69-727] c22 A69-33483
Angular grid spacing resolution near poles effect tests in global prediction model for geophysical fluid dynamics, investigating forecast height and wind fields
c20 A69-43066
Water rejection dynamics in hydrogen oxygen fuel cells
[NASA-TN-D-4956] c03 N69-14518
Turbulent mixing of compressible air in supersonic and subsonic coaxial jet flows
[NASA-TN-D-5315] c02 N69-30727

FLUID FLOW
Nondimensional Jeffreys number as ratio of Reynolds to Froude number for gravitational motion of viscous masses, with application to lunar maria and plastic ice
c30 A69-19262
Impulsive fluid motion on flat plates pulsed with uniform heat flux
[NASA-TN-D-5249] c33 N69-26236
Computerized simulation of low frequency dynamics of liquid hydrogen flow in nuclear rocket engine
[NASA-TN-D-5312] c22 N69-30070
Comparison of predicted nozzle coolant side heat transfer and fluid flow with experimental values from Phoebus 2A nuclear tests
[NASA-TM-X-1881] c33 N69-36806
Integral relations solution for radiating, nonadiabatic, inviscid flow over blunt body
[NASA-TN-D-5480] c33 N69-40356

FLUID INJECTION
Skin friction drag reducing high polymer solution injected into turbulent boundary layer to test effectiveness on marine vehicles
c12 A69-33254
Numerical analysis of laminar and turbulent mixing region for two dimensional jet injected at angle to moving stream
[NASA-TN-D-5531] c12 N69-41213

FLUID MECHANICS
Gaseous reactor fluid mechanics for nuclear rocket engines, discussing experiments on geometries used in open cycle engine for acceptable uranium loss rate
[AIAA PAPER 69-477] c22 A69-32728
Fluid mechanical problems related with subsonic and supersonic aircraft
[NASA-SP-183] c12 N69-10693
Summaries of recent gaseous reactor fluid mechanics experiments
[NASA-TM-X-1847] c12 N69-31888

FLUIDICS
Fluidic proportional thruster system for sounding rocket control
[ASME PAPER 68-WA/FE-32] c14 A69-16105
Fluidic type temperature sensor for total temperature measurement for hypersonic aircraft in atmosphere
c14 A69-16755
Fluidic oscillator use as molecular weight sensor for gas mixtures
[NASA-TM-X-1698] c03 N69-13246
Flight tests of fluidic flight control system for aircraft
[NASA-TN-D-5298] c21 N69-30946

FLUORESCENCE
Energy spectrum of secondary electrons and fluorescent efficiency in 3914 A band, obtaining ionization cross section
c29 A69-32315
Detection and spectral examination of trace porphyrin complexes by demetallation with methanesulfonic acid and spectrofluorometry, compared to absorption spectrophotometry
c06 A69-42557

FLUORIDES
Friction and wear tests with graphite fluoride lubricant
[NASA-TN-D-5097] c15 N69-20939
Rare earth fluorides and oxides used as solid lubricants at high temperatures
[NASA-TN-D-5301] c15 N69-29568

FLUORINATION
Elemental fluorine reactions with Ni, Cu, Fe, Ti, Be-Al, Zr and Ag, giving reaction rate constants, activation energies, etc
c06 A69-39706

FLUORINE
Safety planning for use of reactive cryogens in large volume, noting FLOX and liquid fluorine
c27 A69-14468
Thermionic converter with fluorine vapor deposited tungsten emitter etched to expose crystal planes
[NASA-CR-1381] c03 N69-35689

FLUORINE ORGANIC COMPOUNDS
Fluorinated polyurethanes synthesis for liquid oxygen environments and cryogenic structural utility, noting structural effects on LCX compatibility
c06 A69-16498
Sugars identification as trifluoethylacetyl polyol derivatives by gas-liquid chromatography
c04 A69-31539

FLUOROCARBONS
Steel ball bearing high temperature fatigue life tested with synthetic paraffinic oil, fluorocarbon and polyphenyl ether
[ASME PAPER 69-LUBS-18] c15 A69-34378
Surface tension, viscosity, and density of fluorocarbon solvents as function of temperature
[NASA-TM-X-1862] c18 N69-34134

FLUOROHYDROCARBONS
Real gas effects on hypersonic aerodynamics of blunt vehicles simulated with tetrafluoromethane
[NASA-TR-R-312] c01 N69-29270

FLUTTER ANALYSIS
Anomalous spacecraft OGO-D motion explained by open section boom thermally induced oscillations, discussing corrective measures
c32 A69-18331
Flutter design charts for isotropic panels stressed to verge of buckling for typical values of structural damping
c32 A69-25524
Semiempirical stability boundary for flutter of simply supported cylinders for various length-radius and radius-thickness ratios
c32 A69-41914
Effects of structural damping on flutter of stressed panels
[NASA-TN-D-4990] c32 N69-16091
Wind tunnel study of deflected elevator flutter encountered on T-tail airplane
[NASA-TN-D-5024] c32 N69-16211
Measured static aerodynamic forces for hypersonic flutter analysis on airfoil models in helium flow
[NASA-TN-D-5233] c01 N69-26271
Thermal flutter analysis of booms with open cross section
[NASA-TN-D-5222] c32 N69-29589
Wind tunnel stability tests to determine flutter characteristics of Saturn S-4B stage panel
[NASA-TN-D-5439] c32 N69-38808

FLUX (RATE)
Kim-Anderson flux flow theory for materials with kappa nearly equal to 1, discussing pinning forces and sites
c26 A69-33754
Prediction of thermal neutron flux perturbation effects in cylinders during irradiation tests
[NASA-TN-D-4949] c22 N69-14481
Quadrature variations in discrete-ordinates calculation
[NASA-TM-X-1887] c20 N69-36976

FLUX DENSITY
Ring current particle energy density distribution for symmetric portion of magnetic storm derived from current magnetic field profile measurements
c29 A69-11227
Amplitude equations for magnetoacoustic and entropy waves diverging from normal MHD shock, obtaining energy flux ratios associated with incident and transmitted waves

c25 A69-38242
Nonlinear flux flow in single crystal niobium
[NASA-TN-D-5198] c26 N69-24916
Penetration flux calculation for multiwall structure on Lunar Orbiter spacecraft missions
[NASA-TN-D-5455] c32 N69-41229
FLYBY MISSIONS
Midcourse maneuvers in interplanetary guidance, considering spin stabilized spacecraft flyby for Jupiter mission
c30 A69-28504
Scientific findings from interplanetary spacecraft radio propagation experiments, particularly Mariner 5 data
c07 A69-35940
Direct flight and Jupiter swingby heliocentric trajectory modes of elliptic capture orbits compared for unmanned missions to outer planets
[AAS PAPER 68-105] c30 A69-39221
Perturbative effects of Jupiter moons on spacecraft flyby and postencounter heliocentric trajectories, noting precision targeting
[AIAA PAPER 69-932] c30 A69-39361
Venus swingby and direct Mercury trajectories analysis for optical imaging from flyby missions
[AAS PAPER 69-258] c30 A69-42860
FLYING PERSONNEL
Theory and practice of aircraft navigation - textbook
[NASA-TT-F-524] c21 N69-17788
FOCUSING
Night sky Cerenkov light detectors observations of pulsars CP 1133, NP 0532 and NP 0527, noting instrumental limitation in detecting ultrashort light pulses
c30 A69-34994
N shaped shock wave line focusing simulating sonic superbooms
[NASA-TN-D-5306] c02 N69-31874
FOG
Research on warm fog properties, and dispersal concepts
[NASA-SP-212] c20 N69-39526
FOIL BEARINGS
High speed foil bearing rotor support system
[NASA-CR-1157] c15 N69-14214
FORBIDDEN TRANSITIONS
Intensity ratios effect of forbidden Fe and Ca transitions in solar corona on Fe/Ca ratio, noting cascading configurations
c30 A69-36219
FORCE DISTRIBUTION
Accelerated boundary layers classified in terms of integral balance of pressure, inertia, wall friction forces and entrainment momenta
[AIAA PAPER 69-666] c12 A69-33462
Wind tunnel tests of opening characteristics of all flexible parawing
[NASA-TN-D-5031] c02 N69-17700
FORCED CONVECTION
Acceleration effects on forced convection in turbulent boundary layer, noting heat transfer history and rates prediction
c12 A69-21480
Penetration model explanation for turbulent forced convection heat transfer in near-critical fluids
[NASA-TN-D-5522] c33 N69-40437
FORM FACTORS
Tabulated values of configuration factors between two spheres and parts of two spheres
[NASA-SP-3050] c30 N69-37777
FORMULAS
Low order Runge-Kutta formulas with step control for heat transfer problems
[NASA-TR-R-315] c19 N69-30753
FORTRAN
Users manual on FORTRAN 4 COMPUTE program for IBM 360/67 time sharing system
[NASA-TN-D-4917] c08 N69-10098
FORTRAN 4 subroutines to generate printed plots as normal output
[NASA-TM-X-1700] c08 N69-13566
FORTRAN computer program for spline fit curve with function valves
[NASA-TM-X-1707] c19 N69-14002
FORTRAN 4 subroutines for calculating critical flow factor to determine mass flow rate of gaseous helium and nitrogen through critical flow nozzles
[NASA-SP-3046] c12 N69-16098
FORTRAN programs for calculating wind tunnel boundary interference factors
[NASA-TM-X-1740] c01 N69-17818
Conversational approach to matrix calculations on computers
[NASA-TM-X-1749] c08 N69-18954
FORTRAN 4 program for estimating off-design performance of radial inflow turbines
[NASA-TN-D-5059] c03 N69-19829
FORTRAN program for radiation shield optimization using steepest descent method
[NASA-TM-X-1769] c22 N69-20854
FORTRAN program for computing principal mass moments of inertia of spacecraft treated as composite bodies
[NASA-TM-X-1754] c23 N69-20870
FORTRAN program for calculating velocities and streamlines on blade to blade stream surfaces of turbomachinery
[NASA-TN-D-5044] c01 N69-21811
Sonic boom propagation in stratified atmosphere using FORTRAN computer program with integral and differential equations
[NASA-CR-1299] c02 N69-22546
FORTRAN computer program for providing mission design data for elliptical orbits around Mars and Venus
[NASA-TN-D-5104] c30 N69-22571
Computer program for dimensional analysis using FORTRAN 4 programming
[NASA-TN-D-5165] c08 N69-22935
FORTRAN computer program for detailed solution of compressible, subsonic, nonviscous flow at leading or trailing edges of blade surface
[NASA-TN-D-5091] c01 N69-22938
Tagged arithmetic system for use with FORTRAN programs
[NASA-TN-D-5370] c08 N69-32556
FORTRAN program for computation of finite group tables
[NASA-TN-D-5402] c08 N69-35569
FOULING
Surface fouling of ASTM jet A fuel heated to 700 deg F in simulated heat exchanger tube
[NASA-TN-D-4958] c28 N69-12831
FOUNDATIONS
Undamped rigid rotor critical speed analysis for firm and flexible foundations, discussing effect of center of gravity and rotor shapes
[ASME PAPER 69-VIBR-49] c32 A69-24184
Frequency and critical speed analysis of rigid rotors on flexible foundations
[NASA-TN-D-4858] c32 N69-29159
Aerodynamic characteristics of blunt space capsules and slender reentry bodies with bulbous bases
[NASA-CR-1339] c01 N69-35521
FOUR BODY PROBLEM
Direct and indirect planetary perturbation effects on motion of natural satellites
[NASA-TN-D-5284] c30 N69-37893
FOURIER ANALYSIS
Selected ordinates for Fourier analysis on periodic curve
[NASA-TN-D-5083] c19 N69-20940
FOURIER SERIES
Solution of differential equations by series of exponential functions
[NASA-CR-1294] c19 N69-17249
FOURIER TRANSFORMATION
Extended source Fourier transform holography for single image synthesis of multiple identical images produced by multiple pinhole camera in X ray astronomy
c14 A69-40019
Carroll Fourier transform method applied to stellar spectra lines to determine small rotational velocities
c30 A69-42404
Modified Fourier transform for calculating human operator describing functions
[NASA-TM-X-1762] c08 N69-21119
Laser optical simulation of spaceborne radio astronomy interferometer experiment
[NASA-TN-D-5357] c30 N69-36892
FOVEA
High oxygen concentration breathing effect on foveal thresholds, using sea level tests on

trained observers
c05 A69-12216
Foveal luminances for chromatic and absolute thresholds for hue identification in case of small targets
c23 A69-19649

FRACTURE MECHANICS
Displacements and stress intensity as function of crack length for compact tension specimen, considering load line and crack edge
c15 A69-21392
Fracture design for airflight vehicles, discussing crack strength requirements and method for serviceability prediction
c32 A69-33563
Engineering fracture design noting temperature effects, brittleness, plane strain fracture toughness, fracture test evaluation
c17 A69-33564
Friction effects in round hole clevis for testing compact tension fracture toughness specimens
[NASA-TM-X-1796] c32 N69-25301
Salt stress corrosion cracking effects on tensile and stress rupture properties of titanium alloy sheet
[NASA-TN-D-5417] c17 N69-36221

FRACTURE STRENGTH
Elastic displacements for edge cracked plate specimens used as crack extension indicator in plane strain fracture toughness measurements
c32 A69-16433
Plain strain fracture toughness tests on two inch thick maraging steel plates of various strengths, using bend and compact tension tests
c32 A69-23057
Inclination effect of fatigue cracks on plane strain fracture toughness of 7075-T651 Al alloy, discussing cantilever bending
c32 A69-25958
Plane strain fracture toughness tests on maraging steel plates for various yield strengths and large dimensions
c17 A69-26496
Plane strain fracture toughness determined for crack notched bend specimens using standard test procedure for specific metallic material property
c17 A69-33566
Radius effect on bulging and fracture of through-cracked cylindrical pressure vessels at cryogenic temperatures
[NASA-TN-D-4951] c32 N69-14480
Friction effects in round hole clevis for testing compact tension fracture toughness specimens
[NASA-TM-X-1796] c32 N69-25301
Crack length and thickness influence in plane strain fracture toughness tests
[NASA-TM-X-1860] c17 N69-34916

FRACTURES (MATERIALS)
Papers on fracture, Volume 5, Fracture design of structures
c32 A69-33559
Cryogenic fracture properties of thin AISI 301 cold reduced sheet at different angles to rolling direction
[NASA-TN-D-5413] c17 N69-35688

FRAGMENTATION
Solar radiation pressure windmill effect in rotational bursting and elimination from solar system of small magnetic celestial bodies
c30 A69-39584

FRAMING CAMERAS
Optical system for recording Schlieren images with continuous writing, ultrahigh speed framing camera
[NASA-TN-D-4986] c14 N69-15381

FRAUNHOFER LINES
Object motion effect in Fraunhofer holography with application to velocity measurements
[NASA-TN-D-5515] c14 N69-40812

FREDHOLM EQUATIONS
Outer and inner curved plates and shell shapes optimized by conformal mapping
[NASA-CR-1357] c32 N69-26559

FREE CONVECTION
Subsonic thermal convection or internal gravity waves from formal scale analysis of equations of motion in plane parallel atmosphere
c13 A69-33155

FREE ELECTRONS
Thermodynamic approach to equation of state of magnetized Fermi gas, deriving energy eigenvalues of free electron in magnetic field
c30 A69-25107
Free electron model for electron work functions and number density distributions and surface potentials in metals
c26 A69-29009
Electric fields and electron work functions, surface potentials and number density distributions in selected metals surfaces determined using free electron model
c26 A69-36045
Laser beam interactions with free electrons
[NASA-TN-D-5205] c16 N69-25357

FREE FALL
Luminous spherical fog layer surrounding burning zirconium droplet during free fall through oxygen containing atmosphere, noting effect on mass and heat transfer processes
c33 A69-28462

FREE FLIGHT
Inflation, drag, and stability characteristics of towed inflatable ballute decelerator at free flight
[NASA-TN-D-4943] c01 N69-17398
Free flight test model measurement of drag, lift, and trim in wind tunnel for Apollo command module
[NASA-TN-D-5276] c30 N69-29557

FREE FLOW
Conducting fluid incompressible flow in entrance of MHD channel by momentum integral method, permitting edge stress existence at boundary layer free stream interface
[AIAA PAPER 69-724] c12 A69-33436
Free stream disturbances influence on hypersonic boundary layer transition Reynolds number in heated and unheated flows
[AIAA PAPER 69-704] c12 A69-33453
Use of photoionization in measuring velocity profile of free stream flow in expansion tube
[NASA-TN-D-4936] c12 N69-13945
Flow field from forward facing nozzles exhausting near large cylindrical body at free-stream Mach numbers of 3.0 and 6.0
[NASA-TN-D-5030] c01 N69-21000
Effects of free stream turbulence and boundary layer trip devices on mixing in jet stream
[NASA-CR-1336] c12 N69-24058

FREE RADICALS
Doublet electronic states of benzyl radical, discussing configuration-interaction calculations and transition predictions
c24 A69-13321

FREE VIBRATION
Transient vibration analysis of liner systems using transition matrices
[NASA-CR-1237] c32 N69-11008
Equilibrium and free vibration problems of centrifugally stabilized disk and shell structures
[NASA-CR-1178] c32 N69-14477
Saturn 5 launch vehicle scale model tests for free vibration during first stage burn
[NASA-TN-D-5159] c32 N69-22932
Theoretical analysis of free vibration of discretely stiffened cylindrical shells with arbitrary end conditions
[NASA-CR-1316] c32 N69-28164

FREEZING
Microscopic time lapse movies in solid/liquid interface profile during melting and freezing of materials for spacecraft thermal control as reversible heat sink
[AIAA PAPER 69-95] c33 A69-18126
Transient condensing with freezing on nonisothermal inclined plate
[NASA-TN-D-5289] c33 N69-29598

FREON
Prediction of thermodynamic effects of developed cavitation based on liquid hydrogen and Freon-114 data in scaled venturis
[NASA-TN-D-4899] c12 N69-10070

FREQUENCY ANALYZERS
Technique for dynamically calibrating turbine flowmeters for small perturbations by means of frequency response tests

[NASA-TM-X-1736] c14 N69-17702
FREQUENCY ASSIGNMENT
NASA program for radio spectrum utilization in aerospace communication systems
c07 A69-42502
FREQUENCY CONTROL
Carbon dioxide laser with two gas absorption cells in cavity for emission wavelength control and HF pulsed mode of operation
c16 A69-21088
FREQUENCY CONVERTERS
Frequency conversion in sheath capacitance of glow discharge plasma contained within metallic coaxial cylinders
c25 A69-14456
Electric control and protection circuits for parallel operation of inverter-converter
[NASA-CR-1225] c10 N69-19003
FREQUENCY DIVISION MULTIPLEXING
Multiplexer network synthesis based on arbitrary divisibility of frequency range and obtainability of input impedance at all frequencies
c09 A69-38530
FREQUENCY MEASUREMENT
Frequency and stability measurements in far IR laser region
c16 A69-18482
Beat frequency measurements in far IR due to harmonic mixing of klystrons, discussing noise role
c23 A69-33674
FREQUENCY MODULATION
Double sideband suppressed carrier FM telemetry system as airborne data recorder, discussing noise, environmental conditions, laboratory and flight tests
c07 A69-19132
FREQUENCY MULTIPLIERS
Computerized design parameters for realizable overdriven bimode varactor frequency doubler based on charge-voltage relationship at break point
c09 A69-37299
FREQUENCY RANGES
Multiplexer network synthesis based on arbitrary divisibility of frequency range and obtainability of input impedance at all frequencies
c09 A69-38530
FREQUENCY RESPONSE
Frequency response of forced flow single tube boiler with inserts and exit restriction
[NASA-TN-D-5023] c12 N69-17779
FREQUENCY SHIFT
Temperature dependent isomer shift and anharmonic binding of Sn 119 in niobium stannide, measuring Mossbauer recoil free fraction
c26 A69-10009
Emission and frequency shift angles of anti-Stokes radiation from trapped filaments of laser light in liquids
c23 A69-10012
Frequency shifts observed in Alouette 2 cyclotron harmonic plasma resonances, noting antenna length and direction
c07 A69-37892
FREQUENCY SHIFT KEYING
Split phase PCM code modulated carrier transmission characteristics determined for amplitude, phase and frequency shift keying, assuming random bit pattern and noncoherent modulation
c07 A69-39451
FREQUENCY STABILITY
Frequency and stability measurements in far IR laser region
c16 A69-18482
FRETTING CORROSION
Modes and mechanisms of wear covering adhesive, abrasive and corrosive wear, surface fatigue and fretting corrosion
c15 A69-27231
FRICTION
Theoretical analysis of pressure distribution, load capacity, attitude angle, and friction force for eccentric Rayleigh step journal bearing - infinite length solution
[NASA-TN-D-4873] c15 N69-10231
Influence of number of slip systems operating in magnesium on friction and effect of orientation of crystals on friction behavior
[NASA-TN-D-4351] c15 N69-10370
Friction effects in round hole clevis for testing compact tension fracture toughness specimens
[NASA-TM-X-1796] c32 N69-25301
FRICTION DRAG
Skin friction drag reducing high polymer solution injected into turbulent boundary layer to test effectiveness on marine vehicles
c12 A69-33254
FRICTION FACTOR
Frictional forces and collision frequencies for ions moving in neutral gases
c13 A69-13328
Earth mantle and core friction interaction suggested as cause of secular change in orbital motion obliquity
c13 A69-27821
FRICTION MEASUREMENT
Internal friction measurement apparatus for nonmetallic solids, noting variations of Young modulus in extremely low loss materials
c14 A69-13108
Physical sputtering deposition of molybdenum disulfide films as solid lubricant on rotating and sliding components, discussing lubrication properties in vacuum
[ASLE PAPER 68-LC-15] c15 A69-19308
Skin friction measurement in aerodynamic tests using thin liquid crystal coatings with changes in maximum light scattering wavelength in response to shearing forces
c11 A69-29029
Sliding friction tests of Cu and Cu-Be alloy plates in contact with various alloy sliders in air and vacuum
[ASLE PAPER 68-LC-5] c15 A69-30610
Contact conformity effects on spinning torque and friction coefficient in angular contact ball bearings from lubricated and unlubricated tests
[ASME PAPER 68-LUB-10] c15 A69-30901
Thermal stability and friction of disulfides, diselenides, and ditellurides of molybdenum and tungsten in ultrahigh vacuum
[NASA-TN-D-5141] c15 N69-22992
FRICTION REDUCTION
Solid film lubricants deposited by DC triode sputtering on Ni, Ni-Cr and Nb surfaces friction tested under ultrahigh vacuum conditions
c15 A69-43126
Development of air bearing lift pads
[NASA-TM-X-1724] c01 N69-16467
FROGS
Weightlessness effects on fertilized frog egg development onboard Gemini 8 and 12 manned orbital flights, discussing cell division, differentiation and embryogeneis
c04 A69-11084
Static pressure-diameter measurements on small pulmonary blood vessels of frogs, analyzing capillary septal area as function of intravascular pressures noting high compliance
c04 A69-40974
FROZEN FOODS
Astronaut feeding in space and NASA criteria for space foods, eliminating foods in metal tubes and directing development efforts to dehydrated foods
c05 A69-31459
FRUSTUMS
Laminar heat transfer distributions for blunted-cone, cone frustum reentry configuration at hypersonic speed using Reynolds number
[NASA-TN-D-5146] c33 N69-22997
FUEL CELLS
Manned spacecraft electrical power systems requirements, noting Gemini and Apollo fuel cell system design and configuration
c03 A69-21035
Manned spacecraft fuel cell selection and design, discussing Gemini ion exchange membrane and Apollo Bacon cell systems
c03 A69-32406
Fuel cell /battery and solar array/ battery systems for manned Apollo Applications Program /AAP/ space vehicles, considering mission and power requirements

c03 A69-42244
Water rejection dynamics in hydrogen oxygen fuel cells
[NASA-TN-D-4956] c03 N69-14518
Effects of temperature and electrolyte concentration on performance of fuel cell
[NASA-TN-D-5154] c03 N69-22940
FUEL COMBUSTION
Gaseous reactant combustion simulation of dimethylhydrazine and hydrazine fuel system for nonequilibrium expansion studies
[NASA-TN-D-5404] c33 N69-35506
FUEL CONSUMPTION
Closed form solution for minimum fuel constant thrust trajectories for vehicle transfer in vacuum between arbitrary boundary conditions
[AIAA PAPER 69-905] c30 A69-39337
Optimal control method based on linear programming for satellite fuel consumption
[NASA-CR-1450] c21 N69-41036
FUEL CONTAMINATION
Oxygen supply inert diluent impurities effect on hydrogen-oxygen fuel cell performance
c03 A69-15310
FUEL CONTROL
Precision flow measurement techniques for low thrust auxiliary propulsion liquid rockets
[NASA-TN-D-4785] c28 N69-16122
Dynamic performance analysis of fast-response fuel control valve for air breathing engine research
[NASA-TN-D-5331] c03 N69-29977
Sound wave pressure for preventing cryogenic propellant sloshing during space flight
[NASA-TN-D-4024] c23 N69-38180
FUEL FLOW
Gas core reactor curved porous walls geometry tested with clear and smoky air injection, noting mass flow ratio in reactor cavity
c22 A69-35181
FUEL INJECTION
Vortex motion enhancement of jet penetration and spreading in supersonic fuel injection into large diameter combustors
[AIAA PAPER 69-664] c12 A69-33437
Effect of angle of attack and injection pressure on jet penetration and spreading from Delta wing in supersonic flow
[NASA-TM-X-1889] c12 N69-37271
FUEL PUMPS
Transient performance of full flow hydraulic turbine driven two speed pump inducer system, formulating computer model
[AIAA PAPER 69-551] c15 A69-34415
FUEL SYSTEMS
Gaseous He bubbles injection into liquid propellant launch vehicle fuel lines to reduce vehicle POGO oscillations by lowering feed system natural frequencies
c31 A69-25498
Optimal control method based on linear programming for satellite fuel consumption
[NASA-CR-1450] c21 N69-41036
FUEL TANK PRESSURIZATION
Pressurant gas requirements for pressurized discharge of liquid hydrogen from propellant tanks for optimum pressurization system designs
[AIAA PAPER 69-526] c28 A69-32737
Volume effects on normal gravity pressurization of spherical liquid hydrogen tanks
[NASA-TN-D-5196] c33 N69-24168
Hydrogen gas pressure requirements during pressurization and transfer of liquid hydrogen from spherical tanks
[NASA-TN-D-5387] c28 N69-33211
FUEL TANKS
Heat transfer to windward side of scale model for graphite lunar module fuel cylinder
[NASA-TN-D-5251] c12 N69-29608
Ramp pressurization tests with gaseous helium in thick walled liquid hydrogen tank
[NASA-TM-X-1870] c28 N69-35712
FUEL TESTS
Surface fouling of ASTM jet A fuel heated to 700 deg F in simulated heat exchanger tube
[NASA-TN-D-4958] c28 N69-12831
FUEL VALVES
LOX prevalve accummulator system with He pressurant for prevention of POGO effect on Saturn 5
c31 A69-15298
FUEL-AIR RATIO
Thermodynamic and transport properties of air, and combustion products of natural gas and air, and jet engine fuel and air
[NASA-TN-D-5452] c33 N69-37936
FUELS
Combustion stability of single swirl can combustor modules using ASTM-A1 liquid fuel
[NASA-TN-D-5436] c28 N69-40080
FUNCTIONAL ANALYSIS
Minimization of unconstrained function of several variables by gradient dependent techniques, discussing applications to boundary value problems in optimal control
[AIAA PAPER 69-951] c19 A69-40333
FUNCTIONS (MATHEMATICS)
Tables and graphs of functions for solving nonlinear constant area fin one dimensional heat transfer problem
[NASA-TN-D-5173] c33 N69-26975
FURNACES
Furnace brazing butt joints in tungsten-uranium dioxide cermet cylinders at 3000 deg C
[NASA-TM-X-1815] c15 N69-28862
FUSELAGES
Turbulent boundary layer of subsonic transport fuselage with pressure gradient, Reynolds number, and angle of attack
[NASA-TN-D-5242] c01 N69-28112
FUSION (MELTING)
Powder metallurgy, fusion and chemical vapor deposition techniques in manufacturing tungsten base alloys
c17 A69-18792
Continental diabases and oceanic tholeiites in light of rare earth and barium abundances and partition coefficients indicating fusion process
c13 A69-20945

G

GALACTIC EVOLUTION
Collisionless computer model performing gravitational experiments with two dimensional galaxy
c30 A69-12271
Structure of matter, physical fields, evolution of earth and universe, solar activity and earth, and interaction of earth biosphere with physical fields
[NASA-TT-F-345] c13 N69-12384
GALACTIC RADIATION
Galactic Jupiter Probes investigating Jupiter atmosphere and emissions and deep space cosmic radiation
c30 A69-12303
Annihilation gamma ray spectra from equilibrium spectra of secondary galactic positrons
c29 A69-29948
Origin of galactic gamma rays, discussing evidence in support of interstellar gas in galactic disk and production of neutral pions and bremsstrahlung
c29 A69-32806
Power spectra of interplanetary magnetic field fluctuations determined from Pioneer 6 satellite data, relating results to galactic cosmic rays modulation
c30 A69-37554
Twenty year wave in diurnal anisotropy component of galactic cosmic rays arriving at earth from asymptotic direction east of sun interpreted as magnetic reconnection
c29 A69-38098
Chemical composition of galactic and solar cosmic rays, discussing differences from universal cosmic abundances, using Cerenkov counters, emulsions, etc
c29 A69-40090
GALACTIC RADIO WAVES
Cosmic radio background noise spectrum near north galactic pole based on Radio Astronomy Explorer satellite experiments
c30 A69-42375
GALLIUM ANTIMONIDES
GaSb-ZnTe heterojunction fabrication method, noting photoresponse, fluorescence and light transmission

c26 A69-12408
GALLIUM ARSENIDE LASERS
GaAs laser tracking system for space guidance, describing equipment and operations
[AIAA PAPER 69-870] c21 A69-39396
GALLIUM ARSENIDES
Negative differential resistance effect producing relaxation type oscillations in n-type gallium arsenide
c26 A69-10557
Current oscillations in semiinsulating O and Cr doped GaAs samples at room temperature, noting photoconductivity excitation spectra
c26 A69-21753
Alloying pairs of metal pellets to n and p type semiinsulating GaAs, discussing photo effects
c26 A69-32824
Proton irradiation effects on minority carrier lifetime in silicon and gallium arsenide semiconductor materials
[NASA-TN-D-5028] c26 N69-18897
GALVANOMAGNETIC EFFECTS
Ac technique using lock-in power amplifier SNR for measuring galvanomagnetic and Shubnikov-de-Haas effects, noting error reduction
c14 A69-36375
GAMMA FUNCTION
Tabulation of high accuracy gamma function values for some rational arguments, noting applications to Gaussian quadrature formulas, fractional Bessel functions and Airy functions
c19 A69-13375
GAMMA RAYS
Radioactive decay of neutral pions generated in metagalactic cosmic ray interactions as source of high energy isotropic gamma rays observed by OSO-3
c29 A69-12092
Angular correlation of inelastically scattered alpha particles and gamma rays emitted from 2-plus state of Sn 120
c24 A69-13098
Angular correlation between inelastically scattered 42 MeV alpha particles and emitted gammas from 2-plus Ni 58
c24 A69-13100
Biological effects on rhesus monkeys of high energy protons compared to effects of cobalt 60 gamma radiation
c04 A69-13498
Polymer films tensile properties after exposure to gamma radiation in vacuum, noting chain scission and cross linking
[ASME PAPER 68-WA/RP-6] c18 A69-16160
Gamma heating rate measured by aqueous dosimeter converted to rate in thin tungsten detector in water shield through transport theory calculations, obtaining correction factors
c22 A69-18825
Gamma ray telescope development for balloon-borne astronomy in search for discrete gamma sources and supernova explosions
[IEEE PAPER 3A-5] c14 A69-19192
Chondrite meteorite fall /1969/ in Mexico, noting opaque and microcrystalline matrices and gamma rays from short lived isotopes
c30 A69-20686
Discrete source hypothesis for interpreting high energy cosmic gamma ray measurements obtained by OSO-3 spacecraft
c29 A69-20699
Cosmic gamma ray spectra from metagalactic proton-antiproton annihilation
c29 A69-21459
Extragalactic gamma ray fluxes predicted, discussing collisions, matter-antimatter annihilation and cosmological implications
c29 A69-24466
Annihilation gamma ray spectra from equilibrium spectra of secondary galactic positrons
c29 A69-29948
Mortality kinetics of Drosophila melanogaster, comparing effects of gamma radiation-induced life shortening and natural aging
c04 A69-30444
Origin of galactic gamma rays, discussing evidence in support of interstellar gas in galactic disk and production of neutral pions and bremsstrahlung
c29 A69-32806
Corrections to previous papers on extragalactic gamma rays, discussing effects on various cosmological models
c29 A69-34168
Radiation damage and recovery of lithium-diffused silicon p-n solar cells, measuring photovoltaic parameters as function of gamma radiation fluence
c03 A69-35694
NASA lunar receiving laboratory for lunar rock samples examination by gamma ray spectrometry for induced radioactive nuclides and naturally occurring isotopes
c11 A69-38271
Cosmic gamma rays spectrum from neutral pions production and decay in metagalactic cosmic ray p-p collisions, deriving models based on Einstein general relativity theory
c29 A69-40641
Viruslike particles in fat body cells and oenocytes of Drosophila melanogasters imagoes, in glial cells of cephalic ganglionic center of flies and in gamma radiated cells
c04 A69-42021
Uranium 233 critical mass requirements, neutron kinetic behavior, and neutron and gamma ray heating rates for nuclear light bulb rocket engine
[NASA-CR-1315] c25 N69-23451
Gamma ray detection from Crab Nebula using digitized spark chamber
[NASA-TR-R-308] c30 N69-24170
Gamma ray transport portion of COHORT 2 Monte Carlo shielding code
[NASA-TM-X-1877] c22 N69-35848
Gamma ray backscattering of radioisotope for measuring Martian atmospheric density
[NASA-TN-D-5431] c24 N69-36931
GAPS
Heat transfer and pressure distributions inside hinge line gap of wedge-flap combination at hypersonic speeds
[NASA-TN-D-4911] c01 N69-11009
GAS ANALYSIS
Planetary atmosphere composition determination using mass spectrometry for neutral components, ion spectrometry for ionic components and data system optimization
[AAS PAPER 68-183] c14 A69-11468
Air pollution monitoring instrumentation developed for aerospace uses surveyed for industrial applications
[NASA-SP-5072] c14 N69-24751
Contaminant and atmospheric sensor for spacecraft cabin environments
[NASA-CR-1375] c14 N69-37876
GAS BEARINGS
Herringbone grooved gas lubricated journal bearing stability, testing effects of geometries and clearances on onset speed for half frequency whirl
[ASME PAPER 68-LUBS-25] c15 A69-27271
Development of air bearing lift pads
[NASA-TM-X-1724] c01 N69-16467
Turboalternator gas bearing system for spacecraft electric power production
[NASA-CR-1292] c15 N69-19775
Performance of two stage axial flow turbogenerator with gas bearing rotor support system
[NASA-CR-1290] c03 N69-21771
Design and performance of gas bearing system for turboalternators
[NASA-CR-1291] c15 N69-21772
Air flow and attitude angle compared with theory for rotating externally pressurized air journal bearings
[NASA-TN-D-5192] c15 N69-27956
Performance of gas bearing Brayton cycle turboalternator
[NASA-TM-X-1820] c03 N69-29707
GAS CHROMATOGRAPHY
Automatic equipment for sampling and preparing gases by dual column gas chromatography for subsequent mass spectral analysis of carbon isotopes during methane metabolism
c06 A69-12603
Sugars identification as trifluoethylacetyl polyol derivatives by gas-liquid chromatography

c04 A69-31539
Heats of adsorption of carbon dioxide on silver /I/ oxide and copper /II/ oxide by gas chromatography
c06 A69-38277

GAS COMPOSITION
Planetary atmosphere composition determination using mass spectrometry for neutral components, ion spectrometry for ionic components and data system optimization
[AAS PAPER 68-183] c14 A69-11468

GAS COOLED REACTORS
Gas core reactor curved porous walls geometry tested with clear and smoky air injection, noting mass flow ratio in reactor cavity
c22 A69-35181

GAS COOLING
Nozzle insert evaluation and gas cooling concept in storable liquid propellant rocket engine
[NASA-TM-X-1756] c28 N69-19782
Boundary layer interaction in cooling tubes of rocket engines tends to lower convective heat transfer
[NASA-TN-D-5168] c33 N69-22931

GAS DISCHARGE TUBES
Helium-neon laser discharge with striation oscillations in relation to pressure and current
[NASA-CR-1387] c08 N69-32350

GAS DISCHARGES
Pulsed glow discharges in He and He-H mixtures for high current density, noting electric field and wall potential distributions
c25 A69-23660

GAS DISSOCIATION
Gas breakdown model for analyzing breakdown of Ce vapor filled crack in thermionic trilayer insulator
c03 A69-21840
Modified model for vibration-dissociation relaxation coupling phenomena in nonequilibrium high temperature gas flow, discussing parameter U variation with kinetic temperature
c12 A69-37208
Stagnation point boundary layer with suction and injection in equilibrium dissociating air
[NASA-TN-D-3889] c12 N69-14314
Nonequilibrium gas dynamics of hydrogen dissociation and recombination
[NASA-CR-1411] c12 N69-34709

GAS DYNAMICS
Transport properties of steam, analyzing selection, correlation and prediction using statistical mechanical theories
c33 A69-10110
Measured effects of gaseous flow system dynamics on acoustic mode combustion instability
[NASA-TN-D-5080] c33 N69-20882
Nonequilibrium gas dynamics of hydrogen dissociation and recombination
[NASA-CR-1411] c12 N69-34709
High temperature properties of gases - gas dynamics, thermodynamics, and combustion physics
[NASA-TT-F-558] c12 N69-35365

GAS EXCHANGE
Ventilation-perfusion inequality increase effects on lung overall gas exchange, using digital model
c05 A69-38388

GAS EXPANSION
Hydrogen and methane combustion to simulate expansion of storable propellants
[AIAA PAPER 68-635] c33 A69-37188
He and Ar arc-heated flows into reservoir and expansion in converging-diverging supersonic nozzles, considering flow equilibrium effect on heat transfer and enthalpy
c33 A69-37198

GAS FLOW
Combustion response of hydrazine-nitrogen tetroxide hypergolic rocket propellants to transverse gas flows, noting coupled and uncoupled oscillations
c33 A69-10112
Transmittance and absorption cross sections of carbon particles suspended in flowing stream of nitrogen gas
c33 A69-17804
Steady axisymmetric gas flow from galactic center, determining supersonic to subsonic transition by equations of motion
c30 A69-22189
He and Ar arc-heated flows into reservoir and expansion in converging-diverging supersonic nozzles, considering flow equilibrium effect on heat transfer and enthalpy
c33 A69-37198
Modified model for vibration-dissociation relaxation coupling phenomena in nonequilibrium high temperature gas flow, discussing parameter U variation with kinetic temperature
c12 A69-37208
Pressure measurements and gas flow analysis during thermal vacuum tests of manned spacecraft indicating adequate space vacuum simulation
[AIAA PAPER 69-1033] c11 A69-40401
Radiation equilibrium temperature measured downstream of transpiration cooled gas flow near slender cone vertex in continuous flow hypersonic tunnel
c01 A69-43588
Laser Doppler velocity instrument for measuring turbulence and mean velocity in subsonic and supersonic gas flows
[R-67-4450] c14 N69-14351
Back flow density from jet plumes in vacuum
[NASA-TN-D-4978] c01 N69-14385
Forced convection heat-transfer data for hydrogen flow through heated parallel hexagonal passages
[NASA-TN-D-4959] c33 N69-14588
Pressure fields and multidimensional gas flow in permeable char layers and effects on ablation
[NASA-TR-R-296] c33 N69-16181
Unstable combustion of hydrazine-nitrogen tetroxide caused by transverse gas flow
[NASA-TN-D-4984] c27 N69-19026
Curved porous wall gas core reactor flow distribution experiment
[NASA-TM-X-1852] c12 N69-32217
Quantitative method for determination of fission gases trapped in irradiated fuel forms
[NASA-TM-X-1893] c22 N69-37225
Thermochemical data from simulated pyrolysis gas flow through ablating char layer
[NASA-TN-D-5464] c33 N69-38271

GAS INJECTION
Gaseous He bubbles injection into liquid propellant launch vehicle fuel lines to reduce vehicle POGO oscillations by lowering feed system natural frequencies
c31 A69-25498
Surface pressure and heat transfer over blunt conical body in hypersonic flow with uniform mass addition of various gases
[AIAA PAPER 69-716] c01 A69-33463
Cone boundary layer transition location and Reynolds number as function of nose bluntness combined effect with Ar, air and He mass injection
[AIAA PAPER 67-706] c12 A69-33476
Stagnation point boundary layer with suction and injection in equilibrium dissociating air
[NASA-TN-D-3889] c12 N69-14314
Force measurements in drag reduction by gas injection into turbulent boundary layer through supersonic wing slots
[NASA-TN-D-5307] c12 N69-31359
Physical parameter effect on pressurant gas requirements during expulsion of liquid hydrogen from spherical tanks
[NASA-TN-D-5336] c28 N69-32318

GAS IONIZATION
Ionizing shock front structure in monatomic gas, considering atom-atom and electron-atom collisional ionization rates
c12 A69-13138
Switch-on ionizing shock waves structure, analyzing condition of downstream state and effect on hydromagnetic wave speed
c25 A69-22045
Atomic nitrogen collisional ionization and recombination rates under assumed quasi-steady nonequilibrium distribution of electron state populations
c24 A69-43700
Experimental measurements of two electron capture for negative ion production in atmospheric gases
[NASA-CR-1406] c24 N69-38564

GAS JETS
Photographic study of bromine jet flowing in coaxial airstream and impinging on stagnation surface
[NASA-TN-D-5209] c12 N69-24800
Gaseous jet interaction and penetration in supersonic flow
[NASA-CR-1386] c12 N69-32480
GAS LASERS
Scanned laser beam display techniques based on cathode ray tube technology, noting flying spot scanner and beam deflection
c14 A69-15028
Proportionality between log-amplitude variance and 7/6 power of wavenumber for horizontal propagation from spherical wave transmitter to point detector
c16 A69-19641
Carbon dioxide laser with two gas absorption cells in cavity for emission wavelength control and HF pulsed mode of operation
c16 A69-21088
Sulfur dioxide-helium laser pulsed and CW submillimeter outputs
c16 A69-24005
Absorption coefficient measurement for hydrocarbon gases for He-Ne laser beam at 3.39 microns, tabulating coefficients, noting variations from spectroscopic data
c16 A69-42192
Laser Doppler velocity instrument for measuring turbulence and mean velocity in subsonic and supersonic gas flows
[R-67-4450] c14 N69-14351
Refractive index computation for free electrons and neutral atoms in cesium plasma at helium neon laser wavelengths
[NASA-TN-D-5328] c25 N69-30622
Helium-neon laser discharge with striation oscillations in relation to pressure and current
[NASA-CR-1387] c08 N69-32350
GAS LUBRICANTS
Small eccentricity stability analysis for externally pressurized gas lubricated bearings with journal rotation
[NASA-TN-D-4934] c15 N69-13256
Power loss experiments on herringbone grooved, gas lubricated journal bearings
[NASA-TN-D-5224] c15 N69-24932
Load and stiffness characteristics of rotating externally pressurized air journal bearings
[NASA-TN-D-5191] c15 N69-27078
Steady-state characteristics of herringbone grooved air lubricated journal bearings
[NASA-TN-D-5386] c15 N69-33258
GAS MIXTURES
Pulsed glow discharges in He and He-H mixtures for high current density, noting electric field and wall potential distributions
c25 A69-23660
Specific impulse deliverable performance of space storable propellant combination flucrine-oxygen/methane and oxygen difluoride/diborane
[AIAA PAPER 69-505] c28 A69-32762
Fluidic oscillator use as molecular weight sensor for gas mixtures
[NASA-TM-X-1698] c03 N69-13246
GAS PRESSURE
Fission product gas pressure calculated for uranium dioxide ceramic fuel elements
[NASA-TN-D-4823] c22 N69-10216
Physical parameter effect on pressurant gas requirements during expulsion of liquid hydrogen from spherical tanks
[NASA-TN-D-5336] c28 N69-32318
Hydrogen gas pressure requirements during pressurization and transfer of liquid hydrogen from spherical tanks
[NASA-TN-D-5387] c28 N69-33211
Pressurized liquid nitrogen inside parametric amplifier structures for input, noise, and temperature improvements
[NASA-TN-D-5509] c09 N69-40079
GAS STREAMS
Analysis of flow stability of thin liquid film adjacent to high speed gas stream
[NASA-TN-D-4976] c12 N69-15630
Oxidation resistance and thermal fatigue cracking of nickel and cobalt base alloys in transonic gas streams
[NASA-TN-D-5376] c17 N69-33307
GAS TURBINE ENGINES
Finite difference method computer programs for calculation of velocities and streamlines on blade to blade surface of revolution of turbomachine
[ASME PAPER 69-GT-48] c01 A69-22495
Radial inflow gas turbine engine performance testing, discussing instrumentation, recording systems and calibration techniques
[ASME PAPER 69-GT-104] c14 A69-22522
Gas turbine engine shaft face seal with self acting lift augmentation preventing rubbing contact, noting disadvantages of labyrinth and conventional seals
[ASLE PICFS PREPRINT 27] c15 A69-30492
Scale models of M-1 rocket engine oxygen and hydrogen pump driven two stage turbines used to determine performance and compact inlet manifolds problems
[AIAA PAPER 69-553] c28 A69-32678
Application of boundary layer control concepts to highly loaded turbine stator blades in annular cascades
[NASA-CR-1219] c01 N69-14211
Performance evaluation of oil lubrication system for antifriction bearing rotor system of Brayton cycle turbomachinery
[NASA-CR-1229] c15 N69-16463
Shaft face seal with self acting lift augmentation for advanced gas turbine engines
[NASA-TN-D-5170] c15 N69-23232
Development and high temperature tests of high strength nickel alloy for stator vanes of gas turbine engines
[NASA-TN-D-5352] c17 N69-31873
Three oxidation-resistant alloy foil claddings for protecting typical gas turbine engine alloys of nickel and cobalt
[NASA-TN-D-5483] c17 N69-38794
GAS TURBINES
Variable stator area effect on performance of single stage turbine suitable for air cooling
[NASA-TM-X-1697] c01 N69-10558
Test performance of radial inflow turbine for Brayton cycle space power system
[NASA-TN-D-5090] c03 N69-20937
Computer analysis of total pressure loss and air flow distribution in annular flow gas turbine combustion chambers
[NASA-TN-D-5385] c33 N69-33314
Rotational effects on isothermal compressible flow across gas turbine sealing dam
[NASA-TN-D-5344] c15 N69-35799
GAS VALVES
Valving concepts and functional approaches for inert gas attitude control thrustor systems providing redundancy safeguards at minimum weight, volume and power costs
[AIAA PAPER 69-843] c28 A69-39373
GAS VISCOSITY
Viscosity, thermal conductivity and diffusion predicted for dilute nonpolar, polar and mixed gases, discussing methods for rotational relaxation collision numbers and resonant correction
c33 A69-38951
GAS-GAS INTERACTIONS
Steady-state interactions between turbojet engine and axisymmetric inlet with induced distortions
[NASA-TM-X-1780] c28 N69-23519
Gaseous jet interaction and penetration in supersonic flow
[NASA-CR-1386] c12 N69-32480
GAS-ION INTERACTIONS
Reaction rate constants of ion-molecule interchange reaction as function of temperature, flow velocity, activation energy and constant part of steric factor P
c06 A69-32312
GAS-METAL INTERACTIONS
Elemental fluorine reactions with Ni, Cu, Fe, Ti, Be-Al, Zr and Ag, giving reaction rate constants, activation energies, etc
c06 A69-39706
GASEOUS DIFFUSION
Viscosity, thermal conductivity and diffusion predicted for dilute nonpolar, polar and mixed

gases, discussing methods for rotational relaxation collision numbers and resonant correction
c33 A69-38951

GASEOUS FISSION REACTORS
Cavity reactor consisting of dilute fuel core surrounded by moderating reflector to attain very high temperatures in gaseous cores
c22 A69-18954
Gaseous reactor fluid mechanics for nuclear rocket engines, discussing experiments on geometries used in open cycle engine for acceptable uranium loss rate
[AIAA PAPER 69-477] c22 A69-32728

GASEOUS ROCKET PROPELLANTS
Gaseous reactor fluid mechanics for nuclear rocket engines, discussing experiments on geometries used in open cycle engine for acceptable uranium loss rate
[AIAA PAPER 69-477] c22 A69-32728
Summaries of recent gaseous reactor fluid mechanics experiments
[NASA-TM-X-1847] c12 N69-31888

GASES
Effect of chemical properties of pyrolysis gases on heat shield mass required for lifting reentry vehicle in typical reentry trajectory
[NASA-TN-D-4975] c32 N69-14306
Removal of acid gases and oxides of nitrogen from spacecraft cabin atmospheres at ambient temperatures
[NASA-CR-1388] c05 N69-37517

GEGENSCHEIN
Gegenschein measurements for determining upper limit on asteroidal debris spatial density
c30 A69-12545

GEMINI FLIGHTS
Weightlessness effects on fertilized frog egg development onboard Gemini 8 and 12 manned orbital flights, discussing cell division, differentiation and embryogeneis
c04 A69-11084
Space suit meteoroid protection for extravehicular activity, discussing Gemini and lunar surface EVA suits and bumper concept
[AIAA-PAPER-69-366] c05 A69-28298
Preflight and postflight leukocyte chromosome aberration analyses of Gemini astronauts
c04 A69-33173
Weightlessness simulation of Gemini extravehicular tasks using neutral-buoyancy underwater techniques
[NASA-TN-D-5235] c05 N69-28024
Color photographs of earth surface taken during Gemini flights 6 through 12
[NASA-SP-171] c14 N69-28909
Preflight optical evaluation of right hand hatch windows in Gemini missions 7, 8, 9, and 12
[NASA-TN-D-5471] c31 N69-40813

GEMINI PROJECT
Gemini and Mercury space flights medical results, summarizing physiological effects noted on body systems
c04 A69-11074
Systems engineering activities in manned space flight involving design, development, manufacture, test and operation of Mercury, Gemini and Apollo flight systems
c31 A69-17602
Gemini program for geologic orbital photography, discussing equipment used
c13 A69-35274
Manned spacecraft waste disposal systems
[NASA-TM-X-1851] c05 N69-33260
Chronological study of design and development of Gemini project
[NASA-SP-4002] c31 N69-36501

GEMINI SPACECRAFT
Guidance and control concepts and hardware for atmospheric entry of Mercury, Gemini and Apollo spacecraft
c21 A69-25724
Manned spacecraft fuel cell selection and design, discussing Gemini ion exchange membrane and Apollo Bacon cell systems
c03 A69-32406
Optical properties and chemical analysis of contaminants on Gemini spacecraft windows
[NASA-TN-D-4916] c31 N69-13232
Correlation study of simulation of Gemini extravehicular activity with flight results
[NASA-CR-1146] c05 N69-19902

GEMINI 11 FLIGHT
Primary cosmic ray nuclei studies during Gemini 2 flight by nuclear emulsion detector with time resolution capability, describing experiment design and equipment operation
c29 A69-38350

GEMINI 12 FLIGHT
Sextant sighting measurements from on board Gemini 12 spacecraft
[NASA-TN-D-4952] c21 N69-14332

GEMINI 5 FLIGHT
Visual acuity and visibility of markings on ground in long duration earth orbital space flight
[NASA-CR-1134] c05 N69-10813

GEMINI 7 FLIGHT
Visual acuity and visibility of markings on ground in long duration earth orbital space flight
[NASA-CR-1134] c05 N69-10813

GENERAL AVIATION AIRCRAFT
Advanced electronic applications to navigation, data transmission, and airborne collision avoidance in general aviation aircraft and to simulated displays for low visibility landing
[NASA-CR-1240] c02 N69-14729
Human survival in flight emergencies involving commercial and general aviation aircraft
[NASA-CR-1262] c02 N69-14763
Aviation pilot reactions and opinions on grooved runways
[NASA-CR-1428] c02 N69-35861

GEOCHEMISTRY
Origin and distribution of elements - Conference, Paris, May 1967
c30 A69-20892
Continental diabases and oceanic tholeiites in light of rare earth and barium abundances and partition coefficients indicating fusion process
c13 A69-20945
Gas chromatographic and mass spectrometric analyses of alicyclic hydrocarbons from Carboniferous organic materials, noting alkane distribution and evolutionary histories
c06 A69-34184
Geochemical synthesis of branched chain acyclic polymers from irradiated isoprene
c04 A69-43750
Biogeochemistry applications in mineral prospecting
[NASA-SP-5056] c13 N69-10492
Organic geochemical laboratories solvent purification procedures
[NASA-TM-X-1746] c06 N69-18962

GEOCORONAL EMISSIONS
Spectral and electrophotometric studies of upper atmosphere - airglows, atomic oxygen, hydroxyl emission, helium line spectra, auroras, and solar cycle effects on magnetosphere
[NASA-TT-F-530] c13 N69-16539

GEODETIC COORDINATES
GEOS 1 tracking station positions on SAO standard earth C-5 model
[NASA-TN-D-5034] c13 N69-28019

GEODETIC SATELLITES
Preprocessing procedures for reduction of electronic data from geodetic satellites
[NASA-CR-1183] c08 N69-11470
Potential use of satellites for enhancing positioning capabilities and for marine geodetic control
[NASA-CR-1253] c13 N69-16645
Magnetically anchored eddy current and eddy current rod dampers for GEOS gravity gradient stabilized satellite
[NASA-CR-1282] c14 N69-18953
Tradeoff analysis on radar and laser space altimeter systems for sea surface geodesy
[NASA-CR-1298] c14 N69-21117
Gravity model comparison using geodetic satellite long arc orbital solutions
[NASA-TN-D-5035] c30 N69-27412

GEODETIC SURVEYS
Survey of six year period of satellite observed tropical Pacific cloud mapping
c20 A69-33001
Gemini program for geologic orbital photography, discussing equipment used

c13 A69-35274

GEOLOGY
X Ray fluorescence of rock samples as applied to geological problems, noting standard deviations for element distribution
c14 A69-10890
Biogeochemistry applications in mineral prospecting
[NASA-SP-5056] c13 N69-10492

GEOMAGNETIC LATITUDE
Diurnal variations of low latitude VLF emissions observed at Hiraiso, Japan
c07 A69-13900
Explorer 32 atmospheric density measurements revealing neutral thermosphere latitudinal variations during geomagnetically undisturbed times
c13 A69-38100

GEOMAGNETIC PULSATIONS
Interplanetary magnetic fields from Explorer 33 magnetometer relationship to surface geomagnetic variations emphasizing unified view
c30 A69-32309

GEOMAGNETISM
Sudden magnetic field increase associated with July 8, 1966 sudden commencement observed by OGO 3 satellite in magnetotail
c13 A69-11226
Solar plasma observations during magnetic storms, discussing shocks and tangential discontinuities, geomagnetic variations and He
c13 A69-11234
Secular change examination in cislunar geomagnetic tail field gradient during summers of 1966 and 1967, using Explorer 33 and 35 results
c13 A69-11237
Outer magnetosphere average magnetic field configuration between 5 and 18 earth radii, noting various maps in equatorial plane
c13 A69-14012
Structure, temporal behavior, shape and length of earth magnetic tail via satellite mapping
c29 A69-19363
Geomagnetic tail topology, reconnection and interaction with moon from Explorer 33 satellite data
c13 A69-19365
Satellite measurements of suprathermal electrons at conjugate sunrise, indicating photoelectron escape from production level and movement along geomagnetic lines into conjugate ionosphere
c29 A69-25144
Solar plasma flow around magnetosphere, discussing plasma velocity, density and temperature and magnetic field space and time variations
c29 A69-26736
Satellite observations of geomagnetic tail in magnetosphere near midnight meridian plane, discussing formation, shape, plasma sheet and models
c13 A69-26739
Solar wind plasma observations in geomagnetospheric wake compared at 1000 and 500 earth radii, considering ion energy spectra and geomagnetic tail
c29 A69-26943
Worldwide changes in geomagnetic field, determining causes by examining magnetic field and plasma data for solar wind and classifying as SSC or SI
c29 A69-31963
Geomagnetic field model /POGO/ to confirm eccentric dipole westward velocity secular decrease predicted by day length changes
c13 A69-37490
Model equatorial electrojet with meridional current system constructed by spherical harmonic expansion for geomagnetic field, noting current loops
c13 A69-38084
Magnetic dip equator position at E layer and gradient with time and altitude, using geomagnetic field models
c13 A69-42428
Measurement of change in plasma potential and magnetic field of hydrogen plasma impinging on magnetic dipole - simulation of solar wind-earth interaction
[NASA-TM-X-1738] c25 N69-19131
Parametric angles of trajectory-determined field line intersects predicting location of artificial auroras in magnetosphere
[NASA-TN-D-5189] c30 N69-32316
Investigation of earth atmospheric composition, geomagnetism, extraterrestrial radiation, solar activity, and planetary atmospheres by satellite experiment and astronomical observations
[NASA-SP-195] c34 N69-38951
Strength and direction data on earth and extraterrestrial magnetic fields for guidance in vehicle design
[NASA-SP-8017] c31 N69-40269

GEOMETRY
Simple equations for temperature distributions in radiating gray gases
[NASA-TN-D-5226] c33 N69-25312

GEOMORPHOLOGY
Detecting geomorphological features over northeast Africa by Nimbus 2 visible and infrared radiation measurements
[NASA-TN-D-4648] c13 N69-14290
Summary of lunar data and scientific observations generated by Surveyor landings on Moon
[NASA-SP-184] c30 N69-36451

GEOPHYSICS
Solar-terrestrial physics, Solar aspects - IQSY/COSPAR Conference, London, July 1967, Part 1
c29 A69-30005

GEOPOTENTIAL
Geopotential resonant orbital perturbations of existing satellites, noting high inclination role
c31 A69-13777

GEOPOTENTIAL HEIGHT
Regression generated radiometric and contour height fields of North American Continent using Nimbus 2 IR equivalent black body temperature and geopotential data
c20 A69-42896

GEOSTROPHIC WIND
Steady state solution of quasi-geostrophic perturbation equations for atmospheric forced response to parametized heating as global monsoon theory
c20 A69-36405

GERMANIUM
Ge films formation by evaporation technique, discussing background O pressure effect
c26 A69-43345

GERMANIUM DIODES
Germanium microwave backward diodes optimum design and performance prediction through computer calculation for important parameters
c09 A69-41224

GIANT STARS
Nucleosynthesis in dynamics of massive star cores, noting element synthesis by neutron capture in supernova explosions
c30 A69-20898
Optical depths of convection related to metal deficiency for main sequence and giant stars
c30 A69-29946

GIMBALS
Fourth angle driving law for different four gimbal systems used for simulation display and inertial platform isolation
c11 A69-26265
Torqued two axis gimbaled boom actuator satellite attitude control
[AIAA PAPER 68-857] c21 A69-43245

GLASS
Polymer glasses low temperature transitions, relating structure and transition temperature
c06 A69-16493
Hypervelocity micrometeor impact sites identification on aluminized glass, using conchoidal pattern as criterion in analysis
c30 A69-34952
Optimum solar cell cover glass systems selected by studying interplanetary space environment effects of proton impact, temperature and concurrent illumination on radiation damage
c03 A69-35702

GLASS COATINGS
Production of glass coatings for molybdenum ion thruster accelerator grids
[NASA-TN-D-5320] c15 N69-30062

GLASS FIBERS
Cryogenic mechanical properties of epoxy resins and glass/epoxy composites
c18 A69-16491
Mechanical behavior of boron-epoxy and glass-epoxy filament-wound cylinders under various loads
[NASA-TN-D-5050] c18 N69-19825
GLASSWARE
Glass vacuum systems grease free assembly method using heat shrinkable polyolefin sleeve tubing connector for compression of O ring joints
c15 A69-20529
GLIDE PATHS
Ground based guidance for land-landing manned spacecraft with low velocity descent systems, discussing high and low altitude glide path intercept and spiral
[AIAA PAPER 69-864] c21 A69-39390
Influence of angle of glide slope on accuracy of performing instrument approaches in simulator tests
[NASA-TN-D-4835] c21 N69-10056
GLOBAL TRACKING NETWORK
International 28-station global instrumentation ground support network for space tracking and data acquisition
[UN PAPER 68-95912] c34 A69-17059
GLOW DISCHARGES
Frequency conversion in sheath capacitance of glow discharge plasma contained within metallic coaxial cylinders
c25 A69-14456
Pulsed glow discharges in He and He-H mixtures for high current density, noting electric field and wall potential distributions
c25 A69-23660
GLYCOLS
Ignition hazards in electrical circuits contaminated by glycol fluids, describing hazard detection by RF methods, decontamination procedures, safety checks, etc
c18 A69-36028
GOLD
Influence of surface films on friction and deformation of single crystal and polycrystalline gold
[NASA-TN-D-4875] c15 N69-10249
Monte Carlo analysis of gold sphere transmission experiments at 24 keV neutron energy using S wave spin state data
[NASA-TN-D-5211] c24 N69-24826
Adhesion of gold on copper planes studied with low energy electron diffraction
[NASA-TN-D-5290] c26 N69-29407
Adhesion of gold to copper and to copper aluminum alloys
[NASA-TN-D-5351] c23 N69-31984
GOLD ALLOYS
Friction, wear, and contact resistance of gold alloys and electroplated electric gold contacts
[NASA-CR-1447] c17 N69-40057
GOLD COATINGS
Gold-underlayer film combinations adhesion to oxide substrates, describing adhesion changes as function of Au and underlayer film thickness, time, environment, etc
c26 A69-28007
Friction, wear, and contact resistance of gold alloys and electroplated electric gold contacts
[NASA-CR-1447] c17 N69-40057
GOVERNMENTS
Federal government contracting, discussing legality of NASA service contracts
c34 A69-15987
In-house research on R and D management in government agencies, discussing manning, training, center programs, case studies, etc
c34 A69-38022
GRADIENTS
Branched trajectory optimization for split rocket vehicles using projected gradient or steepest descent method
[AIAA PAPER 69-917] c30 A69-39346
GRAND TOURS
Jupiter swingby missions to Saturn, Uranus, Neptune, and Pluto
[NASA-SP-35-PT-8] c30 N69-34850
GRANTS
NASA university program, discussing participation in space and aeronautics developed based on project oriented research grants and sustaining university grants
[UN PAPER 68-95413] c34 A69-10506
GRANULAR MATERIALS
Circumstellar grain compositions of stars with various O to C abundance ratios, calculating molecular equilibrium of condensates and gaseous compounds in stellar atmospheres
c30 A69-24103
GRAPHIC ARTS
Computer driven graphical techniques for aerospace design and analysis
[ASME PAPER 69-DE-27] c15 A69-28854
Graphic method determining sounding rocket vehicle attitude
[NASA-TN-D-5172] c30 N69-23782
GRAPHITE
IR radiation of NML Cygnus with O/C ratio close to unity ascribed to circumstellar shell of graphite particles
c30 A69-13775
Extinction efficiency of graphite core interstellar grains with solid hydrogen and ice mantles, using theoretical models
c23 A69-29587
Graphite fiber NOL rings and biaxial wound pressurized cylinders tested at ambient and cryogenic temperatures for tensile and cyclic fatigue properties
c18 A69-35521
Solid para hydrogen coated graphite particles expulsion into interstellar medium from star formation regions, considering mantles stability and particles extinction efficiency, albedo and phase function
c30 A69-37492
X ray crystallographic measurements of selected grades of commercial nonpyrolitic artificial graphite
[NASA-TN-D-4888] c18 N69-10754
Joining ceramics and graphite to other materials
[NASA-SP-5052] c15 N69-14241
Friction and wear tests with graphite fluoride lubricant
[NASA-TN-D-5097] c15 N69-20939
Tensile and cyclic fatigue properties of graphite filament-wound pressure vessels at ambient and cryogenic temperatures
[NASA-TN-D-5354] c32 N69-31300
GRAPHS (CHARTS)
Integrated charged particle energy spectra from gridded electrostatic analyzers, relating retarding potential curve to particle floating potential, kinetic temperature, etc
c25 A69-20521
Comparison of class of orbits in Earth-Moon field and class of Kepler orbits in rotating coordinates by use of concurrent series of graphs
[NASA-TN-D-4903] c30 N69-10470
Selected ordinates for Fourier analysis on periodic curve
[NASA-TN-D-5083] c19 N69-20940
Tables and graphs of functions for solving nonlinear constant area fin one dimensional heat transfer problem
[NASA-TN-D-5173] c33 N69-26975
Pilot ratings of lateral directional handling for wide range of aircraft characteristics - graphs
[NASA-TN-D-5358] c02 N69-35762
Tabular and graphical data on thermal radiative properties for dissemination
[NASA-CR-1431] c33 N69-40455
GRAVITATION
Volume effects on normal gravity pressurization of spherical liquid hydrogen tanks
[NASA-TN-D-5196] c33 N69-24168
GRAVITATIONAL COLLAPSE
Ferromagnetism stable state in degenerate electron gas and magnetic fields in gravitationally collapsed bodies based on total microscopic magnetic moments associated with Landau level electrons
c30 A69-38600
GRAVITATIONAL EFFECTS
Collisionless computer model performing gravitaticnal experiments with two dimensional galaxy

c30 A69-12271
Computer study of collisionless self gravitating system using two dimensional model, obtaining gravitational field by solving Poisson equation
c30 A69-12272
Low degree earth gravity harmonics effect on 12 and 24 hour orbits of high altitude communications satellites
c13 A69-14661
Iterative guidance mode /IGM/ applied to effective gravity vector prediction, acceleration measurement of noise sensistivity and energy limitations
[AIAA PAPER 67-620] c21 A69-15501
Nondimensional Jeffreys number as ratio of Reynolds to Froude number for gravitational motion of viscous masses, with application to lunar maria and plastic ice
c30 A69-19262
Gravitational and magnetic torque effect on rotational motion of triaxial rigid body in regressing orbit about oblate primary mass
c30 A69-32240
Acceleration effects on solid propellant rocket motors combustion characteristics
[AIAA PAPER 68-530] c28 A69-39217
Lateral sloshing in cylinders under low gravity conditions
[NASA-TN-D-5058] c12 N69-19112
Effect of gravitational model variations on accuracy of lunar orbit determinatcn from data arcs
[NASA-TN-D-5105] c30 N69-21018
Origin and terrestrial relief of continents and oceans
[NASA-TT-F-533] c13 N69-29491
Adaptation to hypoxia, acclimatization, and conditioning in human and animal subjects from Space Biology collection
[NASA-TT-F-580] c04 N69-32131
Reynolds number relation to single noncondensable bubble motion under low gravity conditions
[NASA-TN-D-5462] c12 N69-38032

GRAVITATIONAL FIELDS
Lunar mass and gravitational field determined from lunar satellite dynamics, using potential function in terms of spherical harmonics
c30 A69-31405
Suitability of white rats for suborbital studies of behavior in gravity fields
[NASA-CR-1255] c05 N69-14094
Legendre polynomials for gravitational field and orbit perturbation
[NASA-TN-D-5163] c13 N69-26969
Gravity model comparison using geodetic satellite long arc orbital solutions
[NASA-TN-D-5035] c30 N69-27412
Disturbing factors in motion of artificial earth satellites due eccentricity of earth gravitational field
[NASA-TT-F-539] c30 N69-33560

GRAVITY GRADIENT SATELLITES
RAE-A satellite design, simulation and flight performance, discussing gravity gradient stabilization
c31 A69-18328
Semiactive gravity gradient stabilization system design for low altitude earth oriented spacecraft attitude control, using active reaction wheel scanner
c31 A69-18334
System designs for manned spacecraft gravity gradient stabilization of Saturn S-4B stage at 400 km and lunar module at synchronous altitude
c31 A69-18338
Torqued two axis gimbaled boom actuator satellite attitude control
[AIAA PAPER 68-857] c21 A69-43245
Magnetically anchored eddy current and eddy current rod dampers for GEOS gravity gradient stabilized satellite
[NASA-CR-1282] c14 N69-18953
Influence of thermal distortion of booms on attitude of gravity stabilized satellites
[NASA-TN-D-5435] c31 N69-40781

GRAVITY WAVES
Atmospheric density variation measurements by density gages on Explorer 32 satellite confirm wave propagation in neutral thermosphere as free internal gravity waves
c13 A69-16261
Full wave calculation of gravity waves for thermospheric model, describing wave type reflection, transmission, conversion and coupling by scattering matrix elements
c13 A69-25150
Subsonic thermal convection or internal gravity waves from formal scale analysis of equations of motion in plane parallel atmosphere
c13 A69-33155

GREASES
Ball bearing test apparatus for evaluation of greases and solid lubricants at high temperatures
[ASLE PREPRINT 68AM 7C-2] c15 A69-10912

GREEN FUNCTION
Green function solution to Maxwell equations for interplanetary and coronal magnetic fields above photosphere, considering field at source surface
c30 A69-24429

GRIDS
Angular grid spacing resolution near poles effect tests in global prediction model for geophysical fluid dynamics, investigating forecast height and wind fields
c20 A69-43066

GRINDING (COMMINUTION)
Dispersion strengthened nickel produced from ultrafine comminuted powders
[NASA-TN-D-5421] c17 N69-38074

GRINDING MILLS
H release, pressure and oxide layer formed by reaction during ball milling Cr in water
c15 A69-38567

GROOVES
Elastohydrodynamic solution for ball torque spinning without rolling in nonconforming groove, showing increase in torque with stress and spinning and decreasing conformity
[ASME PAPER 69-LUBS-11] c15 A69-34381
Theory and clearance effects on stability of water lubricated herringbone-groove journal bearings
[NASA-TN-D-4883] c15 N69-10228
Power loss experiments on herringbone grooved, gas lubricated journal bearings
[NASA-TN-D-5224] c15 N69-24932
Stability of water lubricated herringbone groove journal bearings
[NASA-TN-D-5264] c15 N69-27955

GROOVING
Runway grooving to improve aircraft tire traction in adverse weather tested by F-4D and Convair 990A under wet conditions
[AIAA PAPER 69-773] c02 A69-35649
Runway and highway pavement grooving and traction studies
[NASA-SP-5073] c11 N69-20451
Steady-state characteristics of herringbone grooved air lubricated journal bearings
[NASA-TN-D-5386] c15 N69-33258

GROUND BASED CONTROL
Electron density profiles from topside ionograms compared to ground based sounding results, discussing error corrections
c07 A69-37865
Ground based guidance for land-landing manned spacecraft with low velocity descent systems, discussing high and low altitude glide path intercept and spiral
[AIAA PAPER 69-864] c21 A69-39390
Onboard processor servicing spacecraft sensors, programmable from ground, discussing functions and applications
c08 A69-39921

GROUND EFFECT
Predicting lift and drag for slender sharp-edge Delta wings in ground proximity
[NASA-TN-D-4891] c01 N69-16180

GROUND EFFECT MACHINES
Performance potential of high speed ocean-going air cushion vehicles with aircraft nuclear power plants
[AIAA PAPER 69-416] c02 A69-30480
Nuclear powered surface effects machine performance estimates, calculating reactor power and payload fraction for various clearance heights, gross weights and velocities
c22 A69-35180

Nuclear power plants based on nuclear aircraft technology to power ocean-going air cushion vehicles
[NASA-TM-X-1871] c22 N69-35723
Performance estimates of high speed peripheral jet nuclear powered ground effects machine
[NASA-TM-X-1888] c22 N69-36757
GROUND STATE
Nonequilibrium nitrogen plasma spectral line intensities calculated assuming optically thin plasma
c24 A69-10960
GROUND STATIONS
Magnetic field data from OGO-2 spacecraft and surface magnetic observatories, noting magnetic storm occurrence and magnetosphere inflation and detection of polar ionospheric currents
c13 A69-11125
Mutual RF interference between satellite and terrestrial telecommunications microwave relay system at shared frequencies
c07 A69-13242
Technological and cost factors of voice broadcasts from satellites to earth
[NASA-TM-X-1747] c07 N69-19025
Summary of operation, communications, and other experiments of Relay 2 satellite
[NASA-SP-151] c31 N69-21065
Solar flare and sunspot effects on VHF communications between synchronous satellite relay and ground stations
[NASA-TN-D-5100] c07 N69-23317
Procurement and construction of automatic picture transmission ground station equipment for ESSA and Nimbus transmission
[NASA-SP-5080] c07 N69-31985
GROUND SUPPORT EQUIPMENT
Short wave bands for earth-space communications, considering propagation anomalies compensated systems and frequency bands availability
c07 A69-13721
High pressure compressible flow systems in space vehicle ground support equipment
[NASA-SP-3045] c12 N69-26987
GROUND SUPPORT SYSTEMS
International 28-station global instrumentation ground support network for space tracking and data acquisition
[UN PAPER 68-95912] c34 A69-17059
Ground based guidance systems for supplementing onboard guidance of manned space vehicles
c21 A69-17580
Radio astronomy Explorer A attitude determination via disk-oriented programming ground support system for reducing and calibrating telemetry data, attitude prediction and command, etc
[AIAA PAPER 69-983] c08 A69-40363
GROUND TESTS
Lifting body stability augmentation systems design, development, ground tests and flight data including frequency response, limit cycle and structural resonance
[AIAA PAPER 69-887] c02 A69-39413
GROUP THEORY
FORTRAN program for computation of finite group tables
[NASA-TN-D-5402] c08 N69-35569
GROUP 6A COMPOUNDS
Ductilizing of Group 6A elements by rhenium and other solutes
[NASA-TN-D-4955] c17 N69-14403
GROWTH
Identity between growth hormone degrading activity of pituitary gland and plasmin
c04 A69-17105
Compensatory hypertrophy effects on adrenal phenylethanolamine n-methyl transferase /PNMT/ activity in rats
c04 A69-41404
GUIDANCE (MOTION)
Iterative guidance mode /IGM/ applied to effective gravity vector prediction, acceleration measurement of noise sensistivity and energy limitations
[AIAA PAPER 67-620] c21 A69-15501
GUIDE VANES
Jet engine inlet noise control by modification of inlet guide vanes
c28 A69-15622
GUNS (ORDNANCE)
Characterization of pressure perturbations induced in rocket combustor by machine gun
[NASA-TN-D-5214] c33 N69-24824
GYROFREQUENCY
Banded chorus, VLF discrete emissions in magnetosphere in single variable frequency band with frequency depending on equatorial electron gyrofrequency
c13 A69-31981
GYROSCOPES
Hydrodynamic conical and spherical spiral grooved grease bearings replacement of gyro ball bearings for extended space missions
[AIAA PAPER 69-836] c15 A69-39367
GYROSCOPIC PENDULUMS
Influence of thermal distortion of booms on attitude of gravity stabilized satellites
[NASA-TN-D-5435] c31 N69-40781

H

H ALPHA LINE
M-2 galaxy as Seyfert-like galaxy seem edge-on, using radio and optical data showing H alpha emission collisionally excited, discussing circular polarization
c30 A69-20051
HAFNIUM
Compatibility tests of molten uranium with tungsten and tungsten-1.5 percent hafnium
[NASA-TN-D-5076] c17 N69-19930
HAFNIUM ALLOYS
Mechanical properties of alloys molybdenum hafnium carbon compounds
[NASA-TN-D-5025] c17 N69-19200
Cyclic heating and thermal shock effects on hafnia stabilized with calcia, magnesia, and yttria
[NASA-TN-D-5279] c18 N69-34547
HAFNIUM CARBIDES
High temperature mechanical properties of polycrystalline hafnium carbide containing 13-volume-percent hafnium diboride
[NASA-TN-D-5008] c17 N69-16380
Effect of rhenium on mechanical properties of hafnium carbide strengthened tungsten alloys
[NASA-TN-D-5348] c17 N69-31977
HAIL
Elastic and plastic analyses of hail damage to aircraft surfaces
[NASA-TN-D-5363] c32 N69-33420
HALIDES
Thermionic converters with chloride and fluoride vapor deposited tungsten emitters, comparing performance characteristics and stability
c03 A69-21819
Feasibility of producing dispersion strengthened chromium by ball milling in hydrogen halides
[NASA-TN-D-4912] c17 N69-10827
Hot-salt stress-corrosion of titanium alloy under simulated turbine engine compressor environment
[NASA-TN-D-5510] c17 N69-40242
HALL EFFECT
Characteristic time on motion of magnetic lines of force in medium with Hall effect
c25 A69-12399
Near cathode magnetic field effect on instability in linear Hall current accelerators, using geometry of field extending from anode to cathode region
[AIAA PAPER 69-381] c28 A69-21731
Measurement and interpretation of Hall coefficient and resistivity of semiconductors
[NASA-TM-X-1711] c26 N69-14086
Nernst-Ettingshausen, thermoelectric power, thermal transverse-even, magnetoresistance, and Hall coefficients in white tin in 3.3 tesla field and cryogenic temperatures
[NASA-TN-D-5227] c26 N69-25412
HALOGENS
Halogen detector for leakage in hermetically sealed devices
[NASA-TN-D-5457] c09 N69-38597
HALOPHILES
Cation concentration requirement of halophilic NADH dehydrogenase for stability and maximum activity
c06 A69-23127

Salts and organic solvents effect on halophile Halobacterium cutirubrum catalase, noting enzyme activity inhibition by cation and anion c04 A69-35291
Flavoprotein/cytochrome b/559/ role as branch of Halobacterium electron transport in DPNH oxidase determined by salt dependence of reduced DPNH c06 A69-37101

HAMILTON-JACOBI EQUATION
Spacecraft optimum low thrust trajectory analyzed by Hamilton-Jacobi perturbation theory, obtaining canonic constants of motion c30 A69-17574

HANDBOOKS
Reliability handbook for silicon monolithic microcircuits - applications [NASA-CR-1346] c09 N69-23225
Reliability handbook for silicon monolithic microcircuits - failure mechanisms [NASA-CR-1347] c09 N69-23226
Soviet handbook of astronautics covering spacecraft and operating problems of near-earth spaceflight [NASA-TT-F-500] c31 N69-24760
Reliability handbook for failure analysis of silicon integrated microcircuits [NASA-CR-1348] c09 N69-25328

HANDWRITING
Recognition program for handwritten information in real time computer operation [NASA-CR-1284] c08 N69-21527

HANSEN LUNAR THEORY
Hansen planetary theory basic function, discussing perturbations expansion into trigonometric series c30 A69-13781
Application of Hansen lunar theory to 10th satellite of Jupiter [NASA-TN-D-4979] c30 N69-14479

HARDWARE
Low thrust mission simulation dependence on hardware definition, discussing power plant characteristics, jet velocity and thrustor efficiency c30 A69-21204
Computer memory reduction through FORTRAN higher level language, discussing tradeoff between costs saved and additional logic hardware [AIAA PAPER 69-963] c08 A69-40344
Hardware-software provisions for multiple precision floating point arithmetic [NASA-TM-X-1885] c08 N69-36918

HARMONIC ANALYSIS
Harmonic content of pressure wave shapes in strong traveling transverse acoustic modes [NASA-TM-X-1716] c12 N69-15371

HARMONIC EXCITATION
Ratio of equilibrium responses to transient responses both having equal excitation levels [NASA-TN-D-5070] c32 N69-17258

HARMONIC OSCILLATION
Inelastic scattering cross sections calculated, comparing results for various nuclear states expressed as Wood-Saxon radial and harmonic oscillator functions c26 A69-29006
Numerical calculation of viscous compressible flow around harmonic oscillating rigid cylinder [NASA-CR-1467] c12 N69-38782

HARMONIC OSCILLATORS
Quantum theory of particle-harmonic oscillator collision applied to gas-surface interactions at cryogenic temperatures [NASA-TN-D-4982] c24 N69-14288

HARNESSES
Design and dynamic characteristics of vertical lunar gravity simulator with six degrees of freedom torso harness [NASA-CR-1234] c05 N69-14979

HARTREE APPROXIMATION
Dipole shielding factor in coupled Hartree-Fock approximation for atomic S state c23 A69-12179
Upper bounds for electromagnetic transition rates for Ne 20 determined using Hartree-Fock wave functions c24 A69-35166
Hartree-Fock method used to study even-even nuclei in 2s-1d shell [NASA-TN-D-5066] c24 N69-17976

HATCHES
Preflight optical evaluation of right hand hatch windows in Gemini missions 7, 8, 9, and 12 [NASA-TN-D-5471] c31 N69-40813

HAZARDS
Explosive hazard evaluation of liquid oxygen liquid hydrogen propellants [NASA-TN-D-5382] c27 N69-35321

HAZE
Multiple light scattering solutions accuracy by diffraction peak omission from cloud and haze analytic phase functions compared for optically thick and thin planetary atmospheres c30 A69-33159

HEAD (FLUID MECHANICS)
Jet pump head rise deterioration parameter for prediction of cavitation c12 A69-15791

HEART
Analytic model resembling thick walled ellipsoid of revolution incorporating three dimensional shape of human left ventricle and ventricular wall thickness effects c05 A69-26235
Pneumatic driving system for heart assist or total replacement pumps, discussing design features and performance characteristics c05 A69-42983

HEART RATE
Real time metabolic rate analysis of suited astronaut using heart rate and O methods during thermal vacuum and extravehicular mobility tests [AIAA PAPER 69-993] c05 A69-40371
Circadian rhythm phase relationships between photoperiodism and heart rate, locomotor activity and deep body temperature /EBT/ in unrestrained monkeys c04 A69-42706

HEAT BALANCE
Nighttime protonosphere thermal balance from Alouette 2 electrostatic probe measurements of electron temperature and concentration in magnetosphere c13 A69-43181

HEAT EXCHANGERS
Design point performance of double containment tantalum and stainless steel mercury boiler for SNAP 8 [NASA-TN-D-4926] c33 N69-12739

HEAT FLUX
Downstream radiation flux distribution calculated for blunt entry bodies, considering self absorption effects c33 A69-12547
Rotating wickless hollow shaft heat pipe utilizing centrifugal acceleration for return pumping of condensate and transferring high heat fluxes [ASME PAPER 69-HT-19] c33 A69-43550
Heat finite propagation velocity effects on temperature distribution and heat flux for step temperature change at semiinfinite body surface [ASME PAPER 69-HT-1] c33 A69-43564
Computer program for computation of thermal radiation heat loads and temperatures of spacecraft orbiting planets or moon [NASA-TR-R-278] c30 N69-14428
Tungsten-184 used as thermal flux monitor at high temperatures in Plum Brook reactor [NASA-TN-D-5113] c22 N69-20795
Impulsive fluid motion on flat plates pulsed with uniform heat flux [NASA-TN-D-5249] c33 N69-26236
Aerodynamic heat flux determined within thermally thick walls for case of rapidly rising heat rates [NASA-TN-D-5309] c33 N69-30726
Infrared heating simulation of Mach 4.63 flight on X-15 horizontal stabilizer [NASA-TN-D-5403] c33 N69-35949

HEAT GENERATION
Heat generation calculations and heat transfer measurements in circulating currents of linear crossed field generators and accelerators [NASA-TN-D-5244] c25 N69-26313

HEAT MEASUREMENT
Heats of adsorption of carbon dioxide on silver /I/ oxide and copper /II/ oxide by gas chromatography

c06 A69-38277
Effect of shock precursor heating on radiative flux to blunt bodies
[NASA-CR-1265] c33 N69-17438
Calorimetric efficiency of cone and column solar energy concentrator
[NASA-TN-D-5109] c03 N69-21088
Calorimetric evaluation of three 1.5-meter diameter inflatable rigidized solar concentrators for solar dynamic cycle power systems
[NASA-TN-D-5234] c03 N69-28123

HEAT PIPES
High power TWT tube cooling in space vehicle, discussing thermal control system based on heat pipe radiator
c09 A69-24747
Vacuum tube with cathode heated directly by external radioisotope source, noting heat pipe providing isothermal heat transfer
c09 A69-24748
Rotating wickless hollow shaft heat pipe utilizing centrifugal acceleration for return pumping of condensate and transferring high heat fluxes
[ASME PAPER 69-HT-19] c33 A69-43550
Nuclear thermionic space power system using rod control and heat pipes
[NASA-TN-D-5250] c22 N69-26270
Heat pipe devices for space suit temperature control
[NASA-CR-1400] c05 N69-38491

HEAT RADIATORS
Radiator transfer functions for SNAP 8 ground test facilities
[NASA-TN-D-4946] c22 N69-14503
Aluminized plastic covers to reduce radiator sink temperatures on lunar surface
[NASA-TM-X-1729] c03 N69-17225
Calculation for study of vertical and horizontal positioned lunar radiators
[NASA-TM-X-1846] c33 N69-32683

HEAT RESISTANT ALLOYS
Columbium alloys properties, discussing creep strength, oxidation resistance, costs, production, etc
c17 A69-18791
Examination of thermal oxidation deposits on heat resistant alloys using X ray diffraction and X ray fluorescence analyses
[NASA-TN-D-5019] c17 N69-17277
Spectrochemical analysis of cobalt-base superalloys by liquid-layer solid-sample spark technique
[NASA-TM-X-1753] c06 N69-20853
Effect of ultrasonic vibration on precipitation hardening of steels and superalloys
[NASA-TN-D-5131] c32 N69-21814
Solubility of refractory metals and alloys in liquid potassium and lithium
[NASA-CR-1371] c17 N69-27059
Three oxidation-resistant alloy foil claddings for protecting typical gas turbine engine alloys of nickel and cobalt
[NASA-TN-D-5483] c17 N69-38794

HEAT SHIELDING
Blunt and conical body optimum heat shield shapes for Jupiter atmospheric entry, noting shallow flight path
[AIAA PAPER 68-1150] c31 A69-13565
Make wire, light pipe and spring wire ablation sensors development for measuring parameters of heat shield materials for reentry vehicles
c14 A69-15428
Charring phenolic nylon ablator material pyrolysis and surface recession for cyclic and constant combined convective and radiative heating
[AIAA PAPER 69-151] c33 A69-18055
Ablation characteristics of heat shield materials measured in arc heated wind tunnels, considering influence of model scale, heating rate and pressure level
c18 A69-26813
Heating facility for testing ablative heat shield material models in combined convective and radiative heating environment with constant or transient heating conditions
[AIAA PAPER 69-342] c11 A69-28278
Ablation heat shields, emphasizing dielectric low cost fabrication and application to entry vehicles
c15 A69-35538
Line source technique for ablative heat shield materials thermal conductivity measurements, comparing vacuum and atmospheric test results
[AIAA PAPER 69-1013] c11 A69-40386
Low density polybenzimidazole composites as ablative heat shields, discussing arc-heated wind tunnel tests of linear and crosslinked structures
c18 A69-41715
Effect of chemical properties of pyrolysis gases on heat shield mass required for lifting reentry vehicle in typical reentry trajectory
[NASA-TN-D-4975] c32 N69-14306
Ablation behavior of heat shield of Apollo command module over wide range of thermal environments
[NASA-TM-X-1778] c33 N69-22933
Wind tunnel study of open-face honeycomb to reduce temperature of hypersonic aircraft structure
[NASA-TN-D-5278] c33 N69-29599
Transient temperature fields in porous shell walls cooled by forced flow
[NASA-TT-F-552] c33 N69-30245
RAM-CA carbon-phenolic heat shield test in rocket engine exhaust
[NASA-TM-X-1841] c31 N69-32713

HEAT SINKS
Aluminized plastic covers to reduce radiator sink temperatures on lunar surface
[NASA-TM-X-1729] c03 N69-17225

HEAT SOURCES
Vacuum tube with cathode heated directly by external radioisotope source, noting heat pipe providing isothermal heat transfer
c09 A69-24748
Brayton-B generator for 2-10 kWe production, describing design, heat source/rejection, efficiencies and preliminary test data analysis
c03 A69-42278

HEAT TOLERANCE
Artificial heat acclimatization effect on orthostatic tolerance in man exposed to stresses of heat, exercise and dehydration
c05 A69-32810

HEAT TRANSFER
Transformation laws for thermodynamic quantities confirming conventional formulation by mechanical model of heat
c23 A69-11288
Venus microwave phase effect analyzed assuming dry massive Venus atmospheric model, discussing heat transfer processes
c30 A69-12108
Telemetry technique utilizing thermocouple sensors for base heating determinations on free flight blunt cone in shock tunnels, noting electrical noise reduction
[AIAA PAPER 68-407] c14 A69-15514
Advances in heat transfer, Volume 5, covering Monte Carlo method, film and transition boiling, convective heat transfer, etc
c33 A69-24456
Monte Carlo method application to heat transfer analysis including radiation, rarefied gas energy transfer and conduction
c33 A69-24457
Pressure and heating rate correlations for rocket exhausts impinging on flat plates and curved panels, generating axisymmetric real gas exhaust plumes
c33 A69-26781
X-15 research aircraft program piloting problems, ground facilities, heat transfer, space flight and steep reentry
c02 A69-26872
Inlet thermal boundary layer thickness effect on conical nozzle heat transfer and boundary layer determined by operating nozzle with cooled/uncooled inlet
[AIAA PAPER 69-474] c33 A69-32780
Optimal design for improving thermal performance of existing spacecraft thermally actuated louver system by increasing open-to-closed emittance ratio
[AIAA PAPER 69-627] c33 A69-33269
He and Ar arc-heated flows into reservoir and expansion in converging-diverging supersonic nozzles, considering flow equilibrium effect on

heat transfer and enthalpy
c33 A69-37198
Instantaneous frozen layer thickness and temperature profile in solidified layer obtained by iteration technique
c33 A69-39433
Hydrodynamic inlet conditions effect on film boiling and near critical hydrogen heat transfer, using data from electrically heated various geometry test sections
[ASME PAPER 69-HT-27] c33 A69-43541
Rotating wickless hollow shaft heat pipe utilizing centrifugal acceleration for return pumping of condensate and transferring high heat fluxes
[ASME PAPER 69-HT-19] c33 A69-43550
Heat finite propagation velocity effects on temperature distribution and heat flux for step temperature change at semiinfinite body surface
[ASME PAPER 69-HT-1] c33 A69-43564
Heat transfer and pressure distribution due to two-dimensional repetitive sine wave distortions on flat plate at Mach 20 in helium
[NASA-TN-D-4907] c12 N69-10804
Heat transfer and pressure distributions inside hinge line gap of wedge-flap combination at hypersonic speeds
[NASA-TN-D-4911] c01 N69-11009
Correlation equations for predicting gas-side heat transfer of axisymmetric rocket engine nozzles
[NASA-TM-X-1748] c33 N69-18898
Calculation of compressible turbulent boundary layers with pressure gradients and heat transfer
[NASA-CR-1303] c12 N69-21653
Stagnation pressure and heat transfer measurements of blunt axisymmetric bodies
[NASA-TN-D-5121] c01 N69-22554
Probability calculations for fuel clad surface temperatures of nuclear reactors
[NASA-TM-X-1802] c22 N69-26231
Heat generation calculations and heat transfer measurements in circulating currents of linear crossed field generators and accelerators
[NASA-TN-D-5244] c25 N69-26313
Tables and graphs of functions for solving nonlinear constant area fin one dimensional heat transfer problem
[NASA-TN-D-5173] c33 N69-26975
Heat transfer and neutronic calculations after fuel emitter separation in uranium oxide fueled thermionic diodes
[NASA-TM-X-1812] c22 N69-28212
Skin friction and heat transfer data for hypersonic turbulent layer on flat plates, wind tunnel wall, and cones
[NASA-TN-D-5089] c12 N69-29144
Bimetallic heat exchanger tube performance in sodium boiling facility
[NASA-TN-D-5323] c33 N69-30064
Properties and uses of liquid metal reactor fuels, including heat transfer processes in variously shaped channels, boiling and condensation of metals, and reactor control equipment
[NASA-TT-F-522] c33 N69-30507
Low order Runge-Kutta formulas with step control for heat transfer problems
[NASA-TR-R-315] c19 N69-30753
Energy thickness in prediction of throat heat transfer in rocket nozzles using nozzle geometries and temperature ratios
[NASA-TN-D-5356] c33 N69-31869
High temperature properties of gases - gas dynamics, thermodynamics, and combustion physics
[NASA-TT-F-558] c12 N69-35365
Pressure and heat transfer on swept Delta wing with trailing-edge flap
[NASA-TN-D-5418] c01 N69-35855
Comparison of predicted nozzle coolant side heat transfer and fluid flow with experimental values from Phoebus 2A nuclear tests
[NASA-TM-X-1881] c33 N69-36806

HEAT TRANSFER COEFFICIENTS
Combined conduction and radiation transfer equations solutions for absorbing-emitting gas, obtaining slip coefficient for diffusion solution correct boundary condition
c33 A69-27784
Heat transfer coefficients for film boiling from submerged spheres
[NASA-TN-D-5124] c33 N69-28318
Convective heat transfer rates on large angle conical bodies at hypersonic speeds
[NASA-TN-D-5526] c33 N69-40780
Temperature response of wall separating two fluids one with oscillating temperature
[NASA-TN-D-5520] c33 N69-40789

HEAT TRANSMISSION
Second breakdown and other thermal instabilities analyzed by heat flow equation, obtaining stability criteria predicting reduced power dissipation for transistor at low currents
c09 A69-31618

HEAT TREATMENT
Film processing effects on cryogenic mechanical properties of polyethylene terephthalate
c18 A69-16490
Surface fouling of ASTM jet A fuel heated to 700 deg F in simulated heat exchanger tube
[NASA-TN-D-4958] c28 N69-12831

HEAVING
Cushioncraft ground effect machine with heave response and control concepts
[NASA-TN-D-5202] c02 N69-23449

HEAVY IONS
Uranyl ions interaction with phospholipid and cholesterol monolayers, using surface pressure and potential measurements
c06 A69-25641

HEAVY WATER
Thermodynamic properties of liquid and gas phase equilibria of water plus heavy water
[NASA-TN-D-5223] c33 N69-26247

HEISENBERG THEORY
Anisotropic Heisenberg antiferromagnetism in spin wave approximation, calculating thermodynamic quantities in terms of elliptic integrals
c26 A69-26500
Anisotropic Heisenberg ferromagnets in random phase and spin wave approximation
[NASA-TN-D-5286] c26 N69-29588

HELICAL FLOW
FASTER computer program modified for tracking neutrons through reactor slabs penetrated by helical voided ducts
[NASA-TM-X-1838] c22 N69-31986

HELICAL INDUCERS
Net positive suction head requirements for helical inducer in liquid hydrogen under varied flow and temperature conditions
[NASA-TM-X-1808] c09 N69-27841

HELICAL WINDINGS
Structural stability of lattice column of longerons and helical braces
[NASA-CR-1301] c32 N69-26234

HELICOPTER CONTROL
Quadratic optimization applied to helicopter flight control design, assuming constant feedback gains and command step input with zero steady state error
c02 A69-43279

HELICOPTER DESIGN
NASA flight test of hingeless rotor compound helicopter to determine lift sharing characteristics, showing rotor lift dependence on airspeed
c02 A69-29702

HELICOPTER PERFORMANCE
NASA flight test of hingeless rotor compound helicopter to determine lift sharing characteristics, showing rotor lift dependence on airspeed
c02 A69-29702

HELICOPTERS
Flight tests with helicopters for studying manueverability
[NASA-TN-D-4931] c02 N69-14008
Theory for predicting rotational and vortex noise of lifting rotors in hovering and forward flight
[NASA-CR-1333] c23 N69-25344
Evaluation of contact analog display in landing approaches with helicopters
[NASA-TN-D-5241] c02 N69-27177
Flight investigation of lightweight helicopter to study feasibility of fixed collective pitch autorotations
[NASA-TN-D-5270] c02 N69-29232
Aerodynamic stability of helicopter rotor in forward flight
[NASA-CR-1332] c32 N69-34744

HELIO AIRCRAFT
Large solar sail vehicle to operate in manner of helicopter rotor
[NASA-CR-1329] c31 N69-28861
HELIUM
Magnetron ionization gauge in helium for low pressure measurement, discussing striking characteristics and time lags
c03 A69-10606
Variable He star HZ29, noting unusually wide and shallow He I lines and possible mass and composition
c30 A69-16931
First Born approximation cross sections for He excitation from ground state by proton impact calculated, using wave functions
c24 A69-17027
Primordial helium and horizontal branch star luminosity, obtaining luminosities in He burning phase for different He and metal abundances from models
c30 A69-22211
Pulsed glow discharges in He and He-H mixtures for high current density, noting electric field and wall potential distributions
c25 A69-23660
Gaseous He bubbles injection into liquid propellant launch vehicle fuel lines to reduce vehicle POGO oscillations by lowering feed system natural frequencies
c31 A69-25498
Leak rate measurement accuracy of rate-of-rise technique for nitrogen, methane and He between millionth and thousandth torr
c14 A69-32326
HD 30353 He binary star invisible component suggested as KO type supergiant from IR photometric data
c30 A69-35348
FORTRAN 4 subroutines for calculating critical flow factor to determine mass flow rate of gaseous helium and nitrogen through critical flow nozzles
[NASA-SP-3046] c12 N69-16098
Pumped helium tests of 51 centimeter bore niobium tin magnetic coils
[NASA-TN-D-5158] c26 N69-22965
Creep rupture data on welded tubes for helium to air heat exchanger design
[NASA-TN-D-5195] c17 N69-23731
Helium penetration and spreading in Mach 2 airstream using Delta wing injector
[NASA-TN-D-5322] c01 N69-30878
Shock shape and surface pressure measurements on hypersonic pointed cones in helium
[NASA-TN-D-5343] c01 N69-31228
Ramp pressurization tests with gaseous helium in thick walled liquid hydrogen tank
[NASA-TM-X-1870] c28 N69-35712
Spectroscopic study of helium arc
[NASA-TN-D-5396] c25 N69-36755
Helium pressurization systems for liquid methane fuel in supersonic transports
[NASA-TN-D-5519] c28 N69-40329
Biochemical and metabolic effects of exposure of mice to helium-oxygen atmosphere
[NASA-CR-1372] c04 N69-40955
HELIUM AFTERGLOW
Electron beam fluorescence probe and afterglow investigation for hypersonic He flow visualization, observing qualitative structure
c11 A69-35722
HELIUM IONS
Light ion abundance measurements of OGO satellites and field aligned diffusive equilibrium theory with temperature and concentration latitudinal variations
c13 A69-25157
Two photon decay of metastable levels of hydrogenic and He-like ions in solar corona, depopulating via proton collisional excitation to 2p level
c29 A69-36218
Explorer 34 observations of hydrogen and He ions in solar wind, noting number density variations and tentative association with geomagnetic storms
c29 A69-40305
Autoionized resonance transitions of He at 206.2-192.2 A using He continuum produced by capillary spark, also producing He II line spectra
c23 A69-42149
HELIUM ISOTOPES
Differential cross sections for elastic scattering of 600 Mev protons from He 3 between 19 and 45 degrees
c24 A69-13464
Cosmic ray deuteron and He 3 secondary origin and determination of cosmic ray path length and residual interplanetary field modulation
c29 A69-20066
He 2 excitation spectrum for interparticle potential using pair Hamiltonian with repulsive core and attractive well
c24 A69-33118
Dilute solution of He 3 in He 4 near absolute zero measured for viscosity, showing temperature effect
c23 A69-39582
Elastic and nonelastic scattering cross sections from 42 MeV alpha particles interacting with helium isctopes
[NASA-TN-D-5530] c24 N69-40979
HELMETS
EEG monitor helmet for aircraft or flight simulator programs, discussing sensing and transmitting system
c05 A69-26553
Relationship between binocular depth perception and optical distortion in Apollo pressure suit helmets and visors
[NASA-TN-D-5162] c05 N69-22990
HELMHOLTZ VORTICITY EQUATION
Helmholtz resonators with variable cavity depths tested with unstable rocket combustor
[NASA-TN-D-5171] c33 N69-23351
HEMATOCRIT RATIO
Repeated blcod sampling effect on plasma cholinesterase, acid phosphatase, alkaline phosphatase and hematocrit ratios in domestic chickens
c04 A69-23158
HEMATOLOGY
Repeated blcod sampling effect on plasma cholinesterase, acid phosphatase, alkaline phosphatase and hematocrit ratios in domestic chickens
c04 A69-23158
HERMETIC SEALS
Sealed and unsealed relay coils temperature rise at simulated outer space air pressure levels
c09 A69-28048
Pump and seal parameters for helical groove, hermetically sealed pump and bearing rotor
[NASA-TN-D-5225] c15 N69-24791
Halogen detector for leakage in hermetically sealed devices
[NASA-TN-D-5457] c09 N69-38597
HIGH ALTITUDE
Base flow field at high altitude for four-engine clustered nozzle configuration
[NASA-TN-D-5164] c12 N69-24936
HIGH ALTITUDE BALLOONS
Winds aloft and wind shear analysis from jimsphere wind sensor balloon-radar data
[NASA-CR-1204] c20 N69-13629
HIGH ALTITUDE TESTS
Structure and mean molecular weight measurement of unknown atmosphere assessed from high altitude tests in earth atmosphere
[AIAA PAPER 68-1054] c30 A69-13699
HIGH ENERGY ELECTRONS
Interplanetary relativistic electrons from solar flare events
c29 A69-15528
Hydrogenic atoms ionization by high energy electrons, discussing cross sections for ejected electrons and total energy
c24 A69-20738
Fast electron diffusion in stochastic magnetic field, obtaining diffusion coefficient as function of ratio of correlation time to Larmor period
c25 A69-20807
Relativistic solar electron detection in interplanetary space during July 7, 1966 proton flare event, noting energy spectrum and time

history
c29 A69-23766
High energy cosmic radiation problems
[NASA-SP-199] c29 N69-29652
HIGH ENERGY INTERACTIONS
High energy scattering approximation valid from small to large angles, discussing errors and proton scattering by He
c24 A69-29008
Photodisintegration of ultrahigh energy cosmic rays by universal radiation field, analyzing implications on origin and propagation time
c29 A69-35006
Proton-antiproton high energy elastic scattering by bosons exchange, introducing vertex functions for nonlocal Lagrangian
c24 A69-39467
HIGH FIELD MAGNETS
Cryogenic solenoids with pure Al conductor for production of strong magnetic fields, discussing softness and strain resistivity problems
c03 A69-26497
Design, construction, testing, and control devices for high-field electromagnets
[NASA-TN-D-4910] c23 N69-10889
HIGH FREQUENCIES
Synchroton radiation HF cut-off resulting from electrons with anisotropic pitch angle distribution for type 4 solar radio bursts
c29 A69-40577
HIGH POLYMERS
Skin friction drag reducing high polymer solution injected into turbulent boundary layer to test effectiveness on marine vehicles
c12 A69-33254
HIGH PRESSURE
Thomas-Fermi approximation applied to calculation of equations of state and thermodynamic functions at high pressure from differential equations of statistical atom model
c24 A69-40186
HIGH RESOLUTION
High resolution and image intensity of field ion microscope at low temperatures
[NASA-TN-D-5125] c14 N69-21408
HIGH STRENGTH ALLOYS
Columbium alloys properties, discussing creep strength, oxidation resistance, costs, production, etc
c17 A69-18791
Crack toughness characteristics of high strength alloys for use in heavy sections of supersonic aircraft
[NASA-TN-D-4998] c32 N69-17275
HIGH TEMPERATURE
Edge notch sensitivity in thin sheet nickel alloys under stress at high temperatures
[NASA-CR-1263] c32 N69-16156
High emittance coating materials for beryllium, niobium-zirconium compounds, and stainless steel used in spacecraft radiators
[NASA-CR-1278] c17 N69-18952
Tungsten-184 used as thermal flux monitor at high temperatures in Plum Brook reactor
[NASA-TN-D-5113] c22 N69-20795
Stress rupture and tensile properties of refractory metal wires at 2000 and 2200 deg F
[NASA-TN-D-5139] c32 N69-22823
Outdoor high temperature corrosion tests for aluminum alloys and titanium alloys, and stainless steels
[NASA-TN-D-5362] c17 N69-32558
Chromium base alloys for high temperature application in jet engines
[NASA-TM-X-1867] c17 N69-35764
Development and inverter circuit tests of high temperature cesium vapor thyratrons
[NASA-CR-1435] c03 N69-36843
Hot-salt stress-corrosion of titanium alloy under simulated turbine engine compressor environment
[NASA-TN-D-5510] c17 N69-40242
HIGH TEMPERATURE AIR
Oxidation behavior of coated molybdenum and niobium alloys in high temperature supersonic air streams
[NASA-TN-D-4877] c17 N69-10764
HIGH TEMPERATURE ENVIRONMENTS
Venus atmosphere origin, discussing high temperature effects and chemical composition via space probe and terrestrial observations
c30 A69-23183
Thermal electromotive force change for thermocouples in high temperature, low pressure environments for 3700 hours
[NASA-TN-D-5287] c14 N69-29196
HIGH TEMPERATURE FLUIDS
Chemical reactions activation energy at high temperature, noting cross section shape role for deducing activation energy from rate data
c06 A69-34443
HIGH TEMPERATURE GASES
Nongray equilibrium radiative heat transfer in viscous radiating shock layer around blunt body entering high temperature nonisothermal carbon dioxide-nitrogen atmosphere
[AIAA PAPER 69-636] c33 A69-33258
Modified model for vibration-dissociation relaxation coupling phenomena in nonequilibrium high temperature gas flow, discussing parameter U variation with kinetic temperature
c12 A69-37208
Quartz-insulated, single-wire thermocouples installed on thin-wall rocket cooling tubes to measure hot-gas-side wall temperatures
[NASA-TN-D-5291] c14 N69-29553
Measurement of thermal accommodation coefficients between liquids and high temperature gases in low pressure reentry communications blackout intervals
[NASA-CR-1330] c07 N69-32721
Empirically determined wind and scale effects on hot gas recirculation characteristics of jet V/STOL aircraft
[NASA-CR-1445] c28 N69-40776
HIGH TEMPERATURE LUBRICANTS
Steel ball bearing high temperature fatigue life tested with synthetic paraffinic oil, fluorocarbon and polyphenyl ether
[ASME PAPER 69-LUBS-18] c15 A69-34378
Oxygen concentration effects on ester lubricant degradation during high temperature bearing test
[NASA-TN-D-5262] c15 N69-26311
Oxygen concentration effects on synthetic paraffinic oil lubricant performance in high temperature bearing tests
[NASA-TN-D-5152] c15 N69-26314
Rare earth fluorides and oxides used as solid lubricants at high temperatures
[NASA-TN-D-5301] c15 N69-29568
Feasibility tests on liquid lubricants for inerted lubrication systems of advanced aircraft engines
[NASA-TN-D-5420] c15 N69-35788
HIGH TEMPERATURE RESEARCH
High temperature fatigue tests conducted to determine bearing life of angular contact ball bearing elements
[NASA-TN-D-5002] c15 N69-16367
Performance and cavitation damage to axial flow pump rotor blades in high temperature liquid sodium
[NASA-TN-D-5138] c15 N69-21773
Soviet research on high temperature strength of materials and machine parts
[NASA-TT-F-508] c17 N69-27300
Burst testing of tungsten tubing at high temperatures
[NASA-TM-X-1843] c17 N69-31889
Mechanical behavior of tantalum T-111 alloy at high temperatures and ultrahigh vacuum
[NASA-CR-1436] c17 N69-36831
HIGH TEMPERATURE TESTS
Superplasticity in W-Re alloys, noting tensile properties, grain size and strain rate sensitivity for various Re contents at high temperatures
c17 A69-22990
Boron nitride and boron nitride composite under high temperatures in air and vacuum for various time periods, discussing thermal shock and oxidation resistance
c18 A69-36208
High purity dielectric materials tested in capacitors at high temperatures
[NASA-CR-1213] c18 N69-14400
Strain-rate sensitivity of three titanium-alloy sheet materials after prolonged exposure to high temperature
[NASA-TN-D-4981] c17 N69-14873

High temperature mechanical properties of polycrystalline hafnium carbide containing 13-volume-percent hafnium diboride
[NASA-TN-D-5008] c17 N69-16380
Calorimetric analyses of metal corrosions in deionized heated water
[NASA-TM-X-1791] c17 N69-25243
Development and high temperature tests of high strength nickel alloy for stator vanes of gas turbine engines
[NASA-TN-D-5352] c17 N69-31873
Cavitation damage and effect of fluid temperature on performance of axial flow pumps in liquid sodium
[NASA-TN-D-5484] c15 N69-38641
Temperature effects on turbofan and turbojet noise radiation
[NASA-CR-1472] c02 N69-40439

HIGH VACUUM
Sliding friction and wear behavior of copper alloys in air and vacuum
[NASA-TN-D-4824] c15 N69-10757

HIGHWAYS
Runway and highway pavement grooving and traction studies
[NASA-SP-5073] c11 N69-20451

HILBERT SPACE
Existence, uniqueness, and stability criteria for linear and nonlinear operational differential equations in Banach and Hilbert spaces
[NASA-CR-1356] c19 N69-28256

HINGES
Heat transfer and pressure distributions inside hinge line gap of wedge-flap combination at hypersonic speeds
[NASA-TN-D-4911] c01 N69-11009
Performance tests on dynamic jettison hinge loads of Centaur nose fairing
[NASA-TM-X-1821] c32 N69-29734

HISTORIES
Historical developments in aviation and astronautics including liquid propellant rocket engine design, electric rocket engines, aircraft engines, and inertial guidance
[NASA-TT-F-540] c34 N69-31836

HODOGRAPHS
Normalized hodographic mapping for constrained trajectory families, discussing mapping concepts, information content and applications
[AIAA PAPER 69-924] c30 A69-39362

HOLES (ELECTRON DEFICIENCIES)
Periodicity of magnetothermal oscillations in pressure annealed pyrolytic graphite compared with hole carriers
c26 A69-29005

HOLOGRAPHY
Holographic displays using ultrasonic vibrations or laser outputs as optical sources, discussing recording materials, responses and computer applications
c14 A69-21394
Extended source Fourier transform holography for single image synthesis of multiple identical images produced by multiple pinhole camera in X ray astronomy
c14 A69-40019
Holographic microscopy for performance prediction and quality control of semiconductor devices and integrated circuits
[NASA-CR-1394] c14 N69-31958
Object motion effect in Fraunhofer holography with application to velocity measurements
[NASA-TN-D-5515] c14 N69-40812

HONEYCOMB STRUCTURES
Multiwall meteoroid protection design in Apollo program, discussing bumper, backup sheet and honeycomb cells insulation
[AIAA PAPER 69-372] c32 A69-28304
Forced convection heat-transfer data for hydrogen flow through heated parallel hexagonal passages
[NASA-TN-D-4959] c33 N69-14588
Wind tunnel study of open-face honeycomb to reduce temperature of hypersonic aircraft structure
[NASA-TN-D-5278] c33 N69-29599
Photographic study on bromine jet boundary shape in coaxial airstream with honeycombs at injection plane
[NASA-TM-X-1900] c12 N69-39303

HORIZON
Horizon radiance profile analysis for determining atmospheric temperature
[NASA-TN-D-5068] c13 N69-19024

HORIZON SCANNERS
Infrared horizon radiance profiles for winter conditions based on Scanner project flight test
[NASA-TN-D-4905] c21 N69-14346
Computer program used to infer atmospheric water-vapor mixing ratio from measured horizon radiance profiles
[NASA-TN-D-5252] c13 N69-27246
Stratospheric and mesospheric temperature and moisture profiles determined from infrared horizon observations
[NASA-CR-1419] c20 N69-35528

HORIZONTAL FLIGHT
Aerodynamic stability of helicopter rotor in forward flight
[NASA-CR-1332] c32 N69-34744

HORIZONTAL TAIL SURFACES
Factors affecting flat spin characteristics of fighter aircraft with horizontal tail surfaces
[NASA-TN-D-5409] c02 N69-36807

HORMONES
Identity between growth hormone degrading activity of pituitary gland and plasmin
c04 A69-17105
Blood sampling for parathyroid hormone and calcium metabolism during weightlessness of space flight
[NASA-CR-1395] c05 N69-38600

HOT CATHODES
Predicting relative sensitivities of hot cathode ionization vacuum gages
[NASA-TN-D-5285] c14 N69-29331

HOT STARS
Structure and pulsational properties of massive stars with helium cores and thin hydrogen poor envelopes
c30 A69-22421
Helium-carbon star BD plus 10 degrees 2179 reanalyzed by grid of constant flux models containing right amount of C
c30 A69-40652

HOT-WIRE FLOWMETERS
Turbulence measurement errors with inclined hot wires described by equations, assuming normal component cooling includes greater tangential cooling
c14 A69-34442

HOTSHOT WIND TUNNELS
Real helium hypersonic flow parameters for pressures to 3600 atmospheres and temperatures to 15,000 deg K applicable to hotshot type wind tunnels
[NASA-TN-D-4869] c12 N69-10443

HOVERING
Theory for predicting rotational and vortex noise of lifting rotors in hovering and forward flight
[NASA-CR-1333] c23 N69-25344
Evaluation of six degrees of freedom motion simulator for Bell X-14A aircraft hovering characteristics
[NASA-TN-D-5383] c11 N69-35359

HOVERING STABILITY
Lift loss and jet decay measurements on hovering vertical takeoff aircraft models
[NASA-CR-1297] c01 N69-21477

HUMAN BEINGS
Gravitational and acceleration effects on man and organisms, and biological effects of radiation
[NASA-TT-F-528] c05 N69-38701
Electro-optical instrument for measuring pointing direction of human eye
[NASA-CR-1422] c05 N69-39212

HUMAN BODY
Human body dynamic response to vibration combined with linear acceleration, noting changes in body mechanical impedance and resonance
c05 A69-11335
Human vestibular system and its connection with oculomotor system and their relation to motion perception, spatial disorientation, and illusions
[NASA-CR-1309] c04 N69-22637
Respiratory system and oxygen metabolism regulation in man and animals
[NASA-TT-F-501] c04 N69-31401

HUMAN CENTRIFUGES
Centrifugation for removal of bullet fragment floating freely in ventricular system of human brain to fixed safe position in left lateral ventricle wall
c04 A69-43372

HUMAN FACTORS ENGINEERING
Modular three dimensional mockup technique for economizing and facilitating design of control and display equipment
c05 A69-11953
Weightless simulators effectiveness for obtaining space systems maintainability criteria, using nonparametric experimental design for performance data
c05 A69-17648
Manned space stations for future space exploration, discussing earth-like environment, artificial gravity, human factors and time dependence
c30 A69-25644
Man-computer speech communication, discussing model and aspects of acoustics, phonetics, linguistics, language training, physiology, psychology, bionics, etc
c08 A69-35099
Human angular acceleration sensitivity using rotation and oculogyral illusion perception as indicators, relating to spatial orientation and flight control task precision
c05 A69-41674
Conference on NASA research in noise reduction of subsonic jet aircraft - nacelle acoustic linings, sound generation in jet engines, and operational noise effects on humans
[NASA-SP-189] c02 N69-11542
Visual sensing and spacecraft guidance for earth orbit rendezvous maneuvers
[NASA-CR-1214] c05 N69-13161
Practice and operator work load effects on acquisition and performance of code transformation /COTRAN/ task
[NASA-CR-1261] c05 N69-14345
Physiological and psychological responses of man to space flight problems
[NASA-TT-F-529] c05 N69-32044

HUMAN PERFORMANCE
Hypohydration effects on isometric muscular strength, noting decreasing trends in maximal strength
c04 A69-15983
Ideal safety system for accident prevention, considering foreseeable and unforeseeable aspects to eliminate individual or collective human error
c34 A69-16836
Human information processing rates during one and two axis compensatory tracking tasks with secondary auditory task
c05 A69-23880
Efficacy of sensory feedback information given during training period for improving human performance in producing memorized movement pattern
[NASA-CR-1251] c05 N69-13926
Small perturbation dynamics of neuromuscular system in tracking tasks
[NASA-CR-1212] c05 N69-14212
Proprioceptor influence on operator performance in manual control situations
[NASA-CR-1248] c05 N69-14768
Modified Fourier transform for calculating human operator describing functions
[NASA-TM-X-1762] c08 N69-21119

HUMAN REACTIONS
Rotational velocity estimates by observers during angular acceleration, noting vestibular function interpretation
c04 A69-15332
Psychophysical methods for determining perception threshold of angular acceleration in man during vertical rotation
c04 A69-15969
Space medicine to characterize nature and degree of changes in human functional capabilities due to space flight environment prolonged exposure
c34 A69-36460
Carbon dioxide levels monitoring in spacesuit research including limits of physiological acceptability
c05 A69-39170
Human physiological responses to angular acceleration during breath holding, Mi, Valsalva and Mueller respiratory maneuvers in hollow spherical simulator
c05 A69-41679
Conference on NASA research in noise reduction of subsonic jet aircraft - nacelle acoustic linings, sound generation in jet engines, and operational noise effects on humans
[NASA-SP-189] c02 N69-11542
Space flight effects on human time perception
[NASA-TT-F-545] c05 N69-26455
Predicting human performance in space environments
[NASA-CR-1370] c05 N69-30168
Coordination of voluntary movements of man in zero gravitational fields
[NASA-TT-F-578] c04 N69-31356

HUMAN TOLERANCES
Artificial heat acclimatization effect on orthostatic tolerance in man exposed to stresses of heat, exercise and dehydration
c05 A69-32810
Human responses to aerospace environment in relation to microwave, light, thermal, and ionizing radiation
[NASA-CR-1205-VOL-1] c04 N69-12434
Human responses to aerospace environment related to acceleration, vibration, sound, and noise
[NASA-CR-1205-VOL-2] c04 N69-12588
Conversion tables for studies of human responses to aerospace environment
[NASA-CR-1205-VOL-4] c04 N69-12600
Operational and structural design criteria for artificial gravity stabilization of rotating space station
[NASA-TN-D-5426] c05 N69-39210

HUMAN WASTES
Material recovery from metabolic and other wastes for long duration manned space missions, discussing carbon dioxide removal, bioregenerative food systems, etc
[AAS PAPER 69-143] c05 A69-42876
Manned spacecraft waste disposal systems
[NASA-TM-X-1851] c05 N69-33260

HYBRID PROPELLANT ROCKET ENGINES
Rocket-scramjet hybrid engines in lifting reusable second stage
[NASA-TN-D-5218] c28 N69-24922

HYDRATION
Hydration, oxidation, and origin of calc-alkali differentiation series of igneous rocks
[NASA-TN-D-5400] c13 N69-40893

HYDRAULIC EQUIPMENT
Transient performance of full flow hydraulic turbine driven two speed pump inducer system, formulating computer model
[AIAA PAPER 69-551] c15 A69-34415
Hydraulic-powered self propelled six degree of freedom loading vehicle moving tests assembly to test chamber with high accuracy positioning
c11 A69-38181
Lubrication performance and thermal shear degradation of polyphenyl ethers and refined mineral oils in high temperature vane pump loop
[NASA-TN-D-5096] c15 N69-20938

HYDRAULIC JETS
Mean drop size generated in vapor pressure regime of liquid water jet, noting effect of water temperature and orifice diameter
c12 A69-21995
Noncavitating and cavitating performance of low area ratio water jet pumps, analyzing efficiency, area ratio, throat length, nozzle spacing and diffuser geometry
c03 A69-35176

HYDRAZINES
Isothiocyanates and phenyl isocyanate reaction with hydrazinoethanol and hydrazinoethyl hydrogen sulfate
c06 A69-31808

HYDROCARBONS
Absorption coefficient measurement for hydrocarbon gases for He-Ne laser beam at 3.39 microns, tabulating coefficients, noting variations from spectroscopic data
c16 A69-42192

HYDRODYNAMIC EQUATIONS
Initial hydrodynamic phase of hypervelocity impact analyzed by computer program using eigenvector approach
[NASA-TR-R-298] c32 N69-24765
HYDRODYNAMICS
Nova outburst dynamics investigation by time dependent hydrodynamics computer program including energy transport by radiation and convection
c30 A69-30769
Momentum integral method treating magnetohydrodynamic and simple hydrodynamic entrance flows
[NASA-TN-D-5215] c25 N69-24920
Hydrodynamic stability of inviscid rotating coaxial jets
[NASA-CR-1363] c12 N69-24926
Survey of incompressible and compressible fluid film hydrostatic and hydrodynamic lubrication
[NASA-SP-5058] c15 N69-28592
HYDROGEN
Pressure and temperature dependence of slow crack growth in hardened steel in gaseous hydrogen environment
c17 A69-10612
Hydrogen absorption coefficients, giving number densities in hydrogen gas or plasma for wide range of temperature and pressure
c24 A69-19165
Cooling requirements for high speed polytetrafluorethylene lubricated ball bearings operating in cold hydrogen gas, developing minimum gas flow rate equation
[ASLE PAPER 68-LC-2] c15 A69-19310
High pressure storage vessels for gaseous hydrogen, discussing failure, manufacturing controls and access for internal nondestructive inspection
[ASM PAPER D8-14.1] c15 A69-19666
Segmented anode, carbon dioxide-hydrogen performance and hollow cathode erosion tests on low power MPD arc thrustor, noting current measurements
[AIAA PAPER 69-242] c28 A69-21236
Pulsed glow discharges in He and He-H mixtures for high current density, noting electric field and wall potential distributions
c25 A69-23660
Nuclear energized pulsational instability of stars based on linear quasi-adiabatic theory, including models with hydrogen burning shells
c30 A69-27576
Hot salt stress corrosion of Ti alloy, discussing hydrogen generation during elevated temperature exposure and embrittlement as manifestation of strain rate
c17 A69-39434
Order-disorder transitions in solid hydrogen, discussing model to explain molecular rotation angular momentum operator fluctuations
c23 A69-43119
Forced convection heat-transfer data for hydrogen flow through heated parallel hexagonal passages
[NASA-TN-D-4959] c33 N69-14588
Thermodynamic properties of erbium hydrogen binary system evaluated for use as low pressure standard
[NASA-CR-1271] c14 N69-16099
Hot salt stress corrosion of titanium alloys - generation of hydrogen and its embrittling effect
[NASA-TN-D-5000] c17 N69-16465
Measurement of liquid and two phase hydrogen densities with capacitance density meter
[NASA-TN-D-5015] c14 N69-23470
Ramp pressurization tests with gaseous helium in thick walled liquid hydrogen tank
[NASA-TM-X-1870] c28 N69-35712
Rapid computation of equilibrium, chemical composition, and thermodynamic properties of argon-oxygen-hydrogen gas system
[NASA-TN-D-5416] c33 N69-36299
Absorption of hydrogen by palladium and electrical resistivity of hydrogen-palladium system
[NASA-TN-D-5441] c26 N69-37272
Interaction energy and dipole moment in collisions of two hydrogen molecules
[NASA-TN-D-5486] c24 N69-39184
HYDROGEN ATOMS
Electron impact ionization cross sections for second quantum level of atomic H, using Born exchange approximation and Vainshtein approximation
c24 A69-17138
Hydrogenic atoms ionization by high energy electrons, discussing cross sections for ejected electrons and total energy
c24 A69-20738
Primary processes leading to atomic and molecular hydrogen formation in hydrogen peroxide photolysis at 1236 A, noting OH formation
c06 A69-23527
HYDROGEN CYANIDES
Simultaneous HCN and HOH laser emission in pulsed discharge through mixture containing H, C, N, and O
c16 A69-26330
HYDROGEN IONS
Elastic scattering of slow electrons by negative H and positive Li ions, calculating differential cross sections and phase shifts
c24 A69-12924
Light ion abundance measurements of OGO satellites and field aligned diffusive equilibrium theory with temperature and concentration latitudinal variations
c13 A69-25157
Dynamical effects in structure of H II equilibrium region left behind expanding ionization front, showing temperature as function of distance from star
c30 A69-35966
Two photon decay of metastable levels of hydrogenic and He-like ions in solar corona, depopulating via proton collisional excitation to 2p level
c29 A69-36218
Photospheric radiation field role in temperature inversion of stellar chromospheres with dominant H ion opacity, postulating mechanical energy dissipation
c30 A69-38173
Explorer 34 observations of hydrogen and He ions in solar wind, noting number density variations and tentative association with geomagnetic storms
c29 A69-40305
Positively charged diatomic hydrogen molecules interstellar extinction and photodissociation cross section in terms of formation mechanisms
c30 A69-42610
HYDROGEN OXYGEN ENGINES
Liquid rocket acoustic instability for hydrogen-oxygen and earth storable propellant combinations
[NASA-TN-D-4968] c28 N69-14384
Measured effects of gaseous flow system dynamics on acoustic mode combustion instability
[NASA-TN-D-5080] c33 N69-20882
Injector radial distribution and thrust chamber geometry effect on acoustic mode instability in hydrogen oxygen engines
[NASA-TN-D-5375] c33 N69-32340
HYDROGEN OXYGEN FUEL CELLS
Water electrolysis, discussing oxygen generators for spacecraft prototype cells and testing
c05 A69-12987
Oxygen supply inert diluent impurities effect on hydrogen-oxygen fuel cell performance
c03 A69-15310
High performance light weight electrodes for hydrogen oxygen fuel cells
[NASA-CR-1216] c03 N69-14397
Performance of prototype hydrogen oxygen electrolytic regenerative fuel cell stack with gas storage tank
[NASA-CR-1244] c03 N69-18885
HYDROGEN PEROXIDE
Primary processes leading to atomic and molecular hydrogen formation in hydrogen peroxide photolysis at 1236 A, noting OH formation
c06 A69-23527
HYDROGEN PLASMA
Hydrogen absorption coefficients, giving number densities in hydrogen gas or plasma for wide range of temperature and pressure
c24 A69-19165

Number densities of hydrogen species in hydrogen plasma - tables
[NASA-TN-D-4993] c25 N69-16466
Measurement of change in plasma potential and magnetic field of hydrogen plasma impinging on magnetic dipole - simulation of solar wind-earth interaction
[NASA-TM-X-1738] c25 N69-19131
Energy transfer and ion cost in hydrogen plasma
[NASA-TN-D-5319] c25 N69-29905
Interim absorption coefficients and opacities for hydrogen plasma at high pressure
[NASA-TM-X-1902] c24 N69-39187

HYDROGEN RECOMBINATIONS
Nonequilibrium gas dynamics of hydrogen dissociation and recombination
[NASA-CR-1411] c12 N69-34709

HYDROGENATION
Optimal growths of silicon carbide polytype crystals by methyltrichlorosilane reduction
[NASA-TN-D-5313] c26 N69-30072

HYDROGENOMONAS
NADH stimulation of ATP dependent carbon dioxide fixation in crude extracts of Hydrogenomonas facilis, considering allosteric regulation of phosphoribulokinase activity
c04 A69-30036
Hydrogenomonas cultures investigated for metabolic waste utilization in aerospace life support systems
[NASA-CR-1296] c05 N69-22766

HYDROSTATICS
Survey of incompressible and compressible fluid film hydrostatic and hydrodynamic lubrication
[NASA-SP-5058] c15 N69-28592

HYDROXYL COMPOUNDS
Primary processes leading to atomic and molecular hydrogen formation in hydrogen peroxide photolysis at 1236 A, noting OH formation
c06 A69-23527

HYPERBOLIC FUNCTIONS
Finite difference techniques used in numerical solutions for inviscid radiating shock layers around spheres at hyperbolic speed in air
[NASA-TR-R-311] c12 N69-26504

HYPERGEOMETRIC FUNCTIONS
Analytic continuation of Appell hypergeometric series into linear combination of four infinite series
c19 A69-26605

HYPERGOLIC ROCKET PROPELLANTS
Combustion response of hydrazine-nitrogen tetroxide hypergolic rocket propellants to transverse gas flows, noting coupled and uncoupled oscillations
c33 A69-10112

HYPEROXIA
High oxygen tension effect on transport and incorporation of exogenous leucine and protein synthesis in Pseudomonas saccharophila cells
c04 A69-13433
Hyperoxia and hypoxia effects on mitotic activity in regenerating and normal rat liver exposed to environmental conditions
c04 A69-43565

HYPERSONIC AIRCRAFT
Fluidic type temperature sensor for total temperature measurement for hypersonic aircraft in atmosphere
c14 A69-16755
Drag influence on mission performance of hypersonic aircraft during climb and cruise, noting payload capacity
c02 A69-37154
Transonic aerodynamic characteristics of two hypersonic cruise configurations
[NASA-TM-X-1816] c01 N69-29231
Experimental and theoretical study of symmetrical and cambered Delta wing configuration between Mach 2.0 and 10.7
[NASA-TN-D-5272] c01 N69-29269
Wind tunnel study of open-face honeycomb to reduce temperature of hypersonic aircraft structure
[NASA-TN-D-5278] c33 N69-29599
Wind tunnel stability tests to determine effect of hypersonic research engine on aerodynamic characteristics of research aircraft
[NASA-TM-X-1840] c01 N69-38612

HYPERSONIC BOUNDARY LAYER
Density and velocity fluctuations in hypersonic turbulent boundary layer based on Wallace data
c12 A69-31908
Free stream disturbances influence on hypersonic boundary layer transition Reynolds number in heated and unheated flows
[AIAA PAPER 69-704] c12 A69-33453
Compressible hypersonic turbulent boundary layers solution by finite difference method, relating mixing length to velocity profile shape factor
[AIAA PAPER 69-684] c12 A69-33474

HYPERSONIC FLOW
Hypersonic flow distribution and separation types over highly swept Delta wing with trailing edge flaps at Mach 6
[AIAA PAPER 68-97] c01 A69-12522
Hypersonic body shaping for minimum drag and improved performance from view of flight regimes, discussing implications of pressure laws
[AIAA PAPER 69-181] c01 A69-18052
Three dimensional hypersonic steady flow around blunt and pointed cones at nonzero angles of attack calculated by method of characteristics
[AIAA PAPER 69-187] c01 A69-18176
Drag coefficients for spheres and sharp cones in rarefied hypersonic air flow obtained in shock tunnel using free flight technique
[AIAA PAPER 69-140] c01 A69-18184
Supersonic Preston tube correlations for Mach number and Reynolds number effects on hypersonic turbulent skin friction on adiabatic surfaces, simplifying correlation
[AIAA PAPER 69-345] c12 A69-28280
Subliming ablation effects on boundary layer transition for cones in hypersonic flow, discussing Reynolds numbers measured in wind tunnel tests
[AIAA PAPER 68-40] c01 A69-31881
Boundary layer trip geometry, size and location effects on position of transition at hypersonic speeds
c12 A69-33249
Surface pressure and heat transfer over blunt conical body in hypersonic flow with uniform mass addition of various gases
[AIAA PAPER 69-716] c01 A69-33463
Electron beam fluorescence probe and afterglow investigation for hypersonic He flow visualization, observing qualitative structure
c11 A69-35722
Mach 42 test measuring surface pressures, surface heat transfer rates and shock wave shapes in strong interaction regime for sharp and blunt plates
[AIAA PAPER 68-720] c01 A69-41886
Radiation equilibrium temperature measured downstream of transpiration cooled gas flow near slender cone vertex in continuous flow hypersonic tunnel
c01 A69-43588
Real helium hypersonic flow parameters for pressures to 3600 atmospheres and temperatures to 15,000 deg K applicable to hotshot type wind tunnels
[NASA-TN-D-4869] c12 N69-10443
Effect of unit Reynolds number, nose bluntness, angle of attack, and roughness on transition on 5 degree half-angle cone at Mach 8
[NASA-TN-D-4961] c01 N69-14872
Series solution for hypersonic flow about blunt bodies
[NASA-CR-1266] c33 N69-18125
Flow field from forward facing nozzles exhausting near large cylindrical body at free-stream Mach numbers of 3.0 and 6.0
[NASA-TN-D-5030] c01 N69-21000
Leading edge effects on laminar flat plate boundary layer and aerodynamic heating at Mach 10.4
[NASA-TN-D-5160] c12 N69-23467
Real gas effects on hypersonic aerodynamics of blunt vehicles simulated with tetrafluoromethane
[NASA-TR-R-312] c01 N69-29270
Boundary layer and chemical reactions in hypersonic gas flow
[NASA-TT-F-549] c33 N69-31947

Aerodynamic drag effects of hypersonic magnetohydrodynamic plasma flow around blunt bodies
[NASA-CR-1393] c25 N69-34897
Minimum drag bodies in hypersonic flow using calculus of variations
[NASA-TN-D-5438] c01 N69-36699
Turbulent boundary layer measurements on axisymmetric hypersonic nozzle walls
[NASA-TN-D-5433] c12 N69-36805
Flow field and drag characteristics of several laminar boundary layer tripping element in hypersonic flow
[NASA-TN-D-5454] c12 N69-38156

HYPERSONIC HEAT TRANSFER
Flow characteristics and wall heat transfer in separated flow region of annular cavity at free stream hypersonic speed and high gas temperature
[AIAA PAPER 68-672] c01 A69-37185
Mach 42 test measuring surface pressures, surface heat transfer rates and shock wave shapes in strong interaction regime for sharp and blunt plates
[AIAA PAPER 68-720] c01 A69-41886

HYPERSONIC REENTRY
Hypervelocity reentry simulation problems for slender and blunt bodies, defining significant parameters
c30 A69-30376

HYPERSONIC SHOCK
Shock shape and surface pressure measurements on hypersonic pointed cones in helium
[NASA-TN-D-5343] c01 N69-31228

HYPERSONIC SPEED
Mach number, cone angle, bluntness and wall to recovery temperature ratio effects on slender cones boundary layer transition measurements at hypersonic speeds
c01 A69-33250
Calculated and experimental hinge moments on trailing-edge flaps of swept Delta wings at hypersonic speeds and positive deflection angles
[NASA-TN-D-4268] c01 N69-10054
Heat transfer and pressure distributions inside hinge line gap of wedge-flap combination at hypersonic speeds
[NASA-TN-D-4911] c01 N69-11009
Hypersonic aerodynamic characteristics of low fineness ratio variable geometry logistics spacecraft model
[NASA-TM-X-1701] c01 N69-13218
Laminar heat transfer distributions for blunted-cone, cone frustum reentry configuration at hypersonic speed using Reynolds number
[NASA-TN-D-5146] c33 N69-22997
Solution for shock layer energy equation with mass and convective heat transfer at hypersonic speed
[NASA-TN-D-5246] c12 N69-33421
Numerical calculation of inviscid adiabatic flow field around blunt bodies at hypersonic speeds
[NASA-TN-D-5434] c12 N69-36830
Upwash patterns on ablating and nonablating cones at hypersonic speeds
[NASA-TN-D-5346] c12 N69-37370
Convective heat transfer rates on large angle conical bodies at hypersonic speeds
[NASA-TN-D-5526] c33 N69-40780

HYPERSONIC TEST APPARATUS
Hypersonic surface measurements and flowfield properties about slender cones in hypersonic viscous interaction regime
[AIAA PAPER 68-2] c01 A69-12520

HYPERSONIC VEHICLES
Cone-conical-frustrum configurations meeting center of gravity requirements for higher hypersonic lift-drag ratios in axisymmetric manned spacecraft
c01 A69-39237

HYPERVELOCITY FLOW
Pressure and temperature surveys of Mach 27-47 nozzle boundary layer at Ames M-50 He tunnel, determining velocity profiles, wall friction coefficient, etc
[AIAA PAPER 69-686] c12 A69-33441
Solution to radiation-coupled stagnating flow with nongray emission over hypervelocity blunt body
[NASA-TR-R-299] c33 N69-16268

HYPERVELOCITY IMPACT
Numerical method for time dependent compressible Navier-Stokes equations applied to axisymmetric flow field produced by hypervelocity impact, examining viscous effects
[AIAA PAPER 69-354] c32 A69-28288
Impact crater cross section in fused silica, describing photomicrographic technique for distinguishing hypervelocity from low energy impacts
[AIAA PAPER 69-367] c32 A69-28299
Hypervelocity micrometeor impact sites identification on aluminized glass, using conchoidal pattern as criterion in analysis
c30 A69-34952
Theoretical prediction of crater size in Al alloy for hypervelocity impact by reduced density particles
[NASA-CR-1196] c32 N69-10225
Projectile shape effects on hypervelocity impact craters in aluminum
[NASA-TN-D-4953] c32 N69-14315
Response of infinite elastic plates to axisymmetric initial velocity distributions with application to hypervelocity impact
[NASA-TN-D-5118] c32 N69-23448
Initial hydrodynamic phase of hypervelocity impact analyzed by computer program using eigenvector approach
[NASA-TR-R-298] c32 N69-24765
Momentum transfer from impact into thin aluminum meteor bumper targets
[NASA-TN-D-5492] c32 N69-38809

HYPERVELOCITY PROJECTILES
Bremsstrahlung spectra from bombardment of typical spacecraft materials by monoenergetic electrons
[NASA-CR-1377] c24 N69-33416

HYPOXIA
Hyperoxia and hypoxia effects on mitotic activity in regenerating and normal rat liver exposed to environmental conditions
c04 A69-43565
Respiratory system and oxygen metabolism regulation in man and animals
[NASA-TT-F-501] c04 N69-31401
Adaptation to hypoxia, acclimatization, and conditioning in human and animal subjects from Space Biology collection
[NASA-TT-F-580] c04 N69-32131

HYSTERESIS
Hysteresis of strain gage absolute pressure transducer
[NASA-TN-D-5327] c14 N69-30506

I

IBM 360 COMPUTER
Minitrack data reduction procedures, with IBM 360 computer program description
[NASA-TN-D-5042] c08 N69-26193

IBM 7040 COMPUTER
Computer experiments on the microscopic behavior of one dimensional electrostatic plasma
[NASA-TN-D-4831] c25 N69-10471

ICE
Critique of paper on water crystal existence on Venus, presenting arguments against existence of clouds of micron sized ice crystals
c30 A69-11292
Absorption of black-body radiation by ice cryodeposits on metal substrates
[NASA-TN-D-5181] c23 N69-22769

IDENTIFYING
Applications of quasi-linearization theory to system identification
[NASA-TN-D-5300] c19 N69-29648

IGNEOUS ROCKS
Partition coefficients between natural melts and plagioclase phenocrysts determined for rare earth elements and barium by mass spectrometry
c13 A69-20944
Hydration, oxidation, and origin of calc-alkali differentiation series of igneous rocks
[NASA-TN-D-5400] c13 N69-40893

IGNITERS
Development and test firing of improved igniter for first stage retrorockets of Atlas Centaur launch vehicle
[NASA-TM-X-1676] c28 N69-13275

IGNITION
Ignition hazards in electrical circuits

contaminated by glycol fluids, describing hazard detection by RF methods, decontamination procedures, safety checks, etc
c18 A69-36028
ILLUMINATING
Illumination in cryogenic or noncryogenic fluids by standard light bulbs
[NASA-TM-X-1654] c14 N69-13176
ILMENITE
Chemical analysis and paragenesis of manganoan ilmenite from Sierran adamellite using electron microprobe
c13 A69-35977
Ilmenite composition in equilibrated ordinary chondrites, analyzing Fe, Mg, Ti and Cr content
c30 A69-42890
IMAGE CONTRAST
Optimizing spacecraft televisions for successive picture overlapping and maximum surface resolution during planetary descent
[NASA-TN-D-5061] c14 N69-17259
IMAGE CONVERTERS
Image converter camera and astronomical telescope arrangement for photographing metal diaphragm openings in shock tube
c14 A69-37227
IMAGE DISSECTOR TUBES
Image dissector meteorological cameras, discussing ATS-3 and Nimbus systems, high resolution camera and multispectral cameras
c14 A69-35101
Electronically scanned star sensor with digital output for orbiting astronomical telescope
[NASA-TN-D-5281] c14 N69-29153
IMAGE INTENSIFIERS
High resolution and image intensity of field ion microscope at low temperatures
[NASA-TN-D-5125] c14 N69-21408
IMAGE ORTHICONS
Rocket trajectory determination by tracking onboard light source against star background with image orthicon TV system
c07 A69-26965
IMAGERY
Conference on motion degraded images and correcting procedures - optical filters and digital methods for blurring removal from photographic imagery
[NASA-SP-193] c14 N69-33322
IMAGING TECHNIQUES
Aerospace sensor systems, discussing adaptive multimode sensors and multispectral sensing, electronic recognition of image components, laser radar and Raman scattering technique
c14 A69-13851
Single and double mirror systems geometrical optical image aberrations noting focal number, angle of field, secondary magnification and mutual position tolerances
c23 A69-24836
Image dissector meteorological cameras, discussing ATS-3 and Nimbus systems, high resolution camera and multispectral cameras
c14 A69-35101
Extended source Fourier transform holography for single image synthesis of multiple identical images produced by multiple pinhole camera in X ray astronomy
c14 A69-40019
Conference on motion degraded images and correcting procedures - optical filters and digital methods for blurring removal from photographic imagery
[NASA-SP-193] c14 N69-33322
IMP
Interplanetary magnetic field fluctuations obtained by IMP 2
c30 A69-16264
Cosmic ray detectors design for medium, low and very low energy events on IMP-1 spacecraft, noting PCM format
c07 A69-41738
IMPACT DAMAGE
Spacecraft sterilization requirements, evaluating viable organisms release probability from spacecraft as function of equipment fracturing
c04 A69-25460
Impact crater cross section in fused silica, describing photomicrographic technique for distinguishing hypervelocity from low energy impacts
[AIAA PAPER 69-367] c32 A69-28299
Experimental and analytical studies of multiple liquid impact erosion of aluminum and stainless steel
[NASA-CR-1288] c15 N69-19786
IMPACT LOADS
Inflatable landing system investigated for impact normal to smooth surface
[NASA-TN-D-5236] c32 N69-26223
Cosmic dust sensor experiment on Pioneer 8 space probe
[NASA-TN-D-5267] c30 N69-31058
IMPACT TESTS
FM/AM telemetry circuits with three axis piezoelectric accelerometer for measurements during impact tests of soft landing models
c07 A69-23279
Aluminum double sheet target penetration resistance determined by studying high velocity pyrex glass impact effects on front/rear sheets and spacing
[AIAA PAPER 69-375] c32 A69-28305
Full scale dynamic landing impact investigation of prototype lunar module landing gear
[NASA-TN-D-5029] c31 N69-20965
Crater characteristics of 11 metal alloys under hypervelocity impact including effects of projectile density and target temperature
[NASA-TN-D-5135] c32 N69-22994
Forces on flexible shells of Apollo command module during water impact
[NASA-TM-X-1781] c32 N69-23697
IMPEDANCE PROBES
High speed compression waves, rarefaction waves and gas interface regions position and velocity measurement in shock tube by sensing electrical impedance
c14 A69-13104
IMPELLERS
Impeller matching effects on flow range and stability operating in liquid hydrogen
[NASA-TM-X-1727] c28 N69-16213
IMPINGEMENT
Impingement forces, moments, and centers of pressure due to air jets in vacuum sphere
[NASA-TN-D-5147] c12 N69-23085
IMPURITIES
Impurity profiles and energy band diagram for cuprous sulfide-CdS heterojunction based on capacitance, Hall and electron microprobe measurements
c03 A69-13075
Impurity profile and energy band diagram for cuprous sulfide-cadmium sulfide heterojunction
[NASA-TN-D-5079] c26 N69-19781
Electrical conductivity of lanthanum fluoride single crystal with calcium impurities
[NASA-TN-D-5505] c26 N69-40056
IN-FLIGHT MONITORING
Radiation protection plan for Apollo lunar mission based on real time monitoring of solar activity and radiation in spacecraft
[AIAA PAPER 69-19] c29 A69-18113
Onboard checkout system concept, discussing philosophy, requirements, underlying considerations, system description, development and techniques of system selection
c11 A69-25081
Jet engine compressor stalls in-flight investigation up to Mach 2 on F-111A by pressure sensors, noting steady state distortion role
[AIAA PAPER 69-488] c28 A69-32706
INCIDENT RADIATION
Solar absorptance and hemispherical emmitance of metals at space conditions determined with cyclic incident radiation technique
[AIAA PAPER 69-60] c17 A69-18154
Lunar surface thermal radiation incident on unit area flat surface located at variable distance and orientation above moon, considering diffusion effects
c30 A69-38973
Photomultiplier tubes performance enhancement by light incidence on photocathode at oblique angles explained by reflection
c23 A69-42194

INCOMPRESSIBLE FLOW
Incompressible two dimensional turbulent boundary layer equations with arbitrary pressure distribution solved by weighted residual method
[AIAA PAPER 69-397] c12 A69-30478
Incompressible turbulent boundary layer analysis by two region characterization for eddy viscosity, using Spalding generalized function and Prandtl free shear flow model
c12 A69-33255
Conducting fluid incompressible flow in entrance of MHD channel by momentum integral method, permitting edge stress existence at boundary layer free stream interface
[AIAA PAPER 69-724] c12 A69-33436
Laminar incompressible viscous flow in short cylindrical vortex chamber with finite swirl ratio
[NASA-TN-D-5132] c12 N69-21400
INCOMPRESSIBLE FLUIDS
Survey of incompressible and compressible fluid film hydrostatic and hydrodynamic lubrication
[NASA-SP-5058] c15 N69-28592
INDEPENDENT VARIABLES
PCM bit synchronizer/signal conditioners performance characteristics and specification
c09 A69-19120
Survey of rocket soundings to 60 km, and 100 km
[NASA-CR-1293] c13 N69-18700
Integral transformations used in time variable parameter estimation
[NASA-TN-D-5194] c19 N69-23788
Hydrogen gas pressure requirements during pressurization and transfer of liquid hydrogen from spherical tanks
[NASA-TN-D-5387] c28 N69-33211
INDEXES (DOCUMENTATION)
NASA scientific and technical information program for building technical data and literature repository for scientists, engineers and technical managers, describing IAA and STAR
[UN PAPER 68-95317] c34 A69-17068
Combined selective listing of NASA scientific and technical reports announced during 1968
[NASA-SP-7033] c34 N69-29492
Indexed and abstracted references to reports and articles on management available in NASA information system
[NASA-SP-7500/03/] c34 N69-32430
Bibliography of systems approach to management
[NASA-SP-7501] c34 N69-34917
Annotated bibliography and indexes on aerospace medicine and biological effects - May 1969
[NASA-SP-7011/64/] c04 N69-38242
INDIAN OCEAN
Tiros 7 monthly maps of infrared radiation over Indian Ocean area
[NASA-TN-D-5101] c13 N69-23318
INDICATING INSTRUMENTS
Leak detection for aerospace hardware, discussing equipment, operations, checkout, etc
c15 A69-30315
INDIUM
Backward diodes in indium arsenide for microwave mixing
[NASA-TN-D-5401] c09 N69-36706
INDUCTANCE
Inductance behavior of coils filled with superconducting lead or niobium dusts
[NASA-TN-D-5137] c26 N69-21500
INDUCTION HEATING
Spectral emission characteristics of gaseous tungsten and uranium in induction heated argon plasmas
[NASA-CR-1314] c25 N69-22920
Technology utilization of induction heating systems up to 5800 deg F
[NASA-SP-5071] c03 N69-23643
INDUCTORS
Analysis and design of inductors for protecting power transistors against current surges in inverter bridge circuits
[NASA-TN-D-4995] c10 N69-16198
Digital computer program for homopolar inductor alternator electromagnetic design analysis
[NASA-TN-D-5072] c03 N69-19799
Motor starting characteristics of two inductor alternators
[NASA-TM-X-1912] c03 N69-40440
INDUSTRIAL SAFETY
Treatment procedure and preventive programs outlined for acute exposure to toxic rocket fuels or oxidizers
c05 A69-12498
INDUSTRIES
Application of NASA mathematical management models and systems analyses in private industry and economy
[NASA-SP-5048] c34 N69-10662
Technology utilization by industries of aerospace sciences and systems - conferences
[NASA-SP-5075] c34 N69-31946
INELASTIC SCATTERING
Angular correlation of inelastically scattered alpha particles and gamma rays emitted from 2-plus state of Sn 120
c24 A69-13098
Angular correlation between inelastically scattered 42 MeV alpha particles and emitted gammas from 2-plus Ni 58
c24 A69-13100
Inelastic scattering cross sections calculated, comparing results for various nuclear states expressed as Wood-Saxon radial and harmonic oscillator functions
c26 A69-29006
Core polarization effects in inelastic scattering cross sections for several nuclei in 2s-1d shell, using Hartree-Fock wave functions and Born approximation
c24 A69-29007
Inelastic proton scattering cross sections for target nuclei in 2s-1d shell calculated in distorted wave Born approximation with projected Hartree-Fock wave functions
c24 A69-41045
INERTIA
Transverse shear deformation and rotary inertia effects in vibrating beams
[NASA-CR-1317] c32 N69-24056
INERTIAL GUIDANCE
Historical developments in aviation and astronautics including liquid propellant rocket engine design, electric rocket engines, aircraft engines, and inertial guidance
[NASA-TT-F-540] c34 N69-31836
INERTIAL NAVIGATION
Guidance and navigation flight tests, demonstrating system performance improvements by onboard inertial system communicating with external navigation aid
[AIAA PAPER 69-842] c21 A69-39429
V/STOL aircraft radar inertial navigation system, describing approach and landing phase flight test results
[AAS PAPER 69-401] c02 A69-42831
Computer-generated computational errors in direction cosine matrix for strapdown inertial system
[NASA-TR-R-304] c21 N69-21402
Vibration induced attitude errors in strapdown inertial navigators
[NASA-CR-1396] c21 N69-34672
INERTIAL PLATFORMS
Fourth angle driving law for different four gimbal systems used for simulation display and inertial platform isolation
c11 A69-26265
INFLATABLE SPACECRAFT
Inflatable landing system investigated for impact normal to smooth surface
[NASA-TN-D-5236] c32 N69-26223
INFLATABLE STRUCTURES
Structural and aerodynamic developments in attached inflatable decelerators for deployment of payload at supersonic speeds
[AIAA PAPER 68-929] c02 A69-39015
Inflation, drag, and stability characteristics of towed inflatable ballute decelerator at free flight
[NASA-TN-D-4943] c01 N69-17398
Wind tunnel tests of inflatable disk-gap-band and modified ringsail parachutes at low dynamic pressure
[NASA-TM-X-1786] c01 N69-23538
Supersonic deployment and extraction of inflatable towed ballute decelerator
[NASA-TM-X-1773] c31 N69-26458

Calorimetric evaluation of three 1.5-meter diameter inflatable rigidized solar concentrators for solar dynamic cycle power systems
[NASA-TN-D-5234] c03 N69-28123
Evaluation of double wall balloon enclosure for thermal control of inertial satellites
[NASA-TN-D-5230] c33 N69-28209
Free flight performance characteristics of ram air inflated recovery balloons with peripheral airscoops
[NASA-TN-D-5186] c21 N69-29595
Large scale wind tunnel investigation of lifting body with inflatable and rigid afterbody
[NASA-TN-D-5468] c01 N69-38775

INFORMATION RETRIEVAL
NASA scientific and technical information program for building technical data and literature repository for scientists, engineers and technical managers, describing IAA and STAR
[UN PAPER 68-95317] c34 A69-17068
NASA current awareness service SCAN /selected current aerospace notices/, promoting selectivity in information transfer to abstract journals, accession lists and bibliographies c34 A69-39581
Remote information retrieval facility description
[NASA-CR-1318] c08 N69-23381

INFORMATION SYSTEMS
NASA current awareness service SCAN /selected current aerospace notices/, promoting selectivity in information transfer to abstract journals, accession lists and bibliographies c34 A69-39581

INFORMATION THEORY
Huffman minimum redundancy coding extension to run-length information based on Poisson distribution, including optimization and data compression applications c07 A69-36262
Communication and information theories for digital and analog systems design
[NASA-TN-D-5472] c07 N69-39176

INFRARED ASTRONOMY
Balloon-borne instrumentation for detection of far IR extended emission regions and bright point sources, describing results of initial flights c30 A69-27599
HgCdTe as IR satellite detector for terrestrial, atmospheric and ocean mapping, IR astronomy and optical communication c26 A69-43666

INFRARED DETECTORS
Earth resources remote sensing from spacecraft noting meteorology, oceanography, forestry, agriculture and IR detection of plant diseases and pollution c34 A69-26978
HgCdTe as IR satellite detector for terrestrial, atmospheric and ocean mapping, IR astronomy and optical communication c26 A69-43666
Mercury cadmium telluride as 1 to 20 micrometer wavelength infrared detector for space applications
[NASA-TN-D-4904] c26 N69-10125
Visible and infrared transmitting properties of epoxy resin suitable for infrared detectors
[NASA-TM-X-1776] c18 N69-23843

INFRARED INSTRUMENTS
Balloon-borne instrumentation for detection of far IR extended emission regions and bright point sources, describing results of initial flights c30 A69-27599

INFRARED LASERS
Frequency and stability measurements in far IR laser region c16 A69-18482
Iodine IR laser, discussing CW emission obtained at various wavelengths and attributed to electronic transitions in atom
[IEEE PAPER T-5] c16 A69-19082

INFRARED PHOTOGRAPHY
HD 30353 He binary star invisible component suggested as KO type supergiant from IR photometric data c30 A69-35348
Surface temperature mapping with infrared photographic pyrometry for turbine cooling investigations
[NASA-TN-D-5179] c14 N69-23895

INFRARED RADIATION
IR radiation of NML Cygnus with O/C ratio close to unity ascribed to circumstellar shell of graphite particles c30 A69-13775
Inverse problems in radiative transfer applied to remote measurements of IR radiation from planetary atmospheres, noting temperature and water vapor inversions c13 A69-17617
Thermal and free-free emission from planetary nebulae based on graphite grain model, discussing IR fluxes c30 A69-27158
Residual interstellar gas from protostar formation detected as high luminosity IR object c29 A69-27593
Water vapor profiles in stratosphere from IR radiometric observations under cloudless conditions, indicating relation to tropospheric meteorological features c13 A69-38261
Thermal calculations of objects near lunar surface, considering IR emission directivity effects c30 A69-43254
Detecting geomorphological features over northeast Africa by Nimbus 2 visible and infrared radiation measurements
[NASA-TN-D-4648] c13 N69-14290
Infrared horizon radiance profiles for winter conditions based on Scanner project flight test
[NASA-TN-D-4905] c21 N69-14346
Nimbus 2 high resolution infrared radiometer data on earth resources of arid and subarid lands
[NASA-TN-D-4647] c13 N69-14450
Thermal and dielectric properties of homogeneous moon based on microwave and infrared temperature observations
[NASA-TM-X-1734] c30 N69-17815
Tiros 7 monthly maps of infrared radiation over Indian Ocean area
[NASA-TN-D-5101] c13 N69-23318
Infrared radiation measurements in space environment simulator using integral equations
[NASA-TN-D-5166] c29 N69-28111
Infrared heating simulation of Mach 4.63 flight on X-15 horizontal stabilizer
[NASA-TN-D-5403] c33 N69-35949

INFRARED REFLECTION
Ice clouds near IR spectral reflectivity dependence on particle size, noting application to planetary atmospheres c13 A69-34283

INFRARED SPECTRA
Atmospheric ozone vertical distribution and total amount determined by radiative transfer and perturbation theory, presenting error analysis c13 A69-28493
Ice clouds near IR spectral reflectivity dependence on particle size, noting application to planetary atmospheres c13 A69-34283
Vertical tropospheric humidity distribution estimation from IR spectra obtained by TIROS satellites c13 A69-34284
IR directional and hemispherical emittance of spacecraft thermal control coatings, comparing values determined by various measurement techniques c14 A69-41633
IR excess of R CrB type variable star RY Sgr, noting visual brightness and radiation in 2.0-3.4 micron range c30 A69-42377

INGREDIENTS
Determination of micromorphic material constants from elastic properties of constituents
[NASA-CR-1320] c32 N69-21569

INHOUR EQUATION
Pulsed neutron source studies to determine shutdown reactivities of unreflected solution reactor
[NASA-TN-D-5487] c22 N69-39186

INITIATORS (EXPLOSIVES)
Pretesting techniques of suppliers and users and

effects on electroexplosive devices
[NASA-CR-1203] c15 N69-10298
INJECTION
Injection of attached inviscid jet at oblique angle to moving stream
[NASA-TN-D-5501] c12 N69-39916
INJECTORS
Double-dead-time model describing chugging to liquid propellant rocket engines having multielement injectors
[NASA-TN-D-5303] c28 N69-29405
Design of injectors and ablative thrust chambers for FLOX propane rocket engine with 1.2 inch throat diameter
[NASA-TN-D-5324] c28 N69-30560
Injector radial distribution and thrust chamber geometry effect on acoustic mode instability in hydrogen oxygen engines
[NASA-TN-D-5375] c33 N69-32340
Dynamic stability and performance of injectors, rocket liners, and supersonic combustors
[NASA-TM-X-1845] c33 N69-32468
INJURIES
Biomechanical factors determining lung damage following explosive decompression of space suits in vacuum test chambers
[NASA-CR-1223] c05 N69-13969
INLET FLOW
Exhaust gas reingestion and inlet flow distortion in V/STOL lift engines, discussing static and wind tunnel testing using fighter configuration models
[AIAA PAPER 68-78] c01 A69-26762
Inlet thermal boundary layer thickness effect on conical nozzle heat transfer and boundary layer determined by operating nozzle with cooled/uncooled inlet
[AIAA PAPER 69-474] c33 A69-32780
Conducting fluid incompressible flow in entrance of MHD channel by momentum integral method, permitting edge stress existence at boundary layer free stream interface
[AIAA PAPER 69-724] c12 A69-33436
Hydrodynamic inlet conditions effect on film boiling and near critical hydrogen heat transfer, using data from electrically heated various geometry test sections
[ASME PAPER 69-HT-27] c33 A69-43541
Performance tests of wind tunnel model inlet for bleed system back pressure and porous area effect of axisymmetric compression
[NASA-TM-X-1710] c01 N69-14075
Theoretical analysis of axisymmetric flow in VTOL lift fan inlets without crossflow
[NASA-TN-D-5065] c01 N69-17831
Performance and stall limits of YTF30-P-1 turbofan engine with uniform compressor inlet flow
[NASA-TM-X-1803] c28 N69-27019
INLET NOZZLES
Large scale axisymmetric inlet systems performance capabilities, reviewing theoretical and experimental programs
[AIAA PAPER 68-580] c28 A69-34018
INLET PRESSURE
Flow analysis to determine turbine efficiency as function of inlet temperature for two stage turbine
[NASA-TM-X-1728] c01 N69-17392
INNER RADIATION BELT
Inner radiation zone including data on electrons, protons and heavier particles and results from high altitude nuclear tests
c29 A69-27144
Model environment of inner belt proton fluxes
[NASA-SP-3024-VOL-5] c24 N69-28911
INPUT
Problem of identifying input-output of pilot by measuring data from flight tests with pilot providing feedback control
[NASA-TN-D-5127] c05 N69-23842
INPUT/OUTPUT ROUTINES
Concepts of theory of fuzzy systems
[NASA-CR-1432] c19 N69-37033
INSECTS
Viruslike particles in fat body cells and oenocytes of Drosophila melanogasters imagoes, in glial cells of cephalic ganglionic center of flies and in gamma radiated cells
c04 A69-42021
INSPECTION
High pressure storage vessels for gaseous hydrogen, discussing failure, manufacturing controls and access for internal nondestructive inspection
[ASM PAPER D8-14.1] c15 A69-19666
INSTRUMENT APPROACH
Influence of angle of glide slope on accuracy of performing instrument approaches in simulator tests
[NASA-TN-D-4835] c21 N69-10056
INSTRUMENT COMPENSATION
Radiation compensating thermocouple for gas temperature measurement, noting advantage over single thermocouples
c14 A69-14916
INSTRUMENT ERRORS
Radiation ccmpensating thermocouple for gas temperature measurement, noting advantage over single thermocouples
c14 A69-14916
Root mean square time delay error with respect to playback time and autocorrelation function of tape recorded sine wave for studying jitter spectra
c14 A69-18827
Error analysis of high resolution balloon-borne temperature sensor and comparison of temperature data with simultaneous rawinsonde measurements
c14 A69-21642
Turbulence measurement errors with inclined hot wires described by equations, assuming normal component cooling includes greater tangential cooling
c14 A69-34442
Precision autocollimating solar sensor design for attitude alignment changes, including detector calibration and sounding rocket flight test results
[AIAA PAPER 69-858] c21 A69-39386
INSTRUMENT FLIGHT RULES
IFR flight tests of Breguet 941 STOL transport
[NASA-TN-D-4939] c02 N69-13252
INSTRUMENT LANDING SYSTEMS
Influence of angle of glide slope on accuracy of performing instrument approaches in simulator tests
[NASA-TN-D-4835] c21 N69-10056
Advanced electronic applications to navigation, data transmission, and airborne collision avoidance in general aviation aircraft and to simulated displays for low visibility landing
[NASA-CR-1240] c02 N69-14729
INSTRUMENT PACKAGES
Magnetometer experiment for Apollo project to measure lunar surface magnetic field, describing mission requirements and instrumentation
[AAS PAPER 68-206] c30 A69-11481
Manned spacecraft systems design optimization for extended space missions replacement modules
c31 A69-16380
Small Scientific Satellite program, discussing payload for investigating magnetosphere and near interplanetary space
[IEEE PAPER 3C-1] c31 A69-19195
Pyrotechnic activated calorimeter for reentry package design of vehicles entering earth atmosphere at lunar return velocities
c11 A69-23026
Simulated manual package transfer in weightless environment of Saturn Orbital Space Station
[NASA-TN-D-5111] c05 N69-21501
INSTRUMENTS
Instrumentation in the aerospace industry - Conference, Boston, June 1968, Volume 14
c11 A69-23245
Instrumentation in aerospace simulation facilities - Conference, Farmingdale, New York, May 1969
c11 A69-35714
INSULATED STRUCTURES
Gas breakdown model for analyzing breakdown of Ce vapor filled crack in thermionic trilayer insulator
c03 A69-21840
Multiwall meteoroid protection design in Apollo program, discussing bumper, backup sheet and honeycomb cells insulation
[AIAA PAPER 69-372] c32 A69-28304

INTAKE SYSTEMS
M 3.5 two dimensional mixed compression inlet system with self restart using flexible variable ramp system
[AIAA PAPER 69-447] c28 A69-32732
Transient performance of full flow hydraulic turbine driven two speed pump inducer system, formulating computer model
[AIAA PAPER 69-551] c15 A69-34415
Effects of boundary layer bleed rate and location on performance of axisymmetric inlet designed for Mach 2.5
[NASA-TM-X-1692] c01 N69-10294
Electron temperature instabilities in entrance region of magnetohydrodynamic generator
[NASA-TM-X-1761] c25 N69-20875
Characteristics study of bicone mixed compression inlet for Mach 1.80 to 2.50
[NASA-TN-D-5084] c01 N69-20914
Steady-state interactions between turbojet engine and axisymmetric inlet with induced distortions
[NASA-TM-X-1780] c28 N69-23519
Tandem bladed inducer tested in water for cavitation corrosion
[NASA-TN-D-5134] c01 N69-23769
Prediction of cavitation performance of centrifugal pumps
[NASA-TN-D-5292] c15 N69-29165
Two phase hydrogen flow in pump inlet line
[NASA-TN-D-5258] c15 N69-29476
Noncavitating and cavitating performance of inducer in liquid hydrogen
[NASA-TM-X-1854] c12 N69-33261
INTEGRAL EQUATIONS
Integral equation method with continuous functions for calculating boundary stress components in plane elasticity
[NASA-CR-1273] c32 N69-19030
Sonic boom propagation in stratified atmosphere using FORTRAN computer program with integral and differential equations
[NASA-CR-1299] c02 N69-22546
Vinti dynamic problem relevance to prediction of satellite orbits using differential and integral equations
[NASA-TR-R-307] c30 N69-22948
Momentum integral method treating magnetohydrodynamic and simple hydrodynamic entrance flows
[NASA-TN-D-5215] c25 N69-24920
Infrared radiation measurements in space environment simulator using integral equations
[NASA-TN-D-5166] c29 N69-28111
Integral relations solution for radiating, nonadiabatic, inviscid flow over blunt body
[NASA-TN-D-5480] c33 N69-40356
INTEGRAL TRANSFORMATIONS
Integral transformations used in time variable parameter estimation
[NASA-TN-D-5194] c19 N69-23788
INTEGRATED CIRCUITS
Hybrid integrated parametric amplifier design considerations for fabrication in microstrip transmission line
c09 A69-10193
Metal oxide semiconductor integrated circuits, showing failure rates and degradation causes
c09 A69-31851
Scanning electron mirror microscope advantages over electron mirror and scanning electron microscopes for examining integrated circuits
c14 A69-32891
Al interconnections discontinuities at integrated circuit contact windows observed by scanning electron microscope, noting catastrophic failure and Si presence
c09 A69-32893
Fluidic integrated circuits for control of pneumatic stepping-motor actuator system
[NASA-TN-D-5155] c03 N69-22896
Reliability handbook for silicon monolithic microcircuits - applications
[NASA-CR-1346] c09 N69-23225
Reliability handbook for silicon monolithic microcircuits - failure mechanisms
[NASA-CR-1347] c09 N69-23226
Reliability handbook for failure analysis of silicon integrated microcircuits
[NASA-CR-1348] c09 N69-25328
Holographic microscopy for performance prediction and quality control of semiconductor devices and integrated circuits
[NASA-CR-1394] c14 N69-31958
INTELLECT
Evaluation of computer aids to augment human intellectual capability
[NASA-CR-1270] c08 N69-16140
INTERATOMIC FORCES
He 2 excitation spectrum for interparticle potential using pair Hamiltonian with repulsive core and attractive well
c24 A69-33118
INTERFACE STABILITY
Cylindrical bubbles stability in vertical pipes from photographs, describing wake, spacing, pressure pulsations and convection cells effects
[ASME PAPER 69-HT-28] c33 A69-43540
INTERFACES
Energetics in solid film lubricants vacuum deposition methods, showing dependence on interfacial and film characteristics
c15 A69-29001
INTERFACIAL TENSION
Influence of surface films on friction and deformation of single crystal and polycrystalline gold
[NASA-TN-D-4875] c15 N69-10249
Droplet wake minimization by surface tension changes
[NASA-CR-1368] c12 N69-24958
Surface tension, viscosity, and density of fluorocarbon solvents as function of temperature
[NASA-TM-X-1862] c18 N69-34134
INTERFERENCE
FORTRAN programs for calculating wind tunnel boundary interference factors
[NASA-TM-X-1740] c01 N69-17818
INTERFERENCE DRAG
Computer program for calculating wall interference factors of V/STOL aircraft and conventional airplanes
[NASA-TR-R-302] c01 N69-19028
Numerical method for evaluation and utilization of supersonic nacelle-wing interference
[NASA-TN-D-5057] c01 N69-19641
INTERFERENCE LIFT
Lift loss and jet decay measurements on hovering vertical takeoff aircraft models
[NASA-CR-1297] c01 N69-21477
INTERFEROMETERS
Navigation satellites system designed for ATC without requirement for onboard transmitter, discussing spectrum occupancy, satellite power, lane ambiguities and computational procedures
c21 A69-19212
INTERGRANULAR CORROSION
Dynamic creep model to determine oxidation effects on high temperature deformation of nickel
[NASA-TN-D-5266] c17 N69-27061
INTERMOLECULAR FORCES
Interaction energy and dipole moment in collisions of two hydrogen molecules
[NASA-TN-D-5486] c24 N69-39184
INTERNAL COMPRESSION INLETS
Numerical analysis of shock control by using perforated walls in internal compression supersonic inlets
[NASA-TR-R-317] c01 N69-32338
INTERNAL FRICTION
Internal friction measurement apparatus for nonmetallic solids, noting variations of Young modulus in extremely low loss materials
c14 A69-13108
INTERNATIONAL COOPERATION
International experimentation with U.S. communications satellites, noting design variations with participants and restraintless information exchange
[UN PAPER 68-95421] c20 A69-10474
NASA programs and opportunities for international cooperation in space
[UN PAPER 68-95367] c34 A69-10516
International liability for damage caused by launching of objects into outer space
[UN PAPER 68-95337] c34 A69-10525
International 28-station global instrumentation ground support network for space tracking and data acquisition

[UN PAPER 68-95912] c34 A69-17059
Summary of operation, communications, and other experiments of Relay 2 satellite
[NASA-SP-151] c31 N69-21065
INTERNATIONAL LAW
International legal liability for personal injury or property damage caused by space activities c34 A69-37127
INTERNATIONAL QUIET SUN YEAR
IQSY low energy galactic and solar cosmic ray observations made by various satellites and space probes, including hydrogen and helium energy spectra c29 A69-30014
INTERPLANETARY FLIGHT
Voyage to planets - Conference, Washington, D.C., March 1967 c30 A69-12301
Interplanetary low thrust mission analysis model, discussing major elements interactions c30 A69-21206
Evaluation method for strapdown spacecraft guidance systems on automated interplanetary missions, using cost and system performance efficiency probability model
[AIAA PAPER 68-828] c21 A69-35953
Direct flight and Jupiter swingby heliocentric trajectory modes of elliptic capture orbits compared for unmanned missions to outer planets
[AAS PAPER 68-105] c30 A69-39221
Interplanetary midcourse velocity correction schedules optimization, discussing timing equations modifications, mission simulation and role of earth based radar c21 A69-39646
Interplanetary space trajectories based on Jupiter swingby flights
[NASA-TN-D-5271] c30 N69-28441
Planetary flight handbook - direct trajectories to Jupiter, Saturn, Uranus, and Neptune
[NASA-SP-35-VOL-3-PT-7] c30 N69-33490
INTERPLANETARY MAGNETIC FIELDS
Interplanetary magnetic field measurements in lunar wake, noting magnetic perturbations pattern and absence of shocks c30 A69-11228
Charged particle dynamics in spiral interplanetary magnetic field model, discussing electric drift velocity, point of origin and distribution c29 A69-14015
Interplanetary magnetic field fluctuations obtained by IMP 2 c30 A69-16264
Cosmic ray deuteron and He 3 secondary origin and determination of cosmic ray path length and residual interplanetary field modulation c29 A69-20066
Sudden commencement associated discontinuities in interplanetary magnetic field observed by IMP 3 satellite, stressing shocks and tangential and rotational discontinuities c30 A69-22183
Simultaneous interplanetary magnetic field measurements by geocentric satellites Explorer 33 and IMP 3 of MHD shock wave associated with July 8, 1966 sudden storm commencement c30 A69-23773
Microscale fluctuations in interplanetary magnetic field, considering proton thermal energy and magnetic field energy densities c30 A69-24100
Green function solution to Maxwell equations for interplanetary and coronal magnetic fields above photosphere, considering field at source surface c30 A69-24429
Interplanetary sector structure during rising portion of 1966-1967 sunspot cycle, giving recurrence period of interplanetary field c30 A69-28957
Discontinuities in interplanetary magnetic field direction presented on mesoscale from Pioneer 6 observation, emphasizing distribution in time c30 A69-29970
Solar wind existence verified by direct measurements of interplanetary magnetic field and plasma, reviewing solar corona studies by satellites and space probes c30 A69-30010
Lunar dynamic response to discontinuities in interplanetary magnetic field to determine electrical conductivity and internal temperature c30 A69-31442
Interplanetary magnetic fields from Explorer 33 magnetometer relationship to surface geomagnetic variations emphasizing unified view c30 A69-32309
Earth bow shock waves in far upstream interplanetary medium observed from magnetic data of Explorer 34 satellite c30 A69-34941
Power spectra of interplanetary magnetic field fluctuations determined from Pioneer 6 satellite data, relating results to galactic cosmic rays modulation c30 A69-37554
Solar wind plasma effects on lunar wake umbral and penumbral interplanetary magnetic field anomalies, evaluating roles of electrons and ions c30 A69-38095
High energy cosmic radiation problems
[NASA-SP-199] c29 N69-29652
INTERPLANETARY MEDIUM
Interplanetary magnetic field measurements in lunar wake, noting magnetic perturbations pattern and absence of shocks c30 A69-11228
Discontinuities in interplanetary magnetic field direction presented on mesoscale from Pioneer 6 observation, emphasizing distribution in time c30 A69-29970
Solar wind existence verified by direct measurements of interplanetary magnetic field and plasma, reviewing solar corona studies by satellites and space probes c30 A69-30010
Interplanetary shock waves structure and evolution, discussing propagation in collision free media by wave-particle interactions c30 A69-42394
High energy cosmic radiation problems
[NASA-SP-199] c29 N69-29652
INTERPLANETARY SPACE
Optimum solar cell cover glass systems selected by studying interplanetary space environment effects of proton impact, temperature and concurrent illumination on radiation damage c03 A69-35702
IMP 4 satellite measurements of cosmic ray electrons in interplanetary space compared to predictions of electron intensity from interstellar proton-electron collisions c29 A69-42667
Translunar abort technique for nonfree-return missions
[NASA-TM-X-1806] c30 N69-29569
Meteoroid environment model for cometary origin near earth to lunar surface
[NASA-SP-8013] c30 N69-40326
INTERPLANETARY SPACECRAFT
Interplanetary Pioneer spacecraft development and systems engineering aspects c31 A69-17605
Advanced reconnaissance electric planetary spacecraft /AREPS/ concept for repeated coverage of Mars or Venus surface, using solar-photovoltaic system
[AIAA PAPER 69-253] c30 A69-21244
Spacecraft sterilization requirements, evaluating viable organisms release probability from spacecraft as function of equipment fracturing c04 A69-25460
Nuclear solid core rocket engine performance for interplanetary orbital launch of spacecraft by multiorbit injection
[AIAA PAPER 69-535] c22 A69-32660
Minimal electric propulsion systems for interplanetary spacecraft, discussing payload, reduced trip time and low thrust systems for Jupiter flyby
[AIAA PAPER 69-499] c28 A69-32714
Scientific findings from interplanetary spacecraft radio propagation experiments, particularly Mariner 5 data c07 A69-35940
Propulsion system performance relationship to manned planetary mission capability, discussing

anticipated performance of advanced propulsion concepts
c28 A69-38118
Optimum structural design for Martian entry capsule configurations
[NASA-CR-1414] c33 N69-35516

INTERPLANETARY TRAJECTORIES
Midcourse maneuvers in interplanetary guidance, considering spin stabilized spacecraft flyby for Jupiter mission
c30 A69-28504
Recurrent Lagrange multipliers for optimal low thrust earth-Jupiter transfers, using three dimensional solar system model
c30 A69-41896
Matched conic solutions to round trip interplanetary trajectory problems for use in guidance and navigation simulation
[NASA-TN-D-4942] c30 N69-14861
Interplanetary probe missions with solar electric propulsion systems
[NASA-TN-D-5293] c30 N69-29738

INTERPLANETARY TRANSFER ORBITS
Direct flight and Jupiter swingby heliocentric trajectory modes of elliptic capture orbits compared for unmanned missions to outer planets
[AAS PAPER 68-105] c30 A69-39221
Thrust requirements for correcting Keplerian orbits with interplanetary guidance application
[NASA-TN-D-4945] c21 N69-14399

INTERPOLATION
Graphical interpolation charts of local skin friction from compressible velocity profiles
[NASA-SP-3048] c01 N69-25391

INTERSTELLAR GAS
Steady axisymmetric gas flow from galactic center, determining supersonic to subsonic transition by equations of motion
c30 A69-22189
Residual interstellar gas from protostar formation detected as high luminosity IR object
c29 A69-27593
Origin of galactic gamma rays, discussing evidence in support of interstellar gas in galactic disk and production of neutral pions and bremsstrahlung
c29 A69-32806
Dynamical effects in structure of H II equilibrium region left behind expanding ionization front, showing temperature as function of distance from star
c30 A69-35966
Positively charged diatomic hydrogen molecules interstellar extinction and photodissociation cross section in terms of formation mechanisms
c30 A69-42610

INTERSTELLAR MATTER
Cosmic ray propagation, discussing interstellar matter effect on composition and diffusion effect necessary to study radiation models
c29 A69-16361
Far IR source in galactic center detected at 100 microns, noting thermal emission of interstellar dust grains as possible mechanism
c30 A69-22264
Interstellar extinction models of classical Mie particles and quantum mechanical polycyclic aromatic molecules
c30 A69-23679
Extinction efficiency of graphite core interstellar grains with solid hydrogen and ice mantles, using theoretical models
c23 A69-29587
Solid para hydrogen coated graphite particles expulsion into interstellar medium from star formation regions, considering mantles stability and particles extinction efficiency, albedo and phase function
c30 A69-37492

INTERSTELLAR RADIATION
Interstellar extinction in UV from zeta and epsilon Persei spectra obtained with scanner attached to telescope mounted in pointed Aerobee rocket
c30 A69-40772

INTERSTITIALS
Internal friction, Young modulus and resistivity measurements for stage I interstitials in electron irradiated tungsten
c17 A69-28682

INTRAMOLECULAR STRUCTURES
Rotational spectrum of ethylene episulfoxide to determine molecular structure, particularly orientation of C sub 2 S ring
c06 A69-20535

INVERTERS
Development and inverter circuit tests of high temperature cesium vapor thyratrons
[NASA-CR-1435] c03 N69-36843

INVISCID FLOW
One strip method of integral relations applied to inviscid supersonic blunt body problem
c01 A69-21972
Inviscid flow of two parallel slot jets impinging normally on surface
[NASA-TN-D-4957] c12 N69-14316
Hydrodynamic stability of inviscid rotating coaxial jets
[NASA-CR-1363] c12 N69-24926
Numerical calculation of inviscid adiabatic flow field around blunt bodies at hypersonic speeds
[NASA-TN-D-5434] c12 N69-36830
Analytical solution for inviscid separated jet injection at oblique angle into moving stream
[NASA-TN-D-5460] c12 N69-37965
Injection of attached inviscid jet at oblique angle to moving stream
[NASA-TN-D-5501] c12 N69-39916
Integral relations solution for radiating, nonadiabatic, inviscid flow over blunt body
[NASA-TN-D-5480] c33 N69-40356
Numerical analysis of laminar and turbulent mixing region for two dimensional jet injected at angle to moving stream
[NASA-TN-D-5531] c12 N69-41213

IODINE
Iodine IR laser, discussing CW emission obtained at various wavelengths and attributed to electronic transitions in atom
[IEEE PAPER T-5] c16 A69-19082
Three crystal sodium iodide pair spectrometers
[NASA-TM-X-1857] c14 N69-34628

IODINE ISOTOPES
Iodine 123 decay via gamma ray emission, noting energies of several transitions
c24 A69-13099
Excited states of xenon nuclei formed in beta decay of iodine and cesium isotopes
[NASA-TN-D-5329] c24 N69-30074

ION ATOM INTERACTIONS
Frictional forces and collision frequencies for ions moving in neutral gases
c13 A69-13328

ION BEAMS
Ion accelerators design for Kaufman thrustors in terms of beam optics and grid lifetime, using digital computer and electrolytic tank analog
[AIAA PAPER 69-261] c28 A69-21261

ION CURRENTS
Cesium contact ion microthrustor experiment onboard ATS 4, measuring emission currents and spacecraft potentials
[AIAA PAPER 69-297] c28 A69-21218

ION CYCLOTRON RADIATION
Ion cyclotron wave generation in RF self sustained mode improved by installing grid structures in plasma near magnetic mirrors
c25 A69-13113
Wave fields and coupling of RF power to ion cyclotron waves in finite length thermal collisional plasma column
c25 A69-13114

ION DENSITY (CONCENTRATION)
Mars lower ionosphere ionization from spectroscopic and Mariner 4 occultation data, discussing various ionization sources
c30 A69-18607
Light ion abundance measurements of OGO satellites and field aligned diffusive equilibrium theory with temperature and concentration latitudinal variations
c13 A69-25157

ION DISTRIBUTION
Earth thermal plasmasphere contraction subsequent to solar flare obtained from ion mass spectrometers on OGO satellites
c13 A69-23777

Ion, electron and neutral temperatures from ion composition distribution, assuming no change in vertical distribution within horizontal distance between upleg and downleg measurements
c29 A69-31990

ION EMISSION
Cesium contact ion microthrustor experiment onboard ATS 4, measuring emission currents and spacecraft potentials
[AIAA PAPER 69-297] c28 A69-21218

ION ENGINES
Mercury ion thrusters and facilities automatic controls durability testing, discussing vacuum chamber systems, unattended operation and control
[AIAA PAPER 68-576] c11 A69-12385
High voltage mercury electron bombardment ion thruster power efficiency
[ECS PAPER 170D] c28 A69-16233
Cesium contact ion microthrustor experiment onboard ATS 4, measuring emission currents and spacecraft potentials
[AIAA PAPER 69-297] c28 A69-21218
30 cm diameter mercury bombardment low impulse thrustor development for potential space applications, discussing performance and control
[AIAA PAPER 69-238] c28 A69-21256
Research and development program in annular slit colloid thrustor technology, proving thrustor feasibility by performance tests
[AIAA PAPER 69-287] c28 A69-21257
Ion accelerators design for Kaufman thrustors in terms of beam optics and grid lifetime, using digital computer and electrolytic tank analog
[AIAA PAPER 69-261] c28 A69-21261
Discharge chamber plasma processes in electron bombardment ion thrustors, considering factors affecting thrustor performance
[AIAA PAPER 69-494] c28 A69-32735
Electric propulsion systems for manned planetary exploration flights, discussing arc jet, ion and plasma engines
c28 A69-35108
Power conditioner for use with SERT 2 mercury ion thrustor, describing electrical and mechanical design and operation
c03 A69-42301
Uranium dioxide vent loss in externally fueled thermionic reactor concept
[NASA-TN-D-4922] c22 N69-10099
Performance of various oxide magazine cathodes in Kaufman thrusters
[NASA-TN-D-5074] c28 N69-19980
Production of glass coatings for molybdenum ion thruster accelerator grids
[NASA-TN-D-5320] c15 N69-30062
Performance of two electron bombardment thrusters with axial magnetic field and superimposed cusp magnetic field
[NASA-TN-D-5448] c28 N69-36844

ION EXCHANGE MEMBRANE ELECTROLYTES
Manned spacecraft fuel cell selection and design, discussing Gemini ion exchange membrane and Apollo Bacon cell systems
c03 A69-32406

ION EXCHANGING
Free lysine and dinitrophenyl /DNP/ derivatives determined quantitatively by ion exchange chromatography
c06 A69-33651

ION IRRADIATION
Plasma electron beam for welding, deriving beam current from secondary emission by ion bombardment, discussing gas pressure, equipment and applications
c15 A69-35555

ION MICROSCOPES
High resolution and image intensity of field ion microscope at low temperatures
[NASA-TN-D-5125] c14 N69-21408

ION MOTION
Electric field variations in vicinity of auroral forms from motions of Ba vapor clouds released from Nike-Tomahawk rockets
c13 A69-34935

ION PRODUCTION RATES
Experimental measurements of two electron capture for negative ion production in atmospheric gases
[NASA-CR-1406] c24 N69-38564

ION PUMPS
Tritium contamination reduction in small ion accelerators for neutron production, discussing pumping problems and vacuum systems
c11 A69-26499

ION RECOMBINATION
Lower auroral ionosphere rocket measurements of electrons, positive ions and energy particles, deriving height variation of ion pair production and ion-ion recombination
c13 A69-32187

ION SOURCES
Experimental measurements of two electron capture for negative ion production in atmospheric gases
[NASA-CR-1406] c24 N69-38564

ION TEMPERATURE
Electron, ion and neutral particle temperatures of upper atmosphere
c13 A69-14975
Ion temperature diurnal variations at 250-475 km obtained from Thomson scatter spectra
c13 A69-16407
Ion composition and charged particle temperatures at 300-600 km from sounding rocket and topside sounder Alouette 2 measurements
c13 A69-18839
Ion, electron and neutral temperatures from ion composition distribution, assuming no change in vertical distribution within horizontal distance between upleg and downleg measurements
c29 A69-31990
Ionospheric parameters of ion and electron density and temperature and ionic species compared by direct measurement probes on Explorer 31 satellite
c13 A69-37882

ION TRAPS (INSTRUMENTATION)
Planar thermal ion and electron trap experiments on Explorer 31 satellite, measuring ion and electron density and temperature and ionic composition
c14 A69-37878

IONIC COLLISIONS
Ion-molecule collisions of Ar-Co and N-No pairs, discussing charge exchange reaction rates and spiraling nature
c24 A69-16428
Computer made movies and time history plots for ion-dipole collisions involving polar molecules /CO, HCL and acetonitrile/
c24 A69-43124
Numerical analysis of spiraling in ion molecule collisions with polar targets using computer plotting techniques
[NASA-TN-D-5407] c24 N69-35508

IONIC DIFFUSION
Light ion abundance measurements of OGO satellites and field aligned diffusive equilibrium theory with temperature and concentration latitudinal variations
c13 A69-25157
Applicability and limitations of diffusive equilibrium in topside ionosphere, noting plasma density distribution along magnetic field line
c13 A69-37887

IONIZATION COEFFICIENTS
Rational approximation for coefficients used in calculating hydrogenic photoionization Gaunt factors
c24 A69-20153

IONIZATION CROSS SECTIONS
Atomic Li photoionization cross sections calculated with Brueckner-Goldstone many body perturbation theory
c24 A69-17134
Electron impact ionization cross sections for second quantum level of atomic H, using Born exchange approximation and Vainshtein approximation
c24 A69-17138
Cross sections computed for excitation and ionization of atoms and ions by electrons, using peaking approximation to evaluate Coulomb-Born matrix approximation
c24 A69-20206
Hydrogenic atoms ionization by high energy electrons, discussing cross sections for ejected electrons and total energy
c24 A69-20738

Electron impact cross sections for diatomic molecule ionization and excitation from modified Gryzinski theory, discussing results from molecular models
c24 A69-22249
Energy spectrum of secondary electrons and fluorescent efficiency in 3914 A band, obtaining ionization cross section
c29 A69-32315
Chemical reactions activation energy at high temperature, noting cross section shape role for deducing activation energy from rate data
c06 A69-34443

IONIZATION FREQUENCIES
High latitude ionization spikes observed by POGO spacecraft, noting frequency correlation with magnetic disturbances and development by high energy electron injections
c29 A69-28950

IONIZATION GAGES
Magnetron ionization gauge in helium for low pressure measurement, discussing striking characteristics and time lags
c03 A69-10606
Buried collector ionization gage for measurements in 100 billionth torr pressure range using shielded collector to lower X ray current
c14 A69-32324
Bent beam ionization gage linearity from calibrated nude Modulated Bayard-Alpert /MBA/ gage, discussing buried collector and tabulated magnetron gages
c14 A69-41216
Low pressure application of orbitron and ion gage designs
[NASA-CR-1300] c14 N69-28402
Predicting relative sensitivities of hot cathode ionization vacuum gages
[NASA-TN-D-5285] c14 N69-29331

IONIZATION POTENTIALS
Approximate ionization potentials for high ionization stages of elements with atomic numbers 31 to 92 obtained by binding energy calculations
c24 A69-29923
Ionization rate limiting processes behind strong shock waves in pure N, plotting electron density profile diagrams
c12 A69-43367

IONIZED GASES
Frictional forces and collision frequencies for ions moving in neutral gases
c13 A69-13328
Collisional theory of longitudinal wave propagation for two fluid viscous ionized plasmas formulated from coupled Maxwell and Boltzmann equations
c25 A69-20796
Electron number density LF oscillations for ionized gas identified with periodic solutions to neutral and charged particle plasma continuity equations
c25 A69-24315
Moving striations as plasma oscillations arising from transit time delays of neutral and charged particles moving through ionized gas, using continuity equation
c25 A69-43122
Electron density oscillations in ionized neon, helium, and deuterium gases
[NASA-TN-D-4950] c25 N69-14525

IONIZING RADIATION
Solar ionizing radiation increase during flares of 21 and 23 May 1967 determined from ionospheric electron density concentrations
c29 A69-37558

IONOGRAMS
Electron density profiles from topside ionograms compared to ground based sounding results, discussing error corrections
c07 A69-37865
Propagation characteristic model study of kinked Z trace observed on topside ionograms and explained by magnetoionic theory
c13 A69-37893
Computation of topside ionograms from electron concentration profiles
[NASA-TN-D-5052] c13 N69-23557

IONOSPHERE
Suprathermal electrons energy distributions as function of magnetic latitude in polar ionosphere obtained by Explorer 31 satellite observation
c29 A69-28963
Significant achievements in space sciences for 1967, including stellar astronomy, bioscience, ionospheres, planetology, particles and fields, solar physics, and planetary atmospheres
[NASA-SP-167] c30 N69-25460

IONOSPHERIC COMPOSITION
Plasmapause and relation to ion composition in topside ionosphere, using Bohm coefficient for turbulent diffusion
c13 A69-12741
Simultaneous solution of continuity and heat conduction equations for ionospheric plasma consisting of electrons, atomic O ions and neutral gas species, discussing varying solar flux effects
c29 A69-32082
Simultaneous solution of continuity and heat conduction equations for ionospheric electrons, ions and neutral species for studying F region magnetic storm behavior
c13 A69-32083
Ionospheric parameters of ion and electron density and temperature and ionic species compared by direct measurement probes on Explorer 31 satellite
c13 A69-37882
Rocket measurements of diurnal variations of F region concentrations and temperature of molecular N and O, showing disagreement with satellite drag data
c13 A69-40515

IONOSPHERIC CURRENTS
Magnetic field data from OGO-2 spacecraft and surface magnetic observatories, noting magnetic storm occurrence and magnetosphere inflation and detection of polar ionospheric currents
c13 A69-11125
Electric field variations in vicinity of auroral forms from motions of Ba vapor clouds released from Nike-Tomahawk rockets
c13 A69-34935
High latitude magnetospheric convection patterns determined from ionospheric current distribution using magnetic disturbance plots
c13 A69-38503
Ionospheric currents geophysical dc electric field measurement from sounding rockets, indicating anticorrelation with auroral luminosity
c13 A69-38508

IONOSPHERIC DISTURBANCES
Ionospheric irregularities effect on accurate satellite position determination in near real time
c07 A69-42549

IONOSPHERIC DRIFT
Causal and semiphenomenological theories concerning equatorial F 2 region, discussing electrodynamic drift theory and transequatorial winds
c13 A69-37888

IONOSPHERIC ELECTRON DENSITY
Nocturnal electron concentrations and temperature at Manitoba measured by rocket-borne Langmuir probe, compared with F 1 region
c29 A69-14008
Simultaneous rocket measurements of D region temperatures and electron densities on anomalous winter day
c13 A69-16411
Magnetic storm time variations of electron concentrations in upper ionosphere near north geomagnetic pole, discussing magnetic time, altitude and latitude dependence
c29 A69-28939
Rocket sounding measurements of ionospheric D region electron density profile during 20 May 1966 solar eclipse, discussing D region ionization source
c13 A69-29116
Rocket measurements of upper F region electron temperature and density profiles, for particle and energy balance of ionosphere topside, noting diffusive equilibrium

c29 A69-31975
Solar ionizing radiation increase during flares of 21 and 23 May 1967 determined from ionospheric electron density concentrations
c29 A69-37558
Topside ionogram reduction for ionospheric electron density determination, using geomagnetic strength at all heights, iteration and change of variables
c13 A69-37864
Electron density profiles from topside ionograms compared to ground based sounding results, discussing error corrections
c07 A69-37865
Global electron density distribution morphology in topside ionosphere during sunspot minimum from Alouette 1 and 2 ionograms
c13 A69-37867
Cylindrical electrostatic probes on Alouette 2 and Explorer 31 satellites used in intersatellite comparison of directly measured ionospheric electron temperature and density
c14 A69-37876
Ionospheric parameters of ion and electron density and temperature and ionic species compared by direct measurement probes on Explorer 31 satellite
c13 A69-37882
Topside ionosphere response to magnetic storms, using Explorer 22 satellite electron concentration and temperature measurements
c13 A69-42438

IONOSPHERIC ION DENSITY
Spectrometric rocket measurements of ion concentrations between 200 and 630 km
c13 A69-31974
Rocket measurements of upper F region electron temperature and density profiles, for particle and energy balance of ionosphere topside, noting diffusive equilibrium
c29 A69-31975
Ion depletion in high latitude exosphere, considering OGO 2 simultaneous observations of positive ion concentration, VLF signal propagation and whistlers
c29 A69-34939
Ionospheric parameters of ion and electron density and temperature and ionic species compared by direct measurement probes on Explorer 31 satellite
c13 A69-37882
Plasma temperature and ion concentration profiles determined from simultaneous measurements by Alouette 2 and Explorer 31 satellites of electron density, temperature and ion abundance
c13 A69-37896
Diurnal and seasonal variations of primary atmospheric ions in topside ionosphere correlated with solar zenith angle, using ion mass spectrometer on Explorer 32
c13 A69-38087
Distributions, seasonal variations and ionospheric implications of mesospheric nitric oxide concentration
c13 A69-38364

IONOSPHERIC PROPAGATION
Sudden magnetic field increase associated with July 8, 1966 sudden commencement observed by OGO 3 satellite in magnetotail
c13 A69-11226
Propagation characteristic model study of kinked Z trace observed on topside ionograms and explained by magnetoionic theory
c13 A69-37893
Polar cap ionospheric response to solar cosmic ray events observed by Mariners 2 and 4 solar proton measurements used to test magnetosphere models
c29 A69-43621

IONOSPHERIC SOUNDING
Nonvertical propagation effects on high altitude topside ionosphere sounder data reduction, using ray tracing
c13 A69-18838
Ion composition and charged particle temperatures at 300-600 km from sounding rocket and topside sounder Alouette 2 measurements
c13 A69-18839
Ionospheric satellites objectives and development resulting from topside sounder and ISIS programs
c13 A69-37855
Cylindrical electrostatic probes on Alouette 2 and Explorer 31 satellites used in intersatellite comparison of directly measured ionospheric electron temperature and density
c14 A69-37876
Plasma temperature and ion concentration profiles determined from simultaneous measurements by Alouette 2 and Explorer 31 satellites of electron density, temperature and ion abundance
c13 A69-37896
Antenna reactance from sounding rocket in ionosphere, showing variations relationship to rocket spin period
c13 A69-39964
Alouette 2 sounding data for magnetospheric field aligned propagation duct model
[NASA-TN-D-5332] c13 N69-34891

IONOSPHERIC TEMPERATURE
Ion temperature diurnal variations at 250-475 km obtained from Thomson scatter spectra
c13 A69-16407
Simultaneous rocket measurements of D region temperatures and electron densities on anomalous winter day
c13 A69-16411
Radar backscatter and rocket profiles of ionospheric electron temperature, noting agreement in daytime flight measurements
c29 A69-25162
Simultaneous solution of continuity and heat conduction equations for ionospheric plasma consisting of electrons, atomic O ions and neutral gas species, discussing varying solar flux effects
c29 A69-32082
Rocket measurements of diurnal variations of F region concentrations and temperature of molecular N and O, showing disagreement with satellite drag data
c13 A69-40515

IONS
Energy transfer and ion cost in hydrogen plasma
[NASA-TN-D-5319] c25 N69-29905
Technique for measuring ion energy loss in vapor deposited materials
[NASA-TN-D-5430] c24 N69-36929

IRISES (MECHANICAL APERTURES)
Thin film microwave irises with capacitive reactance
[NASA-CR-1364] c26 N69-28096

IRON
Iron line absence in emission spectrum of thermal X ray sources, constraining proposed thermal models
c29 A69-22231
Oscillator strengths and wavelengths of X ray and EUV transitions in highly ionized iron line spectra
c29 A69-27554
Intensity ratios effect of forbidden Fe and Ca transitions in solar corona on Fe/Ca ratio, noting cascading configurations
c30 A69-36219
Mass dependence of self diffusion in Fe by serial sectioning in alpha, gamma and delta phases, determining isotope effect with Fe radioactive isotopes
c17 A69-36440

IRON ISOTOPES
Mass dependence of self diffusion in Fe by serial sectioning in alpha, gamma and delta phases, determining isotope effect with Fe radioactive isotopes
c17 A69-36440

IRON METEORITES
Electron microprobe analysis of potassium feldspar in Weekerco Station meteorite
c30 A69-14979
Kodaikanal iron meteorite measurements for cosmogenic rare gases and K-Ar isotopes ages for glass inclusions
c30 A69-22047
Iron meteorites genetic classification based on parent body cooling rate and Ga-Ge trace element content
c30 A69-36129
Fe-Ni-P phase diagram studies applied to schreibersite and rhabdite formation in iron

meteorites
c30 A69-36132

IRRADIANCE
Solar spectral irradiance measured by airborne instruments, discussing construction, calibration, etc, of photoelectric filter radiometer and Leiss monochromator
c30 A69-32261

IRRADIATION
Luminescence effects on apparent size and shape of foveally fixated targets of various forms
c04 A69-36458
Prediction of thermal neutron flux perturbation effects in cylinders during irradiation tests
[NASA-TN-D-4949] c22 N69-14481
Uranium carbides irradiation tests for control of nuclear fuels fission gas swelling
[NAA-SR-12629] c22 N69-22946
Irradiation of encapsulated fuel and fast neutron fluxes that simulate thermionic reactor conditions
[NASA-TM-X-1858] c22 N69-33273
Properties of irradiated polyethylene memory materials
[NASA-CR-1384] c18 N69-36762
Quantitative method for determination of fission gases trapped in irradiated fuel forms
[NASA-TM-X-1893] c22 N69-37225
Effects of reactor irradiation at cryogenic temperatures on tensile properties of titanium and titanium-base alloys
[NASA-TN-D-5442] c17 N69-37436

ISIS SATELLITES
Ionospheric satellites objectives and development resulting from topside sounder and ISIS programs
c13 A69-37855

ISOCYANATES
Isothiocyanates and phenyl isocyanate reaction with hydrazinoethanol and hydrazinoethyl hydrogen sulfate
c06 A69-31808

ISOLATION
Optical carrier single channel telemetry system providing complete electrical isolation between shock tube data acquisition and data recording instrumentation
c14 A69-29561

ISOMERS
Temperature dependent isomer shift and anharmonic binding of Sn 119 in niobium stannide, measuring Mossbauer recoil free fraction
c26 A69-10009

ISOSTASY
Lunar gravitational anomalies from internal density variation viewpoint, discussing isostasy in maria
c30 A69-14631

ISOTHERMAL FLOW
Computer program for steady laminar, subsonic, and isothermal compressible flow across sealing dam
[NASA-TN-D-5373] c15 N69-33281

ISOTHERMAL PROCESSES
Isothermal diode as study basis for internal complex controlling thermionic energy conversion
c03 A69-21827
Transient condensing with freezing on nonisothermal inclined plate
[NASA-TN-D-5289] c33 N69-29598
Cyclic life calculations of materials subjected to isothermal stress considering fatigue and creep
[NASA-TN-D-5317] c32 N69-29672

ISOTOPE EFFECT
Mass dependence of self diffusion in Fe by serial sectioning in alpha, gamma and delta phases, determining isotope effect with Fe radioactive isotopes
c17 A69-36440

ISOTOPE SEPARATION
Thermal neutron capture cross section at high temperature irradiations determined for W 184, describing radiochemical separation and flux counting techniques
c14 A69-43192

ISOTOPIC LABELING
Z-micron sections removed from metal specimens by microtome for radiotracer study of mass dependence of self diffusion
c14 A69-36490

ITERATION
Iterative solution of boundary value problem for rapid optimization of multiple-burn rocket flights
[NASA-CR-1430] c30 N69-36439

ITERATIVE SOLUTION
Iterative guidance mode /IGM/ applied to effective gravity vector prediction, acceleration measurement of noise sensistivity and energy limitations
[AIAA PAPER 67-620] c21 A69-15501
Adaptive random search algorithm utilizing boundary cost-function hypersurfaces measurement to implement Pontryagin maximum principle, discussing hybrid computer use, iterative solution and convergence properties
c08 A69-33745
Instantaneous frozen layer thickness and temperature profile in solidified layer obtained by iteration technique
c33 A69-39433
Computational method for time optimal space rendezvous between rocket vehicle and circular orbit target
[NASA-TN-D-5017] c30 N69-16210
Second order errors in linearized velocity corrections and their effects on rate of convergence of iterative solutions
[NASA-TN-D-5037] c21 N69-17780
Applications of quasi-linearization theory to system identification
[NASA-TN-D-5300] c19 N69-29648

J

J-85 ENGINE
Inlet produced dynamic distortion and effects on stall margin of J-85 turbojet engine from supersonic wind tunnel tests
[AIAA PAPER 69-487] c28 A69-32676
Steady state airflow and afterburning performance characteristics of four J85-GE-13 turbojet engines
[NASA-TM-X-1742] c28 N69-17781

JAPAN
Comparisons of wind and temperature data obtained by Japanese MT-135 and American ARCAS meteorological rocket systems in closely spaced launchings
[NASA-TM-X-1726] c20 N69-17772

JET AIRCRAFT
Calculated and flight measured handling quality factors of three subsonic jet transports
[NASA-TN-D-4832] c02 N69-10495
Variation in engine noise for two landing approach configurations of jet transport aircraft
[NASA-TM-X-1896] c02 N69-38104
Aerodynamics and flight dynamics of turbojet aircraft
[NASA-TT-F-542] c01 N69-38670
Empirically determined wind and scale effects on hot gas recirculation characteristics of jet V/STOL aircraft
[NASA-CR-1445] c28 N69-40776

JET AIRCRAFT NOISE
Jet engine inlet noise control by modification of inlet guide vanes
c28 A69-15622
Technology trends in airbreathing propulsion, discussing noise control for subsonic jet transports, turbine blade cooling, etc
[AIAA PAPER 69-774] c02 A69-35648
Conference on NASA research in noise reduction of subsonic jet aircraft - nacelle acoustic linings, sound generation in jet engines, and operational noise effects on humans
[NASA-SP-189] c02 N69-11542
Optimum takeoff and climbout trajectory calculation technique for jet aircraft noise abatement
[NASA-TN-D-5182] c02 N69-26194
Effects of aerodynamic forces on jet engine noise from rigid flow spoilers
[NASA-CR-1340] c23 N69-26307
Operational limitations in flying noise abatement approaches
[NASA-TN-D-5497] c02 N69-39188
Temperature effects on turbofan and turbojet noise radiation

[NASA-CR-1472] c02 N69-40439
JET BOUNDARIES
FORTRAN programs for calculating wind tunnel boundary interference factors
[NASA-TM-X-1740] c01 N69-17818
Photographic study on bromine jet boundary shape in coaxial airstream with honeycombs at injection plane
[NASA-TM-X-1900] c12 N69-39303
JET ENGINE FUELS
Surface fouling of ASTM jet A fuel heated to 700 deg F in simulated heat exchanger tube
[NASA-TN-D-4958] c28 N69-12831
Thermodynamic and transport properties of air, and combustion products of natural gas and air, and jet engine fuel and air
[NASA-TN-D-5452] c33 N69-37936
JET ENGINES
Shorter combustors for high temperature jet engines of high speed aircraft, considering lifetime, shroud scoops, overheating, warpage, etc
c28 A69-29433
Jet engine compressor stalls in-flight investigation up to Mach 2 on F-111A by pressure sensors, noting steady state distortion role
[AIAA PAPER 69-488] c28 A69-32706
Wind tunnel tests for V/STOL aircraft having direct-lift and lift-cruise jet nozzles
[NASA-TM-X-1758] c01 N69-20016
Chromium base alloys for high temperature application in jet engines
[NASA-TM-X-1867] c17 N69-35764
Jet velocity and axial location of nozzle exit on performance of twin-jet afterbody model
[NASA-TN-D-5393] c28 N69-36932
JET EXHAUST
Path and shape of jet directed at large angles to subsonic free stream
[NASA-TN-D-4919] c01 N69-11634
Back flow density from jet plumes in vacuum
[NASA-TN-D-4978] c01 N69-14385
Scaled lunar landing module jet erosion of simulated moon surfaces
[NASA-TN-D-5051] c31 N69-22630
Jet exhaust location effects on longitudinal aerodynamic characteristics of jet V/STOL model
[NASA-TN-D-5333] c01 N69-33210
Exhaust recirculation effects produced by two heated jets impinging on ground plane
[NASA-CR-1307] c01 N69-34703
JET FLAPS
Trailing-edge flap system with boundary layer control and external jet augmentation for subsonic jet transport
[NASA-TN-D-5129] c01 N69-30722
Wind tunnel tests of static longitudinal and lateral characteristics of short takeoff aircraft with external flow jet flap
[NASA-TN-D-5364] c01 N69-33275
Static and dynamic stability derivatives of model jet transport equipped with external flow jet augmented flaps
[NASA-TN-D-5408] c02 N69-36258
Performance tests of jet flapped blade in six blade annular cascade
[NASA-CR-1423] c28 N69-36680
JET FLOW
Reduction of noise from underexpanded axisymmetric jet flows using radial jet flow impingement
[AIAA PAPER 68-81] c12 A69-28212
Path and shape of jet directed at large angles to subsonic free stream
[NASA-TN-D-4919] c01 N69-11634
Wind tunnel tests of large jet transport aircraft model with external flow jet flap
[NASA-TN-D-4928] c01 N69-14000
Conformal mapping of two dimensional jet flow from two nozzles striking plane surfaces
[NASA-TN-D-5064] c01 N69-17816
Impingement forces, moments, and centers of pressure due to air jets in vacuum sphere
[NASA-TN-D-5147] c12 N69-23085
Effects of free stream turbulence and boundary layer trip devices on mixing in jet stream
[NASA-CR-1336] c12 N69-24058
Photographic study of bromine jet flowing in coaxial airstream and impinging on stagnation surface
[NASA-TN-D-5209] c12 N69-24800
Jet effects on boattail pressure drag of isolated ejector nozzles at Mach 0.60 to 1.47
[NASA-TM-X-1785] c01 N69-26976
Turbulent mixing of compressible air in supersonic and subsonic coaxial jet flows
[NASA-TN-D-5315] c02 N69-30727
Helium penetration and spreading in Mach 2 airstream using Delta wing injector
[NASA-TN-D-5322] c01 N69-30878
Dynamic response of liquid jet atomization to acoustic oscillations
[NASA-TN-D-5339] c28 N69-30980
Exhaust recirculation effects produced by two heated jets impinging on ground plane
[NASA-CR-1307] c01 N69-34703
Injection of attached inviscid jet at oblique angle to moving stream
[NASA-TN-D-5501] c12 N69-39916
JET IMPINGEMENT
Pressure and heating rate correlations for rocket exhausts impinging on flat plates and curved panels, generating axisymmetric real gas exhaust plumes
c33 A69-26781
Reduction of noise from underexpanded axisymmetric jet flows using radial jet flow impingement
[AIAA PAPER 68-81] c12 A69-28212
Inviscid flow of two parallel slot jets impinging normally on surface
[NASA-TN-D-4957] c12 N69-14316
Conformal mapping of two dimensional jet flow from two nozzles striking plane surfaces
[NASA-TN-D-5064] c01 N69-17816
Analysis of two dimensional inviscid model jet impingement under verticle takeoff airplane
[NASA-TN-D-5288] c01 N69-29479
Exhaust recirculation effects produced by two heated jets impinging on ground plane
[NASA-CR-1307] c01 N69-34703
JET LIFT
Wind tunnel investigation of static stability characteristics of model jet-lift V/STOL research airplane
[NASA-TM-X-1835] c02 N69-30633
JET MIXING FLOW
Vortex motion enhancement of jet penetration and spreading in supersonic fuel injection into large diameter combustors
[AIAA PAPER 69-664] c12 A69-33437
Turbulence in mixing region of ducted coaxial flow of air-air and air-Freon 12 combination
[NASA-CR-1335] c12 N69-30728
Model analysis for viscosity in jet mixing flows
[NASA-CR-1382] c12 N69-31887
Analytical solution for inviscid separated jet injection at oblique angle into moving stream
[NASA-TN-D-5460] c12 N69-37965
Photographic study on bromine jet boundary shape in coaxial airstream with honeycombs at injection plane
[NASA-TM-X-1900] c12 N69-39303
JET NOZZLES
Flow field from forward facing nozzles exhausting near large cylindrical body at free-stream Mach numbers of 3.0 and 6.0
[NASA-TN-D-5030] c01 N69-21000
Base flow field at high altitude for four-engine clustered nozzle configuration
[NASA-TN-D-5164] c12 N69-24935
JET PROPULSION
Effect of angle of attack and injection pressure on jet penetration and spreading from Delta wing in supersonic flow
[NASA-TM-X-1889] c12 N69-37271
JET PUMPS
Jet pump head rise deterioration parameter for prediction of cavitation
c12 A69-15791
Noncavitating and cavitating performance of low area ratio water jet pumps, analyzing efficiency, area ratio, throat length, nozzle spacing and diffuser geometry
c03 A69-35176
Noncavitating and cavitating performance of low area ratio water jet pumps having throat lengths of 3.54 diameters
[NASA-TN-D-5095] c03 N69-20797

JETTISON SYSTEMS
Performance tests on dynamic jettison hinge loads of Centaur nose fairing
[NASA-TM-X-1821] c32 N69-29734
JOINTS (JUNCTIONS)
Joining ceramics and graphite to other materials
[NASA-SP-5052] c15 N69-14241
Space suit design with pressure stabilizer for force assisted elbow joint
[NASA-TN-D-5221] c05 N69-26259
JOURNAL BEARINGS
Herringbone grooved gas lubricated journal bearing stability, testing effects of geometries and clearances on onset speed for half frequency whirl
[ASME PAPER 68-LUBS-25] c15 A69-27271
Theory and clearance effects on stability of water lubricated herringbone-groove journal bearings
[NASA-TN-D-4883] c15 N69-10228
Theoretical analysis of pressure distribution, load capacity, attitude angle, and friction force for eccentric Rayleigh step journal bearing - infinite length solution
[NASA-TN-D-4873] c15 N69-10231
Small eccentricity stability analysis for externally pressurized gas lubricated bearings with journal rotation
[NASA-TN-D-4934] c15 N69-13256
Power loss experiments on herringbone grooved, gas lubricated journal bearings
[NASA-TN-D-5224] c15 N69-24932
Load and stiffness characteristics of rotating externally pressurized air journal bearings
[NASA-TN-D-5191] c15 N69-27078
Stability of water lubricated herringbone groove journal bearings
[NASA-TN-D-5264] c15 N69-27955
Air flow and attitude angle compared with theory for rotating externally pressurized air journal bearings
[NASA-TN-D-5192] c15 N69-27956
Steady-state characteristics of herringbone grooved air lubricated journal bearings
[NASA-TN-D-5386] c15 N69-33258
JUNCTION DIODES
Observation of photocurrents generated in Schottky barrier diodes on barium titanate, suggesting practical utility of photon-to-electron conversion efficiencies
c09 A69-18905
High performance silicon carbide backward diode, discussing device design and operational characteristics
c09 A69-22787
JUPITER (PLANET)
Photovoltaic properties of CdS thin film solar cells and silicon cells at Jupiter temperature and solar intensity
c03 A69-13076
Midcourse maneuvers in interplanetary guidance, considering spin stabilized spacecraft flyby for Jupiter mission
c30 A69-28504
Hansen method applied to Jupiter tenth satellite orbit correction and perturbations, describing computer program and formulas used
c30 A69-37529
Perturbative effects of Jupiter moons on spacecraft flyby and postencounter heliocentric trajectories, noting precision targeting
[AIAA PAPER 69-932] c30 A69-39361
Recurrent Lagrange multipliers for optimal low thrust earth-Jupiter transfers, using three dimensional solar system model
c30 A69-41896
Pioneer F/G mission to Jupiter by NASA for exploring interplanetary medium, asteroid belt, planet and environment
[AAS PAPER 69-290] c30 A69-42863
Application of Hansen lunar theory to 10th satellite of Jupiter
[NASA-TN-D-4979] c30 N69-14479
Analytical evaluation of space storable propellants for unmanned Jupiter and Saturn orbiter missions
[NASA-TM-X-1793] c31 N69-24942
Planetary flight handbook - direct trajectories to Jupiter, Saturn, Uranus, and Neptune
[NASA-SP-35-VOL-3-PT-7] c30 N69-33490
Jupiter swingby missions to Saturn, Uranus, Neptune, and Pluto
[NASA-SP-35-PT-8] c30 N69-34850
JUPITER ATMOSPHERE
Galactic Jupiter Probes investigating Jupiter atmosphere and emissions and deep space cosmic radiation
c30 A69-12303
Blunt and conical body optimum heat shield shapes for Jupiter atmospheric entry, noting shallow flight path
[AIAA PAPER 68-1150] c31 A69-13565

K

KALMAN-SCHMIDT FILTERING
Kalman filter simulation for estimating aircraft position and velocity from airborne digital computer data in zero-zero landing system
[AIAA PAPER 69-944] c21 A69-40327
Suboptimal estimator to Kalman filter containing scalar weighting factors
[NASA-TN-D-5082] c10 N69-21123
KEELS
Wind tunnel investigation of twin keel parawing aerodynamic characteristics
[NASA-TN-D-5199] c01 N69-23781
KEPLER LAWS
Comparison of class of orbits in Earth-Moon field and class of Kepler orbits in rotating coordinates by use of concurrent series of graphs
[NASA-TN-D-4903] c30 N69-10470
KINETIC ENERGY
Energetics in solid film lubricants vacuum deposition methods, showing dependence on interfacial and film characteristics
c15 A69-29001
KINETIC EQUATIONS
Coupled kinetic equations for inhomogeneous systems treated as simultaneous equations in time, obtaining solutions by successive approximation
c25 A69-30913
KINETIC THEORY
Kinetic theory model of plasma sheath transition, analyzing sheath structure in unignited mode of thermionic converter
c03 A69-13125
Kinetic theory model of plasma sheath transition applied to sheath structure in unignited mode of thermionic converter
c03 A69-21828
Coupled kinetic equations for inhomogeneous systems treated as simultaneous equations in time, obtaining solutions by successive approximation
c25 A69-30913
KINETICS
Uranium 233 critical mass requirements, neutron kinetic behavior, and neutron and gamma ray heating rates for nuclear light bulb rocket engine
[NASA-CR-1315] c25 N69-23451
KLYSTRONS
Beat frequency measurements in far IR due to harmonic mixing of klystrons, discussing noise role
c23 A69-33674

L

LABORATORIES
Design and operation of high temperature loads calibration laboratory
[NASA-TM-X-1868] c11 N69-36224
LABORATORY EQUIPMENT
Design and equipment requirements for manned earth orbiting biotechnology laboratory
[NASA-CR-1408] c05 N69-35541
LAGRANGE MULTIPLIERS
Recurrent Lagrange multipliers for optimal low thrust earth-Jupiter transfers, using three dimensional solar system model
c30 A69-41896
LAMINAR BOUNDARY LAYER
Nonsimilar laminar boundary layer solutions with negative pressure gradient compared to experimental boundary layer velocity profiles,

momentum and displacement thicknesses
[AIAA PAPER 69-35] c12 A69-18094
Amplified boundary layer oscillations and transition at swept flat nosed wing attachment line with/without boundary layer suction analyzed by wind tunnel tests
c01 A69-33251
Leading edge effects on laminar flat plate boundary layer and aerodynamic heating at Mach 10.4
[NASA-TN-D-5160] c12 N69-23467
Flow field and drag characteristics of several laminar boundary layer tripping element in hypersonic flow
[NASA-TN-D-5454] c12 N69-38156

LAMINAR FLOW
Flow characteristics and wall heat transfer in separated flow region of annular cavity at free stream hypersonic speed and high gas temperature
[AIAA PAPER 68-672] c01 A69-37185
Laminar incompressible viscous flow in short cylindrical vortex chamber with finite swirl ratio
[NASA-TN-D-5132] c12 N69-21400
Computer program for steady laminar, subsonic, and isothermal compressible flow across sealing dam
[NASA-TN-D-5373] c15 N69-33281
Laminar heating rate from wind tunnel tests using angle of attack and Reynolds number
[NASA-TN-D-5450] c12 N69-37604

LAMINAR HEAT TRANSFER
Laminar heat transfer distributions for blunted-cone, cone frustum reentry configuration at hypersonic speed using Reynolds number
[NASA-TN-D-5146] c33 N69-22997
Heat transfer to windward side of scale model for graphite lunar module fuel cylinder
[NASA-TN-D-5251] c12 N69-29608

LAMINAR MIXING
Numerical analysis of laminar and turbulent mixing region for two dimensional jet injected at angle to moving stream
[NASA-TN-D-5531] c12 N69-41213

LAMINATES
Cryogenic flexibility of thin polymeric film plies for use as spacecraft positive expulsion bladders
c15 A69-16486
Synthesis of Pyrrone laminates from sulfone dianhydride
[NASA-CR-1404] c30 N69-31960

LAND
Multispectral orbital photography used to obtain urban land-use data
[AAS PAPER 69-483] c13 A69-42837

LANDING
Evaluation of contact analog display in landing approaches with helicopters
[NASA-TN-D-5241] c02 N69-27177
Systems developed for reducing pilot workload and tracking accuracy improvements during noise abatement landing approaches
[NASA-CR-1427] c02 N69-38657

LANDING AIDS
Ground based guidance for land-landing manned spacecraft with low velocity descent systems, discussing high and low altitude glide path intercept and spiral
[AIAA PAPER 69-864] c21 A69-39390
Kalman filter simulation for estimating aircraft position and velocity from airborne digital computer data in zero-zero landing system
[AIAA PAPER 69-944] c21 A69-40327
Indirect optical viewing system in F-104B for simulated lifting-body approach and landing tasks
[NASA-TN-D-5299] c14 N69-29730

LANDING GEAR
Steerable landing gear system consisting of freely castoring corotating wheel nose gear, tiltable axle and main gear skids for lifting body spacecraft
[AIAA PAPER 69-790] c02 A69-35639
Full scale dynamic landing impact investigation of prototype lunar module landing gear
[NASA-TN-D-5029] c31 N69-20965

LANDING LOADS
Effect of heat shield flexibility on water landing loads of Apollo spacecraft models
[NASA-TN-D-5108] c32 N69-21042

LANDING MODULES
Inflatable landing system investigated for impact normal to smooth surface
[NASA-TN-D-5236] c32 N69-26223

LANDING SIMULATION
Optical simulation landing system for evaluating pilot controlled flexible parawing and Apollo capsule combination performance during landing
[NASA-TN-D-5049] c21 N69-20936

LANDING SITES
Longitudinal range dispersion of unmanned Mars landers using VM-8 and VM-9 atmospheric models, discussing Syrtis Major as possible landing site
c30 A69-12390

LANGUAGE PROGRAMMING
NASA computer language CLASP coordinated with evolution of SPL /Space Programming Language/ for aeronautics and space programming
[AIAA PAPER 69-957] c08 A69-40339
Computer memory reduction through FORTRAN higher level language, discussing tradeoff between costs saved and additional logic hardware
[AIAA PAPER 69-963] c08 A69-40344
Evaluation of computer aids to augment human intellectual capability
[NASA-CR-1270] c08 N69-16140

LANTHANUM FLUORIDES
Electrical conductivity of lanthanum fluoride single crystal with calcium impurities
[NASA-TN-D-5505] c26 N69-40056

LANTHANUM ISOTOPES
Lanthanum isotopes beta decay, analyzing excitation of near spherical daughter nuclei of barium isotopes
c24 A69-10100

LARGE SCALE INTEGRATION
Computer organization design employing distributed processor to provide general purpose computing while taking advantage of large scale integration
c34 A69-39133

LASER MODES
Carbon dioxide laser with two gas absorption cells in cavity for emission wavelength control and HF pulsed mode of operation
c16 A69-21088
Low energy ultrafast flashlamp systems as optical pumps for lasers using fast decaying fluorescent materials /organic dyes/
c16 A69-42187

LASER OUTPUTS
Emission and frequency shift angles of anti-Stokes radiation from trapped filaments of laser light in liquids
c23 A69-10012
Organic dye laser frequency variation with temperature, noting absorption and fluorescence spectra
c16 A69-12617
Sinusoidal phase modulation role in spectral broadening observed in trapped filaments of laser and Raman light
c16 A69-14189
Mie total and differential backscattering cross sections at laser wavelengths for Junge size distribution aerosol models
c16 A69-14290
Ammonium perchlorate high temperature decomposition by using carbon dioxide laser pyrolysis/mass spectrometry
[AIAA PAPER 69-143] c06 A69-18111
Iodine IR laser, discussing CW emission obtained at various wavelengths and attributed to electronic transitions in atom
[IEEE PAPER T-5] c16 A69-19082
Proportionality between log-amplitude variance and 7/6 power of wavenumber for horizontal propagation from spherical wave transmitter to point detector
c16 A69-19641
Picosecond light pulse measurement by two photon excitation of photographic film
c14 A69-20165
Holographic displays using ultrasonic vibrations or laser outputs as optical sources, discussing recording materials, responses and computer applications
c14 A69-21394

Three dimensional laser Doppler velocity instrument for mean velocity and turbulence measurements in subsonic jet shear layer
[SAE PAPER 690266] c14 A69-21555
Optical parametric noise in water by ruby laser beam for phase matched four photon process
c23 A69-21751
Sulfur dioxide-helium laser pulsed and CW submillimeter outputs
c16 A69-24005
Simultaneous HCN and HOH laser emission in pulsed discharge through mixture containing H, C, N, and O
c16 A69-26330
Laser Doppler flowmeter for heterodyne detection of laser light scattered from moving fluid applied to fluid velocity and velocity distribution measurements
c14 A69-26546
Absorption coefficient measurement for hydrocarbon gases for He-Ne laser beam at 3.39 microns, tabulating coefficients, noting variations from spectroscopic data
c16 A69-42192
Mie scattering calculations on laser wavelengths and atmospheric aerosols
[NASA-TN-D-5110] c23 N69-20905
Helium-neon laser discharge with striation oscillations in relation to pressure and current
[NASA-CR-1387] c08 N69-32350
Theoretical feasibility of detecting laser radiation scattered from plasma
[NASA-TN-D-5311] c25 N69-36939

LASERS
Microwave and optical generation and amplification - Conference, Hamburg, September 1968
c09 A69-18420
Intersatellite microwave laser communication system for ATS-F and ATS-G, discussing experiment, functional design and parameters
c07 A69-41758
Lunar laser beam retroreflection observations, showing agreement with predicted ephemeris and signal strength
c30 A69-43197
Design and performance of traveling wave phototube for coherent light demodulation
[NASA-TT-F-430] c09 N69-15441
Laser beam interactions with free electrons
[NASA-TN-D-5205] c16 N69-25357
Laser optical simulation of spaceborne radio astronomy interferometer experiment
[NASA-TN-D-5357] c30 N69-36892

LATERAL CONTROL
Pilot ratings of lateral directional handling for wide range of aircraft characteristics - graphs
[NASA-TN-D-5358] c02 N69-35762
Flight evaluation of tip turbine driven fans for lateral control in hovering VTOL aircraft
[NASA-TN-D-5491] c02 N69-38807

LATERAL OSCILLATION
Longitudinal structural vibration and lateral bending response mass and spring coupling in Saturn AS-502 during boost with longitudinal excitation by POGO effect
[AIAA PAPER 69-58] c31 A69-18204
Effects of lateral cable oscillations on dynamic response of cable-connected space station
[NASA-TN-D-5107] c31 N69-21111

LATERAL STABILITY
Instability of eccentrically stiffened cylindrical shells under axial compression and lateral pressure
[NASA-CR-1280] c32 N69-15378
Full scale wind tunnel investigation of lateral and longitudinal stability and control characteristics of light twin engine airplane
[NASA-TN-D-4983] c02 N69-17303
Lateral bending dynamic tests of Atlas Centaur Surveyor launch vehicle
[NASA-TM-X-1837] c31 N69-30631
Jet fighter aircraft lateral directional stability at high angles of attack
[NASA-TN-D-5361] c02 N69-32337
Wind tunnel tests of static longitudinal and lateral characteristics of short takeoff aircraft with external flow jet flap
[NASA-TN-D-5364] c01 N69-33275

LATTICE PARAMETERS
Effects of lithium and oxygen losses on magnetic and crystallographic properties of spinel lithium ferrite
[NASA-TR-R-305] c06 N69-20775

LAUNCH DATES
Launch opportunity and window constraints, considering injection energy and precision, reference body occultation, communications range, etc
c31 A69-37287

LAUNCH ESCAPE SYSTEMS
Aerodynamic loads on deployed canard surfaces and rocket nose section of Apollo launch escape vehicle
[NASA-TN-D-5260] c31 N69-28166
Aerodynamic characteristics determined during development of Apollo launch escape vehicle configuration in wind tunnel tests
[NASA-TN-D-5208] c01 N69-29027

LAUNCH VEHICLE CONFIGURATIONS
Cryogenic core concept for flexible and economical delivery system
[AIAA PAPER 68-812] c31 A69-39753

LAUNCH VEHICLES
Future space programs as governed by cost limitations, suggesting development of economical launch vehicle for shuttling between earth and orbital space stations
c30 A69-12680
Launch vehicle upper stage requirements in space missions, discussing space engine for lunar, planetary and interplanetary exploration
[AAS PAPER 69-359] c34 A69-42828
Cost analysis in low cost launch vehicle studies emphasizing sustaining engineering and plant economics
c31 A69-43120
Analysis of aeroelastic divergence phenomena in unguided launch vehicles
[NASA-TN-D-4846] c32 N69-10297
Wind tunnel test of aerodynamic characteristics of scale model of Tomahawk launch vehicle at Mach speeds
[NASA-TM-X-1684] c01 N69-10732
Prediction curves for launch vehicle vibration levels in region of spacecraft adaptor
[NASA-CR-1227] c31 N69-16155
Mathematical models for optimal three dimensional launch vehicle trajectories with attitude and attitude rate constraints
[NASA-TN-D-5117] c30 N69-20810
Longitudinal mass spring modeling of launch vehicles
[NASA-TN-D-5371] c32 N69-34970
Statistical effects of wind and atmospheric turbulence on launch vehicles
[NASA-CR-1410] c20 N69-35570

LAUNCH WINDOWS
Launch opportunity and window constraints, considering injection energy and precision, reference body occultation, communications range, etc
c31 A69-37287
Computer program for launch window determination from star illumination of night sky background
[NASA-TM-X-1772] c21 N69-22969
Performance of Atlas-Agena vehicle from lift off through Agena posigrade maneuver
[NASA-TM-X-1826] c31 N69-29594

LAUNCHING
International liability for damage caused by launching of objects into outer space
[UN PAPER 68-95337] c34 A69-10525

LAUNCHING SITES
Failure data role in management of launch operations reliability program
c11 A69-36022

LAW (JURISPRUDENCE)
Federal government contracting, discussing legality of NASA service contracts
c34 A69-15987

LC CIRCUITS
Delta functions spectrum in reciprocal time domain for LC and RC structures due to impulse response in distributed parameters
c10 A69-21327

LEADING EDGES
Leading edge effects on laminar flat plate

boundary layer and aerodynamic heating at Mach 10.4
[NASA-TN-D-5160] c12 N69-23467
LEAKAGE
Leak detection for aerospace hardware, discussing equipment, operations, checkout, etc
c15 A69-30315
Leak rate measurement accuracy of rate-of-rise technique for nitrogen, methane and He between millionth and thousandth torr
c14 A69-32326
Containment vessel leakage due to penetrations
[NASA-TM-X-1735] c22 N69-17701
Source and cause of fuel element fisson product leakage in reactor cooling water system at Plum Brook Reactor
[NASA-TN-D-5374] c22 N69-32317
Torque and leakage rates of various lubricated lip seal designs at peripheral velocity of 120 feet per second
[NASA-TN-D-5411] c15 N69-35769
Halogen detector for leakage in hermetically sealed devices
[NASA-TN-D-5457] c09 N69-38597
LEAST SQUARES METHOD
Damping factor automatic determination by use of second derivatives of residuals for damped least squares method of optical design
c23 A69-14295
Nonlinear least squares optimization program applied to atmospheric temperature sounding, solving for temperatures at various altitudes from simulated carbon dioxide intensity measurements
c13 A69-33156
Analytic approximations for application to spacecraft optical navigation system where position fixes are taken over short trajectory arcs
[NASA-TN-D-4863] c21 N69-10372
LEGAL LIABILITY
International liability for damage caused by launching of objects into outer space
[UN PAPER 68-95337] c34 A69-10525
International legal liability for personal injury or property damage caused by space activities
c34 A69-37127
LEGENDRE FUNCTIONS
Legendre polynomials for gravitational field and orbit perturbation
[NASA-TN-D-5163] c13 N69-26969
LEUCINE
High oxygen tension effect on transport and incorporation of exogenous leucine and protein synthesis in Pseudomonas saccharophila cells
c04 A69-13433
LEUKOCYTES
Preflight and postflight leukocyte chromosome aberration analyses of Gemini astronauts
c04 A69-33173
LEVITATION
Magnetic performance properties of air cooled solenoids applied to one component support and balance system
[NASA-CR-1352] c11 N69-24089
LIBRATIONAL MOTION
Libration point relay satellites for continuous communication link between earth and lunar far side, discussing trajectories and halo orbit stationkeeping
c30 A69-30188
LIFE (DURABILITY)
SERT 2 thrustor hollow cathode durability tested in bell jar
[AIAA PAPER 69-304] c28 A69-21224
Plasma electron beam for welding, deriving beam current from secondary emission by ion bombardment, discussing gas pressure, equipment and applications
c15 A69-35555
High temperature fatigue tests conducted to determine bearing life of angular contact ball bearing elements
[NASA-TN-D-5002] c15 N69-16367
LIFE DETECTORS
Mars biological exploration, discussing life detection, chemical and biological experimental strategy
[AIAA PAPER 68-1122] c04 A69-13700
Extraterrestrial life detection experiments integrated into single multipurpose space laboratory, including chemical analyses, metabolism identification, observation for molecular and/or cellular growth and replication
c05 A69-32970
Sequential analyses of planetary surface sample for extraterrestrial life detection, discussing chemistry, morphology, growth and metabolism for life attributes
c30 A69-41623
LIFE SCIENCES
Life sciences and space research - COSPAR Conference, London, July 1967
c04 A69-11073
Life sciences and space research on biological effects of radiation in space - COSPAR Conference, Tokyo, May 1968
c04 A69-37612
LIFE SPAN
Mortality kinetics of Drosophila melanogaster, comparing effects of gamma radiation-induced life shortening and natural aging
c04 A69-30444
LIFE SUPPORT SYSTEMS
Water electrolysis, discussing oxygen generators for spacecraft prototype cells and testing
c05 A69-12987
Lithium peroxide utilization feasibility for oxygen supply and carbon dioxide control in extravehicular portable life support systems
[AIAA PAPER 69-620] c05 A69-33303
Regenerative life support system development, considering synthesized organic compounds and microorganisms as foods for long duration space missions
c04 A69-37623
Unstabilized astronaut, hand-held and integrated life support EVA maneuvering units tested in gimbaled six degree of freedom servo driven moving base simulator
[AAS PAPER 69-516] c05 A69-42850
Material recovery from metabolic and other wastes for long duration manned space missions, discussing carbon dioxide removal, bioregenerative food systems, etc
[AAS PAPER 69-143] c05 A69-42876
Hydrogenomonas cultures investigated for metabolic waste utilization in aerospace life support systems
[NASA-CR-1296] c05 N69-22766
Astronaut capability to maintain life support systems and cabin habitability in weightlessness
[NASA-CR-1405] c05 N69-36709
LIFT
Flight tests of modified aileron direct lift control system during approach and landing of F8-C aircraft
[NASA-TN-D-4854] c02 N69-10371
Predicting lift and drag for slender sharp-edge Delta wings in ground proximity
[NASA-TN-D-4891] c01 N69-16180
Transonic wind tunnel tests of aerodynamic drag and lift forces on circular cylinder in two dimensional flow at high Reynolds number
[NASA-TR-R-300] c01 N69-17304
Rocket-scramjet hybrid engines in lifting reusable second stage
[NASA-TN-D-5218] c28 N69-24922
Free flight test model measurement of drag, lift, and trim in wind tunnel for Apollo command module
[NASA-TN-D-5276] c30 N69-29557
LIFT AUGMENTATION
Gas turbine engine shaft face seal with self acting lift augmentation preventing rubbing contact, noting disadvantages of labyrinth and conventional seals
[ASLE PICFS PREPRINT 27] c15 A69-30492
Shaft face seal with self acting lift augmentation for advanced gas turbine engines
[NASA-TN-D-5170] c15 N69-23232
LIFT DEVICES
Subsonic lifting surface theory including leading edge, discussing singularities in solution of integral equation for determination of aerodynamic properties
[AIAA PAPER 69-37] c01 A69-18167

Development of air bearing lift pads
[NASA-TM-X-1724] c01 N69-16467

LIFT DRAG RATIO
Cone-conical-frustrum configurations meeting center of gravity requirements for higher hypersonic lift-drag ratios in axisymmetric manned spacecraft
c01 A69-39237
Hypersonic aerodynamic characteristics of low fineness ratio variable geometry logistics spacecraft model
[NASA-TM-X-1701] c01 N69-13218
Newtonian aerodynamics for circular cones modified to produce lift at zero angle of attack
[NASA-TN-D-5193] c01 N69-23926

LIFT FANS
Theoretical analysis of axisymmetric flow in VTOL lift fan inlets without crossflow
[NASA-TN-D-5065] c01 N69-17831
Wind tunnel tests of subsonic aerodynamic characteristics of large scale tip turbine cruise fan with 1.075 pressure ratio at angle of attack
[NASA-TN-D-5316] c28 N69-34575

LIFTING BODIES
Subsonic lifting surface theory including leading edge, discussing singularities in solution of integral equation for determination of aerodynamic properties
[AIAA PAPER 69-37] c01 A69-18167
Lifting body stability augmentation systems design, development, ground tests and flight data including frequency response, limit cycle and structural resonance
[AIAA PAPER 69-887] c02 A69-39413
Transonic wind tunnel evaluation of variable stabilizer configuration effects on hypersonic elliptical lifting body dynamics
[NASA-TM-X-1789] c01 N69-25244
Indirect optical viewing system in F-104B for simulated lifting-body approach and landing tasks
[NASA-TN-D-5299] c14 N69-29730
Load distribution calculations for subsonic compressible flow of arbitrary wings and lifting surfaces
[NASA-TN-D-5335] c01 N69-31337
Three dimensional pressure distribution functions for lifting surfaces with trailing-edge controls based on integral equations for subsonic flow
[NASA-TN-D-5419] c01 N69-38768
Large scale wind tunnel investigation of lifting body with inflatable and rigid afterbody
[NASA-TN-D-5468] c01 N69-38775
Aerodynamic characteristics of large-angle cones in supersonic lifting capabilities
[NASA-TN-D-5499] c01 N69-40026
Longitudinal dynamics of lifting vehicle in orbital flight
[NASA-CR-1449] c30 N69-40062

LIFTING REENTRY VEHICLES
Lifting body type M2-F1 and M2-F2 aircraft enabling astronauts to make own landings at choice airport
c02 A69-13367
Lifting body entry vehicles in low speed flight test program for determining handling qualities, discussing M2-F2 glide flights
c02 A69-15571
Steerable landing gear system consisting of freely castoring corotating wheel nose gear, tiltable axle and main gear skids for lifting body spacecraft
[AIAA PAPER 69-790] c02 A69-35639
Aerodynamic performance tests of autorotative unpowered rotor entry vehicle model at various Mach numbers and angles of attack
[AIAA PAPER 68-950] c01 A69-37155

LIFTING ROTORS
Theory for predicting rotational and vortex noise of lifting rotors in hovering and forward flight
[NASA-CR-1333] c23 N69-25344
Wind tunnel investigation of steady state aerodynamics of composite lift VTOL aircraft model combining rotary and fixed wings
[NASA-TN-D-5232] c02 N69-28097

LIGHT (VISIBLE RADIATION)
Picosecond light pulse measurement by two photon excitation of photographic film
c14 A69-20165
Optical parametric noise in water by ruby laser beam for phase matched four photon process
c23 A69-21751
Light effects on circadian rhythms in monkeys, describing changes in deep body temperature and locomotor activity phase relationships
c04 A69-31336
Night sky Cerenkov light detectors observations of pulsars CP 1133, NP 0532 and NP 0527, noting instrumental limitation in detecting ultrashort light pulses
c30 A69-34994
Detecting geomorphological features over northeast Africa by Nimbus 2 visible and infrared radiation measurements
[NASA-TN-D-4648] c13 N69-14290
Visible and infrared transmitting properties of epoxy resin suitable for infrared detectors
[NASA-TM-X-1776] c18 N69-23843
Spectral emission of visible from Q switched dye lasers
[NASA-CR-1374] c16 N69-29934

LIGHT AIRCRAFT
Light aircraft hazards due to trailing vortex generated by heavy transport aircraft, suggesting specific procedures for takeoff, landing and flight phase
[SAE PAPER 680220] c02 A69-14930
Light rigid civil aircraft response to continuous atmospheric turbulence estimated using two rigid body degrees of freedom method for vertical and lateral gusts
[AIAA PAPER 69-766] c32 A69-35657
Full scale wind tunnel investigation of lateral and longitudinal stability and control characteristics of light twin engine airplane
[NASA-TN-D-4983] c02 N69-17303
Potential structural materials and design concepts for light aircraft
[NASA-CR-1285] c02 N69-20848

LIGHT BEAMS
Scanned laser beam display techniques based on cathode ray tube technology, noting flying spot scanner and beam deflection
c14 A69-15028
Self modulation, self steepening and spectral development of light in small scale trapped filaments, noting influence of relaxation time
c23 A69-20745
Laser beam interactions with free electrons
[NASA-TN-D-5205] c16 N69-25357

LIGHT ELEMENTS
Intermediate energy protons elastic and quasi-elastic scattering from light nuclei, correlating p-D, p-He-3, p-p and p-He-4 data with various scattering models
c24 A69-43123
Differential cross section and polarization measurements for elastic scattering of high energy protons from light nuclei
c24 A69-43125

LIGHT EMISSION
Ionospheric currents geophysical dc electric field measurement from sounding rockets, indicating anticorrelation with auroral luminosity
c13 A69-38508

LIGHT MODULATION
Automatic closed loop distortionless control of magnetic field modulation using light sensitive resistor as one leg of attenuator
c09 A69-17708
Self modulation, self steepening and spectral development of light in small scale trapped filaments, noting influence of relaxation time
c23 A69-20745

LIGHT SCATTERING
Multiple light scattering in planetary atmospheres, discussing diffuse reflection and transmission by atmosphere of particles with anisotropic scattering pattern
c30 A69-12105
Unicellular microorganisms size and concentration estimates based on light scattering measurements of suspensions in spectrophotometer cuvette compartment
c04 A69-25643
Multiple light scattering solutions accuracy by diffraction peak omission from cloud and haze

analytic phase functions compared for optically thick and thin planetary atmospheres
c30 A69-33159
Computer analysis of light scattering data from polymer solutions
[NASA-TN-D-5177] c06 N69-22991
LIGHT SOURCES
Detection time to light point source noting response to dark, star field and glare source backgrounds
c05 A69-17215
Rotating and oscillating magnetic neutron stars causing pulsars radio and optical signals, stressing UV line emissions theory
c30 A69-20624
Dual beam white or nearly monochromatic light source providing programmed repetitive sample illumination with variable intensity, pulse duration and sequence for photosynthesis research
c14 A69-36378
Optical system for recording Schlieren images with continuous writing, ultrahigh speed framing camera
[NASA-TN-D-4986] c14 N69-15381
LIGHT TRANSMISSION
Optical absorption coefficients for triphenylmethylarsonium tetracyanoquinodimethan complex single crystal, evaluating reflectance
c26 A69-10934
Multiple light scattering in planetary atmospheres, discussing diffuse reflection and transmission by atmosphere of particles with anisotropic scattering pattern
c30 A69-12105
Self modulation, self steepening and spectral development of light in small scale trapped filaments, noting influence of relaxation time
c23 A69-20745
Reflection and transmission measurements on as grown surfaces of tetracyanoquinodimethan, obtaining optical constants by Kramer-Kronig method
c26 A69-35477
LIMITER CIRCUITS
Filtering optimization prior to limiting digital signals in strong noise, detailing bandwidth choice of single pole low pass filter
c07 A69-39450
LIMITS (MATHEMATICS)
Relationship between complex covariance and covariances of envelopes of Rician fading communication channels
[NASA-TN-D-4825] c07 N69-11011
LINE SPECTRA
Red, blue and no bias light effects on spectral response of copper sulfide-cadmium sulfide cell, using model incorporating photoconductive layer
c26 A69-16358
Doppler shift measurements of axial and rotational velocities in MPD arc, using reference lines from iron arc
[AIAA PAPER 69-110] c25 A69-18171
Subdwarf HD 25329 studied with model atmosphere approach, using H alpha, Na I and Mg I profiles for effective temperature
c30 A69-22199
Cloud scattering corrections added to synthetic spectrum analysis of carbon dioxide bands and water vapor line in Venus spectrum
c30 A69-33161
Computer program to predict spectra from electronic transitions of diatomic molecules and atoms, noting line intensity distribution by Voigt profile
c24 A69-35239
Interferometrically measured wavelengths tabulated for Th lines in 2747-4572 A range, using liquid nitrogen cooled hollow cathode lamp and Fabry-Perot interferometer
c23 A69-42150
Carroll Fourier transform method applied to stellar spectra lines to determine small rotational velocities
c30 A69-42404
Theoretical molecular line absorption of carbon monoxide in late spectral type stellar atmospheres
[NASA-TN-D-4798] c24 N69-14448
Composition and line emission characteristics of ionized tungsten, uranium, and argon
[NASA-CR-1313] c25 N69-21124
Spectral analysis of solar activity, including solar electromagnetic phenomena, facula structure, and periodic variations in chromospheric flares and solar cycles
[NASA-TT-F-581] c29 N69-33401
LINEAR ACCELERATORS
Heat generation calculations and heat transfer measurements in circulating currents of linear crossed field generators and accelerators
[NASA-TN-D-5244] c25 N69-26313
LINEAR EQUATIONS
Finite difference method for symmetric positive linear differential equations, discussing methods to solve finite difference equations generated
c19 A69-13370
Buckling equations solved for equatorial segment of spherical shell loaded in axial direction by own weight
[NASA-TN-D-4921] c32 N69-13034
Generalized averaging method for linear differential equations with almost periodic coefficients
[NASA-TN-D-5167] c19 N69-22988
Nonlinear compressible flow problems - half-space of ideal compressible fluid motion due to arbitrary pressure front
[NASA-TT-F-560] c12 N69-27168
Existence, uniqueness, and stability criteria for linear and nonlinear operational differential equations in Banach and Hilbert spaces
[NASA-CR-1356] c19 N69-28256
LINEAR PREDICTION
Linear prediction of structural failure criteria for uniaxial fiber composites
[NASA-TN-D-5367] c18 N69-33321
LINEAR SYSTEMS
Linear state variable feedback to obtain asymptotic stabilization of linear dynamic systems
c10 A69-17947
Stochastic saturating systems optimal control computation, considering attitude control and tracking system design by elliptical differential equation of dynamic programming
c10 A69-30601
Model performance index /PI/ providing criterion for approximating one dynamic flight control system by another based on geometrical representation of linear autonomous systems
[AIAA PAPER 69-885] c21 A69-39410
Transient vibration analysis of liner systems using transition matrices
[NASA-CR-1237] c32 N69-11008
Determination of stability indicative function for linear systems with multiple time delays
[NASA-TR-R-301] c31 N69-17801
LINEARITY
Second order errors in linearized velocity corrections and their effects on rate of convergence of iterative solutions
[NASA-TN-D-5037] c21 N69-17780
LINEARIZATION
Applications of quasi-linearization theory to system identification
[NASA-TN-D-5300] c19 N69-29648
LINES OF FORCE
Characteristic time on motion of magnetic lines of force in medium with Hall effect
c25 A69-12399
LININGS
Conference on NASA research in noise reduction of subsonic jet aircraft - nacelle acoustic linings, sound generation in jet engines, and operational noise effects on humans
[NASA-SP-189] c02 N69-11542
Parameters of acoustic liner for maximum liner damping for rocket engines
[NASA-TM-X-1720] c28 N69-16152
LIPID METABOLISM
Acetate carbon 14 utilization in centrifuged rats, analyzing metabolism by measuring plasma glucose, FFA and lipids synthesis
c04 A69-19429
LIPIDS
Uranyl ions interaction with phospholipid and

cholesterol monolayers, using surface pressure and potential measurements
c06 A69-25641

LIQUID AMMONIA
Reaction rate and mechanism for low temperature reaction between lithium hydride and liquid ammonia, noting chemisorbed ammonia dissociation at interface
c06 A69-11285
ATS 3 spacecraft ammonia-fueled resistojet engine test performance
[AIAA PAPER 68-553] c28 A69-39754

LIQUID ATOMIZATION
Mean drop size generated in vapor pressure regime of liquid water jet, noting effect of water temperature and orifice diameter
c12 A69-21995

LIQUID COOLING
Instantaneous frozen layer thickness and temperature profile in solidified layer obtained by iteration technique
c33 A69-39433

LIQUID CRYSTALS
Skin friction measurement in aerodynamic tests using thin liquid crystal coatings with changes in maximum light scattering wavelength in response to shearing forces
c11 A69-29029

LIQUID HELIUM
Velocity of 1 MHz sound waves in He 4 along isotherms just above critical temperature, noting specific heat ratio for 4.5 and 5 K isotherms
c23 A69-17142

LIQUID HYDROGEN
Ball bearings lubrication and wear in cryogenic hydrogen turbopumps by transfer films provided from self lubricating cage
c15 A69-10109
Pressurant gas requirements for pressurized discharge of liquid hydrogen from propellant tanks for optimum pressurization system designs
[AIAA PAPER 69-526] c28 A69-32737
Hydrodynamic inlet conditions effect on film boiling and near critical hydrogen heat transfer, using data from electrically heated various geometry test sections
[ASME PAPER 69-HT-27] c33 A69-43541
Prediction of thermodynamic effects of developed cavitation based on liquid hydrogen and Freon-114 data in scaled venturis
[NASA-TN-D-4899] c12 N69-10070
Impeller matching effects on flow range and stability operating in liquid hydrogen
[NASA-TM-X-1727] c28 N69-16213
Friction and wear of polymers with various fillers in liquid hydrogen
[NASA-TN-D-5073] c15 N69-19800
Lightweight polyurethane insulation for liquid hydrogen tanks of space vehicles
[NASA-TN-D-5114] c18 N69-20790
Volume effects on normal gravity pressurization of spherical liquid hydrogen tanks
[NASA-TN-D-5196] c33 N69-24168
Venting of spherical liquid hydrogen tankage
[NASA-TN-D-5263] c33 N69-27620
Net positive suction head requirements for helical inducer in liquid hydrogen under varied flow and temperature conditions
[NASA-TM-X-1808] c09 N69-27841
Two phase hydrogen flow in pump inlet line
[NASA-TN-D-5258] c15 N69-29476
Computerized simulation of low frequency dynamics of liquid hydrogen flow in nuclear rocket engine
[NASA-TN-D-5312] c22 N69-30070
Physical parameter effect on pressurant gas requirements during expulsion of liquid hydrogen from spherical tanks
[NASA-TN-D-5336] c28 N69-32318
Hydrogen gas pressure requirements during pressurization and transfer of liquid hydrogen from spherical tanks
[NASA-TN-D-5387] c28 N69-33211
Noncavitating and cavitating performance of inducer in liquid hydrogen
[NASA-TM-X-1854] c12 N69-33261
Low speed characteristics of liquid hydrogen centrifugal turbopumps
[NASA-TM-X-1861] c28 N69-33806
Explosive hazard evaluation of liquid oxygen liquid hydrogen propellants
[NASA-TN-D-5382] c27 N69-35321
Heat transfer characteristics of water/cryogenic hydrogen heat exchanger for nuclear rocket reactor
[NASA-TN-D-5429] c33 N69-36701

LIQUID INJECTION
Wind profile developed for calculation of deflection impulse for rocket with liquid injection thrust vector control
[NASA-TM-X-1708] c31 N69-14033

LIQUID LASERS
Organic dye laser frequency variation with temperature, noting absorption and fluorescence spectra
c16 A69-12617

LIQUID METALS
Luminous spherical fog layer surrounding burning zirconium droplet during free fall through oxygen containing atmosphere, noting effect on mass and heat transfer processes
c33 A69-28462
Compatibility tests of molten uranium with tungsten and tungsten-1.5 percent hafnium
[NASA-TN-D-5076] c17 N69-19930
Performance tests on liquid metal pumps for sodium potassium loops
[NASA-TM-X-1765] c15 N69-22970
Liquid-metal centrifugal pump at mercury loop
[NASA-TM-X-1766] c15 N69-23768
Properties and uses of liquid metal reactor fuels, including heat transfer processes in variously shaped channels, boiling and condensation of metals, and reactor control equipment
[NASA-TT-F-522] c33 N69-30507

LIQUID NITROGEN
Spontaneous Raman band shapes and depolarization ratios in liquid nitrogen and oxygen measured and compared to gas, discussing time dependence of rotational motion
c24 A69-17817
Film-nucleate boiling transition for liquid nitrogen in vertical forced flow in electrically heated tube, discussing conduction model and agreement with visual experiment
[ASME PAPER 69-HT-26] c33 A69-43542
Pressurized liquid nitrogen inside parametric amplifier structures for input, noise, and temperature improvements
[NASA-TN-D-5509] c09 N69-40079

LIQUID OXYGEN
LOX prevalve accummulator system with He pressurant for prevention of POGO effect on Saturn 5
c31 A69-15298
Vulcanizable elastomers suitable for contact with liquid oxygen, discussing preparation, mechanical properties, transition temperature and structure
c06 A69-16497
Fluorinated polyurethanes synthesis for liquid oxygen environments and cryogenic structural utility, noting structural effects on LOX compatibility
c06 A69-16498
Spontaneous Raman band shapes and depolarization ratios in liquid nitrogen and oxygen measured and compared to gas, discussing time dependence of rotational motion
c24 A69-17817
Explosive hazard evaluation of liquid oxygen liquid hydrogen propellants
[NASA-TN-D-5382] c27 N69-35321

LIQUID PHASES
Thermodynamic properties of liquid and gas phase equilibria of water plus heavy water
[NASA-TN-D-5223] c33 N69-26247

LIQUID POTASSIUM
Solubility of vanadium in liquid potassium
[NASA-TN-D-5093] c17 N69-20789
Solubility of refractory metals and alloys in liquid potassium and lithium
[NASA-CR-1371] c17 N69-27059
Molybdenum and tungsten solubility in liquid potassium
[NASA-TN-D-5504] c17 N69-40053

LIQUID PROPELLANT ROCKET ENGINES
Gaseous He bubbles injection into liquid

propellant launch vehicle fuel lines to reduce vehicle POGO oscillations by lowering feed system natural frequencies
c31 A69-25498
Precision flow measurement techniques for low thrust auxiliary propulsion liquid rockets
[NASA-TN-D-4785] c28 N69-16122
Nozzle insert evaluation and gas cooling concept in storable liquid propellant rocket engine
[NASA-TM-X-1756] c28 N69-19782
Double-dead-time model describing chugging to liquid propellant rocket engines having multielement injectors
[NASA-TN-D-5303] c28 N69-29405
Dynamic response of liquid jet atomization to acoustic oscillations
[NASA-TN-D-5339] c28 N69-30980
Historical developments in aviation and astronautics including liquid propellant rocket engine design, electric rocket engines, aircraft engines, and inertial guidance
[NASA-TT-F-540] c34 N69-31836

LIQUID ROCKET PROPELLANTS
Characteristics of liquid propellant explosions, analyzing detonation, shock wave formation and deflagration
c27 A69-14474
Saturn fireball thermal environment associated with liquid propellant explosions, using analytical model
c27 A69-14475
Yield and combustion physics of liquid propellant explosions determined from analytic charts
c27 A69-14477
Performance of bipropellant fractional-pound rocket thrustor
[NASA-TM-X-1699] c28 N69-13237
Liquid rocket acoustic instability for hydrogen-oxygen and earth storable propellant combinations
[NASA-TN-D-4968] c28 N69-14384
Analytical model for use in design of pump inlet accumulators for prevention of liquid rocket longitudinal oscillation
[NASA-TN-D-5394] c28 N69-33319
Development of barium chemical release system
[NASA-CR-1415] c13 N69-35660
Historical development of liquid propellant rocket engines and aviation models
[NASA-TT-F-537] c34 N69-36314

LIQUID SLOSHING
Propellant slosh load criteria for design of space vehicles
[NASA-SP-8009] c32 N69-14553
Lateral sloshing in cylinders under low gravity conditions
[NASA-TN-D-5058] c12 N69-19112
Sound wave pressure for preventing cryogenic propellant sloshing during space flight
[NASA-TN-D-4024] c23 N69-38180

LIQUID SODIUM
Performance and cavitation damage to axial flow pump rotor blades in high temperature liquid sodium
[NASA-TN-D-5138] c15 N69-21773
Effect of temperature and pressure on cavitation damage to cobalt base alloy in sodium
[NASA-TN-D-5273] c17 N69-28863
Cavitation damage and effect of fluid temperature on performance of axial flow pumps in liquid sodium
[NASA-TN-D-5484] c15 N69-38641

LIQUID-SOLID INTERFACES
Microscopic time lapse movies in solid/liquid interface profile during melting and freezing of materials for spacecraft thermal control as reversible heat sink
[AIAA PAPER 69-95] c33 A69-18126

LIQUID-VAPOR INTERFACES
Cylindrical bubbles stability in vertical pipes from photographs, describing wake, spacing, pressure pulsations and convection cells effects
[ASME PAPER 69-HT-28] c33 A69-43540
Observations of interface behavior during inflow to elliptical ended cylinder in weightlessness
[NASA-TM-X-1719] c12 N69-15473
Flow rate effect on dynamic contact angle for wetting liquids in weightless environment
[NASA-TN-D-5115] c12 N69-20794
Vapor ingestion phenomenon during draining in weightlessness
[NASA-TN-D-5210] c12 N69-24917
Liquid-vapor interface during outflow in weightlessness
[NASA-TM-X-1811] c12 N69-27954

LIQUIDS
Analysis of flow stability of thin liquid film adjacent to high speed gas stream
[NASA-TN-D-4976] c12 N69-15630
Combustion stability of single swirl can combustor modules using ASTM-A1 liquid fuel
[NASA-TN-D-5436] c28 N69-40080

LITHIUM
Elastic scattering of slow electrons by negative H and positive Li ions, calculating differential cross sections and phase shifts
c24 A69-12924
Atomic Li photoionization cross sections calculated with Brueckner-Goldstone many body perturbation theory
c24 A69-17134
Vacuum distillation determination of O in Li, evaluating accuracy through O additions and recoveries, method blank and residue identification
c06 A69-40932
Electron irradiation effect on resolution of lithium-drifted silicon semiconductor detectors
[NASA-TN-D-4901] c14 N69-10933
Fabrication and testing of lithium-drifted detectors as low energy photon spectrometers
[NASA-TN-D-5056] c24 N69-19828
Vacuum distillation determination of oxygen in lithium
[NASA-TN-D-5197] c06 N69-23706
Solubility of refractory metals and alloys in liquid potassium and lithium
[NASA-CR-1371] c17 N69-27059

LITHIUM COMPOUNDS
Effects of lithium and oxygen losses on magnetic and crystallographic properties of spinel lithium ferrite
[NASA-TR-R-305] c06 N69-20775

LITHIUM COOLED REACTOR EXPERIMENT
Systems analysis of Rankine cycle nuclear-electric potassium space power system using Li cooled fast reactor and high temperature turbine inlet
c22 A69-42266

LITHIUM HYDRIDES
Reaction rate and mechanism for low temperature reaction between lithium hydride and liquid ammonia, noting chemisorbed ammonia dissociation at interface
c06 A69-11285
Compton profile from single crystal of LiH measured with X ray scattering, noting valence-electron momentum distribution role
c26 A69-40730
Transport study of neutron and photon attenuation through lithium hydride and tungsten spheres
[NASA-TN-D-4989] c24 N69-15375

LITHIUM OXIDES
Lithium peroxide utilization feasibility for oxygen supply and carbon dioxide control in extravehicular portable life support systems
[AIAA PAPER 69-620] c05 A69-33303

LIVER
Acetate-2-C 14 conversion to C 14 carbon dioxide and C 14 fatty acids in rats with 2/3 of liver removed
c04 A69-35976
Hyperoxia and hypoxia effects on mitotic activity in regenerating and normal rat liver exposed to environmental conditions
c04 A69-43565

LOAD DISTRIBUTION (FORCES)
Spherical caps axisymmetric static and dynamic buckling under load, using axisymmetric nonlinear elastic shell theory approximation and finite difference equations
[AIAA PAPER 69-89] c32 A69-18133
Flexible rotor blade dynamic response to radially moving force, emphasizing helicopter rotor vibration characteristics associated with tip-vortex impingement
[AIAA PAPER 69-203] c02 A69-19546

User manual for computer program 55VD for computation of minimum induced drag and load distribution of nonplanar wings
[NASA-CR-1218-SUPPL] c01 N69-12286
Propellant slosh load criteria for design of space vehicles
[NASA-SP-8009] c32 N69-14553
Load distribution calculations for subsonic compressible flow of arbitrary wings and lifting surfaces
[NASA-TN-D-5335] c01 N69-31337

LOADING OPERATIONS
Hydraulic-powered self propelled six degree of freedom loading vehicle moving tests assembly to test chamber with high accuracy positioning
c11 A69-38181

LOADS (FORCES)
Turbine blade loading in terms of surface diffusion and loading factors, discussing tandem and jet flap blades and vortex generators
[ASME PAPER 68-WA/GT-11] c28 A69-16136
Forces on flexible shells of Apollo command module during water impact
[NASA-TM-X-1781] c32 N69-23697
Design calculations for conical shells and elastic systems subject to antisymmetric loads
[NASA-TT-F-518] c32 N69-30754
Drag and stability characteristics of towed, conical decelerator
[NASA-TM-X-1833] c02 N69-38598

LOCOMOTION
Light effects on circadian rhythms in monkeys, describing changes in deep body temperature and locomotor activity phase relationships
c04 A69-31336

LOGIC CIRCUITS
Magnetic core logic circuit system for bidirectional stepping motor drive voltage power supply control in proper phase and time sequence
c09 A69-11000

LOGIC DESIGN
Computer organization design employing distributed processor to provide general purpose computing while taking advantage of large scale integration
c34 A69-39133
Computer memory reduction through FORTRAN higher level language, discussing tradeoff between costs saved and additional logic hardware
[AIAA PAPER 69-963] c08 A69-40344

LOGISTICS
Logistics management developed for Apollo Applications Program of NASA Manned Spacecraft Center
[AAS PAPER 69-204] c34 A69-42812

LONG TERM EFFECTS
Atmospheric model development relating temperature, density, moisture and energy measurements from satellite observations for long term weather forecasting
[UN PAPER 68-95397] c20 A69-10463
Secular change examination in cislunar geomagnetic tail field gradient during summers of 1966 and 1967, using Explorer 33 and 35 results
c13 A69-11237
Earth mantle and core friction interaction suggested as cause of secular change in orbital motion obliquity
c13 A69-27821

LONGERONS
Structural stability of lattice column of longerons and helical braces
[NASA-CR-1301] c32 N69-26234

LONGITUDE MEASUREMENT
Longitudinal mass spring modeling of launch vehicles
[NASA-TN-D-5371] c32 N69-34970

LONGITUDINAL CONTROL
Flight investigation of lightweight helicopter to study feasibility of fixed collective pitch autorotations
[NASA-TN-D-5270] c02 N69-29232

LONGITUDINAL STABILITY
Gaseous He bubbles injection into liquid propellant launch vehicle fuel lines to reduce vehicle POGO oscillations by lowering feed system natural frequencies
c31 A69-25498
Saturn 5 longitudinal instability /POGO/ precluded by lowering S-1C stage propulsion system resonance below structural frequency
[AIAA PAPER 69-548] c31 A69-32658
Large scale wind tunnel tests to improve longitudinal stability of supersonic transports with variable swept wings
[NASA-TN-D-5005] c02 N69-16384
Full scale wind tunnel investigation of lateral and longitudinal stability and control characteristics of light twin engine airplane
[NASA-TN-D-4983] c02 N69-17303
Jet exhaust location effects on longitudinal aerodynamic characteristics of jet V/STOL model
[NASA-TN-D-5333] c01 N69-33210
Wind tunnel tests of static longitudinal and lateral characteristics of short takeoff aircraft with external flow jet flap
[NASA-TN-D-5364] c01 N69-33275
Longitudinal dynamics of lifting vehicle in orbital flight
[NASA-CR-1449] c30 N69-40062

LONGITUDINAL WAVES
Collisional theory of longitudinal wave propagation for two fluid viscous ionized plasmas formulated from coupled Maxwell and Boltzmann equations
c25 A69-20796
Longitudinal plasma waves collision damping calculations using Rostoker test particle method
c25 A69-34439

LOOPS
Cb-1Zr pumped sodium loop tests to evaluate loop components, EM pump, pressure transducers, and instrumentation techniques
[NASA-CR-1135] c03 N69-11373

LOSSES
Flow angle and throat Reynolds number effects on loss characteristics of two dimensional supersonic nozzle
[NASA-TM-X-1823] c01 N69-31360

LOUVERS
Optimal design for improving thermal performance of existing spacecraft thermally actuated louver system by increasing open-to-closed emittance ratio
[AIAA PAPER 69-627] c33 A69-33269

LOW ALTITUDE
Parachute load distribution measurements with tensiometer during low altitude drop tests
[NASA-TM-X-1832] c14 N69-32682

LOW DENSITY FLOW
Flight test performance of supersonic parachutes in low density environment
[NASA-TN-D-5296] c01 N69-30063

LOW DENSITY MATERIALS
Low density polybenzimidazole composites as ablative heat shields, discussing arc-heated wind tunnel tests of linear and crosslinked structures
c18 A69-41715

LOW FREQUENCIES
Electron number density LF oscillations for ionized gas identified with periodic solutions to neutral and charged particle plasma continuity equations
c25 A69-24315

LOW NOISE
Error analysis of input noise temperature measurements of low noise amplifiers
[NASA-TN-D-4997] c07 N69-16162

LOW PASS FILTERS
Filtering optimization prior to limiting digital signals in strong noise, detailing bandwidth choice of single pole low pass filter
c07 A69-39450
Cataloged pulse response curves for different types of conventional low pass filters
[NASA-TN-D-5494] c07 N69-40099

LOW PRESSURE
Thermodynamic properties of erbium hydrogen binary system evaluated for use as low pressure standard
[NASA-CR-1271] c14 N69-16099
Low pressure application of orbitron and ion gage designs
[NASA-CR-1300] c14 N69-28402
Thermal electromotive force change for thermocouples in high temperature, low pressure

environments for 3700 hours
[NASA-TN-D-5287] c14 N69-29196
LOW SPEED
Low speed characteristics of liquid hydrogen centrifugal turbopumps
[NASA-TM-X-1861] c28 N69-33806
LOW SPEED STABILITY
Test facilities and techniques for low speed flight problems of aircraft handling qualities, stability, control and performance
c11 A69-15575
Low speed static and dynamic longitudinal, and lateral stability of scale model of supersonic transport in wind tunnel tests
[NASA-TN-D-4726] c02 N69-10733
LOW TEMPERATURE
Radius effect on bulging and fracture of through-cracked cylindrical pressure vessels at cryogenic temperatures
[NASA-TN-D-4951] c32 N69-14480
High resolution and image intensity of field ion microscope at low temperatures
[NASA-TN-D-5125] c14 N69-21408
Tensile and cyclic fatigue properties of graphite filament-wound pressure vessels at ambient and cryogenic temperatures
[NASA-TN-D-5354] c32 N69-31300
Emissivity coatings for low temperature space radiators
[NASA-CR-1420] c17 N69-36723
LOW TEMPERATURE ENVIRONMENTS
Solar absorptance, total hemispherical emittance and absorptance/emittance ratio for metals at cryogenic temperatures measured simultaneously with sinusoidally perturbed incident radiation
c33 A69-10847
Cryogenic behavior of adhesive materials used in fabrication of liquid hydrogen/liquid oxygen powered Saturn S-4B stage
c18 A69-16487
Film processing effects on cryogenic mechanical properties of polyethylene terephthalate
c18 A69-16490
Cryogenic mechanical properties of epoxy resins and glass/epoxy composites
c18 A69-16491
Mechanical behavior of polyethylene terephthalate at cryogenic temperatures
c18 A69-16494
Molecular motion in polytetrafluoroethylene crystals at cryogenic temperatures, noting crystal defect permitting angular displacements of chain segments
c24 A69-16495
Vulcanizable elastomers suitable for contact with liquid oxygen, discussing preparation, mechanical properties, transition temperature and structure
c06 A69-16497
Fluorinated polyurethanes synthesis for liquid oxygen environments and cryogenic structural utility, noting structural effects on LOX compatibility
c06 A69-16498
LOW TEMPERATURE PHYSICS
Fermi surface topology effects on Nernst-Ettingshausen coefficient from measurements in magnetic fields to 3.3 tesla and 1.2-4.2 K temperatures in metallic tin
c26 A69-16357
Cryogenic behavior of adhesive materials used in fabrication of liquid hydrogen/liquid oxygen powered Saturn S-4B stage
c18 A69-16487
Mechanical relaxation of poly 4 methyl pentene 1 at cryogenic temperatures, discussing temperature dispersion curve and secondary absorption associated with thermal motion of side chains
c18 A69-16492
Polymer glasses low temperature transitions, relating structure and transition temperature
c06 A69-16493
Molecular motion in polytetrafluoroethylene crystals at cryogenic temperatures, noting crystal defect permitting angular displacements of chain segments
c24 A69-16495
LOW TEMPERATURE TESTS
Cryogenic mechanical properties of epoxy resins and glass/epoxy composites
c18 A69-16491
Cooling requirements for high speed polytetrafluorethylene lubricated ball bearings operating in cold hydrogen gas, developing minimum gas flow rate equation
[ASLE PAPER 68-LC-2] c15 A69-19310
LOW THRUST PROPULSION
Spacecraft optimum low thrust trajectory analyzed by Hamiltcn-Jacobi perturbation theory, obtaining canonic constants of motion
c30 A69-17574
Low thrust mission simulation dependence on hardware definition, discussing power plant characteristics, jet velocity and thrustor efficiency
c30 A69-21204
Interplanetary low thrust mission analysis model, discussing major elements interactions
c30 A69-21206
30 cm diameter mercury bombardment low impulse thrustor development for potential space applications, discussing performance and control
[AIAA PAPER 69-238] c28 A69-21256
Low thrust trajectories for minimum time rendezvous between continuous thrust interceptor and passive target vehicle, comparing calculus of variations and steepest ascent analyses
c30 A69-32177
Minimal electric propulsion systems for interplanetary spacecraft, discussing payload, reduced trip time and low thrust systems for Jupiter flyby
[AIAA PAPER 69-499] c28 A69-32714
Precision flow measurement techniques for low thrust auxiliary propulsion liquid rockets
[NASA-TN-D-4785] c28 N69-16122
Current computer programs for low thrust trajectory analysis using flyby and rendezvous trajectories
[NASA-TM-X-1824] c08 N69-30014
Mechanics of low thrust space flight
[NASA-TT-F-507] c28 N69-33354
LOWER ATMOSPHERE
Mars lower atmospheric pressure, temperature and composition, noting consistency between photometric, spectroscopic and occultation techniques
c30 A69-12104
Optical radar studies of lower atmosphere, giving Mie theory calculations of clear atmosphere volume backscattering cross sections for four laser wavelengths
c07 A69-27001
LOWER IONOSPHERE
Mars lower ionosphere ionization from spectroscopic and Mariner 4 occultation data, discussing various ionization sources
c30 A69-18607
LUBRICANT TESTS
Steel ball bearing high temperature fatigue life tested with synthetic paraffinic oil, fluorocarbon and polyphenyl ether
[ASME PAPER 69-LUBS-18] c15 A69-34378
Oxygen concentration effects on oxidation of synthetic paraffinic and type II ester lubricants determined from ball bearing tests at 400 and 450 degrees F
c15 A69-35177
LUBRICANTS
Lubrication performance and thermal shear degradation of polyphenyl ethers and refined mineral oils in high temperature vane pump loop
[NASA-TN-D-5096] c15 N69-20938
Friction and contact resistance during sliding in vacuum of low resistivity metals lubricated with sputtered molybdenum disulfide
[NASA-TN-D-5349] c15 N69-31884
LUBRICATING OILS
Hydrodynamic conical and spherical spiral grooved grease bearings replacement of gyro ball bearings for extended space missions
[AIAA PAPER 69-836] c15 A69-39367
Performance evaluation of oil lubrication system for antifriction bearing rotor system of Brayton cycle turbomachinery
[NASA-CR-1229] c15 N69-16463

LUBRICATION
Ball bearings lubrication and wear in cryogenic hydrogen turbopumps by transfer films provided from self lubricating cage
c15 A69-10109
Elastohydrodynamic lubrication, discussing film thickness and dependence on fluid hydrodynamics and contact zone deformation
c15 A69-11324
Contact conformity effects on spinning torque and friction coefficient in angular contact ball bearings from lubricated and unlubricated tests
[ASME PAPER 68-LUB-10] c15 A69-30901
Elastohydrodynamic solution for ball torque spinning without rolling in nonconforming groove, showing increase in torque with stress and spinning and decreasing conformity
[ASME PAPER 69-LUBS-11] c15 A69-34381
Theory and clearance effects on stability of water lubricated herringbone-groove journal bearings
[NASA-TN-D-4883] c15 N69-10228
High speed foil bearing rotor support system
[NASA-CR-1157] c15 N69-14214
Survey of incompressible and compressible fluid film hydrostatic and hydrodynamic lubrication
[NASA-SP-5058] c15 N69-28592
LUBRICATION SYSTEMS
Performance and analysis of seals for nitrogen inerted lubrication systems of turbine engines
[NASA-TN-D-4761] c15 N69-10055
Performance tests of SNAP 8 lubrication and cooling subsystem
[NASA-TM-X-1731] c03 N69-20828
LUMINAIRES
Illumination in cryogenic or noncryogenic fluids by standard light bulbs
[NASA-TM-X-1654] c14 N69-13176
LUMINANCE
Foveal luminances for chromatic and absolute thresholds for hue identification in case of small targets
c23 A69-19649
LUMINESCENCE
Luminescence spectra of aromatic polymers, monomers and dimers under high energy electron excitation using molecular resonance model
c26 A69-32792
Luminescence effects on apparent size and shape of foveally fixated targets of various forms
c04 A69-36458
LUMINOUS INTENSITY
Minimal angle of resolution /MAR/ between point and extended circular source and between point source and simulated horizon, studying irradiation effects on manual navigation
c21 A69-19208
Star twinkling absence for lunar observation laboratory, noting star distance measurement and laser action in stellar atmospheres
c30 A69-27172
Intensity ratios effect of forbidden Fe and Ca transitions in solar corona on Fe/Ca ratio, noting cascading configurations
c30 A69-36219
IR excess of R CrB type variable star RY Sgr, noting visual brightness and radiation in 2.0-3.4 micron range
c30 A69-42377
LUNAR BASES
Lunar surface power plants, considering weight constraint for various systems using nuclear power, solar cell/fuel cells and H-O reactant regeneration
c03 A69-11396
Lunar colony development, detailing construction of permanent lunar bases taking into account oxygen, food, water, power and transportation
c11 A69-27906
Lunar soil as building material and extraction of water, oxygen and rocket propellants from lunar materials for lunar colony needs
c30 A69-27907
Apollo 11 mission and future space exploration prospects including moon base, manned space station, reusable shuttle vehicles, etc
c30 A69-41477
Lunar environment, bases, exploration, and extraterrestrial resources
[NASA-SP-177] c30 N69-22226
LUNAR COMMUNICATION
Lunar surface transmission loss for Apollo astronaut point-to-point communications
[NASA-TN-D-4915] c07 N69-13301
LUNAR COMPOSITION
Lunar composition analysis by measuring atomic and nuclear radiation emission from orbiter
[AAS PAPER 68-197] c30 A69-11475
Surveyor 5 Mare Tranquillitatis landing site similarity to Oceanus Procellarum sites, discussing surface material elemental composition and lunar structure
c30 A69-12224
Possible evolution of earth continents and ocean basin, considering ultrabasic, basic, and intermediate to acidic lunar highlands chemical composition
c30 A69-17006
LUNAR CRATERS
Collapse theory of dimple craters, analogies with terrestrial sink holes and dimple craters as channels for gas escape from interior
c30 A69-15589
Regolith thickness distribution at Lunar Orbiter sites, correlating thickness directly with cratering density
c30 A69-18604
Module landing effects on lunar surface, deriving erosion law from Surveyor 5 engine firing test and vacuum test data
c30 A69-41388
LUNAR CRUST
Lunar surface mechanical properties at Surveyor 5 site
c30 A69-12225
Regolith thickness distribution at Lunar Orbiter sites, correlating thickness directly with cratering density
c30 A69-18604
LUNAR ECHOES
Lunar laser beam retroreflection observations, showing agreement with predicted ephemeris and signal strength
c30 A69-43197
LUNAR EFFECTS
Interplanetary magnetic field measurements in lunar wake, noting magnetic perturbations pattern and absence of shocks
c30 A69-11228
LUNAR ENVIRONMENT
Manned testing of EVA equipment in thermal-vacuum environment for qualification of Apollo extravehicular mobility unit, using lunar surface thermal simulator
[AIAA PAPER 69-992] c05 A69-40370
Thermal and dielectric properties of homogeneous moon based on microwave and infrared temperature observations
[NASA-TM-X-1734] c30 N69-17815
LUNAR EVOLUTION
Chemical composition of Earth, Venus, Mars, Mercury and Moon calculated from mathematical models, constructing approximate equations of state at high pressure
c30 A69-29878
Lunar origin theories, considering moon/earth mass ratio, earth-moon system angular momentum deficiency and differential volatilization in earth
c30 A69-29882
LUNAR EXPLORATION
Lunar colony development, detailing construction of permanent lunar bases taking into account oxygen, food, water, power and transportation
c11 A69-27906
Lunar soil as building material and extraction of water, oxygen and rocket propellants from lunar materials for lunar colony needs
c30 A69-27907
Vehicles for lunar surface exploration and transportation including flying machines and wheeled vehicles
c30 A69-27908
Space travel and lunar exploration medical problems
c04 A69-27909
Lunar environment, bases, exploration, and extraterrestrial resources
[NASA-SP-177] c30 N69-22226

Manned space flight capabilities for lunar and planetary explorations and earth orbiting stations
[NASA-SP-196-VOL-1] c34 N69-22510
Proposed electromagnetic exploration of moon
[NASA-SP-174] c30 N69-33595
LUNAR FAR SIDE
Libration point relay satellites for continuous communication link between earth and lunar far side, discussing trajectories and halo orbit stationkeeping
c30 A69-30188
LUNAR FLIGHT
Navigation state vector update effect on lunar mission completion capability for Saturn 5, emphasizing hardware and scheme errors and accelerometer failure
[AIAA PAPER 69-883] c21 A69-39409
LUNAR GEOLOGY
NASA lunar receiving laboratory for lunar rock samples examination by gamma ray spectrometry for induced radioactive nuclides and naturally occurring isotopes
c11 A69-38271
Tektite origin theories, discussing Surveyor experiments effects on lunar geology and Tektite origin
c30 A69-40086
Apollo lunar sample collection and analysis, discussing astronauts activity and equipment, sample types, laboratories for radioactive counting and gas analysis, etc
c11 A69-40191
Summary of lunar data and scientific observations generated by Surveyor landings on Moon
[NASA-SP-184] c30 N69-36451
LUNAR GRAVITATION
Lunar gravitational anomalies from internal density variation viewpoint, discussing isostasy in maria
c30 A69-14631
Lunar mass and gravitational field determined from lunar satellite dynamics, using potential function in terms of spherical harmonics
c30 A69-31405
Lunar gravity effects on mans locomotion on moon
[NASA-CR-1403] c05 N69-36271
LUNAR GRAVITY SIMULATOR
Prototype lunar gravity simulator using magnetic air bearings and spring motors
[NASA-CR-1233-VOL-1] c05 N69-11675
Magnetic air bearings for use as low friction overhead support fixtures in vertical lunar gravity simulator
[NASA-CR-1235] c05 N69-14213
Design and dynamic characteristics of vertical lunar gravity simulator with six degrees of freedom torso harness
[NASA-CR-1234] c05 N69-14979
LUNAR LANDING
Module landing effects on lunar surface, deriving erosion law from Surveyor 5 engine firing test and vacuum test data
c30 A69-41388
LUNAR LANDING MODULES
Lunar colony development, detailing construction of permanent lunar bases taking into account oxygen, food, water, power and transportation
c11 A69-27906
Concepts of acceptance testing lunar and planetary vehicles
[NASA-TN-D-4924] c11 N69-14507
Scaled lunar landing module jet erosion of simulated moon surfaces
[NASA-TN-D-5051] c31 N69-22630
Translunar abort technique for nonfree-return missions
[NASA-TM-X-1806] c30 N69-29569
LUNAR LANDING SITES
Surveyor 5 Mare Tranquillitatis landing site similarity to Oceanus Procellarum sites, discussing surface material elemental composition and lunar structure
c30 A69-12224
Lunar surface mechanical properties at Surveyor 5 site
c30 A69-12225
Photographic results of Lunar Orbiter program noting possible Apollo sites
c30 A69-15858
Regolith thickness distribution at Lunar Orbiter sites, correlating thickness directly with cratering density
c30 A69-18604
NASA lunar survey and mapping for generating Apollo satellite landing navigation control, using analytic photogrammetry, camera position and altitude data of lunar topography
c14 A69-36931
Summary of lunar data and scientific observations generated by Surveyor landings on Moon
[NASA-SP-184] c30 N69-36451
LUNAR MAGNETIC FIELDS
Interplanetary magnetic field measurements in lunar wake, noting magnetic perturbations pattern and absence of shocks
c30 A69-11228
Secular change examination in cislunar geomagnetic tail field gradient during summers of 1966 and 1967, using Explorer 33 and 35 results
c13 A69-11237
Magnetometer experiment for Apollo project to measure lunar surface magnetic field, describing mission requirements and instrumentation
[AAS PAPER 68-206] c30 A69-11481
Lunar magnetic moment and surface field, discussing Explorer 35 field measurements
c30 A69-14005
Solar wind plasma effects on lunar wake umbral and penumbral interplanetary magnetic field anomalies, evaluating roles of electrons and ions
c30 A69-38095
Lunar Explorer 35 measurements of lunar surface electromagnetic properties, magnetic fields and solar wind-moon interactions
c30 A69-38379
LUNAR MARIA
Surveyor 5 Mare Tranquillitatis landing site similarity to Oceanus Procellarum sites, discussing surface material elemental composition and lunar structure
c30 A69-12224
Lunar gravitational anomalies from internal density variation viewpoint, discussing isostasy in maria
c30 A69-14631
Nondimensional Jeffreys number as ratio of Reynolds to Froude number for gravitational motion of viscous masses, with application to lunar maria and plastic ice
c30 A69-19262
LUNAR MODULE
System designs for manned spacecraft gravity gradient stabilization of Saturn S-4B stage at 400 km and lunar module at synchronous altitude
c31 A69-18338
Thermal Vacuum /TV/ manned test operations related to Apollo lunar module in simulated space environment
c05 A69-30394
Module landing effects on lunar surface, deriving erosion law from Surveyor 5 engine firing test and vacuum test data
c30 A69-41388
Full scale dynamic landing impact investigation of prototype lunar module landing gear
[NASA-TN-D-5029] c31 N69-20965
LUNAR ORBIT AND LANDING SIMULATORS
Full scale dynamic landing impact investigation of prototype lunar module landing gear
[NASA-TN-D-5029] c31 N69-20965
Human transfer functions applied in systems analysis of manually controlled lunar landing simulator
[NASA-TN-D-5478] c05 N69-39183
LUNAR ORBITER
Lunar composition analysis by measuring atomic and nuclear radiation emission from orbiter
[AAS PAPER 68-197] c30 A69-11475
Lunar Orbiter mission objectives and orbit design
[AIAA PAPER 68-47] c30 A69-15503
Photographic results of Lunar Orbiter program noting possible Apollo sites
c30 A69-15858
Telecommunications performance of two lunar relay satellite system /LRSS/, determining operation capabilities with Apollo communications system

c07 A69-42508
Telemetry data from image-motion compensation sensor on Lunar Orbiter 1 spacecraft for determining radius of moon
[NASA-TN-D-5231] c30 N69-29115
Flight performance of Atlas Agena launch vehicles in support of Lunar Orbiter missions 3, 4, and 5
[NASA-TM-X-1859] c31 N69-37281
Lunar Orbiter 1 terrain assessment photographs and preliminary selenodesy, micrometeoroid, and radiation data
[NASA-SP-197] c30 N69-39213
Penetration flux calculation for multiwall structure on Lunar Orbiter spacecraft missions
[NASA-TN-D-5455] c32 N69-41229

LUNAR ORBITS
Explorer 35 measurements of low energy plasma in lunar orbit made by planar multigrid sensor programmed as retarding potential analyzer
c30 A69-16278
Real time targeting for Apollo lunar orbit insertion maneuver burn, discussing impulsive maneuvers for flight control
[AIAA PAPER 68-848] c31 A69-39760
Effect of gravitational model variations on accuracy of lunar orbit determination from data arcs
[NASA-TN-D-5105] c30 N69-21018
Lunar and artificial satellite theories treated by generalization of Von Zeipel procedure
[NASA-TN-D-5459] c30 N69-38145
Entry aerodynamics at lunar return conditions from command module of Apollo 4 flight
[NASA-TN-D-5399] c31 N69-38820

LUNAR PHOTOGRAPHS
NASA photogrammetric lunar activities, discussing imagery and control data by Lunar Orbiter and photogrammetric data reduction for preparing manned lunar landing
c14 A69-34336

LUNAR PHOTOGRAPHY
Lunar Orbiter mission objectives and orbit design
[AIAA PAPER 68-47] c30 A69-15503
Photographic results of Lunar Orbiter program noting possible Apollo sites
c30 A69-15858
NASA lunar survey and mapping for generating Apollo satellite landing navigation control, using analytic photogrammetry, camera position and altitude data of lunar topography
c14 A69-36931
NASA Lunar Orbiter Program of lunar photography from orbiting spacecraft
c30 A69-38377
Photogrammetric camera system developed from NASA requirements to document lunar surface environment during manned space flight exploration
c14 A69-40989
Lunar Orbiter 1 terrain assessment photographs and preliminary selenodesy, micrometeoroid, and radiation data
[NASA-SP-197] c30 N69-39213

LUNAR PROBES
Lunar orbital mission plans intended to optimize spacecraft procurement, flight schedules, science objectives and available funds
c30 A69-34362

LUNAR RADIATION
Lunar surface thermal radiation incident on unit area flat surface located at variable distance and orientation above moon, considering diffusion effects
c30 A69-38973
Thermal calculations of objects near lunar surface, considering IR emission directivity effects
c30 A69-43254

LUNAR RECEIVING LABORATORY
NASA lunar receiving laboratory for lunar rock samples examination by gamma ray spectrometry for induced radioactive nuclides and naturally occurring isotopes
c11 A69-38271
NASA Lunar Receiving Laboratory functional areas and physical, chemical, biological and quarantine activities for crew and lunar samples
c11 A69-38896

LUNAR SATELLITES
Lunar mass and gravitational field determined from lunar satellite dynamics, using potential function in terms of spherical harmonics
c30 A69-31405
Short term motion of lunar satellite, discussing third body disturbing functions and perturbation solution of nonsingular orbit elements
c30 A69-35934
Semianalytic theory for lunar satellite motion including perturbative effects
[NASA-TN-D-5043] c30 N69-28050

LUNAR SHADOW
Moon effect on intensity and angular distribution of energetic electron and proton shadowing as observed by Explorer satellites
c30 A69-16252

LUNAR SOIL
Module landing effects on lunar surface, deriving erosion law from Surveyor 5 engine firing test and vacuum test data
c30 A69-41388

LUNAR SPACECRAFT
Chronology of Apollo spacecraft program to 7 Nov. 1962
[NASA-SP-4009] c31 N69-32021

LUNAR SURFACE VEHICLES
Flight test evaluation of small one man lunar flying device /POGO/, discussing vehicle control, pressure suit factors and piloting differences
[AIAA PAPER 68-240] c11 A69-12379
Vehicles for lunar surface exploration and transportation including flying machines and wheeled vehicles
c30 A69-27908

LUNAR TEMPERATURE
Lunar dynamic response to discontinuities in interplanetary magnetic field to determine electrical conductivity and internal temperature
c30 A69-31442
Lunar temperature prediction with emphasis on variable property models, noting assumptions about physical properties appearing in heat conduction equations
c30 A69-34374

LUNAR TIDES
Ocean circulation as climate regulator, discussing role in redistributing climate-changing energy input from solar radiation or lunar tidal friction into atmosphere
c13 A69-26333

LUNAR TOPOGRAPHY
Magnetometer experiment for Apollo project to measure lunar surface magnetic field, describing mission requirements and instrumentation
[AAS PAPER 68-206] c30 A69-11481
Electron beam meter application as lunar surface electric field detector, discussing breadboard model and performance characteristics
c14 A69-13221
Photographic results of Lunar Orbiter program noting possible Apollo sites
c30 A69-15858
Possible evolution of earth continents and ocean basin, considering ultrabasic, basic, and intermediate to acidic lunar highlands chemical composition
c30 A69-17006
Gaussian particle size distribution with porosity and surface irregularity corrections used to determine mean particle size of lunar surface material at Surveyor sites
c30 A69-26371
Vehicles for lunar surface exploration and transportation including flying machines and wheeled vehicles
c30 A69-27908
NASA lunar survey and mapping for generating Apollo satellite landing navigation control, using analytic photogrammetry, camera position and altitude data of lunar topography
c14 A69-36931
Aluminized plastic covers to reduce radiator sink temperatures on lunar surface
[NASA-TM-X-1729] c03 N69-17225
Lunar topography statistics determined by Zond 3 space probe
[NASA-TT-F-514] c30 N69-24206

Spectral reflectance of planetary atmospheres, lunar topography, and planetary surface analyses
[NASA-TT-F-502] c30 N69-31989
Calculation for study of vertical and horizontal positioned lunar radiators
[NASA-TM-X-1846] c33 N69-32683
Simulation of astronaut locomotion on lunar surface to determine metabolic costs
[NASA-CR-1402] c05 N69-37964

LUNGS
Ventilation-perfusion inequality increase effects on lung overall gas exchange, using digital model
c05 A69-38388
Biomechanical factors determining lung damage following explosive decompression of space suits in vacuum test chambers
[NASA-CR-1223] c05 N69-13969

LYMAN SPECTRA
Rocket spectrographic observations of Alpha Virginis noting hydrogen Lyman absorption lines
c30 A69-27555

LYRAE CONSTELLATION
Individual properties of RR Lyrae stars
[NASA-TT-F-562] c30 N69-27169

LYSINE
Time of heating effect on thermal polymerization of L-lysine free base
c06 A69-28439
Free lysine and dinitrophenyl /DNP/ derivatives determined quantitatively by ion exchange chromatography
c06 A69-33651

M

M-1 ENGINE
Scale models of M-1 rocket engine oxygen and hydrogen pump driven two stage turbines used to determine performance and compact inlet manifolds problems
[AIAA PAPER 69-553] c28 A69-32678
Structural failures of high pressure, gaseous hydrogen storage tanks for M-1 engines
[NASA-CR-1305] c17 N69-19831

M-2 LIFTING BODY
Lifting body type M2-F1 and M2-F2 aircraft enabling astronauts to make own landings at choice airport
c02 A69-13367

MACH NUMBER
Oblique shock wave properties with free stream Mach number and flow deflection angle as independent variables, noting explicit solution
c01 A69-25378
Mach number, cone angle, bluntness and wall to recovery temperature ratio effects on slender cones boundary layer transition measurements at hypersonic speeds
c01 A69-33250
Large scale axisymmetric inlet systems performance capabilities, reviewing theoretical and experimental programs
[AIAA PAPER 68-580] c28 A69-34018
Effect of unit Reynolds number, nose bluntness, angle of attack, and roughness on transition on 5 degree half-angle cone at Mach 8
[NASA-TN-D-4961] c01 N69-14872
Experimental surface pressure distributions on spherically blunted cone at Mach numbers from 1.50 to 4.63
[NASA-TM-X-1730] c01 N69-16209
Performance test from Mach 2.58 to 1.98 of axisymmetric mixed-compression inlet system with 60 percent internal contraction
[NASA-TM-X-1739] c01 N69-19130
Effects of cone angle, base flare angle, and corner radius on Mach 3 aerodynamic characteristics of large angle cones
[NASA-TN-D-5048] c01 N69-19926
Characteristics study of bicone mixed compression inlet for Mach 1.80 to 2.50
[NASA-TN-D-5084] c01 N69-20914
Antenna effects on aerodynamic characteristics of 0.410 scale model Cajun rocket at Mach numbers from 2.30 to 4.63
[NASA-TM-X-1771] c01 N69-21106
Aerodynamic characteristics of blunted cones, tension shell, and attached inflatable decelerator models
[NASA-TN-D-5219] c31 N69-26570
Aerodynamic investigation of sharp cone-cylinder spikes on 120 degree blunted cones at Mach numbers of 3, 4.5, and 6
[NASA-TN-D-5201] c01 N69-29154
Aerodynamic characteristics effected by parallel-staged simple aerodynamic configurations at Mach numbers of 3 and 6
[NASA-TN-D-5379] c01 N69-33302
Fluctuating properties of turbulent boundary layers for Mach numbers up to 9
[NASA-TN-D-5496] c12 N69-40137

MACHINE ORIENTED LANGUAGES
Interactive experimenter computer system software and hardware design considerations based on astronaut-machine/experimenter question-answer interactions
[AIAA PAPER 69-953] c08 A69-40335

MACHINE TOOLS
Soviet research on high temperature strength of materials and machine parts
[NASA-TT-F-508] c17 N69-27300

MACROSCOPIC EQUATIONS
Relation between ellipsoidal velocity distribution function and macroscopic flow equations
[NASA-TN-D-5026] c12 N69-17827

MAGNESIUM
Influence of number of slip systems operating in magnesium on friction and effect of orientation of crystals on friction behavior
[NASA-TN-D-4351] c15 N69-10370
Cyclic heating and thermal shock effects on hafnia stabilized with calcia, magnesia, and yttria
[NASA-TN-D-5279] c18 N69-34547

MAGNETIC ANOMALIES
Solar wind plasma effects on lunar wake umbral and penumbral interplanetary magnetic field anomalies, evaluating roles of electrons and ions
c30 A69-38095

MAGNETIC CIRCUITS
Magnetic core logic circuit system for bidirectional stepping motor drive voltage power supply control in proper phase and time sequence
c09 A69-11000

MAGNETIC COILS
Cryogenic solenoids with pure Al conductor for production of strong magnetic fields, discussing softness and strain resistivity problems
c03 A69-26497
Sealed and unsealed relay coils temperature rise at simulated outer space air pressure levels
c09 A69-28048
Pumped helium tests of 51 centimeter bore niobium tin magnetic coils
[NASA-TN-D-5158] c26 N69-22965
Wind tunnel magnetic support and balance system for measuring sphere drag
[NASA-CR-1353] c11 N69-25343
Thermal outgassing tests on epoxy impregnated magnet coil
[NASA-TM-X-1813] c18 N69-28203

MAGNETIC CONTROL
Automatic closed loop distortionless control of magnetic field modulation using light sensitive resistor as one leg of attenuator
c09 A69-17708

MAGNETIC CORES
Inductance behavior of coils filled with superconducting lead or niobium dusts
[NASA-TN-D-5137] c26 N69-21500

MAGNETIC DIPOLES
Outer magnetosphere average magnetic field configuration between 5 and 18 earth radii, noting various maps in equatorial plane
c13 A69-14012
Geomagnetic field model /POGO/ to confirm eccentric dipole westward velocity secular decrease predicted by day length changes
c13 A69-37490
Hydromagnetic radiation characteristics of electric and magnetic dipoles in homogeneous anisotropic cold plasma, obtaining field components and wave propagation modes
c13 A69-42905
Measurement of change in plasma potential and magnetic field of hydrogen plasma impinging on magnetic dipole - simulation of solar wind-earth

interaction
[NASA-TM-X-1738] c25 N69-19131
MAGNETIC DISPERSION
Physical properties of magnetic base ferrofluids
[NASA-CR-1407] c06 N69-33493
MAGNETIC DISTURBANCES
Sudden magnetic field increase associated with July 8, 1966 sudden commencement observed by OGO 3 satellite in magnetotail
c13 A69-11226
High latitude ionization spikes observed by POGO spacecraft, noting frequency correlation with magnetic disturbances and development by high energy electron injections
c29 A69-28950
High latitude magnetospheric convection patterns determined from ionospheric current distribution using magnetic disturbance plots
c13 A69-38503
MAGNETIC EFFECTS
Quiet solar wind model with magnetic field numerically calculated, obtaining coronal electron densities and angular momentum near earth
c29 A69-34301
Strength and direction data on earth and extraterrestrial magnetic fields for guidance in vehicle design
[NASA-SP-8017] c31 N69-40269
MAGNETIC EQUATOR
Magnetic dip equator position at E layer and gradient with time and altitude, using geomagnetic field models
c13 A69-42428
MAGNETIC FIELDS
Magnetic field data from OGO-2 spacecraft and surface magnetic observatories, noting magnetic storm occurrence and magnetosphere inflation and detection of polar ionospheric currents
c13 A69-11125
Ring current particle energy density distribution for symmetric portion of magnetic storm derived from current magnetic field profile measurements
c29 A69-11227
Characteristic time on motion of magnetic lines of force in medium with Hall effect
c25 A69-12399
Fermi surface topology effects on Nernst-Ettingshausen coefficient from measurements in magnetic fields to 3.3 tesla and 1.2-4.2 K temperatures in metallic tin
c26 A69-16357
Automatic closed loop distortionless control of magnetic field modulation using light sensitive resistor as one leg of attenuator
c09 A69-17708
Steady shock discontinuity in perfectly conducting gas flow in arbitrarily oriented magnetic field for various Mach numbers
c25 A69-19988
Plasma oscillation modes perpendicular to magnetic field used to study energy conversion by wave coupling across density discontinuity
c25 A69-20795
Fast electron diffusion in stochastic magnetic field, obtaining diffusion coefficient as function of ratio of correlation time to Larmor period
c25 A69-20807
Rotating plasma disturbances onset in MPD arc, determining magnetic field dependence on mass flow, background pressure and propellant
[AIAA PAPER 69-232] c28 A69-21225
Background pressure and magnetic field shape effect on MPD thrustor performance, testing radiation cooled thrustors
[AIAA PAPER 69-243] c28 A69-21239
Near cathode magnetic field effect on instability in linear Hall current accelerators, using geometry of field extending from anode to cathode region
[AIAA PAPER 69-381] c28 A69-21731
Electrothermal instabilities of ionization region of nonequilibrium MHD generator in presence of magnetic field
c25 A69-21919
Thermodynamic approach to equation of state of magnetized Fermi gas, deriving energy eigenvalues of free electron in magnetic field
c30 A69-25107
Electric relays requirements for spacecraft with magnetic field constraints
c09 A69-28046
Severe magnetosphere distortions in north-south direction with parallel/antiparallel magnetosheath to magnetospheric field ascribed to solar wind property changes from Explorer 12 observations
c13 A69-34947
Twenty year wave in diurnal anisotropy component of galactic cosmic rays arriving at earth from asymptotic direction east of sun interpreted as magnetic reconnection
c29 A69-38098
Ferromagnetism stable state in degenerate electron gas and magnetic fields in gravitationally collapsed bodies based on total microscopic magnetic moments associated with Landau level electrons
c30 A69-38600
Dirac equation in external electromagnetic fields, deriving solution for constant orthogonal electric and magnetic fields encountered in plasma transport
c23 A69-41357
Convected balanced electric arcs in transverse magnetic fields
[NASA-CR-1267] c25 N69-18041
Plasma accelerator with magnetic field producing divergent-nozzle effect
[NASA-TN-D-5122] c25 N69-22942
Physical model for plasma containment simulation in magnetic fields
[NASA-TN-D-5217] c25 N69-25394
Eddy current torques on bodies rotating relative to uniform magnetic field
[NASA-TN-D-5086] c23 N69-29477
Magnetic torque resulting from interaction between magnetic properties of spacecraft and ambient magnetic field
[NASA-SP-8018] c31 N69-30339
Parametric angles of trajectory-determined field line intersects predicting location of artificial auroras in magnetosphere
[NASA-TN-D-5189] c30 N69-32316
Hydrodynamic stability and vortex containment of two fluid wheel flow to helical disturbances contained by axial magnetic field
[NASA-TN-D-5372] c12 N69-32377
Performance tests of silicon and germanium transistors in intense magnetic fields
[NASA-TN-D-5428] c09 N69-36710
Performance of two electron bombardment thrusters with axial magnetic field and superimposed cusp magnetic field
[NASA-TN-D-5448] c28 N69-36844
Energy conversion and distribution of spiraling electron beam using retarding field analyzer
[NASA-TN-D-5490] c09 N69-41208
MAGNETIC FLUX
Interplanetary magnetic field fluctuations obtained by IMP 2
c30 A69-16264
MAGNETIC FORMING
Decoupling force exerted by magnetic forming Be coil assembly on metallic plate during forming
c14 A69-25310
MAGNETIC MATERIALS
Evaluation of magnetic materials for static inverters and converters, tested under square wave excitation and direct current excitation
[NASA-CR-1226] c03 N69-17765
MAGNETIC MEASUREMENT
Ac technique using lock-in power amplifier SNR for measuring galvanomagnetic and Shubnikov-de-Haas effects, noting error reduction
c14 A69-36375
Shock discontinuities in solar wind measured by magnetic field and plasma instruments on Explorer 34, applying Rankine-Hugoniot relations
c30 A69-40304
Spectral analysis of solar activity, including solar electromagnetic phenomena, facula structure, and periodic variations in chromospheric flares and solar cycles
[NASA-TT-F-581] c29 N69-33401
Physical properties of magnetic base ferrofluids
[NASA-CR-1407] c06 N69-33493

MAGNETIC MIRRORS
Ion cyclotron wave generation in RF self sustained mode improved by installing grid structures in plasma near magnetic mirrors
c25 A69-13113
MAGNETIC MOMENTS
Lunar magnetic moment and surface field, discussing Explorer 35 field measurements
c30 A69-14005
Quantum theory of electron gas with anomalous magnetic moments in intense magnetic fields, noting pair creation from thermodynamic energy in system
c24 A69-19782
Ferromagnetism stable state in degenerate electron gas and magnetic fields in gravitationally collapsed bodies based on total microscopic magnetic moments associated with Landau level electrons
c30 A69-38600
Effects of lithium and oxygen losses on magnetic and crystallographic properties of spinel lithium ferrite
[NASA-TR-R-305] c06 N69-20775
MAGNETIC PROPERTIES
Magnetically anchored eddy current and eddy current rod dampers for GEOS gravity gradient stabilized satellite
[NASA-CR-1282] c14 N69-18953
Magnetic performance properties of air cooled solenoids applied to one component support and balance system
[NASA-CR-1352] c11 N69-24089
MAGNETIC STORMS
Magnetic field data from OGO-2 spacecraft and surface magnetic observatories, noting magnetic storm occurrence and magnetosphere inflation and detection of polar ionospheric currents
c13 A69-11125
Ring current particle energy density distribution for symmetric portion of magnetic storm derived from current magnetic field profile measurements
c29 A69-11227
Solar plasma observations during magnetic storms, discussing shocks and tangential discontinuities, geomagnetic variations and He
c13 A69-11234
Sudden commencement associated discontinuities in interplanetary magnetic field observed by IMP 3 satellite, stressing shocks and tangential and rotational discontinuities
c30 A69-22183
Simultaneous interplanetary magnetic field measurements by geocentric satellites Explorer 33 and IMP 3 of MHD shock wave associated with July 8, 1966 sudden storm commencement
c30 A69-23773
Magnetic storm time variations of electron concentrations in upper ionosphere near north geomagnetic pole, discussing magnetic time, altitude and latitude dependence
c29 A69-28939
Worldwide changes in geomagnetic field, determining causes by examining magnetic field and plasma data for solar wind and classifying as SSC or SI
c29 A69-31963
Simultaneous solution of continuity and heat conduction equations for ionospheric electrons, ions and neutral species for studying F region magnetic storm behavior
c13 A69-32083
Interplanetary magnetic fields from Explorer 33 magnetometer relationship to surface geomagnetic variations emphasizing unified view
c30 A69-32309
Electron temperature, density and magnetic disturbances measurements at 1000 km compared with visual observations during 25-26 May 1967 magnetic storm and aurora
c13 A69-34954
Explorer 34 observations of hydrogen and He ions in solar wind, noting number density variations and tentative association with geomagnetic storms
c29 A69-40305
Topside ionosphere response to magnetic storms, using Explorer 22 satellite electron concentration and temperature measurements
c13 A69-42438
MAGNETIC SURVEYS
Structure, temporal behavior, shape and length of earth magnetic tail via satellite mapping
c29 A69-19363
Interplanetary magnetic fields from Explorer 33 magnetometer relationship to surface geomagnetic variations emphasizing unified view
c30 A69-32309
MAGNETIC TAPES
Root mean square time delay error with respect to playback time and autocorrelation function of tape recorded sine wave for studying jitter spectra
c14 A69-18827
MAGNETIC VARIATIONS
Solar plasma observations during magnetic storms, discussing shocks and tangential discontinuities, geomagnetic variations and He
c13 A69-11234
Secular change examination in cislunar geomagnetic tail field gradient during summers of 1966 and 1967, using Explorer 33 and 35 results
c13 A69-11237
Interplanetary magnetic field fluctuations obtained by IMP 2
c30 A69-16264
Microscale fluctuations in interplanetary magnetic field, considering proton thermal energy and magnetic field energy densities
c30 A69-24100
Electron concentration enhancement in upper atmosphere at polar latitudes, noting three independent zones and relation to magnetic local time
c29 A69-28938
Geomagnetic field model /POGO/ to confirm eccentric dipole westward velocity secular decrease predicted by day length changes
c13 A69-37490
MAGNETICALLY TRAPPED PARTICLES
Trapped particles drift velocity in time dependent meridional magnetic and perpendicular electric field
c25 A69-20809
Time dependent convection electric fields as agents for diffusing trapped magnetospheric radiation inward toward earth, discussing one dimensional diffusion equation
c29 A69-28936
MAGNETOACOUSTICS
Amplitude equations for magnetoacoustic and entropy waves diverging from normal MHD shock, obtaining energy flux ratios associated with incident and transmitted waves
c25 A69-38242
MAGNETOACTIVITY
Radiation fields from energetic electron moving in helical orbit in magnetoactive plasma, using Maxwell equations
c30 A69-39965
MAGNETOHYDRODYNAMIC FLOW
Steady shock discontinuity in perfectly conducting gas flow in arbitrarily oriented magnetic field for various Mach numbers
c25 A69-19988
Solar plasma flow around magnetosphere, discussing plasma velocity, density and temperature and magnetic field space and time variations
c29 A69-26736
Fluid dynamic simulation of gas core nuclear rocket chamber for separating light and heavy gas via centrifugal force produced by MHD-driven rotational flow
[AIAA PAPER 69-727] c22 A69-33483
Dirac equation in external electromagnetic fields, deriving solution for constant orthogonal electric and magnetic fields encountered in plasma transport
c23 A69-41357
Measurement of change in plasma potential and magnetic field of hydrogen plasma impinging on magnetic dipole - simulation of solar wind-earth interaction
[NASA-TM-X-1738] c25 N69-19131
Momentum integral method treating magnetohydrodynamic and simple hydrodynamic entrance flows
[NASA-TN-D-5215] c25 N69-24920

Aerodynamic drag effects of hypersonic magnetohydrodynamic plasma flow around blunt bodies
[NASA-CR-1393] c25 N69-34897
MAGNETOHYDRODYNAMIC GENERATORS
Doppler shift measurements of axial and rotational velocities in MPD arc, using reference lines from iron arc
[AIAA PAPER 69-110] c25 A69-18171
Electrothermal instabilities of ionization region of nonequilibrium MHD generator in presence of magnetic field
c25 A69-21919
Conducting fluid incompressible flow in entrance of MHD channel by momentum integral method, permitting edge stress existence at boundary layer free stream interface
[AIAA PAPER 69-724] c12 A69-33436
Comparison of Brayton and Rankine cycle magnetogasdynamic space power generation systems for use with nuclear heat source
[NASA-TN-D-5085] c03 N69-20852
Electron temperature instabilities in entrance region of magnetohydrodynamic generator
[NASA-TM-X-1761] c25 N69-20875
Physical model for behavior of thermionic arc spots on MHD generator cathode
[NASA-TN-D-5414] c25 N69-35732
MAGNETOHYDRODYNAMIC STABILITY
Relationship between instabilities and turbulence in plasma, using spectrum of plasma fluctuations
c25 A69-13115
Rotating plasma disturbances onset in MPD arc, determining magnetic field dependence on mass flow, background pressure and propellant
[AIAA PAPER 69-232] c28 A69-21225
Near cathode magnetic field effect on instability in linear Hall current accelerators, using geometry of field extending from anode to cathode region
[AIAA PAPER 69-381] c28 A69-21731
Electrothermal instabilities of ionization region of nonequilibrium MHD generator in presence of magnetic field
c25 A69-21919
Dynamics, stability and approach to equilibrium of bounded one dimensional collisionless plasma representing minimum energy states with nonlinear Vlasov equation solutions
c25 A69-24305
Alternating current plasma arc coaxial flow stabilization
[AIAA PAPER 68-706] c25 A69-28232
Plasma instabilities in astrophysics - Conference, Monterey, October 1968
c30 A69-42681
Electrothermal instabilities effects on Brayton and Rankine cycle magnetohydrodynamic space power generation systems
[NASA-TN-D-5461] c03 N69-37883
MAGNETOHYDRODYNAMIC WAVES
Collisionless plasma heating by hydromagnetic waves in solar wind
c29 A69-12714
Steady shock discontinuity in perfectly conducting gas flow in arbitrarily oriented magnetic field for various Mach numbers
c25 A69-19988
Quasi-linear theory of hydromagnetic waves in nonrelativistic collisionless plasma, noting resonant diffusion effect on plasma heating mode
c25 A69-20797
Switch-on ionizing shock waves structure, analyzing condition of downstream state and effect on hydromagnetic wave speed
c25 A69-22045
Collisionless plasma heating by damping hydromagnetic waves applied to solar wind qualitative model, discussing magnetoacoustic wave energy
c30 A69-22426
Simultaneous interplanetary magnetic field measurements by geocentric satellites Explorer 33 and IMP 3 of MHD shock wave associated with July 8, 1966 sudden storm commencement
c30 A69-23773
Transmission of Alfven waves through earth bow shock based on hydromagnetic shocks theory, discussing amplitude amplification
c13 A69-32099
Amplitude equations for magnetoacoustic and entropy waves diverging from normal MHD shock, obtaining energy flux ratios associated with incident and transmitted waves
c25 A69-38242
Hydromagnetic radiation characteristics of electric and magnetic dipoles in homogeneous anisotropic cold plasma, obtaining field components and wave propagation modes
c13 A69-42905
MAGNETOHYDRODYNAMICS
MHD Rankine-Hugoniot equations for ion density, thermal pressure and convective velocity magnitude and orientation during Pioneer 6 traversal of earth bow shock
c30 A69-42417
MAGNETOIONICS
Conjugate echoes in Alouette 2 topside sounder ionograms explained by multiple reflections between conjugate points of field line, noting magnetospheric waveguides role
c07 A69-20045
Propagation characteristic model study of kinked Z trace observed on topside ionograms and explained by magnetoionic theory
c13 A69-37893
MAGNETOMETERS
Magnetometer experiment for Apollo project to measure lunar surface magnetic field, describing mission requirements and instrumentation
[AAS PAPER 68-206] c30 A69-11481
MAGNETORESISTIVITY
Nernst-Ettingshausen, thermoelectric power, thermal transverse-even, magnetoresistance, and Hall coefficients in white tin in 3.3 tesla field and cryogenic temperatures
[NASA-TN-D-5227] c26 N69-25412
MAGNETOSPHERE
Outer magnetosphere average magnetic field configuration between 5 and 18 earth radii, noting various maps in equatorial plane
c13 A69-14012
Magnetosphere - Conference, Boston College, June 1967
c29 A69-19351
Solar wind flow past earth and magnetosphere correspondence to external aerodynamics of round nosed bodies in supersonic stream
c13 A69-19360
Structure, temporal behavior, shape and length of earth magnetic tail via satellite mapping
c29 A69-19363
Magnetospheric plasma probe results with Pioneer 6 and 7, discussing plasma fluctuations and solar wind interaction with geomagnetic field
c13 A69-19364
Geomagnetic tail topology, reconnection and interaction with moon from Explorer 33 satellite data
c13 A69-19365
Modified first order theory of magnetosphere boundary shape incorporating effects of neutral sheet currents of extended geomagnetic tail
c13 A69-21661
Solar protons in magnetospheric tail after flare of July 7, 1966 with isotropic pitch angle distribution, expressing energy spectrum as exponential in rigidity
c29 A69-21699
Earth thermal plasmasphere contraction subsequent to solar flare obtained from ion mass spectrometers on OGO satellites
c13 A69-23777
Plasma-pause position measurements by ion mass spectrometers and broadband VLF receivers on OGO 1 and OGO 3 and by broadband recordings at Antarctica
c13 A69-25153
Light ion abundance measurements of OGO satellites and field aligned diffusive equilibrium theory with temperature and concentration latitudinal variations
c13 A69-25157
Solar plasma flow around magnetosphere, discussing plasma velocity, density and temperature and magnetic field space and time variations
c29 A69-26736

Satellite observations of geomagnetic tail in magnetosphere near midnight meridian plane, discussing formation, shape, plasma sheet and models
c13 A69-26739
Solar wind plasma observations in geomagnetospheric wake compared at 1000 and 500 earth radii, considering ion energy spectra and geomagnetic tail
c29 A69-26943
Time dependent convection electric fields as agents for diffusing trapped magnetospheric radiation inward toward earth, discussing one dimensional diffusion equation
c29 A69-28936
Banded chorus, VLF discrete emissions in magnetosphere in single variable frequency band with frequency depending on equatorial electron gyrofrequency
c13 A69-31981
Low energy solar protons entry into magnetosphere on 26 May 1967 showing diffusion control
c29 A69-31984
High latitude magnetospheric convection patterns determined from ionospheric current distribution using magnetic disturbance plots
c13 A69-38503
Polar cap ionospheric response to solar cosmic ray events observed by Mariners 2 and 4 solar proton measurements used to test magnetosphere models
c29 A69-43621
Parametric angles of trajectory-determined field line intersects predicting location of artificial auroras in magnetosphere
[NASA-TN-D-5189] c30 N69-32316
Strength and direction data on earth and extraterrestrial magnetic fields for guidance in vehicle design
[NASA-SP-8017] c31 N69-40269

MAGNETOSPHERIC ELECTRON DENSITY
Nighttime protonosphere thermal balance from Alouette 2 electrostatic probe measurements of electron temperature and concentration in magnetosphere
c13 A69-43181

MAGNETOSPHERIC INSTABILITY
Severe magnetosphere distortions in north-south direction with parallel/antiparallel magnetosheath to magnetospheric field ascribed to solar wind property changes from Explorer 12 observations
c13 A69-34947

MAGNETOSPHERIC ION DENSITY
Alouette 2 sounding data for magnetospheric field aligned propagation duct model
[NASA-TN-D-5332] c13 N69-34891

MAGNETOSPHERIC PROTON DENSITY
Solar protons in magnetospheric tail after flare of July 7, 1966 with isotropic pitch angle distribution, expressing energy spectrum as exponential in rigidity
c29 A69-21699

MAGNETRONS
Magnetron ionization gauge in helium for low pressure measurement, discussing striking characteristics and time lags
c03 A69-10606
Bent beam ionization gage linearity from calibrated nude Modulated Bayard-Alpert /MBA/ gage, discussing buried collector and tabulated magnetron gages
c14 A69-41216

MAGNETS
Magnetic air bearings for use as low friction overhead support fixtures in vertical lunar gravity simulator
[NASA-CR-1235] c05 N69-14213

MAGNITUDE
Spectral classes and photographic magnitudes determined for region Lacerta OB1
[NASA-TN-D-5060] c30 N69-26235

MAGNONS
Anisotropic Heisenberg antiferromagnetism in spin wave approximation, calculating thermodynamic quantities in terms of elliptic integrals
c26 A69-26500
Anisotropic Heisenberg ferromagnets in random phase and spin wave approximation
[NASA-TN-D-5286] c26 N69-29588

MAIN SEQUENCE STARS
Atmospheric models for metal deficient stars of K and G spectral type, studying reduced metal abundance effect on atmospheric structure
c30 A69-22055
Optical depths of convection related to metal deficiency for main sequence and giant stars
c30 A69-29946

MAINTAINABILITY
Weightless simulators effectiveness for obtaining space systems maintainability criteria, using nonparametric experimental design for performance data
c05 A69-17648
Reliability and maintainability - Conference, Denver, July 1969
c15 A69-35999

MAMMALS
Micro lagoon technique for culture and observation of isolated mammalian cells
[NASA-TN-D-4906] c04 N69-11056

MAN MACHINE SYSTEMS
Roll-motion cues for man-vehicle control in compensatory tracking task with disturbance input
c05 A69-23879
Man-computer speech communication, discussing model and aspects of acoustics, phonetics, linguistics, language training, physiology, psychology, bionics, etc
c08 A69-35099
Synthesis methods for manual aerospace control systems using digital programming and man machine performance data with application to supersonic transport design
[NASA-CR-1208] c02 N69-13185
Measurement of pilot describing functions in single controller multiloop tasks
[NASA-CR-1238] c05 N69-15372
Predictive display systems using repetitive, fast time, on-line computation
[NASA-CR-1274] c05 N69-17738
Conversational approach to matrix calculations on computers
[NASA-TM-X-1749] c08 N69-18954
Engineering problems survey on teleoperator control systems
[NASA-SP-5070] c05 N69-21478
Physiological and psychological responses of man to space flight problems
[NASA-TT-F-529] c05 N69-32044

MANAGEMENT
Indexed and abstracted references to reports and articles on management available in NASA information system
[NASA-SP-7500/03/] c34 N69-32430

MANAGEMENT PLANNING
Electromagnetic interference /EMI/ created by noise coupling through conductive paths, discussing responsibility for control within systems management
c07 A69-18944
NASA long range planning of primary electric propulsion for automated space program
[AIAA PAPER 69-247] c28 A69-21251
In-house research on R and D management in government agencies, discussing manning, training, center programs, case studies, etc
c34 A69-38022
Logistics management developed for Apollo Applications Program of NASA Manned Spacecraft Center
[AAS PAPER 69-204] c34 A69-42812
Space program planning, noting market requirements, acceptability and future characteristics
[AAS PAPER 69-083] c34 A69-42820
Communication in large organizations, describing internal communication model
c34 A69-42930
Application of NASA mathematical management models and systems analyses in private industry and economy
[NASA-SP-5048] c34 N69-10662
Computer program for research and engineering management of spacecraft projects
[NASA-CR-1275] c34 N69-18057
Bibliography of systems approach to management
[NASA-SP-7501] c34 N69-34917

Chronological study of design and development of Gemini project
[NASA-SP-4002] c31 N69-36501
MANEUVERABILITY
Flight tests with helicopters for studying manueverability
[NASA-TN-D-4931] c02 N69-14008
MANEUVERS
Unstabilized astronaut, hand-held and integrated life support EVA maneuvering units tested in gimbaled six degree of freedom servo driven moving base simulator
[AAS PAPER 69-516] c05 A69-42850
MANGANESE COMPOUNDS
Chemical analysis and paragenesis of manganoan ilmenite from Sierran adamellite using electron microprobe
c13 A69-35977
MANIFOLDS
Scale models of M-1 rocket engine oxygen and hydrogen pump driven two stage turbines used to determine performance and compact inlet manifolds problems
[AIAA PAPER 69-553] c28 A69-32678
MANIPULATORS
Manipulation errors in finite element analysis of structures
[NASA-CR-1385] c19 N69-34360
MANNED ORBITAL LABORATORIES
Earth-orbiting manned space station as single facility base for power, volume, logistics, experimental equipment and data communications
c31 A69-36464
MANNED ORBITAL RESEARCH LABORATORIES
Experiment requirements for manned earth orbiting biotechnology laboratory
[NASA-CR-1409] c05 N69-35540
Design and equipment requirements for manned earth orbiting biotechnology laboratory
[NASA-CR-1408] c05 N69-35541
MANNED ORBITAL TELESCOPES
Equations of motion computerized simulation for attitude stabilization of orbiting telescope coupled to crew compartment
c14 A69-27952
Electronically scanned star sensor with digital output for orbiting astronomical telescope
[NASA-TN-D-5281] c14 N69-29153
MANNED SPACE FLIGHT
Manned Mars and Venus missions role in overall planetary exploration program
c30 A69-12304
Future space programs as governed by cost limitations, suggesting development of economical launch vehicle for shuttling between earth and orbital space stations
c30 A69-12680
Microbiology of water management subsystem for manned space flight, discussing sterilization by heat and tests inside Integrated Life Support System /ILSS/
[SAE PAPER 680718] c05 A69-13441
German analysis of preparatory technology of U.S. space programs, noting effects of hardware development for manned space travel on future planning
c34 A69-15576
Manned spacecraft systems design optimization for extended space missions replacement modules
c31 A69-16380
Manned space flight programs, discussing U.S. technological, scientific and practical contributions
c30 A69-17074
Ground based guidance systems for supplementing onboard guidance of manned space vehicles
c21 A69-17580
Systems engineering activities in manned space flight involving design, development, manufacture, test and operation of Mercury, Gemini and Apollo flight systems
c31 A69-17602
Space travel and lunar exploration medical problems
c04 A69-27909
Earth orbital manned space astronomy, discussing long range program, instruments, facilities and data processing
c11 A69-27947
Thermal Vacuum /TV/ manned test operations related to Apollo lunar module in simulated space environment
c05 A69-30394
Design philcsophy for cost reductions on future space transportation systems, exemplifying applicatcn to booster system for earth orbital lcgistics
[AIAA PAPER 69-439] c34 A69-32654
Navigation, guidance and control developments for manned space missions, discussing earth orbital exploratcn bases
c21 A69-35801
Propulsion system performance relationship to manned planetary mission capability, discussing anticipated performance of advanced propulsion concepts
c28 A69-38118
Reducing cost of space transportation - AAS Conference, Washington, D.C., March 1969
c34 A69-39686
Crew and passenger transportation to and from space station orbits, discussing cost reduction possibilities with current or future technology
c31 A69-39691
Real time digital computer hardware simulation of Apollo Telescope Mount /ATM/ mission
[AIAA PAPER 69-940] c11 A69-40323
Photogrammetric camera system developed from NASA requirements to document lunar surface environment during manned space flight exploratcn
c14 A69-40989
Space research in past and expected scientific knowledge from manned and automated earth orbital science missions
[AAS PAPER 69-036] c30 A69-42825
Management system for safety in NASA Manned Space Flight Prcgram, discussing hazard analyses and reduction precedence sequence
[AAS PAPER 69-522] c34 A69-42851
Manned space flight history and spacecraft development
[AAS PAPER 69-501] c30 A69-42852
Material recovery from metabolic and other wastes for long duration manned space missions, discussing carbon dioxide removal, bioregenerative food systems, etc
[AAS PAPER 69-143] c05 A69-42876
NASA contributions to bioinstrumentation system - survey
[NASA-SP-5054] c04 N69-14860
Research prcblems in atmospheric entry and landing of manned planetary space flights to Mars and Venus
[NASA-TN-D-4977] c31 N69-15634
Manned space flight capabilities for lunar and planetary explorations and earth orbiting stations
[NASA-SP-196-VOL-1] c34 N69-22510
Space flight effects on human time perception
[NASA-TT-F-545] c05 N69-26455
Manned spacecraft control system requirements for abort problems
[NASA-CR-835] c31 N69-27299
Solid electrolyte electrolysis of carbon dioxide and water as oxygen regeneration system for long manned space flights
[NASA-CR-1359] c05 N69-28099
Propulsion systems for manned exploration of solar system
[NASA-TM-X-1864] c28 N69-34674
MANNED SPACECRAFT
Meteorological satellite research program, including unmanned satellite observations and possibilities with meteorologist on board manned spacecraft
[UN PAPER 68-95350] c20 A69-10483
Lifting body type M2-F1 and M2-F2 aircraft enabling astronauts to make own landings at choice airport
c02 A69-13367
Photographic control system requirements for Project Apollo manned launches, considering extreme heat, vibration and sound pressure environment
[SMPTE PAPER 104-20] c14 A69-14360
Manned spacecraft systems design optimization for extended space missions replacement modules

c31 A69-16380
Life in spacecraft - Conference, Belgrade, September 1967
c05 A69-17642
System designs for manned spacecraft gravity gradient stabilization of Saturn S-4B stage at 400 km and lunar module at synchronous altitude
c31 A69-18338
Communications for Apollo Applications Program, considering extended duration manned missions in low earth orbit and Gemini, Saturn and Apollo hardware
c07 A69-19124
Displays and controls requirements in manned spacecraft to integrate man into vehicle system, noting man capability for task diversity
c14 A69-19968
Manned spacecraft electrical power systems requirements, noting Gemini and Apollo fuel cell system design and configuration
c03 A69-21035
Manned spacecraft developments, considering Apollo Applications Program, space station establishment, space shuttle operations and payload cost
c31 A69-22866
Weight estimation and forecast in manned spacecraft design, noting size and weight relationship
[SAWE PAPER 793] c31 A69-34864
Low cost rate transportation as mandatory goal for future space program, discussing recovery and reuse, launch system costs, hardware development, etc
c31 A69-38117
Cone-conical-frustrum configurations meeting center of gravity requirements for higher hypersonic lift-drag ratios in axisymmetric manned spacecraft
c01 A69-39237
Ground based guidance for land-landing manned spacecraft with low velocity descent systems, discussing high and low altitude glide path intercept and spiral
[AIAA PAPER 69-864] c21 A69-39390
Statistical error analysis of autonomous manned spacecraft navigation in long duration eccentric Mars orbits
[AIAA PAPER 69-880] c21 A69-39406
Flexible parawing lifting decelerator research data from wind tunnel and flight tests, noting manned space vehicle recovery and aircraft escape systems
[AIAA PAPER 68-967] c02 A69-43715
Visual sensing and spacecraft guidance for earth orbit rendezvous maneuvers
[NASA-CR-1214] c05 N69-13161
Effect of spacecraft onboard radar range and range rate data and accuracy on unmanned probe entry guidance corridor
[NASA-TN-D-4852] c21 N69-16503

MANUAL CONTROL

Flight test evaluation of small one man lunar flying device /POGO/, discussing vehicle control, pressure suit factors and piloting differences
[AIAA PAPER 68-240] c11 A69-12379
Minimal angle of resolution /MAR/ between point and extended circular source and between point source and simulated horizon, studying irradiation effects on manual navigation
c21 A69-19208
Roll-motion cues for man-vehicle control in compensatory tracking task with disturbance input
c05 A69-23879
Manual procedures for midcourse and terminal guidance, discussing onboard optical measurements and calculations
c21 A69-35792
Manual guidance and control of Saturn launch vehicles, considering feasibility, reliability and hardware implementation
[AIAA PAPER 69-876] c31 A69-39402
Synthesis methods for manual aerospace control systems using digital programming and man machine performance data with application to supersonic transport design
[NASA-CR-1208] c02 N69-13185
Proprioceptor influence on operator performance in manual control situations
[NASA-CR-1248] c05 N69-14768
Optical simulation landing system for evaluating pilot controlled flexible parawing and Apollo capsule combination performance during landing
[NASA-TN-D-5049] c21 N69-20936
Simulator program for defining in-flight experiment to evaluate manual control system for Saturn 1
[NASA-TN-D-5150] c21 N69-22936
Evaluation of pilot describing function method applied to manual control analysis of large flexible booster in Saturn 5 launch vehicle simulator
[NASA-TN-D-5149] c21 N69-22996
Reliability study of Saturn 5 launch vehicle manual backup control system
[NASA-TN-D-5261] c21 N69-28018
Multimodality pilot model for visual and motion feedbacks derived from simulator program
[NASA-CR-1325] c05 N69-28071

MANUALS

Users manual on FORTRAN 4 COMPUTE program for IBM 360/67 time sharing system
[NASA-TN-D-4917] c08 N69-10098
User manual for computer program 55VD for computation of minimum induced drag and load distribution of nonplanar wings
[NASA-CR-1218-SUPPL] c01 N69-12286

MANUFACTURING

Space manufacturing operations program, discussing zero gravity effect during earth orbit flight, Apollo Applications Program Orbital Workshop Flight 2, etc
c31 A69-35067
Space manufacturing processes for orbital low and zero gravity environment, discussing buoyancy and thermal convection sensitive and molecular forces controlled methods
[AAS PAPER 69-486] c30 A69-42844

MANY BODY PROBLEM

Computer study of collisionless self gravitating system using two dimensional model, obtaining gravitational field by solving Poisson equation
c30 A69-12272
Atomic Li photoionization cross sections calculated with Brueckner-Goldstone many body perturbation theory
c24 A69-17134
Trajectory error propagation upper bounds in many body field for impulsive initial error, relating error to mission tolerances
c30 A69-21937

MAPPING

Survey of six year period of satellite observed tropical Pacific cloud mapping
c20 A69-33001
Color coded area sensitivity maps of photomultiplier tubes by multicolor display technique, noting focus electrode voltage
c14 A69-35724
Normalized hodographic mapping for constrained trajectory families, discussing mapping concepts, information content and applications
[AIAA PAPER 69-924] c30 A69-39362
Orbit selection rules for planetary cartographic spacecraft derived from relations connecting camera angle, view field and imaging resolution
[AIAA PAPER 69-879] c21 A69-39405

MARAGING STEELS

Plain strain fracture toughness tests on two inch thick maraging steel plates of various strengths, using bend and compact tension tests
c32 A69-23057
Plane strain fracture toughness tests on maraging steel plates for various yield strengths and large dimensions
c17 A69-26496
Metallurgy, behavior, and application of 18 percent nickel maraging steels
[NASA-SP-5051] c17 N69-14193

MARINER SPACE PROBES

Orbital Experimental Capsule /OEC/ as subsatellite concept for Martian fields and particles measurements, noting Voyager exploring vehicle applications
c30 A69-39215

MARKETING
Space program planning, noting market requirements, acceptability and future characteristics
[AAS PAPER 69-083] c34 A69-42820

MARKING
Cross hatching on various body surfaces due to periodic surface pressure fluctuations, discussing origin from counter-rotating longitudinal vortices in boundary layer
[AIAA PAPER 69-11] c12 A69-18213

MARS (PLANET)
Extraterrestrial life possibility in solar system, noting Martian atmosphere and terrestrial life adaption to Mars simulations
c04 A69-11770
Manned Mars and Venus missions role in overall planetary exploration program
c30 A69-12304
Entry and terminal deceleration systems for unmanned Martian landers, discussing parachute landing and lifting entry vehicles
[AIAA PAPER 68-1147] c31 A69-13670
Mars biological exploration, discussing life detection, chemical and biological experimental strategy
[AIAA PAPER 68-1122] c04 A69-13700
Chemical composition of Earth, Venus, Mars, Mercury and Moon calculated from mathematical models, constructing approximate equations of state at high pressure
c30 A69-29878
Statistical error analysis of autonomous manned spacecraft navigation in long duration eccentric Mars orbits
[AIAA PAPER 69-880] c21 A69-39406
Mars exploration for life by Mariner flybys and orbiters and 1973 Viking landers
c30 A69-41611
Research problems in atmospheric entry and landing of manned planetary space flights to Mars and Venus
[NASA-TN-D-4977] c31 N69-15634
Observations and theoretical studies on Mars properties
[NASA-SP-179] c30 N69-16571
FORTRAN computer program for providing mission design data for elliptical orbits around Mars and Venus
[NASA-TN-D-5104] c30 N69-22571

MARS ATMOSPHERE
Extraterrestrial life possibility in solar system, noting Martian atmosphere and terrestrial life adaption to Mars simulations
c04 A69-11770
Mars lower atmospheric pressure, temperature and composition, noting consistency between photometric, spectroscopic and occultation techniques
c30 A69-12104
Deceleration control system for aerobraking and skipout to orbit at Mars
[AIAA PAPER 68-1146] c31 A69-13564
Dynamic stability derivatives of large angle blunted conical spacecraft near transonic speed in simulated Mars environment for various angles of attack
[AIAA PAPER 69-104] c31 A69-18210
Mars lower ionosphere ionization from spectroscopic and Mariner 4 occultation data, discussing various ionization sources
c30 A69-18607
Atmospheric models for exospheric temperatures of Mars and Venus based on photoionization heating efficiency
c30 A69-26020
UV solar radiation variation effects on Mars and Venus upper atmosphere temperatures
c30 A69-37136
Dynamic stability derivatives of large angle blunted conical spacecraft near transonic speed in simulated Mars environment for various angles of attack
c31 A69-40550
Mars atmospheric features from measurements during entry and after landing, discussing atmospheric state properties, diurnal variability, clouds and winds
c30 A69-41617
Requirement estimates and performance predictions for Martian television experiment onboard spacecraft in three point-mass descent trajectories
[NASA-TN-D-5062] c14 N69-17944
Optimum structural design for Martian entry capsule configurations
[NASA-CR-1414] c33 N69-35516
Gamma ray backscattering of radioisotope for measuring Martian atmospheric density
[NASA-TN-D-5431] c24 N69-36931
Physical properties of Martian atmosphere using solar occultation seen from artificial satellite
[NASA-TN-D-5443] c30 N69-38658

MARS PROBES
Longitudinal range dispersion of unmanned Mars landers using VM-8 and VM-9 atmospheric models, discussing Syrtis Major as possible landing site
c30 A69-12390
Mars exploration for life by Mariner flybys and orbiters and 1973 Viking landers
c30 A69-41611
Mars atmospheric features from measurements during entry and after landing, discussing atmospheric state properties, diurnal variability, clouds and winds
c30 A69-41617

MARS SURFACE
Mars surface photometric and spectrophotometric measurements, relating opposition effect details with corresponding laboratory sample measurements
c30 A69-18601
Adenosine triphosphate /ATP/ content of terrestrial soils, based on firefly bioluminescent reaction, for Mars soil problems
c04 A69-37567

MASKING
Auditory temporal masking of tonal signal by narrow band noise and perception of temporal order noting effects of intensity, frequency and time
c05 A69-24795

MASS
Nuclear level density and mass shell corrections relationship for deformed and undeformed nuclei
c24 A69-29337
Radio galaxy Messier 87 mass determined using virial theorem for nucleus velocity dispersion
c30 A69-30883
Effect of chemical properties of pyrolysis gases on heat shield mass required for lifting reentry vehicle in typical reentry trajectory
[NASA-TN-D-4975] c32 N69-14306

MASS DISTRIBUTION
Lunar mass and gravitational field determined from lunar satellite dynamics, using potential function in terms of spherical harmonics
c30 A69-31405
Einstein field equations solutions generated via static spherically symmetric mass and charge distributions
c23 A69-32053
Operational analysis of mass measuring system in orbiting spacecraft
[NASA-TN-D-5039] c04 N69-19115
FORTRAN program for computing principal mass moments of inertia of spacecraft treated as composite bodies
[NASA-TM-X-1754] c23 N69-20870
Weighting factor for correction of photographic bias caused by variation in mass and velocity of sporadic meteoroids
[NASA-TN-D-5245] c30 N69-26239

MASS FLOW RATE
FORTRAN 4 subroutines for calculating critical flow factor to determine mass flow rate of gaseous helium and nitrogen through critical flow nozzles
[NASA-SP-3046] c12 N69-16098

MASS RATIOS
Lunar origin theories, considering moon/earth mass ratio, earth-moon system angular momentum deficiency and differential volatilization in earth
c30 A69-29882

MASS SPECTROMETERS
Contaminant and atmospheric sensor for spacecraft cabin environments

[NASA-CR-1375] c14 N69-37876
MASS SPECTROSCOPY
Planetary atmosphere composition determination using mass spectrometry for neutral components, ion spectrometry for ionic components and data system optimization
[AAS PAPER 68-183] c14 A69-11468
Automatic equipment for sampling and preparing gases by dual column gas chromatography for subsequent mass spectral analysis of carbon isotopes during methane metabolism
c06 A69-12603
Ammonium perchlorate high temperature decomposition by using carbon dioxide laser pyrolysis/mass spectrometry
[AIAA PAPER 69-143] c06 A69-18111
Partition coefficients between natural melts and plagioclase phenocrysts determined for rare earth elements and barium by mass spectrometry
c13 A69-20944
MASS TRANSFER
Ablation product absorption and line transitions effects on shock layer radiative transport around blunt body
[NASA-CR-1264] c33 N69-19117
Solution for shock layer energy equation with mass and convective heat transfer at hypersonic speed
[NASA-TN-D-5246] c12 N69-33421
MATERIALS
Structures, structural dynamics, materials and aeroelasticity - ASME-AIAA Conference, New Orleans, April 1969
c32 A69-25492
MATERIALS RECOVERY
Material recovery from metabolic and other wastes for long duration manned space missions, discussing carbon dioxide removal, bioregenerative food systems, etc
[AAS PAPER 69-143] c05 A69-42876
MATERIALS SCIENCE
Cryogenic properties of polymers - NASA/Case Conference, Cleveland, April 1967
c18 A69-16485
Materials compatibility for space requirements, discussing shape retention, ductility, tensile strength, dissimilar materials stability, etc
c17 A69-17872
Aerospace material investigation and fabrication techniques - Conference, Cocoa Beach, November 1968
c15 A69-22301
Structures, structural dynamics and materials - AIAA-ASME Conference, New Orleans, April 1969
c32 A69-26807
Kim-Anderson flux flow theory for materials with kappa nearly equal to 1, discussing pinning forces and sites
c26 A69-33754
Materials and processes for aerospace applications in 1970s - Conference, Los Angeles, April- May 1969
c15 A69-35501
Materials research structural design cycle, discussing simultaneous optimization, constituent materials, fabrication process, load environment and mission constraints
c32 A69-42991
MATERIALS TESTS
Ablation characteristics of heat shield materials measured in arc heated wind tunnels, considering influence of model scale, heating rate and pressure level
c18 A69-26813
Unfilled Pyrrone prepared from powder into molded parts for flexural tests at elevated temperatures observed for stability to electron irradiation in air
c18 A69-35529
Design and performance prediction of calorimetric apparatus for measuring total hemispherical emittance of materials
[NASA-TN-D-5106] c14 N69-20941
MATHEMATICAL LOGIC
Mathematical model for measurement scale forms
[NASA-TN-D-5277] c19 N69-29141
MATHEMATICAL MODELS
Radiation models using discrete radiator ensembles having applications to analysis of forward and backscatter from rough surfaces, clutter and chaff models, etc
c07 A69-10556
Collisionless computer model performing gravitaticnal experiments with two dimensional galaxy
c30 A69-12271
Computer study of collisionless self gravitating system using two dimensional model, obtaining gravitaticnal field by solving Poisson equation
c30 A69-12272
Space-station-centrifuge configuration dynamic stability exhibiting instabilities at lower and higher centrifuge rotational speeds
[AIAA PAPER 68-142] c31 A69-12373
Explorer 40 satellite mathematical model and verification testing for close spacecraft flight temperature predictions
[SAE PAPER 690202] c33 A69-18305
Four terminal silicon planar p-n-p-n model operating as semiconductor small signal linear tetrode amplifier, discussing properties and mathematical models
c09 A69-35293
Model performance index /PI/ providing criterion for approximating one dynamic flight control system by another based on geometrical representation of linear autonomous systems
[AIAA PAPER 69-885] c21 A69-39410
Theoretical prediction of crater size in Al alloy for hypervelocity impact by reduced density particles
[NASA-CR-1196] c32 N69-10225
Effects of structural damping on flutter of stressed panels
[NASA-TN-D-4990] c32 N69-16091
Calculating equilibrium and kinetically limited performance using one dimensional model
[NASA-TN-D-4991] c27 N69-16153
Development of air bearing lift pads
[NASA-TM-X-1724] c01 N69-16467
Effect of shock precursor heating on radiative flux to blunt bodies
[NASA-CR-1265] c33 N69-17438
Photoviscoelastic method for stress analysis of two dimensional viscoelastic models
[NASA-CR-1289] c32 N69-17770
Thermal and dielectric properties of homogeneous moon based on microwave and infrared temperature observaticns
[NASA-TM-X-1734] c30 N69-17815
Mathematical model for determining total drag of pointed body of revolution in supersonic flow with turbulent boundary layer
[NASA-TN-D-5046] c01 N69-19925
Mathematical models for optimal three dimensional launch vehicle trajectories with attitude and attitude rate constraints
[NASA-TN-D-5117] c30 N69-20810
Effect of gravitational model variations on accuracy of lunar orbit determination from data arcs
[NASA-TN-D-5105] c30 N69-21018
Boundedness theorem, thresholds, and stationary values in modified Huxley-Hodgkin model for electric current flow through cell membrane
[NASA-CR-1272] c19 N69-21143
Estimating sound intensity from stationary and moving sources using mathematical models
[NASA-CR-1338] c23 N69-22545,
Development of lattice model for composite materials
[NASA-CR-1322] c32 N69-22982
Semiempirical collision model for plasmas
[NASA-TR-R-310] c25 N69-23787
Mitchell strain criterion for minimum weight structures using mathematical models
[NASA-TN-D-4345] c32 N69-25001
Systematic investigation of mathematical models by comparison of experimental and analytical regression coefficients
[NASA-TM-X-1797] c19 N69-25311
Gravity model comparison using geodetic satellite long arc orbital solutions
[NASA-TN-D-5035] c30 N69-27412
Mathematical model for measurement scale forms
[NASA-TN-D-5277] c19 N69-29141
Analytic time function models of stochastic processes of noise and modulation
[NASA-TR-R-314] c07 N69-29230

Model analysis for viscosity in jet mixing flows
[NASA-CR-1382] c12 N69-31887
Analytical model for use in design of pump inlet accumulators for prevention of liquid rocket longitudinal oscillation
[NASA-TN-D-5394] c28 N69-33319
Mathematical model for quantitative wind and turbulence effects on design and operation of launch vehicles
[NASA-CR-1418] c20 N69-36222
Comparison of fourth order Runge-Kutta numerical integration technique with two numerical integration formulas in mathematical models used for computing rigid body trajectories
[NASA-TN-D-5425] c30 N69-38769
Mathematical simulation model for rigid body rotational kinematics
[NASA-TN-D-5302] c23 N69-39178
Flow model for vortex shedding from slender body in coning motion
[NASA-CR-1448] c12 N69-40200

MATHEMATICAL TABLES
Tabulation of high accuracy gamma function values for some rational arguments, noting applications to Gaussian quadrature formulas, fractional Bessel functions and Airy functions
c19 A69-13375
Tabulated bending moment transfer coefficients for helicopter rotor blades
[NASA-CR-1441] c32 N69-40359

MATRICES (MATHEMATICS)
Coulomb approximation for dipole and quadrupole transitions, calculating tables for radial matrix elements
c24 A69-10901
Matrix Riccati and matrix quadratic equations in problems of stochastic control and filtering
c10 A69-16601
Transient vibration analysis of liner systems using transition matrices
[NASA-CR-1237] c32 N69-11008
Stiffness matrices analysis of thin flat plates
[NASA-TN-D-4927] c32 N69-14169
Conversational approach to matrix calculations on computers
[NASA-TM-X-1749] c08 N69-18954
Existence theorem using Pade approximation and matrices
[NASA-CR-1319] c19 N69-26248

MATRIX METHODS
Finite element method for computing natural frequencies and mode shapes of thin shells of revolution
[NASA-TN-D-4972] c32 N69-16469
Identification of structural systems using near resonance testing
[NASA-TN-D-5069] c32 N69-17737

MATRIX THEORY
Matrix theorem and application to establishing independent coordinates for complex dynamical systems with constraints
[NASA-TR-R-326] c19 N69-38655

MATTER (PHYSICS)
Extragalactic gamma ray fluxes predicted, discussing collisions, matter-antimatter annihilation and cosmological implications
c29 A69-24466
Structure of matter, physical fields, evolution of earth and universe, solar activity and earth, and interaction of earth biosphere with physical fields
[NASA-TT-F-345] c13 N69-12384

MAXWELL EQUATION
Radiation fields from energetic electron moving in helical orbit in magnetoactive plasma, using Maxwell equations
c30 A69-39965

MEASURING INSTRUMENTS
Make wire, light pipe and spring wire ablation sensors development for measuring parameters of heat shield materials for reentry vehicles
c14 A69-15428
Three dimensional laser Doppler velocity instrument for mean velocity and turbulence measurements in subsonic jet shear layer
[SAE PAPER 690266] c14 A69-21555
Radial inflow gas turbine engine performance testing, discussing instrumentation, recording systems and calibration techniques
[ASME PAPER 69-GT-104] c14 A69-22522
Earth orbital manned space astronomy, discussing long range program, instruments, facilities and data processing
c11 A69-27947
Multiple function combination probe design for compressor and turbine air flow research
c11 A69-31917
Self contained hand held battery operated aerosol particle analyzer, measuring aerosol concentration and size distribution for laboratory and space flight applications
c14 A69-34691
Design and performance of flueric shock position sensor for mixed compression supersonic inlets
[NASA-TM-X-1733] c14 N69-16382
Mathematical analysis of Fitzgerald apparatus measuring solids dynamic mechanical properties
[NASA-TN-D-5116] c18 N69-21384
Cosmic dust sensor experiment on Pioneer 8 space probe
[NASA-TN-D-5267] c30 N69-31058

MECHANICAL DRIVES
Mechanical characteristics of flexible drive shaft coupling
[NASA-CR-1241] c15 N69-16104

MECHANICAL IMPEDANCE
Human body dynamic response to vibration combined with linear acceleration, noting changes in body mechanical impedance and resonance
c05 A69-11335
Analysis of Fitzgerald apparatus for extraneous resonant modes, dynamic compliance, and mechanical impedance
[NASA-TN-D-5103] c26 N69-20798
Vibration test fixture design for mount impedance simulation of aerospace structures
[NASA-CR-1351] c32 N69-26315

MECHANICAL MEASUREMENT
Plain strain fracture toughness tests on two inch thick maraging steel plates of various strengths, using bend and compact tension tests
c32 A69-23057
Plane strain fracture toughness tests on maraging steel plates for various yield strengths and large dimensions
c17 A69-26496
Development of automatic quality control device for measuring welded joints
[NASA-TN-D-5304] c15 N69-33800

MECHANICAL PROPERTIES
Lunar surface mechanical properties at Surveyor 5 site
c30 A69-12225
Cryogenic behavior of adhesive materials used in fabrication of liquid hydrogen/liquid oxygen powered Saturn S-4B stage
c18 A69-16487
Film processing effects on cryogenic mechanical properties of polyethylene terephthalate
c18 A69-16490
Cryogenic mechanical properties of epoxy resins and glass/epoxy composites
c18 A69-16491
Mechanical behavior of polyethylene terephthalate at cryogenic temperatures
c18 A69-16494
Vulcanizable elastomers suitable for contact with liquid oxygen, discussing preparation, mechanical properties, transition temperature and structure
c06 A69-16497
Materials compatibility for space requirements, discussing shape retention, ductility, tensile strength, dissimilar materials stability, etc
c17 A69-17872
Powder metallurgy, fusion and chemical vapor deposition techniques in manufacturing tungsten base alloys
c17 A69-18792
In situ vacuum testing requirement for valid measurement of vacuum induced changes in mechanical and thermal properties of various filled elastomers
c11 A69-22008
Mechanical properties associated with 55-Nitinol memory effect, presenting stress-strain and electrical resistivity as function of temperature

c17 A69-35523
Mission sequential environment effects on Dacron parachute material mechanical properties
[AIAA PAPER 69-1018] c11 A69-40390
High temperature mechanical properties of polycrystalline hafnium carbide containing 13-volume-percent hafnium diboride
[NASA-TN-D-5008] c17 N69-16380
Mechanical properties of alloys molybdenum hafnium carbon compounds
[NASA-TN-D-5025] c17 N69-19200
Mechanical behavior of boron-epoxy and glass-epoxy filament-wound cylinders under various loads
[NASA-TN-D-5050] c18 N69-19825
Mechanical properties and column behavior of thin wall beryllium-aluminum alloy tubing
[NASA-TN-D-5145] c17 N69-23004
Soviet research on high temperature strength of materials and machine parts
[NASA-TT-F-508] c17 N69-27300
Effect of rhenium on mechanical properties of hafnium carbide strengthened tungsten alloys
[NASA-TN-D-5348] c17 N69-31977
Physical, mechanical, and electrical properties of 55-Nitinol - nickel-titanium alloy
[NASA-CR-1433] c17 N69-36367
Summary of lunar data and scientific observations generated by Surveyor landings on Moon
[NASA-SP-184] c30 N69-36451
Properties of irradiated polyethylene memory materials
[NASA-CR-1384] c18 N69-36762
Mechanical behavior of tantalum T-111 alloy at high temperatures and ultrahigh vacuum
[NASA-CR-1436] c17 N69-36831

MEDICAL EQUIPMENT
Soviet handbook on operation principles, use, and installation of electrocardiographs and electromedical apparatus for therapeutics
[NASA-TT-F-523] c05 N69-27577

MEDICAL SCIENCE
Aeromedical developments by NASA biomedical applications program applied to general medical equipment including cardiac sensors, surgical sterilization, ballistocardiograph, etc
c34 A69-32430
Centrifugation for removal of bullet fragment floating freely in ventricular system of human brain to fixed safe position in left lateral ventricle wall
c04 A69-43372

MEDIUM SCALE INTEGRATION
Spacecraft onboard data handling system with MSI complementary MOS arrays, describing various components
c08 A69-41739

MELTING
Microscopic time lapse movies in solid/liquid interface profile during melting and freezing of materials for spacecraft thermal control as reversible heat sink
[AIAA PAPER 69-95] c33 A69-18126

MEMORY
Efficacy of sensory feedback information given during training period for improving human performance in producing memorized movement pattern
[NASA-CR-1251] c05 N69-13926

MENTAL PERFORMANCE
Evaluation of computer aids to augment human intellectual capability
[NASA-CR-1270] c08 N69-16140

MERCURY (METAL)
Liquid mercury cathode thrustors characteristics satisfying constraints imposed by solar flux variations with distance from sun
[AIAA PAPER 69-237] c28 A69-21246
Design point performance of double containment tantalum and stainless steel mercury boiler for SNAP 8
[NASA-TN-D-4926] c33 N69-12739
Liquid-metal centrifugal pump at mercury loop
[NASA-TM-X-1766] c15 N69-23768
Corrosion in cobalt alloy two phase mercury loop
[NASA-TN-D-5326] c17 N69-31065

MERCURY (PLANET)
Mercury atmospheric models for preliminary environmental criteria to be used in spacecraft design and engineering trade-off studies
[AIAA PAPER 69-54] c30 A69-18042
Chemical composition of Earth, Venus, Mars, Mercury and Moon calculated from mathematical models, constructing approximate equations of state at high pressure
c30 A69-29878
Resonant spin and anomalous rotation of Mercury, analyzing influence of tidal degradation and permanent deformation of planet
c30 A69-39568
Venus swingby and direct Mercury trajectories analysis for optical imaging from flyby missions
[AAS PAPER 69-258] c30 A69-42860

MERCURY ARCS
Mercury ion thrusters and facilities automatic controls durability testing, discussing vacuum chamber systems, unattended operation and control
[AIAA PAPER 68-576] c11 A69-12385

MERCURY FLIGHTS
Manned spacecraft waste disposal systems
[NASA-TM-X-1851] c05 N69-33260

MERCURY PROJECT
Gemini and Mercury space flights medical results, summarizing physiological effects noted on body systems
c04 A69-11074
Systems engineering activities in manned space flight involving design, development, manufacture, test and operation of Mercury, Gemini and Apollo flight systems
c31 A69-17602

MERCURY SPACECRAFT
Guidance and control concepts and hardware for atmospheric entry of Mercury, Gemini and Apollo spacecraft
c21 A69-25724

MERCURY TELLURIDES
HgCdTe as IR satellite detector for terrestrial, atmospheric and ocean mapping, IR astronomy and optical communication
c26 A69-43666
Mercury cadmium telluride as 1 to 20 micrometer wavelength infrared detector for space applications
[NASA-TN-D-4904] c26 N69-10125

MERCURY VAPOR
Study of discharge from mercury vapor fed hollow cathode
[NASA-TN-D-4966] c28 N69-17847

MERIDIONAL FLOW
Model equatorial electrojet with meridional current system constructed by spherical harmonic expansion for geomagnetic field, noting current loops
c13 A69-38084

MESH
Variable mesh multistep methods for numerical solution of nonlinear differential equations
[NASA-CR-1247] c19 N69-11419

MESOPAUSE
Mesopause wind measurements at high latitude locations by sounding rockets noting relation to noctilucent clouds
c20 A69-28466

MESOSPHERE
Distributions, seasonal variations and ionospheric implications of mesospheric nitric oxide concentration
c13 A69-38364
Theoretical comparison of beads, wires, and films as rocketsonde temperature sensors in mesosphere
[NASA-CR-1286] c13 N69-18126
Stratospheric and mesospheric temperature and moisture profiles determined from infrared horizon observations
[NASA-CR-1419] c20 N69-35528

MESSAGES
Variable length codes for alphabets containing messages with assigned weighted information content
[NASA-TN-D-4962] c07 N69-15373

METABOLIC WASTES
Hydrogenomonas cultures investigated for metabolic waste utilization in aerospace life support systems
[NASA-CR-1296] c05 N69-22766

METABOLISM
Extraterrestrial life detection experiments

integrated into single multipurpose space laboratory, including chemical analyses, metabolism identification, observation for molecular and/or cellular growth and replication c05 A69-32970
Real time metabolic rate analysis of suited astronaut using heart rate and O methods during thermal vacuum and extravehicular mobility tests [AIAA PAPER 69-993] c05 A69-40371
Lunar gravity effects on mans locomotion on moon [NASA-CR-1403] c05 N69-36271
Simulation of astronaut locomotion on lunar surface to determine metabolic costs [NASA-CR-1402] c05 N69-37964
Biochemical and metabolic effects of exposure of mice to helium-oxygen atmosphere [NASA-CR-1372] c04 N69-40955

METAL BONDING
Quartz fiber adhesion to Re measured in LEED /low energy electron diffraction/ apparatus for clean and O layer surfaces, noting brittle fracture c17 A69-35182
Joining ceramics and graphite to other materials [NASA-SP-5052] c15 N69-14241

METAL COATINGS
High emittance coating materials for beryllium, niobium-zirconium compounds, and stainless steel used in spacecraft radiators [NASA-CR-1278] c17 N69-18952
Emittance properties of hafnium oxide, cerium oxide, and iron titanate coatings on platinum rhodium alloy substrates [NASA-CR-1413] c17 N69-35514
Corrosion and heat resistant coatings for oxidation protection of tungsten [NASA-TT-F-583] c17 N69-35836

METAL COMPOUNDS
Crater characteristics of 11 metal alloys under hypervelocity impact including effects of projectile density and target temperature [NASA-TN-D-5135] c32 N69-22994

METAL CRYSTALS
Fiber-metal matrix composites fabrication, applications, mechanical properties and powder metallurgy c17 A69-20204
Internal friction, Young modulus and resistivity measurements for stage I interstitials in electron irradiated tungsten c17 A69-28682

METAL FILMS
Gold-underlayer film combinations adhesion to oxide substrates, describing adhesion changes as function of Au and underlayer film thickness, time, environment, etc c26 A69-28007
Ge films formation by evaporation technique, discussing background O pressure effect c26 A69-43345

METAL FOILS
Resonance absorption integrals for rhenium 185, rhenium 187, and natural rhenium in foils and thin films [NASA-TN-D-4938] c24 N69-13152
Three oxidation-resistant alloy foil claddings for protecting typical gas turbine engine alloys of nickel and cobalt [NASA-TN-D-5483] c17 N69-38794

METAL IONS
Uranyl ions interaction with phospholipid and cholesterol monolayers, using surface pressure and potential measurements c06 A69-25641
Oscillator strengths and wavelengths of X ray and EUV transitions in highly ionized iron line spectra c29 A69-27554

METAL JOINTS
Dielectric overcoating effects on electromigration Al interconnections, showing dependence on thickness and surface passivation c09 A69-32889

METAL MATRIX COMPOSITES
Tensile data and photomicrographs of explosively bonded metal matrix composites interfaces c15 A69-43452

METAL OXIDE SEMICONDUCTORS
Electric field effects on thermal annealing of electron irradiation damage in p-channel MOSFET device c09 A69-16562
Electron radiation damage in MOSFET devices using bias temperature treatments c26 A69-16877
Metal oxide semiconductor integrated circuits, showing failure rates and degradation causes c09 A69-31851
Spacecraft onboard data handling system with MSI complementary MOS arrays, describing various components c08 A69-41739
Spacecraft analog to digital conversion system employing metal oxide semiconductor field effect transistors [NASA-TN-D-5228] c08 N69-29478

METAL OXIDES
H release, pressure and oxide layer formed by reaction during ball milling Cr in water c15 A69-38567

METAL PLATES
Plain strain fracture toughness tests on two inch thick maraging steel plates of various strengths, using bend and compact tension tests c32 A69-23057
Decoupling force exerted by magnetic forming Be coil assembly on metallic plate during forming c14 A69-25310
Plane strain fracture toughness tests on maraging steel plates for various yield strengths and large dimensions c17 A69-26496
Force penetration characteristics of sand horizontally penetrated by various geometrically shaped models [NASA-CR-1252] c18 N69-14764

METAL POWDER
Ductile metal powder chemical reactions during comminution in pure or oxygenated water c06 A69-27762
Inductance behavior of coils filled with superconducting lead or niobium dusts [NASA-TN-D-5137] c26 N69-21500

METAL SHEETS
Aluminum double sheet target penetration resistance determined by studying high velocity pyrex glass impact effects on front/rear sheets and spacing [AIAA PAPER 69-375] c32 A69-28305
Axial load fatigue crack propagation tests on Al alloy sheets for stress ratio effects c17 A69-36435
Stress ratio effects on fatigue crack growth in sheet aluminum alloys [NASA-TN-D-5390] c17 N69-34704

METAL SURFACES
Work function and desorption energy measurements of alkali metals from metallic substrates with modulated molecular beam, noting surface contamination c26 A69-21808
Free electron model for electron work functions and number density distributions and surface potentials in metals c26 A69-29009
Quartz fiber adhesion to Re measured in LEED /low energy electron diffraction/ apparatus for clean and O layer surfaces, noting brittle fracture c17 A69-35182
Electric fields and electron work functions, surface potentials and number density distributions in selected metals surfaces determined using free electron model c26 A69-36045
Solid film lubricants deposited by DC triode sputtering on Ni, Ni-Cr and Nb surfaces friction tested under ultrahigh vacuum conditions c15 A69-43126
Compressive properties and weight saving of metals reinforced on surface with resin bonded fibers [NASA-TN-D-4878] c17 N69-11012
Theory and method for characterizing surface cleanliness of nickel during adhesion testing [NASA-TN-D-5055] c17 N69-19827
Absorption of black-body radiation by ice cryodeposits on metal substrates [NASA-TN-D-5181] c23 N69-22769

METAL VAPORS
Electric field variations in vicinity of auroral

forms from motions of Ba vapor clouds released from Nike-Tomahawk rockets
c13 A69-34935

METALLURGY
Refractory metal alloys metallurgy and technology - Conference, Washington, D. C., April 1968
c17 A69-18790
Z-micron sections removed from metal specimens by microtome for radiotracer study of mass dependence of self diffusion
c14 A69-36490
Metallurgy, behavior, and application of 18 percent nickel maraging steels
[NASA-SP-5051] c17 N69-14193

METALS
Solar absorptance, total hemispherical emittance and absorptance/emittance ratio for metals at cryogenic temperatures measured simultaneously with sinusoidally perturbed incident radiation
c33 A69-10847
Solar absorptance and hemispherical emmitance of metals at space conditions determined with cyclic incident radiation technique
[AIAA PAPER 69-60] c17 A69-18154
Atmospheric models for metal deficient stars of K and G spectral type, studying reduced metal abundance effect on atmospheric structure
c30 A69-22055
Optical depths of convection related to metal deficiency for main sequence and giant stars
c30 A69-29946
Atmospheric models for specified effective temperatures, hydrogen-to-metal ratios and surface gravities in studying metal deficiency effect on stellar atmosphere
c30 A69-36338
Calorimetric analyses of metal corrosions in deionized heated water
[NASA-TM-X-1791] c17 N69-25243
Solar absorptances and spectral reflectances of metals
[NASA-TN-D-5353] c17 N69-31895

METASTABLE STATE
Two photon decay of metastable levels of hydrogenic and He-like ions in solar corona, depopulating via proton collisional excitation to 2p level
c29 A69-36218

METEOR TRAILS
Visual observation of meteor and train microstructure obtained by refractor
c30 A69-41058

METEORITE CRATERS
Moldavites and Ries crater material, studying Rb-Sr isochronal relationship
c13 A69-41341

METEORITES
Meteorite research - Conference, Vienna, August 1968
c30 A69-36072

METEORITIC COMPOSITION
Electron microprobe analysis of potassium feldspar in Weekeroo Station meteorite
c30 A69-14979
Electron microprobe analysis of vanadium in presence of titanium by compositional measurement of chromite in chondritic meteorites
c06 A69-18419
Chondrite meteorite fall /1969/ in Mexico, noting opaque and microcrystalline matrices and gamma rays from short lived isotopes
c30 A69-20686
Kodaikanal iron meteorite measurements for cosmogenic rare gases and K-Ar isotopes ages for glass inclusions
c30 A69-22047
Oxide composition of silicate spherules from forest area devastated by Tunguka meteorite explosion using electron microprobe analysis
c30 A69-28869
Bjurbole chrondrules composition and density, discussing formation of homogeneous olivines and pyroxenes
c30 A69-36090
Ca-rich achondrites genesis implied from rare earth and Ba absolute and relative concentrations
c30 A69-36091
Iron meteorites genetic classification based on parent body cooling rate and Ga-Ge trace element content
c30 A69-36129
Abundance compilations of elements due to nuclear processes, discussing carbonaceous chondrites character
c29 A69-38812
Tektite origin theories, discussing Surveyor experiments effects on lunar geology and Tektite origin
c30 A69-40086
Moldavites and Ries crater material, studying Rb-Sr isochronal relationship
c13 A69-41341
Rb-Sr isotope patterns in tekites from Southeast Australian strewn field, studying Rb volatilization role in Rb-Sr isochron production
c13 A69-41342
Ivory Coast microtektites chemical composition from electron microprobe analysis
c30 A69-41351
Ilmenite composition in equilibrated ordinary chondrites, analyzing Fe, Mg, Ti and Cr content
c30 A69-42890

METEORITIC DAMAGE
Hypervelocity micrometeor impact sites identification on aluminized glass, using conchoidal pattern as criterion in analysis
c30 A69-34952
Simulated micrometeoroid impact effect on silicon and cadmium sulfide solar cell performances
[NASA-TN-D-5133] c03 N69-21016
Penetration flux calculation for multiwall structure on Lunar Orbiter spacecraft missions
[NASA-TN-D-5455] c32 N69-41229

METEORITIC MICROSTRUCTURES
Chondrite meteorite fall /1969/ in Mexico, noting opaque and microcrystalline matrices and gamma rays from short lived isotopes
c30 A69-20686
Fe-Ni-P phase diagram studies applied to schreibersite and rhabdite formation in iron meteorites
c30 A69-36132

METEOROID CONCENTRATION
Determination of meteoroid environments from photographic meteor data
[NASA-TR-R-322] c30 N69-39336
Meteoroid environment model for cometary origin near earth to lunar surface
[NASA-SP-8013] c30 N69-40326

METEOROID HAZARDS
Meteoroid environment model for cometary origin near earth to lunar surface
[NASA-SP-8013] c30 N69-40326

METEOROID PROTECTION
Space suit meteoroid protection for extravehicular activity, discussing Gemini and lunar surface EVA suits and bumper concept
[AIAA-PAPER-69-366] c05 A69-28298
Multiwall meteoroid protection design in Apollo program, discussing bumper, backup sheet and honeycomb cells insulation
[AIAA PAPER 69-372] c32 A69-28304
Momentum transfer from impact into thin aluminum meteor bumper targets
[NASA-TN-D-5492] c32 N69-38809

METEOROIDS
Visual observation of meteor and train microstructure obtained by refractor
c30 A69-41058

METEOROLOGICAL BALLOONS
All weather wing profile monitoring system using FPS-16 radar/jimsphere system and flight simulation for protection of space vehicle and missile launches
c20 A69-13852
Error analysis of high resolution balloon-borne temperature sensor and comparison of temperature data with simultaneous rawinsonde measurements
c14 A69-21642

METEOROLOGICAL CHARTS
Tiros 7 monthly maps of infrared radiation over Indian Ocean area
[NASA-TN-D-5101] c13 N69-23318
Synoptic analysis of Southern Hemisphere stratosphere
[NASA-TM-X-1814] c13 N69-33555

METEOROLOGICAL PARAMETERS
Daily simultaneous solar measurements of microwave atmospheric absorption and emission to determine frequency correlation between meteorological phenomena and atmospheric parameters
c13 A69-39747
Mars atmospheric features from measurements during entry and after landing, discussing atmospheric state properties, diurnal variability, clouds and winds
c30 A69-41617
METEOROLOGICAL RADAR
All weather wing profile monitoring system using FPS-16 radar/jimsphere system and flight simulation for protection of space vehicle and missile launches
c20 A69-13852
METEOROLOGICAL SATELLITES
Atmospheric model development relating temperature, density, moisture and energy measurements from satellite observations for long term weather forecasting
[UN PAPER 68-95397] c20 A69-10463
Space applications program including communications and navigation meteorology, earth resources survey and geodesy
[UN PAPER 68-95437] c34 A69-10472
Meteorological satellite research program, including unmanned satellite observations and possibilities with meteorologist on board manned spacecraft
[UN PAPER 68-95350] c20 A69-10483
Atmospheric measurements from satellites, discussing ATS-1 cloud images for definition of wind and use of WEFAX through ATS 2 satellites for data transmission
[AIAA PAPER 69-158] c20 A69-18038
Image dissector meteorological cameras, discussing ATS-3 and Nimbus systems, high resolution camera and multispectral cameras
c14 A69-35101
Satellite-based meteorological observation system for global atmospheric research program, discussing wind measurement, IR and microwave sounding possibilities, etc
[AAS PAPER 69-120] c13 A69-42817
Exametnet meteorological rocket launchings and data dissemination, 1967 - tables
[NASA-SP-176] c20 N69-22570
METEOROLOGICAL SERVICES
WEFAX /Weather Facsimile/ experiment to explore operational feasibility of direct meteorological data transmission via satellite relay from central station to remote stations
c11 A69-13240
METEOROLOGY
Meteorological satellite research program, including unmanned satellite observations and possibilities with meteorologist on board manned spacecraft
[UN PAPER 68-95350] c20 A69-10483
METHANE
Leak rate measurement accuracy of rate-of-rise technique for nitrogen, methane and He between millionth and thousandth torr
c14 A69-32326
Real gas effects on hypersonic aerodynamics of blunt vehicles simulated with tetrafluoromethane
[NASA-TR-R-312] c01 N69-29270
Helium pressurization systems for liquid methane fuel in supersonic transports
[NASA-TN-D-5519] c28 N69-40329
METHOD OF CHARACTERISTICS
Three dimensional hypersonic steady flow around blunt and pointed cones at nonzero angles of attack calculated by method of characteristics
[AIAA PAPER 69-187] c01 A69-18176
FORTRAN computer program for designing supersonic inlets by characteristic theory
[NASA-TN-D-4960] c01 N69-14566
Characteristics method for determining three dimensional supersonic flow around inclined body of revolution
[NASA-TN-D-5341] c12 N69-39177
MICE
Centrifugation effects on body composition and growth of mice
c04 A69-33746
Biochemical and metabolic effects of exposure of mice to helium-oxygen atmosphere
[NASA-CR-1372] c04 N69-40955
MICHELL THEOREM
Mitchell strain criterion for minimum weight structures using mathematical models
[NASA-TN-D-4345] c32 N69-25001
MICROBIOLOGY
Microbiology of water management subsystem for manned space flight, discussing sterilization by heat and tests inside Integrated Life Support System /ILSS/
[SAE PAPER 680718] c05 A69-13441
MICROELECTRONICS
Hybrid integrated parametric amplifier design considerations for fabrication in microstrip transmission line
c09 A69-10193
Neutral buoyancy microelectrode for prolonged recording from single nerve units
c05 A69-11865
Microelectronic data and remote control function transmission system for wind tunnel testing of aircraft dynamic response to gusts and turbulence
c11 A69-23283
Reliability handbook for silicon monolithic microcircuits - applications
[NASA-CR-1346] c09 N69-23225
Reliability handbook for silicon monolithic microcircuits - failure mechanisms
[NASA-CR-1347] c09 N69-23226
Reliability handbook for failure analysis of silicon integrated microcircuits
[NASA-CR-1348] c09 N69-25328
MICROFILMS
Micromation and micrographics, discussing nonimpact printing in computer avoiding output imbalance by high speed microfilm recorder
c34 A69-35059
MICROMETEOROIDS
Stony meteoric particles size and velocity during passage through atmosphere
c30 A69-26341
Meteoritic dust particles collections prediction in atmosphere for low and high entry fluxes
c30 A69-26342
Hypervelocity micrometeor impact sites identification on aluminized glass, using conchoidal pattern as criterion in analysis
c30 A69-34952
Pegasus and Explorer 23 detector panels calibrated by determining particle perforation mass and velocity
[NASA-TR-R-321] c14 N69-36985
Lunar Orbiter 1 terrain assessment photographs and preliminary selenodesy, micrometeoroid, and radiation data
[NASA-SP-197] c30 N69-39213
MICROORGANISMS
Spacecraft sterilization techniques for space exploration, discussing mathematical models for planetary quarantine and contamination by nonlanding vehicles
c05 A69-15935
Spacecraft sterilization requirements, evaluating viable organisms release probability from spacecraft as function of equipment fracturing
c04 A69-25460
Unicellular microorganisms size and concentration estimates based on light scattering measurements of suspensions in spectrophotometer cuvette compartment
c04 A69-25643
Regenerative life support system development, considering synthesized organic compounds and microorganisms as foods for long duration space missions
c04 A69-37623
Gravitational and acceleration effects on man and organisms, and biological effects of radiation
[NASA-TT-F-528] c05 N69-38701
MICROROCKET ENGINES
Valving concepts and functional approaches for inert gas attitude control thrustor systems providing redundancy safeguards at minimum weight, volume and power costs
[AIAA PAPER 69-843] c28 A69-39373

MICROSCOPY
Holographic microscopy for performance prediction and quality control of semiconductor devices and integrated circuits
[NASA-CR-1394] c14 N69-31958
MICROSTRUCTURE
Visual observation of meteor and train microstructure obtained by refractor
c30 A69-41058
Sigma phase formation and its effect on stress rupture properties of nickel base alloy IN-100
[NASA-TN-D-5185] c17 N69-23465
MICROTHRUST
Cesium contact ion microthrustor experiment onboard ATS 4, measuring emission currents and spacecraft potentials
[AIAA PAPER 69-297] c28 A69-21218
MICROTOMY
Z-micron sections removed from metal specimens by microtome for radiotracer study of mass dependence of self diffusion
c14 A69-36490
MICROWAVE AMPLIFIERS
Microwave and optical generation and amplification - Conference, Hamburg, September 1968
c09 A69-18420
MICROWAVE ANTENNAS
Omnidirectional microwave parallel plate waveguide fed antenna design for flush mounted broadband spacecraft, noting equatorial and polar patterns
c09 A69-40697
MICROWAVE EQUIPMENT
Microwave power applications to propulsion, noting spacecraft launching, aircraft takeoff thrust assistance and power transmission in space
[IMPI PAPER D2] c28 A69-15000
Microwave and optical generation and amplification - Conference, Hamburg, September 1968
c09 A69-18420
Germanium microwave backward diodes optimum design and performance prediction through computer calculation for important parameters
c09 A69-41224
Thin film microwave irises with capacitive reactance
[NASA-CR-1364] c26 N69-28096
MICROWAVE FREQUENCIES
Daily simultaneous solar measurements of microwave atmospheric absorption and emission to determine frequency correlation between meteorological phenomena and atmospheric parameters
c13 A69-39747
MICROWAVE INTERFEROMETERS
Electron density measurement technique for dense thick steady state plasmas using swept microwave interferometer
c25 A69-12349
MICROWAVE RADIOMETERS
Microwave radiometric sensor operational principles and capabilities, discussing antennas and radiometric receivers
c07 A69-26976
Clear air turbulence detection in troposphere by multifrequency radiometric sensor, noting multibeam system for supersonic aircraft
c09 A69-42536
Microwave radiometric techniques for reentry plasma measurements
[NASA-TN-D-5274] c25 N69-29600
MICROWAVE SPECTRA
Microwave thermal emission by water measured from aircraft, studying radiation dependence on surface roughness
c13 A69-34421
MICROWAVE TRANSMISSION
Mutual RF interference between satellite and terrestrial telecommunications microwave relay system at shared frequencies
c07 A69-13242
Intersatellite microwave laser communication system for ATS-F and ATS-G, discussing experiment, functional design and parameters
c07 A69-41758
Parametric analysis of microwave and laser systems for communication and tracking - summary
[NASA-TR-R-309] c07 N69-23642
Statistical correlation between optical microwave propagation reliability, fade margin, path length, and geographic location
[NASA-CR-1442] c07 N69-39282
MICROWAVES
Venus microwave phase effect analyzed assuming dry massive Venus atmospheric model, discussing heat transfer processes
c30 A69-12108
Microwave power applications to propulsion, noting spacecraft launching, aircraft takeoff thrust assistance and power transmission in space
[IMPI PAPER D2] c28 A69-15000
Solar microwave radiation burst of 29 October 1968 from active region behind west limb
c30 A69-32811
Thermal and dielectric properties of homogeneous moon based on microwave and infrared temperature observations
[NASA-TM-X-1734] c30 N69-17815
Transfer of microwave radiation in atmosphere and underlying surfaces measured by aircraft instruments
[NASA-TT-F-590] c13 N69-31851
Backward diodes in indium arsenide for microwave mixing
[NASA-TN-D-5401] c09 N69-36706
MIDCOURSE GUIDANCE
Midcourse maneuvers in interplanetary guidance, considering spin stabilized spacecraft flyby for Jupiter mission
c30 A69-28504
Manual procedures for midcourse and terminal guidance, discussing onboard optical measurements and calculations
c21 A69-35792
Interplanetary midcourse velocity correction schedules optimization, discussing timing equations modifications, mission simulation and role of earth based radar
c21 A69-39646
MIDLATITUDE ATMOSPHERE
Electron cooling rates in midlatitude and auroral zone thermosphere measured by probe rockets
c13 A69-16267
Midlatitude neutral thermosphere density and temperature measurements, noting effect of atomic oxygen adsorption by instruments
c13 A69-16268
MIE SCATTERING
Mie total and differential backscattering cross sections at laser wavelengths for Junge size distribution aerosol models
c16 A69-14290
Interstellar extinction models of classical Mie particles and quantum mechanical polycyclic aromatic molecules
c30 A69-23679
Optical radar studies of lower atmosphere, giving Mie theory calculations of clear atmosphere volume backscattering cross sections for four laser wavelengths
c07 A69-27001
Particle albedos and extinction cross sections computed by Mie theory showing dependence on refractivity, considering thermal radiation from cloudy planetary atmospheres
c30 A69-38255
Mie scattering calculations on laser wavelengths and atmospheric aerosols
[NASA-TN-D-5110] c23 N69-20905
MILITARY AIRCRAFT
Spin-tunnel investigation of scale model of straight wing, twin boom counter insurgency airplane
[NASA-TM-X-1602] c02 N69-34988
MILITARY HELICOPTERS
NASA flight test of hingeless rotor compound helicopter to determine lift sharing characteristics, showing rotor lift dependence on airspeed
c02 A69-29702
MILKY WAY GALAXY
Far IR source in galactic center detected at 100 microns, noting thermal emission of interstellar dust grains as possible mechanism
c30 A69-22264
MILLIMETER WAVES
Short wave bands for earth-space communications, considering propagation anomalies compensated systems and frequency bands availability
c07 A69-13721

Background radiation intensity upper limits for mm and submillimeter wavelengths in interstellar medium, noting intense flux in far IR
c30 A69-19404
Radiometric techniques applicable to measurement of solar activity and atmospheric attenuation at millimeter wavelengths
[NASA-TR-R-306] c07 N69-22951
Cyclotron resonance oscillators as sources of millimeter waves
[NASA-TN-D-5237] c10 N69-28121

MILLING (MACHINING)
Feasibility of producing dispersion strengthened chromium by ball milling in hydrogen halides
[NASA-TN-D-4912] c17 N69-10827

MINERAL OILS
Lubrication performance and thermal shear degradation of polyphenyl ethers and refined mineral oils in high temperature vane pump loop
[NASA-TN-D-5096] c15 N69-20938

MINITRACK SYSTEM
Minitrack data reduction procedures, with IBM 360 computer program description
[NASA-TN-D-5042] c08 N69-26193

MINORITY CARRIERS
Proton irradiation effects on minority carrier lifetime in silicon and gallium arsenide semiconductor materials
[NASA-TN-D-5028] c26 N69-18897

MIRRORS
Single and double mirror systems geometrical optical image aberrations noting focal number, angle of field, secondary magnification and mutual position tolerances
c23 A69-24836
Control system for thin diffraction limited orbiting astronomical telescope mirror based on structural analysis of static deflections
c14 A69-27951
Second surface mirror used as coating for spacecraft thermal control
c33 A69-37290
Thermal control coatings, windows and mirrors for 1973 Mars Viking Lander vehicles under simulated Martian surface conditions
[AIAA PAPER 69-1023] c11 A69-40393

MISSILE CONFIGURATIONS
Wind tunnel tests to determine static aerodynamic characteristics of cruciform wing-body missiles at transonic and supersonic speeds
[NASA-TM-X-1839] c01 N69-31875

MISSION PLANNING
Iterative guidance mode /IGM/ applied to effective gravity vector prediction, acceleration measurement of noise sensistivity and energy limitations
[AIAA PAPER 67-620] c21 A69-15501
German analysis of preparatory technology of U.S. space programs, noting effects of hardware development for manned space travel on future planning
c34 A69-15576
Astrodynamical data compilation for use by system engineer for mission planning
[AIAA PAPER 69-124] c30 A69-18090
Low thrust mission simulation dependence on hardware definition, discussing power plant characteristics, jet velocity and thrustor efficiency
c30 A69-21204
Interplanetary low thrust mission analysis model, discussing major elements interactions
c30 A69-21206
SERT 2 thrustor system performance over expected mission parameters, noting operational lifetime excess over mission requirements
[AIAA PAPER 69-235] c28 A69-21255
Space exploration plans adaptation, considering spacecraft design, programs, costs and schedules flexibility
c34 A69-22863
Lunar orbital mission plans intended to optimize spacecraft procurement, flight schedules, science objectives and available funds
c30 A69-34362
General aviation missions in national transportation system /1968, 1975, 1980/, considering fuel taxes, overall system economics, ground facilities, etc
[AIAA PAPER 69-818] c34 A69-35624
Worldwide cloud cover simulation procedure providing data for computer simulation of earth oriented space missions, describing computer program using Monte Carlo mission simulation
c20 A69-38120
Direct flight and Jupiter swingby heliocentric trajectory modes of elliptic capture orbits compared for unmanned missions to outer planets
[AAS PAPER 68-105] c30 A69-39221
Space power systems analysis, using computer program to correlate systems characteristics with mission parameters for automated satellite repair vehicle and space stations
c03 A69-42240
Space program planning, noting market requirements, acceptability and future characteristics
[AAS PAPER 69-083] c34 A69-42820
Objectives, current programs, and future mission options in space sciences and applications
[NASA-SP-162] c30 N69-13844
Engineering models of Venus atmosphere for design and mission planning for spacecrafts
[NASA-SP-8011] c30 N69-20916
Lunar environment, bases, exploration, and extraterrestrial resources
[NASA-SP-177] c30 N69-22226
Parametric analysis of microwave and laser systems for communication and tracking - summary
[NASA-TR-R-309] c07 N69-23642
Interplanetary probe missions with solar electric propulsion systems
[NASA-TN-D-5293] c30 N69-29738

MITOSIS
Hyperoxia and hypoxia effects on mitotic activity in regenerating and normal rat liver exposed to environmental conditions
c04 A69-43565
Mitotic synchronization of fibroblasts with metabolic retardants by chronophotography
[NASA-TN-D-5021] c04 N69-17248
Osmotically induced coalescence of sarcoma cells through intercellular bridges in vitro
[NASA-TN-D-5022] c04 N69-17782

MIXING LENGTH FLOW THEORY
Compressible hypersonic turbulent boundary layers solution by finite difference method, relating mixing length to velocity profile shape factor
[AIAA PAPER 69-684] c12 A69-33474

MODAL RESPONSE
Dynamic instability of solid bodies, using modal vibration method to establish criteria on basis of equivalent energy conditions
c32 A69-16742
Adaptive simulation using modal clustering and method of potential functions
[NASA-CR-1179] c08 N69-10316
Frequency and critical speed analysis of rigid rotors on flexible foundations
[NASA-TN-D-4858] c32 N69-29159

MODELS
GEOS 1 tracking station positions on SAO standard earth C-5 model
[NASA-TN-D-5034] c13 N69-28019
Double-dead-time model describing chugging to liquid propellant rocket engines having multielement injectors
[NASA-TN-D-5303] c28 N69-29405
Longitudinal mass spring modeling of launch vehicles
[NASA-TN-D-5371] c32 N69-34970

MODULUS OF ELASTICITY
Static pressure-diameter measurements on small pulmonary blood vessels of frogs, analyzing capillary septal area as function of intravascular pressures noting high compliance
c04 A69-40974
Analysis of Fitzgerald apparatus for extraneous resonant modes, dynamic compliance, and mechanical impedance
[NASA-TN-D-5103] c26 N69-20798

MOLDAVITE
Moldavites and Ries crater material, studying Rb-Sr isochronal relationship
c13 A69-41341

MOLDING MATERIALS
Compression molding of molecular salt-like intermediate Pyrrone powders by two pressure

method, noting volatiles elimination
c18 A69-29415
MOLECULAR ABSORPTION
Theoretical molecular line absorption of carbon monoxide in late spectral type stellar atmospheres
[NASA-TN-D-4798] c24 N69-14448
MOLECULAR BEAMS
High and medium energy molecular beams - Conference, Cannes, July 1969
c24 A69-36171
Satellite-borne experiments of neutral molecular beam-solid surface interactions, describing Molsink chamber, densitometer, sphere and paddlewheel satellites
c24 A69-36182
Cryogenic molecular beam system with pressure attenuation
[NASA-TN-D-5308] c24 N69-31338
MOLECULAR CHAINS
Molecular orientation and mechanical isotropy in polyethylene, polypropylene, and polyethylene terephthalate films
[NASA-TN-D-5380] c18 N69-34708
MOLECULAR COLLISIONS
Frictional forces and collision frequencies for ions moving in neutral gases
c13 A69-13328
Ion-molecule collisions of Ar-Co and N-No pairs, discussing charge exchange reaction rates and spiraling nature
c24 A69-16428
Computer made movies and time history plots for ion-dipole collisions involving polar molecules /CO, HCL and acetonitrile/
c24 A69-43124
Rotational relaxation times for calculating rotational collision numbers in polar gases
[NASA-TN-D-5321] c24 N69-30073
Numerical analysis of spiraling in ion molecule collisions with polar targets using computer plotting techniques
[NASA-TN-D-5407] c24 N69-35508
Interaction energy and dipole moment in collisions of two hydrogen molecules
[NASA-TN-D-5486] c24 N69-39184
MOLECULAR ENERGY LEVELS
Doublet electronic states of benzyl radical, discussing configuration-interaction calculations and transition predictions
c24 A69-13321
Rate coefficient for primary process in removing molecular nitrogen in high vibrational levels from active nitrogen by N atoms
c24 A69-36424
MOLECULAR GASES
Rocket measurements of diurnal variations of F region concentrations and temperature of molecular N and O, showing disagreement with satellite drag data
c13 A69-40515
MOLECULAR OSCILLATIONS
Molecular vibration absorption spectra from variation of field emitted electron energy distribution due to inelastic electron-molecule interaction at metal-vacuum interface
c24 A69-26097
MOLECULAR RELAXATION
Mechanical relaxation of poly 4 methyl pentene 1 at cryogenic temperatures, discussing temperature dispersion curve and secondary absorption associated with thermal motion of side chains
c18 A69-16492
MOLECULAR ROTATION
Molecular motion in polytetrafluoroethylene crystals at cryogenic temperatures, noting crystal defect permitting angular displacements of chain segments
c24 A69-16495
Spontaneous Raman band shapes and depolarization ratios in liquid nitrogen and oxygen measured and compared to gas, discussing time dependence of rotational motion
c24 A69-17817
Diatomic molecules rotational excitation calculated from electron molecule elastic scattering parameters in fixed nuclei approximation
c24 A69-39665
Order-disorder transitions in solid hydrogen, discussing model to explain molecular rotation angular momentum operator fluctuations
c23 A69-43119
Electron beam technique of measuring molecular rotational and vibrational temperatures of nitrogen in hypersonic tunnel using air as test gas
[NASA-TN-D-4892] c33 N69-10932
Rotational relaxation times for calculating rotational collision numbers in polar gases
[NASA-TN-D-5321] c24 N69-30073
MOLECULAR SPECTRA
Electronic transition moment for C /Swan/ bands measured in shock tube in carbon dioxide and argon mixtures
c24 A69-12833
Computer program to predict spectra from electronic transitions of diatomic molecules and atoms, noting line intensity distribution by Voigt profile
c24 A69-35239
Molecular vibration spectra from field emission energy distributions
[NASA-TN-D-5423] c24 N69-36924
MOLECULAR STRUCTURE
Europium complexes high resolution emission spectra in relation to molecular configuration
c06 A69-10893
Mechanical anisotropy of polyethylene terephthalate and relation to molecular structure and cold drawing
c18 A69-16489
Rotational spectrum of ethylene episulfoxide to determine molecular structure, particularly orientation of C sub 2 S ring
c06 A69-20535
Constitutive equation variation effect on near wall flow pattern of dilute polymer solutions
c12 A69-33257
MOLECULAR WEIGHT
Structure and mean molecular weight measurement of unknown atmosphere assessed from high altitude tests in earth atmosphere
[AIAA PAPER 68-1054] c30 A69-13699
Ultrahigh molecular weight polyethylene terephthalate synthesis from commercial solid state materials, noting effects of several parameters
c24 A69-16496
Fluidic oscillator use as molecular weight sensor for gas mixtures
[NASA-TM-X-1698] c03 N69-13246
MOLTEN SALT ELECTROLYTES
Electrochemical behavior of the aluminum electrode in molten salt electrolytes
[NASA-TN-D-5503] c06 N69-40240
MOLYBDENUM
Neutron interaction behavior of beryllium oxide and molybdenum reflectors for nuclear reactors
[NASA-TM-X-1822] c22 N69-29593
Production of glass coatings for molybdenum ion thruster accelerator grids
[NASA-TN-D-5320] c15 N69-30062
Molybdenum and tungsten solubility in liquid potassium
[NASA-TN-D-5504] c17 N69-40053
MOLYBDENUM ALLOYS
Oxidation behavior of coated molybdenum and niobium alloys in high temperature supersonic air streams
[NASA-TN-D-4877] c17 N69-10764
Ductilizing of Group 6A elements by rhenium and other solutes
[NASA-TN-D-4955] c17 N69-14403
Mechanical properties of alloys molybdenum hafnium carbon compounds
[NASA-TN-D-5025] c17 N69-19200
Stress rupture and tensile properties of refractory metal wires at 2000 and 2200 deg F
[NASA-TN-D-5139] c32 N69-22823
Dynamic strain aging during creep and tensile tests of molybdenum-titanium-carbon alloys
[NASA-TN-D-5169] c17 N69-22993
Dynamic strain aging in carbide strengthened molybdenum alloys
[NASA-TN-D-5355] c17 N69-31883

Creep rate equations for refractory metal alloys of tantalum molybdenum, and columbium
[NASA-TN-D-5424] c17 N69-36653
MOLYBDENUM COMPOUNDS
Impregnation of polytetrafluoroethylene with hexaflourides of rhenium, molybdenum, and tungsten
[NASA-TN-D-4886] c06 N69-10126
Thermal stability and friction of disulfides, diselenides, and ditellurides of molybdenum and tungsten in ultrahigh vacuum
[NASA-TN-D-5141] c15 N69-22992
MOLYBDENUM DISULFIDES
Physical sputtering deposition of molybdenum disulfide films as solid lubricant on rotating and sliding components, discussing lubrication properties in vacuum
[ASLE PAPER 68-LC-15] c15 A69-19308
Friction and contact resistance during sliding in vacuum of low resistivity metals lubricated with sputtered molybdenum disulfide
[NASA-TN-D-5349] c15 N69-31884
MOMENTS OF INERTIA
FORTRAN program for computing principal mass moments of inertia of spacecraft treated as composite bodies
[NASA-TM-X-1754] c23 N69-20870
MOMENTUM
Accelerated boundary layers classified in terms of integral balance of pressure, inertia, wall friction forces and entrainment momenta
[AIAA PAPER 69-666] c12 A69-33462
Momentum diffusion between two supersonic airstreams passing through oblique shock waves
[NASA-TN-D-4974] c12 N69-15631
Momentum integral method treating magnetohydrodynamic and simple hydrodynamic entrance flows
[NASA-TN-D-5215] c25 N69-24920
MOMENTUM TRANSFER
Interphase momentum transfer during propagation of infinitesimal pressure pulse through bubbly flow two phase mixture
c33 A69-43511
Impulsive fluid motion on flat plates pulsed with uniform heat flux
[NASA-TN-D-5249] c33 N69-26236
Electron-cesium atom collision probability for momentum transfer
[NASA-TM-X-1897] c24 N69-38773
Momentum transfer from impact into thin aluminum meteor bumper targets
[NASA-TN-D-5492] c32 N69-38809
MONATOMIC GASES
Radiation attenuation cross sections of monatomic and diatomic xenon gas from UV absorption measurements near resonance line
c24 A69-12551
Ionizing shock front structure in monatomic gas, considering atom-atom and electron-atom collisional ionization rates
c12 A69-13138
MONKEYS
Biological effects on rhesus monkeys of high energy protons compared to effects of cobalt 60 gamma radiation
c04 A69-13498
Light effects on circadian rhythms in monkeys, describing changes in deep body temperature and locomotor activity phase relationships
c04 A69-31336
Circadian rhythm phase relationships between photoperiodism and heart rate, locomotor activity and deep body temperature /DBT/ in unrestrained monkeys
c04 A69-42706
MONOCHROMATIC RADIATION
Dual beam white or nearly monochromatic light source providing programmed repetitive sample illumination with variable intensity, pulse duration and sequence for photosynthesis research
c14 A69-36378
MONOCHROMATORS
Solar spectral irradiance measured by airborne instruments, discussing construction, calibration, etc, of photoelectric filter radiometer and Leiss monochromator
c30 A69-32261
Minimization of optical resonance scattering by adjustment of monochromator slit geometry
[NASA-TM-X-1702] c24 N69-13210
MONOCULAR VISION
Landing performance in T-33A aircraft with loss of binocular vision compared to performance with both eyes
c05 A69-41675
MONOMERS
Luminescence spectra of aromatic polymers, monomers and dimers under high energy electron excitation using molecular resonance model
c26 A69-32792
MONOMOLECULAR FILMS
Uranyl ions interaction with phospholipid and cholesterol monolayers, using surface pressure and potential measurements
c06 A69-25641
MONOPOLE ANTENNAS
Apollo astronaut, backpack monopole antenna and its radiation patterns
[NASA-TN-D-5081] c07 N69-23882
MONOPULSE ANTENNAS
Multiplicative feed system for monopulse angle tracking antennas, discussing influence of sidelobe and backlobe responses on control function slope determining antenna bearing angle
c11 A69-37704
Parabolic antenna properties generated by dual band circularly polarized focused two channel monopulse feed system, discussing tracking data from helicopter, Apollo 8 and Cassiopeia A
c07 A69-41752
MONSOONS
Steady state solution of quasi-geostrophic perturbation equations for atmospheric forced response to parametized heating as global monsoon theory
c20 A69-36405
MONTE CARLO METHOD
Monte Carlo method application to heat transfer analysis including radiation, rarefied gas energy transfer and conduction
c33 A69-24457
COHORT-2 Monte Carlo computer program written in FORTRAN 4 to model radiation shielding problems
c08 A69-29004
Monte Carlo method application to neutron streaming in hemispherical air-filled ducts in water tank to determine leakage through nuclear reactor shields
c22 A69-35178
Monte Carlo relaxation method for physically self consistent model stellar atmospheres, discussing stability, accuracy and convergence of solution
c30 A69-36337
Comparison of ray trace methods for estimating sound intensity variations due to atmospheric variability as determined by Monte Carlo methods
[NASA-CR-1337] c23 N69-23199
Monte Carlo analysis of gold sphere transmission experiments at 24 keV neutron energy using S wave spin state data
[NASA-TN-D-5211] c24 N69-24826
Monte Carlo method for estimating costs and optimal testing of Explorer size spacecraft
[NASA-TN-D-5283] c34 N69-31333
Gamma ray transport portion of COHORT 2 Monte Carlo shielding code
[NASA-TM-X-1877] c22 N69-35848
MOON
Geomagnetic tail topology, reconnection and interaction with moon from Explorer 33 satellite data
c13 A69-19365
Lunar dynamic response to discontinuities in interplanetary magnetic field to determine electrical conductivity and internal temperature
c30 A69-31442
Computer program for computation of thermal radiation heat loads and temperatures of spacecraft orbiting planets or moon
[NASA-TR-R-278] c30 N69-14428
Space communications system for earth moon radio link
[NASA-TT-F-527] c07 N69-14973
Telemetry data from image-motion compensation sensor on Lunar Orbiter 1 spacecraft for determining radius of moon

[NASA-TN-D-5231] c30 N69-29115
MORPHOLOGY
Determination of micromorphic material constants from elastic properties of constituents
[NASA-CR-1320] c32 N69-21569
MOSSBAUER EFFECT
Temperature dependent isomer shift and anharmonic binding of Sn 119 in niobium stannide, measuring Mossbauer recoil free fraction
c26 A69-10009
MOTION
Differential thresholds for rotary and linear motion in the periphery
[NASA-CR-1439] c05 N69-36925
MOTION STABILITY
Boussinesq approximation for compressible fluids, discussing perturbation pressure and velocities and vertical scale motions
c12 A69-26013
Numerical solution of coupled, nonlinear, equation of motion for rigid blade to simulate response sensitivity and blade-motion stability of fully articulated rotor
[NASA-TN-D-5032] c01 N69-17289
Motion stabilization criteria for aircraft during spatial maneuvers
[NASA-TT-F-555] c02 N69-24761
MOTIVATION
Science education and training, discussing student motivation
[UN PAPER 68-95809] c34 A69-10515
MOTORS
Dynamic analysis and maximum stepping rate prediction for permanent magnet motor
[NASA-TN-D-5094] c03 N69-20780
Fluidic integrated circuits for control of pneumatic stepping-motor actuator system
[NASA-TN-D-5155] c03 N69-22896
MULTIPHASE FLOW
Wind tunnel tests of distortion dynamics in Mach three mixed compression inlet
[NASA-TM-X-1706] c01 N69-13154
Dynamic response of supersonic mixed compression inlet coupled to cold pipe or turbojet engine
[NASA-TN-D-5338] c28 N69-31336
MULTIPLIERS
Stability of time varying systems by construction of multipliers with prescribed phase characteristics
c10 A69-16598
Vector integral extension to optimal trajectory coordinate multiplier systems with constant of motion demonstrated for coast-arc problem
[AIAA PAPER 69-907] c30 A69-39339
MULTIPOLAR FIELDS
Coulomb approximation for dipole and quadrupole transitions, calculating tables for radial matrix elements
c24 A69-10901
MULTISTAGE ROCKET VEHICLES
Multistage rocket trajectories optimized by second order numerical technique and digital computer program, considering coasting, vacuum flight and transition times
c30 A69-32154
MUSCULAR FUNCTION
Exercise prescription for hypokinetic airline pilots to prevent physiological deterioration and maintain performance, discussing predictive tests, tolerance evaluation, training regimens, etc
c05 A69-41800
Small perturbation dynamics of neuromuscular system in tracking tasks
[NASA-CR-1212] c05 N69-14212
Coordination of voluntary movements of man in zero gravitational fields
[NASA-TT-F-578] c04 N69-31356
MUSCULAR STRENGTH
Hypohydration effects on isometric muscular strength, noting decreasing trends in maximal strength
c04 A69-15983
MYLAR (TRADEMARK)
Proton induced voltage breakdowns in polymeric materials
[NASA-TM-X-1688] c18 N69-10066

N

N-TYPE SEMICONDUCTORS
Negative differential resistance effect producing relaxation type oscillations in n-type gallium arsenide
c26 A69-10557
NACELLES
Conference on NASA research in noise reduction of subsonic jet aircraft - nacelle acoustic linings, sound generation in jet engines, and operational noise effects on humans
[NASA-SP-189] c02 N69-11542
Numerical method for evaluation and utilization of supersonic nacelle-wing interference
[NASA-TN-D-5057] c01 N69-19641
NASA PROGRAMS
Scientific advances from space research in communications astronomy, electronics, transportation, etc
c30 A69-10498
NASA university program, discussing participation in space and aeronautics developed based on project oriented research grants and sustaining university grants
[UN PAPER 68-95413] c34 A69-10506
NASA Technology Utilization Program, discussing information dissemination
[UN PAPER 68-95313] c34 A69-10512
NASA programs and opportunities for international cooperation in space
[UN PAPER 68-95367] c34 A69-10516
NASA programs impact on U.S. education
[UN PAPER 68-95291] c34 A69-10519
NASA Planetary Exploration Program to gather data on origin of solar system and life, discussing planetary evolution and extraterrestrial life
c04 A69-12804
NASA Plum Brook Reactor Facility /PBRF/ for determining radiation tolerance to support nuclear power application in space for propulsion and power
c22 A69-13128
NASA Space Application Program strategy, discussing research and development trend toward complexity, versatility and multidisciplinary use of larger spacecraft
c30 A69-13427
NASA research on flexible and stiffened flexible wings, discussing range of applicability, aerodynamic characteristics and wind tunnel results
c02 A69-15568
Federal government contracting, discussing legality of NASA service contracts
c34 A69-15987
Proton beams uniformity available at NASA synchrocyclotron designed for radiation biology research by simulating space radiation environment
c11 A69-15992
NASA civil aviation electronics research program, discussing feasibility of V/STOL aircraft all-weather operations
c34 A69-16718
NASA scientific and technical information program for building technical data and literature repository for scientists, engineers and technical managers, describing IAA and STAR
[UN PAPER 68-95317] c34 A69-17068
Manned space flight programs, discussing U.S. technological, scientific and practical contributions
c30 A69-17074
Multifunction Receiver System rationale, concepts, background requirements and technical justifications for tracking, telemetry and ranging data acquisition by Goddard Center
c07 A69-19101
Small Scientific Satellite program, discussing payload for investigating magnetosphere and near interplanetary space
[IEEE PAPER 3C-1] c31 A69-19195
NASA flight safety research, discussing size effects on aircraft handling and built-in response to failure modes
c02 A69-19764

NASA program in electric propulsion, noting applications for spacecraft position control and for small automated interplanetary spacecraft
[AIAA PAPER 69-248] c28 A69-21216
NASA long range planning of primary electric propulsion for automated space program
[AIAA PAPER 69-247] c28 A69-21251
Ablation characteristics of heat shield materials measured in arc heated wind tunnels, considering influence of model scale, heating rate and pressure level
c18 A69-26813
NASA manned aerospace simulation techniques and equipment as used at Ames Research Center, noting applications to various types of manned vehicles
[ASME PAPER 69-DE-56] c11 A69-28844
NASA flight test of hingeless rotor compound helicopter to determine lift sharing characteristics, showing rotor lift dependence on airspeed
c02 A69-29702
Aeromedical developments by NASA biomedical applications program applied to general medical equipment including cardiac sensors, surgical sterilization, ballistocardiograph, etc
c34 A69-32430
Commercial utilization of space technology, discussing cost reduction and role of NASA Apollo Program
c30 A69-34044
NASA photogrammetric lunar activities, discussing imagery and control data by Lunar Orbiter and photogrammetric data reduction for preparing manned lunar landing
c14 A69-34336
Professional programs for aeronautics, rocketry and astronautics development
c34 A69-34552
Space exploration influence on science education, showing NASA instructional materials for teachers in biology, chemistry, physics, mathematics, industrial arts, etc
c34 A69-35077
NASA technology utilization program for civilian economy benefit, discussing scientific and technical documentation and transfer across industrial, disciplinary and regional boundaries
c34 A69-35105
NASA planetary entry parachute program for rocket launched and balloon deployment tests
[AIAA PAPER 68-934] c02 A69-35952
NASA Earth Resources Survey Aircraft Program, describing aircraft and remote sensors characteristics
c14 A69-36259
NASA Lunar Orbiter Program of lunar photography from orbiting spacecraft
c30 A69-38377
NASA current awareness service SCAN /selected current aerospace notices/, promoting selectivity in information transfer to abstract journals, accession lists and bibliographies
c34 A69-39581
Telemetry data processing, describing designation, tasks and possibilities of data reduction laboratory attached to NASA Goddard Space Flight Center
c11 A69-40352
NASA program for radio spectrum utilization in aerospace communication systems
c07 A69-42502
Planetary exploration and NASA program objectives
[AAS PAPER 69-286] c30 A69-42810
Logistics management developed for Apollo Applications Program of NASA Manned Spacecraft Center
[AAS PAPER 69-204] c34 A69-42812
Launch vehicle upper stage requirements in space missions, discussing space engine for lunar, planetary and interplanetary exploration
[AAS PAPER 69-359] c34 A69-42828
Management system for safety in NASA Manned Space Flight Program, discussing hazard analyses and reduction precedence sequence
[AAS PAPER 69-522] c34 A69-42851
Pioneer F/G mission to Jupiter by NASA for exploring interplanetary medium, asteroid belt, planet and environment
[AAS PAPER 69-290] c30 A69-42863
NASA programs for development of high temperature alloys for advanced air breathing engines emphasizing cast Ni-base alloy
[ICAS PAPER 68-26] c17 A69-43718
Application of NASA mathematical management models and systems analyses in private industry and economy
[NASA-SP-5048] c34 N69-10662
Selected conference papers on NASA technology utilization for electric power industry
[NASA-SP-5057] c03 N69-12575
Objectives, current programs, and future mission options in space sciences and applications
[NASA-SP-162] c30 N69-13844
NASA contributions to bioinstrumentation system - survey
[NASA-SP-5054] c04 N69-14860
NASA Small Astronomy Satellite /SAS/ program for radiation source detection
[NASA-TN-D-5099] c31 N69-21017
Combined selective listing of NASA scientific and technical reports announced during 1968
[NASA-SP-7033] c34 N69-29492
Potential for advancement of astronomy by space programs
[NASA-SP-213] c30 N69-41150

NATURAL SATELLITES
Hansen method applied to Jupiter tenth satellite orbit correction and perturbations, describing computer program and formulas used
c30 A69-37529
Perturbative effects of Jupiter moons on spacecraft flyby and postencounter heliocentric trajectories, noting precision targeting
[AIAA PAPER 69-932] c30 A69-39361
Application of Hansen lunar theory to 10th satellite of Jupiter
[NASA-TN-D-4979] c30 N69-14479
Direct and indirect planetary perturbation effects on motion of natural satellites
[NASA-TN-D-5284] c30 N69-37893

NAVIER-STOKES EQUATION
Algorithm for Navier-Stokes and continuity equations used to derive curvilinear coordinate system
c08 A69-14858
Numerical method for time dependent compressible Navier-Stokes equations applied to axisymmetric flow field produced by hypervelocity impact, examining viscous effects
[AIAA PAPER 69-354] c32 A69-28288
Nonlinear disturbance decay in unbounded viscous fluid
[NASA-TN-D-4947] c12 N69-14483

NAVIGATION
Minimal angle of resolution /MAR/ between point and extended circular source and between point source and simulated horizon, studying irradiation effects on manual navigation
c21 A69-19208
Theory and practice of aircraft navigation - textbook
[NASA-TT-F-524] c21 N69-17788
Prediction methods for angular line-of-sight deviations induced by spacecraft window
[NASA-TN-D-5238] c21 N69-31227

NAVIGATION AIDS
Artificial satellites as navigation aids, describing angle, range and range-angle systems, discussing orbital mechanics and communications difficulties
c21 A69-34855
Guidance and navigation flight tests, demonstrating system performance improvements by onboard inertial system communicating with external navigation aid
[AIAA PAPER 69-842] c21 A69-39429
Advanced electronic applications to navigation, data transmission, and airborne collision avoidance in general aviation aircraft and to simulated displays for low visibility landing
[NASA-CR-1240] c02 N69-14729
Design and development of boresighted star tracker
[NASA-CR-976] c21 N69-21502

NAVIGATION INSTRUMENTS
Navigation-aids identification decoder and display device for general aviation aircraft
[NASA-TN-D-5445] c09 N69-38852

NAVIGATION SATELLITES
Space applications program including communications and navigation meteorology, earth resources survey and geodesy
[UN PAPER 68-95437] c34 A69-10472
Navigation services satellite systems including position determination, communication and telemetry for ships and aircraft
[UN PAPER 68-95363] c21 A69-10479
Navigation satellites system designed for ATC without requirement for onboard transmitter, discussing spectrum occupancy, satellite power, lane ambiguities and computational procedures
c21 A69-19212
Artificial satellites as navigation aids, describing angle, range and range-angle systems, discussing orbital mechanics and communications difficulties
c21 A69-34855
Optical measurements on secondary satellite for determining perturbation parameters of orbiting spacecraft
[NASA-CR-1412] c30 N69-35513

NEAR INFRARED RADIATION
Ice clouds near IR spectral reflectivity dependence on particle size, noting application to planetary atmospheres
c13 A69-34283
Two-micron sky survey catalog of celestial objects
[NASA-SP-3047-REV] c30 N69-37993

NEGATIVE CONDUCTANCE
Negative differential resistance effect producing relaxation type oscillations in n-type gallium arsenide
c26 A69-10557

NEON ISOTOPES
Upper bounds for electromagnetic transition rates for Ne 20 determined using Hartree-Fock wave functions
c24 A69-35166

NEPTUNE (PLANET)
Planetary flight handbook - direct trajectories to Jupiter, Saturn, Uranus, and Neptune
[NASA-SP-35-VOL-3-PT-7] c30 N69-33490

NERNST-ETTINGSHAUSEN EFFECT
Fermi surface topology effects on Nernst-Ettingshausen coefficient from measurements in magnetic fields to 3.3 tesla and 1.2-4.2 K temperatures in metallic tin
c26 A69-16357
Nernst-Ettingshausen, thermoelectric power, thermal transverse-even, magnetoresistance, and Hall coefficients in white tin in 3.3 tesla field and cryogenic temperatures
[NASA-TN-D-5227] c26 N69-25412

NERVES
Neutral buoyancy microelectrode for prolonged recording from single nerve units
c05 A69-11865

NETWORK ANALYSIS
Passive circuit to transform voltage of indefinitely repeated positive or negative pulses using transistors, diodes and magnetic cores
c09 A69-10564
Voltage divider network board composed of composite carbon resistors for measurement of terminal voltage of 3 MeV Dynamitron electron accelerator recalibration
c11 A69-17705
Feedback systems analysis, considering single phase and polyphase coupled and uncoupled commutation networks in forward loop and linear transfer function feedback loop
c10 A69-19853
Delta functions spectrum in reciprocal time domain for LC and RC structures due to impulse response in distributed parameters
c10 A69-21327
Scanning electron mirror microscope advantages over electron mirror and scanning electron microscopes for examining integrated circuits
c14 A69-32891
Circuits and systems - Conference, Pacific Grove, California, October-November 1968
c10 A69-34671
Multiloop feedback in active distributed RC networks for low parameter sensitivity with low amplifier gain compared to single loop circuits
c10 A69-34679
N-terminal parent networks with symmetry constraints derived for nonredundant one port configurations through combinatorial functions test patterns, using computer algorithm
c08 A69-42524

NETWORK SYNTHESIS
Circuits and systems - Conference, Pacific Grove, California, October-November 1968
c10 A69-34671
Multiplexer network synthesis based on arbitrary divisibility of frequency range and obtainability of input impedance at all frequencies
c09 A69-38530
Computer program for generation of test patterns for multiterminal devices and networks
c08 A69-39604
Time varying resistance wire to arrest oscillations in pulsed capacitor discharge circuit, deriving over, under and critical damping conditions
c09 A69-41228

NEUROMUSCULAR TRANSMISSION
Small perturbation dynamics of neuromuscular system in tracking tasks
[NASA-CR-1212] c05 N69-14212

NEURONS
Neutral buoyancy microelectrode for prolonged recording from single nerve units
c05 A69-11865

NEUTRAL PARTICLES
Radioactive decay of neutral pions generated in metagalactic cosmic ray interactions as source of high energy isotropic gamma rays observed by OSO-3
c29 A69-12092
Electron, ion and neutral particle temperatures of upper atmosphere
c13 A69-14975

NEUTRINOS
Red supergiants as old derivatives of main sequence O and B stars, discussing neutrino emissions and carbon core contraction
c30 A69-24125

NEUTRON ABSORBERS
Neutron interaction behavior of beryllium oxide and molybdenum reflectors for nuclear reactors
[NASA-TM-X-1822] c22 N69-29593
Multigroup calculations of resonance neutron capture in thick slab of depleted U-238
[NASA-TM-X-1878] c24 N69-36901

NEUTRON COUNTERS
Improved delayed neutron fission product monitor for operation in reactor coolant system
[NASA-TM-X-1886] c14 N69-38766

NEUTRON CROSS SECTIONS
Group cross section generating techniques to calculate neutron capture rates and spatial capture distribution in depleted thick U slab, using GARCL program
c24 A69-35179
Thermal neutron capture cross section at high temperature irradiations determined for W 184, describing radiochemical separation and flux counting techniques
c14 A69-43192

NEUTRON DISTRIBUTION
Group cross section generating techniques to calculate neutron capture rates and spatial capture distribution in depleted thick U slab, using GARCL program
c24 A69-35179

NEUTRON EMISSION
Monte Carlo method application to neutron streaming in hemispherical air-filled ducts in water tank to determine leakage through nuclear reactor shields
c22 A69-35178
Heat transfer and neutronic calculations after fuel emitter separation in uranium oxide fueled thermionic diodes
[NASA-TM-X-1812] c22 N69-28212

NEUTRON FLUX DENSITY
Boron 10 absorption cross sections from counting ratios measurements of boron trifluoride proportional counter used to monitor neutron fluxes
c24 A69-33753

Thermal neutron flux perturbations in cylinders in test reactors, using regression analysis to obtain polynomials for flux perturbation, depression, self shielding factors, etc
c22 A69-38274
Thermal neutron capture cross section at high temperature irradiations determined for W 184, describing radiochemical separation and flux counting techniques
c14 A69-43192

NEUTRON IRRADIATION
Effects of neutron irradiation on silicon voltage regulator Zener diodes
[NASA-TN-D-4923] c09 N69-10250

NEUTRON SOURCES
Pulsed neutron source studies to determine shutdown reactivities of unreflected solution reactor
[NASA-TN-D-5487] c22 N69-39186

NEUTRON SPECTRA
FASTER code for significantly reducing ducted reactor shield computation time for neutron number spectrum
[NASA-TM-X-1828] c22 N69-29671
FASTER computer program modified for tracking neutrons through reactor slabs penetrated by helical voided ducts
[NASA-TM-X-1838] c22 N69-31986

NEUTRON STARS
Rotating and oscillating magnetic neutron stars causing pulsars radio and optical signals, stressing UV line emissions theory
c30 A69-20624
Radio emission from magnetic neutron stars as possible model for pulsars, noting optical and IR emission bands
c30 A69-20729
Instability of stellar structures intermediate between white dwarfs and neutron stars shown by stellar models, discussing pulsar signals periodicities
c30 A69-20770
Rotational energy conversion of neutron star into relativistic electrons energy suggested by increasing period of pulsating radio source in Crab Nebula
c30 A69-21454
Spin down effects on neutron stars, discussing decrease of period of PSR 0833-45 as result of differential rotation instability
c30 A69-32803
Radial pulsations of neutron star losing mass, interpreting Crab Nebula pulsar observed period and secular increase of period
c30 A69-37573
Crab Nebula pulsars radio properties, possible neutron star origin, interstellar gas and magnetic fields, etc
c30 A69-42556

NEUTRONS
Tritium contamination reduction in small ion accelerators for neutron production, discussing pumping problems and vacuum systems
c11 A69-26499
Transport study of neutron and photon attenuation through lithium hydride and tungsten spheres
[NASA-TN-D-4989] c24 N69-15375
One megawatt reactor design for Brayton cycle space power application - neutronics design
[NASA-TN-D-5014] c22 N69-17314

NEWTON THEORY
Newtonian aerodynamics for circular cones modified to produce lift at zero angle of attack
[NASA-TN-D-5193] c01 N69-23926

NEWTON-RAPHSON METHOD
Newton-Raphson technique development for determining stability derivatives from flight data, noting use of a priori wind tunnel information
[AIAA PAPER 69-315] c02 A69-22379

NICKEL
Angular correlation between inelastically scattered 42 MeV alpha particles and emitted gammas from 2-plus Ni 58
c24 A69-13100
Size effect on tensile strength of polycrystalline nickel wires
[NASA-TN-D-4884] c17 N69-10226
Radiation induced reduction of ammoniacal nickel /2/ sulfate to metallic nickel
[NASA-TN-D-5213] c06 N69-24940
Low energy electron diffraction study of adhesion of various materials to nickel surface
[NASA-TN-D-5247] c17 N69-26258
Dynamic creep model to determine oxidation effects on high temperature deformation of nickel
[NASA-TN-D-5266] c17 N69-27061
Effects of nickel on performance of n on p silicon solar cells
[NASA-TN-D-5366] c03 N69-31844
Internal stress and deposit hardness of nickel electrodeposited containing controlled quantities of meta-benzenedisulfonic acid
[NASA-TN-D-5188] c17 N69-36697

NICKEL ALLOYS
Tungsten alloy fiber reinforced nickel base alloy composites stress-rupture strength, oxidation and impact resistance for high temperature turbojet engine buckets
c17 A69-29010
Mechanical properties associated with 55-Nitinol memory effect, presenting stress-strain and electrical resistivity as function of temperature
c17 A69-35523
NASA programs for development of high temperature alloys for advanced air breathing engines emphasizing cast Ni-base alloy
[ICAS PAPER 68-26] c17 A69-43718
Physical properties of near stoichiometric nickel-titanium alloy Nitinol and some structural-mechanical applications employing these properties
[NASA-CR-1232] c17 N69-11420
Edge notch sensitivity in thin sheet nickel alloys under stress at high temperatures
[NASA-CR-1263] c32 N69-16156
Sigma phase formation and its effect on stress rupture properties of nickel base alloy IN-100
[NASA-TN-D-5185] c17 N69-23465
Extruded prealloyed powder evaluation for two nickel-base alloys
[NASA-TN-D-5248] c17 N69-26192
Development and high temperature tests of high strength nickel alloy for stator vanes of gas turbine engines
[NASA-TN-D-5352] c17 N69-31873
Oxidation resistance and thermal fatigue cracking of nickel and cobalt base alloys in transonic gas streams
[NASA-TN-D-5376] c17 N69-33307
Physical, mechanical, and electrical properties of 55-Nitinol - nickel-titanium alloy
[NASA-CR-1433] c17 N69-36367
Dispersion strengthened nickel produced from ultrafine comminuted powders
[NASA-TN-D-5421] c17 N69-38074

NICKEL CADMIUM BATTERIES
Signal electrode charge control of sealed Ni-Cd batteries, discussing signal voltage for overcharge control
c03 A69-23993

NICKEL COMPOUNDS
Three oxidation-resistant alloy foil claddings for protecting typical gas turbine engine alloys of nickel and cobalt
[NASA-TN-D-5483] c17 N69-38794

NICKEL STEELS
Metallurgy, behavior, and application of 18 percent nickel maraging steels
[NASA-SP-5051] c17 N69-14193

NIGHT SKY
Day sky brightness at altitude above 100 km obtained during rocket flight compared to night sky viewed from ground
c30 A69-33664
Spectral and electrophotometric studies of upper atmosphere - airglows, atomic oxygen, hydroxyl emission, helium line spectra, auroras, and solar cycle effects on magnetosphere
[NASA-TT-F-530] c13 N69-16539
Computer program for launch window determination from star illumination of night sky background
[NASA-TM-X-1772] c21 N69-22969

NIMBUS PROJECT
NIMBUS program individual missions characteristics emphasizing NIMBUS 3 results and weather

forecasting improvements
[AAS PAPER 69-421] c31 A69-42835
NIMBUS SATELLITES
Regression generated radiometric and contour height fields of North American Continent using Nimbus 2 IR equivalent black body temperature and geopotential data
c20 A69-42896
Procurement and construction of automatic picture transmission ground station equipment for ESSA and Nimbus transmission
[NASA-SP-5080] c07 N69-31985
NIMBUS 2 SATELLITE
Detecting geomorphological features over northeast Africa by Nimbus 2 visible and infrared radiation measurements
[NASA-TN-D-4648] c13 N69-14290
Nimbus 2 high resolution infrared radiometer data on earth resources of arid and subarid lands
[NASA-TN-D-4647] c13 N69-14450
Nimbus 2 flight evaluation and engineering report covering launch through orbit 5275
[NASA-TN-D-4881] c31 N69-17851
NIMBUS 3 SATELLITE
NIMBUS program individual missions characteristics emphasizing NIMBUS 3 results and weather forecasting improvements
[AAS PAPER 69-421] c31 A69-42835
NIOBIUM
Rhenium-niobium cylindrical thermionic converters with mechanically polished or electroetched emitters, comparing performance
c03 A69-13126
Nonlinear flux flow in single crystal niobium
[NASA-TN-D-5198] c26 N69-24916
NIOBIUM ALLOYS
Columbium alloys properties, discussing creep strength, oxidation resistance, costs, production, etc
c17 A69-18791
Oxidation behavior of coated molybdenum and niobium alloys in high temperature supersonic air streams
[NASA-TN-D-4877] c17 N69-10764
Absorption rate sticking probabilities for oxygen on niobium and dilute niobium-zirconium alloys
[NASA-TN-D-4885] c17 N69-10931
Stress rupture and tensile properties of refractory metal wires at 2000 and 2200 deg F
[NASA-TN-D-5139] c32 N69-22823
Creep rate equations for refractory metal alloys of tantalum molybdenum, and columbium
[NASA-TN-D-5424] c17 N69-36653
NIOBIUM COMPOUNDS
Nuclear magnetic resonance of epsilon and delta phases in NbN system with nitrogen mole fractions
c26 A69-36445
Cb-1Zr pumped sodium loop tests to evaluate loop components, EM pump, pressure transducers, and instrumentation techniques
[NASA-CR-1135] c03 N69-11373
High emittance coating materials for beryllium, niobium-zirconium compounds, and stainless steel used in spacecraft radiators
[NASA-CR-1278] c17 N69-18952
NIOBIUM STANNIDES
Temperature dependent isomer shift and anharmonic binding of Sn 119 in niobium stannide, measuring Mossbauer recoil free fraction
c26 A69-10009
Superconductive 14-tesla magnet system with 15-cm bore and niobium stanide ribbon
[NASA-CR-1260] c03 N69-15382
Pumped helium tests of 51 centimeter bore niobium tin magnetic coils
[NASA-TN-D-5158] c26 N69-22965
NITRATION
Protective coatings for chromium alloys for use in advanced air breathing applications
[NASA-TN-D-5157] c17 N69-23084
NITRIC OXIDE
Distributions, seasonal variations and ionospheric implications of mesospheric nitric oxide concentration
c13 A69-38364
NITRIDES
Nuclear magnetic resonance of epsilon and delta phases in NbN system with nitrogen mole fractions
c26 A69-36445
NITROGEN
Leak rate measurement accuracy of rate-of-rise technique for nitrogen, methane and He between millionth and thousandth torr
c14 A69-32326
Rocket measurements of diurnal variations of F region concentrations and temperature of molecular N and O, showing disagreement with satellite drag data
c13 A69-40515
Ionization rate limiting processes behind strong shock waves in pure N, plotting electron density profile diagrams
c12 A69-43367
Performance and analysis of seals for nitrogen inerted lubrication systems of turbine engines
[NASA-TN-D-4761] c15 N69-10055
FORTRAN 4 subroutines for calculating critical flow factor to determine mass flow rate of gaseous helium and nitrogen through critical flow nozzles
[NASA-SP-3046] c12 N69-16098
NITROGEN ATOMS
Rate coefficient for primary process in removing molecular nitrogen in high vibrational levels from active nitrogen by N atoms
c24 A69-36424
Atomic nitrogen collisional ionization and recombination rates under assumed quasi-steady nonequilibrium distribution of electron state populations
c24 A69-43700
NITROGEN IONS
Energy spectrum of secondary electrons and fluorescent efficiency in 3914 A band, obtaining ionization cross section
c29 A69-32315
NITROGEN PLASMA
Nonequilibrium nitrogen plasma spectral line intensities calculated assuming optically thin plasma
c24 A69-10960
NITROGEN TETROXIDE
Liquid rocket acoustic instability for hydrogen-oxygen and earth storable propellant combinations
[NASA-TN-D-4968] c28 N69-14384
NOBLE METALS
Less common refractory metals /rhenium, technetium, hafnium, noble metals/ properties, phase equilibria, etc
c17 A69-18793
NOCTILUCENT CLOUDS
Mesopause wind measurements at high latitude locations by sounding rockets noting relation to noctilucent clouds
c20 A69-28466
Noctilucent clouds with wave movement, chemical composition, and water vapor
[NASA-TT-F-546] c13 N69-25013
NOISE (SOUND)
Auditory temporal masking of tonal signal by narrow band noise and perception of temporal order noting effects of intensity, frequency and time
c05 A69-24795
Systems developed for reducing pilot workload and tracking accuracy improvements during noise abatement landing approaches
[NASA-CR-1427] c02 N69-38657
NOISE INTENSITY
Cosmic radio noise intensity measurements by ATS 2 satellite-borne radiometer
c30 A69-19715
Conference on NASA research in noise reduction of subsonic jet aircraft - nacelle acoustic linings, sound generation in jet engines, and operational noise effects on humans
[NASA-SP-189] c02 N69-11542
Estimating sound intensity from stationary and moving sources using mathematical models
[NASA-CR-1338] c23 N69-22545
Temperature effects on turbofan and turbojet noise radiation
[NASA-CR-1472] c02 N69-40439
NOISE PROPAGATION
Estimating sound intensity from stationary and

moving sources using mathematical models
[NASA-CR-1338] c23 N69-22545
Noise in axisymmetric convergent electron beams
[NASA-TN-D-5212] c10 N69-24918
NOISE REDUCTION
Telemetry technique utilizing thermocouple sensors for base heating determinations on free flight blunt cone in shock tunnels, noting electrical noise reduction
[AIAA PAPER 68-407] c14 A69-15514
Jet engine inlet noise control by modification of inlet guide vanes
c28 A69-15622
Reduction of noise from underexpanded axisymmetric jet flows using radial jet flow impingement
[AIAA PAPER 68-81] c12 A69-28212
Technology trends in airbreathing propulsion, discussing noise control for subsonic jet transports, turbine blade cooling, etc
[AIAA PAPER 69-774] c02 A69-35648
Conference on NASA research in noise reduction of subsonic jet aircraft - nacelle acoustic linings, sound generation in jet engines, and operational noise effects on humans
[NASA-SP-189] c02 N69-11542
Optimum takeoff and climbout trajectory calculation technique for jet aircraft noise abatement
[NASA-TN-D-5182] c02 N69-26194
Analytical and experimental studies for predicting noise attenuation in acoustically treated ducts for turbofan engines
[NASA-CR-1373] c23 N69-36974
Operational limitations in flying noise abatement approaches
[NASA-TN-D-5497] c02 N69-39188
Pressurized liquid nitrogen inside parametric amplifier structures for input, noise, and temperature improvements
[NASA-TN-D-5509] c09 N69-40079
NOISE SPECTRA
Photon bunching effect in spatially coherent noise field enhanced by superposing monochromatic coherent signal and/or shaping incident noise spectra
c07 A69-31694
Beat frequency measurements in far IR due to harmonic mixing of klystrons, discussing noise role
c23 A69-33674
NOISE TOLERANCE
Conference on NASA research in noise reduction of subsonic jet aircraft - nacelle acoustic linings, sound generation in jet engines, and operational noise effects on humans
[NASA-SP-189] c02 N69-11542
Tone and duration effects on perceived noisiness
[NASA-CR-1283] c04 N69-18722
NONDESTRUCTIVE TESTS
Nondestructive testing methods for Saturn 5 space vehicle with emphasis on NDT equipment for Apollo program
c15 A69-23050
Cb-1Zr pumped sodium loop tests to evaluate loop components, EM pump, pressure transducers, and instrumentation techniques
[NASA-CR-1135] c03 N69-11373
Pumped helium tests of 51 centimeter bore niobium tin magnetic coils
[NASA-TN-D-5158] c26 N69-22965
NONEQUILIBRIUM CONDITIONS
Nonequilibrium performance of oxygen difluoride diborane rocket propellant
[NASA-TN-D-4992] c27 N69-16195
Gaseous reactant combustion simulation of dimethylhydrazine and hydrazine fuel system for nonequilibrium expansion studies
[NASA-TN-D-5404] c33 N69-35506
NONEQUILIBRIUM FLOW
Compressible hypersonic turbulent boundary layers solution by finite difference method, relating mixing length to velocity profile shape factor
[AIAA PAPER 69-684] c12 A69-33474
Modified model for vibration-dissociation relaxation coupling phenomena in nonequilibrium high temperature gas flow, discussing parameter U variation with kinetic temperature
c12 A69-37208
Aerodynamic and thermodynamic calibration of nonequilibrium air flow in Ames 1-foot shock tunnel
[NASA-TN-D-4985] c11 N69-15633
Numerical difficulties in integrating equations for one dimensional nonequilibrium nozzle flow of gas
[NASA-TN-D-5176] c19 N69-23355
Nonequilibrium gas dynamics of hydrogen dissociation and recombination
[NASA-CR-1411] c12 N69-34709
NONEQUILIBRIUM PLASMAS
Nonequilibrium nitrogen plasma spectral line intensities calculated assuming optically thin plasma
c24 A69-10960
Electrothermal instabilities of ionization region of nonequilibrium MHD generator in presence of magnetic field
c25 A69-21919
NONGRAY ATMOSPHERES
Correlations of stagnation point radiative heat transfer for earth reentry, noting use of nongray absorption coefficient models
c33 A69-14736
Nongray equilibrium radiative heat transfer in viscous radiating shock layer around blunt body entering high temperature nonisothermal carbon dioxide-nitrogen atmosphere
[AIAA PAPER 69-636] c33 A69-33258
Nongray absorption and radiation cooling on smooth symmetric blunt bodies included in modified Maslen flow field method for radiation and large blowing
[AIAA PAPER 69-637] c01 A69-33290
NONLINEAR EQUATIONS
Existence, uniqueness, and stability criteria for linear and nonlinear operational differential equations in Banach and Hilbert spaces
[NASA-CR-1356] c19 N69-28256
NONLINEAR FEEDBACK
Stochastic saturating systems optimal control computation, considering attitude control and tracking system design by elliptical differential equation of dynamic programming
c10 A69-30601
NONLINEAR FILTERS
Continuous time nonlinear dynamical system states variables estimated suboptimally from discrete noisy measurements with second order nonlinear filter, deriving dynamical equations
c10 A69-17939
NONLINEAR PROGRAMMING
Nonlinear least squares optimization program applied to atmospheric temperature sounding, solving for temperatures at various altitudes from simulated carbon dioxide intensity measurements
c13 A69-33156
NONLINEAR SYSTEMS
Continuous time nonlinear dynamical system states variables estimated suboptimally from discrete noisy measurements with second order nonlinear filter, deriving dynamical equations
c10 A69-17939
Stability of systems with sector nonlinearities determined by converting feedback equation into positive operators equation and by introducing appropriate multiplier
c10 A69-25450
Computer oriented error analysis of electrical circuits and nonlinear system performance
[NASA-TN-D-5112] c10 N69-22919
Computation of regions of constrained stability for nonlinear control systems
[NASA-CR-1328] c19 N69-28196
Chebyshev series solution of nonlinear ordinary differential equations - initial value problems
[NASA-TM-X-1882] c19 N69-36923
NONLINEARITY
Nonlinear disturbance decay in unbounded viscous fluid
[NASA-TN-D-4947] c12 N69-14483
Nonlinear flux flow in single crystal niobium
[NASA-TN-D-5198] c26 N69-24916
NONNEWTONIAN FLUIDS
Quasi-linear ordinary differential equations solutions for steady two dimensional stagnation point flows of nonNewtonian power law fluids

c12 A69-39674
NONPOLAR GASES
Viscosity, thermal conductivity and diffusion predicted for dilute nonpolar, polar and mixed gases, discussing methods for rotational relaxation collision numbers and resonant correction
c33 A69-38951
NONRELATIVISTIC MECHANICS
Scattering, reactions, and decay in nonrelativistic quantum mechanics
[NASA-TT-F-510] c24 N69-25848
NONUNIFORM MAGNETIC FIELDS
Magnetic field nonuniformity and its effect on stability of theta pinch plasma
[NASA-TR-R-303] c25 N69-20997
NORMAL DENSITY FUNCTIONS
Gaussian particle size distribution with porosity and surface irregularity corrections used to determine mean particle size of lunar surface material at Surveyor sites
c30 A69-26371
NORTH AMERICA
Regression generated radiometric and contour height fields of North American Continent using Nimbus 2 IR equivalent black body temperature and geopotential data
c20 A69-42896
NORTHERN HEMISPHERE
Low energy electron precipitation data at northern high latitudes obtained from satellite low altitude polar orbit
c29 A69-28964
Two-micron sky survey catalog of celestial objects
[NASA-SP-3047-REV] c30 N69-37993
NOSE CONES
Cone boundary layer transition location and Reynolds number as function of nose bluntness combined effect with Ar, air and He mass injection
[AIAA PAPER 67-706] c12 A69-33476
Surface pressure distribution on spherical blunted cones, and correlation of Mach numbers, cone angle, and angle of attack
[NASA-TN-D-5204] c01 N69-24764
Upwash patterns on ablating and nonablating cones at hypersonic speeds
[NASA-TN-D-5346] c12 N69-37370
NOSE WHEELS
Steerable landing gear system consisting of freely castoring corotating wheel nose gear, tiltable axle and main gear skids for lifting body spacecraft
[AIAA PAPER 69-790] c02 A69-35639
NOSES (FOREBODIES)
Performance tests on dynamic jettison hinge loads of Centaur nose fairing
[NASA-TM-X-1821] c32 N69-29734
NOTCH SENSITIVITY
Edge notch sensitivity in thin sheet nickel alloys under stress at high temperatures
[NASA-CR-1263] c32 N69-16156
NOTCH STRENGTH
Ultrasonic detection and measurement of fatigue cracks in notched cylinders subjected to reversed axial cyclic loading
c14 A69-10113
Load and temperature effects on fatigue strength of notched titanium alloy sheet for supersonic transport operation
[NASA-TN-D-5294] c32 N69-29607
NOTCH TESTS
Plane strain fracture toughness determined for crack notched bend specimens using standard test procedure for specific metallic material property
c17 A69-33566
NOTCHES
Elastoplastic stress-strain behavior at notch roots in sheet specimens under constant amplitude loading
[NASA-TN-D-5253] c32 N69-28038
NOVAE
Nova outburst dynamics investigation by time dependent hydrodynamics computer program including energy transport by radiation and convection
c30 A69-30769
NOZZLE DESIGN
Location effect of power plants on aft-mounted supersonic cruise exhaust nozzles at transonic speeds in flight and wind tunnel
[AIAA PAPER 69-427] c01 A69-32769
Jet velocity and axial location of nozzle exit on performance of twin-jet afterbody model
[NASA-TN-D-5393] c28 N69-36932
NOZZLE EFFICIENCY
Noncavitating and cavitating performance of low area ratio water jet pumps, analyzing efficiency, area ratio, throat length, nozzle spacing and diffuser geometry
c03 A69-35176
Static tests of nozzle efficiency and pumping characteristics of conical turbojet plug nozzle with translating primary and secondary shrouds at Mach 0 to 2.0
[NASA-TM-X-1777] c28 N69-21648
NOZZLE FLOW
Jet pump head rise deterioration parameter for prediction of cavitation
c12 A69-15791
Pressure and temperature surveys of Mach 27-47 nozzle boundary layer at Ames M-50 He tunnel, determining velocity profiles, wall friction coefficient, etc
[AIAA PAPER 69-686] c12 A69-33441
FORTRAN 4 subroutines for calculating critical flow factor to determine mass flow rate of gaseous helium and nitrogen through critical flow nozzles
[NASA-SP-3046] c12 N69-16098
Conformal mapping of two dimensional jet flow from two nozzles striking plane surfaces
[NASA-TN-D-5064] c01 N69-17816
Numerical difficulties in integrating equations for one dimensional nonequilibrium nozzle flow of gas
[NASA-TN-D-5176] c19 N69-23355
Jet effects on boattail pressure drag of isolated ejector nozzles at Mach 0.60 to 1.47
[NASA-TM-X-1785] c01 N69-26976
Flow angle and throat Reynolds number effects on loss characteristics of two dimensional supersonic nozzle
[NASA-TM-X-1823] c01 N69-31360
Comparison of predicted nozzle coolant side heat transfer and fluid flow with experimental values from Phoebus 2A nuclear tests
[NASA-TM-X-1881] c33 N69-36806
Discharge nozzle coefficients for thick plate orifices with approach flow perpendicular and inclined to orifice axis
[NASA-TN-D-5467] c12 N69-38012
NOZZLE GEOMETRY
Plug and shroud geometry variables on plug nozzle performance at transonic speeds
[NASA-TN-D-5098] c28 N69-21463
Performance characteristics of truncated, conical plug nozzle with cylindrical outer shroud
[NASA-TM-X-1807] c26 N69-27840
Energy thickness in prediction of throat heat transfer in rocket nozzles using nozzle geometries and temperature ratios
[NASA-TN-D-5356] c33 N69-31869
NOZZLE INSERTS
Nozzle insert evaluation and gas cooling concept in storable liquid propellant rocket engine
[NASA-TM-X-1756] c28 N69-19782
Throat and nozzle insert design for ablative rocket engine using storable propellants
[NASA-TN-D-4964] c32 N69-33481
NOZZLE WALLS
Turbulent boundary layer measurements on axisymmetric hypersonic nozzle walls
[NASA-TN-D-5433] c12 N69-36805
NOZZLES
Wind tunnel tests for V/STOL aircraft having direct-lift and lift-cruise jet nozzles
[NASA-TM-X-1758] c01 N69-20016
NUCLEAR BINDING ENERGY
Approximate ionization potentials for high ionization stages of elements with atomic numbers 31 to 92 obtained by binding energy calculations
c24 A69-29923
NUCLEAR ELECTRIC POWER GENERATION
Space nuclear electric power systems applications

and development, summarizing current status and near future programs
[AAS PAPER 69-305] c28 A69-42865
NUCLEAR ELECTRIC PROPULSION
Performance boundaries of space propulsion systems containing nuclear electric stages
[AIAA PAPER 69-249] c22 A69-21249
Space nuclear electric power systems applications and development, summarizing current status and near future programs
[AAS PAPER 69-305] c28 A69-42865
NUCLEAR EMULSIONS
Density measurements of particle tracks in nuclear emulsions utilizing digitized video scan, discussing operation and instrumentation
[IEEE PAPER 2A-7] c14 A69-19185
Primary cosmic ray nuclei studies during Gemini 2 flight by nuclear emulsion detector with time resolution capability, describing experiment design and equipment operation
c29 A69-38350
NUCLEAR ENGINE FOR ROCKET VEHICLES
Nuclear rocket program status and plans, presenting NERVA reactor and engine system tests
[AIAA PAPER 68-610] c22 A69-39219
NUCLEAR EXPLOSIONS
Inner radiation zone including data on electrons, protons and heavier particles and results from high altitude nuclear tests
c29 A69-27144
NUCLEAR FUEL ELEMENTS
Uranium dioxide vent loss in externally fueled thermionic reactor concept
[NASA-TN-D-4922] c22 N69-10099
Rate of loss of uranium dioxide or uranium mononitride from vented nuclear fuel element
[NASA-TN-D-4913] c22 N69-10734
Fabrication of cermets of uranium nitride and tungsten or molybdenum from mixed powders and from coated particles for nuclear fuel elements
[NASA-TN-D-5136] c17 N69-21404
Analysis of cylindrical reactor fuel pin for clad stress caused by fission gases
[NASA-TN-D-5178] c22 N69-24802
Source and cause of fuel element fisson product leakage in reactor cooling water system at Plum Brook Reactor
[NASA-TN-D-5374] c22 N69-32317
Irradiation of encapsulated fuel and fast neutron fluxes that simulate thermionic reactor conditions
[NASA-TM-X-1858] c22 N69-33273
Quantitative method for determination of fission gases trapped in irradiated fuel forms
[NASA-TM-X-1893] c22 N69-37225
NUCLEAR FUELS
Nuclear reactor space power system concept using thermionic diodes, heat pipes and rod control, emphasizing neutronic aspects and feasibility
c22 A69-14799
Nondestructive methods for fuel density determination in uranium dioxide
[NASA-TM-X-1779] c22 N69-22555
Uranium carbides irradiation tests for control of nuclear fuels fission gas swelling
[NAA-SR-12629] c22 N69-22946
NUCLEAR FUSION
Nucleosynthesis in dynamics of massive star cores, noting element synthesis by neutron capture in supernova explosions
c30 A69-20898
NUCLEAR MAGNETIC RESONANCE
Nuclear magnetic resonance of epsilon and delta phases in NbN system with nitrogen mole fractions
c26 A69-36445
Nuclear magnetic resonance and electron paramagnetic resonance techniques for aprotic electrolytes
[NASA-CR-1425] c06 N69-36413
NUCLEAR PARTICLES
High energy cosmic radiation problems
[NASA-SP-199] c29 N69-29652
NUCLEAR POWER PLANTS
Solar and nuclear electric power technology for electric propulsion
[AIAA PAPER 69-826] c03 A69-32709
Nuclear aircraft power plant, discussing safety, economy and obstacles
[AIAA PAPER 69-554] c22 A69-32761
Nuclear power plants based on nuclear aircraft technology to power ocean-going air cushion vehicles
[NASA-TM-X-1871] c22 N69-35723
NUCLEAR POWER REACTORS
Nuclear reactor space power system concept using thermionic diodes, heat pipes and rod control, emphasizing neutronic aspects and feasibility
c22 A69-14799
Systems analysis of Rankine cycle nuclear-electric potassium space power system using Li cooled fast reactor and high temperature turbine inlet
c22 A69-42266
NUCLEAR POWERED SHIPS
Performance potential of high speed ocean-going air cushion vehicles with aircraft nuclear power plants
[AIAA PAPER 69-416] c02 A69-30480
NUCLEAR PROPELLED AIRCRAFT
Performance potential of high speed ocean-going air cushion vehicles with aircraft nuclear power plants
[AIAA PAPER 69-416] c02 A69-30480
Nuclear aircraft power plant, discussing safety, economy and obstacles
[AIAA PAPER 69-554] c22 A69-32761
Nuclear power plants based on nuclear aircraft technology to power ocean-going air cushion vehicles
[NASA-TM-X-1871] c22 N69-35723
NUCLEAR PROPULSION
Solar and nuclear electric power technology for electric propulsion
[AIAA PAPER 69-826] c03 A69-32709
Nuclear powered surface effects machine performance estimates, calculating reactor power and payload fraction for various clearance heights, gross weights and velocities
c22 A69-35180
Performance estimates of high speed peripheral jet nuclear powered ground effects machine
[NASA-TM-X-1888] c22 N69-36757
Steam cycle analysis for nuclear powered turbofan engine
[NASA-TM-X-1907] c22 N69-40060
NUCLEAR RADIATION
NERVA control drum actuator tests in cryogenic temperature, nuclear radiation, and vacuum environments
[NASA-TN-D-5347] c22 N69-31870
NUCLEAR REACTIONS
Absolute cross sections for coincidence detection of deuteron breakup by 42 MeV alpha particles, showing He 5 and Li 5 final state interaction peaks
c24 A69-13469
Nuclear energized pulsational instability of stars based on linear quasi-adiabatic theory, including models with hydrogen burning shells
c30 A69-27576
Abundance compilations of elements due to nuclear processes, discussing carbonaceous chondrites character
c29 A69-38812
Angular distributions for Sc 45 Ti 46 nuclear reactions involving 41 MeV alpha particles bombardment described by Born approximation
c24 A69-41044
Alpha particle-triton reaction on scandium 45 at 41 MeV
[NASA-TN-D-5216] c24 N69-24919
NUCLEAR REACTOR CONTROL
Nuclear reactor space power system concept using thermionic diodes, heat pipes and rod control, emphasizing neutronic aspects and feasibility
c22 A69-14799
Linear multivariable control system design using modern control theory, and application to coupled core reactor control
[NASA-CR-1345] c19 N69-29268
Reflector based poison drum control on equal size reactor cores fueled with U-233 and U-235
[NASA-TM-X-1883] c22 N69-36756
NUCLEAR REACTORS
NASA Plum Brook Reactor Facility /PBRF/ for determining radiation tolerance to support nuclear power application in space for

propulsion and power
c22 A69-13128
Monte Carlo method application to neutron streaming in hemispherical air-filled ducts in water tank to determine leakage through nuclear reactor shields
c22 A69-35178
Initial radio frequency gas heating experiments to simulate thermal environment in nuclear light bulb reactor
[NASA-CR-1311] c22 N69-23450
Radial power tailoring for uranium dioxide-T-111 clad reactor with contained fission product gases
[NASA-TM-X-1795] c22 N69-25305
Probability calculations for fuel clad surface temperatures of nuclear reactors
[NASA-TM-X-1802] c22 N69-26231
Effects of reactor irradiation at cryogenic temperatures on tensile properties of titanium and titanium-base alloys
[NASA-TN-D-5442] c17 N69-37436

NUCLEAR RESEARCH AND TEST REACTORS
Cavity reactor consisting of dilute fuel core surrounded by moderating reflector to attain very high temperatures in gaseous cores
c22 A69-18954
Performance testing of SNAP 8 experimental power system
[NASA-TM-X-1732] c03 N69-20868

NUCLEAR ROCKET ENGINES
Nuclear rockets as Saturn 5 third stages, emphasizing increased payload or velocity utility and resulting engine and stage requirements
[AIAA PAPER 69-555] c31 A69-31849
Nuclear solid core rocket engine performance for interplanetary orbital launch of spacecraft by multiorbit injection
[AIAA PAPER 69-535] c22 A69-32660
Gaseous reactor fluid mechanics for nuclear rocket engines, discussing experiments on geometries used in open cycle engine for acceptable uranium loss rate
[AIAA PAPER 69-477] c22 A69-32728
Fluid dynamic simulation of gas core nuclear rocket chamber for separating light and heavy gas via centrifugal force produced by MHD-driven rotational flow
[AIAA PAPER 69-727] c22 A69-33483
Characteristics, performance potential, and problems of solid, liquid, and gas core nuclear rocket engines
[NASA-TM-X-1685] c22 N69-10067
Uranium dioxide vent loss in externally fueled thermionic reactor concept
[NASA-TN-D-4922] c22 N69-10099
Initial radio frequency gas heating experiments to simulate thermal environment in nuclear light bulb reactor
[NASA-CR-1311] c22 N69-23450
Uranium 233 critical mass requirements, neutron kinetic behavior, and neutron and gamma ray heating rates for nuclear light bulb rocket engine
[NASA-CR-1315] c25 N69-23451
Computerized simulation of low frequency dynamics of liquid hydrogen flow in nuclear rocket engine
[NASA-TN-D-5312] c22 N69-30070
Summaries of recent gaseous reactor fluid mechanics experiments
[NASA-TM-X-1847] c12 N69-31888

NUCLEAR SCATTERING
Asymmetry of polarized protons scattered from He 4 at 540 MeV for laboratory angles between 4 and 42 degrees
c24 A69-14966
Inelastic scattering cross sections calculated, comparing results for various nuclear states expressed as Wood-Saxon radial and harmonic oscillator functions
c26 A69-29006
Core polarization effects in inelastic scattering cross sections for several nuclei in 2s-1d shell, using Hartree-Fock wave functions and Born approximation
c24 A69-29007
High energy scattering approximation valid from small to large angles, discussing errors and proton scattering by He
c24 A69-29008
Intermediate energy protons elastic and quasi-elastic scattering from light nuclei, correlating p-D, p-He-3, p-p and p-He-4 data with varicus scattering models
c24 A69-43123

NUCLEAR STRUCTURE
Hartree-Fock method used to study even-even nuclei in 2s-1d shell
[NASA-TN-D-5066] c24 N69-17976

NUCLEATE BOILING
Film-nucleate boiling transition for liquid nitrogen in vertical forced flow in electrically heated tube, discussing conduction model and agreement with visual experiment
[ASME PAPER 69-HT-26] c33 A69-43542

NUCLEI
Inelastic proton scattering cross sections for target nuclei in 2s-1d shell calculated in distorted wave Born approximation with projected Hartree-Fock wave functions
c24 A69-41045

NUCLEI (NUCLEAR PHYSICS)
Iodine 123 decay via gamma ray emission, noting energies of several transitions
c24 A69-13099
Energy spectra of carbon and oxygen nuclei in primary cosmic radiation, comparing results to earlier measurements and satellite observation
c29 A69-20632
Core polarization effects in inelastic scattering cross sections for several nuclei in 2s-1d shell, using Hartree-Fock wave functions and Born approximation
c24 A69-29007
Nuclear level density and mass shell corrections relationship for deformed and undeformed nuclei
c24 A69-29337
Elastic scattering cross sections for 21-MeV incident protons measured for nuclei differing in mass, determining optical model potential
c24 A69-35489
Primary cosmic ray nuclei studies during Gemini 2 flight by nuclear emulsion detector with time resolution capability, describing experiment design and equipment operation
c29 A69-38350
Differential cross section and polarization measurements for elastic scattering of high energy protons from light nuclei
c24 A69-43125

NUCLEON POTENTIAL
He 2 excitation spectrum for interparticle potential using pair Hamiltonian with repulsive core and attractive well
c24 A69-33118

NUMERICAL ANALYSIS
Complex chemical equilibrium calculation, analyzing thermodynamic principles and solution to nonlinear equations
c06 A69-10588
Tabulation of high accuracy gamma function values for some rational arguments, noting applications to Gaussian quadrature formulas, fractional Bessel functions and Airy functions
c19 A69-13375
Aerodynamic coefficients from observed motion of body in flight, eliminating need for closed form solutions by employing numerical solutions to equations of motion
[AIAA PAPER 69-134] c01 A69-18161
Numerical analysis of periodic solutions of restricted three body problem in sun-Jupiter system, noting genealogy of periodic orbits
c30 A69-19874
Numerical method for time dependent compressible Navier-Stokes equations applied to axisymmetric flow field produced by hypervelocity impact, examining viscous effects
[AIAA PAPER 69-354] c32 A69-28288
Multistage rocket trajectories optimized by second order numerical technique and digital computer program, considering coasting, vacuum flight and transition times
c30 A69-32154
Variable mesh multistep methods for numerical solution of nonlinear differential equations
[NASA-CR-1247] c19 N69-11419

Analysis of flow stability of thin liquid film adjacent to high speed gas stream
[NASA-TN-D-4976] c12 N69-15630
Numerical solution of coupled, nonlinear, equation of motion for rigid blade to simulate response sensitivity and blade-motion stability of fully articulated rotor
[NASA-TN-D-5032] c01 N69-17289
Numerical method for evaluation and utilization of supersonic nacelle-wing interference
[NASA-TN-D-5057] c01 N69-19641
Wind tunnel and analytical study of conversion from wing lift to rotor lift on composite lift VTOL aircraft
[NASA-TN-D-5256] c02 N69-28044
Numerical method and computer program for computing deflection response of thin shells
[NASA-CR-1376] c32 N69-29558
Numerical analysis of shock control by using perforated walls in internal compression supersonic inlets
[NASA-TR-R-317] c01 N69-32338
Computer analysis of total pressure loss and air flow distribution in annular flow gas turbine combustion chambers
[NASA-TN-D-5385] c33 N69-33314
Numerical analysis of spiraling in ion molecule collisions with polar targets using computer plotting techniques
[NASA-TN-D-5407] c24 N69-35508
Evaluation of height and time based meteorological rocket wind reduction techniques
[NASA-TM-X-1850] c20 N69-35523
Numerical calculation of inviscid adiabatic flow field around blunt bodies at hypersonic speeds
[NASA-TN-D-5434] c12 N69-36830
Theoretical feasibility of detecting laser radiation scattered from plasma
[NASA-TN-D-5311] c25 N69-36939
Numerical calculation of viscous compressible flow around harmonic oscillating rigid cylinder
[NASA-CR-1467] c12 N69-38782
Numerical analysis of laminar and turbulent mixing region for two dimensional jet injected at angle to moving stream
[NASA-TN-D-5531] c12 N69-41213

NUMERICAL INTEGRATION
Recursive formulas for numerical evaluation of real convolution integral for simulation of control systems and electrical networks on digital computer
c19 A69-17250
Parasitic eigenvalue in integration of equations governing one dimensional flow of chemically reactive gas
c12 A69-18317
Encke type analytical-numerical integration for solving differential equations of modified set of Lagrange planetary equations, obtaining satellite ephemeris for orbit prediction
[AIAA PAPER 69-908] c30 A69-39340
Numerical integration techniques for real time digital flight simulation
[NASA-TN-D-4900] c11 N69-11371
Comparison of fourth order Runge-Kutta numerical integration technique with two numerical integration formulas in mathematical models used for computing rigid body trajectories
[NASA-TN-D-5425] c30 N69-38769

NUMERICAL WEATHER FORECASTING
Angular grid spacing resolution near poles effect tests in global prediction model for geophysical fluid dynamics, investigating forecast height and wind fields
c20 A69-43066

NUTRITIONAL REQUIREMENTS
Biological, psychological and technological requirements in astronaut nutrition programs, examining preservation and reconstitution techniques
c05 A69-15388
Human responses to spacecraft cabin atmosphere, pressure, and contamination, and water supply, diet, and anthropometry
[NASA-CR-1205-VOL-3] c04 N69-12592

NYQUIST DIAGRAM
Apollo-Saturn 5 propulsion and structure feedback loop, analyzing POGO components and Nyquist plot application
[AIAA PAPER 69-877] c31 A69-39403
Pilots and flight simulator used in study of human visual sampling study
[NASA-CR-1258] c05 N69-14145

O

O RING SEALS
Glass vacuum systems grease free assembly method using heat shrinkable polyolefin sleeve tubing connector for compression of O ring joints
c15 A69-20529

OAO
Orbiting Astronomical Observatory thermal test and evaluation program, discussing equipment and role in experimental design
[AIAA PAPER 69-995] c11 A69-40373
Spaceborne stored program computer design for OAO-C, noting auxiliary command storage, spacecraft monitoring and malfunction reporting, etc
c08 A69-41736

OBLIQUE SHOCK WAVES
Linear wave interaction with oblique shock waves, noting dependence of transmission, reflection and generation coefficients on Mach number
c12 A69-13137
Oblique shock wave properties with free stream Mach number and flow deflection angle as independent variables, noting explicit solution
c01 A69-25378

OBSERVATION AIRCRAFT
NASA Earth Resources Survey Aircraft Program, describing aircraft and remote sensors characteristics
c14 A69-36259

OCEANOGRAPHY
Orbiting satellite global all-weather oceanographic data acquisition to complement higher resolution data from ships, buoys and aircraft remote sensors
[UN PAPER 68-95878] c13 A69-10491
Ocean circulation as climate regulator, discussing role in redistributing climate-changing energy input from solar radiation or lunar tidal friction into atmosphere
c13 A69-26333

OCEANS
Origin and terrestrial relief of continents and oceans
[NASA-TT-F-533] c13 N69-29491
Nuclear power plants based on nuclear aircraft technology to power ocean-going air cushion vehicles
[NASA-TM-X-1871] c22 N69-35723

OCULOGRAVIC ILLUSIONS
Human angular acceleration sensitivity using rotation and oculogyral illusion perception as indicators, relating to spatial orientation and flight control task precision
c05 A69-41674

OGO
Magnetic field data from OGO-2 spacecraft and surface magnetic observatories, noting magnetic storm occurrence and magnetosphere inflation and detection of polar ionospheric currents
c13 A69-11125
Deployable appendages of OGO attitude controlled spacecraft design
c31 A69-17606
OGO program failure rate analysis with respect to cost, schedule and performance tradeoffs, considering component and systems design and reliability, prelaunch feedback, etc
c31 A69-34519
OGO for conducting diversified measurements to study earth atmosphere, earth-sun relationship, etc
c31 A69-36674

OGO-F
Solid state detector for electron spatial distribution measurements on OGO-F satellite, discussing design emphasizing reliability
c09 A69-36676

OILS
Diffusion pump oil reflectance and absorption coefficients measured in three thicknesses using light source, monochromator and detector
c23 A69-23647

OMEGA NAVIGATION SYSTEM
OMEGA position location equipment /OPLE/ test data to demonstrate feasibility of using OMEGA navigational system in conjunction with synchronous satellites
c21 A69-19135

OMNIDIRECTIONAL ANTENNAS
Omnidirectional microwave parallel plate waveguide fed antenna design for flush mounted broadband spacecraft, noting equatorial and polar patterns
c09 A69-40697
Simple antenna with good circular polarization over wide space sector, showing geometry, normalized orthogonal field distributions and beamwidth range, considering slot combinations
c09 A69-41590

OMNIDIRECTIONAL RADIO RANGES
Navigation-aids identification decoder and display device for general aviation aircraft
[NASA-TN-D-5445] c09 N69-38852

ON-LINE PROGRAMMING
On-line central data processing system connected to time shared computer for recording data from test facilities, discussing hardware configuration, software considerations and advantages
c08 A69-33106
Predictive display systems using repetitive, fast time, on-line computation
[NASA-CR-1274] c05 N69-17738

ONBOARD EQUIPMENT
Onboard checkout system concept, discussing philoscphy, requirements, underlying considerations, system description, development and techniques of system selection
c11 A69-25081
Manual procedures for midcourse and terminal guidance, discussing onboard optical measurements and calculations
c21 A69-35792
Operational analysis of mass measuring system in orbiting spacecraft
[NASA-TN-D-5039] c04 N69-19115

ONE DIMENSIONAL FLOW
Parasitic eigenvalue in integration of equations governing one dimensional flow of chemically reactive gas
c12 A69-18317
Normal stress effects in viscoelastic fluid theories applied to one dimensional Burgers model of weak turbulence predicting drag reduction
c12 A69-33256
Calculating equilibrium and kinetically limited performance using one dimensional model
[NASA-TN-D-4991] c27 N69-16153
Numerical difficulties in integrating equations for one dimensional nonequilibrium nozzle flow of gas
[NASA-TN-D-5176] c19 N69-23355

OPACITY
Interim absorption coefficients and opacities for hydrogen plasma at high pressure
[NASA-TM-X-1902] c24 N69-39187

OPERATIONS RESEARCH
Computer program for research and engineering management of spacecraft projects
[NASA-CR-1275] c34 N69-18057
Design and operation of high temperature loads calibration laboratory
[NASA-TM-X-1868] c11 N69-36224

OPERATOR PERFORMANCE
Weightless simulators effectiveness for obtaining space systems maintainability criteria, using nonparametric experimental design for performance data
c05 A69-17648
Small perturbation dynamics of neuromuscular system in tracking tasks
[NASA-CR-1212] c05 N69-14212
Practice and operator work load effects on acquisition and performance of code transformation /COTRAN/ task
[NASA-CR-1261] c05 N69-14345
Aspects of human operator performance in low order compensatory control tasks studied with regression analysis
[NASA-CR-1259] c05 N69-16212
Engineering problems survey on teleoperator control systems
[NASA-SP-5070] c05 N69-21478

OPERATORS (MATHEMATICS)
Stability of systems with sector nonlinearities determined by converting feedback equation into positive operators equation and by introducing appropriate multiplier
c10 A69-25450

OPTICAL COMMUNICATION
Intersatellite microwave laser communication system for ATS-F and ATS-G, discussing experiment, functional design and parameters
c07 A69-41758
HgCdTe as IR satellite detector for terrestrial, atmospheric and ocean mapping, IR astronomy and optical communication
c26 A69-43666
Parametric analysis of microwave and laser systems for communication and tracking - summary
[NASA-TR-R-309] c07 N69-23642
Quantum communication systems performance evaluated by communication efficiency parameter
[NASA-TR-R-320] c07 N69-39264

OPTICAL CORRECTION PROCEDURE
Remote sensing cross-beam cross correlation methods of determining spatially resolved average thermodynamic properties
[AIAA PAPER 67-149] c14 A69-31868
Conference on motion degraded images and correcting procedures - optical filters and digital methods for blurring removal from photographic imagery
[NASA-SP-193] c14 N69-33322

OPTICAL EQUIPMENT
Apollo optics system ground and flight performance tests results, suggesting possible design changes for sunlit space environments
c14 A69-35796
Analytic approximations for application to spacecraft optical navigation system where position fixes are taken over short trajectory arcs
[NASA-TN-D-4863] c21 N69-10372
Development of optical pilot warning indicator system for aircraft detection
[NASA-TN-D-5174] c14 N69-27267
Derivation of transfer function for optical system relating image intensity to spatial autocorrelation
[NASA-CR-1443] c21 N69-38041

OPTICAL FILTERS
Rocket-borne photoelectric photometers for UV observations of Saturn, using interference filters
c30 A69-22216
Laser optical simulation of spaceborne radio astronomy interferometer experiment
[NASA-TN-D-5357] c30 N69-36892

OPTICAL MEASUREMENT
Unicellular microorganisms size and concentration estimates based on light scattering measurements of suspensions in spectrophotometer cuvette compartment
c04 A69-25643
Manual procedures for midcourse and terminal guidance, discussing onboard optical measurements and calculations
c21 A69-35792
Optical measurements on secondary satellite for determining perturbation parameters of orbiting spacecraft
[NASA-CR-1412] c30 N69-35513

OPTICAL MEASURING INSTRUMENTS
Optical carrier single channel telemetry system providing complete electrical isolation between shock tube data acquisition and data recording instrumentation
c14 A69-29561
Indirect optical viewing system in F-104B for simulated lifting-body approach and landing tasks
[NASA-TN-D-5299] c14 N69-29730
Electro-optical instrument for measuring pointing direction of human eye
[NASA-CR-1422] c05 N69-39212

OPTICAL PATHS
Statistical correlation between optical microwave propagation reliability, fade margin, path

length, and geographic location
[NASA-CR-1442] c07 N69-39282
OPTICAL PROPERTIES
Diffusion pump oil reflectance and absorption coefficients measured in three thicknesses using light source, monochromator and detector
c23 A69-23647
Optical properties and chemical analysis of contaminants on Gemini spacecraft windows
[NASA-TN-D-4916] c31 N69-13232
Horizon radiance profile analysis for determining atmospheric temperature
[NASA-TN-D-5068] c13 N69-19024
Prediction methods for angular line-of-sight deviations induced by spacecraft window
[NASA-TN-D-5238] c21 N69-31227
Preflight optical evaluation of right hand hatch windows in Gemini missions 7, 8, 9, and 12
[NASA-TN-D-5471] c31 N69-40813
OPTICAL PUMPING
Time dependent emission spectra from flashlamp pumped organic dye lasers recorded with image converter, comparing dyes characteristics
c16 A69-17901
Microwave and optical generation and amplification - Conference, Hamburg, September 1968
c09 A69-18420
Low energy ultrafast flashlamp systems as optical pumps for lasers using fast decaying fluorescent materials /organic dyes/
c16 A69-42187
OPTICAL RADAR
Optical radar studies of lower atmosphere, giving Mie theory calculations of clear atmosphere volume backscattering cross sections for four laser wavelengths
c07 A69-27001
GaAs laser tracking system for space guidance, describing equipment and operations
[AIAA PAPER 69-870] c21 A69-39396
OPTICAL REFLECTION
Reflection and transmission measurements on as grown surfaces of tetracyanoquinodimethan, obtaining optical constants by Kramer-Kronig method
c26 A69-35477
Photomultiplier tubes performance enhancement by light incidence on photocathode at oblique angles explained by reflection
c23 A69-42194
OPTICAL RESONANCE
Minimization of optical resonance scattering by adjustment of monochromator slit geometry
[NASA-TM-X-1702] c24 N69-13210
OPTICAL SCANNERS
Scanned laser beam display techniques based on cathode ray tube technology, noting flying spot scanner and beam deflection
c14 A69-15028
Density measurements of particle tracks in nuclear emulsions utilizing digitized video scan, discussing operation and instrumentation
[IEEE PAPER 2A-7] c14 A69-19185
Visual simulation image generation using flying spot scanner
[NASA-TN-D-5151] c11 N69-23194
OPTICAL THICKNESS
Nonequilibrium nitrogen plasma spectral line intensities calculated assuming optically thin plasma
c24 A69-10960
Radiative transfer by doubling very thin layers in problem of diffuse reflection from plane-parallel atmosphere eliminates numerically solving transfer equation
c33 A69-20064
Optical depths of convection related to metal deficiency for main sequence and giant stars
c30 A69-29946
OPTICAL TRACKING
GaAs laser tracking system for space guidance, describing equipment and operations
[AIAA PAPER 69-870] c21 A69-39396
Optical simulation landing system for evaluating pilot controlled flexible parawing and Apollo capsule combination performance during landing
[NASA-TN-D-5049] c21 N69-20936
OPTICS
Damping factor automatic determination by use of second derivatives of residuals for damped least squares method of optical design
c23 A69-14295
Single and double mirror systems geometrical optical image aberrations noting focal number, angle of field, secondary magnification and mutual position tolerances
c23 A69-24836
OPTIMAL CONTROL
Optimal stochastic control of small dynamic systems described by random differential equations, noting selective bibliography on several subjects
c10 A69-14697
Optimal stochastic control, discussing dynamic mathematical models described by differential equations
c10 A69-22567
Adaptive random search algorithm utilizing boundary cost-function hypersurfaces measurement to implement Pontryagin maximum principle, discussing hybrid computer use, iterative solution and convergence properties
c08 A69-33745
Minimization of unconstrained function of several variables by gradient dependent techniques, discussing applications to boundary value problems in optimal control
[AIAA PAPER 69-951] c19 A69-40333
Quadratic optimization applied to helicopter flight control design, assuming constant feedback gains and command step input with zero steady state error
c02 A69-43279
Computation of optimal branched trajectories using classical variational problem of Bolza
[NASA-CR-1331] c30 N69-24950
Optimal control method based on linear programming for satellite fuel consumption
[NASA-CR-1450] c21 N69-41036
OPTIMIZATION
Digital computers in space flight simulation and vehicle performance optimization, examining mission analysis
c30 A69-14519
Hypersonic body shaping for minimum drag and improved performance from view of flight regimes, discussing implications of pressure laws
[AIAA PAPER 69-181] c01 A69-18052
Huffman minimum redundancy coding extension to run-length information based on Poisson distribution, including optimization and data compression applications
c07 A69-36262
Filtering optimization prior to limiting digital signals in strong noise, detailing bandwidth choice of single pole low pass filter
c07 A69-39450
Minimization of unconstrained function of several variables by gradient dependent techniques, discussing applications to boundary value problems in optimal control
[AIAA PAPER 69-951] c19 A69-40333
Computer optimization of spacecraft optical coatings for temperature control, using finite element analysis and matrix inversion
[AIAA PAPER 69-979] c33 A69-40359
Germanium microwave backward diodes optimum design and performance prediction through computer calculation for important parameters
c09 A69-41224
Spacecraft solar cell near-maximum power operation by tracking optimum value with array temperature sensor
c03 A69-42303
Materials research structural design cycle, discussing simultaneous optimization, constituent materials, fabrication process, load environment and mission constraints
c32 A69-42991
Optimum thickness of dynamically stable composite superconducting tapes determined for substrate thickness as function of current density
c26 A69-43121
Optimum design of binary phase shift keyed communication links with noisy phase reference
[NASA-TN-D-4895] c07 N69-13155

Variational methods for determining optimum design and flight of rockets
[NASA-TR-R-297] c31 N69-15374
FORTRAN program for radiation shield optimization using steepest descent method
[NASA-TM-X-1769] c22 N69-20854
Analytical solutions of optimum orbit modifications
[NASA-CR-1379] c30 N69-31362
Optimal structural design for sandwich-shaped and ring-stiffened loaded shells of revolution
[NASA-CR-1424] c32 N69-35515
Optimum structural design for Martian entry capsule configurations
[NASA-CR-1414] c33 N69-35516
Optimal rendezvous and transfers between close elliptical orbits
[NASA-TT-F-554] c30 N69-40592

ORBIT CALCULATION
Autonomous solution to orbital navigation problem yielding direct measure of orbital parameters
c21 A69-11005
Lunar Orbiter mission objectives and orbit design
[AIAA PAPER 68-47] c30 A69-15503
Impulsive orbit transfer optimization using accelerated gradient program based on Newtonian algorithm for digital computer method
c30 A69-35956
Hansen method applied to Jupiter tenth satellite orbit correction and perturbations, describing computer program and formulas used
c30 A69-37529
Encke type analytical-numerical integration for solving differential equations of modified set of Lagrange planetary equations, obtaining satellite ephemeris for orbit prediction
[AIAA PAPER 69-908] c30 A69-39340
Thrust requirements for correcting Keplerian orbits with interplanetary guidance application
[NASA-TN-D-4945] c21 N69-14399
Accuracy and speed comparison between drag-free and numerical satellite orbit prediction methods
[NASA-TN-D-5203] c30 N69-26252
Optical measurements on secondary satellite for determining perturbation parameters of orbiting spacecraft
[NASA-CR-1412] c30 N69-35513
Unified form of Lambert theorem valid for orbits
[NASA-TN-D-5368] c30 N69-36930

ORBIT PERTURBATION
Geopotential resonant orbital perturbations of existing satellites, noting high inclination role
c31 A69-13777
Perturbative effects of Jupiter moons on spacecraft flyby and postencounter heliocentric trajectories, noting precision targeting
[AIAA PAPER 69-932] c30 A69-39361
Thrust requirements for correcting Keplerian orbits with interplanetary guidance application
[NASA-TN-D-4945] c21 N69-14399
Vinti dynamic problem relevance to prediction of satellite orbits using differential and integral equations
[NASA-TR-R-307] c30 N69-22948
Legendre polynomials for gravitational field and orbit perturbation
[NASA-TN-D-5163] c13 N69-26969
Semianalytic theory for lunar satellite motion including perturbative effects
[NASA-TN-D-5043] c30 N69-28050
Optical measurements on secondary satellite for determining perturbation parameters of orbiting spacecraft
[NASA-CR-1412] c30 N69-35513
Direct and indirect planetary perturbation effects on motion of natural satellites
[NASA-TN-D-5284] c30 N69-37893

ORBITAL ASSEMBLY
Configurations for extravehicular activity work platforms for astronaut use in orbital assembly
[NASA-CR-1361] c31 N69-26993

ORBITAL ELEMENTS
Thrust requirements for correcting Keplerian orbits with interplanetary guidance application
[NASA-TN-D-4945] c21 N69-14399
Application of Hansen lunar theory to 10th satellite of Jupiter
[NASA-TN-D-4979] c30 N69-14479

ORBITAL LAUNCHING
Nuclear solid core rocket engine performance for interplanetary orbital launch of spacecraft by multiorbit injection
[AIAA PAPER 69-535] c22 A69-32660

ORBITAL MECHANICS
Hansen planetary theory basic function, discussing perturbations expansion into trigonometric series
c30 A69-13781
Numerical analysis of periodic solutions of restricted three body problem in sun-Jupiter system, noting genealogy of periodic orbits
c30 A69-19874
Gravitational and magnetic torque effect on rotational motion of triaxial rigid body in regressing orbit about oblate primary mass
c30 A69-32240
Short term motion of lunar satellite, discussing third body disturbing functions and perturbation solution of nonsingular orbit elements
c30 A69-35934
Encke type analytical-numerical integration for solving differential equations of modified set of Lagrange planetary equations, obtaining satellite ephemeris for orbit prediction
[AIAA PAPER 69-908] c30 A69-39340
Satellites resonant perturbations analysis, deriving mean mean motion formulas
c31 A69-39968
Effect of gravitational model variations on accuracy of lunar orbit determination from data arcs
[NASA-TN-D-5105] c30 N69-21018
Vinti dynamic problem relevance to prediction of satellite orbits using differential and integral equations
[NASA-TR-R-307] c30 N69-22948
Longitudinal dynamics of lifting vehicle in orbital flight
[NASA-CR-1449] c30 N69-40062

ORBITAL SPACE STATIONS
Future space programs as governed by cost limitations, suggesting development of economical launch vehicle for shuttling between earth and orbital space stations
c30 A69-12680
Manned space stations for future space exploration, discussing earth-like environment, artificial gravity, human factors and time dependence
c30 A69-25644
Space manufacturing operations program, discussing zero gravity effect during earth orbit flight, Apollo Applications Program Orbital Workshop Flight 2, etc
c31 A69-35067
Navigation, guidance and control developments for manned space missions, discussing earth orbital exploration bases
c21 A69-35801
Earth-orbiting manned space station as single facility base for power, volume, logistics, experimental equipment and data communications
c31 A69-36464
Mass expulsion and momentum systems for orbiting space station attitude control optimized, considering reaction jet and control moment gyro systems
[AIAA PAPER 69-846] c31 A69-39376
Apollo 11 mission and future space exploration prospects including moon base, manned space station, reusable shuttle vehicles, etc
c30 A69-41477
Apollo Applications Program /AAP/ spacecraft, describing contributions to space station engineering
[AAS PAPER 69-491] c31 A69-42838
Simulated manual package transfer in weightless environment of Saturn Orbital Space Station
[NASA-TN-D-5111] c05 N69-21501
Manned space flight capabilities for lunar and planetary explorations and earth orbiting stations
[NASA-SP-196-VOL-1] c34 N69-22510

ORBITER PROJECT
NASA Lunar Orbiter Program of lunar photography from orbiting spacecraft
c30 A69-38377

ORBITS
Comparison of class of orbits in Earth-Moon field and class of Kepler orbits in rotating coordinates by use of concurrent series of graphs
[NASA-TN-D-4903] c30 N69-10470
Analytical solutions of optimum orbit modifications
[NASA-CR-1379] c30 N69-31362
Unified form of Lambert theorem valid for orbits
[NASA-TN-D-5368] c30 N69-36930

ORDER-DISORDER TRANSFORMATIONS
Order-disorder transitions in solid hydrogen, discussing model to explain molecular rotation angular momentum operator fluctuations
c23 A69-43119

ORGANIC COMPOUNDS
Regenerative life support system development, considering synthesized organic compounds and microorganisms as foods for long duration space missions
c04 A69-37623
Electrochemical evaluation of electrode organic electrolyte combinations for rechargeable battery systems
[NASA-CR-1434] c03 N69-36829
Physical density and enzyme activity in coacervate biogenic molecular compounds
[NASA-TT-F-525] c04 N69-40324

ORGANIC LASERS
Organic dye laser frequency variation with temperature, noting absorption and fluorescence spectra
c16 A69-12617
Time dependent emission spectra from flashlamp pumped organic dye lasers recorded with image converter, comparing dyes characteristics
c16 A69-17901
Low energy ultrafast flashlamp systems as optical pumps for lasers using fast decaying fluorescent materials /organic dyes/
c16 A69-42187

ORGANIC LIQUIDS
Feasibility tests on liquid lubricants for inerted lubrication systems of advanced aircraft engines
[NASA-TN-D-5420] c15 N69-35788

ORGANIC MATERIALS
Gas chromatographic and mass spectrometric analyses of alicyclic hydrocarbons from Carboniferous organic materials, noting alkane distribution and evolutionary histories
c06 A69-34184

ORGANIZATIONS
Communication in large organizations, describing internal communication model
c34 A69-42930

ORGANOMETALLIC COMPOUNDS
Optical absorption coefficients for triphenylmethylarsonium tetracyanoquinodimethan complex single crystal, evaluating reflectance
c26 A69-10934

ORIENTATION
Feasibility of using roll and yaw compensation to reduce inclination error of Scout launch vehicle
[NASA-CR-1209] c31 N69-16221

ORIFICE FLOW
Discharge nozzle coefficients for thick plate orifices with approach flow perpendicular and inclined to orifice axis
[NASA-TN-D-5467] c12 N69-38012

ORTHOGONAL FUNCTIONS
First-order solutions for mutual coupling between waveguides which propagate two orthogonal modes
[NASA-TN-D-5180] c07 N69-24051

ORTHOSTATIC TOLERANCE
Artificial heat acclimatization effect on orthostatic tolerance in man exposed to stresses of heat, exercise and dehydration
c05 A69-32810

ORTHOTROPIC SHELLS
Finite element method for computing natural frequencies and mode shapes of thin shells of revolution
[NASA-TN-D-4972] c32 N69-16469

OSCILLATING FLOW
Amplified boundary layer oscillations and transition at swept flat nosed wing attachment line with/without boundary layer suction analyzed by wind tunnel tests
c01 A69-33251

OSCILLATION DAMPERS
Time varying resistance wire to arrest oscillations in pulsed capacitor discharge circuit, deriving over, under and critical damping conditions
c09 A69-41228

OSCILLATIONS
Individual properties of RR Lyrae stars
[NASA-TT-F-562] c30 N69-27169
Oscillations in pulse modulated satellite attitude control systems
[NASA-CR-1369] c21 N69-29967
Analytical model for use in design of pump inlet accumulators for prevention of liquid rocket longitudinal oscillation
[NASA-TN-D-5394] c28 N69-33319
Magnetothermal oscillations in pressure annealed pyrolytic graphite
[NASA-TN-D-5488] c26 N69-39239

OSCILLATORS
Small signal and saturation characteristics for X band cyclotron resonance oscillator, discussing device design and configuration
c09 A69-22786
Fluidic oscillator use as molecular weight sensor for gas mixtures
[NASA-TM-X-1698] c03 N69-13246
Cyclotron resonance oscillators as sources of millimeter waves
[NASA-TN-D-5237] c10 N69-28121

OSEEN APPROXIMATION
Nature of outside boundary layer on liquid sphere in steady, uniform stream
[NASA-CR-1362] c12 N69-24877

OSMOSIS
Transient electro-osmosis of water in capillary tubes for pumping and generation modes, analyzing response to step change in pressure or voltage change under external loading
c06 A69-14862
Osmotically induced coalescence of sarcoma cells through intercellular bridges in vitro
[NASA-TN-D-5022] c04 N69-17782

OSO-C
Solar extreme UV, soft and hard solar X rays, cosmic X rays and gamma rays, cosmic ray particles and near earth visible radiation observed by OSO-3
c29 A69-22167
Solar X ray and extreme UV spectra during flares, attributing intense emissions to optical transitions
c29 A69-22169

OUTGASSING
Leak rate measurement accuracy of rate-of-rise technique for nitrogen, methane and He between millionth and thousandth torr
c14 A69-32326
Rate of rise outgassing measurement technique in vacuums
[NASA-TN-D-4973] c14 N69-16097
Thermal outgassing tests on epoxy impregnated magnet coil
[NASA-TM-X-1813] c18 N69-28203

OUTPUT
Problem of identifying input-output of pilot by measuring data from flight tests with pilot providing feedback control
[NASA-TN-D-5127] c05 N69-23842

OVERPRESSURE
Design method for far field sonic boom shock strength and impulse independent of body length and volume
[NASA-TN-D-5148] c01 N69-23927

OXIDATION
Oxygen concentration effects on oxidation of synthetic paraffinic and type II ester lubricants determined from ball bearing tests at 400 and 450 degrees F
c15 A69-35177
Oxidation behavior of coated molybdenum and niobium alloys in high temperature supersonic air streams
[NASA-TN-D-4877] c17 N69-10764
Flow reduction due to oxidation of wire-form porous materials for transpiration cooled turbine blades
[NASA-TN-D-5001] c17 N69-16383

Protective coatings for chromium alloys for use in advanced air breathing applications
[NASA-TN-D-5157] c17 N69-23084
Dynamic creep model to determine oxidation effects on high temperature deformation of nickel
[NASA-TN-D-5266] c17 N69-27061
Hydration, oxidation, and origin of calc-alkali differentiation series of igneous rocks
[NASA-TN-D-5400] c13 N69-40893
OXIDATION RESISTANCE
Columbium alloys properties, discussing creep strength, oxidation resistance, costs, production, etc
c17 A69-18791
Ductile metal clads and coatings of silicides, aluminides and noble metals to protect Cr alloys against nitrogen embrittlement and air oxidation
c17 A69-26495
Boron nitride and boron nitride composite under high temperatures in air and vacuum for various time periods, discussing thermal shock and oxidation resistance
c18 A69-36208
Examination of thermal oxidation deposits on heat resistant alloys using X ray diffraction and X ray fluorescence analyses
[NASA-TN-D-5019] c17 N69-17277
Oxidation resistance and thermal fatigue cracking of nickel and cobalt base alloys in transonic gas streams
[NASA-TN-D-5376] c17 N69-33307
Corrosion and heat resistant coatings for oxidation protection of tungsten
[NASA-TT-F-583] c17 N69-35836
Three oxidation-resistant alloy foil claddings for protecting typical gas turbine engine alloys of nickel and cobalt
[NASA-TN-D-5483] c17 N69-38794
OXIDES
Oxide composition of silicate spherules from forest area devastated by Tunguka meteorite explosion using electron microprobe analysis
c30 A69-28869
Rare earth fluorides and oxides used as solid lubricants at high temperatures
[NASA-TN-D-5301] c15 N69-29568
OXYGEN
Oxygen concentration effects on oxidation of synthetic paraffinic and type II ester lubricants determined from ball bearing tests at 400 and 450 degrees F
c15 A69-35177
Ge films formation by evaporation technique, discussing background O pressure effect
c26 A69-43345
Absorption rate sticking probabilities for oxygen on niobium and dilute niobium-zirconium alloys
[NASA-TN-D-4885] c17 N69-10931
Evaluation of various laboratory determination of oxygen in potassium and sodium
[NASA-TN-D-4971] c06 N69-14180
Solubility of oxygen in tantalum determined by resistivity technique
[NASA-CR-1276] c17 N69-19886
Vacuum distillation determination of oxygen in lithium
[NASA-TN-D-5197] c06 N69-23706
Controlled oxygen additions to refractory metal alloys
[NASA-TM-X-1799] c17 N69-26952
Rapid computation of equilibrium, chemical composition, and thermodynamic properties of argon-oxygen-hydrogen gas system
[NASA-TN-D-5416] c33 N69-36299
OXYGEN ANALYZERS
Vacuum distillation determination of O in Li, evaluating accuracy through O additions and recoveries, method blank and residue identification
c06 A69-40932
OXYGEN ATOMS
Atomic oxygen density role in ionospheric E and F region magnetic stability, noting heat loss effect of atomic excitation
c13 A69-32314
OXYGEN CONSUMPTION
Oxygen depletion effect in chemical reactions between pyrolysis gases and air stream on surface recession of charring ablators
[AIAA PAPER 68-302] c33 A69-21982
Real time metabolic rate analysis of suited astronaut using heart rate and O methods during thermal vacuum and extravehicular mobility tests
[AIAA PAPER 69-993] c05 A69-40371
OXYGEN FLUORIDES
Specific impulse deliverable performance of space storable propellant combination fluorine-oxygen/methane and oxygen difluoride/diborane
[AIAA PAPER 69-505] c28 A69-32762
OXYGEN METABOLISM
Respiratory system and oxygen metabolism regulation in man and animals
[NASA-TT-F-501] c04 N69-31401
OXYGEN REGULATORS
Respiratory system and oxygen metabolism regulation in man and animals
[NASA-TT-F-501] c04 N69-31401
OXYGEN SUPPLY EQUIPMENT
Water electrolysis, discussing oxygen generators for spacecraft prototype cells and testing
c05 A69-12987
Oxygen supply inert diluent impurities effect on hydrogen-oxygen fuel cell performance
c03 A69-15310
Lithium peroxide utilization feasibility for oxygen supply and carbon dioxide control in extravehicular portable life support systems
[AIAA PAPER 69-620] c05 A69-33303
Solid electrolyte electrolysis of carbon dioxide and water as oxygen regeneration system for long manned space flights
[NASA-CR-1359] c05 N69-28099
OXYGEN TENSION
High oxygen concentration breathing effect on foveal thresholds, using sea level tests on trained observers
c05 A69-12216
High oxygen tension effect on transport and incorporation of exogenous leucine and protein synthesis in Pseudomonas saccharophila cells
c04 A69-13433
OXYGENATION
Oxygen concentration effects on synthetic paraffinic oil lubricant performance in high temperature bearing tests
[NASA-TN-D-5152] c15 N69-26314
OZONOMETRY
Atmospheric ozone vertical distribution and total amount determined by radiative transfer and perturbation theory, presenting error analysis
c13 A69-28493
OZONOSPHERE
Atmospheric ozone vertical distribution and total amount determined by radiative transfer and perturbation theory, presenting error analysis
c13 A69-28493

P

P-N JUNCTIONS
Radiation damage and recovery of lithium-diffused silicon p-n solar cells, measuring photovoltaic parameters as function of gamma radiation fluence
c03 A69-35694
Potential electrical response of p-n junction to mechanical strain
[NASA-CR-1366] c26 N69-29724
Effects of nickel on performance of n on p silicon solar cells
[NASA-TN-D-5366] c03 N69-31844
P-N-P-N JUNCTIONS
Four terminal silicon planar p-n-p-n model operating as semiconductor small signal linear tetrode amplifier, discussing properties and mathematical models
c09 A69-35293
P-TYPE SEMICONDUCTORS
Strong p-type conductivity of silicon doped with beryllium by thermal diffusion, giving electrical and optical measurements
c26 A69-21652
PACIFIC OCEAN
Survey of six year period of satellite observed tropical Pacific cloud mapping
c20 A69-33001
PACKAGING
Astronaut feeding in space and NASA criteria for

space foods, eliminating foods in metal tubes and directing development efforts to dehydrated foods
c05 A69-31459

PACKINGS (SEALS)
Torque and leakage rates of various lubricated lip seal designs at peripheral velocity of 120 feet per second
[NASA-TN-D-5411] c15 N69-35769

PADE APPROXIMATION
Existence theorem using Pade approximation and matrices
[NASA-CR-1319] c19 N69-26248

PAINTS
Computer optimization of spacecraft optical coatings for temperature control, using finite element analysis and matrix inversion
[AIAA PAPER 69-979] c33 A69-40359
Investigation of SA-501 S-4B auxiliary propulsion system anomalies
[NASA-TN-D-5207] c28 N69-26224

PAIR PRODUCTION
Quantum theory of electron gas with anomalous magnetic moments in intense magnetic fields, noting pair creation from thermodynamic energy in system
c24 A69-19782
Lower auroral ionosphere rocket measurements of electrons, positive ions and energy particles, deriving height variation of ion pair production and ion-ion recombination
c13 A69-32187

PALEONTOLOGY
Gas chromatographic and mass spectrometric analyses of alicyclic hydrocarbons from Carboniferous organic materials, noting alkane distribution and evolutionary histories
c06 A69-34184

PALLADIUM
Deuterium concentration effect on electrical resistivity of palladium-deuterium system
[NASA-TN-D-4970] c26 N69-14565
Comparison of extraction procedures using 1-nitroso 2-naphthol and dimethylglyoxime for spectrophotometric determination of palladium in titanium alloys
[NASA-TM-X-1767] c06 N69-20801
Absorption of hydrogen by palladium and electrical resistivity of hydrogen-palladium system
[NASA-TN-D-5441] c26 N69-37272

PANEL FLUTTER
Flutter design charts for isotropic panels stressed to verge of buckling for typical values of structural damping
c32 A69-25524
Effects of structural damping on flutter of stressed panels
[NASA-TN-D-4990] c32 N69-16091
Flutter investigation at Mach 3 of rotationally restrained panels and comparison with theory
[NASA-TN-D-5508] c32 N69-40087

PARA HYDROGEN
Solid para hydrogen coated graphite particles expulsion into interstellar medium from star formation regions, considering mantles stability and particles extinction efficiency, albedo and phase function
c30 A69-37492

PARABOLIC ANTENNAS
Parabolic antenna properties generated by dual band circularly polarized focused two channel monopulse feed system, discussing tracking data from helicopter, Apollo 8 and Cassiopeia A
c07 A69-41752

PARABOLIC REFLECTORS
Parametric analysis of surface temperatures and distortions of paraboloidal solar concentrators
[NASA-TN-D-5144] c03 N69-23356

PARACHUTE DESCENT
NASA planetary entry parachute program for rocket launched and balloon deployment tests
[AIAA PAPER 68-934] c02 A69-35952
Experimental verification of scale factors for parawing opening characteristics with dimensional ratios from 1/1.3 to 1/3
[NASA-TN-D-5071] c02 N69-19950
Parachute load distribution measurements with tensiometer during low altitude drop tests
[NASA-TM-X-1832] c14 N69-32682

PARACHUTE FABRICS
Mission sequential environment effects on Dacron parachute material mechanical properties
[AIAA PAPER 69-1018] c11 A69-40390

PARACHUTES
Equation of motion for predicting dynamic behavior of parachute payload system
[NASA-TN-D-4859] c02 N69-14504
Wind tunnel tests of inflatable disk-gap-band and modified ringsail parachutes at low dynamic pressure
[NASA-TM-X-1786] c01 N69-23538
Flight test performance of supersonic parachutes in low density environment
[NASA-TN-D-5296] c01 N69-30063

PARAFFINS
Steel ball bearing high temperature fatigue life tested with synthetic paraffinic oil, fluorocarbon and polyphenyl ether
[ASME PAPER 69-LUBS-18] c15 A69-34378
Oxygen concentration effects on oxidation of synthetic paraffinic and type II ester lubricants determined from ball bearing tests at 400 and 450 degrees F
c15 A69-35177
Oxygen concentration effects on synthetic paraffinic oil lubricant performance in high temperature bearing tests
[NASA-TN-D-5152] c15 N69-26314

PARALLEL PLATES
Admittance of parallel plate waveguide aperture with infinite flange illuminating metal sheet, using wedge diffraction theory and integral transform method
c09 A69-12328
Reflection coefficient of symmetric parallel plate waveguide operating in TEM mode illuminating lossless dielectric layer, using wedge diffraction and geometrical optics methods
c09 A69-34802
Omnidirectional microwave parallel plate waveguide fed antenna design for flush mounted broadband spacecraft, noting equatorial and polar patterns
c09 A69-40697
Admittance of parallel plate aperture illuminating displaced dielectric-dielectric boundary
[NASA-TN-D-5038] c07 N69-19114
Symmetric parallel plate waveguide reflection coefficient analyzed
[NASA-CR-1327] c07 N69-24059
Slope diffraction analysis of TEM parallel plate guide patterns
[NASA-CR-1326] c07 N69-26273

PARAMETERIZATION
Real helium hypersonic flow parameters for pressures to 3600 atmospheres and temperatures to 15,000 deg K applicable to hotshot type wind tunnels
[NASA-TN-D-4869] c12 N69-10443

PARAMETRIC AMPLIFIERS
Hybrid integrated parametric amplifier design considerations for fabrication in microstrip transmission line
c09 A69-10193
Error analysis of input noise temperature measurements of low noise amplifiers
[NASA-TN-D-4997] c07 N69-16162
Pressurized liquid nitrogen inside parametric amplifier structures for input, noise, and temperature improvements
[NASA-TN-D-5509] c09 N69-40079

PARAWINGS
Flexible parawing lifting decelerator research data from wind tunnel and flight tests, noting manned space vehicle recovery and aircraft escape systems
[AIAA PAPER 68-967] c02 A69-43715
Wind tunnel tests of opening characteristics of all flexible parawing
[NASA-TN-D-5031] c02 N69-17700
Experimental verification of scale factors for parawing opening characteristics with dimensional ratios from 1/1.3 to 1/3
[NASA-TN-D-5071] c02 N69-19950
Optical simulation landing system for evaluating pilot controlled flexible parawing and Apollo capsule combination performance during landing
[NASA-TN-D-5049] c21 N69-20936

Wind tunnel investigation of twin keel parawing aerodynamic characteristics
[NASA-TN-D-5199] c01 N69-23781
PARKING ORBITS
Two burn spacecraft trajectories for escaping earth parking orbit
[NASA-TN-D-5011] c30 N69-17305
PARTIAL DIFFERENTIAL EQUATIONS
Boundary conditions for Tricomi equation in symmetric positive form, showing analytical and finite difference solutions
c19 A69-42792
PARTICLE ACCELERATION
Solar cosmic radiation, particle acceleration, energetic particles as sample of sun and propagation of particles from sun tc earth
c29 A69-12934
Rocket measurements of primary auroral particles energy spectra indicating spectral structure acceleration peaks associated with electrostatic fields
c13 A69-38490
PARTICLE ACCELERATORS
Tritium contamination reduction in small ion accelerators for neutron production, discussing pumping problems and vacuum systems
c11 A69-26499
PARTICLE COLLISIONS
Collisional theory of longitudinal wave propagation for two fluid viscous ionized plasmas formulated from coupled Maxwell and Boltzmann equations
c25 A69-20796
Extragalactic gamma ray fluxes predicted, discussing collisions, matter-antimatter annihilation and cosmological implications
c29 A69-24466
Longitudinal plasma waves collision damping calculations using Rostoker test particle method
c25 A69-34439
Cosmic X ray bremsstrahlung due to collisions of suprathermal protons with ambient electron, giving clue about diffuse sky background of X rays
c29 A69-40643
Quantum theory of particle-harmonic oscillator collision applied to gas-surface interactions at cryogenic temperatures
[NASA-TN-D-4982] c24 N69-14288
Electron-cesium atom collision probability for momentum transfer
[NASA-TM-X-1897] c24 N69-38773
PARTICLE DENSITY (CONCENTRATION)
Transmittance and absorption cross sections of carbon particles suspended in flowing stream of nitrogen gas
c33 A69-17804
Unicellular microorganisms size and concentration estimates based on light scattering measurements of suspensions in spectrophotometer cuvette compartment
c04 A69-25643
Meteoritic dust particles collections prediction in atmosphere for low and high entry fluxes
c30 A69-26342
Self contained hand held battery operated aerosol particle analyzer, measuring aerosol concentration and size distribution for laboratory and space flight applications
c14 A69-34691
Back flow density from jet plumes in vacuum
[NASA-TN-D-4978] c01 N69-14385
PARTICLE DIFFUSION
Charged particle dynamics in spiral interplanetary magnetic field model, discussing electric drift velocity, point of origin and distribution
c29 A69-14015
Equation describing statistically trapped particle motion under influence of fields varying in time and space
c29 A69-19375
Low energy solar protons entry into magnetosphere on 26 May 1967 showing diffusion control
c29 A69-31984
PARTICLE EMISSION
Solid para hydrogen coated graphite particles expulsion into interstellar medium from star formation regions, considering mantles stability and particles extinction efficiency, albedo and phase function
c30 A69-37492
Atmospheric emissions - NATO Conference, Norway, July-August 1968
c13 A69-38482
PARTICLE ENERGY
Ring current particle energy density distribution for symmetric portion of magnetic storm derived from current magnetic field profile measurements
c29 A69-11227
Inner radiation zone including data on electrons, protons and heavier particles and results from high altitude nuclear tests
c29 A69-27144
High and medium energy molecular beams - Conference, Cannes, July 1969
c24 A69-36171
Cosmic ray detectors design for medium, low and very low energy events on IMP-1 spacecraft, noting PCM format
c07 A69-41738
PARTICLE INTERACTIONS
Ion-molecule collisions of Ar-Co and N-No pairs, discussing charge exchange reaction rates and spiraling nature
c24 A69-16428
Maximum number of binary collisions for three particles with zero range forces in relativistic rescattering singularities studies
c24 A69-19788
Computer experiments on the microscopic behavior of one dimensional electrostatic plasma
[NASA-TN-D-4831] c25 N69-10471
PARTICLE MOTION
Solar cosmic radiation, particle acceleration, energetic particles as sample of sun and propagation of particles from sun to earth
c29 A69-12934
Charged particle dynamics in spiral interplanetary magnetic field model, discussing electric drift velocity, point of origin and distribution
c29 A69-14015
PARTICLE PRODUCTION
Tritium contamination reduction in small ion accelerators for neutron production, discussing pumping problems and vacuum systems
c11 A69-26499
Cosmic gamma rays spectrum from neutral pions production and decay in metagalactic cosmic ray p-p collisions, deriving models based on Einstein general relativity theory
c29 A69-40641
PARTICLE SIZE DISTRIBUTION
Mie total and differential backscattering cross sections at laser wavelengths for Junge size distribution aerosol models
c16 A69-14290
Stony meteoric particles size and velocity during passage through atmosphere
c30 A69-26341
Gaussian particle size distribution with porosity and surface irregularity corrections used to determine mean particle size of lunar surface material at Surveyor sites
c30 A69-26371
Ice clouds near IR spectral reflectivity dependence on particle size, noting application to planetary atmospheres
c13 A69-34283
Self contained hand held battery operated aerosol particle analyzer, measuring aerosol concentration and size distribution for laboratory and space flight applications
c14 A69-34691
Particle albedos and extinction cross sections computed by Mie theory showing dependence on refractivity, considering thermal radiation from cloudy planetary atmospheres
c30 A69-38255
Sorting particles by shape using sieving equipment, noting results with crushed gravel
c15 A69-38950
PARTICLE TELESCOPES
Gamma ray telescope development for balloon-borne astronomy in search for discrete gamma sources and supernova explosions
[IEEE PAPER 3A-5] c14 A69-19192
PARTICLE THEORY
Computer experiment on 9000 particle plasma to

test temporal echo theoretical prediction
c25 A69-38713
PARTICLE TRAJECTORIES
Density measurements of particle tracks in nuclear emulsions utilizing digitized video scan, discussing operation and instrumentation
[IEEE PAPER 2A-7] c14 A69-19185
Trapped particles drift velocity in time dependent meridional magnetic and perpendicular electric field
c25 A69-20809
PARTITIONS (MATHEMATICS)
Partition coefficients between natural melts and plagioclase phenocrysts determined for rare earth elements and barium by mass spectrometry
c13 A69-20944
PATHOLOGICAL EFFECTS
Adaptation to hypoxia, acclimatization, and conditioning in human and animal subjects from Space Biology collection
[NASA-TT-F-580] c04 N69-32131
PAYLOAD MASS RATIO
Nuclear rockets as Saturn 5 third stages, emphasizing increased payload or velocity utility and resulting engine and stage requirements
[AIAA PAPER 69-555] c31 A69-31849
PAYLOADS
Onboard SDP-3 computer data system core for IMP spacecraft, considering payload
c08 A69-13243
Manned spacecraft developments, considering Apollo Applications Program, space station establishment, space shuttle operations and payload cost
c31 A69-22866
Balloon flights with space available for secondary experiments, discussing launching agencies and experiment design restrictions
c02 A69-40807
Equation of motion for predicting dynamic behavior of parachute payload system
[NASA-TN-D-4859] c02 N69-14504
PCM TELEMETRY
PCM bit synchronizer/signal conditioners performance characteristics and specification
c09 A69-19120
Spectral null from spectral characteristics and statistical properties of PCM signals used to estimate SNR
c07 A69-19122
Ground data handling equipment characteristics for PCM telemetry link utilizing convolutional coding
c07 A69-36267
Stored program data processor used as PCM telemetry data acquisition system for postApollo applications, considering format and bit rate changes
c07 A69-36280
PEGASUS SATELLITES
Pegasus and Explorer 23 detector panels calibrated by determining particle perforation mass and velocity
[NASA-TR-R-321] c14 N69-36985
PENETRATION
Force penetration characteristics of sand horizontally penetrated by various geometrically shaped models
[NASA-CR-1252] c18 N69-14764
Containment vessel leakage due to penetrations
[NASA-TM-X-1735] c22 N69-17701
Gaseous jet interaction and penetration in supersonic flow
[NASA-CR-1386] c12 N69-32480
Penetration flux calculation for multiwall structure on Lunar Orbiter spacecraft missions
[NASA-TN-D-5455] c32 N69-41229
PEPTIDES
Substrate specificity of cathepsin C derived from rat liver, describing polymeric structure and behavior as acidic protein
c04 A69-37577
PERFORATED PLATES
Numerical analysis of shock control by using perforated walls in internal compression supersonic inlets
[NASA-TR-R-317] c01 N69-32338
PERFORMANCE
Large scale axisymmetric inlet systems performance capabilities, reviewing theoretical and experimental programs
[AIAA PAPER 68-580] c28 A69-34018
Noncavitating and cavitating performance of low area ratio water jet pumps having throat lengths of 3.54 diameters
[NASA-TN-D-5095] c03 N69-20797
Performance characteristics of 14.3 kVA modified Lundell alternator for 1200 Hz Brayton cycle space power system
[NASA-TN-D-5405] c03 N69-35537
PERFORMANCE PREDICTION
Jet pump head rise deterioration parameter for prediction of cavitation
c12 A69-15791
Performance boundaries of space propulsion systems containing nuclear electric stages
[AIAA PAPER 69-249] c22 A69-21249
SERT 2 thrustor system performance over expected mission parameters, noting operational lifetime excess over mission requirements
[AIAA PAPER 69-235] c28 A69-21255
Supersonic compressor blade sections performance prediction near maximum pressure ratio and efficiency by analyzing flow processes
[AIAA PAPER 69-522] c28 A69-32711
Nuclear powered surface effects machine performance estimates, calculating reactor power and payload fraction for various clearance heights, gross weights and velocities
c22 A69-35180
Propulsion system performance relationship to manned planetary mission capability, discussing anticipated performance of advanced propulsion concepts
c28 A69-38118
Germanium microwave backward diodes optimum design and performance prediction through computer calculation for important parameters
c09 A69-41224
Analytical method for predicting performance of centrifugal pumps during pressurized startup
[NASA-TN-D-4967] c15 N69-14082
Equation of motion for predicting dynamic behavior of parachute payload system
[NASA-TN-D-4859] c02 N69-14504
Calculating equilibrium and kinetically limited performance using one dimensional model
[NASA-TN-D-4991] c27 N69-16153
Nonequilibrium performance of oxygen difluoride diborane rocket propellant
[NASA-TN-D-4992] c27 N69-16195
Steady state airflow and afterburning performance characteristics of four J85-GE-13 turbojet engines
[NASA-TM-X-1742] c28 N69-17781
Requirement estimates and performance predictions for Martian television experiment onboard spacecraft in three point-mass descent trajectories
[NASA-TN-D-5062] c14 N69-17944
Correlation equations for predicting gas-side heat transfer of axisymmetric rocket engine nozzles
[NASA-TM-X-1748] c33 N69-18898
Dynamic analysis and maximum stepping rate prediction for permanent magnet motor
[NASA-TN-D-5094] c03 N69-20780
Design and performance prediction of calorimetric apparatus for measuring total hemispherical emittance of materials
[NASA-TN-D-5106] c14 N69-20941
Accuracy and speed comparison between drag-free and numerical satellite orbit prediction methods
[NASA-TN-D-5203] c30 N69-26252
Design effects on performance of two dimensional mixed-compression supersonic inlets with low angle cowls
[NASA-TN-D-5330] c01 N69-30060
Predicting human performance in space environments
[NASA-CR-1370] c05 N69-30168
Performance estimates of high speed peripheral jet nuclear powered ground effects machine
[NASA-TM-X-1888] c22 N69-36757
Multistage turbocompressor simulation applied to performance prediction of axial flow instabilities
[NASA-TM-X-1880] c28 N69-36998

Creep rupture data for predicting thermal fatigue cracking of turbine blades or disks
[NASA-TN-D-5489] c32 N69-39393
Performance prediction for fast reactor with axially moving reflector control system
[NASA-TM-X-1911] c22 N69-40061
PERFORMANCE TESTS
Rhenium-niobium cylindrical thermionic converters with mechanically polished or electroetched emitters, comparing performance
c03 A69-13126
Optical design of Wolter type 1 glancing incidence X ray telescope for 6-100 A wavelength region, describing results of laboratory and rocket flight tests of prototype
c14 A69-21087
Segmented anode, carbon dioxide-hydrogen performance and hollow cathode erosion tests on low power MPD arc thrustor, noting current measurements
[AIAA PAPER 69-242] c28 A69-21236
Research and development program in annular slit colloid thrustor technology, proving thrustor feasibility by performance tests
[AIAA PAPER 69-287] c28 A69-21257
Thermionic converters with chloride and fluoride vapor deposited tungsten emitters, comparing performance characteristics and stability
c03 A69-21819
Turbine stator blade performance determination from total pressure surveys downstream of blade row, noting problems in pressure measurement
[ASME PAPER 69-GT-103] c01 A69-22521
Radial inflow gas turbine engine performance testing, discussing instrumentation, recording systems and calibration techniques
[ASME PAPER 69-GT-104] c14 A69-22522
Apollo optics system ground and flight performance tests results, suggesting possible design changes for sunlit space environments
c14 A69-35796
Aerodynamic performance tests of autorotative unpowered rotor entry vehicle model at various Mach numbers and angles of attack
[AIAA PAPER 68-950] c01 A69-37155
Guidance and navigation flight tests, demonstrating system performance improvements by onboard inertial system communicating with external navigation aid
[AIAA PAPER 69-842] c21 A69-39429
Photomultiplier tubes performance enhancement by light incidence on photocathode at oblique angles explained by reflection
c23 A69-42194
Variable stator area effect on performance of single stage turbine suitable for air cooling
[NASA-TM-X-1697] c01 N69-10558
Blast shields testing
[NASA-TN-D-4894] c11 N69-10888
Design point performance of double containment tantalum and stainless steel mercury boiler for SNAP 8
[NASA-TN-D-4926] c33 N69-12739
Performance of bipropellant fractional-pound rocket thrustor
[NASA-TM-X-1699] c28 N69-13237
Performance evaluation of tandem rotor blade of single stage turbine
[NASA-CR-1254] c01 N69-13621
Performance tests of wind tunnel model inlet for bleed system back pressure and porous area effect of axisymmetric compression
[NASA-TM-X-1710] c01 N69-14075
High performance light weight electrodes for hydrogen oxygen fuel cells
[NASA-CR-1216] c03 N69-14397
Design and performance of flueric shock position sensor for mixed compression supersonic inlets
[NASA-TM-X-1733] c14 N69-16382
Experimental and analytical study of dynamics of single tube counterflow boiler
[NASA-CR-1230] c12 N69-17751
Water electrolysis rocket engine performance tests
[NASA-TM-X-1737] c28 N69-19017
Performance test from Mach 2.58 to 1.98 of axisymmetric mixed-compression inlet system with 60 percent internal contraction
[NASA-TM-X-1739] c01 N69-19130
Performance tests of SNAP 8 lubrication and cooling subsystem
[NASA-TM-X-1731] c03 N69-20828
Performance testing of SNAP 8 experimental power system
[NASA-TM-X-1732] c03 N69-20868
Flight performance of PW-4D solid propellant rocket motor on third stage of Delta 50 launch vehicle
[NASA-TN-D-4987] c28 N69-20876
Results of endurance tests of SNAP 8 turbine alternator
[NASA-TM-X-1741] c03 N69-20913
Lubrication performance and thermal shear degradation of polyphenyl ethers and refined mineral oils in high temperature vane pump loop
[NASA-TN-D-5096] c15 N69-20938
Performance of two stage axial flow turbogenerator with gas bearing rotor support system
[NASA-CR-1290] c03 N69-21771
Design and performance of gas bearing system for turboalternators
[NASA-CR-1291] c15 N69-21772
Performance and cavitation damage to axial flow pump rotor blades in high temperature liquid sodium
[NASA-TN-D-5138] c15 N69-21773
Tests of bending strength on full scale model of Atlas LV-3C booster
[NASA-TN-D-5156] c31 N69-22937
Effects of temperature and electrolyte concentration on performance of fuel cell
[NASA-TN-D-5154] c03 N69-22940
Performance tests on liquid metal pumps for sodium potassium loops
[NASA-TM-X-1765] c15 N69-22970
Wind tunnel tests of inflatable disk-gap-band and modified ringsail parachutes at low dynamic pressure
[NASA-TM-X-1786] c01 N69-23538
Load and stiffness characteristics of rotating externally pressurized air journal bearings
[NASA-TN-D-5191] c15 N69-27078
Performance of Atlas-Agena vehicle from lift off through Agena posigrade maneuver
[NASA-TM-X-1826] c31 N69-29594
Free flight performance characteristics of ram air inflated recovery balloons with peripheral airscoops
[NASA-TN-D-5186] c21 N69-29595
Performance of gas bearing Brayton cycle turboalternator
[NASA-TM-X-1820] c03 N69-29707
Performance tests on dynamic jettison hinge loads of Centaur nose fairing
[NASA-TM-X-1821] c32 N69-29734
Outdoor high temperature corrosion tests for aluminum alloys and titanium alloys, and stainless steels
[NASA-TN-D-5362] c17 N69-32558
Performance of turbine driven V/STOL cruise fan propulsion system at subsonic Mach numbers
[NASA-TN-D-5314] c28 N69-35526
Design, development, and testing of 1000 pound thrust FLOX-propane ablative rocket engine
[NASA-TM-X-1873] c28 N69-35847
Performance tests of jet flapped blade in six blade annular cascade
[NASA-CR-1423] c28 N69-36680
Performance of two electron bombardment thrusters with axial magnetic field and superimposed cusp magnetic field
[NASA-TN-D-5448] c28 N69-36844
Jet velocity and axial location of nozzle exit on performance of twin-jet afterbody model
[NASA-TN-D-5393] c28 N69-36932
Thermal, acoustical, and acceleration environments of XB-70 airplane crew compartment in airworthiness tests
[NASA-TN-D-5449] c25 N69-38010
Derivation of transfer function for optical system relating image intensity to spatial autocorrelation
[NASA-CR-1443] c21 N69-38041
Stator performance with cooling by air ejection from trailing edges of blades
[NASA-TM-X-1901] c03 N69-39335
Performance of radiation cooled magnetoplasmadynamic arc thrustors

[NASA-TM-X-1908] c28 N69-40058
Outlet annulus area blockage configuration effects on performance of axial flow compressor rotor
[NASA-TN-D-5506] c28 N69-40078
PERIODIC FUNCTIONS
Numerical analysis of periodic solutions of restricted three body problem in sun-Jupiter system, noting genealogy of periodic orbits
c30 A69-19874
Generalized averaging method for linear differential equations with almost periodic coefficients
[NASA-TN-D-5167] c19 N69-22988
PERIODIC VARIATIONS
Interplanetary sector structure during rising portion of 1966-1967 sunspot cycle, giving recurrence period of interplanetary field
c30 A69-28957
Periodicity of magnetothermal oscillations in pressure annealed pyrolytic graphite compared with hole carriers
c26 A69-29005
Twenty year wave in diurnal anisotropy component of galactic cosmic rays arriving at earth from asymptotic direction east of sun interpreted as magnetic reconnection
c29 A69-38098
Individual properties of RR Lyrae stars
[NASA-TT-F-562] c30 N69-27169
Statistical analysis of satellite position with tracking error inclusion
[NASA-TN-D-5259] c30 N69-30611
PERIPHERAL JET FLOW
Nuclear powered surface effects machine performance estimates, calculating reactor power and payload fraction for various clearance heights, gross weights and velocities
c22 A69-35180
Performance estimates of high speed peripheral jet nuclear powered ground effects machine
[NASA-TM-X-1888] c22 N69-36757
PERISCOPES
Indirect optical viewing system in F-104B for simulated lifting-body approach and landing tasks
[NASA-TN-D-5299] c14 N69-29730
PERMALLOYS (TRADEMARK)
Transformer for unilateral energy transfer using single domain uniaxial Permalloy film
c09 A69-39454
PERTURBATION
Thermal neutron flux perturbations in cylinders in test reactors, using regression analysis to obtain polynomials for flux perturbation, depression, self shielding factors, etc
c22 A69-38274
Prediction of thermal neutron flux perturbation effects in cylinders during irradiation tests
[NASA-TN-D-4949] c22 N69-14481
Technique for dynamically calibrating turbine flowmeters for small perturbations by means of frequency response tests
[NASA-TM-X-1736] c14 N69-17702
Characterization of pressure perturbations induced in rocket combustor by machine gun
[NASA-TN-D-5214] c33 N69-24824
PERTURBATION THEORY
Hansen planetary theory basic function, discussing perturbations expansion into trigonometric series
c30 A69-13781
Atomic Li photoionization cross sections calculated with Brueckner-Goldstone many body perturbation theory
c24 A69-17134
Spacecraft optimum low thrust trajectory analyzed by Hamilton-Jacobi perturbation theory, obtaining canonic constants of motion
c30 A69-17574
Boussinesq approximation for compressible fluids, discussing perturbation pressure and velocities and vertical scale motions
c12 A69-26013
Atmospheric ozone vertical distribution and total amount determined by radiative transfer and perturbation theory, presenting error analysis
c13 A69-28493
Correction and calculation methods for second and first order Plutonian perturbations with respect to perturbing masses, and new Pluto elements
[NASA-TT-F-491] c30 N69-14943
Correction and calculation methods for first order Plutonian perturbations with respect to perturbing masses
[NASA-TT-F-490] c30 N69-14944
Semianalytic theory for lunar satellite motion including perturbative effects
[NASA-TN-D-5043] c30 N69-28050
PETROGRAPHY
Chemical analysis and paragenesis of manganoan ilmenite from Sierran adamellite using electron microprobe
c13 A69-35977
PETROLOGY
Hydration, oxidation, and origin of calc-alkali differentiation series of igneous rocks
[NASA-TN-D-5400] c13 N69-40893
PHASE COHERENCE
Split phase PCM code modulated carrier transmission characteristics determined for amplitude, phase and frequency shift keying, assuming random bit pattern and noncoherent modulation
c07 A69-39451
PHASE DIAGRAMS
Fe-Ni-P phase diagram studies applied to schreibersite and rhabdite formation in iron meteorites
c30 A69-36132
PHASE LOCK DEMODULATORS
Phase-lock loop demodulator ability to acquire and remain locked on signal under noise and pulse interference
c10 A69-42230
PHASE MODULATION
Sinusoidal phase modulation role in spectral broadening observed in trapped filaments of laser and Raman light
c16 A69-14189
Subcarrier phase modulated single sideband sinusoidal carrier synthesis, discussing signal power ratios, signal efficiency, design sensitivity, etc
c07 A69-29489
PHASE SHIFT KEYING
Split phase PCM code modulated carrier transmission characteristics determined for amplitude, phase and frequency shift keying, assuming random bit pattern and noncoherent modulation
c07 A69-39451
Optimum design of binary phase shift keyed communication links with noisy phase reference
[NASA-TN-D-4895] c07 N69-13155
PHASE TRANSFORMATIONS
Polymer glasses low temperature transitions, relating structure and transition temperature
c06 A69-16493
Sigma phase formation and its effect on stress rupture properties of nickel base alloy IN-100
[NASA-TN-D-5185] c17 N69-23465
PHASE VELOCITY
Axial waves in blood vessels, determining phase velocities and damping, noting anisotropic behavior of artery wall
[SESA PAPER 1350] c04 A69-19726
PHASED ARRAYS
Gain measurement of two element phased array aperture antenna during ATS-C tracking
c07 A69-36254
PHENOLIC RESINS
Ablative effectiveness of low density phenolic nylon materials
[NASA-TN-D-5257] c33 N69-28440
PHENOLS
RAM-CA carbon-phenolic heat shield test in rocket engine exhaust
[NASA-TM-X-1841] c31 N69-32713
PHENYLS
Free lysine and dinitrophenyl /DNP/ derivatives determined quantitatively by ion exchange chromatography
c06 A69-33651
Compensatory hypertrophy effects on adrenal phenylethanolamine n-methyl transferase /PNMT/ activity in rats
c04 A69-41404

PHOEBUS NUCLEAR REACTOR
Comparison of predicted nozzle coolant side heat transfer and fluid flow with experimental values from Phoebus 2A nuclear tests
[NASA-TM-X-1881] c33 N69-36806
PHONONS
Phonons, electrons and protons in ferro-paraelectrics and hydrogen bonded ferroelectrics, examining higher frequency optical and lower frequency dielectric properties
c26 A69-32262
PHOSPHATES
Uranyl ions interaction with phospholipid and cholesterol monolayers, using surface pressure and potential measurements
c06 A69-25641
PHOSPHORS
Superlinear and sublinear phosphors combined for producing single gun color cathode ray tubes
[NASA-CR-1228] c09 N69-14256
PHOTOCONDUCTIVITY
Current oscillations in semiinsulating O and Cr doped GaAs samples at room temperature, noting photoconductivity excitation spectra
c26 A69-21753
PHOTODECOMPOSITION
Photodegradation of organic polymers by UV radiation exposure, emphasizing polyvinyl chloride photochemistry and radiation stabilization
c18 A69-10861
PHOTODISSOCIATION
Primary processes leading to atomic and molecular hydrogen formation in hydrogen peroxide photolysis at 1236 A, noting OH formation
c06 A69-23527
Positively charged diatomic hydrogen molecules interstellar extinction and photodissociation cross section in terms of formation mechanisms
c30 A69-42610
PHOTOELECTRIC EFFECT
Alloying pairs of metal pellets to n and p type semiinsulating GaAs, discussing photo effects
c26 A69-32824
PHOTOELECTRIC EMISSION
Observation of photocurrents generated in Schottky barrier diodes on barium titanate, suggesting practical utility of photon-to-electron conversion efficiencies
c09 A69-18905
PHOTOELECTRICITY
Photoelectronic commutation by dc torquer-driven reaction wheel for spacecraft attitude control
[NASA-TN-D-5265] c03 N69-30945
PHOTOELECTRONS
Auger and photoelectron spectroscopy for chemical analysis, noting effects of sample thickness, sample potential, surface contamination and X ray incident angle
c06 A69-19775
Satellite measurements of suprathermal electrons at conjugate sunrise, indicating photoelectron escape from production level and movement along geomagnetic lines into conjugate ionosphere
c29 A69-25144
PHOTOGRAMMETRY
Photogrammetry - Conference, Washington, D.C., March 1969
c14 A69-34334
NASA photogrammetric lunar activities, discussing imagery and control data by Lunar Orbiter and photogrammetric data reduction for preparing manned lunar landing
c14 A69-34336
Heights of cloud bases and convective cloud tops determined by stereoscopic photogrammetry of Apollo 6 mission
c20 A69-36926
NASA lunar survey and mapping for generating Apollo satellite landing navigation control, using analytic photogrammetry, camera position and altitude data of lunar topography
c14 A69-36931
Photogrammetric camera system developed from NASA requirements to document lunar surface environment during manned space flight exploration
c14 A69-40989
PHOTOGRAPHIC EQUIPMENT
Photographic control system requirements for Project Apollo manned launches, considering extreme heat, vibration and sound pressure environment
[SMPTE PAPER 104-20] c14 A69-14360
PHOTOGRAPHIC FILM
Design, fabrication, assembly of planetary film reconnaissance system
[NASA-CR-1358] c14 N69-28023
PHOTOGRAPHIC MEASUREMENT
Photographic control system requirements for Project Apollo manned launches, considering extreme heat, vibration and sound pressure environment
[SMPTE PAPER 104-20] c14 A69-14360
Picosecond light pulse measurement by two photon excitation of photographic film
c14 A69-20165
Image converter camera and astronomical telescope arrangement for photographing metal diaphragm openings in shock tube
c14 A69-37227
Determination of meteoroid environments from photographic meteor data
[NASA-TR-R-322] c30 N69-39336
PHOTOGRAPHIC RECORDING
Holographic displays using ultrasonic vibrations or laser outputs as optical sources, discussing recording materials, responses and computer applications
c14 A69-21394
Optical system for recording Schlieren images with continuous writing, ultrahigh speed framing camera
[NASA-TN-D-4986] c14 N69-15381
Tuft-grid photographic survey of flow field about low speed Delta wings
[NASA-TN-D-5045] c01 N69-19027
Photographic study of bromine jet flowing in coaxial airstream and impinging on stagnation surface
[NASA-TN-D-5209] c12 N69-24800
Conference on motion degraded images and correcting procedures - optical filters and digital methods for blurring removal from photographic imagery
[NASA-SP-193] c14 N69-33322
PHOTOGRAPHS
Color photographs of earth surface taken during Gemini flights 6 through 12
[NASA-SP-171] c14 N69-28909
PHOTOGRAPHY
Flash X ray unit with special film transport devices to obtain sequenced dynamic radiographs of ablating models during reentry simulation tests
c11 A69-35720
Weighting factor for correction of photographic bias caused by variation in mass and velocity of sporadic meteoroids
[NASA-TN-D-5245] c30 N69-26239
PHOTOINTERPRETATION
Day sky brightness at altitude above 100 km obtained during rocket flight compared to night sky viewed from ground
c30 A69-33664
Multispectral orbital photography used to obtain urban land-use data
[AAS PAPER 69-483] c13 A69-42837
PHOTOIONIZATION
Atomic Li photoionization cross sections calculated with Brueckner-Goldstone many body perturbation theory
c24 A69-17134
Rational approximation for coefficients used in calculating hydrogenic photoionization Gaunt factors
c24 A69-20153
Use of photoionization in measuring velocity profile of free stream flow in expansion tube
[NASA-TN-D-4936] c12 N69-13945
PHOTOLYSIS
Primary processes leading to atomic and molecular hydrogen formation in hydrogen peroxide photolysis at 1236 A, noting OH formation
c06 A69-23527
PHOTOMICROGRAPHY
Impact crater cross section in fused silica,

describing photomicrographic technique for distinguishing hypervelocity from low energy impacts
[AIAA PAPER 69-367] c32 A69-28299
Micromation and micrographics, discussing nonimpact printing in computer avoiding output imbalance by high speed microfilm recorder c34 A69-35059

PHOTOMULTIPLIER TUBES
Photomultipliers response to energetic particles in terms of background current using data from OGO experiments c14 A69-16932
Color coded area sensitivity maps of photomultiplier tubes by multicolor display technique, noting focus electrode voltage c14 A69-35724
Photomultiplier tubes performance enhancement by light incidence on photocathode at oblique angles explained by reflection c23 A69-42194
Degradation of multiplier phototubes exposed to spatial radiations
[NASA-CR-1304] c14 N69-20777

PHOTON BEAMS
Theoretical feasibility of detecting laser radiation scattered from plasma
[NASA-TN-D-5311] c25 N69-36939

PHOTONS
Photon bunching effect in spatially coherent noise field enhanced by superposing monochromatic coherent signal and/or shaping incident noise spectra c07 A69-31694
Two photon decay of metastable levels of hydrogenic and He-like ions in solar corona, depopulating via proton collisional excitation to 2p level c29 A69-36218
Transport study of neutron and photon attenuation through lithium hydride and tungsten spheres
[NASA-TN-D-4989] c24 N69-15375
Fabrication and testing of lithium-drifted detectors as low energy photon spectrometers
[NASA-TN-D-5056] c24 N69-19828

PHOTORECONNAISSANCE
Design, fabrication, assembly of planetary film reconnaissance system
[NASA-CR-1358] c14 N69-28023

PHOTOSENSITIVITY
Color coded area sensitivity maps of photomultiplier tubes by multicolor display technique, noting focus electrode voltage c14 A69-35724

PHOTOSPHERE
Photospheric radiation field role in temperature inversion of stellar chromospheres with dominant H ion opacity, postulating mechanical energy dissipation c30 A69-38173

PHOTOSYNTHESIS
Dual beam white or nearly monochromatic light source providing programmed repetitive sample illumination with variable intensity, pulse duration and sequence for photosynthesis research c14 A69-36378

PHOTOVISCOELASTICITY
Photoviscoelastic method for stress analysis of two dimensional viscoelastic models
[NASA-CR-1289] c32 N69-17770

PHOTOVOLTAGES
Cadmium sulfide films with larger than bandgap photovoltages, analyzing photovoltage decay and temperature and light intensity effects c26 A69-17772

PHOTOVOLTAIC CELLS
Photovoltaic solar cell power technology application to space use and exploration
[ASME PAPER 68-WA/SOL-1] c03 A69-16158
Red, blue and no bias light effects on spectral response of copper sulfide-cadmium sulfide cell, using model incorporating photoconductive layer c26 A69-16358
Radiation damage and recovery of lithium-diffused silicon p-n solar cells, measuring photovoltaic parameters as function of gamma radiation fluence c03 A69-35694

PHOTOVOLTAIC CONVERSION
Photovoltaic properties of CdS thin film solar cells and silicon cells at Jupiter temperature and solar intensity c03 A69-13076
Advanced reconnaissance electric planetary spacecraft /AREPS/ concept for repeated coverage of Mars or Venus surface, using solar-photovoltaic system
[AIAA PAPER 69-253] c30 A69-21244
Liquid mercury cathode thrustors characteristics satisfying constraints imposed by solar flux variations with distance from sun
[AIAA PAPER 69-237] c28 A69-21246

PHOTOVOLTAIC EFFECT
Photovoltaics - IEEE Conference, Pasadena, November 1968 c03 A69-35678

PHYSICAL EXAMINATIONS
NASA Lunar Receiving Laboratory functional areas and physical, chemical, biological and quarantine activities for crew and lunar samples c11 A69-38896

PHYSICAL EXERCISE
Exercise prescription for hypokinetic airline pilots to prevent physiological deterioration and maintain performance, discussing predictive tests, tolerance evaluation, training regimens, etc c05 A69-41800

PHYSICAL PROPERTIES
Physical model for plasma containment simulation in magnetic fields
[NASA-TN-D-5217] c25 N69-25394
Physical, mechanical, and electrical properties of 55-Nitinol - nickel-titanium alloy
[NASA-CR-1433] c17 N69-36367
Physical properties of Martian atmosphere using solar occultation seen from artificial satellite
[NASA-TN-D-5443] c30 N69-38658
Physical density and enzyme activity in coacervate biogenic molecular compounds
[NASA-TT-F-525] c04 N69-40324

PHYSICS
Physics applications to earth and planetary interiors - NATO Conference, Newcastle-upon-Tyne, England, March-April 1967 c30 A69-40172

PHYSIOLOGICAL EFFECTS
Gemini and Mercury space flights medical results, summarizing physiological effects noted on body systems c04 A69-11074
Transensor implantation, sham implantation, no implantation and lighting effects on rat body composition, noting fat and water content c04 A69-26557
Light effects on circadian rhythms in monkeys, describing changes in deep body temperature and locomotor activity phase relationships c04 A69-31336
Carbon dioxide levels monitoring in spacesuit research including limits of physiological acceptability c05 A69-39170
Human responses to aerospace environment in relation to microwave, light, thermal, and ionizing radiation
[NASA-CR-1205-VOL-1] c04 N69-12434
Summary of potential adverse effects of artificial gravity and weightlessness on astronaut physiological processes and performance in aerospace environment
[NASA-TN-D-4980] c05 N69-15629
Aerospace Medicine and Biology bibliography on biological, physiological, psychological, and environmental effects on man during aerospace flight
[NASA-SP-7011/57/] c04 N69-16537

PHYSIOLOGICAL FACTORS
Space medicine to characterize nature and degree of changes in human functional capabilities due to space flight environment prolonged exposure c34 A69-36460

PHYSIOLOGICAL RESPONSES
Meaningful comparisons between single stimulus EEG records and average evoked potential c05 A69-40163

Human physiological responses to angular acceleration during breath holding, Mi, Valsalva and Meuller respiratory maneuvers in hollow spherical simulator
c05 A69-41679
Gravitational and acceleration effects on man and organisms, and biological effects of radiation
[NASA-TT-F-528] c05 N69-38701

PHYSIOLOGICAL TESTS
Exercise prescription for hypokinetic airline pilots to prevent physiological deterioration and maintain performance, discussing predictive tests, tolerance evaluation, training regimens, etc
c05 A69-41800
Suitability of white rats for suborbital studies of behavior in gravity fields
[NASA-CR-1255] c05 N69-14094

PIEZOELECTRIC GAGES
FM/AM telemetry circuits with three axis piezoelectric accelerometer for measurements during impact tests of soft landing models
c07 A69-23279

PIEZORESISTIVE TRANSDUCERS
Simplified theory and transducer potentialities of pinch effect in semiconductors
[NASA-TN-D-5130] c26 N69-22573

PIGMENTS
Test program simulating solar wind outside magnetosphere to evaluate high melting point high density ceramic oxides as white thermal control coating pigments
[AIAA PAPER 69-641] c18 A69-33762
Meteorites pigments identification as porphyrins for extraterrestrial life evidence, noting sample analyses of Orgueil, Murray, Cold Bokkeveld and Mokoia carbonaceous chondrites
c30 A69-39889

PILOT PERFORMANCE
Error reduction in identifying pilot describing function from flight test data by shifting input signal by pilot delay time in simulated computer model
c05 A69-11950
Landing performance in T-33A aircraft with loss of binocular vision compared to performance with both eyes
c05 A69-41675
Exercise prescription for hypokinetic airline pilots to prevent physiological deterioration and maintain performance, discussing predictive tests, tolerance evaluation, training regimens, etc
c05 A69-41800
Pilots and flight simulator used in study of human visual sampling study
[NASA-CR-1258] c05 N69-14145
Peripheral vision displays for presenting dynamic control information
[NASA-CR-1239] c05 N69-14478
Measurement of pilot describing functions in single controller multiloop tasks
[NASA-CR-1238] c05 N69-15372
Human transfer characteristics in flight and ground simulation for roll tracking task
[NASA-TN-D-5007] c05 N69-17814
Pilot rating scales and their use in assessing aircraft handling qualities
[NASA-TN-D-5153] c02 N69-22539
Indirect optical viewing system in F-104B for simulated lifting-body approach and landing tasks
[NASA-TN-D-5299] c14 N69-29730
Human transfer functions applied in systems analysis of manually controlled lunar landing simulator
[NASA-TN-D-5478] c05 N69-39183

PILOTS (PERSONNEL)
Evaluation of pilot describing function method applied to manual control analysis of large flexible booster in Saturn 5 launch vehicle simulator
[NASA-TN-D-5149] c21 N69-22996
Problem of identifying input-output of pilot by measuring data from flight tests with pilot providing feedback control
[NASA-TN-D-5127] c05 N69-23842
Development of optical pilot warning indicator system for aircraft detection
[NASA-TN-D-5174] c14 N69-27267
Pilot ratings of lateral directional handling for wide range of aircraft characteristics - graphs
[NASA-TN-D-5358] c02 N69-35762
Aviation pilot reactions and opinions on grooved runways
[NASA-CR-1428] c02 N69-35861

PINCH EFFECT
Simplified theory and transducer potentialities of pinch effect in semiconductors
[NASA-TN-D-5130] c26 N69-22573

PION BEAMS
Origin of galactic gamma rays, discussing evidence in support of interstellar gas in galactic disk and production of neutral pions and bremsstrahlung
c29 A69-32806

PIONEER PROJECT
Interplanetary Pioneer spacecraft development and systems engineering aspects
c31 A69-17605
Pioneer F/G mission to Jupiter by NASA for exploring interplanetary medium, asteroid belt, planet and environment
[AAS PAPER 69-290] c30 A69-42863
Monograph on Pioneer spacecraft program, discussing mission objectives, spacecraft design, etc
[AAS PAPER 69-066] c30 A69-42883

PIONEER SPACE PROBES
Magnetospheric plasma probe results with Pioneer 6 and 7, discussing plasma fluctuations and solar wind interaction with geomagnetic field
c13 A69-19364
Monograph on Pioneer spacecraft program, discussing mission objectives, spacecraft design, etc
[AAS PAPER 69-066] c30 A69-42883

PIONEER 8 SPACE PROBE
Cosmic dust sensor experiment on Pioneer 8 space probe
[NASA-TN-D-5267] c30 N69-31058

PIONEER 9 SPACE PROBE
Pioneer 9 deep space probe with telemetry link operated in coded mode with sequential decoding, discussing ground and flight test data
c07 A69-42522

PIONS
Radioactive decay of neutral pions generated in metagalactic cosmic ray interactions as source of high energy isotropic gamma rays observed by OSO-3
c29 A69-12092
Cosmic gamma rays spectrum from neutral pions production and decay in metagalactic cosmic ray p-p collisions, deriving models based on Einstein general relativity theory
c29 A69-40641

PIPE FLOW
Turbulence measurements and roughness effects on viscous drag reduction with polymer solution in pipe flow, discussing friction factor, wall velocity profile, etc
c12 A69-33252
Concentration, flow rate and tube diameter effects on viscous drag reduction in nonpolar soap solutions, using pressure drop measurements to observe turbulent flow behavior
c12 A69-33253
Cylindrical bubbles stability in vertical pipes from photographs, describing wake, spacing, pressure pulsations and convection cells effects
[ASME PAPER 69-HT-28] c33 A69-43540
Film-nucleate boiling transition for liquid nitrogen in vertical forced flow in electrically heated tube, discussing conduction model and agreement with visual experiment
[ASME PAPER 69-HT-26] c33 A69-43542
Effects of aerodynamic forces on jet engine noise from rigid flow spoilers
[NASA-CR-1340] c23 N69-26307

PIPES (TUBES)
Use of photoionization in measuring velocity profile of free stream flow in expansion tube
[NASA-TN-D-4936] c12 N69-13945
Impact energy absorbing strut using tube cutting
[NASA-TN-D-4941] c32 N69-14506
Mechanical properties and column behavior of thin wall beryllium-aluminum alloy tubing

[NASA-TN-D-5145] c17 N69-23004
Subsonic expansion tube evaluation as device for studying particle drag in subsonic compressible slip flow
[NASA-CR-1354] c11 N69-28095
Structural response of tubular beryllium and beryllium aluminum alloy truss-type structures to dynamic and static loads
[NASA-TN-D-5254] c32 N69-28658
Burst testing of tungsten tubing at high temperatures
[NASA-TM-X-1843] c17 N69-31889

PISTONS
Fast response electrohydraulic valve-controlled piston servo systems
[NASA-TN-D-5388] c03 N69-34652

PITCHING MOMENTS
Aerodynamics of bodies of revolution in nonplanar motion using nonlinear functional analysis of moments for motion about center of gravity
[AIAA PAPER 68-20] c01 A69-14714

PITOT TUBES
Supersonic Preston tube correlations for Mach number and Reynolds number effects on hypersonic turbulent skin friction on adiabatic surfaces, simplifying correlation
[AIAA PAPER 69-345] c12 A69-28280
Baronti-Libby transformation and Preston tube calibrations used to determine skin friction from turbulent velocity profiles
[NASA-TN-D-4853] c12 N69-10472

PITUITARY GLAND
Identity between growth hormone degrading activity of pituitary gland and plasmin
c04 A69-17105
Adrenal epinephrine and phenylethanolamine n-methyl transferase /PNMT/ activity in rat bearing transplantable pituitary tumor
c04 A69-20374
Rats adrenal corticosterone concentrations changes in response to ACTH, determining response sensitivity dependence on time after hypophysectomy
c04 A69-39871

PLANETARY ATMOSPHERES
Planetary atmosphere composition determination using mass spectrometry for neutral components, ion spectrometry for ionic components and data system optimization
[AAS PAPER 68-183] c14 A69-11468
Multiple light scattering in planetary atmospheres, discussing diffuse reflection and transmission by atmosphere of particles with anisotropic scattering pattern
c30 A69-12105
Structure and mean molecular weight measurement of unknown atmosphere assessed from high altitude tests in earth atmosphere
[AIAA PAPER 68-1054] c30 A69-13699
Inverse problems in radiative transfer applied to remote measurements of IR radiation from planetary atmospheres, noting temperature and water vapor inversions
c13 A69-17617
Model ion-exosphere for nonrotating planet with static dipole magnetic field generalized by permitting density and temperature variations over baropause
c13 A69-25284
Multiple light scattering solutions accuracy by diffraction peak omission from cloud and haze analytic phase functions compared for optically thick and thin planetary atmospheres
c30 A69-33159
Ice clouds near IR spectral reflectivity dependence on particle size, noting application to planetary atmospheres
c13 A69-34283
Particle albedos and extinction cross sections computed by Mie theory showing dependence on refractivity, considering thermal radiation from cloudy planetary atmospheres
c30 A69-38255
Neutral exosphere model for nonrotating planet permitting barosphere uniform rotation at certain angular velocity, determining velocity distribution and density
c30 A69-40524
Significant achievements in space sciences for 1967, including stellar astronomy, bioscience, ionospheres, planetology, particles and fields, solar physics, and planetary atmospheres
[NASA-SP-167] c30 N69-25460
Spectral reflectance of planetary atmospheres, lunar topography, and planetary surface analyses
[NASA-TT-F-502] c30 N69-31989
Investigation of earth atmospheric composition, geomagnetism, extraterrestrial radiation, solar activity, and planetary atmospheres by satellite experiment and astronomical observations
[NASA-SP-195] c34 N69-38951

PLANETARY COMPOSITION
Mars surface photometric and spectrophotometric measurements, relating opposition effect details with corresponding laboratory sample measurements
c30 A69-18601
Chemical composition of Earth, Venus, Mars, Mercury and Moon calculated from mathematical models, constructing approximate equations of state at high pressure
c30 A69-29878
Observations and theoretical studies on Mars properties
[NASA-SP-179] c30 N69-16571

PLANETARY EVOLUTION
NASA Planetary Exploration Program to gather data on origin of solar system and life, discussing planetary evolution and extraterrestrial life
c04 A69-12804
Possible evolution of earth continents and ocean basin, considering ultrabasic, basic, and intermediate to acidic lunar highlands chemical composition
c30 A69-17006
Resonant spin and anomalous rotation of Mercury, analyzing influence of tidal degradation and permanent deformation of planet
c30 A69-39568
Cosmological forces in planetary evolution
[NASA-TT-F-532] c13 N69-28983

PLANETARY LANDING
Longitudinal range dispersion of unmanned Mars landers using VM-8 and VM-9 atmospheric models, discussing Syrtis Major as possible landing site
c30 A69-12390
Entry and terminal deceleration systems for unmanned Martian landers, discussing parachute landing and lifting entry vehicles
[AIAA PAPER 68-1147] c31 A69-13670
Research problems in atmospheric entry and landing of manned planetary space flights to Mars and Venus
[NASA-TN-D-4977] c31 N69-15634
Optimizing spacecraft televisions for successive picture overlapping and maximum surface resolution during planetary descent
[NASA-TN-D-5061] c14 N69-17259
Manned space flight capabilities for lunar and planetary explorations and earth orbiting stations
[NASA-SP-196-VOL-1] c34 N69-22510

PLANETARY MAGNETIC FIELDS
Model ion-exosphere for nonrotating planet with static dipole magnetic field generalized by permitting density and temperature variations over baropause
c13 A69-25284
Orbital Experimental Capsule /OEC/ as subsatellite concept for Martian fields and particles measurements, noting Voyager exploring vehicle applications
c30 A69-39215
Strength and direction data on earth and extraterrestrial magnetic fields for guidance in vehicle design
[NASA-SP-8017] c31 N69-40269

PLANETARY MASS
Correction and calculation methods for second and first order Plutonian perturbations with respect to perturbing masses, and new Pluto elements
[NASA-TT-F-491] c30 N69-14943
Correction and calculation methods for first order Plutonian perturbations with respect to perturbing masses
[NASA-TT-F-490] c30 N69-14944

PLANETARY NEBULAE
Thermal and free-free emission from planetary nebulae based on graphite grain model, discussing IR fluxes
c30 A69-27158
Nebulosity around FG Sagittae for origin and evolution of planetary nebulae, suggesting ejection of nebular shell
c30 A69-42887
PLANETARY ORBITS
Numerical analysis of periodic solutions of restricted three body problem in sun-Jupiter system, noting genealogy of periodic orbits
c30 A69-19874
Analytical evaluation of space storable propellants for unmanned Jupiter and Saturn orbiter missions
[NASA-TM-X-1793] c31 N69-24942
Direct and indirect planetary perturbation effects on motion of natural satellites
[NASA-TN-D-5284] c30 N69-37893
PLANETARY RADIATION
Working breadboard model of planet tracker under various illuminating conditions, discussing hardware and closed loop tracking error analysis accounting for signal to noise effects
c21 A69-13214
Visual ashen light observation on Venus possibly attributable to solar particle bombardment from dark side emission detection by spectroscopic and photometric studies
c30 A69-32300
Orbital Experimental Capsule /OEC/ as subsatellite concept for Martian fields and particles measurements, noting Voyager exploring vehicle applications
c30 A69-39215
PLANETARY ROTATION
Model ion-exosphere for nonrotating planet with static dipole magnetic field generalized by permitting density and temperature variations over baropause
c13 A69-25284
Resonant spin and anomalous rotation of Mercury, analyzing influence of tidal degradation and permanent deformation of planet
c30 A69-39568
PLANETARY SURFACES
Hard space suit for use on planetary surfaces and extravehicular activity, discussing design, fabrication and mobility
c05 A69-12993
Orbit selection rules for planetary cartographic spacecraft derived from relations connecting camera angle, view field and imaging resolution
[AIAA PAPER 69-879] c21 A69-39405
Sequential analyses of planetary surface sample for extraterrestrial life detection, discussing chemistry, morphology, growth and metabolism for life attributes
c30 A69-41623
Terrain bias error analysis in pulse modulated planetary radar altimeters
[NASA-TN-D-5220] c21 N69-26195
Spectral reflectance of planetary atmospheres, lunar topography, and planetary surface analyses
[NASA-TT-F-502] c30 N69-31989
PLANETARY TEMPERATURE
Photovoltaic properties of CdS thin film solar cells and silicon cells at Jupiter temperature and solar intensity
c03 A69-13076
Scaled solar and gray-body temperature distribution models compared to determine stellar atmosphere
c30 A69-14626
Atmospheric models for exospheric temperatures of Mars and Venus based on photoionization heating efficiency
c30 A69-26020
PLANETOLOGY
Boundary conditions for theory of solar system origin, discussing planetary atmospheres, surfaces, magnetic fields, composition and early solar wind
c30 A69-36209
Physics applications to earth and planetary interiors - NATO Conference, Newcastle-upon-Tyne, England, March-April 1967
c30 A69-40172
Planetary exploration and NASA program objectives
[AAS PAPER 69-286] c30 A69-42810
PLANETS
Computer program for computation of thermal radiation heat loads and temperatures of spacecraft orbiting planets or moon
[NASA-TR-R-278] c30 N69-14428
PLASMA ACCELERATORS
Particle free path estimates for axisymmetric high specific impulse plasma accelerators, discussing collisionless plasma simulated by computer
[AIAA PAPER 69-278] c28 A69-21233
Near cathode magnetic field effect on instability in linear Hall current accelerators, using geometry of field extending from anode to cathode region
[AIAA PAPER 69-381] c28 A69-21731
Plasma accelerator with magnetic field producing divergent-nozzle effect
[NASA-TN-D-5122] c25 N69-22942
PLASMA ARC WELDING
Plasma electron beam for welding, deriving beam current from secondary emission by ion bombardment, discussing gas pressure, equipment and applications
c15 A69-35555
PLASMA COMPOSITION
High temperature properties of gases - gas dynamics, thermodynamics, and combustion physics
[NASA-TT-F-558] c12 N69-35365
PLASMA CONDUCTIVITY
Coaxial three coil probe measuring local electrical conductivity and velocity in plasma streams, discussing operations in electrolytes and axisymmetric plasma stream
[AIAA PAPER 69-327] c25 A69-28264
PLASMA CONTROL
Theoretical population inversion in decaying nitrogen plasma column free from external fields and confined motionless in circular cylinder
[AIAA PAPER 69-48] c25 A69-18145
Physical model for plasma containment simulation in magnetic fields
[NASA-TN-D-5217] c25 N69-25394
PLASMA CYLINDERS
Theoretical population inversion in decaying nitrogen plasma column free from external fields and confined motionless in circular cylinder
[AIAA PAPER 69-48] c25 A69-18145
PLASMA DECAY
Theoretical population inversion in decaying nitrogen plasma column free from external fields and confined motionless in circular cylinder
[AIAA PAPER 69-48] c25 A69-18145
PLASMA DENSITY
Plasma oscillation modes perpendicular to magnetic field used to study energy conversion by wave coupling across density discontinuity
c25 A69-20795
Theoretical feasibility of detecting laser radiation scattered from plasma
[NASA-TN-D-5311] c25 N69-36939
PLASMA DIAGNOSTICS
Electron density measurement technique for dense thick steady state plasmas using swept microwave interferometer
c25 A69-12349
SERT 2 mercury vapor fed hollow cathode operated in bell jar, determining volt-ampere characteristics and flow rates for plasma diagnostics
[AIAA PAPER 69-258] c28 A69-21221
Solar wind plasma observations in geomagnetospheric wake compared at 1000 and 500 earth radii, considering ion energy spectra and geomagnetic tail
c29 A69-26943
Coupled set of differential equations describing generalized Volterra problem of conflicting populations and application to plasma oscillations
c19 A69-41260
Microwave radiometric techniques for reentry plasma measurements
[NASA-TN-D-5274] c25 N69-29600
PLASMA DIFFUSION
Quasi-linear theory of hydromagnetic waves in nonrelativistic collisionless plasma, noting

resonant diffusion effect on plasma heating mode
c25 A69-20797
Applicability and limitations of diffusive equilibrium in topside ionosphere, noting plasma density distribution along magnetic field line
c13 A69-37887

PLASMA DYNAMICS
Dynamics, stability and approach to equilibrium of bounded one dimensional collisionless plasma representing minimum energy states with nonlinear Vlasov equation solutions
c25 A69-24305
Coupled kinetic equations for inhomogeneous systems treated as simultaneous equations in time, obtaining solutions by successive approximation
c25 A69-30913
Helium-neon laser discharge with striation oscillations in relation to pressure and current
[NASA-CR-1387] c08 N69-32350
Performance of radiation cooled magnetoplasmadynamic arc thrustors
[NASA-TM-X-1908] c28 N69-40058

PLASMA ELECTRODES
Segmented anode, carbon dioxide-hydrogen performance and hollow cathode erosion tests on low power MPD arc thrustor, noting current measurements
[AIAA PAPER 69-242] c28 A69-21236

PLASMA ENGINES
Background pressure and magnetic field shape effect on MPD thrustor performance, testing radiation cooled thrustors
[AIAA PAPER 69-243] c28 A69-21239
Axial velocities in ammonia MPD thrustor exhaust by measuring Doppler shifts of spectral lines emitted by plasma constituents
c28 A69-31890
Electric propulsion systems for manned planetary exploration flights, discussing arc jet, ion and plasma engines
c28 A69-35108

PLASMA GENERATORS
Plasma generation using large V-groove cathode discharge
[NASA-TN-D-5269] c25 N69-29140

PLASMA HEATING
Collisionless plasma heating by hydromagnetic waves in solar wind
c29 A69-12714
Electron emitter cooling and plasma heating of thermionic converters noting effects of plasma density, diode spacing, etc
c03 A69-13127
Quasi-linear theory of hydromagnetic waves in nonrelativistic collisionless plasma, noting resonant diffusion effect on plasma heating mode
c25 A69-20797
Collisionless plasma heating by damping hydromagnetic waves applied to solar wind qualitative model, discussing magnetoacoustic wave energy
c30 A69-22426

PLASMA INTERACTIONS
Magnetospheric plasma probe results with Pioneer 6 and 7, discussing plasma fluctuations and solar wind interaction with geomagnetic field
c13 A69-19364
Solar plasma flow around magnetosphere, discussing plasma velocity, density and temperature and magnetic field space and time variations
c29 A69-26736
Comet interaction with solar wind, assuming field tail coupling of ionized comet material to solar wind ions
c30 A69-27817

PLASMA JETS
Frequency conversion in sheath capacitance of glow discharge plasma contained within metallic coaxial cylinders
c25 A69-14456
Doppler shift measurements of axial and rotational velocities in MPD arc, using reference lines from iron arc
[AIAA PAPER 69-110] c25 A69-18171
SERT 2 mercury vapor fed hollow cathode operated in bell jar, determining volt-ampere characteristics and flow rates for plasma diagnostics
[AIAA PAPER 69-258] c28 A69-21221
Alternating current plasma arc coaxial flow stabilization
[AIAA PAPER 68-706] c25 A69-28232
Discharge chamber plasma processes in electron bombardment ion thrustors, considering factors affecting thrustor performance
[AIAA PAPER 69-494] c28 A69-32735
Comparative evaluation of ablative materials in arc plasma jets
[NASA-CR-1207] c33 N69-14171

PLASMA LAYERS
Plasmapause and relation to ion composition in topside ionosphere, using Bohm coefficient for turbulent diffusion
c13 A69-12741

PLASMA OSCILLATIONS
Relationship between instabilities and turbulence in plasma, using spectrum of plasma fluctuations
c25 A69-13115
Plasma oscillation modes perpendicular to magnetic field used to study energy conversion by wave coupling across density discontinuity
c25 A69-20795
Rotating plasma disturbances onset in MPD arc, determining magnetic field dependence on mass flow, background pressure and propellant
[AIAA PAPER 69-232] c28 A69-21225
Electron number density LF oscillations for ionized gas identified with periodic solutions to neutral and charged particle plasma continuity equations
c25 A69-24315
LF oscillations in electron number density of ionized deuterium, Ne and He identified from particle continuity equation
c24 A69-40759
Moving striations as plasma oscillations arising from transit time delays of neutral and charged particles moving through ionized gas, using continuity equation
c25 A69-43122
Possible applications of continuity equation plasma oscillations to other periodic astrophysical phenomena
[NASA-TN-D-5078] c25 N69-19783

PLASMA PHYSICS
Characteristic time on motion of magnetic lines of force in medium with Hall effect
c25 A69-12399
Ion cyclotron wave generation in RF self sustained mode improved by installing grid structures in plasma near magnetic mirrors
c25 A69-13113
Computer experiment on 9000 particle plasma to test temporal echo theoretical prediction
c25 A69-38713
Nonthermal phenomena of astrophysics in relation to plasma physics, considering planetary and stellar regions, supernova envelopes, interstellar medium, cosmic rays, radio galaxies, etc
c30 A69-42682

PLASMA POTENTIALS
Integrated charged particle energy spectra from gridded electrostatic analyzers, relating retarding potential curve to particle floating potential, kinetic temperature, etc
c25 A69-20521
Measurement of change in plasma potential and magnetic field of hydrogen plasma impinging on magnetic dipole - simulation of solar wind-earth interaction
[NASA-TM-X-1738] c25 N69-19131

PLASMA PROBES
Explorer 35 measurements of low energy plasma in lunar orbit made by planar multigrid sensor programmed as retarding potential analyzer
c30 A69-16278
Magnetospheric plasma probe results with Pioneer 6 and 7, discussing plasma fluctuations and solar wind interaction with geomagnetic field
c13 A69-19364
Coaxial three coil probe measuring local electrical conductivity and velocity in plasma streams, discussing operations in electrolytes and axisymmetric plasma stream
[AIAA PAPER 69-327] c25 A69-28264

Refractive index computation for free electrons and neutral atoms in cesium plasma at helium neon laser wavelengths
[NASA-TN-D-5328] c25 N69-30622
PLASMA PROPULSION
Mercury ion thrusters and facilities automatic controls durability testing, discussing vacuum chamber systems, unattended operation and control
[AIAA PAPER 68-576] c11 A69-12385
Rotating plasma disturbances onset in MPD arc, determining magnetic field dependence on mass flow, background pressure and propellant
[AIAA PAPER 69-232] c28 A69-21225
Segmented anode, carbon dioxide-hydrogen performance and hollow cathode erosion tests on low power MPD arc thrustor, noting current measurements
[AIAA PAPER 69-242] c28 A69-21236
Electrothermal instabilities for explanation of MPD arc thrustor rotating spoke phenomenon, noting agreement with experimental results
[AIAA PAPER 69-231] c28 A69-21254
PLASMA RADIATION
Hydromagnetic radiation characteristics of electric and magnetic dipoles in homogeneous anisotropic cold plasma, obtaining field components and wave propagation modes
c13 A69-42905
Microwave radiometric techniques for reentry plasma measurements
[NASA-TN-D-5274] c25 N69-29600
PLASMA RESONANCE
Frequency shifts observed in Alouette 2 cyclotron harmonic plasma resonances, noting antenna length and direction
c07 A69-37892
PLASMA SHEATHS
Kinetic theory model of plasma sheath transition, analyzing sheath structure in unignited mode of thermionic converter
c03 A69-13125
Frequency conversion in sheath capacitance of glow discharge plasma contained within metallic coaxial cylinders
c25 A69-14456
Kinetic theory model of plasma sheath transition applied to sheath structure in unignited mode of thermionic converter
c03 A69-21828
Severe magnetosphere distortions in north-south direction with parallel/antiparallel magnetosheath to magnetospheric field ascribed to solar wind property changes from Explorer 12 observations
c13 A69-34947
PLASMA TEMPERATURE
Plasma temperature and ion concentration profiles determined from simultaneous measurements by Alouette 2 and Explorer 31 satellites of electron density, temperature and ion abundance
c13 A69-37896
PLASMA TURBULENCE
Relationship between instabilities and turbulence in plasma, using spectrum of plasma fluctuations
c25 A69-13115
PLASMA WAVES
Wave fields and coupling of RF power to ion cyclotron waves in finite length thermal collisional plasma column
c25 A69-13114
Collisional theory of longitudinal wave propagation for two fluid viscous ionized plasmas formulated from coupled Maxwell and Boltzmann equations
c25 A69-20796
Longitudinal plasma waves collision damping calculations using Rostoker test particle method
c25 A69-34439
PLASMA-PARTICLE INTERACTIONS
Backscattering due to collisions for electrons from emitter accelerated through positive ion sheath into plasma in thermionic diodes
c09 A69-17773
Radiation fields from energetic electron moving in helical orbit in magnetoactive plasma, using Maxwell equations
c30 A69-39965
Moving striations as plasma oscillations arising from transit time delays of neutral and charged particles moving through ionized gas, using continuity equation
c25 A69-43122
PLASMAS (PHYSICS)
Computer experiments on the microscopic behavior of one dimensional electrostatic plasma
[NASA-TN-D-4831] c25 N69-10471
Magnetic field nonuniformity and its effect on stability of theta pinch plasma
[NASA-TR-R-303] c25 N69-20997
Radio frequency induction heated plasmas with power deposition and energy removal
[NASA-CR-1312] c25 N69-22638
Semiempirical collision model for plasmas
[NASA-TR-R-310] c25 N69-23787
PLASTIC COATINGS
Plastic backing films removal from carbon electron microscope replicas by maintaining specimens in horizontal position
c14 A69-21651
PLASTIC DEFORMATION
Plastic deformation of corrosion resistant steel, CER-VIT 101, and fused silica as function of applied torsional stress
[NASA-CR-1257] c14 N69-16100
Digital computer program for analyzing elastic and plastic deformations and creep strains in solid and hollow cylindrical bodies
[NASA-TM-X-1723] c32 N69-16115
Elastic and plastic analyses of hail damage to aircraft surfaces
[NASA-TN-D-5363] c32 N69-33420
PLASTIC MEMORY
Mechanical properties associated with 55-Nitinol memory effect, presenting stress-strain and electrical resistivity as function of temperature
c17 A69-35523
Properties of irradiated polyethylene memory materials
[NASA-CR-1384] c18 N69-36762
PLASTIC PROPERTIES
Superplasticity in W-Re alloys, noting tensile properties, grain size and strain rate sensitivity for various Re contents at high temperatures
c17 A69-22990
PLASTICS
Plastics engineering - Conference, Chicago, May 1969
c18 A69-29411
Plastics applications in Apollo-Saturn 5 program, considering foam, honeycomb, conformal coatings, embedment compounds, dielectrics, damping compounds, adhesives, sealants and gaskets
c18 A69-38533
Design and construction of plastic model of prestressed segmented spherical shell
[NASA-CR-1231] c32 N69-11010
Dies for imprinting microscopic lagoon fields in plastic surfaces for use in cell and tissue culture
[NASA-TN-D-5255] c04 N69-29195
Toxicity of plastic hardware containing biological space flight experiment
[NASA-TM-X-1818] c04 N69-29723
PLATE THEORY
Statistical theories of turbulence applied to thermal convection between infinite slippery plates at large Prandtl number
c33 A69-24283
Mach 42 test measuring surface pressures, surface heat transfer rates and shock wave shapes in strong interaction regime for sharp and blunt plates
[AIAA PAPER 68-720] c01 A69-41886
PLATES (STRUCTURAL MEMBERS)
Dynamic response of uniform beams and plates exposed to sonic booms
[NASA-CR-1281] c32 N69-21403
PLATINUM ALLOYS
Emittance properties of hafnium oxide, cerium oxide, and iron titanate coatings on platinum rhodium alloy substrates
[NASA-CR-1413] c17 N69-35514
PLOTTERS
Data distortion elimination by improved

superimposing of sinusoidal audio frequency signal on dc voltage of automatic Langmuir probe second derivative plotters
c14 A69-32855
High speed printer for hard copy alphanumeric listings and digital data plots
[NASA-TN-D-5474] c08 N69-38654

PLOTTING
Numerical analysis of spiraling in ion molecule collisions with polar targets using computer plotting techniques
[NASA-TN-D-5407] c24 N69-35508

PLUG NOZZLES
Performance of 10 deg conical turbojet plug nozzle with iris primary and translating shroud for supersonic cruise applications
[NASA-TM-X-1709] c28 N69-14313
Plug and shroud geometry variables on plug nozzle performance at transonic speeds
[NASA-TN-D-5098] c28 N69-21463
Static tests of nozzle efficiency and pumping characteristics of conical turbojet plug nozzle with translating primary and secondary shrouds at Mach 0 to 2.0
[NASA-TM-X-1777] c28 N69-21648
Performance characteristics of truncated, conical plug nozzle with cylindrical outer shroud
[NASA-TM-X-1807] c26 N69-27840

PLUM BROOK REACTOR
Beryllium reflector distortion in Plum Brook Reactor due to neutron embrittlement and gas formation, noting material surveillance, replacement, etc
c22 A69-13131
Tungsten-184 used as thermal flux monitor at high temperatures in Plum Brook reactor
[NASA-TN-D-5113] c22 N69-20795
Beryllium swelling and replacement in Plum Brook reactor
[NASA-TM-X-1794] c22 N69-26233
Source and cause of fuel element fission product leakage in reactor cooling water system at Plum Brook Reactor
[NASA-TN-D-5374] c22 N69-32317
NASA Plum Brook Reactor Facility experimental program
[NASA-TM-X-1853] c22 N69-33132

PLUMES
Back flow density from jet plumes in vacuum
[NASA-TN-D-4978] c01 N69-14385

PLUTO (PLANET)
Correction and calculation methods for second and first order Plutonian perturbations with respect to perturbing masses, and new Pluto elements
[NASA-TT-F-491] c30 N69-14943
Correction and calculation methods for first order Plutonian perturbations with respect to perturbing masses
[NASA-TT-F-490] c30 N69-14944

PNEUMATIC CONTROL
Pneumatic driving system for heart assist or total replacement pumps, discussing design features and performance characteristics
c05 A69-42983

PNEUMATIC EQUIPMENT
Fluidic integrated circuits for control of pneumatic stepping-motor actuator system
[NASA-TN-D-5155] c03 N69-22896

POINT DEFECTS
Internal friction, Young modulus and resistivity measurements for stage I interstitials in electron irradiated tungsten
c17 A69-28682
Point defect calculations for tungsten
[NASA-TN-D-4918] c22 N69-13309

POINT SOURCES
Minimal angle of resolution /MAR/ between point and extended circular source and between point source and simulated horizon, studying irradiation effects on manual navigation
c21 A69-19208

POINT TO POINT COMMUNICATIONS
Lunar surface transmission loss for Apollo astronaut point-to-point communications
[NASA-TN-D-4915] c07 N69-13301

POISSON DENSITY FUNCTIONS
Huffman minimum redundancy coding extension to run-length information based on Poisson distribution, including optimization and data compression applications
c07 A69-36262

POLAR CAP ABSORPTION
Time history of July 7-10 1966 PCA event analyzed using 16 riometers and concurrent satellite observations of solar cosmic radiation
c13 A69-23770
Polar cap ionospheric response to solar cosmic ray events observed by Mariners 2 and 4 solar proton measurements used to test magnetosphere models
c29 A69-43621

POLAR COORDINATES
Numerical integration for continuously thrusting spacecraft optimal trajectory, considering rectangular Cartesian and polar cylindrical coordinates characteristics
[AIAA PAPER 69-903] c30 A69-38546
Graphic method determining sounding rocket vehicle attitude
[NASA-TN-D-5172] c30 N69-23782

POLAR GASES
Viscosity, thermal conductivity and diffusion predicted for dilute nonpolar, polar and mixed gases, discussing methods for rotational relaxation collision numbers and resonant correction
c33 A69-38951
Computer made movies and time history plots for ion-dipole collisions involving polar molecules /CO, HCL and acetonitrile/
c24 A69-43124
Rotational relaxation times for calculating rotational collision numbers in polar gases
[NASA-TN-D-5321] c24 N69-30073

POLAR REGIONS
Electron concentration enhancement in upper atmosphere at polar latitudes, noting three independent zones and relation to magnetic local time
c29 A69-28938
Magnetic storm time variations of electron concentrations in upper ionosphere near north geomagnetic pole, discussing magnetic time, altitude and latitude dependence
c29 A69-28939
Suprathermal electrons energy distributions as function of magnetic latitude in polar ionosphere obtained by Explorer 31 satellite observation
c29 A69-28963
Polar exosphere near solar maximum investigation by Explorer 19 and Explorer 24 drag satellites, considering density and atomic oxygen concentration measurements
c13 A69-31351
Ion depletion in high latitude exosphere, considering OGO 2 simultaneous observations of positive ion concentration, VLF signal propagation and whistlers
c29 A69-34939

POLARIZATION
Polarization, differential cross section, and total reaction cross section data for proton scattering
[NASA-TN-D-5067] c24 N69-22934

POLARIZATION (SPIN ALIGNMENT)
Asymmetry of polarized protons scattered from He 4 at 540 MeV for laboratory angles between 4 and 42 degrees
c24 A69-14966
Differential cross section and polarization measurements for elastic scattering of high energy protons from light nuclei
c24 A69-43125
Numerical analysis of spiraling in ion molecule collisions with polar targets using computer plotting techniques
[NASA-TN-D-5407] c24 N69-35508

POLARIZATION CHARACTERISTICS
Core polarization effects in inelastic scattering cross sections for several nuclei in 2s-1d shell, using Hartree-Fock wave functions and Born approximation
c24 A69-29007

POLARONS
Polarons large to nearly small transitions, studying ground state mass dependence on bare electron mass, electron-phonon interactions model, superconducting strontium titanate, etc

c26 A69-37280

POLYAMIDE RESINS
Ablative effectiveness of low density phenolic nylon materials
[NASA-TN-D-5257] c33 N69-28440

POLYBENZIMIDAZOLE
Low density polybenzimidazole composites as ablative heat shields, discussing arc-heated wind tunnel tests of linear and crosslinked structures
c18 A69-41715

POLYCRYSTALS
High temperature mechanical properties of polycrystalline hafnium carbide containing 13-volume-percent hafnium diboride
[NASA-TN-D-5008] c17 N69-16380
Optimal growths of silicon carbide polytype crystals by methyltrichlorosilane reduction
[NASA-TN-D-5313] c26 N69-30072

POLYETHYLENE TEREPHTHALATE
Mechanical anisotropy of polyethylene terephthalate and relation to molecular structure and cold drawing
c18 A69-16489
Film processing effects on cryogenic mechanical properties of polyethylene terephthalate
c18 A69-16490
Mechanical behavior of polyethylene terephthalate at cryogenic temperatures
c18 A69-16494
Ultrahigh molecular weight polyethylene terephthalate synthesis from commercial solid state materials, noting effects of several parameters
c24 A69-16496
Molecular orientation and mechanical isotropy in polyethylene, polypropylene, and polyethylene terephthalate films
[NASA-TN-D-5380] c18 N69-34708

POLYETHYLENES
Proton induced voltage breakdowns in polymeric materials
[NASA-TM-X-1688] c18 N69-10066
Molecular orientation and mechanical isotropy in polyethylene, polypropylene, and polyethylene terephthalate films
[NASA-TN-D-5380] c18 N69-34708
Properties of irradiated polyethylene memory materials
[NASA-CR-1384] c18 N69-36762

POLYIMIDES
Blocked polyimide precursor resistance to thermal imidization compared to polyamic acid
[NASA-TN-D-5184] c06 N69-23353

POLYISOPRENES
Geochemical synthesis of branched chain acyclic polymers from irradiated isoprene
c04 A69-43750

POLYMER CHEMISTRY
Photodegradation of organic polymers by UV radiation exposure, emphasizing polyvinyl chloride photochemistry and radiation stabilization
c18 A69-10861
Ultrahigh molecular weight polyethylene terephthalate synthesis from commercial solid state materials, noting effects of several parameters
c24 A69-16496
Geochemical synthesis of branched chain acyclic polymers from irradiated isoprene
c04 A69-43750
Syntheses and properties of pyrrone polymers
[NASA-CR-1310] c18 N69-26448

POLYMER PHYSICS
Mechanical anisotropy of polyethylene terephthalate and relation to molecular structure and cold drawing
c18 A69-16489
Polymer glasses low temperature transitions, relating structure and transition temperature
c06 A69-16493

POLYMERIC FILMS
Polymer films tensile properties after exposure to gamma radiation in vacuum, noting chain scission and cross linking
[ASME PAPER 68-WA/RP-6] c18 A69-16160
Cryogenic flexibility of thin polymeric film plies for use as spacecraft positive expulsion bladders
c15 A69-16486
Film processing effects on cryogenic mechanical properties of polyethylene terephthalate
c18 A69-16490
Plastic backing films removal from carbon electron microscope replicas by maintaining specimens in horizontal position
c14 A69-21651
Molecular orientation and mechanical isotropy in polyethylene, polypropylene, and polyethylene terephthalate films
[NASA-TN-D-5380] c18 N69-34708
Transmission effects on plastic films irradiated with ultraviolet light in vacuum
[NASA-TM-X-1905] c18 N69-40339

POLYMERIZATION
Time of heating effect on thermal polymerization of L-lysine free base
c06 A69-28439
Blocked polyimide precursor resistance to thermal imidizatiCn compared to polyamic acid
[NASA-TN-D-5184] c06 N69-23353

POLYMERS
Cryogenic properties of polymers - NASA/Case Conference, Cleveland, April 1967
c18 A69-16485
Luminescence spectra of aromatic polymers, monomers and dimers under high energy electron excitation using molecular resonance model
c26 A69-32792
Turbulence measurements and roughness effects on viscous drag reduction with polymer solution in pipe flow, discussing friction factor, wall velocity profile, etc
c12 A69-33252
Constitutive equation variation effect on near wall flow pattern of dilute polymer solutions
c12 A69-33257
Unfilled Pyrrone prepared from powder into molded parts for flexural tests at elevated temperatures observed for stability to electron irradiation in air
c18 A69-35529
Computer analysis of light scattering data from polymer sclutions
[NASA-TN-D-5177] c06 N69-22991

POLYPHENYL ETHER
Steel ball bearing high temperature fatigue life tested with synthetic paraffinic oil, fluorocarbon and polyphenyl ether
[ASME PAPER 69-LUBS-18] c15 A69-34378
Lubrication performance and thermal shear degradation of polyphenyl ethers and refined mineral oils in high temperature vane pump loop
[NASA-TN-D-5096] c15 N69-20938

POLYPROPYLENE
Molecular orientation and mechanical isotropy in polyethylene, polypropylene, and polyethylene terephthalate films
[NASA-TN-D-5380] c18 N69-34708

POLYTETRAFLUOROETHYLENE
Molecular motion in polytetrafluoroethylene crystals at cryogenic temperatures, noting crystal defect permitting angular displacements of chain segments
c24 A69-16495
Impregnation of polytetrafluoroethylene with hexaflourides of rhenium, molybdenum, and tungsten
[NASA-TN-D-4886] c06 N69-10126

POLYURETHANE FOAM
Ablative materials thermal protection characteristics at low heating rates evaluated by convective heating tests, stressing polyurethane foam composite
c18 A69-35536
Polyurethane foam composites for low heating rate thermal protection, noting astroquartz fiber additive effect on performance
c18 A69-39236
Lightweight polyurethane insulation for liquid hydrogen tanks of space vehicles
[NASA-TN-D-5114] c18 N69-20790

POLYURETHANE RESINS
Fluorinated polyurethanes synthesis for liquid oxygen environments and cryogenic structural utility, noting structural effects on LOX compatibility

c06 A69-16498
POLYVINYL CHLORIDE
Photodegradation of organic polymers by UV radiation exposure, emphasizing polyvinyl chloride photochemistry and radiation stabilization
c18 A69-10861
PONTRYAGIN PRINCIPLE
Adaptive random search algorithm utilizing boundary cost-function hypersurfaces measurement to implement Pontryagin maximum principle, discussing hybrid computer use, iterative solution and convergence properties
c08 A69-33745
POPULATION INVERSION
Theoretical population inversion in decaying nitrogen plasma column free from external fields and confined motionless in circular cylinder
[AIAA PAPER 69-48] c25 A69-18145
POROSITY
Performance tests of wind tunnel model inlet for bleed system back pressure and porous area effect of axisymmetric compression
[NASA-TM-X-1710] c01 N69-14075
POROUS MATERIALS
Flow reduction due to oxidation of wire-form porous materials for transpiration cooled turbine blades
[NASA-TN-D-5001] c17 N69-16383
POROUS WALLS
Gas core reactor curved porous walls geometry tested with clear and smoky air injection, noting mass flow ratio in reactor cavity
c22 A69-35181
Transient temperature fields in porous shell walls cooled by forced flow
[NASA-TT-F-552] c33 N69-30245
PORPHYRINS
Meteorites pigments identification as porphyrins for extraterrestrial life evidence, noting sample analyses of Orgueil, Murray, Cold Bokkeveld and Mokoia carbonaceous chondrites
c30 A69-39889
Detection and spectral examination of trace porphyrin complexes by demetallation with methanesulfonic acid and spectrofluorometry, compared to absorption spectrophotometry
c06 A69-42557
PORTABLE EQUIPMENT
Portable integrating sphere reflectometer, describing optical system, construction, etc
[AIAA PAPER 69-599] c14 A69-33264
Lithium peroxide utilization feasibility for oxygen supply and carbon dioxide control in extravehicular portable life support systems
[AIAA PAPER 69-620] c05 A69-33303
Self contained hand held battery operated aerosol particle analyzer, measuring aerosol concentration and size distribution for laboratory and space flight applications
c14 A69-34691
POSITION (LOCATION)
Plasma-pause position measurements by ion mass spectrometers and broadband VLF receivers on OGO 1 and OGO 3 and by broadband recordings at Antarctica
c13 A69-25153
Magnetic dip equator position at E layer and gradient with time and altitude, using geomagnetic field models
c13 A69-42428
GEOS 1 tracking station positions on SAO standard earth C-5 model
[NASA-TN-D-5034] c13 N69-28019
POSITION ERRORS
OMEGA position location equipment /OPLE/ test data to demonstrate feasibility of using OMEGA navigational system in conjunction with synchronous satellites
c21 A69-19135
Ionospheric irregularities effect on accurate satellite position determination in near real time
c07 A69-42549
POSITION INDICATORS
High speed compression waves, rarefaction waves and gas interface regions position and velocity measurement in shock tube by sensing electrical impedance
c14 A69-13104
OMEGA position location equipment /OPLE/ test data to demonstrate feasibility of using OMEGA navigational system in conjunction with synchronous satellites
c21 A69-19135
Electronic position indicator for latching solenoid valves in SNAP 8 ground test facility
[NASA-TM-X-1760] c14 N69-20874
POSITIONING
Potential use of satellites for enhancing positioning capabilities and for marine geodetic control
[NASA-CR-1253] c13 N69-16645
POSITIONING DEVICES (MACHINERY)
Hydraulic-powered self propelled six degree of freedom loading vehicle moving tests assembly to test chamber with high accuracy positioning
c11 A69-38181
POSITRONS
Annihilation gamma ray spectra from equilibrium spectra of secondary galactic positrons
c29 A69-29948
POSTFLIGHT ANALYSIS
Optical properties and chemical analysis of contaminants on Gemini spacecraft windows
[NASA-TN-D-4916] c31 N69-13232
Nimbus 2 flight evaluation and engineering report covering launch through orbit 5275
[NASA-TN-D-4881] c31 N69-17851
Correlation study of simulation of Gemini extravehicular activity with flight results
[NASA-CR-1146] c05 N69-19902
Systems analysis of Atlas-Centaur AC-11 flight performance for Surveyor 4
[NASA-TM-X-1768] c31 N69-21399
Postflight analysis of flight performance of Atlas Agena launch vehicle for Applications Technology Satellite ATS-2 mission
[NASA-TM-X-1800] c31 N69-27260
POTASSIUM
Work function and desorption energy measurements of alkali metals from metallic substrates with modulated molecular beam, noting surface contamination
c26 A69-21808
Evaluation of various laboratory determination of oxygen in potassium and sodium
[NASA-TN-D-4971] c06 N69-14180
POTENTIAL ENERGY
Vacancy relaxations in bcc crystals using energy dependence on radial displacements from defect of nearest neighbor sets, discussing crystal size and shape
c26 A69-16529
POTENTIAL GRADIENTS
Simplified theory and transducer potentialities of pinch effect in semiconductors
[NASA-TN-D-5130] c26 N69-22573
POTENTIAL THEORY
Adaptive simulation using modal clustering and method of potential functions
[NASA-CR-1179] c08 N69-10316
POWDER (PARTICLES)
Measurement of radiative thermal conduction of ideal powder as function of temperature
[NASA-TN-D-5063] c33 N69-20008
Extruded prealloyed powder evaluation for two nickel-base alloys
[NASA-TN-D-5248] c17 N69-26192
POWDER METALLURGY
Powder metallurgy, fusion and chemical vapor deposition techniques in manufacturing tungsten base alloys
c17 A69-18792
Yttrium effect on rate of thermal decomposition of silver carbonate powder and pressed pellets by isothermogravimetric analysis, examining water vapor, Co 60 gamma radiation and temperature effects
c06 A69-30442
Creep rate-stress-temperature relations for powder metallurgy rhenium, discussing activation energy
c17 A69-34186
H release, pressure and oxide layer formed by reaction during ball milling Cr in water
c15 A69-38567
Fabrication of cermets of uranium nitride and tungsten or molybdenum from mixed powders and

from coated particles for nuclear fuel elements
[NASA-TN-D-5136] c17 N69-21404
Dispersion strengthened nickel produced from ultrafine comminuted powders
[NASA-TN-D-5421] c17 N69-38074
POWER CONDITIONING
Modularized static ac and dc inverters and converters for aerospace electrical power conditioning systems, discussing circuit functions and performance tests
c03 A69-42292
Power conditioner for use with SERT 2 mercury ion thrustor, describing electrical and mechanical design and operation
c03 A69-42301
POWER EFFICIENCY
High voltage mercury electron bombardment ion thruster power efficiency
[ECS PAPER 170D] c28 A69-16233
Power loss experiments on herringbone grooved, gas lubricated journal bearings
[NASA-TN-D-5224] c15 N69-24932
POWER GAIN
Gain measurement of two element phased array aperture antenna during ATS-C tracking
c07 A69-36254
POWER LIMITED SPACECRAFT
Mechanics of low thrust space flight
[NASA-TT-F-507] c28 N69-33354
POWER SPECTRA
Power spectra of interplanetary magnetic field fluctuations determined from Pioneer 6 satellite data, relating results to galactic cosmic rays modulation
c30 A69-37554
POWER SUPPLIES
Magnetic core logic circuit system for bidirectional stepping motor drive voltage power supply control in proper phase and time sequence
c09 A69-11000
PRANDTL NUMBER
Statistical theories of turbulence applied to thermal convection between infinite slippery plates at large Prandtl number
c33 A69-24283
PRECIPITATION (METEOROLOGY)
Transfer of microwave radiation in atmosphere and underlying surfaces measured by aircraft instruments
[NASA-TT-F-590] c13 N69-31851
PRECIPITATION HARDENING
Effect of ultrasonic vibration on precipitation hardening of steels and superalloys
[NASA-TN-D-5131] c32 N69-21814
Dynamic strain aging during creep and tensile tests of molybdenum-titanium-carbon alloys
[NASA-TN-D-5169] c17 N69-22993
Dispersion strengthened nickel produced from ultrafine comminuted powders
[NASA-TN-D-5421] c17 N69-38074
PRECISION
Hardware-software provisions for multiple precision floating point arithmetic
[NASA-TM-X-1885] c08 N69-36918
PREDICTION RECORDING
Predictive display systems using repetitive, fast time, on-line computation
[NASA-CR-1274] c05 N69-17738
PREDICTIONS
Adaptive compression system for predicting and encoding video data for transmission in noiseless channel
c14 A69-12869
Prediction curves for launch vehicle vibration levels in region of spacecraft adaptor
[NASA-CR-1227] c31 N69-16155
Summary of random vibration prediction procedures for aerospace vehicles, with bibliography
[NASA-CR-1302] c32 N69-23096
Theory for predicting rotational and vortex noise of lifting rotors in hovering and forward flight
[NASA-CR-1333] c23 N69-25344
Prediction methods for angular line-of-sight deviations induced by spacecraft window
[NASA-TN-D-5238] c21 N69-31227
PREFLIGHT ANALYSIS
Preflight optical evaluation of right hand hatch windows in Gemini missions 7, 8, 9, and 12
[NASA-TN-D-5471] c31 N69-40813
PRELAUNCH TESTS
OGO program failure rate analysis with respect to cost, schedule and performance tradeoffs, considering component and systems design and reliability, prelaunch feedback, etc
c31 A69-34519
PRESSURE
Magnetothermal oscillations in pressure annealed pyrolytic graphite
[NASA-TN-D-5488] c26 N69-39239
PRESSURE DISTRIBUTION
Aircraft created pressure patterns responsible for sonic boom, discussing design techniques for noise reduction
c02 A69-30369
Incompressible two dimensional turbulent boundary layer equations with arbitrary pressure distribution solved by weighted residual method
[AIAA PAPER 69-397] c12 A69-30478
Flow and pressure fields for spiral grooved pumping seal with specified groove dimensions and Reynolds number
[ASLE PICFS PREPRINT 30] c15 A69-30481
Surface pressure and heat transfer over blunt conical body in hypersonic flow with uniform mass addition of various gases
[AIAA PAPER 69-716] c01 A69-33463
Equations for pressure signature of supersonic projectile in stratified atmosphere
[NASA-TN-D-4890] c02 N69-10087
Computational method for surface pressures on blunt bodies of revolution at small angles of attack in supersonic flow
[NASA-TN-D-4865] c01 N69-10215
Heat transfer and pressure distribution due to two-dimensional repetitive sine wave distortions on flat plate at Mach 20 in helium
[NASA-TN-D-4907] c12 N69-10804
Heat transfer and pressure distributions inside hinge line gap of wedge-flap combination at hypersonic speeds
[NASA-TN-D-4911] c01 N69-11009
Pressure fields and multidimensional gas flow in permeable char layers and effects on ablation
[NASA-TR-R-296] c33 N69-16181
Experimental surface pressure distributions on spherically blunted cone at Mach numbers from 1.50 to 4.63
[NASA-TM-X-1730] c01 N69-16209
Experimental pressure distributions on 120 deg cone at Mach 2.96 to 4.63 and angles of attack from 0 deg to 20 deg
[NASA-TN-D-5054] c01 N69-19826
Surface pressure distribution on spherical blunted cones, and correlation of Mach numbers, cone angle, and angle of attack
[NASA-TN-D-5204] c01 N69-24764
Initial hydrodynamic phase of hypervelocity impact analyzed by computer program using eigenvector approach
[NASA-TR-R-298] c32 N69-24765
Space suit design with pressure stabilizer for force assisted elbow joint
[NASA-TN-D-5221] c05 N69-26259
Wind tunnel tests of subsonic aerodynamic characteristics of large scale tip turbine cruise fan with 1.075 pressure ratio at angle of attack
[NASA-TN-D-5316] c28 N69-34575
Pressure distributions for blunt body wind tunnel models at supersonic speeds and angles of attack from 0 to 15 degrees
[NASA-TN-D-5392] c01 N69-35300
Pressure and heat transfer on swept Delta wing with trailing-edge flap
[NASA-TN-D-5418] c01 N69-35855
Three dimensional pressure distribution functions for lifting surfaces with trailing-edge controls based on integral equations for subsonic flow
[NASA-TN-D-5419] c01 N69-38768
Aerodynamic pressure distribution on semispan tilting wing-propeller combination of V/STOL aircraft
[NASA-TN-D-5481] c01 N69-40876
PRESSURE DRAG
Determination of drag of fabrication-type surface roughness in turbulent boundary layer at transonic speeds
[NASA-TN-D-5004] c01 N69-16460

Jet effects on boattail pressure drag of isolated ejector nozzles at Mach 0.60 to 1.47
[NASA-TM-X-1785] c01 N69-26976

PRESSURE EFFECTS
Pressure and temperature dependence of slow crack growth in hardened steel in gaseous hydrogen environment
c17 A69-10612
Cross hatching on various body surfaces due to periodic surface pressure fluctuations, discussing origin from counter-rotating longitudinal vortices in boundary layer
[AIAA PAPER 69-11] c12 A69-18213
Background pressure and magnetic field shape effect on MPD thrustor performance, testing radiation cooled thrustors
[AIAA PAPER 69-243] c28 A69-21239
Pressure and heating rate correlations for rocket exhausts impinging on flat plates and curved panels, generating axisymmetric real gas exhaust plumes
c33 A69-26781
Compression molding of molecular salt-like intermediate Pyrrone powders by two pressure method, noting volatiles elimination
c18 A69-29415
Jet engine compressor stalls in-flight investigation up to Mach 2 on F-111A by pressure sensors, noting steady state distortion role
[AIAA PAPER 69-488] c28 A69-32706
Supersonic compressor blade sections performance prediction near maximum pressure ratio and efficiency by analyzing flow processes
[AIAA PAPER 69-522] c28 A69-32711
Thermal contact resistance measurement at various ambient pressures compared with theoretical predictions with each parameter analyzed over interface by computer program
[AIAA PAPER 69-629] c33 A69-33299
Temperature and pressure effect on cobalt base alloy cavitation in liquid sodium, using vibratory apparatus and loss rate contour diagram
c17 A69-35184
Ge films formation by evaporation technique, discussing background O pressure effect
c26 A69-43345
Force penetration characteristics of sand horizontally penetrated by various geometrically shaped models
[NASA-CR-1252] c18 N69-14764
Instability of eccentrically stiffened cylindrical shells under axial compression and lateral pressure
[NASA-CR-1280] c32 N69-15378
Load and stiffness characteristics of rotating externally pressurized air journal bearings
[NASA-TN-D-5191] c15 N69-27078
Effect of temperature and pressure on cavitation damage to cobalt base alloy in sodium
[NASA-TN-D-5273] c17 N69-28863
Pressure and velocity coupling effects on combustion stability in solid propellant burning
[NASA-TN-D-5395] c33 N69-34892
Sound wave pressure for preventing cryogenic propellant sloshing during space flight
[NASA-TN-D-4024] c23 N69-38180

PRESSURE GRADIENTS
Nonsimilar laminar boundary layer solutions with negative pressure gradient compared to experimental boundary layer velocity profiles, momentum and displacement thicknesses
[AIAA PAPER 69-35] c12 A69-18094
Lower solar corona composition changes due to pressure and thermal gradients calculated with multicomponent diffusion equations
c30 A69-33059
Calculation of compressible turbulent boundary layers with pressure gradients and heat transfer
[NASA-CR-1303] c12 N69-21653
Turbulent boundary layer of subsonic transport fuselage with pressure gradient, Reynolds number, and angle of attack
[NASA-TN-D-5242] c01 N69-28112
Thermal outgassing tests on epoxy impregnated magnet coil
[NASA-TM-X-1813] c18 N69-28203
Respiratory system and oxygen metabolism regulation in man and animals
[NASA-TT-F-501] c04 N69-31401

PRESSURE HEADS
Net positive suction head requirements for helical inducer in liquid hydrogen under varied flow and temperature conditions
[NASA-TM-X-1808] c09 N69-27841

PRESSURE MEASUREMENTS
Turbine stator blade performance determination from total pressure surveys downstream of blade row, noting problems in pressure measurement
[ASME PAPER 69-GT-103] c01 A69-22521
Buried collector ionization gage for measurements in 100 billionth torr pressure range using shielded collector to lower X ray current
c14 A69-32324
Pressure and temperature surveys of Mach 27-47 nozzle boundary layer at Ames M-50 He tunnel, determining velocity profiles, wall friction coefficient, etc
[AIAA PAPER 69-686] c12 A69-33441
Pressure measurements and gas flow analysis during thermal vacuum tests of manned spacecraft indicating adequate space vacuum simulation
[AIAA PAPER 69-1033] c11 A69-40401
Variability in sonic boom signatures measured along 8000 foot linear microphone array
[NASA-TN-D-5040] c02 N69-17279
Wind tunnel force and pressure tests of rocket engine nozzle extensions on X-15-2 model at supersonic and hypersonic speeds
[NASA-TM-X-1759] c01 N69-20873
Low pressure application of orbitron and ion gage designs
[NASA-CR-1300] c14 N69-28402
Shock shape and surface pressure measurements on hypersonic pointed cones in helium
[NASA-TN-D-5343] c01 N69-31228

PRESSURE PULSES
Elastic behavior of large blood vessels in canine aorta by measuring dispersion and attenuation of artificially induced pressure waves
c04 A69-14692
Interphase momentum transfer during propagation of infinitesimal pressure pulse through bubbly flow two phase mixture
c33 A69-43511

PRESSURE REDUCTION
Concentration, flow rate and tube diameter effects on viscous drag reduction in nonpolar soap solutions, using pressure drop measurements to observe turbulent flow behavior
c12 A69-33253
Performance tests of wind tunnel model inlet for bleed system back pressure and porous area effect of axisymmetric compression
[NASA-TM-X-1710] c01 N69-14075
Computer analysis of total pressure loss and air flow distribution in annular flow gas turbine combustion chambers
[NASA-TN-D-5385] c33 N69-33314

PRESSURE SENSORS
Single channel pressure telemetry unit for chronic implantation into cardiac chambers or major blood vessels in unrestrained animals for measuring ventricular pressure
c05 A69-25642
Fixed position pressure probe for measuring subsonic flow direction over range of Reynolds number, Mach number and flow angle
c14 A69-33107
Potential electrical response of p-n junction to mechanical strain
[NASA-CR-1366] c26 N69-29724

PRESSURE SUITS
Flight test evaluation of small one man lunar flying device /POGO/, discussing vehicle control, pressure suit factors and piloting differences
[AIAA PAPER 68-240] c11 A69-12379
Relationship between binocular depth perception and optical distortion in Apollo pressure suit helmets and visors
[NASA-TN-D-5162] c05 N69-22990

PRESSURE VESSELS
Glass, boron and graphite filament wound resin composites and liners for cryogenic pressure vessels
c18 A69-16488

High pressure storage vessels for gaseous hydrogen, discussing failure, manufacturing controls and access for internal nondestructive inspection
[ASM PAPER D8-14.1] c15 A69-19666
Graphite fiber NOL rings and biaxial wound pressurized cylinders tested at ambient and cryogenic temperatures for tensile and cyclic fatigue properties
c18 A69-35521
Radius effect on bulging and fracture of through-cracked cylindrical pressure vessels at cryogenic temperatures
[NASA-TN-D-4951] c32 N69-14480
Containment vessel leakage due to penetrations
[NASA-TM-X-1735] c22 N69-17701

PRESSURIZING
Ramp pressurization tests with gaseous helium in thick walled liquid hydrogen tank
[NASA-TM-X-1870] c28 N69-35712
Helium pressurization systems for liquid methane fuel in supersonic transports
[NASA-TN-D-5519] c28 N69-40329

PRESTRESSING
Design and construction of plastic model of prestressed segmented spherical shell
[NASA-CR-1231] c32 N69-11010

PRIMARY COSMIC RAYS
Energy spectra of carbon and oxygen nuclei in primary cosmic radiation, comparing results to earlier measurements and satellite observation
c29 A69-20632
Primary cosmic ray nuclei studies during Gemini 2 flight by nuclear emulsion detector with time resolution capability, describing experiment design and equipment operation
c29 A69-38350

PRIMATES
Circadian rhythms in nonhuman primates - Conference, Atlanta, July 1968
c04 A69-42701

PRINTERS (DATA PROCESSING)
Alphanumeric listing and digital data x-y plotting by high speed printer, describing equipment modifications and control software
c08 A69-33108
Micromation and micrographics, discussing nonimpact printing in computer avoiding output imbalance by high speed microfilm recorder
c34 A69-35059
High speed printer for hard copy alphanumeric listings and digital data plots
[NASA-TN-D-5474] c08 N69-38654

PRINTOUTS
FORTRAN 4 subroutines to generate printed plots as normal output
[NASA-TM-X-1700] c08 N69-13566

PROBABILITY DENSITY FUNCTIONS
Statistical method for evaluating goodness of fit between data set and theoretical distribution of random variables
[NASA-TR-R-313] c19 N69-30610

PROBABILITY DISTRIBUTION FUNCTIONS
Recursive equation for estimating variance of sequential random numbers
[NASA-TN-D-5465] c19 N69-38178

PROBABILITY THEORY
Evaluation method for strapdown spacecraft guidance systems on automated interplanetary missions, using cost and system performance efficiency probability model
[AIAA PAPER 68-828] c21 A69-35953
Log-a-posteriori probability metric for use in sequential decoding
[NASA-TN-D-4930] c07 N69-23163
Probability calculations for fuel clad surface temperatures of nuclear reactors
[NASA-TM-X-1802] c22 N69-26231
Statistical effects of wind and atmospheric turbulence on launch vehicles
[NASA-CR-1410] c20 N69-35570

PROBLEM SOLVING
Practice and operator work load effects on acquisition and performance of code transformation /COTRAN/ task
[NASA-CR-1261] c05 N69-14345
Nonlinear compressible flow problems - half-space of ideal compressible fluid motion due to arbitrary pressure front
[NASA-TT-F-560] c12 N69-27168
Analytical solutions of optimum orbit modifications
[NASA-CR-1379] c30 N69-31362
Chebyshev series solution of nonlinear ordinary differential equations - initial value problems
[NASA-TM-X-1882] c19 N69-36923

PRODUCT DEVELOPMENT
Development and test firing of improved igniter for first stage retrorockets of Atlas Centaur launch vehicle
[NASA-TM-X-1676] c28 N69-13275
Disk radiometer for use in space vacuum-thermal environmental studies
[NASA-TN-D-4925] c14 N69-13311
Performance evaluation of tandem rotor blade of single stage turbine
[NASA-CR-1254] c01 N69-13621
Mechanical characteristics of flexible drive shaft coupling
[NASA-CR-1241] c15 N69-16104
Development of static inverters or converters operating electrically in parallel for space vehicle applications
[NASA-CR-1224] c03 N69-16379
Development of optical pilot warning indicator system for aircraft detection
[NASA-TN-D-5174] c14 N69-27267
Design, development, integration, and testing of Small Scientific Satellites
[NASA-TN-D-4988] c32 N69-33232
Development of automatic quality control device for measuring welded joints
[NASA-TN-D-5304] c15 N69-33800
Development and inverter circuit tests of high temperature cesium vapor thyratrons
[NASA-CR-1435] c03 N69-36843
Computer program for designing compressor blades
[NASA-TN-D-5437] c28 N69-36882

PRODUCTION ENGINEERING
Flat conductor cable technology, discussing design, manufacture, specifications, etc
[ASME PAPER 69-DE-8] c03 A69-28855
Production of glass coatings for molybdenum ion thruster accelerator grids
[NASA-TN-D-5320] c15 N69-30062

PROGRAMS
German analysis of preparatory technology of U.S. space programs, noting effects of hardware development for manned space travel on future planning
c34 A69-15576

PROJECT MANAGEMENT
Interplanetary Pioneer spacecraft development and systems engineering aspects
c31 A69-17605
Failure data role in management of launch operations reliability program
c11 A69-36022
Management system for safety in NASA Manned Space Flight Program, discussing hazard analyses and reduction precedence sequence
[AAS PAPER 69-522] c34 A69-42851
Objectives, current programs, and future mission options in space sciences and applications
[NASA-SP-162] c30 N69-13844

PROJECTILE CRATERING
Numerical method for time dependent compressible Navier-Stokes equations applied to axisymmetric flow field produced by hypervelocity impact, examining viscous effects
[AIAA PAPER 69-354] c32 A69-28288
Hypervelocity micrometeor impact sites identification on aluminized glass, using conchoidal pattern as criterion in analysis
c30 A69-34952
Theoretical prediction of crater size in Al alloy for hypervelocity impact by reduced density particles
[NASA-CR-1196] c32 N69-10225
Projectile shape effects on hypervelocity impact craters in aluminum
[NASA-TN-D-4953] c32 N69-14315
Crater characteristics of 11 metal alloys under hypervelocity impact including effects of projectile density and target temperature
[NASA-TN-D-5135] c32 N69-22994
Momentum transfer from impact into thin aluminum meteor bumper targets

[NASA-TN-D-5492] c32 N69-38809
PROPAGATION MODES
Air gap tolerances effect on admittance of TEM mode dielectric and plasma coated slot antennas determined by variational method
c09 A69-24986
Propagation characteristic model study of kinked Z trace observed on topside ionograms and explained by magnetoionic theory
c13 A69-37893
Equatorial radiation pattern of parallel plate TEM mode axial slot on elliptical conducting cylinders, using wedge diffraction and creeping wave theory
c09 A69-40703
PROPAGATION VELOCITY
Heat finite propagation velocity effects on temperature distribution and heat flux for step temperature change at semiinfinite body surface
[ASME PAPER 69-HT-1] c33 A69-43564
PROPANE
Design, development, and testing of 1000 pound thrust FLOX-propane ablative rocket engine
[NASA-TM-X-1873] c28 N69-35847
PROPELLANT CHEMISTRY
Propellant condensation on surfaces near electric rocket exhaust, calculating particle arrival rates, backflow and desorption energies
[AIAA PAPER 69-270] c28 A69-21252
PROPELLANT COMBUSTION
Characteristics of liquid propellant explosions, analyzing detonation, shock wave formation and deflagration
c27 A69-14474
Saturn fireball thermal environment associated with liquid propellant explosions, using analytical model
c27 A69-14475
Yield and combustion physics of liquid propellant explosions determined from analytic charts
c27 A69-14477
Ammonium perchlorate high temperature decomposition by using carbon dioxide laser pyrolysis/mass spectrometry
[AIAA PAPER 69-143] c06 A69-18111
Shorter combustors for high temperature jet engines of high speed aircraft, considering lifetime, shroud scoops, overheating, warpage, etc
c28 A69-29433
Hydrogen and methane combustion to simulate expansion of storable propellants
[AIAA PAPER 68-635] c33 A69-37188
Acceleration effects on solid propellant rocket motors combustion characteristics
[AIAA PAPER 68-530] c28 A69-39217
Steady state acceleration effects on combustion characteristics of aluminized composite solid propellant
[NASA-TN-D-4914] c33 N69-13231
PROPELLANT PROPERTIES
Characteristics of liquid propellant explosions, analyzing detonation, shock wave formation and deflagration
c27 A69-14474
PROPELLANT STORABILITY
Analytical evaluation of space storable propellants for unmanned Jupiter and Saturn orbiter missions
[NASA-TM-X-1793] c31 N69-24942
PROPELLANT STORAGE
Liquid rocket acoustic instability for hydrogen-oxygen and earth storable propellant combinations
[NASA-TN-D-4968] c28 N69-14384
PROPELLANT TESTS
Short duration tube wind tunnel supersonic testing, noting Saturn S-1C base heating and solid propellant rocket base burning tests
[AIAA PAPER 69-335] c11 A69-28271
Acceleration effects on solid propellant rocket motors combustion characteristics
[AIAA PAPER 68-530] c28 A69-39217
Explosive hazard evaluation of liquid oxygen liquid hydrogen propellants
[NASA-TN-D-5382] c27 N69-35321
PROPELLANT TRANSFER
Cryogenic flexibility of thin polymeric film plies for use as spacecraft positive expulsion bladders
c15 A69-16486
Pressurant gas requirements for pressurized discharge of liquid hydrogen from propellant tanks for optimum pressurization system designs
[AIAA PAPER 69-526] c28 A69-32737
Excessive extrapolation limitations in applying transient data to low gravity fluid behavior for orbital refueling systems, presenting orbital fluid transfer experiment
[AIAA PAPER 69-566] c31 A69-32755
Hydrogen gas pressure requirements during pressurization and transfer of liquid hydrogen from spherical tanks
[NASA-TN-D-5387] c28 N69-33211
PROPELLER BLADES
Numerical sclution of coupled, nonlinear, equation of motion for rigid blade to simulate response sensitivity and blade-motion stability of fully articulated rotor
[NASA-TN-D-5032] c01 N69-17289
PROPELLER DRIVE
Aerodynamic characteristics of large semi-span V/STOL tilt-wing with single propeller tested for modes of propeller rotation
[NASA-TN-D-5016] c01 N69-17312
PROPORTIONAL CONTROL
Fluidic proportional thruster system for sounding rocket control
[ASME PAPER 68-WA/FE-32] c14 A69-16105
PROPORTIONAL COUNTERS
Boron 10 absorption cross sections from counting ratios measurements of boron trifluoride proportional counter used to monitor neutron fluxes
c24 A69-33753
PROPRIOCEPTORS
Proprioceptor influence on operator performance in manual control situations
[NASA-CR-1248] c05 N69-14768
PROPULSION SYSTEM CONFIGURATIONS
Interplanetary probe missions with solar electric propulsion systems
[NASA-TN-D-5293] c30 N69-29738
PROPULSION SYSTEM PERFORMANCE
High voltage mercury electron bombardment ion thruster power efficiency
[ECS PAPER 170D] c28 A69-16233
Particle free path estimates for axisymmetric high specific impulse plasma accelerators, discussing collisionless plasma simulated by computer
[AIAA PAPER 69-278] c28 A69-21233
Background pressure and magnetic field shape effect on MPD thrustor performance, testing radiation cooled thrustors
[AIAA PAPER 69-243] c28 A69-21239
Performance boundaries of space propulsion systems containing nuclear electric stages
[AIAA PAPER 69-249] c22 A69-21249
30 cm diameter mercury bombardment low impulse thrustor development for potential space applications, discussing performance and control
[AIAA PAPER 69-238] c28 A69-21256
Performance potential of high speed ocean-going air cushion vehicles with aircraft nuclear power plants
[AIAA PAPER 69-416] c02 A69-30480
Nuclear rockets as Saturn 5 third stages, emphasizing increased payload or velocity utility and resulting engine and stage requirements
[AIAA PAPER 69-555] c31 A69-31849
Nuclear solid core rocket engine performance for interplanetary orbital launch of spacecraft by multiorbit injection
[AIAA PAPER 69-535] c22 A69-32660
Stator setting effect on single stage turbine performance, considering blade loss and surface velocity distribution
[AIAA PAPER 69-525] c28 A69-32686
Discharge chamber plasma processes in electron bombardment ion thrustors, considering factors affecting thrustor performance
[AIAA PAPER 69-494] c28 A69-32735
Steady state and dynamic distortion influence on performance and stall of turbofan engine, discussing compressor instrumentation, tests and simulation data
c28 A69-35175

Propulsion system performance relationship to manned planetary mission capability, discussing anticipated performance of advanced propulsion concepts
c28 A69-38118
ATS 3 spacecraft ammonia-fueled resistojet engine test performance
[AIAA PAPER 68-553] c28 A69-39754
Characteristics, performance potential, and problems of solid, liquid, and gas core nuclear rocket engines
[NASA-TM-X-1685] c22 N69-10067
Investigation of SA-501 S-4B auxiliary propulsion system anomalies
[NASA-TN-D-5207] c28 N69-26224
Propulsion systems for manned exploration of solar system
[NASA-TM-X-1864] c28 N69-34674

PROPULSIVE EFFICIENCY
Performance evaluation of plain rotor blade with plow type vortex generators
[NASA-CR-1342] c28 N69-24223
Performance characteristics of truncated, conical plug nozzle with cylindrical outer shroud
[NASA-TM-X-1807] c26 N69-27840

PROTECTIVE COATINGS
Plastic backing films removal from carbon electron microscope replicas by maintaining specimens in horizontal position
c14 A69-21651
Ductile metal clads and coatings of silicides, aluminides and noble metals to protect Cr alloys against nitrogen embrittlement and air oxidation
c17 A69-26495
UV irradiation effects on ZnO spacecraft thermal control coating pigments, discussing photo-Hall, luminescence and electron paramagnetic resonance measurements
[AIAA PAPER 69-639] c18 A69-33288
Second surface mirror used as coating for spacecraft thermal control
c33 A69-37290
Computer optimization of spacecraft optical coatings for temperature control, using finite element analysis and matrix inversion
[AIAA PAPER 69-979] c33 A69-40359
Vacuum integrating sphere for measuring solar absorptance in space environment to determine thermal control coatings qualifications
[AIAA PAPER 69-1021] c11 A69-40392
IR directional and hemispherical emittance of spacecraft thermal control coatings, comparing values determined by various measurement techniques
c14 A69-41633
Integral coverslip development for Si solar cells, considering borosilicate glass fusing on cell surface and RF and high vacuum ion beam sputtering
c03 A69-42272
Protective coatings for chromium alloys for use in advanced air breathing applications
[NASA-TN-D-5157] c17 N69-23084

PROTEINS
High oxygen tension effect on transport and incorporation of exogenous leucine and protein synthesis in Pseudomonas saccharophila cells
c04 A69-13433
Dynamic differential thermal analysis with He flow performed on biological specimens, proteins and starches, showing discrete decomposition peaks monitoring pyrolysis process
c06 A69-31807

PROTON BEAMS
Proton beams uniformity available at NASA synchrocyclotron designed for radiation biology research by simulating space radiation environment
c11 A69-15992
Elastic scattering cross sections for 21-MeV incident protons measured for nuclei differing in mass, determining optical model potential
c24 A69-35489

PROTON BELTS
Inner radiation zone including data on electrons, protons and heavier particles and results from high altitude nuclear tests
c29 A69-27144
Proton dose in receiver behind combination electromagnetic and material shield, calculating dose for Van Allen and solar proton event spectra
c22 A69-31522
Nighttime protonosphere thermal balance from Alouette 2 electrostatic probe measurements of electron temperature and concentration in magnetosphere
c13 A69-43181
Model environment of inner belt proton fluxes
[NASA-SP-3024-VOL-5] c24 N69-28911

PROTON ENERGY
Microscale fluctuations in interplanetary magnetic field, considering proton thermal energy and magnetic field energy densities
c30 A69-24100
Low energy solar protons entry into magnetosphere on 26 May 1967 showing diffusion control
c29 A69-31984
Cosmic X ray bremsstrahlung due to collisions of suprathermal protons with ambient electron, giving clue about diffuse sky background of X rays
c29 A69-40643
Intermediate energy protons elastic and quasi-elastic scattering from light nuclei, correlating p-D, p-He-3, p-p and p-He-4 data with various scattering models
c24 A69-43123

PROTON FLUX DENSITY
Ground based solar proton monitoring, considering particle intensities and radiation dose rates from riometer absorption as function of time
c29 A69-32321

PROTON IMPACT
First Born approximation cross sections for He excitation from ground state by proton impact calculated, using wave functions
c24 A69-17027

PROTON IRRADIATION
Biological effects on rhesus monkeys of high energy protons compared to effects of cobalt 60 gamma radiation
c04 A69-13498
Proton induced voltage breakdowns in polymeric materials
[NASA-TM-X-1688] c18 N69-10066
Analysis of annealed and proton irradiated silicon
[NASA-TN-D-5119] c26 N69-22552

PROTON SCATTERING
Differential cross sections for elastic scattering of 600 Mev protons from He 3 between 19 and 45 degrees
c24 A69-13464
Asymmetry of polarized protons scattered from He 4 at 540 MeV for laboratory angles between 4 and 42 degrees
c24 A69-14966
High energy scattering approximation valid from small to large angles, discussing errors and proton scattering by He
c24 A69-29008
Inelastic proton scattering cross sections for target nuclei in 2s-1d shell calculated in distorted wave Born approximation with projected Hartree-Fock wave functions
c24 A69-41045
Intermediate energy protons elastic and quasi-elastic scattering from light nuclei, correlating p-D, p-He-3, p-p and p-He-4 data with various scattering models
c24 A69-43123
Differential cross section and polarization measurements for elastic scattering of high energy protons from light nuclei
c24 A69-43125
Polarization, differential cross section, and total reaction cross section data for proton scattering
[NASA-TN-D-5067] c24 N69-22934

PROTONS
Cosmic gamma ray spectra from metagalactic proton-antiproton annihilation
c29 A69-21459
Phonons, electrons and protons in ferroelectrics and hydrogen bonded ferroelectrics, examining higher frequency optical and lower frequency dielectric

properties
c26 A69-32262
Proton-antiproton high energy elastic scattering by bosons exchange, introducing vertex functions for nonlocal Lagrangian
c24 A69-39467
Elastic scattering of 21 MeV protons from nitrogen 14, oxygen 16, argon 40, nickel 58, and tin 116
[NASA-TN-D-4932] c24 N69-12840
Diffraction dissociation of protons on complex nuclei of photoemulsion
[NASA-TT-F-535] c29 N69-24924

PROTOSTARS
Residual interstellar gas from protostar formation detected as high luminosity IR object
c29 A69-27593
Primitive solar nebula physical model considered under angular momentum conservation in collapsing fragment
c30 A69-36074

PROTOTYPES
Optical design of Wolter type 1 glancing incidence X ray telescope for 6-100 A wavelength region, describing results of laboratory and rocket flight tests of prototype
c14 A69-21087
Prototype lunar gravity simulator using magnetic air bearings and spring motors
[NASA-CR-1233-VOL-1] c05 N69-11675
Performance of prototype hydrogen oxygen electrolytic regenerative fuel cell stack with gas storage tank
[NASA-CR-1244] c03 N69-18885
Full scale dynamic landing impact investigation of prototype lunar module landing gear
[NASA-TN-D-5029] c31 N69-20965
Monte Carlo method for estimating costs and optimal testing of Explorer size spacecraft
[NASA-TN-D-5283] c34 N69-31333

PSEUDOMONAS
High oxygen tension effect on transport and incorporation of exogenous leucine and protein synthesis in Pseudomonas saccharophila cells
c04 A69-13433

PSYCHOLOGICAL EFFECTS
Aerospace Medicine and Biology bibliography on biological, physiological, psychological, and environmental effects on man during aerospace flight
[NASA-SP-7011/57/] c04 N69-16537

PSYCHOLOGICAL FACTORS
Biological, psychological and technological requirements in astronaut nutrition programs, examining preservation and reconstitution techniques
c05 A69-15388

PSYCHOMOTOR PERFORMANCE
Circadian rhythm phase relationships between photoperiodism and heart rate, locomotor activity and deep body temperature /DBT/ in unrestrained monkeys
c04 A69-42706
Efficacy of sensory feedback information given during training period for improving human performance in producing memorized movement pattern
[NASA-CR-1251] c05 N69-13926

PSYCHOPHYSICS
Psychophysical methods for determining perception threshold of angular acceleration in man during vertical rotation
c04 A69-15969

PULMONARY CIRCULATION
Static pressure-diameter measurements on small pulmonary blood vessels of frogs, analyzing capillary septal area as function of intravascular pressures noting high compliance
c04 A69-40974

PULSARS
Rotating and oscillating magnetic neutron stars causing pulsars radio and optical signals, stressing UV line emissions theory
c30 A69-20624
Radio emission from magnetic neutron stars as possible model for pulsars, noting optical and IR emission bands
c30 A69-20729
Instability of stellar structures intermediate between white dwarfs and neutron stars shown by stellar models, discussing pulsar signals periodicities
c30 A69-20770
Spin down effects on neutron stars, discussing decrease of period of PSR 0833-45 as result of differential rotation instability
c30 A69-32803
Night sky Cerenkov light detectors observations of pulsars CP 1133, NP 0532 and NP 0527, noting instrumental limitation in detecting ultrashort light pulses
c30 A69-34994
Radial pulsations of neutron star losing mass, interpreting Crab Nebula pulsar observed period and secular increase of period
c30 A69-37573
Pulsed X ray emission associated with pulsar NP 0532 in Crab Nebula measured by six element detector on Aerobee 150 rocket
c29 A69-37574
Crab Nebula pulsars radio properties, possible neutron star origin, interstellar gas and magnetic fields, etc
c30 A69-42556

PULSE AMPLITUDE
High latitude ionization spikes observed by POGO spacecraft, noting frequency correlation with magnetic disturbances and development by high energy electron injections
c29 A69-28950
Cataloged pulse response curves for different types of conventional low pass filters
[NASA-TN-D-5494] c07 N69-40099

PULSE CODE MODULATION
PCM data handling system for NASA Space Tracking and Data Acquisition Network with explanation for output capabilities, noting BIOSAT project
c07 A69-36242
Split phase PCM code modulated carrier transmission characteristics determined for amplitude, phase and frequency shift keying, assuming random bit pattern and noncoherent modulation
c07 A69-39451
Log-a-posteriori probability metric for use in sequential decoding
[NASA-TN-D-4930] c07 N69-23163

PULSE DURATION
Radial pulsation mode of convective envelopes in adiabatic equilibrium for variable M red supergiant stars
c30 A69-30766
Night sky Cerenkov light detectors observations of pulsars CP 1133, NP 0532 and NP 0527, noting instrumental limitation in detecting ultrashort light pulses
c30 A69-34994
Cataloged pulse response curves for different types of conventional low pass filters
[NASA-TN-D-5494] c07 N69-40099

PULSE FREQUENCY MODULATION
Oscillations in pulse modulated satellite attitude control systems
[NASA-CR-1369] c21 N69-29967

PULSE MODULATION
Terrain bias error analysis in pulse modulated planetary radar altimeters
[NASA-TN-D-5220] c21 N69-26195

PULSE RATE
Ultrasonic pulse velocity and attenuation measurement in presence of noise, using coherent detection and signal averaging
c14 A69-29564

PULSED JET ENGINES
Multipulse thruster module design and development tests for spacecraft attitude control, noting micropulse solid propellant rocket motor
c03 A69-11762

PULSED LASERS
Carbon dioxide laser with two gas absorption cells in cavity for emission wavelength control and HF pulsed mode of operation
c16 A69-21088
Sulfur dioxide-helium laser pulsed and CW submillimeter outputs
c16 A69-24005
Simultaneous HCN and HOH laser emission in pulsed discharge through mixture containing H, C, N, and O

c16 A69-26330
PULSED RADIATION
Thermodielectric radiometer for transient radiant flux short duration pulse measurement, using thermally induced depolarization of polymer film dielectric
[AIAA PAPER 68-403] c14 A69-12392
Picosecond light pulse measurement by two photon excitation of photographic film
c14 A69-20165
Nuclear energized pulsational instability of stars based on linear quasi-adiabatic theory, including models with hydrogen burning shells
c30 A69-27576
PUMP SEALS
Flow and pressure fields for spiral grooved pumping seal with specified groove dimensions and Reynolds number
[ASLE PICFS PREPRINT 30] c15 A69-30481
PUMPS
Pneumatic driving system for heart assist or total replacement pumps, discussing design features and performance characteristics
c05 A69-42983
Two phase hydrogen flow in pump inlet line
[NASA-TN-D-5258] c15 N69-29476
Analytical model for use in design of pump inlet accumulators for prevention of liquid rocket longitudinal oscillation
[NASA-TN-D-5394] c28 N69-33319
PURIFICATION
Organic geochemical laboratories solvent purification procedures
[NASA-TM-X-1746] c06 N69-18962
PYRIDINE NUCLEOTIDES
Flavoprotein/cytochrome b/559/ role as branch of Halobacterium electron transport in DPNH oxidase determined by salt dependence of reduced DPNH
c06 A69-37101
PYROLYSIS
Charring phenolic nylon ablator material pyrolysis and surface recession for cyclic and constant combined convective and radiative heating
[AIAA PAPER 69-151] c33 A69-18055
Yttrium effect on rate of thermal decomposition of silver carbonate powder and pressed pellets by isothermogravimetric analysis, examining water vapor, Co 60 gamma radiation and temperature effects
c06 A69-30442
Dynamic differential thermal analysis with He flow performed on biological specimens, proteins and starches, showing discrete decomposition peaks monitoring pyrolysis process
c06 A69-31807
Effect of chemical properties of pyrolysis gases on heat shield mass required for lifting reentry vehicle in typical reentry trajectory
[NASA-TN-D-4975] c32 N69-14306
Chemical equilibrium of ablation materials including condensed species
[NASA-TN-D-5391] c33 N69-34966
PYROLYTIC GRAPHITE
Periodicity of magnetothermal oscillations in pressure annealed pyrolytic graphite compared with hole carriers
c26 A69-29005
Magnetcthermal oscillations in pressure annealed pyrolytic graphite
[NASA-TN-D-5488] c26 N69-39239
PYROLYTIC MATERIALS
High temperature capacitor consisting of thin wafers of pyrolytic boron nitride noting fabrication, dissipation factor and capacitance
c03 A69-15299
Thermochemical data from simulated pyrolysis gas flow through ablating char layer
[NASA-TN-D-5464] c33 N69-38271
PYROTECHNICS
Pyrotechnic and explosive elements in space systems - Conference, Tarbes, France, July 1968
c27 A69-23003
Pyrotechnic activated calorimeter for reentry package design of vehicles entering earth atmosphere at lunar return velocities
c11 A69-23026
PYRROLES
Syntheses and properties of pyrrone polymers
[NASA-CR-1310] c18 N69-26448
Electrical properties and high energy radiation effect on Pyrrone polymers
[NASA-CR-1367] c18 N69-29559
Synthesis of Pyrrone laminates from sulfone dianhydride
[NASA-CR-1404] c30 N69-31960

Q

Q SWITCHED LASERS
Spectral emission of visible from Q switched dye lasers
[NASA-CR-1374] c16 N69-29934
QUALITY CONTROL
Electromagnetic interference /EMI/ created by noise coupling through conductive paths, discussing responsibility for control within systems management
c07 A69-18944
High pressure storage vessels for gaseous hydrogen, discussing failure, manufacturing controls and access for internal nondestructive inspection
[ASM PAPER D8-14.1] c15 A69-19666
Computer program for component quality control and reliability data analysis
[NASA-TN-D-5009] c15 N69-17988
Development of automatic quality control device for measuring welded joints
[NASA-TN-D-5304] c15 N69-33800
QUANTITATIVE ANALYSIS
X Ray fluorescence of rock samples as applied to geological problems, noting standard deviations for element distribution
c14 A69-10890
Quantitative method for determination of fission gases trapped in irradiated fuel forms
[NASA-TM-X-1893] c22 N69-37225
QUANTUM ELECTRODYNAMICS
Interstellar extinction models of classical Mie particles and quantum mechanical polycyclic aromatic molecules
c30 A69-23679
QUANTUM MECHANICS
Scattering, reactions, and decay in nonrelativistic quantum mechanics
[NASA-TT-F-510] c24 N69-25848
QUANTUM THEORY
Quantum theory of electron gas with anomalous magnetic moments in intense magnetic fields, noting pair creation from thermodynamic energy in system
c24 A69-19782
Quantum theory of particle-harmonic oscillator collision applied to gas-surface interactions at cryogenic temperatures
[NASA-TN-D-4982] c24 N69-14288
Quantum communication systems performance evaluated by communication efficiency parameter
[NASA-TR-R-320] c07 N69-39264
QUARTZ
Quartz fiber adhesion to Re measured in LEED /low energy electron diffraction/ apparatus for clean and O layer surfaces, noting brittle fracture
c17 A69-35182
Low energy electron diffraction analysis of quartz fiber adhesion to rhenium crystal surface
[NASA-TN-D-5229] c17 N69-25363
Quartz-insulated, single-wire thermocouples installed on thin-wall rocket cooling tubes to measure hot-gas-side wall temperatures
[NASA-TN-D-5291] c14 N69-29553

R

RADAR DATA
Effect of spacecraft onboard radar range and range rate data and accuracy on unmanned probe entry guidance corridor
[NASA-TN-D-4852] c21 N69-16503
Exametnet meteorological rocket launchings and data dissemination, 1967 - tables
[NASA-SP-176] c20 N69-22570
RADAR DETECTION
Radar attitude sensing system for determining vehicle roll, pitch, yaw, altitude and velocity of earth and lunar orbital vehicles
c07 A69-13183

RADAR MEASUREMENT
Temperature profiles and associated wind profiles obtained with Jimsphere/FPS-16 radar system at Cape Kennedy, discussing remote CAT detector assessment
c20 A69-33739
Tradeoff analysis on radar and laser space altimeter systems for sea surface geodesy
[NASA-CR-1298] c14 N69-21117
RADAR NAVIGATION
V/STOL aircraft radar inertial navigation system, describing approach and landing phase flight test results
[AAS PAPER 69-401] c02 A69-42831
RADAR SCATTERING
Radar backscatter and rocket profiles of ionospheric electron temperature, noting agreement in daytime flight measurements
c29 A69-25162
RADAR TRACKING
Regression analysis procedures for evaluating tracking system measurement errors
[NASA-TN-D-4826] c19 N69-14476
Radar observations and radiophysical investigations of Venus
[NASA-TT-F-536] c30 N69-38643
RADIAL FLOW
FORTRAN 4 program for estimating off-design performance of radial inflow turbines
[NASA-TN-D-5059] c03 N69-19829
Test performance of radial inflow turbine for Brayton cycle space power system
[NASA-TN-D-5090] c03 N69-20937
Approximative solution for dynamic response of flexible rotor blade to radially moving force
[NASA-TN-D-5410] c32 N69-36220
RADIANCE
Infrared horizon radiance profiles for winter conditions based on Scanner project flight test
[NASA-TN-D-4905] c21 N69-14346
Horizon radiance profile analysis for determining atmospheric temperature
[NASA-TN-D-5068] c13 N69-19024
RADIANT COOLING
Nongray absorption and radiation cooling on smooth symmetric blunt bodies included in modified Maslen flow field method for radiation and large blowing
[AIAA PAPER 69-637] c01 A69-33290
RADIANT FLUX DENSITY
Thermodielectric radiometer for transient radiant flux short duration pulse measurement, using thermally induced depolarization of polymer film dielectric
[AIAA PAPER 68-403] c14 A69-12392
Radiation measurements inside Apollo 4 and 6 command modules during passage through trapped radiation belts
[AIAA PAPER 69-17] c05 A69-18202
Background radiation intensity upper limits for mm and submillimeter wavelengths in interstellar medium, noting intense flux in far IR
c30 A69-19404
Cosmic ray intensity during solar cycles, considering minima relationship to Bartel index maxima and solar wind modulation theory
c29 A69-29967
Radiant energy transfer measurements in air plasma in reflected region of arc-driven shock tube
[NASA-CR-1390] c25 N69-38227
Large thin film cadmium sulfide solar cell electrical characteristics over ranging temperatures and radiant intensities
[NASA-TM-X-1899] c03 N69-38767
RADIANT HEATING
Initial radio frequency gas heating experiments to simulate thermal environment in nuclear light bulb reactor
[NASA-CR-1311] c22 N69-23450
RADIATION ABSORPTION
Radiation attenuation cross sections of monatomic and diatomic xenon gas from UV absorption measurements near resonance line
c24 A69-12551
Nongray absorption and radiation cooling on smooth symmetric blunt bodies included in modified Maslen flow field method for radiation and large blowing
[AIAA PAPER 69-637] c01 A69-33290
Vacuum integrating sphere for measuring solar absorptance in space environment to determine thermal control coatings qualifications
[AIAA PAPER 69-1021] c11 A69-40392
Interstellar extinction in UV from zeta and epsilon Persei spectra obtained with scanner attached to telescope mounted in pointed Aerobee rocket
c30 A69-40772
Absorption of black-body radiation by ice cryodeposits on metal substrates
[NASA-TN-D-5181] c23 N69-22769
Simple equations for temperature distributions in radiating gray gases
[NASA-TN-D-5226] c33 N69-25312
RADIATION BELTS
Radiation measurements inside Apollo 4 and 6 command modules during passage through trapped radiation belts
[AIAA PAPER 69-17] c05 A69-18202
RADIATION COUNTERS
NASA lunar receiving laboratory for lunar rock samples examination by gamma ray spectrometry for induced radioactive nuclides and naturally occurring isotopes
c11 A69-38271
RADIATION DAMAGE
Radiation damage and recovery of lithium-diffused silicon p-n solar cells, measuring photovoltaic parameters as function of gamma radiation fluence
c03 A69-35694
Solar cell radiation damage during 416.8 days in synchronous orbit on satellite ATS 1, discussing radiation shields
c03 A69-35704
Diffusion lengths of silicon solar cells after radiation damage and annealing by X ray method
[NASA-TM-X-1894] c03 N69-37827
RADIATION DETECTORS
Cosmic ray detectors design for medium, low and very low energy events on IMP-1 spacecraft, noting PCM format
c07 A69-41738
Theoretical feasibility of detecting laser radiation scattered from plasma
[NASA-TN-D-5311] c25 N69-36939
RADIATION DISTRIBUTION
Emission and frequency shift angles of anti-Stokes radiation from trapped filaments of laser light in liquids
c23 A69-10012
Radiating collinear open ended waveguides and near field coupling analyzed using simultaneous integral equations and Fourier series expansion of aperture field
c09 A69-24984
Radiation fields from energetic electron moving in helical orbit in magnetoactive plasma, using Maxwell equations
c30 A69-39965
Computer program for line-by-line calculation of spectra from diatomic molecules and atoms assuming Voigt line profile
[NASA-TN-D-5088] c24 N69-21462
Tabulated values of configuration factors between two spheres and parts of two spheres
[NASA-SP-3050] c30 N69-37777
RADIATION DOSAGE
Radiation measurements inside Apollo 4 and 6 command modules during passage through trapped radiation belts
[AIAA PAPER 69-17] c05 A69-18202
Proton dose in receiver behind combination electromagnetic and material shield, calculating dose for Van Allen and solar proton event spectra
c22 A69-31522
Ground based solar proton monitoring, considering particle intensities and radiation dose rates from riometer absorption as function of time
c29 A69-32321
RADIATION EFFECTS
Photodegradation of organic polymers by UV radiation exposure, emphasizing polyvinyl chloride photochemistry and radiation stabilization
c18 A69-10861

Biological effects on rhesus monkeys of high energy protons compared to effects of cobalt 60 gamma radiation
c04 A69-13498
Polymer films tensile properties after exposure to gamma radiation in vacuum, noting chain scission and cross linking
[ASME PAPER 68-WA/RP-6] c18 A69-16160
Electric field effects on thermal annealing of electron irradiation damage in p-channel MOSFET device
c09 A69-16562
Electron radiation damage in MOSFET devices using bias temperature treatments
c26 A69-16877
Annealing temperature of radiation defects in phosphorus doped silicon, discussing isochronal recovery characteristics of solar cells with different donor and oxygen concentrations
c26 A69-24006
Mortality kinetics of Drosophila melanogaster, comparing effects of gamma radiation-induced life shortening and natural aging
c04 A69-30444
UV irradiation effects on ZnO spacecraft thermal control coating pigments, discussing photo-Hall, luminescence and electron paramagnetic resonance measurements
[AIAA PAPER 69-639] c18 A69-33288
Photodisintegration of ultrahigh energy cosmic rays by universal radiation field, analyzing implications on origin and propagation time
c29 A69-35006
Optimum solar cell cover glass systems selected by studying interplanetary space environment effects of proton impact, temperature and concurrent illumination on radiation damage
c03 A69-35702
UV solar radiation variation effects on Mars and Venus upper atmosphere temperatures
c30 A69-37136
Life sciences and space research on biological effects of radiation in space - COSPAR Conference, Tokyo, May 1968
c04 A69-37612
Photospheric radiation field role in temperature inversion of stellar chromospheres with dominant H ion opacity, postulating mechanical energy dissipation
c30 A69-38173
Thermal calculations of objects near lunar surface, considering IR emission directivity effects
c30 A69-43254
Effects of neutron irradiation on silicon voltage regulator Zener diodes
[NASA-TN-D-4923] c09 N69-10250
Human responses to aerospace environment in relation to microwave, light, thermal, and ionizing radiation
[NASA-CR-1205-VOL-1] c04 N69-12434
Proton irradiation effects on minority carrier lifetime in silicon and gallium arsenide semiconductor materials
[NASA-TN-D-5028] c26 N69-18897
Degradation of multiplier phototubes exposed to spatial radiations
[NASA-CR-1304] c14 N69-20777
Radiation induced reduction of ammoniacal nickel /2/ sulfate to metallic nickel
[NASA-TN-D-5213] c06 N69-24940
Electrical properties and high energy radiation effect on Pyrrone polymers
[NASA-CR-1367] c18 N69-29559

RADIATION LAWS

Radiation models using discrete radiator ensembles having applications to analysis of forward and backscatter from rough surfaces, clutter and chaff models, etc
c07 A69-10556

RADIATION MEASUREMENT

Energy spectra of carbon and oxygen nuclei in primary cosmic radiation, comparing results to earlier measurements and satellite observation
c29 A69-20632
Pulsed X ray emission associated with pulsar NP 0532 in Crab Nebula measured by six element detector on Aerobee 150 rocket
c29 A69-37574
Infrared radiation measurements in space environment simulator using integral equations
[NASA-TN-D-5166] c29 N69-28111
Lunar Orbiter 1 terrain assessment photographs and preliminary selenodesy, micrometeoroid, and radiation data
[NASA-SP-197] c30 N69-39213

RADIATION MEASURING INSTRUMENTS

Lunar composition analysis by measuring atomic and nuclear radiation emission from orbiter
[AAS PAPER 68-197] c30 A69-11475
Vacuum ultraviolet detector-spectroscopy systems for capsule reentry measurements
[NASA-CR-1268] c09 N69-18761

RADIATION MEDICINE

Gravitational and acceleration effects on man and organisms, and biological effects of radiation
[NASA-TT-F-528] c05 N69-38701

RADIATION PRESSURE

Solar radiation pressure windmill effect in rotational bursting and elimination from solar system of small magnetic celestial bodies
c30 A69-39584

RADIATION PROTECTION

Radiation protection plan for Apollo lunar mission based on real time monitoring of solar activity and radiation in spacecraft
[AIAA PAPER 69-19] c29 A69-18113
Integral coverslip development for Si solar cells, considering borosilicate glass fusing on cell surface and RF and high vacuum ion beam sputtering
c03 A69-42272

RADIATION SHIELDING

Radiation compensating thermocouple for gas temperature measurement, noting advantage over single thermocouples
c14 A69-14916
COHORT-2 Monte Carlo computer program written in FORTRAN 4 to model radiation shielding problems
c08 A69-29004
Proton dose in receiver behind combination electromagnetic and material shield, calculating dose for Van Allen and solar proton event spectra
c22 A69-31522
Monte Carlo method application to neutron streaming in hemispherical air-filled ducts in water tank to determine leakage through nuclear reactor shields
c22 A69-35178
Solar cell radiation damage during 416.8 days in synchronous orbit on satellite ATS 1, discussing radiation shields
c03 A69-35704
FORTRAN program for radiation shield optimization using steepest descent method
[NASA-TM-X-1769] c22 N69-20854
Neutron interaction behavior of beryllium oxide and molybdenum reflectors for nuclear reactors
[NASA-TM-X-1822] c22 N69-29593
Tungsten and depleted uranium in mimimum weight, layered shield comparisons for space power reactor
[NASA-TM-X-1874] c22 N69-35817
Gamma ray transport portion of COHORT 2 Monte Carlo shielding code
[NASA-TM-X-1877] c22 N69-35848

RADIATION SOURCES

Discrete source hypothesis for interpreting high energy cosmic gamma ray measurements obtained by OSO-3 spacecraft
c29 A69-20699
Iron line absence in emission spectrum of thermal X ray sources, constraining proposed thermal models
c29 A69-22231
Far IR source in galactic center detected at 100 microns, noting thermal emission of interstellar dust grains as possible mechanism
c30 A69-22264
X ray sources model, describing possible ring of matter around white dwarf near end of active evolution
c29 A69-35204
NASA Small Astronomy Satellite /SAS/ program for radiation source detection
[NASA-TN-D-5099] c31 N69-21017

RADIATION SPECTRA
Annihilation gamma ray spectra from equilibrium spectra of secondary galactic positrons
c29 A69-29948
Cosmic gamma rays spectrum from neutral pions production and decay in metagalactic cosmic ray p-p collisions, deriving models based on Einstein general relativity theory
c29 A69-40641
RADIATION THERAPY
Soviet handbook on operation principles, use, and installation of electrocardiographs and electromedical apparatus for therapeutics
[NASA-TT-F-523] c05 N69-27577
RADIATION TOLERANCE
NASA Plum Brook Reactor Facility /PBRF/ for determining radiation tolerance to support nuclear power application in space for propulsion and power
c22 A69-13128
Unfilled Pyrrone prepared from powder into molded parts for flexural tests at elevated temperatures observed for stability to electron irradiation in air
c18 A69-35529
Radiation resistance of cylindrical shells in ideal compressible acoustic medium
[NASA-CR-1437] c32 N69-40935
RADIATIVE HEAT TRANSFER
Downstream radiation flux distribution calculated for blunt entry bodies, considering self absorption effects
c33 A69-12547
Correlations of stagnation point radiative heat transfer for earth reentry, noting use of nongray absorption coefficient models
c33 A69-14736
Inverse problems in radiative transfer applied to remote measurements of IR radiation from planetary atmospheres, noting temperature and water vapor inversions
c13 A69-17617
Combined radiation and conduction heat transfer equation applied to temperature profile around opaque hollow sphere and in solid condensed gas layer
[SAE PAPER 690197] c33 A69-18303
Combined conduction and radiation transfer equations solutions for absorbing-emitting gas, obtaining slip coefficient for diffusion solution correct boundary condition
c33 A69-27784
Atmospheric ozone vertical distribution and total amount determined by radiative transfer and perturbation theory, presenting error analysis
c13 A69-28493
Nongray equilibrium radiative heat transfer in viscous radiating shock layer around blunt body entering high temperature nonisothermal carbon dioxide-nitrogen atmosphere
[AIAA PAPER 69-636] c33 A69-33258
Perturbation solution to blunt body stagnation region flow of radiating gas with radiation heat transfer
[NASA-TR-R-295] c12 N69-10788
Solution to radiation-coupled stagnating flow with nongray emission over hypervelocity blunt body
[NASA-TR-R-299] c33 N69-16268
Effect of shock precursor heating on radiative flux to blunt bodies
[NASA-CR-1265] c33 N69-17438
Ablation product absorption and line transitions effects on shock layer radiative transport around blunt body
[NASA-CR-1264] c33 N69-19117
Measurement of radiative thermal conduction of ideal powder as function of temperature
[NASA-TN-D-5063] c33 N69-20008
Thermal radiation exchange between surfaces and enclosures
[NASA-SP-164-VOL-2] c33 N69-30317
Calculation for study of vertical and horizontal positioned lunar radiators
[NASA-TM-X-1846] c33 N69-32683
Tabulated values of configuration factors between two spheres and parts of two spheres
[NASA-SP-3050] c30 N69-37777
Integral relations solution for radiating, nonadiabatic, inviscid flow over blunt body
[NASA-TN-D-5480] c33 N69-40356
RADIATORS
Radiation models using discrete radiator ensembles having applications to analysis of forward and backscatter from rough surfaces, clutter and chaff models, etc
c07 A69-10556
RADII
Radius effect on bulging and fracture of through-cracked cylindrical pressure vessels at cryogenic temperatures
[NASA-TN-D-4951] c32 N69-14480
Telemetry data from image-motion compensation sensor on Lunar Orbiter 1 spacecraft for determining radius of moon
[NASA-TN-D-5231] c30 N69-29115
RADIO ALTIMETERS
Terrain bias error analysis in pulse modulated planetary radar altimeters
[NASA-TN-D-5220] c21 N69-26195
RADIO ANTENNAS
Microwave radiometric sensor operational principles and capabilities, discussing antennas and radiometric receivers
c07 A69-26976
Transmission loss and effects on antenna radiation patterns and impedance produced by thermally degraded ablation materials
[NASA-TN-D-4879] c07 N69-10885
RADIO ASTRONOMY
Laser optical simulation of spaceborne radio astronomy interferometer experiment
[NASA-TN-D-5357] c30 N69-36892
RADIO ASTRONOMY EXPLORER SATELLITE
RAE-A satellite design, simulation and flight performance, discussing gravity gradient stabilization
c31 A69-18328
Radio astronomy Explorer A attitude determination via disk-oriented programming ground support system for reducing and calibrating telemetry data, attitude prediction and command, etc
[AIAA PAPER 69-983] c08 A69-40363
Cosmic radio background noise spectrum near north galactic pole based on Radio Astronomy Explorer satellite experiments
c30 A69-42375
RADIO ATTENUATION
Flow field predictions for radio attenuation measurements on blunt reentry cone
[NASA-CR-1308] c07 N69-28223
RADIO ECHOES
Conjugate echoes in Alouette 2 topside sounder ionograms explained by multiple reflections between conjugate points of field line, noting magnetospheric waveguides role
c07 A69-20045
RADIO EMISSION
Venus microwave phase effect analyzed assuming dry massive Venus atmospheric model, discussing heat transfer processes
c30 A69-12108
Galactic Jupiter Probes investigating Jupiter atmosphere and emissions and deep space cosmic radiation
c30 A69-12303
Diurnal variations of low latitude VLF emissions observed at Hiraiso, Japan
c07 A69-13900
Radio emission from magnetic neutron stars as possible model for pulsars, noting optical and IR emission bands
c30 A69-20729
Radio emission from Sco XR-1 shown as synchroton radiation of relativistic electrons in low density region surrounding denser core producing X ray
c30 A69-37334
Crab Nebula pulsars radio properties, possible neutron star origin, interstellar gas and magnetic fields, etc
c30 A69-42556
RADIO FREQUENCIES
Extragalactic gamma ray fluxes predicted, discussing collisions, matter-antimatter annihilation and cosmological implications
c29 A69-24466
Radio frequency transmission characteristics of ablation materials for planetary entry vehicle

heat shields
[NASA-TN-D-4920] c07 N69-13158
Radio frequency induction heated plasmas with power deposition and energy removal
[NASA-CR-1312] c25 N69-22638
RADIO FREQUENCY INTERFERENCE
Mutual RF interference between satellite and terrestrial telecommunications microwave relay system at shared frequencies
c07 A69-13242
RFI effects of earth based emitters on operation of geosynchronous satellites for data relay from near earth orbiting satellites, noting frequency assignments
c07 A69-41757
Experiment design for measuring radio frequency interference between communication satellite and terrestrial microwave relay system
[NASA-TN-D-5041] c07 N69-26272
RADIO GALAXIES
M-2 galaxy as Seyfert-like galaxy seem edge-on, using radio and optical data showing H alpha emission collisionally excited, discussing circular polarization
c30 A69-20051
Radio galaxy Messier 87 mass determined using virial theorem for nucleus velocity dispersion
c30 A69-30883
RADIO INTERFEROMETERS
Laser optical simulation of spaceborne radio astronomy interferometer experiment
[NASA-TN-D-5357] c30 N69-36892
RADIO PHYSICS
Radar observations and radiophysical investigations of Venus
[NASA-TT-F-536] c30 N69-38643
RADIO RECEIVERS
Microwave radiometric sensor operational principles and capabilities, discussing antennas and radiometric receivers
c07 A69-26976
RADIO RELAY SYSTEMS
Mutual RF interference between satellite and terrestrial telecommunications microwave relay system at shared frequencies
c07 A69-13242
RADIO SOURCES (ASTRONOMY)
Balloon-borne instrumentation for detection of far IR extended emission regions and bright point sources, describing results of initial flights
c30 A69-27599
RADIO SPECTRA
Cosmic radio background noise spectrum near north galactic pole based on Radio Astronomy Explorer satellite experiments
c30 A69-42375
NASA program for radio spectrum utilization in aerospace communication systems
c07 A69-42502
RADIO TELEMETRY
Laboratory and flight tests of airborne solid state UHF telemetry transmitter, discussing miniaturized coaxial hardware from RF power conservation viewpoint
c07 A69-35996
Pioneer 9 deep space probe with telemetry link operated in coded mode with sequential decoding, discussing ground and flight test data
c07 A69-42522
Computerized telemetry filter design
[NASA-SP-3049] c08 N69-35816
RADIO TELESCOPES
Structural technology for large radio and radar telescope systems - Conference, Cambridge, Mass., October 1967
c11 A69-42120
RADIO TRANSMISSION
Scientific findings from interplanetary spacecraft radio propagation experiments, particularly Mariner 5 data
c07 A69-35940
Split phase PCM code modulated carrier transmission characteristics determined for amplitude, phase and frequency shift keying, assuming random bit pattern and noncoherent modulation
c07 A69-39451
Lunar surface transmission loss for Apollo astronaut point-to-point communications
[NASA-TN-D-4915] c07 N69-13301
RADIO TRANSMITTERS
Laboratory and flight tests of airborne solid state UHF telemetry transmitter, discussing miniaturized coaxial hardware from RF power conservation viewpoint
c07 A69-35996
RADIOACTIVE AGE DETERMINATION
Kodaikanal iron meteorite measurements for cosmogenic rare gases and K-Ar isotopes ages for glass inclusions
c30 A69-22047
RADIOACTIVE DECAY
Lanthanum isotopes beta decay, analyzing excitation of near spherical daughter nuclei of barium isotopes
c24 A69-10100
Radioactive decay of neutral pions generated in metagalactic cosmic ray interactions as source of high energy isotropic gamma rays observed by OSO-3
c29 A69-12092
Iodine 123 decay via gamma ray emission, noting energies of several transitions
c24 A69-13099
RADIOACTIVE ISOTOPES
Chondrite meteorite fall /1969/ in Mexico, noting opaque and microcrystalline matrices and gamma rays from short lived isotopes
c30 A69-20686
Vacuum tube with cathode heated directly by external radioisotope source, noting heat pipe providing isothermal heat transfer
c09 A69-24748
NASA lunar receiving laboratory for lunar rock samples examination by gamma ray spectrometry for induced radioactive nuclides and naturally occurring isotopes
c11 A69-38271
Gamma ray backscattering of radioisotope for measuring Martian atmospheric density
[NASA-TN-D-5431] c24 N69-36931
RADIOBIOLOGY
Proton beams uniformity available at NASA synchrocyclotron designed for radiation biology research by simulating space radiation environment
c11 A69-15992
Gravitational and acceleration effects on man and organisms, and biological effects of radiation
[NASA-TT-F-528] c05 N69-38701
RADIOGRAPHY
Flash X ray unit with special film transport devices to obtain sequenced dynamic radiographs of ablating models during reentry simulation tests
c11 A69-35720
RADIOISOTOPE BATTERIES
Planar radioisotope thermoelectric generator system for NASA deep space missions and integrated spacecraft power supply
c03 A69-42254
RADIOLYSIS
Blocked two level factorial experiment to measure radiolysis of water in water cooled reactors
[NASA-TN-D-5369] c19 N69-32319
RADIOMETEOROGRAPHS
Radiometric measurements of atmospheric attenuation in electromagnetic spectrum
[NASA-TN-D-5087] c07 N69-22949
RADIOMETERS
Thermodielectric radiometer for transient radiant flux short duration pulse measurement, using thermally induced depolarization of polymer film dielectric
[AIAA PAPER 68-403] c14 A69-12392
Cosmic radio noise intensity measurements by ATS 2 satellite-borne radiometer
c30 A69-19715
Solar spectral irradiance measured by airborne instruments, discussing construction, calibration, etc, of photoelectric filter radiometer and Leiss monochromator
c30 A69-32261
Radiometer for measuring solar flux variations, discussing design, performance tests and use for spacecraft measurements
[AAS PAPER 69-254] c14 A69-42858

Regression generated radiometric and contour height fields of North American Continent using Nimbus 2 IR equivalent black body temperature and geopotential data
c20 A69-42896
Disk radiometer for use in space vacuum-thermal environmental studies
[NASA-TN-D-4925] c14 N69-13311
Nimbus 2 high resolution infrared radiometer data on earth resources of arid and subarid lands
[NASA-TN-D-4647] c13 N69-14450
Radiometric techniques applicable to measurement of solar activity and atmospheric attenuation at millimeter wavelengths
[NASA-TR-R-306] c07 N69-22951
Design, calibration, and use of radiometers to measure spectral emission in ballistic range and shock tube experiments
[NASA-TN-D-5360] c14 N69-38144

RAMAN SPECTRA
Emission and frequency shift angles of anti-Stokes radiation from trapped filaments of laser light in liquids
c23 A69-10012
Sinusoidal phase modulation role in spectral broadening observed in trapped filaments of laser and Raman light
c16 A69-14189
Spontaneous Raman band shapes and depolarization ratios in liquid nitrogen and oxygen measured and compared to gas, discussing time dependence of rotational motion
c24 A69-17817

RAMPS (STRUCTURES)
M 3.5 two dimensional mixed compression inlet system with self restart using flexible variable ramp system
[AIAA PAPER 69-447] c28 A69-32732

RANDOM NOISE
Analytic time function models of stochastic processes of noise and modulation
[NASA-TR-R-314] c07 N69-29230
Quantum communication systems performance evaluated by communication efficiency parameter
[NASA-TR-R-320] c07 N69-39264

RANDOM PROCESSES
Fast electron diffusion in stochastic magnetic field, obtaining diffusion coefficient as function of ratio of correlation time to Larmor period
c25 A69-20807
Anisotropic Heisenberg ferromagnets in random phase and spin wave approximation
[NASA-TN-D-5286] c26 N69-29588

RANDOM VARIABLES
Statistical method for evaluating goodness of fit between data set and theoretical distribution of random variables
[NASA-TR-R-313] c19 N69-30610

RANDOM VIBRATION
Summary of random vibration prediction procedures for aerospace vehicles, with bibliography
[NASA-CR-1302] c32 N69-23096

RANGE AND RANGE RATE TRACKING
Effect of spacecraft onboard radar range and range rate data and accuracy on unmanned probe entry guidance corridor
[NASA-TN-D-4852] c21 N69-16503
Evaluation of Goddard range and range rate system at Rosman by intercomparison with GEOS 1 long-arc orbital solutions
[NASA-TN-D-5036] c13 N69-28442

RANGE ERRORS
Longitudinal range dispersion of unmanned Mars landers using VM-8 and VM-9 atmospheric models, discussing Syrtis Major as possible landing site
c30 A69-12390
Prediction methods for angular line-of-sight deviations induced by spacecraft window
[NASA-TN-D-5238] c21 N69-31227

RANGEFINDING
Navigation satellites system designed for ATC without requirement for onboard transmitter, discussing spectrum occupancy, satellite power, lane ambiguities and computational procedures
c21 A69-19212

RANGES (FACILITIES)
Wind velocity profiles by smoke trail method for eastern test range
[NASA-TN-D-4880] c20 N69-14505

RANKINE CYCLE
Systems analysis of Rankine cycle nuclear-electric potassium space power system using Li cooled fast reactor and high temperature turbine inlet
c22 A69-42266
Comparison of Brayton and Rankine cycle magnetogasdynamic space power generation systems for use with nuclear heat source
[NASA-TN-D-5085] c03 N69-20852
Electrothermal instabilities effects on Brayton and Rankine cycle magnetohydrodynamic space power generation systems
[NASA-TN-D-5461] c03 N69-37883

RANKINE-HUGONIOT RELATION
MHD Rankine-Hugoniot equations for ion density, thermal pressure and convective velocity magnitude and orientation during Pioneer 6 traversal of earth bow shock
c30 A69-42417

RARE EARTH COMPOUNDS
Rare earth fluorides and oxides used as solid lubricants at high temperatures
[NASA-TN-D-5301] c15 N69-29568

RARE EARTH ELEMENTS
Partition coefficients between natural melts and plagioclase phenocrysts determined for rare earth elements and barium by mass spectrometry
c13 A69-20944
Continental diabases and oceanic tholeiites in light of rare earth and barium abundances and partition coefficients indicating fusion process
c13 A69-20945
Ca-rich achondrites genesis implied from rare earth and Ba absolute and relative concentrations
c30 A69-36091

RARE GASES
Kodaikanal iron meteorite measurements for cosmogenic rare gases and K-Ar isotopes ages for glass inclusions
c30 A69-22047
Valving concepts and functional approaches for inert gas attitude control thrustor systems providing redundancy safeguards at minimum weight, volume and power costs
[AIAA PAPER 69-843] c28 A69-39373

RAREFIED GAS DYNAMICS
Monte Carlo method application to heat transfer analysis including radiation, rarefied gas energy transfer and conduction
c33 A69-24457

RAREFIED GASES
Viscosity, thermal conductivity and diffusion predicted for dilute nonpolar, polar and mixed gases, discussing methods for rotational relaxation collision numbers and resonant correction
c33 A69-38951
Quantum theory of particle-harmonic oscillator collision applied to gas-surface interactions at cryogenic temperatures
[NASA-TN-D-4982] c24 N69-14288

RATES (PER TIME)
Rate of rise outgassing measurement technique in vacuums
[NASA-TN-D-4973] c14 N69-16097

RATINGS
Pilot rating scales and their use in assessing aircraft handling qualities
[NASA-TN-D-5153] c02 N69-22539

RATIOS
Gamma heating rate measured by aqueous dosimeter converted to rate in thin tungsten detector in water shield through transport theory calculations, obtaining correction factors
c22 A69-18825
Volume-ratio system for vacuum gage calibration from 10 to minus 8 to 10 torr
[NASA-TN-D-5406] c14 N69-35265

RATS
Critical body temperature for intracranial self stimulation in white rats
c04 A69-13897
Acetate carbon 14 utilization in centrifuged rats, analyzing metabolism by measuring plasma glucose, FFA and lipids synthesis
c04 A69-19429

Adrenal epinephrine and phenylethanolamine n-methyl transferase /PNMT/ activity in rat bearing transplantable pituitary tumor
c04 A69-20374

Transensor implantation, sham implantation, no implantation and lighting effects on rat body composition, noting fat and water content
c04 A69-26557

Acetate-2-C 14 conversion to C 14 carbon dioxide and C 14 fatty acids in rats with 2/3 of liver removed
c04 A69-35976

Rats adrenal corticosterone concentrations changes in response to ACTH, determining response sensitivity dependence on time after hypophysectomy
c04 A69-39871

Compensatory hypertrophy effects on adrenal phenylethanolamine n-methyl transferase /PNMT/ activity in rats
c04 A69-41404

Hyperoxia and hypoxia effects on mitotic activity in regenerating and normal rat liver exposed to environmental conditions
c04 A69-43565

Suitability of white rats for suborbital studies of behavior in gravity fields
[NASA-CR-1255] c05 N69-14094

RAY TRACING

Nonvertical propagation effects on high altitude topside ionosphere sounder data reduction, using ray tracing
c13 A69-18838

Propagation characteristic model study of kinked Z trace observed on topside ionograms and explained by magnetoionic theory
c13 A69-37893

Comparison of ray trace methods for estimating sound intensity variations due to atmospheric variability as determined by Monte Carlo methods
[NASA-CR-1337] c23 N69-23199

RAYLEIGH-RITZ METHOD

Theoretical analysis of free vibration of discretely stiffened cylindrical shells with arbitrary end conditions
[NASA-CR-1316] c32 N69-28164

RC CIRCUITS

Delta functions spectrum in reciprocal time domain for LC and RC structures due to impulse response in distributed parameters
c10 A69-21327

Multiloop feedback in active distributed RC networks for low parameter sensitivity with low amplifier gain compared to single loop circuits
c10 A69-34679

REACTANCE

Antenna reactance from sounding rocket in ionosphere, showing variations relationship to rocket spin period
c13 A69-39964

Thin film microwave irises with capacitive reactance
[NASA-CR-1364] c26 N69-28096

REACTION KINETICS

Reaction rate and mechanism for low temperature reaction between lithium hydride and liquid ammonia, noting chemisorbed ammonia dissociation at interface
c06 A69-11285

Reaction rate constants of ion-molecule interchange reaction as function of temperature, flow velocity, activation energy and constant part of steric factor P
c06 A69-32312

Chemical reactions activation energy at high temperature, noting cross section shape role for deducing activation energy from rate data
c06 A69-34443

Rate coefficient for primary process in removing molecular nitrogen in high vibrational levels from active nitrogen by N atoms
c24 A69-36424

Elemental fluorine reactions with Ni, Cu, Fe, Ti, Be-Al, Zr and Ag, giving reaction rate constants, activation energies, etc
c06 A69-39706

Computerized Arrhenius equation component reliability extrapolation techniques
[NASA-TN-D-4902] c19 N69-13368

Boundary layer and chemical reactions in hypersonic gas flow
[NASA-TT-F-549] c33 N69-31947

REACTION TIME

Yttrium effect on rate of thermal decomposition of silver carbonate powder and pressed pellets by isothermogravimetric analysis, examining water vapor, Co 60 gamma radiation and temperature effects
c06 A69-30442

REACTION WHEELS

Semiactive gravity gradient stabilization system design for low altitude earth oriented spacecraft attitude control, using active reaction wheel scanner
c31 A69-18334

Photoelectronic commutation by dc torquer-driven reaction wheel for spacecraft attitude control
[NASA-TN-D-5265] c03 N69-30945

REACTIVITY

Pulsed neutron source studies to determine shutdown reactivities of unreflected solution reactor
[NASA-TN-D-5487] c22 N69-39186

REACTOR CORES

Beryllium reflector distortion in Plum Brook Reactor due to neutron embrittlement and gas formation, noting material surveillance, replacement, etc
c22 A69-13131

Cavity reactor consisting of dilute fuel core surrounded by moderating reflector to attain very high temperatures in gaseous cores
c22 A69-18954

Thermal neutron flux perturbations in cylinders in test reactors, using regression analysis to obtain polynomials for flux perturbation, depression, self shielding factors, etc
c22 A69-38274

Characteristics, performance potential, and problems of solid, liquid, and gas core nuclear rocket engines
[NASA-TM-X-1685] c22 N69-10067

Elastic-plastic and creep analysis predictions of core movement during operation of fast nuclear reactor
[NASA-TN-D-5012] c22 N69-16381

One megawatt reactor design for Brayton cycle space power application - thermal analysis and core design
[NASA-TN-D-5013] c22 N69-17313

Beryllium swelling and replacement in Plum Brook reactor
[NASA-TM-X-1794] c22 N69-26233

Curved porous wall gas core reactor flow distribution experiment
[NASA-TM-X-1852] c12 N69-32217

Reflector based poison drum control on equal size reactor cores fueled with U-233 and U-235
[NASA-TM-X-1883] c22 N69-36756

REACTOR DESIGN

Cavity reactor consisting of dilute fuel core surrounded by moderating reflector to attain very high temperatures in gaseous cores
c22 A69-18954

Gas core reactor curved porous walls geometry tested with clear and smoky air injection, noting mass flow ratio in reactor cavity
c22 A69-35181

Brayton-B generator for 2-10 kWe production, describing design, heat source/rejection, efficiencies and preliminary test data analysis
c03 A69-42278

One megawatt reactor design for Brayton cycle space power application - thermal analysis and core design
[NASA-TN-D-5013] c22 N69-17313

One megawatt reactor design for Brayton cycle space power application - neutronics design
[NASA-TN-D-5014] c22 N69-17314

REACTOR MATERIALS

Properties and uses of liquid metal reactor fuels, including heat transfer processes in variously shaped channels, boiling and condensation of metals, and reactor control equipment
[NASA-TT-F-522] c33 N69-30507

REACTOR SAFETY

Improved delayed neutron fission product monitor for operation in reactor coolant system

[NASA-TM-X-1886] c14 N69-38766

REACTOR TECHNOLOGY
Pulsed neutron source studies to determine shutdown reactivities of unreflected solution reactor
[NASA-TN-D-5487] c22 N69-39186

REAL GASES
Shock wave propagation in real gases
[NASA-TT-F-585] c12 N69-40824

REAL TIME OPERATION
Radiation protection plan for Apollo lunar mission based on real time monitoring of solar activity and radiation in spacecraft
[AIAA PAPER 69-19] c29 A69-18113
Real time targeting for Apollo lunar orbit insertion maneuver burn, discussing impulsive maneuvers for flight control
[AIAA PAPER 68-848] c31 A69-39760
Real time digital computer hardware simulation of Apollo Telescope Mount /ATM/ mission
[AIAA PAPER 69-940] c11 A69-40323
Real time telemetry, tracking and command links by synchronous satellite relay, describing ATS-Nimbus E S band experiment
c07 A69-41759
Ionospheric irregularities effect on accurate satellite position determination in near real time
c07 A69-42549
Numerical integration techniques for real time digital flight simulation
[NASA-TN-D-4900] c11 N69-11371
Predictive display systems using repetitive, fast time, on-line computation
[NASA-CR-1274] c05 N69-17738
Iterative solution of boundary value problem for rapid optimization of multiple-burn rocket flights
[NASA-CR-1430] c30 N69-36439

RECOMBINATION COEFFICIENT
Atomic nitrogen collisional ionization and recombination rates under assumed quasi-steady nonequilibrium distribution of electron state populations
c24 A69-43700

RECOVERABLE SPACECRAFT
Flexible parawing lifting decelerator research data from wind tunnel and flight tests, noting manned space vehicle recovery and aircraft escape systems
[AIAA PAPER 68-967] c02 A69-43715

RECTANGLES
Flow characteristics in two dimensional channel with rectangular cavity
[NASA-CR-1245] c12 N69-14095

RECTANGULAR GUIDES
Waveguide fed rectangular aperture antenna with dielectric plug load, describing admittance resonant perturbation due to excited TE mode
c09 A69-41589

RECTANGULAR PANELS
Influence of fabrication methods on compressive strength of titanium alloy skin stringer panels
[NASA-TN-D-5389] c15 N69-34707
Flutter investigation at Mach 3 of rotationally restrained panels and comparison with theory
[NASA-TN-D-5508] c32 N69-40087

RECTANGULAR WINGS
Spin-tunnel investigation of scale model of straight wing, twin boom counter insurgency airplane
[NASA-TM-X-1602] c02 N69-34988

RECURSIVE FUNCTIONS
Recursive formulas for numerical evaluation of real convolution integral for simulation of control systems and electrical networks on digital computer
c19 A69-17250
Recursive equation for estimating variance of sequential random numbers
[NASA-TN-D-5465] c19 N69-38178

RED SHIFT
Red shift-magnitude relation for universe model and observational data
[NASA-TN-D-5398] c30 N69-34884

REDUCED GRAVITY
Excessive extrapolation limitations in applying transient data to low gravity fluid behavior for orbital refueling systems, presenting orbital fluid transfer experiment
[AIAA PAPER 69-566] c31 A69-32755
Space manufacturing processes for orbital low and zero gravity environment, discussing buoyancy and thermal convection sensitive and molecular forces controlled methods
[AAS PAPER 69-486] c30 A69-42844
Natural frequency of liquids in annular cylinders under low gravity conditions
[NASA-TN-D-5412] c12 N69-35842
Reynolds number relation to single noncondensable bubble motion under low gravity conditions
[NASA-TN-D-5462] c12 N69-38032

REDUCTION (CHEMISTRY)
Radiation induced reduction of ammoniacal nickel /2/ sulfate to metallic nickel
[NASA-TN-D-5213] c06 N69-24940

REDUNDANCY ENCODING
Huffman minimum redundancy coding extension to run-length information based on Poisson distribution, including optimization and data compression applications
c07 A69-36262

REDUNDANT COMPONENTS
Valving concepts and functional approaches for inert gas attitude control thrustor systems providing redundancy safeguards at minimum weight, volume and power costs
[AIAA PAPER 69-843] c28 A69-39373

REENTRY COMMUNICATION
Measurements of mutual interference heating for probe antenna mounted on Apollo reentry configuration
[NASA-TM-X-1787] c01 N69-29318
Measurement of thermal accommodation coefficients between liquids and high temperature gases in low pressure reentry communications blackout intervals
[NASA-CR-1330] c07 N69-32721

REENTRY EFFECTS
Flash X ray unit with special film transport devices to obtain sequenced dynamic radiographs of ablating models during reentry simulation tests
c11 A69-35720
Flow field predictions for radio attenuation measurements on blunt reentry cone
[NASA-CR-1308] c07 N69-28223
Microwave radiometric techniques for reentry plasma measurements
[NASA-TN-D-5274] c25 N69-29600

REENTRY GUIDANCE
Reentry and planetary entry physics and technology 2, advanced concepts, experiments, guidance-control and technology
c31 A69-25718
Guidance and navigation for atmospheric entry phase of vehicles
[NASA-SP-8015] c21 N69-19518

REENTRY PHYSICS
Correlations of stagnation point radiative heat transfer for earth reentry, noting use of nongray absorption coefficient models
c33 A69-14736
Reentry and planetary entry physics and technology 2, advanced concepts, experiments, guidance-control and technology
c31 A69-25718
Apollo afterbody heat transfer, studying ablation effects for various reentry angles of attack
c33 A69-43680
Vacuum ultraviolet detector-spectroscopy systems for capsule reentry measurements
[NASA-CR-1268] c09 N69-18761

REENTRY SHIELDING
Apollo thermal protection system, noting low density ablation, flight and ground tests
[AIAA PAPER 68-1142] c31 A69-13558

REENTRY TRAJECTORIES
Computer mechanization of reentry equations with four degrees of freedom
[NASA-CR-1249] c30 N69-13300

REENTRY VEHICLES
Make wire, light pipe and spring wire ablation sensors development for measuring parameters of heat shield materials for reentry vehicles
c14 A69-15428
Pyrotechnic activated calorimeter for reentry package design of vehicles entering earth

atmosphere at lunar return velocities
c11 A69-23026
Hypervelocity reentry simulation problems for slender and blunt bodies, defining significant parameters
c30 A69-30376
Collection of papers on thermal design principles of spacecraft and entry bodies
c33 A69-34372
Aerodynamic and flight characteristics of variable geometry entry spacecraft during subsonic wing deployment and landing
[AIAA PAPER 69-742] c01 A69-34407
Ablation heat shields, emphasizing dielectric low cost fabrication and application to entry vehicles
c15 A69-35538
Guidance and navigation for atmospheric entry phase of vehicles
[NASA-SP-8015] c21 N69-19518

REFLECTANCE
Diffusion pump oil reflectance and absorption coefficients measured in three thicknesses using light source, monochromator and detector
c23 A69-23647
Reflection coefficient of symmetric parallel plate waveguide operating in TEM mode illuminating lossless dielectric layer, using wedge diffraction and geometrical optics methods
c09 A69-34802
Bidirectional reflectance of earth atmosphere and cloud formation above equatorial Pacific observed by synchronous satellite as function of angular dependence
c20 A69-43154
Symmetric parallel plate waveguide reflection coefficient analyzed
[NASA-CR-1327] c07 N69-24059
Solar absorptances and spectral reflectances of metals
[NASA-TN-D-5353] c17 N69-31895

REFLECTING TELESCOPES
Single and double mirror systems geometrical optical image aberrations noting focal number, angle of field, secondary magnification and mutual position tolerances
c23 A69-24836

REFLECTOMETERS
Portable integrating sphere reflectometer, describing optical system, construction, etc
[AIAA PAPER 69-599] c14 A69-33264
ATS 3 satellite reflectometer experiment carrying test samples to measure specular reflectance, noting silica shield effects
[AIAA PAPER 69-644] c33 A69-33270

REFLECTORS
Beryllium reflector distortion in Plum Brook Reactor due to neutron embrittlement and gas formation, noting material surveillance, replacement, etc
c22 A69-13131
Reflector based poison drum control on equal size reactor cores fueled with U-233 and U-235
[NASA-TM-X-1883] c22 N69-36756
Performance prediction for fast reactor with axially moving reflector control system
[NASA-TM-X-1911] c22 N69-40061

REFRACTIVITY
Refractive index computation for free electrons and neutral atoms in cesium plasma at helium neon laser wavelengths
[NASA-TN-D-5328] c25 N69-30622

REFRACTORY MATERIALS
High temperature capacitor consisting of thin wafers of pyrolytic boron nitride noting fabrication, dissipation factor and capacitance
c03 A69-15299
Refractory cone models made of copper and Co coated Be for force tests in high enthalpy hypersonic arc tunnels at high simulated attitudes
c11 A69-26796

REFRACTORY METAL ALLOYS
Refractory metal alloys metallurgy and technology - Conference, Washington, D. C., April 1968
c17 A69-18790
NASA programs for development of high temperature alloys for advanced air breathing engines emphasizing cast Ni-base alloy
[ICAS PAPER 68-26] c17 A69-43718
Controlled oxygen additions to refractory metal alloys
[NASA-TM-X-1799] c17 N69-26952

REFRACTORY METALS
Less common refractory metals /rhenium, technetium, hafnium, noble metals/ properties, phase equilibria, etc
c17 A69-18793
Crack initiation prediction in high temperature components subjected to arbitrary thermal-mechanical cycling
c32 A69-28252
Solubility of refractory metals and alloys in liquid potassium and lithium
[NASA-CR-1371] c17 N69-27059
Performance prediction for fast reactor with axially moving reflector control system
[NASA-TM-X-1911] c22 N69-40061

REFUELING
Excessive extrapolation limitations in applying transient data to low gravity fluid behavior for orbital refueling systems, presenting orbital fluid transfer experiment
[AIAA PAPER 69-566] c31 A69-32755

REGENERATION (PHYSIOLOGY)
Regenerative life support system development, considering synthesized organic compounds and microorganisms as foods for long duration space missions
c04 A69-37623
Conference on bone diseases and regeneration, cellular differentiation, and homeostasis of calcium
[NASA-SP-161] c04 N69-10444

REGENERATIVE COOLING
Heat transfer characteristics of water/cryogenic hydrogen heat exchanger for nuclear rocket reactor
[NASA-TN-D-5429] c33 N69-36701

REGENERATIVE FUEL CELLS
Performance of prototype hydrogen oxygen electrolytic regenerative fuel cell stack with gas storage tank
[NASA-CR-1244] c03 N69-18885
Electrochemical evaluation of electrode organic electrolyte combinations for rechargeable battery systems
[NASA-CR-1434] c03 N69-36829

REGRESSION ANALYSIS
Regression generated radiometric and contour height fields of North American Continent using Nimbus 2 IR equivalent black body temperature and geopotential data
c20 A69-42896
Regression analysis procedures for evaluating tracking system measurement errors
[NASA-TN-D-4826] c19 N69-14476
Aspects of human operator performance in low order compensatory control tasks studied with regression analysis
[NASA-CR-1259] c05 N69-16212

REGRESSION COEFFICIENTS
Systematic investigation of mathematical models by comparison of experimental and analytical regression coefficients
[NASA-TM-X-1797] c19 N69-25311

REINFORCED PLASTICS
Compressive behavior of uniaxial filament reinforced epoxy tubes for aerospace structures, using hand layup method with Teflon mandrel and sleeve
c15 A69-22339
Lightly loaded truss structures fabricated from Be, Be-Al alloy and uniaxial B filament reinforced epoxy tubing for unmanned spacecraft applications
c17 A69-35504

REINFORCED SHELLS
Dynamic analysis of axisymmetric ring stiffened shells with attached asymmetric elastic structures, noting vibration modes
c32 A69-25525
Computer program determination of barreling effect on strength of ring and stringer stiffened shells designed to support axial compression loads
c32 A69-43671

Structural synthesis of cylindrical shell reinforced with rectangular cross section stiffeners
[NASA-CR-1217] c32 N69-14254
Predicting buckling of thin walled, uniform stiffened and unstiffened circular cylindrical shells under static loading
[NASA-SP-8007] c32 N69-23320

REINFORCEMENT (STRUCTURES)
Optimal structural design for sandwich-shaped and ring-stiffened loaded shells of revolution
[NASA-CR-1424] c32 N69-35515

REINFORCING FIBERS
Glass, boron and graphite filament wound resin composites and liners for cryogenic pressure vessels
c18 A69-16488
Fiber-metal matrix composites fabrication, applications, mechanical properties and powder metallurgy
c17 A69-20204
Failure criteria for predicting filamentary composite strength under uniaxial and combined stresses from properties and fabrication process considerations
c32 A69-21479
Tungsten alloy fiber reinforced nickel base alloy composites stress-rupture strength, oxidation and impact resistance for high temperature turbojet engine buckets
c17 A69-29010
Tensile data and photomicrographs of explosively bonded metal matrix composites interfaces
c15 A69-43452
Compressive properties and weight saving of metals reinforced on surface with resin bonded fibers
[NASA-TN-D-4878] c17 N69-11012
Mechanical behavior of boron-epoxy and glass-epoxy filament-wound cylinders under various loads
[NASA-TN-D-5050] c18 N69-19825
Theory and test results of tensile strength of epoxy rings and belts reinforced by boron filaments
[NASA-TN-D-5053] c18 N69-19918
Zero thermal expansion composites of high strength and stiffness
[NASA-CR-1324] c32 N69-24876

REJECTION
Water rejection dynamics in hydrogen oxygen fuel cells
[NASA-TN-D-4956] c03 N69-14518

RELATIVISTIC PARTICLES
Interplanetary relativistic electrons from solar flare events
c29 A69-15528
Maximum number of binary collisions for three particles with zero range forces in relativistic rescattering singularities studies
c24 A69-19788
Rotational energy conversion of neutron star into relativistic electrons energy suggested by increasing period of pulsating radio source in Crab Nebula
c30 A69-21454
Relativistic solar electron detection in interplanetary space during July 7, 1966 proton flare event, noting energy spectrum and time history
c29 A69-23766

RELATIVITY
Einstein field equations solutions generated via static spherically symmetric mass and charge distributions
c23 A69-32053

RELAXATION (MECHANICS)
Mechanical relaxation of poly 4 methyl pentene 1 at cryogenic temperatures, discussing temperature dispersion curve and secondary absorption associated with thermal motion of side chains
c18 A69-16492
Vacancy relaxations in bcc crystals using energy dependence on radial displacements from defect of nearest neighbor sets, discussing crystal size and shape
c26 A69-16529
Modified model for vibration-dissociation relaxation coupling phenomena in nonequilibrium high temperature gas flow, discussing parameter U variation with kinetic temperature
c12 A69-37208
Steady state stress relaxation analysis of turbine blade cooling designs
[NASA-TN-D-5282] c28 N69-29321
Turbulent boundary layer measurements on axisymmetric hypersonic nozzle walls
[NASA-TN-D-5433] c12 N69-36805

RELAXATION METHOD (MATHEMATICS)
Monte Carlo relaxation method for physically self consistent model stellar atmospheres, discussing stability, accuracy and convergence of solution
c30 A69-36337

RELAXATION OSCILLATORS
Negative differential resistance effect producing relaxation type oscillations in n-type gallium arsenide
c26 A69-10557

RELAY SATELLITES
Data relay satellite systems for support of NASA R and D missions, discussing communications between satellites and to mission control
c07 A69-25296
Libration point relay satellites for continuous communication link between earth and lunar far side, discussing trajectories and halo orbit stationkeeping
c30 A69-30188
Tracking and Data Relay Satellite System with synchronous orbit satellites to relay data between low altitude earth orbital spacecraft and mission control centers
c07 A69-41755
RFI effects of earth based emitters on operation of geosynchronous satellites for data relay from near earth orbiting satellites, noting frequency assignments
c07 A69-41757
Real time telemetry, tracking and command links by synchronous satellite relay, describing ATS-Nimbus E S band experiment
c07 A69-41759
Telecommunications performance of two lunar relay satellite system /LRSS/, determining operation capabilities with Apollo communications system
c07 A69-42508

RELAY 2 SATELLITE
Summary of operation, communications, and other experiments of Relay 2 satellite
[NASA-SP-151] c31 N69-21065

RELIABILITY
Reliability handbook for failure analysis of silicon integrated microcircuits
[NASA-CR-1348] c09 N69-25328
Upgrading of electronic power supply for greater reliability in aerospace use
[NASA-TM-X-1875] c03 N69-35763

RELIABILITY ENGINEERING
Reliability - Conference, Chicago, January 1969
c15 A69-34476
Scanning electron microscopy for reliability studies in semiconductor devices
c26 A69-35788
Reliability and maintainability - Conference, Denver, July 1969
c15 A69-35999
Failure data role in management of launch operations reliability program
c11 A69-36022
Pretesting techniques of suppliers and users and effects on electroexplosive devices
[NASA-CR-1203] c15 N69-10298
Reliability handbook for silicon monolithic microcircuits - applications
[NASA-CR-1346] c09 N69-23225
Reliability handbook for silicon monolithic microcircuits - failure mechanisms
[NASA-CR-1347] c09 N69-23226
Reliability study of Saturn 5 launch vehicle manual backup control system
[NASA-TN-D-5261] c21 N69-28018
Clean room technologies for control of contaminants for component reliability
[NASA-SP-5074] c05 N69-33775

REMOTE HANDLING
Engineering problems survey on teleoperator control systems
[NASA-SP-5070] c05 N69-21478

Remote information retrieval facility description
[NASA-CR-1318] c08 N69-23381
REMOTE SENSORS
Remote sensing of environment - Conference, University of Michigan, Ann Arbor, April 1968
c14 A69-26974
Microwave radiometric sensor operational principles and capabilities, discussing antennas and radiometric receivers
c07 A69-26976
Earth resources remote sensing from spacecraft noting meteorology, oceanography, forestry, agriculture and IR detection of plant diseases and pollution
c34 A69-26978
Optical radar studies of lower atmosphere, giving Mie theory calculations of clear atmosphere volume backscattering cross sections for four laser wavelengths
c07 A69-27001
Temperature profiles and associated wind profiles obtained with Jimsphere/FPS-16 radar system at Cape Kennedy, discussing remote CAT detector assessment
c20 A69-33739
NASA Earth Resources Survey Aircraft Program, describing aircraft and remote sensors characteristics
c14 A69-36259
RENDEZVOUS GUIDANCE
Visual sensing and spacecraft guidance for earth orbit rendezvous maneuvers
[NASA-CR-1214] c05 N69-13161
RENDEZVOUS TRAJECTORIES
Low thrust trajectories for minimum time rendezvous between continuous thrust interceptor and passive target vehicle, comparing calculus of variations and steepest ascent analyses
c30 A69-32177
Computational method for time optimal space rendezvous between rocket vehicle and circular orbit target
[NASA-TN-D-5017] c30 N69-16210
Current computer programs for low thrust trajectory analysis using flyby and rendezvous trajectories
[NASA-TM-X-1824] c08 N69-30014
REPLICAS
Plastic backing films removal from carbon electron microscope replicas by maintaining specimens in horizontal position
c14 A69-21651
RESEARCH AIRCRAFT
Wind tunnel stability tests to determine effect of hypersonic research engine on aerodynamic characteristics of research aircraft
[NASA-TM-X-1840] c01 N69-38612
RESEARCH AND DEVELOPMENT
30 cm diameter mercury bombardment low impulse thrustor development for potential space applications, discussing performance and control
[AIAA PAPER 69-238] c28 A69-21256
Research and development program in annular slit colloid thrustor technology, proving thrustor feasibility by performance tests
[AIAA PAPER 69-287] c28 A69-21257
In-house research on R and D management in government agencies, discussing manning, training, center programs, case studies, etc
c34 A69-38022
Materials research structural design cycle, discussing simultaneous optimization, constituent materials, fabrication process, load environment and mission constraints
c32 A69-42991
RESEARCH FACILITIES
Scientific advances from space research in communications astronomy, electronics, transportation, etc
c30 A69-10498
Flight simulator with large lateral motion for large and supersonic transport aircraft, emphasizing reproduction of cockpit accelerations due to supersonic engine thrust loss
c11 A69-43044
NASA Plum Brook Reactor Facility experimental program
[NASA-TM-X-1853] c22 N69-33132
RESEARCH PROJECTS
NASA Space Application Program strategy, discussing research and development trend toward complexity, versatility and multidisciplinary use of larger spacecraft
c30 A69-13427
NASA civil aviation electronics research program, discussing feasibility of V/STOL aircraft all-weather operations
c34 A69-16718
Experiment requirements for manned earth orbiting biotechnology laboratory
[NASA-CR-1409] c05 N69-35540
RESIDUAL GAS
Residual interstellar gas from protostar formation detected as high luminosity IR object
c29 A69-27593
RESIDUAL STRESS
Internal stress and deposit hardness of nickel electrodeposited containing controlled quantities of meta-benzenedisulfonic acid
[NASA-TN-D-5188] c17 N69-36697
RESISTOJET ENGINES
Ammonia resistojet stationkeeping subsystem onboard ATS 4 satellite, noting flight test data agreement with ground tests
[AIAA PAPER 69-296] c28 A69-21212
ATS 3 spacecraft ammonia-fueled resistojet engine test performance
[AIAA PAPER 68-553] c28 A69-39754
RESISTORS
Voltage divider network board composed of composite carbon resistors for measurement of terminal voltage of 3 MeV Dynamitron electron accelerator recalibration
c11 A69-17705
Composite carbon resistor characteristics used for accelerator terminal voltage measurement
[NASA-TM-X-1718] c24 N69-14398
RESOLUTION
Electron irradiation effect on resolution of lithium-drifted silicon semiconductor detectors
[NASA-TN-D-4901] c14 N69-10933
Atmospheric turbulence limits on resolution of manned aerospace observations of ground
[NASA-TN-D-4940] c20 N69-12934
RESONANCE
Resonance absorption integrals for rhenium 185, rhenium 187, and natural rhenium in foils and thin films
[NASA-TN-D-4938] c24 N69-13152
Analysis of Fitzgerald apparatus for extraneous resonant modes, dynamic compliance, and mechanical impedance
[NASA-TN-D-5103] c26 N69-20798
Multigroup calculations of resonance neutron capture in thick slab of depleted U-238
[NASA-TM-X-1878] c24 N69-36901
RESONANCE SCATTERING
Minimization of optical resonance scattering by adjustment of monochromator slit geometry
[NASA-TM-X-1702] c24 N69-13210
RESONANCE TESTING
Identification of structural systems using near resonance testing
[NASA-TN-D-5069] c32 N69-17737
RESONANT FREQUENCIES
Gaseous He bubbles injection into liquid propellant launch vehicle fuel lines to reduce vehicle POGO oscillations by lowering feed system natural frequencies
c31 A69-25498
Saturn 5 longitudinal instability /POGO/ precluded by lowering S-1C stage propulsion system resonance below structural frequency
[AIAA PAPER 69-548] c31 A69-32658
Rosman I reflector antenna for collecting data from earth orbiting satellites, discussing dynamic analysis of structural response to natural frequencies
c32 A69-42133
Loss factor and resonant frequency of viscoelastic shear damped structural composites
[NASA-CR-1269] c32 N69-17766
Natural vibration modal analysis as related to space vehicle design criteria
[NASA-SP-8012] c32 N69-22773
Effect of shallow meridional curvature on vibration of nearly cylindrical shells

[NASA-TN-D-5143] c32 N69-22821
Transient response of coupled acoustic cavity resonators
[NASA-CR-1421] c23 N69-35286
Natural frequency of liquids in annular cylinders under low gravity conditions
[NASA-TN-D-5412] c12 N69-35842

RESPIRATORY PHYSIOLOGY
Human physiological responses to angular acceleration during breath holding, Mi, Valsalva and Mueller respiratory maneuvers in hollow spherical simulator
c05 A69-41679
Respiratory system and oxygen metabolism regulation in man and animals
[NASA-TT-F-501] c04 N69-31401

RESPIRATORY SYSTEM
Respiratory system and oxygen metabolism regulation in man and animals
[NASA-TT-F-501] c04 N69-31401

RETROREFLECTION
Lunar laser beam retroreflection observations, showing agreement with predicted ephemeris and signal strength
c30 A69-43197

RETROROCKET ENGINES
Development and test firing of improved igniter for first stage retrorockets of Atlas Centaur launch vehicle
[NASA-TM-X-1676] c28 N69-13275

RETURN TO EARTH SPACE FLIGHT
Pyrotechnic activated calorimeter for reentry package design of vehicles entering earth atmosphere at lunar return velocities
c11 A69-23026
Entry aerodynamics at lunar return conditions from command module of Apollo 4 flight
[NASA-TN-D-5399] c31 N69-38820

REUSABLE SPACECRAFT
Low cost rate transportation as mandatory goal for future space program, discussing recovery and reuse, launch system costs, hardware development, etc
c31 A69-38117
Apollo 11 mission and future space exploration prospects including moon base, manned space station, reusable shuttle vehicles, etc
c30 A69-41477

REVERSED FLOW
Flow field throughout wind tunnel containing rotor with sharply defected blades, noting reversed flow effect in front of wake
c11 A69-35228

REYNOLDS NUMBER
Subliming ablation effects on boundary layer transition for cones in hypersonic flow, discussing Reynolds numbers measured in wind tunnel tests
[AIAA PAPER 68-40] c01 A69-31881
Free stream disturbances influence on hypersonic boundary layer transition Reynolds number in heated and unheated flows
[AIAA PAPER 69-704] c12 A69-33453
Cone boundary layer transition location and Reynolds number as function of nose bluntness combined effect with Ar, air and He mass injection
[AIAA PAPER 67-706] c12 A69-33476
Effect of unit Reynolds number, nose bluntness, angle of attack, and roughness on transition on 5 degree half-angle cone at Mach 8
[NASA-TN-D-4961] c01 N69-14872
Transonic wind tunnel studies on airfoil to determine effects of Reynolds number and boundary layer transition location on shock induced separated flow
[NASA-TN-D-5003] c01 N69-16121
Laminar heat transfer distributions for blunted-cone, cone frustum reentry configuration at hypersonic speed using Reynolds number
[NASA-TN-D-5146] c33 N69-22997
Turbulent boundary layer of subsonic transport fuselage with pressure gradient, Reynolds number, and angle of attack
[NASA-TN-D-5242] c01 N69-28112
Laminar heating rate from wind tunnel tests using angle of attack and Reynolds number
[NASA-TN-D-5450] c12 N69-37604
Reynolds number relation to single noncondensable bubble motion under low gravity conditions
[NASA-TN-D-5462] c12 N69-38032

RHENIUM
Rhenium-niobium cylindrical thermionic converters with mechanically polished or electroetched emitters, comparing performance
c03 A69-13126
Vacuum arc melted W and W-Re alloys mechanical properties, noting Re additions effects
c17 A69-20190
Creep rate-stress-temperature relations for powder metallurgy rhenium, discussing activation energy
c17 A69-34186
Quartz fiber adhesion to Re measured in LEED /low energy electron diffraction/ apparatus for clean and O layer surfaces, noting brittle fracture
c17 A69-35182
Resonance absorption integrals for rhenium 185, rhenium 187, and natural rhenium in foils and thin films
[NASA-TN-D-4938] c24 N69-13152
Ductilizing of Group 6A elements by rhenium and other solutes
[NASA-TN-D-4955] c17 N69-14403
Low energy electron diffraction analysis of quartz fiber adhesion to rhenium crystal surface
[NASA-TN-D-5229] c17 N69-25363

RHENIUM ALLOYS
Superplasticity in W-Re alloys, noting tensile properties, grain size and strain rate sensitivity for various Re contents at high temperatures
c17 A69-22990
Stress rupture and tensile properties of refractory metal wires at 2000 and 2200 deg F
[NASA-TN-D-5139] c32 N69-22823
Effect of rhenium on mechanical properties of hafnium carbide strengthened tungsten alloys
[NASA-TN-D-5348] c17 N69-31977

RHENIUM COMPOUNDS
Impregnation of polytetrafluoroethylene with hexaflourides of rhenium, molybdenum, and tungsten
[NASA-TN-D-4886] c06 N69-10126

RHODIUM ALLOYS
Emittance properties of hafnium oxide, cerium oxide, and iron titanate coatings on platinum rhodium alloy substrates
[NASA-CR-1413] c17 N69-35514

RICCATI EQUATION
Matrix Riccati and matrix quadratic equations in problems of stochastic control and filtering
c10 A69-16601

RIGID ROTORS
Undamped rigid rotor critical speed analysis for firm and flexible foundations, discussing effect of center of gravity and rotor shapes
[ASME PAPER 69-VIBR-49] c32 A69-24184
NASA flight test of hingeless rotor compound helicopter to determine lift sharing characteristics, showing rotor lift dependence on airspeed
c02 A69-29702
Frequency and critical speed analysis of rigid rotors on flexible foundations
[NASA-TN-D-4858] c32 N69-29159

RIGID STRUCTURES
Light rigid civil aircraft response to continuous atmospheric turbulence estimated using two rigid body degrees of freedom method for vertical and lateral gusts
[AIAA PAPER 69-766] c32 A69-35657
Calorimetric evaluation of three 1.5-meter diameter inflatable rigidized solar concentrators for solar dynamic cycle power systems
[NASA-TN-D-5234] c03 N69-28123
Equations of motion for rigid body rotor in linearized bearings
[NASA-CR-1391] c15 N69-36349
Comparison of fourth order Runge-Kutta numerical integration technique with two numerical integration formulas in mathematical models used for computing rigid body trajectories
[NASA-TN-D-5425] c30 N69-38769

RING CURRENTS
Ring current particle energy density distribution for symmetric portion of magnetic storm derived

from current magnetic field profile measurements
c29 A69-11227

RING STRUCTURES
Rotational spectrum of ethylene episulfoxide to determine molecular structure, particularly orientation of C sub 2 S ring
c06 A69-20535
Graphite fiber NOL rings and biaxial wound pressurized cylinders tested at ambient and cryogenic temperatures for tensile and cyclic fatigue properties
c18 A69-35521
Computer program determination of barreling effect on strength of ring and stringer stiffened shells designed to support axial compression loads
c32 A69-43671

RIOMETERS
Ground based solar proton monitoring, considering particle intensities and radiation dose rates from riometer absorption as function of time
c29 A69-32321

RLC CIRCUITS
Time varying resistance wire to arrest oscillations in pulsed capacitor discharge circuit, deriving over, under and critical damping conditions
c09 A69-41228

ROCKET ENGINE CASES
Rocket motor integration into Scout vehicle to improve performance
c31 A69-12384

ROCKET ENGINE CONTROL
Fluidic proportional thruster system for sounding rocket control
[ASME PAPER 68-WA/FE-32] c14 A69-16105

ROCKET ENGINE DESIGN
Ion accelerators design for Kaufman thrustors in terms of beam optics and grid lifetime, using digital computer and electrolytic tank analog
[AIAA PAPER 69-261] c28 A69-21261
Cryogenic core concept for flexible and economical delivery system
[AIAA PAPER 68-812] c31 A69-39753
Parameters of acoustic liner for maximum liner damping for rocket engines
[NASA-TM-X-1720] c28 N69-16152

ROCKET ENGINES
Fluidic proportional thruster system for sounding rocket control
[ASME PAPER 68-WA/FE-32] c14 A69-16105
Research and development program in annular slit colloid thrustor technology, proving thrustor feasibility by performance tests
[AIAA PAPER 69-287] c28 A69-21257
Performance of bipropellant fractional-pound rocket thrustor
[NASA-TM-X-1699] c28 N69-13237
Water electrolysis rocket engine performance tests
[NASA-TM-X-1737] c28 N69-19017
Wind tunnel force and pressure tests of rocket engine nozzle extensions on X-15-2 model at supersonic and hypersonic speeds
[NASA-TM-X-1759] c01 N69-20873
Boundary layer interaction in cooling tubes of rocket engines tends to lower convective heat transfer
[NASA-TN-D-5168] c33 N69-22931
Design of injectors and ablative thrust chambers for FLOX propane rocket engine with 1.2 inch throat diameter
[NASA-TN-D-5324] c28 N69-30560
Throat and nozzle insert design for ablative rocket engine using storable propellants
[NASA-TN-D-4964] c32 N69-33481
Design, development, and testing of 1000 pound thrust FLOX-propane ablative rocket engine
[NASA-TM-X-1873] c28 N69-35847
Historical development of liquid propellant rocket engines and aviation models
[NASA-TT-F-537] c34 N69-36314
Performance of radiation cooled magnetoplasmadynamic arc thrustors
[NASA-TM-X-1908] c28 N69-40058

ROCKET EXHAUST
Propellant condensation on surfaces near electric rocket exhaust, calculating particle arrival rates, backflow and desorption energies
[AIAA PAPER 69-270] c28 A69-21252
Pressure and heating rate correlations for rocket exhausts impinging on flat plates and curved panels, generating axisymmetric real gas exhaust plumes
c33 A69-26781
RAM-CA carbon-phenolic heat shield test in rocket engine exhaust
[NASA-TM-X-1841] c31 N69-32713

ROCKET FLIGHT
Rocket trajectory determination by tracking onboard light source against star background with image orthicon TV system
c07 A69-26965

ROCKET LAUNCHING
Exametnet meteorological rocket launchings and data dissemination, 1967 - tables
[NASA-SP-176] c20 N69-22570

ROCKET LININGS
Helmholtz resonators with variable cavity depths tested with unstable rocket combustor
[NASA-TN-D-5171] c33 N69-23351
Dynamic stability and performance of injectors, rocket liners, and supersonic combustors
[NASA-TM-X-1845] c33 N69-32468

ROCKET NOSE CONES
Aerodynamic loads on deployed canard surfaces and rocket nose section of Apollo launch escape vehicle
[NASA-TN-D-5260] c31 N69-28166

ROCKET NOZZLES
Hydrogen and methane combustion to simulate expansion of storable propellants
[AIAA PAPER 68-635] c33 A69-37188
Rocket engine evaluation of erosion and char as functions of fabric orientation for silica reinforced nozzle materials
[NASA-TM-X-1721] c28 N69-15475
Correlation equations for predicting gas-side heat transfer of axisymmetric rocket engine nozzles
[NASA-TM-X-1748] c33 N69-18898
Energy thickness in prediction of throat heat transfer in rocket nozzles using nozzle geometries and temperature ratios
[NASA-TN-D-5356] c33 N69-31869

ROCKET OXIDIZERS
Treatment procedure and preventive programs outlined for acute exposure to toxic rocket fuels or oxidizers
c05 A69-12498

ROCKET PROPELLANTS
Treatment procedure and preventive programs outlined for acute exposure to toxic rocket fuels or oxidizers
c05 A69-12498
Mercury electron bombardment thrusters, discussing mission, design, ground tests, components and thrust vectoring
c28 A69-26787
Lunar soil as building material and extraction of water, oxygen and rocket propellants from lunar materials for lunar colony needs
c30 A69-27907
Nonequilibrium performance of oxygen difluoride diborane rocket propellant
[NASA-TN-D-4992] c27 N69-16195

ROCKET SOUNDING
Simultaneous rocket measurements of D region temperatures and electron densities on anomalous winter day
c13 A69-16411
Radar backscatter and rocket profiles of ionospheric electron temperature, noting agreement in daytime flight measurements
c29 A69-25162
Rocket spectrographic observations of Alpha Virginis noting hydrogen Lyman absorption lines
c30 A69-27555
Spectrometric rocket measurements of ion concentrations between 200 and 630 km
c13 A69-31974
Ionospheric currents geophysical dc electric field measurement from sounding rockets, indicating anticorrelation with auroral luminosity
c13 A69-38508
Survey of rocket soundings to 60 km, and 100 km
[NASA-CR-1293] c13 N69-18700

ROCKET TEST FACILITIES
Short duration tube wind tunnel supersonic testing, noting Saturn S-1C base heating and

solid propellant rocket base burning tests
[AIAA PAPER 69-335] c11 A69-28271
ROCKET VEHICLES
Ballistically effective atmospheric parameters for rocket vehicle design manuals involving application of climatological concepts of meteorology
c31 A69-26874
Wind profile developed for calculation of deflection impulse for rocket with liquid injection thrust vector control
[NASA-TM-X-1708] c31 N69-14033
Aerodynamic characteristics in pitch of scale model of two and three stage rocket configuration at Mach numbers of 0.4 to 4.63
[NASA-TN-D-5378] c01 N69-34986
ROCKET-BORNE INSTRUMENTS
Nocturnal electron concentrations and temperature at Manitoba measured by rocket-borne Langmuir probe, compared with F 1 region
c29 A69-14008
Rocket-borne spectroheliograph for monochromatic solar photography in Mg II 2802.7 A line noting filter bandwidth, film polarizers and temperature control
c14 A69-24838
Spinning rockets UV spectrophotometry of early type stars, discussing instrumentation, calibration, data recording and stellar spectra
c30 A69-25812
ROCKET-BORNE PHOTOGRAPHY
Rocket-borne spectroheliograph for monochromatic solar photography in Mg II 2802.7 A line noting filter bandwidth, film polarizers and temperature control
c14 A69-24838
ROCKETS
Professional programs for aeronautics, rocketry and astronautics development
c34 A69-34552
Variational methods for determining optimum design and flight of rockets
[NASA-TR-R-297] c31 N69-15374
ROCKS
X Ray fluorescence of rock samples as applied to geological problems, noting standard deviations for element distribution
c14 A69-10890
RODS
Magnetically anchored eddy current and eddy current rod dampers for GEOS gravity gradient stabilized satellite
[NASA-CR-1282] c14 N69-18953
ROLL
Feasibility of using roll and yaw compensation to reduce inclination error of Scout launch vehicle
[NASA-CR-1209] c31 N69-16221
Human transfer characteristics in flight and ground simulation for roll tracking task
[NASA-TN-D-5007] c05 N69-17814
ROLLER BEARINGS
Design of Brayton rotating unit with roller bearings for space power system
[NASA-CR-1401] c15 N69-33450
ROLLING MOMENTS
Aerodynamics of bodies of revolution in nonplanar motion using nonlinear functional analysis of moments for motion about center of gravity
[AIAA PAPER 68-20] c01 A69-14714
Motion stabilization criteria for aircraft during spatial maneuvers
[NASA-TT-F-555] c02 N69-24761
ROOT-MEAN-SQUARE ERRORS
Root mean square time delay error with respect to playback time and autocorrelation function of tape recorded sine wave for studying jitter spectra
c14 A69-18827
ROTARY STABILITY
Herringbone grooved gas lubricated journal bearing stability, testing effects of geometries and clearances on onset speed for half frequency whirl
[ASME PAPER 68-LUBS-25] c15 A69-27271
Theory and clearance effects on stability of water lubricated herringbone-groove journal bearings
[NASA-TN-D-4883] c15 N69-10228
Operational and structural design criteria for artificial gravity stabilization of rotating space station
[NASA-TN-D-5426] c05 N69-39210
ROTARY WING AIRCRAFT
Aerodynamics of rotary wing and V/STOL aircraft - Conference, Buffalo, June 1969, Volume 3
c01 A69-41369
Wind tunnel investigation of steady state aerodynamics of composite lift VTOL aircraft model combining rotary and fixed wings
[NASA-TN-D-5232] c02 N69-28097
ROTARY WINGS
Flexible rotor blade dynamic response to radially moving force, emphasizing helicopter rotor vibration characteristics associated with tip-vortex impingement
[AIAA PAPER 69-203] c02 A69-19546
Aerodynamics of rotary wing and V/STOL aircraft-Conference, Buffalo, June 1969, Volume 2, Wind tunnel testing, new concepts in rotor control
c01 A69-35226
Flow field throughout wind tunnel containing rotor with sharply defected blades, noting reversed flow effect in front of wake
c11 A69-35228
Aerodynamic performance tests of autorotative unpowered rotor entry vehicle model at various Mach numbers and angles of attack
[AIAA PAPER 68-950] c01 A69-37155
Rotor aerodynamics research in terms of theoretical and experimental data comparison, rotor blade flow visualization and blade section camber
c01 A69-41372
Aerodynamic stability of helicopter rotor in forward flight
[NASA-CR-1332] c32 N69-34744
Approximative solution for dynamic response of flexible rotor blade to radially moving force
[NASA-TN-D-5410] c32 N69-36220
Tabulated bending moment transfer coefficients for helicopter rotor blades
[NASA-CR-1441] c32 N69-40359
ROTATING BODIES
Gravitational and magnetic torque effect on rotational motion of triaxial rigid body in regressing orbit about oblate primary mass
c30 A69-32240
Antenna reactance from sounding rocket in ionosphere, showing variations relationship to rocket spin period
c13 A69-39964
Air flow and attitude angle compared with theory for rotating externally pressurized air journal bearings
[NASA-TN-D-5192] c15 N69-27956
Eddy current torques on bodies rotating relative to uniform magnetic field
[NASA-TN-D-5086] c23 N69-29477
Mathematical simulation model for rigid body rotational kinematics
[NASA-TN-D-5302] c23 N69-39178
ROTATING CYLINDERS
Equations formulated for space vehicle reaction to rotating machinery and internal mass motion, evaluating dynamics of cylindrical space station rotating about major axis
c30 A69-16476
ROTATING ENVIRONMENTS
Rotational velocity estimates by observers during angular acceleration, noting vestibular function interpretation
c04 A69-15332
ROTATING FLUIDS
Fluid dynamic simulation of gas core nuclear rocket chamber for separating light and heavy gas via centrifugal force produced by MHD-driven rotational flow
[AIAA PAPER 69-727] c22 A69-33483
Hydrodynamic stability and vortex containment of two fluid wheel flow to helical disturbances contained by axial magnetic field
[NASA-TN-D-5372] c12 N69-32377
ROTATING PLASMAS
Rotating plasma disturbances onset in MPD arc, determining magnetic field dependence on mass flow, background pressure and propellant
[AIAA PAPER 69-232] c28 A69-21225
ROTATING SHAFTS
Rotating wickless hollow shaft heat pipe utilizing

centrifugal acceleration for return pumping of condensate and transferring high heat fluxes
[ASME PAPER 69-HT-19] c33 A69-43550
Single shaft Brayton rotating unit for 2 to 10 kilowatt space power generation system
[NASA-TM-X-1869] c03 N69-39238
ROTATION
Rotational effects on isothermal compressible flow across gas turbine sealing dam
[NASA-TN-D-5344] c15 N69-35799
ROTOR AERODYNAMICS
Flow field throughout wind tunnel containing rotor with sharply defected blades, noting reversed flow effect in front of wake
c11 A69-35228
Rotor aerodynamics research in terms of theoretical and experimental data comparison, rotor blade flow visualization and blade section camber
c01 A69-41372
ROTOR BLADES
Theoretical study of discrete frequency noise generated by turbocompressors and blades
[NASA-CR-1287] c28 N69-21476
Tabulated bending moment transfer coefficients for helicopter rotor blades
[NASA-CR-1441] c32 N69-40359
ROTOR BLADES (TURBOMACHINERY)
Performance evaluation of tandem rotor blade of single stage turbine
[NASA-CR-1254] c01 N69-13621
Performance comparisons of supersonic compressor rotor blades
[NASA-CR-1256] c28 N69-14210
Performance evaluation of oil lubrication system for antifriction bearing rotor system of Brayton cycle turbomachinery
[NASA-CR-1229] c15 N69-16463
Effect of rotor tip clearance on performance of 5-inch single-stage axial flow turbine
[NASA-TM-X-1757] c03 N69-20883
Performance and cavitation damage to axial flow pump rotor blades in high temperature liquid sodium
[NASA-TN-D-5138] c15 N69-21773
FORTRAN computer program for detailed solution of compressible, subsonic, nonviscous flow at leading or trailing edges of blade surface
[NASA-TN-D-5091] c01 N69-22938
Performance evaluation of plain rotor blade with plow type vortex generators
[NASA-CR-1342] c28 N69-24223
Prediction of cavitation performance of centrifugal pumps
[NASA-TN-D-5292] c15 N69-29165
Noncavitating and cavitating performance of inducer in liquid hydrogen
[NASA-TM-X-1854] c12 N69-33261
ROTOR LIFT
NASA flight test of hingeless rotor compound helicopter to determine lift sharing characteristics, showing rotor lift dependence on airspeed
c02 A69-29702
Wind tunnel and analytical study of conversion from wing lift to rotor lift on composite lift VTOL aircraft
[NASA-TN-D-5256] c02 N69-28044
ROTOR SPEED
Frequency and critical speed analysis of rigid rotors on flexible foundations
[NASA-TN-D-4858] c32 N69-29159
ROTORS
High speed foil bearing rotor support system
[NASA-CR-1157] c15 N69-14214
Large solar sail vehicle to operate in manner of helicopter rotor
[NASA-CR-1329] c31 N69-28861
ROUND TRIP TRAJECTORIES
Matched conic solutions to round trip interplanetary trajectory problems for use in guidance and navigation simulation
[NASA-TN-D-4942] c30 N69-14861
RUBBER
Reverted rubber during skidding of aircraft tires
[NASA-CR-1398] c02 N69-34915
RUBIDIUM
Moldavites and Ries crater material, studying Rb-Sr isochronal relationship
c13 A69-41341
RUBIDIUM ISOTOPES
Rb-Sr isotope patterns in tekites from Southeast Australian strewn field, studying Rb volatilization role in Rb-Sr isochron production
c13 A69-41342
RUBY LASERS
Optical parametric noise in water by ruby laser beam for phase matched four photon process
c23 A69-21751
RUNGE-KUTTA METHOD
Low order Runge-Kutta formulas with step control for heat transfer problems
[NASA-TR-R-315] c19 N69-30753
Comparison of fourth order Runge-Kutta numerical integration technique with two numerical integration formulas in mathematical models used for computing rigid body trajectories
[NASA-TN-D-5425] c30 N69-38769
RUNWAY CONDITIONS
Runway grooving to improve aircraft tire traction in adverse weather tested by F-4D and Convair 990A under wet conditions
[AIAA PAPER 69-773] c02 A69-35649
Aviation pilot reactions and opinions on grooved runways
[NASA-CR-1428] c02 N69-35861
Airplane response to ground roughness from three-track runway and taxiway profiles by elevation angle measurements
[NASA-TN-D-5444] c02 N69-38770
RUNWAYS
Runway and highway pavement grooving and traction studies
[NASA-SP-5073] c11 N69-20451

S

S MATRIX THEORY
Full wave calculation of gravity waves for thermospheric model, describing wave type reflection, transmission, conversion and coupling by scattering matrix elements
c13 A69-25150
S WAVES
Monte Carlo analysis of gold sphere transmission experiments at 24 keV neutron energy using S wave spin state data
[NASA-TN-D-5211] c24 N69-24826
SAFETY DEVICES
Pilot warning indicators to equip all aircraft at low cost, discussing Doppler system
c21 A69-16726
SAFETY FACTORS
Safety planning for use of reactive cryogens in large volume, noting FLOX and liquid fluorine
c27 A69-14468
Management system for safety in NASA Manned Space Flight Program, discussing hazard analyses and reduction precedence sequence
[AAS PAPER 69-522] c34 A69-42851
SAGITTARIUS CONSTELLATION
Nebulosity around FG Sagittae for origin and evolution of planetary nebulae, suggesting ejection of nebular shell
c30 A69-42887
SALT BATHS
Hot salt stress corrosion of Ti alloy, discussing hydrogen generation during elevated temperature exposure and embrittlement as manifestation of strain rate
c17 A69-39434
SALT SPRAY TESTS
Salt stress corrosion cracking effects on tensile and stress rupture properties of titanium alloy sheet
[NASA-TN-D-5417] c17 N69-36221
SALTS
Salts and organic solvents effect on halophile Halobacterium cutirubrum catalase, noting enzyme activity inhibition by cation and anion
c04 A69-35291
Electron transport chain of monovalent and divalent cations and of polyamines, studying effects on menadione reductase activity to determine salt dependence
c04 A69-41077
SAMPLES
Apollo lunar sample collection and analysis,

discussing astronauts activity and equipment, sample types, laboratories for radioactive counting and gas analysis, etc
c11 A69-40191

SAMPLING
Statistical method for evaluating goodness of fit between data set and theoretical distribution of random variables
[NASA-TR-R-313] c19 N69-30610
Recursive equation for estimating variance of sequential random numbers
[NASA-TN-D-5465] c19 N69-38178

SANDS
Force penetration characteristics of sand horizontally penetrated by various geometrically shaped models
[NASA-CR-1252] c18 N69-14764

SANDWICH STRUCTURES
Structural design of conical and tension shells using sandwich structures
[NASA-CR-1365] c32 N69-36357

SATELLITE ANTENNAS
Directional solar thermal field /sunlight/ effect on coupled nonplanar transverse and torsional vibrations of satellite cylindrical antennas in orbit
c32 A69-25534

SATELLITE ATTITUDE CONTROL
Multipulse thruster module design and development tests for spacecraft attitude control, noting micropulse solid propellant rocket motor
c03 A69-11762
Multijet electrothermal systems for attitude control and stationkeeping of synchronous communications satellite
[AIAA PAPER 67-723] c28 A69-12375
Semiactive gravity gradient stabilization system design for low altitude earth oriented spacecraft attitude control, using active reaction wheel scanner
c31 A69-18334
Biosatellite attitude control systems design development and flight test results for payload perturbing effects, discussing simulation activity
c31 A69-35094
Valving concepts and functional approaches for inert gas attitude control thrustor systems providing redundancy safeguards at minimum weight, volume and power costs
[AIAA PAPER 69-843] c28 A69-39373
Mass expulsion and momentum systems for orbiting space station attitude control optimized, considering reaction jet and control moment gyro systems
[AIAA PAPER 69-846] c31 A69-39376
Spacecraft wide angle attitude control system stability analysis, using air bearing table simulation
[AIAA PAPER 69-856] c31 A69-39384
Radio astronomy Explorer A attitude determination via disk-oriented programming ground support system for reducing and calibrating telemetry data, attitude prediction and command, etc
[AIAA PAPER 69-983] c08 A69-40363
Torqued two axis gimbaled boom actuator satellite attitude control
[AIAA PAPER 68-857] c21 A69-43245
Oscillations in pulse modulated satellite attitude control systems
[NASA-CR-1369] c21 N69-29967
Spinning satellite attitude stability
[NASA-TN-D-5268] c31 N69-32298
Optimal control method based on linear programming for satellite fuel consumption
[NASA-CR-1450] c21 N69-41036

SATELLITE CONFIGURATIONS
Small astronomy satellite /SAS/ design, power, command, telemetry and control systems
c31 A69-19126

SATELLITE CONTROL
Radar attitude sensing system for determining vehicle roll, pitch, yaw, altitude and velocity of earth and lunar orbital vehicles
c07 A69-13183
Small astronomy satellite /SAS/ design, power, command, telemetry and control systems
c31 A69-19126
NASA lunar survey and mapping for generating Apollo satellite landing navigation control, using analytic photogrammetry, camera position and altitude data of lunar topography
c14 A69-36931

SATELLITE DESIGN
RAE-A satellite design, simulation and flight performance, discussing gravity gradient stabilization
c31 A69-18328
Small astronomy satellite /SAS/ design, power, command, telemetry and control systems
c31 A69-19126
Small Scientific Satellite program, discussing payload for investigating magnetosphere and near interplanetary space
[IEEE PAPER 3C-1] c31 A69-19195
OGO for conducting diversified measurements to study earth atmosphere, earth-sun relationship, etc
c31 A69-36674
Orbital Experimental Capsule /OEC/ as subsatellite concept for Martian fields and particles measurements, noting Voyager exploring vehicle applications
c30 A69-39215

SATELLITE DRAG
Polar exosphere near solar maximum investigation by Explorer 19 and Explorer 24 drag satellites, considering density and atomic oxygen concentration measurements
c13 A69-31351

SATELLITE INSTRUMENTS
Small Scientific Satellite program, discussing payload for investigating magnetosphere and near interplanetary space
[IEEE PAPER 3C-1] c31 A69-19195
Satellite-borne experiments of neutral molecular beam-solid surface interactions, describing Molsink chamber, densitometer, sphere and paddlewheel satellites
c24 A69-36182
HgCdTe as IR satellite detector for terrestrial, atmospheric and ocean mapping, IR astronomy and optical communication
c26 A69-43666

SATELLITE NAVIGATION SYSTEMS
Artificial satellites as navigation aids, describing angle, range and range-angle systems, discussing orbital mechanics and communications difficulties
c21 A69-34855

SATELLITE NETWORKS
Navigation services satellite systems including position determination, communication and telemetry for ships and aircraft
[UN PAPER 68-95363] c21 A69-10479
Data relay satellite systems for support of NASA R and D missions, discussing communications between satellites and to mission control
c07 A69-25296
Tracking and data acquisition networks and communications systems for support of space missions, studying data processing, unified S Band System and Data Relay Satellite System
c07 A69-25933
Real time telemetry, tracking and command links by synchronous satellite relay, describing ATS-Nimbus E S band experiment
c07 A69-41759

SATELLITE OBSERVATION
Atmospheric model development relating temperature, density, moisture and energy measurements from satellite observations for long term weather forecasting
[UN PAPER 68-95397] c20 A69-10463
Orbiting satellite global all-weather oceanographic data acquisition to complement higher resolution data from ships, buoys and aircraft remote sensors
[UN PAPER 68-95878] c13 A69-10491
Magnetic field data from OGO-2 spacecraft and surface magnetic observatories, noting magnetic storm occurrence and magnetosphere inflation and detection of polar ionospheric currents
c13 A69-11125
Sudden magnetic field increase associated with July 8, 1966 sudden commencement observed by OGO 3 satellite in magnetotail

c13 A69-11226
Solar plasma observations during magnetic storms, discussing shocks and tangential discontinuities, geomagnetic variations and He
c13 A69-11234
Vela 3A and Explorer 33 elapsed time observations of earth bow shock
c13 A69-12299
Moon effect on intensity and angular distribution of energetic electron and proton shadowing as observed by Explorer satellites
c30 A69-16252
Explorer 35 measurements of low energy plasma in lunar orbit made by planar multigrid sensor programmed as retarding potential analyzer
c30 A69-16278
Photomultipliers response to energetic particles in terms of background current using data from OGO experiments
c14 A69-16932
Atmospheric measurements from satellites, discussing ATS-1 cloud images for definition of wind and use of WEFAX through ATS 2 satellites for data transmission
[AIAA PAPER 69-158] c20 A69-18038
Structure, temporal behavior, shape and length of earth magnetic tail via satellite mapping
c29 A69-19363
Geomagnetic tail topology, reconnection and interaction with moon from Explorer 33 satellite data
c13 A69-19365
Cosmic radio noise intensity measurements by ATS 2 satellite-borne radiometer
c30 A69-19715
Solar extreme UV, soft and hard solar X rays, cosmic X rays and gamma rays, cosmic ray particles and near earth visible radiation observed by OSO-3
c29 A69-22167
Sudden commencement associated discontinuities in interplanetary magnetic field observed by IMP 3 satellite, stressing shocks and tangential and rotational discontinuities
c30 A69-22183
Spectral intensity of high energy solar X rays observed during July 7, 1966 polar event with satellite OGO 3, suggesting nonthermal bremsstrahlung origin
c29 A69-23753
Simultaneous interplanetary magnetic field measurements by geocentric satellites Explorer 33 and IMP 3 of MHD shock wave associated with July 8, 1966 sudden storm commencement
c30 A69-23773
Satellite measurements of suprathermal electrons at conjugate sunrise, indicating photoelectron escape from production level and movement along geomagnetic lines into conjugate ionosphere
c29 A69-25144
Satellite observations of geomagnetic tail in magnetosphere near midnight meridian plane, discussing formation, shape, plasma sheet and models
c13 A69-26739
Earth resources remote sensing from spacecraft noting meteorology, oceanography, forestry, agriculture and IR detection of plant diseases and pollution
c34 A69-26978
Star twinkling absence for lunar observation laboratory, noting star distance measurement and laser action in stellar atmospheres
c30 A69-27172
High latitude ionization spikes observed by POGO spacecraft, noting frequency correlation with magnetic disturbances and development by high energy electron injections
c29 A69-28950
Suprathermal electrons energy distributions as function of magnetic latitude in polar ionosphere obtained by Explorer 31 satellite observation
c29 A69-28963
Discontinuities in interplanetary magnetic field direction presented on mesoscale from Pioneer 6 observation, emphasizing distribution in time
c30 A69-29970
Solar wind Helmholtz-type velocity discontinuities, noting plasma density and temperature stabilities from Explorer 34 observations
c29 A69-29971
Solar wind existence verified by direct measurements of interplanetary magnetic field and plasma, reviewing solar corona studies by satellites and space probes
c30 A69-30010
IQSY low energy galactic and solar cosmic ray observations made by various satellites and space probes, including hydrogen and helium energy spectra
c29 A69-30014
Banded chorus, VLF discrete emissions in magnetosphere in single variable frequency band with frequency depending on equatorial electron gyrofrequency
c13 A69-31981
Interplanetary magnetic fields from Explorer 33 magnetometer relationship to surface geomagnetic variations emphasizing unified view
c30 A69-32309
Survey of six year period of satellite observed tropical Pacific cloud mapping
c20 A69-33001
Vertical tropospheric humidity distribution estimation from IR spectra obtained by TIROS satellites
c13 A69-34284
Ion depletion in high latitude exosphere, considering OGO 2 simultaneous observations of positive ion concentration, VLF signal propagation and whistlers
c29 A69-34939
Earth bow shock waves in far upstream interplanetary medium observed from magnetic data of Explorer 34 satellite
c30 A69-34941
OGO for conducting diversified measurements to study earth atmosphere, earth-sun relationship, etc
c31 A69-36674
Solid state detector for electron spatial distribution measurements on OGO-F satellite, discussing design emphasizing reliability
c09 A69-36676
Power spectra of interplanetary magnetic field fluctuations determined from Pioneer 6 satellite data, relating results to galactic cosmic rays modulation
c30 A69-37554
Electron density profiles from topside ionograms compared to ground based sounding results, discussing error corrections
c07 A69-37865
Global electron density distribution morphology in topside ionosphere during sunspot minimum from Alouette 1 and 2 ionograms
c13 A69-37867
Cylindrical electrostatic probe measurements on Alouette 2 and Explorer 31, considering implications for future missions
c14 A69-37877
Planar thermal ion and electron trap experiments on Explorer 31 satellite, measuring ion and electron density and temperature and ionic composition
c14 A69-37878
Suprathermal electron flux in lower latitudes and polar region analyzed from measurements by retarding potential analyzers on Explorer 31 satellite
c29 A69-37880
Frequency shifts observed in Alouette 2 cyclotron harmonic plasma resonances, noting antenna length and direction
c07 A69-37892
Explorer 32 atmospheric density measurements revealing neutral thermosphere latitudinal variations during geomagnetically undisturbed times
c13 A69-38100
Lunar Explorer 35 measurements of lunar surface electromagnetic properties, magnetic fields and solar wind-moon interactions
c30 A69-38379

Shock discontinuities in solar wind measured by magnetic field and plasma instruments on Explorer 34, applying Rankine-Hugoniot relations c30 A69-40304
Explorer 34 observations of hydrogen and He ions in solar wind, noting number density variations and tentative association with geomagnetic storms c29 A69-40305
Topside ionosphere response to magnetic storms, using Explorer 22 satellite electron concentration and temperature measurements c13 A69-42438
IMP 4 satellite measurements of cosmic ray electrons in interplanetary space compared to predictions of electron intensity from interstellar proton-electron collisions c29 A69-42667
Satellite-based meteorological observation system for global atmospheric research program, discussing wind measurement, IR and microwave sounding possibilities, etc
[AAS PAPER 69-120] c13 A69-42817
Venus swingby and direct Mercury trajectories analysis for optical imaging from flyby missions
[AAS PAPER 69-258] c30 A69-42860
Bidirectional reflectance of earth atmosphere and cloud formation above equatorial Pacific observed by synchronous satellite as function of angular dependence c20 A69-43154
Nighttime protonosphere thermal balance from Alouette 2 electrostatic probe measurements of electron temperature and concentration in magnetosphere c13 A69-43181
Solar flare soft X ray and EUV emission spectra data obtained on OSO-3 satellite compared with centimetric radio bursts c29 A69-43609
Preprocessing procedures for reduction of electronic data from geodetic satellites
[NASA-CR-1183] c08 N69-11470
Air pollution detection using satellite observation
[GDC-DBE-68-011] c13 N69-31961

SATELLITE ORBITS
Geopotential resonant orbital perturbations of existing satellites, noting high inclination role c31 A69-13777
Artificial satellites as navigation aids, describing angle, range and range-angle systems, discussing orbital mechanics and communications difficulties c21 A69-34855
Satellites resonant perturbations analysis, deriving mean mean motion formulas c31 A69-39968
Ionospheric irregularities effect on accurate satellite position determination in near real time c07 A69-42549
Accuracy and speed comparison between drag-free and numerical satellite orbit prediction methods
[NASA-TN-D-5203] c30 N69-26252
Semianalytic theory for lunar satellite motion including perturbative effects
[NASA-TN-D-5043] c30 N69-28050

SATELLITE PERTURBATION
Anomalous spacecraft OGO-D motion explained by open section boom thermally induced oscillations, discussing corrective measures c32 A69-18331
Lunar mass and gravitational field determined from lunar satellite dynamics, using potential function in terms of spherical harmonics c30 A69-31405
Short term motion of lunar satellite, discussing third body disturbing functions and perturbation solution of nonsingular orbit elements c30 A69-35934
Hansen method applied to Jupiter tenth satellite orbit correction and perturbations, describing computer program and formulas used c30 A69-37529
Satellites resonant perturbations analysis, deriving mean mean motion formulas c31 A69-39968
Application of Hansen lunar theory to 10th satellite of Jupiter
[NASA-TN-D-4979] c30 N69-14479

SATELLITE ROTATION
Spinning satellite attitude stability
[NASA-TN-D-5268] c31 N69-32298

SATELLITE TRACKING
Computer programming of satellite orbit tracking angles for automatic picture transmission receiving stations c07 A69-14917
Gain measurement of two element phased array aperture antenna during ATS-C tracking c07 A69-36254
Tracking and Data Relay Satellite System with synchronous orbit satellites to relay data between low altitude earth orbital spacecraft and mission control centers c07 A69-41755
Real time telemetry, tracking and command links by synchronous satellite relay, describing ATS-Nimbus E S band experiment c07 A69-41759
Rosman I reflector antenna for collecting data from earth orbiting satellites, discussing dynamic analysis of structural response to natural frequencies c32 A69-42133
Preprocessing procedures for reduction of electronic data from geodetic satellites
[NASA-CR-1183] c08 N69-11470
Minitrack data reduction procedures, with IBM 360 computer program description
[NASA-TN-D-5042] c08 N69-26193
Statistical analysis of satellite position with tracking error inclusion
[NASA-TN-D-5259] c30 N69-30611

SATELLITE TRANSMISSION
International experimentation with U.S. communications satellites, noting design variations with participants and restraintless information exchange
[UN PAPER 68-95421] c20 A69-10474
WEFAX /Weather Facsimile/ experiment to explore operational feasibility of direct meteorological data transmission via satellite relay from central station to remote stations c11 A69-13240
Conjugate echoes in Alouette 2 topside sounder ionograms explained by multiple reflections between conjugate points of field line, noting magnetospheric waveguides role c07 A69-20045
Image dissector meteorological cameras, discussing ATS-3 and Nimbus systems, high resolution camera and multispectral cameras c14 A69-35101
Procurement and construction of automatic picture transmission ground station equipment for ESSA and Nimbus transmission
[NASA-SP-5080] c07 N69-31985

SATELLITE-BORNE PHOTOGRAPHY
Gemini program for geologic orbital photography, discussing equipment used c13 A69-35274
Multispectral orbital photography used to obtain urban land-use data
[AAS PAPER 69-483] c13 A69-42837

SATELLITE-BORNE RADAR
Radar attitude sensing system for determining vehicle roll, pitch, yaw, altitude and velocity of earth and lunar orbital vehicles c07 A69-13183

SATURN (PLANET)
Rocket-borne photoelectric photometers for UV observations of Saturn, using interference filters c30 A69-22216
Analytical evaluation of space storable propellants for unmanned Jupiter and Saturn orbiter missions
[NASA-TM-X-1793] c31 N69-24942
Planetary flight handbook - direct trajectories to Jupiter, Saturn, Uranus, and Neptune
[NASA-SP-35-VOL-3-PT-7] c30 N69-33490

SATURN LAUNCH VEHICLES
Saturn fireball thermal environment associated with liquid propellant explosions, using analytical model

c27 A69-14475
Manual guidance and control of Saturn launch vehicles, considering feasibility, reliability and hardware implementation
[AIAA PAPER 69-876] c31 A69-39402
SATURN S-1C STAGE
Short duration tube wind tunnel supersonic testing, noting Saturn S-1C base heating and solid propellant rocket base burning tests
[AIAA PAPER 69-335] c11 A69-28271
Saturn 5 longitudinal instability /POGO/ precluded by lowering S-1C stage propulsion system resonance below structural frequency
[AIAA PAPER 69-548] c31 A69-32658
SATURN S-4B STAGE
Cryogenic behavior of adhesive materials used in fabrication of liquid hydrogen/liquid oxygen powered Saturn S-4B stage
c18 A69-16487
System designs for manned spacecraft gravity gradient stabilization of Saturn S-4B stage at 400 km and lunar module at synchronous altitude
c31 A69-18338
Investigation of SA-501 S-4B auxiliary propulsion system anomalies
[NASA-TN-D-5207] c28 N69-26224
Wind tunnel stability tests to determine flutter characteristics of Saturn S-4B stage panel
[NASA-TN-D-5439] c32 N69-38808
SATURN STAGES
Nuclear rockets as Saturn 5 third stages, emphasizing increased payload or velocity utility and resulting engine and stage requirements
[AIAA PAPER 69-555] c31 A69-31849
SATURN 1 LAUNCH VEHICLES
Simulator program for defining in-flight experiment to evaluate manual control system for Saturn 1
[NASA-TN-D-5150] c21 N69-22936
SATURN 1B LAUNCH VEHICLES
Wind tunnel investigation for determination of subsonic and transonic aerodynamic characteristics of Saturn 1B launch vehicle
[NASA-TM-X-1848] c31 N69-33380
SATURN 5 LAUNCH VEHICLES
LOX prevalve accummulator system with He pressurant for prevention of POGO effect on Saturn 5
c31 A69-15298
Nondestructive testing methods for Saturn 5 space vehicle with emphasis on NDT equipment for Apollo program
c15 A69-23050
Saturn 5 longitudinal instability /POGO/ precluded by lowering S-1C stage propulsion system resonance below structural frequency
[AIAA PAPER 69-548] c31 A69-32658
Plastics applications in Apollo-Saturn 5 program, considering foam, honeycomb, conformal coatings, embedment compounds, dielectrics, damping compounds, adhesives, sealants and gaskets
c18 A69-38533
Apollo-Saturn 5 propulsion and structure feedback loop, analyzing POGO components and Nyquist plot application
[AIAA PAPER 69-877] c31 A69-39403
Navigation state vector update effect on lunar mission completion capability for Saturn 5, emphasizing hardware and scheme errors and accelerometer failure
[AIAA PAPER 69-883] c21 A69-39409
Vibration characteristics of 1/40 scale model of Saturn 5 launch vehicle and umbilical tower configuration
[NASA-TN-D-4870] c31 N69-10775
Direct stiffness method of computing vibrational characteristics of dynamic model of Apollo-Saturn 5 vehicle - umbilical tower configuration
[NASA-TN-D-4871] c31 N69-10934
Lateral vibration characteristics of dynamic model of Apollo-Saturn 5 launch vehicle
[NASA-TN-D-4872] c31 N69-11007
Identification of structural systems using near resonance testing
[NASA-TN-D-5069] c32 N69-17737
Saturn 5 launch vehicle scale model tests for free vibration during first stage burn
[NASA-TN-D-5159] c32 N69-22932
Evaluation of pilot describing function method applied to manual control analysis of large flexible booster in Saturn 5 launch vehicle simulator
[NASA-TN-D-5149] c21 N69-22996
Investigation of SA-501 S-4B auxiliary propulsion system anomalies
[NASA-TN-D-5207] c28 N69-26224
Reliability study of Saturn 5 launch vehicle manual backup control system
[NASA-TN-D-5261] c21 N69-28018
SCALE (CORROSION)
Examination of thermal oxidation deposits on heat resistant alloys using X ray diffraction and X ray fluorescence analyses
[NASA-TN-D-5019] c17 N69-17277
SCALE (RATIO)
Mathematical model for measurement scale forms
[NASA-TN-D-5277] c19 N69-29141
SCALE EFFECT
Experimental verification of scale factors for parawing opening characteristics with dimensional ratios from 1/1.3 to 1/3
[NASA-TN-D-5071] c02 N69-19950
SCALE MODELS
Scaled solar and gray-body temperature distribution models compared to determine stellar atmosphere
c30 A69-14626
Scale models of M-1 rocket engine oxygen and hydrogen pump driven two stage turbines used to determine performance and compact inlet manifolds problems
[AIAA PAPER 69-553] c28 A69-32678
Wind tunnel test of aerodynamic characteristics of scale model of Tomahawk launch vehicle at Mach speeds
[NASA-TM-X-1684] c01 N69-10732
Low speed static and dynamic longitudinal, and lateral stability of scale model of supersonic transport in wind tunnel tests
[NASA-TN-D-4726] c02 N69-10733
Identification of structural systems using near resonance testing
[NASA-TN-D-5069] c32 N69-17737
Effect of heat shield flexibility on water landing loads of Apollo spacecraft models
[NASA-TN-D-5108] c32 N69-21042
Antenna effects on aerodynamic characteristics of 0.410 scale model Cajun rocket at Mach numbers from 2.30 to 4.63
[NASA-TM-X-1771] c01 N69-21106
Lift loss and jet decay measurements on hovering vertical takeoff aircraft models
[NASA-CR-1297] c01 N69-21477
Scaled lunar landing module jet erosion of simulated moon surfaces
[NASA-TN-D-5051] c31 N69-22630
Tests of bending strength on full scale model of Atlas LV-3C booster
[NASA-TN-D-5156] c31 N69-22937
Physical model for plasma containment simulation in magnetic fields
[NASA-TN-D-5217] c25 N69-25394
Heat transfer to windward side of scale model for graphite lunar module fuel cylinder
[NASA-TN-D-5251] c12 N69-29608
Aerodynamic characteristics in pitch of scale model of two and three stage rocket configuration at Mach numbers of 0.4 to 4.63
[NASA-TN-D-5378] c01 N69-34986
Spin-tunnel investigation of scale model of straight wing, twin boom counter insurgency airplane
[NASA-TM-X-1602] c02 N69-34988
Performance of turbine driven V/STOL cruise fan propulsion system at subsonic Mach numbers
[NASA-TN-D-5314] c28 N69-35526
Spin and recovery characteristics of 1/30 scale subsonic attack aircraft model determined in wind tunnel tests
[NASA-TM-X-1788] c02 N69-37976
Empirically determined wind and scale effects on hot gas recirculation characteristics of jet V/STOL aircraft
[NASA-CR-1445] c28 N69-40776
Design and structural model of thin film solar cell array
[NASA-TM-X-1913] c03 N69-40787

Wind tunnel studies of scaled model of multijet cargo airplane
[NASA-TN-D-5538] c02 N69-40937
SCANDIUM ISOTOPES
Angular distributions for Sc 45 Ti 46 nuclear reactions involving 41 MeV alpha particles bombardment described by Born approximation
c24 A69-41044
Alpha particle-triton reaction on scandium 45 at 41 MeV
[NASA-TN-D-5216] c24 N69-24919
SCANNER PROJECT
Infrared horizon radiance profiles for winter conditions based on Scanner project flight test
[NASA-TN-D-4905] c21 N69-14346
SCANNERS
Scanning electron mirror microscope advantages over electron mirror and scanning electron microscopes for examining integrated circuits
c14 A69-32891
Scanning electron microscopy for reliability studies in semiconductor devices
c26 A69-35788
SCANNING
Celestial sphere scanning by passive method applicable to space missions requiring long lifetime and moderate pointing accuracies
[AIAA PAPER 68-854] c21 A69-39764
SCATTER PROPAGATION
Mie scattering calculations on laser wavelengths and atmospheric aerosols
[NASA-TN-D-5110] c23 N69-20905
SCATTERING
Scattering, reactions, and decay in nonrelativistic quantum mechanics
[NASA-TT-F-510] c24 N69-25848
Gamma ray transport portion of COHORT 2 Monte Carlo shielding code
[NASA-TM-X-1877] c22 N69-35848
SCATTERING CROSS SECTIONS
Differential cross sections for elastic scattering of 600 MeV protons from He 3 between 19 and 45 degrees
c24 A69-13464
Mie total and differential backscattering cross sections at laser wavelengths for Junge size distribution aerosol models
c16 A69-14290
First Born approximation cross sections for He excitation from ground state by proton impact calculated, using wave functions
c24 A69-17027
Inelastic scattering cross sections calculated, comparing results for various nuclear states expressed as Wood-Saxon radial and harmonic oscillator functions
c26 A69-29006
Core polarization effects in inelastic scattering cross sections for several nuclei in 2s-1d shell, using Hartree-Fock wave functions and Born approximation
c24 A69-29007
Elastic scattering cross sections for 21-MeV incident protons measured for nuclei differing in mass, determining optical model potential
c24 A69-35489
Inelastic proton scattering cross sections for target nuclei in 2s-1d shell calculated in distorted wave Born approximation with projected Hartree-Fock wave functions
c24 A69-41045
Differential cross section and polarization measurements for elastic scattering of high energy protons from light nuclei
c24 A69-43125
Absolute cross sections for scattering of 42 MeV alpha particles from even isotopes of cadmium
[NASA-TN-D-4948] c24 N69-14482
Polarization, differential cross section, and total reaction cross section data for proton scattering
[NASA-TN-D-5067] c24 N69-22934
Theoretical feasibility of detecting laser radiation scattered from plasma
[NASA-TN-D-5311] c25 N69-36939
Elastic and nonelastic scattering cross sections from 42 MeV alpha particles interacting with helium isotopes
[NASA-TN-D-5530] c24 N69-40979
SCATTERING FUNCTIONS
Maximum number of binary collisions for three particles with zero range forces in relativistic rescattering singularities studies
c24 A69-19788
SCHLIEREN PHOTOGRAPHY
Optical system for recording Schlieren images with continuous writing, ultrahigh speed framing camera
[NASA-TN-D-4986] c14 N69-15381
SCHREIBERSITE
Fe-Ni-P phase diagram studies applied to schreibersite and rhabdite formation in iron meteorites
c30 A69-36132
SCIENTIFIC SATELLITES
Stored program computer for small scientific spacecraft, noting program and data memory capacities
c08 A69-15472
Small Scientific Satellite program, discussing payload for investigating magnetosphere and near interplanetary space
[IEEE PAPER 3C-1] c31 A69-19195
OGO for conducting diversified measurements to study earth atmosphere, earth-sun relationship, etc
c31 A69-36674
Programmable data handling and telemetry systems for scientific satellites, noting system checkout, spacecraft integration, software and ground data processing
c08 A69-41735
Space research in past and expected scientific knowledge from manned and automated earth orbital science missions
[AAS PAPER 69-036] c30 A69-42825
Design, development, integration, and testing of Small Scientific Satellites
[NASA-TN-D-4988] c32 N69-33232
SCIENTISTS
Bibliography of works of Soviet engineer F. A. Tsander
[NASA-TT-F-541] c34 N69-26112
SCINTILLATION
Proportionality between log-amplitude variance and 7/6 power of wavenumber for horizontal propagation from spherical wave transmitter to point detector
c16 A69-19641
SCORPIUS CONSTELLATION
Radio emission from Sco XR-1 shown as synchroton radiation of relativistic electrons in low density region surrounding denser core producing X ray
c30 A69-37334
SCOUT LAUNCH VEHICLE
Rocket motor integration into Scout vehicle to improve performance
c31 A69-12384
Feasibility of using roll and yaw compensation to reduce inclination error of Scout launch vehicle
[NASA-CR-1209] c31 N69-16221
SEA URCHINS
Toxicity of plastic hardware containing biological space flight experiment
[NASA-TM-X-1818] c04 N69-29723
SEA WATER
Tradeoff analysis on radar and laser space altimeter systems for sea surface geodesy
[NASA-CR-1298] c14 N69-21117
SEALERS
Computer program for steady laminar, subsonic, and isothermal compressible flow across sealing dam
[NASA-TN-D-5373] c15 N69-33281
SEALING
Gas turbine compressor end seals, discussing air leakage paths, primary and secondary seals, design and efficiency
[ASLE PREPRINT 68AM 4B-4] c15 A69-27366
SEALS (STOPPERS)
Gas turbine engine shaft face seal with self acting lift augmentation preventing rubbing contact, noting disadvantages of labyrinth and conventional seals
[ASLE PICFS PREPRINT 27] c15 A69-30492
Performance and analysis of seals for nitrogen inerted lubrication systems of turbine engines
[NASA-TN-D-4761] c15 N69-10055

Shaft face seal with self acting lift augmentation for advanced gas turbine engines
[NASA-TN-D-5170] c15 N69-23232
Vibration of shaft face seals and stabilizing effect of viscous and friction damping
[NASA-TN-D-5161] c15 N69-23466
Rotational effects on isothermal compressible flow across gas turbine sealing dam
[NASA-TN-D-5344] c15 N69-35799

SEARCHING
Adaptive random search algorithm utilizing boundary cost-function hypersurfaces measurement to implement Pontryagin maximum principle, discussing hybrid computer use, iterative solution and convergence properties
c08 A69-33745

SEAS
Microwave thermal emission by water measured from aircraft, studying radiation dependence on surface roughness
c13 A69-34421

SECONDARY EMISSION
Plasma electron beam for welding, deriving beam current from secondary emission by ion bombardment, discussing gas pressure, equipment and applications
c15 A69-35555

SEGMENTS
Design and construction of plastic model of prestressed segmented spherical shell
[NASA-CR-1231] c32 N69-11010

SELENIDES
Thermal stability and friction of disulfides, diselenides, and ditellurides of molybdenum and tungsten in ultrahigh vacuum
[NASA-TN-D-5141] c15 N69-22992

SELENOGRAPHY
Gaussian particle size distribution with porosity and surface irregularity corrections used to determine mean particle size of lunar surface material at Surveyor sites
c30 A69-26371
Lunar Orbiter 1 terrain assessment photographs and preliminary selenodesy, micrometeoroid, and radiation data
[NASA-SP-197] c30 N69-39213

SELENOLOGY
Regolith thickness distribution at Lunar Orbiter sites, correlating thickness directly with cratering density
c30 A69-18604

SELF ABSORPTION
Downstream radiation flux distribution calculated for blunt entry bodies, considering self absorption effects
c33 A69-12547

SELF LUBRICATING MATERIALS
Cooling requirements for high speed polytetrafluorethylene lubricated ball bearings operating in cold hydrogen gas, developing minimum gas flow rate equation
[ASLE PAPER 68-LC-2] c15 A69-19310

SELF STIMULATION
Critical body temperature for intracranial self stimulation in white rats
c04 A69-13897

SEMICONDUCTING FILMS
Cadmium sulfide films with larger than bandgap photovoltages, analyzing photovoltage decay and temperature and light intensity effects
c26 A69-17772

SEMICONDUCTOR DEVICES
Delta functions spectrum in reciprocal time domain for LC and RC structures due to impulse response in distributed parameters
c10 A69-21327
Four terminal silicon planar p-n-p-n model operating as semiconductor small signal linear tetrode amplifier, discussing properties and mathematical models
c09 A69-35293
Scanning electron microscopy for reliability studies in semiconductor devices
c26 A69-35788
Electron irradiation effect on resolution of lithium-drifted silicon semiconductor detectors
[NASA-TN-D-4901] c14 N69-10933
Simplified theory and transducer potentialities of pinch effect in semiconductors
[NASA-TN-D-5130] c26 N69-22573

SEMICONDUCTOR JUNCTIONS
GaSb-ZnTe heterojunction fabrication method, noting photoresponse, fluorescence and light transmission
c26 A69-12408
Impurity profiles and energy band diagram for cuprous sulfide-CdS heterojunction based on capacitance, Hall and electron microprobe measurements
c03 A69-13075

SEMICONDUCTORS (MATERIALS)
Current oscillations in semiinsulating O and Cr doped GaAs samples at room temperature, noting photoconductivity excitation spectra
c26 A69-21753
Computerized Arrhenius equation component reliability extrapolation techniques
[NASA-TN-D-4902] c19 N69-13368
Measurement and interpretation of Hall coefficient and resistivity of semiconductors
[NASA-TM-X-1711] c26 N69-14086
Breaking of semiconductor single crystal wafer into chips
[NASA-TM-X-1892] c09 N69-38774

SEMIEMPIRICAL EQUATIONS
Semiempirical fracture analysis for semielliptical surface crack in plate
[NASA-TN-D-5340] c32 N69-31056

SEMISPAN MODELS
Aerodynamic characteristics of large semi-span V/STOL tilt-wing with single propeller tested for modes of propeller rotation
[NASA-TN-D-5016] c01 N69-17312

SENSITIVITY
Predicting relative sensitivities of hot cathode ionization vacuum gages
[NASA-TN-D-5285] c14 N69-29331

SENSORS
Make wire, light pipe and spring wire ablation sensors development for measuring parameters of heat shield materials for reentry vehicles
c14 A69-15428
Transensor implantation, sham implantation, no implantation and lighting effects on rat body composition, noting fat and water content
c04 A69-26557

SENSORY FEEDBACK
Efficacy of sensory feedback information given during training period for improving human performance in producing memorized movement pattern
[NASA-CR-1251] c05 N69-13926
Multimodality pilot model for visual and motion feedbacks derived from simulator program
[NASA-CR-1325] c05 N69-28071

SENSORY PERCEPTION
Human vestibular system and its connection with oculomotor system and their relation to motion perception, spatial disorientation, and illusions
[NASA-CR-1309] c04 N69-22637
Human perception of multiple-point tactile and visual stimuli
[NASA-CR-1389] c05 N69-39211

SENSORY STIMULATION
Critical body temperature for intracranial self stimulation in white rats
c04 A69-13897

SEPARATED FLOW
Flow characteristics and wall heat transfer in separated flow region of annular cavity at free stream hypersonic speed and high gas temperature
[AIAA PAPER 68-672] c01 A69-37185
Transonic wind tunnel studies on airfoil to determine effects of Reynolds number and boundary layer transition location on shock induced separated flow
[NASA-TN-D-5003] c01 N69-16121
Statistical analysis of pressure fluctuations in separated turbulent boundary layer
[NASA-TN-D-5440] c12 N69-36940

SEQUENCING
Determining sequential decoding performance and metric sensitivity by computer simulation
[NASA-TR-R-294] c07 N69-16196

SEQUENTIAL ANALYSIS
Auditory temporal masking of tonal signal by narrow band noise and perception of temporal

order noting effects of intensity, frequency and time
c05 A69-24795
Sequential analyses of planetary surface sample for extraterrestrial life detection, discussing chemistry, morphology, growth and metabolism for life attributes
c30 A69-41623
Log-a-posteriori probability metric for use in sequential decoding
[NASA-TN-D-4930] c07 N69-23163
Sequential stochastic techniques for trajectory estimation
[NASA-CR-1360] c30 N69-40325
SEQUENTIAL COMPUTERS
SDP-3 small serial computer for engineering experiment on IMP spacecraft, discussing design modifications to improve performance
c08 A69-41737
SERIES (MATHEMATICS)
Analytic continuation of Appell hypergeometric series into linear combination of four infinite series
c19 A69-26605
Series solution for hypersonic flow about blunt bodies
[NASA-CR-1266] c33 N69-18125
Chebyshev series solution of nonlinear ordinary differential equations - initial value problems
[NASA-TM-X-1882] c19 N69-36923
SERVICE LIFE
SERT 2 thrustor system performance over expected mission parameters, noting operational lifetime excess over mission requirements
[AIAA PAPER 69-235] c28 A69-21255
High performance light weight electrodes for hydrogen oxygen fuel cells
[NASA-CR-1216] c03 N69-14397
SERVOAMPLIFIERS
Design and analysis of modular servoamplifier for fast response electrohydraulic control systems
[NASA-TN-D-4898] c03 N69-10068
SERVOCONTROL
Three axis attitude servomechanism design to adjust attitude and angular velocity of spacecraft
c21 A69-17589
Fast response electrohydraulic valve-controlled piston servo systems
[NASA-TN-D-5388] c03 N69-34652
SET THEORY
Shape preserving expansion and contraction of objects in E 3
[NASA-TN-D-5240] c19 N69-31303
Concepts of theory of fuzzy systems
[NASA-CR-1432] c19 N69-37033
SEXTANTS
Sextant sighting measurements from on board Gemini 12 spacecraft
[NASA-TN-D-4952] c21 N69-14332
Sextant sighting performance concerned with training and monochromatic stars
[NASA-TN-D-5190] c05 N69-35024
SHADOWS
Thermal analysis of shadow shields and structural members in space environment
[NASA-TN-D-4876] c33 N69-10473
SHAFTS (MACHINE ELEMENTS)
Shaft face seal with self acting lift augmentation for advanced gas turbine engines
[NASA-TN-D-5170] c15 N69-23232
Torque and leakage rates of various lubricated lip seal designs at peripheral velocity of 120 feet per second
[NASA-TN-D-5411] c15 N69-35769
Vibrations of turbomachine rotors and methods for determining optimal hydraulic damping mounts, vibrations of systems with friction, and self induced vibrations of compressor blades
[NASA-TT-F-547] c02 N69-36326
SHAPES
Hypersonic body shaping for minimum drag and improved performance from view of flight regimes, discussing implications of pressure laws
[AIAA PAPER 69-181] c01 A69-18052
Sorting particles by shape using sieving equipment, noting results with crushed gravel
c15 A69-38950
Harmonic content of pressure wave shapes in strong traveling transverse acoustic modes
[NASA-TM-X-1716] c12 N69-15371
Theoretical comparison of beads, wires, and films as rocketsonde temperature sensors in mesosphere
[NASA-CR-1286] c13 N69-18126
SHEAR FLOW
Direction of maximum turbulent vorticity in turbulent shear flow, determining alignment
c12 A69-25282
Incompressible turbulent boundary layer analysis by two region characterization for eddy viscosity, using Spalding generalized function and Prandtl free shear flow model
c12 A69-33255
SHEAR LAYERS
Three dimensional laser Doppler velocity instrument for mean velocity and turbulence measurements in subsonic jet shear layer
[SAE PAPER 690266] c14 A69-21555
SHEAR PROPERTIES
Transverse shear deformation and rotary inertia effects in vibrating beams
[NASA-CR-1317] c32 N69-24056
SHEAR STRENGTH
Dislocation model of strength of elastically inhomogeneous crystalline materials based on elastic interactions between dislocations and periodic fluctuations of shear modulus
c17 A69-20557
SHEAR STRESS
Normal stress effects in viscoelastic fluid theories applied to one dimensional Burgers model of weak turbulence predicting drag reduction
c12 A69-33256
SHEARING
Skin friction measurement in aerodynamic tests using thin liquid crystal coatings with changes in maximum light scattering wavelength in response to shearing forces
c11 A69-29029
SHEETS
Elastoplastic stress-strain behavior at notch roots in sheet specimens under constant amplitude loading
[NASA-TN-D-5253] c32 N69-28038
SHELL STABILITY
Recent advances in shell buckling, discussing imperfection sensitivity, boundary conditions and wall configuration
[AIAA PAPER 68-103] c32 A69-12516
Computer program determination of barreling effect on strength of ring and stringer stiffened shells designed to support axial compression loads
c32 A69-43671
Structural synthesis of cylindrical shell reinforced with rectangular cross section stiffeners
[NASA-CR-1217] c32 N69-14254
SHELL THEORY
Spherical caps axisymmetric static and dynamic buckling under load, using axisymmetric nonlinear elastic shell theory approximation and finite difference equations
[AIAA PAPER 69-89] c32 A69-18133
SHELLS (STRUCTURAL FORMS)
Equilibrium and free vibration problems of centrifugally stabilized disk and shell structures
[NASA-CR-1178] c32 N69-14477
Forces on flexible shells of Apollo command module during water impact
[NASA-TM-X-1781] c32 N69-23697
Transient temperature fields in porous shell walls cooled by forced flow
[NASA-TT-F-552] c33 N69-30245
Design calculations for conical shells and elastic systems subject to antisymmetric loads
[NASA-TT-F-518] c32 N69-30754
Optimal structural design for sandwich-shaped and ring-stiffened loaded shells of revolution
[NASA-CR-1424] c32 N69-35515
SHIELDING
Thermal analysis of shadow shields and structural members in space environment
[NASA-TN-D-4876] c33 N69-10473

SHIPS
Skin friction drag reducing high polymer solution injected into turbulent boundary layer to test effectiveness on marine vehicles
c12 A69-33254
SHOCK ABSORBERS
Impact energy absorbing strut using tube cutting
[NASA-TN-D-4941] c32 N69-14506
SHOCK DISCONTINUITY
Steady shock discontinuity in perfectly conducting gas flow in arbitrarily oriented magnetic field for various Mach numbers
c25 A69-19988
Shock discontinuities in solar wind measured by magnetic field and plasma instruments on Explorer 34, applying Rankine-Hugoniot relations
c30 A69-40304
SHOCK FRONTS
Ionizing shock front structure in monatomic gas, considering atom-atom and electron-atom collisional ionization rates
c12 A69-13138
SHOCK HEATING
Flight measurement of optical radiation from shock heated air with Trailblazer 2 reentry vehicle
[NASA-TN-D-4937] c33 N69-14501
Effect of shock precursor heating on radiative flux to blunt bodies
[NASA-CR-1265] c33 N69-17438
SHOCK LAYERS
Nongray equilibrium radiative heat transfer in viscous radiating shock layer around blunt body entering high temperature nonisothermal carbon dioxide-nitrogen atmosphere
[AIAA PAPER 69-636] c33 A69-33258
Effects of angle of attack and bluntness on shock layer properties of cones at supersonic speeds
[NASA-TN-D-4909] c01 N69-10789
Ablation product absorption and line transitions effects on shock layer radiative transport around blunt body
[NASA-CR-1264] c33 N69-19117
Finite difference techniques used in numerical solutions for inviscid radiating shock layers around spheres at hyperbolic speed in air
[NASA-TR-R-311] c12 N69-26504
Solution for shock layer energy equation with mass and convective heat transfer at hypersonic speed
[NASA-TN-D-5246] c12 N69-33421
SHOCK LOADS
Numerical analysis of shock control by using perforated walls in internal compression supersonic inlets
[NASA-TR-R-317] c01 N69-32338
SHOCK SIMULATORS
Design and performance of sonic boom simulator
[NASA-CR-1378] c02 N69-31959
SHOCK SPECTRA
Radiant energy transfer measurements in air plasma in reflected region of arc-driven shock tube
[NASA-CR-1390] c25 N69-38227
SHOCK TUBES
Electronic transition moment for C /Swan/ bands measured in shock tube in carbon dioxide and argon mixtures
c24 A69-12833
High speed compression waves, rarefaction waves and gas interface regions position and velocity measurement in shock tube by sensing electrical impedance
c14 A69-13104
Optical carrier single channel telemetry system providing complete electrical isolation between shock tube data acquisition and data recording instrumentation
c14 A69-29561
Image converter camera and astronomical telescope arrangement for photographing metal diaphragm openings in shock tube
c14 A69-37227
High temperature properties of gases - gas dynamics, thermodynamics, and combustion physics
[NASA-TT-F-558] c12 N69-35365
Design, calibration, and use of radiometers to measure spectral emission in ballistic range and shock tube experiments
[NASA-TN-D-5360] c14 N69-38144
SHOCK TUNNELS
Digital data acquisition system with ultrahigh sampling rate for Ames electric arc shock tunnel, describing analog to digital conversion, data storage, system performance, etc
c11 A69-35744
Aerodynamic and thermodynamic calibration of nonequilibrium air flow in Ames 1-foot shock tunnel
[NASA-TN-D-4985] c11 N69-15633
Exploding wire initiation and electrical operation of 40 kV system for arc heated drivers up to 10 feet long
[NASA-TN-D-5126] c11 N69-22989
SHOCK WAVE INTERACTION
Hypersonic surface measurements and flowfield properties about slender cones in hypersonic viscous interaction regime
[AIAA PAPER 68-2] c01 A69-12520
Linear wave interaction with oblique shock waves, noting dependence of transmission, reflection and generation coefficients on Mach number
c12 A69-13137
Amplitude equations for magnetoacoustic and entropy waves diverging from normal MHD shock, obtaining energy flux ratios associated with incident and transmitted waves
c25 A69-38242
Mach 42 test measuring surface pressures, surface heat transfer rates and shock wave shapes in strong interaction regime for sharp and blunt plates
[AIAA PAPER 68-720] c01 A69-41886
SHOCK WAVE PROFILES
Switch-on ionizing shock waves structure, analyzing condition of downstream state and effect on hydromagnetic wave speed
c25 A69-22045
Interplanetary shock waves structure and evolution, discussing propagation in collision free media by wave-particle interactions
c30 A69-42394
SHOCK WAVE PROPAGATION
Transmission of Alfven waves through earth bow shock based on hydromagnetic shocks theory, discussing amplitude amplification
c13 A69-32099
Interplanetary shock waves structure and evolution, discussing propagation in collision free media by wave-particle interactions
c30 A69-42394
Ionization rate limiting processes behind strong shock waves in pure N, plotting electron density profile diagrams
c12 A69-43367
High temperature properties of gases - gas dynamics, thermodynamics, and combustion physics
[NASA-TT-F-558] c12 N69-35365
SHOCK WAVES
Vela 3A and Explorer 33 elapsed time observations of earth bow shock
c13 A69-12299
Steady shock discontinuity in perfectly conducting gas flow in arbitrarily oriented magnetic field for various Mach numbers
c25 A69-19988
Simultaneous interplanetary magnetic field measurements by geocentric satellites Explorer 33 and IME 3 of MHD shock wave associated with July 8, 1966 sudden storm commencement
c30 A69-23773
Earth bow shock waves in far upstream interplanetary medium observed from magnetic data of Explorer 34 satellite
c30 A69-34941
MHD Rankine-Hugoniot equations for ion density, thermal pressure and convective velocity magnitude and orientation during Pioneer 6 traversal of earth bow shock
c30 A69-42417
Estimated supersonic flow field shock waves and sonic boom effects for cones and axisymmetric bodies
[NASA-TN-D-4935] c01 N69-13238
Momentum diffusion between two supersonic airstreams passing through oblique shock waves
[NASA-TN-D-4974] c12 N69-15631
Transonic wind tunnel studies on airfoil to determine effects of Reynolds number and boundary layer transition location on shock induced separated flow

[NASA-TN-D-5003] c01 N69-16121
Design and performance of flueric shock position sensor for mixed compression supersonic inlets
[NASA-TM-X-1733] c14 N69-16382
Vacuum ultraviolet detector-spectroscopy systems for capsule reentry measurements
[NASA-CR-1268] c09 N69-18761
N shaped shock wave line focusing simulating sonic superbooms
[NASA-TN-D-5306] c02 N69-31874
Supersonic aerodynamic characteristics and shock standoff distances for large angle cones with and without cylindrical afterbodies
[NASA-TN-D-5334] c01 N69-33237
Shock wave propagation in real gases
[NASA-TT-F-585] c12 N69-40824

SHORT TAKEOFF AIRCRAFT
IFR flight tests of Breguet 941 STOL transport
[NASA-TN-D-4939] c02 N69-13252
Wind tunnel tests of static longitudinal and lateral characteristics of short takeoff aircraft with external flow jet flap
[NASA-TN-D-5364] c01 N69-33275

SHORT WAVE RADIO TRANSMISSION
Short wave bands for earth-space communications, considering propagation anomalies compensated systems and frequency bands availability
c07 A69-13721

SHROUDED NOZZLES
Plug and shroud geometry variables on plug nozzle performance at transonic speeds
[NASA-TN-D-5098] c28 N69-21463
Static tests of nozzle efficiency and pumping characteristics of conical turbojet plug nozzle with translating primary and secondary shrouds at Mach 0 to 2.0
[NASA-TM-X-1777] c28 N69-21648

SIDELOBES
Multiplicative feed system for monopulse angle tracking antennas, discussing influence of sidelobe and backlobe responses on control function slope determining antenna bearing angle
c11 A69-37704

SIEVES
Sorting particles by shape using sieving equipment, noting results with crushed gravel
c15 A69-38950

SIGNAL ANALYSIS
Spectral null from spectral characteristics and statistical properties of PCM signals used to estimate SNR
c07 A69-19122
Subcarrier phase modulated single sideband sinusoidal carrier synthesis, discussing signal power ratios, signal efficiency, design sensitivity, etc
c07 A69-29489

SIGNAL DETECTION
Proportionality between log-amplitude variance and 7/6 power of wavenumber for horizontal propagation from spherical wave transmitter to point detector
c16 A69-19641
Phase-lock loop demodulator ability to acquire and remain locked on signal under noise and pulse interference
c10 A69-42230
Lunar laser beam retroreflection observations, showing agreement with predicted ephemeris and signal strength
c30 A69-43197

SIGNAL ENCODING
Ground data handling equipment characteristics for PCM telemetry link utilizing convolutional coding
c07 A69-36267

SIGNAL FADING
Relationship between complex covariance and covariances of envelopes of Rician fading communication channels
[NASA-TN-D-4825] c07 N69-11011

SIGNAL MEASUREMENT
Experiment design for measuring radio frequency interference between communication satellite and terrestrial microwave relay system
[NASA-TN-D-5041] c07 N69-26272

SIGNAL PROCESSING
Photon bunching effect in spatially coherent noise field enhanced by superposing monochromatic coherent signal and/or shaping incident noise spectra
c07 A69-31694

SIGNAL RECEPTION
Multifunction Receiver System rationale, concepts, background requirements and technical justifications for tracking, telemetry and ranging data acquisition by Goddard Center
c07 A69-19101

SIGNAL TO NOISE RATIOS
Working breadboard model of planet tracker under various illuminating conditions, discussing hardware and closed loop tracking error analysis accounting for signal to noise effects
c21 A69-13214
Spectral null from spectral characteristics and statistical properties of PCM signals used to estimate SNR
c07 A69-19122
Double sideband suppressed carrier FM telemetry system as airborne data recorder, discussing noise, environmental conditions, laboratory and flight tests
c07 A69-19132
Ultrasonic pulse velocity and attenuation measurement in presence of noise, using coherent detection and signal averaging
c14 A69-29564
Beat frequency measurements in far IR due to harmonic mixing of klystrons, discussing noise role
c23 A69-33674
Ac technique using lock-in power amplifier SNR for measuring galvanomagnetic and Shubnikov-de-Haas effects, noting error reduction
c14 A69-36375
Filtering optimization prior to limiting digital signals in strong noise, detailing bandwidth choice of single pole low pass filter
c07 A69-39450
Phase-lock loop demodulator ability to acquire and remain locked on signal under noise and pulse interference
c10 A69-42230

SIGNAL TRANSMISSION
Adaptive compression system for predicting and encoding video data for transmission in noiseless channel
c14 A69-12869

SIGNATURES
Equations for pressure signature of supersonic projectile in stratified atmosphere
[NASA-TN-D-4890] c02 N69-10087

SILICA GLASS
Impact crater cross section in fused silica, describing photomicrographic technique for distinguishing hypervelocity from low energy impacts
[AIAA PAPER 69-367] c32 A69-28299

SILICON
Strong p-type conductivity of silicon doped with beryllium by thermal diffusion, giving electrical and optical measurements
c26 A69-21652
Annealing temperature of radiation defects in phosphorus doped silicon, discussing isochronal recovery characteristics of solar cells with different donor and oxygen concentrations
c26 A69-24006
Electron irradiation effect on resolution of lithium-drifted silicon semiconductor detectors
[NASA-TN-D-4901] c14 N69-10933
Proton irradiation effects on minority carrier lifetime in silicon and gallium arsenide semiconductor materials
[NASA-TN-D-5028] c26 N69-18897
Energy and angular distribution of electrons transmitted through silicon targets
[NASA-TN-D-5075] c24 N69-19113
Analysis of annealed and proton irradiated silicon
[NASA-TN-D-5119] c26 N69-22552
Effects of nickel on performance of n on p silicon solar cells
[NASA-TN-D-5366] c03 N69-31844

SILICON CARBIDES
Cubic /beta/ silicon carbide films deposition by volatilization in presence of acetylene
c26 A69-21350

Chemical processes in silicon carbide due to reactive deposition and chemical conversion, noting silicon growth mechanism involving outward diffusion
c26 A69-21351
High performance silicon carbide backward diode, discussing device design and operational characteristics
c09 A69-22787
Figures of merit for experimental silicon carbide backward diode operable to 1000 degrees K
[NASA-TN-D-5183] c09 N69-23556
Optimal growths of silicon carbide polytype crystals by methyltrichlorosilane reduction
[NASA-TN-D-5313] c26 N69-30072

SILICON DIOXIDE
Single crystal growth by controlled diffusion in silica gel using metathetical and decomplexation reactions
c06 A69-23371
Rocket engine evaluation of erosion and char as functions of fabric orientation for silica reinforced nozzle materials
[NASA-TM-X-1721] c28 N69-15475
Plastic deformation of corrosion resistant steel, CER-VIT 101, and fused silica as function of applied torsional stress
[NASA-CR-1257] c14 N69-16100

SILICON JUNCTIONS
Al interconnections discontinuities at integrated circuit contact windows observed by scanning electron microscope, noting catastrophic failure and Si presence
c09 A69-32893
Radiation damage and recovery of lithium-diffused silicon p-n solar cells, measuring photovoltaic parameters as function of gamma radiation fluence
c03 A69-35694
Simulated micrometeoroid impact effect on silicon and cadmium sulfide solar cell performances
[NASA-TN-D-5133] c03 N69-21016
Potential electrical response of p-n junction to mechanical strain
[NASA-CR-1366] c26 N69-29724

SILICON RADIATION DETECTORS
Fabrication and testing of lithium-drifted detectors as low energy photon spectrometers
[NASA-TN-D-5056] c24 N69-19828

SILVER COMPOUNDS
Yttrium effect on rate of thermal decomposition of silver carbonate powder and pressed pellets by isothermogravimetric analysis, examining water vapor, Co 60 gamma radiation and temperature effects
c06 A69-30442

SIMILITUDE LAW
Model design for simulation of space capsule landing on soils using similitude law
[NASA-CR-1210] c34 N69-13159

SIMULATION
Fourth angle driving law for different four gimbal systems used for simulation display and inertial platform isolation
c11 A69-26265
Flow simulation on wind tunnel test models for aerodynamic characteristics of aircraft design, discussing boundary layer and external flow coupling
[AIAA PAPER 69-660] c11 A69-33471
Evaluating performance of swirl can turbojet combustor at simulated supersonic inlet conditions
[NASA-TN-D-4996] c28 N69-16154
Gaseous reactant combustion simulation of dimethylhydrazine and hydrazine fuel system for nonequilibrium expansion studies
[NASA-TN-D-5404] c33 N69-35506
Multistage turbocompressor simulation applied to performance prediction of axial flow instabilities
[NASA-TM-X-1880] c28 N69-36998
Simulation of astronaut locomotion on lunar surface to determine metabolic costs
[NASA-CR-1402] c05 N69-37964

SIMULATORS
Rendezvous and station keeping simulator with fly around capability and virtual image viewing
[NASA-TN-D-5123] c11 N69-22629

SIMULTANEOUS EQUATIONS
Coupled kinetic equations for inhomogeneous systems treated as simultaneous equations in time, obtaining solutions by successive approximation
c25 A69-30913

SINE WAVES
Sinusoidal phase modulation role in spectral broadening observed in trapped filaments of laser and Raman light
c16 A69-14189
Heat transfer and pressure distribution due to two-dimensional repetitive sine wave distortions on flat plate at Mach 20 in helium
[NASA-TN-D-4907] c12 N69-10804

SINGLE CRYSTALS
Single crystal growth by controlled diffusion in silica gel using metathetical and decomplexation reactions
c06 A69-23371
Compton profile from single crystal of LiH measured with X ray scattering, noting valence-electron momentum distribution role
c26 A69-40730
Nonlinear flux flow in single crystal niobium
[NASA-TN-D-5198] c26 N69-24916
Breaking of semiconductor single crystal wafer into chips
[NASA-TM-X-1892] c09 N69-38774
Tungsten and tungsten alloy single crystal deformations determined as function of alloying, strain, and temperature
[NASA-TN-D-5493] c17 N69-39182
Electrical conductivity of lanthanum fluoride single crystal with calcium impurities
[NASA-TN-D-5505] c26 N69-40056

SINGLE SIDEBAND TRANSMISSION
Subcarrier phase modulated single sideband sinusoidal carrier synthesis, discussing signal power ratios, signal efficiency, design sensitivity, etc
c07 A69-29489
Analytic function theory applications to analysis of single-sideband angle modulated systems
[NASA-TN-D-5446] c07 N69-37602

SINTERING
Effects of lithium and oxygen losses on magnetic and crystallographic properties of spinel lithium ferrite
[NASA-TR-R-305] c06 N69-20775

SITE DATA PROCESSORS
IMP-1 experiment, describing design and applications of SDP-3 computer
c08 A69-36265
SDP-3-A general purpose stored program computer designed for small scientific spacecraft onboard data system, noting computerized simulation
c08 A69-37385

SIZE (DIMENSIONS)
Plane strain fracture toughness tests on maraging steel plates for various yield strengths and large dimensions
c17 A69-26496
Weight estimation and forecast in manned spacecraft design, noting size and weight relationship
[SAWE PAPER 793] c31 A69-34864
Size effect on tensile strength of polycrystalline nickel wires
[NASA-TN-D-4884] c17 N69-10226

SIZE DETERMINATION
Unicellular microorganisms size and concentration estimates based on light scattering measurements of suspensions in spectrophotometer cuvette compartment
c04 A69-25643

SIZE SEPARATION
Sorting particles by shape using sieving equipment, noting results with crushed gravel
c15 A69-38950

SKID LANDINGS
Steerable landing gear system consisting of freely castoring corotating wheel nose gear, tiltable axle and main gear skids for lifting body spacecraft
[AIAA PAPER 69-790] c02 A69-35639

SKIDDING
Reverted rubber during skidding of aircraft tires
[NASA-CR-1398] c02 N69-34915

SKIN FRICTION
Supersonic Preston tube correlations for Mach number and Reynolds number effects on hypersonic turbulent skin friction on adiabatic surfaces, simplifying correlation
[AIAA PAPER 69-345] c12 A69-28280
Skin friction measurement in aerodynamic tests using thin liquid crystal coatings with changes in maximum light scattering wavelength in response to shearing forces
c11 A69-29029
Baronti-Libby transformation and Preston tube calibrations used to determine skin friction from turbulent velocity profiles
[NASA-TN-D-4853] c12 N69-10472
Graphical interpolation charts of local skin friction from compressible velocity profiles
[NASA-SP-3048] c01 N69-25391
Direct measurement of skin friction in wind tunnel testing by using cholesteric liquid crystals
[NASA-TM-X-1774] c12 N69-26956
Skin friction and heat transfer data for hypersonic turbulent layer on flat plates, wind tunnel wall, and cones
[NASA-TN-D-5089] c12 N69-29144
SKIN TEMPERATURE (NON-BIOLOGICAL)
Computer program for computation of thermal radiation heat loads and temperatures of spacecraft orbiting planets or moon
[NASA-TR-R-278] c30 N69-14428
Parametric analysis of surface temperatures and distortions of paraboloidal solar concentrators
[NASA-TN-D-5144] c03 N69-23356
SKY BRIGHTNESS
Day sky brightness at altitude above 100 km obtained during rocket flight compared to night sky viewed from ground
c30 A69-33664
SKY RADIATION
Cosmic X ray bremsstrahlung due to collisions of suprathermal protons with ambient electron, giving clue about diffuse sky background of X rays
c29 A69-40643
SLABS
Group cross section generating techniques to calculate neutron capture rates and spatial capture distribution in depleted thick U slab, using GAROL program
c24 A69-35179
Multigroup calculations of resonance neutron capture in thick slab of depleted U-238
[NASA-TM-X-1878] c24 N69-36901
SLEEVES
Glass vacuum systems grease free assembly method using heat shrinkable polyolefin sleeve tubing connector for compression of O ring joints
c15 A69-20529
SLENDER BODIES
Hypervelocity reentry simulation problems for slender and blunt bodies, defining significant parameters
c30 A69-30376
Aerodynamic characteristics of blunt space capsules and slender reentry bodies with bulbous bases
[NASA-CR-1339] c01 N69-35521
Flow model for vortex shedding from slender body in coning motion
[NASA-CR-1448] c12 N69-40200
SLENDER CONES
Hypersonic surface measurements and flowfield properties about slender cones in hypersonic viscous interaction regime
[AIAA PAPER 68-2] c01 A69-12520
Ballistic range tests to study ablation effects on aerodynamic characteristics of ablating and nonablating slender cones
[AIAA PAPER 69-179] c33 A69-18083
Drag coefficients for spheres and sharp cones in rarefied hypersonic air flow obtained in shock tunnel using free flight technique
[AIAA PAPER 69-140] c01 A69-18184
Mach number, cone angle, bluntness and wall to recovery temperature ratio effects on slender cones boundary layer transition measurements at hypersonic speeds
c01 A69-33250
Radiation equilibrium temperature measured downstream of transpiration cooled gas flow near slender cone vertex in continuous flow hypersonic tunnel
c01 A69-43588
Experimental pressure distributions on 120 deg cone at Mach 2.96 to 4.63 and angles of attack from 0 deg to 20 deg
[NASA-TN-D-5054] c01 N69-19826
SLIDING FRICTION
Gas turbine engine shaft face seal with self acting lift augmentation preventing rubbing contact, noting disadvantages of labyrinth and conventional seals
[ASLE PICFS PREPRINT 27] c15 A69-30492
Sliding friction tests of Cu and Cu-Be alloy plates in contact with various alloy sliders in air and vacuum
[ASLE PAPER 68-LC-5] c15 A69-30610
Solid solutions atomic ordering effect on friction and wear in vacuum, using CuAu and FeCo systems
c15 A69-35183
Influence of surface films on friction and deformation of single crystal and polycrystalline gold
[NASA-TN-D-4875] c15 N69-10249
Sliding friction and wear behavior of copper alloys in air and vacuum
[NASA-TN-D-4824] c15 N69-10757
Effect of orientation and presence of surface active materials on friction and wear of aluminum
[NASA-TN-D-4994] c15 N69-16197
Friction and wear of polymers with various fillers in liquid hydrogen
[NASA-TN-D-5073] c15 N69-19800
Vibration of shaft face seals and stabilizing effect of viscous and friction damping
[NASA-TN-D-5161] c15 N69-23466
Structure, interactions, and topography of solid surfaces, sliding friction, adhesion, wear, and boundary lubrication conference topics
[NASA-SP-181] c15 N69-30401
Friction and contact resistance during sliding in vacuum of low resistivity metals lubricated with sputtered molybdenum disulfide
[NASA-TN-D-5349] c15 N69-31884
SLIP FLOW
Subsonic expansion tube evaluation as device for studying particle drag in subsonic compressible slip flow
[NASA-CR-1354] c11 N69-28095
SLITS
Minimization of optical resonance scattering by adjustment of monochromator slit geometry
[NASA-TM-X-1702] c24 N69-13210
SLOPES
Transient condensing with freezing on nonisothermal inclined plate
[NASA-TN-D-5289] c33 N69-29598
SLOT ANTENNAS
Air gap tolerances effect on admittance of TEM mode dielectric and plasma coated slot antennas determined by variational method
c09 A69-24986
Radiation pattern of axial slot on circular conducting cylinder based on wedge diffraction and creeping wave theory
c07 A69-24993
Equatorial radiation pattern of parallel plate TEM mode axial slot on elliptical conducting cylinders, using wedge diffraction and creeping wave theory
c09 A69-40703
Edge diffraction effects in TEM axially slotted finite ground plane on radiation pattern in waveguides of different geometries
c07 A69-41588
Simple antenna with good circular polarization over wide space sector, showing geometry, normalized orthogonal field distributions and beamwidth range, considering slot combinations
c09 A69-41590
SLOTS
Inviscid flow of two parallel slot jets impinging normally on surface
[NASA-TN-D-4957] c12 N69-14316
SMOKE TRAILS
Wind velocity profiles by smoke trail method for

eastern test range
[NASA-TN-D-4880] c20 N69-14505
SNAP 8
Design point performance of double containment tantalum and stainless steel mercury boiler for SNAP 8
[NASA-TN-D-4926] c33 N69-12739
Radiator transfer functions for SNAP 8 ground test facilities
[NASA-TN-D-4946] c22 N69-14503
Performance tests of SNAP 8 lubrication and cooling subsystem
[NASA-TM-X-1731] c03 N69-20828
Performance testing of SNAP 8 experimental power system
[NASA-TM-X-1732] c03 N69-20868
Electronic position indicator for latching solenoid valves in SNAP 8 ground test facility
[NASA-TM-X-1760] c14 N69-20874
Results of endurance tests of SNAP 8 turbine alternator
[NASA-TM-X-1741] c03 N69-20913
SOAPS
Concentration, flow rate and tube diameter effects on viscous drag reduction in nonpolar soap solutions, using pressure drop measurements to observe turbulent flow behavior
c12 A69-33253
SOCIAL FACTORS
Aerospace technology role in economic and social benefits
[UN PAPER 68-95321] c34 A69-10467
Space, technology and society - Conference, Cocoa Beach, Florida, March 1969, Volume 2
c34 A69-35055
Space, technology and society - Conference, Cocoa Beach, Florida, March 1969, Volume 1
c34 A69-35070
SODIUM
Cb-1Zr pumped sodium loop tests to evaluate loop components, EM pump, pressure transducers, and instrumentation techniques
[NASA-CR-1135] c03 N69-11373
Evaluation of various laboratory determination of oxygen in potassium and sodium
[NASA-TN-D-4971] c06 N69-14180
SODIUM CHLORIDES
Hot salt stress corrosion of titanium alloys - generation of hydrogen and its embrittling effect
[NASA-TN-D-5000] c17 N69-16465
Analysis of sodium chloride deposits on compressor blades of flight gas turbine engines
[NASA-TN-D-4999] c28 N69-17276
Research on warm fog properties, and dispersal concepts
[NASA-SP-212] c20 N69-39526
SODIUM COMPOUNDS
Three crystal sodium iodide pair spectrometers
[NASA-TM-X-1857] c14 N69-34628
SODIUM COOLING
Properties and uses of liquid metal reactor fuels, including heat transfer processes in variously shaped channels, boiling and condensation of metals, and reactor control equipment
[NASA-TT-F-522] c33 N69-30507
SODIUM VAPOR
Bimetallic heat exchanger tube performance in sodium boiling facility
[NASA-TN-D-5323] c33 N69-30064
SOFT LANDING
FM/AM telemetry circuits with three axis piezoelectric accelerometer for measurements during impact tests of soft landing models
c07 A69-23279
Model design for simulation of space capsule landing on soils using similitude law
[NASA-CR-1210] c34 N69-13159
SOFT LANDING SPACECRAFT
Vehicles for lunar surface exploration and transportation including flying machines and wheeled vehicles
c30 A69-27908
SOIL SCIENCE
Adenosine triphosphate /ATP/ content of terrestrial soils, based on firefly bioluminescent reaction, for Mars soil problems
c04 A69-37567
SOLAR ACTIVITY
Polar exosphere near solar maximum investigation by Explorer 19 and Explorer 24 drag satellites, considering density and atomic oxygen concentration measurements
c13 A69-31351
Structure of matter, physical fields, evolution of earth and universe, solar activity and earth, and interaction of earth biosphere with physical fields
[NASA-TT-F-345] c13 N69-12384
Radiometric techniques applicable to measurement of solar activity and atmospheric attenuation at millimeter wavelengths
[NASA-TR-R-306] c07 N69-22951
Investigation of earth atmospheric composition, geomagnetism, extraterrestrial radiation, solar activity, and planetary atmospheres by satellite experiment and astronomical observations
[NASA-SP-195] c34 N69-38951
SOLAR ACTIVITY EFFECTS
Radiation protection plan for Apollo lunar mission based on real time monitoring of solar activity and radiation in spacecraft
[AIAA PAPER 69-19] c29 A69-18113
Time history of July 7-10 1966 PCA event analyzed using 16 riometers and concurrent satellite observations of solar cosmic radiation
c13 A69-23770
Cosmic ray intensity during solar cycles, considering minima relationship to Bartel index maxima and solar wind modulation theory
c29 A69-29967
Simultaneous solution of continuity and heat conduction equations for ionospheric plasma consisting of electrons, atomic O ions and neutral gas species, discussing varying solar flux effects
c29 A69-32082
Solar radiation pressure windmill effect in rotational bursting and elimination from solar system of small magnetic celestial bodies
c30 A69-39584
Spectral and electrophotometric studies of upper atmosphere - airglows, atomic oxygen, hydroxyl emission, helium line spectra, auroras, and solar cycle effects on magnetosphere
[NASA-TT-F-530] c13 N69-16539
SOLAR ATMOSPHERE
Type 3 solar radio bursts observed during April - October 1967 for two alternative models of active region streamers in outer corona
c29 A69-40300
SOLAR CELLS
Thermal cycling tests showing improvement in cadmium sulfide solar cell stability, noting effect of thermal cycling stresses
c03 A69-13074
Photovoltaic properties of CdS thin film solar cells and silicon cells at Jupiter temperature and solar intensity
c03 A69-13076
Photovoltaic solar cell power technology application to space use and exploration
[ASME PAPER 68-WA/SOL-1] c03 A69-16158
Annealing temperature of radiation defects in phosphorus doped silicon, discussing isochronal recovery characteristics of solar cells with different donor and oxygen concentrations
c26 A69-24006
Photovoltaics - IEEE Conference, Pasadena, November 1968
c03 A69-35678
Radiation damage and recovery of lithium-diffused silicon p-n solar cells, measuring photovoltaic parameters as function of gamma radiation fluence
c03 A69-35694
Optimum solar cell cover glass systems selected by studying interplanetary space environment effects of proton impact, temperature and concurrent illumination on radiation damage
c03 A69-35702
Solar cell radiation damage during 416.8 days in synchronous orbit on satellite ATS 1, discussing radiation shields
c03 A69-35704
Fuel cell /battery and solar array/ battery systems for manned Apollo Applications Program

/AAP/ space vehicles, considering mission and power requirements
c03 A69-42244
Integral coverslip development for Si solar cells, considering borosilicate glass fusing on cell surface and RF and high vacuum ion beam sputtering
c03 A69-42272
Spacecraft solar cell near-maximum power operation by tracking optimum value with array temperature sensor
c03 A69-42303
Effects of preparation techniques on thin film CdS solar cells
[NASA-TM-X-1722] c03 N69-15397
Simulated micrometeoroid impact effect on silicon and cadmium sulfide solar cell performances
[NASA-TN-D-5133] c03 N69-21016
Thermal shock cycling of Kapton, copper, and molybdenum thin film cadmium sulfide solar cell
[NASA-TM-X-1819] c03 N69-29555
Effects of nickel on performance of n on p silicon solar cells
[NASA-TN-D-5366] c03 N69-31844
Simulated space environmental effects on full and fractional size cadmium sulfide thin film solar cells
[NASA-TM-X-1884] c03 N69-36758
Diffusion lengths of silicon solar cells after radiation damage and annealing by X ray method
[NASA-TM-X-1894] c03 N69-37827
Large thin film cadmium sulfide solar cell electrical characteristics over ranging temperatures and radiant intensities
[NASA-TM-X-1899] c03 N69-38767
Design and structural model of thin film solar cell array
[NASA-TM-X-1913] c03 N69-40787

SOLAR COLLECTORS
Calorimetric, optical, and vibration investigation of stretch-formed aluminum solar concentrators for thermionic converters
[NASA-TN-D-4889] c03 N69-10708
Calorimetric efficiency of cone and column solar energy concentrator
[NASA-TN-D-5109] c03 N69-21088
Calorimetric evaluation of three 1.5-meter diameter inflatable rigidized solar concentrators for solar dynamic cycle power systems
[NASA-TN-D-5234] c03 N69-28123

SOLAR CONSTANT
Solar electromagnetic radiation spectral distribution from ground level, rocket and satellite observations to obtain value of energy received at top of atmosphere
c29 A69-21645
Solar irradiance spectral distribution data normalized and combined with spectral absorptance of satellite surface coatings, obtaining absorbed energy for spectral range
c29 A69-21646
Solar constant and spectral irradiance curve for zero air mass obtained from aircraft measurements
c30 A69-42191

SOLAR CORONA
Green function solution to Maxwell equations for interplanetary and coronal magnetic fields above photosphere, considering field at source surface
c30 A69-24429
Solar wind existence verified by direct measurements of interplanetary magnetic field and plasma, reviewing solar corona studies by satellites and space probes
c30 A69-30010
Lower solar corona composition changes due to pressure and thermal gradients calculated with multicomponent diffusion equations
c30 A69-33059
Quiet solar wind model with magnetic field numerically calculated, obtaining coronal electron densities and angular momentum near earth
c29 A69-34301
Primitive solar nebula physical model considered under angular momentum conservation in collapsing fragment
c30 A69-36074
Two photon decay of metastable levels of hydrogenic and He-like ions in solar corona, depopulating via proton collisional excitation to 2p level
c29 A69-36218
Intensity ratios effect of forbidden Fe and Ca transitions in solar corona on Fe/Ca ratio, noting cascading configurations
c30 A69-36219
Type 3 solar radio bursts observed during April - October 1967 for two alternative models of active region streamers in outer corona
c29 A69-40300

SOLAR COSMIC RAYS
Solar cosmic radiation, particle acceleration, energetic particles as sample of sun and propagation of particles from sun to earth
c29 A69-12934
Time history of July 7-10 1966 PCA event analyzed using 16 riometers and concurrent satellite observations of solar cosmic radiation
c13 A69-23770
Chemical composition of galactic and solar cosmic rays, discussing differences from universal cosmic abundances, using Cerenkov counters, emulsions, etc
c29 A69-40090
Polar cap ionospheric response to solar cosmic ray events observed by Mariners 2 and 4 solar proton measurements used to test magnetosphere models
c29 A69-43621
High energy cosmic radiation problems
[NASA-SP-199] c29 N69-29652

SOLAR CYCLES
Cosmic ray intensity during solar cycles, considering minima relationship to Bartel index maxima and solar wind modulation theory
c29 A69-29967
Solar cycle and slowly varying components correlation with soft X ray radiation based on spacecraft measurements
c29 A69-40504
Diurnal and solar cycle variations of thermosphere density and temperature generated by solar EUV input and tidal wave, using two dimensional model
c29 A69-43003

SOLAR ECLIPSES
Rocket sounding measurements of ionospheric D region electron density profile during 20 May 1966 solar eclipse, discussing D region ionization source
c13 A69-29116
Physical properties of Martian atmosphere using solar occultation seen from artificial satellite
[NASA-TN-D-5443] c30 N69-38658

SOLAR ENERGY
Liquid mercury cathode thrustors characteristics satisfying constraints imposed by solar flux variations with distance from sun
[AIAA PAPER 69-237] c28 A69-21246

SOLAR ENERGY ABSORBERS
Solar irradiance spectral distribution data normalized and combined with spectral absorptance of satellite surface coatings, obtaining absorbed energy for spectral range
c29 A69-21646
Solar absorptances and spectral reflectances of metals
[NASA-TN-D-5353] c17 N69-31895

SOLAR FLARES
Interplanetary relativistic electrons from solar flare events
c29 A69-15528
Charge and energy composition of particles in solar flare, discussing rigidity spectra of singly and multiply charged nuclei
c29 A69-17280
Solar protons in magnetospheric tail after flare of July 7, 1966 with isotropic pitch angle distribution, expressing energy spectrum as exponential in rigidity
c29 A69-21699
Solar X ray and extreme UV spectra during flares, attributing intense emissions to optical transitions
c29 A69-22169
Synchrotron and X ray emission generation from upper chromosphere electrons during solar flares

c29 A69-22203
Spectral intensity of high energy solar X rays observed during July 7, 1966 polar event with satellite OGO 3, suggesting nonthermal bremsstrahlung origin
c29 A69-23753
Relativistic solar electron detection in interplanetary space during July 7, 1966 proton flare event, noting energy spectrum and time history
c29 A69-23766
Earth thermal plasmasphere contraction subsequent to solar flare obtained from ion mass spectrometers on OGO satellites
c13 A69-23777
Sunspots magnetic structure producing solar proton flares, considering role of sunspots rotational motion on photospheric surface
c29 A69-35415
Solar flares microwave and hard X ray bursts, discussing gyrosynchroton plasma, nonthermal electron bremsstrahlung and electron relaxation
c29 A69-37551
Solar ionizing radiation increase during flares of 21 and 23 May 1967 determined from ionospheric electron density concentrations
c29 A69-37558
Solar flare and space research - COSPAR Conference, Tokyo, May 1968
c29 A69-43603
Solar flare soft X ray and EUV emission spectra data obtained on OSO-3 satellite compared with centimetric radio bursts
c29 A69-43609
Solar flare and sunspot effects on VHF communications between synchronous satellite relay and ground stations
[NASA-TN-D-5100] c07 N69-23317
Spectral analysis of solar activity, including solar electromagnetic phenomena, facula structure, and periodic variations in chromospheric flares and solar cycles
[NASA-TT-F-581] c29 N69-33401

SOLAR FLUX
Photovoltaic properties of CdS thin film solar cells and silicon cells at Jupiter temperature and solar intensity
c03 A69-13076

SOLAR FLUX DENSITY
Liquid mercury cathode thrustors characteristics satisfying constraints imposed by solar flux variations with distance from sun
[AIAA PAPER 69-237] c28 A69-21246
Radiometer for measuring solar flux variations, discussing design, performance tests and use for spacecraft measurements
[AAS PAPER 69-254] c14 A69-42858

SOLAR GENERATORS
Solar and nuclear electric power technology for electric propulsion
[AIAA PAPER 69-826] c03 A69-32709
Transient solidification outside cocled pipe with application to solar Brayton heat receiver
[NASA-TN-D-4897] c33 N69-10227

SOLAR HEATING
Empirical determination of heating efficiency of extreme solar UV radiation interacting with carbon dioxide atmosphere of Mars and Venus
c30 A69-26019

SOLAR MAGNETIC FIELD
Green function solution to Maxwell equations for interplanetary and coronal magnetic fields above photosphere, considering field at source surface
c30 A69-24429
Sunspots magnetic structure producing solar proton flares, considering role of sunspots rotational motion on photospheric surface
c29 A69-35415
Spectral analysis of solar activity, including solar electromagnetic phenomena, facula structure, and periodic variations in chromospheric flares and solar cycles
[NASA-TT-F-581] c29 N69-33401

SOLAR ORBITS
Perturbative effects of Jupiter moons on spacecraft flyby and postencounter heliocentric trajectories, noting precision targeting
[AIAA PAPER 69-932] c30 A69-39361
Correction and calculation methods for second and first order Plutonian perturbations with respect to perturbing masses, and new Pluto elements
[NASA-TT-F-491] c30 N69-14943
Correction and calculation methods for first order Plutonian perturbations with respect to perturbing masses
[NASA-TT-F-490] c30 N69-14944
Direct and indirect planetary perturbation effects on motion of natural satellites
[NASA-TN-D-5284] c30 N69-37893

SOLAR PHYSICS
Solar-terrestrial physics, Solar aspects - IQSY/COSPAR Conference, London, July 1967, Part 1
c29 A69-30005
Significant achievements in space sciences for 1967, including stellar astronomy, bioscience, ionospheres, planetology, particles and fields, solar physics, and planetary atmospheres
[NASA-SP-167] c30 N69-25460

SOLAR POSITION
Diurnal and seasonal variations of primary atmospheric ions in topside ionosphere correlated with solar zenith angle, using ion mass spectrometer on Explorer 32
c13 A69-38087

SOLAR PROBES
Spacecraft central data system for deep space solar probe data management
c08 A69-42621

SOLAR PROPULSION
Advanced reconnaissance electric planetary spacecraft /AREPS/ concept for repeated coverage of Mars or Venus surface, using solar-photovoltaic system
[AIAA PAPER 69-253] c30 A69-21244
Solar and nuclear electric power technology for electric propulsion
[AIAA PAPER 69-826] c03 A69-32709
Interplanetary probe missions with solar electric propulsion systems
[NASA-TN-D-5293] c30 N69-29738

SOLAR PROTONS
Solar protons in magnetospheric tail after flare of July 7, 1966 with isotropic pitch angle distribution, expressing energy spectrum as exponential in rigidity
c29 A69-21699
Spectral intensity of high energy solar X rays observed during July 7, 1966 polar event with satellite OGO 3, suggesting nonthermal bremsstrahlung origin
c29 A69-23753
Relativistic solar electron detection in interplanetary space during July 7, 1966 proton flare event, noting energy spectrum and time history
c29 A69-23766
Proton dose in receiver behind combination electromagnetic and material shield, calculating dose for Van Allen and solar proton event spectra
c22 A69-31522
Low energy solar protons entry into magnetosphere on 26 May 1967 showing diffusion control
c29 A69-31984
Ground based solar proton monitoring, considering particle intensities and radiation dose rates from riometer absorption as function of time
c29 A69-32321
Sunspots magnetic structure producing solar proton flares, considering role of sunspots rotational motion on photospheric surface
c29 A69-35415

SOLAR RADIATION
Solar absorptance, total hemispherical emittance and absorptance/emittance ratio for metals at cryogenic temperatures measured simultaneously with sinusoidally perturbed incident radiation
c33 A69-10847
Moon effect on intensity and angular distribution of energetic electron and proton shadowing as observed by Explorer satellites
c30 A69-16252
Charge and energy composition of particles in solar flare, discussing rigidity spectra of singly and multiply charged nuclei
c29 A69-17280

Solar absorptance and hemispherical emmitance of metals at space conditions determined with cyclic incident radiation technique
[AIAA PAPER 69-60] c17 A69-18154
Albedo over Antarctic, measuring solar radiation reflected by surface and atmosphere by Eppley radiometer
c13 A69-21404
Solar electromagnetic radiation spectral distribution from ground level, rocket and satellite observations to obtain value of energy received at top of atmosphere
c29 A69-21645
Solar extreme UV, soft and hard solar X rays, cosmic X rays and gamma rays, cosmic ray particles and near earth visible radiation observed by OSO-3
c29 A69-22167
Empirical determination of heating efficiency of extreme solar UV radiation interacting with carbon dioxide atmosphere of Mars and Venus
c30 A69-26019
Ocean circulation as climate regulator, discussing role in redistributing climate-changing energy input from solar radiation or lunar tidal friction into atmosphere
c13 A69-26333
Visual ashen light observation on Venus possibly attributable to solar particle bombardment from dark side emission detection by spectroscopic and photometric studies
c30 A69-32300
UV solar radiation variation effects on Mars and Venus upper atmosphere temperatures
c30 A69-37136
Solar ionizing radiation increase during flares of 21 and 23 May 1967 determined from ionospheric electron density concentrations
c29 A69-37558
Solar radiation pressure windmill effect in rotational bursting and elimination from solar system of small magnetic celestial bodies
c30 A69-39584
Vacuum integrating sphere for measuring solar absorptance in space environment to determine thermal control coatings qualifications
[AIAA PAPER 69-1021] c11 A69-40392

SOLAR RADIO BURSTS
Solar microwave radiation burst of 29 October 1968 from active region behind west limb
c30 A69-32811
Solar flares microwave and hard X ray bursts, discussing gyrosynchroton plasma, nonthermal electron bremsstrahlung and electron relaxation
c29 A69-37551
Synchroton radiation HF cut-off resulting from electrons with anisotropic pitch angle distribution for type 4 solar radio bursts
c29 A69-40577
Solar flare soft X ray and EUV emission spectra data obtained on OSO-3 satellite compared with centimetric radio bursts
c29 A69-43609

SOLAR RADIO EMISSION
Synchrotron and X ray emission generation from upper chromosphere electrons during solar flares
c29 A69-22203
Solar cycle and slowly varying components correlation with soft X ray radiation based on spacecraft measurements
c29 A69-40504

SOLAR SAILS
Large solar sail vehicle to operate in manner of helicopter rotor
[NASA-CR-1329] c31 N69-28861

SOLAR SENSORS
Precision autocollimating solar sensor design for attitude alignment changes, including detector calibration and sounding rocket flight test results
[AIAA PAPER 69-858] c21 A69-39386

SOLAR SIMULATION
Handbook of solar simulation for thermal vacuum testing, discussing space environment, thermal control coatings, radiation sources, optical components, etc
c11 A69-38894

SOLAR SIMULATORS
Solar simulator with xenon and krypton lamps designed for thermal balance tests, power conversion and material degradation experiments
c11 A69-30383
Spectral and operational characteristics of high intensity carbon arc solar simulator
[NASA-TM-X-1825] c11 N69-29737

SOLAR SPECTRA
Solar electromagnetic radiation spectral distribution from ground level, rocket and satellite observations to obtain value of energy received at top of atmosphere
c29 A69-21645
Solar irradiance spectral distribution data normalized and combined with spectral absorptance of satellite surface coatings, obtaining absorbed energy for spectral range
c29 A69-21646
Solar X ray and extreme UV spectra during flares, attributing intense emissions to optical transitions
c29 A69-22169
Rocket-borne spectroheliograph for monochromatic solar photography in Mg II 2802.7 A line noting filter bandwidth, film polarizers and temperature control
c14 A69-24838
Solar spectral irradiance measured by airborne instruments, discussing construction, calibration, etc, of photoelectric filter radiometer and Leiss monochromator
c30 A69-32261
Solar Na D lines analysis by direct inversion of line source function, finding Doppler core dependence on frequency
c30 A69-38479
Solar X rays observations, describing instrumentation, radiation characteristics, association with flares, spectrum analysis, etc
c29 A69-39506
Solar constant and spectral irradiance curve for zero air mass obtained from aircraft measurements
c30 A69-42191

SOLAR SYSTEM
NASA Planetary Exploration Program to gather data on origin of solar system and life, discussing planetary evolution and extraterrestrial life
c04 A69-12804
Solar system elements abundance compilation based on carbonaceous chondrites and nucleosynthesis in stars
c30 A69-20903
Boundary conditions for theory of solar system origin, discussing planetary atmospheres, surfaces, magnetic fields, composition and early solar wind
c30 A69-36209
Propulsion systems for manned exploration of solar system
[NASA-TM-X-1864] c28 N69-34674

SOLAR WIND
Solar plasma observations during magnetic storms, discussing shocks and tangential discontinuities, geomagnetic variations and He
c13 A69-11234
Collisionless plasma heating by hydromagnetic waves in solar wind
c29 A69-12714
Solar wind flow past earth and magnetosphere correspondence to external aerodynamics of round nosed bodies in supersonic stream
c13 A69-19360
Magnetospheric plasma probe results with Pioneer 6 and 7, discussing plasma fluctuations and solar wind interaction with geomagnetic field
c13 A69-19364
Collisionless plasma heating by damping hydromagnetic waves applied to solar wind qualitative model, discussing magnetoacoustic wave energy
c30 A69-22426
Solar plasma flow around magnetosphere, discussing plasma velocity, density and temperature and magnetic field space and time variations
c29 A69-26736
Solar wind plasma observations in geomagnetospheric wake compared at 1000 and 500 earth radii, considering ion energy spectra and geomagnetic tail

c29 A69-26943
Comet interaction with solar wind, assuming field tail coupling of ionized comet material to solar wind ions
c30 A69-27817
Cosmic ray intensity during solar cycles, considering minima relationship tc Bartel index maxima and solar wind modulation theory
c29 A69-29967
Solar wind Helmholtz-type velocity discontinuities, noting plasma density and temperature stabilities from Explorer 34 observations
c29 A69-29971
Solar wind existence verified by direct measurements of interplanetary magnetic field and plasma, reviewing solar corona studies by satellites and space probes
c30 A69-30010
Worldwide changes in geomagnetic field, determining causes by examining magnetic field and plasma data for solar wind and classifying as SSC or SI
c29 A69-31963
Test program simulating solar wind outside magnetosphere to evaluate high melting point high density ceramic oxides as white thermal ccntrol coating pigments
[AIAA PAPER 69-641] c18 A69-33762
Quiet solar wind model with magnetic field numerically calculated, obtaining coronal electron densities and angular momentum near earth
c29 A69-34301
Severe magnetosphere distortions in north-south direction with parallel/antiparallel magnetosheath to magnetospheric field ascribed to solar wind property changes from Explorer 12 observations
c13 A69-34947
Boundary conditions for theory of solar system origin, discussing planetary atmospheres, surfaces, magnetic fields, composition and early solar wind
c30 A69-36209
Solar wind plasma effects on lunar wake umbral and penumbral interplanetary magnetic field anomalies, evaluating roles of electrons and ions
c30 A69-38095
Lunar Explorer 35 measurements of lunar surface electromagnetic properties, magnetic fields and solar wind-moon interactions
c30 A69-38379
Shock discontinuities in solar wind measured by magnetic field and plasma instruments on Explorer 34, applying Rankine-Hugoniot relations
c30 A69-40304
Explorer 34 observations of hydrogen and He ions in solar wind, noting number density variations and tentative association with geomagnetic storms
c29 A69-40305
Measurement of change in plasma potential and magnetic field of hydrogen plasma impinging on magnetic dipole - simulation of solar wind-earth interaction
[NASA-TM-X-1738] c25 N69-19131
Significant achievements in space sciences for 1967, including stellar astronomy, bioscience, ionospheres, planetology, particles and fields, solar physics, and planetary atmospheres
[NASA-SP-167] c30 N69-25460

SOLAR X-RAYS
Solar X ray and extreme UV spectra during flares, attributing intense emissions to optical transitions
c29 A69-22169
Synchrotron and X ray emission generation from upper chromosphere electrons during sclar flares
c29 A69-22203
Spectral intensity of high energy solar X rays observed during July 7, 1966 polar event with satellite OGO 3, suggesting nonthermal bremsstrahlung origin
c29 A69-23753
Solar flares microwave and hard X ray bursts, discussing gyrosynchroton plasma, nonthermal electron bremsstrahlung and electron relaxation
c29 A69-37551
Solar X rays observations, describing instrumentation, radiation characteristics, association with flares, spectrum analysis, etc
c29 A69-39506
Solar cycle and slowly varying components correlation with soft X ray radiation based on spacecraft measurements
c29 A69-40504
Solar flare soft X ray and EUV emission spectra data obtained on OSO-3 satellite compared with centimetric radio bursts
c29 A69-43609

SOLENOIDS
Cryogenic sclenoids with pure Al conductor for production of strong magnetic fields, discussing softness and strain resistivity problems
c03 A69-26497
Electronic position indicator for latching sclenoid valves in SNAP 8 ground test facility
[NASA-TM-X-1760] c14 N69-20874
Magnetic performance properties of air cooled solenoids applied to one component support and balance system
[NASA-CR-1352] c11 N69-24089

SOLID LUBRICANTS
Ball bearing test apparatus for evaluation of greases and solid lubricants at high temperatures
[ASLE PREPRINT 68AM 7C-2] c15 A69-10912
Physical sputtering deposition of molybdenum disulfide films as solid lubricant on rotating and sliding components, discussing lubrication properties in vacuum
[ASLE PAPER 68-LC-15] c15 A69-19308
Energetics in solid film lubricants vacuum deposition methods, showing dependence on interfacial and film characteristics
c15 A69-29001
Solid film lubricants deposited by DC triode sputtering on Ni, Ni-Cr and Nb surfaces friction tested under ultrahigh vacuum conditions
c15 A69-43126
Friction and wear tests with graphite flucride lubricant
[NASA-TN-D-5097] c15 N69-20939

SOLID PHASES
Mass dependence of self diffusion in Fe by serial sectioning in alpha, gamma and delta phases, determining isotope effect with Fe radioactive isotopes
c17 A69-36440
Nuclear magnetic resonance of epsilon and delta phases in NbN system with nitrogen mcle fractions
c26 A69-36445

SOLID PROPELLANT ROCKET ENGINES
Multipulse thruster module design and development tests for spacecraft attitude ccntrol, noting micropulse solid propellant rocket motor
c03 A69-11762
Acceleration effects on solid propellant rocket motors combustion characteristics
[AIAA PAPER 68-530] c28 A69-39217
Flight perfcrmance of FW-4D solid propellant rocket motor on third stage of Delta 50 launch vehicle
[NASA-TN-D-4987] c28 N69-20876

SOLID PROPELLANTS
Pressure and velocity coupling effects on combustion stability in solid propellant burning
[NASA-TN-D-5395] c33 N69-34892
Aluminum size and loading effects on burning rate of centrifugal accelerated solid propellants
[NASA-TN-D-5397] c27 N69-36225

SOLID ROCKET PROPELLANTS
Steady state acceleration effects on combustion characteristics of aluminized composite solid propellant
[NASA-TN-D-4914] c33 N69-13231

SOLID SOLUTIONS
Solid solutions atomic ordering effect on friction and wear in vacuum, using CuAu and FeCo systems
c15 A69-35183

SOLID STATE DEVICES
Laboratory and flight tests of airborne solid state UHF telemetry transmitter, discussing miniaturized coaxial hardware from RF power conservation viewpoint

c07 A69-35996
Solid state detector for electron spatial distribution measurements on OGO-F satellite, discussing design emphasizing reliability
c09 A69-36676

SOLID SURFACES
Structure, interactions, and topography of solid surfaces, sliding friction, adhesion, wear, and boundary lubrication conference topics
[NASA-SP-181] c15 N69-30401

SOLIDIFICATION
Transient solidification outside cooled pipe with application to solar Brayton heat receiver
[NASA-TN-D-4897] c33 N69-10227

SOLIDIFIED GASES
Solid para hydrogen coated graphite particles expulsion into interstellar medium from star formation regions, considering mantles stability and particles extinction efficiency, albedo and phase function
c30 A69-37492
Order-disorder transitions in solid hydrogen, discussing model to explain molecular rotation angular momentum operator fluctuations
c23 A69-43119

SOLIDS
Compatibility conditions for strain measures of theory of micromorphic elastic solids
[NASA-CR-1236] c26 N69-10817
Mathematical analysis of Fitzgerald apparatus measuring solids dynamic mechanical properties
[NASA-TN-D-5116] c18 N69-21384

SOLUBILITY
Solubility of oxygen in tantalum determined by resistivity technique
[NASA-CR-1276] c17 N69-19886
Solubility of vanadium in liquid potassium
[NASA-TN-D-5093] c17 N69-20789
Solubility of refractory metals and alloys in liquid potassium and lithium
[NASA-CR-1371] c17 N69-27059
Molybdenum and tungsten solubility in liquid potassium
[NASA-TN-D-5504] c17 N69-40053

SOLUTIONS
Computer analysis of light scattering data from polymer solutions
[NASA-TN-D-5177] c06 N69-22991

SOLVENTS
Organic geochemical laboratories solvent purification procedures
[NASA-TM-X-1746] c06 N69-18962

SONIC BOOMS
Aircraft created pressure patterns responsible for sonic boom, discussing design techniques for noise reduction
c02 A69-30369
Equations for pressure signature of supersonic projectile in stratified atmosphere
[NASA-TN-D-4890] c02 N69-10087
Estimated supersonic flow field shock waves and sonic boom effects for cones and axisymmetric bodies
[NASA-TN-D-4935] c01 N69-13238
Variability in sonic boom signatures measured along 8000 foot linear microphone array
[NASA-TN-D-5040] c02 N69-17279
Dynamic response of uniform beams and plates exposed to sonic booms
[NASA-CR-1281] c32 N69-21403
Sonic boom propagation in stratified atmosphere using FORTRAN computer program with integral and differential equations
[NASA-CR-1299] c02 N69-22546
Design method for far field sonic boom shock strength and impulse independent of body length and volume
[NASA-TN-D-5148] c01 N69-23927
N shaped shock wave line focusing simulating sonic superbooms
[NASA-TN-D-5306] c02 N69-31874
Design and performance of sonic boom simulator
[NASA-CR-1378] c02 N69-31959

SOUND GENERATORS
Acoustic energy generation for helium rich stars, discussing X ray radiation from helium star corona
c29 A69-20645

SOUND INTENSITY
Comparison of ray trace methods for estimating sound intensity variations due to atmospheric variability as determined by Monte Carlo methods
[NASA-CR-1337] c23 N69-23199
Prediction of loudness from frequency characteristics of sound
[NASA-TN-D-5422] c23 N69-37028

SOUND PRESSURE
Prediction of loudness from frequency characteristics of sound
[NASA-TN-D-5422] c23 N69-37028
Thermal, acoustical, and acceleration environments of XB-70 airplane crew compartment in airworthiness tests
[NASA-TN-D-5449] c25 N69-38010
Sound wave pressure for preventing cryogenic propellant sloshing during space flight
[NASA-TN-D-4024] c23 N69-38180

SOUND WAVES
Linear wave interaction with oblique shock waves, noting dependence of transmission, reflection and generation coefficients on Mach number
c12 A69-13137
Stellar atmospheres acoustic energy generation rate calculations, studying corona mass ejection effects on stellar rotation
c30 A69-39521
Dynamic response of liquid jet atomization to acoustic oscillations
[NASA-TN-D-5339] c28 N69-30980
Temperature effects on turbofan and turbojet noise radiation
[NASA-CR-1472] c02 N69-40439
Radiation resistance of cylindrical shells in ideal compressible acoustic medium
[NASA-CR-1437] c32 N69-40935

SOUNDING ROCKETS
Fluidic proportional thruster system for sounding rocket control
[ASME PAPER 68-WA/FE-32] c14 A69-16105
Antenna reactance from sounding rocket in ionosphere, showing variations relationship to rocket spin period
c13 A69-39964
Theoretical comparison of beads, wires, and films as rocketsonde temperature sensors in mesosphere
[NASA-CR-1286] c13 N69-18126
Graphic method determining sounding rocket vehicle attitude
[NASA-TN-D-5172] c30 N69-23782
Evaluation of height and time based meteorological rocket wind reduction techniques
[NASA-TM-X-1850] c20 N69-35523

SOUTHERN HEMISPHERE
Synoptic analysis of Southern Hemisphere stratosphere
[NASA-TM-X-1814] c13 N69-33555

SPACE CAPSULES
Model design for simulation of space capsule landing on soils using similitude law
[NASA-CR-1210] c34 N69-13159
Astronaut capability to maintain life support systems and cabin habitability in weightlessness
[NASA-CR-1405] c05 N69-36709

SPACE COMMUNICATION
Short wave bands for earth-space communications, considering propagation anomalies compensated systems and frequency bands availability
c07 A69-13721
NASA program for radio spectrum utilization in aerospace communication systems
c07 A69-42502
Space communications system for earth moon radio link
[NASA-TT-F-527] c07 N69-14973
Analytic function theory applications to analysis of single-sideband angle modulated systems
[NASA-TN-D-5446] c07 N69-37602

SPACE DEBRIS
Gegenschein measurements for determining upper limit on asteroidal debris spatial density
c30 A69-12545

SPACE ELECTRIC ROCKET TESTS
SERT 2 mercury vapor fed hollow cathode operated in bell jar, determining volt-ampere characteristics and flow rates for plasma diagnostics
[AIAA PAPER 69-258] c28 A69-21221

SERT 2 thrustor system performance over expected mission parameters, noting operational lifetime excess over mission requirements
[AIAA PAPER 69-235] c28 A69-21255
Mercury electron bombardment thrusters, discussing mission, design, ground tests, components and thrust vectoring
c28 A69-26787
Power conditioner for use with SERT 2 mercury ion thrustor, describing electrical and mechanical design and operation
c03 A69-42301
Performance of various oxide magazine cathodes in Kaufman thrusters
[NASA-TN-D-5074] c28 N69-19980

SPACE ENVIRONMENT SIMULATION
Sealed and unsealed relay coils temperature rise at simulated outer space air pressure levels
c09 A69-28048
Space suit meteoroid protection for extravehicular activity, discussing Gemini and lunar surface EVA suits and bumper concept
[AIAA-PAPER-69-366] c05 A69-28298
Thermal Vacuum /TV/ manned test operations related to Apollo lunar module in simulated space environment
c05 A69-30394
Test program simulating solar wind outside magnetosphere to evaluate high melting point high density ceramic oxides as white thermal control coating pigments
[AIAA PAPER 69-641] c18 A69-33762
Instrumentation in aerospace simulation facilities - Conference, Farmingdale, New York, May 1969
c11 A69-35714
Flash X ray unit with special film transport devices to obtain sequenced dynamic radiographs of ablating models during reentry simulation tests
c11 A69-35720
Handbook of solar simulation for thermal vacuum testing, discussing space environment, thermal control coatings, radiation sources, optical components, etc
c11 A69-38894
Pressure measurements and gas flow analysis during thermal vacuum tests of manned spacecraft indicating adequate space vacuum simulation
[AIAA PAPER 69-1033] c11 A69-40401
Degradation of multiplier phototubes exposed to spatial radiations
[NASA-CR-1304] c14 N69-20777
Predicting human performance in space environments
[NASA-CR-1370] c05 N69-30168
Lunar gravity effects on mans locomotion on moon
[NASA-CR-1403] c05 N69-36271
Simulated space environmental effects on full and fractional size cadmium sulfide thin film solar cells
[NASA-TM-X-1884] c03 N69-36758
Laser optical simulation of spaceborne radio astronomy interferometer experiment
[NASA-TN-D-5357] c30 N69-36892

SPACE EXPLORATION
Life sciences and space research - COSPAR Conference, London, July 1967
c04 A69-11073
Manned Mars and Venus missions role in overall planetary exploration program
c30 A69-12304
Structural design options for decelerative aeroshell configurations for atmospheric entry on unmanned planetary explorations
[AIAA PAPER 68-344] c32 A69-15507
Spacecraft sterilization techniques for space exploration, discussing mathematical models for planetary quarantine and contamination by nonlanding vehicles
c05 A69-15935
Manned space flight programs, discussing U.S. technological, scientific and practical contributions
c30 A69-17074
Interplanetary Pioneer spacecraft development and systems engineering aspects
c31 A69-17605
Space exploration plans adaptation, considering spacecraft design, programs, costs and schedules flexibility
c34 A69-22863
Manned space stations for future space exploration, discussing earth-like environment, artificial gravity, human factors and time dependence
c30 A69-25644
Commercial utilization of space technology, discussing cost reduction and role of NASA Apollo Program
c30 A69-34044
Advanced space experiments - AAS Conference, Ann Arbor, September 1968
c30 A69-34359
Space, technology and society - Conference, Cocoa Beach, Florida, March 1969, Volume 2
c34 A69-35055
Space exploration influence on science education, showing NASA instructional materials for teachers in biology, chemistry, physics, mathematics, industrial arts, etc
c34 A69-35077
Scientific findings from interplanetary spacecraft radio propagation experiments, particularly Mariner 5 data
c07 A69-35940
Propulsion system performance relationship to manned planetary mission capability, discussing anticipated performance of advanced propulsion concepts
c28 A69-38118
Apollo 11 mission and future space exploration prospects including moon base, manned space station, reusable shuttle vehicles, etc
c30 A69-41477
Mars exploration for life by Mariner flybys and orbiters and 1973 Viking landers
c30 A69-41611
Planetary exploration and NASA program objectives
[AAS PAPER 69-286] c30 A69-42810
Space research in past and expected scientific knowledge from manned and automated earth orbital science missions
[AAS PAPER 69-036] c30 A69-42825
Launch vehicle upper stage requirements in space missions, discussing space engine for lunar, planetary and interplanetary exploration
[AAS PAPER 69-359] c34 A69-42828
Manned space flight history and spacecraft development
[AAS PAPER 69-501] c30 A69-42852
Pioneer F/G mission to Jupiter by NASA for exploring interplanetary medium, asteroid belt, planet and environment
[AAS PAPER 69-290] c30 A69-42863
Monograph on Pioneer spacecraft program, discussing mission objectives, spacecraft design, etc
[AAS PAPER 69-066] c30 A69-42883
Interplanetary space trajectories based on Jupiter swingby flights
[NASA-TN-D-5271] c30 N69-28441
Propulsion systems for manned exploration of solar system
[NASA-TM-X-1864] c28 N69-34674

SPACE FLIGHT
Digital computers in space flight simulation and vehicle performance optimization, examining mission analysis
c30 A69-14519
X-15 research aircraft program piloting problems, ground facilities, heat transfer, space flight and steep reentry
c02 A69-26872
Soviet handbook of astronautics covering spacecraft and operating problems of near-earth spaceflight
[NASA-TT-F-500] c31 N69-24760
Bibliography of works of Soviet engineer F. A. Tsander
[NASA-TT-F-541] c34 N69-26112
Physiological and psychological responses of man to space flight problems
[NASA-TT-F-529] c05 N69-32044
Mechanics of low thrust space flight
[NASA-TT-F-507] c28 N69-33354
Bibliography on aerospace medicine and related biological research
[NASA-SP-7011/66/] c04 N69-37909

Blood sampling for parathyroid hormone and calcium metabolism during weightlessness of space flight
[NASA-CR-1395] c05 N69-38600
SPACE FLIGHT FEEDING
Biological, psychological and technological requirements in astronaut nutrition programs, examining preservation and reconstitution techniques
c05 A69-15388
Astronaut feeding in space and NASA criteria for space foods, eliminating foods in metal tubes and directing development efforts to dehydrated foods
c05 A69-31459
Regenerative life support system development, considering synthesized organic compounds and microorganisms as foods for long duration space missions
c04 A69-37623
SPACE FLIGHT STRESS
Gemini and Mercury space flights medical results, summarizing physiological effects noted on body systems
c04 A69-11074
Gravitational and acceleration effects on man and organisms, and biological effects of radiation
[NASA-TT-F-528] c05 N69-38701
SPACE LABORATORIES
Space station design requirements, Apollo applications program and various experimental programs
c31 A69-11395
Extraterrestrial life detection experiments integrated into single multipurpose space laboratory, including chemical analyses, metabolism identification, observation for molecular and/or cellular growth and replication
c05 A69-32970
Space manufacturing processes for orbital low and zero gravity environment, discussing buoyancy and thermal convection sensitive and molecular forces controlled methods
[AAS PAPER 69-486] c30 A69-42844
SPACE LAW
International liability for damage caused by launching of objects into outer space
[UN PAPER 68-95337] c34 A69-10525
Space law - Conference, New York, October 1968
c34 A69-37102
International legal liability for personal injury or property damage caused by space activities
c34 A69-37127
SPACE MAINTENANCE
Space manufacturing operations program, discussing zero gravity effect during earth orbit flight, Apollo Applications Program Orbital Workshop Flight 2, etc
c31 A69-35067
Tools and equipment for extravehicular and intravehicular activities in space and on lunar surface
[AAS PAPER 69-438] c15 A69-42802
Space manufacturing processes for orbital low and zero gravity environment, discussing buoyancy and thermal convection sensitive and molecular forces controlled methods
[AAS PAPER 69-486] c30 A69-42844
SPACE MISSIONS
Lunar Orbiter mission objectives and orbit design
[AIAA PAPER 68-47] c30 A69-15503
Apollo 4, 5 and 6 space missions, with preview of Apollo 7, 8 and 9 missions
c31 A69-17672
Worldwide cloud cover simulation procedure providing data for computer simulation of earth oriented space missions, describing computer program using Monte Carlo mission simulation
c20 A69-38120
Celestial sphere scanning by passive method applicable to space missions requiring long lifetime and moderate pointing accuracies
[AIAA PAPER 68-854] c21 A69-39764
Aerodynamic deceleration systems for space missions, considering deployment of subsonic parachute and inflatable configuration following atmospheric entry
[AIAA PAPER 68-1081] c31 A69-40542
Parametric analysis of microwave and laser systems for communication and tracking - summary
[NASA-TR-R-309] c07 N69-23642
SPACE NAVIGATION
Autonomous solution to orbital navigation problem yielding direct measure of orbital parameters
c21 A69-11005
Ground based guidance systems for supplementing onboard guidance of manned space vehicles
c21 A69-17580
Space navigation - Conference, Houston, April 1969
c21 A69-35789
Navigation, guidance and control developments for manned space missions, discussing earth orbital exploration bases
c21 A69-35801
Statistical error analysis of autonomous manned spacecraft navigation in long duration eccentric Mars orbits
[AIAA PAPER 69-880] c21 A69-39406
Navigation state vector update effect on lunar mission completion capability for Saturn 5, emphasizing hardware and scheme errors and accelerometer failure
[AIAA PAPER 69-883] c21 A69-39409
Analytic approximations for application to spacecraft optical navigation system where position fixes are taken over short trajectory arcs
[NASA-TN-D-4863] c21 N69-10372
Sextant sighting measurements from on board Gemini 12 spacecraft
[NASA-TN-D-4952] c21 N69-14332
Matched conic solutions to round trip interplanetary trajectory problems for use in guidance and navigation simulation
[NASA-TN-D-4942] c30 N69-14861
Soviet handbook of astronautics covering spacecraft and operating problems of near-earth spaceflight
[NASA-TT-F-500] c31 N69-24760
SPACE PERCEPTION
Luminescence effects on apparent size and shape of foveally fixated targets of various forms
c04 A69-36458
Relationship between binocular depth perception and optical distortion in Apollo pressure suit helmets and visors
[NASA-TN-D-5162] c05 N69-22990
Space flight effects on human time perception
[NASA-TT-F-545] c05 N69-26455
SPACE POWER UNIT REACTORS
Lunar surface power plants, considering weight constraint for various systems using nuclear power, solar cell/fuel cells and H-O reactant regeneration
c03 A69-11396
Comparison of Brayton and Rankine cycle magnetogasdynamic space power generation systems for use with nuclear heat source
[NASA-TN-D-5085] c03 N69-20852
Nuclear thermionic space power system using rod control and heat pipes
[NASA-TN-D-5250] c22 N69-26270
Design of Brayton rotating unit with roller bearings for space power system
[NASA-CR-1401] c15 N69-33450
Tungsten and depleted uranium in minimum weight, layered shield comparisons for space power reactor
[NASA-TM-X-1874] c22 N69-35817
SPACE PROBES
IQSY low energy galactic and solar cosmic ray observations made by various satellites and space probes, including hydrogen and helium energy spectra
c29 A69-30014
SPACE PROGRAMS
Space applications program including communications and navigation meteorology, earth resources survey and geodesy
[UN PAPER 68-95437] c34 A69-10472
Meteorological satellite research program, including unmanned satellite observations and possibilities with meteorologist on board manned spacecraft
[UN PAPER 68-95350] c20 A69-10483
NASA university program, discussing participation in space and aeronautics developed based on project oriented research grants and sustaining university grants

[UN PAPER 68-95413] c34 A69-10506
NASA programs and opportunities for international cooperation in space
[UN PAPER 68-95367] c34 A69-10516
Galactic Jupiter Probes investigating Jupiter atmosphere and emissions and deep space cosmic radiation
c30 A69-12303
Future space programs as governed by cost limitations, suggesting development of economical launch vehicle for shuttling between earth and orbital space stations
c30 A69-12680
NASA Space Application Program strategy, discussing research and development trend toward complexity, versatility and multidisciplinary use of larger spacecraft
c30 A69-13427
Space exploration plans adaptation, considering spacecraft design, programs, costs and schedules flexibility
c34 A69-22863
Earth orbital manned space astronomy, discussing long range program, instruments, facilities and data processing
c11 A69-27947
Commercial utilization of space - Conference, Dallas, May 1967
c30 A69-34043
Space manufacturing operations program, discussing zero gravity effect during earth orbit flight, Apollo Applications Program Orbital Workshop Flight 2, etc
c31 A69-35067
Low cost rate transportation as mandatory goal for future space program, discussing recovery and reuse, launch system costs, hardware development, etc
c31 A69-38117
Nuclear rocket program status and plans, presenting NERVA reactor and engine system tests
[AIAA PAPER 68-610] c22 A69-39219
Space program planning, noting market requirements, acceptability and future characteristics
[AAS PAPER 69-083] c34 A69-42820
Space research in past and expected scientific knowledge from manned and automated earth orbital science missions
[AAS PAPER 69-036] c30 A69-42825
Potential for advancement of astronomy by space programs
[NASA-SP-213] c30 N69-41150

SPACE RENDEZVOUS
Low thrust trajectories for minimum time rendezvous between continuous thrust interceptor and passive target vehicle, comparing calculus of variations and steepest ascent analyses
c30 A69-32177

SPACE SIMULATORS
Unstabilized astronaut, hand-held and integrated life support EVA maneuvering units tested in gimbaled six degree of freedom servo driven moving base simulator
[AAS PAPER 69-516] c05 A69-42850

SPACE STATIONS
Space station design requirements, Apollo applications program and various experimental programs
c31 A69-11395
Space-station-centrifuge configuration dynamic stability exhibiting instabilities at lower and higher centrifuge rotational speeds
[AIAA PAPER 68-142] c31 A69-12373
Equations formulated for space vehicle reaction to rotating machinery and internal mass motion, evaluating dynamics of cylindrical space station rotating about major axis
c30 A69-16476
Crew and passenger transportation to and from space station orbits, discussing cost reduction possibilities with current or future technology
c31 A69-39691
Space station safety, discussing damage containment and control, escape and rescue, etc
[AAS PAPER 69-518] c31 A69-42842
Effects of lateral cable oscillations on dynamic response of cable-connected space station
[NASA-TN-D-5107] c31 N69-21111
Rendezvous and station keeping simulator with fly around capability and virtual image viewing
[NASA-TN-D-5123] c11 N69-22629
Operational and structural design criteria for artificial gravity stabilization of rotating space station
[NASA-TN-D-5426] c05 N69-39210

SPACE STORAGE
Specific impulse deliverable performance of space storable propellant combination fluorine-oxygen/methane and oxygen difluoride/diborane
[AIAA PAPER 69-505] c28 A69-32762
Shadow shields for thermal protection of cryogenic tanks in space
[NASA-TN-D-4887] c33 N69-10420
Analytical evaluation of space storable propellants for unmanned Jupiter and Saturn orbiter missions
[NASA-TM-X-1793] c31 N69-24942

SPACE SUITS
Hard space suit for use on planetary surfaces and extravehicular activity, discussing design, fabrication and mobility
c05 A69-12993
Space suit meteoroid protection for extravehicular activity, discussing Gemini and lunar surface EVA suits and bumper concept
[AIAA-PAPER-69-366] c05 A69-28298
Carbon dioxide levels monitoring in spacesuit research including limits of physiological acceptability
c05 A69-39170
Manned testing of EVA equipment in thermal-vacuum environment for qualification of Apollo extravehicular mobility unit, using lunar surface thermal simulator
[AIAA PAPER 69-992] c05 A69-40370
Real time metabolic rate analysis of suited astronaut using heart rate and O methods during thermal vacuum and extravehicular mobility tests
[AIAA PAPER 69-993] c05 A69-40371
Cardiovascular conditioning suit to provide transmural pressure gradient in circulatory system during weightlessness
[NASA-CR-1206] c05 N69-13202
Biomechanical factors determining lung damage following explosive decompression of space suits in vacuum test chambers
[NASA-CR-1223] c05 N69-13969
Space suit design with pressure stabilizer for force assisted elbow joint
[NASA-TN-D-5221] c05 N69-26259
Heat pipe devices for space suit temperature control
[NASA-CR-1400] c05 N69-38491

SPACE SURVEILLANCE (SPACEBORNE)
Earth resources remote sensing from spacecraft noting meteorology, oceanography, forestry, agriculture and IR detection of plant diseases and pollution
c34 A69-26978

SPACE TOOLS
Tools and equipment for extravehicular and intravehicular activities in space and on lunar surface
[AAS PAPER 69-438] c15 A69-42802

SPACE VEHICLE CHECKOUT PROGRAM
Onboard checkout system concept, discussing philosophy, requirements, underlying considerations, system description, development and techniques of system selection
c11 A69-25081

SPACE-TIME FUNCTIONS
Equation describing statistically trapped particle motion under influence of fields varying in time and space
c29 A69-19375
Metric state-time dynamical polysystem with sequentially compact topological space, noting sliding state trajectories
c19 A69-40573

SPACEBORNE PHOTOGRAPHY
Photographic results of Lunar Orbiter program noting possible Apollo sites
c30 A69-15858
NASA photogrammetric lunar activities, discussing imagery and control data by Lunar Orbiter and photogrammetric data reduction for preparing manned lunar landing

c14 A69-34336
Design, fabrication, assembly of planetary film reconnaissance system
[NASA-CR-1358] c14 N69-28023
SPACECRAFT
Propellant slosh load criteria for design of space vehicles
[NASA-SP-8009] c32 N69-14553
Development of static inverters or converters operating electrically in parallel for space vehicle applications
[NASA-CR-1224] c03 N69-16379
Spacecraft analog to digital conversion system employing metal oxide semiconductor field effect transistors
[NASA-TN-D-5228] c08 N69-29478
SPACECRAFT ANTENNAS
Antenna reactance from sounding rocket in ionosphere, showing variations relationship to rocket spin period
c13 A69-39964
Omnidirectional microwave parallel plate waveguide fed antenna design for flush mounted broadband spacecraft, noting equatorial and polar patterns
c09 A69-40697
Measurements of mutual interference heating for probe antenna mounted on Apollo reentry configuration
[NASA-TM-X-1787] c01 N69-29318
SPACECRAFT CABIN ATMOSPHERES
Human responses to spacecraft cabin atmosphere, pressure, and contamination, and water supply, diet, and anthropometry
[NASA-CR-1205-VOL-3] c04 N69-12592
Removal of acid gases and oxides of nitrogen from spacecraft cabin atmospheres at ambient temperatures
[NASA-CR-1388] c05 N69-37517
Contaminant and atmospheric sensor for spacecraft cabin environments
[NASA-CR-1375] c14 N69-37876
SPACECRAFT CABIN SIMULATORS
Apollo mission simulation, discussing Command Module Simulator /CMS/, onboard computer system and dynamic visual presentation via infinity-optics display
[SMPTE PAPER 105-74] c11 A69-25768
Evaluation of pilot describing function method applied to manual control analysis of large flexible booster in Saturn 5 launch vehicle simulator
[NASA-TN-D-5149] c21 N69-22996
SPACECRAFT COMMUNICATION
Communications for Apollo Applications Program, considering extended duration manned missions in low earth orbit and Gemini, Saturn and Apollo hardware
c07 A69-19124
Data relay satellite systems for support of NASA R and D missions, discussing communications between satellites and to mission control
c07 A69-25296
Tracking and data acquisition networks and communications systems for support of space missions, studying data processing, unified S Band System and Data Relay Satellite System
c07 A69-25933
Artificial satellites as navigation aids, describing angle, range and range-angle systems, discussing orbital mechanics and communications difficulties
c21 A69-34855
Ground data handling equipment characteristics for PCM telemetry link utilizing convolutional coding
c07 A69-36267
Intersatellite microwave laser communication system for ATS-F and ATS-G, discussing experiment, functional design and parameters
c07 A69-41758
Telecommunications performance of two lunar relay satellite system /LRSS/, determining operation capabilities with Apollo communications system
c07 A69-42508
Solar flare and sunspot effects on VHF communications between synchronous satellite relay and ground stations
[NASA-TN-D-5100] c07 N69-23317
Parametric analysis of microwave and laser systems for communication and tracking - summary
[NASA-TR-R-309] c07 N69-23642
SPACECRAFT CONFIGURATIONS
Entry phase flight data of Missions AS-202, Apollo 4 and 6 compared with wind tunnel aerodynamics data
[AIAA PAPER 68-1143] c31 A69-13556
Structural design options for decelerative aeroshell configurations for atmospheric entry on unmanned planetary explorations
[AIAA PAPER 68-344] c32 A69-15507
Configuration, trajectory planning, instrumentation, calorimetry and aerodynamic heating for planetary atmosphere entry
c31 A69-25719
Cone-conical-frustrum configurations meeting center of gravity requirements for higher hypersonic lift-drag ratios in axisymmetric manned spacecraft
c01 A69-39237
FORTRAN program for computing principal mass moments of inertia of spacecraft treated as composite bodies
[NASA-TM-X-1754] c23 N69-20870
Engineering models of Venus atmosphere for design and mission planning for spacecrafts
[NASA-SP-8011] c30 N69-20916
SPACECRAFT CONSTRUCTION MATERIALS
Cryogenic behavior of adhesive materials used in fabrication of liquid hydrogen/liquid oxygen powered Saturn S-4B stage
c18 A69-16487
Materials compatibility for space requirements, discussing shape retention, ductility, tensile strength, dissimilar materials stability, etc
c17 A69-17872
High emittance coating materials for beryllium, niobium-zirconium compounds, and stainless steel used in spacecraft radiators
[NASA-CR-1278] c17 N69-18952
Bremsstrahlung spectra from bombardment of typical spacecraft materials by monoenergetic electrons
[NASA-CR-1377] c24 N69-33416
SPACECRAFT CONTAMINATION
Spacecraft sterilization requirements, evaluating viable organisms release probability from spacecraft as function of equipment fracturing
c04 A69-25460
Human responses to spacecraft cabin atmosphere, pressure, and contamination, and water supply, diet, and anthropometry
[NASA-CR-1205-VOL-3] c04 N69-12592
SPACECRAFT CONTROL
Deceleration control system for aerobraking and skipout to orbit at Mars
[AIAA PAPER 68-1146] c31 A69-13564
Astrodynamics, guidance and control - Conference, Belgrade, September 1967, Volume 1
c30 A69-17560
Three axis attitude servomechanism design to adjust attitude and angular velocity of spacecraft
c21 A69-17589
Microscopic time lapse movies in solid/liquid interface profile during melting and freezing of materials for spacecraft thermal control as reversible heat sink
[AIAA PAPER 69-95] c33 A69-18126
Space guidance and control system components, noting control moment gyro, actuator, brushless dc motor, electrically supported gyro and laser gyro
c14 A69-22434
Spacecraft design for minimization of structure interaction with control system, noting susceptibility of extendible booms to solar environment
c31 A69-25500
Reentry and planetary entry physics and technology 2, advanced concepts, experiments, guidance-control and technology
c31 A69-25718
Guidance and control concepts and hardware for atmospheric entry of Mercury, Gemini and Apollo spacecraft
c21 A69-25724
Navigation, guidance and control developments for manned space missions, discussing earth orbital

exploration bases
c21 A69-35801
Manual guidance and control of Saturn launch vehicles, considering feasibility, reliability and hardware implementation
[AIAA PAPER 69-876] c31 A69-39402
Orbit selection rules for planetary cartographic spacecraft derived from relations connecting camera angle, view field and imaging resolution
[AIAA PAPER 69-879] c21 A69-39405
Guidance and control in space - Conference, Warsaw, June 1969
c21 A69-39644
Real time targeting for Apollo lunar orbit insertion maneuver burn, discussing impulsive maneuvers for flight control
[AIAA PAPER 68-848] c31 A69-39760
Responsiveness of three axis, large angle attitude control systems of highly maneuverable spacecraft capable of tracking time-varying target attitudes
[NASA-TN-D-4896] c30 N69-10756
Manned spacecraft control system requirements for abort problems
[NASA-CR-835] c31 N69-27299
Reliability study of Saturn 5 launch vehicle manual backup control system
[NASA-TN-D-5261] c21 N69-28018
Magnetic torque resulting from interaction between magnetic properties of spacecraft and ambient magnetic field
[NASA-SP-8018] c31 N69-30339

SPACECRAFT DESIGN
Space station design requirements, Apollo applications program and various experimental programs
c31 A69-11395
Entry corridor thermal entry limits for Apollo spacecraft defined for design of thermal protection system
[AIAA PAPER 68-1144] c31 A69-13673
Structural design options for decelerative aeroshell configurations for atmospheric entry on unmanned planetary explorations
[AIAA PAPER 68-344] c32 A69-15507
Manned spacecraft systems design optimization for extended space missions replacement modules
c31 A69-16380
Equations formulated for space vehicle reaction to rotating machinery and internal mass motion, evaluating dynamics of cylindrical space station rotating about major axis
c30 A69-16476
Spacecraft systems, education - Conference, Belgrade, September 1967
c31 A69-17596
Interplanetary Pioneer spacecraft development and systems engineering aspects
c31 A69-17605
Deployable appendages of OGO attitude controlled spacecraft design
c31 A69-17606
Mercury atmospheric models for preliminary environmental criteria to be used in spacecraft design and engineering trade-off studies
[AIAA PAPER 69-54] c30 A69-18042
Explorer 40 satellite mathematical model and verification testing for close spacecraft flight temperature predictions
[SAE PAPER 690202] c33 A69-18305
Semiactive gravity gradient stabilization system design for low altitude earth oriented spacecraft attitude control, using active reaction wheel scanner
c31 A69-18334
Propellant condensation on surfaces near electric rocket exhaust, calculating particle arrival rates, backflow and desorption energies
[AIAA PAPER 69-270] c28 A69-21252
Space exploration plans adaptation, considering spacecraft design, programs, costs and schedules flexibility
c34 A69-22863
Spacecraft design for minimization of structure interaction with control system, noting susceptibility of extendible booms to solar environment
c31 A69-25500
Electric relays requirements for spacecraft with magnetic field constraints
c09 A69-28046
Lunar orbital mission plans intended to optimize spacecraft procurement, flight schedules, science objectives and available funds
c30 A69-34362
Collection of papers on thermal design principles of spacecraft and entry bodies
c33 A69-34372
Weight estimation and forecast in manned spacecraft design, noting size and weight relationship
[SAWE PAPER 793] c31 A69-34864
Low cost efficient shuttle system for personnel and cargo transport to earth orbit for NASA and DOD needs
c31 A69-39695
Manned space flight history and spacecraft development
[AAS PAPER 69-501] c30 A69-42852
Statistical analysis on influential aspects of wind profile disturbance design and dynamic response of space vehicles
[NASA-TN-D-4963] c32 N69-15632
Prediction curves for launch vehicle vibration levels in region of spacecraft adaptor
[NASA-CR-1227] c31 N69-16155
Natural vibration modal analysis as related to space vehicle design criteria
[NASA-SP-8012] c32 N69-22773
Design, development, integration, and testing of Small Scientific Satellites
[NASA-TN-D-4988] c32 N69-33232
Design and test criteria regarding structural flexibility effects on spacecraft stability and control systems
[NASA-SP-8016] c31 N69-37030

SPACECRAFT DOCKING
Space vehicle docking dynamics and matrix equations of motion amenable to numerical solution on digital computer, using Hamilton principle and Lagrange multipliers
c31 A69-25501

SPACECRAFT ELECTRONIC EQUIPMENT
High temperature capacitor consisting of thin wafers of pyrolytic boron nitride noting fabrication, dissipation factor and capacitance
c03 A69-15299
Spacecraft electronics - Conference, Chicago, December 1968
c09 A69-22433
High power TWT tube cooling in space vehicle, discussing thermal control system based on heat pipe radiator
c09 A69-24747
Electric relays requirements for spacecraft with magnetic field constraints
c09 A69-28046
Onboard spacecraft computer design, programming and operation based on dual bussing system
c08 A69-37384
SDP-3-A general purpose stored program computer designed for small scientific spacecraft onboard data system, noting computerized simulation
c08 A69-37385
Spacecraft onboard data handling system with MSI complementary MOS arrays, describing various components
c08 A69-41739

SPACECRAFT ENVIRONMENTS
UV irradiation effects on ZnO spacecraft thermal control coating pigments, discussing photo-Hall, luminescence and electron paramagnetic resonance measurements
[AIAA PAPER 69-639] c18 A69-33288
Optimum solar cell cover glass systems selected by studying interplanetary space environment effects of proton impact, temperature and concurrent illumination on radiation damage
c03 A69-35702
Space medicine to characterize nature and degree of changes in human functional capabilities due to space flight environment prolonged exposure
c34 A69-36460
Back flow density from jet plumes in vacuum
[NASA-TN-D-4978] c01 N69-14385

SPACECRAFT GUIDANCE
Astrodynamics, guidance and control - Conference,

Belgrade, September 1967, Volume 1
c30 A69-17560
Ground based guidance systems for supplementing onboard guidance of manned space vehicles
c21 A69-17580
Trajectory error propagation upper bounds in many body field for impulsive initial error, relating error to mission tolerances
c30 A69-21937
Space guidance and control system components, noting control moment gyro, actuator, brushless dc motor, electrically supported gyro and laser gyro
c14 A69-22434
Guidance and control concepts and hardware for atmospheric entry of Mercury, Gemini and Apollo spacecraft
c21 A69-25724
Tracking and data acquisition systems for spacecraft and ground link through command, telemetry and tracking, noting data relay satellites, etc
c07 A69-33371
Manual procedures for midcourse and terminal guidance, discussing onboard optical measurements and calculations
c21 A69-35792
Navigation, guidance and control developments for manned space missions, discussing earth orbital exploration bases
c21 A69-35801
Evaluation method for strapdown spacecraft guidance systems on automated interplanetary missions, using cost and system performance efficiency probability model
[AIAA PAPER 68-828] c21 A69-35953
GaAs laser tracking system for space guidance, describing equipment and operations
[AIAA PAPER 69-870] c21 A69-39396
Manual guidance and control of Saturn launch vehicles, considering feasibility, reliability and hardware implementation
[AIAA PAPER 69-876] c31 A69-39402
Guidance and control in space - Conference, Warsaw, June 1969
c21 A69-39644
Visual sensing and spacecraft guidance for earth orbit rendezvous maneuvers
[NASA-CR-1214] c05 N69-13161
Matched conic solutions to round trip interplanetary trajectory problems for use in guidance and navigation simulation
[NASA-TN-D-4942] c30 N69-14861
Effect of spacecraft onboard radar range and range rate data and accuracy on unmanned probe entry guidance corridor
[NASA-TN-D-4852] c21 N69-16503

SPACECRAFT INSTRUMENTS
Aerospace sensor systems, discussing adaptive multimode sensors and multispectral sensing, electronic recognition of image components, laser radar and Raman scattering technique
c14 A69-13851
Sterilization techniques for instruments and materials as applied to space research - COSPAR Conference, London, July 1967
c05 A69-15934
Spaceborne optical telescopes requirements and development including mirror material and construction, optical design, servocontrol, etc
c14 A69-27946
Apollo optics system ground and flight performance tests results, suggesting possible design changes for sunlit space environments
c14 A69-35796
Onboard processor servicing spacecraft sensors, programmable from ground, discussing functions and applications
c08 A69-39921
Operational analysis of mass measuring system in orbiting spacecraft
[NASA-TN-D-5039] c04 N69-19115

SPACECRAFT LANDING
Aerodynamic and flight characteristics of variable geometry entry spacecraft during subsonic wing deployment and landing
[AIAA PAPER 69-742] c01 A69-34407
Ground based guidance for land-landing manned spacecraft with low velocity descent systems, discussing high and low altitude glide path intercept and spiral
[AIAA PAPER 69-864] c21 A69-39390

SPACECRAFT LAUNCHING
All weather wing profile monitoring system using FPS-16 radar/jimsphere system and flight simulation for protection of space vehicle and missile launches
c20 A69-13852
Photographic control system requirements for Project Apollo manned launches, considering extreme heat, vibration and sound pressure environment
[SMPTE PAPER 104-20] c14 A69-14360
Microwave power applications to propulsion, noting spacecraft launching, aircraft takeoff thrust assistance and power transmission in space
[IMPI PAPER D2] c28 A69-15000
Longitudinal structural vibration and lateral bending response mass and spring coupling in Saturn AS-502 during boost with longitudinal excitation by POGO effect
[AIAA PAPER 69-58] c31 A69-18204
Launch opportunity and window constraints, considering injection energy and precision, reference body occultation, communications range, etc
c31 A69-37287
Low cost rate transportation as mandatory goal for future space program, discussing recovery and reuse, launch system costs, hardware development, etc
c31 A69-38117
Nimbus 2 flight evaluation and engineering report covering launch through orbit 5275
[NASA-TN-D-4881] c31 N69-17851

SPACECRAFT MANEUVERS
Ground based guidance systems for supplementing onboard guidance of manned space vehicles
c21 A69-17580
Midcourse maneuvers in interplanetary guidance, considering spin stabilized spacecraft flyby for Jupiter mission
c30 A69-28504
Real time targeting for Apollo lunar orbit insertion maneuver burn, discussing impulsive maneuvers for flight control
[AIAA PAPER 68-848] c31 A69-39760

SPACECRAFT MODELS
Model design for simulation of space capsule landing on soils using similitude law
[NASA-CR-1210] c34 N69-13159
Data from thermal vacuum tests of flight model spacecraft
[NASA-TN-D-4908] c31 N69-14010
Engineering models of Venus atmosphere for design and mission planning for spacecrafts
[NASA-SP-8011] c30 N69-20916

SPACECRAFT ORBITS
Orbit selection rules for planetary cartographic spacecraft derived from relations connecting camera angle, view field and imaging resolution
[AIAA PAPER 69-879] c21 A69-39405
Statistical error analysis of autonomous manned spacecraft navigation in long duration eccentric Mars orbits
[AIAA PAPER 69-880] c21 A69-39406
Celestial sphere scanning by passive method applicable to space missions requiring long lifetime and moderate pointing accuracies
[AIAA PAPER 68-854] c21 A69-39764
Computer program for computation of thermal radiation heat loads and temperatures of spacecraft orbiting planets or moon
[NASA-TR-R-278] c30 N69-14428

SPACECRAFT PERFORMANCE
Digital computers in space flight simulation and vehicle performance optimization, examining mission analysis
c30 A69-14519
RAE-A satellite design, simulation and flight performance, discussing gravity gradient stabilization
c31 A69-18328
Navigation state vector update effect on lunar mission completion capability for Saturn 5, emphasizing hardware and scheme errors and accelerometer failure
[AIAA PAPER 69-883] c21 A69-39409

Summary of operation, communications, and other experiments of Relay 2 satellite
[NASA-SP-151] c31 N69-21065
SPACECRAFT POSITION INDICATORS
Navigation satellites system designed for ATC without requirement for onboard transmitter, discussing spectrum occupancy, satellite power, lane ambiguities and computational procedures c21 A69-19212
SPACECRAFT POWER SUPPLIES
Photovoltaic solar cell power technology application to space use and exploration
[ASME PAPER 68-WA/SOL-1] c03 A69-16158
Manned spacecraft electrical power systems requirements, noting Gemini and Apollo fuel cell system design and configuration c03 A69-21035
Electrochemical generators for space applications - Conference, Paris, December 1967 c03 A69-32405
Manned spacecraft fuel cell selection and design, discussing Gemini ion exchange membrane and Apollo Bacon cell systems c03 A69-32406
Space power systems analysis, using computer program to correlate systems characteristics with mission parameters for automated satellite repair vehicle and space stations c03 A69-42240
Fuel cell /battery and solar array/ battery systems for manned Apollo Applications Program /AAP/ space vehicles, considering mission and power requirements c03 A69-42244
Planar radioisotope thermoelectric generator system for NASA deep space missions and integrated spacecraft power supply c03 A69-42254
Systems analysis of Rankine cycle nuclear-electric potassium space power system using Li cooled fast reactor and high temperature turbine inlet c22 A69-42266
Argon turboalternator design and testing for Brayton cycle space power system, discussing inlet operating temperature and shaft bearings and rotation c03 A69-42279
Modularized static ac and dc inverters and converters for aerospace electrical power conditioning systems, discussing circuit functions and performance tests c03 A69-42292
Power conditioner for use with SERT 2 mercury ion thruster, describing electrical and mechanical design and operation c03 A69-42301
Spacecraft solar cell near-maximum power operation by tracking optimum value with array temperature sensor c03 A69-42303
Space nuclear electric power systems applications and development, summarizing current status and near future programs
[AAS PAPER 69-305] c28 A69-42865
Design, fabrication, and testing of 12-kilowatt inductor alternator, voltage regulator-exciter, and parasitic loading speed controller - summary
[NASA-TN-D-4874] c03 N69-10088
One megawatt reactor design for Brayton cycle space power application - thermal analysis and core design
[NASA-TN-D-5013] c22 N69-17313
One megawatt reactor design for Brayton cycle space power application - neutronics design
[NASA-TN-D-5014] c22 N69-17314
Calorimetric evaluation of three 1.5-meter diameter inflatable rigidized solar concentrators for solar dynamic cycle power systems
[NASA-TN-D-5234] c03 N69-28123
Performance characteristics of 14.3 kVA modified Lundell alternator for 1200 Hz Brayton cycle space power system
[NASA-TN-D-5405] c03 N69-35537
Electrothermal instabilities effects on Brayton and Rankine cycle magnetohydrodynamic space power generation systems
[NASA-TN-D-5461] c03 N69-37883
SPACECRAFT PROPULSION
Rocket motor integration into Scout vehicle to improve performance c31 A69-12384
Microwave power applications to propulsion, noting spacecraft launching, aircraft takeoff thrust assistance and power transmission in space
[IMPI PAPER D2] c28 A69-15000
Spacecraft optimum low thrust trajectory analyzed by Hamiltcn-Jacobi perturbation theory, obtaining canonic constants of motion c30 A69-17574
SERT 2 thrustor hollow cathode durability tested in bell jar
[AIAA PAPER 69-304] c28 A69-21224
Background pressure and magnetic field shape effect on MPD thrustor performance, testing radiation cooled thrustors
[AIAA PAPER 69-243] c28 A69-21239
Performance boundaries of space propulsion systems containing nuclear electric stages
[AIAA PAPER 69-249] c22 A69-21249
NASA long range planning of primary electric propulsion for automated space program
[AIAA PAPER 69-247] c28 A69-21251
Minimal electric propulsion systems for interplanetary spacecraft, discussing payload, reduced trip time and low thrust systems for Jupiter flyby
[AIAA PAPER 69-499] c28 A69-32714
Electric propulsion systems for manned planetary exploration flights, discussing arc jet, ion and plasma engines c28 A69-35108
Launch vehicle upper stage requirements in space missions, discussing space engine for lunar, planetary and interplanetary exploration
[AAS PAPER 69-359] c34 A69-42828
Mechanics of low thrust space flight
[NASA-TT-F-507] c28 N69-33354
SPACECRAFT RADIATORS
Emissivity coatings for low temperature space radiators
[NASA-CR-1420] c17 N69-36723
SPACECRAFT RECOVERY
Cloud cover effects on selection of recovery sites for future earth orbital missions
[NASA-TN-D-5120] c30 N69-22939
Free flight performance characteristics of ram air inflated recovery balloons with peripheral airscoops
[NASA-TN-D-5186] c21 N69-29595
SPACECRAFT REENTRY
Apollo thermal protection system, noting low density ablation, flight and ground tests
[AIAA PAPER 68-1142] c31 A69-13558
NASA planetary entry parachute program for rocket launched and balloon deployment tests
[AIAA PAPER 68-934] c02 A69-35952
SPACECRAFT RELIABILITY
Electric relays requirements for spacecraft with magnetic field constraints c09 A69-28046
Orbiting Astronomical Observatory thermal test and evaluation program, discussing equipment and role in experimental design
[AIAA PAPER 69-995] c11 A69-40373
Space station safety, discussing damage containment and control, escape and rescue, etc
[AAS PAPER 69-518] c31 A69-42842
Design, development, integration, and testing of Small Scientific Satellites
[NASA-TN-D-4988] c32 N69-33232
SPACECRAFT SHIELDING
Multiwall meteoroid protection design in Apollo program, discussing bumper, backup sheet and honeycomb cells insulation
[AIAA PAPER 69-372] c32 A69-28304
Second surface mirror used as coating for spacecraft thermal control c33 A69-37290
Computer optimization of spacecraft optical coatings for temperature control, using finite element analysis and matrix inversion
[AIAA PAPER 69-979] c33 A69-40359
IR directional and hemispherical emittance of spacecraft thermal control coatings, comparing values determined by various measurement techniques

c14 A69-41633
SPACECRAFT STABILITY
Dynamic stability derivatives of large angle blunted conical spacecraft near transonic speed in simulated Mars environment for various angles of attack
[AIAA PAPER 69-104] c31 A69-18210
RAE-A satellite design, simulation and flight performance, discussing gravity gradient stabilization
c31 A69-18328
System designs for manned spacecraft gravity gradient stabilization of Saturn S-4B stage at 400 km and lunar module at synchronous altitude
c31 A69-18338
Differential synthesis technique application to design of multiaxis stability augmentation systems for aerospace vehicles
[AIAA PAPER 68-834] c31 A69-37156
Apollo-Saturn 5 propulsion and structure feedback loop, analyzing POGO components and Nyquist plot application
[AIAA PAPER 69-877] c31 A69-39403
Dynamic stability derivatives of large angle blunted conical spacecraft near transonic speed in simulated Mars environment for various angles of attack
c31 A69-40550
Design and test criteria regarding structural flexibility effects on spacecraft stability and control systems
[NASA-SP-8016] c31 N69-37030
SPACECRAFT STERILIZATION
Sterilization techniques for instruments and materials as applied to space research - COSPAR Conference, London, July 1967
c05 A69-15934
Spacecraft sterilization techniques for space exploration, discussing mathematical models for planetary quarantine and contamination by nonlanding vehicles
c05 A69-15935
Spacecraft sterilization requirements, evaluating viable organisms release probability from spacecraft as function of equipment fracturing
c04 A69-25460
Spacecraft sterilization by destructive heating with thermite or high velocity entry friction before entering planet atmosphere
c05 A69-31472
SPACECRAFT STRUCTURES
Spacecraft design for minimization of structure interaction with control system, noting susceptibility of extendible booms to solar environment
c31 A69-25500
Lightly loaded truss structures fabricated from Be, Be-Al alloy and uniaxial B filament reinforced epoxy tubing for unmanned spacecraft applications
c17 A69-35504
Penetration flux calculation for multiwall structure on Lunar Orbiter spacecraft missions
[NASA-TN-D-5455] c32 N69-41229
SPACECRAFT TELEVISION
Optimizing spacecraft televisions for successive picture overlapping and maximum surface resolution during planetary descent
[NASA-TN-D-5061] c14 N69-17259
SPACECRAFT TRACKING
Multifunction Receiver System rationale, concepts, background requirements and technical justifications for tracking, telemetry and ranging data acquisition by Goddard Center
c07 A69-19101
Tracking and data acquisition systems for spacecraft and ground link through command, telemetry and tracking, noting data relay satellites, etc
c07 A69-33371
Regression analysis procedures for evaluating tracking system measurement errors
[NASA-TN-D-4826] c19 N69-14476
Parametric analysis of microwave and laser systems for communication and tracking - summary
[NASA-TR-R-309] c07 N69-23642
SPACECRAFT TRAJECTORIES
Multistage rocket trajectories optimized by second order numerical technique and digital computer program, considering coasting, vacuum flight and transition times
c30 A69-32154
Numerical integration for continuously thrusting spacecraft optimal trajectory, considering rectangular Cartesian and polar cylindrical coordinates characteristics
[AIAA PAPER 69-903] c30 A69-38546
Closed form solution for minimum fuel constant thrust trajectories for vehicle transfer in vacuum between arbitrary boundary conditions
[AIAA PAPER 69-905] c30 A69-39337
Branched trajectory optimization for split rocket vehicles using projected gradient or steepest descent method
[AIAA PAPER 69-917] c30 A69-39346
Perturbative effects of Jupiter moons on spacecraft flyby and postencounter heliocentric trajectories, noting precision targeting
[AIAA PAPER 69-932] c30 A69-39361
Venus swingby and direct Mercury trajectories analysis for optical imaging from flyby missions
[AAS PAPER 69-258] c30 A69-42860
Two burn spacecraft trajectories for escaping earth parking orbit
[NASA-TN-D-5011] c30 N69-17305
Requirement estimates and performance predictions for Martian television experiment onboard spacecraft in three point-mass descent trajectories
[NASA-TN-D-5062] c14 N69-17944
Semianalytic theory for lunar satellite motion including perturbative effects
[NASA-TN-D-5043] c30 N69-28050
Planetary flight handbook - direct trajectories to Jupiter, Saturn, Uranus, and Neptune
[NASA-SP-35-VOL-3-PT-7] c30 N69-33490
SPARE PARTS
Manned spacecraft systems design optimization for extended space missions replacement modules
c31 A69-16380
SPARK CHAMBERS
Gamma ray detection from Crab Nebula using digitized spark chamber
[NASA-TR-R-308] c30 N69-24170
SPARK GAPS
Parameters affecting firing time of simultaneously triggered trigatron spark gap switches
[NASA-TN-D-5077] c09 N69-20888
SPATIAL DISTRIBUTION
Gegenschein measurements for determining upper limit on asteroidal debris spatial density
c30 A69-12545
SPATIAL FILTERING
Mechanical collimator using random aperture arrays for celestial observation at extreme UV and X rays
c14 A69-36489
SPECIES DIFFUSION
Z-micron sections removed from metal specimens by microtome for radiotracer study of mass dependence of self diffusion
c14 A69-36490
SPECIFIC IMPULSE
Specific impulse deliverable performance of space storable propellant combination fluorine-oxygen/methane and oxygen difluoride/diborane
[AIAA PAPER 69-505] c28 A69-32762
SPECTRA
Flight measurement of optical radiation from shock heated air with Trailblazer 2 reentry vehicle
[NASA-TN-D-4937] c33 N69-14501
Bremsstrahlung spectra from bombardment of typical spacecraft materials by monoenergetic electrons
[NASA-CR-1377] c24 N69-33416
SPECTRAL BANDS
Banded chorus, VLF discrete emissions in magnetosphere in single variable frequency band with frequency depending on equatorial electron gyrofrequency
c13 A69-31981
Energy spectrum of secondary electrons and fluorescent efficiency in 3914 A band, obtaining ionization cross section
c29 A69-32315
Limb radiance calculation model for atmospheric carbon dioxide bands with pressure and temperature gradients
[NASA-TN-D-5495] c21 N69-40055

SPECTRAL EMISSION
Autoionized resonance transitions of He at 206.2-192.2 A using He continuum produced by capillary spark, also producing He 2 line spectra
c23 A69-42149
Spectral emission characteristics of gaseous tungsten and uranium in induction heated argon plasmas
[NASA-CR-1314] c25 N69-22920
Spectral emission of visible from Q switched dye lasers
[NASA-CR-1374] c16 N69-29934
Design, calibration, and use of radiometers to measure spectral emission in ballistic range and shock tube experiments
[NASA-TN-D-5360] c14 N69-38144

SPECTRAL ENERGY DISTRIBUTION
Solar irradiance spectral distribution data normalized and combined with spectral absorptance of satellite surface coatings, obtaining absorbed energy for spectral range
c29 A69-21646
Rocket measurements of primary auroral particles energy spectra indicating spectral structure acceleration peaks associated with electrostatic fields
c13 A69-38490
Spectral and operational characteristics of high intensity carbon arc solar simulator
[NASA-TM-X-1825] c11 N69-29737
Radiant energy transfer measurements in air plasma in reflected region of arc-driven shock tube
[NASA-CR-1390] c25 N69-38227

SPECTRAL LINE WIDTH
Nonequilibrium nitrogen plasma spectral line intensities calculated assuming optically thin plasma
c24 A69-10960
Sinusoidal phase modulation role in spectral broadening observed in trapped filaments of laser and Raman light
c16 A69-14189
Self modulation, self steepening and spectral development of light in small scale trapped filaments, noting influence of relaxation time
c23 A69-20745

SPECTRAL REFLECTANCE
Spectral reflectance of planetary atmospheres, lunar topography, and planetary surface analyses
[NASA-TT-F-502] c30 N69-31989

SPECTRAL RESOLUTION
Europium complexes high resolution emission spectra in relation to molecular configuration
c06 A69-10893

SPECTROHELIOGRAPHS
Rocket-borne spectroheliograph for monochromatic solar photography in Mg II 2802.7 A line noting filter bandwidth, film polarizers and temperature control
c14 A69-24838

SPECTROMETERS
Fabrication and testing of lithium-drifted detectors as low energy photon spectrometers
[NASA-TN-D-5056] c24 N69-19828
Computer program for line-by-line calculation of spectra from diatomic molecules and atoms assuming Voigt line profile
[NASA-TN-D-5088] c24 N69-21462
Three crystal sodium iodide pair spectrometers
[NASA-TM-X-1857] c14 N69-34628

SPECTROPHOTOMETRY
Mars surface photometric and spectrophotometric measurements, relating opposition effect details with corresponding laboratory sample measurements
c30 A69-18601
Electron transport of Halobacterium cutirubrum, discussing spectrophotometric identification of cytochromes
c04 A69-19481
Detection and spectral examination of trace porphyrin complexes by demetallation with methanesulfonic acid and spectrofluorometry, compared to absorption spectrophotometry
c06 A69-42557
Comparison of extraction procedures using 1-nitroso 2-naphthol and dimethylglyoxime for spectrophotometric determination of palladium in titanium alloys
[NASA-TM-X-1767] c06 N69-20801

SPECTROSCOPIC ANALYSIS
Spectrochemical analysis of cobalt-base superalloys by liquid-layer solid-sample spark technique
[NASA-TM-X-1753] c06 N69-20853

SPECTROSCOPY
Auger and photoelectron spectroscopy for chemical analysis, noting effects of sample thickness, sample potential, surface contamination and X ray incident angle
c06 A69-19775
Remote sensing cross-beam cross correlation methods of determining spatially resolved average thermodynamic properties
[AIAA PAPER 67-149] c14 A69-31868
Spectroscopic study of helium arc
[NASA-TN-D-5396] c25 N69-36755

SPECTRUM ANALYSIS
Spectra of close binary systems, analyzing abundance anomalies, noting metallicity results
c30 A69-15854
Ion temperature diurnal variations at 250-475 km obtained from Thomson scatter spectra
c13 A69-16407
Rotating and oscillating magnetic neutron stars causing pulsars radio and optical signals, stressing UV line emissions theory
c30 A69-20624
Doublet structure suppression in mixtures of cesium and foreign gases, discussing absorption observations
c24 A69-20736
Oscillator strengths and wavelengths of X ray and EUV transitions in highly ionized iron line spectra
c29 A69-27554
Luminescence spectra of aromatic polymers, monomers and dimers under high energy electron excitation using molecular resonance model
c26 A69-32792
Cloud scattering corrections added to synthetic spectrum analysis of carbon dioxide bands and water vapor line in Venus spectrum
c30 A69-33161
Solar Na D lines analysis by direct inversion of line source function, finding Doppler core dependence on frequency
c30 A69-38479
Autoionized resonance transitions of He at 206.2-192.2 A using He continuum produced by capillary spark, also producing He II line spectra
c23 A69-42149
Spectral and electrophotometric studies of upper atmosphere - airglows, atomic oxygen, hydroxyl emission, helium line spectra, auroras, and solar cycle effects on magnetosphere
[NASA-TT-F-530] c13 N69-16539
Spectral classes and photographic magnitudes determined for region Lacerta OB1
[NASA-TN-D-5060] c30 N69-26235

SPECULAR REFLECTION
ATS 3 satellite reflectometer experiment carrying test samples to measure specular reflectance, noting silica shield effects
[AIAA PAPER 69-644] c33 A69-33270

SPEED INDICATORS
Supersonic Preston tube correlations for Mach number and Reynolds number effects on hypersonic turbulent skin friction on adiabatic surfaces, simplifying correlation
[AIAA PAPER 69-345] c12 A69-28280
Baronti-Libby transformation and Preston tube calibrations used to determine skin friction from turbulent velocity profiles
[NASA-TN-D-4853] c12 N69-10472

SPHERES
Drag coefficients for spheres and sharp cones in rarefied hypersonic air flow obtained in shock tunnel using free flight technique
[AIAA PAPER 69-140] c01 A69-18184
Force penetration characteristics of sand horizontally penetrated by various geometrically shaped models
[NASA-CR-1252] c18 N69-14764
Wind tunnel magnetic support and balance system for measuring sphere drag
[NASA-CR-1353] c11 N69-25343

Heat transfer coefficients for film boiling from submerged spheres
[NASA-TN-D-5124] c33 N69-28318
Wind tunnel drag measurements on subsonic sphere
[NASA-CR-1392] c01 N69-30609
Tabulated values of configuration factors between two spheres and parts of two spheres
[NASA-SP-3050] c30 N69-37777

SPHERICAL CAPS
Spherical caps axisymmetric static and dynamic buckling under load, using axisymmetric nonlinear elastic shell theory approximation and finite difference equations
[AIAA PAPER 69-89] c32 A69-18133
Surface pressure distribution on spherical blunted cones, and correlation of Mach numbers, cone angle, and angle of attack
[NASA-TN-D-5204] c01 N69-24764

SPHERICAL SHELLS
Design and construction of plastic model of prestressed segmented spherical shell
[NASA-CR-1231] c32 N69-11010
Buckling equations solved for equatorial segment of spherical shell loaded in axial direction by own weight
[NASA-TN-D-4921] c32 N69-13034
Monte Carlo analysis of gold sphere transmission experiments at 24 keV neutron energy using S wave spin state data
[NASA-TN-D-5211] c24 N69-24826

SPHERICAL TANKS
Volume effects on normal gravity pressurization of spherical liquid hydrogen tanks
[NASA-TN-D-5196] c33 N69-24168
Venting of spherical liquid hydrogen tankage
[NASA-TN-D-5263] c33 N69-27620
Physical parameter effect on pressurant gas requirements during expulsion of liquid hydrogen from spherical tanks
[NASA-TN-D-5336] c28 N69-32318
Hydrogen gas pressure requirements during pressurization and transfer of liquid hydrogen from spherical tanks
[NASA-TN-D-5387] c28 N69-33211

SPHERICAL WAVES
Proportionality between log-amplitude variance and 7/6 power of wavenumber for horizontal propagation from spherical wave transmitter to point detector
c16 A69-19641

SPHERULES
Oxide composition of silicate spherules from forest area devastated by Tunguska meteorite explosion using electron microprobe analysis
c30 A69-28869

SPIKES
High latitude ionization spikes observed by POGO spacecraft, noting frequency correlation with magnetic disturbances and development by high energy electron injections
c29 A69-28950

SPIN DYNAMICS
Celestial sphere scanning by passive method applicable to space missions requiring long lifetime and moderate pointing accuracies
[AIAA PAPER 68-854] c21 A69-39764
Elastohydrodynamic analysis and experimental speed effects on ball spinning friction coefficients and torque
[NASA-TN-D-5527] c15 N69-41210

SPIN REDUCTION
Resonant spin and anomalous rotation of Mercury, analyzing influence of tidal degradation and permanent deformation of planet
c30 A69-39568

SPIN STABILIZATION
Spin-tunnel investigation of scale model of straight wing, twin boom counter insurgency airplane
[NASA-TM-X-1602] c02 N69-34988
Spin and recovery characteristics of 1/30 scale subsonic attack aircraft model determined in wind tunnel tests
[NASA-TM-X-1788] c02 N69-37976

SPIRALS
Energy conversion and distribution of spiraling electron beam using retarding field analyzer
[NASA-TN-D-5490] c09 N69-41208

SPLINE FUNCTIONS
FORTRAN computer program for spline fit curve with function valves
[NASA-TM-X-1707] c19 N69-14002

SPOILERS
Effects of aerodynamic forces on jet engine noise from rigid flow spoilers
[NASA-CR-1340] c23 N69-26307

SPORADIC METEOROIDS
Weighting factor for correction of photographic bias caused by variation in mass and velocity of sporadic meteoroids
[NASA-TN-D-5245] c30 N69-26239

SPRINGS (ELASTIC)
Longitudinal mass spring modeling of launch vehicles
[NASA-TN-D-5371] c32 N69-34970

SPUTTERING
Physical sputtering deposition of molybdenum disulfide films as solid lubricant on rotating and sliding components, discussing lubrication properties in vacuum
[ASLE PAPER 68-LC-15] c15 A69-19308
Friction and contact resistance during sliding in vacuum of low resistivity metals lubricated with sputtered molybdenum disulfide
[NASA-TN-D-5349] c15 N69-31884

STABILITY
Stability of time varying systems by construction of multipliers with prescribed phase characteristics
c10 A69-16598
Digital simulation computer stability analysis scheme premised on use of perturbed transient responses
c10 A69-32899
Determination of stability indicative function for linear systems with multiple time delays
[NASA-TR-R-301] c31 N69-17801
Computation of regions of constrained stability for nonlinear control systems
[NASA-CR-1328] c19 N69-28196
Combustion stability of single swirl can combustor modules using ASTM-A1 liquid fuel
[NASA-TN-D-5436] c28 N69-40080

STABILITY DERIVATIVES
Newton-Raphson technique development for determining stability derivatives from flight data, noting use of a priori wind tunnel information
[AIAA PAPER 69-315] c02 A69-22379

STABILITY TESTS
Thermal cycling tests showing improvement in cadmium sulfide solar cell stability, noting effect of thermal cycling stresses
c03 A69-13074
Design and test criteria regarding structural flexibility effects on spacecraft stability and control systems
[NASA-SP-8016] c31 N69-37030

STABILIZATION
Lifting body stability augmentation systems design, development, ground tests and flight data including frequency response, limit cycle and structural resonance
[AIAA PAPER 69-887] c02 A69-39413

STABILIZERS (FLUID DYNAMICS)
Infrared heating simulation of Mach 4.63 flight on X-15 horizontal stabilizer
[NASA-TN-D-5403] c33 N69-35949

STACKS
Performance of prototype hydrogen oxygen electrolytic regenerative fuel cell stack with gas storage tank
[NASA-CR-1244] c03 N69-18885

STADAN (SATELLITE TRACKING NETWORK)
International 28-station global instrumentation ground support network for space tracking and data acquisition
[UN PAPER 68-95912] c34 A69-17059
Tracking and data acquisition networks and communications systems for support of space missions, studying data processing, unified S Band System and Data Relay Satellite System
c07 A69-25933
PCM data handling system for NASA Space Tracking and Data Acquisition Network with explanation for output capabilities, noting BIOSAT project
c07 A69-36242

Data systems coordinating standards developed from experience with STADAN, discussing operating environment and administrative decisions influence on implementation
c08 A69-41769

STAGE SEPARATION
Launch vehicle upper stage requirements in space missions, discussing space engine for lunar, planetary and interplanetary exploration
[AAS PAPER 69-359] c34 A69-42828
Rocket-scramjet hybrid engines in lifting reusable second stage
[NASA-TN-D-5218] c28 N69-24922
Aerodynamic characteristics in pitch of scale model of two and three stage rocket configuration at Mach numbers of 0.4 to 4.63
[NASA-TN-D-5378] c01 N69-34986

STAGNATION FLOW
Quasi-linear ordinary differential equations solutions for steady two dimensional stagnation point flows of nonNewtonian power law fluids
c12 A69-39674
Solution to radiation-coupled stagnating flow with nongray emission over hypervelocity blunt body
[NASA-TR-R-299] c33 N69-16268

STAGNATION POINT
Correlations of stagnation point radiative heat transfer for earth reentry, noting use of nongray absorption coefficient models
c33 A69-14736
Perturbation solution to blunt body stagnation region flow of radiating gas with radiation heat transfer
[NASA-TR-R-295] c12 N69-10788
Stagnation point boundary layer with suction and injection in equilibrium dissociating air
[NASA-TN-D-3889] c12 N69-14314
Stagnation pressure and heat transfer measurements of blunt axisymmetric bodies
[NASA-TN-D-5121] c01 N69-22554
Photographic study of bromine jet flowing in coaxial airstream and impinging on stagnation surface
[NASA-TN-D-5209] c12 N69-24800

STAINLESS STEELS
High emittance coating materials for beryllium, niobium-zirconium compounds, and stainless steel used in spacecraft radiators
[NASA-CR-1278] c17 N69-18952
Experimental and analytical studies of multiple liquid impact erosion of aluminum and stainless steel
[NASA-CR-1288] c15 N69-19786
Fabrication of counterflow double wall tantalum-stainless steel mercury boiler
[NASA-TN-D-5092] c33 N69-23707
Outdoor high temperature corrosion tests for aluminum alloys and titanium alloys, and stainless steels
[NASA-TN-D-5362] c17 N69-32558

STANDARD DEVIATION
X Ray fluorescence of rock samples as applied to geological problems, noting standard deviations for element distribution
c14 A69-10890
Approximation for mean and standard deviation of magnitude of statistical velocity correction vector
[NASA-TN-D-5381] c30 N69-36143

STANDARDS
Data systems coordinating standards developed from experience with STADAN, discussing operating environment and administrative decisions influence on implementation
c08 A69-41769
Thermodynamic properties of erbium hydrogen binary system evaluated for use as low pressure standard
[NASA-CR-1271] c14 N69-16099

STANDING WAVES
Multiple scattering in Kapitza-Dirac effect describing electron scattering by standing electromagnetic wave, noting transition probability less than unity
c23 A69-25323

STAR CLUSTERS
Computer study of collisionless self gravitating system using two dimensional model, obtaining gravitational field by solving Poisson equation
c30 A69-12272
Lacerta OB1 stellar spectral classes and photographic magnitudes, analyzing clusters and distributions in concentrated and dispersed areas
c30 A69-25813
Residual interstellar gas from protostar formation detected as high luminosity IR object
c29 A69-27593

STAR DISTRIBUTION
Lacerta OB1 stellar spectral classes and photographic magnitudes, analyzing clusters and distributions in concentrated and dispersed areas
c30 A69-25813

STAR TRACKERS
Working breadboard model of planet tracker under various illuminating conditions, discussing hardware and closed loop tracking error analysis accounting for signal to noise effects
c21 A69-13214
Design and development of boresighted star tracker
[NASA-CR-976] c21 N69-21502
Electronically scanned star sensor with digital output for orbiting astronomical telescope
[NASA-TN-D-5281] c14 N69-29153
Derivation of transfer function for optical system relating image intensity to spatial autocorrelation
[NASA-CR-1443] c21 N69-38041

STARCHES
Dynamic differential thermal analysis with He flow performed on biological specimens, proteins and starches, showing discrete decomposition peaks monitoring pyrolysis process
c06 A69-31807

STARK EFFECT
Europium complexes high resolution emission spectra in relation to molecular configuration
c06 A69-10893

STARS
Individual properties of RR Lyrae stars
[NASA-TT-F-562] c30 N69-27169
Sextant sighting performance concerned with training and monochromatic stars
[NASA-TN-D-5190] c05 N69-35024

STARTING
Analytical method for predicting performance of centrifugal pumps during pressurized startup
[NASA-TN-D-4967] c15 N69-14082

STATIC AERODYNAMIC CHARACTERISTICS
Wind tunnel tests to determine static aerodynamic characteristics of cruciform wing-body missiles at transonic and supersonic speeds
[NASA-TM-X-1839] c01 N69-31875
Wind tunnel stability tests to determine effect of hypersonic research engine on aerodynamic characteristics of research aircraft
[NASA-TM-X-1840] c01 N69-38612

STATIC INVERTERS
Modularized static ac and dc inverters and converters for aerospace electrical power conditioning systems, discussing circuit functions and performance tests
c03 A69-42292
Development of static inverters or converters operating electrically in parallel for space vehicle applications
[NASA-CR-1224] c03 N69-16379
Evaluation of magnetic materials for static inverters and converters, tested under square wave excitation and direct current excitation
[NASA-CR-1226] c03 N69-17765
Electric control and protection circuits for parallel operation of inverter-converter
[NASA-CR-1225] c10 N69-19003

STATIC LOADS
Predicting buckling of thin walled, uniform stiffened and unstiffened circular cylindrical shells under static loading
[NASA-SP-8007] c32 N69-23320
Buckling of thin walled truncated conical shells under static loads
[NASA-SP-8019] c32 N69-24131

STATIC PRESSURE
Flow direction measurement with fixed-position probes
[NASA-TM-X-1904] c14 N69-40059

STATIC STABILITY
Spherical caps axisymmetric static and dynamic buckling under load, using axisymmetric nonlinear elastic shell theory approximation and finite difference equations
[AIAA PAPER 69-89] c32 A69-18133
Small eccentricity stability analysis for externally pressurized gas lubricated bearings with journal rotation
[NASA-TN-D-4934] c15 N69-13256
Wind tunnel investigation of static stability characteristics of model jet-lift V/STOL research airplane
[NASA-TM-X-1835] c02 N69-30633
STATIONKEEPING
Multijet electrothermal systems for attitude control and stationkeeping of synchronous communications satellite
[AIAA PAPER 67-723] c28 A69-12375
Ammonia resistojet stationkeeping subsystem onboard ATS 4 satellite, noting flight test data agreement with ground tests
[AIAA PAPER 69-296] c28 A69-21212
STATISTICAL ANALYSIS
Spectral null from spectral characteristics and statistical properties of PCM signals used to estimate SNR
c07 A69-19122
Statistical theories of turbulence applied to thermal convection between infinite slippery plates at large Prandtl number
c33 A69-24283
Statistical error analysis of autonomous manned spacecraft navigation in long duration eccentric Mars orbits
[AIAA PAPER 69-880] c21 A69-39406
Statistical analysis on influential aspects of wind profile disturbance design and dynamic response of space vehicles
[NASA-TN-D-4963] c32 N69-15632
Statistical analysis of satellite position with tracking error inclusion
[NASA-TN-D-5259] c30 N69-30611
Approximation for mean and standard deviation of magnitude of statistical velocity correction vector
[NASA-TN-D-5381] c30 N69-36143
Creep rate equations for refractory metal alloys of tantalum molybdenum, and columbium
[NASA-TN-D-5424] c17 N69-36653
Statistical analysis of pressure fluctuations in separated turbulent boundary layer
[NASA-TN-D-5440] c12 N69-36940
Determination of meteoroid environments from photographic meteor data
[NASA-TR-R-322] c30 N69-39336
STATISTICAL CORRELATION
Lunar topography statistics determined by Zond 3 space probe
[NASA-TT-F-514] c30 N69-24206
Statistical method for evaluating goodness of fit between data set and theoretical distribution of random variables
[NASA-TR-R-313] c19 N69-30610
Statistical correlation between optical microwave propagation reliability, fade margin, path length, and geographic location
[NASA-CR-1442] c07 N69-39282
STATISTICAL MECHANICS
Transport properties of steam, analyzing selection, correlation and prediction using statistical mechanical theories
c33 A69-10110
STATOR BLADES
Turbine stator blade performance determination from total pressure surveys downstream of blade row, noting problems in pressure measurement
[ASME PAPER 69-GT-103] c01 A69-22521
Variable stator area effect on performance of single stage turbine suitable for air cooling
[NASA-TM-X-1697] c01 N69-10558
Application of boundary layer control concepts to highly loaded turbine stator blades in annular cascades
[NASA-CR-1219] c01 N69-14211
Theoretical study of discrete frequency noise generated by turbocompressors and blades
[NASA-CR-1287] c28 N69-21476
Aerodynamic characteristics of annular cascade of blades
[NASA-CR-1323] c01 N69-25327
Stator performance with cooling by air ejection from trailing edges of blades
[NASA-TM-X-1901] c03 N69-39335
STATORS
Stator setting effect on single stage turbine performance, considering blade loss and surface velocity distribution
[AIAA PAPER 69-525] c28 A69-32686
Effect of variable stator with area design of 70 percent on performance of single stage turbine suitable for air cooling
[NASA-TM-X-1696] c28 N69-10296
Development and high temperature tests of high strength nickel alloy for stator vanes of gas turbine engines
[NASA-TN-D-5352] c17 N69-31873
STEADY FLOW
Three dimensional hypersonic steady flow around blunt and pointed cones at nonzero angles of attack calculated by method of characteristics
[AIAA PAPER 69-187] c01 A69-18176
STEAM FLOW
Transport properties of steam, analyzing selection, correlation and prediction using statistical mechanical theories
c33 A69-10110
Steam cycle analysis for nuclear powered turbofan engine
[NASA-TM-X-1907] c22 N69-40060
STEELS
Pressure and temperature dependence of slow crack growth in hardened steel in gaseous hydrogen environment
c17 A69-10612
Plastic deformation of corrosion resistant steel, CER-VIT 101, and fused silica as function of applied torsional stress
[NASA-CR-1257] c14 N69-16100
Effect of ultrasonic vibration on precipitation hardening of steels and superalloys
[NASA-TN-D-5131] c32 N69-21814
STEEPEST DESCENT METHOD
Branched trajectory optimization for split rocket vehicles using projected gradient or steepest descent method
[AIAA PAPER 69-917] c30 A69-39346
FORTRAN program for radiation shield optimization using steepest descent method
[NASA-TM-X-1769] c22 N69-20854
STEERING
Steerable landing gear system consisting of freely castoring corotating wheel nose gear, tiltable axle and main gear skids for lifting body spacecraft
[AIAA PAPER 69-790] c02 A69-35639
STELLAR ATMOSPHERES
Scaled solar and gray-body temperature distribution models compared to determine stellar atmosphere
c30 A69-14626
Acoustic energy generation for helium rich stars, discussing X ray radiation from helium star corona
c29 A69-20645
Aurigae star HD 35620 with respect to epsilon Virginis using model atmosphere and high dispersion spectra
c30 A69-20913
Density inversion in convective zone of stellar photospheres occurring in Eridani atmospheric model under certain conditions
c30 A69-21843
Atmospheric models for metal deficient stars of K and G spectral type, studying reduced metal abundance effect on atmospheric structure
c30 A69-22055
Subdwarf HD 25329 studied with model atmosphere approach, using H alpha, Na I and Mg I profiles for effective temperature
c30 A69-22199
Circumstellar grain compositions of stars with various O to C abundance ratios, calculating molecular equilibrium of condensates and gaseous compounds in stellar atmospheres
c30 A69-24103

Star twinkling absence for lunar observation laboratory, noting star distance measurement and laser action in stellar atmospheres
c30 A69-27172
Radial pulsation mode of convective envelopes in adiabatic equilibrium for variable M red supergiant stars
c30 A69-30766
Monte Carlo relaxation method for physically self consistent model stellar atmospheres, discussing stability, accuracy and convergence of solution
c30 A69-36337
Atmospheric models for specified effective temperatures, hydrogen-to-metal ratios and surface gravities in studying metal deficiency effect on stellar atmosphere
c30 A69-36338
Stellar atmospheres acoustic energy generation rate calculations, studying corona mass ejection effects on stellar rotation
c30 A69-39521
Helium-carbon star BD plus 10 degrees 2179 reanalyzed by grid of constant flux models containing right amount of C
c30 A69-40652
Theoretical molecular line absorption of carbon monoxide in late spectral type stellar atmospheres
[NASA-TN-D-4798] c24 N69-14448

STELLAR EVOLUTION
Computer study of collisionless self gravitating system using two dimensional model, obtaining gravitational field by solving Poisson equation
c30 A69-12272
Primordial helium and horizontal branch star luminosity, obtaining luminosities in He burning phase for different He and metal abundances from models
c30 A69-22211
Red supergiants as old derivatives of main sequence O and B stars, discussing neutrino emissions and carbon core contraction
c30 A69-24125
Residual interstellar gas from protostar formation detected as high luminosity IR object
c29 A69-27593
X ray sources model, describing possible ring of matter around white dwarf near end of active evolution
c29 A69-35204
Primitive solar nebula physical model considered under angular momentum conservation in collapsing fragment
c30 A69-36074
Nebulosity around FG Sagittae for origin and evolution of planetary nebulae, suggesting ejection of nebular shell
c30 A69-42887

STELLAR LUMINOSITY
Relation between amplitude of light and radial velocity variations of beta Canis Majoris stars
c30 A69-14126
Primordial helium and horizontal branch star luminosity, obtaining luminosities in He burning phase for different He and metal abundances from models
c30 A69-22211
Red supergiants as old derivatives of main sequence O and B stars, discussing neutrino emissions and carbon core contraction
c30 A69-24125
Lacerta OB1 stellar spectral classes and photographic magnitudes, analyzing clusters and distributions in concentrated and dispersed areas
c30 A69-25813
Computer program for launch window determination from star illumination of night sky background
[NASA-TM-X-1772] c21 N69-22969
Two-micron sky survey catalog of celestial objects
[NASA-SP-3047-REV] c30 N69-37993

STELLAR MASS
Structure and pulsational properties of massive stars with helium cores and thin hydrogen poor envelopes
c30 A69-22421
Radial pulsation mode of convective envelopes in adiabatic equilibrium for variable M red supergiant stars
c30 A69-30766

STELLAR MASS EJECTION
Stellar rotation braking due to mass loss from coronae through stellar wind based on calculation of acoustic energy generation from convective zone
c30 A69-20644
Radial pulsations of neutron star losing mass, interpreting Crab Nebula pulsar observed period and secular increase of period
c30 A69-37573
Stellar atmospheres acoustic energy generation rate calculations, studying corona mass ejection effects on stellar rotation
c30 A69-39521

STELLAR MOTIONS
Relation between amplitude of light and radial velocity variations of beta Canis Majoris stars
c30 A69-14126

STELLAR RADIATION
Radio emission from magnetic neutron stars as possible model for pulsars, noting optical and IR emission bands
c30 A69-20729
Nuclear energized pulsational instability of stars based on linear quasi-adiabatic theory, including models with hydrogen burning shells
c30 A69-27576
Interstellar extinction in UV from zeta and epsilon Persei spectra obtained with scanner attached to telescope mounted in pointed Aerobee rocket
c30 A69-40772
IR excess of R CrB type variable star RY Sgr, noting visual brightness and radiation in 2.0-3.4 micron range
c30 A69-42377

STELLAR ROTATION
Stellar rotation braking due to mass loss from coronae through stellar wind based on calculation of acoustic energy generation from convective zone
c30 A69-20644
Rotational energy conversion of neutron star into relativistic electrons energy suggested by increasing period of pulsating radio source in Crab Nebula
c30 A69-21454
Spin down effects on neutron stars, discussing decrease of period of PSR 0833-45 as result of differential rotation instability
c30 A69-32803
Stellar atmospheres acoustic energy generation rate calculations, studying corona mass ejection effects on stellar rotation
c30 A69-39521
Carroll Fourier transform method applied to stellar spectra lines to determine small rotational velocities
c30 A69-42404

STELLAR SPECTRA
Spectra of close binary systems, analyzing abundance anomalies, noting metallicity results
c30 A69-15854
Aurigae star HD 35620 with respect to epsilon Virginis using model atmosphere and high dispersion spectra
c30 A69-20913
Atmospheric models for metal deficient stars of K and G spectral type, studying reduced metal abundance effect on atmospheric structure
c30 A69-22055
Subdwarf HD 25329 studied with model atmosphere approach, using H alpha, Na I and Mg I profiles for effective temperature
c30 A69-22199
Spinning rockets UV spectrophotometry of early type stars, discussing instrumentation, calibration, data recording and stellar spectra
c30 A69-25812
Lacerta OB1 stellar spectral classes and photographic magnitudes, analyzing clusters and distributions in concentrated and dispersed areas
c30 A69-25813
Rocket spectrographic observations of Alpha Virginis noting hydrogen Lyman absorption lines
c30 A69-27555

Curve of growth analysis for close binary HR 5317 indicating Mg, Mn, Ca and Sr overabundance respecting standard star 110 Her
c30 A69-34297
Variable stars blue sequence, proposing mu mechanism and beta mechanism as explanation for radial pulsations
c30 A69-40650
Helium-carbon star BD plus 10 degrees 2179 reanalyzed by grid of constant flux models containing right amount of C
c30 A69-40652
Carroll Fourier transform method applied to stellar spectra lines to determine small rotational velocities
c30 A69-42404

STELLAR SPECTROPHOTOMETRY
Spinning rockets UV spectrophotometry of early type stars, discussing instrumentation, calibration, data recording and stellar spectra
c30 A69-25812
Lacerta OB1 stellar spectral classes and photographic magnitudes, analyzing clusters and distributions in concentrated and dispersed areas
c30 A69-25813
HD 30353 He binary star invisible component suggested as KO type supergiant from IR photometric data
c30 A69-35348
Spectral classes and photographic magnitudes determined for region Lacerta OB1
[NASA-TN-D-5060] c30 N69-26235

STELLAR STRUCTURE
Instability of stellar structures intermediate between white dwarfs and neutron stars shown by stellar models, discussing pulsar signals periodicities
c30 A69-20770
Structure and pulsational properties of massive stars with helium cores and thin hydrogen poor envelopes
c30 A69-22421

STELLAR WINDS
Stellar rotation braking due to mass loss from coronae through stellar wind based on calculation of acoustic energy generation from convective zone
c30 A69-20644

STEP FUNCTIONS
Dynamic analysis and maximum stepping rate prediction for permanent magnet motor
[NASA-TN-D-5094] c03 N69-20780
Low order Runge-Kutta formulas with step control for heat transfer problems
[NASA-TR-R-315] c19 N69-30753

STEREOPHOTOGRAPHY
Heights of cloud bases and convective cloud tops determined by stereoscopic photogrammetry of Apollo 6 mission
c20 A69-36926

STIFFNESS
Direct stiffness method of computing vibrational characteristics of dynamic model of Apollo-Saturn 5 vehicle - umbilical tower configuration
[NASA-TN-D-4871] c31 N69-10934
Stiffness matrices analysis of thin flat plates
[NASA-TN-D-4927] c32 N69-14169
Instability of eccentrically stiffened cylindrical shells under axial compression and lateral pressure
[NASA-CR-1280] c32 N69-15378
Theoretical analysis of free vibration of discretely stiffened cylindrical shells with arbitrary end conditions
[NASA-CR-1316] c32 N69-28164
Beam stiffness determined for thin walled truncated cones under bending loads
[NASA-TN-D-5536] c32 N69-41141

STOCHASTIC PROCESSES
Stochastic problems in control - Conference, Ann Arbor, June 1968
c10 A69-14693
Optimal stochastic control of small dynamic systems described by random differential equations, noting selective bibliography on several subjects
c10 A69-14697
Matrix Riccati and matrix quadratic equations in problems of stochastic control and filtering
c10 A69-16601
Optimal stochastic control, discussing dynamic mathematical models described by differential equations
c10 A69-22567
Stochastic saturating systems optimal control computation, considering attitude control and tracking system design by elliptical differential equation of dynamic programming
c10 A69-30601
Analytic time function models of stochastic processes of noise and modulation
[NASA-TR-R-314] c07 N69-29230
Sequential stochastic techniques for trajectory estimation
[NASA-CR-1360] c30 N69-40325

STOICHIOMETRY
Physical properties of near stoichiometric nickel-titanium alloy Nitinol and some structural-mechanical applications employing these properties
[NASA-CR-1232] c17 N69-11420

STOKES LAW (FLUID MECHANICS)
Nature of outside boundary layer on liquid sphere in steady, uniform stream
[NASA-CR-1362] c12 N69-24877

STONY METEORITES
Stony meteoric particles size and velocity during passage through atmosphere
c30 A69-26341

STORABLE PROPELLANTS
Specific impulse deliverable performance of space storable propellant combination fluorine-oxygen/methane and oxygen difluoride/diborane
[AIAA PAPER 69-505] c28 A69-32762
Hydrogen and methane combustion to simulate expansion of storable propellants
[AIAA PAPER 68-635] c33 A69-37188
Nozzle insert evaluation and gas cooling concept in storable liquid propellant rocket engine
[NASA-TM-X-1756] c28 N69-19782
Throat and nozzle insert design for ablative rocket engine using storable propellants
[NASA-TN-D-4964] c32 N69-33481
Gaseous reactant combustion simulation of dimethylhydrazine and hydrazine fuel system for nonequilibrium expansion studies
[NASA-TN-D-5404] c33 N69-35506

STORAGE TANKS
High pressure storage vessels for gaseous hydrogen, discussing failure, manufacturing controls and access for internal nondestructive inspection
[ASM PAPER D8-14.1] c15 A69-19666
Structural failures of high pressure, gaseous hydrogen storage tanks for M-1 engines
[NASA-CR-1305] c17 N69-19831
Lightweight polyurethane insulation for liquid hydrogen tanks of space vehicles
[NASA-TN-D-5114] c18 N69-20790

STRAIN GAGES
Hysteresis of strain gage absolute pressure transducer
[NASA-TN-D-5327] c14 N69-30506
Design and operation of high temperature loads calibration laboratory
[NASA-TM-X-1868] c11 N69-36224

STRAIN HARDENING
Dynamic strain aging in carbide strengthened molybdenum alloys
[NASA-TN-D-5355] c17 N69-31883
Internal stress and deposit hardness of nickel electrodeposited containing controlled quantities of meta-benzenedisulfonic acid
[NASA-TN-D-5188] c17 N69-36697

STRAIN RATE
Strain-rate sensitivity of three titanium-alloy sheet materials after prolonged exposure to high temperature
[NASA-TN-D-4981] c17 N69-14873

STRAPDOWN INERTIAL GUIDANCE
Computer-generated computational errors in direction cosine matrix for strapdown inertial system
[NASA-TR-R-304] c21 N69-21402
Vibration induced attitude errors in strapdown inertial navigators

[NASA-CR-1396] c21 N69-34672
Algorithm for computing direction cosine matrix of strapdown inertial system
[NASA-TN-D-5384] c21 N69-36997
STRATOSPHERE
Water vapor profiles in stratosphere from IR radiometric observations under cloudless conditions, indicating relation to tropospheric meteorological features
c13 A69-38261
Synoptic analysis of Southern Hemisphere stratosphere
[NASA-TM-X-1814] c13 N69-33555
Stratospheric and mesospheric temperature and moisture profiles determined from infrared horizon observations
[NASA-CR-1419] c20 N69-35528
STREAMLINING
FORTRAN program for calculating velocities and streamlines on blade to blade stream surfaces of turbomachinery
[NASA-TN-D-5044] c01 N69-21811
STREAMS
Injection of attached inviscid jet at oblique angle to moving stream
[NASA-TN-D-5501] c12 N69-39916
STRESS (PHYSIOLOGY)
Artificial heat acclimatization effect on orthostatic tolerance in man exposed to stresses of heat, exercise and dehydration
c05 A69-32810
STRESS ANALYSIS
Creep rate-stress-temperature relations for powder metallurgy rhenium, discussing activation energy
c17 A69-34186
Photoviscoelastic method for stress analysis of two dimensional viscoelastic models
[NASA-CR-1289] c32 N69-17770
Integral equation method with continuous functions for calculating boundary stress components in plane elasticity
[NASA-CR-1273] c32 N69-19030
Structural response of tubular beryllium and beryllium aluminum alloy truss-type structures to dynamic and static loads
[NASA-TN-D-5254] c32 N69-28658
STRESS CONCENTRATION
Geometrically exact finite element for thin shells of revolution, using approximation to predict boundary layer stress distribution during vibration
[AIAA PAPER 69-56] c32 A69-18193
Displacements and stress intensity as function of crack length for compact tension specimen, considering load line and crack edge
c15 A69-21392
Inclination effect of fatigue cracks on plane strain fracture toughness of 7075-T651 Al alloy, discussing cantilever bending
c32 A69-25958
Analysis of cylindrical reactor fuel pin for clad stress caused by fission gases
[NASA-TN-D-5178] c22 N69-24802
Stress concentration around broken filaments in filament stiffened sheet
[NASA-TN-D-5453] c32 N69-38642
STRESS CORROSION
Hot salt stress corrosion of Ti alloy, discussing hydrogen generation during elevated temperature exposure and embrittlement as manifestation of strain rate
c17 A69-39434
Hot salt stress corrosion of titanium alloys - generation of hydrogen and its embrittling effect
[NASA-TN-D-5000] c17 N69-16465
Analysis of sodium chloride deposits on compressor blades of flight gas turbine engines
[NASA-TN-D-4999] c28 N69-17276
Salt stress corrosion cracking effects on tensile and stress rupture properties of titanium alloy sheet
[NASA-TN-D-5417] c17 N69-36221
Hot-salt stress-corrosion of titanium alloy under simulated turbine engine compressor environment
[NASA-TN-D-5510] c17 N69-40242
STRESS CYCLES
Factors influencing low cycle crack growth of aluminum sheet specimens
[NASA-TN-D-5140] c32 N69-21392
Cyclic life calculations of materials subjected to isothermal stress considering fatigue and creep
[NASA-TN-D-5317] c32 N69-29672
STRESS RATIO
Axial load fatigue crack propagation tests on Al alloy sheets for stress ratio effects
c17 A69-36435
Stress ratio effects on fatigue crack growth in sheet aluminum alloys
[NASA-TN-D-5390] c17 N69-34704
STRESS-STRAIN DIAGRAMS
Elastoplastic stress-strain behavior at notch roots in sheet specimens under constant amplitude loading
[NASA-TN-D-5253] c32 N69-28038
STRESSED-SKIN STRUCTURES
Influence of fabrication methods on compressive strength of titanium alloy skin stringer panels
[NASA-TN-D-5389] c15 N69-34707
STRESSES
Edge notch sensitivity in thin sheet nickel alloys under stress at high temperatures
[NASA-CR-1263] c32 N69-16156
STRETCH FORMING
Calorimetric, optical, and vibration investigation of stretch-formed aluminum solar concentrators for thermionic converters
[NASA-TN-D-4889] c03 N69-10708
STRIATION
Moving striations as plasma oscillations arising from transit time delays of neutral and charged particles moving through ionized gas, using continuity equation
c25 A69-43122
Helium-neon laser discharge with striation oscillations in relation to pressure and current
[NASA-CR-1387] c08 N69-32350
STRINGERS
Influence of fabrication methods on compressive strength of titanium alloy skin stringer panels
[NASA-TN-D-5389] c15 N69-34707
STRONTIUM
Moldavites and Ries crater material, studying Rb-Sr isochronal relationship
c13 A69-41341
STRONTIUM ISOTOPES
Rb-Sr isotope patterns in tekites from Southeast Australian strewn field, studying Rb volatilization role in Rb-Sr isochron production
c13 A69-41342
STRONTIUM TITANATES
Zr doped superconducting ceramic strontium titanate, noting effective electron mass variations and transition temperature
c26 A69-27400
Polarons large to nearly small transitions, studying ground state mass dependence on bare electron mass, electron-phonon interactions model, superconducting strontium titanate, etc
c26 A69-37280
STRUCTURAL ANALYSIS
Control system for thin diffraction limited orbiting astronomical telescope mirror based on structural analysis of static deflections
c14 A69-27951
Rosman I reflector antenna for collecting data from earth orbiting satellites, discussing dynamic analysis of structural response to natural frequencies
c32 A69-42133
Structural synthesis of cylindrical shell reinforced with rectangular cross section stiffeners
[NASA-CR-1217] c32 N69-14254
Transient thermal analysis and structural analysis for synthesis of ablating thermostructural panels in planetary entry environment
[NASA-CR-1215] c32 N69-16114
Outer and inner curved plates and shell shapes optimized by conformal mapping
[NASA-CR-1357] c32 N69-26559
Manipulation errors in finite element analysis of structures
[NASA-CR-1385] c19 N69-34360
Differential equations for compression loaded axisymmetric cylindrical structures
[NASA-CR-1444] c32 N69-38781

STRUCTURAL DESIGN
Structural design options for decelerative aeroshell configurations for atmospheric entry on unmanned planetary explorations
[AIAA PAPER 68-344] c32 A69-15507
Flutter design charts for isotropic panels stressed to verge of buckling for typical values of structural damping
c32 A69-25524
Papers on fracture, Volume 5, Fracture design of structures
c32 A69-33559
Fracture design for airflight vehicles, discussing crack strength requirements and method for serviceability prediction
c32 A69-33563
Structural and aerodynamic developments in attached inflatable decelerators for deplcyment of payload at supersonic speeds
[AIAA PAPER 68-929] c02 A69-39015
Structural technology for large radio and radar telescope systems - Conference, Cambridge, Mass., October 1967
c11 A69-42120
Materials research structural design cycle, discussing simultaneous optimization, constituent materials, fabrication process, load environment and mission constraints
c32 A69-42991
Design and construction of plastic model of prestressed segmented spherical shell
[NASA-CR-1231] c32 N69-11010
Conference on NASA research in noise reduction of subsonic jet aircraft - nacelle acoustic linings, sound generation in jet engines, and operational noise effects on humans
[NASA-SP-189] c02 N69-11542
Propellant slosh load criteria for design of space vehicles
[NASA-SP-8009] c32 N69-14553
Variational methods for determining optimum design and flight of rockets
[NASA-TR-R-297] c31 N69-15374
Design and performance prediction of calorimetric apparatus for measuring total hemispherical emittance of materials
[NASA-TN-D-5106] c14 N69-20941
Design and development of boresighted star tracker
[NASA-CR-976] c21 N69-21502
Vibration test fixture design for mount impedance simulation of aerospace structures
[NASA-CR-1351] c32 N69-26315
Wind tunnel study of open-face honeycomb to reduce temperature of hypersonic aircraft structure
[NASA-TN-D-5278] c33 N69-29599
Design effects on performance of two dimensional mixed-compression supersonic inlets with low angle cowls
[NASA-TN-D-5330] c01 N69-30060
Design calculations for conical shells and elastic systems subject to antisymmetric loads
[NASA-TT-F-518] c32 N69-30754
Design and performance of sonic boom simulator
[NASA-CR-1378] c02 N69-31959
Design of Brayton rotating unit with roller bearings for space power system
[NASA-CR-1401] c15 N69-33450
Optimal structural design for sandwich-shaped and ring-stiffened loaded shells of revclution
[NASA-CR-1424] c32 N69-35515
Optimum structural design for Martian entry capsule configurations
[NASA-CR-1414] c33 N69-35516
Design and equipment requirements for manned earth orbiting biotechnology laboratory
[NASA-CR-1408] c05 N69-35541
Structural design of conical and tension shells using sandwich structures
[NASA-CR-1365] c32 N69-36357
Modified structural design of high temperature cesium vapor thyratrons
[NASA-CR-1417] c03 N69-36411
Drag and stability characteristics of towed, conical decelerator
[NASA-TM-X-1833] c02 N69-38598
STRUCTURAL FAILURE
High pressure storage vessels for gaseous hydrogen, discussing failure, manufacturing controls and access for internal nondestructive inspection
[ASM PAPER D8-14.1] c15 A69-19666
Failure criteria for predicting filamentary composite strength under uniaxial and combined stresses from properties and fabrication process considerations
c32 A69-21479
Structural failures of high pressure, gaseous hydrogen storage tanks for M-1 engines
[NASA-CR-1305] c17 N69-19831
STRUCTURAL MEMBERS
Computer program for one dimensional elastic wave problems connected with structural members
[NASA-CR-1306] c32 N69-22983
STRUCTURAL STABILITY
Instability of eccentrically stiffened cylindrical shells under axial compression and lateral pressure
[NASA-CR-1280] c32 N69-15378
Structural stability of lattice column of longerons and helical braces
[NASA-CR-1301] c32 N69-26234
STRUCTURAL STRAIN
Plane strain fracture toughness determined for crack notched bend specimens using standard test procedure for specific metallic material property
c17 A69-33566
STRUCTURAL VIBRATION
LOX prevalve accummulator system with He pressurant for prevention of POGO effect on Saturn 5
c31 A69-15298
Longitudinal structural vibration and lateral bending response mass and spring coupling in Saturn AS-502 during boost with longitudinal excitation by POGO effect
[AIAA PAPER 69-58] c31 A69-18204
Flexible rotor blade dynamic response to radially moving force, emphasizing helicopter rotor vibration characteristics associated with tip-vortex impingement
[AIAA PAPER 69-203] c02 A69-19546
Dynamic analysis of axisymmetric ring stiffened shells with attached asymmetric elastic structures, noting vibration modes
c32 A69-25525
Saturn 5 longitudinal instability /POGO/ precluded by lowering S-1C stage propulsion system resonance below structural frequency
[AIAA PAPER 69-548] c31 A69-32658
Natural vibration modal analysis as related to space vehicle design criteria
[NASA-SP-8012] c32 N69-22773
Effect of shallow meridional curvature on vibration of nearly cylindrical shells
[NASA-TN-D-5143] c32 N69-22821
STRUCTURAL WEIGHT
Weight estimation and forecast in manned spacecraft design, noting size and weight relationship
[SAWE PAPER 793] c31 A69-34864
Compressive properties and weight saving of metals reinforced on surface with resin bonded fibers
[NASA-TN-D-4878] c17 N69-11012
STRUTS
Thermal analysis of shadow shields and structural members in space environment
[NASA-TN-D-4876] c33 N69-10473
Impact energy absorbing strut using tube cutting
[NASA-TN-D-4941] c32 N69-14506
SUBMERGED BODIES
Heat transfer coefficients for film boiling from submerged spheres
[NASA-TN-D-5124] c33 N69-28318
SUBMILLIMETER WAVES
Background radiation intensity upper limits for mm and submillimeter wavelengths in interstellar medium, ncting intense flux in far IR
c30 A69-19404
Sulfur dioxide-helium laser pulsed and CW submillimeter outputs
c16 A69-24005
SUBORBITAL FLIGHT
Suitability of white rats for suborbital studies of behavior in gravity fields
[NASA-CR-1255] c05 N69-14094
SUBROUTINES
FORTRAN 4 subroutines to generate printed plots as

normal output
[NASA-TM-X-1700] c08 N69-13566
FASTER computer program modified for tracking neutrons through reactor slabs penetrated by helical voided ducts
[NASA-TM-X-1838] c22 N69-31986
SUBSONIC AIRCRAFT
Calculated and flight measured handling quality factors of three subsonic jet transports
[NASA-TN-D-4832] c02 N69-10495
Fluid mechanical problems related with subsonic and supersonic aircraft
[NASA-SP-183] c12 N69-10693
Conference on NASA research in noise reduction of subsonic jet aircraft - nacelle acoustic linings, sound generation in jet engines, and operational noise effects on humans
[NASA-SP-189] c02 N69-11542
SUBSONIC FLOW
Subsonic lifting surface theory including leading edge, discussing singularities in solution of integral equation for determination of aerodynamic properties
[AIAA PAPER 69-37] c01 A69-18167
Fixed position pressure probe for measuring subsonic flow direction over range of Reynolds number, Mach number and flow angle
c14 A69-33107
FORTRAN computer program for detailed solution of compressible, subsonic, nonviscous flow at leading or trailing edges of blade surface
[NASA-TN-D-5091] c01 N69-22938
Subsonic expansion tube evaluation as device for studying particle drag in subsonic compressible slip flow
[NASA-CR-1354] c11 N69-28095
Load distribution calculations for subsonic compressible flow of arbitrary wings and lifting surfaces
[NASA-TN-D-5335] c01 N69-31337
Computer program for steady laminar, subsonic, and isothermal compressible flow across sealing dam
[NASA-TN-D-5373] c15 N69-33281
Wind tunnel investigation for determination of subsonic and transonic aerodynamic characteristics of Saturn 1B launch vehicle
[NASA-TM-X-1848] c31 N69-33380
Wind tunnel tests of subsonic aerodynamic characteristics of large scale tip turbine cruise fan with 1.075 pressure ratio at angle of attack
[NASA-TN-D-5316] c28 N69-34575
Three dimensional pressure distribution functions for lifting surfaces with trailing-edge controls based on integral equations for subsonic flow
[NASA-TN-D-5419] c01 N69-38768
SUBSONIC SPEED
Aerodynamic and flight characteristics of variable geometry entry spacecraft during subsonic wing deployment and landing
[AIAA PAPER 69-742] c01 A69-34407
C-5A aircraft model high subsonic speed tests, correlating data from three transonic wind tunnels
[AIAA PAPER 69-794] c01 A69-35636
SUBSONIC WIND TUNNELS
Wind tunnel wall constraints effects at extreme force coefficients during V/STOL testing shown different from effects in conventional aircraft testing
c11 A69-15574
Test facilities and techniques for low speed flight problems of aircraft handling qualities, stability, control and performance
c11 A69-15575
Wind tunnel drag measurements on subsonic sphere
[NASA-CR-1392] c01 N69-30609
SUBSTRATES
Gold-underlayer film combinations adhesion to oxide substrates, describing adhesion changes as function of Au and underlayer film thickness, time, environment, etc
c26 A69-28007
Substrate specificity of cathepsin C derived from rat liver, describing polymeric structure and behavior as acidic protein
c04 A69-37577
SUBZERO TEMPERATURE
Cryogenic fracture properties of thin AISI 301 cold reduced sheet at different angles to rolling direction
[NASA-TN-D-5413] c17 N69-35688
SUCTION
Amplified boundary layer oscillations and transition at swept flat nosed wing attachment line with/without boundary layer suction analyzed by wind tunnel tests
c01 A69-33251
Stagnation point boundary layer with suction and injection in equilibrium dissociating air
[NASA-TN-D-3889] c12 N69-14314
SUDDEN IONOSPHERIC DISTURBANCES
Sudden magnetic field increase associated with July 8, 1966 sudden commencement observed by OGO 3 satellite in magnetotail
c13 A69-11226
Sudden commencement associated discontinuities in interplanetary magnetic field observed by IMP 3 satellite, stressing shocks and tangential and rotational discontinuities
c30 A69-22183
Worldwide changes in geomagnetic field, determining causes by examining magnetic field and plasma data for solar wind and classifying as SSC or SI
c29 A69-31963
SUGARS
Sugars identification as trifluoethylacetyl polyol derivatives by gas-liquid chromatography
c04 A69-31539
SULFONES
Synthesis of Pyrrone laminates from sulfone dianhydride
[NASA-CR-1404] c30 N69-31960
SUNLIGHT
Directional solar thermal field /sunlight/ effect on coupled nonplanar transverse and torsional vibrations of satellite cylindrical antennas in orbit
c32 A69-25534
SUNSPOT CYCLE
Interplanetary sector structure during rising portion of 1966-1967 sunspot cycle, giving recurrence period of interplanetary field
c30 A69-28957
Global electron density distribution morphology in topside ionosphere during sunspot minimum from Alouette 1 and 2 ionograms
c13 A69-37867
SUNSPOTS
Sunspots magnetic structure producing solar proton flares, considering role of sunspots rotational motion on photospheric surface
c29 A69-35415
Solar flare and sunspot effects on VHF communications between synchronous satellite relay and ground stations
[NASA-TN-D-5100] c07 N69-23317
SUPERCONDUCTING MAGNETS
Variable voltage dc power supplies for energizing cryogenically cooled and superconductive electromagnets
c03 A69-26498
Design, construction, testing, and control devices for high-field electromagnets
[NASA-TN-D-4910] c23 N69-10889
Superconductive 14-tesla magnet system with 15-cm bore and niobium stanide ribbon
[NASA-CR-1260] c03 N69-15382
SUPERCONDUCTIVITY
Polarons large to nearly small transitions, studying ground state mass dependence on bare electron mass, electron-phonon interactions model, superconducting strontium titanate, etc
c26 A69-37280
SUPERCONDUCTORS
Zr doped superconducting ceramic strontium titanate, noting effective electron mass variations and transition temperature
c26 A69-27400
Optimum thickness of dynamically stable composite superconducting tapes determined for substrate thickness as function of current density
c26 A69-43121
Inductance behavior of coils filled with superconducting lead or niobium dusts
[NASA-TN-D-5137] c26 N69-21500

SUPERGIANT STARS
Red supergiants as old derivatives of main sequence O and B stars, discussing neutrino emissions and carbon core contraction
c30 A69-24125
Radial pulsation mode of convective envelopes in adiabatic equilibrium for variable M red supergiant stars
c30 A69-30766
HD 30353 He binary star invisible component suggested as KO type supergiant from IR photometric data
c30 A69-35348
SUPERNOVAE
Gamma ray telescope development for balloon-borne astronomy in search for discrete gamma sources and supernova explosions
[IEEE PAPER 3A-5] c14 A69-19192
Nucleosynthesis in dynamics of massive star cores, noting element synthesis by neutron capture in supernova explosions
c30 A69-20898
SUPERSONIC AIRCRAFT
Fluid mechanical problems related with subsonic and supersonic aircraft
[NASA-SP-183] c12 N69-10693
Crack toughness characteristics of high strength alloys for use in heavy sections of supersonic aircraft
[NASA-TN-D-4998] c32 N69-17275
Conditions for supersonic aircraft entering critical stall and spin regimes
[NASA-TT-F-526] c02 N69-31917
Helium pressurization systems for liquid methane fuel in supersonic transports
[NASA-TN-D-5519] c28 N69-40329
SUPERSONIC AIRFOILS
Performance comparisons of supersonic compressor rotor blades
[NASA-CR-1256] c28 N69-14210
SUPERSONIC COMBUSTION
Dynamic stability and performance of injectors, rocket liners, and supersonic combustors
[NASA-TM-X-1845] c33 N69-32468
SUPERSONIC COMBUSTION RAMJET ENGINES
Rocket-scramjet hybrid engines in lifting reusable second stage
[NASA-TN-D-5218] c28 N69-24922
SUPERSONIC COMPRESSORS
Supersonic compressor blade sections performance prediction near maximum pressure ratio and efficiency by analyzing flow processes
[AIAA PAPER 69-522] c28 A69-32711
Steady state and dynamic distortion influence on performance and stall of turbofan engine, discussing compressor instrumentation, tests and simulation data
c28 A69-35175
SUPERSONIC DRAG
Drag coefficients for spheres and sharp cones in rarefied hypersonic air flow obtained in shock tunnel using free flight technique
[AIAA PAPER 69-140] c01 A69-18184
Numerical method for evaluation and utilization of supersonic nacelle-wing interference
[NASA-TN-D-5057] c01 N69-19641
Force measurements in drag reduction by gas injection into turbulent boundary layer through supersonic wing slots
[NASA-TN-D-5307] c12 N69-31359
SUPERSONIC FLIGHT
Evaluating performance of swirl can turbojet combustor at simulated supersonic inlet conditions
[NASA-TN-D-4996] c28 N69-16154
Aerodynamic characteristics of large-angle cones in supersonic lifting capabilities
[NASA-TN-D-5499] c01 N69-40026
SUPERSONIC FLOW
Solar wind flow past earth and magnetosphere correspondence to external aerodynamics of round nosed bodies in supersonic stream
c13 A69-19360
One strip method of integral relations applied to inviscid supersonic blunt body problem
c01 A69-21972
Vortex motion enhancement of jet penetration and spreading in supersonic fuel injection into large diameter combustors
[AIAA PAPER 69-664] c12 A69-33437
Computational method for surface pressures on blunt bodies of revolution at small angles of attack in supersonic flow
[NASA-TN-D-4865] c01 N69-10215
Oxidation behavior of coated molybdenum and niobium alloys in high temperature supersonic air streams
[NASA-TN-D-4877] c17 N69-10764
Estimated supersonic flow field shock waves and sonic boom effects for cones and axisymmetric bodies
[NASA-TN-D-4935] c01 N69-13238
Momentum diffusion between two supersonic airstreams passing through oblique shock waves
[NASA-TN-D-4974] c12 N69-15631
Experimental pressure distributions on 120 deg cone at Mach 2.96 to 4.63 and angles of attack from 0 deg to 20 deg
[NASA-TN-D-5054] c01 N69-19826
Mathematical model for determining total drag of pointed body of revolution in supersonic flow with turbulent boundary layer
[NASA-TN-D-5046] c01 N69-19925
Flow field from forward facing nozzles exhausting near large cylindrical body at free-stream Mach numbers of 3.0 and 6.0
[NASA-TN-D-5030] c01 N69-21000
Finite difference techniques used in numerical solutions for inviscid radiating shock layers around spheres at hyperbolic speed in air
[NASA-TR-R-311] c12 N69-26504
Flow field measurements on flat plate with attached protuberances in supersonic turbulent boundary layer
[NASA-TN-D-5297] c12 N69-30071
Supersonic flow characteristics in wake of blunt cones
[NASA-TN-D-5365] c01 N69-32299
Gaseous jet interaction and penetration in supersonic flow
[NASA-CR-1386] c12 N69-32480
Turbulent boundary layer temperature and velocity measurements in supersonic water-cooled conical nozzle
[NASA-TN-D-5377] c12 N69-33353
Mathematical analysis of wave structure in supersonic flow
[NASA-CR-1438] c04 N69-37062
Effect of angle of attack and injection pressure on jet penetration and spreading from Delta wing in supersonic flow
[NASA-TM-X-1889] c12 N69-37271
Characteristics method for determining three dimensional supersonic flow around inclined body of revolution
[NASA-TN-D-5341] c12 N69-39177
SUPERSONIC INLETS
M 3.5 two dimensional mixed compression inlet system with self restart using flexible variable ramp system
[AIAA PAPER 69-447] c28 A69-32732
Large scale axisymmetric inlet systems performance capabilities, reviewing theoretical and experimental programs
[AIAA PAPER 68-580] c28 A69-34018
Wind tunnel tests of distortion dynamics in Mach three mixed compression inlet
[NASA-TM-X-1706] c01 N69-13154
Approximate mathematical analysis of supersonic inlet dynamics
[NASA-TN-D-4969] c01 N69-14289
FORTRAN computer program for designing supersonic inlets by characteristic theory
[NASA-TN-D-4960] c01 N69-14566
Design and performance of flueric shock position sensor for mixed compression supersonic inlets
[NASA-TM-X-1733] c14 N69-16382
Performance test from Mach 2.58 to 1.98 of axisymmetric mixed-compression inlet system with 60 percent internal contraction
[NASA-TM-X-1739] c01 N69-19130
Restart and high response terminal shock control for axisymmetric mixed-compression inlet with internal contraction
[NASA-TM-X-1792] c28 N69-24938
Design effects on performance of two dimensional mixed-compression supersonic inlets with low angle cowls

[NASA-TN-D-5330] c01 N69-30060
Dynamic response of supersonic mixed compression inlet coupled to cold pipe or turbojet engine
[NASA-TN-D-5338] c28 N69-31336
Numerical analysis of shock control by using perforated walls in internal compression supersonic inlets
[NASA-TR-R-317] c01 N69-32338

SUPERSONIC NOZZLES
Flow angle and throat Reynolds number effects on loss characteristics of two dimensional supersonic nozzle
[NASA-TM-X-1823] c01 N69-31360

SUPERSONIC SPEEDS
Structural and aerodynamic developments in attached inflatable decelerators for deployment of payload at supersonic speeds
[AIAA PAPER 68-929] c02 A69-39015
Effects of boundary layer bleed rate and location on performance of axisymmetric inlet designed for Mach 2.5
[NASA-TM-X-1692] c01 N69-10294
Effects of angle of attack and bluntness on shock layer properties of cones at supersonic speeds
[NASA-TN-D-4909] c01 N69-10789
Performance of 10 deg conical turbojet plug nozzle with iris primary and translating shroud for supersonic cruise applications
[NASA-TM-X-1709] c28 N69-14313
Aerodynamic characteristics of blunted cones, tension shell, and attached inflatable decelerator models
[NASA-TN-D-5219] c31 N69-26570
Flight test performance of supersonic parachutes in low density environment
[NASA-TN-D-5296] c01 N69-30063
Pressure distributions for blunt body wind tunnel models at supersonic speeds and angles of attack from 0 to 15 degrees
[NASA-TN-D-5392] c01 N69-35300
Feasibility tests on liquid lubricants for inerted lubrication systems of advanced aircraft engines
[NASA-TN-D-5420] c15 N69-35788

SUPERSONIC TRANSPORTS
Location effect of power plants on aft-mounted supersonic cruise exhaust nozzles at transonic speeds in flight and wind tunnel
[AIAA PAPER 69-427] c01 A69-32769
XB-70 aircraft test data as applied to SST safety, describing aircraft design, flight characteristics, instrumentation, takeoff and landing, etc
c02 A69-41143
Flight simulator with large lateral motion for large and supersonic transport aircraft, emphasizing reproduction of cockpit accelerations due to supersonic engine thrust loss
c11 A69-43044
Low speed static and dynamic longitudinal, and lateral stability of scale model of supersonic transport in wind tunnel tests
[NASA-TN-D-4726] c02 N69-10733
Simulation studies of supersonic transports in future air traffic control systems
[NASA-TN-D-4944] c21 N69-14382
Large scale wind tunnel tests to improve longitudinal stability of supersonic transports with variable swept wings
[NASA-TN-D-5005] c02 N69-16384
Supersonic transport performance during real time simulated operations in future air traffic control system environments
[NASA-TN-D-5018] c02 N69-17257
Aerodynamic characteristics and ground effects of supersonic transport with double Delta wing
[NASA-TN-D-5102] c02 N69-21020
Supersonic transport instrumentation and flight simulation
[NASA-TN-D-5280] c14 N69-32286

SUPERSONIC WAKES
Supersonic flow characteristics in wake of blunt cones
[NASA-TN-D-5365] c01 N69-32299

SUPERSONIC WIND TUNNELS
Short duration tube wind tunnel supersonic testing, noting Saturn S-1C base heating and solid propellant rocket base burning tests
[AIAA PAPER 69-335] c11 A69-28271
Inlet produced dynamic distortion and effects on stall margin of J-85 turbojet engine from supersonic wind tunnel tests
[AIAA PAPER 69-487] c28 A69-32676

SUPERSONICS
Supersonic aerodynamic characteristics and shock standoff distances for large angle cones with and without cylindrical afterbodies
[NASA-TN-D-5334] c01 N69-33237

SUPPORT SYSTEMS
Data relay satellite systems for support of NASA R and D missions, discussing communications between satellites and to mission control
c07 A69-25296
Tracking and data acquisition networks and communications systems for support of space missions, studying data processing, unified S Band System and Data Relay Satellite System
c07 A69-25933
High speed foil bearing rotor support system
[NASA-CR-1157] c15 N69-14214

SUPPORTS
Vibration test fixture design for mount impedance simulation of aerospace structures
[NASA-CR-1351] c32 N69-26315

SURFACE CRACKS
Gas breakdown model for analyzing breakdown of Ce vapor filled crack in thermionic trilayer insulator
c03 A69-21840
Semiempirical fracture analysis for semielliptical surface crack in plate
[NASA-TN-D-5340] c32 N69-31056

SURFACE DIFFUSION
Turbine blade loading in terms of surface diffusion and loading factors, discussing tandem and jet flap blades and vortex generators
[ASME PAPER 68-WA/GT-11] c28 A69-16136
Lunar surface thermal radiation incident on unit area flat surface located at variable distance and orientation above moon, considering diffusion effects
c30 A69-38973

SURFACE DISTORTION
Heat transfer and pressure distribution due to two-dimensional repetitive sine wave distortions on flat plate at Mach 20 in helium
[NASA-TN-D-4907] c12 N69-10804
Parametric analysis of surface temperatures and distortions of paraboloidal solar concentrators
[NASA-TN-D-5144] c03 N69-23356

SURFACE ENERGY
Free electron model for electron work functions and number density distributions and surface potentials in metals
c26 A69-29009

SURFACE NAVIGATION
Potential use of satellites for enhancing positioning capabilities and for marine geodetic control
[NASA-CR-1253] c13 N69-16645

SURFACE PROPERTIES
Rhenium-niobium cylindrical thermionic converters with mechanically polished or electroetched emitters, comparing performance
c03 A69-13126
Lunar magnetic moment and surface field, discussing Explorer 35 field measurements
c30 A69-14005
Cross hatching on various body surfaces due to periodic surface pressure fluctuations, discussing origin from counter-rotating longitudinal vortices in boundary layer
[AIAA PAPER 69-11] c12 A69-18213
Albedo over Antarctic, measuring solar radiation reflected by surface and atmosphere by Eppley radiometer
c13 A69-21404
Nonlinear compressible flow problems - half-space of ideal compressible fluid motion due to arbitrary pressure front
[NASA-TT-F-560] c12 N69-27168
Summary of lunar data and scientific observations generated by Surveyor landings on Moon
[NASA-SP-184] c30 N69-36451

SURFACE REACTIONS
Propellant condensation on surfaces near electric rocket exhaust, calculating particle arrival rates, backflow and desorption energies

[AIAA PAPER 69-270] c26 A69-21252
Oxygen depletion effect in chemical reactions between pyrolysis gases and air stream on surface recession of charring ablators
[AIAA PAPER 68-302] c33 A69-21982
Uranyl ions interaction with phospholipid and cholesterol monolayers, using surface pressure and potential measurements
c06 A69-25641
Modes and mechanisms of wear covering adhesive, abrasive and corrosive wear, surface fatigue and fretting corrosion
c15 A69-27231
Dielectric overcoating effects on electromigration Al interconnections, showing dependence on thickness and surface passivation
c09 A69-32889
Quartz fiber adhesion to Re measured in LEED /low energy electron diffraction/ apparatus for clean and O layer surfaces, noting brittle fracture
c17 A69-35182
Satellite-borne experiments of neutral molecular beam-solid surface interactions, describing Molsink chamber, densitometer, sphere and paddlewheel satellites
c24 A69-36182
Quantum theory of particle-harmonic oscillator collision applied to gas-surface interactions at cryogenic temperatures
[NASA-TN-D-4982] c24 N69-14288
Thermal radiation exchange between surfaces and enclosures
[NASA-SP-164-VOL-2] c33 N69-30317

SURFACE ROUGHNESS
Radiation models using discrete radiator ensembles having applications to analysis of forward and backscatter from rough surfaces, clutter and chaff models, etc
c07 A69-10556
Turbulence characteristics up to 150 m above ground, noting surface roughness length directional dependence, longitudinal turbulence spectra and turbulent energy budget
c20 A69-10695
Experimental verification of surface vehicle dynamics
[NASA-CR-1399] c11 N69-37022
Airplane response to ground roughness from three-track runway and taxiway profiles by elevation angle measurements
[NASA-TN-D-5444] c02 N69-38770

SURFACE ROUGHNESS EFFECTS
Turbulence measurements and roughness effects on viscous drag reduction with polymer solution in pipe flow, discussing friction factor, wall velocity profile, etc
c12 A69-33252
Microwave thermal emission by water measured from aircraft, studying radiation dependence on surface roughness
c13 A69-34421
Effect of unit Reynolds number, nose bluntness, angle of attack, and roughness on transition on 5 degree half-angle cone at Mach 8
[NASA-TN-D-4961] c01 N69-14872
Determination of drag of fabrication-type surface roughness in turbulent boundary layer at transonic speeds
[NASA-TN-D-5004] c01 N69-16460

SURFACE TEMPERATURE
Venus atmosphere chemical composition, surface temperature and pressure obtained by Venera 4 and Mariner 5
c30 A69-26129
Heat finite propagation velocity effects on temperature distribution and heat flux for step temperature change at semiinfinite body surface
[ASME PAPER 69-HT-1] c33 A69-43564
Surface temperature mapping with infrared photographic pyrometry for turbine cooling investigations
[NASA-TN-D-5179] c14 N69-23895
Probability calculations for fuel clad surface temperatures of nuclear reactors
[NASA-TM-X-1802] c22 N69-26231

SURFACE VEHICLES
Experimental verification of surface vehicle dynamics
[NASA-CR-1399] c11 N69-37022

SURFACES
Subsonic lifting surface theory including leading edge, discussing singularities in solution of integral equation for determination of aerodynamic properties
[AIAA PAPER 69-37] c01 A69-18167
Three dimensional pressure distribution functions for lifting surfaces with trailing-edge controls based on integral equations for subsonic flow
[NASA-TN-D-5419] c01 N69-38768

SURGES
Analysis and design of inductors for protecting power transistors against current surges in inverter bridge circuits
[NASA-TN-D-4995] c10 N69-16198

SURVEYOR LUNAR PROBES
Summary of lunar data and scientific observations generated by Surveyor landings on Moon
[NASA-SP-184] c30 N69-36451

SURVEYOR 3 LUNAR PROBE
Flight performance evaluation of Atlas Centaur launch vehicle AC-12 carrying Surveyor 3 lunar probe
[NASA-TM-X-1678] c31 N69-10295

SURVEYOR 4 LUNAR PROBE
Systems analysis of Atlas-Centaur AC-11 flight performance for Surveyor 4
[NASA-TM-X-1768] c31 N69-21399

SURVIVAL
Human survival in flight emergencies involving commercial and general aviation aircraft
[NASA-CR-1262] c02 N69-14763

SWAN BANDS
Electronic transition moment for C /Swan/ bands measured in shock tube in carbon dioxide and argon mixtures
c24 A69-12833

SWEAT COOLING
Radiation equilibrium temperature measured downstream of transpiration cooled gas flow near slender cone vertex in continuous flow hypersonic tunnel
c01 A69-43588
Flow reduction due to oxidation of wire-form porous materials for transpiration cooled turbine blades
[NASA-TN-D-5001] c17 N69-16383

SWEEP FREQUENCY
Dynamic tests for air breathing engines using sweep frequency techniques
[NASA-TN-D-5485] c28 N69-39185

SWELLING
Uranium carbides irradiation tests for control of nuclear fuels fission gas swelling
[NAA-SR-12629] c22 N69-22946
Beryllium swelling and replacement in Plum Brook reactor
[NASA-TM-X-1794] c22 N69-26233

SWEPT WINGS
Amplified boundary layer oscillations and transition at swept flat nosed wing attachment line with/without boundary layer suction analyzed by wind tunnel tests
c01 A69-33251

SWINGBY TECHNIQUE
Venus swingby and direct Mercury trajectories analysis for optical imaging from flyby missions
[AAS PAPER 69-258] c30 A69-42860
Interplanetary space trajectories based on Jupiter swingby flights
[NASA-TN-D-5271] c30 N69-28441
Jupiter swingby missions to Saturn, Uranus, Neptune, and Pluto
[NASA-SP-35-PT-8] c30 N69-34850

SYMMETRY
Response of infinite elastic plates to axisymmetric initial velocity distributions with application to hypervelocity impact
[NASA-TN-D-5118] c32 N69-23448
Noise in axisymmetric convergent electron beams
[NASA-TN-D-5212] c10 N69-24918
Restart and high response terminal shock control for axisymmetric mixed-compression inlet with internal contraction
[NASA-TM-X-1792] c28 N69-24938

SYNCHROCYCLOTRONS
Proton beams uniformity available at NASA synchrocyclotron designed for radiation biology research by simulating space radiation

environment
c11 A69-15992
SYNCHRONISM
Mitotic synchronization of fibroblasts with metabolic retardants by chronophotography
[NASA-TN-D-5021] c04 N69-17248
SYNCHRONOUS MOTORS
Motor starting characteristics of two inductor alternators
[NASA-TM-X-1912] c03 N69-40440
SYNCHRONOUS SATELLITES
Multijet electrothermal systems for attitude control and stationkeeping of synchronous communications satellite
[AIAA PAPER 67-723] c28 A69-12375
OMEGA position location equipment /OPLE/ test data to demonstrate feasibility of using OMEGA navigational system in conjunction with synchronous satellites
c21 A69-19135
Solar cell radiation damage during 416.8 days in synchronous orbit on satellite ATS 1, discussing radiation shields
c03 A69-35704
Tracking and Data Relay Satellite System with synchronous orbit satellites to relay data between low altitude earth orbital spacecraft and mission control centers
c07 A69-41755
RFI effects of earth based emitters on operation of geosynchronous satellites for data relay from near earth orbiting satellites, noting frequency assignments
c07 A69-41757
Solar flare and sunspot effects on VHF communications between synchronous satellite relay and ground stations
[NASA-TN-D-5100] c07 N69-23317
SYNCHROTRON RADIATION
Synchrotron and X ray emission generation from upper chromosphere electrons during solar flares
c29 A69-22203
Radio emission from Sco XR-1 shown as synchroton radiation of relativistic electrons in low density region surrounding denser core producing X ray
c30 A69-37334
Synchroton radiation HF cut-off resulting from electrons with anisotropic pitch angle distribution for type 4 solar radio bursts
c29 A69-40577
SYNOPTIC METEOROLOGY
Synoptic analysis of Southern Hemisphere stratosphere
[NASA-TM-X-1814] c13 N69-33555
SYNTHETIC ARRAYS
Mechanical collimator using random aperture arrays for celestial observation at extreme UV and X rays
c14 A69-36489
SYNTHETIC RUBBERS
Stable crack propagation in viscoelastic strip of polyurethane rubber
[NASA-CR-1279] c30 N69-21506
SYSTEM FAILURES
Metal oxide semiconductor integrated circuits, showing failure rates and degradation causes
c09 A69-31851
Failure data role in management of launch operations reliability program
c11 A69-36022
Computer oriented error analysis of electrical circuits and nonlinear system performance
[NASA-TN-D-5112] c10 N69-22919
SYSTEMS ANALYSIS
Stability of time varying systems by construction of multipliers with prescribed phase characteristics
c10 A69-16598
Digital simulation computer stability analysis scheme premised on use of perturbed transient responses
c10 A69-32899
Evaluation method for strapdown spacecraft guidance systems on automated interplanetary missions, using cost and system performance efficiency probability model
[AIAA PAPER 68-828] c21 A69-35953
Space power systems analysis, using computer program to correlate systems characteristics with mission parameters for automated satellite repair vehicle and space stations
c03 A69-42240
Systems analysis of Rankine cycle nuclear-electric potassium space power system using Li cooled fast reactor and high temperature turbine inlet
c22 A69-42266
Systems analysis of Atlas-Centaur AC-11 flight performance for Surveyor 4
[NASA-TM-X-1768] c31 N69-21399
Human transfer functions applied in systems analysis of manually controlled lunar landing simulator
[NASA-TN-D-5478] c05 N69-39183
Quantum communication systems performance evaluated by communication efficiency parameter
[NASA-TR-R-320] c07 N69-39264
Application of control theory to production engineering, transportation systems, urban development, biological oceanography, mass communications, and socio-economic problems
[NASA-SP-211] c34 N69-39957
Modern network theory applications to analysis of complex systems
[NASA-TN-D-5511] c19 N69-40088
SYSTEMS ENGINEERING
Navigation services satellite systems including position determination, communication and telemetry for ships and aircraft
[UN PAPER 68-95363] c21 A69-10479
Nuclear reactor space power system concept using thermionic diodes, heat pipes and rod control, emphasizing neutronic aspects and feasibility
c22 A69-14799
Systems engineering activities in manned space flight involving design, development, manufacture, test and operation of Mercury, Gemini and Apollo flight systems
c31 A69-17602
Interplanetary Pioneer spacecraft development and systems engineering aspects
c31 A69-17605
Astrodynamical data compilation for use by system engineer for mission planning
[AIAA PAPER 69-124] c30 A69-18090
High performance silicon carbide backward diode, discussing device design and operational characteristics
c09 A69-22787
Onboard checkout system concept, discussing philosophy, requirements, underlying considerations, system description, development and techniques of system selection
c11 A69-25081
Spacecraft design for minimization of structure interaction with control system, noting susceptibility of extendible booms to solar environment
c31 A69-25500
Fourth angle driving law for different four gimbal systems used for simulation display and inertial platform isolation
c11 A69-26265
Spaceborne optical telescopes requirements and development including mirror material and construction, optical design, servocontrol, etc
c14 A69-27946
Solar simulator with xenon and krypton lamps designed for thermal balance tests, power conversion and material degradation experiments
c11 A69-30383
Design philosophy for cost reductions on future space transportation systems, exemplifying application to booster system for earth orbital logistics
[AIAA PAPER 69-439] c34 A69-32654
Optimal design for improving thermal performance of existing spacecraft thermally actuated louver system by increasing open-to-closed emittance ratio
[AIAA PAPER 69-627] c33 A69-33269
OGO program failure rate analysis with respect to cost, schedule and performance tradeoffs, considering component and systems design and reliability, prelaunch feedback, etc
c31 A69-34519

Biosatellite attitude control systems design development and flight test results for paylcad perturbing effects, discussing simulation activity c31 A69-35094
Nuclear rocket program status and plans, presenting NERVA reactor and engine system tests [AIAA PAPER 68-610] c22 A69-39219
Model performance index /PI/ providing criterion for approximating one dynamic flight control system by another based on geometrical representation of linear autonomous systems [AIAA PAPER 69-885] c21 A69-39410
Lifting body stability augmentation systems design, development, ground tests and flight data including frequency response, limit cycle and structural resonance [AIAA PAPER 69-887] c02 A69-39413
SDP-3 small serial computer for engineering experiment on IMP spacecraft, discussing design modifications to improve performance c08 A69-41737
Pneumatic driving system for heart assist or total replacement pumps, discussing design features and performance characteristics c05 A69-42983
Design and analysis of modular servoamplifier for fast response electrohydraulic control systems [NASA-TN-D-4898] c03 N69-10068
Effect of variable stator with area design of 70 percent on performance of single stage turbine suitable for air cooling [NASA-TM-X-1696] c28 N69-10296
Synthesis methods for manual aerospace control systems using digital programming and man machine performance data with application to supersonic transport design [NASA-CR-1208] c02 N69-13185
Concepts of acceptance testing lunar and planetary vehicles [NASA-TN-D-4924] c11 N69-14507
Evaluation of computer aids to augment human intellectual capability [NASA-CR-1270] c08 N69-16140
Design and performance of flueric shock position sensor for mixed compression supersonic inlets [NASA-TM-X-1733] c14 N69-16382
Nimbus 2 flight evaluation and engineering report covering launch through orbit 5275 [NASA-TN-D-4881] c31 N69-17851
Design and performance of gas bearing system for turboalternators [NASA-CR-1291] c15 N69-21772
Low pressure application of orbitron and ion gage designs [NASA-CR-1300] c14 N69-28402
Communication and information theories for digital and analog systems design [NASA-TN-D-5472] c07 N69-39176

SYSTEMS STABILITY
Spacecraft wide angle attitude control system stability analysis, using air bearing table simulation [AIAA PAPER 69-856] c31 A69-39384

T

T TAIL SURFACES
Wind tunnel study of deflected elevator flutter encountered on T-tail airplane [NASA-TN-D-5024] c32 N69-16211

TABLES (DATA)
Solar system elements abundance compilation based on carbonaceous chondrites and nucleosynthesis in stars c30 A69-20903
Approximate ionization potentials for high ionization stages of elements with atomic numbers 31 to 92 obtained by binding energy calculations c24 A69-29923
Interferometrically measured wavelengths tabulated for Th lines in 2747-4572 A range, using liquid nitrogen cooled hollow cathode lamp and Fabry-Perot interferometer c23 A69-42150
Data from thermal vacuum tests of flight model spacecraft [NASA-TN-D-4908] c31 N69-14010
Rocket sounding meteorological data of Exametnet for 1966 [NASA-SP-175] c20 N69-16214
Exametnet meteorological rocket launchings and data dissemination, 1967 - tables [NASA-SP-176] c20 N69-22570
Performance data for high tip speed compressor rotor operated with radial and inlet airflow distortions [NASA-TM-X-1798] c01 N69-26312
Tables and graphs of functions for solving nonlinear constant area fin one dimensional heat transfer problem [NASA-TN-D-5173] c33 N69-26975
Model environment of inner belt proton fluxes [NASA-SP-3024-VOL-5] c24 N69-28911
Pressure distributions for blunt body wind tunnel models at supersonic speeds and angles of attack from 0 to 15 degrees [NASA-TN-D-5392] c01 N69-35300
FORTRAN program for computation of finite group tables [NASA-TN-D-5402] c08 N69-35569
Thermochemical data from simulated pyrolysis gas flow through ablating char layer [NASA-TN-D-5464] c33 N69-38271
Tabular and graphical data on thermal radiative properties for dissemination [NASA-CR-1431] c33 N69-40455
Aerodynamic pressure distribution on semispan tilting wing-propeller combination of V/STOL aircraft [NASA-TN-D-5481] c01 N69-40876

TACTILE DISCRIMINATION
Human perception of multiple-point tactile and visual stimuli [NASA-CR-1389] c05 N69-39211

TAIL ASSEMBLIES
Aerodynamic characteristics of COIN aircraft model with boundary layer control on inverted V-tail [NASA-TN-D-4856] c02 N69-10935
Factors affecting flat spin characteristics of fighter aircraft with horizontal tail surfaces [NASA-TN-D-5409] c02 N69-36807

TAKEOFF
Optimum takeoff and climbout trajectory calculation technique for jet aircraft noise abatement [NASA-TN-D-5182] c02 N69-26194

TANTALUM
Fabrication of counterflow double wall tantalum-stainless steel mercury boiler [NASA-TN-D-5092] c33 N69-23707

TANTALUM ALLOYS
Solubility of oxygen in tantalum determined by resistivity technique [NASA-CR-1276] c17 N69-19886
Creep rate equations for refractory metal alloys of tantalum molybdenum, and columbium [NASA-TN-D-5424] c17 N69-36653
Mechanical behavior of tantalum T-111 alloy at high temperatures and ultrahigh vacuum [NASA-CR-1436] c17 N69-36831

TARGET RECOGNITION
Luminescence effects on apparent size and shape of foveally fixated targets of various forms c04 A69-36458

TARGET THICKNESS
Aluminum double sheet target penetration resistance determined by studying high velocity pyrex glass impact effects on front/rear sheets and spacing [AIAA PAPER 69-375] c32 A69-28305

TARGETS
Responsiveness of three axis, large angle attitude control systems of highly maneuverable spacecraft capable of tracking time-varying target attitudes [NASA-TN-D-4896] c30 N69-10756
Crater characteristics of 11 metal alloys under hypervelocity impact including effects of projectile density and target temperature [NASA-TN-D-5135] c32 N69-22994

TASK COMPLEXITY
Displays and controls requirements in manned spacecraft to integrate man into vehicle system, noting man capability for task diversity c14 A69-19968

Human information processing rates during one and two axis compensatory tracking tasks with secondary auditory task
c05 A69-23880
TASKS
Practice and operator work load effects on acquisition and performance of code transformation /COTRAN/ task
[NASA-CR-1261] c05 N69-14345
TAYLOR INSTABILITY
Cylindrical bubbles stability in vertical pipes from photographs, describing wake, spacing, pressure pulsations and convection cells effects
[ASME PAPER 69-HT-28] c33 A69-43540
TECHNOLOGY UTILIZATION
Aerospace technology role in economic and social benefits
[UN PAPER 68-95321] c34 A69-10467
Space applications program including communications and navigation meteorology, earth resources survey and geodesy
[UN PAPER 68-95437] c34 A69-10472
NASA Technology Utilization Program, discussing information dissemination
[UN PAPER 68-95313] c34 A69-10512
NASA Space Application Program strategy, discussing research and development trend toward complexity, versatility and multidisciplinary use of larger spacecraft
c30 A69-13427
Photovoltaic solar cell power technology application to space use and exploration
[ASME PAPER 68-WA/SOL-1] c03 A69-16158
Manned space flight programs, discussing U.S. technological, scientific and practical contributions
c30 A69-17074
Refractory metal alloys metallurgy and technology - Conference, Washington, D. C., April 1968
c17 A69-18790
Spaceborne optical telescopes requirements and development including mirror material and construction, optical design, servocontrol, etc
c14 A69-27946
Aeromedical developments by NASA biomedical applications program applied to general medical equipment including cardiac sensors, surgical sterilization, ballistocardiograph, etc
c34 A69-32430
Commercial utilization of space - Conference, Dallas, May 1967
c30 A69-34043
Commercial utilization of space technology, discussing cost reduction and role of NASA Apollo Program
c30 A69-34044
Space, technology and society - Conference, Cocoa Beach, Florida, March 1969, Volume 2
c34 A69-35055
Space, technology and society - Conference, Cocoa Beach, Florida, March 1969, Volume 1
c34 A69-35070
Space exploration influence on science education, showing NASA instructional materials for teachers in biology, chemistry, physics, mathematics, industrial arts, etc
c34 A69-35077
NASA technology utilization program for civilian economy benefit, discussing scientific and technical documentation and transfer across industrial, disciplinary and regional boundaries
c34 A69-35105
Nuclear rocket program status and plans, presenting NERVA reactor and engine system tests
[AIAA PAPER 68-610] c22 A69-39219
Application of NASA mathematical management models and systems analyses in private industry and economy
[NASA-SP-5048] c34 N69-10662
Selected conference papers on NASA technology utilization for electric power industry
[NASA-SP-5057] c03 N69-12575
Metallurgy, behavior, and application of 18 percent nickel maraging steels
[NASA-SP-5051] c17 N69-14193
Technology utilization of induction heating systems up to 5800 deg F
[NASA-SP-5071] c03 N69-23643
Air pollution monitoring instrumentation developed for aerospace uses surveyed for industrial applications
[NASA-SP-5072] c14 N69-24751
Survey of incompressible and compressible fluid film hydrostatic and hydrodynamic lubrication
[NASA-SP-5058] c15 N69-28592
Technology transfer and utilization - bibliography
[NASA-CR-1355] c34 N69-28868
Technology utilization by industries of aerospace sciences and systems - conferences
[NASA-SP-5075] c34 N69-31946
Indexed and abstracted references to reports and articles on management available in NASA information system
[NASA-SP-7500/03/] c34 N69-32430
TECTONICS
Origin and terrestrial relief of continents and oceans
[NASA-TT-F-533] c13 N69-29491
TEFLON (TRADEMARK)
Proton induced voltage breakdowns in polymeric materials
[NASA-TM-X-1688] c18 N69-10066
TEKTITES
Tektite origin theories, discussing Surveyor experiments effects on lunar geology and Tektite origin
c30 A69-40086
Rb-Sr isotope patterns in tekites from Southeast Australian strewn field, studying Rb volatilization role in Rb-Sr isochron production
c13 A69-41342
Ivory Coast microtektites chemical composition from electron microprobe analysis
c30 A69-41351
TELECOMMUNICATION
Communications - IEEE Conference, Boulder, June 1969
c07 A69-42500
Relationship between complex covariance and covariances of envelopes of Rician fading communication channels
[NASA-TN-D-4825] c07 N69-11011
Requirement estimates and performance predictions for Martian television experiment onboard spacecraft in three point-mass descent trajectories
[NASA-TN-D-5062] c14 N69-17944
Summary of operation, communications, and other experiments of Relay 2 satellite
[NASA-SP-151] c31 N69-21065
Communication and information theories for digital and analog systems design
[NASA-TN-D-5472] c07 N69-39176
TELEMETRY
Telemetering - Conference, Los Angeles, October 1968
c07 A69-19092
Multifunction Receiver System rationale, concepts, background requirements and technical justifications for tracking, telemetry and ranging data acquisition by Goddard Center
c07 A69-19101
Double sideband suppressed carrier FM telemetry system as airborne data recorder, discussing noise, environmental conditions, laboratory and flight tests
c07 A69-19132
FM/AM telemetry circuits with three axis piezoelectric accelerometer for measurements during impact tests of soft landing models
c07 A69-23279
Space electronics, telemetry, antennas, computers - IEEE Conference, Cocoa Beach, Florida, November 1968
c07 A69-25288
Single channel pressure telemetry unit for chronic implantation into cardiac chambers or major blood vessels in unrestrained animals for measuring ventricular pressure
c05 A69-25642
Optical carrier single channel telemetry system providing complete electrical isolation between shock tube data acquisition and data recording instrumentation
c14 A69-29561
Tracking and data acquisition systems for spacecraft and ground link through command,

telemetry and tracking, noting data relay satellites, etc
c07 A69-33371
Telemetering - IEEE Conference, Washington, D.C., April 1969
c07 A69-36237
Backfire antenna radiation characteristics and physical dimensions for tracking and telemetry applications, including five element array model
c07 A69-36251
Telemetry data processing, describing designation, tasks and possibilities of data reduction laboratory attached to NASA Goddard Space Flight Center
c11 A69-40352
Telemetering - Conference, Washington, D.C., September 1969
c07 A69-41734
Programmable data handling and telemetry systems for scientific satellites, noting system checkout, spacecraft integration, software and ground data processing
c08 A69-41735
Digital telemetry link coding as English language analogy, developing block code scheme combining bit, word and block error detection and correction methods
c07 A69-41745
Telemetry data from image-motion compensation sensor on Lunar Orbiter 1 spacecraft for determining radius of moon
[NASA-TN-D-5231] c30 N69-29115

TELEVISION CAMERAS
Rocket trajectory determination by tracking onboard light source against star background with image orthicon TV system
c07 A69-26965
Image dissector meteorological cameras, discussing ATS-3 and Nimbus systems, high resolution camera and multispectral cameras
c14 A69-35101
Visual simulation image generation using flying spot scanner
[NASA-TN-D-5151] c11 N69-23194

TELEVISION TRANSMISSION
Optimizing spacecraft televisions for successive picture overlapping and maximum surface resolution during planetary descent
[NASA-TN-D-5061] c14 N69-17259
Requirement estimates and performance predictions for Martian television experiment onboard spacecraft in three point-mass descent trajectories
[NASA-TN-D-5062] c14 N69-17944

TELLURIDES
Thermal stability and friction of disulfides, diselenides, and ditellurides of molybdenum and tungsten in ultrahigh vacuum
[NASA-TN-D-5141] c15 N69-22992

TEMPERATURE CONTROL
Electron emitter cooling and plasma heating of thermionic converters noting effects of plasma density, diode spacing, etc
c03 A69-13127
Explorer 40 satellite mathematical model and verification testing for close spacecraft flight temperature predictions
[SAE PAPER 690202] c33 A69-18305
High power TWT tube cooling in space vehicle, discussing thermal control system based on heat pipe radiator
c09 A69-24747
UV irradiation effects on ZnO spacecraft thermal control coating pigments, discussing photo-Hall, luminescence and electron paramagnetic resonance measurements
[AIAA PAPER 69-639] c18 A69-33288
Second surface mirror used as coating for spacecraft thermal control
c33 A69-37290
Computer optimization of spacecraft optical coatings for temperature control, using finite element analysis and matrix inversion
[AIAA PAPER 69-979] c33 A69-40359
Thermal control coatings, windows and mirrors for 1973 Mars Viking Lander vehicles under simulated Martian surface conditions
[AIAA PAPER 69-1023] c11 A69-40393
Aluminized plastic covers to reduce radiator sink temperatures on lunar surface
[NASA-TM-X-1729] c03 N69-17225
Evaluation of double wall balloon enclosure for thermal control of inertial satellites
[NASA-TN-D-5230] c33 N69-28209
Heat pipe devices for space suit temperature control
[NASA-CR-1400] c05 N69-38491

TEMPERATURE DISTRIBUTION
Scaled solar and gray-body temperature distribution models compared to determine stellar atmosphere
c30 A69-14626
Electron, ion and neutral particle temperatures of upper atmosphere
c13 A69-14975
Atmospheric models for exospheric temperatures of Mars and Venus based on photoionization heating efficiency
c30 A69-26020
Periodicity of magnetothermal oscillations in pressure annealed pyrolytic graphite compared with hole carriers
c26 A69-29005
Dynamical effects in structure of H II equilibrium region left behind expanding ionization front, showing temperature as function of distance from star
c30 A69-35966
Instantaneous frozen layer thickness and temperature profile in solidified layer obtained by iteration technique
c33 A69-39433
Heat finite propagation velocity effects on temperature distribution and heat flux for step temperature change at semiinfinite body surface
[ASME PAPER 69-HT-1] c33 A69-43564
Simple equations for temperature distributions in radiating gray gases
[NASA-TN-D-5226] c33 N69-25312
Transient temperature fields in porous shell walls cooled by forced flow
[NASA-TT-F-552] c33 N69-30245

TEMPERATURE EFFECTS
Temperature dependent isomer shift and anharmonic binding of Sn 119 in niobium stannide, measuring Mossbauer recoil free fraction
c26 A69-10009
Pressure and temperature dependence of slow crack growth in hardened steel in gaseous hydrogen environment
c17 A69-10612
Ball bearing test apparatus for evaluation of greases and solid lubricants at high temperatures
[ASLE PREPRINT 68AM 7C-2] c15 A69-10912
Organic dye laser frequency variation with temperature, noting absorption and fluorescence spectra
c16 A69-12617
Rhenium Nb cylindrical thermionic converter, measuring efficiency and power density in emitter temperature range 1600-2050 K and collector temperature range 873-1173 K
c03 A69-16359
Electron radiation damage in MOSFET devices using bias temperature treatments
c26 A69-16877
Venus atmosphere origin, discussing high temperature effects and chemical composition via space probe and terrestrial observations
c30 A69-23183
Reaction rate constants of ion-molecule interchange reaction as function of temperature, flow velocity, activation energy and constant part of steric factor P
c06 A69-32312
Al interconnections discontinuities at integrated circuit contact windows observed by scanning electron microscope, noting catastrophic failure and Si presence
c09 A69-32893
Creep rate-stress-temperature relations for powder metallurgy rhenium, discussing activation energy
c17 A69-34186
Temperature and pressure effect on cobalt base alloy cavitation in liquid sodium, using vibratory apparatus and loss rate contour

diagram
c17 A69-35184
Mechanical properties associated with 55-Nitinol memory effect, presenting stress-strain and electrical resistivity as function of temperature
c17 A69-35523
Unfilled Pyrrone prepared from powder into molded parts for flexural tests at elevated temperatures observed for stability to electron irradiation in air
c18 A69-35529
Ablative materials thermal protection characteristics at low heating rates evaluated by convective heating tests, stressing polyurethane foam composite
c18 A69-35536
Dilute solution of He 3 in He 4 near absolute zero measured for viscosity, showing temperature effect
c23 A69-39582
Pressure measurements and gas flow analysis during thermal vacuum tests of manned spacecraft indicating adequate space vacuum simulation
[AIAA PAPER 69-1033] c11 A69-40401
Flow analysis to determine turbine efficiency as function of inlet temperature for two stage turbine
[NASA-TM-X-1728] c01 N69-17392
Compatibility tests of molten uranium with tungsten and tungsten-1.5 percent hafnium
[NASA-TN-D-5076] c17 N69-19930
Measurement of radiative thermal conduction of ideal powder as function of temperature
[NASA-TN-D-5063] c33 N69-20008
Effects of temperature and electrolyte concentration on performance of fuel cell
[NASA-TN-D-5154] c03 N69-22940
Effect of temperature and pressure on cavitation damage to cobalt base alloy in sodium
[NASA-TN-D-5273] c17 N69-28863
Load and temperature effects on fatigue strength of notched titanium alloy sheet for supersonic transport operation
[NASA-TN-D-5294] c32 N69-29607
Fluid temperature effect on cavitation performance of axial flow pump
[NASA-TN-D-5318] c15 N69-30069
Hydrogen gas pressure requirements during pressurization and transfer of liquid hydrogen from spherical tanks
[NASA-TN-D-5387] c28 N69-33211
Large thin film cadmium sulfide solar cell electrical characteristics over ranging temperatures and radiant intensities
[NASA-TM-X-1899] c03 N69-38767
Influence of thermal distortion of booms on attitude of gravity stabilized satellites
[NASA-TN-D-5435] c31 N69-40781

TEMPERATURE GRADIENTS
Lower solar corona composition changes due to pressure and thermal gradients calculated with multicomponent diffusion equations
c30 A69-33059
Thermal outgassing tests on epoxy impregnated magnet coil
[NASA-TM-X-1813] c18 N69-28203
Surface tension, viscosity, and density of fluorocarbon solvents as function of temperature
[NASA-TM-X-1862] c18 N69-34134

TEMPERATURE INVERSIONS
Photospheric radiation field role in temperature inversion of stellar chromospheres with dominant H ion opacity, postulating mechanical energy dissipation
c30 A69-38173

TEMPERATURE MEASUREMENT
Radiation compensating thermocouple for gas temperature measurement, noting advantage over single thermocouples
c14 A69-14916
Midlatitude neutral thermosphere density and temperature measurements, noting effect of atomic oxygen adsorption by instruments
c13 A69-16268
Ion temperature diurnal variations at 250-475 km obtained from Thomson scatter spectra
c13 A69-16407
Pressure and temperature surveys of Mach 27-47 nozzle boundary layer at Ames M-50 He tunnel, determining velocity profiles, wall friction coefficient, etc
[AIAA PAPER 69-686] c12 A69-33441
Thermal calculations of objects near lunar surface, considering IR emission directivity effects
c30 A69-43254
Radiation equilibrium temperature measured downstream of transpiration cooled gas flow near slender cone vertex in continuous flow hypersonic tunnel
c01 A69-43588
Electron beam technique of measuring molecular rotational and vibrational temperatures of nitrogen in hypersonic tunnel using air as test gas
[NASA-TN-D-4892] c33 N69-10932
Error analysis of input noise temperature measurements of low noise amplifiers
[NASA-TN-D-4997] c07 N69-16162
Surface temperature mapping with infrared photographic pyrometry for turbine cooling investigations
[NASA-TN-D-5179] c14 N69-23895
Turbulent boundary layer temperature and velocity measurements in supersonic water-cooled conical nozzle
[NASA-TN-D-5377] c12 N69-33353

TEMPERATURE MEASURING INSTRUMENTS
Telemetry technique utilizing thermocouple sensors for base heating determinations on free flight blunt cone in shock tunnels, noting electrical noise reduction
[AIAA PAPER 68-407] c14 A69-15514
Fluidic type temperature sensor for total temperature measurement for hypersonic aircraft in atmosphere
c14 A69-16755

TEMPERATURE PROBES
Thermodielectric radiometer for transient radiant flux short duration pulse measurement, using thermally induced depolarization of polymer film dielectric
[AIAA PAPER 68-403] c14 A69-12392

TEMPERATURE PROFILES
Combined radiation and conduction heat transfer equation applied to temperature profile around opaque hollow sphere and in solid condensed gas layer
[SAE PAPER 690197] c33 A69-18303
Sealed and unsealed relay coils temperature rise at simulated outer space air pressure levels
c09 A69-28048
Nonlinear least squares optimization program applied to atmospheric temperature sounding, solving for temperatures at various altitudes from simulated carbon dioxide intensity measurements
c13 A69-33156
Temperature profiles and associated wind profiles obtained with Jimsphere/FPS-16 radar system at Cape Kennedy, discussing remote CAT detector assessment
c20 A69-33739
Thermosphere temperature shape parameters from probe flights, showing dependence on hour angle
c13 A69-38088
Comparisons of wind and temperature data obtained by Japanese MT-135 and American ARCAS meteorological rocket systems in closely spaced launchings
[NASA-TM-X-1726] c20 N69-17772

TEMPERATURE SENSORS
Fluidic type temperature sensor for total temperature measurement for hypersonic aircraft in atmosphere
c14 A69-16755
Error analysis of high resolution balloon-borne temperature sensor and comparison of temperature data with simultaneous rawinsonde measurements
c14 A69-21642
Spacecraft solar cell near-maximum power operation by tracking optimum value with array temperature sensor
c03 A69-42303

TENSILE PROPERTIES
Polymer films tensile properties after exposure to

gamma radiation in vacuum, noting chain scission and cross linking
[ASME PAPER 68-WA/RP-6] c18 A69-16160
Strain-rate sensitivity of three titanium-alloy sheet materials after prolonged exposure to high temperature
[NASA-TN-D-4981] c17 N69-14873
Tensile properties and creep strength of aluminum alloys
[NASA-TN-D-5010] c17 N69-19203
Tensile and cyclic fatigue properties of graphite filament-wound pressure vessels at ambient and cryogenic temperatures
[NASA-TN-D-5354] c32 N69-31300
Salt stress corrosion cracking effects on tensile and stress rupture properties of titanium alloy sheet
[NASA-TN-D-5417] c17 N69-36221
Effects of reactor irradiation at cryogenic temperatures on tensile properties of titanium and titanium-base alloys
[NASA-TN-D-5442] c17 N69-37436

TENSILE STRENGTH
Failure criteria for predicting filamentary composite strength under uniaxial and combined stresses from properties and fabrication process considerations
c32 A69-21479
Graphite fiber NOL rings and biaxial wound pressurized cylinders tested at ambient and cryogenic temperatures for tensile and cyclic fatigue properties
c18 A69-35521
Size effect on tensile strength of polycrystalline nickel wires
[NASA-TN-D-4884] c17 N69-10226
Physical properties of near stoichiometric nickel-titanium alloy Nitinol and some structural-mechanical applications employing these properties
[NASA-CR-1232] c17 N69-11420
Theory and test results of tensile strength of epoxy rings and belts reinforced by boron filaments
[NASA-TN-D-5053] c18 N69-19918
Stress rupture and tensile properties of refractory metal wires at 2000 and 2200 deg F
[NASA-TN-D-5139] c32 N69-22823

TENSILE STRESS
Displacements and stress intensity as function of crack length for compact tension specimen, considering load line and crack edge
c15 A69-21392
Tensile properties and creep strength of aluminum alloys
[NASA-TN-D-5010] c17 N69-19203

TENSILE TESTS
Dynamic strain aging during creep and tensile tests of molybdenum-titanium-carbon alloys
[NASA-TN-D-5169] c17 N69-22993

TENSOR ANALYSIS
Suboptimal estimator to Kalman filter containing scalar weighting factors
[NASA-TN-D-5082] c10 N69-21123

TERMINAL BALLISTICS
Aluminum double sheet target penetration resistance determined by studying high velocity pyrex glass impact effects on front/rear sheets and spacing
[AIAA PAPER 69-375] c32 A69-28305
Pegasus and Explorer 23 detector panels calibrated by determining particle perforation mass and velocity
[NASA-TR-R-321] c14 N69-36985

TERMINAL FACILITIES
Remote information retrieval facility description
[NASA-CR-1318] c08 N69-23381

TERMINAL GUIDANCE
Manual procedures for midcourse and terminal guidance, discussing onboard optical measurements and calculations
c21 A69-35792

TERMINAL VELOCITY
Entry and terminal deceleration systems for unmanned Martian landers, discussing parachute landing and lifting entry vehicles
[AIAA PAPER 68-1147] c31 A69-13670

TERRAIN ANALYSIS
Gemini program for geologic orbital photography, discussing equipment used
c13 A69-35274

TEST CHAMBERS
Hydraulic-powered self propelled six degree of freedom loading vehicle moving tests assembly to test chamber with high accuracy positioning
c11 A69-38181

TEST EQUIPMENT
Ball bearing test apparatus for evaluation of greases and solid lubricants at high temperatures
[ASLE PREPRINT 68AM 7C-2] c15 A69-10912
EEG monitor helmet for aircraft or flight simulator programs, discussing sensing and transmitting system
c05 A69-26553
Hydraulic-powered self propelled six degree of freedom loading vehicle moving tests assembly to test chamber with high accuracy positioning
c11 A69-38181

TEST FACILITIES
NASA Plum Brook Reactor Facility /PBRF/ for determining radiation tolerance to support nuclear power application in space for propulsion and power
c22 A69-13128
Heating facility for testing ablative heat shield material models in combined convective and radiative heating environment with constant or transient heating conditions
[AIAA PAPER 69-342] c11 A69-28278
On-line central data processing system connected to time shared computer for recording data from test facilities, discussing hardware configuration, software considerations and advantages
c08 A69-33106
Telemetry data processing, describing designation, tasks and possibilities of data reduction laboratory attached to NASA Goddard Space Flight Center
c11 A69-40352
Vacuum integrating sphere for measuring solar absorptance in space environment to determine thermal control coatings qualifications
[AIAA PAPER 69-1021] c11 A69-40392
Concepts of acceptance testing lunar and planetary vehicles
[NASA-TN-D-4924] c11 N69-14507
High enthalpy arc tunnel at Langley Research Center for simulating aerodynamic heating and forces during spacecraft reentry
[NASA-TN-D-5295] c11 N69-29981

TEST FIRING
Development and test firing of improved igniter for first stage retrorockets of Atlas Centaur launch vehicle
[NASA-TM-X-1676] c28 N69-13275
Rocket engine evaluation of erosion and char as functions of fabric orientation for silica reinforced nozzle materials
[NASA-TM-X-1721] c28 N69-15475

TEST STANDS
Test facilities and techniques for low speed flight problems of aircraft handling qualities, stability, control and performance
c11 A69-15575

TEST VEHICLES
Monte Carlo method for estimating costs and optimal testing of Explorer size spacecraft
[NASA-TN-D-5283] c34 N69-31333

TETHERED BALLOONS
Aerostatic and aerodynamic characteristics of Dart Vee tethered balloon system
c02 A69-40813

TETRODES
Four terminal silicon planar p-n-p-n model operating as semiconductor small signal linear tetrode amplifier, discussing properties and mathematical models
c09 A69-35293

TEXTBOOKS
Theory and practice of aircraft navigation - textbook
[NASA-TT-F-524] c21 N69-17788

THEOREM PROVING
Shape preserving expansion and contraction of objects in E 3
[NASA-TN-D-5240] c19 N69-31303

THEORIES
Flutter investigation at Mach 3 of rotationally restrained panels and comparison with theory
[NASA-TN-D-5508] c32 N69-40087
Modern network theory applications to analysis of complex systems
[NASA-TN-D-5511] c19 N69-40088

THERMAL ABSORPTION
Solar absorptances and spectral reflectances of metals
[NASA-TN-D-5353] c17 N69-31895

THERMAL BOUNDARY LAYER
Inlet thermal boundary layer thickness effect on conical nozzle heat transfer and boundary layer determined by operating nozzle with cooled/uncooled inlet
[AIAA PAPER 69-474] c33 A69-32780

THERMAL CONDUCTIVITY
Subject classification bibliography for thermal contact resistance
[ASME PAPER 68-WA/HT-18] c33 A69-16122
Thermal contact resistance measurement at various ambient pressures compared with theoretical predictions with each parameter analyzed over interface by computer program
[AIAA PAPER 69-629] c33 A69-33299
Viscosity, thermal conductivity and diffusion predicted for dilute nonpolar, polar and mixed gases, discussing methods for rotational relaxation collision numbers and resonant correction
c33 A69-38951
Line source technique for ablative heat shield materials thermal conductivity measurements, comparing vacuum and atmospheric test results
[AIAA PAPER 69-1013] c11 A69-40386
Transient thermal analysis and structural analysis for synthesis of ablating thermostructural panels in planetary entry environment
[NASA-CR-1215] c32 N69-16114
Thermodynamic and transport properties of air, and combustion products of natural gas and air, and jet engine fuel and air
[NASA-TN-D-5452] c33 N69-37936

THERMAL CYCLING TESTS
Thermal cycling tests showing improvement in cadmium sulfide solar cell stability, noting effect of thermal cycling stresses
c03 A69-13074
Crack initiation prediction in high temperature components subjected to arbitrary thermal-mechanical cycling
c32 A69-28252

THERMAL DEGRADATION
Oxygen concentration effects on ester lubricant degradation during high temperature bearing test
[NASA-TN-D-5262] c15 N69-26311

THERMAL DIFFUSIVITY
Thermal and dielectric properties of homogeneous moon based on microwave and infrared temperature observations
[NASA-TM-X-1734] c30 N69-17815

THERMAL EMISSION
Far IR source in galactic center detected at 100 microns, noting thermal emission of interstellar dust grains as possible mechanism
c30 A69-22264
Thermal and free-free emission from planetary nebulae based on graphite grain model, discussing IR fluxes
c30 A69-27158
Microwave thermal emission by water measured from aircraft, studying radiation dependence on surface roughness
c13 A69-34421

THERMAL ENERGY
Microscale fluctuations in interplanetary magnetic field, considering proton thermal energy and magnetic field energy densities
c30 A69-24100

THERMAL ENVIRONMENTS
Saturn fireball thermal environment associated with liquid propellant explosions, using analytical model
c27 A69-14475
Optimal design for improving thermal performance of existing spacecraft thermally actuated louver system by increasing open-to-closed emittance ratio
[AIAA PAPER 69-627] c33 A69-33269
Orbiting Astronomical Observatory thermal test and evaluation program, discussing equipment and role in experimental design
[AIAA PAPER 69-995] c11 A69-40373
Disk radiometer for use in space vacuum-thermal environmental studies
[NASA-TN-D-4925] c14 N69-13311
Ablation behavior of heat shield of Apollo command module over wide range of thermal environments
[NASA-TM-X-1778] c33 N69-22933
Initial radio frequency gas heating experiments to simulate thermal environment in nuclear light bulb reactor
[NASA-CR-1311] c22 N69-23450
Thermal, acoustical, and acceleration environments of XB-70 airplane crew compartment in airworthiness tests
[NASA-TN-D-5449] c25 N69-38010

THERMAL EXPANSION
Zero thermal expansion composites of high strength and stiffness
[NASA-CR-1324] c32 N69-24876

THERMAL FATIGUE
Crack initiation prediction in high temperature components subjected to arbitrary thermal-mechanical cycling
c32 A69-28252
Oxidation resistance and thermal fatigue cracking of nickel and cobalt base alloys in transonic gas streams
[NASA-TN-D-5376] c17 N69-33307

THERMAL INSTABILITY
Electrothermal instabilities for explanation of MPD arc thrustor rotating spoke phenomenon, noting agreement with experimental results
[AIAA PAPER 69-231] c28 A69-21254
Pressure and velocity coupling effects on combustion stability in solid propellant burning
[NASA-TN-D-5395] c33 N69-34892

THERMAL INSULATION
Lightweight polyurethane insulation for liquid hydrogen tanks of space vehicles
[NASA-TN-D-5114] c18 N69-20790

THERMAL NEUTRONS
Thermal neutron flux perturbations in cylinders in test reactors, using regression analysis to obtain polynomials for flux perturbation, depression, self shielding factors, etc
c22 A69-38274
Thermal neutron capture cross section at high temperature irradiations determined for W 184, describing radiochemical separation and flux counting techniques
c14 A69-43192
Prediction of thermal neutron flux perturbation effects in cylinders during irradiation tests
[NASA-TN-D-4949] c22 N69-14481

THERMAL NOISE
Error analysis of input noise temperature measurements of low noise amplifiers
[NASA-TN-D-4997] c07 N69-16162

THERMAL PLASMAS
Wave fields and coupling of RF power to ion cyclotron waves in finite length thermal collisional plasma column
c25 A69-13114
Earth thermal plasmasphere contraction subsequent to solar flare obtained from ion mass spectrometers on OGO satellites
c13 A69-23777
Suprathermal electron flux in lower latitudes and polar region analyzed from measurements by retarding potential analyzers on Explorer 31 satellite
c29 A69-37880

THERMAL PROTECTION
Apollo thermal protection system, noting low density ablation, flight and ground tests
[AIAA PAPER 68-1142] c31 A69-13558
Entry corridor thermal entry limits for Apollo spacecraft defined for design of thermal protection system
[AIAA PAPER 68-1144] c31 A69-13673
Collection of papers on thermal design principles of spacecraft and entry bodies
c33 A69-34372
Ablative materials thermal protection characteristics at low heating rates evaluated

by convective heating tests, stressing polyurethane foam composite
c18 A69-35536
Polyurethane foam composites for low heating rate thermal protection, noting astroquartz fiber additive effect on performance
c18 A69-39236
IR directional and hemispherical emittance of spacecraft thermal control coatings, comparing values determined by various measurement techniques
c14 A69-41633
Shadow shields for thermal protection of cryogenic tanks in space
[NASA-TN-D-4887] c33 N69-10420
Thermal analysis of shadow shields and structural members in space environment
[NASA-TN-D-4876] c33 N69-10473

THERMAL RADIATION
Solar absorptance, total hemispherical emittance and absorptance/emittance ratio for metals at cryogenic temperatures measured simultaneously with sinusoidally perturbed incident radiation
c33 A69-10847
Solar absorptance and hemispherical emmitance of metals at space conditions determined with cyclic incident radiation technique
[AIAA PAPER 69-60] c17 A69-18154
Gamma heating rate measured by aqueous dosimeter converted to rate in thin tungsten detector in water shield through transport theory calculations, obtaining correction factors
c22 A69-18825
Iron line absence in emission spectrum of thermal X ray sources, constraining proposed thermal models
c29 A69-22231
Microwave thermal emission by water measured from aircraft, studying radiation dependence on surface roughness
c13 A69-34421
Lunar surface thermal radiation incident on unit area flat surface located at variable distance and orientation above moon, considering diffusion effects
c30 A69-38973
Computer program for computation of thermal radiation heat loads and temperatures of spacecraft orbiting planets or moon
[NASA-TR-R-278] c30 N69-14428
Thermal radiation exchange between surfaces and enclosures
[NASA-SP-164-VOL-2] c33 N69-30317
Tabular and graphical data on thermal radiative properties for dissemination
[NASA-CR-1431] c33 N69-40455

THERMAL RESISTANCE
Subject classification bibliography for thermal contact resistance
[ASME PAPER 68-WA/HT-18] c33 A69-16122

THERMAL SHOCK
Boron nitride and boron nitride composite under high temperatures in air and vacuum for various time periods, discussing thermal shock and oxidation resistance
c18 A69-36208
Restart and high response terminal shock control for axisymmetric mixed-compression inlet with internal contraction
[NASA-TM-X-1792] c28 N69-24938
Thermal shock cycling of Kapton, copper, and molybdenum thin film cadmium sulfide solar cell
[NASA-TM-X-1819] c03 N69-29555

THERMAL SIMULATION
Handbook of solar simulation for thermal vacuum testing, discussing space environment, thermal control coatings, radiation sources, optical components, etc
c11 A69-38894

THERMAL STABILITY
Second breakdown and other thermal instabilities analyzed by heat flow equation, obtaining stability criteria predicting reduced power dissipation for transistor at low currents
c09 A69-31618
Electron temperature instabilities in entrance region of magnetohydrodynamic generator
[NASA-TM-X-1761] c25 N69-20875
Thermal stability and friction of disulfides, diselenides, and ditellurides of molybdenum and tungsten in ultrahigh vacuum
[NASA-TN-D-5141] c15 N69-22992
Cyclic heating and thermal shock effects on hafnia stabilized with calcia, magnesia, and yttria
[NASA-TN-D-5279] c18 N69-34547

THERMAL STRESSES
Directional solar thermal field /sunlight/ effect on coupled nonplanar transverse and torsional vibrations of satellite cylindrical antennas in orbit
c32 A69-25534
Creep rupture data for predicting thermal fatigue cracking of turbine blades or disks
[NASA-TN-D-5489] c32 N69-39393
Influence of thermal distortion of booms on attitude of gravity stabilized satellites
[NASA-TN-D-5435] c31 N69-40781

THERMAL VACUUM TESTS
Thermal Vacuum /TV/ manned test operations related to Apollo lunar module in simulated space environment
c05 A69-30394
Manned testing of EVA equipment in thermal-vacuum environment for qualification of Apollo extravehicular mobility unit, using lunar surface thermal simulator
[AIAA PAPER 69-992] c05 A69-40370
Line source technique for ablative heat shield materials thermal conductivity measurements, comparing vacuum and atmospheric test results
[AIAA PAPER 69-1013] c11 A69-40386
Pressure measurements and gas flow analysis during thermal vacuum tests of manned spacecraft indicating adequate space vacuum simulation
[AIAA PAPER 69-1033] c11 A69-40401

THERMIONIC CATHODES
Physical model for behavior of thermionic arc spots on MHD generator cathode
[NASA-TN-D-5414] c25 N69-35732

THERMIONIC CONVERTERS
Kinetic theory model of plasma sheath transition, analyzing sheath structure in unignited mode of thermionic converter
c03 A69-13125
Rhenium-niobium cylindrical thermionic converters with mechanically polished or electroetched emitters, comparing performance
c03 A69-13126
Electron emitter cooling and plasma heating of thermionic converters noting effects of plasma density, diode spacing, etc
c03 A69-13127
Rhenium Nb cylindrical thermionic converter, measuring efficiency and power density in emitter temperature range 1600-2050 K and collector temperature range 873-1173 K
c03 A69-16359
Thermionic conversion - Conference, Framingham, Mass., October 1968
c03 A69-21806
Thermionic converters with chloride and fluoride vapor deposited tungsten emitters, comparing performance characteristics and stability
c03 A69-21819
Isothermal diode as study basis for internal complex controlling thermionic energy conversion
c03 A69-21827
Kinetic theory model of plasma sheath transition applied to sheath structure in unignited mode of thermionic converter
c03 A69-21828
Gas breakdown model for analyzing breakdown of Ce vapor filled crack in thermionic trilayer insulator
c03 A69-21840
Calorimetric, optical, and vibration investigation of stretch-formed aluminum solar concentrators for thermionic converters
[NASA-TN-D-4889] c03 N69-10708
Nuclear thermionic space power system using rod control and heat pipes
[NASA-TN-D-5250] c22 N69-26270

THERMIONIC DIODES
Nuclear reactor space power system concept using thermionic diodes, heat pipes and rod control, emphasizing neutronic aspects and feasibility
c22 A69-14799

Heat transfer and neutronic calculations after fuel emitter separation in uranium oxide fueled thermionic diodes
[NASA-TM-X-1812] c22 N69-28212

THERMIONIC EMITTERS
Thermionic converters with chloride and fluoride vapor deposited tungsten emitters, comparing performance characteristics and stability
c03 A69-21819

THERMIONIC POWER GENERATION
Rhenium Nb cylindrical thermionic converter, measuring efficiency and power density in emitter temperature range 1600-2050 K and collector temperature range 873-1173 K
c03 A69-16359
Thermionic converter with chloride vapor deposited tungsten emitter and nickel collector
[NASA-CR-1416] c03 N69-32553

THERMISTORS
Theoretical comparison of beads, wires, and films as rocketsonde temperature sensors in mesosphere
[NASA-CR-1286] c13 N69-18126

THERMOCHEMICAL PROPERTIES
Time of heating effect on thermal polymerization of L-lysine free base
c06 A69-28439

THERMOCOUPLE PYROMETERS
Radiation compensating thermocouple for gas temperature measurement, noting advantage over single thermocouples
c14 A69-14916

THERMOCOUPLES
Thermal electromotive force change for thermocouples in high temperature, low pressure environments for 3700 hours
[NASA-TN-D-5287] c14 N69-29196
Quartz-insulated, single-wire thermocouples installed on thin-wall rocket cooling tubes to measure hot-gas-side wall temperatures
[NASA-TN-D-5291] c14 N69-29553

THERMODYNAMIC CYCLES
Steam cycle analysis for nuclear powered turbofan engine
[NASA-TM-X-1907] c22 N69-40060

THERMODYNAMIC EFFICIENCY
Rhenium Nb cylindrical thermionic converter, measuring efficiency and power density in emitter temperature range 1600-2050 K and collector temperature range 873-1173 K
c03 A69-16359

THERMODYNAMIC EQUILIBRIUM
Light ion abundance measurements of OGO satellites and field aligned diffusive equilibrium theory with temperature and concentration latitudinal variations
c13 A69-25157
Dynamical effects in structure of H II equilibrium region left behind expanding ionization front, showing temperature as function of distance from star
c30 A69-35966

THERMODYNAMIC PROPERTIES
Complex chemical equilibrium calculation, analyzing thermodynamic principles and solution to nonlinear equations
c06 A69-10588
In situ vacuum testing requirement for valid measurement of vacuum induced changes in mechanical and thermal properties of various filled elastomers
c11 A69-22008
Anisotropic Heisenberg antiferromagnetism in spin wave approximation, calculating thermodynamic quantities in terms of elliptic integrals
c26 A69-26500
Remote sensing cross-beam cross correlation methods of determining spatially resolved average thermodynamic properties
[AIAA PAPER 67-149] c14 A69-31868
Thomas-Fermi approximation applied to calculation of equations of state and thermodynamic functions at high pressure from differential equations of statistical atom model
c24 A69-40186
Prediction of thermodynamic effects of developed cavitation based on liquid hydrogen and Freon-114 data in scaled venturis
[NASA-TN-D-4899] c12 N69-10070
NASA development work on high efficiency batteries for space electric power systems
[NASA-SP-172] c03 N69-18042
Test performance of radial inflow turbine for Brayton cycle space power system
[NASA-TN-D-5090] c03 N69-20937
Investigation of SA-501 S-4B auxiliary propulsion system anomalies
[NASA-TN-D-5207] c28 N69-26224
Thermodynamic properties of liquid and gas phase equilibria of water plus heavy water
[NASA-TN-D-5223] c33 N69-26247
Computerized simulation of low frequency dynamics of liquid hydrogen flow in nuclear rocket engine
[NASA-TN-D-5312] c22 N69-30070
Rapid computation of equilibrium, chemical composition, and thermodynamic properties of argon-oxygen-hydrogen gas system
[NASA-TN-D-5416] c33 N69-36299
Magnetothermal oscillations in pressure annealed pyrolytic graphite
[NASA-TN-D-5488] c26 N69-39239

THERMODYNAMICS
Transformation laws for thermodynamic quantities confirming conventional formulation by mechanical model of heat
c23 A69-11288
Thermodynamic approach to equation of state of magnetized Fermi gas, deriving energy eigenvalues of free electron in magnetic field
c30 A69-25107
Aerodynamic and thermodynamic calibration of nonequilibrium air flow in Ames 1-foot shock tunnel
[NASA-TN-D-4985] c11 N69-15633
High pressure compressible flow systems in space vehicle ground support equipment
[NASA-SP-3045] c12 N69-26987
High temperature properties of gases - gas dynamics, thermodynamics, and combustion physics
[NASA-TT-F-558] c12 N69-35365

THERMOELASTICITY
Anomalous spacecraft OGO-D motion explained by open section boom thermally induced oscillations, discussing corrective measures
c32 A69-18331
Thermal flutter analysis of booms with open cross section
[NASA-TN-D-5222] c32 N69-29589

THERMOELECTRIC GENERATORS
Planar radioisotope thermoelectric generator system for NASA deep space missions and integrated spacecraft power supply
c03 A69-42254

THERMOELECTRIC POWER GENERATION
Nernst-Ettingshausen, thermoelectric power, thermal transverse-even, magnetoresistance, and Hall coefficients in white tin in 3.3 tesla field and cryogenic temperatures
[NASA-TN-D-5227] c26 N69-25412

THERMONUCLEAR POWER GENERATION
Comparison of Brayton and Rankine cycle magnetogasdynamic space power generation systems for use with nuclear heat source
[NASA-TN-D-5085] c03 N69-20852

THERMONUCLEAR REACTIONS
Primordial helium and horizontal branch star luminosity, obtaining luminosities in He burning phase for different He and metal abundances from models
c30 A69-22211

THERMOPHYSICAL PROPERTIES
Mars atmospheric features from measurements during entry and after landing, discussing atmospheric state properties, diurnal variability, clouds and winds
c30 A69-41617

THERMOSETTING RESINS
Synthesis of Pyrrone laminates from sulfone dianhydride
[NASA-CR-1404] c30 N69-31960

THERMOSPHERE
Atmospheric density variation measurements by density gages on Explorer 32 satellite confirm wave propagation in neutral thermosphere as free internal gravity waves
c13 A69-16261
Electron cooling rates in midlatitude and auroral zone thermosphere measured by probe rockets

c13 A69-16267
Midlatitude neutral thermosphere density and temperature measurements, noting effect of atomic oxygen adsorption by instruments
c13 A69-16268
Full wave calculation of gravity waves for thermospheric model, describing wave type reflection, transmission, conversion and coupling by scattering matrix elements
c13 A69-25150
Characteristic plane harmonic free internal neutral atmospheric wave oblique propagation through horizontally stratified quiet atmosphere for various thermospheric parameters
c13 A69-26101
Thermosphere temperature shape parameters from probe flights, showing dependence on hour angle
c13 A69-38088
Explorer 32 atmospheric density measurements revealing neutral thermosphere latitudinal variations during geomagnetically undisturbed times
c13 A69-38100
Diurnal and solar cycle variations of thermosphere density and temperature generated by solar EUV input and tidal wave, using two dimensional model
c29 A69-43003

THETA PINCH
Magnetic field nonuniformity and its effect on stability of theta pinch plasma
[NASA-TR-R-303] c25 N69-20997

THICK WALLS
Analytic model resembling thick walled ellipsoid of revolution incorporating three dimensional shape of human left ventricle and ventricular wall thickness effects
c05 A69-26235
Aerodynamic heat flux determined within thermally thick walls for case of rapidly rising heat rates
[NASA-TN-D-5309] c33 N69-30726
Ramp pressurization tests with gaseous helium in thick walled liquid hydrogen tank
[NASA-TM-X-1870] c28 N69-35712
Discharge nozzle coefficients for thick plate orifices with approach flow perpendicular and inclined to orifice axis
[NASA-TN-D-5467] c12 N69-38012

THICKNESS
Optimum thickness of dynamically stable composite superconducting tapes determined for substrate thickness as function of current density
c26 A69-43121

THIN FILMS
Cryogenic flexibility of thin polymeric film plies for use as spacecraft positive expulsion bladders
c15 A69-16486
Film processing effects on cryogenic mechanical properties of polyethylene terephthalate
c18 A69-16490
X ray fluorescence and electron microprobe for determining thin film thickness
c09 A69-19582
Cubic /beta/ silicon carbide films deposition by volatilization in presence of acetylene
c26 A69-21350
Energetics in solid film lubricants vacuum deposition methods, showing dependence on interfacial and film characteristics
c15 A69-29001
Transformer for unilateral energy transfer using single domain uniaxial Permalloy film
c09 A69-39454
Solid film lubricants deposited by DC triode sputtering on Ni, Ni-Cr and Nb surfaces friction tested under ultrahigh vacuum conditions
c15 A69-43126
Thin film formation, deposition methods and relation to film structure and properties
c26 A69-43344
Resonance absorption integrals for rhenium 185, rhenium 187, and natural rhenium in foils and thin films
[NASA-TN-D-4938] c24 N69-13152
Effects of preparation techniques on thin film CdS solar cells
[NASA-TM-X-1722] c03 N69-15397
Thin film microwave irises with capacitive reactance
[NASA-CR-1364] c26 N69-28096
Thermal shock cycling of Kapton, copper, and molybdenum thin film cadmium sulfide solar cell
[NASA-TM-X-1819] c03 N69-29555
Friction and contact resistance during sliding in vacuum of low resistivity metals lubricated with sputtered molybdenum disulfide
[NASA-TN-D-5349] c15 N69-31884
Simulated space environmental effects on full and fractional size cadmium sulfide thin film solar cells
[NASA-TM-X-1884] c03 N69-36758
Large thin film cadmium sulfide solar cell electrical characteristics over ranging temperatures and radiant intensities
[NASA-TM-X-1899] c03 N69-38767
Design and structural model of thin film solar cell array
[NASA-TM-X-1913] c03 N69-40787

THIN PLATES
Stiffness matrices analysis of thin flat plates
[NASA-TN-D-4927] c32 N69-14169
Cryogenic fracture properties of thin AISI 301 cold reduced sheet at different angles to rolling direction
[NASA-TN-D-5413] c17 N69-35688

THIN WALLED SHELLS
Recent advances in shell buckling, discussing imperfection sensitivity, boundary conditions and wall configuration
[AIAA PAPER 68-103] c32 A69-12516
Geometrically exact finite element for thin shells of revolution, using approximation to predict boundary layer stress distribution during vibration
[AIAA PAPER 69-56] c32 A69-18193
Finite element method for computing natural frequencies and mode shapes of thin shells of revolution
[NASA-TN-D-4972] c32 N69-16469
Predicting buckling of thin walled, uniform stiffened and unstiffened circular cylindrical shells under static loading
[NASA-SP-8007] c32 N69-23320
Numerical method and computer program for computing deflection response of thin shells
[NASA-CR-1376] c32 N69-29558

THIN WALLS
Buckling of thin walled truncated conical shells under static loads
[NASA-SP-8019] c32 N69-24131
Quartz-insulated, single-wire thermocouples installed on thin-wall rocket cooling tubes to measure hot-gas-side wall temperatures
[NASA-TN-D-5291] c14 N69-29553

THOMAS-FERMI MODEL
Thomas-Fermi approximation applied to calculation of equations of state and thermodynamic functions at high pressure from differential equations of statistical atom model
c24 A69-40186

THORIUM
Interferometrically measured wavelengths tabulated for Th lines in 2747-4572 A range, using liquid nitrogen cooled hollow cathode lamp and Fabry-Perot interferometer
c23 A69-42150

THREE BODY PROBLEM
Numerical analysis of periodic solutions of restricted three body problem in sun-Jupiter system, noting genealogy of periodic orbits
c30 A69-19874
Short term motion of lunar satellite, discussing third body disturbing functions and perturbation solution of nonsingular orbit elements
c30 A69-35934

THREE DIMENSIONAL FLOW
Three dimensional hypersonic steady flow around blunt and pointed cones at nonzero angles of attack calculated by method of characteristics
[AIAA PAPER 69-187] c01 A69-18176
Characteristics method for determining three dimensional supersonic flow around inclined body of revolution
[NASA-TN-D-5341] c12 N69-39177

THREE DIMENSIONAL MOTION
Mathematical models for optimal three dimensional

launch vehicle trajectories with attitude and attitude rate constraints
[NASA-TN-D-5117] c30 N69-20810
Evaluation of six degrees of freedom motion simulator for Bell X-14A aircraft hovering characteristics
[NASA-TN-D-5383] c11 N69-35359
THRESHOLDS (PERCEPTION)
Psychophysical methods for determining perception threshold of angular acceleration in man during vertical rotation
c04 A69-15969
Foveal luminances for chromatic and absolute thresholds for hue identification in case of small targets
c23 A69-19649
Differential thresholds for rotary and linear motion in the periphery
[NASA-CR-1439] c05 N69-36925
THROATS
Throat and nozzle insert design for ablative rocket engine using storable propellants
[NASA-TN-D-4964] c32 N69-33481
THRUST CHAMBERS
Mercury ion thrusters and facilities automatic controls durability testing, discussing vacuum chamber systems, unattended operation and control
[AIAA PAPER 68-576] c11 A69-12385
Discharge chamber plasma processes in electron bombardment ion thrustors, considering factors affecting thrustor performance
[AIAA PAPER 69-494] c28 A69-32735
Characterization of pressure perturbations induced in rocket combustor by machine gun
[NASA-TN-D-5214] c33 N69-24824
Design of injectors and ablative thrust chambers for FLOX propane rocket engine with 1.2 inch throat diameter
[NASA-TN-D-5324] c28 N69-30560
Injector radial distribution and thrust chamber geometry effect on acoustic mode instability in hydrogen oxygen engines
[NASA-TN-D-5375] c33 N69-32340
THRUST CONTROL
Mercury ion thrusters and facilities automatic controls durability testing, discussing vacuum chamber systems, unattended operation and control
[AIAA PAPER 68-576] c11 A69-12385
Wind profile developed for calculation of deflection impulse for rocket with liquid injection thrust vector control
[NASA-TM-X-1708] c31 N69-14033
THRUST PROGRAMMING
Optimal rendezvous and transfers between close elliptical orbits
[NASA-TT-F-554] c30 N69-40592
THRUST VECTOR CONTROL
Flight test evaluation of small one man lunar flying device /POGO/, discussing vehicle control, pressure suit factors and piloting differences
[AIAA PAPER 68-240] c11 A69-12379
Thrust requirements for correcting Keplerian orbits with interplanetary guidance application
[NASA-TN-D-4945] c21 N69-14399
THYRATRONS
Modified structural design of high temperature cesium vapor thyratrons
[NASA-CR-1417] c03 N69-36411
Development and inverter circuit tests of high temperature cesium vapor thyratrons
[NASA-CR-1435] c03 N69-36843
TIDES
Resonant spin and anomalous rotation of Mercury, analyzing influence of tidal degradation and permanent deformation of planet
c30 A69-39568
TILT WING AIRCRAFT
Aerodynamic pressure distribution on semispan tilting wing-propeller combination of V/STOL aircraft
[NASA-TN-D-5481] c01 N69-40876
TIME CONSTANT
Characteristic time on motion of magnetic lines of force in medium with Hall effect
c25 A69-12399
TIME DEPENDENCE
Time dependent emission spectra from flashlamp pumped organic dye lasers recorded with image converter, comparing dyes characteristics
c16 A69-17901
Trapped particles drift velocity in time dependent meridional magnetic and perpendicular electric field
c25 A69-20809
Delta functions spectrum in reciprocal time domain for LC and RC structures due to impulse response in distributed parameters
c10 A69-21327
Time of heating effect on thermal polymerization of L-lysine free base
c06 A69-28439
Time dependent convection electric fields as agents for diffusing trapped magnetospheric radiation inward toward earth, discussing one dimensional diffusion equation
c29 A69-28936
Electron concentration enhancement in upper atmosphere at polar latitudes, noting three independent zones and relation to magnetic local time
c29 A69-28938
Discontinuities in interplanetary magnetic field direction presented on mesoscale from Pioneer 6 observation, emphasizing distribution in time
c30 A69-29970
Coupled kinetic equations for inhomogeneous systems treated as simultaneous equations in time, obtaining solutions by successive approximation
c25 A69-30913
Ground based solar proton monitoring, considering particle intensities and radiation dose rates from riometer absorption as function of time
c29 A69-32321
Computer experiment on 9000 particle plasma to test temporal echo theoretical prediction
c25 A69-38713
TIME DISCRIMINATION
Auditory temporal masking of tonal signal by narrow band noise and perception of temporal order noting effects of intensity, frequency and time
c05 A69-24795
Space flight effects on human time perception
[NASA-TT-F-545] c05 N69-26455
TIME FUNCTIONS
Stability of time varying systems by construction of multipliers with prescribed phase characteristics
c10 A69-16598
Integral transformations used in time variable parameter estimation
[NASA-TN-D-5194] c19 N69-23788
Analytic time function models of stochastic processes of noise and modulation
[NASA-TR-R-314] c07 N69-29230
TIME LAG
Magnetron ionization gauge in helium for low pressure measurement, discussing striking characteristics and time lags
c03 A69-10606
Root mean square time delay error with respect to playback time and autocorrelation function of tape recorded sine wave for studying jitter spectra
c14 A69-18827
Moving striations as plasma oscillations arising from transit time delays of neutral and charged particles moving through ionized gas, using continuity equation
c25 A69-43122
Determination of stability indicative function for linear systems with multiple time delays
[NASA-TR-R-301] c31 N69-17801
TIME MEASUREMENT
Picosecond light pulse measurement by two photon excitation of photographic film
c14 A69-20165
TIME OPTIMAL CONTROL
Stochastic saturating systems optimal control computation, considering attitude control and tracking system design by elliptical differential equation of dynamic programming
c10 A69-30601

Interplanetary midcourse velocity correction schedules optimization, discussing timing equations modifications, mission simulation and role of earth based radar
c21 A69-39646
Computational method for time optimal space rendezvous between rocket vehicle and circular orbit target
[NASA-TN-D-5017] c30 N69-16210

TIME RESPONSE
Detection time to light point source noting response to dark, star field and glare source backgrounds
c05 A69-17215

TIME SHARING
On-line central data processing system connected to time shared computer for recording data from test facilities, discussing hardware configuration, software considerations and advantages
c08 A69-33106
Users manual on FORTRAN 4 COMPUTE program for IBM 360/67 time sharing system
[NASA-TN-D-4917] c08 N69-10098
COMPUTE time sharing calculator program for numerical calculations
[NASA-TN-D-5350] c08 N69-32685

TIN
Temperature dependent isomer shift and anharmonic binding of Sn 119 in niobium stannide, measuring Mossbauer recoil free fraction
c26 A69-10009
Angular correlation of inelastically scattered alpha particles and gamma rays emitted from 2-plus state of Sn 120
c24 A69-13098
Fermi surface topology effects on Nernst-Ettingshausen coefficient from measurements in magnetic fields to 3.3 tesla and 1.2-4.2 K temperatures in metallic tin
c26 A69-16357
Nernst-Ettingshausen, thermoelectric power, thermal transverse-even, magnetoresistance, and Hall coefficients in white tin in 3.3 tesla field and cryogenic temperatures
[NASA-TN-D-5227] c26 N69-25412

TIP DRIVEN ROTORS
Wind tunnel tests of subsonic aerodynamic characteristics of large scale tip turbine cruise fan with 1.075 pressure ratio at angle of attack
[NASA-TN-D-5316] c28 N69-34575

TIP SPEED
Performance data for high tip speed compressor rotor operated with radial and inlet airflow distortions
[NASA-TM-X-1798] c01 N69-26312

TIROS 7 SATELLITE
Tiros 7 monthly maps of infrared radiation over Indian Ocean area
[NASA-TN-D-5101] c13 N69-23318

TITANIUM
Electron microprobe analysis of vanadium in presence of titanium by compositional measurement of chromite in chondritic meteorites
c06 A69-18419
Angular distributions for Sc 45 Ti 46 nuclear reactions involving 41 MeV alpha particles bombardment described by Born approximation
c24 A69-41044

TITANIUM ALLOYS
Mechanical properties associated with 55-Nitinol memory effect, presenting stress-strain and electrical resistivity as function of temperature
c17 A69-35523
Hot salt stress corrosion of Ti alloy, discussing hydrogen generation during elevated temperature exposure and embrittlement as manifestation of strain rate
c17 A69-39434
Physical properties of near stoichiometric nickel-titanium alloy Nitinol and some structural-mechanical applications employing these properties
[NASA-CR-1232] c17 N69-11420
Strain-rate sensitivity of three titanium-alloy sheet materials after prolonged exposure to high temperature
[NASA-TN-D-4981] c17 N69-14873
Hot salt stress corrosion of titanium alloys - generation of hydrogen and its embrittling effect
[NASA-TN-D-5000] c17 N69-16465
Comparison of extraction procedures using 1-nitroso 2-naphthol and dimethylglyoxime for spectrophotometric determination of palladium in titanium alloys
[NASA-TM-X-1767] c06 N69-20801
Dynamic strain aging during creep and tensile tests of molybdenum-titanium-carbon alloys
[NASA-TN-D-5169] c17 N69-22993
Load and temperature effects on fatigue strength of notched titanium alloy sheet for supersonic transport operation
[NASA-TN-D-5294] c32 N69-29607
Outdoor high temperature corrosion tests for aluminum alloys and titanium alloys, and stainless steels
[NASA-TN-D-5362] c17 N69-32558
Influence of fabrication methods on compressive strength of titanium alloy skin stringer panels
[NASA-TN-D-5389] c15 N69-34707
Salt stress corrosion cracking effects on tensile and stress rupture properties of titanium alloy sheet
[NASA-TN-D-5417] c17 N69-36221
Physical, mechanical, and electrical properties of 55-Nitinol - nickel-titanium alloy
[NASA-CR-1433] c17 N69-36367
Effects of reactor irradiation at cryogenic temperatures on tensile properties of titanium and titanium-base alloys
[NASA-TN-D-5442] c17 N69-37436
Hot-salt stress-corrosion of titanium alloy under simulated turbine engine compressor environment
[NASA-TN-D-5510] c17 N69-40242

TITANIUM NITRIDES
Dissociation energy of gaseous titanium nitride
[NASA-TN-D-5027] c06 N69-19129

TOPOLOGY
Fermi surface topology effects on Nernst-Ettingshausen coefficient from measurements in magnetic fields to 3.3 tesla and 1.2-4.2 K temperatures in metallic tin
c26 A69-16357

TOROIDS
Radiation view factors for toroid calculated by digital computer
[NASA-TN-D-5006] c33 N69-23471

TORQUE
Contact conformity effects on spinning torque and friction coefficient in angular contact ball bearings from lubricated and unlubricated tests
[ASME PAPER 68-LUB-10] c15 A69-30901
Gravitational and magnetic torque effect on rotational motion of triaxial rigid body in regressing orbit about oblate primary mass
c30 A69-32240
Elastohydrodynamic solution for ball torque spinning without rolling in nonconforming groove, showing increase in torque with stress and spinning and decreasing conformity
[ASME PAPER 69-LUBS-11] c15 A69-34381
Calculated and experimental hinge moments on trailing-edge flaps of swept Delta wings at hypersonic speeds and positive deflection angles
[NASA-TN-D-4268] c01 N69-10054
Eddy current torques on bodies rotating relative to uniform magnetic field
[NASA-TN-D-5086] c23 N69-29477
Magnetic torque resulting from interaction between magnetic properties of spacecraft and ambient magnetic field
[NASA-SP-8018] c31 N69-30339
Torque and leakage rates of various lubricated lip seal designs at peripheral velocity of 120 feet per second
[NASA-TN-D-5411] c15 N69-35769
Elastohydrodynamic analysis and experimental speed effects on ball spinning friction coefficients and torque
[NASA-TN-D-5527] c15 N69-41210

TORQUE MOTORS
Design and analysis of modular servoamplifier for fast response electrohydraulic control systems
[NASA-TN-D-4898] c03 N69-10068

TORQUERS
Photoelectronic commutation by dc torquer-driven reaction wheel for spacecraft attitude control
[NASA-TN-D-5265] c03 N69-30945
TORSIONAL STRESS
Plastic deformation of corrosion resistant steel, CER-VIT 101, and fused silica as function of applied torsional stress
[NASA-CR-1257] c14 N69-16100
Mechanical characteristics of flexible drive shaft coupling
[NASA-CR-1241] c15 N69-16104
TORSIONAL VIBRATION
Anomalous spacecraft OGO-D motion explained by open section boom thermally induced oscillations, discussing corrective measures
c32 A69-18331
Directional solar thermal field /sunlight/ effect on coupled nonplanar transverse and torsional vibrations of satellite cylindrical antennas in orbit
c32 A69-25534
TOUGHNESS
Crack length and thickness influence in plane strain fracture toughness tests
[NASA-TM-X-1860] c17 N69-34916
TOXIC HAZARDS
Treatment procedure and preventive programs outlined for acute exposure to toxic rocket fuels or oxidizers
c05 A69-12498
TOXICITY
Toxicity of plastic hardware containing biological space flight experiment
[NASA-TM-X-1818] c04 N69-29723
TRACE ELEMENTS
Detection and spectral examination of trace porphyrin complexes by demetallation with methanesulfonic acid and spectrofluorometry, compared to absorption spectrophotometry
c06 A69-42557
TRACKING (POSITION)
Working breadboard model of planet tracker under various illuminating conditions, discussing hardware and closed loop tracking error analysis accounting for signal to noise effects
c21 A69-13214
Small perturbation dynamics of neuromuscular system in tracking tasks
[NASA-CR-1212] c05 N69-14212
Modified Fourier transform for calculating human operator describing functions
[NASA-TM-X-1762] c08 N69-21119
Systems developed for reducing pilot workload and tracking accuracy improvements during noise abatement landing approaches
[NASA-CR-1427] c02 N69-38657
TRACKING NETWORKS
Tracking and Data Relay Satellite System with synchronous orbit satellites to relay data between low altitude earth orbital spacecraft and mission control centers
c07 A69-41755
TRACKING STATIONS
GEOS 1 tracking station positions on SAC standard earth C-5 model
[NASA-TN-D-5034] c13 N69-28019
TRACTION
Runway grooving to improve aircraft tire traction in adverse weather tested by F-4D and Convair 990A under wet conditions
[AIAA PAPER 69-773] c02 A69-35649
Runway and highway pavement grooving and traction studies
[NASA-SP-5073] c11 N69-20451
TRAILBLAZER 2 REENTRY VEHICLE
Flight measurement of optical radiation from shock heated air with Trailblazer 2 reentry vehicle
[NASA-TN-D-4937] c33 N69-14501
TRAILING EDGES
Stator performance with cooling by air ejection from trailing edges of blades
[NASA-TM-X-1901] c03 N69-39335
TRAILING-EDGE FLAPS
Hypersonic flow distribution and separation types over highly swept Delta wing with trailing edge flaps at Mach 6
[AIAA PAPER 68-97] c01 A69-12522
Calculated and experimental hinge moments on trailing-edge flaps of swept Delta wings at hypersonic speeds and positive deflection angles
[NASA-TN-D-4268] c01 N69-10054
Trailing-edge flap system with boundary layer control and external jet augmentation for subsonic jet transport
[NASA-TN-D-5129] c01 N69-30722
Pressure and heat transfer on swept Delta wing with trailing-edge flap
[NASA-TN-D-5418] c01 N69-35855
Three dimensional pressure distribution functions for lifting surfaces with trailing-edge controls based on integral equations for subsonic flow
[NASA-TN-D-5419] c01 N69-38768
Boundary layer control and trailing edge flaps for direct-lift control
[NASA-CR-1426] c02 N69-38819
TRAINING SIMULATORS
Flight simulation requirements for reducing aircraft training flight time, discussing control system and instrument motion characteristics, visual simulation and critical maneuvers motion
c11 A69-41139
TRAJECTORY ANALYSIS
Autonomous solution to orbital navigation problem yielding direct measure of orbital parameters
c21 A69-11005
Longitudinal range dispersion of unmanned Mars landers using VM-8 and VM-9 atmospheric models, discussing Syrtis Major as possible landing site
c30 A69-12390
Trajectory error propagation upper bounds in many body field for impulsive initial error, relating error to mission tolerances
c30 A69-21937
Configuration, trajectory planning, instrumentation, calorimetry and aerodynamic heating for planetary atmosphere entry
c31 A69-25719
Normalized hodographic mapping for constrained trajectory families, discussing mapping concepts, information content and applications
[AIAA PAPER 69-924] c30 A69-39362
Metric state-time dynamical polysystem with sequentially compact topological space, noting sliding state trajectories
c19 A69-40573
Computation of optimal branched trajectories using classical variational problem of Bolza
[NASA-CR-1331] c30 N69-24950
Gravity model comparison using geodetic satellite long arc orbital solutions
[NASA-TN-D-5035] c30 N69-27412
Interplanetary space trajectories based on Jupiter swingby flights
[NASA-TN-D-5271] c30 N69-28441
Current computer programs for low thrust trajectory analysis using flyby and rendezvous trajectories
[NASA-TM-X-1824] c08 N69-30014
Comparison of fourth order Runge-Kutta numerical integration technique with two numerical integration formulas in mathematical models used for computing rigid body trajectories
[NASA-TN-D-5425] c30 N69-38769
Sequential stochastic techniques for trajectory estimation
[NASA-CR-1360] c30 N69-40325
TRAJECTORY CONTROL
Numerical integration for continuously thrusting spacecraft optimal trajectory, considering rectangular Cartesian and polar cylindrical coordinates characteristics
[AIAA PAPER 69-903] c30 A69-38546
Performance of Atlas-Agena vehicle from lift off through Agena posigrade maneuver
[NASA-TM-X-1826] c31 N69-29594
TRAJECTORY MEASUREMENT
Rocket trajectory determination by tracking onboard light source against star background with image orthicon TV system
c07 A69-26965
TRAJECTORY OPTIMIZATION
Iterative guidance mode /IGM/ applied to effective gravity vector prediction, acceleration measurement of noise sensistivity and energy limitations

[AIAA PAPER 67-620] c21 A69-15501
Spacecraft optimum low thrust trajectory analyzed by Hamilton-Jacobi perturbation theory, obtaining canonic constants of motion c30 A69-17574
Multistage rocket trajectories optimized by second order numerical technique and digital computer program, considering coasting, vacuum flight and transition times c30 A69-32154
Low thrust trajectories for minimum time rendezvous between continuous thrust interceptor and passive target vehicle, comparing calculus of variations and steepest ascent analyses c30 A69-32177
Impulsive orbit transfer optimization using accelerated gradient program based on Newtonian algorithm for digital computer method c30 A69-35956
Numerical integration for continuously thrusting spacecraft optimal trajectory, considering rectangular Cartesian and polar cylindrical coordinates characteristics
[AIAA PAPER 69-903] c30 A69-38546
Closed form solution for minimum fuel constant thrust trajectories for vehicle transfer in vacuum between arbitrary boundary conditions
[AIAA PAPER 69-905] c30 A69-39337
Vector integral extension to optimal trajectory coordinate multiplier systems with constant of motion demonstrated for coast-arc problem
[AIAA PAPER 69-907] c30 A69-39339
Branched trajectory optimization for split rocket vehicles using projected gradient or steepest descent method
[AIAA PAPER 69-917] c30 A69-39346
Recurrent Lagrange multipliers for optimal low thrust earth-Jupiter transfers, using three dimensional solar system model c30 A69-41896
Generation of ideal coordinate systems for analysis of optimal trajectories
[NASA-CR-1250] c30 N69-13274
Computational method for time optimal space rendezvous between rocket vehicle and circular orbit target
[NASA-TN-D-5017] c30 N69-16210
Optimum takeoff and climbout trajectory calculation technique for jet aircraft noise abatement
[NASA-TN-D-5182] c02 N69-26194

TRANSDUCERS
Cb-1Zr pumped sodium loop tests to evaluate loop components, EM pump, pressure transducers, and instrumentation techniques
[NASA-CR-1135] c03 N69-11373
Hysteresis of strain gage absolute pressure transducer
[NASA-TN-D-5327] c14 N69-30506

TRANSFER FUNCTIONS
Radiator transfer functions for SNAP 8 ground test facilities
[NASA-TN-D-4946] c22 N69-14503
Measurement of pilot describing functions in single controller multiloop tasks
[NASA-CR-1238] c05 N69-15372
Experimental and analytical study of dynamics of single tube counterflow boiler
[NASA-CR-1230] c12 N69-17751
Derivation of transfer function for optical system relating image intensity to spatial autocorrelation
[NASA-CR-1443] c21 N69-38041
Human transfer functions applied in systems analysis of manually controlled lunar landing simulator
[NASA-TN-D-5478] c05 N69-39183

TRANSFER ORBITS
Impulsive orbit transfer optimization using accelerated gradient program based on Newtonian algorithm for digital computer method c30 A69-35956
Recurrent Lagrange multipliers for optimal low thrust earth-Jupiter transfers, using three dimensional solar system model c30 A69-41896
Optimal rendezvous and transfers between close elliptical orbits
[NASA-TT-F-554] c30 N69-40592

TRANSFERRING
Simulated manual package transfer in weightless environment of Saturn Orbital Space Station
[NASA-TN-D-5111] c05 N69-21501

TRANSFORMATIONS (MATHEMATICS)
Transformation laws for thermodynamic quantities confirming conventional formulation by mechanical model of heat c23 A69-11288
Computation of topside ionograms from electron concentration profiles
[NASA-TN-D-5052] c13 N69-23557

TRANSFORMERS
Passive circuit to transform voltage of indefinitely repeated positive or negative pulses using transistors, diodes and magnetic cores c09 A69-10564
Transformer for unilateral energy transfer using single domain uniaxial Permalloy film c09 A69-39454
Transformer of closely spaced pulsed waveforms having nonzero average value
[NASA-TN-D-5473] c09 N69-38776

TRANSIENT HEATING
Charring phenolic nylon ablator material pyrolysis and surface recession for cyclic and constant combined convective and radiative heating
[AIAA PAPER 69-151] c33 A69-18055
Heating facility for testing ablative heat shield material models in combined convective and radiative heating environment with constant or transient heating conditions
[AIAA PAPER 69-342] c11 A69-28278
Transient solidification outside cooled pipe with application to solar Brayton heat receiver
[NASA-TN-D-4897] c33 N69-10227

TRANSIENT RESPONSE
Transient electro-osmosis of water in capillary tubes for pumping and generation modes, analyzing response to step change in pressure or voltage change under external loading c06 A69-14862
Digital simulation computer stability analysis scheme premised on use of perturbed transient responses c10 A69-32899
Transient performance of full flow hydraulic turbine driven two speed pump inducer system, formulating computer model
[AIAA PAPER 69-551] c15 A69-34415
Ratio of equilibrium responses to transient responses both having equal excitation levels
[NASA-TN-D-5070] c32 N69-17258
Identification of structural systems using near resonance testing
[NASA-TN-D-5069] c32 N69-17737
Transient response of coupled acoustic cavity resonators
[NASA-CR-1421] c23 N69-35286
Cataloged pulse response curves for different types of conventional low pass filters
[NASA-TN-D-5494] c07 N69-40099

TRANSISTORS
Second breakdown and other thermal instabilities analyzed by heat flow equation, obtaining stability criteria predicting reduced power dissipation for transistor at low currents c09 A69-31618
Analysis and design of inductors for protecting power transistors against current surges in inverter bridge circuits
[NASA-TN-D-4995] c10 N69-16198
Performance tests of silicon and germanium transistors in intense magnetic fields
[NASA-TN-D-5428] c09 N69-36710
Transformer of closely spaced pulsed waveforms having nonzero average value
[NASA-TN-D-5473] c09 N69-38776

TRANSITION FLOW
Linear amplification, nonlinear limiting and secondary instability induced by unsteady effects illustrated for various transitional flows, including roughness and streamwise vorticity c12 A69-33248

TRANSITION LAYERS
Plasmapause and relation to ion composition in topside ionosphere, using Bohm coefficient for

turbulent diffusion
c13 A69-12741
TRANSITION METALS
Vacuum distillation technique for isolation and recovery of alkali metal reaction products with Ta, Ni, V and oxygen
c14 A69-10927
TRANSMISSION CIRCUITS
Microelectronic data and remote control function transmission system for wind tunnel testing of aircraft dynamic response to gusts and turbulence
c11 A69-23283
TRANSMISSION LOSS
Transmission loss and effects on antenna radiation patterns and impedance produced by thermally degraded ablation materials
[NASA-TN-D-4879] c07 N69-10885
Lunar surface transmission loss for Apollo astronaut point-to-point communications
[NASA-TN-D-4915] c07 N69-13301
TRANSMISSIVITY
Radio frequency transmission characteristics of ablation materials for planetary entry vehicle heat shields
[NASA-TN-D-4920] c07 N69-13158
Transmission effects on plastic films irradiated with ultraviolet light in vacuum
[NASA-TM-X-1905] c18 N69-40339
TRANSMITTANCE
Transmittance and absorption cross sections of carbon particles suspended in flowing stream of nitrogen gas
c33 A69-17804
Visible and infrared transmitting properties of epoxy resin suitable for infrared detectors
[NASA-TM-X-1776] c18 N69-23843
TRANSONIC FLOW
Oxidation resistance and thermal fatigue cracking of nickel and cobalt base alloys in transonic gas streams
[NASA-TN-D-5376] c17 N69-33307
Wind tunnel investigation for determination of subsonic and transonic aerodynamic characteristics of Saturn 1B launch vehicle
[NASA-TM-X-1848] c31 N69-33380
Finite difference theory for transonic velocity calculations on blade-to-blade stream surface of turbomachine
[NASA-TN-D-5427] c01 N69-37521
TRANSONIC FLUTTER
Wind tunnel study of deflected elevator flutter encountered on T-tail airplane
[NASA-TN-D-5024] c32 N69-16211
TRANSONIC SPEED
Location effect of power plants on aft-mounted supersonic cruise exhaust nozzles at transonic speeds in flight and wind tunnel
[AIAA PAPER 69-427] c01 A69-32769
Determination of drag of fabrication-type surface roughness in turbulent boundary layer at transonic speeds
[NASA-TN-D-5004] c01 N69-16460
Plug and shroud geometry variables on plug nozzle performance at transonic speeds
[NASA-TN-D-5098] c28 N69-21463
Transonic aerodynamic characteristics of two hypersonic cruise configurations
[NASA-TM-X-1816] c01 N69-29231
TRANSONIC WIND TUNNELS
Microelectronic data and remote control function transmission system for wind tunnel testing of aircraft dynamic response to gusts and turbulence
c11 A69-23283
Transonic wind tunnel tests of aerodynamic drag and lift forces on circular cylinder in two dimensional flow at high Reynolds number
[NASA-TR-R-300] c01 N69-17304
Transonic wind tunnel evaluation of variable stabilizer configuration effects on hypersonic elliptical lifting body dynamics
[NASA-TM-X-1789] c01 N69-25244
TRANSPORT AIRCRAFT
Light aircraft hazards due to trailing vortex generated by heavy transport aircraft, suggesting specific procedures for takeoff, landing and flight phase
[SAE PAPER 680220] c02 A69-14930
Drag influence on mission performance of hypersonic aircraft during climb and cruise, noting payload capacity
c02 A69-37154
Flight simulator with large lateral motion for large and supersonic transport aircraft, emphasizing reproduction of cockpit accelerations due to supersonic engine thrust loss
c11 A69-43044
Calculated and flight measured handling quality factors of three subsonic jet transports
[NASA-TN-D-4832] c02 N69-10495
Wind tunnel tests of large jet transport aircraft model with external flow jet flap
[NASA-TN-D-4928] c01 N69-14000
Trailing-edge flap system with boundary layer control and external jet augmentation for subsonic jet transport
[NASA-TN-D-5129] c01 N69-30722
Auxiliary flap system tests using Boeing 367-80 transport aircraft and wind tunnels
[NASA-TN-D-5128-REV] c02 N69-31962
Static and dynamic stability derivatives of model jet transport equipped with external flow jet augmented flaps
[NASA-TN-D-5408] c02 N69-36258
Variation in engine noise for two landing approach configurations of jet transport aircraft
[NASA-TM-X-1896] c02 N69-38104
TRANSPORT PROPERTIES
Transport properties of steam, analyzing selection, correlation and prediction using statistical mechanical theories
c33 A69-10110
Laser ignited combustion of 365 micron Zr droplets falling in ultrapure oxygen using spectroscopic and photographic techniques, discussing vapor phase transport phenomena
[WSCI PAPER 69-4] c27 A69-32345
Thermodynamic and transport properties of air, and combustion products of natural gas and air, and jet engine fuel and air
[NASA-TN-D-5452] c33 N69-37936
TRANSPORT THEORY
Gamma heating rate measured by aqueous dosimeter converted to rate in thin tungsten detector in water shield through transport theory calculations, obtaining correction factors
c22 A69-18825
Transport study of neutron and photon attenuation through lithium hydride and tungsten spheres
[NASA-TN-D-4989] c24 N69-15375
Quadrature variations in discrete-ordinates calculation
[NASA-TM-X-1887] c20 N69-36976
TRANSPORT VEHICLES
Concepts of acceptance testing lunar and planetary vehicles
[NASA-TN-D-4924] c11 N69-14507
TRANSPORTATION
Design philosophy for cost reductions on future space transportation systems, exemplifying application to booster system for earth orbital logistics
[AIAA PAPER 69-439] c34 A69-32654
Reducing cost of space transportation - AAS Conference, Washington, D.C., March 1969
c34 A69-39686
TRANSVERSE WAVES
Air gap tolerances effect on admittance of TEM mode dielectric and plasma coated slot antennas determined by variational method
c09 A69-24986
Reflection coefficient of symmetric parallel plate waveguide operating in TEM mode illuminating lossless dielectric layer, using wedge diffraction and geometrical optics methods
c09 A69-34802
Edge diffraction effects in TEM axially slotted finite ground plane on radiation pattern in waveguides of different geometries
c07 A69-41588
Harmonic content of pressure wave shapes in strong traveling transverse acoustic modes
[NASA-TM-X-1716] c12 N69-15371
TRAPPED PARTICLES
Equation describing statistically trapped particle motion under influence of fields varying in time

and space
c29 A69-19375
TRAVELING WAVE MODULATION
Design and performance of traveling wave phototube for coherent light demodulation
[NASA-TT-F-430] c09 N69-15441
TRAVELING WAVE TUBES
High power TWT tube cooling in space vehicle, discussing thermal control system based on heat pipe radiator
c09 A69-24747
Design and performance of traveling wave phototube for coherent light demodulation
[NASA-TT-F-430] c09 N69-15441
TRAVELING WAVES
Harmonic content of pressure wave shapes in strong traveling transverse acoustic modes
[NASA-TM-X-1716] c12 N69-15371
TRIGATRONS
Parameters affecting firing time of simultaneously triggered trigatron spark gap switches
[NASA-TN-D-5077] c09 N69-20888
TRIGONOMETRIC FUNCTIONS
Algorithm for computing direction cosine matrix of strapdown inertial system
[NASA-TN-D-5384] c21 N69-36997
TRITIUM
Tritium contamination reduction in small ion accelerators for neutron production, discussing pumping problems and vacuum systems
c11 A69-26499
TRITONS
Alpha particle-triton reaction on scandium 45 at 41 MeV
[NASA-TN-D-5216] c24 N69-24919
TROPICAL METEOROLOGY
Survey of six year period of satellite observed tropical Pacific cloud mapping
c20 A69-33001
Causal and semiphenomenological theories concerning equatorial F 2 region, discussing electrodynamic drift theory and transequatorial winds
c13 A69-37888
TROPICAL REGIONS
Bidirectional reflectance of earth atmosphere and cloud formation above equatorial Pacific observed by synchronous satellite as function of angular dependence
c20 A69-43154
TROPOSPHERE
Vertical tropospheric humidity distribution estimation from IR spectra obtained by TIROS satellites
c13 A69-34284
Water vapor profiles in stratosphere from IR radiometric observations under cloudless conditions, indicating relation to tropospheric meteorological features
c13 A69-38261
Clear air turbulence detection in troposphere by multifrequency radiometric sensor, noting multibeam system for supersonic aircraft
c09 A69-42536
TRUSSES
Lightly loaded truss structures fabricated from Be, Be-Al alloy and uniaxial B filament reinforced epoxy tubing for unmanned spacecraft applications
c17 A69-35504
Structural response of tubular beryllium and beryllium aluminum alloy truss-type structures to dynamic and static loads
[NASA-TN-D-5254] c32 N69-28658
TUBE CATHODES
SERT 2 mercury vapor fed hollow cathode operated in bell jar, determining volt-ampere characteristics and flow rates for plasma diagnostics
[AIAA PAPER 69-258] c28 A69-21221
Vacuum tube with cathode heated directly by external radioisotope source, noting heat pipe providing isothermal heat transfer
c09 A69-24748
TUBE HEAT EXCHANGERS
Creep rupture data on welded tubes for helium to air heat exchanger design
[NASA-TN-D-5195] c17 N69-23731
Bimetallic heat exchanger tube performance in sodium boiling facility
[NASA-TN-D-5323] c33 N69-30064
Heat transfer characteristics of water/cryogenic hydrogen heat exchanger for nuclear rocket reactor
[NASA-TN-D-5429] c33 N69-36701
TUBES
Tube techniques - IEEE Conference, New York, September 1968
c09 A69-24740
TUMBLING MOTION
Multimodality pilot model for visual and motion feedbacks derived from simulator program
[NASA-CR-1325] c05 N69-28071
TUMORS
Adrenal epinephrine and phenylethanolamine n-methyl transferase /PNMT/ activity in rat bearing transplantable pituitary tumor
c04 A69-20374
TUNGSTEN
Work function and desorption energy measurements of alkali metals from metallic substrates with modulated molecular beam, noting surface contamination
c26 A69-21808
Thermionic converters with chloride and fluoride vapor deposited tungsten emitters, comparing performance characteristics and stability
c03 A69-21819
Internal friction, Young modulus and resistivity measurements for stage I interstitials in electron irradiated tungsten
c17 A69-28682
Thermal neutron capture cross section at high temperature irradiations determined for W 184, describing radiochemical separation and flux counting techniques
c14 A69-43192
Point defect calculations for tungsten
[NASA-TN-D-4918] c22 N69-13309
Transport study of neutron and photon attenuation through lithium hydride and tungsten spheres
[NASA-TN-D-4989] c24 N69-15375
Compatibility tests of molten uranium with tungsten and tungsten-1.5 percent hafnium
[NASA-TN-D-5076] c17 N69-19930
Tungsten-184 used as thermal flux monitor at high temperatures in Plum Brook reactor
[NASA-TN-D-5113] c22 N69-20795
Composition and line emission characteristics of ionized tungsten, uranium, and argon
[NASA-CR-1313] c25 N69-21124
Spectral emission characteristics of gaseous tungsten and uranium in induction heated argon plasmas
[NASA-CR-1314] c25 N69-22920
Furnace brazing butt joints in tungsten-uranium dioxide cermet cylinders at 3000 deg C
[NASA-TM-X-1815] c15 N69-28862
Burst testing of tungsten tubing at high temperatures
[NASA-TM-X-1843] c17 N69-31889
Thermionic converter with fluorine vapor deposited tungsten emitter etched to expose crystal planes
[NASA-CR-1381] c03 N69-35689
Tungsten and depleted uranium in mimimum weight, layered shield comparisons for space power reactor
[NASA-TM-X-1874] c22 N69-35817
Corrosion and heat resistant coatings for oxidation protection of tungsten
[NASA-TT-F-583] c17 N69-35836
Tungsten and tungsten alloy single crystal deformations determined as function of alloying, strain, and temperature
[NASA-TN-D-5493] c17 N69-39182
Molybdenum and tungsten solubility in liquid potassium
[NASA-TN-D-5504] c17 N69-40053
TUNGSTEN ALLOYS
Powder metallurgy, fusion and chemical vapor deposition techniques in manufacturing tungsten base alloys
c17 A69-18792
Vacuum arc melted W and W-Re alloys mechanical properties, noting Re additions effects
c17 A69-20190

Superplasticity in W-Re alloys, noting tensile properties, grain size and strain rate sensitivity for various Re contents at high temperatures
c17 A69-22990
Tungsten alloy fiber reinforced nickel base alloy composites stress-rupture strength, oxidation and impact resistance for high temperature turbojet engine buckets
c17 A69-29010
Ductilizing of Group 6A elements by rhenium and other solutes
[NASA-TN-D-4955] c17 N69-14403
Effect of rhenium on mechanical properties of hafnium carbide strengthened tungsten alloys
[NASA-TN-D-5348] c17 N69-31977
Tungsten and tungsten alloy single crystal deformations determined as function of alloying, strain, and temperature
[NASA-TN-D-5493] c17 N69-39182

TUNGSTEN CHLORIDES
Thermionic converter with chloride vapor deposited tungsten emitter and nickel collector
[NASA-CR-1416] c03 N69-32553

TUNGSTEN COMPOUNDS
Impregnation of polytetrafluoroethylene with hexaflourides of rhenium, molybdenum, and tungsten
[NASA-TN-D-4886] c06 N69-10126
Thermal stability and friction of disulfides, diselenides, and ditellurides of molybdenum and tungsten in ultrahigh vacuum
[NASA-TN-D-5141] c15 N69-22992

TUNGUSK METEORITE
Oxide composition of silicate spherules from forest area devastated by Tunguka meteorite explosion using electron microprobe analysis
c30 A69-28869

TUNING
VHF cavity backed cylindrical gap antenna input tuning impedance and equatorial radiation patterns controlled by cavity adjustments
c09 A69-40698

TUNNEL DIODES
Germanium microwave backward diodes optimum design and performance prediction through computer calculation for important parameters
c09 A69-41224
Backward diodes in indium arsenide for microwave mixing
[NASA-TN-D-5401] c09 N69-36706

TURBINE BLADES
Turbine blade loading in terms of surface diffusion and loading factors, discussing tandem and jet flap blades and vortex generators
[ASME PAPER 68-WA/GT-11] c28 A69-16136
Turbine stator blade performance determination from total pressure surveys downstream of blade row, noting problems in pressure measurement
[ASME PAPER 69-GT-103] c01 A69-22521
Technology trends in airbreathing propulsion, discussing noise control for subsonic jet transports, turbine blade cooling, etc
[AIAA PAPER 69-774] c02 A69-35648
Performance evaluation of tandem rotor blade of single stage turbine
[NASA-CR-1254] c01 N69-13621
Flow reduction due to oxidation of wire-form porous materials for transpiration cooled turbine blades
[NASA-TN-D-5001] c17 N69-16383
Performance of tandem turbine blade and its influence on flow separation and visualization
[NASA-CR-1341] c01 N69-23892
Steady state stress relaxation analysis of turbine blade cooling designs
[NASA-TN-D-5282] c28 N69-29321
Flow and wake characteristics on turbine tandem blades in two dimensional cascade tunnel
[NASA-TM-X-1836] c01 N69-30632

TURBINE ENGINES
Performance and analysis of seals for nitrogen inerted lubrication systems of turbine engines
[NASA-TN-D-4761] c15 N69-10055

TURBINE INSTRUMENTS
Technique for dynamically calibrating turbine flowmeters for small perturbations by means of frequency response tests
[NASA-TM-X-1736] c14 N69-17702

TURBINE PUMPS
Ball bearings lubrication and wear in cryogenic hydrogen turbopumps by transfer films provided from self lubricating cage
c15 A69-10109
Transient performance of full flow hydraulic turbine driven two speed pump inducer system, formulating computer model
[AIAA PAPER 69-551] c15 A69-34415
Low speed characteristics of liquid hydrogen centrifugal turbopumps
[NASA-TM-X-1861] c28 N69-33806

TURBINE WHEELS
Vibrations of turbomachine rotors and methods for determining optimal hydraulic damping mounts, vibrations of systems with friction, and self induced vibrations of compressor blades
[NASA-TT-F-547] c02 N69-36326

TURBINES
Multiple function combination probe design for compressor and turbine air flow research
c11 A69-31917
Stator setting effect on single stage turbine performance, considering blade loss and surface velocity distribution
[AIAA PAPER 69-525] c28 A69-32686
Effect of variable stator with area design of 70 percent on performance of single stage turbine suitable for air cooling
[NASA-TM-X-1696] c28 N69-10296
FORTRAN 4 program for estimating off-design performance of radial inflow turbines
[NASA-TN-D-5059] c03 N69-19829
Surface temperature mapping with infrared photographic pyrometry for turbine cooling investigations
[NASA-TN-D-5179] c14 N69-23895

TURBOCOMPRESSORS
Gas turbine compressor end seals, discussing air leakage paths, primary and secondary seals, design and efficiency
[ASLE PREPRINT 68AM 4B-4] c15 A69-27366
Analog simulation of closed loop Braytcn cycle test facility
[NASA-TM-X-1715] c03 N69-14312
Theoretical study of discrete frequency noise generated by turbocompressors and blades
[NASA-CR-1287] c28 N69-21476
Multistage turbocompressor simulation applied to performance prediction of axial flow instabilities
[NASA-TM-X-1880] c28 N69-36998
Hot-salt stress-corrosion of titanium alloy under simulated turbine engine compressor environment
[NASA-TN-D-5510] c17 N69-40242

TURBOFAN ENGINES
Steady state and dynamic distortion influence on performance and stall of turbofan engine, discussing compressor instrumentation, tests and simulation data
c28 A69-35175
Conference cn NASA research in noise reduction of subsonic jet aircraft - nacelle acoustic linings, sound generation in jet engines, and operational noise effects on humans
[NASA-SP-189] c02 N69-11542
Performance and stall limits of YTF30-P-1 turbofan engine with uniform compressor inlet flow
[NASA-TM-X-1803] c28 N69-27019
Analytical and experimental studies for predicting noise attenuation in acoustically treated ducts for turbofan engines
[NASA-CR-1373] c23 N69-36974
Steam cycle analysis for nuclear powered turbofan engine
[NASA-TM-X-1907] c22 N69-40060

TURBOFANS
Flight evaluation of tip turbine driven fans for lateral control in hovering VTOL aircraft
[NASA-TN-D-5491] c02 N69-38807

TURBOGENERATORS
Argon turboalternator design and testing for Brayton cycle space power system, discussing inlet operating temperature and shaft bearings and rotation
c03 A69-42279
Turboalternator gas bearing system for spacecraft electric power production
[NASA-CR-1292] c15 N69-19775

Results of endurance tests of SNAP 8 turbine alternator
[NASA-TM-X-1741] c03 N69-20913
Performance of two stage axial flow turbogenerator with gas bearing rotor support system
[NASA-CR-1290] c03 N69-21771
Design and performance of gas bearing system for turboalternators
[NASA-CR-1291] c15 N69-21772
Performance of gas bearing Brayton cycle turbcalternator
[NASA-TM-X-1820] c03 N69-29707

TURBOJET ENGINES
Tungsten alloy fiber reinforced nickel base alloy composites stress-rupture strength, oxidation and impact resistance for high temperature turbojet engine buckets
c17 A69-29010
Performance of 10 deg conical turbojet plug nozzle with iris primary and translating shroud for supersonic cruise applications
[NASA-TM-X-1709] c28 N69-14313
Evaluating performance of swirl can turbojet combustor at simulated supersonic inlet conditions
[NASA-TN-D-4996] c28 N69-16154
Static tests of nozzle efficiency and pumping characteristics of conical turbojet plug nozzle with translating primary and secondary shrouds at Mach 0 to 2.0
[NASA-TM-X-1777] c28 N69-21648
Steady-state interactions between turbcjet engine and axisymmetric inlet with induced distortions
[NASA-TM-X-1780] c28 N69-23519
Dynamic distortion of supersonic wind tunnel for turbojet engines
[NASA-TM-X-1842] c28 N69-38599
Aerodynamics and flight dynamics of turbojet aircraft
[NASA-TT-F-542] c01 N69-38670

TURBOMACHINE BLADES
Tungsten alloy fiber reinforced nickel base alloy composites stress-rupture strength, oxidation and impact resistance for high temperature turbojet engine buckets
c17 A69-29010
FORTRAN program for calculating velocities and streamlines on blade to blade stream surfaces of turbomachinery
[NASA-TN-D-5044] c01 N69-21811
Computer program for aerodynamic analysis of turbomachine blades
[NASA-TM-X-1764] c01 N69-22553
Tandem bladed inducer tested in water for cavitation corrosion
[NASA-TN-D-5134] c01 N69-23769
Performance tests of jet flapped blade in six blade annular cascade
[NASA-CR-1423] c28 N69-36680

TURBOMACHINERY
Finite difference theory for transonic velocity calculations on blade-to-blade stream surface of turbomachine
[NASA-TN-D-5427] c01 N69-37521

TURBOSHAFTS
Gas turbine engine shaft face seal with self acting lift augmentation preventing rubbing contact, noting disadvantages of labyrinth and conventional seals
[ASLE PICFS PREPRINT 27] c15 A69-30492

TURBULENCE
Statistical theories of turbulence applied to thermal convection between infinite slippery plates at large Prandtl number
c33 A69-24283

TURBULENCE EFFECTS
Statistical effects of wind and atmospheric turbulence on launch vehicles
[NASA-CR-1410] c20 N69-35570

TURBULENCE METERS
Turbulence measurement errors with inclined hot wires described by equations, assuming normal component cooling includes greater tangential cooling
c14 A69-34442

TURBULENT BOUNDARY LAYER
Acceleration effects on forced convection in turbulent boundary layer, noting heat transfer history and rates prediction
c12 A69-21480
Incompressible two dimensional turbulent boundary layer equations with arbitrary pressure distribution solved by weighted residual method
[AIAA PAPER 69-397] c12 A69-30478
Density and velocity fluctuations in hypersonic turbulent boundary layer based on Wallace data
c12 A69-31908
Boundary layer trip geometry, size and location effects on position of transition at hypersonic speeds
c12 A69-33249
Skin friction drag reducing high polymer solution injected into turbulent boundary layer to test effectiveness on marine vehicles
c12 A69-33254
Incompressible turbulent boundary layer analysis by two region characterization for eddy viscosity, using Spalding generalized function and Prandtl free shear flow model
c12 A69-33255
Compressible hypersonic turbulent boundary layers solution by finite difference method, relating mixing length to velocity profile shape factor
[AIAA PAPER 69-684] c12 A69-33474
Determination of drag of fabrication-type surface roughness in turbulent boundary layer at transonic speeds
[NASA-TN-D-5004] c01 N69-16460
Mathematical model for determining total drag of pointed body of revolution in supersonic flow with turbulent boundary layer
[NASA-TN-D-5046] c01 N69-19925
Calculation of compressible turbulent boundary layers with pressure gradients and heat transfer
[NASA-CR-1303] c12 N69-21653
Turbulent boundary layer of subsonic transport fuselage with pressure gradient, Reynolds number, and angle of attack
[NASA-TN-D-5242] c01 N69-28112
Skin friction and heat transfer data for hypersonic turbulent layer on flat plates, wind tunnel wall, and cones
[NASA-TN-D-5089] c12 N69-29144
Flow field measurements on flat plate with attached protuberances in supersonic turbulent boundary layer
[NASA-TN-D-5297] c12 N69-30071
Turbulent boundary layer temperature and velocity measurements in supersonic water-cooled conical nozzle
[NASA-TN-D-5377] c12 N69-33353
Statistical analysis of pressure fluctuations in separated turbulent boundary layer
[NASA-TN-D-5440] c12 N69-36940
Fluctuating properties of turbulent boundary layers for Mach numbers up to 9
[NASA-TN-D-5496] c12 N69-40137

TURBULENT DIFFUSION
Plasmapause and relation to ion composition in topside ionosphere, using Bohm coefficient for turbulent diffusion
c13 A69-12741

TURBULENT FLOW
Direction of maximum turbulent vorticity in turbulent shear flow, determining alignment
c12 A69-25282
Supersonic Preston tube correlations for Mach number and Reynolds number effects on hypersonic turbulent skin friction on adiabatic surfaces, simplifying correlation
[AIAA PAPER 69-345] c12 A69-28280
Linear amplification, nonlinear limiting and secondary instability induced by unsteady effects illustrated for various transitional flows, including roughness and streamwise vorticity
c12 A69-33248
Turbulence measurements and roughness effects on viscous drag reduction with polymer solution in pipe flow, discussing friction factor, wall velocity profile, etc
c12 A69-33252
Concentration, flow rate and tube diameter effects on viscous drag reduction in nonpolar soap solutions, using pressure drop measurements to observe turbulent flow behavior
c12 A69-33253

Baronti-Libby transformation and Preston tube calibrations used to determine skin friction from turbulent velocity profiles
[NASA-TN-D-4853] c12 N69-10472
Nonlinear disturbance decay in unbounded viscous fluid
[NASA-TN-D-4947] c12 N69-14483
Turbulent boundary layer measurements on axisymmetric hypersonic nozzle walls
[NASA-TN-D-5433] c12 N69-36805
Flow model for vortex shedding from slender body in coning motion
[NASA-CR-1448] c12 N69-40200

TURBULENT HEAT TRANSFER
Acceleration effects on forced convection in turbulent boundary layer, noting heat transfer history and rates prediction
c12 A69-21480
Penetration model explanation for turbulent forced convection heat transfer in near-critical fluids
[NASA-TN-D-5522] c33 N69-40437

TURBULENT JETS
Three dimensional laser Doppler velocity instrument for mean velocity and turbulence measurements in subsonic jet shear layer
[SAE PAPER 690266] c14 A69-21555

TURBULENT MIXING
Effects of free stream turbulence and boundary layer trip devices on mixing in jet stream
[NASA-CR-1336] c12 N69-24058
Turbulent mixing of compressible air in supersonic and subsonic coaxial jet flows
[NASA-TN-D-5315] c02 N69-30727
Turbulence in mixing region of ducted coaxial flow of air-air and air-Freon 12 combination
[NASA-CR-1335] c12 N69-30728
Numerical analysis of laminar and turbulent mixing region for two dimensional jet injected at angle to moving stream
[NASA-TN-D-5531] c12 N69-41213

TURBULENT WAKES
Light aircraft hazards due to trailing vortex generated by heavy transport aircraft, suggesting specific procedures for takeoff, landing and flight phase
[SAE PAPER 680220] c02 A69-14930
Flow field throughout wind tunnel containing rotor with sharply defected blades, noting reversed flow effect in front of wake
c11 A69-35228

TURNING FLIGHT
Direct side-force maneuvering system on deflected X-14A jet VTOL aircraft without changing bank angle
[NASA-TN-D-5175] c02 N69-22572

TWENTY-FOUR HOUR ORBITS
Low degree earth gravity harmonics effect on 12 and 24 hour orbits of high altitude communications satellites
c13 A69-14661

TWENTY-SEVEN DAY VARIATION
Solar cycle and slowly varying components correlation with soft X ray radiation based on spacecraft measurements
c29 A69-40504

TWILIGHT GLOW
Spectral and electrophotometric studies of upper atmosphere - airglows, atomic oxygen, hydroxyl emission, helium line spectra, auroras, and solar cycle effects on magnetosphere
[NASA-TT-F-530] c13 N69-16539

TWO BODY PROBLEM
Second order errors in linearized velocity corrections and their effects on rate of convergence of iterative solutions
[NASA-TN-D-5037] c21 N69-17780

TWO DIMENSIONAL BODIES
Flow characteristics in two dimensional channel with rectangular cavity
[NASA-CR-1245] c12 N69-14095
Photoviscoelastic method for stress analysis of two dimensional viscoelastic models
[NASA-CR-1289] c32 N69-17770

TWO DIMENSIONAL FLOW
Unsteady two dimensional flow in square cavity with fluid initially at rest and constant velocity upper surface of cavity, noting vortex center
[AICHE PAPER 25C] c12 A69-14510
Finite difference method computer programs for calculation of velocities and streamlines on blade to blade surface of revolution of turbomachine
[ASME PAPER 69-GT-48] c01 A69-22495
Incompressible two dimensional turbulent boundary layer equations with arbitrary pressure distribution solved by weighted residual method
[AIAA PAPER 69-397] c12 A69-30478
Quasi-linear ordinary differential equations solutions for steady two dimensional stagnation point flows of nonNewtonian power law fluids
c12 A69-39674
Transonic wind tunnel tests of aerodynamic drag and lift forces on circular cylinder in two dimensional flow at high Reynolds number
[NASA-TR-R-300] c01 N69-17304
Conformal mapping of two dimensional jet flow from two nozzles striking plane surfaces
[NASA-TN-D-5064] c01 N69-17816

TWO DIMENSIONAL JETS
Analytical solution for inviscid separated jet injection at oblique angle into moving stream
[NASA-TN-D-5460] c12 N69-37965

TWO FLUID MODELS
Hydrodynamic stability and vortex containment of two fluid wheel flow to helical disturbances contained by axial magnetic field
[NASA-TN-D-5372] c12 N69-32377

TWO PHASE FLOW
Interphase momentum transfer during propagation of infinitesimal pressure pulse through bubbly flow two phase mixture
c33 A69-43511
Measurement of liquid and two phase hydrogen densities with capacitance density meter
[NASA-TN-D-5015] c14 N69-23470
Two phase hydrogen flow in pump inlet line
[NASA-TN-D-5258] c15 N69-29476
Corrosion in cobalt alloy two phase mercury loop
[NASA-TN-D-5326] c17 N69-31065

TWO REFLECTOR ANTENNAS
Rosman I reflector antenna for collecting data from earth orbiting satellites, discussing dynamic analysis of structural response to natural frequencies
c32 A69-42133

TWO STAGE TURBINES
Scale models of M-1 rocket engine oxygen and hydrogen pump driven two stage turbines used to determine performance and compact inlet manifolds problems
[AIAA PAPER 69-553] c28 A69-32678
Flow analysis to determine turbine efficiency as function of inlet temperature for two stage turbine
[NASA-TM-X-1728] c01 N69-17392
Performance of two stage axial flow turbogenerator with gas bearing rotor support system
[NASA-CR-1290] c03 N69-21771

TYPE 3 BURSTS
Type 3 solar radio bursts observed during April - October 1967 for two alternative models of active region streamers in outer corona
c29 A69-40300

TYPE 4 BURSTS
Synchroton radiation HF cut-off resulting from electrons with anisotropic pitch angle distribution for type 4 solar radio bursts
c29 A69-40577

U

U.S.S.R.
Bibliography of works of Soviet engineer F. A. Tsander
[NASA-TT-F-541] c34 N69-26112
Soviet research on high temperature strength of materials and machine parts
[NASA-TT-F-508] c17 N69-27300
Adaptation to hypoxia, acclimatization, and conditioning in human and animal subjects from Space Biology collection
[NASA-TT-F-580] c04 N69-32131

ULTRAHIGH FREQUENCIES
Transfer of microwave radiation in atmosphere and underlying surfaces measured by aircraft instruments
[NASA-TT-F-590] c13 N69-31851

ULTRAHIGH VACUUM
Thermal stability and friction of disulfides, diselenides, and ditellurides of molybdenum and tungsten in ultrahigh vacuum
[NASA-TN-D-5141] c15 N69-22992
Mechanical behavior of tantalum T-111 alloy at high temperatures and ultrahigh vacuum
[NASA-CR-1436] c17 N69-36831
ULTRASONIC RADIATION
Velocity of 1 MHz sound waves in He 4 along isotherms just above critical temperature, noting specific heat ratio for 4.5 and 5 K isotherms
c23 A69-17142
Holographic displays using ultrasonic vibrations or laser outputs as optical sources, discussing recording materials, responses and computer applications
c14 A69-21394
ULTRASONIC TESTS
Ultrasonic detection and measurement of fatigue cracks in notched cylinders subjected to reversed axial cyclic loading
c14 A69-10113
Effect of ultrasonic vibration on precipitation hardening of steels and superalloys
[NASA-TN-D-5131] c32 N69-21814
ULTRASONICS
Ultrasonic pulse velocity and attenuation measurement in presence of noise, using coherent detection and signal averaging
c14 A69-29564
ULTRAVIOLET PHOTOMETRY
Rocket-borne photoelectric photometers for UV observations of Saturn, using interference filters
c30 A69-22216
ULTRAVIOLET RADIATION
Photodegradation of organic polymers by UV radiation exposure, emphasizing polyvinyl chloride photochemistry and radiation stabilization
c18 A69-10861
Rocket-borne spectroheliograph for monochromatic solar photography in Mg II 2802.7 A line noting filter bandwidth, film polarizers and temperature control
c14 A69-24838
Empirical determination of heating efficiency of extreme solar UV radiation interacting with carbon dioxide atmosphere of Mars and Venus
c30 A69-26019
UV irradiation effects on ZnO spacecraft thermal control coating pigments, discussing photo-Hall, luminescence and electron paramagnetic resonance measurements
[AIAA PAPER 69-639] c18 A69-33288
Transmission effects on plastic films irradiated with ultraviolet light in vacuum
[NASA-TM-X-1905] c18 N69-40339
ULTRAVIOLET SPECTROPHOTOMETERS
Spinning rockets UV spectrophotometry of early type stars, discussing instrumentation, calibration, data recording and stellar spectra
c30 A69-25812
Interstellar extinction in UV from zeta and epsilon Persei spectra obtained with scanner attached to telescope mounted in pointed Aerobee rocket
c30 A69-40772
ULTRAVIOLET SPECTROSCOPY
Vacuum ultraviolet detector-spectroscopy systems for capsule reentry measurements
[NASA-CR-1268] c09 N69-18761
UMBILICAL TOWERS
Vibration characteristics of 1/40 scale model of Saturn 5 launch vehicle and umbilical tower configuration
[NASA-TN-D-4870] c31 N69-10775
Direct stiffness method of computing vibrational characteristics of dynamic model of Apollo-Saturn 5 vehicle - umbilical tower configuration
[NASA-TN-D-4871] c31 N69-10934
UNDERWATER TESTS
Correlation study of simulation of Gemini extravehicular activity with flight results
[NASA-CR-1146] c05 N69-19902
Weightlessness simulation of Gemini extravehicular tasks using neutral-buoyancy underwater techniques
[NASA-TN-D-5235] c05 N69-28024
UNIFORM FLOW
Performance and stall limits of YTF30-P-1 turbofan engine with uniform compressor inlet flow
[NASA-TM-X-1803] c28 N69-27019
UNITED STATES OF AMERICA
Federal government contracting, discussing legality of NASA service contracts
c34 A69-15987
UNITS OF MEASUREMENT
Mathematical model for measurement scale forms
[NASA-TN-D-5277] c19 N69-29141
UNIVERSE
Radioactive decay of neutral pions generated in metagalactic cosmic ray interactions as source of high energy isotropic gamma rays observed by OSO-3
c29 A69-12092
Cosmic gamma rays spectrum from neutral pions production and decay in metagalactic cosmic ray p-p collisions, deriving models based on Einstein general relativity theory
c29 A69-40641
Red shift-magnitude relation for universe model and observational data
[NASA-TN-D-5398] c30 N69-34884
UNIVERSITY PROGRAM
NASA university program, discussing participation in space and aeronautics developed based on project oriented research grants and sustaining university grants
[UN PAPER 68-95413] c34 A69-10506
UNMANNED SPACECRAFT
Meteorological satellite research program, including unmanned satellite observations and possibilities with meteorologist on board manned spacecraft
[UN PAPER 68-95350] c20 A69-10483
Longitudinal range dispersion of unmanned Mars landers using VM-8 and VM-9 atmospheric models, discussing Syrtis Major as possible landing site
c30 A69-12390
Effect of spacecraft onboard radar range and range rate data and accuracy on unmanned probe entry guidance corridor
[NASA-TN-D-4852] c21 N69-16503
UNSTEADY FLOW
Unsteady two dimensional flow in square cavity with fluid initially at rest and constant velocity upper surface of cavity, noting vortex center
[AICHE PAPER 25C] c12 A69-14510
Linear amplification, nonlinear limiting and secondary instability induced by unsteady effects illustrated for various transitional flows, including roughness and streamwise vorticity
c12 A69-33248
Unstable combustion of hydrazine-nitrogen tetroxide caused by transverse gas flow
[NASA-TN-D-4984] c27 N69-19026
UPGRADING
Upgrading of electronic power supply for greater reliability in aerospace use
[NASA-TM-X-1875] c03 N69-35763
UPPER ATMOSPHERE
Electron, ion and neutral particle temperatures of upper atmosphere
c13 A69-14975
Semiannual density variations in thermosphere and exosphere as function of mixtopause height variations
c13 A69-26012
Electron concentration enhancement in upper atmosphere at polar latitudes, noting three independent zones and relation to magnetic local time
c29 A69-28938
UV solar radiation variation effects on Mars and Venus upper atmosphere temperatures
c30 A69-37136
Spectral and electrophotometric studies of upper atmosphere - airglows, atomic oxygen, hydroxyl emission, helium line spectra, auroras, and solar cycle effects on magnetosphere
[NASA-TT-F-530] c13 N69-16539
Survey of rocket soundings to 60 km, and 100 km
[NASA-CR-1293] c13 N69-18700

UPPER IONOSPHERE
Nonvertical propagation effects on high altitude topside ionosphere sounder data reduction, using ray tracing
c13 A69-18838
Ion composition and charged particle temperatures at 300-600 km from sounding rocket and topside sounder Alouette 2 measurements
c13 A69-18839
Satellite measurements of suprathermal electrons at conjugate sunrise, indicating photoelectron escape from production level and movement along geomagnetic lines into conjugate ionosphere
c29 A69-25144
Ionospheric satellites objectives and development resulting from topside sounder and ISIS programs
c13 A69-37855
Topside ionogram reduction for ionospheric electron density determination, using geomagnetic strength at all heights, iteration and change of variables
c13 A69-37864
Global electron density distribution morphology in topside ionosphere during sunspot minimum from Alouette 1 and 2 ionograms
c13 A69-37867
Applicability and limitations of diffusive equilibrium in topside ionosphere, noting plasma density distribution along magnetic field line
c13 A69-37887
Diurnal and seasonal variations of primary atmospheric ions in topside ionosphere correlated with solar zenith angle, using ion mass spectrometer on Explorer 32
c13 A69-38087
Topside ionosphere response to magnetic storms, using Explorer 22 satellite electron concentration and temperature measurements
c13 A69-42438
Computation of topside ionograms from electron concentration profiles
[NASA-TN-D-5052] c13 N69-23557
UPWASH
Upwash patterns on ablating and nonablating cones at hypersonic speeds
[NASA-TN-D-5346] c12 N69-37370
URANIUM
Gaseous reactor fluid mechanics for nuclear rocket engines, discussing experiments on geometries used in open cycle engine for acceptable uranium loss rate
[AIAA PAPER 69-477] c22 A69-32728
Group cross section generating techniques to calculate neutron capture rates and spatial capture distribution in depleted thick U slab, using GAROL program
c24 A69-35179
Compatibility tests of molten uranium with tungsten and tungsten-1.5 percent hafnium
[NASA-TN-D-5076] c17 N69-19930
Composition and line emission characteristics of ionized tungsten, uranium, and argon
[NASA-CR-1313] c25 N69-21124
Spectral emission characteristics of gaseous tungsten and uranium in induction heated argon plasmas
[NASA-CR-1314] c25 N69-22920
Tungsten and depleted uranium in minimum weight, layered shield comparisons for space power reactor
[NASA-TM-X-1874] c22 N69-35817
URANIUM CARBIDES
Uranium carbides irradiation tests for control of nuclear fuels fission gas swelling
[NAA-SR-12629] c22 N69-22946
URANIUM COMPOUNDS
Uranyl ions interaction with phospholipid and cholesterol monolayers, using surface pressure and potential measurements
c06 A69-25641
Fabrication of cermets of uranium nitride and tungsten or molybdenum from mixed powders and from coated particles for nuclear fuel elements
[NASA-TN-D-5136] c17 N69-21404
URANIUM OXIDES
Uranium dioxide vent loss in externally fueled thermionic reactor concept
[NASA-TN-D-4922] c22 N69-10099
Fission product gas pressure calculated for uranium dioxide ceramic fuel elements
[NASA-TN-D-4823] c22 N69-10216
Rate of loss of uranium dioxide or uranium mononitride from vented nuclear fuel element
[NASA-TN-D-4913] c22 N69-10734
Nondestructive methods for fuel density determination in uranium dioxide
[NASA-TM-X-1779] c22 N69-22555
Radial power tailoring for uranium dioxide-T-111 clad reactor with contained fission product gases
[NASA-TM-X-1795] c22 N69-25305
Heat transfer and neutronic calculations after fuel emitter separation in uranium oxide fueled thermionic diodes
[NASA-TM-X-1812] c22 N69-28212
Furnace brazing butt joints in tungsten-uranium dioxide cermet cylinders at 3000 deg C
[NASA-TM-X-1815] c15 N69-28862
URANIUM 233
Uranium 233 critical mass requirements, neutron kinetic behavior, and neutron and gamma ray heating rates for nuclear light bulb rocket engine
[NASA-CR-1315] c25 N69-23451
Reflector based poison drum control on equal size reactor cores fueled with U-233 and U-235
[NASA-TM-X-1883] c22 N69-36756
URANIUM 235
Reflector based poison drum control on equal size reactor cores fueled with U-233 and U-235
[NASA-TM-X-1883] c22 N69-36756
URANIUM 238
Multigroup calculations of resonance neutron capture in thick slab of depleted U-238
[NASA-TM-X-1878] c24 N69-36901
URANUS (PLANET)
Planetary flight handbook - direct trajectories to Jupiter, Saturn, Uranus, and Neptune
[NASA-SP-35-VOL-3-PT-7] c30 N69-33490
URBAN DEVELOPMENT
Multispectral orbital photography used to obtain urban land-use data
[AAS PAPER 69-483] c13 A69-42837

V

V GROOVES
Herringbone grooved gas lubricated journal bearing stability, testing effects of geometries and clearances on onset speed for half frequency whirl
[ASME PAPER 68-LUBS-25] c15 A69-27271
Plasma generation using large V-groove cathode discharge
[NASA-TN-D-5269] c25 N69-29140
V/STOL AIRCRAFT
V/STOL aircraft characteristics, emphasizing propeller, ducted fan and turbojet types
c02 A69-15563
Wind tunnel wall constraints effects at extreme force coefficients during V/STOL testing shown different from effects in conventional aircraft testing
c11 A69-15574
Exhaust gas reingestion and inlet flow distortion in V/STOL lift engines, discussing static and wind tunnel testing using fighter configuration models
[AIAA PAPER 68-78] c01 A69-26762
Aerodynamics of rotary wing and V/STOL aircraft-Conference, Buffalo, June 1969, Volume 2, Wind tunnel testing, new concepts in rotor control
c01 A69-35226
V/STOL aircraft radar inertial navigation system, describing approach and landing phase flight test results
[AAS PAPER 69-401] c02 A69-42831
Instrument display devices for landing VTOL aircraft
[NASA-TN-D-4861] c21 N69-10069
Aerodynamic characteristics of large semi-span V/STOL tilt-wing with single propeller tested for modes of propeller rotation
[NASA-TN-D-5016] c01 N69-17312
Computer program for calculating wall interference factors of V/STOL aircraft and conventicnal airplanes

[NASA-TR-R-302] c01 N69-19028
Wind tunnel tests for V/STOL aircraft having direct-lift and lift-cruise jet nozzles
[NASA-TM-X-1758] c01 N69-20016
Wind tunnel investigation of static stability characteristics of model jet-lift V/STOL research airplane
[NASA-TM-X-1835] c02 N69-30633
Jet exhaust location effects on longitudinal aerodynamic characteristics of jet V/STOL model
[NASA-TN-D-5333] c01 N69-33210
Performance of turbine driven V/STOL cruise fan propulsion system at subsonic Mach numbers
[NASA-TN-D-5314] c28 N69-35526
Empirically determined wind and scale effects on hot gas recirculation characteristics of jet V/STOL aircraft
[NASA-CR-1445] c28 N69-40776

VACUUM
Disk radiometer for use in space vacuum-thermal environmental studies
[NASA-TN-D-4925] c14 N69-13311
Rate of rise outgassing measurement technique in vacuums
[NASA-TN-D-4973] c14 N69-16097
Impingement forces, moments, and centers of pressure due to air jets in vacuum sphere
[NASA-TN-D-5147] c12 N69-23085
NERVA control drum actuator tests in cryogenic temperature, nuclear radiation, and vacuum environments
[NASA-TN-D-5347] c22 N69-31870

VACUUM APPARATUS
Vacuum distillation technique for isolation and recovery of alkali metal reaction products with Ta, Ni, V and oxygen
c14 A69-10927
Vacuum distillation determination of O in Li, evaluating accuracy through O additions and recoveries, method blank and residue identification
c06 A69-40932

VACUUM CHAMBERS
In situ vacuum testing requirement for valid measurement of vacuum induced changes in mechanical and thermal properties of various filled elastomers
c11 A69-22008
Solid solutions atomic ordering effect on friction and wear in vacuum, using CuAu and FeCo systems
c15 A69-35183
Pressure measurements and gas flow analysis during thermal vacuum tests of manned spacecraft indicating adequate space vacuum simulation
[AIAA PAPER 69-1033] c11 A69-40401
Biomechanical factors determining lung damage following explosive decompression of space suits in vacuum test chambers
[NASA-CR-1223] c05 N69-13969

VACUUM DEPOSITION
Physical sputtering deposition of molybdenum disulfide films as solid lubricant on rotating and sliding components, discussing lubrication properties in vacuum
[ASLE PAPER 68-LC-15] c15 A69-19308
Energetics in solid film lubricants vacuum deposition methods, showing dependence on interfacial and film characteristics
c15 A69-29001
Thin film formation, deposition methods and relation to film structure and properties
c26 A69-43344

VACUUM EFFECTS
Polymer films tensile properties after exposure to gamma radiation in vacuum, noting chain scission and cross linking
[ASME PAPER 68-WA/RP-6] c18 A69-16160
In situ vacuum testing requirement for valid measurement of vacuum induced changes in mechanical and thermal properties of various filled elastomers
c11 A69-22008
Sliding friction tests of Cu and Cu-Be alloy plates in contact with various alloy sliders in air and vacuum
[ASLE PAPER 68-LC-5] c15 A69-30610
Solid film lubricants deposited by DC triode sputtering on Ni, Ni-Cr and Nb surfaces friction tested under ultrahigh vacuum conditions
c15 A69-43126
Transmission effects on plastic films irradiated with ultraviolet light in vacuum
[NASA-TM-X-1905] c18 N69-40339

VACUUM GAGES
Volume-ratio system for vacuum gage calibration from 10 to minus 8 to 10 torr
[NASA-TN-D-5406] c14 N69-35265

VACUUM MELTING
Vacuum arc melted W and W-Re alloys mechanical properties, noting Re additions effects
c17 A69-20190

VACUUM SPECTROSCOPY
Vacuum ultraviolet detector-spectroscopy systems for capsule reentry measurements
[NASA-CR-1268] c09 N69-18761

VACUUM SYSTEMS
Magnetron ionization gauge in helium for low pressure measurement, discussing striking characteristics and time lags
c03 A69-10606
Glass vacuum systems grease free assembly method using heat shrinkable polyolefin sleeve tubing connector for compression of O ring joints
c15 A69-20529
Vacuum distillation determination of oxygen in lithium
[NASA-TN-D-5197] c06 N69-23706
Cryogenic molecular beam system with pressure attenuation
[NASA-TN-D-5308] c24 N69-31338
Quantitative method for determination of fission gases trapped in irradiated fuel forms
[NASA-TM-X-1893] c22 N69-37225

VACUUM TUBES
Vacuum tube with cathode heated directly by external radioisotope source, noting heat pipe providing isothermal heat transfer
c09 A69-24748

VALVES
Fast response electrohydraulic valve-controlled piston servo systems
[NASA-TN-D-5388] c03 N69-34652

VANADIUM
Electron microprobe analysis of vanadium in presence of titanium by compositional measurement of chromite in chondritic meteorites
c06 A69-18419
Solubility of vanadium in liquid potassium
[NASA-TN-D-5093] c17 N69-20789

VAPOR DEPOSITION
Powder metallurgy, fusion and chemical vapor deposition techniques in manufacturing tungsten base alloys
c17 A69-18792
Cubic /beta/ silicon carbide films deposition by volatilization in presence of acetylene
c26 A69-21350
Chemical processes in silicon carbide due to reactive deposition and chemical conversion, noting silicon growth mechanism involving outward diffusion
c26 A69-21351
Ge films formation by evaporation technique, discussing background O pressure effect
c26 A69-43345
Thermionic converter with chloride vapor deposited tungsten emitter and nickel collector
[NASA-CR-1416] c03 N69-32553
Technique for measuring ion energy loss in vapor deposited materials
[NASA-TN-D-5430] c24 N69-36929

VAPOR PHASES
Oxygen depletion effect in chemical reactions between pyrolysis gases and air stream on surface recession of charring ablators
[AIAA PAPER 68-302] c33 A69-21982
Laser ignited combustion of 365 micron Zr droplets falling in ultrapure oxygen using spectroscopic and photographic techniques, discussing vapor phase transport phenomena
[WSCI PAPER 69-4] c27 A69-32345
Dissociation energy of gaseous titanium nitride
[NASA-TN-D-5027] c06 N69-19129
Thermodynamic properties of liquid and gas phase equilibria of water plus heavy water
[NASA-TN-D-5223] c33 N69-26247
Computer program used to infer atmospheric water-vapor mixing ratio from measured horizon

radiance profiles
[NASA-TN-D-5252] c13 N69-27246
Net positive suction head requirements for helical inducer in liquid hydrogen under varied flow and temperature conditions
[NASA-TM-X-1808] c09 N69-27841
Transient condensing with freezing on nonisothermal inclined plate
[NASA-TN-D-5289] c33 N69-29598

VAPOR PRESSURE
Mean drop size generated in vapor pressure regime of liquid water jet, noting effect of water temperature and orifice diameter
c12 A69-21995

VAPORS
Vapor ingestion phenomenon during draining in weightlessness
[NASA-TN-D-5210] c12 N69-24917

VARACTOR DIODES
Computerized design parameters for realizable overdriven bimode varactor frequency doubler based on charge-voltage relationship at break point
c09 A69-37299

VARIABLE GEOMETRY STRUCTURES
Aerodynamic and flight characteristics of variable geometry entry spacecraft during subsonic wing deployment and landing
[AIAA PAPER 69-742] c01 A69-34407
Hypersonic aerodynamic characteristics of low fineness ratio variable geometry logistics spacecraft model
[NASA-TM-X-1701] c01 N69-13218
Transonic wind tunnel evaluation of variable stabilizer configuration effects on hypersonic elliptical lifting body dynamics
[NASA-TM-X-1789] c01 N69-25244

VARIABLE STARS
Variable He star HZ29, noting unusually wide and shallow He I lines and possible mass and composition
c30 A69-16931
Star twinkling absence for lunar observation laboratory, noting star distance measurement and laser action in stellar atmospheres
c30 A69-27172
Radial pulsation mode of convective envelopes in adiabatic equilibrium for variable M red supergiant stars
c30 A69-30766
Variable stars blue sequence, proposing mu mechanism and beta mechanism as explanation for radial pulsations
c30 A69-40650
IR excess of R CrB type variable star RY Sgr, noting visual brightness and radiation in 2.0-3.4 micron range
c30 A69-42377

VARIABLE SWEEP WINGS
Large scale wind tunnel tests to improve longitudinal stability of supersonic transports with variable swept wings
[NASA-TN-D-5005] c02 N69-16384

VARIANCE (STATISTICS)
Recursive equation for estimating variance of sequential random numbers
[NASA-TN-D-5465] c19 N69-38178

VARIATIONS
Comparison of ray trace methods for estimating sound intensity variations due to atmospheric variability as determined by Monte Carlo methods
[NASA-CR-1337] c23 N69-23199
Fluctuating properties of turbulent boundary layers for Mach numbers up to 9
[NASA-TN-D-5496] c12 N69-40137

VECTOR ANALYSIS
Vector integral extension to optimal trajectory coordinate multiplier systems with constant of motion demonstrated for coast-arc problem
[AIAA PAPER 69-907] c30 A69-39339
Computer mechanization of reentry equations with four degrees of freedom
[NASA-CR-1249] c30 N69-13300

VECTORS (MATHEMATICS)
Approximation for mean and standard deviation of magnitude of statistical velocity correction vector
[NASA-TN-D-5381] c30 N69-36143

VELOCITY
Fluctuating properties of turbulent boundary layers for Mach numbers up to 9
[NASA-TN-D-5496] c12 N69-40137

VELOCITY DISTRIBUTION
Unsteady two dimensional flow in square cavity with fluid initially at rest and constant velocity upper surface of cavity, noting vortex center
[AICHE PAPER 25C] c12 A69-14510
Stony meteoric particles size and velocity during passage through atmosphere
c30 A69-26341
Solar wind Helmholtz-type velocity discontinuities, noting plasma density and temperature stabilities from Explorer 34 observations
c29 A69-29971
Radio galaxy Messier 87 mass determined using virial theorem for nucleus velocity dispersion
c30 A69-30883
Density and velocity fluctuations in hypersonic turbulent boundary layer based on Wallace data
c12 A69-31908
Baronti-Libby transformation and Preston tube calibrations used to determine skin friction from turbulent velocity profiles
[NASA-TN-D-4853] c12 N69-10472
Use of photoionization in measuring velocity profile of free stream flow in expansion tube
[NASA-TN-D-4936] c12 N69-13945
Response of infinite elastic plates to axisymmetric initial velocity distributions with application to hypervelocity impact
[NASA-TN-D-5118] c32 N69-23448
Graphical interpolation charts of local skin friction from compressible velocity profiles
[NASA-SP-3048] c01 N69-25391
Weighting factor for correction of photographic bias caused by variation in mass and velocity of sporadic meteoroids
[NASA-TN-D-5245] c30 N69-26239
Torque and leakage rates of various lubricated lip seal designs at peripheral velocity of 120 feet per second
[NASA-TN-D-5411] c15 N69-35769
Elastohydrodynamic analysis and experimental speed effects on ball spinning friction coefficients and torque
[NASA-TN-D-5527] c15 N69-41210

VELOCITY ERRORS
Interplanetary midcourse velocity correction schedules optimization, discussing timing equations modifications, mission simulation and role of earth based radar
c21 A69-39646
Second order errors in linearized velocity corrections and their effects on rate of convergence of iterative solutions
[NASA-TN-D-5037] c21 N69-17780
Approximation for mean and standard deviation of magnitude of statistical velocity correction vector
[NASA-TN-D-5381] c30 N69-36143

VELOCITY MEASUREMENT
High speed compression waves, rarefaction waves and gas interface regions position and velocity measurement in shock tube by sensing electrical impedance
c14 A69-13104
Doppler shift measurements of axial and rotational velocities in MPD arc, using reference lines from iron arc
[AIAA PAPER 69-110] c25 A69-18171
Three dimensional laser Doppler velocity instrument for mean velocity and turbulence measurements in subsonic jet shear layer
[SAE PAPER 690266] c14 A69-21555
Coaxial three coil probe measuring local electrical conductivity and velocity in plasma streams, discussing operations in electrolytes and axisymmetric plasma stream
[AIAA PAPER 69-327] c25 A69-28264
Ultrasonic pulse velocity and attenuation measurement in presence of noise, using coherent detection and signal averaging
c14 A69-29564
Axial velocities in ammonia MPD thrustor exhaust by measuring Doppler shifts of spectral lines

emitted by plasma constituents
c28 A69-31890
Laser Doppler velocity instrument for measuring turbulence and mean velocity in subsonic and supersonic gas flows
[R-67-4450] c14 N69-14351
FORTRAN program for calculating velocities and streamlines on blade to blade stream surfaces of turbomachinery
[NASA-TN-D-5044] c01 N69-21811
Turbulent boundary layer temperature and velocity measurements in supersonic water-cooled conical nozzle
[NASA-TN-D-5377] c12 N69-33353
Object motion effect in Fraunhofer holography with application to velocity measurements
[NASA-TN-D-5515] c14 N69-40812

VENTILATION
Ventilation-perfusion inequality increase effects on lung overall gas exchange, using digital model
c05 A69-38388

VENTING
Rate of loss of uranium dioxide or uranium mononitride from vented nuclear fuel element
[NASA-TN-D-4913] c22 N69-10734
Venting of spherical liquid hydrogen tankage
[NASA-TN-D-5263] c33 N69-27620

VENTURI TUBES
Venturi meter with separable diffuser and radial outward step at transition from throat to diffuser, noting effect of step on efficiency
[ASME PAPER 68-WA/FM-2] c14 A69-16135
Prediction of thermodynamic effects of developed cavitation based on liquid hydrogen and Freon-114 data in scaled venturis
[NASA-TN-D-4899] c12 N69-10070

VENUS (PLANET)
Critique of paper on water crystal existence on Venus, presenting arguments against existence of clouds of micron sized ice crystals
c30 A69-11292
Manned Mars and Venus missions role in overall planetary exploration program
c30 A69-12304
Chemical composition of Earth, Venus, Mars, Mercury and Moon calculated from mathematical models, constructing approximate equations of state at high pressure
c30 A69-29878
Research problems in atmospheric entry and landing of manned planetary space flights to Mars and Venus
[NASA-TN-D-4977] c31 N69-15634
FORTRAN computer program for providing mission design data for elliptical orbits around Mars and Venus
[NASA-TN-D-5104] c30 N69-22571
Radar observations and radiophysical investigations of Venus
[NASA-TT-F-536] c30 N69-38643

VENUS ATMOSPHERE
Venus microwave phase effect analyzed assuming dry massive Venus atmospheric model, discussing heat transfer processes
c30 A69-12108
Venus exospheric temperature for various composition models, discussing carbon dioxide concentration effects
c30 A69-12109
Venus atmosphere origin, discussing high temperature effects and chemical composition via space probe and terrestrial observations
c30 A69-23183
Atmospheric models for exospheric temperatures of Mars and Venus based on photoionization heating efficiency
c30 A69-26020
Venus atmosphere chemical composition, surface temperature and pressure obtained by Venera 4 and Mariner 5
c30 A69-26129
Visual ashen light observation on Venus possibly attributable to solar particle bombardment from dark side emission detection by spectroscopic and photometric studies
c30 A69-32300
Cloud scattering corrections added to synthetic spectrum analysis of carbon dioxide bands and water vapor line in Venus spectrum
c30 A69-33161
UV solar radiation variation effects on Mars and Venus upper atmosphere temperatures
c30 A69-37136
Engineering models of Venus atmosphere for design and mission planning for spacecrafts
[NASA-SP-8011] c30 N69-20916

VENUS PROBES
Venus atmosphere origin, discussing high temperature effects and chemical composition via space probe and terrestrial observations
c30 A69-23183

VERTICAL DISTRIBUTION
Radar backscatter and rocket profiles of ionospheric electron temperature, noting agreement in daytime flight measurements
c29 A69-25162
Semiannual density variations in thermosphere and exosphere as function of mixtopause height variations
c13 A69-26012
Spectrometric rocket measurements of ion concentrations between 200 and 630 km
c13 A69-31974
Ion, electron and neutral temperatures from ion composition distribution, assuming no change in vertical distribution within horizontal distance between upleg and downleg measurements
c29 A69-31990
Nonlinear least squares optimization program applied to atmospheric temperature sounding, solving for temperatures at various altitudes from simulated carbon dioxide intensity measurements
c13 A69-33156
Vertical tropospheric humidity distribution estimation from IR spectra obtained by TIROS satellites
c13 A69-34284

VERTICAL TAKEOFF AIRCRAFT
Aerodynamics of rotary wing and V/STOL aircraft - Conference, Buffalo, June 1969, Volume 3
c01 A69-41369
Theoretical analysis of axisymmetric flow in VTOL lift fan inlets without crossflow
[NASA-TN-D-5065] c01 N69-17831
Lift loss and jet decay measurements on hovering vertical takeoff aircraft models
[NASA-CR-1297] c01 N69-21477
Direct side-force maneuvering system on deflected X-14A jet VTOL aircraft without changing bank angle
[NASA-TN-D-5175] c02 N69-22572
Wind tunnel and analytical study of conversion from wing lift to rotor lift on composite lift VTOL aircraft
[NASA-TN-D-5256] c02 N69-28044
Wind tunnel investigation of steady state aerodynamics of composite lift VTOL aircraft model combining rotary and fixed wings
[NASA-TN-D-5232] c02 N69-28097
Analysis of two dimensional inviscid model jet impingement under verticle takeoff airplane
[NASA-TN-D-5288] c01 N69-29479
In-flight simulation to evaluate simultaneous use of attitude control for jet VTOL maneuvering
[NASA-TN-D-5342] c02 N69-32110
Flight evaluation of tip turbine driven fans for lateral control in hovering VTOL aircraft
[NASA-TN-D-5491] c02 N69-38807

VERY HIGH FREQUENCIES
Solar flare and sunspot effects on VHF communications between synchronous satellite relay and ground stations
[NASA-TN-D-5100] c07 N69-23317

VESTIBULAR TESTS
Human vestibular system and its connection with oculomotor system and their relation to motion perception, spatial disorientation, and illusions
[NASA-CR-1309] c04 N69-22637

VESTIBULES
Rotational velocity estimates by observers during angular acceleration, noting vestibular function interpretation
c04 A69-15332

VHF OMNIRANGE NAVIGATION
Navigation-aids identification decoder and display

device for general aviation aircraft
[NASA-TN-D-5445] c09 N69-38852
VIBRATION
Electron beam technique of measuring molecular rotational and vibrational temperatures of nitrogen in hypersonic tunnel using air as test gas
[NASA-TN-D-4892] c33 N69-10932
Direct stiffness method of computing vibrational characteristics of dynamic model of Apollo-Saturn 5 vehicle - umbilical tower configuration
[NASA-TN-D-4871] c31 N69-10934
Human responses to aerospace environment related to acceleration, vibration, sound, and noise
[NASA-CR-1205-VOL-2] c04 N69-12588
Prediction curves for launch vehicle vibration levels in region of spacecraft adaptor
[NASA-CR-1227] c31 N69-16155
VIBRATION DAMPING
Axial waves in blood vessels, determining phase velocities and damping, noting anisotropic behavior of artery wall
[SESA PAPER 1350] c04 A69-19726
Flutter design charts for isotropic panels stressed to verge of buckling for typical values of structural damping
c32 A69-25524
Effects of structural damping on flutter of stressed panels
[NASA-TN-D-4990] c32 N69-16091
Vibrations of turbomachine rotors and methods for determining optimal hydraulic damping mounts, vibrations of systems with friction, and self induced vibrations of compressor blades
[NASA-TT-F-547] c02 N69-36326
VIBRATION EFFECTS
Human body dynamic response to vibration combined with linear acceleration, noting changes in body mechanical impedance and resonance
c05 A69-11335
Effect of ultrasonic vibration on precipitation hardening of steels and superalloys
[NASA-TN-D-5131] c32 N69-21814
Vibration of shaft face seals and stabilizing effect of viscous and friction damping
[NASA-TN-D-5161] c15 N69-23466
Dynamic stability of mechanisms with elastic couplings under vibratory impact
[NASA-TT-F-534] c15 N69-35859
Vibrations of turbomachine rotors and methods for determining optimal hydraulic damping mounts, vibrations of systems with friction, and self induced vibrations of compressor blades
[NASA-TT-F-547] c02 N69-36326
VIBRATION MODE
Dynamic instability of solid bodies, using modal vibration method to establish criteria on basis of equivalent energy conditions
c32 A69-16742
Geometrically exact finite element for thin shells of revolution, using approximation to predict boundary layer stress distribution during vibration
[AIAA PAPER 69-56] c32 A69-18193
Plasma oscillation modes perpendicular to magnetic field used to study energy conversion by wave coupling across density discontinuity
c25 A69-20795
Dynamic analysis of axisymmetric ring stiffened shells with attached asymmetric elastic structures, noting vibration modes
c32 A69-25525
Finite element method for computing natural frequencies and mode shapes of thin shells of revolution
[NASA-TN-D-4972] c32 N69-16469
Natural vibration modal analysis as related to space vehicle design criteria
[NASA-SP-8012] c32 N69-22773
Effect of shallow meridional curvature on vibration of nearly cylindrical shells
[NASA-TN-D-5143] c32 N69-22821
Longitudinal mass spring modeling of launch vehicles
[NASA-TN-D-5371] c32 N69-34970
VIBRATION SIMULATORS
Temperature and pressure effect on cobalt base alloy cavitation in liquid sodium, using vibratory apparatus and loss rate contour diagram
c17 A69-35184
Vibration test fixture design for mount impedance simulation of aerospace structures
[NASA-CR-1351] c32 N69-26315
VIBRATION TESTS
Vibration characteristics of 1/40 scale model of Saturn 5 launch vehicle and umbilical tower configuration
[NASA-TN-D-4870] c31 N69-10775
Lateral vibration characteristics of dynamic model of Apollo-Saturn 5 launch vehicle
[NASA-TN-D-4872] c31 N69-11007
Saturn 5 launch vehicle scale model tests for free vibration during first stage burn
[NASA-TN-D-5159] c32 N69-22932
VIBRATIONAL SPECTRA
Molecular vibration absorption spectra from variation of field emitted electron energy distribution due to inelastic electron-molecule interaction at metal-vacuum interface
c24 A69-26097
Rate coefficient for primary process in removing molecular nitrogen in high vibrational levels from active nitrogen by N atoms
c24 A69-36424
Molecular vibration spectra from field emission energy distributions
[NASA-TN-D-5423] c24 N69-36924
VIDEO DATA
Adaptive compression system for predicting and encoding video data for transmission in noiseless channel
c14 A69-12869
VIDEO EQUIPMENT
Density measurements of particle tracks in nuclear emulsions utilizing digitized video scan, discussing operation and instrumentation
[IEEE PAPER 2A-7] c14 A69-19185
VIEW EFFECTS
Evaluation of contact analog display in landing approaches with helicopters
[NASA-TN-D-5241] c02 N69-27177
VIKING LANDER SPACECRAFT
Thermal control coatings, windows and mirrors for 1973 Mars Viking Lander vehicles under simulated Martian surface conditions
[AIAA PAPER 69-1023] c11 A69-40393
VINTI THEORY
Vinti dynamic problem relevance to prediction of satellite orbits using differential and integral equations
[NASA-TR-R-307] c30 N69-22948
VIRIAL THEOREM
Radio galaxy Messier 87 mass determined using virial theorem for nucleus velocity dispersion
c30 A69-30883
VIRUSES
Viruslike particles in fat body cells and oenocytes of Drosophila melanogasters imagoes, in glial cells of cephalic ganglionic center of flies and in gamma radiated cells
c04 A69-42021
VISCOELASTICITY
Normal stress effects in viscoelastic fluid theories applied to one dimensional Burgers model of weak turbulence predicting drag reduction
c12 A69-33256
Stable crack propagation in viscoelastic strip of polyurethane rubber
[NASA-CR-1279] c30 N69-21506
VISCOPUMPS
Pump and seal parameters for helical groove, hermetically sealed pump and bearing rotor
[NASA-TN-D-5225] c15 N69-24791
VISCOSITY
Dilute solution of He 3 in He 4 near absolute zero measured for viscosity, showing temperature effect
c23 A69-39582
Model analysis for viscosity in jet mixing flows
[NASA-CR-1382] c12 N69-31887
Surface tension, viscosity, and density of fluorocarbon solvents as function of temperature
[NASA-TM-X-1862] c18 N69-34134
VISCOUS DAMPING
Loss factor and resonant frequency of viscoelastic shear damped structural composites

[NASA-CR-1269] c32 N69-17766
Vibration of shaft face seals and stabilizing effect of viscous and friction damping
[NASA-TN-D-5161] c15 N69-23466
VISCOUS DRAG
Viscous drag reduction - Conference, Dallas, September 1968
c12 A69-33247
Turbulence measurements and roughness effects on viscous drag reduction with polymer solution in pipe flow, discussing friction factor, wall velocity profile, etc
c12 A69-33252
Concentration, flow rate and tube diameter effects on viscous drag reduction in nonpolar soap solutions, using pressure drop measurements to observe turbulent flow behavior
c12 A69-33253
VISCOUS FLOW
Numerical method for time dependent compressible Navier-Stokes equations applied to axisymmetric flow field produced by hypervelocity impact, examining viscous effects
[AIAA PAPER 69-354] c32 A69-28288
Relation between ellipsoidal velocity distribution function and macroscopic flow equations
[NASA-TN-D-5026] c12 N69-17827
Laminar incompressible viscous flow in short cylindrical vortex chamber with finite swirl ratio
[NASA-TN-D-5132] c12 N69-21400
Numerical calculation of viscous compressible flow around harmonic oscillating rigid cylinder
[NASA-CR-1467] c12 N69-38782
VISCOUS FLUIDS
Nondimensional Jeffreys number as ratio of Reynolds to Froude number for gravitational motion of viscous masses, with application to lunar maria and plastic ice
c30 A69-19262
Nonlinear disturbance decay in unbounded viscous fluid
[NASA-TN-D-4947] c12 N69-14483
Physical properties of magnetic base ferrofluids
[NASA-CR-1407] c06 N69-33493
VISIBILITY
Visual acuity and visibility of markings on ground in long duration earth orbital space flight
[NASA-CR-1134] c05 N69-10813
VISUAL ACUITY
Minimal angle of resolution /MAR/ between point and extended circular source and between point source and simulated horizon, studying irradiation effects on manual navigation
c21 A69-19208
Visual acuity and visibility of markings on ground in long duration earth orbital space flight
[NASA-CR-1134] c05 N69-10813
VISUAL DISCRIMINATION
Human perception of multiple-point tactile and visual stimuli
[NASA-CR-1389] c05 N69-39211
VISUAL OBSERVATION
Visual ashen light observation on Venus possibly attributable to solar particle bombardment from dark side emission detection by spectroscopic and photometric studies
c30 A69-32300
Visual observation of meteor and train microstructure obtained by refractor
c30 A69-41058
Atmospheric turbulence limits on resolution of manned aerospace observations of ground
[NASA-TN-D-4940] c20 N69-12934
Pilots and flight simulator used in study of human visual sampling study
[NASA-CR-1258] c05 N69-14145
VISUAL PERCEPTION
High oxygen concentration breathing effect on foveal thresholds, using sea level tests on trained observers
c05 A69-12216
Detection time to light point source noting response to dark, star field and glare source backgrounds
c05 A69-17215
Luminescence effects on apparent size and shape of foveally fixated targets of various forms
c04 A69-36458
Visual sensing and spacecraft guidance for earth orbit rendezvous maneuvers
[NASA-CR-1214] c05 N69-13161
Peripheral vision displays for presenting dynamic control information
[NASA-CR-1239] c05 N69-14478
Differential thresholds for rotary and linear motion in the periphery
[NASA-CR-1439] c05 N69-36925
VISUAL SIGNALS
Visual simulation image generation using flying spot scanner
[NASA-TN-D-5151] c11 N69-23194
VISUAL STIMULI
Human perception of multiple-point tactile and visual stimuli
[NASA-CR-1389] c05 N69-39211
VISUAL TASKS
Minimal angle of resolution /MAR/ between point and extended circular source and between point source and simulated horizon, studying irradiation effects on manual navigation
c21 A69-19208
Human information processing rates during one and two axis compensatory tracking tasks with secondary auditory task
c05 A69-23880
Indirect optical viewing system in F-104B for simulated lifting-body approach and landing tasks
[NASA-TN-D-5299] c14 N69-29730
VOICE COMMUNICATION
Technological and cost factors of voice broadcasts from satellites to earth
[NASA-TM-X-1747] c07 N69-19025
VOICE DATA PROCESSING
Man-computer speech communication, discussing model and aspects of acoustics, phonetics, linguistics, language training, physiology, psychology, bionics, etc
c08 A69-35099
VOIGT EFFECT
Computer program to predict spectra from electronic transitions of diatomic molecules and atoms, noting line intensity distribution by Voigt profile
c24 A69-35239
Computer program for line-by-line calculation of spectra from diatomic molecules and atoms assuming Voigt line profile
[NASA-TN-D-5088] c24 N69-21462
VOLT-AMPERE CHARACTERISTICS
SERT 2 mercury vapor fed hollow cathode operated in bell jar, determining volt-ampere characteristics and flow rates for plasma diagnostics
[AIAA PAPER 69-258] c28 A69-21221
Current oscillations in semiinsulating O and Cr doped GaAs samples at room temperature, noting photoconductivity excitation spectra
c26 A69-21753
Composite carbon resistor characteristics used for accelerator terminal voltage measurement
[NASA-TM-X-1718] c24 N69-14398
VOLTAGE REGULATORS
Passive circuit to transform voltage of indefinitely repeated positive or negative pulses using transistors, diodes and magnetic cores
c09 A69-10564
Magnetic core logic circuit system for bidirectional stepping motor drive voltage power supply control in proper phase and time sequence
c09 A69-11000
Variable voltage dc power supplies for energizing cryogenically cooled and superconductive electromagnets
c03 A69-26498
VOLTERRA EQUATIONS
Coupled set of differential equations describing generalized Volterra problem of conflicting populations and application to plasma oscillations
c19 A69-41260
VOLUME
Volume effects on normal gravity pressurization of spherical liquid hydrogen tanks
[NASA-TN-D-5196] c33 N69-24168

Volume-ratio system for vacuum gage calibration from 10 to minus 8 to 10 torr
[NASA-TN-D-5406] c14 N69-35265
VON ZEIPEL METHOD
Lunar and artificial satellite theories treated by generalization of Von Zeipel procedure
[NASA-TN-D-5459] c30 N69-38145
VORTEX GENERATORS
Performance evaluation of plain rotor blade with plow type vortex generators
[NASA-CR-1342] c28 N69-24223
Flow model for vortex shedding from slender body in coning motion
[NASA-CR-1448] c12 N69-40200
VORTEX INJECTORS
Vortex motion enhancement of jet penetration and spreading in supersonic fuel injection into large diameter combustors
[AIAA PAPER 69-664] c12 A69-33437
Helium penetration and spreading in Mach 2 airstream using Delta wing injector
[NASA-TN-D-5322] c01 N69-30878
VORTICES
Unsteady two dimensional flow in square cavity with fluid initially at rest and constant velocity upper surface of cavity, acting vortex center
[AICHE PAPER 25C] c12 A69-14510
Light aircraft hazards due to trailing vortex generated by heavy transport aircraft, suggesting specific procedures for takeoff, landing and flight phase
[SAE PAPER 680220] c02 A69-14930
Cross hatching on various body surfaces due to periodic surface pressure fluctuations, discussing origin from counter-rotating longitudinal vortices in boundary layer
[AIAA PAPER 69-11] c12 A69-18213
Flexible rotor blade dynamic response to radially moving force, emphasizing helicopter rotor vibration characteristics associated with tip-vortex impingement
[AIAA PAPER 69-203] c02 A69-19546
Laminar incompressible viscous flow in short cylindrical vortex chamber with finite swirl ratio
[NASA-TN-D-5132] c12 N69-21400
Hydrodynamic stability and vortex containment of two fluid wheel flow to helical disturbances contained by axial magnetic field
[NASA-TN-D-5372] c12 N69-32377
VORTICITY
Direction of maximum turbulent vorticity in turbulent shear flow, determining alignment
c12 A69-25282
Linear amplification, nonlinear limiting and secondary instability induced by unsteady effects illustrated for various transitional flows, including roughness and streamwise vorticity
c12 A69-33248
VULCANIZED ELASTOMERS
Vulcanizable elastomers suitable for contact with liquid oxygen, discussing preparation, mechanical properties, transition temperature and structure
c06 A69-16497

W

WAFERS
Breaking of semiconductor single crystal wafer into chips
[NASA-TM-X-1892] c09 N69-38774
WAKES
Droplet wake minimization by surface tension changes
[NASA-CR-1368] c12 N69-24958
Flow and wake characteristics on turbine tandem blades in two dimensional cascade tunnel
[NASA-TM-X-1836] c01 N69-30632
WALL FLOW
Computer program for calculating wall interference factors of V/STOL aircraft and conventional airplanes
[NASA-TR-R-302] c01 N69-19028
WALL TEMPERATURE
Mach number, cone angle, bluntness and wall to recovery temperature ratio effects on slender cones boundary layer transition measurements at hypersonic speeds
c01 A69-33250
Correlation equations for predicting gas-side heat transfer of axisymmetric rocket engine nozzles
[NASA-TM-X-1748] c33 N69-18898
Quartz-insulated, single-wire thermocouples installed on thin-wall rocket cooling tubes to measure hot-gas-side wall temperatures
[NASA-TN-D-5291] c14 N69-29553
Transient temperature fields in porous shell walls cooled by forced flow
[NASA-TT-F-552] c33 N69-30245
Aerodynamic heat flux determined within thermally thick walls for case of rapidly rising heat rates
[NASA-TN-D-5309] c33 N69-30726
Temperature response of wall separating two fluids one with oscillating temperature
[NASA-TN-D-5520] c33 N69-40789
WARNING SYSTEMS
Pilot warning indicators to equip all aircraft at low cost, discussing Doppler system
c21 A69-16726
Development of optical pilot warning indicator system for aircraft detection
[NASA-TN-D-5174] c14 N69-27267
WASTE DISPOSAL
Manned spacecraft waste disposal systems
[NASA-TM-X-1851] c05 N69-33260
WASTE UTILIZATION
Material recovery from metabolic and other wastes for long duration manned space missions, discussing carbon dioxide removal, bioregenerative food systems, etc
[AAS PAPER 69-143] c05 A69-42876
Hydrogenomonas cultures investigated for metabolic waste utilization in aerospace life support systems
[NASA-CR-1296] c05 N69-22766
WATER
Optical parametric noise in water by ruby laser beam for phase matched four photon process
c23 A69-21751
Simultaneous HCN and HOH laser emission in pulsed discharge through mixture containing H, C, N, and O
c16 A69-26330
Water rejection dynamics in hydrogen oxygen fuel cells
[NASA-TN-D-4956] c03 N69-14518
Tandem bladed inducer tested in water for cavitation corrosion
[NASA-TN-D-5134] c01 N69-23769
Calorimetric analyses of metal corrosions in deionized heated water
[NASA-TM-X-1791] c17 N69-25243
Stability of water lubricated herringbone groove journal bearings
[NASA-TN-D-5264] c15 N69-27955
Solid electrolyte electrolysis of carbon dioxide and water as oxygen regeneration system for long manned space flights
[NASA-CR-1359] c05 N69-28099
WATER BALANCE
Transient electro-osmosis of water in capillary tubes for pumping and generation modes, analyzing response to step change in pressure or voltage change under external loading
c06 A69-14862
WATER COOLED REACTORS
FASTER computer program modified for tracking neutrons through reactor slabs penetrated by helical voided ducts
[NASA-TM-X-1838] c22 N69-31986
Blocked two level factorial experiment to measure radiolysis of water in water cooled reactors
[NASA-TN-D-5369] c19 N69-32319
WATER FLOW
Water flow and cavitation in convergent-divergent boiler inlet nozzles
[NASA-TM-X-1689] c12 N69-10293
WATER INJECTION
Mean drop size generated in vapor pressure regime of liquid water jet, noting effect of water temperature and orifice diameter
c12 A69-21995
WATER LANDING
Effect of heat shield flexibility on water landing

loads of Apollo spacecraft models
[NASA-TN-D-5108] c32 N69-21042
Forces on flexible shells of Apollo command module during water impact
[NASA-TM-X-1781] c32 N69-23697

WATER RECLAMATION
Microbiology of water management subsystem for manned space flight, discussing sterilization by heat and tests inside Integrated Life Support System /ILSS/
[SAE PAPER 680718] c05 A69-13441

WATER VAPOR
Water vapor profiles in stratosphere from IR radiometric observations under cloudless conditions, indicating relation to tropospheric meteorological features
c13 A69-38261
Noctilucent clouds with wave movement, chemical composition, and water vapor
[NASA-TT-F-546] c13 N69-25013

WAVE ATTENUATION
Elastic behavior of large blood vessels in canine aorta by measuring dispersion and attenuation of artificially induced pressure waves
c04 A69-14692
Longitudinal plasma waves collision damping calculations using Rostoker test particle method
c25 A69-34439

WAVE DIFFRACTION
Radiation pattern of axial slot on circular conducting cylinder based on wedge diffraction and creeping wave theory
c07 A69-24993

WAVE DISPERSION
Elastic behavior of large blood vessels in canine aorta by measuring dispersion and attenuation of artificially induced pressure waves
c04 A69-14692

WAVE EXCITATION
Evaluation of magnetic materials for static inverters and converters, tested under square wave excitation and direct current excitation
[NASA-CR-1226] c03 N69-17765

WAVE FUNCTIONS
Inelastic scattering cross sections calculated, comparing results for various nuclear states expressed as Wood-Saxon radial and harmonic oscillator functions
c26 A69-29006
Upper bounds for electromagnetic transition rates for Ne 20 determined using Hartree-Fock wave functions
c24 A69-35166
Equatorial radiation pattern of parallel plate TEM mode axial slot on elliptical conducting cylinders, using wedge diffraction and creeping wave theory
c09 A69-40703

WAVE GENERATION
Ion cyclotron wave generation in RF self sustained mode improved by installing grid structures in plasma near magnetic mirrors
c25 A69-13113
Stellar atmospheres acoustic energy generation rate calculations, studying corona mass ejection effects on stellar rotation
c30 A69-39521

WAVE INTERACTION
Plasma oscillation modes perpendicular to magnetic field used to study energy conversion by wave coupling across density discontinuity
c25 A69-20795

WAVE PROPAGATION
High speed compression waves, rarefaction waves and gas interface regions position and velocity measurement in shock tube by sensing electrical impedance
c14 A69-13104
Atmospheric density variation measurements by density gages on Explorer 32 satellite confirm wave propagation in neutral thermosphere as free internal gravity waves
c13 A69-16261
Axial waves in blood vessels, determining phase velocities and damping, noting anisotropic behavior of artery wall
[SESA PAPER 1350] c04 A69-19726
Self modulation, self steepening and spectral development of light in small scale trapped filaments, noting influence of relaxation time
c23 A69-20745
Collisional theory of longitudinal wave propagation for two fluid viscous ionized plasmas formulated from coupled Maxwell and Boltzmann equations
c25 A69-20796
Full wave calculation of gravity waves for thermospheric model, describing wave type reflection, transmission, conversion and coupling by scattering matrix elements
c13 A69-25150
Characteristic plane harmonic free internal neutral atmospheric wave oblique propagation through horizontally stratified quiet atmosphere for various thermospheric parameters
c13 A69-26101
Interphase momentum transfer during propagation of infinitesimal pressure pulse through bubbly flow two phase mixture
c33 A69-43511
Continuum theory for wave propagation in elastic composite solid with elastic microinclusions
[NASA-CR-1321] c32 N69-21401
First-order solutions for mutual coupling between waveguides which propagate two orthogonal modes
[NASA-TN-D-5180] c07 N69-24051
Analytical and experimental studies for predicting noise attenuation in acoustically treated ducts for turbofan engines
[NASA-CR-1373] c23 N69-36974
Shock wave propagation in real gases
[NASA-TT-F-585] c12 N69-40824

WAVE REFLECTION
Radiative transfer by doubling very thin layers in problem of diffuse reflection from plane-parallel atmosphere eliminates numerically solving transfer equation
c33 A69-20064

WAVEFORMS
N shaped shock wave line focusing simulating sonic superbooms
[NASA-TN-D-5306] c02 N69-31874
Mathematical analysis of wave structure in supersonic flow
[NASA-CR-1438] c04 N69-37062
Transformer of closely spaced pulsed waveforms having nonzero average value
[NASA-TN-D-5473] c09 N69-38776

WAVEGUIDE ANTENNAS
Omnidirectional microwave parallel plate waveguide fed antenna design for flush mounted broadband spacecraft, noting equatorial and polar patterns
c09 A69-40697
Slope diffraction analysis of TEM parallel plate guide patterns
[NASA-CR-1326] c07 N69-26273

WAVEGUIDES
Admittance of parallel plate waveguide aperture with infinite flange illuminating metal sheet, using wedge diffraction theory and integral transform method
c09 A69-12328
Conjugate echoes in Alouette 2 topside sounder ionograms explained by multiple reflections between conjugate points of field line, noting magnetospheric waveguides role
c07 A69-20045
Radiating collinear open ended waveguides and near field coupling analyzed using simultaneous integral equations and Fourier series expansion of aperture field
c09 A69-24984
Reflection coefficient of symmetric parallel plate waveguide operating in TEM mode illuminating lossless dielectric layer, using wedge diffraction and geometrical optics methods
c09 A69-34802
Edge diffraction effects in TEM axially slotted finite ground plane on radiation pattern in waveguides of different geometries
c07 A69-41588
Symmetric parallel plate waveguide reflection coefficient analyzed
[NASA-CR-1327] c07 N69-24059

WEAR
Ball bearings lubrication and wear in cryogenic hydrogen turbopumps by transfer films provided from self lubricating cage

c15 A69-10109
Modes and mechanisms of wear covering adhesive, abrasive and corrosive wear, surface fatigue and fretting corrosion
c15 A69-27231
Effect of orientation and presence of surface active materials on friction and wear of aluminum
[NASA-TN-D-4994] c15 N69-16197
Friction and wear of polymers with various fillers in liquid hydrogen
[NASA-TN-D-5073] c15 N69-19800
Structure, interactions, and topography of solid surfaces, sliding friction, adhesion, wear, and boundary lubrication conference topics
[NASA-SP-181] c15 N69-30401

WEAR TESTS
Modes and mechanisms of wear covering adhesive, abrasive and corrosive wear, surface fatigue and fretting corrosion
c15 A69-27231
Solid solutions atomic ordering effect on friction and wear in vacuum, using CuAu and FeCo systems
c15 A69-35183
Friction and wear tests with graphite fluoride lubricant
[NASA-TN-D-5097] c15 N69-20939

WEATHER FORECASTING
Atmospheric model development relating temperature, density, moisture and energy measurements from satellite observations for long term weather forecasting
[UN PAPER 68-95397] c20 A69-10463
Satellite-based meteorological observation system for global atmospheric research program, discussing wind measurement, IR and microwave sounding possibilities, etc
[AAS PAPER 69-120] c13 A69-42817
NIMBUS program individual missions characteristics emphasizing NIMBUS 3 results and weather forecasting improvements
[AAS PAPER 69-421] c31 A69-42835

WEDGES
Heat transfer and pressure distributions inside hinge line gap of wedge-flap combination at hypersonic speeds
[NASA-TN-D-4911] c01 N69-11009

WEIGHT (MASS)
Mitchell strain criterion for minimum weight structures using mathematical models
[NASA-TN-D-4345] c32 N69-25001

WEIGHT ANALYSIS
Lunar surface power plants, considering weight constraint for various systems using nuclear power, solar cell/fuel cells and H-C reactant regeneration
c03 A69-11396
Weight estimation and forecast in manned spacecraft design, noting size and weight relationship
[SAWE PAPER 793] c31 A69-34864

WEIGHT MEASUREMENT
Operational analysis of mass measuring system in orbiting spacecraft
[NASA-TN-D-5039] c04 N69-19115

WEIGHTING FUNCTIONS
Variable length codes for alphabets containing messages with assigned weighted information content
[NASA-TN-D-4962] c07 N69-15373
Suboptimal estimator to Kalman filter containing scalar weighting factors
[NASA-TN-D-5082] c10 N69-21123
Weighting factor for correction of photographic bias caused by variation in mass and velocity of sporadic meteoroids
[NASA-TN-D-5245] c30 N69-26239

WEIGHTLESS FLUIDS
Excessive extrapolation limitations in applying transient data to low gravity fluid behavior for orbital refueling systems, presenting orbital fluid transfer experiment
[AIAA PAPER 69-566] c31 A69-32755

WEIGHTLESSNESS
Weightlessness effects on fertilized frog egg development onboard Gemini 8 and 12 manned orbital flights, discussing cell division, differentiation and embryogeneis
c04 A69-11084
Space manufacturing operations program, discussing zero gravity effect during earth orbit flight, Apollo Applications Program Orbital Workshop Flight 2, etc
c31 A69-35067
Space manufacturing processes for orbital low and zero gravity environment, discussing buoyancy and thermal convection sensitive and molecular forces controlled methods
[AAS PAPER 69-486] c30 A69-42844
Cardiovascular conditioning suit to provide transmural pressure gradient in circulatory system during weightlessness
[NASA-CR-1206] c05 N69-13202
Observations of interface behavior during inflow to elliptical ended cylinder in weightlessness
[NASA-TM-X-1719] c12 N69-15473
Summary of potential adverse effects of artificial gravity and weightlessness on astronaut physiological processes and performance in aerospace environment
[NASA-TN-D-4980] c05 N69-15629
Vapor ingestion phenomenon during draining in weightlessness
[NASA-TN-D-5210] c12 N69-24917
Liquid-vapor interface during outflow in weightlessness
[NASA-TM-X-1811] c12 N69-27954
Coordination of voluntary movements of man in zero gravitational fields
[NASA-TT-F-578] c04 N69-31356
Astronaut capability to maintain life support systems and cabin habitability in weightlessness
[NASA-CR-1405] c05 N69-36709
Blood sampling for parathyroid hormone and calcium metabolism during weightlessness of space flight
[NASA-CR-1395] c05 N69-38600

WEIGHTLESSNESS SIMULATION
Weightless simulators effectiveness for obtaining space systems maintainability criteria, using nonparametric experimental design for performance data
c05 A69-17648
Correlation study of simulation of Gemini extravehicular activity with flight results
[NASA-CR-1146] c05 N69-19902
Simulated manual package transfer in weightless environment of Saturn Orbital Space Station
[NASA-TN-D-5111] c05 N69-21501
Astronaut extravehicular work performance under simulated weightlessness conditions
[NASA-CR-1334] c05 N69-27266
Weightlessness simulation of Gemini extravehicular tasks using neutral-buoyancy underwater techniques
[NASA-TN-D-5235] c05 N69-28024

WELDED JOINTS
Development of automatic quality control device for measuring welded joints
[NASA-TN-D-5304] c15 N69-33800

WETTING
Flow rate effect on dynamic contact angle for wetting liquids in weightless environment
[NASA-TN-D-5115] c12 N69-20794

WHISKERS (SINGLE CRYSTALS)
Fiber-metal matrix composites fabrication, applications, mechanical properties and powder metallurgy
c17 A69-20204

WHITE DWARF STARS
Instability of stellar structures intermediate between white dwarfs and neutron stars shown by stellar models, discussing pulsar signals periodicities
c30 A69-20770
X ray sources model, describing possible ring of matter around white dwarf near end of active evolution
c29 A69-35204

WIND (METEOROLOGY)
Rocket sounding meteorological data of Exametnet for 1966
[NASA-SP-175] c20 N69-16214

WIND EFFECTS
Statistical effects of wind and atmospheric turbulence on launch vehicles
[NASA-CR-1410] c20 N69-35570
Mathematical model for quantitative wind and turbulence effects on design and operation of

launch vehicles
[NASA-CR-1418] c20 N69-36222
Empirically determined wind and scale effects on hot gas recirculation characteristics of jet V/STOL aircraft
[NASA-CR-1445] c28 N69-40776

WIND MEASUREMENT
Atmospheric measurements from satellites, discussing ATS-1 cloud images for definition of wind and use of WEFAX through ATS 2 satellites for data transmission
[AIAA PAPER 69-158] c20 A69-18038
Mesopause wind measurements at high latitude locations by sounding rockets noting relation to noctilucent clouds
c20 A69-28466
Angular grid spacing resolution near poles effect tests in global prediction model for geophysical fluid dynamics, investigating forecast height and wind fields
c20 A69-43066
Evaluation of height and time based meteorological rocket wind reduction techniques
[NASA-TM-X-1850] c20 N69-35523

WIND PROFILES
All weather wing profile monitoring system using FPS-16 radar/jimsphere system and flight simulation for protection of space vehicle and missile launches
c20 A69-13852
Temperature profiles and associated wind profiles obtained with Jimsphere/FPS-16 radar system at Cape Kennedy, discussing remote CAT detector assessment
c20 A69-33739
Winds aloft and wind shear analysis from jimsphere wind sensor balloon-radar data
[NASA-CR-1204] c20 N69-13629
Wind profile developed for calculation of deflection impulse for rocket with liquid injection thrust vector control
[NASA-TM-X-1708] c31 N69-14033
Wind velocity profiles by smoke trail method for eastern test range
[NASA-TN-D-4880] c20 N69-14505
Statistical analysis on influential aspects of wind profile disturbance design and dynamic response of space vehicles
[NASA-TN-D-4963] c32 N69-15632
Comparisons of wind and temperature data obtained by Japanese MT-135 and American ARCAS meteorological rocket systems in closely spaced launchings
[NASA-TM-X-1726] c20 N69-17772

WIND TUNNEL APPARATUS
Factors influencing development of both wind tunnel and flight test technology for determining aerodynamic derivatives of aircraft motions
c11 A69-15572
Wind tunnel magnetic support and balance system for measuring sphere drag
[NASA-CR-1353] c11 N69-25343

WIND TUNNEL DRIVES
Exploding wire initiation and electrical operation of 40 kV system for arc heated drivers up to 10 feet long
[NASA-TN-D-5126] c11 N69-22989

WIND TUNNEL MODELS
Factors influencing development of both wind tunnel and flight test technology for determining aerodynamic derivatives of aircraft motions
c11 A69-15572
Refractory cone models made of copper and Co coated Be for force tests in high enthalpy hypersonic arc tunnels at high simulated attitudes
c11 A69-26796
Flow simulation on wind tunnel test models for aerodynamic characteristics of aircraft design, discussing boundary layer and external flow coupling
[AIAA PAPER 69-660] c11 A69-33471
C-5A aircraft model high subsonic speed tests, correlating data from three transonic wind tunnels
[AIAA PAPER 69-794] c01 A69-35636
Aerodynamic performance tests of autorotative unpowered rotor entry vehicle model at various Mach numbers and angles of attack
[AIAA PAPER 68-950] c01 A69-37155
Experimental surface pressure distributions on spherically blunted cone at Mach numbers from 1.50 to 4.63
[NASA-TM-X-1730] c01 N69-16209
Wind tunnel study of deflected elevator flutter encountered on T-tail airplane
[NASA-TN-D-5024] c32 N69-16211
Wind tunnel tests of opening characteristics of all flexible parawing
[NASA-TN-D-5031] c02 N69-17700
Effects of cone angle, base flare angle, and corner radius on Mach 3 aerodynamic characteristics of large angle cones
[NASA-TN-D-5048] c01 N69-19926
Wind tunnel force and pressure tests of rocket engine nozzle extensions on X-15-2 model at supersonic and hypersonic speeds
[NASA-TM-X-1759] c01 N69-20873
Aerodynamic characteristics and ground effects of supersonic transport with double Delta wing
[NASA-TN-D-5102] c02 N69-21020
Measured static aerodynamic forces for hypersonic flutter analysis on airfoil models in helium flow
[NASA-TN-D-5233] c01 N69-26271
Measurements of mutual interference heating for probe antenna mounted on Apollo reentry configuration
[NASA-TM-X-1787] c01 N69-29318
Free flight test model measurement of drag, lift, and trim in wind tunnel for Apollo command module
[NASA-TN-D-5276] c30 N69-29557
Jet exhaust location effects on longitudinal aerodynamic characteristics of jet V/STOL model
[NASA-TN-D-5333] c01 N69-33210
Wind tunnel investigation for determination of subsonic and transonic aerodynamic characteristics of Saturn 1B launch vehicle
[NASA-TM-X-1848] c31 N69-33380
Spin-tunnel investigation of scale model of straight wing, twin boom counter insurgency airplane
[NASA-TM-X-1602] c02 N69-34988
Pressure distributions for blunt body wind tunnel models at supersonic speeds and angles of attack from 0 to 15 degrees
[NASA-TN-D-5392] c01 N69-35300
Jet velocity and axial location of nozzle exit on performance of twin-jet afterbody model
[NASA-TN-D-5393] c28 N69-36932
Upwash patterns on ablating and nonablating cones at hypersonic speeds
[NASA-TN-D-5346] c12 N69-37370
Wind tunnel study of aerodynamic pressures on Apollo command module configuration
[NASA-TN-D-5514] c01 N69-40345
Wind tunnel studies of scaled model of multijet cargo airplane
[NASA-TN-D-5538] c02 N69-40937

WIND TUNNEL NOZZLES
Pressure and temperature surveys of Mach 27-47 nozzle boundary layer at Ames M-50 He tunnel, determining velocity profiles, wall friction coefficient, etc
[AIAA PAPER 69-686] c12 A69-33441

WIND TUNNEL STABILITY TESTS
Entry phase flight data of Missions AS-202, Apollo 4 and 6 compared with wind tunnel aerodynamics data
[AIAA PAPER 68-1143] c31 A69-13556
Amplified boundary layer oscillations and transition at swept flat nosed wing attachment line with/without boundary layer suction analyzed by wind tunnel tests
c01 A69-33251
Flow field throughout wind tunnel containing rotor with sharply defected blades, noting reversed flow effect in front of wake
c11 A69-35228
Low speed static and dynamic longitudinal, and lateral stability of scale model of supersonic transport in wind tunnel tests
[NASA-TN-D-4726] c02 N69-10733

Large scale wind tunnel tests to improve longitudinal stability of supersonic transports with variable swept wings
[NASA-TN-D-5005] c02 N69-16384
Full scale wind tunnel investigation of lateral and longitudinal stability and control characteristics of light twin engine airplane
[NASA-TN-D-4983] c02 N69-17303
Aerodynamic characteristics of full scale model sailwing with aspect ratio 5.9
[NASA-TN-D-5047] c01 N69-19243
Wind tunnel tests for V/STOL aircraft having direct-lift and lift-cruise jet nozzles
[NASA-TM-X-1758] c01 N69-20016
Wind tunnel investigation of twin keel parawing aerodynamic characteristics
[NASA-TN-D-5199] c01 N69-23781
Wind tunnel and analytical study of conversion from wing lift to rotor lift on composite lift VTOL aircraft
[NASA-TN-D-5256] c02 N69-28044
Wind tunnel investigation of steady state aerodynamics of composite lift VTOL aircraft model combining rotary and fixed wings
[NASA-TN-D-5232] c02 N69-28097
Wind tunnel investigation of static stability characteristics of model jet-lift V/STOL research airplane
[NASA-TM-X-1835] c02 N69-30633
Wind tunnel tests to determine static aerodynamic characteristics of cruciform wing-body missiles at transonic and supersonic speeds
[NASA-TM-X-1839] c01 N69-31875
Wind tunnel tests of static longitudinal and lateral characteristics of short takeoff aircraft with external flow jet flap
[NASA-TN-D-5364] c01 N69-33275
Wind tunnel investigation for determination of subsonic and transonic aerodynamic characteristics of Saturn 1B launch vehicle
[NASA-TM-X-1848] c31 N69-33380
Spin and recovery characteristics of 1/30 scale subsonic attack aircraft model determined in wind tunnel tests
[NASA-TM-X-1788] c02 N69-37976
Wind tunnel stability tests to determine effect of hypersonic research engine on aerodynamic characteristics of research aircraft
[NASA-TM-X-1840] c01 N69-38612
Large scale wind tunnel investigation of lifting body with inflatable and rigid afterbody
[NASA-TN-D-5468] c01 N69-38775
Wind tunnel stability tests to determine flutter characteristics of Saturn S-4B stage panel
[NASA-TN-D-5439] c32 N69-38808

WIND TUNNEL WALLS
Wind tunnel wall constraints effects at extreme force coefficients during V/STOL testing shown different from effects in conventional aircraft testing
c11 A69-15574
Skin friction and heat transfer data for hypersonic turbulent layer on flat plates, wind tunnel wall, and cones
[NASA-TN-D-5089] c12 N69-29144

WIND TUNNELS
FORTRAN programs for calculating wind tunnel boundary interference factors
[NASA-TM-X-1740] c01 N69-17818
Direct measurement of skin friction in wind tunnel testing by using cholesteric liquid crystals
[NASA-TM-X-1774] c12 N69-26956
Aerodynamic characteristics determined during development of Apollo launch escape vehicle configuration in wind tunnel tests
[NASA-TN-D-5208] c01 N69-29027
Auxiliary flap system tests using Boeing 367-80 transport aircraft and wind tunnels
[NASA-TN-D-5128-REV] c02 N69-31962
Aerodynamic characteristics effected by parallel-staged simple aerodynamic configurations at Mach numbers of 3 and 6
[NASA-TN-D-5379] c01 N69-33302
Laminar heating rate from wind tunnel tests using angle of attack and Reynolds number
[NASA-TN-D-5450] c12 N69-37604
Dynamic distortion of supersonic wind tunnel for turbojet engines
[NASA-TM-X-1842] c28 N69-38599
Langmuir and interferometric measurements on electron concentration in arc heated wind tunnel using air and nitrogen
[NASA-TN-D-5500] c25 N69-39302

WIND VARIATIONS
Turbulence characteristics up to 150 m above ground, noting surface roughness length directional dependence, longitudinal turbulence spectra and turbulent energy budget
c20 A69-10695

WINDOWS (APERTURES)
Thermal control coatings, windows and mirrors for 1973 Mars Viking Lander vehicles under simulated Martian surface conditions
[AIAA PAPER 69-1023] c11 A69-40393
Optical properties and chemical analysis of contaminants on Gemini spacecraft windows
[NASA-TN-D-4916] c31 N69-13232
Preflight optical evaluation of right hand hatch windows in Gemini missions 7, 8, 9, and 12
[NASA-TN-D-5471] c31 N69-40813

WING CAMBER
Rotor aerodynamics research in terms of theoretical and experimental data comparison, rotor blade flow visualization and blade section camber
c01 A69-41372

WING LOADING
Computing span loads and stability derivatives due to sideslip, yawing, and rolling for wings in compressible flow
[NASA-TN-D-4929] c01 N69-14001

WING PROFILES
Experimental and theoretical study of symmetrical and cambered Delta wing configuration between Mach 2.0 and 10.7
[NASA-TN-D-5272] c01 N69-29269

WING SLOTS
Force measurements in drag reduction by gas injection into turbulent boundary layer through supersonic wing slots
[NASA-TN-D-5307] c12 N69-31359

WINGS
Numerical solution for minimum induced drag, and associated loading, of nonplanar wings
[NASA-CR-1218] c01 N69-10343
User manual for computer program 55VD for computation of minimum induced drag and load distribution of nonplanar wings
[NASA-CR-1218-SUPPL] c01 N69-12286
Wind tunnel and analytical study of conversion from wing lift to rotor lift on composite lift VTOL aircraft
[NASA-TN-D-5256] c02 N69-28044
Load distribution calculations for subsonic compressible flow of arbitrary wings and lifting surfaces
[NASA-TN-D-5335] c01 N69-31337

WINTER
Infrared horizon radiance profiles for winter conditions based on Scanner project flight test
[NASA-TN-D-4905] c21 N69-14346

WIRE
Size effect on tensile strength of polycrystalline nickel wires
[NASA-TN-D-4884] c17 N69-10226
Stress rupture and tensile properties of refractory metal wires at 2000 and 2200 deg F
[NASA-TN-D-5139] c32 N69-22823

WIRE CLOTH
Flow reduction due to oxidation of wire-form porous materials for transpiration cooled turbine blades
[NASA-TN-D-5001] c17 N69-16383

WORK FUNCTIONS
Observation of photocurrents generated in Schottky barrier diodes on barium titanate, suggesting practical utility of photon-to-electron conversion efficiencies
c09 A69-18905
Work function and desorption energy measurements of alkali metals from metallic substrates with modulated molecular beam, noting surface contamination
c26 A69-21808
Free electron model for electron work functions and number density distributions and surface potentials in metals
c26 A69-29009

Electric fields and electron work functions, surface potentials and number density distributions in selected metals surfaces determined using free electron model
c26 A69-36045

X

X RAY ANALYSIS
Diffusion lengths of silicon solar cells after radiation damage and annealing by X ray method
[NASA-TM-X-1894] c03 N69-37827
X RAY ASTRONOMY
Acoustic energy generation for helium rich stars, discussing X ray radiation from helium star corona
c29 A69-20645
Discrete source hypothesis for interpreting high energy cosmic gamma ray measurements obtained by OSO-3 spacecraft
c29 A69-20699
Iron line absence in emission spectrum of thermal X ray sources, constraining proposed thermal models
c29 A69-22231
X ray energy spectrum from Crab Nebula and diffuse background on celestial sphere near galactic anticenter, noting spectral index
c29 A69-30759
X ray sources model, describing possible ring of matter around white dwarf near end of active evolution
c29 A69-35204
Pulsed X ray emission associated with pulsar NP 0532 in Crab Nebula measured by six element detector on Aerobee 150 rocket
c29 A69-37574
Solar X rays observations, describing instrumentation, radiation characteristics, association with flares, spectrum analysis, etc
c29 A69-39506
Extended source Fourier transform holography for single image synthesis of multiple identical images produced by multiple pinhole camera in X ray astronomy
c14 A69-40019
X RAY DIFFRACTION
X ray crystallographic measurements of selected grades of commercial nonpyrolitic artificial graphite
[NASA-TN-D-4888] c18 N69-10754
Examination of thermal oxidation deposits on heat resistant alloys using X ray diffraction and X ray fluorescence analyses
[NASA-TN-D-5019] c17 N69-17277
X RAY FLUORESCENCE
X Ray fluorescence of rock samples as applied to geological problems, noting standard deviations for element distribution
c14 A69-10890
X ray fluorescence and electron microprobe for determining thin film thickness
c09 A69-19582
Examination of thermal oxidation deposits on heat resistant alloys using X ray diffraction and X ray fluorescence analyses
[NASA-TN-D-5019] c17 N69-17277
X RAY SCATTERING
Compton profile from single crystal of LiH measured with X ray scattering, noting valence-electron momentum distribution role
c26 A69-40730
X RAY SPECTROSCOPY
Spectral intensity of high energy solar X rays observed during July 7, 1966 polar event with satellite OGO 3, suggesting nonthermal bremsstrahlung origin
c29 A69-23753
X RAY TELESCOPES
Optical design of Wolter type 1 glancing incidence X ray telescope for 6-100 A wavelength region, describing results of laboratory and rocket flight tests of prototype
c14 A69-21087
X RAYS
Solar extreme UV, soft and hard solar X rays, cosmic X rays and gamma rays, cosmic ray particles and near earth visible radiation observed by OSO-3
c29 A69-22167
Oscillator strengths and wavelengths of X ray and EUV transitions in highly ionized iron line spectra
c29 A69-27554
Radio emission from Sco XR-1 shown as synchroton radiation of relativistic electrons in low density region surrounding denser core producing X ray
c30 A69-37334
Cosmic X ray bremsstrahlung due to collisions of suprathermal protons with ambient electron, giving clue about diffuse sky background of X rays
c29 A69-40643
X-Y PLOTTERS
Alphanumeric listing and digital data x-y plotting by high speed printer, describing equipment modifications and control software
c08 A69-33108
X-14 AIRCRAFT
Direct side-force maneuvering system on deflected X-14A jet VTOL aircraft without changing bank angle
[NASA-TN-D-5175] c02 N69-22572
Evaluation of six degrees of freedom motion simulator for Bell X-14A aircraft hovering characteristics
[NASA-TN-D-5383] c11 N69-35359
X-15 AIRCRAFT
X-15 research aircraft program piloting problems, ground facilities, heat transfer, space flight and steep reentry
c02 A69-26872
Wind tunnel force and pressure tests of rocket engine nozzle extensions on X-15-2 model at supersonic and hypersonic speeds
[NASA-TM-X-1759] c01 N69-20873
Infrared heating simulation of Mach 4.63 flight on X-15 horizontal stabilizer
[NASA-TN-D-5403] c33 N69-35949
Aerodynamic drag of external fuel tanks attached to X-15-2 airplane at Mach numbers of 1.6 to 2.3
[NASA-TM-X-1895] c01 N69-38065
XENON
Radiation attenuation cross sections of monatomic and diatomic xenon gas from UV absorption measurements near resonance line
c24 A69-12551
Excited states of xenon nuclei formed in beta decay of iodine and cesium isotopes
[NASA-TN-D-5329] c24 N69-30074

Y

YAW
Feasibility of using roll and yaw compensation to reduce inclination error of Scout launch vehicle
[NASA-CR-1209] c31 N69-16221
YIELD STRENGTH
Vacuum arc melted W and W-Re alloys mechanical properties, noting Re additions effects
c17 A69-20190
Plain strain fracture toughness tests on two inch thick maraging steel plates of various strengths, using bend and compact tension tests
c32 A69-23057
Plane strain fracture toughness tests on maraging steel plates for various yield strengths and large dimensions
c17 A69-26496
YTTRIUM
Yttrium effect on rate of thermal decomposition of silver carbonate powder and pressed pellets by isothermogravimetric analysis, examining water vapor, Co 60 gamma radiation and temperature effects
c06 A69-30442
Cyclic heating and thermal shock effects on hafnia stabilized with calcia, magnesia, and yttria
[NASA-TN-D-5279] c18 N69-34547

Z

ZERO ANGLE OF ATTACK
Newtonian aerodynamics for circular cones modified to produce lift at zero angle of attack
[NASA-TN-D-5193] c01 N69-23926

ZINC OXIDES
UV irradiation effects on ZnO spacecraft thermal control coating pigments, discussing photo-Hall, luminescence and electron paramagnetic resonance measurements
[AIAA PAPER 69-639] c18 A69-33288
ZINC TELLURIDES
GaSb-ZnTe heterojunction fabrication method, noting photoresponse, fluorescence and light transmission
c26 A69-12408
ZIRCONIUM
Zr doped superconducting ceramic strontium titanate, noting effective electron mass variations and transition temperature
c26 A69-27400
Luminous spherical fog layer surrounding burning zirconium droplet during free fall through oxygen containing atmosphere, noting effect on mass and heat transfer processes
c33 A69-28462
Laser ignited combustion of 365 micron Zr droplets falling in ultrapure oxygen using spectroscopic and photographic techniques, discussing vapor phase transport phenomena
[WSCI PAPER 69-4] c27 A69-32345
ZIRCONIUM ALLOYS
Absorption rate sticking probabilities for oxygen on niobium and dilute niobium-zirconium alloys
[NASA-TN-D-4885] c17 N69-10931
ZIRCONIUM COMPOUNDS
Cb-1Zr pumped sodium loop tests to evaluate loop components, EM pump, pressure transducers, and instrumentation techniques
[NASA-CR-1135] c03 N69-11373
ZOND 3 SPACE PROBE
Lunar topography statistics determined by Zond 3 space probe
[NASA-TT-F-514] c30 N69-24206

PERSONAL AUTHOR INDEX

NASA SCIENTIFIC AND TECHNICAL REPORTS AND PUBLICATIONS FOR 1969

A Selected Listing

Typical Personal Author Index Listing

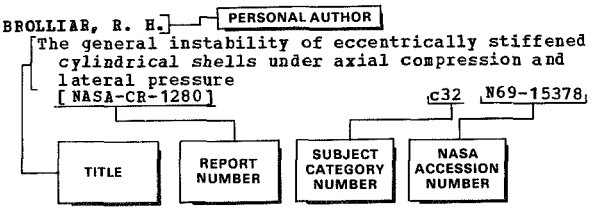

Listings in this index are arranged alphabetically by personal author. The title of the document provides the user with a brief description of the subject matter. The report number helps to indicate the type of document cited (e.g., NASA report, NASA contractor report). The subject category number indicates the subject category in the abstract section in which the citation is located. The accession number denotes the number by which the citation is identified within the subject category. The titles are arranged under each personal author in ascending accession number order. "A" items precede "N" items in this index.

A

ABBOTT, D. E.
Analytical prediction of the incompressible turbulent boundary layer with arbitrary pressure distribution.
[AIAA PAPER 69-397] c12 A69-30478

ABBOTT, W. H.
Research on metallurgical characteristics and performance of materials used for sliding electrical contacts Summary report, 1 May 1968 - 30 Apr. 1969
[NASA-CR-1447] c17 N69-40057

ABDALLA, K. L.
Vapor ingestion phenomenon in weightlessness
[NASA-TN-D-5210] c12 N69-24917
The liquid-vapor interface during outflow in weightlessness
[NASA-TM-X-1811] c12 N69-27954

ABEL, I.
Evaluation of a technique for determining airplane aileron effectiveness and roll rate by using an aeroelastically scaled model
[NASA-TN-D-5538] c02 N69-40937

ACAMPORA, F. L.
High photovoltages in cadmium sulfide films.
c26 A69-17772

ADAMS, B. H.
Computer experiments on the microscopic behavior of one-dimensional plasmas
[NASA-TN-D-4831] c25 N69-10471

ADAMS, D. W.
A procedure for furnace brazing butt joints in tungsten-uranium dioxide cermet cylinders at 3000 deg C
[NASA-TM-X-1815] c15 N69-28862
Heat-transfer characteristics of a water-to-cryogenic-hydrogen heat exchanger
[NASA-TN-D-5429] c33 N69-36701

ADAMS, G. W.
Riometer measurements, solar proton intensities and radiation dose rates.
c29 A69-32321

ADAMS, J. J.
Application of human transfer functions to system analysis
[NASA-TN-D-5478] c05 N69-39183

ADAMS, M. C.
The aerospace stimulus to technological advance.
[ON PAPER 68-95321] c34 A69-10467

ADAMS, W. M., JR.
Analytic approximations for application to spacecraft optical navigation on short data arcs
[NASA-TN-D-4863] c21 N69-10372

ADAMSKY, R. F.
Effect of oxygen on the formation of germanium films.
c26 A69-43345

ADELFANG, S. I.
A study of jimsphere wind profiles as related to space vehicle design and operations
[NASA-CR-1204] c20 N69-13629

ADELMAN, H. M.
A geometrically exact finite element for thin shells of revolution.
[AIAA PAPER 69-56] c32 A69-18193
Vibration analysis of a 1/40-scale dynamic model of Saturn 5 launch platform-umbilical tower configuration
[NASA-TN-D-4871] c31 N69-10934
A method for computation of vibration modes and frequencies of orthotropic thin shells of revolution having general meridional curvature
[NASA-TN-D-4972] c32 N69-16469

ADKINS, E. J.
Variation in engine noise for two landing-approach configurations of a jet transport aircraft
[NASA-TM-X-1896] c02 N69-38104

ADLER, I.
An integrated experiment for compositional analysis from an orbiter.
[AAS PAPER 68-197] c30 A69-11475
Some parameters affecting Auger and photoelectron spectroscopy as an analytical technique.
c06 A69-19775

ADLON, G. L.
Effects of simulated Mars dust erosion environment on thermal control coatings.
[AIAA PAPER 69-1023] c11 A69-40393

AGGSON, T. L.
Probe measurements of electric fields in space.
c13 A69-38508

AHRENS, L. H.
Origin and Distribution of the Elements, Proceedings of the International Symposium, Paris, France, May 8-11, 1967.
c30 A69-20892

AIKIN, A. C.
The lower ionosphere of Mars.
c30 A69-18607

AKIN, C. M.
Combined effects of mass addition and nose bluntness on boundary-layer transition.
[AIAA PAPER 67-706] c12 A69-33476

ALBERS, J. A.
Design-point performance of a double containment tantalum and stainless steel mercury boiler for SNAP-8
[NASA-TN-D-4926] c33 N69-12739

ALBERS, L. U.
Noise in axisymmetric convergent electron beams
[NASA-TN-D-5212] c10 N69-24918

ALDRIDGE, M. D.
Enhancement of photon-bunching effects.
c07 A69-31694

ALEKSEYEV, B. V.
Boundary layer and chemical reactions
[NASA-TT-F-549] c33 N69-31947

ALEX, F. R.
Experiments and a model for pilot dynamics with visual and motion inputs
[NASA-CR-1325] c05 N69-28071

ALEXANDER, J. K.
Measurements in the ionosphere of the aspect dependence of antenna reactance. I - Variations arising from the inhomogeneous plasma distribution about the vehicle.

c13 A69-39964
Type III radio bursts in the outer corona.
c29 A69-40300
The spectrum of the cosmic radio background between 0.4 and 6.5 MHz.
c30 A69-42375
ALGER, D. L.
A solution to tritium pump contamination for small accelerators.
c11 A69-26499
ALI, D. E.
Measurements of negative ion production in atmospheric gases
[NASA-CR-1406] c24 N69-38564
ALKSNE, A. Y.
External aerodynamics of the magnetosphere.
c13 A69-19360
Effect of neutral sheet currents on the shape and magnetic field of the magnetosphere tail.
c13 A69-21661
Plasma flow around the magnetosphere.
c29 A69-26736
ALLARIO, F.
Onset of rotating disturbance in the interelectrode region and exhaust jet of an MPD arc.
[AIAA PAPER 69-232] c28 A69-21225
Onset of rotating disturbance in linear Hall current accelerator.
[AIAA PAPER 69-381] c28 A69-21731
Electric-field distribution in pulsed high-current-density discharges in helium and helium-hydrogen mixtures.
c25 A69-23660
ALLEN, C. W.
Elastohydrodynamic lubrication of a spinning ball in a nonconforming groove.
[ASME PAPER 69-LUBS-11] c15 A69-34381
ALLEN, G.
Viscosity measurements of dilute solutions of helium-3 in superfluid helium-4 between 0.1 and 1.2 deg K.
c23 A69-39582
FORTRAN program for machine computation of group tables of finite groups
[NASA-TN-D-5402] c08 N69-35569
ALLEN, H. W.
Characteristics of a 2.17-megawatt fast- spectrum reactor concept using an axially moving reflector control system
[NASA-TM-X-1911] c22 N69-40061
ALLEN, J. L.
Conceptual study of rocket-scramjet hybrid engines in a lifting reusable second stage
[NASA-TN-D-5218] c28 N69-24922
ALLEN, J. M.
Use of Baronti-Libby transformation and Preston tube calibrations to determine skin friction from turbulent velocity profiles
[NASA-TN-D-4853] c12 N69-10472
Charts for interpolation of local skin friction from experimental turbulent velocity profiles
[NASA-SP-3048] c01 N69-25391
ALLEN, W. H.
Irradiation and manual navigation.
c21 A69-19208
ALLENBY, R. J.
Lunar orbital mission plans.
c30 A69-34362
ALLISON, L. J.
Satellite mapping of the Pacific tropical cloudiness.
c20 A69-33001
An atlas of Tiros 7 monthly maps of emitted radiation in the 8-12 micron atmospheric window over the Indian Ocean area
[NASA-TN-D-5101] c13 N69-23318
ALLUISI, E. A.
Effects of practice and work load on the performance of a code transformation task /COTRAN/
[NASA-CR-1261] c05 N69-14345
AMICONE, R. G.
Study of pretesting effects on electroexplosive devices
[NASA-CR-1203] c15 N69-10298
AMMANN, C.
Properties of high emittance materials
[NASA-CR-1278] c17 N69-18952
Testing of high-emittance coatings
[NASA-CR-1413] c17 N69-35514
ANAGNOSTOU, E.
Transmission effects on plastic films irradiated with ultraviolet light, electrons, and protons
[NASA-TM-X-1905] c18 N69-40339
ANDERSON, B. H.
Design of supersonic inlets by a computer program incorporating the method of characteristics
[NASA-TN-D-4960] c01 N69-14566
Characteristics study of a bicone mixed-compression inlet for Mach 1.80 to 2.50
[NASA-TN-D-5084] c01 N69-20914
Characteristic design study of mixed- compression two-dimensional inlets with low-angle cowls for the Mach number range 2.70 to 1.80
[NASA-TN-D-5330] c01 N69-30060
ANDERSON, D. L.
An exploratory study of the interplanetary environmental effects on solar-cell cover glasses.
c03 A69-35702
ANDERSON, H. R.
A lunar-surface electric-field detector.
c14 A69-13221
ANDERSON, J. L.
A nuclear thermionic space power concept using rod control and heat pipes.
c22 A69-14799
A nuclear thermionic space power concept using rod control and heat pipes
[NASA-TN-D-5250] c22 N69-26270
ANDERSON, K. F.
NASA high temperature loads calibration laboratory
[NASA-TM-X-1868] c11 N69-36224
ANDERSON, S. B.
A review of facilities and test techniques used in low-speed flight.
c11 A69-15575
ANDERSON, W. C.
Environmental control for radiation testing of lunar rock samples.
c11 A69-38271
ANDERSON, W. E.
A two-dimensional, mixed-compression inlet system designed to self-restart at a Mach number of 3.5.
[AIAA PAPER 69-447] c28 A69-32732
ANDERSON, W. J.
EHD lubrication.
c15 A69-11324
Experimental stability studies of the herringbone-grooved gas-lubricated journal bearing.
[ASME PAPER 68-LUBS-25] c15 A69-27271
Contact conformity effects on spinning torque and friction.
[ASME PAPER 68-LUB-10] c15 A69-30901
Effect of three advanced lubricants on high-temperature bearing life.
[ASME PAPER 69-LUBS-18] c15 A69-34378
Experiments on the stability of water lubricated herringbone-groove journal bearings. 1 - Theoretical considerations and clearance effects
[NASA-TN-D-4883] c15 N69-10228
Incompressibly lubricated Rayleigh step journal bearing. 2 - Infinite-length solution
[NASA-TN-D-4873] c15 N69-10231
Stability analysis for unloaded externally pressurized gas-lubricated bearings with journal rotation
[NASA-TN-D-4934] c15 N69-13256
Rolling-element bearing life from 400 deg to 600 F
[NASA-TN-D-5002] c15 N69-16367
Experiments on power loss in herringbone grooved, gas-lubricated journal bearings
[NASA-TN-D-5224] c15 N69-24932
Experiments on rotating externally pressurized air journal bearings. Part 1 - Load capacity and stiffness
[NASA-TN-D-5191] c15 N69-27078
Experiments on the stability of water lubricated herringbone-groove journal bearings. 2 - Effects of configuration and groove to ridge clearance ratio
[NASA-TN-D-5264] c15 N69-27955
Experiments on rotating externally pressurized air journal bearings. Part 2 - Attitude angle and air flow

[NASA-TN-D-5192] c15 N69-27956
Experiments on the steady state characteristics of herringbone-grooved air-lubricated journal bearings
[NASA-TN-D-5386] c15 N69-33258
ANDERSON, W. W.
On lateral cable oscillations of cable- connected space stations
[NASA-TN-D-5107] c31 N69-21111
ANDERTON, H. L.
Progress in pilot warning indicators.
c21 A69-16726
ANDREWS, W. H.
Summary of XB-70 airplane cockpit environmental data
[NASA-TN-D-5449] c25 N69-38010
ANDRUS, A. M. G.
Tracking and data relay satellite system.
c07 A69-41755
ANGELE, W.
Flat conductor cable technology.
[ASME PAPER 69-DE-8] c03 A69-28855
ANGLIN, E. L.
Analysis of lateral directional stability characteristics of a twin jet fighter airplane at high angles of attack
[NASA-TN-D-5361] c02 N69-32337
Analysis of the flat-spin characteristics of a twin-jet swept-wing fighter airplane
[NASA-TN-D-5409] c02 N69-36807
ANGUS, J. C.
Application of the laser Doppler flowmeter to fluid flow measurements.
c14 A69-26546
ANLIKER, M.
Dispersion and attenuation of small artificial pressure waves in the canine aorta.
c04 A69-14692
Transmission characteristics of axial waves in blood vessels.
[SESA PAPER 1350] c04 A69-19726
ANSTEAD, R. J.
Thermal effects on the integrity of aluminum to silicon contacts in silicon integrated circuits.
c09 A69-32893
Current status of scanning electron microscopy in semiconductor device reliability physics.
c26 A69-35788
ANTL, R. J.
Steady-state airflow and afterburning performance characteristics of four J85-GE-13 turbojet engines
[NASA-TM-X-1742] c28 N69-17781
AOKI, S.
Friction between mantle and core of the earth as a cause of the secular change in obliquity.
c13 A69-27821
AOYAGI, K.
Investigation of a 0.3-scale jet-transport model having a jet-augmented boundary-layer- control flap with direct-lift control capability
[NASA-TN-D-5129] c01 N69-30722
ARCHER, J. S.
Natural vibration modal analysis
[NASA-SP-8012] c32 N69-22773
ARGENTIERO, P. D.
The X sup 2 statistic and the goodness of fit test
[NASA-TR-R-313] c19 N69-30610
On the shape preserving expansion and contraction of objects in E sup 3
[NASA-TN-D-5240] c19 N69-31303
ARIAS, A.
Chemical reactions of ductile metals during comminution.
c06 A69-27762
The release of hydrogen on ball milling chromium in water.
c15 A69-38567
Feasibility of producing dispersion strengthened chromium by ball-milling in hydrogen halides
[NASA-TN-D-4912] c17 N69-10827
ARMENIADES, C. D.
Mechanical behavior of poly/ethylene terephthalate/ at cryogenic temperatures.
c18 A69-16494
ARMSTEAD, B. J.
Tagged arithmetic
[NASA-TN-D-5370] c08 N69-32556
ARMSTRONG, E. S.
A computational method for time-optimal space rendezvous
[NASA-TN-D-5017] c30 N69-16210
ARNDT, G. D.
An analysis of the telecommunications performance of a lunar relay satellite system.
c07 A69-42508
ARNETT, G. M.
Optical absorption in tetracyanoquinodimethan.
c26 A69-35477
ARNETT, W. D.
Nucleosynthesis in supernova explosions.
c30 A69-20898
ARNO, R. D.
Computer analysis of space power systems for mission analysis.
c03 A69-42240
ARNOLD, J. O.
A shock tube determination of the electronic transition moment of the C sub 2.
c24 A69-12833
Line by line calculation of spectra from diatomic molecules and atoms assuming a Voigt line profile.
c24 A69-35239
A computer program for a line by line calculation of spectra from diatomic molecules and atoms assuming a Voigt line profile
[NASA-TN-D-5088] c24 N69-21462
ARRINGTON, J. P.
Heat transfer and pressure distributions due to sinusoidal distortions on a flat plate at Mach 20 in helium
[NASA-TN-D-4907] c12 N69-10804
ARVESEN, J.
Handbook of Solar Simulation for Thermal Vacuum Testing.
c11 A69-38894
ASADOURIAN, A. S.
Results of endurance tests of a SNAP 8 turbine-alternator
[NASA-TM-X-1741] c03 N69-20913
ASANO, N.
Primordial helium and the luminosity of horizontal-branch stars.
c30 A69-22211
ASHBROOK, R. L.
A survey of salt deposits in compressors of flight gas turbine engines
[NASA-TN-D-4999] c28 N69-17276
Sigma phase formation and its effect on stress-rupture properties of IN-100
[NASA-TN-D-5185] c17 N69-23465
Evaluation of two nickel-base alloys, alloy 713C and NASA TAZ-8A, produced by extrusion of prealloyed powders
[NASA-TN-D-5248] c17 N69-26192
Oxidation and thermal fatigue cracking of nickel- and cobalt-base alloys in a high velocity gas stream
[NASA-TN-D-5376] c17 N69-33307
ASHBURN, E. V.
A study of jimsphere wind profiles as related to space vehicle design and operations
[NASA-CR-1204] c20 N69-13629
ASHBY, G. C., JR.
Some topics in hypersonic body shaping.
[AIAA PAPER 69-181] c01 A69-18052
Calculated and experimental hinge moments on a trailing-edge flap of a 75 deg swept delta wing at Mach 6
[NASA-TN-D-4268] c01 N69-10054
ASTRIN, R.
Hydrogen-oxygen electrolytic regenerative fuel cells
[NASA-CR-1244] c03 N69-18885
ATHANS, M.
Suboptimal state estimation for continuous-time nonlinear systems from discrete noisy measurements.
c10 A69-17939
ATKINS, H.
Subject classification bibliography for thermal contact resistance studies.
[ASME PAPER 68-WA/HT-18] c33 A69-16122
ATLAN, H.
Differences between radiation-induced life shortening and natural aging in Drosophila

melanogaster.
c04 A69-30444
Viruslike particles in the fat body, oenocytes, and central nervous tissue of Drosophila melanogaster imagoes.
c04 A69-42021
AUSTIN, R. W.
Experiments on visual acuity and the visibility of markings on the ground in long-duration earth-orbital space flight
[NASA-CR-1134] c05 N69-10813
AWOSHIKA, K.
An application of similitude to model design of a soil-projectile system
[NASA-CR-1210] c34 N69-13159
AXELROD, A. R.
Adaptive simulation using mode identification
[NASA-CR-1179] c08 N69-10316
AXFORD, W. I.
Solar modulation of galactic cosmic rays. I.
c29 A69-43169
AYDELOTT, J. C.
Effect of size on normal-gravity self-pressurization of spherical liquid hydrogen tankage
[NASA-TN-D-5196] c33 N69-24168
Venting of liquid hydrogen tankage
[NASA-TN-D-5263] c33 N69-27620
AZIMOV, S. A.
Some problems of the physics of high energies and cosmic rays
[NASA-TT-F-535] c29 N69-24924

B

BABB, G. R., JR.
Translunar abort techniques for nonfree-return missions
[NASA-TM-X-1806] c30 N69-29569
BABCOCK, J. E.
Micromation and micrographics.
c34 A69-35059
BACKE, R. J.
Relay coil temperature rise at simulated outer space pressure levels.
c09 A69-28048
BACON, J. W., JR.
Amplified laminar boundary layer oscillations and transition at the front attachment line of a 45 deg swept flat-nosed wing with and without boundary layer suction.
c01 A69-33251
BAE, M. S.
Degradation of multiplier phototubes exposed to spatial radiations
[NASA-CR-1304] c14 N69-20777
BAER, E.
Mechanical behavior of poly/ethylene terephthalate/ at cryogenic temperatures.
c18 A69-16494
BAGDOEV, A. G.
Nonlinear problems of compressible flow
[NASA-TT-F-560] c12 N69-27168
BAILEY, E. E.
Experimental data for two 1400-feet per second tip speed compressor rotors operated with inlet flow distortions
[NASA-TM-X-1798] c01 N69-26312
BAILEY, H. E.
Integration of the equations governing the one-dimensional flow of a chemically reactive gas.
c12 A69-18317
On some numerical difficulties in integrating the equations for one-dimensional nonequilibrium nozzle flow
[NASA-TN-D-5176] c19 N69-23355
BAILEY, P.
A neutral buoyancy micro-electrode for prolonged recording from single nerve units.
c05 A69-11865
BAKER, B. L.
Porphyrins in meteorites - Metal complexes in Orgueil, Murray, Cold Bokkeveld, and Mokoia carbonaceous chondrites.
c30 A69-39889
Trace porphyrin complexes - Fluorescence detection by demetallation with methanesulfonic acid.
c06 A69-42557
BAKER, J. C.
Temporal plasma echoes.
c25 A69-38713
BALANIS, C. A.
Analysis of aperture radiation from an axially slotted circular conducting cylinder using geometrical theory of diffraction.
c07 A69-24993
Aperture radiation from an axially slotted elliptical conducting cylinder using geometrical theory of diffraction.
c09 A69-40703
Equatorial plane pattern of an axial-TEM slot on a finite size ground plane.
c07 A69-41588
BALASUBRAHMANYAN, V. K.
Solar activity and the 11-year modulation of cosmic rays.
c29 A69-29967
BALL, L. L.
The use of super 184 W as a thermal flux monitor at high temperatures.
c14 A69-43192
Use of tungsten-184 as a thermal flux monitor at high temperatures
[NASA-TN-D-5113] c22 N69-20795
BALL, R. H.
Prediction of geomagnetic secular change confirmed.
c13 A69-37490
BALLANCE, J. O.
In-situ molecular beam experiments in earth orbit.
c24 A69-36182
BAMBAKIDIS, G.
Electrical resistivity as a function of deuterium concentration in palladium
[NASA-TN-D-4970] c26 N69-14565
BAMBERGER, E. N.
Effect of three advanced lubricants on high-temperature bearing life.
[ASME PAPER 69-LUBS-18] c15 A69-34378
Rolling-element bearing life from 400 deg to 600 F
[NASA-TN-D-5002] c15 N69-16367
BANDEEN, W. R.
Observations of the reflection properties of the earth-atmosphere system and the cloud formation above the equatorial Pacific from a synchronous satellite.
c20 A69-43154
BANKS, B. A.
A fabrication process for glass coated electron-bombardment ion thruster grids
[NASA-TN-D-5320] c15 N69-30062
BANNISTER, J. R.
Space flight nutrition.
c05 A69-15388
BANNISTER, T. C.
Microscopic observation of interfacial phenomena.
[AIAA PAPER 69-95] c33 A69-18126
BAR-TOUV, J.
Inelastic scattering calculations with Wood- Saxon Hartree-Fock wave functions.
c26 A69-29006
BARAONA, C. R.
Effects of nickel on the performance of N on P silicon scar cells
[NASA-TN-D-5366] c03 N69-31844
BARCHAS, J. D.
Adrenal epinephrine and phenylethanolamine n-methyl transferase /PNMT/ activity in the rat bearing a transplantable pituitary tumor.
c04 A69-20374
Compensatory hypertrophy and phenylethanolamine n-methyl transferase /PNMT/ activity in the rat adrenal.
c04 A69-41404
BARDUSCH, R. E.
A rendezvous and station-keeping simulator with fly around capability and virtual image viewing
[NASA-TN-D-5123] c11 N69-22629
BARGER, R. L.
Development of sonic-boom signatures in a stratified atmosphere
[NASA-TN-D-4890] c02 N69-10087
Investigation of a class of bodies that generate far-field sonic boom shock strength and impulse independent of body length and volume
[NASA-TN-D-5148] c01 N69-23927

BARKLEY, H. B., JR.
Significant experiences of the NASA Plum Brook Reactor Facility. c22 A69-13128
Significant experiences of the NASA Plum Brook reactor facility [NASA-TM-X-1853] c22 N69-33132
BARNA, G. J.
Study of a 300 kWe Rankine cycle advanced nuclear-electric space power system. c22 A69-42266
BARNES, A.
Collisionless heating of the solar-wind plasma. I. c29 A69-12714
Quasilinear theory of hydromagnetic waves in collisionless plasma. c25 A69-20797
Collisionless heating of the solar-wind plasma. II. c30 A69-22426
BARNES, R. M.
Preliminary development of spectrochemical analysis of superalloys with the liquid-layer solid-sample spark technique [NASA-TM-X-1753] c06 N69-20853
BARNETT, T. L.
Application of a nonlinear least-squares method to atmospheric temperature sounding. c13 A69-33156
BARNOSKI, R. L.
Summary of random vibration prediction procedures [NASA-CR-1302] c32 N69-23096
BARNWELL, R. W.
Inviscid radiating shock layers about spheres traveling at hyperbolic speeds in air [NASA-TR-R-311] c12 N69-26504
BARON, N.
Alpha-gamma angular correlations in super 120 Sn. c24 A69-13098
Alpha-gamma angular correlations on super 58 Ni. c24 A69-13100
Elastic scattering of 21-MeV protons from nitrogen-14, oxygen-16, argon-40, nickel-58, and tin-116. c24 A69-35489
Elastic scattering of 21-MeV protons from nitrogen 14, oxygen 16, argon 40, nickel 58, and tin 116 [NASA-TN-D-4932] c24 N69-12840
Scattering of 42 MeV /6.7-pJ/ alpha particles from even isotopes of cadmium. Supplement 1 - Absolute cross sections [NASA-TN-D-4948] c24 N69-14482
BARRACK, J. P.
Reingestion characteristics and inlet flow distortion of V/STOL lift-engine fighter configurations. [AIAA PAPER 68-78] c01 A69-26762
BARRETT, C. A.
Absorption rate sticking probabilities for oxygen on columbium and dilute columbium- zirconium alloys [NASA-TN-D-4885] c17 N69-10931
Evaluation of the results of a round robin analysis for oxygen in potassium and sodium [NASA-TN-D-4971] c06 N69-14180
Controlled oxygen additions to refractory metals [NASA-TM-X-1799] c17 N69-26952
BARRITT, P. F.
Data relay satellites for support of NASA R and D missions. c07 A69-25296
Tracking and data relay satellite system. c07 A69-41755
BARTHLOME, D. E.
The equipotential space suit design concept and its application to a space suit elbow joint [NASA-TN-D-5221] c05 N69-26259
BARTLE, R.
Study of air pollutant detection by remote sensors [GDC-DBE-68-011] c13 N69-31961
BARTLETT, E. S.
Research on metallurgical characteristics and performance of materials used for sliding electrical contacts Summary report, 1 May 1968 - 30 Apr. 1969 [NASA-CR-1447] c17 N69-40057
BARTLETT, R. O.
Cesium contact ion microthruster experiment aboard applications technology satellite /ATS/ IV. [AIAA PAPER 69-297] c28 A69-21218
BARTOO, E. R.
Experimental studies on shadow shields for thermal protection of cryogenic tanks in space [NASA-TN-D-4887] c33 N69-10420
BASHARK, L. T.
Techniques for generation of control and guidance signals derived from optical fields [NASA-CR-1443] c21 N69-38041
BASHE, R.
Planetary film reconnaissance system [NASA-CR-1358] c14 N69-28023
BASS, M.
A program to evaluate dye lasers as high power, pulsed, visible light sources [NASA-CR-1374] c16 N69-29934
BATSON, B. H.
Transmission characteristics of split-phase PCM codes. c07 A69-39451
An analysis of the telecommunications performance of a lunar relay satellite system. c07 A69-42508
BATTERSON, S. A.
Principal science results from Surveyor 5. c30 A69-12224
Lunar surface mechanical properties. c30 A69-12225
BATTERTON, P. G.
Dynamic performance analysis of a fuel-control valve for use in airbreathing engine research [NASA-TN-D-5331] c03 N69-29977
BATY, D. L.
Human information processing rates during certain multiaxis tracking tasks with a concurrent auditory task. c05 A69-23880
BAUCOM, R. M.
Strain rate sensitivity of three titanium alloy sheet materials after prolonged exposure at 550 deg F /561 deg K/ [NASA-TN-D-4981] c17 N69-14873
Mechanical behavior of boron-epoxy and glass-epoxy filament-wound cylinders under various loads [NASA-TN-D-5050] c18 N69-19825
Tensile behavior of boron filament reinforced epoxy rings and belts [NASA-TN-D-5053] c18 N69-19918
BAUER, P.
Batteries for space power systems [NASA-SP-172] c03 N69-18042
BAUER, S. F.
Power conditioning development for the Sert II ion thrustor. c03 A69-42301
BAUER, S. J.
Diffusive equilibrium in the topside ionosphere. c13 A69-37887
BAUMANN, R. C.
Design techniques for small scientific satellite structures [NASA-TN-D-4988] c32 N69-33232
BAUMEISTER, K. J.
Hyperbolic heat-conduction equation - A solution for the semi-infinite body problem. [ASME PAPER 69-HT-1] c33 A69-43564
Lighting in cryogenic and noncryogenic fluids [NASA-TM-X-1654] c14 N69-13176
Film boiling from submerged spheres [NASA-TN-D-5124] c33 N69-28318
BAYLESS, J. W.
Analytic function models of noise and modulation [NASA-TR-R-314] c07 N69-29230
BAZ, A. I.
Scattering, reactions and decay in nonrelativistic quantum mechanics [NASA-TT-F-510] c24 N69-25848
BAZHENOVA, T. V.
Shock waves in real gases [NASA-TT-F-585] c12 N69-40824
BEAM, B. H.
Thermodielectric radiometer. [AIAA PAPER 68-403] c14 A69-12392
Hydrocarbon gas absorption by a He Ne laser beam at a 3.39-mu wavelength. c16 A69-42192
BEAM, R. M.
On the phenomenon of thermoelastic instability /thermal flutter/ of booms with open cross

section
[NASA-TN-D-5222] c32 N69-29589
BEARD, T. W.
Deployable elements of the orbiting geophysical observatories.
c31 A69-17606
BEASLEY, G. P.
Simulation of Gemini extravehicular tasks by neutral-buoyancy techniques
[NASA-TN-D-5235] c05 N69-28024
BEASLEY, W. D.
Investigation of a plasma accelerator with magnetic field arranged to produce a divergent-nozzle effect
[NASA-TN-D-5122] c25 N69-22942
A laboratory investigation of N-wave focusing
[NASA-TN-D-5306] c02 N69-31874
BEATTY, M. E., III
Changes in minority-carrier lifetime in silicon and gallium arsenide resulting from irradiation with 22 and 40 MeV protons
[NASA-TN-D-5028] c26 N69-18897
Annealing of 22, 40, and 158 MeV proton damage in n-type and p-type silicon
[NASA-TN-D-5119] c26 N69-22552
BEAUCHENE, J. H.
The design and performance of a versatile 25 solar constant simulator.
c11 A69-30383
BECHTEL, R. T.
Performance and control of a 30-centimeter diameter, low impulse Kaufman thruster.
[AIAA PAPER 69-238] c28 A69-21256
BECK, A. J.
Models of Venus atmosphere, 1968
[NASA-SP-8011] c30 N69-20916
BECK, S. M.
Lithium-drifted silicon detectors as low-energy photon spectrometers
[NASA-TN-D-5056] c24 N69-19828
BECKER, H. S.
Adapting space plans to changing times.
c34 A69-22863
Planning future space programs - Are we on the right track?
[AAS PAPER 69-083] c34 A69-42820
BECKER, J. V.
The X-15 program in retrospect.
c02 A69-26872
BECKWITH, I. E.
Calculation of nonequilibrium hypersonic turbulent boundary layers and comparisons with experimental data.
[AIAA PAPER 69-684] c12 A69-33474
Fluctuating properties of turbulent boundary layers for Mach numbers up to 9
[NASA-TN-D-5496] c12 N69-40137
BEEBEE, W. S.
Design of strapdown gyroscopes for a dynamic environment Interim scientific report
[NASA-CR-1396] c21 N69-34672
BEGGS, J. E.
Nonelectric cathode heating.
c09 A69-24748
BEGLEY, R. T.
Refractory Metal Alloys- Metallurgy and Technology, Proceedings of a Symposium on Metallurgy and Technology of Refractory Metals, Washington, D.C., April 25, 26, 1968.
c17 A69-18790
BEHANNON, K. W.
Measurements of the perturbed-interplanetary magnetic field in the lunar wake.
c30 A69-11228
Intrinsic magnetic properties of the lunar body.
c30 A69-14005
Satellite studies of the earth's magnetic tail.
c29 A69-19363
BEHNING, F. P.
Cold air investigation of a turbine with stator-blade trailing-edge coolant ejection. Part 1 - Overall stator performance
[NASA-TM-X-1901] c03 N69-39335
BEHRENDT, D. R.
Resonant mode analysis of the Fitzgerald apparatus
[NASA-TN-D-5103] c26 N69-20798
Mathematical analysis of the Fitzgerald apparatus
[NASA-TN-D-5116] c18 N69-21384
BEHRNDT, K. H.
Adhesion mechanism of gold-underlayer film combinations to oxide substrates.
c26 A69-28007
Film formation and structure-sensitive properties - An introduction.
c26 A69-43344
Effect of oxygen on the formation of germanium films.
c26 A69-43345
BELL, M. L.
Current research on regenerative systems.
c04 A69-37623
BELL, V. L.
Preparation and compression molding of salt- like intermediate Pyrrone /BTDA-EG-DAB/.
c18 A69-29415
Radiation stability of unfilled pyrrone moldings.
c18 A69-35529
BELLMAN, D. R.
The flight investigation of pressure phenomena in the air intake of an F-111A airplane.
[AIAA PAPER 69-488] c28 A69-32706
BELLO, L. M.
Central data system concepts for spacecraft data management.
c08 A69-42621
BELTRACCHI, L.
Design, simulation and flight performance of the Radio Astronomy Explorer-A satellite.
c31 A69-18328
BENDURA, R. J.
Dynamic stability characteristics of large-size 120 deg blunted conical spacecraft in a simulated Martian environment.
[AIAA PAPER 69-104] c31 A69-18210
Damping derivatives of 120 deg conical spacecraft from flights in a low-density environment.
c31 A69-40550
Inflation and performance of three parachute configurations from supersonic flight tests in a low-density environment
[NASA-TN-D-5296] c01 N69-30063
BENNETT, R. A.
Nuclear magnetic resonance study of the niobium-nitrogen system NbN sub x.
c26 A69-36445
BENNIGHT, J. D.
An investigation of the decoupling effects in a magnetic forming beryllium coil assembly.
c14 A69-25310
BENNING, F. N.
Handbook of Solar Simulation for Thermal Vacuum Testing.
c11 A69-38894
BENSON, H. E.
Lunar surface mechanical properties.
c30 A69-12225
BENSON, R. F.
Frequency shifts observed in the Alouette I cyclotron harmonic plasma resonances.
c07 A69-37892
BENTLEY, S. B.
Shock ionization kinetics of pure nitrogen.
c12 A69-43367
BENVENISTE, J. E.
Dynamic response of structural elements exposed to sonic booms
[NASA-CR-1281] c32 N69-21403
BERCAW, R. W.
Deuteron break-up by 42 Mev alpha particles.
c24 A69-13469
BERENYI, S. G.
Vapor ingestion phenomenon in weightlessness
[NASA-TN-D-5210] c12 N69-24917
The liquid-vapor interface during outflow in weightlessness
[NASA-TM-X-1811] c12 N69-27954
BERG, O. E.
A new criterion for the identification of micrometeor impact sites on aluminized glass.
c30 A69-34952
The Pioneer 8 cosmic dust experiment
[NASA-TN-D-5267] c30 N69-31058
BERGER, R. L.
A laboratory investigation of N-wave focusing
[NASA-TN-D-5306] c02 N69-31874
BERNARDO, J. V.
Educational materials produced by the space

program.
[UN PAPER 68-95291] c34 A69-10519
The influence of space exploration on science education.
c34 A69-35077
BERNER, D. C.
Nondestructive determination of uranium 235 distribution by fixed position gamma scanning
[NASA-TM-X-1779] c22 N69-22555
BERNOT, P. T.
Center-of-gravity requirements for trim of several axisymmetric bodies.
c01 A69-39237
BERNSTEIN, M. I.
Hand-printed input for on-line systems
[NASA-CR-1284] c08 N69-21527
BERRIER, B. L.
Effect of plug and shroud geometry variables on plug-nozzle performance at transonic speeds
[NASA-TN-D-5098] c28 N69-21463
Effect of jet velocity and axial location of nozzle exit on the performance of a twin-jet afterbody model at Mach numbers up to 2.2
[NASA-TN-D-5393] c28 N69-36932
BERRY, C. A.
The medical legacy of Gemini.
c04 A69-11074
Preliminary clinical report of the medical aspects of Apollos VII and VIII.
c05 A69-22542
Lunar medicine.
c04 A69-27909
Chromosome analyses of Gemini astronauts.
c04 A69-33173
Status report on space medicine in the United States.
c34 A69-36460
BERRY, R. L.
Real-time targeting for the Apollo lunar orbit insertion maneuver.
[AIAA PAPER 68-848] c31 A69-39760
BERRY, W. H.
Sequential processing techniques for trajectory estimation
[NASA-CR-1360] c30 N69-40325
BERSOFF, E. H.
CLASP, computer language for aeronautics and space programming.
[AIAA PAPER 69-957] c08 A69-40339
BERTOLINI, A.
Suboptimal state estimation for continuous-time nonlinear systems from discrete noisy measurements.
c10 A69-17939
BESS, L.
A suboptimal approximation to the Kalman filter
[NASA-TN-D-5082] c10 N69-21123
BETHEA, R. M.
Removal of acid gases and oxides of nitrogen from space cabin atmospheres
[NASA-CR-1388] c05 N69-37517
BETTINGER, P. J.
Tagged arithmetic
[NASA-TN-D-5370] c08 N69-32556
BETTNER, J. L.
Experimental investigation in an annular cascade sector of highly loaded turbine stator blading. Volume 1 - Analysis and design
[NASA-CR-1219] c01 N69-14211
Experimental investigation in an annular cascade sector of highly loaded turbine stator blading. Volume 3 - Performance of tandem blade
[NASA-CR-1341] c01 N69-23892
Experimental investigation in an annular cascade sector of highly loaded turbine stator blading. Volume 2 - Performance of plain blade and effect of vortex generators
[NASA-CR-1323] c01 N69-25327
Experimental investigation in an angular cascade sector of highly loaded turbine stator blading. Volume 4 - Performance of a jet- flapped blade
[NASA-CR-1423] c28 N69-36680
BEVANS, J. T.
Thermal Design Principles of Spacecraft and Entry Bodies.
c33 A69-34372
BIDER, B.
Effect of variable stator area on performance of a single-stage turbine suitable for air cooling. 5 - Stator detailed losses with 70 percent design area
[NASA-TM-X-1696] c28 N69-10296
BIEN, D. D.
A method for reducing the equivalent sink temperature of a vertically oriented radiator on the lunar surface
[NASA-TM-X-1729] c03 N69-17225
BILLIG, F. S.
The interaction and penetration of gaseous jets in supersonic flow
[NASA-CR-1386] c12 N69-32480
BILLINGSLEY, D. G.
A real-time processing system for determination of metabolic rates of a suited astronaut.
[AIAA PAPER 69-993] c05 A69-40371
BILLMAN, K. W.
Temperature tuning of an organic dye laser.
c16 A69-12617
Picosecond pulse measurement by two-photon excitation of photographic film.
c14 A69-20165
BILLUPS, C. W.
Attitude control of a manned earth orbiting space station.
[AIAA PAPER 69-846] c31 A69-39376
BINKLEY, W. O.
Millimeter wavelengths for space communications?
c07 A69-13721
BINNARD, R.
Differences between radiation-induced life shortening and natural aging in Drosophila melanogaster.
c04 A69-30444
BIRD, J. D.
An investigation of the optimum design and flight of rockets
[NASA-TR-R-297] c31 N69-15374
Tuft-grid surveys at low speeds for delta wings
[NASA-TN-D-5045] c01 N69-19027
BIRMINGHAM, T. J.
Charged particle diffusion by violation of the third adiabatic invariant.
c29 A69-19375
Guiding center drifts in time-dependent meridional magnetic fields.
c25 A69-20809
Convection electric fields and the diffusion of trapped magnetospheric radiation.
c29 A69-28936
BIRYUKOV, YU. V.
Transactions of the Ninth Scientific Conference of Graduate Students and Junior Scientific Associates of the Institute for the History of Natural Science and Technology, Section on the History of Aviation and Cosmonautics
[NASA-TT-F-540] c34 N69-31836
Transactions of the Tenth Scientific Conference of the Institute of History of Natural Science and Technology
[NASA-TT-F-537] c34 N69-36314
BISHOP, A. R.
Effect of electrothermal instabilities on Brayton- and Rankine-cycle magnetohydrodynamic space-power generation systems
[NASA-TN-D-5461] c03 N69-37883
BISSON, E. E.
Various modes of wear and their controlling factors.
c15 A69-27231
BITTKER, D. A.
Nonequilibrium calculations of methane fluorine oxygen and butene-1-fluorine oxygen rocket performance
[NASA-TN-D-4991] c27 N69-16153
Theoretical nonequilibrium performance of oxygen difluoride-diborane rocket propellant
[NASA-TN-D-4992] c27 N69-16195
BJERKLIE, J. W.
Configurations for gas turbine compressor end seals.
[ASLE PREPRINT 68AM 4B-4] c15 A69-27366
BJERKNES, J.
Satellite mapping of the Pacific tropical cloudiness.
c20 A69-33001
BJORKLUND, S.
Fluorescence spectra of homogeneous and mixed europium complexes.

c06 A69-10893
BLACKADAR, A. K.
Investigation of the turbulent wind field below 150-meter altitude at the eastern test range
[NASA-CR-1410] c20 N69-35570
BLACKSHEAR, W. T.
Results on the mass and the gravitaticnal field of the moon as determined from dynamics of lunar satellites.
c30 A69-31405
BLACKWELL, J. A., JR.
Preliminary study of effects of Reynolds number and boundary-layer transition location on shock-induced separation
[NASA-TN-D-5003] c01 N69-16121
A finite-step method for calculation of theoretical load distributions for arbitrary lifting surface arrangements at subsonic speeds
[NASA-TN-D-5335] c01 N69-31337
BLACKWOOD, D.
Pulse motor for spacecraft attitude control.
c03 A69-11762
BLAHA, B. J.
Flight and wind tunnel investigation of installation effects on supersonic cruise exhaust nozzles at transonic speeds.
[AIAA PAPER 69-427] c01 A69-32769
BLAHA, R. J.
An analog computer study of the low-frequency flow dynamics of two nuclear rocket cold-flow engine systems
[NASA-TN-D-5312] c22 N69-30070
BLAISE, H. T.
Development of air bearing lift pads
[NASA-TM-X-1724] c01 N69-16467
BLAMONT, J. E.
Effects of energetic particles on photomultipliers in earth orbits up to 1500 km.
c14 A69-16932
BLANCHARD, D. L.
Design, simulation and flight performance of the Radio Astronomy Explorer-A satellite.
c31 A69-18328
BLANCHARD, R. C.
A unified form of Lambert's theorem
[NASA-TN-D-5368] c30 N69-36930
BLANCHARD, U. J.
Full-scale dynamic landing-impact investigation of a prototype lunar module landing gear
[NASA-TN-D-5029] c31 N69-20965
BLAND, D.
A computer program for calculating external thermal-radiation heat loads and temperatures of spacecraft orbiting the planets or the moon
[NASA-TR-R-278] c30 N69-14428
BLESS, R. C.
Filter photometry of Saturn in the spectral region lambda lambda 2950-2450.
c30 A69-22216
BLISS, J. C.
Characteristics of the tactile information channel
[NASA-CR-1389] c05 N69-39211
BLOCHER, M.
Elastic scattering of 600 MeV protons from He super 3.
c24 A69-13464
BLOCK, A.
Design considerations for an integrated 1.8- GHz parametric amplifier.
c09 A69-10193
BLOCK, H. B.
Performance of the SNAP-8 lubrication and coolant subsystem
[NASA-TM-X-1731] c03 N69-20828
BLOCKLEY, B. V.
Preliminary evaluation test of the Langley cardiovascular conditioning suit concept
[NASA-CR-1206] c05 N69-13202
BLOOMER, H. E.
Liquid rocket acoustic-mode-instability studies at a nominal thrust of 20000 pounds
[NASA-TN-D-4968] c28 N69-14384
BLOOMFIELD, H. S.
Evaluation of the COHORT 2 Monte Carlo shielding code - Gamma ray transport using source direction biasing
[NASA-TM-X-1877] c22 N69-35848
BLOOMQUIST, C. E.
Spacecraft failure rates - Where are we?
c31 A69-34519
BLUE, J. W.
Another study of the decay of I super 123.
c24 A69-13099
BLUM, H. A.
Subject classification bibliography for thermal contact resistance studies.
[ASME PAPER 68-WA/HT-18] c33 A69-16122
BLUM, R. E.
Buckling of an equatorial segment of a spherical shell loaded by its own weight
[NASA-TN-D-4921] c32 N69-13034
BLUME, H.-J. C.
Error analysis of input-noise-temperature measurements of low-noise amplifiers
[NASA-TN-D-4997] c07 N69-16162
Application of pressurized liquid nitrogen inside parametric-amplifier structures for input-noise-temperature improvement
[NASA-TN-D-5509] c09 N69-40079
BODLEY, C.
A method for digital computation of spacecraft response in the docking maneuver.
c31 A69-25501
BOECKEL, J. H.
Test plan optimization for an Explorer-size spacecraft
[NASA-TN-D-5283] c34 N69-31333
BOEDEKER, L.
Theoretical investigations of RF induction heated plasmas
[NASA-CR-1312] c25 N69-22638
BOGARD, D. D.
Cosmogenic rare gases and the super 40 K-super 40 Ar age of the Kodaikanal iron meteorite.
c30 A69-22047
BOGART, D.
Measurement of the super 10 B/n, alpha/ super 7 Li, super 7 Li relative cross sections in the keV region.
c24 A69-33753
Resonance integrals of rhenium for a wide range of sample sizes
[NASA-TN-D-4938] c24 N69-13152
BOGGS, F. W.
Relationship between flow pattern, constitutive equation and molecular structure.
c12 A69-33257
BOGUE, R. K.
Advanced air data sensing techniques.
c14 A69-16755
BOHON, H. L.
Development status of attached inflatable decelerators.
[AIAA PAPER 68-929] c02 A69-39015
BOIES, D.
Detection and minimization of chemically induced ignition hazards of glycol fluids.
c18 A69-36028
BOLDMAN, D. R.
Heat transfer and thermal boundary layer in a conical nozzle.
[AIAA PAPER 69-474] c33 A69-32780
The use of energy thickness in prediction of throat heat transfer in rocket nozzle
[NASA-TN-D-5356] c33 N69-31869
Experimental and theoretical turbulent boundary layer development in a Mach 4.4 water-cooled conical nozzle
[NASA-TN-D-5377] c12 N69-33353
BOLDT, E. A.
Iron line emission from X-ray sources.
c29 A69-22231
Two-twenty keV spectrum of X-rays from the Crab Nebula and the diffuse background near galactic anticenter.
c29 A69-30759
Pulsed X-ray emission of NP 0532 in March 1968.
c29 A69-37574
Cosmic X-ray bremsstrahlung associated with suprathermal protons.
c29 A69-40643
BOLGER, P. H.
System safety - A management system for safety used in manned space flight.
[AAS PAPER 69-522] c34 A69-42851
BOLLENBACHER, G.
Description and evaluation of digital-computer design-analysis program for homopolar inductor

alternators
[NASA-TN-D-5072] c03 N69-19799
BOLTZ, F. W.
Minimum thrust for correcting Keplerian orbits with application to interplanetary guidance
[NASA-TN-D-4945] c21 N69-14399
BONAVITO, N. L.
An accuracy and speed comparison of the Vinti and Brouwer orbit prediction methods
[NASA-TN-D-5203] c30 N69-26252
An analysis of satellite positional uncertainty by statistical mechanics
[NASA-TN-D-5259] c30 N69-30611
BOND, G. H.
Plasma enzyme responses to blood withdrawal in chickens.
c04 A69-23158
BOND, V. R.
Matched conic solutions to round trip interplanetary trajectory problems that insure state-vector continuity at all boundaries
[NASA-TN-D-4942] c30 N69-14861
BONNER, F. M.
Ion depletion in the high-latitude exosphere - Simultaneous OGO 2 observations of the light ion trough and the VLF cutoff.
c29 A69-34939
BONNER, G. P.
Postflight optical evaluation of the right- hand and left-hand windows of Gemini missions 4, 5, 6, and 7
[NASA-TN-D-4916] c31 N69-13232
Preflight optical evaluation of the right-hand hatch windows of Gemini missions 7, 8, 9, and 12
[NASA-TN-D-5471] c31 N69-40813
BONNEVILLE, J. M.
Propulsion assisted by microwave power.
[IMPI PAPER D2] c28 A69-15000
BONOMO, P. J.
RAE-A attitude determination ground support system.
[AIAA PAPER 69-983] c08 A69-40363
BOOTH, S.
Laser Doppler velocity instrument
[R-67-4450] c14 N69-14351
BOREK, R. W.
Flight and laboratory tests of an ''L-band'' telemetry RF system.
c07 A69-35996
BORELLI, M. T.
Analysis of commutated networks employing feedback circuits.
c10 A69-19853
Analysis of commutated networks employing feedback circuits
[NASA-TN-D-4893] c10 N69-10755
BORING, K. L.
Plasma electron beam development for welding applications.
c15 A69-35555
BORN, G. H.
An approximate solution for the short-term motion of a lunar satellite.
c30 A69-35934
An Encke-type special perturbation method.
[AIAA PAPER 69-908] c30 A69-39340
BORTOLOT, V. J., JR.
Upper limits to the intensity of background radiation at lambda equals 1.32, 0.559, and 0.359 mm.
c30 A69-19404
BOSCHITZ, E. T.
Elastic scattering of 600 MeV protons from He super 3.
c24 A69-13464
Polarization in proton super 4 He scattering at 540 MeV.
c24 A69-14966
The interaction of intermediate energy protons with light nuclei.
c24 A69-43123
Elastic scattering of 600 MeV protons from light nuclei.
c24 A69-43125
Optical model analysis of proton scattering in the range 16 to 22 MeV
[NASA-TN-D-5067] c24 N69-22934
Interaction of 42-MeV alpha particles with helium-3
[NASA-TN-D-5530] c24 N69-40979
BOSCO, J. S.
Effects of progressive hypohydration on maximal isometric muscular strength.
c04 A69-15983
Orthostatic intolerance after artificial heat acclimatization in physically fit subjects.
c05 A69-32810
BOSSLER, R. B., JR.
The Bossler coupling
[NASA-CR-1241] c15 N69-16104
BOSTROM, C. O.
Proton entry into the magnetosphere on May 26, 1967.
c29 A69-31984
BOTHE, G. G.
Auditory temporal masking and the perception of order.
c05 A69-24795
BOUGHNER, R. E.
Theoretical predictions of nongray radiant heat transfer in high-temperature nonisothermal CO sub 2 -N sub 2 mixtures.
[AIAA PAPER 69-636] c33 A69-33258
BOURQUE, D. J.
Ground-based guidance for land-landing manned spacecraft equipped with low-velocity descent systems.
[AIAA PAPER 69-864] c21 A69-39390
BOWEN, F. E.
Aerodynamic characteristics determined during development of the Apollo launch escape vehicle configuration
[NASA-TN-D-5208] c01 N69-29027
BOWKER, D. E.
Investigations of the unique memory properties of 55-Nitinol alloy.
c17 A69-35523
BOWMAN, J. S., JR.
Analysis of the flat-spin characteristics of a twin-jet swept-wing fighter airplane
[NASA-TN-D-5409] c02 N69-36807
BOWMAN, R. L.
Performance of N/p silicon and cadmium sulfide solar cells as affected by hypervelocity particle impact
[NASA-TN-D-5133] c03 N69-21016
Solar absorptances and spectral reflectances of 12 metals for temperatures ranging from 300 to 500 K
[NASA-TN-D-5353] c17 N69-31895
BOXER, E.
A method for predicting the performance of high reaction supersonic compressor blade sections.
[AIAA PAPER 69-522] c28 A69-32711
BOYLE, J. C.
Experimental determination of eddy-current torques on bodies rotating relative to a uniform magnetic field
[NASA-TN-D-5086] c23 N69-29477
BOYLE, R. J.
Thermal analysis of shadow shields and structural members in a vacuum
[NASA-TN-D-4876] c33 N69-10473
BOZEK, J. M.
Effects of sample preparation on photomicrographs of cadmium sulfide thin-film solar cells
[NASA-TM-X-1722] c03 N69-15397
BRACE, L. H.
Langmuir probe evidence for a nocturnal ionization source at Fort Churchill.
c29 A69-14008
Measurements of electron cooling rates in the mid-latitude and auroral-zone thermosphere.
c13 A69-16267
Radar backscatter and rocket probe measurements of electron temperature above Arecibo.
c29 A69-25162
Electron measurements bearing on the energy and particle balance of the upper F region.
c29 A69-31975
Ionospheric and magnetic observations at 1000 kilometers during the geomagnetic storm and aurora of May 25-26, 1967.
c13 A69-34954
Cylindrical electrostatic probes employed on Alouette II and Explorer XXXI satellites.
c14 A69-37876

Comparison of cylindrical electrostatic probe measurements on Alouette II and Explorer XXXI satellites.
c14 A69-37877
Comparison of results of Explorer XXXI direct measurement probes.
c13 A69-37882
Response of the 1000-kilometer ionosphere to magnetic storms.
c13 A69-42438
Latitudinal observations of the thermal balance in the nighttime protonosphere.
c13 A69-43181

BRACKETT, R. L.
Geometric properties of a prestressed segmented spherical shell
[NASA-CR-1231] c32 N69-11010

BRADFORD, J. M., JR.
A method for characterizing the surface cleanliness during adhesion testing
[NASA-TN-D-5055] c17 N69-19827

BRADY, S. W.
Boundedness theorems and other mathematical studies of a Hodgkin-Huxley type system of differential equations - Numerical treatment of thresholds and stationary values
[NASA-CR-1272] c19 N69-21143

BRAINARD, W. A.
The influence of ordering on the friction and wear of metals in vacuum.
c15 A69-35183
The thermal stability and friction of the disulfides, diselenides, and ditellurides of molybdenum and tungsten in vacuum
[NASA-TN-D-5141] c15 N69-22992

BRAITHWAITE, W. M.
Performance and stall limits of a YTF30-P-1 turbofan engine with uniform inlet flow
[NASA-TM-X-1803] c28 N69-27019

BRALEY, R. C.
Inelastic scattering calculations with Wood- Saxon Hartree-Fock wave functions.
c26 A69-29006
Core polarization effects in inelastic scattering.
c24 A69-29007
E2 transition rates for super 20 Ne.
c24 A69-35166
Inelastic scattering calculations with projected Hartree-Fock wave functions.
c24 A69-41045
Hartree-Fock calculations with Wood-Saxon basis functions
[NASA-TN-D-5066] c24 N69-17976

BRANCAZIO, P. J.
Relation between nuclear level density parameters and mass shell.
c24 A69-29337

BRANCHFLOWER, G. A.
A review of the image dissector meteorological cameras and a view of their future.
c14 A69-35101

BRANDHORST, H. W., JR.
Impurity profile and energy band diagram for the Cu sub 2 S-CdS heterojunction.
c03 A69-13075
Effect of bias light on the spectral response of Cu sub 2 S-CdS cells.
c26 A69-16358
High photovoltages in cadmium sulfide films.
c26 A69-17772
Impurity profile and energy band diagram for the cuprous sulfide-cadmium sulfide heterojunction
[NASA-TN-D-5079] c26 N69-19781

BRANDT, J. C.
The lower atmosphere of Mars - A progress report.
c30 A69-12104
OSO-III - Preliminary scientific results.
c29 A69-22167
Messier 87 - The galaxy of greatest known mass.
c30 A69-30883
Interplanetary gas. XVI.
c29 A69-34301

BRASHEARS, S. S.
Effects of electric fields on annealing of radiation damage in MOSFET's.
c09 A69-16562
Investigation of radiation damage in MOSFETs using bias-temperature treatments.
c26 A69-16877

BRAUN, W.
Injection of an inviscid separated jet at an oblique angle to a moving stream
[NASA-TN-D-5460] c12 N69-37965
Injection of an attached inviscid jet at an oblique angle to a moving stream
[NASA-TN-D-5501] c12 N69-39916
Analysis of the mixing region for a two-dimensional jet injected at an angle to a moving stream
[NASA-TN-D-5531] c12 N69-41213

BRAY, C. W.
An experimental and theoretical investigation of striations in a He-Ne laser
[NASA-CR-1387] c08 N69-32350

BRAYTON, D.
Solubility and diffusion of oxygen in tantalum
[NASA-CR-1276] c17 N69-19886

BREAKWELL, J. V.
Sequential processing techniques for trajectory estimation
[NASA-CR-1360] c30 N69-40325

BREITWIESER, R.
Electron cooling and plasma heating of thermionic converters.
c03 A69-13127

BRESNAHAN, D. L.
Experimental investigation of a 10 deg conical turbojet plug nozzle with iris primary and translating shroud at Mach numbers from 0 to 2.0
[NASA-TM-X-1709] c28 N69-14313
Experimental investigation of a 10 deg conical turbojet plug nozzle with translating primary and secondary shrouds at Mach numbers from 0 to 2.0
[NASA-TM-X-1777] c28 N69-21648

BREWE, D. E.
Lubrication and wear of ball bearings in cryogenic hydrogen.
c15 A69-10109
Cooling studies with high-speed ball bearings operating in cold hydrogen gas.
[ASLE PAPER 68-LC-2] c15 A69-19310

BREWER, E. B.
Experimental investigation of base flow field at high altitude for a four engine clustered nozzle configuration
[NASA-TN-D-5164] c12 N69-24935

BREWER, G. W.
Lunar Orbiter 1, preliminary results - Lunar terrain assessment and selenodesy, micrometecroid, and radiation measurements
[NASA-SP-197] c30 N69-39213

BREWER, W. D.
Effect of the chemical state of pyrolysis gases on heat-shield mass
[NASA-TN-D-4975] c32 N69-14306

BRIAN, E.
Direct entry longitudinal range dispersion of unmanned Mars landers.
c30 A69-12390

BRICKLEN, R. H.
Causes, measurement, and elimination of fuel element fission product leakage at the NASA Plum Brook reactor
[NASA-TN-D-5374] c22 N69-32317

BRIGGS, R. W.
Power conditioning development for the Sert II ion thrustor.
c03 A69-42301

BRINKLEY, K. L.
Chemical equilibrium of ablation materials including condensed species
[NASA-TN-D-5391] c33 N69-34966

BRINTON, H. C.
Evidence of contraction of the earth's thermal plasmasphere subsequent to the solar flare events of 7 and 9 July 1966.
c13 A69-23777
Multi-experiment detection of the plasmapause from EOGO satellites and antarctic ground stations.
c13 A69-25153
Implications for ionospheric chemistry and dynamics of a direct measurement of ion composition in the F 2 region.
c13 A69-31974
Ion depletion in the high-latitude exosphere - Simultaneous OGO 2 observations of the light ion trough and the VLF cutoff.

c29 A69-34939
Diurnal and seasonal variation of atmospheric ion composition, correlation with solar zenith angle.
c13 A69-38087

BROCKER, D. H.
Study of a global search algorithm for optimal control.
c08 A69-33745

BRODERSON, A. B.
An investigation of the suitability of white rats for sub-orbital studies of behavior in a gravity field
[NASA-CR-1255] c05 N69-14094

BROGAN, W. T.
Effect of oxygen on the formation of germanium films.
c26 A69-43345

BROKAW, R. S.
Statistical mechanical theories of transport properties.
c33 A69-10110
Predicting transport properties of dilute gases.
c33 A69-38951

BROLLIAR, R. H.
The general instability of eccentrically stiffened cylindrical shells under axial compression and lateral pressure
[NASA-CR-1280] c32 N69-15378

BROOKS, J. D.
Investigation of a plasma accelerator with magnetic field arranged to produce a divergent-nozzle effect
[NASA-TN-D-5122] c25 N69-22942
A laboratory investigation of N-wave focusing
[NASA-TN-D-5306] c02 N69-31874

BROOKS, R. L.
GEOS I tracking station positions on the SAO standard earth /C-5/
[NASA-TN-D-5034] c13 N69-28019

BROUSSARD, P. H.
Experiments in hydrodynamic grease bearings.
[AIAA PAPER 69-836] c15 A69-39367

BROWN, A. H.
Life Sciences and Space Research VI, COSPAR, Plenary Meeting, 10th, Open Meeting of Working Group V, London, England, July 27, 28, 1967, Proceedings.
c04 A69-11073

BROWN, D. D.
Inlet effects on boiling and near critical hydrogen heat transfer.
[ASME PAPER 69-HT-27] c33 A69-43541

BROWN, G. V.
High-field cryogenic magnets with pure aluminum conductor.
c03 A69-26497
Excitation spectrum for a Bose gas with repulsive core and attractive well.
c24 A69-33118
Thickness optimization for dynamically stable superconducting tapes.
c26 A69-43121
Pumped helium tests of a 51-centimeter bore niobium-tin magnet
[NASA-TN-D-5158] c26 N69-22965

BROWN, K. R.
Rapid optimization of multiple-burn rocket flights, 8 March 1968 - 8 March 1969
[NASA-CR-1430] c30 N69-36439

BROWN, L. W.
The spectrum of the cosmic radio background between 0.4 and 6.5 MHz.
c30 A69-42375

BROWN, M. J.
Degradation of multiplier phototubes exposed to spatial radiations
[NASA-CR-1304] c14 N69-20777

BROWN, R. L.
Thermionic fuel irradiation experiment description
[NASA-TM-X-1858] c22 N69-33273

BROWN, S. C.
A cloud-cover simulation procedure.
c20 A69-38120

BROWN, W.
Effects of various respiratory maneuvers on the physiological response to angular acceleration.
c05 A69-41679

BROWN, W. E., III
Analysis of a multiplicative feed system for monopulse tracking applications.
c11 A69-37704
The simultaneous investigation of attenuation and emission by the earth's atmosphere at wavelengths from 4 centimeters to 8 millimeters.
c13 A69-39747
A 60-GHz multifrequency radiometric sensor for detecting clear air turbulence in the troposphere.
c09 A69-42536
A laboratory study of microwave radiometric techniques for re-entry plasma measurements
[NASA-TN-D-5274] c25 N69-29600

BROWN, W. E., JR.
Principal science results from Surveyor 5.
c30 A69-12224

BROWN, W. F., JR.
Crack toughness characteristics of several alloys for use in heavy sections of high speed aircraft
[NASA-TN-D-4998] c32 N69-17275
Clevis design for compact tension specimens used in plane-strain fracture toughness testing
[NASA-TM-X-1796] c32 N69-25301
The influence of crack length and thickness in plane strain fracture toughness tests
[NASA-TM-X-1860] c17 N69-34916

BROWN, W. J.
Brayton-B power system - A progress report.
c03 A69-42278

BROWNE, I. D.
Cloud height contouring from Apollo 6 photography.
c20 A69-36926

BROWNE, L. E.
A study of astronauts' extravehicular work capabilities in weightless conditions
[NASA-CR-1334] c05 N69-27266
Man's capability for self-locomotion on the moon. Volume 2 - Summary report
[NASA-CR-1403] c05 N69-36271
Man's capability for self-locomotion on the moon. Volume 1 - Detailed report
[NASA-CR-1402] c05 N69-37964

BRUCE, M. M.
Estimation of variance by a recursive equation
[NASA-TN-D-5465] c19 N69-38178

BRUNK, W. E.
Photographic results of the Lunar Orbiter program.
c30 A69-15858
The Lunar Orbiter program.
c30 A69-38377

BRYAN, J. W.
RFI characteristics of a delay relay satellite system.
c07 A69-41757

BUBSEY, R. T.
Crack toughness characteristics of several alloys for use in heavy sections of high speed aircraft
[NASA-TN-D-4998] c32 N69-17275
Clevis design for compact tension specimens used in plane-strain fracture toughness testing
[NASA-TM-X-1796] c32 N69-25301

BUCHELE, D. R.
Damping factor for the least-squares method of optical design.
c23 A69-14295

BUCKELEW, V. L.
Iterative guidance applied to generalized missions.
[AIAA PAPER 67-620] c21 A69-15501

BUCKINGHAM, A. G.
Satellite attitude control using a torqued, 2-axis-gimbaled boom as the actuator.
[AIAA PAPER 68-857] c21 A69-43245

BUCKLEY, D. H.
A study of adhesion to a rhenium surface with LEED.
c17 A69-35182
The influence of ordering on the friction and wear of metals in vacuum.
c15 A69-35183
Influence of surface films on friction and deformation of single-crystal and polycrystalline gold
[NASA-TN-D-4875] c15 N69-10249
Influence of number of operable slip systems on friction characteristics of single-crystal and polycrystalline magnesium

[NASA-TN-D-4351] c15 N69-10370
The effect of orientation and the presence of surface active materials on the friction, deformation and wear of aluminum
[NASA-TN-D-4994] c15 N69-16197
LEED studies of adhesion to a rhenium surface
[NASA-TN-D-5229] c17 N69-25363
LEED study of the adhesion of various materials to the /iii/ surface of nickel
[NASA-TN-D-5247] c17 N69-26258
Adhesion of gold to various planes of copper studied with LEED
[NASA-TN-D-5290] c26 N69-29407
A LEED study of the adhesion of gold to copper and copper-aluminum alloys
[NASA-TN-D-5351] c23 N69-31984

BUCKLEY, J.
Test parameters, material characterization, and the white thermal control coating stability problem.
[AIAA PAPER 69-641] c18 A69-33762

BUCKLEY, J. D.
Static oxidation and compatibility of boron nitride and boron nitride composite to 2000 deg C.
c18 A69-36208
Effects of cyclic heating and thermal shock on hafnia stabilized with calcia, magnesia, and yttria
[NASA-TN-D-5279] c18 N69-34547

BUDURKA, W. J.
RAE-A attitude determination ground support system.
[AIAA PAPER 69-983] c08 A69-40363

BUDY, A. M.
Biology of hard tissue
[NASA-SP-161] c04 N69-10444

BUELL, C. E.
Variability of sound propagation prediction due to atmospheric variability
[NASA-CR-1338] c23 N69-22545

BUFTON, J. L.
Wavelength dependence of laser-beam scintillation.
c16 A69-19641

BUGNA, E.
The effect of time of heating on the thermal polymerization of L-lysine.
c06 A69-28439
Determination of the water-soluble dinitrophenylamino acids by ion-exchange chromatography.
c06 A69-33651

BULLARD, T. R.
Rat body composition - Sensor implantation and lighting effects.
c04 A69-26557

BUNCH, T. E.
Potassium feldspar in Weekeroo Station, Kodaikanal, and Colomera iron meteorites.
c30 A69-14979
Electron microprobe analysis of vanadium in the presence of titanium.
c06 A69-18419

BUNDGAARD, R. C.
The effects of atmospheric fluctuations and representation upon propagated sound
[NASA-CR-1337] c23 N69-23199

BURA, P.
Design considerations for an integrated 1.8- GHz parametric amplifier.
c09 A69-10193

BURCH, J. L.
Experiments in hydrodynamic grease bearings.
[AIAA PAPER 69-836] c15 A69-39367

BURCHER, E.
Radar attitude sensing system.
c07 A69-13183

BURCHER, E. E.
A flight measurement of optical radiation from shock-heated air by using a Trailblazer 2 vehicle
[NASA-TN-D-4937] c33 N69-14501

BURGESS, W.
A family of portable versatile aerosol particle analyzers.
c14 A69-34691

BURGETT, A. L.
A study of human operator performance using regression analysis
[NASA-CR-1259] c05 N69-16212

BURK, S. M., JR.
Low-speed deployment, inflation, and steady-descent characteristics of ram-air-inflated balloon recovery systems with peripheral airscoop
[NASA-TN-D-5186] c21 N69-29595

BURKHART, J. A.
Segmented anode, CO sub 2 -H sub 2 performance and hollow cathode erosion tests on a low power MPD arc thruster.
[AIAA PAPER 69-242] c28 A69-21236

BURLAGA, L. F.
Plasma observations on Explorer 34.
c13 A69-11234
Microscale fluctuations in the interplanetary magnetic field.
c30 A69-24100
Directional discontinuities in the interplanetary magnetic field.
c30 A69-29970
Large velocity discontinuities in the solar wind.
c29 A69-29971
Causes of sudden commencements and sudden impulses.
c29 A69-31963
Hydromagnetic shocks in the solar wind.
c30 A69-40304

BURLEY-MEAD, J.
Survey of the region of Lacerta OB1.
c30 A69-25813

BURLEY, R. R.
Steady-state airflow and afterburning performance characteristics of four J85-GE-13 turbojet engines
[NASA-TM-X-1742] c28 N69-17781

BURNETT, D. S.
Cosmogenic rare gases and the super 40 K-super 40 Ar age of the Kodaikanal iron meteorite.
c30 A69-22047

BURNHAM, D. C.
Temperature tuning of an organic dye laser.
c16 A69-12617
Picosecond pulse measurement by two-photon excitation of photographic film.
c14 A69-20165

BURNS, E. A.
An experimental feasibility study for the preparation of thermo-oxidatively stable Pyrrone laminates
[NASA-CR-1404] c30 N69-31960

BURNS, J. A.
Dynamics of a charged particle in a spiral field.
c29 A69-14015

BURNS, R. K.
Downstream radiation flux to blunt entry vehicles.
c33 A69-12547

BURNSIDE, W. D.
The admittance of a parallel-plate waveguide aperture illuminating a metal sheet.
c09 A69-12328
Reflection coefficient of a TEM mode symmetric parallel-plate waveguide illuminating a dielectric layer.
c09 A69-34802

BURROWS, K.
The application of the image orthicon television system to rocket trajectory determination.
c07 A69-26965

BURROWS, M. C.
Hydrazine-nitrogen tetroxide combustion response to transverse gas flows.
c33 A69-10112
Dynamic response of hydrazine-nitrogen tetroxide combustion to transverse gas flow
[NASA-TN-D-4984] c27 N69-19026

BURROWS, R. R.
Optimal continuous low-thrust trajectories for co-altitude rendezvous.
c30 A69-32177

BURTIS, W. J.
Banded chorus - A new type of VLF radiation observed in the magnetosphere by OGO 1 and OGO 3.
c13 A69-31981

BURTON, W. M.
Airbreathing propulsion system testing using sweep frequency techniques
[NASA-TN-D-5485] c28 N69-39185

BUSH, H. G.
Multidimensional gas flow through permeable char layers and its effects on ablation
[NASA-TR-R-296] c33 N69-16181
BUSHNELL, D. M.
Measurement of mean drop sizes for sprays from superheated waterjets.
c12 A69-21995
Velocity fluctuation intensities in a hypersonic turbulent boundary layer.
c12 A69-31908
Calculation of nonequilibrium hypersonic turbulent boundary layers and comparisons with experimental data.
[AIAA PAPER 69-684] c12 A69-33474
Comparison of prediction methods and studies of relaxation in hypersonic turbulent nozzle-wall boundary layers
[NASA-TN-D-5433] c12 N69-36805
Fluctuating properties of turbulent boundary layers for Mach numbers up to 9
[NASA-TN-D-5496] c12 N69-40137
BUTLER, D. H.
An evaluation test of a full scale replica of the RAM-CA flight heat shield in a rocket engine exhaust
[NASA-TM-X-1841] c31 N69-32713
BUTLER, T. G.
Rosman I dynamic analysis.
c32 A69-42133
BUTZE, H. F.
Performance of swirl-can turbojet combustors at simulated supersonic combustor-inlet conditions
[NASA-TN-D-4996] c28 N69-16154
BYERS, D. C.
An experimental investigation of a high-voltage electron-bombardment ion thruster.
[ECS PAPER 170D] c28 A69-16233
SERT II flight-type thruster system performance.
[AIAA PAPER 69-235] c28 A69-21255
Performance of various oxide-magazine cathodes in Kaufman thrusters
[NASA-TN-D-5074] c28 N69-19980
BYRD, P. F.
High accuracy gamma function values for some rational arguments.
c19 A69-13375
Chebyshev series solution of nonlinear ordinary differential equations - Initial-value problems
[NASA-TM-X-1882] c19 N69-36923
BYUSHGENS, G. S.
Dynamics of the spatial motion of an aircraft
[NASA-TT-F-555] c02 N69-24761

C

CABRA, O., JR.
Onboard checkout system concept and philosophy.
c11 A69-25081
CAHILL, L. J., JR.
Ring current particle distributions derived from ring current magnetic field measurements.
c29 A69-11227
CAIN, J. C.
OGO-2 magnetic field observations during the magnetic storm of March 13-15, 1966.
c13 A69-11125
Prediction of geomagnetic secular change confirmed.
c13 A69-37490
The location of the dip equator at E-layer altitude.
c13 A69-42428
CAKE, J. E.
A FORTRAN code for computing the principle mass movements of inertia of composite bodies
[NASA-TM-X-1754] c23 N69-20870
CALFO, F. D.
Cryogenic fracture properties of thin AISI 301 60-percent cold-reduced sheet at various angles to the rolling direction
[NASA-TN-D-5413] c17 N69-35688
CALLENS, R. A.
Ammonia Resistojet station keeping subsystem aboard applications technolcgy satellite /ATS/ IV.
[AIAA PAPER 69-296] c28 A69-21212
CALLIS, L. B.
Solutions of blunt-body stagnation-region flows with nongray emission and absorption of radiation by a time-asymptotic technique
[NASA-TR-R-299] c33 N69-16268
CALOGERAS, J. E.
Supersonic wind tunnel investigation of inlet-engine compatibility.
[AIAA PAPER 69-487] c28 A69-32676
Experimental investigation of dynamic distortion in a Mach 2.50 inlet with 60 percent internal contraction and its effect on turbojet stall margin
[NASA-TM-X-1842] c28 N69-38599
CALVERT, T. A.
Thermal and dielectric properties of a homogeneous moon based on microwave and infrared temperature observations
[NASA-TM-X-1734] c30 N69-17815
CAMBEL, A. B.
Experimental investigation of magnetoaerodynamic flow around blunt bodies
[NASA-CR-1393] c25 N69-34897
CAMERON, A. G. W.
The instability of stellar structures intermediate between white dwarfs and neutron stars.
c30 A69-20770
Nucleosynthesis in supernova explosions.
c30 A69-20898
A new table of abundances of the elements in the solar system.
c30 A69-20903
Infrared radiation associated with protostars.
c29 A69-27593
Relation between nuclear level density parameters and mass shell.
c24 A69-29337
Spin down effects in neutron stars.
c30 A69-32803
A schematic model for certain X-ray sources.
c29 A69-35204
Physical conditions in the primitive solar nebula.
c30 A69-36074
Fundamental problems of the solar system.
c30 A69-36209
Abundances of the elements.
c29 A69-38812
Progress report on pulsars.
c30 A69-42556
Nonthermal phenomena of astrophysics and their relation to plasma physics.
c30 A69-42682
CAMISA, R.
Design considerations for an integrated 1.8- GHz parametric amplifier.
c09 A69-10193
CAMNITZ, H. G.
Ground wind characteristics at Kennedy Space Center Final report
[NASA-CR-1418] c20 N69-36222
CAMP, D. W.
High resolution balloonborne temperature sensor.
c14 A69-21642
Detailed wind and temperature profiles.
c20 A69-33739
CAMPBELL, J. F.
Pressure distributions on 140 deg, 160 deg, and 180 deg cones at Mach numbers from 2.30 to 4.63 and angles of attack from 0 deg to 20 deg
[NASA-TN-D-5204] c01 N69-24764
Experimental flow properties in the wake of a 120 deg cone at Mach number 2.20
[NASA-TN-D-5365] c01 N69-32299
Supersonic aerodynamic characteristics and shock standoff distances for large-angle cones with and without cylindrical afterbodies
[NASA-TN-D-5334] c01 N69-33237
Supersonic lifting capabilities of large-angle cones
[NASA-TN-D-5499] c01 N69-40026
CAMPBELL, J. P.
V/STOL session introductory and review paper.
c02 A69-15563
CAMPBELL, T.
An approach to cost analysis in low cost launch vehicle studies.
c31 A69-43120
CAMPBELL, T. G.
Radiation characteristics of a cavity-backed cylindrical gap antenna.
c09 A69-40698

CANAVOS, G. C.
Influence of angle of glide slope on the accuracy of performing instrument approaches in a simulator
[NASA-TN-D-4835] c21 N69-10056
CANCRO, C. A.
Cosmic ray experiments source-encoding in the IMP-I spacecraft.
c07 A69-41738
CANN, M. W. P.
Determination of thermodynamic properties with optical cross-correlation methods.
[AIAA PAPER 67-149] c14 A69-31868
Evaluation of vacuum UV detector-spectroscopy systems for capsule reentry measurements
[NASA-CR-1268] c09 N69-18761
CANNIFF, J.
Flight test report of experiments in inertial navigation system updating.
[AIAA PAPER 69-842] c21 A69-39429
CANRIGHT, R. B., JR.
Computer-made movies and plotting descriptions of ion-molecule collisions with polar targets.
c24 A69-43124
A conversational approach to matrix calculations, concepts and implementation
[NASA-TM-X-1749] c08 N69-18954
Implementation and structure of COMPUTE, a time-sharing calculator program
[NASA-TN-D-5350] c08 N69-32685
CANUTO, V.
Quantum theory of an electron gas with anomalous magnetic moments in intense magnetic fields.
c24 A69-19782
Nature of radio and optical emissions from pulsars.
c30 A69-20624
Radio emission from magnetic neutron stars - A possible model for pulsars.
c30 A69-20729
Thermodynamic approach to the equation of state of a magnetized Fermi gas.
c30 A69-25107
New state of ferromagnetism in degenerate electron gas and magnetic fields in collapsed bodies.
c30 A69-38600
Solution of the Dirac equation in orthogonal electric and magnetic fields.
c23 A69-41357
CAPLAN, F. E.
High resolution balloonborne temperature sensor.
c14 A69-21642
CAPONE, F. J.
Subsonic aerodynamic characteristics of a large-scale 1.075-pressure-ratio tip-turbine cruise-fan propulsion system at angle of attack
[NASA-TN-D-5316] c28 N69-34575
Subsonic performance characteristics of a large-scale 1.075-pressure-ratio tip-turbine cruise-fan propulsion system
[NASA-TN-D-5314] c28 N69-35526
CARBONELL, J. R.
Human visual sampling processes - A simulation validation study
[NASA-CR-1258] c05 N69-14145
CARIGNAN, G. R.
Measurements of electron cooling rates in the mid-latitude and auroral-zone thermosphere.
c13 A69-16267
CARLSON, G. A.
Circulating currents in linear crossed-field generators and accelerators
[NASA-TN-D-5244] c25 N69-26313
CARLSON, H. C.
Radar backscatter and rocket probe measurements of electron temperature above Arecibo.
c29 A69-25162
CARLSON, H. W.
Sonic booms - Fundamental characteristics.
c02 A69-30369
CARLSON, T. B.
An experimental and theoretical investigation of striations in a He-Ne laser
[NASA-CR-1387] c08 N69-32350
CARMICHAEL, R. L.
An experimental and theoretical investigation of a symmetrical and a cambered delta wing configuration at Mach numbers from 2.0 to 10.7
[NASA-TN-D-5272] c01 N69-29269
CARON, P. R.
A technique for measuring the electron density of dense, thick, steady-state plasmas.
c25 A69-12349
Plasma generation using a large V-groove cathode discharge
[NASA-TN-D-5269] c25 N69-29140
A laboratory study of microwave radiometric techniques for re-entry plasma measurements
[NASA-TN-D-5274] c25 N69-29600
CAROVILLANO, R. L.
Physics of the Magnetosphere, Proceedings of the Conference, Boston College, Chestnut Hill, Mass., June 19-28, 1967.
c29 A69-19351
CARPENTER, D. L.
Multi-experiment detection of the plasmapause from EOGO satellites and antarctic ground stations.
c13 A69-25153
Ion depletion in the high-latitude exosphere - Simultaneous OGO 2 observations of the light ion trough and the VLF cutoff.
c29 A69-34939
CARPENTER, J. D.
The impact of biosciences requirements on biosatellite attitude control.
c31 A69-35094
CARPENTER, L. H.
Periodic orbits in the restricted three-body problem in the neighborhood of resonances of type /k plus 1//k /Ueber periodische Bahnen im eingeschraenkten Dreikoerperproblem und in der Naehe der Kommensurabilitaeten vom Typus /k plus 1//k/.
c30 A69-19874
CARRION, W.
Laser beam directed at the lunar retro- reflector array - Observations of the first returns.
c30 A69-43197
CARTER, A. W.
Effects of jet exhaust longitudinal aerodynamic characteristics of a jet V/STOL model
[NASA-TN-D-5333] c01 N69-33210
CARUSO, A. J.
Production of an intense helium continuum below 230 angstrom units.
c23 A69-42149
CARUSO, P., JR.
The Orbiting Astronomical Observatory thermal test program.
[AIAA PAPER 69-995] c11 A69-40373
CASAL, F. G.
A method for obtaining performance boundaries of complete space propulsion systems containing nuclear-electric stages.
[AIAA PAPER 69-249] c22 A69-21249
CASHMAN, W. F.
A computational approach to optimal control of stochastic saturating systems.
c10 A69-30601
CASSEY, H. N.
An experimental feasibility study for the preparation of thermo-oxidatively stable Pyrrone laminates
[NASA-CR-1404] c30 N69-31960
CASSIDY, J. F.
Thermal contact resistance measurements at ambient pressures of one atmosphere to 3 x 10 super minus super 12 mm Hg and comparison with theoretical predictions.
[AIAA PAPER 69-629] c33 A69-33299
CASSINELLI, J. P.
Interplanetary gas. XVI.
c29 A69-34301
CASTELLANO, C. R.
An experimental and theoretical investigation of a symmetrical and a cambered delta wing configuration at Mach numbers from 2.0 to 10.7
[NASA-TN-D-5272] c01 N69-29269
CASTELLI, V.
High performance turboalternator and associated hardware. 3. Design of backup gas bearings
[NASA-CR-1292] c15 N69-19775
CASTELLOW, S. L., JR.
Radiofrequency transmission characteristics of several ablation materials
[NASA-TN-D-4879] c07 N69-10885
CASTLE, B. L.
Effects of acute exposure to high-energy protons

on primates.
c04 A69-13498
Pressure-diameter relations of capillaries and small blood vessels in frog lung.
c04 A69-40974
CASTLE, J. A.
Handbook of Solar Simulation for Thermal Vacuum Testing.
c11 A69-38894
CATALDO, C. E.
Recent experience in high pressure gaseous hydrogen equipment operated at room temperature.
[ASM PAPER D8-14.1] c15 A69-19666
CATHERINES, D. S.
A geometrically exact finite element for thin shells of revolution.
[AIAA PAPER 69-56] c32 A69-18193
A method for computation of vibration modes and frequencies of orthotropic thin shells of revolution having general meridional curvature
[NASA-TN-D-4972] c32 N69-16469
CATHERINES, J. J.
Experimental vibration characteristics of a 1/40-scale dynamic model of the Saturn 5 launch umbilical tower configuration
[NASA-TN-D-4870] c31 N69-10775
Lateral vibration characteristics of a 1/40-scale dynamic model of Apollo-Saturn 5 launch vehicle
[NASA-TN-D-4872] c31 N69-11007
CATO, R. E., JR.
The impact of failure data on management of a launch operations reliability program.
c11 A69-36022
CAUGHEY, D. A.
Second-order wave structure in supersonic flows
[NASA-CR-1438] c04 N69-37062
CAVICCHI, R. H.
Comparison of flexible- and firm-foundation rotor critical-speed analyses.
[ASME PAPER 69-VIBR-49] c32 A69-24184
Critical-speed analysis of rigid rotors on flexible foundations
[NASA-TN-D-4858] c32 N69-29159
CAYREL DE STROBEL, G.
Detailed analysis of the star phi Aurigae.
c30 A69-20913
CECCON, H. L.
Time dependent spectroscopy of flashlamp pumped dye lasers.
c16 A69-17901
Optical pumps for organic dye lasers.
c16 A69-42187
CHADWICK, G. G.
A 17-1 dual band circularly polarized focused two-channel monopulse tracking system.
c07 A69-41752
CHAMBERS, J. R.
Analysis of lateral directional stability characteristics of a twin jet fighter airplane at high angles of attack
[NASA-TN-D-5361] c02 N69-32337
Analysis of the flat-spin characteristics of a twin-jet swept-wing fighter airplane
[NASA-TN-D-5409] c02 N69-36807
CHAMIS, C. C.
Failure criteria for filamentary composites.
c32 A69-21479
Closing materials research structural design cycle.
c32 A69-42991
Failure criteria for filamentary composites
[NASA-TN-D-5367] c18 N69-33321
CHAMPINE, R. A.
Flying quality factors currently limiting helicopter nap of the earth maneuverability as identified by flight investigation
[NASA-TN-D-4931] c02 N69-14008
CHAMPION, K. S. W.
Space Research IX, COSPAR Plenary Meeting, 11th, Tokyo, Japan, May 9-21, 1968, Proceedings.
c13 A69-38334
CHAN, K.-L.
Storm-time variations of the electron concentration in the polar topside ionosphere.
c29 A69-28939
Global electron density distributions from topside soundings.
c13 A69-37867
Model studies of the kinked Z trace in topside ionograms.
c13 A69-37893
Computation of topside ionograms from N/h/ profiles
[NASA-TN-D-5052] c13 N69-23557
CHANDLER, D. C.
Iterative guidance applied to generalized missions.
[AIAA PAPER 67-620] c21 A69-15501
CHANDRA, S.
The influence of varying solar flux on ionospheric temperatures and densities - A theoretical study.
c29 A69-32082
F-region ionization and heating during magnetic storms.
c13 A69-32083
The role of atomic oxygen in the ionospheric E- and F-region behavior.
c13 A69-32314
CHANG, E. S.
Dipole shielding factor in Hartree-Fock theory.
c23 A69-12179
Photo-ionization of lithium - A many-body calculation.
c24 A69-17134
Rotational excitation of diatomic molecules by electron impact.
c24 A69-39665
CHANG, S.
Studies on the formation and transformation of esters. IXXX.
c06 A69-31808
CHANG, T. Y.
A lattice model for composite materials
[NASA-CR-1322] c32 N69-22982
CHAPLIN, A.
Investigation of the turbulent wind field below 150-meter altitude at the eastern test range
[NASA-CR-1410] c20 N69-35570
CHAPMAN, A. J.
Radiofrequency transmission characteristics of candidate ablation materials for planetary-entry-vehicle heat shields
[NASA-TN-D-4920] c07 N69-13158
CHAPMAN, D. R.
Sr isotope patterns within the Southeast Australasian strewn-field.
c13 A69-41342
CHAPMAN, G. T.
Ballistic range tests of ablating and nonablating slender cones.
[AIAA PAPER 69-179] c33 A69-18083
A new method for extracting aerodynamic coefficients from free-flight data.
[AIAA PAPER 69-134] c01 A69-18161
CHAPMAN, R. D.
Rational approximations to Gaunt factors.
c24 A69-20153
Oscillator strengths and wavelengths of some X-ray and extreme-ultraviolet spectrum lines of highly ionized iron.
c29 A69-27554
CHAPPELLE, E. W.
ATP assay of terrestrial soils - A test of an exobiological experiment.
c04 A69-37567
CHARNOW, M.
Application of Hansen's method to the X super th satellite of Jupiter.
c30 A69-37529
Application of Hansen's method to the 10th satellite of Jupiter
[NASA-TN-D-4979] c30 N69-14479
CHASE, C. E.
Velocity of sound at 1 MHz near the He super 4 critical point.
c23 A69-17142
CHAUVIN, L. T.
Apollo thermal-protection system development.
[AIAA PAPER 68-1142] c31 A69-13558
CHENEY, L.
Spacecraft oceanography - Its scientific and economic implications for the next decade.
[UN PAPER 68-95878] c13 A69-10491
CHENG, D. H.
Dynamic response of structural elements exposed to sonic booms

[NASA-CR-1281] c32 N69-21403
CHENG, D. H.
A novel use of a telescope to photograph metal diaphragm openings. c14 A69-37227
Application of a variable resistance to arrest oscillations in a pulsed capacitor discharge circuit. c09 A69-41228
CHENG, H. S.
Configurations for gas turbine compressor end seals.
[ASLE PREPRINT 68AM 4B-4] c15 A69-27366
CHERNIGOVSKIY, V. N.
Problems of space biology. Volume 7 - Operational activity, problems of habitability and biotechnology
[NASA-TT-F-529] c05 N69-32044
Problems of space biology. Volume 8 - Adaptation to hypoxia and resistance of an organism
[NASA-TT-F-580] c04 N69-32131
CHESTNUTT, D.
Jet engine inlet noise control. c28 A69-15622
CHEYNEY, H.
Comments on the paper by D. G. Rea and B. T. O'Leary, "On the composition of the Venus clouds." c30 A69-11292
Theoretical spectral scattering of ice clouds in the near infrared. c13 A69-34283
CHILDRESS, J. D.
Effects of lithium and oxygen losses on the magnetic and crystallographic properties of spinel lithium ferrite
[NASA-TR-R-305] c06 N69-20775
CHILDS, S. B.
Applications of quasi-linearization theory to system identification
[NASA-TN-D-5300] c19 N69-29648
CHILTON, E. A.
Design and development of a multipurpose, boresighted star tracker
[NASA-CR-976] c21 N69-21502
CHISEL, D. M.
A fluidic proportional thruster system for sounding rocket applications.
[ASME PAPER 68-WA/FE-32] c14 A69-16105
New functional approaches for redundant inert gas thruster systems.
[AIAA PAPER 69-843] c28 A69-39373
CHIU, H.-Y.
Quantum theory of an electron gas with anomalous magnetic moments in intense magnetic fields. c24 A69-19782
Nature of radio and optical emissions from pulsars. c30 A69-20624
Radio emission from magnetic neutron stars - A possible model for pulsars. c30 A69-20729
Thermodynamic approach to the equation of state of a magnetized Fermi gas. c30 A69-25107
New state of ferromagnetism in degenerate electron gas and magnetic fields in collapsed bodies. c30 A69-38600
CHIUDERI, C.
New state of ferromagnetism in degenerate electron gas and magnetic fields in collapsed bodies. c30 A69-38600
Solution of the Dirac equation in orthogonal electric and magnetic fields. c23 A69-41357
CHKHAIDZE, L. V.
Coordination of the voluntary movements of man in a zero gravitational field /under weightlessness/
[NASA-TT-F-578] c04 N69-31356
CHOATE, R.
Lunar surface mechanical properties. c30 A69-12225
CHOBY, D. A.
Steady-state interactions from Mach 1.98 to 2.58 between a turbojet engine and an axisymmetric inlet with 60-percent internal area contraction
[NASA-TM-X-1780] c28 N69-23519
CHOU, Y. S.
Series solution for hypersonic flow about blunt bodies
[NASA-CR-1266] c33 N69-18125
CHRISTENSEN, E. M.
Principal science results from Surveyor 5. c30 A69-12224
Lunar surface mechanical properties. c30 A69-12225
CHRISTENSON, H. H.
Test of sodium boiling in a single tube-in- shell heat exchanger over the range 1720 deg to 1980 deg F /1211 to 1355 K/
[NASA-TN-D-5323] c33 N69-30064
CHU, T. W.
High performance turboalternator and associated hardware. 3. Design of backup gas bearings
[NASA-CR-1292] c15 N69-19775
CHUAN, R. L.
In-situ molecular beam experiments in earth orbit. c24 A69-36182
CHUBB, D. L.
Ionizing shock structure in a monatomic gas. c12 A69-13138
Laboratory simulation of solar wind - earth interaction
[NASA-TM-X-1738] c25 N69-19131
CHYU, W. J.
Power- and cross-spectra and space-time correlations of surface fluctuating pressures at Mach numbers between 1.6 and 2.5
[NASA-TN-D-5440] c12 N69-36940
CIARANELLO, R. D.
Adrenal epinephrine and phenylethanolamine n-methyl transferase /PNMT/ activity in the rat bearing a transplantable pituitary tumor. c04 A69-20374
Compensatory hypertrophy and phenylethanolamine n-methyl transferase /PNMT/ activity in the rat adrenal. c04 A69-41404
CINCOTTA, J. J.
Aerodynamic forces on a stationary and oscillating circular cylinder at high Reynolds numbers
[NASA-TR-R-300] c01 N69-17304
CLARK, B.
Magnitude estimates of rotational velocity during and following prolonged increasing, constant, and zero angular acceleration. c04 A69-15332
Comparison of three methods to determine thresholds for perception of angular acceleration. c04 A69-15969
Effects of angular acceleration on man - Thresholds for the perception of rotation and the oculogyral illusion. c05 A69-41674
CLARK, C. F.
Ablative characterization of seven heat shield materials - A review of the NASA-SRI Round-Robin program. c18 A69-26813
Comparative evaluation of ablating materials in arc plasma jets
[NASA-CR-1207] c33 N69-14171
CLARK, E. S.
Molecular motion in polytetrafluoroethylene at cryogenic temperatures. c24 A69-16495
CLARK, M.
Analysis of integrated charged particle energy spectra from gridded electrostatic analyzers. c25 A69-20521
CLARK, M., JR.
Feasibility of detecting radiation scattered from a plasma
[NASA-TN-D-5311] c25 N69-36939
CLARK, R. K.
Effect of the chemical state of pyrolysis gases on heat-shield mass
[NASA-TN-D-4975] c32 N69-14306
Simulation of pyrolysis-gas flow through a char layer during ablation
[NASA-TN-D-5464] c33 N69-38271
CLARK, R. N.
Analysis of oscillations in pulse-modulated satellite attitude control systems
[NASA-CR-1369] c21 N69-29967

CLARK, S. K.
Laboratory experiments on reverted rubber friction
[NASA-CR-1398] c02 N69-34915
CLARK, T. A.
The spectrum of the cosmic radio background between 0.4 and 6.5 MHz.
c30 A69-42375
CLARKE, J. F.
Galactic Jupiter probes.
c30 A69-12303
CLARKE, J. M.
Pulse interference effects in a phase-lock loop.
c10 A69-42230
Radio spectrum utilization in aerospace communication systems.
c07 A69-42502
CLAUSEN, O. W.
Thermal tests of an improved louver system for spacecraft thermal control.
[AIAA PAPER 69-627] c33 A69-33269
CLAUSER, J. F.
Upper limits to the intensity of background radiation at lambda equals 1.32, 0.559, and 0.359 mm.
c30 A69-19404
CLAUSI, J.
Design of Brayton rotating unit on rolling-element bearings
[NASA-CR-1401] c15 N69-33450
CLEARY, J. W.
Theoretical and experimental study of supersonic steady flow around inclined bodies of revolution.
[AIAA PAPER 69-187] c01 A69-18176
Effects of angle of attack and bluntness on the shock-layer properties of a 15 deg cone at a Mach number of 10.6
[NASA-TN-D-4909] c01 N69-10789
Effects of angle of attack and bluntness on laminar heating-rate distributions of a 15 deg cone at a Mach number of 10.6
[NASA-TN-D-5450] c12 N69-37604
CLEARY, R. E.
Properties of high emittance materials
[NASA-CR-1278] c17 N69-18952
Testing of high-emittance coatings
[NASA-CR-1413] c17 N69-35514
CLEMONS, L.
Monte Carlo calculations of a hemispherical duct neutron streaming experiment.
c22 A69-35178
CLEMONS, L. C., JR.
COHORT-II - A Monte Carlo general purpose shielding computer code.
c08 A69-29004
CLEMONS, L., JR.
Evaluation of the COHORT 2 Monte Carlo shielding code - Gamma ray transport using source direction biasing
[NASA-TM-X-1877] c22 N69-35848
CLIFF, R. A.
The SDP-3 - A computer for use on board small scientific spacecraft.
c08 A69-13243
The SDP-1 stored-program computer.
c08 A69-15472
The IMP-I computer experiment.
c08 A69-36265
The SDP-3 - A computer designed for data systems of small scientific spacecraft.
c08 A69-37385
Recent improvements in the SDP-3 computer.
c08 A69-41737
CLINE, J. E.
X-ray fluorescence and electron microprobe techniques for determination of thin-film thicknesses.
c09 A69-19582
Scanning electron mirror microscopy and scanning electron microscopy of integrated circuits.
c14 A69-32891
CLINE, T. L.
Relativistic electrons from solar flares.
c29 A69-15528
On the generation of synchroton and X-ray emission from electrons with energy below Mc super 2 in solar flares.
c29 A69-22203
Very high energy solar X-rays observed during the proton event of 7 July 1966.
c29 A69-23753
Relativistic solar electrons detected during the 7 July 1966 proton flare event.
c29 A69-23766
CLOUGH, N.
Crater characteristics of 11 metal alloys under hyper-velocity impact including effects of projectile density and target temperature
[NASA-TN-D-5135] c32 N69-22994
CLUA, A. L.
Interferometrically measured thorium lines between 2747 and 4572 angstrom units.
c23 A69-42150
COAKLEY, T. J.
A generalized averaging method for linear differential equations with almost periodic coefficients
[NASA-TN-D-5167] c19 N69-22988
COATE, R. E.
Manned aerospace simulation.
[ASME PAPER 69-DE-56] c11 A69-28844
COATES, K.
Investigation of SA-501 S-4B auxiliary
[NASA-TN-D-5207] c28 N69-26224
COATES, R. J.
Tracking and data acquisition for space exploration.
c07 A69-33371
Why data system standards?
c08 A69-41769
COCKRELL, C. R.
An omnidirectional microwave antenna for use on spacecraft.
c09 A69-40697
CODE, A. D.
Filter photometry of Saturn in the spectral region lambda lambda 2950-2450.
c30 A69-22216
COE, H. H.
Lubrication and wear of ball bearings in cryogenic hydrogen.
c15 A69-10109
Cooling studies with high-speed ball bearings operating in cold hydrogen gas.
[ASLE PAPER 68-LC-2] c15 A69-19310
COFER, W. R., III
High temperature decomposition of ammonium perchlorate using CO sub 2 laser-mass spectrometry.
[AIAA PAPER 69-143] c06 A69-18111
COHEN, A. J.
An electron bombardment thruster operated with a cusped magnetic field
[NASA-TN-D-5448] c28 N69-36844
COHEN, G.
Effects of various respiratory maneuvers on the physiological response to angular acceleration.
c05 A69-41679
COHEN, G. A.
Structural optimization of sandwich and ring-stiffened 120 degree conical shells subjected to external pressure
[NASA-CR-1424] c32 N69-35515
Evaluation of configuration changes on optimum structural designs for a Mars entry capsule
[NASA-CR-1414] c33 N69-35516
Synthesis of optimum structural designs for conical and tension shell Mars entry capsules
[NASA-CR-1365] c32 N69-36357
COHEN, J. D.
Biochemical and metabolic effects of a six- month exposure of small animals to a helium- oxygen atmosphere
[NASA-CR-1372] c04 N69-40955
COHEN, J. M.
The instability of stellar structures intermediate between white dwarfs and neutron stars.
c30 A69-20770
Exact fields of charge and mass distributions in general relativity.
c23 A69-32053
COHEN, M. D.
Exact fields of charge and mass distributions in general relativity.
c23 A69-32053
COHEN, M. K.
Approach guidance planet tracker.

c21 A69-13214
COHEN, R.
Brayton-cycle turbomachinery rolling-element bearings
[NASA-CR-1229] c15 N69-16463
High performance turboalternator and associated hardware. 1 - Design of turboalternator
[NASA-CR-1290] c03 N69-21771
Design of Brayton rotating unit on rolling-element bearings
[NASA-CR-1401] c15 N69-33450
COLBURN, D. S.
Earth's bow shock - Elapsed-time observations by two closely spaced satellites.
c13 A69-12299
The geomagnetic tail - Topology, reconnection and interaction with the moon.
c13 A69-19365
Interplanetary sector structure in the rising portion of the sunspot cycle.
c30 A69-28957
Interplanetary field and geomagnetic variations - A unified view.
c30 A69-32309
COLE, G. L.
Restart and high response terminal shock control for an axisymmetric mixed-compression inlet with 60-percent internal contraction
[NASA-TM-X-1792] c28 N69-24938
COLE, J. M.
Delta-T curves for measuring magnetic tape link jitter.
c14 A69-18827
COLES, W. D.
Pumped helium tests of a 51-centimeter bore niobium-tin magnet
[NASA-TN-D-5158] c26 N69-22965
COLIN, L.
Ray tracing studies for the topside ionosphere.
c13 A69-18838
An interpretation of OGO light ion abundance measurements.
c13 A69-25157
Morphology of electron concentration enhancement at a height of 1000 kilometers at polar latitudes.
c29 A69-28938
Global electron density distributions from topside soundings.
c13 A69-37867
Model studies of the kinked Z trace in topside ionograms.
c13 A69-37893
Temperature and ion abundance profiles deduced from simultaneous Explorer XXXI and Alouette II data.
c13 A69-37896
Computation of topside ionograms from N/h/ profiles
[NASA-TN-D-5052] c13 N69-23557
COLLARD, H. R.
Preliminary comparison of solar wind plasma observations in the geomagnetospheric wake at 1000 and 500 earth radii.
c29 A69-26943
COLLINS, M.
Progress report on Apollo program.
c31 A69-17672
COLMAN, W. P.
High-performance light-weight electrodes for hydrogen-oxygen fuel cells
[NASA-CR-1216] c03 N69-14397
COLTRIN, R. E.
Supersonic wind tunnel investigation of inlet-engine compatibility.
[AIAA PAPER 69-487] c28 A69-32676
Preliminary investigation of distortion dynamics in a Mach 3 mixed compression inlet
[NASA-TM-X-1706] c01 N69-13154
Steady-state interactions from Mach 1.98 to 2.58 between a turbojet engine and an axisymmetric inlet with 60-percent internal area contraction
[NASA-TM-X-1780] c28 N69-23519
COMPARIN, R. A.
In situ vacuum testing - A must for certain elastomeric materials.
c11 A69-22008
Application of the line-source technique for vacuum thermal conductivity measurements.
[AIAA PAPER 69-1013] c11 A69-40386
COMPSTON, W.
Sr isotope patterns within the Southeast Australasian strewn-field.
c13 A69-41342
COMPTON, E. C.
An optical system for recording schlieren images with continuous writing ultra high speed framing camera
[NASA-TN-D-4986] c14 N69-15381
COMPTON, H. R.
Determination of lunar equatorial radius using image-motion compensation sensor data from Lunar Orbiter I
[NASA-TN-D-5231] c30 N69-29115
CONANT, C. W.
Experience with and improvements in containment vessel penetrations
[NASA-TM-X-1735] c22 N69-17701
CONAWAY, J.
Microwave observations of sea state from aircraft.
c13 A69-34421
CONE, C. D., JR.
A micro lagoon technique for the culture and observation of isolated mammalian cells
[NASA-TN-D-4906] c04 N69-11056
Mitotic synchronization of L-strain fibroblasts with 5-aminouracil as determined by time-lapse cinephotography
[NASA-TN-D-5021] c04 N69-17248
Osmotically induced coalescence of sarcoma cells through intercellular bridges in vitro
[NASA-TN-D-5022] c04 N69-17782
A process for imprinting micro lagoon fields in plastic surfaces for use in cell and tissue culture
[NASA-TN-D-5255] c04 N69-29195
CONEY, T. A.
Effect of flow rate on the dynamic contact angle for wetting liquids
[NASA-TN-D-5115] c12 N69-20794
Surface tension, viscosity, and density measurements of two fluorocarbon solvents, FC-43 and FC-78
[NASA-TM-X-1862] c18 N69-34134
CONLEY, C. C.
Effects of acute exposure to high-energy protons on primates.
c04 A69-13498
CONNELLY, R. E.
Investigation of two-phase hydrogen flow in pump inlet line
[NASA-TN-D-5258] c15 N69-29476
CONNOLLY, D. J.
The effect of background pressure and magnetic field shape on MPD thruster performance.
[AIAA PAPER 69-243] c28 A69-21239
A study of the axial velocities in an ammonia MPD thruster.
c28 A69-31890
Performance of radiation-cooled magnetoplasmadynamic arc thrusters
[NASA-TM-X-1908] c28 N69-40058
CONNORS, M. M.
The effect of breathing 100 percent oxygen on foveal thresholds.
c05 A69-12216
Luminance requirements for hue identification in small targets.
c23 A69-19649
CONRAD, E. W.
Liquid rocket acoustic-mode-instability studies at a nominal thrust of 20000 pounds
[NASA-TN-D-4968] c28 N69-14384
Characterization of pressure perturbations induced in a rocket combustor by a machine gun
[NASA-TN-D-5214] c33 N69-24824
CONRATH, B. J.
Inverse problems in radiative transfer - A review.
c13 A69-17617
On the estimation of relative humidity profiles from medium-resolution infrared spectra obtained from a satellite.
c13 A69-34284
CONWAY, B. A.
An analysis of the operation of a mass measuring system in an orbiting spacecraft
[NASA-TN-D-5039] c04 N69-19115

CONWAY, E. C.
Cooling of a high-power electron tube in a space vehicle.
c09 A69-24747
Nonelectric cathode heating.
c09 A69-24748
COOHRAN, T. H.
Impulsive motion on a flat plate pulsed with uniform heat flux
[NASA-TN-D-5249] c33 N69-26236
COOK, A. M.
Large scale wind tunnel investigation to improve the low speed longitudinal stability at high lift of a supersonic transport with variable-sweep wings
[NASA-TN-D-5005] c02 N69-16384
Flight-determined aerodynamic properties of a jet-augmented, auxiliary-flap, direct-lift-control system including correlation with wind-tunnel results
[NASA-TN-D-5128-REV] c02 N69-31962
COOK, G. R.
A coaxial, three-coil probe for measuring local values of electrical conductivity and velocity in plasma streams.
[AIAA PAPER 69-327] c25 A69-28264
COOLIDGE, A. W., JR.
Reduction of recovery time in high-temperature cesium vapor thyratrons
[NASA-CR-1417] c03 N69-36411
Development and inverter testing of high temperature cesium-vapor thyratrons
[NASA-CR-1435] c03 N69-36843
COOPER, G. E.
The use of pilot rating in the evaluation of aircraft handling qualities
[NASA-TN-D-5153] c02 N69-22539
COOPER, J. E.
Investigations of the unique memory properties of 55-Nitinol alloy.
c17 A69-35523
COOPER, P. A.
Effect of shallow meridional curvature on the vibration of nearly cylindrical shells
[NASA-TN-D-5143] c32 N69-22821
COOPERSMITH, M. H.
Excitation spectrum for a Bose gas with repulsive core and attractive well.
c24 A69-33118
CORCORAN, C. S.
Summary of electrical component development for a 400-hertz Brayton energy conversion system
[NASA-TN-D-4874] c03 N69-10088
Motor-starting characteristics of two inductor alternators
[NASA-TM-X-1912] c03 N69-40440
CORLISS, W. R.
Teleoperator control An AEC-NASA technology survey
[NASA-SP-5070] c05 N69-21478
CORRINGTON, L. C.
The nuclear rocket program - Its status and plans.
[AIAA PAPER 68-610] c22 A69-39219
CORSIGLIA, V. R.
Large-scale tests of an airplane model with a double-delta wing, including longitudinal and lateral characteristics and ground effects
[NASA-TN-D-5102] c02 N69-21020
COSGROVE, W. J.
Empirically determined wind and scale effects on hot gas recirculation characteristics of jet V/STOL aircraft
[NASA-CR-1445] c28 N69-40776
COSTELLO, F. A.
The selection of spacecraft optical coatings for temperature control.
[AIAA PAPER 69-979] c33 A69-40359
COTA, R. A.
Compressed gas handbook
[NASA-SP-3045] c12 N69-26987
COUCH, L. M.
Flow-field measurements downstream of two protuberances on a flat plate submerged in a turbulent boundary layer at Mach 2.49 and 4.44
[NASA-TN-D-5297] c12 N69-30071
COUR-PALAIS, B. G.
Meteoroid protection by multiwall structures.
[AIAA PAPER 69-372] c32 A69-28304
NASA space vehicle design criteria- environment. Meteorid environment model - 1969 /near earth to lunar surface/
[NASA-SP-8013] c30 N69-40326
COURT, A.
A study of jimsphere wind profiles as related to space vehicle design and operations
[NASA-CR-1204] c20 N69-13629
COX, J. E.
The effect of oxygen-supply impurities on the performance of a hydrogen-oxygen fuel cell.
c03 A69-15310
COX, W. R.
An application of similitude to model design of a soil-projectile system
[NASA-CR-1210] c34 N69-13159
Force-penetration characteristics of a sand horizontally penetrated by plates, cones, and spherical segments
[NASA-CR-1252] c18 N69-14764
COYNE, G.
Survey of the region of Lacerta OB1.
c30 A69-25813
Statistics of the region of Lacerta OB1
[NASA-TN-D-5060] c30 N69-26235
CRABILL, N. L.
Lunar Orbiter mission design.
[AIAA PAPER 68-47] c30 A69-15503
CRAGGS, A.
Transient vibration analysis of linear systems using transition matrices
[NASA-CR-1237] c32 N69-11008
The transient response of coupled acousto-mechanical systems
[NASA-CR-1421] c23 N69-35286
CRAIG, R. A.
Absolute radiometers for use in ballistic- range and shock-tube experiments
[NASA-TN-D-5360] c14 N69-38144
CRAIG, S. J.
Measurement of pilot describing functions in single-controller multiloop tasks
[NASA-CR-1238] c05 N69-15372
CRANE, D. F.
The use of integral transforms in the estimation of time variable parameters
[NASA-TN-D-5194] c19 N69-23788
CRANSTON, G. E.
General-aviation pilot reactions to and opinions on grooved runways
[NASA-CR-1428] c02 N69-35861
CRAVEN, C. E.
Experimental investigation of base flow field at high altitude for a four engine clustered nozzle configuration
[NASA-TN-D-5164] c12 N69-24935
CRAVENS, J. E.
Cost plus award fee contracting.
c34 A69-30426
CRAWFORD, A. M.
ATP assay of terrestrial soils - A test of an exobiological experiment.
c04 A69-37567
CRAWFORD, R. F.
Investigation of a coilable lattice column
[NASA-CR-1301] c32 N69-26234
CREEDON, J. F.
Evaluation of multipoint interaction in the design of a thin diffraction-limited active mirror.
c14 A69-27951
CREER, B. Y.
Evaluation of a pilot describing function method applied to the manual control analysis of a large flexible booster
[NASA-TN-D-5149] c21 N69-22996
CRESPO, A. N.
Development of three-dimensional pressure-distribution functions for lifting surfaces with trailing-edge controls based on the integral equation for subsonic flow
[NASA-TN-D-5419] c01 N69-38768
CREWS, J. H., JR.
Elastoplastic stress-strain behavior at notch roots in sheet specimens under constant-amplitude loading
[NASA-TN-D-5253] c32 N69-28038
CRIDLIN, M. S.
An in situ facility for the determination of the effects of a space environment on the solar

absorptance of materials.
[AIAA PAPER 69-1021] c11 A69-40392
CRIMI, P.
A method for analyzing the aeroelastic stability of a helicopter rotor in forward flight
[NASA-CR-1332] c32 N69-34744
CROSBY, M. J.
Restart and high response terminal shock control for an axisymmetric mixed-compression inlet with 60-percent internal contraction
[NASA-TM-X-1792] c28 N69-24938
CROSS, W. B.
Investigations of the unique memory properties of 55-Nitinol alloy.
c17 A69-35523
Nitinol characterization study
[NASA-CR-1433] c17 N69-36367
CROSWELL, W. F.
An omnidirectional microwave antenna for use on spacecraft.
c09 A69-40697
Radiofrequency transmission characteristics of several ablation materials
[NASA-TN-D-4879] c07 N69-10885
CROUCH, R. K.
An investigation of ablation behavior of Avcoat 5026/39M over a wide range of thermal environments
[NASA-TM-X-1778] c33 N69-22933
CROUSE, J. E.
A computer program for composing compressor blading from simulated circular-arc elements on conical surfaces
[NASA-TN-D-5437] c28 N69-36882
CROWDER, V. D.
Integration of a rocket motor into the Scout vehicle.
c31 A69-12384
CROWNFIELD, F. R., JR.
Mie total and differential backscattering cross sections at laser wavelengths for Junge aerosol models.
c16 A69-14290
CRUM, R. J.
Gamma heating in thin heavy-element absorbers.
c22 A69-18825
CSIKY, G. A.
Investigation of a hollow cathode discharge plasma.
[AIAA PAPER 69-258] c28 A69-21221
Measurements of some properties of a discharge from a hollow cathode
[NASA-TN-D-4966] c28 N69-17847
CUBBISON, R. W.
Study of a family of supersonic inlet systems.
[AIAA PAPER 68-580] c28 A69-34018
Effect of porous bleed in a high performance axisymmetric, mixed compression inlet at Mach 2.50
[NASA-TM-X-1692] c01 N69-10294
Effect of bleed-system back pressure and porous area on the performance of an axisymmetric mixed-compression inlet at Mach 2.50
[NASA-TM-X-1710] c01 N69-14075
Performance characteristics from Mach 2.58 to 1.98 of an axisymmetric mixed-compression inlet system with 60-percent internal contraction
[NASA-TM-X-1739] c01 N69-19130
CUNNAN, W. S.
Performance and cavitation damage of an axial-flow pump in 1500 deg F /1089 K/ liquid sodium
[NASA-TN-D-5138] c15 N69-21773
Effect of fluid temperature on the cavitation performance of a high hub-tip ratio axial flow pump in water to 250 degrees F /394 K/
[NASA-TN-D-5318] c15 N69-30069
Cavitation damage and the effect of fluid temperature on the performance of an axial- flow pump in liquid sodium
[NASA-TN-D-5484] c15 N69-38641
CUNNINGHAM, H. J.
Development of three-dimensional pressure-distribution functions for lifting surfaces with trailing-edge controls based on the integral equation for subsonic flow
[NASA-TN-D-5419] c01 N69-38768
CUNNINGHAM, R. E.
Experimental stability studies of the herringbone-grooved gas-lubricated journal bearing.
[ASME PAPER 68-LUBS-25] c15 A69-27271
Stability analysis for unloaded externally pressurized gas-lubricated bearings with journal rotation
[NASA-TN-D-4934] c15 N69-13256
Experiments on power loss in herringbone grooved, gas-lubricated journal bearings
[NASA-TN-D-5224] c15 N69-24932
Experiments on rotating externally pressurized air journal bearings. Part 1 - Load capacity and stiffness
[NASA-TN-D-5191] c15 N69-27078
Experiments on rotating externally pressurized air journal bearings. Part 2 - Attitude angle and air flow
[NASA-TN-D-5192] c15 N69-27956
Experiments on the steady state characteristics of herringbone-grooved air-lubricated journal bearings
[NASA-TN-D-5386] c15 N69-33258
CUNNINGHAM, W.
Stars that do not twinkle outside the earth's atmosphere.
c30 A69-27172
CUNNINGTON, G. R.
Emissivity coatings for low-temperature space radiators
[NASA-CR-1420] c17 N69-36723
CURRERI, J. S.
Preliminary performance characteristics of a gas-bearing turboalternator
[NASA-TM-X-1820] c03 N69-29707
CURRIE, R. G.
The geomagnetic tail - Topology, reconnection and interaction with the moon.
c13 A69-19365
CURRY, D. M.
Definition of entry corridor thermal limits for Apollo spacecraft.
[AIAA PAPER 68-1144] c31 A69-13673
CURWEN, P. W.
High-performance turboalternator and associated hardware. 2 - Design of gas bearings
[NASA-CR-1291] c15 N69-21772
CUSICK, J. P.
Resonant mode analysis of the Fitzgerald apparatus
[NASA-TN-D-5103] c26 N69-20798
Mathematical analysis of the Fitzgerald apparatus
[NASA-TN-D-5116] c18 N69-21384
CZARNECKI, K. R.
Roughness drag due to two-dimensional fabrication-type surface roughness on an ogive cylinder from force tests at transonic speeds
[NASA-TN-D-5004] c01 N69-16460
Drag reduction due to gas injection through various discrete slots on a three-dimensional wing at Mach 2.01
[NASA-TN-D-5307] c12 N69-31359

D

DA ROSA, A. V.
Enhancement of ionizing radiation during a solar flare.
c29 A69-37558
DAILEY, C. C.
The versatility of electrically propelled spacecraft for planetary missions.
[AIAA PAPER 69-253] c30 A69-21244
DALLAS, T.
Design studies on the effect of orientation, lunation, and location of the performance of lunar radiators
[NASA-TM-X-1846] c33 N69-32683
DALTON, B. P.
Factors affecting the cation requirement of a halophilic NADH dehydrogenase.
c06 A69-23127
DALTON, C. C.
Determination of meteoroid environments from photographic meteor data
[NASA-TR-R-322] c30 N69-39336
DAMATO, R.
Static and dynamic stability derivatives of a model of a jet transport equipped with external-flow jet-augmented flaps
[NASA-TN-D-5408] c02 N69-36258

DAN, C., JR.
The Orbiting Astronomical Observatory thermal test program.
[AIAA PAPER 69-995] c11 A69-40373
DANA, W. H.
Evaluation of an indirect viewing system for lifting-body terminal-area navigation and landing tasks
[NASA-TN-D-5299] c14 N69-29730
DANCE, W. E.
Investigation of bremsstrahlung production in spacecraft materials
[NASA-CR-1377] c24 N69-33416
DANCHENKO, V.
Effects of electric fields on annealing of radiation damage in MOSFET's.
c09 A69-16562
Investigation of radiation damage in MOSFETs using bias-temperature treatments.
c26 A69-16877
DANE, D. H.
Development of air bearing lift pads
[NASA-TM-X-1724] c01 N69-16467
DANIEL, R. R.
Cosmic Ray Studies in Relation to Recent Developments in Astronomy and Astrophysics, Tata Institute of Fundamental Research, Colloquium, Bombay, India, November 11-16, 1968, Proceedings.
c29 A69-38811
DANIELE, C. J.
A wind profile for generating control requirements for rocket vehicles using liquid-injection control systems
[NASA-TM-X-1708] c21 N69-14033
DANIELS, G. E.
Measurement of gas temperature and the radiation compensating thermocouple.
c14 A69-14916
DANILOWICZ, R. L.
Point defect calculations in tungsten
[NASA-TN-D-4918] c22 N69-13309
DANNENBERG, R. E.
Microsecond response system for measuring shock arrival by changes in stream electrical impedance in a shock tube.
c14 A69-13104
An application of optical telemetry to shock tube measurements.
c14 A69-29561
A novel use of a telescope to photograph metal diaphragm openings.
c14 A69-37227
Exploding wire initiation and electrical operation of a 40-kV system for arc-heated drivers up to 10 feet long
[NASA-TN-D-5126] c11 N69-22989
DARIA, M. D.
GEOS I tracking station positions on the SAO standard earth /C-5/
[NASA-TN-D-5034] c13 N69-28019
DATNOW, B.
Single-channel pressure telemetry unit.
c05 A69-25642
DAUBERT, D. L.
Power systems for the Apollo Applications Program.
c03 A69-42244
DAVENPORT, E. E.
Static longitudinal aerodynamic characteristics of some supersonic decelerator models at Mach numbers of 2.30 and 4.63
[NASA-TN-D-5219] c31 N69-26570
DAVIES, W. O.
Determination of thermodynamic properties with optical cross-correlation methods.
[AIAA PAPER 67-149] c14 A69-31868
DAVIS, A. B.
Causes, measurement, and elimination of fuel element fission product leakage at the NASA Plum Brook reactor
[NASA-TN-D-5374] c22 N69-32317
DAVIS, D. D., JR.
A pyrotechnic-activated calorimeter for flight research at lunar return velocity.
c11 A69-23026
DAVIS, J. A.
Research and development of a single gun color CRT, phase 1 Final report
[NASA-CR-1228] c09 N69-14256
DAVIS, J. G., JR.
Fabrication of uniaxial filament-reinforced epoxy tubes for structural applications.
c15 A69-22339
Application of advanced materials to truss structures.
c17 A69-35504
DAVIS, M. E.
An investigation of the decoupling effects in a magnetic forming beryllium coil assembly.
c14 A69-25310
DAVIS, M. J.
Enhancement of ionizing radiation during a solar flare.
c29 A69-37558
DAVIS, R. E.
Infrared horizon profiles for winter conditions from Project Scanner
[NASA-TN-D-4905] c21 N69-14346
A limb radiance calculation approach for model atmospheres containing horizontal gradients of temperature and pressure
[NASA-TN-D-5495] c21 N69-40055
DAVIS, R. M.
Design, simulation and flight performance of the Radio Astronomy Explorer-A satellite.
c31 A69-18328
DAVIS, W. F.
A comparison of two spectrophotometric methods for the determination of palladium in titanium-base alloys
[NASA-TM-X-1767] c06 N69-20801
DAVIS, W. S.
ATS-III resistojet thruster system performance.
[AIAA PAPER 68-553] c28 A69-39754
DAVISON, H. W.
The fuel-emitter separation problem in externally fueled thermionic diodes
[NASA-TM-X-1812] c22 N69-28212
DAVY, W. C.
Absolute radiometers for use in ballistic- range and shock-tube experiments
[NASA-TN-D-5360] c14 N69-38144
DAY, M. S.
Cooperation through the exchange of scientific and technical information.
[UN PAPER 68-95317] c34 A69-17068
Rationale of the NASA biomedical applications program.
c34 A69-32430
DAYTON, J. A., JR.
Survey of electron-cesium collision probabilities - Momentum transfer collisions
[NASA-TM-X-1897] c24 N69-38773
DE ANGELIS, V. M.
Flight measurements of canard loads, canard buffeting, and elevon and wing tip hinge moments on the XB-70 aircraft including comparisons with predictions
[NASA-TN-D-5359] c02 N69-32284
DE CHOUDHURY, P.
Rigid rotor dynamics
[NASA-CR-1391] c15 N69-36349
DE ROSE, C. E.
Trim attitude, lift and drag of the Apollo command module with offset center-of-gravity positions at Mach numbers to 29
[NASA-TN-D-5276] c30 N69-29557
DE WITT, D. P.
A comprehensive program for the compilation and analysis of thermal radiative properties data
[NASA-CR-1431] c33 N69-40455
DE WITT, R. L.
Gaseous-hydrogen pressurant requirements for the discharge of liquid hydrogen from a 3.96 meter /13 ft/ diameter spherical tank
[NASA-TN-D-5387] c28 N69-33211
DEAL, P. L.
Flight investigation of the wing-rotor lift-sharing characteristics of a hingeless rotor compound helicopter.
c02 A69-29702
DEAN, L. W., III
Analytical and experimental studies for predicting noise attenuation in acoustically treated ducts for turbofan engines
[NASA-CR-1373] c23 N69-36974
DEARING, J. D.
Heat-transfer and pressure distributions inside

the hinge-line gap of a wedge-flap combination at Mach number 10.4
[NASA-TN-D-4911] c01 N69-11009
Laminar heat-transfer distributions for a blunted-cone, cone-frustum reentry configuration at Mach 10
[NASA-TN-D-5146] c33 N69-22997

DECARLO, V. J.
Vacuum-ultraviolet photochemistry. IX - Primary and chain processes in the photolysis of hydrogen peroxide.
c06 A69-23527

DECKER, J. P.
Aerodynamic interference effects caused by parallel-staged simple aerodynamic configurations at Mach numbers of 3 and 6
[NASA-TN-D-5379] c01 N69-33302

DEERKOSKI, L. F.
A performance evaluation of a two-element large aperture antenna array.
c07 A69-36254

DEERWESTER, J. M.
Jupiter swingby missions to nonspecific locaticns in interplanetary space
[NASA-TN-D-5271] c30 N69-28441

DEESE, J. H.
A systematic approach for the analytical analysis and prediction of the yield from liquid propellant explosions.
c27 A69-14477

DEISSLER, R. G.
Direction of maximum turbulent vorticity in a shear flow.
c12 A69-25282
Nonlinear decay of a disturbance in an unbounded viscous fluid
[NASA-TN-D-4947] c12 N69-14483

DEIWERT, G. S.
Analytical prediction of the incompressible turbulent boundary layer with arbitrary pressure distribution.
[AIAA PAPER 69-397] c12 A69-30478

DEL DUCA, B. S.
The use of a heat shrinkable sleeve in a lubricant-free connector for glass vacuum systems.
c15 A69-20529
Electrochemical behavior of the aluminum electrode in molten salt electrolytes
[NASA-TN-D-5503] c06 N69-40240

DELLNER, L. T.
A set of 360 FORTRAN /level G or H/ subroutines for generating printed plots
[NASA-TM-X-1700] c08 N69-13566

DELVIGS, P.
The synthesis of a novel polymide precursor
[NASA-TN-D-5184] c06 N69-23353

DEMBLING, P. B.
International liability for damages caused by the launching of objects into outer space.
c34 A69-37127

DEMBLING, P. G.
International liability for damages caused by the launching of objects into outer space - Theory and applications.
[UN PAPER 68-95337] c34 A69-10525

DEMBROW, D.
Flight performance of FW-4D solid-propellant rocket motor on Delta 50 /AIMP-E/
[NASA-TN-D-4987] c28 N69-20876

DEMIDOV, V. YE.
Radio bridge - ''Earth-moon-earth''
[NASA-TT-F-527] c07 N69-14973

DENARDO, B. P.
Projectile shape effects on hypervelocity impact craters in aluminum
[NASA-TN-D-4953] c32 N69-14315
Experimental investigation of the momentum transfer associated with impact into thin aluminum targets
[NASA-TN-D-5492] c32 N69-38809

DENERY, D. G.
Evaluation of a pilot describing functicn method applied to the manual control analysis of a large flexible booster
[NASA-TN-D-5149] c21 N69-22996

DENISON, R. D.
Manned aerospace simulation.
[ASME PAPER 69-DE-56] c11 A69-28844

DERBY, T. F.
Loss factor and resonant frequency of viscoelastic shear-damped structural composites
[NASA-CR-1269] c32 N69-17766

DEROSHIA, C. W.
Mechanisms of action of light on circadian rhythms in the monkey.
c04 A69-31336

DESAI, U. D.
Effects of electric fields on annealing of radiation damage in MOSFET's.
c09 A69-16562
Two-twenty keV spectrum of X-rays from the Crab Nebula and the diffuse background near galactic anticenter.
c29 A69-30759
Pulsed X-ray emission of NP 0532 in March 1968.
c29 A69-37574

DETHLEFSEN, R.
Experiments on a high power, pulsed, constricted arc heater
[GDC-DBE-68-008] c25 N69-17212

DETWILER, D. P.
Apparatus for the precision measurement of internal friction.
c14 A69-13108

DEUTSCH, T.
A program to evaluate dye lasers as high power, pulsed, visible light sources
[NASA-CR-1374] c16 N69-29934

DEUTSCH, T. F.
Iodine infrared laser.
[IEEE PAPER T-5] c16 A69-19082

DEVANEY, A. J.
Laser display systems. I - Scanners.
c14 A69-15028
Laser display systems. II.
c14 A69-21394

DEVEIKIS, W. D.
Effects of cone angle, base flare angle, and corner radius on Mach 3.0 aerodynamic characteristics of large-angle cones
[NASA-TN-D-5048] c01 N69-19926

DEWITT, R. L.
Pressurant gas requirements for the pressurized discharge of liquid hydrogen from propellant tanks.
[AIAA PAPER 69-526] c28 A69-32737
Gaseous hydrogen requirements for the discharge of liquid hydrogen from a 1.52 meter /5 ft/ diameter spherical tank
[NASA-TN-D-5336] c28 N69-32318

DEXTER, C. B.
Analytical investigation of an inflatable landing system having omnidirectional and multiple impact capabilities
[NASA-TN-D-5236] c32 N69-26223

DEXTER, H. B.
Compressive properties and column efficiency of metals reinforced on the surface with bonded filaments
[NASA-TN-D-4878] c17 N69-11012

DI BATTISTA, J. D.
Shock-wave pressure decay in polycarbonate targets impacted by cylindrical polycarbonate projectiles
[NASA-TN-D-4864] c32 N69-10057

DIAGUILA, A. J.
Design studies on the effect of orientation, lunation, and location of the performance of lunar radiators
[NASA-TM-X-1846] c33 N69-32683

DICARLO, J. A.
Stage-I interstitials in electron-irradiated tungsten.
c17 A69-28682

DICKEY, R. R.
Effects of pyrolysis-gas chemical reactions on surface recession of charring ablators.
[AIAA PAPER 68-302] c33 A69-21982
The development of polybenzimidazole composites as ablative heat shields.
c18 A69-41715

DICKINSON, S. O.
Investigation of a 0.3-scale jet-transport model having a jet-augmented boundary-layer- control flap with direct-lift control capability
[NASA-TN-D-5129] c01 N69-30722

DICKSON, J.
The centrifuge as a therapeutic device. c04 A69-43372

DICKSON, J. N.
The general instability of eccentrically stiffened cylindrical shells under axial compression and lateral pressure
[NASA-CR-1280] c32 N69-15378

DIETRICH, M. W.
Contact conformity effects on spinning torque and friction.
[ASME PAPER 68-LUB-10] c15 A69-30901
Speed effects on ball spinning torque
[NASA-TN-D-5527] c15 N69-41210

DILLON, J. L.
Data-reduction technique for determining rapidly rising heating rates to thermally thick walls
[NASA-TN-D-5309] c33 N69-30726

DISHMAN, B. H.
Air bearing table mechanization and verification of a spacecraft wide angle attitude control system.
[AIAA PAPER 69-856] c31 A69-39384

DIXON, F. P.
Manned expeditions to Mars and Venus. c30 A69-12304

DIXON, G. V.
Heave response of a plenum air cushion including passive and active control concepts
[NASA-TN-D-5202] c02 N69-23449

DIXON, S. C.
Flutter boundary for simply supported unstiffened cylinders. c32 A69-41914

DOAN, A. S., JR.
The formation of phosphides in iron meteorites. c30 A69-36132

DOBROWOLSKI, A.
Conceptual study of rocket-scramjet hybrid engines in a lifting reusable second stage
[NASA-TN-D-5218] c28 N69-24922

DOBRZELECKI, A. J.
Non-linear longitudinal dynamics of an orbital lifting vehicle
[NASA-CR-1449] c30 N69-40062

DOD, L. R.
Backfire antennas for telemetry and tracking applications. c07 A69-36251

DOEBBLER, G. F.
Biochemical and metabolic effects of a six- month exposure of small animals to a helium- oxygen atmosphere
[NASA-CR-1372] c04 N69-40955

DONALD, E.
Investigation of SA-501 S-4B auxiliary
[NASA-TN-D-5207] c28 N69-26224

DONCHIN, E.
Discriminant analysis in average evoked response studies - The study of single trial data. c05 A69-40163

DONLEY, J. L.
Photoelectron flux in the topside ionosphere measured by retarding potential analyzers. c29 A69-25144
The thermal ion and electron trap experiments on the Explorer XXXI satellite. c14 A69-37878
Comparison of results of Explorer XXXI direct measurement probes. c13 A69-37882

DONN, B.
Extinction by interstellar grains, Mie particles and polycyclic aromatic molecules. c30 A69-23679
Ionization and ray formation in comets. c30 A69-27817

DONOHUE, J. H.
Thermoelastic instability of open section booms. c32 A69-18331

DONOVAN, L. F.
A numerical solution of unsteady flow in a two-dimensional square cavity.
[AICHE PAPER 25C] c12 A69-14510

DOOLEN, G.
Maximum number of binary collisions for three relativistic point particles. c24 A69-19788

DOSANJH, D. S.
Underexpanded jet noise reduction using radial flow impingement.
[AIAA PAPER 68-81] c12 A69-28212

DOTSON, W. P., JR.
The effect of object motion in Fraunhofer holography with application to velocity measurements
[NASA-TN-D-5515] c14 N69-40812

DOUGHMAN, C. L.
Inverter-converter automatic paralleling and protection
[NASA-CR-1225] c10 N69-19003

DOUGLAS, B. C.
Resonant perturbations of existing satellites. c31 A69-13777
Perturbations of existing resonant satellites. c31 A69-39968

DOW, M. B.
Multidimensional gas flow through permeable char layers and its effects on ablation
[NASA-TR-R-296] c33 N69-16181

DOW, N. F.
Zero thermal expansion composites of high strength and stiffness
[NASA-CR-1324] c32 N69-24876

DOWNS, W. R.
Detection and minimization of chemically induced ignition hazards of glycol fluids. c18 A69-36028

DOWTY, J. R.
Synthesis of optimum structural designs for conical and tension shell Mars entry capsules
[NASA-CR-1365] c32 N69-36357

DOYLE, R. O.
A long-range program in space astronomy - Position paper of the Astronomy Missions Board
[NASA-SP-213] c30 N69-41150

DRAIN, D. I.
Airbreathing propulsion system testing using sweep frequency techniques
[NASA-TN-D-5485] c28 N69-39185

DRAKE, H. M.
Mission analysis of general aviation in the 1970's.
[AIAA PAPER 69-818] c34 A69-35624

DRESHFIELD, R. L.
Sigma phase formation and its effect on stress-rupture properties of IN-100
[NASA-TN-D-5185] c17 N69-23465

DRESSER, H.
Theoretical flow field calculations for Project RAM
[NASA-CR-1308] c07 N69-28223

DRESSER, K. J.
Evaluation of lithium peroxide for oxygen supply and carbon dioxide control.
[AIAA PAPER 69-620] c05 A69-33303

DRISCOLL, L. C.
Concept of an interactive system as an experimenter.
[AIAA PAPER 69-953] c08 A69-40335

DROPPLEMAN, J. D.
A lunar-surface electric-field detector. c14 A69-13221

DUCK, K. I.
MEPSIS - Minimal electric propulsion systems for interplanetary spacecraft.
[AIAA PAPER 69-499] c28 A69-32714

DUCKETT, R. J.
Free-stream electron concentration in an arc-heated wind tunnel and correlation of Langmuir probe and microwave interferometer measurements
[NASA-TN-D-5500] c25 N69-39302

DUDZINSKI, T. J.
Venturi meter with separable diffuser.
[ASME PAPER 68-WA/FM-2] c14 A69-16135
Multiple-function probe for airflow research. c11 A69-31917
Flow-direction measurement with fixed-position probes in subsonic flow over a range of Reynolds numbers. c14 A69-33107
Flow-direction measurement with fixed-position probes
[NASA-TM-X-1904] c14 N69-40059

DUFOUR, S. W.
An interpretation of OGO light ion abundance

measurements.
c13 A69-25157
Temperature and ion abundance profiles deduced from simultaneous Explorer XXXI and Alouette II data.
c13 A69-37896
DUGAN, J. F., JR.
Future technology trends in airbreathing propulsion.
[AIAA PAPER 69-774] c02 A69-35648
DUGAN, J. V., JR.
On the nature of ion-molecule collisions.
c24 A69-16428
Computer-made movies and plotting descriptions of ion-molecule collisions with polar targets.
c24 A69-43124
A computer plotting description of ion-molecule collisions with long-lived capture complexes
[NASA-TN-D-5407] c24 N69-35508
DUGOFF, L.
NASA Technology Utilization Program.
c34 A69-35105
DUNAVANT, J. C.
Downstream cooling effectiveness of massive upstream transpiration from a slender cone.
c01 A69-43588
DUNCAN, C. H.
Solar irradiance measurements from a research aircraft.
c30 A69-42191
DUNCAN, J. R., JR.
The astrodynamicist's role vis-a-vis the systems engineer.
[AIAA PAPER 69-124] c30 A69-18090
DUNCAN, R. C.
Display requirements for advanced manned spacecraft.
c14 A69-19968
Guidance and control for atmospheric entry.
c21 A69-25724
Satellite navigation aids.
c21 A69-34855
DUNHAM, R. E., JR.
Evaluation of a contact-analog display in landing approaches with a helicopter
[NASA-TN-D-5241] c02 N69-27177
DUNKELMAN, L.
Airglow and star photographs in the daytime from a rocket.
c30 A69-33664
DUNNING, J. W., JR.
Application of the laser Doppler flowmeter to fluid flow measurements.
c14 A69-26546
DUNTLEY, S. Q.
Experiments on visual acuity and the visibility of markings on the ground in long-duration earth-orbital space flight
[NASA-CR-1134] c05 N69-10813
DURGAPRASAD, N.
Composition of the 2nd September 1966 solar particle event.
c29 A69-17280
Composition of cosmic rays measured in Gemini XI.
c29 A69-38350
DURLING, B. J.
A method for computing the response of a general axisymmetric shell with an attached asymmetric structure.
c32 A69-25525
DUST, D. C.
Manned aerospace simulation.
[ASME PAPER 69-DE-56] c11 A69-28844
DUSTERBERRY, J. C.
The simulator to match the transports to come.
c11 A69-43044
DUSTIN, M. O.
Design and performance of two integrated circuits for fluidic-controlled pneumatic stepping motor system
[NASA-TN-D-5155] c03 N69-22896
DUTTON, J. A.
Approximate equations of motion for gases and liquids.
c12 A69-26013
Investigation of the turbulent wind field below 150-meter altitude at the eastern test range
[NASA-CR-1410] c20 N69-35570
DWORNIK, S. E.
Principal science results from Surveyor 5.
c30 A69-12224
DYAL, P.
Magnetometer experiment.
[AAS PAPER 68-206] c30 A69-11481
DYSON, P. L.
Ionospheric and magnetic observations at 1000 kilometers during the geomagnetic storm and aurora of May 25-26, 1967.
c13 A69-34954

E

EAGLES, D. M.
Effective masses in Zr-doped superconducting ceramic SrTiO sub 3.
c26 A69-27400
Theory of transitions from large to nearly- small polarons, with application to Zr-doped superconducting SrTiO sub 3.
c26 A69-37280
EASTER, R. W.
Experimental investigation of the dynamics of water rejection from a matrix type of hydrogen-oxygen fuel cell
[NASA-TN-D-4956] c03 N69-14518
ECKERT, R. E.
Effect of film processing on cryogenic properties of poly/ethylene terephthalate/.
c18 A69-16490
ECKSTROM, C. V.
Flight-test results from supersonic deployment of an 18-foot-diameter /5.49 meter/ towed ballute decelerator
[NASA-TM-X-1773] c31 N69-26458
EDGECOMBE, D. S.
Problems in planning for the introduction of primary electric propulsion.
[AIAA PAPER 69-247] c28 A69-21251
EDKIN, R. A.
Performance characteristics of a 14.3-kilovolt-ampere modified Lundell alternator for 1200 hertz Brayton-cycle space-power system
[NASA-TN-D-5405] c03 N69-35537
EDWARDS, F. G.
Measurement of pilot describing functions from flight test data with an example from Gemini X.
c05 A69-11950
A technique for identifying pilot describing functions from routine flight-test records
[NASA-TN-D-5127] c05 N69-23842
EDWARDS, R.
Application of the laser Doppler flowmeter to fluid flow measurements.
c14 A69-26546
EGGER, A.
Central data system concepts for spacecraft data management.
c08 A69-42621
EGGERS, J. M.
An experimental investigation of the mixing of compressible-air jets in a coaxial configuration
[NASA-TN-D-5315] c02 N69-30727
EGLE, D. M.
An approximate theory for transverse shear deformation and rotatory inertia effects in vibrating beams
[NASA-CR-1317] c32 N69-24056
A theoretical analysis of the free vibration of discretely stiffened cylindrical shells with arbitrary end conditions
[NASA-CR-1316] c32 N69-28164
EHLERS, H. K. F.
Pressure measurements and gas-flow analysis in chambers A and B during thermal vacuum tests of spacecraft 2TV-1 and LTA-8.
[AIAA PAPER 69-1033] c11 A69-40401
EHLERS, R. C.
Experimental and theoretical turbulent boundary layer development in a Mach 4.4 water-cooled conical nozzle
[NASA-TN-D-5377] c12 N69-33353
EHRLICH, E.
The general utility and character of prospective navigation services satellite systems.
[UN PAPER 68-95363] c21 A69-10479
EHRMANN, C. H.
Computer analysis of tracks in nuclear emulsion

utilizing digitized video scan.
[IEEE PAPER 2A-7] c14 A69-19185
A gamma ray telescope utilizing large area wire spark chambers.
[IEEE PAPER 3A-5] c14 A69-19192
EICHBLATT, D. L.
Experimental verification of scale factors for parawing opening characteristics with dimensional ratios from 1/1.3 to 1/3
[NASA-TN-D-5071] c02 N69-19950
EICHELBERGER, R. L.
Solubility of refractory metals and alloys in potassium and in lithium
[NASA-CR-1371] c17 N69-27059
EISENBERG, J. D.
Helium pressurization systems for liquid- methane fuel in supersonic transports
[NASA-TN-D-5519] c28 N69-40329
ELDRIDGE, J. S.
Meteorite fall at Pueblito de Allende, Chihuahua, Mexico - Preliminary information.
c30 A69-20686
ELFNER, L. F.
Auditory temporal masking and the perception of order.
c05 A69-24795
ELIKAN, L.
Solid electrolyte system for oxygen regeneration
[NASA-CR-1359] c05 N69-28099
ELLIS, S.
Identity between the growth hormone degrading activity of the pituitary gland and plasmin.
c04 A69-17105
New observations on the substrate specificity of cathepsin C /dipeptidyl aminopeptidase I/ including the degradation of beta-corticotropin and other peptide hormones.
c04 A69-37577
ELLISON, J. C.
Experimental stagnation point velocity gradients and heat transfer coefficients for a family of blunt bodies at Mach 8 and angles of attack
[NASA-TN-D-5121] c01 N69-22554
EMANUELSON, R.
Properties of high emittance materials
[NASA-CR-1278] c17 N69-18952
EMME, E. M.
Aeronautics, rocketry, and astronautics.
c34 A69-34552
ENGELBART, D. C.
Human intellect augmentation techniques Final report
[NASA-CR-1270] c08 N69-16140
ERB, R. B.
Apollo thermal-protection system development.
[AIAA PAPER 68-1142] c31 A69-13558
ERICKSON, W. D.
Some aspects of interplanetary earth-entry simulation.
c30 A69-30376
ERICSSON, L. E.
Aerodynamic effects of bulbous bases
[NASA-CR-1339] c01 N69-35521
ERINGEN, A. C.
Compatibility conditions of the theory of micromorphic elastic solids
[NASA-CR-1236] c26 N69-10817
A lattice model for composite materials
[NASA-CR-1322] c32 N69-22982
ERNSBERGER, G. W.
Inverter-converter parallel operation
[NASA-CR-1224] c03 N69-16379
ERNULL, R. E.
Utilization of ground-based guidance systems to supplement onboard guidance of space vehicles.
c21 A69-17580
ERTEL, I. D.
The Apollo spacecraft. Volume 1 - A chronology
[NASA-SP-4009] c31 N69-32021
ERZBERGER, H.
Technique for calculating optimum takeoff and climb out trajectories for noise abatement
[NASA-TN-D-5182] c02 N69-26194
ESHEL, A.
Study, fabrication and testing of a foil-bearing rotor support system
[NASA-CR-1157] c15 N69-14214
ESTOK, G. K.
Differential thermal analysis of some biological specimens, proteins, and starches.
c06 A69-31807
ETTELSON, B.
NASA contributions to bioinstrumentation systems - A survey
[NASA-SP-5054] c04 N69-14860
ETZEL, J. G.
Development of a weld quality monitor
[NASA-TN-D-5304] c15 N69-33800
EUL, W. A.
Shear strain properties to 10 sup -10 of selected optical materials
[NASA-CR-1257] c14 N69-16100
EVANS, A., JR.
Fouling characteristics of ASTM jet A fuel when heated to 700 deg F in a simulated heat exchanger tube
[NASA-TN-D-4958] c28 N69-12831
EVANS, D. C.
Airglow and star photographs in the daytime from a rocket.
c30 A69-33664
EVANS, D. D.
FORTRAN program for machine computation of group tables of finite groups
[NASA-TN-D-5402] c08 N69-35569
EVANS, D. S.
Fine structure in the energy spectrum of low energy auroral electrons.
c13 A69-38490
EVANS, R. C.
Preliminary investigation of a single-shaft Brayton rotating unit designed for a 2 to 10-kilowatt space power generation system
[NASA-TM-X-1869] c03 N69-39238
EVANS, R. M.
Joining ceramics and graphite to other materials
[NASA-SP-5052] c15 N69-14241
EVERSMAN, W.
Some equilibrium and free vibration problems associated with centrifugally stabilized disk and shell structures
[NASA-CR-1178] c32 N69-14477
EVVARD, J. C.
Atmospheric limits on the observational capabilities of aerospacecraft
[NASA-TN-D-4940] c20 N69-12934
EWEN, H. I.
Microwave radiometric capabilities and techniques.
c07 A69-26976
EXPOSITO, L. F.
Biochemical and metabolic effects of a six- month exposure of small animals to a helium- oxygen atmosphere
[NASA-CR-1372] c04 N69-40955
EXTON, R. J.
Doublet suppression in the principal series of cesium.
c24 A69-20736

F

FAELTHAMMAR, C.-G.
Charged particle diffusion by violation of the third adiabatic invariant.
c29 A69-19375
FAETH, P. A.
Research and development of a single gun color CRT, phase 1 Final report
[NASA-CR-1228] c09 N69-14256
FAINBERG, J.
Measurements in the ionosphere of the aspect dependence of antenna reactance. I - Variations arising from the inhomogeneous plasma distribution about the vehicle.
c13 A69-39964
FAIRBANKS, J. W.
Evaluation of integral covers on silicon solar cells.
c03 A69-42272
FAIRFIELD, D. H.
Average magnetic field configuration of the outer magnetosphere.
c13 A69-14012
Microscale fluctuations in the interplanetary magnetic field.
c30 A69-24100
Bow shock associated waves observed in the far upstream interplanetary medium.

c30 A69-34941
FAISON, R. W.
Ratios of steady-state responses to various transient responses, both having equal maximum excitation levels
[NASA-TN-D-5070] c32 N69-17258
Analytical and experimental investigation of end-plane rotations of truncated cones under bending loads
[NASA-TN-D-5536] c32 N69-41141
FAKEN, J. C.
Application of modern network theory to analysis of complex systems
[NASA-TN-D-5511] c19 N69-40088
FALARSKI, M. D.
Large-scale wind-tunnel investigation of an M1-L lifting body with an inflatable and a rigid afterbody
[NASA-TN-D-5468] c01 N69-38775
FALLER, J.
Laser beam directed at the lunar retro- reflector array - Observations of the first returns.
c30 A69-43197
FANG, A. C.
Digital simulation of rotational kinematics
[NASA-TN-D-5302] c23 N69-39178
FANG, P. H.
Impurity effects on annealing of radiation defects in silicon.
c26 A69-24006
Gamma irradiation of lithium silicon solar cells.
c03 A69-35694
FARBER, E. A.
A systematic approach for the analytical analysis and prediction of the yield from liquid propellant explosions.
c27 A69-14477
FARNSWORTH, D.
Test parameters, material characterization, and the white thermal control coating stability problem.
[AIAA PAPER 69-641] c18 A69-33762
FARQUHAR, J.
Transient pumping performance of a two speed, hydraulic turbine driven inducer system.
[AIAA PAPER 69-551] c15 A69-34415
FARQUHAR, R. W.
Future missions for libration-point satellites.
c30 A69-30188
FARRELL, R.
A SiC backward diode.
c09 A69-22787
Development of an experimental silicon carbide backward diode operable to 1000 deg K
[NASA-TN-D-5183] c09 N69-23556
FASSIO-CANUTO, L.
Quantum theory of an electron gas with anomalous magnetic moments in intense magnetic fields.
c24 A69-19782
Nature of radio and optical emissions from pulsars.
c30 A69-20624
Thermodynamic approach to the equation of state of a magnetized Fermi gas.
c30 A69-25107
One-boson-exchange contributions to high-energy proton antiproton elastic scattering in a nonlocal field theory.
c24 A69-39467
FAVORITE, F. G.
Life Sciences and Space Research VI, COSPAR, Plenary Meeting, 10th, Open Meeting of Working Group V, London, England, July 27, 28, 1967, Proceedings.
c04 A69-11073
Life Sciences and Space Research VII COSPAR, Plenary meeting, 11th, Open Meeting of Working Group V and Symposium on Biological Effects of Radiation in Space, Tokyo, Japan, May 14-16, 1968 and May 10, 1968, Proceedings.
c04 A69-37612
FEAST, M. W.
Infrared excess of RY Sgr.
c30 A69-42377
FECYCH, W.
Experiences with beryllium swelling and replacement in the Plum Brook Reactor.
c22 A69-13131
Experiences with beryllium swelling and replacement in the Plum Brook reactor
[NASA-TM-X-1794] c22 N69-26233
FEDCHIN, S. S.
Aircraft navigation
[NASA-TT-F-524] c21 N69-17788
FEDER, E.
Analytical and experimental studies for predicting noise attenuation in acoustically treated ducts for turbofan engines
[NASA-CR-1373] c23 N69-36974
FEDERLINE, M. F.
Explorer 35 attitude control system
[NASA-TN-D-5187] c21 N69-27268
FEDOR, J. V.
Explorer 35 attitude control system
[NASA-TN-D-5187] c21 N69-27268
FEDYNSKII, V. V.
The earth in the universe
[NASA-TT-F-345] c13 N69-12384
FEHLBERG, E.
Low-order classical Runge-Kutta formulas with stepsize control and their application to some heat transfer problems
[NASA-TR-R-315] c19 N69-30753
FEHRS, D. L.
Measurements of the work function and desorption energy of cesium and potassium on /100/ tungsten.
c26 A69-21808
FEINBERG, P.
Use of computers and programmable telemetry systems on scientific satellies.
c08 A69-41735
FEISTEL, T. W.
An investigation of a direct side-force maneuvering system on a deflected jet VTOL aircraft
[NASA-TN-D-5175] c02 N69-22572
FEIX, M. R.
Diffusion of fast electrons in stochastic magnetic fields.
c25 A69-20807
FELLER, D. D.
In vivo utilization of acetate-1-C super 14 in centrifuged rats.
c04 A69-19429
Conversion of acetate-2 -super 14 C to super 14 CO sub 2 and super 14 C-fatty acids in the partially hepatectomized rat /33627/.
c04 A69-35976
Effects of hyperoxia and hypoxia on mitosis in the normal and regenerating rat liver.
c04 A69-43565
FELLER, W. V.
Comparison of prediction methods and studies of relaxation in hypersonic turbulent nozzle-wall boundary layers
[NASA-TN-D-5433] c12 N69-36805
FELSENTREGER, T. L.
A semi-analytic theory for the motion of a lunar satellite
[NASA-TN-D-5043] c30 N69-28050
FELTON, L. P.
Geometric properties of a prestressed segmented spherical shell
[NASA-CR-1231] c32 N69-11010
FESSLER, T. E.
Decay of super 136 La and super 134 La.
c24 A69-10100
Excited states of barium 136 and barium 134
[NASA-TN-D-4933] c24 N69-12778
Excited states of xenon-130 populated by beta decay
[NASA-TN-D-5329] c24 N69-30074
FICHTEL, C. E.
Energetic solar particles.
c29 A69-12934
Cosmic-ray propagation.
c29 A69-16361
Composition of the 2nd September 1966 solar particle event.
c29 A69-17280
A gamma ray telescope utilizing large area wire spark chambers.
[IEEE PAPER 3A-5] c14 A69-19192
Composition of cosmic rays measured in Gemini XI.
c29 A69-38350

FICHTER, W. B.
Stress concentration around broken filaments in a filament-stiffened sheet
[NASA-TN-D-5453] c32 N69-38642
FICHTL, G. H.
Characteristics of turbulence observed at the NASA 150-m meteorological tower.
c20 A69-10695
Approximate equations of motion for gases and liquids.
c12 A69-26013
Detailed wind and temperature profiles.
c20 A69-33739
FIELDER, W. L.
Ionic conductivity of lanthanum fluoride
[NASA-TN-D-5505] c26 N69-40056
FIELDS, R. A.
Evaluation of an infrared heating simulation of a Mach 4.63 flight on an X 15 horizontal stabilizer
[NASA-TN-D-5403] c33 N69-35949
FIENO, D.
Transport study of neutron and photon attenuation through lithium hydride and tungsten spherical media
[NASA-TN-D-4989] c24 N69-15375
Analysis and experiments with a pulsed neutron source for an unreflected solution reactor up to 50 dollars shutdown
[NASA-TN-D-5487] c22 N69-39186
FILIPESCU, N.
Fluorescence spectra of homogeneous and mixed europium complexes.
c06 A69-10893
FINNELL, R. O.
Central data system concepts for spacecraft data management.
c08 A69-42621
FINCH, H. L.
A computer program for calculating external thermal-radiation heat loads and temperatures of spacecraft orbiting the planets or the moon
[NASA-TR-R-278] c30 N69-14428
FINDLAY, J. A.
Electron measurements bearing on the energy and particle balance of the upper F region.
c29 A69-31975
Ionospheric and magnetic observations at 1000 kilometers during the geomagnetic storm and aurora of May 25-26, 1967.
c13 A69-34954
Cylindrical electrostatic probes employed on Alouette II and Explorer XXXI satellites.
c14 A69-37876
Comparison of cylindrical electrostatic probe measurements on Alouette II and Explorer XXXI satellites.
c14 A69-37877
Comparison of results of Explorer XXXI direct measurement probes.
c13 A69-37882
FINGER, F. G.
A comparison of data obtained by the MT-135 and ARCAS meteorological rocket systems
[NASA-TM-X-1726] c20 N69-17772
Synoptic analysis of the Southern Hemisphere stratosphere
[NASA-TM-X-1814] c13 N69-33555
FINK, M. P.
Wind-tunnel investigation of a large jet transport model equipped with an external-flow jet flap
[NASA-TN-D-4928] c01 N69-14000
Full-scale wind-tunnel investigation of static longtudinal and lateral characteristics of a light twin-engine airplane
[NASA-TN-D-4983] c02 N69-17303
Aerodynamic data on large semispan tilting wing with 0.4-diameter chord, single-slotted flap, and single propeller 0.22 chord below wing
[NASA-TN-D-5016] c01 N69-17312
Full-scale investigation of the aerodynamic characteristics of a sailwing of aspect ratio 5.9
[NASA-TN-D-5047] c01 N69-19243
Pressure distribution of a large semispan tilting wing with 0.4-diameter-chord, single- slotted flap, and a single propeller 0.22 chord below wing
[NASA-TN-D-5481] c01 N69-40876
FINK, R.
Handbook of Solar Simulation for Thermal Vacuum Testing.
c11 A69-38894
FINKEL, M. W.
Portable reflectometer.
[AIAA PAPER 69-599] c14 A69-33264
FINZI, A.
Possible conversion of rotational energy of the neutron star in the Crab Nebula into energy of relativistic electrons.
c30 A69-21454
FISCHLER, S.
GaSb-ZnTe heterojunction.
c26 A69-12408
FISHBACK, L. H.
A steam cycle for aircraft nuclear propulsion
[NASA-TM-X-1907] c22 N69-40060
FISHER, D. F.
Flight-measured aerodynamic drag of two large external tanks attached to the X-15-2 airplane at Mach numbers of 1.6 to 2.3
[NASA-TM-X-1895] c01 N69-38065
FISHER, D. M.
Note on inclination of fatigue cracks in plane strain fracture toughness test specimens.
c32 A69-25958
FISK, L. A.
Solar modulation of galactic cosmic rays. I.
c29 A69-43169
FITZGERALD, D. F.
A study of 2 GHz electromagnetic wave propagation over optical paths in three geographical regions of the United States
[NASA-CR-1442] c07 N69-39282
FITZGERALD, R. T.
Why data system standards?
c08 A69-41769
FITZMAURICE, M. W.
Wavelength dependence of laser-beam scintillation.
c16 A69-19641
FLAHERTY, R. E.
Impact characteristics in fused silica.
[AIAA PAPER 69-367] c32 A69-28299
FLATLEY, T. W.
Explorer 35 attitude control system
[NASA-TN-D-5187] c21 N69-27268
Attitude stability of a class of partially flexible spinning satellites
[NASA-TN-D-5268] c31 N69-32298
FLAX, L.
Spin wave approximation for anisotropic Heisenberg antiferromagnet.
c26 A69-26500
Theory of phase transitions in solid hydrogen.
c23 A69-43119
Random phase approximation for the anisotropic Heisenberg ferromagnet
[NASA-TN-D-5286] c26 N69-29588
FLECHNER, S. G.
Transonic aerodynamic characteristics of a Saturn 1B Manned Orbiting Research Labcratory launch vehicle
[NASA-TM-X-1848] c31 N69-33380
FLEENOR, E. N., JR.
A process for imprinting micro lagoon fields in plastic surfaces for use in cell and tissue culture
[NASA-TN-D-5255] c04 N69-29195
FLEIG, A. J., JR.
A passive method for scanning the celestial sphere.
[AIAA PAPER 68-854] c21 A69-39764
FLEMING, D. P.
Experimental stability studies of the herringbone-grooved gas-lubricated journal bearing.
[ASME PAPER 68-LUBS-25] c15 A69-27271
Experiments on the stability of water lubricated herringbone-groove journal bearings. 1 - Theoretical considerations and clearance effects
[NASA-TN-D-4883] c15 N69-10228
Stability analysis for unloaded externally pressurized gas-lubricated bearings with journal rotation
[NASA-TN-D-4934] c15 N69-13256
Experiments on power loss in herringbone grooved, gas-lubricated journal bearings
[NASA-TN-D-5224] c15 N69-24932

Experiments on rotating externally pressurized air journal bearings. Part 1 - Load capacity and stiffness
[NASA-TN-D-5191] c15 N69-27078
Experiments on the stability of water lubricated herringbone-groove journal bearings. 2 - Effects of configuration and groove to ridge clearance ratio
[NASA-TN-D-5264] c15 N69-27955
Experiments on rotating externally pressurized air journal bearings. Part 2 - Attitude angle and air flow
[NASA-TN-D-5192] c15 N69-27956
Experiments on the steady state characteristics of herringbone-grooved air-lubricated journal bearings
[NASA-TN-D-5386] c15 N69-33258

FLETCHER, J.
Effects of various respiratory maneuvers on the physiological response to angular acceleration. c05 A69-41679

FLETCHER, R. F.
Characteristics of liquid propellant explosions. c27 A69-14474

FLOOD, D. J.
Molecular vibration spectra from field emission energy distributions. c24 A69-26097
Magnetothermal oscillations in pressure- annealed pyrolytic graphite. c26 A69-29005
Molecular vibration spectra from field emission energy distributions
[NASA-TN-D-5423] c24 N69-36924
Magnetothermal oscillations in pressure- annealed, pyrolytic graphite
[NASA-TN-D-5488] c26 N69-39239

FLORA, C. C.
A flight investigation of systems developed for reducing pilot workload and improving tracking accuracy during noise-abatement landing approaches
[NASA-CR-1427] c02 N69-38657

FLOYD, S. R.
Thermal effects on the integrity of aluminum to silicon contacts in silicon integrated circuits. c09 A69-32893
Current status of scanning electron microscopy in semiconductor device reliability physics. c26 A69-35788

FLUEGGE-LOTZ, I.
Minimum fuel attitude control of a nonlinear satellite system with bounded control by a method based on linear programming
[NASA-CR-1450] c21 N69-41036

FOGARTY, L. E.
Computer mechanization of six-degree of freedom flight equations
[NASA-CR-1344] c21 N69-26232

FOLKESTAD, K.
Results of rocket measurements in the lower auroral ionosphere. c13 A69-32187

FORD, C. H.
Analysis and experiments with a pulsed neutron source for an unreflected sclution reactor up to 50 dollars shutdown
[NASA-TN-D-5487] c22 N69-39186

FORD, F. E.
Auxiliary electrode charge control. c03 A69-23993

FORD, W. F.
Inelastic scattering calculations with Wood- Saxon Hartree-Fock wave functions. c26 A69-29006
Core polarization effects in inelastic scattering. c24 A69-29007
A large-angle approximation for high-energy scattering. c24 A69-29008
E2 transition rates for super 20 Ne. c24 A69-35166
Inelastic scattering calculations with projected Hartree-Fock wave functions. c24 A69-41045
Hartree-Fock calculations with Wood-Saxon basis functions
[NASA-TN-D-5066] c24 N69-17976

FORDYCE, S. W.
Communications for the Apollo Applications Program. c07 A69-19124

FORESTIERI, A. F.
Observations on CdS solar cell stability. c03 A69-13074
On the resolution and image intensity of the field-ion microscope
[NASA-TN-D-5125] c14 N69-21408

FOSTER, J. F.
Systems approach to evaluating Hydrogenomonas cultures
[NASA-CR-1296] c05 N69-22766

FOSTER, J. N.
Properties of nonaqueous electrolytes
[NASA-CR-1425] c06 N69-36413

FOSTER, R. M.
Synthesis of optimum structural designs for conical and tension shell Mars entry capsules
[NASA-CR-1365] c32 N69-36357

FOURNIER, R. H.
Aerodynamic characteristics in pitch of a 1/7-scale model of a two- and three-stage rocket configuration at Mach numbers of 0.4 to 4.63
[NASA-TN-D-5378] c01 N69-34986

FOWKE, J. G.
Lightweight, high-thermal-capacity force models for use in arc tunnels. c11 A69-26796

FOWLER, W. B.
Effects of energetic particles on photomultipliers in earth orbits up to 1500 km. c14 A69-16932

FOWLER, W. T.
Recurrent nature of Lagrange multipliers for optimal low-thrust earth-Jupiter transfers. c30 A69-41896

FOWLKES, C. W.
Photoviscoelastic model testing
[NASA-CR-1289] c32 N69-17770

FOX, C. H., JR.
Prediction of lift and drag for slender sharp-edge delta wings in ground proximity
[NASA-TN-D-4891] c01 N69-16180
Transonic aerodynamic characteristics of hypersonic low-wave-drag elliptical body-tail combinations as affected by changes in stabilizer configuration
[NASA-TM-X-1789] c01 N69-25244

FOX, H. W., JR.
An analog computer study of the low-frequency flow dynamics of two nuclear rocket cold-flow engine systems
[NASA-TN-D-5312] c22 N69-30070

FOX, T. A.
Analysis and experiments with a pulsed neutron source for an unreflected solution reactor up to 50 dollars shutdown
[NASA-TN-D-5487] c22 N69-39186

FRANK, R. G.
Recent advances in columbium alloys. c17 A69-18791

FRANKS, H. J., JR.
STADAN PCM data handling systems. c07 A69-36242

FRANKS, R. K.
Beryllium as an acceptor in silicon. c26 A69-21652

FRASCO, L. A.
Communication system design
[NASA-TN-D-5472] c07 N69-39176

FRAZIER, N. A.
Satellite applications to marine geodesy
[NASA-CR-1253] c13 N69-16645

FRECHE, J. C.
Ultrasonic detection and measurement of fatigue cracks in notched specimens. c14 A69-10113
NASA programs for development of high- temperature alloys for advanced engines.
[ICAS PAPER 68-26] c17 A69-43718
Evaluation of two nickel-base alloys, alloy 713C and NASA TAZ-8A, produced by extrusion of prealloyed powders
[NASA-TN-D-5248] c17 N69-26192
A nickel base alloy, WAZ-20, with improved strength in the 2000 deg to 2200 deg F range
[NASA-TN-D-5352] c17 N69-31873

FREDEN, S. C.
Inner-belt Van Allen radiation.
c29 A69-27144
FREDERICK, C. L.
Far-infrared observation of the galactic-center region at 100 microns.
c30 A69-22264
A far infrared sky survey.
c30 A69-27599
FREDGA, K.
Rocket spectroheliograph for the Mg II line at 2802.7 angstrom units.
c14 A69-24838
FREEDMAN, M. I.
Logarithmic variation criteria for the stability of systems with time-varying gains.
c10 A69-13073
L sub 2 -stability of time-varying systems - Construction of multipliers with prescribed phase characteristics.
c10 A69-16598
FREEMAN, D. C., JR.
Low subsonic flight and force investigation of a supersonic transport model with a variable-sweep wing
[NASA-TN-D-4726] c02 N69-10733
Wind-tunnel investigation of a large jet transport model equipped with an external-flow jet flap
[NASA-TN-D-4928] c01 N69-14000
Full-scale wind-tunnel investigation of static longtudinal and lateral characteristics of a light twin-engine airplane
[NASA-TN-D-4983] c02 N69-17303
Static and dynamic stability derivatives of a model of a jet transport equipped with external-flow jet-augmented flaps
[NASA-TN-D-5408] c02 N69-36258
FREEMAN, J. W.
Sensitivity of the creep-rupture properties of nickel-base superalloy sheet to sharp edge-notches in the temperature range of 1000 deg F - 1400 deg F
[NASA-CR-1263] c32 N69-16156
FREMMING, P. D.
Roll and yaw compensation feasibility study
[NASA-CR-1209] c31 N69-16221
FRENKEL, L.
Methods for the measurement of frequency and stability of laser generators in the infrared.
c16 A69-18482
Frequency measurements in the far infrared - Limitations imposed by the noise spectrum in harmonic mixing.
c23 A69-33674
FREUNDLICH, M. M.
Exobiology- The Search for Extraterrestrial Life, American Astronautical Society and American Association for the Advancement of Science, Symposium, New York, N.Y., December 30, 1967, Proceedings.
c04 A69-32967
FRICK, V.
Hydrogen gas pressure vessel problems in the M-1 facilities
[NASA-CR-1305] c17 N69-19831
FRIED, W. R.
Avionics Navigation Systems.
c21 A69-34843
FRIEDLANDER, S. L.
Preliminary evaluation test of the Langley cardiovascular conditioning suit concept
[NASA-CR-1206] c05 N69-13202
FRIEDMAN, J.
Space storable propellant performance demonstration.
[AIAA PAPER 69-505] c28 A69-32762
FRIEDMAN, R.
Expansion of simulated storable propellants in a supersonic nozzle.
[AIAA PAPER 68-635] c33 A69-37188
Experimental measurements of expanding storable-propellant products simulated by combustion of gaseous reactants
[NASA-TN-D-5404] c33 N69-35506
FRIEND, E. L.
Flight measurements of canard loads, canard buffeting, and elevon and wing tip hinge moments on the XB-70 aircraft including comparisons with predictions
[NASA-TN-D-5359] c02 N69-32284
FRIESEN, W. J.
Use of photoionization in measuring velocity profile of free-stream flow in Langley pilot model expansion tube
[NASA-TN-D-4936] c12 N69-13945
FRISCH, H. P.
Thermoelastic instability of open section booms.
c32 A69-18331
Thermally induced vibrations of long thin- walled cylinders of open section.
c32 A69-25534
FROST, A.
High-performance turboalternator and associated hardware. 2 - Design of gas bearings
[NASA-CR-1291] c15 N69-21772
FROST, R. M.
Evaluation of magnetic materials for static inverters and converters
[NASA-CR-1226] c03 N69-17765
FROST, W. O.
Errors resulting from channel filters and adjacent channel crosstalk in DSB/SC telemetry systems.
c07 A69-19130
FRUTKIN, A. W.
NASA programs and opportunities for international cooperation in space.
[UN PAPER 68-95367] c34 A69-10516
FRY, E. B.
An investigation of a direct side-force maneuvering system on a deflected jet VTOL aircraft
[NASA-TN-D-5175] c02 N69-22572
Use of a six-degrees-of-freedom motion simulator for VTOL hovering tasks
[NASA-TN-D-5383] c11 N69-35359
FRYE, R. J.
Electronic position indicator for latching solenoid valves
[NASA-TM-X-1760] c14 N69-20874
Results of endurance tests of a SNAP 8 turbine-alternator
[NASA-TM-X-1741] c03 N69-20913
FRYER, T. B.
Single-channel pressure telemetry unit.
c05 A69-25642
FULCHER, R.
A brushless dc torquer-driven reaction wheel for spacecraft attitude control
[NASA-TN-D-5265] c03 N69-30945
FULLER, C. E.
Application of laser Doppler velocity instrumentation to the measurement of jet turbulence.
[SAE PAPER 690266] c14 A69-21555
FULLER, F. B.
On some numerical difficulties in integrating the equations for one-dimensional nonequilibrium nozzle flow
[NASA-TN-D-5176] c19 N69-23355
FULTON, F.
Lessons from the B-70 to be applied to SST safety.
c02 A69-41143
FULTON, R. E.
Axisymmetric static and dynamic buckling of spherical caps due to centrally distributed pressures.
[AIAA PAPER 69-89] c32 A69-18133
FUNK, J.
Application of nuclear solid-core rockets to interplanetary orbital launch by multiorbit injection.
[AIAA PAPER 69-535] c22 A69-32660
FURUMOTO, H.
Time dependent spectroscopy of flashlamp pumped dye lasers.
c16 A69-17901
FURUMOTO, H. W.
Optical pumps for organic dye lasers.
c16 A69-42187
FUSARO, R. L.
Preliminary investigation of graphite fluoride /CF sub x/ sut n as a solid lubricant
[NASA-TN-D-5097] c15 N69-20939
FUTRAL, S. M.
Instrumentation used to define performance of small size, low power gas turbines.
[ASME PAPER 69-GT-104] c14 A69-22522

FUTRAL, S. M., JR.
A FORTRAN 4 program to estimate the off-design performance of radial-inflow turbines
[NASA-TN-D-5059] c03 N69-19829
Effect of rotor tip clearance on the performance of a 5-inch single stage axial flow turbine
[NASA-TM-X-1757] c03 N69-20883

G

GADDIS, J. L.
A model for large eddy contributions in incompressible turbulent boundary layers.
c12 A69-33255
GADEBERG, B. L.
Methods for predicting spacecraft-window- induced line-of-sight deviations
[NASA-TN-D-5238] c21 N69-31227
GAGLIARDI, R. M.
Radiation models using discrete radiator ensembles.
c07 A69-10556
GAHN, R. F.
Vacuum distillation technique for recovery of alkali-metal reaction products.
c14 A69-10927
Determination of oxygen in lithium by the vacuum distillation method.
c06 A69-40932
Determination of oxygen in lithium by the vacuum distillation method
[NASA-TN-D-5197] c06 N69-23706
GAIDSICK, H. G.
Evaluation of an indirect viewing system for lifting-body terminal-area navigation and landing tasks
[NASA-TN-D-5299] c14 N69-29730
GAINER, T. G.
Status of research on parawing lifting decelerators.
[AIAA PAPER 68-967] c02 A69-43715
Investigation of opening characteristics of an all-flexible parawing
[NASA-TN-D-5031] c02 N69-17700
GALANT, D. C.
High accuracy gamma function values for some rational arguments.
c19 A69-13375
GALLAGHER, J. D.
Performance of the SNAP-8 lubrication and coolant subsystem
[NASA-TM-X-1731] c03 N69-20828
GALLANT, R. P.
Flight tests under IFR with an STOL transport aircraft
[NASA-TN-D-4939] c02 N69-13252
GALLO, W. F.
A study of the nonsimilar nature of the laminar boundary layer in a region of adverse pressure gradient.
[AIAA PAPER 69-35] c12 A69-18094
GALLOWAY, T. L.
Mission analysis of general aviation in the 1970's.
[AIAA PAPER 69-818] c34 A69-35624
GAMBELE, J. D.
A mathematical model for calculating the flight dynamics of a general parachute-payload system
[NASA-TN-D-4859] c02 N69-14504
GAPCYNSKI, J. P.
Results on the mass and the gravitational field of the moon as determined from dynamics of lunar satellites.
c30 A69-31405
GARCIA, J. G.
Cloud height contouring from Apollo 6 photography.
c20 A69-36926
GARDINER, R. A.
Guidance and control considerations for advanced manned space missions.
c21 A69-35801
GARDNER, H.
New approach to logistics management.
[AAS PAPER 69-204] c34 A69-42812
GARDNER, J. E.
Influence of various fabrication methods on the compressive strength of titanium skin- stringer panels
[NASA-TN-D-5389] c15 N69-34707
GARFINKLE, M.
Superplasticity in tungsten-rhenium alloys.
c17 A69-22990
GARRETT, L. B.
A modified method of integral relations approach to the blunt-body equilibrium air flow field, including comparisons with inverse solutions
[NASA-TN-D-5434] c12 N69-36830
GARRIOTT, O. K.
Enhancement of ionizing radiation during a solar flare.
c29 A69-37558
GARY, H. R.
Hot-salt stress-corrosion of titanium alloys - Generation of hydrogen and its embrittling effect
[NASA-TN-D-5000] c17 N69-16465
GATES, W. J.
X-ray and extreme ultraviolet /1-400 angstrom units/ spectroscopy of the sun, from OSO-III.
c29 A69-22169
GATLIN, J. A.
Satellite attitude control using a torqued, 2-axis-gimbaled boom as the actuator.
[AIAA PAPER 68-857] c21 A69-43245
GAUGLER, R. E.
Expansion of simulated storable propellants in a supersonic nozzle.
[AIAA PAPER 68-635] c33 A69-37188
Experimental measurements of expanding storable-propellant products simulated by combustion of gaseous reactants
[NASA-TN-D-5404] c33 N69-35506
GAULT, D. E.
Principal science results from Surveyor 5.
c30 A69-12224
GAUNTNER, D. J.
Characteristics of composite carbon resistors used for measuring accelerator terminal voltages.
c11 A69-17705
Characteristics of composite carbon resistors used for measuring accelerator terminal voltages
[NASA-TM-X-1718] c24 N69-14398
GAUTHIER, P. R.
Manned test operations related to the Apollo lunar module in the simulated space environment.
c05 A69-30394
GEBBEN, V. D.
A multipurpose ventricular actuating system.
c05 A69-42983
GEDEON, L.
Analysis of cylindrical reactor fuel pin for clad stress caused by fission gases
[NASA-TN-D-5178] c22 N69-24802
GEDNEY, R. T.
Inviscid flow analysis of two parallel slot jets impinging normally on a surface
[NASA-TN-D-4957] c12 N69-14316
GEDWILL, M. A.
An evaluation of three oxidation-resistant alloy claddings for IN 100 and WI 52 superalloys
[NASA-TN-D-5483] c17 N69-38794
GEE, S. W.
Flight investigation of a fluidic autopilot system
[NASA-TN-D-5298] c21 N69-30946
GELLMAN, L.
Memory reduction through higher level language hardware.
[AIAA PAPER 69-963] c08 A69-40344
GELOPULOS, D. P.
Computation of regions of constrained stability for nonlinear control systems
[NASA-CR-1328] c19 N69-28196
GENTRY, G. L., JR.
Aerodynamic characteristics of twin propeller deflected slipstream STOL airplane model with boundary layer control on inverted V-tail
[NASA-TN-D-4856] c02 N69-10935
GERA, J.
Branched trajectory optimization by the projected gradient technique.
[AIAA PAPER 69-917] c30 A69-39346
GERDES, R. D. M.
Use of a six-degrees-of-freedom motion simulator for VTOL hovering tasks
[NASA-TN-D-5383] c11 N69-35359
GERDES, R. M.
An investigation of a direct side-force maneuvering system on a deflected jet VTOL

aircraft
[NASA-TN-D-5175] c02 N69-22572
A detailed study of manual backup control systems for the Saturn 5 launch vehicle
[NASA-TN-D-5261] c21 N69-28018
Flight evaluation of tip-turbine-driven fans for lateral control in a hovering VTOL aircraft
[NASA-TN-D-5491] c02 N69-38807
GERSHBERG, D.
High-performance light-weight electrodes for hydrogen-oxygen fuel cells
[NASA-CR-1216] c03 N69-14397
GERTSMA, L. W.
Design and fabrication of a counterflow double-containment tantalum-stainless steel mercury boiler
[NASA-TN-D-5092] c33 N69-23707
GERUS, T. F.
Experimental lateral bending dynamics of the Atlas-Centaur-Surveyor launch vehicle
[NASA-TM-X-1837] c31 N69-30631
GHAFFARI, A.
Multiple midcourse maneuvers in interplanetary guidance.
c30 A69-28504
GHISTA, D. N.
A dislocation model pertaining to the strength of elastically inhomogeneous materials.
c17 A69-20557
An analytic elastic-viscoelastic model for the shape and the forces in the left ventricle.
c05 A69-26235
Development of Michell minimum weight structures
[NASA-TN-D-4345] c32 N69-25001
GIACAGLIA, G. E. O.
A semi-analytic theory for the motion of a lunar satellite
[NASA-TN-D-5043] c30 N69-28050
GILBERT, J. L.
Analytical and experimental investigation of end-plane rotations of truncated cones under bending loads
[NASA-TN-D-5536] c32 N69-41141
GILLIS, C. L.
Deployable aerodynamic decelerators for space missions.
[AIAA PAPER 68-1081] c31 A69-40542
GILMAN, R. C.
On the composition of circumstellar grains.
c30 A69-24103
GILMER, J. R.
Commercial Utilization of Space, American Astronautical Society, Annual Meeting, 13th, Dallas, Tex., May 1-3, 1967, Proceedings.
c30 A69-34043
GILREATH, M. C.
Radiofrequency transmission characteristics of several ablation materials
[NASA-TN-D-4879] c07 N69-10885
Radiofrequency transmission characteristics of candidate ablation materials for planetary-entry-vehicle heat shields
[NASA-TN-D-4920] c07 N69-13158
GILROY, W. K.
High performance turboalternator and associated hardware. 1 - Design of turboalternator
[NASA-CR-1290] c03 N69-21771
GILRUTH, R. R.
Why space stations?
c31 A69-11395
Manned space missions - Gateway to our future in space.
c30 A69-25644
Manned space stations.
c31 A69-36464
GILVARRY, J. J.
Equations of state at high pressure from the Thomas-Fermi atom model.
c24 A69-40186
GLASER, R. F.
Longitudinal mass-spring modeling of launch vehicles
[NASA-TN-D-5371] c32 N69-34970
GLASS, B. P.
Silicate spherules from Tunguska impact area - Electron microprobe analysis.
c30 A69-28869
Chemical composition of Ivory Coast microtektites.
c30 A69-41351
GLASSMAN, A. J.
Advanced concepts to increase turbine blade loading.
[ASME PAPER 68-WA/GT-11] c28 A69-16136
GLASSTONE, S.
The book of Mars
[NASA-SP-179] c30 N69-16571
GLAWE, G. E.
Multiple-function probe for airflow research.
c11 A69-31917
GLORIA, H. R.
A survey of the photodegradation of organic polymers exposed to ultraviolet radiation.
c18 A69-10861
GLUYAS, R. E.
Calculation of fuel loss from vented nuclear fuel elements for space power reactors
[NASA-TN-D-4913] c22 N69-10734
GNOS, A. V.
A study of the nonsimilar nature of the laminar boundary layer in a region of adverse pressure gradient.
[AIAA PAPER 69-35] c12 A69-18094
GODSHALL, F. A.
Satellite mapping of the Pacific tropical cloudiness.
c20 A69-33001
GOERNER, E. E.
Lox prevalve to prevent Pogo effect on Saturn 5.
c31 A69-15298
GOETZ, R. C.
Hypersonic flutter analysis using measured static aerodynamic derivatives, and comparison with experiment
[NASA-TN-D-5233] c01 N69-26271
GOLAND, A. N.
Stage-I interstitials in electron-irradiated tungsten.
c17 A69-28682
GOLDBERG, F. N.
Use of time-sharing computer to support several large test facilities.
c08 A69-33106
GOLDBERG, R. A.
A review of the theories concerning the equatorial F2 region ionosphere.
c13 A69-37888
GOLDBURG, A.
Clear Air Turbulence and its Detection, Boeing Company, Symposium, Seattle, Wash., August 14-16, 1968, Proceedings.
c20 A69-33732
GOLDEN, T. S.
A note on the effects of the ionosphere on satellite orbital corrections in near-real time.
c07 A69-42549
GOLDMAN, L. J.
Analytical investigation of two-dimensional loss characteristics of supersonic turbine stator blades
[NASA-TM-X-1823] c01 N69-31360
GOLDSTEIN, H. E.
Ablative thermal protection at low heating rates.
c18 A69-35536
GOLDSTEIN, J. I.
The classification of iron meteorites.
c30 A69-36129
The formation of phosphides in iron meteorites.
c30 A69-36132
GOLDSTEIN, M. E.
Effective slip coefficients for coupled conduction-radiation problems.
c33 A69-27784
Two dimensional inviscid jet flow from two nozzles at an angle to a plane surface
[NASA-TN-D-5064] c01 N69-17816
Analysis of two dimensional inviscid model of jet impingement under vertical-takeoff airplane
[NASA-TN-D-5288] c01 N69-29479
Injection of an inviscid separated jet at an oblique angle to a moving stream
[NASA-TN-D-5460] c12 N69-37965
Injection of an attached inviscid jet at an oblique angle to a moving stream
[NASA-TN-D-5501] c12 N69-39916
Analysis of the mixing region for a two-dimensional jet injected at an angle to a moving stream
[NASA-TN-D-5531] c12 N69-41213

GOMERSALL, E. W.
An advanced cryogenic core concept for a flexible and economical delivery system.
[AIAA PAPER 68-812] c31 A69-39753
GOOCH, P. C.
Chromosome analyses of Gemini astronauts.
c04 A69-33173
GOODE, M. W.
Flight test evaluation of a small one-man lunar flying device.
[AIAA PAPER 68-240] c11 A69-12379
Application of human transfer functions to system analysis
[NASA-TN-D-5478] c05 N69-39183
GOODELL, P. D.
Sensitivity of the creep-rupture properties of nickel-base superalloy sheet to sharp edge-notches in the temperature range of 1000 deg F - 1400 deg F
[NASA-CR-1263] c32 N69-16156
GOODERUM, P. B.
Measurement of mean drop sizes for sprays from superheated waterjets.
c12 A69-21995
GOODYKOONTZ, J. H.
Frequency response of a forced flow single tube boiler with inserts and exit restriction
[NASA-TN-D-5023] c12 N69-17779
GOORVITCH, D.
Interferometrically measured thorium lines between 2747 and 4572 angstrom units.
c23 A69-42150
GORDON, C. G.
Correlation of fluctuating forces with the sound radiation from rigid flow spoilers
[NASA-CR-1340] c23 N69-26307
GORDON, S.
Calculation of complex chemical equilibria.
c06 A69-10588
GORLAND, S. H.
Performance of an experimental SNAP 8 power conversion system
[NASA-TM-X-1732] c03 N69-20868
Performance and evaluation of two liquid-metal pumps for sodium-potassium service
[NASA-TM-X-1765] c15 N69-22970
Performance and evaluation of a liquid-metal pump for mercury service
[NASA-TM-X-1766] c15 N69-23768
GORSTEIN, M.
Approach guidance planet tracker.
c21 A69-13214
GOSNELL, R.
Synthesis of fluorinated polyurethanes.
c06 A69-16498
GOSSELIN, C. M.
Study of low pressure application of new orbitron and iron gauge designs
[NASA-CR-1300] c14 N69-28402
GOSTELOW, J. P.
Performance comparisons of high Mach number compressor rotor blading
[NASA-CR-1256] c28 N69-14210
GOTOW, K.
Elastic scattering of 600 MeV protons from He super 3.
c24 A69-13464
Polarization in proton super 4 He scattering at 540 MeV.
c24 A69-14966
GOUGH, D. O.
The anelastic approximation for thermal convection.
c13 A69-33155
GOURASH, F.
Modularization of high-power inverters and converters.
c03 A69-42292
Analysis and design of inductors for protecting power transistors against current surges in inverter bridge circuits
[NASA-TN-D-4995] c10 N69-16198
GOWEN, F. E.
The Ames combined heating facility.
[AIAA PAPER 69-342] c11 A69-28278
GRACEY, W.
Comparison of information display concepts for landing of VTOL aircraft
[NASA-TN-D-4861] c21 N69-10069
GRAFF, C. B.
Power systems for the Apollo Applications Program.
c03 A69-42244
GRAFTON, S. B.
Static and dynamic stability derivatives of a model of a jet transport equipped with external-flow jet-augmented flaps
[NASA-TN-D-5408] c02 N69-36258
GRAHAM, D.
Mass dependence of self-diffusion in iron.
c17 A69-36440
Tracer diffusion studies on metals using a microtome.
c14 A69-36490
GRAHAM, R. R.
Removal of acid gases and oxides of nitrogen from space cabin atmospheres
[NASA-CR-1388] c05 N69-37517
GRAHAM, R. W.
The effect of acceleration on heat transfer in a turbulent boundary layer.
c12 A69-21480
Heat transfer and thermal boundary layer in a conical nozzle.
[AIAA PAPER 69-474] c33 A69-32780
The use of energy thickness in prediction of throat heat transfer in rocket nozzle
[NASA-TN-D-5356] c33 N69-31869
Penetration model explanation for turbulent forced-convection heat transfer observed in near-critical fluids
[NASA-TN-D-5522] c33 N69-40437
GRAMMER, J. R.
Emissivity coatings for low-temperature space radiators
[NASA-CR-1420] c17 N69-36723
GRANA, D. C.
Microbiological studies on a water management subsystem for manned space flight.
[SAE PAPER 680718] c05 A69-13441
GRANT, D. J.
Precision flow measurement techniques for low-thrust auxiliary-propulsion liquid rockets
[NASA-TN-D-4785] c28 N69-16122
GRAULING, C. R.
Laser display systems. I - Scanners.
c14 A69-15028
Laser display systems. II.
c14 A69-21394
GRAVES, E. B.
Effect of hypersonic research engine installation on aerodynamic characteristics of 0.0667-scale model of X-15A-2 airplane at Mach numbers from 1.75 to 4.63
[NASA-TM-X-1840] c01 N69-38612
GRAY, D. L.
Application of quadratic optimization to helicopter flight control.
c02 A69-43279
GRAY, E. Z.
Manned expeditions to Mars and Venus.
c30 A69-12304
GRAY, H. R.
Hot salt stress corrosion of a titanium alloy - Generation of hydrogen and its embrittling effect.
c17 A69-39434
Hot-salt stress-corrosion of a titanium alloy under a simulated turbine-engine compressor environment
[NASA-TN-D-5510] c17 N69-40242
GRAY, V. H.
The rotating heat pipe - A wickless, hollow shaft for transferring high heat fluxes.
[ASME PAPER 69-HT-19] c33 A69-43550
GRAYZEL, A. I.
Design parameters for overdriven varactor frequency doublers using punch-through or bimode varactors.
c09 A69-37299
A fundamental multiplexer theorem.
c09 A69-38530
GREAVES, J. R.
Solar effects on VHF communications between a synchronous satellite relay and earth ground stations
[NASA-TN-D-5100] c07 N69-23317
GREEN, I. M.
Earth's bow shock - Elapsed-time observations by

two closely spaced satellites.
c13 A69-12299
GREEN, R. N.
Investigation of occultation and imagery problems for orbital missions to Venus and Mars
[NASA-TN-D-5104] c30 N69-22571
GREEN, W. D., JR.
The impact of Apollo application on space station engineering.
[AAS PAPER 69-491] c31 A69-42838
GREENE, A. N.
Photographic control system for Project Apollo launches.
[SMPTE PAPER 104-20] c14 A69-14360
GREENE, R. F., JR.
Generalized approach to the thermal analysis of orbiting spacecraft.
[SAE PAPER 690202] c33 A69-18305
GREENLEAF, J. E.
Effects of progressive hypohydration on maximal isometric muscular strength.
c04 A69-15983
Orthostatic intolerance after artificial heat acclimatization in physically fit subjects.
c05 A69-32810
GREENSHIELDS, D. H.
Apollo thermal-protection system development.
[AIAA PAPER 68-1142] c31 A69-13558
GREENSITE, A. L.
Analysis and design of space vehicle flight control systems. Volume 16 - Abort
[NASA-CR-835] c31 N69-27299
GREENSTADT, E. W.
Earth's bow shock - Elapsed-time observations by two closely spaced satellites.
c13 A69-12299
GREENSTEIN, G. S.
Spin down effects in neutron stars.
c30 A69-32803
GREENWOOD, L. R.
In situ vacuum testing - A must for certain elastomeric materials.
c11 A69-22008
Application of the line-source technique for vacuum thermal conductivity measurements.
[AIAA PAPER 69-1013] c11 A69-40386
GREER, D.
An investigation of the basic properties of irradiated polyethylene memory materials
[NASA-CR-1384] c18 N69-36762
GREGORY, G. L.
Experimental evaluation of the rate-of-rise method for measuring outgassing rates of three gases between 10 super minus super 6 and 10 super minus super 3 torr.
c14 A69-32326
Experimental study in vacuum of the rate-of-rise outgassing-measurement technique
[NASA-TN-D-4973] c14 N69-16097
GREIF, R. K.
Use of a six-degrees-of-freedom motion simulator for VTOL hovering tasks
[NASA-TN-D-5383] c11 N69-35359
GREYERBIEHL, J. M.
Experimental determination of eddy-current torques on bodies rotating relative to a uniform magnetic field
[NASA-TN-D-5086] c23 N69-29477
GRIENEISEN, P. H.
Evidence for sinusoidal phase modulation in small self-trapped filaments.
c16 A69-14189
GRIER, N. T.
Back flow from jet plumes in vacuum
[NASA-TN-D-4978] c01 N69-14385
View factors for toroids and their parts
[NASA-TN-D-5006] c33 N69-23471
Tabulations of configuration factors between any two spheres and their parts
[NASA-SP-3050] c30 N69-37777
GRIFFIN, W. S.
Design and performance of flueric shock position sensor for a mixed-compression supersonic inlet
[NASA-TM-X-1733] c14 N69-16382
GRIFFITH, J. G.
Environmental control for radiation testing of lunar rock samples.
c11 A69-38271
GRIFFITH, J. S.
Handbook of Solar Simulation for Thermal Vacuum Testing.
c11 A69-38894
GRIGGS, M.
Study of air pollutant detection by remote sensors
[GDC-DBE-68-011] c13 N69-31961
GRIM, D.
Cost data for economical orbital transportation system design.
[AIAA PAPER 69-439] c34 A69-32654
GRIMES, H. H.
Vacancy relaxations in b.c.c. crystals.
c26 A69-16529
GRIMWOOD, J. M.
Project Gemini technology and operations - A chronology
[NASA-SP-4002] c31 N69-36501
GRINDELAND, R. E.
Identity between the growth hormone degrading activity of the pituitary gland and plasmin.
c04 A69-17105
GRISAFFE, S. J.
Protective coatings for chromium alloys.
c17 A69-26495
Examination of oxide scales on heat resisting alloys
[NASA-TN-D-5019] c17 N69-17277
GRISSETT, F. R.
Attitude control of a manned earth orbiting space station.
[AIAA PAPER 69-846] c31 A69-39376
GROBMAN, J.
Analysis of total-pressure loss and airflow distribution for annular gas turbine combustors
[NASA-TN-D-5385] c33 N69-33314
GRODZOVSKII, G. L.
Mechanics of spaceflight low-thrust
[NASA-TT-F-507] c28 N69-33354
GROENEWEG, J. F.
Measured effects of gaseous flow system dynamics on acoustic-mode combustion instability
[NASA-TN-D-5080] c33 N69-20882
Analysis of the dynamic response of liquid jet atomization to acoustic oscillations
[NASA-TN-D-5339] c28 N69-30980
GROESBECK, D. E.
Test of sodium boiling in a single tube-in- shell heat exchanger over the range 1720 deg to 1980 deg F /1211 to 1355 K/
[NASA-TN-D-5323] c33 N69-30064
GROSCH, C. B.
Method of deriving orbital perturbing parameters from onboard optical measurements of an ejected probe or a natural satellite
[NASA-CR-1412] c30 N69-35513
GROSS, B.
Elastic displacements for various edge-cracked plate specimens.
c32 A69-16433
GROSS, E. E.
A study of 2 GHz electromagnetic wave propagation over optical paths in three geographical regions of the United States
[NASA-CR-1442] c07 N69-39282
GROSS, J. E., III
Preprocessing electronic satellite observations
[NASA-CR-1183] c08 N69-11470
GROSS, S. H.
On the exospheric temperature of Venus.
c30 A69-12109
GROSS, W. H.
Power systems for the Apollo Applications Program.
c03 A69-42244
GROSSMAN, K.
Multiple light scattering in planetary atmospheres.
c30 A69-12105
GROW, J. W.
Experimental flow properties in the wake of a 120 deg cone at Mach number 2.20
[NASA-TN-D-5365] c01 N69-32299
GRUENDEMAN, P.
Evaluation of the Goddard research and engineering management exercise simulation
[NASA-CR-1275] c34 N69-18057
GUALTIEROTTI, T.
A neutral buoyancy micro-electrode for prolonged recording from single nerve units.

c05 A69-11865
GUENTERT, D. C.
A method for reducing the equivalent sink temperature of a vertically oriented radiator on the lunar surface
[NASA-TM-X-1729] c03 N69-17225
GUGELOT, P. C.
Elastic scattering of 600 MeV protons from He super 3.
c24 A69-13464
Polarization in proton super 4 He scattering at 540 MeV.
c24 A69-14966
GULLY, A. J.
Removal of acid gases and oxides of nitrogen from space cabin atmospheres
[NASA-CR-1388] c05 N69-37517
GUNN, K.
Compilation of data from related technologies in the development of an optical pilot warning indicator system
[NASA-TN-D-5174] c14 N69-27267
GUNTER, E. J., JR.
Rigid rotor dynamics
[NASA-CR-1391] c15 N69-36349
GUPTA, S. C.
Domain analysis and measurement techniques for distributed RC structures. I - Analysis in the reciprocal time domain.
c10 A69-21327
Analytic function models of noise and modulation
[NASA-TR-R-314] c07 N69-29230
GUSS, D. E.
Composition of the 2nd September 1966 solar particle event.
c29 A69-17280
Composition of cosmic rays measured in Gemini XI.
c29 A69-38350
GUSSOW, S.
Computer-aided filter design manual
[NASA-SP-3049] c08 N69-35816
GUSTAFSON, F. B.
Notes on rotor aerodynamic research.
c01 A69-41372
GUSTAFSON, T. K.
Self-modulation, self-steepening, and spectral development of light in small-scale trapped filaments.
c23 A69-20745
GUY, L. D.
Structural and decelerator design options for Mars entry.
[AIAA PAPER 68-344] c32 A69-15507
GYORGAK, C. A.
Burst testing of tungsten tubing at temperatures from 3000 deg to 4500 deg F /1650 deg to 2480 deg C/
[NASA-TM-X-1843] c17 N69-31889

H

HAAK, F. A.
Simultaneous HCN and H sub 2 O laser emission in mixtures containing H, C, N, and O.
c16 A69-26330
HABIP, L. M.
A continuum theory for an elastic solid with elastic micro-inclusions
[NASA-CR-1321] c32 N69-21401
HACKER, B. C.
Project Gemini technology and operations - A chronology
[NASA-SP-4002] c31 N69-36501
HADY, W. F.
Lubrication with some polyphenyl ethers and superrefined mineral oils in a 600 deg F /316 deg C/ inerted vane pump loop
[NASA-TN-D-5096] c15 N69-20938
HAEFELI, R. C.
Sonic boom propagation in a stratified atmosphere, with computer program
[NASA-CR-1299] c02 N69-22546
HAGENBUCH, K. M.
Simple model for a rotating neutral planetary exosphere.
c30 A69-40524
HAGERMAN, J. R.
Data correlation from investigations of a high-subsonic speed transport aircraft model in three major transonic wind tunnels.
[AIAA PAPER 69-794] c01 A69-35636
HAGGARD, J. B., JR.
Motion of single bubbles under low gravitational conditions
[NASA-TN-D-5462] c12 N69-38032
HAHN, M.
Experimental investigation of separated flow over a cavity at hypersonic speed.
[AIAA PAPER 68-672] c01 A69-37185
HAHNE, G. E.
Analytic continuation of Appell's hypergeometric series F sub 2 to the vicinity of the singular point x equals 1, y equals 1.
c19 A69-26605
HAINES, R. F.
Detection time to a point source of light appearing on a star field background with and without a glare source present.
c05 A69-17215
Irradiation and manual navigation.
c21 A69-19208
Changes in perceived size of high luminance targets.
c04 A69-36458
HAKURA, Y.
The polar-cap absorption on 7-10 July 1966.
c13 A69-23770
HALBERG, F.
Rat body composition - Sensor implantation and lighting effects.
c04 A69-26557
HALDON, R. A.
Transitions in glasses at low temperatures.
c06 A69-16493
HALE, D. P.
The versatility of electrically propelled spacecraft for planetary missions.
[AIAA PAPER 69-253] c30 A69-21244
HALEY, F. A.
Effect of nuclear radiation at cryogenic temperatures on the tensile properties of titanium and titanium-base alloys
[NASA-TN-D-5442] c17 N69-37436
HALEY, R. L.
Meteorological satellites - Beyond the first nine years.
[AAS PAPER 69-421] c31 A69-42835
HALL, A. M.
The metallurgy, behavior, and application of the 18-percent nickel maraging steels A survey
[NASA-SP-5051] c17 N69-14193
HALL, A. W.
Three-track runway and taxiway profiles measured at international airports A and B
[NASA-TN-D-5444] c02 N69-38770
HALL, C. F.
Development and management of the interplanetary Pioneer spacecraft.
c31 A69-17605
The Pioneer mission to Jupiter.
[AAS PAPER 69-290] c30 A69-42863
HALL, C. J.
New approach to logistics management.
[AAS PAPER 69-204] c34 A69-42812
HALL, G. R.
Recirculation effects produced by a pair of heated jets impinging on a ground plane
[NASA-CR-1307] c01 N69-34703
HALL, J. M.
A precision autocollimating solar sensor.
[AIAA PAPER 69-858] c21 A69-39386
HALL, L. B.
The importance of sterilization techniques in space exploration.
c05 A69-15935
Potential effects of recent findings on spacecraft sterilization requirements.
c04 A69-25460
Spacecraft sterilization by destructive heating.
c05 A69-31472
HALL, R. W.
NASA programs for development of high- temperature alloys for advanced engines.
[ICAS PAPER 68-26] c17 A69-43718
HALLOCK, J. N.
Fourier analysis by the method of selected ordinates
[NASA-TN-D-5083] c19 N69-20940

HALLUM, C. E.
New functional approaches for redundant inert gas thruster systems.
[AIAA PAPER 69-843] c28 A69-39373
HALPERN, G.
Dynamics of a charged particle in a spiral field.
c29 A69-14015
HAMER, H. A.
A concept of midcourse and terminal guidance with single position fixes obtained from onboard optical measurements.
c21 A69-35792
Effect of gravitational-model selection on accuracy of lunar orbit determination from short data arcs
[NASA-TN-D-5105] c30 N69-21018
HAMILL, T. D.
Hyperbolic heat-conduction equation - A solution for the semi-infinite body problem.
[ASME PAPER 69-HT-1] c33 A69-43564
HAMILTON, D. A.
Forces on a flexible shell during water impact
[NASA-TM-X-1781] c32 N69-23697
HAMILTON, H. H.
Heat-transfer and pressure distributions inside the hinge-line gap of a wedge-flap combination at Mach number 10.4
[NASA-TN-D-4911] c01 N69-11009
HAMILTON, R. W., JR.
Biochemical and metabolic effects of a six- month exposure of small animals to a helium- oxygen atmosphere
[NASA-CR-1372] c04 N69-40955
HAMITER, L. C., JR.
How reliable are MOS ICs - As good as bipolars, says NASA.
c09 A69-31851
HAMROCK, B. J.
Incompressibly lubricated Rayleigh step journal bearing. 2 - Infinite-length solution
[NASA-TN-D-4873] c15 N69-10231
HANEMAN, F.
Microwave radiometric capabilities and techniques.
c07 A69-26976
HANKS, B. R.
The use of helium bubbles as a pogo fix in launch vehicle propellant lines.
c31 A69-25498
HANLY, R. D.
Power- and cross-spectra and space-time correlations of surface fluctuating pressures at Mach numbers between 1.6 and 2.5
[NASA-TN-D-5440] c12 N69-36940
HANNA, W. T.
Transient electro-osmosis in capillary tubes.
c06 A69-14862
Performance of an experimental SNAP 8 power conversion system
[NASA-TM-X-1732] c03 N69-20868
HANNUM, N. P.
On the design of acoustic liners for rocket engines - Helmholtz resonators evaluated with a rocket combustor
[NASA-TN-D-5171] c33 N69-23351
HANSELL, J. D.
A new method for treatment of uncertainties in nuclear reactor heat transfer calculations
[NASA-TM-X-1802] c22 N69-26231
HANSEN, C. P.
Apparent activation energy of chemical reactions at high temperature.
c06 A69-34443
HANSEN, J. E.
Comments on the paper by D. G. Rea and E. T. O'Leary, "On the composition of the Venus clouds."
c30 A69-11292
Radiative transfer by doubling very thin layers.
c33 A69-20064
Exact and approximate solutions for multiple scattering by cloudy and hazy planetary atmospheres.
c30 A69-33159
Theoretical spectral scattering of ice clouds in the near infrared.
c13 A69-34283
HANSON, D. C.
Properties of nonaqueous electrolytes
[NASA-CR-1425] c06 N69-36413
HANSON, M. P.
Glass- boron-, and graphite-filament-wound resin composites and liners for cryogenic pressure vessels.
c18 A69-16488
Tensile and cyclic fatigue properties of graphite filament-wound pressure vessels at ambient and cryogenic temperatures.
c18 A69-35521
Tensile and cyclic fatigue properties of graphite filament-wound pressure vessels at ambient and cryogenic temperatures
[NASA-TN-D-5354] c32 N69-31300
HANST, P. L.
Iodine infrared laser.
[IEEE PAPER T-5] c16 A69-19082
A wavelength-selective, repetitively pulsed CO sub 2 laser.
c16 A69-21088
HAPP, W. W.
Domain analysis and measurement techniques for distributed RC structures. I - Analysis in the reciprocal time domain.
c10 A69-21327
Coding schemes for run-length information based on Poisson distribution.
c07 A69-36262
Programmed test patterns for multiterminal devices.
c08 A69-39604
Algorithms for test patterns in multiterminal devices with symmetry constraints.
c08 A69-42524
Examples of coding schemes based on strategic value
[NASA-TN-D-4962] c07 N69-15373
Symbol-oriented failure analysis in multicomponent systems
[NASA-TN-D-5112] c10 N69-22919
Computer program for dimensional analysis
[NASA-TN-D-5165] c08 N69-22935
HAQ, K. E.
Reactive deposition of cubic silicon carbide.
c26 A69-21350
Chemical processes in SiC formation by reactive deposition and chemical conversion.
c26 A69-21351
Adhesion mechanism of gold-underlayer film combinations to oxide substrates.
c26 A69-28007
HARD, T. M.
Sulfur dioxide submillimeter laser.
c16 A69-24005
Simultaneous HCN and H sub 2 O laser emission in mixtures containing H, C, N, and O.
c16 A69-26330
HARDY, A. C.
Apollo 4 and 6 radiation analysis.
[AIAA PAPER 69-17] c05 A69-18202
HARDY, G. H.
Man's role in launch vehicle guidance and control.
[AIAA PAPER 69-876] c31 A69-39402
Simulation studies for planning an in-flight experiment to define manual guidance and control techniques for large launch vehicles
[NASA-TN-D-5150] c21 N69-22936
A detailed study of manual backup control systems for the Saturn 5 launch vehicle
[NASA-TN-D-5261] c21 N69-28018
HARDY, R.
Cost data for economical orbital transportation system design.
[AIAA PAPER 69-439] c34 A69-32654
HARNEY, P. F.
Flight and laboratory testing of a double sideband FM telemetry system.
c07 A69-19132
HAROULES, G.
A laboratory study of microwave radiometric techniques for re-entry plasma measurements
[NASA-TN-D-5274] c25 N69-29600
HAROULES, G. G.
Analysis of a multiplicative feed system for monopulse tracking applications.
c11 A69-37704
The simultaneous investigation of attenuation and emission by the earth's atmosphere at wavelengths from 4 centimeters to 8 millimeters.
c13 A69-39747

A 60-GHz multifrequency radiometric sensor for detecting clear air turbulence in the troposphere.
c09 A69-42536
A review of radiometric measurements of atmospheric attenuation at wavelengths from 75 centimeters to 2 millimeters
[NASA-TN-D-5087] c07 N69-22949
Radiometric techniques applicable to the measurement of solar activity and atmospheric attenuation at millimeter wavelengths
[NASA-TR-R-306] c07 N69-22951

HARPER, C. W.
NASA and flight safety research.
c02 A69-19764

HARPER, R. P., JR.
The use of pilot rating in the evaluation of aircraft handling qualities
[NASA-TN-D-5153] c02 N69-22539

HARPER, T. P.
The selection of spacecraft optical coatings for temperature control.
[AIAA PAPER 69-979] c33 A69-40359

HARRINGTON, D. E.
Jet effects on boattail pressure drag of isolated ejector nozzles at Mach numbers from 0.60 to 1.47
[NASA-TM-X-1785] c01 N69-26976

HARRINGTON, R. F.
An analysis of terrain bias error in planetary radar altimeters
[NASA-TN-D-5220] c21 N69-26195

HARRIS, G.
Conductive EMI - Responsibility and control.
c07 A69-18944

HARRIS, I.
On the semiannual variation of the upper atmosphere.
c13 A69-26012

HARRIS, J. L.
Experiments on visual acuity and the visibility of markings on the ground in long-duration earth-orbital space flight
[NASA-CR-1134] c05 N69-10813

HARRISON, D. R.
Heat-transfer telemetry for models using thermocouple sensors.
[AIAA PAPER 68-407] c14 A69-15514
FM/AM telemetry to measure impact accelerations.
c07 A69-23279

HARRISON, E. F.
Direct entry longitudinal range dispersion of unmanned Mars landers.
c30 A69-12390
Evaluation of entry and terminal deceleration systems for unmanned Martian landers.
[AIAA PAPER 68-1147] c31 A69-13670

HARRISON, J. K.
Non-diffuse infrared emission from the lunar surface.
c30 A69-38973
Effect of the moon's infrared emission on thermal calculations.
c30 A69-43254

HARROLD, E. F.
Rapid optimization of multiple-burn rocket flights, 8 March 1968 - 8 March 1969
[NASA-CR-1430] c30 N69-36439

HART, F. D.
The radiation resistance of cylindrical shells
[NASA-CR-1437] c32 N69-40935

HART, J. D.
Recurrent nature of Lagrange multipliers for optimal low-thrust earth-Jupiter transfers.
c30 A69-41896

HARTENSTEIN, R.
On-board spacecraft processor.
c08 A69-39921
An on-board processor for OAO-C.
c08 A69-41736

HARTLE, R. E.
Ion-exosphere with variable conditions at the baropause.
c13 A69-25284
Simple model for a rotating neutral planetary exosphere.
c30 A69-40524

HARTNETT, J. P.
Advances in Heat Transfer. Volume 5.
c33 A69-24456

HARTON, E. E., JR.
Safety planning for the use of reactive cryogens in large volume.
c27 A69-14468

HARVEY, W. D.
Velocity fluctuation intensities in a hypersonic turbulent boundary layer.
c12 A69-31908
Comparison of prediction methods and studies of relaxation in hypersonic turbulent nozzle-wall boundary layers
[NASA-TN-D-5433] c12 N69-36805
Fluctuating properties of turbulent boundary layers for Mach numbers up to 9
[NASA-TN-D-5496] c12 N69-40137

HATCH, H. G., JR.
Application of differential synthesis to design of multiaxis stability augmentation systems.
[AIAA PAPER 68-834] c31 A69-37156

HATCHER, D. M.
Radiofrequency transmission characteristics of candidate ablation materials for planetary-entry-vehicle heat shields
[NASA-TN-D-4920] c07 N69-13158

HATHAWAY, M. E.
Effects of bottom-structure flexibility on water landing loads of Apollo spacecraft models
[NASA-TN-D-5108] c32 N69-21042
Analytical investigation of an inflatable landing system having omnidirectional and multiple impact capabilities
[NASA-TN-D-5236] c32 N69-26223

HAUGHEY, J. W.
Problems in planning for the introduction of primary electric propulsion.
[AIAA PAPER 69-247] c28 A69-21251

HAUS, H. A.
Self-modulation, self-steepening, and spectral development of light in small-scale trapped filaments.
c23 A69-20745

HAY, G. M.
Correlation study of the simulation of Gemini extravehicular activity with flight results
[NASA-CR-1146] c05 N69-19902
Study of the astronaut's capabilities to maintain life support systems and cabin habitability in weightless conditions
[NASA-CR-1405] c05 N69-36709

HAYAT, G. S.
X-ray imaging with multiple-pinhole cameras using a postericri holographic image synthesis.
c14 A69-40019

HAYDUK, R. J.
Response of an infinite elastic plate to axisymmetric initial velocity distributions with application to hypervelocity impact
[NASA-TN-D-5118] c32 N69-23448
An analytical evaluation of the denting of airplane surfaces by hail
[NASA-TN-D-5363] c32 N69-33420

HAYES, J. D.
Studies of ultraviolet irradiation effects in ZnO-type thermal control coating pigments.
[AIAA PAPER 69-639] c18 A69-33288

HAYES, J. M.
Studies on the formation and transformation of esters. LXXX.
c06 A69-31808
Solvent purification procedures used in organic geochemistry laboratories
[NASA-TM-X-1746] c06 N69-18962

HAYES, R. J.
NASA aviation electronics research.
c34 A69-16718

HAYES, W. D.
Sonic boom propagation in a stratified atmosphere, with computer program
[NASA-CR-1299] c02 N69-22546

HAYMAKER, W.
Effects of acute exposure to high-energy protons on primates.
c04 A69-13498

HEANEY, J. B.
Results from the ATS-3 reflectometer experiment.
[AIAA PAPER 69-644] c33 A69-33270

HEATH, G. L.
A new method for treatment of uncertainties in

nuclear reactor heat transfer calculations
[NASA-TM-X-1802] c22 N69-26231
HEATH, R. W.
Test of improved ignitor for first stage separation rockets for the Atlas-Centaur launch vehicle
[NASA-TM-X-1676] c28 N69-13275
HEBERT, J. O., JR.
A study of 2 GHz electromagnetic wave propagation over optical paths in three geographical regions of the United States
[NASA-CR-1442] c07 N69-39282
HECKELMAN, J. D.
An improved delayed neutron fission product monitor
[NASA-TM-X-1886] c14 N69-38766
HECKER, T. P.
Performance and evaluation of two liquid-metal pumps for sodium-potassium service
[NASA-TM-X-1765] c15 N69-22970
Performance and evaluation of a liquid-metal pump for mercury service
[NASA-TM-X-1766] c15 N69-23768
HEDGEPETH, J. M.
Heliogyro solar sailer Summary report
[NASA-CR-1329] c31 N69-28861
Axisymmetric and cylindrical isostabiloids
[NASA-CR-1444] c32 N69-38781
HEFFERNAN, P. J.
The S-band Telemetry, Tracking, and Command Experiment.
c07 A69-41759
HEIDMANN, M. F.
Empirical characterization of some pressure wave shapes in strong traveling transverse acoustic modes
[NASA-TM-X-1716] c12 N69-15371
Analysis of the dynamic response of liquid jet atomization to acoustic oscillations
[NASA-TN-D-5339] c28 N69-30980
HEIDT, M. F.
Postflight optical evaluation of the right- hand and left-hand windows of Gemini missions 4, 5, 6, and 7
[NASA-TN-D-4916] c31 N69-13232
Preflight optical evaluation of the right-hand hatch windows of Gemini missions 7, 8, 9, and 12
[NASA-TN-D-5471] c31 N69-40813
HEINEMAN, W., JR.
A total perspective weight technique for advanced manned spacecraft.
[SAWE PAPER 793] c31 A69-34864
HEINRICH, M. R.
The effect of time of heating on the thermal polymerization of L-lysine.
c06 A69-28439
Determination of the water-soluble dinitrophenylamino acids by ion-exchange chromatography.
c06 A69-33651
HEINS, J. F.
Modularization of high-power inverters and converters.
c03 A69-42292
HELLER, H. H.
Correlation of fluctuating forces with the sound radiation from rigid flow spoilers
[NASA-CR-1340] c23 N69-26307
HELLER, J. A.
Study of a 300 kWe Rankine cycle advanced nuclear-electric space power system.
c22 A69-42266
HELLIWELL, R. A.
Banded chorus - A new type of VLF radiation observed in the magnetosphere by OGO 1 and OGO 3.
c13 A69-31981
HEMAMI, H.
Techniques for generation of control and guidance signals derived from optical fields
[NASA-CR-1443] c21 N69-38041
HENDERSHOT, K. C.
Applications of a tube wind tunnel in supersonic testing.
[AIAA PAPER 69-335] c11 A69-28271
HENDERSON, A., JR.
Influence of measured free-stream disturbances on hypersonic boundary-layer transition.
[AIAA PAPER 69-704] c12 A69-33453
Electron beam flow visualization in hypersonic helium flow.
c11 A69-35722
HENDERSON, H. R.
Variability in sonic-boom signatures measured along an 8000-foot linear array
[NASA-TN-D-5040] c02 N69-17279
HENDERSON, M.
A dual-beam source of actinic light for photosynthesis research.
c14 A69-36378
One component, magnetic, support and balance system for wind tunnel models
[NASA-CR-1353] c11 N69-25343
HENDRICKS, H. D.
A study to determine the presence of voltage breakdown due to proton irradiation in polymeric materials
[NASA-TM-X-1688] c18 N69-10066
Resolution changes in lithium-drifted silicon semiconductor detectors irradiated with 0.5, 1.0, 2.0, and 3.0 MeV electrons
[NASA-TN-D-4901] c14 N69-10933
HENDRICKS, R. C.
Lighting in cryogenic and noncryogenic fluids
[NASA-TM-X-1654] c14 N69-13176
Film boiling from submerged spheres
[NASA-TN-D-5124] c33 N69-28318
HENIZE, K. G.
A comment on the nebulosity about FG Sagittae.
c30 A69-42887
HENNING, A. B.
Dynamic stability characteristics of large-size 120 deg blunted conical spacecraft in a simulated Martian environment.
[AIAA PAPER 69-104] c31 A69-18210
Damping derivatives of 120 deg conical spacecraft from flights in a low-density environment.
c31 A69-40550
HENRY, A. S.
Improvement of an integral equation method in plane elasticity through modification of source density representation
[NASA-CR-1273] c32 N69-19030
HENRY, R. C.
Flight tests of a direct lift control system during approach and landing
[NASA-TN-D-4854] c02 N69-10371
HENRY, R. E.
Pressure wave propagation in two-phase mixtures.
c33 A69-43511
HENRY, R. M.
Wind velocity profiles measured by the smoke-trail method at the eastern test range, 1963
[NASA-TN-D-4880] c20 N69-14505
HENRY, V. F.
Radio frequency interference experiment design for the Applications Technology Satellite.
c07 A69-13242
Radio frequency interference experiment design for the applications technology satellite
[NASA-TN-D-5041] c07 N69-26272
HEPPNER, J. P.
Propagation of the sudden commencement of July 8, 1966, to the magnetotail.
c13 A69-11226
Electric fields in the vicinity of auroral forms from motions of barium vapor releases.
c13 A69-34935
Magnetospheric convection patterns inferred from high latitude activity.
c13 A69-38503
HERMAN, J. R.
Conjugate echoes in Alouette-2 topside-sounder data.
c07 A69-20045
The influence of varying solar flux on ionospheric temperatures and densities - A theoretical study.
c29 A69-32082
F-region ionization and heating during magnetic storms.
c13 A69-32083
The role of atomic oxygen in the ionospheric E- and F-region behavior.
c13 A69-32314
HERNICZ, R. S.
A comprehensive program for the compilation and analysis of thermal radiative properties data

[NASA-CR-1431] c33 N69-40455
HERR, P. N.
Space storable propellant performance demonstration.
[AIAA PAPER 69-505] c28 A69-32762
HERRING, H. W.
Mechanical behavior of boron-epoxy and glass-epoxy filament-wound cylinders under various loads
[NASA-TN-D-5050] c18 N69-19825
HERRING, J. R.
Statistical theory of thermal convection at large Prandtl number.
c33 A69-24283
HERRMANN, P. F.
Comparison of tungsten and depleted uranium in minimum-weight, layered shields for a space power reactor
[NASA-TM-X-1874] c22 N69-35817
HERSCH, M.
Vortex enhancement of jet penetration in supersonic flow.
[AIAA PAPER 69-664] c12 A69-33437
A study of helium penetration and spreading in a Mach 2 airstream using a delta wing injector
[NASA-TN-D-5322] c01 N69-30878
Effect of angle of attack and injection pressure on jet penetration and spreading from a delta wing in supersonic flow
[NASA-TM-X-1889] c12 N69-37271
HERZOG, J. H.
Proprioceptive cues and their influence on operator performance in manual control
[NASA-CR-1248] c05 N69-14768
HESLIN, T. M.
Apparatus for the precision measurement of internal friction.
c14 A69-13108
HESS, H. L.
Analytical and experimental study of the dynamics of a single-tube counterflow boiler
[NASA-CR-1230] c12 N69-17751
HESS, R. V.
Onset of rotating disturbance in the interelectrode region and exhaust jet of an MPD arc.
[AIAA PAPER 69-232] c28 A69-21225
Onset of rotating disturbance in linear Hall current accelerator.
[AIAA PAPER 69-381] c28 A69-21731
HESS, W. N.
Generation of an artificial aurora.
c13 A69-34365
HETHERINGTON, N. W.
Mechanisms of action of light on circadian rhythms in the monkey.
c04 A69-31336
HETTEL, H. J.
Further experiments on ion-cyclotron-wave generation in the RF self-sustained mode.
c25 A69-13113
Molecular hydrogen inelastic electron impact cross sections - A semiclassical method.
c24 A69-22249
HEYBORNE, R. L.
Ion depletion in the high-latitude exosphere - Simultaneous OGO 2 observations of the light ion trough and the VLF cutoff.
c29 A69-34939
HEYDA, J. F.
Theoretical prediction of crater size for hypervelocity impact by reduced-density particles, 18 May 1966 - 17 August 1967
[NASA-CR-1196] c32 N69-10225
HEYER, R. E.
Carbon dioxide build-up characteristics in spacesuits.
c05 A69-39170
HEYL, P.
Brayton-cycle turbomachinery rolling-element bearings
[NASA-CR-1229] c15 N69-16463
HEYMAN, J. S.
Evaluation of a technique for measuring ion energy loss in vapor-deposited materials
[NASA-TN-D-5430] c24 N69-36929
HEYSON, H. H.
Wind-tunnel wall effects at extreme force coefficients.
c11 A69-15574
The flow throughout a wind tunnel containing a rotor with a sharply deflected wake.
c11 A69-35228
FORTRAN programs for calculating wind-tunnel boundary interference
[NASA-TM-X-1740] c01 N69-17818
Use of superposition in digital computers to obtain wind tunnel interference factors for arbitrary configurations, with particular reference to V/STOL models
[NASA-TR-R-302] c01 N69-19028
HIBBARD, R. R.
Fouling characteristics of ASTM jet A fuel when heated to 700 deg F in a simulated heat exchanger tube
[NASA-TN-D-4958] c28 N69-12831
HICKEL, R. O.
Surface temperature mapping with infrared photographic pyrometry for turbine cooling investigations
[NASA-TN-D-5179] c14 N69-23895
HIERS, R. S., JR.
Analysis of nonequilibrium air streams in the Ames 1-foot shock tunnel
[NASA-TN-D-4985] c11 N69-15633
HIESTER, N. K.
Ablative characterization of seven heat shield materials - A review of the NASA-SRI Round-Robin program.
c18 A69-26813
Comparative evaluation of ablating materials in arc plasma jets
[NASA-CR-1207] c33 N69-14171
HIGGINS, D. M.
Pulse-response curves of conventional low-pass filters
[NASA-TN-D-5494] c07 N69-40099
HIGH, R. W.
The Saturn fireball.
c27 A69-14475
Some liquid oxygen/liquid hydrogen explosive effects in controlled failure-mode tests
[NASA-TN-D-5382] c27 N69-35321
HILBISH, R. T.
Frequency conversion in the sheath capacitance of a glow discharge plasma.
c25 A69-14456
HILL, G. F.
Uniformity of proton beams available at the NASA synchrocyclotron /SREL/.
c11 A69-15992
Annealing of 22, 40, and 158 MeV proton damage in n-type and p-type silicon
[NASA-TN-D-5119] c26 N69-22552
HILL, J. C.
Equations for errors in turbulence measurements with inclined hot wires.
c14 A69-34442
HILL, J. W.
Characteristics of the tactile information channel
[NASA-CR-1389] c05 N69-39211
HILL, R. D.
Saturn V longitudinal oscillation /POGO/ solution.
[AIAA PAPER 69-548] c31 A69-32658
HILLJE, E. R.
Status of the aerodynamic characteristics of the Apollo entry configuration.
[AIAA PAPER 68-1143] c31 A69-13556
Entry aerodynamics at lunar return conditions obtained from the flight of Apollo 4 /AS-501/
[NASA-TN-D-5399] c31 N69-38820
HILLS, F. A.
Computer-generated graphics in aerospace design and analysis.
[ASME PAPER 69-DE-27] c15 A69-28854
HINSON, W. F.
Aerodynamic characteristics in pitch of a 1/7-scale model of a two- and three-stage rocket configuration at Mach numbers of 0.4 to 4.63
[NASA-TN-D-5378] c01 N69-34986
HIRSHBERG, J.
Interplanetary field and geomagnetic variations - A unified view.
c30 A69-32309
HISTAND, M. B.
Dispersion and attenuation of small artificial pressure waves in the canine aorta.
c04 A69-14692

HITT, E. F.
Evaluation of strapdown guidance systems on interplanetary missions.
[AIAA PAPER 68-828] c21 A69-35953
HOBURG, J. F.
MCDIT 21 - A computer code for one-dimensional elastic wave problems
[NASA-CR-1306] c32 N69-22983
HOCHSTEIN, L. I.
Factors affecting the cation requirement of a halophilic NADH dehydrogenase.
c06 A69-23127
HOCKNEY, R. W.
Gravitational experiments with a cylindrical galaxy.
c30 A69-12271
HODARA, H.
Radiation characteristics of a cavity-backed cylindrical gap antenna.
c09 A69-40698
HODGSON, G. W.
Porphyrins in meteorites - Metal complexes in Orgueil, Murray, Cold Bokkeveld, and Mokoia carbonaceous chondrites.
c30 A69-39889
Trace porphyrin complexes - Fluorescence detection by demetallation with methanesulfonic acid.
c06 A69-42557
HOELKER, R. F.
A comparison of a class of earth-moon orbits with a class of rotating Kepler orbits
[NASA-TN-D-4903] c30 N69-10470
HOFFMAN, A. C.
Power conditioning development for the Sert II ion thrustor.
c03 A69-42301
HOFFMAN, E. E.
Cb-1Zr pumped sodium loop
[NASA-CR-1135] c03 N69-11373
HOFFMAN, I. S.
Evaluation of a parachute load distribution measuring system during low altitude drop tests
[NASA-TM-X-1832] c14 N69-32682
HOFFMAN, J. H.
Comparison of results of Explorer XXXI direct measurement probes.
c13 A69-37882
HOFFMAN, L. H.
Approximation to the statistics of midcourse velocity corrections
[NASA-TN-D-5381] c30 N69-36143
HOFFMAN, R. A.
Ring current particle distributions derived from ring current magnetic field measurements.
c29 A69-11227
Low-energy electron precipitation at high latitudes.
c29 A69-28964
HOFFMAN, S.
Forces and moments due to air jets exhausting parallel to large flat plates in a near vacuum
[NASA-TN-D-5147] c12 N69-23085
HOFFMANN, W. F.
Far-infrared observation of the galactic-center region at 100 microns.
c30 A69-22264
A far infrared sky survey.
c30 A69-27599
HOFSTETTER, W. R.
Data correlation from investigations of a high-subsonic speed transport aircraft model in three major transonic wind tunnels.
[AIAA PAPER 69-794] c01 A69-35636
HOGAN, J. S.
Empirical determination of heating efficiencies in the Mars and Venus atmospheres.
c30 A69-26019
Exospheric temperatures on Mars and Venus.
c30 A69-26020
Ocean circulation and climatic changes.
c13 A69-26333
Solar cycle variation of exospheric temperatures on Mars and Venus - A prediction for Mariner 6 and 7.
c30 A69-37136
HOHL, F.
Computer solutions of the gravitational n-body problem.
c30 A69-12272
Minimum energy property of a bounded one-dimensional plasma.
c25 A69-24305
Computer simulation of a cylindrical galaxy
[NASA-TN-D-5200] c30 N69-23708
HOLANDA, R.
Evaluation of a volume-ratio system for vacuum gage calibration from 10 to the minus 8 power to 10 torr
[NASA-TN-D-5406] c14 N69-35265
HOLDAHL, J. H.
Satellite applications to marine geodesy
[NASA-CR-1253] c13 N69-16645
HOLDEN, S. J.
Apparatus for the precision measurement of internal friction.
c14 A69-13108
HOLESKI, D. E.
Effect of rotor tip clearance on the performance of a 5-inch single stage axial flow turbine
[NASA-TM-X-1757] c03 N69-20883
HOLLAND, R. L.
A first-order theory for the rotational motion of a triaxial rigid body orbiting an oblate primary.
c30 A69-32240
HOLLAND, W.
A method for digital computation of spacecraft response in the docking maneuver.
c31 A69-25501
HOLLANDER, J.
Synthesis of fluorinated polyurethanes.
c06 A69-16498
HOLLENDER, H. A.
Food technology problems related to space feeding.
c05 A69-31459
HOLLIS, J. M.
Federal Government contracting - The legal debate regarding NASA service contracts.
c34 A69-15987
HOLLOWAY, P. F.
Effects of cloud cover on selection of recovery sites for future earth orbital missions
[NASA-TN-D-5120] c30 N69-22939
HOLMES, R. A.
Frequency conversion in the sheath capacitance of a glow discharge plasma.
c25 A69-14456
HOLMS, A. G.
Design of experiments as doubly telescoping sequences of blocks with application to a nuclear reactor experiment
[NASA-TN-D-5369] c19 N69-32319
HOLOWACH, J.
Cb-1Zr pumped sodium loop
[NASA-CR-1135] c03 N69-11373
HOLT, S. S.
On the generation of synchroton and X-ray emission from electrons with energy below Mc super 2 in solar flares.
c29 A69-22203
Iron line emission from X-ray sources.
c29 A69-22231
Very high energy solar X-rays observed during the proton event of 7 July 1966.
c29 A69-23753
Two-twenty keV spectrum of X-rays from the Crab Nebula and the diffuse background near galactic anticenter.
c29 A69-30759
Microwave and hard X-ray bursts from solar flares.
c29 A69-37551
Pulsed X-ray emission of NP 0532 in March 1968.
c29 A69-37574
HOLZHAUSER, C. A.
Flight tests under IFR with an STOL transport aircraft
[NASA-TN-D-4939] c02 N69-13252
HOLZMANN, E. G.
Approximating properties of linear models for input-output descriptions
[NASA-CR-1319] c19 N69-26248
HOMICK, J. L.
Auditory temporal masking and the perception of order.
c05 A69-24795
HON, J. F.
Properties of nonaqueous electrolytes
[NASA-CR-1425] c06 N69-36413

HONAKER, W. C.
Uniformity of proton beams available at the NASA synchrocyclotron /SREL/.
c11 A69-15992
HONES, E. W., JR.
Very high energy solar X-rays observed during the proton event of 7 July 1966.
c29 A69-23753
HOOPER, A. T.
Satellite applications to marine geodesy
[NASA-CR-1253] c13 N69-16645
HOOPER, H. O.
Nuclear magnetic resonance study of the niobium-nitrogen system NbN sub x.
c26 A69-36445
HOOPER, J. R.
Analytical and experimental study of the dynamics of a single-tube counterflow boiler
[NASA-CR-1230] c12 N69-17751
HOOVER, R. B.
X-ray imaging with multiple-pinhole cameras using a posteriori holographic image synthesis.
c14 A69-40019
HOPKINS, E. J.
Use of Preston tubes for measuring hypersonic turbulent skin friction.
[AIAA PAPER 69-345] c12 A69-28280
Summary and correlation of skin-friction and heat-transfer data for a hypersonic turbulent boundary layer on simple shapes
[NASA-TN-D-5089] c12 N69-29144
HOPKINS, J. B.
Optimum design of germanium microwave backward diodes.
c09 A69-41224
Fabrication and characteristics of microwave backward diodes in indium arsenide
[NASA-TN-D-5401] c09 N69-36706
HOPPE, C. H.
Experimental verification of surface vehicle dynamics
[NASA-CR-1399] c11 N69-37022
HOPPE, J. C.
Rotational and vibrational temperature measurements in the 12-inch hypersonic ceramic-heated tunnel
[NASA-TN-D-4892] c33 N69-10932
HORIUCHI, H. S.
Preliminary experiment results from the Omega position location equipment /OPLE/.
c21 A69-19135
HORN, H. J.
Iterative guidance applied to generalized missions.
[AIAA PAPER 67-620] c21 A69-15501
HORNBECK, R. W.
Viscous flow in a short cylindrical vortex chamber with a finite swirl ratio
[NASA-TN-D-5132] c12 N69-21400
HOROWITZ, R.
Atmospheric densities measured by the Explorer 17 density gauges - Analysis of errors and their effects upon the measurements
[NASA-TN-D-5447] c13 N69-40924
HORSTMAN, C. C.
Hypersonic viscous interaction on slender cones.
[AIAA PAPER 68-2] c01 A69-12520
Cone drag in rarefied hypersonic flow.
[AIAA PAPER 69-140] c01 A69-18184
HOSHIZAKI, H.
Effect of ablation product absorption and line transitions on shock layer radiative transport
[NASA-CR-1264] c33 N69-19117
HOTT, A. C.
Preparation of UC and UC-W specimens for an irradiation test of the value of a fine-particle dispersion in the control of fission gas swelling /EXP-NRX-9-101 experiment/
[NAA-SR-12629] c22 N69-22946
HOUSE, F. B.
Inference of stratospheric temperature and moisture profiles from observations of the infrared horizon Final report
[NASA-CR-1419] c20 N69-35528
HOWARD, J. C.
An algorithm for deriving the equations of mathematical physics by symbolic manipulation.
c08 A69-14858
HOWARD, W. H.
Effects of acute exposure to high-energy protons on primates.
c04 A69-13498
HOWE, J. T.
Some fluid mechanical problems related to subsonic and supersonic aircraft
[NASA-SP-183] c12 N69-10693
HOWE, R. M.
Computer mechanization of reentry equations with four degrees of freedom
[NASA-CR-1249] c30 N69-13300
Computer mechanization of six-degree of freedom flight equations
[NASA-CR-1344] c21 N69-26232
HOWELL, D. T.
Experimental pressure distributions for a family of blunt bodies at Mach numbers from 2.49 to 4.63 and angles of attack from 0 deg to 15 deg
[NASA-TN-D-5392] c01 N69-35300
Supersonic lifting capabilities of large-angle cones
[NASA-TN-D-5499] c01 N69-40026
HOWELL, H. L.
Hand-printed input for on-line systems
[NASA-CR-1284] c08 N69-21527
HOWELL, H. R.
Inverter-converter parallel operation
[NASA-CR-1224] c03 N69-16379
HOWELL, J. R.
Application of Monte Carlo to heat transfer problems.
c33 A69-24457
Effective slip coefficients for coupled conduction-radiation problems.
c33 A69-27784
Thermal radiation heat transfer. Volume 2 - Radiation exchange between surfaces and in exclosures
[NASA-SP-164-VOL-2] c33 N69-30317
HOWELL, R. R.
Exploratory study of open-face honeycomb to reduce temperature of hypersonic aircraft structure
[NASA-TN-D-5278] c33 N69-29599
HOWELL, W. E.
A study of the performance of low-density phenolic-nylon ablators
[NASA-TN-D-5257] c33 N69-28440
HOWES, W. L.
Phenomenological theory of loudness
[NASA-TN-D-5422] c23 N69-37028
HOWLETT, J. T.
Identification of structural systems by use of near-resonance testing
[NASA-TN-D-5069] c32 N69-17737
HSU, L.-C.
Synthesis of ultrahigh molecular weight poly/ethylene terephthalate/.
c24 A69-16496
The synthesis of a novel polymide precursor
[NASA-TN-D-5184] c06 N69-23353
HSU, Y. Y.
Stability of cylindrical bubbles in a vertical pipe.
[ASME PAPER 69-HT-28] c33 A69-43540
HU, W. W.
Transient solidification outside a cooled pipe with application to a solar Brayton heat receiver
[NASA-TN-D-4897] c33 N69-10227
HUCK, F. O.
An analytical procedure for optimizing television systems for planetary descent missions
[NASA-TN-D-5061] c14 N69-17259
Requirements of a Martian television experiment for three point-mass descent trajectories
[NASA-TN-D-5062] c14 N69-17944
HUCKEL, V.
Variability in sonic-boom signatures measured along an 8000-foot linear array
[NASA-TN-D-5040] c02 N69-17279
HUDELSON, J. C.
Vibration of shaft face seals and stabilizing effect of viscous and friction damping
[NASA-TN-D-5161] c15 N69-23466
HUDICK, M. G.
Apparatus for the precision measurement of internal friction.
c14 A69-13108

HUDSON, C. M.
Effect of stress ratio on fatigue-crack growth in 7075-T6 aluminum-alloy sheet. c17 A69-36435
Effect of stress ratio on fatigue-crack growth in 7075-T6 and 2024-T3 aluminum-alloy specimens [NASA-TN-D-5390] c17 N69-34704
HUDSON, M. L.
Flutter boundary for simply supported unstiffened cylinders. c32 A69-41914
HUDSON, W. R.
Flux flow in materials where kappa approximates 1. c26 A69-33754
Nonlinear flux flow in single crystal niobium [NASA-TN-D-5198] c26 N69-24916
Transistor performance in intense magnetic fields [NASA-TN-D-5428] c09 N69-36710
HUFF, R. G.
Variation of convective heat-transfer coefficient around a simulated rocket cooling tube section [NASA-TN-D-5168] c33 N69-22931
A thermocouple technique for measuring hot-gas-side wall temperatures in rocket engines [NASA-TN-D-5291] c14 N69-29553
Convective heat-transfer coefficients from a solution of the conduction equation for a wall separating two fluids, one having an oscillating temperature [NASA-TN-D-5520] c33 N69-40789
HUFFAKER, R. M.
Application of laser Doppler velocity instrumentation to the measurement of jet turbulence. [SAE PAPER 690266] c14 A69-21555
HUGHES, D. L.
The flight investigation of pressure phenomena in the air intake of an F-111A airplane. [AIAA PAPER 69-488] c28 A69-32706
HUGHES, J. K.
Lunar Orbiter 1, preliminary results - Lunar terrain assessment and selenodesy, micrometeoroid, and radiation measurements [NASA-SP-197] c30 N69-39213
HUGHES, R. F.
Experimental verification of surface vehicle dynamics [NASA-CR-1399] c11 N69-37022
HUGHES, T. F.
Experimental verification of scale factors for parawing opening characteristics with dimensional ratios from 1/1.3 to 1/3 [NASA-TN-D-5071] c02 N69-19950
HUGHES, W. E.
Current controlled negative resistance in n-type gallium arsenide. c26 A69-10557
HUI, P. S.
Implementation of a semi-active gravity gradient controller. c31 A69-18334
HUMBERT, G. F.
A real-time processing system for determination of metabolic rates of a suited astronaut. [AIAA PAPER 69-993] c05 A69-40371
HUMES, D. H.
Calculation of the penetration flux for a multiwall structure on the Lunar Orbiter spacecraft [NASA-TN-D-5455] c32 N69-41229
HUMPHRY, D. E.
Microsecond response system for measuring shock arrival by changes in stream electrical impedance in a shock tube. c14 A69-13104
HUNGER, K.
The atmosphere of the helium-carbon star BD plus 10 deg 2179. c30 A69-40652
HUNT, J. L.
Use of tetrafluoromethane to simulate real-gas effects on the hypersonic aerodynamics of blunt vehicles [NASA-TR-R-312] c01 N69-29270
Measurements of mutual interference heating for a probe antenna mounted on an Apollo reentry configuration [NASA-TM-X-1787] c01 N69-29318
Heat transfer to the windward side of a fineness-ratio-2.9 cylinder with nearly spherical ends at a Mach number of 6 and angles of attack of 50 deg, 70 deg, and 90 deg [NASA-TN-D-5251] c12 N69-29608
HUNT, L. R.
Exploratory study of open-face honeycomb to reduce temperature of hypersonic aircraft structure [NASA-TN-D-5278] c33 N69-29599
HUNTER, R. E.
Cesium contact ion microthruster experiment aboard applications technology satellite /ATS/ IV. [AIAA PAPER 69-297] c28 A69-21218
HURLBURT, R. W.
A 17-1 dual band circularly polarized focused two-channel monopulse tracking system. c07 A69-41752
HURT, C. R.
Fluorescence spectra of homogeneous and mixed europium complexes. c06 A69-10893
HURWITZ, M. G.
Geometric optical image aberrations of single and double mirrors. c23 A69-24836
HUSTAD, P. A.
Force-penetration characteristics of a sand horizontally penetrated by plates, cones, and spherical segments [NASA-CR-1252] c18 N69-14764
HUSTON, R. J.
A wind-tunnel and analytical study of the conversion from wing lift to rotor lift on a composite-lift V/TOL aircraft [NASA-TN-D-5256] c02 N69-28044
Wind-tunnel investigation of steady-state aerodynamics of a composite-lift VTOL aircraft model [NASA-TN-D-5232] c02 N69-28097
HUTTON, R. E.
Lunar surface mechanical properties. c30 A69-12225
HYLAND, R. E.
Cavity reactor critical experiments. c22 A69-18954
HYMOWITZ, E. W.
Galactic Jupiter probes. c30 A69-12303

I

ILES, P.
Impurity effects on annealing of radiation defects in silicon. c26 A69-24006
ILIFF, K. W.
Experience using Balakrishnan's epsilon technique to compute optimum flight profiles. [AIAA PAPER 69-75] c02 A69-18058
A comparison of Newton-Raphson and other methods for determining stability derivatives from flight data. [AIAA PAPER 69-315] c02 A69-22379
Fixed-base simulator pilot rating surveys for predicting lateral-directional handling qualities and pilot rating variability [NASA-TN-D-5358] c02 N69-35762
ILLG, W.
Fatigue of notched Ti-8Al-1Mo-1V titanium alloy at room temperature and 550 deg F /560 deg K/ with flight-by-flight loading representative of a supersonic transport [NASA-TN-D-5294] c32 N69-29607
IMIG, L. A.
Fatigue of notched Ti-8Al-1Mo-1V titanium alloy at room temperature and 550 deg F /560 deg K/ with flight-by-flight loading representative of a supersonic transport [NASA-TN-D-5294] c32 N69-29607
INGELS, F. M.
A study of 2 GHz electromagnetic wave propagation over optical paths in three geographical regions of the United States [NASA-CR-1442] c07 N69-39282
INGRAO, H. C.
Space-borne optical telescopes - An introduction. c14 A69-27946
INNIS, R. C.
Flight tests under IFR with an STOL transport

aircraft
[NASA-TN-D-4939] c02 N69-13252
Flight-determined aerodynamic properties of a jet-augmented, auxiliary-flap, direct-lift-control system including correlation with wind-tunnel results
[NASA-TN-D-5128-REV] c02 N69-31962

INOUYE, M.
Summary and correlation of skin-friction and heat-transfer data for a hypersonic turbulent boundary layer on simple shapes
[NASA-TN-D-5089] c12 N69-29144
Shock shapes and pressure distributions for large angle pointed cones in helium at Mach numbers of 8 and 20
[NASA-TN-D-5343] c01 N69-31228

INTRIERI, P. F.
Ballistic range tests of ablating and nonablating slender cones.
[AIAA PAPER 69-179] c33 A69-18083

INTRILIGATOR, D. S.
Preliminary comparison of solar wind plasma observations in the geomagnetospheric wake at 1000 and 500 earth radii.
c29 A69-26943

IRVINE, T. F., JR.
Advances in Heat Transfer. Volume 5.
c33 A69-24456

IRWIN, K. S.
Summary of XB-70 airplane cockpit environmental data
[NASA-TN-D-5449] c25 N69-38010

ISLEY, W. C.
Optimal control application for electrothermal multijet systems on synchronous earth spacecraft.
[AIAA PAPER 67-723] c28 A69-12375
MEPSIS - Minimal electric propulsion systems for interplanetary spacecraft.
[AIAA PAPER 69-499] c28 A69-32714

ISOZAKI, S.
Characteristics of low-latitude VLF emissions.
c07 A69-13900

IVANOV, V. YE.
High temperature oxidation protection of tungsten
[NASA-TT-F-583] c17 N69-35836

IVANOV, YU. N.
Mechanics of spaceflight low-thrust
[NASA-TT-F-507] c28 N69-33354

J

JACK, J. R.
Experimental measurements of thermal radiation properties by cyclic incident radiation.
c33 A69-10847
Solar absorptance and hemispherical emittance of various metals at space conditions.
[AIAA PAPER 69-60] c17 A69-18154
Performance of N/p silicon and cadmium sulfide solar cells as affected by hypervelocity particle impact
[NASA-TN-D-5133] c03 N69-21016
Spectral and operational characteristics of a high-intensity carbon arc solar simulator
[NASA-TM-X-1825] c11 N69-29737
Solar absorptances and spectral reflectances of 12 metals for temperatures ranging from 300 to 500 K
[NASA-TN-D-5353] c17 N69-31895
Electrical characteristics of a large area thin film CdS solar cell
[NASA-TM-X-1899] c03 N69-38767

JACKSON, C. M., JR.
A method for determining surface pressures on blunt bodies of revolution at small angles of attack in supersonic flow
[NASA-TN-D-4865] c01 N69-10215
A method for determining the total drag of a pointed body of revolution in supersonic flow with turbulent boundary layer
[NASA-TN-D-5046] c01 N69-19925

JACKSON, J. E.
Objectives, history, and principal achievements of the topside sounder and ISIS programs.
c13 A69-37855
The reduction of topside ionograms to electron-density profiles.
c13 A69-37864
Comparisons between topside and ground-based soundings.
c07 A69-37865

JACOBS, D. L.
Simulation of Gemini extravehicular tasks by neutral-buoyancy techniques
[NASA-TN-D-5235] c05 N69-28024

JAFFE, L.
Overview of space applications programs.
[UN PAPER 68-95437] c34 A69-10472
International experimentation with communications satellites.
[UN PAPER 68-95421] c20 A69-10474

JAFFE, L. D.
Principal science results from Surveyor 5.
c30 A69-12224
Lunar surface mechanical properties.
c30 A69-12225

JAHNKE, L.
Cellular localization of acetyl-coenzyme A synthetase in yeast.
c04 A69-15333

JAMES, E. L.
Cesium contact ion microthruster experiment aboard applications technology satellite /ATS/ IV.
[AIAA PAPER 69-297] c28 A69-21218

JANETZKE, D. C.
A computer program for composing compressor blading from simulated circular-arc elements on conical surfaces
[NASA-TN-D-5437] c28 N69-36882

JANNICHE, P. J., JR.
Cosmic ray experiments source-encoding in the IMP-I spacecraft.
c07 A69-41738

JANOS, J. J.
Forces and moments due to air jets exhausting parallel to large flat plates in a near vacuum
[NASA-TN-D-5147] c12 N69-23085

JANOW, C.
Guidance and control components for space applications.
c14 A69-22434

JAQUET, B. M.
Fixed-base visual simulation of pilot controlled descents of an advanced Apollo spacecraft with an all-flexible parawing
[NASA-TN-D-5049] c21 N69-20936

JARRETT, O., JR.
Onset of rotating disturbance in the interelectrode region and exhaust jet of an MPD arc.
[AIAA PAPER 69-232] c28 A69-21225

JARVINEN, W.
A study of Saturn AS-502 coupling longitudinal structural vibration and lateral bending response during boost.
[AIAA PAPER 69-58] c31 A69-18204

JASTROW, R.
Education and training.
[UN PAPER 68-95809] c34 A69-10515

JAYNES, D. N.
Hydrocarbon gas absorption by a He Ne laser beam at a 3.39-mu wavelength.
c16 A69-42192

JEFFRIES, K. S.
Transfer functions for radiator dynamics in the SNAP-8 system
[NASA-TN-D-4946] c22 N69-14503
Performance of an experimental SNAP 8 power conversion system
[NASA-TM-X-1732] c03 N69-20868

JELLISON, J.
Sliding friction of copper alloys in vacuum.
[ASLE PAPER 68-LC-5] c15 A69-30610
Sliding friction of copper alloys in vacuum
[NASA-TN-D-4824] c15 N69-10757

JENKINS, J. L., JR.
Flight investigation of the wing-rotor lift-sharing characteristics of a hingeless rotor compound helicopter.
c02 A69-29702
A parametric study of blade-motion stability boundaries for an articulated rotor
[NASA-TN-D-5032] c01 N69-17289

JENKINS, J. M.
Flight measurements of canard loads, canard buffeting, and elevon and wing tip hinge moments on the XB-70 aircraft including comparisons with

predictions
[NASA-TN-D-5359] c02 N69-32284
JERNELL, L. S.
Aerodynamic characteristics of 0.25-scale model of Tomahawk launch vehicle at Mach numbers from 2.30 to 4.63
[NASA-TM-X-1684] c01 N69-10732
Antenna effects on the aerodynamic characteristics of a 0.410-scale model of the Cajun rocket at Mach numbers from 2.30 to 4.63
[NASA-TM-X-1771] c01 N69-21106
JESSEE, W. P.
Experimental investigation of the effect of aluminum size and loading on the burning rate of solid propellants under acceleration
[NASA-TN-D-5397] c27 N69-36225
JEX, D. W.
Calibration of Pegasus and Explorer 23 detector panels
[NASA-TR-R-321] c14 N69-36985
JEZEWSKI, D. J.
A closed-form solution for minimum-fuel, constant thrust trajectories.
[AIAA PAPER 69-905] c30 A69-39337
JHA, S.
Excited states of xenon-130 populated by beta decay
[NASA-TN-D-5329] c24 N69-30074
JIRBERG, R. J.
Automatic distortionless control of magnetic field modulation.
c09 A69-17708
Variable-voltage, direct-current power supplies for energizing cryogenically cooled and superconductive electromagnets.
c03 A69-26498
Flux flow in materials where kappa approximates 1.
c26 A69-33754
Superconductive dust cores for inductive elements
[NASA-TN-D-5137] c26 N69-21500
Nonlinear flux flow in single crystal niobium
[NASA-TN-D-5198] c26 N69-24916
JOHNS, A. L.
Quiescent-air performance of a truncated turbojet plug nozzle with shroud and plug base flows from a common source
[NASA-TM-X-1807] c26 N69-27840
JOHNSEN, E. G.
Teleoperator control An AEC-NASA technology survey
[NASA-SP-5070] c05 N69-21478
JOHNSON, B. A.
Corrosion of metals in deionized water at 30 deg C /100 deg F/
[NASA-TM-X-1791] c17 N69-25243
JOHNSON, B. G.
Solubility of refractory metals and alloys in potassium and in lithium
[NASA-CR-1371] c17 N69-27059
JOHNSON, C. B.
Comparison of prediction methods and studies of relaxation in hypersonic turbulent nozzle-wall boundary layers
[NASA-TN-D-5433] c12 N69-36805
JOHNSON, C. E.
Development of electric power supplies for electric propulsion.
[AIAA PAPER 69-826] c03 A69-32709
JOHNSON, C. L.
Calibration of Pegasus and Explorer 23 detector panels
[NASA-TR-R-321] c14 N69-36985
JOHNSON, D. F.
A precision autocollimating solar sensor.
[AIAA PAPER 69-858] c21 A69-39386
Effect of porous bleed in a high performance axisymmetric, mixed compression inlet at Mach 2.50
[NASA-TM-X-1692] c01 N69-10294
Performance characteristics from Mach 2.58 to 1.98 of an axisymmetric mixed-compression inlet system with 60-percent internal contraction
[NASA-TM-X-1739] c01 N69-19130
JOHNSON, E. J.
Characterization of ribulose diphosphate carboxylase and phosphoribulokinase from Thiobacillus thioparus and Thiobacillus neapolitanus.
c04 A69-11866
Control of ATP-dependent CO sub 2 fixation in extracts of Hydrogenomonas facilis - NADH regulation of phosphoribulokinase.
c04 A69-30036
JOHNSON, G. W.
Rapid optimization of multiple-burn rocket flights, 8 March 1968 - 8 March 1969
[NASA-CR-1430] c30 N69-36439
JOHNSON, I. L., JR.
Impulsive orbit transfer optimization by an accelerated gradient method.
c30 A69-35956
JOHNSON, K. G.
Effect of gravitational-model selection on accuracy of lunar orbit determination from short data arcs
[NASA-TN-D-5105] c30 N69-21018
JOHNSON, M. K.
Characterization of ribulose diphosphate carboxylase and phosphoribulokinase from Thiobacillus thioparus and Thiobacillus neapolitanus.
c04 A69-11866
Control of ATP-dependent CO sub 2 fixation in extracts of Hydrogenomonas facilis - NADH regulation of phosphoribulokinase.
c04 A69-30036
JOHNSON, P.
Nuclear rocket applications - Mission and launch-vehicle versatility.
[AIAA PAPER 69-555] c31 A69-31849
JOHNSON, R. C.
Venturi meter with separable diffuser.
[ASME PAPER 68-WA/FM-2] c14 A69-16135
Real-gas effects in critical flow through nozzles and thermodynamic properties of nitrogen and helium at pressures to 300 times 10 sup 5. Newtons per square meter /approx. 300 ATM/
[NASA-SP-3046] c12 N69-16098
JOHNSON, R. D.
Extraterrestrial biology - Prospects and problems in the early 1970's.
[AIAA PAPER 68-1122] c04 A69-13700
JOHNSON, R. L.
Preliminary evaluation of greases to 600 F and solid lubricants to 1500 F in ball bearings.
[ASLE PREPRINT 68AM 7C-2] c15 A69-10912
Shaft face seal with self-acting lift augmentation for advanced gas turbine engines.
[ASLE PREPRINT 27] c15 A69-30492
Performance and analysis of seals for inerted lubrication systems of turbine engines
[NASA-TN-D-4761] c15 N69-10055
Friction and wear of nine selected polymers with various fillers in liquid hydrogen
[NASA-TN-D-5073] c15 N69-19800
Shaft face seal with self-acting lift augmentation for advanced gas turbine engines
[NASA-TN-D-5170] c15 N69-23232
Experimental study of pump and seal characteristics of helical groove geometry incorporated in a combined bearing and pump
[NASA-TN-D-5225] c15 N69-24791
Torque and leakage rates of various lubricated lip seal designs at a peripheral velocity of 120 feet per second
[NASA-TN-D-5411] c15 N69-35769
Lubricants for inerted lubrication systems in engines for advanced aircraft
[NASA-TN-D-5420] c15 N69-35788
JOHNSON, R. W.
Water electrolysis - Prospect for the future.
c05 A69-12987
The lunar colony.
c11 A69-27906
JOHNSON, T. S.
Laser beam directed at the lunar retro- reflector array - Observations of the first returns.
c30 A69-43197
JOHNSTON, J. R.
Effect of temperature and pressure on cavitation damage to a cobalt base alloy in sodium.
c17 A69-35184
Effect of temperature and pressure on cavitation damage to a cobalt base alloy in sodium
[NASA-TN-D-5273] c17 N69-28863
Oxidation and thermal fatigue cracking of nickel- and cobalt-base alloys in a high velocity gas stream

[NASA-TN-D-5376] c17 N69-33307
Hot-salt stress-corrosion of a titanium alloy under a simulated turbine-engine compressor environment
[NASA-TN-D-5510] c17 N69-40242
JONES, B. P.
Predicting lunar temperatures.
c30 A69-34374
JONES, D. G.
Large scale wind tunnel investigation to improve the low speed longitudinal stability at high lift of a supersonic transport with variable-sweep wings
[NASA-TN-D-5005] c02 N69-16384
JONES, F. C.
Relativity, heat and ''fictitious'' forces.
c23 A69-11288
JONES, G. W., JR.
Aerodynamic forces on a stationary and oscillating circular cylinder at high Reynolds numbers
[NASA-TR-R-300] c01 N69-17304
JONES, J. C.
The effect of oxygen-supply impurities on the performance of a hydrogen-oxygen fuel cell.
c03 A69-15310
JONES, J. E.
The admittance of a parallel-plate waveguide aperture illuminating a metal sheet.
c09 A69-12328
The influence of air-gap tolerances on the admittance of a dielectric-coated slot antenna.
c09 A69-24986
Reflection coefficient of a TEM mode symmetric parallel-plate waveguide illuminating a dielectric layer.
c09 A69-34802
The admittance of a parallel-plate aperture illuminating a displaced dielectric-dielectric boundary
[NASA-TN-D-5038] c07 N69-19114
JONES, J. L.
Problems of flow simulation in wind tunnels.
[AIAA PAPER 69-660] c11 A69-33471
JONES, L. E., III
Space, Technology, and Society, Canaveral Council of Technical Societies, Space Congress, 6th, Cocoa Beach, Fla., March 17-19, 1969, Proceedings. Volume 2.
c34 A69-35055
Space, Technology, and Society, Canaveral Council of Technical Societies, Space Congress, 6th, Cocoa Beach, Fla., March 17-19, 1969, Proceedings. Volume 1.
c34 A69-35070
JONES, M. H.
Clevis design for compact tension specimens used in plane-strain fracture toughness testing
[NASA-TM-X-1796] c32 N69-25301
The influence of crack length and thickness in plane strain fracture toughness tests
[NASA-TM-X-1860] c17 N69-34916
JONES, R. A.
Use of tetrafluoromethane to simulate real-gas effects on the hypersonic aerodynamics of blunt vehicles
[NASA-TR-R-312] c01 N69-29270
Measurements of mutual interference heating for a probe antenna mounted on an Apollo reentry configuration
[NASA-TM-X-1787] c01 N69-29318
JONES, R. E.
Combustion stability of single swirl-can combustor modules using ASTM-A1 liquid fuel
[NASA-TN-D-5436] c28 N69-40080
JONES, R. H.
Lunar surface mechanical properties.
c30 A69-12225
JONES, R. J.
An experimental feasibility study for the preparation of thermo-oxidatively stable Pyrrone laminates
[NASA-CR-1404] c30 N69-31960
JONES, W. L., JR.
Free-stream electron concentration in an arc-heated wind tunnel and correlation of Langmuir probe and microwave interferometer measurements
[NASA-TN-D-5500] c25 N69-39302
JONES, W. R., JR.
Lubrication with some polyphenyl ethers and superrefined mineral oils in a 600 deg F /316 deg C/ inerted vane pump loop
[NASA-TN-D-5096] c15 N69-20938
JORDAN, F. L., JR.
Investigation of a class of bodies that generate far-field sonic boom shock strength and impulse independent of body length and volume
[NASA-TN-D-5148] c01 N69-23927
JORDAN, J. W.
Direction cosine computational error
[NASA-TR-R-304] c21 N69-21402
An accurate strapdown direction cosine algorithm
[NASA-TN-D-5384] c21 N69-36997
JORDAN, S. D.
Why the temperature rise does not occur in radiative equilibrium in stellar chromospheres of dominant H super minus opacity.
c30 A69-38173
JORDAN, T. M.
Use of ''FASTER'' code for significantly reducing ducted reactor shield computation time
[NASA-TM-X-1828] c22 N69-29671
Helical duct geometry routine for the shielding computer program ''FASTER''
[NASA-TM-X-1838] c22 N69-31986
JOSEPH, J. A.
Spacecraft failure rates - Where are we?
c31 A69-34519
JOYNER, U. T.
Steerable landing gear for vehicles with main gear skids.
[AIAA PAPER 69-790] c02 A69-35639
Recent studies on effects of runway grooving on airplane operations.
[AIAA PAPER 69-773] c02 A69-35649
JUDAY, R. D.
Riometer measurements, solar proton intensities and radiation dose rates.
c29 A69-32321
JULIAN, G. M.
Decay of super 136 La and super 134 La.
c24 A69-10100
Excited states of barium 136 and barium 134
[NASA-TN-D-4933] c24 N69-12778
Excited states of xenon-130 populated by beta decay
[NASA-TN-D-5329] c24 N69-30074
JUN, E. T.
Impulsive motion on a flat plate pulsed with uniform heat flux
[NASA-TN-D-5249] c33 N69-26236
JUNKIN, B. G.
Regression analysis procedures for the evaluation of tracking system measurement errors
[NASA-TN-D-4826] c19 N69-14476

K

KAHLBAUM, W. M.
A rendezvous and station-keeping simulator with fly around capability and virtual image viewing
[NASA-TN-D-5123] c11 N69-22629
KAHLE, A. B.
Prediction of geomagnetic secular change confirmed.
c13 A69-37490
KAHN, D.
Wave coupling across a density discontinuity in a magnetized plasma.
c25 A69-20795
Longitudinal wave propagation in viscous fully ionized plasmas.
c25 A69-20796
KAIL, L. T.
Requirements study for a biotechnology laboratory for manned earth orbiting missions. Volume 2 - Summary of individual experiments requirements
[NASA-CR-1409] c05 N69-35540
Requirements study for a biotechnology laboratory for manned earth orbiting missions Volume 1 - Results, recommendations and requirements
[NASA-CR-1408] c05 N69-35541
KAISER, R.
Study of ferromagnetic liquid
[NASA-CR-1407] c06 N69-33493
KALAFUS, R. M.
Microwave radiometric capabilities and techniques.

c07 A69-26976
KALIL, F.
Parametric analysis of microwave and laser systems for communication and tracking - A summary
[NASA-TR-R-309] c07 N69-23642
KALINOWSKI, C. A.
Concept of an interactive system as an experimenter.
[AIAA PAPER 69-953] c08 A69-40335
KANE, J. A.
D-region electron density measurements during the solar eclipse of May 20, 1966.
c13 A69-29116
Results of rocket measurements in the lower auroral ionosphere.
c13 A69-32187
KANNING, G.
The influence of thermal distortion on the performance of gravity-stabilized satellites
[NASA-TN-D-5435] c31 N69-40781
KARIOTIS, A. H.
Nitinol characterization study
[NASA-CR-1433] c17 N69-36367
KARP, S.
Radiation models using discrete radiator ensembles.
c07 A69-10556
Communication efficiencey of quantum systems
[NASA-TR-R-320] c07 N69-39264
KARRE, L. E.
Development and processing of pyronne polymers
[NASA-CR-1310] c18 N69-26448
KASCAK, A. F.
The potential of nuclear power for high-speed ocean-going air-cushion vehicles.
[AIAA PAPER 69-416] c02 A69-30480
Parametric study of large nuclear surface effects machines.
c22 A69-35180
Simple equations for calculating temperature distributions in radiating gray gases
[NASA-TN-D-5226] c33 N69-25312
The potential of nuclear power for high-speed ocean-going air-cushion vehicles
[NASA-TM-X-1871] c22 N69-35723
Parametric study of large nuclear surface effects machines
[NASA-TM-X-1888] c22 N69-36757
KASCAK, T. J.
A comparison of the performance of two rhenium, niobium cylindrical thermionic converters.
c03 A69-13126
The performance of a rhenium, niobium cylindrical thermionic converter.
c03 A69-16359
KASHIWAGI, Y.
The determination of a stability indicative function for linear systems with multiple delays
[NASA-TR-R-301] c31 N69-17801
KASKEY, A. G.
An impact energy-absorbing strut employing tube cutting
[NASA-TN-D-4941] c32 N69-14506
KASSEL, P. C., JR.
Flash X-ray technique for recession measurements in ablating models.
c11 A69-35720
KASTNER, S. O.
Approximate higher ionization potentials for the heavier elements.
c24 A69-29923
KASZUBINSKI, L. J.
Thermionic fuel irradiation experiment description
[NASA-TM-X-1858] c22 N69-33273
KATSANIS, T.
Numerical solution of symmetric positive differential equations.
c19 A69-13370
Programs for computation of velocities and stream-lines on a blade-to-blade surface of a turbomachine.
[ASME PAPER 69-GT-48] c01 A69-22495
Numerical solution of Tricomi equation using theory of symmetric positive differential equations.
c19 A69-42792
FORTRAN program for spline fit curve
[NASA-TM-X-1707] c19 N69-14002
FORTRAN program for calculating velocities and streamlines on a blade-to-blade stream surface of a tandem blade turbomachine
[NASA-TN-D-5044] c01 N69-21811
Revised FORTRAN program for calculating velocities and streamlines on a blade to blade stream surface of a turbomachine
[NASA-TM-X-1764] c01 N69-22553
FORTRAN program for calculating velocities in a magnified region on a blade to blade stream surface of a turbomachine
[NASA-TN-D-5091] c01 N69-22938
FORTRAN program for calculating transonic velocities on a blade-to-blade stream surface of a turbomachine
[NASA-TN-D-5427] c01 N69-37521
KATTERFELD, G. N.
The face of the earth and its origin
[NASA-TT-F-533] c13 N69-29491
KATZ, L.
The versatility of electrically propelled spacecraft for planetary missions.
[AIAA PAPER 69-253] c30 A69-21244
KATZMAN, H.
An application of optical telemetry to shock tube measurements.
c14 A69-29561
KAUFMAN, A.
Analytical study of flow reduction due to oxidation of wire-form porous sheet for transpiration cooled turbine blades
[NASA-TN-D-5001] c17 N69-16383
Steady-state stress relaxation analysis of turbine blade cooling designs
[NASA-TN-D-5282] c28 N69-29321
KAUFMAN, B.
The effects of the Galilean moons on Jupiter flyby trajectories.
[AIAA PAPER 69-932] c30 A69-39361
KAUFMAN, H. R.
Analysis of electron analog simulation of ion containment in magnetic fields
[NASA-TN-D-5217] c25 N69-25394
KAUFMAN, M.
Survey of the region of Lacerta OB1.
c30 A69-25813
Statistics of the region of Lacerta OB1
[NASA-TN-D-5060] c30 N69-26235
KAUFMAN, W. F.
New functional approaches for redundant inert gas thruster systems.
[AIAA PAPER 69-843] c28 A69-39373
KAUFMANN, R. L.
Explorer 12 magnetopause observations - Large-scale nonuniform motion.
c13 A69-34947
KAVANAUGH, W. P.
Study of a global search algorithm for optimal control.
c08 A69-33745
KAWASAKI, N.
Mechanical relaxation of poly-4-methyl-pentene- 1 at cryogenic temperatures.
c18 A69-16492
KAWASHIMA, N.
Analysis of fluctuations in the interplanetary magnetic field obtained by IMP 2.
c30 A69-16264
KAYTON, M.
Avionics Navigation Systems.
c21 A69-34843
KEAFER, L. S., JR.
A flight measurement of optical radiation from shock-heated air by using a Trailblazer 2 vehicle
[NASA-TN-D-4937] c33 N69-14501
KEANE, L. M.
Recent progress in navigation satellites.
c21 A69-19212
KEATING, G. M.
The polar exosphere near solar maximum.
c13 A69-31351
KEATING, J. C.
Night sky background conditions and launch windows for research experiments
[NASA-TM-X-1772] c21 N69-22969
KECKLER, C. R.
Description of a real-time digital full-scale CMG control system simulation for manned spacecraft.

[AIAA PAPER 69-940] c11 A69-40323
KEENER, E. R.
Use of Preston tubes for measuring hypersonic turbulent skin friction.
[AIAA PAPER 69-345] c12 A69-28280
Summary and correlation of skin-friction and heat-transfer data for a hypersonic turbulent boundary layer on simple shapes
[NASA-TN-D-5089] c12 N69-29144
KEIL, K.
Electron microprobe analysis of vanadium in the presence of titanium.
c06 A69-18419
Ilmenite in ordinary chondrites.
c30 A69-42890
KEIL, L. C.
Changes in growth and body composition of mice exposed to chronic centrifugation.
c04 A69-33746
KEIPERT, F. A.
A new approach to telemetry data processing - The data reduction laboratory.
c11 A69-40352
KELLEHER, J. J.
Radio frequency interference experiment design for the Applications Technology Satellite.
c07 A69-13242
Millimeter wavelengths for space communications?
c07 A69-13721
Radio frequency interference experiment design for the applications technology satellite
[NASA-TN-D-5041] c07 N69-26272
KELLER, L. B.
Development and processing of pyronne polymers
[NASA-CR-1310] c18 N69-26448
KELLER, R.
Properties of nonaqueous electrolytes
[NASA-CR-1425] c06 N69-36413
KELLEY, H. J.
Rocket trajectory optimization by a second- order numerical technique.
c30 A69-32154
KELLEY, H. L.
Flying quality factors currently limiting helicopter nap of the earth maneuverability as identified by flight investigation
[NASA-TN-D-4931] c02 N69-14008
KELLEY, M. J.
Nonelectric cathode heating.
c09 A69-24748
KELLEY, P. L.
Self-modulation, self-steepening, and spectral development of light in small-scale trapped filaments.
c23 A69-20745
KELLY, M. G.
Study of pretesting effects on electroexplosive devices
[NASA-CR-1203] c15 N69-10298
KELLY, R. J.
A real-time processing system for determination of metabolic rates of a suited astronaut.
[AIAA PAPER 69-993] c05 A69-40371
KEMMERER, W. W., JR.
Physical, chemical, and biological activities at the Lunar Receiving Laboratory.
c11 A69-38896
A review of spacecraft waste-management systems
[NASA-TM-X-1851] c05 N69-33260
KEMP, J. H., JR.
Preliminary results from an experimental investigation of nozzle wall boundary layer at Mach numbers ranging from 27 to 47.
[AIAA PAPER 69-686] c12 A69-33441
Hypersonic viscous interaction on sharp and blunt inclined plates.
[AIAA PAPER 68-720] c01 A69-41886
KENDALL, J. S.
Initial radio-frequency gas heating experiments to simulate the thermal environment in a nuclear light bulb reactor
[NASA-CR-1311] c22 N69-23450
KENNEDY, D. W.
Laser display systems. I - Scanners.
c14 A69-15028
Laser display systems. II.
c14 A69-21394
KENNOY, J.
A study of Saturn AS-502 coupling longitudinal structural vibration and lateral bending response during boost.
[AIAA PAPER 69-58] c31 A69-18204
KENYON, G. C.
Mission analysis of general aviation in the 1970's.
[AIAA PAPER 69-818] c34 A69-35624
KERNER, H.
Memory reduction through higher level language hardware.
[AIAA PAPER 69-963] c08 A69-40344
KERSLAKE, W. R.
Durability of the SERT II hollow cathode and future applications of hollow cathodes.
[AIAA PAPER 69-304] c28 A69-21224
Bombardment thruster investigations at the Lewis Research Center.
c28 A69-26787
KERWIN, P. T.
A 1-megawatt reactor design for Brayton-cycle space power application. Part 1 - Thermal analysis and core design
[NASA-TN-D-5013] c22 N69-17313
A 1-megawatt reactor design for Brayton-cycle space power application Part 2 - Neutronics design
[NASA-TN-D-5014] c22 N69-17314
KERWIN, W. J.
Multiloop distributed RC active networks for low parameter sensitivity with low amplifier gain.
c10 A69-34679
KESAREV, V. V.
Motive forces in the development of the earth and planets
[NASA-TT-F-532] c13 N69-28983
KESSLER, D. J.
Upper limit on the spatial density of asteroidal debris.
c30 A69-12545
KEUSCH, P.
An investigation of the basic properties of irradiated polyethylene memory materials
[NASA-CR-1384] c18 N69-36762
KEYES, J. W.
Flow phenomena and separation over delta wings with trailing-edge flaps at Mach 6.
[AIAA PAPER 68-97] c01 A69-12522
Calculated and experimental hinge moments on a trailing-edge flap of a 75 deg swept delta wing at Mach 6
[NASA-TN-D-4268] c01 N69-10054
Pressures and heat transfer on a 75 degree swept delta wing with trailing-edge flap at Mach 6 and angles of attack to 90 degrees
[NASA-TN-D-5418] c01 N69-35855
KHARE, S. P.
Energy spectrum of the secondary electrons and the fluorescent efficiency of electrons in the 3914-angstrom units band.
c29 A69-32315
KIDWELL, R.
The selection of spacecraft optical coatings for temperature control.
[AIAA PAPER 69-979] c33 A69-40359
KIEFLING, L. A.
A study of Saturn AS-502 coupling longitudinal structural vibration and lateral bending response during boost.
[AIAA PAPER 69-58] c31 A69-18204
KILLIANY, J. M.
Effects of electric fields on annealing of radiation damage in MOSFET's.
c09 A69-16562
KIM, H. H.
Iodine infrared laser.
[IEEE PAPER T-5] c16 A69-19082
KIM, K. H.
Uniformity of proton beams available at the NASA synchrocyclotron /SREL/.
c11 A69-15992
KINCAID, W. K., JR.
Visual sensing of spacecraft guidance information. Earth orbit rendezvous maneuvers
[NASA-CR-1214] c05 N69-13161
KING, A. W.
The influential aspects of atmospheric disturbances on space vehicle design using statistical approaches for analysis
[NASA-TN-D-4963] c32 N69-15632

KING, C. B.
Dielectric processing for low-cost ablation heat shields.
c15 A69-35538
KING, E. A., JR.
Meteorite fall at Pueblito de Allende, Chihuahua, Mexico - Preliminary information.
c30 A69-20686
KING, E. L.
Multifunction receiver system for integrated tracking, telemetry and ranging data acquisition.
cC7 A69-19101
KING, H. J.
Systems characteristics of liquid mercury cathode thrusters.
[AIAA PAPER 69-237] c28 A69-21246
KING, J. M.
Biochemical and metabolic effects of a six- month exposure of small animals to a helium- oxygen atmosphere
[NASA-CR-1372] c04 N69-40955
KINGSBURY, J.
Plastics in space flight programs.
c18 A69-38533
KIRILLOV, P. L.
Liquid metals
[NASA-TT-F-522] c33 N69-30507
KIRK, D. B.
Ballistic range tests of ablating and nonablating slender cones.
[AIAA PAPER 69-179] c33 A69-18083
A new method for extracting aerodynamic coefficients from free-flight data.
[AIAA PAPER 69-134] c01 A69-18161
KIRK, J. V.
Reingestion characteristics and inlet flow distortion of V/STOL lift-engine fighter configurations.
[AIAA PAPER 68-78] c01 A69-26762
KIRKPATRICK, J. P.
The design and performance of a versatile 25 solar constant simulator.
c11 A69-30383
Thermal tests of an improved louver system for spacecraft thermal control.
[AIAA PAPER 69-627] c33 A69-33269
KLAGSBRUN, M.
NASA contributions to bioinstrumentation systems - A survey
[NASA-SP-5054] c04 N69-14860
KLASSEN, H.
Analog simulation of a closed loop Brayton cycle test facility
[NASA-TM-X-1715] c03 N69-14312
KLASSEN, H. A.
Preliminary investigation of a single-shaft Brayton rotating unit designed for a 2 to 10-kilowatt space power generation system
[NASA-TM-X-1869] c03 N69-39238
KLEIN, E. J.
Exploratory investigation on the measurement of skin friction by means of liquid crystals.
c11 A69-29029
Exploratory investigation on the measurement of skin friction by means of liquid crystals
[NASA-TM-X-1774] c12 N69-26956
KLEIN, H. P.
Some biological problems in the search for extraterrestrial life.
c04 A69-11770
Extraterrestrial biology - Prospects and problems in the early 1970's.
[AIAA PAPER 68-1122] c04 A69-13700
Cellular localization of acetyl-coenzyme A synthetase in yeast.
c04 A69-15333
KLEIN, M.
Hydrogen-oxygen electrolytic regenerative fuel cells
[NASA-CR-1244] c03 N69-18885
KLICKA, M. V.
Food technology problems related to space feeding.
c05 A69-31459
KLIMA, S. J.
Ultrasonic detection and measurement of fatigue cracks in notched specimens.
c14 A69-10113
KLINE, J. F.
Aerodynamic studies of scale model turbines for the M-1 engine.
[AIAA PAPER 69-553] c28 A69-32678
Two-dimensional cascade investigation of a turbine tandem blade design
[NASA-TM-X-1836] c01 N69-30632
KLINE, R. C.
Potential effects of recent findings on spacecraft sterilization requirements.
c04 A69-25460
KLINGENBERGER, J. L.
Inverter-converter parallel operation
[NASA-CR-1224] c03 N69-16379
KLINGLESMITH, D.
The atmosphere of the helium-carbon star BD plus 10 deg 2179.
c30 A69-40652
KLOPP, W. D.
Superplasticity in tungsten-rhenium alloys.
c17 A69-22990
Review of ductilizing of group 6A elements by rhenium and other solutes
[NASA-TN-D-4955] c17 N69-14403
Exploratory study of silicide, aluminide, and boride coatings for nitridation-oxidation protection of chromium alloys
[NASA-TN-D-5157] c17 N69-23084
Mechanical properties of arc-melted tungsten-rhenium-hafnium-carbon alloys
[NASA-TN-D-5348] c17 N69-31977
Recent developments in chromium and chromium alloys
[NASA-TM-X-1867] c17 N69-35764
KLUCHER, T. M.
Effects of simulated space environment on full, half, and quarter-size cadmium sulfide thin-film solar cells
[NASA-TM-X-1884] c03 N69-36758
KNIAZZEH, A.
Theory of gas breakdown in hot cracks with application to thermionic trilayer insulation.
c03 A69-21840
KNIFFEN, D. A.
A gamma ray telescope utilizing large area wire spark chambers.
[IEEE PAPER 3A-5] c14 A69-19192
A search for gamma-rays from the Crab nebula using a digitized spark chamber
[NASA-TR-R-308] c30 N69-24170
KNIGHT, J. R.
Synthesis methods for manual aerospace control systems with applications to SST design
[NASA-CR-1208] c02 N69-13185
KNOLL, R. H.
Experimental studies on shadow shields for thermal protection of cryogenic tanks in space
[NASA-TN-D-4887] c33 N69-10420
Thermal analysis of shadow shields and structural members in a vacuum
[NASA-TN-D-4876] c33 N69-10473
KO, H. Y.
Lunar surface mechanical properties.
c30 A69-12225
KOBIN, I.
Adhesion mechanism of gold-underlayer film combinations to oxide substrates.
c26 A69-28007
KOBRINSKIY, A. YE.
Mechanisms with elastic couplings - Dynamics and stability
[NASA-TT-F-534] c15 N69-35859
KOCHER, W.
A survey of current debugging concepts
[NASA-CR-1397] c08 N69-35613
KOCZELA, L. J.
The design of a highly parallel computer organization.
c34 A69-39133
KOENIG, D. G.
Large-scale tests of an airplane model with a double-delta wing, including longitudinal and lateral characteristics and ground effects
[NASA-TN-D-5102] c02 N69-21020
KOENIG, E. W.
A review of the image dissector meteorological cameras and a view of their future.
c14 A69-35101

KOENIG, J. L.
Cryogenic Properties of Polymers, Proceedings of the NASA-Case Conference on the Properties of Polymers at Cryogenic Temperatures, NASA Lewis Research Center and Case-Western-Reserve University, Cleveland, Ohio, April 25-27, 1967. c18 A69-16485
KOENIG, R. W.
Influence of high-turbine inlet temperature engines in a methane-fueled SST when takeoff jet noise limits are considered
[NASA-TN-D-4965] c28 N69-14386
KOENKE, E. J.
Evaluation of strapdown guidance systems on interplanetary missions.
[AIAA PAPER 68-828] c21 A69-35953
KOFSKEY, M.
Instrumentation used to define performance of small size, low power gas turbines.
[ASME PAPER 69-GT-104] c14 A69-22522
KOFSKEY, M. G.
Cold performance evaluation of 4.97-inch radial-inflow turbine design for single-shaft Brayton cycle space-power system
[NASA-TN-D-5090] c03 N69-20937
KOGELSCHATZ, U.
Doppler-shift measurements of axial and rotational velocities in an MPD arc.
[AIAA PAPER 69-110] c25 A69-18171
KOHL, F. J.
The dissociation energy of gaseous titanium mononitride
[NASA-TN-D-5027] c06 N69-19129
KOHL, W. H.
The compatibility of materials. c17 A69-17872
KOLCHINSKAYA, A. Z.
The Oxygen Regime of the Organism and Its Regulation /Symposium/
[NASA-TT-F-501] c04 N69-31401
KOLKER, M.
Space geodesy altimetry study
[NASA-CR-1298] c14 N69-21117
KONDO, Y.
Investigation of possible abundance anomalies in close binaries of spectral types A0-A2 and F5-F6. c30 A69-15854
Curve-of-growth analysis for the close binary Hr 5317. c30 A69-34297
KONDRATEV, N. YA.
Handbook of astronautics
[NASA-TT-F-500] c31 N69-24760
KONRADI, A.
One-hundred thirty-five-1650 keV solar protons after the flare of July 1966, observed in the magnetotail and magnetosheath. c29 A69-21699
Explorer 12 magnetopause observations - Large-scale nonuniform motion. c13 A69-34947
KOOKER, D. E.
Heat-transfer and pressure analysis of rocket exhaust impingement on flat plates and curved panels. c33 A69-26781
KOPIA, L. P.
Requirements of a Martian television experiment for three point-mass descent trajectories
[NASA-TN-D-5062] c14 N69-17944
KORKAN, K.
Theoretical flow field calculations for Project RAM
[NASA-CR-1308] c07 N69-28223
KORNBLUM, J. J.
Micrometeoroid interaction with the atmosphere. c30 A69-26341
Concentration and collection of meteoric dust in the atmosphere. c30 A69-26342
KOSHAHL, H. G.
Noise in axisymmetric convergent electron beams
[NASA-TN-D-5212] c10 N69-24918
KOTFILIA, R. P.
Design, development, and flight test experience with lifting body stability augmentation systems.
[AIAA PAPER 69-887] c02 A69-39413
KOTIK, M. G.
Critical regimes of supersonic jet aircraft-stall and spin
[NASA-TT-F-526] c02 N69-31917
KOTILA, C. L.
Postflight optical evaluation of the right- hand and left-hand windows of Gemini missions 4, 5, 6, and 7
[NASA-TN-D-4916] c31 N69-13232
Preflight optical evaluation of the right-hand hatch windows of Gemini missions 7, 8, 9, and 12
[NASA-TN-D-5471] c31 N69-40813
KOUTSANDREAS, J. D.
Surveying earth resources with remote sensors. c14 A69-36259
KOVAL, I. K.
Physics of the moon and planets
[NASA-TT-F-502] c30 N69-31989
KOVALENKO, A. D.
The design of conical shells subjected to antisymmetric loadings
[NASA-TT-F-518] c32 N69-30754
KOVICH, G.
Effect of fluid temperature on the cavitation performance of a high hub-tip ratio axial flow pump in water to 250 degrees F /394 K/
[NASA-TN-D-5318] c15 N69-30069
KRABACHER, K. W.
Performance comparisons of high Mach number compressor rotor blading
[NASA-CR-1256] c28 N69-14210
KRAFT, G. A.
Influence of high-turbine inlet temperature engines in a methane-fueled SST when takeoff jet noise limits are considered
[NASA-TN-D-4965] c28 N69-14386
KRAMER, F.
Acceptance testing lunar and planetary vehicles /a concept/
[NASA-TN-D-4924] c11 N69-14507
Pressure effect of a sound wave on a cryogenic fluid
[NASA-TN-D-4024] c23 N69-38180
KRANC, S.
Experimental investigation of magnetoaerodynamic flow around blunt bodies
[NASA-CR-1393] c25 N69-34897
KRASCELLA, N. L.
Theoretical investigation of the composition and line emission characteristics of argon-tungsten and argon-uranium plasmas
[NASA-CR-1313] c25 N69-21124
Experimental investigation of the spectral emission characteristics of argon-tungsten and argon-uranium induction heated plasmas
[NASA-CR-1314] c25 N69-22920
KRASOVSKIY, V. I.
Aurorae and airglow. Results of the research on the international geophysical projects. Collection of articles, no. 13
[NASA-TT-F-530] c13 N69-16539
KRAUSE, F. R.
Determination of thermodynamic properties with optical cross-correlation methods.
[AIAA PAPER 67-149] c14 A69-31868
KRAUSE, L. N.
Venturi meter with separable diffuser.
[ASME PAPER 68-WA/FM-2] c14 A69-16135
Multiple-function probe for airflow research. c11 A69-31917
Flow-direction measurement with fixed-position probes in subsonic flow over a range of Reynolds numbers. c14 A69-33107
Flow-direction measurement with fixed-position probes
[NASA-TM-X-1904] c14 N69-40059
KRAWEC, R.
Further experiments on ion-cyclotron-wave generation in the RF self-sustained mode. c25 A69-13113
Improved method of injecting the audio signal in automatic Langmuir probe second derivative plotters. c14 A69-32855
KREEZER, G. L.
Visual sensing of spacecraft guidance information. Earth orbit rendezvous maneuvers
[NASA-CR-1214] c05 N69-13161

KREINS, E. R.
Satellite mapping of the Pacific tropical cloudiness. c20 A69-33001
An atlas of Tiros 7 monthly maps of emitted radiation in the 8-12 micron atmospheric window over the Indian Ocean area
[NASA-TN-D-5101] c13 N69-23318
KREJSA, E. A.
Frequency response of a forced flow single tube boiler with inserts and exit restriction
[NASA-TN-D-5023] c12 N69-17779
KRIECHBAUM, G. K. L.
A flight investigation of systems developed for reducing pilot workload and improving tracking accuracy during noise-abatement landing approaches
[NASA-CR-1427] c02 N69-38657
KRIER, G. E.
Flight research program. XIV - Landing performance in jet aircraft after the loss of binocular vision. c05 A69-41675
KRISHNA SWAMY, K. S.
Inversion of density in the convective zone. c30 A69-21843
Atmospheres of metal-deficient stars - Main sequence stars. c30 A69-22055
Extinction by interstellar grains, Mie particles and polycyclic aromatic molecules. c30 A69-23679
Thermal emission by grains and the free-free emission from planetary nebulae. c30 A69-27158
Strengths of the fundamental bands of ice and solid hydrogen in composite grains. c23 A69-29587
KROES, R. L.
Studies of ultraviolet irradiation effects in ZnO-type thermal control coating pigments.
[AIAA PAPER 69-639] c18 A69-33288
KRONICK, P. L.
Electrical characteristics of Pyrrole polymers
[NASA-CR-1367] c18 N69-29559
KROSS, D. A.
A study of stiffness matrices for the analysis of flat plates
[NASA-TN-D-4927] c32 N69-14169
KRUCHOWY, R.
Performance of the SNAP-8 lubrication and coolant subsystem
[NASA-TM-X-1731] c03 N69-20828
Preliminary performance characteristics of a gas-bearing turboalternator
[NASA-TM-X-1820] c03 N69-29707
KRUGER, R.
Solar irradiance measurements from a research aircraft. c30 A69-42191
KRYLOV, I. A.
Motion of artificial satellites in the earth's gravitational field
[NASA-TT-F-539] c30 N69-33560
KU, P. M.
Interdisciplinary approach to friction and wear Conference proceedings
[NASA-SP-181] c15 N69-30401
KUBOKAWA, C. C.
Instant modular 3-D mockup for configuring control and display equipment. c05 A69-11953
Space tool state-of-the-art, and considerations for future space tool-equipment design.
[AAS PAPER 69-438] c15 A69-42802
KUCHTA, B. J.
Aerodynamic and flight characteristics of several variable geometry entry spacecraft during subsonic wing deployment and landing.
[AIAA PAPER 69-742] c01 A69-34407
KUHN, G. D.
Calculation of compressible turbulent boundary layers with pressure gradients and heat transfer
[NASA-CR-1303] c12 N69-21653
Theoretical study of vortex shedding from bodies of revolution undergoing coning motion
[NASA-CR-1448] c12 N69-40200
KUHN, P.
Fracture design analysis for airflight vehicles. c32 A69-33563
KUHN, P. M.
Infrared measurements of variations in stratospheric water vapour. c13 A69-38261
KUHN, R. E.
Factors influencing the choice of facilities and techniques for aeronautical development. c11 A69-15572
KUHNER, M. B.
Techniques for generation of control and guidance signals derived from optical fields
[NASA-CR-1443] c21 N69-38041
KUHNS, P. W.
Feasibility studies of direct voice broadcast satellites
[NASA-TM-X-1747] c07 N69-19025
KULIK, R. A.
Effect of free stream turbulence on coaxial mixing
[NASA-CR-1336] c12 N69-24058
Turbulence in the mixing region between ducted coaxial streams
[NASA-CR-1335] c12 N69-30728
KULKE, B.
Small-signal and saturation characteristics of an X-band cyclotron-resonance oscillator. c09 A69-22786
Design considerations for cyclotron resonance oscillators
[NASA-TN-D-5237] c10 N69-28121
Energy distribution of a spiraling electron beam
[NASA-TN-D-5490] c09 N69-41208
KULSHRESHTHA, A. P.
Studies of ultraviolet irradiation effects in ZnO-type thermal control coating pigments.
[AIAA PAPER 69-639] c18 A69-33288
KULSRUD, H. E.
Sonic boom propagation in a stratified atmosphere, with computer program
[NASA-CR-1299] c02 N69-22546
KUNDE, V. G.
Theoretical molecular line absorption of CO in late spectral type atmospheres
[NASA-TN-D-4798] c24 N69-14448
KUNKLE, J. S.
Compressed gas handbook
[NASA-SP-3045] c12 N69-26987
KUNZE, J. F.
Cavity reactor critical experiments. c22 A69-18954
KURIYAMA, I.
Mechanical behavior of poly/ethylene terephthalate/ at cryogenic temperatures. c18 A69-16494
KURKOWSKI, R. L.
A detailed study of manual backup control systems for the Saturn 5 launch vehicle
[NASA-TN-D-5261] c21 N69-28018
KURZIUS, S. C.
Vaporization and decomposition kinetics of candidate re-entry blackout suppressants in low-pressure flames
[NASA-CR-1330] c07 N69-32721
KUSSOY, M. I.
Hypersonic viscous interaction on slender cones.
[AIAA PAPER 68-2] c01 A69-12520
Cone drag in rarefied hypersonic flow.
[AIAA PAPER 69-140] c01 A69-18184
KUTZ, R. L.
Adaptive data compression for video signals. c14 A69-12869
KUZMIN, A. D.
Radiophysics - Radiophysical investigations of Venus, 1965 - 1966
[NASA-TT-F-536] c30 N69-38643
KVENVOLDEN, K. A.
Solvent purification procedures used in organic geochemistry laboratories
[NASA-TM-X-1746] c06 N69-18962
KYLE, H. L.
Electron-impact ionization of H/2s/ and H/2p/. c24 A69-17138
On a peaking approximation in scattering theory. c24 A69-20206
KYLE, R. G.
Description of a real-time digital full-scale CMG control system simulation for manned spacecraft.
[AIAA PAPER 69-940] c11 A69-40323

L

LABUS, T. L.
Natural frequency of liquids in annular cylinders under low gravitational conditions
[NASA-TN-D-5412] c12 N69-35842

LACOVIC, R.
A comparison of experimental and calculated helium requirements for the pressurization of a Centaur liquid hydrogen tank
[NASA-TM-X-1870] c28 N69-35712

LAFLEUR, J. D., JR.
Applications and development of space nuclear electric power systems.
[AAS PAPER 69-305] c28 A69-42865

LAHTI, G. P.
Resonance neutron capture in a thick slab of depleted uranium.
c24 A69-35179
OPEX 2 - A radiation shield optimization code
[NASA-TM-X-1769] c22 N69-20854
Comparison of tungsten and depleted uranium in minimum-weight, layered shields for a space power reactor
[NASA-TM-X-1874] c22 N69-35817
Multigroup calculations of resonance neutron capture in a thick slab of depleted uranium
[NASA-TM-X-1878] c24 N69-36901

LAIDLEY, R. A.
X-ray fluorescence of rock samples as applied to geological problems.
c14 A69-10890

LAKSHMI, D. R.
Response of the 1000-kilometer ionosphere to magnetic storms.
c13 A69-42438

LAMB, G.
A study of astronauts' extravehicular work capabilities in weightless conditions
[NASA-CR-1334] c05 N69-27266

LAMB, J. P.
A model for large eddy contributions in incompressible turbulent boundary layers.
c12 A69-33255

LAMBIOTTE, J. J., JR.
A technique to infer atmospheric temperature from horizon radiance profiles
[NASA-TN-D-5068] c13 N69-19024
A technique to infer atmospheric water-vapor mixing ratio from measured horizon radiance profiles
[NASA-TN-D-5252] c13 N69-27246

LAMNECK, J. H., JR.
Diffusion lengths in silicon obtained by an X-ray method
[NASA-TM-X-1894] c03 N69-37827

LAMOTHE, R.
Some parameters affecting Auger and photoelectron spectroscopy as an analytical technique.
c06 A69-19775

LAMPKIN, B. A.
Sextant sighting measurements from on board the Gemini 12 spacecraft
[NASA-TN-D-4952] c21 N69-14332

LAMPKIN, E. C.
Effects of differing amounts of training and of monochromatic targets on sextant sighting performance
[NASA-TN-D-5190] c05 N69-35024

LANCASHIRE, R. B.
Refractive index - Particle density nonequilibrium cesium plasmas probed by a multifrequency helium-neon laser
[NASA-TN-D-5328] c25 N69-30622

LANCASTER, E. R.
A unified form of Lambert's theorem
[NASA-TN-D-5368] c30 N69-36930

LAND, N. S.
A feasibility study of a technique for sorting particles by shape.
c15 A69-38950
Scaled lunar module jet erosion experiments
[NASA-TN-D-5051] c31 N69-22630

LANDES, H. S.
The thin film iris
[NASA-CR-1364] c26 N69-28096

LANDGREBE, A. J.
Simplified procedures for estimating flapwise bending moments on helicopter rotor blades. Part 2 - Tables
[NASA-CR-1441] c32 N69-40359

LANDMARK, B.
Results of rocket measurements in the lower auroral ionosphere.
c13 A69-32187

LANGE, K. O.
An investigation of the suitability of white rats for sub-orbital studies of behavior in a gravity field
[NASA-CR-1255] c05 N69-14094

LANGEL, R. A.
OGO-2 magnetic field observations during the magnetic storm of March 13-15, 1966.
c13 A69-11125

LANGHANS, R. A.
Transonic aerodynamic characteristics of two hypersonic cruise configurations
[NASA-TM-X-1816] c01 N69-29231
Transonic aerodynamic characteristics of a Saturn 1B Manned Orbiting Research Laboratory launch vehicle
[NASA-TM-X-1848] c31 N69-33380
Aerodynamic characteristics in pitch of a 1/7-scale model of a two- and three-stage rocket configuration at Mach numbers of 0.4 to 4.63
[NASA-TN-D-5378] c01 N69-34986

LANTZ, E.
A nuclear thermionic space power concept using rod control and heat pipes.
c22 A69-14799
A nuclear thermionic space power concept using rod control and heat pipes
[NASA-TN-D-5250] c22 N69-26270

LANTZ, P. A.
A 17-1 dual band circularly polarized focused two-channel monopulse tracking system.
c07 A69-41752

LANYI, J. K.
Studies of the electron transport chain of extremely halophilic bacteria. I - Spectrophotometric identification of the cytochromes of halobacterium cutirubrum.
c04 A69-19481
Effect of salts and organic solvents on the activity of Halobacterium cutirubrum catalase.
c04 A69-35291
Studies of the electron transport chain of extremely halophilic bacteria. II - Salt dependence of reduced diphosphopyridine nucleotide oxidase.
c06 A69-37101
Studies of the electron transport chain of extremely halophilic bacteria. III - Mechanism of the effect of salt on menadione reductase.
c04 A69-41077

LANZO, C. D.
Experimental transmittance and absorption cross sections of carbon particles suspended in a jet.
c33 A69-17804
Coaxial-flow stabilization of an alternating-current plasma arc.
[AIAA PAPER 68-706] c25 A69-28232
Some recent gaseous reactor fluid mechanics experiments.
[AIAA PAPER 69-477] c22 A69-32728
A flow experiment on a curved-porous-wall gas-core reactor geometry.
c22 A69-35181
Summary of recent gaseous reactor fluid mechanics experiments
[NASA-TM-X-1847] c12 N69-31888
A flow experiment on a curved-porous-wall gas-core reactor geometry
[NASA-TM-X-1852] c12 N69-32217

LARK, R. F.
Cryogenic positive expulsion bladders.
c15 A69-16486

LARSON, C. A.
Rotating space station stabilization criteria for artificial gravity
[NASA-TN-D-5426] c05 N69-39210

LARSON, H. K.
Unusual boundary-layer transition results on cones in hypersonic flow.
[AIAA PAPER 68-40] c01 A69-31881

LASAGNA, P. L.
Variation in engine noise for two landing-

approach configurations of a jet transport aircraft
[NASA-TM-X-1896] c02 N69-38104
LASHER, L. E.
Effect of shock precursor heating on radiative flux to blunt bodies
[NASA-CR-1265] c33 N69-17438
LASSITER, W. S.
Striking characteristics and time lags of the magnetron gauge in helium from 1.9 x 10 super -7 torr to 7 x 10 super -10 torr.
c03 A69-10606
In situ vacuum testing - A must for certain elastomeric materials.
c11 A69-22008
Gauge comparison study of the magnetron, buried collector, bent-beam, and nude modulated Bayard-Alpert gauges.
c14 A69-41216
LATHAM, T. S.
Nuclear studies of the nuclear light bulb rocket engine
[NASA-CR-1315] c25 N69-23451
LATHEM, W. C.
Ion accelerator designs for Kaufman thrusters.
[AIAA PAPER 69-261] c28 A69-21261
LAUER, N. V.
The Oxygen Regime of the Organism and Its Regulation /Symposium/
[NASA-TT-F-501] c04 N69-31401
LAURENCE, J. C.
Variable-voltage, direct-current power supplies for energizing cryogenically cooled and superconductive electromagnets.
c03 A69-26498
High-field electromagnets at NASA Lewis Research Center
[NASA-TN-D-4910] c23 N69-10889
LAVAKARE, P. J.
Cosmic Ray Studies in Relation to Recent Developments in Astronomy and Astrophysics, Tata Institute of Fundamental Research, Colloquium, Bombay, India, November 11-16, 1968, Proceedings.
c29 A69-38811
LAVAN, Z.
Flow in a two-dimensional channel with a rectangular cavity
[NASA-CR-1245] c12 N69-14095
LAVINE, J. P.
Models of the trapped radiation environment. Volume 5 - Inner belt protons
[NASA-SP-3024-VOL-5] c24 N69-28911
LAWLOR, E. A.
Design, simulation and flight performance of the Radio Astronomy Explorer-A satellite.
c31 A69-18328
LAWRENCE, J.
Characteristics of a thermionic converter with a fluoride vapor deposited tungsten emitter etched to preferentially expose the 110 crystal planes
[NASA-CR-1381] c03 N69-35689
LAWRENCE, J. D., JR.
Mie total and differential backscattering cross sections at laser wavelengths for Junge aerosol models.
c16 A69-14290
Optical radar studies of the atmosphere.
c07 A69-27001
Tables of Mie scattering functions for particles with refractive index 1.5
[NASA-TN-D-5110] c23 N69-20905
LAWRENCE, T. R.
Application of laser Doppler velocity instrumentation to the measurement of jet turbulence.
[SAE PAPER 690266] c14 A69-21555
LAWS, J. S.
Hydrogen gas pressure vessel problems in the M-1 facilities
[NASA-CR-1305] c17 N69-19831
LAZAR, J.
Review of the NASA program in electric propulsion.
[AIAA PAPER 69-248] c28 A69-21216
LE BEL, P. J.
Analysis of the gamma-ray-backscatter technique for direct measurement of the density of the Martian atmosphere
[NASA-TN-D-5431] c24 N69-36931
LE ROY, M. J., JR.
Evaluation of a fluidic oscillator as a molecular weight sensor for gas mixtures
[NASA-TM-X-1698] c03 N69-13246
LEA, W. A.
The impact of speech communication with computer.
c08 A69-35099
A formalization of measurement scale forms
[NASA-TN-D-5277] c19 N69-29141
LEAK, J.
Instrumentation in the Aerospace Industry. Volume 14 - Instrument Society of America, International Aerospace Instrumentation Symposium, 14th, Boston, Mass., June 3-5, 1968, Proceedings.
c11 A69-23245
LEARN, A. J.
Reactive deposition of cubic silicon carbide.
c26 A69-21350
Chemical processes in SiC formation by reactive deposition and chemical conversion.
c26 A69-21351
LEATHERMAN, A. F.
Induction heating advances - Applications to 5800 deg F
[NASA-SP-5071] c03 N69-23643
LEATHERWOOD, J. D.
Heave response of a plenum air cushion including passive and active control concepts
[NASA-TN-D-5202] c02 N69-23449
LEBAN, M.
Heats of adsorption of carbon dioxide on silver
c06 A69-38277
LEBEL, P. J.
Entry vehicle instrumentation for heat shield ablation measurements.
c14 A69-15428
LEDERER, J.
Ideal safety system for accident prevention.
c34 A69-16836
LEDLEY, B. G.
Propagation of the sudden commencement of July 8, 1966, to the magnetotail.
c13 A69-11226
LEE, G.
Effects of mass addition of various gases on the heat transfer and surface pressures on a blunt cone in hypersonic flow.
[AIAA PAPER 69-716] c01 A69-33463
Ablation effects on the Apollo afterbody heat transfer.
c33 A69-43680
LEE, H. A.
Spin-tunnel investigation of a 1/20-scale model of a straight-wing, twin-boom, counter-insurgency airplane
[NASA-TM-X-1602] c02 N69-34988
Spin-tunnel investigation of a 1/30-scale model of a subsonic attack airplane
[NASA-TM-X-1788] c02 N69-37976
LEE, H. J.
New state of ferromagnetism in degenerate electron gas and magnetic fields in collapsed bodies.
c30 A69-38600
LEE, H. Q.
Technique for calculating optimum takeoff and climb out trajectories for noise abatement
[NASA-TN-D-5182] c02 N69-26194
LEE, J. G. K.
Computation of topside ionograms from N/h/ profiles
[NASA-TN-D-5052] c13 N69-23557
LEE, K. L.
Chebyshev series solution of nonlinear ordinary differential equations - Initial-value problems
[NASA-TM-X-1882] c19 N69-36923
LEE, S. Y.
A study of 2 GHz electromagnetic wave propagation over optical paths in three geographical regions of the United States
[NASA-CR-1442] c07 N69-39282
LEE, T. A.
Infrared photometry of a helium star, HD 30353.
c30 A69-35348
Infrared excess of RY Sgr.
c30 A69-42377
LEE, T. J.
Measurements of the work function and desorption energy of cesium and potassium on /100/

tungsten.
c26 A69-21808
LEIBECKI, H.
Observations on permeation of polytetrafluoroethylene by compounds of rhenium, molybdenum, and tungsten
[NASA-TN-D-4886] c06 N69-10126
LEIBOVICH, S.
Hydrodynamic stability of inviscid rotating coaxial jets
[NASA-CR-1363] c12 N69-24926
LEIGHTON, R. B.
Two-micron sky survey - A preliminary catalog
[NASA-SP-3047-REV] c30 N69-37993
LEITHEM, J. J.
Effect of free stream turbulence on coaxial mixing
[NASA-CR-1336] c12 N69-24058
Turbulence in the mixing region between ducted coaxial streams
[NASA-CR-1335] c12 N69-30728
LEKO, R. W.
Transfer functions for radiator dynamics in the SNAP-8 system
[NASA-TN-D-4946] c22 N69-14503
LENHART, N. D.
Inverter-converter automatic paralleling and protection
[NASA-CR-1225] c10 N69-19003
LENN, P.
Handbook of Solar Simulation for Thermal Vacuum Testing.
c11 A69-38894
LEONARD, H. W.
Longitudinal vibration characteristics of 1/10-scale Apollo/Saturn 5 replica model
[NASA-TN-D-5159] c32 N69-22932
LEONARD, L.
Effect of ultrasonic vibration on precipitation hardening of steels and superalloys
[NASA-TN-D-5131] c32 N69-21814
LEONARD, R. F.
Alpha-gamma angular correlations in super 120 Sn.
c24 A69-13098
Alpha-gamma angular correlations on super 58 Ni.
c24 A69-13100
Elastic scattering of 21-MeV protons from nitrogen-14, oxygen-16, argon-40, nickel-58, and tin-116.
c24 A69-35489
Elastic scattering of 21-MeV protons from nitrogen 14, oxygen 16, argon 40, nickel 58, and tin 116
[NASA-TN-D-4932] c24 N69-12840
Scattering of 42 MeV /6.7-pJ/ alpha particles from even isotopes of cadmium. Supplement 1 - Absolute cross sections
[NASA-TN-D-4948] c24 N69-14482
LEONOV, A. A.
Perception of space and time in outer space
[NASA-TT-F-545] c05 N69-26455
LERCH, F. J.
Gravity model comparison using GEOS 1 long- arc orbital solutions
[NASA-TN-D-5035] c30 N69-27412
GEOS I tracking station positions on the SAO standard earth /C-5/
[NASA-TN-D-5034] c13 N69-28019
Evaluation of the Goddard range and range rate system at Rosman by intercomparison with GEOS 1 long-arc orbital solutions
[NASA-TN-D-5036] c13 N69-28442
LESHER, R. L.
The Government role in technology utilization programs.
[UN PAPER 68-95313] c34 A69-10512
LESNIEWSKI, R. J.
A complementary MOS spacecraft data handling system.
c08 A69-41739
LESSING, H. C.
The use of integral transforms in the estimation of time variable parameters
[NASA-TN-D-5194] c19 N69-23788
LESSOFF, H.
Effects of lithium and oxygen losses on the magnetic and crystallographic properties of spinel lithium ferrite
[NASA-TR-R-305] c06 N69-20775
LESTER, H. C.
A dynamic stability study of a centrifuge-equipped space station.
[AIAA PAPER 68-142] c31 A69-12373
LEUNG, K.-C.
On the relation between the amplitude of light and radial velocity variations of beta Canis Majoris stars.
c30 A69-14126
LEVENSON, M. M.
A simple antenna with good circular polarization.
c09 A69-41590
LEVENTHAL, A.
Spacecraft failure rates - Where are we?
c31 A69-34519
LEVIN, A. D.
Experimental aerodynamics of a rotor entry vehicle.
[AIAA PAPER 68-950] c01 A69-37155
LEVINE, J. S.
The ashen light - An auroral phenomenon on Venus.
c30 A69-32300
LEVY, L. L., JR.
Influence of drag on the mission performance of hypersonic aircraft.
c02 A69-37154
LEWALLEN, J. M.
Coordinate system influence on the regularized trajectory optimization problem.
[AIAA PAPER 69-903] c30 A69-38546
Recurrent nature of Lagrange multipliers for optimal low-thrust earth-Jupiter transfers.
c30 A69-41896
LEWANDOWSKI, K.
Thermodynamic and transport properties of air and the combustion products of natural gas and of ASTM-A-1 fuel with air
[NASA-TN-D-5452] c33 N69-37936
LEWIS, C. E., JR.
Flight research program. XIV - Landing performance in jet aircraft after the loss of binocular vision.
c05 A69-41675
A simple technique for automatic computer editing of biodata
[NASA-TN-D-5275] c08 N69-29592
LEWIS, G. W., JR.
Effects of three outlet-annulus area blockage configurations on the performance of a 20-inch /50.8-CM/ axial-flow compressor rotor
[NASA-TN-D-5506] c28 N69-40078
LEWIS, J. P.
Test of sodium boiling in a single tube-in- shell heat exchanger over the range 1720 deg to 1980 deg F /1211 to 1355 K/
[NASA-TN-D-5323] c33 N69-30064
LEWIS, R. D.
Performance of two models of commercial unbonded strain-gage-type absolute pressure transducer at 260 deg C
[NASA-TN-D-5327] c14 N69-30506
LEWIS, W.
Simplified analytical model for use in design of pump-inlet accumulators for the prevention of liquid-rocket longitudinal oscillation /POGO/
[NASA-TN-D-5394] c28 N69-33319
LEZBERG, E. A.
Expansion of simulated storable propellants in a supersonic nozzle.
[AIAA PAPER 68-635] c33 A69-37188
Experimental measurements of expanding storable-propellant products simulated by combustion of gaseous reactants
[NASA-TN-D-5404] c33 N69-35506
LIBBY, L. M.
Stars that do not twinkle outside the earth's atmosphere.
c30 A69-27172
LICHT, L.
Study, fabrication and testing of a foil-bearing rotor support system
[NASA-CR-1157] c15 N69-14214
LIEBERMAN, A.
Air pollution monitoring instrumentation A survey
[NASA-SP-5072] c14 N69-24751
LIEBERT, C. H.
Solar cell performance at Jupiter temperature and solar intensity.
c03 A69-13076
LIEBLEIN, S.
Theoretical analysis of flow in VTOL lift fan

inlets without crossflow
[NASA-TN-D-5065] c01 N69-17831
Crater characteristics of 11 metal alloys under hyper-velocity impact including effects of projectile density and target temperature
[NASA-TN-D-5135] c32 N69-22994
LIEBOWITZ, H.
Fracture- An Advanced Treatise. Volume 4 - Engineering Fracture Design.
c17 A69-33564
Structures Technology for Large Radio and Radar Telescope Systems, Proceedings of the International Symposium, Massachusetts Institute of Technology, Cambridge, Mass., October 18-20, 1967.
c11 A69-42120
LIEPINS, A. A.
Asymmetric nonlinear dynamic response and buckling of shallow spherical shells
[NASA-CR-1376] c32 N69-29558
LIETZKE, A. F.
Analysis of cylindrical reactor fuel pin for clad stress caused by fission gases
[NASA-TN-D-5178] c22 N69-24802
LIFSITZ, J. R.
Anti-Stokes generation in trapped filaments of light.
c23 A69-10012
Evidence for sinusoidal phase modulation in small self-trapped filaments.
c16 A69-14189
Self-modulation, self-steepening, and spectral development of light in small-scale trapped filaments.
c23 A69-20745
LIGUM, T. I.
Aerodynamics and flight dynamics of turbojet aircraft
[NASA-TT-F-542] c01 N69-38670
LILLYWHITE, M.
Handbook of Solar Simulation for Thermal Vacuum Testing.
c11 A69-38894
LINA, L. J.
Influence of angle of glide slope on the accuracy of performing instrument approaches in a simulator
[NASA-TN-D-4835] c21 N69-10056
LIND, D. A.
Elastic scattering of 21-MeV protons from nitrogen-14, oxygen-16, argon-40, nickel-58, and tin-116.
c24 A69-35489
Elastic scattering of 21-MeV protons from nitrogen 14, oxygen 16, argon 40, nickel 58, and tin 116
[NASA-TN-D-4932] c24 N69-12840
LINDBERG, R. A.
High-temperature capacitors from pyrolytic boron nitride.
c03 A69-15299
LINDLEY, B. K.
Transient pumping performance of a two speed, hydraulic turbine driven inducer system.
[AIAA PAPER 69-551] c15 A69-34415
LINDSEY, J. F., III
Lunar surface transmission loss for the Apollo astronaut
[NASA-TN-D-4915] c07 N69-13301
Performance characteristics of the Apollo astronaut backpack antenna
[NASA-TN-D-5081] c07 N69-23882
LINGENFELTER, R. E.
Cosmic-ray deuterium and helium-3 of secondary origin and the residual modulation of cosmic rays.
c29 A69-20066
LINK, F. J.
A complementary MOS spacecraft data handling system.
c08 A69-41739
LINK, J. M.
Differential thresholds for motions in the periphery
[NASA-CR-1439] c05 N69-36925
LINTON, R. C.
A radiometer for measuring solar flux variations.
[AAS PAPER 69-254] c14 A69-42858
LINTOTT, J. A.
Postflight optical evaluation of the right- hand and left-hand windows of Gemini missions 4, 5, 6, and 7
[NASA-TN-D-4916] c31 N69-13232
Preflight optical evaluation of the right-hand hatch windows of Gemini missions 7, 8, 9, and 12
[NASA-TN-D-5471] c31 N69-40813
LIPANA, J. G.
Effects of various respiratory maneuvers on the physiological response to angular acceleration.
c05 A69-41679
LIPPE, P.
The centrifuge as a therapeutic device.
c04 A69-43372
LIPSKIY, YU. N.
Atlas of the reverse side of the moon, part 2
[NASA-TT-F-514] c30 N69-24206
LITANT, I.
Leak detection in hermetically sealed devices
[NASA-TN-D-5457] c09 N69-38597
A method for separating a semiconductor wafer into individual chips
[NASA-TM-X-1892] c09 N69-38774
LITCHFIELD, J. H.
Systems approach to evaluating Hydrogenomonas cultures
[NASA-CR-1296] c05 N69-22766
LITCHFORD, G. B.
Study of advanced electronic applications to aeronautical display and control problems
[NASA-CR-1240] c02 N69-14729
LITTLE, J. C.
Environmental control for radiation testing of lunar rock samples.
c11 A69-38271
LIVENTSEV, N. M.
Electromedical apparatus - Principles of operation, installation, and use
[NASA-TT-F-523] c05 N69-27577
LOATS, H. L., JR.
Correlation study of the simulation of Gemini extravehicular activity with flight results
[NASA-CR-1146] c05 N69-19902
Study of the astronaut's capabilities to maintain life support systems and cabin habitability in weightless conditions
[NASA-CR-1405] c05 N69-36709
LOCK, W. P.
Flight investigation of a fluidic autopilot system
[NASA-TN-D-5298] c21 N69-30946
LOCKMAN, W. K.
Heat-transfer telemetry for models using thermocouple sensors.
[AIAA PAPER 68-407] c14 A69-15514
LOCKWOOD, L. W.
Apollo mission simulation with visual presentation.
[SMPTE PAPER 105-74] c11 A69-25768
LOEWY, R. G.
A theory for predicting the rotational and vortex noise of lifting rotors in hover and forward flight
[NASA-CR-1333] c23 N69-25344
LOH, W. H. T.
Re-entry and Planetary Entry Physics and Technology. II - Advanced Concepts, Experiments, Guidance-Control and Technology.
c31 A69-25718
LOJKO, M. S.
Infrared measurements of variations in stratospheric water vapour.
c13 A69-38261
LOKERSON, D. C.
A spacecraft analog-to-digital conversion system employing MOSFETS
[NASA-TN-D-5228] c08 N69-29478
LOMAX, H.
On some numerical difficulties in integrating the equations for one-dimensional nonequilibrium nozzle flow
[NASA-TN-D-5176] c19 N69-23355
LONG, L.
A family of portable versatile aerosol particle analyzers.
c14 A69-34691
LOOMIS, W. R.
Performance and analysis of seals for inerted lubrication systems of turbine engines
[NASA-TN-D-4761] c15 N69-10055

Lubricants for inerted lubrication systems in engines for advanced aircraft
[NASA-TN-D-5420] c15 N69-35788
LOPER, L. R.
The relationship between optical distortion and binocular depth perception
[NASA-TN-D-5162] c05 N69-22990
LOPEZ, M. D.
Radiation plan for the Apollo lunar mission.
[AIAA PAPER 69-19] c29 A69-18113
LORENZO, C. F.
Digital simulation stability criterion.
c10 A69-32899
LOTTIG, R. A.
Performance and evaluation of two liquid-metal pumps for sodium-potassium service
[NASA-TM-X-1765] c15 N69-22970
Performance and evaluation of a liquid-metal pump for mercury service
[NASA-TM-X-1766] c15 N69-23768
LOUAPRE, M. E.
Microwave radiometric capabilities and techniques.
c07 A69-26976
LOVE, E. S.
Some topics in hypersonic body shaping.
[AIAA PAPER 69-181] c01 A69-18052
Toward efficient shuttle service to earth orbit.
c31 A69-39695
LOVE, W. L.
An experiment on the MHD-driven flow for a gas core nuclear rocket.
[AIAA PAPER 69-727] c22 A69-33483
LOVINGOOD, J. A.
A special class of dynamical polysystems.
c19 A69-40573
LOW, F. J.
A far infrared sky survey.
c30 A69-27599
LOWDERMILK, W. H.
Corrosion in a cobalt alloy, two-phase mercury loop
[NASA-TN-D-5326] c17 N69-31065
LOWELL, C. E.
Examination of oxide scales on heat resisting alloys
[NASA-TN-D-5019] c17 N69-17277
LOWES, F. B.
Autonomous navigation in long-duration, highly eccentric orbits about Mars.
[AIAA PAPER 69-880] c21 A69-39406
LOWMAN, P. D., JR.
Composition of the lunar highlands - Possible implications for evolution of the earth's crust.
c30 A69-17006
The moon's resources.
c30 A69-27907
Geologic orbital photography - Experience from the Gemini program.
c13 A69-35274
LOWSON, M. V.
Theoretical studies of compressor noise
[NASA-CR-1287] c28 N69-21476
LUBOWITZ, H. R.
An experimental feasibility study for the preparation of thermo-oxidatively stable Pyrrone laminates
[NASA-CR-1404] c30 N69-31960
LUCAS, J. W.
Principal science results from Surveyor 5.
c30 A69-12224
LUCY, M. H.
Effects of acceleration upon solid-rocket performance.
[AIAA PAPER 68-530] c28 A69-39217
LUDWIG, C. B.
Study of air pollutant detection by remote sensors
[GDC-DBE-68-011] c13 N69-31961
LUDWIG, F. A.
Electrochemical characterization of nonaqueous systems for secondary battery application
[NASA-CR-1434] c03 N69-36829
LUDWIG, L. P.
Configurations for gas turbine compressor end seals.
[ASLE PREPRINT 68AM 4B-4] c15 A69-27366
Shaft face seal with self-acting lift augmentation for advanced gas turbine engines.
[ASLE FICFS PREPRINT 27] c15 A69-30492
Performance and analysis of seals for inerted lubrication systems of turbine engines
[NASA-TN-D-4761] c15 N69-10055
Shaft face seal with self-acting lift augmentation for advanced gas turbine engines
[NASA-TN-D-5170] c15 N69-23232
Vibration of shaft face seals and stabilizing effect of viscous and friction damping
[NASA-TN-D-5161] c15 N69-23466
Experimental study of pump and seal characteristics of helical groove geometry incorporated in a combined bearing and pump
[NASA-TN-D-5225] c15 N69-24791
Torque and leakage rates of various lubricated lip seal designs at a peripheral velocity of 120 feet per second
[NASA-TN-D-5411] c15 N69-35769
Investigation of isothermal, compressible flow across a rotating sealing dam. 1 - Analysis
[NASA-TN-D-5344] c15 N69-35799
LUEDERS, H. G.
Experimental investigation of advanced concepts to increase turbine blade loading. 3 - Performance evaluation of tandem rotor blade
[NASA-CR-1254] c01 N69-13621
Experimental investigation of advanced concepts to increase turbine blade loading. 4 - Performance evaluation of plain rotor blade with plow type vortex generators
[NASA-CR-1342] c28 N69-24223
LUIDENS, R. W.
An estimate of the supersonic flow field about an axisymmetric body with an N wave pressure trace
[NASA-TN-D-4935] c01 N69-13238
LUMB, D. R.
Test and preliminary flight results on the sequential decoding of convolutional encoded data from Pioneer IX.
c07 A69-42522
LUNC, M.
International Astronautical Federation, International Astronautical Congress, 18th, Belgrade, Yugoslavia, September 24-30, 1967, Proceedings. Volume 1 - Astrodynamics, Guidance and Control, Miscellanea.
c30 A69-17560
International Astronautical Federation, International Astronautical Congress, 18th, Belgrade, Yugoslavia, September 24-30, 1967, Proceedings. Volume 2 - Spacecraft Systems, Education.
c31 A69-17596
International Astronautical Federation, International Astronautical Congress, 18th, Belgrade, Yugoslavia, September 24-30, 1967, Proceedings. Volume 4 - Life in Spacecraft.
c05 A69-17642
LUND, J. W.
High-performance turboalternator and associated hardware. 2 - Design of gas bearings
[NASA-CR-1291] c15 N69-21772
LUND, W.
ATS-III resistojet thruster system performance.
[AIAA PAPER 68-553] c28 A69-39754
LUNDELL, J. H.
Comparison of the performance of a charring ablator under transient and constant combined convective and radiative heating.
[AIAA PAPER 69-151] c33 A69-18055
Effects of pyrolysis-gas chemical reactions on surface recession of charring ablators.
[AIAA PAPER 68-302] c33 A69-21982
The development of polybenzimidazole composites as ablative heat shields.
c18 A69-41715
LUNDIN, C. E.
The use of thermodynamic properties of metal-gas systems as reduced-pressure standards
[NASA-CR-1271] c14 N69-16099
LUNDRY, J. L.
A numerical solution for the minimum induced drag, and the corresponding loading, of nonplanar wings Final report
[NASA-CR-1218] c01 N69-10343
A numerical solution for the minimum induced drag, and the corresponding loading, of nonplanar wings. 1 - User's manual for computer program 55VD. 2 - Descriptive manual for computer program 55VD

[NASA-CR-1218-SUPPL] c01 N69-12286
LUOMA, W.
Properties of high emittance materials
[NASA-CR-1278] c17 N69-18952
LYLE, G. C.
Line by line calculation of spectra from diatomic molecules and atoms assuming a Voigt line profile.
c24 A69-35239
A computer program for a line by line calculation of spectra from diatomic molecules and atoms assuming a Voigt line profile
[NASA-TN-D-5088] c24 N69-21462
LYNCH, J. H.
Gamma heating in thin heavy-element absorbers.
c22 A69-18825
Measured thermal-neutron-flux perturbations in cylinders in a test reactor.
c22 A69-38274
Predictive equations for thermal neutron flux perturbation effects in cylinders
[NASA-TN-D-4949] c22 N69-14481
A systematic approach to model development by comparison of experimental and analytical regression coefficients
[NASA-TM-X-1797] c19 N69-25311
LYNES, L. L.
Calculation of compressible turbulent boundary layers with pressure gradients and heat transfer
[NASA-CR-1303] c12 N69-21653

M

MAAG, W. L.
Statistical analysis of high-temperature creep-rate data for alloys of tantalum, molybdenum, and columbium
[NASA-TN-D-5424] c17 N69-36653
MAAHS, H. G.
Crystallographic data on selected artificial graphites with comments on the role of the degree of crystal development in oxidation
[NASA-TN-D-4888] c18 N69-10754
MAC NEAL, R. H.
Heliogyro solar sailer Summary report
[NASA-CR-1329] c31 N69-28861
MACCORMACK, R. W.
The effect of viscosity in hypervelocity impact cratering.
[AIAA PAPER 69-354] c32 A69-28288
MACELROY, R. D.
Characterization of ribulose diphosphate carboxylase and phosphoribulokinase from Thiobacillus thioparus and Thiobacillus neapolitanus.
c04 A69-11866
Control of ATP-dependent CO sub 2 fixation in extracts of Hydrogenomonas facilis - NADH regulation of phosphoribulokinase.
c04 A69-30036
MACHLIN, I.
Refractory Metal Alloys- Metallurgy and Technology, Proceedings of a Symposium on Metallurgy and Technology of Refractory Metals, Washington, D.C., April 25, 26, 1968.
c17 A69-18790
MACK, R. J.
A numerical method for evaluation and utilization of supersonic nacelle-wing interference
[NASA-TN-D-5057] c01 N69-19641
MACKAY, J. S.
Space mission analysis.
c30 A69-14519
MACLEOD, N. H.
ATP assay of terrestrial soils - A test of an exobiological experiment.
c04 A69-37567
MACOSKO, R. P.
Performance of an experimental SNAP 8 power conversion system
[NASA-TM-X-1732] c03 N69-20868
Results of endurance tests of a SNAP 8 turbine-alternator
[NASA-TM-X-1741] c03 N69-20913
MADDALON, D. V.
Influence of measured free-stream disturbances on hypersonic boundary-layer transition.
[AIAA PAPER 69-704] c12 A69-33453
MADDEN, R.
Hypervelocity impact analysis by the method of characteristics
[NASA-TR-R-298] c32 N69-24765
MADEY, J. M.
Design techniques for small scientific satellite structures
[NASA-TN-D-4988] c32 N69-33232
MADIGAN, R. J.
Flight test report of experiments in inertial navigation system updating.
[AIAA PAPER 69-842] c21 A69-39429
Flight evaluation of radar-inertial systems.
[AAS PAPER 69-401] c02 A69-42831
MAGDALENO, R. P.
Small perturbation dynamics of the neuromuscular system in tracking tasks
[NASA-CR-1212] c05 N69-14212
MAGEE, J. L.
On the nature of ion-molecule collisions.
c24 A69-16428
Computer-made movies and plotting descriptions of ion-molecule collisions with polar targets.
c24 A69-43124
MAGGIN, B.
NASA space program possibilities and upper stage implications.
[AAS PAPER 69-359] c34 A69-42828
MAGLIERI, D. J.
Variability in sonic-boom signatures measured along an 8000-foot linear array
[NASA-TN-D-5040] c02 N69-17279
MAHAJAN, K. K.
Diurnal variation of the ion temperature.
c13 A69-16407
Radar backscatter and rocket probe measurements of electron temperature above Arecibo.
c29 A69-25162
Latitudinal observations of the thermal balance in the nighttime protonosphere.
c13 A69-43181
MAIER, E. J. R.
Sounding rocket measurements of ion composition and charged particle temperatures in the topside ionosphere.
c13 A69-18839
Suprathermal electrons in the polar ionosphere.
c29 A69-28963
Explorer XXXI total current monitor experiments.
c29 A69-37880
MAILLOUX, R.
Microwave radiometric capabilities and techniques.
c07 A69-26976
MAILLOUX, R. J.
Radiation and near-field coupling between two collinear open-ended waveguides.
c09 A69-24984
A simple antenna with good circular polarization.
c09 A69-41590
First-order solutions for mutual coupling between waveguides which propagate two orthogonal modes
[NASA-TN-D-5180] c07 N69-24051
MALITSON, H. H.
The solar electromagnetic radiation environment.
c29 A69-21645
Type III radio bursts in the outer corona.
c29 A69-40300
MALLARY, W. E.
The stored program data processor for post- Apollo applications.
c07 A69-36280
MALLOY, J. E.
Gaseous hydrogen requirements for the discharge of liquid hydrogen from a 1.52 meter /5 ft/ diameter spherical tank
[NASA-TN-D-5336] c28 N69-32318
Gaseous-hydrogen pressurant requirements for the discharge of liquid hydrogen from a 3.96 meter /13 ft/ diameter spherical tank
[NASA-TN-D-5387] c28 N69-33211
MALONEY, J. E.
Pressure-diameter relations of capillaries and small blood vessels in frog lung.
c04 A69-40974
MALTE, P. C.
Experimental evaluation of a subsonic expansion tube
[NASA-CR-1354] c11 N69-28095

MALTZ, J.
The less common refractory metals /rhenium, technetium, hafnium, noble metals/.
c17 A69-18793
MANDEL, A. D.
Current research on regenerative systems.
c04 A69-37623
MANGUS, J. D.
Optical design of a glancing incidence X-ray telescope.
c14 A69-21087
MANKA, R. H.
A lunar-surface electric-field detector.
c14 A69-13221
MANN, J. D.
An in situ facility for the determination of the effects of a space environment on the solar absorptance of materials.
[AIAA PAPER 69-1021] c11 A69-40392
MANNELLA, G. G.
Aerospace sensor systems.
c14 A69-13851
Quenching of N sub 2
c24 A69-36424
MANNING, J. C.
Wind velocity profiles measured by the smoke-trail method at the eastern test range, 1963
[NASA-TN-D-4880] c20 N69-14505
MANNING, L. A.
Investigation of an early flyby sequence for imaging of the planet Mercury.
[AAS PAPER 69-258] c30 A69-42860
MANOS, A. M.
Tagged arithmetic
[NASA-TN-D-5370] c08 N69-32556
MANRY, C. E.
Results of ground and flight tests of the Apollo optics.
c14 A69-35796
MANTENIEKS, M. A.
Analytical and experimental studies of MHD generator cathodes emitting in a ''spot'' mode
[NASA-TN-D-5414] c25 N69-35732
MANUS, E. A.
The thin film iris
[NASA-CR-1364] c26 N69-28096
MAPLES, H. E.
Engineering and operational experiences related to lunar-surface thermal-vacuum qualification of the Apollo extravehicular mobility unit.
[AIAA PAPER 69-992] c05 A69-40370
MAR, J. W.
Structures Technology for Large Radio and Radar Telescope Systems, Proceedings of the International Symposium, Massachusetts Institute of Technology, Cambridge, Mass., October 18-20, 1967.
c11 A69-42120
MARAN, S. P.
Progress report on pulsars.
c30 A69-42556
MARCHAL, C.
Analytical solutions of a class of optimum orbit modifications
[NASA-CR-1379] c30 N69-31362
MAREC, J. P.
Optimal transfers between close elliptical orbits
[NASA-TT-F-554] c30 N69-40592
MARGASON, R. J.
Aerodynamic characteristics of twin propeller deflected slipstream STOL airplane model with boundary layer control on inverted V-tail
[NASA-TN-D-4856] c02 N69-10935
The path of a jet directed at large angles to a subsonic free stream
[NASA-TN-D-4919] c01 N69-11634
MARGOZZI, A. P.
Exploratory investigation on the measurement of skin friction by means of liquid crystals.
c11 A69-29029
A dual-beam source of actinic light for photosynthesis research.
c14 A69-36378
Exploratory investigation on the measurement of skin friction by means of liquid crystals
[NASA-TM-X-1774] c12 N69-26956
MARINO, B. A.
Inverter-converter automatic paralleling and protection
[NASA-CR-1225] c10 N69-19003
MARK, H.
Thermal contact resistance measurements at ambient pressures of one atmosphere to 3 x 10 super minus super 12 mm Hg and comparison with theoretical predictions.
[AIAA PAPER 69-629] c33 A69-33299
MARKHAM, J.
The centrifuge as a therapeutic device.
c04 A69-43372
MARKOS, A. T.
A computational method for time-optimal space rendezvous
[NASA-TN-D-5017] c30 N69-16210
MARSH, J. G.
Gravity model comparison using GEOS 1 long- arc orbital solutions
[NASA-TN-D-5035] c30 N69-27412
GEOS I tracking station positions on the SAO standard earth /C-5/
[NASA-TN-D-5034] c13 N69-28019
Evaluation of the Goddard range and range rate system at Rosman by intercomparison with GEOS 1 long-arc orbital solutions
[NASA-TN-D-5036] c13 N69-28442
MARSHALL, R. L.
Luminous fog layer surrounding a zirconium droplet burning in an oxygen-containing atmosphere.
c33 A69-28462
Vapor-phase combustion phenomena when Zr droplets burn in oxygen.
[WSCI PAPER 69-4] c27 A69-32345
MARSIK, S. J.
Radiation induced reduction of ammoniacal nickel /2/ sulfate to metallic nickel
[NASA-TN-D-5213] c06 N69-24940
MARTENEY, P. J.
Experimental investigation of the spectral emission characteristics of argon-tungsten and argon-uranium induction heated plasmas
[NASA-CR-1314] c25 N69-22920
MARTIN, F. L.
Statistical specification of the 500-mb height fields using smoothed medium-resolution radiometric fields of Nimbus II.
c20 A69-42896
MARTIN, J. A.
Exploratory investigation of flow field resulting from forward-facing nozzles exhausting near a large cylindrical body at free-stream Mach numbers of 3.0 and 6.0
[NASA-TN-D-5030] c01 N69-21000
MARVIN, J. G.
A study of the nonsimilar nature of the laminar boundary layer in a region of adverse pressure gradient.
[AIAA PAPER 69-35] c12 A69-18094
Combined effects of mass addition and nose bluntness on boundary-layer transition.
[AIAA PAPER 67-706] c12 A69-33476
Convective heat-transfer rates on large-angle conical bodies at hypersonic speeds
[NASA-TN-D-5526] c33 N69-40780
MARXER, W. L.
Prescription of exercise for the hypokinetic airline pilot.
c05 A69-41800
MASCITTI, V. R.
A closed-form solution to oblique shock-wave properties.
c01 A69-25378
A procedure for rapid computation of equilibrium chemical composition and thermodynamic properties of the generalized argon-nitrogen-oxygen-hydrogen gas system
[NASA-TN-D-5416] c33 N69-36299
MASCY, A. C.
Low-thrust mission simulation - Feedback to hardware definition.
c30 A69-21204
A compilation of current computer programs for low-thrust trajectory analysis
[NASA-TM-X-1824] c08 N69-30014
MASICA, W. J.
Lateral sloshing in cylinders under low-gravity conditions
[NASA-TN-D-5058] c12 N69-19112
Effect of flow rate on the dynamic contact angle for wetting liquids

[NASA-TN-D-5115] c12 N69-20794
Motion of single bubbles under low gravitational conditions
[NASA-TN-D-5462] c12 N69-38032
MASON, C. C.
Particle size distribution of lunar surface material.
c30 A69-26371
An empirically derived erosion law and its application to Lunar Module landing.
c30 A69-41388
MASON, J. A.
Physical, chemical, and biological activities at the Lunar Receiving Laboratory.
c11 A69-38896
MASON, J. D.
Some optimal branched trajectories
[NASA-CR-1331] c30 N69-24950
MASON, J. L.
E-type photodemodulators for coherent light signals Final technical report
[NASA-TT-F-430] c09 N69-15441
MASSEL, G. A.
Diffusion of fast electrons in stochastic magnetic fields.
c25 A69-20807
MASSER, C. C.
Photographic study of a bromine jet flowing in a coaxial airstream and impinging on a stagnation surface
[NASA-TN-D-5209] c12 N69-24800
A photographic study of a bromine jet in a coaxial airstream with honeycombs at the injection plane
[NASA-TM-X-1900] c12 N69-39303
MASTERS, P. A.
Gaseous hydrogen requirements for the discharge of liquid hydrogen from a 1.52 meter /5 ft/ diameter spherical tank
[NASA-TN-D-5336] c28 N69-32318
Gaseous-hydrogen pressurant requirements for the discharge of liquid hydrogen from a 3.96 meter /13 ft/ diameter spherical tank
[NASA-TN-D-5387] c28 N69-33211
MASUR, E. F.
Some general principles of dynamic instability of solid bodies.
c32 A69-16742
MATEER, G. C.
Summary and correlation of skin-friction and heat-transfer data for a hypersonic turbulent boundary layer on simple shapes
[NASA-TN-D-5089] c12 N69-29144
MATEER, G. G.
Unusual boundary-layer transition results on cones in hypersonic flow.
[AIAA PAPER 68-40] c01 A69-31881
MATEL, A. F.
Handbook of Solar Simulation for Thermal Vacuum Testing.
c11 A69-38894
MATHEWS, C. W.
Systems engineering, manned space flight.
c31 A69-17602
MATSUDA, K.
Collision damping of longitudinal plasma waves.
c25 A69-34439
MATTHEWS, C. W.
A numerical analysis of the use of perforated walls to control shock location and movement in an internal compression supersonic inlet
[NASA-TR-R-317] c01 N69-32338
MATTHEWS, H. F.
The Pioneer mission to Jupiter.
[AAS PAPER 69-290] c30 A69-42863
MATTINGLY, G. S.
Correlation study of the simulation of Gemini extravehicular activity with flight results
[NASA-CR-1146] c05 N69-19902
MATTSON, W. F.
Heat-transfer coefficients for hydrogen flowing through parallel hexagonal passages at surface temperatures to 2275 K
[NASA-TN-D-4959] c33 N69-14588
Statistical analysis of high-temperature creep-rate data for alloys of tantalum, molybdenum, and columbium
[NASA-TN-D-5424] c17 N69-36653
MAULDIN, L. E., III
An optical system for recording schlieren images with continuous writing ultra high speed framing camera
[NASA-TN-D-4986] c14 N69-15381
MAURY, J. L.
Application of Hansen's method to the X super th satellite of Jupiter.
c30 A69-37529
Application of Hansen's method to the 10th satellite of Jupiter
[NASA-TN-D-4979] c30 N69-14479
MAXWELL, M.
Use of computers and programmable telemetry systems on scientific satellies.
c08 A69-41735
MAY, C. B.
The effectiveness of weightless simulators for obtaining maintainability criteria for space systems.
c05 A69-17648
MAYE, R. F.
On the determination of micromorphic material constants from properties of the constituents
[NASA-CR-1320] c32 N69-21569
MAYER, J. J.
NERVA control drum actuator irradiation test program
[NASA-TN-D-5347] c22 N69-31870
MAYER, J. P.
Utilization of ground-based guidance systems to supplement onboard guidance of space vehicles.
c21 A69-17580
MAYERJAK, R. J.
The Bossler coupling
[NASA-CR-1241] c15 N69-16104
MAYHUE, J. J.
Flight-test results from supersonic deployment of an 18-foot-diameter /5.49 meter/ towed ballute decelerator
[NASA-TM-X-1773] c31 N69-26458
MAYO, A. M.
Commercial Utilization of Space, American Astronautical Society, Annual Meeting, 13th, Dallas, Tex., May 1-3, 1967, Proceedings.
c30 A69-34043
MAYO, A. P.
Analytic approximations for application to spacecraft optical navigation on short data arcs
[NASA-TN-D-4863] c21 N69-10372
MAYO, W.
Radial power tailoring for a uranium dioxide T-111 clad reactor with contained fission product gases
[NASA-TM-X-1795] c22 N69-25305
Neutronic comparison of beryllium oxide and molybdenum for movable reflector control of a fast-spectrum reactor
[NASA-TM-X-1822] c22 N69-29593
Reflector-based poison-drum control on equal-size reactor cores fueled with uranium-233 and with uranium-235
[NASA-TM-X-1883] c22 N69-36756
Characteristics of a 2.17-megawatt fast- spectrum reactor concept using an axially moving reflector control system
[NASA-TM-X-1911] c22 N69-40061
MAYO, W. L.
Lunar Orbiter mission design.
[AIAA PAPER 68-47] c30 A69-15503
MAYR, H. G.
The plasmapause and its relation to the ion composition in the topside ionosphere.
c13 A69-12741
Measurements of electron cooling rates in the mid-latitude and auroral-zone thermosphere.
c13 A69-16267
Implications for ionospheric chemistry and dynamics of a direct measurement of ion composition in the F 2 region.
c13 A69-31974
Electron measurements bearing on the energy and particle balance of the upper F region.
c29 A69-31975
MAZER, L.
A 500,000 sample per second digital recorder for the Ames electric arc shock tunnel.
c11 A69-35744
MC CABE, J. T.
High performance turboalternator and associated hardware. 3. Design of backup gas bearings

[NASA-CR-1292] c15 N69-19775
MC COMB, H. G., JR.
Buckling of an equatorial segment of a spherical shell loaded by its own weight
[NASA-TN-D-4921] c32 N69-13034
MC CONAUGHY, D.
Evaluation of the Goddard research and engineering management exercise simulation
[NASA-CR-1275] c34 N69-18057
MC CONNELL, J.
Hydrogen gas pressure vessel problems in the M-1 facilities
[NASA-CR-1305] c17 N69-19831
MC CORMICK, M. P.
Tables of Mie scattering functions for particles with refractive index 1.5
[NASA-TN-D-5110] c23 N69-20905
MC CRACKEN, H. C.
Evaluation of an indirect viewing system for lifting-body terminal-area navigation and landing tasks
[NASA-TN-D-5299] c14 N69-29730
MC DEVITT, J. B.
Upwash patterns on ablating and nonablating cones at hypersonic speeds
[NASA-TN-D-5346] c12 N69-37370
MC GEHEE, J. R.
Analytical investigation of an inflatable landing system having omnidirectional and multiple impact capabilities
[NASA-TN-D-5236] c32 N69-26223
MC GHEE, R. J.
Exploratory investigation of flow field resulting from forward-facing nozzles exhausting near a large cylindrical body at free-stream Mach numbers of 3.0 and 6.0
[NASA-TN-D-5030] c01 N69-21000
Aerodynamic investigation of sharp cone- cylinder spikes on 120 degree blunted cones at Mach numbers of 3.00, 4.50, and 6.00
[NASA-TN-D-5201] c01 N69-29154
MC KEE, T. B.
Infrared horizon profiles for winter conditions from Project Scanner
[NASA-TN-D-4905] c21 N69-14346
A technique to infer atmospheric temperature from horizon radiance profiles
[NASA-TN-D-5068] c13 N69-19024
A technique to infer atmospheric water-vapor mixing ratio from measured horizon radiance profiles
[NASA-TN-D-5252] c13 N69-27246
MC KISSON, H. L.
Solubility of refractory metals and alloys in potassium and in lithium
[NASA-CR-1371] c17 N69-27059
MC LAUGHLIN, M. D.
Simulation studies of the supersonic transport in future air traffic control systems
[NASA-TN-D-4944] c21 N69-14382
Supersonic transport operating practices during simulated operations in future air traffic control system environments
[NASA-TN-D-5018] c02 N69-17257
MC LEAN, J. D.
Second order errors in linearized velocity corrections and their effects on the rate of convergence of iterative solutions
[NASA-TN-D-5037] c21 N69-17780
MC LEOD, N. J.
Variability in sonic-boom signatures measured along an 8000-foot linear array
[NASA-TN-D-5040] c02 N69-17279
Variation in engine noise for two landing-approach configurations of a jet transport aircraft
[NASA-TM-X-1896] c02 N69-38104
MC MILLEN, A. R.
Crater characteristics of 11 metal alloys under hyper-velocity impact including effects of projectile density and target temperature
[NASA-TN-D-5135] c32 N69-22994
MC NALLY, W. D.
FORTRAN program for calculating velocities and streamlines on a blade-to-blade stream surface of a tandem blade turbomachine
[NASA-TN-D-5044] c01 N69-21811
Revised FORTRAN program for calculating velocities and streamlines on a blade to blade stream surface of a turbomachine
[NASA-TM-X-1764] c01 N69-22553
FORTRAN program for calculating velocities in a magnified region on a blade to blade stream surface of a turbomachine
[NASA-TN-D-5091] c01 N69-22938
MC NANEY, J. J.
Nimbus 2 flight evaluation and engineering report, launch through orbit 5275
[NASA-TN-D-4881] c31 N69-17851
MC NEILL, W. E.
Calculated and flight measured handling- qualities factors of three subsonic jet transports
[NASA-TN-D-4832] c02 N69-10495
MC RAE, R.
Solubility and diffusion of oxygen in tantalum
[NASA-CR-1276] c17 N69-19886
MC RUER, D. T.
Small perturbation dynamics of the neuromuscular system in tracking tasks
[NASA-CR-1212] c05 N69-14212
MC VAY, R. E.
Evaluation of magnetic materials for static inverters and converters
[NASA-CR-1226] c03 N69-17765
MC VEHIL, G. E.
Ground wind characteristics at Kennedy Space Center Final report
[NASA-CR-1418] c20 N69-36222
MCADOO, S. F., JR.
Application of nuclear solid-core rockets to interplanetary orbital launch by multiorbit injection.
[AIAA PAPER 69-535] c22 A69-32660
MCALLUM, W. E.
Development of meteoroid protection for extravehicular-activity space suits.
[AIAA-PAPER-69-366] c05 A69-28298
MCAVOY, N.
Fluorescence spectra of homogeneous and mixed europium complexes.
c06 A69-10893
10.6-micrometer laser communication system experiment for ATS-F and ATS-G.
c07 A69-41758
MCBRYAR, H.
Fuel cell systems for manned spacecraft.
c03 A69-21035
Fuel cell systems for manned spacecraft.
c03 A69-32406
MCCAFFERTY, R. D.
Apollo mission simulation with visual presentation.
[SMPTE PAPER 105-74] c11 A69-25768
MCCLAY, J. F.
Physics of the Magnetosphere, Proceedings of the Conference, Boston College, Chestnut Hill, Mass., June 19-28, 1967.
c29 A69-19351
MCCLUSKEY, G. E., JR.
Curve-of-growth analysis for the close binary Hr 5317.
c30 A69-34297
MCCONNELL, D. G.
Combined radiation and conduction heat transfer - Application in design.
[SAE PAPER 690197] c33 A69-18303
MCCORMAC, B. M.
Atmospheric Emissions, Proceedings of the NATO Advanced Study Institute, Agricultural College of Norway, As, Norway, July 29-August 9, 1968.
c13 A69-38482
MCCORMICK, M. P.
Mie total and differential backscattering cross sections at laser wavelengths for Junge aerosol models.
c16 A69-14290
Optical radar studies of the atmosphere.
c07 A69-27001
MCCOY, J. E.
High-latitude ionization spikes observed by the POGO ion chamber experiment.
c29 A69-28950
MCCULLEY, G.
Ray tracing studies for the topside ionosphere.
c13 A69-18838
MCDONALD, F. B.
Relativistic electrons from solar flares.
c29 A69-15528

Relativistic solar electrons detected during the 7 July 1966 proton flare event. c29 A69-23766
IQSY observations of low-energy galactic and solar cosmic rays. c29 A69-30014
The chemical composition of galactic and solar cosmic rays. c29 A69-40090
Observations of cosmic-ray electrons between 2.7 and 21.5 MeV. c29 A69-42667

MCDONALD, J. K.
New observations on the substrate specificity of cathepsin C /dipeptidyl aminopeptidase I/ including the degradation of beta-corticotropin and other peptide hormones. c04 A69-37577

MCDOWELL, M. R. C.
Elastic scattering of slow electrons by two-electron ions. c24 A69-12924
Photo-ionization of lithium - A many-body calculation. c24 A69-17134
On a peaking approximation in scattering theory. c24 A69-20206

MCELROY, J. H.
10.6-micrometer laser communication system experiment for ATS-F and ATS-G. c07 A69-41758

MCFALL, J. C., JR.
Some test results from the NASA planetary entry parachute program.
[AIAA PAPER 68-934] c02 A69-35952
Secondary experiment space available on balloon flights - 1969. c02 A69-40807

MCGOVERN, W. E.
On the exospheric temperature of Venus. c30 A69-12109
Albedo measurements over the Antarctic. c13 A69-21404
Wind measurements in noctilucent clouds. c20 A69-28466

MCGOWAN, W. A.
Trailing vortex hazard.
[SAE PAPER 680220] c02 A69-14930

MCGUNIGAL, T. E.
10.6-micrometer laser communication system experiment for ATS-F and ATS-G. c07 A69-41758

MCINTOSH, F. J.
Programmed test patterns for multiterminal devices. c08 A69-39604

MCKAY, S. S., II
Rocket trajectory optimization by a second- order numerical technique. c30 A69-32154

MCKENZIE, J. F.
Interaction of linear waves with oblique shock waves. c12 A69-13137
Transmission of Alfven waves through the earth's bow shock. c13 A69-32099
Interaction of magnetoacoustic and entropy waves with normal magnetohydrodynamic shock waves. c25 A69-38242

MCKIBBIN, D. D.
Review of Ames Research Center plasma-probe results from Pioneers 6 and 7. c13 A69-19364
Preliminary comparison of solar wind plasma observations in the geomagnetospheric wake at 1000 and 500 earth radii. c29 A69-26943

MCNALLY, W. D.
Programs for computation of velocities and stream-lines on a blade-to-blade surface of a turbomachine.
[ASME PAPER 69-GT-48] c01 A69-22495

MCPHERSON, W. B.
Recent experience in high pressure gaseous hydrogen equipment operated at room temperature.
[ASM PAPER D8-14.1] c15 A69-19666

MCTIGUE, J. G.
Lifting-body research vehicles in a low-speed flight test program. c02 A69-15571

MEAD, J. B.
Statistics of the region of Lacerta OB1
[NASA-TN-D-5060] c30 N69-26235

MEADOR, M. C.
Removal of acid gases and oxides of nitrogen from space cabin atmospheres
[NASA-CR-1388] c05 N69-37517

MEADOR, W. E.
A semiempirical collision model for plasmas
[NASA-TR-R-310] c25 N69-23787

MEANS, H.
Brayton-cycle turbomachinery rolling-element bearings
[NASA-CR-1229] c15 N69-16463

MECHTLY, E. A.
Coordinated rocket measurements on the D-region winter anomaly. I - Experimental results. c13 A69-16411

MEDENICA, W. V.
Blast shields testing
[NASA-TN-D-4894] c11 N69-10888

MEDWID, D. W.
Design and fabrication of a counterflow double-containment tantalum-stainless steel mercury boiler
[NASA-TN-D-5092] c33 N69-23707

MEHTA, U. B.
Flow in a two-dimensional channel with a rectangular cavity
[NASA-CR-1245] c12 N69-14095

MEISSNER, C. W., JR.
A navigation-aids identification decoder and display for general-aviation aircraft
[NASA-TN-D-5445] c09 N69-38852

MEISTER, K.
Laser Doppler velocity instrument
[E-67-4450] c14 N69-14351

MELEASON, E. T.
Effect of porous bleed in a high performance axisymmetric, mixed compression inlet at Mach 2.50
[NASA-TM-X-1692] c01 N69-10294
Performance characteristics from Mach 2.58 to 1.98 of an axisymmetric mixed-compression inlet system with 60-percent internal contraction
[NASA-TM-X-1739] c01 N69-19130

MELFI, L. T., JR.
Buried collector gauge for measurements in the 10 super minus super 11 torr pressure range. c14 A69-32324

MELFI, S. H.
Optical radar studies of the atmosphere. c07 A69-27001

MELLENTHIN, J. A.
Upwash patterns on ablating and nonablating cones at hypersonic speeds
[NASA-TN-D-5346] c12 N69-37370

MELOSH, R. J.
Manipulation errors in finite element analysis of structures
[NASA-CR-1385] c19 N69-34360

MELUGIN, R. K.
A precision autocollimating solar sensor.
[AIAA PAPER 69-858] c21 A69-39386

MENG, P. R.
Cavitation performance of 80.6 deg helical inducer in liquid hydrogen
[NASA-TM-X-1808] c09 N69-27841
Investigation of two-phase hydrogen flow in pump inlet line
[NASA-TN-D-5258] c15 N69-29476
Cavitation performance of line-mounted 80.6 deg helical inducer in hydrogen
[NASA-TM-X-1854] c12 N69-33261

MENGERS, D.
The Orbiting Astronomical Observatory thermal test program.
[AIAA PAPER 69-995] c11 A69-40373

MENNELLA, R. A.
Unusual 1 to 5 GHz solar radio emission of 29 October 1968. c30 A69-32811

MENSING, A. E.
Theoretical investigations of RF induction heated plasmas
[NASA-CR-1312] c25 N69-22638

Experimental investigation of the spectral emission characteristics of argon-tungsten and argon-uranium induction heated plasmas
[NASA-CR-1314] c25 N69-22920
MERCHANT, J.
Laboratory oculometer
[NASA-CR-1422] c05 N69-39212
MEREK, E. L.
Estimating the size and concentration of unicellular microorganisms by light scattering.
c04 A69-25643
MERRICK, R. B.
A simplified Kalman estimator for an aircraft landing display.
[AIAA PAPER 69-944] c21 A69-40327
MERRIFIELD, R. B.
A historical note on the genesis of manned interplanetary flight.
[AAS PAPER 69-501] c30 A69-42852
MERRILL, R. B.
Thermal conduction through an evacuated idealized powder over the temperature range of 100 deg K to 500 deg K
[NASA-TN-D-5063] c33 N69-20008
MERSMAN, W. A.
A unified treatment of lunar theory and artificial satellite theory
[NASA-TN-D-5459] c30 N69-38145
MERTEL, M. H.
Sequential processing techniques for trajectory estimation
[NASA-CR-1360] c30 N69-40325
MERZHANOVA, R. F.
Motion of artificial satellites in the earth's gravitational field
[NASA-TT-F-539] c30 N69-33560
METGER, G. W.
Discharge coefficients for thick plate orifices with approach flow perpendicular and inclined to the orifice axis
[NASA-TN-D-5467] c12 N69-38012
METZGER, J. R.
Explorer 35 attitude control system
[NASA-TN-D-5187] c21 N69-27268
MEYER, A. J.
Exploration of the moon.
c30 A69-27908
MEYER, G.
The design of a large angle three-axis attitude servomechanism for spacecraft.
c21 A69-17589
Response envelope - A global description of three-axis large angle spacecraft attitude control systems
[NASA-TN-D-4896] c30 N69-10756
MEYN, E. H.
Variable-voltage, direct-current power supplies for energizing cryogenically cooled and superconductive electromagnets.
c03 A69-26498
Pumped helium tests of a 51-centimeter bore niobium-tin magnet
[NASA-TN-D-5158] c26 N69-22965
Transistor performance in intense magnetic fields
[NASA-TN-D-5428] c09 N69-36710
MICHAEL, W. H., JR.
Results on the mass and the gravitational field of the moon as determined from dynamics of lunar satellites.
c30 A69-31405
MICHEL, E. L.
Carbon dioxide build-up characteristics in spacesuits.
c05 A69-39170
MICKELWAIT, A. B.
Development and management of the interplanetary Pioneer spacecraft.
c31 A69-17605
MIGRA, R. P.
Thermionic fuel irradiation experiment description
[NASA-TM-X-1858] c22 N69-33273
MIHALOV, J. D.
The cislunar geomagnetic tail gradient in 1967.
c13 A69-11237
The geomagnetic tail - Topology, reconnection and interaction with the moon.
c13 A69-19365
MHD Rankine-Hugoniot equations applied to earth's bow shock.
c30 A69-42417
MIKHAYLOV, M. D.
Transient temperature fields in shells
[NASA-TT-F-552] c33 N69-30245
MIKULAS, M. M., JR.
Development status of attached inflatable decelerators.
[AIAA PAPER 68-929] c02 A69-39015
MILDER, N. L.
A survey and evaluation of research on the discharge chamber plasma of a Kaufman thruster.
[AIAA PAPER 69-494] c28 A69-32735
Analysis of electron analog simulation of ion containment in magnetic fields
[NASA-TN-D-5217] c25 N69-25394
MILLARD, J. P.
A comparison of infrared-emittance measurements and measurement techniques.
c14 A69-41633
MILLER, A. J.
A comparison of data obtained by the MT-135 and ARCAS meteorological rocket systems
[NASA-TM-X-1726] c20 N69-17772
Synoptic analysis of the Southern Hemisphere stratosphere
[NASA-TM-X-1814] c13 N69-33555
Response characteristics of meteorological rocket wind reduction techniques
[NASA-TM-X-1850] c20 N69-35523
MILLER, C. D.
Unaccelerated geocentric velocities and influx rates of sporadic photographic meteors
[NASA-TN-D-5245] c30 N69-26239
MILLER, C. F., JR.
A graphic method for determining the absolute attitude of sounding rocket vehicles
[NASA-TN-D-5172] c30 N69-23782
MILLER, C. G., III
Real-helium hypersonic flow parameters for pressures to 3600 atmospheres and temperatures to 15,000 deg K
[NASA-TN-D-4869] c12 N69-10443
MILLER, G. K., JR.
Fixed-base visual simulation of pilot controlled descents of an advanced Apollo spacecraft with an all-flexible parawing
[NASA-TN-D-5049] c21 N69-20936
MILLER, H. B.
A radiometer for use in thermal studies of spacecraft
[NASA-TN-D-4925] c14 N69-13311
MILLER, I. M.
An evaluation of coated molybdenum and columbium alloys in high-temperature supersonic airstreams
[NASA-TN-D-4877] c17 N69-10764
MILLER, J. V.
Characteristics of a 2.17-megawatt fast- spectrum reactor concept using an axially moving reflector control system
[NASA-TM-X-1911] c22 N69-40061
MILLER, L. J.
Development and processing of pyronne polymers
[NASA-CR-1310] c18 N69-26448
MILLER, M.
The application of the image orthicon television system to rocket trajectory determination.
c07 A69-26965
MILLER, M. J.
Overall performance of a tandem-bladed inducer tested in water
[NASA-TN-D-5134] c01 N69-23769
MILLER, R. P.
Experimental bending strength of an Atlas LV-3C booster beyond compressive skin wrinkling
[NASA-TN-D-5156] c31 N69-22937
Experimental lateral bending dynamics of the Atlas-Centaur-Surveyor launch vehicle
[NASA-TM-X-1837] c31 N69-30631
MILLER, R. W.
Wind velocity profiles measured by the smoke-trail method at the eastern test range, 1963
[NASA-TN-D-4880] c20 N69-14505
MILLER, W. E.
A study to determine the presence of voltage breakdown due to proton irradiation in polymeric materials
[NASA-TM-X-1688] c18 N69-10066
MILLETT, D. A.
A lunar gravity simulator, volume 3

[NASA-CR-1235] c05 N69-14213
MILLMAN, P. M.
Meteorite Research, Proceedings of the Symposium, Vienna, Austria, August 7-13, 1968. c30 A69-36072
MINER, W. E.
The Hamilton-Jacobi method applied to the low-thrust trajectory problem. c30 A69-17574
Optimal trajectory coordinate-multiplier systems with constant of the motion components.
[AIAA PAPER 69-907] c30 A69-39339
MINOTT, P. O.
Wavelength dependence of laser-beam scintillation. c16 A69-19641
MIQUEL, J.
Differences between radiation-induced life shortening and natural aging in Drosophila melanogaster. c04 A69-30444
Viruslike particles in the fat body, cenocytes, and central nervous tissue of Drosophila melanogaster imagoes. c04 A69-42021
MIRTICH, M. J.
Performance of N/p silicon and cadmium sulfide solar cells as affected by hypervelccity particle impact
[NASA-TN-D-5133] c03 N69-21016
MITCHELL, G. A.
Preliminary investigation of distortion dynamics in a Mach 3 mixed compression inlet
[NASA-TM-X-1706] c01 N69-13154
MITRA, A. P.
Nitric oxide in the mesosphere and its variations. c13 A69-38364
MODISETTE, J. L.
Radiation plan for the Apollo lunar mission.
[AIAA PAPER 69-19] c29 A69-18113
MOECKEL, W. E.
Propulsion systems for manned exploration of the solar system. c28 A69-38118
Propulsion systems for manned exploration of the solar system
[NASA-TM-X-1864] c28 N69-34674
MOFFITT, T. P.
Some measurement problems encountered when determining the performance of certain turbine stator blades from total pressure surveys.
[ASME PAPER 69-GT-103] c01 A69-22521
Performance of a single-stage turbine as affected by variable stator area.
[AIAA PAPER 69-525] c28 A69-32686
Effect of variable stator area on performance of a single-stage turbine suitable for air cooling. 5 - Stator detailed losses with 70 percent design area
[NASA-TM-X-1696] c28 N69-10296
MOLHO, R.
Mechanical properties of epoxy resins and glass/epoxy composites at cryogenic temperatures. c18 A69-16491
MOLLS, F. B.
Three-phase heat transfer - Transient condensing with freezing on a nonisothermal inclined plane
[NASA-TN-D-5289] c33 N69-29598
MONAGHAN, R. C.
Flight measurements of canard loads, canard buffeting, and elevon and wing tip hinge moments on the XB-70 aircraft including comparisons with predictions
[NASA-TN-D-5359] c02 N69-32284
MONDRE, E.
Relationship between complex- and envelope-covariance for Rician fading communication channels
[NASA-TN-D-4825] c07 N69-11011
MONNIN, C. F.
Molecular hydrogen inelastic electron impact cross sections - A semiclassical method. c24 A69-22249
Energy transfer and ion cost in a hydrogen plasma
[NASA-TN-D-5319] c25 N69-29905
Stability of two-fluid wheel flows with an imposed uniform axial magnetic field
[NASA-TN-D-5372] c12 N69-32377
MONROE, R. E.
Joining ceramics and graphite to other materials
[NASA-SP-5052] c15 N69-14241
MONTA, W. J.
Roughness drag due to two-dimensional fabrication-type surface roughness on an ogive cylinder from force tests at transonic speeds
[NASA-TN-D-5004] c01 N69-16460
MONTEGANI, F. J.
Underexpanded jet noise reduction using radial flow impingement.
[AIAA PAPER 68-81] c12 A69-28212
MONTGOMERY, R. C.
Application of differential synthesis to design of multiaxis stability augmentation systems.
[AIAA PAPER 68-834] c31 A69-37156
MONTGOMERY, R. M.
Frequency conversion in the sheath capacitance of a glow discharge plasma. c25 A69-14456
MONTOYA, E. J.
Wind-tunnel force and pressure tests of rocket-engine nozzle extensions on the 0.0667-scale X-15-2 model at supersonic and hypersonic speeds
[NASA-TM-X-1759] c01 N69-20873
MOOKHERJI, T.
Optical absorption in triphenylmethylarsonium tetracyanoquinodimethan single crystals. c26 A69-10934
Studies of ultraviolet irradiation effects in ZnO-type thermal control coating pigments.
[AIAA PAPER 69-639] c18 A69-33288
Optical absorption in tetracyanoquinodimethan. c26 A69-35477
MOORE, C. J., JR.
Subject classification bibliography for thermal contact resistance studies.
[ASME PAPER 68-WA/HT-18] c33 A69-16122
MOORE, D. W.
On the flow of gas from the galactic center. c30 A69-22189
MOORE, F. K.
Comments on the nature of the outside boundary layer on a liquid sphere in a steady, uniform stream
[NASA-CR-1362] c12 N69-24877
On minimizing the wake of droplets
[NASA-CR-1368] c12 N69-24958
MOORE, G. P.
Small perturbation dynamics of the neuromuscular system in tracking tasks
[NASA-CR-1212] c05 N69-14212
MOORE, J. E.
Numerical integration in a rigid-body trajectory program
[NASA-TN-D-5425] c30 N69-38769
MOORE, R. D.
Prediction of thermodynamic effects of developed cavitation based on liquid-hydrogen and Freon-114 data on scaled venturis
[NASA-TN-D-4899] c12 N69-10070
Cavitation performance of 80.6 deg helical inducer in liquid hydrogen
[NASA-TM-X-1808] c09 N69-27841
Method for prediction of pump cavitation performance for various liquids, liquid temperatures, and rotative speeds
[NASA-TN-D-5292] c15 N69-29165
Cavitation performance of line-mounted 80.6 deg helical inducer in hydrogen
[NASA-TM-X-1854] c12 N69-33261
MOORE, R. H.
Experimental verification of scale factors for parawing opening characteristics with dimensional ratios from 1/1.3 to 1/3
[NASA-TN-D-5071] c02 N69-19950
MOORE, T. J.
A procedure for furnace brazing butt joints in tungsten-uranium dioxide cermet cylinders at 3000 deg C
[NASA-TM-X-1815] c15 N69-28862
MOORJANI, K.
Fluorescence spectra of homogeneous and mixed europium complexes. c06 A69-10893
MORAN, F. J.
Air bearing table mechanization and verification of a spacecraft wide angle attitude control

system.
[AIAA PAPER 69-856] c31 A69-39384
MORAR, J. W.
A review of spacecraft waste-management systems
[NASA-TM-X-1851] c05 N69-33260
MOREHOUSE, L. E.
Prescription of exercise for the hypokinetic airline pilot.
c05 A69-41800
MORELLI, J. P.
Large-scale tests of an airplane model with a double-delta wing, including longitudinal and lateral characteristics and ground effects
[NASA-TN-D-5102] c02 N69-21020
MORGAN, B. B., JR.
Effects of practice and work load on the performance of a code transformation task /COTRAN/
[NASA-CR-1261] c05 N69-14345
MORGAN, C. J.
Effect of injection element radial distribution and chamber geometry on acoustic mode instability in a hydrogen oxygen rocket
[NASA-TN-D-5375] c33 N69-32340
MORGEN, R. J.
A lunar gravity simulator, volume 2
[NASA-CR-1234] c05 N69-14979
MORIARTY, T. F.
The conformal mapping of the interior of the unit circle onto the interior of a class of smooth curves
[NASA-CR-1357] c32 N69-26559
MORIN, S.
Wave coupling across a density discontinuity in a magnetized plasma.
c25 A69-20795
MORIOKA, S.
Magnetohydrodynamic shock waves in non-aligned flow.
c25 A69-19988
MORITZ, W. E.
Transmission characteristics of axial waves in blood vessels.
[SESA PAPER 1350] c04 A69-19726
MORKOVIN, M. V.
On the many faces of transition.
c12 A69-33248
MOROSOW, G.
A method for digital computation of spacecraft response in the docking maneuver.
c31 A69-25501
MORREAL, J. A.
A wavelength-selective, repetitively pulsed CO sub 2 laser.
c16 A69-21088
MORRELL, F. R.
Precise attitude stabilization of a large orbiting telescope coupled to a crew compartment.
c14 A69-27952
MORRIS, E.
Study of the astronaut's capabilities to maintain life support systems and cabin habitability in weightless conditions
[NASA-CR-1405] c05 N69-36709
MORRIS, J. F.
Reflections of electron beams in thermionic diodes.
c09 A69-17773
Isothermal diode '68.
c03 A69-21827
MORRIS, J. M.
Scanning electron mirror microscopy and scanning electron microscopy of integrated circuits.
c14 A69-32891
MORRIS, J. P.
Solid electrolyte system for oxygen regeneration
[NASA-CR-1359] c05 N69-28099
MORRIS, R. A.
The X sup 2 statistic and the goodness of fit test
[NASA-TR-R-313] c19 N69-30610
MORRIS, R. E.
Creep-rupture data for welded N-155 tubes
[NASA-TN-D-5195] c17 N69-23731
MORRISETTE, E. L.
Boundary-layer tripping with emphasis on hypersonic flows.
c12 A69-33249
MORRISON, D. D.
Sequential processing techniques for trajectory estimation
[NASA-CR-1360] c30 N69-40325
MORROW, W. M., II
Structural synthesis of a stiffened cylinder
[NASA-CR-1217] c32 N69-14254
MORSE, M. L.
The Apollo spacecraft. Volume 1 - A chronology
[NASA-SP-4009] c31 N69-32021
MORT, K. W.
Large-scale wind-tunnel investigation of an M1-L lifting body with an inflatable and a rigid afterbody
[NASA-TN-D-5468] c01 N69-38775
MORTENSEN, R. E.
Sequential processing techniques for trajectory estimation
[NASA-CR-1360] c30 N69-40325
MORTIMER, R. W.
MCDIT 21 - A computer code for one-dimensional elastic wave problems
[NASA-CR-1306] c32 N69-22983
MOSELEY, W. C., JR.
Aerodynamic loads on deployed canard surfaces and rocket nose section of the Apollo launch escape vehicle
[NASA-TN-D-5260] c31 N69-28166
Aerodynamic characteristics determined during development of the Apollo launch escape vehicle configuration
[NASA-TN-D-5208] c01 N69-29027
Wind-tunnel investigation of the aerodynamic pressures on the Apollo command module configuration
[NASA-TN-D-5514] c01 N69-40345
MOSHER, E. J.
Experimental determination of eddy-current torques on bodies rotating relative to a uniform magnetic field
[NASA-TN-D-5086] c23 N69-29477
MOSKOWITZ, S.
An approach to autonomous orbital navigation.
c21 A69-11005
Guidance and control parameters of a planetary cartographic probe.
[AIAA PAPER 69-879] c21 A69-39405
MOSS, J. N.
A study of the performance of low-density phenolic-nylon ablators
[NASA-TN-D-5257] c33 N69-28440
MOSS, T. A.
Study of a 300 kWe Rankine cycle advanced nuclear-electric space power system.
c22 A69-42266
MOURAD, A. G.
Satellite applications to marine geodesy
[NASA-CR-1253] c13 N69-16645
MOYER, H. M.
Performance of swirl-can turbojet combustors at simulated supersonic combustor-inlet conditions
[NASA-TN-D-4996] c28 N69-16154
MRAZEK, W. A.
The various stages of development of astronautics in the U.S. - Technological and economic aspects
c34 A69-15576
MUELLER, G. E.
Manned space flight - The future.
c30 A69-12680
Contributions and results of manned space flight programs.
c30 A69-17074
The new future for manned spacecraft developments.
c31 A69-22866
Commercial exploitation of space technology.
c30 A69-34044
Apollo and beyond.
c30 A69-41477
MUELLER, H.-K.
Stable crack propagation in a viscoelastic strip
[NASA-CR-1279] c30 N69-21506
MUELLER, J. N.
Lightweight, high-thermal-capacity force models for use in arc tunnels.
c11 A69-26796
MUELLER, R. A.
Analysis and experiments with a pulsed neutron source for an unreflected solution reactor up to 50 dollars shutdown
[NASA-TN-D-5487] c22 N69-39186

MUELLER, R. F.
Planetary probe - Origin of atmosphere of Venus. c30 A69-23183
Hydration, oxidation, and the origin of the calc-alkali series
[NASA-TN-D-5400] c13 N69-40893
MUGLER, J. P., JR.
In situ vacuum testing - A must for certain elastomeric materials. c11 A69-22008
MUINZER, M. C.
A comprehensive program for the compilation and analysis of thermal radiative properties data
[NASA-CR-1431] c33 N69-40455
MUIRHEAD, J. S.
Properties of nonaqueous electrolytes
[NASA-CR-1425] c06 N69-36413
MULLER, R. M.
On-board processor. I - Philosophy, design and operation. c08 A69-37384
Coding - An engineering tool for the digital telemetry link. c07 A69-41745
MULLIGAN, J. C.
Downstream cooling effectiveness of massive upstream transpiration from a slender cone. c01 A69-43588
MULLINS, J. A.
The polar exosphere near solar maximum. c13 A69-31351
MUNDAY, C.
Synthesis of acyclic isoprenoids by the gamma-irradiation of isoprene. c04 A69-43750
MUNFORD, J. A.
Development of a weld quality monitor
[NASA-TN-D-5304] c15 N69-33800
Evaluation of meta-benzenedisulfonic acid as a stress-reducing additive in a Watts nickel electroplating bath
[NASA-TN-D-5188] c17 N69-36697
MURPHY, G. L.
Saturn V longitudinal oscillation /POGO/ solution.
[AIAA PAPER 69-548] c31 A69-32658
MURPHY, J. P.
A semi-analytic theory for the motion of a lunar satellite
[NASA-TN-D-5043] c30 N69-28050
MURPHY, W. J.
Development of a barium chemical release system
[NASA-CR-1415] c13 N69-35660
MURRELL, J. D.
Power systems for the Apollo Applications Program. c03 A69-42244
MURROW, H. N.
Some test results from the NASA planetary entry parachute program.
[AIAA PAPER 68-934] c02 A69-35952
MURTAGH, T. B.
Optimum interplanetary midcourse velocity-correction schedules. c21 A69-39646
Planetary probe guidance accuracy influence factors for conjunction-class missions
[NASA-TN-D-4852] c21 N69-16503
MUSEN, P.
Investigations in Hansen's planetary theory. c30 A69-13781
Application of Hansen's method to the X super th satellite of Jupiter. c30 A69-37529
Application of Hansen's method to the 10th satellite of Jupiter
[NASA-TN-D-4979] c30 N69-14479
Planetary effects in the motion of natural satellites
[NASA-TN-D-5284] c30 N69-37893
MUSTEL, E. R.
Solar activity, no. 3 Collection of articles
[NASA-TT-F-581] c29 N69-33401

N

NACHTSHEIM, P. R.
Analysis of the stability of a thin liquid film adjacent to a high-speed gas stream
[NASA-TN-D-4976] c12 N69-15630
NAKADA, M. P.
A study of the composition of the lower solar corona. c30 A69-33059
NARASINGA RAO, B. C.
Photoelectron flux in the topside ionosphere measured by retarding potential analyzers. c29 A69-25144
Ion, electron, and neutral temperatures derived from ion composition distribution. c29 A69-31990
NARIAI, K.
Mass loss from coronae and its effect upon stellar rotation. c30 A69-20644
Coronae around helium stars and X-ray sources. c29 A69-20645
Infrared photometry of a helium star, HD 30353. c30 A69-35348
Mass loss from coronae and its effect upon stellar rotation. c30 A69-39521
NAUGLE, J. E.
Objectives and goals in space science and applications 1968
[NASA-SP-162] c30 N69-13844
NAUMANN, R. J.
Calibration of Pegasus and Explorer 23 detector panels
[NASA-TR-R-321] c14 N69-36985
NEINER, G. H.
Restart and high response terminal shock control for an axisymmetric mixed-compression inlet with 60-percent internal contraction
[NASA-TM-X-1792] c28 N69-24938
NELMS, W. P., JR.
An experimental and theoretical investigation of a symmetrical and a cambered delta wing configuration at Mach numbers from 2.0 to 10.7
[NASA-TN-D-5272] c01 N69-29269
NELSON, A.
NASA space program possibilities and upper stage implications.
[AAS PAPER 69-359] c34 A69-42828
NELSON, C. B.
Simulation of package transfer concepts for Saturn 1 Orbital Workshop
[NASA-TN-D-5111] c05 N69-21501
NELSON, L. A.
Handbook of Solar Simulation for Thermal Vacuum Testing. c11 A69-38894
NELSON, L. S.
Luminous fog layer surrounding a zirconium droplet burning in an oxygen-containing atmosphere. c33 A69-28462
NELSON, W.
Rat body composition - Sensor implantation and lighting effects. c04 A69-26557
NESS, N. F.
Measurements of the perturbed-interplanetary magnetic field in the lunar wake. c30 A69-11228
Particle shadowing by the moon. c30 A69-16252
Satellite studies of the earth's magnetic tail. c29 A69-19363
Observations of the interplanetary magnetic field, 4-12 July 1966. c30 A69-23773
A model of interplanetary and coronal magnetic fields. c30 A69-24429
The geomagnetic tail. c13 A69-26739
Direct measurements of interplanetary magnetic fields and plasmas. c30 A69-30010
The electrical conductivity and internal temperature of the moon. c30 A69-31442
Power spectra of the interplanetary magnetic field. c30 A69-37554
Dependence of the lunar wake on solar wind plasma characteristics. c30 A69-38095

Lunar Explorer 35.
c30 A69-38379
NEUGEBAUER, G.
Two-micron sky survey - A preliminary catalog
[NASA-SP-3047-REV] c30 N69-37993
NEUPERT, W. M.
X-ray and extreme ultraviolet /1-400 angstrom units/ spectroscopy of the sun, from OSO-III.
c29 A69-22169
X rays from the sun.
c29 A69-39506
Observations of the solar flare soft X-ray spectrum and comparison with centimetric radio bursts.
c29 A69-43609
NEUSCHAEFER, R. W.
Assuring Saturn quality through nondestructive testing.
c15 A69-23050
NEVILLE, E. D.
In vivo utilization of acetate-1-C super 14 in centrifuged rats.
c04 A69-19429
Conversion of acetate-2 -super 14 C tc super 14 CO sub 2 and super 14 C-fatty acids in the partially hepatectomized rat /33627/.
c04 A69-35976
Effects of hyperoxia and hypoxia on mitosis in the normal and regenerating rat liver.
c04 A69-43565
NEWELL, F. D.
Human transfer characteristics in flight and ground simulation for a roll tracking task
[NASA-TN-D-5007] c05 N69-17814
NEWELL, H. E.
Contributions and results of space science programs.
c30 A69-10498
Current program and considerations of the future for earth resources survey.
c34 A69-26978
NEWTON, G. P.
Direct in situ measurements of wave propagation in the neutral thermosphere.
c13 A69-16261
Midlatitude neutral thermosphere density and temperature measurements.
c13 A69-16268
Latitudinal variations in the neutral atmospheric density.
c13 A69-38100
Atmospheric densities measured by the Explorer 17 density gauges - Analysis of errors and their effects upon the measurements
[NASA-TN-D-5447] c13 N69-40924
NICHOLLS, J. A.
Subsonic sphere drag measurements at intermediate Reynolds numbers
[NASA-CR-1392] c01 N69-30609
NICHOLS, C. D.
Microelectronic data and control transmission system for dynamic wind-tunnel testing.
c11 A69-23283
NICHOLS, C. E.
Automatic controls for facilities and Mercury ion thrusters in durability testing.
[AIAA PAPER 68-576] c11 A69-12385
NICHOLS, F. H.
The Ames combined heating facility.
[AIAA PAPER 69-342] c11 A69-28278
NICHOLS, J. J.
Saturn 5, S-4B panel flutter qualification test Final report
[NASA-TN-D-5439] c32 N69-38808
NICHOLS, L. D.
Comparison of Brayton and Rankine cycle magnetogasdynamic space-power generation systems
[NASA-TN-D-5085] c03 N69-20852
Analytical and experimental studies of MHD generator cathodes emitting in a ''spot'' mode
[NASA-TN-D-5414] c25 N69-35732
Effect of electrothermal instabilities on Brayton- and Rankine-cycle magnetohydrodynamic space-power generation systems
[NASA-TN-D-5461] c03 N69-37883
NICHOLS, L. L.
Measurement of the super 10 B/n, alpha/ super 7 Li, super 7 Li relative cross sections in the keV region.
c24 A69-33753
NICOLAI, L. M.
An experimental and theoretical analysis of the convected balanced arc
[NASA-CR-1267] c25 N69-18041
NICOLETTA, C. A.
An in situ facility for the determination of the effects of a space environment on the solar absorptance of materials.
[AIAA PAPER 69-1021] c11 A69-40392
NIEDRA, J. M.
A passive isolating transformer of repeated positive cr negative voltage pulses.
c09 A69-10564
A transformer of closely spaced pulsed wave forms having a nonzero average value
[NASA-TN-D-5473] c09 N69-38776
NIEDZWIECKI, R. W.
Combustion stability of single swirl-can combustor modules using ASTM-A1 liquid fuel
[NASA-TN-D-5436] c28 N69-40080
NIELSEN, J. N.
Calculation of compressible turbulent boundary layers with pressure gradients and heat transfer
[NASA-CR-1303] c12 N69-21653
Theoretical study of vortex shedding from bodies of revolution undergoing coning motion
[NASA-CR-1448] c12 N69-40200
NIESSEN, F. R.
Simultaneous usage of attitude control for VTOL maneuvering determined by in-flight simulation
[NASA-TN-D-5342] c02 N69-32110
NIX, W. D.
A dislocatien model pertaining to the strength of elastically inhomogeneous materials.
c17 A69-20557
NIXON, D. D.
Attitude control of a manned earth orbiting space station.
[AIAA PAPER 69-846] c31 A69-39376
NOLL, R. B.
Minimizing spacecraft structure control-system interactien.
c31 A69-25500
NORDBERG, W.
Atmospheric structure research for long-term forecasting.
[UN PAPER 68-95397] c20 A69-10463
Microwave observations of sea state from aircraft.
c13 A69-34421
NORDMEYER, E. F.
An empirically derived erosion law and its applicatien to Lunar Module landing.
c30 A69-41388
NORMAN, P. E.
Out-of-this-world photogrammetry.
c14 A69-34336
Out-of-this-world photogrammetry.
c14 A69-36931
NORMAN, S. M.
Unmanned outer planet capture missions.
[AAS PAPER 68-105] c30 A69-39221
NORTHAM, G. B.
Effects of acceleration upon solid-rocket performance.
[AIAA PAPER 68-530] c28 A69-39217
Effects of steady-state acceleration on combustion characteristics of an aluminized composite solid propellant
[NASA-TN-D-4914] c33 N69-13231
Experimental investigation of the effect of aluminum size and loading on the burning rate of solid propellants under acceleration
[NASA-TN-D-5397] c27 N69-36225
NORTHROP, T. G.
Charged particle diffusion by violation of the third adiabatic invariant.
c29 A69-19375
NORTON, H. T., JR.
Subsonic performance characteristics of a large-scale 1.075-pressure-ratio tip-turbine cruise-fan propulsion system
[NASA-TN-D-5314] c28 N69-35526
NORTON, R. H.
Principal science results from Surveyor 5.
c30 A69-12224
NORWOOD, J., JR.
Causes of magnetic-field nonuniformity and its effect on stability of theta-pinch plasma

[NASA-TR-R-303] c25 N69-20997
NOSEK, S. M.
Two-dimensional cascade investigation of a turbine tandem blade design
[NASA-TM-X-1836] c01 N69-30632
NOVELLO, J.
On-board spacecraft processor.
c08 A69-39921
NOVOSAD, S. W.
An analysis of the telecommunications performance of a lunar relay satellite system.
c07 A69-42508
NOVOTNY, J. E.
Postflight optical evaluation of the right- hand and left-hand windows of Gemini missions 4, 5, 6, and 7
[NASA-TN-D-4916] c31 N69-13232
Preflight optical evaluation of the right-hand hatch windows of Gemini missions 7, 8, 9, and 12
[NASA-TN-D-5471] c31 N69-40813
NOYES, J.
The centrifuge as a therapeutic device.
c04 A69-43372
NUENKE, J. M.
Identity between the growth hormone degrading activity of the pituitary gland and plasmin.
c04 A69-17105
NUGENT, J.
Wind-tunnel force and pressure tests of rocket-engine nozzle extensions on the 0.0667-scale X-15-2 model at supersonic and hypersonic speeds
[NASA-TM-X-1759] c01 N69-20873
NURRE, G. S.
Application of gravity gradient stabilization to large manned space vehicles.
c31 A69-18338
NUSBAUM, W. J.
Cold performance evaluation of 4.97-inch radial-inflow turbine design for single-shaft Brayton cycle space-power system
[NASA-TN-D-5090] c03 N69-20937
NUSSLE, R. C.
Observations of interface behavior during inflow to an elliptical ended cylinder in weightlessness
[NASA-TM-X-1719] c12 N69-15473
NYBAKKEN, G. H.
Laboratory experiments on reverted rubber friction
[NASA-CR-1398] c02 N69-34915
NYSMITH, C. R.
An experimental impact investigation of aluminum double-sheet structures.
[AIAA PAPER 69-375] c32 A69-28305
Experimental investigation of the momentum transfer associated with impact into thin aluminum targets
[NASA-TN-D-5492] c32 N69-38809

O

OATES, R. W.
Human survival in aircraft emergencies
[NASA-CR-1262] c02 N69-14763
OBERBECK, V. R.
Genetic implications of lunar regolith thickness variations.
c30 A69-18604
OBLOY, S. J.
Automatic controls for facilities and Mercury ion thrusters in durability testing.
[AIAA PAPER 68-576] c11 A69-12385
OBRIEN, R. M.
Saturn V navigation update.
[AIAA PAPER 69-883] c21 A69-39409
OCHELTREE, S. L.
Electron beam flow visualization in hypersonic helium flow.
c11 A69-35722
ODELL, F. W.
Composition of cosmic rays measured in Gemini XI.
c29 A69-38350
ODONNELL, P. M.
The fluorination of metals.
c06 A69-39706
ODUM, R.
A study of Saturn AS-502 coupling longitudinal structural vibration and lateral bending response during boost.
[AIAA PAPER 69-58] c31 A69-18204
OEGELMAN, H.
Discrete source interpretation of recent high energy cosmic gamma ray measurements.
c29 A69-20699
Search for ultra-short light pulses from pulsars.
c30 A69-34994
OEGELMAN, H. B.
A gamma ray telescope utilizing large area wire spark chambers.
[IEEE PAPER 3A-5] c14 A69-19192
OEGELMANN, H. P.
Lectures in high energy astrophysics
[NASA-SP-199] c29 N69-29652
OEHMAN, W. I.
Bodies of revolution having minimum total drag in hypersonic flow
[NASA-TN-D-5438] c01 N69-36699
OERTEL, G. K.
Tables for the calculation of radial multipole matrix elements by the Coulomb approximation.
c24 A69-10901
OGAWA, T.
Radiation fields of energetic electrons in helical orbits within a magnetoactive plasma.
c30 A69-39965
OGDEN, E.
Dispersion and attenuation of small artificial pressure waves in the canine aorta.
c04 A69-14692
Transmission characteristics of axial waves in blood vessels.
[SESA PAPER 1350] c04 A69-19726
OGILVIE, K. W.
Plasma observations on Explorer 34.
c13 A69-11234
Microscale fluctuations in the interplanetary magnetic field.
c30 A69-24100
Causes of sudden commencements and sudden impulses.
c29 A69-31963
Dependence of the lunar wake on solar wind plasma characteristics.
c30 A69-38095
Hydromagnetic shocks in the solar wind.
c30 A69-40304
Helium abundance in the solar wind.
c29 A69-40305
OGLEBAY, J. C.
Analytical evaluation of space storable propellants for unmanned Jupiter and Saturn orbiter missions
[NASA-TM-X-1793] c31 N69-24942
OGLESBEE, J. W.
A device for printing alphanumeric listings and digital data plots.
c08 A69-33108
A device for producing both hard copy alphanumeric listings and digital data plots
[NASA-TN-D-5474] c08 N69-38654
OHLHABER, R. L.
Evaluation of vacuum UV detector-spectroscopy systems for capsule reentry measurements
[NASA-CR-1268] c09 N69-18761
OHRING, G.
Inference of stratospheric temperature and moisture profiles from observations of the infrared horizon Final report
[NASA-CR-1419] c20 N69-35528
OKEEFE, J. A.
Isostasy on the moon.
c30 A69-14631
Collapse theory of dimple craters.
c30 A69-15589
Water on the moon and a new nondimensional number.
c30 A69-19262
Origin of the moon.
c30 A69-29882
Origin of tektites.
c30 A69-40086
OLDHAM, W. J. B., JR.
Excitation of the n super 1 S states of helium by proton impact.
c24 A69-17027
Temporal plasma echoes.
c25 A69-38713
OLDRIEVE, R. E.
Protective coatings for chromium alloys.

c17 A69-26495
OLEARY, B. T.
The opposition effect of Mars and its implications.
c30 A69-18601
OLIVER, C. C.
Downstream radiation flux to blunt entry vehicles.
c33 A69-12547
Theoretical predictions of nongray radiant heat transfer in high-temperature nonisothermal CO sub 2 -N sub 2 mixtures.
[AIAA PAPER 69-636] c33 A69-33258
OLIVIER, J. R.
A program plan for earth orbital space astronomy.
c11 A69-27947
OLSEN, E.
Potassium feldspar in Weekeroo Station, Kodaikanal, and Colomera iron meteorites.
c30 A69-14979
OLSEN, W. A., JR.
Three-phase heat transfer - Transient condensing with freezing on a nonisothermal inclined plane
[NASA-TN-D-5289] c33 N69-29598
OLSON, D.
Predicting human performance in space environments
[NASA-CR-1370] c05 N69-30168
OLSON, K. E.
High-performance light-weight electrodes for hydrogen-oxygen fuel cells
[NASA-CR-1216] c03 N69-14397
OLSTAD, W. B.
Correlations for stagnation-point radiative heat transfer.
c33 A69-14736
Nongray radiating flow about smooth symmetric bodies with large blowing.
[AIAA PAPER 69-637] c01 A69-33290
Blunt body stagnation region flow with nongray radiation heat transfer - A singular perturbation solution
[NASA-TR-R-295] c12 N69-10788
OMATHUNA, D.
The Vinti dynamical problem and the geopotential
[NASA-TR-R-307] c30 N69-22948
OMHOLT, A.
Atmospheric Emissions, Proceedings of the NATO Advanced Study Institute, Agricultural College of Norway, As, Norway, July 29-August 9, 1968.
c13 A69-38482
OMIDVAR, K.
Electron-impact ionization of H/2s/ and H/2p/.
c24 A69-17138
Behavior of the ionization cross section in collisions of high-energy electrons with hydrogenic atoms.
c24 A69-20738
ONDOH, T.
Characteristics of low-latitude VLF emissions.
c07 A69-13900
ONEILL, B.
Gravity model comparison using GEOS 1 long- arc orbital solutions
[NASA-TN-D-5035] c30 N69-27412
Evaluation of the Goddard range and range rate system at Rosman by intercomparison with GEOS 1 long-arc orbital solutions
[NASA-TN-D-5036] c13 N69-28442
ORANGE, T. W.
A semiempirical fracture analysis for small surface cracks
[NASA-TN-D-5340] c32 N69-31056
ORGAN, S. L.
Analytical and experimental study of the dynamics of a single-tube counterflow boiler
[NASA-CR-1230] c12 N69-17751
ORMES, J. F.
The relative energy spectra of carbon and oxygen nuclei in the primary cosmic radiation.
c29 A69-20632
ORTH, R. C.
The interaction and penetration of gaseous jets in supersonic flow
[NASA-CR-1386] c12 N69-32480
OSBORN, W. M.
Effects of three outlet-annulus area blockage configurations on the performance of a 20-inch /50.8-CM/ axial-flow compressor rotor
[NASA-TN-D-5506] c28 N69-40078
OSTERLE, J. F.
Transient electro-osmosis in capillary tubes.
c06 A69-14862
OSTROFF, A. J.
Design of an electronically scanned star sensor with digital output
[NASA-TN-D-5281] c14 N69-29153
OTERO, R. J.
Pulse interference effects in a phase-lock loop.
c10 A69-42230
Radio spectrum utilization in aerospace communication systems.
c07 A69-42502
OTTERSON, D. A.
Electrical resistivity as a function of deuterium concentration in palladium
[NASA-TN-D-4970] c26 N69-14565
Absorption of hydrogen by palladium and electrical resistivity up to hydrogen- palladium atom ratios of 0.97
[NASA-TN-D-5441] c26 N69-37272
OYAMA, V. I.
Automatic apparatus for sampling and preparing gases for mass spectral analysis in studies of carbon isotope fractionation during methane metabolism.
c06 A69-12603
Differential thermal analysis of some biological specimens, proteins, and starches.
c06 A69-31807

P

PAANANEN, R. A.
Iodine infrared laser.
[IEEE PAPER T-5] c16 A69-19082
Compilation of data from related technologies in the development of an optical pilot warning indicator system
[NASA-TN-D-5174] c14 N69-27267
PACE, N.
Phase relationships between circadian rhythms and photoperiodism in the monkey.
c04 A69-42706
PACKARD, R. D.
Mercury cadmium telluride as a 1-20 microns wavelength infrared detector for space applications.
c26 A69-43666
Mercury cadmium telluride as a 1- to 20-micro-meter wavelength infrared detector for space applications
[NASA-TN-D-4904] c26 N69-10125
A bonding material for optically immersing infrared detectors from 2 to 14 micro-meters
[NASA-TM-X-1776] c18 N69-23843
PADDACK, S. J.
Rotational bursting of small celestial bodies - Effects of radiation pressure.
c30 A69-39584
PAETZNICK, H. R.
Method of deriving orbital perturbing parameters from onboard optical measurements of an ejected probe or a natural satellite
[NASA-CR-1412] c30 N69-35513
PAEZ, O. A.
Electrochemical characterization of nonaqueous systems for secondary battery application
[NASA-CR-1434] c03 N69-36829
PAINTER, J. H.
Synthesis techniques for a class of SSB-AM-PM signals.
c07 A69-29489
On filtering prior to limiting digital signals in strong noise.
c07 A69-39450
Analytic function models of noise and modulation
[NASA-TR-R-314] c07 N69-29230
Applications of analytic function theory to analysis of single-sideband angle-modulated systems
[NASA-TN-D-5446] c07 N69-37602
PAINTER, W. D.
Design, development, and flight test experience with lifting body stability augmentation systems.
[AIAA PAPER 69-887] c02 A69-39413
PALACOL, E. L.
Manipulation errors in finite element analysis of

structures
[NASA-CR-1385] c19 N69-34360
PALLSON, W. A.
Estimation of fission-product gas pressure in uranium dioxide ceramic fuel elements
[NASA-TN-D-4823] c22 N69-10216
PALMER, B. A.
Nimbus 2 flight evaluation and engineering report, launch through orbit 5275
[NASA-TN-D-4881] c31 N69-17851
PALMER, R. W.
Computer-made movies and plotting descriptions of ion-molecule collisions with polar targets.
c24 A69-43124
PALUDAN, C. T. N.
Potential contributions of orbital earth resources data to urban planning.
[AAS PAPER 69-483] c13 A69-42837
PAN, W. Y.
Design considerations for an integrated 1.8- GHz parametric amplifier.
c09 A69-10193
PANOFSKY, H. A.
Investigation of the turbulent wind field below 150-meter altitude at the eastern test range
[NASA-CR-1410] c20 N69-35570
PAO, C.-V.
Stability theory of nonlinear operational differential equations in Hilbert space
[NASA-CR-1356] c19 N69-28256
PAO, H.-H.
Clear Air Turbulence and its Detection, Boeing Company, Symposium, Seattle, Wash., August 14-16, 1968, Proceedings.
c20 A69-33732
PAPADOPOULOS, J. G.
A study of Saturn AS-502 coupling longitudinal structural vibration and lateral bending response during boost.
[AIAA PAPER 69-58] c31 A69-18204
PAPE, R.
Solubility and diffusion of oxygen in tantalum
[NASA-CR-1276] c17 N69-19886
PAPELL, S. S.
Inlet effects on boiling and near critical hydrogen heat transfer.
[ASME PAPER 69-HT-27] c33 A69-43541
PAPPAS, C. C.
Effects of mass addition of various gases on the heat transfer and surface pressures on a blunt cone in hypersonic flow.
[AIAA PAPER 69-716] c01 A69-33463
PARK, C.
Spectral line intensities in a nonequilibrium nitrogen plasma.
c24 A69-10960
Theoretical population inversion in a decaying nitrogen plasma column.
[AIAA PAPER 69-48] c25 A69-18145
An experiment on the MHD-driven flow for a gas core nuclear rocket.
[AIAA PAPER 69-727] c22 A69-33483
Collisional ionization and recombination rates of atomic nitrogen.
c24 A69-43700
PARK, C. G.
Multi-experiment detection of the plasmapause from EOGO satellites and antarctic ground stations.
c13 A69-25153
PARK, S.
Degradation of multiplier phototubes exposed to spatial radiations
[NASA-CR-1304] c14 N69-20777
PARKER, A. J., JR.
Thermal model of a 75 watt.
c03 A69-42254
PARKER, C. D.
A feasibility study of a miniature solid-state pressure transducer
[NASA-CR-1366] c26 N69-29724
PARKER, J. A.
Ablative thermal protection at low heating rates.
c18 A69-35536
Experimental evaluation of polyurethane foam composites for low-heating-rate thermal protection.
c18 A69-39236
The development of polybenzimidazole composites as ablative heat shields.
c18 A69-41715
PARKER, R. J.
Contact conformity effects on spinning torque and friction.
[ASME PAPER 68-LUB-10] c15 A69-30901
Effect of oxygen concentration on synthetic paraffinic and advanced ester base lubricants in bearing tests at 400 deg and 450 deg F.
c15 A69-35177
Rolling-element fatigue life of ausformed M-50 steel balls
[NASA-TN-D-4954] c15 N69-14383
Effect of oxygen concentration on an advanced ester lubricant in bearing tests at 400 deg and 450 deg F
[NASA-TN-D-5262] c15 N69-26311
Effect of oxygen concentration on the performance of synthetic paraffinic oils in short term bearing tests from 400 deg to 500 deg F
[NASA-TN-D-5152] c15 N69-26314
PARKMAN, M.
Solubility and diffusion of oxygen in tantalum
[NASA-CR-1276] c17 N69-19886
PARLETT, L. P.
Wind-tunnel investigation of a large jet transport model equipped with an external-flow jet flap
[NASA-TN-D-4928] c01 N69-14000
Wind-tunnel investigation of a STOL aircraft configuration equipped with an external-flow jet flap
[NASA-TN-D-5364] c01 N69-33275
PARTEN, R. P.
Utilization of ground-based guidance systems to supplement onboard guidance of space vehicles.
c21 A69-17580
PATCH, R. W.
Absorption coefficients for hydrogen. I.
c24 A69-19165
Components of a hydrogen plasma including minor species
[NASA-TN-D-4993] c25 N69-16466
Calculated interaction energy and dipole moment in collisions of two hydrogen molecules
[NASA-TN-D-5486] c24 N69-39184
Interim absorption coefficients and opacities for hydrogen plasma at high pressure
[NASA-TM-X-1902] c24 N69-39187
PATTEE, H. E.
Joining ceramics and graphite to other materials
[NASA-SP-5052] c15 N69-14241
PATTERSON, G. N.
Exploratory drag reduction studies in non-polar soap systems.
c12 A69-33253
PATTON, J. M.
Flight tests of a direct lift control system during approach and landing
[NASA-TN-D-4854] c02 N69-10371
PAUL, F. W.
Optical constants of some pump oils in the vacuum ultraviolet.
c23 A69-23647
PAULI, A. J.
Design, development, and testing of a 1000 pound /4450 N/ thrust FLOX-propane ablative rocket engine
[NASA-TM-X-1873] c28 N69-35847
PAULL, S.
The IMP-I computer experiment.
c08 A69-36265
PAULOVICH, F. J.
Airbreathing propulsion system testing using sweep frequency techniques
[NASA-TN-D-5485] c28 N69-39185
PAVLI, A. J.
Design of injectors and ablative thrust chambers for a flox-propane rocket engine with a 1.2-inch throat diameter
[NASA-TN-D-5324] c28 N69-30560
PAVLOSKY, J. E.
Apollo thermal-protection system development.
[AIAA PAPER 68-1142] c31 A69-13558
PAVLOVIC, D. M.
Evaluation of magnetic materials for static inverters and converters
[NASA-CR-1226] c03 N69-17765
PEARSON, O. L.
Manned test operations related to the Apollo lunar module in the simulated space environment.

c05 A69-30394
PEARSONS, K. S.
Combination effects of tone and duration parameters on perceived noisiness
[NASA-CR-1283] c04 N69-18722
PEAVEY, B.
Performance characteristics and specification of PCM bit synchronizer/signal conditioners.
c09 A69-19120
PEAVEY, R. C.
Commercial Utilization of Space, American Astronautical Society, Annual Meeting, 13th, Dallas, Tex., May 1-3, 1967, Proceedings.
c30 A69-34043
PEDDREW, K. M.
A micro lagoon technique for the culture and observation of isolated mammalian cells
[NASA-TN-D-4906] c04 N69-11056
PEELE, E. L.
A simplified method of estimating the response of light aircraft to continuous atmospheric turbulence.
[AIAA PAPER 69-766] c32 A69-35657
PEGG, R. J.
Flying quality factors currently limiting helicopter nap of the earth maneuverability as identified by flight investigation
[NASA-TN-D-4931] c02 N69-14008
A flight investigation of a lightweight helicopter to study the feasibility of fixed-collective-pitch autorotations
[NASA-TN-D-5270] c02 N69-29232
PELLETT, G. L.
High temperature decomposition of ammonium perchlorate using CO sub 2 laser-mass spectrometry.
[AIAA PAPER 69-143] c06 A69-18111
Vapor-phase combustion phenomena when Zr droplets burn in oxygen.
[WSCI PAPER 69-4] c27 A69-32345
PELLIGRA, R.
The centrifuge as a therapeutic device.
c04 A69-43372
PELZ, D. T.
Direct in situ measurements of wave propagation in the neutral thermosphere.
c13 A69-16261
Midlatitude neutral thermosphere density and temperature measurements.
c13 A69-16268
Latitudinal variations in the neutral atmospheric density.
c13 A69-38100
PENTZ, N. E.
A large-angle approximation for high-energy scattering.
c24 A69-29008
PEOPLES, J. A.
Transport study of neutron and photon attenuation through lithium hydride and tungsten spherical media
[NASA-TN-D-4989] c24 N69-15375
PEPPER, S. V.
Enhanced photoemission by attenuated total reflection.
c23 A69-42194
Absorption of infrared radiation by ice cryodeposits
[NASA-TN-D-5181] c23 N69-22769
PERDRISAT, C. F.
Elastic scattering of 600 MeV protons from He super 3.
c24 A69-13464
Polarization in proton super 4 He scattering at 540 MeV.
c24 A69-14966
PEREK, L.
Highlights of Astronomy, International Astronomical Union, General Assembly, 13th, Prague, Czechoslovakia, August 22-31, 1967, Proceedings.
c30 A69-15834
PERING, K.
Alicyclic hydrocarbons from an unusual deposit in Derbyshire, England - A study in possible diagenesis.
c06 A69-34184
Synthesis of acyclic isoprenoids by the gamma-irradiation of isoprene.
c04 A69-43750
PERKINS, J. N.
A modified method of integral relations approach to the blunt-body equilibrium air flow field, including comparisons with inverse solutions
[NASA-TN-D-5434] c12 N69-36830
PERSON, L. H., JR.
Flight test evaluation of a small one-man lunar flying device.
[AIAA PAPER 68-240] c11 A69-12379
PERZ, D. A.
Preliminary performance characteristics of a gas-bearing turboalternator
[NASA-TM-X-1820] c03 N69-29707
PETERS, L. E., JR.
Analysis of aperture radiation from an axially slotted circular conducting cylinder using geometrical theory of diffraction.
c07 A69-24993
Measured thermal-neutron-flux perturbations in cylinders in a test reactor.
c22 A69-38274
Aperture radiation from an axially slotted elliptical conducting cylinder using geometrical theory of diffraction.
c09 A69-40703
Equatorial plane pattern of an axial-TEM slot on a finite size ground plane.
c07 A69-41588
Predictive equations for thermal neutron flux perturbation effects in cylinders
[NASA-TN-D-4949] c22 N69-14481
PETERS, R. A.
Dynamics of the vestibular system and their relation to motion perception, spatial disorientation, and illusions
[NASA-CR-1309] c04 N69-22637
Experiments and a model for pilot dynamics with visual and motion inputs
[NASA-CR-1325] c05 N69-28071
PETERSEN, E. W.
Infrared measurements of variations in stratospheric water vapour.
c13 A69-38261
PETERSON, D. A.
Rocket engine evaluation of erosion and char as functions of fabric orientation for silica-reinforced nozzle materials
[NASA-TM-X-1721] c28 N69-15475
Evaluation of 7.8-inch-throat-diameter inserts and a unique cooling concept in a storable-propellant rocket engine
[NASA-TM-X-1756] c28 N69-19782
Design of injectors and ablative thrust chambers for a flox-propane rocket engine with a 1.2-inch throat diameter
[NASA-TN-D-5324] c28 N69-30560
Development of improved throat inserts for ablative rocket engines
[NASA-TN-D-4964] c32 N69-33481
Design, development, and testing of a 1000 pound /4450 N/ thrust FLOX-propane ablative rocket engine
[NASA-TM-X-1873] c28 N69-35847
PETERSON, E.
Trace porphyrin complexes - Fluorescence detection by demetallation with methanesulfonic acid.
c06 A69-42557
PETERSON, J. P.
Buckling of thin-walled circular cylinders
[NASA-SP-8007] c32 N69-23320
PETERSON, V. L.
Aerodynamics of bodies of revolution in coning motion.
[AIAA PAPER 68-20] c01 A69-14714
PETRASEK, D. W.
Tungsten alloy fiber reinforced nickel base alloy composites for high temperature turbojet engine applications.
c17 A69-29010
Stress-rupture and tensile properties of refractory-metal wires at 2000 deg and 2200 deg F /1093 deg and 1204 deg C/
[NASA-TN-D-5139] c32 N69-22823
PEW, R. W.
Skill training for the production of a memorized movement pattern
[NASA-CR-1251] c05 N69-13926

PFEIFFER, C. G.
Sequential processing techniques for trajectory estimation
[NASA-CR-1360] c30 N69-40325
PFENNINGER, W.
Amplified laminar boundary layer oscillations and transition at the front attachment line of a 45 deg swept flat-nosed wing with and without boundary layer suction.
c01 A69-33251
PHARO, M. W., III
Evidence of contraction of the earth's thermal plasmasphere subsequent to the solar flare events of 7 and 9 July 1966.
c13 A69-23777
Implications for ionospheric chemistry and dynamics of a direct measurement of ion composition in the F 2 region.
c13 A69-31974
PHILIPP, W. H.
Radiation induced reduction of ammoniacal nickel /2/ sulfate to metallic nickel
[NASA-TN-D-5213] c06 N69-24940
PHILLIPS, B.
On the design of acoustic liners for rocket engines - Maximum damping as a design objective
[NASA-TM-X-1720] c28 N69-16152
On the design of acoustic liners for rocket engines - Helmholtz resonators evaluated with a rocket combustor
[NASA-TN-D-5171] c33 N69-23351
PHILLIPS, B. S.
Aerodynamic loads on deployed canard surfaces and rocket nose section of the Apollo launch escape vehicle
[NASA-TN-D-5260] c31 N69-28166
PHILLIPS, D. H.
Doublet electronic states of the benzyl radical.
c24 A69-13321
Luminescence from aromatic polymers, monomers, and dimers under high-energy electron excitation.
c26 A69-32792
Resolution changes in lithium-drifted silicon semiconductor detectors irradiated with 0.5, 1.0, 2.0, and 3.0 MeV electrons
[NASA-TN-D-4901] c14 N69-10933
PHILLIPS, E. P.
Effect of outdoor exposure at elevated temperature on the fatigue life of Ti-8Al-1Mo-1V titanium alloy and AM 350 stainless steel sheet
[NASA-TN-D-5362] c17 N69-32558
PHILLIPS, W. C.
Compton profile of LiH.
c26 A69-40730
PHILLIPS, W. P.
Recent studies on effects of runway grooving on airplane operations.
[AIAA PAPER 69-773] c02 A69-35649
PHILPOTT, D. E.
Viruslike particles in the fat body, oenocytes, and central nervous tissue of Drosophila melanogaster imagoes.
c04 A69-42021
PHILPOTTS, J. A.
Partition coefficients of rare-earth elements and barium between igneous matrix material and rock-forming-mineral phenocrysts. I.
c13 A69-20944
Genesis of continental diabases and oceanic tholeiites considered in light of rare-earth and barium abundances and partition coefficients.
c13 A69-20945
Genesis of the calcium-rich achondrites in light of rare-earth and barium concentrations.
c30 A69-36091
Rubidium-strontium correlation study of moldavites and Ries Crater material.
c13 A69-41341
PICKARD, R. H.
The S-band Telemetry, Tracking, and Command Experiment.
c07 A69-41759
PICKETT, R. A.
Diurnal and seasonal variation of atmospheric ion composition, correlation with solar zenith angle.
c13 A69-38087
PIERCE, C. R.
Resonance integrals of rhenium for a wide range of sample sizes
[NASA-TN-D-4938] c24 N69-13152
PIERCE, W. S.
Effect of radius on bulging and fracture of through-cracked cylindrical pressure vessels at cryogenic temperatures
[NASA-TN-D-4951] c32 N69-14480
Factors influencing low cycle crack growth in 2014-T6 aluminum sheet at minus 320 deg F /77 K/
[NASA-TN-D-5140] c32 N69-21392
PIERSOL, A. G.
A method for predicting launch vehicle vibration levels in the region of the spacecraft adaptor
[NASA-CR-1227] c31 N69-16155
Summary of random vibration prediction procedures
[NASA-CR-1302] c32 N69-23096
PILAND, W. M.
Potential problems related to weightlessness and artificial gravity
[NASA-TN-D-4980] c05 N69-15629
PINCOCK, G. D.
Cavity reactor critical experiments.
c22 A69-18954
PINSON, L. D.
Longitudinal vibration characteristics of 1/10-scale Apollo/Saturn 5 replica model
[NASA-TN-D-5159] c32 N69-22932
PINSON, W. H., JR.
Rubidium-strontium correlation study of moldavites and Ries Crater material.
c13 A69-41341
PISARENKO, G. S.
High temperature strength of materials
[NASA-TT-F-508] c17 N69-27300
PITTELLI, E. E.
Simplified theory and transducer potentialities of the "pinch effect" in semiconductors
[NASA-TN-D-5130] c26 N69-22573
PITTMAN, P. F.
Modularization of high-power inverters and converters.
c03 A69-42292
PITTS, D. E.
A mathematical technique for programming automatic picture transmission tracking angles.
c07 A69-14917
PITTS, G. C.
Rat body composition - Sensor implantation and lighting effects.
c04 A69-26557
PLATT, R. J., JR.
A parametric analysis of surface temperatures of paraboloidal solar concentrators in space
[NASA-TN-D-5144] c03 N69-23356
PLEASANTS, W. H.
Satellite attitude control using a torqued, 2-axis-gimbaled boom as the actuator.
[AIAA PAPER 68-857] c21 A69-43245
PLUMBLEE, H. E.
Effect of jet temperature on jet and pure tone noise radiation
[NASA-CR-1472] c02 N69-40439
PODKULSKI, S. P.
Characteristics of a thermionic converter with a chloride vapor deposited tungsten emitter /110/ and a nickel collector
[NASA-CR-1416] c03 N69-32553
POFFEL, D. J.
Thermodynamic and transport properties of air and the combustion products of natural gas and of ASTM-A-1 fuel with air
[NASA-TN-D-5452] c33 N69-37936
POLAK, L. F.
The design and performance of a versatile 25 solar constant simulator.
c11 A69-30383
POLAND, W. B., JR.
Delta-T curves for measuring magnetic tape link jitter.
c14 A69-18827
Why data system standards?
c08 A69-41769
POLEK, T. E.
Summary and correlation of skin-friction and heat-transfer data for a hypersonic turbulent boundary layer on simple shapes
[NASA-TN-D-5089] c12 N69-29144
POLLACK, F. G.
Surface temperature mapping with infrared

photographic pyrometry for turbine cooling investigations
[NASA-TN-D-5179] c14 N69-23895
POLLACK, M. A.
Methods for the measurement of frequency and stability of laser generators in the infrared.
c16 A69-18482
POLSTORFF, W. K.
Dynamics of a rotating space station.
c30 A69-16476
PONNAMPERUMA, C.
Alicyclic hydrocarbons from an unusual deposit in Derbyshire, England - A study in possible diagenesis.
c06 A69-34184
Synthesis of acyclic isoprenoids by the gamma-irradiation of isoprene.
c04 A69-43750
PONTING, R. L.
Minimization of optical scattering effects through use of optimal monochromator slit geometry
[NASA-TM-X-1702] c24 N69-13210
POORMAN, R. M.
Plasma electron beam development for welding applications.
c15 A69-35555
POPE, R. B.
Ablative thermal protection at low heating rates.
c18 A69-35536
Stagnation-point heat transfer in arc-heated helium and argon.
c33 A69-37198
Experimental evaluation of polyurethane foam composites for low-heating-rate thermal protection.
c18 A69-39236
POPOVIC, P.
Critical temperature for intracranial self-stimulation in white rats.
c04 A69-13897
POPOVIC, V. P.
Critical temperature for intracranial self-stimulation in white rats.
c04 A69-13897
POROS, D. J.
An improved model equatorial electrojet with a meridional current system.
c13 A69-38084
POSCH, R. E.
A coaxial, three-coil probe for measuring local values of electrical conductivity and velocity in plasma streams.
[AIAA PAPER 69-327] c25 A69-28264
POSGAY, R. G.
Definition of entry corridor thermal limits for Apollo spacecraft.
[AIAA PAPER 68-1144] c31 A69-13673
POST, R. E.
Effects of temperature and electrolyte concentration on performance of a fuel cell of the Bacon type
[NASA-TN-D-5154] c03 N69-22940
POTTER, A. E., JR.
Effect of bias light on the spectral response of Cu sub 2 S-CdS cells.
c26 A69-16358
High photovoltages in cadmium sulfide films.
c26 A69-17772
POTTER, J. F.
Effect of cloud scattering on line formation in the atmosphere of Venus.
c30 A69-33161
POULARIKAS, A. D.
A note on the effects of the ionosphere on satellite orbital corrections in near-real time.
c07 A69-42549
POUQUET, J.
A preliminary study of the detection of geomorphological features over northeast Africa by satellite radiation measurements in the visible and infrared
[NASA-TN-D-4648] c13 N69-14290
An approach to the remote detection of earth resources in sub-arid lands
[NASA-TN-D-4647] c13 N69-14450
POVINELLI, F. P.
Vortex enhancement of jet penetration in supersonic flow.
[AIAA PAPER 69-664] c12 A69-33437
A study of helium penetration and spreading in a Mach 2 airstream using a delta wing injector
[NASA-TN-D-5322] c01 N69-30878
Effect of angle of attack and injection pressure on jet penetration and spreading from a delta wing in supersonic flow
[NASA-TM-X-1889] c12 N69-37271
POVINELLI, L. A.
Vortex enhancement of jet penetration in supersonic flow.
[AIAA PAPER 69-664] c12 A69-33437
A study of helium penetration and spreading in a Mach 2 airstream using a delta wing injector
[NASA-TN-D-5322] c01 N69-30878
Solid-propellant combustion instability and the role of velocity coupling
[NASA-TN-D-5395] c33 N69-34892
Effect of angle of attack and injection pressure on jet penetration and spreading from a delta wing in supersonic flow
[NASA-TM-X-1889] c12 N69-37271
POVOLNY, J. H.
Stall and distortion investigation of a YTF30- p-1 turbofan engine.
c28 A69-35175
POWELL, C. A., JR.
The calculated response of a three-crystal pair spectrometer
[NASA-TM-X-1857] c14 N69-34628
POWELL, J. A.
Growth of 2H silicon carbide crystals
[NASA-TN-D-5313] c26 N69-30072
POWERS, B. G.
A comparison of Newton-Raphson and other methods for determining stability derivatives from flight data.
[AIAA PAPER 69-315] c02 A69-22379
POWERS, W. F.
The Hamilton-Jacobi method applied to the low-thrust trajectory problem.
c30 A69-17574
Optimal trajectory coordinate-multiplier systems with constant of the motion components.
[AIAA PAPER 69-907] c30 A69-39339
On the generation of ideal coordinate systems for the analysis of optimal trajectories
[NASA-CR-1250] c30 N69-13274
PRABHAKARA, C.
Feasibility of determining atmospheric ozone from outgoing infrared energy.
c13 A69-28493
PREDMORE, R.
Sliding friction of copper alloys in vacuum.
[ASLE PAPER 68-LC-5] c15 A69-30610
Sliding friction of copper alloys in vacuum
[NASA-TN-D-4824] c15 N69-10757
PREDVODITELEV, A. S.
High-temperature properties of gases. Physical gas dynamics, thermodynamics, and physics of combustion
[NASA-TT-F-558] c12 N69-35365
PREISWERK, P. R.
Axisymmetric and cylindrical isostabiloids
[NASA-CR-1444] c32 N69-38781
PRESCOTT, J. R.
International Conference on Cosmic Rays, 10th, Calgary, Canada, June 19-30, 1967, Proceedings. Part A - Invited and Rapporteur Papers.
c29 A69-12928
PRICE, D. B.
Fixed-base visual simulation of pilot controlled descents of an advanced Apollo spacecraft with an all-flexible parawing
[NASA-TN-D-5049] c21 N69-20936
PRICE, H. L.
Effect of gamma radiation in vacuum on the tensile properties of polymer films.
[ASME PAPER 68-WA/RP-6] c18 A69-16160
Preparation and compression molding of salt- like intermediate Pyrrone /BTDA-EG-DAB/.
c18 A69-29415
Radiation stability of unfilled pyrrone moldings.
c18 A69-35529
Molecular orientation and mechanical anisotropy in polyethylene, polypropylene, and poly/ethylene terephthalate/ films
[NASA-TN-D-5380] c18 N69-34708
PRICE, J. C.
Kinetic theory of inhomogeneous systems.

c25 A69-30913
PRICE, J. W.
Tables and graphs of functions necessary for solving nonlinear heat transfer constant area fin problems with examples on their use
[NASA-TN-D-5173] c33 N69-26975
PRICE, M. J.
A relaxation method for the computation of model stellar atmospheres.
c30 A69-36337
PRIDE, R. A.
Mechanical behavior of boron-epoxy and glass-epoxy filament-wound cylinders under various loads
[NASA-TN-D-5050] c18 N69-19825
Influence of various fabrication methods on the compressive strength of titanium skin- stringer panels
[NASA-TN-D-5389] c15 N69-34707
PRIERSON, W. B.
Protection against toxic rocket fuels.
c05 A69-12498
PRIEST, J. R.
Study of the Sc super 45 /alpha,t/ Ti super 46 reaction at 41 MeV.
c24 A69-41044
Study of the /alpha, t/ reaction on scandium-45 at 41 MeV
[NASA-TN-D-5216] c24 N69-24919
PRIESTER, W.
On the semiannual variation of the upper atmosphere.
c13 A69-26012
PRINCE, R. N.
Evaluation of lithium peroxide for oxygen supply and carbon dioxide control.
[AIAA PAPER 69-620] c05 A69-33303
PRIOR, E. J.
The polar exosphere near solar maximum.
c13 A69-31351
PRIVETTE, C. A.
A subsatellite concept for Martian fields and particles measurements.
c30 A69-39215
PROBST, H. B.
High temperature mechanical properties of polycrystalline hafnium carbide and hafnium carbide containing 13-volume-percent hafnium diboride
[NASA-TN-D-5008] c17 N69-16380
PROCTOR, T. G.
A family of solutions of certain nonautonomous differential equations by series of exponential functions
[NASA-CR-1294] c19 N69-17249
PROGAR, D. J.
The design and uncertainty analysis of an improved total hemispherical emittance transient calorimeter
[NASA-TN-D-5106] c14 N69-20941
PROK, G. M.
Molecular hydrogen inelastic electron impact cross sections - A semiclassical method.
c24 A69-22249
Energy transfer and ion cost in a hydrogen plasma
[NASA-TN-D-5319] c25 N69-29905
PROKOPIUS, P. R.
Experimental investigation of the dynamics of water rejection from a matrix type cf hydrogen-oxygen fuel cell
[NASA-TN-D-4956] c03 N69-14518
PROTOPAPA, S.
Compilation of data from related technologies in the development of an optical pilot warning indicator system
[NASA-TN-D-5174] c14 N69-27267
PRUST, H. W., JR.
Some measurement problems encountered when determining the performance of certain turbine stator blades from total pressure surveys.
[ASME PAPER 69-GT-103] c01 A69-22521
Effect of variable stator area on performance of a single-stage turbine suitable for air cooling. 5 - Stator detailed losses with 70 percent design area
[NASA-TM-X-1696] c28 N69-10296
Effect of variable stator area on performance of a single-stage turbine suitable for air cooling. 6 - Turbine performance with 70-percent design stator area
[NASA-TM-X-1697] c01 N69-10558
PRZYBYSZEWSKI, J. S.
Friction and contact resistance during sliding in vacuum of some-low-resistivity metals lubricated with sputtered molybdenum disulfide films
[NASA-TN-D-5349] c15 N69-31884
PUGMIRE, T. K.
Ammonia Resistojet station keeping subsystem aboard applications technology satellite /ATS/ IV.
[AIAA PAPER 69-296] c28 A69-21212
ATS-III resistojet thruster system performance.
[AIAA PAPER 68-553] c28 A69-39754
PUTHOFF, R. L.
A digital computer program for determining the elastic-plastic deformation and creep strains in cylindrical rods, tubes and vessels
[NASA-TM-X-1723] c32 N69-16115
Reactivity changes of a fast reactor core due to elastic-plastic strain and creep
[NASA-TN-D-5012] c22 N69-16381
PUTT, C. W.
Use of time-sharing computer to support several large test facilities.
c08 A69-33106

Q

QUAIDE, W. L.
Genetic implications of lunar regolith thickness variations.
c30 A69-18604
QUANN, J. J.
A new approach to telemetry data processing - The data reduction laboratory.
c11 A69-40352
QUANTINETZ, M.
Dispersion-strengthened nickel produced from ultrafine comminuted powders
[NASA-TN-D-5421] c17 N69-38074
QUATTRONE, P. D.
Current research on regenerative systems.
c04 A69-37623
QUEIJO, M. J.
Theory for computing span loads and stability derivatives due to sideslip, yawing, and rolling for wings in subsonic compressible flow
[NASA-TN-D-4929] c01 N69-14001
QUIROZ, R. S.
Meteorological rocket research since 1959 and current requirements for observations and analysis above 60 kilometers
[NASA-CR-1293] c13 N69-18700
QUITTER, J. P.
The improvement of an electronic power supply for greater reliability in aerospace use
[NASA-TM-X-1875] c03 N69-35763

R

RAAB, F. H.
Vaporization and decomposition kinetics of candidate re-entry blackout suppressants in low-pressure flames
[NASA-CR-1330] c07 N69-32721
RABINOVICI, B.
A unilateral transformer.
c09 A69-39454
RABINOWITZ, J.
Studies on the formation and transformation of esters. LXXX.
c06 A69-31808
RADFORD, W. E.
Ionospheric and magnetic observations at 1000 kilometers during the geomagnetic storm and aurora of May 25-26, 1967.
c13 A69-34954
RADIN, I.
Exploratory drag reduction studies in non-polar soap systems.
c12 A69-33253
RADNOR, M.
In-house research on the management of R and D in government agencies.
c34 A69-38022
RADOS, R. M.
Atmospheric measurements from satellites.
[AIAA PAPER 69-158] c20 A69-18038

RADOSKI, H. R.
Physics of the Magnetosphere, Proceedings of the Conference, Boston College, Chestnut Hill, Mass., June 19-28, 1967. c29 A69-19351
RAFFO, P. L.
Yielding and fracture in tungsten and tungsten-rhenium alloys. c17 A69-20190
Creep of powder metallurgy rhenium at 0.43 to 0.72 T sub m. c17 A69-34186
Exploratory study of mechanical properties and heat treatment of molybdenum-hafnium-carbon alloys
[NASA-TN-D-5025] c17 N69-19200
Dynamic strain aging during the creep and tensile testing of a molybdenum-titanium- carbon alloy
[NASA-TN-D-5169] c17 N69-22993
Dynamic strain aging in carbide strengthened molybdenum alloys
[NASA-TN-D-5355] c17 N69-31883
RAGSDALE, R. G.
Some recent gaseous reactor fluid mechanics experiments.
[AIAA PAPER 69-477] c22 A69-32728
Simple equations for calculating temperature distributions in radiating gray gases
[NASA-TN-D-5226] c33 N69-25312
Summary of recent gaseous reactor fluid mechanics experiments
[NASA-TM-X-1847] c12 N69-31888
RAHE, J.
Ionization and ray formation in comets. c30 A69-27817
RAHLMANN, D. F.
Phase relationships between circadian rhythms and photoperiodism in the monkey. c04 A69-42706
RAICH, J. C.
Spin wave approximation for anisotropic Heisenberg antiferromagnet. c26 A69-26500
Random phase approximation for the anisotropic Heisenberg ferromagnet
[NASA-TN-D-5286] c26 N69-29588
RAINEY, R. W.
Some topics in hypersonic body shaping.
[AIAA PAPER 69-181] c01 A69-18052
Center-of-gravity requirements for trim of several axisymmetric bodies. c01 A69-39237
RAINWATER, W. J.
Investigation of bremsstrahlung production in spacecraft materials
[NASA-CR-1377] c24 N69-33416
RAKICH, J. V.
Theoretical and experimental study of supersonic steady flow around inclined bodies of revolution.
[AIAA PAPER 69-187] c01 A69-18176
A method of characteristics for steady three-dimensional supersonic flow with application to inclined bodies of revolution
[NASA-TN-D-5341] c12 N69-39177
RAMADURAI, S.
Cosmic Ray Studies in Relation to Recent Developments in Astronomy and Astrophysics, Tata Institute of Fundamental Research, Colloquium, Bombay, India, November 11-16, 1968, Proceedings. c29 A69-38811
RAMASASTRY, J.
Conjugate echoes in Alouette-2 topside-sounder data. c07 A69-20045
Magnetospheric duct propagation research using Alouette-2 topside-sounder observations
[NASA-TN-D-5332] c13 N69-34891
RAMATY, R.
Cosmic-ray deuterium and helium-3 of secondary origin and the residual modulation of cosmic rays. c29 A69-20066
Physical properties of the radio-emitting region in sCo XR-1. c30 A69-37334
Microwave and hard X-ray bursts from solar flares. c29 A69-37551
On the nature of the high-frequency cutoffs of type IV solar radio bursts. c29 A69-40577
RAMEY, R. L.
The thin film iris
[NASA-CR-1364] c26 N69-28096
RAND, E.
Thermal decomposition of yttrium-doped silver carbonate. c06 A69-30442
RANDALL, C. A., JR.
Extra-Terrestrial Matter, Central States Universities and Argonne National Laboratory, Conference, Argonne, Ill., March 7, 8, 1968, Proceedings. c30 A69-40083
RANDLE, R. J.
Effects of differing amounts of training and of monochromatic targets on sextant sighting performance
[NASA-TN-D-5190] c05 N69-35024
RANEY, J. P.
Identification of structural systems by use of near-resonance testing
[NASA-TN-D-5069] c32 N69-17737
RAPARELLI, R.
Theoretical flow field calculations for Project RAM
[NASA-CR-1308] c07 N69-28223
RASCHKE, E.
Observations of the reflection properties of the earth-atmosphere system and the cloud formation above the equatorial Pacific from a synchronous satellite. c20 A69-43154
A preliminary study of the detection of geomorphological features over northeast Africa by satellite radiation measurements in the visible and infrared
[NASA-TN-D-4648] c13 N69-14290
RASOOL, S. I.
On the exospheric temperature of Venus. c30 A69-12109
Albedo measurements over the Antarctic. c13 A69-21404
The planet Venus, after Mariner-5. c30 A69-26129
Ocean circulation and climatic changes. c13 A69-26333
RATAJCZAK, A. F.
Effects of simulated space environment on full, half, and quarter-size cadmium sulfide thin-film solar cells
[NASA-TM-X-1884] c03 N69-36758
RAWLIN, V. K.
Durability of the SERT II hollow cathode and future applications of hollow cathodes.
[AIAA PAPER 69-304] c28 A69-21224
REA, D. G.
The opposition effect of Mars and its implications. c30 A69-18601
Exobiology and the exploration of Mars. c30 A69-41611
READER, P. D.
Systems characteristics of liquid mercury cathode thrusters.
[AIAA PAPER 69-237] c28 A69-21246
REAMES, D. V.
Cosmic-ray propagation. c29 A69-16361
Composition of the 2nd September 1966 solar particle event. c29 A69-17280
Computer analysis of tracks in nuclear emulsion utilizing digitized video scan.
[IEEE PAPER 2A-7] c14 A69-19185
Composition of cosmic rays measured in Gemini XI. c29 A69-38350
REDDY, B. M.
Response of the 1000-kilometer ionosphere to magnetic storms. c13 A69-42438
REDDY, N. M.
A modified model for vibration-dissociation coupling phenomena. c12 A69-37208
REDIESS, H. A.
A new model performance index for the engineering

design of flight control systems.
[AIAA PAPER 69-885] c21 A69-39410
REDING, J. P.
Aerodynamic effects of bulbous bases
[NASA-CR-1339] c01 N69-35521
REECE, O. Y.
Explosive bonding of metal matrix composites.
c15 A69-43452
REED, E. I.
Effects of energetic particles on photomultipliers in earth orbits up to 1500 km.
c14 A69-16932
REED, I. S.
Radiation models using discrete radiator ensembles.
c07 A69-10556
REED, L.
Solubility and diffusion of oxygen in tantalum
[NASA-CR-1276] c17 N69-19886
REEDER, J. P.
What's important in simulation?
c11 A69-41139
REEMSNYDER, D. C.
Performance and cavitation damage of an axial-flow pump in 1500 deg F /1089 K/ liquid sodium
[NASA-TN-D-5138] c15 N69-21773
Effect of fluid temperature on the cavitation performance of a high hub-tip ratio axial flow pump in water to 250 degrees F /394 K/
[NASA-TN-D-5318] c15 N69-30069
Cavitation damage and the effect of fluid temperature on the performance of an axial- flow pump in liquid sodium
[NASA-TN-D-5484] c15 N69-38641
REES, M. H.
Langmuir probe evidence for a nocturnal ionization source at Fort Churchill.
c29 A69-14008
REID, J. H.
Unusual 1 to 5 GHz solar radio emission of 29 October 1968.
c30 A69-32811
REIFF, G. A.
Radio propagation experiments with interplanetary spacecraft.
c07 A69-35940
The Pioneer spacecraft program.
[AAS PAPER 69-066] c30 A69-42883
REILLY, H. J.
Gamma heating in thin heavy-element absorbers.
c22 A69-18825
A new method for treatment of uncertainties in nuclear reactor heat transfer calculations
[NASA-TM-X-1802] c22 N69-26231
REILLY, T. J.
New observations on the substrate specificity of cathepsin C /dipeptidyl aminopeptidase I/ including the degradation of beta-corticotropin and other peptide hormones.
c04 A69-37577
REINISCH, R. F.
A survey of the photodegradation of organic polymers exposed to ultraviolet radiation.
c18 A69-10861
REINMANN, J. J.
Power coupling and wave fields of ion-cyclotron waves in a finite length system.
c25 A69-13114
Stability of two-fluid wheel flows with an imposed uniform axial magnetic field
[NASA-TN-D-5372] c12 N69-32377
REISIG, G. H. R.
Development of the ballistic rocket concept for rocket climatology
c31 A69-26874
REISS, E.
Analyses and measurements of blood samples
[NASA-CR-1395] c05 N69-38600
REIST, P.
A family of portable versatile aerosol particle analyzers.
c14 A69-34691
RELLER, J. O., JR.
Analysis of nonequilibrium air streams in the Ames 1-foot shock tunnel
[NASA-TN-D-4985] c11 N69-15633
REMPFER, P. S.
Application of quadratic optimization to helicopter flight control.
c02 A69-43279
RENKEL, H. E.
Numerical solutions for the flow and pressure fields in an idealized spiral grooved pumping seal.
[ASLE PICFS PREPRINT 30] c15 A69-30481
RENTON, C. A.
A unilateral transformer.
c09 A69-39454
REPAS, D. S.
Description and evaluation of digital-computer design-analysis program for homopolar inductor alternators
[NASA-TN-D-5072] c03 N69-19799
Performance characteristics of a 14.3-kilovolt-ampere modified Lundell alternator for 1200 hertz Brayton-cycle space-power system
[NASA-TN-D-5405] c03 N69-35537
Motor-starting characteristics of two inductor alternators
[NASA-TM-X-1912] c03 N69-40440
REPKO, A. J.
Note on inclination of fatigue cracks in plane strain fracture toughness test specimens.
c32 A69-25958
RESNIKOFF, M. M.
Development of Michell minimum weight structures
[NASA-TN-D-4345] c32 N69-25001
RESTER, D. H.
An experimental study of electron transmission and bremsstrahlung production
[NASA-CR-1383] c24 N69-34541
REUCROFT, P. J.
Electrical characteristics of Pyrrole polymers
[NASA-CR-1367] c18 N69-29559
REYNOLDS, R. T.
Calculations on the composition of the terrestrial planets.
c30 A69-29878
REYNOLDS, T. W.
Propellant condensation on surfaces near an electric rocket exhaust.
[AIAA PAPER 69-270] c28 A69-21252
RHODES, M. D.
Calorimetric, optical, and vibration investigations of stretch-formed aluminum solar concentrators
[NASA-TN-D-4889] c03 N69-10708
Calorimetric evaluation of two cone-column solar-energy concentrations
[NASA-TN-D-5109] c03 N69-21088
Calorimetric evaluation of three 1.5-meter-diameter inflatable rigidized solar concentrators
[NASA-TN-D-5234] c03 N69-28123
RIBBLE, G. H., JR.
Experimental study of low-speed operating characteristics of a liquid hydrogen centrifugal turbopump
[NASA-TM-X-1861] c28 N69-33806
RICCITIELLO, S. R.
Ablative thermal protection at low heating rates.
c18 A69-35536
Experimental evaluation of polyurethane foam composites for low-heating-rate thermal protection.
c18 A69-39236
RICE, J. H.
On the nature of ion-molecule collisions.
c24 A69-16428
Vacancy relaxations in b.c.c. crystals.
c26 A69-16529
A computer plotting description of ion-molecule collisions with long-lived capture complexes
[NASA-TN-D-5407] c24 N69-35508
RICHARD, B. E.
Microscopic observation of interfacial phenomena.
[AIAA PAPER 69-95] c33 A69-18126
RICHARDS, H. L.
10.6-micrometer laser communication system experiment for ATS-F and ATS-G.
c07 A69-41758
RICHARDS, H. T.
Discharge coefficients for thick plate orifices with approach flow perpendicular and inclined to the orifice axis
[NASA-TN-D-5467] c12 N69-38012
RICHARDS, W. E.
10.6-micrometer laser communication system

experiment for ATS-F and ATS-G.
c07 A69-41758

RICHARDS, W. H.
Analytical and experimental investigation of end-plane rotations of truncated cones under bending loads
[NASA-TN-D-5536] c32 N69-41141

RICHARDSON, F. F.
The Pioneer 8 cosmic dust experiment
[NASA-TN-D-5267] c30 N69-31058

RICHARDSON, K. A.
Meteorite fall at Pueblito de Allende, Chihuahua, Mexico - Preliminary information.
c30 A69-20686
Environmental control for radiation testing of lunar rock samples.
c11 A69-38271

RICHARDSON, N. L.
Luminous fog layer surrounding a zirconium droplet burning in an oxygen-containing atmosphere.
c33 A69-28462

RICHARDSON, P. J.
The use of super 184 W as a thermal flux monitor at high temperatures.
c14 A69-43192
Use of tungsten-184 as a thermal flux monitor at high temperatures
[NASA-TN-D-5113] c22 N69-20795
Nondestructive determination of uranium 235 distribution by fixed position gamma scanning
[NASA-TM-X-1779] c22 N69-22555

RICHARDSON, R. B.
Flight and laboratory testing of a double sideband FM telemetry system.
c07 A69-19132
Flight and laboratory tests of an ''L-band'' telemetry RF system.
c07 A69-35996

RICHLEY, E. A.
Propellant condensation on surfaces near an electric rocket exhaust.
[AIAA PAPER 69-270] c28 A69-21252
Bombardment thruster investigations at the Lewis Research Center.
c28 A69-26787

RIDGLEY, D. H.
Effects of lithium and oxygen losses on the magnetic and crystallographic properties of spinel lithium ferrite
[NASA-TR-R-305] c06 N69-20775

RIEGLER, G. R.
Physical properties of the radio-emitting region in sCo XR-1.
c30 A69-37334

RIM, K.
Improvement of an integral equation method in plane elasticity through modification of source density representation
[NASA-CR-1273] c32 N69-19030

RINDNER, W.
Simplified theory and transducer potentialities of the ''pinch effect'' in semiconductors
[NASA-TN-D-5130] c26 N69-22573

RINEY, T. D.
Theoretical prediction of crater size for hypervelocity impact by reduced-density particles, 18 May 1966 - 17 August 1967
[NASA-CR-1196] c32 N69-10225

RITTER, G. D.
A detailed study of manual backup control systems for the Saturn 5 launch vehicle
[NASA-TN-D-5261] c21 N69-28018

ROBB, M.
Skill training for the production of a memorized movement pattern
[NASA-CR-1251] c05 N69-13926

ROBERTS, E., JR.
Elastic displacements for various edge-cracked plate specimens.
c32 A69-16433
Elastic crack-edge displacements for the compact tension specimen.
c15 A69-21392

ROBERTS, L.
Transportation to earth orbit - 1975-1985.
c31 A69-39691

ROBERTS, W. K.
Elastic scattering of 600 MeV protons from He super 3.
c24 A69-13464
Polarization in proton super 4 He scattering at 540 MeV.
c24 A69-14966

ROBERTSON, H. J.
Evaluation of multipoint interaction in the design of a thin diffraction-limited active mirror.
c14 A69-27951

ROBERTSON, J. B.
Beryllium as an acceptor in silicon.
c26 A69-21652

ROBERTSON, W. G.
A study of astronauts' extravehicular work capabilities in weightless conditions
[NASA-CR-1334] c05 N69-27266
Man's capability for self-locomotion on the moon. Volume 2 - Summary report
[NASA-CR-1403] c05 N69-36271
Man's capability for self-locomotion on the moon. Volume 1 - Detailed report
[NASA-CR-1402] c05 N69-37964

ROBINSON, D. J.
Dynamic analysis of permanent magnet stepping motors
[NASA-TN-D-5094] c03 N69-20780
NERVA control drum actuator irradiation test program
[NASA-TN-D-5347] c22 N69-31870

ROBINSON, L.
Laser beam directed at the lunar retro- reflector array - Observations of the first returns.
c30 A69-43197

ROCHELLE, W. C.
Heat-transfer and pressure analysis of rocket exhaust impingement on flat plates and curved panels.
c33 A69-26781

ROE, J. M.
Mechanical behavior of poly/ethylene terephthalate/ at cryogenic temperatures.
c18 A69-16494

ROGALLO, F. M.
NASA research on flexible wings.
c02 A69-15568

ROGERS, D. P.
NASA's developing strategy of space applications.
c30 A69-13427

ROGERS, J. F.
Infrared spectral irradiance measurements in a space environment simulator
[NASA-TN-D-5166] c29 N69-28111

ROGERS, J. W.
An investigation of the decoupling effects in a magnetic forming beryllium coil assembly.
c14 A69-25310

ROGERS, K. H.
Recirculation effects produced by a pair of heated jets impinging on a ground plane
[NASA-CR-1307] c01 N69-34703

ROHDE, J. E.
Discharge coefficients for thick plate orifices with approach flow perpendicular and inclined to the orifice axis
[NASA-TN-D-5467] c12 N69-38012

ROHLFING, D. L.
The effect of time of heating on the thermal polymerization of L-lysine.
c06 A69-28439

ROHLIK, H. E.
Instrumentation used to define performance of small size, low power gas turbines.
[ASME PAPER 69-GT-104] c14 A69-22522

ROLFE, E.
Laser Doppler velocity instrument
[R-67-4450] c14 N69-14351

ROLLBUHLER, R. J.
Performance investigation of bipropellant fractional-pound thrusters
[NASA-TM-X-1699] c28 N69-13237
Experimental performance of a water- electrolysis rocket
[NASA-TM-X-1737] c28 N69-19017

ROLLS, L. S.
Flight-determined aerodynamic properties of a jet-augmented, auxiliary-flap, direct-lift-control system including correlation with wind-tunnel results
[NASA-TN-D-5128-REV] c02 N69-31962

Flight evaluation of tip-turbine-driven fans for lateral control in a hovering VTOL aircraft
[NASA-TN-D-5491] c02 N69-38807
ROM, F. E.
The potential of nuclear power for high-speed ocean-going air-cushion vehicles.
[AIAA PAPER 69-416] c02 A69-30480
Status of the nuclear powered airplane.
[AIAA PAPER 69-554] c22 A69-32761
Nuclear-rocket propulsion
[NASA-TM-X-1685] c22 N69-10067
The potential of nuclear power for high-speed ocean-going air-cushion vehicles
[NASA-TM-X-1871] c22 N69-35723
ROMAN, W. C.
Initial radio-frequency gas heating experiments to simulate the thermal environment in a nuclear light bulb reactor
[NASA-CR-1311] c22 N69-23450
ROMANCZYK, K. C.
Design of an electronically scanned star sensor with digital output
[NASA-TN-D-5281] c14 N69-29153
ROOSEN, R. G.
Messier 87 - The galaxy of greatest known mass.
c30 A69-30883
ROSE, D. C.
International Conference on Cosmic Rays, 10th, Calgary, Canada, June 19-30, 1967, Proceedings. Part A - Invited and Rapporteur Papers.
c29 A69-12928
ROSE, R. K.
A fluidic proportional thruster system for sounding rocket applications.
[ASME PAPER 68-WA/RE-32] c14 A69-16105
ROSELAND, L. M.
Adhesives for cryogenic applications.
c18 A69-16487
ROSEN, A.
Explicit upper bounds for error propagation in the n-body field.
c30 A69-21937
ROSEN, B. W.
Zero thermal expansion composites of high strength and stiffness
[NASA-CR-1324] c32 N69-24876
ROSENBLATT, L. S.
Plasma enzyme responses to blood withdrawal in chickens.
c04 A69-23158
Mechanisms of action of light on circadian rhythms in the monkey.
c04 A69-31336
ROSENBLUM, E.
A family of portable versatile aerosol particle analyzers.
c14 A69-34691
ROSENBLUM, L.
Effect of bias light on the spectral response of Cu sub 2 S-CdS cells.
c26 A69-16358
Corrosion in a cobalt alloy, two-phase mercury loop
[NASA-TN-D-5326] c17 N69-31065
ROSENSWEIG, R. E.
Study of ferromagnetic liquid
[NASA-CR-1407] c06 N69-33493
ROSS, R. W.
A gamma ray telescope utilizing large area wire spark chambers.
[IEEE PAPER 3A-5] c14 A69-19192
ROSTAFINSKI, W. A.
Transient pumping performance of a two speed, hydraulic turbine driven inducer system.
[AIAA PAPER 69-551] c15 A69-34415
An analytical method for predicting the performance of centrifugal pumps during pressurized startup
[NASA-TN-D-4967] c15 N69-14082
ROTH, E. M.
Compendium of human responses to the aerospace environment. Volume 1 - Sections 1-6
[NASA-CR-1205-VOL-1] c04 N69-12434
Compendium of human responses to the aerospace environment. Volume 2 - Sections 7-9
[NASA-CR-1205-VOL-2] c04 N69-12588
Compendium of human responses to the aerospace environment. Volume 3 - Sections 10-16
[NASA-CR-1205-VOL-3] c04 N69-12592
Compendium of human responses to the aerospace environment. Volume 4 - Conversion tables alphabetic index
[NASA-CR-1205-VOL-4] c04 N69-12600
Rapid /explosive/ decompression emergencies in pressure-suited subjects
[NASA-CR-1223] c05 N69-13969
ROTH, J. R.
Analysis of integrated charged particle energy spectra from gridded electrostatic analyzers.
c25 A69-20521
Experimental observation of low-frequency oscillations described by the plasma continuity equations.
c25 A69-24315
Experimental observation of continuity-equation oscillations in slightly ionized deuterium, neon and helium gas.
c24 A69-40759
Periodic small-amplitude solutions to Volterra's problem of two conflicting populations and their application to the plasma continuity equations.
c19 A69-41260
A theory of moving striations based on the continuity-equation plasma oscillation.
c25 A69-43122
Experimental observation of oscillations described by the continuity equations of slightly ionized deuterium, neon, and helium gas
[NASA-TN-D-4950] c25 N69-14525
Possible applications of the continuity- equation plasma oscillation to pulsars and other periodic astrophysical phenomena
[NASA-TN-D-5078] c25 N69-19783
ROUDEBUSH, W. H.
Shorter combustors for high-temperature jet engines.
c28 A69-29433
ROWE, A. J.
Evaluation of the Goddard research and engineering management exercise simulation
[NASA-CR-1275] c34 N69-18057
ROY, R.
Adaptive simulation using mode identification
[NASA-CR-1179] c08 N69-10316
ROY, U.
Nuclear magnetic resonance study of the niobium-nitrogen system NbN sub x.
c26 A69-36445
ROYSTER, D. M.
Tensile properties and creep strength of three aluminum alloys exposed up to 25000 hours at 200 deg to 400 deg F /370 deg to 480 deg K/
[NASA-TN-D-5010] c17 N69-19203
Influence of various fabrication methods on the compressive strength of titanium skin- stringer panels
[NASA-TN-D-5389] c15 N69-34707
Hot-salt-stress-corrosion cracking and its effect on tensile and stress-rupture properties of Ti-6Al-4V titanium-alloy sheet
[NASA-TN-D-5417] c17 N69-36221
ROZENBERSKY, J.
An investigation of the basic properties of irradiated polyethylene memory materials
[NASA-CR-1384] c18 N69-36762
ROZOVSKIY, I. L.
High-velocity hydrodynamics, no. 4
[NASA-TT-F-577] c12 N69-29235
RUBENSTEIN, L. S.
Effect of size on tensile strength of fine polycrystalline nickel wires
[NASA-TN-D-4884] c17 N69-10226
RUBESIN, M. W.
Summary and correlation of skin-friction and heat-transfer data for a hypersonic turbulent boundary layer on simple shapes
[NASA-TN-D-5089] c12 N69-29144
RUBEY, R. J.
CLASP, computer language for aeronautics and space programming.
[AIAA PAPER 69-957] c08 A69-40339
RUBIN, B.
The growth of single crystals by controlled diffusion in silica gel.
c06 A69-23371
RUCH, R. B.
Uranium dioxide vent loss in an externally fueled thermionic reactor concept

[NASA-TN-D-4922] c22 N69-10099
RUDDUCK, R. C.
The admittance of a parallel-plate waveguide aperture illuminating a metal sheet. c09 A69-12328
Reflection coefficient of a TEM mode symmetric parallel-plate waveguide illuminating a dielectric layer. c09 A69-34802
The Te-d1 mode reflection coefficient of a ground-plane mounted parallel-plate waveguide illuminating a reflecting sheet [NASA-CR-1327] c07 N69-24059
Slope diffraction analysis of TEM parallel- plate guide patterns [NASA-CR-1326] c07 N69-26273
RUDY, S. L.
Experimental and analytical investigations on multiple liquid impact erosion [NASA-CR-1288] c15 N69-19786
RUGGERI, R. S.
Prediction of thermodynamic effects of developed cavitation based on liquid-hydrogen and Freon-114 data on scaled venturis [NASA-TN-D-4899] c12 N69-10070
Experimental data for two 1400-feet per second tip speed compressor rotors operated with inlet flow distortions [NASA-TM-X-1798] c01 N69-26312
Method for prediction of pump cavitation performance for various liquids, liquid temperatures, and rotative speeds [NASA-TN-D-5292] c15 N69-29165
RUHLIN, C. L.
Wind-tunnel study of deflected-elevator flutter encountered on a T-tail airplane [NASA-TN-D-5024] c32 N69-16211
RULE, G. W.
Cost plus award fee contracting. c34 A69-30426
RUMMLER, D. R.
Application of advanced materials to truss structures. c17 A69-35504
Mechanical properties and column behavior of thin wall Be-38Al alloy tubing [NASA-TN-D-5145] c17 N69-23004
Design, fabrication, and tests of tubular beryllium and Be-38Al alloy truss-type structures [NASA-TN-D-5254] c32 N69-28658
RUNCORN, S. K.
The Application of Modern Physics to the Earth and Planetary Interiors, Proceedings of the NATO Advanced Study Institute, University of Newcastle-upon-Tyne, Newcastle-upon-Tyne, England, March 29- April 4, 1967. c30 A69-40172
RUNKLE, C. J.
The radiation resistance of cylindrical shells [NASA-CR-1437] c32 N69-40935
RUPP, E.
Radar attitude sensing system. c07 A69-13183
RUSERT, E. L.
Effects of simulated Mars dust erosion environment on thermal control coatings. [AIAA PAPER 69-1023] c11 A69-40393
RUSSELL, J. M.
Entry vehicle instrumentation for heat shield ablation measurements. c14 A69-15428
RUSSELL, L. D.
Thermodielectric radiometer. [AIAA PAPER 68-403] c14 A69-12392
RUSSELL, L. M.
On the design of acoustic liners for rocket engines - Helmholtz resonators evaluated with a rocket combustor [NASA-TN-D-5171] c33 N69-23351
RUSSO, F.
A technique for measuring the electron density of dense, thick, steady-state plasmas. c25 A69-12349
A laboratory study of microwave radiometric techniques for re-entry plasma measurements [NASA-TN-D-5274] c25 N69-29600
RUTLAND, C.
Cost data for economical orbital transportation system design. [AIAA PAPER 69-439] c34 A69-32654
RUTTENBERG, S.
Some systems possibilities for global atmospheric research program. [AAS PAPER 69-120] c13 A69-42817
RUZICKA, J. E.
Loss factor and resonant frequency of viscoelastic shear-damped structural composites [NASA-CR-1269] c32 N69-17766
RYAN, B. M.
Lifting-body research vehicles in a low-speed flight test program. c02 A69-15571
RYAN, J. A.
Analysis of light-scattering data from polymer solutions [NASA-TN-D-5177] c06 N69-22991
RYAN, P. E.
Empirically determined wind and scale effects on hot gas recirculation characteristics of jet V/STOL aircraft [NASA-CR-1445] c28 N69-40776
RYAN, R.
Compilation of data from related technologies in the development of an optical pilot warning indicator system [NASA-TN-D-5174] c14 N69-27267
RYAN, R. S.
A study of Saturn AS-502 coupling longitudinal structural vibration and lateral bending response during boost. [AIAA PAPER 69-58] c31 A69-18204
Attitude control of a manned earth orbiting space station. [AIAA PAPER 69-846] c31 A69-39376
The influential aspects of atmospheric disturbances on space vehicle design using statistical approaches for analysis [NASA-TN-D-4963] c32 N69-15632

S

SACCHI, C. A.
Anti-Stokes generation in trapped filaments of light. c23 A69-10012
SADLER, S. G.
A theory for predicting the rotational and vortex noise of lifting rotors in hover and forward flight [NASA-CR-1333] c23 N69-25344
SAGERMAN, G. D.
Analytical evaluation of space storable propellants for unmanned Jupiter and Saturn orbiter missions [NASA-TM-X-1793] c31 N69-24942
SAKURAI, K.
Note on the times characteristic on the motion of magnetic lines of force. c25 A69-12399
Magnetic structure of sunspot groups which produce solar proton flares. c29 A69-35415
Radiation fields of energetic electrons in helical orbits within a magnetoactive plasma. c30 A69-39965
SALIGA, T. V.
A comparsion of sequential decoding metrics by computer simulation [NASA-TR-R-294] c07 N69-16196
The log-a-posteriori probability metric for use in sequential decoding [NASA-TN-D-4930] c07 N69-23163
SALOMON, M.
Thermodynamic properties of liquid H sub 2 O and D sub 2 O and their mixtures [NASA-TN-D-5223] c33 N69-26247
SALTER, W. E.
Errors resulting from channel filters and adjacent channel crosstalk in DSB/SC telemetry systems. c07 A69-19130
SALTSMAN, J. F.
Design studies on the effect of orientation, lunation, and location of the performance of lunar radiators [NASA-TM-X-1846] c33 N69-32683
SALTZMAN, B.
On a steady state theory of global monsoons.

c20 A69-36405
SALZMAN, J. A.
Lateral sloshing in cylinders under low-gravity conditions
[NASA-TN-D-5058] c12 N69-19112
SAMANICH, N. E.
Flight and wind tunnel investigation of installation effects on supersonic cruise exhaust nozzles at transonic speeds.
[AIAA PAPER 69-427] c01 A69-32769
SAMOYLOVICH, G. V.
Motion of artificial satellites in the earth's gravitational field
[NASA-TT-F-539] c30 N69-33560
SAMUELS, R. D.
Experimental investigation of the turbulent boundary layer on a typical subsonic transport fuselage
[NASA-TN-D-5242] c01 N69-28112
SAMUELSON, R. E.
The thermal radiation field emitted by anisotropically scattering cloudy planetary atmospheres.
c30 A69-38255
SANBORN, W. G.
Man's capability for self-locomotion on the moon. Volume 2 - Summary report
[NASA-CR-1403] c05 N69-36271
Man's capability for self-locomotion on the moon. Volume 1 - Detailed report
[NASA-CR-1402] c05 N69-37964
SANDERS, B. W.
Effect of bleed-system back pressure and porous area on the performance of an axisymmetric mixed-compression inlet at Mach 2.50
[NASA-TM-X-1710] c01 N69-14075
SANDERS, N. D.
Integral balance of forces and momenta in accelerated boundary layers.
[AIAA PAPER 69-666] c12 A69-33462
SANDERS, R. E.
Engineering and operational experiences related to lunar-surface thermal-vacuum qualification of the Apollo extravehicular mobility unit.
[AIAA PAPER 69-992] c05 A69-40370
SANDERS, W. A.
High temperature mechanical properties of polycrystalline hafnium carbide and hafnium carbide containing 13-volume-percent hafnium diboride
[NASA-TN-D-5008] c17 N69-16380
SANDFORD, M. C.
Wind-tunnel study of deflected-elevator flutter encountered on a T-tail airplane
[NASA-TN-D-5024] c32 N69-16211
SANDLER, H.
Single-channel pressure telemetry unit.
c05 A69-25642
An analytic elastic-viscoelastic model for the shape and the forces in the left ventricle.
c05 A69-26235
SANGER, N. L.
A jet pump cavitation prediction parameter.
c12 A69-15791
An experimental investigation of several low-area-ratio water jet pumps.
c03 A69-35176
Noncavitating and cavitating performance of several low area ratio water jet pumps having throat lengths of 3.54 diameters
[NASA-TN-D-5095] c03 N69-20797
SANKAR-RAO, M.
On a steady state theory of global monsoons.
c20 A69-36405
Tests of the effect of grid resolution in a global prediction model.
c20 A69-43066
SARACHIK, E. S.
The interaction of intense laser beams with free electrons
[NASA-TN-D-5205] c16 N69-25357
SARI, J. W.
Power spectra of the interplanetary magnetic field.
c30 A69-37554
SATCHELL, L. F.
Drag reduction due to gas injection through various discrete slots on a three-dimensional wing at Mach 2.01
[NASA-TN-D-5307] c12 N69-31359
SATO, T.
Morphology of electron concentration enhancement at a height of 1000 kilometers at polar latitudes.
c29 A69-28938
Storm-time variations of the electron concentration in the polar topside ionosphere.
c29 A69-28939
SAVAGE, R.
Status of the aerodynamic characteristics of the Apollo entry configuration.
[AIAA PAPER 68-1143] c31 A69-13556
SAVINO, J. M.
An analytical solution for solidification of a moving warm liquid onto an isothermal cold wall.
c33 A69-39433
SAWYER, D. E.
GaSb-ZnTe heterojunction.
c26 A69-12408
Photosensitive barium titanate Schottky diodes.
c09 A69-18905
SAWYER, J. C.
Mechanical behavior of tantalum-base T-111 alloy at elevated temperature
[NASA-CR-1436] c17 N69-36831
SAWYER, J. W.
Effects of cone angle, base flare angle, and corner radius on Mach 3.0 aerodynamic characteristics of large-angle cones
[NASA-TN-D-5048] c01 N69-19926
SAWYER, R. H.
Simulation studies of the supersonic transport in future air traffic control systems
[NASA-TN-D-4944] c21 N69-14382
Supersonic transport operating practices during simulated operations in future air traffic control system environments
[NASA-TN-D-5018] c02 N69-17257
Operational limitations in flying noise- abatement approaches
[NASA-TN-D-5497] c02 N69-39188
SAWYER, W. C.
A method for determining surface pressures on blunt bodies of revolution at small angles of attack in supersonic flow
[NASA-TN-D-4865] c01 N69-10215
Experimental surface-pressure distributions on a 9 deg spherically blunted cone at Mach numbers from 1.50 to 4.63
[NASA-TM-X-1730] c01 N69-16209
SCALZOTT, L. L.
Digital simulation stability criterion.
c10 A69-32899
SCAMMON, L. W.
Induction plasma heating - High power, low frequency operation and pure hydrogen heating
[NASA-CR-1343] c22 N69-24055
SCARDINA, J. T.
Effect of stress ratio on fatigue-crack growth in 7075-T6 aluminum-alloy sheet.
c17 A69-36435
SCHAEFER, W. T., JR.
Operational limitations in flying noise- abatement approaches
[NASA-TN-D-5497] c02 N69-39188
SCHAELCHLIN, J. W.
The improvement of an electronic power supply for greater reliability in aerospace use
[NASA-TM-X-1875] c03 N69-35763
SCHALKOWSKY, S.
Potential effects of recent findings on spacecraft sterilization requirements.
c04 A69-25460
SCHALLA, R. L.
Effect of bias light on the spectral response of Cu sub 2 S-CdS cells.
c26 A69-16358
SCHAPPERT, G. T.
Temperature tuning of an organic dye laser.
c16 A69-12617
Multiple scattering in the Kapitza-Dirac effect.
c23 A69-25323
SCHATTEN, K. H.
A model of interplanetary and coronal magnetic fields.
c30 A69-24429
Direction of the nearby galactic magnetic field inferred from a cosmic-ray diurnal anisotropy.

c29 A69-38098
SCHELL, W. J.
Transitions in glasses at low temperatures.
c06 A69-16493
SCHERRER, V. E.
Spectroscopic study of a helium arc
[NASA-TN-D-5396] c25 N69-36755
SCHERTLER, R. J.
Outgassing characteristics of an expoxy-impregnated magnet coil
[NASA-TM-X-1813] c18 N69-28203
SCHETZ, J. A.
Unified analysis of turbulent jet mixing
[NASA-CR-1382] c12 N69-31887
The interaction and penetration of gaseous jets in supersonic flow
[NASA-CR-1386] c12 N69-32480
SCHEUERMANN, C. M.
Corrosion in a cobalt alloy, two-phase mercury loop
[NASA-TN-D-5326] c17 N69-31065
SCHIFF, L. B.
Aerodynamics of bodies of revolution in coning motion.
[AIAA PAPER 68-20] c01 A69-14714
SCHIFFER, R. A.
Models of Venus atmosphere, 1968
[NASA-SP-8011] c30 N69-20916
SCHIPMA, P.
Air pollution monitoring instrumentation A survey
[NASA-SP-5072] c14 N69-24751
SCHLEY, C. H.
Adaptive simulation using mode identification
[NASA-CR-1179] c08 N69-10316
SCHMID, P. E.
The S-band Telemetry, Tracking, and Command Experiment.
c07 A69-41759
SCHMIDT, J. F.
Experimental and theoretical turbulent boundary layer development in a Mach 4.4 water-cooled conical nozzle
[NASA-TN-D-5377] c12 N69-33353
SCHMIEDLIN, R. F.
Test of improved ignitor for first stage separation rockets for the Atlas-Centaur launch vehicle
[NASA-TM-X-1676] c28 N69-13275
SCHMIT, L. A., JR.
Structural synthesis of a stiffened cylinder
[NASA-CR-1217] c32 N69-14254
The structural synthesis of an ablating thermostructural panel
[NASA-CR-1215] c32 N69-16114
SCHMITZ, E. W.
High-performance light-weight electrodes for hydrogen-oxygen fuel cells
[NASA-CR-1216] c03 N69-14397
SCHNEIDER, R. A.
An approach to cost analysis in low cost launch vehicle studies.
c31 A69-43120
SCHNETZLER, C. C.
Partition coefficients of rare-earth elements and barium between igneous matrix material and rock-forming-mineral phenocrysts. I.
c13 A69-20944
Genesis of continental diabases and oceanic tholeiites considered in light of rare-earth and barium abundances and partition coefficients.
c13 A69-20945
Genesis of the calcium-rich achondrites in light of rare-earth and barium concentrations.
c30 A69-36091
Rubidium-strontium correlation study of moldavites and Ries Crater material.
c13 A69-41341
SCHOLL, H. F.
Scaled lunar module jet erosion experiments
[NASA-TN-D-5051] c31 N69-22630
SCHONFELD, E.
Meteorite fall at Pueblito de Allende, Chihuahua, Mexico - Preliminary information.
c30 A69-20686
SCHRADER, E. R.
Superconductive magnet system, 14-Tesla, 15-cm-bore
[NASA-CR-1260] c03 N69-15382
Pumped helium tests of a 51-centimeter bore niobium-tin magnet
[NASA-TN-D-5158] c26 N69-22965
SCHRADER, J. H.
Microelectronic data and control transmission system for dynamic wind-tunnel testing.
c11 A69-23283
SCHRECK, W.
A study of astronauts' extravehicular work capabilities in weightless conditions
[NASA-CR-1334] c05 N69-27266
SCHREINER, H. R.
Biochemical and metabolic effects of a six- month exposure of small animals to a helium- oxygen atmosphere
[NASA-CR-1372] c04 N69-40955
SCHRENK, G. L.
The selection of spacecraft optical coatings for temperature control.
[AIAA PAPER 69-979] c33 A69-40359
SCHROERS, L. G.
A review of facilities and test techniques used in low-speed flight.
c11 A69-15575
SCHUERCH, H. U.
Certain physical properties and applications of Nitinol
[NASA-CR-1232] c17 N69-11420
Heliogyro solar sailer Summary report
[NASA-CR-1329] c31 N69-28861
Axisymmetric and cylindrical isostabiloids
[NASA-CR-1444] c32 N69-38781
SCHUG, J. C.
Doublet electronic states of the benzyl radical.
c24 A69-13321
Luminescence from aromatic polymers, monomers, and dimers under high-energy electron excitation.
c26 A69-32792
SCHULLER, F. T.
Experiments on the stability of water lubricated herringbone-groove journal bearings. 1 - Theoretical considerations and clearance effects
[NASA-TN-D-4883] c15 N69-10228
Experiments on the stability of water lubricated herringbone-groove journal bearings. 2 - Effects of configuration and groove to ridge clearance ratio
[NASA-TN-D-5264] c15 N69-27955
SCHULMAN, F.
Lunar power systems - A long view.
c03 A69-11396
Development of electric power supplies for electric propulsion.
[AIAA PAPER 69-826] c03 A69-32709
Applications and development of space nuclear electric power systems.
[AAS PAPER 69-305] c28 A69-42865
SCHULTZ, C. W.
Transistor performance in intense magnetic fields
[NASA-TN-D-5428] c09 N69-36710
SCHULTZ, D. G.
Computation of regions of constrained stability for nonlinear control systems
[NASA-CR-1328] c19 N69-28196
The design of linear multivariable control systems using modern control theory /with applications to coupled core reactor control/
[NASA-CR-1345] c19 N69-29268
SCHUM, H. J.
Some measurement problems encountered when determining the performance of certain turbine stator blades from total pressure surveys.
[ASME PAPER 69-GT-103] c01 A69-22521
Performance of a single-stage turbine as affected by variable stator area.
[AIAA PAPER 69-525] c28 A69-32686
Effect of variable stator area on performance of a single-stage turbine suitable for air cooling. 6 - Turbine performance with 70-percent design stator area
[NASA-TM-X-1697] c01 N69-10558
SCHUMAN, P. D.
Development of vulcanizable elastomers suitable for use in contact with liquid oxygen.
c06 A69-16497
SCHWARTZ, I.
Planetary film reconnaissance system
[NASA-CR-1358] c14 N69-28023

SCHWARTZ, M. D.
International Astronautical Federation, Colloquium on the Law of Outer Space, 11th, New York, N.Y., October 17, 18, 1968, Proceedings. c34 A69-37102
SCHWARTZ, S.
The effects of dielectric overcoating on electromigration in aluminum interconnections. c09 A69-32889
Scanning electron mirror microscopy and scanning electron microscopy of integrated circuits. c14 A69-32891
SCHWAUSCH, O. A.
Coordinate system influence on the regularized trajectory optimization problem. [AIAA PAPER 69-903] c30 A69-38546
SCHWIRIAN, R. E.
A new momentum-integral method for treating MHD and simple hydrodynamic entrance flows. [AIAA PAPER 69-724] c12 A69-33436
A new momentum integral method for treating magnetohydrodynamic and simple hydrodynamic entrance flows [NASA-TN-D-5215] c25 N69-24920
A computer program for composing compressor blading from simulated circular-arc elements on conical surfaces [NASA-TN-D-5437] c28 N69-36882
SCHY, A. A.
Deceleration-control system for aerobraking and skipout to orbit at Mars. [AIAA PAPER 68-1146] c31 A69-13564
SCIBBE, H. W.
Lubrication and wear of ball bearings in cryogenic hydrogen. c15 A69-10109
Cooling studies with high-speed ball bearings operating in cold hydrogen gas. [ASLE PAPER 68-LC-2] c15 A69-19310
SCIULLI, J. A.
Adaptive data compression for video signals. c14 A69-12869
SCOTT, H.
Electrical characteristics of Pyrrole polymers [NASA-CR-1367] c18 N69-29559
SCOTT, R. F.
Principal science results from Surveyor 5. c30 A69-12224
SCOTTO, M.
Molecular motion and Raman band shapes in liquid nitrogen and oxygen. c24 A69-17817
SCULL, W. E.
Deployable elements of the orbiting geophysical observatories. c31 A69-17606
The orbiting geophysical observatories. c31 A69-36674
SEBESTA, P. D.
Rat body composition - Sensor implantation and lighting effects. c04 A69-26557
SECHRIST, C. F., JR.
Coordinated rocket measurements on the D-region winter anomaly. I - Experimental results. c13 A69-16411
SECRETAN, L.
A new criterion for the identification of micrometeor impact sites on aluminized glass. c30 A69-34952
SEEGMILLER, H. L.
A 500,000 sample per second digital recorder for the Ames electric arc shock tunnel. c11 A69-35744
SEFIC, W. J.
NASA high temperature loads calibration laboratory [NASA-TM-X-1868] c11 N69-36224
SEIDE, P.
Buckling of thin-walled circular cylinders [NASA-SP-8007] c32 N69-23320
Buckling of thin-walled truncated cones [NASA-SP-8019] c32 N69-24131
SEIDENSTEIN, S.
Visual sensing of spacecraft guidance information. Earth orbit rendezvous maneuvers [NASA-CR-1214] c05 N69-13161
SEIFF, A.
Measurements in the atmosphere of Mars. c30 A69-41617
SEKAS, N. J.
Water flow and cavitation in converging- diverging boiler-inlet nozzle [NASA-TM-X-1689] c12 N69-10293
SELDNER, K.
Multistage compressor simulation applied to the prediction of axial flow instabilities [NASA-TM-X-1880] c28 N69-36998
SELL, H. G.
Advanced processing technology and high temperature mechanical properties of tungsten base alloys c17 A69-18792
SEMENCHUK, K.
An improved delayed neutron fission product monitor [NASA-TM-X-1886] c14 N69-38766
SEMLER, T. T.
Analysis of gold sphere transmission experiments at 24-keV neutron energy using spin-dependent S-wave statistics [NASA-TN-D-5211] c24 N69-24826
SENDERS, J. W.
Human visual sampling processes - A simulation validation study [NASA-CR-1258] c05 N69-14145
SERAFIN, F. L.
Electrical characteristics of Pyrrole polymers [NASA-CR-1367] c18 N69-29559
SERAFINI, J. S.
Some observations on the relationship between instabilities and turbulence in plasma. c25 A69-13115
SERAFINI, T. T.
Cryogenic Properties of Polymers, Proceedings of the NASA-Case Conference on the Properties of Polymers at Cryogenic Temperatures, NASA Lewis Research Center and Case-Western-Reserve University, Cleveland, Ohio, April 25-27, 1967. c18 A69-16485
Effect of film processing on cryogenic properties of poly/ethylene terephthalate/. c18 A69-16490
The synthesis of a novel polymide precursor [NASA-TN-D-5184] c06 N69-23353
SERBU, G. P.
Explorer 35 measurements of low-energy plasma in lunar orbit. c30 A69-16278
SERLEMITSOS, P. J.
Iron line emission from X-ray sources. c29 A69-22231
Pulsed X-ray emission of NP 0532 in March 1968. c29 A69-37574
Cosmic X-ray bremsstrahlung associated with suprathermal protons. c29 A69-40643
SERREZE, H.
GaSb-ZnTe heterojunction. c26 A69-12408
SHAFER, J. W.
Preflight optical evaluation of the right-hand hatch windows of Gemini missions 7, 8, 9, and 12 [NASA-TN-D-5471] c31 N69-40813
SHAFFER, C. V.
Multiloop distributed RC active networks for low parameter sensitivity with low amplifier gain. c10 A69-34679
SHAFFER, H. W.
Multifunction receiver system for integrated tracking, telemetry and ranging data acquisition. c07 A69-19101
SHAH, D. O.
Interaction of uranyl ions with phospholipid and cholesterol monolayers. c06 A69-25641
SHANLEY, F. R.
Geometric properties of a prestressed segmented spherical shell [NASA-CR-1231] c32 N69-11010
SHAPIRA, J.
Identification of sugars as their trifluoroacetyl polyol derivatives. c04 A69-31539
Current research on regenerative systems. c04 A69-37623
Recent advances in closed life support system concepts.

[AAS PAPER 69-143] c05 A69-42876
SHAPIRO, M. M.
Composition of cosmic rays measured in Gemini XI. c29 A69-38350
SHAPIRO, R.
Nimbus 2 flight evaluation and engineering report, launch through orbit 5275
[NASA-TN-D-4881] c31 N69-17851
SHAPIRO, W.
High performance turboalternator and associated hardware. 3. Design of backup gas bearings
[NASA-CR-1292] c15 N69-19775
SHARAF, SH. G.
Theory of motion of the planet Pluto. Part 2 - Plutonian perturbation of the second order with respect to perturbing masses. Part 3 - Recalculation of first- order Plutonian perturbations with respect to perturbing masses. Part 4 - New elements of Pluto
[NASA-TT-F-491] c30 N69-14943
Theory of motion of the planet Pluto. Part 1 - Plutonian perturbations of the first order with respect to perturbing masses
[NASA-TT-F-490] c30 N69-14944
SHARDANAND
Attenuation cross sections of Xe and Xe sub 2 near resonance line 1469.6 angstrom units. c24 A69-12551
Production of an intense helium continuum below 230 angstrom units. c23 A69-42149
SHARMA, H. S.
Carbon dioxide build-up characteristics in spacesuits. c05 A69-39170
SHAUGHNESSY, J. D.
The determination of a stability indicative function for linear systems with multiple delays
[NASA-TR-R-301] c31 N69-17801
SHAW, M.
Electrochemical characterization of nonaqueous systems for secondary battery application
[NASA-CR-1434] c03 N69-36829
SHAW, R.
Ammonia Resistojet station keeping subsystem aboard applications technology satellite /ATS/ IV.
[AIAA PAPER 69-296] c28 A69-21212
SHEATS, J. P.
Saturn V navigation update.
[AIAA PAPER 69-883] c21 A69-39409
SHEERAN, W. J.
Applications of a tube wind tunnel in supersonic testing.
[AIAA PAPER 69-335] c11 A69-28271
SHEETZ, N. W., JR.
Ballistics range boundary-layer transition measurements on cones at hypersonic speeds. c01 A69-33250
SHEFFLER, K. D.
Mechanical behavior of tantalum-base T-111 alloy at elevated temperature
[NASA-CR-1436] c17 N69-36831
SHEHADEH, N. M.
Transmission characteristics of split-phase PCM codes. c07 A69-39451
SHEIBLEY, D. W.
The use of super 184 W as a thermal flux monitor at high temperatures. c14 A69-43192
Use of tungsten-184 as a thermal flux monitor at high temperatures
[NASA-TN-D-5113] c22 N69-20795
A simple method for determination of fission gases trapped in irradiated fuel forms
[NASA-TM-X-1893] c22 N69-37225
SHELTON, R. D.
Advantages of using a combination electromagnetic and material shield. c22 A69-31522
SHERMAN, B. W.
A lunar-surface electric-field detector. c14 A69-13221
SHERMAN, J. W.
Spacecraft oceanography - Its scientific and economic implications for the next decade.
[UN PAPER 68-95878] c13 A69-10491
SHERMAN, W. L.
The red-shift magnitude relation and observational data
[NASA-TN-D-5398] c30 N69-34884
SHIEH, R. C.
Some general principles of dynamic instability of solid bodies. c32 A69-16742
SHIER, J. S.
Temperature-dependent isomer shift and anharmonic binding of Sn super 119 in Nb sub 3 Sn from Moessbauer-effect measurements. c26 A69-10009
SHIFRIN, K. S.
Transfer of microwave radiation in the atmosphere
[NASA-TT-F-590] c13 N69-31851
SHINN, A. M., JR.
Rocket engine evaluation of erosion and char as functions of fabric orientation for silica-reinforced nozzle materials
[NASA-TM-X-1721] c28 N69-15475
SHIRKE, J. S.
Coordinated rocket measurements on the D-region winter anomaly. I - Experimental results. c13 A69-16411
SHIRLEY, R. S.
Motion cues in man-vehicle control. c05 A69-23879
Application of a modified fast Fourier transform to calculate human operator describing functions
[NASA-TM-X-1762] c08 N69-21119
SHIVERS, J. P.
A wind-tunnel and analytical study of the conversion from wing lift to rotor lift on a composite-lift V/TOL aircraft
[NASA-TN-D-5256] c02 N69-28044
Wind-tunnel investigation of a STOL aircraft configuration equipped with an external-flow jet flap
[NASA-TN-D-5364] c01 N69-33275
SHLOSINGER, A. P.
Heat pipe devices for space suit temperature control Research report, 30 Jun. 1966 - 1 Sep. 1968
[NASA-CR-1400] c05 N69-38491
SHMOYS, J.
Ray tracing studies for the topside ionosphere. c13 A69-18838
SHOFNER, F. M.
An experimental and theoretical investigation of striations in a He-Ne laser
[NASA-CR-1387] c08 N69-32350
SHOMO, L. P.
Tables for the calculation of radial multipole matrix elements by the Coulomb approximation. c24 A69-10901
SHOOK, D. F.
Monte Carlo calculations of a hemispherical duct neutron streaming experiment. c22 A69-35178
Resonance integrals of rhenium for a wide range of sample sizes
[NASA-TN-D-4938] c24 N69-13152
SHORE, C. P.
Flutter design charts for stressed isotropic panels. c32 A69-25524
Effects of structural damping on flutter of stressed panels
[NASA-TN-D-4990] c32 N69-16091
Experimental investigation of flutter at Mach 3 of rotationally restrained panels and comparison with theory
[NASA-TN-D-5508] c32 N69-40087
SHORT, B. J.
Newtonian aerodynamics for circular cones modified to produce lift at zero angle of attack
[NASA-TN-D-5193] c01 N69-23926
SHOUMAN, A. R.
Tables and graphs of functions necessary for solving nonlinear heat transfer constant area fin problems with examples on their use
[NASA-TN-D-5173] c33 N69-26975
SHUMPERT, P. K.
Model tests of jet induced lift effects on a VTOL aircraft in hover
[NASA-CR-1297] c01 N69-21477
SHURTLEFF, W. O.
Reliability handbook for silicon monolithic

microcircuits. Volume 2 - Failure mechanisms of monolithic microcircuits
[NASA-CR-1347] c09 N69-23226
SIDIK, S. M.
Design of experiments as doubly telescoping sequences of blocks with application to a nuclear reactor experiment
[NASA-TN-D-5369] c19 N69-32319
SIDNEY, B. D.
Onset of rotating disturbance in linear Hall current accelerator.
[AIAA PAPER 69-381] c28 A69-21731
SIEGEL, R.
An analytical solution for solidification of a moving warm liquid onto an isothermal cold wall.
c33 A69-39433
Inviscid flow analysis of two parallel slot jets impinging normally on a surface
[NASA-TN-D-4957] c12 N69-14316
Two dimensional inviscid jet flow from two nozzles at an angle to a plane surface
[NASA-TN-D-5064] c01 N69-17816
Analysis of two dimensional inviscid model of jet impingement under vertical-takeoff airplane
[NASA-TN-D-5288] c01 N69-29479
Thermal radiation heat transfer. Volume 2 - Radiation exchange between surfaces and in exclosures
[NASA-SP-164-VOL-2] c33 N69-30317
SIGMAN, D. R.
Power coupling and wave fields of ion-cyclotron waves in a finite length system.
c25 A69-13114
SIGNORELLI, R. A.
Tungsten alloy fiber reinforced nickel base alloy composites for high temperature turbojet engine applications.
c17 A69-29010
Stress-rupture and tensile properties of refractory-metal wires at 2000 deg and 2200 deg F /1093 deg and 1204 deg C/
[NASA-TN-D-5139] c32 N69-22823
SILBERBERG, R.
Composition of cosmic rays measured in Gemini XI.
c29 A69-38350
SILBERT, M. N.
Performance characteristics of a tethered balloon system.
c02 A69-40813
SILK, J.
Predictions of extragalactic gamma ray fluxes between 1 and 100 MeV
c29 A69-24466
SILK, J. K.
Laser Doppler velocity instrument
[R-67-4450] c14 N69-14351
SILSBY, N. S.
Simulation studies of the supersonic transport in future air traffic control systems
[NASA-TN-D-4944] c21 N69-14382
Simulation studies of some supersonic transport instrumentation requirements and operating problems
[NASA-TN-D-5280] c14 N69-32286
SILVA, A. F.
Exploding wire initiation and electrical operation of a 40-kV system for arc-heated drivers up to 10 feet long
[NASA-TN-D-5126] c11 N69-22989
SILVER, A. B.
Critical temperature for intracranial self-stimulation in white rats.
c04 A69-13897
SILVERBERG, R. F.
Pulsed X-ray emission of NP 0532 in March 1968.
c29 A69-37574
SILVERMAN, B. D.
Phonons, electrons, and protons in ferroelectric materials.
c26 A69-32262
SILVERMAN, J. R.
Use of computers and programmable telemetry systems on scientific satellies.
c08 A69-41735
SILVERMAN, M. P.
Automatic apparatus for sampling and preparing gases for mass spectral analysis in studies of carbon isotope fractionation during methane metabolism.
c06 A69-12603
SIMHA, R.
Transitions in glasses at low temperatures.
c06 A69-16493
SINNETT, G. M.
Observations of cosmic-ray electrons between 2.7 and 21.5 MeV.
c29 A69-42667
SIMON, F. F.
Stability of cylindrical bubbles in a vertical pipe.
[ASME PAPER 69-HT-28] c33 A69-43540
Transition from film to nucleate boiling in vertical forced flow.
[ASME PAPER 69-HT-26] c33 A69-43542
SIMON, N. R.
Pulsational instabilities in hydrogen-poor massive blue stars. I.
c30 A69-22421
A criterion for nuclear-energized pulsational instability.
c30 A69-27576
An explanation for the blue sequence of variable stars.
c30 A69-40650
SIMONEAU, R. J.
Transition from film to nucleate boiling in vertical forced flow.
[ASME PAPER 69-HT-26] c33 A69-43542
SINGH, J. J.
Transmission of 2.43 MeV electrons through thick silicon targets
[NASA-TN-D-5075] c24 N69-19113
SISAKYAN, N. M.
Problems of Space Biology, volume 6
[NASA-TT-F-528] c05 N69-38701
SISNEROS, T. E.
Research and development of a single gun color CRT, phase 1 Final report
[NASA-CR-1228] c09 N69-14256
SIVIER, K. R.
Magnetic field properties related to the design of a one-component magnetic support-and-balance system
[NASA-CR-1352] c11 N69-24089
One component, magnetic, support and balance system for wind tunnel models
[NASA-CR-1353] c11 N69-25343
Experimental evaluation of a subsonic expansion tube
[NASA-CR-1354] c11 N69-28095
Subsonic sphere drag measurements at intermediate Reynolds numbers
[NASA-CR-1392] c01 N69-30609
SKILLMAN, T. L.
Propagation of the sudden commencement of July 8, 1966, to the magnetotail.
c13 A69-11226
SKOLKA, E. J.
Spacecraft loader has all-hydraulic, all-direction positioning.
c11 A69-38181
SKRETTINGLAND, K.
The centrifuge as a therapeutic device.
c04 A69-43372
SKUBACHEVSKIY, G. S.
Investigation of vibration and stability of aircraft engine components
[NASA-TT-F-547] c02 N69-36326
SLABY, J. G.
Heat-transfer coefficients for hydrogen flowing through parallel hexagonal passages at surface temperatures to 2275 K
[NASA-TN-D-4959] c33 N69-14588
SLEEMAN, W. C., JR.
Status of research on parawing lifting decelerators.
[AIAA PAPER 68-967] c02 A69-43715
SLEEPER, R. K.
A dynamic stability study of a centrifuge-equipped space station.
[AIAA PAPER 68-142] c31 A69-12373
SLEICHER, C. A.
Equations for errors in turbulence measurements with inclined hot wires.
c14 A69-34442
SLEMP, W. S.
Effects of simulated Mars dust erosion environment on thermal control coatings.

[AIAA PAPER 69-1023] c11 A69-40393
SLINEY, H. E.
Preliminary evaluation of greases to 600 F and solid lubricants to 1500 F in ball bearings.
[ASLE PREPRINT 68AM 7C-2] c15 A69-10912
Preliminary investigation of graphite fluoride /CF sub x/ sub n as a solid lubricant
[NASA-TN-D-5097] c15 N69-20939
Rare earth fluorides and oxides - An exploratory study of their use as solid lubricants at temperatures to 1800 deg F /1000 deg C/
[NASA-TN-D-5301] c15 N69-29568
SLIVINSKY, C. R.
The design of linear multivariable control systems using modern control theory /with applications to coupled core reactor control/
[NASA-CR-1345] c19 N69-29268
SLOAN, A. D.
Computer program for dimensional analysis
[NASA-TN-D-5165] c08 N69-22935
SLOCUMB, T. H., JR.
Evaluation of entry and terminal deceleration systems for unmanned Martian landers.
[AIAA PAPER 68-1147] c31 A69-13670
SLOOP, J. L.
The aerospace stimulus to technological advance.
[UN PAPER 68-95321] c34 A69-10467
SLOVLI, G.
Results of rocket measurements in the lower auroral ionosphere.
c13 A69-32187
SLUNDER, C. J.
The metallurgy, behavior, and application of the 18-percent nickel maraging steels A survey
[NASA-SP-5051] c17 N69-14193
SLYE, R. E.
An advanced cryogenic core concept for a flexible and economical delivery system.
[AIAA PAPER 68-812] c31 A69-39753
SMELTZER, D. B.
Study of a family of supersonic inlet systems.
[AIAA PAPER 68-580] c28 A69-34018
SMITH-ROSE, R. L.
Space Research IX, COSPAR Plenary Meeting, 11th, Tokyo, Japan, May 9-21, 1968, Proceedings.
c13 A69-38334
SMITH, A.
Status of photovoltaic power technology.
[ASME PAPER 68-WA/SOL-1] c03 A69-16158
Analysis of a molecular beam system utilizing a known pressure source
[NASA-TN-D-5308] c24 N69-31338
SMITH, A. H.
Lunar power systems - A long view.
c03 A69-11396
Development of electric power supplies for electric propulsion.
[AIAA PAPER 69-826] c03 A69-32709
SMITH, A. M.
Rocket spectrographic observations of alpha Virginis.
c30 A69-27555
SMITH, C. C., JR.
Pressure distribution of a large semispan tilting wing with 0.4-diameter-chord, single- slotted flap, and a single propeller 0.22 chord below wing
[NASA-TN-D-5481] c01 N69-40876
SMITH, D. W.
Sextant sighting measurements from on board the Gemini 12 spacecraft
[NASA-TN-D-4952] c21 N69-14332
SMITH, E. W.
Development of a barium chemical release system
[NASA-CR-1415] c13 N69-35660
SMITH, F. B.
The NASA University Program.
[UN PAPER 68-95413] c34 A69-10506
SMITH, F. J.
Emissivity coatings for low-temperature space radiators
[NASA-CR-1420] c17 N69-36723
SMITH, G. L.
Some aspects of interplanetary earth-entry simulation.
c30 A69-30376
Data-reduction technique for determining rapidly rising heating rates to thermally thick walls
[NASA-TN-D-5309] c33 N69-30726
SMITH, H. J.
Experience using Balakrishnan's epsilon technique to compute optimum flight profiles.
[AIAA PAPER 69-75] c02 A69-18058
Future manned and automated earth orbital science missions.
[AAS PAPER 69-036] c30 A69-42825
Human transfer characteristics in flight and ground simulation for a roll tracking task
[NASA-TN-D-5007] c05 N69-17814
SMITH, J. D.
Quantum theory of a particle oscillator collision applied to gas-surface interactions at cryogenic temperatures
[NASA-TN-D-4982] c24 N69-14288
SMITH, J. M.
Electrothermal instability - An explanation of the MPD arc thruster rotating spoke phenomenon.
[AIAA PAPER 69-231] c28 A69-21254
Electrothermal instabilities in the entrance region of an MHD generator.
c25 A69-21919
Electrothermal instabilities in the entrance region of an MHD generator
[NASA-TM-X-1761] c25 N69-20875
SMITH, J. R.
Self-consistent many-electron theory of electron work functions and surface potential characteristics for selected metals.
c26 A69-29009
Self-consistent many-electron theory of electron work functions and surface potential characteristics for selected metals.
c26 A69-36045
SMITH, K. H.
Biochemical and metabolic effects of a six- month exposure of small animals to a helium- oxygen atmosphere
[NASA-CR-1372] c04 N69-40955
SMITH, L. H., JR.
Performance comparisons of high Mach number compressor rotor blading
[NASA-CR-1256] c28 N69-14210
SMITH, M. C.
Food technology problems related to space feeding.
c05 A69-31459
The stored program data processor for post- Apollo applications.
c07 A69-36280
SMITH, P. A.
Space Research IX, COSPAR Plenary Meeting, 11th, Tokyo, Japan, May 9-21, 1968, Proceedings.
c13 A69-38334
SMITH, P. J.
Computer program for viscous, isothermal compressible flow across a sealing dam with small tilt angle
[NASA-TN-D-5373] c15 N69-33281
SMITH, R. C.
Experimental aerodynamics of a rotor entry vehicle.
[AIAA PAPER 68-950] c01 A69-37155
SMITH, R. J.
Electrical resistivity as a function of deuterium concentration in palladium
[NASA-TN-D-4970] c26 N69-14565
Absorption of hydrogen by palladium and electrical resistivity up to hydrogen- palladium atom ratios of 0.97
[NASA-TN-D-5441] c26 N69-37272
SMITH, R. S.
A method for determining surface pressures on blunt bodies of revolution at small angles of attack in supersonic flow
[NASA-TN-D-4865] c01 N69-10215
Experimental surface-pressure distributions on a 9 deg spherically blunted cone at Mach numbers from 1.50 to 4.63
[NASA-TM-X-1730] c01 N69-16209
A method for determining the total drag of a pointed body of revolution in supersonic flow with turbulent boundary layer
[NASA-TN-D-5046] c01 N69-19925
SMITH, T. S.
Two-photon processes in the solar X-ray spectrum.
c29 A69-36218
On the interpretation of intensity ratios of forbidden iron and calcium transitions in the solar corona.

c30 A69-36219
SMITH, W. S.
Wind measurements in noctilucent clouds.
c20 A69-28466
SMITHRICK, J. J.
Effects of thermal-shock cycling on thin-film cadmium sulfide solar cells
[NASA-TM-X-1819] c03 N69-29555
SNEAD, C. L., JR.
Stage-I interstitials in electron-irradiated tungsten.
c17 A69-28682
SNEATH, P. H. A.
Sterilization Techniques for Instruments and Materials as applied to Space Research, COSPAR, Symposium, London, England, July 18-22, 1967, Proceedings /COSPAR Technique Manual Series. Number 4/.
c05 A69-15934
SNETSINGER, K. G.
Electron microprobe analysis of vanadium in the presence of titanium.
c06 A69-18419
Manganoan ilmenite from a Sierran adamellite.
c13 A69-35977
Ilmenite in ordinary chondrites.
c30 A69-42890
SNEYD, J. M.
Experimental verification of surface vehicle dynamics
[NASA-CR-1399] c11 N69-37022
SNYDER, J. W.
Radiation plan for the Apollo lunar mission.
[AIAA PAPER 69-19] c29 A69-18113
SNYDER, R. W.
Measurement of liquid and two-phase hydrogen densities with a capacitance density meter
[NASA-TN-D-5015] c14 N69-23470
SNYDER, W. J.
The dynamic response of a flexible rotor blade to a tip-vortex induced moving force.
[AIAA PAPER 69-203] c02 A69-19546
SOBIESKI, S.
Search for ultra-short light pulses from pulsars.
c30 A69-34994
SOCKOL, P. M.
Sheath structure in the unignited mode.
c03 A69-13125
Sheath structure in the unignited mode.
c03 A69-21828
SODD, V. J.
Another study of the decay of I super 123.
c24 A69-13099
SODER, K. E., JR.
A theoretical analysis of the free vibration of discretely stiffened cylindrical shells with arbitrary end conditions
[NASA-CR-1316] c32 N69-28164
SODERMAN, P. T.
Investigation of a 0.3-scale jet-transport model having a jet-augmented boundary-layer- control flap with direct-lift control capability
[NASA-TN-D-5129] c01 N69-30722
SOEDER, R. H.
Design-point performance of a double containment tantalum and stainless steel mercury boiler for SNAP-8
[NASA-TN-D-4926] c33 N69-12739
SOFFER, L.
COHORT-II - A Monte Carlo general purpose shielding computer code.
c08 A69-29004
SOFFER, L. M.
Mechanical properties of epoxy resins and glass/epoxy composites at cryogenic temperatures.
c18 A69-16491
SOFIA, S.
Dynamical study of an H II region.
c30 A69-35966
SOHARTON, T. D.
Development of impedance simulation fixtures for spacecraft vibration tests
[NASA-CR-1351] c32 N69-26315
SOKOLOWSKI, D. E.
Characterization of pressure perturbations induced in a rocket combustor by a machine gun
[NASA-TN-D-5214] c33 N69-24824
SOLINGER, A. B.
The galaxy M82. I - Analysis of the observations.
c30 A69-20051
SOLTIS, R. F.
Overall performance of a tandem-bladed inducer tested in water
[NASA-TN-D-5134] c01 N69-23769
SOMERLOCK, C. E.
Cosmic radio noise intensity from 0.45 to 3.0 MHz observed by the ATS II satellite.
c30 A69-19715
SOMEROSKI, F. W.
Satellite applications to marine geodesy
[NASA-CR-1253] c13 N69-16645
SOMMER, R. W.
Evaluation of a contact-analog display in landing approaches with a helicopter
[NASA-TN-D-5241] c02 N69-27177
SOMMER, S. C.
An experiment to determine the structure of a planetary atmosphere.
[AIAA PAPER 68-1054] c30 A69-13699
SOMMERS, R. D.
View factors for toroids and their parts
[NASA-TN-D-5006] c33 N69-23471
SOMMERVILLE, D.
A computer program for calculating external thermal-radiation heat loads and temperatures of spacecraft orbiting the planets or the moon
[NASA-TR-R-278] c30 N69-14428
SONDHAUS, C. A.
Effects of acute exposure to high-energy protons on primates.
c04 A69-13498
SONETT, C. P.
The cislunar geomagnetic tail gradient in 1967.
c13 A69-11237
Magnetometer experiment.
[AAS PAPER 68-206] c30 A69-11481
The geomagnetic tail - Topology, reconnection and interaction with the moon.
c13 A69-19365
Resonant spin states and the anomalous rotation of Mercury.
c30 A69-39568
Interplanetary shock waves. I - Gross structure.
c30 A69-42394
MHD Rankine-Hugoniot equations applied to earth's bow shock.
c30 A69-42417
SORENSEN, N. E.
Study of a family of supersonic inlet systems.
[AIAA PAPER 68-580] c28 A69-34018
SORRELLS, R. B., III
Drag reduction due to gas injection through various discrete slots on a three-dimensional wing at Mach 2.01
[NASA-TN-D-5307] c12 N69-31359
SOS, J. Y.
Delta-T curves for measuring magnetic tape link jitter.
c14 A69-18827
The signal-to-noise ratio estimation techniques for PCM signals.
c07 A69-19122
Data handling equipment requirements for convolutional PCM telemetry.
c07 A69-36267
SOUTH, J. C., JR.
New features of the method of integral relations for the blunt body problem.
c01 A69-21972
SOVEL, M. T.
Technology transfer - A selected bibliography
[NASA-CR-1355] c34 N69-28868
SOVIE, R. J.
The effect of background pressure and magnetic field shape on MPD thruster performance.
[AIAA PAPER 69-243] c28 A69-21239
A study of the axial velocities in an ammonia MPD thruster.
c28 A69-31890
Performance of radiation-cooled magnetoplasmadynamic arc thrusters
[NASA-TM-X-1908] c28 N69-40058
SOWA, W. A.
Apparatus for the precision measurement of internal friction.
c14 A69-13108

SPADIN, P.
Laser beam directed at the lunar retro- reflector array - Observations of the first returns. c30 A69-43197
SPAKOWSKI, A. E.
Observations on CdS solar cell stability. c03 A69-13074
Transmission effects on plastic films irradiated with ultraviolet light, electrons, and protons [NASA-TM-X-1905] c18 N69-40339
SPALVINS, T.
Deposition of MoS sub 2 films by physical sputtering and their lubrication properties in vacuum. [ASLE PAPER 68-LC-15] c15 A69-19308
Energetics in vacuum deposition methods for depositing solid film lubricants. c15 A69-29001
Sputtering of solid lubricants. c15 A69-43126
Friction and contact resistance during sliding in vacuum of some-low-resistivity metals lubricated with sputtered molybdenum disulfide films [NASA-TN-D-5349] c15 N69-31884
SPANGLER, J. G.
Studies of viscous drag reduction with polymers including turbulence measurements and roughness effects. c12 A69-33252
SPANGLER, S. B.
Theoretical study of vortex shedding from bodies of revolution undergoing coning motion [NASA-CR-1448] c12 N69-40200
SPARKS, W. M.
Dynamical models of novae. c30 A69-30769
SPEARMAN, M. L.
Effects of wing planform on the static aerodynamics of a cruciform wing-body missile for Mach numbers up to 4.63 [NASA-TM-X-1839] c01 N69-31875
SPENCE, D. C.
Effects of mission environments on the mechanical properties of dacron parachute material. [AIAA PAPER 69-1018] c11 A69-40390
SPENCER, B., JR.
Aerodynamic and flight characteristics of several variable geometry entry spacecraft during subsonic wing deployment and landing. [AIAA PAPER 69-742] c01 A69-34407
Hypersonic aerodynamic characteristics of a model of a low-fineness-ratio variable geometry logistics spacecraft concept [NASA-TM-X-1701] c01 N69-13218
Transonic aerodynamic characteristics of hypersonic low-wave-drag elliptical body-tail combinations as affected by changes in stabilizer configuration [NASA-TM-X-1789] c01 N69-25244
SPENCER, N. W.
Planetary atmosphere mass spectrometry. [AAS PAPER 68-183] c14 A69-11468
Temperatures of the earth's upper atmosphere. c13 A69-14975
SPENCER, R. L.
Lunar surface mechanical properties. c30 A69-12225
SPENCER, W. B.
High performance turboalternator and associated hardware. 1 - Design of turboalternator [NASA-CR-1290] c03 N69-21771
SPENNY, C. H.
Minimizing spacecraft structure control-system interaction. c31 A69-25500
SPERA, D. A.
The calculation of thermal-fatigue life based on accumulated creep damage. c32 A69-28252
The calculation of elevated temperature cyclic life considering low cycle fatigue and creep [NASA-TN-D-5317] c32 N69-29672
Calculation of thermal-fatigue life based on accumulated creep damage [NASA-TN-D-5489] c32 N69-39393
SPERLING, H. J.
A first-order theory for the rotational motion of a triaxial rigid body orbiting an oblate primary. c30 A69-32240
SPIEGEL, E. A.
On the flow of gas from the galactic center. c30 A69-22189
SPIERS, R. B., JR.
Requirements of a Martian television experiment for three point-mass descent trajectories [NASA-TN-D-5062] c14 N69-17944
SPINELLI, R. A.
On the O.D.E. of stagnation point flows of power law fluids. c12 A69-39674
SPINRAD, H.
The lower atmosphere of Mars - A progress report. c30 A69-12104
SPISZ, E. W.
Experimental measurements of thermal radiation properties by cyclic incident radiation. c33 A69-10847
Solar absorptance and hemispherical emittance of various metals at space conditions. [AIAA PAPER 69-60] c17 A69-18154
Spectral and operational characteristics of a high-intensity carbon arc solar simulator [NASA-TM-X-1825] c11 N69-29737
Solar absorptances and spectral reflectances of 12 metals for temperatures ranging from 300 to 500 K [NASA-TN-D-5353] c17 N69-31895
Electrical characteristics of a large area thin film CdS solar cell [NASA-TM-X-1899] c03 N69-38767
SPITZER, S. M.
Thermal instabilities limiting power dissipation in transistors. c09 A69-31618
The effects of dielectric overcoating on electromigration in aluminum interconnections. c09 A69-32889
SPREITER, J. R.
External aerodynamics of the magnetosphere. c13 A69-19360
Magnetohydrodynamic shock waves in non-aligned flow. c25 A69-19988
Effect of neutral sheet currents on the shape and magnetic field of the magnetosphere tail. c13 A69-21661
Plasma flow around the magnetosphere. c29 A69-26736
SPRINGBORN, R. H.
Estimation of fission-product gas pressure in uranium dioxide ceramic fuel elements [NASA-TN-D-4823] c22 N69-10216
SPUCKLER, C. M.
Effect of size on normal-gravity self-pressurization of spherical liquid hydrogen tankage [NASA-TN-D-5196] c33 N69-24168
Venting of liquid hydrogen tankage [NASA-TN-D-5263] c33 N69-27620
SPURLOCK, O. F.
Optimal three dimensional launch vehicle trajectories with attitude and attitude rate constraints [NASA-TN-D-5117] c30 N69-20810
SRAWLEY, J. E.
Elastic displacements for various edge-cracked plate specimens. c32 A69-16433
Plane strain fracture toughness tests on two-inch-thick maraging steel plate at various strength levels. c32 A69-23057
Plane strain fracture toughness tests on two-inch-thick maraging steel plate at various strength levels. c17 A69-26496
Plane strain fracture toughness. c17 A69-33566
SREEKANTH, A. K.
Preliminary results from an experimental investigation of nozzle wall boundary layer at Mach numbers ranging from 27 to 47. [AIAA PAPER 69-686] c12 A69-33441
STABE, R. G.
Aerodynamic studies of scale model turbines for the M-1 engine. [AIAA PAPER 69-553] c28 A69-32678

STAFFANSON, F. L.
Theoretical comparison of beads, wires, and films as rocketsonde temperature sensors in the mesosphere
[NASA-CR-1286] c13 N69-18126
STAFSUDD, O. M.
Simultaneous HCN and H sub 2 O laser emission in mixtures containing H, C, N, and O.
c16 A69-26330
STAGGS, J. F.
SERT II flight-type thruster system performance.
[AIAA PAPER 69-235] c28 A69-21255
STAINBACK, P. C.
Effect of unit Reynolds number, nose bluntness, angle of attack, and roughness on transition on a 5 deg half-angle cone at Mach 8
[NASA-TN-D-4961] c01 N69-14872
STALLINGS, R. L., JR.
Experimental pressure distributions on a 120 deg cone at Mach numbers from 2.96 to 4.63 and angles of attack from 0 deg to 20 deg
[NASA-TN-D-5054] c01 N69-19826
Experimental pressure distributions for a family of blunt bodies at Mach numbers from 2.49 to 4.63 and angles of attack from 0 deg to 15 deg
[NASA-TN-D-5392] c01 N69-35300
STAMPFL, R. A.
Adaptive data compression for video signals.
c14 A69-12869
STANKIEWICZ, N.
The ellipsoidal velocity distribution function
[NASA-TN-D-5026] c12 N69-17827
STANLEY, W. D.
An analysis of terrain bias error in planetary radar altimeters
[NASA-TN-D-5220] c21 N69-26195
Pulse-response curves of conventional low-pass filters
[NASA-TN-D-5494] c07 N69-40099
STAPLEFORD, R. L.
Measurement of pilot describing functions in single-controller multiloop tasks
[NASA-CR-1238] c05 N69-15372
Experiments and a model for pilot dynamics with visual and motion inputs
[NASA-CR-1325] c05 N69-28071
STAPLES, R. J.
Laboratory experiments on reverted rubber friction
[NASA-CR-1398] c02 N69-34915
STAPLETON, R. E.
High-temperature capacitors from pyrolytic boron nitride.
c03 A69-15299
High-temperature capacitor feasibility
[NASA-CR-1213] c18 N69-14400
STARK, K. W.
Design and development of an annular slit colloid thruster.
[AIAA PAPER 69-287] c28 A69-21257
STASSINOPOULOS, E. G.
Parametric angles of trajectory determined field line intersects predicting the location of artificial auroras
[NASA-TN-D-5189] c30 N69-32316
STATHAM, C. L.
Apollo thermal-protection system development.
[AIAA PAPER 68-1142] c31 A69-13558
STAUGAITIS, C. L.
Sliding friction of copper alloys in vacuum.
[ASLE PAPER 68-LC-5] c15 A69-30610
Sliding friction of copper alloys in vacuum
[NASA-TN-D-4824] c15 N69-10757
STAYLOR, W. F.
Aerodynamic investigation of sharp cone- cylinder spikes on 120 degree blunted cones at Mach numbers of 3.00, 4.50, and 6.00
[NASA-TN-D-5201] c01 N69-29154
STEARNS, C. A.
The dissociation energy of gaseous titanium mononitride
[NASA-TN-D-5027] c06 N69-19129
STECHER, T. P.
Ultraviolet spectrophotometry of early-type stars.
c30 A69-25812
Interstellar extinction in the ultraviolet. II.
c30 A69-40772
The interstellar H super plus sub 2 molecule.
c30 A69-42610
STECKER, F. W.
Isotropic gamma radiation and the metagalactic cosmic ray intensity.
c29 A69-12092
Cosmic gamma rays from metagalactic proton-antiproton annihilation.
c29 A69-21459
Predictions of extragalactic gamma ray fluxes between 1 and 100 MeV
c29 A69-24466
Equilibrium spectra of secondary cosmic-ray positrons in the Galaxy and the spectrum of cosmic gamma-rays resulting from their annihilation.
c29 A69-29948
Origin of galactic gamma-rays.
c29 A69-32806
Corrections to two previous articles on extragalactic gamma rays and implications of the corrected results.
c29 A69-34168
Photodisintegration of ultrahigh-energy cosmic rays by the universal radiation field.
c29 A69-35006
The cosmic gamma-ray spectrum from secondary-particle production in the metagalaxy.
c29 A69-40641
STECURA, S.
Solubilities of vanadium, titanium, and zirconium in liquid potassium
[NASA-TN-D-5093] c17 N69-20789
Solubilities of molybdenum and tungsten in liquid potassium
[NASA-TN-D-5504] c17 N69-40053
STEEVES, E. C.
A method for computing the response of a general axisymmetric shell with an attached asymmetric structure.
c32 A69-25525
Vibration analysis of a 1/40-scale dynamic model of Saturn 5 launch platform-umbilical tower configuration
[NASA-TN-D-4871] c31 N69-10934
Lateral vibration characteristics of a 1/40-scale dynamic model of Apollo-Saturn 5 launch vehicle
[NASA-TN-D-4872] c31 N69-11007
A new matrix theorem and its application for establishing independent coordinates for complex dynamical systems with constraints
[NASA-TR-R-326] c19 N69-38655
STEIGERWALD, E. A.
Mechanical behavior of tantalum-base T-111 alloy at elevated temperature
[NASA-CR-1436] c17 N69-36831
STEIN, M.
Some recent advances in the investigation of shell buckling.
[AIAA PAPER 68-103] c32 A69-12516
STEIN, S.
The centrifuge as a therapeutic device.
c04 A69-43372
STEINBERG, R.
A solution to tritium pump contamination for small accelerators.
c11 A69-26499
STEINBRECHER, D. H.
Microwave radiometric capabilities and techniques.
c07 A69-26976
STEINER, R.
A simplified method of estimating the response of light aircraft to continuous atmospheric turbulence.
[AIAA PAPER 69-766] c32 A69-35657
STEINLE, F. W.
Data correlation from investigations of a high-subsonic speed transport aircraft model in three major transonic wind tunnels.
[AIAA PAPER 69-794] c01 A69-35636
STEINMETZ, G. G.
Analysis of numerical integration techniques for real-time digital flight simulation
[NASA-TN-D-4900] c11 N69-11371
STENGER, F. J.
Conceptual design and structural model of a 560-watt thin-film solar-cell array
[NASA-TM-X-1913] c03 N69-40787
STEPHENS, D. G.
The use of helium bubbles as a pogo fix in launch vehicle propellant lines.

c31 A69-25498
Heave response of a plenum air cushion including passive and active control concepts
[NASA-TN-D-5202] c02 N69-23449
STEPHENS, J. R.
Exploratory study of silicide, aluminide, and boride coatings for nitridation-oxidation protection of chromium alloys
[NASA-TN-D-5157] c17 N69-23084
STEPHENS, W. B.
Axisymmetric static and dynamic buckling of spherical caps due to centrally distributed pressures.
[AIAA PAPER 69-89] c32 A69-18133
STEPHENS, W. E.
A novel use of a telescope to photograph metal diaphragm openings.
c14 A69-37227
STERN, H. E.
Advantages of using a combination electromagnetic and material shield.
c22 A69-31522
STEVENS, G. H.
Dynamic calibration of turbine flowmeters by means of frequency response tests
[NASA-TM-X-1736] c14 N69-17702
Frequency response of a forced flow single tube boiler with inserts and exit restriction
[NASA-TN-D-5023] c12 N69-17779
STEVENS, J. R.
Dislocation structures in single crystal tungsten and tungsten alloys
[NASA-TN-D-5493] c17 N69-39182
STEVENSON, F. R.
Characteristics of composite carbon resistors used for measuring accelerator terminal voltages.
c11 A69-17705
Characteristics of composite carbon resistors used for measuring accelerator terminal voltages
[NASA-TM-X-1718] c24 N69-14398
STEVENSON, J.
Effect of salts and organic solvents on the activity of Halobacterium cutirubrum catalase.
c04 A69-35291
STEVENSON, L.
Application of quadratic optimization to helicopter flight control.
c02 A69-43279
STEWART, D. A.
Shock shapes and pressure distributions for large angle pointed cones in helium at Mach numbers of 8 and 20
[NASA-TN-D-5343] c01 N69-31228
Convective heat-transfer rates on large-angle conical bodies at hypersonic speeds
[NASA-TN-D-5526] c33 N69-40780
STEWART, E. C.
Study of a global search algorithm for optimal control.
c08 A69-33745
STEWART, J. D.
Magnitude estimates of rotational velocity during and following prolonged increasing, constant, and zero angular acceleration.
c04 A69-15332
Comparison of three methods to determine thresholds for perception of angular acceleration.
c04 A69-15969
Effects of angular acceleration on man - Thresholds for the perception of rotation and the oculogyral illusion.
c05 A69-41674
STEWART, R. W.
Empirical determination of heating efficiencies in the Mars and Venus atmospheres.
c30 A69-26019
Exospheric temperatures on Mars and Venus.
c30 A69-26020
Solar cycle variation of exospheric temperatures on Mars and Venus - A prediction for Mariner 6 and 7.
c30 A69-37136
STEWART, W. L.
Advanced concepts to increase turbine blade loading.
[ASME PAPER 68-WA/GT-11] c28 A69-16136
STEWART, W. M.
Alpha-gamma angular correlations in super 120 Sn.
c24 A69-13098
Alpha-gamma angular correlations on super 58 Ni.
c24 A69-13100
Scattering of 42 MeV /6.7-pJ/ alpha particles from even isotopes of cadmium. Supplement 1 - Absolute cross sections
[NASA-TN-D-4948] c24 N69-14482
STICKLAND, A. C.
Solar-Terrestrial Physics- Solar Aspects, International Years of the Quiet Sun and COSPAR, Joint Symposium, London, England, July 17-22, 1967, Proceedings. Part 1.
c29 A69-30005
STICKLE, J. W.
Flight tests of a direct lift control system during approach and landing
[NASA-TN-D-4854] c02 N69-10371
STICKNEY, R. E.
Measurements of the work function and desorption energy of cesium and potassium on /100/ tungsten.
c26 A69-21808
STIEF, L. J.
Vacuum-ultraviolet photochemistry. IX - Primary and chain processes in the photolysis of hydrogen peroxide.
c06 A69-23527
STILLER, B.
Composition of cosmic rays measured in Gemini XI.
c29 A69-38350
STIMLER, F. J.
Nitinol characterization study
[NASA-CR-1433] c17 N69-36367
STINNETT, G. W.
Simulation studies for planning an in-flight experiment to define manual guidance and control techniques for large launch vehicles
[NASA-TN-D-5150] c21 N69-22936
A detailed study of manual backup control systems for the Saturn 5 launch vehicle
[NASA-TN-D-5261] c21 N69-28018
STOCHL, R. J.
Pressurant gas requirements for the pressurized discharge of liquid hydrogen from propellant tanks.
[AIAA PAPER 69-526] c28 A69-32737
Gaseous hydrogen requirements for the discharge of liquid hydrogen from a 1.52 meter /5 ft/ diameter spherical tank
[NASA-TN-D-5336] c28 N69-32318
Gaseous-hydrogen pressurant requirements for the discharge of liquid hydrogen from a 3.96 meter /13 ft/ diameter spherical tank
[NASA-TN-D-5387] c28 N69-33211
STOCKMAN, N. O.
Theoretical analysis of flow in VTOL lift fan inlets without crossflow
[NASA-TN-D-5065] c01 N69-17831
STOKES, C. S.
Development of a barium chemical release system
[NASA-CR-1415] c13 N69-35660
STOKES, R. C.
Preflight optical evaluation of the right-hand hatch windows of Gemini missions 7, 8, 9, and 12
[NASA-TN-D-5471] c31 N69-40813
STOLARIK, J. D.
The application of the image orthicon television system to rocket trajectory determination.
c07 A69-26965
Electric fields in the vicinity of auroral forms from motions of barium vapor releases.
c13 A69-34935
STOLOV, H. L.
Polar cap ionospheric response to solar cosmic ray events observed by Mariners 2 and 4.
c29 A69-43621
STONE, D. G.
Entry flight research and experimentation.
c31 A69-25719
STONE, D. R.
Boundary-layer tripping with emphasis on hypersonic flows.
c12 A69-33249
STONE, H. W.
The leading-edge effects on the laminar flat-plate boundary layer and the aerodynamic heating at Mach 10.4
[NASA-TN-D-5160] c12 N69-23467

STONE, J. R.
Water flow and cavitation in converging- diverging boiler-inlet nozzle
[NASA-TM-X-1689] c12 N69-10293
STONE, R. G.
Cosmic radio noise intensity from 0.45 to 3.0 MHz observed by the ATS II satellite.
c30 A69-19715
Measurements in the ionosphere of the aspect dependence of antenna reactance. I - Variations arising from the inhomogeneous plasma distribution about the vehicle.
c13 A69-39964
Type III radio bursts in the outer corona.
c29 A69-40300
The spectrum of the cosmic radio backgrcund between 0.4 and 6.5 MHz.
c30 A69-42375
STONE, R. W., JR.
Potential problems related to weightlessness and artificial gravity
[NASA-TN-D-4980] c05 N69-15629
STOOLZ, J. M.
A closed-form solution for minimum-fuel, constant thrust trajectories.
[AIAA PAPER 69-905] c30 A69-39337
STORY, A.
Compilation of data from related technologies in the development of an optical pilot warning indicator system
[NASA-TN-D-5174] c14 N69-27267
STOTHERS, R.
An interpretation of the peculiar helium star HZ 29.
c30 A69-16931
Pulsational instabilities in hydrogen-poor massive blue stars. I.
c30 A69-22421
Red supergiants and neutrino emission.
c30 A69-24125
A criterion for nuclear-energized pulsational instability.
c30 A69-27576
On the pulsation hypothesis for massive red supergiants.
c30 A69-30766
Mass loss from pulsating neutron stars.
c30 A69-37573
An explanation for the blue sequence of variable stars.
c30 A69-40650
STOUT, R. C.
The relationship between optical distortion and binocular depth perception
[NASA-TN-D-5162] c05 N69-22990
STRACK, W. C.
Interplanetary low-thrust mission analysis.
c30 A69-21206
STRAETER, T. A.
A comparison of gradient dependent techniques for the minimization of an unconstrained function of several variables.
[AIAA PAPER 69-951] c19 A69-40333
STREED, E. R.
Passive thermal control by second-surface mirrcr.
c33 A69-37290
A comparison of infrared-emittance measurements and measurement techniques.
c14 A69-41633
STRETCHBERRY, D. M.
A summary of the measurement and interpretation of the Hall coefficient and resistivity cf semiconductors
[NASA-TM-X-1711] c26 N69-14086
STROKE, G. W.
X-ray imaging with multiple-pinhole cameras using a posteriori holographic image synthesis.
c14 A69-40019
STROM, T. N.
Vibration of shaft face seals and stabilizing effect of viscous and friction damping
[NASA-TN-D-5161] c15 N69-23466
Experimental study of pump and seal characteristics of helical groove geometry incorporated in a combined bearing and pump
[NASA-TN-D-5225] c15 N69-24791
Torque and leakage rates of various lubricated lip seal designs at a peripheral velocity of 120 feet per second
[NASA-TN-D-5411] c15 N69-35769
STRONG, J. P., III
Optical simulation of a radio-astronomy interferometer experiment
[NASA-TN-D-5357] c30 N69-36892
STROUD, C. W.
Effect of the chemical state of pyrolysis gases on heat-shield mass
[NASA-TN-D-4975] c32 N69-14306
Chemical equilibrium of ablation materials including condensed species
[NASA-TN-D-5391] c33 N69-34966
STROUD, W. J.
Minimum-weight stiffened shells with slight meridional curvature designed to support axial compressive loads.
c32 A69-43671
STROUHAL, G.
Definition cf entry corridor thermal limits for Apollo spacecraft.
[AIAA PAPER 68-1144] c31 A69-13673
STUBBE, P.
Frictional forces and collision frequencies between mcving ion and neutral gases.
c13 A69-13328
Temperature dependence of the rate constants for the reactions O super plus plus O sub 2 goes to O sub 2 super plus plus O and O super plus plus N sub 2 gces to NO super plus plus N.
c06 A69-32312
STUBBS, S. M.
Effects of bottom-structure flexibility on water landing loads of Apollo spacecraft mcdels
[NASA-TN-D-5108] c32 N69-21042
STUHLINGER, E.
The versatility of electrically propelled spacecraft for planetary missions.
[AIAA PAPER 69-253] c30 A69-21244
Electric space propulsion.
c28 A69-35108
STUMP, E. C.
Development of vulcanizable elastomers suitable for use in contact with liquid oxygen.
c06 A69-16497
STUMPF, J. J.
A rendezvous and station-keeping simulator with fly around capability and virtual image viewing
[NASA-TN-D-5123] c11 N69-22629
STUMPFF, K.
Periodic orbits in the restricted three-body problem in the neighborhood of resonances of type /k plus 1//k /Ueber periodische Bahnen im eingeschraenkten Dreikoerperproblem und in der Naehe der Kommensurabilitaeten vom Typus /k plus 1//k/.
c30 A69-19874
STUTZ, D. E.
Induction heating advances - Applications to 5800 deg F
[NASA-SP-5071] c03 N69-23643
SUBER, H. H.
A family of solutions of certain nonautonomous differential equations by series of exponential functions
[NASA-CR-1294] c19 N69-17249
SUDDETH, D.
Pulse motor for spacecraft attitude control.
c03 A69-11762
SUGIMOTO, D.
Primordial helium and the luminosity of horizontal-branch stars.
c30 A69-22211
SUGIURA, M.
Propagation of the sudden commencement of July 8, 1966, to the magnetotail.
c13 A69-11226
An improved model equatorial electrojet with a meridional current system.
c13 A69-38084
SULLIVAN, E. M.
Some aspects of interplanetary earth-entry simulation.
c30 A69-30376
SULLIVAN, R. E.
Quadrature variations in discrete-ordinates calculations
[NASA-TM-X-1887] c20 N69-36976
SULLIVAN, T.
Frequency measurements in the far infrared -

Limitations imposed by the noise spectrum in harmonic mixing.
c23 A69-33674

SULLIVAN, T. L.
Effect of radius on bulging and fracture of through-cracked cylindrical pressure vessels at cryogenic temperatures
[NASA-TN-D-4951] c32 N69-14480
Factors influencing low cycle crack growth in 2014-T6 aluminum sheet at minus 320 deg F /77 K/
[NASA-TN-D-5140] c32 N69-21392

SUMMER, I. E.
Low-density foam for insulating liquid- hydrogen tanks
[NASA-TN-D-5114] c18 N69-20790

SUMMERS, A. L.
External aerodynamics of the magnetosphere.
c13 A69-19360
Calculations on the composition of the terrestrial planets.
c30 A69-29878

SUMMERS, R. L.
Empirical observations on the sensitivity of hot cathode ionization type vacuum gages
[NASA-TN-D-5285] c14 N69-29331

SUMMIT, R. K.
Remote information retrieval facility
[NASA-CR-1318] c08 N69-23381

SUMNER, B. S.
Comments on the nature of the outside boundary layer on a liquid sphere in a steady, uniform stream
[NASA-CR-1362] c12 N69-24877

SUN, F. T.
On the normalized hodographic mapping for constrained trajectory families.
[AIAA PAPER 69-924] c30 A69-39362

SUNDARAM, A. K.
Hydromagnetic radiation from electric and magnetic dipoles in the magnetosphere.
c13 A69-42905

SUSSMAN, M.
Tracking solar array maximum power by sensing array temperature.
c03 A69-42303

SUTHERLAND, A. A., JR.
Design of strapdown gyroscopes for a dynamic environment Interim scientific report
[NASA-CR-1396] c21 N69-34672

SUTTLES, J. T.
Some aspects of interplanetary earth-entry simulation.
c30 A69-30376
A modified method of integral relations approach to the blunt-body equilibrium air flow field, including comparisons with inverse solutions
[NASA-TN-D-5434] c12 N69-36830
A method of integral relations sclution for radiating, nonadiabatic, inviscid flow over a blunt body
[NASA-TN-D-5480] c33 N69-40356

SUTTON, K.
An evaluation test of a full scale replica of the RAM-CA flight heat shield in a rocket engine exhaust
[NASA-TM-X-1841] c31 N69-32713

SVEHLA, R. A.
Thermodynamic and transport properties of air and the combustion products of natural gas and of ASTM-A-1 fuel with air
[NASA-TN-D-5452] c33 N69-37936

SWAMY, K. S. K.
Graphite particle model for NML Cygnus.
c30 A69-13775
Line blanketing in stars.
c30 A69-14626
Analysis of subdwarf HD 25329.
c30 A69-22199
Convection in normal stars and metal-deficient stars.
c30 A69-29946
Atmospheres of extreme metal-deficient stars.
c30 A69-36338
Solid hydrogen coated graphite particles in the interstellar medium. I.
c30 A69-37492

SWAROOP, R.
A simple technique for automatic computer editing of biodata
[NASA-TN-D-5275] c08 N69-29592

SWARTZ, C. K.
Effects of simulated space environment on full, half, and quarter-size cadmium sulfide thin-film solar cells
[NASA-TM-X-1884] c03 N69-36758

SWARTZ, M.
X-ray and extreme ultraviolet /1-400 angstrom units/ spectroscopy of the sun, from OSO-III.
c29 A69-22169
Observations of the solar flare soft X-ray spectrum and comparison with centimetric radio bursts.
c29 A69-43609

SWEET, G. E.
A radiometer for use in thermal studies of spacecraft
[NASA-TN-D-4925] c14 N69-13311
An experimental and analytical investigation of balloon-type enclcsures for thermal control of satellites
[NASA-TN-D-5230] c33 N69-28209

SWENSON, B. L.
Spacecraft sterilization by destructive heating.
c05 A69-31472

SWENSON, G. R.
Temperature shape parameter of the thermosphere determined from probe data.
c13 A69-38088
Diurnal variations in the thermosphere from a series of Marshall-University-of-Michigan probes.
c13 A69-40515

SWENSON, L. W.
Polarization in proton super 4 He scattering at 540 MeV.
c24 A69-14966

SWETT, C. C.
Further experiments on ion-cyclotron-wave generation in the RF self-sustained mode.
c25 A69-13113

SWIDERSKI, E. F.
Power conditioning development for the Sert II ion thrustor.
c03 A69-42301

SWIFT, C. T.
The admittance of a parallel-plate waveguide aperture illuminating a metal sheet.
c09 A69-12328
Radiation characteristics of a cavity-backed cylindrical gap antenna.
c09 A69-40698
Admittance of a waveguide-fed aperture loaded with a dielectric plug.
c09 A69-41589

SWIGERT, P.
COMPUTE - A time-sharing desk calculator program
[NASA-TN-D-4917] c08 N69-10098
Implementation and structure of COMPUTE, a time-sharing calculator program
[NASA-TN-D-5350] c08 N69-32685
FORTRAN program for machine computation of group tables of finite groups
[NASA-TN-D-5402] c08 N69-35569

SWIKERT, M. A.
Lubrication with some polyphenyl ethers and superrefined mineral oils in a 600 deg F /316 deg C/ inerted vane pump loop
[NASA-TN-D-5096] c15 N69-20938

SWYLER, J. L.
Requirements for relays in spacecraft having magnetic field constraints.
c09 A69-28046

SYKES, N. P.
Minimum-weight stiffened shells with slight meridional curvature designed to support axial compressive loads.
c32 A69-43671

SYMONS, E. P.
Observations of interface behavior during inflow to an elliptical ended cylinder in weightlessness
[NASA-TM-X-1719] c12 N69-15473

SYNOR, H.
Test of improved ignitor for first stage separation rockets for the Atlas-Centaur launch vehicle
[NASA-TM-X-1676] c28 N69-13275

SYVERTSON, C. A.
Aircraft without wings.
c02 A69-13367
Research problems in atmosphere entry and landing for manned planetary missions
[NASA-TN-D-4977] c31 N69-15634
SZANCA, E. M.
Effect of variable stator area on performance of a single-stage turbine suitable for air cooling. 6 - Turbine performance with 70-percent design stator area
[NASA-TM-X-1697] c01 N69-10558
Cold air investigation of a turbine with stator-blade trailing-edge coolant ejection. Part 1 - Overall stator performance
[NASA-TM-X-1901] c03 N69-39335
SZANISZLO, A. J.
Thermal electromotive force change for 87Pt13Rh/Pt thermocouples in 1530 K, 10 to the minus 8 torr environment for 3700 hours
[NASA-TN-D-5287] c14 N69-29196
SZUCH, J. R.
Application of a double-dead-time model describing chugging to liquid propellant rocket engines having multielement injectors
[NASA-TN-D-5303] c28 N69-29405

T

TACINA, R. R.
Analysis of total-pressure loss and airflow distribution for annular gas turbine combustors
[NASA-TN-D-5385] c33 N69-33314
TAKAYANAGI, M.
Mechanical relaxation of poly-4-methyl-pentene- 1 at cryogenic temperatures.
c18 A69-16492
TAKETA, S. T.
Effects of acute exposure to high-energy protons on primates.
c04 A69-13498
TAKKUNEN, P. D.
Compatibility tests of molten uranium with tungsten and tungsten - 1.5 percent hafnium
[NASA-TN-D-5076] c17 N69-19930
Fabrication of cermets of uranium nitride and tungsten or molybdenum from mixed powders and from coated particles
[NASA-TN-D-5136] c17 N69-21404
TALARICO, K. S.
Conversion of acetate-2 -super 14 C to super 14 CO sub 2 and super 14 C-fatty acids in the partially hepatectomized rat /33627/.
c04 A69-35976
Effects of hyperoxia and hypoxia on mitosis in the normal and regenerating rat liver.
c04 A69-43565
TANG, H. M.
Analysis of dynamic jettison hinge forces for Centaur nose fairing
[NASA-TM-X-1821] c32 N69-29734
TANNER, R. I.
Normal-stress effects in drag-reducing fluids.
c12 A69-33256
TAPLEY, B. D.
The Hamiltcn-Jacobi method applied to the low-thrust trajectory problem.
c30 A69-17574
An approximate solution for the short-term motion of a lunar satellite.
c30 A69-35934
Coordinate system influence on the regularized trajectory optimization problem.
[AIAA PAPER 69-903] c30 A69-38546
TARAN, J. P.
Self-modulation, self-steepening, and spectral development of light in small-scale trapped filaments.
c23 A69-20745
TASHJIAN, H.
An algorithm for deriving the equatiens of mathematical physics by symbolic manipulation.
c08 A69-14858
TAUBER, M. E.
Atmospheric entry into the major planets with emphasis on Jupiter.
[AIAA PAPER 68-1150] c31 A69-13565
TAUCHERT, T. R.
A lattice model for composite materials
[NASA-CR-1322] c32 N69-22982
TAYLOR, C. R., JR.
Flight test results of a trailing edge flap designed for direct-lift control
[NASA-CR-1426] c02 N69-38819
TAYLOR, D. J.
Filter photometry of Saturn in the spectral region lambda lambda 2950-2450.
c30 A69-22216
TAYLOR, H. A., JR.
Evidence of contraction of the earth's thermal plasmasphere subsequent to the solar flare events of 7 and 9 July 1966.
c13 A69-23777
Multi-experiment detection of the plasmapause from EOGO satellites and antarctic ground stations.
c13 A69-25153
Implications for ionospheric chemistry and dynamics of a direct measurement of ion compositicn in the F 2 region.
c13 A69-31974
Ion depleticn in the high-latitude exosphere - Simultaneous OGO 2 observations of the light ion trough and the VLF cutoff.
c29 A69-34939
Diurnal and seasonal variation of atmospheric ion compositicn, correlation with solar zenith angle.
c13 A69-38087
TAYLOR, H. E.
Measurements of the perturbed-interplanetary magnetic field in the lunar wake.
c30 A69-11228
Sudden commencement associated discontinuities in the interplanetary magnetic field observed by IMP 3.
c30 A69-22183
Observations of the interplanetary magnetic field, 4-12 July 1966.
c30 A69-23773
TAYLOR, H. P.
Analysis of a multiplicative feed system for monopulse tracking applicatiens.
c11 A69-37704
TAYLOR, J. H.
Experiments on visual acuity and the visibility of markings cn the ground in long-duration earth-orbital space flight
[NASA-CR-1134] c05 N69-10813
TAYLOR, L. W., JR.
Experience using Balakrishnan's epsilon technique to compute optimum flight profiles.
[AIAA PAPER 69-75] c02 A69-18058
A comparison of Newton-Raphson and other methods for determining stability derivatives from flight data.
[AIAA PAPER 69-315] c02 A69-22379
Fixed-base simulator pilot rating surveys for predicting lateral-directional handling qualities and pilot rating variability
[NASA-TN-D-5358] c02 N69-35762
TAYLOR, M. F.
Photographic study of a bromine jet flowing in a coaxial airstream and impinging on a stagnation surface
[NASA-TN-D-5209] c12 N69-24800
Comparison of predicted nozzle coolant side heat transfer and fluid flow with experimental values from Phoetus-2A nuclear tests
[NASA-TM-X-1881] c33 N69-36806
TAYLOR, R. D.
Temperature-dependent isomer shift and anharmonic binding of Sn super 119 in Nb sub 3 Sn from Mcessbauer-effect measurements.
c26 A69-10009
TAYLOR, T. D.
On-board spacecraft processor.
c08 A69-39921
An on-board processor for OAO-C.
c08 A69-41736
TEICHNER, W. H.
Predicting human performance in space environments
[NASA-CR-1370] c05 N69-30168
TEMKIN, A.
Rotational excitation of diatomic molecules by electron impact.
c24 A69-39665
TENDYS, J.
Study of the structure of switch-on ionizing shock

waves.
c25 A69-22045
TENNANT, J. A.
Measurement of pilot describing functions in single-controller multiloop tasks
[NASA-CR-1238] c05 N69-15372
TEPPER, M.
Weather research satellites.
[UN PAPER 68-95350] c20 A69-10483
Some systems possibilities for global atmospheric research program.
[AAS PAPER 69-120] c13 A69-42817
TEREN, F.
A wind profile for generating control requirements for rocket vehicles using liquid-injection control systems
[NASA-TM-X-1708] c31 N69-14033
Optimal three dimensional launch vehicle trajectories with attitude and attitude rate constraints
[NASA-TN-D-5117] c30 N69-20810
TERJUNG, R. L.
Effects of progressive hypohydration on maximal isometric muscular strength.
c04 A69-15983
TERRY, M. C.
A lunar-surface electric-field detector.
c14 A69-13221
THADDEUS, P.
The dry massive model of the atmosphere of Venus and the microwave phase effect.
c30 A69-12108
Upper limits to the intensity of background radiation at lambda equals 1.32, 0.559, and 0.359 mm.
c30 A69-19404
Microwave observations of sea state from aircraft.
c13 A69-34421
THARPE, M.
On-board spacecraft processor.
c08 A69-39921
THEKAEKARA, M. P.
Solar irradiance curves and absorptance of satellite coatings.
c29 A69-21646
Solar irradiance measurements from a research aircraft.
c30 A69-42191
THEON, J. S.
Coordinated rocket measurements on the D-region winter anomaly. I - Experimental results.
c13 A69-16411
Wind measurements in noctilucent clouds.
c20 A69-28466
THIRUVENGADAM, A.
Experimental and analytical investigations on multiple liquid impact erosion
[NASA-CR-1288] c15 N69-19786
THOLLOT, P. A.
Design-point performance of a double containment tantalum and stainless steel mercury boiler for SNAP-8
[NASA-TN-D-4926] c33 N69-12739
THOMAS, E. T.
The impact of biosciences requirements on biosatellite attitude control.
c31 A69-35094
THOME, G. D.
Enhancement of ionizing radiation during a solar flare.
c29 A69-37558
THOME, P. G.
The challenge of planetary exploration.
[AAS PAPER 69-286] c30 A69-42810
THOMPSON, P. A.
Superconductive magnet system, 14-Tesla, 15-cm-bore
[NASA-CR-1260] c03 N69-15382
THOMPSON, R. E.
A 2-1/4- by 2-1/4-inch photogrammetric camera system for the moon.
c14 A69-40989
THOMPSON, W. I., III
A review of radiometric measurements of atmospheric attenuation at wavelengths from 75 centimeters to 2 millimeters
[NASA-TN-D-5087] c07 N69-22949
THOMSON, M. H.
The Royal Astronomical Society of Canada 1968.
c30 A69-41058
THOMSON, R. G.
An analytical evaluation of the denting of airplane surfaces by hail
[NASA-TN-D-5363] c32 N69-33420
THORNTON, W. A.
The structural synthesis of an ablating thermostructural panel
[NASA-CR-1215] c32 N69-16114
THORNWALL, J. C.
A stepping motor drive circuit using magnetic core logic.
c09 A69-11000
THORPE, M. L.
Induction plasma heating - High power, low frequency operation and pure hydrogen heating
[NASA-CR-1343] c22 N69-24055
TIBBETTS, J. G.
Model tests of jet induced lift effects on a VTOL aircraft in hover
[NASA-CR-1297] c01 N69-21477
TIDMAN, D. A.
Plasma Instabilities in Astrophysics, Proceedings of the Conference, Monterey, Calif., October 14-17, 1968.
c30 A69-42681
TIFFANY, O. L.
Advanced Space Experiments, American Astronautical Society, Conference, Ann Arbor, Mich., September 16-18, 1968, Proceedings.
c30 A69-34359
TIMMINS, A. R.
Time required for an adequate thermal-vacuum test of flight model spacecraft
[NASA-TN-D-4908] c31 N69-14010
Test plan optimization for an Explorer-size spacecraft
[NASA-TN-D-5283] c34 N69-31333
TISCHLER, A. O.
A commentary on low-cost transportation.
c31 A69-38117
TOBAK, M.
Aerodynamics of bodies of revolution in coning motion.
[AIAA PAPER 68-20] c01 A69-14714
Hypothesis for the origin of cross-hatching.
[AIAA PAPER 69-11] c12 A69-18213
TOBEY, W. H.
EVA maneuvering unit comparison.
[AAS PAPER 69-516] c05 A69-42850
TODD, C. A.
A FORTRAN 4 program to estimate the off-design performance of radial-inflow turbines
[NASA-TN-D-5059] c03 N69-19829
TOKAREV, V. V.
Mechanics of spaceflight low-thrust
[NASA-TT-F-507] c28 N69-33354
TOLSON, R. H.
The X sup 2 statistic and the goodness of fit test
[NASA-TR-R-313] c19 N69-30610
TOMBOULIAN, R.
Research and development of a sonic boom simulation device
[NASA-CR-1378] c02 N69-31959
TONGIER, M., JR.
Mitotic synchronization of L-strain fibroblasts with 5-aminouracil as determined by time-lapse cinephotography
[NASA-TN-D-5021] c04 N69-17248
Osmotically induced coalescence of sarcoma cells through intercellular bridges in vitro
[NASA-TN-D-5022] c04 N69-17782
TORRENCE, M. G.
An experimental investigation of the mixing of compressible-air jets in a coaxial configuration
[NASA-TN-D-5315] c02 N69-30727
TOWNES, C. H.
Anti-Stokes generation in trapped filaments of light.
c23 A69-10012
TOWNSEND, D.
Configurations for gas turbine compressor end seals.
[ASLE PREPRINT 68AM 4B-4] c15 A69-27366
TOWNSEND, D. P.
Elastohydrodynamic lubrication of a spinning ball in a nonconforming groove.
[ASME PAPER 69-LUBS-11] c15 A69-34381

Lubricants for inerted lubrication systems in engines for advanced aircraft
[NASA-TN-D-5420] c15 N69-35788
Speed effects on ball spinning torque
[NASA-TN-D-5527] c15 N69-41210
TOWNSEND, M. R.
The Small Astronomy Satellite /SAS/ program.
c31 A69-19126
The Small Astronomy Satellite /SAS/ program
[NASA-TN-D-5099] c31 N69-21017
TOYE, C. R.
Computerized Arrhenius reliability extrapolation techniques
[NASA-TN-D-4902] c19 N69-13368
Introduction to computer aided reliability data analysis
[NASA-TN-D-5009] c15 N69-17988
TRAINOR, J. H.
Galactic Jupiter probes.
c30 A69-12303
Design of a long-life reliable nuclear experiment for space flight.
c09 A69-36676
TRAUBOTH, H. H.
Recursive formulas for the evaluation of the convolution integral.
c19 A69-17250
TREMOR, J. W.
Weightlessness and the developing frog egg.
c04 A69-11084
Rat body composition - Sensor implantation and lighting effects.
c04 A69-26557
TREON, S. L.
Data correlation from investigations of a high-subsonic speed transport aircraft model in three major transonic wind tunnels.
[AIAA PAPER 69-794] c01 A69-35636
TRESCOT, C. D., JR.
Effects of wing planform on the static aerodynamics of a cruciform wing-body missile for Mach numbers up to 4.63
[NASA-TM-X-1839] c01 N69-31875
TREVATHAN, C. E.
On-board spacecraft processor.
c08 A69-39921
An on-board processor for OAO-C.
c08 A69-41736
TREXLER, C. A.
Preliminary investigation of momentum diffusion between two supersonic airstreams in the presence of shock waves
[NASA-TN-D-4974] c12 N69-15631
TROMBKA, J.
An integrated experiment for compositional analysis from an orbiter.
[AAS PAPER 68-197] c30 A69-11475
TROUT, A. M.
Performance of swirl-can turbojet combustors at simulated supersonic combustor-inlet conditions
[NASA-TN-D-4996] c28 N69-16154
TROUT, O. F., JR.
Simulation of Gemini extravehicular tasks by neutral-buoyancy techniques
[NASA-TN-D-5235] c05 N69-28024
TRULIO, J. G.
Numerical calculation of viscous compressible fluid flow around an oscillating rigid cylinder
[NASA-CR-1467] c12 N69-38782
TURAN, J. W.
Nucleosynthesis in supernova explosions.
c30 A69-20898
TRUSZYNSKI, G. M.
International benefits of cooperative tracking and data acquisition agreements.
[UN PAPER 68-95912] c34 A69-17059
Communications for space research.
c07 A69-25933
TRYON, H. B.
Hot performance characteristics of a gas bearing Brayton cycle turboalternator.
c03 A69-42279
Preliminary performance characteristics of a gas-bearing turboalternator
[NASA-TM-X-1820] c03 N69-29707
TSAI, L. L.
The admittance of a parallel-plate waveguide aperture illuminating a metal sheet.
c09 A69-12328
Reflection coefficient of a TEM mode symmetric parallel-plate waveguide illuminating a dielectric layer.
c09 A69-34802
The Te-d1 mode reflection coefficient of a ground-plane mounted parallel-plate waveguide illuminating a reflecting sheet
[NASA-CR-1327] c07 N69-24059
TSANDER, F. A.
From a scientific heritage
[NASA-TT-F-541] c34 N69-26112
TSAO, C. H.
Composition of cosmic rays measured in Gemini XI.
c29 A69-38350
TSCHUNKO, H. F. A.
Geometric optical image aberrations of single and double mirrors.
c23 A69-24836
TSESEVICH, V. P.
RR Lyrae stars
[NASA-TT-F-562] c30 N69-27169
TSURUTA, S.
Nucleosynthesis in supernova explosions.
c30 A69-20898
TUDOR, D. H.
Experimental pressure distributions on a 120 deg cone at Mach numbers from 2.96 to 4.63 and angles of attack from 0 deg to 20 deg
[NASA-TN-D-5054] c01 N69-19826
Pressure distributions on 140 deg, 160 deg, and 180 deg cones at Mach numbers from 2.30 to 4.63 and angles of attack from 0 deg to 20 deg
[NASA-TN-D-5204] c01 N69-24764
Charts for interpolation of local skin friction from experimental turbulent velocity profiles
[NASA-SP-3048] c01 N69-25391
TURNER, L. R.
Hardware /or software/ provisions for multiple precision floating-point arithmetic
[NASA-TM-X-1885] c08 N69-36918
TURNER, R. E.
Generalized approach to the thermal analysis of orbiting spacecraft.
[SAE PAPER 690202] c33 A69-18305
TURNEY, G. E.
Measurement of liquid and two-phase hydrogen densities with a capacitance density meter
[NASA-TN-D-5015] c14 N69-23470
Experimental study of low-speed operating characteristics of a liquid hydrogen centrifugal turbopump
[NASA-TM-X-1861] c28 N69-33806

U

UHAINES, R. F.
Changes in perceived size of high luminance targets.
c04 A69-36458
UKKESTAD, D.
NASA contributions to bioinstrumentation systems - A survey
[NASA-SP-5054] c04 N69-14860
UMSCHEID, L., JR.
Tests of the effect of grid resolution in a global prediction model.
c20 A69-43066
UNDERWOOD, J. H.
Optical design of a glancing incidence X-ray telescope.
c14 A69-21087
An improved collimator for extreme ultraviolet and X rays.
c14 A69-36489
X-ray imaging with multiple-pinhole cameras using a posteriori holographic image synthesis.
c14 A69-40019
URASEK, D. C.
Investigation of flow range and stability of three inducer-impeller pump combinations operating in liquid hydrogen
[NASA-TM-X-1727] c28 N69-16213
Overall performance of a tandem-bladed inducer tested in water
[NASA-TN-D-5134] c01 N69-23769
Investigation of two-phase hydrogen flow in pump inlet line
[NASA-TN-D-5258] c15 N69-29476

URCIS, S.
A subsatellite concept for Martian fields and particles measurements.
c30 A69-39215
USELLER, J. W.
Clean room technology
[NASA-SP-5074] c05 N69-33775
USRY, J. W.
Performance of a towed, 48-inch-diameter /121.92-cm/ ballute decelerator tested in free flight at Mach numbers from 4.2 tc 0.4
[NASA-TN-D-4943] c01 N69-17398
Results of a free-flight test to determine the performance characteristics of a towed, conical decelerator
[NASA-TM-X-1833] c02 N69-38598
UTTER, D. H.
Visual sensing of spacecraft guidance information. Earth orbit rendezvous maneuvers
[NASA-CR-1214] c05 N69-13161
UZZELL, B. R.
Rocket trajectory optimization by a second- order numerical technique.
c30 A69-32154

V

VALENTINE, H. H.
Analytical evaluation of space storable propellants for unmanned Jupiter and Saturn orbiter missions
[NASA-TM-X-1793] c31 N69-24942
VALERO, F. P. J.
Interferometrically measured thorium lines between 2747 and 4572 angstrom units.
c23 A69-42150
VALGORA, M. E.
Hot performance characteristics of a gas bearing Brayton cycle turboalternator.
c03 A69-42279
Preliminary performance characteristics of a gas-bearing turboalternator
[NASA-TM-X-1820] c03 N69-29707
Motor-starting characteristics of two inductor alternators
[NASA-TM-X-1912] c03 N69-40440
VALLERIE, L. L.
Peripheral vision displays, phase 2 report
[NASA-CR-1239] c05 N69-14478
Differential thresholds for motions in the periphery
[NASA-CR-1439] c05 N69-36925
VAN ALLEN, J. A.
Particle shadowing by the moon.
c30 A69-16252
VAN ATTA, L. C.
A simple antenna with good circular polarization.
c09 A69-41590
VAN CLEAVE, R.
Transmission characteristics of split-phase PCM codes.
c07 A69-39451
VAN DE HULST, H. C.
Multiple light scattering in planetary atmospheres.
c30 A69-12105
VAN DENSEN, B. D.
Experimental verification of surface vehicle dynamics
[NASA-CR-1399] c11 N69-37022
VAN DER LAAN, W. F.
A method for predicting launch vehicle vibration levels in the region of the spacecraft adaptor
[NASA-CR-1227] c31 N69-16155
Summary of random vibration predictien procedures
[NASA-CR-1302] c32 N69-23096
VAN ESS, J. C.
The impact of biosciences requirements on biosatellite attitude control.
c31 A69-35094
VAN LIGTEN, R. F.
Holographic microscopy for the determination of failure mechanisms in monolithic circuits
[NASA-CR-1394] c14 N69-31958
VAN WYK, R.
Variable mesh methods for differential equations
[NASA-CR-1247] c19 N69-11419
VANCO, M. R.
Analytical investigation of two-dimensional loss characteristics of supersonic turbine stator blades
[NASA-TM-X-1823] c01 N69-31360
VANO, A.
Evaluation of an infrared heating simulation of a Mach 4.63 flight on an X 15 horizontal stabilizer
[NASA-TN-D-5403] c33 N69-35949
VARY, A.
Corrosion in a cobalt alloy, two-phase mercury loop
[NASA-TN-D-5326] c17 N69-31065
VAUGHAN, O. H., JR.
Model atmospheres of Mercury.
[AIAA PAPER 69-54] c30 A69-18042
VAUGHAN, R. W.
An experimental feasibility study for the preparatien of thermo-oxidatively stable Pyrrone laminates
[NASA-CR-1404] c30 N69-31960
VAUGHAN, W. W.
New wind-monitoring system protects R and D launches.
c20 A69-13852
Detailed wind and temperature profiles.
c20 A69-33739
VENDELL, E. W.
A coaxial, three-coil probe for measuring local values of electrical conductivity and velocity in plasma streams.
[AIAA PAPER 69-327] c25 A69-28264
VERMILLION, C. H.
Weather satellite picture receiving stations - Inexpensive construction of automatic picture transmission ground equipment
[NASA-SP-5080] c07 N69-31985
VERNIKOS-DANELLIS, J.
Adrenal epinephrine and phenylethanolamine n-methyl transferase /PNMT/ activity in the rat bearing a transplantable pituitary tumor.
c04 A69-20374
Sensitivity of the adrenal corticosterone response to ACTH as a function of time after hypophysectomy.
c04 A69-39871
Compensatory hypertrophy and phenylethanolamine n-methyl transferase /PNMT/ activity in the rat adrenal.
c04 A69-41404
VERNON, R. W.
Results of endurance tests of a SNAP 8 turbine-alternator
[NASA-TM-X-1741] c03 N69-20913
VETTE, J. I.
Models of the trapped radiation environment. Volume 5 - Inner belt protons
[NASA-SP-3024-VOL-5] c24 N69-28911
VIEHMANN, W.
Current oscillations in photoexcited gallium-arsenide.
c26 A69-21753
Differential photo effects in gallium arsenide-metal junctions.
c26 A69-32824
VILLMAN, CH. I.
Observations of noctilucent clouds
[NASA-TT-F-546] c13 N69-25013
VINCENT, D. W.
Liquid rocket acoustic-mode-instability studies at a nominal thrust of 20000 pounds
[NASA-TN-D-4968] c28 N69-14384
Characterization of pressure perturbations induced in a rocket combustor by a machine gun
[NASA-TN-D-5214] c33 N69-24824
Stability and performance characteristics of several hydrazine and nitrogen tetroxide hot gas generators for large scale supersonic combustor testing
[NASA-TM-X-1845] c33 N69-32468
VINCENT, J. P.
Engineering and operational experiences related to lunar-surface thermal-vacuum qualification of the Apollo extravehicular mobility unit.
[AIAA PAPER 69-992] c05 A69-40370
VINCENT, J. S.
Elastic scattering of 600 MeV protons from He super 3.
c24 A69-13464

Polarization in proton super 4 He scattering at 540 MeV.
c24 A69-14966
Study of the Sc super 45 /alpha,t/ Ti super 46 reaction at 41 MeV.
c24 A69-41044
Study of the /alpha, t/ reaction on scandium-45 at 41 MeV
[NASA-TN-D-5216] c24 N69-24919
Interaction of 42-MeV alpha particles with helium-3
[NASA-TN-D-5530] c24 N69-40979

VINH, N. X.
Analytical solutions of a class of optimum orbit modifications
[NASA-CR-1379] c30 N69-31362
Non-linear longitudinal dynamics of an orbital lifting vehicle
[NASA-CR-1449] c30 N69-40062

VISHNIAC, W.
Life Sciences and Space Research VII COSPAR, Plenary meeting, 11th, Open Meeting of Working Group V and Symposium on Biological Effects of Radiation in Space, Tokyo, Japan, May 14-16, 1968 and May 10, 1968, Proceedings.
c04 A69-37612

VOGT, P. G.
Initial radio-frequency gas heating experiments to simulate the thermal environment in a nuclear light bulb reactor
[NASA-CR-1311] c22 N69-23450

VOGT, R.
A computer program for calculating external thermal-radiation heat loads and temperatures of spacecraft orbiting the planets or the moon
[NASA-TR-R-278] c30 N69-14428

VOJVODICH, N. S.
Ablative characterization of seven heat shield materials - A review of the NASA-SRI Round-Robin program.
c18 A69-26813

VOLLAND, H.
Direct in situ measurements of wave propagation in the neutral thermosphere.
c13 A69-16261
Full wave calculations of gravity wave propagation through the thermosphere.
c13 A69-25150
The upper atmosphere as a multiply refractive medium for neutral air motions.
c13 A69-26101
A theory of thermosphere dynamics. I - Diurnal and solar cycle variations.
c29 A69-43003

VOLLMAR, W. R.
Performance and stall limits of a YTF30-P-1 turbofan engine with uniform inlet flow
[NASA-TM-X-1803] c28 N69-27019

VON GLAHN, U. H.
Correlation of gas-side heat transfer for axisymmetric rocket engine nozzles
[NASA-TM-X-1748] c33 N69-18898

VON PRAGENAU, G. L.
Stability analysis of Apollo-Saturn V propulsion and structure feedback loop.
[AIAA PAPER 69-877] c31 A69-39403

VON PUTTKAMER, J.
Survey and comparative analysis of current geophysical models
[NASA-TN-D-5163] c13 N69-26969

VON ROSENVINGE, T. T.
The relative energy spectra of carbon and oxygen nuclei in the primary cosmic radiation.
c29 A69-20632

VORZIMER, P. J.
Project Gemini technology and operations - A chronology
[NASA-SP-4002] c31 N69-36501

VOULGARIS, N. C.
Linear operation of a p-n-p-n tetrode.
c09 A69-35293

VYKUKAL, H. C.
Dynamic response of the human body to vibration when combined with various magnitudes of linear acceleration.
c05 A69-11335
Advanced developments in hard space suit technology.
c05 A69-12993

W

WADDEL, R. C.
Solar cell radiation damage on synchronous satellite ATS-I.
c03 A69-35704

WADE, W. R.
The design and uncertainty analysis of an improved total hemispherical emittance transient calorimeter
[NASA-TN-D-5106] c14 N69-20941

WAGNER, B. M.
Exobiology- The Search for Extraterrestrial Life, American Astronautical Society and American Association for the Advancement of Science, Symposium, New York, N.Y., December 30, 1967, Proceedings.
c04 A69-32967

WAGNER, C. A.
Resonant perturbations of existing satellites.
c31 A69-13777
Combined solution for low degree longitude harmonics of gravity from 12- and 24-hour satellites.
c13 A69-14661
Perturbations of existing resonant satellites.
c31 A69-39968
Visual simulation image generation using a flying-spot scanner
[NASA-TN-D-5151] c11 N69-23194

WAGNER, D. E.
Optimum packaging design and sparing levels for extended manned space missions.
c31 A69-16380

WAGNER, L. S.
Enhancement of ionizing radiation during a solar flare.
c29 A69-37558

WAGNER, R. D., JR.
Influence of measured free-stream disturbances on hypersonic boundary-layer transition.
[AIAA PAPER 69-704] c12 A69-33453
Electron beam flow visualization in hypersonic helium flow.
c11 A69-35722

WAGNER, S.
On the singularity method of subsonic lifting-surface theory.
[AIAA PAPER 69-37] c01 A69-18167

WAINFAN, N.
Electric-field distribution in pulsed high-current-density discharges in helium and helium-hydrogen mixtures.
c25 A69-23660

WAKEFIELD, R. M.
Comparison of the performance of a charring ablator under transient and constant combined convective and radiative heating.
[AIAA PAPER 69-151] c33 A69-18055
Effects of pyrolysis-gas chemical reactions on surface recession of charring ablators.
[AIAA PAPER 68-302] c33 A69-21982

WALBERG, G. D.
An investigation of ablation behavior of Avcoat 5026/39M over a wide range of thermal environments
[NASA-TM-X-1778] c33 N69-22933

WALDEN, H.
An accuracy and speed comparison of the Vinti and Brouwer orbit prediction methods
[NASA-TN-D-5203] c30 N69-26252

WALDMAN, B. J.
Space storable propellant performance demonstration.
[AIAA PAPER 69-505] c28 A69-32762

WALITT, L.
Numerical calculation of viscous compressible fluid flow around an oscillating rigid cylinder
[NASA-CR-1467] c12 N69-38782

WALKER, G. H.
Improved method of removing plastic backing films from carbon electron microscope replicas.
c14 A69-21651

WALKER, J. C. G.
Langmuir probe evidence for a nocturnal ionization source at Fort Churchill.
c29 A69-14008

Temperatures of the earth's upper atmosphere.
c13 A69-14975
WALKER, R. W.
Aerodynamic forces on a stationary and oscillating circular cylinder at high Reynolds numbers
[NASA-TR-R-300] c01 N69-17304
WALLACE, S. A.
Bodies of revolution having minimum total drag in hypersonic flow
[NASA-TN-D-5438] c01 N69-36699
WALLHAGEN, R. E.
Design and performance of two integrated circuits for fluidic-controlled pneumatic stepping motor system
[NASA-TN-D-5155] c03 N69-22896
WALLIO, H. A.
A feasibility study of determining physical properties of the Martian atmosphere by use of solar occultation as seen from an artificial satellite
[NASA-TN-D-5443] c30 N69-38658
WALSH, E. J.
Conjugate echoes in Alouette-2 topside-sounder data.
c07 A69-20045
Magnetospheric duct propagation research using Alouette-2 topside-sounder observations
[NASA-TN-D-5332] c13 N69-34891
WALTER, L. S.
The major-element composition of individual chondrules of the Bjurboele meteorite.
c30 A69-36090
WALTON, B. A.
A new approach to telemetry data processing - The data reduction laboratory.
c11 A69-40352
WALTON, W. C., JR.
A geometrically exact finite element for thin shells of revolution.
[AIAA PAPER 69-56] c32 A69-18193
A method for computing the response of a general axisymmetric shell with an attached asymmetric structure.
c32 A69-25525
A method for computation of vibration modes and frequencies of orthotropic thin shells of revolution having general meridional curvature
[NASA-TN-D-4972] c32 N69-16469
A new matrix theorem and its application for establishing independent coordinates for complex dynamical systems with constraints
[NASA-TR-R-326] c19 N69-38655
WAMPLER, E. J.
Laser beam directed at the lunar retro- reflector array - Observations of the first returns.
c30 A69-43197
WANBAUGH, W. C.
Pulse interference effects in a phase-lock loop.
c10 A69-42230
Radio spectrum utilization in aerospace communication systems.
c07 A69-42502
WANG, C.-C.
Performance of chloride and fluoride vapor-deposited tungsten emitters in thermionic converters.
c03 A69-21819
WANG, G. Y.
The design of a highly parallel computer organization.
c34 A69-39133
WANHAINEN, J. P.
Liquid rocket acoustic-mode-instability studies at a nominal thrust of 20000 pounds
[NASA-TN-D-4968] c28 N69-14384
Effect of injection element radial distribution and chamber geometry on acoustic mode instability in a hydrogen oxygen rocket
[NASA-TN-D-5375] c33 N69-32340
Stability and performance characteristics of several hydrazine and nitrogen tetroxide hot gas generators for large scale supersonic combustor testing
[NASA-TM-X-1845] c33 N69-32468
WARD, I. M.
The mechanical behavior of poly/ethylene terephthalate/.
c18 A69-16489
WARD, J. F.
The dynamic response of a flexible rotor blade to a tip-vortex induced moving force.
[AIAA PAPER 69-203] c02 A69-19546
The dynamic response of a flexible rotor blade to a concentrated force moving from tip to root
[NASA-TN-D-5410] c32 N69-36220
WARD, J. J.
Performance of chloride and fluoride vapor-deposited tungsten emitters in thermionic converters.
c03 A69-21819
Uranium dioxide vent loss in an externally fueled thermionic reactor concept
[NASA-TN-D-4922] c22 N69-10099
WARD, J. L.
Human visual sampling processes - A simulation validation study
[NASA-CR-1258] c05 N69-14145
WARE, G. M.
Wind-tunnel investigation of the aerodynamic characteristics of a twin-keel parawing
[NASA-TN-D-5199] c01 N69-23781
WARNECKE, G.
Satellite mapping of the Pacific tropical cloudiness.
c20 A69-33001
WARNER, J. D. S.
A fundamental study of predictive display systems
[NASA-CR-1274] c05 N69-17738
WARNER, R. E.
Deuteron break-up by 42 Mev alpha particles.
c24 A69-13469
WARNER, R. W.
An impact energy-absorbing strut employing tube cutting
[NASA-TN-D-4941] c32 N69-14506
WARREN, E. D.
Prescription of exercise for the hypokinetic airline pilot.
c05 A69-41800
WARREN, E. S.
Objectives, history, and principal achievements of the topside sounder and ISIS programs.
c13 A69-37855
WARSHAWSKY, I.
Kinetics of the reaction between lithium hydride and liquid ammonia at -78 deg C.
c06 A69-11285
WASSERBAUER, J. F.
Dynamic response of a Mach 2.5 axisymmetric inlet with engine or cold pipe and utilizing 60 percent supersonic internal area contraction
[NASA-TN-D-5338] c28 N69-31336
WASSERBURG, G. J.
Cosmogenic rare gases and the super 40 K-super 40 Ar age of the Kodaikanal iron meteorite.
c30 A69-22047
WATERS, W. J.
Evaluation of two nickel-base alloys, alloy 713C and NASA TAZ-8A, produced by extrusion of prealloyed powders
[NASA-TN-D-5248] c17 N69-26192
A nickel base alloy, WAZ-20, with improved strength in the 2000 deg to 2200 deg F range
[NASA-TN-D-5352] c17 N69-31873
WATKINS, E. R., JR.
Preprocessing of Minitrack data
[NASA-TN-D-5042] c08 N69-26193
WATSON, D. M.
Simulation studies for planning an in-flight experiment to define manual guidance and control techniques for large launch vehicles
[NASA-TN-D-5150] c21 N69-22936
WATSON, N. D.
Generalized approach to the thermal analysis of orbiting spacecraft.
[SAE PAPER 690202] c33 A69-18305
WATSON, S.
An accuracy and speed comparison of the Vinti and Brouwer orbit prediction methods
[NASA-TN-D-5203] c30 N69-26252
WATSON, V. R.
A collisionless model for high specific impulse accelerators.
[AIAA PAPER 69-278] c28 A69-21233
WATT, J. J.
Fouling characteristics of ASTM jet A fuel when heated to 700 deg F in a simulated heat

exchanger tube
[NASA-TN-D-4958] c28 N69-12831
WATT, W. S.
Nonequilibrium gasdynamics
[NASA-CR-1411] c12 N69-34709
WATTS, H. V.
Evaluation of vacuum UV detector-spectroscopy systems for capsule reentry measurements
[NASA-CR-1268] c09 N69-18761
WATTS, J. W.
Advantages of using a combination electromagnetic and material shield.
c22 A69-31522
WAYLAND, J. R., JR.
Lectures in high energy astrophysics
[NASA-SP-199] c29 N69-29652
WEATHERS, G.
Computer-aided filter design manual
[NASA-SP-3049] c08 N69-35816
WEAVER, E. C.
A dual-beam source of actinic light for photosynthesis research.
c14 A69-36378
WEAVER, L. E.
The design of linear multivariable control systems using modern control theory /with applications to coupled core reactor control/
[NASA-CR-1345] c19 N69-29268
WEBB, H., JR.
Theoretical flow field calculations for Project RAM
[NASA-CR-1308] c07 N69-28223
WEBB, J. A., JR.
A multipurpose ventricular actuating system.
c05 A69-42983
WEBB, J. J.
Solar spectral irradiance measured from 38,000 feet with a Leiss monochromator and a photoelectric filter radiometer.
c30 A69-32261
WEBB, L. D.
Advanced air data sensing techniques.
c14 A69-16755
WEBBER, W. R.
The relative energy spectra of carbon and oxygen nuclei in the primary cosmic radiation.
c29 A69-20632
WEBELER, R. W. H.
Viscosity measurements of dilute solutions of helium-3 in superfluid helium-4 between 0.1 and 1.2 deg K.
c23 A69-39582
WEBER, M.
A program to evaluate dye lasers as high power, pulsed, visible light sources
[NASA-CR-1374] c16 N69-29934
WEBER, R. R.
Cosmic radio noise intensity from 0.45 to 3.0 MHz observed by the ATS II satellite.
c30 A69-19715
The spectrum of the cosmic radio background between 0.4 and 6.5 MHz.
c30 A69-42375
WEETON, J. W.
Fiber-metal matrix composites.
c17 A69-20204
Dispersion-strengthened nickel produced from ultrafine comminuted powders
[NASA-TN-D-5421] c17 N69-38074
WEGER, R. M.
Power conditioning development for the Sert II ion thrustor.
c03 A69-42301
WEGER, W. C.
Reliability handbook for silicon monolithic microcircuits. Volume 1 - Application of monolithic microcircuits
[NASA-CR-1346] c09 N69-23225
WEIBEL, J.
Viruslike particles in the fat body, oenocytes, and central nervous tissue of Drosophila melanogaster imagoes.
c04 A69-42021
WEIDNER, D. K.
Diurnal variations in the thermosphere from a series of Marshall-University-of-Michigan probes.
c13 A69-40515
WEIDNER, J. P.
Preliminary investigation of momentum diffusion between two supersonic airstreams in the presence of shock waves
[NASA-TN-D-4974] c12 N69-15631
WEIGAND, A. J.
Solar absorptances and spectral reflectances of 12 metals for temperatures ranging from 300 to 500 K
[NASA-TN-D-5353] c17 N69-31895
WEIGEL, C.
Performance and cavitation damage of an axial-flow pump in 1500 deg F /1089 K/ liquid sodium
[NASA-TN-D-5138] c15 N69-21773
WEILAND, W. F., JR.
Heat-transfer characteristics of a water-to-cryogenic-hydrogen heat exchanger
[NASA-TN-D-5429] c33 N69-36701
WEINBERG, D. L.
Four-photon optical parametric noise in water.
c23 A69-21751
WEINGARTEN, V. I.
Buckling of thin-walled circular cylinders
[NASA-SP-8007] c32 N69-23320
Buckling of thin-walled truncated cones
[NASA-SP-8019] c32 N69-24131
WEINREB, M. P.
Quenching of N sub 2
c24 A69-36424
WEINSTEIN, H.
Effect of free stream turbulence on coaxial mixing
[NASA-CR-1336] c12 N69-24058
Turbulence in the mixing region between ducted coaxial streams
[NASA-CR-1335] c12 N69-30728
WEINSTEIN, L. M.
Influence of measured free-stream disturbances on hypersonic boundary-layer transition.
[AIAA PAPER 69-704] c12 A69-33453
Electron beam flow visualization in hypersonic helium flow.
c11 A69-35722
WEINSTEIN, M. C.
Symbol-oriented failure analysis in multicomponent systems
[NASA-TN-D-5112] c10 N69-22919
WEINSTEIN, R. H.
Computer experiments on the microscopic behavior of one-dimensional plasmas
[NASA-TN-D-4831] c25 N69-10471
WEINSTEIN, S. T.
The effects of reactor radiation on 22-volt silicon voltage-regulator diodes
[NASA-TN-D-4923] c09 N69-10250
WEISERT, E. D.
Refractory Metal Alloys- Metallurgy and Technology, Proceedings of a Symposium on Metallurgy and Technology of Refractory Metals, Washington, D.C., April 25, 26, 1968.
c17 A69-18790
WEISS, E.
Space geodesy altimetry study
[NASA-CR-1298] c14 N69-21117
WEISS, G.
Delta-T curves for measuring magnetic tape link jitter.
c14 A69-18827
WEISS, R. J.
Compton profile of LiH.
c26 A69-40730
WEITZENFELD, A. S.
Algorithms for test patterns in multiterminal devices with symmetry constraints.
c08 A69-42524
WEIZER, V. G.
On the resolution and image intensity of the field-ion microscope
[NASA-TN-D-5125] c14 N69-21408
WELLS, B. J.
Wind-tunnel investigation of the aerodynamic pressures on the Apollo command module configuration
[NASA-TN-D-5514] c01 N69-40345
WELLS, C. S.
Viscous Drag Reduction, Proceedings of the Symposium, Dallas, Tex., September 24, 25, 1968.
c12 A69-33247
An analysis of uniform injection of a drag-reducing fluid into a turbulent boundary layer.

c12 A69-33254
WELLS, F. E.
A survey of leak detection for aerospace hardware.
c15 A69-30315
WELLS, W. L.
Description of the high-enthalpy arc tunnel at the Langley Research Center including test- stream conditions at selected operating points
[NASA-TN-D-5295] c11 N69-29981
WELLS, W. R.
Determination of lunar equatorial radius using image-motion compensation sensor data from Lunar Orbiter I
[NASA-TN-D-5231] c30 N69-29115
WELTMAN, G.
NASA contributions to bioinstrumentation systems - A survey
[NASA-SP-5054] c04 N69-14860
WEMPE, T. E.
Human information processing rates during certain multiaxis tracking tasks with a concurrent auditory task.
c05 A69-23880
WENDE, C. D.
Correlation of solar microwave and soft X-ray radiation. I - The solar cycle and slowly varying components.
c29 A69-40504
WENTE, V. A.
Operating experience with NASA/SCAN - A large scale selective announcement service.
c34 A69-39581
WENTZEL, D. G.
Plasma Instabilities in Astrophysics, Proceedings of the Conference, Monterey, Calif., October 14-17, 1968.
c30 A69-42681
WERKING, R. D.
RAE-A attitude determination ground support system.
[AIAA PAPER 69-983] c08 A69-40363
WESCOTT, E. M.
Electric fields in the vicinity of auroral forms from motions of barium vapor releases.
c13 A69-34935
WEST, J. B.
Ventilation-perfusion inequality and overall gas exchange in computer models of the lung.
c05 A69-38388
WEST, K. A.
A simple technique for automatic computer editing of biodata
[NASA-TN-D-5275] c08 N69-29592
WEST, W. S.
Thermal model of a 75 watt.
c03 A69-42254
WESTBROOK, R. M.
EEG sensing and transmitting system contained in a flight helmet.
c05 A69-26553
WESTFALL, R. M.
Radial power tailoring for a uranium dioxide T-111 clad reactor with contained fission product gases
[NASA-TM-X-1795] c22 N69-25305
Reflector-based poison-drum control on equal-size reactor cores fueled with uranium-233 and with uranium-235
[NASA-TM-X-1883] c22 N69-36756
WESTMORELAND, G.
Development of vulcanizable elastomers suitable for use in contact with liquid oxygen.
c06 A69-16497
WESTON, K. C.
The stagnation-point boundary layer with suction and injection in equilibrium dissociating air
[NASA-TN-D-3889] c12 N69-14314
WESTPHAL, K. O.
Interaction of linear waves with oblique shock waves.
c12 A69-13137
Transmission of Alfven waves through the earth's bow shock.
c13 A69-32099
Interaction of magnetoacoustic and entropy waves with normal magnetohydrodynamic shock waves.
c25 A69-38242
WEYGANDT, P. C.
Application of gravity gradient stabilization to large manned space vehicles.
c31 A69-18338
WHEADON, W. C.
The impact of failure data on management of a launch operations reliability program.
c11 A69-36022
WHITAKER, H. P.
A new model performance index for the engineering design of flight control systems.
[AIAA PAPER 69-885] c21 A69-39410
WHITE, J. A.
Deceleration-control system for aerobraking and skipout to orbit at Mars.
[AIAA PAPER 68-1146] c31 A69-13564
WHITE, K. C.
Methods for predicting spacecraft-window- induced line-of-sight deviations
[NASA-TN-D-5238] c21 N69-31227
WHITE, M. D.
The simulator to match the transports to come.
c11 A69-43044
WHITE, P. H.
Summary of random vibration prediction procedures
[NASA-CR-1302] c32 N69-23096
WHITE, T. T.
Apollo 4 and 6 radiation analysis.
[AIAA PAPER 69-17] c05 A69-18202
WHITE, W. A.
X-ray and extreme ultraviolet /1-400 angstrom units/ spectroscopy of the sun, from OSO-III.
c29 A69-22169
Observations of the solar flare soft X-ray spectrum and comparison with centimetric radio bursts.
c29 A69-43609
WHITE, W. F.
Rotational spectrum of ethylene episulfoxide.
c06 A69-20535
WHITEHEAD, A. H., JR.
Flow phenomena and separation over delta wings with trailing-edge flaps at Mach 6.
[AIAA PAPER 68-97] c01 A69-12522
Boundary-layer tripping with emphasis on hypersonic flows.
c12 A69-33249
Flow-field and drag characteristics of several boundary-layer tripping elements in hypersonic flow
[NASA-TN-D-5454] c12 N69-38156
WHITEHEAD, V. S.
Cloud height contouring from Apollo 6 photography.
c20 A69-36926
WHITFIELD, C. E.
Evaluation of meta-benzenedisulfonic acid as a stress-reducing additive in a Watts nickel electroplating bath
[NASA-TN-D-5188] c17 N69-36697
WHITING, E. E.
Line by line calculation of spectra from diatomic molecules and atoms assuming a Voigt line profile.
c24 A69-35239
A computer program for a line by line calculation of spectra from diatomic molecules and atoms assuming a Voigt line profile
[NASA-TN-D-5088] c24 N69-21462
WHITLOCK, C. H.
Dynamic stability characteristics of large-size 120 deg blunted conical spacecraft in a simulated Martian environment.
[AIAA PAPER 69-104] c31 A69-18210
Damping derivatives of 120 deg conical spacecraft from flights in a low-density environment.
c31 A69-40550
Wind tunnel investigation of inflation of disk-gap-band and modified ringsail parachutes at dynamic pressures between 0.24 and 7.07 pounds per square foot
[NASA-TM-X-1786] c01 N69-23538
Inflation and performance of three parachute configurations from supersonic flight tests in a low-density environment
[NASA-TN-D-5296] c01 N69-30063
WHITMAN, R. I.
Infrared horizon profiles for winter conditions from Project Scanner
[NASA-TN-D-4905] c21 N69-14346
A technique to infer atmospheric temperature from horizon radiance profiles

[NASA-TN-D-5068] c13 N69-19024
A technique to infer atmospheric water-vapor mixing ratio from measured horizon radiance profiles
[NASA-TN-D-5252] c13 N69-27246
WHITMARSH, C. L., JR.
A 1-megawatt reactor design for Brayton-cycle space power application. Part 1 - Thermal analysis and core design
[NASA-TN-D-5013] c22 N69-17313
A 1-megawatt reactor design for Brayton-cycle space power application Part 2 - Neutronics design
[NASA-TN-D-5014] c22 N69-17314
Neutronic comparison of beryllium oxide and molybdenum for movable reflector control of a fast-spectrum reactor
[NASA-TM-X-1822] c22 N69-29593
Characteristics of a 2.17-megawatt fast- spectrum reactor concept using an axially moving reflector control system
[NASA-TM-X-1911] c22 N69-40061
WHITNEY, W. J.
Performance of a single-stage turbine as affected by variable stator area.
[AIAA PAPER 69-525] c28 A69-32686
Analytical investigation of the effect of cooling air on two-stage turbine performance
[NASA-TM-X-1728] c01 N69-17392
Cold air investigation of a turbine with stator-blade trailing-edge coolant ejection. Part 1 - Overall stator performance
[NASA-TM-X-1901] c03 N69-39335
WHITSETT, C. E., JR.
EVA maneuvering unit comparison.
[AAS PAPER 69-516] c05 A69-42850
WICHOREK, G. R.
Design, fabrication, and tests of tubular beryllium and Be-38Al alloy truss-type structures
[NASA-TN-D-5254] c32 N69-28658
WICKRAMASINGHE, N. C.
Graphite particle model for NML Cygnus.
c30 A69-13775
Strengths of the fundamental bands of ice and solid hydrogen in composite grains.
c23 A69-29587
Solid hydrogen coated graphite particles in the interstellar medium. I.
c30 A69-37492
WIDNALL, S. E.
Correlation of fluctuating forces with the sound radiation from rigid flow spoilers
[NASA-CR-1340] c23 N69-26307
WIEBER, D.
Laser beam directed at the lunar retro- reflector array - Observations of the first returns.
c30 A69-43197
WIER, D. D.
An investigation of the decoupling effects in a magnetic forming beryllium coil assembly.
c14 A69-25310
WIERWILLE, W. W.
Synthesis methods for manual aerospace control systems with applications to SST design
[NASA-CR-1208] c02 N69-13185
WIESMAN, W.
Organizational communication.
c34 A69-42930
WILBER, B. M.
Characteristics of the tactile information channel
[NASA-CR-1389] c05 N69-39211
WILBUR, A. C.
An exploratory study of the interplanetary environmental effects on solar-cell cover glasses.
c03 A69-35702
WILCOCK, D. F.
Configurations for gas turbine compressor end seals.
[ASLE PREPRINT 68AM 4B-4] c15 A69-27366
WILCOX, F. A.
Flight and wind tunnel investigation of installation effects on supersonic cruise exhaust nozzles at transonic speeds.
[AIAA PAPER 69-427] c01 A69-32769
WILCOX, J. M.
A model of interplanetary and coronal magnetic fields.
c30 A69-24429
Interplanetary sector structure in the rising portion of the sunspot cycle.
c30 A69-28957
Direction of the nearby galactic magnetic field inferred from a cosmic-ray diurnal anisotropy.
c29 A69-38098
WILD, J. W.
Safety for large space stations.
[AAS PAPER 69-518] c31 A69-42842
WILDER, D. R.
Effects of cyclic heating and thermal shock on hafnia stabilized with calcia, magnesia, and yttria
[NASA-TN-D-5279] c18 N69-34547
WILDER, S. E.
Real-helium hypersonic flow parameters for pressures to 3600 atmospheres and temperatures to 15,000 deg K
[NASA-TN-D-4869] c12 N69-10443
WILEY, R. F.
Real-time targeting for the Apollo lunar orbit insertion maneuver.
[AIAA PAPER 68-848] c31 A69-39760
WILKERSON, T. D.
Plasma observations on Explorer 34.
c13 A69-11234
Helium abundance in the solar wind.
c29 A69-40305
WILKINS, J. R.
Microbiological studies on a water management subsystem for manned space flight.
[SAE PAPER 680718] c05 A69-13441
WILLIAMS, B. L.
Improved method of removing plastic backing films from carbon electron microscope replicas.
c14 A69-21651
WILLIAMS, D. A.
The interstellar H super plus sub 2 molecule.
c30 A69-42610
WILLIAMS, D. J.
The Small Scientific Satellite
[IEEE PAPER 3C-1] c31 A69-19195
Proton entry into the magnetosphere on May 26, 1967.
c29 A69-31984
Design of a long-life reliable nuclear experiment for space flight.
c09 A69-36676
WILLIAMS, D. P.
Comments on slow crack growth of steels in hydrogen and water environments.
c17 A69-10612
WILLIAMS, J. R.
Space manufacturing modules.
c31 A69-35067
A feasibility study of determining physical properties of the Martian atmosphere by use of solar occultation as seen from an artificial satellite
[NASA-TN-D-5443] c30 N69-38658
WILLIAMS, M. D.
Parameters affecting firing time of simultaneously triggered trigatron spark gap switches
[NASA-TN-D-5077] c09 N69-20888
WILLIAMS, R. M.
A comparison of the performance of two rhenium, niobium cylindrical thermionic converters.
c03 A69-13126
The performance of a rhenium, niobium cylindrical thermionic converter.
c03 A69-16359
WILLIAMS, W. L.
In-house research on the management of R and D in government agencies.
c34 A69-38022
WILLIAMSON, R. C.
Velocity of sound at 1 MHz near the He super 4 critical point.
c23 A69-17142
Measurement of the velocity and attenuation of ultrasonic pulses in the presence of noise.
c14 A69-29564
WILLICH, W.
A flight investigation of systems developed for reducing pilot workload and improving tracking accuracy during noise-abatement landing approaches
[NASA-CR-1427] c02 N69-38657

WILLIS, C. M.
Calorimetric, optical, and vibration investigations of stretch-formed aluminum solar concentrators
[NASA-TN-D-4889] c03 N69-10708
Calorimetric evaluation of two cone-column solar-energy concentrations
[NASA-TN-D-5109] c03 N69-21088
WILLIS, E. A., JR.
Two-burn escape maneuvers with an intermediate coasting ellipse
[NASA-TN-D-5011] c30 N69-17305
WILLOH, R. G.
A mathematical analysis of supersonic inlet dynamics
[NASA-TN-D-4969] c01 N69-14289
Multistage compressor simulation applied to the prediction of axial flow instabilities
[NASA-TM-X-1880] c28 N69-36998
WILLOUGHBY, D. S.
An interpretation of OGO light ion abundance measurements.
c13 A69-25157
Temperature and ion abundance profiles deduced from simultaneous Explorer XXXI and Alouette II data.
c13 A69-37896
WILLOUGHBY, R.
Toxicity problems in plastic hardware designed for biological space-flight experiments
[NASA-TM-X-1818] c04 N69-29723
WILMARTH, R. W.
Small-signal and saturation characteristics of an X-band cyclotron-resonance oscillator.
c09 A69-22786
Cooling of a high-power electron tube in a space vehicle.
c09 A69-24747
Nonelectric cathode heating.
c09 A69-24748
WILMARTH, V. R.
Apollo lunar sample analysis program - A progress report.
c11 A69-40191
WILSON, A.
Carroll's method applied to small stellar rotations.
c30 A69-42404
WILSON, A. M.
An analysis of the solar sodium D lines.
c30 A69-38479
WILSON, B. G.
International Conference on Cosmic Rays, 10th, Calgary, Canada, June 19-30, 1967, Proceedings. Part A - Invited and Rapporteur Papers.
c29 A69-12928
WILSON, D. J.
Sensitivity of the creep-rupture properties of nickel-base superalloy sheet to sharp edge-notches in the temperature range of 1000 deg F - 1400 deg F
[NASA-CR-1263] c32 N69-16156
WILSON, H. B., JR.
Applications of a tube wind tunnel in supersonic testing.
[AIAA PAPER 69-335] c11 A69-28271
WILSON, J. W.
Four-gimbal systems for simulation display.
c11 A69-26265
Analysis of numerical integration techniques for real-time digital flight simulation
[NASA-TN-D-4900] c11 N69-11371
WILSON, K. H.
Effect of shock precursor heating on radiative flux to blunt bodies
[NASA-CR-1265] c33 N69-17438
Effect of ablation product absorption and line transitions on shock layer radiative transport
[NASA-CR-1264] c33 N69-19117
Radiant energy transfer measurements in air
[NASA-CR-1390] c25 N69-38227
WILSON, M. D.
International Conference on Cosmic Rays, 10th, Calgary, Canada, June 19-30, 1967, Proceedings. Part A - Invited and Rapporteur Papers.
c29 A69-12928
WILSON, S. D.
Compressed gas handbook
[NASA-SP-3045] c12 N69-26987
WILSON, V. C.
Characteristics of a thermionic converter with a chloride vapor deposited tungsten emitter /110/ and a nickel collector
[NASA-CR-1416] c03 N69-32553
Characteristics of a thermionic converter with a fluoride vapor deposited tungsten emitter etched to preferentially expose the 110 crystal planes
[NASA-CR-1381] c03 N69-35689
WIMMER, H. L.
Electronic position indicator for latching solenoid valves
[NASA-TM-X-1760] c14 N69-20874
WINER, I.
Laser beam directed at the lunar retro- reflector array - Observations of the first returns.
c30 A69-43197
WINGET, C. M.
Plasma enzyme responses to blood withdrawal in chickens.
c04 A69-23158
Mechanisms of action of light on circadian rhythms in the monkey.
c04 A69-31336
Phase relationships between circadian rhythms and photoperiodism in the monkey.
c04 A69-42706
WINGROVE, R. C.
Measurement of pilot describing functions from flight test data with an example from Gemini X.
c05 A69-11950
A technique for identifying pilot describing functions from routine flight-test records
[NASA-TN-D-5127] c05 N69-23842
WINSTON, B. P.
A comparison of a class of earth-moon orbits with a class of rotating Kepler orbits
[NASA-TN-D-4903] c30 N69-10470
WINSTON, M. M.
Wind-tunnel data from a 0.16-scale V/STOL model with direct-lift and lift-cruise jets
[NASA-TM-X-1758] c01 N69-20016
Wind-tunnel investigation of steady-state aerodynamics of a composite-lift VTOL aircraft model
[NASA-TN-D-5232] c02 N69-28097
Static stability characteristics of a 0.16- scale model of a jet-lift V/STOL research airplane in cruise
[NASA-TM-X-1835] c02 N69-30633
WINTER, E. F.
Summary of random vibration prediction procedures
[NASA-CR-1302] c32 N69-23096
WINTER, J. M.
Rocket engine evaluation of erosion and char as functions of fabric orientation for silica-reinforced nozzle materials
[NASA-TM-X-1721] c28 N69-15475
Evaluation of 7.8-inch-throat-diameter inserts and a unique cooling concept in a storable-propellant rocket engine
[NASA-TM-X-1756] c28 N69-19782
Design of injectors and ablative thrust chambers for a flox-propane rocket engine with a 1.2-inch throat diameter
[NASA-TN-D-5324] c28 N69-30560
Development of improved throat inserts for ablative rocket engines
[NASA-TN-D-4964] c32 N69-33481
Design, development, and testing of a 1000 pound /4450 N/ thrust FLOX-propane ablative rocket engine
[NASA-TM-X-1873] c28 N69-35847
WINZIG, C. H.
Preliminary investigation of a single-shaft Brayton rotating unit designed for a 2 to 10-kilowatt space power generation system
[NASA-TM-X-1869] c03 N69-39238
WISANDER, D. W.
Friction and wear of nine selected polymers with various fillers in liquid hydrogen
[NASA-TN-D-5073] c15 N69-19800
WISHNA, S.
WEFAX - Weather data relay communications experiment.
c11 A69-13240
Solar effects on VHF communications between a synchronous satellite relay and earth ground stations

[NASA-TN-D-5100] c07 N69-23317
WISHNER, R. P.
Suboptimal state estimation for continuous-time nonlinear systems from discrete noisy measurements. c10 A69-17939
WITZKE, W. R.
Superplasticity in tungsten-rhenium alloys. c17 A69-22990
Creep of powder metallurgy rhenium at 0.43 to 0.72 T sub m. c17 A69-34186
Mechanical properties of arc-melted tungsten-rhenium-hafnium-carbon alloys
[NASA-TN-D-5348] c17 N69-31977
WOELLER, F.
Studies on the formation and transformation of esters. LXXX. c06 A69-31808
WOHL, M. L.
Use of ''FASTER'' code for significantly reducing ducted reactor shield computation time
[NASA-TM-X-1828] c22 N69-29671
Helical duct geometry routine for the shielding computer program ''FASTER''
[NASA-TM-X-1838] c22 N69-31986
WOLBERS, H. L.
A program plan for earth orbital space astronomy. c11 A69-27947
WOLF, J. S.
A proposed model for the effect of oxidation on the high-temperature deformation of nickel
[NASA-TN-D-5266] c17 N69-27061
WOLF, R. A.
Possible conversion of rotational energy of the neutron star in the Crab Nebula into energy of relativistic electrons. c30 A69-21454
WOLFE, J. H.
Review of Ames Research Center plasma-probe results from Pioneers 6 and 7. c13 A69-19364
Preliminary comparison of solar wind plasma observations in the geomagnetospheric wake at 1000 and 500 earth radii. c29 A69-26943
MHD Rankine-Hugoniot equations applied to earth's bow shock. c30 A69-42417
WOLFF, C.
Interplanetary gas. XVI. c29 A69-34301
WOLLRAB, J. E.
Rotational spectrum of ethylene episulfoxide. c06 A69-20535
WOLOVICH, W. A.
On the stabilization of controllable systems. c10 A69-17947
WOLSKE, G. D.
Minimum fuel attitude control of a nonlinear satellite system with bounded control by a method based on linear programming
[NASA-CR-1450] c21 N69-41036
WONG, N. D.
A two-dimensional, mixed-compression inlet system designed to self-restart at a Mach number of 3.5.
[AIAA PAPER 69-447] c28 A69-32732
WONG, R. Y.
Preliminary investigation of a single-shaft Brayton rotating unit designed for a 2 to 10-kilowatt space power generation system
[NASA-TM-X-1869] c03 N69-39238
WONHAM, W. M.
Optimal stochastic control. c10 A69-14697
On a matrix Riccati equation of stochastic control. c10 A69-16601
Optimal stochastic control. c10 A69-22567
A computational approach to optimal control of stochastic saturating systems. c10 A69-30601
WOOD, A. D.
Radiant energy transfer measurements in air
[NASA-CR-1390] c25 N69-38227
WOOD, C.
A pyrotechnic-activated calorimeter for flight research at lunar return velocity. c11 A69-23026
WOOD, C. C.
Evaluation of experimental and analytical data for orbital refueling systems.
[AIAA PAPER 69-566] c31 A69-32755
WOOD, F. H., JR.
Effect of jet velocity and axial location of nozzle exit on the performance of a twin-jet afterbody model at Mach numbers up to 2.2
[NASA-TN-D-5393] c28 N69-36932
WOOD, G. A.
Optimal continuous low-thrust trajectories for co-altitude rendezvous. c30 A69-32177
WOOD, J. C.
Hot performance characteristics of a gas bearing Brayton cycle turboalternator. c03 A69-42279
Preliminary performance characteristics of a gas-bearing turboalternator
[NASA-TM-X-1820] c03 N69-29707
WOODMAN, D. P.
Optical radar studies of the atmosphere. c07 A69-27001
WOODS, W. C.
Some topics in hypersonic body shaping.
[AIAA PAPER 69-181] c01 A69-18052
WOODS, W. W.
Shear strain properties to 10 sup -10 of selected optical materials
[NASA-CR-1257] c14 N69-16100
WOOLEY, B. C.
Physical, chemical, and biological activities at the Lunar Receiving Laboratory. c11 A69-38896
WOOLF, H. M.
A comparison of data obtained by the MT-135 and ARCAS meteorological rocket systems
[NASA-TM-X-1726] c20 N69-17772
WOOLF, N. J.
A far infrared sky survey. c30 A69-27599
WOOLLAM, J. A.
Thermomagnetic effects and Fermi surface topology - Results in metallic tin at low temperatures. c26 A69-16357
A simple A.C. technique for galvanomagnetic and Shubnikov-de Haas measurements. c14 A69-36375
Galvanomagnetic and thermomagnetic effects in white tin in fields to 3.3 tesla and at temperatures between 1.2 and 4.2 K
[NASA-TN-D-5227] c26 N69-25412
WORKMAN, W. L.
Reliability handbook for silicon monolithic microcircuits. Volume 3 - Failure analysis of monolithic microcircuits
[NASA-CR-1348] c09 N69-25328
WORLEY, H. E.
Attitude control of a manned earth orbiting space station.
[AIAA PAPER 69-846] c31 A69-39376
WORLEY, W. J.
The conformal mapping of the interior of the unit circle onto the interior of a class of smooth curves
[NASA-CR-1357] c32 N69-26559
WORLOCK, R. M.
Cesium contact ion microthruster experiment aboard applications technology satellite /ATS/ IV.
[AIAA PAPER 69-297] c28 A69-21218
WORLUND, A. L.
Saturn V longitudinal oscillation /POGO/ solution.
[AIAA PAPER 69-548] c31 A69-32658
WORONOWICZ, T. J.
Apparatus for the precision measurement of internal friction. c14 A69-13108
WORRALL, G.
An analysis of the solar sodium D lines. c30 A69-38479
WORTZ, E. C.
A study of astronauts' extravehicular work capabilities in weightless conditions
[NASA-CR-1334] c05 N69-27266
Man's capability for self-locomotion on the moon. Volume 2 - Summary report
[NASA-CR-1403] c05 N69-36271

Man's capability for self-locomotion on the moon. Volume 1 - Detailed report
[NASA-CR-1402] c05 N69-37964
WRENN, G. L.
Comparison of results of Explorer XXXI direct measurement probes.
c13 A69-37882
WRIGHT, R. D.
Laser display systems. I - Scanners.
c14 A69-15028
Laser display systems. II.
c14 A69-21394
WRIGHT, R. L.
Data-reduction technique for determining rapidly rising heating rates to thermally thick walls
[NASA-TN-D-5309] c33 N69-30726
WRIGHTS, G. N.
Monte Carlo calculations of a hemispherical duct neutron streaming experiment.
c22 A69-35178
WU, D. C. F.
Slope diffraction analysis of TEM parallel- plate guide patterns
[NASA-CR-1326] c07 N69-26273
WUDELL, A. E.
EVA maneuvering unit comparison.
[AAS PAPER 69-516] c05 A69-42850
WUENSCHER, H. F.
Space manufacturing unique to zero gravity environment.
[AAS PAPER 69-486] c30 A69-42844
WYDEVEN, T.
Water electrolysis - Prospect for the future.
c05 A69-12987
Thermal decomposition of yttrium-doped silver carbonate.
c06 A69-30442
Heats of adsorption of carbon dioxide on silver
c06 A69-38277
WYER, R. R.
NERVA control drum actuator irradiation test program
[NASA-TN-D-5347] c22 N69-31870
WYMAN, C. L.
An advanced laser tracking technique for future space guidance systems.
[AIAA PAPER 69-870] c21 A69-39396
WYNNE, G. A.
Effect of jet temperature on jet and pure tone noise radiation
[NASA-CR-1472] c02 N69-40439

X

XENAKIS, G.
Guidance and control considerations for advanced manned space missions.
c21 A69-35801

Y

YAGELOWICH, H.
10.6-micrometer laser communication system experiment for ATS-F and ATS-G.
c07 A69-41758
YAGER, T. J.
Recent studies on effects of runway grooving on airplane operations.
[AIAA PAPER 69-773] c02 A69-35649
YAGHMAI, S.
Incremental analysis of large deformations in mechanics of solids with applications to axisymmetric shells of revolution
[NASA-CR-1350] c32 N69-28624
YAMINY, R. R.
A 17-1 dual band circularly polarized focused two-channel monopulse tracking system.
c07 A69-41752
YANG, E. S.
Linear operation of a p-n-p-n tetrode.
c09 A69-35293
YEAGER, L. J.
Summary of electrical component development for a 400-hertz Brayton energy conversion system
[NASA-TN-D-4874] c03 N69-10088
YEE, L.
An experiment to determine the structure of a planetary atmosphere.
[AIAA PAPER 68-1054] c30 A69-13699
YEVREINOVA, T. N.
Concentration of matter and action of enzymes in coacervates
[NASA-TT-F-525] c04 N69-40324
YEVTUSHENKO, YU. G.
Motion of artificial satellites in the earth's gravitational field
[NASA-TT-F-539] c30 N69-33560
YIN, L. I.
Some parameters affecting Auger and photoelectron spectroscopy as an analytical technique.
c06 A69-19775
YOSHIKAWA, K. K.
Linearized theory of stagnation point heat and mass transfer at hypersonic speeds
[NASA-TN-D-5246] c12 N69-33421
YOST, C. A.
Human survival in aircraft emergencies
[NASA-CR-1262] c02 N69-14763
YOUNG, C. P., JR.
Analysis of the aeroelastic divergence of two experimental unguided launch vehicles
[NASA-TN-D-4846] c32 N69-10297
YOUNG, E.
The Orbiting Astronomical Observatory thermal test program.
[AIAA PAPER 69-995] c11 A69-40373
YOUNG, G. A.
Operating experience with NASA/SCAN - A large scale selective announcement service.
c34 A69-39581
YOUNG, G. R.
Approximation to the statistics of midcourse velocity corrections
[NASA-TN-D-5381] c30 N69-36143
YOUNG, H. L.
Uptake and incorporation of exogenous leucine in bacterial cells under high oxygen tension.
c04 A69-13433
YOUNG, L. R.
Motion cues in man-vehicle control.
c05 A69-23879
YOUNG, R. M.
X-ray and extreme ultraviolet /1-400 angstrom units/ spectroscopy of the sun, from OSO-III.
c29 A69-22169
Observations of the solar flare soft X-ray spectrum and comparison with centimetric radio bursts.
c29 A69-43609
Laser Doppler velocity instrument
[R-67-4450] c14 N69-14351
YOUNG, R. S.
Weightlessness and the developing frog egg.
c04 A69-11084
The search for life - Planetary evolution.
c04 A69-12804
Life detection techniques.
c05 A69-32970
Extraterrestrial life detection.
c30 A69-41623
YOUNG, S. G.
Effect of temperature and pressure on cavitation damage to a cobalt base alloy in sodium.
c17 A69-35184
Effect of ultrasonic vibration on precipitation hardening of steels and superalloys
[NASA-TN-D-5131] c32 N69-21814
Effect of temperature and pressure on cavitation damage to a cobalt base alloy in sodium
[NASA-TN-D-5273] c17 N69-28863
YOUNGBLUTH, O., JR.
Photomultiplier area sensitivity measurements using a multicolor display technique.
c14 A69-35724
YOUNGER, C. L.
Effect of nuclear radiation at cryogenic temperatures on the tensile properties of titanium and titanium-base alloys
[NASA-TN-D-5442] c17 N69-37436
YUAN, S.
Design considerations for an integrated 1.8- GHz parametric amplifier.
c09 A69-10193
YUEN, M. C.
Experimental investigation of magnetoaerodynamic flow around blunt bodies
[NASA-CR-1393] c25 N69-34897

Z

ZADEH, L. A.
Toward a theory of fuzzy systems
[NASA-CR-1432] c19 N69-37033

ZAITZEFF, E. M.
Advanced Space Experiments, American Astronautical Society, Conference, Ann Arbor, Mich., September 16-18, 1968, Proceedings.
c30 A69-34359

ZAKIN, J. L.
Exploratory drag reduction studies in non-polar soap systems.
c12 A69-33253

ZAMES, G.
Logarithmic variation criteria for the stability of systems with time-varying gains.
c10 A69-13073
Stability of systems with sector nonlinearities - a comparison of various inequalities.
c10 A69-25450

ZAREMBA, J. G.
Implementation of a semi-active gravity gradient controller.
c31 A69-18334

ZARETSKY, E. V.
EHD lubrication.
c15 A69-11324
Contact conformity effects on spinning torque and friction.
[ASME PAPER 68-LUB-10] c15 A69-30901
Elastohydrodynamic lubrication of a spinning ball in a nonconforming groove.
[ASME PAPER 69-LUBS-11] c15 A69-34381
Effect of oxygen concentration on synthetic paraffinic and advanced ester base lubricants in bearing tests at 400 deg and 450 deg F.
c15 A69-35177
Rolling-element fatigue life of ausformed M-50 steel balls
[NASA-TN-D-4954] c15 N69-14383
Rolling-element bearing life from 400 deg to 600 F
[NASA-TN-D-5002] c15 N69-16367
Effect of oxygen concentration on an advanced ester lubricant in bearing tests at 400 deg and 450 deg F
[NASA-TN-D-5262] c15 N69-26311
Effect of oxygen concentration on the performance of synthetic paraffinic oils in short term bearing tests from 400 deg to 500 deg F
[NASA-TN-D-5152] c15 N69-26314
Speed effects on ball spinning torque
[NASA-TN-D-5527] c15 N69-41210

ZEITMAN, B. B.
New observations on the substrate specificity of cathepsin C /dipeptidyl aminopeptidase I/ including the degradation of beta-corticotropin and other peptide hormones.
c04 A69-37577

ZELEZNIK, F. J.
Calculation of complex chemical equilibria.
c06 A69-10588
A comparison of rotational collision numbers obtained from different definitions
[NASA-TN-D-5321] c24 N69-30073

ZELLARS, G. R.
Evaluation of the results of a round robin analysis for oxygen in potassium and sodium
[NASA-TN-D-4971] c06 N69-14180

ZELLER, J. R.
Design and analysis of a modular servoamplifier for fast-response electrohydraulic control systems
[NASA-TN-D-4898] c03 N69-10068
Dynamic performance analysis of a fuel-control valve for use in airbreathing engine research
[NASA-TN-D-5331] c03 N69-29977
Analysis of dynamic performance limitations of fast response /150 to 200 Hz/ electrohydraulic servos
[NASA-TN-D-5388] c03 N69-34652

ZENDER, G. W.
Compressive properties and column efficiency of metals reinforced on the surface with bonded filaments
[NASA-TN-D-4878] c17 N69-11012

ZIMMERMAN, B. G.
Digital simulation of rotational kinematics
[NASA-TN-D-5302] c23 N69-39178

ZINN, B. T.
Effect of jet temperature on jet and pure tone noise radiation
[NASA-CR-1472] c02 N69-40439

ZITO, G. V.
Design and development of a multipurpose, boresighted star tracker
[NASA-CR-976] c21 N69-21502

ZMUDA, A. J.
Ionospheric and magnetic observations at 1000 kilometers during the geomagnetic storm and aurora of May 25-26, 1967.
c13 A69-34954

ZOBY, E. V.
An evaluation test of a full scale replica of the RAM-CA flight heat shield in a rocket engine exhaust
[NASA-TM-X-1841] c31 N69-32713

ZOLA, C. L.
Interplanetary probe missions with solar- electric propulsion systems
[NASA-TN-D-5293] c30 N69-29738

ZRUBEK, W. E.
Optimum design of communication links with noisy phase reference
[NASA-TN-D-4895] c07 N69-13155

ZUCCARO, J. J.
EEG sensing and transmitting system contained in a flight helmet.
c05 A69-26553

ZUK, J.
Numerical solutions for the flow and pressure fields in an idealized spiral grooved pumping seal.
[ASLE PREPRINT 30] c15 A69-30481
Computer program for viscous, isothermal compressible flow across a sealing dam with small tilt angle
[NASA-TN-D-5373] c15 N69-33281
Investigation of isothermal, compressible flow across a rotating sealing dam. 1 - Analysis
[NASA-TN-D-5344] c15 N69-35799

ZUMOFF, J.
Fluorescence spectra of homogeneous and mixed europium complexes.
c06 A69-10893

ZUPP, G. A., JR.
Applications of quasi-linearization theory to system identification
[NASA-TN-D-5300] c19 N69-29648

ZWEIGBAUM, H.
Launch constraints.
c31 A69-37287

CORPORATE SOURCE INDEX

NASA SCIENTIFIC AND TECHNICAL REPORTS AND PUBLICATIONS FOR 1969

A Selected Listing

Typical Corporate Source Index Listing

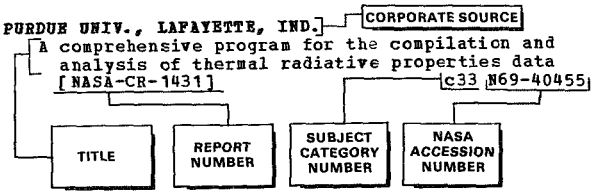

Listings in this index are arranged alphabetically by corporate source. The title of the document provides the user with a brief description of the subject matter. The report number helps to indicate the type of document cited (e.g., NASA report, translation, NASA contractor report). The subject category number indicates the subject category in the abstract section in which the citation is located. The accession number denotes the number by which the citation is identified within the subject category. The titles are arranged under each personal author in ascending accession number order. There are no "A" items in this index because AIAA does not use the Corporate Source entry.

A

AEROCHEM RESEARCH LABS., INC., PRINCETON, N. J.
Vaporization and decomposition kinetics of candidate re-entry blackout suppressants in low-pressure flames
[NASA-CR-1330] c07 N69-32721

AEROJET-GENERAL CORP., SACRAMENTO, CALIF.
Hydrogen gas pressure vessel problems in the M-1 facilities
[NASA-CR-1305] c17 N69-19831

AERONAUTICAL RESEARCH ASSOCIATES OF PRINCETON, INC., N. J.
Sonic boom propagation in a stratified atmosphere, with computer program
[NASA-CR-1299] c02 N69-22546

AIRESEARCH MFG. CO., LOS ANGELES, CALIF.
Man's capability for self-locomotion on the moon. Volume 2 - Summary report
[NASA-CR-1403] c05 N69-36271
Man's capability for self-locomotion on the moon. Volume 1 - Detailed report
[NASA-CR-1402] c05 N69-37964

ALI /DELORES E./, BERKELEY, CALIF.
Measurements of negative ion production in atmospheric gases
[NASA-CR-1406] c24 N69-38564

AMERICAN CYANAMID CO., STAMFORD, CONN.
High-performance light-weight electrodes for hydrogen-oxygen fuel cells
[NASA-CR-1216] c03 N69-14397

AMERICAN OPTICAL CO., FRAMINGHAM, MASS.
Holographic microscopy for the determination of failure mechanisms in monolithic circuits
[NASA-CR-1394] c14 N69-31958

ANPEX CORP., REDWOOD CITY, CALIF.
Study, fabrication and testing of a foil-bearing rotor support system
[NASA-CR-1157] c15 N69-14214

ANALYTIC SCIENCES CORP., READING, MASS.
Design of strapdown gyroscopes for a dynamic environment Interim scientific report
[NASA-CR-1396] c21 N69-34672

APPLIED PHYSICS LAB., JOHNS HOPKINS UNIV., SILVER SPRING, MD.
Unified analysis of turbulent jet mixing
[NASA-CR-1382] c12 N69-31887
The interaction and penetration of gaseous jets in supersonic flow
[NASA-CR-1386] c12 N69-32480

APPLIED THEORY, SANTA MONICA, CALIF.
Numerical calculation of viscous compressible fluid flow around an oscillating rigid cylinder
[NASA-CR-1467] c12 N69-38782

ARIZONA UNIV., TUCSON.
Computation of regions of constrained stability for nonlinear control systems
[NASA-CR-1328] c19 N69-28196
The design of linear multivariable control systems using modern control theory /with applications to coupled core reactor control/
[NASA-CR-1345] c19 N69-29268

ASTRO RESEARCH CORP., SANTA BARBARA, CALIF.
Certain physical properties and applications of Nitinol
[NASA-CR-1232] c17 N69-11420
Investigation of a coilable lattice column
[NASA-CR-1301] c32 N69-26234
Heliogyro solar sailer Summary report
[NASA-CR-1329] c31 N69-28861
Axisymmetric and cylindrical isostabiloids
[NASA-CR-1444] c32 N69-38781

ATOMICS INTERNATIONAL, CANOGA PARK, CALIF.
Preparation of UC and UC-W specimens for an irradiation test of the value of a fine-particle dispersion in the control of fission gas swelling /EXP-NRX-9-101 experiment/
[NAA-SR-12629] c22 N69-22946
Solubility of refractory metals and alloys in potassium and in lithium
[NASA-CR-1371] c17 N69-27059

AVCO CORP., LOWELL, MASS.
Study of ferromagnetic liquid
[NASA-CR-1407] c06 N69-33493

AZTEC SCHOOL OF LANGUAGES, INC., ACTON, MASS.
Radio bridge - ''Earth-moon-earth''
[NASA-TT-F-527] c07 N69-14973
Aurorae and airglow. Results of the research on the international geophysical projects. Collection of articles, no. 13
[NASA-TT-F-530] c13 N69-16539
Observations of noctilucent clouds
[NASA-TT-F-546] c13 N69-25013
Perception of space and time in outer space
[NASA-TT-F-545] c05 N69-26455
Electromedical apparatus - Principles of operation, installation, and use
[NASA-TT-F-523] c05 N69-27577
Motive forces in the development of the earth and planets
[NASA-TT-F-532] c13 N69-28983
Critical regimes of supersonic jet aircraft-stall and spin
[NASA-TT-F-526] c02 N69-31917
Boundary layer and chemical reactions
[NASA-TT-F-549] c33 N69-31947
Transactions of the Tenth Scientific Conference of the Institute of History of Natural Science and Technology
[NASA-TT-F-537] c34 N69-36314
Problems of Space Biology, volume 6
[NASA-TT-F-528] c05 N69-38701

AZTEC SCHOOL OF LANGUAGES, INC., MAYNARD, MASS.
Coordination of the voluntary movements of man in a zero gravitational field /under weightlessness/
[NASA-TT-F-578] c04 N69-31356
Transactions of the Ninth Scientific Conference of Graduate Students and Junior Scientific Associates of the Institute for the History of Natural Science and Technology, Section on the History of Aviation and Cosmonautics
[NASA-TT-F-540] c34 N69-31836
Transfer of microwave radiation in the atmosphere
[NASA-TT-F-590] c13 N69-31851
Problems of space biology. Volume 8 - Adaptation to hypoxia and resistance of an organism
[NASA-TT-F-580] c04 N69-32131

Solar activity, no. 3 Collection of articles
[NASA-TT-F-581] c29 N69-33401
High temperature oxidation protection of tungsten
[NASA-TT-F-583] c17 N69-35836

B

BARRY WRIGHT CORP., WATERTOWN, MASS.
Loss factor and resonant frequency of viscoelastic shear-damped structural composites
[NASA-CR-1269] c32 N69-17766
BATTELLE MEMORIAL INST., COLUMBUS, OHIO.
Satellite applications to marine geodesy
[NASA-CR-1253] c13 N69-16645
Systems approach to evaluating Hydrogenomonas cultures
[NASA-CR-1296] c05 N69-22766
Research on metallurgical characteristics and performance of materials used for sliding electrical contacts Summary report, 1 May 1968 - 30 Apr. 1969
[NASA-CR-1447] c17 N69-40057
BELL AEROSYSTEMS CO., BUFFALO, N. Y.
Empirically determined wind and scale effects on hot gas recirculation characteristics of jet V/STOL aircraft
[NASA-CR-1445] c28 N69-40776
BENDIX CORP., MISHAWAKA, IND.
Study of a modular extravehicular activity work platform
[NASA-CR-1361] c31 N69-26993
BENDIX CORP., TETERBORO, N. J.
Design and development of a multipurpose, boresighted star tracker
[NASA-CR-976] c21 N69-21502
BOEING CO., SEATTLE, WASH.
Shear strain properties to 10 sup -10 of selected optical materials
[NASA-CR-1257] c14 N69-16100
A flight investigation of systems developed for reducing pilot workload and improving tracking accuracy during noise-abatement landing approaches
[NASA-CR-1427] c02 N69-38657
Flight test results of a trailing edge flap designed for direct-lift control
[NASA-CR-1426] c02 N69-38819
BOLT, BERANEK, AND NEWMAN, INC., CAMBRIDGE, MASS.
Human visual sampling processes - A simulation validation study
[NASA-CR-1258] c05 N69-14145
Correlation of fluctuating forces with the sound radiation from rigid flow spoilers
[NASA-CR-1340] c23 N69-26307
BOLT, BERANEK, AND NEWMAN, INC., VAN NUYS, CALIF.
Combination effects of tone and duration parameters on perceived noisiness
[NASA-CR-1283] c04 N69-18722
Development of impedance simulation fixtures for spacecraft vibration tests
[NASA-CR-1351] c32 N69-26315
BROWN ENGINEERING CO., INC., HUNTSVILLE, ALA.
The general instability of eccentrically stiffened cylindrical shells under axial compression and lateral pressure
[NASA-CR-1280] c32 N69-15378

C

CALIFORNIA INST. OF TECH., PASADENA.
Stable crack propagation in a viscoelastic strip
[NASA-CR-1279] c30 N69-21506
Two-micron sky survey - A preliminary catalog
[NASA-SP-3047-REV] c30 N69-37993
CALIFORNIA UNIV., BERKELEY.
Incremental analysis of large deformations in mechanics of solids with applications to axisymmetric shells of revolution
[NASA-CR-1350] c32 N69-28624
Toward a theory of fuzzy systems
[NASA-CR-1432] c19 N69-37033
CALIFORNIA UNIV., LOS ANGELES.
Geometric properties of a prestressed segmented spherical shell
[NASA-CR-1231] c32 N69-11010
CALIFORNIA UNIV., SAN DIEGO.
Experiments on visual acuity and the visibility of markings on the ground in long-duration earth-orbital space flight
[NASA-CR-1134] c05 N69-10813
CASE WESTERN RESERVE UNIV., CLEVELAND, OHIO.
A lunar gravity simulator, volume 1
[NASA-CR-1233-VOL-1] c05 N69-11675
A lunar gravity simulator, volume 3
[NASA-CR-1235] c05 N69-14213
Structural synthesis of a stiffened cylinder
[NASA-CR-1217] c32 N69-14254
A lunar gravity simulator, volume 2
[NASA-CR-1234] c05 N69-14979
The structural synthesis of an ablating thermostructural panel
[NASA-CR-1215] c32 N69-16114
CHRYSLER CORP., DETROIT, MICH.
Experimental verification of surface vehicle dynamics
[NASA-CR-1399] c11 N69-37022
CITY COLL. OF THE CITY OF NEW YORK.
Dynamic response of structural elements exposed to sonic booms
[NASA-CR-1281] c32 N69-21403
CLEMSON COLL., S. C.
A family of solutions of certain nonautonomous differential equations by series of exponential functions
[NASA-CR-1294] c19 N69-17249
COMMUNICATIONS AND SYSTEMS, INC., FALLS CHURCH, VA.
Analysis of two alternate damping systems for GEOS gravity gradient stabilized satellite
[NASA-CR-1282] c14 N69-18953
CONTROL DATA CORP., MINNEAPOLIS, MINN.
Method of deriving orbital perturbing parameters from onboard optical measurements of an ejected probe or a natural satellite
[NASA-CR-1412] c30 N69-35513
CORNELL AERONAUTICAL LAB., INC., BUFFALO, N. Y.
Synthesis methods for manual aerospace control systems with applications to SST design
[NASA-CR-1208] c02 N69-13185
Nonequilibrium gasdynamics
[NASA-CR-1411] c12 N69-34709
Ground wind characteristics at Kennedy Space Center Final report
[NASA-CR-1418] c20 N69-36222
CORNELL UNIV., ITHACA, N. Y.
Comments on the nature of the outside boundary layer on a liquid sphere in a steady, uniform stream
[NASA-CR-1362] c12 N69-24877
Hydrodynamic stability of inviscid rotating coaxial jets
[NASA-CR-1363] c12 N69-24926
On minimizing the wake of droplets
[NASA-CR-1368] c12 N69-24958

D

DENVER UNIV., COLO.
The use of thermodynamic properties of metal-gas systems as reduced-pressure standards
[NASA-CR-1271] c14 N69-16099
Technology transfer - A selected bibliography
[NASA-CR-1355] c34 N69-28868
DREXEL INST. OF TECH., PHILADELPHIA, PA.
MCDIT 21 - A computer code for one-dimensional elastic wave problems
[NASA-CR-1306] c32 N69-22983
DUNLAP AND ASSOCIATES, INC., DARIEN, CONN.
Peripheral vision displays, phase 2 report
[NASA-CR-1239] c05 N69-14478
Differential thresholds for motions in the periphery
[NASA-CR-1439] c05 N69-36925
DYNATECH CORP., CAMBRIDGE, MASS.
Asymmetric nonlinear dynamic response and buckling of shallow spherical shells
[NASA-CR-1376] c32 N69-29558

E

ELECTRO-OPTICAL SYSTEMS, INC., PASADENA, CALIF.
Hydrogen-oxygen electrolytic regenerative fuel cells
[NASA-CR-1244] c03 N69-18885
ENVIRONMENTAL RESEARCH ASSOCIATES, RANDALLSTOWN, MD.
Correlation study of the simulation of Gemini extravehicular activity with flight results
[NASA-CR-1146] c05 N69-19902

Study of the astronaut's capabilities to maintain life support systems and cabin habitability in weightless conditions
[NASA-CR-1405] c05 N69-36709

F

FAIRCHILD CAMERA AND INSTRUMENT CORP., SYOSSET, N. Y.
Planetary film reconnaissance system
[NASA-CR-1358] c14 N69-28023
FLIGHT SAFETY FOUNDATION, INC., ARLINGTON, VA.
General-aviation pilot reactions to and opinions on grooved runways
[NASA-CR-1428] c02 N69-35861
FRANKLIN INST., PHILADELPHIA, PA.
Study of pretesting effects on electroexplosive devices
[NASA-CR-1203] c15 N69-10298
High performance turboalternator and associated hardware. 3. Design of backup gas bearings
[NASA-CR-1292] c15 N69-19775
NASA contributions to fluid-film lubrication - A survey
[NASA-SP-5058] c15 N69-28592
Electrical characteristics of Pyrrole polymers
[NASA-CR-1367] c18 N69-29559

G

GARRETT CORP., LOS ANGELES, CALIF.
A study of astronauts' extravehicular work capabilities in weightless conditions
[NASA-CR-1334] c05 N69-27266
GCA CORP., BEDFORD, MASS.
Inference of stratospheric temperature and moisture profiles from observations of the infrared horizon Final report
[NASA-CR-1419] c20 N69-35528
GENERAL APPLIED SCIENCE LABS., INC., WESTBURY, N. Y.
Research and development of a sonic boom simulation device
[NASA-CR-1378] c02 N69-31959
GENERAL DYNAMICS CORP., SAN DIEGO, CALIF.
Experiments on a high power, pulsed, constricted arc heater
[GDC-DBE-68-008] c25 N69-17212
Study of air pollutant detection by remote sensors
[GDC-DBE-68-011] c13 N69-31961
GENERAL DYNAMICS/CONVAIR, SAN DIEGO, CALIF.
Analysis and design of space vehicle flight control systems. Volume 16 - Abort
[NASA-CR-835] c31 N69-27299
GENERAL DYNAMICS/FORT WORTH, TEX.
Space flight handbooks, volume 3. Planetary flight handbook, part 7 - Direct trajectories to Jupiter, Saturn, Uranus, and Neptune. General discussion, contour charts and related graphical information
[NASA-SP-35-VOL-3-PT-7] c30 N69-33490
Planetary Flight Handbook. Part 8 - Jupiter swingby missions to Saturn, Uranus, Neptune, and Pluto
[NASA-SP-35-PT-8] c30 N69-34850
GENERAL ELECTRIC CO., CINCINNATI, OHIO.
Cb-1Zr pumped sodium loop
[NASA-CR-1135] c03 N69-11373
GENERAL ELECTRIC CO., LYNN, MASS.
Performance comparisons of high Mach number compressor rotor blading
[NASA-CR-1256] c28 N69-14210
GENERAL ELECTRIC CO., PHILADELPHIA, PA.
Theoretical prediction of crater size for hypervelocity impact by reduced-density particles, 18 May 1966 - 17 August 1967
[NASA-CR-1196] c32 N69-10225
Zero thermal expansion composites of high strength and stiffness
[NASA-CR-1324] c32 N69-24876
GENERAL ELECTRIC CO., SCHENECTADY, N. Y.
Characteristics of a thermionic converter with a chloride vapor deposited tungsten emitter /110/ and a nickel collector
[NASA-CR-1416] c03 N69-32553
Characteristics of a thermionic converter with a fluoride vapor deposited tungsten emitter etched to preferentially expose the 110 crystal planes
[NASA-CR-1381] c03 N69-35689
Reduction of recovery time in high-temperature cesium vapor thyratrons
[NASA-CR-1417] c03 N69-36411
Development and inverter testing of high temperature cesium-vapor thyratrons
[NASA-CR-1435] c03 N69-36843
GENERAL MOTORS CORP., INDIANAPOLIS, IND.
Experimental investigation of advanced concepts to increase turbine blade loading. 3 - Performance evaluation of tandem rotor blade
[NASA-CR-1254] c01 N69-13621
Experimental investigation in an annular cascade sector of highly loaded turbine stator blading. Volume 1 - Analysis and design
[NASA-CR-1219] c01 N69-14211
Experimental investigation in an annular cascade sector of highly loaded turbine stator blading. Volume 3 - Performance of tandem blade
[NASA-CR-1341] c01 N69-23892
Experimental investigation of advanced concepts to increase turbine blade loading. 4 - Performance evaluation of plain rotor blade with plow type vortex generators
[NASA-CR-1342] c28 N69-24223
Experimental investigation in an annular cascade sector of highly loaded turbine stator blading. Volume 2 - Performance of plain blade and effect of vortex generators
[NASA-CR-1323] c01 N69-25327
Experimental investigation in an angular cascade sector of highly loaded turbine stator blading. Volume 4 - Performance of a jet- flapped blade
[NASA-CR-1423] c28 N69-36680
GENERAL TECHNOLOGY CORP., LAWRENCEVILLE, N. J.
Compatibility conditions of the theory of micromorphic elastic solids
[NASA-CR-1236] c26 N69-10817
A continuum theory for an elastic solid with elastic micro-inclusions
[NASA-CR-1321] c32 N69-21401
On the determination of micromorphic material constants from properties of the constituents
[NASA-CR-1320] c32 N69-21569
A lattice model for composite materials
[NASA-CR-1322] c32 N69-22982
GOODYEAR AEROSPACE CORP., AKRON, OHIO.
Nitinol characterization study
[NASA-CR-1433] c17 N69-36367

H

HARVARD UNIV., BOSTON, MASS.
Predicting human performance in space environments
[NASA-CR-1370] c05 N69-30168
HONEYWELL, INC., LEXINGTON, MASS.
Laboratory cculometer
[NASA-CR-1422] c05 N69-39212
HUGHES AIRCRAFT CO., CULVER CITY, CALIF.
Development and processing of pyrcnne polymers
[NASA-CR-1310] c18 N69-26448
HUMPHREYS CORP., CONCORD, N. H.
Induction plasma heating - High power, low frequency operation and pure hydrogen heating
[NASA-CR-1343] c22 N69-24055
HYDRONAUTICS, INC., LAUREL, MD.
Experimental and analytical investigations on multiple liquid impact erosion
[NASA-CR-1288] c15 N69-19786

I

IIT RESEARCH INST., CHICAGO, ILL.
Flow in a two-dimensional channel with a rectangular cavity
[NASA-CR-1245] c12 N69-14095
Evaluation of vacuum UV detector-spectroscopy systems fcr capsule reentry measurements
[NASA-CR-1268] c09 N69-18761
Effect of free stream turbulence on coaxial mixing
[NASA-CR-1336] c12 N69-24058
Air pollution monitoring instrumentation A survey
[NASA-SP-5072] c14 N69-24751
Turbulence in the mixing region between ducted coaxial streams
[NASA-CR-1335] c12 N69-30728
ILLINOIS UNIV., URBANA.
The conformal mapping of the interior of the unit circle onto the interior of a class of smooth curves
[NASA-CR-1357] c32 N69-26559

INTERNATIONAL BUSINESS MACHINES CORP., CAMBRIDGE, MASS.
Rapid optimization of multiple-burn rocket flights, 8 March 1968 - 8 March 1969
[NASA-CR-1430] c30 N69-36439
INTERNATIONAL INFORMATION, INC., PHILADELPHIA, PA.
Theory of motion of the planet Pluto. Part 2 - Plutonian perturbation of the second order with respect to perturbing masses. Part 3 - Recalculation of first- order Plutonian perturbations with respect to perturbing masses. Part 4 - New elements of Pluto
[NASA-TT-F-491] c30 N69-14943
Theory of motion of the planet Pluto. Part 1 - Plutonian perturbations of the first order with respect to perturbing masses
[NASA-TT-F-490] c30 N69-14944
IOWA UNIV., IOWA CITY.
Improvement of an integral equation method in plane elasticity through modification of source density representation
[NASA-CR-1273] c32 N69-19030
ISRAEL PROGRAM FOR SCIENTIFIC TRANSLATIONS, LTD., JERUSALEM.
The earth in the universe
[NASA-TT-F-345] c13 N69-12384
Handbook of astronautics
[NASA-TT-F-500] c31 N69-24760
Scattering, reactions and decay in nonrelativistic quantum mechanics
[NASA-TT-F-510] c24 N69-25848
Nonlinear problems of compressible flow
[NASA-TT-F-560] c12 N69-27168
RR Lyrae stars
[NASA-TT-F-562] c30 N69-27169
High temperature strength of materials
[NASA-TT-F-508] c17 N69-27300
The Oxygen Regime of the Organism and Its Regulation /Symposium/
[NASA-TT-F-501] c04 N69-31401
Mechanics of spaceflight low-thrust
[NASA-TT-F-507] c28 N69-33354
High-temperature properties of gases. Physical gas dynamics, thermodynamics, and physics of combustion
[NASA-TT-F-558] c12 N69-35365
ITT INDUSTRIAL LABS., FORT WAYNE, IND.
Research and development of a single gun color CRT, phase 1 Final report
[NASA-CR-1228] c09 N69-14256

K

KAMAN AIRCRAFT CORP., BLOOMFIELD, CONN.
The Bossler coupling
[NASA-CR-1241] c15 N69-16104
KAMAN NUCLEAR, COLORADO SPRINGS, COLO.
Variability of sound propagation prediction due to atmospheric variability
[NASA-CR-1338] c23 N69-22545
KAMAN SCIENCES CORP., COLORADO SPRINGS, COLO.
The effects of atmospheric fluctuations and representation upon propagated sound
[NASA-CR-1337] c23 N69-23199
KENTUCKY UNIV., LEXINGTON.
An investigation of the suitability of white rats for sub-orbital studies of behavior in a gravity field
[NASA-CR-1255] c05 N69-14094

L

LING-TEMCO-VOUGHT, INC., DALLAS, TEX.
Roll and yaw compensation feasibility study
[NASA-CR-1209] c31 N69-16221
Investigation of bremsstrahlung production in spacecraft materials
[NASA-CR-1377] c24 N69-33416
An experimental study of electron transmission and bremsstrahlung production
[NASA-CR-1383] c24 N69-34541
LITCHFORD SYSTEMS, NORTHPORT, N. Y.
Study of advanced electronic applications to aeronautical display and control problems
[NASA-CR-1240] c02 N69-14729
LOCKHEED AIRCRAFT CORP., SUNNYVALE, CALIF.
Emissivity coatings for low-temperature space radiators
[NASA-CR-1420] c17 N69-36723
LOCKHEED MISSILES AND SPACE CO., PALO ALTO, CALIF.
Effect of shock precursor heating on radiative flux to blunt bodies
[NASA-CR-1265] c33 N69-17438
Series solution for hypersonic flow about blunt bodies
[NASA-CR-1266] c33 N69-18125
Effect of ablation product absorption and line transitions on shock layer radiative transport
[NASA-CR-1264] c33 N69-19117
Remote information retrieval facility
[NASA-CR-1318] c08 N69-23381
Radiant energy transfer measurements in air
[NASA-CR-1390] c25 N69-38227
LOCKHEED MISSILES AND SPACE CO., SUNNYVALE, CALIF.
Visual sensing of spacecraft guidance information. Earth orbit rendezvous maneuvers
[NASA-CR-1214] c05 N69-13161
Aerodynamic effects of bulbous bases
[NASA-CR-1339] c01 N69-35521
LOCKHEED-CALIFORNIA CO., BURBANK.
A study of jimsphere wind profiles as related to space vehicle design and operations
[NASA-CR-1204] c20 N69-13629
LOCKHEED-GEORGIA CO., MARIETTA.
Model tests of jet induced lift effects on a VTOL aircraft in hover
[NASA-CR-1297] c01 N69-21477
Effect of jet temperature on jet and pure tone noise radiation
[NASA-CR-1472] c02 N69-40439
LOUISVILLE UNIV., KY.
Effects of practice and work load on the performance of a code transformation task /COTRAN/
[NASA-CR-1261] c05 N69-14345
LOVELACE FOUNDATION FOR MEDICAL EDUCATION AND RESEARCH, ALBUQUERQUE, N. MEX.
Compendium of human responses to the aerospace environment. Volume 1 - Sections 1-6
[NASA-CR-1205-VOL-1] c04 N69-12434
Compendium of human responses to the aerospace environment. Volume 2 - Sections 7-9
[NASA-CR-1205-VOL-2] c04 N69-12588
Compendium of human responses to the aerospace environment. Volume 3 - Sections 10-16
[NASA-CR-1205-VOL-3] c04 N69-12592
Compendium of human responses to the aerospace environment. Volume 4 - Conversion tables alphabetic index
[NASA-CR-1205-VOL-4] c04 N69-12600
Rapid /explosive/ decompression emergencies in pressure-suited subjects
[NASA-CR-1223] c05 N69-13969

M

MARYLAND UNIV., COLLEGE PARK.
Unified analysis of turbulent jet mixing
[NASA-CR-1382] c12 N69-31887
MATHEMATICS AND BIOLOGY CORP., BENTON, KANS.
Boundedness theorems and other mathematical studies of a Hodgkin-Huxley type system of differential equations - Numerical treatment of thresholds and stationary values
[NASA-CR-1272] c19 N69-21143
MCDONNELL-DOUGLAS CO., HUNTINGTON BEACH, CALIF.
Requirements study for a biotechnology laboratory for manned earth orbiting missions. Volume 2 - Summary of individual experiments requirements
[NASA-CR-1409] c05 N69-35540
Requirements study for a biotechnology laboratory for manned earth orbiting missions Volume 1 - Results, recommendations and requirements
[NASA-CR-1408] c05 N69-35541
MCDONNELL-DOUGLAS CO., LONG BEACH, CALIF.
A numerical solution for the minimum induced drag, and the corresponding loading, of nonplanar wings Final report
[NASA-CR-1218] c01 N69-10343
A numerical solution for the minimum induced drag, and the corresponding loading, of nonplanar wings. 1 - User's manual for computer program 55VD. 2 - Descriptive manual for computer program 55VD
[NASA-CR-1218-SUPPL] c01 N69-12286
MEASUREMENT ANALYSIS CORP., LOS ANGELES, CALIF.
A method for predicting launch vehicle vibration levels in the region of the spacecraft adaptor

[NASA-CR-1227] c31 N69-16155
Summary of random vibration prediction procedures
[NASA-CR-1302] c32 N69-23096
MECHANICAL TECHNOLOGY, INC., LATHAM, N. Y.
High-performance turboalternator and associated hardware. 2 - Design of gas bearings
[NASA-CR-1291] c15 N69-21772
MICHAEL REESE HOSPITAL AND MEDICAL CENTER, CHICAGO, ILL.
Analyses and measurements of blood samples
[NASA-CR-1395] c05 N69-38600
MICHIGAN UNIV., ANN ARBOR.
On the generation of ideal coordinate systems for the analysis of optimal trajectories
[NASA-CR-1250] c30 N69-13274
Computer mechanization of reentry equations with four degrees of freedom
[NASA-CR-1249] c30 N69-13300
Skill training for the production of a memorized movement pattern
[NASA-CR-1251] c05 N69-13926
Proprioceptive cues and their influence on operator performance in manual control
[NASA-CR-1248] c05 N69-14768
E-type photodemodulators for coherent light signals Final technical report
[NASA-TT-F-430] c09 N69-15441
Sensitivity of the creep-rupture properties of nickel-base superalloy sheet to sharp edge-notches in the temperature range of 1000 deg F - 1400 deg F
[NASA-CR-1263] c32 N69-16156
A study of human operator performance using regression analysis
[NASA-CR-1259] c05 N69-16212
A fundamental study of predictive display systems
[NASA-CR-1274] c05 N69-17738
An experimental and theoretical analysis of the convected balanced arc
[NASA-CR-1267] c25 N69-18041
Magnetic field properties related to the design of a one-component magnetic support-and-balance system
[NASA-CR-1352] c11 N69-24089
One component, magnetic, support and balance system for wind tunnel models
[NASA-CR-1353] c11 N69-25343
Computer mechanization of six-degree of freedom flight equations
[NASA-CR-1344] c21 N69-26232
Experimental evaluation of a subsonic expansion tube
[NASA-CR-1354] c11 N69-28095
Subsonic sphere drag measurements at intermediate Reynolds numbers
[NASA-CR-1392] c01 N69-30609
Analytical solutions of a class of optimum orbit modifications
[NASA-CR-1379] c30 N69-31362
Laboratory experiments on reverted rubber friction
[NASA-CR-1398] c02 N69-34915
Non-linear longitudinal dynamics of an orbital lifting vehicle
[NASA-CR-1449] c30 N69-40062
MIDWEST RESEARCH INST., KANSAS CITY, MO.
Study of low pressure application of new orbitron and iron gauge designs
[NASA-CR-1300] c14 N69-28402
MISSISSIPPI STATE UNIV., STATE COLLEGE.
A study of 2 GHz electromagnetic wave propagation over optical paths in three geographical regions of the United States
[NASA-CR-1442] c07 N69-39282

N

NATIONAL AERONAUTICS AND SPACE ADMINISTRATION. AMES RESEARCH CENTER, MOFFETT FIELD, CALIF.
Calculated and flight measured handling- qualities factors of three subsonic jet transports
[NASA-TN-D-4832] c02 N69-10495
Response envelope - A global description of three-axis large angle spacecraft attitude control systems
[NASA-TN-D-4896] c30 N69-10756
Effects of angle of attack and bluntness on the shock-layer properties of a 15 deg cone at a Mach number of 10.6
[NASA-TN-D-4909] c01 N69-10789

Flight tests under IFR with an STOL transport aircraft
[NASA-TN-D-4939] c02 N69-13252
Projectile shape effects on hypervelocity impact craters in aluminum
[NASA-TN-D-4953] c32 N69-14315
Sextant sighting measurements from on board the Gemini 12 spacecraft
[NASA-TN-D-4952] c21 N69-14332
Minimum thrust for correcting Keplerian orbits with application to interplanetary guidance
[NASA-TN-D-4945] c21 N69-14399
An impact energy-absorbing strut employing tube cutting
[NASA-TN-D-4941] c32 N69-14506
Analysis of the stability of a thin liquid film adjacent to a high-speed gas stream
[NASA-TN-D-4976] c12 N69-15630
Analysis of nonequilibrium air streams in the Ames 1-foot shock tunnel
[NASA-TN-D-4985] c11 N69-15633
Research problems in atmosphere entry and landing for manned planetary missions
[NASA-TN-D-4977] c31 N69-15634
Large scale wind tunnel investigation to improve the low speed longitudinal stability at high lift of a supersonic transport with variable-sweep wings
[NASA-TN-D-5005] c02 N69-16384
Second order errors in linearized velocity corrections and their effects on the rate of convergence of iterative solutions
[NASA-TN-D-5037] c21 N69-17780
Solvent purification procedures used in organic geochemistry laboratories
[NASA-TM-X-1746] c06 N69-18962
Large-scale tests of an airplane model with a double-delta wing, including longitudinal and lateral characteristics and ground effects
[NASA-TN-D-5102] c02 N69-21020
A computer program for a line by line calculation of spectra from diatomic molecules and atoms assuming a Voigt line profile
[NASA-TN-D-5088] c24 N69-21462
The use of pilot rating in the evaluation of aircraft handling qualities
[NASA-TN-D-5153] c02 N69-22539
An investigation of a direct side-force maneuvering system on a deflected jet VTOL aircraft
[NASA-TN-D-5175] c02 N69-22572
Simulation studies for planning an in-flight experiment to define manual guidance and control techniques for large launch vehicles
[NASA-TN-D-5150] c21 N69-22936
A generalized averaging method for linear differential equations with almost periodic coefficients
[NASA-TN-D-5167] c19 N69-22988
Exploding wire initiation and electrical operation of a 40-kV system for arc-heated drivers up to 10 feet long
[NASA-TN-D-5126] c11 N69-22989
Evaluation of a pilot describing function method applied to the manual control analysis of a large flexible booster
[NASA-TN-D-5149] c21 N69-22996
On some numerical difficulties in integrating the equations for one-dimensional nonequilibrium nozzle flow
[NASA-TN-D-5176] c19 N69-23355
Computation of topside ionograms from N/h/ profiles
[NASA-TN-D-5052] c13 N69-23557
The use of integral transforms in the estimation of time variable parameters
[NASA-TN-D-5194] c19 N69-23788
A technique for identifying pilot describing functions from routine flight-test records
[NASA-TN-D-5127] c05 N69-23842
Newtonian aerodynamics for circular cones modified to produce lift at zero angle of attack
[NASA-TN-D-5193] c01 N69-23926
Development of Michell minimum weight structures
[NASA-TN-D-4345] c32 N69-25001
Technique for calculating optimum takeoff and climb out trajectories for noise abatement
[NASA-TN-D-5182] c02 N69-26194

Circulating currents in linear crossed-field generators and accelerators
[NASA-TN-D-5244] c25 N69-26313
Exploratory investigation on the measurement of skin friction by means of liquid crystals
[NASA-TM-X-1774] c12 N69-26956
A detailed study of manual backup control systems for the Saturn 5 launch vehicle
[NASA-TN-D-5261] c21 N69-28018
Jupiter swingby missions to nonspecific locaticns in interplanetary space
[NASA-TN-D-5271] c30 N69-28441
Summary and correlation of skin-friction and heat-transfer data for a hyperscnic turbulent boundary layer on simple shapes
[NASA-TN-D-5089] c12 N69-29144
An experimental and theoretical investigation of a symmetrical and a cambered delta wing configuration at Mach numbers from 2.0 to 10.7
[NASA-TN-D-5272] c01 N69-29269
Trim attitude, lift and drag of the Apollc command module with offset center-of-gravity positions at Mach numbers to 29
[NASA-TN-D-5276] c30 N69-29557
On the phenomenon of thermoelastic instability /thermal flutter/ of booms with open cross section
[NASA-TN-D-5222] c32 N69-29589
Toxicity problems in plastic hardware designed for biological space-flight experiments
[NASA-TM-X-1818] c04 N69-29723
A compilation of current computer programs for low-thrust trajectory analysis
[NASA-TM-X-1824] c08 N69-30014
Investigation of a 0.3-scale jet-transport model having a jet-augmented boundary-layer- control flap with direct-lift control capability
[NASA-TN-D-5129] c01 N69-30722
Methods for predicting spacecraft-window- induced line-of-sight deviations
[NASA-TN-D-5238] c21 N69-31227
Shock shapes and pressure distributicns for large angle pointed cones in helium at Mach numbers of 8 and 20
[NASA-TN-D-5343] c01 N69-31228
Flight-determined aerodynamic properties of a jet-augmented, auxiliary-flap, direct-lift-control system including correlation with wind-tunnel results
[NASA-TN-D-5128-REV] c02 N69-31962
Linearized theory of stagnation point heat and mass transfer at hypersonic speeds
[NASA-TN-D-5246] c12 N69-33421
Conference on Electromagnetic Exploration of the Moon, 11-13 June 1968. Report of the Program Evaluation Committee
[NASA-SP-174] c30 N69-33595
Effects of differing amounts of training and of monochromatic targets on sextant sighting performance
[NASA-TN-D-5190] c05 N69-35024
Use of a six-degrees-of-freedom motion simulator for VTOL hovering tasks
[NASA-TN-D-5383] c11 N69-35359
Chebyshev series solution of nonlinear ordinary differential equations - Initial-value problems
[NASA-TM-X-1882] c19 N69-36923
Power- and cross-spectra and space-time correlations of surface fluctuating pressures at Mach numbers between 1.6 and 2.5
[NASA-TN-D-5440] c12 N69-36940
Upwash patterns on ablating and nonablating cones at hypersonic speeds
[NASA-TN-D-5346] c12 N69-37370
Effects of angle of attack and bluntness on laminar heating-rate distributions cf a 15 deg cone at a Mach number of 10.6
[NASA-TN-D-5450] c12 N69-37604
Absolute radiometers for use in ballistic- range and shock-tube experiments
[NASA-TN-D-5360] c14 N69-38144
A unified treatment of lunar theory and artificial satellite theory
[NASA-TN-D-5459] c30 N69-38145
Large-scale wind-tunnel investigation of an M1-L lifting body with an inflatable and a rigid afterbody
[NASA-TN-D-5468] c01 N69-38775
Flight evaluation of tip-turbine-driven fans for lateral control in a hovering VTOL aircraft
[NASA-TN-D-5491] c02 N69-38807
Experimental investigation of the momentum transfer associated with impact into thin aluminum targets
[NASA-TN-D-5492] c32 N69-38809
A method of characteristics for steady three-dimensional supersonic flow with application to inclined bodies of revolution
[NASA-TN-D-5341] c12 N69-39177
Convective heat-transfer rates on large-angle conical bcdies at hypersonic speeds
[NASA-TN-D-5526] c33 N69-40780
The influence of thermal distortion on the performance of gravity-stabilized satellites
[NASA-TN-D-5435] c31 N69-40781

NATIONAL AERONAUTICS AND SPACE ADMINISTRATION. ELECTRONICS RESEARCH CENTER, CAMBRIDGE, MASS.

Mercury cadmium telluride as a 1- to 20-micro-meter wavelength infrared detector for space applications
[NASA-TN-D-4904] c26 N69-10125
A comparison of a class of earth-moon orbits with a class of rotating Kepler orbits
[NASA-TN-D-4903] c30 N69-10470
Examples of coding schemes based on strategic value
[NASA-TN-D-4962] c07 N69-15373
Introduction to computer aided reliability data analysis
[NASA-TN-D-5009] c15 N69-17988
Effects of lithium and oxygen losses on the magnetic and crystallographic properties of spinel lithium ferrite
[NASA-TR-R-305] c06 N69-20775
Fourier analysis by the method of selected ordinates
[NASA-TN-D-5083] c19 N69-20940
Application of a modified fast Fourier transform to calculate human operator describing functions
[NASA-TM-X-1762] c08 N69-21119
A suboptimal approximation to the Kalman filter
[NASA-TN-D-5082] c10 N69-21123
Direction ccsine computational error
[NASA-TR-R-304] c21 N69-21402
Simplified theory and transducer potentialities of the ''pinch effect'' in semiconductors
[NASA-TN-D-5130] c26 N69-22573
Symbol-oriented failure analysis in multicomponent systems
[NASA-TN-D-5112] c10 N69-22919
Computer program for dimensional analysis
[NASA-TN-D-5165] c08 N69-22935
The Vinti dynamical problem and the geopotential
[NASA-TR-R-307] c30 N69-22948
A review of radiometric measurements of atmospheric attenuation at wavelengths from 75 centimeters to 2 millimeters
[NASA-TN-D-5087] c07 N69-22949
Radiometric techniques applicable to the measurement of solar activity and atmospheric attenuation at millimeter wavelengths
[NASA-TR-R-306] c07 N69-22951
Development of an experimental silicon carbide backward diode operable to 1000 deg K
[NASA-TN-D-5183] c09 N69-23556
A bonding material for optically immersing infrared detectors from 2 to 14 micro-meters
[NASA-TM-X-1776] c18 N69-23843
First-order solutions for mutual coupling between waveguides which propagate two orthogonal modes
[NASA-TN-D-5180] c07 N69-24051
The interaction of intense laser beams with free electrons
[NASA-TN-D-5205] c16 N69-25357
Thermodynamic properties of liquid H sub 2 O and D sub 2 O and their mixtures
[NASA-TN-D-5223] c33 N69-26247
Compilation of data from related technologies in the develcpment of an optical pilot warning indicator system
[NASA-TN-D-5174] c14 N69-27267
Design considerations for cyclotron resonance oscillators
[NASA-TN-D-5237] c10 N69-28121
Plasma generation using a large V-groove cathode discharge
[NASA-TN-D-5269] c25 N69-29140

A formalization of measurement scale forms
[NASA-TN-D-5277] c19 N69-29141
A laboratory study of microwave radiometric techniques for re-entry plasma measurements
[NASA-TN-D-5274] c25 N69-29600
Spacecraft magnetic torques
[NASA-SP-8018] c31 N69-30339
Magnetospheric duct propagation research using Alouette-2 topside-sounder observations
[NASA-TN-D-5332] c13 N69-34891
Fabrication and characteristics of microwave backward diodes in indium arsenide
[NASA-TN-D-5401] c09 N69-36706
Spectroscopic study of a helium arc
[NASA-TN-D-5396] c25 N69-36755
Feasibility of detecting radiation scattered from a plasma
[NASA-TN-D-5311] c25 N69-36939
An accurate strapdown direction cosine algorithm
[NASA-TN-D-5384] c21 N69-36997
Leak detection in hermetically sealed devices
[NASA-TN-D-5457] c09 N69-38597
A method for separating a semiconductor wafer into individual chips
[NASA-TM-X-1892] c09 N69-38774
Communication system design
[NASA-TN-D-5472] c07 N69-39176
Communication efficiencey of quantum systems
[NASA-TR-R-320] c07 N69-39264
Future fields of control application
[NASA-SP-211] c34 N69-39957
Energy distribution of a spiraling electron beam
[NASA-TN-D-5490] c09 N69-41208

NATIONAL AERONAUTICS AND SPACE ADMINISTRATION. FLIGHT RESEARCH CENTER, EDWARDS, CALIF.

Human transfer characteristics in flight and ground simulation for a roll tracking task
[NASA-TN-D-5007] c05 N69-17814
Wind-tunnel force and pressure tests of rocket-engine nozzle extensions on the 0.0667-scale X-15-2 model at supersonic and hypersonic speeds
[NASA-TM-X-1759] c01 N69-20873
Visual simulation image generation using a flying-spot scanner
[NASA-TN-D-5151] c11 N69-23194
A simple technique for automatic computer editing of biodata
[NASA-TN-D-5275] c08 N69-29592
Evaluation of an indirect viewing system for lifting-body terminal-area navigation and landing tasks
[NASA-TN-D-5299] c14 N69-29730
Flight investigation of a fluidic autopilot system
[NASA-TN-D-5298] c21 N69-30946
Flight measurements of canard loads, canard buffeting, and elevon and wing tip hinge moments on the XB-70 aircraft including comparisons with predictions
[NASA-TN-D-5359] c02 N69-32284
Fixed-base simulator pilot rating surveys for predicting lateral-directional handling qualities and pilot rating variability
[NASA-TN-D-5358] c02 N69-35762
Evaluation of an infrared heating simulation of a Mach 4.63 flight on an X 15 horizontal stabilizer
[NASA-TN-D-5403] c33 N69-35949
NASA high temperature loads calibration laboratory
[NASA-TM-X-1868] c11 N69-36224
Summary of XB-70 airplane cockpit environmental data
[NASA-TN-D-5449] c25 N69-38010
Flight-measured aerodynamic drag of two large external tanks attached to the X-15-2 airplane at Mach numbers of 1.6 to 2.3
[NASA-TM-X-1895] c01 N69-38065
Variation in engine noise for two landing-approach configurations of a jet transport aircraft
[NASA-TM-X-1896] c02 N69-38104

NATIONAL AERONAUTICS AND SPACE ADMINISTRATION. GODDARD SPACE FLIGHT CENTER, GREENBELT, MD.

Sliding friction of copper alloys in vacuum
[NASA-TN-D-4824] c15 N69-10757
Relationship between complex- and envelope-covariance for Rician fading communication channels
[NASA-TN-D-4825] c07 N69-11011

Time required for an adequate thermal-vacuum test of flight model spacecraft
[NASA-TN-D-4908] c31 N69-14010
A preliminary study of the detection of geomorphological features over northeast Africa by satellite radiation measurements in the visible and infrared
[NASA-TN-D-4648] c13 N69-14290
Theoretical molecular line absorption of CO in late spectral type atmospheres
[NASA-TN-D-4798] c24 N69-14448
An approach to the remote detection of earth resources in sub-arid lands
[NASA-TN-D-4647] c13 N69-14450
Application of Hansen's method to the 10th satellite of Jupiter
[NASA-TN-D-4979] c30 N69-14479
Precision flow measurement techniques for low-thrust auxiliary-propulsion liquid rockets
[NASA-TN-D-4785] c28 N69-16122
A comparsion of sequential decoding metrics by computer simulation
[NASA-TR-R-294] c07 N69-16196
Nimbus 2 flight evaluation and engineering report, launch through orbit 5275
[NASA-TN-D-4881] c31 N69-17851
Flight performance of FW-4D solid-propellant rocket motor on Delta 50 /AIMP-E/
[NASA-TN-D-4987] c28 N69-20876
The Small Astronomy Satellite /SAS/ program
[NASA-TN-D-5099] c31 N69-21017
Relay program Final report
[NASA-SP-151] c31 N69-21065
The log-a-posteriori probability metric for use in sequential decoding
[NASA-TN-D-4930] c07 N69-23163
Solar effects on VHF communications between a synchronous satellite relay and earth ground stations
[NASA-TN-D-5100] c07 N69-23317
An atlas of Tiros 7 monthly maps of emitted radiation in the 8-12 micron atmospheric window over the Indian Ocean area
[NASA-TN-D-5101] c13 N69-23318
Parametric analysis of microwave and laser systems for communication and tracking - A summary
[NASA-TR-R-309] c07 N69-23642
A graphic method for determining the absolute attitude of sounding rocket vehicles
[NASA-TN-D-5172] c30 N69-23782
A search for gamma-rays from the Crab nebula using a digitized spark chamber
[NASA-TR-R-308] c30 N69-24170
Preprocessing of Minitrack data
[NASA-TN-D-5042] c08 N69-26193
Statistics of the region of Lacerta OB1
[NASA-TN-D-5060] c30 N69-26235
An accuracy and speed comparison of the Vinti and Brouwer orbit prediction methods
[NASA-TN-D-5203] c30 N69-26252
Radio frequency interference experiment design for the applications technology satellite
[NASA-TN-D-5041] c07 N69-26272
Explorer 35 attitude control system
[NASA-TN-D-5187] c21 N69-27268
Gravity model comparison using GEOS 1 long- arc orbital solutions
[NASA-TN-D-5035] c30 N69-27412
GEOS I tracking station positions on the SAO standard earth /C-5/
[NASA-TN-D-5034] c13 N69-28019
A semi-analytic theory for the motion of a lunar satellite
[NASA-TN-D-5043] c30 N69-28050
Infrared spectral irradiance measurements in a space environment simulator
[NASA-TN-D-5166] c29 N69-28111
Evaluation of the Goddard range and range rate system at Rosman by intercomparison with GEOS 1 long-arc orbital solutions
[NASA-TN-D-5036] c13 N69-28442
Models of the trapped radiation environment. Volume 5 - Inner belt protons
[NASA-SP-3024-VOL-5] c24 N69-28911
Experimental determination of eddy-current torques on bodies rotating relative to a uniform magnetic field
[NASA-TN-D-5086] c23 N69-29477

A spacecraft analog-to-digital conversion system employing MOSFETS
[NASA-TN-D-5228] c08 N69-29478
Lectures in high energy astrophysics
[NASA-SP-199] c29 N69-29652
The X sup 2 statistic and the goodness of fit test
[NASA-TR-R-313] c19 N69-30610
An analysis of satellite positional uncertainty by statistical mechanics
[NASA-TN-D-5259] c30 N69-30611
A brushless dc torquer-driven reaction wheel for spacecraft attitude control
[NASA-TN-D-5265] c03 N69-30945
The Picneer 8 cosmic dust experiment
[NASA-TN-D-5267] c30 N69-31058
On the shape preserving expansion and contraction of objects in E sup 3
[NASA-TN-D-5240] c19 N69-31303
Test plan optimization for an Explorer-size spacecraft
[NASA-TN-D-5283] c34 N69-31333
Attitude stability of a class of partially flexible spinning satellites
[NASA-TN-D-5268] c31 N69-32298
Parametric angles of trajectory determined field line intersects predicting the location of artificial auroras
[NASA-TN-D-5189] c30 N69-32316
Design techniques for small scientific satellite structures
[NASA-TN-D-4988] c32 N69-33232
Development of a weld quality monitor
[NASA-TN-D-5304] c15 N69-33800
Evaluation of meta-benzenedisulfonic acid as a stress-reducing additive in a Watts nickel electroplating bath
[NASA-TN-D-5188] c17 N69-36697
Optical simulation of a radio-astronomy interferometer experiment
[NASA-TN-D-5357] c30 N69-36892
A unified form of Lambert's theorem
[NASA-TN-D-5368] c30 N69-36930
Planetary effects in the motion of natural satellites
[NASA-TN-D-5284] c30 N69-37893
Significant accomplishments in science, 1968
[NASA-SP-195] c34 N69-38951
Digital simulation of rotational kinematics
[NASA-TN-D-5302] c23 N69-39178
NASA space vehicle design criteria- environment. Magnetic fields - Earth and terrestrial
[NASA-SP-8017] c31 N69-40269
Hydration, oxidation, and the origin of the calc-alkali series
[NASA-TN-D-5400] c13 N69-40893
Atmospheric densities measured by the Explorer 17 density gauges - Analysis of errors and their effects upon the measurements
[NASA-TN-D-5447] c13 N69-40924

NATIONAL AERONAUTICS AND SPACE ADMINISTRATION. LANGLEY RESEARCH CENTER, LANGLEY STATION, VA.

Calculated and experimental hinge moments on a trailing-edge flap of a 75 deg swept delta wing at Mach 6
[NASA-TN-D-4268] c01 N69-10054
Influence of angle of glide slope on the accuracy of performing instrument approaches in a simulator
[NASA-TN-D-4835] c21 N69-10056
Shock-wave pressure decay in polycarbonate targets impacted by cylindrical polycarbonate projectiles
[NASA-TN-D-4864] c32 N69-10057
A study to determine the presence of voltage breakdown due to proton irradiation in polymeric materials
[NASA-TM-X-1688] c18 N69-10066
Comparison of information display concepts for landing of VTOL aircraft
[NASA-TN-D-4861] c21 N69-10069
Development of sonic-boom signatures in a stratified atmosphere
[NASA-TN-D-4890] c02 N69-10087
A method for determining surface pressures on blunt bodies of revolution at small angles of attack in supersonic flow
[NASA-TN-D-4865] c01 N69-10215
Analysis of the aeroelastic divergence of two experimental unguided launch vehicles
[NASA-TN-D-4846] c32 N69-10297
Flight tests of a direct lift control system during approach and landing
[NASA-TN-D-4854] c02 N69-10371
Analytic approximations for application to spacecraft optical navigation on short data arcs
[NASA-TN-D-4863] c21 N69-10372
Real-helium hypersonic flow parameters for pressures to 3600 atmospheres and temperatures to 15,000 deg K
[NASA-TN-D-4869] c12 N69-10443
Computer experiments on the microscopic behavior of one-dimensional plasmas
[NASA-TN-D-4831] c25 N69-10471
Use of Baronti-Libby transformation and Preston tube calibrations to determine skin friction from turbulent velocity profiles
[NASA-TN-D-4853] c12 N69-10472
Calorimetric, optical, and vibration investigations of stretch-formed aluminum solar concentrators
[NASA-TN-D-4889] c03 N69-10708
Aerodynamic characteristics of 0.25-scale model of Tomahawk launch vehicle at Mach numbers from 2.30 to 4.63
[NASA-TM-X-1684] c01 N69-10732
Crystallographic data on selected artificial graphites with comments on the role of the degree of crystal development in oxidation
[NASA-TN-D-4888] c18 N69-10754
An evaluation of coated molybdenum and columbium alloys in high-temperature supersonic airstreams
[NASA-TN-D-4877] c17 N69-10764
Experimental vibration characteristics of a 1/40-scale dynamic model of the Saturn 5 launch umbilical tower configuration
[NASA-TN-D-4870] c31 N69-10775
Blunt body stagnation region flow with nongray radiation heat transfer - A singular perturbation solution
[NASA-TR-R-295] c12 N69-10788
Heat transfer and pressure distributions due to sinusoidal distortions on a flat plate at Mach 20 in helium
[NASA-TN-D-4907] c12 N69-10804
Radiofrequency transmission characteristics of several ablation materials
[NASA-TN-D-4879] c07 N69-10885
Rotational and vibrational temperature measurements in the 12-inch hypersonic ceramic-heated tunnel
[NASA-TN-D-4892] c33 N69-10932
Resolution changes in lithium-drifted silicon semiconductor detectors irradiated with 0.5, 1.0, 2.0, and 3.0 MeV electrons
[NASA-TN-D-4901] c14 N69-10933
Vibration analysis of a 1/40-scale dynamic model of Saturn 5 launch platform-umbilical tower configuration
[NASA-TN-D-4871] c31 N69-10934
Aerodynamic characteristics of twin propeller deflected slipstream STOL airplane model with boundary layer control on inverted V-tail
[NASA-TN-D-4856] c02 N69-10935
Lateral vibration characteristics of a 1/40-scale dynamic model of Apollo-Saturn 5 launch vehicle
[NASA-TN-D-4872] c31 N69-11007
Heat-transfer and pressure distributions inside the hinge-line gap of a wedge-flap combination at Mach number 10.4
[NASA-TN-D-4911] c01 N69-11009
Compressive properties and column efficiency of metals reinforced on the surface with bonded filaments
[NASA-TN-D-4878] c17 N69-11012
A micro lagoon technique for the culture and observation of isolated mammalian cells
[NASA-TN-D-4906] c04 N69-11056
Analysis of numerical integration techniques for real-time digital flight simulation
[NASA-TN-D-4900] c11 N69-11371
The path of a jet directed at large angles to a subsonic free stream
[NASA-TN-D-4919] c01 N69-11634
Buckling of an equatorial segment of a spherical shell loaded by its own weight
[NASA-TN-D-4921] c32 N69-13034
Radiofrequency transmission characteristics of candidate ablation materials for

planetary-entry-vehicle heat shields
[NASA-TN-D-4920] c07 N69-13158
Hypersonic aerodynamic characteristics of a model of a low-fineness-ratio variable geometry logistics spacecraft concept
[NASA-TM-X-1701] c01 N69-13218
Effects of steady-state acceleration on combustion characteristics of an aluminized composite solid propellant
[NASA-TN-D-4914] c33 N69-13231
A radiometer for use in thermal studies of spacecraft
[NASA-TN-D-4925] c14 N69-13311
Use of photoionization in measuring velocity profile of free-stream flow in Langley pilot model expansion tube
[NASA-TN-D-4936] c12 N69-13945
Wind-tunnel investigation of a large jet transport model equipped with an external-flow jet flap
[NASA-TN-D-4928] c01 N69-14000
Theory for computing span loads and stability derivatives due to sideslip, yawing, and rolling for wings in subsonic compressible flow
[NASA-TN-D-4929] c01 N69-14001
Flying quality factors currently limiting helicopter nap of the earth maneuverability as identified by flight investigation
[NASA-TN-D-4931] c02 N69-14008
Effect of the chemical state of pyrolysis gases on heat-shield mass
[NASA-TN-D-4975] c32 N69-14306
Infrared horizon profiles for winter conditions from Project Scanner
[NASA-TN-D-4905] c21 N69-14346
A flight measurement of optical radiation from shock-heated air by using a Trailblazer 2 vehicle
[NASA-TN-D-4937] c33 N69-14501
Wind velocity profiles measured by the smoke-trail method at the eastern test range, 1963
[NASA-TN-D-4880] c20 N69-14505
Effect of unit Reynolds number, nose bluntness, angle of attack, and roughness on transition on a 5 deg half-angle cone at Mach 8
[NASA-TN-D-4961] c01 N69-14872
Strain rate sensitivity of three titanium alloy sheet materials after prolonged exposure at 550 deg F /561 deg K/
[NASA-TN-D-4981] c17 N69-14873
An investigation of the optimum design and flight of rockets
[NASA-TR-R-297] c31 N69-15374
An optical system for recording schlieren images with continuous writing ultra high speed framing camera
[NASA-TN-D-4986] c14 N69-15381
Potential problems related to weightlessness and artificial gravity
[NASA-TN-D-4980] c05 N69-15629
Preliminary investigation of momentum diffusion between two supersonic airstreams in the presence of shock waves
[NASA-TN-D-4974] c12 N69-15631
Effects of structural damping on flutter of stressed panels
[NASA-TN-D-4990] c32 N69-16091
Experimental study in vacuum of the rate-of-rise outgassing-measurement technique
[NASA-TN-D-4973] c14 N69-16097
Preliminary study of effects of Reynolds number and boundary-layer transition location on shock-induced separation
[NASA-TN-D-5003] c01 N69-16121
Error analysis of input-noise-temperature measurements of low-noise amplifiers
[NASA-TN-D-4997] c07 N69-16162
Prediction of lift and drag for slender sharp-edge delta wings in ground proximity
[NASA-TN-D-4891] c01 N69-16180
Multidimensional gas flow through permeable char layers and its effects on ablation
[NASA-TR-R-296] c33 N69-16181
Experimental surface-pressure distributions on a 9 deg spherically blunted cone at Mach numbers from 1.50 to 4.63
[NASA-TM-X-1730] c01 N69-16209
A computational method for time-optimal space rendezvous
[NASA-TN-D-5017] c30 N69-16210
Wind-tunnel study of deflected-elevator flutter encountered on a T-tail airplane
[NASA-TN-D-5024] c32 N69-16211
Solutions of blunt-body stagnation-region flows with nongray emission and absorption of radiation by a time-asymptotic technique
[NASA-TR-R-299] c33 N69-16268
Roughness drag due to two-dimensional fabrication-type surface roughness on an ogive cylinder from force tests at transonic speeds
[NASA-TN-D-5004] c01 N69-16460
A method for computation of vibration modes and frequencies of orthotropic thin shells of revolution having general meridional curvature
[NASA-TN-D-4972] c32 N69-16469
Mitotic synchronization of L-strain fibroblasts with 5-aminouracil as determined by time-lapse cinephotography
[NASA-TN-D-5021] c04 N69-17248
Supersonic transport operating practices during simulated operations in future air traffic control system environments
[NASA-TN-D-5018] c02 N69-17257
Ratios of steady-state responses to various transient responses, both having equal maximum excitation levels
[NASA-TN-D-5070] c32 N69-17258
An analytical procedure for optimizing television systems for planetary descent missions
[NASA-TN-D-5061] c14 N69-17259
Variability in sonic-boom signatures measured along an 8000-foot linear array
[NASA-TN-D-5040] c02 N69-17279
A parametric study of blade-motion stability boundaries for an articulated rotor
[NASA-TN-D-5032] c01 N69-17289
Full-scale wind-tunnel investigation of static longtudinal and lateral characteristics of a light twin-engine airplane
[NASA-TN-D-4983] c02 N69-17303
Aerodynamic forces on a stationary and oscillating circular cylinder at high Reynolds numbers
[NASA-TR-R-300] c01 N69-17304
Aerodynamic data on large semispan tilting wing with 0.4-diameter chord, single-slotted flap, and single propeller 0.22 chord below wing
[NASA-TN-D-5016] c01 N69-17312
Performance of a towed, 48-inch-diameter /121.92-cm/ ballute decelerator tested in free flight at Mach numbers from 4.2 to 0.4
[NASA-TN-D-4943] c01 N69-17398
Investigation of opening characteristics of an all-flexible parawing
[NASA-TN-D-5031] c02 N69-17700
Identification of structural systems by use of near-resonance testing
[NASA-TN-D-5069] c32 N69-17737
Osmotically induced coalescence of sarcoma cells through intercellular bridges in vitro
[NASA-TN-D-5022] c04 N69-17782
The determination of a stability indicative function for linear systems with multiple delays
[NASA-TR-R-301] c31 N69-17801
FORTRAN programs for calculating wind-tunnel boundary interference
[NASA-TM-X-1740] c01 N69-17818
Requirements of a Martian television experiment for three point-mass descent trajectories
[NASA-TN-D-5062] c14 N69-17944
Changes in minority-carrier lifetime in silicon and gallium arsenide resulting from irradiation with 22 and 40 MeV protons
[NASA-TN-D-5028] c26 N69-18897
A technique to infer atmospheric temperature from horizon radiance profiles
[NASA-TN-D-5068] c13 N69-19024
Tuft-grid surveys at low speeds for delta wings
[NASA-TN-D-5045] c01 N69-19027
Use of superposition in digital computers to obtain wind tunnel interference factors for arbitrary configurations, with particular reference to V/STOL models
[NASA-TR-R-302] c01 N69-19028
Transmission of 2.43 MeV electrons through thick silicon targets
[NASA-TN-D-5075] c24 N69-19113
The admittance of a parallel-plate aperture illuminating a displaced dielectric-dielectric boundary

[NASA-TN-D-5038] c07 N69-19114
An analysis of the operation of a mass measuring system in an orbiting spacecraft
[NASA-TN-D-5039] c04 N69-19115
Tensile properties and creep strength of three aluminum alloys exposed up to 25000 hours at 200 deg to 400 deg F /370 deg to 480 deg K/
[NASA-TN-D-5010] c17 N69-19203
Full-scale investigation of the aerodynamic characteristics of a sailwing of aspect ratio 5.9
[NASA-TN-D-5047] c01 N69-19243
A numerical method for evaluation and utilization of supersonic nacelle-wing interference
[NASA-TN-D-5057] c01 N69-19641
Mechanical behavior of boron-epoxy and glass-epoxy filament-wound cylinders under various loads
[NASA-TN-D-5050] c18 N69-19825
Experimental pressure distributions on a 120 deg cone at Mach numbers from 2.96 tc 4.63 and angles of attack from 0 deg to 20 deg
[NASA-TN-D-5054] c01 N69-19826
A method for characterizing the surface cleanliness during adhesion testing
[NASA-TN-D-5055] c17 N69-19827
Lithium-drifted silicon detectors as low-energy photcn spectrometers
[NASA-TN-D-5056] c24 N69-19828
Tensile behavicr of boron filament reinforced epoxy rings and belts
[NASA-TN-D-5053] c18 N69-19918
A method for determining the total drag of a pointed body of revolution in supersonic flow with turbulent boundary layer
[NASA-TN-D-5046] c01 N69-19925
Effects of cone angle, base flare angle, and corner radius on Mach 3.0 aerodynamic characteristics of large-angle cones
[NASA-TN-D-5048] c01 N69-19926
Wind-tunnel data from a 0.16-scale V/STOL model with direct-lift and lift-cruise jets
[NASA-TM-X-1758] c01 N69-20016
Parameters affecting firing time of simultaneously triggered trigatron spark gap switches
[NASA-TN-D-5077] c09 N69-20888
Tables of Mie scattering functions for particles with refractive index 1.5
[NASA-TN-D-5110] c23 N69-20905
Fixed-base visual simulation of pilot ccntrolled descents of an advanced Apollo spacecraft with an all-flexible parawing
[NASA-TN-D-5049] c21 N69-20936
The design and uncertainty analysis of an improved total hemispherical emittance transient calorimeter
[NASA-TN-D-5106] c14 N69-20941
Full-scale dynamic landing-impact investigation of a prototype lunar module landing gear
[NASA-TN-D-5029] c31 N69-20965
Causes of magnetic-field nonuniformity and its effect on stability of theta-pinch plasma
[NASA-TR-R-303] c25 N69-20997
Exploratory investigation of flow field resulting from forward-facing nozzles exhausting near a large cylindrical body at free-stream Mach numbers of 3.0 and 6.0
[NASA-TN-D-5030] c01 N69-21000
Effect of gravitational-model selection on accuracy of lunar orbit determinatien from short data arcs
[NASA-TN-D-5105] c30 N69-21018
Effects of bottom-structure flexibility on water landing loads of Apollo spacecraft models
[NASA-TN-D-5108] c32 N69-21042
Calorimetric evaluation of two cone-column solar-energy concentrations
[NASA-TN-D-5109] c03 N69-21088
Antenna effects on the aerodynamic characteristics of a 0.410-scale model of the Cajun rocket at Mach numbers from 2.30 to 4.63
[NASA-TM-X-1771] c01 N69-21106
On lateral cable oscillations of cable- connected space stations
[NASA-TN-D-5107] c31 N69-21111
Effect of plug and shroud geometry variables on plug-nozzle performance at transonic speeds
[NASA-TN-D-5098] c28 N69-21463
Annealing of 22, 40, and 158 MeV prcton damage in n-type and p-type silicon
[NASA-TN-D-5119] c26 N69-22552
Experimental stagnation point velocity gradients and heat transfer coefficients for a family of blunt bodies at Mach 8 and angles of attack
[NASA-TN-D-5121] c01 N69-22554
Investigation of occultation and imagery problems for orbital missions to Venus and Mars
[NASA-TN-D-5100] c30 N69-22571
A rendezvous and station-keeping simulator with fly around capability and virtual image viewing
[NASA-TN-D-5123] c11 N69-22629
Scaled lunar module jet erosion experiments
[NASA-TN-D-5051] c31 N69-22630
Natural vibration modal analysis
[NASA-SP-8012] c32 N69-22773
Effect of shallow meridional curvature on the vibration of nearly cylindrical shells
[NASA-TN-D-5143] c32 N69-22821
Longitudinal vibration characteristics of 1/10-scale Apollo/Saturn 5 replica model
[NASA-TN-D-5159] c32 N69-22932
An investigation of ablation behavior of Avcoat 5026/39M cver a wide range of thermal environments
[NASA-TM-X-1778] c33 N69-22933
Effects of cloud cover on selection of recovery sites for future earth orbital missions
[NASA-TN-D-5120] c30 N69-22939
Investigatien of a plasma accelerator with magnetic field arranged to produce a divergent-nozzle effect
[NASA-TN-D-5122] c25 N69-22942
Night sky background conditions and launch windows for research experiments
[NASA-TM-X-1772] c21 N69-22969
Laminar heat-transfer distributions for a blunted-cone, cone-frustum reentry configuration at Mach 10
[NASA-TN-D-5146] c33 N69-22997
Mechanical properties and column behavior of thin wall Be-38Al alloy tubing
[NASA-TN-D-5145] c17 N69-23004
Forces and moments due to air jets exhausting parallel to large flat plates in a near vacuum
[NASA-TN-D-5147] c12 N69-23085
Buckling of thin-walled circular cylinders
[NASA-SP-8007] c32 N69-23320
A parametric analysis of surface temperatures of paraboloidal solar concentrators in space
[NASA-TN-D-5144] c03 N69-23356
Response of an infinite elastic plate to axisymmetric initial velocity distributions with applicatien to hypervelocity impact
[NASA-TN-D-5118] c32 N69-23448
Heave response of a plenum air cushion including passive and active control concepts
[NASA-TN-D-5202] c02 N69-23449
The leading-edge effects on the laminar flat-plate boundary layer and the aerodynamic heating at Mach 10.4
[NASA-TN-D-5160] c12 N69-23467
Wind tunnel investigation of inflation of disk-gap-band and modified ringsail parachutes at dynamic pressures between 0.24 and 7.07 pounds per square foot
[NASA-TM-X-1786] c01 N69-23538
Computer simulation of a cylindrical galaxy
[NASA-TN-D-5200] c30 N69-23708
Wind-tunnel investigation of the aerodynamic characteristics of a twin-keel parawing
[NASA-TN-D-5199] c01 N69-23781
A semiempirical collision model for plasmas
[NASA-TR-R-310] c25 N69-23787
Investigation of a class of bodies that generate far-field sonic boom shock strength and impulse independent of body length and volume
[NASA-TN-D-5148] c01 N69-23927
Buckling of thin-walled truncated cones
[NASA-SP-8019] c32 N69-24131
Pressure distributions on 140 deg, 160 deg, and 180 deg cones at Mach numbers from 2.30 to 4.63 and angles of attack from 0 deg to 20 deg
[NASA-TN-D-5204] c01 N69-24764
Hypervelocity impact analysis by the methcd of characteristics
[NASA-TR-R-298] c32 N69-24765
Transonic aerodynamic characteristics of hypersonic low-wave-drag elliptical body-tail combinations as affected by changes in

stabilizer configuration
[NASA-TM-X-1789] c01 N69-25244
Charts for interpolation of local skin friction from experimental turbulent velocity profiles
[NASA-SP-3048] c01 N69-25391
An analysis of terrain bias error in planetary radar altimeters
[NASA-TN-D-5220] c21 N69-26195
Analytical investigation of an inflatable landing system having omnidirectional and multiple impact capabilities
[NASA-TN-D-5236] c32 N69-26223
The equipotential space suit design concept and its application to a space suit elbow joint
[NASA-TN-D-5221] c05 N69-26259
Hypersonic flutter analysis using measured static aerodynamic derivatives, and comparison with experiment
[NASA-TN-D-5233] c01 N69-26271
Flight-test results from supersonic deployment of an 18-foot-diameter /5.49 meter/ towed ballute decelerator
[NASA-TM-X-1773] c31 N69-26458
Inviscid radiating shock layers about spheres traveling at hyperbolic speeds in air
[NASA-TR-R-311] c12 N69-26504
Static longitudinal aerodynamic characteristics of some supersonic decelerator models at Mach numbers of 2.30 and 4.63
[NASA-TN-D-5219] c31 N69-26570
Evaluation of a contact-analog display in landing approaches with a helicopter
[NASA-TN-D-5241] c02 N69-27177
A technique to infer atmospheric water-vapor mixing ratio from measured horizon radiance profiles
[NASA-TN-D-5252] c13 N69-27246
Simulation of Gemini extravehicular tasks by neutral-buoyancy techniques
[NASA-TN-D-5235] c05 N69-28024
Elastoplastic stress-strain behavior at notch roots in sheet specimens under constant-amplitude loading
[NASA-TN-D-5253] c32 N69-28038
A wind-tunnel and analytical study of the conversion from wing lift to rotor lift on a composite-lift V/TOL aircraft
[NASA-TN-D-5256] c02 N69-28044
Wind-tunnel investigation of steady-state aerodynamics of a composite-lift VTOL aircraft model
[NASA-TN-D-5232] c02 N69-28097
Experimental investigation of the turbulent boundary layer on a typical subsonic transport fuselage
[NASA-TN-D-5242] c01 N69-28112
Calorimetric evaluation of three 1.5-meter-diameter inflatable rigidized solar concentrators
[NASA-TN-D-5234] c03 N69-28123
An experimental and analytical investigation of balloon-type enclosures for thermal control of satellites
[NASA-TN-D-5230] c33 N69-28209
A study of the performance of low-density phenolic-nylon ablators
[NASA-TN-D-5257] c33 N69-28440
Design, fabrication, and tests of tubular beryllium and Be-38Al alloy truss-type structures
[NASA-TN-D-5254] c32 N69-28658
Determination of lunar equatorial radius using image-motion compensation sensor data from Lunar Orbiter I
[NASA-TN-D-5231] c30 N69-29115
Design of an electronically scanned star sensor with digital output
[NASA-TN-D-5281] c14 N69-29153
Aerodynamic investigation of sharp cone- cylinder spikes on 120 degree blunted cones at Mach numbers of 3.00, 4.50, and 6.00
[NASA-TN-D-5201] c01 N69-29154
A process for imprinting micro lagoon fields in plastic surfaces for use in cell and tissue culture
[NASA-TN-D-5255] c04 N69-29195
Analytic function models of noise and modulation
[NASA-TR-R-314] c07 N69-29230
Transonic aerodynamic characteristics of two hypersonic cruise configurations
[NASA-TM-X-1816] c01 N69-29231
A flight investigation of a lightweight helicopter to study the feasibility of fixed-collective-pitch autorotations
[NASA-TN-D-5270] c02 N69-29232
Use of tetrafluoromethane to simulate real-gas effects on the hypersonic aerodynamics of blunt vehicles
[NASA-TR-R-312] c01 N69-29270
Measurements of mutual interference heating for a probe antenna mounted on an Apollo reentry configuration
[NASA-TM-X-1787] c01 N69-29318
Low-speed deployment, inflation, and steady-descent characteristics of ram-air-inflated balloon recovery systems with peripheral airscoop
[NASA-TN-D-5186] c21 N69-29595
Exploratory study of open-face honeycomb to reduce temperature of hypersonic aircraft structure
[NASA-TN-D-5278] c33 N69-29599
Fatigue of notched Ti-8Al-1Mo-1V titanium alloy at room temperature and 550 deg F /560 deg K/ with flight-by-flight loading representative of a supersonic transport
[NASA-TN-D-5294] c32 N69-29607
Heat transfer to the windward side of a fineness-ratio-2.9 cylinder with nearly spherical ends at a Mach number of 6 and angles of attack of 50 deg, 70 deg, and 90 deg
[NASA-TN-D-5251] c12 N69-29608
Description of the high-enthalpy arc tunnel at the Langley Research Center including test- stream conditions at selected operating points
[NASA-TN-D-5295] c11 N69-29981
Inflation and performance of three parachute configurations from supersonic flight tests in a low-density environment
[NASA-TN-D-5296] c01 N69-30063
Flow-field measurements downstream of two protuberances on a flat plate submerged in a turbulent boundary layer at Mach 2.49 and 4.44
[NASA-TN-D-5297] c12 N69-30071
Static stability characteristics of a 0.16- scale model of a jet-lift V/STOL research airplane in cruise
[NASA-TM-X-1835] c02 N69-30633
Data-reduction technique for determining rapidly rising heating rates to thermally thick walls
[NASA-TN-D-5309] c33 N69-30726
An experimental investigation of the mixing of compressible-air jets in a coaxial configuration
[NASA-TN-D-5315] c02 N69-30727
A finite-step method for calculation of theoretical load distributions for arbitrary lifting surface arrangements at subsonic speeds
[NASA-TN-D-5335] c01 N69-31337
Analysis of a molecular beam system utilizing a known pressure source
[NASA-TN-D-5308] c24 N69-31338
Drag reduction due to gas injection through various discrete slots on a three-dimensional wing at Mach 2.01
[NASA-TN-D-5307] c12 N69-31359
A laboratory investigation of N-wave focusing
[NASA-TN-D-5306] c02 N69-31874
Effects of wing planform on the static aerodynamics of a cruciform wing-body missile for Mach numbers up to 4.63
[NASA-TM-X-1839] c01 N69-31875
Simultaneous usage of attitude control for VTOL maneuvering determined by in-flight simulation
[NASA-TN-D-5342] c02 N69-32110
Simulation studies of some supersonic transport instrumentation requirements and operating problems
[NASA-TN-D-5280] c14 N69-32286
Experimental flow properties in the wake of a 120 deg cone at Mach number 2.20
[NASA-TN-D-5365] c01 N69-32299
Analysis of lateral directional stability characteristics of a twin jet fighter airplane at high angles of attack
[NASA-TN-D-5361] c02 N69-32337
A numerical analysis of the use of perforated walls to control shock location and movement in an internal compression supersonic inlet

[NASA-TR-R-317] c01 N69-32338
Effect of outdoor exposure at elevated temperature on the fatigue life of Ti-8Al-1Mo-1V titanium alloy and AM 350 stainless steel sheet
[NASA-TN-D-5362] c17 N69-32558
Evaluation of a parachute load distribution measuring system during low altitude drop tests
[NASA-TM-X-1832] c14 N69-32682
An evaluation test of a full scale replica of the RAM-CA flight heat shield in a rocket engine exhaust
[NASA-TM-X-1841] c31 N69-32713
Effects of jet exhaust longitudinal aerodynamic characteristics of a jet V/STOL model
[NASA-TN-D-5333] c01 N69-33210
Supersonic aerodynamic characteristics and shock standoff distances for large-angle cones with and without cylindrical afterbodies
[NASA-TN-D-5334] c01 N69-33237
Wind-tunnel investigation of a STOL aircraft configuration equipped with an external-flow jet flap
[NASA-TN-D-5364] c01 N69-33275
Aerodynamic interference effects caused by parallel-staged simple aerodynamic configurations at Mach numbers of 3 and 6
[NASA-TN-D-5379] c01 N69-3330
Transonic aerodynamic characteristics of a Saturn 1B Manned Orbiting Research Laboratory launch vehicle
[NASA-TM-X-1848] c31 N69-33380
An analytical evaluation of the denting of airplane surfaces by hail
[NASA-TN-D-5363] c32 N69-33420
Effects of cyclic heating and thermal shock on hafnia stabilized with calcia, magnesia, and yttria
[NASA-TN-D-5279] c18 N69-34547
Subsonic aerodynamic characteristics of a large-scale 1.075-pressure-ratio tip-turbine cruise-fan propulsion system at angle of attack
[NASA-TN-D-5316] c28 N69-34575
The calculated response of a three-crystal pair spectrometer
[NASA-TM-X-1857] c14 N69-34628
Effect of stress ratio on fatigue-crack growth in 7075-T6 and 2024-T3 aluminum-alloy specimens
[NASA-TN-D-5390] c17 N69-34704
Influence of various fabrication methods on the compressive strength of titanium skin- stringer panels
[NASA-TN-D-5389] c15 N69-34707
Molecular orientation and mechanical anisotropy in polyethylene, polypropylene, and poly/ethylene terephthalate/ films
[NASA-TN-D-5380] c18 N69-34708
The red-shift magnitude relation and observational data
[NASA-TN-D-5398] c30 N69-34884
Chemical equilibrium of ablation materials including condensed species
[NASA-TN-D-5391] c33 N69-34966
Aerodynamic characteristics in pitch of a 1/7-scale model of a two- and three-stage rocket configuration at Mach numbers of 0.4 to 4.63
[NASA-TN-D-5378] c01 N69-34986
Spin-tunnel investigation of a 1/20-scale model of a straight-wing, twin-boom, counter-insurgency airplane
[NASA-TM-X-1602] c02 N69-34988
Experimental pressure distributions for a family of blunt bodies at Mach numbers from 2.49 to 4.63 and angles of attack from 0 deg to 15 deg
[NASA-TN-D-5392] c01 N69-35300
Subsonic performance characteristics of a large-scale 1.075-pressure-ratio tip-turbine cruise-fan propulsion system
[NASA-TN-D-5314] c28 N69-35526
Pressures and heat transfer on a 75 degree swept delta wing with trailing-edge flap at Mach 6 and angles of attack to 90 degrees
[NASA-TN-D-5418] c01 N69-35855
The dynamic response of a flexible rotor blade to a concentrated force moving from tip to root
[NASA-TN-D-5410] c32 N69-36220
Hot-salt-stress-corrosion cracking and its effect on tensile and stress-rupture properties of Ti-6Al-4V titanium-alloy sheet
[NASA-TN-D-5417] c17 N69-36221
Experimental investigation of the effect of aluminum size and loading on the burning rate of solid propellants under acceleration
[NASA-TN-D-5397] c27 N69-36225
Static and dynamic stability derivatives of a model of a jet transport equipped with external-flow jet-augmented flaps
[NASA-TN-D-5408] c02 N69-36258
A procedure for rapid computation of equilibrium chemical composition and thermodynamic properties of the generalized argon-nitrogen-oxygen-hydrogen gas system
[NASA-TN-D-5416] c33 N69-36299
Bodies of revolution having minimum total drag in hypersonic flow
[NASA-TN-D-5438] c01 N69-36699
Comparison of prediction methods and studies of relaxation in hypersonic turbulent nozzle-wall boundary layers
[NASA-TN-D-5433] c12 N69-36805
Analysis of the flat-spin characteristics of a twin-jet swept-wing fighter airplane
[NASA-TN-D-5409] c02 N69-36807
A modified method of integral relations approach to the blunt-body equilibrium air flow field, including comparisons with inverse solutions
[NASA-TN-D-5434] c12 N69-36830
Evaluation of a technique for measuring ion energy loss in vapor-deposited materials
[NASA-TN-D-5430] c24 N69-36929
Analysis of the gamma-ray-backscatter technique for direct measurement of the density of the Martian atmosphere
[NASA-TN-D-5431] c24 N69-36931
Effect of jet velocity and axial location of nozzle exit on the performance of a twin-jet afterbody model at Mach numbers up tc 2.2
[NASA-TN-D-5393] c28 N69-36932
Applications of analytic function theory to analysis of single-sideband angle-modulated systems
[NASA-TN-D-5446] c07 N69-37602
Spin-tunnel investigation of a 1/30-scale model of a subsonic attack airplane
[NASA-TM-X-1788] c02 N69-37976
Flow-field and drag characteristics of several boundary-layer tripping elements in hypersonic flow
[NASA-TN-D-5454] c12 N69-38156
Estimation of variance by a recursive equation
[NASA-TN-D-5465] c19 N69-38178
Simulation of pyrolysis-gas flow through a char layer during ablation
[NASA-TN-D-5464] c33 N69-38271
Results of a free-flight test to determine the performance characteristics of a towed, conical decelerator
[NASA-TM-X-1833] c02 N69-38598
Effect of hypersonic research engine installation on aerodynamic characteristics of 0.0667-scale model of X-15A-2 airplane at Mach numbers from 1.75 to 4.63
[NASA-TM-X-1840] c01 N69-38612
Stress concentration around broken filaments in a filament-stiffened sheet
[NASA-TN-D-5453] c32 N69-38642
A new matrix theorem and its application for establishing independent coordinates for complex dynamical systems with constraints
[NASA-TR-R-326] c19 N69-38655
A feasibility study of determining physical properties of the Martian atmosphere by use of solar occultation as seen from an artificial satellite
[NASA-TN-D-5443] c30 N69-38658
Development of three-dimensional pressure-distribution functions for lifting surfaces with trailing-edge controls based on the integral equation for subsonic flow
[NASA-TN-D-5419] c01 N69-38768
Three-track runway and taxiway profiles measured at international airports A and B
[NASA-TN-D-5444] c02 N69-38770
A navigation-aids identification decoder and display for general-aviation aircraft
[NASA-TN-D-5445] c09 N69-38852
Application of human transfer functions to system analysis
[NASA-TN-D-5478] c05 N69-39183

Operational limitations in flying noise- abatement approaches
[NASA-TN-D-5497] c02 N69-39188
Lunar Orbiter 1, preliminary results - Lunar terrain assessment and selenodesy, micrometeoroid, and radiation measurements
[NASA-SP-197] c30 N69-39213
Free-stream electron concentration in an arc-heated wind tunnel and correlation of Langmuir probe and microwave interferometer measurements
[NASA-TN-D-5500] c25 N69-39302
Supersonic lifting capabilities of large-angle cones
[NASA-TN-D-5499] c01 N69-40026
A limb radiance calculation approach for model atmospheres containing horizontal gradients of temperature and pressure
[NASA-TN-D-5495] c21 N69-40055
Application of pressurized liquid nitrogen inside parametric-amplifier structures for input-noise-temperature improvement
[NASA-TN-D-5509] c09 N69-40079
Experimental investigation of flutter at Mach 3 of rotationally restrained panels and comparison with theory
[NASA-TN-D-5508] c32 N69-40087
Pulse-response curves of conventional low-pass filters
[NASA-TN-D-5494] c07 N69-40099
Fluctuating properties of turbulent boundary layers for Mach numbers up to 9
[NASA-TN-D-5496] c12 N69-40137
A method of integral relations solution for radiating, nonadiabatic, inviscid flow over a blunt body
[NASA-TN-D-5480] c33 N69-40356
Pressure distribution of a large semispan tilting wing with 0.4-diameter-chord, single- slotted flap, and a single propeller 0.22 chord below wing
[NASA-TN-D-5481] c01 N69-40876
Evaluation of a technique for determining airplane aileron effectiveness and roll rate by using an aeroelastically scaled model
[NASA-TN-D-5538] c02 N69-40937
Analytical and experimental investigation of end-plane rotations of truncated cones under bending loads
[NASA-TN-D-5536] c32 N69-41141
Calculation of the penetration flux for a multiwall structure on the Lunar Orbiter spacecraft
[NASA-TN-D-5455] c32 N69-41229

NATIONAL AERONAUTICS AND SPACE ADMINISTRATION. LEWIS RESEARCH CENTER, CLEVELAND, OHIO.

Performance and analysis of seals for inerted lubrication systems of turbine engines
[NASA-TN-D-4761] c15 N69-10055
Nuclear-rocket propulsion
[NASA-TM-X-1685] c22 N69-10067
Design and analysis of a modular servoamplifier for fast-response electrohydraulic control systems
[NASA-TN-D-4898] c03 N69-10068
Prediction of thermodynamic effects of developed cavitation based on liquid-hydrogen and Freon-114 data on scaled venturis
[NASA-TN-D-4899] c12 N69-10070
Summary of electrical component development for a 400-hertz Brayton energy conversion system
[NASA-TN-D-4874] c03 N69-10088
COMPUTE - A time-sharing desk calculator program
[NASA-TN-D-4917] c08 N69-10098
Uranium dioxide vent loss in an externally fueled thermionic reactor concept
[NASA-TN-D-4922] c22 N69-10099
Observations on permeation of polytetrafluoroethylene by compounds of rhenium, molybdenum, and tungsten
[NASA-TN-D-4886] c06 N69-10126
Estimation of fission-product gas pressure in uranium dioxide ceramic fuel elements
[NASA-TN-D-4823] c22 N69-10216
Effect of size on tensile strength of fine polycrystalline nickel wires
[NASA-TN-D-4884] c17 N69-10226
Transient solidification outside a cooled pipe with application to a solar Brayton heat receiver
[NASA-TN-D-4897] c33 N69-10227
Experiments on the stability of water lubricated herringbone-groove journal bearings. 1 - Theoretical considerations and clearance effects
[NASA-TN-D-4883] c15 N69-10228
Incompressibly lubricated Rayleigh step journal bearing. 2 - Infinite-length solution
[NASA-TN-D-4873] c15 N69-10231
Influence of surface films on friction and deformation of single-crystal and polycrystalline gold
[NASA-TN-D-4875] c15 N69-10249
The effects of reactor radiation on 22-volt silicon voltage-regulator diodes
[NASA-TN-D-4923] c09 N69-10250
Water flow and cavitation in converging- diverging boiler-inlet nozzle
[NASA-TM-X-1689] c12 N69-10293
Effect of porous bleed in a high performance axisymmetric, mixed compression inlet at Mach 2.50
[NASA-TM-X-1692] c01 N69-10294
Atlas-Centaur AC-12 flight performance for Surveyor 3
[NASA-TM-X-1678] c31 N69-10295
Effect of variable stator area on performance of a single-stage turbine suitable for air cooling. 5 - Stator detailed losses with 70 percent design area
[NASA-TM-X-1696] c28 N69-10296
Influence of number of operable slip systems on friction characteristics of single-crystal and polycrystalline magnesium
[NASA-TN-D-4351] c15 N69-10370
Experimental studies on shadow shields for thermal protection of cryogenic tanks in space
[NASA-TN-D-4887] c33 N69-10420
Thermal analysis of shadow shields and structural members in a vacuum
[NASA-TN-D-4876] c33 N69-10473
Effect of variable stator area on performance of a single-stage turbine suitable for air cooling. 6 - Turbine performance with 70-percent design stator area
[NASA-TM-X-1697] c01 N69-10558
Calculation of fuel loss from vented nuclear fuel elements for space power reactors
[NASA-TN-D-4913] c22 N69-10734
Feasibility of producing dispersion strengthened chromium by ball-milling in hydrogen halides
[NASA-TN-D-4912] c17 N69-10827
High-field electromagnets at NASA Lewis Research Center
[NASA-TN-D-4910] c23 N69-10889
Absorption rate sticking probabilities for oxygen on columbium and dilute columbium- zirconium alloys
[NASA-TN-D-4885] c17 N69-10931
Selected technology for the electric power industry
[NASA-SP-5057] c03 N69-12575
Design-point performance of a double containment tantalum and stainless steel mercury boiler for SNAP-8
[NASA-TN-D-4926] c33 N69-12739
Excited states of barium 136 and barium 134
[NASA-TN-D-4933] c24 N69-12778
Fouling characteristics of ASTM jet A fuel when heated to 700 deg F in a simulated heat exchanger tube
[NASA-TN-D-4958] c28 N69-12831
Elastic scattering of 21-MeV protons from nitrogen 14, oxygen 16, argon 40, nickel 58, and tin 116
[NASA-TN-D-4932] c24 N69-12840
Atmospheric limits on the observational capabilities of aerospacecraft
[NASA-TN-D-4940] c20 N69-12934
Resonance integrals of rhenium for a wide range of sample sizes
[NASA-TN-D-4938] c24 N69-13152
Preliminary investigation of distortion dynamics in a Mach 3 mixed compression inlet
[NASA-TM-X-1706] c01 N69-13154
Lighting in cryogenic and noncryogenic fluids
[NASA-TM-X-1654] c14 N69-13176
Minimization of optical scattering effects through use of optimal monochromator slit geometry
[NASA-TM-X-1702] c24 N69-13210

Performance investigation of bipropellant fractional-pound thrusters
[NASA-TM-X-1699] c28 N69-13237
An estimate of the supersonic flow field about an axisymmetric body with an N wave pressure trace
[NASA-TN-D-4935] c01 N69-13238
Evaluation of a fluidic oscillator as a molecular weight sensor for gas mixtures
[NASA-TM-X-1698] c03 N69-13246
Stability analysis for unloaded externally pressurized gas-lubricated bearings with journal rotation
[NASA-TN-D-4934] c15 N69-13256
Test of improved ignitor for first stage separation rockets for the Atlas-Centaur launch vehicle
[NASA-TM-X-1676] c28 N69-13275
Point defect calculations in tungsten
[NASA-TN-D-4918] c22 N69-13309
A set of 360 FORTRAN /level G or H/ subroutines for generating printed plots
[NASA-TM-X-1700] c08 N69-13566
FORTRAN program for spline fit curve
[NASA-TM-X-1707] c19 N69-14002
A wind profile for generating control requirements for rocket vehicles using liquid-injection control systems
[NASA-TM-X-1708] c31 N69-14033
Effect of bleed-system back pressure and porous area on the performance of an axisymmetric mixed-compression inlet at Mach 2.50
[NASA-TM-X-1710] c01 N69-14075
An analytical method for predicting the performance of centrifugal pumps during pressurized startup
[NASA-TN-D-4967] c15 N69-14082
A summary of the measurement and interpretation of the Hall coefficient and resistivity of semiconductors
[NASA-TM-X-1711] c26 N69-14086
Evaluation of the results of a round robin analysis for oxygen in potassium and sodium
[NASA-TN-D-4971] c06 N69-14180
Quantum theory of a particle oscillator collision applied to gas-surface interactions at cryogenic temperatures
[NASA-TN-D-4982] c24 N69-14288
A mathematical analysis of supersonic inlet dynamics
[NASA-TN-D-4969] c01 N69-14289
Analog simulation of a closed loop Brayton cycle test facility
[NASA-TM-X-1715] c03 N69-14312
Experimental investigation of a 10 deg conical turbojet plug nozzle with iris primary and translating shroud at Mach numbers from 0 to 2.0
[NASA-TM-X-1709] c28 N69-14313
Inviscid flow analysis of two parallel slot jets impinging normally on a surface
[NASA-TN-D-4957] c12 N69-14316
Simulation studies of the supersonic transport in future air traffic control systems
[NASA-TN-D-4944] c21 N69-14382
Rolling-element fatigue life of ausformed M-50 steel balls
[NASA-TN-D-4954] c15 N69-14383
Liquid rocket acoustic-mode-instability studies at a nominal thrust of 20000 pounds
[NASA-TN-D-4968] c28 N69-14384
Back flow from jet plumes in vacuum
[NASA-TN-D-4978] c01 N69-14385
Influence of high-turbine inlet temperature engines in a methane-fueled SST when takeoff jet noise limits are considered
[NASA-TN-D-4965] c28 N69-14386
Characteristics of composite carbon resistors used for measuring accelerator terminal voltages
[NASA-TM-X-1718] c24 N69-14398
Review of ductilizing of group 6A elements by rhenium and other solutes
[NASA-TN-D-4955] c17 N69-14403
Effect of radius on bulging and fracture of through-cracked cylindrical pressure vessels at cryogenic temperatures
[NASA-TN-D-4951] c32 N69-14480
Predictive equations for thermal neutron flux perturbation effects in cylinders
[NASA-TN-D-4949] c22 N69-14481
Scattering of 42 MeV /6.7-pJ/ alpha particles from even isotopes of cadmium. Supplement 1 - Absolute cross sections
[NASA-TN-D-4948] c24 N69-14482
Nonlinear decay of a disturbance in an unbounded viscous fluid
[NASA-TN-D-4947] c12 N69-14483
Transfer functions for radiator dynamics in the SNAP-8 system
[NASA-TN-D-4946] c22 N69-14503
Experimental investigation of the dynamics of water rejection from a matrix type of hydrogen-oxygen fuel cell
[NASA-TN-D-4956] c03 N69-14518
Experimental observation of oscillations described by the continuity equations of slightly ionized deuterium, neon, and helium gas
[NASA-TN-D-4950] c25 N69-14525
Electrical resistivity as a function of deuterium concentration in palladium
[NASA-TN-D-4970] c26 N69-14565
Design of supersonic inlets by a computer program incorporating the method of characteristics
[NASA-TN-D-4960] c01 N69-14566
Heat-transfer coefficients for hydrogen flowing through parallel hexagonal passages at surface temperatures to 2275 K
[NASA-TN-D-4959] c33 N69-14588
Empirical characterization of some pressure wave shapes in strong traveling transverse acoustic modes
[NASA-TM-X-1716] c12 N69-15371
Transport study of neutron and photon attenuation through lithium hydride and tungsten spherical media
[NASA-TN-D-4989] c24 N69-15375
Effects of sample preparation on photomicrographs of cadmium sulfide thin-film solar cells
[NASA-TM-X-1722] c03 N69-15397
Observations of interface behavior during inflow to an elliptical ended cylinder in weightlessness
[NASA-TM-X-1719] c12 N69-15473
Rocket engine evaluation of erosion and char as functions of fabric orientation for silica-reinforced nozzle materials
[NASA-TM-X-1721] c28 N69-15475
Real-gas effects in critical flow through nozzles and thermodynamic properties of nitrogen and helium at pressures to 300 times 10 sup 5. Newtons per square meter /approx. 300 ATM/
[NASA-SP-3046] c12 N69-16098
A digital computer program for determining the elastic-plastic deformation and creep strains in cylindrical rods, tubes and vessels
[NASA-TM-X-1723] c32 N69-16115
On the design of acoustic liners for rocket engines - Maximum damping as a design objective
[NASA-TM-X-1720] c28 N69-16152
Nonequilibrium calculations of methane fluorine oxygen and butene-1-fluorine oxygen rocket performance
[NASA-TN-D-4991] c27 N69-16153
Performance of swirl-can turbojet combustors at simulated supersonic combustor-inlet conditions
[NASA-TN-D-4996] c28 N69-16154
Theoretical nonequilibrium performance of oxygen difluoride-diborane rocket propellant
[NASA-TN-D-4992] c27 N69-16195
The effect of orientation and the presence of surface active materials on the friction, deformation and wear of aluminum
[NASA-TN-D-4994] c15 N69-16197
Analysis and design of inductors for protecting power transistors against current surges in inverter bridge circuits
[NASA-TN-D-4995] c10 N69-16198
Investigation of flow range and stability of three inducer-impeller pump combinations operating in liquid hydrogen
[NASA-TM-X-1727] c28 N69-16213
Rolling-element bearing life from 400 deg to 600 F
[NASA-TN-D-5002] c15 N69-16367
High temperature mechanical properties of polycrystalline hafnium carbide and hafnium carbide containing 13-volume-percent hafnium diboride
[NASA-TN-D-5008] c17 N69-16380

Reactivity changes of a fast reactor core due to elastic-plastic strain and creep
[NASA-TN-D-5012] c22 N69-16381
Design and performance of flueric shock position sensor for a mixed-compression supersonic inlet
[NASA-TM-X-1733] c14 N69-16382
Analytical study of flow reduction due to oxidation of wire-form porous sheet for transpiration cooled turbine blades
[NASA-TN-D-5001] c17 N69-16383
Hot-salt stress-corrosion of titanium alloys - Generation of hydrogen and its embrittling effect
[NASA-TN-D-5000] c17 N69-16465
Components of a hydrogen plasma including minor species
[NASA-TN-D-4993] c25 N69-16466
A method for reducing the equivalent sink temperature of a vertically oriented radiator on the lunar surface
[NASA-TM-X-1729] c03 N69-17225
Crack toughness characteristics of several alloys for use in heavy sections of high speed aircraft
[NASA-TN-D-4998] c32 N69-17275
A survey of salt deposits in compressors of flight gas turbine engines
[NASA-TN-D-4999] c28 N69-17276
Examination of oxide scales on heat resisting alloys
[NASA-TN-D-5019] c17 N69-17277
Two-burn escape maneuvers with an intermediate coasting ellipse
[NASA-TN-D-5011] c30 N69-17305
A 1-megawatt reactor design for Brayton-cycle space power application. Part 1 - Thermal analysis and core design
[NASA-TN-D-5013] c22 N69-17313
A 1-megawatt reactor design for Brayton-cycle space power application Part 2 - Neutronics design
[NASA-TN-D-5014] c22 N69-17314
Analytical investigation of the effect of cooling air on two-stage turbine performance
[NASA-TM-X-1728] c01 N69-17392
Experience with and improvements in containment vessel penetrations
[NASA-TM-X-1735] c22 N69-17701
Dynamic calibration of turbine flowmeters by means of frequency response tests
[NASA-TM-X-1736] c14 N69-17702
Frequency response of a forced flow single tube boiler with inserts and exit restriction
[NASA-TN-D-5023] c12 N69-17779
Steady-state airflow and afterburning performance characteristics of four J85-GE-13 turbojet engines
[NASA-TM-X-1742] c28 N69-17781
Two dimensional inviscid jet flow from two nozzles at an angle to a plane surface
[NASA-TN-D-5064] c01 N69-17816
The ellipsoidal velocity distribution function
[NASA-TN-D-5026] c12 N69-17827
Theoretical analysis of flow in VTOL lift fan inlets without crossflow
[NASA-TN-D-5065] c01 N69-17831
Measurements of some properties of a discharge from a hollow cathode
[NASA-TN-D-4966] c28 N69-17847
Hartree-Fock calculations with Wood-Saxon basis functions
[NASA-TN-D-5066] c24 N69-17976
Correlation of gas-side heat transfer for axisymmetric rocket engine nozzles
[NASA-TM-X-1748] c33 N69-18898
A conversational approach to matrix calculations, concepts and implementation
[NASA-TM-X-1749] c08 N69-18954
Experimental performance of a water- electrolysis rocket
[NASA-TM-X-1737] c28 N69-19017
Feasibility studies of direct voice broadcast satellites
[NASA-TM-X-1747] c07 N69-19025
Dynamic response of hydrazine-nitrogen tetroxide combustion to transverse gas flow
[NASA-TN-D-4984] c27 N69-19026
Lateral sloshing in cylinders under low-gravity conditions
[NASA-TN-D-5058] c12 N69-19112
The dissociation energy of gaseous titanium mononitride
[NASA-TN-D-5027] c06 N69-19129
Performance characteristics from Mach 2.58 to 1.98 of an axisymmetric mixed-compression inlet system with 60-percent internal contraction
[NASA-TM-X-1739] c01 N69-19130
Laboratory simulation of solar wind - earth interaction
[NASA-TM-X-1738] c25 N69-19131
Exploratory study of mechanical properties and heat treatment of molybdenum-hafnium-carbon alloys
[NASA-TN-D-5025] c17 N69-19200
Impurity profile and energy band diagram for the cuprous sulfide-cadmium sulfide heterojunction
[NASA-TN-D-5079] c26 N69-19781
Evaluation of 7.8-inch-throat-diameter inserts and a unique cooling concept in a storable-propellant rocket engine
[NASA-TM-X-1756] c28 N69-19782
Possible applications of the continuity- equation plasma oscillation to pulsars and other periodic astrophysical phenomena
[NASA-TN-D-5078] c25 N69-19783
Description and evaluation of digital-computer design-analysis program for homopolar inductor alternators
[NASA-TN-D-5072] c03 N69-19799
Friction and wear of nine selected polymers with various fillers in liquid hydrogen
[NASA-TN-D-5073] c15 N69-19800
A FORTRAN 4 program to estimate the off-design performance of radial-inflow turbines
[NASA-TN-D-5059] c03 N69-19829
Compatibility tests of molten uranium with tungsten and tungsten - 1.5 percent hafnium
[NASA-TN-D-5076] c17 N69-19930
Performance of various oxide-magazine cathodes in Kaufman thrusters
[NASA-TN-D-5074] c28 N69-19980
Dynamic analysis of permanent magnet stepping motors
[NASA-TN-D-5094] c03 N69-20780
Solubilities of vanadium, titanium, and zirconium in liquid potassium
[NASA-TN-D-5093] c17 N69-20789
Low-density foam for insulating liquid- hydrogen tanks
[NASA-TN-D-5114] c18 N69-20790
Effect of flow rate on the dynamic contact angle for wetting liquids
[NASA-TN-D-5115] c12 N69-20794
Use of tungsten-184 as a thermal flux monitor at high temperatures
[NASA-TN-D-5113] c22 N69-20795
Noncavitating and cavitating performance of several low area ratio water jet pumps having throat lengths of 3.54 diameters
[NASA-TN-D-5095] c03 N69-20797
Resonant mode analysis of the Fitzgerald apparatus
[NASA-TN-D-5103] c26 N69-20798
A comparison of two spectrophotometric methods for the determination of palladium in titanium-base alloys
[NASA-TM-X-1767] c06 N69-20801
Optimal three dimensional launch vehicle trajectories with attitude and attitude rate constraints
[NASA-TN-D-5117] c30 N69-20810
Performance of the SNAP-8 lubrication and coolant subsystem
[NASA-TM-X-1731] c03 N69-20828
Comparison of Brayton and Rankine cycle magnetogasdynamic space-power generation systems
[NASA-TN-D-5085] c03 N69-20852
Preliminary development of spectrochemical analysis of superalloys with the liquid-layer solid-sample spark technique
[NASA-TM-X-1753] c06 N69-20853
OPEX 2 - A radiation shield optimization code
[NASA-TM-X-1769] c22 N69-20854
Performance of an experimental SNAP 8 power conversion system
[NASA-TM-X-1732] c03 N69-20868
A FORTRAN code for computing the principle mass movements of inertia of composite bodies
[NASA-TM-X-1754] c23 N69-20870

Electronic position indicator for latching solenoid valves
[NASA-TM-X-1760] c14 N69-20874
Electrothermal instabilities in the entrance region of an MHD generator
[NASA-TM-X-1761] c25 N69-20875
Measured effects of gaseous flow system dynamics on acoustic-mode combustion instability
[NASA-TN-D-5080] c33 N69-20882
Effect of rotor tip clearance on the performance of a 5-inch single stage axial flow turbine
[NASA-TM-X-1757] c03 N69-20883
Results of endurance tests of a SNAP 8 turbine-alternator
[NASA-TM-X-1741] c03 N69-20913
Characteristics study of a bicone mixed-compression inlet for Mach 1.80 to 2.50
[NASA-TN-D-5084] c01 N69-20914
Cold performance evaluation of 4.97-inch radial-inflow turbine design for single-shaft Brayton cycle space-power system
[NASA-TN-D-5090] c03 N69-20937
Lubrication with some polyphenyl ethers and superrefined mineral oils in a 600 deg F /316 deg C/ inerted vane pump loop
[NASA-TN-D-5096] c15 N69-20938
Preliminary investigation of graphite fluoride /CF sub x/ sub n as a solid lubricant
[NASA-TN-D-5097] c15 N69-20939
Performance of N/p silicon and cadmium sulfide solar cells as affected by hypervelocity particle impact
[NASA-TN-D-5133] c03 N69-21016
Mathematical analysis of the Fitzgerald apparatus
[NASA-TN-D-5116] c18 N69-21384
Factors influencing low cycle crack growth in 2014-T6 aluminum sheet at minus 320 deg F /77 K/
[NASA-TN-D-5140] c32 N69-21392
Atlas-Centaur AC-11 flight performance for Surveyor 4
[NASA-TM-X-1768] c31 N69-21399
Viscous flow in a short cylindrical vortex chamber with a finite swirl ratio
[NASA-TN-D-5132] c12 N69-21400
Fabrication of cermets of uranium nitride and tungsten or molybdenum from mixed powders and from coated particles
[NASA-TN-D-5136] c17 N69-21404
On the resolution and image intensity of the field-ion microscope
[NASA-TN-D-5125] c14 N69-21408
Superconductive dust cores for inductive elements
[NASA-TN-D-5137] c26 N69-21500
Experimental investigation of a 10 deg conical turbojet plug nozzle with translating primary and secondary shrouds at Mach numbers from 0 to 2.0
[NASA-TM-X-1777] c28 N69-21648
Performance and cavitation damage of an axial-flow pump in 1500 deg F /1089 K/ liquid sodium
[NASA-TN-D-5138] c15 N69-21773
FORTRAN program for calculating velocities and streamlines on a blade-to-blade stream surface of a tandem blade turbomachine
[NASA-TN-D-5044] c01 N69-21811
Effect of ultrasonic vibration on precipitation hardening of steels and superalloys
[NASA-TN-D-5131] c32 N69-21814
Revised FORTRAN program for calculating velocities and streamlines on a blade to blade stream surface of a turbomachine
[NASA-TM-X-1764] c01 N69-22553
Nondestructive determination of uranium 235 distribution by fixed position gamma scanning
[NASA-TM-X-1779] c22 N69-22555
Absorption of infrared radiation by ice cryodeposits
[NASA-TN-D-5181] c23 N69-22769
Stress-rupture and tensile properties of refractory-metal wires at 2000 deg and 2200 deg F /1093 deg and 1204 deg C/
[NASA-TN-D-5139] c32 N69-22823
Design and performance of two integrated circuits for fluidic-controlled pneumatic stepping motor system
[NASA-TN-D-5155] c03 N69-22896
Variation of convective heat-transfer coefficient around a simulated rocket cooling tube section
[NASA-TN-D-5168] c33 N69-22931
Optical model analysis of proton scattering in the range 16 to 22 MeV
[NASA-TN-D-5067] c24 N69-22934
Experimental bending strength of an Atlas LV-3C booster beyond compressive skin wrinkling
[NASA-TN-D-5156] c31 N69-22937
FORTRAN program for calculating velocities in a magnified region on a blade to blade stream surface of a turbomachine
[NASA-TN-D-5091] c01 N69-22938
Effects of temperature and electrolyte concentration on performance of a fuel cell of the Bacon type
[NASA-TN-D-5154] c03 N69-22940
Pumped helium tests of a 51-centimeter bore niobium-tin magnet
[NASA-TN-D-5158] c26 N69-22965
Performance and evaluation of two liquid-metal pumps for sodium-potassium service
[NASA-TM-X-1765] c15 N69-22970
Analysis of light-scattering data from polymer solutions
[NASA-TN-D-5177] c06 N69-22991
The thermal stability and friction of the disulfides, diselenides, and ditellurides of molybdenum and tungsten in vacuum
[NASA-TN-D-5141] c15 N69-22992
Dynamic strain aging during the creep and tensile testing of a molybdenum-titanium- carbon alloy
[NASA-TN-D-5169] c17 N69-22993
Crater characteristics of 11 metal alloys under hyper-velocity impact including effects of projectile density and target temperature
[NASA-TN-D-5135] c32 N69-22994
Exploratory study of silicide, aluminide, and boride coatings for nitridation-oxidation protection of chromium alloys
[NASA-TN-D-5157] c17 N69-23084
Shaft face seal with self-acting lift augmentation for advanced gas turbine engines
[NASA-TN-D-5170] c15 N69-23232
On the design of acoustic liners for rocket engines - Helmholtz resonators evaluated with a rocket combustor
[NASA-TN-D-5171] c33 N69-23351
The synthesis of a novel polymide precursor
[NASA-TN-D-5184] c06 N69-23353
Sigma phase formation and its effect on stress-rupture properties of IN-100
[NASA-TN-D-5185] c17 N69-23465
Vibration of shaft face seals and stabilizing effect of viscous and friction damping
[NASA-TN-D-5161] c15 N69-23466
Measurement of liquid and two-phase hydrogen densities with a capacitance density meter
[NASA-TN-D-5015] c14 N69-23470
View factors for toroids and their parts
[NASA-TN-D-5006] c33 N69-23471
Steady-state interactions from Mach 1.98 to 2.58 between a turbojet engine and an axisymmetric inlet with 60-percent internal area contraction
[NASA-TM-X-1780] c28 N69-23519
Determination of oxygen in lithium by the vacuum distillation method
[NASA-TN-D-5197] c06 N69-23706
Design and fabrication of a counterflow double-containment tantalum-stainless steel mercury boiler
[NASA-TN-D-5092] c33 N69-23707
Creep-rupture data for welded N-155 tubes
[NASA-TN-D-5195] c17 N69-23731
Performance and evaluation of a liquid-metal pump for mercury service
[NASA-TM-X-1766] c15 N69-23768
Overall performance of a tandem-bladed inducer tested in water
[NASA-TN-D-5134] c01 N69-23769
Surface temperature mapping with infrared photographic pyrometry for turbine cooling investigations
[NASA-TN-D-5179] c14 N69-23895
Atlas-Agena flight performance for the Applications Technology Satellite ATS-1 mission
[NASA-TM-X-1784] c31 N69-24038
Effect of size on normal-gravity self-pressurization of spherical liquid hydrogen tankage
[NASA-TN-D-5196] c33 N69-24168

Experimental study of pump and seal characteristics of helical groove geometry incorporated in a combined bearing and pump
[NASA-TN-D-5225] c15 N69-24791
Photographic study of a bromine jet flowing in a coaxial airstream and impinging on a stagnation surface
[NASA-TN-D-5209] c12 N69-24800
Analysis of cylindrical reactor fuel pin for clad stress caused by fission gases
[NASA-TN-D-5178] c22 N69-24802
Characterization of pressure perturbations induced in a rocket combustor by a machine gun
[NASA-TN-D-5214] c33 N69-24824
Analysis of gold sphere transmission experiments at 24-keV neutron energy using spin-dependent S-wave statistics
[NASA-TN-D-5211] c24 N69-24826
Nonlinear flux flow in single crystal niobium
[NASA-TN-D-5198] c26 N69-24916
Vapor ingestion phenomenon in weightlessness
[NASA-TN-D-5210] c12 N69-24917
Noise in axisymmetric convergent electron beams
[NASA-TN-D-5212] c10 N69-24918
Study of the /alpha, t/ reaction on scandium-45 at 41 MeV
[NASA-TN-D-5216] c24 N69-24919
A new momentum integral method for treating magnetohydrodynamic and simple hydrodynamic entrance flows
[NASA-TN-D-5215] c25 N69-24920
Conceptual study of rocket-scramjet hybrid engines in a lifting reusable second stage
[NASA-TN-D-5218] c28 N69-24922
Experiments on power loss in herringbone grooved, gas-lubricated journal bearings
[NASA-TN-D-5224] c15 N69-24932
Restart and high response terminal shock control for an axisymmetric mixed-compression inlet with 60-percent internal contraction
[NASA-TM-X-1792] c28 N69-24938
Radiation induced reduction of ammoniacal nickel /2/ sulfate to metallic nickel
[NASA-TN-D-5213] c06 N69-24940
Analytical evaluation of space storable propellants for unmanned Jupiter and Saturn orbiter missions
[NASA-TM-X-1793] c31 N69-24942
Corrosion of metals in deionized water at 30 deg C /100 deg F/
[NASA-TM-X-1791] c17 N69-25243
Clevis design for compact tension specimens used in plane-strain fracture toughness testing
[NASA-TM-X-1796] c32 N69-25301
Radial power tailoring for a uranium dioxide T-111 clad reactor with contained fission product gases
[NASA-TM-X-1795] c22 N69-25305
A systematic approach to model development by comparison of experimental and analytical regression coefficients
[NASA-TM-X-1797] c19 N69-25311
Simple equations for calculating temperature distributions in radiating gray gases
[NASA-TN-D-5226] c33 N69-25312
LEED studies of adhesion to a rhenium surface
[NASA-TN-D-5229] c17 N69-25363
Analysis of electron analog simulation of ion containment in magnetic fields
[NASA-TN-D-5217] c25 N69-25394
Galvanomagnetic and thermomagnetic effects in white tin in fields to 3.3 tesla and at temperatures between 1.2 and 4.2 K
[NASA-TN-D-5227] c26 N69-25412
Evaluation of two nickel-base alloys, alloy 713C and NASA TAZ-8A, produced by extrusion of prealloyed powders
[NASA-TN-D-5248] c17 N69-26192
A new method for treatment of uncertainties in nuclear reactor heat transfer calculations
[NASA-TM-X-1802] c22 N69-26231
Experiences with beryllium swelling and replacement in the Plum Brook reactor
[NASA-TM-X-1794] c22 N69-26233
Impulsive motion on a flat plate pulsed with uniform heat flux
[NASA-TN-D-5249] c33 N69-26236
Unaccelerated geocentric velocities and influx rates of sporadic photographic meteors
[NASA-TN-D-5245] c30 N69-26239
LEED study of the adhesion of various materials to the /iii/ surface of nickel
[NASA-TN-D-5247] c17 N69-26258
A nuclear thermionic space power concept using rod control and heat pipes
[NASA-TN-D-5250] c22 N69-26270
Effect of oxygen concentration on an advanced ester lubricant in bearing tests at 400 deg and 450 deg F
[NASA-TN-D-5262] c15 N69-26311
Experimental data for two 1400-feet per second tip speed compressor rotors operated with inlet flow distortions
[NASA-TM-X-1798] c01 N69-26312
Effect of oxygen concentration on the performance of synthetic paraffinic oils in short term bearing tests from 400 deg to 500 deg F
[NASA-TN-D-5152] c15 N69-26314
Controlled oxygen additions to refractory metals
[NASA-TM-X-1799] c17 N69-26952
Jet effects on boattail pressure drag of isolated ejector nozzles at Mach numbers from 0.60 to 1.47
[NASA-TM-X-1785] c01 N69-26976
Performance and stall limits of a YTF30-P-1 turbofan engine with uniform inlet flow
[NASA-TM-X-1803] c28 N69-27019
A proposed model for the effect of oxidation on the high-temperature deformation of nickel
[NASA-TN-D-5266] c17 N69-27061
Experiments on rotating externally pressurized air journal bearings. Part 1 - Load capacity and stiffness
[NASA-TN-D-5191] c15 N69-27078
Atlas-Agena flight performance for the Applications Technology Satellite ATS-2 mission
[NASA-TM-X-1800] c31 N69-27260
Venting of liquid hydrogen tankage
[NASA-TN-D-5263] c33 N69-27620
Quiescent-air performance of a truncated turbojet plug nozzle with shroud and plug base flows from a common source
[NASA-TM-X-1807] c26 N69-27840
Cavitation performance of 80.6 deg helical inducer in liquid hydrogen
[NASA-TM-X-1808] c09 N69-27841
The liquid-vapor interface during outflow in weightlessness
[NASA-TM-X-1811] c12 N69-27954
Experiments on the stability of water lubricated herringbone-groove journal bearings. 2 - Effects of configuration and groove to ridge clearance ratio
[NASA-TN-D-5264] c15 N69-27955
Experiments on rotating externally pressurized air journal bearings. Part 2 - Attitude angle and air flow
[NASA-TN-D-5192] c15 N69-27956
Outgassing characteristics of an expoxy-impregnated magnet coil
[NASA-TM-X-1813] c18 N69-28203
The fuel-emitter separation problem in externally fueled thermionic diodes
[NASA-TM-X-1812] c22 N69-28212
Film boiling from submerged spheres
[NASA-TN-D-5124] c33 N69-28318
A procedure for furnace brazing butt joints in tungsten-uranium dioxide cermet cylinders at 3000 deg C
[NASA-TM-X-1815] c15 N69-28862
Effect of temperature and pressure on cavitation damage to a cobalt base alloy in sodium
[NASA-TN-D-5273] c17 N69-28863
Critical-speed analysis of rigid rotors on flexible foundations
[NASA-TN-D-4858] c32 N69-29159
Method for prediction of pump cavitation performance for various liquids, liquid temperatures, and rotative speeds
[NASA-TN-D-5292] c15 N69-29165
Thermal electromotive force change for 87Pt13Rh/Pt thermocouples in 1530 K, 10 to the minus 8 torr environment for 3700 hours
[NASA-TN-D-5287] c14 N69-29196
Steady-state stress relaxation analysis of turbine blade cooling designs
[NASA-TN-D-5282] c28 N69-29321

Empirical observations on the sensitivity of hot cathode ionization type vacuum gages
[NASA-TN-D-5285] c14 N69-29331
Application of a double-dead-time model describing chugging to liquid propellant rocket engines having multielement injectors
[NASA-TN-D-5303] c28 N69-29405
Adhesion of gold to various planes of copper studied with LEED
[NASA-TN-D-5290] c26 N69-29407
Investigation of two-phase hydrogen flow in pump inlet line
[NASA-TN-D-5258] c15 N69-29476
Analysis of two dimensional inviscid model of jet impingement under vertical-takeoff airplane
[NASA-TN-D-5288] c01 N69-29479
A thermocouple technique for measuring hot-gas-side wall temperatures in rocket engines
[NASA-TN-D-5291] c14 N69-29553
Effects of thermal-shock cycling on thin-film cadmium sulfide solar cells
[NASA-TM-X-1819] c03 N69-29555
Rare earth fluorides and oxides - An exploratory study of their use as solid lubricants at temperatures to 1800 deg F /1000 deg C/
[NASA-TN-D-5301] c15 N69-29568
Random phase approximation for the anisotropic Heisenberg ferromagnet
[NASA-TN-D-5286] c26 N69-29588
Neutronic comparison of beryllium oxide and molybdenum for movable reflector control of a fast-spectrum reactor
[NASA-TM-X-1822] c22 N69-29593
Atlas-Agena performance for the 1967 Mariner Venus mission
[NASA-TM-X-1826] c31 N69-29594
Three-phase heat transfer - Transient condensing with freezing on a nonisothermal inclined plane
[NASA-TN-D-5289] c33 N69-29598
Use of ''FASTER'' code for significantly reducing ducted reactor shield computation time
[NASA-TM-X-1828] c22 N69-29671
The calculation of elevated temperature cyclic life considering low cycle fatigue and creep
[NASA-TN-D-5317] c32 N69-29672
Preliminary performance characteristics of a gas-bearing turboalternator
[NASA-TM-X-1820] c03 N69-29707
Analysis of dynamic jettison hinge forces for Centaur nose fairing
[NASA-TM-X-1821] c32 N69-29734
Spectral and operational characteristics of a high-intensity carbon arc solar simulator
[NASA-TM-X-1825] c11 N69-29737
Interplanetary probe missions with solar- electric propulsion systems
[NASA-TN-D-5293] c30 N69-29738
Energy transfer and ion cost in a hydrogen plasma
[NASA-TN-D-5319] c25 N69-29905
Dynamic performance analysis of a fuel-control valve for use in airbreathing engine research
[NASA-TN-D-5331] c03 N69-29977
Characteristic design study of mixed- compression two-dimensional inlets with low-angle cowls for the Mach number range 2.70 to 1.80
[NASA-TN-D-5330] c01 N69-30060
A fabrication process for glass coated electron-bombardment ion thruster grids
[NASA-TN-D-5320] c15 N69-30062
Test of sodium boiling in a single tube-in- shell heat exchanger over the range 1720 deg to 1980 deg F /1211 to 1355 K/
[NASA-TN-D-5323] c33 N69-30064
Effect of fluid temperature on the cavitation performance of a high hub-tip ratio axial flow pump in water to 250 degrees F /394 K/
[NASA-TN-D-5318] c15 N69-30069
An analog computer study of the low-frequency flow dynamics of two nuclear rocket cold-flow engine systems
[NASA-TN-D-5312] c22 N69-30070
Growth of 2H silicon carbide crystals
[NASA-TN-D-5313] c26 N69-30072
A comparison of rotational collision numbers obtained from different definitions
[NASA-TN-D-5321] c24 N69-30073
Excited states of xenon-130 populated by beta decay
[NASA-TN-D-5329] c24 N69-30074
Thermal radiation heat transfer. Volume 2 - Radiation exchange between surfaces and in exclosures
[NASA-SP-164-VOL-2] c33 N69-30317
Performance of two models of commercial unbonded strain-gage-type absolute pressure transducer at 260 deg C
[NASA-TN-D-5327] c14 N69-30506
Design of injectors and ablative thrust chambers for a flox-propane rocket engine with a 1.2-inch throat diameter
[NASA-TN-D-5324] c28 N69-30560
Refractive index - Particle density nonequilibrium cesium plasmas probed by a multifrequency helium-neon laser
[NASA-TN-D-5328] c25 N69-30622
Experimental lateral bending dynamics of the Atlas-Centaur-Surveyor launch vehicle
[NASA-TM-X-1837] c31 N69-30631
Two-dimensional cascade investigation of a turbine tandem blade design
[NASA-TM-X-1836] c01 N69-30632
A study of helium penetration and spreading in a Mach 2 airstream using a delta wing injector
[NASA-TN-D-5322] c01 N69-30878
Analysis of the dynamic response of liquid jet atomization to acoustic oscillations
[NASA-TN-D-5339] c28 N69-30980
A semiempirical fracture analysis for small surface cracks
[NASA-TN-D-5340] c32 N69-31056
Corrosion in a cobalt alloy, two-phase mercury loop
[NASA-TN-D-5326] c17 N69-31065
Tensile and cyclic fatigue properties of graphite filament-wound pressure vessels at ambient and cryogenic temperatures
[NASA-TN-D-5354] c32 N69-31300
Dynamic response of a Mach 2.5 axisymmetric inlet with engine or cold pipe and utilizing 60 percent supersonic internal area contraction
[NASA-TN-D-5338] c28 N69-31336
Analytical investigation of two-dimensional loss characteristics of supersonic turbine stator blades
[NASA-TM-X-1823] c01 N69-31360
Effects of nickel on the performance of N on P silicon soar cells
[NASA-TN-D-5366] c03 N69-31844
The use of energy thickness in prediction of throat heat transfer in rocket nozzle
[NASA-TN-D-5356] c33 N69-31869
NERVA control drum actuator irradiation test program
[NASA-TN-D-5347] c22 N69-31870
A nickel base alloy, WAZ-20, with improved strength in the 2000 deg to 2200 deg F range
[NASA-TN-D-5352] c17 N69-31873
Dynamic strain aging in carbide strengthened molybdenum alloys
[NASA-TN-D-5355] c17 N69-31883
Friction and contact resistance during sliding in vacuum of some-low-resistivity metals lubricated with sputtered molybdenum disulfide films
[NASA-TN-D-5349] c15 N69-31884
Summary of recent gaseous reactor fluid mechanics experiments
[NASA-TM-X-1847] c12 N69-31888
Burst testing of tungsten tubing at temperatures from 3000 deg to 4500 deg F /1650 deg to 2480 deg C/
[NASA-TM-X-1843] c17 N69-31889
Solar absorptances and spectral reflectances of 12 metals for temperatures ranging from 300 to 500 K
[NASA-TN-D-5353] c17 N69-31895
Mechanical properties of arc-melted tungsten-rhenium-hafnium-carbon alloys
[NASA-TN-D-5348] c17 N69-31977
A LEED study of the adhesion of gold to copper and copper-aluminum alloys
[NASA-TN-D-5351] c23 N69-31984
Helical duct geometry routine for the shielding computer program ''FASTER''
[NASA-TM-X-1838] c22 N69-31986
A flow experiment on a curved-porous-wall gas-core reactor geometry
[NASA-TM-X-1852] c12 N69-32217

Causes, measurement, and elimination of fuel element fission product leakage at the NASA Plum Brook reactor
[NASA-TN-D-5374] c22 N69-32317
Gaseous hydrogen requirements for the discharge of liquid hydrogen from a 1.52 meter /5 ft/ diameter spherical tank
[NASA-TN-D-5336] c28 N69-32318
Design of experiments as doubly telescoping sequences of blocks with application to a nuclear reactor experiment
[NASA-TN-D-5369] c19 N69-32319
Effect of injection element radial distribution and chamber geometry on acoustic mode instability in a hydrogen oxygen rocket
[NASA-TN-D-5375] c33 N69-32340
Stability of two-fluid wheel flows with an imposed uniform axial magnetic field
[NASA-TN-D-5372] c12 N69-32377
Stability and performance characteristics of several hydrazine and nitrogen tetroxide hot gas generators for large scale supersonic combustor testing
[NASA-TM-X-1845] c33 N69-32468
Tagged arithmetic
[NASA-TN-D-5370] c08 N69-32556
Design studies on the effect of orientation, lunation, and location of the performance of lunar radiators
[NASA-TM-X-1846] c33 N69-32683
Implementation and structure of COMPUTE, a time-sharing calculator program
[NASA-TN-D-5350] c08 N69-32685
Significant experiences of the NASA Plum Brook reactor facility
[NASA-TM-X-1853] c22 N69-33132
Gaseous-hydrogen pressurant requirements for the discharge of liquid hydrogen from a 3.96 meter /13 ft/ diameter spherical tank
[NASA-TN-D-5387] c28 N69-33211
Experiments on the steady state characteristics of herringbone-grooved air-lubricated journal bearings
[NASA-TN-D-5386] c15 N69-33258
Cavitation performance of line-mounted 80.6 deg helical inducer in hydrogen
[NASA-TM-X-1854] c12 N69-33261
Thermionic fuel irradiation experiment description
[NASA-TM-X-1858] c22 N69-33273
Computer program for viscous, isothermal compressible flow across a sealing dam with small tilt angle
[NASA-TN-D-5373] c15 N69-33281
Oxidation and thermal fatigue cracking of nickel- and cobalt-base alloys in a high velocity gas stream
[NASA-TN-D-5376] c17 N69-33307
Analysis of total-pressure loss and airflow distribution for annular gas turbine combustors
[NASA-TN-D-5385] c33 N69-33314
Simplified analytical model for use in design of pump-inlet accumulators for the prevention of liquid-rocket longitudinal oscillation /POGO/
[NASA-TN-D-5394] c28 N69-33319
Failure criteria for filamentary composites
[NASA-TN-D-5367] c18 N69-33321
Experimental and theoretical turbulent boundary layer development in a Mach 4.4 water-cooled conical nozzle
[NASA-TN-D-5377] c12 N69-33353
Development of improved throat inserts for ablative rocket engines
[NASA-TN-D-4964] c32 N69-33481
Clean room technology
[NASA-SP-5074] c05 N69-33775
Experimental study of low-speed operating characteristics of a liquid hydrogen centrifugal turbopump
[NASA-TM-X-1861] c28 N69-33806
Surface tension, viscosity, and density measurements of two fluorocarbon solvents, FC-43 and FC-78
[NASA-TM-X-1862] c18 N69-34134
Analysis of dynamic performance limitations of fast response /150 to 200 Hz/ electrohydraulic servos
[NASA-TN-D-5388] c03 N69-34652
Propulsion systems for manned exploration of the solar system
[NASA-TM-X-1864] c28 N69-34674
Solid-propellant combustion instability and the role of velocity coupling
[NASA-TN-D-5395] c33 N69-34892
The influence of crack length and thickness in plane strain fracture toughness tests
[NASA-TM-X-1860] c17 N69-34916
Evaluation of a volume-ratio system for vacuum gage calibration from 10 to the minus 8 power to 10 torr
[NASA-TN-D-5406] c14 N69-35265
Experimental measurements of expanding storable-propellant products simulated by combustion of gaseous reactants
[NASA-TN-D-5404] c33 N69-35506
A computer plotting description of ion-molecule collisions with long-lived capture complexes
[NASA-TN-D-5407] c24 N69-35508
Performance characteristics of a 14.3-kilovolt-ampere modified Lundell alternator for 1200 hertz Brayton-cycle space-power system
[NASA-TN-D-5405] c03 N69-35537
FORTRAN program for machine computation of group tables of finite groups
[NASA-TN-D-5402] c08 N69-35569
Cryogenic fracture properties of thin AISI 301 60-percent cold-reduced sheet at various angles to the rolling direction
[NASA-TN-D-5413] c17 N69-35688
A comparison of experimental and calculated helium requirements for the pressurization of a Centaur liquid hydrogen tank
[NASA-TM-X-1870] c28 N69-35712
The potential of nuclear power for high-speed ocean-going air-cushion vehicles
[NASA-TM-X-1871] c22 N69-35723
Analytical and experimental studies of MHD generator cathodes emitting in a ''spot'' mode
[NASA-TN-D-5414] c25 N69-35732
The improvement of an electronic power supply for greater reliability in aerospace use
[NASA-TM-X-1875] c03 N69-35763
Recent developments in chromium and chromium alloys
[NASA-TM-X-1867] c17 N69-35764
Torque and leakage rates of various lubricated lip seal designs at a peripheral velocity of 120 feet per second
[NASA-TN-D-5411] c15 N69-35769
Lubricants for inerted lubrication systems in engines for advanced aircraft
[NASA-TN-D-5420] c15 N69-35788
Investigation of isothermal, compressible flow across a rotating sealing dam. 1 - Analysis
[NASA-TN-D-5344] c15 N69-35799
Comparison of tungsten and depleted uranium in minimum-weight, layered shields for a space power reactor
[NASA-TM-X-1874] c22 N69-35817
Natural frequency of liquids in annular cylinders under low gravitational conditions
[NASA-TN-D-5412] c12 N69-35842
Design, development, and testing of a 1000 pound /4450 N/ thrust FLOX-propane ablative rocket engine
[NASA-TM-X-1873] c28 N69-35847
Evaluation of the COHORT 2 Monte Carlo shielding code - Gamma ray transport using source direction biasing
[NASA-TM-X-1877] c22 N69-35848
Statistical analysis of high-temperature creep-rate data for alloys of tantalum, molybdenum, and columbium
[NASA-TN-D-5424] c17 N69-36653
Heat-transfer characteristics of a water-to-cryogenic-hydrogen heat exchanger
[NASA-TN-D-5429] c33 N69-36701
Transistor performance in intense magnetic fields
[NASA-TN-D-5428] c09 N69-36710
Reflector-based poison-drum control on equal-size reactor cores fueled with uranium-233 and with uranium-235
[NASA-TM-X-1883] c22 N69-36756
Parametric study of large nuclear surface effects machines
[NASA-TM-X-1888] c22 N69-36757
Effects of simulated space environment on full, half, and quarter-size cadmium sulfide thin-film solar cells

[NASA-TM-X-1884] c03 N69-36758
Comparison of predicted nozzle coolant side heat transfer and fluid flow with experimental values from Phoebus-2A nuclear tests
[NASA-TM-X-1881] c33 N69-36806
An electron bombardment thruster operated with a cusped magnetic field
[NASA-TN-D-5448] c28 N69-36844
A computer program for composing compressor blading from simulated circular-arc elements on conical surfaces
[NASA-TN-D-5437] c28 N69-36882
Multigroup calculations of resonance neutron capture in a thick slab of depleted uranium
[NASA-TM-X-1878] c24 N69-36901
Hardware /or software/ provisions for multiple precision floating-point arithmetic
[NASA-TM-X-1885] c08 N69-36918
Molecular vibration spectra from field emission energy distributions
[NASA-TN-D-5423] c24 N69-36924
Quadrature variations in discrete-ordinates calculations
[NASA-TM-X-1887] c20 N69-36976
Multistage compressor simulation applied to the prediction of axial flow instabilities
[NASA-TM-X-1880] c28 N69-36998
Phenomenological theory of loudness
[NASA-TN-D-5422] c23 N69-37028
A simple method for determination of fission gases trapped in irradiated fuel forms
[NASA-TM-X-1893] c22 N69-37225
Effect of angle of attack and injection pressure on jet penetration and spreading from a delta wing in supersonic flow
[NASA-TM-X-1889] c12 N69-37271
Absorption of hydrogen by palladium and electrical resistivity up to hydrogen- palladium atom ratios of 0.97
[NASA-TN-D-5441] c26 N69-37272
Flight performance of Atlas-Agena launch vehicles in support of the Lunar Orbiter missions 3, 4, and 5
[NASA-TM-X-1859] c31 N69-37281
Effect of nuclear radiation at cryogenic temperatures on the tensile properties of titanium and titanium-base alloys
[NASA-TN-D-5442] c17 N69-37436
FORTRAN program for calculating transonic velocities on a blade-to-blade stream surface of a turbomachine
[NASA-TN-D-5427] c01 N69-37521
Tabulations of configuration factors between any two spheres and their parts
[NASA-SP-3050] c30 N69-37777
Diffusion lengths in silicon obtained by an X-ray method
[NASA-TM-X-1894] c03 N69-37827
Flight performance of the Atlas-Agena launch vehicle in support of the Applications Technology Satellite ATS-3
[NASA-TM-X-1879] c31 N69-37840
Effect of electrothermal instabilities on Brayton- and Rankine-cycle magnetohydrodynamic space-power generation systems
[NASA-TN-D-5461] c03 N69-37883
Thermodynamic and transport properties of air and the combustion products of natural gas and of ASTM-A-1 fuel with air
[NASA-TN-D-5452] c33 N69-37936
Injection of an inviscid separated jet at an oblique angle to a moving stream
[NASA-TN-D-5460] c12 N69-37965
Discharge coefficients for thick plate orifices with approach flow perpendicular and inclined to the orifice axis
[NASA-TN-D-5467] c12 N69-38012
Motion of single bubbles under low gravitational conditions
[NASA-TN-D-5462] c12 N69-38032
Dispersion-strengthened nickel produced from ultrafine comminuted powders
[NASA-TN-D-5421] c17 N69-38074
Experimental investigation of dynamic distortion in a Mach 2.50 inlet with 60 percent internal contraction and its effect on turbojet stall margin
[NASA-TM-X-1842] c28 N69-38599
Cavitation damage and the effect of fluid temperature on the performance of an axial- flow pump in liquid sodium
[NASA-TN-D-5484] c15 N69-38641
A device for producing both hard copy alphanumeric listings and digital data plots
[NASA-TN-D-5474] c08 N69-38654
An improved delayed neutron fission product monitor
[NASA-TM-X-1886] c14 N69-38766
Electrical characteristics of a large area thin film CdS solar cell
[NASA-TM-X-1899] c03 N69-38767
Survey of electron-cesium collision probabilities - Momentum transfer collisions
[NASA-TM-X-1897] c24 N69-38773
A transformer of closely spaced pulsed wave forms having a nonzero average value
[NASA-TN-D-5473] c09 N69-38776
An evaluation of three oxidation-resistant alloy claddings for IN 100 and WI 52 superalloys
[NASA-TN-D-5483] c17 N69-38794
Dislocation structures in single crystal tungsten and tungsten alloys
[NASA-TN-D-5493] c17 N69-39182
Calculated interaction energy and dipole moment in collisions of two hydrogen molecules
[NASA-TN-D-5486] c24 N69-39184
Airbreathing propulsion system testing using sweep frequency techniques
[NASA-TN-D-5485] c28 N69-39185
Analysis and experiments with a pulsed neutron source for an unreflected solution reactor up to 50 dollars shutdown
[NASA-TN-D-5487] c22 N69-39186
Interim absorption coefficients and opacities for hydrogen plasma at high pressure
[NASA-TM-X-1902] c24 N69-39187
Preliminary investigation of a single-shaft Brayton rotating unit designed for a 2 to 10-kilowatt space power generation system
[NASA-TM-X-1869] c03 N69-39238
Magnetothermal oscillations in pressure- annealed, pyrolytic graphite
[NASA-TN-D-5488] c26 N69-39239
A photographic study of a bromine jet in a coaxial airstream with honeycombs at the injection plane
[NASA-TM-X-1900] c12 N69-39303
Cold air investigation of a turbine with stator-blade trailing-edge coolant ejection. Part 1 - Overall stator performance
[NASA-TM-X-1901] c03 N69-39335
Calculation of thermal-fatigue life based on accumulated creep damage
[NASA-TN-D-5489] c32 N69-39393
Injection of an attached inviscid jet at an oblique angle to a moving stream
[NASA-TN-D-5501] c12 N69-39916
Solubilities of molybdenum and tungsten in liquid potassium
[NASA-TN-D-5504] c17 N69-40053
Ionic conductivity of lanthanum fluoride
[NASA-TN-D-5505] c26 N69-40056
Performance of radiation-cooled magnetoplasmadynamic arc thrusters
[NASA-TM-X-1908] c28 N69-40058
Flow-direction measurement with fixed-position probes
[NASA-TM-X-1904] c14 N69-40059
A steam cycle for aircraft nuclear propulsion
[NASA-TM-X-1907] c22 N69-40060
Characteristics of a 2.17-megawatt fast- spectrum reactor concept using an axially moving reflector control system
[NASA-TM-X-1911] c22 N69-40061
Effects of three outlet-annulus area blockage configurations on the performance of a 20-inch /50.8-CM/ axial-flow compressor rotor
[NASA-TN-D-5506] c28 N69-40078
Combustion stability of single swirl-can combustor modules using ASTM-A1 liquid fuel
[NASA-TN-D-5436] c28 N69-40080
Application of modern network theory to analysis of complex systems
[NASA-TN-D-5511] c19 N69-40088
Electrochemical behavior of the aluminum electrode in molten salt electrolytes
[NASA-TN-D-5503] c06 N69-40240

Hot-salt stress-corrosion of a titanium alloy under a simulated turbine-engine compressor environment
[NASA-TN-D-5510] c17 N69-40242
Helium pressurization systems for liquid- methane fuel in supersonic transports
[NASA-TN-D-5519] c28 N69-40329
Transmission effects on plastic films irradiated with ultraviolet light, electrons, and protons
[NASA-TM-X-1905] c18 N69-40339
Penetration model explanation for turbulent forced-convection heat transfer observed in near-critical fluids
[NASA-TN-D-5522] c33 N69-40437
Motor-starting characteristics of two inductor alternators
[NASA-TM-X-1912] c03 N69-40440
Conceptual design and structural model of a 560-watt thin-film solar-cell array
[NASA-TM-X-1913] c03 N69-40787
Convective heat-transfer coefficients from a solution of the conduction equation for a wall separating two fluids, one having an oscillating temperature
[NASA-TN-D-5520] c33 N69-40789
Interaction of 42-MeV alpha particles with helium-3
[NASA-TN-D-5530] c24 N69-40979
Speed effects on ball spinning torque
[NASA-TN-D-5527] c15 N69-41210
Analysis of the mixing region for a two-dimensional jet injected at an angle to a moving stream
[NASA-TN-D-5531] c12 N69-41213

NATIONAL AERONAUTICS AND SPACE ADMINISTRATION. MANNED SPACECRAFT CENTER, HOUSTON, TEX.

Optimum design of communication links with noisy phase reference
[NASA-TN-D-4895] c07 N69-13155
Postflight optical evaluation of the right- hand and left-hand windows of Gemini missions 4, 5, 6, and 7
[NASA-TN-D-4916] c31 N69-13232
Lunar surface transmission loss for the Apollo astronaut
[NASA-TN-D-4915] c07 N69-13301
The stagnation-point boundary layer with suction and injection in equilibrium dissociating air
[NASA-TN-D-3889] c12 N69-14314
A computer program for calculating external thermal-radiation heat loads and temperatures of spacecraft orbiting the planets or the moon
[NASA-TR-R-278] c30 N69-14428
A mathematical model for calculating the flight dynamics of a general parachute-payload system
[NASA-TN-D-4859] c02 N69-14504
Matched conic solutions to round trip interplanetary trajectory problems that insure state-vector continuity at all boundaries
[NASA-TN-D-4942] c30 N69-14861
Planetary probe guidance accuracy influence factors for conjunction-class missions
[NASA-TN-D-4852] c21 N69-16503
Experimental verification of scale factors for parawing opening characteristics with dimensional ratios from 1/1.3 to 1/3
[NASA-TN-D-5071] c02 N69-19950
The relationship between optical distortion and binocular depth perception
[NASA-TN-D-5162] c05 N69-22990
Forces on a flexible shell during water impact
[NASA-TM-X-1781] c32 N69-23697
Performance characteristics of the Apollo astronaut backpack antenna
[NASA-TN-D-5081] c07 N69-23882
Aerodynamic loads on deployed canard surfaces and rocket nose section of the Apollo launch escape vehicle
[NASA-TN-D-5260] c31 N69-28166
Aerodynamic characteristics determined during development of the Apollo launch escape vehicle configuration
[NASA-TN-D-5208] c01 N69-29027
Translunar abort techniques for nonfree-return missions
[NASA-TM-X-1806] c30 N69-29569
Applications of quasi-linearization theory to system identification
[NASA-TN-D-5300] c19 N69-29648

A review of spacecraft waste-management systems
[NASA-TM-X-1851] c05 N69-33260
Some liquid oxygen/liquid hydrogen explosive effects in controlled failure-mode tests
[NASA-TN-D-5382] c27 N69-35321
Entry aerodynamics at lunar return conditions obtained from the flight of Apollo 4 /AS-501/
[NASA-TN-D-5399] c31 N69-38820
Wind-tunnel investigation of the aerodynamic pressures on the Apollo command module configuration
[NASA-TN-D-5514] c01 N69-40345
The effect of object motion in Fraunhofer holography with application to velocity measurements
[NASA-TN-D-5515] c14 N69-40812
Preflight optical evaluation of the right-hand hatch windows of Gemini missions 7, 8, 9, and 12
[NASA-TN-D-5471] c31 N69-40813

NATIONAL AERONAUTICS AND SPACE ADMINISTRATION. MANNED SPACECRAFT CENTER, LANGLEY STATION, VA.

Low subsonic flight and force investigation of a supersonic transport model with a variable-sweep wing
[NASA-TN-D-4726] c02 N69-10733

NATIONAL AERONAUTICS AND SPACE ADMINISTRATION. MARSHALL SPACE FLIGHT CENTER, HUNTSVILLE, ALA.

Analysis of commutated networks employing feedback circuits
[NASA-TN-D-4893] c10 N69-10755
Blast shields testing
[NASA-TN-D-4894] c11 N69-10888
A study of stiffness matrices for the analysis of flat plates
[NASA-TN-D-4927] c32 N69-14169
Regression analysis procedures for the evaluation of tracking system measurement errors
[NASA-TN-D-4826] c19 N69-14476
Acceptance testing lunar and planetary vehicles /a concept/
[NASA-TN-D-4924] c11 N69-14507
The influential aspects of atmospheric disturbances on space vehicle design using statistical approaches for analysis
[NASA-TN-D-4963] c32 N69-15632
Development of air bearing lift pads
[NASA-TM-X-1724] c01 N69-16467
Thermal and dielectric properties of a homogeneous moon based on microwave and infrared temperature observations
[NASA-TM-X-1734] c30 N69-17815
Thermal conduction through an evacuated idealized powder over the temperature range of 100 deg K to 500 deg K
[NASA-TN-D-5063] c33 N69-20008
Simulation of package transfer concepts for Saturn 1 Orbital Workshop
[NASA-TN-D-5111] c05 N69-21501
Scientific experiments for the Apollo telescope mount
[NASA-TN-D-5020] c30 N69-21526
Experimental investigation of base flow field at high altitude for a four engine clustered nozzle configuration
[NASA-TN-D-5164] c12 N69-24935
Investigation of SA-501 S-4B auxiliary
[NASA-TN-D-5207] c28 N69-26224
Survey and comparative analysis of current geophysical models
[NASA-TN-D-5163] c13 N69-26969
Tables and graphs of functions necessary for solving nonlinear heat transfer constant area fin problems with examples on their use
[NASA-TN-D-5173] c33 N69-26975
Low-order classical Runge-Kutta formulas with stepsize control and their application to some heat transfer problems
[NASA-TR-R-315] c19 N69-30753
Longitudinal mass-spring modeling of launch vehicles
[NASA-TN-D-5371] c32 N69-34970
Calibration of Pegasus and Explorer 23 detector panels
[NASA-TR-R-321] c14 N69-36985
Pressure effect of a sound wave on a cryogenic fluid
[NASA-TN-D-4024] c23 N69-38180
Numerical integration in a rigid-body trajectory program

[NASA-TN-D-5425] c30 N69-38769
Saturn 5, S-4B panel flutter qualification test Final report
[NASA-TN-D-5439] c32 N69-38808
Rotating space station stabilization criteria for artificial gravity
[NASA-TN-D-5426] c05 N69-39210
Determination of meteoroid environments from photographic meteor data
[NASA-TR-R-322] c30 N69-39336

NATIONAL AERONAUTICS AND SPACE ADMINISTRATION. WALLOPS STATION, WALLOPS ISLAND, VA.

EXAMETNET Data Report series - Annual report, 1967
[NASA-SP-176] c20 N69-22570

NATIONAL AERONAUTICS AND SPACE ADMINISTRATION, WASHINGTON, D. C.

Biology of hard tissue
[NASA-SP-161] c04 N69-10444
Applications of systems analysis models - A survey
[NASA-SP-5048] c34 N69-10662
Some fluid mechanical problems related to subsonic and supersonic aircraft
[NASA-SP-183] c12 N69-10693
Progress of NASA research relating tc noise alleviation of large subsonic jet aircraft
[NASA-SP-189] c02 N69-11542
Aerospace Medicine and Biology - A continuing bibliography with indexes
[NASA-SP-7011/55/] c04 N69-11695
Computerized Arrhenius reliability extrapolation techniques
[NASA-TN-D-4902] c19 N69-13368
Objectives and goals in space science and applications 1968
[NASA-SP-162] c30 N69-13844
The metallurgy, behavior, and application of the 18-percent nickel maraging steels A survey
[NASA-SP-5051] c17 N69-14193
Joining ceramics and graphite to other materials
[NASA-SP-5052] c15 N69-14241
Aerospace Medicine and Biology
[NASA-SP-7011/56/] c04 N69-14387
NASA space vehicle design criteria /structures/ - Propellant slosh loads
[NASA-SP-8009] c32 N69-14553
NASA contributions to bioinstrumentation systems - A survey
[NASA-SP-5054] c04 N69-14860
Aerospace medicine and biology - A continuing bibliography with indexes
[NASA-SP-7011/57/] c04 N69-16537
The book of Mars
[NASA-SP-179] c30 N69-16571
A comparison of data obtained by the MT-135 and ARCAS meteorological rocket systems
[NASA-TM-X-1726] c20 N69-17772
Aircraft navigation
[NASA-TT-F-524] c21 N69-17788
Aerospace Medicine and Biology - A continuing bibliography with indexes, December 1968
[NASA-SP-7011/58/] c04 N69-19023
Guidance and navigation for entry vehicles
[NASA-SP-8015] c21 N69-19518
Aerospace Medicine and Biology. A continuing bibliography with indexes
[NASA-SP-7011/60/] c04 N69-19714
Pavement grooving and traction studies
[NASA-SP-5073] c11 N69-20451
Models of Venus atmosphere, 1968
[NASA-SP-8011] c30 N69-20916
Teleoperatcr control An AEC-NASA technology survey
[NASA-SP-5070] c05 N69-21478
Sixth Annual Meeting of the Working Group on Extraterrestrial Resources
[NASA-SP-177] c30 N69-22226
NASA Science and Technology Advisory Committee for Manned Space Flight. Winter Study on Uses of Manned Space Flight, 1975-1985. Volume 1 - Proceedings
[NASA-SP-196-VOL-1] c34 N69-22510
Aerospace Medicine and Biology - A continuing bibliography with indexes
[NASA-SP-7011/61/] c04 N69-23126
Induction heating advances - Applications to 5800 deg F
[NASA-SP-5071] c03 N69-23643
Aerospace Medicine and Biology - A cumulative index to the 1968 issues of a continuing bibliography
[NASA-SP-7011/59/] c04 N69-24752
Dynamics of the spatial motion of an aircraft
[NASA-TT-F-555] c02 N69-24761
Aerospace Medicine and Biology. A continuing bibliography with indexes, March 1969
[NASA-SP-7011/62/] c04 N69-24822
Significant achievements in space science, 1967
[NASA-SP-167] c30 N69-25460
Compressed gas handbook
[NASA-SP-3045] c12 N69-26987
Earth photographs from Gemini 6 through 12
[NASA-SP-171] c14 N69-28909
The face of the earth and its origin
[NASA-TT-F-533] c13 N69-29491
NASA scientific and technical reports for 1968. A selected listing
[NASA-SP-7033] c34 N69-29492
Interdisciplinary approach to friction and wear Conference proceedings
[NASA-SP-181] c15 N69-30401
The design of conical shells subjected to antisymmetric loadings
[NASA-TT-F-518] c32 N69-30754
Aerospace medicine and biology - A continuing bibliography with indexes
[NASA-SP-7011/65/] c04 N69-31923
Aerospace related technology for industry
[NASA-SP-5075] c34 N69-31946
Weather satellite picture receiving stations - Inexpensive construction of automatic picture transmission ground equipment
[NASA-SP-5080] c07 N69-31985
The Apollo spacecraft. Volume 1 - A chronology
[NASA-SP-4009] c31 N69-32021
Management - A continuing literature survey with indexes
[NASA-SP-7500/03/] c34 N69-32430
Evaluation cf motion-degraded images
[NASA-SP-193] c14 N69-33322
Synoptic analysis of the Southern Hemisphere stratosphere
[NASA-TM-X-1814] c13 N69-33555
The systems approach to management. An annotated bibliography, with indexes
[NASA-SP-7501] c34 N69-34917
Investigation of vibration and stability of aircraft engine components
[NASA-TT-F-547] c02 N69-36326
Surveyor program results Final report
[NASA-SP-184] c30 N69-36451
Project Gemini technology and operations - A chronology
[NASA-SP-4002] c31 N69-36501
Effects of structural flexibility on spacecraft control systems
[NASA-SP-8016] c31 N69-37030
Aerospace Medicine and Biology Continuing bibliography with indexes, Aug. 1969
[NASA-SP-7011/67/] c04 N69-37887
Aerospace Medicine and Biology Continuing bibliography with indexes, Jul. 1969
[NASA-SP-7011/66/] c04 N69-37909
Aerospace Medicine and Biology A continuing bibliography with indexes, Apr. 1969
[NASA-SP-7011/63/] c04 N69-38235
Aerospace Medicine and Biology A continuing bibliography with indexes, May 1969
[NASA-SP-7011/64/] c04 N69-38242
Aerodynamics and flight dynamics of turbojet aircraft
[NASA-TT-F-542] c01 N69-38670
Progress of NASA research on warm fog properties and modification concepts Symposium proceedings
[NASA-SP-212] c20 N69-39526
Concentration of matter and action of enzymes in ccacervates
[NASA-TT-F-525] c04 N69-40324
NASA space vehicle design criteria- environment. Meteorid environment model - 1969 /near earth to lunar surface/
[NASA-SP-8013] c30 N69-40326
Shock waves in real gases
[NASA-TT-F-585] c12 N69-40824
A long-range program in space astronomy - Position paper of the Astronomy Missions Board
[NASA-SP-213] c30 N69-41150

NATIONAL AERONAUTICS AND SPACE COUNCIL, WASHINGTON, D. C.

Response characteristics of meteorolcgical rocket wind reduction techniques
[NASA-TM-X-1850] c20 N69-35523
NATIONAL METEOROLOGICAL CENTER, SUITLAND, MD.
Meteorological rocket research since 1959 and current requirements for observations and analysis above 60 kilometers
[NASA-CR-1293] c13 N69-18700
NIELSEN ENGINEERING AND RESEARCH, INC., PALO ALTO, CALIF.
Calculation of compressible turbulent boundary layers with pressure gradients and heat transfer
[NASA-CR-1303] c12 N69-21653
Theoretical study of vortex shedding from bodies of revolution undergoing coning motion
[NASA-CR-1448] c12 N69-40200
NORTH AMERICAN ROCKWELL CORP., CANOGA PARK, CALIF.
Variable mesh methods for differential equations
[NASA-CR-1247] c19 N69-11419
NORTH AMERICAN ROCKWELL CORP., DOWNEY, CALIF.
Theoretical flow field calculations for Project RAM
[NASA-CR-1308] c07 N69-28223
NORTH CAROLINA STATE UNIV., RALEIGH.
The radiation resistance of cylindrical shells
[NASA-CR-1437] c32 N69-40935
NORTHROP CORP., HAWTHORNE, CALIF.
Recirculation effects produced by a pair of heated jets impinging on a ground plane
[NASA-CR-1307] c01 N69-34703
NORTHWESTERN UNIV., EVANSTON, ILL.
Experimental investigation of magnetoaerodynamic flow around blunt bodies
[NASA-CR-1393] c25 N69-34897

O

OHIO STATE UNIV., COLUMBUS.
Preprocessing electronic satellite observations
[NASA-CR-1183] c08 N69-11470
The Te-d1 mode reflection coefficient of a ground-plane mounted parallel-plate waveguide illuminating a reflecting sheet
[NASA-CR-1327] c07 N69-24059
Slope diffraction analysis of TEM parallel- plate guide patterns
[NASA-CR-1326] c07 N69-26273
Techniques for generation of control and guidance signals derived from optical fields
[NASA-CR-1443] c21 N69-38041
OKLAHOMA UNIV., NORMAN.
An approximate theory for transverse shear deformation and rotatory inertia effects in vibrating beams
[NASA-CR-1317] c32 N69-24056
A theoretical analysis of the free vibration of discretely stiffened cylindrical shells with arbitrary end conditions
[NASA-CR-1316] c32 N69-28164

P

PENNSYLVANIA STATE UNIV., UNIVERSITY PARK.
Investigation of the turbulent wind field below 150-meter altitude at the eastern test range
[NASA-CR-1410] c20 N69-35570
PERKIN-ELMER CORP., POMONA, CALIF.
Analytical study of contaminant and atmospheric sensor, phase 1
[NASA-CR-1375] c14 N69-37876
PHILCO-FORD CORP., NEWPORT BEACH, CALIF.
Structural optimization of sandwich and ring-stiffened 120 degree conical shells subjected to external pressure
[NASA-CR-1424] c32 N69-35515
Evaluation of configuration changes on optimum structural designs for a Mars entry capsule
[NASA-CR-1414] c33 N69-35516
Synthesis of optimum structural designs for conical and tension shell Mars entry capsules
[NASA-CR-1365] c32 N69-36357
PHILCO-FORD CORP., PALO ALTO, CALIF.
Manipulation errors in finite element analysis of structures
[NASA-CR-1385] c19 N69-34360
PITTSBURGH UNIV., PA.
Stability theory of nonlinear operational differential equations in Hilbert space
[NASA-CR-1356] c19 N69-28256
PRATT AND WHITNEY AIRCRAFT, EAST HARTFORD, CONN.
Analytical and experimental study of the dynamics of a single-tube counterflow boiler
[NASA-CR-1230] c12 N69-17751
High performance turboalternator and associated hardware. 3. Design of backup gas bearings
[NASA-CR-1292] c15 N69-19775
High performance turboalternator and associated hardware. 1 - Design of turboalternator
[NASA-CR-1290] c03 N69-21771
High-performance turboalternator and associated hardware. 2 - Design of gas bearings
[NASA-CR-1291] c15 N69-21772
Design of Brayton rotating unit on rolling-element bearings
[NASA-CR-1401] c15 N69-33450
Testing of high-emittance coatings
[NASA-CR-1413] c17 N69-35514
Analytical and experimental studies for predicting noise attenuation in acoustically treated ducts for turbofan engines
[NASA-CR-1373] c23 N69-36974
PRINCETON UNIV., N. J.
Second-order wave structure in supersonic flows
[NASA-CR-1438] c04 N69-37062
PURDUE UNIV., LAFAYETTE, IND.
A comprehensive program for the compilation and analysis of thermal radiative properties data
[NASA-CR-1431] c33 N69-40455

R

RADIO CORP. OF AMERICA, HARRISON, N. J.
Superconductive magnet system, 14-Tesla, 15-cm-bore
[NASA-CR-1260] c03 N69-15382
RAI RESEARCH CORP., LONG ISLAND CITY, N. Y.
An investigation of the basic properties of irradiated polyethylene memory materials
[NASA-CR-1384] c18 N69-36762
RAYTHEON CO., SUDBURY, MASS.
Laser Doppler velocity instrument
[R-67-4450] c14 N69-14351
Space geodesy altimetry study
[NASA-CR-1298] c14 N69-21117
RAYTHEON CO., WALTHAM, MASS.
A program to evaluate dye lasers as high power, pulsed, visible light sources
[NASA-CR-1374] c16 N69-29934
RENSSELAER POLYTECHNIC INST., TROY, N. Y.
Adaptive simulation using mode identification
[NASA-CR-1179] c08 N69-10316
RESEARCH TRIANGLE INST., DURHAM, N. C.
A feasibility study of a miniature solid-state pressure transducer
[NASA-CR-1366] c26 N69-29724
ROCHESTER APPLIED SCIENCE ASSOCIATES, INC., N. Y.
A theory for predicting the rotational and vortex noise of lifting rotors in hover and forward flight
[NASA-CR-1333] c23 N69-25344
A method for analyzing the aeroelastic stability of a helicopter rotor in forward flight
[NASA-CR-1332] c32 N69-34744
ROCKETDYNE, CANOGA PARK, CALIF.
Application of biogeochemistry to mineral prospecting A survey
[NASA-SP-5056] c13 N69-10492
Properties of nonaqueous electrolytes
[NASA-CR-1425] c06 N69-36413

S

SAN DIEGO AIRCRAFT ENGINEERING, INC., CALIF.
Potential structural materials and design concepts for light aircraft
[NASA-CR-1285] c02 N69-20848
SCIENTIFIC TRANSLATION SERVICE, LA CANADA, CALIF.
Atlas of the reverse side of the moon, part 2
[NASA-TT-F-514] c30 N69-24206
SCRIPTA TECHNICA, INC., WASHINGTON, D. C.
Transient temperature fields in shells
[NASA-TT-F-552] c33 N69-30245
Liquid metals
[NASA-TT-F-522] c33 N69-30507
Physics of the moon and planets
[NASA-TT-F-502] c30 N69-31989
Problems of space biology. Volume 7 - Operational activity, problems of habitability and

biotechnology
[NASA-TT-F-529] c05 N69-32044
SOUTHAMPTON UNIV. /ENGLAND/.
Transient vibration analysis of linear systems using transition matrices
[NASA-CR-1237] c32 N69-11008
The transient response of coupled acousto-mechanical systems
[NASA-CR-1421] c23 N69-35286
SPERRY RAND CORP., HUNTSVILLE, ALA.
Computer-aided filter design manual
[NASA-SP-3049] c08 N69-35816
STANFORD RESEARCH INST., MENLO PARK, CALIF.
Comparative evaluation of ablating materials in arc plasma jets
[NASA-CR-1207] c33 N69-14171
Human intellect augmentation techniques Final report
[NASA-CR-1270] c08 N69-16140
Characteristics of the tactile information channel
[NASA-CR-1389] c05 N69-39211
STANFORD UNIV., CALIF.
Approximating properties of linear models for input-output descriptions
[NASA-CR-1319] c18 N69-26248
Analysis of oscillations in pulse-modulated satellite attitude control systems
[NASA-CR-1369] c21 N69-29967
Minimum fuel attitude control of a nonlinear satellite system with bounded control by a method based on linear programming
[NASA-CR-1450] c21 N69-41036
STENCEL AERO ENGINEERING CORP., ASHEVILLE, N. C.
Human survival in aircraft emergencies
[NASA-CR-1262] c02 N69-14763
SYSTEM DEVELOPMENT CORP., SANTA MONICA, CALIF.
Hand-printed input for on-line systems
[NASA-CR-1284] c08 N69-21527
SYSTEMS TECHNOLOGY, INC., HAWTHORNE, CALIF.
Small perturbation dynamics of the neuromuscular system in tracking tasks
[NASA-CR-1212] c05 N69-14212
Measurement of pilot describing functions in single-controller multiloop tasks
[NASA-CR-1238] c05 N69-15372
Dynamics of the vestibular system and their relation to motion perception, spatial disorientation, and illusions
[NASA-CR-1309] c04 N69-22637
Experiments and a model for pilot dynamics with visual and motion inputs
[NASA-CR-1325] c05 N69-28071

T

TECHTRAN CORP., GLEN BURNIE, MD.
Some problems of the physics of high energies and cosmic rays
[NASA-TT-F-535] c29 N69-24924
From a scientific heritage
[NASA-TT-F-541] c34 N69-26112
High-velocity hydrodynamics, no. 4
[NASA-TT-F-577] c12 N69-29235
Motion of artificial satellites in the earth's gravitational field
[NASA-TT-F-539] c30 N69-33560
Mechanisms with elastic couplings - Dynamics and stability
[NASA-TT-F-534] c15 N69-35859
Radiophysics - Radiophysical investigations of Venus, 1965 - 1966
[NASA-TT-F-536] c30 N69-38643
Optimal transfers between close elliptical orbits
[NASA-TT-F-554] c30 N69-40592
TEMPLE UNIV. RESEARCH INST., PHILADELPHIA, PA.
Development of a barium chemical release system
[NASA-CR-1415] c13 N69-35660
TENNESSEE UNIV., TULLAHOMA.
An experimental and theoretical investigation of striations in a He-Ne laser
[NASA-CR-1387] c08 N69-32350
TEXAS INSTRUMENTS, INC., DALLAS.
Reliability handbook for silicon monolithic microcircuits. Volume 1 - Application of monolithic microcircuits
[NASA-CR-1346] c09 N69-23225
Reliability handbook for silicon monolithic microcircuits. Volume 2 - Failure mechanisms of monolithic microcircuits
[NASA-CR-1347] c09 N69-23226
Reliability handbook for silicon monolithic microcircuits. Volume 3 - Failure analysis of monolithic microcircuits
[NASA-CR-1348] c09 N69-25328
TEXAS TECHNOLOGICAL COLL., LUBBOCK.
Removal of acid gases and oxides of nitrogen from space cabin atmospheres
[NASA-CR-1388] c05 N69-37517
TEXAS UNIV., AUSTIN.
An application of similitude to model design of a soil-projectile system
[NASA-CR-1210] c34 N69-13159
Force-penetration characteristics of a sand horizontally penetrated by plates, cones, and spherical segments
[NASA-CR-1252] c18 N69-14764
TEXAS WESTERN COLL., EL PASO.
Exametnet data report series Annual report, 1966
[NASA-SP-175] c20 N69-16214
TRW SYSTEMS GROUP, REDONDO BEACH, CALIF.
An experimental feasibility study for the preparation of thermo-oxidatively stable Pyrrone laminates
[NASA-CR-1404] c30 N69-31960
Heat pipe devices for space suit temperature control Research report, 30 Jun. 1966 - 1 Sep. 1968
[NASA-CR-1400] c05 N69-38491
Sequential processing techniques for trajectory estimation
[NASA-CR-1360] c30 N69-40325
TRW SYSTEMS, REDONDO BEACH, CALIF.
Batteries for space power systems
[NASA-SP-172] c03 N69-18042
Some optimal branched trajectories
[NASA-CR-1331] c30 N69-24950
TRW, INC., CLEVELAND, OHIO.
Mechanical behavior of tantalum-base T-111 alloy at elevated temperature
[NASA-CR-1436] c17 N69-36831

U

UNION CARBIDE CORP., TONAWANDA, N. Y.
Biochemical and metabolic effects of a six- month exposure of small animals to a helium- oxygen atmosphere
[NASA-CR-1372] c04 N69-40955
UNITED AIRCRAFT CORP., EAST HARTFORD, CONN.
Brayton-cycle turbomachinery rolling-element bearings
[NASA-CR-1229] c15 N69-16463
Properties of high emittance materials
[NASA-CR-1278] c17 N69-18952
Theoretical investigation of the composition and line emission characteristics of argon-tungsten and argon-uranium plasmas
[NASA-CR-1313] c25 N69-21124
Theoretical investigations of RF induction heated plasmas
[NASA-CR-1312] c25 N69-22638
Experimental investigation of the spectral emission characteristics of argon-tungsten and argon-uranium induction heated plasmas
[NASA-CR-1314] c25 N69-22920
Initial radio-frequency gas heating experiments to simulate the thermal environment in a nuclear light bulb reactor
[NASA-CR-1311] c22 N69-23450
Nuclear studies of the nuclear light bulb rocket engine
[NASA-CR-1315] c25 N69-23451
Simplified procedures for estimating flapwise bending moments on helicopter rotor blades. Part 2 - Tables
[NASA-CR-1441] c32 N69-40359
UNIVERSITY OF SOUTHERN CALIF., LOS ANGELES.
Evaluation of the Goddard research and engineering management exercise simulation
[NASA-CR-1275] c34 N69-18057
UTAH UNIV., SALT LAKE CITY.
Theoretical comparison of beads, wires, and films as rocketsonde temperature sensors in the mesosphere
[NASA-CR-1286] c13 N69-18126

V

VARIAN ASSOCIATES, SAN CARLOS, CALIF.
Solubility and diffusion of oxygen in tantalum
[NASA-CR-1276] c17 N69-19886
VIRGINIA UNIV., CHARLOTTESVILLE.
The thin film iris
[NASA-CR-1364] c26 N69-28096
Rigid rotor dynamics
[NASA-CR-1391] c15 N69-36349

W

WASHINGTON UNIV., SEATTLE.
Photoviscoelastic model testing
[NASA-CR-1289] c32 N69-17770
WEBB ASSOCIATES, MALIBU, CALIF.
Preliminary evaluation test of the Langley cardiovascular conditioning suit concept
[NASA-CR-1206] c05 N69-13202
WESTINGHOUSE ELECTRIC CORP., LIMA, OHIO.
High-temperature capacitor feasibility
[NASA-CR-1213] c18 N69-14400
Inverter-converter parallel operation
[NASA-CR-1224] c03 N69-16379
Evaluation of magnetic materials for static inverters and converters
[NASA-CR-1226] c03 N69-17765
Inverter-converter automatic paralleling and protection
[NASA-CR-1225] c10 N69-19003
WESTINGHOUSE ELECTRIC CORP., PITTSBURGH, PA.
Solid electrolyte system for oxygen regeneration
[NASA-CR-1359] c05 N69-28099
WESTON INSTRUMENTS, INC., COLLEGE PARK, MD.
Degradation of multiplier phototubes exposed to spatial radiations
[NASA-CR-1304] c14 N69-20777
WHITTAKER CORP., SAN DIEGO, CALIF.
Electrochemical characterization of nonaqueous systems for secondary battery application
[NASA-CR-1434] c03 N69-36829
WICHITA STATE UNIV., KANS.
Some equilibrium and free vibration problems associated with centrifugally stabilized disk and shell structures
[NASA-CR-1178] c32 N69-14477
WOLF RESEARCH AND DEVELOPMENT CORP., BLADENSBURG, MD.
A survey of current debugging concepts
[NASA-CR-1397] c08 N69-35613
WYLE LABS., INC., HUNTSVILLE, ALA.
Theoretical studies of compressor noise
[NASA-CR-1287] c28 N69-21476

REPORT/ACCESSION NUMBER INDEX

NASA SCIENTIFIC AND TECHNICAL REPORTS AND PUBLICATIONS FOR 1969

A Selected Listing

Typical Report/Accession Number Index Listing

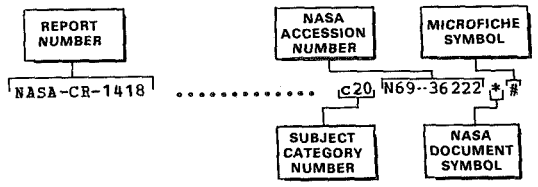

Listings in this index are arranged alphanumerically by report number. The subject category number indicates the subject category in the abstract section in which the citation is located. The accession number denotes the number by which the citation is identified within the subject category. An asterisk (*) indicates that the item is a NASA report. A pound sign (#) indicates that the item is available on microfiche.

A-2894 ..... c01 N69-38775*#
A-3252 ..... c32 N69-38809*#
A-3299 ..... c02 N69-38807*#

AI-68-110 ..... c17 N69-27059*#

APO-68-1101 ..... c17 N69-19886*#

ARC-R-280 ..... c17 N69-11420*#
ARC-R-297 ..... c31 N69-28861*#
ARC-R-299 ..... c32 N69-38781*#
ARC-R-310 ..... c32 N69-26234*#

BAC-2099-956005 ..... c28 N69-40776*#

BBN-1681 ..... c05 N69-14145*#
BBN-1703 ..... c32 N69-26315*#
BBN-1734 ..... c23 N69-26307*#

BMSD-6182 ..... c31 N69-26993*#

BSD-68-643 ..... c05 N69-14478*#
BSD-69-701 ..... c05 N69-36925*#

C-78 ..... c07 N69-39264*#
C-85 ..... c09 N69-38774*#

CAL-AD-1689-A-10 ..... c12 N69-34709*#

CAL-IM-2429-B-1 ..... c02 N69-13185*#

DAC-58155 ..... c05 N69-35541*#
DAC-58156 ..... c05 N69-35540*#
DAC-66900 ..... c01 N69-10343*#

DAD-66898 ..... c01 N69-12286*
DAD-66899 ..... c01 N69-12286*

E-4863 ..... c08 N69-38654*#
E-4919 ..... c22 N69-36757*#
E-4950 ..... c32 N69-39393*#
E-5011 ..... c17 N69-38794*#
E-5032 ..... c26 N69-39239*#
E-5075 ..... c24 N69-39184*#
E-5079 ..... c22 N69-35817*#
E-5098 ..... c17 N69-39182*#
E-5102 ..... c28 N69-38599*#
E-5106 ..... c12 N69-39916*#
E-5130 ..... c03 N69-39238*#
E-5144 ..... c28 N69-39185*#
E-5147 ..... c24 N69-39187*#
E-5154 ..... c24 N69-38773*#
E-5163 ..... c12 N69-41213*#
E-5182 ..... c03 N69-39335*#
E-5185 ..... c09 N69-38776*#
E-5190 ..... c12 N69-39303*#

EDR-4909-VOL-4 ..... c28 N69-24223*#
EDR-5315-VOL-2 ..... c01 N69-25327*#
EDR-5315-VOL-4 ..... c28 N69-36680*#

EE-4012-111-69U ..... c26 N69-28096*#

ER-7365 ..... c17 N69-36831*#

ERA-67-7 ..... c05 N69-19902*#
ERA-68-1 ..... c05 N69-36709*#

ERL-69-2 ..... c19 N69-37033*#

F-B2263 ..... c15 N69-19775*#

F-C1859 ..... c15 N69-10298*#

G-910091-17 ..... c22 N69-23450*#
G-910091-18 ..... c25 N69-22638*#
G-910092-10 ..... c25 N69-21124*#
G-910092-11 ..... c25 N69-22920*#
G-910375-3 ..... c25 N69-23451*#

GASL-TR-713 ..... c02 N69-31959*#

GCA-TR-69-5-N ..... c20 N69-35528*#

GDC-DBE-68-008 ..... c25 N69-17212*#
GDC-DBE-68-011 ..... c13 N69-31961*#

GDC-DDE-68-001 ..... c31 N69-27299*#

GER-14188 ..... c17 N69-36367*#

GESP-9001 ..... c03 N69-32553*#

GEST-2107 ..... c03 N69-35689*#

IBM-150 ..... c30 N69-36439*#

IITRI-V6045 ..... c09 N69-18761*#

ISR-2 ..... c21 N69-34672*#

KAMAN-R-741 ..... c15 N69-16104*#

KN-67-698-2 ..... c23 N69-23199*#
KN-68-698-4 ..... c23 N69-22545*#

L-6019 ..... c32 N69-41141*#
L-6052 ..... c19 N69-38655*#
L-6260 ..... c02 N69-39188*#
L-6382 ..... c05 N69-39183*#
L-6383 ..... c33 N69-29599*#
L-6679 ..... c25 N69-39302*#
L-6695 ..... c02 N69-40937*#

LMSC-4-17-68-4 ..... c01 N69-35521*#
LMSC-681796 ..... c25 N69-38227*#

LR-21588 ..... c20 N69-13629*#

M-146 ..... c30 N69-39336*#

MAC-709-10 ..... c31 N69-16155*#

MTI-67TR29 ..... c15 N69-21772*#

N-07-68-1 ..... c08 N69-23381*#

REPORT NUMBER INDEX

NAA-SR-12629	c22	N69-22946 #
NASA-CR-835	c31	N69-27299*#
NASA-CR-976	c21	N69-21502*#
NASA-CR-1134	c05	N69-10813*#
NASA-CR-1135	c03	N69-11373*#
NASA-CR-1146	c05	N69-19902*#
NASA-CR-1157	c15	N69-14214*#
NASA-CR-1178	c32	N69-14477*#
NASA-CR-1179	c08	N69-10316*#
NASA-CR-1183	c08	N69-11470*#
NASA-CR-1196	c32	N69-10225*#
NASA-CR-1203	c15	N69-10298*#
NASA-CR-1204	c20	N69-13629*#
NASA-CR-1205-VOL-1	c04	N69-12434*#
NASA-CR-1205-VOL-2	c04	N69-12588*#
NASA-CR-1205-VOL-3	c04	N69-12592*#
NASA-CR-1205-VOL-4	c04	N69-12600*#
NASA-CR-1206	c05	N69-13202*#
NASA-CR-1207	c33	N69-14171*#
NASA-CR-1208	c02	N69-13185*#
NASA-CR-1209	c31	N69-16221*#
NASA-CR-1210	c34	N69-13159*#
NASA-CR-1212	c05	N69-14212*#
NASA-CR-1213	c18	N69-14400*#
NASA-CR-1214	c05	N69-13161*#
NASA-CR-1215	c32	N69-16114*#
NASA-CR-1216	c03	N69-14397*#
NASA-CR-1217	c32	N69-14254*#
NASA-CR-1218	c01	N69-10343*#
NASA-CR-1218-SUPPL	c01	N69-12286*
NASA-CR-1219	c01	N69-14211*#
NASA-CR-1223	c05	N69-13969*#
NASA-CR-1224	c03	N69-16379*#
NASA-CR-1225	c10	N69-19003*#
NASA-CR-1226	c03	N69-17765*#
NASA-CR-1227	c31	N69-16155*#
NASA-CR-1228	c09	N69-14256*#
NASA-CR-1229	c15	N69-16463*#
NASA-CR-1230	c12	N69-17751*#
NASA-CR-1231	c32	N69-11010*#
NASA-CR-1232	c17	N69-11420*#
NASA-CR-1233-VOL-1	c05	N69-11675*#
NASA-CR-1234	c05	N69-14979*#
NASA-CR-1235	c05	N69-14213*#
NASA-CR-1236	c26	N69-10817*#
NASA-CR-1237	c32	N69-11008*#
NASA-CR-1238	c05	N69-15372*#
NASA-CR-1239	c05	N69-14478*#
NASA-CR-1240	c02	N69-14729*#
NASA-CR-1241	c15	N69-16104*#
NASA-CR-1244	c03	N69-18885*#
NASA-CR-1245	c12	N69-14095*#
NASA-CR-1247	c19	N69-11419*#
NASA-CR-1248	c05	N69-14768*#
NASA-CR-1249	c30	N69-13300*#
NASA-CR-1250	c30	N69-13274*#
NASA-CR-1251	c05	N69-13926*#
NASA-CR-1252	c18	N69-14764*#
NASA-CR-1253	c13	N69-16645*#
NASA-CR-1254	c01	N69-13621*#
NASA-CR-1255	c05	N69-14094*#
NASA-CR-1256	c28	N69-14210*#
NASA-CR-1257	c14	N69-16100*#
NASA-CR-1258	c05	N69-14145*#
NASA-CR-1259	c05	N69-16212*#
NASA-CR-1260	c03	N69-15382*#
NASA-CR-1261	c05	N69-14345*#
NASA-CR-1262	c02	N69-14763*#
NASA-CR-1263	c32	N69-16156*#
NASA-CR-1264	c33	N69-19117*#
NASA-CR-1265	c33	N69-17438*#
NASA-CR-1266	c33	N69-18125*#
NASA-CR-1267	c25	N69-18041*#
NASA-CR-1268	c09	N69-18761*#
NASA-CR-1269	c32	N69-17766*#
NASA-CR-1270	c08	N69-16140*#
NASA-CR-1271	c14	N69-16099*#
NASA-CR-1272	c19	N69-21143*#
NASA-CR-1273	c32	N69-19030*#
NASA-CR-1274	c05	N69-17738*#
NASA-CR-1275	c34	N69-18057*#
NASA-CR-1276	c17	N69-19886*#
NASA-CR-1278	c17	N69-18952*#
NASA-CR-1279	c30	N69-21506*#
NASA-CR-1280	c32	N69-15378*#
NASA-CR-1281	c32	N69-21403*#
NASA-CR-1282	c14	N69-18953*#
NASA-CR-1283	c04	N69-18722*#
NASA-CR-1284	c08	N69-21527*#
NASA-CR-1285	c02	N69-20848*#
NASA-CR-1286	c13	N69-18126*#
NASA-CR-1287	c28	N69-21476*#
NASA-CR-1288	c15	N69-19786*#
NASA-CR-1289	c32	N69-17770*#
NASA-CR-1290	c03	N69-21771*#
NASA-CR-1291	c15	N69-21772*#
NASA-CR-1292	c15	N69-19775*#
NASA-CR-1293	c13	N69-18700*#
NASA-CR-1294	c19	N69-17249*#
NASA-CR-1296	c05	N69-22766*#
NASA-CR-1297	c01	N69-21477*#
NASA-CR-1298	c14	N69-21117*#
NASA-CR-1299	c02	N69-22546*#
NASA-CR-1300	c14	N69-28402*#
NASA-CR-1301	c32	N69-26234*#
NASA-CR-1302	c32	N69-23096*#
NASA-CR-1303	c12	N69-21653*#
NASA-CR-1304	c14	N69-20777*#
NASA-CR-1305	c17	N69-19831*#
NASA-CR-1306	c32	N69-22983*#
NASA-CR-1307	c01	N69-34703*#
NASA-CR-1308	c07	N69-28223*#
NASA-CR-1309	c04	N69-22637*#
NASA-CR-1310	c18	N69-26448*#
NASA-CR-1311	c22	N69-23450*#
NASA-CR-1312	c25	N69-22638*#
NASA-CR-1313	c25	N69-21124*#
NASA-CR-1314	c25	N69-22920*#
NASA-CR-1315	c25	N69-23451*#
NASA-CR-1316	c32	N69-28164*#
NASA-CR-1317	c32	N69-24056*#
NASA-CR-1318	c08	N69-23381*#
NASA-CR-1319	c19	N69-26248*#
NASA-CR-1320	c32	N69-21569*#
NASA-CR-1321	c32	N69-21401*#
NASA-CR-1322	c32	N69-22982*#
NASA-CR-1323	c01	N69-25327*#
NASA-CR-1324	c32	N69-24876*#
NASA-CR-1325	c05	N69-28071*#
NASA-CR-1326	c07	N69-26273*#
NASA-CR-1327	c07	N69-24059*#
NASA-CR-1328	c19	N69-28196*#
NASA-CR-1329	c31	N69-28861*#
NASA-CR-1330	c07	N69-32721*#
NASA-CR-1331	c30	N69-24950*#
NASA-CR-1332	c32	N69-34744*#
NASA-CR-1333	c23	N69-25344*#
NASA-CR-1334	c05	N69-27266*#
NASA-CR-1335	c12	N69-30728*#
NASA-CR-1336	c12	N69-24058*#
NASA-CR-1337	c23	N69-23199*#
NASA-CR-1338	c23	N69-22545*#
NASA-CR-1339	c01	N69-35521*#
NASA-CR-1340	c23	N69-26307*#
NASA-CR-1341	c01	N69-23892*#
NASA-CR-1342	c28	N69-24223*#
NASA-CR-1343	c22	N69-24055*#
NASA-CR-1344	c21	N69-26232*#
NASA-CR-1345	c19	N69-29268*#
NASA-CR-1346	c09	N69-23225*#
NASA-CR-1347	c09	N69-23226*#
NASA-CR-1348	c09	N69-25328*#
NASA-CR-1350	c32	N69-28624*#
NASA-CR-1351	c32	N69-26315*#
NASA-CR-1352	c11	N69-24089*#
NASA-CR-1353	c11	N69-25343*#
NASA-CR-1354	c11	N69-28095*#
NASA-CR-1355	c34	N69-28868*#
NASA-CR-1356	c19	N69-28256*#
NASA-CR-1357	c32	N69-26559*#
NASA-CR-1358	c14	N69-28023*#
NASA-CR-1359	c05	N69-28099*#
NASA-CR-1360	c30	N69-40325*#
NASA-CR-1361	c31	N69-26993*#
NASA-CR-1362	c12	N69-24877*#
NASA-CR-1363	c12	N69-24926*#
NASA-CR-1364	c26	N69-28096*#
NASA-CR-1365	c32	N69-36357*#
NASA-CR-1366	c26	N69-29724*#
NASA-CR-1367	c18	N69-29559*#
NASA-CR-1368	c12	N69-24958*#
NASA-CR-1369	c21	N69-29967*#
NASA-CR-1370	c05	N69-30168*#
NASA-CR-1371	c17	N69-27059*#
NASA-CR-1372	c04	N69-40955*#
NASA-CR-1373	c23	N69-36974*#

NASA-CR-1374 ..... c16 N69-29934*#
NASA-CR-1375 ..... c14 N69-37876*#
NASA-CR-1376 ..... c32 N69-29558*#
NASA-CR-1377 ..... c24 N69-33416*#
NASA-CR-1378 ..... c02 N69-31959*#
NASA-CR-1379 ..... c30 N69-31362*#
NASA-CR-1381 ..... c03 N69-35689*#
NASA-CR-1382 ..... c12 N69-31887*#
NASA-CR-1383 ..... c24 N69-34541*#
NASA-CR-1384 ..... c18 N69-36762*#
NASA-CR-1385 ..... c19 N69-34360*#
NASA-CR-1386 ..... c12 N69-32480*#
NASA-CR-1387 ..... c08 N69-32350*#
NASA-CR-1388 ..... c05 N69-37517*#
NASA-CR-1389 ..... c05 N69-39211*#
NASA-CR-1390 ..... c25 N69-38227*#
NASA-CR-1391 ..... c15 N69-36349*#
NASA-CR-1392 ..... c01 N69-30609*#
NASA-CR-1393 ..... c25 N69-34897*#
NASA-CR-1394 ..... c14 N69-31958*#
NASA-CR-1395 ..... c05 N69-38600*#
NASA-CR-1396 ..... c21 N69-34672*#
NASA-CR-1397 ..... c08 N69-35613*#
NASA-CR-1398 ..... c02 N69-34915*#
NASA-CR-1399 ..... c11 N69-37022*#
NASA-CR-1400 ..... c05 N69-38491*#
NASA-CR-1401 ..... c15 N69-33450*#
NASA-CR-1402 ..... c05 N69-37964*#
NASA-CR-1403 ..... c05 N69-36271*#
NASA-CR-1404 ..... c30 N69-31960*#
NASA-CR-1405 ..... c05 N69-36709*#
NASA-CR-1406 ..... c24 N69-38564*#
NASA-CR-1407 ..... c06 N69-33493*#
NASA-CR-1408 ..... c05 N69-35541*#
NASA-CR-1409 ..... c05 N69-35540*#
NASA-CR-1410 ..... c20 N69-35570*#
NASA-CR-1411 ..... c12 N69-34709*#
NASA-CR-1412 ..... c30 N69-35513*#
NASA-CR-1413 ..... c17 N69-35514*#
NASA-CR-1414 ..... c33 N69-35516*#
NASA-CR-1415 ..... c13 N69-35660*#
NASA-CR-1416 ..... c03 N69-32553*#
NASA-CR-1417 ..... c03 N69-36411*#
NASA-CR-1418 ..... c20 N69-36222*#
NASA-CR-1419 ..... c20 N69-35528*#
NASA-CR-1420 ..... c17 N69-36723*#
NASA-CR-1421 ..... c23 N69-35286*#
NASA-CR-1422 ..... c05 N69-39212*#
NASA-CR-1423 ..... c28 N69-36680*#
NASA-CR-1424 ..... c32 N69-35515*#
NASA-CR-1425 ..... c06 N69-36413*#
NASA-CR-1426 ..... c02 N69-38819*#
NASA-CR-1427 ..... c02 N69-38657*#
NASA-CR-1428 ..... c02 N69-35861*#
NASA-CR-1430 ..... c30 N69-36439*#
NASA-CR-1431 ..... c33 N69-40455*#
NASA-CR-1432 ..... c19 N69-37033*#
NASA-CR-1433 ..... c17 N69-36367*#
NASA-CR-1434 ..... c03 N69-36829*#
NASA-CR-1435 ..... c03 N69-36843*#
NASA-CR-1436 ..... c17 N69-36831*#
NASA-CR-1437 ..... c32 N69-40935*#
NASA-CR-1438 ..... c04 N69-37062*#
NASA-CR-1439 ..... c05 N69-36925*#
NASA-CR-1441 ..... c32 N69-40359*#
NASA-CR-1442 ..... c07 N69-39282*#
NASA-CR-1443 ..... c21 N69-38041*#
NASA-CR-1444 ..... c32 N69-38781*#
NASA-CR-1445 ..... c28 N69-40776*#
NASA-CR-1447 ..... c17 N69-40057*#
NASA-CR-1448 ..... c12 N69-40200*#
NASA-CR-1449 ..... c30 N69-40062*#
NASA-CR-1450 ..... c21 N69-41036*#
NASA-CR-1467 ..... c12 N69-38782*#
NASA-CR-1472 ..... c02 N69-40439*#

NASA-SP-35-PT-8 ..... c30 N69-34850*#
NASA-SP-35-VOL-3-PT-7 ..... c30 N69-33490*#
NASA-SP-151 ..... c31 N69-21065*#
NASA-SP-161 ..... c04 N69-10444*#
NASA-SP-162 ..... c30 N69-13844*#
NASA-SP-164-VOL-2 ..... c33 N69-30317*#
NASA-SP-167 ..... c30 N69-25460*#
NASA-SP-171 ..... c14 N69-28909*
NASA-SP-172 ..... c03 N69-18042*#
NASA-SP-174 ..... c30 N69-33595*#
NASA-SP-175 ..... c20 N69-16214*#
NASA-SP-176 ..... c20 N69-22570*#
NASA-SP-177 ..... c30 N69-22226*#

NASA-SP-179 ..... c30 N69-16571*#
NASA-SP-181 ..... c15 N69-30401*#
NASA-SP-183 ..... c12 N69-10693*#
NASA-SP-184 ..... c30 N69-36451*#
NASA-SP-189 ..... c02 N69-11542*#
NASA-SP-193 ..... c14 N69-33322*#
NASA-SP-195 ..... c34 N69-38951*#
NASA-SP-196-VOL-1 ..... c34 N69-22510*#
NASA-SP-197 ..... c30 N69-39213*#
NASA-SP-199 ..... c29 N69-29652*#
NASA-SP-211 ..... c34 N69-39957*#
NASA-SP-212 ..... c20 N69-39526*#
NASA-SP-213 ..... c30 N69-41150*#
NASA-SP-3024-VOL-5 ..... c24 N69-28911*#
NASA-SP-3045 ..... c12 N69-26987*#
NASA-SP-3046 ..... c12 N69-16098*#
NASA-SP-3047-REV ..... c30 N69-37993*#
NASA-SP-3048 ..... c01 N69-25391*#
NASA-SP-3049 ..... c08 N69-35816*#
NASA-SP-3050 ..... c30 N69-37777*#
NASA-SP-4002 ..... c31 N69-36501*#
NASA-SP-4009 ..... c31 N69-32021*#
NASA-SP-5048 ..... c34 N69-10662*#
NASA-SP-5051 ..... c17 N69-14193*#
NASA-SP-5052 ..... c15 N69-14241*#
NASA-SP-5054 ..... c04 N69-14860*#
NASA-SP-5056 ..... c13 N69-10492*#
NASA-SP-5057 ..... c03 N69-12575*#
NASA-SP-5058 ..... c15 N69-28592*#
NASA-SP-5070 ..... c05 N69-21478*#
NASA-SP-5071 ..... c03 N69-23643*#
NASA-SP-5072 ..... c14 N69-24751*#
NASA-SP-5073 ..... c11 N69-20451*#
NASA-SP-5074 ..... c05 N69-33775*#
NASA-SP-5075 ..... c34 N69-31946*#
NASA-SP-5080 ..... c07 N69-31985*#
NASA-SP-7011/55/ ..... c04 N69-11695*#
NASA-SP-7011/56/ ..... c04 N69-14387*#
NASA-SP-7011/57/ ..... c04 N69-16537*#
NASA-SP-7011/58/ ..... c04 N69-19023*#
NASA-SP-7011/59/ ..... c04 N69-24752*#
NASA-SP-7011/60/ ..... c04 N69-19714*#
NASA-SP-7011/61/ ..... c04 N69-23126*#
NASA-SP-7011/62/ ..... c04 N69-24822*#
NASA-SP-7011/63/ ..... c04 N69-38235*#
NASA-SP-7011/64/ ..... c04 N69-38242*#
NASA-SP-7011/65/ ..... c04 N69-31923*#
NASA-SP-7011/66/ ..... c04 N69-37909*#
NASA-SP-7011/67/ ..... c04 N69-37887*#
NASA-SP-7033 ..... c34 N69-29492*#
NASA-SP-7500/03/ ..... c34 N69-32430*#
NASA-SP-7501 ..... c34 N69-34917*#
NASA-SP-8007 ..... c32 N69-23320*#
NASA-SP-8009 ..... c32 N69-14553*#
NASA-SP-8011 ..... c30 N69-20916*#
NASA-SP-8012 ..... c32 N69-22773*#
NASA-SP-8013 ..... c30 N69-40326*#
NASA-SP-8015 ..... c21 N69-19518*#
NASA-SP-8016 ..... c31 N69-37030*#
NASA-SP-8017 ..... c31 N69-40269*#
NASA-SP-8018 ..... c31 N69-30339*#
NASA-SP-8019 ..... c32 N69-24131*#

NASA-TM-X-1602 ..... c02 N69-34988*#
NASA-TM-X-1654 ..... c14 N69-13176*#
NASA-TM-X-1676 ..... c28 N69-13275*#
NASA-TM-X-1678 ..... c31 N69-10295*#
NASA-TM-X-1684 ..... c01 N69-10732*#
NASA-TM-X-1685 ..... c22 N69-10067*#
NASA-TM-X-1688 ..... c18 N69-10066*#
NASA-TM-X-1689 ..... c12 N69-10293*#
NASA-TM-X-1692 ..... c01 N69-10294*#
NASA-TM-X-1696 ..... c28 N69-10296*#
NASA-TM-X-1697 ..... c01 N69-10558*#
NASA-TM-X-1698 ..... c03 N69-13246*#
NASA-TM-X-1699 ..... c28 N69-13237*#
NASA-TM-X-1700 ..... c08 N69-13566*#
NASA-TM-X-1701 ..... c01 N69-13218*#
NASA-TM-X-1702 ..... c24 N69-13210*#
NASA-TM-X-1706 ..... c01 N69-13154*#
NASA-TM-X-1707 ..... c19 N69-14002*#
NASA-TM-X-1708 ..... c31 N69-14033*#
NASA-TM-X-1709 ..... c28 N69-14313*#
NASA-TM-X-1710 ..... c01 N69-14075*#
NASA-TM-X-1711 ..... c26 N69-14086*#
NASA-TM-X-1715 ..... c03 N69-14312*#
NASA-TM-X-1716 ..... c12 N69-15371*#
NASA-TM-X-1718 ..... c24 N69-14398*#
NASA-TM-X-1719 ..... c12 N69-15473*#

REPORT NUMBER INDEX

NASA-TM-X-1720 ..... c28 N69-16152*#
NASA-TM-X-1721 ..... c28 N69-15475*#
NASA-TM-X-1722 ..... c03 N69-15397*#
NASA-TM-X-1723 ..... c32 N69-16115*#
NASA-TM-X-1724 ..... c01 N69-16467*#
NASA-TM-X-1726 ..... c20 N69-17772*#
NASA-TM-X-1727 ..... c28 N69-16213*#
NASA-TM-X-1728 ..... c01 N69-17392*#
NASA-TM-X-1729 ..... c03 N69-17225*#
NASA-TM-X-1730 ..... c01 N69-16209*#
NASA-TM-X-1731 ..... c03 N69-20828*#
NASA-TM-X-1732 ..... c03 N69-20868*#
NASA-TM-X-1733 ..... c14 N69-16382*#
NASA-TM-X-1734 ..... c30 N69-17815*#
NASA-TM-X-1735 ..... c22 N69-17701*#
NASA-TM-X-1736 ..... c14 N69-17702*#
NASA-TM-X-1737 ..... c28 N69-19017*#
NASA-TM-X-1738 ..... c25 N69-19131*#
NASA-TM-X-1739 ..... c01 N69-19130*#
NASA-TM-X-1740 ..... c01 N69-17818*#
NASA-TM-X-1741 ..... c03 N69-20913*#
NASA-TM-X-1742 ..... c28 N69-17781*#
NASA-TM-X-1746 ..... c06 N69-18962*#
NASA-TM-X-1747 ..... c07 N69-19025*#
NASA-TM-X-1748 ..... c33 N69-18898*#
NASA-TM-X-1749 ..... c08 N69-18954*#
NASA-TM-X-1753 ..... c06 N69-20853*#
NASA-TM-X-1754 ..... c23 N69-20870*#
NASA-TM-X-1756 ..... c28 N69-19782*#
NASA-TM-X-1757 ..... c03 N69-20883*#
NASA-TM-X-1758 ..... c01 N69-20016*#
NASA-TM-X-1759 ..... c01 N69-20873*#
NASA-TM-X-1760 ..... c14 N69-20874*#
NASA-TM-X-1761 ..... c25 N69-20875*#
NASA-TM-X-1762 ..... c08 N69-21119*#
NASA-TM-X-1764 ..... c01 N69-22553*#
NASA-TM-X-1765 ..... c15 N69-22970*#
NASA-TM-X-1766 ..... c15 N69-23768*#
NASA-TM-X-1767 ..... c06 N69-20801*#
NASA-TM-X-1768 ..... c31 N69-21399*#
NASA-TM-X-1769 ..... c22 N69-20854*#
NASA-TM-X-1771 ..... c01 N69-21106*#
NASA-TM-X-1772 ..... c21 N69-22969*#
NASA-TM-X-1773 ..... c31 N69-26458*#
NASA-TM-X-1774 ..... c12 N69-26956*#
NASA-TM-X-1776 ..... c18 N69-23843*#
NASA-TM-X-1777 ..... c28 N69-21648*#
NASA-TM-X-1778 ..... c33 N69-22933*#
NASA-TM-X-1779 ..... c22 N69-22555*#
NASA-TM-X-1780 ..... c28 N69-23519*#
NASA-TM-X-1781 ..... c32 N69-23697*#
NASA-TM-X-1784 ..... c31 N69-24038*#
NASA-TM-X-1785 ..... c01 N69-26976*#
NASA-TM-X-1786 ..... c01 N69-23538*#
NASA-TM-X-1787 ..... c01 N69-29318*#
NASA-TM-X-1788 ..... c02 N69-37976*#
NASA-TM-X-1789 ..... c01 N69-25244*#
NASA-TM-X-1791 ..... c17 N69-25243*#
NASA-TM-X-1792 ..... c28 N69-24938*#
NASA-TM-X-1793 ..... c31 N69-24942*#
NASA-TM-X-1794 ..... c22 N69-26233*#
NASA-TM-X-1795 ..... c22 N69-25305*#
NASA-TM-X-1796 ..... c32 N69-25301*#
NASA-TM-X-1797 ..... c19 N69-25311*#
NASA-TM-X-1798 ..... c01 N69-26312*#
NASA-TM-X-1799 ..... c17 N69-26952*#
NASA-TM-X-1800 ..... c31 N69-27260*#
NASA-TM-X-1802 ..... c22 N69-26231*#
NASA-TM-X-1803 ..... c28 N69-27019*#
NASA-TM-X-1806 ..... c30 N69-29569*#
NASA-TM-X-1807 ..... c26 N69-27840*#
NASA-TM-X-1808 ..... c09 N69-27841*#
NASA-TM-X-1811 ..... c12 N69-27954*#
NASA-TM-X-1812 ..... c22 N69-28212*#
NASA-TM-X-1813 ..... c18 N69-28203*#
NASA-TM-X-1814 ..... c13 N69-33555*#
NASA-TM-X-1815 ..... c15 N69-28862*#
NASA-TM-X-1816 ..... c01 N69-29231*#
NASA-TM-X-1818 ..... c04 N69-29723*#
NASA-TM-X-1819 ..... c03 N69-29555*#
NASA-TM-X-1820 ..... c03 N69-29707*#
NASA-TM-X-1821 ..... c32 N69-29734*#
NASA-TM-X-1822 ..... c22 N69-29593*#
NASA-TM-X-1823 ..... c01 N69-31360*#
NASA-TM-X-1824 ..... c08 N69-30014*#
NASA-TM-X-1825 ..... c11 N69-29737*#
NASA-TM-X-1826 ..... c31 N69-29594*#
NASA-TM-X-1828 ..... c22 N69-29671*#
NASA-TM-X-1832 ..... c14 N69-32682*#
NASA-TM-X-1833 ..... c02 N69-38598*#
NASA-TM-X-1835 ..... c02 N69-30633*#
NASA-TM-X-1836 ..... c01 N69-30632*#
NASA-TM-X-1837 ..... c31 N69-30631*#
NASA-TM-X-1838 ..... c22 N69-31986*#
NASA-TM-X-1839 ..... c01 N69-31875*#
NASA-TM-X-1840 ..... c01 N69-38612*#
NASA-TM-X-1841 ..... c31 N69-32713*#
NASA-TM-X-1842 ..... c28 N69-38599*#
NASA-TM-X-1843 ..... c17 N69-31889*#
NASA-TM-X-1845 ..... c33 N69-32468*#
NASA-TM-X-1846 ..... c33 N69-32683*#
NASA-TM-X-1847 ..... c12 N69-31888*#
NASA-TM-X-1848 ..... c31 N69-33380*#
NASA-TM-X-1850 ..... c20 N69-35523*#
NASA-TM-X-1851 ..... c05 N69-33260*#
NASA-TM-X-1852 ..... c12 N69-32217*#
NASA-TM-X-1853 ..... c22 N69-33132*#
NASA-TM-X-1854 ..... c12 N69-33261*#
NASA-TM-X-1857 ..... c14 N69-34628*#
NASA-TM-X-1858 ..... c22 N69-33273*#
NASA-TM-X-1859 ..... c31 N69-37281*#
NASA-TM-X-1860 ..... c17 N69-34916*#
NASA-TM-X-1861 ..... c28 N69-33806*#
NASA-TM-X-1862 ..... c18 N69-34134*#
NASA-TM-X-1864 ..... c28 N69-34674*#
NASA-TM-X-1867 ..... c17 N69-35764*#
NASA-TM-X-1868 ..... c11 N69-36224*#
NASA-TM-X-1869 ..... c03 N69-39238*#
NASA-TM-X-1870 ..... c28 N69-35712*#
NASA-TM-X-1871 ..... c22 N69-35723*#
NASA-TM-X-1873 ..... c28 N69-35847*#
NASA-TM-X-1874 ..... c22 N69-35817*#
NASA-TM-X-1875 ..... c03 N69-35763*#
NASA-TM-X-1877 ..... c22 N69-35848*#
NASA-TM-X-1878 ..... c24 N69-36901*#
NASA-TM-X-1879 ..... c31 N69-37840*#
NASA-TM-X-1880 ..... c28 N69-36998*#
NASA-TM-X-1881 ..... c33 N69-36806*#
NASA-TM-X-1882 ..... c19 N69-36923*#
NASA-TM-X-1883 ..... c22 N69-36756*#
NASA-TM-X-1884 ..... c03 N69-36758*#
NASA-TM-X-1885 ..... c08 N69-36918*#
NASA-TM-X-1886 ..... c14 N69-38766*#
NASA-TM-X-1887 ..... c20 N69-36976*#
NASA-TM-X-1888 ..... c22 N69-36757*#
NASA-TM-X-1889 ..... c12 N69-37271*#
NASA-TM-X-1892 ..... c09 N69-38774*#
NASA-TM-X-1893 ..... c22 N69-37225*#
NASA-TM-X-1894 ..... c03 N69-37827*#
NASA-TM-X-1895 ..... c01 N69-38065*#
NASA-TM-X-1896 ..... c02 N69-38104*#
NASA-TM-X-1897 ..... c24 N69-38773*#
NASA-TM-X-1899 ..... c03 N69-38767*#
NASA-TM-X-1900 ..... c12 N69-39303*#
NASA-TM-X-1901 ..... c03 N69-39335*#
NASA-TM-X-1902 ..... c24 N69-39187*#
NASA-TM-X-1904 ..... c14 N69-40059*#
NASA-TM-X-1905 ..... c18 N69-40339*#
NASA-TM-X-1907 ..... c22 N69-40060*#
NASA-TM-X-1908 ..... c28 N69-40058*#
NASA-TM-X-1911 ..... c22 N69-40061*#
NASA-TM-X-1912 ..... c03 N69-40440*#
NASA-TM-X-1913 ..... c03 N69-40787*#

NASA-TN-D-3889 ..... c12 N69-14314*#
NASA-TN-D-4024 ..... c23 N69-38180*#
NASA-TN-D-4268 ..... c01 N69-10054*#
NASA-TN-D-4345 ..... c32 N69-25001*#
NASA-TN-D-4351 ..... c15 N69-10370*#
NASA-TN-D-4647 ..... c13 N69-14450*#
NASA-TN-D-4648 ..... c13 N69-14290*#
NASA-TN-D-4726 ..... c02 N69-10733*#
NASA-TN-D-4761 ..... c15 N69-10055*#
NASA-TN-D-4785 ..... c28 N69-16122*#
NASA-TN-D-4798 ..... c24 N69-14448*#
NASA-TN-D-4823 ..... c22 N69-10216*#
NASA-TN-D-4824 ..... c15 N69-10757*#
NASA-TN-D-4825 ..... c07 N69-11011*#
NASA-TN-D-4826 ..... c19 N69-14476*#
NASA-TN-D-4831 ..... c25 N69-10471*#
NASA-TN-D-4832 ..... c02 N69-10495*#
NASA-TN-D-4835 ..... c21 N69-10056*#
NASA-TN-D-4846 ..... c32 N69-10297*#
NASA-TN-D-4852 ..... c21 N69-16503*#
NASA-TN-D-4853 ..... c12 N69-10472*#
NASA-TN-D-4854 ..... c02 N69-10371*#
NASA-TN-D-4856 ..... c02 N69-10935*#
NASA-TN-D-4858 ..... c32 N69-29159*#

NASA-TN-D-4859 ..... c02 N69-14504*#
NASA-TN-D-4861 ..... c21 N69-10069*#
NASA-TN-D-4863 ..... c21 N69-10372*#
NASA-TN-D-4864 ..... c32 N69-10057*#
NASA-TN-D-4865 ..... c01 N69-10215*#
NASA-TN-D-4869 ..... c12 N69-10443*#
NASA-TN-D-4870 ..... c31 N69-10775*#
NASA-TN-D-4871 ..... c31 N69-10934*#
NASA-TN-D-4872 ..... c31 N69-11007*#
NASA-TN-D-4873 ..... c15 N69-10231*#
NASA-TN-D-4874 ..... c03 N69-10088*#
NASA-TN-D-4875 ..... c15 N69-10249*#
NASA-TN-D-4876 ..... c33 N69-10473*#
NASA-TN-D-4877 ..... c17 N69-10764*#
NASA-TN-D-4878 ..... c17 N69-11012*#
NASA-TN-D-4879 ..... c07 N69-10885*#
NASA-TN-D-4880 ..... c20 N69-14505*#
NASA-TN-D-4881 ..... c31 N69-17851*#
NASA-TN-D-4883 ..... c15 N69-10228*#
NASA-TN-D-4884 ..... c17 N69-10226*#
NASA-TN-D-4885 ..... c17 N69-10931*#
NASA-TN-D-4886 ..... c06 N69-10126*#
NASA-TN-D-4887 ..... c33 N69-10420*#
NASA-TN-D-4888 ..... c18 N69-10754*#
NASA-TN-D-4889 ..... c03 N69-10708*#
NASA-TN-D-4890 ..... c02 N69-10087*#
NASA-TN-D-4891 ..... c01 N69-16180*#
NASA-TN-D-4892 ..... c33 N69-10932*#
NASA-TN-D-4893 ..... c10 N69-10755*#
NASA-TN-D-4894 ..... c11 N69-10888*#
NASA-TN-D-4895 ..... c07 N69-13155*#
NASA-TN-D-4896 ..... c30 N69-10756*#
NASA-TN-D-4897 ..... c33 N69-10227*#
NASA-TN-D-4898 ..... c03 N69-10068*#
NASA-TN-D-4899 ..... c12 N69-10070*#
NASA-TN-D-4900 ..... c11 N69-11371*#
NASA-TN-D-4901 ..... c14 N69-10933*#
NASA-TN-D-4902 ..... c19 N69-13368*#
NASA-TN-D-4903 ..... c30 N69-10470*#
NASA-TN-D-4904 ..... c26 N69-10125*#
NASA-TN-D-4905 ..... c21 N69-14346*#
NASA-TN-D-4906 ..... c04 N69-11056*#
NASA-TN-D-4907 ..... c12 N69-10804*#
NASA-TN-D-4908 ..... c31 N69-14010*#
NASA-TN-D-4909 ..... c01 N69-10789*#
NASA-TN-D-4910 ..... c23 N69-10889*#
NASA-TN-D-4911 ..... c01 N69-11009*#
NASA-TN-D-4912 ..... c17 N69-10827*#
NASA-TN-D-4913 ..... c22 N69-10734*#
NASA-TN-D-4914 ..... c33 N69-13231*#
NASA-TN-D-4915 ..... c07 N69-13301*#
NASA-TN-D-4916 ..... c31 N69-13232*#
NASA-TN-D-4917 ..... c08 N69-10098*#
NASA-TN-D-4918 ..... c22 N69-13309*#
NASA-TN-D-4919 ..... c01 N69-11634*#
NASA-TN-D-4920 ..... c07 N69-13158*#
NASA-TN-D-4921 ..... c32 N69-13034*#
NASA-TN-D-4922 ..... c22 N69-10099*#
NASA-TN-D-4923 ..... c09 N69-10250*#
NASA-TN-D-4924 ..... c11 N69-14507*#
NASA-TN-D-4925 ..... c14 N69-13311*#
NASA-TN-D-4926 ..... c33 N69-12739*#
NASA-TN-D-4927 ..... c32 N69-14169*#
NASA-TN-D-4928 ..... c01 N69-14000*#
NASA-TN-D-4929 ..... c01 N69-14001*#
NASA-TN-D-4930 ..... c07 N69-23163*#
NASA-TN-D-4931 ..... c02 N69-14008*#
NASA-TN-D-4932 ..... c24 N69-12840*#
NASA-TN-D-4933 ..... c24 N69-12778*#
NASA-TN-D-4934 ..... c15 N69-13256*#
NASA-TN-D-4935 ..... c01 N69-13238*#
NASA-TN-D-4936 ..... c12 N69-13945*#
NASA-TN-D-4937 ..... c33 N69-14501*#
NASA-TN-D-4938 ..... c24 N69-13152*#
NASA-TN-D-4939 ..... c02 N69-13252*#
NASA-TN-D-4940 ..... c20 N69-12934*#
NASA-TN-D-4941 ..... c32 N69-14506*#
NASA-TN-D-4942 ..... c30 N69-14861*#
NASA-TN-D-4943 ..... c01 N69-17398*#
NASA-TN-D-4944 ..... c21 N69-14382*#
NASA-TN-D-4945 ..... c21 N69-14399*#
NASA-TN-D-4946 ..... c22 N69-14503*#
NASA-TN-D-4947 ..... c12 N69-14483*#
NASA-TN-D-4948 ..... c24 N69-14482*#
NASA-TN-D-4949 ..... c22 N69-14481*#
NASA-TN-D-4950 ..... c25 N69-14525*#
NASA-TN-D-4951 ..... c32 N69-14480*#
NASA-TN-D-4952 ..... c21 N69-14332*#
NASA-TN-D-4953 ..... c32 N69-14315*#
NASA-TN-D-4954 ..... c15 N69-14383*#
NASA-TN-D-4955 ..... c17 N69-14403*#
NASA-TN-D-4956 ..... c03 N69-14518*#
NASA-TN-D-4957 ..... c12 N69-14316*#
NASA-TN-D-4958 ..... c28 N69-12831*#
NASA-TN-D-4959 ..... c33 N69-14588*#
NASA-TN-D-4960 ..... c01 N69-14566*#
NASA-TN-D-4961 ..... c01 N69-14872*#
NASA-TN-D-4962 ..... c07 N69-15373*#
NASA-TN-D-4963 ..... c32 N69-15632*#
NASA-TN-D-4964 ..... c32 N69-33481*#
NASA-TN-D-4965 ..... c28 N69-14386*#
NASA-TN-D-4966 ..... c28 N69-17847*#
NASA-TN-D-4967 ..... c15 N69-14082*#
NASA-TN-D-4968 ..... c28 N69-14384*#
NASA-TN-D-4969 ..... c01 N69-14289*#
NASA-TN-D-4970 ..... c26 N69-14565*#
NASA-TN-D-4971 ..... c06 N69-14180*#
NASA-TN-D-4972 ..... c32 N69-16469*#
NASA-TN-D-4973 ..... c14 N69-16097*#
NASA-TN-D-4974 ..... c12 N69-15631*#
NASA-TN-D-4975 ..... c32 N69-14306*#
NASA-TN-D-4976 ..... c12 N69-15630*#
NASA-TN-D-4977 ..... c31 N69-15634*#
NASA-TN-D-4978 ..... c01 N69-14385*#
NASA-TN-D-4979 ..... c30 N69-14479*#
NASA-TN-D-4980 ..... c05 N69-15629*#
NASA-TN-D-4981 ..... c17 N69-14873*#
NASA-TN-D-4982 ..... c24 N69-14288*#
NASA-TN-D-4983 ..... c02 N69-17303*#
NASA-TN-D-4984 ..... c27 N69-19026*#
NASA-TN-D-4985 ..... c11 N69-15633*#
NASA-TN-D-4986 ..... c14 N69-15381*#
NASA-TN-D-4987 ..... c28 N69-20876*#
NASA-TN-D-4988 ..... c32 N69-33232*#
NASA-TN-D-4989 ..... c24 N69-15375*#
NASA-TN-D-4990 ..... c32 N69-16091*#
NASA-TN-D-4991 ..... c27 N69-16153*#
NASA-TN-D-4992 ..... c27 N69-16195*#
NASA-TN-D-4993 ..... c25 N69-16466*#
NASA-TN-D-4994 ..... c15 N69-16197*#
NASA-TN-D-4995 ..... c10 N69-16198*#
NASA-TN-D-4996 ..... c28 N69-16154*#
NASA-TN-D-4997 ..... c07 N69-16162*#
NASA-TN-D-4998 ..... c32 N69-17275*#
NASA-TN-D-4999 ..... c28 N69-17276*#
NASA-TN-D-5000 ..... c17 N69-16465*#
NASA-TN-D-5001 ..... c17 N69-16383*#
NASA-TN-D-5002 ..... c15 N69-16367*#
NASA-TN-D-5003 ..... c01 N69-16121*#
NASA-TN-D-5004 ..... c01 N69-16460*#
NASA-TN-D-5005 ..... c02 N69-16384*#
NASA-TN-D-5006 ..... c33 N69-23471*#
NASA-TN-D-5007 ..... c05 N69-17814*#
NASA-TN-D-5008 ..... c17 N69-16380*#
NASA-TN-D-5009 ..... c15 N69-17988*#
NASA-TN-D-5010 ..... c17 N69-19203*#
NASA-TN-D-5011 ..... c30 N69-17305*#
NASA-TN-D-5012 ..... c22 N69-16381*#
NASA-TN-D-5013 ..... c22 N69-17313*#
NASA-TN-D-5014 ..... c22 N69-17314*#
NASA-TN-D-5015 ..... c14 N69-23470*#
NASA-TN-D-5016 ..... c01 N69-17312*#
NASA-TN-D-5017 ..... c30 N69-16210*#
NASA-TN-D-5018 ..... c02 N69-17257*#
NASA-TN-D-5019 ..... c17 N69-17277*#
NASA-TN-D-5020 ..... c30 N69-21526*#
NASA-TN-D-5021 ..... c04 N69-17248*#
NASA-TN-D-5022 ..... c04 N69-17782*#
NASA-TN-D-5023 ..... c12 N69-17779*#
NASA-TN-D-5024 ..... c32 N69-16211*#
NASA-TN-D-5025 ..... c17 N69-19200*#
NASA-TN-D-5026 ..... c12 N69-17827*#
NASA-TN-D-5027 ..... c06 N69-19129*#
NASA-TN-D-5028 ..... c26 N69-18897*#
NASA-TN-D-5029 ..... c31 N69-20965*#
NASA-TN-D-5030 ..... c01 N69-21000*#
NASA-TN-D-5031 ..... c02 N69-17700*#
NASA-TN-D-5032 ..... c01 N69-17289*#
NASA-TN-D-5034 ..... c13 N69-28019*#
NASA-TN-D-5035 ..... c30 N69-27412*#
NASA-TN-D-5036 ..... c13 N69-28442*#
NASA-TN-D-5037 ..... c21 N69-17780*#
NASA-TN-D-5038 ..... c07 N69-19114*#
NASA-TN-D-5039 ..... c04 N69-19115*#
NASA-TN-D-5040 ..... c02 N69-17279*#
NASA-TN-D-5041 ..... c07 N69-26272*#
NASA-TN-D-5042 ..... c08 N69-26193*#
NASA-TN-D-5043 ..... c30 N69-28050*#

REPORT NUMBER INDEX

NASA-TN-D-5044 ..... c01 N69-21811*#
NASA-TN-D-5045 ..... c01 N69-19027*#
NASA-TN-D-5046 ..... c01 N69-19925*#
NASA-TN-D-5047 ..... c01 N69-19243*#
NASA-TN-D-5048 ..... c01 N69-19926*#
NASA-TN-D-5049 ..... c21 N69-20936*#
NASA-TN-D-5050 ..... c18 N69-19825*#
NASA-TN-D-5051 ..... c31 N69-22630*#
NASA-TN-D-5052 ..... c13 N69-23557*#
NASA-TN-D-5053 ..... c18 N69-19918*#
NASA-TN-D-5054 ..... c01 N69-19826*#
NASA-TN-D-5055 ..... c17 N69-19827*#
NASA-TN-D-5056 ..... c24 N69-19828*#
NASA-TN-D-5057 ..... c01 N69-19641*#
NASA-TN-D-5058 ..... c12 N69-19112*#
NASA-TN-D-5059 ..... c03 N69-19829*#
NASA-TN-D-5060 ..... c30 N69-26235*#
NASA-TN-D-5061 ..... c14 N69-17259*#
NASA-TN-D-5062 ..... c14 N69-17944*#
NASA-TN-D-5063 ..... c33 N69-20008*#
NASA-TN-D-5064 ..... c01 N69-17816*#
NASA-TN-D-5065 ..... c01 N69-17831*#
NASA-TN-D-5066 ..... c24 N69-17976*#
NASA-TN-D-5067 ..... c24 N69-22934*#
NASA-TN-D-5068 ..... c13 N69-19024*#
NASA-TN-D-5069 ..... c32 N69-17737*#
NASA-TN-D-5070 ..... c32 N69-17258*#
NASA-TN-D-5071 ..... c02 N69-19950*#
NASA-TN-D-5072 ..... c03 N69-19799*#
NASA-TN-D-5073 ..... c15 N69-19800*#
NASA-TN-D-5074 ..... c28 N69-19980*#
NASA-TN-D-5075 ..... c24 N69-19113*#
NASA-TN-D-5076 ..... c17 N69-19930*#
NASA-TN-D-5077 ..... c09 N69-20888*#
NASA-TN-D-5078 ..... c25 N69-19783*#
NASA-TN-D-5079 ..... c26 N69-19781*#
NASA-TN-D-5080 ..... c33 N69-20882*#
NASA-TN-D-5081 ..... c07 N69-23882*#
NASA-TN-D-5082 ..... c10 N69-21123*#
NASA-TN-D-5083 ..... c19 N69-20940*#
NASA-TN-D-5084 ..... c01 N69-20914*#
NASA-TN-D-5085 ..... c03 N69-20852*#
NASA-TN-D-5086 ..... c23 N69-29477*#
NASA-TN-D-5087 ..... c07 N69-22949*#
NASA-TN-D-5088 ..... c24 N69-21462*#
NASA-TN-D-5089 ..... c12 N69-29144*#
NASA-TN-D-5090 ..... c03 N69-20937*#
NASA-TN-D-5091 ..... c01 N69-22938*#
NASA-TN-D-5092 ..... c33 N69-23707*#
NASA-TN-D-5093 ..... c17 N69-20789*#
NASA-TN-D-5094 ..... c03 N69-20780*#
NASA-TN-D-5095 ..... c03 N69-20797*#
NASA-TN-D-5096 ..... c15 N69-20938*#
NASA-TN-D-5097 ..... c15 N69-20939*#
NASA-TN-D-5098 ..... c28 N69-21463*#
NASA-TN-D-5099 ..... c31 N69-21017*#
NASA-TN-D-5100 ..... c07 N69-23317*#
NASA-TN-D-5101 ..... c13 N69-23318*#
NASA-TN-D-5102 ..... c02 N69-21020*#
NASA-TN-D-5103 ..... c26 N69-20798*#
NASA-TN-D-5104 ..... c30 N69-22571*#
NASA-TN-D-5105 ..... c30 N69-21018*#
NASA-TN-D-5106 ..... c14 N69-20941*#
NASA-TN-D-5107 ..... c31 N69-21111*#
NASA-TN-D-5108 ..... c32 N69-21042*#
NASA-TN-D-5109 ..... c03 N69-21088*#
NASA-TN-D-5110 ..... c23 N69-20905*#
NASA-TN-D-5111 ..... c05 N69-21501*#
NASA-TN-D-5112 ..... c10 N69-22919*#
NASA-TN-D-5113 ..... c22 N69-20795*#
NASA-TN-D-5114 ..... c18 N69-20790*#
NASA-TN-D-5115 ..... c12 N69-20794*#
NASA-TN-D-5116 ..... c18 N69-21384*#
NASA-TN-D-5117 ..... c30 N69-20810*#
NASA-TN-D-5118 ..... c32 N69-23448*#
NASA-TN-D-5119 ..... c26 N69-22552*#
NASA-TN-D-5120 ..... c30 N69-22939*#
NASA-TN-D-5121 ..... c01 N69-22554*#
NASA-TN-D-5122 ..... c25 N69-22942*#
NASA-TN-D-5123 ..... c11 N69-22629*#
NASA-TN-D-5124 ..... c33 N69-28318*#
NASA-TN-D-5125 ..... c14 N69-21408*#
NASA-TN-D-5126 ..... c11 N69-22989*#
NASA-TN-D-5127 ..... c05 N69-23842*#
NASA-TN-D-5128-REV ..... c02 N69-31962*#
NASA-TN-D-5129 ..... c01 N69-30722*#
NASA-TN-D-5130 ..... c26 N69-22573*#
NASA-TN-D-5131 ..... c32 N69-21814*#
NASA-TN-D-5132 ..... c12 N69-21400*#
NASA-TN-D-5133 ..... c03 N69-21016*#
NASA-TN-D-5134 ..... c01 N69-23769*#
NASA-TN-D-5135 ..... c32 N69-22994*#
NASA-TN-D-5136 ..... c17 N69-21404*#
NASA-TN-D-5137 ..... c26 N69-21500*#
NASA-TN-D-5138 ..... c15 N69-21773*#
NASA-TN-D-5139 ..... c32 N69-22823*#
NASA-TN-D-5140 ..... c32 N69-21392*#
NASA-TN-D-5141 ..... c15 N69-22992*#
NASA-TN-D-5143 ..... c32 N69-22821*#
NASA-TN-D-5144 ..... c03 N69-23356*#
NASA-TN-D-5145 ..... c17 N69-23004*#
NASA-TN-D-5146 ..... c33 N69-22997*#
NASA-TN-D-5147 ..... c12 N69-23085*#
NASA-TN-D-5148 ..... c01 N69-23927*#
NASA-TN-D-5149 ..... c21 N69-22996*#
NASA-TN-D-5150 ..... c21 N69-22936*#
NASA-TN-D-5151 ..... c11 N69-23194*#
NASA-TN-D-5152 ..... c15 N69-26314*#
NASA-TN-D-5153 ..... c02 N69-22539*#
NASA-TN-D-5154 ..... c03 N69-22940*#
NASA-TN-D-5155 ..... c03 N69-22896*#
NASA-TN-D-5156 ..... c31 N69-22937*#
NASA-TN-D-5157 ..... c17 N69-23084*#
NASA-TN-D-5158 ..... c26 N69-22965*#
NASA-TN-D-5159 ..... c32 N69-22932*#
NASA-TN-D-5160 ..... c12 N69-23467*#
NASA-TN-D-5161 ..... c15 N69-23466*#
NASA-TN-D-5162 ..... c05 N69-22990*#
NASA-TN-D-5163 ..... c13 N69-26969*#
NASA-TN-D-5164 ..... c12 N69-24935*#
NASA-TN-D-5165 ..... c08 N69-22935*#
NASA-TN-D-5166 ..... c29 N69-28111*#
NASA-TN-D-5167 ..... c19 N69-22988*#
NASA-TN-D-5168 ..... c33 N69-22931*#
NASA-TN-D-5169 ..... c17 N69-22993*#
NASA-TN-D-5170 ..... c15 N69-23232*#
NASA-TN-D-5171 ..... c33 N69-23351*#
NASA-TN-D-5172 ..... c30 N69-23782*#
NASA-TN-D-5173 ..... c33 N69-26975*#
NASA-TN-D-5174 ..... c14 N69-27267*#
NASA-TN-D-5175 ..... c02 N69-22572*#
NASA-TN-D-5176 ..... c19 N69-23355*#
NASA-TN-D-5177 ..... c06 N69-22991*#
NASA-TN-D-5178 ..... c22 N69-24802*#
NASA-TN-D-5179 ..... c14 N69-23895*#
NASA-TN-D-5180 ..... c07 N69-24051*#
NASA-TN-D-5181 ..... c23 N69-22769*#
NASA-TN-D-5182 ..... c02 N69-26194*#
NASA-TN-D-5183 ..... c09 N69-23556*#
NASA-TN-D-5184 ..... c06 N69-23353*#
NASA-TN-D-5185 ..... c17 N69-23465*#
NASA-TN-D-5186 ..... c21 N69-29595*#
NASA-TN-D-5187 ..... c21 N69-27268*#
NASA-TN-D-5188 ..... c17 N69-36697*#
NASA-TN-D-5189 ..... c30 N69-32316*#
NASA-TN-D-5190 ..... c05 N69-35024*#
NASA-TN-D-5191 ..... c15 N69-27078*#
NASA-TN-D-5192 ..... c15 N69-27956*#
NASA-TN-D-5193 ..... c01 N69-23926*#
NASA-TN-D-5194 ..... c19 N69-23788*#
NASA-TN-D-5195 ..... c17 N69-23731*#
NASA-TN-D-5196 ..... c33 N69-24168*#
NASA-TN-D-5197 ..... c06 N69-23706*#
NASA-TN-D-5198 ..... c26 N69-24916*#
NASA-TN-D-5199 ..... c01 N69-23781*#
NASA-TN-D-5200 ..... c30 N69-23708*#
NASA-TN-D-5201 ..... c01 N69-29154*#
NASA-TN-D-5202 ..... c02 N69-23449*#
NASA-TN-D-5203 ..... c30 N69-26252*#
NASA-TN-D-5204 ..... c01 N69-24764*#
NASA-TN-D-5205 ..... c16 N69-25357*#
NASA-TN-D-5207 ..... c28 N69-26224*#
NASA-TN-D-5208 ..... c01 N69-29027*#
NASA-TN-D-5209 ..... c12 N69-24800*#
NASA-TN-D-5210 ..... c12 N69-24917*#
NASA-TN-D-5211 ..... c24 N69-24826*#
NASA-TN-D-5212 ..... c10 N69-24918*#
NASA-TN-D-5213 ..... c06 N69-24940*#
NASA-TN-D-5214 ..... c33 N69-24824*#
NASA-TN-D-5215 ..... c25 N69-24920*#
NASA-TN-D-5216 ..... c24 N69-24919*#
NASA-TN-D-5217 ..... c25 N69-25394*#
NASA-TN-D-5218 ..... c28 N69-24922*#
NASA-TN-D-5219 ..... c31 N69-26570*#
NASA-TN-D-5220 ..... c21 N69-26195*#
NASA-TN-D-5221 ..... c05 N69-26259*#
NASA-TN-D-5222 ..... c32 N69-29589*#
NASA-TN-D-5223 ..... c33 N69-26247*#

NASA-TN-D-5224 ..... c15 N69-24932*#
NASA-TN-D-5225 ..... c15 N69-24791*#
NASA-TN-D-5226 ..... c33 N69-25312*#
NASA-TN-D-5227 ..... c26 N69-25412*#
NASA-TN-D-5228 ..... c08 N69-29478*#
NASA-TN-D-5229 ..... c17 N69-25363*#
NASA-TN-D-5230 ..... c33 N69-28209*#
NASA-TN-D-5231 ..... c30 N69-29115*#
NASA-TN-D-5232 ..... c02 N69-28097*#
NASA-TN-D-5233 ..... c01 N69-26271*#
NASA-TN-D-5234 ..... c03 N69-28123*#
NASA-TN-D-5235 ..... c05 N69-28024*#
NASA-TN-D-5236 ..... c32 N69-26223*#
NASA-TN-D-5237 ..... c10 N69-28121*#
NASA-TN-D-5238 ..... c21 N69-31227*#
NASA-TN-D-5240 ..... c19 N69-31303*#
NASA-TN-D-5241 ..... c02 N69-27177*#
NASA-TN-D-5242 ..... c01 N69-28112*#
NASA-TN-D-5244 ..... c25 N69-26313*#
NASA-TN-D-5245 ..... c30 N69-26239*#
NASA-TN-D-5246 ..... c12 N69-33421*#
NASA-TN-D-5247 ..... c17 N69-26258*#
NASA-TN-D-5248 ..... c17 N69-26192*#
NASA-TN-D-5249 ..... c33 N69-26236*#
NASA-TN-D-5250 ..... c22 N69-26270*#
NASA-TN-D-5251 ..... c12 N69-29608*#
NASA-TN-D-5252 ..... c13 N69-27246*#
NASA-TN-D-5253 ..... c32 N69-28038*#
NASA-TN-D-5254 ..... c32 N69-28658*#
NASA-TN-D-5255 ..... c04 N69-29195*#
NASA-TN-D-5256 ..... c02 N69-28044*#
NASA-TN-D-5257 ..... c33 N69-28440*#
NASA-TN-D-5258 ..... c15 N69-29476*#
NASA-TN-D-5259 ..... c30 N69-30611*#
NASA-TN-D-5260 ..... c31 N69-28166*#
NASA-TN-D-5261 ..... c21 N69-28018*#
NASA-TN-D-5262 ..... c15 N69-26311*#
NASA-TN-D-5263 ..... c33 N69-27620*#
NASA-TN-D-5264 ..... c15 N69-27955*#
NASA-TN-D-5265 ..... c03 N69-30945*#
NASA-TN-D-5266 ..... c17 N69-27061*#
NASA-TN-D-5267 ..... c30 N69-31058*#
NASA-TN-D-5268 ..... c31 N69-32298*#
NASA-TN-D-5269 ..... c25 N69-29140*#
NASA-TN-D-5270 ..... c02 N69-29232*#
NASA-TN-D-5271 ..... c30 N69-28441*#
NASA-TN-D-5272 ..... c01 N69-29269*#
NASA-TN-D-5273 ..... c17 N69-28863*#
NASA-TN-D-5274 ..... c25 N69-29600*#
NASA-TN-D-5275 ..... c08 N69-29592*#
NASA-TN-D-5276 ..... c30 N69-29557*#
NASA-TN-D-5277 ..... c19 N69-29141*#
NASA-TN-D-5278 ..... c33 N69-29599*#
NASA-TN-D-5279 ..... c18 N69-34547*#
NASA-TN-D-5280 ..... c14 N69-32286*#
NASA-TN-D-5281 ..... c14 N69-29153*#
NASA-TN-D-5282 ..... c28 N69-29321*#
NASA-TN-D-5283 ..... c34 N69-31333*#
NASA-TN-D-5284 ..... c30 N69-37893*#
NASA-TN-D-5285 ..... c14 N69-29331*#
NASA-TN-D-5286 ..... c26 N69-29588*#
NASA-TN-D-5287 ..... c14 N69-29196*#
NASA-TN-D-5288 ..... c01 N69-29479*#
NASA-TN-D-5289 ..... c33 N69-29598*#
NASA-TN-D-5290 ..... c26 N69-29407*#
NASA-TN-D-5291 ..... c14 N69-29553*#
NASA-TN-D-5292 ..... c15 N69-29165*#
NASA-TN-D-5293 ..... c30 N69-29738*#
NASA-TN-D-5294 ..... c32 N69-29607*#
NASA-TN-D-5295 ..... c11 N69-29981*#
NASA-TN-D-5296 ..... c01 N69-30063*#
NASA-TN-D-5297 ..... c12 N69-30071*#
NASA-TN-D-5298 ..... c21 N69-30946*#
NASA-TN-D-5299 ..... c14 N69-29730*#
NASA-TN-D-5300 ..... c19 N69-29648*#
NASA-TN-D-5301 ..... c15 N69-29568*#
NASA-TN-D-5302 ..... c23 N69-39178*#
NASA-TN-D-5303 ..... c28 N69-29405*#
NASA-TN-D-5304 ..... c15 N69-33800*#
NASA-TN-D-5806 ..... c02 N69-31874*#
NASA-TN-D-5307 ..... c12 N69-31359*#
NASA-TN-D-5308 ..... c24 N69-31338*#
NASA-TN-D-5309 ..... c33 N69-30726*#
NASA-TN-D-5311 ..... c25 N69-36939*#
NASA-TN-D-5312 ..... c22 N69-30070*#
NASA-TN-D-5313 ..... c26 N69-30072*#
NASA-TN-D-5314 ..... c28 N69-35526*#
NASA-TN-D-5315 ..... c02 N69-30727*#
NASA-TN-D-5316 ..... c28 N69-34575*#
NASA-TN-D-5317 ..... c32 N69-29672*#
NASA-TN-D-5318 ..... c15 N69-30069*#
NASA-TN-D-5319 ..... c25 N69-29905*#
NASA-TN-D-5320 ..... c15 N69-30062*#
NASA-TN-D-5321 ..... c24 N69-30073*#
NASA-TN-D-5322 ..... c01 N69-30878*#
NASA-TN-D-5323 ..... c33 N69-30064*#
NASA-TN-D-5324 ..... c28 N69-30560*#
NASA-TN-D-5326 ..... c17 N69-31065*#
NASA-TN-D-5327 ..... c14 N69-30506*#
NASA-TN-D-5328 ..... c25 N69-30622*#
NASA-TN-D-5329 ..... c24 N69-30074*#
NASA-TN-D-5330 ..... c01 N69-30060*#
NASA-TN-D-5331 ..... c03 N69-29977*#
NASA-TN-D-5332 ..... c13 N69-34891*#
NASA-TN-D-5333 ..... c01 N69-33210*#
NASA-TN-D-5334 ..... c01 N69-33237*#
NASA-TN-D-5335 ..... c01 N69-31337*#
NASA-TN-D-5336 ..... c28 N69-32318*#
NASA-TN-D-5338 ..... c28 N69-31336*#
NASA-TN-D-5339 ..... c28 N69-30980*#
NASA-TN-D-5340 ..... c32 N69-31056*#
NASA-TN-D-5341 ..... c12 N69-39177*#
NASA-TN-D-5342 ..... c02 N69-32110*#
NASA-TN-D-5343 ..... c01 N69-31228*#
NASA-TN-D-5344 ..... c15 N69-35799*#
NASA-TN-D-5346 ..... c12 N69-37370*#
NASA-TN-D-5347 ..... c22 N69-31870*#
NASA-TN-D-5348 ..... c17 N69-31977*#
NASA-TN-D-5349 ..... c15 N69-31884*#
NASA-TN-D-5350 ..... c08 N69-32685*#
NASA-TN-D-5351 ..... c23 N69-31984*#
NASA-TN-D-5352 ..... c17 N69-31873*#
NASA-TN-D-5353 ..... c17 N69-31895*#
NASA-TN-D-5354 ..... c32 N69-31300*#
NASA-TN-D-5355 ..... c17 N69-31883*#
NASA-TN-D-5356 ..... c33 N69-31869*#
NASA-TN-D-5357 ..... c30 N69-36892*#
NASA-TN-D-5358 ..... c02 N69-35762*#
NASA-TN-D-5359 ..... c02 N69-32284*#
NASA-TN-D-5360 ..... c14 N69-38144*#
NASA-TN-D-5361 ..... c02 N69-32337*#
NASA-TN-D-5362 ..... c17 N69-32558*#
NASA-TN-D-5363 ..... c32 N69-33420*#
NASA-TN-D-5364 ..... c01 N69-33275*#
NASA-TN-D-5365 ..... c01 N69-32299*#
NASA-TN-D-5366 ..... c03 N69-31844*#
NASA-TN-D-5367 ..... c18 N69-33321*#
NASA-TN-D-5368 ..... c30 N69-36930*#
NASA-TN-D-5369 ..... c19 N69-32319*#
NASA-TN-D-5370 ..... c08 N69-32556*#
NASA-TN-D-5371 ..... c32 N69-34970*#
NASA-TN-D-5372 ..... c12 N69-32377*#
NASA-TN-D-5373 ..... c15 N69-33281*#
NASA-TN-D-5374 ..... c22 N69-32317*#
NASA-TN-D-5375 ..... c33 N69-32340*#
NASA-TN-D-5376 ..... c17 N69-33307*#
NASA-TN-D-5377 ..... c12 N69-33353*#
NASA-TN-D-5378 ..... c01 N69-34986*#
NASA-TN-D-5379 ..... c01 N69-33302*#
NASA-TN-D-5380 ..... c18 N69-34708*#
NASA-TN-D-5381 ..... c30 N69-36143*#
NASA-TN-D-5382 ..... c27 N69-35321*#
NASA-TN-D-5383 ..... c11 N69-35359*#
NASA-TN-D-5384 ..... c21 N69-36997*#
NASA-TN-D-5385 ..... c33 N69-33314*#
NASA-TN-D-5386 ..... c15 N69-33258*#
NASA-TN-D-5387 ..... c28 N69-33211*#
NASA-TN-D-5388 ..... c03 N69-34652*#
NASA-TN-D-5389 ..... c15 N69-34707*#
NASA-TN-D-5390 ..... c17 N69-34704*#
NASA-TN-D-5391 ..... c33 N69-34966*#
NASA-TN-D-5392 ..... c01 N69-35300*#
NASA-TN-D-5393 ..... c28 N69-36932*#
NASA-TN-D-5394 ..... c28 N69-33319*#
NASA-TN-D-5395 ..... c33 N69-34892*#
NASA-TN-D-5396 ..... c25 N69-36755*#
NASA-TN-D-5397 ..... c27 N69-36225*#
NASA-TN-D-5398 ..... c30 N69-34884*#
NASA-TN-D-5399 ..... c31 N69-38820*#
NASA-TN-D-5400 ..... c13 N69-40893*#
NASA-TN-D-5401 ..... c09 N69-36706*#
NASA-TN-D-5402 ..... c08 N69-35569*#
NASA-TN-D-5403 ..... c33 N69-35949*#
NASA-TN-D-5404 ..... c33 N69-35506*#
NASA-TN-D-5405 ..... c03 N69-35537*#
NASA-TN-D-5406 ..... c14 N69-35265*#
NASA-TN-D-5407 ..... c24 N69-35508*#
NASA-TN-D-5408 ..... c02 N69-36258*#

NASA-TN-D-5409 ..... c02 N69-36807*#
NASA-TN-D-5410 ..... c32 N69-36220*#
NASA-TN-D-5411 ..... c15 N69-35769*#
NASA-TN-D-5412 ..... c12 N69-35842*#
NASA-TN-D-5413 ..... c17 N69-35688*#
NASA-TN-D-5414 ..... c25 N69-35732*#
NASA-TN-D-5416 ..... c33 N69-36299*#
NASA-TN-D-5417 ..... c17 N69-36221*#
NASA-TN-D-5418 ..... c01 N69-35855*#
NASA-TN-D-5419 ..... c01 N69-38768*#
NASA-TN-D-5420 ..... c15 N69-35788*#
NASA-TN-D-5421 ..... c17 N69-38074*#
NASA-TN-D-5422 ..... c23 N69-37028*#
NASA-TN-D-5423 ..... c24 N69-36924*#
NASA-TN-D-5424 ..... c17 N69-36653*#
NASA-TN-D-5425 ..... c30 N69-38769*#
NASA-TN-D-5426 ..... c05 N69-39210*#
NASA-TN-D-5427 ..... c01 N69-37521*#
NASA-TN-D-5428 ..... c09 N69-36710*#
NASA-TN-D-5429 ..... c33 N69-36701*#
NASA-TN-D-5430 ..... c24 N69-36929*#
NASA-TN-D-5431 ..... c24 N69-36931*#
NASA-TN-D-5433 ..... c12 N69-36805*#
NASA-TN-D-5434 ..... c12 N69-36830*#
NASA-TN-D-5435 ..... c31 N69-40781*#
NASA-TN-D-5436 ..... c28 N69-40080*#
NASA-TN-D-5437 ..... c28 N69-36882*#
NASA-TN-D-5438 ..... c01 N69-36699*#
NASA-TN-D-5439 ..... c32 N69-38808*#
NASA-TN-D-5440 ..... c12 N69-36940*#
NASA-TN-D-5441 ..... c26 N69-37272*#
NASA-TN-D-5442 ..... c17 N69-37436*#
NASA-TN-D-5443 ..... c30 N69-38658*#
NASA-TN-D-5444 ..... c02 N69-38770*#
NASA-TN-D-5445 ..... c09 N69-38852*#
NASA-TN-D-5446 ..... c07 N69-37602*#
NASA-TN-D-5447 ..... c13 N69-40924*#
NASA-TN-D-5448 ..... c28 N69-36844*#
NASA-TN-D-5449 ..... c25 N69-38010*#
NASA-TN-D-5450 ..... c12 N69-37604*#
NASA-TN-D-5452 ..... c33 N69-37936*#
NASA-TN-D-5453 ..... c32 N69-38642*#
NASA-TN-D-5454 ..... c12 N69-38156*#
NASA-TN-D-5455 ..... c32 N69-41229*#
NASA-TN-D-5457 ..... c09 N69-38597*#
NASA-TN-D-5459 ..... c30 N69-38145*#
NASA-TN-D-5460 ..... c12 N69-37965*#
NASA-TN-D-5461 ..... c03 N69-37883*#
NASA-TN-D-5462 ..... c12 N69-38032*#
NASA-TN-D-5464 ..... c33 N69-38271*#
NASA-TN-D-5465 ..... c19 N69-38178*#
NASA-TN-D-5467 ..... c12 N69-38012*#
NASA-TN-D-5468 ..... c01 N69-38775*#
NASA-TN-D-5471 ..... c31 N69-40813*#
NASA-TN-D-5472 ..... c07 N69-39176*#
NASA-TN-D-5473 ..... c09 N69-38776*#
NASA-TN-D-5474 ..... c08 N69-38654*#
NASA-TN-D-5478 ..... c05 N69-39183*#
NASA-TN-D-5480 ..... c33 N69-40356*#
NASA-TN-D-5481 ..... c01 N69-40876*#
NASA-TN-D-5483 ..... c17 N69-38794*#
NASA-TN-D-5484 ..... c15 N69-38641*#
NASA-TN-D-5485 ..... c28 N69-39185*#
NASA-TN-D-5486 ..... c24 N69-39184*#
NASA-TN-D-5487 ..... c22 N69-39186*#
NASA-TN-D-5488 ..... c26 N69-39239*#
NASA-TN-D-5489 ..... c32 N69-39393*#
NASA-TN-D-5490 ..... c09 N69-41208*#
NASA-TN-D-5491 ..... c02 N69-38807*#
NASA-TN-D-5492 ..... c32 N69-38809*#
NASA-TN-D-5493 ..... c17 N69-39182*#
NASA-TN-D-5494 ..... c07 N69-40099*#
NASA-TN-D-5495 ..... c21 N69-40055*#
NASA-TN-D-5496 ..... c12 N69-40137*#
NASA-TN-D-5497 ..... c02 N69-39188*#
NASA-TN-D-5499 ..... c01 N69-40026*#
NASA-TN-D-5500 ..... c25 N69-39302*#
NASA-TN-D-5501 ..... c12 N69-39916*#
NASA-TN-D-5503 ..... c06 N69-40240*#
NASA-TN-D-5504 ..... c17 N69-40053*#
NASA-TN-D-5505 ..... c26 N69-40056*#
NASA-TN-D-5506 ..... c28 N69-40078*#
NASA-TN-D-5508 ..... c32 N69-40087*#
NASA-TN-D-5509 ..... c09 N69-40079*#
NASA-TN-D-5510 ..... c17 N69-40242*#
NASA-TN-D-5511 ..... c19 N69-40088*#
NASA-TN-D-5514 ..... c01 N69-40345*#
NASA-TN-D-5515 ..... c14 N69-40812*#
NASA-TN-D-5519 ..... c28 N69-40329*#

NASA-TN-D-5520 ..... c33 N69-40789*#
NASA-TN-D-5522 ..... c33 N69-40437*#
NASA-TN-D-5526 ..... c33 N69-40780*#
NASA-TN-D-5527 ..... c15 N69-41210*#
NASA-TN-D-5530 ..... c24 N69-40979*#
NASA-TN-D-5531 ..... c12 N69-41213*#
NASA-TN-D-5536 ..... c32 N69-41141*#
NASA-TN-D-5538 ..... c02 N69-40937*#

NASA-TR-R-278 ..... c30 N69-14428*#
NASA-TR-R-294 ..... c07 N69-16196*#
NASA-TR-R-295 ..... c12 N69-10788*#
NASA-TR-R-296 ..... c33 N69-16181*#
NASA-TR-R-297 ..... c31 N69-15374*#
NASA-TR-R-298 ..... c32 N69-24765*#
NASA-TR-R-299 ..... c33 N69-16268*#
NASA-TR-R-300 ..... c01 N69-17304*#
NASA-TR-R-301 ..... c31 N69-17801*#
NASA-TR-R-302 ..... c01 N69-19028*#
NASA-TR-R-303 ..... c25 N69-20997*#
NASA-TR-R-304 ..... c21 N69-21402*#
NASA-TR-R-305 ..... c06 N69-20775*#
NASA-TR-R-306 ..... c07 N69-22951*#
NASA-TR-R-307 ..... c30 N69-22948*#
NASA-TR-R-308 ..... c30 N69-24170*#
NASA-TR-R-309 ..... c07 N69-23642*#
NASA-TR-R-310 ..... c25 N69-23787*#
NASA-TR-R-311 ..... c12 N69-26504*#
NASA-TR-R-312 ..... c01 N69-29270*#
NASA-TR-R-313 ..... c19 N69-30610*#
NASA-TR-R-314 ..... c07 N69-29230*#
NASA-TR-R-315 ..... c19 N69-30753*#
NASA-TR-R-317 ..... c01 N69-32338*#
NASA-TR-R-320 ..... c07 N69-39264*#
NASA-TR-R-321 ..... c14 N69-36985*#
NASA-TR-R-322 ..... c30 N69-39336*#
NASA-TR-R-326 ..... c19 N69-38655*#

NASA-TT-F-345 ..... c13 N69-12384*#
NASA-TT-F-430 ..... c09 N69-15441 #
NASA-TT-F-490 ..... c30 N69-14944*#
NASA-TT-F-491 ..... c30 N69-14943*#
NASA-TT-F-500 ..... c31 N69-24760*#
NASA-TT-F-501 ..... c04 N69-31401*#
NASA-TT-F-502 ..... c30 N69-31989*#
NASA-TT-F-507 ..... c28 N69-33354*#
NASA-TT-F-508 ..... c17 N69-27300*#
NASA-TT-F-510 ..... c24 N69-25848*#
NASA-TT-F-514 ..... c30 N69-24206*#
NASA-TT-F-518 ..... c32 N69-30754*#
NASA-TT-F-522 ..... c33 N69-30507*#
NASA-TT-F-523 ..... c05 N69-27577*#
NASA-TT-F-524 ..... c21 N69-17788*#
NASA-TT-F-525 ..... c04 N69-40324*#
NASA-TT-F-526 ..... c02 N69-31917*#
NASA-TT-F-527 ..... c07 N69-14973*#
NASA-TT-F-528 ..... c05 N69-38701*#
NASA-TT-F-529 ..... c05 N69-32044*#
NASA-TT-F-530 ..... c13 N69-16539*#
NASA-TT-F-532 ..... c13 N69-28983*#
NASA-TT-F-533 ..... c13 N69-29491*#
NASA-TT-F-534 ..... c15 N69-35859*#
NASA-TT-F-535 ..... c29 N69-24924*#
NASA-TT-F-536 ..... c30 N69-38643*#
NASA-TT-F-537 ..... c34 N69-36314*#
NASA-TT-F-539 ..... c30 N69-33560*#
NASA-TT-F-540 ..... c34 N69-31836*#
NASA-TT-F-541 ..... c34 N69-26112*#
NASA-TT-F-542 ..... c01 N69-38670*#
NASA-TT-F-545 ..... c05 N69-26455*#
NASA-TT-F-546 ..... c13 N69-25013*#
NASA-TT-F-547 ..... c02 N69-36326*#
NASA-TT-F-549 ..... c33 N69-31947*#
NASA-TT-F-552 ..... c33 N69-30245*#
NASA-TT-F-554 ..... c30 N69-40592*#
NASA-TT-F-555 ..... c02 N69-24761*#
NASA-TT-F-558 ..... c12 N69-35365*#
NASA-TT-F-560 ..... c12 N69-27168 #
NASA-TT-F-562 ..... c30 N69-27169 #
NASA-TT-F-577 ..... c12 N69-29235*#
NASA-TT-F-578 ..... c04 N69-31356*#
NASA-TT-F-580 ..... c04 N69-32131*#
NASA-TT-F-581 ..... c29 N69-33401*#
NASA-TT-F-583 ..... c17 N69-35836*#
NASA-TT-F-585 ..... c12 N69-40824*#
NASA-TT-F-590 ..... c13 N69-31851*#

NEAR-TR-6 ..... c12 N69-21653*#
NEAR-TR-14 ..... c12 N69-40200*#

P68-148 ..... c18 N69-26448*#

PWA-3070-VOL-1 ..... c03 N69-21771*#
PWA-3070-VOL-2 ..... c15 N69-21772*#
PWA-3070-VOL-3 ..... c15 N69-19775*#
PWA-3486 ..... c23 N69-36974*#
PWA-3549 ..... c15 N69-33450*#

R-67-4450 ..... c14 N69-14351*#
R-68-4459 ..... c14 N69-21117*#
R-4035-30-1 ..... c14 N69-18953*#
R-7491 ..... c19 N69-11419*#
R-7703 ..... c06 N69-36413*#

RAI-397 ..... c18 N69-36762*#

RASA-68-10 ..... c32 N69-34744*#

REPT-0-71100/8R-18 ..... c24 N69-33416*#
REPT-0-71100/9R-1 ..... c24 N69-34541*#
REPT-03-67-04-VOL-1 ..... c09 N69-23225*#
REPT-03-67-04-VOL-2 ..... c09 N69-23226*#
REPT-3-32000/7R-36 ..... c31 N69-16221*#
REPT-68-2 ..... c32 N69-17770*#
REPT-68-23 ..... c32 N69-11010*#
REPT-68-3986-REV-1 ..... c05 N69-37964*#
REPT-340-2 ..... c32 N69-22983*#
REPT-8800-67 ..... c17 N69-19831*#

RF-2421 ..... c21 N69-38041*#

RR-68-2 ..... c15 N69-14214*#

S-1112 ..... c16 N69-29934*#

SIO-REF-68-6 ..... c05 N69-10813*#

SPO-20224 ..... c14 N69-37876*#

SUDAAR-361 ..... c21 N69-29967*#
SUDAAR-374 ..... c21 N69-41036*#

TI-03-67-04 ..... c09 N69-25328*#

TP-181 ..... c07 N69-32721*#

TR-7 ..... c02 N69-34915*#
TR-8-5 ..... c26 N69-10817*#
TR-8-6 ..... c32 N69-21569*#
TR-8-7 ..... c32 N69-21401*#
TR-8-8 ..... c32 N69-22982*#
TR-101-4 ..... c21 N69-34672*#
TR-154-1 ..... c05 N69-14212*#
TR-167-1 ..... c05 N69-15372*#
TR-168-1 ..... c04 N69-22637*#
TR-168-2 ..... c05 N69-28071*#
TR-719-1 ..... c15 N69-19786*#
TR-1691-29 ..... c07 N69-26273*#
TR-1691-30 ..... c07 N69-24059*#

TRW-06462-6005-R0-00 ..... c05 N69-38491*#
TRW-11433-6005-R0-00 ..... c30 N69-31960*#

TT-66-51025 ..... c13 N69-12384*#
TT-67-51213 ..... c09 N69-15441 #
TT-68-50301 ..... c28 N69-33354*#
TT-68-50302 ..... c04 N69-31401*#
TT-68-50304 ..... c31 N69-24760*#
TT-68-50308 ..... c17 N69-27300*#
TT-68-50309 ..... c24 N69-25848*#
TT-69-55023 ..... c12 N69-27168 #
TT-69-55025 ..... c30 N69-27169 #

UTEC-MR-67-055 ..... c13 N69-18126*#

WAED-67.24E ..... c18 N69-14400*#

WR-68-15 ..... c28 N69-21476*#

ACCESSION/REPORT NUMBER INDEX

NASA SCIENTIFIC AND TECHNICAL REPORTS AND PUBLICATIONS FOR 1969

A Selected Listing

Typical Accession/Report Number Index Listing

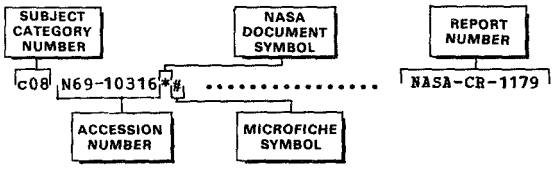

Listings in this index are arranged numerically by IAA and NASA accession numbers. The subject category number indicates the subject category in the abstract section in which the citation is located. The accession number denotes the number by which the citation is identified within the subject category. An asterisk (*) indicates that the item is a NASA report. A pound sign (#) indicates that the item is available on microfiche. The report numbers are the identification numbers that have been assigned to the item by the issuing body or other agency.

c26 A69-10009* ..... NO REPORT NUMBER
c23 A69-10012* ..... NO REPORT NUMBER
c24 A69-10100* ..... NO REPORT NUMBER
c15 A69-10109*# ..... NO REPORT NUMBER
c33 A69-10110*# ..... NO REPORT NUMBER
c33 A69-10112*# ..... NO REPORT NUMBER
c14 A69-10113*# ..... NO REPORT NUMBER
c09 A69-10193* ..... NO REPORT NUMBER
c20 A69-10463*# ..... NO REPORT NUMBER
c34 A69-10467*# ..... NO REPORT NUMBER
c34 A69-10472*# ..... NO REPORT NUMBER
c20 A69-10474*# ..... NO REPORT NUMBER
c21 A69-10479*# ..... NO REPORT NUMBER
c20 A69-10483*# ..... NO REPORT NUMBER
c13 A69-10491*# ..... NO REPORT NUMBER
c30 A69-10498*# ..... NO REPORT NUMBER
c34 A69-10506*# ..... NO REPORT NUMBER
c34 A69-10512*# ..... NO REPORT NUMBER
c34 A69-10515*# ..... NO REPORT NUMBER
c34 A69-10516*# ..... NO REPORT NUMBER
c34 A69-10519*# ..... NO REPORT NUMBER
c34 A69-10525*# ..... NO REPORT NUMBER
c07 A69-10556* ..... NO REPORT NUMBER
c26 A69-10557* ..... NO REPORT NUMBER
c09 A69-10564* ..... NO REPORT NUMBER
c06 A69-10588* ..... NO REPORT NUMBER
c03 A69-10606* ..... NO REPORT NUMBER
c17 A69-10612* ..... NO REPORT NUMBER
c20 A69-10695*# ..... NO REPORT NUMBER
c33 A69-10847* ..... NO REPORT NUMBER
c18 A69-10861* ..... NO REPORT NUMBER
c14 A69-10890* ..... NO REPORT NUMBER
c06 A69-10893* ..... NO REPORT NUMBER
c24 A69-10901* ..... NO REPORT NUMBER
c15 A69-10912* ..... NO REPORT NUMBER
c14 A69-10927* ..... NO REPORT NUMBER
c26 A69-10934* ..... NO REPORT NUMBER
c24 A69-10960* ..... NO REPORT NUMBER
c09 A69-11000* ..... NO REPORT NUMBER
c21 A69-11005* ..... NO REPORT NUMBER
c04 A69-11073 ..... NO REPORT NUMBER
c04 A69-11074* ..... NO REPORT NUMBER
c04 A69-11084* ..... NO REPORT NUMBER
c13 A69-11125* ..... NO REPORT NUMBER
c13 A69-11226* ..... NO REPORT NUMBER
c29 A69-11227* ..... NO REPORT NUMBER
c30 A69-11228* ..... NO REPORT NUMBER
c13 A69-11234* ..... NO REPORT NUMBER
c13 A69-11237* ..... NO REPORT NUMBER
c06 A69-11285* ..... NO REPORT NUMBER
c23 A69-11288* ..... NO REPORT NUMBER
c30 A69-11292* ..... NO REPORT NUMBER
c15 A69-11324* ..... NO REPORT NUMBER
c05 A69-11335* ..... NO REPORT NUMBER
c31 A69-11395*# ..... NO REPORT NUMBER
c03 A69-11396*# ..... NO REPORT NUMBER
c14 A69-11468* ..... NO REPORT NUMBER
c30 A69-11475* ..... NO REPORT NUMBER
c30 A69-11481* ..... NO REPORT NUMBER
c11 A69-11755 ..... NO REPORT NUMBER
c03 A69-11762* ..... NO REPORT NUMBER
c04 A69-11770* ..... NO REPORT NUMBER
c05 A69-11865* ..... NO REPORT NUMBER
c04 A69-11866* ..... NO REPORT NUMBER
c05 A69-11950* ..... NO REPORT NUMBER
c05 A69-11953* ..... NO REPORT NUMBER
c29 A69-12092* ..... NO REPORT NUMBER
c30 A69-12104*# ..... NO REPORT NUMBER
c30 A69-12105*# ..... NO REPORT NUMBER
c30 A69-12108*# ..... NO REPORT NUMBER
c30 A69-12109*# ..... NO REPORT NUMBER
c23 A69-12179* ..... NO REPORT NUMBER
c05 A69-12216* ..... NO REPORT NUMBER
c30 A69-12224* ..... NO REPORT NUMBER
c30 A69-12225* ..... NO REPORT NUMBER
c30 A69-12271* ..... NO REPORT NUMBER
c30 A69-12272* ..... NO REPORT NUMBER
c13 A69-12299* ..... NO REPORT NUMBER
c30 A69-12301 ..... NO REPORT NUMBER
c30 A69-12303* ..... NO REPORT NUMBER
c30 A69-12304* ..... NO REPORT NUMBER
c09 A69-12328* ..... NO REPORT NUMBER
c25 A69-12349* ..... NO REPORT NUMBER
c31 A69-12373*# ..... NO REPORT NUMBER
c28 A69-12375*# ..... NO REPORT NUMBER
c11 A69-12379*# ..... NO REPORT NUMBER
c31 A69-12384*# ..... NO REPORT NUMBER
c11 A69-12385*# ..... NO REPORT NUMBER
c30 A69-12390*# ..... NO REPORT NUMBER
c14 A69-12392*# ..... NO REPORT NUMBER
c25 A69-12399*# ..... NO REPORT NUMBER
c26 A69-12408*# ..... NO REPORT NUMBER
c05 A69-12498* ..... NO REPORT NUMBER
c32 A69-12516*# ..... NO REPORT NUMBER
c01 A69-12520*# ..... NO REPORT NUMBER
c01 A69-12522*# ..... NO REPORT NUMBER
c30 A69-12545*# ..... NO REPORT NUMBER
c33 A69-12547*# ..... NO REPORT NUMBER
c24 A69-12551* ..... NO REPORT NUMBER
c06 A69-12603* ..... NO REPORT NUMBER
c16 A69-12617* ..... NO REPORT NUMBER
c30 A69-12680* ..... NO REPORT NUMBER
c29 A69-12714* ..... NO REPORT NUMBER
c13 A69-12741* ..... NO REPORT NUMBER
c30 A69-12801 ..... NO REPORT NUMBER
c04 A69-12804* ..... NO REPORT NUMBER
c24 A69-12833* ..... NO REPORT NUMBER
c14 A69-12869* ..... NO REPORT NUMBER
c24 A69-12924* ..... NO REPORT NUMBER
c29 A69-12928 ..... NO REPORT NUMBER
c29 A69-12934*# ..... NO REPORT NUMBER
c05 A69-12987*# ..... NO REPORT NUMBER
c05 A69-12993*# ..... NO REPORT NUMBER
c10 A69-13073* ..... NO REPORT NUMBER
c03 A69-13074*# ..... NO REPORT NUMBER
c03 A69-13075*# ..... NO REPORT NUMBER
c03 A69-13076*# ..... NO REPORT NUMBER
c24 A69-13098*# ..... NO REPORT NUMBER
c24 A69-13099*# ..... NO REPORT NUMBER
c24 A69-13100*# ..... NO REPORT NUMBER
c14 A69-13104*# ..... NO REPORT NUMBER
c14 A69-13108 # ..... NO REPORT NUMBER
c25 A69-13113*# ..... NO REPORT NUMBER
c25 A69-13114*# ..... NO REPORT NUMBER
c25 A69-13115*# ..... NO REPORT NUMBER
c03 A69-13125*# ..... NO REPORT NUMBER
c03 A69-13126*# ..... NO REPORT NUMBER

c03 A69-13127*# ..... NO REPORT NUMBER
c22 A69-13128*# ..... NO REPORT NUMBER
c22 A69-13131*# ..... NO REPORT NUMBER
c12 A69-13137* ..... NO REPORT NUMBER
c12 A69-13138 ..... NO REPORT NUMBER
c07 A69-13176 ..... NO REPORT NUMBER
c07 A69-13183* ..... NO REPORT NUMBER
c21 A69-13214* ..... NO REPORT NUMBER
c14 A69-13221* ..... NO REPORT NUMBER
c11 A69-13240* ..... NO REPORT NUMBER
c07 A69-13242* ..... NO REPORT NUMBER
c08 A69-13243* ..... NO REPORT NUMBER
c24 A69-13321* ..... NO REPORT NUMBER
c13 A69-13328* ..... NO REPORT NUMBER
c02 A69-13367* ..... NO REPORT NUMBER
c19 A69-13370* ..... NO REPORT NUMBER
c19 A69-13375* ..... NO REPORT NUMBER
c30 A69-13427* ..... NO REPORT NUMBER
c04 A69-13433* ..... NO REPORT NUMBER
c05 A69-13441* ..... NO REPORT NUMBER
c24 A69-13464*# ..... NO REPORT NUMBER
c24 A69-13469 ..... NO REPORT NUMBER
c04 A69-13498* ..... NO REPORT NUMBER
c31 A69-13556*# ..... NO REPORT NUMBER
c31 A69-13558*# ..... NO REPORT NUMBER
c31 A69-13564*# ..... NO REPORT NUMBER
c31 A69-13565*# ..... NO REPORT NUMBER
c31 A69-13670*# ..... NO REPORT NUMBER
c31 A69-13673*# ..... NO REPORT NUMBER
c30 A69-13699*# ..... NO REPORT NUMBER
c04 A69-13700*# ..... NO REPORT NUMBER
c07 A69-13721* ..... NO REPORT NUMBER
c30 A69-13775* ..... NO REPORT NUMBER
c31 A69-13777* ..... NO REPORT NUMBER
c30 A69-13781* ..... NO REPORT NUMBER
c14 A69-13851*# ..... NO REPORT NUMBER
c20 A69-13852*# ..... NO REPORT NUMBER
c04 A69-13897* ..... NO REPORT NUMBER
c07 A69-13900*# ..... NO REPORT NUMBER
c30 A69-14005* ..... NO REPORT NUMBER
c29 A69-14008* ..... NO REPORT NUMBER
c13 A69-14012* ..... NO REPORT NUMBER
c29 A69-14015* ..... NO REPORT NUMBER
c30 A69-14126* ..... NO REPORT NUMBER
c16 A69-14189*# ..... NO REPORT NUMBER
c16 A69-14290* ..... NO REPORT NUMBER
c23 A69-14295* ..... NO REPORT NUMBER
c14 A69-14360* ..... NO REPORT NUMBER
c25 A69-14456 # ..... NO REPORT NUMBER
c27 A69-14468* ..... NO REPORT NUMBER
c27 A69-14474* ..... NO REPORT NUMBER
c27 A69-14475* ..... NO REPORT NUMBER
c27 A69-14477* ..... NO REPORT NUMBER
c12 A69-14510*# ..... AICHE PAPER 25C
c30 A69-14519* ..... NO REPORT NUMBER
c30 A69-14626* ..... NO REPORT NUMBER
c30 A69-14631* ..... NO REPORT NUMBER
c13 A69-14661* ..... NO REPORT NUMBER
c04 A69-14692* ..... NO REPORT NUMBER
c10 A69-14693 ..... NO REPORT NUMBER
c10 A69-14697* ..... NO REPORT NUMBER
c01 A69-14714*# ..... NO REPORT NUMBER
c33 A69-14736*# ..... NO REPORT NUMBER
c22 A69-14799* ..... NO REPORT NUMBER
c08 A69-14858* ..... NO REPORT NUMBER
c06 A69-14862* ..... NO REPORT NUMBER
c14 A69-14916*# ..... NO REPORT NUMBER
c07 A69-14917*# ..... NO REPORT NUMBER
c02 A69-14930* ..... SAE PAPER 680220
c24 A69-14966* ..... NO REPORT NUMBER
c13 A69-14975* ..... NO REPORT NUMBER
c30 A69-14979* ..... NO REPORT NUMBER
c28 A69-15000* ..... NO REPORT NUMBER
c14 A69-15028* ..... NO REPORT NUMBER
c31 A69-15298* ..... NO REPORT NUMBER
c03 A69-15299* ..... NO REPORT NUMBER
c03 A69-15310* ..... NO REPORT NUMBER
c04 A69-15332* ..... NO REPORT NUMBER
c04 A69-15333* ..... NO REPORT NUMBER
c05 A69-15388*# ..... NO REPORT NUMBER
c14 A69-15428* ..... NO REPORT NUMBER
c08 A69-15472* ..... NO REPORT NUMBER
c21 A69-15501*# ..... NO REPORT NUMBER
c30 A69-15503*# ..... NO REPORT NUMBER
c32 A69-15507*# ..... NO REPORT NUMBER
c14 A69-15514*# ..... NO REPORT NUMBER
c29 A69-15528* ..... NO REPORT NUMBER
c02 A69-15563* ..... NO REPORT NUMBER
c02 A69-15568* ..... NO REPORT NUMBER
c02 A69-15571* ..... NO REPORT NUMBER
c11 A69-15572* ..... NO REPORT NUMBER
c11 A69-15574* ..... NO REPORT NUMBER
c11 A69-15575* ..... NO REPORT NUMBER
c34 A69-15576* ..... NO REPORT NUMBER
c30 A69-15589*# ..... NO REPORT NUMBER
c28 A69-15622* ..... NO REPORT NUMBER
c12 A69-15791*# ..... NO REPORT NUMBER
c30 A69-15834 ..... NO REPORT NUMBER
c30 A69-15854* ..... NO REPORT NUMBER
c30 A69-15858* ..... NO REPORT NUMBER
c05 A69-15934 ..... NO REPORT NUMBER
c05 A69-15935*# ..... NO REPORT NUMBER
c04 A69-15969* ..... NO REPORT NUMBER
c04 A69-15983* ..... NO REPORT NUMBER
c34 A69-15987* ..... NO REPORT NUMBER
c11 A69-15992* ..... NO REPORT NUMBER
c14 A69-16105*# ..... NO REPORT NUMBER
c33 A69-16122*# ..... NO REPORT NUMBER
c14 A69-16135*# ..... NO REPORT NUMBER
c28 A69-16136*# ..... NO REPORT NUMBER
c03 A69-16158*# ..... NO REPORT NUMBER
c18 A69-16160*# ..... NO REPORT NUMBER
c28 A69-16233* ..... ECS PAPER 170D
c30 A69-16252* ..... NO REPORT NUMBER
c13 A69-16261* ..... NO REPORT NUMBER
c30 A69-16264* ..... NO REPORT NUMBER
c13 A69-16267* ..... NO REPORT NUMBER
c13 A69-16268* ..... NO REPORT NUMBER
c30 A69-16278* ..... NO REPORT NUMBER
c26 A69-16357*# ..... NO REPORT NUMBER
c26 A69-16358*# ..... NO REPORT NUMBER
c03 A69-16359*# ..... NO REPORT NUMBER
c29 A69-16361* ..... NO REPORT NUMBER
c31 A69-16380*# ..... NO REPORT NUMBER
c13 A69-16407* ..... NO REPORT NUMBER
c13 A69-16411* ..... NO REPORT NUMBER
c24 A69-16428* ..... NO REPORT NUMBER
c32 A69-16433* ..... NO REPORT NUMBER
c30 A69-16476* ..... NO REPORT NUMBER
c18 A69-16485* ..... NO REPORT NUMBER
c15 A69-16486* ..... NO REPORT NUMBER
c18 A69-16487* ..... NO REPORT NUMBER
c18 A69-16488* ..... NO REPORT NUMBER
c18 A69-16489 ..... NO REPORT NUMBER
c18 A69-16490* ..... NO REPORT NUMBER
c18 A69-16491* ..... NO REPORT NUMBER
c18 A69-16492 ..... NO REPORT NUMBER
c06 A69-16493* ..... NO REPORT NUMBER
c18 A69-16494 ..... NO REPORT NUMBER
c24 A69-16495 ..... NO REPORT NUMBER
c24 A69-16496* ..... NO REPORT NUMBER
c06 A69-16497* ..... NO REPORT NUMBER
c06 A69-16498* ..... NO REPORT NUMBER
c26 A69-16529* ..... NO REPORT NUMBER
c09 A69-16562* ..... NO REPORT NUMBER
c10 A69-16598* ..... NO REPORT NUMBER
c10 A69-16601 ..... NO REPORT NUMBER
c21 A69-16716 ..... NO REPORT NUMBER
c34 A69-16718*# ..... NO REPORT NUMBER
c21 A69-16726*# ..... NO REPORT NUMBER
c32 A69-16742 ..... NO REPORT NUMBER
c14 A69-16755*# ..... NO REPORT NUMBER
c34 A69-16836* ..... NO REPORT NUMBER
c26 A69-16877* ..... NO REPORT NUMBER
c30 A69-16931* ..... NO REPORT NUMBER
c14 A69-16932 # ..... NO REPORT NUMBER
c30 A69-17006* ..... NO REPORT NUMBER
c24 A69-17027* ..... NO REPORT NUMBER
c34 A69-17059*# ..... NO REPORT NUMBER
c34 A69-17068*# ..... NO REPORT NUMBER
c30 A69-17074*# ..... NO REPORT NUMBER
c04 A69-17105* ..... NO REPORT NUMBER
c24 A69-17134* ..... NO REPORT NUMBER
c24 A69-17138* ..... NO REPORT NUMBER
c23 A69-17142 ..... NO REPORT NUMBER
c05 A69-17215* ..... NO REPORT NUMBER
c19 A69-17250* ..... NO REPORT NUMBER
c29 A69-17268 ..... NO REPORT NUMBER
c29 A69-17280*# ..... NO REPORT NUMBER
c30 A69-17560 ..... NO REPORT NUMBER
c30 A69-17574* ..... NO REPORT NUMBER
c21 A69-17580* ..... NO REPORT NUMBER
c21 A69-17589* ..... NO REPORT NUMBER
c31 A69-17596 ..... NO REPORT NUMBER
c31 A69-17602* ..... NO REPORT NUMBER
c31 A69-17605* ..... NO REPORT NUMBER
c31 A69-17606* ..... NO REPORT NUMBER
c13 A69-17617* ..... NO REPORT NUMBER

c05 A69-17642 ..... NO REPORT NUMBER
c05 A69-17648* ..... NO REPORT NUMBER
c31 A69-17672* ..... NO REPORT NUMBER
c11 A69-17705*# ..... NO REPORT NUMBER
c09 A69-17708*# ..... NO REPORT NUMBER
c26 A69-17772*# ..... NO REPORT NUMBER
c09 A69-17773*# ..... NO REPORT NUMBER
c33 A69-17804*# ..... NO REPORT NUMBER
c24 A69-17817* ..... NO REPORT NUMBER
c17 A69-17872* ..... NO REPORT NUMBER
c16 A69-17901*# ..... NO REPORT NUMBER
c10 A69-17939* ..... NO REPORT NUMBER
c10 A69-17947* ..... NO REPORT NUMBER
c20 A69-18038*# ..... NO REPORT NUMBER
c30 A69-18042*# ..... NO REPORT NUMBER
c01 A69-18052*# ..... NO REPORT NUMBER
c33 A69-18055*# ..... NO REPORT NUMBER
c02 A69-18058*# ..... NO REPORT NUMBER
c33 A69-18083*# ..... NO REPORT NUMBER
c30 A69-18090*# ..... NO REPORT NUMBER
c12 A69-18094*# ..... NO REPORT NUMBER
c06 A69-18111*# ..... NO REPORT NUMBER
c29 A69-18113*# ..... NO REPORT NUMBER
c33 A69-18126*# ..... NO REPORT NUMBER
c32 A69-18133*# ..... NO REPORT NUMBER
c25 A69-18145*# ..... NO REPORT NUMBER
c17 A69-18154*# ..... NO REPORT NUMBER
c01 A69-18161*# ..... NO REPORT NUMBER
c01 A69-18167*# ..... NO REPORT NUMBER
c25 A69-18171*# ..... NO REPORT NUMBER
c01 A69-18176*# ..... NO REPORT NUMBER
c01 A69-18184*# ..... NO REPORT NUMBER
c32 A69-18193*# ..... NO REPORT NUMBER
c05 A69-18202*# ..... NO REPORT NUMBER
c31 A69-18204*# ..... NO REPORT NUMBER
c31 A69-18210*# ..... NO REPORT NUMBER
c12 A69-18213*# ..... NO REPORT NUMBER
c33 A69-18303* ..... NO REPORT NUMBER
c33 A69-18305* ..... NO REPORT NUMBER
c12 A69-18317*# ..... NO REPORT NUMBER
c31 A69-18328*# ..... NO REPORT NUMBER
c32 A69-18331*# ..... NO REPORT NUMBER
c31 A69-18334*# ..... NO REPORT NUMBER
c31 A69-18338*# ..... NO REPORT NUMBER
c06 A69-18419* ..... NO REPORT NUMBER
c09 A69-18420 ..... NO REPORT NUMBER
c16 A69-18482* ..... NO REPORT NUMBER
c30 A69-18601* ..... NO REPORT NUMBER
c30 A69-18604* ..... NO REPORT NUMBER
c30 A69-18607* ..... NO REPORT NUMBER
c17 A69-18790* ..... NO REPORT NUMBER
c17 A69-18791 ..... NO REPORT NUMBER
c17 A69-18792 ..... NO REPORT NUMBER
c17 A69-18793* ..... NO REPORT NUMBER
c22 A69-18825* ..... NO REPORT NUMBER
c14 A69-18827* ..... NO REPORT NUMBER
c13 A69-18838* ..... NO REPORT NUMBER
c13 A69-18839* ..... NO REPORT NUMBER
c09 A69-18905*# ..... NO REPORT NUMBER
c07 A69-18944* ..... NO REPORT NUMBER
c22 A69-18954* ..... NO REPORT NUMBER
c16 A69-19082* ..... NO REPORT NUMBER
c07 A69-19092 ..... NO REPORT NUMBER
c07 A69-19101* ..... NO REPORT NUMBER
c09 A69-19120* ..... NO REPORT NUMBER
c07 A69-19122* ..... NO REPORT NUMBER
c07 A69-19124* ..... NO REPORT NUMBER
c31 A69-19126* ..... NO REPORT NUMBER
c07 A69-19130* ..... NO REPORT NUMBER
c07 A69-19132* ..... NO REPORT NUMBER
c21 A69-19135* ..... NO REPORT NUMBER
c24 A69-19165* ..... NO REPORT NUMBER
c14 A69-19185* ..... NO REPORT NUMBER
c14 A69-19192* ..... NO REPORT NUMBER
c31 A69-19195* ..... NO REPORT NUMBER
c21 A69-19208* ..... NO REPORT NUMBER
c21 A69-19212* ..... NO REPORT NUMBER
c30 A69-19262* ..... NO REPORT NUMBER
c15 A69-19308* ..... NO REPORT NUMBER
c15 A69-19310* ..... NO REPORT NUMBER
c29 A69-19351 ..... NO REPORT NUMBER
c13 A69-19360* ..... NO REPORT NUMBER
c29 A69-19363* ..... NO REPORT NUMBER
c13 A69-19364* ..... NO REPORT NUMBER
c13 A69-19365* ..... NO REPORT NUMBER
c29 A69-19375* ..... NO REPORT NUMBER
c30 A69-19404* ..... NO REPORT NUMBER
c04 A69-19429* ..... NO REPORT NUMBER
c04 A69-19481* ..... NO REPORT NUMBER
c02 A69-19546*# ..... NO REPORT NUMBER
c09 A69-19582* ..... NO REPORT NUMBER
c16 A69-19641*# ..... NO REPORT NUMBER
c23 A69-19649*# ..... NO REPORT NUMBER
c15 A69-19666* ..... NO REPORT NUMBER
c30 A69-19715* ..... NO REPORT NUMBER
c04 A69-19726* ..... NO REPORT NUMBER
c02 A69-19764* ..... NO REPORT NUMBER
c06 A69-19775* ..... NO REPORT NUMBER
c24 A69-19782* ..... NO REPORT NUMBER
c24 A69-19788* ..... NO REPORT NUMBER
c10 A69-19853* ..... NO REPORT NUMBER
c30 A69-19874*# ..... NO REPORT NUMBER
c14 A69-19968* ..... NO REPORT NUMBER
c25 A69-19988*# ..... NO REPORT NUMBER
c07 A69-20045* ..... NO REPORT NUMBER
c30 A69-20051 ..... NO REPORT NUMBER
c33 A69-20064* ..... NO REPORT NUMBER
c29 A69-20066* ..... NO REPORT NUMBER
c24 A69-20153* ..... NO REPORT NUMBER
c14 A69-20165*# ..... NO REPORT NUMBER
c17 A69-20190* ..... NO REPORT NUMBER
c17 A69-20204* ..... NO REPORT NUMBER
c24 A69-20206* ..... NO REPORT NUMBER
c04 A69-20374* ..... NO REPORT NUMBER
c25 A69-20521* ..... NO REPORT NUMBER
c15 A69-20529*# ..... NO REPORT NUMBER
c06 A69-20535* ..... NO REPORT NUMBER
c17 A69-20557 ..... NO REPORT NUMBER
c30 A69-20624* ..... NO REPORT NUMBER
c29 A69-20632* ..... NO REPORT NUMBER
c30 A69-20644* ..... NO REPORT NUMBER
c29 A69-20645* ..... NO REPORT NUMBER
c30 A69-20686* ..... NO REPORT NUMBER
c29 A69-20699* ..... NO REPORT NUMBER
c30 A69-20729* ..... NO REPORT NUMBER
c24 A69-20736* ..... NO REPORT NUMBER
c24 A69-20738* ..... NO REPORT NUMBER
c23 A69-20745 ..... NO REPORT NUMBER
c30 A69-20770* ..... NO REPORT NUMBER
c25 A69-20795* ..... NO REPORT NUMBER
c25 A69-20796* ..... NO REPORT NUMBER
c25 A69-20797* ..... NO REPORT NUMBER
c25 A69-20807* ..... NO REPORT NUMBER
c25 A69-20809* ..... NO REPORT NUMBER
c30 A69-20892 ..... NO REPORT NUMBER
c30 A69-20898* ..... NO REPORT NUMBER
c30 A69-20903* ..... NO REPORT NUMBER
c30 A69-20913* ..... NO REPORT NUMBER
c13 A69-20944* ..... NO REPORT NUMBER
c13 A69-20945* ..... NO REPORT NUMBER
c03 A69-21034 ..... NO REPORT NUMBER
c03 A69-21035* ..... NO REPORT NUMBER
c14 A69-21087* ..... NO REPORT NUMBER
c16 A69-21088* ..... NO REPORT NUMBER
c30 A69-21204*# ..... NO REPORT NUMBER
c30 A69-21206*# ..... NO REPORT NUMBER
c28 A69-21212*# ..... NO REPORT NUMBER
c28 A69-21216*# ..... NO REPORT NUMBER
c28 A69-21218*# ..... NO REPORT NUMBER
c28 A69-21221*# ..... NO REPORT NUMBER
c28 A69-21224*# ..... NO REPORT NUMBER
c28 A69-21225*# ..... NO REPORT NUMBER
c28 A69-21233*# ..... NO REPORT NUMBER
c28 A69-21236*# ..... NO REPORT NUMBER
c28 A69-21239*# ..... NO REPORT NUMBER
c30 A69-21244*# ..... NO REPORT NUMBER
c28 A69-21246*# ..... NO REPORT NUMBER
c22 A69-21249*# ..... NO REPORT NUMBER
c28 A69-21251*# ..... NO REPORT NUMBER
c28 A69-21252*# ..... NO REPORT NUMBER
c28 A69-21254*# ..... NO REPORT NUMBER
c28 A69-21255*# ..... NO REPORT NUMBER
c28 A69-21256*# ..... NO REPORT NUMBER
c28 A69-21257*# ..... NO REPORT NUMBER
c28 A69-21261*# ..... NO REPORT NUMBER
c10 A69-21327*# ..... NO REPORT NUMBER
c26 A69-21350*# ..... NO REPORT NUMBER
c26 A69-21351*# ..... NO REPORT NUMBER
c15 A69-21392* ..... NO REPORT NUMBER
c14 A69-21394* ..... NO REPORT NUMBER
c13 A69-21404*# ..... NO REPORT NUMBER
c30 A69-21454* ..... NO REPORT NUMBER
c29 A69-21459* ..... NO REPORT NUMBER
c32 A69-21479 # ..... NO REPORT NUMBER
c12 A69-21480*# ..... NO REPORT NUMBER
c14 A69-21555* ..... NO REPORT NUMBER
c14 A69-21642*# ..... NO REPORT NUMBER
c29 A69-21645* ..... NO REPORT NUMBER

c29 A69-21646* ..... NO REPORT NUMBER
c14 A69-21651*# ..... NO REPORT NUMBER
c26 A69-21652* ..... NO REPORT NUMBER
c13 A69-21661* ..... NO REPORT NUMBER
c29 A69-21699* ..... NO REPORT NUMBER
c28 A69-21731*# ..... NO REPORT NUMBER
c23 A69-21751*# ..... NO REPORT NUMBER
c26 A69-21753*# ..... NO REPORT NUMBER
c03 A69-21806 ..... NO REPORT NUMBER
c26 A69-21808* ..... NO REPORT NUMBER
c03 A69-21819* ..... NO REPORT NUMBER
c03 A69-21827* ..... NO REPORT NUMBER
c03 A69-21828* ..... NO REPORT NUMBER
c03 A69-21840* ..... NO REPORT NUMBER
c30 A69-21843*# ..... NO REPORT NUMBER
c25 A69-21919*# ..... NO REPORT NUMBER
c30 A69-21937*# ..... NO REPORT NUMBER
c01 A69-21972*# ..... NO REPORT NUMBER
c33 A69-21982*# ..... NO REPORT NUMBER
c12 A69-21995*# ..... NO REPORT NUMBER
c11 A69-22008*# ..... NO REPORT NUMBER
c25 A69-22045* ..... NO REPORT NUMBER
c30 A69-22047* ..... NO REPORT NUMBER
c30 A69-22055* ..... NO REPORT NUMBER
c29 A69-22167* ..... NO REPORT NUMBER
c29 A69-22169* ..... NO REPORT NUMBER
c30 A69-22183* ..... NO REPORT NUMBER
c30 A69-22189* ..... NO REPORT NUMBER
c30 A69-22199* ..... NO REPORT NUMBER
c29 A69-22203* ..... NO REPORT NUMBER
c30 A69-22211* ..... NO REPORT NUMBER
c30 A69-22216* ..... NO REPORT NUMBER
c29 A69-22231* ..... NO REPORT NUMBER
c24 A69-22249* ..... NO REPORT NUMBER
c30 A69-22264* ..... NO REPORT NUMBER
c15 A69-22301 ..... NO REPORT NUMBER
c15 A69-22339 # ..... NO REPORT NUMBER
c02 A69-22379*# ..... NO REPORT NUMBER
c30 A69-22421* ..... NO REPORT NUMBER
c30 A69-22426* ..... NO REPORT NUMBER
c09 A69-22433 ..... NO REPORT NUMBER
c14 A69-22434* ..... NO REPORT NUMBER
c01 A69-22495*# ..... NO REPORT NUMBER
c01 A69-22521*# ..... NO REPORT NUMBER
c14 A69-22522*# ..... NO REPORT NUMBER
c05 A69-22542* ..... NO REPORT NUMBER
c10 A69-22567* ..... NO REPORT NUMBER
c09 A69-22786* ..... NO REPORT NUMBER
c09 A69-22787* ..... NO REPORT NUMBER
c34 A69-22863*# ..... NO REPORT NUMBER
c31 A69-22866*# ..... NO REPORT NUMBER
c17 A69-22990* ..... NO REPORT NUMBER
c27 A69-23003 ..... NO REPORT NUMBER
c11 A69-23026* ..... NO REPORT NUMBER
c15 A69-23050*# ..... NO REPORT NUMBER
c32 A69-23057*# ..... NO REPORT NUMBER
c06 A69-23127* ..... NO REPORT NUMBER
c04 A69-23158* ..... NO REPORT NUMBER
c30 A69-23183* ..... NO REPORT NUMBER
c11 A69-23245 ..... NO REPORT NUMBER
c07 A69-23279* ..... NO REPORT NUMBER
c11 A69-23283* ..... NO REPORT NUMBER
c06 A69-23371* ..... NO REPORT NUMBER
c06 A69-23527*# ..... NO REPORT NUMBER
c23 A69-23647*# ..... NO REPORT NUMBER
c25 A69-23660 # ..... NO REPORT NUMBER
c30 A69-23679* ..... NO REPORT NUMBER
c29 A69-23753* ..... NO REPORT NUMBER
c29 A69-23766* ..... NO REPORT NUMBER
c13 A69-23770* ..... NO REPORT NUMBER
c30 A69-23773* ..... NO REPORT NUMBER
c13 A69-23777* ..... NO REPORT NUMBER
c05 A69-23879* ..... NO REPORT NUMBER
c05 A69-23880* ..... NO REPORT NUMBER
c03 A69-23993* ..... NO REPORT NUMBER
c16 A69-24005*# ..... NO REPORT NUMBER
c26 A69-24006*# ..... NO REPORT NUMBER
c30 A69-24100* ..... NO REPORT NUMBER
c30 A69-24103* ..... NO REPORT NUMBER
c30 A69-24125* ..... NO REPORT NUMBER
c32 A69-24184*# ..... NO REPORT NUMBER
c33 A69-24283*# ..... NO REPORT NUMBER
c25 A69-24305*# ..... NO REPORT NUMBER
c25 A69-24315*# ..... NO REPORT NUMBER
c30 A69-24429* ..... NO REPORT NUMBER
c33 A69-24456 ..... NO REPORT NUMBER
c33 A69-24457* ..... NO REPORT NUMBER
c29 A69-24466* ..... NO REPORT NUMBER
c09 A69-24740 ..... NO REPORT NUMBER
c09 A69-24747* ..... NO REPORT NUMBER
c09 A69-24748* ..... NO REPORT NUMBER
c05 A69-24795 # ..... NO REPORT NUMBER
c23 A69-24836* ..... NO REPORT NUMBER
c14 A69-24838* ..... NO REPORT NUMBER
c09 A69-24984* ..... NO REPORT NUMBER
c09 A69-24986* ..... NO REPORT NUMBER
c07 A69-24993* ..... NO REPORT NUMBER
c11 A69-25081* ..... NO REPORT NUMBER
c30 A69-25107* ..... NO REPORT NUMBER
c29 A69-25144* ..... NO REPORT NUMBER
c13 A69-25150* ..... NO REPORT NUMBER
c13 A69-25153* ..... NO REPORT NUMBER
c13 A69-25157* ..... NO REPORT NUMBER
c29 A69-25162* ..... NO REPORT NUMBER
c12 A69-25282*# ..... NO REPORT NUMBER
c13 A69-25284*# ..... NO REPORT NUMBER
c07 A69-25288 ..... NO REPORT NUMBER
c07 A69-25296*# ..... NO REPORT NUMBER
c14 A69-25310*# ..... NO REPORT NUMBER
c23 A69-25323*# ..... NO REPORT NUMBER
c01 A69-25378*# ..... NO REPORT NUMBER
c10 A69-25450* ..... NO REPORT NUMBER
c04 A69-25460* ..... NO REPORT NUMBER
c32 A69-25492 ..... NO REPORT NUMBER
c31 A69-25498*# ..... NO REPORT NUMBER
c31 A69-25500*# ..... NO REPORT NUMBER
c31 A69-25501*# ..... NO REPORT NUMBER
c32 A69-25524*# ..... NO REPORT NUMBER
c32 A69-25525*# ..... NO REPORT NUMBER
c32 A69-25534*# ..... NO REPORT NUMBER
c06 A69-25641 ..... NO REPORT NUMBER
c05 A69-25642* ..... NO REPORT NUMBER
c04 A69-25643* ..... NO REPORT NUMBER
c30 A69-25644*# ..... NO REPORT NUMBER
c31 A69-25718 ..... NO REPORT NUMBER
c31 A69-25719* ..... NO REPORT NUMBER
c21 A69-25724* ..... NO REPORT NUMBER
c11 A69-25768* ..... NO REPORT NUMBER
c30 A69-25812* ..... NO REPORT NUMBER
c30 A69-25813* ..... NO REPORT NUMBER
c07 A69-25933* ..... NO REPORT NUMBER
c32 A69-25958* ..... NO REPORT NUMBER
c13 A69-26012*# ..... NO REPORT NUMBER
c12 A69-26013 # ..... NO REPORT NUMBER
c30 A69-26019*# ..... NO REPORT NUMBER
c30 A69-26020*# ..... NO REPORT NUMBER
c24 A69-26097*# ..... NO REPORT NUMBER
c13 A69-26101* ..... NO REPORT NUMBER
c30 A69-26129 # ..... NO REPORT NUMBER
c05 A69-26235* ..... NO REPORT NUMBER
c11 A69-26265* ..... NO REPORT NUMBER
c16 A69-26330* ..... NO REPORT NUMBER
c13 A69-26333*# ..... NO REPORT NUMBER
c30 A69-26341* ..... NO REPORT NUMBER
c30 A69-26342* ..... NO REPORT NUMBER
c30 A69-26371* ..... NO REPORT NUMBER
c17 A69-26495*# ..... NO REPORT NUMBER
c17 A69-26496*# ..... NO REPORT NUMBER
c03 A69-26497*# ..... NO REPORT NUMBER
c03 A69-26498*# ..... NO REPORT NUMBER
c11 A69-26499*# ..... NO REPORT NUMBER
c26 A69-26500 # ..... NO REPORT NUMBER
c14 A69-26546*# ..... NO REPORT NUMBER
c05 A69-26553* ..... NO REPORT NUMBER
c04 A69-26557* ..... NO REPORT NUMBER
c19 A69-26605*# ..... NO REPORT NUMBER
c29 A69-26736* ..... NO REPORT NUMBER
c13 A69-26739* ..... NO REPORT NUMBER
c01 A69-26762*# ..... NO REPORT NUMBER
c33 A69-26781*# ..... NO REPORT NUMBER
c28 A69-26787*# ..... NO REPORT NUMBER
c11 A69-26796*# ..... NO REPORT NUMBER
c32 A69-26807 ..... NO REPORT NUMBER
c18 A69-26813* ..... NO REPORT NUMBER
c02 A69-26872 ..... NO REPORT NUMBER
c31 A69-26874* ..... NO REPORT NUMBER
c29 A69-26943* ..... NO REPORT NUMBER
c07 A69-26965* ..... NO REPORT NUMBER
c14 A69-26974 ..... NO REPORT NUMBER
c07 A69-26976*# ..... NO REPORT NUMBER
c34 A69-26978*# ..... NO REPORT NUMBER
c07 A69-27001*# ..... NO REPORT NUMBER
c29 A69-27144* ..... NO REPORT NUMBER
c30 A69-27158* ..... NO REPORT NUMBER
c30 A69-27172* ..... NO REPORT NUMBER
c15 A69-27231* ..... NO REPORT NUMBER
c15 A69-27271*# ..... NO REPORT NUMBER
c15 A69-27366* ..... NO REPORT NUMBER

c26 N69-27400* ..... NO REPORT NUMBER
c29 N69-27554* ..... NO REPORT NUMBER
c30 N69-27555* ..... NO REPORT NUMBER
c30 N69-27576* ..... NO REPORT NUMBER
c29 N69-27593*# ..... NO REPORT NUMBER
c30 N69-27599*# ..... NO REPORT NUMBER
c06 N69-27762* ..... NO REPORT NUMBER
c33 N69-27784*# ..... NO REPORT NUMBER
c30 N69-27817* ..... NO REPORT NUMBER
c13 N69-27821* ..... NO REPORT NUMBER
c11 N69-27906* ..... NO REPORT NUMBER
c30 N69-27907* ..... NO REPORT NUMBER
c30 N69-27908* ..... NO REPORT NUMBER
c04 N69-27909* ..... NO REPORT NUMBER
c14 N69-27946* ..... NO REPORT NUMBER
c11 N69-27947* ..... NO REPORT NUMBER
c14 N69-27951* ..... NO REPORT NUMBER
c14 N69-27952* ..... NO REPORT NUMBER
c26 N69-28007* ..... NO REPORT NUMBER
c09 N69-28042 ..... NO REPORT NUMBER
c09 N69-28046* ..... NO REPORT NUMBER
c09 N69-28048* ..... NO REPORT NUMBER
c12 N69-28212*# ..... NO REPORT NUMBER
c25 N69-28232*# ..... NO REPORT NUMBER
c32 N69-28252*# ..... NO REPORT NUMBER
c25 N69-28264*# ..... NO REPORT NUMBER
c11 N69-28271*# ..... NO REPORT NUMBER
c11 N69-28278*# ..... NO REPORT NUMBER
c12 N69-28280*# ..... NO REPORT NUMBER
c32 N69-28288*# ..... NO REPORT NUMBER
c05 N69-28298*# ..... NO REPORT NUMBER
c32 N69-28299*# ..... NO REPORT NUMBER
c32 N69-28304*# ..... NO REPORT NUMBER
c32 N69-28305*# ..... NO REPORT NUMBER
c06 N69-28439* ..... NO REPORT NUMBER
c33 N69-28462* ..... NO REPORT NUMBER
c20 N69-28466* ..... NO REPORT NUMBER
c13 N69-28493*# ..... NO REPORT NUMBER
c30 N69-28504* ..... NO REPORT NUMBER
c17 N69-28682* ..... NO REPORT NUMBER
c11 N69-28844*# ..... NO REPORT NUMBER
c15 N69-28854*# ..... NO REPORT NUMBER
c03 N69-28855*# ..... NO REPORT NUMBER
c30 N69-28869* ..... NO REPORT NUMBER
c29 N69-28936* ..... NO REPORT NUMBER
c29 N69-28938* ..... NO REPORT NUMBER
c29 N69-28939* ..... NO REPORT NUMBER
c29 N69-28950* ..... NO REPORT NUMBER
c30 N69-28957* ..... NO REPORT NUMBER
c29 N69-28963* ..... NO REPORT NUMBER
c29 N69-28964* ..... NO REPORT NUMBER
c15 N69-29001*# ..... NO REPORT NUMBER
c08 N69-29004*# ..... NO REPORT NUMBER
c26 N69-29005*# ..... NO REPORT NUMBER
c26 N69-29006*# ..... NO REPORT NUMBER
c24 N69-29007*# ..... NO REPORT NUMBER
c24 N69-29008*# ..... NO REPORT NUMBER
c26 N69-29009*# ..... NO REPORT NUMBER
c17 N69-29010*# ..... NO REPORT NUMBER
c12 N69-29011 ..... NO REPORT NUMBER
c11 N69-29029* ..... NO REPORT NUMBER
c13 N69-29116* ..... NO REPORT NUMBER
c24 N69-29337 ..... NO REPORT NUMBER
c18 N69-29411 ..... NO REPORT NUMBER
c18 N69-29415*# ..... NO REPORT NUMBER
c28 N69-29433* ..... NO REPORT NUMBER
c07 N69-29489* ..... NO REPORT NUMBER
c14 N69-29561*# ..... NO REPORT NUMBER
c14 N69-29564*# ..... NO REPORT NUMBER
c23 N69-29587*# ..... NO REPORT NUMBER
c02 N69-29702* ..... NO REPORT NUMBER
c30 N69-29878* ..... NO REPORT NUMBER
c30 N69-29882* ..... NO REPORT NUMBER
c24 N69-29923*# ..... NO REPORT NUMBER
c30 N69-29946* ..... NO REPORT NUMBER
c29 N69-29948* ..... NO REPORT NUMBER
c29 N69-29967* ..... NO REPORT NUMBER
c30 N69-29970* ..... NO REPORT NUMBER
c29 N69-29971* ..... NO REPORT NUMBER
c29 N69-30005 ..... NO REPORT NUMBER
c30 N69-30010* ..... NO REPORT NUMBER
c29 N69-30014* ..... NO REPORT NUMBER
c04 N69-30036 ..... NO REPORT NUMBER
c30 N69-30188*# ..... NO REPORT NUMBER
c15 N69-30315* ..... NO REPORT NUMBER
c11 N69-30356 ..... NO REPORT NUMBER
c02 N69-30369* ..... NO REPORT NUMBER
c30 N69-30376* ..... NO REPORT NUMBER
c11 N69-30383* ..... NO REPORT NUMBER
c05 N69-30394* ..... NO REPORT NUMBER
c34 N69-30426* ..... NO REPORT NUMBER
c06 N69-30442* ..... NO REPORT NUMBER
c04 N69-30444* ..... NO REPORT NUMBER
c12 N69-30478*# ..... NO REPORT NUMBER
c02 N69-30480*# ..... NO REPORT NUMBER
c15 N69-30481* ..... NO REPORT NUMBER
c15 N69-30492* ..... NO REPORT NUMBER
c10 N69-30601* ..... NO REPORT NUMBER
c15 N69-30610* ..... NO REPORT NUMBER
c29 N69-30759* ..... NO REPORT NUMBER
c30 N69-30766* ..... NO REPORT NUMBER
c30 N69-30769* ..... NO REPORT NUMBER
c30 N69-30883* ..... NO REPORT NUMBER
c15 N69-30901*# ..... NO REPORT NUMBER
c25 N69-30913*# ..... NO REPORT NUMBER
c04 N69-31336*# ..... NO REPORT NUMBER
c13 N69-31351*# ..... NO REPORT NUMBER
c30 N69-31405*# ..... NO REPORT NUMBER
c30 N69-31442*# ..... NO REPORT NUMBER
c05 N69-31459*# ..... NO REPORT NUMBER
c05 N69-31472*# ..... NO REPORT NUMBER
c22 N69-31522* ..... NO REPORT NUMBER
c04 N69-31539* ..... NO REPORT NUMBER
c09 N69-31618* ..... NO REPORT NUMBER
c07 N69-31694*# ..... NO REPORT NUMBER
c06 N69-31807* ..... NO REPORT NUMBER
c06 N69-31808* ..... NO REPORT NUMBER
c31 N69-31849*# ..... NO REPORT NUMBER
c09 N69-31851* ..... NO REPORT NUMBER
c14 N69-31868*# ..... NO REPORT NUMBER
c01 N69-31881*# ..... NO REPORT NUMBER
c28 N69-31890*# ..... NO REPORT NUMBER
c12 N69-31908*# ..... NO REPORT NUMBER
c11 N69-31917*# ..... NO REPORT NUMBER
c29 N69-31963* ..... NO REPORT NUMBER
c13 N69-31974* ..... NO REPORT NUMBER
c29 N69-31975* ..... NO REPORT NUMBER
c13 N69-31981* ..... NO REPORT NUMBER
c29 N69-31984* ..... NO REPORT NUMBER
c29 N69-31990* ..... NO REPORT NUMBER
c23 N69-32053* ..... NO REPORT NUMBER
c29 N69-32082* ..... NO REPORT NUMBER
c13 N69-32083* ..... NO REPORT NUMBER
c13 N69-32099* ..... NO REPORT NUMBER
c30 N69-32154*# ..... NO REPORT NUMBER
c30 N69-32177*# ..... NO REPORT NUMBER
c13 N69-32187 ..... NO REPORT NUMBER
c30 N69-32240* ..... NO REPORT NUMBER
c30 N69-32261*# ..... NO REPORT NUMBER
c26 N69-32262* ..... NO REPORT NUMBER
c30 N69-32300* ..... NO REPORT NUMBER
c30 N69-32309* ..... NO REPORT NUMBER
c06 N69-32312* ..... NO REPORT NUMBER
c13 N69-32314* ..... NO REPORT NUMBER
c29 N69-32315* ..... NO REPORT NUMBER
c29 N69-32321* ..... NO REPORT NUMBER
c14 N69-32324* ..... NO REPORT NUMBER
c14 N69-32326* ..... NO REPORT NUMBER
c27 N69-32345*# ..... NO REPORT NUMBER
c03 N69-32405 ..... NO REPORT NUMBER
c03 N69-32406* ..... NO REPORT NUMBER
c34 N69-32430* ..... NO REPORT NUMBER
c34 N69-32654*# ..... NO REPORT NUMBER
c31 N69-32658*# ..... NO REPORT NUMBER
c22 N69-32660*# ..... NO REPORT NUMBER
c28 N69-32676*# ..... NO REPORT NUMBER
c28 N69-32678*# ..... NO REPORT NUMBER
c28 N69-32686*# ..... NO REPORT NUMBER
c28 N69-32706*# ..... NO REPORT NUMBER
c03 N69-32709*# ..... NO REPORT NUMBER
c28 N69-32711*# ..... NO REPORT NUMBER
c28 N69-32714*# ..... NO REPORT NUMBER
c22 N69-32728*# ..... NO REPORT NUMBER
c28 N69-32732*# ..... NO REPORT NUMBER
c28 N69-32735*# ..... NO REPORT NUMBER
c28 N69-32737*# ..... NO REPORT NUMBER
c31 N69-32755*# ..... NO REPORT NUMBER
c22 N69-32761*# ..... NO REPORT NUMBER
c28 N69-32762*# ..... NO REPORT NUMBER
c01 N69-32769*# ..... NO REPORT NUMBER
c33 N69-32780*# ..... NO REPORT NUMBER
c26 N69-32792 # ..... NO REPORT NUMBER
c30 N69-32803* ..... NO REPORT NUMBER
c29 N69-32806* ..... NO REPORT NUMBER
c05 N69-32810* ..... NO REPORT NUMBER
c30 N69-32811* ..... NO REPORT NUMBER
c26 N69-32824* ..... NO REPORT NUMBER
c14 N69-32855*# ..... NO REPORT NUMBER

c09 A69-32889* ..... NO REPORT NUMBER
c14 A69-32891* ..... NO REPORT NUMBER
c09 A69-32893* ..... NO REPORT NUMBER
c10 A69-32899* ..... NO REPORT NUMBER
c04 A69-32967 ..... NO REPORT NUMBER
c05 A69-32970* ..... NO REPORT NUMBER
c20 A69-33001*# ..... NO REPORT NUMBER
c30 A69-33059* ..... NO REPORT NUMBER
c08 A69-33106*# ..... NO REPORT NUMBER
c14 A69-33107*# ..... NO REPORT NUMBER
c08 A69-33108*# ..... NO REPORT NUMBER
c24 A69-33118* ..... NO REPORT NUMBER
c13 A69-33155*# ..... NO REPORT NUMBER
c13 A69-33156*# ..... NO REPORT NUMBER
c30 A69-33159*# ..... NO REPORT NUMBER
c30 A69-33161*# ..... NO REPORT NUMBER
c04 A69-33173* ..... NO REPORT NUMBER
c12 A69-33247* ..... NO REPORT NUMBER
c12 A69-33248 ..... NO REPORT NUMBER
c12 A69-33249* ..... NO REPORT NUMBER
c01 A69-33250 ..... NO REPORT NUMBER
c01 A69-33251 ..... NO REPORT NUMBER
c12 A69-33252* ..... NO REPORT NUMBER
c12 A69-33253* ..... NO REPORT NUMBER
c12 A69-33254 ..... NO REPORT NUMBER
c12 A69-33255 ..... NO REPORT NUMBER
c12 A69-33256* ..... NO REPORT NUMBER
c12 A69-33257* ..... NO REPORT NUMBER
c33 A69-33258*# ..... NO REPORT NUMBER
c14 A69-33264*# ..... NO REPORT NUMBER
c33 A69-33269*# ..... NO REPORT NUMBER
c33 A69-33270*# ..... NO REPORT NUMBER
c18 A69-33288*# ..... NO REPORT NUMBER
c01 A69-33290*# ..... NO REPORT NUMBER
c33 A69-33299*# ..... NO REPORT NUMBER
c05 A69-33303*# ..... NO REPORT NUMBER
c07 A69-33371* ..... NO REPORT NUMBER
c12 A69-33436*# ..... NO REPORT NUMBER
c12 A69-33437*# ..... NO REPORT NUMBER
c12 A69-33441*# ..... NO REPORT NUMBER
c12 A69-33453*# ..... NO REPORT NUMBER
c12 A69-33462*# ..... NO REPORT NUMBER
c01 A69-33463*# ..... NO REPORT NUMBER
c11 A69-33471*# ..... NO REPORT NUMBER
c12 A69-33474*# ..... NO REPORT NUMBER
c12 A69-33476*# ..... NO REPORT NUMBER
c22 A69-33483*# ..... NO REPORT NUMBER
c32 A69-33559 ..... NO REPORT NUMBER
c32 A69-33563* ..... NO REPORT NUMBER
c17 A69-33564 ..... NO REPORT NUMBER
c17 A69-33566* ..... NO REPORT NUMBER
c06 A69-33651* ..... NO REPORT NUMBER
c30 A69-33664* ..... NO REPORT NUMBER
c23 A69-33674* ..... NO REPORT NUMBER
c20 A69-33732 ..... NO REPORT NUMBER
c20 A69-33739* ..... NO REPORT NUMBER
c08 A69-33745*# ..... NO REPORT NUMBER
c04 A69-33746* ..... NO REPORT NUMBER
c24 A69-33753* ..... NO REPORT NUMBER
c26 A69-33754* ..... NO REPORT NUMBER
c18 A69-33762*# ..... NO REPORT NUMBER
c28 A69-34018*# ..... NO REPORT NUMBER
c30 A69-34043 ..... NO REPORT NUMBER
c30 A69-34044* ..... NO REPORT NUMBER
c29 A69-34168* ..... NO REPORT NUMBER
c06 A69-34184* ..... NO REPORT NUMBER
c17 A69-34186* ..... NO REPORT NUMBER
c13 A69-34283* ..... NO REPORT NUMBER
c13 A69-34284* ..... NO REPORT NUMBER
c30 A69-34297* ..... NO REPORT NUMBER
c29 A69-34301* ..... NO REPORT NUMBER
c14 A69-34334 ..... NO REPORT NUMBER
c14 A69-34336* ..... NO REPORT NUMBER
c30 A69-34359 ..... NO REPORT NUMBER
c30 A69-34362* ..... NO REPORT NUMBER
c13 A69-34365* ..... NO REPORT NUMBER
c33 A69-34372 ..... NO REPORT NUMBER
c30 A69-34374* ..... NO REPORT NUMBER
c15 A69-34378*# ..... NO REPORT NUMBER
c15 A69-34381*# ..... NO REPORT NUMBER
c01 A69-34407*# ..... NO REPORT NUMBER
c15 A69-34415*# ..... NO REPORT NUMBER
c13 A69-34421*# ..... NO REPORT NUMBER
c25 A69-34439*# ..... NO REPORT NUMBER
c14 A69-34442 # ..... NO REPORT NUMBER
c06 A69-34443*# ..... NO REPORT NUMBER
c15 A69-34476 ..... NO REPORT NUMBER
c31 A69-34519* ..... NO REPORT NUMBER
c34 A69-34552* ..... NO REPORT NUMBER
c10 A69-34671 ..... NO REPORT NUMBER
c10 A69-34679* ..... NO REPORT NUMBER
c14 A69-34691* ..... NO REPORT NUMBER
c09 A69-34802* ..... NO REPORT NUMBER
c21 A69-34843 ..... NO REPORT NUMBER
c21 A69-34855* ..... NO REPORT NUMBER
c31 A69-34864* ..... NO REPORT NUMBER
c13 A69-34935* ..... NO REPORT NUMBER
c29 A69-34939* ..... NO REPORT NUMBER
c30 A69-34941* ..... NO REPORT NUMBER
c13 A69-34947 ..... NO REPORT NUMBER
c30 A69-34952* ..... NO REPORT NUMBER
c13 A69-34954 ..... NO REPORT NUMBER
c30 A69-34994* ..... NO REPORT NUMBER
c29 A69-35006* ..... NO REPORT NUMBER
c34 A69-35055 ..... NO REPORT NUMBER
c34 A69-35059*# ..... NO REPORT NUMBER
c31 A69-35067*# ..... NO REPORT NUMBER
c34 A69-35070 ..... NO REPORT NUMBER
c34 A69-35077*# ..... NO REPORT NUMBER
c31 A69-35094*# ..... NO REPORT NUMBER
c08 A69-35099*# ..... NO REPORT NUMBER
c14 A69-35101*# ..... NO REPORT NUMBER
c34 A69-35105*# ..... NO REPORT NUMBER
c28 A69-35108* ..... NO REPORT NUMBER
c24 A69-35166* ..... NO REPORT NUMBER
c28 A69-35175*# ..... NO REPORT NUMBER
c03 A69-35176*# ..... NO REPORT NUMBER
c15 A69-35177*# ..... NO REPORT NUMBER
c22 A69-35178*# ..... NO REPORT NUMBER
c24 A69-35179*# ..... NO REPORT NUMBER
c22 A69-35180*# ..... NO REPORT NUMBER
c22 A69-35181*# ..... NO REPORT NUMBER
c17 A69-35182*# ..... NO REPORT NUMBER
c15 A69-35183*# ..... NO REPORT NUMBER
c17 A69-35184*# ..... NO REPORT NUMBER
c29 A69-35204* ..... NO REPORT NUMBER
c01 A69-35226 ..... NO REPORT NUMBER
c11 A69-35228*# ..... NO REPORT NUMBER
c24 A69-35239* ..... NO REPORT NUMBER
c13 A69-35274* ..... NO REPORT NUMBER
c04 A69-35291* ..... NO REPORT NUMBER
c09 A69-35293* ..... NO REPORT NUMBER
c30 A69-35348*# ..... NO REPORT NUMBER
c29 A69-35415*# ..... NO REPORT NUMBER
c26 A69-35477*# ..... NO REPORT NUMBER
c24 A69-35489 ..... NO REPORT NUMBER
c15 A69-35501 ..... NO REPORT NUMBER
c17 A69-35504* ..... NO REPORT NUMBER
c18 A69-35521* ..... NO REPORT NUMBER
c17 A69-35523* ..... NO REPORT NUMBER
c18 A69-35529* ..... NO REPORT NUMBER
c18 A69-35536* ..... NO REPORT NUMBER
c15 A69-35538* ..... NO REPORT NUMBER
c15 A69-35555* ..... NO REPORT NUMBER
c34 A69-35624*# ..... NO REPORT NUMBER
c01 A69-35636*# ..... NO REPORT NUMBER
c02 A69-35639*# ..... NO REPORT NUMBER
c02 A69-35648*# ..... NO REPORT NUMBER
c02 A69-35649*# ..... NO REPORT NUMBER
c32 A69-35657*# ..... NO REPORT NUMBER
c03 A69-35678 ..... NO REPORT NUMBER
c03 A69-35694* ..... NO REPORT NUMBER
c03 A69-35702* ..... NO REPORT NUMBER
c03 A69-35704* ..... NO REPORT NUMBER
c11 A69-35714 ..... NO REPORT NUMBER
c11 A69-35720* ..... NO REPORT NUMBER
c11 A69-35722* ..... NO REPORT NUMBER
c14 A69-35724* ..... NO REPORT NUMBER
c11 A69-35744* ..... NO REPORT NUMBER
c09 A69-35781 ..... NO REPORT NUMBER
c26 A69-35788*# ..... NO REPORT NUMBER
c21 A69-35789 ..... NO REPORT NUMBER
c21 A69-35792*# ..... NO REPORT NUMBER
c14 A69-35796*# ..... NO REPORT NUMBER
c21 A69-35801*# ..... NO REPORT NUMBER
c30 A69-35934*# ..... NO REPORT NUMBER
c07 A69-35940*# ..... NO REPORT NUMBER
c02 A69-35952*# ..... NO REPORT NUMBER
c21 A69-35953*# ..... NO REPORT NUMBER
c30 A69-35956*# ..... NO REPORT NUMBER
c30 A69-35966* ..... NO REPORT NUMBER
c04 A69-35976* ..... NO REPORT NUMBER
c13 A69-35977* ..... NO REPORT NUMBER
c07 A69-35996* ..... NO REPORT NUMBER
c15 A69-35999 ..... NO REPORT NUMBER
c11 A69-36022* ..... NO REPORT NUMBER
c18 A69-36028* ..... NO REPORT NUMBER
c26 A69-36045* ..... NO REPORT NUMBER

c30 A69-36072 ..... NO REPORT NUMBER
c30 A69-36074* ..... NO REPORT NUMBER
c30 A69-36090* ..... NO REPORT NUMBER
c30 A69-36091* ..... NO REPORT NUMBER
c30 A69-36129* ..... NO REPORT NUMBER
c30 A69-36132* ..... NO REPORT NUMBER
c24 A69-36171 ..... NO REPORT NUMBER
c24 A69-36182*# ..... NO REPORT NUMBER
c18 A69-36208* ..... NO REPORT NUMBER
c30 A69-36209* ..... NO REPORT NUMBER
c29 A69-36218*# ..... NO REPORT NUMBER
c30 A69-36219*# ..... NO REPORT NUMBER
c07 A69-36237 ..... NO REPORT NUMBER
c07 A69-36242* ..... NO REPORT NUMBER
c07 A69-36251* ..... NO REPORT NUMBER
c07 A69-36254* ..... NO REPORT NUMBER
c14 A69-36259* ..... NO REPORT NUMBER
c07 A69-36262* ..... NO REPORT NUMBER
c08 A69-36265* ..... NO REPORT NUMBER
c07 A69-36267* ..... NO REPORT NUMBER
c07 A69-36280* ..... NO REPORT NUMBER
c30 A69-36337* ..... NO REPORT NUMBER
c30 A69-36338* ..... NO REPORT NUMBER
c14 A69-36375* ..... NO REPORT NUMBER
c14 A69-36378* ..... NO REPORT NUMBER
c20 A69-36405 # ..... NO REPORT NUMBER
c24 A69-36424*# ..... NO REPORT NUMBER
c17 A69-36435* ..... NO REPORT NUMBER
c17 A69-36440*# ..... NO REPORT NUMBER
c26 A69-36445 # ..... NO REPORT NUMBER
c04 A69-36458* ..... NO REPORT NUMBER
c34 A69-36460* ..... NO REPORT NUMBER
c31 A69-36464* ..... NO REPORT NUMBER
c14 A69-36489*# ..... NO REPORT NUMBER
c14 A69-36490*# ..... NO REPORT NUMBER
c31 A69-36674* ..... NO REPORT NUMBER
c09 A69-36676* ..... NO REPORT NUMBER
c20 A69-36926*# ..... NO REPORT NUMBER
c14 A69-36931* ..... NO REPORT NUMBER
c06 A69-37101* ..... NO REPORT NUMBER
c34 A69-37102 ..... NO REPORT NUMBER
c34 A69-37127*# ..... NO REPORT NUMBER
c30 A69-37136* ..... NO REPORT NUMBER
c02 A69-37154*# ..... NO REPORT NUMBER
c01 A69-37155*# ..... NO REPORT NUMBER
c31 A69-37156*# ..... NO REPORT NUMBER
c01 A69-37185*# ..... NO REPORT NUMBER
c33 A69-37188*# ..... NO REPORT NUMBER
c33 A69-37198*# ..... NO REPORT NUMBER
c12 A69-37208*# ..... NO REPORT NUMBER
c14 A69-37227*# ..... NO REPORT NUMBER
c26 A69-37280* ..... NO REPORT NUMBER
c31 A69-37287* ..... NO REPORT NUMBER
c33 A69-37290* ..... NO REPORT NUMBER
c09 A69-37299* ..... NO REPORT NUMBER
c30 A69-37334* ..... NO REPORT NUMBER
c08 A69-37377 ..... NO REPORT NUMBER
c08 A69-37384* ..... NO REPORT NUMBER
c08 A69-37385* ..... NO REPORT NUMBER
c13 A69-37490* ..... NO REPORT NUMBER
c30 A69-37492*# ..... NO REPORT NUMBER
c30 A69-37529* ..... NO REPORT NUMBER
c29 A69-37551* ..... NO REPORT NUMBER
c30 A69-37554* ..... NO REPORT NUMBER
c29 A69-37558* ..... NO REPORT NUMBER
c04 A69-37567* ..... NO REPORT NUMBER
c30 A69-37573* ..... NO REPORT NUMBER
c29 A69-37574* ..... NO REPORT NUMBER
c04 A69-37577* ..... NO REPORT NUMBER
c04 A69-37612 ..... NO REPORT NUMBER
c04 A69-37623* ..... NO REPORT NUMBER
c11 A69-37704* ..... NO REPORT NUMBER
c13 A69-37855* ..... NO REPORT NUMBER
c13 A69-37864* ..... NO REPORT NUMBER
c07 A69-37865* ..... NO REPORT NUMBER
c13 A69-37867* ..... NO REPORT NUMBER
c14 A69-37876* ..... NO REPORT NUMBER
c14 A69-37877* ..... NO REPORT NUMBER
c14 A69-37878* ..... NO REPORT NUMBER
c29 A69-37880* ..... NO REPORT NUMBER
c13 A69-37882* ..... NO REPORT NUMBER
c13 A69-37887* ..... NO REPORT NUMBER
c13 A69-37888* ..... NO REPORT NUMBER
c07 A69-37892* ..... NO REPORT NUMBER
c13 A69-37893* ..... NO REPORT NUMBER
c13 A69-37896* ..... NO REPORT NUMBER
c34 A69-38022* ..... NO REPORT NUMBER
c13 A69-38084* ..... NO REPORT NUMBER
c13 A69-38087* ..... NO REPORT NUMBER
c13 A69-38088* ..... NO REPORT NUMBER
c30 A69-38095* ..... NO REPORT NUMBER
c29 A69-38098* ..... NO REPORT NUMBER
c13 A69-38100* ..... NO REPORT NUMBER
c31 A69-38117*# ..... NO REPORT NUMBER
c28 A69-38118*# ..... NO REPORT NUMBER
c20 A69-38120*# ..... NO REPORT NUMBER
c30 A69-38173* ..... NO REPORT NUMBER
c11 A69-38181* ..... NO REPORT NUMBER
c25 A69-38242*# ..... NO REPORT NUMBER
c30 A69-38255* ..... NO REPORT NUMBER
c13 A69-38261* ..... NO REPORT NUMBER
c11 A69-38271* ..... NO REPORT NUMBER
c22 A69-38274* ..... NO REPORT NUMBER
c06 A69-38277* ..... NO REPORT NUMBER
c13 A69-38334 ..... NO REPORT NUMBER
c29 A69-38350* ..... NO REPORT NUMBER
c13 A69-38364* ..... NO REPORT NUMBER
c30 A69-38377* ..... NO REPORT NUMBER
c30 A69-38379* ..... NO REPORT NUMBER
c05 A69-38388* ..... NO REPORT NUMBER
c30 A69-38479* ..... NO REPORT NUMBER
c13 A69-38482 ..... NO REPORT NUMBER
c13 A69-38490* ..... NO REPORT NUMBER
c13 A69-38503* ..... NO REPORT NUMBER
c13 A69-38508* ..... NO REPORT NUMBER
c09 A69-38530* ..... NO REPORT NUMBER
c18 A69-38533* ..... NO REPORT NUMBER
c30 A69-38546*# ..... NO REPORT NUMBER
c15 A69-38567* ..... NO REPORT NUMBER
c30 A69-38600 ..... NO REPORT NUMBER
c25 A69-38713*# ..... NO REPORT NUMBER
c29 A69-38811 ..... NO REPORT NUMBER
c29 A69-38812*# ..... NO REPORT NUMBER
c11 A69-38894* ..... NO REPORT NUMBER
c11 A69-38896* ..... NO REPORT NUMBER
c15 A69-38950* ..... NO REPORT NUMBER
c33 A69-38951* ..... NO REPORT NUMBER
c30 A69-38973* ..... NO REPORT NUMBER
c02 A69-39015*# ..... NO REPORT NUMBER
c34 A69-39133* ..... NO REPORT NUMBER
c05 A69-39170* ..... NO REPORT NUMBER
c30 A69-39215*# ..... NO REPORT NUMBER
c28 A69-39217*# ..... NO REPORT NUMBER
c22 A69-39219*# ..... NO REPORT NUMBER
c30 A69-39221*# ..... NO REPORT NUMBER
c18 A69-39236*# ..... NO REPORT NUMBER
c01 A69-39237*# ..... NO REPORT NUMBER
c30 A69-39337*# ..... NO REPORT NUMBER
c30 A69-39339*# ..... NO REPORT NUMBER
c30 A69-39340*# ..... NO REPORT NUMBER
c30 A69-39346*# ..... NO REPORT NUMBER
c30 A69-39361*# ..... NO REPORT NUMBER
c30 A69-39362*# ..... NO REPORT NUMBER
c15 A69-39367*# ..... NO REPORT NUMBER
c28 A69-39373*# ..... NO REPORT NUMBER
c31 A69-39376*# ..... NO REPORT NUMBER
c31 A69-39384*# ..... NO REPORT NUMBER
c21 A69-39386*# ..... NO REPORT NUMBER
c21 A69-39390*# ..... NO REPORT NUMBER
c21 A69-39396*# ..... NO REPORT NUMBER
c31 A69-39402*# ..... NO REPORT NUMBER
c31 A69-39403*# ..... NO REPORT NUMBER
c21 A69-39405*# ..... NO REPORT NUMBER
c21 A69-39406*# ..... NO REPORT NUMBER
c21 A69-39409*# ..... NO REPORT NUMBER
c21 A69-39410*# ..... NO REPORT NUMBER
c02 A69-39413*# ..... NO REPORT NUMBER
c21 A69-39429*# ..... NO REPORT NUMBER
c33 A69-39433* ..... NO REPORT NUMBER
c17 A69-39434* ..... NO REPORT NUMBER
c07 A69-39437 ..... NO REPORT NUMBER
c07 A69-39450* ..... NO REPORT NUMBER
c07 A69-39451* ..... NO REPORT NUMBER
c09 A69-39454* ..... NO REPORT NUMBER
c24 A69-39467 ..... NO REPORT NUMBER
c29 A69-39506* ..... NO REPORT NUMBER
c30 A69-39521* ..... NO REPORT NUMBER
c30 A69-39568* ..... NO REPORT NUMBER
c34 A69-39581* ..... NO REPORT NUMBER
c23 A69-39582*# ..... NO REPORT NUMBER
c30 A69-39584* ..... NO REPORT NUMBER
c08 A69-39604* ..... NO REPORT NUMBER
c21 A69-39644 ..... NO REPORT NUMBER
c21 A69-39646*# ..... NO REPORT NUMBER
c24 A69-39665* ..... NO REPORT NUMBER
c12 A69-39674* ..... NO REPORT NUMBER
c34 A69-39686 ..... NO REPORT NUMBER
c31 A69-39691* ..... NO REPORT NUMBER

c31 A69-39695* ..... NO REPORT NUMBER
c06 A69-39706*# ..... NO REPORT NUMBER
c13 A69-39747* ..... NO REPORT NUMBER
c31 A69-39753*# ..... NO REPORT NUMBER
c28 A69-39754*# ..... NO REPORT NUMBER
c31 A69-39760*# ..... NO REPORT NUMBER
c21 A69-39764*# ..... NO REPORT NUMBER
c04 A69-39871* ..... NO REPORT NUMBER
c30 A69-39889* ..... NO REPORT NUMBER
c08 A69-39921* ..... NO REPORT NUMBER
c13 A69-39964* ..... NO REPORT NUMBER
c30 A69-39965* ..... NO REPORT NUMBER
c31 A69-39968* ..... NO REPORT NUMBER
c14 A69-40019*# ..... NO REPORT NUMBER
c30 A69-40083 ..... NO REPORT NUMBER
c30 A69-40086* ..... NO REPORT NUMBER
c29 A69-40090* ..... NO REPORT NUMBER
c05 A69-40163* ..... NO REPORT NUMBER
c30 A69-40172 ..... NO REPORT NUMBER
c24 A69-40186* ..... NO REPORT NUMBER
c11 A69-40191* ..... NO REPORT NUMBER
c29 A69-40300* ..... NO REPORT NUMBER
c30 A69-40304* ..... NO REPORT NUMBER
c29 A69-40305* ..... NO REPORT NUMBER
c11 A69-40323*# ..... NO REPORT NUMBER
c21 A69-40327*# ..... NO REPORT NUMBER
c19 A69-40333*# ..... NO REPORT NUMBER
c08 A69-40335*# ..... NO REPORT NUMBER
c08 A69-40339*# ..... NO REPORT NUMBER
c08 A69-40344*# ..... NO REPORT NUMBER
c11 A69-40352*# ..... NO REPORT NUMBER
c33 A69-40359*# ..... NO REPORT NUMBER
c08 A69-40363*# ..... NO REPORT NUMBER
c05 A69-40370*# ..... NO REPORT NUMBER
c05 A69-40371*# ..... NO REPORT NUMBER
c11 A69-40373*# ..... NO REPORT NUMBER
c11 A69-40386*# ..... NO REPORT NUMBER
c11 A69-40390*# ..... NO REPORT NUMBER
c11 A69-40392*# ..... NO REPORT NUMBER
c11 A69-40393*# ..... NO REPORT NUMBER
c11 A69-40401*# ..... NO REPORT NUMBER
c29 A69-40504* ..... NO REPORT NUMBER
c13 A69-40515* ..... NO REPORT NUMBER
c30 A69-40524*# ..... NO REPORT NUMBER
c31 A69-40542*# ..... NO REPORT NUMBER
c31 A69-40550*# ..... NO REPORT NUMBER
c19 A69-40573* ..... NO REPORT NUMBER
c29 A69-40577* ..... NO REPORT NUMBER
c29 A69-40641* ..... NO REPORT NUMBER
c29 A69-40643* ..... NO REPORT NUMBER
c30 A69-40650* ..... NO REPORT NUMBER
c30 A69-40652* ..... NO REPORT NUMBER
c09 A69-40697* ..... NO REPORT NUMBER
c09 A69-40698* ..... NO REPORT NUMBER
c09 A69-40703* ..... NO REPORT NUMBER
c26 A69-40730* ..... NO REPORT NUMBER
c24 A69-40759* ..... NO REPORT NUMBER
c30 A69-40772* ..... NO REPORT NUMBER
c02 A69-40803 ..... NO REPORT NUMBER
c02 A69-40807*# ..... NO REPORT NUMBER
c02 A69-40813*# ..... NO REPORT NUMBER
c06 A69-40932* ..... NO REPORT NUMBER
c04 A69-40974* ..... NO REPORT NUMBER
c14 A69-40989* ..... NO REPORT NUMBER
c24 A69-41044* ..... NO REPORT NUMBER
c24 A69-41045* ..... NO REPORT NUMBER
c30 A69-41058 # ..... NO REPORT NUMBER
c04 A69-41077* ..... NO REPORT NUMBER
c02 A69-41127 ..... NO REPORT NUMBER
c11 A69-41139*# ..... NO REPORT NUMBER
c02 A69-41143*# ..... NO REPORT NUMBER
c14 A69-41216* ..... NO REPORT NUMBER
c09 A69-41224* ..... NO REPORT NUMBER
c09 A69-41228*# ..... NO REPORT NUMBER
c19 A69-41260*# ..... NO REPORT NUMBER
c13 A69-41341* ..... NO REPORT NUMBER
c13 A69-41342* ..... NO REPORT NUMBER
c30 A69-41351* ..... NO REPORT NUMBER
c23 A69-41357* ..... NO REPORT NUMBER
c01 A69-41369 ..... NO REPORT NUMBER
c01 A69-41372*# ..... NO REPORT NUMBER
c30 A69-41388* ..... NO REPORT NUMBER
c04 A69-41404* ..... NO REPORT NUMBER
c30 A69-41477* ..... NO REPORT NUMBER
c07 A69-41588* ..... NO REPORT NUMBER
c09 A69-41589* ..... NO REPORT NUMBER
c09 A69-41590* ..... NO REPORT NUMBER
c30 A69-41611* ..... NO REPORT NUMBER
c30 A69-41617* ..... NO REPORT NUMBER
c30 A69-41623* ..... NO REPORT NUMBER
c14 A69-41633* ..... NO REPORT NUMBER
c05 A69-41674* ..... NO REPORT NUMBER
c05 A69-41675* ..... NO REPORT NUMBER
c05 A69-41679 ..... NO REPORT NUMBER
c18 A69-41715* ..... NO REPORT NUMBER
c07 A69-41734 ..... NO REPORT NUMBER
c08 A69-41735* ..... NO REPORT NUMBER
c08 A69-41736* ..... NO REPORT NUMBER
c08 A69-41737* ..... NO REPORT NUMBER
c07 A69-41738* ..... NO REPORT NUMBER
c08 A69-41739* ..... NO REPORT NUMBER
c07 A69-41745* ..... NO REPORT NUMBER
c07 A69-41752* ..... NO REPORT NUMBER
c07 A69-41755* ..... NO REPORT NUMBER
c07 A69-41757* ..... NO REPORT NUMBER
c07 A69-41758* ..... NO REPORT NUMBER
c07 A69-41759* ..... NO REPORT NUMBER
c08 A69-41769* ..... NO REPORT NUMBER
c05 A69-41783 ..... NO REPORT NUMBER
c05 A69-41800* ..... NO REPORT NUMBER
c01 A69-41886*# ..... NO REPORT NUMBER
c30 A69-41896*# ..... NO REPORT NUMBER
c32 A69-41914*# ..... NO REPORT NUMBER
c04 A69-42021* ..... NO REPORT NUMBER
c11 A69-42120 ..... NO REPORT NUMBER
c32 A69-42133* ..... NO REPORT NUMBER
c23 A69-42149*# ..... NO REPORT NUMBER
c23 A69-42150*# ..... NO REPORT NUMBER
c16 A69-42187* ..... NO REPORT NUMBER
c30 A69-42191* ..... NO REPORT NUMBER
c16 A69-42192* ..... NO REPORT NUMBER
c23 A69-42194* ..... NO REPORT NUMBER
c09 A69-42215 ..... NO REPORT NUMBER
c10 A69-42230* ..... NO REPORT NUMBER
c03 A69-42236 ..... NO REPORT NUMBER
c03 A69-42240* ..... NO REPORT NUMBER
c03 A69-42244* ..... NO REPORT NUMBER
c03 A69-42254* ..... NO REPORT NUMBER
c22 A69-42266* ..... NO REPORT NUMBER
c03 A69-42272* ..... NO REPORT NUMBER
c03 A69-42278* ..... NO REPORT NUMBER
c03 A69-42279* ..... NO REPORT NUMBER
c03 A69-42292* ..... NO REPORT NUMBER
c03 A69-42301* ..... NO REPORT NUMBER
c03 A69-42303* ..... NO REPORT NUMBER
c30 A69-42375* ..... NO REPORT NUMBER
c30 A69-42377* ..... NO REPORT NUMBER
c30 A69-42394* ..... NO REPORT NUMBER
c30 A69-42404*# ..... NO REPORT NUMBER
c30 A69-42417*# ..... NO REPORT NUMBER
c13 A69-42428* ..... NO REPORT NUMBER
c13 A69-42438* ..... NO REPORT NUMBER
c07 A69-42500 ..... NO REPORT NUMBER
c07 A69-42502* ..... NO REPORT NUMBER
c07 A69-42508* ..... NO REPORT NUMBER
c07 A69-42522* ..... NO REPORT NUMBER
c08 A69-42524* ..... NO REPORT NUMBER
c09 A69-42536* ..... NO REPORT NUMBER
c07 A69-42549* ..... NO REPORT NUMBER
c30 A69-42556* ..... NO REPORT NUMBER
c06 A69-42557* ..... NO REPORT NUMBER
c30 A69-42610* ..... NO REPORT NUMBER
c08 A69-42621* ..... NO REPORT NUMBER
c29 A69-42667* ..... NO REPORT NUMBER
c30 A69-42681 ..... NO REPORT NUMBER
c30 A69-42682*# ..... NO REPORT NUMBER
c04 A69-42701 ..... NO REPORT NUMBER
c04 A69-42706* ..... NO REPORT NUMBER
c19 A69-42792* ..... NO REPORT NUMBER
c15 A69-42802*# ..... NO REPORT NUMBER
c30 A69-42810*# ..... NO REPORT NUMBER
c34 A69-42812*# ..... NO REPORT NUMBER
c13 A69-42817*# ..... NO REPORT NUMBER
c34 A69-42820*# ..... NO REPORT NUMBER
c30 A69-42825*# ..... NO REPORT NUMBER
c34 A69-42828*# ..... NO REPORT NUMBER
c02 A69-42831*# ..... NO REPORT NUMBER
c31 A69-42835*# ..... NO REPORT NUMBER
c13 A69-42837*# ..... NO REPORT NUMBER
c31 A69-42838*# ..... NO REPORT NUMBER
c31 A69-42842*# ..... NO REPORT NUMBER
c30 A69-42844*# ..... NO REPORT NUMBER
c05 A69-42850*# ..... NO REPORT NUMBER
c34 A69-42851*# ..... NO REPORT NUMBER
c30 A69-42852*# ..... NO REPORT NUMBER
c14 A69-42858*# ..... NO REPORT NUMBER
c30 A69-42860*# ..... NO REPORT NUMBER

c30 A69-42863*# ..... NO REPORT NUMBER
c28 A69-42865*# ..... NO REPORT NUMBER
c05 A69-42876*# ..... NO REPORT NUMBER
c30 A69-42883*# ..... NO REPORT NUMBER
c30 A69-42887* ..... NO REPORT NUMBER
c30 A69-42890* ..... NO REPORT NUMBER
c20 A69-42896 # ..... NO REPORT NUMBER
c13 A69-42905* ..... NO REPORT NUMBER
c34 A69-42930* ..... NO REPORT NUMBER
c05 A69-42983*# ..... NO REPORT NUMBER
c32 A69-42991 # ..... NO REPORT NUMBER
c29 A69-43003* ..... NO REPORT NUMBER
c11 A69-43044*# ..... NO REPORT NUMBER
c20 A69-43066*# ..... NO REPORT NUMBER
c23 A69-43119*# ..... NO REPORT NUMBER
c31 A69-43120*# ..... NO REPORT NUMBER
c26 A69-43121*# ..... NO REPORT NUMBER
c25 A69-43122*# ..... NO REPORT NUMBER
c24 A69-43123*# ..... NO REPORT NUMBER
c24 A69-43124*# ..... NO REPORT NUMBER
c24 A69-43125*# ..... NO REPORT NUMBER
c15 A69-43126*# ..... NO REPORT NUMBER
c20 A69-43154* ..... NO REPORT NUMBER
c29 A69-43169* ..... NO REPORT NUMBER
c13 A69-43181* ..... NO REPORT NUMBER
c14 A69-43192* ..... NO REPORT NUMBER
c30 A69-43197* ..... NO REPORT NUMBER
c21 A69-43245*# ..... NO REPORT NUMBER
c30 A69-43254*# ..... NO REPORT NUMBER
c10 A69-43267 ..... NO REPORT NUMBER
c02 A69-43279* ..... NO REPORT NUMBER
c26 A69-43344* ..... NO REPORT NUMBER
c26 A69-43345* ..... NO REPORT NUMBER
c12 A69-43367*# ..... NO REPORT NUMBER
c04 A69-43369 ..... NO REPORT NUMBER
c04 A69-43372*# ..... NO REPORT NUMBER
c15 A69-43416 ..... NO REPORT NUMBER
c15 A69-43452* ..... NO REPORT NUMBER
c33 A69-43511*# ..... NO REPORT NUMBER
c33 A69-43540*# ..... NO REPORT NUMBER
c33 A69-43541*# ..... NO REPORT NUMBER
c33 A69-43542*# ..... NO REPORT NUMBER
c33 A69-43550*# ..... NO REPORT NUMBER
c33 A69-43564*# ..... NO REPORT NUMBER
c04 A69-43565* ..... NO REPORT NUMBER
c01 A69-43588*# ..... NO REPORT NUMBER
c29 A69-43603 ..... NO REPORT NUMBER
c29 A69-43609* ..... NO REPORT NUMBER
c29 A69-43621* ..... NO REPORT NUMBER
c26 A69-43666*# ..... NO REPORT NUMBER
c32 A69-43671*# ..... NO REPORT NUMBER
c33 A69-43680*# ..... NO REPORT NUMBER
c24 A69-43700*# ..... NO REPORT NUMBER
c02 A69-43715*# ..... NO REPORT NUMBER
c17 A69-43718*# ..... NO REPORT NUMBER
c04 A69-43750* ..... NO REPORT NUMBER
c01 N69-10054*# NASA-TN-D-4268
c15 N69-10055*# NASA-TN-D-4761
c21 N69-10056*# NASA-TN-D-4835
c32 N69-10057*# NASA-TN-D-4864
c18 N69-10066*# NASA-TM-X-1688
c22 N69-10067*# NASA-TM-X-1685
c03 N69-10068*# NASA-TN-D-4898
c21 N69-10069*# NASA-TN-D-4861
c12 N69-10070*# NASA-TN-D-4899
c02 N69-10087*# NASA-TN-D-4890
c03 N69-10088*# NASA-TN-D-4874
c08 N69-10098*# NASA-TN-D-4917
c22 N69-10099*# NASA-TN-D-4922
c26 N69-10125*# NASA-TN-D-4904
c06 N69-10126*# NASA-TN-D-4886
c01 N69-10215*# NASA-TN-D-4865
c22 N69-10216*# NASA-TN-D-4823
c32 N69-10225*# NASA-CR-1196
c17 N69-10226*# NASA-TN-D-4884
c33 N69-10227*# NASA-TN-D-4897
c15 N69-10228*# NASA-TN-D-4883
c15 N69-10231*# NASA-TN-D-4873
c15 N69-10249*# NASA-TN-D-4875
c09 N69-10250*# NASA-TN-D-4923
c12 N69-10293*# NASA-TM-X-1689
c01 N69-10294*# NASA-TM-X-1692
c31 N69-10295*# NASA-TM-X-1678
c28 N69-10296*# NASA-TM-X-1696
c32 N69-10297*# NASA-TN-D-4846
c15 N69-10298*# F-C1859
NASA-CR-1203
c08 N69-10316*# NASA-CR-1179
c01 N69-10343*# DAC-66900
NASA-CR-1218
c15 N69-10370*# NASA-TN-D-4351
c02 N69-10371*# NASA-TN-D-4854
c21 N69-10372*# NASA-TN-D-4863
c33 N69-10420*# NASA-TN-D-4887
c12 N69-10443*# NASA-TN-D-4869
c04 N69-10444*# NASA-SP-161
c30 N69-10470*# NASA-TN-D-4903
c25 N69-10471*# NASA-TN-D-4831
c12 N69-10472*# NASA-TN-D-4853
c33 N69-10473*# NASA-TN-D-4876
c13 N69-10492*# NASA-SP-5056
c02 N69-10495*# NASA-TN-D-4832
c01 N69-10558*# NASA-TM-X-1697
c34 N69-10662*# NASA-SP-5048
c12 N69-10693*# NASA-SP-183
c03 N69-10708*# NASA-TN-D-4889
c01 N69-10732*# NASA-TM-X-1684
c02 N69-10733*# NASA-TN-D-4726
c22 N69-10734*# NASA-TN-D-4913
c18 N69-10754*# NASA-TN-D-4888
c10 N69-10755*# NASA-TN-D-4893
c30 N69-10756*# NASA-TN-D-4896
c15 N69-10757*# NASA-TN-D-4824
c17 N69-10764*# NASA-TN-D-4877
c31 N69-10775*# NASA-TN-D-4870
c12 N69-10788*# NASA-TR-R-295
c01 N69-10789*# NASA-TN-D-4909
c12 N69-10804*# NASA-TN-D-4907
c05 N69-10813*# NASA-CR-1134
SIO-REF-68-6
c26 N69-10817*# NASA-CR-1236
TR-8-5
c17 N69-10827*# NASA-TN-D-4912
c07 N69-10885*# NASA-TN-D-4879
c11 N69-10888*# NASA-TN-D-4894
c23 N69-10889*# NASA-TN-D-4910
c17 N69-10931*# NASA-TN-D-4885
c33 N69-10932*# NASA-TN-D-4892
c14 N69-10933*# NASA-TN-D-4901
c31 N69-10934*# NASA-TN-D-4871
c02 N69-10935*# NASA-TN-D-4856
c31 N69-11007*# NASA-TN-D-4872
c32 N69-11008*# NASA-CR-1237
c01 N69-11009*# NASA-TN-D-4911
c32 N69-11010*# NASA-CR-1231
REPT-68-23
c07 N69-11011*# NASA-TN-D-4825
c17 N69-11012*# NASA-TN-D-4878
c04 N69-11056*# NASA-TN-D-4906
c11 N69-11371*# NASA-TN-D-4900
c03 N69-11373*# NASA-CR-1135
c19 N69-11419*# NASA-CR-1247
R-7491
c17 N69-11420*# ARC-R-280
NASA-CR-1232
c08 N69-11470*# NASA-CR-1183
c02 N69-11542*# NASA-SP-189
c01 N69-11634*# NASA-TN-D-4919
c05 N69-11675*# NASA-CR-1233-VOL-1
c04 N69-11695*# NASA-SP-7011/55/
c01 N69-12286* DAD-66898
DAD-66899
NASA-CR-1218-SUPPL
c13 N69-12384*# NASA-TT-F-345
TT-66-51025
c04 N69-12434*# NASA-CR-1205-VOL-1
c03 N69-12575*# NASA-SP-5057
c04 N69-12588*# NASA-CR-1205-VOL-2
c04 N69-12592*# NASA-CR-1205-VOL-3
c04 N69-12600*# NASA-CR-1205-VOL-4
c33 N69-12739*# NASA-TN-D-4926
c24 N69-12778*# NASA-TN-D-4933
c28 N69-12831*# NASA-TN-D-4958
c24 N69-12840*# NASA-TN-D-4932
c20 N69-12934*# NASA-TN-D-4940
c32 N69-13034*# NASA-TN-D-4921
c24 N69-13152*# NASA-TN-D-4938
c01 N69-13154*# NASA-TM-X-1706
c07 N69-13155*# NASA-TN-D-4895
c07 N69-13158*# NASA-TN-D-4920
c34 N69-13159*# NASA-CR-1210
c05 N69-13161*# NASA-CR-1214
c14 N69-13176*# NASA-TM-X-1654
c02 N69-13185*# CAL-IM-2429-B-1
NASA-CR-1208
c05 N69-13202*# NASA-CR-1206
c24 N69-13210*# NASA-TM-X-1702
c01 N69-13218*# NASA-TM-X-1701
c33 N69-13231*# NASA-TN-D-4914
c31 N69-13232*# NASA-TN-D-4916
c28 N69-13237*# NASA-TM-X-1699
c01 N69-13238*# NASA-TN-D-4935
c03 N69-13246*# NASA-TM-X-1698

c02 N69-13252*# NASA-TN-D-4939
c15 N69-13256*# NASA-TN-D-4934
c30 N69-13274*# NASA-CR-1250
c28 N69-13275*# NASA-TM-X-1676
c30 N69-13300*# NASA-CR-1249
c07 N69-13301*# NASA-TN-D-4915
c22 N69-13309*# NASA-TN-D-4918
c14 N69-13311*# NASA-TN-D-4925
c19 N69-13368*# NASA-TN-D-4902
c08 N69-13566*# NASA-TM-X-1700
c01 N69-13621*# NASA-CR-1254
c20 N69-13629*# LR-21588
NASA-CR-1204
c30 N69-13844*# NASA-SP-162
c05 N69-13926*# NASA-CR-1251
c12 N69-13945*# NASA-TN-D-4936
c05 N69-13969*# NASA-CR-1223
c01 N69-14000*# NASA-TN-D-4928
c01 N69-14001*# NASA-TN-D-4929
c19 N69-14002*# NASA-TM-X-1707
c02 N69-14008*# NASA-TN-D-4931
c31 N69-14010*# NASA-TN-D-4908
c31 N69-14033*# NASA-TM-X-1708
c01 N69-14075*# NASA-TM-X-1710
c15 N69-14082*# NASA-TN-D-4967
c26 N69-14086*# NASA-TM-X-1711
c05 N69-14094*# NASA-CR-1255
c12 N69-14095*# NASA-CR-1245
c05 N69-14145*# BBN-1681
NASA-CR-1258
c32 N69-14169*# NASA-TN-D-4927
c33 N69-14171*# NASA-CR-1207
c06 N69-14180*# NASA-TN-D-4971
c17 N69-14193*# NASA-SP-5051
c28 N69-14210*# NASA-CR-1256
c01 N69-14211*# NASA-CR-1219
c05 N69-14212*# NASA-CR-1212
TR-154-1
c05 N69-14213*# NASA-CR-1235
c15 N69-14214*# NASA-CR-1157
RR-68-2
c15 N69-14241*# NASA-SP-5052
c32 N69-14254*# NASA-CR-1217
c09 N69-14256*# NASA-CR-1228
c24 N69-14288*# NASA-TN-D-4982
c01 N69-14289*# NASA-TN-D-4969
c13 N69-14290*# NASA-TN-D-4648
c32 N69-14306*# NASA-TN-D-4975
c03 N69-14312*# NASA-TM-X-1715
c28 N69-14313*# NASA-TM-X-1709
c12 N69-14314*# NASA-TN-D-3889
c32 N69-14315*# NASA-TN-D-4953
c12 N69-14316*# NASA-TN-D-4957
c21 N69-14332*# NASA-TN-D-4952
c05 N69-14345*# NASA-CR-1261
c21 N69-14346*# NASA-TN-D-4905
c14 N69-14351*# R-67-4450
c21 N69-14382*# NASA-TN-D-4944
c15 N69-14383*# NASA-TN-D-4954
c28 N69-14384*# NASA-TN-D-4968
c01 N69-14385*# NASA-TN-D-4978
c28 N69-14386*# NASA-TN-D-4965
c04 N69-14387*# NASA-SP-7011/56/
c03 N69-14397*# NASA-CR-1216
c24 N69-14398*# NASA-TM-X-1718
c21 N69-14399*# NASA-TN-D-4945
c18 N69-14400*# NASA-CR-1213
WAED-67.24E
c17 N69-14403*# NASA-TN-D-4955
c30 N69-14428*# NASA-TR-R-278
c24 N69-14448*# NASA-TN-D-4798
c13 N69-14450*# NASA-TN-D-4647
c19 N69-14476*# NASA-TN-D-4826
c32 N69-14477*# NASA-CR-1178
c05 N69-14478*# BSD-68-643
NASA-CR-1239
c30 N69-14479*# NASA-TN-D-4979
c32 N69-14480*# NASA-TN-D-4951
c22 N69-14481*# NASA-TN-D-4949
c24 N69-14482*# NASA-TN-D-4948
c12 N69-14483*# NASA-TN-D-4947
c33 N69-14501*# NASA-TN-D-4937
c22 N69-14503*# NASA-TN-D-4946
c02 N69-14504*# NASA-TN-D-4859
c20 N69-14505*# NASA-TN-D-4880
c32 N69-14506*# NASA-TN-D-4941
c11 N69-14507*# NASA-TN-D-4924
c03 N69-14518*# NASA-TN-D-4956
c25 N69-14525*# NASA-TN-D-4950
c32 N69-14553*# NASA-SP-8009
c26 N69-14565*# NASA-TN-D-4970
c01 N69-14566*# NASA-TN-D-4960
c33 N69-14588*# NASA-TN-D-4959
c02 N69-14729*# NASA-CR-1240
c02 N69-14763*# NASA-CR-1262
c18 N69-14764*# NASA-CR-1252
c05 N69-14768*# NASA-CR-1248
c04 N69-14860*# NASA-SP-5054
c30 N69-14861*# NASA-TN-D-4942
c01 N69-14872*# NASA-TN-D-4961
c17 N69-14873*# NASA-TN-D-4981
c30 N69-14943*# NASA-TT-F-491
c30 N69-14944*# NASA-TT-F-490
c07 N69-14973*# NASA-TT-F-527
c05 N69-14979*# NASA-CR-1234
c12 N69-15371*# NASA-TM-X-1716
c05 N69-15372*# NASA-CR-1238
TR-167-1
c07 N69-15373*# NASA-TN-D-4962
c31 N69-15374*# NASA-TR-R-297
c24 N69-15375*# NASA-TN-D-4989
c32 N69-15378*# NASA-CR-1280
c14 N69-15381*# NASA-TN-D-4986
c03 N69-15382*# NASA-CR-1260
c03 N69-15397*# NASA-TM-X-1722
c09 N69-15441 # NASA-TT-F-430
TT-67-51213
c12 N69-15473*# NASA-TM-X-1719
c28 N69-15475*# NASA-TM-X-1721
c05 N69-15629*# NASA-TN-D-4980
c12 N69-15630*# NASA-TN-D-4976
c12 N69-15631*# NASA-TN-D-4974
c32 N69-15632*# NASA-TN-D-4963
c11 N69-15633*# NASA-TN-D-4985
c31 N69-15634*# NASA-TN-D-4977
c32 N69-16091*# NASA-TN-D-4990
c14 N69-16097*# NASA-TN-D-4973
c12 N69-16098*# NASA-SP-3046
c14 N69-16099*# NASA-CR-1271
c14 N69-16100*# NASA-CR-1257
c15 N69-16104*# KAMAN-R-741
NASA-CR-1241
c32 N69-16114*# NASA-CR-1215
c32 N69-16115*# NASA-TM-X-1723
c01 N69-16121*# NASA-TN-D-5003
c28 N69-16122*# NASA-TN-D-4785
c08 N69-16140*# NASA-CR-1270
c28 N69-16152*# NASA-TM-X-1720
c27 N69-16153*# NASA-TN-D-4991
c28 N69-16154*# NASA-TN-D-4996
c31 N69-16155*# MAC-709-10
NASA-CR-1227
c32 N69-16156*# NASA-CR-1263
c07 N69-16162*# NASA-TN-D-4997
c01 N69-16180*# NASA-TN-D-4891
c33 N69-16181*# NASA-TR-R-296
c27 N69-16195*# NASA-TN-D-4992
c07 N69-16196*# NASA-TR-R-294
c15 N69-16197*# NASA-TN-D-4994
c10 N69-16198*# NASA-TN-D-4995
c01 N69-16209*# NASA-TM-X-1730
c30 N69-16210*# NASA-TN-D-5017
c32 N69-16211*# NASA-TN-D-5024
c05 N69-16212*# NASA-CR-1259
c28 N69-16213*# NASA-TM-X-1727
c20 N69-16214*# NASA-SP-175
c31 N69-16221*# NASA-CR-1209
REPT-3-32000/7R-36
c33 N69-16268*# NASA-TR-R-299
c15 N69-16367*# NASA-TN-D-5002
c03 N69-16379*# NASA-CR-1224
c17 N69-16380*# NASA-TN-D-5008
c22 N69-16381*# NASA-TN-D-5012
c14 N69-16382*# NASA-TM-X-1733
c17 N69-16383*# NASA-TN-D-5001
c02 N69-16384*# NASA-TN-D-5005
c01 N69-16460*# NASA-TN-D-5004
c15 N69-16463*# NASA-CR-1229
c17 N69-16465*# NASA-TN-D-5000
c25 N69-16466*# NASA-TN-D-4993
c01 N69-16467*# NASA-TM-X-1724
c32 N69-16469*# NASA-TN-D-4972
c21 N69-16503*# NASA-TN-D-4852
c04 N69-16537*# NASA-SP-7011/57/
c13 N69-16539*# NASA-TT-F-530
c30 N69-16571*# NASA-SP-179
c13 N69-16645*# NASA-CR-1253
c25 N69-17212*# GDC-DBE-68-008

c03 N69-17225*# NASA-TM-X-1729
c04 N69-17248*# NASA-TN-D-5021
c19 N69-17249*# NASA-CR-1294
c02 N69-17257*# NASA-TN-D-5018
c32 N69-17258*# NASA-TN-D-5070
c14 N69-17259*# NASA-TN-D-5061
c32 N69-17275*# NASA-TN-D-4998
c28 N69-17276*# NASA-TN-D-4999
c17 N69-17277*# NASA-TN-D-5019
c02 N69-17279*# NASA-TN-D-5040
c01 N69-17289*# NASA-TN-D-5032
c02 N69-17303*# NASA-TN-D-4983
c01 N69-17304*# NASA-TR-R-300
c30 N69-17305*# NASA-TN-D-5011
c01 N69-17312*# NASA-TN-D-5016
c22 N69-17313*# NASA-TN-D-5013
c22 N69-17314*# NASA-TN-D-5014
c01 N69-17392*# NASA-TM-X-1728
c01 N69-17398*# NASA-TN-D-4943
c33 N69-17438*# NASA-CR-1265
c02 N69-17700*# NASA-TN-D-5031
c22 N69-17701*# NASA-TM-X-1735
c14 N69-17702*# NASA-TM-X-1736
c32 N69-17737*# NASA-TN-D-5069
c05 N69-17738*# NASA-CR-1274
c12 N69-17751*# NASA-CR-1230
c03 N69-17765*# NASA-CR-1226
c32 N69-17766*# NASA-CR-1269
c32 N69-17770*# NASA-CR-1289
REPT-68-2
c20 N69-17772*# NASA-TM-X-1726
c12 N69-17779*# NASA-TN-D-5023
c21 N69-17780*# NASA-TN-D-5037
c28 N69-17781*# NASA-TM-X-1742
c04 N69-17782*# NASA-TN-D-5022
c21 N69-17788*# NASA-TT-F-524
c31 N69-17801*# NASA-TR-R-301
c05 N69-17814*# NASA-TN-D-5007
c30 N69-17815*# NASA-TM-X-1734
c01 N69-17816*# NASA-TN-D-5064
c01 N69-17818*# NASA-TM-X-1740
c12 N69-17827*# NASA-TN-D-5026
c01 N69-17831*# NASA-TN-D-5065
c28 N69-17847*# NASA-TN-D-4966
c31 N69-17851*# NASA-TN-D-4881
c14 N69-17944*# NASA-TN-D-5062
c24 N69-17976*# NASA-TN-D-5066
c15 N69-17988*# NASA-TN-D-5009
c25 N69-18041*# NASA-CR-1267
c03 N69-18042*# NASA-SP-172
c34 N69-18057*# NASA-CR-1275
c33 N69-18125*# NASA-CR-1266
c13 N69-18126*# NASA-CR-1286
UTEC-MR-67-055
c13 N69-18700*# NASA-CR-1293
c04 N69-18722*# NASA-CR-1283
c09 N69-18761*# IITRI-V6045
NASA-CR-1268
c03 N69-18885*# NASA-CR-1244
c26 N69-18897*# NASA-TN-D-5028
c33 N69-18898*# NASA-TM-X-1748
c17 N69-18952*# NASA-CR-1278
c14 N69-18953*# NASA-CR-1282
R-4035-30-1
c08 N69-18954*# NASA-TM-X-1749
c06 N69-18962*# NASA-TM-X-1746
c10 N69-19003*# NASA-CR-1225
c28 N69-19017*# NASA-TM-X-1737
c04 N69-19023*# NASA-SP-7011/58/
c13 N69-19024*# NASA-TN-D-5068
c07 N69-19025*# NASA-TM-X-1747
c27 N69-19026*# NASA-TN-D-4984
c01 N69-19027*# NASA-TN-D-5045
c01 N69-19028*# NASA-TR-R-302
c32 N69-19030*# NASA-CR-1273
c12 N69-19112*# NASA-TN-D-5058
c24 N69-19113*# NASA-TN-D-5075
c07 N69-19114*# NASA-TN-D-5038
c04 N69-19115*# NASA-TN-D-5039
c33 N69-19117*# NASA-CR-1264
c06 N69-19129*# NASA-TN-D-5027
c01 N69-19130*# NASA-TM-X-1739
c25 N69-19131*# NASA-TM-X-1738
c17 N69-19200*# NASA-TN-D-5025
c17 N69-19203*# NASA-TN-D-5010
c01 N69-19243*# NASA-TN-D-5047
c21 N69-19518*# NASA-SP-8015
c01 N69-19641*# NASA-TN-D-5057
c04 N69-19714*# NASA-SP-7011/60/
c15 N69-19775*# F-B2263
NASA-CR-1292
PWA-3070-VOL-3
c26 N69-19781*# NASA-TN-D-5079
c28 N69-19782*# NASA-TM-X-1756
c25 N69-19783*# NASA-TN-D-5078
c15 N69-19786*# NASA-CR-1288
TR-719-1
c03 N69-19799*# NASA-TN-D-5072
c15 N69-19800*# NASA-TN-D-5073
c18 N69-19825*# NASA-TN-D-5050
c01 N69-19826*# NASA-TN-D-5054
c17 N69-19827*# NASA-TN-D-5055
c24 N69-19828*# NASA-TN-D-5056
c03 N69-19829*# NASA-TN-D-5059
c17 N69-19831*# NASA-CR-1305
REPT-8800-67
c17 N69-19886*# APO-68-1101
NASA-CR-1276
c05 N69-19902*# ERA-67-7
NASA-CR-1146
c18 N69-19918*# NASA-TN-D-5053
c01 N69-19925*# NASA-TN-D-5046
c01 N69-19926*# NASA-TN-D-5048
c17 N69-19930*# NASA-TN-D-5076
c02 N69-19950*# NASA-TN-D-5071
c28 N69-19980*# NASA-TN-D-5074
c33 N69-20008*# NASA-TN-D-5063
c01 N69-20016*# NASA-TM-X-1758
c11 N69-20451*# NASA-SP-5073
c06 N69-20775*# NASA-TR-R-305
c14 N69-20777*# NASA-CR-1304
c03 N69-20780*# NASA-TN-D-5094
c17 N69-20789*# NASA-TN-D-5093
c18 N69-20790*# NASA-TN-D-5114
c12 N69-20794*# NASA-TN-D-5115
c22 N69-20795*# NASA-TN-D-5113
c03 N69-20797*# NASA-TN-D-5095
c26 N69-20798*# NASA-TN-D-5103
c06 N69-20801*# NASA-TM-X-1767
c30 N69-20810*# NASA-TN-D-5117
c03 N69-20828*# NASA-TM-X-1731
c02 N69-20848*# NASA-CR-1285
c03 N69-20852*# NASA-TN-D-5085
c06 N69-20853*# NASA-TM-X-1753
c22 N69-20854*# NASA-TM-X-1769
c03 N69-20868*# NASA-TM-X-1732
c23 N69-20870*# NASA-TM-X-1754
c01 N69-20873*# NASA-TM-X-1759
c14 N69-20874*# NASA-TM-X-1760
c25 N69-20875*# NASA-TM-X-1761
c28 N69-20876*# NASA-TN-D-4987
c33 N69-20882*# NASA-TN-D-5080
c03 N69-20883*# NASA-TM-X-1757
c09 N69-20888*# NASA-TN-D-5077
c23 N69-20905*# NASA-TN-D-5110
c03 N69-20913*# NASA-TM-X-1741
c01 N69-20914*# NASA-TN-D-5084
c30 N69-20916*# NASA-SP-8011
c21 N69-20936*# NASA-TN-D-5049
c03 N69-20937*# NASA-TN-D-5090
c15 N69-20938*# NASA-TN-D-5096
c15 N69-20939*# NASA-TN-D-5097
c19 N69-20940*# NASA-TN-D-5083
c14 N69-20941*# NASA-TN-D-5106
c31 N69-20965*# NASA-TN-D-5029
c25 N69-20997*# NASA-TR-R-303
c01 N69-21000*# NASA-TN-D-5030
c03 N69-21016*# NASA-TN-D-5133
c31 N69-21017*# NASA-TN-D-5099
c30 N69-21018*# NASA-TN-D-5105
c02 N69-21020*# NASA-TN-D-5102
c32 N69-21042*# NASA-TN-D-5108
c31 N69-21065*# NASA-SP-151
c03 N69-21088*# NASA-TN-D-5109
c01 N69-21106*# NASA-TM-X-1771
c31 N69-21111*# NASA-TN-D-5107
c14 N69-21117*# NASA-CR-1298
R-68-4459
c08 N69-21119*# NASA-TM-X-1762
c10 N69-21123*# NASA-TN-D-5082
c25 N69-21124*# G-910092-10
NASA-CR-1313
c19 N69-21143*# NASA-CR-1272
c18 N69-21384*# NASA-TN-D-5116
c32 N69-21392*# NASA-TN-D-5140
c31 N69-21399*# NASA-TM-X-1768
c12 N69-21400*# NASA-TN-D-5132
c32 N69-21401*# NASA-CR-1321

TR-8-7
c21 N69-21402*# NASA-TR-R-304
c32 N69-21403*# NASA-CR-1281
c17 N69-21404*# NASA-TN-D-5136
c14 N69-21408*# NASA-TN-D-5125
c24 N69-21462*# NASA-TN-D-5088
c28 N69-21463*# NASA-TN-D-5098
c28 N69-21476*# NASA-CR-1287
WR-68-15
c01 N69-21477*# NASA-CR-1297
c05 N69-21478*# NASA-SP-5070
c26 N69-21500*# NASA-TN-D-5137
c05 N69-21501*# NASA-TN-D-5111
c21 N69-21502*# NASA-CR-976
c30 N69-21506*# NASA-CR-1279
c30 N69-21526*# NASA-TN-D-5020
c08 N69-21527*# NASA-CR-1284
c32 N69-21569*# NASA-CR-1320
TR-8-6
c28 N69-21648*# NASA-TM-X-1777
c12 N69-21653*# NASA-CR-1303
NEAR-TR-6
c03 N69-21771*# NASA-CR-1290
PWA-3070-VOL-1
c15 N69-21772*# MTI-67TR29
NASA-CR-1291
PWA-3070-VOL-2
c15 N69-21773*# NASA-TN-D-5138
c01 N69-21811*# NASA-TN-D-5044
c32 N69-21814*# NASA-TN-D-5131
c30 N69-22226*# NASA-SP-177
c34 N69-22510*# NASA-SP-196-VOL-1
c02 N69-22539*# NASA-TN-D-5153
c23 N69-22545*# KN-68-698-4
NASA-CR-1338
c02 N69-22546*# NASA-CR-1299
c26 N69-22552*# NASA-TN-D-5119
c01 N69-22553*# NASA-TM-X-1764
c01 N69-22554*# NASA-TN-D-5121
c22 N69-22555*# NASA-TM-X-1779
c20 N69-22570*# NASA-SP-176
c30 N69-22571*# NASA-TN-D-5104
c02 N69-22572*# NASA-TN-D-5175
c26 N69-22573*# NASA-TN-D-5130
c11 N69-22629*# NASA-TN-D-5123
c31 N69-22630*# NASA-TN-D-5051
c04 N69-22637*# NASA-CR-1309
TR-168-1
c25 N69-22638*# G-910091-18
NASA-CR-1312
c05 N69-22766*# NASA-CR-1296
c23 N69-22769*# NASA-TN-D-5181
c32 N69-22773*# NASA-SP-8012
c32 N69-22821*# NASA-TN-D-5143
c32 N69-22823*# NASA-TN-D-5139
c03 N69-22896*# NASA-TN-D-5155
c10 N69-22919*# NASA-TN-D-5112
c25 N69-22920*# G-910092-11
NASA-CR-1314
c33 N69-22931*# NASA-TN-D-5168
c32 N69-22932*# NASA-TN-D-5159
c33 N69-22933*# NASA-TM-X-1778
c24 N69-22934*# NASA-TN-D-5067
c08 N69-22935*# NASA-TN-D-5165
c21 N69-22936*# NASA-TN-D-5150
c31 N69-22937*# NASA-TN-D-5156
c01 N69-22938*# NASA-TN-D-5091
c30 N69-22939*# NASA-TN-D-5120
c03 N69-22940*# NASA-TN-D-5154
c25 N69-22942*# NASA-TN-D-5122
c22 N69-22946 # NAA-SR-12629
c30 N69-22948*# NASA-TR-R-307
c07 N69-22949*# NASA-TN-D-5087
c07 N69-22951*# NASA-TR-R-306
c26 N69-22965*# NASA-TN-D-5158
c21 N69-22969*# NASA-TM-X-1772
c15 N69-22970*# NASA-TM-X-1765
c32 N69-22982*# NASA-CR-1322
TR-8-8
c32 N69-22983*# NASA-CR-1306
REPT-340-2
c19 N69-22988*# NASA-TN-D-5167
c11 N69-22989*# NASA-TN-D-5126
c05 N69-22990*# NASA-TN-D-5162
c06 N69-22991*# NASA-TN-D-5177
c15 N69-22992*# NASA-TN-D-5141
c17 N69-22993*# NASA-TN-D-5169
c32 N69-22994*# NASA-TN-D-5135
c21 N69-22996*# NASA-TN-D-5149
c33 N69-22997*# NASA-TN-D-5146
c17 N69-23004*# NASA-TN-D-5145
c17 N69-23084*# NASA-TN-D-5157
c12 N69-23085*# NASA-TN-D-5147
c32 N69-23096*# NASA-CR-1302
c04 N69-23126*# NASA-SP-7011/61/
c07 N69-23163*# NASA-TN-D-4930
c11 N69-23194*# NASA-TN-D-5151
c23 N69-23199*# KN-67-698-2
NASA-CR-1337
c09 N69-23225*# NASA-CR-1346
REPT-03-67-04-VOL-1
c09 N69-23226*# NASA-CR-1347
REPT-03-67-04-VOL-2
c15 N69-23232*# NASA-TN-D-5170
c07 N69-23317*# NASA-TN-D-5100
c13 N69-23318*# NASA-TN-D-5101
c32 N69-23320*# NASA-SP-8007
c33 N69-23351*# NASA-TN-D-5171
c06 N69-23353*# NASA-TN-D-5184
c19 N69-23355*# NASA-TN-D-5176
c03 N69-23356*# NASA-TN-D-5144
c08 N69-23381*# N-07-68-1
NASA-CR-1318
c32 N69-23448*# NASA-TN-D-5118
c02 N69-23449*# NASA-TN-D-5202
c22 N69-23450*# G-910091-17
NASA-CR-1311
c25 N69-23451*# G-910375-3
NASA-CR-1315
c17 N69-23465*# NASA-TN-D-5185
c15 N69-23466*# NASA-TN-D-5161
c12 N69-23467*# NASA-TN-D-5160
c14 N69-23470*# NASA-TN-D-5015
c33 N69-23471*# NASA-TN-D-5006
c28 N69-23519*# NASA-TM-X-1780
c01 N69-23538*# NASA-TM-X-1786
c09 N69-23556*# NASA-TN-D-5183
c13 N69-23557*# NASA-TN-D-5052
c07 N69-23642*# NASA-TR-R-309
c03 N69-23643*# NASA-SP-5071
c32 N69-23697*# NASA-TM-X-1781
c06 N69-23706*# NASA-TN-D-5197
c33 N69-23707*# NASA-TN-D-5092
c30 N69-23708*# NASA-TN-D-5200
c17 N69-23731*# NASA-TN-D-5195
c15 N69-23768*# NASA-TM-X-1766
c01 N69-23769*# NASA-TN-D-5134
c01 N69-23781*# NASA-TN-D-5199
c30 N69-23782*# NASA-TN-D-5172
c25 N69-23787*# NASA-TR-R-310
c19 N69-23788*# NASA-TN-D-5194
c05 N69-23842*# NASA-TN-D-5127
c18 N69-23843*# NASA-TM-X-1776
c07 N69-23882*# NASA-TN-D-5081
c01 N69-23892*# NASA-CR-1341
c14 N69-23895*# NASA-TN-D-5179
c01 N69-23926*# NASA-TN-D-5193
c01 N69-23927*# NASA-TN-D-5148
c31 N69-24038*# NASA-TM-X-1784
c07 N69-24051*# NASA-TN-D-5180
c22 N69-24055*# NASA-CR-1343
c32 N69-24056*# NASA-CR-1317
c12 N69-24058*# NASA-CR-1336
c07 N69-24059*# NASA-CR-1327
TR-1691-30
c11 N69-24089*# NASA-CR-1352
c32 N69-24131*# NASA-SP-8019
c33 N69-24168*# NASA-TN-D-5196
c30 N69-24170*# NASA-TR-R-308
c30 N69-24206*# NASA-TT-F-514
c28 N69-24223*# EDR-4909-VOL-4
NASA-CR-1342
c14 N69-24751*# NASA-SP-5072
c04 N69-24752*# NASA-SP-7011/59/
c31 N69-24760*# NASA-TT-F-500
TT-68-50304
c02 N69-24761*# NASA-TT-F-555
c01 N69-24764*# NASA-TN-D-5204
c32 N69-24765*# NASA-TR-R-298
c15 N69-24791*# NASA-TN-D-5225
c12 N69-24800*# NASA-TN-D-5209
c22 N69-24802*# NASA-TN-D-5178
c04 N69-24822*# NASA-SP-7011/62/
c33 N69-24824*# NASA-TN-D-5214
c24 N69-24826*# NASA-TN-D-5211
c32 N69-24876*# NASA-CR-1324
c12 N69-24877*# NASA-CR-1362
c26 N69-24916*# NASA-TN-D-5198

c12 N69-24917*# NASA-TN-D-5210
c10 N69-24918*# NASA-TN-D-5212
c24 N69-24919*# NASA-TN-D-5216
c25 N69-24920*# NASA-TN-D-5215
c28 N69-24922*# NASA-TN-D-5218
c29 N69-24924*# NASA-TT-F-535
c12 N69-24926*# NASA-CR-1363
c15 N69-24932*# NASA-TN-D-5224
c12 N69-24935*# NASA-TN-D-5164
c28 N69-24938*# NASA-TM-X-1792
c06 N69-24940*# NASA-TN-D-5213
c31 N69-24942*# NASA-TM-X-1793
c30 N69-24950*# NASA-CR-1331
c12 N69-24958*# NASA-CR-1368
c32 N69-25001*# NASA-TN-D-4345
c13 N69-25013*# NASA-TT-F-546
c17 N69-25243*# NASA-TM-X-1791
c01 N69-25244*# NASA-TM-X-1789
c32 N69-25301*# NASA-TM-X-1796
c22 N69-25305*# NASA-TM-X-1795
c19 N69-25311*# NASA-TM-X-1797
c33 N69-25312*# NASA-TN-D-5226
c01 N69-25327*# EDR-5315-VOL-2
NASA-CR-1323
c09 N69-25328*# NASA-CR-1348
TI-03-67-04
c11 N69-25343*# NASA-CR-1353
c23 N69-25344*# NASA-CR-1333
c16 N69-25357*# NASA-TN-D-5205
c17 N69-25363*# NASA-TN-D-5229
c01 N69-25391*# NASA-SP-3048
c25 N69-25394*# NASA-TN-D-5217
c26 N69-25412*# NASA-TN-D-5227
c30 N69-25460*# NASA-SP-167
c24 N69-25848*# NASA-TT-F-510
TT-68-50309
c34 N69-26112*# NASA-TT-F-541
c17 N69-26192*# NASA-TN-D-5248
c08 N69-26193*# NASA-TN-D-5042
c02 N69-26194*# NASA-TN-D-5182
c21 N69-26195*# NASA-TN-D-5220
c32 N69-26223*# NASA-TN-D-5236
c28 N69-26224*# NASA-TN-D-5207
c22 N69-26231*# NASA-TM-X-1802
c21 N69-26232*# NASA-CR-1344
c22 N69-26233*# NASA-TM-X-1794
c32 N69-26234*# ARC-R-310
NASA-CR-1301
c30 N69-26235*# NASA-TN-D-5060
c33 N69-26236*# NASA-TN-D-5249
c30 N69-26239*# NASA-TN-D-5245
c33 N69-26247*# NASA-TN-D-5223
c19 N69-26248*# NASA-CR-1319
c30 N69-26252*# NASA-TN-D-5203
c17 N69-26258*# NASA-TN-D-5247
c05 N69-26259*# NASA-TN-D-5221
c22 N69-26270*# NASA-TN-D-5250
c01 N69-26271*# NASA-TN-D-5233
c07 N69-26272*# NASA-TN-D-5041
c07 N69-26273*# NASA-CR-1326
TR-1691-29
c23 N69-26307*# BBN-1734
NASA-CR-1340
c15 N69-26311*# NASA-TN-D-5262
c01 N69-26312*# NASA-TM-X-1798
c25 N69-26313*# NASA-TN-D-5244
c15 N69-26314*# NASA-TN-D-5152
c32 N69-26315*# BBN-1703
NASA-CR-1351
c18 N69-26448*# NASA-CR-1310
P68-148
c05 N69-26455*# NASA-TT-F-545
c31 N69-26458*# NASA-TM-X-1773
c12 N69-26504*# NASA-TR-R-311
c32 N69-26559*# NASA-CR-1357
c31 N69-26570*# NASA-TN-D-5219
c17 N69-26952*# NASA-TM-X-1799
c12 N69-26956*# NASA-TM-X-1774
c13 N69-26969*# NASA-TN-D-5163
c33 N69-26975*# NASA-TN-D-5173
c01 N69-26976*# NASA-TM-X-1785
c12 N69-26987*# NASA-SP-3045
c31 N69-26993*# BMSD-6182
NASA-CR-1361
c28 N69-27019*# NASA-TM-X-1803
c17 N69-27059*# AI-68-110
NASA-CR-1371
c17 N69-27061*# NASA-TN-D-5266
c15 N69-27078*# NASA-TN-D-5191
c12 N69-27168 # NASA-TT-F-560
TT-69-55023
c30 N69-27169 # NASA-TT-F-562
TT-69-55025
c02 N69-27177*# NASA-TN-D-5241
c13 N69-27246*# NASA-TN-D-5252
c31 N69-27260*# NASA-TM-X-1800
c05 N69-27266*# NASA-CR-1334
c14 N69-27267*# NASA-TN-D-5174
c21 N69-27268*# NASA-TN-D-5187
c31 N69-27299*# GDC-DDE-68-001
NASA-CR-835
c17 N69-27300*# NASA-TT-F-508
TT-68-50308
c30 N69-27412*# NASA-TN-D-5035
c05 N69-27577*# NASA-TT-F-523
c33 N69-27620*# NASA-TN-D-5263
c26 N69-27840*# NASA-TM-X-1807
c09 N69-27841*# NASA-TM-X-1808
c12 N69-27954*# NASA-TM-X-1811
c15 N69-27955*# NASA-TN-D-5264
c15 N69-27956*# NASA-TN-D-5192
c21 N69-28018*# NASA-TN-D-5261
c13 N69-28019*# NASA-TN-D-5034
c14 N69-28023*# NASA-CR-1358
c05 N69-28024*# NASA-TN-D-5235
c32 N69-28038*# NASA-TN-D-5253
c02 N69-28044*# NASA-TN-D-5256
c30 N69-28050*# NASA-TN-D-5043
c05 N69-28071*# NASA-CR-1325
TR-168-2
c11 N69-28095*# NASA-CR-1354
c26 N69-28096*# EE-4012-111-69U
NASA-CR-1364
c02 N69-28097*# NASA-TN-D-5232
c05 N69-28099*# NASA-CR-1359
c29 N69-28111*# NASA-TN-D-5166
c01 N69-28112*# NASA-TN-D-5242
c10 N69-28121*# NASA-TN-D-5237
c03 N69-28123*# NASA-TN-D-5234
c32 N69-28164*# NASA-CR-1316
c31 N69-28166*# NASA-TN-D-5260
c19 N69-28196*# NASA-CR-1328
c18 N69-28203*# NASA-TM-X-1813
c33 N69-28209*# NASA-TN-D-5230
c22 N69-28212*# NASA-TM-X-1812
c07 N69-28223*# NASA-CR-1308
c19 N69-28256*# NASA-CR-1356
c33 N69-28318*# NASA-TN-D-5124
c14 N69-28402*# NASA-CR-1300
c33 N69-28440*# NASA-TN-D-5257
c30 N69-28441*# NASA-TN-D-5271
c13 N69-28442*# NASA-TN-D-5036
c15 N69-28592*# NASA-SP-5058
c32 N69-28624*# NASA-CR-1350
c32 N69-28658*# NASA-TN-D-5254
c31 N69-28861*# ARC-R-297
NASA-CR-1329
c15 N69-28862*# NASA-TM-X-1815
c17 N69-28863*# NASA-TN-D-5273
c34 N69-28868*# NASA-CR-1355
c14 N69-28909* NASA-SP-171
c24 N69-28911*# NASA-SP-3024-VOL-5
c13 N69-28983*# NASA-TT-F-532
c01 N69-29027*# NASA-TN-D-5208
c30 N69-29115*# NASA-TN-D-5231
c25 N69-29140*# NASA-TN-D-5269
c19 N69-29141*# NASA-TN-D-5277
c12 N69-29144*# NASA-TN-D-5089
c14 N69-29153*# NASA-TN-D-5281
c01 N69-29154*# NASA-TN-D-5201
c32 N69-29159*# NASA-TN-D-4858
c15 N69-29165*# NASA-TN-D-5292
c04 N69-29195*# NASA-TN-D-5255
c14 N69-29196*# NASA-TN-D-5287
c07 N69-29230*# NASA-TR-R-314
c01 N69-29231*# NASA-TM-X-1816
c02 N69-29232*# NASA-TN-D-5270
c12 N69-29235*# NASA-TT-F-577
c19 N69-29268*# NASA-CR-1345
c01 N69-29269*# NASA-TN-D-5272
c01 N69-29270*# NASA-TR-R-312
c01 N69-29318*# NASA-TM-X-1787
c28 N69-29321*# NASA-TN-D-5282
c14 N69-29331*# NASA-TN-D-5285
c28 N69-29405*# NASA-TN-D-5303
c26 N69-29407*# NASA-TN-D-5290
c15 N69-29476*# NASA-TN-D-5258
c23 N69-29477*# NASA-TN-D-5086

c08 N69-29478*# NASA-TN-D-5228
c01 N69-29479*# NASA-TN-D-5288
c13 N69-29491*# NASA-TT-F-533
c34 N69-29492*# NASA-SP-7033
c14 N69-29553*# NASA-TN-D-5291
c03 N69-29555*# NASA-TM-X-1819
c30 N69-29557*# NASA-TN-D-5276
c32 N69-29558*# NASA-CR-1376
c18 N69-29559*# NASA-CR-1367
c15 N69-29568*# NASA-TN-D-5301
c30 N69-29569*# NASA-TM-X-1806
c26 N69-29588*# NASA-TN-D-5286
c32 N69-29589*# NASA-TN-D-5222
c08 N69-29592*# NASA-TN-D-5275
c22 N69-29593*# NASA-TM-X-1822
c31 N69-29594*# NASA-TM-X-1826
c21 N69-29595*# NASA-TN-D-5186
c33 N69-29598*# NASA-TN-D-5289
c33 N69-29599*# L-6383
NASA-TN-D-5278
c25 N69-29600*# NASA-TN-D-5274
c32 N69-29607*# NASA-TN-D-5294
c12 N69-29608*# NASA-TN-D-5251
c19 N69-29648*# NASA-TN-D-5300
c29 N69-29652*# NASA-SP-199
c22 N69-29671*# NASA-TM-X-1828
c32 N69-29672*# NASA-TN-D-5317
c03 N69-29707*# NASA-TM-X-1820
c04 N69-29723*# NASA-TM-X-1818
c26 N69-29724*# NASA-CR-1366
c14 N69-29730*# NASA-TN-D-5299
c32 N69-29734*# NASA-TM-X-1821
c11 N69-29737*# NASA-TM-X-1825
c30 N69-29738*# NASA-TN-D-5293
c25 N69-29905*# NASA-TN-D-5319
c16 N69-29934*# NASA-CR-1374
S-1112
c21 N69-29967*# NASA-CR-1369
SUDAAR-361
c03 N69-29977*# NASA-TN-D-5331
c11 N69-29981*# NASA-TN-D-5295
c08 N69-30014*# NASA-TM-X-1824
c01 N69-30060*# NASA-TN-D-5330
c15 N69-30062*# NASA-TN-D-5320
c01 N69-30063*# NASA-TN-D-5296
c33 N69-30064*# NASA-TN-D-5323
c15 N69-30069*# NASA-TN-D-5318
c22 N69-30070*# NASA-TN-D-5312
c12 N69-30071*# NASA-TN-D-5297
c26 N69-30072*# NASA-TN-D-5313
c24 N69-30073*# NASA-TN-D-5321
c24 N69-30074*# NASA-TN-D-5329
c05 N69-30168*# NASA-CR-1370
c33 N69-30245*# NASA-TT-F-552
c33 N69-30317*# NASA-SP-164-VOL-2
c31 N69-30339*# NASA-SP-8018
c15 N69-30401*# NASA-SP-181
c14 N69-30506*# NASA-TN-D-5327
c33 N69-30507*# NASA-TT-F-522
c28 N69-30560*# NASA-TN-D-5324
c01 N69-30609*# NASA-CR-1392
c19 N69-30610*# NASA-TR-R-313
c30 N69-30611*# NASA-TN-D-5259
c25 N69-30622*# NASA-TN-D-5328
c31 N69-30631*# NASA-TM-X-1837
c01 N69-30632*# NASA-TM-X-1836
c02 N69-30633*# NASA-TM-X-1835
c01 N69-30722*# NASA-TN-D-5129
c33 N69-30726*# NASA-TN-D-5309
c02 N69-30727*# NASA-TN-D-5315
c12 N69-30728*# NASA-CR-1335
c19 N69-30753*# NASA-TR-R-315
c32 N69-30754*# NASA-TT-F-518
c01 N69-30878*# NASA-TN-D-5322
c03 N69-30945*# NASA-TN-D-5265
c21 N69-30946*# NASA-TN-D-5298
c28 N69-30980*# NASA-TN-D-5339
c32 N69-31056*# NASA-TN-D-5340
c30 N69-31058*# NASA-TN-D-5267
c17 N69-31065*# NASA-TN-D-5326
c21 N69-31227*# NASA-TN-D-5238
c01 N69-31228*# NASA-TN-D-5343
c32 N69-31300*# NASA-TN-D-5354
c19 N69-31303*# NASA-TN-D-5240
c34 N69-31333*# NASA-TN-D-5283
c28 N69-31336*# NASA-TN-D-5338
c01 N69-31337*# NASA-TN-D-5335
c24 N69-31338*# NASA-TN-D-5308
c04 N69-31356*# NASA-TT-F-578
c12 N69-31359*# NASA-TN-D-5307
c01 N69-31360*# NASA-TM-X-1823
c30 N69-31362*# NASA-CR-1379
c04 N69-31401*# NASA-TT-F-501
TT-68-50302
c34 N69-31836*# NASA-TT-F-540
c03 N69-31844*# NASA-TN-D-5366
c13 N69-31851*# NASA-TT-F-590
c33 N69-31869*# NASA-TN-D-5356
c22 N69-31870*# NASA-TN-D-5347
c17 N69-31873*# NASA-TN-D-5352
c02 N69-31874*# NASA-TN-D-5306
c01 N69-31875*# NASA-TM-X-1839
c17 N69-31883*# NASA-TN-D-5355
c15 N69-31884*# NASA-TN-D-5349
c12 N69-31887*# NASA-CR-1382
c12 N69-31888*# NASA-TM-X-1847
c17 N69-31889*# NASA-TM-X-1843
c17 N69-31895*# NASA-TN-D-5353
c02 N69-31917*# NASA-TT-F-526
c04 N69-31923*# NASA-SP-7011/65/
c34 N69-31946*# NASA-SP-5075
c33 N69-31947*# NASA-TT-F-549
c14 N69-31958*# NASA-CR-1394
c02 N69-31959*# GASL-TR-713
NASA-CR-1378
c30 N69-31960*# NASA-CR-1404
TRW-11433-6005-R0-00
c13 N69-31961*# GDC-DBE-68-011
c02 N69-31962*# NASA-TN-D-5128-REV
c17 N69-31977*# NASA-TN-D-5348
c23 N69-31984*# NASA-TN-D-5351
c07 N69-31985*# NASA-SP-5080
c22 N69-31986*# NASA-TM-X-1838
c30 N69-31989*# NASA-TT-F-502
c31 N69-32021*# NASA-SP-4009
c05 N69-32044*# NASA-TT-F-529
c02 N69-32110*# NASA-TN-D-5342
c04 N69-32131*# NASA-TT-F-580
c12 N69-32217*# NASA-TM-X-1852
c02 N69-32284*# NASA-TN-D-5359
c14 N69-32286*# NASA-TN-D-5280
c31 N69-32298*# NASA-TN-D-5268
c01 N69-32299*# NASA-TN-D-5365
c30 N69-32316*# NASA-TN-D-5189
c22 N69-32317*# NASA-TN-D-5374
c28 N69-32318*# NASA-TN-D-5336
c19 N69-32319*# NASA-TN-D-5369
c02 N69-32337*# NASA-TN-D-5361
c01 N69-32338*# NASA-TR-R-317
c33 N69-32340*# NASA-TN-D-5375
c08 N69-32350*# NASA-CR-1387
c12 N69-32377*# NASA-TN-D-5372
c34 N69-32430*# NASA-SP-7500/03/
c33 N69-32468*# NASA-TM-X-1845
c12 N69-32480*# NASA-CR-1386
c03 N69-32553*# GESP-9001
NASA-CR-1416
c08 N69-32556*# NASA-TN-D-5370
c17 N69-32558*# NASA-TN-D-5362
c14 N69-32682*# NASA-TM-X-1832
c33 N69-32683*# NASA-TM-X-1846
c08 N69-32685*# NASA-TN-D-5350
c31 N69-32713*# NASA-TM-X-1841
c07 N69-32721*# NASA-CR-1330
TP-181
c22 N69-33132*# NASA-TM-X-1853
c01 N69-33210*# NASA-TN-D-5333
c28 N69-33211*# NASA-TN-D-5387
c32 N69-33232*# NASA-TN-D-4988
c01 N69-33237*# NASA-TN-D-5334
c15 N69-33258*# NASA-TN-D-5386
c05 N69-33260*# NASA-TM-X-1851
c12 N69-33261*# NASA-TM-X-1854
c22 N69-33273*# NASA-TM-X-1858
c01 N69-33275*# NASA-TN-D-5364
c15 N69-33281*# NASA-TN-D-5373
c01 N69-33302*# NASA-TN-D-5379
c17 N69-33307*# NASA-TN-D-5376
c33 N69-33314*# NASA-TN-D-5385
c28 N69-33319*# NASA-TN-D-5394
c18 N69-33321*# NASA-TN-D-5367
c14 N69-33322*# NASA-SP-193
c12 N69-33353*# NASA-TN-D-5377
c28 N69-33354*# NASA-TT-F-507
TT-68-50301
c31 N69-33380*# NASA-TM-X-1848
c29 N69-33401*# NASA-TT-F-581
c24 N69-33416*# NASA-CR-1377

REPT-0-71100/8R-18
c32 N69-33420*# NASA-TN-D-5363
c12 N69-33421*# NASA-TN-D-5246
c15 N69-33450*# NASA-CR-1401
PWA-3549
c32 N69-33481*# NASA-TN-D-4964
c30 N69-33490*# NASA-SP-35-VOL-3-PT-7
c06 N69-33493*# NASA-CR-1407
c13 N69-33555*# NASA-TM-X-1814
c30 N69-33560*# NASA-TT-F-539
c30 N69-33595*# NASA-SP-174
c05 N69-33775*# NASA-SP-5074
c15 N69-33800*# NASA-TN-D-5304
c28 N69-33806*# NASA-TM-X-1861
c18 N69-34134*# NASA-TM-X-1862
c19 N69-34360*# NASA-CR-1385
c24 N69-34541*# NASA-CR-1383
REPT-0-71100/9R-1
c18 N69-34547*# NASA-TN-D-5279
c28 N69-34575*# NASA-TN-D-5316
c14 N69-34628*# NASA-TM-X-1857
c03 N69-34652*# NASA-TN-D-5388
c21 N69-34672*# ISR-2
NASA-CR-1396
TR-101-4
c28 N69-34674*# NASA-TM-X-1864
c01 N69-34703*# NASA-CR-1307
c17 N69-34704*# NASA-TN-D-5390
c15 N69-34707*# NASA-TN-D-5389
c18 N69-34708*# NASA-TN-D-5380
c12 N69-34709*# CAL-AD-1689-A-10
NASA-CR-1411
c32 N69-34744*# NASA-CR-1332
RASA-68-10
c30 N69-34850*# NASA-SP-35-PT-8
c30 N69-34884*# NASA-TN-D-5398
c13 N69-34891*# NASA-TN-D-5332
c33 N69-34892*# NASA-TN-D-5395
c25 N69-34897*# NASA-CR-1393
c02 N69-34915*# NASA-CR-1398
TR-7
c17 N69-34916*# NASA-TM-X-1860
c34 N69-34917*# NASA-SP-7501
c33 N69-34966*# NASA-TN-D-5391
c32 N69-34970*# NASA-TN-D-5371
c01 N69-34986*# NASA-TN-D-5378
c02 N69-34988*# NASA-TM-X-1602
c05 N69-35024*# NASA-TN-D-5190
c14 N69-35265*# NASA-TN-D-5406
c23 N69-35286*# NASA-CR-1421
c01 N69-35300*# NASA-TN-D-5392
c27 N69-35321*# NASA-TN-D-5382
c11 N69-35359*# NASA-TN-D-5383
c12 N69-35365*# NASA-TT-F-558
c33 N69-35506*# NASA-TN-D-5404
c24 N69-35508*# NASA-TN-D-5407
c30 N69-35513*# NASA-CR-1412
c17 N69-35514*# NASA-CR-1413
c32 N69-35515*# NASA-CR-1424
c33 N69-35516*# NASA-CR-1414
c01 N69-35521*# LMSC-4-17-68-4
NASA-CR-1339
c20 N69-35523*# NASA-TM-X-1850
c28 N69-35526*# NASA-TN-D-5314
c20 N69-35528*# GCA-TR-69-5-N
NASA-CR-1419
c03 N69-35537*# NASA-TN-D-5405
c05 N69-35540*# DAC-58156
NASA-CR-1409
c05 N69-35541*# DAC-58155
NASA-CR-1408
c08 N69-35569*# NASA-TN-D-5402
c20 N69-35570*# NASA-CR-1410
c08 N69-35613*# NASA-CR-1397
c13 N69-35660*# NASA-CR-1415
c17 N69-35688*# NASA-TN-D-5413
c03 N69-35689*# GEST-2107
NASA-CR-1381
c28 N69-35712*# NASA-TM-X-1870
c22 N69-35723*# NASA-TM-X-1871
c25 N69-35732*# NASA-TN-D-5414
c02 N69-35762*# NASA-TN-D-5358
c03 N69-35763*# NASA-TM-X-1875
c17 N69-35764*# NASA-TM-X-1867
c15 N69-35769*# NASA-TN-D-5411
c15 N69-35788*# NASA-TN-D-5420
c15 N69-35799*# NASA-TN-D-5344
c08 N69-35816*# NASA-SP-3049
c22 N69-35817*# E-5079
NASA-TM-X-1874
c17 N69-35836*# NASA-TT-F-583
c12 N69-35842*# NASA-TN-D-5412
c28 N69-35847*# NASA-TM-X-1873
c22 N69-35848*# NASA-TM-X-1877
c01 N69-35855*# NASA-TN-D-5418
c15 N69-35859*# NASA-TT-F-534
c02 N69-35861*# NASA-CR-1428
c33 N69-35949*# NASA-TN-D-5403
c30 N69-36143*# NASA-TN-D-5381
c32 N69-36220*# NASA-TN-D-5410
c17 N69-36221*# NASA-TN-D-5417
c20 N69-36222*# NASA-CR-1418
c11 N69-36224*# NASA-TM-X-1868
c27 N69-36225*# NASA-TN-D-5397
c02 N69-36258*# NASA-TN-D-5408
c05 N69-36271*# NASA-CR-1403
c33 N69-36299*# NASA-TN-D-5416
c34 N69-36314*# NASA-TT-F-537
c02 N69-36326*# NASA-TT-F-547
c15 N69-36349*# NASA-CR-1391
c32 N69-36357*# NASA-CR-1365
c17 N69-36367*# GER-14188
NASA-CR-1433
c03 N69-36411*# NASA-CR-1417
c06 N69-36413*# NASA-CR-1425
R-7703
c30 N69-36439*# IBM-150
NASA-CR-1430
c30 N69-36451*# NASA-SP-184
c31 N69-36501*# NASA-SP-4002
c17 N69-36653*# NASA-TN-D-5424
c28 N69-36680*# EDR-5315-VOL-4
NASA-CR-1423
c17 N69-36697*# NASA-TN-D-5188
c01 N69-36699*# NASA-TN-D-5438
c33 N69-36701*# NASA-TN-D-5429
c09 N69-36706*# NASA-TN-D-5401
c05 N69-36709*# ERA-68-1
NASA-CR-1405
c09 N69-36710*# NASA-TN-D-5428
c17 N69-36723*# NASA-CR-1420
c25 N69-36755*# NASA-TN-D-5396
c22 N69-36756*# NASA-TM-X-1883
c22 N69-36757*# E-4919
NASA-TM-X-1888
c03 N69-36758*# NASA-TM-X-1884
c18 N69-36762*# NASA-CR-1384
RAI-397
c12 N69-36805*# NASA-TN-D-5433
c33 N69-36806*# NASA-TM-X-1881
c02 N69-36807*# NASA-TN-D-5409
c03 N69-36829*# NASA-CR-1434
c12 N69-36830*# NASA-TN-D-5434
c17 N69-36831*# ER-7365
NASA-CR-1436
c03 N69-36843*# NASA-CR-1435
c28 N69-36844*# NASA-TN-D-5448
c28 N69-36882*# NASA-TN-D-5437
c30 N69-36892*# NASA-TN-D-5357
c24 N69-36901*# NASA-TM-X-1878
c08 N69-36918*# NASA-TM-X-1885
c19 N69-36923*# NASA-TM-X-1882
c24 N69-36924*# NASA-TN-D-5423
c05 N69-36925*# BSD-69-701
NASA-CR-1439
c24 N69-36929*# NASA-TN-D-5430
c30 N69-36930*# NASA-TN-D-5368
c24 N69-36931*# NASA-TN-D-5431
c28 N69-36932*# NASA-TN-D-5393
c25 N69-36939*# NASA-TN-D-5371
c12 N69-36940*# NASA-TN-D-5440
c23 N69-36974*# NASA-CR-1373
PWA-3486
c20 N69-36976*# NASA-TM-X-1887
c14 N69-36985*# NASA-TR-R-321
c21 N69-36997*# NASA-TN-D-5384
c28 N69-36998*# NASA-TM-X-1880
c11 N69-37022*# NASA-CR-1399
c23 N69-37028*# NASA-TN-D-5422
c31 N69-37030*# NASA-SP-8016
c19 N69-37033*# ERL-69-2
NASA-CR-1432
c04 N69-37062*# NASA-CR-1438
c22 N69-37225*# NASA-TM-X-1893
c12 N69-37271*# NASA-TM-X-1889
c26 N69-37272*# NASA-TN-D-5441
c31 N69-37281*# NASA-TM-X-1859
c12 N69-37370*# NASA-TN-D-5346

c17 N69-37436*# NASA-TN-D-5442
c05 N69-37517*# NASA-CR-1388
c01 N69-37521*# NASA-TN-D-5427
c07 N69-37602*# NASA-TN-D-5446
c12 N69-37604*# NASA-TN-D-5450
c30 N69-37777*# NASA-SP-3050
c03 N69-37827*# NASA-TM-X-1894
c31 N69-37840*# NASA-TM-X-1879
c14 N69-37876*# NASA-CR-1375
SPO-20224
c03 N69-37883*# NASA-TN-D-5461
c04 N69-37887*# NASA-SP-7011/67/
c30 N69-37893*# NASA-TN-D-5284
c04 N69-37909*# NASA-SP-7011/66/
c33 N69-37936*# NASA-TN-D-5452
c05 N69-37964*# NASA-CR-1402
REPT-68-3986-REV-1
c12 N69-37965*# NASA-TN-D-5460
c02 N69-37976*# NASA-TM-X-1788
c30 N69-37993*# NASA-SP-3047-REV
c25 N69-38010*# NASA-TN-D-5449
c12 N69-38012*# NASA-TN-D-5467
c12 N69-38032*# NASA-TN-D-5462
c21 N69-38041*# NASA-CR-1443
RF-2421
c01 N69-38065*# NASA-TM-X-1895
c17 N69-38074*# NASA-TN-D-5421
c02 N69-38104*# NASA-TM-X-1896
c14 N69-38144*# NASA-TN-D-5360
c30 N69-38145*# NASA-TN-D-5459
c12 N69-38156*# NASA-TN-D-5454
c19 N69-38178*# NASA-TN-D-5465
c23 N69-38180*# NASA-TN-D-4024
c25 N69-38227*# LMSC-681796
NASA-CR-1390
c04 N69-38235*# NASA-SP-7011/63/
c04 N69-38242*# NASA-SP-7011/64/
c33 N69-38271*# NASA-TN-D-5464
c05 N69-38491*# NASA-CR-1400
TRW-06462-6005-R0-00
c24 N69-38564*# NASA-CR-1406
c09 N69-38597*# NASA-TN-D-5457
c02 N69-38598*# NASA-TM-X-1833
c28 N69-38599*# E-5102
NASA-TM-X-1842
c05 N69-38600*# NASA-CR-1395
c01 N69-38612*# NASA-TM-X-1840
c15 N69-38641*# NASA-TN-D-5484
c32 N69-38642*# NASA-TN-D-5453
c30 N69-38643*# NASA-TT-F-536
c08 N69-38654*# E-4863
NASA-TN-D-5474
c19 N69-38655*# L-6052
NASA-TR-R-326
c02 N69-38657*# NASA-CR-1427
c30 N69-38658*# NASA-TN-D-5443
c01 N69-38670*# NASA-TT-F-542
c05 N69-38701*# NASA-TT-F-528
c14 N69-38766*# NASA-TM-X-1886
c03 N69-38767*# NASA-TM-X-1899
c01 N69-38768*# NASA-TN-D-5419
c30 N69-38769*# NASA-TN-D-5425
c02 N69-38770*# NASA-TN-D-5444
c24 N69-38773*# E-5154
NASA-TM-X-1897
c09 N69-38774*# C-85
NASA-TM-X-1892
c01 N69-38775*# A-2894
NASA-TN-D-5468
c09 N69-38776*# E-5185
NASA-TN-D-5473
c32 N69-38781*# ARC-R-299
NASA-CR-1444
c12 N69-38782*# NASA-CR-1467
c17 N69-38794*# E-5011
NASA-TN-D-5483
c02 N69-38807*# A-3299
NASA-TN-D-5491
c32 N69-38808*# NASA-TN-D-5439
c32 N69-38809*# A-3252
NASA-TN-D-5492
c02 N69-38819*# NASA-CR-1426
c31 N69-38820*# NASA-TN-D-5399
c09 N69-38852*# NASA-TN-D-5445
c34 N69-38951*# NASA-SP-195
c07 N69-39176*# NASA-TN-D-5472
c12 N69-39177*# NASA-TN-D-5341
c23 N69-39178*# NASA-TN-D-5302
c17 N69-39182*# E-5098
NASA-TN-D-5493
c05 N69-39183*# L-6382
NASA-TN-D-5478
c24 N69-39184*# E-5075
NASA-TN-D-5486
c28 N69-39185*# E-5144
NASA-TN-D-5485
c22 N69-39186*# NASA-TN-D-5487
c24 N69-39187*# E-5147
NASA-TM-X-1902
c02 N69-39188*# L-6260
NASA-TN-D-5497
c05 N69-39210*# NASA-TN-D-5426
c05 N69-39211*# NASA-CR-1389
c05 N69-39212*# NASA-CR-1422
c30 N69-39213*# NASA-SP-197
c03 N69-39238*# E-5130
NASA-TM-X-1869
c26 N69-39239*# E-5032
NASA-TN-D-5488
c07 N69-39264*# C-78
NASA-TR-R-320
c07 N69-39282*# NASA-CR-1442
c25 N69-39302*# L-6679
NASA-TN-D-5500
c12 N69-39303*# E-5190
NASA-TM-X-1900
c03 N69-39335*# E-5182
NASA-TM-X-1901
c30 N69-39336*# M-146
NASA-TR-R-322
c32 N69-39393*# E-4950
NASA-TN-D-5489
c20 N69-39526*# NASA-SP-212
c12 N69-39916*# E-5106
NASA-TN-D-5501
c34 N69-39957*# NASA-SP-211
c01 N69-40026*# NASA-TN-D-5499
c17 N69-40053*# NASA-TN-D-5504
c21 N69-40055*# NASA-TN-D-5495
c26 N69-40056*# NASA-TN-D-5505
c17 N69-40057*# NASA-CR-1447
c28 N69-40058*# NASA-TM-X-1908
c14 N69-40059*# NASA-TM-X-1904
c22 N69-40060*# NASA-TM-X-1907
c22 N69-40061*# NASA-TM-X-1911
c30 N69-40062*# NASA-CR-1449
c28 N69-40078*# NASA-TN-D-5506
c09 N69-40079*# NASA-TN-D-5509
c28 N69-40080*# NASA-TN-D-5436
c32 N69-40087*# NASA-TN-D-5508
c19 N69-40088*# NASA-TN-D-5511
c07 N69-40099*# NASA-TN-D-5494
c12 N69-40137*# NASA-TN-D-5496
c12 N69-40200*# NASA-CR-1448
NEAR-TR-14
c06 N69-40240*# NASA-TN-D-5503
c17 N69-40242*# NASA-TN-D-5510
c31 N69-40269*# NASA-SP-8017
c04 N69-40324*# NASA-TT-F-525
c30 N69-40325*# NASA-CR-1360
c30 N69-40326*# NASA-SP-8013
c28 N69-40329*# NASA-TN-D-5519
c18 N69-40339*# NASA-TM-X-1905
c01 N69-40345*# NASA-TN-D-5514
c33 N69-40356*# NASA-TN-D-5480
c32 N69-40359*# NASA-CR-1441
c33 N69-40437*# NASA-TN-D-5522
c02 N69-40439*# NASA-CR-1472
c03 N69-40440*# NASA-TM-X-1912
c33 N69-40455*# NASA-CR-1431
c30 N69-40592*# NASA-TT-F-554
c28 N69-40776*# BAC-2099-956005
NASA-CR-1445
c33 N69-40780*# NASA-TN-D-5526
c31 N69-40781*# NASA-TN-D-5435
c03 N69-40787*# NASA-TM-X-1913
c33 N69-40789*# NASA-TN-D-5520
c14 N69-40812*# NASA-TN-D-5515
c31 N69-40813*# NASA-TN-D-5471
c12 N69-40824*# NASA-TT-F-585
c01 N69-40876*# NASA-TN-D-5481
c13 N69-40893*# NASA-TN-D-5400
c13 N69-40924*# NASA-TN-D-5447
c32 N69-40935*# NASA-CR-1437
c02 N69-40937*# L-6695
NASA-TN-D-5538
c04 N69-40955*# NASA-CR-1372
c24 N69-40979*# NASA-TN-D-5530

c21 N69-41036*# NASA-CR-1450
SUDAAR-374
c32 N69-41141*# L-6019
NASA-TN-D-5536
c30 N69-41150*# NASA-SP-213
c09 N69-41208*# NASA-TN-D-5490
c15 N69-41210*# NASA-TN-D-5527
c12 N69-41213*# E-5163
NASA-TN-D-5531
c32 N69-41229*# NASA-TN-D-5455

☆ U. S. GOVERNMENT PRINTING OFFICE : 1970 O - 384-822

PUBLIC COLLECTIONS OF NASA DOCUMENTS

DOMESTIC

NASA deposits its technical documents and bibliographic tools in eleven Federal Regional Technical Report Centers located in the organizations listed below. Each center is prepared to furnish the public such services as reference assistance, interlibrary loans, photocopy service, and assistance in obtaining copies of NASA documents for retention.

CALIFORNIA
University of California, Berkeley

COLORADO
University of Colorado, Boulder

DISTRICT OF COLUMBIA
Library of Congress

GEORGIA
Georgia Institute of Technology, Atlanta

ILLINOIS
The John Crerar Library, Chicago

MASSACHUSETTS
Massachusetts Institute of Technology, Cambridge

MISSOURI
Linda Hall Library, Kansas City

NEW YORK
Columbia University, New York

PENNSYLVANIA
Carnegie Library of Pittsburgh

TEXAS
Southern Methodist University, Dallas

WASHINGTON
University of Washington, Seattle

NASA publications (those indicated by an "*" following the accession number) are also received by the following public and free libraries:

CALIFORNIA
Los Angeles Public Library
San Diego Public Library

COLORADO
Denver Public Library

CONNECTICUT
Hartford Public Library

DELAWARE
Wilmington Institute Free Library, Wilmington

MARYLAND
Enoch Pratt Free Library, Baltimore

MASSACHUSETTS
Boston Public Library

MICHIGAN
Detroit Public Library

MINNESOTA
Minneapolis Public Library
James Jerome Hill Reference Library, St. Paul

MISSOURI
Kansas City Public Library
St. Louis Public Library

NEW JERSEY
Trenton Public Library

NEW YORK
Brooklyn Public Library
Buffalo and Erie County Public Library
Rochester Public Library
New York Public Library

OHIO
Akron Public Library
Cincinnati Public Library
Cleveland Public Library
Dayton Public Library
Toledo Public Library

OKLAHOMA
Oklahoma County Libraries, Oklahoma City

TENNESSEE
Cossitt-Goodwin Libraries, Memphis

TEXAS
Dallas Public Library
Fort Worth Public Library

WASHINGTON
Seattle Public Library

WISCONSIN
Milwaukee Public Library

An extensive collection of NASA and NASA-sponsored documents and aerospace publications available to the public for reference purposes is maintained by the American Institute of Aeronautics and Astronautics, Technical Information Service, 750 Third Avenue, New York, New York, 10017.

EUROPEAN

An extensive collection of NASA and NASA-sponsored publications is maintained by the National Lending Library for Science and Technology, Boston Spa, Yorkshire, England. By virtue of arrangements other than with NASA, the National Lending Library also has available many of the non-NASA publications cited in *STAR*. European requesters may purchase facsimile copy or microfiche of NASA and NASA-sponsored documents, those identified by both the symbols "#" and "*", from: ESRO/ELDO Space Documentation Service, European Space Research Organization, 114, av de Neuilly, 92-Neuilly-sur-Seine, France.

NATIONAL AERONAUTICS AND SPACE ADMINISTRATION
WASHINGTON, D.C. 20546

OFFICIAL BUSINESS

FIRST CLASS MAIL

POSTAGE AND FEES PAID
NATIONAL AERONAUTICS AND
SPACE ADMINISTRATION

POSTMASTER: If Undeliverable (Section 158 Postal Manual) Do Not Return

"The aeronautical and space activities of the United States shall be conducted so as to contribute . . . to the expansion of human knowledge of phenomena in the atmosphere and space. The Administration shall provide for the widest practicable and appropriate dissemination of information concerning its activities and the results thereof."

—NATIONAL AERONAUTICS AND SPACE ACT OF 1958

NASA SCIENTIFIC AND TECHNICAL PUBLICATIONS

TECHNICAL REPORTS: Scientific and technical information considered important, complete, and a lasting contribution to existing knowledge.

TECHNICAL NOTES: Information less broad in scope but nevertheless of importance as a contribution to existing knowledge.

TECHNICAL MEMORANDUMS: Information receiving limited distribution because of preliminary data, security classification, or other reasons.

CONTRACTOR REPORTS: Scientific and technical information generated under a NASA contract or grant and considered an important contribution to existing knowledge.

TECHNICAL TRANSLATIONS: Information published in a foreign language considered to merit NASA distribution in English.

SPECIAL PUBLICATIONS: Information derived from or of value to NASA activities. Publications include conference proceedings, monographs, data compilations, handbooks, sourcebooks, and special bibliographies.

TECHNOLOGY UTILIZATION PUBLICATIONS: Information on technology used by NASA that may be of particular interest in commercial and other non-aerospace applications. Publications include Tech Briefs, Technology Utilization Reports, and Technology Surveys.

Details on the availability of these publications may be obtained from:

SCIENTIFIC AND TECHNICAL INFORMATION DIVISION

NATIONAL AERONAUTICS AND SPACE ADMINISTRATION

Washington, D.C. 20546